Natriuretic Peptides and their Receptors

Lincoln R. Potter
University of Minnesota, Minneapolis, Minnesota, USA

Natriuretic peptides are an ancient family of hormones/paracrine factors that regulate blood pressure, cardiovascular homeostasis, and bone growth. The mammalian family consists of atrial natriuretic peptide, brain natriuretic peptide, and C-type natriuretic peptide. All three peptides are derived from separate genes, but share a common 17-amino-acid disulfide ring that is required for biological activity. A family of three cell surface receptors mediates their cellular effects: two are receptor guanylyl cyclases, enzymes that catalyze the synthesis of the intracellular second messenger, cGMP, whereas one is a decoy receptor that lacks enzymatic activity. In this article, the structure, function, and regulation of each hormone and receptor are discussed.

Natriuretic Peptides

Atrial Natriuretic Peptide

The first natriuretic peptide to be identified was atrial natriuretic peptide (ANP), which was originally called atrial natriuretic factor (ANF) because of its unknown structure. It was discovered by de Bold and co-workers in 1981. They found that intravenous infusion of atrial, but not ventricular, homogenates into rats caused a rapid and dramatic increase in renal sodium and water excretion that was accompanied by reduced blood pressure. Subsequently, a smooth muscle relaxing activity was shown to cofractionate with the natriuretic activity. The peptide responsible for both blood pressure lowering properties was purified and sequenced from multiple species by several laboratories. The structure of the polypeptide precursor of the mature peptide was derived from cDNA sequence, which like the peptide sequence was obtained from a number of different species by several different laboratories.

All natriuretic peptides are synthesized as preprohormones. Human preproANP is 151 amino acids in length. Proteolytic removal of the amino-terminal signal sequence yields a 126 residue proANP peptide, which is the predominant storage form found in dense atrial granules. Upon secretion, proANP is cleaved by corin, a transmembrane serine protease, to a 98 residue amino-terminal peptide and a 28 residue carboxyl-terminal peptide. Both fragments circulate in the plasma and are elevated under conditions where vascular volume is increased, such as congestive heart failure. The carboxyl terminal 28 amino-acid peptide is the mature biologically active form of ANP that mediates the known biological effects associated with the ANP gene (Figure 1).

The majority of ANP gene expression occurs in the cardiac atria, but there is low-level expression in extra-atrial tissues, e.g., central nervous system, adrenal gland, kidney, and ventricles. Expression in the latter tissue is generally only observed in early life or during ventricular hypertrophy. Hence, ANP mRNA expression has become a universal marker for ventricular remodeling that results from prolonged hypertension or other forms of cardiovascular insult. Differential processing of ANP in the kidney produces a variant containing four additional amino-terminal amino acids called urodilatin. It has been reported to be more potent than ANP, possibly because it is less sensitive to proteolytic degradation by neutral endopeptidases (NEPs). Atrial-wall stretch, reflecting increased intravascular volume, is the dominant stimulus for ANP release. However, several hormones and neurotransmitters – such as endothelin, arginine vasopressin, and catecholamines – also stimulate its secretion.

In addition to stimulating natriuresis, diuresis, and vasorelaxation, ANP also inhibits renin, vasopressin, and aldosterone release. It decreases cell proliferation and hypertrophy as well. Hence, ANP's short-term (natriuresis, diuresis, vasorelaxation) and long-term (antimitogenesis) effects are generally considered beneficial.

Transgenic mice exhibiting lifelong elevated plasma ANP levels display reduced blood pressure and heart size. In contrast, mice lacking ANP are hypertensive. The initial report describing these animals suggested that ANP regulates blood pressure in a salt-sensitive manner, but a subsequent communication indicated that these same mice were also hypertensive when fed a very low

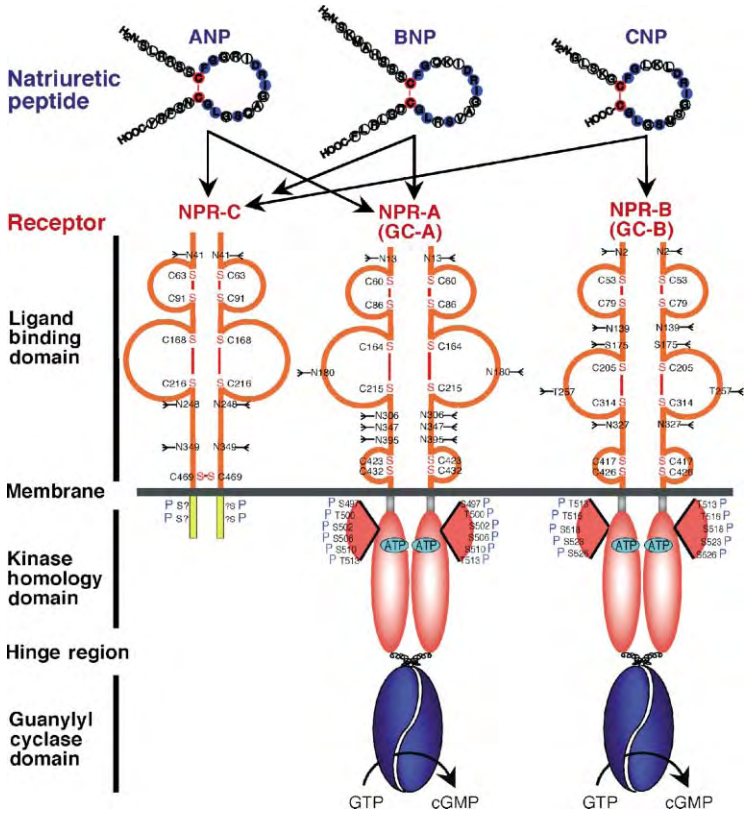

FIGURE 1 Schematic representation of natriuretic peptides and their receptors. Black arrows indicate which receptors each natriuretic peptide binds. Note that each peptide can bind more than one receptor. Blue circles in natriuretic peptide structures indicate conserved residues. Red lines indicate disulfide bonds. Black branched lines indicate N-linked glycosylation sites. Blue Ps indicate phosphorylation sites. ANP, atrial natriuretic peptide; BNP, brain natriuretic peptide; CNP, C-type natriuretic peptide; cGMP, cyclic guanosine monophosphate; GC-A, guanylyl cyclase A; GC-B, guanylyl cyclase B; GTP, guanosine triphosphate; NPR-A, natriuretic peptide receptor A; NPR-B, natriuretic peptide receptor B; NPR-C, natriuretic peptide receptor C.

salt diet (0.008% NaCl), consistent with ANP mediating its effects independently of body sodium chloride levels.

ANP is degraded outside and inside the cell by extracellular proteases and NPR-C-dependent internalization and degradation, respectively. The extracellular NEP 24.11 is a metallopeptidase that degrades all three natriuretic peptides. Recently, compounds have been developed that inhibit both angiotensin converting enzyme (ACE) and NEP. Omapatrilat, the most studied of these so-called vasopeptidase inhibitors, has the combined benefit of prolonging the blood pressure decreasing effects of natriuretic peptides while inhibiting the blood pressure increasing effects of the angiotensin system. Although early indications from clinical trials suggested that these drugs are beneficial to some patients with hypertension and/or congestive heart failure, very recent studies indicate that patients receiving vasopeptidase inhibitors experience more angioedema than patients treated with ACE inhibitors. Therefore, further development is needed before vasopeptidase inhibitors are viable alternatives to current therapies.

Brain Natriuretic Peptide

Although brain natriuretic peptide (BNP) was originally isolated from porcine brain, it was subsequently found to be more abundant in cardiac ventricles. Of all the natriuretic peptides, the amino-acid sequence of BNP varies most among species. For instance, in human, pig, and rat, mature BNP is 32, 26, and 45 amino acids in length, respectively.

Human BNP cDNA encodes a 132 amino-acid preprohormone that is processed to a 105-residue prohormone by removal of the signal peptide. Both corin and the endopeptidase, furin, have been shown to cleave the prohormone into the 32 amino-acid mature peptide. In the myocyte, BNP mRNA levels are regulated transcriptionally and posttranscriptionally in response to increased ventricular filling pressures or mechanical stretch. BNP is functionally similar to ANP

with respect to its vasorelaxant, natriuretic, and diuretic properties, but normal plasma BNP levels are only one-seventeenth of ANP levels. In contrast to ANP, ventricular BNP is not stored in secretory granules, instead it is released in a constitutive fashion following synthesis. Transgenic mice overexpressing BNP exhibited reduced blood pressure and cardiac weight accompanied by an elevation of plasma cGMP concentrations. They also exhibit increased long bone growth that most likely results from cross-activation of NPR-B. BNP null mice have normal blood pressures, but display pressure-sensitive cardiac fibrosis, proliferation of interstitial fibroblasts, and elevated ventricular extracellular matrix proteins. Hence, BNP's main function may be to regulate the cardiac ventricles.

BNP release is directly proportional to ventricular volume expansion and pressure overload. Although ANP is elevated in patients with congestive heart failure, BNP levels correlate more closely with left ventricular pressure, amount of dyspnea, and the state of neurohormonal modulation. Therefore, BNP, more than ANP, is an excellent indicator of heart failure. A rapid, whole-blood BNP assay (Triage BNP Test, Biosite Inc., San Diego, CA) that allows quick evaluation of patient plasma BNP levels was recently approved by the US Food and Drug Administration. Normal human plasma levels of BNP are <40 pg ml^{-1} and levels greater than 100 pg ml^{-1} are highly correlated with congestive heart failure. The high negative predictive value of this measurement suggests that it may be extremely useful in ruling out cardiac abnormalities in patients with dyspnea.

Recombinant B-type natriuretic peptide, whose clinical and trade names are Nesiritide and Natrecor, respectively, mimics the actions of endogenous BNP. It has been studied in more than 1700 patients with acute decompensated heart failure and has been shown to cause potent, dose-related vasodilation that is rapid in onset and sustained for the duration of drug infusion. It was approved for the treatment of acute decompensated congestive heart failure by the Food and Drug Administration in 2001.

C-Type Natriuretic Peptide

Like BNP, C-type natriuretic peptide (CNP) was first isolated from porcine brain. It is the most highly expressed natriuretic peptide in this tissue. Similarly in cerebrospinal fluid, CNP is $\sim$2 pM, which is about tenfold higher than ANP or BNP. BNP is also found at high concentrations in cytokine-treated endothelial cells and bone tissue. Because it is barely detectable in plasma, CNP is expected to signal primarily in a paracrine manner.

The primary structure of CNP is similar to ANP and BNP, but it lacks a C-terminal tail (Figure 1). It has higher amino-acid identity between species than ANP and BNP. For example, the structures of CNP from humans, pigs, and rats are identical. The 103 amino acid CNP propeptide is processed to either 53 or 22 amino acid forms. Furin, but not corin, has been suggested to mediate this final cleavage step. Both the 53 and 22 amino acid forms have been identified *in vivo* and the 22-amino-acid peptide predominates in the central nervous system, anterior pituitary, kidney, vascular endothelial cells, and plasma. Unlike ANP, CNP is not stored in granules. Instead, it is regulated at the level of transcription by various signaling molecules, such as transforming growth factor-β, tumor necrosis factor-α, and shear stress.

CNP relaxes vascular smooth muscle and is a more potent dilator of veins than ANP or BNP. It is not a potent inducer of diuresis and natriuresis. Like ANP, CNP has been shown to inhibit the proliferation of various cultured cell lines. A potential clinical benefit of this antimitogenic property was demonstrated in a rodent model when CNP treatment was shown to dramatically inhibit the normal vascular intimal thickening that accompanies balloon angioplasty.

Homozygous deletion of the gene-encoding CNP in mice caused more than half of the offspring to die during postnatal development. Surviving animals exhibited shortened body length and defects in endochondral bone development, which is analogous to human dwarfism. Importantly, cGMP-dependent protein kinase II (PKGII) knockout mice also develop dwarfism as a result of impaired endochondral ossification, suggesting that PKGII mediates the CNP-dependent skeletal effects. Consistent with a linear CNP/cGMP/PKGII pathway, the targeted expression of CNP in growth plate chondrocytes cannot increase the longitudinal bone growth or chondrocytic proliferation and hypertrophy in PKGII knockout mice.

Natriuretic Peptide Receptors

There are three known natriuretic peptide receptors. Natriuretic peptide receptor A (NPR-A) (also known as guanylyl cyclase A (GC-A)) and natriuretic peptide receptor B (NPR-B) (also known as guanylyl cyclase B (GC-B)) are receptor guanylyl cyclases, whereas the natriuretic peptide clearance receptor (NPR-C) does not possess any known enzymatic activity. Instead, NPR-C controls the local concentration of natriuretic peptides that are available to bind NPR-A and NPR-B through receptor-mediated internalization and degradation.

Guanylyl Cyclase-Linked Natriuretic Peptide Receptors

The ligand selectivity for NPR-A is ANP > BNP ≫ CNP, whereas the ligand selectivity for NPR-B is CNP ≫ ANP > BNP. Mice lacking NPR-A are hypertensive and develop cardiac hypertrophy and ventricular fibrosis. In addition, they are completely unresponsive to the renal and vasorelaxing effects of ANP and BNP, consistent with NPR-A being the sole signaling receptor for these peptides. A promoter mutation resulting in reduced transcription of the human NPR-A gene was recently identified and shown to be highly correlated with essential hypertension or ventricular hypertrophy.

Both NPR-A and NPR-B consist of an ~450-amino-acid extracellular ligand-binding domain, a 21-residue hydrophobic membrane-spanning region, and a 566- or 568-amino-acid intracellular domain, respectively (Figure 1). The latter can be divided into a ~250-amino-acid kinase homology domain (KHD), a 41-amino-acid hinge-dimerization region, and a 250-amino-acid C-terminal guanylyl cyclase catalytic domain. Like adenylyl cyclases and soluble guanylyl cyclases, a dimer is believed to be the minimal catalytic unit for both NPR-A and NPR-B.

The NPR-A extracellular domain contains three intramolecular but no intermolecular disulfide bonds (Figure 1). Similar Cys are conserved in the extracellular domain of NPR-B. Both NPR-A and NPR-B are highly glycosylated, and several studies suggest that glycosylation is required for proper receptor folding and/or transport of the receptor to the cell surface, but is not required for hormone binding. The crystal structure of the glycosylated, unliganded, dimerized hormone-binding domain of NPR-A has been solved at 2.0Å resolution. It reveals that the monomer consists of two interconnected subdomains, each encompassing a central β-sheet flanked by α-helices and the dimerization results from juxtaposition of 2×2 parallel helices that bring the two protruding C termini in close proximity. The crystal structure of an ANP–NPR-A complex has not been solved.

Activation of the guanylyl-cyclase-linked natriuretic peptide receptors is incompletely understood. Both receptors are homooligomers in the absence and presence of their respective ligands, indicating that receptor activation does not simply result from ligand-dependent dimerization. However, ANP binding does cause a conformational change in NPR-A that brings the extracellular juxtamembrane regions of each monomer closer together. In addition to natriuretic peptides, ATP is also required to maximally activate these receptors in broken cell preparations. Since receptors lacking the kinase homology domain are constitutively active and are not further stimulated by ATP, it has been suggested that the ATP binding to the kinase homology domain may relieve the basal repression of the guanylyl cyclase domain. No direct binding data have been presented to confirm this hypothesis, but ATP has been shown to modulate ANP binding and cyclase activity in purified receptor preparations, which is consistent with a direct binding model. On the other hand, the ATP effect observed with purified preparations is significantly less than that seen in crude membranes, which is consistent with a hypothesis where membranes contain an ATP-binding factor that is only partially removed during the purification procedure.

In the resting state, both NPR-A and NPR-B are highly phosphorylated on serines and threonines within their KHD domains. NPR-A isolated from resting 293 cells is phosphorylated on Ser497, Thr500, Ser502, Ser506, Ser510, and Thr513, which are located within a 17-residue stretch that contains the glycine-rich elbow and putative ATP-binding region of its KHD. Mutation of any of these phosphorylated residues to alanine in order to mimic a dephosphorylated serine or threonine results in decreased ANP-dependent guanylyl cyclase activities. Furthermore, receptors containing alanine substitutions at four or more phosphorylation sites are completely unresponsive to hormone. NPR-B is phosphorylated on Thr513, Thr51, Ser518, Ser523, and Ser526 in a similar region of its KHD. Four of these five sites are conserved between NPR-A and NPR-B. Phosphorylation of NPR-B is also required for ligand-dependent activation.

With respect to the mechanism by which an activated receptor is turned off, a process commonly referred to as desensitization, a number of theories have been put forth. Initial *in vitro* data suggested that direct phosphorylation of NPR-A by protein kinase C mediated its desensitization, but subsequent studies conducted in live cells indicated that desensitization in response to chronic natriuretic peptide exposure (homologous desensitization) or activators of protein kinase C results in the loss of phosphate from NPR-A and NPR-B. The role of phosphorylation/dephosphorylation in the regulation of these receptors was later clarified when mutations that mimic phosphorylated or dephosphorylated receptors were shown to be active or inactive, respectively. These experiments revealed for the first time a clear positive correlation between the phosphorylation state and enzymatic activity of NPR-A and NPR-B.

In contrast to the protein phosphorylation, the role of ligand-dependent internalization and degradation of NPR-A is unclear. Pandey and co-workers have reported many times that NPR-A undergoes this process, whereas Maack and co-workers contend that NPR-A is a constitutively membrane resident protein that is not internalized.

The Natriuretic Peptide Clearance Receptor

In addition to NPR-A and NPR-B, all three natriuretic peptides bind to a third receptor called the natriuretic peptide clearance receptor (NPR-C). NPR-C migrates as a 60 and 120 kDa protein when fractionated by reducing or nonreducing SDS-PAGE, respectively. It is found on the cell surface as a disulfide-linked homodimer. NPR-C has a large amino-terminal extracellular ligand-binding domain, a single transmembrane domain, and an intracellular domain that contains only 37 amino acids and possesses no known enzymatic activity (Figure 1). It binds ANP, BNP, and CNP with similar affinities, but it can also bind tightly to several smaller carboxyl-terminal and ring-deleted peptide analogues that do not bind well to NPR-A or NPR-B. C-ANF, the prototypical form of these peptides, is sometimes used to distinguish NPR-C from NPR-A in both binding and cGMP stimulation assays. The crystal structure of both the apo form and CNP bound form of NPR-C has been determined. In contrast to the 2:2 stoichiometry that was suggested for the ANP–NPR-A complex, the stoichiometry of binding of CNP to NPR-C was determined to be 1:2.

NPR-C is the most abundant natriuretic peptide receptor on the cell surface, and its primary function is to remove natriuretic peptides from the circulation via receptor mediated internalization and degradation, thereby controlling the local concentrations of the natriuretic peptides that are available to bind NPR-A and NPR-B. Like many nutrient receptors, NPR-C internalization is constitutive, i.e., it is not increased by natriuretic peptide binding. In addition to its clearance role, NPR-C has also been implicated in signaling, possibly in a G-protein-dependent manner. However, mice lacking NPR-C displayed a reduced ability to clear ^{125}I-ANP from the circulation, but no reduction in known signaling functions. In fact, pathways activated by NPR-A and NPR-B, blood pressure, and bone growth, respectively, are increased in these animals. Nonetheless, it remains possible that NPR-C may signal as yet unidentified processes.

See Also the Following Articles

Aminopeptidases • Calcium/Calmodulin-Dependent Protein Kinase II • Metalloproteases • Protein Kinase C Family • Vasopressin/Oxytocin Receptor Family

Glossary

cyclic GMP A cyclic mononucleotide of guanosine that acts as an intracellular second messenger for hormones, such as natriuretic peptides, guanylin, and nitric oxide.

guanylyl cyclase An enzyme that catalyzes the synthesis of cyclic GMP and pyrophosphate from guanosine triphosphate.

natriuresis Urinary sodium excretion.

protein phosphorylation Covalent addition of a phosphate molecule to the side chain of an amino acid, usually serine, threonine, or tyrosine in mammalian cells.

Further Reading

Levin, E. R., Gardner, D. G., and Samson, W. K. (1998). Natriuretic peptides. *N. Engl. J. Med.* **339**, 321–328.

Potter, L. R., and Hunter, T. (2001). Guanylyl cyclase-linked natriuretic peptide receptors: Structure and function. *J. Biol. Chem.* **276**, 6057–6060.

Schreiner, G. F., and Protter, A. A. (2002). B-type natriuretic peptide for the treatment of congestive heart failure. *Curr. Opin. Pharmacol.* **2**, 142–147.

Biography

Lincoln Potter earned his B.S. in biology/chemistry from David Lipscomb University in Nashville. He received his Ph.D. under the direction of David Garbers from Vanderbilt University in 1994 and then conducted postdoctoral studies with Tony Hunter at the Salk Institute in San Diego. In the fall of 1999, he joined the Department of Biochemistry, Molecular Biology and Biophysics at the University of Minnesota as a tenure-track assistant professor, which is his current position.

N-End Rule

Alexander Varshavsky
California Institute of Technology, Pasadena, California, USA

The N-end rule relates the *in vivo* half-life of a protein to the identity of its N-terminal residue The N-end rule stems from the activity of a universally present proteolytic pathway called the N-end rule pathway.

Proteolysis

Proteolysis, or protein degradation, is a set of processes that result in the hydrolysis of one or more of the peptide bonds in a protein. Proteolysis is a part of protein turnover, in which the molecules of specific proteins are first made through ribosome-mediated translation, and are eventually destroyed, in ways and at rates that are specific for the protein in question and depend on the state of an organism. The *in vivo* half-lives of intracellular proteins vary from a few seconds to many days. Two major functions of intracellular proteolysis are the selective destruction of damaged or otherwise abnormal proteins, and the regulated destruction of normal proteins whose concentrations must vary depending on the cell's state. Metabolic instability (a short *in vivo* half-life) is a property of many regulatory proteins. These proteins evolved not only to carry out their primary functions, for example, those of a phosphokinase or a repressor of transcription, but also to be rapidly destroyed *in vivo*. A short half-life of a regulator provides a way to generate its spatial gradients and allows for rapid adjustments of its concentration through changes in the rate of its synthesis. A protein can also be conditionally unstable, i.e., long-lived or short-lived depending on the state of molecular circuit of which the protein is a part. This fact, and also a faster (in general) destruction of the newly formed molecules of a protein in comparison to older, conformationally mature molecules of the same protein result in complex degradation kinetics, so that a single "half-life" of specific protein is at best an approximation of its actual decay curve *in vivo* (Figure 1).

The Ubiquitin System

A major set of pathways that target and destroy specific intracellular proteins is the ubiquitin (Ub) system, also called the Ub-proteasome system. In eukaryotes, the N-end rule pathway (Figure 2) is one pathway of the Ub system. Ub, a highly conserved 76-residue protein, is conjugated to ε-amino groups of lysine residues of other proteins (including other Ub molecules) through the action of three enzymes, E1, E2, and E3. The selectivity of ubiquitylation is determined by E3, which recognizes a substrate's degradation signal (degron). The term "Ub ligase" denotes either an E2–E3 complex or its E3 component. A ubiquitylated protein substrate bears a covalently attached poly-Ub chain, which mediates the binding of substrate to the 26S proteasome, an ATP-dependent protease that processively destroys the bound protein, yielding short peptides. The rate of degradation of specific proteins is regulated through modulation of the structure or steric exposure of their degrons, and also through the control of activity of Ub ligases. Physiological functions of the Ub system encompass enormous range: the regulation of cell differentiation, cell cycle, embryogenesis, apoptosis, signal transduction, DNA transcription, replication, repair and recombination, transmembrane and vesicular transport, stress responses (including the immune response), functions of the nervous system, and many other processes.

The N-End Rule Pathway

The multiple proteolytic pathways of the Ub system have in common their dependence on Ub conjugation and the proteasome, and differ largely through their utilization of distinct E2–E3 complexes. The Ub ligase of the N-end rule pathway targets proteins bearing specific (destabilizing) N-terminal residues (Figure 2). The corresponding degron, called the N-degron, consists of a substrate's destabilizing N-terminal residue and an internal lysine residue, the latter being the site of formation of a substrate-linked poly-Ub chain. Because an N-degron must be produced through a proteolytic cleavage that yields a destabilizing N-terminal residue, a nascent N-end rule substrate contains a cryptic N-degron, called pro-N-degron. In the yeast *Saccharomyces cerevisiae*, the two substrate-binding

Residue X	Half life of X-βgal	
	E. coli	*S. cerevisiae*
Arg	2 min	2 min
Lys	2 min	3 min
Phe	2 min	3 min
Leu	2 min	3 min
Trp	2 min	3 min
Tyr	2 min	10 min
His	> 10 h	3 min
Ile	> 10 h	30 min
Asp	> 10 h	3 min
Glu	> 10 h	30 min
Asn	> 10 h	3 min
Gln	> 10 h	10 min
Cys	> 10 h	> 30 h
Ala	> 10 h	> 30 h
Ser	> 10 h	> 30 h
Thr	> 10 h	> 30 h
Gly	> 10 h	> 30 h
Val	> 10 h	> 30 h
Pro	> 10 h	> 30 h
Met	> 10 h	> 30 h

FIGURE 1 The N-end rules of the prokaryote *E. coli* and the eukaryote (yeast) *S. cerevisiae*. Approximate *in vivo* half-lives of X-β-galactosidase (X-βgal) test proteins in *E. coli* at 36°C and in *S. cerevisiae* at 30°C. The N-end rule pathway is Ub-dependent in eukaryotes, and is also present in prokaryotes, which lack the Ub system.

sites of the 225-kDa Ub ligase UBR1 recognize (bind to) primary destabilizing N-terminal residues of two types: basic (type 1: Arg, Lys, His) and bulky hydrophobic (type 2: Phe, Trp, Leu, Tyr, Ile) (Figure 2B). Several other N-terminal residues function as tertiary (Asn, Gln) and secondary (Asp, Glu) destabilizing residues, in that they are recognized by UBR1 only after their enzymatic conjugation to Arg, a primary destabilizing residue (Figure 2). In the case of N-terminal Asn and Gln, the conjugation of Arg is preceded by enzymatic deamidation, to yield N-terminal Asp and Glu. In animals (but not in fungi such as *S. cerevisiae*), N-terminal Cys is yet another tertiary destabilizing residue, in that the arginylation of Cys is preceded by its oxidation. These covalent modification/conjugation reactions of N-terminal residues are required for the "downstream" step of Ub conjugation to N-end rule substrates that bear N-terminal Asn, Gln, Asp, Glu, or Cys (Figure 2A).

The UBR1 Ub ligase of the N-end rule pathway contains yet another, third substrate-binding site that recognizes a specific internal (non-N-terminal) degron in pathway's substrates. The only physiological substrate of this class that had been identified thus far is the 35-kDa homeodomain transcriptional repressor CUP9 of *S. cerevisiae*. Among the genes repressed by CUP9 is *PTR2*, which encodes a di- and tripeptide transporter. CUP9 is a short-lived protein targeted by the N-end rule pathway through an internal degron near the C terminus of CUP9. Dipeptides with destabilizing N-terminal residues allosterically activate UBR1, leading to accelerated *in vivo* degradation of CUP9 and the resulting induction of PTR2 expression (Figure 3). Through this positive feedback, *S. cerevisiae* can sense the presence of extracellular peptides and react by accelerating their uptake. Thus, the type 1 and type 2 sites of UBR1 function not only as substrate-binding sites, but also as nutritional sensors, making possible the adaptive regulation of peptide import (Figure 3). The mechanism of activation by dipeptides involves a conformational transition in UBR1, induced by the binding of dipeptides, that exposes the previously inactive (sterically inaccessible) CUP9-binding site of UBR1.

Another function of the *S. cerevisiae* N-end rule pathway is the maintenance of chromosome stability. At the metaphase–anaphase transition, the *ESP1*- encoded protease, called separase, cleaves SCC1, a subunit of cohesin complexes that hold together sister chromatids of replicated chromosomes. The resulting 33-kDa C-terminal fragment of SCC1 bears N-terminal Arg and is rapidly degraded by the N-end rule pathway. A failure to degrade this fragment of SCC1 in *ubr1*Δ cells (which lack the pathway's Ub ligase) results in a greatly increased frequency of chromosome loss, presumably because the retention of cohesin's fragment perturbs the assembly of intact cohesin complexes in subsequent cell cycles. Thus, the type 1 binding site of the UBR1 Ub ligase has a dual function of both a dipeptide-binding nutritional sensor (Figure 3) and a site that recognizes proteins with destabilizing N-terminal residues, targeting these proteins for Ub-dependent degradation.

Methionine aminopeptidases (MetAPs), the proteases that are specific for N-terminal Met (every nascent protein bears N-terminal Met), would remove this Met residue if, and only if, the second residue after Met is a stabilizing residue in the N-end rule. The only exceptions, in the mammalian N-end rule, are destabilizing residues Cys, Ala, Ser, and Thr (Figure 2A). Other destabilizing residues can be exposed at the N termini of proteins only through cleavage by proteases other than MetAPs. One such protease is separase, which cleaves the SCC1 subunit of cohesin, as stated before. A large class of proteases that can also produce, *in vivo*, a destabilizing residue at the N terminus of a protein are deubiquitylating enzymes (DUBs). One reaction catalyzed by these proteases is the cleavage of a linear Ub-X-polypeptide fusion at the Ub-X junction; this cotranslational cleavage can take place irrespective of the identity of a residue X at the junction, proline being a single exception. A method, called the Ub fusion technique, that takes advantage of

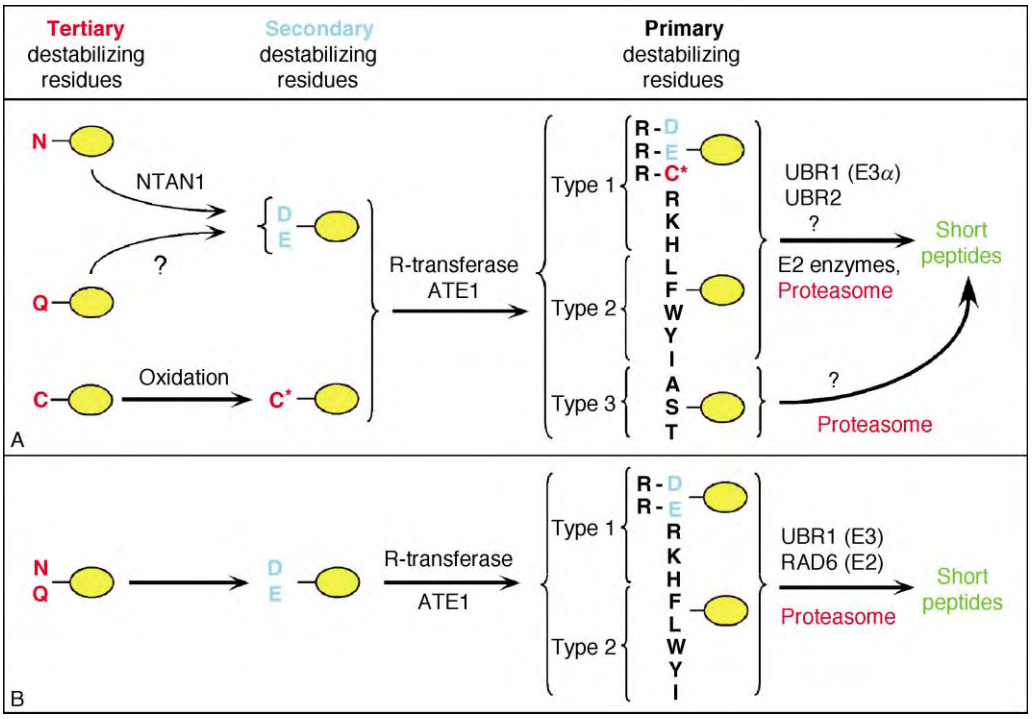

FIGURE 2 The N-end rule pathway in mammals (A) and the yeast *S. cerevisiae* (B). N-terminal residues are indicated by single-letter abbreviations. The ovals denote the rest of a protein substrate. In mammals (A), the Asn-specific N-terminal amidase NTAN1 converts N-terminal Asn into Asp. N-terminal Gln is deamidated by another (unidentified) amidase. N-terminal Asp, Glu, and Cys are conjugated to Arg by Arg-tRNA-protein transferases (R-transferases), encoded by the *ATE1* gene. N-terminal Cys is arginylated after its oxidation to either sulfinic or cysteic acid (A), a reaction that does not take place in yeast (B). The primary destabilizing N-terminal residues Arg, Lys, His (type 1 residues), as well as Phe, Leu, Trp, Tyr, and Ile (type 2 residues) are recognized in yeast (B) by the UBR1 E3, in a complex with the RAD6 E2 enzyme. In mammals (A), the same residues are recognized by UBR1 and UBR2, and by another Ub ligase that remains to be identified. In mammals but not in yeast, Ala (A), Ser (S), and Thr (T) are primary (type 3) destabilizing residues, recognized by a distinct Ub ligase that remains to be characterized.

this property of DUBs, has made it possible to produce different residues at the N termini of otherwise identical test proteins *in vivo*, and led, in 1986, to the discovery of the N-end rule.

Besides CUP9 and SCC1, several other proteins were also found to be substrates of the N-end rule pathway. These proteins include Sindbis virus RNA polymerase (and homologous polymerases of other alphaviruses), the integrase of the human immunodeficiency virus (HIV), a bacterial protein p60, which is secreted by *Listeria monocytogenes* into the cytosol of infected mammalian cells, the mammalian GTPase-activating proteins (GAP) RGS4 and RGS16, the *S. cerevisiae GPA1*-encoded Gα protein, and the encephalomyocarditis (EMC) virus 3C protease. Physiological functions, if any, of the degradation of these proteins by the N-end rule pathway are either unknown or have not been established definitively.

The N-end rule pathway of multicellular eukaryotes is organized similarly to that in *S. cerevisiae*, with several additional features. Among them is the presence of at least three functionally overlapping Ub ligases that target pathway's substrates, in contrast to a single such ligase, UBR1, in *S. cerevisiae* (Figure 2). Molecular genetic analyses in the mouse have demonstrated, through the deletion of *ATE1*, which encodes Arg-tRNA-protein transferases (R-transferases), that the arginylation branch of the mammalian N-end rule pathway (Figure 2A) is essential for cardiovascular development. It was also discovered that the mammalian N-end rule pathway is essential for meiosis in spermatocytes: in the absence of UBR2 (one of the pathway's Ub ligases), spermatocytes fail to form synaptonemal complexes and die, rendering the male *UBR2* $^{-/-}$ mice infertile. The corresponding molecular circuits, as well as physiological N-end rule substrates whose metabolic stabilization causes the cardiovascular and meiotic phenotypes in these mutants are unknown. Yet another function of the N-end rule pathway is regulation of apoptosis (programmed cell death) in the fruit fly *Drosophila melanogaster*. Specifically, the activated caspases (specific proteases that mediate apoptosis) cleave DIAP1, the inhibitor of apoptosis, producing a large C-terminal fragment of DIAP1 that bears Asn, a tertiary destabilizing residue in the N-end rule (Figure 2A). The degradation of this fragment by the N-end rule pathway down-regulates

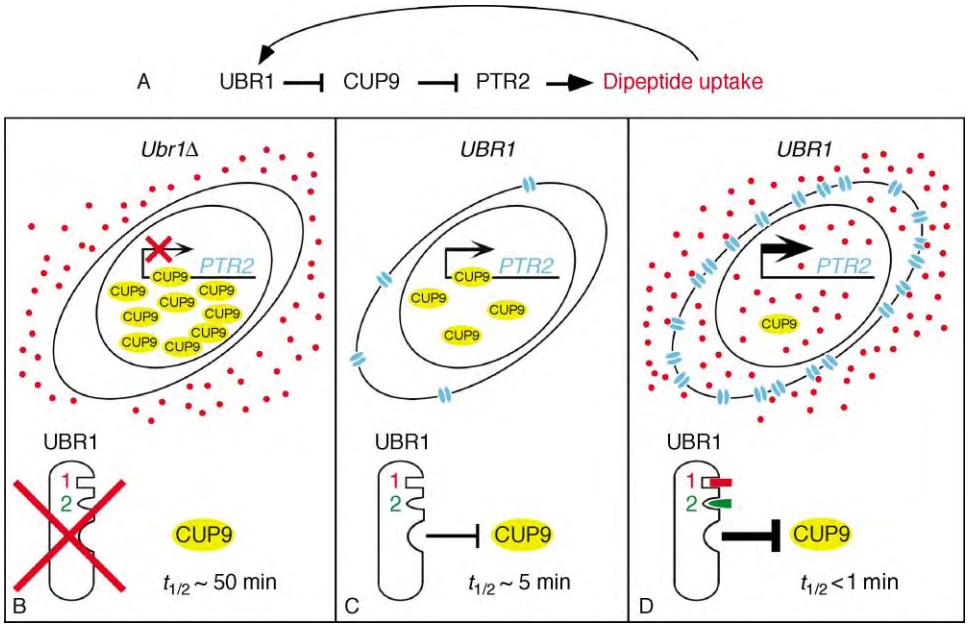

FIGURE 3 Ubiquitin-dependent activation of peptide import in *S. cerevisiae*. (A) Genetic diagram of the peptide transport circuit. (B) UBR1 is required for dipeptide uptake. In the absence of UBR1 (*ubr1*Δ), the transcriptional repressor CUP9 is long-lived, accumulates to high levels, and extinguishes the expression of peptide transporter, encoded by *PTR2*. *ubr1*Δ cells cannot import dipeptides (small dots). (C) In a *UBR1* cell growing in the absence of extracellular dipeptides, UBR1 targets CUP9 for degradation ($t_{1/2}$ ~ 5 min), resulting in a lower steady-state concentration of CUP9 and weak but significant expression of the PTR2 transporter (double ovals). (D) In *UBR1* cells growing in the presence of extracellular dipeptides some of which bear destabilizing N-terminal residues, the imported dipeptides bind to the basic (type 1) or hydrophobic (type 2) residue-binding sites of UBR1. These peptides are denoted as a rectangle and a wedge, respectively. Binding of either type of dipeptide to UBR1 allosterically increases the rate of UBR1-mediated degradation of CUP9. The resulting decrease of the half-life of CUP9 from ~5 min to less than 1 min leads to a further decrease in CUP9 levels, and consequently to a strong induction of the PTR2 transporter.

the apoptosis in *Drosophila*, presumably through the concomitant destruction of DIAP1-associated activators of apoptosis. The set of proteases that produce physiological N-end rule substrates is unlikely to be confined to MetAPs, caspases, and separases. For example, the cleavage specificity of calcium-activated proteases called calpains and the properties of other, less well-characterized cytosolic and/or nuclear proteases suggest that they, too, may function as upstream components of the N-end rule pathway. Although many functions of the N-end rule pathway remain to be discovered, the functions that have already emerged – peptide import, chromosome stability, cardiovascular development, meiosis, and apoptosis – are strikingly diverse. The broad functional range of the N-end rule pathway thus resembles, in a microcosm, the vastly greater span of the Ub system at large.

See Also the Following Articles

Aminopeptidases • Proteasomes, Overview • Ubiquitin System • Ubiquitin-Like Proteins

Glossary

degrons, or degradation signals Features of proteins that confer metabolic instability (short *in vivo* half-lives) on these proteins.

polyubiquitin chain A chain of covalently linked Ub moieties in which the C-terminal Gly residue of one moiety is conjugated to a specific lysine residue (usually, but not always, Lys-48) of adjacent Ub moieties. Protein-linked poly-Ub chains of different topologies (mediated by different, but unique for a given chain, lysine residues of Ub) underlie distinct roles of the Ub system, including its nonproteolytic functions. Poly-Ub can also exist as linear, head-to-tail chains of DNA-encoded Ub repeats produced through the ribosome-mediated translation. Such chains, the natural precursors of mature Ub, are called linear poly-Ub.

spermatocytes Germ cells in the testes of animals that are engaged in meiosis.

synaptonemal complex Two chromosome-length, closely apposed structures that mediate the pairing of two homologous chromosomes in meiosis.

ubiquitin ligase A complex of E2 and E3 enzymes, or an E3 enzyme alone.

ubiquitylation Conjugation of Ub to other proteins, including other Ub molecules. Ub whose C-terminal (Gly-76) carboxyl group is covalently linked to another compound is called the *ubiquityl* moiety.

Further Reading

Bachmair, A., Finley, D., and Varshavsky, A. (1986). *In vivo* half-life of a protein is a function of its N-terminal residue. *Science* **234**, 179–186.

Ditzel, M., Wilson, R., Tenev, T., Zachariou, A., Paul, A., Deas, E., and Meier, P. (2003). Degradation of DIAP1 by the N-end rule pathway is essential for regulating apoptosis. *Nat. Cell Biol.* **5**, 467–473.

Du, F., Navarro-Garcia, F., Xia, Z., Tasaki, T., and Varshavsky, A. (2002). Pairs of dipeptides activate the binding of substrate by ubiquitin ligase through dissociation of its autoinhibitory domain. *Proc. Natl. Acad. Sci. USA* **99**, 14110–14115.

Hershko, A., Ciechanover, A., and Varshavsky, A. (2000). The ubiquitin system. *Nat. Med.* **6**, 1073–1081.

Kwon, Y. T., Kashina, A. S., Davydov, I. V., Hu, R.-G., An, J. Y., Seo, J. W., Du, F., and Varshavsky, A. (2002). An essential role of N-terminal arginylation in cardiovascular development. *Science* **297**, 96–99.

Kwon, Y. T., Xia, Z., An, J. Y., Tasaki, T., Davydov, I. V., Seo, J. W., Sheng, J., Xie, and Varshavsky, A. (2003). Female lethality and apoptosis of spermatocytes in mice lacking the UBR2 ubiquitin ligase of the N-end rule pathway. *Mol. Cell. Biol.* **23**, 8255–8271.

Rao, H., Uhlmann, F., Nasmyth, K., and Varshavsky, A. (2001). Degradation of a cohesin subunit by the N-end rule pathway is essential for chromosome stability. *Nature* **410**, 955–960.

Turner, G. C., Du, F., and Varshavsky, A. (2000). Peptides accelerate their uptake by activating a ubiquitin-dependent proteolytic pathway. *Nature* **405**, 579–583.

Varshavsky, A. (1996). The N-end rule: Functions, mysteries, uses. *Proc. Natl. Acad. Sci. USA* **93**, 12142–12149.

Varshavsky, A. (2003). The N-end rule and regulation of apoptosis. *Nat. Cell Biol.* **5**, 373–376.

Biography

Alexander Varshavsky is Smits Professor of Cell Biology at the California Institute of Technology, in Pasadena. He is a member of the US National Academy of Sciences, and has received a number of scientific awards, including the Gairdner Award, the Lasker Award, the Sloan Prize, the Merck Award, the Wolf Prize, the Horwitz Prize, the Max Planck Prize, the Pasarow Award, the Massry Prize, and the Wilson Medal.

Neoglycoproteins

Y. C. Lee and Reiko T. Lee
The Johns Hopkins University, Baltimore, Maryland, USA

The term neoglycoproteins refers to proteins modified with chemical or enzymatic means to acquire structurally defined carbohydrates. The carbohydrates can be monosaccharides, oligosaccharides, or even polysaccharides.

Preparation

Direct Coupling of Oligosaccharides to Proteins

The easiest method is to attach naturally available oligosaccharides to the amino groups of proteins. This process does not require any chemical manipulations other than the conjugation process by reductive amination. Some of the readily available di- and oligosaccharides are: lactose, maltose, cellobiose, melibiose, N-acetyl-lactosamine, di-N-acetyl-chitobiose, and a number of milk oligosaccharides. An example of coupling of lactose by reductive amination to protein using sodium cyanoborohydride or pyridine borane as reducing agent, which preferentially reduces aldimine (Schiffs base) over aldehyde, is shown in Figure 1. This method relies on the fact that reducing sugars in acyclic aldehydo form, although present in a very minor proportion, are in equilibrium with the cyclic forms. As the aldehydo form of oligosaccharide is consumed, more will become available by conversion from the cyclic forms. However, the conjugation by this simple method is a very slow process, requiring several days or longer, because of the low concentration of the aldehyde form of oligosaccharide in solution.

The reductive amination converts the primary amino groups of N terminus and lysine side chains to secondary amines initially, and eventually to tertiary amines (with two sugar groups attached to a single nitrogen), if both oligosaccharide and reducing agent are present in excess. It is important to note that after such a reaction, the reducing terminal sugar of the oligosaccharide will become acyclic, and for this reason, conjugation with monosaccharide is meaningless. The shortcoming of this approach, in addition to long reaction time mentioned above, is the limited availability of suitable oligosaccharides. However, the number of commercially available oligosaccharides that are naturally derived or synthetically prepared has been steadily increasing.

Using Synthetic Carbohydrate Derivatives

Neoglycoproteins prepared by direct conjugation of oligosaccharides sometimes can be disadvantageous, due to sugar residues that are recognition target being too close to the protein surface. Synthetic carbohydrate derivatives would expand the scope of neoglycoprotein considerably both in terms of sugar structure and its disposition on the protein surface. The procedures can be totally synthetic or can be chemical modifications of naturally available glycans either in a free sugar form or linked to a group such as peptide. A few of the popular procedures are presented below.

Aromatic Glycosides

Commercially available *p*-aminophenyl glycosides are convenient derivatives for making neoglycoproteins either by diazo-coupling to tyrosine side chains or via transformation into isothiocyanate (reaction with thiophosgen), which then reacts with amino groups. *p*-Nitrophenyl glycosides, commonly used chromogenic glycosides, are available in even wider variety, and can be easily reduced to the corresponding *p*-aminophenyl glycosides. A shortcoming of these derivatives is that they can increase the hydrophobicity of product neoglycoprotein considerably and consequently may alter the nature of protein and give anomalous results in the probing of carbohydrate function.

Nonaromatic Glycosides

The problem of excessive hydrophobicity can be alleviated by the use of derivatives which do not contain aromatic rings and are not as hydrophobic as aromatic glycosides (e.g., Figure 2). Some of these derivatives are thioglycosides, which have the advantage of being more resistant to most exoglycosidases and also specifically cleavable with mercuric salts. Examples shown in Figure 2 are: (A) sugar imidate reacting with amino groups of protein to produce amidino-type (AI)

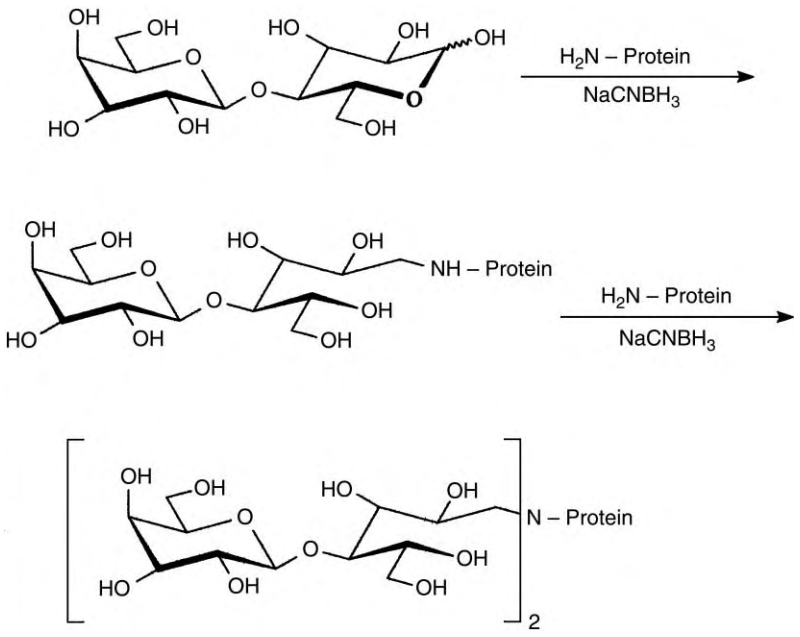

FIGURE 1 Conjugation of lactose via reductive amination.

neoglycoproteins; (B) an ω-aldehydo glycoside being coupled to protein via reductive amination; and (C) an ω-aminoalkyl glycosides converted to squaric acid derivative which can react with amino groups of protein. In both (B) and (C), the length of a glycon can be varied.

Reduced and Periodate-Oxidized Natural Oligosaccharides

Synthesis of oligosaccharides having complex structure is still a tedious and difficult task. Therefore, it is prudent sometimes to utilize naturally isolable oligosaccharides, if the quantity of neoglycoprotein needed is not too large. Natural oligosaccharides, pre-existing or obtained from natural glycoconjugates by enzymatic cleavage, can be made more reactive by first reducing them with sodium borohydride (to convert the reducing sugar residue into acyclic alditol) followed by mild periodate oxidation (e.g., 10 mM $NaIO_4$ for 10 min at room temperature), which will preferentially oxidize acyclic glycols to generate aldehydo group(s) without affecting the rest of the cyclic sugar residues. The newly generated aldehyde can be used in the reductive amination reaction as described above.

Using Other Functional Groups of Proteins

Most of the conjugation methods described above utilize amino groups of proteins for conjugation, which are often abundant and reactive because of the distance from the protein backbone. However, other functional groups such as phenolic, sulfhydryl, and carboxyl groups can also be used for conjugation. Diazo coupling of aryl glycosides to tyrosine side chain has been mentioned earlier. Thiol groups of protein are easy target for oligosaccharide attachment, since chemically mild, thiol-specific reactions are readily available. For example, a heterobifunctional linker with an amino-reacting group on one end and a maleimido or iodoacetamido group on the other end is reacted first to an Asn-oligosaccharide (or other glycopeptide) via its amino terminus, which is then reacted with protein thiol groups to produce neoglycoprotein in high yield. Bovine serum albumin has a single sulfhydryl group which can be utilized in this way to produce a neoglycoprotein carrying a single oligosaccharide chain of defined structure. An interesting approach is to react glycosylthiol with protein thiol group to form a disulfide bond. This will result in a product quite similar in structure to the natural N-glycosylated protein in terms of linkage length.

Use of Glycosyl Transferases

As the number of glycosyl transferases available commercially increases steadily, these enzymes have become a powerful synthetic tool in neoglycoprotein synthesis. The advantage of glycosyl transferases, is their exquisite specificity for anomeric configuration as well as the position of attachment. Thus, these enzymes are especially suited for modifying a pre-existing glycan structure (even a monosaccharide) at a specific position. Attachment of terminal α-L-fucosyl group or sialic acid group is a prime example. The enzymatic reaction can be carried out on the oligosaccharide before conjugation or after the conjugation to proteins.

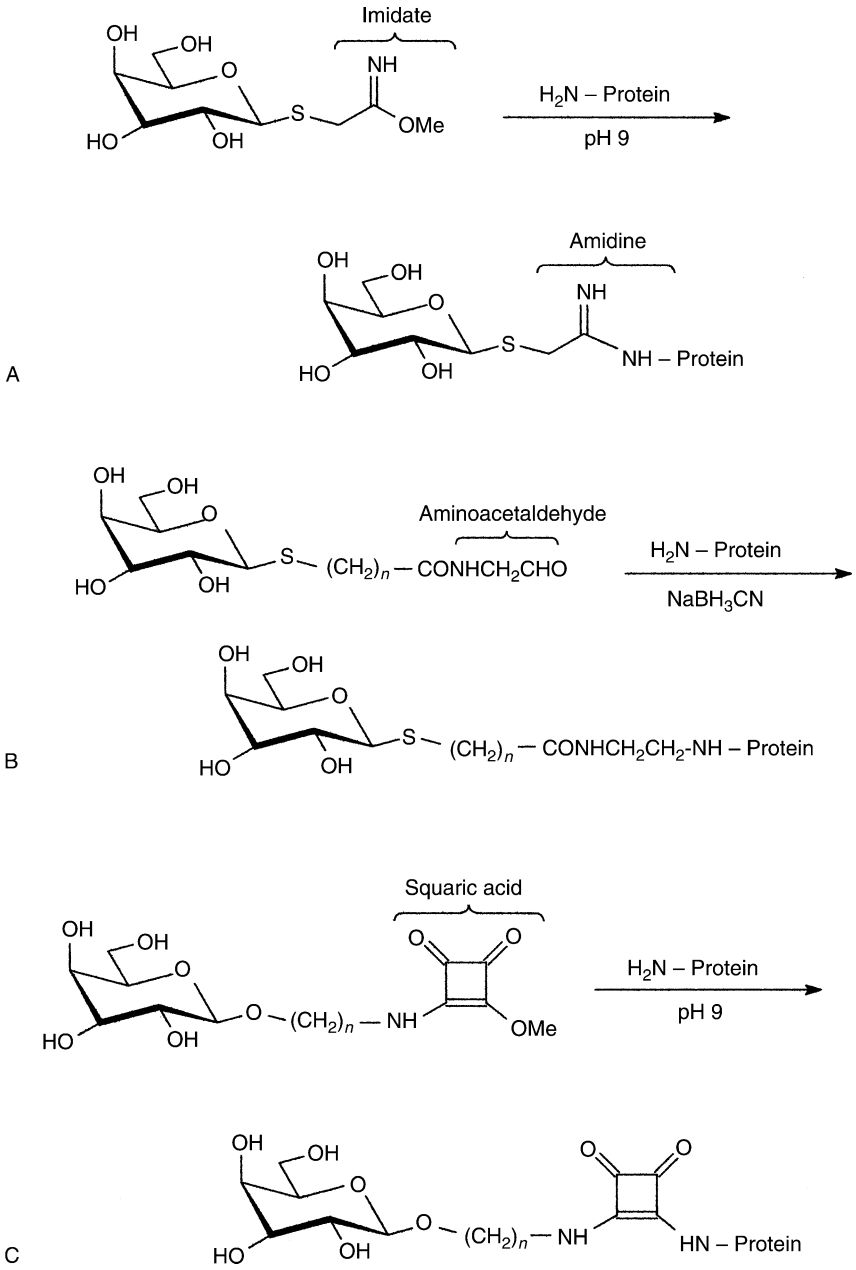

FIGURE 2 Example of synthetic methods for neoglycoprotein preparations.

Conjugation of Glycopeptides

For the conjugation of glycan structures from glycoprotein, sometimes it is easier to generate glycopeptide than to generate reducing oligosaccharide. A heterobifunctional crosslinker with a hydrazide and an acetal groups at two ends of molecule was devised to react first with amino groups of glycopeptide (or any other amino-terminated carbohydrate derivatives) via azide reaction, which is followed by generation of aldehydo function and then coupling to protein via reductive amination.

In all of these reactions, the level of sugars on neoglycoproteins can be controlled either by the ratio of reagent to protein or by the length of reaction. It should be borne in mind that these modifications generally produce a distribution of different sugar substitution in terms of both position and number. However, the ability to vary the degree of substitution turned out to be a great advantage for probing of carbohydrate function in many biological systems that is not readily available in natural glycoproteins. This is because recognition of carbohydrates often requires multivalency (Glycoside Clustering Effect) in order to manifest its function unequivocally. Neoglycoproteins can readily provide multivalency and thus are powerful ligands for carbohydrate binding.

In addition, neoglycoproteins can be radioiodinated (using the tyrosine side chain) or modified with fluorescent groups, such as fluorescein (using available ε-amino group) for easy monitoring.

Applications

Carbohydrate Receptor Analyses

Using neoglycoproteins, one can easily survey sugar-binding receptors (or lectins) in biological specimen. For example, a series of neoglycoproteins have been used to determine that alligator hepatic receptor has binding specificity for mannose and L-fucose. The binding of tagged neoglycoproteins (e.g., ^{125}I-labeled) to receptors can be probed both in solution phase and solid phase. Properly labeled neoglycoproteins can be used as cytochemical markers.

Affinant for Isolation

Neoglycoproteins can serve as effective affinant for isolation of lectins and receptors. For such a purpose, a neoglycoprotein can be conveniently immobilized to a suitable solid phase (e.g., Sepharose). In an alternate case, a protein (such as BSA) is immobilized first and then modified with one of the reagents mentioned above to form neoglycoproteins on solid phase.

Substrates for Enzymes

Neoglycoproteins can be used as convenient substrate for enzymes. For example, GlcNAc-BSA adsorbed on microtiter wells was used conveniently as substrate to assay β-galactosyl transferase with great sensitivity, which in turn can be used to assay α-fucosyl transferase.

Targeting Device

Neoglycoproteins can be used to target drugs and other materials to specific organs. For example, Gal- or GalNAc-containing neoglycoproteins, when properly conjugated to drug or anti-sense materials, can be used to target such materials to mammalian liver.

Examination of Glycoprotein Structure/Function Relationship

Carbohydrate chains of glycoprotein can have biological and biochemical function unrelated to specific sugar–lectin interaction. One of the better documented cases is the glycan in the Fc domain of IgG, which is required for interaction with Fc receptor. Neoglycoproteins were prepared by disulfide formation between Cys (in lieu of Asn) in the Fc domain and glycosylthiols of various structures to examine the effect of glycan structure on Fc receptor binding activity. Moreover, if the amino acid sequence and X-ray structure are known, one can place a Cys at different surface locations by genetic engineering, which would provide more latitude in examination of the role of carbohydrates on glycoproteins.

See Also the Following Articles

DNA Ligases: Mechanism and Functions • DNA Ligases: Structures • DNA Mismatch Repair and the DNA Damage Response • Glycoprotein Folding and Processing Reactions • Glycoproteins, N-linked • Glycosylation, Congenital Disorders of • Immunoglobulin (Fc) Receptors • Nonhomologous Recombination: Bacterial Transposons • Nonhomologous Recombination: Retrotransposons • Glycoprotein-Mediated Cell Interactions, O-Linked • Protein Glycosylation Inhibitors • Protein Glycosylation, Overview • Protein Kinase C Family

Glossary

BSA Bovine serum albumin.

glycoside clustering effect When glycosides are bundled together at proper distances, the total effect can be much greater ($>10^6$-fold) than the simple sum of individual glycoside.

neoglycoconjugates The original term of neoglycoproteins has now been expanded, and the term neoglycoconjugates has been introduced to encompass all the glyco-modified materials.

Further Reading

Lee, R. T., and Lee, Y. C. (1997). Neoglycoproteins. In *Glycoproteins II* (J. Montreuil, J. F. G. Vliegenthart and H. Schachter, eds.) pp. 601–620. Elsevier, Amsterdam, The Netherlands.

Lee, Y. C., and Lee, R. T. (1994). *Methods in Enzymology, Vol. 247. Neoglycoconjugates: Part A. Synthesis*. Academic Press, San Diego, CA.

Lee, Y. C., and Lee, R. T. (1994). *Methods in Enzymology, Vol. 242. Neoglycoconjugates: Part B. Biomedical Applications*. Academic Press, San Diego, CA.

Lee, Y. C., and Lee, R. T. (1994). *Neoglycoconjugates: Preparation and Applications*. Academic Press, San Diego, CA.

Macindoe, W. M., Van Oijen, A. H., and Boons, G. J. (1998). A unique and highly facile method for synthesizing disulfide linked neoglycoconjugates: A new approach for remodelling of peptides and proteins. *Chem. Commun.* **7**, 847–848.

Monsigny, M., Midoux, P., Mayer, R., and Roche, A. C. (1999). Glycotargeting: Influence of the sugar moiety on both the uptake and the intracellular trafficking of nucleic acid carried by glycosylated polymers. *Biosci. Rep.* **19**, 125–132.

Monsigny, M., Mayer, R., and Roche, A. C. (2000). Sugar–lectin interactions: Sugar clusters, lectin multivalency and avidity. *Carbohydr. Lett.* **4**, 35–52.

Biography

Y. C. Lee is Professor of Biology at the Johns Hopkins University in Baltimore, Maryland. He received his Ph.D. from the University of Iowa. His principal research interests are chemistry and biochemistry of glycoconjugates, especially biological interactions involving carbohydrates. He developed the field of neoglycoproteins as well as discovered glycoside clustering effect. He has published nearly 400 papers and book chapters, and received the Claude Hudson Award of the American Chemical Society in 2001.

Reiko Lee also received her Ph.D. from University of Iowa and is a Research Scientist in Biology Department of the Johns Hopkins University. She has coedited several volumes of books on the topics of neoglycoconjugates and recognition of carbohydrates in biological systems.

Neuronal Calcium Signal

Hilmar Bading
University of Heidelberg, Heidelberg, Germany

Neurons initiate many changes in gene expression in response to a synaptic or electrical stimulus. Calcium is the principal second messenger bridging the gap between the synapse and the nucleus. To couple synaptic events to specific genomic responses, neurons exploit the spatial diversity of calcium signals associated with the stimulus. Dendritic calcium signals, activating the MAP kinase (extracellular signal-regulated kinase, ERK1/2) signaling cascade, stimulate gene expression mediated by the serum response element. Calcium signals in the cell nucleus activate the transcription factor CRE-binding protein (CREB) and the coactivator CREB-binding protein (CBP). Nuclear calcium may, in particular, initiate and govern gene-expression-dependent forms of neuronal adaptations, including survival, learning, and memory.

Calcium Ions, Key Regulators of Electrical-Activity-Dependent Gene Expression

The generation of calcium signals following electrical activation is a fundamental property of neurons that controls many processes in the developing and the adult nervous system. Activity-induced increases in the intracellular calcium concentration result from calcium entering neurons from the extracellular space through ligand- and/or voltage-gated ion channels; these calcium transients can be amplified through calcium release from intracellular calcium stores. The N-methyl-D-aspartate (NMDA) receptor, a calcium permeable, glutamate-gated ion channel, plays a particularly important role in the mammalian central nervous system. Calcium entry through NMDA receptors, triggered by electrical activity, stimulates mechanisms that affect synaptic connectivity and neuronal network behavior leading to information storage; NMDA receptor-mediated calcium entry can also promote neuronal survival or cause cell death. For the consolidation of these activity-induced responses it is important that calcium signals, generated initially at the plasma membrane, are transduced to the cell nucleus where they stimulate the expression of particular genes. Thus, neurons use calcium ions to couple electrical signals to specific genomic events. Among the target genes of calcium signaling are neurotrophic factors, cytoskeletal proteins, and transcription factors (see below).

Spatial Calcium Signaling in Synapse-to-Nucleus Communication

The use of calcium as a universal signal mediator raises the issue of specificity: what mechanism allows neurons to use a single second messenger to convert a diverse range of electrical stimuli into distinct gene expression responses? Neurons appear to achieve this by using a calcium code: a given electrical stimulus is transformed into a calcium signal with particular spatial and temporal properties. Thus, an activity-induced neuronal calcium signal is a signature of the stimulus; it functions as its intracellular representation and links the stimulus to a gene expression response. The amplitude and the duration of the calcium signal, two features that transcriptional regulators decode, primarily control the magnitude of the increase in transcription. The site of calcium entry also matters; indeed, calcium entry through synaptic NMDA receptors and through extrasynaptic NMDA receptors has opposing effects on the activation of a crucial transcription factor (see below). However, most importantly, the genomic response depends on which part of the neuron is invaded by the calcium transient (Figure 1). For example, a weak synaptic input may generate a calcium signal that is confined to the submembranous space in the immediate vicinity of the site of calcium entry; following a stronger stimulus, calcium increases may reach further into the dendritic tree. Under certain conditions the calcium signal can invade the cell body and the nucleus. It is important for the specification of the gene expression response exactly which subcellular compartment (i.e., submembranous space, dendritic tree and somatic cytoplasm, and cell nucleus) undergoes a change in the calcium concentration. Thus, the "dialogue between genes and synapses" (to use a phrase from Eric Kandel) exploits the spatial and temporal diversity of calcium

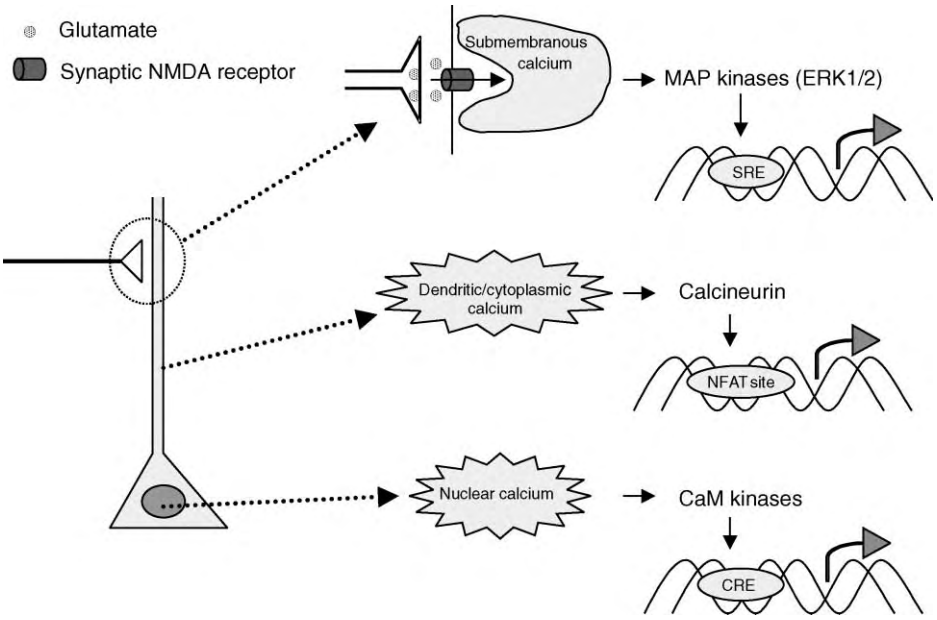

FIGURE 1 Schematic drawing of a neuron and the intracellular signaling pathways that mediate the induction of gene expression following neuronal activity. Three spatially distinct calcium signals (submembranous, cytoplasmic, and nuclear) are illustrated. Each type of calcium signal couples to a specific effector mechanism with distinct genomic targets. The decoding, by transcriptional regulators, of spatial information contained in activity-induced calcium transients allows neuronal impulse patterns to specify gene expression responses.

transients associated with electrical activation. Transcriptional regulation and the neuronal responses depend on how calcium enters the neurons, the amplitude of the signal, how long the signal lasts and what subcellular compartment it invades.

Regulators of Calcium-Induced Gene Expression

Much knowledge of the mechanisms of electrical-activity-dependent gene expression comes from studies of the *c-fos* gene. This gene is induced, without the need for new protein synthesis, within minutes after the stimulation. The *c-fos* gene encodes a DNA binding protein; together with members of the Jun transcription factor family it forms the AP-1 complex that is involved in the regulation of many genes. *c-fos* was the first gene found to be induced by membrane depolarization and calcium influx into excitable cell lines and primary neurons.

SRE AND CRE

Analysis of the *c-fos* promoter revealed that calcium influx-induced gene transcription is mediated by two distinct DNA regulatory elements: the cAMP response element (CRE) and the serum response element (SRE). The CRE and the SRE were previously known to mediate gene induction upon increasing intracellular levels of cAMP or following the addition of serum to serum-starved fibroblasts, respectively. Analysis of calcium regulation of SRE-dependent and CRE-dependent transcription uncovered the importance of the intracellular localization of the calcium signal: an increase in cytoplasmic calcium activates gene expression mediated by the SRE; in contrast, activation of the CRE and the CRE-binding protein (CREB) require increases in the nuclear calcium concentration. Thus, a single second messenger can, depending on its intracellular localization, induce distinct responses.

NFAT AND DREAM

Calcium-responsive regulators of transcription, other than the SRE and CREB, include the Nuclear Factor of Activated T-cells (NFAT) and the downstream regulatory element (DRE)-binding protein, DREAM (DRE-Antagonist Modulator). NFAT is important in the immune system; it mediates in activated T-cells the induction of interleukin-2 expression, a critical step in the response to antigen stimulation. DREAM is a multifunctional calcium-binding protein that can act as a repressor of gene transcription. The importance of spatial calcium signaling in the regulation of the SRE, the CRE, NFAT, and DREAM is outlined in the following section.

Calcium Signals in Different Subcellular Compartments

Calcium brings about biological responses through activating effector molecules such as protein kinases or protein phosphatases. Exactly which calcium-regulated molecule is stimulated depends on the subcellular localization of the calcium transient.

Submembranous Calcium Signals

A calcium microdomain restricted to the submembranous space near synaptic NMDA receptors serves as the "on-switch" of the MAP kinase (ERK1/2) cascade following synaptic activity. This signaling pathway is a major route for intracellular communication. The actions of MAP kinases (ERK1/2), both in the vicinity of calcium entry sites and in the nucleus, are involved in controlling many different brain functions ranging from learning to neuronal survival and light-induced shifts in the circadian rhythm.

One important target of the MAP kinase (ERK1/2) cascade is the nucleus. The MAP kinase (ERK1/2) signal propagates to the nucleus independently of global (i.e., cell-wide) increases in the calcium concentration and stimulates gene expression mediated by the SRE. It can also lead to the phosphorylation of CREB on its activator site, serine 133. Although this phosphorylation is necessary for inducing CREB-mediated transcription, it is not sufficient; a second regulatory event is required that involves stimulation of the activity of the CREB coactivator CBP by nuclear calcium and nuclear calcium/calmodulin (CaM)-dependent protein kinases. Nevertheless, the MAP kinase (ERK1/2) cascade acts as an auxiliary pathway that promotes at least one of several activating steps that control CREB-dependent gene expression. CREB target genes include *c-fos* and the brain-derived neurotrophic factor (BDNF).

Dendritic/Cytoplasmic Calcium Signals

The second calcium pool with a role in transcription regulation by neuronal activity is localized to the dendrites and the cytoplasm of the cell body. One of the targets of dendritic/cytoplasmic calcium is calcineurin (CaN). CaN is a cytoplasmic serine/threonine phosphatase that, upon activation by calcium/CaM, catalyzes the dephosphorylation of NFAT, which unmasks a NFAT nuclear localization signal. The activated CaN/NFAT complex is subsequently imported into the nucleus to activate gene transcription. Possible target genes of the CaN/NFAT signaling module are genes involved in regulating calcium homeostasis; this includes the IP_3 receptor and plasma membrane calcium ATPases (calcium pumps).

Once calcium concentrations have returned to basal levels, the NFAT/CaN complex dissociates, NFAT is exported from the nucleus and transcription is rapidly shut off. Thus, the magnitude of the transcriptional response is a function of the duration of the calcium signal; only prolonged increases in intracellular calcium efficiently activate NFAT-mediated gene expression. In addition, increases in nuclear calcium are required to maintain NFAT in the nucleus and to sustain transcription. Such calcium signals (i.e., elevated calcium plateaus in the cytoplasm and the nucleus) are typically seen in antigen-stimulated T-cells that require NFAT activation for the immune response (see above). In neurons, synaptic activity often generates only transient increases in intracellular calcium that may induce a less robust NFAT activation.

Nuclear Calcium Signals

The third player in electrical-activity-dependent gene expression is nuclear calcium. Synaptically evoked calcium transients can be amplified by calcium release from intracellular stores and are propagated, possibly in the form of a regenerative wave, to the nucleus. Nuclear calcium is a central regulator of neuronal gene expression. It activates nuclear calcium/CaM-dependent protein kinases and is the principal regulator of gene expression by the CREB/CBP complex. Activation of gene expression by CREB/CBP requires at least two regulatory events: phosphorylation of CREB on its activator site serine 133, which allows CBP to be recruited to CREB. The second event is the stimulation of CBP activity. The first regulatory step can be catalyzed by several protein kinases, including kinases of the MAP kinase (ERK1/2) signaling pathway (triggered by submembranous calcium; see above) and nuclear calcium-induced CaM kinases. Induction of CBP activity, however, depends upon increases in the nuclear calcium concentration and the activation of nuclear CaM kinases.

The only other second messenger known to stimulate CBP activity and to increase CREB/CBP-mediated gene expression is cAMP. Global increases in the intracellular concentration of cAMP stimulate the cAMP-dependent protein kinase (PKA); upon binding of cAMP to the PKA regulatory subunit, the catalytic subunit of PKA translocates to the cell nucleus to activate the CREB/CBP complex. A large body of literature suggests that cAMP and PKA are important for certain long-term, gene-expression-dependent forms of plasticity and learning in *Aplysia californica* and *Drosophila melanogaster*. Mammalian neurons are also capable of increasing intracellular levels of cAMP

following synaptic activity through a process that involves calcium/CaM-dependent adenylyl cyclases. However, electrical activity does not appear to elevate global levels of cAMP sufficiently high to stimulate the CREB/CBP complex, although it may increase cAMP and PKA activity locally leading to the phosphorylation of neurotransmitter receptors or other proteins in the post-synaptic space. Thus, the cAMP-PKA system may be important for localized dendritic signaling in the mammalian nervous system, but the stimulation of CREB/CBP-dependent gene expression following synaptic activity appears to be controlled by nuclear calcium signals.

CBP is a coactivator of CREB, but it also interacts with several other DNA-binding proteins, thereby conferring calcium inducibility. One example is the transcription factor c-Jun that can function as a calcium-regulated activator. Thus, control of CBP activity by nuclear calcium and nuclear CaM kinases provides a general mechanism through which electrical activity regulates an entire class of transcription factors and, consequently, many genes. This may be important in activity-dependent neuronal adaptation including information storage and memory that are likely to require up-regulation (or down-regulation) of many genes. Indeed, CREB (presumably as a CREB/CBP complex) has been implicated in synaptic plasticity and learning-related event in *Aplysia californica*, *Drosophila melanogaster*, and mice. Nuclear calcium may be essential for these processes.

A second type of transcriptional regulation by nuclear calcium involves DREAM. Rather than being controlled by calcium/CaM-dependent enzymes, the ability of DREAM to modulate transcription is directly controlled by nuclear calcium. DREAM is a calcium-binding protein that, in the absence of calcium, interacts with the DRE and represses transcription. Increases in nuclear calcium lead to the formation of a calcium/DREAM complex; calcium-bound DREAM dissociates from the DNA, allowing transcription to take place. Potential DREAM-binding sites are present in many different genes; the involvement of DREAM is best documented for the prodynorphin gene.

CREB Shut-Off Pathway

The genomic responses (and their effects on survival and plasticity programs) induced by calcium flux through synaptic NMDA receptors are antagonized by a signaling pathway stimulated by the addition of glutamate to the extracellular medium. Bath glutamate application stimulates both synaptic and extrasynaptic NMDA receptors as well as other types of glutamate receptors. Pharmacological experiments revealed that calcium flux through extrasynaptic NMDA receptors is responsible for this nuclear signaling mechanism that negatively regulates gene expression; this pathway also couples to neuronal cell death. The target transcription factor inactivated following calcium entry through extrasynaptic NMDA receptors is CREB; the CREB shut-off is brought about by a rapid dephosphorylation of CREB on its activator site, serine 133.

Extrasynaptic NMDA Receptors Antagonize Nuclear Calcium Signaling and BDNF Gene Expression

After calcium entry through extrasynaptic NMDA receptors, one of the consequences of the CREB shut-off is the suppression of BDNF gene expression. BDNF, a neurotrophic factor, activates intracellular signaling pathways through binding to TrkB, a receptor tyrosine kinase; BDNF also acts as a fast neurotransmitter and can rapidly depolarize neurons. BDNF has many functions in neuronal plasticity and cell survival. BDNF gene transcription is electrical-activity-dependent and controlled, antagonistically, by two calcium signaling pathways: calcium flux through synaptic NMDA receptors (or through L-type voltage-gate calcium channels) stimulates BNDF gene transcription; in contrast, calcium flux through extrasynaptic NMDA receptors antagonizes increases in BDNF expression. The BDNF gene's promoter is complex and provides binding sites for many transcription factors; however, a key factor is CREB, which may explain the opposing action of synaptic and extrasynaptic NMDA receptors on influencing BDNF gene transcription. Activation of synaptic NMDA receptors (or L-type voltage-gate calcium channels) strongly promotes CREB activity, whereas CREB function is shut off following activation of extrasynaptic NMDA receptors. Thus, the dialogue between the synapse and the nucleus is modulated by extrasynaptic NMDA receptors; those receptors trigger a CREB shut-off signal and antagonize increases in BDNF transcription induced by calcium entry through synaptic NMDA receptors. This underscores the importance of the intracellular localization of the calcium signal for the specification of the neuronal response.

See Also the Following Articles

Chaperones, Molecular • Proteasomes, Overview • Ubiquitin System • Ubiquitin-Like Proteins

Glossary

calcium Principal second messenger in the control of gene expression by electrical activity in neurons.

CBP (CREB binding protein) Transcriptional coactivator regulated by cAMP and calcium signaling pathway; interacts with CREB and many transcription factors thereby conferring calcium- and cAMP-inducibility.

CRE (cAMP response element) DNA regulatory element present in the promoter of many genes.

CREB (CRE binding protein) CRE-interacting transcription factor that is a target of cAMP and calcium signaling pathways; mediates gene induction upon synaptic activity and nuclear calcium transients.

MAP kinases/extracellular signal-regulated kinases (ERK 1/2) Important intracellular signaling pathway; activated by electrical activity-induced submembranous calcium signals.

spatial calcium signaling Electrical activity can induce calcium signals in different intracellular compartments; submembranous, cytoplasmic, and nuclear calcium activate gene expression through different mechanisms and have distinct genomic targets.

SRE (serum response element) DNA regulatory element regulated by signaling pathway, activated by growth factors, serum, or calcium; nuclear target of MAP kinases (ERK 1/2) signaling pathway.

Further Reading

Bading, H. (2000). Transcription-dependent neuronal plasticity: The nuclear calcium hypothesis. *Eur. J. Biochem.* **267**, 5280–5283.

Carafoli, E., and Klee, C. B. (1999). *Calcium as a Cellular Regulator.* Oxford University Press, New York.

Hardingham, G. E., and Bading, H. (2003). The yin and yang of NMDA receptor signalling. *Trends Neurosci.* **26**, 81–89.

Kandel, E. R. (2001). The molecular biology of memory storage: A dialogue between genes and synapses. *Science* **294**, 1030–1038.

West, A. E., Griffith, E. C., and Greenberg, M. E. (2002). Regulation of transcription factors by neuronal activity. *Nat. Rev. Neurosci.* **3**, 921–931.

Biography

Hilmar Bading is Professor of Neurobiology and Director of the Neurobiology Institute at the Interdisciplinary Center for Neurosciences at Heidelberg University, Germany. He holds an M.D. from Heidelberg University, received postdoctoral training at the Max Plank Institute in Berlin and Harvard Medical School, and was a staff scientist at the MRC Laboratory of Molecular Biology, Cambridge, United Kingdom. His principal research interest is neuronal calcium signaling and how this affects gene regulation and plasticity. His work highlighted the spatial aspects of calcium signals and the importance of nuclear calcium in governing activity-dependent gene expression in neurons.

Neuronal Intermediate Filaments

Ronald K. H. Liem
Columbia University College of Physicians and Surgeons, New York, USA

Neuronal intermediate filaments (IFs) are 10–12 nm filaments that are expressed in the nervous system. IF proteins belong to a large gene family and the expression of different IF proteins is tissue specific. In the nervous system, different neuronal IFs are expressed in neuroepithelial stem cells, the central nervous system (CNS) and peripheral nervous system (PNS). In addition, the expression patterns of these neuronal IFs are developmentally regulated. There are six neuronal IFs that will be described in this section. These are the three neurofilament triplet proteins (NFTPs), α-internexin, peripherin, and nestin.

Introduction

The cytoskeleton of most eukaryotic cells is composed of microtubules, microfilaments, and IFs. Microtubules are 25 nm in diameter and are composed of two subunit proteins called α- and β-tubulin, as well as a number of associated proteins, microfilaments are 6–8 nm in diameter and made up of a protein called actin. IFs are intermediate in size between the microtubules and microfilaments. All IF proteins contain a central α-helical rod domain flanked by nonhelical N-terminal head and C-terminal tail domains. The rod domain contains hydrophobic repeats (called heptad repeats) that mediate dimerization by allowing two α-helices to wrap around each other forming a "coiled coil." Subsequent polymerization into filaments involves the formation of tetramers and higher-order structures for which the N-terminal head domain is particularly important. Based on their protein sequence similarities and their gene structure, the IF protein family is separated into six or seven types. In the nervous system, IFs are expressed in both neurons and glial cells. In the CNS, astroglial cells express the glial fibrillary acidic protein (GFAP), whereas oligodendrocytes appear to be one of the few cell types that express no cytoplasmic IFs. In the PNS, Schwann cells express the more ubiquitous IF protein vimentin. Vimentin and GFAP are quite similar in sequence and gene structure and are part of a subfamily of IFs called type III IFs.

Neuronal IFs are the major and most visible filamentous structures in the axons. The number of neuronal IFs is correlated with axon diameter and they are believed to be primary determinants of axonal diameter. The NFTPs are the most ubiquitous IF proteins in neurons; they are present in both central and peripheral nerves. The NFTPs and α-internexin are more closely related to each other than to other IF proteins and are classified together as a subfamily called type IV IFs. The expression of peripherin predominates in the PNS. Although peripherin is expressed exclusively in neurons, based on its protein sequence homologies and its gene structure, peripherin is more similar to vimentin and GFAP and is therefore considered a type III IF. Nestin is the IF protein found in neuroepithelial stem cells, as well as muscle progenitor cells. The protein sequence of nestin is quite unique and nestin is sometimes considered to be a separate type VI IF. However, on the basis of its gene structure, it resembles the other type IV neuronal IFs.

One of the hallmarks of a number of neurodegenerative diseases is the accumulation of neuronal IFs in the form of axonal spheroids. These axonal spheroids have been observed in amyotropic lateral sclerosis (ALS, also called Lou Gehrig's disease) as well as other neuropathies. A number of recent studies from transgenic mice have indicated that the disorganization of neuronal IFs, especially in the forms of axonal spheroids, can lead to neurodegeneration. The relationship between the various neuronal IF proteins and neurodegeneration will be discussed below.

The Neurofilament Triplet Proteins

The NFTPs are composed of three proteins called NFL, NFM, and NFH for neurofilament light, medium, and heavy chain. NFTPs have been identified in all mammals and birds. The identification of the NFTPs was first done on the basis of studies on the transport of proteins in the axon. To study the transport of particular proteins, early studies used radioactive amino acids to label the newly synthesized proteins, and the nerves were then analyzed to determine the rates at which different proteins move. The slowest moving fraction moved at 0.1–1 mm per day and were believed to be the structural components. There were five major proteins, α- and β-tubulin and three

proteins with apparent molecular weights of 68, 145, and 200 kDa. Since actin, the component of the microfilaments, moved somewhat faster than these five proteins, the three unidentified proteins were identified as the subunits of the other structural element, the neurofilaments. Biochemical verification came when neurofilaments were purified and isolated and the contaminating astroglial filaments were removed. Each subunit was purified and the ability of the purified proteins to assemble *in vitro* was determined and assayed by examining the assembled filaments under the electron microscope. These *in vitro* assembly studies showed that the 68 kDa protein, later called NFL, was necessary and sufficient for IF formation. The 145 kDa (NFM) and 200 kDa (NFH) proteins coassembled with NFL and their long C-terminal tails appeared to form the links that can be observed between filaments in the electron microscope. The actual sequences of each of these proteins were determined by protein sequencing and later by cDNA cloning. They are shown schematically in Figure 1. Like all other IFs they contain a central α-helical rod domain flanked by nonhelical N-terminal head and C-terminal tail. The rod domain contains α-helical segments that are represented as cylinders. The rod domain of NFL can be divided into three separate segments (1A, 1B, and 2), whereas those of NFM and NFH are separated into two segments. The NF proteins have variable size C-terminal tails. The lengths of the C-terminal tails determine the ultimate sizes of the three proteins.

The tails of NFM and NFH contain multiple lysine-serine protein (KSP) repeats (shown as yellow circles), which are sites for phosphorylation as described below. As mentioned above, NFL is necessary for filament formation. Using various assays to study protein–protein interactions, it has been demonstrated that NFL can form homodimers and heterodimers with NFM and NFH. These results are consistent with the earlier observations from *in vitro* assembly studies that NFL can form a filament, whereas the other two proteins require NFL to assemble into filaments. Interestingly, transfection studies have shown that rat or mouse NFL needed either NFM or NFH to form a filamentous network *in vivo*, indicating that rodent neurofilaments are obligate heteropolymers. Human NFL can self-assemble in the transfected cells, but this assembly is not very efficient. The other neuronal IF proteins, peripherin, and α-internexin are able to self-assemble into homopolymers *in vitro* and *in vivo*, although NFM appears to have an inhibitory effect on the ability of peripherin to assemble into a filamentous network.

Neurofilaments have been suggested to play a role in regulating axonal caliber and thereby influencing axonal conduction velocity. This role has been confirmed by studies of the Japanese *quiver* quail, which has a premature termination codon in its NFL gene and consequently no neurofilaments in its axons. Normal radial growth is severely inhibited in the large caliber fibers. When the NFL gene was deleted in NFL knockout mice, no visible IFs were observed and there was axonal hypotrophy. There was also a substantial decrease in NFM and NFH in the NFL knockout mice, presumably because they were unstable, since they could not polymerize into filaments. Curiously, in spite of this hypotrophy, the NFL deficient mice developed normally and showed no obvious neurological problems. NFM and NFH knockouts have an even less severe phenotype. NFM knockouts also resulted in some reduction of the caliber of large axons and some axonal loss, whereas NFH knockouts resulted in an even more modest reduction in axonal caliber. Overexpression of NFL and either NFH or NFM in transgenic mice resulted in an increase in the number of neurofilaments as well as axonal caliber, consistent with the role of neurofilaments in regulating axonal calibers.

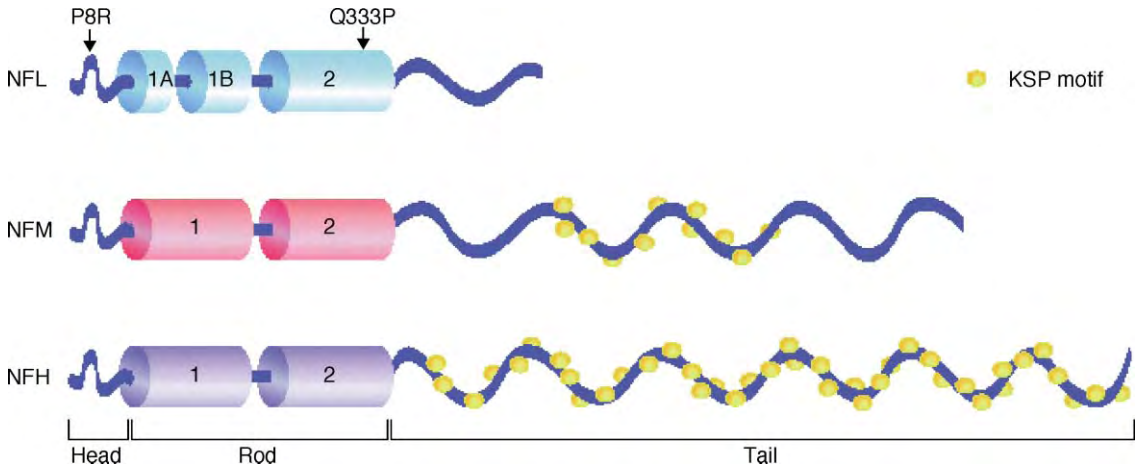

FIGURE 1 Diagrammatic representation of the NFTPs. Note that the size of the proteins are dependent on the lengths of the C-terminal tails. The a-helical rod regions are shown as cylinders. The KSP phosphorylation sites in the tail regions are shown as yellow circles. The first two mutations linked to CMT disease in NFL are indicated.

NFs are characterized by their phosphorylation, a post-translational mechanism that is thought to regulate their functions. NFM and NFH are phosphorylated mainly in the (KSP) repeats located in their C-terminal tail domains. These phosphorylation sites are depicted in the tail domains seen in Figure 1. NFH has 44–51 KSP residues, whereas NFM has 5–14 of these residues, depending on species. Phosphorylation of NFs induces extension of their side arms from the filament backbone, apparently increasing the spacing between individual filaments and ultimately the axonal caliber. Phosphorylated NFs are found in axons, while the nonphosphorylated forms are found in neuronal cell bodies and dendrites. A number of different kinases have been shown to phosphorylate the KSP residues of NFM and NFH. Phosphorylation of the KSP residues has been proposed to be important for the increase of the radial growth of axons by increasing the nearest neighbor distances between the neurofilaments, possibly through electrostatic repulsion between the neurofilament sidearms. The evidence for this proposal came from electron microscopy studies that showed that dephosphorylated neurofilaments were more closely spaced together than phosphorylated neurofilaments. In the dysmyelinated *Trembler* mouse mutant, there is a decrease in neurofilament phosphorylation and smaller axonal diameter. When segments of *Trembler* sciatic nerves were grafted onto control nerves, the *Trembler* segments still maintained their smaller diameters and dephosphorylated neurofilaments, whereas adjacent regions showed normal diameters and neurofilament phosphorylation. These studies were considered as strong evidence that phosphorylation of neurofilaments (especially of NFH) is a determinant of axonal diameter. It therefore came as a surprise that the NFH knockout mice showed only a slight decrease in nearest neighbor spacing of neurofilaments and did not change the axon caliber, indicating that NFH phosphorylation may be less important for the determination of axonal caliber than was predicted. To test this particular property of NFH more rigorously, the NFH gene was replaced in transgenic mice with one deleted in the NFH tail. The results showed that the loss of the NFH tail and all of its phosphorylation sites did not affect the interfilament spacing of the neurofilaments. In contrast, the NFM tail and its state of phosphorylation may be more important for radial growth, even though it contains considerably fewer phosphorylation sites.

As described before, neurofilament proteins are synthesized in the cell body and have been found to move down the axon as part of the slow component of axonal transport with a velocity of $\sim 0.1–1$ mm day^{-1}. The initial hypothesis was that the entire axoplasm moved as a coherent block, but more recent work has shown that the entire axoplasm in its totality does not move. Neuronal IFs are now thought to move as monomeric and polymeric units. Studies using proteins tagged with green fluorescent protein and live-video microscopy have demonstrated that neuronal IFs undergo rapid, intermittent, and nonsynchronous transport in both directions, with predominance of the anterograde transport and long pauses in between movements along the axons. These studies indicate that slow transport is actually the result of fast motions interrupted by long pauses. This fast transport is likely to utilize one of the many motors that have been identified for fast transport. These motor proteins could also be responsible for some of the cross-links observed between IFs and microtubules. Other potential cross-linkers are members of the plakin family of proteins that were first identified in junctions in epithelial cells. Recent studies have indicated that some plakins are also expressed in the nervous system. Plakins have distinct domains that include microtubule, microfilament, and IF-binding domains and could therefore be important in the formation of cross-links between these cytoskeletal elements. The phosphorylation of the side chains of the neurofilaments described above has also been considered to be important for the regulation of transport of neurofilaments through axons. Two recent studies have provided different conclusions regarding the role of NFH side arm phosphorylation in neurofilament transport. In one study, all the potential phosphorylation sites of NFH were mutated either to preclude phosphorylation or mimic permanent phosphorylation of the NFH side arms. These mutants displayed altered rates of transport in a bulk transport assay. The mutant mimicking permanent phosphorylation spent a higher proportion of time pausing than one that could not be phosphorylated, indicating that NFH phosphorylation slows neurofilament transport. In contrast, in transgenic mice, where the endogenous NFH was replaced by a tailless NFH, there were no changes in the rate of bulk transport. These studies indicate that the mouse studies are not always consistent with the studies in cultured cells, in part due to additional compensatory mechanisms that may exist in the mouse. In any case, some of these aspects of neurofilament transport will become clearer when the specific motors that move neurofilaments are identified.

Overexpression of neuronal IFs in transgenic mouse models results in the formation of mislocalized protein aggregates, which affect neuronal function and survival. This has been shown in the case of human NFH, mouse NFL, peripherin, and rat α-internexin. The relationship between misexpression, disrupted transport, and mislocalization of neuronal IFs to neurodegeneration is also apparent from the appearance of axonal neurofilamentous accumulations in a number of neurodegenerative diseases. In particular, aggregation of IFs in motor neurons and alteration in their axonal transport has been reported in amyotrophic lateral sclerosis (ALS).

It appears likely that mutations in neurofilament proteins would also lead to neurodegeneration. When an assembly disrupting NFL mutant was produced in a transgenic mouse model, the mutant NFL caused massive degeneration of motor nerves. Recently, several mutations have been identified in neurofilament proteins that lead to neurodegenerative diseases. Deletions and insertions in the tail domain of NFH have been reported in 1–2% of patients with sporadic ALS. More strikingly, a number of mutations in the NFL gene have now been linked to Charcot-Marie-Tooth neuropathy type 2E. Two of these mutations (P8R and Q333P) are shown in Figure 1. When these same mutations are introduced in an NFL cDNA and the mutant NFL constructs are expressed in cultured cells, defects in assembly and transport of NFL are observed. It appears therefore that these mutations in NFL might alter axonal transport, which in turn would cause neurodegeneration. This notion is consistent with the hypothesis that alterations in axonal transport (in which neuronal IFs could be directly or indirectly involved) play a role in the pathogenesis of other neurodegenerative diseases.

α-Internexin

α-Internexin was first isolated from optic nerve and spinal cord and found to be particularly abundant in the developing nervous system. α-Internexin has an apparent molecular weight of 66 kDa and is therefore a little smaller than the NFTPs. Although it is present in both the CNS and PNS early in development, it is mainly CNS specific in the mature mammalian nervous system. Consistent with its expression early in development in the absence of other IFs, α-internexin has been shown to be able to self-assemble both *in vitro* and in transfected cells. α-Internexin is closely related to the NFTPs and is therefore also classified as a type IV IF protein. α-Internexin is the first neuronal IF expressed in neurons after they are committed to the neuronal lineage. The expression of α-internexin is high early in development and then decreases after the axon matures. In the PNS, the level of α-internexin decreases significantly in adulthood, although it persists especially in thinner unmyelinated axons. In the CNS, α-internexin expression is also lower after the axon matures. Of particular interest is the fact that α-internexin is the only neuronal IF expressed in some neurons, e.g., the granule cell neurons in the cerebellum. The axons of these neurons are thinner in diameter than the ones that express the NFTPs suggesting that α-internexin is not important for maintaining axonal diameter. The early expression of α-internexin led to the suggestion that it might be important for axon outgrowth. Although this idea was supported by antisense inhibition experiments in cultured cells, the α-internexin knockout mice have no obvious phenotype. No compensatory changes in the levels of other neuronal IFs were observed and it appears that α-internexin is not necessary for axon outgrowth in these mice. Unfortunately, these knockout studies tell us little about other potential functions of this protein. Overexpression of α-internexin in transgenic mice results in the formation of cerebellar torpedoes. These torpedoes are swellings in Purkinje cell axons. The presence of these torpedoes results in the degeneration and ultimate death of the Purkinje cell. There is a dysfunction of the cell as determined behaviorally from the transgenic mice before the cells die.

Peripherin

Peripherin was first identified as an IF protein from neuroblastoma and its cDNA was cloned from a cell line that can be induced to grow neuronal processes by the addition of nerve growth factor, called PC12 cells. Peripherin has a molecular weight of 57 kDa and belongs to the type III IF proteins, which also consists of vimentin, the glial specific GFAP, and the muscle specific IF protein called desmin. Peripherin is therefore the only type III neuronal IF protein, since all the other neuronal IFs are in the type IV category. The significance of this difference is not known. Like all the other type III IFs, peripherin can self-assemble into a filamentous network. Peripherin can also coassemble with other neuronal IFs. Peripherin is predominantly found in the PNS (hence its name), but some CNS neurons also express peripherin. As described above, peripherin was identified as a gene that was increased in PC12 cells upon stimulation by nerve growth factor. Peripherin has also been shown to be up-regulated following axonal injury. These studies suggested that peripherin may play a role in axon outgrowth and elongation. Peripherin depletion experiments with anti-sense technologies yielded conflicting results: initial studies showed that anti-sense oligonucleotides did not inhibit neurite outgrowth, whereas more recent studies using small interfering RNAs (siRNAs) showed that peripherin siRNA inhibits the initiation, extension and maintenance of neurites in PC12 cells. The reason for this discrepancy is not clear. Peripherin knock-out mice have normal caliber axons and show no axonal loss. Some interesting observations have led to the possibility that misexpression of peripherin can lead to neurodegenerative disease. Peripherin has been found in axonal spheroids in patients with ALS. Furthermore, overexpression of peripherin by four to seven fold in transgenic mice leads to late onset progressive motor neuron disease, which is accelerated in mice that lack NFL.

Nestin

Nestin was first described as a marker of neuroepithelial stem cells. Subsequent cDNA cloning showed that a large IF protein encoded this marker. Nestin has the basic hallmarks of an IF protein with a α-helical rod, capable of forming coiled coil dimers, a very short head domain and a very long tail domain. Nestin has little homology to the other mammalian IF proteins, but its genomic structure is similar to the NFTPs and α-internexin. As a result, nestin is placed either as a separate type of IF (type VI), or as a type IV IF along with the NFTPs and α-internexin. During early development, nestin is expressed in neuroepithelial cells and muscle progenitor cells. Transgenic mouse studies have indicated that different regulatory elements in the nestin gene are responsible for directing gene expression in developing muscle and neural precursor cells, respectively. Nestin is not able to self-polymerize, but requires vimentin to form a filamentous network. There have been no published reports of a nestin knockout mouse.

See Also the Following Articles

Actin Assembly/Disassembly • Actin-Capping and -Severing Proteins • Actin-Related Proteins • Intermediate Filament Linker Proteins: Plectin and BPAG1 • Intermediate Filaments • Microtubule-Associated Proteins • Rho GTPases and Actin Cytoskeleton Dynamics • Tubulin and its Isoforms

Glossary

axonal spheroids Accumulations of protein aggregates in axons, usually containing neurofilamentous structures.

axonal transport The movements of vesicles, mitochondria, and other cytoplasmic structures down the axon, necessitated by the fact that most protein synthesis occurs in the axon and the proteins must sometimes travel long distances to reach the end of the axon. This transport generally occurs by way of motor proteins along microtubules and microfilaments.

Charcot–Marie–Tooth (CMT) disease An inherited neurological disorder that affects the peripheral nerves. It is named after the three physicians who described it. CMT patients slowly lose the normal use of their limbs as the nerves to the extremities degenerate. There are a large number of different causes for the disease, including the recently identified neurofilament mutations.

cytoskeleton A network of interconnected cytoplasmic filaments that consists of microtubules, microfilaments and IFs.

transgenic mouse A mouse that has been genetically altered to express a gene that is not normally expressed or to have a gene deleted (also called a knockout mouse).

Further Reading

Coulombe, P. A., Ma, L., Yamada, S., and Wawersik, M. (2001). Intermediate filaments at a glance. *J. Cell Sci.* **114**, 4345–4347.

Helfand, B. T., Chang, L., and Goldman, R. D. (2003). The dynamic and motile properties of intermediate filaments. *Annu. Rev. Cell Dev. Biol.* **19**, 445–467.

Lariviere, R. C., and Julien, J. P. (2004). Functions of intermediate filaments in neuronal development and disease. *J. Neurobiol.* **58**, 131–148.

Leung, C. L., and Liem, R. K. H. (2003). Neuronal intermediate filament overexpression and neurodegeneration in transgenic mice. *Exp. Neur.* **184**, 3–8.

Leung, C. L., Flores, R. G., and Liem, R. K. H. (1998). The complexity of intermediate filaments in the nervous system. In *Intermediate Filaments* (H. Herrmann and R. Warton, eds.) pp. 497–526. Plenum Press.

Leung, C. L., Green, K. J., and Liem, R. K. H. (2002). Plakins: A family of versatile cytolinker proteins. *Trends Cell Biol.* **12**, 37–45.

Shah, J. V., and Cleveland, D. W. (2002). Slow axonal transport: Fast motors in the slow lane. *Curr. Opin. Cell Biol.* **14**, 58–62.

Biography

Ronald K. H. Liem is a Professor of Pathology and Anatomy and Cell Biology at Columbia University College of Physicians and Surgeons. Dr. Liem's primary research interest is in the cell and molecular biology of the neuronal cytoskeleton and its involvement in neurodegenerative diseases. His contributions include the biochemical identification of the neurofilament triplet proteins, the first identification and cDNA cloning of α-internexin and the characterization of the plakins, the major cytoskeletal linker proteins in the nervous system.

Neuropeptide Y Receptors

Eric M. Parker
Schering-Plough Research Institute, Kenilworth, New Jersey, USA

Neuropeptide Y (NPY) is a 36 amino acid neuropeptide that is widely distributed in both the central and peripheral nervous systems. NPY is a member of the pancreatic polypeptide family, which also includes the structurally related peptides peptide YY (PYY) and pancreatic polypeptide (PP). Neurons containing NPY typically coexpress and cosecrete classical neurotransmitters and/or other neuropeptides (e.g., norepinephrine, γ-aminobutyric acid, somatostatin, corticotrophin releasing hormone); hence, NPY probably acts in concert with other neurotransmitters and neuropeptides in either a cotransmitter or modulatory role. As expected from its ubiquitous distribution and colocalization with other neurotransmitters and neuropeptides, NPY has been implicated in a wide variety of physiological effects, including the regulation of body weight, neuronal excitability, circadian rhythms, mood, ethanol consumption, nociception, cognition, endocrine function, cardiovascular function, gastrointestinal function, and bone formation. The effects of NPY on energy homeostasis have been most extensively studied in recent years. NPY increases body weight via stimulation of food intake and reduction of energy expenditure and also induces metabolic abnormalities associated with obesity, including hyperinsulinemia, hyperglycemia, and hypercortisolemia.

Neuropeptide Y (NPY) produces its physiological effects by interacting with at least six distinct G-protein-coupled receptors designated Y_1, Y_2, Y_3, Y_4, Y_5, and y_6. With the exception of the Y_3 receptor, genes and/or cDNAs encoding each of these receptors have been cloned. Pharmacological tools that activate (agonists) or inhibit (antagonists) each of the NPY receptors have also been identified (Table 1, Figure 1). Although all the NPY receptors are G-protein-coupled receptors with high affinity for NPY, their primary sequences are not highly related to one another (Figure 2). Site-directed mutagenesis studies suggest that NPY, NPY-related peptides, and nonpeptide NPY receptor antagonists have overlapping (although not entirely identical) binding sites, composed primarily of residues in the extracellular domains and in the extracellular side of the transmembrane domains.

The NPY Y_1 Receptor

The NPY Y_1 receptor is pharmacologically characterized by its high affinity for [Pro^{34}]NPY and [D-Arg^{25}]NPY; its low affinity for N-terminally truncated NPY analogues; and its high affinity for nonpeptide antagonists such as 1229U91, BIBP3226, and BIBO3304 (Table 1, Figure 1). Structurally, the receptor is related to the NPY Y_4 and NPY y_6 receptors (Figure 2). NPY Y_1 receptor mRNA is expressed at highest levels in brain (especially cortex, hippocampus, thalamus, and hypothalamus), vascular smooth muscle, heart, kidney, spleen, skeletal muscle, lung, testis, adrenal gland, placenta, bone marrow, and gastrointestinal tract. NPY Y_1 receptor protein distribution mirrors mRNA distribution fairly closely with the notable exception that low levels of receptor are detected in most hippocampal regions. The NPY Y_1 receptor is coupled to multiple signal transduction pathways via pertussis toxin sensitive G proteins (G_i and/or G_o), including reduction of cyclic AMP (cAMP) formation, an increase in intracellular calcium, an increase in MAP kinase activity, and activation of GIRK K^+ channels and L-type Ca^{2+} channels. The NPY Y_1 receptor mediates several biological effects of NPY, including contraction of vascular smooth muscle, stimulation of food intake and body weight gain, inhibition of insulin secretion, anxiolytic and antidepressant effects, regulation of pituitary hormone secretion (reduction of growth hormone and thyroid stimulating hormone secretion, stimulation of luteinizing hormone secretion), regulation of ethanol consumption, nociception, and neurogenic inflammation. Activation of the NPY Y_1 receptor acutely stimulates food intake and body weight gain, and acute treatment with NPY Y_1 receptor antagonists often has the opposite effect. As expected from acute experiments, mice lacking the NPY Y_1 receptor are hypophagic, hyperinsulinemic and have slightly reduced NPY- and deprivation-induced food intake. However, NPY Y_1 receptor-deficient mice are also obese, perhaps due to hyperinsulinemia, reduced locomotor activity, and/or reduced metabolic rate.

TABLE 1

Potencies of Standard Agonist and Antagonist Ligands for the Known NPY Receptors

Peptide	Y_1	Y_2	Y_3	Y_4	Y_5	y_6
NPY	0.14	1.2	1.8	>1000	0.96	1.9
PYY	0.70	0.58	7200	>1000	1.0	0.8
NPY (2–36)	3.4	1.6		>1000	1.2	1.4
NPY (3–36)	110	2.4		>1000	2.8	4.9
NPY (13–36)	300	2.2		>1000	20	16.1
[Pro^{34}] PYY	0.37	>1000		6.0	1.3	
Human PP	150	>1000		0.037	1.4	>1000
Rat PP	>1000	>1000		0.060	170	>1000
[D-Arg^{25}]NPY	0.2	28.1		577	118	
1229U91	**0.063**	**> 1000**		**3**	**> 1000**	**0.8**
BIBP3226	**5.1**	**> 1000**	**> 1000**	**> 1000**	**> 1000**	**> 1000**
BIBO3304	**0.38**	**> 1000**		**> 1000**	**> 1000**	
BIIE0246	**> 1000**	**15**		**> 1000**	**> 1000**	
[D-Trp^{32}]NPY	>1000	>1000		>1000	43	164
[D-Trp^{34}]NPY	363	>1000		525	15	186
[Ala^{31}, Aib^{32}]NPY	>1000	>1000		>1000	29	
CGP-71684A	**> 1000**	**> 1000**		**> 1000**	**0.72**	**> 1000**

EC_{50} (nM) (Agonists; normal text) or **K_i (nM) (Antagonists; bold text)**.

The NPY Y_2 Receptor

The NPY Y_2 receptor is structurally quite distinct from the other NPY receptors (Figure 2) and is pharmacologically characterized by its high affinity for N-terminally truncated NPY analogues, its low affinity for [Pro^{34}]NPY, and its high affinity for the nonpeptide antagonist BIIE0246 (Table 1). The NPY Y_2 receptor is localized primarily in the brain, but is also expressed at low levels in the gastrointestinal tract and peripheral nerve terminals. In the brain, highest levels of NPY Y_2 receptor mRNA are found in hippocampus, piriform cortex, olfactory tubercle, hypothalamus, thalamus, inferior olive, and lateral reticular nucleus. NPY Y_2 receptor protein is detected at highest levels in subfornical organ, thalamus, hypothalamus, substantia nigra, and area postrema. NPY-containing neurons in the brain express the NPY Y_2 receptor and the NPY Y_2 receptor antagonist BIIE0246 increases depolarization-evoked NPY release from brain slices, suggesting that the NPY Y_2 receptor acts as an autoreceptor. Similarly, pharmacological studies have shown that the receptor is localized on sympathetic, parasympathetic, and sensory nerve terminals where it functions as both an autoreceptor and a heteroreceptor to regulate neurotransmitter/neuropeptide release. The NPY Y_2 receptor couples to pertussis toxin-sensitive G proteins (G_i and/or G_o) leading to a reduction of cAMP formation, an increase in intracellular calcium mediated by activation of phospholipase C, an increase in MAP kinase activity, an activation of K^+ channels (e.g., Kv4, GIRK, and Ca^{2+} activated K^+ channels), and an inhibition of voltage-gated (N and P/Q type) Ca^{2+} channels. The NPY Y_2 receptor also apparently increases intracellular calcium via a phospholipase C-independent pathway that utilizes a pertussis-toxin insensitive G protein. The NPY Y_2 receptor is involved in several physiological processes, including reduction of neuronal excitability and seizure activity, regulation of circadian rhythms, regulation of body weight and energy metabolism, improvement in learning and memory, regulation of ethanol consumption, reduction of bone formation, reduction of gastrointestinal motility, intestinal secretory activity and stimulation of angiogenesis and wound healing. The precise role of the NPY Y_2 receptor in the regulation of body weight is currently unclear. Selective NPY Y_2 receptor peptide agonists do not alter food intake, suggesting that this receptor does not mediate the orexigenic effects of NPY. In fact, the NPY Y_2 receptor peptide agonist PYY3-36, which is released postprandially, actually decreases food intake and body weight in humans. Variable effects of genetic deletion of the NPY Y_2 receptor in mice have been reported. Further studies are needed to definitively determine the role of the NPY Y_2 receptor in the regulation of body weight.

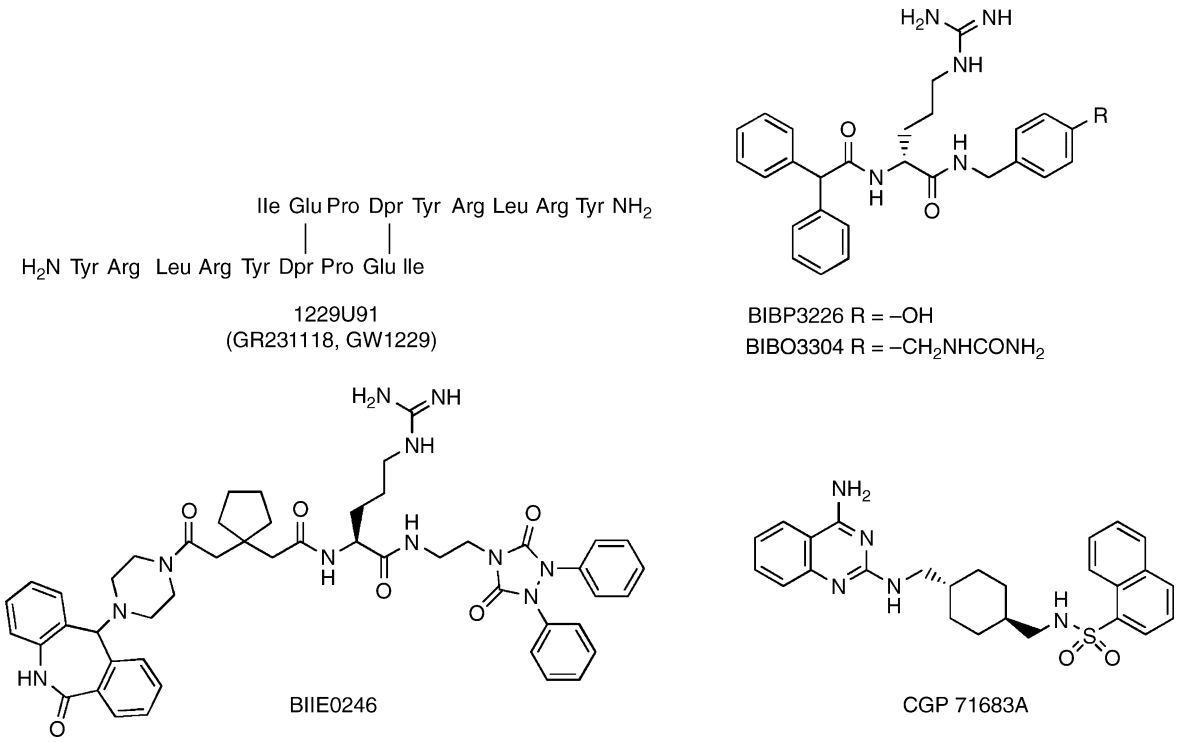

FIGURE 1 Structures of standard NPY receptor antagonists.

The NPY Y_3 Receptor

The NPY Y_3 receptor has been pharmacologically characterized in bovine adrenal chromaffin cells and in the rat heart, colon, lung, hippocampus, and brainstem. The distinguishing pharmacological feature of this receptor is its higher affinity for NPY than for PYY. Activation of the NPY Y_3 receptor has been shown to decrease cAMP formation and increase intracellular calcium concentration. Application of NPY to the brainstem decreases blood pressure and heart rate, effects that may be mediated by activation of the NPY Y_3 receptor. Although pharmacological evidence supports the existence of this receptor in rats and cows, there is no evidence that this receptor exists in humans, and a gene or cDNA encoding the receptor has not been cloned. Molecular characterization of the NPY Y_3 receptor is required to unequivocally validate its existence and determine its physiological role.

The NPY Y_4 Receptor

The NPY Y_4 receptor is structurally related to the NPY Y_1 and NPY y_6 receptors (Figure 2), but has distinct pharmacological properties (Table 1). Specifically, the NPY Y_4 receptor has high affinity for human and rat pancreatic polypeptide (PP), but has low affinity for NPY (Table 1). Indeed, this receptor would be more accurately classified as a PP receptor rather than as an NPY receptor. Interestingly, the rat and human NPY Y_4 receptors display some significant pharmacological differences, perhaps due to the fact that these species orthologues are only 75% identical to one another. Very low levels of NPY Y_4 receptor mRNA are expressed in the brain, primarily in the brainstem and hypothalamus. There are also species differences in the expression pattern of the NPY Y_4 receptor in the periphery. In rat, the receptor is expressed primarily in testis and lung, whereas in human the receptor is expressed primarily in colon, small intestine, prostate, and pancreas. Activation of the NPY Y_4 receptor decreases cAMP formation and increases intracellular calcium. Pharmacological studies have shown that, the NPY Y_4 receptor mediates the ability of PP to increase pancreatic secretion and increase intestinal motility. Mice lacking the NPY Y_4 receptor suggest that this receptor is involved in aggressive behavior and in maintaining sympathetic nervous system activity. In addition, genetically obese *ob*/*ob* mice lacking the NPY Y_4 receptor have improved fertility relative to *ob*/*ob* mice with an intact NPY Y_4 receptor, suggesting that this receptor mediates at least some of the negative effects of NPY and/or PP on fertility and on the hypothalamic–pituitary–gonad axis.

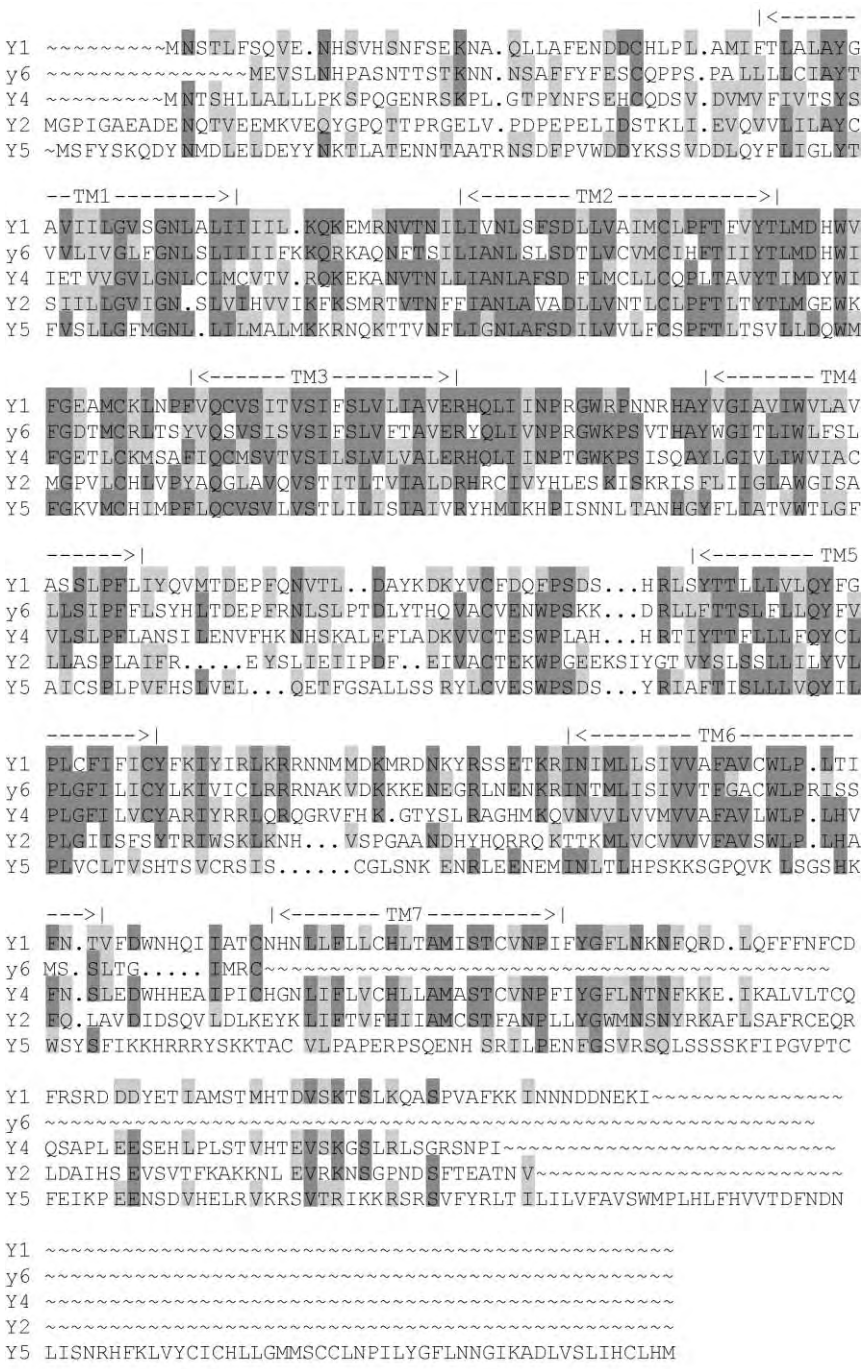

FIGURE 2 Alignment of the primary sequences of the NPY receptors. Amino acids that are identical in ≥3 NPY receptors are shaded dark while conservative amino acid substitutions in >3 NPY receptors are shaded light. The approximate location of the seven transmembrane domains is indicated over the sequences.

The NPY Y_5 Receptor

The NPY Y_5 receptor is a structurally and pharmacologically unique NPY receptor (Figure 2) characterized by high affinity for N-terminally truncated NPY analogues [Pro^{34}]NPY, [D-Trp^{32}]NPY, [D-Trp^{34}]NPY, and [Ala^{31}, Aib^{32}]NPY (Table 1). This receptor also has high affinity for several recently disclosed nonpeptide antagonists such as CGP-71684A (Figure 1). The NPY Y_5 receptor is discretely localized in brain, primarily in hypothalamus, hippocampus, piriform cortex, and olfactory tubercle. Interestingly, NPY Y_5 receptor mRNA is almost always localized in neurons that also express NPY Y_1 mRNA. Since the

genes encoding the NPY Y_1 and Y_5 receptors overlap on chromosome 4q31, this may reflect a regulatory mechanism inherent to this gene locus. In the periphery, NPY Y_5 receptor mRNA has been detected in testis, spleen, pancreas, gastrointestinal tract, vascular smooth muscles, and cardiomyocytes. Like the other NPY receptors, the NPY Y_5 receptor couples to multiple G protein-mediated pathways (primarily pertussis toxin-sensitive G proteins G_i and/or G_o) to decrease cAMP formation, increase intracellular calcium concentration, and activate MAP kinase pathways. There is evidence that the NPY Y_5 receptor utilizes a somewhat different signaling pathway to activate MAP kinase than do the other NPY receptors. Evidence suggests that this receptor is involved in the regulation of body weight (stimulation of food intake and reduction of energy expenditure), control of glucose homeostasis, regulation of pituitary hormone secretion (stimulation of adrenocorticotropin secretion, inhibition of thyroid stimulating hormone secretion, inhibition of luteinizing hormone secretion), regulation of ethanol consumption, control of neuronal excitability and seizure activity, circadian rhythms, diuresis, and natriuresis. Although selective NPY Y_5 receptor peptide agonists have been shown to stimulate food intake and decrease energy expenditure, selective NPY Y_5 receptor antagonists generally do not affect food intake, energy expenditure, or body weight. Furthermore, mice lacking the NPY Y_5 receptor have normal food intake, energy expenditure, and body weight. Thus, the role of the NPY Y_5 receptor in the regulation of body weight remains unclear.

The NPY y_6 Receptor

The NPY y_6 receptor is structurally related to the NPY Y_1 and Y_4 receptors. It is pharmacologically very similar to the NPY Y_1 receptor, although it tends to bind N-terminally truncated NPY analogues with somewhat higher affinity than the NPY Y_1 receptor. The NPY y_6 receptor couples to G_i and inhibits cAMP formation. Interestingly, a functional NPY y_6 receptor is found in mice and rabbits, but not in rats and primates. In the case of rats, a gene encoding the NPY y_6 gene cannot be detected, whereas in primates the gene is a nonfunctional pseudogene. The lack of a functional NPY y_6 receptor in primates has resulted in the adoption of a lower case designation for this receptor. In mice, NPY y_6 receptor mRNA has been detected in kidney, testis, and brain, particularly in the hypothalamus. Although the NPY y_6 receptor clearly does not contribute to the effects of NPY in humans, this receptor must be taken into account when considering the physiological effects of NPY in mice. To date, however, no physiological effect of NPY in mice has been linked to activation of the NPY y_6 receptor.

Regulation of NPY Receptors

As is the case for most G-protein-coupled receptors, NPY receptors are subject to various mechanisms of regulation. The NPY Y_1, Y_2, and Y_5 receptors have recently been shown to exist as homodimers in the plasma membrane, although the extent of homodimerization was not affected by the binding of NPY to the receptors or by the coupling of the receptors to G proteins. NPY receptors have also been shown to be subject to both homologous and heterologous desensitization. These desensitization processes are typically mediated by phosphorylation of the receptor and subsequent association of the phosphorylated receptor with arrestins. Over a longer period of time, receptors can internalize and be recycled or degraded. Changes in receptor gene expression can also occur. NPY Y_1 receptors rapidly desensitize after NPY treatment by phosphorylation of the receptor and rapid internalization of the receptor via clathrin coated pits. Conversely, NPY Y_2 receptors are internalized very slowly. The NPY Y_1, Y_2, Y_4, and Y_5 receptors also associate with β-arrestin 2, with the Y_1 receptor again showing the most rapid association rate and NPY Y_2 receptors showing the slowest association rate. With respect to heterologous desensitization, NPY Y_2 receptors have been shown to desensitize after exposure of LN319 cells to bradykinin.

See Also the Following Articles

G Protein-Coupled Receptor Kinases and Arrestins • Neurotensin Receptors • Neurotransmitter Transporters • Phospholipase C

Glossary

G protein A heterotrimeric GTP binding protein consisting of α-, β-, and γ-subunits. G proteins link G-protein-coupled receptors to a wide variety of effector molecules in signal transduction pathways by alternately binding and hydrolyzing GTP in response to receptor and effector activation.

G-protein-coupled receptors (GPCRs) A family of ~500 neurotransmitter and neuropeptide receptors (as well as several hundred odorant receptors) that are structurally characterized by seven transmembrane domains, an extracellular amino terminus, and a cytoplasmic carboxy terminus. This receptor family is functionally characterized by the ability to bind and activate G proteins upon binding of their cognate ligand.

Further Reading

Berglund, M. M., Hipskind, P. A., and Gehlert, D. R. (2003). Recent developments in our understanding of the physiological

role of PP-fold peptide receptor subtypes. *Exp. Biol. Med.* **228**, 217–244.

Parker, E., van Heek, M., and Stamford, A. (2002). Neuropeptide Y receptors as targets for anti-obesity drug development: perspective and current status. *Eur. J. Pharmacol.* **440**, 173–187.

Thorsell, A., and Heilig, M. (2002). Diverse functions of neuropeptide Y revealed using genetically modified animals. *Neuropeptides* **36**, 182–193.

Biography

Eric Parker is Group Director of Central Nervous System Research at the Schering-Plough Research Institute. His research interests include the molecular pathogenesis of Alzheimer's disease and neuropeptide and neurotransmitter receptors involved in the etiology of obesity and psychiatric disease. He holds a Ph.D. in pharmacology from the University of North Carolina at Chapel Hill.

Neurotensin Receptors

William Rostène, Patrick Kitabgi and Didier Pélaprat
INSERM, Paris, France

Peptides are now well-recognized as important modulators of central and peripheral functions. Among the considerable number of peptides which has been discovered in various species, neurotensin (NT) has been found to play an essential role in specific brain and neuroendocrine functions and more recently in cancer. These effects of NT have been related to an interaction of this 13 aminoacid peptide with receptors belonging to the family of G protein-coupled receptors (GPCRs) with seven transmembrane domains. Very recently a new NT receptor with a single transmembrane domain has been discovered. Cloning of these receptors has permitted to develop agonists and antagonists for NT, the more recent developments being focused on the potential therapeutical usefulness of nonpeptide and peptido-mimetic substances able to cross the blood–brain barrier.

Neurotensin

The discovery of Neurotensin (NT), a 13 aminoacid peptide, occurred during the isolation of another peptide, substance P, from bovine hypothalamus, by Susan Leeman and Robert Carraway in 1973. It was the simple observation of a characteristic vasodilatation occurring around the face and ears after intravenous injection of the isolated material which allowed the purification of NT. Rapidly after its primary structure in aminoacids was known, antibodies were raised, a strategy used for several peptides in order to develop sensitive radio-immunoassays and immunocytochemical approaches which provided useful information on the physiology, content, distribution, and anatomical localization of NT in fluids and tissues. Though NT was first found in the brain, 90% of the peptide is located in the gut.

The main *in vivo* biological activities of NT following peripheral administration include a strong vasodilatation and hypotension, an increase in vascular permeability via histamine released by the mast cells, a hyperglycemia involving glucagon, insulin and histamine, inhibition of gastric acid and pepsin secretion and of gastric motility. Strong neuroendocrine effects on the release of pituitary hormones such as ACTH, LH, FSH, GH, and prolactin have been particularly evidenced. Central injection of NT induced hypothermia, release of the neurotransmitter dopamine (DA), inhibition of feeding in fasted animals, and analgesic effects which are not mediated by opiates. Finally, high-fat meal and drugs affecting the brain DA systems have been reported to produce strong release of NT in plasma and brain, respectively.

Neurotensin Receptors

The relatively simple amino acid sequence of NT allowed structure-activity studies which showed that the C-terminal part (aa 8–13) of the peptide contained the whole activity of NT. Thus, design of small peptide molecules and modifications both in the N- and C-terminal portions of NT rapidly led to NT analogues which could be labeled with tritium or iodine in order to carry out binding studies. Such experiments demonstrated that high affinity NT binding sites could be observed in several tissues and various cell lines including human cancer cells. From these binding studies, it became obvious that NT could bind to several receptors as already shown for other neuropeptides.

Up to now indeed, three NT receptors – NTS1, NTS2, and NTS3 – have been identified and their biochemical and pharmacological properties recently reviewed. We will thus briefly outline their main characteristics (Table I).

NTS1

NTS1 has been cloned from rat and human and belongs to the family of G protein-coupled receptors (GPCRs) with seven transmembrane domains. It seems to be involved in the majority of the physiological effects of NT reported so far. NTS1 is a Gq-preferring receptor suggesting that binding of NT to NTS1 induces activation of phospholipase C, increase in inositol phosphate, and intracellular calcium concentration. In parallel, in transfected cell systems, NTS1 has been also reported to be linked to Gi/o or Gs, leading to inhibition or stimulation of cyclic AMP production, respectively, and to stimulation of more distal transduction pathways such as mitogen-activated protein kinases. Interestingly, the most recent data indicate that different intracellular

TABLE I

Characteristics of Cloned Neurotensin Receptors

Receptor subtype	Structure	Signal transduction pathway	Protein size amino acids	Agonists	Antagonists
NTS1	7 transmembrane domains	G_q/G_{11}, calcium mobilization	418 (h[a])	Neurotensin	SR 48692
		G_S, increase cAMP	424 (r[b])	NL-69L	SR 142948A
NTS2	7 transmembrane domains	Calcium mobilization	410 (h)	SR 48692 SR 142948A	Neurotensin Levocabastine
			416 (r)	Neurotensin SR 48692 Levocabastine	
NTS3 also termed sortilin	A single transmembrane domain	Unknown	831 (h) 825 (m[c])		

[a] Human.
[b] Rat.
[c] Mouse.

domains of the receptor are involved in coupling to the various G-proteins and suggest the existence of multiple agonist-selective conformations, which may lead to the preferential activation of either of the corresponding signaling pathways. These results open the possibility of designing agonists selective for one of the pathways associated with a given NTS receptor.

Although the development of selective NT agonists may be important for a better understanding of the physiological relevances of this peptide, random screening and chemical optimization led to the achievement of nonpeptide antagonists, which have proved extremely useful to study the role of endogenous NT associated with NTS1. The first nonpeptide antagonist, SR 48692, developed by Sanofi-Synthelabo, as well as the recent development of knock-out mice for NTS1 confirmed that most of the NT effects reported above can be attributed to NTS1. More recently, another nonpeptide NTS1 antagonist, SR 142948A, but with less selectivity for NTS1 than SR 48692, has been described.

Elegant strategies of mutagenesis and modeling of NTS1 have provided useful information about the molecular determinants of NT and SR 48692 binding sites on NTS1 demonstrating that on the 424 aminoacid protein sequence of rat NTS1, the third extracellular domain and residues in the sixth and seventh transmembrane domains were essential for both NT and SR 48692 binding. Some residues such as Trp339, Phe344, and Tyr347 (all of them aromatic aminoacids) located in the third extracellular loop of NTS1 are implicated in NT binding, Tyr324, Tyr351, Thr354, Phe358, and Tyr359 are involved in antagonist binding only, and Met208, Phe331, and Arg327 interact with both agonist and antagonist. The third intracellular loop of the NTS1 and the first half of the C-terminal intracellular domain are involved in Gq and Gi/o coupling respectively, whereas the C terminus is essential for NT-induced NTS1 internalization, an observation important for NT targeting, as it will be discussed later (Figure 1).

NTS2

NTS2 which is also a GPCR shares 60% sequence similarity with NTS1. It has been cloned from mouse, rat, and human, and corresponds to the low NT affinity sites originally described and able to bind the nonpeptide histamine H1 antagonist levocabastine. Most of the physiolological implications of NTS2 are unknown, but several arguments suggest that it mediates the analgesic effect of NT reported in the mouse. Surprisingly, depending on the species studied, NT, SR 48692, and levocabastine behave differently on transduction signaling pathway activation. In summary, SR 48692, an antagonist of the NTS1, behaves as a potent agonist on NTS2, whereas NT or levocabastine have no effect or antagonize the effect of SR 48692, for instance, on inositol phosphate production. These results suggest that an endogenous activator for NTS2 other than NT may exist and remains to be discovered. Though mutagenesis studies have not been carried out as extensively for NTS2 as that for NTS1, it was recently reported that a single tyrosine residue in position 237 in the third intracellular loop of the mouse and human NTS2 was responsible for receptor phosphorylation and essential for receptor recycling.

NTS3

In contrast to both NTS1 and NTS2, this more recently discovered NT receptor subtype belongs to the family of proteins characterized by a single-transmembrane domain, a cystein-rich domain, a signal peptide, a furin cleavage site, and a short cytoplasmic C-terminal

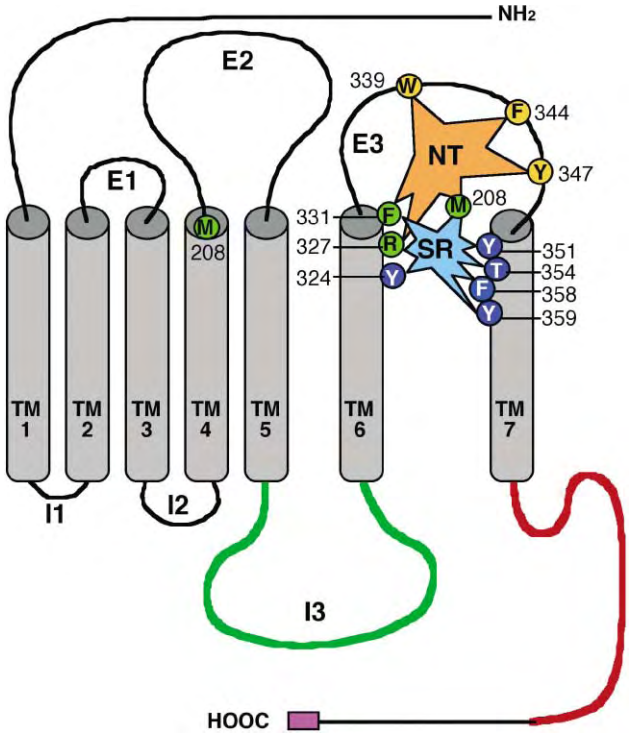

FIGURE 1 Molecular properties of the rat NTS1 (color illustration). The rat NTS1 is a 424 amino acid proteins with seven transmembrane (TM) domains. The SR 48692 (SR, light blue) and NT (orange) binding domains were established by mutagenesis and modeling studies. The residues that play a role in agonist and antagonist binding can be grouped in three categories: Met208, Phe331, Arg327 that interact with both NT and SR 48692 (green); Tyr324, Tyr351, Thr354, Phe358, and Tyr359 that are involved in antagonist binding only (blue); and Trp339, Phe344, and Tyr347 in extracellular loop 3 (E3) that interact with NT only (yellow). The C terminus of the NTS1 (magenta box) is essential for agonist-induced receptor internalization. Intracellular loop 3 (I3, in green) and the first half of the C-terminal intracellular domain (in red) are involved in Gq and Gi/o coupling, respectively.

tail. This 100 kDa protein shares 100% with sortilin, a protein involved in molecule sorting between the cell surface and intracellular compartments. Thus, it was recently observed that NTS3 could interfere with NT-induced intracellular trafficking of NTS1. Brain distribution of NTS3 demonstrates an extensive overlap of NTS3 with NTS1 and NTS2 subtypes, suggesting that NTS3 might interact with the other NT receptors to mediate central effects of NT. Recent evidence suggests that NT3 can mediate the effect of NT on microglial migration.

Receptor-Mediated Physiological Effects of NT

Although NT has been implicated in several central and peripheral effects as reported above, studies have been extensively focused on two main orientations. On the one hand, the brain involvement of NT in the regulation of central dopaminergic systems. On the other hand, in the periphery, its implication in cancer.

The main conclusions of these studies and their potential implication in therapeutics are reported here.

Neurotensin Receptor Implication in Brain Functions

Neurotensin and Dopamine Interaction

More than twenty years ago, it was observed that some behavioral and biochemical effects of centrally administered NT were similar to those exhibited by antipsychotic drugs, and that these drugs stimulated NT expression in brain regions where there are mesocorticolimbic and nigrostriatal DA neuronal projections. These observations led to the hypothesis that NT may act as an endogenous neuroleptic, and stimulated the research on NT–DA interactions. Moreover, autoradiographic binding studies showing that central DA neuronal pathways could be mapped using radiolabeled NT further suggested that NT could regulate DA transmission.

Subsequent studies confirmed that NT compounds targeting NTS1 might represent a new class of antipsychotic drugs. However, there is still a debate as to whether an NTS1 agonist or an antagonist such as SR 48692 would be more suitable as an antipsychotic and have fewer side effects than the antipsychotic drugs used in clinics. Such controversial issue has recently been addressed in two complementary reviews.

Part of the discrepancies is based on the fact that NT exerts opposite effects on DA transmission depending on the site of injection in the brain. Administered into the nucleus accumbens where the mesolimbic DA system projects, NT produced a neuroleptic-like effect. By contrast, injection of the peptide in the ventral tegmental area, the region of the mesolimbic DA cell bodies, elicits psychostimulant-like effects. Similarly, though several data demonstrate that NT facilitates DA synthesis and DA transmission (an effect blocked by SR 48692), suggesting a psychostimulant action of NT, the observation that SR142948A disrupted acquisition of latent inhibition in rat, an animal model of schizophrenia, is in favor of NT mediating the effects of antipsychotic drugs. Finally, a pseudopeptide analogue of NT able to cross the blood brain barrier, NL-69L, was recently reported to exhibit antipsychotic-like effects after peripheral administration in rat.

Overall, final answer to whether an NT agonist or antagonist may be useful for the treatment of psychotic disorders such as schizophrenia will need clear-cut results in human trials.

Another field in which interaction between NT and DA has been proved to be potently and clinically

interesting is the treatment of stress and drug abuse. On the one hand, SR48692 has been shown to blunt stress-induced DA release and stimulation of the hypothalamo-pituitary adrenal axis; on the other hand, very recent data clearly report that NT neurons play a key role in the modulation of DA mesolimbic system in reward, blockade of NTS1 by SR 48692 inducing an inhibition of both amphetamine and cocaine-induced increase in locomotor activity and addiction.

NT and Pain Modulation

Whereas NTS1 seems to be implicated in NT–DA interaction, strong evidence suggests the involvement of NTS2 in the mediation of NT antinociceptive effects. Pharmacological studies have demonstrated that the NT antagonist SR 142948A does not distinguish between NTS1 and NTS2, blocks NT-induced nociception, whereas the NTS1-specific antagonist SR 48692 does not. Recent data on NTS1 and NTS2 knockout mice suggest the implication of NTS2 in the analgesic effects of NT. Supporting this, levocabastine and NTS2 antisense oligonucleotides were both found to inhibit the antinociceptive effects of intracerebroventricular administration of NT. Furthermore, brain structures associated with every single sensory system, in particular those implicated in the descending control of nociceptive inputs (e.g., the periaqueductal gray or raphe nuclei), contain a strong NTS2 immunoreactivity. However, since the distribution of brain NTS2 largely exceeds that of NT terminal fields, it suggests that NT may not be the only endogenous ligand for this receptor subtype. More work has to be done to clarify the pharmacology and physiological relevance of NTS2 in that context.

Neurotensin Receptor Implication in Cancer

Increasing evidence demonstrates that proNT and NTS1 are deregulated in several human cancers such as colon, pancreatic, prostate, and lung cancer, suggesting that NT may exert an autocrine activation of its own NTS1 receptor in cancer. Thus, the use of NT receptor antagonists to block the proliferative effect of NT on cancer cells is one of the promising prospects in cancer therapy. In this respect, it has been recently reported that SR 48692 could inhibit NT-stimulated growth of human colon, pancreatic, and lung cancer cell lines and, when administered alone to nude mice grafted with human NTS1-expressing colon cancer cells, could induce a reduction in tumor volume. It also seems that the proliferative effect of NT can be mediated not only by NTS1 but also by NTS3 since several of the cancer cells coexpressed both receptor subtypes. Selective NTS3 antagonists may thus be of particular interest in cancer therapy.

Not only NT antagonists but also NT agonists may be useful in cancer. Since NT receptors can be overexpressed in cancer tissues, this property can be used positively to target NTS-expressing cancer cells. Like most GPCRs, NTS1 undergoes internalization of the agonist into the target cell. Because NTS1-agonist complexes readily internalize, radiolabeled NT analogues targeting NTS1-expressing cancer cells have been recently developed. Pseudopeptide NT 8–13 stable analogues radiolabeled with 99mTechnecium have been developed for diagnostic purpose in cancer. Recently a strategy using the simultaneous detection of an antigen specifically expressed on cancer cells, carcinoembryonic antigen, with NTS1 using an 111Indium labeled NT hapten-bearing analogue has been shown to be an extremely promising approach to enhance selectivity to target tumor cells as compared to cells only expressing the cell surface receptor. This approach could allow the development of radiopharmaceuticals labeled with isotopes suitable not only for diagnostic but also for radiotherapy.

See Also the Following Articles

Dopamine Receptors • G Protein-Coupled Receptor Kinases and Arrestins • Neuropeptide Y Receptors

Glossary

antipsychotic and **psychostimulant drugs** Synthetic molecules which affect brain dopamine transmission. Neuroleptics are antipsychotics and psychostimulant drugs of abuse.

dopamine A neurotransmitter synthesized in specific cells from tyrosine, by means of a rate-specific enzyme, tyrosine hydroxylase. Dopamine is implicated in motor activity, mood behavior, and emotion. It is considered as a "pleasure" molecule.

EISAI, NT-69-L, JMV 449, JMV 431 NT analogues used for the characterization of NTS.

GPCR G protein-coupled receptors, receptor family of heptahelical transmembrane proteins that trigger intracellular signaling cascade via G proteins when stimulated by a variety of stimuli including light, odorant molecules, neurotransmitters, hormones, and peptides. They represent targets for more than 40% of all marketed drugs and around 10% of the human genome.

levocabastine A nonpeptide histamine H1 antagonist that binds NTS2; developed by Janssen Laboratories, Beerse, Belgium.

neuropeptides Peptides that work as neurotransmitters or neuromodulators on brain and neuroendocrine functions. More than 100 have been described so far.

neurotensin A 13 amino acid peptide found mainly in both the brain and the gut. Synthetized as part of a precursor protein (pro-NT) from which it is excised by prohormone convertases in the regulated secretory pathway of neuroendocrine cells. Its primary structure is: pGlu-Leu-Tyr-Glu-Asn-Lys-Pro-Arg-Arg-Pro-Tyr-Ileu-Leu.

SR 48692 and SR 142948A Synthetic molecules which are nonpeptide antagonists of NTS1 and agonists of NTS2 developed by Sanofi Synthelabo, France.

Further Reading

Bérod, A., and Rostène, W. (2002). Neurotensin: An endogenous psychostimulant? *Curr. Opin. Pharmacol.* **2**, 93–98.

Betancur, C., Azzi, M., and Rostène, W. (1997). Nonpeptide antagonists of neuropeptide receptors: Tools for research and therapy. *Trends Pharmacol. Sci.* **18**, 372–386.

Dal Farra, C., Sarret, P., Navarro, V., Botto, J. M., Mazella, J., and Vincent, J. P. (2001). Involvement of the neurotensin receptor subtype NTR3 in the growth effect of neurotensin on cancer cell lines. *Int. J. Cancer* **92**, 503–509.

Hillairet De Boisferon, M., Raguin, O., Thiercelin, C., Dussaillant, M., Rostene, W., Barbet, J., Pelegrin, A., and Gruaz-Guyon, A. (2002). Improved tumor selectivity of radiolabeled peptides by receptor and antigen dual targeting in the neurotensin receptor model. *Biocong. Chem.* **13**, 654–662.

Kitabgi, P. (2002). Targeting neurotensin receptors with agonists and antagonists for therapeutic purposes. *Curr. Opin. Drug Discov. Develop.* **5**, 764–776.

Kinkead, B., and Nemeroff, C. B. (2002). An endogenous antipsychotic? *Curr. Opin. Pharmacol.* **2**, 99–103.

Martin, S., Vincent, J. P., and Mazella, J. (2003). Involvement of the neurotensin receptor-3 in the neurotensin-induced migration of human microglia. *J. Neurosci.* **23**, 1198–1205.

Rostène, W., and Alexander, M. J. (1997). Neurotensin and neuroendocrine regulation. *Front Neuroendocrinol* **18**, 115–173.

Sarret, P., Gendron, L., Kilian, P., Nguyen, N. H., Gallo-Payet, N., Payet, M. D., and Beaudet, A. (2002). Pharmacology and functional properties of NTS2 neurotensin receptors in cerebellar granule cells. *J. Biol. Chem.* **277**, 36233–36243.

Vincent, J. P., Mazella, J., and Kitabgi, P. (1999). Neurotensin and neurotensin receptors. *Trends Pharmacol. Sci.* **20**, 302–309.

Biography

William Rostène is Research Director at INSERM, France. He was head of the INSERM Unit 339 in Paris (1991–2002). He qualified as a neuroendocrinologist and was President of the French Society for Neuroendocrinology (1997–2000). He is one of the pioneers in the development of autoradiography and image analysis for neuropeptide receptors and has carried out extensive work on two neuropeptides, neurotensin and VIP.

Patrick Kitabgi is Research Director at INSERM, France. He is currently Head of INSERM E0350 in Paris. He has devoted most of his scientific career to the study of neurotensin starting in 1974 in the laboratory of Susan Leeman who discovered neurotensin.

Didier Pélaprat is Research Director at INSERM, France. He qualified as an organic chemist and then a neurobiologist. His work particularly focused on functional consequences of ligand–receptor interactions and modulation of dopaminergic systems by neuropeptides such as cholecystokinin and neurotensin.

Neurotransmitter Transporters

Aurelio Galli, Randy D. Blakely and Louis J. DeFelice
Vanderbilt University, Nashville, Tennessee, USA

Neurotransmitters are chemical messengers that neurons use to communicate with each other. Timely removal of neurotransmitters from the synaptic cleft is critical for synaptic neurotransmission. If released neurotransmitter molecules remain in the synaptic cleft, the synapse would become nonresponsive due to continued exposure of neurotransmitter. Removal of neurotransmitter from the synaptic cleft occurs by three mechanisms: diffusion, enzymatic degradation, and reuptake. Transporter proteins localized in nerve and glial cell membranes mediate high affinity reuptake for the released neurotransmitters, and under many circumstances reuptake is the dominant mechanism for the termination of synaptic signaling. This mechanism not only serves to clear extracellular neurotransmitter, but it also recaptures transmitter molecules for possible reuse. In addition, significant ionic currents are associated with transport, and these may contribute substantially to the excitability of the cell.

Neurotransmitter transporters utilize the electrochemical energy derived from the inward movement of ions, particularly sodium, to drive the intracellular accumulation of neurotransmitter. Neurotransmitter transporters are thus designated as cotransporters. In the early 1990s, several of these membrane proteins were cloned and two broad families have been identified. The first, which includes the norepinephrine (NE), dopamine (DA), γ-aminobutyric acid (GABA) and serotonin (5HT) transporters, shares no significant sequence homology with the second, which includes transporters for glutamate. After the "cloning" decade, several intriguing and exiting questions related to their structure and function are being raised: What is the molecular mechanism of transport? How does the protein structure define these mechanisms? What are the cellular signals and determinants that regulate transporter expression and function? Are there disease states related to neurotransmitter transporter dysfunction? This article will be restricted to GABA transporters and the monoamine transporters; discussion of vesicular transporters, glutamate transporters and sodium-dependent glucose transporters will be omitted.

Mechanisms of Transport

Reuptake

Neurotransmitter transporters operate by coupling the transmembrane translocation of substrate to the movement of driving ions down pre-established electrochemical gradients (cotransport). Members of this family include the membrane carriers for dopamine (DAT), serotonin (SERT), norepinephrine (NET), and γ-aminobutyric acid (GAT1–3). The most widely held concept of how cotransporters function is founded on the "alternating access model," in which the binding sites for substrates and cosubstrates are alternately exposed to extracellular or cytoplasmic environments via conformational changes in the transporter protein. The thermodynamic work of the transporter is accomplished by coupling the flux of substrate to the movement of cotransported ions down their electrochemical gradients. The stoichiometry inferred from radiolabeled transport studies on neurotransmitter transporter-expressing cells and membrane vesicles is two Na^+, one Cl^-, and one molecule of substrate for DAT and GAT1. For NET the proposed stoichiometry is one Na^+, one Cl^-, and one molecule of NE. With the exception of mammalian SERT, which is proposed to be electroneutral due to additional counter ion flow, the neurotransmitter transporter process is electrogenic meaning that the transport cycle moves net charges across the plasma membrane. Indeed, in cell lines stably transfected with the cDNA of neurotransmitter transporters, it is possible to record electrical currents generated by their activity using the patch clamp technique in the whole-cell configuration. However, these currents are generally too large to be explained entirely by fixed stoichiometry models (see Figure 1).

Recent electrophysiological studies of both native and cloned neurotransmitter transporters revealed that transporters can have brief and rare channel-like openings comparable to those generated by ligand-gated ion channels. Models for this exiting mode of the neurotransmitter transporters have been established, in which substrate, Na^+ and Cl^- induce the carrier to transport in the alternating access mode (Figure 1A, 1B), and rarely switching to a channel-like mode (Figure 1C). The alternating access model assumes that the substrate permeation occurs through a state transition (A ↔ B) and results in the transport of a single neurotransmitter molecule (Figures 1A and 1B). The channel-like mode (Figure 1C) is a low probability event that consists of hundreds of ions

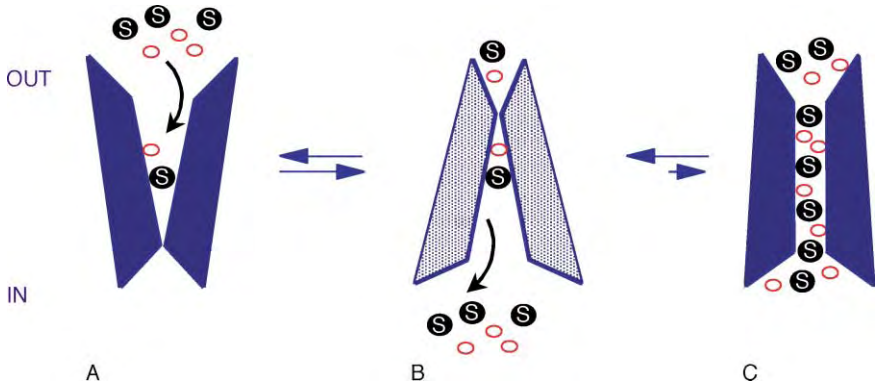

FIGURE 1 Model for neurotransmitter transporter function.

crossing the membrane (using a transporter pore), down their electrochemical gradients. These models have been recently refined and expanded based on new data.

Efflux

In addition to mediating the reuptake of neurotransmitter into nerve terminals, transporters can also cause non-Ca^{2+}-mediated efflux of the transmitter from the nerve terminal. There are essentially two mechanisms by which to elicit reverse transport from neurons: first, by changing the transmembrane ion gradients and voltage; and, second, for monoamine transporters, via the actions of pharmacological compounds such as amphetamine that may stabilize an efflux competent conformation, modulate ion gradients or both. In the case of glutamate transporters, nonvesicular neurotransmitter release is thought to play a role in pathophysiological conditions causing membrane depolarization such as epilepsy, or excitotoxicity such as stroke.

Structure and Function

A milestone in the advancement of knowledge of neurotransmitter transporters was achieved in 1990 when the first cDNAs encoding the GABA transporters were cloned and sequenced. As a consequence neurotransmitter transporters cDNAs for NET and SERT were soon cloned, and the list grew. The gene products of the Na^+/Cl^- neurotransmitter transporter family are highly conserved. Monoamine and GABA transporters show a common structure of a predicted 12 transmembrane (TM) domains with a single large loop in the external side of the plasma membrane with potential glycosylation sites. Each TM domain contains predominantly hydrophobic amino acid residues. The TM domains are connected by extracellular or intracellular loops located on either side of the plasma membrane in which the residues are mostly hydrophilic. Because high-resolution structures, such as the ones obtained by X-ray crystallography, are difficult to gain for integral membrane proteins, most of the structural information for neurotransmitter transporters obtained in recent years has been obtained by chemical modification with labeling reagents. In particular, the cysteine accessibility method (SCAM) has been used to gather information on the topology and the mechanism of transport. With this technique, a particular residue in the sequence is replaced usually with a cysteine residue. Then, chemical modifications of the cysteine are performed to measure its accessibility by evaluating, for example, changes in transporter function induced by the chemical modification. Cysteines are well tolerated as a replacement for a particular amino acid in the sequence of most membrane transporter proteins. By using different types of reagents, and, depending on the reagent used, the accessibility of a residue may provide information about its location and function. Use of these methodologies allowed researchers to measure the level of exposure of predicted extracellular loops in SERT, DAT, and other neurotransmitter transporters. Because the kinetics of reactivity for cysteine substitutions in TM domains and loops are expected to be different, SCAM can also provide information on the location of the end and the beginning of a particular transmembrane domain. Furthermore, cysteine substitutions whose chemical reactions result in a robust modification in transporter activity can elucidate the relationship between structure and function. For example, if the change in transporter activity resulting from the chemical modification of a cysteine can be altered by the presence of an inhibitor or a substrate, there is the possibility that this cysteine is part of the substrate-inhibitor binding site. With this experimental strategy, Rudnick and co-workers suggested that the Ile in position 172 and Tyr in position 176 of the TM domain 3 of the rat

SERT are in proximity to the binding site for 5-HT and cocaine. A relevant transporter (lactose permease of *Escherichia coli*) structure from another gene family has recently appeared.

Regulation

It is not surprising that molecules regulating the spatial and temporal dimension of synaptic events are tightly regulated. Several reports have shown that various signaling molecules can rapidly regulate many of the neurotransmitter transporters. Regulators of neurotransmitter transporter activity include G protein-coupled receptors such as the D_2 and mGluR5 receptors, kinases such as protein kinase C, phosphatidylinositol 3-kinase, tyrosine kinase, and Ca^{2+}/calmodulin kinase, protein kinase B, protein kinase C, and neurotrophic factors. In addition to transporter rates, many studies suggested that the regulation of neurotransmitter transport capacity might originate from a change in their cell surface expression. In this context, it is important to point out that transporter interacting proteins finely control plasma membrane expression level of neurotransmitter transporters. For example, in addition to PKC and other signaling pathways, cell surface expression and activity of GAT1 and NET are regulated by syntaxin 1A, a protein involved in synaptic vesicle fusion to the plasma membrane. Similarly, DAT surface expression can be influenced by its PDZ-mediated protein–protein interaction with PICK1, a PKC-binding protein. Although it is still not clear whether this transporter family shares common regulating factors, it is becoming evident that the trafficking of neurotransmitter transporters represents a new paradigm by which neurons control their ability to reuptake neurotransmitter. Other regulators of DAT and SERT cell surface expression include psychostimulants such as AMPH and cocaine.

The general process of transporter trafficking, that involves endocytosis, intracellular sorting, and exocytosis of these membrane proteins, is acquiring great interest for neuroscientists. Indeed, researchers studying transporter cell surface redistribution are envisioning the possibility of discovering new cellular targets to cure specific neurological disorders.

Relationships Between Disease States and Neurotransmitter Transporters

The ability of the neurotransmitter transporters to regulate normal synaptic signaling implies that functional modification of transporter activity might contribute to the etiology of multiple neurobiological diseases. Indeed, many studies have suggested for years, largely on the basis of pharmacology, that the monoamine transporters NET, DAT, and SERT play an important role in regulating mood, learning, and motor activity, while GABA transporters have been implicated in neuronal excitability dysfunction such as epilepsy. Indeed, a decade of innovative pharmacology resulted in the development of compounds that, by targeting neurotransmitter transporters, alleviate the symptoms of neurological diseases such as drug abuse and attention deficit/hyperactivity disorder. New hopes for the cure of these conditions are coming from studying the gene organization and polymorphisms of these membrane proteins. It has been shown that variations in the human neurotransmitter transporter sequences, known as polymorphisms, may alter transporter expression level, activity, or regulation that ultimately may influence the levels of extracellular neurotransmitter. The cloning of the neurotransmitter transporter genes has provided the tool for examining transporter genetic variations and possibly to correlate them to human diseases. This is particularly true for the monoamine transporters (SERT, DAT, NET) each encoded by a single gene. Therefore, the impact of polymorphisms could have far-reaching consequences due to a limited opportunity for compensation from other genes. Finding an association of a polymorphism with disease is clearly the first of many steps toward understanding how genetics shape the neurobiological diseases. A recent example of such an effort is the identification of a NET coding variant, A457P, in subjects with orthostatic intolerance.

See Also the Following Articles

Calcium/Calmodulin-Dependent Protein Kinase II • Calcium/Calmodulin-Dependent Protein Kinases • Dopamine Receptors • $GABA_A$ Receptor • $GABA_B$ Receptors • Protein Kinase C Family • Serotonin Receptor Signaling

Glossary

neurotransmitters Message chemicals released from one neuron at the presynaptic nerve terminal.

polymorphism A genetic variance that appears at least in 1% of the population.

synaptic cleft A gap between the pre-and postsynaptic membranes.

Further Reading

Abramson, J., Smirnova, I., Kasho, V., Verner, G., Kaback, H. R., and Iwata, S. (2003). Structure and mechanism of the lactose permease of *Escherichia coli*. *Science* **301**, 610–615.

Beckman, M. L., and Quick, M. W. (1998). Neurotransmitter transporters: Regulators of function and functional regulation. *J. Membr. Biol.* **164**, 1–10.

Chen, J. G., Sachpatzidis, A., and Rudnick, G. (1997). The third transmembrane domain of the serotonin transporter contains residues associated with substrate and cocaine binding. *J. Biol. Chem.* **272**, 28321–28327.

DeFelice, L. J., and Galli, A. (1998). Fluctuation analysis of norepinephrine and serotonin transporter currents. *Methods Enzymol.* **296**, 578–593.

Guastella, J., Nelson, N., Nelson, H., Czyzyk, L., Keynan, S., Miedel, M. C., Davidson, N., Lester, H. A., and Kanner, B. I. (1990). Cloning and expression of a rat brain GABA transporter. *Science* **249**, 1303–1306.

Jardetzky, O. (1966). Simple allosteric model for membrane pumps. *Nature* **211**, 969–970.

Javitch, J. A. (1998). Probing structure of neurotransmitter transporters by substituted-cysteine accessibility method. *Methods Enzymol.* **296**, 331–346.

Rudnick, G. (1998). Bioenergetics of neurotransmitter transport. *J.Bioenerg. Biomembr.* **30**, 173–185.

Saunders, C., Ferrer, J. V., Shi, L., Chen, J., Merrill, G., Lamb, M. E., Leeb-Lundberg, L. M. F., Carvelli, L., Javitch, J. A., and Galli, A. (2000). Amphetamine-Induced Loss of Human Dopamine Transporter Activity: An Internalization-Dependent and Cocaine-Sensitive Mechanism. *Proc. Natl Acad. Sci. USA* **97**, 6850–6855.

Shannon, J. R., Flattem, N. L., Jordan, J., Jacob, G., Black, B. K., Biaggioni, I., Blakely, R. D., and Robertson, D. (2000). Orthostatic intolerance and tachycardia associated with norepinephrine-transporter deficiency. *N. Engl. J. Med.* **342**, 541–549.

BIOGRAPHY

Aurelio Galli received his Ph.D. from the University of Milan in 1994. He is now a faculty member in the Department of Molecular Physiology and Biophysics at Vanderbilt University in Nashville, Tennessee. His principal research interest is to study the regulation by psychostimulants of neurotransmitter transporter function.

Randy Blakely received his doctorate in Neuroscience from the Johns Hopkins School of Medicine and then pursued postdoctoral studies at Yale University. Following a faculty position at Emory University, he became the Alan D. Bass Professor of Pharmacology at Vanderbilt. His major interest is in the molecular regulation of neurotransmitter transporter.

Louis J. DeFelice received his Ph.D. in Physics in Calgary, Alberta, Canada in 1967. He is now a Professor of Pharmacology and Neuroscience at Vanderbilt University. His principal research interest is the molecular mechanism of ion tansport across membranes, including ion channels and co-transporters.

Neurotrophin Receptor Signaling

Jennifer J. Gentry and Bruce D. Carter
Vanderbilt University, Nashville, Tennessee, USA

The purification of nerve growth factor (NGF) during the 1950s, based on its ability to promote the survival of sensory and sympathetic neurons, led to the discovery of a family of related trophic factors referred to as the neurotrophins. The members of the neurotrophin family include NGF, brain-derived neurotrophic factor (BDNF), neurotrophin 3 (NT3), and neurotrophin 4 (NT4), and each is essential for the survival of specific, but overlapping, populations of neurons during development. Given that nearly half of the neurons generated during mammalian ontogenesis undergo programmed cell death, it is clear that the neurotrophins have a major role in determining the ultimate population size for a given group of neurons. Moreover, the neurotrophins not only promote survival, but also regulate differentiation, axon guidance, synaptogenesis and neurite branching, and elongation; thus, this family of trophic factors has a wide spectrum of actions that are key for the proper sculpting of the mammalian nervous system. In addition to their role in development, this family of proteins also has important effects on maintenance of the nervous system, including such processes as learning and memory, neurogenesis in the adult and response to injury. This article will focus on the molecular-signaling mechanisms activated by the binding of neurotrophins to their receptors, with particular emphasis on the regulation of cell viability.

Introduction

The diversity in neurotrophin function is likely a reflection of the variety of signaling pathways that are influenced by activation of their receptors. The neurotrophin receptors consist of a family of tyrosine kinase receptors, the Trks, and a member of the tumor necrosis factor receptor family, p75NTR. Neurotrophin binding to the Trks promotes survival and differentiation while activation of p75NTR can also enhance cell viability or, paradoxically, induce apoptosis. Although activation of the Trks or p75NTR can initiate discrete signal transduction pathways, the two receptor types are frequently coexpressed on a given cell. Thus, it is the complex interactions between these receptors and crosstalk between their signaling pathways that ultimately determines the fate of the cell. In addition, a number of other receptors are modulated by the neurotrophins or can regulate neurotrophin signaling, either through interaction between receptors or cross talk between signaling pathways.

Neurotrophin Activation of Trk Receptors

The most well-studied actions of neurotrophins are mediated through activation of a family of tyrosine kinase receptors, the Trks. There are three members of the Trk family, TrkA, TrkB, and TrkC. Each receptor binds to specific members of the neurotrophin family preferentially with nerve growth factor (NGF) having the highest affinity for TrkA, BDNF, and NT4/5 for TrkB, and NT-3 for TrkC. Binding of a neurotrophin, which exist as dimers, to a Trk receptor triggers receptor dimerization and activation of intrinsic tyrosine kinase activity. Like other tyrosine kinase receptors, autophosphorylation of specific residues within the intracellular domain of the receptor leads to the recruitment of a wide variety of signaling molecules (Figure 1). In particular, these phosphotyrosines serve as docking sites for proteins containing Shc homolog 2 (SH2) or phosphotyrosine-binding (PTB) domains, including phospholipase C-γ (PLC-γ) and the adaptor proteins Shc, Frs-2, rAPS and SH2-B. These receptor-binding proteins initiate several signal transduction cascades.

Association of Trk with PLC-γ activates this enzyme, resulting in cleavage of phosphatidylinositol (4,5) bisphosphate to release the second messengers inositol-1,4,5-triphosphate (IP3) and diacylglycerol (DAG). DAG activates a number of isoforms of protein kinase C (PKC) while IP3 triggers the release of Ca^{2+} from intracellular stores, which activates a variety of pathways, including calmodulin kinases and Ca^{2+} regulated isoforms of PKC. The maintenance of calcium homeostasis has been well documented as key for regulating neuronal survival. Indeed, a role for PKC in prosurvival effects of the neurotrophins has been suggested; however, recent data suggests that this pathway has a more significant role in regulating spatial learning and

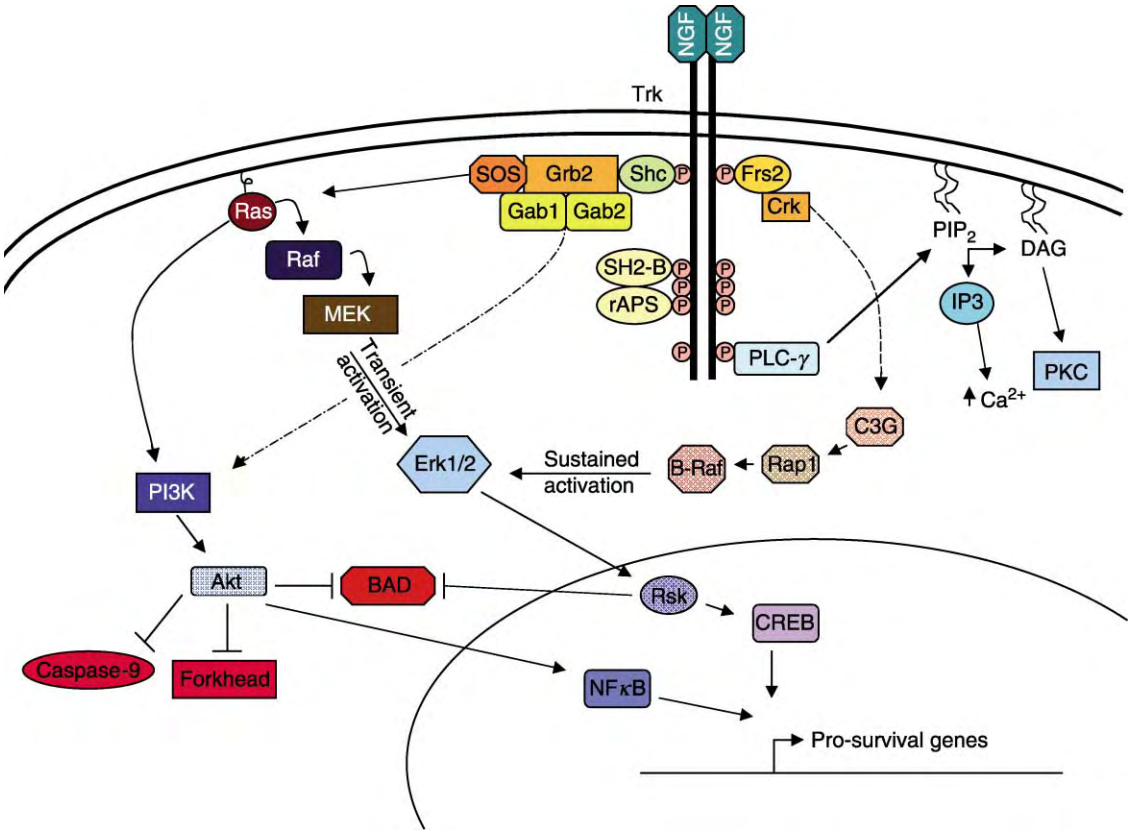

FIGURE 1 Neurotrophin signaling through the Trk receptor.

memory. Analysis of transgenic, knock-in mice lacking the docking site for PLC-γ on the TrkB receptor has not revealed any defects in neuronal survival, but the animals do display deficiencies in hippocampal long-term potentiation (LTP), which is a model for spatial memory.

Another signaling cascade activated by the Trk receptors is the Ras–MAP kinase pathway (Figure 1). The phosphorylation of the membrane proximal tyrosine (Y490 on TrkA) recruits the protein Shc, leading to docking of the adaptor proteins Gab1, Gab2, and Grb2. Grb2 associates with the guanine-nucleotide-exchange factor SOS, which facilitates activation of Ras, an activator of several pathways. The activated, GTP-bound form of Ras recruits the serine/threonine kinase Raf to the plasma membrane, thereby facilitating its activation. Raf then phosphorylates MEK1 and/or MEK2 and these kinases phosphorylate the MAP kinases Erk1 and 2. The activated Erks translocate into the nucleus where they phosphorylate a variety of substrates, including the kinase Rsk, which can phosphorylate and inactivate the proapoptotic protein Bad. Rsk also phosphorylates the transcription factor CREB, resulting in its activation and the subsequent up-regulation of downstream genes such as the prosurvival gene Bcl-2. In addition, the Ras–MAP kinase pathway is also important for neurotrophin mediated differentiation, including the induction of neurite outgrowth. For example, expression of activated Raf, in the absence of neurotrophin, induced neurite elongation in sensory neurons and constitutively active MEK up-regulated p35, leading to cdk5 activation, which increases neurite extension.

The ability of neurotrophins to promote differentiation appears, in part, to depend on prolonged Erk1/2 activation, as opposed to the transient activation of the kinases induced by other growth factors such as EGF. The longer kinetics are a result of phospho-Trk associating with the adaptor, Crk, through interaction with the fibroblast growth factor receptor substrate-2 (Frs2). Crk binds to the nucleotide-exchange factor C3G, thereby stimulating the small GTP-binding protein Rap1. The kinase B-Raf is then activated by Rap1, resulting in sustained Erk1/2 activation (Figure 1).

The activation of Ras also leads to activation of the lipid kinase, phosphatidylinositol 3 kinase (PI3K). In addition, PI3K can be activated independent of Ras through Grb2 binding to the adaptor Gab1/2, which facilitates Trk stimulation of the kinase. PI3K produces phosphatidylinositides phosphorylated on the third position of the inositol and these serve to indirectly

activate the serine/threonine kinase Akt. Akt acts on a number of signaling proteins that are critical regulators of cellular survival. The kinase activity of Akt leads to activation of the transcription factor NFκB, which can serve as a prosurvival factor in the nervous system, and inhibition of the proapoptotic proteins Bad, Forkhead, GSK3β, and caspase 9. Numerous studies have demonstrated a requirement for the PI3K-Akt pathway in neurotrophin mediated survival; however, this pathway also promotes protein translation and neurite branching (Figure 1).

Adding to the complexity of Trk signaling is the presence of several splice variants of all of these receptors. Among these isoforms, both Trk B and Trk C exist as truncated receptors lacking the intracellular kinase domain. While there is evidence that loss of the kinase domain can function to abrogate Trk signaling by competitively binding the available neurotrophin or forming inactive complexes with full length receptor, there is also evidence that these truncated Trks may function to display bound neurotrophin to adjacent cells. In addition, recent findings suggest that the truncated receptors can initiate signaling within astrocytes, leading to IP3-dependent calcium release. A second type of splice variant observed for all of the Trks is a form of the receptor lacking a small portion of the extracellular domain in the juxtamembrane region. Expression of these isoforms more stringently restricts the responsiveness of a given Trk for its cognate neurotrophin and may be one mechanism to insure the elimination of neurons making connections to an inappropriate target tissue.

One important aspect of neurotrophin signaling that needs to be considered is the spatial limitations of a neuron. Typically, it is the axonal tip that encounters the neurotrophins, while the regulation of survival involves transcriptional activity; hence, the signal must be retrogradely transported some distance back to the neuron soma. Although it has long been known that neurotrophins are retrogradely transported, it was only recently demonstrated that it is essential that the factor be transported with the active receptor, although this requirement has been contended by Campenot and colleagues. TrkA and NGF are not transported alone, rather, an entire complex of signaling proteins associated with an internalized vesicle, referred to as a signalosome, has been shown to undergo transport from neuronal endings back to the cell body.

Neurotrophin Activation of the p75NTR Receptor

While p75NTR was the first neurotrophin receptor identified and the founding member of the TNF receptor family, only recently has its importance for neurotrophin action been appreciated. With that appreciation, a wave of research highlighting both the mechanisms and functional consequences of its signal transduction pathway has been generated. p75NTR is important for neuronal development through its regulation of programmed cell death. In addition, accumulating evidence indicates that p75NTR also plays an important role in injury response within the nervous system.

Like many members of the TNF receptor family, p75NTR can activate the transcription factor NFκB and the stress activated kinase JNK (c-Jun N-terminal kinase) (Figure 2). The activation of NFκB by p75NTR has been shown to promote survival, thus providing a mechanism by which this receptor can function together with Trk to keep cells alive. In contrast, the activation of JNK is a proapoptotic signal in many contexts. For example, p75NTR-mediated apoptosis has been demonstrated to play a role in the normal elimination of neurons during development of the mouse retina, spinal cord, basal forebrain, and sympathetic ganglia. One of the major roles for cell death induced by this receptor may be after nerve injury. Following a spinal cord lesion in rodents, oligodendrocytes undergo p75NTR-dependent apoptosis. Similarly, pilocarpine-induced seizures cause mouse hippocampal neurons to die through a process dependent on p75NTR. Given that p75NTR is highly up-regulated following a large number of insults, it is likely that future studies will continue to reveal a role for this receptor in the associated cell death.

In addition to its activation of NFκB and JNK, p75NTR has been shown to regulate the small GTP-binding proteins Rac and Rho (Figure 2). Rac has been suggested as an upstream activator for JNK, thus playing an essential role in the apoptotic signal; however, Rac and Rho are best known for their ability to alter the cytoskeletal architecture. It is through modulation of these G proteins that p75NTR alters neurite extension, either promoting it following binding of neurotrophin, or causing growth cone collapse upon association with ligand-bound Nogo receptor.

Although the downstream signals activated by p75NTR are similar to other members of the TNF receptor family (NFκB and JNK), the receptor-proximal mechanisms used appear to be somewhat different. This is not entirely surprising given that p75NTR is the only member of the TNF receptor family that is activated by a dimeric ligand, rather than the trimeric ligands (e.g., TNFα and Fas ligand) that create trimeric receptor complexes and recruit trimeric adaptor proteins. Recently, much effort has been focused on understanding the transduction mechanism of this unique pathway. This work has resulted in the identification of a large number of p75NTR interacting factors whose sheer

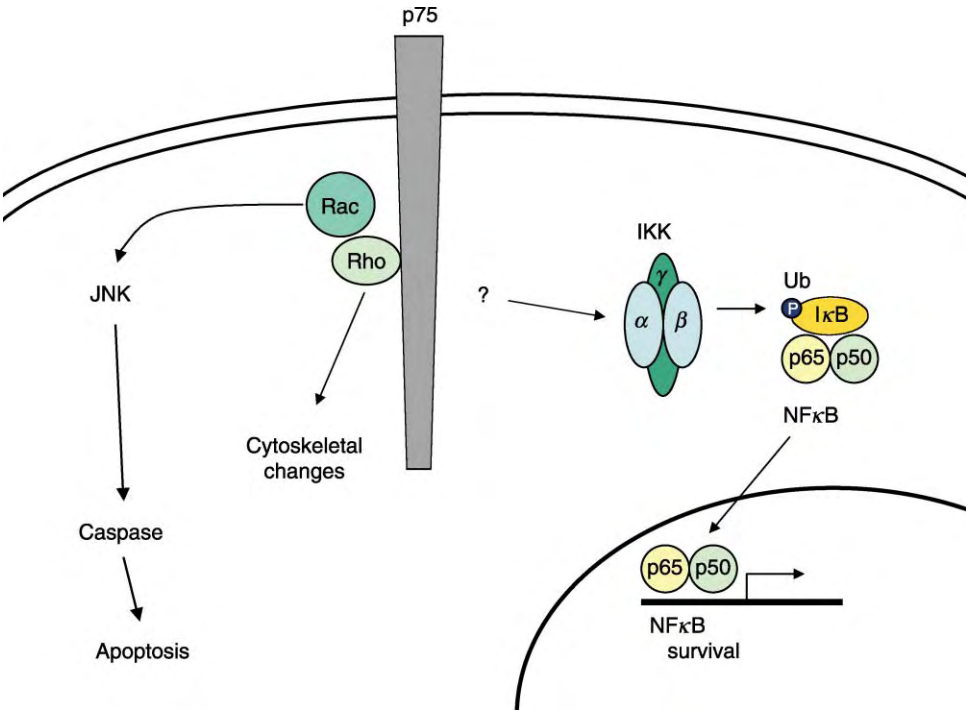

FIGURE 2 Neurotrophin signaling through p75NTR. Neurotrophin binding to this receptor activates the stress kinase JNK, the transcription factor NFκB, and regulates the GTP-binding proteins Rac and Rho. Not depicted are the numerous receptor-binding proteins that have been reported, since how they participate in p75NTR signaling has yet to be elucidated.

numbers will require some time to sort through to understand how they fit into p75NTR signaling under various conditions.

A long-standing conundrum in understanding the physiological role of p75NTR has been the high levels of neurotrophin needed to activate the receptor. *In vivo*, the neurotrophins are typically found at very low levels, usually at or below the K_D for p75NTR. Recently, the group of B. Hempstead made an important discovery that may resolve this dilemma. They found that the unprocessed, proform of the neurotrophins bind p75NTR with high affinity and activate downstream pathways more effectively than the mature neurotrophins. Hence, a mechanism exists for selective activation of p75NTR, since the proneurotrophins do not bind or activate the Trks. This discovery has renewed interest in studying the regulation of neurotrophin processing and release, as these are likely to be key for modulating neuronal survival during development and after injury.

Crosstalk Between p75NTR and the Trks

It is clear that neurotrophin binding to either p75NTR or members of the Trk family of receptors can initiate distinct signal transduction pathways, but these receptors are often coexpressed in the same cells. When both neurotrophin receptors are present, they interact to form a very selective, high-affinity complex. Given the limiting quantities of neurotrophin present in typical target tissues, such a binding site provides neurons expressing both receptors, in the proper ratio, with a competitive advantage during development. Moreover, the interaction between p75NTR and Trk leads to enhanced Trk tyrosine kinase activity and more robust activation of downstream survival signals. The binding of mature neurotrophin to the p75NTR–Trk complex also represses the p75NTR apoptotic signal; for example, Trk activation of Ras has been shown to inhibit p75NTR activation of JNK. Thus, the two receptors synergize to increase neuronal viability. A lack of the p75NTR–Trk receptor interaction has been proposed to explain the significant loss of sensory neurons in the p75NTR −/− mice.

Interaction Between p75NTR and the Nogo Receptor

Although p75NTR responds to binding of the neurotrophins, this receptor can also be activated by an additional group of ligands typically expressed on central nervous system myelin, including Nogo, myelin associated glycoprotein (MAG) and oligodendrocyte

myelin glycoprotein (OMgp). These myelin proteins inhibit neurite outgrowth and are, in part, responsible for preventing regeneration of CNS axons after nerve injury. They all bind to a GPI-linked receptor referred to as the Nogo receptor (NgR), which interacts with p75NTR. Association of NgR with p75NTR results in activation of Rho, which causes changes in the actin-cytoskeleton resulting in growth cone collapse. Interestingly, the association of NgR with p75NTR activates Rho and inhibits Rac, while the binding of neurotrophin to p75NTR has the opposite effects on these G proteins. The mechanisms by which these opposing signals are generated have yet to be fully resolved.

Crosstalk Between Trk and Non-Neurotrophin Receptors

The Trk receptors also interact with a number of non-neurotrophin receptors, although this is primarily an indirect interaction. Several G protein-coupled receptors can transactivate Trk and thereby stimulate downstream signaling pathways. For example, the adenosine receptor and the pituitary adenylate cyclase activating polypeptide (PACAP) receptor can induce phosphorylation of TrkA through a mechanism that does not involve neurotrophins. Such crosstalk is likely involved in the neuroprotective effects of these ligands.

Alternatively, neurotrophin binding to Trk can cross-stimulate the tyrosine kinase c-Ret, a component of the receptor complex for the glial cell line-derived neurotrophic factor (GDNF) family. Although c-Ret is normally activated by GDNF family members, it can also be phosphorylated in mature sympathetic neurons following NGF binding to TrkA. This indirect activation of c-Ret is required for these neurons to maintain their metabolic status and somal size. Similarly, BDNF stimulation of TrkB can transactivate a subunit of the NMDA receptor, which is essential for the formation of LTP. Since BDNF is known to enhance LTP, Trk-NMDA receptor crosstalk may be the mechanism underlying this effect.

See Also the Following Articles

Caspases and Cell Death • Neurotransmitter Transporters • Nuclear Factor kappaB • Phospholipase C

Glossary

neurotrophin A member of a family of homologous growth factors that promote the survival and differentiation of neurons.

nuclear factor kappa B (NFκB) A transcription factor.

phosphatidyl-inositol 3 kinase (PI3K) Kinase that phosphorylates inositol lipids on the third position of the sugar.

PLC-γ An enzyme that cleaves phosphatidyl inositol (4,5) bisphosphate to release inositol-3-phosphate (IP3) and diacylglycerol (DAG).

p75NTR The 75 kDa neurotrophin receptor.

Trk The tyrosine kinase neurotrophin receptor.

Further Reading

Chao, M. V. (2003). Neurotrophins and their receptors: A convergence point for many signalling pathways. *Nat. Rev. Neurosci.* **4**, 299–309.

Dechant, G., and Barde, Y. A. (2002). The neurotrophin receptor p75(NTR): Novel functions and implications for diseases of the nervous system. *Nat. Neurosci.* **5**, 1131–1136.

Ginty, D. D., and Segal, R. A. (2002). Retrograde neurotrophin signaling: Trk-ing along the axon. *Curr. Opin. Neurobiol.* **12**, 268–274.

Hempstead, B. L. (2002). The many faces of p75NTR. *Curr. Opin. Neurobiol.* **12**, 260–267.

Huang, E. J., and Reichardt, L. F. (2001). Neurotrophins: Roles in neuronal development and function. *Annu. Rev. Neurosci.* **24**, 677–736.

Huang, E. J., and Reichardt, L. F. (2003). Trk receptors: Roles in neuronal signal transduction. *Annu. Rev. Biochem.* **72**, 609–642.

Lee, F. S., Rajagopal, R., and Chao, M. V. (2002). Distinctive features of Trk neurotrophin receptor transactivation by G protein-coupled receptors. *Cytokine Growth Factor Rev.* **13**, 11–17.

Biography

Dr. Bruce Carter is an Associate Professor of Biochemistry in the School of Medicine at Vanderbilt University. His principal area of research is on the mechanisms by which the neurotrophins regulate neuronal survival. He holds a Ph.D. degree from the University of Michigan and received postdoctoral training at the Max Planck Institute in Munich, Germany and at Cornell Medical School.

Dr. Jennifer Gentry received her Ph.D. from Vanderbilt University and is currently a postdoctoral Fellow at Harvard Medical School.

Nicotinamide Nucleotide Transhydrogenase

Jan Rydström
Göteborg University, Göteborg, Sweden

Membrane-bound nicotinamide nucleotide is located in the bacterial plasma membrane and mitochondrial inner membrane and catalyzes the reversible reduction of $NADP^+$ by NADH. The reaction is linked to the electrochemical proton gradient across the membrane, generating NADPH essential for, e.g., detoxification of peroxides. In its isolated form the enzyme is a proton pump where proton translocation is driven by the catalytic reaction, mediated by conformational changes. Extensive investigations of the structure–function relationships especially of the substrate-binding domains have established their structures and roles. The membrane domain, in which the proton channel resides, has been structurally predicted, but remains to be determined structurally at the atomic level. Models for the molecular proton translocation mechanism are therefore beginning to emerge.

Introduction

Proton-pumping nicotinamide nucleotide transhydrogenase (E.C. 1.6.1.2) is an integral membrane protein found in most species except some yeasts, plants, and certain bacteria. It is located in the inner membrane of mitochondria and in the plasma membrane of bacteria. The enzyme catalyzes the reversible reduction of $NADP^+$ by a hydride ion, donated by NADH, which is linked to proton translocation across the membrane according to the reaction

$$H^+_{out} + NADH + NADP^+ \rightleftharpoons H^+_{in} + NAD^+ + NADPH \quad [1]$$

In the absence of an electrochemical proton gradient (Δp), the reaction from left to right (the forward reaction) is approximately fivefold slower than the reverse reaction. Under these nonphysiological conditions, the overall reaction proceeds to an equilibrium constant of close to 1. In the presence of a Δp, i.e., under more physiological conditions, the forward reaction is increased five- to tenfold and the apparent equilibrium constant is increased to ~ 500, with one proton translocated per NADPH formed. The net effect of the transhydrogenase (TH) reaction is therefore probably to provide NADPH at the expense of NADH and Δp. Thus, this suggests important roles of TH in mitochondrial/cellular redox regulation including biosynthesis, detoxication (via the glutathione/thioredoxin systems), and apoptosis. TH is globally expressed in eukaryotes, e.g., human, mouse, and *C. elegans*.

Proton-translocating THs from eukaryotes are homodimeric proteins with a relatively large hydrophilic domain composed of the NAD(H)-binding domain I (dI) and the NADP(H)-binding domain III (dIII); part of dI is homologous to alanine dehydrogenase (Figure 1). The hydrophobic part of the enzyme containing the proton channel, denoted domain II (dII), is composed of a variable number of transmembrane helices depending on species. The *Escherichia coli* TH is composed of an α-subunit and a β-subunit, the former subunit containing dI and helices 1–4 of dII and the latter subunit containing dIII and helices 6–14 of dII. Intact *E. coli* TH has the composition $\alpha_2\beta_2$, i.e., it is a tetramer in which $\alpha+\beta$ corresponds to the mitochondrial single polypeptide. dI and dIII can be expressed separately and purified in an active state and, when combined, show catalytic activity. In order to elucidate the coupling mechanism of TH, the enzyme mainly from bovine, human, and *E. coli* has been extensively studied in the purified forms, in cytosolic (plasma membrane) vesicles, as well as reconstituted in liposomal membranes. dI and dIII from bovine, human, and *Rhodospirillum rubrum*, as well as a complex between dI and dIII, have been structurally determined using X-ray crystallography and NMR.

Structure–Function of the Substrate-Binding Domains

Recent advances in structural resolution of the hydrophilic dI and dIII by X-ray crystallography and NMR spectroscopy have dramatically increased our

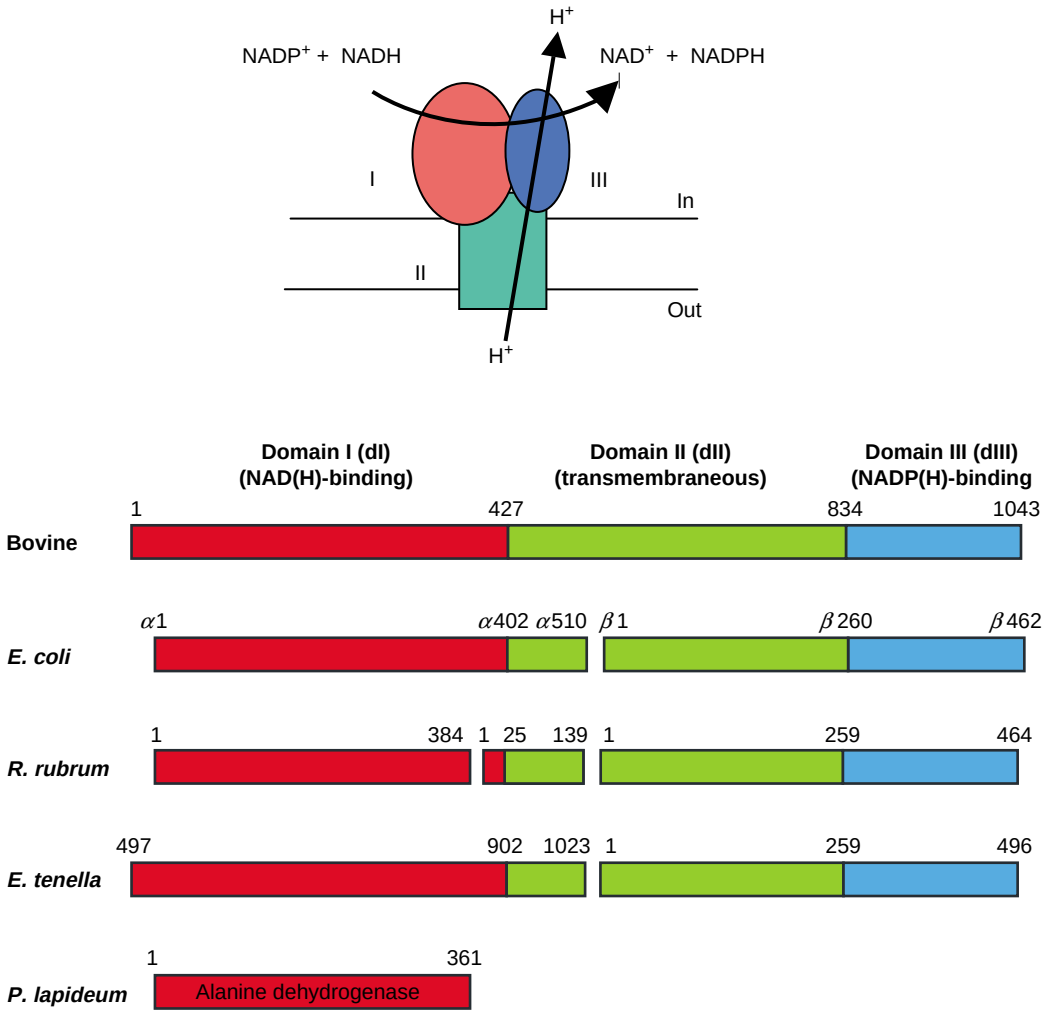

FIGURE 1 Structural organization of proton pumping THs.

knowledge about the structure–function relationships of these domains and their interactions. Thus, the crystal structure of the NAD^+ form of dI from *Rhodospirillum rubrum* solved by Jackson and coworkers and, in the NADH form from the same source later by Hatefi and coworkers, shows that it involves a dimer of a 40 kDa subunit, denoted A and B. Each subunit comprises two subdomains, dI.1 and dI.2, both of which have a Rossmann nucleotide-binding fold composed of a sheet of parallel β-strands flanked by α-helices. The two domains are arranged on the sides of a deep cleft. However, in the crystal structure of the dimer only dI.2(A) contains bound NAD^+ positioned so that its nicotinamide moiety is exposed in the cleft. In contrast, dI.2(B) site contains disordered NAD^+ or no ligand. The arrangement of the monomers in the dimer is such that the nucleotide-binding sites in dI.2(A) and dI.2(B) are pointing away from each other. The potential nucleotide-binding sites in dI.1 (A) and dI.1(B) have no known ligands. It is obvious that in the dI dimer, dI.2(A) and dI.2(B) must have different conformations, since only dI.2(A) contains well-ordered NAD^+. In a dimeric structure of dI with bound NADH, other minor but significant structural changes are observed.

Human and bovine dIII have been structurally resolved by Jackson and co-workers, and Hatefi and coworkers, respectively, using X-ray crystallography. These are structurally close to identical. The structures involve an alternating α/β-structure with a central β-sheet core, and a Rossmann fold in which $NADP^+$ is tightly bound at the C-terminal end of the β-sheet. The molecular mass of dIII is 20 kDa, it is a monomer, and it is isolated with predominantly tightly bound $NADP^+$; the K_d of the NADP(H) bound is in the nM–μM range. A striking difference, however, as compared with other NAD(P)-binding enzymes is that the $NADP^+$ bound to dIII is turned approximately 180°, i.e., the nicotinamide ring is close to α-helix 3 in *E. coli* dIII (corresponding to α-helix B in *R. rubrum* dIII) (Figure 2). A number of

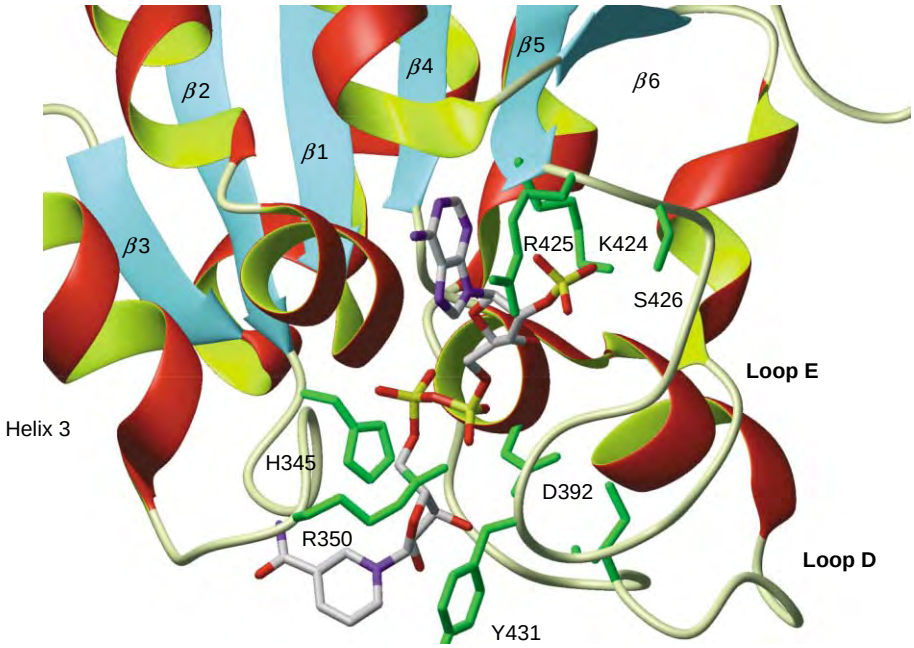

FIGURE 2 The NADP(H)-binding region of dIII. Amino acid residues and loops indicated are directly or indirectly essential in binding NADP(H).

hydrogen bonds stabilize NADP(H) in its binding site, involving, for example, Asp392, Lys424, Arg425, and Ser426. Loops D and E may indeed contribute to the binding and have been proposed to be involved in the Δp-dependent release of NADPH. Interactions between dI and dIII and their regulation by NADP(H)/NAD(H) have been investigated thoroughly by Karlsson and coworkers using NMR spectroscopy.

A crystal structure of a heterotrimer dI_2–dIII complex from *R. rubrum* showed that the dI and dIII structures are essentially identical to those determined separately. However, the dI_2–dIII structure revealed that dIII interacts with the dI.2(B), i.e., the NAD(H)-binding site that contains disordered NAD^+ rather than well-ordered NAD^+. This may be interpreted as indicating that when dIII (with bound $NADP^+$) is interacting with dI_2, it binds the dI.2(B) that has a disorganized NAD^+, not the dI.2(A) that has a well-ordered NAD^+. However, a complicating fact is that, even though an NAD(H) molecule could be modeled in the dI.2(B) site, the two nicotinamide rings are still separated by some 4–6Å, making direct hydride transfer difficult. A possible mechanistic solution to this problem is that the nicotinamide ring of the modeled NAD(H) is changed from an *anti* to a *syn* conformation, leading to a more open exposure of the nicotinamide ring in the cleft, and a direct interaction with the nicotinamide ring of $NADP^+$. Indeed, this rotation may be the very reason why NAD^+ is more mobile in dI.2(B). An additional factor influencing the interaction between dI and dIII, and thus hydride transfer, is the amino acids that make up the interface between the domains. One of these, Gln132 in dI, appears to be essential for activity because it works as a "tether" during the catalytic cycle, holding both NAD(H) and NADP(H) together in the right conformation through H-bonds.

Mechanism of Hydride Transfer

Transfer of the hydride ion between the 4A-hydrogen (*pro-R*) of NADH and the 4B (*pro-S*)-hydrogen of $NADP^+$, while the two substrates are bound to dI and dIII, respectively, occurs directly without any known intermediate and without exchange with bulk protons. Even though NAD^+/NADH are rapidly exchanging with the NAD(H)-binding site in dI throughout the reaction cycle, NADH especially shows different affinities in the open (ordered, high affinity) and closed (disordered, low affinity) states. These affinity changes, and the associated *anti/syn* transitions of NAD(H), are apparently induced by subtle conformational changes in the dI dimer. However, several pieces of evidence together indicate that regulation of hydride transfer by, for example, an electrochemical proton gradient, Δp, occurs mainly at the level of dIII, rather than dI. Essential information in this context was derived from the fact that separately expressed and purified dIII contains tightly bound NADP(H) which, due to a limiting release of the product NADP(H), catalyzes an ~2 orders of

magnitude slower reverse and forward reactions in the presence of purified dI than the wildtype enzyme. Isolated dIII also catalyzes a very fast so-called cyclic reaction, i.e., reduction of 3-acetyl-pyridine-NAD^+ (an NAD^+ analogue) by NADH, mediated by the bound NADP(H). This reaction involves reduction of bound $NADP^+$ by NADH, release of the NAD^+ formed, binding of 3-acetyl-pyridine-NAD^+, reduction of 3-acetyl-pyridine-NAD^+ by the bound NADPH, and release of 3-acetyl-pyridine-NADH. Indeed, it was reasonable to assume that the properties of the isolated dIII reflected an intermediate, the "occluded" state, in the reaction cycle of the intact transhydrogenase (TH). In reaction [1], this is interpreted to indicate that the activity of the forward reaction is limited by NADPH release, a limitation that is alleviated by Δp, allowing the enzyme to be catalytically fully active.

A general reaction scheme for forward reaction catalyzed by the *E. coli* TH may be outlined as follows (Figure 3). Starting with the resting state (state A), $NADP^+$ binds to dIII in the β-subunit generating state B, in which the proton channel and the protonatable group X2 become accessible to the periplasmic space; in state C, the enzyme is protonated at X2, and the β-subunit subsequently changes conformation to state D. In state D the proton moves from X2 to X1 concomitant with hydride transfer from NADH to $NADP^+$, generating state E. States D and E correspond to the "occluded" state. Following a conformational change in dIII, an opening of dIII, and a less tight NAD(H) (state F), the proton dissociates on the cytosolic side generating state G. After dissociation of NADPH, the enzyme returns to the resting state A. During the entire cycle NAD(H) can freely bind to and dissociate from dI. X3 indicates a group on dI that may be regulated by the cytosolic pH.

As further discussed below, at any given time, only half of the sites in the active dimeric enzyme (in the *E. coli* enzyme, $\alpha_2\beta_2$) seem to be available for, for example, NADP(H) binding and reaction with dicyclohexylcarbodiimide. In a recent modification of this principle, an alternating site mechanism has been proposed in which the two dIIIs alternate between an open and a closed ("occluded") state.

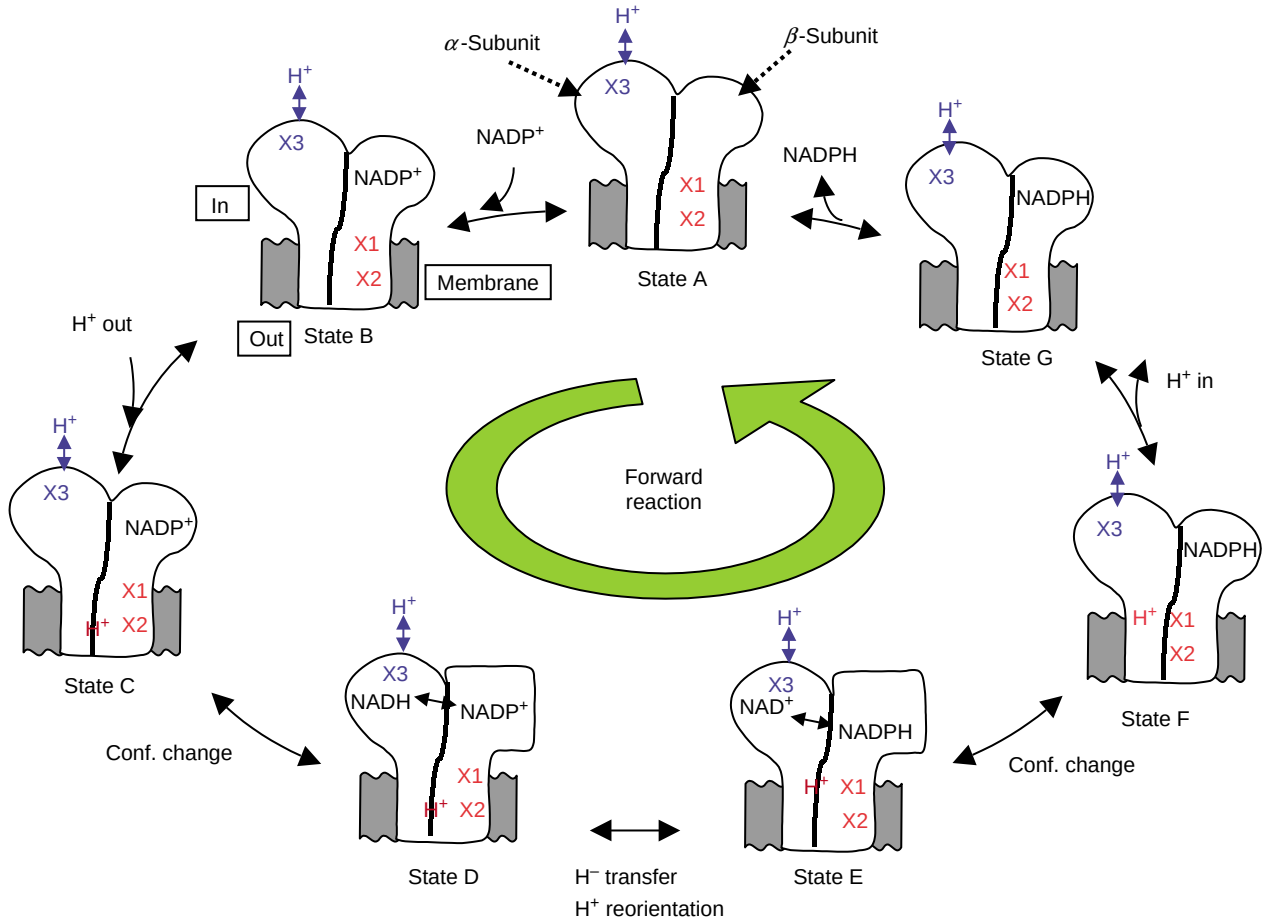

FIGURE 3 Reaction cycle of the forward TH reaction. X1 and X2 denote two protonatable residues in dII, possibly His91 and Asn222, respectively. X3 is a protonatable group in dI unrelated to the proton channel.

Membrane Topology and Helix Packing of the Membrane Domain

dII of the mitochondrial TH was early predicted to be composed of 14 transmembrane α-helices, whereas dII of the *E. coli* TH has been shown to be composed of 13 transmembrane α-helices (Figure 4). However, in contrast to the mitochondrial enzyme, *E. coli* TH consists of two subunits, the α- and β-subunits, which both contribute to dII. For some time, the membrane topology of the *E. coli* enzyme was unclear, especially regarding the region in dII where the two subunits interact. Subsequently, it was shown that the α- and β-subunits can be fused at the gene level, generating a mitochondrial-like TH, provided that the peptide linker is long enough, i.e., as long as the extra helix peptide in the mitochondrial TH; shorter linkers lead to truncated proteins with diminished activities. The C terminus of the α-subunit and the N terminus of the β-subunit are therefore located on different sides of the membrane (Figure 4).

Despite the obvious importance of dII in the overall transhydrogenase reaction, the structure of this domain has subsequently received comparatively little attention. However, a systematic effort to elucidate the packing of dII of the *E. coli* enzyme using cysteine crosslinking of double cysteine mutants in the cysteine-free background has been carried out, with one cysteine located in the α-subunit and the other at various positions in the β-subunit. The results show that, within the $\alpha+\beta$ unit, helices 2 and 4 are close to helix 6, and helix 3 and the C terminus of the α-subunit are close to helix 7. In the $\alpha_2\beta_2$, helices 2 and 4, as well as helix 6, are close to the same helices in the second subunit.

The Proton Channel

Being a proton pump, the membrane domain of THs must contain at least one proton channel, and considering the symmetry of the active $\alpha_2\beta_2$ structure, most likely two identical channels, one in each β-subunit. That the channel resides in the β-subunit is obvious due to the lack of suitable conserved protonatable residues in the α-subunit. However, residues in the α-subunit may contribute to the proton channel. DII of the *E. coli* TH contains few conserved protonatable amino acids, which may form part of a proton channel. Based on the properties of especially the positively charged H91K and N222R mutants (mimicking protonated His91 and Asn222, respectively), located in helix 9 and helix 13 (Figure 4), Bragg and coworkers made the important discovery that these mutants contain tightly bound NADP(H), reminiscent of isolated dIII. Indeed, this was the first piece of evidence indicating that dII not only communicates with dIII, but that the degree of protonation of specific residues, i.e., His91 and Asn222, in dII

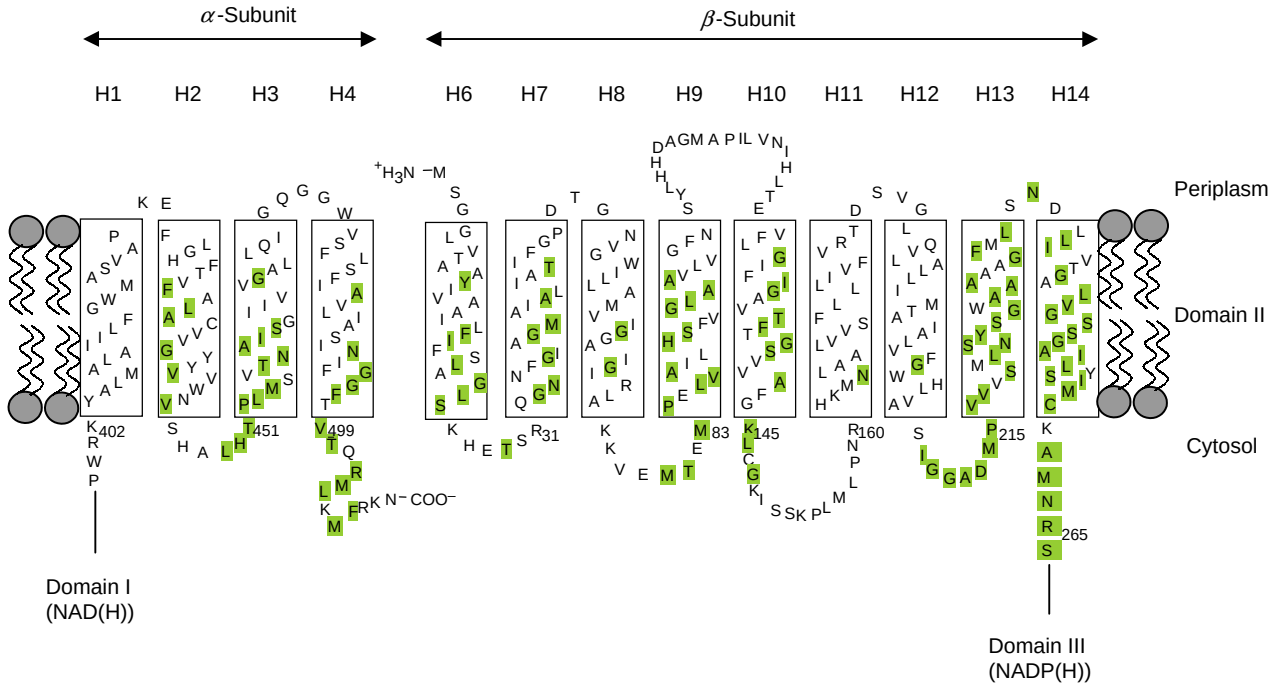

FIGURE 4 Membrane topology of *E. coli* TH. The topology was determined as described by Meuller, J., and Rydström, J. (1999). The membrane topology of proton-pumping *Escherichia coli* transhydrogenase determined by cysteine labeling. *J. Biol. Chem.* **274**, 19072–19080. Residues in green background are at least 80% conserved among 61 THs.

induces conformational changes that affect the dissociation constant for binding of NADP(H) to dIII. Ser139 is another potential component of the proton channel, with Glu85, Asp213, and Glu124 being possible peripheral residues of the channel, located close to the membrane surfaces.

Some mutants of the conserved His91, Asn222, and Ser139 residues still catalyze proton pumping although at reduced rates. This may be due to a compensatory effect of the remaining protonatable residues in the channel. In this context it should be stressed that a proton channel *per se* does not require protonatable residues. It would be sufficient with a chain of bound water molecules in a channel across the membrane to allow protons to "jump" from one water molecule to another. Protonation/deprotonation of protonatable amino acids in the channel induces conformational changes in the channel which link proton passage through the channel to catalytic events in often distantly located domains.

Coupling Mechanism

One of the main mechanistic challenges in past and present TH research is to understand how a Δp can be converted into a high [NADPH][NAD^+]/[NADH][$NADP^+$] ratio and conversely, how a high [NADPH][NAD^+]/[NADH][$NADP^+$] (or a [$NADP^+$][NADH]/[NADPH][NAD^+]) ratio can drive proton pumping. Since the difference in standard redox potential between the NADPH/$NADP^+$ and NADH/NAD^+ pairs is negligible, the main contribution to the redox potential/free energy is derived from the above substrate/product ratios. Because of the water-soluble nature of the TH substrates, and the apparently large distance between the substrate-binding sites and the membrane, it has been generally accepted that some kind of conformational coupling is involved. Such a mechanism is often described as resembling that of ATPase/synthase in which conformationally dependent binding changes are essential. This was also experimentally demonstrated earlier by extensive Δp-dependent changes of Km values for especially NAD(H). As described in the previous section, the single most important finding in this context was that mutating His91 and Asn222 to more positive amino acids lead to tightly bound NADP(H) in the intact mutant enzyme. An important contribution was also the demonstration of tightly bound NADP(H) in isolated dIII, which was assumed to represent an intermediate in the reaction cycle of TH, denoted the "occluded" state, which led to the proposal that both directions of the TH reaction, but especially the Δp-stimulated forward reaction, is limited by dissociation of NADP(H). The term "binding change" mechanism is frequently used in order to stress the role of dissociation/binding of NADP(H).

Despite the known crystal structures of dI, dIII, and the dI–dIII complex, the interface between dII and dI+dIII is unknown, i.e., little is known regarding the communication between dII and dIII. Most cytosolic loops of dII are poorly conserved, which makes it unlikely that dII–dIII signaling occurs via the surfaces of these domains. However, the peptide linking the C-terminal end of dII with dIII is quite conserved, and is highly mobile during catalysis as indicated by the NADP(H)-dependent increased trypsin sensitivity of Arg265 close to transmembrane helix 14 (Figure 4), indicating that this region is potentially important. Subsequently, Arg265 has been suggested to form a functional-salt bridge with Asp213, constituting an essential component ("hinge" region) of a new coupling mechanism. However, communication between this proposed salt bridge and the NADP(H)-binding site remains unknown, although loops D and E close to the NADP(H)-binding site in dIII may be important. Proton-translocating THs, which are all dimers, may work according to an alternate-site-binding change mechanism. According to this mechanism, only half of the intact TH is catalytically active at any given time.

Physiological Role

In 1959 Klingenberg and Slenczka found that the mitochondrial redox level of NADP(H) was at least 90%, and that of NAD(H) ~50–60%. The forward TH reaction (reaction [1]), driven by Δp, is largely responsible for this high redox level of NADPH which, as expected, is sensitive to uncouplers. This also explains the fact that NADPH-dependent detoxification (through glutathione peroxidase) of organic peroxides in intact mitochondria is more effective with NADH-linked substrates than with NADPH-linked substrates. Thus, endogenous $NADP^+$ together with NADH (generated by the added substrate, e.g., β-hydroxybutyrate) provides a higher redox level of NADPH through TH than NADPH-linked substrates. A high level of NADPH is important because it generates reduced glutathione essential for, for example, glutathione peroxidase. NADPH also regulates the redox levels of thioredoxin and protein-bound thiols. Organic peroxides lead to a rapid oxidation of mitochondrial reduced glutathione through the glutathione peroxidase system, which in turn leads to a massive release of Ca^{2+} ions, presumably through the mitochondrial permeability transition pore (MPTP). MPTP may, in turn, contain redox-sensitive protein thiols. Therefore, the high mitochondrial redox level of NADP(H), maintained by TH, is of crucial importance for detoxification, Ca^{2+} homeostasis, cell thiol regulation, and biosynthesis. In liver, but probably not in heart, TH-generated NADPH in the

mitochondrion contributes to cytosolic NADPH through transport in the form of (iso)citrate generated by the NADP-dependent isocitrate dehydrogenase (NADP–ICDH).

A different hypothesis for the physiological role of TH involves a regulation of the citric acid cycle, especially the NAD and the NADP-dependent isocitrate dehydrogenases. The NAD enzyme (NAD–ICDH) is irreversible and strongly regulated by, for example, ADP, whereas NADP–ICDH is reversible and apparently unregulated. Oxidative decarboxylation of isocitrate to α-ketoglutarate, carbon dioxide, and NADH by the NAD–ICDH can be linked to the NADP–ICDH by a reductive carboxylation of α-ketoglutarate, carbon dioxide, and NADPH back to isocitrate. The NADH generated by the NAD–ICDH, together with $NADP^+$, is thus used by TH and Δp to generate NADPH that drives the NADP–ICDH. This nonproductive cycle uses one proton/cycle to slow down or regulate the flux through this step in the citric acid cycle. However, there is no obligatory simultaneous occurrence of TH and NADP-isocitrate dehydrogenase in some species, which casts some doubt on this potentially important regulatory system.

Theoretically, a reversal of reaction [1] can also be used to generate a Δp under, e.g., ischemic conditions. However, it is generally believed that unless a continuous source of $NADP^+$-reducing substrates as well as NAD^+-oxidizing substrates are available, the Δp generated would be transient and short-lived.

See Also the Following Article

Glutathione Peroxidases

Glossary

membrane protein A membrane-associated protein, in this context an integral membrane protein spanning the membrane.

NAD(H) Oxidized (NAD^+) and reduced (NADH) nicotinamide adenine dinucleotide, a common cofactor in cell metabolism, especially catabolism.

NADP(H) Oxidized ($NADP^+$) and reduced (NADPH) nicotinamide adenine dinucleotide phosphate, a common cofactor in cell metabolism, especially anabolism.

proton pump A group of membrane proteins catalyzing a translocation of protons across the membrane, driven either by redox energy, an ion gradient, or ATP.

transhydrogenases A group of enzymes composed of two subgroups: a soluble flavine-containing type and a membrane-bound and proton-translocating type. Both catalyze the transfer of a hydride ion between NAD(H) and NADP(H).

Further Reading

Bergkvist, A., Johansson, C., Johansson, T., Rydstrom, J., and Karlsson, B. G. (2000). Interactions of the NADP(H)-binding domain III of proton-translocating transhydrogenase from *Escherichia coli* with NADP(H) and the NAD(H)-binding domain I studied by NMR and site-directed mutagenesis. *Biochemistry* **39**, 12595–12605.

Bizouarn, T., Fjellström, O., Meuller, J., Axelsson, M., Bergkvist, A., Johansson, C., Karlsson, B. G., and Rydström, J. (2000). Proton translocating nicotinamide nucleotide transhydrogenase from *E. coli*. Mechanism of action deduced from its structural and catalytic properties. *Biochim. Biophys. Acta* **1457**, 211–228.

Bizouarn, T., Althage, M., Pedersen, A., Tigerström, A., Karlsson, J., Johansson, C., and Rydström, J. (2002). The organization of the membrane domain and its interaction with the NADP(H)-binding site in proton-translocating transhydrogenase from *E. coli*. *Biochim. Biophys. Acta* **1555**, 122–127.

Bragg, P. D., and Hou, C. (1999). Mutation of conserved polar residues in the transmembrane domain of the proton-pumping pyridine nucleotide transhydrogenase of *Escherichia coli*. *Biochim. Biophys. Acta* **363**, 182–190.

Buckley, P. A., Jackson, J. B., Schneider, T., White, S. A., Rice, D. W. and Baker, P. J. (2000). Protein–protein recognition, hydride transfer and proton pumping in the transhydrogenase complex. *Structure* **8**, 809–815.

Cotton, N. P., White, S. A., Peake, S. J., McSweeney, S., Jackson, J. B. (2001). The crystals structure of an asymmetric complex of the two nucleotide binding components of proton-translocating transhydrogenase. *Structure* **9**, 165–176.

Glavas, N. A., and Bragg, P. D. (1995). The mechanism of hydride transfer between NADH and 3-acetylpyridine adenine dinucleotide by the pyridine nucleotide transhydrogenase of *Escherichia coli*. *Biochim. Biophys. Acta* **1231**, 297–303.

Hatefi, Y., and Yamaguchi, M. (1996). Nicotinamide nucleotide transhydrogenase: A model for utilization of substrate binding energy for proton translocation. *FASEB J.* **10**, 444–452.

Hoek, J. B., and Rydström, J. (1988). Physiological roles of nicotinamide nucleotide transhydrogenase. *Biochem. J.* **254**, 1–10.

Jackson, J. B., White, S. A., Quirk, P. G., and Venning, J. D. (2002). The alternating site, binding change mechanism for proton translocation by transhydrogenase. *Biochemistry* **41**, 4173–4185.

Meuller, J., and Rydström, J. (1999). The membrane topology of proton-pumping *Escherichia coli* transhydrogenase determined by cysteine labeling. *J. Biol. Chem.* **274**, 19072–19080.

Prasad, G. S., Wahlberg, M., Sridhar, V., Sundaresan, V., Yamaguchi, M., Hatefi, Y., and Stout, C. D. (2002). Crystal structures of transhydrogenase domain I with and without bound NADH. *Biochemistry* **41**, 12745–12754.

Biography

Professor Jan Rydström is Head of Biochemistry and Biophysics, Department of Chemistry, Göteborg University, Sweden. His research interests are focused on structure–function relationship of membrane proteins, especially transport proteins, and biochemical toxicology.

Nicotinic Acetylcholine Receptors

Nivalda O. Rodrigues-Pinguet and Henry A. Lester
California Institute of Technology, Pasadena, California, USA

Ion channels are classified by their gating (opening) mechanisms. Mechano-sensitive channels are activated directly by forces applied to the channel proteins. The superfamily of voltage-gated channels responds to changes in the membrane potential. The ligand-gated or agonist-gated receptors open as they bind specific molecules. The nicotinic acetylcholine receptor (nAChR) is a well-studied member of the superfamily of ligand-gated ion channels (LGICs). The nAChR is the prototype LGIC since its sequence and structure strongly resemble that of glycine, serotonin 5-HT3$_A$, γ-aminobutyric acid (GABA$_A$), and invertebrate glutamate-gated chloride (GluCl) receptors. Since the early twentieth century, researchers have worked to unravel some of the mysteries of this cylindrically shaped macromolecule embedded in the membrane at vertebrate nerve–muscle synapses, at invertebrate nicotinic synapses, and in the vertebrate central nervous system. To date, several nAChR subtypes have been successfully isolated, cloned, purified, imaged, expressed, and unitary currents have been recorded from these channels. There is now a clear picture of the nAChR architecture and function. However, efforts are still underway to understand key functional aspects of this receptor as well as its role in addiction and disease.

Structure

Nigel Unwin and colleagues have resolved the muscle nicotinic acetylcholine receptor (nAChR) structure from *Torpedo* electric organ, which is derived from muscle, to 4Å resolution. The structure of the neuronal nAChR has not been resolved. Yet one expects that many details, certainly including its membrane topology, are identical to the muscle receptor. From Unwin's work, it is now known that the entire muscle nicotinic receptor complex is ~150Å tall (Figure 1A). Biochemical and electron microscopic studies reveal that nicotinic receptors, in peripheral organs (e.g., muscle) and in the central nervous system, are heteromers composed of five subunits that assemble into a barrel-like structure around a central ion pore. The receptor has three main parts: a region found outside of the cell (extracellular), a region located within the membrane (transmembrane), and an intracellular portion (cytoplasmic).

Subunits

Steve Heinemann, Norman Davidson, Shosaku Numa, Jim Patrick, Jim Boulter, and others cloned the nAChR subunits. To date, ten α-subunits and seven β-, γ-, δ-subunits have been cloned. However, additional subunit genes probably await discovery. Each of the five nicotinic subunits is composed of (from N–C terminus) an extracellular domain, four transmembrane domains (referred to as M1–M4) 19–27 amino acids in length, a cytoplasmic loop, and an extracellular C terminus consisting of ~20 amino acid residues (Figure 1A). The fetal or denervated muscle nAChR is a heteromeric pentamer composed of two α-subunits and one β-, γ-, and δ-subunit. In most adult nAChRs, the δ-subunit is replaced with an ε-subunit. Central nicotinic receptors can be either homomeric or heteromeric pentamers composed of α-subunits or, α- and β-subunits, respectively.

The Extracellular Domain

The extracellular domain protrudes ~60Å away from the membrane and has several characteristic structural elements shared by other members of the ligand-gated ion channels (LGICs) superfamily. In 2001, Titia Sixma and co-workers crystallized the acetylcholine-binding protein (AChBP) from a mollusc. Most of the nAChR N-terminal features deduced from X-ray crystallographic, biochemical, and physiological studies have been confirmed with the 2.7Å resolution structure of AChBP. This protein has ~20% homology to the extracellular domain of nicotinic receptors, and it lacks transmembrane, cytoplasmic, and C-terminal domains. Yet Sixma's AChBP crystal structure has given researchers a clearer image of the extracellular region of the nAChR. There are six loops, named with the letters A–F, involved in ligand binding. This region also contains a disulfide bond within loop C and another disulfide bond (the signature loop) located between cysteine residues 123 and 136. Sixma's AChBP crystal structure suggests that the signature disulfide loop present in the nAChR is located at the bottom of the binding domain, where it can interact directly with

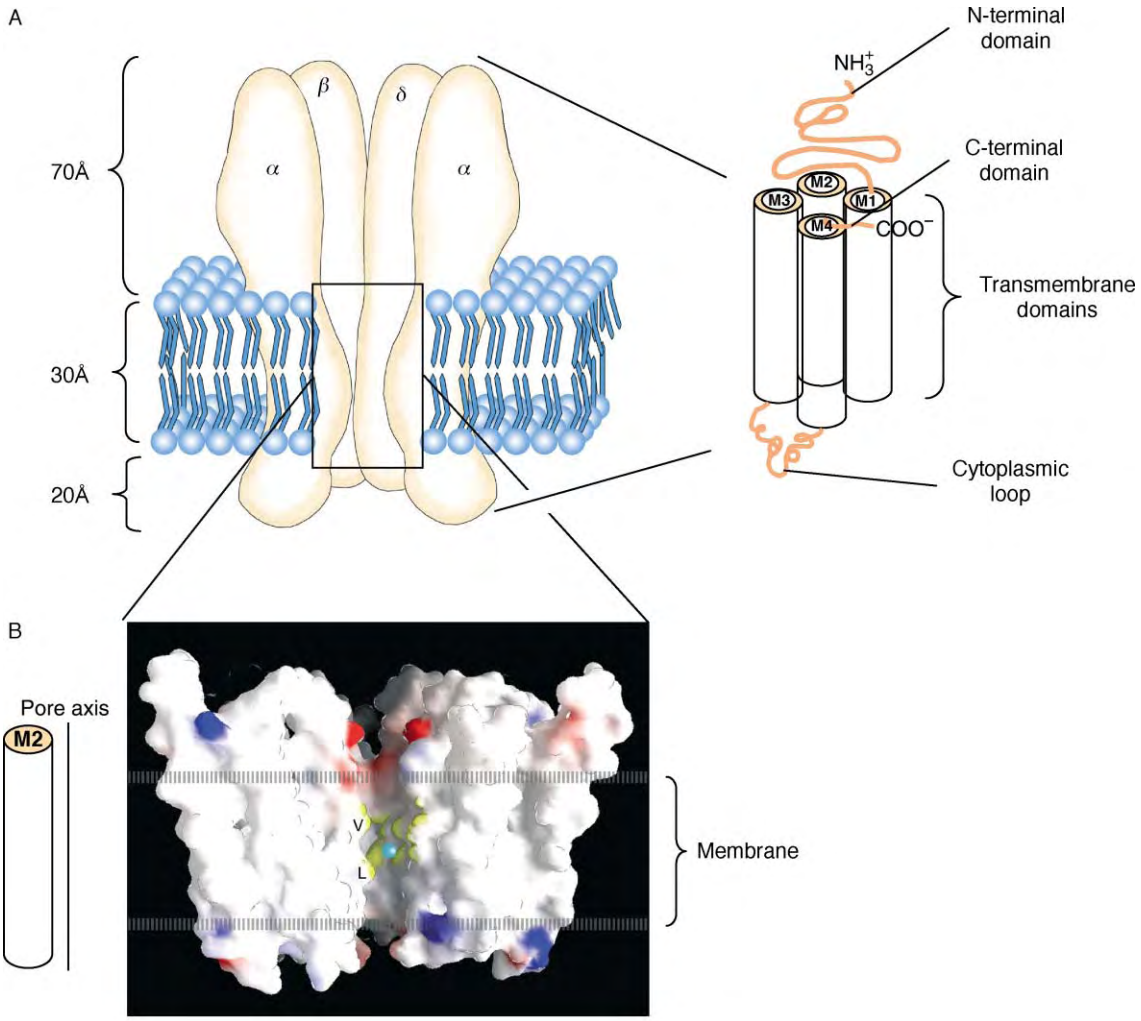

FIGURE 1 (A) The structure of the muscle nicotinic receptor embedded in the plasma membrane (blue), with the front subunit removed. Each subunit is composed of an N-terminal domain, four transmembrane domains (M1–4), a cytoplasmic loop, and a C-terminal domain. (B) The nAChR pore is mostly lined by M2 α-helices. Gray lines represent the plasma membrane, red and blue areas correspond to negative and positive charges, respectively. The channel's gate is expected to be located in hydrophobic regions within the pore (shown in yellow). The blue sphere in the channel represents a sodium ion. (Reproduced from Miyazawa, A., Fujiyoshi, Y., and Unwin, N. (2003). Structure and gating mechanism of the acetylcholine receptor pore. *Nature* **423** (6943), 949–955, with permission from Nature.)

other parts that reside within the membrane, possibly coupling agonist binding with channel opening.

The Agonist Binding Site

The endogenous ligand for the nAChR is acetylcholine (ACh). The open state of the channel is much more likely to be associated with two bound agonist molecules than with a single bound molecule. ACh specifically binds to amino acids at the subunit interface of the extracellular region, within loops A, B, and C in the α-subunit and D, E, and F in the non-α-subunit. The binding site resembles a box that is lined by aromatic amino acid residues (tyrosine and tryptophan) (Figure 2). The positively charged ACh molecule binds to its target site partially via cation–π interactions. In this type of interaction the cation (or positively charged moiety) interacts with the electron density at the face of an aromatic side chain.

The Pore

The nicotinic receptor's pore lies within the membrane ~50Å below the ACh binding site. The central ion channel is mostly lined by the M2 α-helices from the five nicotinic subunits (Figure 1B). Parts of the M1 transmembrane domain from each subunit also protrude into the pore. The M2 domains approach each other most closely midway through the membrane creating a gate, which prevents ions from permeating the channel in the closed conformation. Sliding, rotating, and/or tilting of the M2 α-helices during nearly symmetrical transitions of the pentameric bundle remove this constriction. Once the receptor opens, three rings of

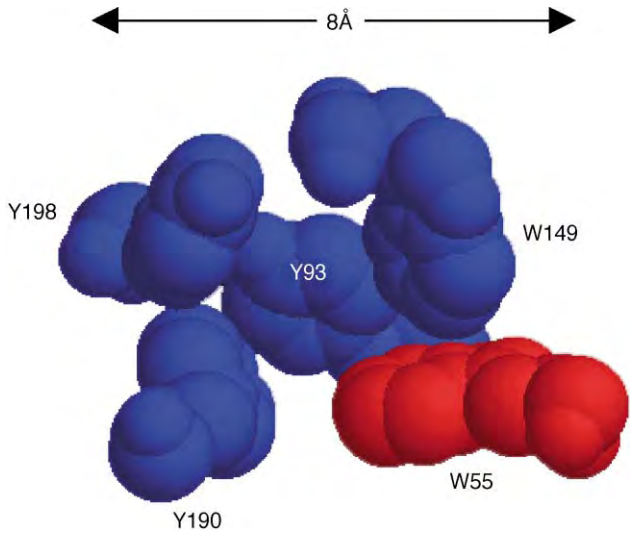

FIGURE 2 The agonist binding site resembles a box lined with five aromatic amino acid residues. Amino acids shown in blue and red are located in the α- and the non-α-subunits, respectively.

negatively charged amino acids within the pore allow the receptor to conduct positively charged sodium, potassium, and calcium ions.

The Cytoplasmic Loop

The M3–M4 cytoplasmic loop in the nAChR varies in both length and sequence among the nicotinic receptor subunits. However, the sequences of the cytoplasmic loops contain consensus phosphorylation sites for various kinases including protein kinase A, C, tyrosine kinase, casein kinase, calmodulin dependent kinase II, and cyclin dependent kinase 5. The M3–M4 loop also contains endoplasmic reticulum retention and export motifs as well as endocytosis motifs. In addition to having phosphorylation sites and targeting motifs, the M3–M4 loop of the muscle nAChR binds to a protein called rapsyn. The muscle nicotinic receptor is anchored to the membrane through its association with this protein.

Channel Activation

The nicotinic acetylcholine receptor has various conformational states including a resting, an active (open channel), and at least two desensitized (non-conducting) states. Upon binding two molecules of ACh in the extracellular region, the receptor undergoes a poorly known conformational change that places the M2 α-helices in the open, cation-conducting state. The channel remains open, or opens several times in succession, for only a few thousandths of a second before one or both agonist molecules dissociate from the binding pocket and the channel closes. If agonist remains present and binds repeatedly, the channel enters a desensitized state.

The Function of nAChRs *in vivo*

Neuromuscular Junction

After the motor nerve muscle is stimulated, the nerve action potential reaches the presynaptic terminal, where it evokes release of prepackaged vesicles containing ACh. The ACh released into the synaptic cleft binds and activates nicotinic receptors located on the postsynaptic muscle membrane. Once the postsynaptic cell is depolarized, voltage-gated sodium channels open, propagating the action potential, and consequently leading to muscle twitches. Presynaptically released ACh remains in the synapse for only about a millisecond before it is broken down by acetylcholinesterase or, more slowly, diffuses away.

Central Nervous System

Researchers have begun by studying the structure and function of the muscle nicotinic receptor. However, the diversity and function of the neuronal nicotinic receptors is being appreciated only now. Despite good efforts, researchers have still not clearly described the various neuronal nAChRs' precise subunit composition, assembly, regulation, and the significance of their heterogeneity.

Neuronal nAChR Composition

Researchers believe that many central nicotinic receptors are heteropentamers composed of at least two α- and three other (α- or β-) subunits. The α7-, α8-, and α9-subunits can form functional homopentameric receptors. There are eight α-subunit (α2–α7, α9, and α10) and three β-subunit (β2–β4) genes expressed in the vertebrate nervous system. An additional α8-subunit gene has been identified in avian species. However, β-, γ-, δ-, and ε-subunits are not expressed in the brain. Although there are literally thousands of different theoretical subunit combinations, only a handful of these produce functional receptors with distinct pharmacological and biophysical properties. Heterologous expression of nAChRs in *Xenopus* oocytes and in mammalian cells has revealed which specific α/β combinations produce functional receptors. The α2-, α3-, and α4-subunits can each form heteropentamers with either β2 or β4. α6β4 receptors express successfully, but similar to the α5- and β3-subunits, α6 expresses best in combination with two other types of subunits. Although the α7-, α8-, and α9-subunits can form functional homopentameric receptors, they can also

form heteropentamers (i.e., $\alpha 7\alpha 8$ and $\alpha 9\alpha 10$ receptors). Evidence for the precise subunit composition of native neuronal receptors is still scant. Although a few major subtypes have been identified (i.e., $\alpha 7$ homopentamers, $\alpha 4\beta 2$, and $\alpha 3\beta 4$), future studies will probably discover other subtypes and perhaps more complex subunit combinations.

The Role of Neuronal nAChRs

Previous work using *in situ* hybridization techniques and radiolabeled ligands shows that nicotinic receptors are present in various brain structures, including the thalamus, cortex, hippocampus, hypothalamus, and cerebellum. Although many neuronal nAChRs are found on the presynaptic terminal, some are located postsynaptically. Brain nAChRs are thought to presynaptically modulate, rather than directly mediate, chemical synaptic transmission. In the retina and striatum, cholinergic (ACh containing) interneurons release ACh and activate nAChRs located on the presynaptic cell. Presynaptic nicotinic receptor activation can positively or negatively affect the release of various neurotransmitters including GABA, glutamate, dopamine, and noradrenaline.

Nicotinic Receptor Agonists and Antagonists

Agonists

In addition to ACh, other compounds can activate nicotinic receptors. In fact, nAChRs are offensive or defensive targets for various organisms. For instance, nicotine, an alkaloid product from tobacco, is the prototypic agonist for nAChRs. Additionally, epibatidine, a powerful analgesic that is purified from the skin of the South American tree frog, *Epipedobates tricolor*, is the most potent nAChR agonist discovered. Other naturally occurring nAChR agonists include choline, cytisine, anabaseine, and (+)-anatoxin A. In an effort to provide greater subtype selectivity and therapeutic efficacy, researchers have also developed a wide range of synthetic compounds that can activate nAChRs. Keep in mind that the muscle and the various neuronal nicotinic receptor subtypes have distinct pharmacological profiles for different natural and synthetic agonists.

Antagonists

Nicotinic receptor inhibitors stabilize the closed-channel conformation and, in the case, of competitive inhibitors, prevent agonist binding. D-tubocurarine (d-TC) is a classic competitive nAChR inhibitor that does not discriminate well between the various types of nicotinic receptors. South American Indians commonly used this poison found in the shrubs of *Chondodendron tomentosum* to coat the tip of their arrows. More selective than d-TC, dihydro-β-erythroidine is an alkaloid that is mostly used to inhibit $\alpha 4\beta 2$ receptors. α-Bungarotoxin (α-Bgt) is a well-established selective competitive nAChR antagonist found in the venom of the Taiwanese banded krait (*Bungarus multicintus*). α-Bgt inhibits muscle nAChRs and $\alpha 7$ homomers, as well as receptors containing $\alpha 8$- and $\alpha 9$-subunits. It does not appear to interact with α/β heteropentamers. Other nAChR noncompetitive inhibitors include α-conotoxins, mecamylamine, steroids, local anesthetics, and such therapeutic agents as MK 801, carbamazepine, buproprion, and chlorpromazine.

Nicotinic Receptors and Disease

Congenital Myasthenic Syndrome

Nicotinic receptors have been implicated in a number of diseases. At the neuromuscular junction, 26 mutations have been identified in the extracellular, transmembrane, and cytoplasmic domains of the nAChR that lead to different forms of congenital myasthenic syndrome (CMS). CMS are presynaptic, synaptic, and postsynaptic in origin. Postsynaptic CMS mutations are divided into two categories, depending on their effects at the endplate region of the muscle membrane. CMS mutations are classified as either slow- or fast-channel syndromes. The slow-channel mutations enhance agonist affinity or gating efficiency. The fast-channel syndrome mutations reduce agonist affinity for the open channel or impair gating. Work from Andrew Engel, Christopher Gomez, Steven Sine and Anthony Auerbach has contributed to the molecular pathophysiology of CMS. Furthermore, their biophysical analyses of the CMS mutations have provided us with some basic insights into the relationship between the structure and function of nAChRs.

Epilepsy

Nicotinic receptors appear to be linked to several forms of inherited epilepsy. Autosomal-dominant nocturnal frontal lobe epilepsy (ADNFLE) is a monogenic disease presently linked to three $\alpha 4$ and two $\beta 2$ mutations. All five of these mutations lie within (or immediately adjacent to) M2 and produce similar clinical symptoms. To date, the mechanism(s) by which these mutations lead to the onset of a partial epileptic seizure remains to be elucidated. However, two effects common to all of the mutations have been identified. (1) The ADNFLE mutants reduce the nAChR's sensitivity to changes in extracellular calcium and (2) the mutations enhance the receptor's sensitivity to ACh. Studies on mouse

models of ADNFLE may be the most appropriate tactic for understanding the pathophysiology of these partial seizures.

Alzheimer's Disease (AD)

AD is a neuro-degenerative disease characterized by the progressive deterioration of higher cognitive functions, including memory loss. Since nicotinic receptors play a critical role in learning and memory, it is not surprising that AD patients lose the cholinergic pathways from the basal forebrain to the hippocampus and the cortex. Moreover, the brains of AD patients have a reduced number of cholinergic cells and presynaptic nAChRs. Since low levels of ACh are believed to lead to the cognitive decline observed in patients, cholinesterase inhibitors (such as tacrine, donepezil, and rivastigmine) are currently used to treat AD.

Parkinson's Disease (PD)

Patients with PD, another neuro-degenerative disorder, have difficulty initiating and sustaining smooth muscle movements. Although loss of dopaminergic neurons defines PD, patients also lose cholinergic cells in the basal forebrain and their high affinity nAChRs. In fact, the reduction in cortical nAChRs correlates well with the degree of dementia. Furthermore, researchers have correlated tobacco use with a lower incidence of PD.

Other Diseases

Nicotinic receptors have also been implicated in other diseases such as schizophrenia, Tourette's syndrome, anxiety, and depression. However, the precise role of the nAChR in the pathology of these diseases remains to be determined.

See Also the Following Articles

Calcium/Calmodulin-Dependent Protein Kinase II • Calcium/Calmodulin-Dependent Protein Kinases • Disulfide Bond Formation • Muscarinic Acetylcholine Receptors • Neurotransmitter Transporters • Protein Kinase C Family

Glossary

acetylcholinesterase The enzyme that breaks down acetylcholine into choline and acetate.

disulfide bond The covalent bond between two thiol groups (S–S) of cysteine residues.

endplate The surface of the muscle fiber at the junction where the motor nerve terminal meets the muscle.

neurotransmitter A chemical released from neurons across the synapse.

postsynaptic Located after the synapse.

presynaptic Located before the synapse.

synapse The extracellular space between the presynaptic and postsynaptic neurons.

Further Reading

Brejc, K., van Dijk, W. J., Klaassen, R. V., Schuurmans, M., van Der Oost, J., Smit, A. B., and Sixma, T. K. (2001). Crystal structure of an ACh-binding protein reveals the ligand-binding domain of nicotinic receptors. *Nature* **411**, 269–276.

Bertrand, D., Picard, F., Le Hellard, S., Weiland, S., Favre, I., Phillips, H., Bertrand, S., Berkovic, S. F., Malafosse, A., and Mulley, J. (2002). How mutations in the nAChRs can cause ADNFLE epilepsy. *Epilepsia* **43**, 112–122.

Engel, A. G., Ohno, K., and Sine, S. (2002). The spectrum of the congenital myasthenic syndromes. *Mol. Neurobiol.* **26**, 347–367.

Hille, B. (2001). Ligand-gated channels of fast chemical synapses. In *Ion Channels of Excitable Membranes*, 3rd edition, pp. 169–199. Sinauer Associates, Massachusetts.

Miyazawa, A., Fujiyoshi, Y., and Unwin, N. (2003). Structure and gating mechanism of the acetylcholine receptor pore. *Nature* **423**, 949–955.

Paterson, D., and Nordberg, A. (2000). Neuronal nicotinic receptors in the human brain. *Prog. Neurobiol.* **61**, 75–111.

Rodrigues-Pinguet, N., Jia, L., Li, M., Figl, A., Klaassen, A., Truong, A., Lester, H. A., and Cohen, B. (2003). Five ADNFLE mutation reduce the Ca^{2+} dependence of the mammalian $\alpha 4\beta 2$ acetylcholine response. *J. Physiol.* **550**, 11–26.

Sharples, C. G. V., and Wonnacott, S. (2001). Neuronal nicotinic receptors. *Tocris Rev.* **19**, 1–12.

Steinlein, O. K. (2002). Channelopathies can cause epilepsy in man. *Eur. J. Pain* **6**(suppl. A), 27–34.

Unwin, N. (2002). Structure of the acetylcholine-gated channel. *The Roy. Soc.* **355**, 1813–1829.

Wonnacott, S. (1997). Presynaptic ACh receptors. *Trends Neurosci.* **20**, 92–98.

Biography

Nivalda O. Rodrigues-Pinguet obtained her Ph.D. in Biomedical Sciences at the University of California, Riverside. She is currently a post-doctoral scholar with Drs. Bruce N. Cohen and Henry A. Lester at the California Institute of Technology. During her graduate tenure, Dr. Rodrigues-Pinguet studied the functional effects of nicotinic receptor mutations linked to autosomal dominant nocturnal frontal lobe epilepsy (ADNFLE).

Henry A. Lester is the Bren Professor of Biology at the California Institute of Technology. He obtained his Ph.D. in Biophysics from Rockefeller University and pursued his postdoctoral training with Dr. Jean-Pierre Changeux, at the Institut Pasteur in Paris, France. Dr. Lester received formal training in physics but has also embraced biochemistry, molecular biology, and neurogenetics. He has worked on nicotinic receptors for 30 years and is an authority on ion channels and molecular neuroscience.

Nitric Oxide Signaling

Michael A. Marletta
University of California, Berkeley, California, USA

The basic components of nitric oxide (NO) signaling involve nitric oxide synthase (NOS) to synthesize NO and the soluble isoform of guanylate cyclase (sGC) to trap NO. Once activated by NO, sGC converts GTP to guanosine 3′5′-cyclic monophosphate (cGMP), leading to cGMP-dependent physiological responses such as vasodilation. Termination of the cGMP signal involves a cyclic nucleotide phosphodiesterase (PDE). There are multiple PDE isoforms, and selective inhibition of specific isoforms has proven to be clinically useful (for example, sidenifil [Viagra] in the treatment of erectile dysfunction). sGC must also be turned off; however, the *in vivo* mechanism for this remains unknown. Catalytic activity of constitutive NOS isoforms involved in signaling is controlled by Ca^{2+} and calmodulin via receptor-mediated events that trigger Ca^{2+} release from intracellular stores or uptake from external sources.

Biological Processes Controlled by Nitric Oxide

First defined as EDRF (endothelium-derived relaxing factor), the biological effects of nitric oxide (NO) have now been definitively characterized in a number of tissues. Smooth muscle is often the target of NO action, leading to vasodilation in blood vessels (Figure 1) and penile erection via NO synthesis in the corpus cavernosum, two well-established functions. Smooth muscle relaxation in the gut is another important function for NO, playing a key role in gastrointestinal tract motility. NO synthesis in the brain is also well established, though the exact role in learning and memory is still under debate. In the CNS, NO acts as a somewhat atypical neurotransmitter in that it is not synthesized and stored and then released with the appropriate signal, but is synthesized on demand. Constitutive nitric oxide synthases (NOSs) are involved in all of these responses and are under the control of Ca^{2+} and calmodulin. Receptor-mediated events that trigger Ca^{2+} release or uptake turn on the specific NOS isoform in the tissue. NOS has also been found in skeletal muscle, in the myocardium, and in many other cells, suggesting that it will play an even more extensive role in physiological control than is currently established. The function of NO in the myocardium is particularly complex, although it appears that novel therapeutics will be an outcome of sorting out the complexity.

Nitric Oxide Synthase

The catalytic activity of the NOS isoforms (constitutive) involved in signaling is controlled by Ca^{2+} and calmodulin (CaM). After stimulation by the appropriate external signal, an increase in intracellular-free Ca^{2+} occurs, which then leads to a Ca^{2+}–calmodulin complex. Each of the four EF hands of calmodulin binds one Ca^{2+}, and then this Ca^{2+}–CaM complex binds to NOS, thereby activating NOS to synthesize NO. The NOS reaction is shown in Figure 2. The enzyme converts L-arginine to citrulline and NO. Co-substrates for the reaction include NADPH and O_2. NOS is composed of two domains: a reductase domain with homology to cytochrome P450 reductase and a heme domain. The reductase domain contains two bound flavins, FAD and FMN, and with analogy to P450 reductase, the electron transfer route is from NADPH to FAD and then to FMN. The heme domain contains a cytochrome P450-type heme (ferric protoporphyrin IX coordinated to cysteine thiol), one equivalent of 6(R)-tetrahydro-L-biopterin (H_4B), and the L-arginine binding site. Crystal structures of the heme domain show it to be dimeric with a tetra-thiolate zinc center at the dimeric interface using two cysteines from each subunit. Catalytic chemistry at the heme domain is dependent on electron transfer from the flavins in the reductase domain, which is triggered by binding of the Ca^{2+}–CaM complex to NOS.

The catalytic chemistry takes place at the P450 heme site; in fact, structures of the oxygenase domain that have been solved in the presence of L-arginine show the substrate positioned over the heme. H_4B also participates in electron transfer at the heme site, using unprecedented one-electron chemistry. The exact details of the involvement of this required bound cofactor are still emerging. As shown in Figure 2, L-arginine is first converted to NHA (N^G-hydroxy-L-arginine) and then NHA is converted to citrulline

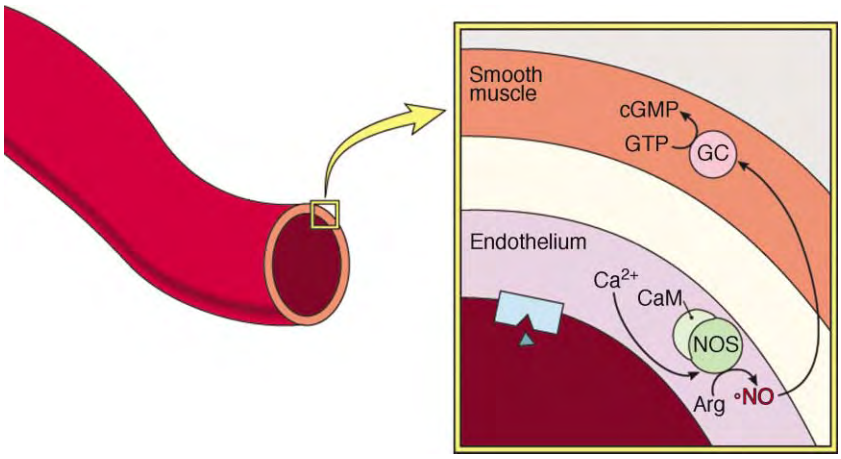

FIGURE 1 Nitric oxide function in blood vessel dilation. In response to a receptor-mediated event (shown schematically), endothelial NOS is activated by Ca^{2+} and calmodulin, leading to the synthesis of NO. NO then diffuses into the adjacent smooth muscle and activates the soluble isoform of guanylate cyclase and the synthesis of cGMP. cGMP, through a signaling cascade, then leads to smooth muscle relaxation.

and NO. NADPH and O_2 are required in both steps of the reactions, as is H_4B. The mechanism of the reaction is complicated and not fully understood, but clearly involves oxidative chemistry at the P450 heme with participation of H_4B.

The Ca^{2+}–CaM complex exerts control over the NOS reaction catalyzed by the constitutive cell-signaling isoforms, eNOS (endothelial NOS) and nNOS (neuronal NOS) by controlling electron transfer from the reductase domain to heme domain. Without this required process, the reaction does not take place, therefore, Ca^{2+}–CaM exerts complete control over the reaction. NO is toxic, and so it is absolutely crucial in NO signaling to strictly control the amount of NO that is made. Tight regulation over Ca^{2+} concentrations in the cell provides this required level of control. In general, nM concentrations of NO are synthesized by the generator cell, and pM concentrations act in the target cell. iNOS (inducible NOS) was first described as a Ca^{2+}–CaM-independent isoform, but subsequent studies showed that Ca^{2+}–CaM co-purified with this isoform. It is, therefore, "constitutively" active. Because the function of iNOS is in the host response to infection, a NOS isoform that is constitutively active and produced at the site of infection conforms to this biological role.

A number of inhibitors of NOS have been developed. The initial molecules were simple derivatives of the substrate L-arginine; however, other non-arginine-related structures were later found that were derived largely from library screens in the pharmaceutical industry, and some demonstrate significant isoform selectivity.

Chemistry of NO

NO is unstable in aqueous, aerobic solution. The stable end products of NO decomposition are nitrite (NO_2^-) and nitrate (NO_3^-). The reaction sequence that leads to these products is shown in Figure 3. This solution chemistry consumes NO as it traverses a path from the generator cell to the target cell, hence the amount that

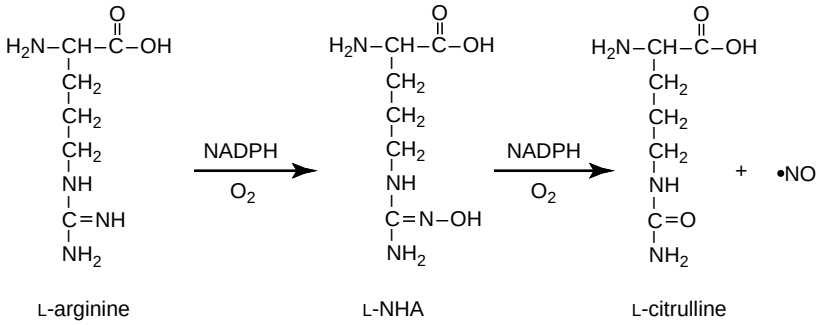

FIGURE 2 The reaction catalyzed by nitric oxide synthase. The substrate for the reaction is the amino acid L-arginine, which is converted to L-NHA and then to citrulline and ·NO. Although it has never been shown, it is assumed that the stereochemistry of citrulline at the α-carbon remains unchanged.

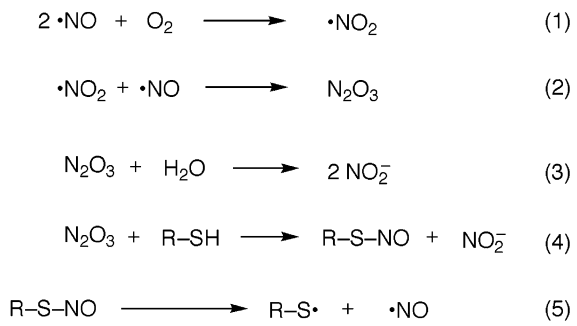

FIGURE 3 Relevant solution chemistry of nitric oxide. NO reacts with O_2 in aqueous solution to produce nitrogen dioxide ($\cdot NO_2$) (Eq. 1). ·NO2 then reacts with another molecule of ·NO to produce dinitrogen trioxide (N_2O_3) (Eq. 2). N_2O_3 can then hydrolyze to yield NO_2^- (Eq. 3) or react with protein or low molecular weight thiols to make the S-nitroso derivative (Eq. 4). The S-nitrosated protein or small molecule is capable of homolytically cleaving to generate the thiol radical and ·NO (Eq. 5).

arrives at the target cell is always lower. An intermediate along the reaction pathway is dinitrogen trioxide (N_2O_3). N_2O_3 can react with water as shown to produce NO_2^- or react with other cellular nucleophiles. The reaction with cysteine residues in proteins or with small cellular sulfur nucleophiles such as glutathione leads to the formation of S-nitrosated species as shown in Figure 3. S-Nitrosated proteins and small molecules are known to decompose to the sulfur radical and NO in a so-called homolytic cleavage (Figure 3); certain biological conditions can accelerate the reaction. The significance of this chemistry is discussed below. NO has 11 valence electrons and, therefore, has one unpaired electron. The radical nature of NO dictates other chemistry, such as the facile reaction of NO with superoxide to give peroxynitrite ($^-$OONO), which then converts very quickly to NO_3^-, and the reaction with oxyhemoglobin to give methemoglobin and NO_3^-, again with the intermediacy of $^-$OONO. Peroxynitrite is a potent oxidant and has been shown to be important in various types of tissue damage associated with the formation of high levels of NO. The decomposition of relatively high concentrations of NO in tissue that occurs under inflammatory conditions leads to nitration chemistry, most frequently seen on tyrosine residues.

Guanylate Cyclase

The soluble isoform of guanylate cyclase (sGC) is the receptor for NO in target cells. Activation of sGC leads to the formation of cGMP, and then through a cascade involving cGMP-dependent kinases, a lowering of intracellular Ca^{2+} occurs, leading to effects such as smooth muscle relaxation (e.g., vasodilation). sGC is a heterodimeric protein composed of two subunits. The best characterized is the physiologically occurring $\alpha1\beta1$ heterodimer, first isolated from lung tissue. The β-subunit contains a unique ferrous heme cofactor that is the receptor for NO. This porphyrin, despite having the same ligation as the globins, does not bind oxygen; rendering it ideally suited to bind NO is the presence of a high competing concentration of oxygen. Upon binding of NO, sGC is activated 300-fold over the basal activity, and a burst of cGMP is produced. cGMP then acts through cGMP-dependent kinases to bring about physiological responses such as vasodilation and other smooth muscle relaxation responses.

Tools to manipulate sGC are emerging and include ODQ (1H-[1,2,4]oxadiazole[4,3-a]quinoxalin-1-one), which inhibits sGC by oxidation of ferrous porphyrin to the ferric oxidation, and a family of activators based on the structure of YC-1 (3-(5′-hydroxymethyl-2′-furyl)-1-benzyl indazole). This compound is a weak activator of sGC; however, YC-1 and CO activate sGC to the same level as NO, and YC-1 acts synergistically with NO. A class of activators based on the YC-1 structure that directly activate and are more potent than YC-1 are entering clinical trials.

Non-cGMP NO-Signaling Pathways

As mentioned previously, N_2O_3 is an intermediate that forms during the aerobic solution decomposition of NO. N_2O_3 is a potent nitrosating agent that reacts with the ω-amino group of lysine and the thiol of cysteine. Formation of S-nitrosated cysteines in proteins can cause a change in the biological activity of the protein. Although increasing studies are directed toward understanding the chemistry and biological activity of the S–NO bond and the formation of these bonds with small molecule thiols and protein thiols, critical aspects remain to be determined. For example, the formation of R–S–NO could occur via the solution reaction of N_2O_3 with the thiol or by an enzyme-catalyzed process. The former path would appear to be too inefficient, and an enzyme to catalyze the latter path has not been isolated. Other hypotheses advanced involve the reversible formation of R–S–NO, where again the R group could be either a low molecular weight species or a protein similar to phosphoryl transfer. The kinase and phosphatase equivalents have yet to be isolated. Confounding all these hypotheses is the chemical reaction of R–SH with N_2O_3, which would be facilitated much beyond what would be expected to occur when nonbiological concentrations of NO are used.

There is another important outcome from the formation of S-nitrosated proteins and low molecular

weight compounds like glutathione. The S-nitroso bond is known to homolytically fragment, forming NO and a thiyl radical. The NO so derived can then function to activate sGC as described above. This mode of generating NO is attractive in that it represents a semi-stable form of this signaling agent and could be a way to store, transport, and deliver NO. There is no question that the decomposition of NO in aerobic aqueous solution will lead to S-nitrosation; rather, the issue is whether the amounts formed *in vivo* are physiologically significant.

See Also the Following Articles

Calcium Signaling: NO Synthase • Flavins • Heme Proteins • Heme Synthesis • Neurotransmitter Transporters

Glossary

domain A compact region of protein structure that is a stable entity.
heterodimer A protein composed of two nonidentical subunits.
kinase An enzyme that transfers a phosphoryl group from a donor (typically ATP) to an acceptor (often a protein in cell signaling pathways).
neurotransmitter A chemical messenger released or synthesized at a synapse.
phosphatase An enzyme that removes a phosphoryl group.
radical A chemical species with an unpaired electron.

Further Reading

Bredt, D. S., and Snyder, S. H. (1994). Nitric oxide: A physiologic messenger molecule. *Annu. Rev. Biochem.* **63**, 175–195.

Denninger, J. W., and Marletta, M. A. (1999). Guanylate cyclase and the NO/cGMP signaling pathway. *Biochim. Biophys. Acta* **1411**, 334–350.

Marletta, M. A. (1994). Nitric oxide synthase: Aspects concerning structure and catalysis. *Cell* **78**, 927–930.

Marletta, M. A. (2001). Another activation switch for endothelial nitric oxide synthase: Why does it have to be so complicated? *Trends Biochem. Sci.* **26**, 519–521.

Moncada, S., Palmer, R. M., and Higgs, E. A. (1991). Nitric oxide: Physiology, pathophysiology, and pharmacology. *Pharmacol. Rev.* **43**, 109–142.

Biography

Michael A. Marletta is the Aldo DeBenedictis Distinguished Professor of Chemistry in the Department of Chemistry, and Professor of Biochemistry in the Department of Molecular and Cell Biology at the University of California, Berkeley. His research interests on protein structure and function relationships have an emphasis on enzymatic catalysis and redox biochemistry. He holds a Ph.D. from the University of California, San Francisco. He is a Fellow of AAAS and was elected to the American Academy of Arts and Sciences and the Institute of Medicine.

N-Linked Glycan Processing Glucosidases and Mannosidases

Linda O. Tremblay and Annette Herscovics
McGill University, Montréal, Québec, Canada

Endoplasmic reticulum (ER) and Golgi glucosidases and mannosidases trim the asparagine-linked glycans (*N*-glycans) attached to newly formed glycoproteins within the secretory pathway. The sequential action of these enzymes yields the substrate(s) required for the biosynthesis of hybrid and complex *N*-glycans which mediate cell–cell interactions during embryogenesis, development, tumor metastasis, lymphocyte trafficking, leukocyte recruitment in inflammation, and many other biological interactions. In addition, the glycosidases participate in glycoprotein folding and quality control.

Abrogation of mammalian glycosidase functions as a consequence of genetic defects in humans or of targeted gene ablation in the mouse results in developmental and multisystemic abnormalities due to anomalous *N*-glycan biosynthesis. Herein the structure, function, and physiological roles of mammalian ER and Golgi processing glucosidases and mannosidases are reviewed, including pertinent studies of yeast and filamentous fungi enzymes.

Glucosidases

Glucosidase I

Glucosidase I is a type-II ER transmembrane protein of 92 kDa that cleaves the terminal α1,2-linked glucose residue of $Glc_3Man_9GlcNAc_2$ immediately following its transfer to nascent polypeptide chains. This inverting glycosidase has been conserved during eukaryotic evolution and, based on sequence similarity, it belongs to glycosylhydrolase family 63. Recently, missense mutations were identified in the human glucosidase I gene of a severely ill neonate that perished shortly after birth (Table I), showing that removal of the terminal glucose residue of $Glc_3Man_9GlcNAc_2$ is essential for human development and viability.

Glucosidase I is inhibited by castanospermine, 1-deoxynojirimycin and its N-methyl and N-butyl-deoxynojirimycin derivatives. These compounds prevent exit of some glycoproteins from the ER. As a result, they affect processes such as myoblast fusion to myotubes, transformation induced by glycoprotein oncogenes, cell surface expression of glycoprotein receptors, and also act as antiviral agents.

Glucosidase II

ER glucosidase II removes the two inner α1,3-linked residues (Figure 1). This glycosidase (glycosylhydrolase family 31) consists of a soluble catalytic α-subunit ($\sim$110 kDa) and a β-subunit ($\sim$80 kDa) which contains the ER retrieval signal HDEL. Glucosidase II is affected by the same inhibitors as glucosidase I, as well as by bromoconduritol.

Endo α-Mannosidase

Endo α-mannosidase is a 52-kDa enzyme present in the intermediate compartment and in the Golgi. It provides an alternate pathway independent of ER glucosidases for glucose removal from $Glc_{1-3}Man_{4-9}GlcNAc_2$, the preferred substrate being $Glc_1Man_9GlcNAc_2$ (Figure 1). Endo α-mannosidase expression is cell-specific and restricted to the chordate phylum; thus, it is likely to have appeared late in evolution. It does not share homology with any other known proteins. Upregulation of endo α-mannosidase was suggested to partially compensate for the glucosidase I deficiency described in the aforementioned patient.

Classification and Properties of Processing α-Mannosidases

Processing mannosidases have been classified into two distinct groups based on their amino acid sequences, different enzymatic mechanisms, and sensitivity to inhibitors. Class-I α1,2-mannosidases (glycosylhydrolase family 47) are inverting enzymes that have been conserved through eukaryotic evolution. They require calcium for activity and are inhibited by 1-deoxymannojirimycin and kifunensine, but not by

TABLE I

Human Glycosidase Genetic Defects and Mouse Glycosidase Gene Ablation Phenotypes

Glycosidase gene	Phenotype
Human diseases	
Glucosidase I	Generalized hypotonia, hypomotility, dysmorphic features, hepatomegaly, hypoventilation, seizures, neonatal lethality
Mannosidase II	Congenital dyserythropoietic anemia (HEMPAS), jaundice, hepatosplenomegaly, diabetes and gallstones
Mouse gene ablations	
Mannosidase II	Dyserythropoietic anemia, splenomegaly, autoimmune disease similar to systemic lupus erythematosus
Mannosidase IIx	Male infertility, hypospermatogenesis, decreased testis size, diminished spermatogenic cell adhesion to Sertoli cells

swainsonine. In contrast, class-II α-mannosidases (glycosylhydrolase family 38) are retaining enzymes that are inhibited by swainsonine, but not by 1-deoxymannojirimycin or kifunensine. The class-II enzymes are involved in *N*-glycan biosynthesis as well as in degradation, and with the exception of the Drosophila Golgi α-mannosidase II, they do not require divalent cations for activity.

Class-I α1,2-Mannosidases

α1,2-Mannosidase Subgroups

The class-I family consists of three subgroups of proteins sequestered by their sequence similarity and distinguished by their enzymatic activity. Subgroup (1) contains yeast and mammalian ER α1,2-mannosidase I that primarily form $Man_8GlcNAc_2$ isomer B; subgroup (2) includes mammalian Golgi α1,2-mannosidases IA, IB and IC as well as filamentous fungi α1,2-mannosidases that readily form $Man_5GlcNAc_2$ from $Man_9GlcNAc_2$ through $Man_8GlcNAc_2$ isomers A and/or C as intermediates; subgroup (3) consists of a group of proteins with amino acid sequence similarity to α1,2-mannosidases, such as mammalian EDEM and yeast Htm1p/Mnl1p, that have no apparent α1,2-mannosidase activity. This latter subgroup of proteins has been implicated in the degradation of misfolded glycoproteins as described in various articles in this encyclopedia.

ER α1,2-Mannosidase I

ER α1,2-mannosidase I is a type-II transmembrane protein of about 80 kDa that absolutely requires calcium for activity. It is the only processing α1,2-mannosidase in the yeast *Saccharomyces cerevisiae*. X-ray crystallographic studies of the yeast catalytic domain as an enzyme–product complex showed that it consists of a novel $(\alpha\alpha)_7$ barrel with one side of the barrel plugged by a β-hairpin forming a cavity of $\sim$15Å. The active site consisting of essential acidic residues and calcium is located at the bottom of the barrel. The structure of the human enzyme in complex with the inhibitors 1-deoxymannojirimycin and kifunensine was also determined. It shows that calcium coordinates with conserved acidic residues and the O2′ and O3′ hydroxyls of the six-membered rings of the inhibitors stabilized in a $^1C_4$ conformation. Although ER α1,2-mannosidase I primary trims the terminal middle arm α1,2-linked mannose residue of $Man_9GlcNAc_2$ to form $Man_8GlcNAc_2$ isomer B (Figure 1), recent studies revealed that ER α1,2-mannosidase I is capable of removing additional mannose residues from $Man_8GlcNAc$, *in vitro* and *in vivo*.

Class-I Golgi α1,2-Mannosidases

There are three mammalian class-I Golgi α1,2-mannosidases, IA, IB, and IC, derived from different genes on different chromosomes. They are type-II transmembrane proteins of about 70 kDa. These enzymes trim the α1,2-linked mannose residues from $Man_8GlcNAc_2$ isomer B to form $Man_5GlcNAc_2$ (Figure 1). When $Man_9GlcNAc_2$ is used as substrate, they readily form $Man_6GlcNAc_2$, but remove the last α1,2-linked mannose residue much more slowly. Their specificity is complementary to that of ER α1,2-mannosidase I since the last residue cleaved from $Man_9GlcNAc_2$ by the Golgi enzymes is the mannose preferred by ER α1,2-mannosidase I. There are small differences in the order of mannose removal by the different Golgi α1,2-mannosidases. X-ray crystallographic and modeling studies of a fungal α1,2-mannosidase with the same specificity as the mammalian Golgi orthologues revealed that the overall protein fold and topology of the active site is identical to that of ER α1,2-mannosidase I, and that the different specificities of these enzymes is determined by the space within the barrel. The fungal enzyme barrel permits binding of multiple oligosaccharide conformations of all three $Man_8GlcNAc_2$ isomers, whereas only a single conformation of $Man_8GlcNAc_2$ isomer B is accommodated by ER α1,2-mannosidase I.

The major difference between the three mammalian Golgi α1,2-mannosidases is their tissue- and cell-specific expression as determined by Northern blots of murine and human tissues and by immunolocalization studies in the male rat reproductive system.

The organization of the three human and murine Golgi α1,2-mannosidase genes is highly conserved with the location of the intron–exon boundaries being nearly identical. Thus, late evolutionary gene duplication is

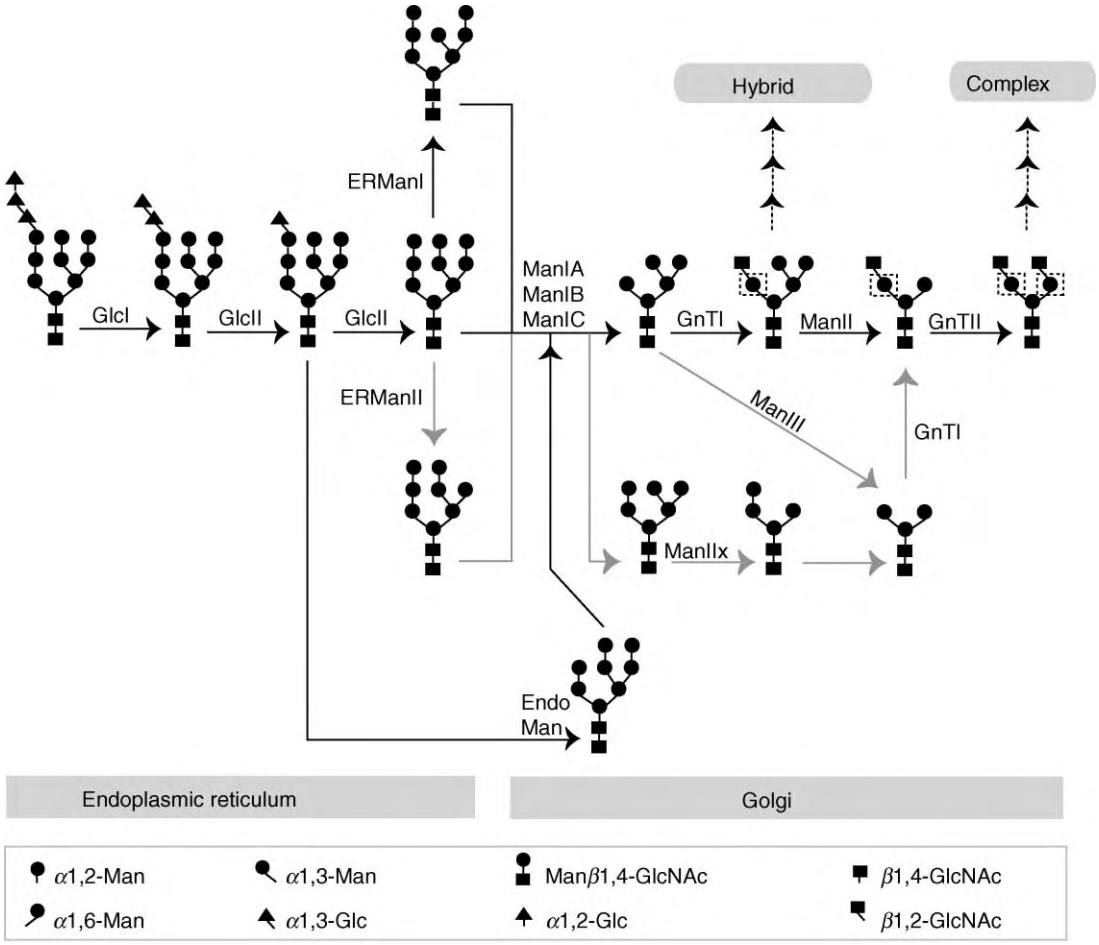

FIGURE 1 Role of glycosidases in mammalian *N*-glycan processing. The $Glc_3Man_9GlcNAc_2$ precursor oligosaccharide attached to asparagine residues of nascent chains (within Asn-X-Ser/Thr where X is any amino acid except Pro) is sequentially modified by processing glycosidases and glycosyltransferases, beginning in the endoplasmic reticulum and continuing in the Golgi. Trimming by α-glucosidases and α1,2-mannosidases is essential for the formation of complex and hybrid *N*-glycans initiated by GnTI. Additional enzymes add other GlcNAc residues to the boxed core mannose residues. Subsequently, glycosyltransferases further elaborate the structures by linking galactose, fucose, and sialic acid. Gray arrows indicate the suggested role of ERManII and the proposed ManIIx- and ManIII-mediated alternate pathways independent of Golgi α-mannosidase II. GlcI, α1,2-glucosidase I; GlcII, α1,3-glucosidase II; ERManI, ER α1,2-mannosidase I; ERManII, ER α1,2-mannosidase II; ManIA, IB, IC, Golgi α1,2-mannosidase IA, IB, IC; Endo Man, endo-α-mannosidase; ManII, IIx, III, α-mannosidase II, IIx, III; GnTI, II, N-acetylglucosaminyltransferase I, II. (Modified from Tremblay, L.O., PhD Thesis, McGill University 2002).

likely to have produced the Golgi α1,2-mannosidase gene family. However, the organization of the Golgi α1,2-mannosidase genes differs from that of the other two class-I α1,2-mannosidase subgroups, suggesting that the genes of the three subgroups may have arisen independently.

Class-II Processing α-Mannosidases

Class II Golgi α-Mannosidases

Golgi α-mannosidase II trims the terminal α1,3- and α1,6-linked mannose residues of $GlcNAc_1Man_5GlcNAc_2$, thus providing the substrate for complex *N*-glycan biosynthesis (Figure 1). It is absolutely dependent upon prior action of N-acetylglucosaminyltransferase I (GnTI) that initiates the first N-acetyllactosamine branch of complex *N*-glycans. The enzyme is a type-II membrane protein of ~130 kDa. The crystal structure of the Drosophila Golgi α-mannosidase II revealed that the active site is on the planar side of the hemi-oval-shaped catalytic domain comprised of an N-terminal α/β-domain, a bundle of three helices, and a C-terminal β-domain. The conformation is stabilized by disulfide bonds and the coordination of a zinc ion. The zinc ion participates directly in the catalytic mechanism and contributes to substrate binding. The terminal GlcNAc of the substrate is anchored in a binding pocket near the active site and is postulated to serve as an anchor

point for substrate rotation within the active site leading to the sequential trimming of the α1,6- and α1,3-linked mannose residues with minimal conformational change.

Ablation of the mouse α-mannosidase II gene indicated that this enzyme plays an important role in the biosynthesis of glycoproteins that maintain erythrocyte membrane integrity. This phenotype resembles congenital dyserythropoietic anemia type II, a rare human disease also known as HEMPAS, caused by a defect in the human Golgi α-mannosidase II gene (Table I). Mice lacking α-mannosidase II also progressively develop autoantibodies indicating that proteins bearing the atypical *N*-glycans produced in these mice can evade self-tolerance. These α1,2-mannosidase II null mice thus provide a model for lupus erythematosus in humans. The fact that complex *N*-glycan biosynthesis occurs in many tissues of mice lacking α-mannosidase II revealed the existence of an alternate biosynthetic pathway mediated by a cobalt-dependent enzyme called α-mannosidase III (Figure 1). However, a gene or cDNA encoding this activity has not yet been identified.

The human and mouse genomes also encode α-mannosidase IIx, a protein that has significant amino acid similarity to α-mannosidase II. The exact specificity of this enzyme remains to be definitively established. However, targeted gene ablation of mouse α-mannosidase IIx indicated that it is required for the biosynthesis of complex *N*-glycans that mediate spermatogenic cell interactions with Sertoli cells in the testis (Table I).

ER α1,2-Mannosidase II

The existence of mammalian ER α1,2-mannosidase II has been proposed from studies with intact cells and membrane preparations, but remains to be confirmed. This activity is distinct from ER α1,2-mannosidase I, since it yields a different $Man_8GlcNAc_2$ isomer (Figure 1) and is inhibited by swainsonine and 1-deoxymannojirimycin but not by kifunensine. Its substrate specificity and sensitivity to inhibitors are similar to those of a class-II cytosolic α-mannosidase involved in glycoprotein degradation. In addition, ER α1,2-mannosidase II cross-reacts with antibodies generated towards the cytosolic α-mannosidase. The existence of a distinct cDNA or gene encoding ER α1,2-mannosidase II has not been described.

In conclusion, the enzymatic specificities and properties of mammalian glycosidases that are involved in *N*-glycan biosynthesis have been well characterized. Current studies are elucidating their functions in glycoprotein folding and in ERAD, but their physiological roles and involvement in genetic diseases remain to be elucidated by further gene ablation studies.

See Also the Following Article

Glycoprotein Folding and Processing Reactions

Glossary

inverting glycosidase Glycosidase that catalyzes hydrolysis with inversion of the anomeric configuration.

retaining glycosidase Glycosidase that catalyzes hydrolysis with retention of the anomeric configuration.

Further Reading

Coutinho, P. M., and Henrissat, B. (1999). Carbohydrate-active enzymes: An integrated database approach. In *Recent Advances in Carbohydrate Bioengineering* (H. J. Gilbert, B. Davies, B. Henrissat and B. Svensson, eds.) pp. 3–12. The Royal Society of Chemistry, Cambridge. http://afmb.cnrs-mrs.fr/CAZY/index.html.

Helenius, A., and Aebi, M. (2001). Intracellular functions of N-linked glycans. *Science* **291**, 2364–2369.

Herscovics, A. (2001). Structure and function of class I α1,2-mannosidases involved in glycoprotein synthesis and endoplasmic reticulum quality control. *Biochimie* **83**, 757–762.

Lobsanov, Y. D., Vallée, F., Imberty, A., Yoshida, T., Yip, P., Herscovics, A., and Howell, P. L. (2002). Structure of *Penicillium citrinum* α1,2-mannosidase reveals the basis for differences in specificity of the ER and Golgi class I enzymes. *J. Biol. Chem.* **277**, 5620–5630.

Moremen, K. W. (2002). Golgi α-mannosidase II deficiency in vertebrate systems: Implications for asparagine-linked oligosaccharide processing in mammals. *Biochim. Biophys. Acta* **1573**, 225–235.

Parodi, A. (2000). Protein glucosylation and its role in protein folding. *Annu. Rev. Biochem.* **69**, 69–93.

Schachter, H. (2001). Congenital disorders involving N-glycosylation of proteins. *Cell Mol. Life Sci.* **58**, 1085–1104.

Tremblay, L. O (2002). *Characterization of Human Class I α1,2 Mannosidases Involved in N-Glycan Biosynthesis and the Role of Murine α1,2-Mannosidase 1B in Embryogenesis and Development*. Thesis, McGill University.

Vallée, F., Lipari, F., Yip, P., Sleno, B., Herscovics, A., and Howell, P. L. (2000). Crystal structure of a class I α1,2-mannosidase involved in *N*-glycan processing and endoplasmic reticulum quality control. *EMBO J.* **19**, 581–588.

Vallée, F., Karaveg, K., Herscovics, A., Moremen, K. W., and Howell, P. L. (2000). Structural basis for catalysis and inhibition of *N*-glycan processing class I α1,2-mannosidases. *J. Biol. Chem.* **275**, 41287–41298.

Biography

Dr. Linda O. Tremblay recently obtained her Ph.D. from McGill University. The focus of her dissertation was on the cloning and characterization of mammalian α1,2-mannosidases.

Dr. Annette Herscovics is a Professor at the McGill Cancer Centre and in the Departments of Medicine, Biochemistry, and Oncology at McGill University. Her main research interests are concerned with the structure and function of enzymes required for eukaryotic glycosylation. She holds a Ph.D. from McGill University and is a Fellow of The Royal Society of Canada.

Non-Homologous End Joining

Penny A. Jeggo
University of Sussex, Brighton, UK

The process of DNA non-homologous end joining (NHEJ) is one of several mechanisms that function to repair DNA double strand breaks (DSBs) in DNA. NHEJ represents the major mechanism for DSB repair in G1 phase cells. If unrepaired, a DSB can lead to loss of genomic material which is likely to result in cell death; a misrepaired DSB can cause genomic rearrangements, a potential initiating event for carcinogenesis. NHEJ, therefore, represents an important mechanism for maintaining genomic stability. Paradoxically, NHEJ also functions during immune development to help create genetic diversity.

Nature of the Rejoining Process

Three mechanisms for DSB rejoining have been described. Homologous recombination (HR) uses an undamaged homologue as a template to repair a DSB and to restore any genetic information lost at the site of the break. Single strand annealing (SSA) uses short direct repeat sequences to hold the broken ends together and then rejoins the two closely located DNA nicks. NHEJ, in contrast, requires no homology or, at most, a few base pairs of microhomology to achieve DSB rejoining. HR has the potential to be highly accurate even if sequence information is lost at the break site. SSA annealing is inherently inaccurate leading to deletions at the break site. The level of accuracy achieved by NHEJ is still unclear. However, cells lacking NHEJ components show increased levels of misrepair observable either as chromosomal rearrangements or in specific assays aimed at detecting misrepair.

Proteins that Function in NHEJ

Six proteins required for NHEJ have been identified in mammalian cells (see Table I). The first component identified was Ku, a heterodimer consisting of two subunits, Ku70 and Ku80. Ku has strong double-strand DNA end-binding activity. Once bound to a DNA end, Ku recruits a large protein kinase to form a complex called the DNA-dependent protein kinase (DNA-PK). The catalytic component of this complex is called the DNA-PK catalytic subunit (DNA-PKcs). A complex of two further proteins, XRCC4 and DNA ligase IV, are required for the rejoining step of NHEJ. More recently, "artemis" has been identified as an additional protein required for some aspects of NHEJ. In the yeasts, *Saccharomyces cerevisciae* and *Schizosaccharomyces pombe*, some additional proteins are required for NHEJ but either homologues of these proteins have not been identified in mammalian cells or the identified homologues do not appear to be required for the process (see Table I). It is noteworthy that there are differences in the requirements for these additional proteins even between the two yeasts. The roles of Sir2, 3, and 4 and Nej1p are regulatory.

The Ku Protein

In addition to being a strong DNA end-binding protein, Ku is able to translocate along the DNA, leading to a DNA substrate with multiple bound Ku molecules. The crystal structure of Ku resembles a basket-shaped structure with two pillars and a handle. A double-stranded DNA end is able to fit through the cavity in the structure allowing Ku to encircle the DNA. The C-terminal region of Ku80 is required for interaction with DNA-PKcs.

DNA-PKcs

DNA-PKcs is a member of a subfamily of phosphoinositol (PI) 3-kinases called PI 3-K-like kinases (PIKKs). This subfamily has protein kinase activity, in contrast to the lipid kinase activity of the PI 3-Ks. DNA-PKcs at 460 kDa is one of the largest PIKKs and other family members include ataxia telangiectasia mutated protein (ATM) and ataxia telengiectasia and Rad 3-like protein (ATR). PI 3-Ks have a conserved kinase domain at the C terminus and PIKKs in addition have a small region at the extreme C terminus that is required for protein kinase activity. Although *in vitro*, DNA-PK can phosphorylate many of the proteins phosphorylated by ATM and ATR, *in vivo*, the three PIKKs have distinct functions. The *in vivo* substrates of DNA-PK have not

TABLE I

Proteins Required for NHEJ in Different Model Systems

	Mammalian cells	*S. cerevisiae*	*S. pombe*
Ku70, Ku80	+	+	+
DNA ligase IV	+	+ (Lig4p)	+ (Lig4p)
XRCC4	+	+ (Lif1p)	+ (Lif1p)
DNA-PKcs	+	No homologue identified	No homologue identified
Artemis	+	No homologue identified	No homologue identified
Mre 11/Rad50/Xrs2	Not required	+	+
Nej1p	No homologue identified	+	No homologue identified
Sir 2, 3, and 4	No homologue identified	+	No role identified

been identified although artemis and XRCC4 are likely substrates. DNA-PK also undergoes autophosphorylation, which is essential for its function in NHEJ. It has been suggested that one role of DNA-PKcs is to regulate the process by phosphorylating NHEJ components. In line with this, autophosphorylation of DNA-PKcs results in release of the protein from the Ku–DNA complex.

XRCC4-DNA Ligase IV

DNA ligase IV has a conserved ligase domain at its N terminus and two BRCT domains at its C terminus. The region between the two BRCT domains is required for interaction with its partner protein, XRCC4. The crystal structure of XRCC4 and the interacting region with DNA ligase IV shows that XRCC4 consists of a globular head domain and a helical tail. A single ligase chain binds to an XRCC4 dimer leading to unwinding of the coiled coil that forms in the uncomplexed molecule. XRCC4 stimulates but is not essential for DNA ligase IV's activity. However, XRCC4 is essential for NHEJ and cells lacking either XRCC4 or DNA ligase IV have identical phenotypes. Ku bound to DNA can recruit the DNA ligase IV-XRCC4 complex, thereby stimulating ligation.

Artemis

Artemis is a member of the metallo-β-lactamase superfamily and, when unphosphorylated, has $5'-3'$ exonuclease activity. Artemis forms a complex with and is phosphorylated by DNA-PKcs, which changes the specificity of its nuclease activity so that it acquires endonucleolytic activity as well as the ability to cleave hairpin structures. A hairpin intermediate is generated during the process of V(D)J recombination and artemis cleaves this hairpin allowing V(D)J recombination to proceed. Consequently, cells and patients lacking artemis are unable to rejoin the coding junctions during V(D)J recombination leading to severe combined immunodeficiency.

Model for NHEJ

Figure 1 presents a model for NHEJ based on a range of biochemical, biophysical, cellular, and molecular studies. The first step of the process is the binding of the Ku heterodimer to DNA ends followed by recruitment of DNA-PKcs and activation of DNA-PK activity. Recruitment of DNA-PKcs causes inward translocation of Ku on the DNA molecule and potentially synapsis of the DNA ends. DNA-PK phosphorylates artemis, which activates its hairpin cleavage activity, a step essential for V(D)J recombination. The specificity of artemis nuclease activity may also be modulated by phosphorylation allowing it to cleave ends that are not amenable to direct ligation. DNA-PKcs may also undergo autophosphorylation enabling it to be released from DNA-bound Ku. Ku then recruits the DNA ligase IV-XRCC4 complex to the DNA end. Subsequent rejoining ensues with the release of the DNA ligase IV-XRCC4 complex.

Roles of NHEJ

Rodent cell lines lacking NHEJ components, as well as the SCID mouse and SCID cell line, have provided invaluable tools to evaluate the function of NHEJ. Complementation analysis of the rodent cells led to the classification of the defective genes as X-ray cross complementing (XRCC). This classification was made prior to cloning, resulting in some of the genes having dual nomenclature (for example, Ku80 is also XRCC5). This nomenclature and the rodent cell lines studied are given in Table II. More recently, mice knocked out for each of the NHEJ components have been generated. The phenotypes observed in the cell lines and mice are shown in Table III. Some phenotypes may represent roles of the proteins separate from their role in NHEJ. For example, Ku70 and 80 knockout mice are growth retarded, die early, and show a severe combined immunodeficient (SCID) phenotype. The latter phenotype reflects the role

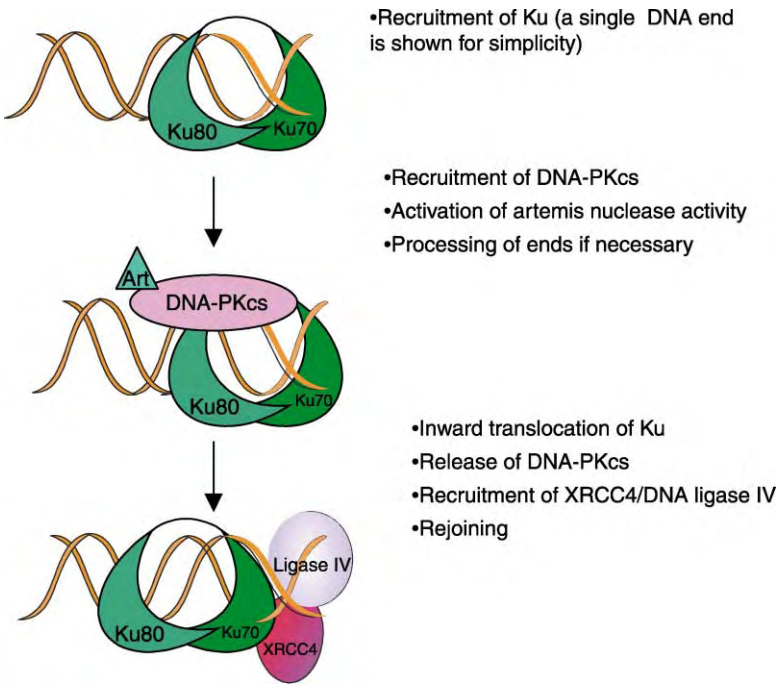

FIGURE 1 Model for DNA NHEJ. Proposed steps involved in the process.

of NHEJ in V(D)J recombination whilst the growth retardation and early senescence are most likely caused by a role of Ku in telomere maintenance, which may be distinct from its role in NHEJ. Mice lacking XRCC4 or DNA ligase IV are embryonic lethal displaying extensive neuronal apoptosis. It is currently unclear whether these differences represent roles for XRCC4 and DNA ligase IV in a process distinct from NHEJ or whether some rejoining can occur in the absence of the other NHEJ components. It has also been suggested that the uncoordinated binding of Ku to DNA ends prevents alternative DSB rejoining mechanisms taking place.

Repair of Radiation Induced DSBs

A DNA DSB is the most biologically significant lethal lesion induced by ionizing radiation. Consequently, all cell lines lacking components of the NHEJ machinery display pronounced radiosensitivity demonstrating that NHEJ represents a major mechanism for the repair of radiation-induced DSBs. Another characteristic feature of Ku, DNA-PKcs, XRCC4, and DNA ligase IV-deficient cells is impaired DSB rejoining monitored by the technique of pulse field gel electrophoresis. Interestingly, artemis-deficient cells repair the majority of their DSBs normally demonstrating that its role is distinct from the other NHEJ components. It is currently unclear if artemis functions downstream of the break rejoining process, for example to relay to the cell that the break has undergone rejoining, or possibly functions to repair a critical subset of breaks that are not detected by the pulse field gel electrophoresis technique. Cytological studies have shown that NHEJ-deficient cells display, not only increased gaps and breaks after irradiation

TABLE II

Nomenclature of Genes Involved in NHEJ and Characterized Cell Lines

Gene	XRCC nomenclature	Rodent cell lines	Human patients
Ku80	XRCC5	xrs 1-6; XRV15-B; XRV9B; sxi-3	None identified
Ku70	XRCC6	sxi-1	None identified
DNA-PKcs/SCID	XRCC7	SCID mouse cell line; V3; M059J glioma cell line; XR-C1; SX9; irs-20	None identified
XRCC4	XRCC4	XR-1	None identified
DNA ligase IV (LIG4)		SX10	LIG4 syndrome
Artemis		None identified	RS-SCID

TABLE III

Phenotypes of Cell Lines and Mice Defective in NHEJ Components

	Cell line deficiency			
Phenotype	**Ku70/Ku80**	**XRCC4/DNA ligase IV**	**DNA-PKcs**	**Artemis**
Cultured cell lines				
Radiosensitivity	Marked sensitivity	Marked sensitivity	Marked sensitivity	Slighly milder sensitivity
DSB rejoining	Defective	Defective	Defective	Normal or mild defect
DNA end-binding activity	Defective	Normal	Normal	Normal
DNA-PK activity	Defective	Normal	Defective	Normal
V(D)J recombination				
Coding joins	Major defect	Major defect	Major defect	Major defect
Signal joins	Major defect	Major defect	Minor defect	No defect
Primary cell lines				
Spontaneous breakage	Increased (also in heterozygotes)	Increased (also in heterozygotes)	Normal	Normal
Mice				
Immunodeficiency	SCID	SCID	SCID	SCID
Growth/viability	Growth retarded senesce early	Embryonic lethal	Normal	Normal
T cell lymphomas	Increase in Ku70−/− mice; no lymphomas in Ku80−/− mice	Mice not viable	Small increase	Increase in patients with hypomorphic mutations

Many of the phenotypes of Ku70-/- and Ku80-/- cell lines and mice are similar and so they have been grouped together. Similarly for XRCC4/DNA ligase IV deficient mice.

indicative of failed rejoining, but also increased chromosomal rearrangements, indicative of misrejoining. Whilst this finding does not address the fidelity of NHEJ, it does suggest that in its absence, there is increased misrejoining. Finally, NHEJ-deficient cells show normal ability to effect cell-cycle checkpoint responses after irradiation demonstrating that the defect lies primarily in the rejoining process rather than in the signalling responses to DSB induction.

Role During Immune Development

In germ line cells, the variable (V), diversity (D), and joining (J) segments are arranged on the DNA as contiguous sequences which become rearranged into distinct V(D)J units during T- and B-cell differentiation via a process called V(D)J recombination. Each V, D, or J segment, termed a coding sequence, is associated with a semi-conserved signal sequence. The initiating event for the recombination process is the generation of a site-specific DSB by two recombination-activating gene proteins (RAG1 and 2). The breaks form between a pair of coding sequences and their adjacent signal sequences and rejoining ensues to create coding and signal junctions from the rejoining of two coding and signal sequences, respectively. A number of additional processes serve to create deletions or insertions at the coding junctions, adding to the diversity of junctions generated. There are distinctions between the rejoining of coding and signal junctions. RAG-mediated cleavage generates hairpin coding ends in contrast to blunt-ended signal ends and the requirements for rejoining of the two ends can be distinguished genetically; coding joint formation requires all six NHEJ components whereas signal joint formation does not require artemis and has only a partial requirement for DNA-PKcs. Current evidence has shown that artemis is the nuclease that cleaves the hairpin end and is activated by DNA-PKcs, providing an explanation for these differences.

Changes in antibody isotype (IgM to IgG/IgA/IgE), an essential feature of the immune response, is achieved by class switch recombination (CSR). Since CSR takes place after V(D)J recombination, it cannot be readily monitored unless V(D)J recombination has taken place. Nonetheless, several novel approaches using transgenes have provided evidence that CSR requires the introduction of a DSB as well as components of the NHEJ machinery.

Role in Maintaining Genomic Stability

Cells constantly incur endogenous DNA damage from reactive oxygen species (ROS) generated as metabolic by-products. DSBs can arise indirectly from ROS following the processing of oxidative damage. DSBs also arise during replication. Current evidence suggests that breaks at the replication fork are repaired

by homologous recombination. Nonetheless, studies of primary cells lacking NHEJ components or even primary cells heterozygous for these proteins have shown elevated chromosome breaks demonstrating that NHEJ also functions to repair endogenously generated damage.

Contribution to Human Disease

Two hereditary syndromes have been shown to be caused by defects in components of the NHEJ machinery. LIG4 syndrome is characterized by pancytopaenia, developmental and growth delay. Hypomorphic mutations in DNA ligase IV have been found in LIG4 syndrome patients, all of which markedly impact upon the protein function. One of the five patients identified developed leukaemia and showed dramatic clinical radiosensitivity. However, the small number of patients precludes an assessment of whether LIG4 syndrome is associated with cancer predisposition.

RS-SCID patients display severe combined immunodeficiency with no additional clinical features. Cell lines derived from the patients show pronounced radiosensitivity. RS-SCID has been shown to be caused by mutations in artemis, many examples of which are loss of function mutational changes. Hypomorphic mutations in artemis have also been described in patients with partial T and B lymphocyte immunodeficiency and a predisposition to EBV-associated lymphomas.

The clinical differences between RS-SCID compared to LIG4 syndrome patients highlights the differing roles of artemis and DNA ligase IV during neuronal development.

See Also the Following Articles

DNA Ligases: Mechanism and Functions • DNA Ligases: Structures • DNA Mismatch Repair and the DNA Damage Response • Homologous Recombination in Meiosis • Immunoglobulin (Fc) Receptors • Nonhomologous Recombination: Bacterial Transposons • Nonhomologous Recombination: Retrotransposons • Protein Kinase C Family

Glossary

DNA damage response mechanisms A number of distinct processes that function to maintain genomic stability. They include pathways of DNA repair and signaling mechanisms that effect cell-cycle checkpoint control and/or apoptosis.

DNA-dependent protein kinase A complex involving Ku, the DNA targeting component, and DNA-PKcs, the catalytic component.

DNA end-binding activity A protein that can bind to double-strand DNA ends. This is normally monitored by electrophoretic mobility shift assays (EMSAs).

genomic rearrangement Joining of two genetic sequences that are not linked in a normal genome. Often visualized cytogentically.

hairpin DNA end A DNA molecule that does not have 5′ and 3′ ends but a continuous looped sequence to the opposite strand. Normally the hairpin involves some unpaired bases.

phenotype The characteristic features of a cell or animal. Contrasts to genotype which describes the genetic status of a cell or animal.

V(D)J recombination A process of recombination that occurs during differentiation of immunoglobulin and T cell receptor genes and serves to enhance their genetic diversity.

Further Reading

Alt, F. W., Oltz, E. M., Young, F., Gorman, J., Taccioli, G., and Chen, J. (1992). VDJ recombination. *Immunol. Today* **13**, 306–314.

Featherstone, C., and Jackson, S. P. (1999). DNA double-strand break repair. *Curr. Biol.* **90**, 759–761.

Jackson, S. (2002). Sensing and repairing DNA double strand breaks. *Carcinogenesis* **23**, 687–696.

Lieber, M. R. (1999). The biochemistry and biological significance of non-homologous DNA end joining: An essential repair process in multicellular eukaryotes. *Genes Cells* **4**, 77–85.

Pastink, A., Eeken, J. C., and Lohman, P. H. (2001). Genomic integrity and the repair of double-strand DNA breaks. *Mutat. Res.* **480-481**, 37–50.

Rouse, J., and Jackson, S. P. (2002). Interfaces between the detection, signaling, and repair of DNA damage. *Science* **297**, 547–551.

Biography

Dr. Penny A. Jeggo is a Senior Scientist and Group Leader at the Genome Damage and Stability Centre, University of Sussex, UK. She holds a Ph.D. from the National Institute of Medical Research, London which she undertook in Dr. Robin Holliday's laboratory. Dr. John Cairns was another significant mentor. Dr. Jeggo played a key role in identifying the first components of the NHEJ machinery. She now has broader interests in damage response mechanisms and the contribution of these processes to human disease.

Nonhomologous Recombination: Bacterial Transposons

Bao Ton Hoang and Michael G. Chandler
Laboratory of Molecular Genetics and Microbiology CNRS, Toulouse, France

Transposable genetic elements (TEs) are small functional segments of DNA capable of translocation into DNA sites within and between genomes and play an important role in horizontal gene transfer. A major division between TEs is whether they translocate via RNA or DNA intermediates. Prokaryotic TEs are probably exclusively limited to those that move using DNA intermediates. They are capable of sequestering and transmitting a variety of genes involved in accessory cell functions such as resistance to antimicrobial agents, catabolism of unusual compounds, and pathogenicity, virulence, or symbiotic functions. They also promote deletions and inversions and their insertion can activate or extinguish gene expression. TEs can constitute an important fraction of bacterial genomes (both chromosomes and plasmids). For example, one class of transposon, bacterial insertion sequences, represents ~7% of the 4 Mbp *Bordetella pertussis* chromosome and ~40% of the 220 kbp *Shigella flexnerii* virulence plasmid pWR100.

Structural Similarities and Diversity

All TEs encode a cognate transposase (Tpase) or recombinase, which recognizes their ends and catalyzes the individual DNA cleavages and strand transfer events necessary for transposition. In bacteria the term transposon (Tn) is limited to elements that carry genes specifying additional functions to those involved in transposition. The large number of TEs which do not include a distinct phenotypic trait are known as insertion sequences (ISs).

Definition of Transposases

Different types of elements can be defined by the nature of their cognate recombinases. In transposition reactions, these enzymes are known as transposases (Tpases). The majority fall into a class generally called DDE transposases because of the presence of three key amino acids, two aspartate residues and a glutamate, as part of the active site. Although DDE enzymes represent the majority of known Tpases, at least three additional types of Tpases have been identified. One class is similar to rolling circle replicases used by certain bacteriophages and plasmids. These are known as Y2 transposases since their catalytic mechanism involves two highly conserved tyrosine residues. The other two classes are members of the site-specific recombinase families. However, while these Tpases show site-specificity for the ends of the donor transposon, they appear more flexible than classic site-specific recombinases in the target DNA sequences they recognize and use. They are known as Y-Tpases and S-Tpases to distinguish them from tyrosine and serine recombinases. A fifth class, which catalyzes sequence-specific integration but does not resemble any of the above groups is represented by a newly discovered class of elements.

Types of Transposable Elements

Insertion Sequences

The smallest autonomous elements known are the bacterial ISs. These have been detected in almost all eubacterial and archaebacterial genomes. They are genetically compact, between 750 bp and 2500 bp in length, are generally flanked by two partially identical and inverted sequences (terminal inverted repeats: IRs) and encode only functions involved in their mobility. The Tpase gene is composed of one or two open reading frames (*orf*s) occupying almost the entire length of the IS (Figure 1A). The IR proximal to the Tpase promoter is defined as IRL. In many ISs with two *orf*s, Tpase is produced as a fusion protein using a programmed −1 translational frameshift between the *orf*s similar to that observed in generating the pol polyprotein in some retro-viruses.

Over 1000 bacterial ISs are known. These have been divided into ~20 groups or families defined by their genetic organization, similarities in their IRs and Tpase sequences, and their preference for given target DNA

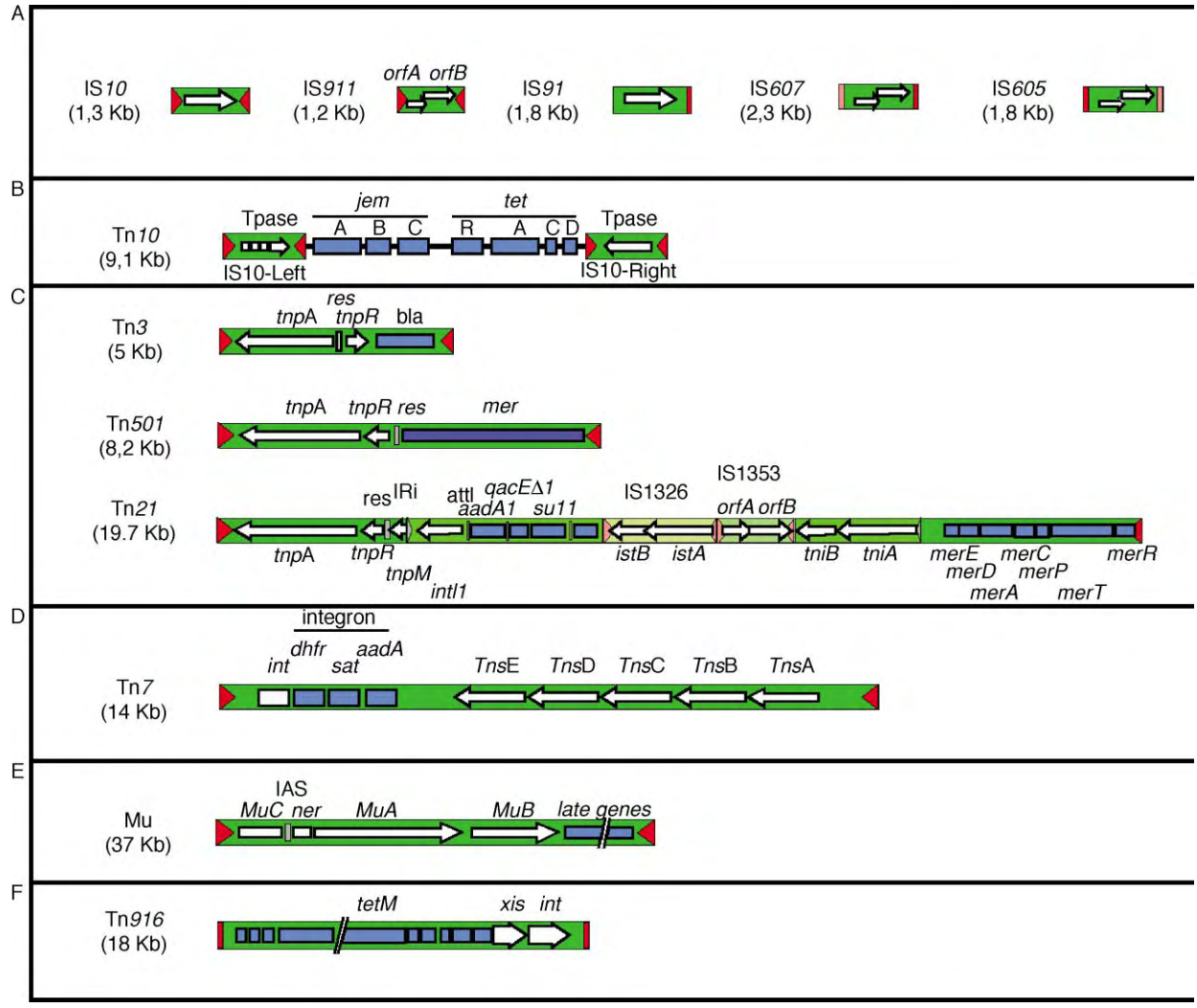

FIGURE 1 Diversity of bacterial transposable elements. The organization of different types of bacterial TE is shown. Terminal repeats (red triangles), transposon ends (red boxes in the case of IS*91*, IS*605*, IS*607* and Tn916 to indicate that they are not inverted repeats), genes whose products are involved in transposition, site-specific integration or recombination (int, xis, R) functions (white boxed arrows), resistance genes and accessory genes (conjugative transfer or phage functions) (blue boxes) are indicated. Grey boxes indicate recombination sites for resolution of cointegrates (*res*) or integron capture of gene cassettes (*att*). *bla*: resistance to β-lactams; *tet*: resistance to tetracycline; *mer*: mercury resistance.

sequences (www-IS.biotoul.fr). The majority (17/20) of these families encode a DDE Tpase, one (IS*91*) encodes a Y2 enzyme, a third (IS*607*) encodes an S-Tpase while a fourth (IS*605*/IS*608*) specifies an enzyme whose mechanism of catalysis is at present unknown (Figure 1A). This classification will undoubtedly continue to evolve as more are characterized.

Miniature Inverted Repeat Transposable Elements

Several bacterial genomes harbor many copies of small DNA segments. Depending on the bacterial species, these are variously called *Rep*, *Box*, *Rup*, or *Correia*. Some resemble ISs, which have been deleted for the transposase. Interestingly, the ends often resemble those of members of the IS*630* family and like these elements are flanked by a directly repeated TA dinucleotide. These were first described in eukaryotic systems.

Compound Transposons

Antibiotic resistance genes in bacteria were often found to be flanked by a pair of similar IS elements. Flanking ISs are capable of mobilizing any interstitial DNA segment. These structures are known as compound transposons. They are widespread and can include resistance to many different antibacterials, to genes involved in bacterial–host interactions as well as to other "accessory" genes, which are important to the host under some conditions of growth. Classical examples are tetracycline resistance transposon, Tn*10*

(flanked by two IS*10* elements in inverse repeat) (Figure 1B), the neomycin resistance transposon, Tn*5* (flanked by two IS*50* elements in inverted repeat) and the chloramphenicol resistance transposon, Tn*9* (flanked by two copies of IS*1* in direct repeat). In some cases the autonomy of the flanking ISs may be reduced in various ways to favor transposition of the entire structure.

Unit Transposons

Another class of bacterial transposons are the unit transposons such as members of the Tn*3* family (Figure 1C). Here, additional genes are contained within the transposable element itself. Large numbers of such transposons have been described carrying antibiotic resistance genes or genes involved in catabolism of unusual substances (including xenobiotics). Tn*3*-family transposons share very similar IRs (~40 bp) and carry highly related DDE transposase genes. They carry a specific site (*res*) and encode a site-specific recombinase (*tnp* R), which promotes recombination in the cointegrate between the two elements at their *res* sites. This leads to separation of donor and target molecules and leaves a single copy of the transposon embedded in each. Many variations on this basic structure have been observed. They include derivatives, which encode only the Tpase with no additional genes and therefore might be included within the IS group.

Tn*3*-family elements can accommodate and accumulate additional genes. For example Tn*21* (Figure 1C) evolved by insertion of a now defective transposon into an ancestral mercury resistance transposon, which has additionally acquired two ISs. Tn*21* also carries a genetic trap, which permits the acquisition of additional genes: the integron system. Integrons include an integrase gene, related to the Y-recombinase of bacteriophage λ. It also carries a flanking site equivalent to the λ attachment site, *att*, at which integration occurs. The acquired genes are generally promoterless and are located on small cassettes, which integrate site-specifically into the *att* site where a resident promoter is appropriately located to drive expression.

Tn*7*

Transposon Tn*7* (Figure 1D) is unusual in that it encodes five proteins necessary for its transposition and uses two transposition pathways: a site-specific insertion pathway and a more random pathway, which recognizes aspects of DNA structure in the target. One of the transposition enzymes (TnsB) is a DDE transposase while a second (TnsA) shows similarity to restriction endonucleases. Two additional proteins (Tns D and E) are involved in target choice for each of the two pathways while the fifth (TnsC) provides a bridge between target protein and the transposase. Tn*7* also carries an integron system, which has permitted it to acquire resistance to trimethoprim among other antibiotic resistances. Other members of this group including different resistance genes have also been described.

Transposable Bacteriophage

The first example of this type to be described was the temperate mutator phage Mu (Figure 1E), so-named because it inserts in a relatively random way and generates mutations during infection. Many different examples of mutator phages have been identified either as phage particles or during annotation of bacterial genome sequences. They are extremely large (>40 kbp) and relatively complex since they must encode for the enzymes and structural proteins involved in the bacteriophage lifestyle. They transpose using DDE enzymes.

Conjugative Transposons

These were first discovered in gram-positive bacteria as elements capable of transmitting tetracycline resistance from cell to cell and between bacterial species. Although they have been called transposons (Ctns for conjugative transposons), they use a site-specific recombination reaction for integration and excision. The enzymes are generally Y-transposases, similar to the site-specific recombinases used by phage λ or the integrons. However, whereas λ and integrons show pronounced sequence specificity for integration, conjugative transposons are much less exacting in their choice of integration sites. They are large and, in addition to the genes involved in integration and excision and in antibiotic resistance, they carry genes required for conjugative transfer. Tn*916* (Figure 1F) and Tn*1545* are the best-characterized transposons of this type. Several examples of Ctns encoding S-transposases have also been described.

Mechanism

DDE Enzymes

Transposition requires precise cleavage at the transposon ends and their coordinated transfer into a target molecule. This is achieved through the assembly of a nucleo-protein complex of defined architecture: the transpososome. This structure involves the Tpase, the transposon ends and target DNA. The signals for recognition and processing by Tpase are located in the transposon ends. Most bacterial ISs carry relatively simple IRs with a single Tpase-binding site. Other transposons show a complex constellation of sites often arranged differently at each end (e.g., phage Mu and Tn*7*).

The majority of known Tpases are structurally related and carry a conserved triad of acidic amino acids, the DDE motif, which coordinate two divalent metal ions central to catalysis. Cleavage at the 3′ ends of the element by an attacking nucleophile (generally H_2O) occurs to expose a free 3′OH group (Figure 2A). This nucleophile then attacks a 5′ phosphate group in the target DNA in a single-step transesterification reaction

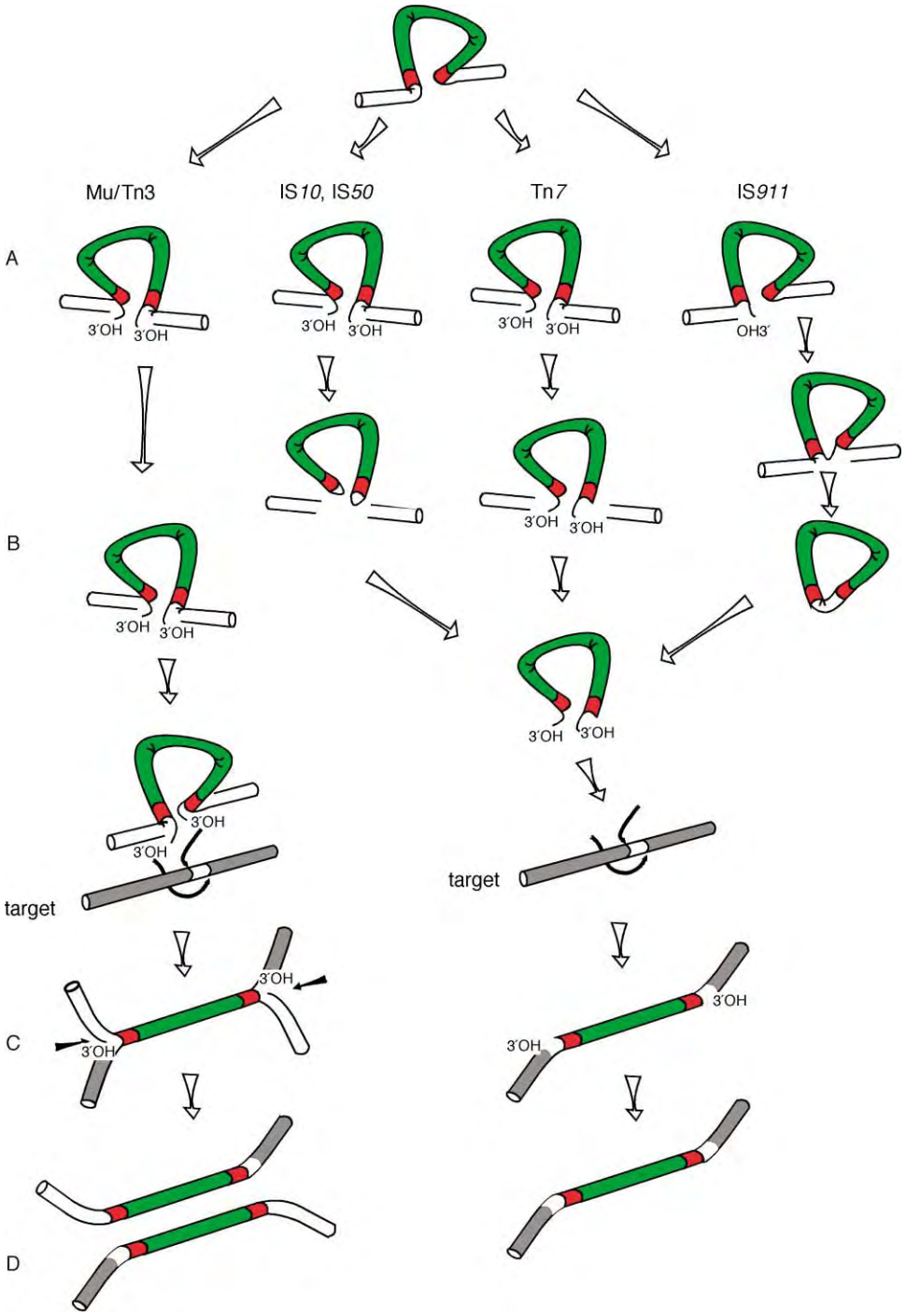

FIGURE 2 Transposition mechanism of DDE elements. Transposon, inverted repeats, and flanking sequences are shown as green, red, and white respectively. In target DNA (grey), direct repetitions (DR) are shown in white. Liberated 3′OH groups involved in subsequent strand joining reactions are shown (A and B). Left column: Replicative transposition as the result of single strand cleavage and transfer to create a replication fork (C). 2nd column: In the IS*10* (IS*50*) reaction pathways the 3′OH liberated in the initial hydrolysis attacks the opposite strand to generate a hairpin intermediate, liberating the transposon from its flanking donor DNA (A). A second hydrolysis regenerates the 3′OH (B). 3rd column: Double strand cleavage using two enzymes (e.g.Tn*7*). 4th column: For members of the IS3 family (e.g., IS*911*), the 3′OH from a single-end hydrolysis directs a strand transfer reaction to the same strand to the other end of the element (A). The branched single-strand circle is resolved into a transposon circle by the host. Single-strand hydrolysis at each 3′end (B) generates a linear transposon, which can integrate in a target.

(Figure 2B). The reaction, analyzed in detail for bacteriophage Mu, HIV, and IS*10*, has been shown to occur as an in-line nucleophilic attack with chiral inversion of the phosphate group. The two metal ions are thought to act respectively as a Lewis acid and base in the reaction.

Concerted transfer of both transposon ends into the target site, while maintaining the correct strand polarity, results in joining each transposon strand to opposite target strands. Since the position of attack in target DNA is generally staggered, this generates short, complementary single strand regions flanking the newly inserted element (Figure 2C). Repair by the appropriate host machinery generates a short duplication (direct repeat or DR) of defined length in the flanking target DNA (Figure 2D). The reactions do not require an external energy source nor do they involve a covalently linked enzyme-substrate intermediate. The donor transposon strand performs the cleavage-ligation steps in the target DNA and no cleaved target molecule is detected in the absence of strand transfer.

DDE enzymes cleave only one of the two DNA strands. An important feature of the transposition reaction is therefore the way in which the 5′ end (second strand) is processed. Some transposons do not process the second strand and are therefore not separated from the donor molecule. Strand transfer generates a structure, which can be used as a replication fork. "Replicative integration" generates cointegrates or replicon fusions where the donor and target replicons are fused and separated at each junction by a directly repeated copy of the element (e.g., bacteriophage Mu, the Tn*3* family; Figure 2 left column). Other elements shed their donor DNA prior to insertion. For some elements, the 3′OH generated by the first hydrolysis attacks the second strand to generate a hairpin form which then undergoes hydrolysis to regenerate an active 3′OH (e.g., IS*10* and IS*50*; Figure 2 second column). Others possess a second enzyme dedicated to cleavage of the second strand (e.g., Tn*7*; Figure 2 third column). For members of several bacterial IS families (e.g., IS*3*, IS*21*, and IS*30*) the 3′OH liberated at one end of the IS attacks the other end on the same strand generating a form in which one IS strand is circularized. The entire transposon is then resolved into a free transient circular form by replication or recombination of the second strand. The transposon circle then undergoes efficient integration after single-strand cleavage at each end (Figure 2 fourth column).

Non-DDE Transposases

The mechanism of transposition mediated by the other classes of transposase is less well detailed than that of the DDE transposases.

Y2 Transposases

The Y2 transposases, at present limited to the IS*91* family, show significant identity to the rolling circle replicases of phage and plasmids in the regions covering their active sites. The characteristics of transposition are strikingly different from those of DDE-mediated events. ISs of this type do not exhibit terminal IRs, do not generate flanking direct repeats and insert into a conserved tetranucleotide, which is required for further transposition events. The right (but not the left) end and the tetranucleotide are essential for transposition. Moreover, deletion of the left end can result in one-ended transposition. In this case, the inserted fragment of donor DNA is flanked at one end (constant end) by the right end and at the other end by a conserved tetranucleotide sequence present elsewhere in the donor plasmid (variable end). In addition, circular single-stranded derivatives of IS*91* have been observed and may represent transposition intermediates. While these data clearly support a polarized rolling circle mechanism, little is known about the strand transfer, which would assure transfer from donor to target site.

Y- and S-Transposases

Again, although site-specific recombination reactions directed by S- and Y- recombinases are known in exquisite detail, the activities of the corresponding transposases remain largely uninvestigated. By analogy, and in contrast to the DDE enzymes, it is assumed that catalysis involves the formation of a covalent enzyme substrate intermediate (Figure 3). In both cases, the element is excised precisely from the donor molecule.

For the Y-transposases, this would involve nucleophilic attack of the target phosphodiester bond by the active site tyrosine to generate a 3′-phosphotyrosyl bond exposing a 5′OH (Figure 3A, left column). In a second step, the 5′OH attacks the phosphotyrosine bond at the opposite end to promote strand exchange (Figure 3B, left column). Note that the reaction of only one strand is shown here. Sequential reactions of cleavage and transfer on the opposite strand would then generate a circular intermediate (Figure 3C, left column). Insertion is thought to occur by reversal of these reactions (Figure 3D, left column).

For the S-transposases recombination occurs by a concerted four strand cleavage (Figure 3A, right column) in which a catalytic serine residue attacks the target phosphodiester bond to generate a 5′ phosphoserine bond and to expose a 3′OH (Figure 3B, right column). Strand transfer to generate a circular intermediate would occur by nucleophilic attacks of the covalent DNA-enzyme bonds by the 3′ hydroxyl ends generated by cleavage (Figure 3C, right column). A second round of similar recombination reactions (Figure 3D, right column)

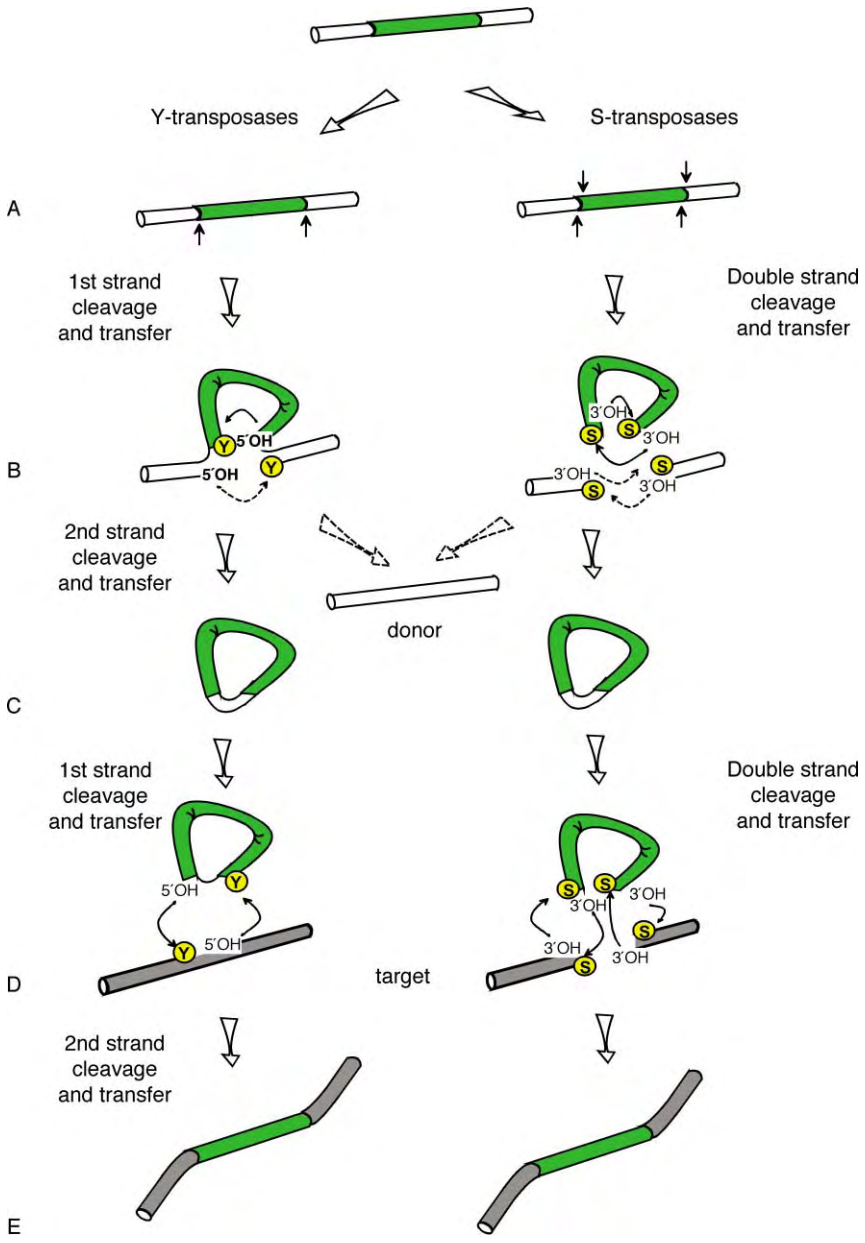

FIGURE 3 Reaction mediated by Y- transposase and S-transposases. Left column: Transposon and flanking sequences are shown as green and white respectively. The active site residue Y or S is shown within a yellow circle. Y-transposase nicks one transposon strand (here on bottom strand) at both ends (A) and forms covalent 3′ phosphotyrosine intermediates (B). The liberated 5′ OH attacks the phosphotyrosine linkage at the other end (arrows) to circularize one transposon strand (B). The same reaction is performed on the top strand to regenerate the donor and a circular intermediate (C). Further cleavage and transfer (D) is presumed to result in an insertion into target DNA (E). In contrast to site-specific recombination, the Y-transposase exhibits low sequence specificity for the target site. Right column: S-transposase catalyzes concerted double-strand breaks at both ends (A), forming covalent 5′ phosphoserine intermediates (B). After a switch of strands, the 3′ OHs attack the phosphoserine bonds in the opposite end (B), resulting in a circular intermediate (C). The same process (D) permits insertion of the element in a target (E). For both pathways, strand transfers reconstituting donor molecule (B and C) are shown by dotted arrows.

would then lead to insertion of the circular transposition intermediates (Figure 3E).

Target Choice

The choice of an insertion site can have important implications both for the transposon and for the host. Insertion into a specific target DNA sequence can provide a secure refuge for the transposon. For example, by using a specific sequence in a highly conserved gene in such a way that insertion does not disrupt the gene, transposon Tn*7* is assured an insertion site, which does not affect the fitness of the host and occurs in many bacterial species. On the other hand, in excluding insertions into other DNA sequences, this strategy precludes the capacity of

the element to generate mutations or to activate or sequester genes and thus to generate genetic diversity. Different transposons exhibit a variety of different strategies for selecting a target. On a genome scale, most transposons appear to insert "randomly". However, when analyzed at the nucleotide level, most show some degree of target preference. Insertion can be sequence-specific, with target sequence lengths varying from a few to many nucleotides, or show regional preferences, for example GC or AT rich DNA segments, probably reflecting more global parameters such as local DNA structure. Other factors which have also been implicated are: the degree of supercoiling, DNA replication, transcription, direction of conjugative transfer, and protein-mediated targeting to, or exclusion from, transcriptional control regions. In addition, some transposons show a preference for insertion close to sequences resembling the transposon end. Others exhibit the converse behavior: exclusion of insertions close to a resident end. This phenomenon, transposition immunity, can act over many kilobases of DNA. For Tn*7* and Mu it has been shown that this is accomplished by a second transposon-encoded protein (in both cases a DNA dependant ATPase), which binds target DNA. Briefly, for phage Mu, the transposase MuA, is capable of stimulating dissociation of the DNA-dependent ATPase, MuB from DNA. Thus, MuA bound to a transposon end resident in the target molecule is thought to provoke disassembly of MuB from neighboring DNA with a probability, which decreases as the distance increases.

Clearly, many insertion preferences must reflect constraints in the architecture of the synaptic complexes formed between the transposon ends, the target DNA and the transposase.

Regulation

Transposable elements are very highly regulated and have evolved a variety of perspicacious regulatory mechanisms. Apart from the temperate transposable bacteriophages, which possess a highly efficient transposition mechanism during their lytic development, transposition is not an efficient event. A given transposable element generally possesses an ensemble of regulatory mechanisms, which can differ in detail from even closely related elements.

Regulation can be at the gene expression level or at the level of Tpase activity. A combination of weak promoters and poor ribosome-binding sites can limit transcription and translation while secondary structures, which sequester translation initiation sites and involve RNA sequences upstream and downstream of the Tpase promoter can be present to prevent accidental activation by impinging transcription (IS*10*, IS*5*). Some elements produce a small antiRNA also capable of sequestering translation initiation signals, which acts as a negative control component (IS*10*). Another mechanism to control transposition activity has been documented in elements whose transposition involves a circular or a dimeric intermediate (IS*911*, IS*2*, IS*30*, IS*21*). Here, the weak endogenous promoter can provide low levels of transposase to enable low frequency formation of the transposon circle. However, the IR–IR junction formed in both transposon dimers and circles creates a strong promoter by virtue of a -10 promoter element oriented inward at one IR and a -35 element oriented outward in the other. This boosts transposase synthesis resulting in cleavage, disassembly of the junction promoter and insertion of the transposon, which then again assumes a low level of Tpase expression from the indigenous promoter. Transcription termination signals within the Tpase *orf* or posttranslational processing might also regulate Tpase expression, although these mechanisms have not been investigated in detail. Another relatively common regulatory mechanism involves programmed translational frameshifting (IS*1* and IS*3* families). Here, the Tpase is distributed over two consecutive *orf*s and frameshifting serves to generate a fusion protein including the products of the upstream *orf*, which generally carries DNA-binding and multimerization functions, and the downstream *orf*, which can include the catalytic site. The product of the upstream frame in these cases generally serves a regulatory role. For certain elements, posttranslational proteolysis might also be used to generate small regulatory proteins. IS*50* also generates a protein, Inh, using a second promoter located downstream from the Tpase promoter and representing an N-terminal truncated derivative of the Tpase. Inh acts as a transposase inhibitor.

Regulation can also occur at the level of transposase activity. The differential arrangement of Tpase-binding sites at each of phage Mu and Tn*7* (and perhaps members of the IS*21* family) permits a functional distinction and presumably favors the use of one left and one right end *in vivo*. Moreover, in many cases, Tpase bound at one end catalyzes strand cleavage at the partner end. This "trans" cleavage assures that the correct complex has been assembled before transposition can take place. For Tn*7*, the cleavage and strand transfer reactions require the presence of the target DNA molecule.

An additional level of control of Tpase activity is reflected in the observation that these enzymes often prefer to act on the copy of the element from which they are synthesized. In other words, they exhibit a preference for activity *in cis*. Several nonexclusive explanations for this behavior are apparent and *cis* activity is likely to involve a combination of different effects. One invokes a, yet untested, cotranslational-binding model in which a nascent Tpase protein is

capable of correctly folding its DNA-binding domain and binding to transposon ends before synthesis of the entire protein is accomplished. A second model invokes Tpase stability and it has been demonstrated in at least one case, IS*903*, that the ion protease plays a crucial role *in cis* activity.

Other host factors can also intervene at different regulatory levels. DAM methylase is involved in regulating Tpase expression and the recombination activity of the ends both IS*10* and IS*50*. DNA architectural proteins such as IHF, Fis and Hu have also been implicated in assuring the correct assembly of the transpososome. Moreover, IHF has been implicated in driving the molecular transitions leading to strand cleavage in IS*10*. Other factors such as RecBC, DnaA, Acyl carrier protein, and ribosomal protein L29 have also been implicated in the transposition behavior of various elements but the exact details remain to be elaborated.

Eukaryotic Transposons

Although this section is devoted to prokaryotic elements, it is important to note that eukaryotes generally carry large numbers of both intact and truncated transposable elements. These constitute over 40% of the human genome and somewhat less in Arabidopsis. There are many similarities between prokaryotic and eukaryotic elements. A major group is the Tc/mariner superfamily whose members are similar to bacterial ISs. They carry terminal inverted repeats and encode a DDE, or in this case, a DDD group transposase and resemble the IS*630* family of bacterial elements. Many eukaryotic genomes, especially those of plants, harbor extremely high numbers of truncated derivatives, similar to those found in bacteria, in which the transposase gene appears to have been deleted leaving both IRs. These elements have been also called miniature inverted repeat transposable elements (MITES) and can presumably be mobilized by the full length copies of the elements located elsewhere in the genome.

Another major group, which is limited to eukaryotes are the retro-viruses and LTR-retro-transposons, which pass through an RNA intermediate during their (viral) life cycle. Integration into the host genome occurs through a double-stranded cDNA intermediate and uses DDE group integrase (IN).

The immunoglobulin V(D)J recombination system represents another important element in vertebrates. Here, rearrangements involve two host proteins, RAG1 and RAG2. The RAG1 recombinase is related to DDE transposases. An interstitial DNA segment (signal sequence) is excised to permit the rejoining of two flanking sequences (coding sequence). In a similar way to IS*10* and IS*50*, recombination involves the formation of a hairpin intermediate. In this case, however, the hairpin is generated on the flanking DNA rather than on the excised fragment.

A third large family of eukaryotic elements is the hAT superfamily. Although the nature of their transposase is not clear and little work has yet been undertaken concerning their transposition (which includes *hobo* and *Hermes* from insects, Ac and Tam3 from plants) it seems probable that they have adopted a V(D)J-type of recombination mechanism.

Eukaryotes also harbor other families of IS-like elements including the P element of *D. melanogaster* whose mode of transposition has received much attention due to its use in mutagenesis, the CACTA family, which includes the plant transposons Tam1 and Tam1, and the En/Spm family.

Other newly recognized classes of eukaryotic elements are the helitrons, which resemble rolling circle transposons of the IS*91* family, and Cryptons, DIRS1, and kangaroo elements, which appear to encode Y-transposases.

In addition to eukaryotic elements, which transpose using a DNA intermediate including the retro-viruses, a large class of transposons, which transpose by a completely novel mechanism have also been identified. These are the target-primed (TP) retro-transposons in which an RNA intermediate is copied into its DNA target via reverse transcription.

See Also the Following Article

Nonhomologous Recombination: Retrotransposons

Glossary

DDE transposases Transposases in which the catalytic site includes two aspartate (D) and one glutamate (E) amino acid residue.

S transposases Transposases that resemble serine (S) site-specific recombinases.

transposases Enzymes that catalyze transposition.

Y transposases Transposases that resemble tyrosine (Y) site-specific recombinases.

Y2 transposases Transposases that resemble rolling circle replicases and in which the catalytic site includes two tyrosine (Y) amino acid residues.

Further Reading

Chandler, M., and Fayet, O. (1993). Translational frameshifting in the control of transposition in bacteria. *Mol. Microbiol.* 7(4), 497–503.

Craig, N. L. (1997). Target site selection in transposition. *Annu. Rev. Biochem.* **66**, 437–474.

Craig, N. L., Craigie, R., Gellert, M., and Lambowitz, A (2002). *Mobile DNA II*. ASM press, Washington DC.

Curcio, M. J., and Derbyshire, K. M. (2003). The outs and ins of transposition: from mu to kangaroo. *Nat. Rev. Mol. Cell Biol.* **4**, 865–877.

Hallet, B., and Sherratt, D. J. (1997). Transposition and site-specific recombination: Adapting DNA cut-and-paste mechanisms to a variety of genetic rearrangements. *FEMS Microbiol. Rev.* **21**(2), 157–178.

Haren, L., Ton-Hoang, B., and Chandler, M. (1999). Integrating DNA: Transposases and retroviral integrases. *Annu. Rev. Microb.* **53**, 245–281.

Mizuuchi, K. (1992). Polynucleotidyl transfer reactions in transpositional DNA recombination. *J. Biol. Chem.* **267**(30), 21273–21276.

Mizuuchi, K. (1997). Polynucleotidyl transfer reactions in site-specific DNA recombination. *Genes Cells* **2**(1), 1–12.

Rice, P., Craigie, R., and Davies, D. R. (1996). Retroviral integrases and their cousins. *Curr. Opin. Struct. Biol.* **6**(1), 76–83.

Biography

Bao Ton Hoang is a Research Scientist with the Centre National de Recherche Scientifique (CNRS) in Toulouse, France. She obtained her Ph.D. from the Université Paul Sabatier and received her postdoctoral training at the Institut National de Recherche Agronomique, Auzeville and the Ecole Veterinaire, Toulouse, France.

Michael Chandler is a Research Director with the CNRS in Toulouse. He obtained his Ph.D. from the University of Leicester (England) and received his postdoctoral training at the University of Geneva (Switzerland). The principal interest of both authors is in genome plasticity and horizontal gene transfer.

Nonhomologous Recombination: Retrotransposons

Siew Loon Ooi and Jef D. Boeke
The Johns Hopkins University School of Medicine, Baltimore, Maryland, USA

Transposons are segments of DNA that can move from one chromosomal locus to another locus on the same or different chromosomes within one cell. DNA transposons transpose via a DNA intermediate, while retrotransposons transpose via an RNA intermediate. Retrotransposons use its own reverse transcriptase protein to make a copy of its DNA from RNA, and the newly-made DNA is then inserted into a new chromosomal location. In this sense, the life cycle of retrotransposons closely resembles that of HIV virus. DNA transposons exist in both prokaryotes and eukaryotes, while retrotransposons are only found in eukaryotes. Interestingly, retrotransposons make up a significant portion of our genome and may play a role in shaping our genome by providing plasticity for evolution.

Genes are typically considered static entities that stably reside at identical loci of chromosomes in the same species. For the most part, this assumption is correct. However, in the 1940s, while studying the genetic basis of variegated pigmentation pattern of maize (Indian corn) kernels (Figure 1), Barbara McClintock proposed that some genes can change position and move from one locus to another locus on the same or different chromosomes, changing the pigmentation patterns of the kernels. She termed these genetic entities that could move into and back out of genes "controlling elements". When a controlling element moves into a gene required for pigment color formation, it disrupts the function of the gene, thus giving rise to a cell that has no color. McClintock's discovery of transposable sequences was ~30 years ahead of its time and was largely ignored mainly because it contradicted the then accepted concept that genes resided at fixed spots on chromosomes. It was not until the 1970s, when transposons were discovered in bacteria, that the general scientific community became more receptive to the concept of transposons.

Transposons

Transposons exist in all forms of life ranging from simple unicellular prokaryotes (e.g., the gut bacterium *Escherichia coli*) and eukaryotes (e.g., yeast *Saccharomyces cerevisiae*) to more complex multicellular eukaryotes including worms, insects, and mammals. Transposons are defined as segments of DNA that can move from one chromosomal locus to another locus on the same or different chromosomes within one cell, without any sequence homology to the insertion site. Transposons are also known as transposable genetic elements, insertion sequences (IS), mobile elements, jumping genes, and nomadic elements. For clarity, the parental copy of the transposon, located in one site of the host genome, is defined as the donor copy (Figure 2A). The new chromosomal site into which the transposon transposes is termed the target site and the new copy of transposon at the target site is termed the newly transposed copy (Figure 2A).

Almost all transposons acquire their abilities to mobilize themselves from the gene(s) encoded in their DNA such as transposase, integrase, and reverse transcriptase. The bacterial IS*50* element is a simple bacterial DNA transposon. IS*50* elements encode transposase required to carry out the transposition reaction and a repressor protein that represses transposition. IS*50* is flanked by a 9 base pair (bp) inverted repeat sequence required for protein binding and recognition by its transposase. Retro transposons are a type of transposon that makes a new copy of itself by copying or "reverse transcribing" an RNA copy of itself. In this way, the life cycle of retro transposons closely resembles that of retro-viruses. Yeast *Ty1*, a long terminal repeat (LTR) retro transposon, is an example of retro transposon (Figure 3A). *Ty1* contains ~340 bp direct LTR repeat that flanks both ends of the retro transposon and its two open reading frames (ORFs) or genes (Figure 3A). The first ORF encodes *GAG*, a structural protein that packages the *Ty1* RNA into a virus-like particle. The second ORF encodes *POL*, a catalytic protein containing activities such as integrase, protease, and reverse transcriptase required for transposition.

FIGURE 1 The discovery of transposons. By studying genetic entities important for pigment formation in maize, Barbara McClintock discovered maize DNA transposons, which can transpose into and out of genes involved in pigment formation and cause corn kernels to have segments with different colors.

Features of Transposons

The size and orientation of repeat elements and the size of the target site duplication are characteristic of individual types of transposons.

Direct Versus Inverted Repeat Elements

Most transposons are flanked by repeat elements ranging in length from a few to more than 300 bp. The 9 bp near-perfect inverted repeat in IS*50* serves as a binding site for the IS*50*-encoded transposase while in *Ty1*, the 340 bp repeat element is required for proper reverse transcription and integrase binding. Repeat elements can exist in either the direct or inverted orientations (Figure 2B). The orientation of the repeat elements is significant because it affects the type of chromosomal rearrangement product resulting from recombination of the repeat sequences. Interestingly, even those transposons flanked by direct repeats such as LTRs are also flanked by short inverted repeats. That is, each LTR itself contains a terminal inverted repeat sequence – in the case of *Ty1* this sequence is TG … CA. Inverted repeat sequences are also known as palindromes. However, palindromes in the "language" of DNA differ from the English palindromes (Figure 2B).

Target Site Duplication

The target site duplication (TSD) is the short "host" DNA sequence that flanks the transposon (Figure 4). For each individual copy of a transposon, the sequence of the TSD will be different, but typically its length is the same. During transposition, the target site is cleaved on both strands by transposase (or for LTR retro transposons, the integrase) followed by insertion of the transposon, resulting in a transposition intermediate structure that must be repaired by DNA synthesis. These repaired gaps that flank both ends of the transposon are identical in sequence, and form the new TSD. Note that TSD is a direct repeat sequence. The size of the TSD is defined by the distance between the two cleavage sites created by the transposase and is unique to each transposon.

"Cut-and-Paste" versus "Copy-and-Paste" Transposition

During conservative transposition, practiced by many but not all DNA transposons, the transposon excises

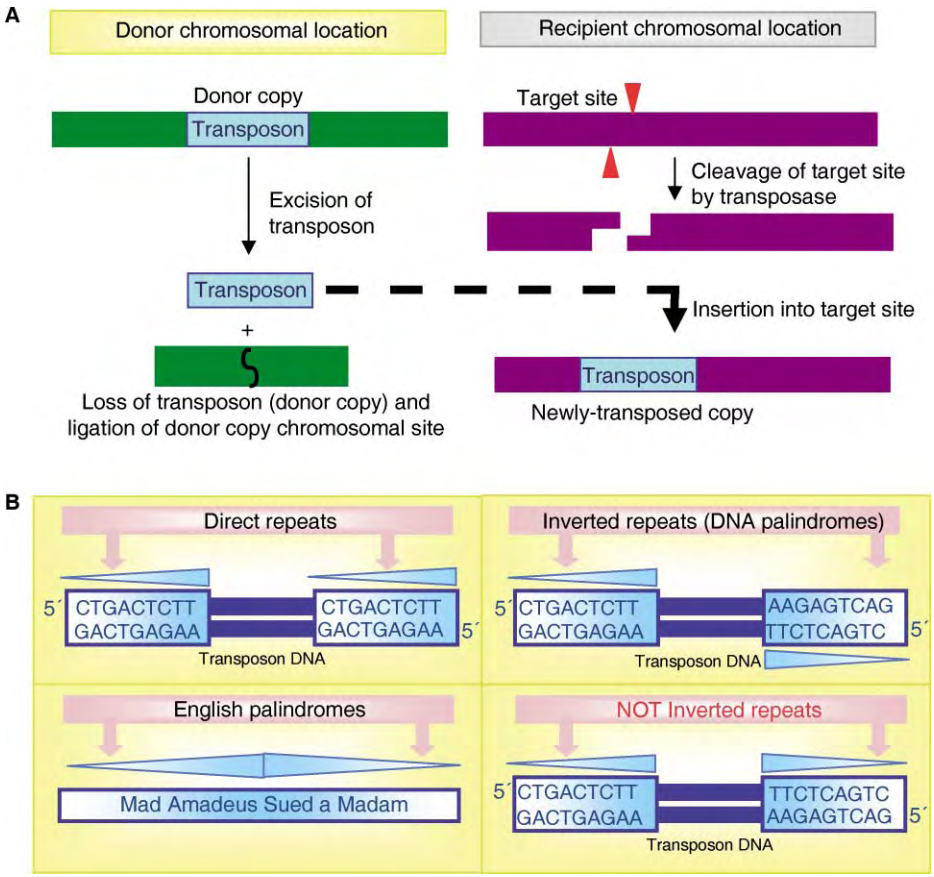

FIGURE 2 (A) Transposition. During transposition, the transposon (donor copy) is first excised from its donor chromosomal location by transposase. Next, transposase cleaves both strands of the DNA at the target site, defined as the chromosomal location into which the transposon will transpose. The transposon inserts itself into the target site, creating a "newly-transposed copy" of the transposon. The yellow background depicts events occurring at the donor chromosomal location while the gray background events occurring at the target site. In this case, the transposon transposes via the "cut-and-paste" mechanism, thus the donor copy of the transposon is lost at the donor chromosomal location. (B) Direct versus inverted repeats. Due to the double-stranded nature of DNA, direct repeats have the same DNA sequence encoded on the same strand, while inverted repeats have the same DNA sequence encoded on opposite strands. Inverted repeats are DNA palindromes, which differ from English palindromes (Reprinted by permission of David R. Godine, from "Mad Amadeus Sued A Madam," by Allan Miller).

itself from the donor site and reinserts itself into the target site. This is also known as "cut-and-paste" transposition. In contrast, retro transposons do not cut themselves out of the donor site. Rather, they copy themselves into RNA (using the cellular RNA polymerase) and then copy that RNA sequence back into DNA using reverse transcriptase. The newly made DNA copy is then inserted into a new site and this process is known as "copy-and-paste" transposition.

RNA- versus DNA-Mediated Transposition: Retro- versus DNA-Transposon

DNA transposons transpose via a DNA intermediate. Transcription of DNA transposons is only needed as a means of expressing the transposon-encoded proteins. In contrast, retro transposons transpose via an RNA intermediate, and transcription of retro transposon is important both for (1) the translation of the retro transposon-encoded proteins and (2) making a full-length RNA copy of its own genome to serve as the template for retro-transposition.

Retrotransposons

In summary, retro transposons differ from DNA transposon mainly because retrotransposons transpose via an RNA intermediate and the "copy-and-paste" mechanism. In addition, retro transposons are only found in eukaryotes including microbes, plants, and animals. Retro transposons can be categorized into long terminal repeats (LTRs) and non-LTR types (Figure 3). They differ primarily in the 5′ and 3′ end structure and in their transposition mechanisms.

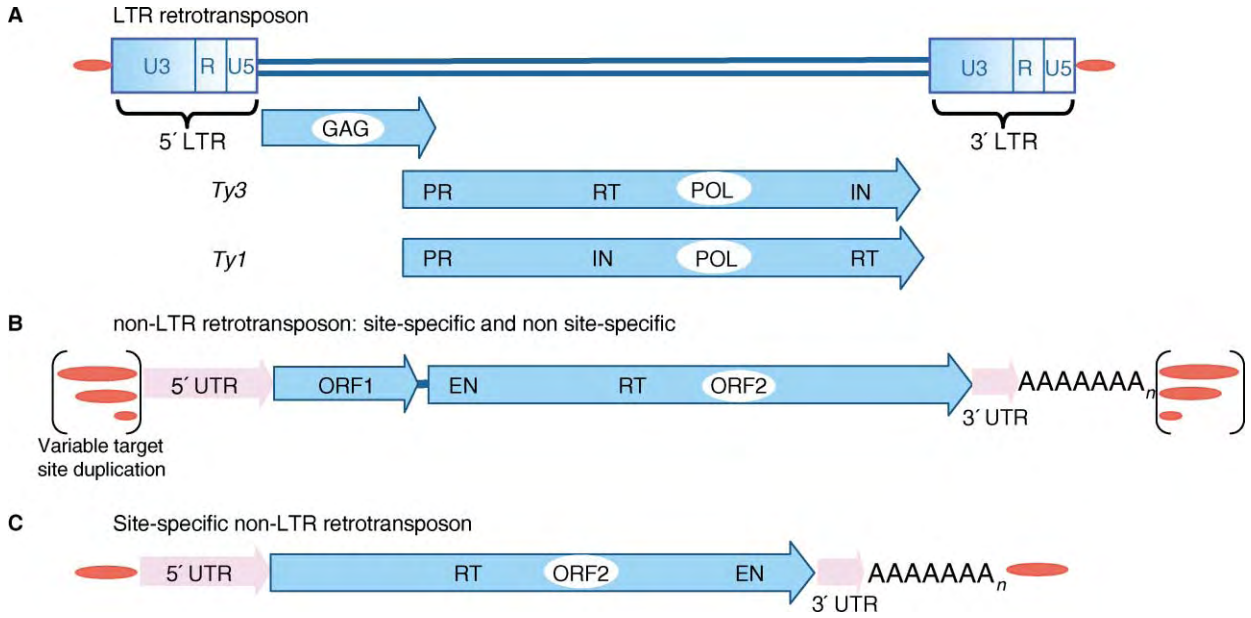

FIGURE 3 Structure of retrotransposons. (A) The long terminal repeat (LTR) of LTR retrotransposon is a few hundred base pair in length and is made up of three distinct segments termed U3, R, and U5. The transposon encodes two ORFs: GAG and POL. In *Ty3*, POL encodes protease (PR), reverse transcriptase (RT) followed by integrase (IN). In *Ty1* POL, the IN domain precedes the RT domain. (B) Non-LTR retrotransposon lacks repeat elements, instead, its 3′ end always ends in stretches of polyA sequences. Non-LTR retrotransposons encode two ORFs: ORF1 and ORF2. ORF1 contains RNA binding activity, while ORF2 encodes for endonuclease (EN), reverse transcriptase (RT) and other unknown functions. (C) Some site-specific non-LTR retrotransposons encode for only one ORF. The red oval denotes the target site duplication, which is variable in length for non-LTR retrotransposons.

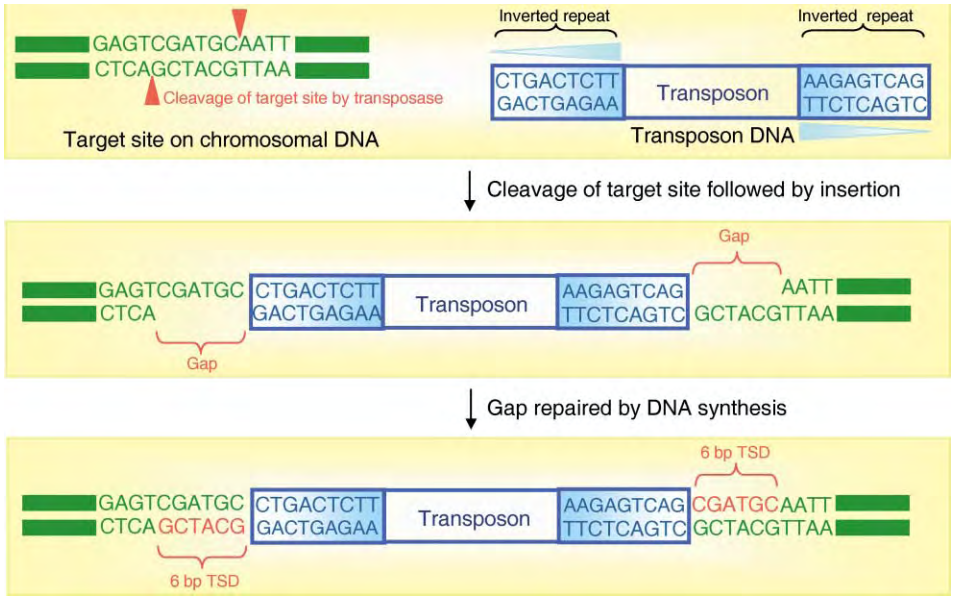

FIGURE 4 The generation of target site duplication (TSD). During transposition, transposase cleaves both strands of the DNA at the target site. The transposon, together with its terminal inverted repeats (arrows) can then insert itself into the new genomic locus. The insertion creates a gap that is usually repaired by DNA synthesis. Once repaired, the 6 bp flanking the transposon is identical in sequence, and is thus termed target site duplication (TSD). The distance between these two cleavage sites defines the size of the TSD. Genomic sequence, transposon and newly synthesized DNA are depicted in green, blue and red respectively.

Long Terminal Repeat (LTR) Retrotransposons

LTR retro transposons resemble retro-viruses such as HIV both in their basic structure and life cycle (Figure 5). Both their DNA structures begin and end with long terminal repeats several hundred bp long and they have similar *Gag* and *Pol* gene structures. The *Pol* gene encodes protease, reverse transcriptase, and integrase (the integrase functions similarly to the transposase of DNA transposons, effecting the reaction outlined in Figure 4). The major difference between LTR retro transposons and retro-viruses is that retro-viruses have a retro-virus-specific *Env* gene, encoding an envelope protein that can bind to receptors on host cells, conferring on retro-viruses the ability to shuttle from cell to cell and thus their infectivity. Retrotransposon life cycles take place within a single host cell, and they are not infectious. Retro-viruses are believed by most scientists to have evolved from the simpler LTR retro transposons.

Non-LTR Retrotransposons

Mammalian genomes contain an additional class of retro transposons that do not have LTRs, suggesting that these retro transposons are quite different from retro-viruses. In human cells for example, the long-interspersed nuclear element (LINE-1 or L1) element is a 6 kilobase (kb) long non-LTR retro transposon. LINE-1 retro transposon consists of a 900 bp 5′ untranslated region (UTR) containing an internal promoter; ORF1, encoding an RNA-binding protein; ORF2, encoding a large protein containing endonuclease, reverse transcriptase and possibly other functions, and a 3′ UTR (Figure 3B). In contrast to LTR retro transposons, the 3′ end of LINE-1 (and similar elements found in other host species) ends in a polyA tail ranging in size from a few nucleotides to ~100 bp long. LINE-1 and related elements lack not only LTRs, but any type of terminal repeats, suggesting a fundamentally different type of insertion mechanisms. Finally, the target site duplication length is variable rather than fixed in LINE-1 retro transposon.

Site-Specific Non-LTR Retrotransposons

Some non-LTR retro transposons such as the insect R1, R2, TRAS1, and SART1 elements are defined as site-specific retro transposons, because they have preferred target sites in the genome. For non-LTR retro transposons, the target site preference is usually defined by a specific host DNA sequence that is repetitive in nature and one that can be recognized and cleaved by the endonuclease encoded by each type of element. R1 and R2 elements target different sequences in ribosomal

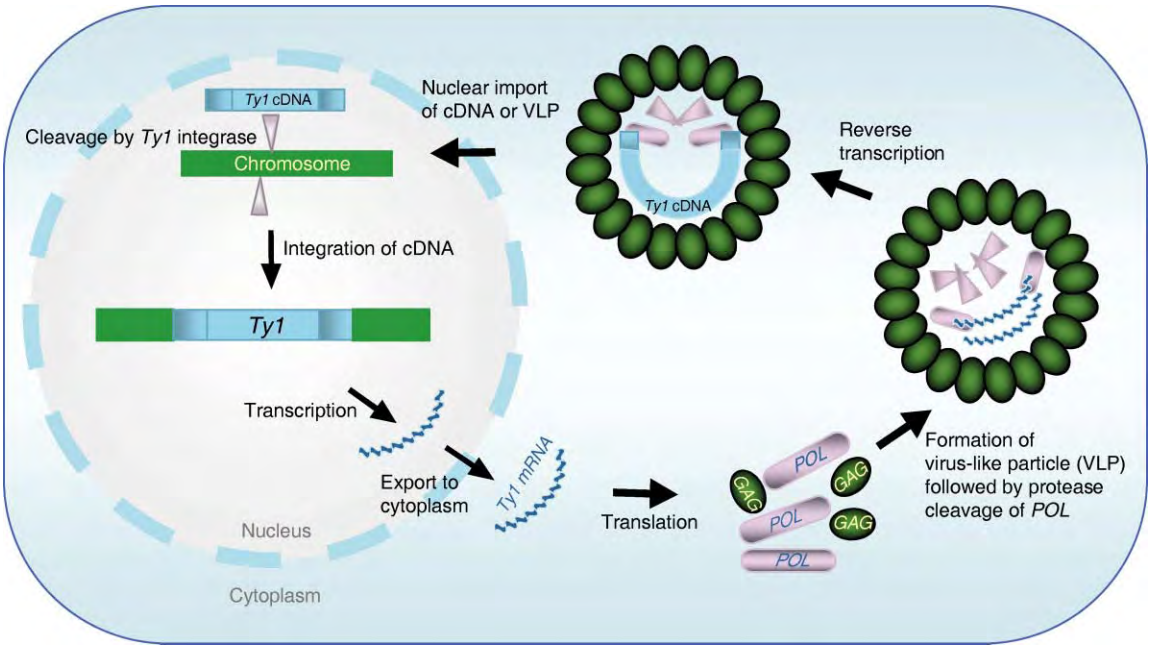

FIGURE 5 The life cycle of *Ty1*. The *Ty1* full length RNA is transcribed in the nucleus and exported to the cytoplasm, which leads to translation of Ty1 protein: *GAG* and *POL*. Full length *Ty1* RNA, together with *GAG* and *Ty1* reverse transcriptase and integrase, is then packaged into a virus-like particle (VLP). *Ty1* protease cleaves *POL* protein into the RT and IN peptides within the VLP. Reverse transcription most likely occurs within the VLP. The newly made *Ty1* cDNA is then imported into the nucleus, and with the help of integrase, which nicks the DNA at the target site, is inserted into a new chromosomal locus to create a new copy of the *Ty1* retrotransposon.

DNA (hundreds of copies per host genome) and TRAS and SART elements target opposite strands of the telomeric repeat sequence (present in hundreds to thousands of copies per host genome). Since the targets are repetitive in nature, such retro transposon insertions are unlikely to harm the host.

Alu Elements

Alu elements are ~300 nucleotide long interspersed elements found only in primate genomes, including the human genome. There are ~1.4 million copies of *Alu* in the human genome, comprising more than 10% of the human genome. Like LINE-1 elements, *Alu*s have 20–100 base pair long polyA tails. *Alu*s elements are too short to encode for proteins required for their transposition. *Alu*s most likely use the transposition machinery of LINE-1 for mobilization, as their 3′ end structures resemble those of LINE-1. Thus, *Alu*s are considered nonautonomous retrotransposons.

Significance

Retrotransposons Make up a Significant Portion of the Human Genome

DNA encodes genetic information required to specify an organism, however, surprisingly, only 2% of the human genome encodes for protein sequences. About 36% of the human genome is comprised of repetitive DNA, of which ~17% are LINE-1 retro transposons and 10% are *Alu* elements. About 8% are LTR elements, and the rest are DNA transposons or unclassified. The genome of multicellular organisms such as primates, fly, and worms contains a very high percentage of noncoding DNA, while the genome of unicellular organism such as yeast and bacteria has a higher percentage of coding DNA. This raises the question of why so much of our genome encodes DNA that does not seem to do anything obvious for the organism.

Are Retrotransposons Selfish DNA or are they One of the Shapers of our Genomes?

Transposon DNAs are often disparaged as junk or selfish DNA since it is not clear what they are doing in our genome. Transposons may have spread simply because they can multiply independently of the host genome. In this view, transposons are purely genomic parasites, selfish DNA that often has detrimental effects on the host. Deleterious insertions are removed from the host species by selection. Elements required for the survival of a species will be selected for. Transposons could play positive evolutionary roles by shaping the genome of host organisms, including our genome, serving as a source of plasticity. LINE-1 sequences sometimes move "chunks" of host genes around in the genome, shuffling gene segments to form new combinations. Their ability to transpose, copy, and rearrange DNA sequences allows the host opportunities to restructure their genome to survive and to adapt to a new environment. There is good evidence that transposons can spread because they confer selective advantages to the cells. Perhaps an organism's ability to evolve and compete effectively directly depends on the flexibility provided by "junk" DNA.

Transposons are Agents of Mutation

If left unchecked, in theory, transposons can colonize an entire genome. To survive, an organism needs to have mechanisms to down-regulate transposition. Full-length human LINE-1 RNA is expressed at very low levels. Worms apparently use RNA interference (RNAi) as one mechanism to defend their genome from transposon invasion by down-regulating transposon RNA expression. Other organisms including mammals may use similar mechanisms. Most of the time, transposons do not cause any detectable phenotypic changes. However, if a transposon inserts itself into coding regions, it can have detrimental effects on the host. There are examples of hemophilia A and other human diseases caused by insertion of LINE-1 sequences into human genes. In *Drosophila*, many spontaneous mutations with visible phenotypes result from insertions of transposable elements.

See Also the Following Article

Nonhomologous Recombination: Bacterial Transposons

Glossary

coding DNA DNA sequence that encodes for protein: the exons of mRNA.

host The organism in whose genome a transposon or retro transposon resides.

integrase A protein required for retro-transposition, in order to make a cleavage in the template DNA so that transposon can insert itself into a new chromosomal locus; analogous to transposase in DNA transposons.

noncoding DNA DNA sequence that does not encode for proteins or any functional RNAs. This includes the promoter element, introns and 3′ untranslated region of mRNAs as well as intergenic regions, which can be extensive.

protease An enzyme that recognizes specific amino acid sequences within a protein and cleaves the protein via hydrolysis of the peptide bonds.

retrotransposon Transposon that transposes via an RNA intermediate using reverse transcriptase.

reverse transcriptase A protein required for retro-transposition and retro-virus multiplication, which uses single stranded RNA as

template to make a double stranded DNA termed complementary DNA (cDNA).

RNA interference (RNAi) A mechanism used by eukaryotes to degrade mRNA via a double stranded RNA intermediate.

target site The DNA sequence in the host genome that the transposon inserts into.

target site duplication (TSD) A short host sequence flanking a transposon that was duplicated during the insertion process.

transposition Movement of a transposon to a new, nonhomologous target site.

transposon Segment of DNA that can move from one chromosomal locus to another locus on the same or different chromosomes within one cell without having any sequence homology to the insertion site.

Further Reading

Boeke, J. D., and Stoye, J. P. (1997). Retrotransposons, endogenous retroviruses, and the evolution of retroelements. In *Retroviruses* (J. M. Coffin, S. H. Hughes and H. E. Varmus, eds.) pp. 343–435. Cold Spring Harbor Laboratory Press, Plainview, NY.

Boeke, J. D., Garfinkel, D. J., Styles, C. A., and Fink, G. R. (1985). Ty elements transpose through an RNA intermediate. *Cell* **40**, 491–500.

Dewannieux, M., Esnault, C., and Heidmann, T. (2003). LINE-mediated retrotransposition of marked Alu sequences. *Nat. Genetics* **35**, 41–48.

Kazazian, Jr. H. H., Wong, C., Youssoufian, H., Scott, A. F., Phillips, D. G., and Antonarakis, S. E. (1988). Haemophilia A resulting from de novo insertion of L1 sequences represents a novel mechanism for mutation in man. *Nature* **332**, 164–166.

Moran, J. V., DeBerardinis, R. J., and Kazazian, Jr. H. H. (1999). Exon shuffling by L1 retrotransposition. *Science* **283**, 1530–1534.

Biography

Jef D. Boeke is a Professor of molecular biology and genetics, Professor of oncology, and Director of the High Throughput Biology Center at the Johns Hopkins University School of Medicine in Baltimore, Maryland. His principal research interests are in retro-transposition, chromatin structure, and yeast genetics and genomics. He holds a Ph.D. from the Rockefeller University and received his postdoctoral training at the Whitehead Institute at the Massachusetts Institute of Technology.

Siew Loon Ooi was a graduate student with Dr. Boeke.

Nuclear Compartmentalization

Kelly P. Smith and Jeanne B. Lawrence
University of Massachusetts Medical School, Worcester, Massachusetts, USA

The eukaryotic nucleus must somehow accommodate diverse tasks ranging from DNA replication to the selective transcription, processing, and transport of different classes of RNA, each requiring its distinct macromolecular machinery. On a gross morphological level the nucleus is composed of a bilayered nuclear envelope, separating the nuclear contents from the cytoplasm, the nucleolus, devoted largely to rRNA metabolism, and the nucleoplasm, which contains the bulk of the genome and the myriad factors essential to its maintenance, replication, and expression. It has now become evident that the nucleoplasm is further differentiated into a number of non-membrane bound "compartments" in which distinct subsets of macromolecules concentrate, presumably for a common function. Despite the significant amount of investigation into these compartments, their functions remain elusive and controversial. Although the list of nucleoplasmic compartments or bodies is incomplete, this article elucidates the current state of knowledge of the most studied of these nucleoplasmic structures, the splicing factor domains, PML nuclear bodies, Cajal bodies and Gemini of Cajal bodies.

Splicing Factor Compartments, "Speckles," or SC35 Domains

In the eukaryotic nucleus, the distribution of pre-mRNA splicing factors is not uniform, but is markedly concentrated at 20–40 sites, with lower levels of factors diffuse throughout the nucleoplasm (Figure 1). Variously referred to as "speckles," "SC35 domains," or "splicing factor compartments (SFCs)," these irregular but discrete domains are most frequently visualized with an antibody directed against the spliceosome assembly factor SC35. Each domain, 0.5–3.0 μm in diameter, corresponds largely, if not entirely, to ultrastructures termed interchromatin granule clusters (IGCs). In addition to spliceosome assembly factor SC35, these domains contain numerous splicing factors and SR proteins, as well as poly(A) RNA, poly(A) RNA-Binding Protein II, hyperphosphorylated RNA polymerase II, lamins, and factors implicated in RNA export. These components are also more diffusely distributed throughout the nucleus. Although the positions of the domains themselves are relatively immobile, they are dynamic structures in that factors within them are in rapid flux dependent upon their phosphorylation state. It is likely that ~150 different proteins localize, at least transiently, to these domains.

As they show relatively little label with uridine incorporation, one hypothesis is that they do not contain mRNA or pre-mRNA but are storage sites of excess splicing components. These components are then "recruited" to nearby active genes, where splicing occurs. However, several active genes have been shown to position directly at the periphery of domains, and RNAs from highly expressed genes have been found within them. The organization of these genes with domains is locus specific and cell-type specific. Evidence now suggests that most, if not all, splicing factor domains associate with numerous genes and contain mRNAs derived from them. The placement of specific genes near these concentrated domains of RNA metabolic factors suggests a specific nuclear organization to the gene relative to the domain which would facilitate the rapid reassembly and use of large RNA metabolic complexes for highly expressed and complex genes (see Figure 2).

PML Nuclear Bodies, ND10

Mammalian nuclei contain 10–30 spherical structures termed PML nuclear bodies (PML NBs) (also termed PODs, ND10 or Kremer bodies) (Figure 3). These 0.3–1 μm bodies were first observed by electron microscopy (EM) and later found to contain the PML protein. Interest in this nuclear body, and nuclear structure in general significantly increased with the discovery that the gene encoding PML is fused to the retinoic acid receptor gene in the t(15;17) translocation of acute promyelocytic leukemia (APL). The resulting PML-retinoic acid receptor fusion protein causes a breakdown of PML domains, a major hallmark of APL. PML bodies are also targeted by many DNA viruses in early infection, and are the site of viral transcription initiation. Subsequently, the viral early proteins localize to and eventually disrupt PML NBs.

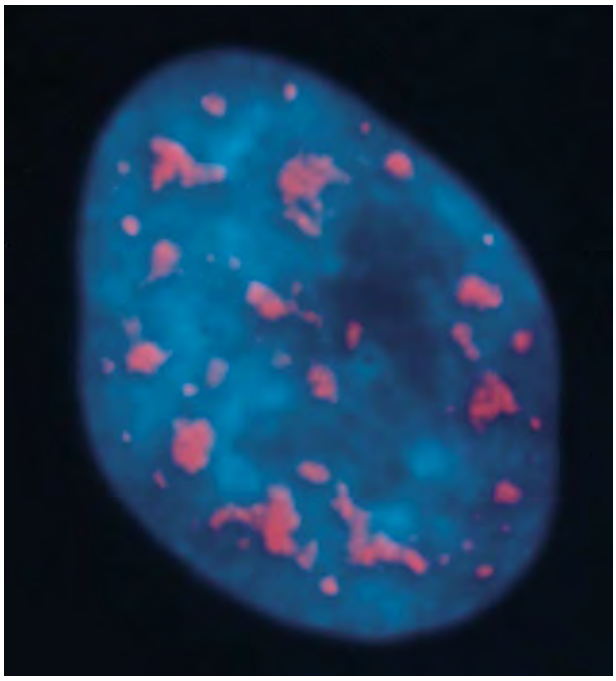

FIGURE 1 Splicing factor rich SC35 domains. Human fibroblast nucleus immunostained using an antibody to the spliceosome assembly factor SC35 (red). The nucleus is stained blue using the DNA stain 4′,6-diamidino-2-phenylindole (DAPI).

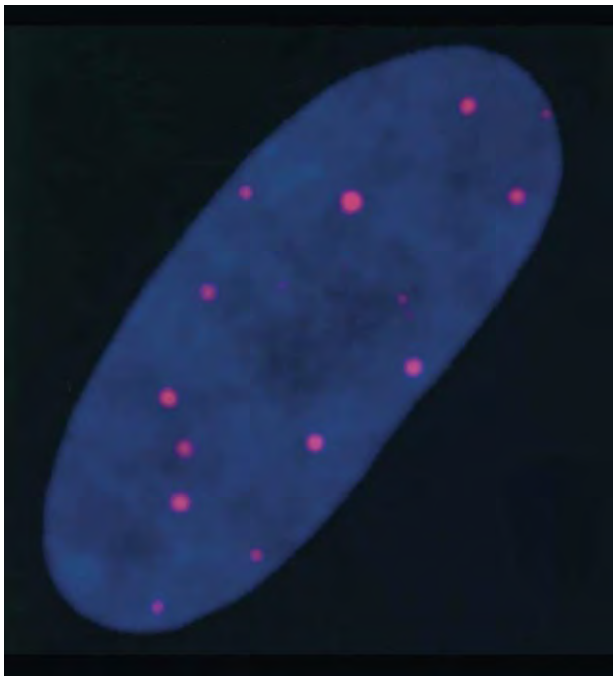

FIGURE 3 PML Nuclear Bodies. Human fibroblast nucleus stained with DAPI (blue) has numerous PML nuclear bodies visualized with an anti-PML antibody (red).

The lynchpin of the PML NB is the PML protein, essential for PML body formation. The PML protein occurs in numerous alternatively spliced isoforms and contains a RING finger, B-box coiled coil (RBCC) motif. This domain allows PML to interact with many of the PML NB proteins (Table I), as well as some proteins such as HDAC that are not concentrated in the PML body, some in an isoform specific manner. The PML NB proteins are involved in a number of different cellular processes including tumor suppression, growth control, apoptosis, immune response, and transcription regulation. A few of the over 40 proteins found within PML NBs are present under all conditions, but many others localize under a variety of conditions such as cell cycle and transient overexpression (see Table I). All of these factors are found at lower levels in the nucleoplasm in addition to the concentrations in PML NBs. Some proteins do not colocalize with all PML NBs or in all cell types, suggesting that different PML NBs may have distinct functions.

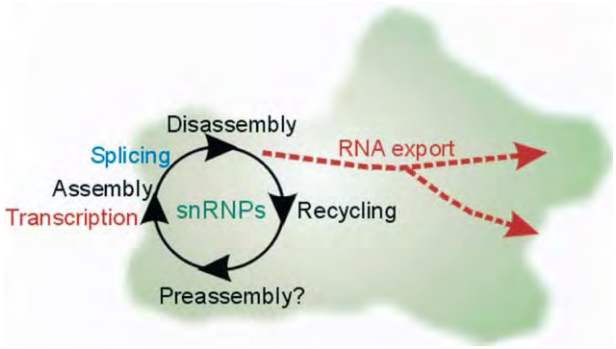

FIGURE 2 SC35 domain model. Domains may function by coupling the completion of mRNA maturation and release for mRNA export with the recycling/preassembly of factors. Because the RNA metabolic machinery requires interaction of such a large number of different factors, their concentration at a site would facilitate recycling and a rapid rate of reuse for expression of adjacent genes. Adapted from Johnson, C. V., Primorac, D., McKinstry, M., McNeil, J., Rowe, D., and Lawrence, J. B., (2000). Tracking COL1A1 RNA in osteogenesis imperfecta. Splice-defective transcripts initiate transport from the gene but are retained within the SC35 domain. *J. Cell Biol.* **150**, 417–431 with permission.

The sheer variety of proteins found in PML bodies has made attribution of a single function almost impossible. The dynamic and diverse nature of these bodies has led to the theory that PML NBs are "nuclear depots" in which numerous proteins are recruited and/or released in response to stimuli such as viral attack or other cell stress. Additionally, PML NBs could be sites for degradation of some nuclear proteins. However, PML NBs may also play a more specific, though indirect, role in transcription, by sequestration and/or modification of transcription factors. Recently, reports have asserted that PML NBs can associate with specific genes such as the p53 locus TP53. Other evidence suggests that, contrary to earlier reports, PML NBs contain newly synthesized RNA. These results are suggestive of a more direct role for PML NBs in gene expression.

TABLE I

Partial List of PML Nuclear Body Components

Component	Function	PML interaction[a]	Conditional association[b]
PML	Essential for NB formation; transcription activator? repressor?	Y	
Transcription			
pRB	Tumor suppressor, transcription factor	Y	Y
p53	Tumor suppressor, transcription factor	Y	Y
CBP	Histone acetylase	Y	Y
Daxx	Transcription regulation, apoptosis	Y	
Sp 100	Transcription factor		
Sp 140	Transcription factor		Y
Sp 110	Transcription factor		
Translation initiation			
eIF-4	Recruits ribosomes to mRNA	Y	Y
INT-6	Promotes ribosomes binding to mRNA		Y
Protein modification			
SUMO-1	Protein modifier	Y	
HAUSP	De-ubiquitination		Y
Ubiquitin	Protein modifier, not with all PML NBs		
Immune response			
PA28	Activates immunoproteasome		
ISG20	Exonuclease, antiviral activity		Y
DNA repair			
BLM	DNA helicase, genome stability		

[a] Factors known to interact with the PML protein.
[b] Factors shown to interact with PML NBs under certain conditions such as cell cycle or interferon treatment.

Cajal (Coiled) Bodies and Gems

First described in 1903 as nucleolar accessory bodies, the Cajal (coiled) bodies (CBs) are usually seen as roughly spherical 0.1–2.0 μM structures numbering one to five per nucleus (see Figure 4A), varying in number and size during the cell cycle and in different cell types. The Cajal bodies are not seen in all cells or tissues, but are especially prominent in highly proliferative cells such as cancer cells or metabolically active cells like neurons. The neuronal CBs, as originally identified, are not round nucleoplasmic bodies, but are found capping the nucleolus as seen in Figure 4B. This localization illustrates the close association between the nucleolus

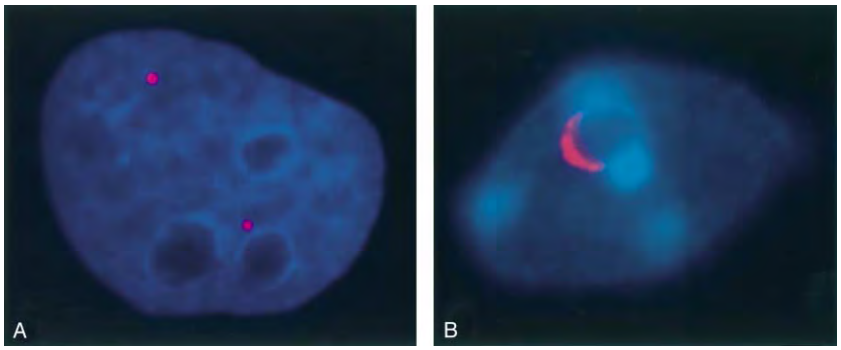

FIGURE 4 Heterogeneity of Cajal Bodies. Cajal bodies, seen using an anti-coilin antibody (red) can appear as round nucleoplasmic bodies in highly proliferative cultured cells like the cervical carcinoma cell HeLa (A) or can be found to cap the nucleolus in mouse brain neurons (B). DNA in nuclei is stained with DAPI.

and the CBs. Whether the CBs capping the nucleolus are functionally distinct from the nucleoplasmic bodies most often seen in cultured cells is unknown.

The coilin protein was first identified using human autoimmune serum and has become the marker most often used to visualize CBs. Although relatively little is known about the function of coilin, studies have indicated that it is the link between CBs and the nucleolus. In addition to coilin, numerous snRNAs and proteins of both nuclear and nucleolar origin are enriched in the CBs. These include factors involved in transcription and/or processing of mRNAs, snRNAs, histone mRNAs, and rRNA (see Table II). CBs have been shown to spatially associate with several U snRNA and histone gene loci, all of which have unusual 3′ processing, suggesting that CBs could have relationship to expression and nuclear metabolism of specific types of RNAs. The CBs contain U7RNA involved in histone RNA processing and have been shown to contain pre-U2RNA, implicating them in snRNA modification or transport. More recent studies have found small Cajal body-specific RNAs (scaRNAs) which catalyze the methylation and pseudouridylation of snRNAs within Cajal bodies.

Like PML bodies, recent work has linked loss of CBs to leukemia. ELL is an RNA polymerase II (pol II) transcriptional elongation factor that interacts with a protein called EAF1. Both ELL and EAF1 are components of Cajal bodies. In acute myeloid leukemia, the (11;19) (q23;p13.1) translocation results in the formation of a chimeric MLL-ELL fusion protein. This fusion mislocalizes ELL and causes the disruption of the Cajal bodies in leukemic cells. The role of ELL in CB formation is unknown.

TABLE II

Reported Coiled Body Components

Component	Function
p80-coilin	Shuttling protein? Interacts with many CB components
mRNA splicing factors	
snRNAs	
U1, U2, U4, U5, U6	General pre-mRNA splicing
U11, U12	Splicing of minor class of introns
U7	3′ processing of histone pre-mRNAs
Sm core proteins	pre-mRNA splicing
U2AF	Splice site selection
SART3/p110	snRNP reassembly after splicing
snRNA modification	
scaRNAs: U85 U93	Modification of spliceosomal snRNAs
Nucleolar factors	
Fibrillarin	rRNA processing, pre-rRNA modification
Nopp 140	Transcription regulation? Nucleolus-cytoplasmic shuttling
Ribosomal protein S6	Ribosome function
Gar1p	pre-rRNA processing
NAP 57	rRNA processing, ribosome assembly
snoRNAs	
U3	Processing of pre-18S ribosomal RNA
U8	Cleavage of pre-rRNA to 5.8S and 28S rRNAs
Transcription factors	
ELL, EAF1	RNA pol II transcription elongation factors
cdk7, cyclin H, MAT1, p62	Subunits of general transcription factor TFIIH
p220(NPAT)	Histone gene transcription factor
PTF	snRNA transcription factor

SMN "Gems" and CBs

Modification of snRNAs may not be the sole function of CBs. The disease Spinal Muscular Atrophy results from deletion of a gene encoding the "survival of *m*otor *n*euron" (SMN) protein. This protein is consistently enriched in foci termed SMN gemini of Cajal bodies (gems), since in the cell line in which they were discovered, gems were often very closely associated or even coincident with CBs (see Figure 5A). However, subsequently in many cultured cells studied, SMN and coilin staining appear to be coincident in CBs (Figure 5B). The SMN protein complexes with a number of other factors, termed gemins. Currently there are six identified geminus, 2–7, in this complex. The SMN complex has been implicated in snRNP assembly, supporting the idea that gems and CBs may be involved in the recycling and/or biogenesis of splicing factors. An extension of this hypothesis is that CBs are sites of preassembly of pols I, II, and III transcription/RNA processing complexes or "transcriptosomes."

The Compartmentalized Nucleus

While this article has focused on some of the most-studied non-nucleolar compartments in the nucleus, there is evidence for the existence of numerous other compartments about which little is known. These include the perinucleolar compartment, Sam68 bodies, cleavage bodies, paraspeckles, and OPT domains. In addition to these compartments, some portions of the genome can form dense, transcriptionally inert regions in the nucleus, often referred to as the heterochromatic compartment. While the nuclear compartments described here all have different components and seemingly different functions, they all do seem to have certain traits in common. First, they are all dynamic structures, varying in composition in different conditions. Additionally, they all appear to associate with specific gene loci. Lastly, PML bodies, CBs, and splicing

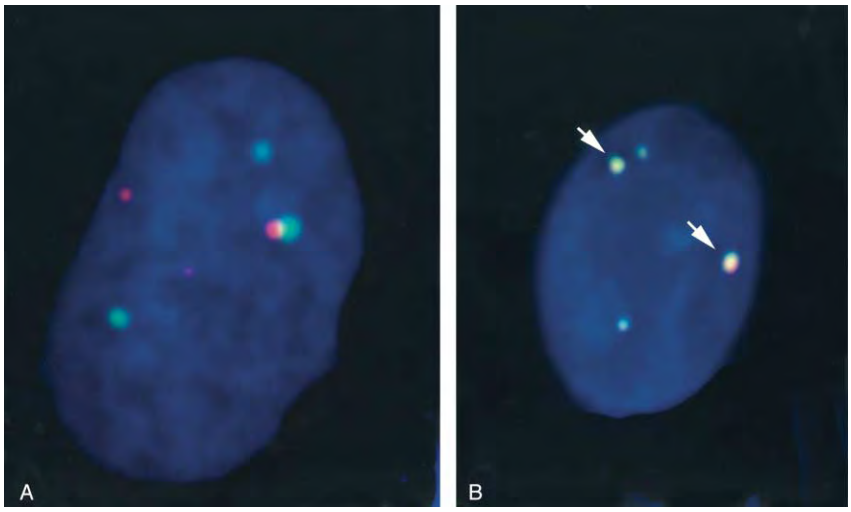

FIGURE 5 SMN gems differ in their association with CBs. By dual staining with anti-SMN antibody (red) and anti-coilin antibody (green), we see that SMN gems are separate from, but often associated with, CBs in some cells such as HeLa (A), but are most often found to be completely coincident with CBs (arrows) as seen in the breast cancer cell HCC1937 (B). Nuclei are stained with DAPI.

factor compartments appear to associate with one another. These commonalities reveal a compartmentalized, functionally integrated nucleus.

See Also the Following Articles

Chromosome Organization and Structure, Overview • mRNA Polyadenylation in Eukaryotes • Nuclear Envelope and Lamins • Nuclear Organization, Chromatin Structure, and Gene Silencing • Nucleolus, Overview

Glossary

Cajal bodies Spherical nuclear bodies (1–5/nucleus) enriched in mRNA, rRNA, and snRNA processing factors.

nuclear compartment A non-membrane-bound subnuclear structure in which a variety of factors accumulate to facilitate specific nuclear processes.

nucleus A membrane-bound cellular structure containing DNA which controls the cell's growth, metabolism, and replication.

PML nuclear bodies Spherical nuclear structures (10–30/nucleus) rich in a variety of factors, many of which are involved in transcription regulation.

SC35 domains 20–40 irregular "speckles" in the nucleus in which numerous factors required for mRNA metabolism accumulate.

SMN gems Nuclear bodies enriched in survival of motor neurons (SMN) protein and other factors involved in snRNP assembly. Gems often associate or coincide with Cajal bodies.

Further Reading

Borden, K. L. (2002). Pondering the promyelocytic leukemia protein (PML) puzzle: Possible functions for PML nuclear bodies. *Mol. Cell Biol.* **22**, 5259–5269.

Gall, J. G. (2000). Cajal bodies: The first 100 years. *Annu. Rev. Cell Develop. Biol.* **16**, 273–300.

Jady, B. E., Darzacq, X., Tucker, K. E., Matera, A. G., Bertrand, E., and Kiss, T. (2003). Modification of Sm small nuclear RNAs occurs in the nucleoplasmic Cajal body following import from the cytoplasm. *EMBO J.* **22**, 1878–1888.

Johnson, C. V., Primorac, D., McKinstry, M., McNeil, J., Rowe, D., and Lawrence, J. B. (2000). Tracking COL1A1 RNA in osteogenesis imperfecta. Splice-defective transcripts initiate transport from the gene but are retained within the SC35 domain. *J. Cell Biol.* **150**, 417–431.

Meister, G., Eggert, C., Fischer, U. (2002). SMN-mediated assembly of RNPs: A complex story. *Trends Cell Biol.* **12**, 472–478.

Misteli, T. (2000). Cell biology of transcription and pre-mRNA splicing: nuclear architecture meets nuclear function. *J. Cell Sci.* **113**, 1841–1849.

Negorev, D., and Maul, G. G. (2001). Cellular proteins localized at and interacting within ND10/PML nuclear bodies/PODs suggest functions of a nuclear depot. *Oncogene* **20**, 7234–7242.

Polak, P. E., Simone, F., Kaberlein, J. J., Luo, R. T., and Thirman, M. J. (2003). ELL and EAF1 are Cajal body components that are disrupted in MLL-ELL leukemia. *Mol. Biol. Cell* **14**, 1517–1528.

Zhong, S., Salomon, P., and Pandolfi, P. P. (2000). The transcriptional role of PML and the nuclear body. *Nat. Cell Biol.* **2**, E85–E90.

Biography

Jeanne B. Lawrence is a Professor of Cell Biology at the University of Massachusetts Medical School in Worcester, Massachusetts. Her research interests bridge the basic cell and developmental biology of nuclear organization with human genetics. She holds an M.S. in Human Genetics and Genetic Counseling from Rutgers University and a Ph.D. in Developmental Biology from Brown University. Dr. Lawrence is a pioneer in the development of fluorescence *in situ* hybridization technology for detection of individual genes and nuclear RNAs.

Nuclear Envelope and Lamins

Bryce M. Paschal
University of Virginia, Charlottesville, Virginia, USA

The nucleus is a prominent cytological feature of eukaryotic cells that is enclosed within a specialized double membrane termed the nuclear envelope. Because of this arrangement, the nuclear envelope provides a physical boundary that separates nuclear processes such as DNA replication and RNA synthesis from cytoplasmic processes such as protein synthesis. Other important functions of the nuclear envelope are mediated by macromolecular structures that are physically integrated into the membrane. Nuclear pore complexes, which are elaborate channels that span the double membrane, provide the passages for transport between the nucleus and the cytoplasm. The nuclear lamina, a meshwork of proteins just beneath the membrane, acts as a scaffold that contributes to nuclear architecture and to the regulation of gene expression. The importance of the nuclear lamina in human biology is underscored by the discoveries of genetic disorders that are caused by mutations in lamina proteins.

Structure of the Nuclear Envelope

The first descriptions of the nuclear envelope were provided by 19th century biologists, notably Fleming, who used light microscopy to examine the nuclei of plants and protozoa. A century later, the application of electron microscopy to the analysis of a variety of intracellular organelles revealed the unique structure and organization of the nuclear envelope. The nuclear envelope consists of two membranes, an inner membrane and an outer membrane, each of which is a bilayer of lipids and proteins (Figure 1). The intermembrane space, or lumen, is a site of calcium storage in the cell, and special channels in the membrane facilitate calcium release and re-uptake upon physiological stimulation. Since the outer nuclear membrane is continuous with the rough endoplasmic reticulum membrane, there is continuity between the lumen of the nuclear envelope and the rough endoplasmic reticulum.

Structure of the Nuclear Lamina

In 1966, Fawcett published a seminal electron microscopy study showing the presence of a "fibrous lamina on the inner aspect of the nuclear envelope" in several cell types. The organization of the lamina as a meshwork of 10 nm diameter filaments adjacent to the inner nuclear membrane was later revealed in samples prepared from frog oocyte nuclei (Figure 1).

Composition of the Lamina

The development of biochemical procedures for isolating nuclei from cells and for preparing the lamina-nuclear pore complex fraction from nuclei set the stage for identifying proteins that comprise the lamina.

Lamins

The major proteins of the nuclear lamina, termed lamins, are members of the intermediate filament protein superfamily. The molecular weights of lamins range from 60–70 kDa depending on the isoform, and all lamins have related primary and secondary structures. The amino- and carboxyl-terminal domains of lamins are globular, the latter encoding a nuclear localization signal. Like other members of the intermediate filament superfamily, lamin proteins contain a central rod domain composed of four α-helical segments that mediate coiled-coil interactions resulting in the formation of lamin dimers (Figure 2). Lamin dimers assemble into tetramers, which, in turn, assemble into 10 nm diameter filaments that comprise the nuclear lamina. The approximately orthogonal arrangement of lamin filaments observed by electron microscopy implies the presence of proteins that mediate inter-filament crosslinks, however, the proteins and interactions that establish and maintain this higher order structure have not yet been identified.

Lamin Genes

Lamins are classified as A-type and B-type. The B-type lamins are expressed in most cell types, whereas A-type lamins, which include lamin C, are generally expressed in differentiated tissues. There is a single lamin A gene (*LMNA*) in mammals that, through alternative

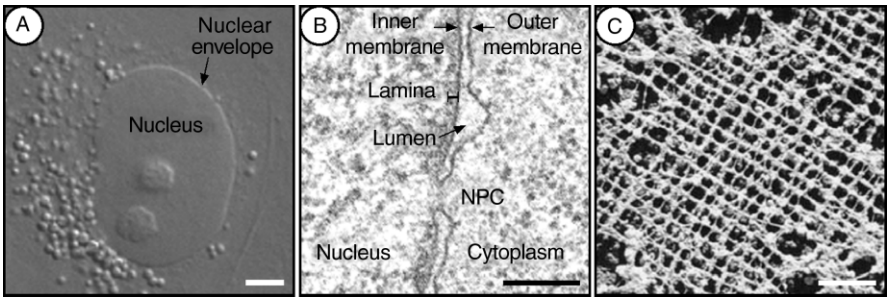

FIGURE 1 The nuclear membrane viewed by light and electron microscopy. (A) Differential interference contrast microscopy of a cell showing the nuclear envelope (scale bar, 5 μm). (B) Thin section electron microscopy showing a small region of the nuclear envelope and associated structures (scale bar, 0.2 μm). (C) Metal-shadowed nuclear lamina from a frog oocyte viewed by electron microscopy (scale bar, 0.5 μm). (Part (C) is modified from Aebi, U., Cohn, J., Buhle, L., and Gerace, L. (1986). The nuclear lamina is a meshwork of intermediate-type filaments. *Nature* **323**, 560–564.

splicing, produces transcripts for two lamin A isoforms and two lamin C isoforms. There are two lamin B genes (*LMNB1* and *LMNB2*) that together encode three lamin isoforms. The phylogenetic distribution of lamins extends to invertebrates, but lamins are absent from plants and fungi.

Lamin-Associated Proteins

A group of integral membrane proteins, which are unique to the inner nuclear membrane, bind directly to nuclear lamins and play critical roles in modulating lamina structure and function. This group includes LAP2, Emerin, Man1, and LBR. These proteins are anchored in the inner nuclear membrane by hydrophobic, membrane-spanning segments, while the rest of the protein projects into the nucleoplasm, where it contacts the lamina. Lamin-associated proteins also interact with DNA-binding proteins such as BAF and GCL that mediate chromatin-attachment to the nuclear membrane.

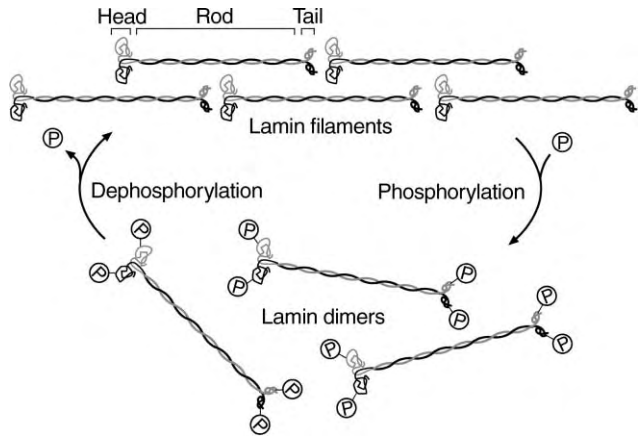

FIGURE 2 Structure of the nuclear lamina is regulated by phosphorylation. Lamin filaments undergo phosphorylation by kinases in mitosis, causing disassembly into lamin dimers. At the end of mitosis, the lamins are dephosphorylated by phosphatases, which return the lamins to an assembly competent state.

Functions of the Lamina

The nuclear lamina performs both structural and regulatory functions. These functions are not mutually exclusive, since alterations in structure can change the capacity of the nuclear lamina to regulate nuclear functions. Characterization of the regulatory functions of the nuclear lamina is a relatively recent area of investigation, and this knowledge base should expand dramatically in the next several years.

Nuclear Envelope Assembly after Mitosis

Disassembly of the nuclear envelope and lamina occurs at prometaphase, a period of the mitotic cell cycle that precedes chromosome segregation. The nuclear envelope fragments into membrane vesicles, and the lamin filaments are disassembled into lamin dimers. Near the end of mitosis in late anaphase, the nuclear envelope-derived vesicles and lamin proteins are reassembled around the chromosomes of the two new daughter cells. The reassembly pathway involves multiple steps, beginning with the binding of lamins and vesicles to the surface of chromosomes. The vesicles then fuse to generate membranes. The incorporation of lamins into the lamina continues after membrane formation by virtue of nuclear import of lamins through newly formed nuclear pore complexes.

Nuclear Size

Experimental manipulation of the nuclear reassembly pathway has shown that lamins and lamina-associated proteins are necessary for the several-fold increase in volume of the nucleus during the cell cycle. The lamina is, therefore, a critical regulator of nuclear size.

Nuclear Shape and Rigidity

The lamina forms a cage-like structure within the nucleus and is tethered to the inner nuclear membrane. As such, the lamina plays a major role in defining nuclear shape. A striking example of how lamins determine the shape of the nucleus is lamin B3, a lamin isoform that was shown by Furukawa and Hotta in 1993 to be responsible for the unusual hook-shape of nuclei in spermatocytes. The lamina also provides rigidity that resists deformation and aids in restoration of shape following deformation. Nuclei from the nematode *Caenorhabditis elegans,* rendered lamin-deficient, show little resistance to deformation, and a failure to restore nuclear shape.

Positioning of Nuclear Pore Complexes

Nuclear pore complexes span both the inner and outer nuclear membranes. Integration of nuclear pore complexes into the membrane is mediated by GP210, an integral membrane protein. The relative spacing of nuclear pore complexes in the two-dimensional plane of the nuclear envelope is maintained by the nuclear lamina. B-type lamins mediate this spacing through direct interactions with nuclear pore complexes. Loss of this functionality results in a failure to maintain the proper distribution of nuclear pore complexes in the nuclear envelope.

Regulation of Gene Expression

Lamins can have a positive or negative influence on gene expression, depending on the context. Lamins and lamina-associated proteins bind to chromatin, resulting in the attachment of a subset of chromatin to the inner nuclear membrane which can be observed by microscopy. Because there is a strong correlation between localization of chromatin at the nuclear periphery and gene silencing, the nuclear lamina has historically been viewed as a scaffold for anchoring transcriptionally inactive heterochromatin. Lamin B is highly concentrated at the inner nuclear membrane, and, together with several DNA-binding proteins that repress transcription, mediates the negative influence on transcription at the nuclear periphery. In contrast, it has been shown that lamin A can turn on expression of muscle-specific genes, a clear indication of positive effects on transcription. Lamin A is found at both the inner nuclear membrane and throughout the nucleoplasm, and the latter pool is thought to promote transcription. Thus, whether lamins influence transcription positively or negatively is dependent on the particular lamin protein, and its subnuclear distribution.

Regulation of DNA Replication

Lamins play an important role in DNA replication by facilitating the recruitment of proteins needed for initiation of replication. The original link between lamins and DNA replication was made by Newport and colleagues in 1990, using a system that reconstitutes nuclear assembly *in vitro*. Depletion of lamin B from the system resulted in small nuclei that failed to initiate DNA synthesis. Subsequent experiments have implicated lamina-associated proteins in DNA replication as well.

Posttranslational Modification of the Lamina

The lamin proteins are subject to modifications that profoundly affect function.

Phosphorylation

Gerace and Blobel showed in 1980 that phosphorylation is used as a molecular switch to control the assembly properties of lamins. Disassembly of lamin filaments at prometaphase is driven by lamin phosphorylation (Figure 2). Lamin disassembly occurs specifically at prometaphase because the kinase that mediates lamin phosphorylation is activated during the mitotic phase of the cell cycle. The phosphorylated lamins are subsequently dephosphorylated by phosphatases, rendering them competent for reassembly into filaments in late anaphase and telophase.

Isoprenylation

A cysteine-containing motif in the carboxyl terminus of lamin B, called a CaaX box, is the site for attachment of an isoprenyl group. This lipid moiety inserts into the inner nuclear membrane, and mediates the stable membrane attachment of lamin B. During mitosis, lamin B remains stably associated with nuclear-envelope-derived vesicles. The isoprenylated carboxyl terminus is cleaved from Lamin A, and Lamin C protein lacks this modification altogether because the CaaX box is not encoded in Lamin C transcripts.

Proteolysis

Lamins are regulated by proteolysis in two functionally distinct pathways. After translation, the carboxyl-terminal 18 amino acids of lamin A are removed by proteolytic cleavage. This cleavage reaction removes the site of isoprenylation and the capacity of lamin A to associate directly with membranes.

During apoptosis, lamins are cleaved by a group of proteases called caspases. Lamin cleavage is a critical step in disassembly and fragmentation of the nucleus, and is commonly used as a biochemical indicator of apoptosis.

Lamins in Human Disease

Certain mutations in lamin A, or in the lamin-associated protein Emerin, cause Emery-Dreifuss muscular dystrophy. Patients display tendon contractures, degeneration of skeletal muscle, and electrical conduction problems in cardiac muscle. Lamin A mutations are also linked to familial partial lipodystrophy, which causes partial loss of fat tissue and late-onset insulin-resistant diabetes. These and other human disorders caused by mutations in the lamin A gene are referred to as laminopathies.

The clinical severity of a particular lamin A mutation often varies, even among members of a given family. This indicates that penetrance of the phenotype can be highly dependent on the genetic background. A major unanswered question is how laminopathies are manifest in specific tissues since lamins are expressed in all cell types. Currently there are two hypotheses addressing the tissue-specific basis of laminopathies. The structural hypothesis proposes that muscular dystrophies result from fragile nuclei that are susceptible to muscle contraction-induced physical damage. The gene expression hypothesis is based on the concept that lamin deficiencies alter nuclear architecture in a manner that changes the pattern of gene expression.

See Also the Following Articles

Chromatin: Physical Organization • Imaging Methods • Metaphase Chromosome • Mitosis • Nuclear Pores and Nuclear Import/Export

Glossary

chromatin Complex of DNA, histones, and nonhistone proteins contained within the nucleus of eukaryotic cells. Heterochromatin is transcriptionally inactive.

electron microscopy A type of microscopy that resolves fine structural details of cells by using a focused beam of electrons to penetrate the specimen.

integral membrane protein Membrane-bound protein containing one or more regions that span the hydrophobic core of the phospholipid bilayer.

lamina Fibrous network of lamins and associated proteins on the inner surface of the nuclear envelope. Lamins are not related to extra-cellular proteins laminins.

nuclear envelope Double membrane structure that surrounds the nucleus.

nuclear pore complex Specialized channels that span the nuclear envelope which are responsible for bidirectional transport of macromolecules between the nucleus and the cytoplasm.

Further Reading

Aebi, U., Cohn, J., Buhle, L., and Gerace, L. (1986). The nuclear lamina is a meshwork of intermediate-type filaments. *Nature* **323**, 560–564.

Burke, B., and Stewart, C. (2002). Life at the edge: The nuclear envelope and human disease. *Nat. Rev. Molecul. Cell Biol.* **3**, 575–585.

Hutchison, C. J. (2002). Lamins: Building blocks or regulators of gene expression? *Nat. Rev. Molecul. Cell Biol.* **3**, 848–858.

Pollard, T. D., and Earnshaw, W. C. (2002). *Cell Biology.* Saunders Press, Philadelphia.

Biography

Bryce M. Paschal is an Associate Professor of Biochemistry and Molecular Genetics in the Center for Cell Signaling at the University of Virginia in Charlottesville. His principal research interests are the mechanisms of transport through the nuclear pore complex. He holds a Ph.D. from the University of Massachusetts Medical School and received his postdoctoral training at The Scripps Research Institute in La Jolla, California. Using biochemical and cell biological approaches, Dr. Paschal has identified several proteins that play major roles in intracellular transport.

Nuclear Factor kappaB

Thomas D. Gilmore
Boston University, Boston, Massachusetts, USA

Nuclear factor kappaB (NFκB) is a family of structurally related DNA-binding proteins that act as transcription factors to regulate the expression of a wide variety of genes involved in many key cellular and organismal processes. The discovery of mammalian NFκB is generally attributed to Ranjan Sen and David Baltimore, who were studying the regulation of expression of a specific immunoglobulin gene; however, it is now clear that earlier researchers studying a viral oncoprotein (v-Rel) and a protein (Dorsal) required for the establishment of *Drosophila* embryonic polarity were also studying an NFκB activity. This entry focuses primarily on the vertebrate NFκB system, although most of the discussion is also applicable to the NFκB system in insects. NFκB activity is controlled by a multicomponent signal transduction pathway, such that in most cells. NFκB is inactive until any of several inducers initiates the signaling pathway that ultimately activates NFκB as a nuclear, DNA-binding protein. Misregulation of NFκB activity has been implicated in a number of human diseases, including several chronic inflammatory diseases and cancer, and the NFκB pathway is modulated by or used by several viruses as part of their pathology or replication. As such, the NFκB pathway is the subject of intense focus for pharmacological intervention.

NFκB Proteins and Protein Structure

The nuclear factor kappaB (NFκB) family is comprised of several evolutionarily conserved proteins that are related through a domain, usually called the Rel homology domain (RHD), which has sequences required for DNA binding, dimerization, and nuclear localization (Figure 1A). In *Drosophila*, there are three known NFκB proteins (Dorsal, Dif, and Relish), whereas in vertebrates, the NFκB protein family is comprised of five proteins: p50/p105, p52/p100, c-Rel, RelA (also called p65), and RelB. There is also an avian retroviral oncoprotein, v-Rel, that is a member of this family. All NFκB proteins contain the ~300 amino acid RHD towards their N termini; however, NFκB proteins can be subdivided into two distinct groups based on sequences C terminal to the RHD. One group (including p50/p105, p52/p100, and Relish) contains C-terminal sequences that fold back to inhibit the RHD, and thus these C-terminal sequences must be removed to release the active DNA-binding protein (i.e., p50 or p52 from the precursors p105 and p100, respectively). A second group (c-Rel, RelA, RelB, Dorsal, Dif) contains C-terminal sequences that are not cleaved and that activate transcription.

NFκB proteins bind to 9–10 bp DNA sites, usually called κB sites, located in the regulatory regions of many cellular and viral promoters. To bind DNA, NFκB proteins must form dimers. These dimers can, with few exceptions, be any combination of homodimer or heterodimer, although the most common NFκB dimer in many cells is a p50–RelA dimer (Figure 1B). The affinity of the various NFκB subunits for one another and the affinity of the various dimers for specific target DNA sites can vary greatly. These considerations provide an array of diversity in the NFκB dimers that are found in different cells, in the DNA sites that can be recognized by different NFκB dimers, and in the genes (and consequently cellular responses) that these dimers regulate.

Regulation of NFκB Activity

In most cells, NFκB is present in the cytoplasm in an inactive state, due to interaction with a family of inhibitor proteins, termed inhibitor of κB (IκB) proteins. IκB proteins include IκBα, IκBβ, IκBϵ, Bcl-3, and the C-terminal sequences of the NFκB precursor proteins p105 and p100. Through a series of ~30 amino acid repeats (called ankyrin repeats), a single IκB protein binds directly to sequences in the RHD of an NFκB dimer. Binding of an IκB to NFκB inhibits the activity of the dimer in two ways: it causes NFκB to be in the cytoplasm and it blocks NFκB DNA binding.

A variety of inducers (Table I), including many cytokines, cell stress, and viral or bacterial infections, can activate NFκB. In almost all cases, NFκB activity is induced through activation of a cellular kinase complex called IκB kinase (IKK). IKK is composed of three subunits: two related kinases (IKKα and IKKβ) and a

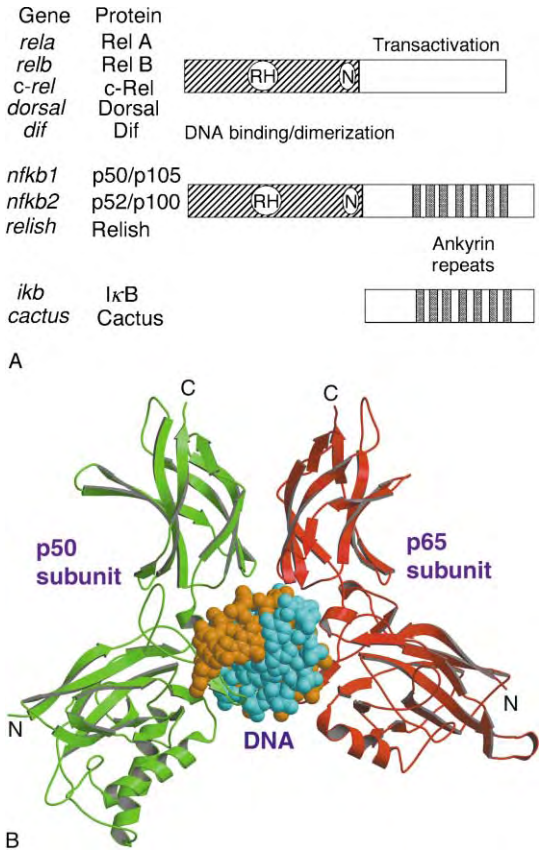

FIGURE 1 NFκB proteins. (A) Shown are the generalized structures, protein names, and genes encoding the two classes of NFκB proteins and the IκB proteins. RH, Rel Homology domain; N, nuclear localization signal; vertical bars, ankyrin repeats. (B) X-ray crystal structure of the NFκB p50–RelA (p65) dimer on DNA. N, N terminus; C, C terminus. Figure provided courtesy of Gourisankar Ghosh.

sensing or scaffold protein called IKKγ. Activation of the IKK complex generally requires phosphorylation of residues in the activation loop of the IKKα or IKKβ kinase, and probably also phosphorylation of IKKγ. Activated IKK then phosphorylates the IκB protein, which in turn signals the IκB sequences for degradation by the ubiquitin–proteasome pathway. The liberated NFκB complex can then enter the nucleus, bind to DNA, and activate specific target gene expression. In many cases, activation of NFκB is transient (perhaps lasting no more than 30 min) primarily because one of the target genes for NFκB is the gene encoding IκB. Therefore, newly synthesized IκB can cause NFκB to be resequestered in an inactive form in the cytoplasm, thus returning the pathway to its original state.

Although the overall pathway of activation is similar (as in Figure 2), there are actually two distinct pathways to activation of NFκB, depending on the nature of the IκB protein and IKK involved. In one pathway, a separate IκB molecule, such as IκBα bound to p50–RelA, is phosphorylated by the IKKβ subunit, which leads to the complete proteolysis of IκBα. In a second activation pathway involving a complex such as p100–RelB, a C-terminal site in p100 is phosphorylated by IKKα, which then leads to the partial proteolysis of the C-terminal ankyrin repeat sequences of p100, ultimately yielding an active p52–RelB dimer, which can also translocate to the nucleus to regulate gene expression.

However, a variety of recent evidence suggests that the NFκB pathway is regulated by mechanisms in addition to interaction with IκB proteins. For example, NFκB proteins can undergo posttranslational modifications

TABLE I

Some Inducers of NFκB Activity

General category	Examples
Bacteria	*Salmonella*, *Staphylococcus*, Lipopolysaccharide
Viruses	HTLV-1, Epstein–Barr virus, hepatitis B virus
Cytokines	Interleukins, tumor necrosis factor
Oxidative stress	Hydrogen peroxide, reperfusion ischemia
Growth factors/ hormones	Platelet-derived growth factor, epidermal growth factor, insulin, transforming growth factor
Drugs	Various chemotherapeutic agents

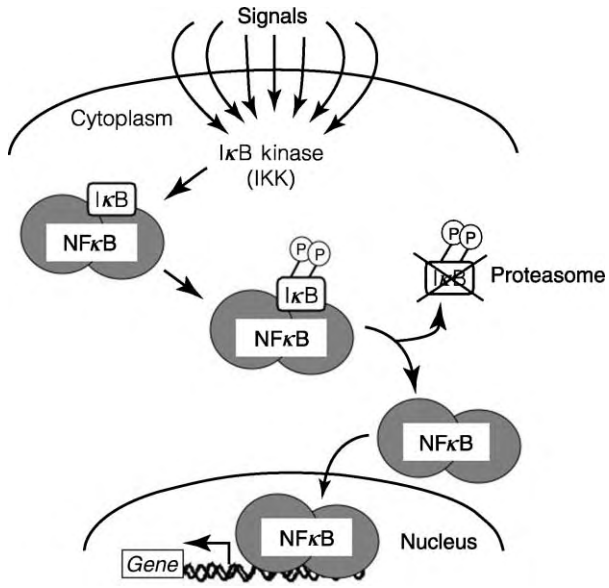

FIGURE 2 The NFκB signal transduction pathway. Under most circumstances, NFκB dimers (e.g., p50–RelA) are located in the cytoplasm of cells bound to inhibitory IκB proteins. Upon receiving an inducing signal, an IκB kinase (IKK) is activated. Active IKK phosphorylates IκB, and phosphorylated IκB then serves as a substrate for the ubiquitin–proteasome degradation pathway. Free NFκB can then enter the nucleus to increase or decrease specific target gene transcription. The system is eventually returned to its resting state through an auto-regulatory system, in that NFκB turns on expression of the gene encoding IκB, and newly synthesized IκB then resequesters NFκB in the cytoplasm.

(such as phosphorylation and acetylation) that affect their activity, they can interact with a variety of other proteins (including many other transcription factors), and the IKK proteins may also have effects on chromatin-binding proteins to affect gene expression from κB site-containing promoters.

Genes and Biological Processes Regulated by NFκB

Normal Biological Roles for NFκB

There are over 300 genes whose transcription is known to be regulated by NFκB activity, and these genes are involved in a multitude of biological processes (Table II). However, a variety of genetic and cellular studies have established that one of the key roles of NFκB is in regulating the innate immune response. In *Drosophila*, the activities of Dorsal, Dif, and Relish are induced to enter the nucleus by bacterial and fungal pathogens. These fly NFκB proteins then bind upstream and increase the expression of a family of genes called cecropins, which encode antifungal and antibacterial peptides. In mammals, it is also clear that many genes that encode antibacterial peptides, cytokines, and interferons are rapidly induced after infection with various pathogens. Moreover, mice in which individual genes for c-Rel, RelB, p50, and p52 are disrupted ("knockout mice") have severe defects in T- and B-cell-mediated immune responses. For example, c-*rel* knockout mice have B cells with greatly reduced survival and proliferation in response to antigen stimulation.

NFκB proteins are, however, also involved in the control of several other genes and processes that are not directly related to immunity. These include certain developmental processes, apoptosis, cell growth, and cell stress. In terms of development, NFκB activity (as directed by Dorsal) is required for the proper establishment of dorsal-ventral polarity in the early *Drosophila* embryo. In mammals, NFκB activity appears to be involved in proper limb development, due to the regulation of a gene called *Twist*.

NFκB transcription factors also regulate cell survival in many contexts, either by promoting or, more often, by inhibiting apoptosis. For example, RelA is required to protect liver cells from apoptosis induced by tumor necrosis factor, and RelA knockout mice die embryonically due to massive liver degeneration. Thus, the genes encoding several inhibitors of apoptosis are activated by NFκB.

TABLE II

Some Biological Processes and Relevant Genes Regulated by NFκB

Biological process	Relevant NFκB target genes
Angiogenesis	Vascular endothelial growth factor (VEGF)
Apoptosis	Bcl-X1, Bfl/A1, Bcl-2, IAP, TRAF, Fas
Cell adhesion	ICAM-1, VCAM-1
Cell growth	Cyclin D1, c-Myc
Stress	Cyclooxygenase, superoxide dismutase, nitric oxide synthetase
Innate immunity	Interleukins, interferon, tumor necrosis factor
Viral promoters	HIV-1, cytomegalovirus

NFκB and Disease

Aberrant NFκB activity has been implicated in several human diseases (Table III), most notably certain cancers and chronic inflammatory diseases, such as inflammatory bowel disease, asthma, and arthritis.

Many cancer cells have constitutively active, nuclear NFκB activity. In certain B-cell lymphomas, notably diffuse large B-cell lymphomas and Hodgkin's lymphomas, NFκB activity is dysregulated due to either amplification of the c-*rel* gene or mutations that inactivate the gene encoding Iκ B. Furthermore, several oncogenic human viruses, such as Epstein-Barr virus (lymphomas, nasopharyngeal carcinomas), HTLV-1 (T-cell leukemias), and Hepatitis B virus (liver cancer), encode proteins that activate NFκB. However, in many other cancers one finds chronic nuclear NFκB activity, which is usually made up of p50–RelA dimers, in the apparent absence of mutations in the NFκB signaling pathway or associated viral infection. That increased NFκB activity is important for the growth and survival of several cancers is emphasized by studies showing that inhibition of NFκB activity often either causes the tumor cells to die (undergo apoptosis) or to become more sensitive to apoptosis-inducing agents.

Because NFκB controls the expression of many cytokines, it is also consistently active in many situations involving acute or chronic inflammation. Moreover, in several animal model systems inhibition of NFκB activity can reduce inflammation. Furthermore, mice with knockouts in the genes encoding p50 or c-Rel are resistant to experimentally induced arthritis.

TABLE III

Some Diseases Associated with Chronic NFκB Activation

Arthritis
Asthma
Cancer
Diabetes
Inflammatory bowel disease
Ischemia/reperfusion damage
Sepsis

Pharmacological Regulation of NFκB Activity

Because of the role played by NFκB in inflammatory diseases and cancer, it has received much attention as a molecular target for pharmacological intervention. As a multicomponent pathway, NFκB activation can be inhibited at a variety of levels, including activation of IKK, IKK-mediated phosphorylation of IκB, ubiquitination and proteasome-mediated degradation of IκB, nuclear translocation of NFκB, and DNA-binding and transactivation by NFκB. Indeed, NFκB inhibitors that act at each of these steps have been described (partial list in Table IV). Nevertheless, to date, most research effort has focused on identifying NFκB inhibitors that target the IKK complex, due to its central role in controlling the NFκB pathway and to successes in identifying specific kinase inhibitors in other systems.

Several natural products with anticancer or anti-inflammatory activities have been shown to inhibit activation of NFκB. Among many others, these natural NFκB inhibitors include gold compounds (anti-arthritis), green tea (anticancer), curcumin (anticancer, anti-inflammation), and various plant extracts (anti-inflammation). In addition, some commonly used anti-inflammatory compounds, such as glucocorticoids, ibuprofen, and aspirin, have been reported to have anti-NFκB activity in experimental model systems. However, in these cases, it is not clear if their biological effects in people are exerted through inhibition of NFκB, due to the fact that doses lower than those required to inhibit NFκB are often still effective in reducing inflammation in humans.

Because NFκB is constitutively active in many cancers, clinical trials are underway with several compounds known to inhibit NFκB. Early clinical trials have reported promising results in the use of a small-molecule inhibitor of the proteasome for the treatment of multiple myeloma, an NFκB-dependent B-cell cancer. Such compounds inhibit activation of NFκB by blocking proteasome-mediated degradation of IκB.

TABLE IV

Some Inhibitors of NFκB Signaling

Inhibitor	Molecular target
Aspirin (high doses)	IKK
Curcumin	IKK
Glucocorticoids	Re1A
Green tea compounds	IKK
PS-341	Proteasome
Sulindac	IKK

See Also the Following Articles

Cell Death by Apoptosis and Necrosis • Cytokines • Proteasomes, Overview • Ubiquitin System • Ubiquitin-Like Proteins

Glossary

apoptosis A programmed cell death pathway that is used by an organism to eliminate unwanted cells or maintain organ size.

cytokines Factors that regulate the growth and activity of blood cells and lymphocytes.

proteasome A cellular complex composed of several proteases that degrades ubiquitinated proteins.

protein kinase An enzyme that can add a phosphate group onto specific residues in a target protein, which then affects the activity of the target protein.

signal transduction A molecular process by which a signal (often an extracellular compound) effects a cellular response. Often this is a multicomponent step-wise intracellular pathway that involves binding of a ligand to a cell-surface receptor, which initiates a cascade of cytoplasmic enzymatic activities that ultimately leads to the activation of a transcription factor that then regulates the expression of a biologically-relevant set of target genes.

transcription factor A protein or protein complex that binds to specific DNA sequences to regulate (increase or decrease) the rate of transcription of a gene.

ubiquitin A small (~8.6 kDa) polypeptide chain that can be conjugated to substrate proteins, which often targets them for degradation by the proteasome.

Further Reading

Beyaert, R. (ed.) (2003). *Nuclear Factor-κB: Regulation and Role in Disease*. Kluwer Academic, The Netherlands.

Ghosh, S., May, M. J., and Kopp, E. B. (1998). NF-κB and rel proteins: Evolutionarily conserved mediators of immune responses. *Annu. Rev. Immunol.* **16**, 225–260.

Gilmore, T. D. (ed.) (1999). NF-κB. *Oncogene*. **18**, 6841–6964.

Gilmore, T. D (2003). Rel/NF-κB transcription factors. http://www.nf-kb.org.

Gilmore, T. D., and Ip, Y. T. (2003). Signal transduction pathways in development and immunity: Rel pathways. In *Nature Encyclopedia of Life Sciences*, Nature Publishing Group, London, ([doi: 10.1038/npg.els.0002332] http://www.els.net).

Karin, M., Cao, Y., Greten, F. R., and Li, Z-W. (2002). NF-κB in cancer: From innocent bystander to major culprit. *Nat. Rev. Cancer* **2**, 301–310.

Silverman, N., and Maniatis, T. (2001). NF-κB signaling pathways in mammalian and insect innate immunity. *Genes and Dev.* **15**, 2321–2342.

Biography

Thomas D. Gilmore is a Professor in the Department of Biology at Boston University. His general research area is in the molecular basis of cancer. He holds a Ph.D. from the University of California (Berkeley) and received postdoctoral training at the University of Wisconsin (Madison). He has authored many research papers and review articles on the role of Rel/NF-κB transcription factors in leukemia and lymphoma, and recently his laboratory was the first to show that human c-Rel has oncogenic activity.

Nuclear Genes in Mitochondrial Function and Biogenesis

Alexander Tzagoloff
Columbia University, New York, USA

Carol L. Dieckmann
University of Arizona, Tucson, Arizona, USA

Only a small fraction of the protein constituents of mitochondria are encoded in the small vestigial genome of the organelle. Most of the genes governing the biogenesis of mitochondria reside in the chromosomal DNA of the nucleus. Referred to as *PET* genes, they represent a sizeable fraction of the total genetic information in the nucleus. *PET* genes code for the enzymes making up the different metabolic pathways housed in mitochondria, for the substrate and protein transport systems, and for the transcriptional and translational machineries involved in expression and regulation of mitochondrial genes.

Historical Background

All life depends on ATP, the universal currency of biological energy. The chemical energy inherent in the structure of this molecule is used to support a large variety of phenomena including chemical, osmotic, electrical, and mechanical work. Most of the ATP in eukaryotic organisms is supplied by the mitochondrion, a complex cellular organelle composed of two membranes (outer and inner) and two soluble compartments (intermembrane space and matrix). Biogenesis of mitochondria occurs by replenishment and addition of newly synthesized proteins and phospholipids to the preexisting organelle. In dividing cells there is a net increase of mitochondrial mass, which is distributed among the progeny. This process is aided by the ability of mitochondria to undergo fusion and fission. Mitochondria, therefore, are not synthesized *de novo* but rather serve as a template for their own faithful replication. The genetic determinants of mitochondria are located in two physically separate compartments of the cell. Most of the information is provided by the *PET* genes of the nucleus, but a small number of genes present in mitochondrial DNA (mtDNA) also play an important role.

The discovery of an extranuclear genetic element (*rho*) in yeast by Boris Ephrussi, and the later demonstration by Gottfried Schatz that this factor corresponds to a unique DNA present in mitochondria, were the foundations for much of the subsequent work aimed at understanding the function of this genome. Despite large variability in the organization, mode of expression, and gene compositions of mtDNA among different members of the plant and animal kingdoms, some general statements can be made nonetheless. More than 100 different mtDNAs have so far been sequenced. In all instances, at least some components of the mitochondrial translational apparatus, such as the genes for the endogenous ribosomal RNAs and tRNAs, are encoded in mtDNA. Another important attribute of this genetic system is that it codes for a small number of mitochondrial proteins that are important for the respiratory and ATP-generating capacities of the organelle. In most organisms, the protein-coding genes of mtDNA specify several subunits of cytochrome oxidase, cytochrome *b*, and one or more subunits of the proton-translocating ATP synthetase/hydrolase. The *rho* zero mutants lacking this set of genes produce mitochondria that are defective in respiration and oxidative phosphorylation because they lack the genes for catalytically important components of the respiratory chain, ATP synthetase, and the ribosomal RNA and tRNAs needed for translation of the endogenous mRNAs.

A much larger share of the information essential for maintaining the structural and functional integrity of mitochondria is contributed by *PET* genes, which are located in the chromosomal DNA of the nucleus.

Origin of Nuclear Gene Products with Functions in Mitochondria

The endosymbiont hypothesis, first proposed by Lynn Margulis in 1968, was a landmark advance in our thinking about how cells evolved in response to major changes in their environment. According to this

hypothesis, many organelles of modern-day eukaryotic cells, including mitochondria and chloroplasts, are stripped down products of what originally were free-living bacteria. In the case of mitochondria, a nucleated cell dependent on glycolysis as its sole source of ATP was invaded by a bacterium with an aerobic mode of energy metabolism. Such a union was advantageous to the host and became fixed during evolution. There is compelling evidence to support the bacterial origin of subcellular structures that inhabit eukaryotic cells. Most notable is the presence in mitochondria and chloroplasts of autonomously replicating genomes, and of all the enzymatic machinery needed to transcribe the organellar genes and translate the resulting RNAs into the encoded protein products. Significantly, the transcriptional and translational machineries of mitochondria and chloroplasts are more closely related to their bacterial counterparts than to those operating in the cytoplasm of eukaryotic cells.

The extent to which the mitochondrial genome contributes towards the propagation of the organelle has been severely reduced due to a continual transfer of genetic information to the host's nuclear DNA. Today, the existence of mitochondria relies in large measure on the expression of gene products encoded in nuclear DNA. The loss of mitochondrial autonomy is clearly evident from the properties of cells that have been depleted of mtDNA. Such genome-less variants termed *rho* zero mutants have been created in yeast and mammalian (e.g., human) cells. Despite the complete absence of mitochondrial DNA, *rho* zero mutants contain subcellular structures with the characteristic morphology and most of the metabolic pathways of mitochondria. These observations point to the nonessentiality of mtDNA for the perpetuity of mitochondria, but do not minimize the importance of this genome for their functional competence.

Number of Mitochondrially Related Nuclear Genes

The number of distinct proteins in mitochondria is still not known precisely but based on currently available data of the unicellular yeast, *Saccharomyces cerevisiae*, a reasonable estimate is in the range of 700–800. This corresponds to ~10–12% of the different proteins known to exist in this organism. Of course, this number will vary in more complex eukaryotes, where depending on their tissue of origin, mitochondria may have specialized and have less complex functions. For example, in mammals, mitochondria of organs like heart and muscle have simpler metabolic profiles than those of liver and consequently are simpler in their protein composition.

Yeast as a Model for Mitochondrial Studies

For practical reasons, *S. cerevisiae* has become an important model for the study of *PET* genes. A vast arsenal of genetic and biochemical tools is directly applicable to the analysis of mitochondria in this organism. Also available are the complete sequences of the 16 nuclear chromosomes and of mtDNA. Finally, because of its status as a facultative anaerobe, this yeast is able to tolerate most mutations that impair mitochondrial function as long as it is supplied with a fermentable source of carbon and energy.

Most of what we presently know about *PET* genes stems from three different sources. An important body of information has been derived from traditional studies of the intermediary metabolism carried out by mitochondria. In some instances, such studies have predated the discovery of mitochondria as the cellular repository of the pathways in question. Genetic analysis has played an equally important role. Respiratory defective mutants of yeast have been instrumental in defining many nuclear genes that impinge on all aspects of mitochondrial function and biogenesis. More recently, the high-throughput proteomic approach has further augmented the list of mitochondrially related gene products, whose functions are yet to be understood.

Gene Functions

Based on the phenotype of the respective mutants, *PET* genes can be either essential or nonessential. Nonessential genes, which make up the larger class, are defined by *pet* mutants. Such strains are viable, but because of their genetic lesions are unable to produce ATP by means of oxidative phosphorylation. The products of *PET* genes have functions that are related either directly or indirectly to mitochondrial metabolism, but not to the continuity of mitochondria as a structural compartment of the cell. The second, less abundant, class consists of essential genes needed for the survival of the cell. Their products provide functions relevant to the structural integrity of mitochondria or to some essential aspect of metabolism. Mutations in the latter prevent growth on both fermentable and nonfermentable substrates.

Nonessential *PET* Genes

These genes encompass a wide range of mitochondrial functions. The most important, from a quantitative point of view, are involved in the expression of the products encoded in mtDNA (Figure 1). They consist of proteins that function in replication of mtDNA, transcription and processing of mitochondrial RNA.

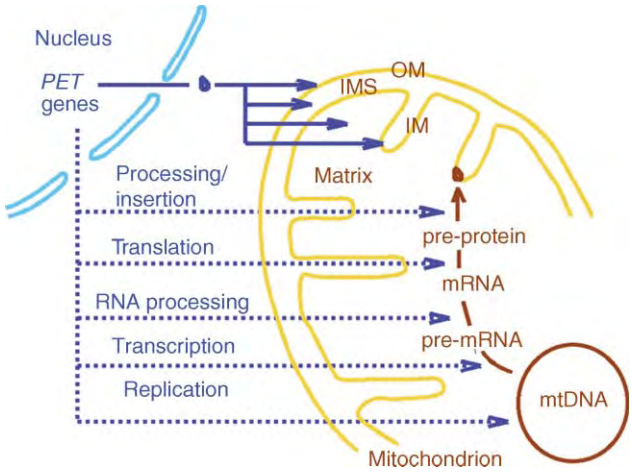

FIGURE 1 Dependence of mitochondrial gene expression on products of *PET* genes. The dashed blue arrows show some of the functions contributed by nuclear DNA for expression of the mitochondrially encoded subunits of the ATPase and respiratory enzymes. In yeast, the pre-mRNAs can be multi-genic transcripts that are matured by excision of intronic sequences and endonucleolytic cleavages. Some proteins are synthesized as precursors (pre-protein) with amino-terminal sequences that are removed by specific proteases. The solid blue arrows denote *PET* gene products targeted to the outer membrane (OM), intermembrane space (IMS), inner membrane (IM), and internal matrix compartment.

They also code for all except one of the mitochondrial ribosomal proteins, as well as most of the tRNA synthetases and translation initiation, elongation, and termination factors. A second important group of genes code for proteins that catalyze most of mitochondrially based metabolism. This includes enzymes of the tricarboxylic acid cycle (TCA cycle), fatty acid metabolism, some aspects of amino acid biosynthesis, and a number of other pathways needed for the synthesis of important cofactors such as hemes A and B, coenzyme Q, and lipoic acid.

The ATP synthetase/hydrolase as well as the enzymes making up the respiratory chain (Figure 2) are all hetero-oligomeric proteins, with more than a dozen different subunit polypeptides in most cases. Assembly of the subunits into the final holoenzymes is a complex process that requires the assistance of nuclearly encoded factors. Some of the chaperones act by facilitating a topologically correct insertion of specific subunits into the inner membrane, by preventing nonproductive interactions of hydrophobic proteins, or by still other unknown mechanisms. Because these chaperones target specific subunits, they represent a substantial fraction of the total number of mitochondrial proteins. For example, some dozen nuclear mutants have been reported to be cytochrome oxidase deficient due to mutations in proteins that affect late events in assembly of this single enzyme. Finally, many *PET* genes, coding for novel proteins still lack functions that can be assigned at this time.

Essential *PET* Genes

The highly regulated metabolism of eukaryotic cells depends on the sequestration of the enzymes making up the various pathways in their appropriate compartments. Proteins translated in the cytoplasm but destined to function in one of the internal compartments of mitochondria are imported and sorted by means of complex

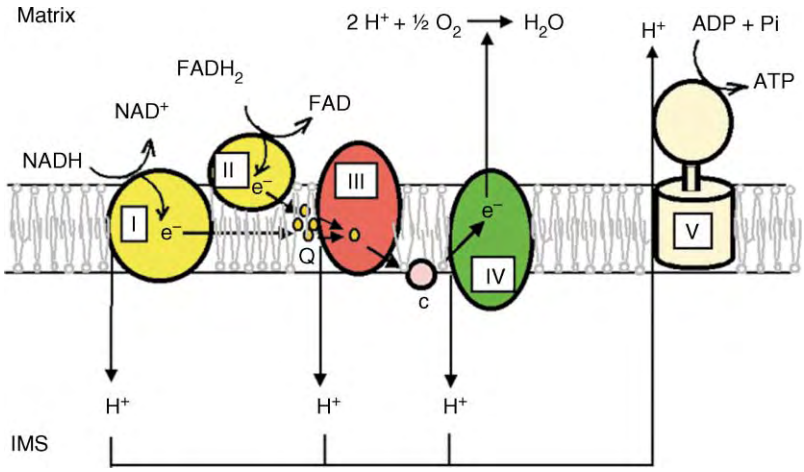

FIGURE 2 Schematic representation of the respiratory complexes and ATP synthetase in the mitochondrial inner membrane. The four complexes of the respiratory chain are: NADH-coenzyme Q reductase or complex I (yellow), succinate-coenzyme Q reductase or complex II (yellow), coenzyme QH_2-cytochrome *c* reductase or complex III (red), and cytochrome *c* oxidase or complex IV (green). Coenzyme Q is denoted by the small orange circles and cytochrome *c* by the pink circle. The ATP synthetase/hydrolase or complex V is shown with the F_1 ATPase protruding into the matrix compartment. In addition to catalyzing the transfer of electrons from NADH and $FADH_2$ to oxygen, three of the complexes promote the vectorial transfer of protons from the matrix to the intermembrane space (IMS). Protons are recycled by the ATP synthetase during synthesis of ATP from ADP and inorganic phosphate.

machines such as the TOM and TIM translocases of the outer and inner membranes, respectively. Mutations in components of either of these protein transport systems are lethal to the cell for several reasons. An immediate effect of the transport defect is a mislocalization of proteins in the cytoplasm. This abrogates the accretion of newly synthesized material by mitochondria, resulting in their eventual disappearance.

Mitochondria house proteins that function in pathways essential for the overall economy of the cell. For example, certain steps of heme B biosynthesis occur in mitochondria. Since heme B is a prosthetic group of enzymes (e.g., P450 hydroxylases) other than those involved in respiration, cells unable to produce heme B are not viable. This also applies to certain enzymes of amino acid biosynthesis located in mitochondria. In animals, carbamoyl synthetase and ornithine transcarbamylase, two important enzymes of arginine biosynthesis, catalyze their respective reactions in the mitochondrial matrix.

In certain instances, nuclear genes may code for proteins that are apportioned in the cytoplasm and mitochondria. This is true for some tRNA modification enzymes and for aminoacyl-tRNA synthetases. In yeast, six mitochondrial aminoacyl-tRNA synthetases are expressed from nuclear genes that also code for the same cytoplasmic enzymes. Therefore, mutations in these essential genes result in cell lethality.

Regulation

Many *PET* genes of yeast are regulated at the level of transcription by oxygen and carbon source. Oxygen stimulates the synthesis of heme in mitochondria mainly at later steps of the pathway catalyzed by oxygenases. Heme activates the binding of the Hap1 transcriptional activator to the upstream activation sites of some genes for respiratory chain proteins such as cytochrome *c*, thereby activating their transcription. Glucose has the opposite effect. It suppresses transcription of genes involved in alternative fuel usage by means of a complex regulatory pathway called catabolite repression. In the absence of glucose, repression is relieved and transcription of glucose-responsive genes is enhanced by the Hap2/3/4/5 transcriptional activator complex.

Mitochondrial gene expression is regulated primarily at the posttranscriptional level by products of *PET* genes. Mitochondrial RNA polymerase recognizes a simple promoter and there is little regulation of its activity except that it is more abundant in the absence of glucose and the presence of oxygen. Most mitochondrial genes are transcribed as long multigenic RNAs. Points of regulation include processing of 5′ and 3′ ends of RNA to the mature length, excision of introns and RNA stability. Initiation of translation is regulated by factors that attract ribosomes to the correct internal translational start sites of mitochondrial mRNAs. Posttranslation modification and assembly of the constituent subunits of the respiratory and ATP synthetase complexes also depend on the intervention of factors encoded by *PET* genes subject to these regulatory systems.

Human Disorders

A growing list of human pathologies has been related to mitochondrial defects and the responsible mutations mapped to RNA and protein-coding genes of mtDNA. Such mutations manifest a wide range of clinical phenotypes including encephalomyopathies, cardiomyopathy, deafness, diabetes, optic neuropathy, and dystonia. Similar presentations are elicited by mutations in nuclear DNA that affect mitochondrial metabolism either directly through lesions in the structural genes for enzymes of the TCA cycle, fatty acid oxidation, and mtDNA integrity; or indirectly by interfering with metabolite and protein import, assembly of respiratory chain complexes, metal homeostasis, and protein turnover. In view of their central role in oxidative metabolism, the list of currently known mitochondrially related diseases will undoubtedly be increased in the future.

See Also the Following Articles

Chaperones, Molecular • Cytochrome bc_1 Complex (Respiratory Chain Complex III) • DNA Replication, Mitochondrial • Mitochondrial DNA • Mitochondrial Genome, Evolution • Mitochondrial Genome, Overview • Mitochondrial Inheritance • The Cytochrome b_6f Complex • Tricarboxylic Acid Cycle

Glossary

ATP synthetase/hydrolase An enzyme of the inner membrane able to form ATP from ADP and inorganic phosphate by utilizing the energy of the proton gradient generated during the oxidation reactions catalyzed by the respiratory chain complexes. It can also form a proton gradient by hydrolyzing ATP to ADP and inorganic phosphate.

chaperones Proteins that promote the folding or unfolding of proteins. In the present context they also facilitate association of subunit polypeptides into hetero-oligomeric proteins.

eukaryotes Organisms with cells having a nucleus enclosed by a membrane.

organelle A structure or membrane enclosed compartment of a cell.

***pet* mutants** Viable mutants able to derive ATP from glycolysis but not from oxidative phosphorylation.

proteome Term used to denote all of the proteins of an organism or compartment of the cell.

respiration In the biochemical sense, the process by which the electrons and protons extracted from reduced fuels such as carbohydrates, fats, and proteins are transferred to oxygen.

***rho* zero mutants** Mutants devoid of mitochondrial DNA.

TIM complex An organized assembly of proteins that mediates the translocation of proteins from the TOM complex to the inner membrane or matrix of mitochondria.

TOM complex An organized assembly of proteins that mediates the translocation of a protein from the cytoplasm to the intermembrane space of mitochondria.

Further Reading

Alberts, B., Bray, D., Lewis, J., Raff, M., Roberts, K., and Watson, J. D. (1994). *Molecular Biology of the Cell*, 3rd edition. Garland Publishing, New York.

Ernster, L., and Schatz, G. (1981). Mitochondria: A historical review. *J. Cell. Biol.* **91**, 227s–255s.

Margulis, I. (1981). *Symbiosis in Cell Evolution*. W. H. Freeman, New York.

Neupert, W., and Brunner, M. (2002). The protein import motor of mitochondria. *Nat. Rev. Mol. Cell Biol.* **3**, 555–565.

Scheffler, I. E. (1999). *Mitochondria*. Wiley-Liss, New York.

Tzagoloff, A., and Dieckmann, C. L. (1990). *PET* genes of *Saccharomyces cerevisiae*. *Microbiol. Rev.* **54**, 211–225.

Biography

Alexander Tzagoloff is a Professor in the Department of Biological Sciences at Columbia University. He received a Ph.D. from Columbia University and postdoctoral training at the Enzyme Institute of the University of Wisconsin. He has used genetics and biochemical approaches to study the roles of mitochondrial and nuclear genes in biogenesis of yeast mitochondria.

Carol L. Dieckmann is a Professor in the Department of Biochemistry and Molecular Biophysics at the University of Arizona. She received a Ph.D. from the University of California, San Diego, and did postdoctoral training at Columbia University. She has used a combination of genetics, molecular biology, and biochemistry to study the regulation of mitochondrial gene expression.

Nuclear Organization, Chromatin Structure, and Gene Silencing

Lori L. Wallrath, John R. Danzer, Oya Yazgan and Pamela K. Geyer
University of Iowa, Iowa City, Iowa, USA

Gene silencing is the process whereby a gene is inactivated due to its chromosomal position. Chromosomal rearrangements that move a gene from a transcriptionally permissive location to a transcriptionally nonpermissive location result in gene silencing. This loss of gene expression is not due to a mutation in a gene itself, but due to the placement of a gene into a chromatin environment that is not favorable for transcription. Chromatin packaging influences whether a chromosomal location will support transcription or result in gene silencing. Eukaryotic genomes are packaged into two types of chromatin, euchromatin and heterochromatin. Euchromatin is represented by single copy, gene-rich DNA sequences located between centromeres and telomeres. These regions are packaged with acetylated histones that foster gene expression. In contrast, heterochromatin is represented by repetitive, gene-poor DNA sequences located near centromeres and telomeres. These regions are packaged with hypoacetylated histones and can cause gene silencing.

The regulation of gene expression involves complex interactions between DNA sequences and protein factors. One mechanism for regulating access of transcription factors to DNA is through chromatin packaging. Double-stranded DNA is wound twice around a histone octamer, forming the fundamental packaging unit, the nucleosome. Nucleosomal DNA is further folded into higher-order chromatin structures that differentiate euchromatin from heterochromatin. A second mechanism for regulating access of transcription factors to DNA involves the spatial positioning of genes within the nucleus. Increasing evidence supports the notion that the nucleus is not a homogenous mixture of DNA and proteins, but is a highly organized environment. For example, chromosome labeling techniques show that certain chromosomes reproducibly localize to specific positions within the nucleus, termed chromosome territories (Figure 1). Thus, a given gene might have a specific address within the nucleus.

Nuclear zones are superimposed on chromosome territories (Figure 1). A zone is defined as a region of the nucleus that is enriched in a particular class of transcription factors. There are two types of zones, those enriched for silencing factors that do not support transcription (inactive zones), and those enriched for activating factors that do support transcription (active zones). Entire chromosomes can be located within a zone, such as the case for the inactive X chromosome (Barr body) of mammalian females that localizes to an inactive zone along the nuclear periphery. Alternatively, smaller regions along a chromosome can attract transcription factors and form a local zone (Figure 1). In addition, regions of similar transcription activity on different chromosomes can come together to form a zone. Thus, regulation of gene expression can occur at many levels involving the local chromatin environment, chromosomal territories, and the nuclear zones.

Establishing a Zone

Zones are established by increasing the local concentrations of transcriptional regulatory factors within an area of the nucleus. This nonuniform distribution of factors occurs by mechanisms involving protein–protein and protein–DNA interactions. As an example, heterochromatin protein 1 (HP1) can direct silent chromatin into the inactive zone at the nuclear periphery. The amino terminal chromo domain of HP1 interacts with a histone modification that is enriched in heterochromatin and the carboxy chromo shadow domain of HP1 interacts with a component of the nuclear envelope. These protein–protein interactions promote the accumulation of heterochromatin and HP1 at the nuclear periphery. The role of protein–DNA interactions is illustrated by studies of yeast telomeres. Repetitive DNA sequences found at yeast telomeres attract the DNA-binding protein Rap1. This protein interacts with Sir proteins that are involved in gene silencing. Through this interaction, the concentration of Sir proteins increases at the nuclear periphery relative to the interior of the nucleus. The concentration gradient of Sir proteins within the nucleus can be "sensed" by reporter transgenes containing Sir-responsive DNA sequences. When such a reporter transgene is

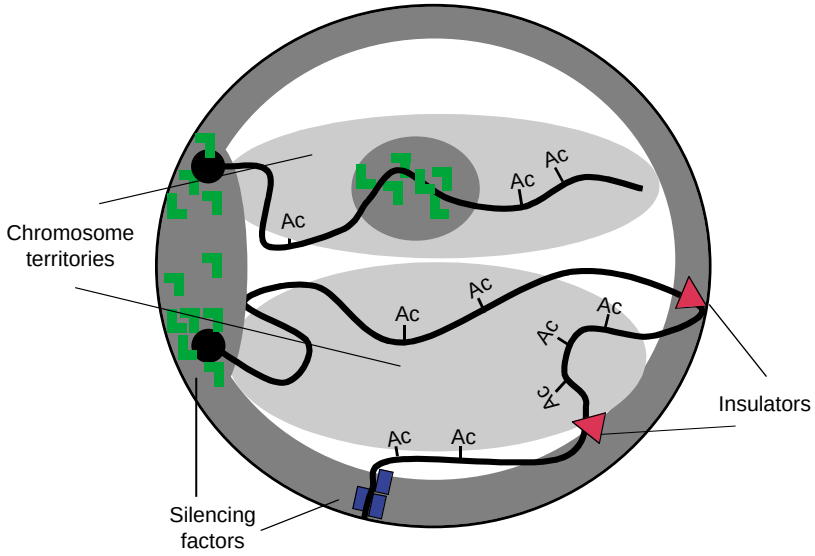

FIGURE 1 Diagram of organization within the nucleus. A nucleus is depicted with chromosome territories (light gray) and silencing zones (dark gray). Histone acetylation (Ac) is shown over active chromatin. Hypoacetylation is associated with inactive chromatin, such as that found at centromeres (black circle) and telomeres. Small domains within a chromosome can acquire properties similar to heterochromatin and form a silencing zone (shaded circle). Silencing factors (green and blue shapes) are involved in chromatin compaction, gene silencing, and tethering to the nuclear periphery. Insulator elements (red triangles) partition chromosomes into transcriptonally related domains and assist in organizing chromatin into zones.

placed at positions close to the telomere, gene silencing is strong. When the same transgene is positioned further from the telomere, gene silencing is weak. Overexpression of Sir proteins produces silencing at internal sites, presumably due to increased levels of Sir proteins within the interior of the nucleus. These studies demonstrate that gene silencing can be modulated by the position of a gene within the nucleus, as well as, the local concentration of regulatory factors.

Organizing DNA into Zones

What mechanisms ensure that chromosome domains remain independent? Specialized DNA elements called insulators may be responsible for maintaining domain autonomy. These DNA elements, 0.2–3 kb in length, associate with specific proteins that limit the scope of regulatory interactions. An insulator located between an enhancer and promoter blocks activated gene expression. Insulator elements flanking a gene "insulate" it from neighboring positive and negative regulatory elements. Several models have been proposed to explain the mechanism of insulator action. One model states that attachment of insulators to the nuclear envelope could result in the formation of looped domains that compartmentalize gene activity (Figure 1). Physical associations with architectural components of the nucleus could serve to anchor chromosomal sites leading to spatial positioning of insulated domains within a zone.

Changes in Gene Expression Correlate with Shifting Zones

The nucleus is a highly dynamic environment in which protein factors and chromosomal domains can change positions within seconds. This mobility allows gene expression to be regulated by shifting zones. Studies on the expression and localization of lymphocyte specific genes demonstrate this point. A set of lymphocyte-specific genes in mice associate with Ikaros, a zinc-finger DNA-binding protein that also associates with centric heterochromatin. When these genes are silenced they localize to discrete foci within B-cell nuclei that correspond to the location of centromeres. Expression of these genes correlates with movement away from the centric foci. A direct role for Ikaros in this process was demonstrated by examining cells that had low levels of Ikaros. In such cells, these genes do not colocalize with centromeres when silenced. These data suggest that Ikaros is not required for silencing but plays a critical role in directing silent genes to an inactive zone. However, it appears that in these examples movement into an inactive zone is not the cause of gene silencing. Therefore, positioning a gene within a silent zone might be a consequence of silencing or assist in the maintenance of the silent state.

Additional studies correlating nuclear position with gene expression have focused on the *brown* gene in the fruit fly *Drosophila*. The *brown* gene is normally positioned at a site distant from centric heterochromatin.

A mutant allele designated *brown*^{Dominant} contains an insertion of a large block of heterochromatin (>1 Mb) in the coding region. Heterochromatin proteins associate with the insertion and are involved in positioning *brown*^{Dominant} near centric heterochromatin. Surprisingly, the wild-type brown allele also becomes silenced. This occurs due to a process called "*trans*-silencing" that results from homologous pairing along the length of *Drosophila* chromosome arms. Silencing of the wild-type *brown* gene demonstrates the impact of positioning within an inactive zone.

In some cases it appears that localization within an inactive zone occurs as the default state. Studies using a mouse *β-globin* transgene demonstrate that a complete enhancer element is required for both gene expression and localization away from inactive zones. Point mutations within the enhancer element that disrupt binding of a transcription factor eliminate gene expression and cause the *β-globin* transgene to localize to inactive zones near centromeres. Interactions between factors bound at enhancer elements and the transcriptional machinery housed within the interior of the nucleus might be responsible for localization within an active zone. Alternatively, factors that bind to enhancer elements might recruit chromatin remodeling machines and/or histone acetyltransferases, generating a chromatin environment that disrupts interactions with silencing proteins in the inactive zone.

Multiple Determinants for Establishing the Activity State of a Gene

The emerging picture is that both nuclear zones and local chromatin structure play essential roles in establishing the transcriptional state of a gene. Silencing at the yeast mating type locus *HMR-E* is dependent upon the recruitment of specific *trans*-acting factors. Deletion of some of their binding sites generates a defective silencer, leading to transcriptional derepression. Tethering an *HMR-E* with a defective silencer to the nuclear periphery restores gene silencing. However, tethering an *HMR-E* in which all binding sites had been removed has no effect on gene expression. These experiments demonstrate that the local chromatin structure, not just the position within a nuclear zone, is necessary to establish the transcriptionally inactive state.

Effects of local chromatin structure and nuclear positioning were further demonstrated by studies involving chromosomal translocations in *Drosophila*. A stock possessing a reporter gene inserted within a region associated with heterochromatin-silencing factors was subjected to X-rays and translocations were recovered. The degree of silencing of the reporter gene was dependent on the location of the translocation breakpoints. Rearrangements that placed the transgene closer to centric heterochromatin showed increased levels of gene silencing. In contrast, rearrangements that placed the transgene at sites distant from centric heterochromatin resulted in decreased gene silencing. Contrasting observations were made when a stock containing the same transgene inserted within a chromosomal region that normally does not associate with heterochromatic silencing factors was subjected to X-rays. Resulting translocations did not alter the expression of the reporter gene, even when the transgene localized near centric heterochromatin. The transgene appeared to be insensitive to positioning in the nucleus. These data suggest that local chromatin structure can influence the response of a gene to placement within a particular nuclear zone.

Nuclear Zones and Human Disease

Studies in model organisms, such as yeast and fruit flies, have clearly demonstrated that nuclear positioning affects gene expression. There is growing evidence in humans that some diseases might result from misregulation of gene expression due to translocations that place a disease-causing gene into an inappropriate zone. Examples include cases of aniridia (absence of the iris), autism, and Burkitt's lymphoma. In these cases the disease-related gene is not damaged by the translocation, in fact, the breakpoints of the translocation map several kilobases or megabases from the gene affected. It is hypothesized that altered expression of the disease gene is due to placement in an inappropriate nuclear zone as a consequence of the translocation. Therefore, understanding the rules of gene regulation has become a three-dimensional problem that will require sophisticated detection of gene expression coupled with high-resolution nuclear imaging.

See Also the Following Articles

Chromatin: Physical Organization • Chromosome Organization and Structure, Overview • Nucleoid Organization of Bacterial Chromosomes • Transcriptional Silencing

Glossary

boundary elements DNA elements that bind specialized nuclear complex that attach to nuclear substructure to delimit chromosome domains.

chromosome territory An area within the nucleus that is occupied by a specific chromosome.

euchromatin Regions of the genome that contain mostly single copy DNA sequence and are relatively gene-rich. These regions replicate early in S phase and decondense during interphase.

heterochromatin Regions of the genome, frequently located near centromeres and telomeres, that contain repetitive DNA sequences and are relatively gene-poor. These regions replicate late in S phase and remain condensed throughout the cell cycle.

histones Small, highly conserved, basic proteins that form a nucleosome.

insulators Specialized DNA sequences that block the effect of enhancers or silencers when placed between a promoter and the regulatory element. When flanking both ends of a gene, they block position effects that arise from neighboring regulatory elements.

nucleosome The fundamental unit of chromatin packaging containing eight histones and ~165 bp of double stranded DNA.

somatic pairing Pairing of two homologous chromosomes during interphase in somatic cells.

Further Reading

Brown, K. E., Guest, S. S., Smale, S. T., Hahm, K., Merkenschlager, M., and Fisher, A. G. (1997). Association of transcriptionally silent genes with Ikaros complexes at centromeric heterochromatin. *Cell* **91**, 845–854.

Cryderman, D. E., Morris, E. J., Biessmann, H., Elgin, S. C. R., and Wallrath, L. L. (1999). Silencing at Drosophila telomeres: Nuclear organization and chromatin structure play critical roles. *EMBO J.* **18**, 3724–3736.

Dernberg, A. F., Broman, K. W., Fung, J. C., Marshall, W. F., Philips, J., Agard, D. A., and Sedat, J. W. (1996). Perturbation of nuclear architecture by long-distance chromosome interactions. *Cell* **85**, 745–759.

Gasser, S. M. (2001). Positions of potential: Nuclear organization and gene expression. *Cell* **104**, 639–642.

Ishii, K., Arib, G., Lin, C., Van Houwe, G., and Laemmli, U. K. (2002). Chromatin boundaries in yeast: The nuclear pore connection. *Cell* **109**, 551–562.

Kleinjan, D.-J., and van Heyningen, V. (1998). Position effect in human genetic disease. *Human Mol. Genet.* **7**, 1611–1618.

Kuhn, M. J., and Geyer, P. K. (2003). Genomic insulators: Connecting properties or mechanism. *Curr. Opin. Cell Biol.* **15**, 259–265.

Mahy, N., Perry, P. E., and Bickmore, W. A. (2002). Gene density and transcription influence the localization of chromatin outside of chromosome territories detectable by FISH. *J. Cell Biol.* **159**, 753–763.

Sass, G. L., and Henikoff, S. (1999). Pairing-dependent mislocalization of a Drosphila *brown* gene reporter to a heterochromatic environment. *Genetics* **152**, 595–604.

Williams, R. R. E. (2003). Transcription and the territory: The ins and outs of gene positioning. *Trends Genet.* **19**, 298–302.

Biography

Lori L. Wallrath and Pamela K. Geyer are faculty members in the Department of Biochemistry at the University of Iowa. Their principal research interest is chromatin structure and gene expression. Dr. Wallrath's research is focused on the molecular mechanisms of gene silencing. Dr. Geyer's research is focused on the role of genomic insulators in gene expression.

John Danzer is a senior Ph.D. student in the Molecular Biology Program, working on the molecular mechanism of heterochromatin spreading.

Dr. Oya Yazgan is a Postdoctoral Fellow researching the role of proteins that associate with insulators.

Nuclear Pores and Nuclear Import/Export

Anita H. Corbett
Emory University School of Medicine, Atlanta, Georgia, USA

The hallmark of a eukaryotic cell is the presence of the nucleus, which separates the chromosomes that encode the genetic information from the protein translation machinery in the cytoplasm. This physical separation requires nuclear transport (import and export) machinery, which is capable of moving macromolecules such as proteins and RNAs rapidly but selectively into and out of the nucleus. There are many processes in eukaryotic cells that require macromolecular exchange between the nucleus and the cytoplasm. The most obvious example is the expression of a gene where the DNA is transcribed to messenger RNA (mRNA) within the nucleus and this mRNA must be transported to the ribosomes, the cytoplasmic protein translation machinery, to be decoded and translated into protein. In addition, many proteins that are created by the cytoplasmic translation machinery enter the nucleus to function in essential nuclear processes such as DNA replication, transcription, DNA repair, and many others. Thus, there is a great deal of traffic between the cytoplasm and the nucleus and these transport events are critical for the proper functioning of a eukaryotic cell.

Nuclear Pores

All transport between the nucleus and the cytoplasm occurs through large protein channels that are embedded in the nuclear membrane. These channels, which are called nuclear pore complexes (NPCs), are composed of proteins referred to as nucleoporins.

Structure

NPCs are large (~30 MDa in yeast and ~60 MDa in vertebrates) structures that span the double membrane, which surrounds the nucleus to provide a transport channel for very large macromolecular cargoes. Many different studies have led to a model for the structure of the NPC (Figure 1). The core of the NPC consists of a cylinder with eightfold rotational symmetry, which spans the nuclear envelope and surrounds a central channel. In addition to this central channel, there are filaments that extend into the cytoplasm and a basket structure that extends into the nucleoplasm. Cargoes that move through the nuclear pores probably interact first with the peripheral structures, move through the central channel, and are then released into their target compartment.

Composition

Sophisticated biochemical studies have revealed the identity of the nucleoporin proteins that make up the NPC. Surprisingly, these studies reveal that both the yeast and vertebrate nuclear pores are composed of only approximately 30 distinct proteins. The pore is large because most of these pore components are present in 16–32 copies per NPC. Many of these nucleoporins contain a characteristic repeat sequence of phenylalanine glycine repeats (FG). These FG-repeat nucleoporins line the central channel of the pore and probably provide the conduit for movement of macromolecules through the pore complex.

Transport Mechanisms: Protein Trafficking

Transport through nuclear pores occurs in both directions, from the nucleus to the cytoplasm and from the cytoplasm to the nucleus. The desired direction of transport generally depends on the cargo to be transported. The cell has developed sophisticated mechanisms to mark cargoes for transport and regulate the direction of the transport processes.

Targeting Signals

As with most intracellular targeting mechanisms, trafficking between the nucleus and the cytoplasm depends on amino acid sequences within the protein cargoes to be transported. However, unlike other targeting mechanisms, such as mitochondrial and ER targeting, nucleocytoplasmic trafficking signals are not

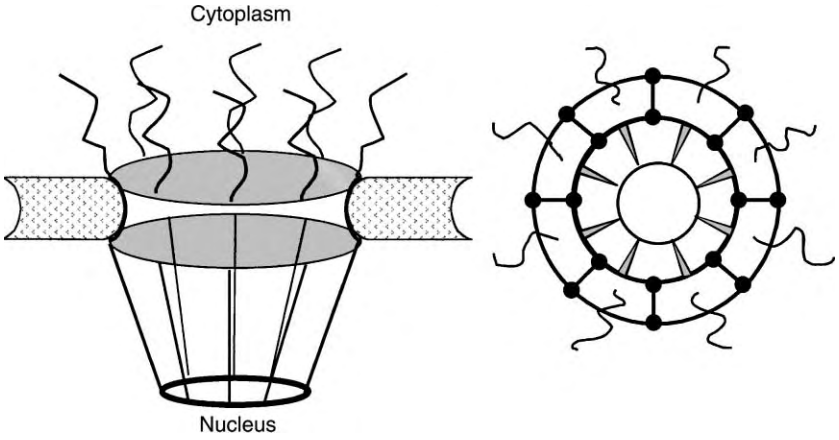

FIGURE 1 Schematic of the nuclear pore complex (NPC). Left: A schematic of the pore in the plane of the membrane is shown. The schematic shows the cytoplasmic filaments and the nuclear basket. Right: A schematic view of the pore looking down from the cytoplasmic face. The eightfold rotational symmetry of the pore is evident.

cleaved and remain an integral part of the protein. This mechanism can allow the cargo proteins to undergo multiple rounds of import and/or export. The nuclear targeting signal within the cargo protein generally mediates a physical interaction with a soluble nuclear transport receptor, which targets the cargo to the nuclear pore for transport.

Canonical signals for both nuclear protein import and nuclear protein export have been identified and studied in some detail. Nuclear import signals are generally termed nuclear localization signals (NLS), while signals that target proteins for export from the nucleus are termed nuclear export signals (NES). The classical NLS consists of either a single cluster of basic amino acid residues (monopartite) or two clusters of basic amino acid residues separated by a 10–13 amino acid linker sequence (bipartite). The monopartite NLS sequence is typified by the NLS found in the simian virus 40 (SV40) large T antigen (PKKKRKV), whereas the bipartite NLS is typified by the nucleoplasmin NLS (**KR**PAATKKAGQA**KKKK**). The classical NES is comprised of a series of hydrophobic amino acids, generally leucine, isoleucine, or valine. Numerous variations on this theme have been identified and thus far the best consensus sequence for an NES is LxxxLxxLxL, where the spacing between the leucines can vary, and, in fact, the leucines can be substituted with virtually any hydrophobic amino acid. Although classical NLS and NES signals are typically identified through computer searches of proteins sequences, it is essential that their function be verified through experimental methods.

Transport Receptors

Targeting signals within cargo proteins are recognized by soluble receptors that direct those cargoes to the nuclear pore for transport. These receptors form a family of structurally related molecules that are generally referred to as importins (for import receptors), exportins (for export receptors), or generally as transport receptors or karyopherins. The family of related receptors is generally referred to as the importin β or karyopherin β-family. One feature of these transport receptors is that they are modulated in such a way that they bind tightly to their cargo in the compartment where the cargo needs to be picked up. However, following the translocation through the NPC to the compartment where the cargo needs to be delivered, the transport receptor undergoes a conformational change that leads to the efficient release and delivery of the cargo. This switch in binding to the cargo is regulated by the small GTPase Ran.

Although most transport cargoes bind directly to their cognate transport receptor, there are examples where an adaptor protein mediates this interaction. The best example of this occurs in nuclear protein import of cargoes that contain a classical NLS sequence. The NLS within these cargoes is recognized by an adaptor protein called importin α or karyopherin α. The importin/karyopherin α recognizes and binds to the cargo and then binds directly to the transport receptor to form a trimeric import complex. This complex is then translocated through the nuclear pore into the nucleus and the NLS cargo is delivered.

Once cargo is released from the transport receptors within the delivery compartment, all the receptors are recycled for another round of transport. Import receptors are recycled back to the cytoplasm and export receptors are recycled back to the nucleus. This recycling of receptors assures that a single receptor can mediate multiple rounds of transport.

The Ran GTPase Cycle

The small GTPase Ran, serves as a molecular switch that modulates the directionality of nuclear transport. As with other GTPases, Ran can exist in two forms, either bound to GDP (RanGDP) or bound to GTP (RanGTP). It is the compartmentalization of these two distinct forms of Ran that regulates cargo/receptor interactions to impart directionality on nuclear transport. This compartmentalization is achieved through the intracellular separation of the two important regulators of the Ran GTPase cycle. The Ran GTPase-Activating Protein (RanGAP), which enhances Ran-mediated GTP hydrolysis, is located in the cytoplasm and the Ran Guanine Nucleotide Exchange Factor (RanGEF), which facilitates exchange of GDP for GTP on Ran, is located in the nucleus. As shown in Figure 2, with the RanGAP in the cytoplasm, any RanGTP that enters the cytoplasm is rapidly converted to RanGDP. Thus, in the cytoplasm the level of RanGDP exceeds the level of RanGTP. In contrast, within the nucleus in the presence of the RanGEF, RanGDP is rapidly converted to RanGTP. Thus, in the nucleus the level of RanGTP is high compared to the level of RanGDP. Due to the asymmetric localization of the Ran regulators, high levels of RanGTP serve as a marker for the nucleus and high levels of RanGDP serve to identify the cytoplasmic compartment.

The different nucleotide bound states of Ran regulate the flow of protein cargoes into and out of the nucleus by regulating the assembly of the import and export complexes (Figure 3). Cargoes to be transported into the nucleus bind to their cognate import receptors in the cytoplasm. These complexes are translocated into the nucleus through NPCs. Once they reach the nucleus, where levels of RanGTP are elevated, RanGTP binds to the import receptor causing a conformational change that releases the import cargo into the nucleus. In contrast, export cargoes bind to their export receptors only in the presence of RanGTP. Export complexes are trimeric complexes that consist of the export receptor, the export cargo, and RanGTP. As with import, the export complex is translocated through NPCs to the cytoplasm. In the cytoplasm, the export complex encounters the RanGAP and the bound RanGTP is converted to RanGDP. This disassembles the export complex and leads to the release of the export cargo into the cytoplasm.

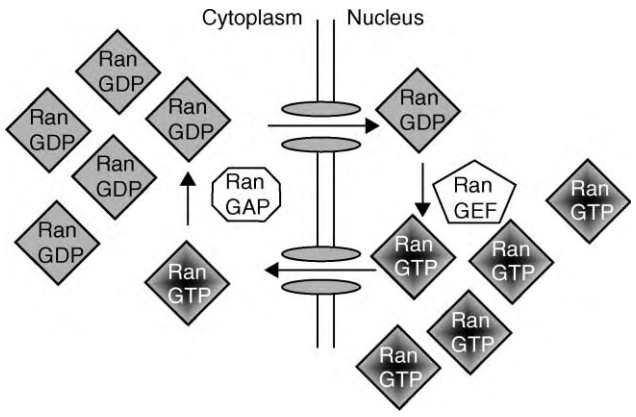

FIGURE 2 The RanGTP gradient. The compartmentalization of the RanGAP to the cytoplasm and the RanGEF to the nucleus results in localized concentrations of RanGDP and RanGTP. In the cytoplasm where the RanGAP enhances the Ran-mediated GTP hydrolysis, levels of RanGDP are high. In the nucleus where the RanGEF facilitates the exchange of GTP for GDP on Ran, the levels of RanGTP are high. This compartmentalization is critical for the identification of the nuclear and cytoplasmic compartments in nuclear transport and in other cellular processes.

Classical NLS-Mediated Protein Import

The best understood nuclear transport process is the import of protein cargoes that contain a classical basic NLS (Figure 4). Thus, this process can be used most readily to illustrate the steps that occur when a transport cargo is moved into or out of the nucleus. Historically, nuclear protein import was divided into two steps, docking at the nuclear pore, an energy-independent step, and translocation into the nucleus, an energy-dependent step. Advances in our understanding of the process and the players now lead us to define at least five distinct steps for import of a cargo that contains a classical NLS: (1) recognition and binding of the NLS cargo to the α/β heterodimeric-import receptor in the cytoplasm; (2) targeting to the nuclear pore through interactions between the importin/karyopherin β nuclear transport receptor and the nuclear pore; (3) translocation through the pore through transient interactions between importin/karyopherin β and the FG-repeat containing nucleoporins; (4) delivery into the nucleus where RanGTP binds to importin/karyopherin β to cause a conformational change that releases α and the NLS cargo; and (5) recycling of importin/karyopherin α to the cytoplasm in a heterotrimeric complex with an importin/karyopherin α export receptor and RanGTP and importin/karyopherin β presumably in complex with RanGTP. Note that the only energy expenditure in this process occurs when the karyopherin proteins are recycled to the cytoplasm and the accompanying RanGTP is hydrolyzed.

Transport Mechanisms: RNA Trafficking

Multiple classes of RNAs, including mRNAs, tRNAs, and U snRNAs are transcribed and processed within

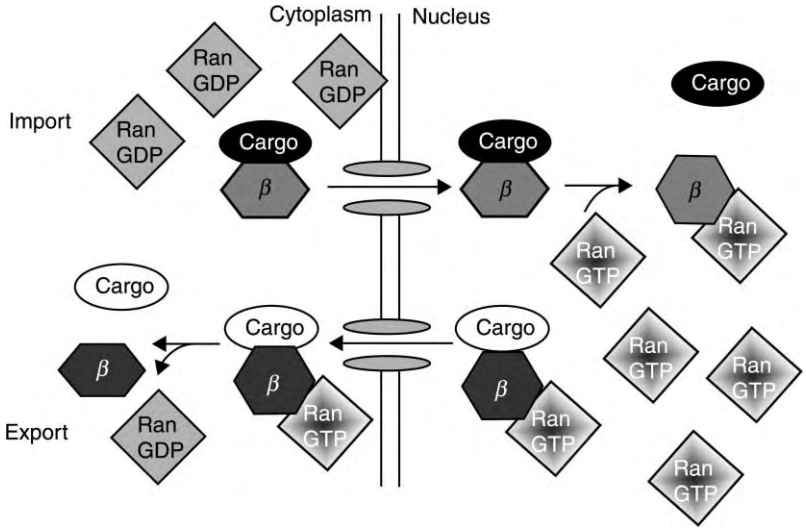

FIGURE 3 Ran regulates the assembly of import and export complexes. Top: For transport into the nucleus (Import), cargoes are recognized in the cytoplasm by an importin/karyopherin β receptor to form an import complex. Once this complex is translocated into the nucleus, it encounters the nuclear RanGTP, which binds tightly to the importin/karyopherin β receptor and causes a conformational change that releases the import cargo. Bottom: For transport out of the nucleus (Export), cargoes are recognized in the nucleus by an importin/karyopherin β receptor. However, in contrast to the import complex, the export complex can only form in the presence of RanGTP. Thus, export complexes are obligate trimeric complexes that consist of the export cargo, the importin/karyopherin β export receptor, and RanGTP. Once the export complex is translocated to the cytoplasm, it encounters the RanGAP. In the presence of the RanGAP, the RanGTP within the complex is converted to RanGDP and the complex dissociates resulting in the release of the export cargo into the cytoplasm. Hence, by controlling complex assembly and disassembly, the different forms of Ran confer directionality on the nuclear transport machinery.

the nucleus and then transported to their sites of action in the cytoplasm. As compared with proteins, RNAs require extensive processing before they reach their mature form and are ready to exit the nucleus. This means that RNA export is intimately linked to RNA processing within the nucleus.

Export of RNA via Classical Nuclear Transport Receptors

The export of tRNA, U snRNA, and rRNA follows pathways analogous to nuclear protein export. For example, tRNA is recognized directly by the importin/karyopherin β family nuclear transport receptor, exportin-t/Los1p and is exported as a complex with RanGTP. As for any classical export process, this trimeric complex is disassembled in the cytoplasm when RanGTP is hydrolyzed to RanGDP. Preferential export of mature tRNAs seems to be achieved at least in part by the specificity of exportin-t for the mature processed, modified, and appropriately aminoacylated tRNAs. U snRNAs are synthesized in the nucleus, transported to the cytoplasm where they associate with protein components of mature small nuclear ribonucleoproteins (snRNPs), and are then reimported to the nucleus where they function in mRNA splicing. Although this export depends on Ran, it is controversial whether Ran plays a direct role in export or whether its activity may be essential for the import of components required for RNP assembly.

mRNA Export

Export of poly (A)+ mRNA remains the least well understood of the RNA export mechanisms. mRNAs are not exported to the cytoplasm as naked nucleic acids, but rather as RNP complexes, and it is generally agreed that the export machinery recognizes signals within the proteins of these complexes rather than the RNA itself. For example, export of intron-containing HIV transcripts from the nucleus is mediated by the HIV protein Rev through its binding to the classical NES receptor, CRM1/exportin. While the HIV virus exploits this mechanism, none of the classical nuclear transport receptors play a central role in cellular mRNA export.

Although the mechanistic details of mRNA export have not yet been fully elucidated, it appears that there are two classes of proteins that are required to achieve export of mature messages. First, there is a family of evolutionarily conserved heterogeneous nuclear ribonucleoproteins (hnRNPs) that interact with poly (A)+ RNA *in vivo*. A number of these hnRNP proteins shuttle between the cytoplasm and the nucleus and escort the poly(A)+ RNAs as they are exported through the NPC. Current models suggest that at least some of the hnRNP proteins may be involved in RNA processing steps that occur cotranscriptionally. The hnRNPs that remain bound to the maturing messages may serve as markers that the different processing steps have been successfully accomplished. The second class of proteins consists of

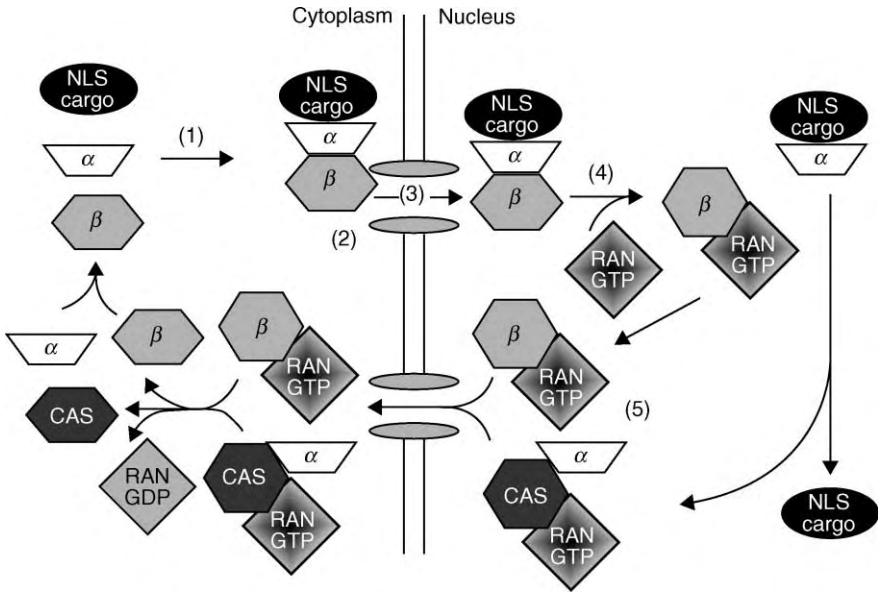

FIGURE 4 Model for classical NLS-mediated protein import into the nucleus. The best-understood transport mechanism is that of classical nuclear protein import mediated by importin/karyopherin β and the NLS binding adapter, importin/karyopherin α. This process can be divided into at least five distinct steps as shown in the model: (1) recognition and binding of the NLS cargo to the α/β heterodimeric import receptor in the cytoplasm; (2) targeting to the nuclear pore through interactions between the importin/karyopherin β nuclear transport receptor and the nuclear pore; (3) translocation through the pore through transient interactions between importin/karyopherin β and the FG-repeat containing nucleoporins; (4) delivery into the nucleus where RanGTP binds to importin/karyopherin β to cause a conformational change that releases α and the NLS cargo; and (5) recycling of importin/karyopherin α to the cytoplasm in a heterotrimeric complex with an importin/karyopherin α export receptor and RanGTP and importin/karyopherin β presumably in complex with RanGTP.

those proteins that have been implicated more directly in the export process; including a helicase, Sub2p/UAP56, and the heterodimeric-export receptor, Mex67p/Mtr2p (TAP/p15 in humans). TAP/Mex67p shuttles between the cytoplasm and the nucleus, and in complex with p15/Mtr2p, binds both to mRNA and to nucleoporins. Thus, it could potentially target bound RNAs directly to the NPC for export.

See Also the Following Articles

mRNA Polyadenylation in Eukaryotes • mRNA Processing and Degradation in Bacteria • Neurotransmitter Transporters • Ran GTPase • RNA Editing

Glossary

cargo Macromolecular substrate to be transported between the nucleus and the cytoplasm.

GTPase Protein that binds to and hydrolyzes the nucleotide GTP.

heterogeneous nuclear ribonucleoprotein (hnRNP) Abundant non-specific poly(A)+ RNA binding protein.

HIV Human immunodeficiency virus.

messenger RNA (mRNA) Class of RNA that carries the information from the DNA to the cytoplasm and serves as the informational blueprint for protein synthesis.

nuclear export signal (NES) An amino acid sequence within a protein that targets that protein for export from the nucleus.

nuclear localization signal (NLS) An amino acid sequence within a protein that targets that protein for import into the nucleus.

nuclear pore complex (NPC) The large proteinaceous channel through which macromolecular cargoes are transported in and out of the nucleus.

nucleoporins Proteins that make up the NPC.

Ran A small GTPase that regulates the directionality of nuclear transport.

RanGAP Cytoplasmic protein that enhances the GTPase activity of Ran.

RanGEF Nuclear protein that facilitates the nucleotide exchange on Ran.

ribosomal RNA (rRNA) Class of RNA that serves as a structural and catalytic component of ribosomes.

transfer RNA (tRNA) Class of RNA that is charged with amino acids to decode the mRNA for protein synthesis.

transport receptor/karyopherin/importin/exportin The receptors that bind to and recognize protein and RNA cargoes that are transported into or out of the nucleus.

U snRNA Small RNAs that participate in splicing.

Further Reading

Damelin, M., Silver, P. A., and Corbett, A. H. (2002). Nuclear protein transport. *Methods Enzymol.* **351**, 587–607.

Dasso, M. (2002). The ran GTPase: Theme and variations. *Curr. Biol.* **12**, R502–R508.

Gorlich, D., and Kutay, U. (1999). Transport between the cell nucleus and the cytoplasm. *Annu. Rev. Cell Develop. Biol.* **15**, 607–660.

Lei, E. P., and Silver, P. A. (2002). Protein and RNA export from the nucleus. *Develop. Cell.* **2**, 261–272.

Quimby, B. B., and Corbett, A. H. (2001). Nuclear transport mechanisms. *Cell Mol. Life Sci.* **58**, 1766–1773.

Rout, M. P., and Aitchison, J. D. (2000). Pore relations: Nuclear pore complexes and nucleocytoplasmic exchange. *Essays Biochem.* **36**, 75–88.

Strom, A. C., and Weis, K. (2001). Importin-beta-like nuclear transport receptors. *Genome Biol.* **2**, Epub 2001 Jun 05.

Suntharalingam, M., and Wente, S. R. (2002). Peering through the pore: Nuclear pore complex structure, assembly, and function. *Develop. Cell.* **4**, 775–789.

Weis, K. (2002). Nucleocytoplasmic transport: Cargo trafficking across the border. *Curr. Opin. Cell Biol.* **14**, 328–335.

Biography

Anita H. Corbett, Ph.D., is an Associate Professor of biochemistry at the Emory University School of Medicine. Her principal research interest is in the area of macromolecular trafficking between the cytoplasm and the nucleus. She utilizes the budding yeast, *Saccharomyces cerevisiae* as a model system for most of her studies. Dr. Corbett holds a Ph.D. in biochemistry from Vanderbilt University. She completed a postdoctoral fellowship at Harvard Medical School before moving to Emory in 1997.

Nucleoid Organization of Bacterial Chromosomes

Charles J. Dorman
Trinity College, Dublin, Ireland

Bacteria do not possess a nuclear membrane, and so have no clearly defined nucleus in the eukaryotic sense. It is for this reason that they are classed as prokaryotes. The term nucleoid is used to describe that part of the bacterial cytoplasm that is occupied by the genetic material. This has been the subject of investigation for several decades now, yet despite intensive study, many details of nucleoid structure and function remain obscure. It seems ironic that our understanding of these so-called "simple" organisms continues to lag behind that of cells in higher organisms in this respect. This article will describe those features of the bacterial nucleoid over which there is general agreement. Much of the material comes from work with *Escherichia coli*, the best-studied prokaryote, and encompasses the organization of the genetic material within the nucleoid and its interactions with those DNA-binding proteins that are thought to impart structure to it.

Organization of DNA in the Nucleoid

When considering the nucleoid, one of the first issues to be confronted concerns the problem of how to package a circular DNA molecule measuring ~1.5 mm in circumference within a cylindrical container with hemispherical ends (the cell) that measures 2 μm in length × 1 μm diameter. Any solution to this problem must take into account the persistence length of the molecule, which for B-DNA is 50 nm (150 bp). This imposes on the circular chromosome a tendency to adopt a disordered globular configuration, resulting in a ball of DNA measuring 10 000 nm in diameter. This structure is at least 10 times too large to fit in the cell. Since bacterial chromosomes clearly do fit in cells, organization at some level must be imposed on this otherwise chaotic arrangement. Organization is also required so that the DNA can participate in transactions such as gene transcription. It seems that this organization occurs at least on two levels. The first concerns an effect on the shape of the DNA itself that is imparted through negative supercoiling, whereas the second involves the interaction of the DNA with so-called nucleoid-associated proteins. Each of these aspects will be considered in turn.

DNA Supercoiling

As with DNA in other types of cells, bacterial DNA is maintained in a negatively supercoiled state. This arises because the double helix in the cell has a deficiency of helical turns; in other words, it is in an under-wound state. The molecule is thus placed in a thermodynamically unfavorable state due to torsional stress. This difficulty is resolved by a structural transition to an energetically more favorable form. In practice, this involves adopting a shape (or topology) that we call supercoiled, in which an already-coiled molecule (the DNA duplex) itself becomes coiled (Figure 1). Supercoiling creates writhing of the DNA helical axis and this results in a more compact molecule. The compaction can arise due to adoption by the DNA of a plectomenic (braided) or a toroidal (doughnut-like) configuration. Depending on how supercoiled the DNA becomes, the structure can also form branches, leading to further compaction. This reduces the diameter of the DNA ball to a value that can be accommodated within the confines of the cell.

The foregoing description of DNA supercoiling and its effects on DNA compaction is highly qualitative. It is possible to treat DNA supercoiling in a quantitative manner, making accurate measurements of how supercoiled DNA molecules are under particular conditions. This is desirable since it allows one to calculate the energetic consequences for DNA of different levels of supercoiling. The under-winding of the DNA duplex that is a characteristic of negatively supercoiled molecules imparts free energy to the DNA, and this energy is available to drive the major transactions in which DNA participates, such as gene transcription. Knowledge of the minimum energy requirements of a particular transaction can be used to estimate the level

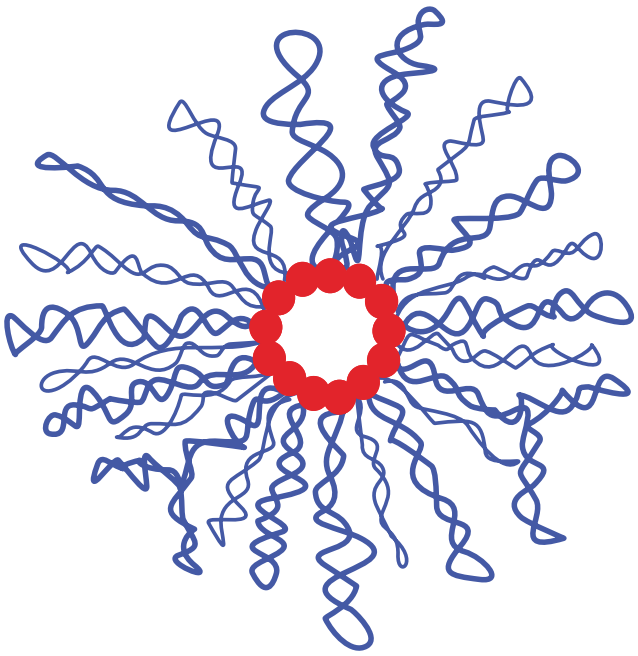

FIGURE 1 Organization of the bacterial nucleoid. A representation of the nucleoid liberated from the cell is shown. The red spheres at the core represent the nucleoprotein complexes that define the ends of the supercoiled domains. These complexes are thought to be composed of nucleoid-associated proteins and possibly topoisomerases. The blue ribbons represent the DNA making up the supercoiled domains. A typical nucleoid from *E. coli* has between 50 and 100 of these.

to which DNA has become supercoiled. When used in conjunction with physical methods based on electrophoretic mobility of covalently closed circular DNA or its sedimentation rates, one can obtain robust measurements of DNA supercoiling.

DNA can be described in terms of three topological parameters: linking number (L), twist (T), and writhe (W). The linking number is a measure of the number of times the two strands of the DNA duplex link with one another. Twist measures the turning of the DNA strands about the helical axis, whereas writhe measures the winding of the helical axis about itself. These properties are related as follows: $L = T + W$ and $\Delta L = \Delta T + \Delta W$. This means that a change in linking number is distributed between the other two parameters, resulting in a change that is manifest: (1) only as altered twist, (2) only as altered writhe, or (3) as a change in both twist and writhe. For very large DNA molecules, such as bacterial chromosomes, measurements of L are cumbersome and largely impractical. Here one employs a parameter such as the superhelical density, σ. This is the average number of superhelical turns per helical turn of DNA:

$$\sigma = 10.5\tau/N$$

where τ is the number of measurable supercoils, N is the number of base pairs in the molecule, and 10.5 refers to the number of base pairs per helical turn in B DNA. The importance of the energetics of supercoiling for DNA-based processes was referred to above. The free energy of supercoiling is related to the change in DNA linking number as follows: $\Delta G = (1050\ RT/N)\ (\Delta L)^2$, where R is the gas constant, T is the temperature in kelvin, and N is the size of the molecule in base pairs. The important point to note about this relationship is that the free energy varies in proportion to the square of the change in the linking number (L). Put qualitatively, this means that even modest changes in the linking number can result in significant variances in the energy imparted to the DNA.

Control of DNA Supercoiling

The level of DNA supercoiling in the bacterial nucleoid is established and maintained largely by the action of specialist enzymes called topoisomerases (Table I). Bacterial DNA gyrase is a type II ATP-dependent topoisomerase that introduces negative supercoils into DNA, reducing its linking number in steps of two. It can also remove positive supercoils using the same enzymatic mechanism. The activity of gyrase is opposed in the cell by DNA topoisomerase I, a type I topoisomerase that removes supercoils from negatively supercoiled DNA by a "swivelase" mechanism, increasing the linking number of the molecule in steps of one. It acts independently of ATP, using the energy stored in the supercoiled DNA molecule to drive the reaction. *E. coli* has two other topoisomerases, III and IV (Table I) that can relax negatively supercoiled DNA, although their main role *in vivo* seems to be to act as decatenases. The promoters of the genes coding for gyrase (*gyrA*, *gyrB*) and topoisomerase I (*topA*) are controlled, *inter alia*, by DNA supercoiling. This provides a useful feedback loop that controls the supply of these proteins. The *gyr* promoters are activated by DNA relaxation (loss of negative supercoiling), whereas the *topA* promoter is repressed by negative supercoiling. An important link between gyrase activity and cellular physiology concerns the dependence of this enzyme on ATP and the fact that gyrase is inhibited by ADP. In this way the major source of negative supercoiling is directly responsive to the energy charge of the cell.

The Domain Structure of the Nucleoid

Physical analysis has indicated that the chromosome within the cell is subdivided into ~50–100 independently supercoiled domains (Figure 1). Evidence comes from experiments in which chemical agents were used to

TABLE I

DNA Topoisomerases of *E. coli*

Enzyme	Gene	Molecular mass (kDa)	Remarks
Topoisomerase I	*topA*	97	Type I enzyme; relaxes negatively supercoiled DNA; cuts one strand of DNA and binds to cut site via a 5′-phospho-tyrosine covalent bond; Mg^{2+} dependent
DNA gyrase (Topoisomerase II)	*gyrA* *gyrB*	105 (GyrA) 95 (GyrB)	Type II enzyme; negatively supercoils relaxed DNA (requires ATP); relaxes positively supercoiled DNA; makes a transient double-stranded cut in DNA and binds via a 5′-phosphotyrosine bond Mg^{2+} dependent
Topoisomerase III	*topB*	73.2	Type I enzyme; can relax negatively supercoiled DNA; decatenase; Mg^{2+} dependent
Topoisomerase IV	*parC* *parE*	75 (ParC) 70 (ParE)	Type II enzyme; with strong sequence homology to gyrase; decatenase; relaxes negative supercoils but cannot create them; requires ATP and Mg^{2+}

nick the DNA. If the chromosome consisted of one continuous domain, a nick anywhere along its length would allow all supercoils to be lost through DNA relaxation. Since 50–100 nicks must be introduced to relax the DNA fully, it has been concluded that subdomains must exist. The possibility that these domains might be supercoiled to different values of σ is an attractive idea since it would allow gene promoters at different locations on the chromosome to experience different degrees of negative superhelicity. This in turn might contribute to differential expression of genes at different locations. However, experiments in which supercoiling-sensitive promoters were placed at different locations in the genome provided no support for this proposal. Therefore, it seems likely that on average each domain of the nucleoid is supercoiled to a similar value of σ.

An important and unresolved issue concerns the nature and locations of the boundaries of the chromosomal domains. Some evidence obtained by promoting long-range interactions in the genome leading to DNA recombination indicates that these boundaries are not fixed in their locations. They may have a transient existence, being dismantled to permit processes such as replication of the DNA to proceed. A favorite hypothesis to explain the nature of the boundaries envisages a role for nucleoid-associated DNA-binding proteins, perhaps acting in combination with topoisomerases (Figure 1).

Nucleoid-Associated Proteins

Bacteria possess DNA-binding proteins that have been described both as "histone-like" and "nucleoid-associated." The former term reflects their function rather than any strong structural similarity to the histones of eukaryotes. The latter name implies that they have a role to play in the organization of the nucleoid. These proteins typically have a low molecular mass, are basic in amino acid composition, and have DNA-binding activity. Depending on the protein, on binding to DNA it can bend or wrap the DNA around itself. DNA wrapping results in the constraining of supercoils. If the DNA is nicked in the absence of the protein, the supercoils are lost; if the protein has wrapped the DNA around itself, the DNA in association with the protein has its supercoils preserved. Measurements of σ for *E. coli* indicate that at any given time ~50% of the DNA in the cell is associated with such proteins while the remainder is in the form of plectonemic supercoils. This is in sharp contrast to the situation in eukaryotes where interaction with histones is the norm. It means that in the bacteria the impact of changes in σ can have more immediate consequences for DNA transactions in these protein-free regions.

The bacteria possess a wide array of histone-like proteins. In *E. coli* the most important include HU, IHF, H-NS, and Fis (Table II). Of these, HU and H-NS are characterized by a lack of a consensus sequence for DNA binding. Instead, they interact with structures in the DNA, such as four-way junctions (HU) or intrinsically curved DNA (H-NS). IHF has a similar amino acid sequence to HU (Fis, HU, and H-NS are structurally distinct) but binds to a clearly defined consensus sequence where it introduces a DNA bend of up to 180°. This gives it a powerful role in local structural organization within the nucleoid, although its action is confined to regions that contain a copy of its binding site. It may also act in conjunction with DNA gyrase to maintain supercoiling at strategically important sites. Fis binds to a rather degenerate consensus sequence and is characterized by having an expression profile that is

TABLE II

Major Nucleoid-Associated Proteins of *E. coli*

Protein	Gene	Molecular mass (kDa)	Remarks
Fis	*fis*	11.2	Fis: factor for inversion stimulation; homodimeric DNA-binding protein; binds to degenerate consensus sequence; bends DNA by between 40° and 90°; organizes local DNA topology; multifunctional and is involved in transcription, DNA replication, recombination, and transposition. Strong growth phase regulation varies protein number/cell over 200–100 000 range
H-NS	*hns*	15.6	H-NS: histone-like nucleoid structuring; oligomeric DNA-binding protein; lacks a consensus sequence for DNA binding but has an affinity for curved DNA; compacts DNA and constrains supercoils; important transcription regulator (usually a repressor); estimated to be 20 000–60 000 H-NS monomers/cell
HU	*hupA* *hupB*	9.5 9.5	HU: heat unstable; abundant heterodimeric DNA-binding protein; 60 000 dimers/cell; lacks a consensus sequence for DNA binding; can constrain DNA supercoils
IHF	*ihfA* *ihfB*	11.2 10.6	IHF: integration host factor; heterodimeric DNA-binding and -bending protein; homologue of HU but binds to well-conserved consensus sequence; bends DNA by up to 180°; between 17 000 and 34 000 monomers/cell

tightly linked to the growth phase of the cell. It is highly abundant in cells exiting lag phase but is present in miniscule amounts in cells in late logarithmic growth. The Fis protein plays a direct role in nucleoid organization by acting as a transcription repressor at the promoters of *gyrA* and *gyrB*, the genes coding for gyrase. It also binds preferentially to DNA with intermediate values of σ and preserves their topology in the face of attempts by topoisomerases to alter σ. Finally, DNA supercoiling controls the supply of Fis at the level of *fis* gene transcription, providing a feedback loop linking expression of this protein to the topological state of the nucleoid. In *E. coli*, the subunit composition of HU and its activities vary with growth phase as the relative amounts of each subunit change in the cell. H-NS is expressed roughly at a constant level throughout growth, but it forms hetero-oligomers with a paralogous protein called StpA at certain periods in the growth cycle and this may alter its properties. IHF also shows a growth-phase-dependent pattern of expression, being most abundant as the cell approaches the stationary phase of growth. This dynamism in the expression of the nucleoid-associated proteins can be expected to have an impact on the structure of the nucleoid as the cell grows and may be reflected in the location and number of domain boundaries and the compactness of the nucleoid.

See Also the Following Articles

Chromosome Organization and Structure, Overview • DNA Supercoiling • DNA Topoisomerases: Type I • DNA Topoisomerases: Type II • Nuclear Organization, Chromatin Structure, and Gene Silencing

Glossary

decatenase An enzyme that unlinks interlinked circular DNA molecules.

par protein A protein involved in DNA partitioning at cell division.

persistence length The average length over which a polymer maintains a straight trajectory when subject to Brownian motion.

Further Reading

Dorman, C. J., and Deighan, P. (2003). Regulation of gene expression by histone-like proteins in bacteria. *Curr. Opin. Genet. Dev.* **13**, 179–184.

Pettijohn, D. E. (1996). The nucleoid. In *Escherichia coli and Salmonella, Cellular and Molecular Biology* (F. C. Neidhardt, R. Curtiss III, J. L. Ingraham, E. C. C. Lin, K. B. Low, B. Magasanik, W. S. Reznikoff, M. Riley, M. Schaechter and H. E. Umbarger, eds.) 2nd edition, Vol 1, pp. 158–166. American Society for Microbiology Press, Washington, DC.

Sinden, R. R. (1994). *DNA Structure and Function.* Academic Press, San Diego.

Trun, N. J., and Marko, J. F. (1998). Architecture of a bacterial chromosome. *ASM News* **64**, 276–283.

Biography

Charles J. Dorman is Professor of Microbiology at the Department of Microbiology, Moyne Institute for Preventive Medicine, University of Dublin, Trinity College. His principal research interest is the regulation of bacterial gene expression by nucleoid-associated proteins and DNA topology. He holds a Ph.D. from the University of Dublin and was a Royal Society Research Fellow in Biochemistry at the University of Dundee. He is editor-in-chief elect of the journal *Microbiology.*

Nucleolus, Overview

Thoru Pederson
University of Massachusetts Medical School, Worcester, Massachusetts, USA

Nucleoli are specialized structures within the nuclei of most eukaryotic cells and are the sites of ribosomal RNA synthesis and the assembly of ribosomes. Nucleoli form around the genes for ribosomal RNA (rRNA), and their structural organization is thought to be a manifestation of ongoing rRNA synthesis and ribosome assembly. The nucleoli are not separated from the rest of the nuclear interior by a membrane, and there is a rapid and diverse traffic of various RNAs and proteins in and out of nucleoli (in addition to the overall export of new ribosomes). There is increasing evidence that nucleoli are involved in functions in addition to ribosome synthesis.

Background

The nucleolus was one of the earliest intracellular structures (and the first within the nucleus) to be observed by microscopy, around 1860. Throughout the early twentieth century, cytologists were struck by the consistent presence of nucleoli inside the nuclei of virtually all cells examined, although the number and shape of nucleoli were quite variable (Figure 1). In the 1930s, it was discovered that the formation of the nucleolus is determined by a distinct genetic locus. This genetic element, termed "the nucleolus organizer," was found in the 1960s to consist of repeated genes for rRNA. It is an interesting historical fact that the rRNA genes were not only the first ones from eukaryotes to be observed at high resolution in the electron microscope, but also they were the first genes to be physically isolated, well before the advent of recombinant DNA techniques.

Although a considerable amount of cytochemical and ultrastructural research had been done on nucleoli up through the 1950s, a major advance occurred when they were first isolated by cell fractionation in the mid-1960s. This opened the door to the investigation of their protein and RNA components, and accelerated the study of rRNA synthesis and processing.

Structure

Although the ultrastructural (electron microscopic) appearance of nucleoli is highly variable, a tripartite organization is generally observed. Fibrillar centers (FCs) are one or more rather small foci within a nucleolus that have a distinctive appearance. Each of these FCs is surrounded (in three dimensions) by a typically much larger zone, called the "dense fibrillar component" (DFC). The remainder of the nucleolus, or at least most of the remainder, displays a distinctly more granular appearance, and is thus called the granular component (GC).

Functional Organization

The tripartite ultrastructural landscape of the nucleolus has been functionally defined (Figure 2). The FCs are the zones where the active rRNA genes themselves are located. The nascent transcripts of pre-rRNA extend out into the juxtaposed DFC, which also contains intermediate RNA species in the rRNA processing pathway. Also present in the DFC are numerous (100–200 or more) small RNA species (and their associated proteins) that serve as guide RNAs for the site-specific modification (2′-*O*-ribose methylation and pseudouridine formation) of many internal nucleotides in pre-rRNA. The GC consists of more mature, assembled ribosomal particles. It is not yet entirely clear whether certain stages of ribosome maturation are sharply restricted to the DFC or the GC or instead have some degree of overlap between them.

Amplified Nucleoli and Missing Nucleoli

One of the most dramatic aspects of the biology of the nucleolus is its selective amplification in the oocytes of certain organisms. In these cells, the rRNA genes are amplified into a large number (typically thousands) of extrachromosomal copies, which form supernumerary nucleoli. Through their activity, the growing oocyte builds up a large reservoir of maternal ribosomes to sustain early embryonic development. Amplified nucleoli are found in the oocytes of several phyletic

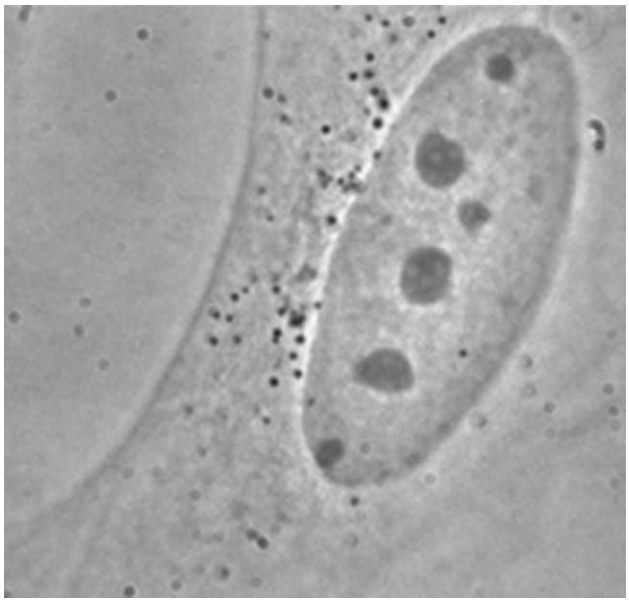

FIGURE 1 Phase contrast micrograph of a portion of a living HeLa (human cervical carcinoma) cell. The dark, spherical objects within the nucleus are the nucleoli. This micrograph was taken by Laura Lewandowski in the author's laboratory. Magnification approx. 3,000x.

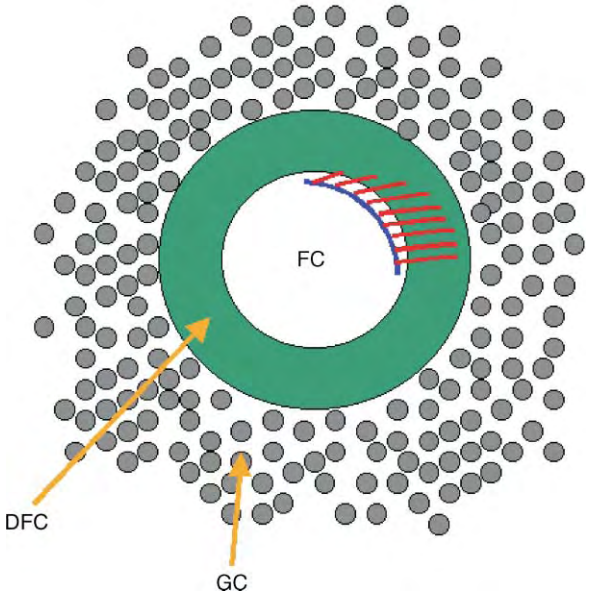

FIGURE 2 A schematic diagram illustrating the relationships of the three major components of the nucleolus. An FC contains the active rRNA genes (blue) with the nascent transcripts of pre-rRNA (red) extending into the surrounding DFC, embedded in the GC. See text for further details. Reproduced with permission from Huang, S. (2002). Building an efficient factory: Where is pre-rRNA synthesized in the nucleolus? *J. Cell Biol.* **157**, 739–741, with copyright permission from the Rockefeller University Press and with the kind consent of the author.

groups, but have been most extensively studied in urodele and anuran Amphibia (salamanders and frogs).

One of the ways the function of the nucleolus in ribosome synthesis was first revealed was by an elegant experiment that involved a frog mutant in which one chromosomal set of rRNA genes is missing. Half the oocytes of females that are heterozygous for this mutation have no rRNA genes whatsoever and, consequently, cannot form amplified nucleoli, nor can anucleolate embryos descended from them synthesize new ribosomes. Accordingly, these embryos die at a time during development when the maternal supply of ribosomes becomes limited. This experiment is one of the classics in the field of eukaryotic gene expression.

Clinical Connections

Two aspects of the nucleolus are significant clinically. For many years pathologists have used nucleolar morphology and number as an important guide in the diagnostic classification of certain malignancies. In addition, a specialized structure called the perinucleolar compartment (PNC) sits as a cap-like disk on the surface of the nucleoli in most malignant cells (both tumor cell lines and actual patient biopsies). The PNC seems to be involved in RNA metabolism, and contains a set of small RNAs that are transcribed by RNA polymerase III. However, its relationship to malignancy is not known.

The Plurifunctional Nucleolus

Since the 1990s a number of clues have begun to suggest that the nucleolus may have functions beyond ribosome synthesis. One line of evidence consists of the observation in nucleoli of various molecules that have no known connection with ribosome biosynthesis. For example, several proteins related to mitogenic cell signaling and cell cycle progression have been found in nucleoli, although these various observations have not yet been drawn together into a coherent framework. In budding yeast, the nucleolus of interphase cells contains a complex that is released and promotes a late stage of mitosis after the nucleolus breaks down, but whether this complex has some role within the interphase nucleolus as well is not known. The RNA subunit of the ribonucleoprotein enzyme telomerase appears to shuttle between the chromosomes and the nucleolus in some cells but, again, the functional meaning of this observation is not clear. The fact that so many of the various ribosome-unrelated molecules and complexes that are increasingly being observed in the nucleolus are related to cell growth is quite intriguing, and this is an important area for future work.

It has also become clear that the life cycle of certain viruses involves the nucleolus in some way. For example, in the replication of the human immunodeficiency virus, certain forms of viral messenger RNAs are associated with the nucleolus during a particular stage in the infectious cycle. However, the functional significance of this and other observations of viral connections with the nucleolus is not presently known.

A third nonribosomal function of the nucleolus is its likely participation in the biosynthesis of the signal recognition particle (SRP). The SRP is an RNA–protein complex that ensures the topologically correct synthesis of membrane and secreted proteins. Both the RNA component of the SRP and some of the SRP's protein components are present in the nucleolus in yeast, amphibian oocytes (i.e., in the amplified nucleoli), and

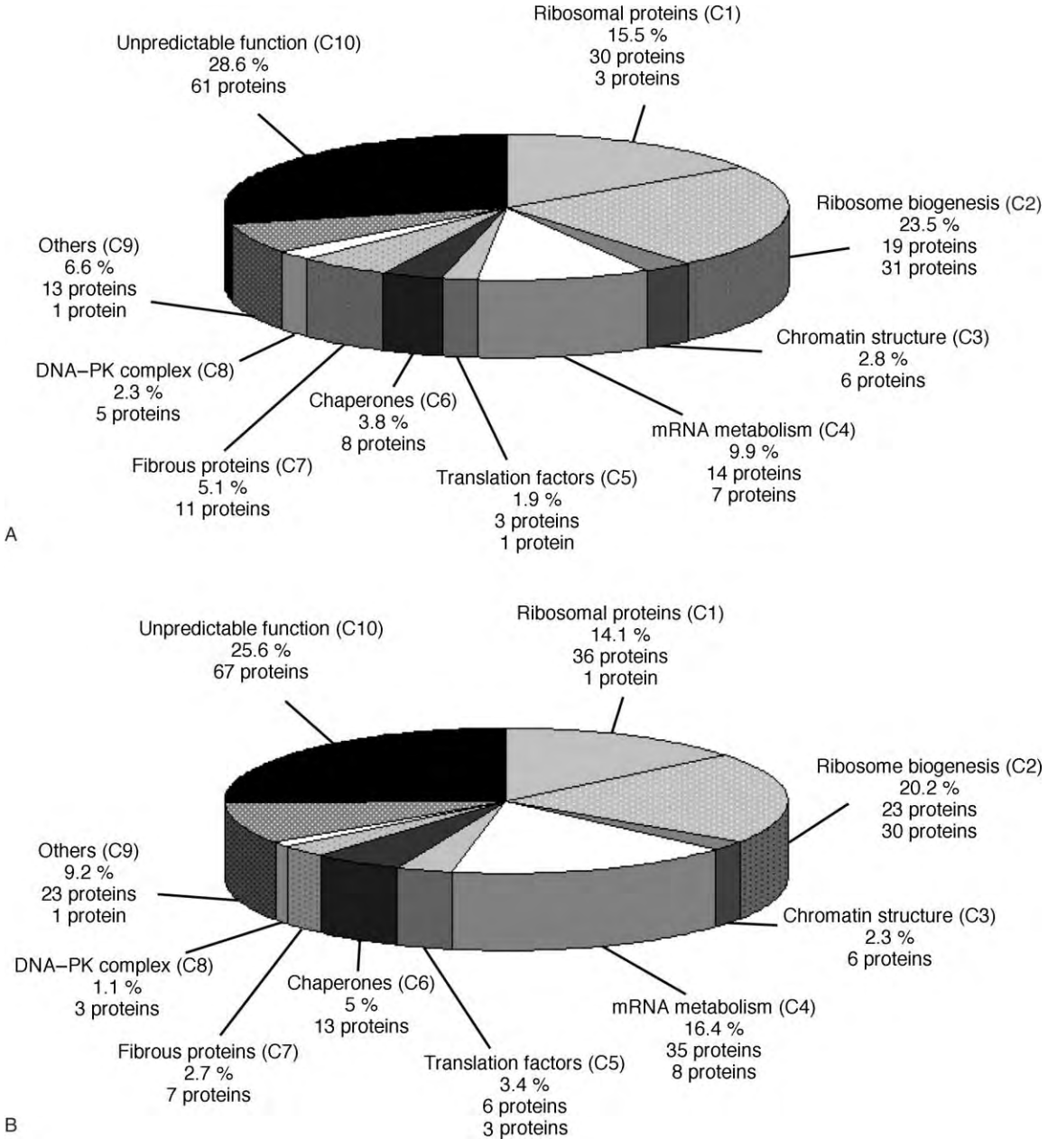

FIGURE 3 Relative occurrence of various classes of proteins in nucleoli purified from HeLa cells, as determined by proteomics. The two panels present the results from two independent studies. Panel A shows the results from Scherl, A., Coute, Y., Deon, C., Calle, K., Kindbeiter, K., Sanchez, J.-D., Greco, A., Hochstrasser, D., and Diaz, J. J. (2002). Functional proteomic analysis of human nucleolus. *Mol. Biol. Cell* **13**, 4100–4109. Panel B shows the results from Andersen, J. S., Lyon, C. E., Fox, A. H., Leung, A. K., Lam, Y. W., Steen, H., Mann, M., and Lamond, A.I. (2002). Directed proteomic analysis of the human nucleolus. *Current Biol.* **12**, 1–12. The figure is reproduced from Scherl, A., Coute, Y., Deon, C., Calle, K., Kindbeiter, K., Sanchez, J.-D., Greco, A., Hochstrasser, D., and Diaz, J.J. (2002). Functional proteomic analysis of human nucleolus. *Mol. Biol. Cell* **13**, 4100–4109, with copyright permission from the American Society for Cell Biology and with the kind consent of the authors. For further details see also Pederson, T. (2002). Proteomics of the nucleolus: more proteins, more functions? *Trends Biochem. Sci.* **27**, 111–112.

mammalian cells, suggesting that this translation-related RNA–protein complex originates in the nucleolus, as do the ribosomes themselves.

Current Trends and Conclusion

At the present time, studies on the nucleolus are being conducted by nucleolar specialists on the one hand, and by an increasing number of cell biologists on the other, who are encountering a nucleolar connection in their work. A nucleolar protein has been implicated in the biology of embryonic stem cells, and a reorganization of the nucleolus in donor somatic cell nuclei appears to be a key factor in the cloning of mammalian animals. Meanwhile, on the analytical front, proteomics studies of purified human nucleoli have identified ~350 proteins that are highly enriched in the isolated fraction (Figure 3). Many of these proteins have no obvious relationship to ribosome biosynthesis. One interesting possibility is that perhaps all of these apparently nonribosome related nucleolar components are indeed related to ribosome biosynthesis after all, not in the constitutive pathway of ribosome synthesis itself (the classical model), but as regulatory components of cellular growth control circuits that intersect in the nucleolus and thus with the biogenesis of the protein synthesis machinery (a neoclassical model).

See Also the Following Articles

Ribosome Assembly • Ribosome Structure • Translation Termination and Ribosome Recycling

Glossary

nucleolus organizer A genetic locus containing genes for ribosomal RNA.

perinucleolar compartment A discoid, cap-like structure situated on the surface of nucleoli in most malignant cells.

proteomics An emergent field of protein sequence determination in complex mixtures, based on a high-resolution analytical method in which the protein components of a subcellular complex or organelle, first separated by electrophoresis or liquid chromatography, is proteolytically cleaved (usually by trpysin) into fragments that are then resolved by matrix-assisted, laser desorption ionization time-of-flight mass spectrometry.

Further Reading

Andersen, J. S., Lyon, C. E., Fox, A. H., Leung, A. K., Lam, Y. W., Steen, H., Mann, M., and Lamond, A. I. (2002). Directed proteomic analysis of the human nucleolus. *Current Biol.* **12**, 1–12.

Brown, D. D., and Gurdon, J. B. (1964). Absence of rRNA synthesis in the anucleolate mutant of *X. laevis*. *Proc. Natl Acad. Sci. USA* **51**, 139–146.

Hernandez-Verdun, D., Roussel, P., and Gebrane-Younes, J. (2002). Emerging concepts of nucleolar assembly. *J. Cell Sci.* **115**, 2265–2270.

Huang, S. (2002). Building an efficient factory: Where is pre-rRNA synthesized in the nucleolus? *J. Cell Biol.* **157**, 739–741.

Olson, M. O., Dundr, M., and Szebeni, A. (2000). The nucleolus: An old factory with unexpected capabilities. *Trends Biochem. Sci.* **10**, 189–196.

Pederson, T. (1998). The plurifunctional nucleolus. *Nucleic Acids Res.* **17**, 3871–3876.

Pederson, T. (2002). Proteomics of the nucleolus: more proteins, more functions? *Trends Biochem. Sci.* **27**, 111–112.

Pederson, T., and Politz, J. C. (2000). The nucleolus and the four ribonucleoproteins of translation. *J. Cell Biol.* **148**, 1091–1095.

Scherl, A., Coute, Y., Deon, C., Calle, K., Kindbeiter, K., Sanchez, J.-D., Greco, A., Hochstrasser, D., and Diaz, J. J. (2002). Functional proteomic analysis of human nucleolus. *Mol. Biol. Cell* **13**, 4100–4109.

Biography

Thoru Pederson is the Vitold Arnett Professor in the Department of Biochemistry and Molecular Pharmacology at the University of Massachusetts Medical School. He received his Ph.D. from Syracuse University and was a Postdoctoral Fellow in Cell Biology at the Albert Einstein College of Medicine. He was at the Worcester Foundation for Biomedical Research throughout his initial career. His research is centered on RNA processing, RNA–protein interactions, and the functional organization of the cell nucleus.

Nucleotide Excision Repair and Human Disease

James E. Cleaver
University of California, San Francisco, California, USA

Nucleotide excision repair, the mechanism of repair of large DNA adducts, has a key role in the development of every organism. This article discusses the types and mechanisms of nucleotide excision repair, and the clinical consequences associated with its deficiencies.

Introduction

DNA repair is an important set of cellular processes that maintain the integrity of the genomes of every organism. Repair genes are found in every sequenced genome, and repair systems are dynamically interrelated to each other and with normal cell metabolism. The mechanism of repair of large DNA adducts especially those produced by ultraviolet (UV) light, known as nucleotide excision repair (NER), plays an important part in the development of the subject. The first connection between repair, specifically NER, and human disease has been found in xeroderma pigmentosum (XP) and details of the disease are in the website – www.xpmutations.org (Table I). XP is predominantly due to a failure of NER in cells that contain UV-induced photoproducts in their DNA (Figure 1). When these photoproducts are unrepaired-replication errors and cytosine deamination leads to characteristic C to T mutations, including especially CC to TT mutations, that are found at very high frequencies in sun-exposed skin and UVB (between 280 and 320 nm wavelength)-induced skin cancers.

Transcribed genes and their transcribed strands are more rapidly repaired than the rest of the DNA in a cell. A specific branch of NER has therefore been named "transcription coupled repair (TCR)" to distinguish it from repair of the remainder of the genome, called "global genome repair (GGR)" (Figure 2). Several components of the basal transcription factor, TFIIH, are also NER enzymes, indicating close integration of the transcription apparatus with repair.

Although in prokaryotes many DNA repair enzymes are inducible in response to damage, in eukaryotes a different strategy appears to predominate. Most of the eukaryotic repair genes are constitutively expressed, except for a small number in human cells that are p53-responsive such as *XPC*, *DDB2*, and *GADD45*. Modification of enzyme activity by phosphorylation, however, represents a major strategy by which eukaryotic cells regulate their response to cellular and DNA damage.

Types of Damage Repaired by NER

The NER system recognizes and repairs DNA damage that consists of UV-induced photoproducts and large DNA adducts. These include the cyclobutane [5–5], [6–6] pyrimidine dimers (CPDs) and the [6–4] pyrimidine pyrimidinone dimers ([6–4]PDs) that can involve T and C pyrimidines (Figure 1). The [6–4]PD can further photoisomerase to the Dewar photoproduct at longer UV wavelengths. Cytosine in dimers has an increased propensity to deaminate causing C to T mutagenesis. Chemical adducts include those produced by N-acetoxy-N-acetyl aminofluorene (AAAF), benzo[a]pyrene, 7,12-dimethyl-1,2-benz[a]anthracene (DMBA) aflatoxin, photoactivated psoralens, and *cis*-platinum. An oxidative purine product, 5′,8-purine cyclodeoxynucleoside, also requires the NER system for repair. The NER system can even recognize DNA triplexes formed by the binding of short oligonucleotides to double-stranded DNA.

Other kinds of damage involving smaller modifications to DNA bases (radiation and oxidative products, alkylations) or DNA breakage require a different suite of enzymes, some of which are involved with immunoglobulin rearrangements and developmental processes. The distinctions between the various repair systems are not absolute, however, and there are overlaps in the substrate specificity of these various repair systems and variations in the efficiencies and sites of action on DNA in differing metabolic states.

TABLE I

The Main Genes and Functions of the NER System

Gene	Chrom location[a]	Protein	Function	Partner(s)	CNS[b]
XPA	9q34.1	273aa	DNA damage binding	RPA	+
XPB	2q21	782aa	3′-5′ helicase	TFIIH	+
XPC	3p25.1	940aa	DNA damage binding	HR23B	−
XPD	19q13.2	760aa	5′-3′ helicase	TFIIH	+
XPE	11p11-12	427aa	DNA damage binding (DDB2)	DBB1(p127)	−
XPF	16p13.3	916aa	Endonuclease 5′ to damage	ERCC1	−
XPG	13q32-33	1186aa	Endonuclease 3′ to damage	Thymine glycosylase (nth)	+
XPV	6p21	713aa	Low fidelity DNA polymerase (pol η)	PCNA	−
CSA	5q11.2	396aa	WD protein, ubiquitination of RNA pol II		+
CSB	10q23	1493aa	DNA dependent ATPase, ubiquitination of RNA pol II		+

[a] For further details on chromosome locations and sequence see www.ensembl.org and for mutations in the genes see www.xpmutations.org.
[b] The presence of central nervous system (CNS) disorders in the majority of the patients in the group is indicated by a " + ," complete absence by a " − ".

Recognition of Damage in Transcriptionally Inactive and Active Regions of the Genome

The initial damage recognition factors uniquely required for GGR are the XPC and XPE DNA binding proteins (Figure 2). XPC is found in association with a cofactor HR23B, one of the two human homologues of the yeast Rad23 gene product. The XPC/HR23B complex is the earliest damage detector to initiate NER in nontranscribed DNA with highest affinity for the [6–4]PD. In XP-C cells that lack this complex, repair is confined to small transcriptionally active islands of the genome, where repair occurs at normal rates, surrounded by oceans of unrepaired transcriptionally silent DNA. The constitutive level of expression of *XPC* is controlled by p53, and the protein can be induced by UV irradiation.

The *XPE* gene product involves a dimeric protein having subunits of 127 kDa (DDB1) and 48 kDa (DDB2) and mutations that are diagnostic for XP-E patients are located in the DDB2 subunit. The XPE protein is mainly involved in repair of mutagenic UV-induced photoproducts.

CPDs are excised more rapidly from actively transcribed genes, especially from the DNA strand used as the template for transcription. The initial damage recognition mechanism for TCR may be the stalled RNA Pol II, itself, although a potentially large number of gene products play a role in mediating the increased rate of repair. Excision can be slow where binding proteins interact with the promoter but increases immediately after the ATG start site for transcription.

Two genes, *CSA* & *CSB*, are involved specifically in TCR. CSA contains WD-repeat motifs that are important for protein–protein interactions. CSB contains an ATPase, helicase motifs, and a nucleotide binding domain, but only the latter is essential for TCR, and CSB does not function as a helicase. Cells lacking either CSA or CSB are unable to ubiquitinate the C-terminal domain of RNA Pol II, that may influence its ability to dissociate or back away from stalling lesions.

The Core Excision Process Common to GGR and TCR

The individual factors of NER associate sequentially and independently on UV photoproducts, *in vivo*, without preassembly of a "repairosome" complex (Figure 2).

Damage Verification

After damage recognition, the initial proteins are replaced by another damage binding complex, XPA and replication protein A (RPA) that acts as a foundation on which many of the other components of the NER process assemble.

DNA Unwinding

The damaged site is unwound by the 3′-5′ (XPB) and 5′-3′ (XPD) helicases of TFIIH and stabilized by the XPA–RPA binding complex.

Excision of the Damaged Strand

An oligonucleotide, 27–29 nucleotides long, containing the photoproduct is excised by enzymatic cleavages, 5 nucleotides on the 3′ side of the photoproduct, and

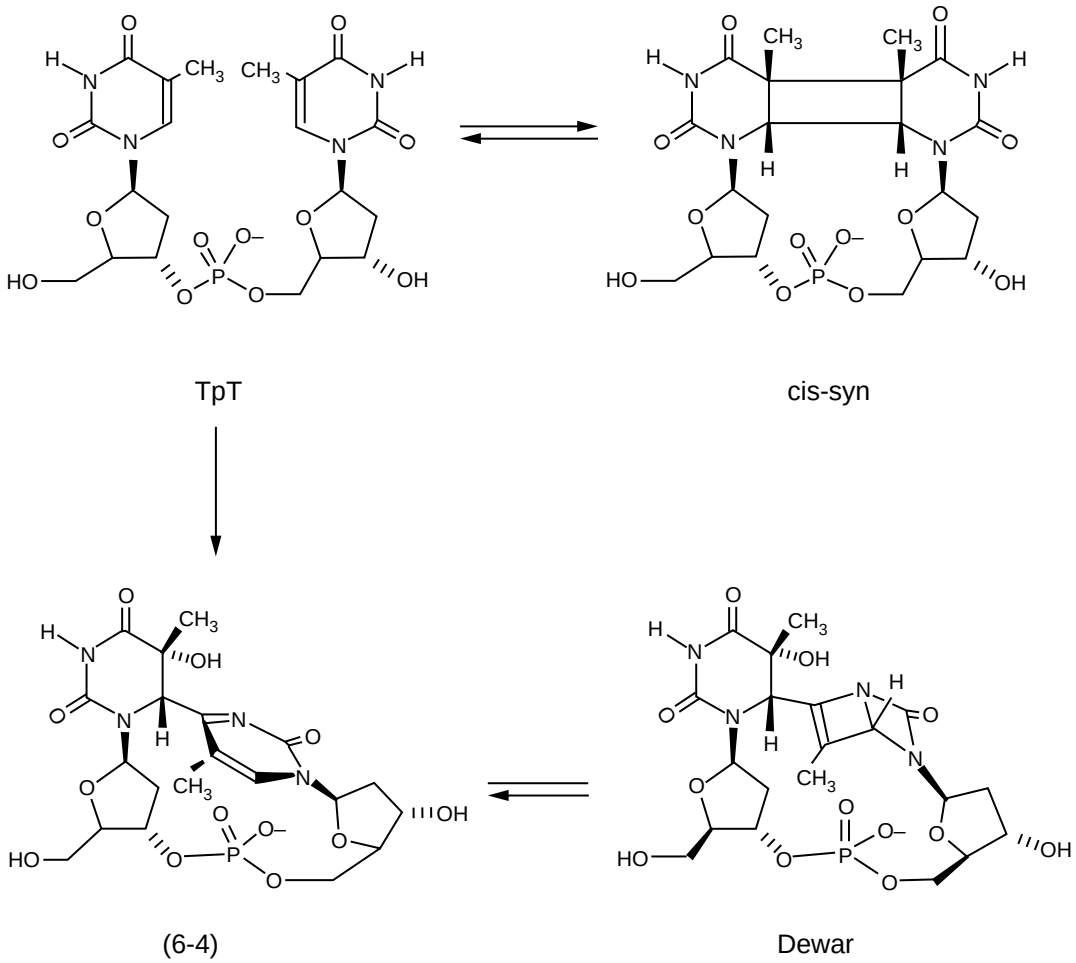

FIGURE 1 Photochemical reactions in a dipyrimidine DNA sequence leading to the formation of a cis-syn CPD (top right) or a [6–4]PD (bottom left) and its photolytic derivative, the Dewar pyrimidine (bottom right). (Reproduced from Cleaver J. E., and Mitchell D. L. (2003). Ultraviolet radiation carcinogenesis. In *Cancer Medicine*, 6th edition, Chap. 20, with permission of B. C. Dekker, London.)

24 nucleotides on the 5′ side. The structure-specific cleavage pattern is determined by binding of RPA to the unwound damaged site, and the excised fragment is close in size to the footprint of RPA on DNA. The XPG nuclease cleaves first on the 3′ side of the damage and interacts with the XPC–HR23B complex and with TFIIH; the XPF–ERCC1 heterodimer then binds to XPA through ERCC1 and cleaves on the 5′ side of the damaged site.

Synthesis of the Repair Patch

The excised region is replaced by the action of a complex similar to that involved in normal DNA replication. Proliferating cell nuclear antigen (PCNA) is loaded onto the DNA by the 5 subunit replication factor C (RFC) complex which then anchors the replicative DNA polymerases, Pol δ or Pol ε. The final closure of the repaired site occurs with DNA ligase I.

Replication of Damaged DNA

NER can remove DNA damage before DNA replication begins, and consequently plays a major role in reducing the amount of damage that becomes fixed as mutations during replication. DNA photoproducts, however, are blocks to the replicative DNA polymerases – alpha, delta and epsilon (Pol α, δ, ε, respectively). Replicative bypass of these photoproducts is achieved instead by damage-specific polymerases with relaxed substrate specificity, now defined as the low-fidelity class Y polymerases. These polymerases have larger active sites that allow them to read-through noninformative sequence information resulting from DNA damage. One adverse consequence of this relaxed specificity is that these polymerases have high error rates of the order of 1% when assayed *in vitro*, and this property must be controlled *in vivo*, otherwise the results would be catastrophic to the cell.

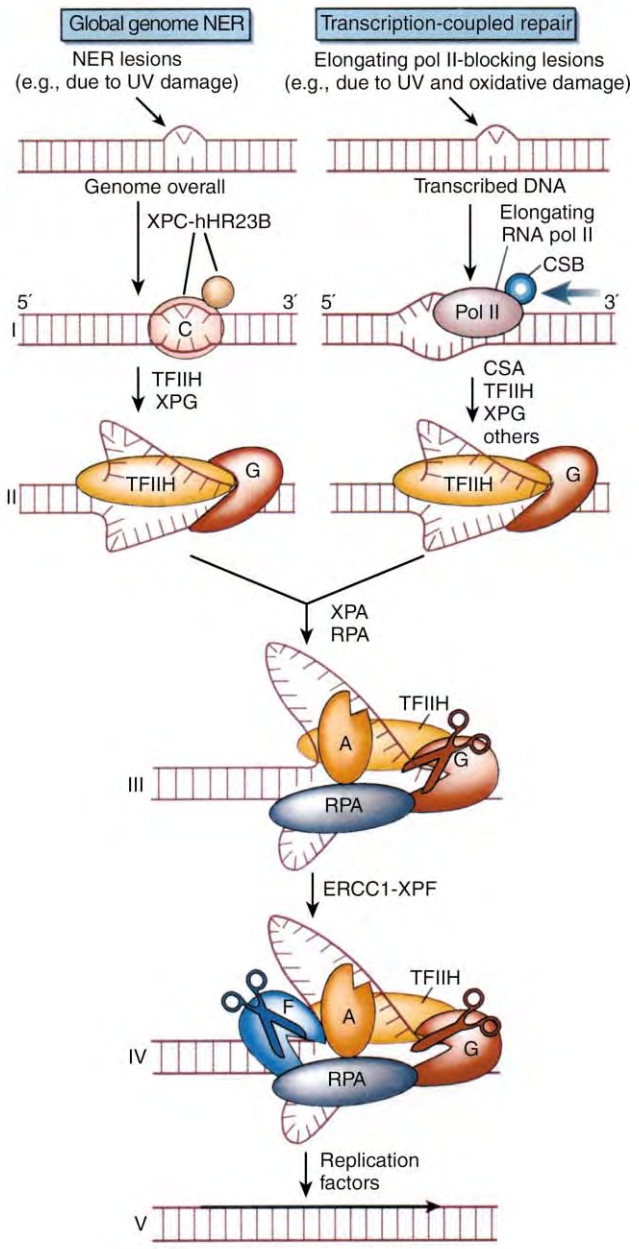

FIGURE 2 The sequence of steps involved in nucleotide excision repair (global genome repair and transcription coupled repair) from damage recognition, verification, unwinding, excision, polymerization and ligation. I, damage recognition; II, DNA unwinding; III, cleavage 3′ to the damaged site; IV, cleavage 5′ to the damaged site; V, repair replication. (Reproduced from Hoeijmakers J.H.J. (2001) Genome maintenance mechanisms for preventing cancer, with permission of Nature.)

Three class Y polymerase genes have been identified in the mammalian genome, *Pol* η, ι, and κ. *Pol* η and ι are close homologues, unique to mammalian cells, and only a single *Pol* η gene is found in yeast. Mutations in *Pol* η result in similar clinical symptoms to those seen in the NER-defective XP patients. Pol η and ι are involved in replication of UV damage but Pol κ replicates other kinds of damage or extends a DNA strand from mis-matched 3′ termini. Pol η preferentially inserts adenines across from thymine-containing photoproducts, resulting in accurate replication of a T-T CPD. Pol ι preferentially inserts guanines across from cytosine-containing photoproducts, resulting in accurate replication of a T–C CPD or [6–4]PD.

Pol η acts distributively to extend nascent DNA chains by one or two bases across from CPDs, and there may be a role for editing by a separate exonuclease. Chain extension then requires the activity of Pol ζ or Pol κ. Pol η is uniformly distributed in the nucleus, and excluded from the replication fork until replication is stalled by UV damage. Pol η then traffics into the nucleus and accumulates with a large number of other proteins in microscopically visible foci at the replication fork. This requires specific sequence motifs in the protein for translocation and for binding to PCNA.

Clinical Consequences of NER Deficiencies – Cancer

Mutations in NER genes are found in XP, and in other cancer, developmental or neurodegenerative diseases such as Cockayne syndrome (CS), trichothiodystrophy (TTD), and Cerebro-Oculo-Facio-Skeletal (COFS) syndrome. These represent only about 10 of the possible 30 genes involved in NER. The other genes are probably essential and mutations are likely to be inconsistent with viability, as has been demonstrated for *ERCC1* and *HR23B*.

XP manifests as a multigenic, multiallelic autosomal-recessive disease but heterozygotes are unaffected. The frequency in the United States is about 1:250 000, but higher in Japan and the Mediterranean, and possibly Central American areas. The disease begins in early life with the first exposures to sunlight, the median age of onset being 1–2 years of age, with skin rapidly exhibiting the signs associated with years of sun exposure. Pigmentation is patchy, and skin shows atrophy and telangiectasia with progressive degeneration of sun-exposed regions of the skin and eyes, usually leading to various forms of cutaneous malignancy (melanoma and nonmelanoma). Cancer incidence for those individuals under 20 years of age is 2000 times that seen in the general population. There may be a reduction in life span associated with the progression of cancer or neurologic degeneration, but a specific effect on aging itself has not been observed. In areas with poor health care, malignant disease may compound other life-threatening conditions (malnutrition, infections etc), but stringent protection from sun-exposure can minimize the development of symptoms dramatically.

The nonmelanoma skin cancers that develop in XP patients contain mutations in the *p53* gene (squamous carcinomas) or *patched* (basal cell carcinoma) that are mainly C to T transitions at dipyrimidine sequences, characteristic of the UV photoproducts that are the substrates for NER (Figure 1). Melanomas are also found at higher frequency in XP patients with a similar body distribution to those in non-XP patients, but UV-specific mutations in relevant genes (*p16*, *BRAF*) have not yet been found.

Clinical Consequences of NER Deficiencies – Neurodegeneration

Progressive neurologic degeneration occurs in a significant number of patients, with NER deficiencies (Table I). Most of these patients have mutations in subset of XP and CS genes, especially those associated with TCR. These include *XPA*, *XPB*, *XPD*, and *XPG*, and the *CSA* and *CSB* genes. Several of these also regulate repair of oxidative damage in transcriptionally active genes. Whether the neurodegeneration and other developmental disorders are due to defects in transcription of critical genes, or defects in repair of oxidative damage in these genes is therefore debatable. Both possibilities may have an element of truth.

In Japan a large fraction of the *XPA* mutations occur at the same splice site, and patients present a fairly uniform neurological disorder involving loss of walking ability and sensoneural deafness.

Patients with one of their *XPA* mutations in exon VI outside the DNA binding region of the gene have much less neurodegeneration. Tunisian patients have a common mutation in this region and have relatively mild symptoms despite their sun exposure. Some neurological dysfunction may, however, appear late in life.

XPD is a particularly complex gene in which mutations can give rise to various diseases and mixed symptoms that correspond to either XP, XP/CS syndrome, XP/TTD, or COFS. Many of these mutations occur in the DNA or RNA helicase "box" regions of the gene or in the 3′ terminal region. Inactivating mutation are lethal, hence all patients so far studied have at least one missense mutation resulting in a change of function, and occasional haplo-insufficiency. Similar XP/CS symptoms are seen in the small number of patients reported with mutations in *XPB*.

TTD is a rare autosomal-recessive disorder characterized by sulfur-deficient brittle hair and ichthyosis. Hair shafts split longitudinally into small fibers, and this brittleness is associated with levels of cysteine/cystine in hair proteins that are 15–50% of those in normal individuals. The hair has characteristic "tiger-tail" banding visible under polarized light. The patients often have an unusual facial appearance, with protruding ears and a receding chin. Mental abilities range from low normal to severe retardation. Several categories of the disease can be recognized on the basis of cellular responses to UV damage and the affected gene. Severe cases have low NER and mutations in *XPB* or *D* as described above. A third category involves another unidentified gene called *TTDA* and lacks major UV sensitivity, but has an unstable TFIIH.

COFS is a particularly severe developmental and neurological expression of mutations in *XPD*, *XPG*, and *CSB*. The disease leads to brain microcephaly and atrophy with calcifications, cataracts, microcornea, optic atrophy, progressive joint contractures, and growth failure.

The XPG nuclease has a particularly complex range of activities, and mutations in *XPG* are often associated with both XP and CS diseases. One patient with a mutation that permits a significant level of repair has been reported who is much milder and has no neurological dysfunction. XPG is an endonuclease in the FEN-1 family that is capable of strand-specific cleavage of a range of DNA substrates that may arise during DNA replication, repair, and recombination. The XPG gene product also interacts with RNA Pol II and facilitates efficient transcription elongation, thereby providing an explanation for the complex symptoms of some XPG patients that show both XP and CS symptoms. XPG is also a cofactor required for the activity of thymine glycosylase (*nth* gene) and is thereby linked to repair of oxidative damage that may also be important in maintaining neural functions that fail in CS.

CS is an autosomal-recessive disease characterized by cachectic dwarfism, retinopathy, microcephaly, deafness, neural defects, and retardation of growth and development after birth. They have a typical facial appearance with sunken eyes and a beaked nose and projecting jaw. CS patients are sensitive to the sun but do not develop cancers, setting this disease apart from XP. Patients who only have CS have mutations in one of two genes, *CSA* and *CSB*, the former being the more common. Cells from CS patients are only defective in TCR. The excision of DNA photoproducts from total genomic DNA of CS cells is normal, but repair of transcriptionally active genes is reduced. Clinically, however, the disease has been classified into type I, II, and others, but no detailed correlation has been made between these classifications and the mutations in *CSA* and *CSB*.

Mouse Models of NER Deficiencies

A series of mouse strains have been developed in which the *XP* or *CS* genes have been knocked out (http://webpath.swmed.edu/mutation/). The knockouts,

in general, exhibit increased cancer rates from treatment with UVB or chemical carcinogens, as expected from their human counterparts.

Xpa and Xpc knockouts, for example, are very sensitive to skin cancer induction. Strikingly, though, mouse knockouts have tended to exaggerate the cancer risks and minimize the neurodegeneration as compared to the corresponding human patients. $Xpa^{-/-}$, $Csa^{-/-}$, $Csb^{-/-}$ mice, for example, show increased skin carcinogenesis from UV light or chemical carcinogens, but have negligible neurodegeneration, whereas the corresponding patients are often severely affected neurologically. Mice that are $Xpa^{-/-}$ or $Csb^{-/-}$ are very sensitive to toxic effects of DMBA, but $Xpc^{-/-}$ survive much better, even though they show increased mutation rates. The severity of the neurological phenotype is greatly enhanced in crosses between Xpa and Csb knockouts, and the double homozygote shows early postnatal ataxia and abnormal cerebellar development.

Homozygous knockouts of the *Xpb* and *Xpd* genes are lethal very early in embryonic cell division because these genes are part of the essential transcription factor TFIIH. Mice with a human TTD mis-sense mutation in the *Xpd* gene are viable and have many of the same symptoms as TTD patients. These TTD mice show increased UVB-induced skin cancer and age prematurely, although TTD patients do not exhibit a corresponding increase in cancer.

Mice lacking Xpg are very severely affected, and exhibit postnatal growth failure and neurological dysfunction especially loss of purkinje cells and early death. Although both Xpg and Xpa mice lack repair completely, Xpa knockouts have a near normal lifespan suggesting important differences in Xpa and Xpg during development.

These studies indicate important differences between the clinical presentation of human patients and corresponding mouse models. One obvious cause is that patients have a variety of mis-sense, chain-terminating, splice site, and deletion mutations, which would not necessarily lead to the same phenotypes as complete knockouts. Another cause may be the difference in NER between human and rodents in the function of the XPE heterodimer. A consensus DNA-binding site for p53 is present in the promoter region of human p48 (DDB2) but the sequence has diverged in the mouse homologue, and is methylated in the hamster. UV-induced expression of DDB2 consequently occurs through p53 transactivation in human, but not mouse or hamster cells. The inactivation of the p53 response element provides a partial explanation for early observations that excision repair was low in some mouse strains and hamster cell strains. Therefore re-expression of DDB2 in mice might confer a phenotype that more closely resembles the human disorders.

Differentiation and Tissue-Specific Expression of DNA Repair Genes

As cells differentiate to a nondividing state their capacity for NER of UV damage declines. The major loss is in the capacity for repair of transcriptionally inactive genes or regions of the genome. Specific down-regulation of repair has been described in the testis due to reduced expression of XPA, rendering testicular tumors more sensitive to cis-platin chemotherapy. In the basal layer of the skin, a small fraction of cells seem to be specifically defective in repair of UV and carcinogen damage and retain photoproducts for long times after irradiation. This represents down-regulation of repair in a few cells distributed among a large population of repair-competent cells.

Polymorphisms in DNA Repair Genes

Polymorphisms that are not directly associated with the XP disease phenotype have been described for many of the NER and other repair genes. Polymorphisms have been found in the *XPA*, *XPC*, and *D* genes. Many of these polymorphisms result in nonconservative amino acid changes that could have an impact on NER function and disease. A large number of alleles present at low frequency individually could combine to create variation in disease frequency in the overall population.

See Also the Following Articles

DNA Helicases: Dimeric Enzyme Action • DNA Helicases: Hexameric Enzyme Action • Nucleotide Excision Repair in Eukaryotes • Nucleotide Excision Repair, Bacterial: The UvrABCD System • Nucleotide Excision Repair: Biology • Transcription-Coupled DNA Repair, Overview • Ubiquitin System • Ubiquitin-Like Proteins

Glossary

DNA damage Any chemical or radiation damage to the bases, deoxyribose and phosphodiester bonds in DNA that interferes with its normal functions.

helicase An enzyme that can unwind double-stranded RNA or DNA in a strand-specific direction.

nucleotide excision repair The process of recognition, removal and resynthesis of a damaged region of DNA.

polymerase An enzyme that copies DNA into RNA (RNA polymerase) or duplicates DNA (DNA polymerase).

polymorphisms Different nucleotides in one position of a gene that give rise to changes in sequence without major alterations in function.

ubiquitin A short peptide that is enzymatically attached to a protein by a set of conjugating enzymes to modify its function or mark it for degradation.

ultraviolet light The wavelengths of solar and artificial light between 240 and 280 nm (UVC), and 280 and 320 nm (UVB) that are strongly absorbed in nucleic acids.

xeroderma pigmentosum A human disease in which hereditary mutations in nucleotide excision repair result in a very high incidence of sunlight-induced skin cancers.

Further Reading

Batty, D. P., and Wood, R. W. (2000). Damage recognition in nucleotide excision repair of DNA. *Gene* **241**, 193–204.

Berg, R. J., Rebel, H., van der Horst, G. T., van Kranen, H. J., Mullenders, L. H., van Vloten, W. A., and de Gruijl, F. R. (2000). Impact of global genome repair versus transcription-coupled repair on ultraviolet carcinogenesis in hairless mice. *Cancer Res.* **60**, 2858–2863.

Bohr, V. A. (1991). Gene specific DNA repair. *Carcinogen.* **12**, 1983–1992.

Bootsma, D., Kraemer, K. H., Cleaver, J. E., and Hoeijmakers, J. H. J. (1998). Nucleotide excision repair syndromes: Xeroderma pigmentosum, Cockayne syndrome, and trichothiodystrophy. In *The Genetic Basis of Human Cancer* (B. Vogelstein and K. W. Kinzler, eds.) pp. 245–274. McGraw-Hill, New York.

Cleaver, J. E., and Mitchell, D. L. (2003). Ultraviolet radiation carcinogenesis. In *Cancer Medicine*, 6th edition, Chap. 20. B. C. Dekker, London.

Cleaver, J. E. (1968). Defective repair replication in xeroderma pigmentosum. *Nature* **218**, 652–656.

Cleaver, J. E., and Mitchell, D. L. (1997). Ultraviolet radiation carcinogenesis. In *Cancer Medicine* (J. F. Holland, R. C., Jr., Bast, D. L. Morton, E. Frei, III, D. W. Kufe and R. R. Weichselbaum, eds.) Vol 1, pp. 307–318. Williams and Wilkins, Baltimore.

Friedberg, E. C., Walker, G., and Siede, W. (1995). *DNA Repair and Mutagenesis*. ASM Press, Washington, DC.

Kraemer, K. H., Lee, M. M., and Scotto, J. (1987). Xeroderma pigmentosum: Cutaneous, ocular and neurological abnormalities in 830 published cases. *Archiv. Dermatol.* **123**, 241–250.

Sancar, A. (1994). Mechanisms of DNA excision repair. *Science* **266**, 1954–1956.

Schaeffer, L., Roy, R., Humbert, S., Moncollin, U., Vermeulen, W., Hoeijmakers, J. H. J., Chambon, P., and Egly, J. M. (1993). DNA repair helicase: A component of BTF2 (TFIIH) basic transcription factor. *Science* **260**, 58–63.

Trincao, J., Johnson, R. E., Escalante, C. R., Prakash, S., Prakash, L., and Aggarwal, A. K. (2001). Structure of the catalytic core of *S. cerevisiae* DNA polymerase η: Implications for translesion synthesis. *Molecul. Cell* **8**, 417–426.

Wood, R. D., Mitchell, M., Sgouros, J., Lindahl, T. (2001). Human D.N.A. repair genes. *Science* **291**, 1284–1289.

Biography

James E. Cleaver is a Professor of dermatology and pharmaceutical chemistry, former Associate Director in the Laboratory of Radiobiology and Environmental Health, and presently Head of the Cutaneous Oncology Program of the UCSF Cancer Center, University of California, San Francisco. His principal research interest is in the field of DNA repair, and he is best known for discovering the repair defect in the human disease xeroderma pigmentosum that linked repair to human cancer. He holds a B.A. and Ph.D. from the University of Cambridge, UK. He has authored over 350 publications and was elected to the National Academy of Sciences in 1999.

Nucleotide Excision Repair in Eukaryotes

Laura A. Lindsey-Boltz and Aziz Sancar
University of North Carolina School of Medicine, Chapel Hill, North Carolina, USA

Eukaryotes possess several repair mechanisms to provide defense against a large variety of DNA alterations. One of these mechanisms, nucleotide excision repair, is responsible for repairing bulky DNA lesions, which if left unrepaired, can result in oncogenesis, developmental abnormalities, and cellular lethality. Humans with hereditary defects in nucleotide excision repair suffer from diseases including xeroderma pigmentosum, Cockayne syndrome, and trichothiodystrophy, with symptoms including elevated sun sensitivity and skin cancers, neurological degeneration, and developmental delays.

Substrates

Two major carcinogens produce the bulky, DNA helix-distorting lesions which are repaired by the nucleotide excision repair system. UV light produces cyclobutane pyrimidine dimers and (6-4) photoproducts, and cigarette smoke produces benzo[a]pyrene-guanine adducts. However, the nucleotide excision repair system is not limited to the repair of bulky DNA lesions. It removes virtually all base lesions tested, including thymine glycols and 8-oxoguanine which are not bulky. Because of the wide substrate range, it is unlikely that the nucleotide excision repair system recognizes the specific chemical groups that make up the lesion, but rather recognizes the changes in the conformation of the phosphodiester backbone created by the damage.

Nucleotide Excision Repair Factors

In eukaryotes, nucleotide excision repair is carried out by six repair factors containing eighteen polypeptides (Table I). The six human nucleotide excision repair factors are RPA, XPA, XPC, TFIIH, XPG, and XPF-ERCC1. With the exception of XPA and XPG, each repair factor consists of 2–9 polypeptides that are in tight complexes, and these complexes are considered to be the subunits of the nucleotide excision repair enzyme (excision nuclease). All eukaryotic organisms whose genomes have been sequenced to date have homologues of the six nucleotide excision repair factors. However, only in the case of human and the budding yeast, *S. cerevisiae*, the excision nuclease has been reconstituted with the purified factors.

The nucleotide excision repair factors were primarily identified by genetic studies in cell lines derived from humans with xeroderma pigmentosum (XP) and UV-sensitive rodent cell lines. Thus, the repair genes have been named *XPA*, *XPB*, etc. or excision repair cross complementary group 1 (*ERCC1*), etc., depending on whether they were cloned by complementing human XP mutants or repair-defective rodent cell lines. In addition to the seven XP proteins, two multifunctional, multi-subunit factors, RPA and TFIIH, have been shown to be required for nucleotide excision repair. Replication protein A(RPA) is a complex of three proteins, and was originally identified and named for its role in replication. TFIIH, a complex of nine proteins, was originally identified as one of the six general transcription factors required for optimal transcription by RNA polymerase II. TFIIH consists of a core complex of proteins containing XPB, XPD, p62, p52, p44, and p34; and the cdk-activating kinase (CAK) subcomplex, consisting of cdk7, cyclinH, and Mat1 (Table I). Only the TFIIH core complex is required for nucleotide excision repair *in vitro*.

Mechanism of Nucleotide Excision Repair

The three basic steps of nucleotide excision repair in eukaryotes are: (1) dual incisions bracketing the lesion in a 24–32 nt-long oligomer; (2) repair synthesis to fill in the resulting gap; and (3) ligation of the newly synthesized DNA (patch) to the old DNA (Figure 1). Of these three steps, the last two are carried out by replication and recombination enzymes, and thus the dual incision (excision) step might be considered the repair reaction proper. Assays for detecting DNA–protein complexes (gel mobility shift and DNAaseI and

TABLE I

The Six Human Nucleotide Excision Repair Factors Consisting of Eighteen Proteins

Factor	Proteins (yeast homolog)	Activity	Role in repair
XPA	XPA/p31 (Rad14)	DNA binding	Damage recognition
RPA	p70	DNA binding	Damage recognition
	p34		
	p11		
XPC	XPC/p125 (Rad4)	DNA binding	• Damage recognition
	HHR23B/p58 (Rad23)		• Stabilization of preincision complex and protection from degradation
TFIIH	XPB/ERCC3/p89 (Rad25)	• DNA-dependent ATPase	• Formation of preincision complex
	XPD/ERCC2/p80 (Rad3)	• Helicase	• Transcription-repair coupling
	p62 (Tfb1)	• General transcription factor	
	p52 (Tfb2)	• Cdk-activating kinase activity	
	p44 (Ssl1)		
	p34 (Tfb4)		
	Cdk7/p41 (Kin28) } CAK sub-complex		
	CyclinH/p38(Ccl1) } CAK sub-complex		
	Mat1/p32 (Tfb3) } CAK sub-complex		
XPF	XPF/ERCC4/p112 (Rad1) ERCC1/p33 (Rad10)	Nuclease	5′ incision
XPG	XPG/ERCC5/p135 (Rad2)	Nuclease	3′ incision

permanganate footprinting) have led to the identification of three high-specificity and high-stability intermediates along the assembly pathway of the excision nuclease. These three intermediates are called preincision complexes (PIC) 1, 2, and 3 and are described in detail below.

Preincision Complex 1

PIC1 consists of DNA, RPA, XPA, XPC, and TFIIH. ATP is required for the formation of this complex. It is hydrolyzed by two helicases in TFIIH, XPB and XPD, which have 3′ to 5′ and 5′ to 3′ helicase activities, respectively. These helicases unwind the DNA by about 20 bp around the lesion in an asymmetric manner with about 15 bp unwound on the 5′ side and 5 bp unwound on the 3′ side of the damage. The overall direction of unwinding with respect to the damaged strand was determined to be 5′ to 3′ based on data with substrates containing an interstrand cross-link.

Preincision Complex 2

XPG enters to form the second complex, which is much more stable than PIC1. As in the case of PIC1, the formation of PIC2 is also dependent on ATP hydrolysis by the XPB and XPD subunits of TFIIH. Interestingly, when the composition of PIC2 was analyzed by gel mobility shift assays it seemed to lack XPC. It appears that XPC leaves the complex after helping to recognize the damage and unwind the duplex, which then enables XPG to enter. The replacement of XPC in PIC1 by XPG in PIC2 is consistent with the findings that TFIIH makes relatively tight complexes with XPC and XPG. Apparently, the binding surfaces of these two factors on TFIIH overlap and therefore the entry of one into the complex is concomitant with the exit of the other. Thus, the composition of PIC2 is RPA XPA XPG TFIIH-DNA.

Preincision Complex 3

Finally, with the entry of XPF ERCC1 into PIC2, the PIC3 forms the complex composed of RPA XPA XPG TFIIH XPF ERCC1-DNA. Within this complex the 3′ incision is made by XPG and the 5′ incision is made by XPF-ERCC1. Following the dual incisions, the excised 24–32 nt-long oligomer carrying the damage is released, and the excision nuclease is dissociated. Replication Factor C (RFC) loads the PCNA trimeric circle onto the DNA, and PCNA recruits DNA Pol δ or Pol ε to fill in the gap in the DNA. Repair is completed by ligation by DNA ligase I.

Damage Recognition and Transcription-Coupled Repair

Recognition of the DNA damage is most likely the rate-limiting step in nucleotide excision repair. The DNA

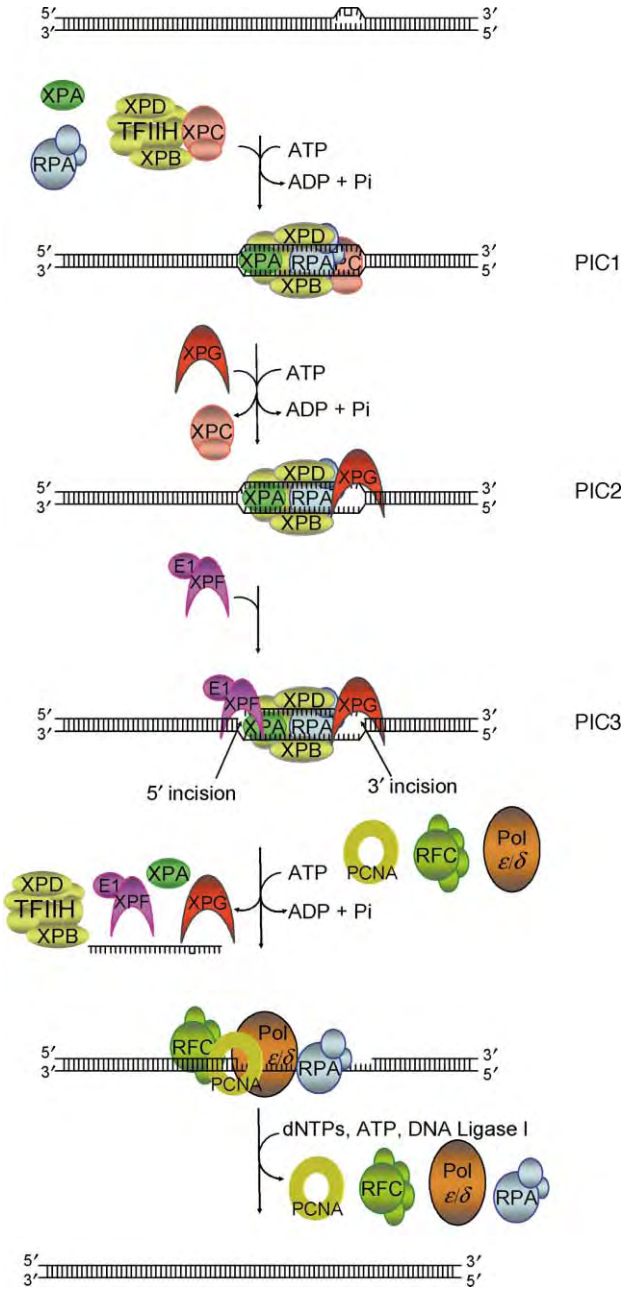

FIGURE 1 Model for nucleotide excision repair in humans. The DNA lesion is bound by RPA, XPA, and TFIIH XPC to form preincision complex (PIC) 1. ATP is hydrolyzed by the XPB and XPD helicase subunits of TFIIH to locally unwind the DNA. XPG enters and XPC exits in the next step which requires ATP hydrolysis by XPB and XPD to form PIC2. After XPF enters to form PIC3, the two endonucleases make incisions in the strand containing the lesion; the 3′ incision is made by XPG and the 5′ incision is made by XPF-ERCC1. Repair synthesis then fills in the single-stranded gap.

lesions must be located among the 3 billion base pairs present in the human genome. The damage recognition factors of the human excision nuclease are RPA, XPA, and XPC. All three proteins are DNA-binding proteins with some preference for damaged DNA, and all three apparently play a role in low-discriminatory damage recognition independent of ATP. However, the precise order of assembly has been difficult to establish with kinetic experiments, resulting in conflicting studies wherein one study concluded that RPA and XPA are the repair factors which make the initial contact, and another study found that XPC makes the initial contact. Nucleotide excision repair appears to operate somewhat differently on DNA that is transcriptionally active (transcription-coupled repair) from that which is transcriptionally silent (global genome repair). Transcribed DNA is repaired at a faster rate than nontranscribed DNA, and this is most likely due to recognition of the RNA polymerase stalled at the damage. In addition to the nucleotide excision repair factors, transcription-coupled repair depends on the CSA and CSB gene products in humans. *In vivo* data indicate that in humans, but not in yeast, XPC is dispensable for transcription-coupled repair. It is thought that the transcription bubble 3′ to the lesion which impedes the progression of RNA polymerase creates a unique damaged DNA structure which can be recognized in the absence of XPC. Indeed, when a cyclobutane thymine dimer is placed adjacent to a 10 nt bubble in a synthetic substrate, it is recognized and excised efficiently in the absence of XPC. Transcription-coupled repair has not been reconstituted *in vitro*, and therefore the mechanism in eukaryotes is currently not known.

See Also the Following Articles

DNA Helicases: Dimeric Enzyme Action • DNA Helicases: Hexameric Enzyme Action • Nucleotide Excision Repair and Human Disease • Nucleotide Excision Repair: Biology

Glossary

Cockayne's syndrome (CS) Human disease caused by defects in proteins involved in coupling transcription to nucleotide excision repair; symptoms include mental retardation, dwarfism, neurological defects, and moderate sensitivity to UV light.

endonuclease Protein that cleaves bonds within a nucleic acid chain, e.g., XPF and XPG.

excision nuclease Enzyme that removes damaged bases by dual incisions bracketing the lesion in the damaged strand.

helicase Protein that uses the energy of ATP hydrolysis to unwind a nucleic acid duplex, e.g., XPB and XPD.

trichothiodystrophy (TTD) Human disease caused by mutations in XPB and XPD which results in defects in both transcription and nucleotide excision repair; symptoms include brittle hair and nails, mental retardation and skeletal abnormalities.

xeroderma pigmentosum (XP) Human disease caused by reduced level of nucleotide excision repair; symptoms include mental retardation, ataxia, deafness, and predisposition to skin cancer caused by sunlight exposure.

Further Reading

Bessho, T., and Sancar, A. (1998). Nucleotide excision repair in man. In *Nucleic Acids and Molecular Biology*, (F. Eckstein and D. M. J. Lilley, eds.) Vol 12, pp. 141–155. Springer, Berlin, Heidelberg.

Cleaver, J. E., and Kraemer, K. H. (1989). Xeroderma pigmentosum and cockayne syndrome. In *The Metabolic and Molecular Bases of Inherited Disease* (C. R. Scriver, A. L. Beaudet, W. S. Sly and D. Valle, eds.) 7th edition, pp. 4393–4419. McGraw-Hill, New York.

Hanawalt, P. C. (1994). Transcription-coupled repair and human disease. *Science* **266**, 1457–1458.

Sancar, A. (1995). Excision repair in mammalian cells. *J. Biol. Chem.* **270**, 15915–15918.

Sancar, A. (1996). DNA excision repair. *Annu. Rev. Biochem.* **65**, 43–81.

Wood, R. D. (1996). DNA repair in eukaryotes. Annu. *Rev. Biochem.* **65**, 135–167.

Biography

Laura Lindsey-Boltz is a Postdoctoral Fellow in Dr. Aziz Sancar's laboratory, and she holds a Ph.D. from Duke University.

Aziz Sancar is a Kenan Professor in the Department of Biochemistry and Biophysics at the University of North Carolina, Chapel Hill. His principal research interests are in the fields of DNA repair, DNA damage checkpoints, and circadian photoreceptors. He holds an M.D. from Istanbul University School of Medicine and a Ph.D. from the University of Texas at Dallas.

Nucleotide Excision Repair, Bacterial: The UvrABCD System

Bennett Van Houten
National Institute of Environmental Health Sciences, Research Triangle Park, North Carolina, USA

Lawrence Grossman
The Johns Hopkins University, Baltimore, Maryland, USA

DNA repair is intrinsic to the evolution of life, and organisms have evolved a large number of complex systems to ensure the integrity of their heredity material. DNA constantly undergoes chemical modification as a result of its intrinsic chemical instability, as well as, endogenous and environmental stresses. The most versatile DNA repair mechanism is nucleotide excision repair (NER), first discovered in *Escherichia coli* in 1964 independently by Setlow and Carrier and Boyce and Howard-Flanders. This bacterial system, like its eukaryotic counterpart, has a very broad spectrum of damage recognition and operates according to the same basic principles in all organisms: (1) repair proteins form macromolecular assemblies in order to locate and activate damage utilizing a number of ATP-hydrolysis-driven nucleoprotein rearrangements; (2) the DNA is incised on both sides of damage; and (3) the incised fragment is displaced with concomitant resynthesis followed by ligation. NER is coupled to other cellular processes, notably, transcription. The sequencing of the complete genomes of over 20 different bacterial species indicates that the NER system is a highly conserved process.

UvrABC Endonuclease

The nucleotide excision repair (NER) pathway consists of five basic steps: damage recognition, incision, excision, repair synthesis, and ligation. In most bacteria the first steps of this process are carried out by an ensemble of three proteins encoded by the *uvrA*, *uvrB*, and *uvrC* genes in an ATP-dependent series of reactions. During the initial characterization of these proteins, the name of this system was shortened to "UvrABC endonuclease" which makes both the 5′ and 3′ incisions to a lesion in a "dual incision" reaction (Figure 1). The UvrABC endonuclease possesses a broad spectrum of substrate specificity and is capable of acting on a wide variety of unrelated DNA damage (Table I).

Genetics and Evolutionary Conservation of *uvr* Genes

It was photobiologists who discovered NER from analyses of ultraviolet radiation (UV) survival curves in some bacterial, most notably *E. coli*. Rather than observing a first-order decline in survival of cells as a function of UV dose there was a shoulder in the survival curves at lower doses. Some *E. coli* mutants, which lacked this shoulder, were sensitive to low doses of UV, and were isolated. All these mutants map at one of three loci on the *E. coli* chromosome designated *uvrA* (92 min), *uvrB* (17 min), and *uvrC* (41.5 min), and are hence, unlinked genes. In species of *Bacillus*, the *uvrA* and *uvrB* genes are within 50 bp of each other on the chromosome.

The *uvr* genes were first cloned, sequenced, and amplified from *E. coli*, which led to a greater understanding of the roles of three proteins in the process of damage recognition and incision. Subsequently, large-scale sequencing efforts have revealed that *uvr* genes are highly conserved among the bacterial species

uvrA

uvrA is one of a series of genes collectively referred to as SOS genes, which are induced to increased levels of transcription by agents that cause DNA damage. A specific binding site for the LexA repressor protein specific for the operator promoter region of the *uvrA* gene (the so-called LexA box or SOS box) has been identified. Sequence analyses reveal that the *uvrA* gene (2.82 kbp) translates into 940 amino acids (Mr = 103,874 Da) and contains two ATP-binding motifs, two zinc-finger motifs and a helix-turn-helix motif.

uvrB

The *uvrB* gene is also a member of the SOS regulon and is inducible by DNA damage. The gene is transcribed

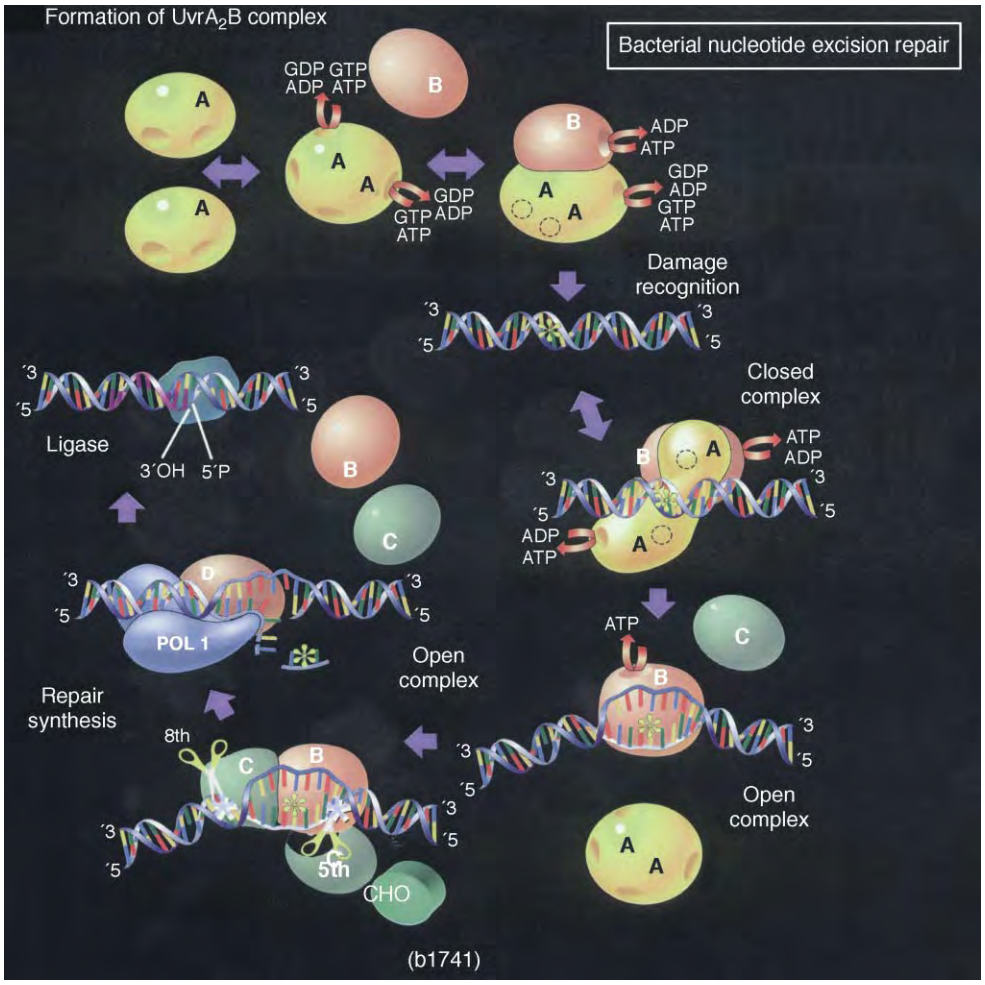

FIGURE 1 Nucleotide excision repair pathway in bacteria. $UvrA_2$ interacts with UvrB, and this $UvrA_2B_1$ complex translocates to the damaged sites. UvrA dissociates and UvrC binds to the UvrB—DNA complex at a damaged site. Dual incision is catalyzed by UvrC. The N-terminal domain is involved in the 3′ incision and the C-terminal domain performs the 5′ incision. UvrD displaces UvrC and an oligonucleotide containing the damage. DNA polymerase I fills the single stranded gap, and DNA ligase seals the nick.

from two overlapping promoters called P1 and P2. A LexA protein-binding site is present in the P2 promoter region. Transcription from P2 is inhibited by LexA repressor protein while that from P1 is unaffected. Sequence analysis revealed that the *uvrB* gene is 2,019 bp, which translates into 673 amino acids (76.6 kDa). The *uvrB* gene product has a consensus Walker-type A nucleotide-binding motif, helicase motifs II–VI as well as coiled-coils consensus sequences.

uvrC

In contrast to *uvrA* and *uvrB*, *uvrC* is not inducible by DNA damage and is not a member of the SOS regulon, although its cellular location is altered during SOS. The sequence analysis shows that the size of *uvrC* is 1,830 bp encoding a polypeptide of 610 amino acids (66 kDa).

Cho

It was quite surprising that a new uvrC homologue, Cho, could be discovered in an organism for which the complete genome sequence was known since 1997. The gene encoding Cho was found to be UV-inducible by Hanawalt and Brown using a high density DNA microarray. Careful inspection of this gene revealed homology to the Tev-homing endonucleases and also the N terminus of uvrC. Goosen and co-workers cloned and overexpressed the Cho protein, and found that the Cho protein will incise a DNA adduct at the tenth phosophodiester bond 3′ to the damaged site. This cutting at a distance was shown to help incise at bulky lesions, which might otherwise block the normal uvrC 3′ incision. They also found that uvrC can complete the incision process by efficient cleavage 5′ to the 3′ incised adduct. Cho is rather rare in the bacterial kingdom (Figure 2).

TABLE I

Range of Substrates of the Bacterial NER UvrABC System

Type	Lesion	UvrABC	ΔM_r	Properties
Single base modification	Thymine glycol	++	+34	
	Dihydrothymine	0	+2	
	Benzo[*a*]pyrene adduct	+++	+171	T_M lowered
	Anthramycin adduct	+++	+191	T_M elevated
	Cross-linked triple strand	+ [72]	~ + 3000	
	O^4-alkyl thymine	+	+14	
	O^6-methyl guanine	+	+14	
	N^6-methyl adenine	0	+14	
	Psoralen adduct	+++	+185	Positive kink
	Base removed (AP site)	+	~ − 130	
Cross-links, intra-strand	*cis*-Pt adduct	+++	+227	Negative kink
	Pyrimidine dimer	++	0	
	6–4 photoproduct	+++	0	
Cross-links, inter-strand	*cis*-Pt adduct	++	+227	
	Nitrogen mustard adduct	+	+69	
	Psoralen bisadduct	+++	+185	Unwound
Natural bases	dsDNA	0	0	
	A-tracts	0	0	Bent
	Mismatches, loops	0[a]	0	
Noncovalent modifications	Caffeine complex	−	+194	Intercalator
	Ditercalinium complex	++[b]	+500	Bisintercalator

[a] Some mismatches are recognized with very low efficiency (<1%).
[b] Futile cycle of spurious repair and subsequent formation of the complex at another site.

A selection of DNA lesions illustrates the lack of a single common property that determines the response of UvrABC to DNA damage. The relative rate of incision for a particular lesion (neglecting the influence of sequence context) by the UvrABC system is indicated by +, ++, and +++; 0 indicates no incision, − indicates inhibition. ΔM_r, change in molecular weight due to the modification.

Properties of UvrA, UvrB, and UvrC Proteins

UvrA

The UvrA protein is a DNA-independent ATPase that binds DNA and is a member of the ABC transporter superfamily characterized by dual ATP binding sites. Soon after UvrA was sequenced, it was noticed that the gene probably arose through multiple duplication events in which a four-cysteine zinc finger was placed between the Walker type A and B nucleotide-binding motifs. Site-directed mutagenesis studies show directly that UvrA has an ATPase activity located in a region centered at lysine residues of two Walker type A nucleotide-binding motifs. UvrA also hydrolyzes GTP. ATPase activity of UvrA is modulated by DNA. High concentrations of UvrA protein and the binding energy of ATP (or poorly hydrolyzable ATP-γ-S) favor dimerization of the protein. UvrA dimers are DNA-binding species. The binding of UvrA to undamaged DNA is $10^3 \sim 10^4$-fold weaker than to the damaged one. The specificity for damaged DNA is abolished by ATP-γ-S, while it enhances nonspecific binding. The dissociation rate for UvrA from damaged sites is fast in the presence of ATP. ATP hydrolysis increases the specificity of binding to the damaged DNA, but lowers the equilibrium binding constant by stimulating dissociation. UvrA contains two zinc atoms per molecule, at least one of which is required for DNA binding. Consistently, C-terminal zinc-finger of UvrA is absolutely essential for nonspecific DNA binding, while N terminal is dispensable. The helix-turn-helix motif as well as C-terminal glycine-rich region appears to contribute into damage recognition by UvrA.

UvrB

The purified protein has no detectable ATPase activity, although it binds ATP with a $K_d \sim 1$ mM. However, ATPase activity is observed when UvrB interacts with UvrA in the presence of DNA. This dramatic appearance is due to activation of the cryptic ATPase when UvrB forms an UvrAB–DNA complex. When UvrB is proteolyzed in a specific region of the C terminus, the resulting ~70 kDa protein is referred to as UvrB*. The "cryptic UvrB ATPase" functional in UvrB*

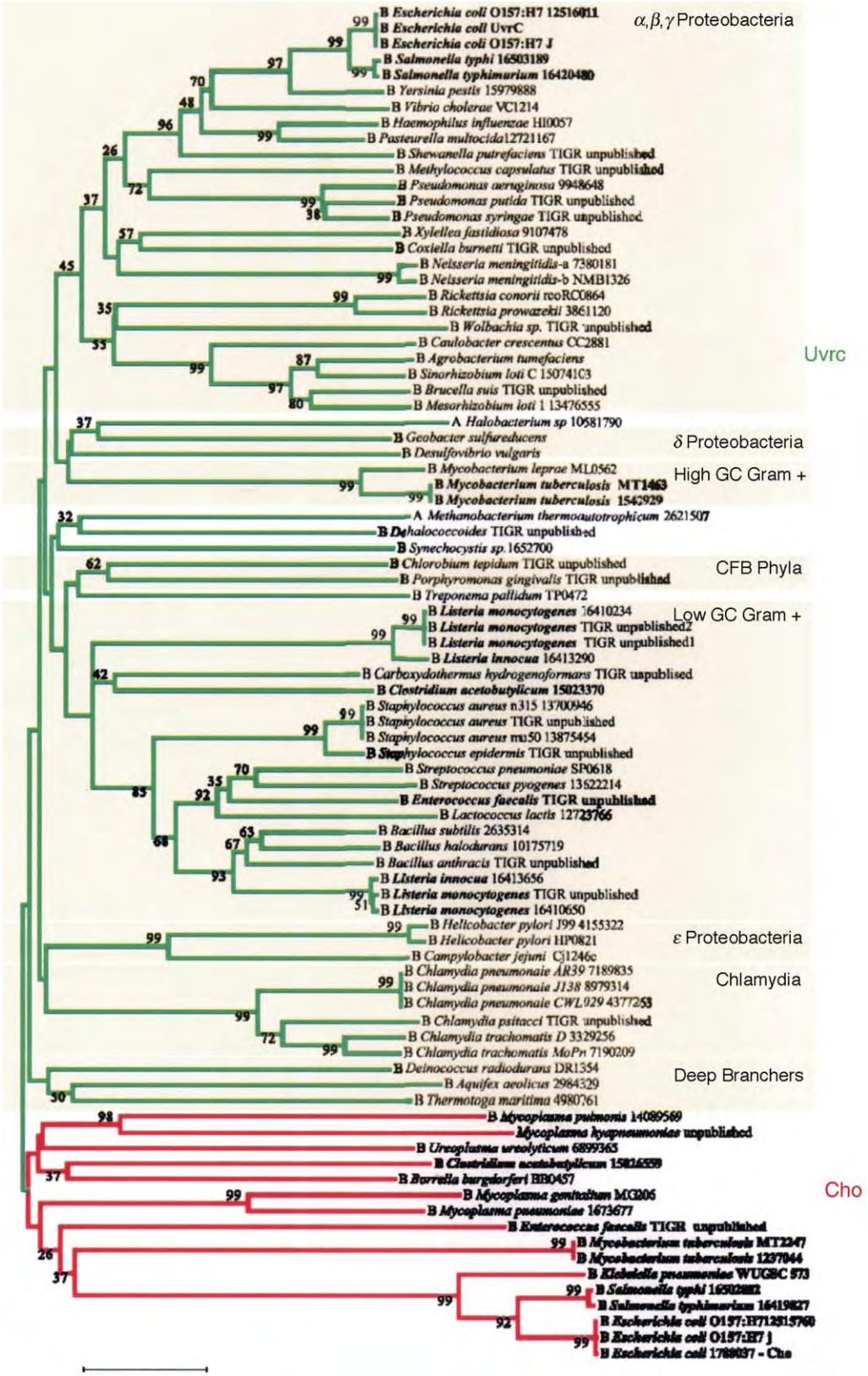

FIGURE 2 Phylogenetic tree of UvrC and Cho in various bacterial species. Phylogenetic tree of UvrC and Cho homologues. Homologues were identified in complete or nearly complete genomes by blastp or blastx searches. Protein sequences were aligned using clustalx. Boostrap values, a measure of statistical support for particular groupings of genes to the right of the number, are shown on the tree when greater than 40%. Reprinted from Van Houten, B., Eisen, J. A., and Hanawalt, P. C. (2002). A cut above: discovery of an alternative excision repair pathway in bacteria. *Proc. Natl Acad. Sci. USA* **99**(5), 2581–2583, with permission of the National Academy of Sciences, U.S.A.

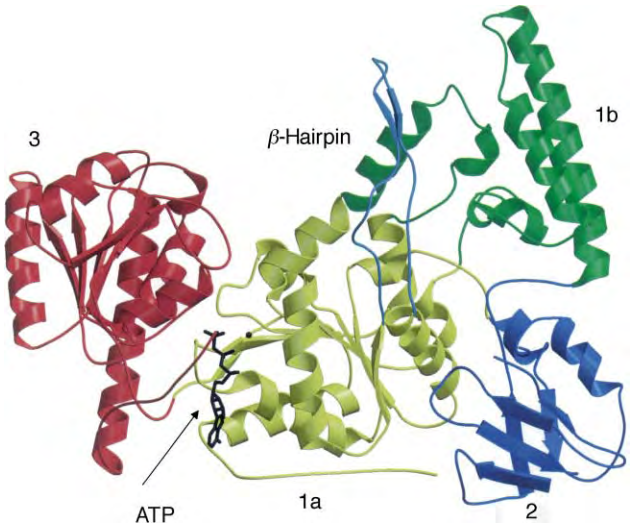

FIGURE 3 Structure of UvrB. Domains 1a, 1b, 2, and 3 are shown in yellow, green, purple and red, respectively. The β-hairpin bridging the gap between domains 1a and 1b is shown in cyan. The ATP molecule bound at the interface between domains 1 and 3 is indicated. (Reprinted from Theis, K., Chen, P. J., Skorvaga, M., Van Houten, B., and Kisker, C. (1999). Crystal structure of UvrB Provides insight into the mechanism of nucleotide excision repair. *EMBO J.* **18**(24), 6899–6907, with permission of Oxford University Press.)

is activated by single stranded DNA or chaotropic salts. UvrB can bind to double stranded DNA only in the presence of UvrA, and binds to single-stranded DNA with a K_d in the micromolar range. The amino acid sequence of the UvrB protein shows homology with two limited stretches of the sequence of the UvrC protein. Three groups have independently solved the crystal structure of UvrB. The structure has revealed that UvrB is folded into four separate domains (Figure 3). Domain 1a includes four helicase motifs: Ia, Ib, II, and III that are required for ATPase activity. Domain two is important for UvrA interaction and domain 3 contains helicase motifs, IV, V, and VI. Sandwiched between domains 1a and 1b is an important β-hairpin motif which is believed to provide important DNA contacts. Further details of the UvrB structure and how it provides function is discussed below.

UvrC

UvrC is a single-strand DNA-binding protein and binds to it with a relatively high affinity. UvrC is a catalytic subunit of the UvrABC endonuclease. Mutations in the C-terminal region of UvrC are extremely sensitive to UV and defective in 5′-incision activity. The 314 C-terminal amino acids of UvrC are sufficient to support dual incision of damaged DNA by the UvrABC endonuclease. UvrC protein associates with a UvrB–DNA complex at damaged site. Recently, the C-terminal part of UvrC was solved by multidimensional NMR and shown to consist of two helix-hairpin-helix (HhH) motifs as predicted previously. Kaptein and co-workers found that this C-terminal region of the protein bound avidly to double-strand/single-strand junctions like those found in bubble substrates containing more than six unpaired bases. Interestingly this is exactly the number of base pairs believed to be unwound during the formation of the UvB–DNA complex.

Damage Recognition and Incision

The broad substrate specificity of the UvrABC endonuclease is achieved through a complex molecular mechanism (Figure 1) identifying some general changes in DNA conformation and dynamics rather than chemically modified bases *per se*.

Molecular Mechanism of Damage Recognition

Molecular recognition proceeds through a series of coordinated Uvr protein–protein and nucleoprotein intermediates characterized by different composition and architecture.

UvrA Dimerization

UvrA forms a dimer in solution with apparent $K_d \sim 10^{-8}$ M. Nucleotide (ATP) binding to UvrA drives UvrA dimerization, whereas the hydrolysis of ATP or the presence of ADP drives monomerization. The UvrA dimer is the active form in binding to undamaged or damaged DNA. Formation of a dimer results in a conformational change of the UvrA protein. UvrA is believed to recognize overall changes in the structure of the DNA helix.

$UvrA_2B_1$ Complex in Solution

The purified UvrA protein associates in solution with UvrB protein (domain 2) in an ATP-dependent manner. The N-terminal 230 amino acids of UvrA are involved in this interaction. UvrB has two UvrA-binding sites: one within amino acids 115–250 and another within C-terminal amino acids 573–673. However, $UvrB^*$ which lacks these C-terminal amino acids can also bind UvrA in solution. The apparent stochiometry of the UvrA–UvrB complex in solution is $UvrA_2UvrB_1$.

$UvrA_2$–DNA Binding

The UvrA dimer binds both damaged and undamaged DNA. ADP decreases the UvrA-binding affinity two- to

threefold and ATP is not required for the specific binding to a damaged site. ATP-γ-S quantitatively inhibits the specific binding while enhancing nonspecific binding. The equilibrium constant for nonspecific binding of UvrA is $(0.7–2.9) \times 10^5\ M^{-1}$. The apparent binding affinity of $UvrA_2$ to damaged DNA is in the range $0.07 \sim 1.0 \times 10^9\ M^{-1}$, depending on the damage type. However, affinity of $UvrA_2$ to damage does not generally correlate with the efficiency of the entire incision reaction.

$UvrA_2B_1$–DNA Complex

This complex provides for more productive damaged DNA-binding intermediates than UvrA dimer. Binding of $UvrA_2B_1$ to DNA results in locally unwound undamaged-DNA between 180° and 220°. Furthermore, it has been proposed that the DNA is wound around the UvrB molecule. The formation of the $UvrA_2B_1$–DNA complex results in a multifold stimulation of ATPase activity apparently through activation of a "cryptic" ATPase of UvrB. Using atomic force microscopy, Goosen and co-workers have recently suggested that UvrA and UvrB can form $UvrA_2UvrB_2$ complex on DNA. Once the UvrAB complex actively engages the damage, UvrA (and possible one molecule of UvrB) dissociate leaving a long-lived salt stable UvrB–DNA complex.

Formation of the UvrB–DNA Intermediate

Previous work by Grossman and co-workers have suggested that the UvrAB complex can track along the DNA helix using a limited helicase activity to create waves of negative and positive supercoiling behind and in front of the damaged site, respectively. This is consistent with the helicase fold of UvrB (shown in Figure 3). However, work from both the Rupp and Van Houten laboratories have argued that the UvrAB complex cannot dissociate damaged DNA strands even as small as 26 bases, and that formation of the UvrB–DNA complex leads to a destabilization of the DNA helix. However, neither UvrB by itself or in complex with UvrA can unwind long tracks of DNA, which is a typical property of proteins with true helicase activity.

Damage-Sensing Mechanism: Padlock Model of Damage Recognition by UvrB

The UvrABC endonuclease does not recognize a specific chemical group or structure in the damaged nucleotide nor does it, in all likelihood, solely recognize a specific backbone deformity in the duplex induced by the varied and unrelated genotoxic chemicals (Table I). Initial damage recognition may occur through direct UvrA–DNA interactions. This triggers structural changes of the preceding $UvrA_2B_1$–DNA complex, so that $UvrA_2$ dissociates, while UvrB is loaded onto a damaged site. Even though the cocrystal structure of the UvrB–DNA complex has not yet been solved, this complex has been observed in footprinting experiments by electron microscopy and gel mobility shifts and the complex is isolated by gel filtration. The formation of this complex requires ATP hydrolysis by both UvrA and UvrB and occurs after the recognition of a damage site by the UvrAB complex. As noted above, Goosen and co-workers have shown that the formation of the UvrB pre-incision complex at damaged sites results in a conformational change of both UvrB and DNA. The DNA molecule in this complex is kinked and the DNA wrapped around the UvrB molecule. Helicase motifs and the β-hairpin motif of UvrB seem to play a role in UvrB–DNA binding at damaged sites (Figure 4). The rate of UvrB loading to DNA is low ($k_{on} = 6–10^{-4}\ M\ s^{-1}$), suggesting that this step may be limiting for damage-specific incision of DNA. Kisker and co-workers have proposed a padlock model of UvrB binding to DNA to help reconcile the earlier helicase-unwinding model of Grossman with the known helicase fold of UvrB. In this model the UvrAB complex uses the UvrB ATPase to make limited motion along the DNA, causing transient opening and closing of the DNA, in which it is believed that the β-hairpin is inserted through the helix. If a DNA lesion is encountered by UvrB, there is a conformational change in the protein–DNA complex leading to the release of UvrA. In this precision complex, UvrB is believed to lock down the nondamaged between the β-hairpin and the wall of domain 1B (Figure 4). In this locked padlock model, the damaged strand wraps in front of the β-hairpin and the hydrophobic tyrosine side-changes at the base of the β-hairpin are believed to bind to or facilitate the damaged nucleotide to flip out of the DNA helix. In this locked down conformation, ATP binding is believed to lead to a large motion of domain 3 which clamps down on the DNA resulting in further deformation of the DNA helix leading to strained structure that is recognized by UvrC.

Dual Incision

The binding of UvrC to the pre-incision UvrB–DNA complex results in the incision of DNA on both sides of the lesion in the damaged strand. DNA sequence context and the type of damage affect the precise location of the 5′ and 3′ incision sites. Usually, it occurs at the 8th phoshodiester bond 5′ to the damage and 4th or 5th phoshodiester bond 3′ to the damage. The C-terminal coiled-coil motif of UvrB (amino acids 636–668) and the N-terminal homologous regions of UvrC (amino acids 214–239) are required for the

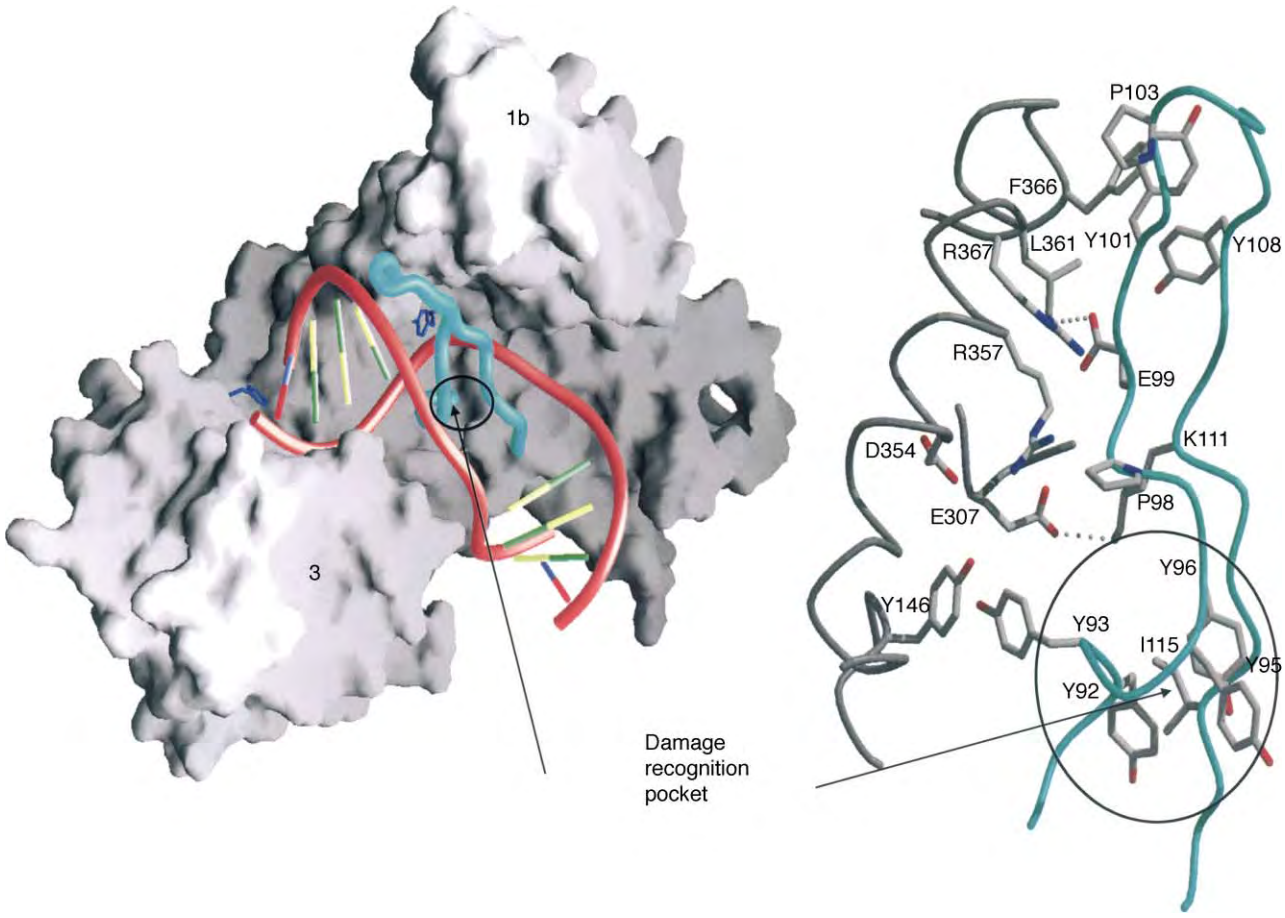

FIGURE 4 Hypothetical model of UvrB–DNA complex showing proposed damage recognition pocket. Left panel, hypothetical model of the UvrB–DNA pre-incision complex. Domains 1b and 3 are indicated. The proposed conformation of DNA is shown as phosphate backbone in red with the undisrupted base pairs shown as spokes. The β-hairpin is depicted in cyan. (Reprinted from Theis, K., Chen, P. J., Skorvaga, M., Van Houten, B., and Kisker, C. (1999). Crystal structure of UvrB Provides insight into the mechanism of nucleotide excision repair. *EMBO J.* **18**(24), 6899–6907, with permission). Right Panel, the β-hairpin and its proposed role in binding to DNA. A Ca-trace of the β-hairpin of bcUvrB cyan and neighboring residues of domain 1b in gray. Hydrophobic residues (Tyr 95–96) believed to be involved in damage recognition are circled. (Modified from Theis, K., Skorvaga, M., Machius, M., Nakagawa, N., Van Houten, B., and Kisker, C. (2000). The nucleotide excision repair protein UvrB, a helicase-like enzyme with a catch. *Mutat. Res.* **460**(3–4), 277–300, with permission from Elsevier.)

formation of UvrBC complex. Site-directed mutagenesis of the UvrC and UvrB proteins has led to the conclusion that the incision process is not a concerted one. The 3′ incision is affected by the N terminus of the UvrC protein, and this incision precedes the 5′ nicking, catalyzed by the C terminus of UvrC protein. There is a conformational change of UvrBC–DNA complex following 3′-incision. The C-terminal region of UvrC (amino acids 555–610) is involved in DNA binding and 5′-incision. Dual incision *per se* does not require ATP hydrolysis; ATP-γ-S can substitute ATP during this step.

Postincision Steps

Following dual incision, the UvrBC complex remains bound to damaged DNA. As a result of the stability of the postincision complex, UvrABC endonuclease does not turnover in an *in vitro* system, which is biochemically reconstituted with only Uvr proteins. Restoration of the DNA primary structure and integrity as well as turnover of the Uvr proteins is accomplished in a series of postincision steps, which require products of two additional genes, uvrD and polA.

UvrD

Its gene maps at 84 min of *E. coli* chromosome. UvrD + is a part of the SOS regulon and is induced by DNA damage. The product of this gene is a 3′–5′ DNA helicase II – a 75 kDa protein which is a DNA-dependent ATPase. DNA helicase II is required for removal of incised damage as a 12–13-mer oligonucleotide fragment. It also effects release of UvrC protein, but not UvrB from the postincision complex.

PolA

Its gene maps at 85 min of *E. coli* genetic map. It encodes a 109 kDa protein, DNA polymerase I. The UvrB protein is not displaced by DNA helicase II and remains bound to gapped DNA. In the presence of deoxyribonucleoside-5′-triphosphates, DNA polymerase I catalyzes repair synthesis, resulting in the filling in of the gap and displacement of the UvrB protein. The size of *in vitro* repair patch is usually ~12 nucleotides in length. Molecular interactions of Uvr proteins, DNA helicase II, and DNA polymerase I during postincision events are not presently known. *E. coli* strains, deficient in uvrD + and polA + are usually significantly less sensitive to the killing effects of UV radiation than Uvr-deficient strains, indicating their auxiliary role in repair. DNA ligase completes NER by catalyzing joining of the last 3′-nucleotide of the patch with the rest of polynucleotide chain.

Transcription-Coupled Repair

Transcription-repair coupling (TRC) allows cells to select some regions of the genome for NER in preference to others. In *E. coli*, as a consequence of a 436-fold induction of β-galactosidase operon, 70% of the UV-induced pyrimidine dimers are removed from the transcribed strand of the induced operon within 5 min, whereas only 50% of dimers are removed from the nontranscribed strand after 20 min of repair. This selective removal of pyrimidine dimers from the transcribed strand of a gene is abolished in the absence of significant levels of transcription. The mechanism of TRC in *E. coli* is a complex one, and may include several subpathways. In one of them, TRC is achieved through the action of transcription-repair coupling factor (TRCF). TRCF is a product of mfd + (for mutation frequency decline) gene, which maps at 25 min on the *E. coli* chromosome. The cloned mfd + gene is translated into a 1148 amino acids protein of ~130 kDa. The Mfd protein has consensus Walker type A nucleotide-binding motif, and, indeed, is a relatively weak ATPase. The Mfd protein can nonspecifically bind dsDNA (and less efficiently ssDNA) in an ATP binding-dependent manner, the ATP hydrolysis promoting its dissociation. The amino acid sequence of Mfd reveals motifs, which are characteristic of a number of DNA and RNA helicases. However, *in vitro* purified Mfd does not show either DNA or RNA helicase activity. The N-terminal 1–378 residues of Mfd, having 140 amino acid region of homology with UvrB, bind UvrA protein. The Mfd protein can also bind different forms of *E. coli* RNA polymerase (RNAP). Amino acids 370–571 of Mfd are involved in this binding. *In vitro*, transcription inhibits NER of damage in a transcribed strand, while it has no effect on the coding strand. This inhibition is thought to result from RNAP stalled at the site of damage. Mfd is able to release stalled RNAP in an ATP hydrolysis-dependent manner. Moreover, Mfd actually stimulates NER on the transcribed strand, so that it becomes faster than on the nontranscribed one. Based on all these observations, it is concluded that TRCF-Mfd carries out preferential repair of the transcribed strand by (1) releasing RNAP stalled at damaged site, and (2) recruiting the $UvrA_2B_1$ complex to damaged site through the high-affinity interaction with UvrA protein. The TRC in *E. coli* is influenced by the rate and conditions of growth as well as the level of gene

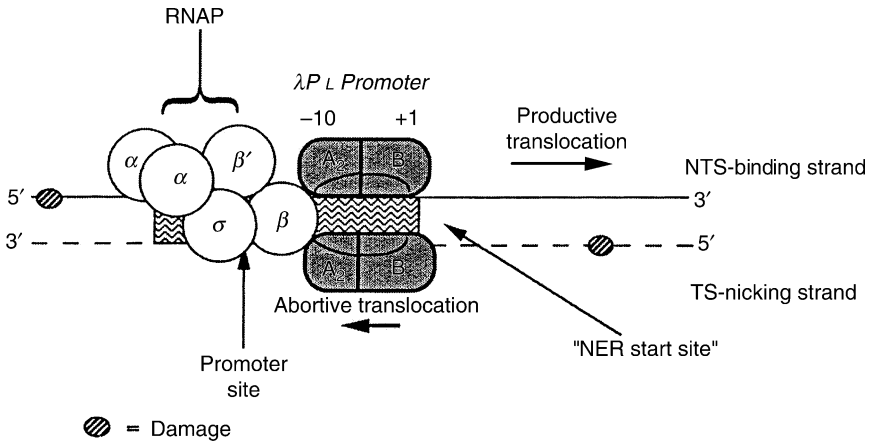

FIGURE 5 Model for strand selectivity by UvrAB helicase. RNA polymerase provides the UvrAB complex a preferred binding site at transcription bubble region via the physical interaction of RNAP with the UvrAB complex. Once the UvrAB complex binds to the promoter region, a competent nucleoprotein complex for helicase action is formed. The UvrAB complex may translocate along the non-transcribed strand in an ATP hydrolysis-dependent reaction. During tanslocation, the DNA damage recognition domain of the UvrA subunit of the UvrAB complex senses damaged sites on the complementary strand. (Reprinted from Ahn, B., and Grossman, L. (1996). RNA polymerase signals UvrAB landing sites. *JBC.* **271**(35), 2153–2161, with permission of The American Society for Biochemistry and Molecular Biology.)

transcription. In the LacZ gene the Mfd-dependent mechanism of preferential repair dominates at basal levels of transcription, while Mfd-independent mechanisms prevail at induced transcription levels. It was shown that in the presence of RNAP, $UvrA_2B_1$ complex is able to specifically bind promoter regions and translocate unidirectionally along coding strand while sensing damage in a transcribed strand. This strand specificity is dictated by the $5'-3'$ directionality of the $UvrA_2B_1$ helicase which can translocate only on the coding strand because the RNAP interferes with that directionality on the transcribed strand (Figure 5). Nicking occurs only on the strand opposite to the strand, along which the $UvrA_2B_1$ complex translocates. Hence, it is the transcribed strand, which is initially repaired. This mechanism could account for the observed Mfd-independent TRC *in vivo*. The Mfd-dependent mode of preferential repair seems to operate at those RNAP molecules which escaped binding of $UvrA_2B_1$ complex at the promoter region and was subsequently stalled at a damaged site.

Conservation of Nucleotide Excision Repair from Bacteria to Man

Nucleotide excision repair (NER) of bacterial, yeast, and mammalian cells have been reconstituted *in vitro* with purified proteins and defined damaged DNA substrates. While it would appear that it takes some 25 proteins in a human cell to complete the process achieved by six bacterial proteins, there is a high degree of conservation of function from bacteria to eukaryotes. Thus NER system of bacteria will certainly serve as a primary model for structure–function studies for years to come.

See Also the Following Articles

DNA Damage: Alkylation • DNA Helicases: Dimeric Enzyme Action • DNA Helicases: Hexameric Enzyme Action • DNA Polymerase I, Bacterial • Zinc Fingers

Glossary

DNA polymerase A protein or protein complex which synthesizes a daughter strand of DNA using a sparental strand as a template.

helicase A protein, which actively separates the two strands of DNA using the energy of ATP hydrolysis.

nucleotide excision repair (NER) A highly conserved multistep process in which several protein machines identify and remove bulky damage from DNA using a dual incision mechanism.

SOS response A number of DNA metabolism genes controlled by the LexA repressor, which is cleaved during genotoxic stress.

***uvr* genes** Genes encoding subunits of NER proteins, which confer sensitivity to killing by UV light.

Zinc Finger A DNA-binding motif consisting of a molecule of zinc bound to four cys found in many DNA-repair proteins.

Further Reading

Friedberg, E. C., Walker, G. C., and Siede, W. (1995). *DNA Repair and Mutagenesis*. ASM Press, Washington, DC.

Goosen, N., and Moolenaar, G. F. (2001). Role of ATP hydrolysis by UvrA and UvrB during nucleotide excision repair. *Res. Microbiol.* **152**(3–4), 401–409.

Goosen, N., Moolenaar, G. F., Visse, R., and van de Putte, P. (1998). Functional domains of the *E. coli* UvrABC proteins in nucleotide excision repair. In *Nucleic Acids and Molecular Biology* (F. Eckstein and D. M. J. Lilley, eds.) Vol 12. Springer, Berlin.

Grossman, L., and Thiagalingam, S. (1993). Nucleotide excision repair, a tracking mechanism in search of damage. *J. Biol. Chem.* **268**, 16871–16874.

Grossman, L., Lin, C.-I. G., and Ahn, B. (1998). Nucleotide excision repair in *Escherichia coli*. In *DNA Damage and Repair* (J. A. Nickoloff and M. F. Hoekstraeds, eds.) Vol 1, pp. 11–27. Humana Press, Totowa, NJ.

Mellon, I., and Hanawalt, P. C. (1989). Induction of the *Escherichia coli* lactose operon selectively increases repair of its transcribed DNA strand. *Nature* **342**, 95–98.

Sancar, A. (1996). DNA excision repair. *Annu. Rev. Biochem.* **65**, 43–81.

Sancar, A., and Rupp, W. D. (1983). A novel repair enzyme: UVRABC excision nuclease of *Escherichia coli* cuts a DNA strand on both sides of the damaged region. *Cell* **33**, 249–260.

Skorvaga, M., Theis, K., Kisker, C., and Van Houten, B. (2002). β-hairpin motif of UvrB is essential for DNA binding, damage processing and UvrC mediated-incisions. *J. Biol. Chem.* **277**(2), 1553–1559.

Theis, K., Chen, P. J., Skorvaga, M., Van Houten, B., and Kisker, C. (1999). Crystal structure of UvrB Provides insight into the mechanism of nucleotide excision repair. *EMBO J.* **18**(24), 6899–6907.

Theis, K., Skorvaga, M., Machius, M., Nakagawa, N., Van Houten, B., and Kisker, C. (2000). The nucleotide excision repair protein UvrB, a helicase-like enzyme with a catch. *Mutat. Res.* **460**(3–4), 277–300.

Van Houten, B. (1990). Nucleotide excision repair in *Escherichia coli*. *Microbiol. Rev.* **54**, 18–51.

Van Houten, B., Eisen, J. A., and Hanawalt, P. C. (2002). A cut above: discovery of an alternative excision repair pathway in bacteria. *Proc. Natl Acad. Sci. USA* **99**(5), 2581–2583.

Biography

Bennett (Ben) Van Houten works at the National Institute of Environmental Health Sciences. His principle research interest is in the structure and function of DNA repair enzymes, and the consequences of mitochondrial DNA damage. He holds a Ph.D. from the University of Tennessee and completed postdoctoral training at the University of North Carolina, and has received the Burroughs Wellcome Toxicology Scholar award.

Lawrence (Larry) Grossman is the University Distinguished Service Professor of Biochemistry in the Department of Biochemistry and Molecular Biology in the Johns Hopkins Bloomberg School of Public Health. His research interests included the chemistry, biochemistry, and enzymology of damaged nucleic acids. He holds a Ph.D. from the University of Southern California and has been a Guggenheim Fellow as well as a Commonwealth Fund Fellow.

Nucleotide Excision Repair: Biology

Errol C. Friedberg
University of Texas Southwestern Medical Center, Dallas, Texas, USA

Nucleotide excision repair (NER) is a fundamental DNA repair process that is ubiquitously distributed from bacteria to man. The process is essential for the enzyme-catalyzed removal of various types of base damage from the nuclear genome, typically those that result in significant distortion of the helical structure of DNA. This article discusses the overview and biology of NER.

The name nucleotide excision repair derives from the fact that during this process damaged bases are excised from the genome as oligonucleotide fragments. This distinguishes nuclear excision repair (NER) from other types of excision repair such as base excision repair (BER), during which damaged bases are excised as free bases, and mismatch excision repair (MMR), during which mismatched nucleotides are removed from the genome as mononucleotides. The oligonucleotide fragments are generated by specific incision of the damaged DNA strand on either side of sites of base damage (bimodal incision) (Figure 1). The gaps (~30 nucleotides in length) generated by oligonucleotide excision are filled in by repair synthesis (Figure 1), using the intact opposite strand as an informational template. When the last nucleotide is inserted, the remaining nick is sealed by DNA ligase (Figure 1).

Modes of Nucleotide Excision Repair

Nucleotide excision repair (NER) transpires in cells in various subforms. Its operation on transcriptionally silent regions of the genome and on the non-transcribed strand of transcriptionally active genes is often referred to as global NER, to distinguish it from NER that specifically operates on the transcribed strand of transcriptionally active genes, so-called transcription-coupled NER (TC-NER). Additionally, both global NER and TC-NER are characterized by incision of the affected DNA strand on either side of sites of base damage (Figure 1), some lower eukaryotes support a form of NER that involves a single incision 5′ to the site of base damage. This process is referred to as specialized NER.

The Biology of NER

Distribution in Nature

As we ascend the evolutionary ladder and encounter increasingly more complex organisms, our information about the cellular biology of NER becomes less precise, even though paradoxically our biochemical understanding has taken leaps and bounds in recent years. Several aspects of the cell biology of higher cells contribute to this paucity of information. Perhaps most importantly, both the structure and organization of the eukaryotic genome is much more complex than that of prokaryotes. Eukaryotic genomes are considerably larger, and the requirements for packaging such large amounts of DNA into the limited confines of the cell nucleus have led to a complex structural organization. A consideration of the distribution of DNA damage in eukaryotes must take into account that nuclear DNA exists in intimate association with both histones and nonhistone chromosomal proteins, and that the structure of chromosomes reflects various levels of folding and coiling of the basic chromatin structural unit, the nucleosome.

Our present understanding of how chromosome structure and nucleosome conformation influence the enzymology of DNA incision and of postincision events during NER in eukaryotes is still scanty. It is certain that structural elements do in fact limit the access of repair enzymes to sites of base damage, and that specific perturbations of chromatin structure are necessary to facilitate NER.

Conventional NER involving the bimodal incision of damaged DNA is operationally and fundamentally similar in all organisms, from bacteria to man. However, there are significant biochemical differences between NER in prokaryotes and eukaryotes. Additionally, the biochemistry of global NER and TC-NER differ in important details during the initial stage of the process. Specifically, during global NER particular proteins are required for the recognition of base damage in DNA. In contrast, during TC-NER the process of arrested RNA polymerase II transcription is believed to provide the mechanism of damage recognition.

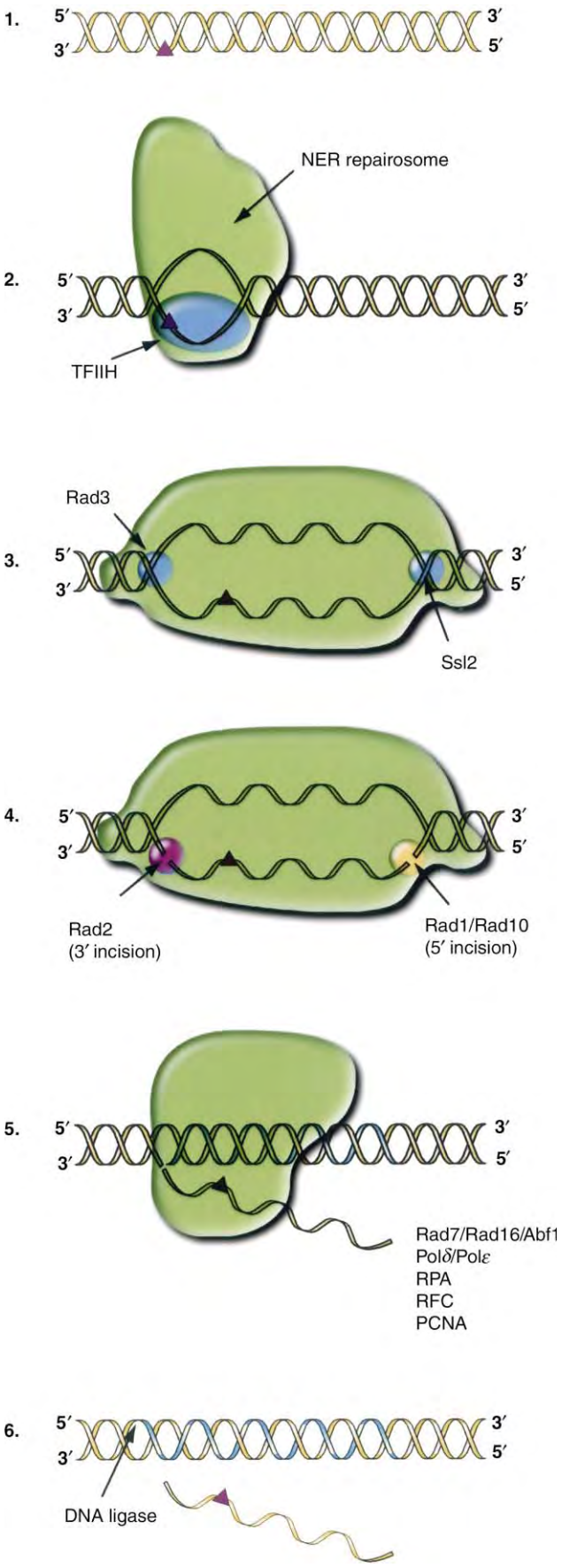

The NER Machinery

NER operates through the assembly of a multiprotein complex. In bacteria this complex comprises about six polypeptides. However, in both lower and higher eukaryotes as many as 30 proteins are required for NER. These comprise proteins that participate in (1) the recognition of base damage, (2) bimodal incision of DNA, (3) oligonucleotide fragment incision, (4) repair synthesis of the gap generated in DNA, and (v) DNA ligation. (Figure 1). In eukaryotes the RNA polymerase II, basal transcription factor IIH (TFIIH) is an integral component of the NER machinery. As noted below, mutations in some of the genes encoding TFIIH subunits can result in disease states with transcription defects.

Substrate Specificity

NER operates primarily on types of base damage that generate conformational distortion of the DNA helical structure. The so-called (6–4) photoproduct, a highly distortive type of base damage in DNA that results from exposure to UV light (Figure 2), as well as cyclobutane pyrimidine dimers (Figure 2), are premier examples of substrates for NER. The NER machinery does not recognize small loops or mismatches in DNA, and small chemical adducts such as those produced by methylation and the oxidation of bases are preferentially recognized by the BER process. The precise mechanism of substrate recognition during NER in eukaryotes remains to be determined.

Detection of NER *in vivo* and *in vitro*

Studies on NER in mammalian cells have historically utilized a variety of increasingly refined experimental strategies and techniques, many of which have been adapted from methods initially developed for studies

FIGURE 1 The general mechanism of nucleotide excision repair (NER) in eukaryotes. In the figure yeast is used as an example. The red triangle represents some type of base damage that is recognized by the transcription-independent NER system. The binding of multiple proteins at or near the site of base damage in an ordered step-wise fashion generates a large multiprotein complex, the NE repairosome, that includes the RNA polymerase II basal transcription factor TFIIH. Two DNA helicase subunits in TFIIH (Rad 3 and Ssl2 in yeast) facilitate the generation of a bubble in the DNA that is ~30 nucleotides in length and that flanks the site of base damage. The double-stranded/single-stranded DNA junctions are then recognized by two structure-specific endonucleases (Rad2 and Rad1/10). These cut the DNA duplex only on the damaged strand, generating an oligonucleotide fragment ~30 nucleotides in length. The Rad7/Rad16/Abf1 protein complex then facilities displacement of the oligonucleotide as a free DNA fragment carrying the damaged base. Replicative DNA polymerases (d and/or e) together with accessory proteins (RPA, RFC, PCNA) fill in the gap formed and DNA ligase seals the damaged DNA strand to restore complete covalent integrity.

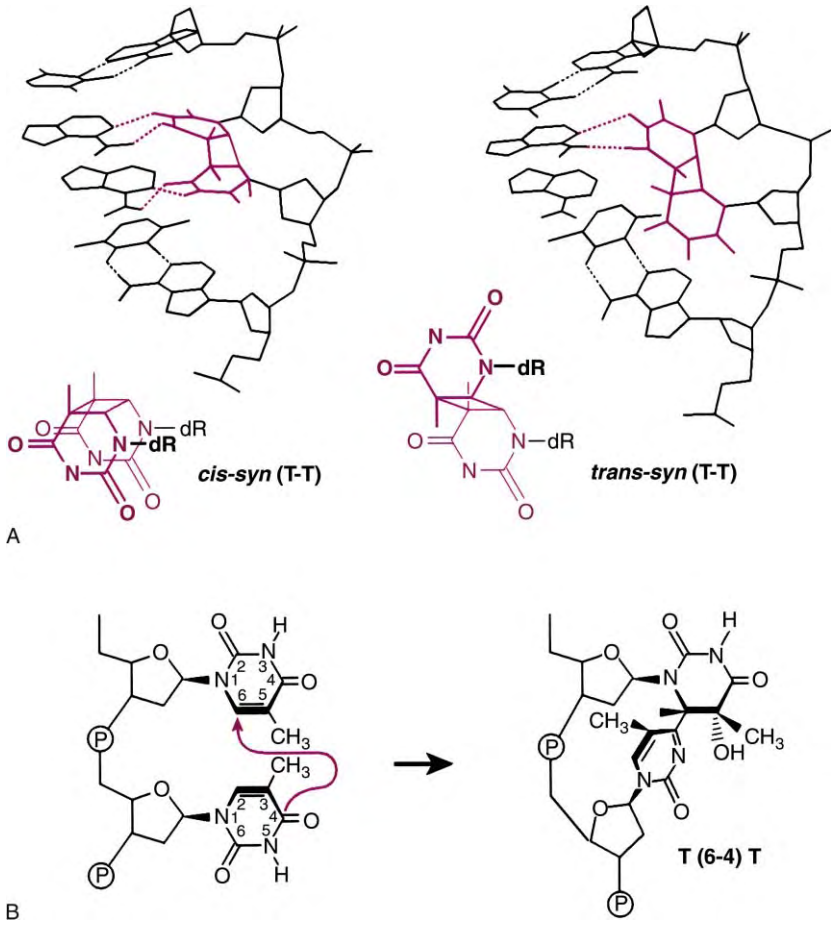

FIGURE 2 Chemical structures of cyclobutane pyrimidine dimers (CPD) (A) and [6–4] photoproducts (B). Both of these photoproducts are generated in large amounts when DNA is exposed to UV light, including sunlight.

with bacteria. Some of these procedures measure the damage-specific incision of DNA, either directly or indirectly. Others measure the physical excision of damaged nucleotides, repair synthesis of DNA, or the rejoining of strand breaks (DNA ligation). A particularly widely used technique for monitoring NER in living cells is referred to as the unscheduled DNA synthesis (UDS) assay, that identifies repair synthesis of DNA. In this procedure cells in monolayer culture are exposed to a DNA damaging agent such as UV radiation and the medium is supplemented with a radiolabeled precursor for DNA synthesis. Repair synthesis of DNA associated with NER is identified by a delicate autoradiographic stippling of nuclei in cells that are outside the S phase of the cell cycle (hence UDS) (Figure 3).

Kinetics of NER

While the application of many of the experimental procedures mentioned above supports the existence of NER in higher organisms, the relative kinetics of specific events associated with NER, such as DNA incision, the excision of specific lesions from high-molecular-weight DNA, and repair synthesis in mammalian cells, are still controversial. In part these controversies have arisen from the use of different experimental procedures, which, though designed to measure the same biological end points, sometimes have optimal reliabilities at different extents of DNA damage and under different experimental conditions, and hence may not be strictly comparable. Nonetheless, some of these apparent "experimental inconsistencies" may actually reflect real distinctions in NER associated with different cell types, different functional states of cells, particular regions of the genome, and different types of DNA damage. It is generally acknowledged that (6–4) photoproducts are removed from the genome of human, and in particular rodent cells, more rapidly than are pyrimidine dimers. It can take many hours before the latter lesions are fully cleared from the genome.

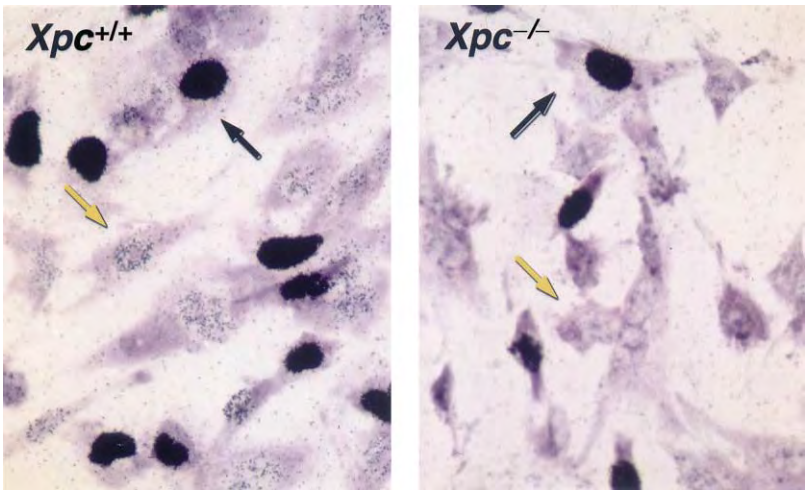

FIGURE 3 The identification of repair synthesis during NER in mammalian cells. The repair synthesis step shown in Figure 1 can be monitored in mammalian cells in monolayer culture. Mouse wild-type ($Xpc^{+/+}$) and NER-defective ($Xpc^{-/-}$) cells are exposed to UV radiation and allowed to incubate in the presence of [^{3}H] thymidine. Cells in S phase of the cell cycle undergo intense autoradiographic labeling by incorporating the radiolabled thymidine (black arrows). However, cells undergoing repair synthesis during NER incorporate much less label which can be identified as a delicate autoradiographic stippling (yellow arrow, $Xpc^{+/+}$). These grains are greatly reduced or absent in the NER-defective $Xpc^{-/-}$ cells.

Defective NER and Human Disease

Several human hereditary diseases have been identified that result from defective NER. The so-called classical xeroderma pigmentosum (XP) is an autosomal-recessive disease that results from defects in both global NER and TC-NER. Affected individuals are extremely sensitive to sunlight and have a markedly increased risk of developing skin cancers. A clinically indistinguishable form of XP called the XP variant form, derives from mutations that affect a different biological response to UV radiation-induced DNA damage. Individuals with mutations in genes required for both NER and RNA polymerase II transcription can develop the clinical features of both XP and a different disease called Cockayne syndrome (CS). Pure CS (unaccompanied by XP) arises from defects in the *CSA* or *CSB* genes that encode proteins required for TC-NER. Unlike XP, CS does not lead to an increased risk of skin cancer in human subjects. Defects in subunits of TFIIH can result in a spectrum of diseases characterized by developmental and neurological defects with or without defective NER, the disease trichothiodystrophy (TTD) being a notable example.

Mouse Models for Defective NER

Mouse models for each of the human hereditary diseases mentioned above have been generated by conventional targeted gene replacement, and sometimes by more refined strategies. In general these mice have proven to mimic the human disease well and have provided much valuable information about the relationships between defective NER and cancer predisposition and pathogenesis.

See Also the Following Articles

DNA Helicases: Dimeric Enzyme Action • DNA Helicases: Hexameric Enzyme Action • RNA Polymerase I and RNA Polymerase III in Eukaryotes • RNA Polymerase II and Basal Transcription Factors in Eukaryotes • RNA Polymerase II Elongation Control in Eukaryotes • RNA Polymerase II Structure in Eukaryotes • Transcription-Coupled DNA Repair, Overview

Glossary

damaged DNA DNA in which the covalent structure, nucleotide sequence, or conformation has been altered.

DNA repair A collection of cellular processes whereby damaged DNA is restored to its normal chemistry, nucleotide sequence, conformation, and function.

eukaryotes One of the kingdoms of life, more highly evolved than bacteria, the cells of which contain a defined nucleus.

oligonucleotides Fragments of one or two DNA strands that can be of any size.

transcriptionally active genes Genes that are in the active process of being transcribed into RNA.

Further Reading

Batty, D. P., and Wood, R. D. (2000). Damage recognition in nucleotide excision repair of DNA. *Gene* **241**, 193–204.

de Boer, J., and Hoeijmakers, J. H. J. (2000). Nucleotide excision repair and human syndromes. *Carcinogenesis* **21**, 453–460.

Friedberg, E. C. (2001). How nucleotide excision repair protects against cancer. *Nat. Rev. Cancer* **1**, 22–33.

Friedberg, E. C., Walker, G. C., and Siede, W. (1995). *DNA Repair and Mutagenesis*. ASM Press, Washington DC.

Norbury, C. J., and Hickson, I. D. (2001). Cellular responses to DNA damage. *Annu. Rev. Pharmacol. Toxicol.* **41**, 367–401.

Biography

Errol C. Friedberg is Professor and Chair in the Department of Pathology, University of Texas Southwestern Medical Center at Dallas. He is the senior author of the textbook *DNA Repair and Mutagenesis* and has published over 300 papers on these topics.

Olfactory Receptors

Sigrun I. Korsching
University of Cologne, Germany

Olfactory receptors mediate the primary interaction of the olfactory brain with the external world. Any odor stimulus is initially represented as activation of one to many different olfactory receptors. Vice versa, anything that binds and activates an olfactory receptor, is as per definition an odor, or odorant, as the single compounds are often called. Olfactory receptors constitute one of the largest families of G protein-coupled receptors. Many large and small clusters of olfactory receptors are distributed throughout the genome. Olfactory receptors are expressed in a highly specific manner and monogenic expression is the general rule, i.e., one neuron–one receptor. The molecular receptive range has been analyzed for several olfactory receptors. Generally, olfactory receptors have been found to exhibit a somewhat relaxed specificity towards ligands. However, some receptors, in particular those for pheromones, show very high specificity. Olfactory receptors signal through specialized trimeric G proteins to open calcium-permeable nonspecific cation channels.

Olfactory Receptors are G Protein-Coupled Heptahelical Receptors

From a modest origin in simple eukaryotes like yeast, G protein-coupled heptahelical receptors (Figure 1) have evolved into the largest superfamily known. As the name indicates, signaling occurs through (trimeric) G proteins, with particular families making use of different G proteins. These receptors transmit biological effects of many hormones, neurotransmitters, chemokines, and diverse sensory stimuli. Chemosensation constitutes an ancient function for this family. Already in yeast a dichotomy between sensing nutrients and sensing pheromones is found.

Whereas simple animals like nematodes possess a single chemosensory sense, in higher animals several specialized systems have evolved, using olfactory and gustatory receptors, respectively. Olfactory receptors may recognize volatile or water-soluble odorants, depending on the species (e.g., mammals versus fish), and the defining difference to taste receptors appears not to be the nature of the ligand, but the outreach of the system. Taste is generally considered to be a contact sense, whereas olfaction delivers long-range information.

Olfactory Receptors Segregate in Several Highly Divergent Groups

Thirteen years ago, the first higher eukaryote chemosensory receptors – mammalian odorant receptors proper (OR) – have been identified. Linda Buck, then a postdoctoral fellow in Richard Axel's laboratory, used short motifs conserved in previously known heptahelical receptors to amplify a group of rat odorant receptors from nasal cDNA via polymerase chain reaction. Like all heptahelicals, odorant receptors exhibit the canonical seven-transmembrane domain structure (Figure 1) and the G protein-interaction motif. Peculiar are the relatively short N and C termini. OR are a highly divergent group, and amino acid homologies below 20% have been reported within one species. Between phyla, homologies have been so low as to be undetectable. Thus, insect and nematode chemosensory receptors have not been identified via homology searches, but by looking for orphan heptahelical receptors in either single cell libraries or genomic databank searches.

Two classes of distantly related receptors have been found in the mid-1990s. They are designated V1R and V2R family, after their occurrence in the mammalian vomeronasal or accessory olfactory system. V1R receptors share the short N and C termini with the OR receptors, whereas the V2R exhibit a large extracellular N-terminal domain, and show some sequence homology to the Ca^{2+}-sensing receptor and the metabotropic glutamate receptor, a neurotransmitter receptor. In mice the V2R family comprises ~100 genes and the V1R family contains ~150 genes, which segregate into 12 subfamilies designated V1Ra, V1Rb etc. Humans and other hominoids have nearly no VR receptors as their accessory olfactory system is derelict and their VR genes suffer ongoing pseudogenization. No intact human V2R is remaining and less than a handful of intact *V1R* genes have been identified in extensive genome searches.

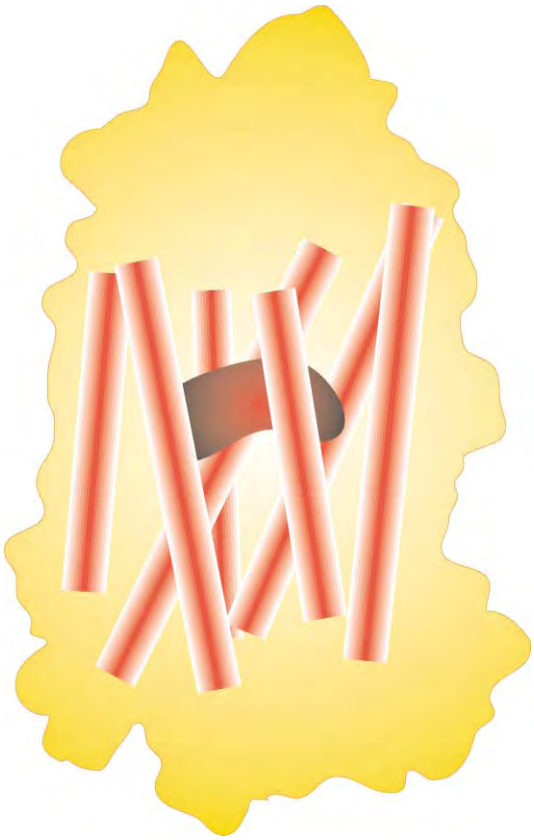

FIGURE 1 Schematical representation of an olfactory receptor. No crystallographical data are available for olfactory receptors. It is assumed that their structure is analogous to that of rhodopsin and the adrenergic receptor, which are more extensively studied. This is supported by some mutational analysis and molecular dynamics modeling. The scheme shown here is based on the structure of rhodopsin, whose crystal structure has been solved in 2000. Seven-transmembrane regions are depicted as cylinders. The binding site for ligands is centrally situated, between several transmembrane domains.

It is commonly assumed but not rigorously shown that OR deal with common odors whereas VR are specialized for detecting pheromones – odors which are relevant in a social context as in kin recognition and mating.

It should be mentioned that there may be another, radically different group of olfactory receptors, a type of membrane-bound guanylate cyclases with a single transmembrane domain. Members of this family are expressed in specific subsets of olfactory receptor neurons. However, no ligands have been identified for them so far.

Gene Structure and Genomic Arrangement of Olfactory Receptors

Vertebrate OR and V1R feature an intronless coding region of ~1 kb that may be preceded by one to several noncoding introns. Alternative splicing is a frequent phenomenon for odorant receptors. Insect olfactory receptors and vertebrate V2R contain several introns within the coding region, as is common for other G protein-coupled receptors.

The OR family size approaches 1300 identified genes in mouse, a species with a completely sequenced genome. About one-fifth are pseudo-genes, a high percentage, which has people speculating about a putative role of the pseudo-genes in the evolution of the gene family. The human OR gene family is of similar size; however, the percentage of pseudo-genes is much higher, so that only ~350 odorant receptors appear functional in humans. Clusters of related genes are a frequent feature and indicate recent expansions of the respective gene lineages. Sometimes other genes may be interspersed, a notable example being the intercalation of MHC genes with odorant receptors reported for the mouse (but not for the human) genome. Overall, olfactory receptors are widely spread throughout the genome, asserting the ancient origin of this gene family.

Family sizes are smaller for lower vertebrates and insects – for *Drosophila* 60 receptor genes have been identified in the complete genome, mosquitoes possess ~80 olfactory receptor genes. For fish estimates range ~100 different OR. However, the occurrence of (smaller) clusters and the overall widespread distribution of receptor genes are equivalent to higher vertebrates. Surprisingly, the nematode *Caenorhabditis elegans* boasts ~1100 different chemosensory receptor genes (including 30% pseudogenes).

Monogenic and Monoallelic Expression of Olfactory Receptor Genes

Nematode chemosensory neurons, like taste receptor cells, express many different receptor genes per cell. Such bundling of receptors may be efficient if many different chemicals should lead to very few behavioral outcomes – mainly the choice between "stay here" and "get out of here" or "swallow this" and "spit it out," respectively. As soon as a chemical sense is used for more sophisticated distinctions, it is imperative that more selective means of expression are used.

Accordingly, the expression of vertebrate and insect olfactory receptors is highly regulated. One particular olfactory receptor neuron expresses only a single type of OR gene or VR gene (Figure 2). This very restricted expression has been christened monogenic expression. In fact, for rodents it has been shown that expression is restricted even to one allele of a particular *OR* or

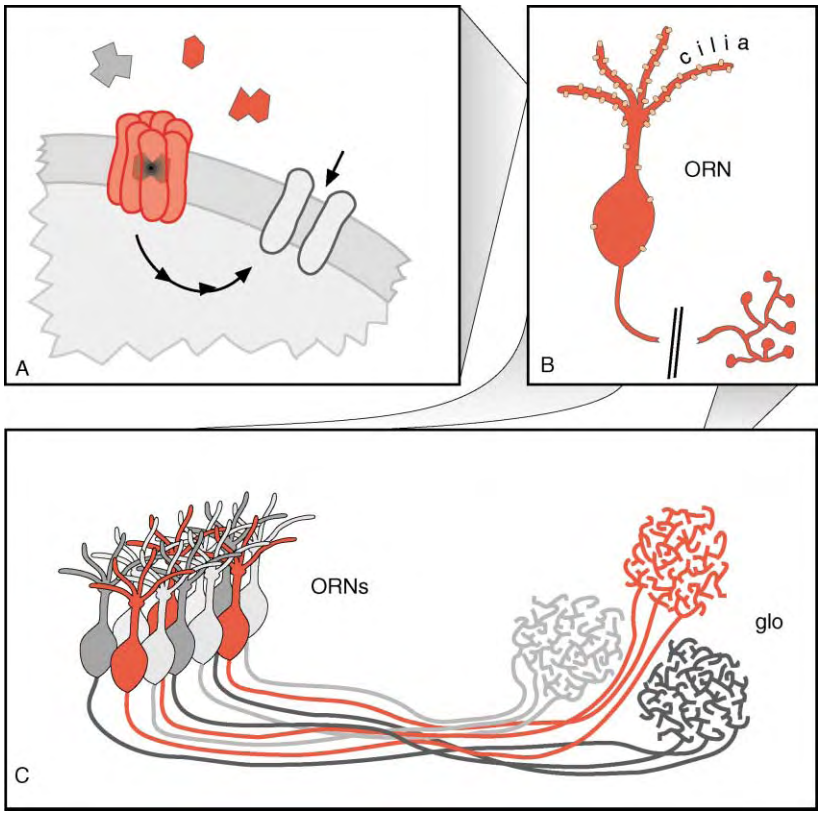

FIGURE 2 Olfactory receptors are part of the olfactory information processing pathway. (A) Olfactory receptors bind odorants and initiate a several step signal processing cascade. As endpoint various channels are opened, leading to depolarization of the olfactory receptor neuron. (B) The olfactory receptors are mainly expressed on the cilia (or microvilli, not shown) of olfactory receptor neurons. These neurons generate action potentials in their axons and propagate them towards their terminals in the so-called glomeruli (glo). Glomeruli are neuropil structures and constitute the first relay station (synapse) in the olfactory processing pathway. (C) Ciliated olfactory receptor neurons expressing the same odorant receptor are distributed within the sensory surface, but converge onto a common glomerulus. Microvillar receptor neurons such as those expressing the *V1R* and *V2R* genes converge onto several microglomeruli (not depicted here).

*VR*gene, reminiscent of the monoallelic expression of immunoglobulin genes.

Some exceptions occur to the rule of one neuron–one gene. Notably a particular insect olfactory receptor, OR83b, has been found to be coexpressed in about two-thirds of all olfactory receptor neurons. This receptor is also highly unusual in that it is strongly conserved between many insect species. It is suspected that such atypical receptors may not have a role in odor detection, but serve another, so far unknown function.

Olfactory Receptor Gene Expression is Regulated by Proximal and Distal Control Regions

A stringent test for specificity of expression relies on the convergence of olfactory receptor neurons expressing the same receptor gene into a single glomerulus at a roughly fixed position (Figure 2). In several cases such a restricted expression pattern could be reproduced faithfully by reporter gene constructs containing variable segments of DNA flanking the coding region. It has been possible to narrow-down control elements to regions of one to a few kilobases, but specific enhancer sites, transcription factors, or combinations thereof are just beginning to be identified. In some cases all control elements appear to be situated close to the gene, whereas for other OR essential regulatory elements have been found in distances of ~100 kb from the coding region.

Selection of an odorant receptor gene for expression is a multilevel process. First, a choice is made for a particular subgroup of genes. Such subgroups feature spatially or temporally limited expression. In a second step, a particular odorant receptor is selected in a stochastic manner and then exerts negative feedback regulation onto all other OR. Thus, monogenic expression of odorant receptors is ensured.

Ligand Spectra have been Established for a Handful of Olfactory Receptors

Although hundreds of olfactory receptors have been cloned to date, ligands are only known for a small percentage of them. The difficulty of guessing potential ligands from among the enormous pool of potential odorants has been a major problem. Also, correct expression in heterologous systems has turned out to be unusually complicated, and has only been possible for some receptors. Most of the receptor molecules synthesized in heterologous systems are not transported to the plasma membrane, but remain in the endoplasmatic reticulum, possibly because some unknown auxiliary molecules are missing. Indeed, for nematode chemosensory receptors a chaperone has been shown to be essential for proper protein translocation and V2R receptors are coexpressed with MHC class 1b molecules that appear to serve as escort molecules. For two OR genes it has been possible to use a viral transfection method to express the recombinant odorant receptor in olfactory receptor neurons. In several cases knockouts of particular olfactory receptors have served to identify receptor ligands, as first shown for the *C. elegans* ODR10 diacetyl receptor. The binding of ligands is not measured directly, but evaluated by a downstream parameter such as a change in membrane potential, or, more commonly, a rise in intracellular calcium levels.

Usually olfactory receptors respond best to a small group of highly related compounds and with lower sensitivity to further odorants. Often a particular functional group is preferred, but in some cases ligands with other functional groups may also activate the same receptor. Many strong ligands identified so far contain an aldehyde or keto group. The most extensive ligand analysis has been performed for the rat odorant receptor I7, which has *n*-octanal as main ligand. Hydrocarbon chain length is another molecular feature that influences ligand efficacy. In the vast majority of cases longer hydrocarbon chains result in more avid binding. From psychophysical experiments it is known that also the shape and rigidity of the ligand molecule determine the olfactory sensation. Enantiomers of known ligands often, but not always, show differential responses. Taken together, a particular olfactory receptor requires a particular combination of molecular features in its cognate ligand/s.

Combinatorial versus Monospecific Representation of Odorants

Due to the monogenic expression of olfactory receptors, the ligand specificity of the olfactory receptor determines the odor responses of the corresponding olfactory receptor neurons (Figure 2). Due to the convergence of olfactory neurons expressing the same receptor in single glomeruli (Figure 2) the ligand specificity of the olfactory receptor determines the odor responses in these glomeruli. This results in a rather direct map of the ligand specificities of the olfactory receptor repertoire on a two-dimensional surface in the corresponding brain region (the olfactory bulb in mammals, the antennal lobe in insects). Interestingly mammalian odorant receptors influence the choice of a target glomerulus of olfactory receptor neurons as shown by gene swap experiments. Insect olfactory receptors, on the other hand, appear not to be involved in selection of the proper target site.

Two complementary principles of odorant representation emerged from ligand binding studies *in situ* and in heterologous systems. Firstly, many odorants activate a small subset of the large repertoire of odorant receptors. Vice versa, any particular OR gets activated by a handful of different compounds, not just by a single compound. This results in a unique combination of activated receptors for each individual odor compound (Figure 3). The theoretical coding capacity of such a combinatorial representation is immense and much higher than needed – even for millions of different odors. In fact, the neuronal representation is sparse – the large majority of receptors does not respond to any given odorant – and thus suboptimal with respect to coding capacity. Nevertheless, humans (trained perfumers, that is) can distinguish and identify several thousand different odors, more than tenfold the number of the functional human OR repertoire.

An alternative principle of neuronal representation seems to be realized for a smaller group of chemicals, including many pheromones. The high sensitivity and specificity of several such olfactory receptors (observed in mammals, fish and insects) appears to indicate a monospecific interaction. A well-known example is the male/female attraction in silk moth, *Bombyx mori* (Figure 3). To integrate labeled line coding with hard-wired behavior appears straightforward. The coding capacity of such a system is low – it equals the number of different olfactory receptors devoted to this strategy – but sufficient for the limited number of potential pheromones. An example for a receptor/ligand pair is the mouse V1Rb2 receptor that specifically recognizes 2-heptanone.

Signal Transduction of Olfactory Receptors

All heptahelical olfactory receptors signal through trimeric G proteins. A controversy surrounding the

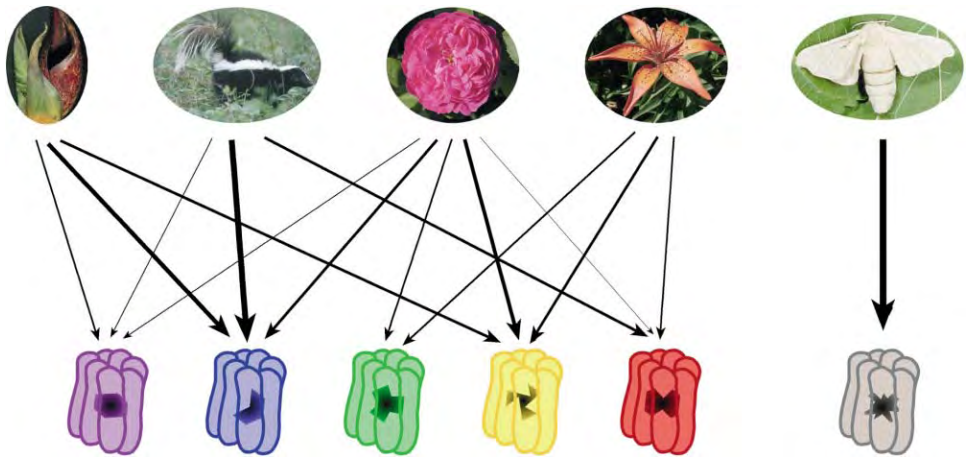

FIGURE 3 Two types of olfactory processing: combinatorial versus monospecific. To the left the combinatorial representation of odorants is depicted. Different odors – here symbolized by various odor sources (skunk cabbage, skunk, rose, lily) – activate overlapping, but distinctive combinations of olfactory receptors. This is also valid for the individual odor components, the odorants. Each odorant activates a particular subset of all olfactory receptors and thus each odorant generates a unique, if overlapping "fingerprint" of olfactory receptor activation. To the right monospecific representation of odorants is shown. A single compound activates a highly specific receptor very selectively, as is often observed for pheromones. Depicted here is a female silk moth, source of an attractive pheromone that is detected with extremely low threshold by the male of that species.

signal transduction by OR has been more or less resolved. Vertebrate OR signal through G_{olf}, a specialized α-subunit, which in turn activates adenylate cyclase type III (Figure 4). The resulting cAMP activates a cyclic nucleotide-gated channel that is a rather nonselective cation channel. Such channels are widespread in the nervous system, their particular gating properties are set by the subunit composition (A2A4B1b in the case of the mammalian olfactory channel). A considerable portion of inward current is carried by calcium (Figure 4). The resulting influx of calcium opens a calcium-gated chloride channel, resulting in chloride efflux, i.e., in further depolarization and thus amplification of the signal (mammals, amphibians, and fish). Finally, the odor-induced signal is switched off by G protein-coupled receptor kinase 3 (GRK3) and binding of arrestin-related molecules to the phosphorylated odorant receptor (Figure 4). Even with a constant odor stimulus the olfactory sensation is down-regulated within seconds, in part due to the peripheral mechanisms mentioned here.

The signal transduction cascade has not been worked out as well in invertebrates. Insects appear to also use cAMP as second messenger. Lobster may additionally employ IP3 as a second signal transduction system that

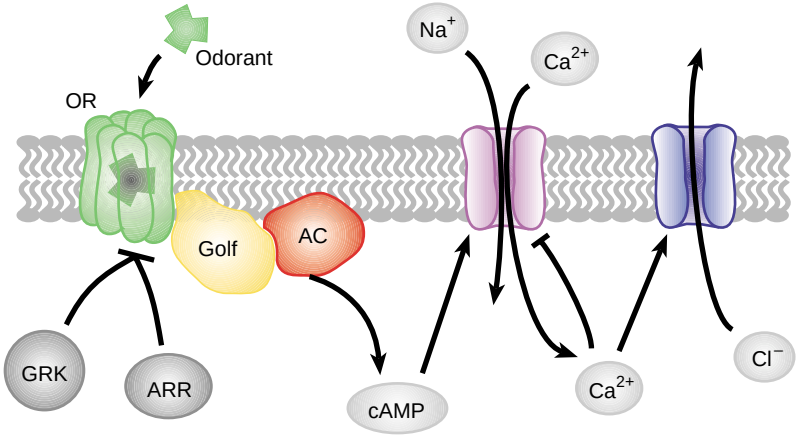

FIGURE 4 Signal transduction and termination of odor responses. A schematical representation of the main signaling pathway. AC, adenylate cyclase type III; ARR, β-arrestin-related molecules; G_{olf}, an α-subunit somewhat specific for the olfactory nervous system; GRK, G protein-coupled receptor kinase; OR, odorant receptor. The cyclic nucleotide-gated channel is permeable for sodium and calcium, but gets blocked by calcium. GRKs phosphorylate the odorant receptor, which subsequently binds β-arrestin, leading to a complete stop of the signal transduction cascade.

opens IP3-gated channels situated in the plasma membrane. Such channels have been described in olfactory receptor neurons of many species, including fish and rodents, but appear to be a minor constituent compared to the number of cyclic nucleotide-gated channels. The effects described for IP3 on olfactory signal transduction in mammals and fish may reflect a modulatory role of this second messenger, conceivably in setting the basal activity level of olfactory receptor neurons. When all the evidence is weighed, a completely independent second signaling pathway for odorant receptors appears not plausible.

Signal transduction for olfactory receptors of the VR type differs both from OR and between V1R and V2R. The emerging picture is that V1R signal via the G_{i2} α-subunit and V2R via the G_o α-subunit. Finally, a transient receptor potential channel, TRP2, is activated by diacylglycerol and allows the influx of cations including calcium.

See Also the Following Articles

Cyclic Nucleotide-Regulated Cation Channels • G Protein-Coupled Receptor Kinases and Arrestins • Taste Receptors

Glossary

chemosensation Any chemical sense, such as olfaction or taste. Very ancient, occurs already in bacteria where it is used for chemotaxis.

glomeruli Globular neuropil, comprises synapses of olfactory receptor neurons.

heptahelical A receptor with seven-transmembrane helices, often, but not exclusively a G protein-coupled receptor.

odorant A chemically pure odor, i.e., a single compound that activates an odorant receptor.

olfactory code The neuronal representation of odors insofar as it is relevant to the encoding of these odors. Often confused with the neuronal representation, which is more commonly studied.

pheromone An odorant that mediates intraspecies communication, eliciting neuroendocrine changes and stereotyped behavioral repertoires.

Further Reading

Breer, H. (2003). Olfactory receptors: Molecular basis for recognition and discrimination of odors. *Anal. Bioanal. Chem.* **377**, 427–433.

Crasto, C., Singer, M. S., and Shepherd, G. M. (2001). The olfactory receptor family album. *Genome Biol.* **2**, 1027.

Halpern, M., and Martinez-Marcos, A. (2003). Structure and function of the vomeronasal system: An update. *Prog. Neurobiol.* **70**, 245–318.

Keller, A., and Vosshall, L. B. (2003). Decoding olfaction in drosophila. *Curr. Opin. Neurobiol.* **13**, 103–110.

Kim, J., and Carlson, J. R. (2002). Gene discovery by E-genetics: Drosophila odor and taste receptors. *J. Cell Sci.* **115**, 1107–1112.

Korsching, S. (2002). Olfactory maps and odor images. *Curr. Opin. Neurobiol.* **12**, 387–392.

Nagao, H., Yamaguchi, M., Takahash, Y., and Mori, K. (2002). Grouping and representation of odorant receptors in domains of the olfactory bulb sensory map. *Microsc. Res. Tech.* **58**, 168–175.

Ronnett, G. V., and Moon, C. (2002). G proteins and olfactory signal transduction. *Annu. Rev. Physiol.* **64**, 189–222.

Touhara, K. (2002). Odor discrimination by G protein-coupled olfactory receptors. *Microsc. Res. Tech.* **58**, 135–141.

Young, J. M., and Trask, B. J. (2002). The sense of smell: Genomics of vertebrate odorant receptors. *Hum Mol. Genet.* **11**, 1153–1160.

Biography

Sigrun Korsching is a Professor at the Institute of Genetics at the University of Cologne in Germany. Her principal research interest is in the field of sensory neurobiology, in particular the sense of smell. She holds a Ph.D. from the Ludwig-Maximilian-Universität in Munich, Germany and received her postdoctoral training at the California Institute of Technology, California. She has authored influential texts in the fields of neurotrophic interactions and olfactory encoding.

Oligosaccharide Analysis by Mass Spectrometry

Andrew J. Hanneman and Vernon N. Reinhold
University of New Hampshire, Durham, New Hampshire, USA

Glycosylation is important for cellular regulation and recognition activities and oligosaccharide structural details are essential determinants of function. In contrast to other biopolymers that are joined by identically positioned functional groups, an oligosaccharide chain is commonly branched, with multiple positions for linkage. The monomer units themselves may exist as isomeric ring conformers (pyrans, furans), with differing spatial orientation of hydroxyl groups. When these hydroxyl groups are involved in linkage between residues (anomers), additional isomeric complexity is introduced. As a consequence, oligosaccharide structure elucidation can be a complicated problem requiring a number of different analytical approaches. Most of the techniques currently available for oligosaccharide analysis are based on mass spectrometry (MS) and we summarize in this report the details of composition, sequence, branching, and inter-residue linkage that can be obtained using small amounts of sample material.

Important Classes of Oligosaccharides

Glycoprotein Glycans

Glycoprotein glycans are branched oligomers having ~5–20 monosaccharides that are added to proteins co- or posttranslationally. Protein glycosylation is primarily based upon two main structural motifs: (1) *N*-linked glycans are linked through the amide bond of asparagine at an amino acid sequence called the consensus site: asparagine-x-serine/threonine (where x can be any amino acid except proline); and (2) *O*-linked glycans, which have no known consensus sequence and are linked through glycosidic bonds to serine and threonine residues on the protein. For both glycan types there are constant core structures proximal to the protein backbone, although numerous variations are known.

Glycosphingolipid Glycans

Glycosphingolipids represent a diverse set of amphipathic molecules comprised of an outer glycan portion linked to a ceramide lipid tail. In glycosphingolipids the ceramide lipid serves as an anchor to the cell membrane and the carbohydrate can present a hydrophilic surface for cell–cell recognition.

Glycosaminoglycans

Glycosaminoglycans (GAGs) are linear carbohydrate chains consisting of repeating disaccharide units, often rich in sulfate groups (e.g., heparin), that make up the carbohydrate portion of high molecular weight protein/carbohydrate assemblages known as proteoglycans. Tissue-specific proteoglycans are inserted into plasma membranes, excreted into the extracellular matrix, or stored in intracellular compartments where they are involved in adhesion, lubrication, and regulatory functions.

Methods and Instrumentation

Obtaining and Preparing Glycans for Mass Spectrometry

Carbohydrates, being less polar, are generally more difficult to ionize than other classes of biological molecules, a feature that is compounded when in the presence of salts and peptides. Consequently, judicious purification steps are required for effective MS analysis of carbohydrates. Purification, including desalting, is often accomplished online using high pressure liquid chromatography (HPLC) prior to electrospray mass spectrometry (ESI). Changing the physical characteristics by derivatization has also proven to be successful, and this is discussed below.

Glycan Release and Purification

Prior to mass spectrometry glycoproteins can be enzymatically cleaved using trypsin or other proteases

resulting in a peptide/glycopeptide mixture; however, glycopeptides ionize poorly within such mixtures and subfractionation is usually advantageous. Consequently, glycans are often enzymatically or chemically released from proteins first and then purified. This approach, however, loses an important feature of structure: the location of the glycan and its consensus sequence on a peptide. Most *N*-linked glycans are conveniently released from proteins using the endoglycosidase enzymes PNGase F or PNGase A. Analogous enzymes for general release of *O*-linked glycans, however, are not known and *O*-linked glycans are typically released using chemical methods including base-release (beta-elimination) and anhydrous hydrazine at low temperature. Hydrazinolysis at higher temperatures is well suited for *N*-linked glycan release, however, at high temperature significant degradation of *O*-glycans is observed.

Glycolipids are obtained from biological materials by extraction with organic solvents, including chloroform: methanol:water (CMW). Glycolipids can be isolated from other lipids using ion exchange or silica gel chromatography and may then be analyzed directly or the oligosaccharide chains are enzymatically or chemically released and extracted.

GAGs are chemically released from proteoglycans and subjected directly to MS analysis or may first be broken down into smaller subunits using GAG-chain-specific enzymes including chondroitinases and heparinases.

Derivatization and Adduction for Ionization

Lacking very polar functional groups many oligosaccharides are not easily ionized. In the positive ion mode naturally occurring oligosaccharides are typically observed as adducts with cations such as sodium or potassium, although numerous cations can be used. Derivatization is another strategy for improving ionization to enhance MS signal. Some of the common derivatization strategies were originally developed to improve the volatility of carbohydrates for gas chromatographic analysis. Complete methylation of hydroxyl groups improves volatility and also assists purification by organic solvent extraction, providing sensitivity enhancement when analyzed by electrospray ionization (ESI) or matrix-assisted laser desorption ionization (MALDI)-MS. Permethylation is also advantageous when structural details are pursued. Other procedures involve covalent attachment of an ionizable functional group such as an amine to the oligosaccharide-reducing end. Some aminated derivatives may include a chromophore or fluorophore to enhance UV/vis or fluorescence detection.

Instrumentation for Glycoconjugate Mass Spectrometry

Mass spectrometry is a gas-phase analytical technique originally limited for use with small molecules that had to be thermally vaporized prior to ionization. The molecular weight obstacle has since been overcome by techniques that combine vaporization and ionization in a single step; these include ESI and MALDI. Both techniques have been interfaced with a variety of mass analyzers, and high-molecular-weight samples now provide no barrier using these techniques.

Gas-phase ions are a long way from detailed structural understanding, thus the recent challenges in mass spectrometry relate to disassembly of large structures within the mass spectrometer. Notwithstanding recent developments, composition analysis of depolymerized oligosaccharides by GCMS has remained an important tool for structure determination.

Ionization Methods for Mass Spectrometry

Electron Impact and Chemical Ionization Electron-impact ionization (EI) and chemical ionization (CI) were the first ionization methods to be widely applied to carbohydrate samples. EI and CI are gas-phase techniques that are readily interfaced with a gas chromatograph (GC) enabling complex mixtures to be efficiently separated by GC with subsequent component identification by MS. EI imparts high energy to the sample resulting in extensive fragmentation. The fragments serve to guide structure determination. Excessive energy and resultant fragmentation in EI often precludes molecular weight determination leaving structural ambiguity if the parent ion is lost from the spectrum. This limitation led to the development of the softer ionization technique CI. CI is an extension of EI wherein energetic electrons are initially directed toward ionizing a gaseous molecule such as methane. The gas-phase analyte is ionized by interaction with the gas (by proton transfer in the case of methane). CI generates a robust molecular ion signal but lacks the information that can be obtained following fragmentation. Modern MS approaches are tailored toward soft ionization to obtain a molecular ion followed by fragmentation step(s) for subsequent structural characterization.

Electrospray Ionization (ESI) Electrospray induces vaporization concurrent with soft ionization making it an extremely useful technique for analysis of biopolymers in solution, including HPLC eluates. Electrospray exploits a high electric field to aerosolize analyte-containing solutions creating a fine mist of charge-dense droplets. A bath gas at ambient pressure serves to vaporize solvent from droplet surfaces reducing their

size and increasing the surface charge density. Electrostatic repulsion ultimately disrupts the droplet surface leading to production of small charged droplets and eventual ejection of gas-phase analyte ions into a high vacuum region for mass analysis.

Matrix-Assisted Laser Desorption Ionization (MALDI) MALDI is a solid-state ionization method that, like ESI, combines ionization and vaporization into a single step thereby providing another convenient interface for biopolymer analysis. In MALDI the sample is dissolved in a matrix solution, spotted onto a stainless steel "target" and dried. The matrix molecules provide a UV-chromophore with an absorbance spectrum tuned to the laser-irradiation source. Laser ablation of the target spot under vacuum results in flash vaporization and ionization of the matrix and embedded sample molecules that can be subsequently directed into the mass analyzer region. In contrast with ESI, which may produce multiply charge ions, MALDI ions are typically singly-charged.

Mass Analyzers

In a mass spectrometer the ionization sector (e.g., ESI, MALDI) is coupled to a mass analyzer. The earliest mass analyzers used magnetic and/or electric sectors to separate ions by their mass-to-charge ratio (*m/z*); more recent instruments use a variety of new designs to accomplish the same task; these include the ion trap (IT), quadrupole mass filter, time-of-flight (TOF) tube, as well as hybrid instruments consisting of a combination of mass analyzers arranged in series for tandem or sequential mass spectrometry.

Complete Structure Elucidation by Mass Spectrometry

Oligosaccharide structure elucidation generally follows an approach consisting of determining the monosaccharide composition, defining monomer sequence and branch points, identifying inter-residue linkage positions, and specifying the anomeric configuration of glycosidic bonds.

Obtaining an MS Profile

After using a specific release, extraction, and cleanup procedure, an oligosaccharide sample is typically profiled by single-stage MS (MALDI, ESI, or HPLC-ESI) to profile the molecular weight(s) of constituent oligosaccharides. With molecular weight in hand, a general composition of monomers may be assigned to each oligosaccharide, i.e., hexose, deoxyhexose, N-acetyl hexosamine, but without indication of specific isomers. When combined with knowledge about the source material, release and purification method, and a composition analysis, a significant component of sequence information can be hypothesized based on the MS profile; however, it remains fraught with holes for potential incorrect assignments. Further characterization is mandatory to accurately assign sequence, branching, and linkage details.

Composition Analysis by GCMS

MALDI and ESI allow most oligosaccharides to be analyzed intact; however, GCMS-based composition analysis has remained a useful method for quantitative determination of monosaccharide composition, offering valuable complementary information. GCMS involves depolymerization into constituent monomers by hydrolysis or methanolysis, followed by volatility-enhancing derivatization. Both the GC retention time and the mass spectrum are used to identify and quantify the constituent monomers. A variety of derivatization or combined depolymerization/derivatization schemes, involving methylation, acetylation, and/or trimethylsilylation are used in composition analyses.

Linkage Analysis

Linkage analysis is used to determine inter residue linkage and branch points. This methodology is an extension of composition analysis wherein the oligosaccharide is permethylated prior to hydrolysis. Following hydrolysis the partially methylated monomers are reduced and acetylated, placing acetyl groups at all the positions opened by hydrolysis and reduction. The resulting alditol acetates have mixed methylation/acetylation substitution patterns depending upon their position in the original polymer, and reduction decreases anomeric heterogeneity in the gas chromatograms. The GC retention times and electron impact fragmentation patterns of partially methylated alditol acetates (PMAA) are used to indicate the type of linkages associated with specific monomers. Because the method involves depolymerization, however, the information that connects one monomer with another is lost making it challenging to use linkage analysis with mixtures.

Tandem Mass Spectrometry (MS/MS) and Sequential Mass Spectrometry (MS^N)

When collision-induced dissociation (CID) is performed on isolated parent ions the fragments produced provide an important strategy for understanding structure. Tandem mass spectrometry is commonly

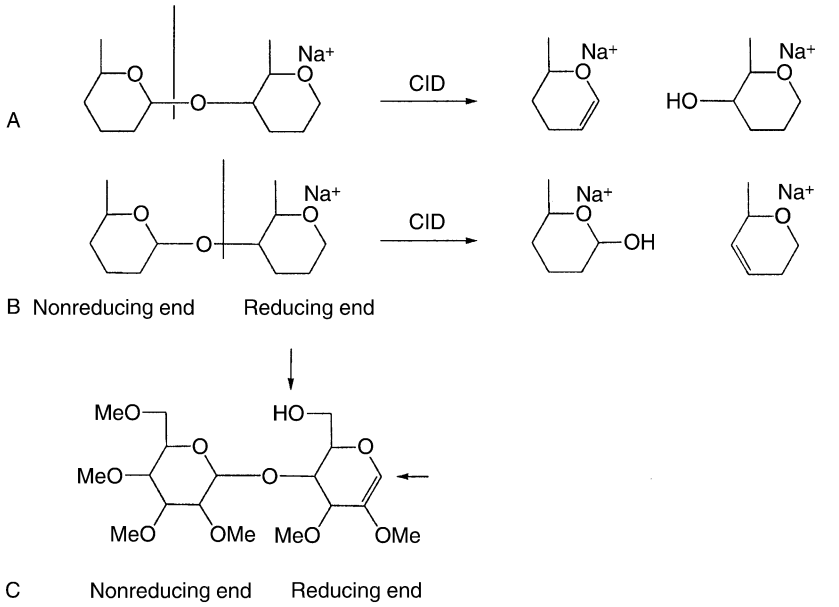

FIGURE 1 (A) and (B) Glycosidic bond cleavages for sodium adducted oligosaccharides. Sodiated fragments representing the reducing and nonreducing ends are observed for breaks on both sides of the glycosidic bond. (C) A branch point fragment; arrows identify the broken bonds.

used in this manner to sequence linear polymers. This straightforward approach has been applied with remarkable success to characterization of peptides but is limited when applied to oligosaccharides. Oligosaccharides are replete with isomeric possibilities that require further decomposition not available by tandem MS.

In order to fully characterize branching and obtain complete understanding of sequence and linkage, sequential steps of collision-induced dissociation must

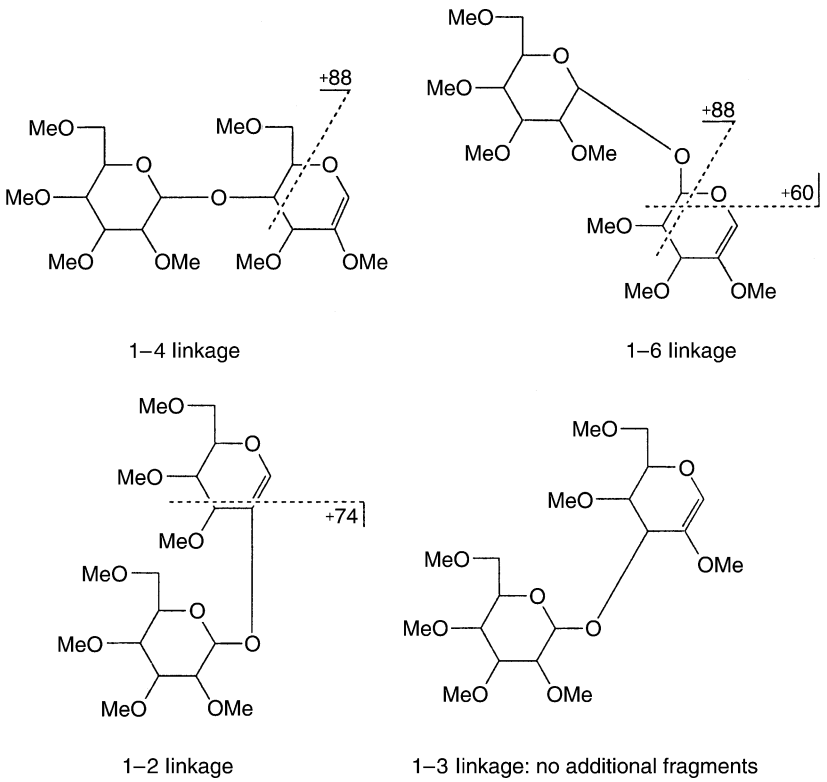

FIGURE 2 Use of cross-ring cleavages in MS^n to identify linkage position on hexoses in permethylated glycans.

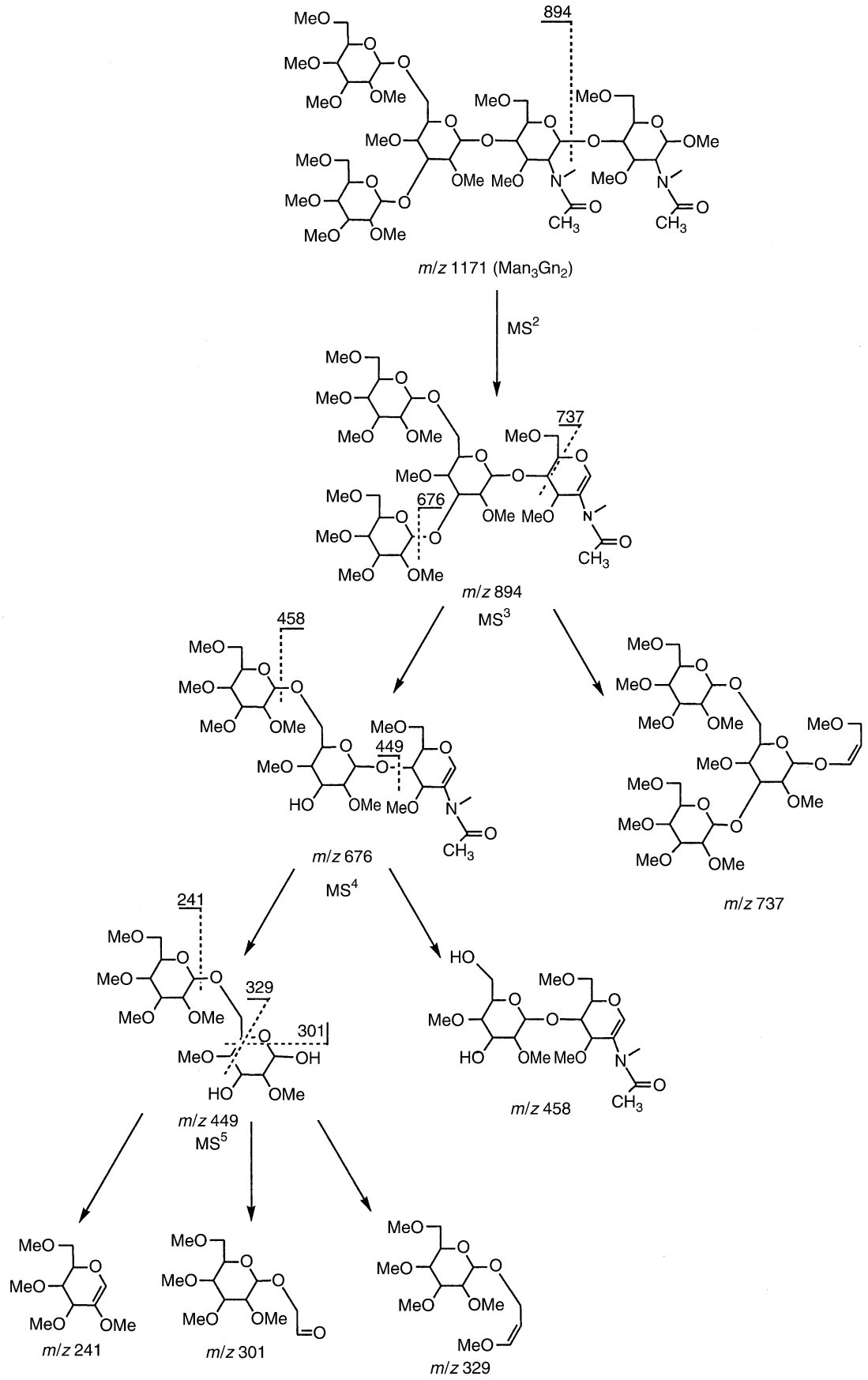

FIGURE 3 Use of MS^n to dissect a typical *N*-linked glycan. Selected CID pathways are shown through MS^5.

be performed using ion trap mass spectrometry (IT-MS). In ion trapping the molecular ion is maintained in a stable oscillatory trajectory within an ion trap via application of electrical fields. Ion trap instruments are programmed to perform sequential rounds of ion isolation sweeping the trap free of all other products. The generated fragments are released from the trap by resonance activation and mass measured, or single product ions may be re-isolated in the same manner and fragmented again. Fragmentation on any isolated ion is accomplished by low-energy collision-induced dissociation (CID) using a neutral gas.

Using MS^n to Identify Oligosaccharide Branching: Glycosidic Bond Rupture

Glycosidic bonds are easily ruptured by CID and fragments representing a single cleavage on either side of the glycosidic oxygen are observed with a mass difference of 18 Da (Figures 1 (A) and 1(B)). Methylation prior to MS analysis uniquely provides identity to reducing and nonreducing termini, as well as an indication of branching when MS peaks appearing at 14 Da lower intervals indicate hydroxyl group exposed during CID (Figure 1 (C)).

Using MS^n for Linkage Analysis: Cross-Ring Cleavages

Monomers within an oligosaccharide sequence are linked through C-1 of a nonreducing end monomer to any one of four hydroxyl groups (2, 3, 4, or 6) on the adjoining reducing end monomer. These subtleties in structure can be identified in an MS/MS spectrum through minor fragment ions in the mass spectrum appearing above the abundant ions indicating glycosidic ruptures. The increment is a consequence of cross-ring fragmentation around the linkage position (88 Da, 4-linkage; 74 Da, 2-linkage; 88 & 60 Da, 6-linkage), (Figure 2). Cross-ring cleavages are not typically observed for 1–3 glycosidic linkages. Diagnostic cleavages observed during MS^n for the *N*-linked glycan Man_3Gn_2 are shown in Figure 3.

Complementary Techniques

Mass spectrometry is typically used to define all oligosaccharide features except for the configuration of anomeric glycosidic bonds. When used in conjunction with MS, anomericity can be approached using enzymes with known activity for specific glycosidic bonds. The enzymes may be employed sequentially or in parallel array and MS and MS^n spectra from before and after treatment are compared to indicate which monomers were lost.

See Also the Following Articles

Glycoprotein-Mediated Cell Interactions, O-Linked • Glycoproteins, N-linked • HPLC Separation of Peptides • Oligosaccharide Chains: Free, *N*-Linked, *O*-Linked • Proteoglycans • Sphingolipid Biosynthesis • Sphingolipid Catabolism

Glossary

glycoside bond An acetal bond linking the monosaccharides in a polymeric carbohydrate chain; originates from carbon-1 of a nonreducing end sugar and may be linked to any of a number of hydroxylated positions on a reducing end sugar.

molecular ion The ion indicating the molecular weight of an intact molecule.

monosaccharide The poly-alcohol units comprising a carbohydrate polymer. In biopolymers monosaccharides are present in the ring-closed form.

oligosaccharide A carbohydrate polymer comprised of a relatively small number of monosaccharides.

reducing end The end of a glycan having a hemi-acetal linkage that can be reduced to an alcohol using a reducing agent. As such, the reducing end is capable of forming linkages to proteins, as in glycoproteins; or with lipids, as in glycolipids.

Further Reading

Cheng, H. S., and Her, G. R. (2002). Determination of linkages of linear and branched oligosaccharides using closed-ring chromophore labeling and negative ion trap mass spectrometry. *J. Am. Soc. Mass Spectrom* **13**, 1322–1330.

Harvey, D. J. (1999). Matrix-assisted laser desorption/ionization mass spectrometry of carbohydrates. *Mass Spec. Rev.* **18**, 349–451.

Reinhold, V. N., and Reinhold, B. B. (1999). Carbohydrate mass spectrometry, a characterization of sequence, linkage and branching using ES-MS and CID. In *Fundamentals and Applications of Gas Phase Ion Chemistry* (K. R. Jennings, ed.) pp. 181–200. Kluwer Academic Publishers, Netherlands.

Sheeley, D. M., and Reinhold, V. N. (1998). Structural characterization of carbohydrate sequence, linkage and branching in a quadrupole ion trap mass spectrometer: Neutral oligosaccharides and N-linked glycans. *Anal. Chem.* **70**(14), 3053–3059.

Varki, A., Cummings, R., Esko, J., Freeze, H., Hart, G., and Marth, J. (eds.) (1999). In *Essentials of Glycobiology.* Cold Springs Harbor Press, Cold Springs Harbor, NY.

Viseux, N., Hoffmann, E. de, and Domon, B. (1998). Structural assignment of permethylated oligosaccharide subunits using sequential tandem mass spectrometry. *Anal. Chem.* **70**, 4951–4959.

Weiskopf, A. S., Vouros, P., and Harvey, D. J. (1997). Characterization of oligosaccharide composition and structure by quadrupole ion trap mass spectrometry. *Rapid Comm. Mass Spectrometry* **11**, 1493–1504.

Biography

Reinhold is a Professor of Chemistry and Biochemistry at the University of New Hampshire in Durham New Hampshire, and Director of the University of New Hampshire Center for Structural Biology (UNH-CSB).

Hanneman is a Bioanalytical Chemist in the Reinhold laboratory.

Oligosaccharide Chains: Free, *N*-Linked, *O*-Linked

Tadashi Suzuki
Osaka University, Osaka, Japan

There is growing evidence that *N*-linked glycans play pivotal roles in protein folding and intra- and intercellular trafficking of *N*-glycosylated proteins. It has been known that during the *N*-glycosylation of proteins, significant amounts of free oligosaccharides (free OSs) are generated in the lumen of the endoplasmic reticulum (ER), possibly by the action of oligosaccharyltransferase. Free OSs are also formed in the cytosol by enzymatic deglycosylation of misfolded glycoproteins, which are destined to be destroyed by a cellular system called ER-associated degradation. Although the precise fate of intracellular free OSs remains obscure, recent biochemical studies have revealed that a novel cellular machinery enables them to be catabolized in a sophisticated manner that involves pumping free OSs from the ER to the cytosol where further processing occurs, followed by their entry into the lysosomes.

Free Oligosaccharides Formed in the Endoplasmic Reticulum

N-Glycosylation is one of the most common co- and posttranslational modifications of eukaryotic proteins occurring in the lumen of the endoplasmic reticulum (ER). During the translocation of proteins in the ER, an enzyme complex called oligosaccharyltransferase (OST) transfers an oligosaccharide (OS) moiety from the dolichol-linked donor substrate to asparagine residues located within the consensus sequence -Asn-Xaa-Ser/Thr- (where Xaa is any amino acid except Pro) to form *N*-linked glycans on the nascent polypeptide chains. Although the biosynthesis of lipid-linked OSs, as well as processing of *N*-linked glycan chains on glycoproteins, is understood in outline, certain aspects of phenomena occurring during *N*-glycosylation reaction remain largely unknown. For instance, biochemical studies have shown that a significant pool of free OSs does occur in the lumen of the ER. It has been proposed that, in the absence of sufficient acceptor sequences, the OST exhibits hydrolytic activity and transfers OSs ($Glc_3Man_9GlcNAc_2$ in most organisms) on dolichol to water, presumably to control the amount of donor substrates when fewer acceptor molecules are around. The OSs formed by OST bear di-*N*-acetylchitobiose (GlcNAcβ1-4GlcNAc) at their reducing termini. Whether there are any other enzyme activities responsible for the release of free oligosaccharides in the lumenal side of the ER is still controversial and has not been unequivocally demonstrated in any organism.

Free Oligosaccharide Transport System from the Endoplasmic Reticulum to the Cytosol

Although it is not known whether free OSs have a physiological role in the ER, one could easily envisage that the accumulation of vast amount of free OSs in the ER could interfere with the quality-control system involving the recognition of the folding state of proteins, export of misfolded lumenal and transmembrane proteins into the cytosol, and degradation of them by the 26S proteasome (see later discussion). Therefore, it is not surprising that cells have machinery to eliminate free glycans from the ER lumen. Using permeabilized mammalian cells, it has been demonstrated that free OSs formed in the ER are, after rapid deglucosylation, exported from the ER into the cytosol. A transporter responsible for the export of free OSs from the ER membrane has not been identified, although biochemical studies show that the export is an ATP- and Ca^{2+}-dependent process. The OS export is also effectively blocked by the addition of low concentrations of mannose and its derivatives, but not by other sugars, suggesting that the transport machinery for free OSs recognizes the mannosyl residues at the nonreducing end, but not the GlcNAc residues at their reducing termini. The main structure of free OSs released from the ER to the cytosol has been shown to be $Man_{8\sim9}GlcNAc_2$ (Figure 1).

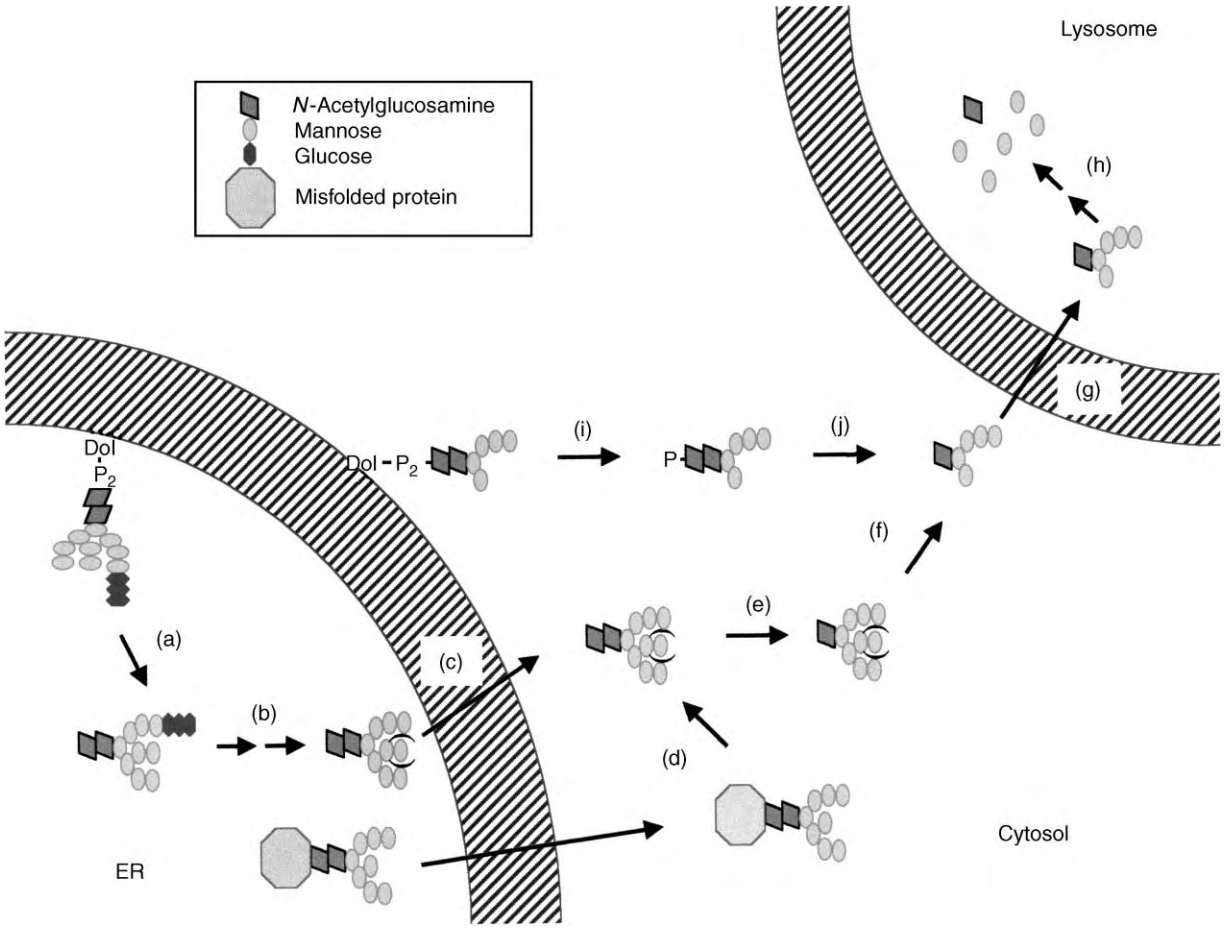

FIGURE 1 Model for the fate of free oligosaccharides generated in and outside of the ER in mammalian cells. Step (a), Free OSs generated in the lumen of the ER by the hydrolytic activity of OST bear di-*N*-acetylchitobiose (two GlcNAc residues) at their reducing termini. Step (b), After quick deglucosylation by α-glucosidase I and II (and sometimes ER α-mannosidase I), (c) $Man_{8\sim9}GlcNAc_2$ is transported into the cytosol by a putative transporter. Step (d), In the cytosol, PNGase removes *N*-linked glycan (most likely a $Man_8GlcNAc_2$ structure because action of an ER α-mannosidase I is prerequisite for the efficient export of misfolded glycoproteins from the ER to the cytosol) from misfolded glycoproteins and thereby releases free OSs bearing di-*N*-acetylchitobiose. Step (e), Once in the cytosol, ENGase (or, in some cases, a chitobiase) forms a free OS with a single GlcNAc at the reducing termini ($Man_{8\sim9}GlcNAc$). Step (f), The free OS with a single GlcNAc is now susceptible to the action of a cytosolic α-mannosidase, giving rise to a $Man_5GlcNAc$ structure. This structure is identical to the last dolichol intermediate present in the cytosolic face. Step (g), The $Man_5GlcNAc$ is transported into the lysosomes by a specific transporter. Step (h), In lysosome, the $Man_5GlcNAc$ is hydrolyzed into monomers (Man and GlcNAc) by lysosomal α- and β-mannosidases. Step (i), Putative pyrophosphatase, whose activity is reported in the cytosolic face of the ER membrane, can also release free OSs from the dolichol-linked OSs (presumably with the structure of $Man_5GlcNAc_2$) in the cytosol. Step (j), probably, this OS-phosphate will be processed by ENGase to give rise to $Man_5GlcNAc$, which is readily transported into lysosome. Note that this scheme cannot be applied to other organisms; for example, *Saccharomyces cerevisiae* does not possess ENGase, so there must be a distinct path.

Free Oligosaccharides Formed in the Cytosol: Its Connection with Endoplasmic-Reticulum-Associated Degradation

Recent evidence clearly shows that the ER has quality-control machinery that differentiates between misfolded (glyco)proteins and correctly folded ones, so that only the latter move from the ER to the Golgi. In this system, proteins that fail to fold or form subunit structures are retained in the ER and interact with various lumenal chaperones that allow them to mature into their native structure before they exit the ER. When proteins consistently fail to acquire the correct state, they eventually are degraded by the mechanism called ER-associated degradation(ERAD). It is now clear that this degradation process involves the retro-translocation of the defective (glyco)proteins from the ER to the cytosol, followed by their degradation in the cytosol by the action of proteasome. Recent growing

evidence shows that glycan chains on glycoproteins play critical roles in monitoring the folding state of glycoproteins in the ER that involves various intracellular lectins.

When the misfolded glycoproteins are retrotranslocated to the cytosol for degradation, protein is ultimately degraded by the action of the 26S proteasome. However, it is reasonable to assume that for glycoproteins to be degraded efficiently by the proteasome, bulky modifications of polypeptide side chains such as *N*-glycan chain may be removed prior to precessive proteolysis by the proteasome. The removal of glycan is achieved by the action of peptide:*N*-glycanase (PNGase), releasing free OSs in the cytosol (Figure 1). PNGase cleaves the amide bond between glycosylated asparagine residues and the proximal GlcNAc residues (Figure 2), and under physiological pH ammonia is released, generating free OSs bearing a di-*N*-acetylchitobiose unit at the reducing termini. The cytosolic PNGase occurs widely from yeast to mammalian cells, and the gene encoding this enzyme has been identified.

Another enzyme that can generate free OSs in the cytosol is a pyrophosphatase that releases OS-phosphate moieties from dolichol-linked OSs (Figure 1). Such cytosol-oriented enzyme activity has been detected in mammalian cells. Another possibility is the action of endo-β-*N*-acetylglucosaminidase (ENGase), which cleaves the glycoside bond in the di-*N*-acetylchitobiose structure, giving rise to free OSs with a single GlcNAc remaining at the reducing termini (Figure 2). This cytoplasmic enzyme is also known to occur widely, but not in yeasts such as *Saccharomyces cerevisiae* or *Schizosaccharomyces pombe*. It is not known whether the cytoplasmic ENGase can directly generate free OSs either from dolichol-linked OS or from glycoproteins *in vivo*.

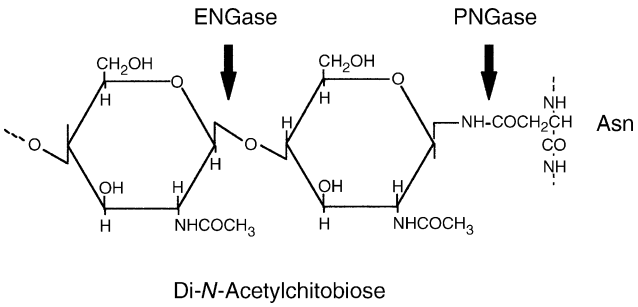

FIGURE 2 Reaction sites for two deglycosylating enzymes acting on *N*-glycosylated peptide. PNGase hydrolyzes the asparaginyl amide bond to give an aspartic acid-containing polypeptide chain and 1-amino-*N*-acetylglucosaminyl oligosaccharide; the latter is subsequently hydrolyzed under neutral pH to *N*-acetylglucosaminyl oligosaccharides and ammonia. On the other hand, ENGase hydrolyzes the glycoside bond in the di-*N*-acetylchitobiose moiety of the core region of *N*-linked glycan, leaving a single *N*-acetylglucosamine on the core peptide.

Cytosolic Processing of Free Oligosaccharides

Irrespective of their source, cytosolic OSs must be further catabolized, possibly to maximize the reuse of the component sugars. In the cytosol, two enzymes mainly contribute to the catabolism of free OSs: β-*N*-acetylglucosaminidase and α-mannosidase. For β-*N*-acetylglucosaminidase, so far two distinct enzyme activities have been reported; one is ENGase and the other is a cytosolic, neutral chitobiase. Although a chitobiase catalyses the same reaction with ENGase, it acts only if the reducing termini of the free OSs are di-*N*-acetylchitobiose, releasing a single GlcNAc from their reducing termini. Therefore, the chitobiase can be called a reducing-end exoglycosidase. Although the gene encoding cytoplasmic ENGase has been identified quite recently, the molecular nature of the cytosolic chitobiase is not known.

It has been shown that the action by a cytosolic α-mannosidase requires that free OSs bear only a single GlcNAc at the reducing ends. The trimming of free OSs by the cytosolic α-mannosidase (α1-2,3,6 mannosidase) results in a different Man_5 structure, yielded by the action of Golgi α-mannosidase I (α1-2 mannosidase), but in the same isomeric conformation with that is present in the dolichol-OS intermediate (Figure 1). The end product of ENGase (or chitobiase) and α-mannosidase in the cytosol, $Man_5GlcNAc$, is then transported into the lysosomes, where further degradation by α- and β-mannosidase can occur (Figure 1). The transporter on the lysosomal membrane seems to be specific to $Man_5GlcNAc$ structure, is ATP-driven, and is inhibited by *N*-acetylglucosamine but not by mannose. The last observation suggests that the reducing terminal structure of free OSs, in sharp contrast to the ER transporter, is crucial for recognition of free OSs by the lysosomal transporter. The molecular nature of the transporter remains to be identified.

Concluding Remarks

Cells possess a variety of enzymes and transporters to handle free OSs generated by several distinct mechanisms. Free OSs collected in the cytosol are processed by ENGase (or a chitobiase) and α-mannosidase before being incorporated into the lysosomes for degradation into monomeric sugars. Why this rather complicated pathway (ER to cytosol to lysosome) is

used for free OS catabolism is a mystery. One notion is that this trafficking route enables them to be removed quickly from the ER, thereby preventing them from interfering with the efficient glycan-dependent quality-control machinery for newly synthesized glycoproteins in the ER. However, it is still possible that a particular free OS itself may play a role in certain cellular processes. Indeed, intracellular free OS derivatives of *N*-glycan chains are known to play a role in the growth, senescence, and ripening of fruits in plants. Although similar bioactivity in other organisms still remains to be detected, the identification of molecules involving the formation, modification, and transport of free OS should provide us with more insight into the mechanism and function of this novel pathway.

See Also the Following Articles

Chaperones, Molecular • Endoplasmic Reticulum-Associated Protein Degradation • Proteasomes, Overview

Glossary

chaperones Molecules that, by associating with substrates, prevent them from aggregation and facilitate their acquiring the correct folding state.

di-*N*-acetylchitobiose A dimer of *N*-acetylglucosamine with β1-4 linkage.

***N*-linked glycan** An oligosaccharide linked by asparagines in the protein/peptide, a common modification in all eukaryotic proteins that go through the secretory pathway.

proteasome A cytoplasmic gigantic protease complex involved in various cellular processes, including the degradation of misfolded proteins and antigen processing.

quality-control machinery A system that maintains the quality of product (i.e., newly synthesized proteins in the endoplasmic reticulum).

Further Reading

Cacan, R., and Verbert, A. (1999). Transport of free and N-linked oligomannoside species across the rough endoplasmic reticulum membranes. *Glycobiology* **10**, 645–648.

Helenius, A. (2001). Quality control in the secretory assembly line. *Philos. Trans. Royal Soc. London B Biol. Sci.* **356**, 146–150.

Moore, S. E. H. (1999). Oligosaccharide transport: Pumping waste from the ER into lysosomes. *Trends Cell Biol.* **9**, 441–446.

Moore, S. E. H., Bauvy, C., and Codogno, P. (1995). Endoplasmic reticulum-to-cytosol transport of free polymannose oligosaccharides in permeabilized HepG2 cells. *EMBO J.* **14**, 6034–6042.

Saint-Pol, A., Bauvy, C., Codogno, P., and Moore, S. E. H. (1997). Transfer to free polymannose-type oligosaccharides from the cytosol to lysosomes in cultured human hepatocellular carcinoma hepG2 cells. *J. Cell Biol.* **136**, 45–59.

Spiro, R. G. (2000). Glucose residues as key determinants in the biosynthesis and quality control of glycoproteins with N-linked oligosaccharides. *J. Biol. Chem.* **275**, 35657–35660.

Suzuki, T., Yan, Q., and Lennarz, W. J. (1998). Complex, two-way traffic of molecules across the membrane of the endoplasmic reticulum. *J. Biol. Chem.* **273**, 10083–10086.

Suzuki, T., Park, H., Hollingsworth, N., Sternglanz, R., and Lennarz, W. J. (2000). *PNG1*, a yeast gene encoding a highly conserved peptide:*N*-glycanse. *J. Cell Biol.* **149**, 1039–1052.

Suzuki, T., Park, H., and Lennarz, W. J. (2002). Cytoplasmic peptide: *N*-glycanase (PNGase) in eukaryotic cells: Occurrence, primary structure, and potential functions. *FASEB J.* **16**, 635–641.

Suzuki, T., Yano, K., Sugimoto, S., Kitajima, K., Lennarz, W. J., Inoue, S., Inoue, Y., and Emori, Y. (2002). Endo-β-*N*-acetylglucosaminidase, an enzyme involved in processing of free oligosaccharides in the cytosol. *Proc. Natl. Acad. Sci. U.S.A.* **99**, 9691–9696.

Biography

Tadashi Suzuki is Visiting Assistant Professor in the Department of Biochemistry, Graduate School of Medicine, Osaka University. His principal research interest is the biological functions of deglycosylating enzymes, including cytoplasmic peptide:*N*-glycanase (PNGase) and endo-β-*N*-acetylglucosaminidase (ENGase) in eukaryotes. He received a D.Sc. degree from the University of Tokyo and served as a Postdoctoral Fellow and Research Assistant Professor at the Department of Biochemistry and Cell Biology, State University of New York at Stony Brook.

Oncocytes

Bernard Tandler and Charles L. Hoppel
Louis Stokes VA Medical Center, Cleveland, Ohio, USA

Oncocytes, first described by H. Hamperl, are large cells possessing a granular, eosinophilic cytoplasm that are present in many glands and various epithelial linings, particularly in humans; they rarely are found in other mammalian species. In humans, they increase in number with age and may come to constitute a sizeable portion of particular organs; e.g., the oxyphil cells of the parathyroid gland are oncocytes. Oncocytes can occur in neoplastic tissues as well as in normal tissues. Oncocytes in normal tissues can themselves undergo neoplastic transformation and, because they are capable of division, result in a tumor composed wholly or partially of oncocytes, e.g., oncocytoma and Warthin's tumor. These generally are benign, but occasionally various oncocytic neoplasms can be malignant, e.g., Hürthle cell carcinoma and malignant oncocytoma. It is clear that oncocyte formation and neoplasia are independent processes that can occur in either sequence.

Structure of Oncocyte Mitochondria

The fundamental morphological nature of oncocytes was firmly established from the earliest examination of these cells by electron microscopy. They are filled with an abundance of mitochondria, which are responsible for the eosinophilic granularity of the cytoplasm as seen by optical microscopy. Other cytoplasmic organelles are inconspicuous, but sparse lysosomes can be revealed by cytochemistry. Special features normally found in specific precursor cell types, such as folded plasma membranes, microvilli, or secretory granules, are reduced or entirely absent. The mitochondria can be regular in form and are usually ovate, but occasionally are discoidal, rod-shaped, or pleomorphic. In some oncocytic cells, various mitochondrial forms co-exist side by side.

The ovate mitochondria frequently contain an unusual number of cristae, which often are arranged in a central stack where they are closely applied to one another (Figures 1 and 2). With transmission electron microscopy (TEM), the cristae appear to be merely simple infoldings of the boundary membrane, but scanning electron microscopy (SEM) reveals that at least some lamelliform cristae are connected to the boundary membrane by several short tubules, the so-called crista junctions. In certain oncocyte mitochondria in Hürthle cell carcinomas, individual cristae may have a lattice-like form. Despite their altered morphology, oncocyte mitochondria are capable of division by medial partition formation.

Those oncocyte mitochondria that are flattened disks often are aggregated like a stack of pancakes. In such organelles, the cristae occasionally are oriented in a longitudinal pile or may appear to be vesicular. Although conventional matrix granules have not been detected in oncocyte mitochondria, these organelles sometimes include in their inner compartment amorphous densities ranging from small to large. Certain mitochondria contain inclusions filled with either α- or β-glycogen; such inclusions are delimited by a single membrane, showing that they truly are intramitochondrial, rather than being cytosolic glycogen aggregates that merely have been engulfed by intact mitochondria. In oncocytes of the parotid gland in the vampire bat, adjacent mitochondria are linked by periodic cross-bridges measuring 10 nm, separated by a 12.5 nm interval. Such linked organelles have not been observed in human oncocytes.

Mitochondrial Biochemistry

The physiological capacity of oncocyte mitochondria is not well established. Histochemical studies of oncocytes and oncocytomas, irrespective of their site of occurrence, invariably show an increase in mitochondrial oxidative enzymatic activity. At the same time, biochemical studies show an increase in the amount of mitochondrial DNA per cell. Both of these phenomena can be accounted for by the increased number of mitochondria (up to 10-fold) in oncocytes. There are no gross alterations in the mitochondrial DNA. A biochemical study of mitochondria isolated from Warthin's tumor of the parotid gland found them to be partially uncoupled. Analysis of mitochondria from thyroid oncocytic tumors showed significant decrease in ATP synthesis, whereas in renal oncocytomas the

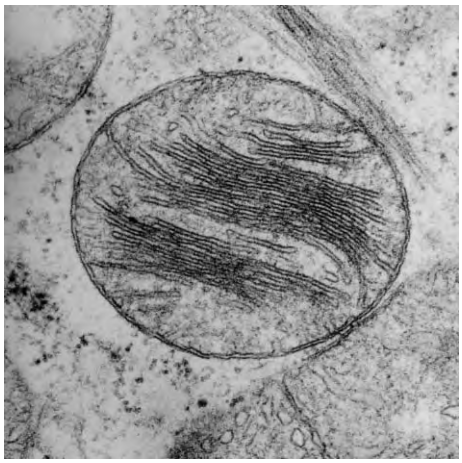

FIGURE 1 Transmission electron microscopy of a typical mitochondrion in an oncocytoma of human parotid gland origin. The abundant cristae are closely packed in a sheaf. Original magnification, ×34,000.

mitochondrial ATPase activity is normal. These data suggest site-specific differences in oncocytic metabolism. The nuclear factor responsible for the increase in mitochondrial number in oncocytes has not been identified. However, this factor does not change in response to decreased respiratory chain activity, decreased ATPase activity, or mitochondrial DNA abnormalities. Study of the biochemistry and genetics of oncocytes is hampered by the comparative rarity of metaplastic or neoplastic aggregates of such cells and by the fact that they occur mostly in humans.

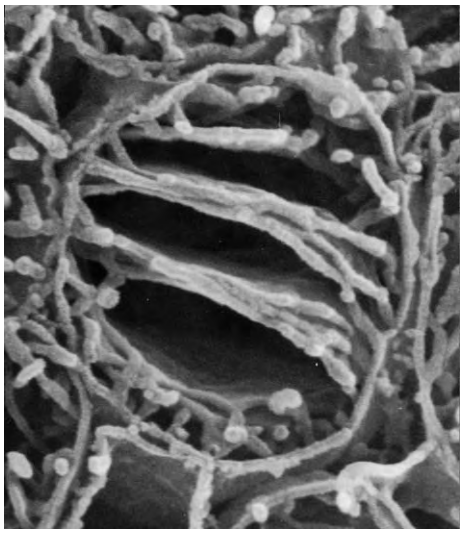

FIGURE 2 A scanning electron microscope micrograph of a mitochondrion from a human oncocyte of submandibular gland origin. All soluble material has been extracted from this specimen, leaving only membranes. A portion of the outer and boundary membranes has been removed from this organelle, allowing the internal sheaf of cristae to become apparent. Original magnification, ×25,000. Micrograph courtesy of Alessandro Riva.

See Also the Following Articles

Imaging Methods • Mitochondrial DNA • Mitochondrial Membranes, Structural Organization • Parathyroid Hormone/Parathyroid Hormone-Related Protein Receptor

Glossary

eosinophilic Stainable by eosin (tetrabromofluorescein), a red dye used to study cell structures.

lysosome A cytoplasmic structure in eukaryotic cells that contains various hydrolytic enzymes and is involved in intracellular digestion.

metaplastic Of or characterized by metaplasia, the transformation of cells from a normal to an abnormal form.

neoplastic Of or characterized by neoplasia, a new and abnormal growth or proliferation of cells.

Further Reading

Ambu, R., Riva, A., Lai, M. L., Loffredo, F., Testa Riva, F., and Tandler, B. (2000). Scanning electron microscopy of the interior of cells in Hürthle cell tumors. *Ultrastruct. Pathol.* **24**, 211–218.

Ebner, D., Rödel, G., Pavenstaedt, I., and Haferkamp, O. (1991). Functional and molecular analysis of mitochondria in thyroid carcinoma. *Virchows Arch. B Cell Pathol.* **60**, 139–144.

Hamperl, H. (1931). Onkocyten un Geschwulste der Speicheldrüsen. *Virchows Arch. Pathol. Anat.* **282**, 724–736.

Heddi, A., Faure-Vigny, H., Wallace, D. C., and Stepien, G. (1996). Coordinate expression of nuclear and mitochondrial genes involved in energy production in carcinoma and oncocytoma. *Biochim. Biophys. Acta* **1316**, 203–209.

Müller-Höcker, J. (1998). Defects of the respiratory chain in hepatic oncocytes. *Virchows Arch.* **432**, 349–356.

Riva, A., and Tandler, B. (2000). Three-dimensional structure of oncocyte mitochondria in human salivary glands. *Ultrastruct. Pathol.* **24**, 145–150.

Tandler, B., and Shipkey, F. H. (1964). Ultrastructure of Warthin's tumor. I. Mitochondria. *J. Ultrastruct. Res.* **11**, 292–305.

Tandler, B., Hutter, R. V. P., and Erlandson, R. A. (1970). Ultrastructure of oncocytoma of the parotid gland. *Lab. Invest.* **23**, 567–580.

Biography

Bernard Tandler was a long-time Professor of Oral Biology and of Anatomy at the Case Western Reserve University Schools of Dentistry and Medicine, where he currently is a Visiting Professor of Oral Diagnosis, as well as a Consultant at the VA Medical Center in Cleveland. He also served as Visiting Professor of Anatomy at Kyushu Dental College and of Biological Sciences at Texas Tech University. His major research interests concern the biogenesis, structure, and physiology of giant mitochondria, as well as the structure, function, and evolution of mammalian salivary glands and of secretory cells in general.

Charles L. Hoppel graduated from Gonzaga University and St. Louis University School of Medicine. He is Professor of Pharmacology, Medicine and Oncology at Case Western Reserve University, Co-Director of the Center for Inherited Disorders of Energy Metabolism at CWRU, and Associate Director, Research in the Geriatric Research, Education, and Clinical Center at the Louis Stokes VA Medical Center, Cleveland. His research interests are in mitochondrial structure and function, mitochondrial fatty acid oxidation, and regulation of carnitine palmitoyltransferase-I.

Opioid Receptors

P.Y. Law and Horace H. Loh
University of Minnesota, Minneapolis, Minnesota, USA

Opioid receptors are transmembrane proteins located at the synaptic membranes that serve as targets of an efficacious pain relief drug: morphine. The identification of these binding sites at neural membrane for plant alkaloids has led to the discovery of the first class of endogenous drug molecules, i.e., the enkephalins and endorphins. These opioid receptors belong to the superfamily of G protein-coupled receptor, and upon activation, the activities of multiple cellular effectors are modulated, leading to inactivation of the ascending and activation of the descending pain pathways. Eventually, pain perception is altered. Unfortunately, with the "good" therapeutic actions of morphine, there are also "bad" side effects of the drug, e.g., tolerance and addiction. Thus, the molecular mechanism in the cellular regulation of these opioid receptors, and the designs of specific agonists for these opioid receptors to be ideal analgesic agents are of great interest in pain medicine development.

Historical Perspectives

For centuries, extracts from the opium poppy, *Papaver somniferum*, have been prescribed for pain relief, to control cough, and to treat diarrhea. However, in addition to its medicinal uses, due to its psychological effects, man has abused opium since the time of the ancient Greeks. The isolation of the principal alkaloid by the German pharmacist, Friedrich W. Serturner in 1805, which he named morphine after the Greek god of dreams, Morpheus, has enabled pharmacologists to determine the relationships between structures and their analgesic activities. From the relatively low concentration of morphine needed to relieve pain in 70% of the patients (10 mg/70 kg body-weight), to the stereoselective requirement for analgesic action of the drug, it is apparent that morphine acts by high-affinity binding to proteins, or specific receptor, located in the central nervous system (CNS). The presence of specific morphine receptor was not demonstrated until 1973, when three research groups: Lars Terenius, Soloman Snyder, and Eric Simon, following the guideline established by Avram Goldstein, independently reported the presence of high affinity and stereoselective binding sites at the synaptic membrane preparations of rodent brain. The affinities of various opiate analgesics for these binding sites and the location of these sites correlated well respectively with the *in vivo* potencies and sites of action of the drug. Thus, the era of the opiate receptor is launched. Immediately, it is apparent that these mammalian CNS binding sites could not be evolved for plant alkaloids. This dichotomy was resolved by the isolation of the endogenous opioid peptide, enkephalin, by John Hughes and Han Kosterlitz in 1975 followed later by the identification of the proenkephalin A gene. The subsequent identification of two other gene products, β-endorphin deriving from the pro-opiomelanocortin gene, and dynorphin deriving from the *prodynorphin*or *proenkephalin B* gene suggests that the *in vivo* actions of morphine and its congeners must be a reflection of these endogenous opioid peptides actions. The presence of multiple endogenous opioid peptides genes also suggests the probable existence of multiple opioid receptors.

Discovery of Multiple Opioid Receptors

In 1976, Bill Martin and his colleagues hypothesized the presence of multiple opioid receptors. Concluding from the physiological responses such as blood pressure and respiration, Martin and co-workers coined the multiple opioid receptors terminology based on the prototypic ligands within each group, with morphine being the mu (μ) agonist, ketocyclazocine being the kappa (κ) agonist, and SKF10 047 being the sigma (σ) agonist. The existence of multiple opioid receptors was further demonstrated by measuring the amount of an opiate antagonist to reverse the agonist effect in two *in vitro* bioassay systems, the guinea pig (GP) ileum and the mouse vas deferens. These bioassays were responsible for the identification of the fourth type of opioid receptor, the delta (δ) with enkaplin being the prototypic agonist. Additional studies such as the cross-tolerance measurements also supported the existence of multiple opioid receptors. In the cross-tolerance studies, animals or the *in vitro* GP ileum were treated with an opioid

receptor-selective agonist. Chronic exposure to the agonist resulted in a loss in response, or tolerance development. However, activities of agonists that are selective for other opioid receptors remained unaltered, or no cross-tolerance was developed. These *in vivo* and *in vitro* experiments support the original hypothesis of multiple opioid receptors.

The implication of the existence of multiple opioid receptors by the animals' studies and bioassays was supported initially by the direct receptor-binding experiments reported by Law and Loh, K.J. Chang, Hans Kosterlitz, and their colleagues. The development of receptor-selective antagonists, such as naltrindole (δ) and nor-binaltorphimine (κ), and the development of ligands that would alkylate receptor selectively, such as β-funaltrexamine (μ), have enabled investigators to characterize the properties of these multiple opioid receptors biochemically further by generating membrane preparations that contain single-receptor type. Only after the molecular cloning of the δ-opioid receptor, concurrently by the groups of Chris Evans and Brigitte Kieffer in 1992, followed by the cloning of μ- and κ-opioid receptors in 1993 by others, is the hypothesis of multiple opioid receptors firmly established. These multiple opioid receptors are products of three separate receptor genes and with high amino acid sequence homology (>60%). Although subtypes of these opioid receptors have been postulated, various gene products that exhibit the reported ligand selectivity of the various opioid receptor subtypes have not been identified. Also, from additional pharmacological and the molecular cloning studies, the sigma (σ) receptor does not belong to the opioid receptor family. Hence, the μ-, κ-, and δ-opioid receptors are the sites that endogenous opioid peptides and exogenous opiate alkaloids exert their actions.

Distribution and Pharmacology of Multiple Opioid Receptors

Prior to the cloning of the opioid receptors, the distribution of the receptors within various brain regions or tissues, was determined with autoradiographic studies using radioactive ligands selective for a specific receptor. These autoradiographic results were later substantiated and extended with the *in situ* hybridization studies using the cloned receptor mRNA and with the histochemical or immunofluorescence studies using the receptor-specific antibodies. In general, these data indicate that the location of the multiple opioid receptors coincides with the pharmacological actions of the drugs. These opioid receptors are mainly localized in the limbic system that are involved in the control of emotion and reward behaviors, the ascending and descending pain pathways that include the different laminae layers of cortex, thalamus, periaqueductal gray, midbrain median raphae and the dorsal horn of the spinal cord, and specific brain regions that are known to control locomotion, emesis, cough, and temperature.

The distributions of the μ- and δ-opioid receptor are very similar but distinct. Although these receptors do not co-localize in the pre- or post-synaptic membrane of the same neuron, they are observed to be located in the same components of the limbic systems such as the nucleus accumbens and the amygdala. Their locations at the cortex, the 4th ventricle and at the substantia gelatinosa of the spinal cord are the reasons why both μ- and δ-opioid receptor selective drugs have strong spinal and supraspinal analgesic effects. Similarities in the distribution of these two opioid receptors suggest the μ- and δ-opioid receptors have similar pharmacological profile (Table I). There are reports using δ-opioid receptor selective antagonist or using mice that the δ-opioid receptor has been genetically deleted that implicate the role of δ-opioid receptor in modulating both the acute and chronic effects of the μ-opioid receptor selective agonist.

On the other hand, distribution of the κ-opioid receptor in the central nervous system is distinct from that of μ- and δ-opioid receptors. The most striking difference is the uniform pre-synaptic location of the κ-opioid receptor in the caudate putamen area. Such location could be the explanation for the observed κ-opioid agonist induced decrease in locomotion and the decrease of dopamine release in this brain area. The inhibition of dopamine release is the basis for the dysphoric effects of the κ-opioid agonists. The brainstem and spinal cord distribution of the κ-opioid receptor resemble that of μ-opioid receptor. Hence, κ-opioid agonists could produce spinal analgesia (Table I).

The multiple opioid receptors are not confined to the central nervous system. The presence of the receptors in the gastrointestinal tract accounts for the constipative

TABLE I

Pharmacological Effects Associated with the Multiple Opioid Receptor

	μ	δ	κ
Analgesia	Supraspinal Spinal	Supraspinal Spinal	 Spinal
Pupil constriction	++	++	–
Respiratory depression	+++	++	+
Diuresis	Antidiuresis	–	++
GI	Constipate	Constipate	–
Smooth muscle	Spasm	Spasm	–
Behavior/effect	Euphoria Sedation ++		Dysphoria Sedation +
Physical dependent	++	++	+

effect of μ- and δ-opioid agonists. The presence of the κ-opioid receptor in the cardiac myocytes could be the reason for the bradycardia effect observed with the κ-opioid agonists, though the bradycardia effect of the opioid agonists is mainly associated with the agonist actions at the brainstem medulla. Opioid receptors have been reported also to be present in the immune cells. The true identities of these receptors are yet to be identified, whether they are the μ-, δ-, or κ-opioid receptor types or the "non-classical" opioid receptors. Nevertheless, the pronounced effects that morphine has in the immune responses of animals, and the fact that intravenous drug users are one of the high risk groups for HIV have led to many studies, and the effects of various opioid agonists and antagonists on the functions of immune cells cannot be ignored.

Opioid Ligands Selectivity for the Multiple Opioid Receptors

With the cloning of the opioid receptors and the subsequent generation of mice in which the transcription of selective opioid receptor gene could be disrupted, it is possible now to delineate the opioid receptor types that various opioid ligands could activate. By expressing the three cloned receptors individually into cells that do not express opioid receptor endogenously, it is possible to generate models that could determine the affinities of the opioid ligands to a specific receptor type accurately. Likewise, by genetically eliminating the *in vivo* expression of an individual opioid receptor type, the loss or gain in functions of a specific opioid agonist can be evaluated *in vivo*. These data in combination with the receptor-selective antagonists studies have determined the selectivity of various opioid ligands and their functions, as summarized in Table II.

It is apparent that morphine and its congeners are agonists in the μ-opioid receptor. Although in the *in vitro* cell line models that express the δ-opioid receptor morphine has partial agonist activities, morphine does not exhibit measurable analgesic activities in mice that do not express the μ-opioid receptor. Since these animals have intact δ- and κ-opioid receptor systems, it is unequivocal that morphine pharmacological effects are mediated via the activation of μ-opioid receptor.

Other opiate alkaloids have been shown to exhibit nonselectivity toward these three opioid receptors. The oripavine derivatives (etorphine and diprenorphine) and the benzomorphans (ketocyclazocine and bremazocine) have been shown by many to have similar affinities for all three opioid receptors. This is surprising since ketocyclazocine was used by Bill Martin to define one of the multiple opioid receptors, the κ-opioid receptor. Such dichotomy may be resolved by the fact that some opiate alkaloids have different activities in different opioid receptor types. For example, nalorphine exhibits antagonistic properties in the μ-and δ-opioid receptors but possesses agonistic activities in the κ-opioid receptor. Another example is pentazocine that possesses both κ-agonistic and μ-antagonistic properties. The mixed agonist-antagonist properties of various alkaloids are being exploited in the clinic so as to minimize the side effects of the drug, most noticeably, the addictive liability of the opiate analgesics.

The endogenous ligands, noticeably the products of the three peptides genes – enkephalin, β-endorphin, and dynorphin do not appear to have specificity toward these multiple opioid receptors. Initially, enkephalin and β-endorphin have been considered to be the prototypic ligands for the δ- and μ-opioid receptors respectively. Dynorphin, with the positively charged amino acids arginine and lysine, has been shown to preferentially interact with the κ-opioid receptor. Since then, it has been shown that Met^5-enkephalin has equal affinity for the μ- and δ-opioid receptor, and that dynorphin has high affinity for the δ-opioid receptor. Only when the peptides are restricted in their rotation is receptor selectivity observed, e.g. the D-penicillamine derivatives of enkephalin, DPDPE. This peptide has been shown

TABLE II

Relative Receptor Selectivity of Various Opioid Ligands and their Functions in Respective Receptors

Opioid ligands	μ	δ	κ
Bemazocine	AG	AG	AG
Buprenorphine	PA		AN
Butrophanol	PA		AG
Diprenorphine	AN	PA	AN
Ethylketocyclazocine		AG	AG
Etorphine	AG	AG	AG
Fentenyl	AG		
β-Funaltrexamine	AN		AG
Levorphanol	AG	PA	
Methadone	AG		
Morphine	AG	PA	
Nalorphine	AN	AN	AG
Naloxone	AN	AN	AN
Naltrexone	AN	AN	AN
Naltrindole		AN	
Nor-Binaltorphimine			AN
NTB		AN	
Pentazocine	PA		AG
Spiradoline			AG
Sufentanyl	AG		
U50,488			AG
U69,593			AG

AG = agonist; PA = partial agonist; AN = antagonist.

in vitro to be selective for the δ-opioid receptor and with minimal activity in the μ-opioid receptor. Hence, the *in vivo* effect of DPDPE has been the hallmark for the δ-opioid receptor activation. However, recent *in vivo* studies using mice lacking the μ- or the δ-opioid receptor, clearly suggest that the DPDPE analgesic effect is mediated by activation of μ-opioid receptor. This conflicting *in vitro* and *in vivo* receptor selectivity of the endogenous peptides and their derivatives requires further detailed investigation.

Molecular Mechanism of Multiple Opioid Receptor Function

A general feature of the opioid agonist is the inhibition of neurotransmitter release. Although there are instances that opioid agonist could increase the neurotransmitter release, it is due to the location of the receptor and the disinhibition of the neurotransmitter release. An excellent example is the dopamine release within the nigrostriatal loop. κ-Opioid agonist inhibits dopamine release by acting directly at the presynaptic dopaminergic terminals, whereas μ- and δ-opioid agonists increase the release by inhibiting the GABAergic interneurons that inhibit the dopamine release. Thus, in either case, the activation of opioid receptor results in the direct inhibition of synaptic transmission.

From the cloning studies, it is unequivocal that the opioid receptors belong to the superfamily of proteins, the G protein-coupled receptors (GPCR) and the subfamily of rhodopsin-like receptors. One common feature of these receptors is that they contain hydrophobic regions that would span the membrane 7 times. Thus these receptors are commonly known as seven-transmembrane receptors. Another common feature is that their signals are mediated by promoting the dissociation of the nucleotide GDP from the α-subunits of the heterotrimeric proteins. The dissociation of GDP allows the association of GTP to the α-subunits resulting in the dissociation of the heterotrimeric proteins into α- and βγ subunits. These subunits will then control the activities of various intracellular or membrane bound proteins and enzymes. For the multiple opioid receptors, the GTP/GDP-binding proteins involved in their actions are the pertussis-toxin-sensitive Gi/Go proteins.

In order for opioid receptors to regulate the neurotransmitter release, two of the proteins that the receptors regulate are the voltage-dependent Ca^{2+} channels and the inward rectifying K^+ channels. By inhibiting the Ca^{2+} channels and thus reducing the influx of Ca^{2+}, opioid agonists could regulate the fusion of vesicles containing the neurotransmitters with the synaptic membrane. Also opioid agonists could activate the voltage-dependent inward rectifying K^+ channels and thus hyperpolarizing the synaptic membrane. By controlling these two ions channels, activation of the opioid receptors would reduce the excitability of the membrane and reduce the transmitter release.

Other prominent proteins and enzymes that are regulated by the multiple opioid receptors are the enzymes responsible for cAMP synthesis, adenylyl cyclase, and that which is involved in the long-term cellular adaptational events, the mitogen-activated protein kinase (MAP kinase). Opioid receptors inhibit the adenylyl cyclase activity, thereby reducing the intracellular cAMP content. This second messenger could control the activities of a protein kinase that, in turn, could regulate the activities of other proteins, such as the ion channels. The MAP kinase has been known to participate in the cellular proliferation and apoptotic events. Thus, it is probable that MAP kinase activation by the multiple opioid receptors could signify their involvement in long-termed potential and learning, two of the probable mechanisms for the basis of chronic drug actions.

Summary and Future Direction

The similarities in the sequence and the molecular action of these multiple opioid receptors are striking. Hence, it is unclear why nature would evolve three different genes coding for three different proteins from the same ancestral gene so as to carry out the same functions. To complicate the picture, there are three endogenous peptides that exhibit selectivity but not specificity among these multiple opioid receptors. It is still unresolved why an endogenous opioid peptide such as Met^5-enkephalin that exhibits *in vitro* agonistic properties in μ-opioid receptor would not produce analgesic effect *in vivo*. There is no debate that endogenous peptides and opiate alkaloids have different recognition motifs within these opioid receptors, and that the cellular regulations of the peptide- and alkaloid-receptor complexes are different. Whether such differences could contribute to the differences in the pharmacological responses of these drugs or simply the spatial distribution of the receptors, remains to be investigated.

In the past, the approach to eliminate the undesirable side effects of the opiate alkaloids was to design drugs that would have selectivity toward one specific opioid receptor. A classic example is the development of drugs that would have κ-opioid receptor selectivity, because the dysphoric effect of κ-opioid receptor activation would reduce the addictive liability of the drug. Unfortunately, drugs marketed thus far do not exhibit the ultimate property of opiate analgesic, i.e., efficacious pain relief with no side effects. The problem lies mainly with the presence of multiple opioid receptors and the selectivity of the drugs for these receptors. Hence new approaches should be taken in

the future for development of pain-management paradigms. With the advent of gene therapy, one could envision the use of receptor engineering in the treatment of pain. If an opioid-receptor mutant could be identified that exhibits distinct phenotype from that of the endogenous receptors, and that this receptor mutant could be delivered to the site of action, e.g., substantia gelatinosa of the spinal cord, then activation of such mutants by a drug that normally would not activate the endogenous receptors, e.g., an opiate antagonist, would result in pain relief. Such an approach would not only provide specificity, but also would eliminate the side effects of the opiate drugs; but this approach could only be accomplished when the molecular basis for the action of the multiple opioid receptors is fully elucidated.

See Also the Following Articles

DNA Damage: Alkylation • DNA Helicases: Dimeric Enzyme Action • DNA Helicases: Hexameric Enzyme Action • DNA Polymerase I, Bacterial • Zinc Fingers

Further Reading

Law, P. Y., Wong, Y. H., and Loh, H. H. (2000). Molecular mechanisms and regulation of opioid receptor signaling. *Annu. Rev. Pharmacol. Toxicol.* **40**, 389–430.

Minami, M., and Satoh, M. (1995). Molecular biology of the opioid receptors: Structures, functions and distributions. *Neurosci. Res.* **23**, 121–145.

Pasternak, G. W. (1988). Multiple morphine and enkephalin receptors and the relief of pain. *J. Amer. Med. Assoc.* **259**, 1362–1367.

Reisine, T., and Pasternak, G. (1996). Opioid analgesics and antagonists. In *The Pharmacological Basis of Therapeutics* (Joel G. Hardman, Lee E. Limbird, Perry B. Molinoff, Raymond W. Ruddon and Alfred G. Gilman, eds.) 9th edition, pp. 521–555. McGraw Hill, New York.

Simon, E. J., and Gioannini, T. L. (1993). Opioid receptor multiplicity: Isolation, purification and chemical characterization of binding sites. In *Opioid I, Handbook of Experimental Pharmacology* (A. Herz, ed.) Vol 104, pp. 3–36. Springer, Berlin.

Biography

P. Y. Law is a Professor in the Department of Pharmacology at the University of Minnesota in Minneapolis. His principal research interests are the cellular control of the opioid receptor signaling. He holds a Ph.D. from the University of Illinois and received his postdoctoral training at the University of California, San Francisco. He has authored numerous research and review articles on the molecular mechanism of opioid receptor actions.

Horace H. Loh is the F. and A. Stark Professor and Head of the Department of Pharmacology at University of Minnesota in Minneapolis. His principal research interests are the neurochemical basis for opiate tolerance and dependence. He holds a Ph.D. from the University of Iowa and received his postdoctoral training from the University of California, San Francisco. He has authored numerous research and review articles on opioid receptors, and has served as an editor on several scientific journals. He is a member of the Chinese National Academy of Sciences.

Ornithine Cycle

Malcolm Watford
Rutgers University, New Brunswick, New Jersey, USA

The ornithine cycle, also known as the urea cycle and the Krebs–Henseleit cycle, is the pathway in mammalian liver that allows the detoxification and excretion of excess nitrogen as urea. Flux through the cycle is driven by the demand to remove excess ammonia derived from the degradation of amino acids that arise either from the diet or from endogenous proteolysis. In a healthy individual, consuming a typical western diet, flux through the ornithine cycle produces some 30–35 g of urea per day but as much as 25% of this can be recycled via hydrolysis to ammonia and bicarbonate by colonic bacteria.

History

Three major systems have evolved for the elimination of excess nitrogen from the body, and animals may be classified according to their major nitrogenous excretion product. Thus most fish are ammoniatelic (ammonia excretion), reptiles and birds are uricotelic (uric acid excretion), and mammals are ureotelic (urea excretion). In addition, urea excretion is seen in some teleost fish, and urea synthesis is also present in elasmobranchs (sharks and rays) where urea functions primarily in an osmotic role, not in nitrogen excretion.

Urea was first described as "substance savoneuse," that yielded ammonia on hydrolysis, isolated from urine by Roulle in 1773 and was obtained in pure form by Proust in 1820. There is evidence that Davy synthesized urea from cabonyl chloride and ammonia in 1812 but he failed to recognize the product. Thus Wholer is credited for achieving the synthesis, in 1828, of urea from ammonia and lead cyanate in what is best remembered as the first synthesis of an organic compound from inorganic substrates. Over the next century many theories were developed to explain urea synthesis but the true pathway was not discovered until 1932. Working with liver slices in incubation Krebs and Henseleit found that the addition of small amounts of ornithine greatly accelerated the synthesis of urea from ammonia and furthermore, that the ornithine could be recovered at the end of the incubation. From this they formulated the idea that ornithine was acting as a "catalyst." They also identified citrulline as an intermediate and described the ornithine cycle as ammonia (together with bicarbonate) and ornithine combining to give citrulline that was then converted to arginine. The final step was hydrolysis of the arginine to urea and with the concomitant regeneration of ornithine. This was the first description of a cyclic biochemical pathway again illustrating the central role urea synthesis has had in the history of biology and chemistry.

Chemistry of the Cycle

Since Krebs and Henseleit's original discovery, the chemistry of the cycle has been completely described and although the ornithine cycle consists only of four enzymes, the need for carbamoyl phosphate means that carbamoyl phosphate synthetase 1 is usually considered an ornithine cycle enzyme.

The complete cycle (Figure 1) is only expressed in liver parenchymal cells with highest activity in those cells near the portal inlet (periportal cells). The substrates for the cycle are ammonia, bicarbonate, aspartate, and three ATP equivalents. In this text the term ammonia refers to the sum of NH_4^+ plus NH_3, and where a specific molecular species is important, it is shown in parentheses. Beginning in the mitochondria ammonia (NH_3) combines with bicarbonate to form carbamoyl phosphate involving 2 ATP and releasing 2 ADP plus inorganic phosphate, through the action of carbamoyl phosphate synthetase 1 (EC 6.3.4.16). The carbamoyl group is then transferred to ornithine via ornithine transcarbamoylase (EC 2.1.3.3) to yield citrulline that leaves the mitochondria in exchange for ornithine on the ORN 1 transporter. In the cytosol, citrulline condenses with aspartate in a reaction, requiring ATP and the formation of a citrulline-AMP intermediate, to give argininosuccinate, AMP, and pyrophosphate via the action of argininosuccinate synthetase (EC 6.3.4.5). The carbon skeleton of the aspartate is then cleaved from argininosuccinate by argininosuccinate lyase (EC 4.3.2.1) to yield fumarate and arginine. The final step is hydrolysis of arginine by arginase (EC 3.5.3.1) to give the end product urea with the regeneration of ornithine that can enter the mitochondria on the ORN 1 transporter and begin another round of the cycle.

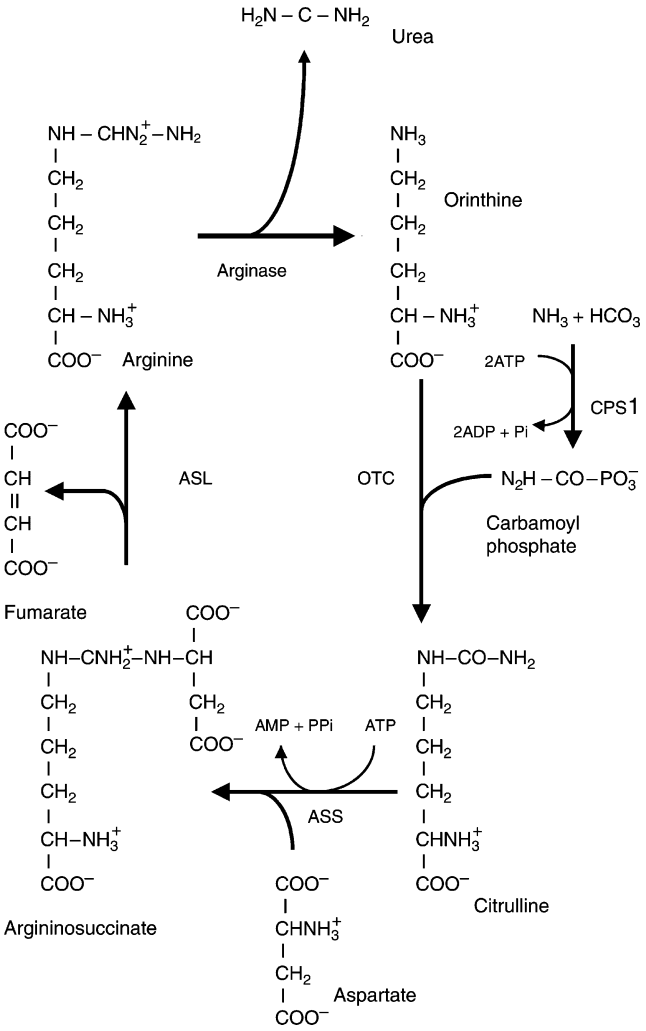

FIGURE 1 The chemistry of the ornithine cycle. CPS 1, carbamoyl phosphate synthetase 1, OTC, ornithine transcarbamoylase, ASS, argininosuccinate synthetase, ASL, argininosuccinate lyase.

Channeling in the Cycle

Although carbamoyl phosphate synthetase 1 and ornithine transcarbamoylase are mitochondrial matrix enzymes, they are localized in very close proximity to the cristae of the inner membrane. This would favor direct transfer of intermediates along the pathway and tracer experiments have shown that extra-mitochondrial ornithine is preferentially utilized for citrulline synthesis over ornithine generated within the mitochondria. Such findings indicate that the ORN 1 transporter, carbamoyl phosphate synthetase 1 and ornithine transcarbamoylase are working efficiently as a unit without free mixing of the intermediates within the mitochondria. In addition, there is evidence of similar channeling within the cytosolic section of the cycle. In permeabilized hepatocytes incubated with ^{14}C labeled bicarbonate, the formation of labeled urea is not significantly diluted by the addition of large amounts of cycle intermediates (arginine, argininosuccinate, or citrulline), again showing no mixing with exogenous intermediates. Therefore all intermediates of the cycle appear to be carefully channeled along the pathway which may be related to the need to ensure removal of the highly toxic substrate, ammonia.

Physiological Aspects of the Cycle

The function of the ornithine cycle is to detoxify excess ammonia in the mammalian body and as such the source of the ammonia must be considered whenever the cycle is discussed in more than simple chemical terms. There are two types of condition when the delivery of ammonia within the liver is high and thus require high rates of urea synthesis. The first is in response to dietary (exogenous) protein when excess amino acids are degraded and the second is in response to increased catabolism of endogenous amino acids, arising from proteolysis, during early starvation and in hypercatabolic states such as those that arise from sepsis and injury. A quantitative analysis of the fate of a typical daily load of dietary amino acids showed that, if those amino acids that must be catabolized within the liver were to undergo complete oxidation then, this would produce more ATP than the liver uses in a day. Since the liver oxidizes other fuels in addition to amino acids, it is evident that the carbon skeletons of the amino acids cannot undergo complete oxidation in the liver. In practice the amino acid carbon skeletons are conserved as either glycogen (indirect pathway of synthesis) or released into the circulation as free glucose. In the case of starvation and hypercatabolic states, the reason the amino acids are being degraded is to provide glucose for the body, and urea synthesis is simply coincidental. Thus the synthesis of urea from amino acids is always linked to the hepatic pathway of gluconeogenesis.

There is currently some debate about how much of the ammonia and aspartate for the cycle are taken up from the circulation directly and how much are synthesized within the liver from ammonia and/or other amino acids. Within the liver however, glutamate dehydrogenase and the major aminotransferases catalyze reactions close to equilibrium which allows the maintenance of a balanced substrate supply to the cycle (Figure 2).

By following the fate of a single amino acid, alanine, through hepatic metabolism, the integrative nature of the ornithine cycle with gluconeogenesis can be seen (Figure 3). Alanine undergoes transamination with α-ketoglutarate in the cytosol and both the pyruvate and glutamate formed enter the mitochondria where the pyruvate is carboxylated to oxaloacetate via the action of pyruvate carboxylase. The glutamate then transaminates with this oxaloacetate to give aspartate and α-ketoglutarate. The latter can then recycle via the

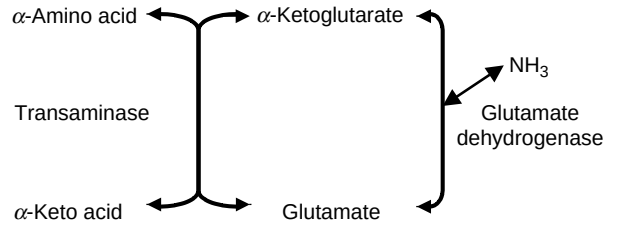

FIGURE 2 The equilibrium nature of glutamate dehydrogenase and the transaminases. Amino acids can transfer their amino group to α-ketoglutarate to produce glutamate via transamination. Glutamate can yield ammonia and α-ketoglutarate through glutamate dehydrogenase. Since glutamate dehydrogenase and the major transminases catalyze reactions close to equilibrium the entire system is freely reversible and thus ensures a balance of substrates, NH3 and aspartate (produced through aspartate aminotransferase) for the ornithine cycle.

cytosol to transaminate with another alanine. The aspartate leaves the mitochondria to be incorporated into the cycle by argininosuccinate synthetase in the cytosol. At the subsequent lyase step the carbon skeleton is released as fumarate. Since fumarate is unable to re-enter the mitochondria, it is metabolized to malate which is oxidized to oxaloacetate with the concomitant generation of NADH in the cytosol. The oxaloacetate is then converted to phosphoenolpyruvate, through the action of cytosolic phosphoenolypyruvate carboxykinase, and enters the gluconeogenic pathway with the utilization of the NADH at the glyceraldehyde 3-phosphate dehydrogenase step. Thus the transport of aspartate out of the mitochondria brings not only the nitrogen required for urea synthesis but also the carbon and the reducing power necessary for gluconeogenesis.

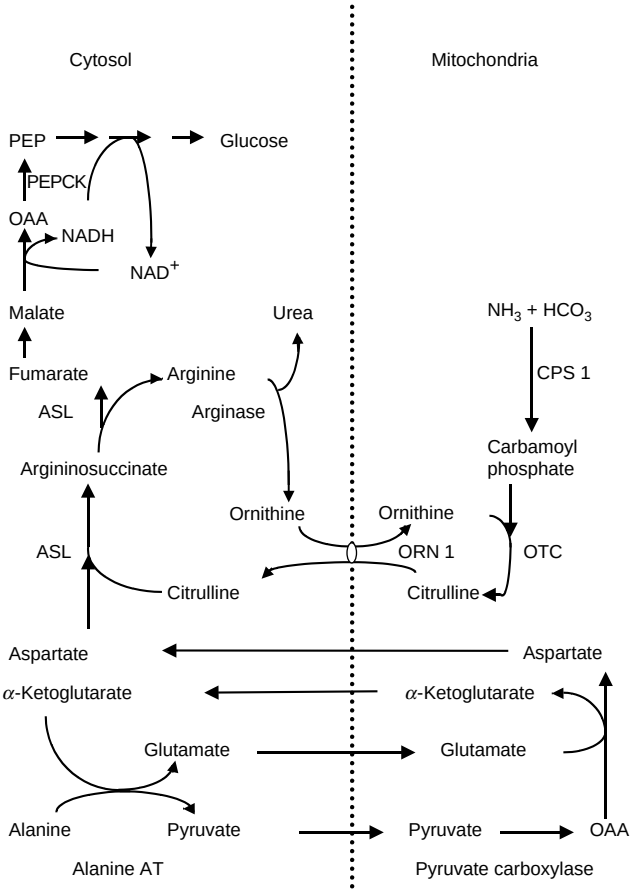

FIGURE 3 The ornithine cycle is linked to gluconeogenesis. CPS 1, carbamoyl phosphate synthetase 1, OTC, ornithine transcarbamoylase, ORN 1, orthine/citrulline transporter, ASL, argininosuccinate synthetase, ASL argininosuccinate lyase, Alanine AT, alanine aminotransferase, PEPCK, phosphoenolpyruvate carboxykinase.

Regulation

In 1905 Otto Folin, carrying out experiments on himself and others, described how urea excretion fluctuated with dietary protein, in particular, he showed how it reached a minimum within two days of consuming a zero protein diet. Thus it is clear that flux through the cycle is highly regulated and as with many biochemical pathways, this involves both short-term (changes in enzyme activity with no change in the amount of enzyme) and long-term (changes in the amount of enzyme) mechanisms. The need for the ornithine cycle is driven solely by the need to remove substrate (ammonia arising from amino acid catabolism), there is never a need for the end product (urea) and thus the cycle is not subject to product feedback regulation. Instead, flux through the cycle must increase rapidly whenever the substrate load increases.

Short-Term Regulation

Quantitative control analysis for the cycle has indicated that carbamoyl phosphate synthetase 1 plays a major regulatory role. In experiments *in vitro* however, where amino acid levels are held constant, the stimulation of carbamoyl phosphate synthetase 1 results in a fall in ammonia levels. This does not occur *in vivo* where the supply of amino acids varies, and at times of increased flux through the cycle, the concentration of ammonia shows little change or even a slight increase. Therefore the role of carbamoyl phosphate synthetase 1 is not to control flux through the cycle, rather it acts to maintain ammonia levels within a very limited range. The intrahepatic concentrations of the intermediates of the cycle are below the K_m for all of the enzymes which means that any increases in the concentration of intermediates, increase flux through the remainder of the cycle. From a teleological viewpoint a possible regulatory scheme would be the simple stimulation of carbamoyl phosphate synthetase 1 by increasing ammonia levels. Since carbamoyl phosphate synthetase 1 shows Michaelis–Menten kinetics towards ammonia

this would mean that a threefold increase in flux through the cycle would require a threefold increase in ammonia concentration. Ammonia levels however, must be held within a very narrow range. If intra-hepatic ammonia levels rise, some will escape from the liver and cause hyperammonemia and neurological toxicity. Conversely, if intra-hepatic ammonia levels decrease, this would disturb the equilibrium nature of the glutamate dehydrogenase and transaminase reactions with resultant dysregulation of non-essential amino acid levels.

Carbamoyl phosphate synthetase 1 has an absolute requirement for an allosteric effector, N-aceyl glutamate, which is made in the mitochondria from glutamate and acetyl CoA by N-acetyl glutamate synthetase (EC 2.3.1.1), and is degraded by an acylase in the cytosol. The synthesis of N-acetyl glutamate is stimulated by arginine and there is evidence that glucagon can increase N-acetyl glutamate levels through inhibition of transport out of the mitochondria thereby decreasing the rate of degradation. The major mechanism responsible for changing N-acetyl glutamate levels however, is substrate supply. Anytime there is an increase in amino acid catabolism this results in increased glutamate supply and a concomitant increase in N-acetyl glutamate levels. This allows carbamoyl phosphate synthetase 1 activity to increase and so prevent the ammonia levels from rising to toxic levels. Thus increased amino acid supply results in not only increased delivery of the direct substrates, ammonia and aspartate of the cycle, but also in the glutamate, and consequently the N-acetyl glutamate, required to allow flux through the cycle to increase and buffer intra-hepatic ammonia levels.

Long-Term Regulation

The urea cycle enzymes are not expressed in mammals until quite late in gestation since there is no need for the fetus to make urea, as the mother can dispose of any potentially toxic waste products. Such changes are also seen in other species, for example, as ammoniatelic tadpoles change to ureotelic frogs there is a dramatic increase in expression of the cycle. In non-carnivorous mammals the levels of all five enzymes can also change with diet and physiological/pathological conditions. Feeding high protein diets, early starvation, and hypercatabolic states are all accompanied by higher amounts of the enzymes, while low protein diets result in lower levels of the enzymes, and Schimke used the kinetics of these responses to develop the quantitative basis of protein turnover. Most of the changes are due to control at the level of gene transcription but the changes in arginase, seen during starvation, also involve changes in the rate of degradation of the arginase protein, and there is evidence that carbamoyl phosphate synthetase 1 expression is also regulated at the translational level. The agents responsible for the changes are predominantly glucagon (cAMP) and glucocorticoids acting to increase expression, with minor roles played by growth hormone, adrenergic hormones, and thyroid hormones. Insulin may act to downregulate expression but the importance *in vivo* is not clear. In addition, transcription of the gene encoding argininosuccinate synthase is suppressed by arginine, but this is likely to be of importance only in non-hepatic cells where the enzyme functions in arginine synthesis.

The half-lives of ornithine cycle enzyme proteins are relatively long, of the order of days, and thus any changes in the amount of protein would take some time to become significant. This means that the long-term changes do not play a role in the acute regulation of the cycle, rather they are adaptive in nature, preparing the body for long-term changes in substrate supply. This fits well with the time course of changes in amino acid catabolism within the body. Excess amino acid supply from a single meal can be readily detoxified through the cycle or temporarily buffered by synthesis of non-essential amino acids such as alanine. However, if the protein content of the diet has undergone a consistent increase then the capacity of the cycle increases to deal with it. Similarly, increased catabolism, of endogenous amino acids in starvation and hypercatabolic states, occurs over the course of days again allowing the cycle time to adapt. Conversely, at times of low protein feeding, expression of the cycle is decreased in order to conserve as much nitrogen as possible. This means that, in retrospect, the experiments of Folin (q.v.) involving the consumption of high protein diets after 14 days of a zero protein diet were potentially highly dangerous. The capacity of the cycle would have been very low and not able to deal with the sudden influx of ammonia. Thus it is important that subjects accustomed to very low protein diets be re-fed relatively small increments of dietary protein until the cycle has increased sufficiently in capacity to avoid hyperammonemia.

Long-term changes in the capacity of the ornithine cycle are always accompanied by similar changes in the expression of a number of genes encoding related hepatic enzymes and transporters. These include, the ORN 1 transporter, various plasma membrane amino acid transporters, tyrosine aminotransferase, glutaminase, and phosphoenolpyruvate carboxykinse. The last is a gluconeogenic enzyme, again illustraing the integrative nature of the entire process of amino acid catabolism.

Extra-Hepatic Expression of Ornithine Cycle Enzymes

The complete ornithine cycle is only found in the liver but some of the enzymes are expressed in other tissues where they function in arginine synthesis. Arginine is not an essential amino acid in non-carnivorous mammals

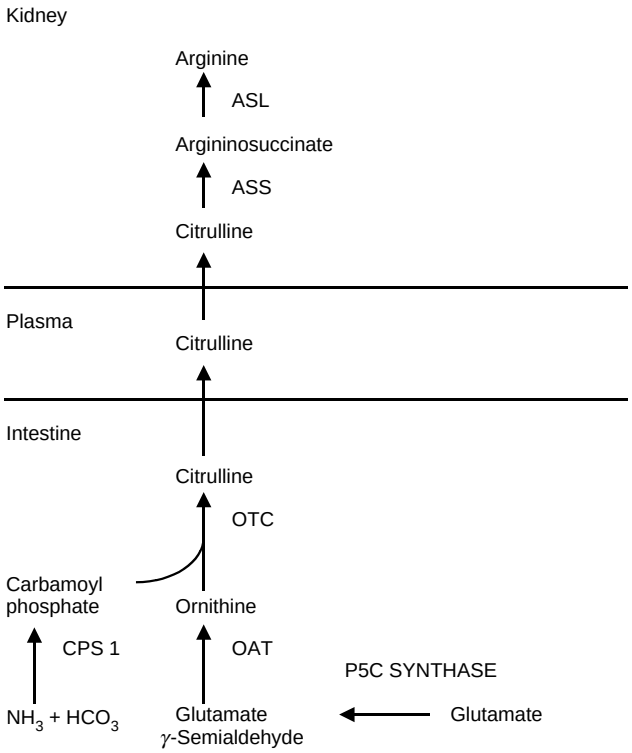

FIGURE 4 Extrahepatic arginine synthesis. ASL, argininosuccinate lyase, ASS, argininosuccinate synthetase, CPS 1, carbamoyl phosphate synthetase 1, OTC, ornithine transcarbomylase, OAT, ornithine aminotransferase, P5C, pyrroline 5-carboxylate.

but the very high arginase activity of the liver means that both dietary arginine and arginine synthesized within the liver are rapidly hydrolyzed and not available to the body. Thus the arginine required for the synthesis of protein, nitric oxide, polyamines, etc. is made in extra-hepatic tissues (Figure 4). The mucosa of the small intestine expresses both carbamoyl phosphate synthetase I and ornithine transcarbamoylase, and together with pyrroline 5-carboxylate synthase and ornithine aminotransferase, this allows the synthesis of citrulline from glutamate and ammonia. This citrulline is released into the circulation to be taken up by the kidney, which expresses both argininosuccinate synthase and argininosuccinate lyase, and used for arginine synthesis. Thus by restricting expression of four enzymes of the ornithine cycle to these two extra-hepatic tissues the body is able to obtain sufficient arginine. Strict carnivores, such as cats and ferrets, lack the intestinal part of this pathway and therefore arginine must be provided in the diet. This is not usually a problem but if, experimentally, they are fed an arginine-free diet, they are unable to generate sufficient ornithine in the liver to allow increased flux through the cycle. This results in hyperammonenia and is one of the very few known cases of acute toxicity arising from a nutritional deficiency.

Inborn Errors of the Ornithine Cycle

As detailed above, the ornithine cycle is not required in utero and thus the genes encoding the cycle enzymes are not expressed until very late in gestation. Therefore it is possible to develop to full term with a misfunctional ornithine cycle gene (inborn errors may arise from a complete lack of a protein, changes in V_{max} or K_M, or the ability to bind cofactors or regulators). Inborn errors for all five cycle enzymes, plus some of the ancillary proteins such as N-acetyl glutamate synthetase and the ORN 1 transporter, have been described. All are characterized by hyperammonemia that is usually accompanied by very high levels of the non-essential amino acids alanine and glutamine. Other intermediates of the cycle accumulate according to the specific enzyme defect. The severity is usually more pronounced with deficiencies of the first two enzymes, carbamoyl phosphate synthetase 1 and ornithine transcarbamoylase, especially if there is a complete lack of activity. The gene encoding ornithine transcarbamoylase is located on the X chromosome and thus boys are most severely affected, however due to Lyonization different alleles are expressed in different cells and some female carriers of a defective gene will present with very low ornithine transcarbamoylase activity. This was traditionally believed to be benign since these women often exhibit protein intolerance and simply self limit their protein intake. It is now recognized however, that times of increased endogenous proteolysis, such as occurs in hypercatabolic states or even pregnancy, can represent a risk for hyperammonemia in such individuals. In classic cases of ornithine transcarbamoylase deficiency, some of the excess carbamoyl phosphate in the mitochondria escapes to the cytosol where it enters the pyrimidine synthesis pathway. This causes production of relatively large amounts of orotic acid which is lost in the urine and the presence of significant orotate excretion is considered definitive evidence for ornithine transcarbamoylase deficiency.

A defect in argininosuccinate synthase results in citrullinemia and excretion of citrulline in the urine. To a limited extent, this lessens the need for urea synthesis and threrefore the ammonemia is not as severe as seen with defects in the first two enzymes. Similarly, with defects of argininosuccinate lyase and argininase, there is excretion of argininosuccinate and arginine, again lowering the need for urea synthesis and the severity of the condition.

The treatment for all inborn errors of the ornithine cycle begins with a limited protein diet to lower the need for urea synthesis. However, depending on the severity of the condition, patients will still encounter periods of hyperammonemia, and additional treatments have been developed. Most commonly, oral benzoic acid or

phenylacetate (or phenylbutyrate) are given since these are detoxified in the liver by conjugation with glycine or glutamine respectively. The amino acid conjugates are excreted which effectively removes nitrogen from the body, again lessening the need for urea synthesis. Recently a number of liver transplants have been carried out and gene therapy trials have been initiated. With inborn errors of the ornithine cycle, except arginase deficiency, arginine becomes an essential amino acid. In cases of argininosuccinate synthase and lyase deficiences, very large amounts of dietary arginine are required to replace the arginine equivalents lost as citrulline and argininosuccinate in the urine. Similarly, while liver transplantion or liver-specific gene therapy will correct the defect in urea synthesis, they do not change the defect in the extra-hepatic arginine synthesis pathway and thus, arginine remains an essential amino acid after such treatments.

See Also the Following Articles

Amino Acid Metabolism • Gluconeogenesis • Urea Cycle, Inborn Defects of

Glossary

ammonia In this context to the sum of NH_3 plus NH_4^+. In the cell, at physiological pH, >99% is present as NH_4^+.

equilibrium An enzyme-catalyzed reaction in which there is little change in Gibbs free energy between the substrates and products. In practice, this means that the reaction is freely reversible and both the direction and magnitude of net flux is determined by the rate of substrate supply and/or product removal.

gluconeogenesis The formation of glucose from non-carbohydrate prescursors such as lactate, glycerol, and amino acids.

hypercatabolic states Conditions in which the body is undergoing extensive catabolism (degradation) of tissues, particularly skeletal muscle, to provide amino acids for acute phase protein synthesis, gluconeogenesis, and tissue repair, after severe injury or infection.

transaminases Enzymes that catalyze the transfer of amino (NH_2) groups between α-amino acids and α-keto acids. Also known as aminotransferases usually glutamate and α-ketoglutarate act as the amino donor or acceptor respectively.

Further Reading

Grisolia, S., Baguena, R., and Mayor, F. (eds.) (1976). *The Urea Cycle*. Wiley-Interscience, New York.

Jungas, R. L., Halperin, M. L., and Brosnan, J. T. (1992). Quantitative analysis of amino acid oxidation and related gluconeogenesis in humans. *Physiol. Rev.* **72**, 419–448.

Krebs, H. A. (1982). The discovery of the ornithine cycle of urea synthesis. *Trends Biochem. Sci.* **7**, 76–78.

Lee, B., and Gross, J. (2001). Long term correction of urea cycle disorders. *J. Pediatr.* **138**, S62–S71.

Meijer, A. J. (1995). Urea synthesis in mammals. In *Nitrogen Metabolism and Excretion* (P. Walsh and P. Wright, eds.) pp. 193–204. CRC Press, Boca Raton, FL.

Morris, S. M. Jr (2002). Regulation of enzymes of the urea cycle and arginine metabolism. *Annu. Rev. Nutr.* **22**, 87–105.

Stipanuk, M. H., and Watford, M. (2000). Amino acid metabolism. In *Biochemical and Physiological Aspects of Human Nutrition* (M. H. Stipanuk, ed.) pp. 233–286, Saunders, Philadelphia, PA.

Watford, M. (1991). The urea cycle: A two-compartment system. *Essays Biochem.* **26**, 49–58.

Watford, M (2003). The urea cycle. *Biochem. Mole. Biol. Education* **31**, 289–297.

Wu, G., and Morris, S. M. Jr (1998). Arginine metabolism; nitric oxide and beyond. *Biochem. J.* **336**, 1–17.

Biography

Malcolm Watford obtained his D.Phil. from the Metabolic Research Laboratory, Oxford, and did postdoctoral work at the University of Montreal and Case Western Reserve University. He is currently on the faculty of the Department of Nutritional Sciences, Rutgers University where he teaches metabolic regulation and carries out research on glutamine metabolism and gluconeogenesis.

Oxygenases

Osamu Hayaishi
Osaka Bioscience Institute, Suita, Osaka, Japan

Oxygenases are a group of oxidative enzymes that catalyze the direct addition or fixation of molecular oxygen into various substrates. The terms "mono" and "di" oxygenases are generally assigned to the enzymes catalyzing the incorporation of either one or two atoms of oxygen per mole of substrate, respectively. Prior to the discovery of "oxygenases" in 1955, the essential characteristics of biological oxidation processes was believed to be the removal or transfer of electrons or hydrogen atoms from a substrate to an appropriate acceptor. These enzymes were termed "dehydrogenases" and when oxygen molecules serve as the immediate electron acceptor, the enzymes have been called "oxidases." Functionally, dehydrogenases and oxidases are mainly involved in energy metabolism whereas oxygenases play major roles in the anabolism and catabolism of biological materials as well as synthetic compounds.

Background

In 1932, Professor Heinrich Wieland, a German Nobel laureate, authored a book entitled "On the Mechanism of Oxidation," in which he proposed the famous "dehydrogenation theory." According to this theory, the principle of biological oxidation processes is the activation and transfer of hydrogen atoms, or their equivalent, from the substrate molecule to an appropriate acceptor such as coenzymes and various dyes. Oxygen molecules may, in some instances, serve as the immediate electron acceptor, and if so, then these enzymes are termed "oxidases." Thus, according to Professor Wieland, molecular oxygen accepts hydrogen atoms and is reduced to water or hydrogen peroxide. However, it is never incorporated into the substrate. When the overall reaction is envisaged as the addition of oxygen, the oxygen atoms are always derived from water molecule rather than from atmospheric oxygen. For example, when aldehydes are converted to acids, aldehydes are hydrated first and then dehydrogenation occurs so that the sum is the addition of oxygen to the substrate X to form XO, but this oxygen atom is derived from water rather than from molecular oxygen. Thus, the direct addition of molecular oxygen to a substrate was considered completely irrelevant to biological oxidation.

In 1955, a set of experiments was performed in which pyrocatechase from a pseudomonad was incubated with its substrate catechol and a heavy oxygen isotope, ^{18}O (oxygen-18), the latter being in its molecular form in air in one flask or in the form of water in the other. The product, muconic acid, was isolated and analyzed for its ^{18}O content by mass spectrometry. Contrary to the then generally held belief, the results clearly demonstrated that the oxygen atoms incorporated into the product molecules were derived exclusively from molecular oxygen and not from the oxygen of the water molecule. Concurrently and independently, the phenolase complex of the mushroom was shown to incorporate 1 atom of molecular oxygen into a substrate, 3, 4-dimethylphenol, to form 4, 5-dimethylcatechol; whereas the other atom of oxygen was reduced to water. These findings together with subsequent work by others established that "oxygen fixation" did occur in biological systems, and revealed a new biological role of molecular oxygen, thus, the new concept of "biological oxygenation" was introduced. These enzymes that catalyze the direct incorporation of molecular oxygen were then named "oxygenases." At first, these oxygenase reactions were generally thought to be rather unusual and were limited to only primitive living organisms such as soil bacteria or mushrooms. It took several years before the ubiquitous existence of oxygenases was confirmed in many laboratories; and during that time a large number of oxygenases were isolated from animals, plants, and microoganisms and were shown to play important roles in the metabolism of various nutrients, hormones, and neurotransmitters as well as synthetic compounds.

Nomenclature, Classification, and General Properties of Oxygenases

Dioxygenases

Dioxygenases are defined as enzymes catalyzing reactions in which both atoms of molecular oxygen are incorporated into substrates. In the many instances where one substrate can act as the oxygen acceptor, the term "intramolecular dioxygenase" may be used.

Pyrocatechase (catechol 1, 2-dioxygenase) (EC 1.13. 11.1) is a typical example. The dioxygenases acting upon two acceptor substrates may be referred to as "intermolecular dioxygenases." One of the two substrates for the latter type has so far been invariably 2-oxoglutarate. Hypoxia-inducible factor 1 (H1F1) is a global regulator of cellular and systemic O_2 homeostasis in animals. Prolyl hydroxylase, also known as procollagen-proline: α-ketoglutarate 4-dioxygenase (EC 1. 14. 11. 2), the enzyme that hydroxylates specific prolyl residues of the collagen chains during their translation and requires 2-oxoglutarate as a cosubstrate in addition to ascorbate and Fe^{2+}, serves as an oxygen sensor. More recent evidence indicates that asparaginyl hydroxylase that hydroxylates the asparagine residues by a similar mechanism also serves as a direct oxygen sensor. A third class of dioxygenases include various enzymes that require NADH or NADPH as an electron donor. Although it is quite possible that reactions of this class may involve a simple dioxygenation reaction followed by a reductive step, these two processes may be coupled in such a way as to justify a separate category. The formation of catechol from anthranilate is an example of this type of reaction.

Prostaglandin endoperoxide synthase (EC 1. 14. 99. 1) is a unique intramolecular dioxygenase catalyzing the sequential addition of two oxygen molecules to a substrate molecule arachidonic acid to produce prostaglandin G_2 followed by the peroxidase reaction to generate prostaglandin H_2. This enzyme is also called cyclooxygenase, abbreviated as COX, and is of great clinical significance as will be discussed.

Some dioxygenases, such as tryptophan 2, 3-dioxygenase, contain heme as the sole prosthetic group; whereas others, such as pyrocatechase, contain nonheme iron, or like quercetinase, contain copper as the prosthetic group.

Monooxygenases

Monooxygenases are defined as a group of enzymes that catalyze the incorporation of one atom of molecular oxygen into a substrate, with the other being reduced to water. Therefore, these enzymes are some times referred to as mixed function oxidases or mixed function oxygenases. The electron donors that serve as coenzymes for these enzymes include reduced forms of pyridine nucleotides, flavin nucleotides, cytochromes, ascorbic acid, and pteridine derivatives. In some cases, the substrate itself may serve as an electron donor.

Internal Monooxygenases

The simplest type of monooxygenase catalyzes the incorporation of a single atom of molecular oxygen concomitant with the reduction of the other oxygen atom by electrons derived from the substrate. Since the reducing agent is internally supplied, these enzymes may be referred to as internal monooxygenases. The first of these enzymes to be crystallized was the lactate oxidative decarboxylase from *Mycobacterium phlei*. This enzyme catalyzes the conversion of lactate to acetate with the incorporation of one atom of oxygen into acetate, the evolution of one mole of CO_2, and the reduction of one atom of oxygen to water.

External Monooxygenases

While the internal monooxygenases do not require external reducing agents, more common types of monooxygenases require various kinds of electron donors. The electron donor (DH_2) serves as a basis for the subclassification of external monooxygenases. Some examples are as follows:

1. Flavoprotein monooxygenases with reduced pyridine nucleotides as DH_2. Salicylate 1-monooxygenase, a flavoprotein, is an example of this type of enzyme and catalyzes the formation of catechol from salicylate.
2. Heme-containing monooxygenases. Aryl 4-monooxygenase (liver microsomal cytochrome p-450) catalyzes the hydroxylation of a variety of substrates with reduced flavin as DH_2.
3. Heme-containing monooxygenases with a reduced iron-sulfur protein as DH_2. Camphor 5-monooxygenase is a typical example of this type of enzyme.
4. Pteridine-linked monooxygenases. Phenylalanine-4-monooxygenase catalyzes the formation of tyrosine from phenylalanine. Nitric oxide (NO) is a ubiquitous bioactive substance and a unique messenger molecule. It is synthesized from L-arginine by NO synthase (NOS), (EC 1, 14, 13, 39) a unique monooxygenase that catalyzes two consecutive monooxygenase reactions and that requires NADPH, tetrahydrobiopterine (BH_4), heme and Ca^{2+}/calmodulin and contains FAD and FMN. The product of the reaction is L-citrulline.
5. External monooxygenases with ascorbate as DH_2. Dopamine β-monooxygenase is an example of this type of enzyme.
6. External monooxygenases with another "substrate" as DH_2. Monophenol monooxygenase is an example of this type. In this case, dopa may be considered as the electron donor in the reaction.

Chemistry of Oxygen Fixation Reactions

Molecular Oxygen as a Substrate

Oxygenases utilize two different species of substrate, namely, molecular oxygen and the oxygen acceptor,

which is called the substrate and may be either an organic or an inorganic compound. It has not yet been clarified whether gaseous oxygen or oxygen dissolved in water is utilized by these enzymes. It is generally believed that the latter type of oxygen is different from the former. In water, oxygen is considered to exist largely in a dimerized form, $O_2{-}O_2$ because of its biradical nature, and probably forms a charge transfer complex with a water molecule. Whatever form is taken by the oxygen dissolved in water, the type of oxygen that serves as a substrate for oxygenases is in rapid equilibrium with gaseous oxygen under normal experimental conditions and can be clearly distinguished through the use of $^{18}O_2$ from the oxygen in water molecules or other compounds in the reaction mixture.

Role of the Substrate that Acts as Oxygen Acceptor

As for the acceptor for molecular oxygen, a great variety of both organic and inorganic compounds can be oxygenated. In general, oxygen-rich and/or hydrophilic compounds such as carbohydrates are not favorable substrates for oxygenases since these usually have many reactive groups containing oxygen, such as the hydroxyl, carbonyl, or formyl, and their biochemical function does not require further oxygenation. On the other hand, hydrophobic compounds such as lipids and aromatic compounds are often metabolized by oxygenases. These oxygen-deficient compounds generally require oxygenation in order to become biologically active or more soluble in water. In contrast, purines and pyrimidines with their hydrophilic ring systems are usually hydroxylated by the addition of water, followed by dehydrogenation.

Reaction Mechanisms and the Nature of Active Oxygen

Evidence generated from a number of laboratories has indicated that the enzyme binds oxygen only in the presence of substrate to form the ternary complex, ESO_2, in which oxygen and substrate interact to form a product. Such a ternary complex was postulated in 1964 on the basis of binding experiments, but more direct experimental evidence was not available until 1967 when a ternary complex of tryptophan 2,3-dioxygenase · tryptophan · O_2 was demonstrated by spectrophotometric experiments. Since that time similar oxygenated intermediates have also been observed, such as those with protocatechuate 3,4-dioxygenase (an iron-sulfur protein dioxygenase), lysine monooxygenase (a flavoprotein), and cytochrome P-450. In each case, the enzyme must bind the organic substrate first, before it can be oxygenated, in contrast to oxygen-carrying pigments such as hemoglobin and hemoerythrin, which are freely and reversibly oxygenated in the absence of any effector or substrate. In fact, several lines of evidence indicate that the substrate tryptophan binds specifically to the heme coenzyme of tryptophan 2,3-dioxygenase; as a consequence, the state of the heme is altered in such a way that its reactivity toward ligands is increased by several orders of magnitude.

The nature of the so-called active form of oxygen in the above-mentioned ternary complexes has been one of the most difficult questions in this field. All oxygenase-catalyzed reactions are exothermic and are therefore irreversible. Nevertheless, molecular oxygen is a rather inert compound and at room temperature reacts slowly with the substrate compounds in the absence of enzymes. This low kinetic reactivity is usually explained on the basis that molecular oxygen is in a triplet ground state. The direct reaction of a triplet molecule with organic molecules in the singlet state is electronically spin forbidden, and therefore a substantial activation energy is required. For this reason singlet oxygen has been suggested as a likely intermediate in many oxygenase-catalyzed reactions; however, definitive evidence is so far unavailable. It has recently been discovered that during enzymic hydroxylation of aromatic substrates the substituent (deuterium, tritium, chlorine, bromine, etc.) displaced by the entering hydroxyl group migrates to an adjacent position in the aromatic ring. On the basis of extensive studies of this phenomenon, called the "NIH shift," the active oxygen species involved in certain monooxygenases was postulated to be oxenoid.

On the other hand, evidence has appeared indicating that $O_2^{\cdot-}$, i.e., the superoxide anion, may be the active form of oxygen in the case of indoleamine 2,3-dioxygenase, and also in the hydroxylation reactions catalyzed by hepatic cytochrome P-450. It is, however, uncertain whether or not the superoxide anion is the general form of active oxygen in all oxygenase-catalyzed reactions or whether these enzymes represent a new class of enzyme that utilizes the superoxide anion rather than molecular oxygen as an oxygenating agent.

Biological Function of Oxygenases

While oxidases and dehydrogenase are mainly involved in energy metabolism, namely, the generation of ATP, oxygenases play important roles in biosynthesis, transformation, and degradation of essential metabolites such as amino acids, lipids, sugars, porphyrins, vitamins, and hormones. They also play a crucial role in the metabolic disposal of foreign compounds such as drugs, insecticides, and carcinogens. Furthermore, they participate in the degradation of various natural and synthetic compounds by soil and airborne microorganisms in

nature and are therefore of great significance in environmental sciences. Therefore, the significance of biological oxygen fixation in medicine, agriculture, and microbiology, and also in food technology, cosmobiology, public health problems, and biochemistry in general, has now been well established.

For example, certain oxygenases fulfill exceptionally important biological functions as exemplified by prolyl and asparaginyl hydroxylases as oxygen sensor as well as NO synthase as already mentioned. Several other examples are being briefly described.

Ribilose 1,5-bisphosphate carboxylase/oxygenase (EC 4. 7. 1 39), also known as "rubisco," catalyzes the CO_2 fixation as well as dioxygenase reaction and is the most abundant naturally occurring catalyst in nature. The global fixation of O_2 by rubisco can be estimated to be $\sim 10^{11}$ metric ton (t) per year.

Tryptophan 2,3-dioxygenase (EC 1. 13. 11. 11), also known as tryptophan pyrrolase, catalyzes the pyrrole ring cleavage by the insertion of two atoms of oxygen to produce L-formylkynurenine. This enzyme is present in the liver and is highly specific for L-tryptophan.

On the other hand, indoleamine 2,3-dioxygenase (EC 1. 13. 11. 42), also known as IDO, shows broad substrate specificity including L- and D-tryptophan, L- and D-5-hydroxytryptophan, serotonin, and so forth and is widely distributed in almost all organs and tissues except in the liver. IDO is induced by interferon and has been implicated in the defence mechanism against infection by depleting tryptophan from the infected tissues and cells. More recently, allogenic fetal rejection was reportedly prevented by tryptophan catabolism by IDO.

The prostaglandin endoperoxide synthases I and II (COX-1 and COX-2) are the major targets of nonsteroidal anti-inflammatory drugs (NSAIDs) including aspirin, indomethacin, ibuprofen, and the new COX-2 inhibitors. These drugs reduce inflammation, pain, and fever and also fatal thrombotic events, colon cancer, and Alzheimer disease.

Another common dioxygenase involved in lipid metabolism and widely distributed in both animals and plants is lipoxygenase (EC 1. 13. 11. 12), which is also known as LOX, lipoxidase, lipoperoxidase, or carotene oxidase. It is a nonheme iron-containing dioxygenase and catalyzes the formation of hydroperoxy derivative of unsaturated fatty acids. Of particular interest is the 5-LOX that catalyzes the dioxygenation of arachidonic acid to produce corresponding cis, trans-diene hydroperoxide followed by the dehydration to generate leukotrien (LT) A_4, another biologically important lipid mediator.

Unspecific monooxygenase is a heme-thiolate enzyme commonly known as cytochrome P450, hepatic microsomal monooxygenase, xenobiotic monooxygenase or aryl-4-monooxygenase (EC 1. 14. 14. 1), and catalyzes hydroxylation of a wide variety of both aromatic and aliphatic compounds. Monooxygenases also catalyze a seemingly diverse group of reactions including epoxide formation, dealkylation, decarboxylation, deamination, and N- or S-oxide formation. Although the overall reactions catalyzed by various monooxygenases appear grossly unlike one another, the primary chemical event is identical, since these processes are all initiated by the incorporation of one atom of molecular oxygen into the substrate.

Oxygenases in Evolution

Primitive Earth is believed to have started with an oxygen-free anaerobic environment. Therefore, the minimum manifestation of life is capable of occurring in the absence of molecular oxygen, as exemplified by the strictly anaerobic microorganisms, which survive and grow solely in the absence of molecular oxygen. With the appearance of oxygen in the Earth's atmosphere, molecular oxygen became a more useful and efficient tool as the terminal electron acceptor. Oxygenases then appeared gradually with the subsequent development of extensive and complicated metabolic pathways for essential components of cell structures and of regulatory mechanisms of metabolism and growth. The appearance of aerobic form of life paved the way for oxygenase-catalyzed reactions by which complicated messengers and structural compounds such as sterols, prostaglandins, and neurotransmitters are efficiently synthesized, while cytochrome P450 plays an essential role in the metabolism of thousands of drugs, carcinogens, and other synthetic compounds and is probably the largest family of proteins that has been cloned and characterized to date. In an evolutionary sense, oxidases preceded oxygenases but the latter appears to be a more advanced oxygen-utilizing catalyst associated with the most advanced and highly specialized life processes.

See Also the Following Articles

Cytochrome P-450 • Dopamine Receptors

Glossary

dehydrogenase The enzyme that catalyzes electron transfer from a substrate to an acceptor.

E.C. numbers and trivial names Enzymes are classified and numbered by the international Enzyme Commission. In this list, the names of the enzymes are formal names whereas trivial names are more common names or informal names. For example, catechol 1, 2-dioxygenase is a formal name while pyrocatechase is a trivial name.

oxidase The dehydrogenase that utilizes molecular oxygen as an immediate electron acceptor.

oxygenase The enzyme that incorporates molecular oxygen into substrates.

Further Reading

Bruick, R. K., and McKnight, S. L. (2001). Oxygen sensing gets a second wind. *Science* **295**, 807–808.

Groves, J. T. (2003). The bioinorganic chemistry of iron in oxygenases and supramolecular assemblies. *Proc. Natl Acad. Sci. USA* **100**, 3569–3574.

Hayaishi, O., Katagiri, M., and Rothberg, S. (1955). Mechanism of the pyrocatechase reaction. *J. Am. Chem. Soc.* **77**, 5450–5451.

Hayaishi, O. (ed.) (1962). *Oxygenases*. Academic Press, New York and London.

Hayaishi, O. (ed.) (1974). *Molecular Mechanism of Oxygen Activation*. Academic Press, New York.

Ishimura, Y., Nozaki, M., Yamamoto, S., Shimizu, T., Narumiya, S., and Mitani, S. (eds.) (2002). *Oxygen and Life-Oxygenases, Oxidases and Lipid Mediators*. Elsevier, Amsterdam.

Mason, H. S., Fowlks, W. L., and Peterson, E. (1955). Oxygen transfer and electron transport of the phenolase complex. *J. Am. Chem. Soc.* **77**, 2914–2915.

Nozaki, M., Yamamoto, S., Ishimura, Y., Coon, M. J., Ernster, L., and Estabrook, R. W. (eds.) (1982). *Oxygenases and Oxygen Metabolism*. Academic Press, New York.

Purich, D. L., and Allison, R. D. (eds.) (2002). *The Enzyme Reference: A Comprehensive Guidebook to Enzyme Nomenclature, Reactions, and Methods*. Academic Press, San Diego, CA.

Solomon, E. I., Decker, A., and Lehnert, N. (2003). Non-heme iron enzymes: Contrasts to heme catalysis. *Proc. Natl. Acad. Sci. USA* **100**, 3589–3594.

Biography

Osamu Hayaishi is a Professor Emeritus of Kyoto University and Osaka Medical College and a Director Emeritus of Osaka Bioscience Institute. His principal research interests are oxygenases and molecular mechanisms of sleep and wakefulness. He is a member of the Japan Academy, the National Academy of Sciences USA, and several other academies and served as President of the International Union of Biochemistry from 1973 to 1976.

P2X Purinergic Receptors

Annmarie Surprenant
University of Sheffield, Sheffield, UK

Inside the cell, adenosine triphosphate (ATP) is the major source of energy for all cellular processes. Outside the cell, ATP has quite distinct actions as a neurotransmitter at nerve–smooth muscle and nerve–nerve synapses, as a chemical stimulant at primary afferent terminals, and as a pro-inflammatory stimulus at immune and endothelial cells. Extracellular ATP acts on two types of membrane receptors: G protein-coupled "metabotropic" P2Y purinergic receptors and "ionotropic" P2X purinergic receptors. They are termed purinergic because ATP is a purine nucleotide. Ionotropic P2X receptors are ion channels opened within ms by extracellular ATP. There are seven members of the P2X receptor family ($P2X_1$–$P2X_7$) which are not related to any other known protein. They show widespread tissue distribution; functional responses to activation of these receptors occur in neurons, glia, endothelia, epithelia, bone, smooth muscle, cardiac muscle, red blood cells, and cells of the immune system.

P2X Receptor Genes

There are seven genes encoding P2X receptor subunits (Figure 1A). In the human genome, $P2X_4$ and $P2X_7$ are adjacent to each other on chromosome 12, an occurrence that probably represents gene duplication. $P2X_1$ and $P2X_5$ receptor genes are also very closely associated on chromosome 13. The remaining genes are located on separate chromosomes. The genes have 11–13 exons and all share a common structure with conserved intron/exon boundaries. Many spliced forms of these receptors have been observed, most due to splicing out of one or more exons. Several non-mammalian homologues of P2X receptors have been identified but no homologous sequences from invertebrates have yet been identified.

P2X Receptor Proteins

P2X receptor proteins range from 384 amino acid residues ($P2X_4$) to 595 amino acids ($P2X_7$). Each subunit comprises a large extracellular domain, two transmembrane domains, and relatively short intracellular amino and carboxy terminal regions (Figure 1B). There are ten cysteines in the extracellular region of the P2X receptor subunit which are conserved through all members of the family. Amino acid residues in the second transmembrane region are involved in ion flux through the channel. The carboxy terminal regions show very little homology among individual P2X receptors, but the remaining amino acids show 40–55% identity with each other among the seven receptors (Figure 1A). There is no amino acid sequence homology between P2X receptors and any known ATP-binding protein, any other ion channel, or any known protein: this places the P2X receptors into their own unique gene/protein family. The receptors assemble in multimeric combinations of subunits, either as homomeric channels (all one subtype) or as heteromeric channels (two or more subtypes). $P2X_1$, $P2X_2$, $P2X_3$, $P2X_4$, and $P2X_7$ exist as homomeric channels but $P2X_2$ and $P2X_3$ also exist as a functionally important heteromeric channel ($P2X_{2/3}$). The current evidence suggests these channels are composed of three, or possibly six, subunits.

P2X Receptor Localization

While other ionotropic ion channels are found mainly on excitable cells (i.e., nerve and muscle), P2X receptor channels are unusual in showing a very widespread distribution in both excitable and nonexcitable cells. There is considerable overlap with multiple receptor subunits found in a single cell, particularly in neurons. However, it is possible and biologically useful to generalize the distribution of these receptors (Table I).

Physiology of P2X Receptors

Release of ATP onto P2X Receptors

Cells release ATP in various ways: ATP is coreleased with noradrenaline from sympathetic nerve endings, or with aceytlcholine from parasympathetic or brain cholinergic neurons. It is rapidly released from vascular endothelial cells during hypoxia which is likely to be present under conditions such as angina or myocardial infarction. ATP is released from red blood cells upon

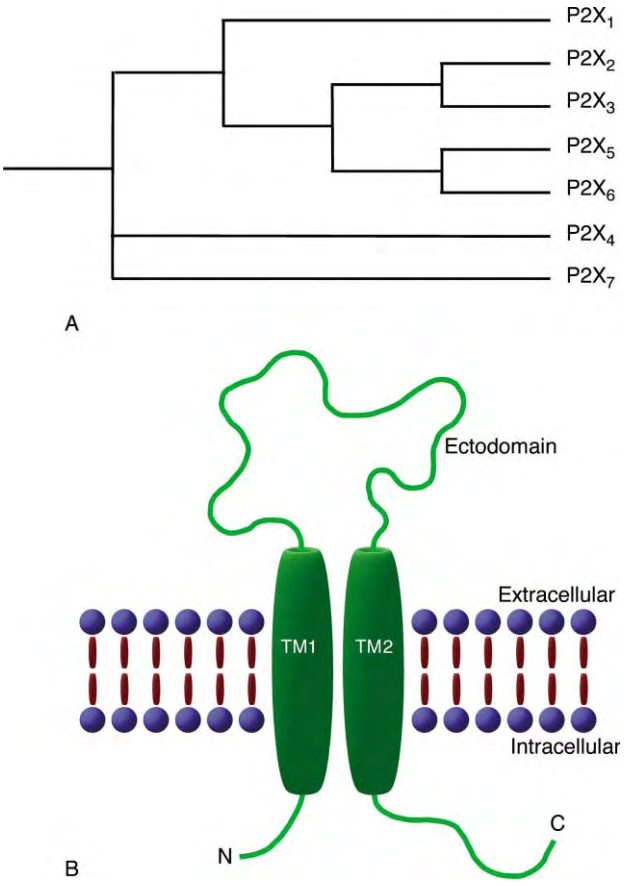

FIGURE 1 Molecular features of purinergic P2X receptor family. In (A) a dendrogram depicts the similarity in amino acid residues among the seven members of the P2X receptor family. $P2X_4$ and $P2X_7$ are the least similar while the pairs of $P2X_2/P2X_3$ and $P2X_5/P2X_6$ are most similar to each other. In (B) a cartoon representation of the likely membrane topology of a P2X receptor subunit shows the receptor protein crossing the lipid bilayer of the cell membrane at two regions (transmembrane TM1 and TM2). The large ectodomain contains the ATP-binding site and the TM2 region forms at least part of the ion channel structure. N and C refer to the intracellular amino (N) and carboxy (C) terminal amino acids.

mechanical distortion. Mechanical deformation of epithelial cells lining the bladder, lung, intestines, and ureter also causes rapid release of ATP. The mechanism by which ATP is released during mechanical displacement of these structures is unclear, but it may be transported from inside to outside by specific ATP transporter proteins or it may be released from storage vesicles by the process of exocytosis. Finally, high concentrations of ATP are released from damaged or dying cells at sites of inflammation and infection.

Activation of P2X Receptor Ion Channels ($P2X_1$ through $P2X_6$)

Although the molecular architecture of P2X receptors (see above) sets this family apart from all other ion channels, their functional properties are generally similar to the other two classes of "fast excitatory neurotransmitter receptors"—the nicotinic and the glutamate receptors. When extracellular ATP binds to specific amino acid residues in the ectodomain of the P2X receptor, a change in the conformation of the protein occurs within milliseconds and this structural alteration allows the influx of sodium ions from the outside concomitant with efflux of potassium ions from the inside. However, chloride or other anions are excluded; thus, the term cation-selective ion channel. This cation flux leads to plasma membrane depolarization and consequent excitation of nerve and muscle, or initiation of other signaling processes in nonexcitable cells. There is also appreciable influx of calcium ions with each P2X receptor allowing different levels of calcium to enter the cell; calcium entry through the $P2X_7$ receptor is several-fold higher than occurs at any other ionotropic (P2X, nicotinic or glutamate) receptor. When a continuous supply of ATP is presented to a cell expressing $P2X_1$ or $P2X_3$ receptors, the cation flux

TABLE I

Overview of Tissue Localization and Functional Role of Individual P2X Purinergic Receptors

Purinergic receptors	Tissue localization	Physiological role	Potential disease involvement
$P2X_1$	Vascular, visceral smooth muscle	Arteriolar vaso-constriction and genito urinary contractility	Male fertility
$P2X_2$	Autonomic neurons	Sympathetic drive	None implicated
$P2X_3$	Afferent neurons	Sensory perception	Neuropathic and visceral pain; bladder dysfunction
$P2X_4$	Epithelia and brain neurons	None identified	
$P2X_5$	Embryonic muscle spinal motor neurons	None identified	
$P2X_6$	Similar to $P2X_4$	None identified	
$P2X_7$	Immune cells	Release of IL-1β	Arthritis, irritable bowel syndrome

(or ionic current) fades away very rapidly (within a few hundred milliseconds) by a process termed desensitization. Desensitization does not occur, or is much slower at the other P2X receptors.

Activation of $P2X_7$ Ion Channels

The $P2X_7$ receptor is a most unusual ion channel in that it not only opens to allow bidirectional flux of cations in a manner similar to that described above for typical ionotropic receptors. However, it also dilates over several seconds to minutes to a size that allows the passage of molecules of either charge with size up to 900 Da. It is not known whether this is due to a true dilatation of the ion-passing pore region within the $P2X_7$ receptor protein itself, or whether the $P2X_7$ receptor couples to another protein which then transports the larger molecules. A further signaling event that is uniquely associated with $P2X_7$ receptor activation includes dramatic, rapid alterations in the cell cytoskeleton due to re-arrangement of the actin filaments within the cell. This causes dynamic membrane blebbing of the cell, visually appearing as though bubbles are continuously forming and retracting. The physiological significance of these membrane blebs are unknown but they have been associated with "programmed" cell death, or apoptosis. The intracellular carboxy-terminal amino acids of the $P2X_7$ receptor are required for the large pore formation and the membrane blebbing but not for its cation-selective ion channel function.

P2X Receptors and Sympathetic Neurotransmission ($P2X_1$ and $P2X_2$ Receptors)

$P2X_1$ receptors are highly expressed on vascular smooth muscle in the gastrointestinal (GI) tract and on visceral smooth muscle of the urogenital system, particularly the bladder, vas deferens, and ureter (Table I). $P2X_2$ receptors are equally highly expressed in the neurons that innervate these tissues, the sympathetic autonomic nerves. The functional role for $P2X_2$ receptors in autonomic neurotransmission is not understood, but $P2X_1$ receptors are now known to be

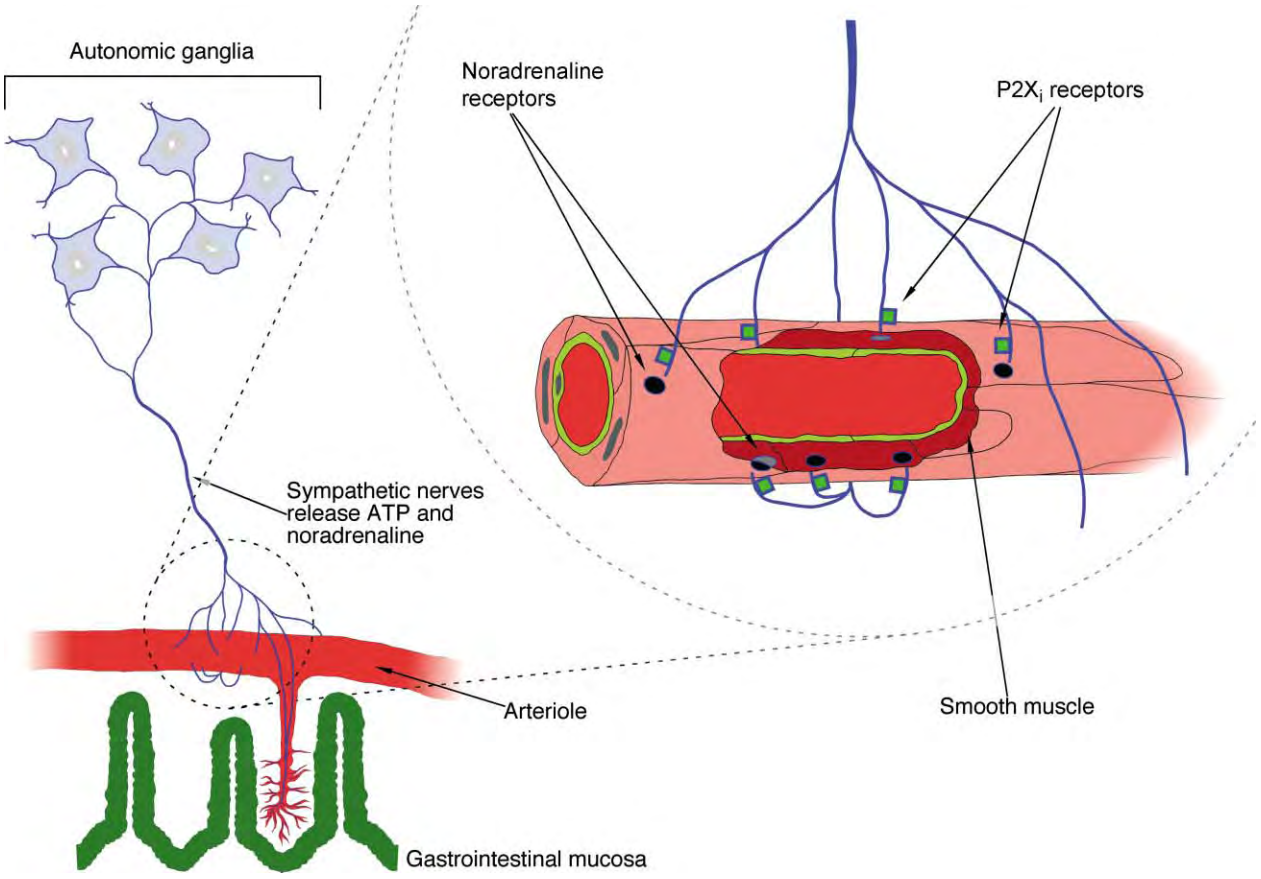

FIGURE 2 Sympathetic innervation to GI blood supply requires P2X receptors. Diagram illustrates the sympathetic nerves supplying the GI vasculature; the sympathetic nerves corelease noradrenaline and ATP. ATP activates postsynaptic $P2X_1$ receptors on the arteriolar smooth muscle to cause vasoconstriction. Noradrenaline released from these nerves acts only on presynaptic noradrenaline receptors which are present on the sympathetic nerve endings; the presynaptic action of noradrenaline alters the subsequent release of ATP.

the primarily, and in some cases, solely responsible for vasoconstriction or visceral smooth muscle contractions caused by sympathetic nerve activity. For example, male mice in which the $P2X_1$ receptor gene has been deleted are infertile, because the sympathetic nerve activity no longer causes smooth muscle of the vas deferens to contract. Thus, no sperm is released from the vas although all other aspects of ejaculation are unaltered. Similarly, in the GI vasculature, the vasoconstriction produced by sympathetic nerve activity is due to the release of ATP onto $P2X_1$ receptors on the vascular smooth muscle. In both of these cases, noradrenaline, which is the cotransmitter along with ATP, continues to be released and act effectively on its receptors. However, the noradrenaline released from these nerves acts on presynaptic noradrenaline receptors to alter the release of both noradrenaline and ATP, but it does not act on postsynaptic noradrenaline receptors present on the smooth muscle (Figure 2).

P2X Receptors and Sensory Pathways ($P2X_3$ and $P2X_{2/3}$)

Pain Pathways

ATP applied to sensory nerve terminals in the skin or tongue has long been known to elicit pain, specifically a tingling or burning sensation in humans. The molecular cloning and subsequent receptor localization studies revealed that the $P2X_3$ receptor subunit is preferentially localized to a specific subset of sensory afferent fibers which innervate skin and viscera. Most of these sensory fibers are nociceptors, i.e., they are activated by noxious stimuli. Both homomeric $P2X_3$ receptors and heteromeric $P2X_{2/3}$ receptors are found at presynaptic and postsynaptic sites in this pathway (Figure 3). When ATP is released as a result of tissue injury, gross visceral distention, or even excess sympathetic activation, it activates the $P2X_3$ and $P2X_{2/3}$ receptors on the nociceptor terminals and initiates excitatory flow to the dorsal horn neurons in the spinal cord. Here, P2X receptors play modulatory roles in further processing of painful stimuli. Presynaptic $P2X_2$ receptors are present on excitatory (glutamate) and inhibitory (glycine or γ-aminobutyrate, GABA) interneurons and can be activated by ATP released from the incoming primary afferents and also when it is coreleased with GABA from GABA interneurons. Activation of these presynaptic P2X receptors increases the further release of transmitters onto the doral horn neurons. There are also postsynaptic P2X receptors on the dorsal horn neurons which can be activated by the release of ATP from the GABA interneurons. These inhibitory and excitatory effects contribute to the "spinal" processing of pain information prior to transmission to central perception areas of the brain (Figure 3).

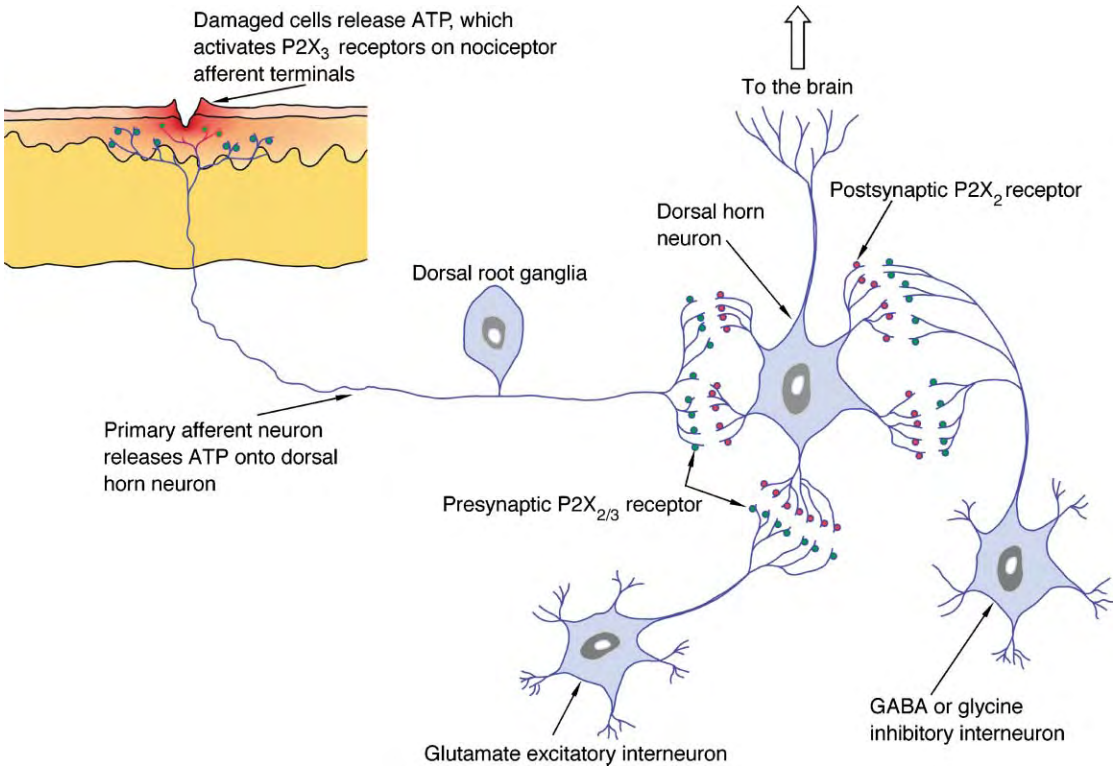

FIGURE 3 P2X receptors and pain pathways $P2X_2$, $P2X_3$, and $P2X_{2/3}$ receptors play a role in pain perception. See text for further description.

Afferent Reflex Pathways

P2X receptors are involved in the proper functioning of several visceral afferent reflexes; the micturation reflex is the best studied. The micturition reflex is initiated by bladder distention and subsequent contraction of the bladder and ureter smooth muscle. This distension releases ATP from the uroepithelium where it activates $P2X_3$ and/or $P2X_{2/3}$ receptors on the urothelial afferent nerve terminals to evoke neural discharge into spinal cord regions which, in turn, activate efferent parasympathetic nerves to bladder and ureter smooth muscle to complete the reflex loop.

P2X Receptors and Immune Cell Function ($P2X_7$)

$P2X_7$ receptors are most abundantly found on immune cells which become activated by tissue damage, inflammation, or infection, i.e., the so-called antigen-presenting cells of the immune system, primarily monocytes, and macrophage. Their synthesis and expression is increased in these cells when the immune response is triggered. Activation of $P2X_7$ receptors by ATP released from damaged cells at sites of inflammation or infection leads to the release of pro-inflammatory mediators (cytokines); the most important of these pro-inflammatory cytokines is interleukin-1β (IL-1β). IL-1β can produce fever, further inflammation, cell, and tissue death. Agents that may block its release are highly sought after with regard to treatment or prevention of diseases such as rheumatoid arthritis and inflammatory bowel disease, and intensive research efforts are currently underway to identify antagonists which selectively target $P2X_7$ receptors.

See Also the Following Articles

Cell Death by Apoptosis and Necrosis • Cytokines • Glutamate Receptors, Ionotropic • Glutamate Receptors, Metabotropic • Neurotransmitter Transporters • Nicotinic Acetylcholine Receptors • P2Y Purinergic Receptors

Glossary

cytokine A protein (usually interleukins or interferons) secreted by lymphoid cells that affects the activity of other cells and is important in controlling inflammatory responses.

dendrogram A diagram showing the relationships of items arranged like the branches of a tree.

exocytosis The release of a substance contained in a small sac (vesicle) within a cell by a process in which the membrane surrounding the vesicle fuses with the membrane forming the outer wall of the cell.

exon A discontinuous sequence of DNA that codes for protein synthesis and carries the genetic code for the final messenger RNA.

intron A length of DNA that is not expressed as an amino acid or messenger RNA.

ionotropic receptors Membrane receptors which are integral ion channels not requiring coupling via intracellular G proteins.

metabotropic receptors Membrane receptors which couple to heterotrimeric G proteins in order to produce an effect.

nociceptor A sensory nerve which subserves the perception of pain.

Further Reading

Burnstock, G. (2000). P2X receptors in sensory neurones. *British J. Anaesthesiol.* **84**, 476–488.

Le Novere, N., and Changeux, J. P. (2001). The ligand-gated ion channel database: An example of a sequence database in neuroscience. *Phil. Trans. Roy. Soc. London, B. Biolog. Sci.* **356**, 1121–1130.

North, R. A. (2002). Molecular physiology of P2X receptors. *Physiol. Rev.* **82**, 1013–1067.

Biography

Annmarie Surprenant is currently a Professor of Cellular Physiology at the University of Sheffield, United Kingdom. She has a long-standing history of research in the area of ion channel physiology. Her lab was the first to demonstrate that extracellular ATP is a synaptic transmitter in the nervous system and that ATP, not noradrenaline, was the neurotransmitter responsible for sympathetically mediated vasoconstriction in arterioles. These sets of findings led to her work over the past decade: the cloning and functional characterization of the ATP-gated P2X receptor-ion channels.

P2Y Purinergic Receptors

George R. Dubyak
Case Western Reserve University, Cleveland, Ohio, USA

P2Y receptors are intrinsic plasma membrane proteins that mediate functional responses of intact cells to extracellular nucleotides, including ATP, ADP, UTP, UDP, and UDP-glucose. P2Y receptors belong to the superfamily of G protein-coupled receptors (GPCR), an exceptionally large group of structurally and functionally related gene products that play critical roles in the transduction of signals between and among different types of cells. In response to the binding of extracellular nucleotides, P2Y receptors undergo conformational changes that facilitate their direct interaction with, and activation of, G proteins. In turn, the activated G proteins couple P2Y receptors to the regulation of enzymes and ion channels that facilitate generation of "second messengers" and intracellular signaling cascades used for the acute or chronic regulation of specific cellular functions. Appreciation of the physiological or pathological functions of P2Y receptors requires some understanding of the general mechanisms by which nucleotides are used as extracellular signaling molecules.

Extracellular Nucleotides as Signaling Molecules

In addition to their critical roles in intracellular energy metabolism and nucleic acid synthesis, nucleotides, such as ATP, and nucleosides, such as adenosine, play important roles as extracellular signaling molecules. Burnstock and his colleagues generated many of the initial hypotheses regarding the roles of purines in nonadrenergic, noncholinergic neurotransmission. They proposed that extracellular nucleotides and nucleosides are utilized for signal transduction at nerve endings in diverse tissues. Implicit in this concept of "purinergic" transmission or signaling was a requirement that ATP (or other nucleotides) be released and metabolized in a highly localized manner at sites of cell-to-cell communication. Given the emphasis on the role of purines in this neuronal signaling, initial characterization focussed on describing the release of nucleotide/nucleosides at neuron-to-neuron synapses, neuron-to-tissue varicosities, or the immediate locale of neuroendocrine cells. Such studies verified that neurons and neuroendocrine cells can release ATP via standard mechanisms involving exocytosis of nucleotides copackaged with biogenic amines or other neurotransmitters in specialized vesicles or granules.

However, subsequent research has resulted in the cloning and characterization of at least 15 distinct ATP/nucleotide receptor genes (including the P2Y receptors), four adenosine receptor genes, and a dozen different ectonucleotidase genes. Analysis of the expression of these genes revealed that most vertebrate cell types express one or more subtypes of nucleotide or nucleoside receptor along with one or more of the ectoenzymes used for metabolizing extracellular nucleotides. Because most cells lack direct proximity to nerve synapses or neuroendocrine cells, the identification of additional sources of extracellular nucleotides is a current area of investigation and speculation. Recent studies indicate that stressed or damaged cells in many tissues can locally release nucleotides via a variety of pathways ranging from irreversible cytolysis to nonlytic export through nucleotide-permeable channels. In turn, the released nucleotides activate autocrine or paracrine signaling cascades that permit those tissues to adapt to the particular stress or injury that precipitated release of the cellular nucleotides.

Regardless of the mechanisms by which ATP or other nucleotides are released from cells, their half-life within extracellular compartments is generally brief due to rapid catabolism by ectonucleotidases. Some of these ectoenzymes serially convert released nucleoside triphosphates (e.g., ATP) to their diphosphate (e.g., ADP) and monophosphate (AMP) forms. Other ectonucleotidases dephosphorylate the nucleoside monophosphates (e.g., AMP) to their corresponding nucleosides (e.g., adenosine). These nucleosides can be reaccumulated and reconverted to intracellular nucleotides via highly conserved nucleotide salvage pathways. In the case of adenosine, nucleosides can additionally function as agonists for G protein-coupled nucleoside receptors that are distinct from the P2Y nucleotide receptors. Thus, the local release of ATP may initially activate ATP-selective P2Y receptor subtypes. Although this hydrolysis of ATP to ADP by ecto-ATPases would act to terminate signaling by these particular P2Y subtypes,

this same extracellular metabolic reaction would result in activation of ADP-selective P2Y receptor subtypes. Further metabolism to adenosine might result to activation of G protein-adenosine receptors in same or adjacent cells. In these ways, ATP release in intact tissues can trigger the serial activation of multiple P2Y and adenosine receptor subtypes to generate complex patterns of positive or negative feedback among the various cell types that comprise the tissue. As a further complication, many cells export nucleoside diphosphokinases that catalyze transphosphorylation reactions between the various extracellular nucleoside tri- and diphosphates. Thus, released ATP may additionally drive the phosphorylation of ambient UDP to locally generate UTP that is a selective agonist for yet other P2Y receptor subtypes.

General Structure of the P2Y Receptors

As members of the GPCR superfamily, all P2Y receptors are intrinsic membrane proteins that consist of a single polypeptide chain with certain invariant structural domains. These include: (1) an extracellular amino terminal tail; (2) seven transmembrane-spanning segments (usually α-helices); (3) three short extracellular loops and three variably sized intracellular loops that connect transmembrane segments; and (4) an intracellular carboxyl terminal tail. The exact protein domains of P2Y receptors that facilitate selective recognition and binding of the extracellular nucleotide agonists have not been identified as yet. Significantly, no single P2Y domain contains amino acid sequences similar to the well-defined nucleotide-binding sites of the many intracellular proteins that interact with ATP (e.g., ATPases, protein kinases, nucleic acid polymerases).

Functional Classification of the P2Y Receptors

Genes encoding P2Y receptors have been identified in the genomes of all vertebrate species examined thus far. In contrast, no obvious P2Y receptor orthologues are apparent in the completely sequenced genomes of the insect, *Drosophila melanogaster*, or the nematode worm, *Caenorhabditis elegens*. At present, genes encoding eight distinct P2Y receptor subtypes have been characterized in a broad range of tissues and cell types from vertebrate organisms. These subtypes can be classified based either on their selective pharmacological recognition of different nucleotides or on their selective functional coupling to particular classes of heterotrimeric G proteins. Table I summarizes both the pharmacological and functional properties of the eight P2Y receptor subtypes.

Based on their functional coupling to G proteins, effector proteins, and second messenger cascades, P2Y receptors can be broadly subdivided into three major groups. The P2Y1, P2Y2, P2Y4, and P2Y6 receptor subtypes predominantly couple to G_q-family G proteins with consequent activation of phosphatidylinositol-specific phospholipase C effector (PI-PLC) enzymes resulting in accumulation of inositol trisphosphate, diacylglycerol, Ca^{2+} as second messengers. The P2Y12, P213, and P2Y14 subtypes activate G_i-family G proteins. As a result, stimulation of these latter receptors most often leads to inhibition of adenylyl cyclase effector enzymes and reduced intracellular levels of cyclic AMP. However, depending on cellular

TABLE I

Receptor subtype	G protein–effector cascade	Selectivity for physiological nucleotide agonists	Tissue/cellular expression
P2Y1	Gq → PI-PLC	ADP > ATP ≫ UDP, UTP	Platelets, Blood Vessels, Brain
P2Y2	Gq → PI-PLC	ATP = UTP ≫ ADP, UDP	Airways, Exocrine Glands, White Blood Cells, Blood Vessels, Brain
P2Y4	Gq → PI-PLC	UTP ≫ ATP, UDP, ADP (human) UTP = ATP ≫ UDP, ADP (rat, mouse)	Small Intestine, Inner Ear
P2Y6	Gq → PI-PLC	UDP > UTP > ADP ≫ ATP	Gallbladder, Airway
P2Y11	Gq → PI-PLC *and* Gs → AC	ADP > ATP ≫ UDP, UTP	Exocrine Glands, Kidney, White Blood Cells
P2Y12	Gi → AC/others	ADP > ATP ≫ UDP, UTP	Platelets, Brain Astrocytes
P2Y13	Gi → AC/others	ADP > ATP ≫ UDP, UTP	Brain Astrocytes
P2Y14	Gi → AC/others	UDP-glucose ≫ UTP, ATP, UDP, ADP	White Blood Cell Precursors, Stem Cells

background, these Gi-coupled P2Y receptor subtypes may also stimulate the activity of G protein-regulated K^+ channels and/or inhibit activity of N-type voltage-gated Ca^{2+} channels. Finally, the P2Y11 receptor represents a subtype that can couple to both G_q- and G_s-dependent signaling pathways; the activation of G_s allows P2Y11 receptors stimulate adenylyl cyclase effector enzymes and thereby induce accumulation of cyclic AMP. Thus, activation of the different P2Y receptor subtypes can variously trigger rapid changes in Ca^{2+}, cyclic AMP, lipid second messengers, and plasma membrane potential. In turn, these acute signals can be integrated within cell-specific transduction networks to regulate particular protein kinases, protein phosphatases, proteases, and transcription factors.

Pharmacological Classification of P2Y Receptors

P2Y receptors can also be categorized by their pharmacological selectivity for particular nucleotide agonists. The P2Y1, P2Y12, and P2Y13 receptors exhibit very high selectivity for ADP over ATP and are virtually insensitive to non-adenine nucleotides. The P2Y2, P2Y4, and P2Y6 subtypes can be effectively activated by uridine nucleotides albeit with subtype-selective preferences. P2Y2 receptors show high affinity for UTP and ATP, but not the corresponding diphosphates. P2Y4 receptors are most potently stimulated by UTP over ATP (but this is species-dependent), while P2Y6 receptors exhibit a preference for UDP. In general, P2Y11 receptors are activated by ADP or ATP, and less effectively by non-adenine nucleotides. The P2Y14 subtype, the most recently identified member of the P2Y family, exhibits a very high selectivity for sugar-conjugates of UDP, such as UDP-glucose. Given the complex and overlapping affinities of the P2Y subtypes for naturally occurring nucleotides, considerable effort is being directed toward generation of synthetic nucleotide agonists and non-nucleotide antagonists that selectively target particular P2Y subtypes. Such subtype-selective reagents may have high potential utility as therapeutic agents in diseases that involve hyperfunctional or hypofunctional P2Y receptors.

Important Physiological or Pathological Functions of P2Y Receptor Subtypes

Understanding of the most important physiological roles for P2Y receptors has been limited by: (1) the relatively recent identification of most P2Y receptor subtypes (post 1995); (2) the current paucity of subtype-selective drugs; and (3) the rather broad expression of P2Y receptors in most tissue types. However, gene-targeting approaches have been recently used to generate "knock-out" mice that lack the expression of P2Y1, P2Y2, P2Y4, or P2Y12 receptors. These mice (or tissues from the mice) exhibit significant deficits in several critical biological responses.

Mice lacking either the P2Y1 or P2Y12 receptor are characterized by abnormalities in the blood-clotting response (also known as hemostasis) that result in prolonged bleeding times. This reflects the synergistic roles of the P2Y1 and P2Y12 receptors in mediating the aggregation of platelets (the key blood cell type in the clotting reaction) in response to ATP/ADP released from damaged blood vessels. Because platelets also release large amounts of ATP/ADP during aggregation induced by other hemostatic factors (such as thrombin), P2Y1 and P2Y12 play additional roles in amplifying and extending the overall blood-clotting response. However, inappropriate platelet aggregation (thrombosis) can lead to interruption of normal blood flow (ischemia) to critical organs, such as the brain or heart, and thereby contribute to acutely life-threatening conditions including stroke and heart attack. For this reason, drugs that specifically block or antagonize P2Y1 and/or P2Y12 receptors are currently being tested for the treatment of thrombotic diseases in humans.

Analyses of other knockout mice strains have revealed important roles for the P2Y2 receptors that are highly expressed in airway cells and the P2Y4 receptors expressed in the jejunal section of the small intestine. Multiple P2Y receptor subtypes are expressed in the epithelial cells from organs such as the airways, lungs, kidneys, and intestines. The major function of epithelial cells and tissues is to act as both a barrier and selectively permeable interface between very different biological compartments. For example, airway epithelial cells comprise an interface between the inspired air compartment (which contains microbes, small particles, and volatile compounds from the outside environment) and the blood compartment. In addition to physically blocking the entry of these airborne particles, microbes, and compounds into the blood, airway epithelial cells secrete water, salt, mucus, and other protective proteins onto their extracellular surface that directly faces the inspired air compartment. While the secreted mucus solution acts to trap the microbes and particles, ciliated protrusions that extend from the epithelial cells beat in a synchronized manner to push the mucus solution – plus the entrapped microbes and particles – back to the nose and upper throat for eventual removal by sneezing or coughing. Activation, by ATP or UTP, of the P2Y2 receptors in different airway epithelial cells can coordinately regulate: (1) the secretion of the water, different salts, and mucus in sufficient amounts to generate

mucus solutions with appropriate viscosity, fluidity, and composition; and (2) the frequency and direction of the ciliary beating required for the appropriate retrograde flow of the mucus back to the upper airways. In airways from the P2Y2 receptor knockout mice, these important epithelial functions are not appropriately regulated. Analysis of small intestine function in P2Y4 receptor–receptor mice has indicated a similar role for this P2Y subtype in the regulation of salt and fluid secretion by intestinal epithelial cells.

Future studies of additional organ- and tissue-specific functions in mice lacking these and other P2Y receptor subtypes will undoubtedly reveal other important *in vivo* roles for these receptors. Insights from these animal studies, coupled with the development of subtype-selective antagonists, should facilitate delineation of how these receptors function in human physiology and pathology.

See Also the Following Articles

Adenylyl Cyclases • G Protein Signaling Regulators • Neurotransmitter Transporters • P2X Purinergic Receptors

Glossary

agonist A molecule that binds to a receptor resulting in functional activation of the receptor.

antagonist A molecule that binds to a receptor and keeps the receptor in a functionally inactive state.

effector protein An intracellular protein, such as an enzyme or ion channel, whose activity is regulated by interaction with G proteins. Effector proteins regulate the production of second messenger signals.

G protein An intracellular protein that becomes active when it binds GTP and becomes inactive when it hydrolyzes the bound GTP to GDP. G proteins act as signal transduction proteins that couple cell surface receptors to the regulation of intracellular effector proteins.

G protein-coupled receptor (GPCR) A cell surface receptor protein for an extracellular signaling molecule; GPCR reversibly interact with G proteins to activate intracellular signal transduction pathways. There are thousands of different GPCR that selectively bind a wide variety of extracellular signaling molecules including many hormones and neurotransmitters.

P2Y receptors A family of related G-protein coupled receptors that become active when bound to extracellular nucleotides such as ATP, ADP, or UTP.

second messenger A small intracellular molecule that is transiently formed in response to the activation of an effector protein by a cell surface receptors, such as a GPCR. Formation of the second messenger acts to relay the signal from the cell surface receptor to the interior of the cell.

Further Reading

Abbracchio, M. P., Boeynaems, J.-M., Barnard, E. A., Boyer, J. L., Kennedy, C., Miras-Portugal, M. T., King, B. F., Gachet, C., Jacobson, K. A., Weisman, G. A., and Burnstock, G. (2003). Characterization of the UDP-glucose receptor (re-named here the P2Y14 receptor) adds diversity to the P2Y receptor family. *Trends Pharmacol. Sci.* **24**, 52–55.

Bhatt, D. L., and Topol, E. J. (2003). Scientific and therapeutic advances in antiplatelet therapy. *Nat. Rev. – Drug Discovery* **2**, 15–28.

Dubyak, G. R. (2003). Knock-out mice reveal tissue-specific roles of P2Y receptor subtypes in different epithelia. *Mol. Pharmacol.* **63**, 773–776.

Lazarowski, E. R., Boucher, R. C., and Harden, T. K. (2003). Mechanisms of release of nucleotides and integration of their actions as P2X-and P2Y-receptor activating molecules. *Mol. Pharmacol.* **64**, 785–795.

Ralevic, V., and Burnstock, G. (1998). Receptors for purines and pyrimidines. *Pharmacol. Rev.* **50**, 413–492.

Von Kugelgen, I., and Wetter, A. (2000). Molecular pharmacology of P2Y receptors. *Naunyn-Schmiedeberg's Arch Pharmacol.* **362**, 310–323.

Zimmermann, H. (2000). Extracellular metabolism of ATP and other nucleotides. *Naunyn-Schmiedeberg's Arch Pharmacol.* **362**, 299–309.

Biography

George R. Dubyak is a Professor in the Department of Physiology and Biophysics at the Case School of Medicine of Case Western Reserve University, Cleveland. His broad research interest is in the field of signal transduction biology with particular focus on the roles of extracellular nucleotides in signal transduction during inflammation and regulation of cardiovascular function. He holds a Ph.D. in physiology from the University of Pennsylvania and received post-doctoral training in biophysics at that university.

p53 Protein

Jamie Hearnes and Jennifer Pietenpol
Vanderbilt University, Nashville, Tennessee, USA

p53 is a tumor suppressor gene that is mutated in over half of all human cancers. The tumor suppressive functions of p53 are dependent, in part, upon its activity as a transcription factor. This protein binds DNA in a sequence-specific manner to regulate the expression of select genes involved in a range of cellular processes including growth arrest, apoptosis, DNA repair, senescence (irreversible growth arrest), and angiogenesis (new blood vessel formation). The p53 protein is activated in response to various cellular stresses, and functions to suppress the transformation of a normal cell to a cancer cell. The p53 protein will continue to be a focus of cancer-based research as it plays a pivotal role in suppressing tumorigenesis.

p53 Functional Domains

The p53 protein was originally identified in 1979, and its name is derived from the apparent molecular weight of the protein (p53 = protein of 53 kDa). This protein consists of 393 amino acids and is divided into three functional domains (Figure 1).

Transcriptional Activation Domain

The transactivation domain is located at the amino terminus of the protein sequence (amino acids 1–73). Numerous proteins can bind to this region of the protein to regulate the function of p53. This region of the protein is constitutively and inducibly phosphorylated, which affects the protein's stability and activity.

DNA-Binding Domain

The central region of the p53 protein is the DNA-binding domain (amino acids 100–293). A majority of tumor-derived p53 mutations occur in the DNA-binding domain. The residues most commonly mutated in the DNA-binding domain either directly contact the DNA or are required for the structural integrity of the protein. Since p53 primarily functions as a transcription factor, these mutations result in a loss of function of the protein.

Oligomerization Domain

The carboxy terminus of the p53 protein (amino acids 293–393) contains an oligomerization domain, which is required for the formation of transcriptionally active dimers and tetramers. The oligomerization domain also contains nuclear localization and export sequences that are required for transport into and out of the nucleus, respectively. The carboxy terminus is also post-translationally modified in a regulatory manner.

p53-Mediated Signaling

p53 functions as a sequence-specific transcription factor regulating select genes (target genes) that are involved in numerous signaling pathways, including cell cycle progression, apoptosis, senescence (irreversible growth arrest), DNA repair, and angiogenesis (new blood vessel formation) (Figure 2). These are the same pathways that become deregulated during cancer progression. The p53 consensus DNA-binding site consists of 2 copies of the DNA sequence RRRCWWGYYY which are separated by a 0–13 base spacer region (R = A/G, W = A/T, Y = T/C). This binding site is present in a majority of p53 target gene regulatory regions. The degeneracy of the consensus DNA-binding site at 8 of the 10 bases is thought to contribute to the selectivity of p53 towards certain genes in response to various stresses. p53 can serve as a transcriptional activator or repressor, depending on the specific gene being regulated.

Growth Arrest and Apoptosis

Human cells are continuously exposed to external agents as well as internal agents that can induce cell damage. Eukaryotic cells have evolved a series of surveillance pathways termed cell-cycle checkpoints to ensure that cells copy and divide their genomes with high fidelity during each replication cycle. These checkpoint signaling pathways execute several tasks: rapid induction of cell-cycle delay, activation of DNA repair, maintenance of cell-cycle arrest until repair is complete, reinitiation of cell cycle progression after completed

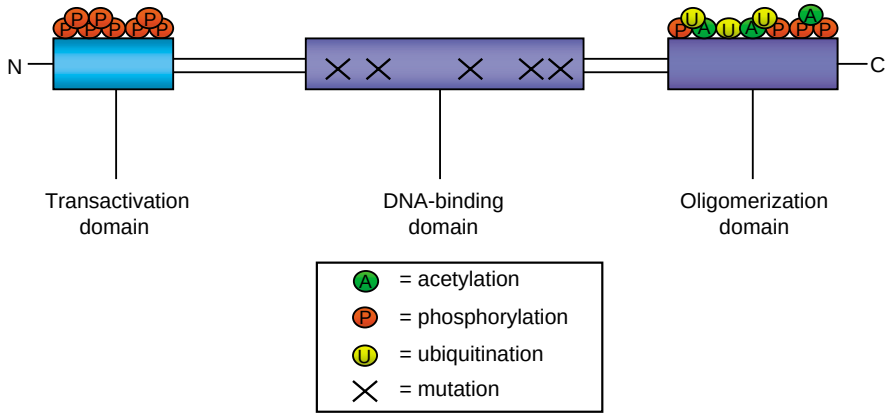

FIGURE 1 Functional domains of p53 are affected by post-translational modifications and mutations. The amino terminus contains the transactivation domain, which becomes phosphorylated in response to certain types of cell damage. The central region of the protein contains the DNA-binding domain that is very commonly mutated in human tumors. The oligomerization domain, which mediates the formation of p53 dimers and tetramers, is present at the carboxy terminus of the protein, and can be modified post-translationally by phosphorylation, acetylation, and ubiquitination.

repair or initiation of apoptosis if the damage is irreparable. These checkpoints provide a fail-safe mechanism by which cells are repaired or eliminated before the damaged DNA is transferred to the daughter cells. Loss of normal cell-cycle checkpoint signaling is a hallmark of tumor cells, and p53 is the most frequently altered cell-cycle checkpoint signaling molecule. One of the major functions of the p53 tumor suppressor protein is to modulate cellular responses to stress and induce cell-cycle arrest or death, as appropriate (Figure 2). Once a cell has been stressed or damaged, p53 initiates cell cycle arrest allowing time for the damage to be repaired or for the stress to dissipate. p53 halts cell growth by selectively activating certain target genes, including $p21^{Waf1/Cip1}$, a protein that inhibits molecules required for cell-cycle progression. If cell damage is extensive and cannot be repaired or the stress is prolonged, the cells may undergo p53-dependent apoptosis. p53 is responsible for both the activation of proapoptotic genes as well as the repression of antiapoptotic genes, and the array of p53-regulated genes involved in apoptosis is quite extensive. Although a given cell in the human body would not benefit from undergoing apoptosis, this process is sometimes necessary for the benefit of the whole organism, to prevent the development of cancer.

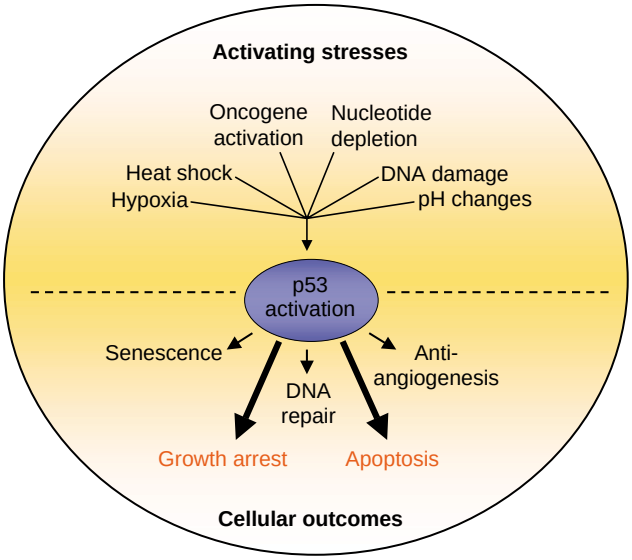

FIGURE 2 p53 signaling pathways. p53 is responsive to many cellular insults (activating stresses) that affect numerous pathways yielding various cellular outcomes. The two primary most well-characterized outcomes of p53 activation are growth arrest and/or apoptosis (thick arrows). However, p53-regulated genes also take part in numerous other signaling pathways (thin arrows).

Other Pathways Regulated by p53

p53 function is not limited to growth arrest and apoptosis. p53 also regulates genes involved in DNA repair, senescence, and angiogenesis (Figure 2). Although the relationships between p53 and these various pathways are not completely understood, future discoveries of novel p53 target genes and protein interactions will further elucidate the signaling networks in which p53 is involved.

p53 Regulation

p53 acts immediately after cell stress occurs, and thus, it is critical that the regulatory mechanism for this protein be fast acting. Following stress, the levels of many proteins in the cell are dictated by transcriptional regulation of the genes encoding the proteins; however, this is not the primary mechanism for p53. Instead, p53

regulation occurs predominantly at the protein level, which allows for rapid induction of p53 activity.

Activating Stresses

In a normal unstressed cell, the p53 protein is present at low levels due to the short half-life of the protein. However, p53 protein levels increase if the cell experiences a stress. There are numerous types of cellular stress and damage that can activate the p53 protein including lack of oxygen (hypoxia), elevated/lowered temperatures (heat/cold shock), DNA damage, metabolic changes, nucleotide depletion, pH changes, and oncogene activation (Figure 2). Cellular stresses trigger signaling pathways that converge on p53, resulting in stabilization and activation of the protein.

Post-translational Modifications

Post-translational modification events are dynamic processes that change protein stability and activity by altering protein–DNA and protein–protein interactions. Depending on the stress, p53 is post-translationally modified with various moieties resulting in diverse effects on the protein's stability, activity, and specificity of DNA binding (Figure 1).

Ubiquitination

Ubiquitination is the addition of ubiquitin molecules to lysine residues of a protein. Following ubiquitination, most proteins are targeted to the 26S proteosome for degradation. This is the mechanism used to rapidly turn over the p53 protein. The ubiquitination system involves numerous proteins, but the specificity of the system depends on the specific E3 ubiquitin ligase enzyme employed, which attaches an ubiquitin molecule to the correct substrate. The mouse double minute 2 (Mdm2) protein is the ligase used to ubiquitinate p53.

Phosphorylation

Phosphorylation of proteins at serine, threonine, and/or tyrosine residues is a common regulatory mechanism in the cell. p53 is phosphorylated at select serine and threonine amino acids in the amino- and carboxy-terminal regions of the protein in response to select cellular stresses. These stresses include exposure of cells to byproducts of cellular metabolism, ultra-violet (UV) radiation, and drugs used in cancer therapy. Numerous kinases have been identified that phosphorylate p53. The specific kinase activated is dependent upon the stress, and each kinase is responsible for phosphorylating a distinct residue(s) on the protein. Phosphorylation of the p53 protein can yield numerous outcomes including protein stabilization, increased transcriptional activity, and alterations in subcellular localization.

Acetylation

Acetylation is a modification that can occur on lysine residues of a protein. Acetylation of a transcription factor can affect the protein's transcriptional activity, either positively or negatively, depending on the specific factor. In response to DNA damage, known transcriptional coactivators acetylate p53 at certain carboxy-terminal lysines, however, the exact role of this modification on p53 activity is not well established.

Protein–Protein Interactions

There are numerous proteins that regulate p53 through a physical interaction. Many of these proteins are involved in post-translationally modifying the protein, but there are also other mechanisms of p53 protein regulation that involve protein–protein interactions. These interactions can both positively and negatively regulate p53.

Mdm2 is a protein that can bind to and ubiquitinate p53, as mentioned above. This p53–Mdm2 interaction results in two outcomes. The first is that Mdm2 inhibits the transcriptional activity of p53 by binding to the amino-terminal transactivation domain of the p53 protein, blocking other interactions that are necessary for p53 activity. The second outcome is p53 ubiquitination, export from the nucleus, and degradation. Mdm2 is responsible for maintaining p53 at low levels in a normal unstressed cell, as well as attenuating the p53 response after stress. Interestingly, Mdm2 is up-regulated by p53 in response to cellular insults, forming an autoregulatory negative feedback loop, which is the primary mechanism of negative regulation for p53.

Viral proteins can also interact with the p53 protein to affect its activity. For instance, the human papilloma virus (HPV) E6 proteins (type 16 and 18) negatively regulate p53 in a manner similar to Mdm2. The E6 protein binds to a protein complex containing p53, which leads to p53 ubiquitination and subsequent degradation.

In addition to protein interactions that negatively regulate p53 activity, there are interactions that have a positive impact on the protein as well. One example of this is the human $p14^{ARF}$ protein. This protein is a tumor suppressor activated in response to oncogenic stimuli. Once activated, $p14^{ARF}$ binds to the p53–Mdm2 complex, which disables Mdm2. This protects p53 from Mdm2-mediated degradation, resulting in p53 activation and subsequent growth suppression or apoptosis of cells that contain activated oncogenes.

p53 Family Members

p53 is a member of a newly identified family of related proteins that includes p73 and p63. p73 was discovered in 1997, with p63 quickly following in 1998. The three family members exhibit a high degree of sequence similarity and conserved functional domains. However, unlike p53 it appears that the functions of p73 and p63 are not restricted to tumor suppression. p73 is involved in neuronal signaling, immune cell apoptosis, and inflammation. p63 is involved in maintaining regenerative cells, and is essential for the normal development of numerous human tissues including the skin, breast, and prostate.

Cancer Therapeutics Involving p53

Since p53 is mutated in over 50% of all human tumors, many therapeutic strategies have been devised to target the p53 signaling pathway, including: (1) transfer of normal p53 genes into mutant p53-containing cancer cells, (2) introduction of small molecules that convert mutant p53 proteins to proteins that are structurally normal in function, (3) identification of small molecules that mimic the function of p53 target genes, and (4) disruption of protein–protein interactions that negatively regulate p53 activity. Due to its central role in preserving genetic stability, deciphering p53 function, regulation, and signaling pathways will continue to be a major focus of cancer-based research.

See Also the Following Articles

Cell Cycle: DNA Damage Checkpoints • Cell Death by Apoptosis and Necrosis • DNA Base Excision Repair • Transcription-Coupled DNA Repair, Overview

Glossary

apoptosis Programmed cell death; an active form of cell suicide.
cell cycle The ordered set of events by which a cell grows and divides.
cell-cycle checkpoint Point in the cell-division cycle where progression through the cycle can be halted until conditions are suitable for the cell to proceed to the next stage.
oncogene A gene whose product has the ability to transform a normal cell into a cancer cell.
tumor suppressor A gene that negatively regulates cell division and when lost allows the cell to progress through the cell cycle in an unrestricted manner.

Further Reading

Alberts, B., Bray, D., Lewis, J., Raff, M., Roberts, K., and Watson, J. D. (eds.) (1994). *Molecular Biology of the Cell*, 3rd edition. Garland Publishing, New York.
Appella, E., and Anderson, C. W. (2001). Post-translational modifications and activation of p53 by genotoxic stresses. *Eur. J. Biochem.* **268**, 2764–2772.
El-Deiry, W. S. (1998). Regulation of p53 downstream genes. *Semin. Cancer Biol.* **8**, 345–357.
Giaccia, A. J., and Kastan, M. B. (1998). The complexity of p53 modulation; emerging patterns from divergent signals. *Genes Dev.* **12**, 2973–2983.
Lane, P. L., and Lain, S. (2002). Therapeutic exploitation of the p53 pathway. *Trends Mol. Med.* **8**, S38–S42.
Lewin, G. (2000). *Genes VII*. Oxford University Press, New York.
May, P., and May, E. (1999). Twenty years of p53 research: Structural and functional aspects of the p53 protein. *Oncogene* **18**, 7621–7636.
Stewart, Z. A., and Pietenpol, J. A. (2001). p53 signaling and cell cycle checkpoints. *Chem. Res. Toxicol.* **14**, 243–263.
Yang, A., and McKeon, F. (2000). p63 and p73: p53 mimics, menaces, and more. *Nat. Rev. Mol. Cell Biol.* **1**, 199–207.

Biography

Jennifer A. Pietenpol, Ph.D., is a Professor of Biochemistry at Vanderbilt University and Associate Director for Basic Research Programs of the Vanderbilt-Ingram Cancer Center. Pietenpol received her Ph.D. in cell biology from Vanderbilt University and pursued postdoctoral studies at Johns Hopkins University. Pietenpol's research is focused on tumor suppressor signaling pathways, with particular focus on p53. A goal of her research is to define molecular changes in tumor cells that can be used as targets for therapeutic intervention.

Jamie Hearnes is a graduate student at Vanderbilt University and will receive her Ph.D. from the Department of Biochemistry. Her research in the Pietenpol Laboratory focuses on the identification of novel p53 target genes.

p70 S6 Kinase/mTOR

Christopher G. Proud
University of Dundee, Dundee, UK

p70 S6 kinase is a protein kinase that is activated by insulin and other stimuli, and which phosphorylates ribosomal protein S6, a component of the small (40S) ribosomal subunit in animal cells. Mammalian target of rapamycin (mTOR) is involved in regulating p70 S6 kinase, and other proteins, and serves to integrate hormonal and nutritional signals.

p70 S6 Kinase

This family of enzymes phosphorylates a series of seryl residues in the C-terminus of S6. It was identified in the 1980s following early work showing that insulin, and a range of other stimuli, led to increased phosphorylation of S6. The p70 S6 kinases were some of the earliest insulin- and mitogen-stimulated kinases to be studied in any detail, largely because the relatively high abundance of S6 means that it appears as a major insulin-stimulated phosphoprotein.

p70 S6 kinases are now believed to be the physiologically relevant S6 kinase. Confusion is possible here however, as a second type of kinase, $p90^{RSK}$, can also phosphorylate S6 *in vitro*. This gives rise to the abbreviation RSK (ribosomal protein S6 kinase) although it is generally thought that $p90^{RSK}$ is not a physiologically relevant S6 kinase. An important reason for favoring the p70 S6 kinases is that their activation and the phosphorylation of S6 are both blocked by rapamycin, while this drug has no effect on $p90^{RSK}$.

Different Isoforms of p70 S6 Kinase Exist in Mammals

In mammals, there are two genes encoding closely related kinases, both of which phosphorylate S6. Here, they are termed p70α S6 kinase (also called S6K1) and p70β S6 kinase (alternative name, S6K2). The overwhelming majority of studies have concerned the α-isoform, which was discovered much earlier than the β. However, the recent studies on S6K2 suggest that it is regulated in a way broadly similar to S6K1. Further diversity in this family is created by alternative splicing: in the cases of p70α and p70β S6 kinases, this gives rise to additional isoforms (p70α1 and p70β1) which are extended at the N-termini (see Figure 1: the shorter versions are termed p70α2 and p70β2). This extension contains a likely nuclear localization signal, which could mediate the transfer of the longer isoforms into the nucleus.

All four isoforms contain a catalytic domain near the N terminus and a regulatory domain towards the C terminus. Phosphorylation within the catalytic domain and at several sites in the C terminus leads to the activation of the S6 kinases (see Figure 1).

p70 S6 Kinase is Activated by a Variety of Stimuli

p70 S6 isoforms are activated by insulin, serum and mitogens, and also by a range of other stimuli including ones that work through G-protein-coupled receptors. A common feature of these stimuli is that they increase the cell's overall rate of protein synthesis. In all cases, activation of p70α S6 kinase involves increased phosphorylation of the protein (Figure 1), and is blocked by rapamycin, indicating a key role for mTOR in activation.

Less effort has so far been devoted to studying the more recently discovered p70β S6 kinase, but the available information suggests that it is also likely to be activated by a wide range of stimuli.

Roles of Nutrients and mTOR in Regulating p70 S6 Kinase

In a number of types of cells, p70α S6 kinase cannot be activated if the cells are deprived of amino acids. Amino acid starvation also results in a fall in the basal activity of the kinase. Readdition of amino acids results, within minutes, in increased basal activity and restoration of the ability of insulin, for example, to activate p70α S6 kinase. This suggests that amino acids provide an important input into the regulation of p70α S6 kinase, and this is discussed further below. The branched-chain amino acid leucine is the most effective amino acid in most cell types tested.

In some cell types, such as hepatoma cells and primary fat cells, the presence of external amino acids

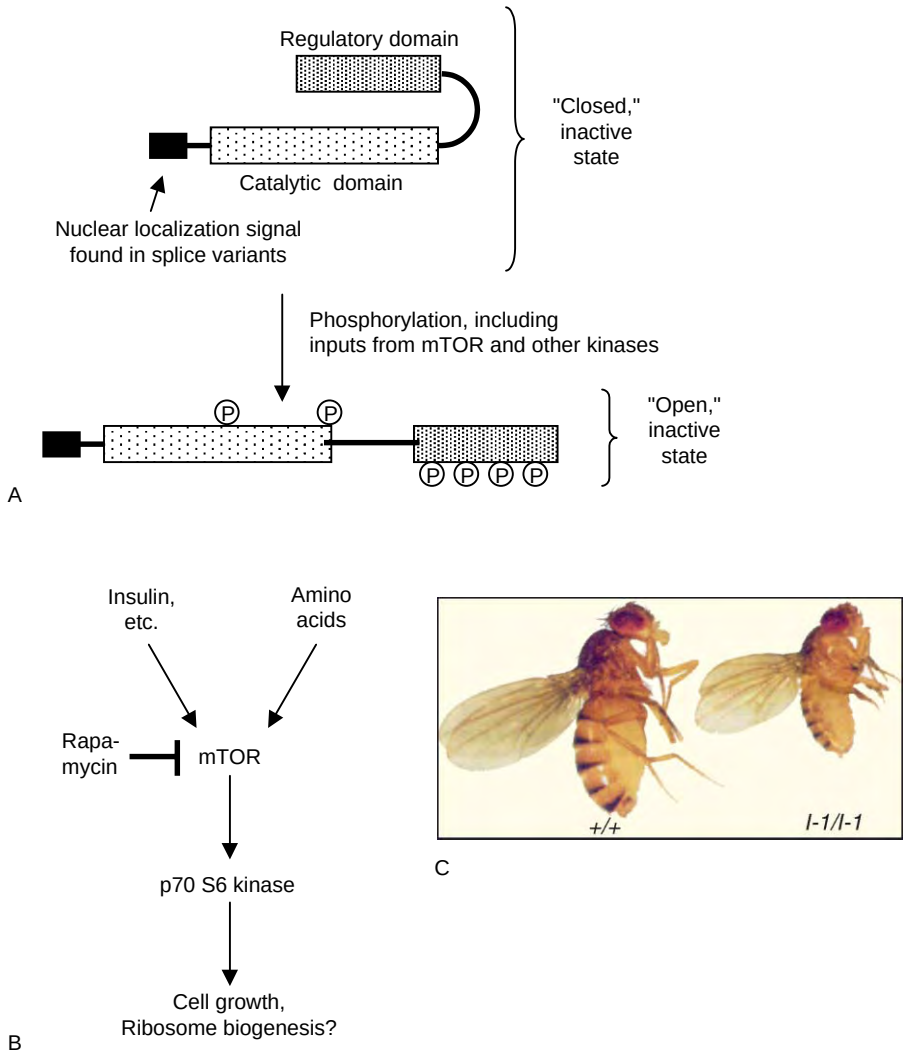

FIGURE 1 p70 S6 kinase. (A) This schematic figure indicates the arrangement of the enzyme into catalytic and regulatory domains. Phosphorylation of the regulatory domain allows the catalytic domain to be phosphorylated too, leading to activation of the enzyme. Phosphorylation involves several kinases and input from mTOR. For further details, see text. (B) Hormones, such as insulin (also growth factors), and amino acids positively regulate p70 S6 kinase via mTOR (its activation is therefore prevented by rapamycin). It has a clear role in regulating cell size, possibly through the control of ribosome biogenesis. (C) Genetic knockout of S6 kinase in *Drosophila melanogaster* dramatically decreases the size of the animals, with all body parts apparently affected to a similar degree: + /+ indicates a wild-type fly, while l-1/l-1 denotes one in which the S6K gene has been disrupted. Reproduced from Montagne, J., Stewart, M. J., Stockes, H., Hafer, E., Kozma, S. C., and Thomas, G. (1999). Drophila S6 kinase: a regulator of cell size. *Science* 285, 2126–2129. Copyright 1999 American Association for the Advancement of Science.

in the medium is not required for regulation of p70α S6 kinase. It is likely that this reflects the presence, within these cells, of sufficient amino acids to support regulation of this enzyme, rather than a fundamental difference in its control in these cells.

Mechanisms Involved in the Activation of p70 S6 Kinase

As noted above, the activation of S6 kinase involves its phosphorylation at several positions. One lies within the catalytic domain and most of the others lie in the C-terminal regulatory domain. It is possible that the C-terminal region blocks access to the catalytic domain, and that this block is alleviated by phosphorylation of the C-terminal sites. The kinases acting at these sites have not been conclusively identified. Since rapamycin blocks the phosphorylation of many sites in p70α S6 kinase, it is conceivable that the relevant kinases are regulated through mTOR, or that mTOR directly phosphorylates p70α S6 kinase, although other explanations are also possible. The proposed mechanism by which p70α S6 kinase is activated is illustrated in Figure 1.

p70 S6 Kinase Plays a Key Role in Growth Control

Genetic studies have revealed a key role for p70 S6 kinases in growth control. The fruit fly, *Drosophila melanogaster*, has just a single p70 S6 kinase gene. Disruption of this gene, to create flies lacking S6 kinase activity, has a dramatic effect on the growth of the flies. S6 kinase-deficient flies are markedly (~50%) smaller than wild-type flies (Figure 1C) and strikingly, this is due primarily to a defect in cell size rather than a reduction in cell number. The mutant flies contain the same number of cells as wild-type flies, but the sizes of these cells are decreased proportionately so that the mutant flies are morphologically very similar to the wild-type flies. This demonstrates a decoupling of cell size from cell proliferation, and implies a key role for S6 kinase in the poorly understood processes that determine cell size. This is discussed further below. A similar effect is observed in mice in which the p70α S6 kinase gene is disrupted, but the magnitude of the reduction in size is smaller, probably because the existence of the second mammalian gene (p70β S6 kinase) compensates to some extent.

Does p70 S6 Kinase Regulate Ribosomal Protein Synthesis?

It has been observed that insulin and serum increase the phosphorylation of ribosomal protein S6 that leads to the identification of the S6 kinases. What role, then, does S6 phosphorylation play? Since it is a ribosomal protein, one would suppose that its role lies in regulating some aspect of mRNA translation (protein synthesis).

In higher animals, the mRNAs encoding the ribosomal proteins all share an unusual feature, a run of pyrimidine nucleotides at the extreme 5′-end of the mRNA. This acts to suppress their translation under basal conditions (e.g., in cells starved of serum or of amino acids). In response to stimulation of cells with serum or amino acids, these mRNAs bind to ribosomes and undergo translation so that ribosomal protein synthesis is switched on. It clearly makes good sense for the production of ribosomes to be stepped up in response to agents that stimulate protein synthesis or cell proliferation, and in parallel with the availability of amino acids, important precursors for ribosome production and for general protein synthesis.

Initial studies showed that rapamycin blocked the activation of the translation of these mRNAs and pointed to a role for p70 S6 kinase in this. However, some more recent studies have questioned the links between p70 S6 kinase/S6 phosphorylation and the activation of the translation of this subset of mRNAs.

Regulation of Other Processes by p70 S6 Kinase

In addition to S6, p70α S6 kinase has also been shown to phosphorylate certain other proteins involved in regulating gene expression. These include a protein involved in the control of gene transcription (the cyclic AMP-response element (CRE) modulator, CREM) and a protein kinase that regulates the elongation stage of protein synthesis (elongation factor 2 kinase). The latter may allow insulin and amino acids to accelerate the rate at which proteins are synthesized. Further substrates for the p70 S6 kinases may, of course, also exist.

mTOR

mTOR is a protein that is implicated in the intracellular signaling events that control a variety of processes in eukaryotic cells. All eukaryotic organisms that have been studied so far contain proteins related to mTOR, and work on the yeast orthologues, TOR1 and TOR2, has been especially fruitful in helping understand TOR signaling.

mTOR Signaling is Inhibited by the Immunosuppressant Drug, Rapamycin

mTOR, and indeed orthologues in many (but perhaps not all) species, are inhibited by rapamycin. Rapamycin is produced by a soil microorganism, *Streptomyces hygroscopicus*, which originates from Easter Island (the indigenous name for this island is Rapa Nui, hence rapamycin). The finding that rapamycin blocks the activation of T-lymphocytes, and thus suppresses the immune response, led to a high level of interest in its mechanism of action. Screening of yeast mutants for strains that are insensitive to the growth-inhibiting effects of this drug led to the identification of TOR1 and TOR2, and to the subsequent identification of related proteins in other organisms, such as mTOR in mammals.

Rapamycin appears to be completely specific for mTOR and its orthologues. Rapamycin binds to mTOR as a complex with a small protein called FKBP12 (FK506-) and rapamycin-binding protein 12: FKBP12 has prolyl *cis/trans* isomerase activity which is inhibited by both rapamycin and FK506, an immunosuppressant (FK506 does not, however, inhibit mTOR). The fact that the binding of the FKBP12/rapamycin complex to mTOR involves contacts with both the drug and the protein probably explains the high specificity. The normal physiological role of FKBP12 is unknown.

mTOR Is a Multidomain Protein

mTOR is a very large protein (about 2500 residues, Figure 2A). Inspection of its sequence reveals a number of potential domains. Its N-terminal section contains multiple "HEAT" domains—such domains are known to be important in protein–protein interactions. Towards its C terminus lies a domain that resembles the catalytic domain of kinases that phosphorylate lipids such as the phosphoinositide (PI) 3-kinases.

The kinase domain of mTOR appears critical to its function since mutants designed to cripple the catalytic domain are not functional *in vivo*. The region with which the FKBP12/rapamycin complex binds and inhibits mTOR function is N-terminal to the kinase domain.

mTOR (and TOR) Regulate Multiple Processes in Eukaryotic Cells

Treatment of cells with rapamycin reveals roles for mTOR/TOR in many important cellular processes such as gene transcription, protein synthesis and degradation, RNA breakdown, nutrient transport, the cell cycle and the organization of the actin cytoskeleton. Recent work with yeast suggests that, in fact, rapamycin may not affect all the functions of yeast TOR2, so that it may have additional roles not revealed by studying the effects of rapamycin. In contrast, the data suggest that all the functions of the other TOR protein in yeast, TOR1, may be blocked by this drug. It was already known that TOR1 and TOR2 had similar, but distinct, functions in yeast.

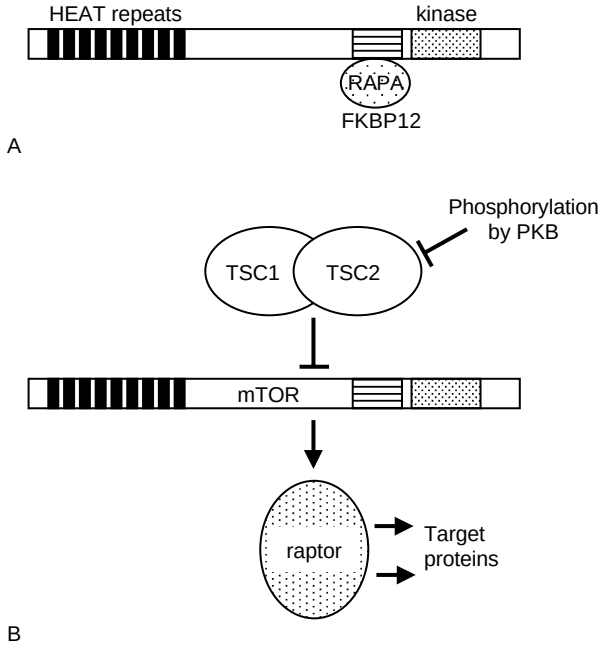

FIGURE 2 mTOR. (A) The figure depicts the principal domains found in mTOR. The complex of rapamycin with FKBP12 binds to and inhibits the function of mTOR. For other details, see text. (B) The complex of TSC1 and TSC2 binds to and inhibits mTOR: inhibition may be removed by phosphorylation of TSC2 by PKB. mTOR also binds a molecular scaffold, raptor, which appears to mediate the regulation of target proteins by mTOR.

The mechanisms by which mTOR/TOR regulates its downstream targets remain unclear. Since, where it has been studied, such regulation often involves changes in the phosphorylation of regulatory proteins, it is likely to be mediated by alterations in the activities of specific protein kinases and phosphatases, and there is evidence for both. In mammals, few of the target proteins that are controlled by mTOR have yet been identified. The best-understood ones are all involved in protein synthesis—they include the p70 S6 kinases, an elongation factor (eEF2) and a repressor of translation initiation, the initiation factor 4E-binding protein, 4E-BP1.

mTOR Interacts with Several Other Proteins

Very recent work has shed important new light on the ways in which mTOR may be regulated and how it signals to its target proteins. The key findings here were that mTOR (and the yeast TOR proteins) interact with other proteins. These interactions may involve the HEAT domains mentioned above. One type of interacting protein ("raptor") appears to be involved in the regulation of targets of mTOR signaling such as 4E-BP1 and the p70 S6 kinases. Others are probably involved in its upstream control.

Like mTOR, raptor is a large protein (1300 amino acids) that contains many motifs that may mediate protein–protein interactions. Related proteins are found in all eukaryotic species studied. Raptor binds to mTOR and also to its target 4E-BP1, and thus appears to act as a molecular scaffold (Figure 2B). The available evidence suggests that it is also required for the regulation of p70α S6 kinase by amino acids. Aspects of mTOR signaling such as raptor are currently a very active area of investigation and further important developments are likely.

Yeast TOR1 and TOR2 have been shown to bind the raptor orthologue in yeast and also to other proteins, although their roles are so far unknown.

mTOR Signaling Is Regulated by Hormones and Nutrients

Recent work has also identified proteins that bind to mTOR and act to regulate it, in response, for example, to insulin. TSC1 and TSC2 are components of the tuberous sclerosis complex, and appear to bind as a complex to mTOR, thereby inhibiting it (Figure 2B).

TSC1 and TSC2 were first identified as the genes that are mutated in tuberous sclerosis, an autosomal dominant disorder, that can lead to the occurrence of benign tumors characterized by excessively large cell size. This is accompanied by increased activity of p70α S6 kinase, consistent with the role described above for p70 S6 kinase in cell growth regulation. The effects of mutations appear to arise because they alleviate the normal inhibitory effect of the TSC1/2 complex on mTOR. The TSC1/2 complex is now also implicated in the normal regulation of mTOR: phosphorylation of TSC2 by a protein kinase B (PKB), which is activated by insulin, is thought to lead to the disruption of the TSC1/2 complex and activation of mTOR. The TSC1/2 complex acts to promote the hydrolysis of GTP on the small G-protein Rheb, which in its GTP-bound state promotes mTOR function. Much remains to be learned about how Rheb activates mTOR, and how other signaling inputs (such as amino acids) activate mTOR.

mTOR Displays Protein Kinase Activity

Although the kinase domain of mTOR resembles those of lipid kinases rather than of protein kinases, mTOR can phosphorylate certain proteins *in vitro*. These include p70α S6 kinase and the translational repressor protein 4E-BP1. However, the activity is weak and requires quite non-physiological conditions, so it is not clear whether this is really a physiological function of mTOR. It is quite conceivable that some of mTOR's partner proteins enhance its kinase activity *in vivo*.

Clinical Implications of mTOR Signaling

As noted above, rapamycin blocks the activation of cells of the immune system and thus acts as an immunosuppressant. As a consequence, rapamycin has found medical applications in combating graft rejection, particularly for recipients of kidney transplants. Very recent work also points to the potential for using rapamycin to treat certain types of cancer. These arise from mutations that inactivate the tumor suppressor protein PTEN and thus lead to unbridled activity of the PI 3-kinase signaling pathway that activates mTOR in response to insulin and many growth factors. Since the mTOR pathway clearly plays a central role in cell and animal growth, it will be of substantial importance for studies on clinical situations characterized by tissue atrophy or hypertrophy.

See Also the Following Articles

Phosphoinositide 3-Kinase • Protein Kinase B

Glossary

elongation/initiation factors Non-ribosomal proteins required for the initiation or elongation stages of protein synthesis.

mTOR The mammalian target of rapamycin, a multidomain protein that plays an important role in linking cellular responses to nutrients and other signals.

orthologue A term used for the distinct proteins found in different species that serve the same function (for example, yeast TOR and mammalian TOR).

ribosomal proteins The proteins that are found in the small and large subunits of the ribosome.

Further Reading

Abraham, R. T. (2002). Identification of TOR signaling complexes: More TORC for the cell growth engine. *Cell* **111**, 9–12.

Avruch, J., Belham, C., Weung, Q. P., Hara, K., and Yorezawa, K. (2001). The p70 S6 kinase integrates nutrient and growth signals to control translational capacity. *Prog. Mol. Subcell. Biol.* **26**, 115–154.

Dennis, P. B., Funagalli, S., and Thomas, G. (1999). Target of rapamycin (TOR): Balancing the opposing forces of protein synthesis and degradation. *Curr. Opin. Genet. Dev* **9**, 49–54.

Monniny, B. D., and Cantley, L. C. (2003). Rheb fills a GAP between TSC and TOR. *Trends Biochem. Sci.* **28**, 573–576.

Montagne, J., Stewart, M. J., Stockes, H., Hafer, E., Kozma, S. C., and Thomas, G. (1999). Drosophila S6 kinase: a regulator of cell size. *Science* **285**, 2126–2129.

Raught, B., Gingras, A. C., and Sorenberg, N. (2001). The target of rapamycin (TOR) proteins. *Proc. Natl Acad. Sci. USA* **98**, 7037–7044.

Rohde, J., Heitman, J., and Cardenas, M. E. (2001). The TOR kinases link nutrient sensing to cell growth. *J. Biol. Chem.* **276**, 9583–9586.

Biography

Christopher Proud is a Professor of Biochemical Physiology in the Faculty of Life Sciences at the University of Dundee. He holds a Ph.D. from the University of Dundee and did his postdoctoral training in Germany and England. His principal research interests are in the regulation of protein synthesis in mammalian cells by hormones and nutrients, and the roles of defects in protein synthesis and its control in the pathogenesis of human diseases.

Parathyroid Hormone/Parathyroid Hormone-Related Protein Receptor

Thomas J. Gardella
Massachusetts General Hospital and Harvard Medical School, Boston, Massachusetts, USA

The parathyroid hormone (PTH)/PTH-related protein (PTHrP) receptor (PPR) is a 593 amino acid, class 2 G protein-coupled receptor that mediates the actions of PTH, the major regulator of blood ionized calcium levels, and PTHrP, a key developmental protein. The PPR is abundantly expressed in bone osteoblasts and in renal tubule cells, the target cells of PTH, and in mesenchymal cells of developing tissues (e.g., skeleton, heart, teeth, and mammary glands), smooth muscle cells, and neurons, the target cells of PTHrP. The PPR binds PTH and PTHrP ligands via a bipartite mechanism involving binding interactions to the amino-terminal extracellular domain of the receptor and signaling interactions to the extracellular loops and seven transmembrane helices. The PPR couples strongly to the adenylyl cyclase (AC)/3′,5′-cyclic-adenosine monophosphate (cAMP)/protein kinase (PK)A signaling cascade, and can also activate the phospholipase (PL)C/inositol triphosphate (IP_3)/intracellular calcium (iCa^{2+})/PKC; PLD/phosphatidic acid/PKC; PLA_2/arachidonic acid/PKC; and MAP kinase pathways. Jansen's metaphyseal chondrodysplasia and Blomstrand's chondrodysplasia are rare diseases of skeletal development and calcium ion homeostasis that are caused by activating and inactivating mutations in the PPR gene, respectively. PTH(1–34) has anabolic effects on bone and is now used to treat osteoporosis.

Background and Physiology

Molecular Cloning of the PPR

The complementary (c)DNA encoding the parathyroid hormone (PTH)/PTH-related protein (PTHrP) receptor (PPR) was first isolated in 1991. This work revealed the classical seven transmembrane domain architecture of the G protein-coupled receptor (GPCR) superfamily (Figure 1). It also revealed that the PPR, along with the receptors for secretin, calcitonin, and several other peptide hormones, form a distinct subgroup – the class 2 GPCRs – which has been well-conserved, evolutionarily, with representatives present in *Drosophila* and *C. elegans*. The cloned PPR expressed in COS-7 cells binds PTH and PTHrP with equal affinities, and, in response to these ligands, activates both the AC/cAMP and PLC/IP_3/iCa^{2+} signaling pathways. It thus appears that the cloned receptor can account for all, or most, of the biological actions of two distinct ligands, PTH and PTHrP.

PTH

Discovery of PTH

Parathyroid hormone was identified as a key calcium-regulating hormone in the 1920s, when it was demonstrated that extracts of the parathyroid glands could modulate blood calcium levels and correct the tetany induced by parathyroid gland removal. The active hormone was purified from glands in 1959 and the complete 84 amino acid sequence of bovine PTH was determined in 1970. In 1971, the N-terminal PTH(1–34) fragment was synthesized and showed to be equipotent to native PTH in *in vitro* and *in vivo* assay systems. Physiological studies performed during this period established that PTH is the most important regulator of ionized calcium (Ca^{2+}) in the blood and extracellular fluids, and that it acts on bone, where it stimulates Ca^{2+} release from the mineralized matrix, and kidney, where it stimulates Ca^{2+} reabsorption from the glomerular filtrate. Related studies established that the secretion of PTH from the glands is regulated in a negative feedback fashion by the levels of extracellular Ca^{2+}; thus increases in blood Ca^{2+} result in decreased PTH secretion and decreases in blood Ca^{2+} result in increased secretion. This Ca^{2+}-mediated regulation of PTH secretion is determined by the actions of the calcium-sensing receptor expressed on the plasma membrane of parathyroid cells, and it is highly sensitive, such that blood Ca^{2+} levels are strictly maintained within the range of 1.1–1.3 mM. PTH is also a key regulator of blood phosphate, the principal Ca^{2+} counter ion, and suppresses the reabsorption of phosphate in the kidney.

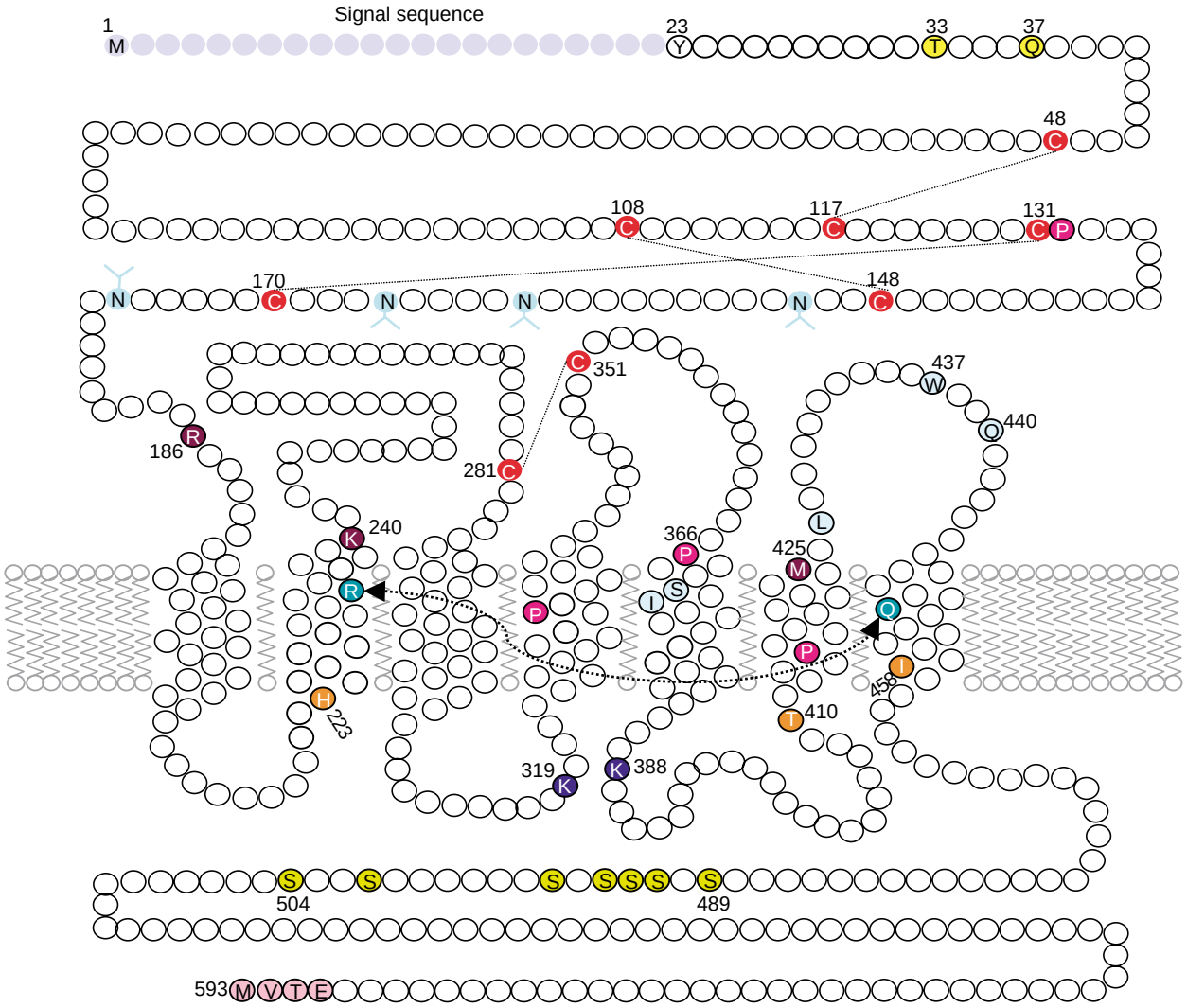

FIGURE 1 The human PTH/PTHrP receptor. Shown is a schematic of the PPR embedded in the lipid bilayer with selected features identified, including the conserved extracellular cysteines and their predicted disulfide linkages; the glycosylated asparagines (N); Thr33 and Gln37, which contribute to PTH(15–34) binding affinity; the probable cross-linking sites for ligand residues 13 (Arg186), 19 (Lys240) and 1 and 2 (Met425); conserved prolines (P), including Pro132, which is mutated to Leu in Blomstrand's chondrodysplasia; a putative inter-helical interaction between Arg233 and Gln451; Ser370, Ile371, Leu427, Trp437, and Gln440, at which mutations alter responsiveness to position 2-modified PTH(1–34) antagonist ligands (also includes Met425); His223, Thr410, and Ile458, which are mutated in Jansen's chondrodysplasia to result in constitutive signaling activity; Lys319 and Lys388, at which mutations impair G_q and G_s/G_q coupling, respectively; serines (S) that are phosphorylated upon agonist activation, and four C-terminal residues (Glu590–Met593) involved in NHERF binding.

PTH Effects in Bone

In bone, the PPR is expressed by osteoblast cells. These bone-forming cells display a variety of responses to PTH, including alterations in the rates of cell proliferation, apoptopsis, and changes in the expression patterns of a number of transcription factors, cytokines and bone-matrix factors. These effects can result in increased rates of bone formation. PTH however, also stimulates the bone-resorbing activity of osteoclastic cells, which are thought to be largely responsible for the calcium-releasing effects of PTH in bone. Osteoclasts, however, do not express the PPR but respond to the hormone via osteoclastogenic factors, such as RANK-ligand, that are expressed by PTH-stimulated osteoblasts. By modulating the activities of both osteoblasts (directly) and osteoclast (indirectly), PTH plays a major role in the continuous process of bone remodeling in the process of bone-remodeling. The mechanisms that control the balance between the anabolic and catabolic effects of PTH on bone are complex and not fully understood; however, it is well documented that intermittent exposure to PTH (once-daily injection) results in net bone formation, whereas continuous exposure (infusion) results in net bone resorption. Consistent with the anabolic effect of intermittent PTH on bone, a large clinical study

completed in 2001 showed that daily administration of PTH(1–34) significantly reduces the risk of bone fracture in patients with osteoporosis. As a result, the peptide is now used in the treatment of this common disease.

PTH Effects in the Kidney

In the kidney, the PPR is expressed by proximal and distal tubule cells. In the distal tubule, PTH stimulates the reabsorption of calcium from the urine, most likely by affecting calcium channel activity. In the proximal tubule, PTH stimulates the synthesis of 1,25-dihydroxy-vitamin D3, which in turn, promotes calcium absorption by the intestine and calcium release from bone. These calcium-regulating effects of vitamin D_3 occur on a longer time scale (days to weeks), than do those of PTH, which occur within seconds to minutes. Also in renal proximal tubule cells PTH suppresses the surface expression of the type II sodium-phosphate co-transporter and thereby decreases the re-uptake of phosphate from the urine.

PTHrP

Discovery of PTHrP

In the late 1980s, much effort was devoted to identifying the hypercalcemia-causing factor that is released by many tumors, and in 1987, the protein factor responsible, PTHrP, was purified from tumor extracts and partially sequenced. This sequence data, in turn, led to the cloning of the corresponding complementary(c) DNA, which revealed a protein of 141 amino acids that has clear N-terminal homology to PTH, as, 8 of the first 13 residues of the two proteins were found to be identical (Figure 2). PTHrP(1–34) peptides were shown to mimic the calciotropic actions of PTH on bone and kidney cells. It seemed clear, however, that PTHrP was not normally a calcium-regulating hormone, as its concentration in the normal circulation was too low (barely detectable). Furthermore, its mRNA was found in a wide variety of tissues (e.g. brain, lung, heart, adrenals, spleen, liver, bladder, skin, stomach, breast, placenta, ovaries, testes), in both adult and fetal life. These observations suggested that PTHrP acts in a paracrine manner, possibly in development.

```
                 1         10        20        30
hPTH(1-34)       SVSEIQLMHNLGKHLNSMERVEWLRKKLQDVHNF
hPTHrP(1-34)     AVSEHQLLHDKGKSIQDLRRFFLHHLIAEIHTA
```

FIGURE 2 PTH and PTHrP. Shown is an alignment of the bioactive (1–34) regions of human PTH and human PTHrP, with conserved residues in bold-faced type.

Genetic Manipulations of PTHrP in Mice

The above hypotheses regarding PTHrP action were largely confirmed in 1994 when mice having homozygous deletion of the *PTHrP* gene were generated and found to die at birth with defects in endochondral bone formation, namely, premature mineralization and short limbs. Subsequent genetic studies in mice determined that PTHrP also plays a role in the development of the mammary glands, hair follicles, and the heart. In 1996, mutant mice lacking the PPR gene were generated, and this established that the PPR mediates the developmental actions of PTHrP. Thus, PPR-deficient mice exhibit nearly the same perinatal lethality and developmental defects as those lacking the *PTHrP* gene.

PTHrP Actions in the Growth Plate

Extensive studies on the cartilaginous growth plates of the fetal tibia and femur in mice vividly demonstrated that PTHrP indeed acts in a paracrine fashion to control the program of events in tissue development. PTHrP is expressed by cells in the periarticular region of the growth plate and acts on prehypertrophic chondrocytes of the central zone to delay their terminal differentiation into hypertrophic chondrocytes. This action of PTHrP in the growth plate is further regulated by at least several other morphogenetic proteins, including Indian hedgehog (Ihh), which is produced by the prehypertrophic chondrocytes and stimulates chondrocyte proliferation. Ihh also induces, as part of a feedback regulatory network, the expression of PTHrP by the periarticular cells. Similar paracrine actions of PTHrP on PPR-expressing cells are also likely to operate in the mesenchyme of other developing tissues (e.g., heart, mammary glands, and hair follicles).

Structure–Activity Relationships in PTH and PTHrP

Functional Domains of PTH(1–34) and PTHrP(1–34)

Both PTH(1–34) and PTHrP(1–34) bind to and activate the PPR with affinities and potencies in the nanomolar range, and the two ligands interact with overlapping sites in the receptor. For both (1–34) ligands, the major determinants of PPR-signaling potency and binding affinity reside within the N-terminal and C-terminal portions, respectively. Based on this physical separation of functional domains, N-terminally truncated analogues, such as [Leu^{11},$DTrp^{12}$]PTHrP(7–34), have been developed as PTH receptor antagonists. The PTH(15–34) fragment represents the minimum-length binding fragment ($K_{dissociation} \sim 1\ \mu M$), and within this

domain, Trp-23, Leu-24, Leu-28, and Val-31 function as key determinants of binding affinity. These residues form the hydrophobic face of a predicted amphipathic α-helix that may contact the receptor. Within the N-terminal signaling domain of PTH, the highly conserved Val-2, plays a key role in PPR activation, as its deletion or replacement by bulky amino acids (e.g., Arg or Trp) confers antagonist behavior to PTH(1–34) analogues. Short amino-terminal fragments, such as PTH(1–14), exhibit little or no binding or signaling activity; however, recent studies have resulted in N-terminal fragment analogues with considerably enhanced binding and signaling capacities. For example, [Aib^{1,3},Gln^{10},Har^{11}, Ala^{12},Trp^{14}]PTH(1–14)NH_2 is ~100 000-fold more potent than native PTH(1–14) for stimulating cAMP formation (EC_{50}s = 2 nM versus 200 μM) and is thus as potent as PTH(1–34) in cell-based assay systems.

Structural Studies of PTH and PTHrP

Solution-phase NMR studies performed on PTH(1–34) analogues suggest that the peptide in solution adopts a bi-helical conformation in which a short N-terminal helix (residues ~3–10) is joined via a turn or flexible linker to a longer more stable C-terminal helix (residues ~17–31). In some studies a U-shaped structure has been proposed for the bi-helical peptide. In 2001, however, the X-ray crystal structure of PTH(1–34) was determined and this revealed a single, slightly bent α-helix that extended from Val-2 to His-32. What is needed now is a direct assessment, by physical methods, of the conformation of the ligand in the receptor-bound state; until this is accomplished, the true bioactive conformation of PTH will likely remain uncertain.

Structure Activity Relationships in the PPR

Molecular Architecture of the PPR

The Amino-Terminal Domain

The PPR contains an amino-terminal extracellular (N) domain of ~167 amino acids (excluding the 23 amino acid signal sequence) (Figure 1). This N domain is Asn-glycosylated at four sites and contains six cysteine residues. These six cysteine residues are very highly conserved among the class 2 GPCRs and they are predicted to form a network of three disulfide bonds that defines a tertiary fold common to the N domains of each of the class 2 receptors. At present, the three-dimensional structure of the N domain of any class 2 GPCR is unknown, but it is clear that for each receptor, the N domain contributes importantly to ligand-binding affinity. For the PPR, the isolated N domain protein, purified and refolded from an *E. coli* expression system, binds PTH(1–34) with micromolar affinity. Protease digestion and mass-spectrometry analysis of this protein reveled the probable disulfide bond arrangement for the PPR N domain (Figure 1), and the same disulfide bond pattern has also been determined for several other class 2 receptor N domain proteins.

The Juxtamembrane Domain

The juxtamembrane (J) region of the PPR is comprised of the heptahelical bundle and the interconnecting loops. The structure of this domain is likely to bear at least some similarity to the heptahelical core region of rhodopsin, the only GPCR for which an X-ray crystal structure is available. Computer models of the PPR J domain have been generated using the rhodopsin X-ray structure as a template, but because there is almost no amino acid sequence homology between rhodopsin, a class 1 GPCR, and the PPR, the accuracy of such models is uncertain. One structural feature that is predicted for the PPR J domain, and for nearly all GPCRs, is a disulfide bond between extracellular loop (ECL)-1 and ECL-2 (Figure 1). Within the transmembrane helices of the PPR there are residues that are well-conserved in the class 2 GPCR family and are likely to help define the topology and functionality of the J domain. These include the prolines in TMs 4, 5, and 6, expected to induce kinks in the helices, and polar residues, such as Arg233 in TM2 and Gln451 in TM7, that are likely to contribute to networks of inter- and intra-helical side-chain interactions. The connecting loops and carboxy-terminal tail (CT) of the PPR also contribute importantly to PPR function, but the structures of these domains are unknown.

The Ligand Interaction Mechanism in the PPR

The Two-Site Model

The ligand-binding mechanism for the PPR has been extensively analyzed by the complementary approaches of photochemical cross-linking and receptor mutagenesis, and the overall results suggest a two-site model. According to this model, the C-terminal binding domain of PTH(1–34) interacts with high affinity with the PPR N domain and this interaction enables the amino-terminal domain of the ligand to interact with lower affinity with the PPR J domain. Thus, the N domain interaction provides the major component of binding energy, while the J domain interaction provides the interactions that induce receptor activation and G protein coupling (Figure 3).

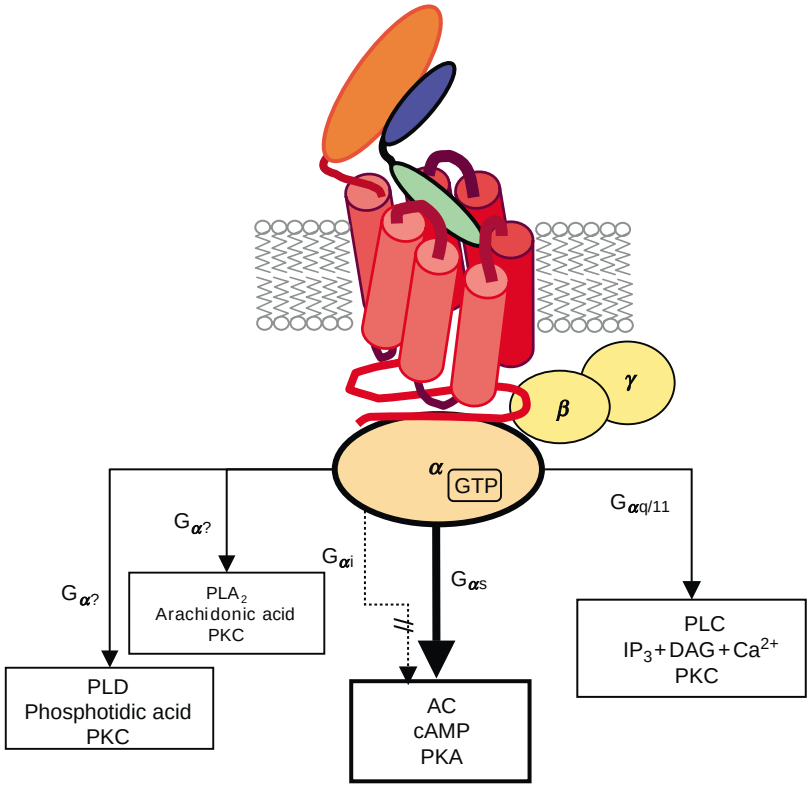

FIGURE 3 Ligand-binding and G protein-coupling mechanisms for the PTH/PTHrP receptor. The ligand, PTH(1–34) or PTHrP(1–34), is shown to interact with the PPR via a bipartite mechanism in which the ligand's C-terminal portion (blue) interacts with the receptor's amino-terminal extracellular domain (orange) to provide binding affinity, and the ligand's N-terminal portion (green) interacts with the receptor's extracellular loops and heptahelical portion (red) to induce receptor activation. The activated PPR can couple to multiple signaling pathways via several different heterotrimeric G proteins. It couples most strongly and in most cells to $G_{\alpha s}$ to stimulate the AC/cAMP/PKA pathway. It can also couple to $G_{\alpha q}$ to stimulate PLC/IP_3/Ca^{2+}/PKC signaling and to a pertussis toxin-sensitive G_i protein to inhibit AC/cAMP activity, but the magnitude of these response are generally less than that of the stimulatory AC/cAMP response. In some cells, the PPR can activate the PLD/phosphotidic acid/PKC and/or PLA_2/arachidonic acid/PKC pathways, but the G proteins involved are unknown.

N Domain Interactions

Cross-linking studies have identified proximities between specific sites in PTH and PTHrP ligands and the PPR. Thus, PTHrP(1–36) analogues modified with the photo-labile amino acid analogue, benzoylphenylalanine (Bpa), at positions 23, 27, 28, and 33 and cross-link to distinct segments of the PPR N domain: (33–40), (96–102), (64–95) and (151–172), respectively. The locations of the important functional contact sites within these N domain regions still need to be determined, but the large segment, residues (61–105), which corresponds precisely to exon E2 of the PPR gene, is not likely to contain such sites, as it can be deleted without affecting ligand-binding affinity. Two possible interaction residues in the N domain of the PPR include Thr33 and Gln37 (Figure 1), as mutation of these residues to alanine results in decreased affinity for PTH(15–34). These two residues are near the Bpa-23 contact site and thus could provide contacts for Trp-23 in the ligand.

J Domain Interactions

Other cross-linking studies identified Met425 at the extracellular end of TM6 as the probable contact site for PTH(1–34) or PTHrP(1–36) ligands modified with Bpa at position 1 or position 2. Interestingly, the Bpa-1-modified analogue (an agonist) and the Bpa-2-modified analogue (a partial antagonist/inverse agonist) cross-linked to overlapping, but not identical, sites at or near Met425, suggesting that the analogues could be used to distinguish between active and inactive receptor conformational states. In further studies, the mutation Met425 → Leu was shown to specifically increase the agonist efficacy (and reduce the inverse agonist efficacy) of [Bpa^2]PTHrP(1–36). These data, combined with earlier data showing that point mutations at the extracellular ends of TM5 (Ser370 → Ala, Ile371 → Val) and, TM6 (Leu427 → Thr) modulate the antagonist properties of [Arg_2]PTH(1–34), and that mutations in ECL-3 (Trp437 → Ala, Gln440 → Ala) impair binding of PTH(1–34) but not that of PTH(3–34), suggest

that residues in the TM5/TM6/ECL-3 region mediate interactions with Val-2 in the ligand that are involved in receptor activation.

Two other contact sites in the PPR J domain identified by cross-linking analyses include Arg186 at the N domain/TM 1 boundary, the probable contact site for ligand residue 13, and Lys240 at the extracellular of TM2, the probable contact site for ligand residue 19. The results of these cross-linking studies, combined with those above for the N-terminally modified ligand analogues, suggest that the portion of the ligand that interacts with the PPR J domain extends from residue 1 to residue 19. Consistent with this, the potencies of PTH(1–20) analogues on a PPR mutant construct (PPR-delNt) that lacks most (residues 23–181) of the N domain are the same as they are on the intact PPR. These studies using the PPR-delNt construct also suggest that the PPR N domain is not required for receptor activation. The PPR N domain is clearly required, however, for achieving full potency and affinity with PTH(1–34), as this ligand is 100-fold weaker on P1R-delNt, as it is on the intact PPR.

PPR Signaling and Regulation

Conformational Changes

As for all GPCRs, it is presumed that PPR activation involves movements in the TM helices and intracellular loops (ICLs), and that these movements result in increased accessibility of the receptor's cyctoplasmic surface to G proteins. The precise conformational changes involved are likely to be complex and are largely unknown. Inter-TM domain movements in the PPR have been analyzed using the Zn(II)-chelation strategy, and these studies have revealed that a movement of TM3 and TM6 away from each other, blocked by the addition of Zn(II), is required for Gs activation. In parallel experiments, a similar movement was also detected in the β2 adrenergic receptor, and has also been observed by this method of analysis in rhodopsin. The activation mechanisms used by the class 1 and class 2 GPCRs may, therefore, be similar. Using conventional mutational methods, specific residues in the IC loops of the PPR have been identified that modulate Gs and/or Gq coupling. These include Lys388 in ICL-3, at which mutations impair both AC/cAMP (G_s) and PLC/IP_3 (G_q) signaling and Lys319 in ICL2, at which mutations selectively impair PLC/IP_3 (G_q) signaling.

The Carboxyl-Terminal Tail

Classical pharmacological studies on PTH action in bone and kidney cells revealed that the PPR desensitizes and internalizes in response to hormone stimulation. More recent molecular studies have shown that the PPR carboxyl-terminal tail plays a major role in this regulation. Upon agonist activation, seven serines within the N-terminal-proximal portion of the tail (Figure 1) are rapidly phosphorylated, most likely by G protein-specific receptor kinase-2. This phosphorylation promotes the binding of β-arrestin and the internalization of the ligand–receptor complex, via clatherin-coated pits, to endosomal vesicles. At least some of the PPR recycles back to the cell membrane in a de-phosphorylated form, resulting in receptor resensitization. The PPR CT also mediates interaction with cytoskeletal scaffolding proteins, including members of the NHERF (Na^+/H^+ exchanger regulatory factor) family of proteins, which were identified in a yeast two-hybrid selection for proteins that bind the PPR CT. The C-terminal four amino acids (Glu-Thr-Val-Met) of the PPR mediate this interaction by binding to one of the PDZ domains of NHERF. The binding of NHERF to the PPR can alter the signaling pathways utilized, resulting in increased PLC signaling and diminished AC/cAMP signaling, and, as suggested by recent data, the internalization properties of the receptor, enabling the internalization of antagonist ligands.

The PPR in Human Disease

Jansen's Metaphyseal Chondrodysplasia

This rare autosomal dominant disease is characterized by short-limbed dwarfism (reflecting the role of PTHrP in the growth plates) and hypercalcemia (reflecting the role of PTH in bone and kidney). In 1995, a mutation in the *PPR* gene that changed His223 at the base of TM2 to Arg was identified in an affected individual. This mutation was then shown to confer high basal cAMP-signaling activity to the receptor expressed in COS-7 cells. Since this time, three other activating mutations in this disease have been identified, each of which alters a residue located near the intracellular termini of a TM helix: Thr410 → Pro and Thr410 → Arg in TM6 and Ile458 → Arg in TM7. In studies performed in transfected COS-7 cells, the antagonist [Leu^{11},$DTrp^{12}$]PTHrP(5–36) was shown to behave as an inverse agonist with the PPRs bearing either the His223Arg or Thr410Pro mutation, while the antagonist [Bpa^2]PTHrP(1–36) behaved as a selective inverse agonist, depressing cAMP signaling only with the His223Arg mutant. These findings with [Bpa^2]PTHrP(1–36) suggest that there may be variable conformational states of the active PPR.

Blomstrand's Chondrodysplasia

This rare perinatal lethal condition is characterized by a severely over-calcified fetal skeleton and short limbs.

Three different PPR-inactivating mutations have been identified in this recessive disorder: a messenger RNA splicing mutation that results in an eleven-amino acid deletion in TM5; a frameshift mutation in ECL-2, and a missense mutation (Pro132 → Leu) in the N domain. The phenotype seen in Blomstrand's chondrodysplasia mirrors that seen in mice having homozygous deletion of the *PPR* gene.

Conclusions

The PPR mediates the biological actions of two key proteins – PTH (calcium and phosphate homeostasis) and PTHrP (development). Disruptions of the PTH/PTHrP/PPR system result in a number of diseases of calcium ion homeostasis and tissue development (Figures 2 and 3). Further unraveling of the molecular mechanisms by which the PPR interacts with PTH and PTHrP is of fundamental biochemical interest and could lead to new therapies for diseases of bone and mineral metabolism.

See Also the Following Articles

Adenylyl Cyclases • Phospholipase C • Steroid/Thyroid Hormone Receptors • Thyroid-Stimulating Hormone/Luteinizing Hormone/Follicle-Stimulating Hormone Receptors • Vitamin D

Glossary

G (guanine nucleotide-binding) protein-coupled receptor (GPCR) An integral membrane protein characterized by seven membrane spanning helical domains and the capacity to activate heterotrimeric G proteins in response to agonist binding.

parathyroid hormone (PTH) An 84 amino acid secreted polypeptide that functions as the major regulator of calcium ion concentrations in blood and extracellular fluids; acts on bone and kidney cells.

PTH/PTHrP receptor (PPR, or PTH-1 receptor) A class 2 GPCR that mediates the actions of PTH and PTHrP. Highly expressed in osteoblasts, renal tubule cells, and a variety of tissues during development.

PTH-related protein (PTHrP) A 141 amino acid polypeptide that acts in a paracrine fashion to control development of the skeleton, heart, teeth, mammary glands, and other tissues. It is highly expressed in breast milk and is the most common mediator of hypercalcemia of malignancy.

Further Reading

Brown, E. M. (2000). Calcium receptor and regulation of parathyroid hormone secretion. *Rev. Endocr. Metab. Disord.* **1**, 307–315.

Gardella, T. J., and Jüppner, H. (2001). Molecular properties of the PTH/PTHrP receptor. *Trends Endocrinol. Metabol.* **12**, 210–217.

Hoare, S. R. J., and Usdin, T. B. (2001). Molecular mechanisms of ligand-recognition by parathyroid hormone 1 (PTH1) and PTH2 receptors. *Curr. Pharm. Design* **7**, 689–713.

Jüppner, H. W., Gardella, T. J., Kronenberg, H. M., and Potts, J. T., Jr. (2001). Parathyroid hormone and parathyroid hormone-related peptide in the regulation of calcium homeostasis and bone regulation. In *Endocrinology* (L. DeGroot and J. Jameson, eds.) Vol 2, pp. 969–1053. Endocrinology, W. B. Saunders, Philadelphia.

Strewler, G. J. (2000). The physiology of parathyroid hormone-related protein. *New England J. Med.* **342**, 177–185.

Biography

Thomas J. Gardella, Ph.D., is an Associate Professor in Medicine with appointments at the Massachusetts General Hospital and Harvard Medical School. He has been a member of the Endocrine Unit of the M.G.H. since 1988, and his research interests focus mainly on the structure–activity relationships of PTH and the PTH receptor. He received his Ph.D. degree in molecular genetics and microbiology from the University of Massachusetts Medical School, Worcester, Massachusetts and a B.S. degree in biochemistry from the University of Massachusetts, Amherst, Massachusetts.

PCR (Polymerase Chain Reaction)

Michael J. Brownstein
National Institute of Mental Health, National Institutes of Health, Bethesda, Maryland, USA

The polymerase chain reaction (PCR) is used to amplify DNA – i.e., to make millions of copies of a particular DNA segment. Invented by Kary Mullis in 1983, the process is simple, fast, and robust. It relies on synthetic oligonucleotide "primers," DNA polymerase(s), nucleotide bases, and a thermal cycler (a programmable instrument that varies and controls the temperature of the solution in which PCRs occur). The enzymes used, among them Taq, Pfu, and Vent polymerases are derived from *Thermus aquaticus*, *Pyrococcus furiosus*, and *Thermococcus litoralis*, respectively. These are bacteria that live in hot springs or undersea vents where the ambient temperature is high. Consequently, the enzymes they synthesize are thermostable. They differ in important ways, however. Taq polymerase, for example, is quite processive. That is, it copies DNA strands very efficiently, but it lacks 3′–5′ exonuclease activity, and is more error prone than Pfu and Vent polymerases, which have exonuclease activity and "proofread" their products. For this reason, enzyme mixtures are sometimes used to catalyze PCR reactions.

The Reaction Cycle

A polymerase chain reaction (PCR) cycle is illustrated in Figure 1. Step one is to melt or unzip the double-stranded DNA templates that will be copied. A thermocycler is used to increase the temperature of the reaction vessel to 90°C or more. At such temperatures most mammalian or bacterial enzymes would be inactivated, but they are well tolerated by the thermostable polymerases described above.

After the DNA strands have been separated, the temperature is dropped to permit short DNA primers to bind (anneal) to complementary sequences on the templates. The polymerases will not copy DNA in the absence of primers, and two are used – one for each of the two template strands that were liberated in step one.

Once they have found their specific target sequences, the polymerases can begin adding bases to the 3′ ends of the primers. Since this process is inefficient at the relatively low annealing temperature, the reaction temperature is increased to ~75°C. Now both of the DNA strands are quickly replicated, beginning at the priming site and ending, in theory, at the end of each template. As the figure shows, there are four DNA strands at the end of the first PCR cycle, instead of the original two. In subsequent cycles, products primed by the two oligonucleotides preferentially accumulate. The length of the "amplicons" is defined by the primers, which form their flanks. After about five PCR cycles have been completed, these amplicons predominate over longer species. It is important to note that at the beginning of a PCR, all of the reagents except for the template are present at high concentrations. Therefore, primer binding is favored over product renaturation, and the amplification is exponential. After many cycles have been completed, this may no longer be the case; product formation becomes linear and finally grinds to a halt. In practice, it is uncommon to use more than 30 reaction cycles.

Applications

PCR can be employed to amplify both DNA and RNA templates. In the latter case, reverse transcriptase (an RNA-directed DNA polymerase) is first used to make complementary DNA from the RNA of interest. DNA produced in this way can be substituted for the double-stranded DNA that served as the starting material in the scheme shown in Figure 1. This process is referred to as reverse transcriptase-PCR (RT-PCR). It allows much smaller amounts of RNA to be measured than can be detected with Northern blotting or RNase protection assays. In fact, real-time RT-PCR has become the method of choice for measuring changes in RNA when large numbers of samples have to be studied. This technique combines PCR with cycle-by-cycle detection of amplicons during the exponential phase of product buildup. Quantitation is based on the fact that many PCR cycles are needed to detect the products of rare targets, while few cycles are required to detect those of abundant ones. The dynamic range of the method spans 6–7 orders of magnitude. It is possible to amplify more than one product at a time with two or more primer pairs (multiplex PCR), and to detect the products with different dyes.

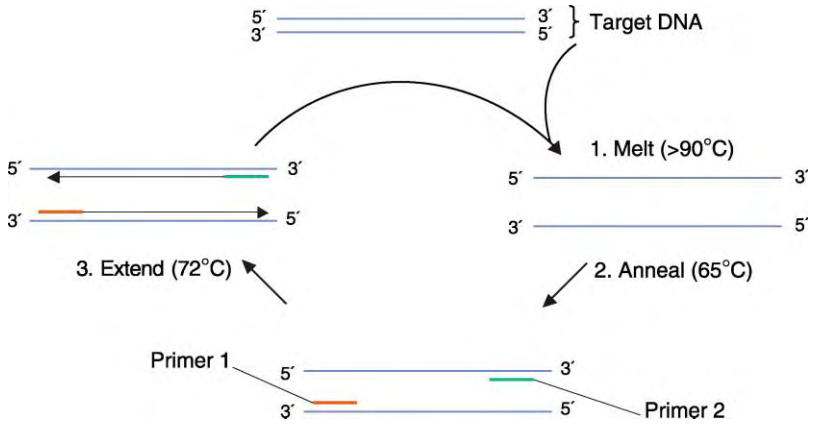

FIGURE 1 The PCR cycle.

It should already be clear that many PCR-based methods have been invented. Some are used for cloning, modifying, and/or sequencing amplicons; others are used for detection or measurement of RNA or DNA. To appreciate these methods, it is important to understand that many sorts of oligonucleotides can be used to prime PCR reactions. Thus, even though it is essential for the primers to be complementary to their targets on their 3′ ends, they can be quite different from the targets on their 5′ ends, where noncomplementary sequences, free amino groups, fluorescent dyes, or molecules like biotin can be added without adversely affecting the amplification process.

One of the earliest uses of PCR was in characterizing families of gene products, e.g., the rhodopsin-like G protein-coupled receptors. In humans there are more than 200 such proteins, exclusive of odorant receptors. After cDNA encoding the first few of these were cloned, it became clear that they were structurally similar, that they shared certain amino acid motifs. "Degenerate" PCR primer mixtures were designed on the basis of the conserved domains and used to amplify fragments of new family members from cDNA templates. Since these fragments lacked the 5′ and 3′ ends of the receptors' open reading frames, another PCR method called rapid amplification of cDNA ends (RACE) was used to identify and isolate the missing 5′ and 3′ termini. Once the sequences of the ends were determined, long-range PCR could be used to amplify the entire open reading frame, using primers with convenient restriction sites on the 5′ ends to facilitate "pasting" the inserts into vectors.

Some scientists were interested in studying the relationship between the structures of receptors (and other proteins) and their functions. To do this, they used PCR to introduce mutations into the receptors or to construct chimeric proteins – half one receptor, and half another, or tagged receptors, which could be used to study protein trafficking in cells. The constructs were sequenced before they were expressed in cells to be sure that no errors were made in producing them. The sequencing reactions were also PCR based. In fact, it is safe to say that the much-heralded sequencing of the human and mouse genomes could not have been accomplished without the method, and DNAs from living species are not the only templates that have been analyzed. PCR has allowed DNA from ancient samples (e.g., insects embedded in amber, tissue from mummies and extinct species like the Quagga) to be characterized.

The instruments used for DNA sequencing can be employed for genotyping as well. To do this, fluorescent PCR primers are used to amplify variable number tandem repeats or single nucleotide polymorphisms that serve as markers for inherited segments of chromosomes. The resulting data are used for linkage analysis, permitting scientists to determine the chromosomal location of disease-causing genes. Once these genes are known, robust screening methods – also based on PCR – can be developed to screen for carriers of deleterious mutations and even to look for mutations in pre-implantation embryos.

Genotyping has other potential uses too. It permits livestock and plants to be improved, and identity, paternity, or culpability of subjects to be determined by forensic scientists.

Finally, PCR is used to detect pathogens in clinical samples, food, and water, and to search for mutations in cancer-causing genes in tumors, or polymorphisms in drug metabolizing enzymes and transporters that affect efficacy/toxicity. It is not unlikely that it will play an important role in the development of personalized medicine in the future. In fact, its use may not be limited to assays of DNA and RNA. PCR-ELISA is an

exquisitely sensitive way to detect any molecule to which an antibody can be raised.

See Also the Following Article

DNA Sequence Recognition by Proteins

Glossary

DNA polymerase An enzyme that catalyzes DNA-directed synthesis of DNA from nucleotide triphosphates.

primer A single-stranded DNA molecule, typically 17–25 nucleotides in length that is required to initiate the synthesis of DNA by polymerase.

reverse transcriptase An enzyme that catalyzes RNA-directed synthesis of DNA from nucleotide triphosphates.

thermocycler A programmable instrument that heats and cools reaction tubes repeatedly allowing the user to move through melting, annealing, and extension steps in the PCR cycle.

Further Reading

McPherson, M. J., and Møller, S. G. (2000). *PCR*. BIOS Scientific, Oxfordshire, UK, http://www.pcrlinks.com/.

Mullis, K. B., and Faloona, F. A. (1987). Specific synthesis of DNA *in vitro* via a polymerase-catalyzed chain reaction. *Methods Enzymol.* **155**, 335–350.

Biography

Michael J. Brownstein is Chief of the Laboratory of Genetics, National Institute of Mental Health, NIH, Bethesda, MD. He received his Ph.D. and M.D. from the University of Chicago and did postdoctoral training with Julius Axelrod. His research has been in the areas of neurobiology, endocrinology, genetics, and genomics.

Pentose Phosphate (Hexose Mono Phosphate) Pathway

Bernard R. Landau
Case Western Reserve University, Cleveland, Ohio, USA

The pentose phosphate pathway is the major source of NADPH for reductive biosynthesis and is the source of ribose-5-P for nucleotide and nucleic acid synthesis. Its reactions are usually viewed in two segments. In the first, glucose-6-P is irreversibly oxidized, generating NADPH and pentose-5-P. In the second, the pentose-5-P is reversibly converted through a series of rearrangements to intermediates of the glycolytic pathway. The pathway is in the cytosol.

History

In 1931, Warburg demonstrated glucose-6-P's oxidation to 6-phosphogluconate with the formation of NADPH. In the following decade, Warburg, Lipmann, Dickens, and others found that the gluconate was decarboxylated to CO_2 and to a pentose phosphate that could then be reconverted to hexose-6-P. Details of the pathways were elucidated in the 1950s by Cohen, Racker, Horecker, and their associates. Figure 1 shows the pentose phosphate pathway.

Reactions

Oxidative Segment

Glucose-6-P oxidation is catalyzed by glucose-6-P dehydrogenase, yielding 6-phosphogluconolactone and NADPH (Figure 2). The spontaneous hydrolysis of the lactone, forms 6-phosphogluconate, catalyzed by a specific lactonase. The gluconate is oxidatively decarboxylated to yield another NADPH and ribulose-5-P. The overall reaction of this segment is then glucose-6-P $\rightarrow$ CO_2 + 2NADPH + ribulose-5-P.

Nonoxidative Segment

The ribulose-5-P is isomerized to ribose-5-P and also epimerized to xylulose-5-P (Figure 3). Transfer of the top 2 carbons as a unit from the xylulose-5-P to ribose-5-P, catalyzed by transketolase, yields seven carbon containing sedohepulose-7-P and glyceraldehyde-3-P. Transfer of the top 3 carbon unit as a unit from the sedohepulose-7-P to the glyceraldehyde-3-P, catalyzed by transaldolase, yields fructose-6-P and 4 carbon containing erythrose-4-P. Transfer of the top 2 carbons as a unit from another xylulose-5-P to the erythrose-4-P, again catalyzed by transketolase, yields fructose-6-P and glyceraldehyde-3-P. Thus, the overall reaction of this segment is 3 pentose-5-P $\leftrightarrow$ 2 fructose-6-P + glyceraldehyde-3-P.

Transketolase requires thiamine pyrophosphate as a cofactor. The 2 carbon unit is transferred via its addition to the thiamine ring of the vitamin. The mechanism is similar to that in the oxidative decarboxylation of pyruvate, catalyzed by the thiamine pyrophosphate containing E_1 subunit of the pyruvate dehydrogenase complex. In the transfer of the 3 carbons unit, catalyzed by transaldolase, a Schiff base is formed between the ketone group of the sedohepulose-7-P and a lysine residue at the active site of the enzyme. The mechanism is similar to that in fructose-1, 6-bisphosphatase aldolase catalysis.

Overall Balance and Carbon Fate

On balance, 3 glucose-6-P (18 carbons) are decarboxylated to yield 3 CO_2 and 3 pentose-5-P (15 carbons) (Figure 4). The rearrangements, catalyzed by transketolase and transaldolase produce 2 fructose-6-P (12 carbons) and glyceraldehyde-3-P (3 carbons). The CO_2 contains carbon 1 of the glucose-6-P (Figure 5). The origin of the top 3 carbons of the 2 fructose-6-P are carbons 2 and 3 of the glucose-6-P.

Mode of Operation

Shunt or Cycle

Since glucose-6-P is converted to fructose-6-P and glyceraldehyde-3-P, the pentose phosphate pathway has been viewed as an alternate route for the conversion

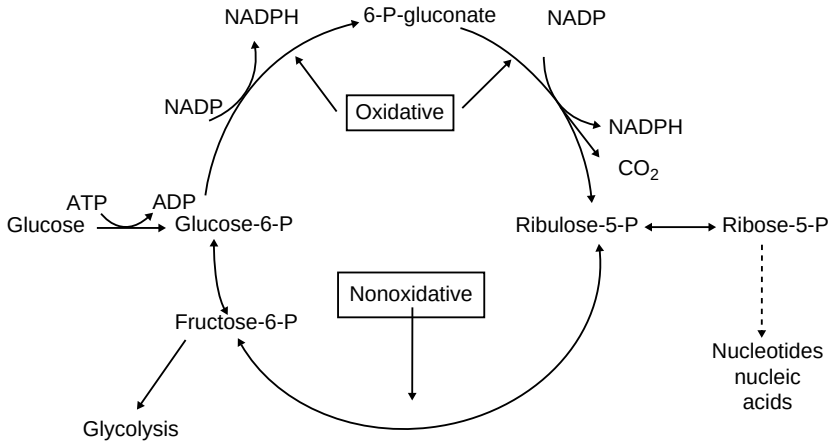

FIGURE 1 Depiction of the pentose phosphate pathway as a cycle composed of oxidative and nonoxidative segments.

of glucose-6-P to intermediates of the glycolytic pathway. Therefore, the pathway has also been called the hexose monophosphate shunt. Since the fructose-6-P can be isomerized to glucose-6-P that can re-enter the pentose phosphate pathway, the pathway has also been viewed as a cycle and called the pentose cycle.

Regulation

The dehydrogenation of glucose-6-P, the first step, is considered to be the rate-limiting step in the oxidative segment. Control is through the activity of glucose-6-P dehydrogenase regulated by the concentration of NADP. NADPH competes with the NADP for binding to the enzyme, thus tightly coupling NADPH production to utilization. When NADPH is utilized (e.g., in fatty acid synthesis), the NADPH is oxidized, increasing NADP and stimulating flux through the oxidative segment. Flux through the nonoxidative segment is determined by the concentration of pentose-5-P. The activity of the pathway is coordinated with that of the pathways utilizing its products. Recent studies identify xylulose-5-P in the pathway as mediating the effect of carbohydrate feeding on the glycolytic pathway and regulating the enzymes required for fatty acid and triglyceride synthesis.

Other Functions

The pentose phosphate pathway is the route by which pentose from food is metabolized. Erythrose-4-P in some organisms is used as an intermediate in the synthesis of the aromatic ring of the amino acids. D-xylulose formed in the glucuronic acid pathway, is further metabolized via the pentose phosphate pathway.

Quantitation

Methods

Estimates of the activity of the pathway rest on measurements of the activities of its enzymes, particularly of glucose-6-P dehydrogenase, and of concentrations of intermediates in the pathway, as well as yields

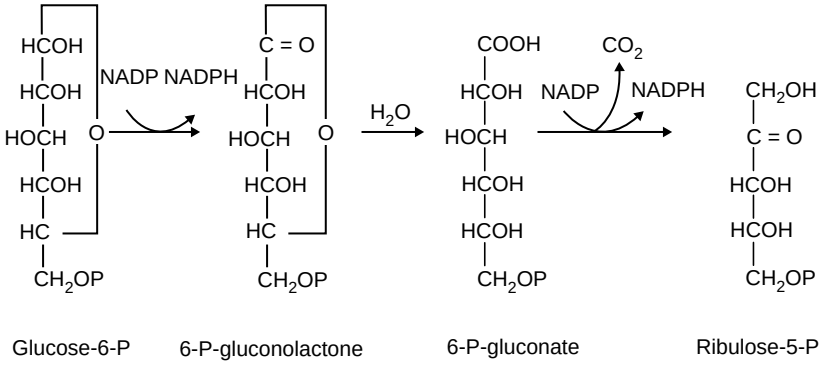

FIGURE 2 Reactions of the oxidative segment of the pentose phosphate pathway.

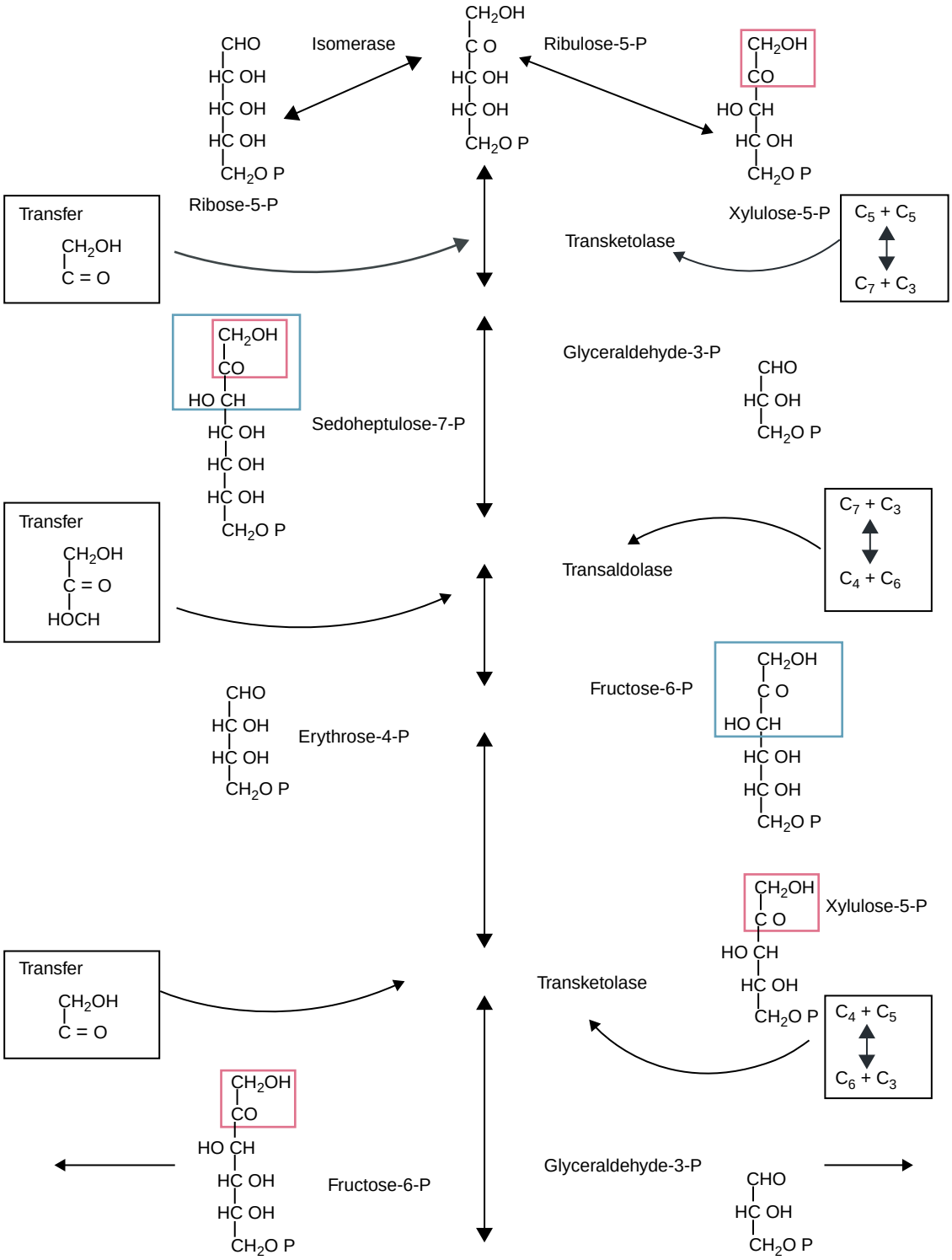

FIGURE 3 Reactions of the nonoxidative segment of the pentose phosphate pathway.

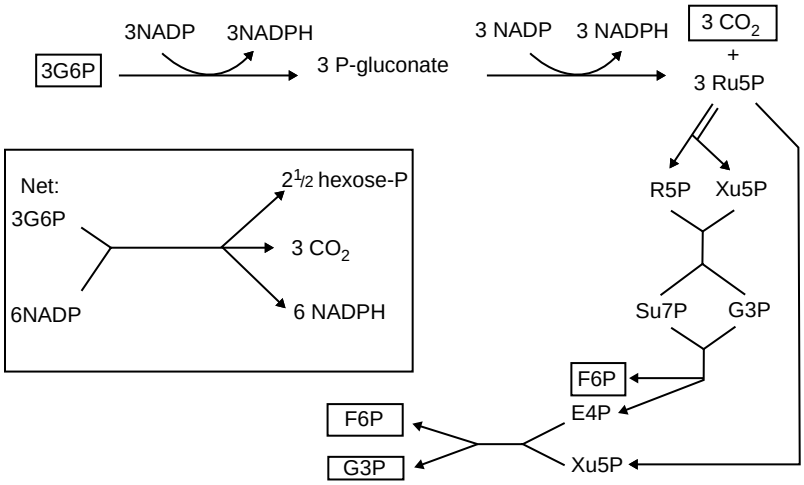

FIGURE 4 Chemical balance in the reactions of the pentose phosphate pathway.

of labeled products after administering labeled substrate and intermediates of the pathway. Specifically, carbon-labeled glucoses have been used to quantitate the amount of glucose utilized by the pathway relative to other pathways utilizing glucose. The quantitations depend on (1) the fact that carbon 1 of every molecule of glucose-6-P entering the pathway is oxidized to CO_2, while via glycolysis and the tricarboxylic acid cycle, carbons 1 and 6 are oxidized to CO_2 to essentially the same extent, or (2) the randomization of carbons 2 and 3 of glucose-6-P occurring in the nonoxidative segment (Figure 5).

The amounts of glucose oxidized and that utilized by the pathway are different. Thus, while the three molecules of glucose-6-P that enter the pathway (Figure 4) are oxidized, and 2 glucose-6-P equivalents are reformed, only a net of 1 glucose-6-P is utilized. It is converted to CO_2 and glyceraldehyde-3-P. If, as can occur in the liver, 2 glyceraldehyde-3-P that are formed are converted to 1 glucose-6-P, the balance becomes 6 glucose-6-P → 12 NADPH + 6 CO_2 + 5 glucose-6-P. Hence, 6 glucose-6-P are oxidized, but only 1 glucose-6-P is utilized (completely oxidized to CO_2).

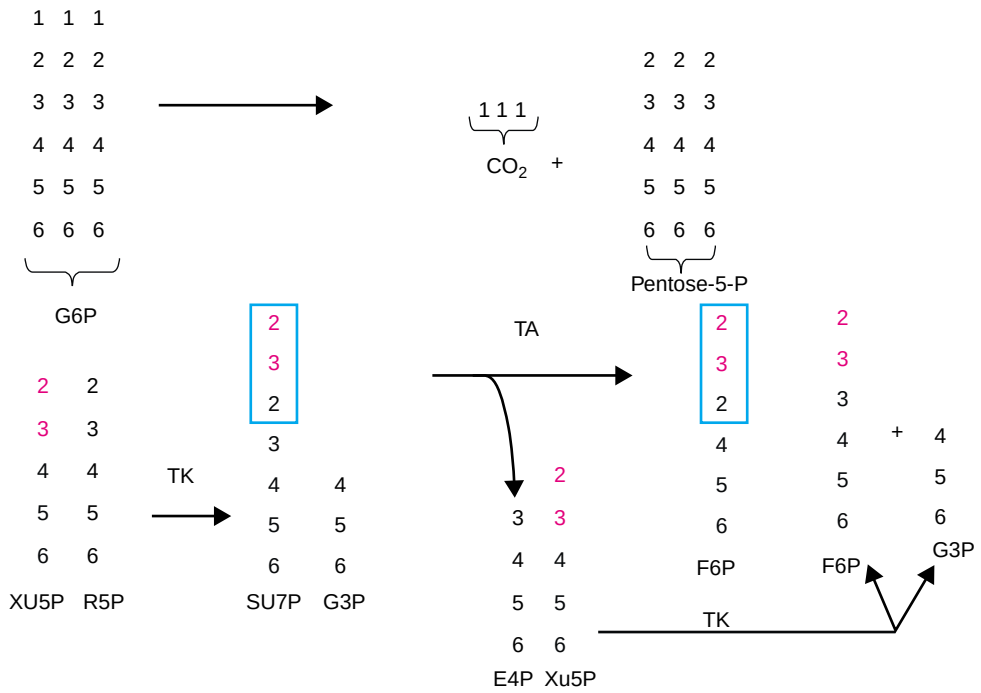

FIGURE 5 Fate of the carbons of the glucose-6-p (g6p) in its metabolism via the pentose phosphate pathway.

Estimates

The pathway is present in all cells. The highest activities are found in tissues where lipogenesis is prominent, e.g., liver, mammary gland, particularly during lactation, and adipose tissue. The pathway is also active in the reproductive glands, adrenal gland, and red blood cells. In those tissues 10–20% of glucose utilization may be via the pathway. The pathway has relatively high activity in growing tissue, e.g., in fetal and newborn tissues and tumors.

Clinical Importance

Maintaining the integrity of the red blood cells depends on having an adequate supply of reduced glutathione to protect the cells from toxic peroxides, as well as maintain hemoglobin in a reduced state. Several hundred million people, mainly in Africa, Asia, and the Mediterranean, have a genetic deficiency of glucose-6-P dehydrogenase. Drugs which increase the formation of peroxide, infections, and other causes of oxidative stress can induce acute hemolysis and hence anemia in those individuals.

The Wernicke–Korsakoff syndrome is a neuropsychiatric disorder occurring in individuals with a dietary deficiency of thiamine. Findings are eyeparalysis, abnormal gait, confabulation, and loss of memory. A genetic defect in transketolase has been suggested as the reason the syndrome is only observed in a small portion of those with thiamine deficiency. A genetic abnormality in transketolase has recently been found in a man with liver cirrhosis.

See Also the Following Articles

Pentose Phosphate Pathway, History of • Sugar Nucleotide Transporters

Glossary

NADPH Reduced form of nicotanamide adenine dinucleotide phosphate; the electron donor in reductive biosynthesis.

pentose phosphate pathway Pathway by which NADPH is generated for reductive biosynthesis and ribose-5-P for nucleotide and nucleic acid formation.

transaldolase Enzyme in the pentose phosphate pathway transferring 3 carbon units via the formation of a Schiff base.

transketolase Enzyme in the pentose phosphate pathway having thiamine as cofactor and transferring 2 carbon units.

Further Reading

Cabezas, H., Raposo, R. R., and Melendez-Hevia, E. (1999). Activity and metabolic roles of the pentose phosphate cycle in several rat tissues. *Mol. Cell. Biochem.* **201**, 57–63.

Horecker, B. L. (2002). The pentose phosphate pathway. *J. Biol. Chem.* **277**, 47965–47971.

Magnusson, I., Chandramouli, V., Schumann, W. C., Kumaran, K., Wahren, J., and Landau, B. R. (1988). Pentose pathway in human liver. *Proc. Natl. Acad. Sci.* **85**, 4682–4685.

Massillon, D., Chen, W., Barzilai, N., Prus-Wertheimer, D., Hawkins, M., Liu, R., Taub, R., and Rossetti, L. (1998). Carbon flux via the pentose pathway regulates the hepatic expression of the glucose-6-phosphatase and phosphoenolpyruvate carboxykinase genes in conscious rats. *J. Biol. Chem.* **273**, 228–234.

Mehta, A., Mason, P. J., and Vulliamy, T. J. (2000). Glucose-6-phosphate dehydrogenase deficiency. *Bailliere's Clin. Haematol.* **13**, 21–38.

Schenk, G., Duggleby, R. G., and Nixon, P. F. (1998). Properties and functions of the thiamin diphosphate dependent enzyme transketolase. *Int. J. Biochem. Cell. Biol.* **30**, 1297–1318.

Veech, R. L. (2003). A humble hexose monophosphate pathway metabolite regulates short- and long-term control of lipogenesis. *Proc. Nat. Acad. Sci.* **100**, 5878–5580.

Verhoeven, N. M., Huck, J. H., Roos, B., Struys, E. A., Salomons, G. S., Douwes, A. C., Van der Knaap, M. S., and Jakobs, C. (2001). Transaldolase deficiency: Liver cirrhosis associated with a new inborn error in the pentose phosphate pathway. *Am. J. Hum. Genet.* **68**, 1086–1092.

Wood, T. (1985). *The Pentose Phosphate Pathway.* Academic Press, Orlando.

Biography

Bernard R. Landau is a Professor of Medicine and Biochemistry at Case Western Reserve University and former Director of the Division of Endocrinology at University Hospitals of Cleveland. His research has focused on carbohydrate and lipid metabolism using radioactive and staple isotope tracer technology. He received a Ph.D. in chemistry from Harvard School of Arts and Sciences and an M.D. from Harvard Medical School.

Pentose Phosphate Pathway, History of

John F. Williams
Australian National University, Canberra, Australia

In this article the oxidative and non-oxidative segments of the pentose pathway (PP) of glucose metabolism are defined. The discovery in 1931–1935 by the German biochemist, Otto Warburg, of the oxidative division of the pathway and of the chemistry and role of a new pyridine nucleotide co-enzyme in its reactions is deliniated.

Background

The successful revelation of many of the reactants and enzymes of the non-oxidative PP was largely achieved by two American biochemists, Bernard L. Horecker and Ephraim Racker who, during 1950–1955, independently accomplished our current text-book knowledge of the classical reaction scheme of PP. A precise reaction order and metabolic map depiction of PP reactions was published by Horecker in 1955 from results of prediction labeling experiments that used variously labeled ^{14}C-ribose 5-phosphate dissimilation by liver and plant tissue extracts. Many PP reactions were also assigned roles in the path of carbon in photosynthesis that was unraveled by Calvin and colleagues during 1945–1954. The above accomplishments briefly terminated fundamental research on the nature of PP which was then replaced by an era (1958–1979) of metabolic pathway measurement.

Joseph Katz and Harland G. Wood were the pioneers who developed theory and methods for quantitative measurement of the contributions of pentose cycle (PC) and other pathways to total glucose metabolism. All of these methods depended on the metabolism of ^{14}C-labeled substrates. PC was measured to a significant level in many animal tissues but made its most notable contribution in adipose tissue, which resulted in the PP being renamed the (fat) F-type PP. Contrary to all expectation, many attempts to quantify PC in liver, the major tissue used by Horecker to establish the reaction scheme for the F-type PP, showed it measured a negligible and therefore puzzling contribution to glucose metabolism.

Based on these latter findings the reaction mechanism of PP was reinvestigated during 1965–1992 by Williams and colleagues in Australia. Liver featured in the investigations because it is a rich source of the enzymes and individual reactions of PP. New octulose and heptulose phosphate reactants and new enzyme activites were discovered. Using specifically ^{14}C-labeled substrates, a revised (liver) L-type PP was identified which quantitatively accounted for 25% of total glucose metabolism. These results aroused criticism and polemic by those defending F-type PC theory and measurement practice. This unsettling state was put to rest in 1993 when the Williams group, using ^{13}C-NMR spectrometry showed that the three group transferring enzymes of the PP, namely transketolase, transaldolase and aldolase catalyzed simultaneous mass transfer and group exchange reactions and in all cases the exchange rates exceeded the mass flux rate. As an example it was found that Transketolase exchange rates in normal and regenerating liver, four different neoplasms, spinach chloroplasts and adipocytes exceeded PP flux rates by 5–600 times. Since the groups being transferred by the above enzymes are ^{14}C-labeled in all of the unraveling investigations that involved F-type and L-type pathways, it is concluded that carbon isotope prediction labeling data are useless for the investigations of the reaction order and measurement of PP. Thus metabolic maps of PP in textbooks of biochemistry are erroneous. A concluding statement that best describes how the PP should now be viewed is given.

All or at least a substantial selection of the reactions of the pentose phosphate (PP) pathway of glucose metabolism occur in the cytoplasmic compartment of most cells. The reaction scheme is in two parts and consists of oxidative (Figure 1) and nonoxidative segments (Figure 2). The reactions of the oxidative segment are few and involve the decarboxylation of glucose-6-phosphate (Glc 6-P) to ribulose 5-phosphate (Ru 5-P) via 6-phosphogluconolactone and 6-phosphogluconate (6-Pg). There is concomitant production of two moles each of reduced nicotinamide-adenine dinucleotide phosphate (NADPH) and proton for each mole of Glc 6-P converted to Ru 5-P by oxidative decarboxylation. The non-oxidative reactions (Figure 2) are classically

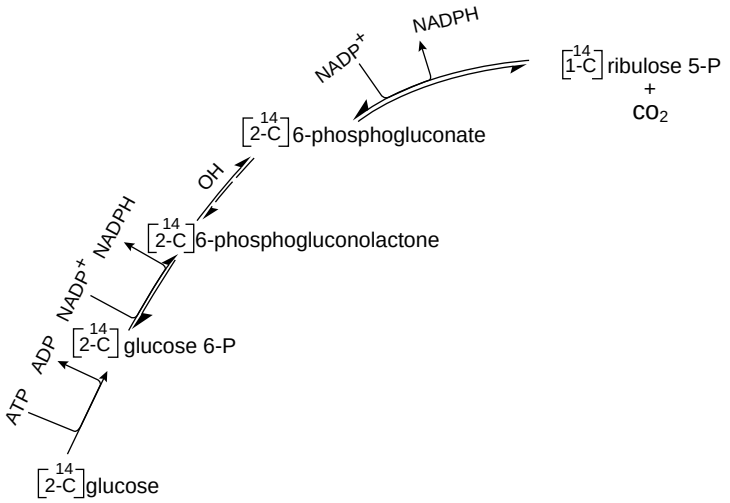

FIGURE 1 Reactions of the oxidative segment of the pentose pathway showing the conversion of [2-^{14}C]-glucose to CO_2 and [1-^{14}C]-ribulose 5-phosphate. Glucose is phosphorylated by hexokinase and oxidatively decarboxylated by the concerted actions of glucose 6-phosphate dehydrogenase, water at pH 7.4 or lactonase and 6-phosphogluconate dehydrogenase (see glossary for equation).

depicted as a diversity of reversible steps for the interconversion and linkage of other pentose phosphate products that arise from Ru 5-P, with triose and hexose phosphates that are also common intermediates in cytoplasm of the higher flux glycolytic pathway of glucose metabolism. The reactions of Figure 2 also show sugar phosphate intermediates (glycolyl units) with 3, 4, 5, 6, and 7 carbon atoms that are generated by the reversible reactions of the nonoxidative segment. There are thus three biosynthetic functions of PP reactions that relate to cellular energetics, growth, and repair: (1) the contribution by the oxidative segment to the provision and maintenance of a high NADPH/$NADP^+$ redox potential and thereby the supply of electrons for some reductive anabolic processes; (2) the formation of ribose 5-phosphate (Rib 5-P) for all nucleotide and nucleic acid biosynthesis; and (3) a storage pool of diverse phosphorylated glycolyl units that may be used in biosynthetic and energy-yielding reactions by other pathways. Finally, selected reactions of the nonoxidative segment are also part of the most extensive synthetic and life-sustaining event on the planet, namely, the photosynthetic reductive path of CO_2 assimilation in all C-3 plants.

Early Discoveries

A summary of the biochemistry of the reactions, enzymes, methods, distributions, and quantitation of the pathways of Figures 1 and 2 in tissues, together with all references cited in this article that relate to the history of the "unraveling" events of the pathway, are given in a comprehensive review of the PP by Williams J. F. *et al.* in 1987. Discoveries which led to the formulation of the classical depiction of the PP (Figures 1 and 2) commenced in 1931 with the discovery of glucose 6-phosphate dehydrogenase (Glc 6-P DH) by Otto Warburg, a German biochemist and a Nobel laureate of extraordinary distinction and influence. Warburg named the enzyme *Zwischenferment* (intermediate enzyme) in order to designate the branching of Glc 6-P away from the pathway of fermentation (glycolysis). In 1935 a second enzyme, 6-phosphogluconate dehydrogenase, was isolated together with a new pyridine nucleotide coenzyme (*Wasserstoffübertragendes*: hydrogen-carrying coferment), which is now called $NADP^+$. Warburg recognized that $NADP^+$ was chemically and functionally different from the NAD^+ coenzyme of glycolysis. With these discoveries Warburg had opened the way into an alternate path of glucose dissimilation. Warburg believed that the NADPH product of these reactions was the substrate of cellular respiration and was thus a prime chemical source of aerobic cellular energy. This view was strongly held and disseminated for the next 20 years, such that the PP was first called the "direct oxidative pathway" in order to distinguish it from the path of fermentation of glucose and lactic acid formation in muscle.

The proposition linking NADPH and respiration (eqns. [1]–[3]) was shared by Erwin Haas, who was a member of Warburg's Berlin-Dahlem laboratory. (Haas fled Germany in 1938 and proceeded to the University of Chicago, where he was joined by Bernard Horecker, a fresh Ph.D. graduate, who was already exhibiting a flair for enzymology.) Haas possessed much of Warburg's data, understood his methods very well, and had a plan of research to test the proposed role of NADPH in respiration. Haas and Horecker set out to isolate a putative NADPH-cytochrome *c* reductase (eqn. [1]) in order to demonstrate the existence and nature of an

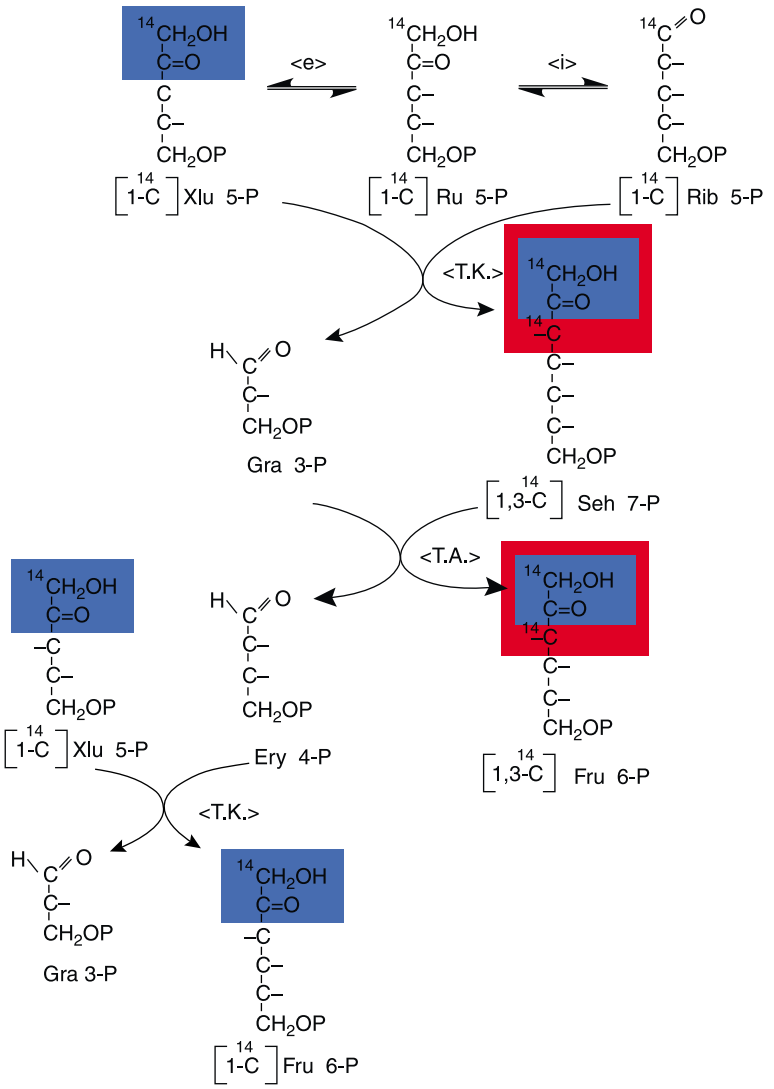

FIGURE 2 The proposed reaction sequence of the non-oxidative segment of the *classical* F-type pentose pathway *in vitro*. The [1-^{14}C]-ribulose 5-P substrate is the labeled product of the Figure 1 reaction scheme and the reactions display the theoretical distributions of ^{14}C-isotope from pentose 5-P into the carbon atoms of labeled intermediates and products. The enzymes catalyzing the reaction steps are: e, ribulose 5-phosphate 3-epimerase, i, ribose 5-phosphate isomerase; TK, transketolase; TA, transaldolase. The blue panels show the two-carbon active *glycolaldehyde* group that is conveyed by TK mass transfer and group exchange. The red panels show the three-carbon *dihydroxyacetone* group that is carried by TA mass transfer and exchange (see text and glossary for other detail).

enzyme that was hypothesized to be the "missing link" in a respiratory pathway between reduced pyridine nucleotide and oxygen via the cytochrome system (eqn. [3]):

$$\mathrm{NADPH + H^+ + Cyt\text{-}cFe^{3+} \xrightarrow{\text{NADPH cytochrome } c \text{ reductase}} NADP^+ + Cyt\text{-}cFe^{2+} + 2H} \quad [1]$$

$$\mathrm{2H + Cyt\text{-}cFe^{2+} + 0.5\ O_2 \xrightarrow{\text{Cytochrome oxidase}} H_2O + Cyt\text{-}cFe^{3+}} \quad [2]$$

Sum reaction:

$$\mathrm{NADPH + H^+ + 0.5\ O_2 \longrightarrow NADP^+ + H_2O.} \quad [3]$$

The search for an enzyme activity was successful and a reasonably pure flavoprotein, NADPH-cytochrome *c* reductase, was isolated from yeast in 1940. Research was interrupted and not taken up again until the end of the Second World War. By 1948, Horecker had returned to the project and soon extensively purified the enzyme from liver. However, by that time, there was growing evidence that the oxidation of NADPH was not the source of reducing equivalents for respiration and the entire proposal was abandoned in 1951, when Albert Lehninger showed that NADH was the "low-redox" respiratory chain substrate for oxidative phosphorylation in mitochondria.

The understandable disappointment with the realization that NADPH-cytochrome *c* reductase had no role in respiratory energy production (it is now known to be part of the cytochrome P-450 hydroxylation-detoxification scheme) directed Horecker's interest to a larger problem, namely, an inquiry into the nature, fate,

and metabolic role of the pentose product of 6-Pg decarboxylation (Figure 1). It is also noteworthy that the British biochemist Frank Dickens (Courtauld Institute, UK) had been making pioneering investigations on this topic since 1936. However, a solution of the problem was made in the USA, where metabolic biochemistry and enzymology were flourishing in the 1950s. The dominant contributions came from the laboratories of Bernard Horecker, Ephraim Racker, and Seymour Cohen. Moreover, a further stimulus was the spectacular investigation made in Melvin Calvin's laboratory at UC Berkeley, which led to a Nobel prize and an understanding of the path of carbon fixation in photosynthesis (PS). Calvin's progress was heavily dependent on success in research by the aforementioned biochemists to resolve the enzymology and chemical problems posed by the reactions of Figure 2.

By 1950 all investigators possessed strong clues which served as signposts for an ultimate elucidation of a PP reaction scheme. (1) There was clear evidence that an alternate path of Glc 6-P dissimilation existed in yeast, red cells, and other animal tissues. (2) Dickens had confirmed that 6-Pg was oxidatively decarboxylated at carbon 1, to yield pentose 5-phosphate and other sugar phosphate products including a putative tetrose-P. He also demonstrated that Rib 5-P was oxidized at 5 times the rates of arabinose 5-phosphate (Ara 5-P) and xylose 5-P (theoretical products of 6-Pg decarboxylation). (3) Finally, as early as 1938, Zacharias Dische, using red cell lysates, found that inosine and inorganic phosphate (P_i) were converted to triose and hexose phosphates. This last important finding of the possible end products of Rib 5-P dissimilation was confirmed in 1946 by Schlenk and Waldvogel, who showed Glc 6-P formation from Rib 5-P using rat liver extracts.

Post Second World War Discoveries of Reactions in the Nonoxidative Segment of the Pentose Pathway

With the above background, between 1950 and 1955, very significant discoveries of enzyme and substrate reactivities followed, which were incorporated into a reaction scheme (mechanism) for the "classical" nonoxidative PP (Figure 2). The diagram in the figure is also designated the F-type (for fat-cell) PP, because it was later shown to uniquely measure a quantitatively large contribution to metabolism when Glc was converted to fatty acid and triglyceride in insulin-stimulated adipocytes. The findings may be summarized in the following temporal conjunction. In 1951 Cohen's group showed that Rib 5-P and Ara 5-P were formed from 6-Pg oxidation. Horecker and his collaborators confirmed Rib 5-P formation and unequivocally established that Ru 5-P was the first pentose-P formed from 6-Pg decarboxylation. They also identified a new enzyme, ribose 5-phosphate isomerase, which catalyzed the interconversion of the two pentose phosphates (see Figure 2). In 1952, Horecker and Smyrniotis, using a liver enzyme preparation, reported the important observation that Rib 5-P was metabolized to sedoheptulose 7-phosphate (Seh 7-P). This seven-carbon ketosugar ester was also found by Andy Benson, in Calvin's laboratory, and was identified as an early product of PS carbon fixation. Seh 7-P was formed by the action of transketolase (TK) (see Figure 2). TK was discovered by Racker and his collaborators in 1951, and it was demonstrated that it catalyzed the transfer of a two-carbon fragment (an active glycolaldehyde group) from appropriately structured ketulose-sugar donors to a wide selection of aldo-sugar acceptors. Two of its donor transfer actions, using different aldo acceptors, are shown as blue rectangular panels in Figure 2. The enzyme requires Mg^{2+} and thiamine pyrophosphate to be active and the list of 15 of its glycolaldehyde acceptor substrates is tabulated. Horecker's group discovered another broad-specificity group transferring enzyme, namely, transaldolase (TA), which catalyzed the reversible transfer of a dihydroxyacetone-enzyme-bound moiety (shown as red panels in Figure 2) from Seh 7-P to glyceraldehyde 3-phosphate (Gra 3-P), thereby forming Fru 6-P and a tetrose phosphate, which was neither isolated nor identified. The availability of synthetic erythrose 4-phosphate (Ery 4-P) enabled Kornberg and Racker to demonstrate the reversal of the TA reaction (eqn. [4]), thus satisfying the reason for its specific inclusion as an intermediate in the reaction scheme of Figure 2. Ery 4-P probably only exists in exceedingly low concentrations in any tissue and to date there is no evidence that it has ever been correctly measured in, or isolated from, any preparation carrying out PP metabolism.

$$\text{Fru 6-P} + \text{Ery 4-P} \longleftrightarrow \text{Seh 7-P} + \text{Gra 3-P}. \quad [4]$$

Finally, in 1954, a third ketopentose ester, xlulose 5-phosphate (Xlu 5-P), was isolated as a product of Rib 5-P metabolism by Ashwell and Hickman. Racker showed that this new intermediate, rather than Ru 5-P, was a definitive substrate of TK. The ribulose 5-phosphate-3′-epimerase (see Figure 2) that catalyzed the formation of the ketosugar imparted the *trans*-configuration to the hydroxyl at C-3, which is the necessary stereochemical condition for substrate reactivity. The 3′-epimerase was simultaneously purified in 1956 by Stumpf and Horecker at NIH and by Dickens and Williamson in the UK (Williamson later became the lifelong collaborator of Hans

Krebs) in the UK. In summary, the above research had uncovered an array of substrates and enzymes that could possibly satisfy the minimum requirements for a new pathway that connected the product of 6-Pg decarboxylation with the formation of hexose and triose phosphates.

Finding a Reaction Sequence for the Nonoxidative Pentose Pathway

It is possible to draw various theoretical schemes that oblige the arithmetic conjunction of five carbon sugars with a summary outcome of sugar products that contain six and three carbon atoms, respectively. That variety is greatly enhanced if reactions by aldolase (Ald) are included. Aldolase occupies the same cellular compartment as the PP; it is a dihydroxyacetone 3-phosphate (DHAP) group transferring enzyme, with a catalytic capacity that is usually much greater than TK or TA (a notable exception is adipose tissue where Ald activity is low and only approximates the activity of TK and TA). Ald also has a broad substrate array of aldo-sugar phosphate acceptors, most of which are the same substrates as those involved in TK and TA reactions. (It has never been clear why the pioneering investigators of the nonoxidative PP assigned aldolase a role of catalytic "silence.")

The results of the two experiments that aimed to identify the reaction sequence (mechanism) of the PP were published by the Horecker group in 1954. Briefly, Horecker adopted a prediction-labeling technique using [1-^{14}C]- and [2,3-^{14}C]-Rib 5-P as substrates and enzyme preparations from rat liver, pea leaf, and pea root tissues to catalyze the formation of ^{14}C-labeled hexose 6-P. It was assumed that the position and degree of any ^{14}C- labeling in Glc 6-P formed from these variously labeled substrates would indicate the nature and order of the reactions involved in Fru 6-P formation (see Figure 2). The enzyme preparations were made from acetone-dried powders of the above tissues. They were therefore free of all nucleotides and thus confined the reactions to a hexose 6-P end point by preventing any possibility of its recycled return through the oxidative segment, with consequent further scrambling of a "predicting" isotope-labeling pattern. Mg^{2+} was also omitted from the reaction mixture in order to inhibit the activity of fructose bisphosphatase and thus the formation of a contaminating Fru 6-P resulting from aldolase manufactured Fru 1,6-P_2 using the triose-P products of TK-catalyzed reactions.

The experiments with liver enzyme preparation were of 17 h duration. Ribose 5-P was rapidly utilized during the initial 3 h and Seh 7-P also accumulated during this early period. Only with the slow decline in Seh 7-P at 6 h was there an increased linear production of Glc 6-P, which was harvested after 17 h and degraded carbon atom by carbon atom to produce the ^{14}C distribution pattern of the whole molecule. The results, using [1-^{14}C]-Rib 5-P as substrate showed that the Glc 6-P product was labeled with ^{14}C isotope in carbons 1 and 3 (see Figure 2) with a C-1/C-3 ratio of 3 (74% of the ^{14}C isotope in C-1 and 24% in C-3). Horecker "tentatively" proposed that the reaction scheme of Figure 2 was consistent with the above isotope distribution. Clearly the consistency is not there, because the pooled [1,3-^{14}C]-Fru 6-P formed in the TA and second TK-catalyzed reactions in Figure 2 impart a ^{14}C content in C-1 and C-3 with a ratio of 2 (twice as much in C-1 as C-3). The difference is serious and the isotope distributions cannot be reconciled with the Figure 2 reaction scheme, nor can the difference be attributed to the tedious analytical and degradative procedures, since the percentage errors in the determination of C-1 are only 2%; C-2, 2.7%; and C-3, 1% with a cumulative percentage error of 12% for the estimate of all carbons of the molecule. The results of the companion experiment conducted by Gibbs and Horecker in1954 used [2,3-^{14}C]-Rib 5-P as substrate and liver, pea root, and pea leaf enzyme preparations made from the acetone-dried powders of these tissues. The results deviated even more radically from the predictions imposed by the sequences of Figure 2 than the above data using [1-^{14}C]-Rib 5-P. It is emphasized that in the publications of these two studies, an ordered series of chemical equations for the nonoxidative PP was only "tentatively" proposed and a metabolic map was not shown. However, in 1955, Horecker authored two important and substantial reviews of carbohydrate metabolism and presented for the first time the diagram illustrating the new metabolic pathway (still with the "tentative" caveat). This illustration (Figure 2) is still the chart of the PP or pentose cycle (PC)—a pathway that has featured in textbooks of general biochemistry since 1956. It is astonishing that such a profound disagreement between practice and theory was so uncritically ignored by the general community of biochemists and glossed over by the very few who drew it to attention in the review literature. This indifference resulted in the prompt inclusion of the scheme of Figure 2 into the canon of metabolic biochemistry without further inquiry. It is also ironic that the participation of a large number of PP reactions into the path of carbon in PS added confidence and prestige to the status of the PP. However, there were two other comprehensive investigations of the mechanism of the PP, one by Joseph Katz and co-workers in 1955 using [1-^{14}C]-Rib metabolism in liver slices and the other by Howard Hiatt in 1957 using the same labeled substrate in mouse liver *in vivo*. These workers did not find ^{14}C distributions in the labeled glucose product with twice as much isotope in C-1 as C-3, but

instead found the carbons equally labeled. These independent early failures to confirm the predictions of Figure 2 were also ignored.

Other than valuable research by Patricia McLean and her collaborators at the Courtauld Institute (UK), who investigated the enzymology, endocrinology, and occurrence of PP reactions in many animal tissues, all fundamental research on the mechanism of the pathway essentially ceased in 1957 and was not taken up again for another decade. Instead the era of the quantitative measurement of pathways of carbohydrate metabolism had dawned and PP measurements featured hugely. This emphasis on quantitation is best summarized in the following statement by Harland G. Wood in 1955. "The determination of the relative role of different pathways in normal living cells is without doubt of the greatest fundamental importance to our understanding of life processes and will in the future require more attention in all fields of metabolism." Wood (Western Reserve University Medical School, Ohio) collaborated with Joseph Katz (Cedars of Lebanon Hospital, Los Angeles) over the next eight years in the development and elaborations of measurement theory for an entity denoted by H. G. Wood and later defined by Wood and Katz as the pentose cycle (PC).

The Quantitation of the Pentose Cycle: Theory and Practice

Between 1958 and 1979 a dozen elegant theoretical papers were published that provided the mathematical basis and formulas for measuring the F-type PC using ^{14}C-labeled substrates. All of these methods depended on a quantitative solution of the problem posed by the recycling of ^{14}C isotope distributions that emerge by the metabolism of the substrates [2-^{14}C]- or [3-^{14} C]-glucose in PC. Calculating the different distributions of labeled carbon to infinite cycles, for all percentage contributions of PC, is a difficult mathematical problem, which was solved by Joe Katz. Katz is not only a gifted biochemist but also an equally talented mathematician and innovative metabolic theorist. The acceptance of a PC definition imposed agreement that all ^{14}C-labeled Fru 6-P formed by the Figure 2 reaction sequence is converted to Glc 6-P and recycled again through the oxidative segment reactions. The quintessence of all measurement methods has involved the development of mathematical expressions describing the rhythmical and ordered redistributions of either carbon 2 or 3 from labeled substrate glucose, into positions 1, 2, and 3 of the hexose 6-P products for any percentage contribution of PC. Such a theoretical distribution is a unique property of the PC. Experimental data for the C-1/C-2 and C-3/C-2 ratios, that have definite limits and values imposed by Katz and Wood theory, measure the degree of redistribution of ^{14}C from the above labeled substrates into the top three carbons of the Glc 6-P product, which is isolated and analyzed for ^{14}C distribution following labeled substrate metabolism. The ratios, in their appropriate measurement equations, express the PC contribution relative to the total metabolism of glucose. The above statements cannot be qualified. They derive from the reaction sequence of Figure 2, which is the mechanistic basis for all the formulas of all the "measurement" papers. The precise values for C-1 and C-3 and the ratio of their isotopic labeling are the "identity" badge of the classically defined PC reaction sequence, which is the foundation of its theories of existence and quantitation. It was therefore intriguing to note, that notwithstanding the initial ambiguities in the establishment of the Figure 2 scheme and the failed efforts of the Katz and Hiatt experiments to support it, that no less than ten independent efforts, over nearly 30 years, have failed to find any significant level of PC in liver using the Katz and Wood method. Liver is a rich source of the enzymes of the PP and it can provide *inter alia* a ready display of the reactions of Figures 1 and 2. Thus, the failure by all measurement investigations to find an F-type PC in liver was mystifying.

The Search for a New Reaction Scheme for the Pentose Pathway

A solution to the mystery was sought in the author's laboratory, with investigations that began in 1965 at the University of New South Wales and later at the Australian National University. Work commenced with the propositions that the scheme of Figure 2 may be an erroneous interpretation of the PP and the coupling of Figures 1 and 2 reactions into a metabolic cycle (PC) was possibly ill-conceived. The following three sets of findings summarize selected aspects of progress in the unraveling of a new PP reaction sequence in liver that does significantly contribute (20–30%) to glucose metabolism.

First, the original experiment performed by Horecker in 1954 was repeated using [1-^{14}C]-Rib 5-P and exactly the same preparation of liver enzymes. However, reaction mixtures were sampled for the labeled Glc 6-P product at a series of much shorter time intervals and right up to the 17 h termination point described in the original work. The results showed a patterned assortment of label distributions in Glc 6-P, that drifted from 8 to 17 h towards the isotope composition in C-1 and C-3 that was originally reported by Horecker. Notably in this study, the C-1/C-3 ratio at 17 h, was the much-sought value of 2. Moreover, in the seven-time

samples, which commenced at 1 min, Glc 6-P was heavily labeled in C-2, C-4, and C-6, while C-1 and C-3 only began to accumulate ^{14}C-isotope after 3 h of reaction. Although this was a study *in vitro*, it is obvious that liver cells *in vivo* do not take between 3 and 17 h to elaborate a path of metabolism and that more enlightening events were being revealed by the isotope distributions in the samples analyzed between 1 and 30 min of reaction. A carbon balance analysis of all compounds in the various reaction mixtures showed that the intermediates of Figure 2 only accounted for 80% of the carbon in the Rib 5-P substrate. The compounds comprising the missing 20% were identified as sugar phosphates, mostly ketuloses (see Figure 3). They were isolated, identified, and shown to be radioactive. These keto-ester sugars were Seh 1,7-P_2, D-*manno*-Heptulose 7-P; D-*glycero*-D-*altro*-octulose 1,8-P_2(D-*g*-D-*a*-Oct); D-*glycero*-D-*ido*-octulose 1,8-P_2(D-*g*-D-*i*-Oct); and a small amount of Ara 5-P (see Figure 3). Octulose (Oct)-, mono- and bisphosphates, and Seh 1,7-P_2 were also isolated and measured in fresh liver. Figure 4 shows the structures and reactions of these sugar esters in a new and much modified reaction scheme for the PP in liver. The new intermediary compounds were easily isolated from all incubations from 30 min to 17 h. The scheme of Figure 4 shows the new PP with prediction ^{14}C-labeling patterns in the intermediates and products of the reactions. The reaction scheme for Figure 4 was initially formulated from the distributions of ^{14}C in the labeled Glc 6-P and D-*g*-D-*i*-Oct 1,8-P_2 formed from [1-^{14}C]-Rib 5-P during the early intervals of the repeat experiment performed by Horecker and co-workers in 1954. The new pathway, called L (liver)-type PP, is distinguished from depictions of the classical F-type PP by the inclusions of Seh-1,7-P_2 and octulose (Oct)-, mono-, and bisphosphates together with Ara 5-P as new intermediates. Aldolase, phosphotransferase (PT), and arabinosephosphate isomerase are new enzymes. Mass transfer catalysis by TA was omitted, but the effects of active TA-exchange reactions (TA_X), which accounted for the 4,6-^{14}C labeling of Glc 6-P, were encountered in all samples. The second TK reaction forming hexose 6-P products in the L-type PP (Figure 4) used D-*g*-D-*i*-Oct 8-P as a substrate and TK was also found to catalyze very active exchange reactions as does aldolase. A clear demonstration that aldolase is a mandatory catalyst in liver PP involved the immunochemical evidence of Bleakly and co-workers in 1984, who showed the cessation of all hexose 6-P formation when liver aldolase antibody titrated the removal of aldolase from the system where Rib 5-P was reacted with the rat liver enzyme preparation that was used to establish the scheme in Figure 2. Irrespective of the other contrary data, this evidence alone showed that there was another reaction mechanism involving Ald in liver PP. The claim that aldolase is an essential enzyme in the PP was also supported by data of Cori and Racker, who, in an *in vitro* "construction" of a PP preparation for the complete oxidation of Glc, noted the formation of Oct-P and the need to include aldolase and sedoheptulose 1,7-bisphosphatase for the construction system to work.

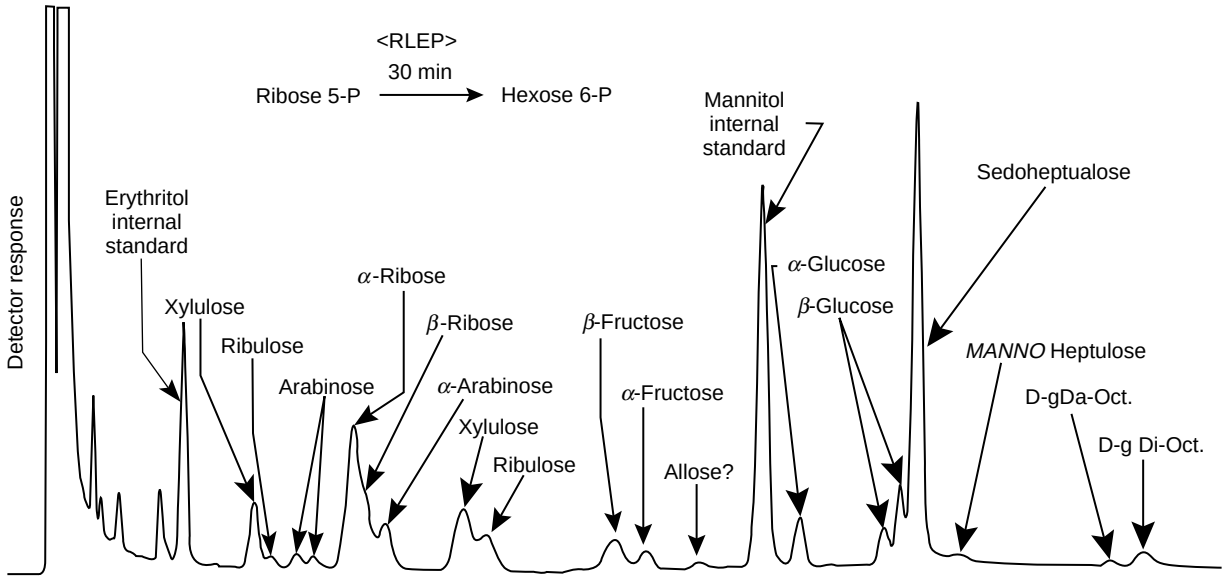

FIGURE 3 Gas liquid chromatogram (GLC) of the dephosphorylated derivatized sugars formed after 30 min reaction of rat liver enzyme preparation with ribose 5-phosphate. The procedures for sample processing and GLC are given in Williams, J. F., Clark, M. G., Arora, K. K., and Reichstein, I. C. (1984) Glucose 6-phosphate formation by L-type pentose pathway reactions of rat liver in vitro: Further evidence. *Seyler's Zeit. Physiol. Chem.* **365**, 1425–1434.

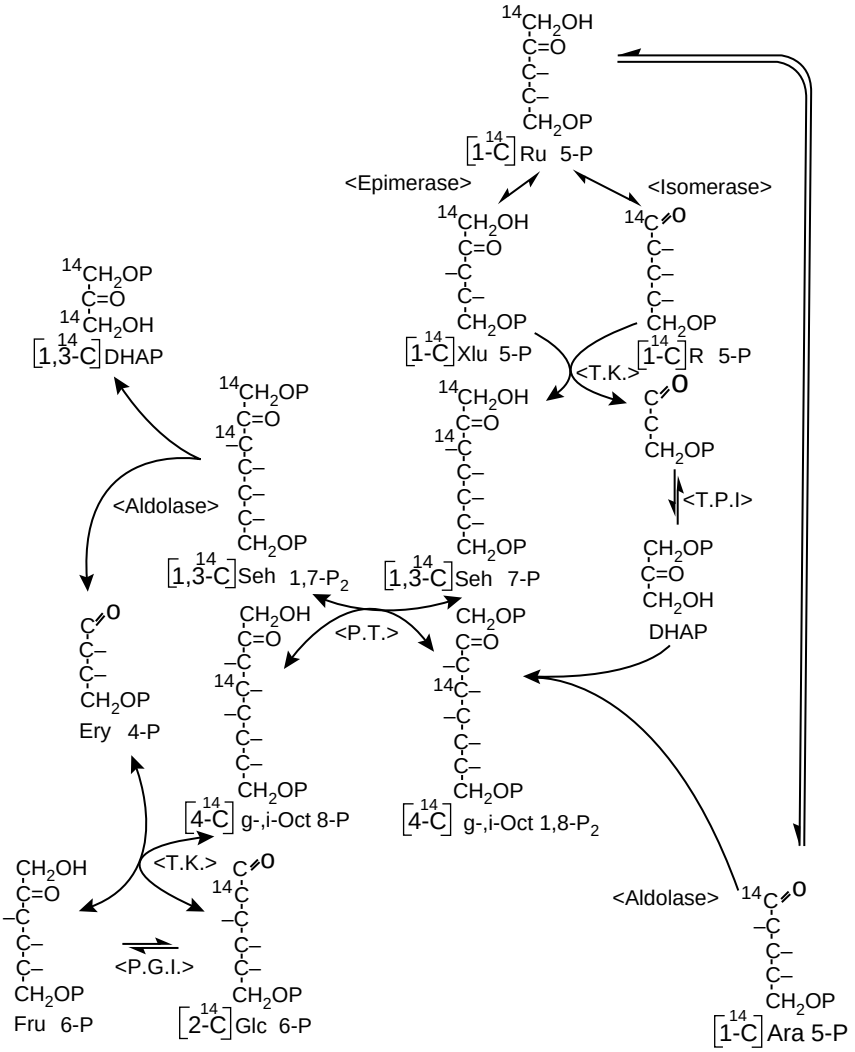

FIGURE 4 The proposed reaction sequence of the nonoxidative segment of the L-type pentose pathway. The [1-^{14}C]-ribulose 5-P substrate is the labeled product of the Figure 1 scheme and the reactions display the theoretical and the found distributions of ^{14}C-isotope from pentose 5-P substrate into labeled Glc, triose and Oct intermediates, and products. The epimerase, isomerase, and TK enzymes are the same catalysts that operate in the F-type pathway. New enzymes are arabinosephosphate isomerase that interconverts arabinose and ribulose 5-phosphates, aldolase, triosephosphate isomerase (EC 5.3.1.1), glucosephosphate isomerase and D-*glycero*-D-*ido*-octulose 1,8-bisphosphate: D-*altro*-Heptulose 7-phosphotransferase, called phosphotransferase (PT) (see Arora, K. K., Cortis, P. A., Bleakley, P. A., and Williams, J. F. (1985) Identification and measurement of D-glycero-D-ido-octulose 1,8-bisphosphate: D-altro heptulose 7-phosphotransferase enzyme in tissues with L-type pentose phosphate pathway activity. *Int. J. Biochem.* **17**, 1329–1337). Besides new enzymes and intermediates, the L-type pathway is distinguished from the F-type pathway by the formation of Glc 6-P labeled in the 2 position by flux and in positions 4 and 6 by group-transfer enzyme exchanges involving the [1,3 ^{14}C]-DHAP product. The triosephosphate formed by the F-type pathway is unlabeled.

Exposing the Problem of Assigning a Reaction Scheme to the Nonoxidative PP

The reactions and enzymes shown in Figure 4 occur in liver cytoplasm and probably in the soluble enzyme compartments of the tissues of most animals (exceptions are adipocytes and possibly lactating mammary gland), plants, and some microorganisms. The failure to uncover "uncontentious" evidence for both F- and L-pathways that permitted the placement of C-3 to C-8 glycolyl phosphates in a reaction order and with stoichiometry that satisfied flux demands of a metabolic pathway or cycle, is the crux of this 50-year-old enigma. Finding an answer to the problem proved to be quick, obvious, and simple. Uncovering irrefutable evidence and proof for the explanation was a more pressing task that was solved by Flanigan *et al.* in 1993. It was the universal use of ^{14}C isotopes in prediction-labeling experiments to both inquire into mechanism and predicate theories for quantifying the F- and L-type

pathways, which was the first fundamental error. The second misjudgment was lack of attention to the consequences of the glycolyl-group exchange reactions that are actively catalyzed by TK_x, TA_x, and Ald_x. The subscript x is used to distinguish exchange catalysis from the mass transfer activity of these enzymes. Moreover, there was an inchoate recognition and warning that both functions were simultaneously active during the unique catalytic roles of these enzymes in PP and PS. The qualitative and partial definition of TK_x and TA_x by Katz and Wood proved to be an insufficient and largely unheeded alarm to the PC measurers.

Flanigan and co-workers used ^{13}C-NMR spectroscopy for their investigations, thus bypassing any controversy concerning results that depended on "wet" chemical methods for the determination of ^{14}C labeling patterns. The maximum catalytic capacities for exchange by the three enzymes were all quantified in reaction mixtures at mass-transfer equilibrium, by measuring, for TA, the rate of exchange of the ^{13}C-TA dihydroxyacetone group with unlabeled Seh 7-P. TK_x was measured by the rate of incorporation of a (2-^{13}C)-TK glycolaldehyde group to unlabeled Fru 6-P and Ald_x by the exchange of an unlabeled DHAP-Ald group from D-*g*-D-*a*-Oct 1,8-P_2 to [1-^{13}C]-Rib 5-P and measurement of the rate of formation of [4-^{13}C]-D-*g*-D-*a*-Oct 1,8-P_2. A comparison of the exchange capacities of these enzymes with the maximum nonoxidative PP flux rates in three liver preparations showed that TK_x and Ald_x exceeded flux by 9–19 times in liver cytosol and acetone-powder enzyme preparations *in vitro* and by 5 in hepatocytes. TA_x was less effective in exchange, only exceeding the flux rate by 1.6 and 5 in liver cytosol and acetone-powder preparations. Values for the ratios of the rates of group exchange and pathway flux are important because of the feature roles of liver and of these preparations in the establishment and status of the schemes of Figures 2 and 4 in biochemistry. The prevalence of exchange activity was also investigated using the dominant TK_x rates relative to the max PP flux rates of normal and regenerating liver, Morris hepatoma, mammary carcinoma, melanoma, colonic epithelium, spinach chloroplasts, and epididymal adipocytes. TK_x rates in these preparations exceeded PP flux by 5–600 times.

Conclusion

It is the conclusion of this brief history that sufficient evidence is on record to show that predictions and calculations based on ^{14}C-distributions in PP products and intermediates are misleading. The isotope patterns cannot reveal the order of the reaction sequences, which can only be measured by an uncompromised net flow of carbon. Instead, the ^{14}C-distributions mainly reflect a composition of disorder, induced by random combinations of group exchanges that scramble, if not obliterate, flux influences. Thus, the description and metabolic map of PP is "in error" in biochemical texts.

How Should We Now View the PP—With or Without Conceptual Structures?

The reactions of Figure 1 are not in contention. The enzymes and intermediates of Figures 2 and 4 are probably present in most tissues, particularly where Ald activity is greater than that of TA. There is, however, no secure evidence that the individual reactions of either Figure 1 or 2 are so linked that they constitute a linear metabolic pathway with ordered reactant and end-product stoichiometry or fixed direction of operational flux. Nor is there uncontentious proof that the PP generally operates as a metabolic cycle. The reaction array is best perceived now as it was in 1958, when the late Prof. Merton Utter (Western Reserve University School of Medicine) so suggested limiting these reactions to an unstructured pool or reservoir of glycolyl phosphates, with as many accessible inputs and exits as there are intermediates in Figures 2 and 4. This includes hexose and triose phosphates that may react reversibly to form or be formed from pentose phosphates by mass action effects and in the process mix with all of the other glycolyl phosphates, which are not constrained by stoichiometric obligation to "connecting" reaction sequences, and which may be freely removed by the needs of other metabolism.

See Also the Following Articles

Pentose Phosphate (Hexose Mono Phosphate) Pathway • Sugar Nucleotide Transporters

Glossary

metabolic pathway A linear sequential order of consecutive enzymatic reactions that proceed from a flux-generating step. The pentose pathway (PP) consists of a set of freely diffusible soluble enzymes, coenzymes, and reactants.

non-oxidative PP (Figures 2 and 4) has the sum reaction of Eqn 1

$$3 \text{ Pentose 5-P} \longleftrightarrow 2 \text{ Fructose 6-P} + 1 \text{ Glyceraldehyde 3-P}. \quad [5]$$

oxidative segment of PP This segment is assigned the stoichiometry of eqn. [6] because of its link with the reactions of Figures 2 and 4.

$$3 \text{ Glc 6-P} + 6 \text{ NADP}^+ \longrightarrow 3 \text{ CO}_2 + 3 \text{ pentose 5-P} + 6 \text{ NADPH} + 6\text{H}^+. \quad [6]$$

pentose cycle (PC) This cycle is a theoretical construct, based on the reactions of Figure 2 for F-type PC and Figure 4 for L-type PC and

the reaction of eqn. [7]. The PC mechanisms permit mathematical treatment of theoretical ^{14}C distributions, generated by a conforming metabolism of labeled glucose, which leads to specific formulae for quantifying the two varieties of PC. The sum of eqns. [5], [6], and [7] is [8], which is the sum reaction of both F-type and L-type PC.

$$2\ \text{Fructose 6-P} \xleftrightarrow{\text{Glucosephosphate isomerase (EC 5.3.1.9)}} 2\ \text{Glucose 6-P}, \qquad [7]$$

$$\text{Glucose 6-P} + 6\ \text{NADP}^+ \longrightarrow 3\ \text{CO}_2 + \text{Gra 3-P} + 6\ \text{NADPH} + 6\ \text{H}^+. \qquad [8]$$

Further Reading

Arora, K. K., Cortis, P. A., Bleakley, P. A., and Williams, J. F. (1985). Identification and measurement of D-glycero-D-ido-octulose 1,8-bisphosphate: D-altro heptulose 7-phosphotransferase enzyme in tissues with L-type pentose phosphate pathway activity. *Int. J. Biochem.* **17**, 1329–1337.

Flanigan, I. L., Grant-Collins, J., Arora, K. K., MacLeod, J. K., and Williams, J. F. (1993). Exchange reactions catalyzed by group transferring enzymes oppose the quantitation and the unravelling of the identity of the pentose pathway. *European J. Biochem.* **213**, 477–485.

Florkin, M. (1979). The pentose phosphate cycle. In *Comprehensive Biochemistry* (M. Florkin and E. H. Stotz, eds.) Vol 33A, Part V, pp. 61–79. Elsevier/North-Holland Biomedical Press, Amsterdam.

Gumma, K. A., and McLean, P. (1971). Factors controlling the flux of glucose through the pentose phosphate pathway. *Post Grad. Med. J.* (June supplement), 403–406.

Horecker, B. L. (1961). Alternative pathways of carbohydrate metabolism in relation to evolutionary development. In *Proc. 5th Int. Congress of Biochemistry*, Vol 111, pp. 86–93. Moscow Pergamon Press, Oxford.

Horecker, B. L. (1982). Cytochrome reductase, the pentose phosphate pathway and Schiff base mechanisms. In *Oxygen, Fuels and Living Matter* (G. Smenza, ed.) Part 2, pp. 59–75. Wiley, Chichester.

Horecker, B. L. (2002). The pentose phosphate pathway. *J. Biol. Chem.* **277**, 47965–47971.

Katz, J. (1961). The use of glucose-^{14}C in the study of the pathways of glucose metabolism in mammalian tissues. In *Radioactive Isotopes in Physiology, Diagnostics and Therapy* (H. Schweigk and F. Turba, eds.) pp. 705–751. Springer, Berlin.

Longnecker, J. P., and Williams, J. F. (1980). Quantitative measurement of the L-type pentose phosphate cycle with [2-14C]-glucose and [5-14C]-glucose in isolated hepatocytes. *Biochem. J.* **188**, 859–865.

Novello, F., and McLean, P. (1968). The pentose phosphate pathway of glucose metabolism: Measurement of the non-oxidative reactions of the cycle. *Biochem. J.* **107**, 775–791.

Utter, M. F. (1958). Carbohydrate metabolism. *Ann. Rev. Biochem.* **27**, 245–284.

Williams, J. F., Clark, M. G., Arora, K. K., and Reichstein, I. C. (1984). Glucose 6-phosphate formation by L-type pentose pathway reactions of rat liver in vitro: Further evidence. *Seyler's Zeit. Physiol. Chem.* **365**, 1425–1434.

Williams, J. F., Arora, K. K., and Longnecker, J. P. (1987). The pentose pathway: a random harvest. Impediments which oppose acceptance of the classical (F-type) pentose cycle for liver, some neoplasms and photosynthetic tissue. The case for the L-type pentose pathway. *Int. J. Biochem.* **19**, 749–817.

Wood, T. (1985). *The Pentose Phosphate Pathway.* Academic Press, Orlando, FL.

Wood, H. G., and Katz, J. (1958). The distribution of 14C in the hexose phosphates and the effect of recycling in the pentose cycle. *J. Biol. Chem.* **233**, 1279–1282.

Biography

John F. Williams is Professor Emeritus and a former Professor and Head of Biochemistry in the faculties at the Australian National University, Canberra. He was a Research Fellow at Merton College, Oxford and is presently Visiting Fellow in The Research School of Chemistry at ANU. His principal research interests are in intermediary metabolism. He holds a Ph.D. from the University of New South Wales and D.Sc. from the ANU, and he received postdoctoral training at Western Reserve University School of Medicine.

Peptide Amidation

Mark J. Niciu, Richard E. Mains and Betty A. Eipper
The University of Connecticut Health Center, Farmington, Connecticut, USA

Generation of a C-terminal α-amide group on a peptide occurs by hydroxylation and cleavage of a C-terminal glycine residue and is a prevalent posttranslational modification essential for the production of many of the peptides that serve as hormones and neurotransmitters. Approximately half of all bioactive peptides are α-amidated, including gonadotropin-releasing hormone (GnRH), corticotropin-releasing hormone (CRH), thyrotropin-releasing hormone (TRH), oxytocin, vasopressin, calcitonin, gastrin, cholecystokinin (CCK), neuropeptide Y (NPY), substance P and pituitary adenylate cyclase-activating polypeptide (PACAP). The α-amide group prevents ionization of the C terminus, which may increase receptor binding, hydrophobicity and/or half-life. In vertebrates, C-terminal α-amidation is accomplished via the activity of peptidylglycine α-amidating monooxygenase (PAM), a bifunctional enzyme localized to large dense core vesicles in neuroendocrine tissues.

Biochemistry and Enzymology of PAM

PAM is composed of two protease-resistant catalytic cores targeted to the lumenal compartment of secretory granules, peptidylglycine α-hydroxylating monooxygenase (PHM; EC 1.14.17.3) and peptidyl-α-hydroxyglycine α-amidating lyase (PAL; EC 4.3.2.5). PHM catalyzes the stereospecific α-hydroxylation of all C-terminally glycine-extended peptide substrates. PAL then catalyzes cleavage of the N–C bond of the α-hydroxylglycine, generating the α-amidated peptide product and glyoxylate (Figure 1).

PAM Structure

Bifunctional PAM is a type I integral membrane protein whose structure is highly conserved in vertebrate phylogeny. From N to C terminus, it contains a signal sequence, proregion, PHM catalytic core, noncatalytic spacer region (exon A), PAL catalytic core, transmembrane domain and cytosolic domain. The hydrophobic signal sequence is cleaved cotranslationally in the endoplasmic reticulum; the prosequence is removed in a post*trans*-Golgi network compartment. Tissue-specific endoproteolytic cleavage at pairs of basic amino acids can remove the pro-region, separate the two catalytic domains, and release the catalytic domains from the transmembrane domain. Poorly conserved linker regions follow both catalytic domains and are susceptible to cleavage by exogenous proteases. Additionally, alternative splicing can generate soluble, monofunctional PHM or soluble, bifunctional PAM. Soluble PAM proteins are secreted with their amidated product peptides while integral membrane PAM proteins undergo endocytosis, guided by routing determinants and phosphorylation at multiple sites in the cytosolic domain (Figure 2).

PAM Substrates

Virtually any peptide with a C-terminal glycine residue can serve as a PAM substrate. PAM generates α-amides of all 20 amino acids. In addition, PAM catalyzes the amidation of nonpeptidergic substrates such as fatty acyl glycines, glutathione, the aspirin metabolite salicylurate, bile acid glycine conjugates and leukotriene C_4. In addition to stereospecific α-hydroxylation of glycine-extended precursors, purified PHM can also catalyze N-dealkylation, O-dealkylation, and sulfoxidation of nonpeptidergic substrates.

Peptidylglycine α-hydroxylating Monooxygenase – PHM

Essential Cofactors

PHM requires the presence of molecular oxygen, a single electron donor (generally ascorbic acid or vitamin C), and copper.

Ascorbic Acid (Vitamin C) Ascorbate is transported across the plasma membrane via a Na^+-dependent transporter enriched in neuroendocrine tissue, SVCT2. How cytosolic ascorbate reaches the lumen of the secretory pathway is currently unclear. Nevertheless, concentrations of ascorbate are five to tenfold higher in the lumen of the secretory pathway than in the cytosol. The mM concentrations of ascorbate in the

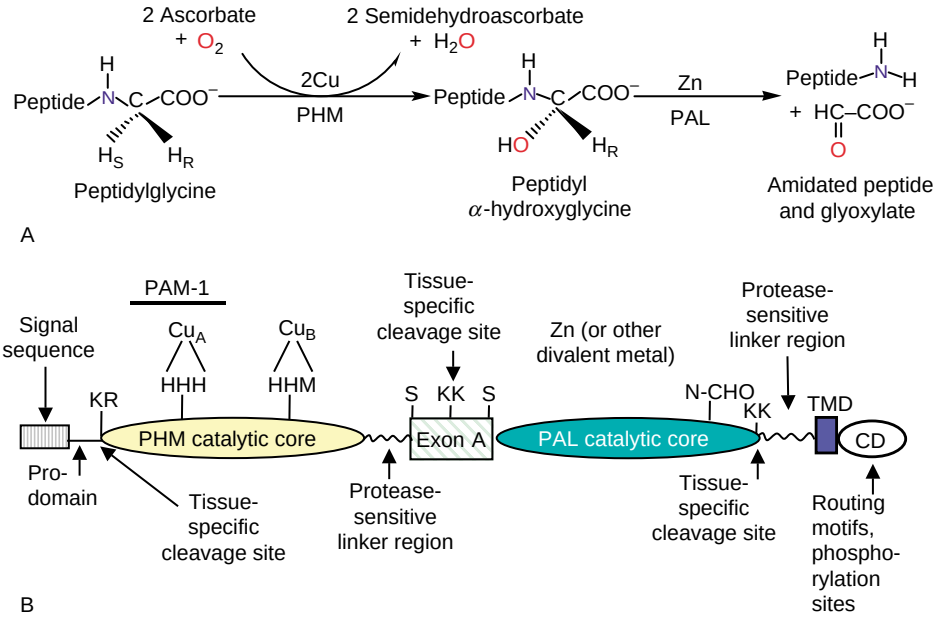

FIGURE 1 PAM reaction and structure. (A) Bifunctional PAM-catalyzed conversion of glycine-extended precursor into hydroxyglycine intermediate and amidated product plus glyoxylate. (B) Domains of integral membrane PAM-1 with salient features: KR and KK lysine-arginine and lysine-lysine dibasic cleavage sites; H, copper-binding histidine; M, copper-binding methionine; N-CHO, N-linked glycosylation site; TMD, transmembrane domain; CD, cytosolic domain; P, phosphorylation sites.

lumenal compartment ensure that lumenal copper is reduced, as required for the enzymatic cleavage of molecular oxygen by PHM. In this oxidation–reduction reaction, PHM converts 2 mol of ascorbate into 2 mol of semidehydroascorbate, which disproportionate to form dehydroascorbate and ascorbate. Other single-electron reductants can substitute for ascorbate to provide reducing equivalents for Cu^{2+}; consistent with this, no ascorbate-specific binding site has been identified on PHM.

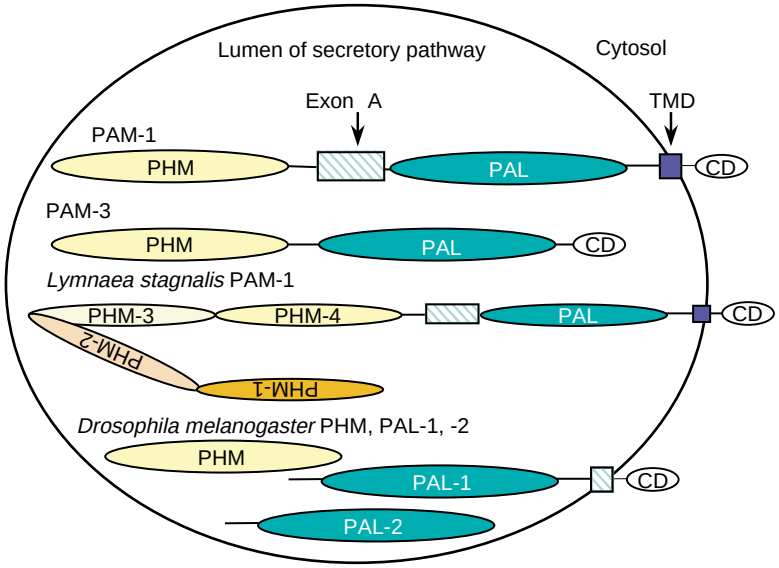

FIGURE 2 PAM in secretory granules. Soluble and membrane PAM isoforms from rat, pond snail and fruit fly in mature secretory granule. Alternative mRNA splicing at "hot spots" generates soluble PAM-3, which lacks exon A and the TMD; it is secreted with the amidated product. *Lymnaea stagnalis* membrane PAM contains four functional PHM domains and an exon A-like linker sequence. *Drosophila* PHM and PAL-1/-2 are encoded on separate genes. PAL-1 is a soluble protein and may be secreted with processed peptide. PAL-2 contains a transmembrane domain and may be recycled via endocytosis to post-Golgi complex compartments.

Copper Copper is required in trace amounts by a limited group of cuproenzymes. However, in excess, copper can support the Fenton reaction, generating reactive oxygen species, that attack cellular constituents with diffusion-limited kinetics. To avoid this problem, copper transporters and copper chaperones deliver this critical metal to these cuproenzymes while preventing toxic intracellular actions. The transport of Cu^{1+} across the plasma membrane requires Ctr1 in mammals. Atox1, a cytosolic copper chaperone, delivers Cu^{1+} to ATP7A and ATP7B, homologous P-type ATPases that pump Cu^{1+} into the lumen of the secretory pathway, where it can be loaded onto lumenal cuproproteins or excreted from the cell.

Structure and Reaction Mechanism

PHM binds two moles of copper, each of which plays a distinct role in the α-hydroxylation reaction. Composed almost entirely of β strands, the catalytic core of PHM consists of two structurally homologous domains (Figure 3). Mutagenesis and phylogenetic comparisons identify a limited number of conserved residues. The copper binding sites are conserved: 3 histidine residues in the N-terminal half of PHM bind Cu_A and two histidines plus one methionine residue in the C-terminal half bind Cu_B. Although reducing equivalents donated by both Cu_A and Cu_B are essential to the reaction, the two Cu ions are separated by a 10Å solvent filled cleft.

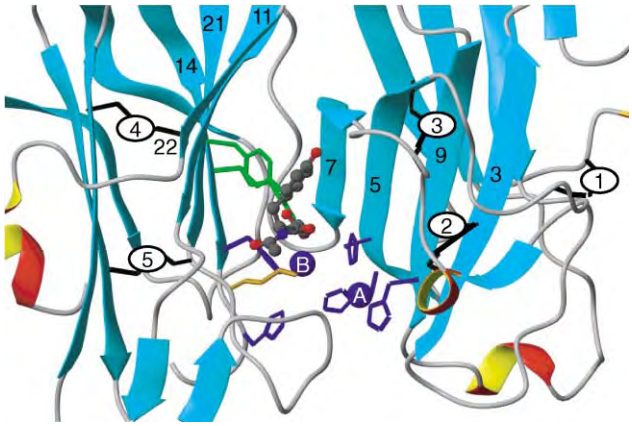

FIGURE 3 PHM active site. The structure determined by crystallization of oxidized PHMcc with its Ac-diiodo-Tyr-Gly substrate is shown to illustrate the structural role played by the disulfide bonds (Prigge, S. T., Mains, R. E., Eipper, B. A., and Amzel, L. M. (2000). New insights into copper monooxygenases and peptide amidation: Structure, mechanism and function. *Cell Mol. Life Sci.* 57, 1236–1259). Histidine ligands to Cu_A and Cu_B are blue; the methionine ligand to Cu_B is gold; substrate binding residues are green; the substrate is shown in ball and stick format. The disulfide bonds in PHM are numbered (except for bond 1, they are totally conserved): 1, Cys^{47}-Cys^{186}; 2, Cys^{81}-Cys^{126}, links β3 to the β5-β6 loop; 3, Cys^{114}-Cys^{131}, links β5 to the β6-β7 loop; 4, Cys^{227}-Cys^{334}, links β13 to β22; 5, Cys^{293}-Cys^{315}, links β19 to β21.

The glycine-extended peptide substrate binds in a conserved, hydrophobic substrate-binding pocket located near Cu_B, placing the α-carbon of the glycine adjacent to molecular oxygen bound to Cu_B with the C terminus of the glycine residue salt bridged to a conserved arginine residue. Several hydrophobic residues near the active site are conserved, along with proline and glycine residues that define the loop regions. The molecular oxygen consumed in the reaction binds only to the enzyme/peptidylglycine complex, and it is not yet clear how electron transfer is accomplished. The reaction is tightly coupled, with little generation of reactive oxygen species, and the two copper ions do not move much closer to each other during catalysis.

Pharmacological Inhibition

Disulfiram, used clinically in the treatment of chronic alcoholism, inhibits PHM activity *in vivo* via its ability to chelate copper. When assayed *in vitro*, after the addition of exogenous copper, the catalytic core of rat PHM displays paradoxically enhanced activity after *in vivo* disulfiram administration. A mechanism-based inhibitor of PHM, trans-styrylacetic acid (phenylbutenoic acid), has also been identified.

Peptidyl-α-Hydroxylglycine α-Amidating Lyase

Limited trypsin digestion and analysis of peptidyl-α-hydroxylglycine α-amidating lyase (PAL) truncation mutants revealed a stable catalytic core with no subdomains. The single N-linked glycosylation site near the COOH terminus of PAL is utilized, although glycosylation is without effect on the catalytic activity of PAL. When treated with divalent metal ion chelators, PAL activity was reduced and its thermal and protease resistance were decreased, suggesting both structural and catalytic roles for divalent metal ions. Approximately 0.7 mol of zinc is bound per mole of enzyme. The four cysteine residues in PAL form disulfide bonds, and conserved histidine, aspartate and glutamate residues are involved in binding zinc, playing both structural and catalytic roles. No reliable mechanism-based small molecule inhibitors of PAL have been characterized. The reaction catalyzed by PAL is most similar to the reaction catalyzed by ureidoglycolate lyase.

Evolutionary Relationships

The process of peptide amidation is highly conserved. In invertebrates like *Drosophila melanogaster* and *Caenorhabditis elegans*, PHM and PAL are encoded by separate genes; a single PHM gene may be accompanied by more than one PAL gene. PHM and PAL homologues

are not found in the genome of *Saccharomyces cerevisiae*. Intriguingly, *Lymnaea stagnalis*, a molluscan pond snail, expresses a huge membrane PAM with four independent, catalytically active PHM domains followed by a single PAL domain. *Schistosoma mansoni*, a nematode and potent human pathogen, expresses a heavily glycosylated, soluble PHM with atypical catalytic features. The copper binding ligands, substrate binding site, disulfide bonds, and selected glycine and proline residues of PHM are conserved across species.

The cofactor requirements of PHM suggest homology to another copper, ascorbate and dioxygen-requiring enzyme, dopamine-β-monooxygenase (DBM; EC 1.14.17.1). DBM converts dopamine to norephinephrine in selected neurons and adrenal chromaffin cells. The catalytic core of PHM is 32% identical to a 291 amino acid stretch in DBM. The Cu_A and Cu_B-binding motifs and disulfide-bonding patterns of PHM are conserved in DBM. *Cnidarians*, such as the sea anemone and *Hydra*, use amidated peptides, not catecholamines like norephinephrine for neural transmission, suggesting that PHM is the more ancestral enzyme. cDNA library screening of human senescent fibroblasts revealed the presence of a third sequence with significant homology to PHM, monooxygenase X (MOX; X13255). No substrates or hydroxylated products have yet been identified for this putative monooxygenase.

PAM Expression

PAM expression is most prevalent in heart atria, the pituitary gland, and peptide-producing neurons of the central and enteric nervous systems. Nevertheless, PAM expression is widespread, as transcripts can be detected in airway and olfactory epithelia, smooth muscle cells, endothelium, brain ependymal cells, astrocytes, and fibroblasts.

During development, PAM is first detected immunohistochemically at embryonic day 9 (E9) in the putative cardiogenic region and at E13 in peptide-producing neurons. PAM is also highly expressed in limb mesoderm and mesenchyme flanking the nasal, maxillary, palatal and dental epithelia during embryonic tissue fusion and remodeling. Most *Drosophila* PHM knockout flies die as young larvae, during the molting process, with malformation of the mouth hooks. A role for PAM in these areas during development is not yet clear.

PAM Molecular Genetics

The human *PAM* gene is located on chromosome 5q14-21 and the mouse *Pam* gene is on chromosome 1. The rat PAM gene contains at least twenty-eight exons encompassing >160 kB. At least two putative promoters upstream of the translational start site and proregion in exon two have been identified. PHM is encoded by exons three to fourteen (excluding exon thirteen). The alternately spliced non-catalytic region between PHM and PAL is encoded by exon sixteen, which is bordered by at least forty kB of intronic sequence. PAL is encoded by exons seventeen to twenty-four. Most of the intron/exon junctions in rat, which preferentially produce bifunctional PAM mRNA transcripts, and *D. melanogaster*, which contains separate PHM and PAL genes, are conserved. Interestingly, rat breeding stocks vary in their alternative splicing of PAM: Harlan Sprague-Dawley rats eliminate the exon A linker in their mRNA transcripts in pituitary, while Charles River Sprague-Dawley rats retain this domain.

Dysregulated Peptide Amidation

Due to the plethora of physiological functions regulated by amidated peptides, deficits in peptide amidation have very detrimental consequences for the organism.

Overexpression of Amidated Peptides

Many amidated peptides, e.g., PACAP, NPY, and gastrin-releasing peptide (GRP), serve as autocrine or paracrine growth factors. Numerous tumors of neuroendocrine origin secrete amidated peptides that serve this function, and PAM expression is concomitantly up-regulated. Amidated peptides secreted by neuroendocrine tumors disrupt normal physiological function. For example, small cell lung carcinomas often secrete GRP, while amidated isoforms of parathyroid hormone related protein (PTHrP) sustain bone growth and produce the hypercalcemia of malignancy. Gastrin-secreting tumors ("gastrinomas") are frequently encountered in Zollinger-Ellison syndrome, which presents clinically as peptic ulceration; vasoactive intestinal polypeptide-secreting tumors ("VIPomas") of pancreatic or duodenal origin present with voluminous watery diarrhea in Verner-Morrison syndrome. Hence, pharmacological inhibition of PAM activity may be a rational therapeutic strategy in the treatment of such amidated peptide-secreting tumors.

Impaired Peptide Amidation

Based on assays of amidated product peptides, peptide amidation is impaired in the context of dietary deficiencies of ascorbate or copper, genetic deficiencies of copper-translocating proteins or targeted gene disruption of the PAM gene.

Impaired Copper Delivery

A reduction in copper delivery to the secretory pathway results in a diminished ability to produce amidated peptides. This can be the result of nutritional deficiencies of copper or ascorbate or genetic malfunctioning of copper transporters. In mammals, ATP7A receives Cu^{+} from the cytosolic chaperone Atox1 and transports it into the lumen of the secretory pathway where the catalytic cores of cuproenzymes like PHM, DBM and tyrosinase reside. Mutations in ATP7A result in the X-linked copper-deficiency disorder, Menkes disease, which presents clinically with profound neurodegeneration. The mottled brindled (Mo^{Br}) mouse, which contains a six base pair in-frame deletion in ATP7A, serves as the mouse model of Menkes disease. Although PAM protein expression is unchanged, the concentrations of amidated neuropeptides, *e.g.*, joining peptide (JP), CCK, and PACAP, are reduced in the pituitary gland and central nervous system of afflicted males relative to age-matched wild type mice.

Targeted Gene Disruption

Insertion of a P-element containing transposon within the *D. melanogaster* PHM transcriptional unit eliminated PHM expression and resulted in early larval lethality with relatively few morphological defects. Recently, PAM null mice have been created. These mice do not survive past embryonic day 14.5, with the most noticeable defect being intractable edema. No PHM or PAL enzymatic activity is detectable in homogenates of null embryos, and heterozygotes display half the wild type level of PHM and PAL activity in age-matched wild type mice. Thus PAM is the only enzyme responsible for C-terminal peptide α-amidation *in vivo*.

See Also the Following Articles

Calcitonin Gene-Related Peptide and Adrenomedullin Receptors • Inorganic Biochemistry • Neuropeptide Y Receptors • P-Type Pumps: Copper Pump • Vasopressin/Oxytocin Receptor Family • Vitamin C

Glossary

large dense core vesicles/secretory granules Membrane-enclosed 300–500 nm diameter peptide-containing storage organelles formed from the *trans*-Golgi network in neuroendocrine cells.

P-type ATPase A family of pumps whose members use the energy of ATP to transport cations uphill across membranes, undergoing a cycle of phosphorylation and dephosphorylation.

type I integral membrane protein A protein that crosses a phosopholipid bilayer once, with its N-terminus projecting into the extracellular environment/lumen of the secretory pathway and a cytosolic C terminus.

Further Reading

Francisco, W. A., Blackburn, N. J., and Klinman, J. P. (2003). Oxygen and hydrogen isotope effects in an active site tyrosine to phenylalanine mutant of peptidylglycine alpha-hydroxylating monooxygenase: Mechanistic implications. *Biochemistry* **42**, 1813–1819.

Iwai, N., Martinez, A., Miller, M.-J., Vos, M., Mulshine, J. L., and Treston, A. M. (1999). Autocrine growth factor loops dependent on peptidyl alpha-amidating enzyme as targets for novel tumor cell growth inhibitors. *Lung Cancer* **23**, 209–222.

Jiang, N., Kolhekar, A. S., Jacobs, P. S., Mains, R. E., Eipper, B. A., and Taghert, P. H. (2000). PHM is required for normal developmental transitions and for biosynthesis of secretory peptides in *Drosophila*. *Develop. Biol.* **226**, 118–136.

Katopodis, A. G., and May, S. W. (1990). Novel substrates and inhibitors of peptidylglycine alpha-amidating monooxygenase. *Biochemistry* **29**, 4541–4548.

Kolhekar, A. S., Bell, J., Shiozaki, E. N., Jin, L., Keutmann, H. T., Hand, T. A., Mains, R. E., and Eipper, B. A. (2002). Essential features of the catalytic core of peptidyl-alpha-hydroxyglycine alpha-amidating lyase. *Biochemistry* **41**, 12384–12394.

Liang, W. J., Johnson, D., and Jarvis, S. M. (2001). Vitamin C transport systems of mammalian cells. *Mol. Membr. Biol.* **18**, 87–95.

Miller, L. A., Baumgart, L. E., Chew, G. H., deLong, M. A., Galloway, L. C., Jung, K. W., Merkler, K. A., Nagle, A. S., Poore, D. D., Yoon, C. H., and Merkler, D. J. (2003). Glutathione, S-substituted glutathiones, and leukotriene C_4 as substrates for peptidylglycine alpha-amidating monooxygenase. *Arch. Biochem. Biophys.* **412**, 3–12.

Prigge, S. T., Mains, R. E., Eipper, B. A., and Amzel, L. M. (2000). New insights into copper monooxygenases and peptide amidation: Structure, mechanism and function. *Cell Mol. Life Sci.* **57**, 1236–1259.

Puig, S., and Thiele, D. J. (2002). Molecular mechanisms of copper uptake and distribution. *Curr. Opin. Chem. Biol.* **6**, 171–180.

Rhames, F. C., Murthy, N. N., Karlin, K. D., and Blackburn, N. J. (2001). Isocyanide binding to the copper(I) centers of the catalytic core of peptidylglycine monooxygenase (PHMcc). *J. Biol. Inorg. Chem.* **6**, 567–577.

Steveson, T. C., Ciccotosto, G. C., Ma, X.-M., Mueller, G. P., Mains, R. E., and Eipper, B. A. (2003). Menkes protein contributes to the function of peptidylglycine alpha-amidating monooxygenase. *Endocrinology* **144**, 188–200.

Biography

Mark Niciu is an M.D.-Ph.D. student and Betty Eipper and Richard Mains are Professors in the Neuroscience Department at the University of Connecticut Health Center in Farmington, CT.

Drs. Eipper and Mains received their Ph.D. from Harvard University and were postdoctoral fellows with Dr. Ed Herbert at the University of Oregon. They developed an interest in peptide amidation when they observed that pituitary cells maintained in serum-free medium failed to amidate the products of proopiomelanocortin processing. Subsequent cloning and characterization of PAM identified ascorbate as the missing factor.

Periplasmic Electron Transport Systems in Bacteria

David J. Richardson
University of East Anglia, Norwich, UK

Gary Sawers
John Innes Centre, Norwich, UK

Rob J.M. Van Spanning
Free University of Amsterdam, The Netherlands

The periplasmic compartment lies between the inner (cytoplasmic) and outer membranes of Gram-negative bacteria. It is frequently termed the "periplasmic space," but this is a misnomer as the term "space" suggests a void and the periplasmic compartment is far from that. In fact, it is a highly metabolically active compartment where many important respiratory electron transfer proteins are located. In bacteria these periplasmic redox proteins result in a great respiratory diversity, as they can facilitate electron transfer between a range of electron donors (e.g., formate, hydrogen, reduced nitrogen species, and reduced sulfur species) and electron acceptors (e.g., nitrogen and sulfur oxyanions, dimethylsulfoxide, and trimethylamine N oxide). This underlies the success of bacteria in colonizing a wide range of the Earth's oxic and anoxic environments and the important contribution of bacteria to critical biogeochemical element cycles, such as the nitrogen, sulfur, and carbon cycles.

Respiratory Electron Transport Systems

In mammalian mitochondrial respiration, electrons flow from low-potential cytoplasmic electron donors (e.g., NADH or succinate) to the high-potential electron acceptor oxygen. The site of oxygen reduction is the aa_3-type cytochrome *c* oxidase that is located within the cytoplasmic membrane (Figure 1). The key postulate of P. Mitchell's chemiosmotic theory is that many energy-consuming reactions catalyzed by integral membrane proteins, such as the ATP synthase, are driven by the energy contained within a transmembrane-proton electrochemical gradient (proton-motive force (PMF)), which is generated by the electron transport system. Proton translocation is achieved via membrane-associated electron transfer proteins. Mitchell described a redox loop mechanism whereby two electrons are transferred from the positive (P, or bacterial periplasmic) side of the membrane to the negative (N, or bacterial cytoplasmic) side of the membrane. There they combine with two protons to reduce a quinone to quinol. The quinol then diffuses back across the membrane where it is reoxidized at the P face releasing protons (Figure 1B). This movement of negative charge from the P to the N side of the membrane, and counter movement of protons, produces a PMF. Structure–function studies of two key integral membrane enzymes of respiration (the structurally defined cytochrome bc_1 complex and the aa_3-type cytochrome *c* oxidase) illustrate yet another three different mechanisms that couple electron transfer to PMF generation. The cytochrome bc_1 complex utilizes a proton-motive Q-cycle mechanism that results in a q^+/e^- ratio of 1 (Figure 1A). The aa_3-type cytochrome *c* oxidase employs two different mechanisms to build up the PMF. Reduction of oxygen at the catalytic site involves proton transfer from the cytoplasm and electron transfer from a periplasmic donor. As a consequence, these charge movements from opposite sides of the membrane give rise to a net charge separation of 1 per electron transferred, $1q^+/e^-$. In addition, it utilizes a proton-pumping mechanism that results in one positive charge being moved across the membrane for each electron ($1\,q^+/e^-$). Therefore, the stoichiometry of charge movements in the oxidases adds up to $2\,q^+/e^-$ transferred from donor to oxygen. It is notable that neither the proton pump mechanism nor the Q-cycle mechanism of energy conservation was originally envisaged by Mitchell.

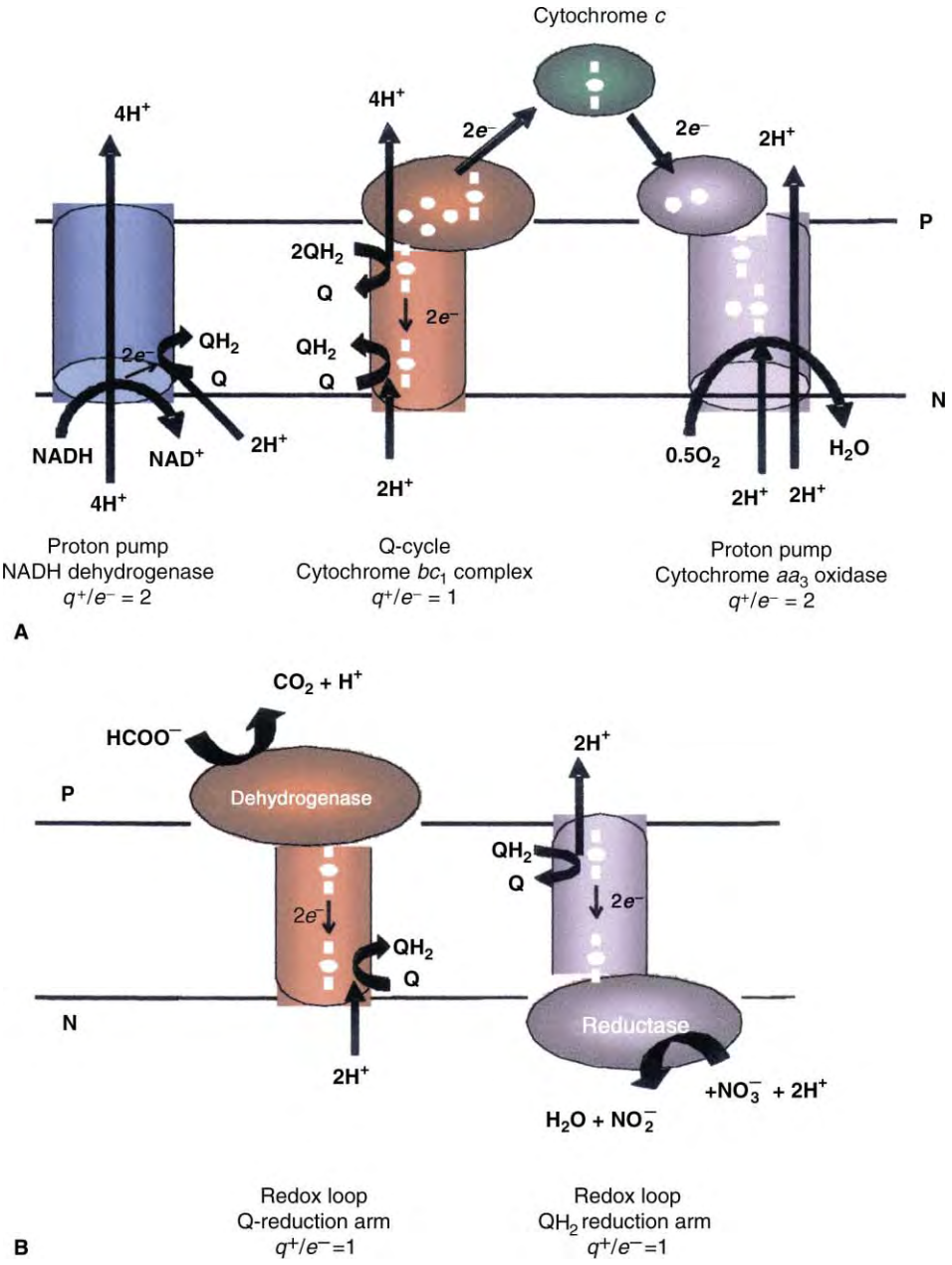

FIGURE 1 Mechanisms of energy conservation in respiration. (A) A basic mammalian mitochondrial electron transport chain illustrating proton pumps and Q-cycle mechanisms of energy conservation. (B) The organization of redox loops using periplasmic electron donors found in some cytochrome bc_1 complex-independent bacterial respiratory systems.

Bacterial Periplasmic Respiratory Electron Transport Systems that are Dependent on the Cytochrome bc_1 Complex

The mammalian mitochondrial-type of electron transport system is present in many aerobic and facultative anaerobic bacteria, for example, the well-studied soil-denitrifying bacterium *Paracoccus denitrificans*. However, many bacteria additionally have alternative electron transport systems that utilize periplasmic electron donors and acceptors. In some cases the periplasmic oxido-reductases will integrate easily into a mitochondrial-type of electron transport chain. For example, in *P. denitrificans* the periplasmic oxido-reductases for the reduction of nitrite or nitrous oxide, which are important reactions of denitrification in the biogeochemical nitrogen cycle, can accept electrons via the cytochrome bc_1 complex (Figure 2). Due to the Q-cycle mechanism of the latter enzyme, the overall

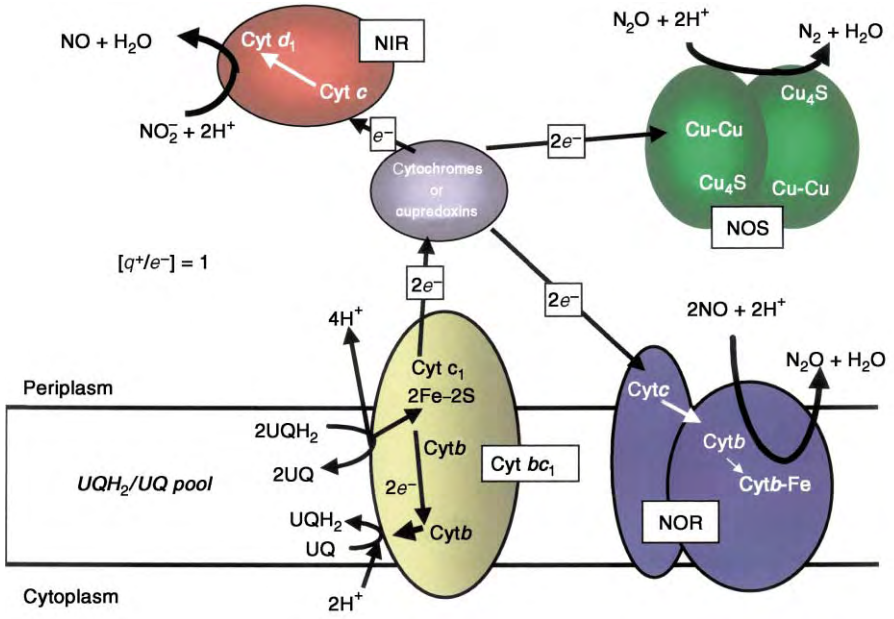

FIGURE 2 Cytochrome bc_1 complex-dependent periplasmic and membrane-bound oxido-reductases involved in denitrification in *Paracoccus* species. NIR, cytochrome cd_1 nitrite reductase dimer. NOR, nitric oxide reductase. NOS, nitrous oxide reductase.

electron transport pathway from quinol to nitrite and nitrous oxide is electrogenic, although the terminal nitrite and nitrous oxide reductases themselves are not. As a consequence, the electron transport from quinol to nitrite is less coupled ($q^+/e^- = 1$) (Figure 2) than electron transfer from quinol to oxygen ($q^+/e^- = 3$) (Figure 1A).

Periplasmic Electron Transport Systems that do not Depend on the Cytochrome bc_1 Complex

Many bacteria (e.g., *Escherichia coli*) do not have genes encoding a cytochrome bc_1 complex. Using periplasmic electron donors and acceptors independently of the cytochrome bc_1 complex can raise interesting questions about the bioenergetics of these systems, particularly with respect to the means by which the electron transfer process is coupled to the generation of a transmembrane electrochemical gradient. The molecular nature of some of these coupling mechanisms has been illuminated by recent structure–function studies on key anaerobic enzymes.

Some of these transmembrane enzymes possess two heme *b* groups at opposite sides of the membrane, which allows transmembrane electron transfer from a periplasmic to a cytoplasmic side. During oxidation of their substrate, two protons are released at the periplasmic side of the membrane while two electrons move inward via the hemes *b* to the cytoplasmic side of the membrane. There they are taken up by the acceptor along with two protons from the cytoplasm. This classical Mitchellian redox loop mechanism results in a net charge separation of one per electron transferred through the enzyme from donor to acceptor molecule ($1q^+/e^-$). Both dehydrogenases, which oxidize their substrate at the periplasmic side and reduce quinone at the cytoplasmic side, and terminal oxido-reductases, which oxidize quinol at the periplasmic site and reduce the acceptor at the cytoplasmic side, may have a redox-loop-type architecture. Examples of such electrogenic dehydrogenase are the HydABC-type hydrogenase and FdhN of *E. coli*, homologues of which are present in many bacteria and archae. An example of such an electrogenic terminal oxido-reductase is membrane-bound nitrate reductase (NarA). Periplasmic or membrane-bound enzymes that are not designed to contribute to the generation of a PMF will dissipate the redox free energy as heat. These enzymes receive their electrons and protons required for reduction of their allocated electron acceptor at the same side of the membrane, either the periplasm (trimethylamine N-oxide reductase (TOR), dimethylsulfoxide reductase (DMS), periplasmic nitrate reductase (Nap), the cytochrome *c* nitrite reductase (Nrf)), or the cytoplasm (succinate dehydrogenase, fumarate reductase). Electron transfer in pathways that are made up of a redox-loop-type dehydrogenase or oxido-reductase along with a non-electrogenic oxido-reductase or dehydrogenase, respectively, will yield a net proton movement of 1 from inside to outside during electron transfer from donor to terminal electron acceptor (q^+/e^- is 1) (Figure 3).

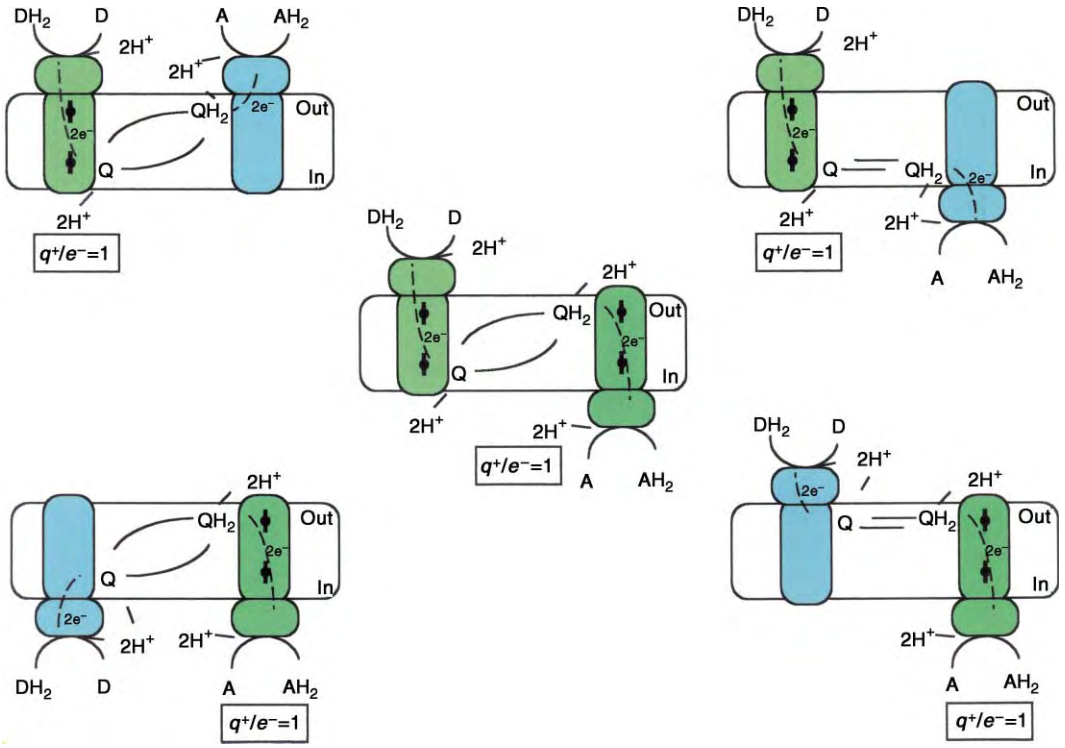

FIGURE 3 Examples of $q/e^- = 1$ and $q/e^- = 2$ redox loop mechanisms.

The most efficient free-energy transducing pathway of electron transfer from donor to acceptor requires the participation of a dehydrogenase and a terminal oxidoreductase, which both have a redox-loop-type architecture (Figure 3). The FdhN to NarA respiratory chain of *E. coli* and the Hyd to NarA (electron transfer from formate or hydrogen to nitrate, q/e^- is 2) are the classical systems used to illustrate such an efficient proton-motive redox loop.

Formate Dehydrogenase N

Formate is an important and widespread electron donor available to bacteria in anaerobic environments. During anaerobic growth with nitrate, *E. coli* can express a membrane-bound formate dehydrogenase (FdhN), which oxidizes formate in the periplasmic compartment and for which a high-resolution structure has been determined. The enzyme is a homo-trimer, with each monomeric unit being composed of an integral membrane di-heme cytochrome subunit (FdhI), a membrane-anchored periplasmic ferredoxin subunit (FdhH), binding four [4Fe–4S] clusters, and a periplasmic catalytic subunit (FdhG), which binds a [4Fe–4S] cluster and catalyzes formate oxidation at a Se-Mo-*bis*-guanine dinucleotide (Se-Mo-MGD) cofactor. Electrons extracted from formate at the periplasmic active site pass down a 90Å redox ladder to a menaquinone reductase site at the cytoplasmic face of the membrane. The redox ladder consists of eight redox centers, Se-Mo-*bis*-MGD, five iron–sulfur clusters, and two hemes. Each of these is within 12Å of its nearest neighbor, and this serves to ensure rapid electron transfer (Figure 4). In considering the whole electron transfer ladder from the Se-Mo-*bis*-MGD to the menaquinone, a notable feature is that the intermediary electron carriers usually function as one-electron transfer centers. However, formate oxidation and menaquinone reduction are two-electron reactions. Thus, the Se-Mo-*bis*-MGD plays a key role in gating electron transfer from formate into the redox ladder and the Q-reductase site is the key to gating the reduction of menaquinone.

Much of the FdhN redox ladder is periplasmic, being located in the extra-membranous periplasmic FdhGH subunits (Figure 4), but the two membrane-intrinsic hemes, bound within the four-helix bundle of FdhI, are critical to charge separation across the membrane. The midpoint redox potential at pH 7 of the formate/CO_2 couple is *c.* −420 mV and that of the MQH_2/MQ couple is *c.* −80 mV. This large, *c.* 340 mV, potential drop allows efficient electron transfer against a negative-inside membrane potential of *c.* 200 mV. The movement of one electron from the periplasmic (P) face to the cytoplasmic (C) face of the membrane and uptake of one proton at the C face gives a coupling stoichiometry of $q^+/e^- = 1$ (Figure 4).

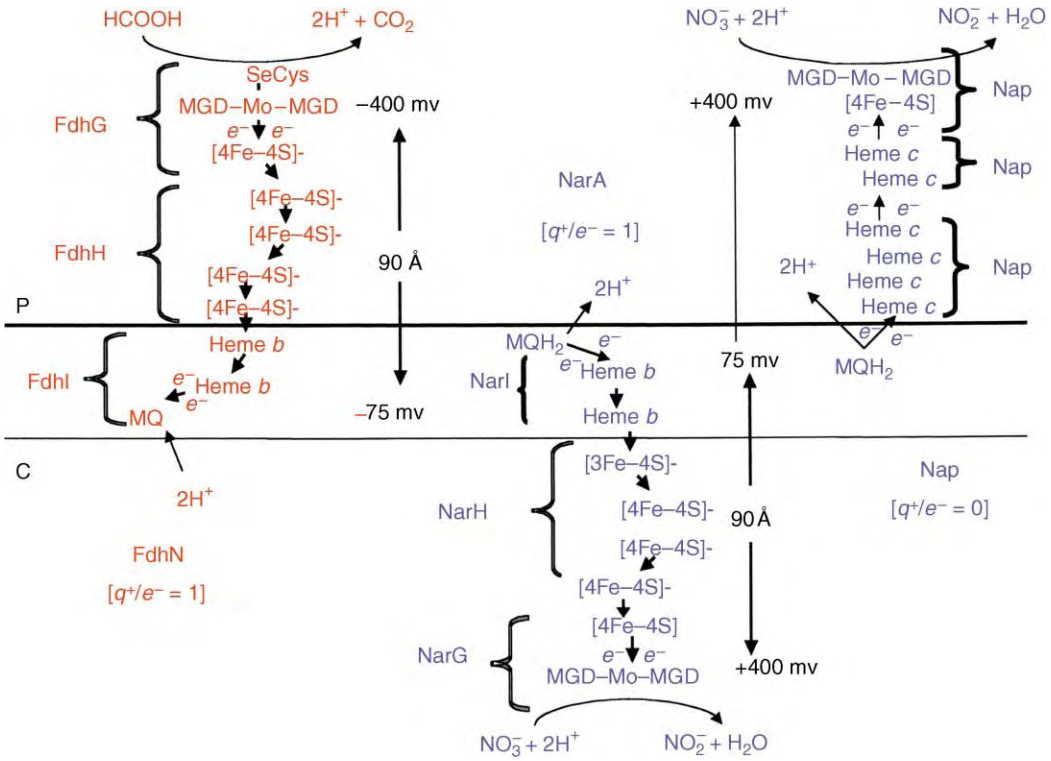

FIGURE 4 The organization of redox ladders involved in periplasmic formate-dependent nitrate reduction in *E. coli*. FdhN, formate dehydrogenase N. NarA, membrane-bound nitrate reductase A. Nap, periplasmic nitrate reductase.

Hydrogenase

Hydrogen is another important periplasmic electron donor for bacteria in anoxic environments. The Hya and Hyb enzymes of *E. coli* catalyze anaerobic hydrogen oxidation. There are no structures for these enzymes, but they are thought to be organized in a manner similar to FdhN. They are composed of three different subunits: an integral membrane di-heme subunit in which the hemes are stacked across the membrane; a periplasmic iron–sulfur protein (anchored by a single transmembrane helix); and a periplasmic catalytic subunit that binds a nickel–iron cofactor at the active side. The bioenergetics of periplasmic hydrogen oxidation are thus predicted to be very similar to that described for formate, with electrons extracted for hydrogen in the periplasm passing through a multi-cofactor redox ladder and combining with protons to reduce quinone at the cytoplasmic face, thus give $q^+/e^- = 1$.

Nitrate Reductase A

In *E. coli*, nitrate reductase A can serve as a second proton-motive arm in electron transfer from the periplasmic active site of FdhN or Hya (Figure 4). NarA is a three-subunit enzyme composed of NarGHI. NarG contains the *bis*-MGD molybdopterin cofactor at its catalytic site and a [4Fe–4S] cluster. NarH contains four additional iron–sulfur centers (one [3Fe–4S] and three [4Fe–4S]). NarGH are located in the cytoplasm and associate with NarI, an integral membrane protein of five transmembrane helices with the N-terminus and two inter-helix loops facing the periplasm. This subunit carries two hemes *b* stacked across the membrane. Oxidation of quinol occurs at the periplasmic side of NarI where the protons are released and the two electrons are moved from the outside low-potential heme *b* to the inside high-potential heme *b*. This charge separation makes the enzyme electrogenic, in that it contributes to the generation of a proton electrochemical gradient across the membrane (two charge separations during transfer of two electrons to nitrate; $q^+/e^- = 1$). Nar is organized in a manner very similar to FdhN, especially with respect to the equivalent FeS-containing NarH and FdhH subunits and Mo-*bis*-MGD NarG and FDHG catalytic subunits. However, the topology of the two systems is opposite (Figure 4), but the redox ladder arrangement of redox centers apparent in FdhN is also present in NarA. The midpoint redox potentials of individual cofactors in this ladder have been determined and suggest that both NarG and FdhN are part of a growing number of electron transfer complexes in bacteria that contain a mixture of endergonic and exergonic electron transfer steps. As in FdhN, the potential difference of *c*. 480 mV between the

MQH_2/MQ and nitrate/nitrite redox couples is sufficient to drive electron transfer across the membrane against the negative-inside PMF (Figure 4).

Non-Proton Motive Cytochrome bc_1 Complex-Independent Periplasmic Electron Transfer

In the FdhN–NarA electron transport system, both the quinone-reducing and quinol-oxidizing arms of the electron transport chain are proton-motive and, when operating together, they yield $q^+/e^- = 2$. However, in principle, only one arm needs to be proton-motive in order for a net PMF ($q^+/e^- = 1$) to be generated. Examples of this can be seen in a periplasmic formate–nitrate electron transport system in which nitrate is reduced by the periplasmic nitrate reductase (Nap) rather than NarA (Figure 3). Such a system operates under nitrate-limited growth conditions in *E. coli*.

The Periplasmic Nitrate Reductase (Nap)

Nap is widespread in many species of denitrifying and non-denitrifying proteobacteria, including both *P. denitrificans* and *E. coli*. Nap is normally found as part of a three-subunit electron transfer system composed of NapABC. NapA is a periplasmic catalytic subunit with a [4Fe–4S] cluster and a *bis*-MGD cofactor. The crystal structure of *Desulfovibrio desulfuricans* NapA reveals that the overall organization is similar to that of the catalytic subunits of the Mo-*bis*-MGD formate dehydrogenases. NapB is a periplasmic di-heme cytochrome *c*, with both hemes having bis-histidinyl ligation. NapC has a single N-terminal transmembrane helix that anchors a globular periplasmic domain with four *c*-type hemes to the periplasmic surface of the cytoplasmic membrane (Figure 4). All four hemes have relatively low midpoint redox potentials (in the region of 0 to −250 mV) and have *bis*-histidinyl axial ligation.

NapC may be made up of two subdomains, each containing a di-heme pair, and it belongs to a large family of bacterial tetra-heme and penta-heme cytochromes. These cytochromes have been proposed to participate in electron transfer between the quinol/quinone pool and periplasmic redox enzymes such as the trimethylamine N-oxide reductase, dimethylsulfoxide reductase, fumarate reductase, nitrite reductases, and hydroxylamine oxido-reductase. For an electron transport pathway from quinol to nitrate through Nap, the enzyme receives electrons from membrane-embedded quinols, which are donated to the tetra-heme periplasmic domain of NapC. From there they flow via the hemes in NapB and the [4Fe–4S] cluster in NapA to the bis-MGD-containing catalytic site of NapA where the two-electron reduction of nitrate to nitrite is catalyzed. As discussed above for NarA and FdhN, this electron transfer system also contains a mixture of endergonic and exergonic electron transfer steps but it is expected that none of the eight redox centers involved will be more than 14Å apart, thus ensuring rapid electron transfer. However, electron transfer from quinol to nitrate via Nap is non-electrogenic ($q^+/e^- = 0$) since both the electrons and the protons required for the reduction of nitrate to nitrite are taken up at the same side of the periplasmic face of the membrane.

Multi-Heme *c*-Type Cytochromes and Periplasmic Electron Transfer

Multi-Heme *c*-Type Cytochromes

In *E. coli* three other illustrative examples of non-electrogenic, quinol-oxidizing periplasmic electron transport systems that include extended redox ladders are illustrated in Figure 5. The cytochrome *c* nitrite reductase (Nrf) is a four-subunit electron transport system that involves 14 redox centers (10 *c*-type hemes and four [4Fe–4S] clusters). The trimethylamine N-oxide reductase (Tor) is a two-subunit system comprising of six redox centers (Mo-*bis*-MGD; and five *c*-type hemes). Finally, the dimethylsulfoxide reductase (Dms) is a three-subunit system containing an integral membrane subunit that is not involved in charge separation, and two periplasmic subunits that bind five redox centers (Mo-*bis*-MGD and four [4Fe–4S] clusters). Consideration of the Nap, Nrf, and Tor systems has revealed the participation of di-, tetra-, and penta-heme cytochromes in electron transfer. In mammalian mitochondria the P-facing cytochrome *c* involved in electron transfer is a small mono-heme protein. However, multi-heme cytochromes are a common feature of bacterial periplasmic electron transport. Other examples not mentioned so far include: (1) the octa-heme hydroxylamine oxido-reductase of nitrifying bacteria (e.g., *Nitrosomonas europeae*) and tetra-heme cytochrome *c554*, which, together with a tetra-heme NapC homologue CycB, mediate non-electrogenic electron transfer from hydroxylamine to quinone; (2) the tetra-heme fumarate reductase of *Shewanella* species that, together with the NapC homologue CymA, reduces fumarate to succinate using electrons drawn from the quinol pool. Structural analysis of these cytochromes and other multi-heme cytochromes such as the penta-heme NrfA reveals that the hemes are closely packed together to allow rapid electron transfer and are frequently arranged in pairs in which the porphyrin planes are nearly parallel or nearly perpendicular.

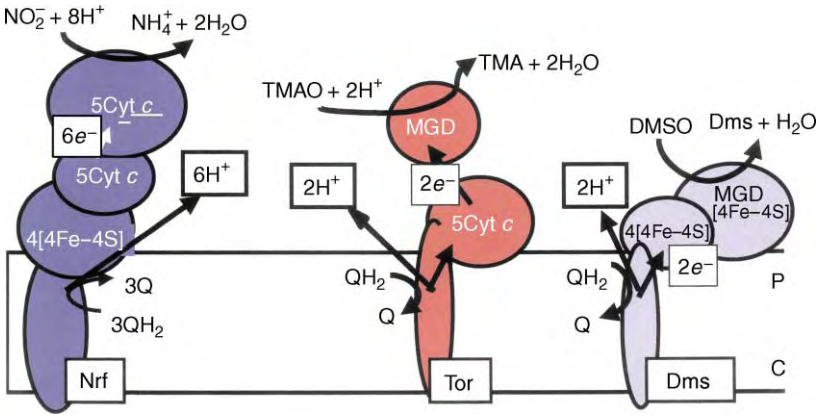

FIGURE 5 The organization of some non-electrogenic periplasmic electron transport systems in *E. coli*. Nrf, cytochrome *c* nitrite reductase, Tor, trimethylamine-N-oxide reductase; Dms, dimethylsulfoxide reductase.

Iron (III) Respiration and Inter-Membrane Periplasmic Electron Transport

Bacterial iron respiration is the process in which the Fe(III) acts as the terminal electron acceptor in an energy-conserving bacterial respiratory electron transport chain. It is an anaerobic process that provides a bacterium with a means of respiration when oxygen is absent and is distinct from the process of iron assimilation, in which iron is taken up into the cell by energy-consuming systems and incorporated into cell biomass. Although not a property of *E. coli*, the capacity for Fe(III) respiration is phylogenetically widespread and the ecological impact in microoxic and anoxic soils and sediments is considerable. A particular problem for gram-negative bacteria is that at neutral pH the speciation of Fe(III) is complex as the cation is present either as insoluble polynuclear oxo/hydroxo-bridged complexes or as soluble organic chelates. Thus, Fe(III) is frequently presented to bacteria in a range of insoluble forms. The best-characterized group of Fe(III)-respiring bacteria are species of the genus *Shewanella*, which are widespread facultative anaerobes of the gamma proteobacterium group. *Shewanella*, species can synthesize a number of periplasmic terminal respiratory reductases, including nitrate, nitrite, fumarate, and trimethylamine N-oxide reductases. During growth under iron-respiring conditions, *de novo* synthesis of a number of multi-heme *c*-type cytochromes that may a play a role in the Fe(III) respiration process occurs and a number of genetic loci that encode multi-heme cytochromes have been implicated as being important for Fe(III) respiration. Critically, these include an inner membrane tetra-heme cytochrome CymA (a NapC homologue), a small periplasmic 10 kDa tetra-heme cytochrome (STC); periplasmic deca-heme cytochromes (e.g., MtrA); and outer membrane cytochromes with deca-heme domains on the cell surface. The different cellular locations of these muti-heme cytochromes is critical to the transfer of electrons from the inner membrane across the periplasm to the outside of the outer-membrane where direct reduction of the insoluble extracellular substrate can occur. The multi-heme nature of the cytochromes may allow the proteins to form a multi-redox-centered electron wire that will be even longer than the redox ladders discussed for FdhN. Similar systems may also operate during the respiration of other insoluble respiratory substrates, such as manganese.

Synthesis of Periplasmic Electron Transport Systems

The periplasmic location of the cofactor-containing periplasmic electron transfer proteins raises the question as to how the organism assembles these proteins. This question is particularly relevant to a large protein complex with multiple redox centers, such as FdhN. In the case of periplasmic cytochromes *c* the protein is translocated in an unfolded state via the Sec pathway and heme is covalently attached using periplasmic or membrane-associated assembly proteins. However, many other classes of periplasmic redox protein possess a signal sequence, processed from the mature enzyme, that includes a twin arginine motif. This motif directs the protein to the twin arginine translocase (Tat), which transports pre-folded proteins with assembled redox cofactors. Some Tat substrates, including FdhGH are very large and consequently the pore of the Tat apparatus must be ~100Å in diameter to accommodate the largest substrates. The structure of the Tat complex is not yet known but there must be a gating mechanism, which maintains an ionic seal upon transport of these large substrates. The translocation process is also energy-driven, consuming PMF. This illustrates how

the overall consideration of the biochemistry and energetics of a periplasmic electron transfer system must take into account not only the operation of the system but also its biogenesis.

See Also the Following Articles

Cytochrome bc_1 Complex (Respiratory Chain Complex III) • Cytochrome *c* • Heme Proteins • Heme Synthesis • Iron–Sulfur Proteins • Photosystem I: F_X, F_A, and F_B Iron–Sulfur Clusters

Glossary

electrogenic Property of a transmembrane electron transport enzyme that generates a PMF.

heme A tetrapyrrole with a coordinated iron that can mediate electron transfer when bound to proteins. In *c*-type cytochromes the heme is covalently bound to the protein.

iron–sulfur cluster A protein cofactor that comprises of inorganic iron and sulfur, which together form a cluster that is often involved in electron transfer.

periplasm A subcellular compartment that lies between the inner (cytoplasmic) and outer membrane of Gram-negative bacteria.

proton-motive force A transmembrane gradient of protons (Δp) that has an electrical component ($\Delta\psi$) and a chemical component (ΔpH). Its magnitude is normally given in units of mV and can be calculated from $\Delta p = \Delta\psi - 60\Delta\text{pH}$.

Further Reading

Bertero, M. G., Rothery, R. A., Palak, M., Hou, C., Lim, D., Blasco, F., Weiner, J. H., Strynadka, N. C. (2003). Insights into the respiratory electron transfer pathway from the structure of nitrate reductase A. *Nat. Struct. Biol.* **10**, 681–687.

Einsle, O., Stach, P., Messerschmidt, A., Simon, J., Kroger, A., Huber, R., Kroneck, P. M. (2000). Cytochrome *c* nitrite reductase from *Wolinella succinogenes*. Structure at 1.6Å resolution, inhibitor binding, and heme-packing motifs. *J. Biol. Chem.* **275**, 39608–39616.

Ferguson, S. J. (2002). Keilin's cytochromes: How bacteria use them, vary them and make them. *Biochem. Soc. Trans.* **29**, 629–640.

Jormakka, M., Tornroth, S., Byrne, B., Iwata, S. (2002). Molecular basis of proton motive force generation: Structure of formate dehydrogenase-N. *Science* **295**, 1863–1868.

Page, C. C., Moser, C. C., Chen, X., Dutton, P. L. (1999). Natural engineering principles of electron tunnelling in biological oxidation–reduction. *Nature* **402**, 47–52.

Palmer, T., and Berks, B. C. (2003). Moving folded proteins across the bacterial cell membrane. *Microbiology* **149**, 547–556.

Potter, L., Angove, H., Richardson, D., Cole, J., (2001). Nitrate reduction in the periplasm of gram-negative bacteria. *Adv. Microb. Physiol.* **45**, 51–112.

Richardson, D. J. (2000). Bacterial respiration: A flexible process for a changing environment. *Microbiology* **146**, 551–571.

Richardson, D. J., and Sawers, G. (2001). PMF through the redox loop. *Science* **295**, 1842–1843.

Sawers, G. (1994). The hydrogenases and formate dehydrogenase of *Escherichia coli*. *Antonie van Leewenhoek* **66**, 57–88.

Simon, J. (2002). Enzymology and bioenergetics of respiratory nitrite ammonification. *FEMS Microbiol. Rev.* **26**, 285–309.

Van Spanning, R. J., Delgado, M. J., and Richardson, D. J. (2003). The nitrogen cycle: Denitrification and relationship to N_2 fixation, In *Nitrogen Fixation* (Newton, W., ed.), pp. 1888–2001. Kluver, Dordrecht, The Netherlands.

Biography

David Richardson is a Professor of Microbial Biochemistry and Director of the Centre for Metalloprotein Spectroscopy in the School of Biological Sciences at the University of East Anglia. He holds a Ph.D. in Biochemistry from the University of Birmingham. His principal research interests are in the field of bacterial respiration, where he studies the regulation, cellular organization, and biochemistry of a range of anaerobic electron transport systems. His contribution to this field was recognized by the Society for General Microbiology in 1999 when he was invited to give the Societies Fleming Lecture. He is on the editorial board of the *Journal of Biological Chemistry* and *Microbiology*.

Gary Sawers is a Project Leader in the Department of Molecular Microbiology at the John Innes Centre. He holds a Ph.D. in Biochemistry from the University of Dundee. His principal research interests include redox-dependent control of gene expression and metabolism in facultative anaerobes and *Streptomyces* and the biochemistry of metalloproteins. He is on the editorial board of *Microbiology*.

Rob van Spanning is an Assistant Professor in the Department of Molecular Cell Physiology at the Free University Amsterdam, The Netherlands. He holds a Ph.D. in Microbial Physiology and Molecular Microbiology from the Free University Amsterdam. His principal research interests are in understanding versatility and adaptive responses of bacterial respiration (from gene to function and back).

Peroxisome Proliferator-Activated Receptors

Mary C. Sugden, Edward A. Sugden and Mark J. Holness
Queen Mary, University of London, London, UK

PPARs (peroxisome proliferator-activated receptors) were originally identified by their ability to induce peroxisome proliferation, leading to the current nomenclaute. It has, however, emerged that PPARs do not induce peroxisome proliferation in man, but have an array of additional functions, most notably as master regulators of genes involved in metabolic control, particularly those involved in whole-body lipid homeostasis. PPARs are transcription factors, activated by binding key metabolic ligands, which exert their effects at the level of DNA to alter gene expression. Through this mechanism, PPARs, once activated, confer distinct properties of lipid handling to the tissues in which they are found, with an overall systemic lipid-lowering effect. There are three PPAR subtypes (α, γ, δ). PPAR subtypes are distributed non-uniformly in tissues. The individual PPARs act to reinforce each other's activities and also have complementary individual activities, all of wich are concerned with the removal of excess lipid from the blood. Acting as a team, the functions of the PPARs include regulation of fat breakdown by oxidation (PPARα and PPARδ), regulation of fat cell differentiation and lipid storage (PPARγ), together with others that include regulation of cholesterol fluxes into and out of cells (PPARγ and PPARδ). The physiological importance of the PPARs resides in lipid management, and the clinical importance of drugs acting via the PPARs lies in their ability to mimic nature's own messengers when harmful lipids accumulate. In this article, which of necessity cannot encompass all the actions of the PPARs, we will focus on how these receptors modulate lipid homeostasis in metabolically active tissues.

Lipids (triacylglycerol, cholesterol, phospholipids, fatty acids, and ketone bodies) are essential for many aspects of cellular processes, whilst also being linked to many pathological processes. Due to the varying demands of individual tissues for lipids, a highly regulated lipoprotein highway transports lipids to and from the periphery. The peroxisome proliferator-activated receptors (PPARs), α, γ, and δ, act as primary "metabolic" transcription factors, responding to fatty acids (FAs) and other metabolic signals to alter gene expression and thereby to confer distinct properties of lipid handling to the tissues in which they are found, with an overall systemic lipid-lowering effect. Thus, the PPARs act as a team with a common goal, but possess different attributes, including regulation of fat breakdown by oxidation (PPARα and PPARδ), regulation of adipocyte differentiation and fat storage (PPARγ), together with other functions that include regulation of cholesterol fluxes into and out of cells (PPARγ and PPARδ).

Lipids are essential for many aspects of cellular processes, including acting as substrates for energy production, steroid hormones and cellular structures. However, the availability and utilization of the various lipids must be carefully regulated since they are also linked to many pathological processes, including the development of obesity. The most familiar biological lipids are the triacylglycerols (TAG), which serve as principal energy stores, and cholesterol, both of which are present in the circulation at detectable levels. Because the hydrophobic lipids do not dissolve in water, moving them around the body requires transport mechanisms that are highly regulated. Due to the variable requirements for these compounds from a wide range of tissues, a lipoprotein highway exists that allows transport of the hydrophobic lipids with water soluble protein escorts enabling the movement of TAG and cholesterol to and from the periphery. TAG-enriched lipoproteins, chylomicrons (containing TAGs made from the re-esterification of newly absorbed FA and monoacylglycerol (MAG) in the gut) and very low density lipoproteins (VLDL) (containing TAG fabricated in the liver), deliver TAG to peripheral tissues for storage and energy production. The utilization by individual tissues of TAG in VLDL and chylomicron is carefully regulated through the expression of lipoprotein lipase (LPL), which is anchored to the outside of the cell in which it is expressed. LPL liberates FA and MAG in TAG for uptake by the tissue. Consequently, individual tissues can regulate their uptake of TAG-derived FA by altering the level of expression of LPL. At the same time, low-density lipoproteins (LDL) deliver cholesterol to tissues so that they can maintain membrane integrity and, in some instance, use it for the production of biologically important compounds, such as steroids.

Cholesterol uptake by cells is also regulated, in this case by the expression of the LDL receptor. In addition to the lipid highway from the liver/gut to peripheral tissues, a contraflow operates in the opposite direction, whereby high-density lipoproteins (HDL) transport surplus cholesterol from cells, such as those of the vessel wall, to the liver, where it can be redeployed to form bile. Gridlock in these lipid transfer and utilisation systems leading to the accumulation of VLDL and LDL in the circulation is integral to the development of metabolic diseases, including type 2 diabetes and cardiovascular disease.

PPARs: A Three-Pronged Attack

Peroxisome proliferator-activated receptors (PPARs) are transcription factors, activated by binding metabolic ligands, which exert their effects at the level of DNA to alter gene expression. There are three PPAR subtypes (α, γ, and δ). PPARs were originally identified by their ability to induce peroxisome proliferation, and this led to the current nomenclature. PPARα was first identified as the intracellular target for a particular class of rodent hepatocarcinogens, which include clofibrate. Clofibrate, a member of the fibrate amphipathic carboxylic acid family, was found to be a potent inducer of proliferation of peroxisomes, cell organelles found in high quantities in the liver, in addition to increasing FA oxidation and lowering lipid levels. Several other "peroxisome proliferating" agents were subsequently cloned. However, it has since emerged that the PPARs do not induce peroxisome proliferation in man, but have an array of additional functions, most notably as master regulators of genes involved in metabolic control, particularly those involved in whole-body lipid homeostasis. Inappropriately, the name PPAR has remained in common use! The PPAR subtypes are distributed non-uniformly in tissues. PPARα is expressed in a wide range of tissues and is highly expressed in liver, kidney, and heart. PPARγ has a more limited tissue distribution and is highly expressed in adipocytes and macrophages. PPARδ is widely expressed. After the PPARs are activated by binding specific ligands and/or by covalent modification (phosphorylation), they consort with another receptor, the 9-cis retinoic acid activated receptor (RXR), and, conjoined and active, recruit co-activators and together bind to peroxisome proliferator response elements (PPRE) to modify the expression of specific genes. This leads to an altered complement of enzymes in the cell, with a resultant alteration in cellular functional characteristics. Through this mechanism, each PPAR can, once activated, confer distinct properties of lipid handling to the tissues in which it is found, with an overall systemic lipid-lowering effect. The individual members of the PPAR gang act to reinforce each other's activities and also have complementary individual activities, all of which are concerned with the removal of excess lipid from the blood. Acting as a team with a common goal but differing attributes, the functions of the PPARs include regulation of fat breakdown by oxidation (PPARα and PPARδ), regulation of adipocyte differentiation and fat storage (PPARγ), together with others that include regulation of cholesterol fluxes in to and out of cells (PPARγ and PPARδ). The molecular messengers that bind to and activate the individual PPARs (the endogenous ligands) are not all identified. However, the close involvement of fat metabolism and lipid homeostasis with the PPAR family members arises, in part, because certain FAs and other lipid-derived molecules, including eicosanoids and arachidonic acid derivatives, can bind to and activate PPARs and are known to be primary natural ligands for these molecules. For example, PPARα is activated by polyunsaturated FAs, and PPARδ by long-chain FAs. Thereby, these lipid-signaling molecules can have power over their own fates by binding to PPARs and changing the expression of genes involved in modulating the patterns of tissue FA handling. The physiological importance of the PPARs thus resides in lipid management, and the clinical importance of drugs acting via the PPARs lies in their ability to mimic nature's own messengers when the task of lipid management becomes too onerous and harmful lipids accumulate. It is now established that the fibrates (e.g., clofibrate) and the anti-diabetic insulin-sensitizing thiazolidinediones (TZDs) both exert their systemic lipid-lowering effects via the PPARs. In this article, which of necessity cannot encompass all the actions of the PPARs, we will focus on how these receptors modulate lipid homeostasis in metabolically active tissues.

PPARα (NR1C1)

Too much FA, TAG or cholesterol circulating in the blood can be hazardous to health. High-fat diets, particularly those rich in very-long-chain FAs and polyunsaturated FAs induce FA oxidation via PPARα. Synthetic ligands for PPARα, in addition to the fibrate drugs, include phthalate ester plasticers, herbicides, and leukotriene D4 receptor antagonists. The fibrate PPARα agonists (clofibrate, gemfibrozil, fenofibrate, bezafibrate, and ciprofibrate) have been in clinical use for over 40 years for the treatment of dylipidemia.

The liver occupies a central position in whole-body lipid handling. In the case of FAs, the liver is capable of either oxidizing, or storing FAs depending on the prevailing requirements. FAs are stored after conversion to the TAG component of VLDL, and this function can be increased when FA delivery is higher than that

required to fuel hepatic ATP requirements via β oxidation. Incoming FAs, derived from the diet or endogenous stores, are re-esterified and stored in the fed state. During starvation, FAs, released from adipose tissue, are taken up by the liver and oxidized to create the water-soluble lipid-derived fuels, the ketone bodies (which are easily transported and oxidized by peripheral tissues), while TAG is incorporated into VLDL which is released into the circulation. These latter metabolic transformations of incoming FAs are enhanced by PPARα, the primary PPAR subtype expressed in liver. PPARα regulates specific genes that code for regulatory proteins involved in almost every stages of hepatic FA utilization, including FA uptake into the cell across the cell membrane, its retention within the cell, and its oxidation leading to ATP production and ketone body formation (Figure 1). PPARα therefore fulfills a critical role in the regulation of hepatic FA handling and, indeed, is essential for the up-regulation of the capacity of the liver for FA utilization in starvation or when lipid delivery is increased by a diet high in fat. This adaptive role is best illustrated by the inadequate response to high-fat feeding seen in PPARα-deficient mice, the Jack Sprats of lipid biochemistry. These animals exhibit an impaired ability to up-regulate hepatic FA oxidation in response to a high-fat diet, despite increases in FA supply, and the liver becomes engorged with lipid. Similarly, PPARα-deficient mice are unable to adapt to starvation, where delivery of FA from adipose tissue is increased. Secondary to impaired FA oxidation, compromised hepatic energy generation results in a low blood glucose concentration (hypoglycemia) when PPARα-deficient mice are fasted. Hypoglycemia arises by virtue of the necessity to continue to use glucose at high rates, rather than to be able to switch to FA or (in extrahepatic tissues) ketone bodies as alternative energy fuels, and because hepatic FA oxidation allows hepatic glucose synthesis (gluconeogenesis) through the generation of ATP and essential cofactors. The accumulation of large amounts of lipid in livers of PPARα-deficient mice, either on fasting or when they are maintained on a high-fat diet demonstrates the critical importance of PPARα-linked functions in matching hepatic FA delivery to FA clearance when the systemic delivery of lipid is increased. Hence, the TAG-lowering action of fibrates and related PPARα-targeted drugs in patients with hyperlipidemia is ascribed to increased FA clearance via oxidation, primarily but not exclusively in liver. Within the liver, PPARα also is heavily involved in the regulation of the synthesis and catabolism of lipoproteins, including some steps of the HDL synthetic pathway. Increased diversion of FA into oxidation decreases the availability of fatty acyl-CoA substrates for TAG synthesis, and thereby decreases VLDL

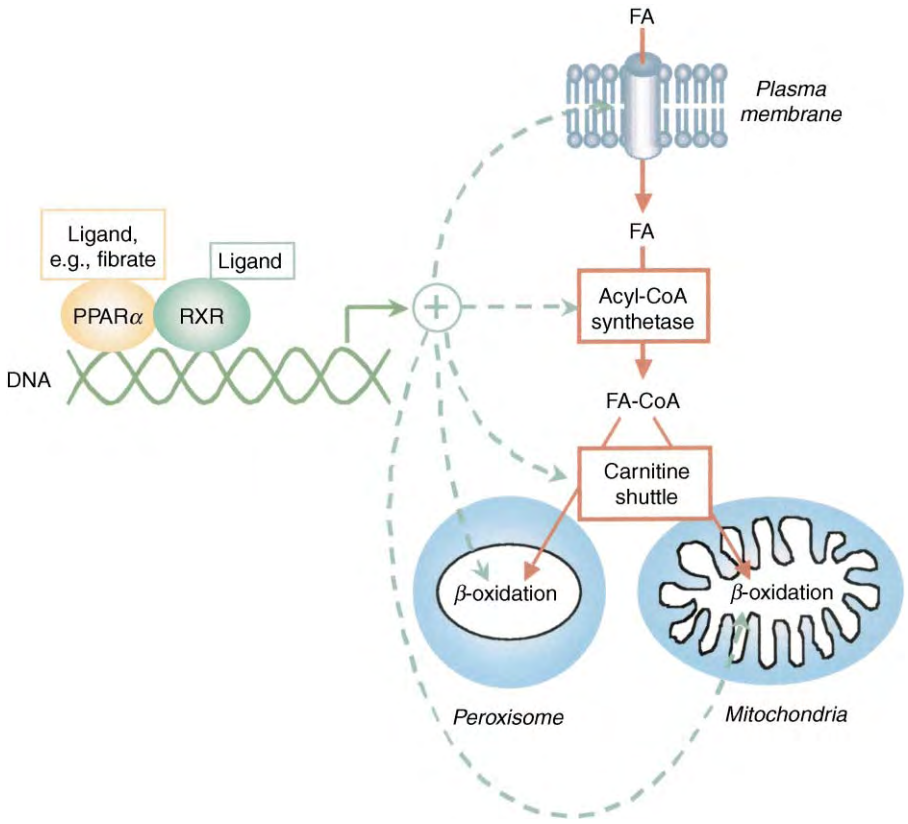

FIGURE 1 Mechanisms whereby activation of PPARα regulates fatty acid uptake, sequestration in the cell and oxidation.

secretion by the liver. In addition, PPARα inhibits expression of apolipoprotein (apo) C-III (a protein that may inhibit the TAG-hydrolysing action of LPL) and so enhances the hydrolysis of TAG contained in lipoproteins, and increases the hepatic uptake of TAG-enriched lipoprotein remnants. This decreases plasma TAG levels further and increases the transfer of other surface components of TAG-rich particles to HDL.

As well as in liver, PPARα is expressed abundantly in other tissues that are normally characterized by high rates of lipid oxidation. It is also present in the artery wall in monocytes/macrophages, vascular smooth muscle cells and endothelial cells. We focus here on the role of PPARα in kidney and heart, tissues which have a high energy demand related to their physiological functions. In these tissues, PPARα activation again enhances the expression of genes involved in FA uptake, activation, and oxidation. PPARα-deficient mice subjected to ischemia/reperfusion injury respond with greater renal cortical necrosis and worse kidney function compared with wild-type controls, indicating the vital role of PPARα in this tissue. PPARα is found predominantly in the renal cortex. Like liver, the renal cortex is a site of gluconeogenesis. Altered renal gluconeogenesis is increasingly recognized as contributing to fasting hyperglycemia in diabetes mellitus, and assumes increasing importance for maintenance of glycaemia after very prolonged food deprivation. Hence, as in liver, PPARα-facilitated gluconeogenesis driven by enhanced FA oxidation is likely.

Although functionally quite distinct from liver and kidney, there is ample evidence for an important role for PPARα in cardiac function in some circumstances. In adulthood, although the heart is a metabolic omnivore using most available fuels, lipids constitute the predominant energy substrate. However, during fetal and early life, in cardiac hypertrophy and in the failing heart, glucose utilization assumes greater importance, possibly as an adaptation to limited oxygen availability. Oxygen is essential for ATP production from FAs, but glucose oxidation needs less oxygen per mole than FA oxidation and glucose utilization can proceed, albeit less efficiently, in the absence of oxygen. The downside is that less ATP is generated per mole of glucose oxidized and when excess dietary lipid can be ingested, as in extrauterine life, the potential exists for myocardial lipid accumulation and lipotoxicity. Accordingly, the importance of PPARα in the adult heart appears relatively limited when the dietary lipid supply or endogenous lipid production is restricted, but PPARα assumes an important role in cardiac lipid management when lipid delivery to the heart is increased. PPARα-deficient mice provided with free access to a high-carbohydrate low-fat diet do not show any obvious cardiac abnormalities, but they accumulate myocardial lipid on starvation or if a high-fat diet is provided. This indicates a vital function for PPARα in allowing cardiac FA oxidation to occur at a rate sufficient to prevent the harmful accumulation of lipid within the heart itself.

Changes in the activity of the PPARα signaling pathway to gene expression characterize many common myocardial diseases. Whether changes in cardiac PPARα signaling are adaptive or causally related to myocardial pathology remains controversial, but there is no doubt that poor lipid management can cause a broken heart! Cardiac PPARα expression and activity are suppressed in the pathologically hypertrophied heart. The resultant decrease in the capacity for FA oxidation is associated with increased rates of glucose utilization and reversion to the fetal pattern of substrate use. Although causality between the reciprocal changes in lipid and glucose utilization has not been established, this metabolic switch may serve to preserve ventricular function within the context of pressure overload. The expression and activity of both PPARα and RXR are also suppressed in the hypoxic cardiac myocyte. To date, there are no reports of worsening of cardiac function in humans with cardiac hypertrophy through the use of the PPARα agonist fibrates. It is interesting that the heart is closely associated with adipose tissue in adult man, and epicardial and pericardial depots can represent a significant fraction of the total mass of the heart, suggesting a possible role as a local FA source. Both neutral lipid and FA adversely affect myofibrillar function. An intriguing possibility is that cardiac adipose tissue may act as a potential local sink for FA, mopping up FA when they are delivered in excess of the cardiac ATP requirement or when they cannot be cleared through oxidation, for example, during cardiac hypertrophy. The heart expresses LPL and, interestingly, LPL activity in cardiac myocytes is inhibited by PPARα activation. This effect may again help protect against a potentially toxic oversupply of FAs to the myocardium.

Epidemiological studies reveal that people with diabetes are at an extraordinary high risk for the development of cardiovascular disease. The heart in uncontrolled diabetes is constrained from switching to glucose oxidation and relies almost exclusively on lipid as an energy source. Cardiac-specific over-expression of PPARα, in the absence of alterations in lipid-fuel delivery, enhances the myocardial capacity for FA oxidation. This, however, is maladaptive, since many of the metabolic abnormalities of the diabetic heart, including decreased glucose utilization and ventricular dysfunction, are recapitulated. In this situation, the profile of myocardial TAG species is similar to the lipid species in the circulation, suggesting that the expanded lipid reservoir reflects increased uptake incompletely balanced by a corresponding increase in oxidation. When mice with cardiac-specific PPARα overexpression are made diabetic, they develop a more severe

cardiomyopathy than wild-type controls. In contrast, PPARα null mice are protected from cardiomyopathy.

PPARγ (NR1C3)

PPARγ, the predominant molecular target for the insulin-sensitizing TZDs and for specific prostanoids, such as 15-deoxy-$\Delta^{12,14}$ prostaglandin J2, is abundantly expressed in adipocytes, macrophages, the placenta and the fetal heart. The role of PPARγ as a critical regulator of adipose tissue development and metabolism is perhaps most well-established of the functions of the PPARs. Adipocytes expand as animals fatten, then shrink when the stored TAGs within them is mobilized because of food scarcity or, in the case of Mrs Sprat or the Atkins diet, lack of carbohydrate. A key feature of the fat cell is its ability to release the FA derived from TAG into the bloodstream: most other tissues are less altruistic and use FA derived from their endogenous TAG themselves. Detectable changes in gene expression in response to PPARγ activation in adipose tissue includes the induction of genes that allow adipose tissue to take up and accumulate lipid (Figure 2). Through this action, PPARγ contributes to lowering of circulating FA and TAG levels and, by sequestering lipid in the adipocyte, reduces the burden of excessive lipid delivery to tissues other than adipose tissue, including heart, skeletal muscle, kidney, and liver, where its accumulation could have deleterious effects. PPARγ can therefore enhance whole-body insulin action even though it is predominantly expressed in adipose tissue (which makes a relatively minor contribution to insulin-stimulated glucose disposal in lean individuals) by limiting the supply of lipid to other insulin-sensitive tissues and reducing the ability of FA to oppose insulin's actions in these tissues.

In addition to effects on genes involved in adipocyte lipid storage, TZDs increase adipocyte expression of the insulin-sensitive glucose transporter GLUT4, which allows increased use of circulating glucose for the synthesis of glycerol-phosphate which, in turn, allows FA esterification to form storage TAG (Figure 2). In addition, the TZDs may actually allow the fat cell to express enzymes that allow glycerol released from TAG breakdown (lipolysis) to be reclaimed or synthesized from circulating lactate, a process termed glyceroneogenesis (Figure 2). The presence of glycerol kinase allows glycerol released via the hydrolysis of stored triglyceride to be converted to glycerol phosphate which, in turn, allows reincorporation of released FA, or of FA derived from exogenous lipoproteins, into storage TAG, albeit at an energetic cost to the adipocyte. However, in obese people, as much as half of the body mass can be adipose tissue due to excessive enlargement of adipocytes and the presence of increased numbers of adipocytes.

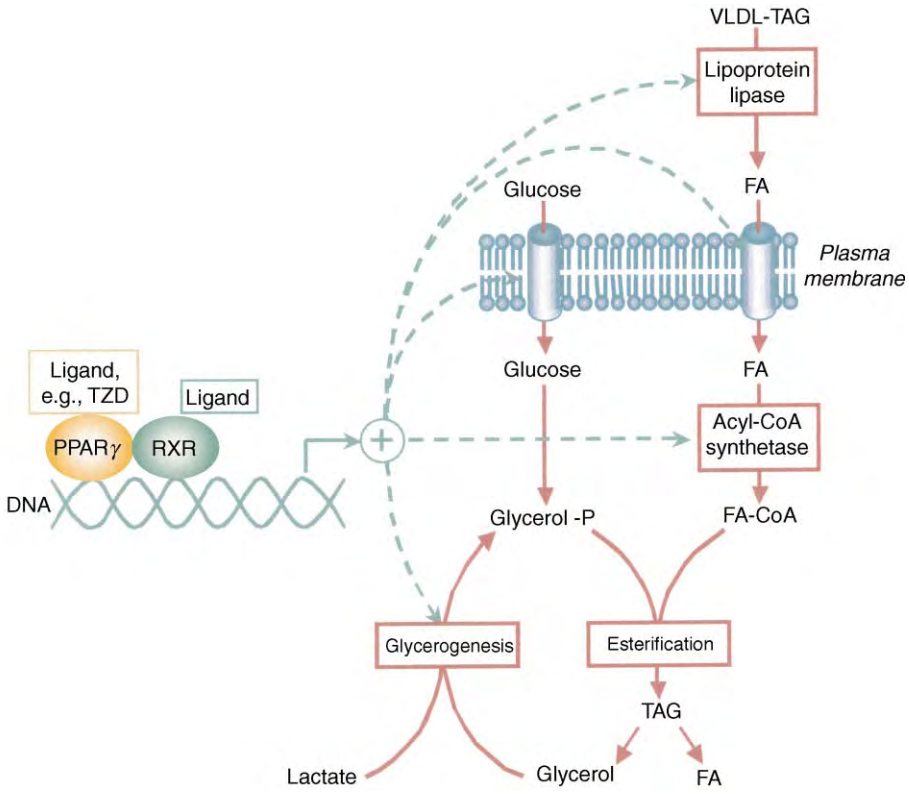

FIGURE 2 Mechanisms whereby activation of PPARγ regulates fatty acid uptake, sequestration and storage and glucose uptake and glycerogenesis in adipocytes.

Obese people invariably become glucose intolerant and insulin resistant, as well as developing other obesity-related complications which increase morbidity and mortality. "We fat all creatures else to fat us, and we fat ourselves for maggots" (Hamlet). It follows that the long-term use of TZDs could actually exacerbate obesity and insulin resistance, despite its more acute beneficial insulin-sensitizing action due to adipose-tissue lipid sequestration.

An additional action of PPARγ activation in adipose tissue is altered rates of secretion of biologically active adipokines (signaling molecules secreted by adipocytes), including leptin and TNFα, which can modulate insulin sensitivity in non-adipose tissue. Both leptin and TNFα have a role in obesity. Samples of adipocytes from obese people produce much more TNFα than those from lean people. Leptin is a molecule that informs the brain that adipose tissue is replete with lipid and signals a need to cease eating. PPARγ suppresses the production of both leptin and TNFα, thereby fooling the adipocyte that enough (lipid) is not enough, and allowing the adipocyte to continue to accumulate even more lipid.

Effects of the TZDs to ameliorate hyperglycemia and hyperlipidemia in fatless mice demonstrate that, although predominantly expressed in adipose tissue, PPARγ ligands may exert their effects via PPARγ in tissues in addition to adipose tissue. PPARγ agonists have been reported to be cardioprotective against ischaemic insult and to modify the cardiac hypertrophic growth response to pressure overload. However, most cardiac effects are likely to be indirect because of the low level of expression of PPARγ in cardiac myocytes themselves in adulthood, although the adipose tissue surrounding the heart itself may be targeted directly and act as a lipid buffer.

Most kinds of mammalian cells synthesize adequate cholesterol for their needs, but the human diet usually contains more than enough to supply our cells. Only the liver can degrade and eliminate cholesterol, so any excess has to be transported there from other tissues. LDL particles are rich in cholesterol. Some LDL leak through the thin lining of major vessels, where they become trapped under the endothelial cells, a process facilitated by hypertension (high blood pressure). Trapped LDL molecules attract macrophages, immune cells that can take up and degrade LDL. Some trapped LDL react with oxygen in the blood. Unfortunately, the oxidized LDL appear to be able to enter the macrophages in almost unlimited quantities, accumulating as pale, greasy particles that resemble the appearance of foam. Death of the lipid-bloated macrophages (foam cells) releases their lipid content forming fatty streaks in the arteries. The endothelial cells over the fatty streaks can become damaged and are replaced with fibrous plaques, narrowing the arteries. In the final stages of cardiovascular disease, the stiff narrow arteries ulcerate, increasing the risk of forming a blood clot, which will plug blood flow completely. The increased risk of cardiovascular disease in diabetic patients has prompted study of PPARγ function in lipid-laden macrophages. It has been reported that activation of PPARγ with the TZDs promotes cholesterol efflux from macrophages, improving the status of the atherosclerotic lesion, whereas macrophages lacking PPARγ are defective in cholesterol efflux and display accelerated lesion progression. Activation of PPARγ by components of oxidized LDL (9-hydroxyoctadecadienoic acid, 13-hydroxyoctadecadienoic acid) however, enhances macrophage lipid accumulation through induction of a scavenger receptor/transporter (FA translocase/CD36).

PPARδ (NR1C2)

Compared with PPARα and PPARγ, relatively little is known about PPARδ (also called PPARβ or FA-activated receptor, FAAR), except that it is relatively ubiquitously expressed. Nevertheless, its importance of PPARδ is established by the observation that most PPARδ-deficient mice die early in embryonic development due to a placental defect and those few that do survive have a reduced fat mass. PPARδ may also be involved in the cellular differentiation and inflammatory response of the epidermis. Importantly, PPARδ has been shown to mediate VLDL signaling to gene expression in the roving macrophages. Exposure of macrophages to VLDL results in enhanced expression of a lipid-droplet-coating protein that is implicated in lipid storage in these cells. Studies of PPARδ-deficient macrophages reveal that the TAG components of VLDL, released by LPL, serve as direct ligands for PPARδ to induce this protein, with accompanying lipid accumulation within the macrophage. These new data reveal a pathway whereby VLDL itself can directly regulate gene expression in atherosclerotic lesions.

Pharmacological activation of PPARδ lowers fasting TAG and LDL levels while increasing levels of HDL (the cardioprotective lipoprotein). It is unclear which tissue is targeted although skeletal muscle, in which PPARδ is highly expressed, is suspected. Slow-twitch oxidative skeletal muscle is a major site of FA catabolism, particularly during starvation and long-term exercise, when circulating lipid delivery increases. However, most evidence suggests that signaling via PPARα impacts predominantly on the regulation of lipid gene expression and fat burning in fast-twitch, not slow-twitch, skeletal muscle, even though fast-twitch muscle does not normally oxidize FA as avidly as slow oxidative muscle. Whereas PPARα ablation in the mouse results in abnormally high accumulation of neutral lipid in heart and liver in response to interventions increasing FA delivery, such as starvation, starvation of

PPARα-deficient mice leads to only minor abnormalities of skeletal-muscle FA metabolism. The lack of accumulation of neutral lipid has been attributed to the findings that PPARδ is the major type of PPAR found in mouse skeletal muscle. PPARδ may therefore assume greater importance in the modulation of lipid metabolism than PPARα in skeletal muscle, a conclusion supported by findings that PPARδ mRNA expression levels in muscle are dramatically increased on fasting, under conditions where FA oxidation by skeletal muscle is increased. Interestingly, PPARδ is also relatively abundant in the heart and exposure of cardiac myocytes to either PPARα- or PPARδ-specific agonists leads to significant induction of PPAR target genes involved in FA uptake and oxidation and both PPARs can be activated by FAs within this system.

Last Words

The question is raised as to why some non-adipose tissues express multiple PPARs, for example, PPARγ and PPARδ in macrophages, PPARα and PPARδ in muscle. Activation of all three PPARs appears to decrease systemic lipid availability and to decrease lipid (TAG and/or cholesterol) storage in non-adipose tissue. One possibility is that each individual PPAR activates overlapping but distinct downstream metabolic pathways. Perhaps more likely, it may be that the physiological ligands (presumably upstream lipid-based messengers) for activation of each of the PPARs are unique and that such ligand distinctness allows specificity of cellular downstream metabolic responses. PPARs are thus jacks of all trades, and masters of (at least) one! Although their individual specific physiological roles still require much further investigation, it is clear that, as ligand-activated transcription factors, the PPARs represent attractive targets for the development of selective therapeutic agents for pharmacological modulation of lipid metabolism.

See Also the Following Articles

Leptin • Lipases • Lipoproteins, HDL/LDL • Peroxisomes

Glossary

fibrates A group of compounds that act as agonists for PPARα.

peroxisome proliferator-activated receptors (PPARs) Are ligand-activated transcription factors, which alter gene expression to confer distinct properties of lipid handling to the tissues in which they are found, with an overall systemic lipid-lowering effect.

thiazolidinediones (TZDs) A group of compounds that act as agonists for PPARγ.

Further Reading

Finck, B. N., and Kelly, D. P. (2002). Peroxisome proliferator-activated receptor alpha (PPARalpha) signaling in the gene regulatory control of energy metabolism in the normal and diseased heart. *J. Molecul. Cell. Cardiology* **34**, 1249–1257.

Francis, G. A., Annicotte, J.-E., and Auwerx, J. (2003). PPAR alpha effects on the heart and other vascular tissues. *Amer. J. Physiol. Heart Circulatory Physiology* **285**, H1–H9.

Fruchart, J. C., Staels, B., and Duriez, P. (2001). PPARs, metabolic disease and atherosclerosis. *Pharmacol. Res.* **44**, 345–352.

Kersten, S., Desvergne, B., and Wahli, W. (2000). Roles of PPARs in health and disease. *Nature* **405**, 421–424.

Lee, C. H., Olson, P., and Evans, R. M. (2003). Lipid metabolism, metabolic diseases, and peroxisome proliferator-activated receptors. *Endocrinology* **144**, 2201–2207.

Biography

Mary C. Sugden is Professor in the Centre for Diabetes and Metabolic Medicine, ICMS at Bart's and the London School of Medicine and Dentistry in London, UK. Her principal research interests lie in the broad fields of insulin secretiion and action and in metabolic regulation, particularly with respect to fuel preference and the regulatory interactions between glucose and fats as energy sources. She holds M.A. and D.Phil. degrees from the University of Oxford and a D.Sc. from the University of London. Edward A. Sugden is associated with the group and assisted with analysis of the accessibility of the text to a lay audience.

Mark J. Holness a Senior Lecturer in the Centre for Diabetes and Metabolic Medicine, ICMS at Bart's and the London School of Medicine and Dentistry in London, UK. He holds B.Sc. and Ph.D. degress from the University of London. His principal research interests include the etiology of insulin resistance elicited by modification of dietary and hormonal status in early life and/or adulthood, the impact of lipid quantity and quality on pancreatic beta cell function and the role of PPARα in mediating changes in insulin sensitivity and secretion.

Peroxisomes

Suresh Subramani
University of California, San Diego, California, USA

Peroxisomes are among the simplest of the subcellular organelles that are characteristic of all eukaryotic cells. With ~60 known enzymes in the matrix and ~45 documented integral or peripheral membrane proteins, it is a reasonable guess that this organelle has only ~125 proteins, which makes it much less complex than other organelles. The peroxisome derives its name from the fact that many metabolic enzymes that generate hydrogen peroxide as a by-product are sequestered here because peroxides are toxic to cells. Within peroxisomes, hydrogen peroxide is degraded by the enzyme, catalase, to water and oxygen. Peroxisomes are surrounded by a single membrane and they range in diameter from 0.1 to 1 μm. They exist either in the form of a network of interconnected tubules (peroxisome reticulum), as in liver cells, or as individual microperoxisomes in other cells such as tissue culture fibroblasts.

Peroxisome-Like Organelles

Peroxisomes are related to specialized peroxisomes called glycosomes in parasites such as Trypanosomes, and to plant glyoxysomes, but are unrelated to hydrogenosomes, mitochondria, and chloroplasts. Collectively, peroxisomes, glyoxysomes, and glycosomes are also referred to as microbodies.

Peroxisome Distribution and Origin

Peroxisomes exist in all eukaryotes from single- and multicellular microorganisms, to plants and animals. Unlike mitochondria, nuclei, and chloroplasts, peroxisomes have no DNA. Consequently all their proteins are encoded by nuclear genes. They are proposed to have originated from endosymbionts that subsequently lost their DNA, but the evidence for an endosymbiont origin is much weaker than it is for mitochondria and chloroplasts.

Regulation of Peroxisome Number, Volume, and Contents

Peroxisomes can be induced to proliferate in many organisms in response to metabolic needs. Examples include the induction of proliferation of hepatic peroxisomes by fibrate drugs, phthalate plasticizers and xenobiotics, or the induction of peroxisomes in the methylotrophic yeast, *Pichia pastoris*, by methanol or oleate. The contents of the organelle are also responsive to the environment, as illustrated by the fact that peroxisomes of yeasts grown on oleate have induced levels of the fatty acid β-oxidation enzymes, whereas methylotrophic yeasts grown on methanol have elevated levels of alcohol oxidase and dihydroxyacetone synthase. Peroxisome volume can also be regulated by proteins such as Pex11p and Pex25p. Some mechanism must also exist for monitoring the need for peroxisomes and their function, because excess peroxisomes can be turned over by autophagic mechanisms involving the lysosome in mammals, or its yeast equivalent, the vacuole.

Functions of Peroxisomes

The principal function of peroxisomes is to house many metabolic pathways that are involved in various aspects of lipid metabolism. These include the following:

1. enzymes involved in the degradative oxidation (e.g., β-oxidation of very long chain fatty acids, 2-methyl-branched fatty acids, dicarboxylic acids, leukotrienes, bile acid intermediates and cholesterol side chains, and both α- and β-oxidation of 3-methyl-branched chain fatty acids);
2. the early steps in the synthesis of ether glycerolipids or plasmalogens;
3. the formation of bile acids, dolichol, and cholesterol; and
4. the catabolism of purines, polyamines, and amino acids, and the detoxification of reactive oxygen species such as hydrogen peroxide, superoxide anions, and epoxides. In methylotrophic yeasts, peroxisomes are also involved in the metabolism of methanol and methyl amines.

Glycosomes contain the glycolytic enzymes, in addition to enzymes common to most peroxisomes, whereas plant gloxysomes have some or all of the

glyoxylate pathway enzymes. Peroxisomes in the leaves of plants also participate in photorespiration.

Despite the fragility of the organelle during biochemical purification, the peroxisome membrane is impermeable to small molecules such as NAD(H), NADP(H), acetyl-CoA, and even protons *in vivo*. Consequently, it is not surprising that the peroxisomal membrane has a number of transporters for fatty acids, fatty-acyl-CoA esters, metabolites, and ATP.

Involvement in Human Disease

There are ~20 peroxisomal disorders, many of which are fatal. These diseases affect either a single metabolic enzyme, or the assembly of the organelle itself (Table I). Almost all of the genes involved in the human peroxisome biogenesis disorders (PBDs) are now known – they fall within the 25 *PEX* genes required for peroxisome biogenesis. Mouse models for human PBDs offer the promise of better insights into the symptoms of these diseases, their diagnoses, and eventually for therapeutic intervention.

Biogenesis of Peroxisomes

Because peroxisomes have no DNA, all their proteins must be imported from genes encoded in the nucleus. Most of proteins that reside in the peroxisome matrix and membrane are synthesized in the cytosol and then imported posttranslationally to the organelle. About 25 *PEX* genes, encoding proteins named peroxins, are necessary for the biogenesis of the organelle. Most of these genes are found in multiple organisms and 13 are conserved in humans (Table II). The general principles of biogenesis appear to be common to organisms across the evolutionary spectrum, but there are indeed organism-specific variations. More recently, additional *PEX* genes (*PEX23–PEX32*) have been defined and many of these are involved in the control of peroxisome division and number, rather than in protein import.

Peroxisomal Matrix Protein Import

Proteins destined for the peroxisome matrix have a few peroxisome targeting signals (PTSs). Most matrix polypeptides have a conserved, C-terminal, tripeptide PTS1 (-SKL in the one letter amino-acid code, or its conserved variants). Others have an N-terminal or internal sequence termed PTS2 [(R/K) (L/V/I))X_5(H/Q) (L/A)]. A few proteins, such *Saccharomyces cerevisiae* acyl-CoA oxidase, either have no canonical PTS1 sequence or have one that is dispensable, suggesting that they may possess other, as yet undefined, features that allow them to be targeted to the peroxisome lumen.

Matrix proteins synthesized in the cytosol are bound by cytosolic receptors – Pex5p in the case of PTS1, and

TABLE I

Human Peroxisomal Disorders Involving Metabolism and Biogenesis

Disease	*Peroxisomal enzyme affected*
Peroxisomal metabolic disorders	
Pseudoneonatal adrenoleukodystrophy	Acyl-CoA oxidase (Acox1)
Multifunctional protein 2 (MFP2) deficiency	MFP2 involved in β-oxidation of very long chain and 2-methylbranched fatty acids
Peroxisomal thiolase deficiency	3-ketoacyl-CoA-thiolase
X-linked adrenoleukodystrophy	ALDp (transporter)
Rhizomelic chondrodysplasia punctata Type 2	Dihydroxyacetonephosphate acyltransferase
Rhizomelic chondrodysplasia punctata Type 3	Alkyl-dihydroxyacetonephosphate synthase
Refsum's disease (classical)	Phytanoyl-CoA hydroxylase
Glutaric aciduria Type 3	Glutaryl-CoA oxidase
Hyperoxaluria Type I	Alanine:glyoxylate aminotransferase
Acatalasaemia	Catalase
Mevalonic aciduria	Mevalonate kinase
Di/trihydroxycholestanoic acidaemia	Trihydroxycholestanoyl-CoA oxidase (Acox2)
Mulibrey nanism	TRIM37
Adult-onset sensory motor neuropathy	2-methylacyl-CoA racemase
Disease	**Peroxin affected**
Peroxisome biogenesis disorders	
Zellweger syndrome	Pex1, Pex2, Pex3, Pex5, Pex6, Pex10, Pex12, Pex13, Pex16, Pex19
Neonatal adrenoleukodystrophy	Several peroxins (Pex1, Pex5, Pex6, Pex10, Pex12, Pex13)
Infantile Refsum's disease	Several peroxins (Pex1, Pex2, Pex5, Pex12)
Rhizomelic chondrodysplasia punctata Type I	Pex7

TABLE II

Proteins Involved in Peroxisome Biogenesis

Pex1	A 100–50 kDa ATPase (AAA family) in yeasts and humans. Interacts with Pex6 and other peroxins. Defects in Pex1 are the most common cause of the PBDs (CGI).
Pex2	A ~40 kDa integral PMP with a carboxy-terminal, cytoplasmically exposed, zinc-binding RING domain. Has been identified in yeasts and humans, interacts with Pex3, Pex10 and Pex12 and is defective in CG10 of the PBDs.
Pex3	A ~40 kDa integral PMP in yeast and humans that binds Pex19 and is defective in CG12 of the PBDs. Needed for assembly/stability of the RING–domain subcomplex comprised of Pex2, Pex10, Pex12 in yeast.
Pex4	A 20–24 kDa peroxisome-associated ubiquitin-conjugating enzyme that interacts with Pex22. Has been identified in several yeast species, but not in any metazoan.
Pex5	A ~70 kDa, predominantly cytoplasmic/partly peroxisomal protein that is found in yeasts, plants and humans. Contains a PTS1-binding, tetratricopeptide-repeat (TPR) domain in its carboxy-terminal half, interacts with several peroxins (Pex7, Pex8, Pex10, Pex12, Pex13 and Pex14) and is defective in CG2 of the PBDs.
Pex6	A ~100 kDa (AAA family) ATPase found in yeasts, plants and humans. Interacts with Pex1 and is defective in CG4 of the PBDs.
Pex7	A ~40 kDa, WD40-repeat-containing protein that binds the PTS2. Defective in CG11 of the PBDs.
Pex8	A variably sized (60–80 kDa), peripheral, but intraperoxisomal, PMP that interacts with Pex5 and the docking subcomplex, found only in yeast. It is an intraperoxisomal organizer of the peroxisomal import machinery in *S. cerevisiae*.
Pex9	A 44 kDa integral PMP found only in the yeast *Yarrowia lipolytica*.
Pex10	A ~35 kDa integral PMP with a carboxy-terminal, cytoplasmically-exposed, zinc binding RING domain. Has been identified in yeasts and humans, interacts with Pex2, Pex3, Pex5 and Pex12, and is defective in CG7 of the PBDs.
Pex11	A ~25 kDa integral PMP required for normal peroxisome abundance. Many species contain several Pex11 genes.
Pex12	A ~40 kDa integral PMP with a carboxy-terminal, cytoplasmically-exposed, zinc-binding RING domain. Has been identified in yeasts and humans, interacts with Pex2, Pex3, Pex5 and Pex10, and is defective in CG3 of the PBDs.
Pex13	A ~44 kDa integral PMP with a carboxy-terminal, cytoplasmically-exposed SH3 domain. Identified in yeasts and humans, interacts with Pex5 and Pex14, and is defective in CG13 of the PBDs.
Pex14	A ~40 kDa PMP of yeasts, plants and humans that interacts with Pex5, Pex8, Pex13 and Pex17.
Pex15	A 44 kDa integral PMP identified only in *Saccharomyces cerevisiae*. Interacts with Pex6 in yeast.
Pex16	In humans, Pex16 is a 36 kDa integral PMP that binds Pex19 and is defective in CG9 of the PBDs.
Pex17	A ~25 kDa integral PMP that interacts with Pex14. Has been identified only in *S. cerevisiae* and *P. pastoris*.
Pex18	A 31 kDa soluble protein involved only in PTS2-protein import. It is highly similar to Pex21, and might act as a Pex7 chaperone. Identified only in *S. cerevisiae*.
Pex19	A 33 kDa farnesylated protein of yeasts and humans. Predominantly cytoplasmic/partly peroxisomal, binds all known integral PMPs and recognizes some, but not all, mPTSs. It is defective in CG14 of the PBDs.
Pex20	A 46 kDa soluble protein involved only in PTS2-protein import. Identified only in *Y. lipolytica*. Substitutes functionally for Pex18/Pex21 in *S. cerevisiae*.
Pex21	A 31 kDa soluble protein involved only in PTS2-protein import, is highly similar to Pex18 and might act as a Pex7 chaperone. Identified only in *S. cerevisiae*.
Pex22	A 20 kDa integral PMP of yeasts that interacts with Pex4 and anchors it on the peroxisomal membrane.
Pex23	A 46 kDa integral PMP. Identified only in *Y. lipolytica*.
Pex24	A 61 kDa integral PMP found in yeasts required for the proper localization of some, but not all, PMPs and matrix proteins.
Pex25	A 45 kDa PMP found in *S. cerevisiae* that regulates peroxisome size and maintenance.

CG, complementation group; SH3, Src-Homology 3.

Pex7p in the case of PTS2 (see Figure 1). These receptor–cargo complexes then move to the peroxisome membrane where they dock with protein subcomplexes that are in or on the membrane. Two such complexes are a docking subcomplex, comprised minimally of peroxins Pex8p, Pex13p, Pex14p, and Pex17p, and a really interesting new gene (RING)–protein subcomplex, consisting of three RING–proteins Pex2p, Pex10p, and Pex12p (and other yeast peroxins, such as Pex3p and Pex8p). The RING–proteins have a characteristic zinc-binding domain and are members of a protein family whose first member was called RING. There is evidence that the protein subcomplexes are dynamic, e.g., the docking and RING–protein subcomplexes can come together as a larger complex during import. The PTS receptors, Pex5p and Pex7p, are believed to shuttle from the cytosol to the peroxisome membrane or lumen of the organelle, where they release their cargo, before they return back to the cytosol for another round of import. This is referred to as the extended shuttle model for matrix protein import. It is unclear at present whether the RING–protein subcomplex (also called the translocation complex in the literature) is involved directly in the translocation of proteins into peroxisomes, or in the shuttling of receptors (e.g., Pex5p) back to the cytosol. Many other peroxins and chaperones such as Djp1p, hsp70, and hsp40 are implicated in matrix protein import, but their precise roles are still under investigation.

The PTS2 pathway, which is dependent on the receptor, Pex7p, requires different additional proteins depending on the organism of its origin. In *S. cerevisiae*, the redundant proteins, Pex18p and Pex21p, fulfill this function, whereas in *Yarrowia lipolytica*, Pex20p is

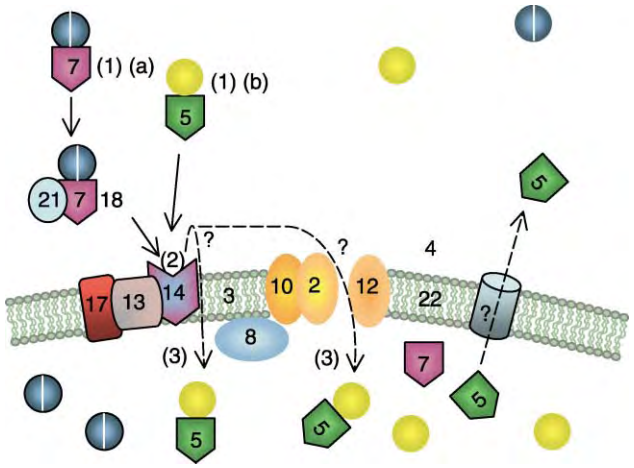

FIGURE 1 Model of peroxisomal matrix enzyme import. Numbers indicate the corresponding Pex protein. Three main steps are outlined: (1) Binding of PTS-containing proteins (yellow and blue circles depict PTS1- and multimeric PTS2-containing proteins, respectively) to the import receptors (Pex5p and Pex7p); (2) transport of receptor–cargo complexes to the peroxisome membrane and interactions with PMPs, such as Pex14p and, perhaps Pex13p, which are in a subcomplex with Pex17p and Pex8p; (3) receptor–cargo translocation through a proteinaceous pore formed either by the docking subcomplex (Pex14p, Pex13p, Pex17p, Pex8p) or the RING–peroxins subcomplex (Pex2p, Pex10p, Pex12p). PTS receptors may deliver cargo while inserted in the peroxisomal membrane or after entry into the lumen. Pex3p and Pex8p have been proposed to bridge proteins in the docking and RING–peroxins subcomplexes.

needed, and in mammals an alternatively spliced form of Pex5p (Pex5pL) is necessary for PTS2 import. However, the docking and RING–proteins are required in common for both PTS1 and PTS2 import pathways, leading to the current view that a common translocation machinery is involved for both these pathways.

Examples of organism-specific variations in the general scheme of biogenesis include the apparent lack of the entire PTS2 pathway (PTS2 proteins and Pex7p, the PTS2 receptor) in worms (*Caenorhabditis elegans*), and the dependence of the PTS2 import pathway on the PTS1 receptor, Pex5p, in mammals, but not in yeasts. However, even where such differences exist, the underlying molecular mechanism is similar. This is illustrated by the point that the proteins Pex18p and Pex21p from *S. cerevisiae*, Pex20p from *Y. lipolytica*, and Pex5pL in mammals all have a conserved motif that allows them to interact with Pex7p and/or PTS2 cargo to facilitate the PTS2 import pathway.

Unlike the transport of unfolded proteins into other organelles, such as the endoplasmic reticulum and mitochondria, folded and oligomeric proteins can be transported across the peroxisomal membrane. How such large multi-subunit complexes are transported across the membrane is unknown, because the translocon in the peroxisomal membrane has not been characterized.

Import of Peroxisomal Membrane Proteins

These proteins have one or more sequences (mPTSs) that direct them to the peroxisomal membrane with the correct topology. Although a dozen or so mPTSs have been defined in several yeast and mammalian peroxisomal membrane proteins (PMPs), they have no simple consensus sequence. The PMP receptor(s), the mechanism of insertion of PMPs into the peroxisomal membrane, and the rules that govern their topology are not completely known, although several peroxins that play a role in PMP biogenesis are defined. Most mutants affecting the import of either peroxisomal matrix or membrane proteins have organelle remnants, in some but perhaps not all, organisms.

Division and Proliferation of Peroxisomes

The division of peroxisomes is compatible with two models. One of these proposes that peroxisomes arise by budding and fission from pre-existing peroxisomes, and may be the one that is used in normal, mitotically dividing cells. The other model is that peroxisomes arise either *de novo* or from some other reservoir of membranes such as the endoplasmic reticulum. Mature peroxisomes are then generated from this membrane reservoir via a variety of biogenesis intermediates. This model may be more applicable to proliferating peroxisomes and to the regeneration of peroxisomes in *pex* mutants complemented by the affected gene.

Acknowledgments

This work was supported by grants NIH DK41737 and NIH DK59844. The author thanks Dr. Sebastien Leon for his help in assembling Table II and Figure 1. He regrets that the format of this article does not permit citation of the many original contributors to this field.

See Also the Following Articles

Fatty Acid Oxidation • Fatty Acid Receptors • Fatty Acid Synthesis and its Regulation • Flavins

Glossary

autophagy Degradation of cytosol and organelles by protein turnover involving the yeast vacuole or the lysosome in mammals.

biogenesis The process of assembly.

microbodies Another name for peroxisomes and similar organelles (glyoxysomes, glycosomes).

organelle A subcellular, membrane-enclosed compartment performing specialized functions.

peroxisomal matrix Lumen of the peroxisome.

peroxisome A subcellular organelle involved in many lipid metabolic pathways.

vacuole or lysosome Organelle in which protein turnover and recycling occurs. The organelle is called the vacuole in yeast and the lysosome in mammalian cells.

Further Reading

Baumgartner, M. R., and Saudubray, J. M. (2002). Peroxisomal disorders. *Semin. Neonatol.* **7**, 85–94.

Hettema, E. H., and Tabak, H. F. (2000). Transport of fatty acids and metabolites across the peroxisomal membrane. *Biochim. Biophys. Acta* **1486**, 18–27.

Purdue, P. E., and Lazarow, P. B. (2001). Peroxisome biogenesis. *Annu. Rev. Cell Develop. Biol.* **17**, 701–752.

Subramani, S., Koller, A., and Snyder, W. B. (2000). Import of peroxisomalmatrix and membrane proteins. *Annu. Rev. Biochem.* **69**, 399–418.

Titorenko, V. I., and Rachubinski, R. A. (1998). The endoplasmic reticulum plays an essential role in peroxisome biogenesis. *Trends Biochem. Sci.* **23**, 231–233.

Van den Bosch, H., Schutgens, R. B., Wanders, R. J., and Tager, J. M. (1992). Biochemistry of peroxisomes. *Annu. Rev. Biochem.* **61**, 157–197.

Biography

Suresh Subramani is a Professor in the Section of Molecular Biology, Division of Biological Sciences, University of California at San Diego. His current research interest is in organelle homeostasis. He holds a doctoral degree in biochemistry from the University of California, Berkeley, and did his postdoctoral work at Stanford University. He has been on the faculty at UCSD since 1982. He and his colleagues have made many important contributions to the field of peroxisome biogenesis and turnover.

Phage Display for Protein Binding

Henry B. Lowman
Genentech, Inc., San Francisco, California, USA

Phage display is a process in which large libraries of protein or peptide variants are prepared as fusion proteins with one of several coat proteins of bacteriophage. Because each phage-displayed variant is both displayed on the surface of the phage particle (virion) and encoded by the DNA packaged within that virion, phage display provides a useful means of purifying rare members of the library with specifically selected binding properties, amplifying the selected members over multiple rounds of selection, determining the sequence of the selected protein, and expressing the protein as a soluble product. Phage display has found many applications in the discovery, engineering, and analysis of peptides and proteins including 1) discovery of novel peptide mimotopes and human(ized) antibodies for binding to proteins and other targets, 2) affinity maturation and mutagenic scanning of antibodies and other proteins, and 3) identification of specific peptide substrates for proteases and other enzymes. Typically, filamentous phage such as Fd, M13 and related phages that infect *Escherichia coli* bacteria are used as vectors for phage display of peptide or protein diversity libraries.

Phage Display Vectors

Phage display is a rapid means for discovery of novel peptides and proteins from large libraries of genetically engineered variants. The process begins with construction of a phage or phagemid vector which encodes either an initial protein "scaffold" or a random peptide as a fusion protein with a phage coat protein. Typical constructs involve a promoter region driving expression of the fusion protein in which a secretion signal sequence (SS) is followed by the display gene and all or part of a phage coat protein, e.g., g3p or g8p (proteins encoded by gene-3 or gene-8 of bacteriophage M13). Alternatively, with appropriate modifications, the displayed protein may be fused at the C terminus of the coat protein. Filamentous phage(mids) are particularly useful vectors because their structure readily adapts to accommodate the size of DNA packaged into the virion.

Polyvalent and Monovalent Phage Display

When many copies of a fusion protein are displayed on each virion, each virion may simultaneously bind to several molecules of the target. In this format, called polyvalent display, even intrinsically weakly binding variants appear to bind tightly because of the avidity effect. As this effect can mask tighter binding (higher intrinsic affinity) interactions, constructs which limit the display of the fusion protein to yield virions that usually display no more than one copy were developed. This format, called monovalent display, facilitates stringent selections for very high-affinity interactions. Statistically, monovalent display vectors allow for display of multiple copies of the fusion protein by a small fraction of the virion population, but the difference between monovalent and polyvalent formats can be dramatic in terms of avidity effects. This difference has been exploited to: (1) identify novel, low-affinity binding peptides in a polyvalent system, followed by (2) "affinity maturation" of the low-affinity peptides through construction of secondary libraries and selection in a monovalent system.

Phage Vectors

Phage vectors consist of an essentially complete phage genome into which is inserted DNA encoding the protein or peptide of interest (Figure 1). Typically, the remainder of the phage genome is left unchanged and provides the other gene products needed for the phage life cycle. For facile growth and propagation of phage in *Escherichia coli*, the function of the fusion protein in the life cycle of the phage must be maintained and this places constraints on the types of fusions that are usually produced using phage vectors. For example, large proteins may be poorly displayed and/or may interfere with phage packaging or infection.

Phagemid Vectors

Phagemid vectors consist of a typical plasmid construct into which a phage origin of replication (ORI), including the phage-packaging region of DNA from the phage genome, and a gene for the displayed fusion protein have been inserted (Figure 1). In this case, the phagemid DNA can be replicated independently of phage production for mutagenesis and amplification. However, for phage

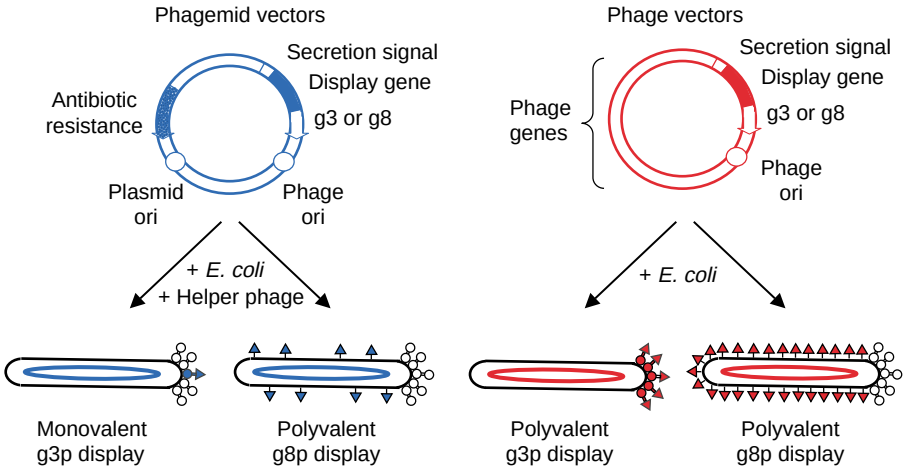

FIGURE 1 Construction of phagemid and phage vectors. Phagemid and phage DNA constructs are shown with appropriate origins of replication (ori), a gene for the protein of interest (shaded) fused the gene-3 or gene-8 encoded coat proteins of filamentous phage and preceded by a secretion-signal sequence, as well as a gene for antibiotic resistance. The remaining genes of the phage vector or helper phage encode other proteins. The DNA is packaged as a single strand in the virion (shown in cartoon form) with many copies of the g8 protein along the length of the particle, a few copies of the g3 protein (two-lobe structure) at one end, and other structural proteins (not shown). The g3p or g8p fusion proteins are shown as filled triangles attached to the corresponding coat protein. In monovalent phage display, expression of the fusion is statistically limited so that very few particles contain more than one copy of the fusion protein, while in polyvalent display, a range of fusion-protein densities is possible.

display, the remaining phage gene functions must be supplied by another construct, usually a "helper phage," which is packaged into virions with lower efficiency than the phagemid itself. When *E. coli* cells transfected with the phagemid, grown under selective pressure with an appropriate antibiotic, are infected with helper phage at an appropriate multiplicity of infection (MOI), both constructs undergo replication, but mature virions predominantly contain phagemid rather than helper-phage DNA. However, both types of particles can display the fusion protein; thus, antibiotic selection of cells containing the desired phagemid is needed. These examples indicate the most commonly used types of phage and phagemid vectors; however, other monovalent and polyvalent displaying phage and phagemid constructs have also been described.

Phage Libraries

A phage library may begin with a "wild-type" protein displayed on phage or with a phage(mid), into which DNA encoding completely novel peptides have been inserted.

Construction of Libraries

The generation of diversity in a phage-display library is usually accomplished by typical site-directed mutagenesis techniques, such as oligodirected single-stranded template mutagenesis, PCR mutagenesis, or cassette mutagenesis using restriction enzymes and DNA ligase to cut out a segment of DNA and replace it with a synthetic piece. Highly diverse DNA sequences can be generated using standard solid-phase deoxynucleotide synthesis techniques in which individual nucleotides are "randomized" by adding to the growing polynucleotide chain a mixture (which may be equimolar or of biased specified composition) of all four nucleotides, or a subset of A, G, C, or T, rather than a single nucleotide (Table I).

TABLE I
Nucleotide Abbreviations for Degenerate Codon Design

Abbreviation	Nucleotide
A	Adenosine
G	Guanosine
C	Cytidine
T	Thymidine
R	A, G
Y	C, T
B	C, G, T
D	A, G, T
H	A, C, T
K	G, T
M	A, C
V	A, C, G
W	A, T
N	A, G, C, T
S	G, C

TABLE II

Codon Degeneracy and the Generation of Diversity in Phage-Display Libraries. The 64 Possible Triplets are Shown, Along with the Corresponding Encoded Amino Acids in the First Two Columns. The Remaining Columns Show Examples of Degenerate Codons (see Table I) Encoding all Amino Acids with 32 Triplets (NNS), and other Selected Sets that Vary in Amino Acid Composition. Often a *sup* E Strain of *E. coli* is used for Phage Propagation, in which Case the Amber Stop Codon (*) is Translated as Gln (Q)

DNA codon	Amino acid	NNS	NYC	NHS	ARS
AAG	Lys (K)	X		X	X
AAC	Asn (N)	X		X	X
AGG	Arg (R)	X			X
AGC	Ser (S)	X			X
ACG	Thr (T)	X		X	
ACC	Thr (T)	X	X	X	
ATG	Met (M)	X		X	
ATC	Ile (I)	X	X	X	
GAG	Glu (E)	X		X	
GAC	Asp (D)	X		X	
GGG	Gly (G)	X			
GGC	Gly (G)	X			
GCG	Ala (A)	X		X	
GCC	Ala (A)	X	X	X	
GTG	Val (V)	X		X	
GTC	Val (V)	X	X	X	
CAG	Gln (Q)	X		X	
CAC	His (H)	X		X	
CGG	Arg (R)	X			
CGC	Arg (R)	X			
CCG	Pro (P)	X		X	
CCC	Pro (P)	X	X	X	
CTG	Leu (L)	X		X	
CTC	Leu (L)	X	X	X	
TAG	Stop*	X		X	
TAC	Tyr (Y)	X		X	
TGG	Trp (W)	X			
TGC	Cys (C)	X			
TCG	Ser (S)	X		X	
TCC	Ser (S)	X	X	X	
TTG	Leu (L)	X		X	
TTC	Phe (F)	X	X	X	
AAA	Lys (K)				
AAT	Asn (N)				
AGA	Arg (R)				
AGT	Ser (S)				
ACA	Thr (T)				
ACT	Thr (T)				
ATA	Ile (I)				
ATT	Ile (I)				
GAA	Glu (E)				
GAT	Asp (D)				
GGA	Gly (G)				
GGT	Gly (G)				
GCA	Ala (A)				
GCT	Ala (A)				
GTA	Val (V)				
GTT	Val (V)				
CAA	Gln (Q)				
CAT	His (H)				
CGA	Arg (R)				
CGT	Arg (R)				
CCA	Pro (P)				
CCT	Pro (P)				
CTA	Leu (L)				
CTT	Leu (L)				
TAA	Stop				
TAT	Tyr (Y)				
TGA	Stop				
TGT	Cys (C)				
TCA	Ser (S)				
TCT	Ser (S)				
TTA	Leu (L)				
TTT	Phe (F)				

(*continues*)

TABLE II

Continued

The degeneracy of the genetic code makes possible the generation of chemically related subsets of codons depending on the amino acids encoded (Table II). Once oligonucleotides with appropriate diversity have been designed and synthesized, mutagenesis is carried out with the phage or phagemid vector on an appropriate scale to yield a sufficient number of DNA molecules (moles of product) to represent the desired diversity as described below. The mutagenesis products are transformed into *E. coli* and propagated in culture (along with helper phage in the case of phagemid vectors) to yield a library of peptide- or protein-displaying phage particles.

Design of Diversity Libraries

The key consideration in the design of diversity libraries is the combinatorial complexity of the DNA and protein resulting from incorporation of random nucleotides at a given number of sites. For example, using NNS codon degeneracy (Table II), all 20 commonly used L-amino acids are encoded by 32 codons. With one NNS codon randomized in this way, the library has a theoretical diversity of 32 at the DNA level and 20 at the protein level. However, this complexity grows quickly as a larger number multiple sites, n, are simultaneously randomized. The experimentally obtained complexity

or diversity of the library is limited to the number of DNA molecules that can be produced at the synthesis and mutagenesis stage, and subsequently transformed into *E. coli* and packaged into a solution of phage(mid) particles. Therefore, the number of randomized codons or the diversity of the degenerate codons may be restricted in order to obtain libraries that completely represent the designed diversity. At the virion level, phage particles are only soluble to a level of $\sim 10^{14}$ particles/ml (10^{17}/l; or 170 nM), presenting an ultimate practical limitation for phage libraries to be produced and used at the laboratory scale. Additional limitations are imposed by the process of transformation of the phage or phagemid construct into *E. coli*, so that libraries are more commonly on the order of 10^9 or 10^{10} as measured by the total number of transformants obtained after mutagenesis and transformation using electroporation or other techniques.

Phage-Binding Selections

Phage libraries yield useful and interesting variants through a process of selection and amplification analogous to affinity-based protein purification (Figure 2).

Preparation of Packaged Virions

Once the products of random mutagenesis have been transformed into *E. coli*, phage amplification occurs through propagation of the infected culture, which in the case of phagemid libraries also includes a helper phage. Since filamentous phage particles are not lytic, large numbers of phage particles are produced during a few hours of culture growth. As the displayed protein is secreted, it is incorporated into the coat of the virion. Once a large number of phage have been produced, they are separated from the *E. coli* host by centrifugation, and often further purified using a series of precipitation and resuspension steps. The final phage stock is a solution of phage particles that are ready for appropriate binding selections.

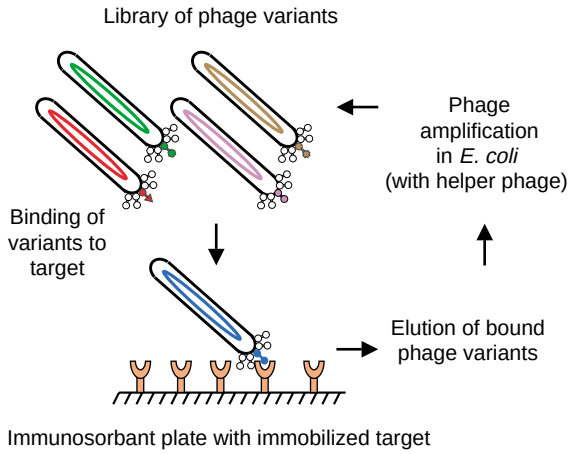

FIGURE 2 Affinity-selection process for binding to an immobilized target protein using a monovalent phagemid vector. One round of binding selection or "panning" is shown. A population of phage particles, each displaying a different peptide or protein variant, is allowed to bind to an immobilized target. After low-affinity variants are washed away, high-affinity variants are eluted and propagated to produce an enriched pool of high-affinity variants, which may be subjected to further rounds of selection.

Phage Binding and Elution

Early phage-binding selections used a simple process for separating variant protein phage that bind to a target molecule from those that do not bind. The target molecule was coated directly onto immunosorbent plastic plates or affixed to chemically activated resins. A variation on this technique involves binding of phage to a labeled target in solution, then capturing the bound phage through use of an affinity matrix that binds to the labeled target. Thereafter, the phage library is allowed to bind to the immobilized target, and then removed. Nonbinding and weakly binding phage variants are washed away, and the remaining tightly bound variants are eluted using affinity-selective reagents (e.g., a competing protein), mild to severe chaotropic agents, ranging from high/low pH buffers to urea, or site-specific proteases. Following elution, phage can be amplified by infecting fresh *E. coli* cells, and the resulting population again subjected to binding selection. This cycle is typically repeated for several rounds, followed by analysis of selectants through DNA sequencing, which may yield nonrandom occurrences of amino acids at p (particular) positions (i.e., a consensus sequence), or through direct binding analysis as described later. As in ELISA experiments, nonspecific binding leads to artifacts in phage display and can be reduced using proteins or detergents that block these typically low-affinity interactions. However, large diversity libraries sometimes contain peptides that can bind to the blocking agent itself. An enrichment ratio, representing the number of phage binding to the intended target versus the number binding to the matrix or blocking agent, is often used to monitor specificity during multiple rounds of binding selection.

Phage-Binding Analysis

The individual clones selected through phage display are often further analyzed in the form of the recombinant phage particles. Beyond the ability to select relatively rare protein variants with specific binding properties from diversity libraries of millions to tens-of-billions of combinatorial variants, phage display is also used to

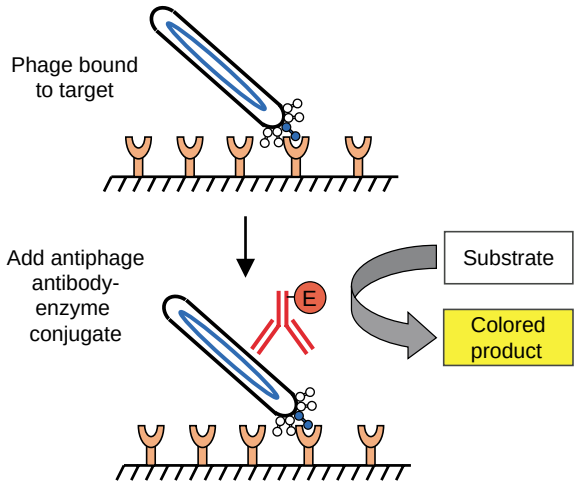

FIGURE 3 Binding assays using phage display. Binding of phage-displayed protein variants is analyzed as in a typical ELISA experiment, with binding of phage to an immobilized target followed by detection with an antiphage antibody conjugated to an appropriate enzyme such as horseradish peroxidase. Relative amounts of bound phage are measured by the amount of color produced when an appropriate substrate is added.

analyze protein–protein-binding interactions without the need to separately purify large numbers of protein variants. For example, to map the binding site on a phage displayed protein for a target protein, the target protein may be coated on an ELISA plate, and mutants or libraries of mutants constructed for phage display. In the case of point-mutation analysis, a phage stock of each mutant is prepared and titrated as in a typical protein-binding ELISA (Figure 3). Alternatively, using libraries of protein variants, the outcome of sequencing many selected variants may be analyzed to determine statistically which amino acids are preferred or disallowed at multiple positions. The utility of phage display has been demonstrated using many systems in which the results of phage selections and binding analysis have been translated into functional proteins whose properties correspond closely to their phage-displayed forms.

See Also the Following Articles

Amino Acid Metabolism • Protein Data Resources

Glossary

degenerate codon A three-nucleotide (triplet) sequence encoding more than one amino acid, realized by synthesis of a pool of triplets having more than one nucleotide at one or more positions. Degenerate codons may be represented in shorthand according to standard abbreviations, e.g., RNS, for (A or G) followed by (A, G, C, or T), followed by (G or C).

elution Process of dissociation which causes the dissociation of bound phage from an immobilized target molecule, for example, using low pH or chaotropic agents.

enrichment Process by which peptide or protein variants with specific binding properties are amplified from a diverse library. An enrichment ratio of the number of phage eluted from an immobilized target divided by the number eluted from a control is often used to measure enrichment.

enzyme-linked immunosorbent assay (ELISA) An assay for binding affinity, typically in which a target molecule is coated onto a plastic plate, a second molecule (the analyte) is added, and a third molecule is used to detect binding of the analyte.

helper phage A bacteriophage which supplies the necessary gene products for packaging of a phagemid construct and is usually deficient in packaging itself into virions.

panning Process of selecting phage for binding to a target protein, especially when the target is coated onto an immunosorbent plastic plate.

phagemid A DNA vector constructed from the combination of replication and other genetic elements from a plasmid with replication, packaging, and other genetic elements from the genome of a bacteriophage.

Further Reading

Barbas, C. F. III, Burton, D. R., Scott, J. K., and Silverman, G. J. (2001). *Phage Display: A Laboratory Manual*. Cold Spring Harbor Laboratory Press, Cold Spring Harbor, New York.

Clackson, T., and Lowman, H. B. (2003). *Phage Display: A Practical Approach*. Oxford University Press, Oxford, UK.

Dower, W. J., and Mattheakis, L. C. (2004). *In vitro* selection as a powerful tool for the applied evolution of proteins and peptides. *Curr. Opin. Chem. Biol.* **6**, 390–398.

Kay, B. K., Winter, J., and McCafferty, J. (1996). *Phage Display of Peptides and Proteins*. Academic Press, San Diego.

Messing, J. M. (1983). New M13 vectors for cloning. *Methods Enzymol.* **101**, 20–78.

Sidhu, S. S., Lowman, H. B., Cunningham, B. C., and Wells, J. A. (2000). Phage display for selection of novel binding peptides. *Methods Enzymol.* **328**, 333–363.

Smith, G. P. (1985). Filamentous fusion phage: Novel expression vectors that display cloned antigens on the virion surface. *Science* **228**, 1315–1317.

Biography

Henry Lowman is a Senior Scientist and Associate Director of Antibody Engineering, with joint appointments in the Departments of Protein Engineering and Immunology, at Genentech, Inc., South San Francisco, California. His research interests are in the structure–function analysis of proteins and the engineering of therapeutic peptides and proteins using structure-based and combinatorial techniques. He holds a Ph.D. from Purdue University and received postdoctoral training as an NIH Postdoctoral Fellow at Genentech, Inc.

Pheromone Receptors (Yeast)

James B. Konopka
State University of New York, Stony Brook, New York, USA

Jeremy W. Thorner
University of California, Berkeley, California, USA

Fungal cells secrete substances (pheromones) that stimulate the ability of haploid cells of different mating types to conjugate, thereby forming diploid cells. Compounds used by various fungal species include terpenes (e.g., *Allomyces* spp.), steroids (e.g., *Achlya* spp.), and peptides (many ascomycetes). The best-characterized fungal pheromone receptors are those for the peptide mating pheromones of the budding yeast, *Saccharomyces cerevisiae*. These receptors are integral membrane proteins that contain seven highly hydrophobic, and potentially α-helical, transmembrane segments. They bind their cognate pheromone at the cell surface, and then activate an intracellular heterotrimeric G protein that initiates a signaling pathway. This pathway induces physiological responses, including the expression of many genes needed to divert cells from the mitotic cell cycle required for vegetative proliferation into a developmental program that permits the fusion of the participating haploid cells. These yeast pheromone receptors are representatives of a very large superfamily that is conserved from yeast to humans.

Pheromone Receptors are Necessary for Conjugation

Pheromone signaling occurs only between cells of different mating type. In *Saccharomyces cerevisiae*, there are two mating types, which are defined by the combination of pheromone and receptor they produce (Figure 1). Haploid cells of the **a**-mating type secrete the **a**-factor pheromone, and express in their plasma membrane, the receptor (Ste2) for α-factor; conversely, haploids of the α-mating type produce α-factor pheromone and, express at their surface, the receptor (Ste3) for **a**-factor. The α-factor is an unmodified 13-residue peptide that is processed from a larger precursor and secreted from cells via the standard secretory pathway. By contrast, **a**-factor is a 12-residue lipopeptide that is modified by farnesylation of the side chain and methyl esterification of the carboxyl group of its C-terminal Cys residue and then exported from cells through the action of a dedicated ATP-driven transporter (Ste6). Cell-type identity is established by genes at the mating type locus (*MAT*) on chromosome III, which encode transcriptional regulators that control expression of the corresponding pheromones and receptors. The gene products required for signaling downstream of the receptors are identical and are expressed in both *MAT***a** and *MAT*α-cells. The genomes of other ascomycetes (i.e., those that pack their spores into an ascus), including the fission yeast, *Schizosaccharomyces pombe*, and the human pathogen, *Candida albicans*, encode homologues of both Ste2 and Ste3. However, in certain basidiomycetes, including the plant rust, *Ustilago maydis*, and the human pathogen, *Cryptococcus neoformans*, the pheromone receptors in the different mating types are all related to Ste3. Furthermore, other groups of fungi, such as many basidiomycetes (including mushrooms), have more than two and often many combinatorial possibilities for distinct mating types and, hence, correspondingly more complex regulation.

Binding of pheromone to a receptor triggers a signal-transduction pathway necessary for eliciting the physiological responses required to differentiate the cells and prepare them for mating. These responses include arrest of cell division in G1 to synchronize the cell cycles of the mating partners, and transcriptional induction of genes that specify proteins required for agglutination, specialized morphogenesis, cell fusion, and nuclear fusion. These proteins and the capacities they confer permit the cells to conjoin, fuse, and form a diploid zygote.

Pheromone Receptors Stimulate a Signal Transduction Pathway

The pheromone receptors induce mating by stimulating a G protein-initiated signaling pathway that has been extensively studied in *S. cerevisiae* and will be described briefly here. Upon binding of the cognate pheromone, an activated pheromone receptor stimulates exchange of GTP for GDP in the α-subunit (Gpa1) of the coupled heterotrimeric G protein. The ensuing conformational

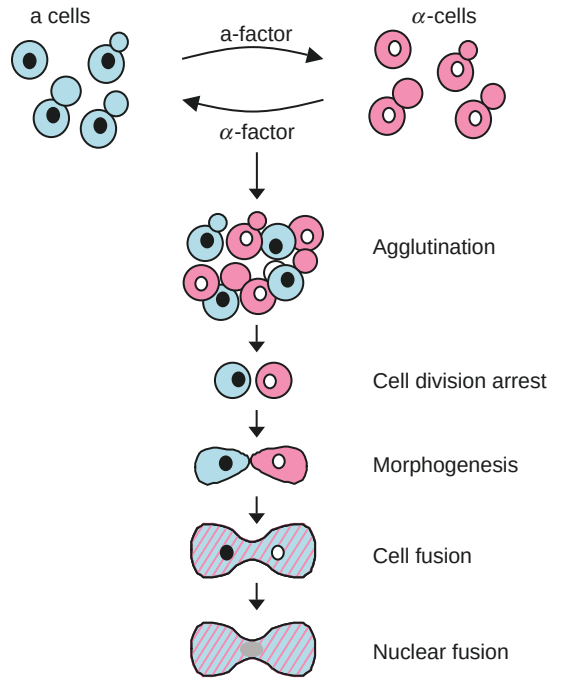

FIGURE 1 Landmark events during conjugation of *S. cerevisiae*. Intercellular communication between cells of mating type **a** and cells of mating type α induces the indicated stages of conjugation, as described in the text.

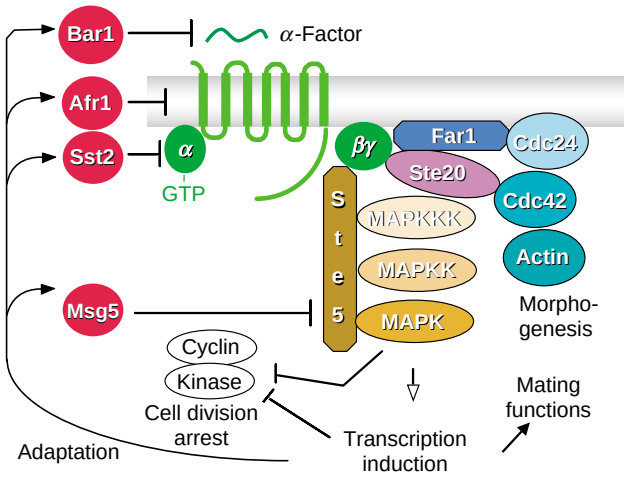

FIGURE 2 Schematic representation of the mating pheromone response pathway in *S. cerevisiae*. A diagram showing the main components involved in transmitting the pheromone signal in *MAT***a** cells. A similar pathway operates in *MAT*α-cells. Activated pheromone receptors stimulate the Gα-subunit to release the G$\beta\gamma$-subunits. The free G$\beta\gamma$-subunits then recruit a scaffold protein, Ste5, to the membrane. Ste5 carries the components of a MAP kinase cascade and places them in proximity to another protein kinase, Ste20. The free G$\beta\gamma$ complex also recruits another scaffold protein, Far1, which carries the activator (Cdc24) of the small GTPase, Cdc42, which is, in turn, the activator of Ste20. Ste20 is further concentrated at these sites because its C terminus also binds to free G$\beta\gamma$-subunits. Conjunction of these components achieved by the pheromone-dependent and receptor-initiated release of G$\beta\gamma$ results in activation of the protein kinase cascade, and ultimately stimulates the pheromone-responsive transcription factor, Ste12, in the nucleus. Activation of Cdc42 also promotes actin polymerization and other aspects of morphogenesis to promote highly polarized growth. Negative regulators of the pathway (shown in red on the left side) are also induced and constitute a negative feedback loop. Bar1 is a secreted protease that degrades α-factor in the medium. Afr1 negatively regulates receptor function. Sst2 is an RGS protein that promotes hydrolysis of the GTP bound to the Gα-subunit. Msg5 is a phosphatase that dephosphorylates and inactivates the terminal MAPK (Fus3).

change in GTP-bound Gpa1 dissociates its associated G$\beta\gamma$ complex (Ste4-Ste18). The free G$\beta\gamma$ complex, which is firmly anchored in the plasma membrane by both C-terminal farnesylation and carboxymethylation of the C-terminal Cys and palmitoylation of the penultimate Cys in Ste18, now exposes surfaces that are able to bind and recruit to the plasma membrane the proteins needed for subsequent events (Figure 2).

One protein that binds to G$\beta\gamma$ is Ste5, which acts as a scaffold by associating with the three protein kinases, Ste11 (MEKK or MAPKKK), Ste7 (MEK or MAPKK), and Fus3 (ERK or MAPK) of a mitogen-activated protein kinase (MAPK) cascade. The existence of such a cascade was first demonstrated unequivocally in *S. cerevisiae*. Phosphorylation and activation of Ste11 requires the action of yet another protein kinase, Ste20. Ste20 is recruited to the membrane in two ways. The activator of Ste20, the small GTPase, Cdc42 (a protein of about 21 kDa), is tethered to the membrane because it is geranylgeranylated and carboxymethylated on its C-terminal Cys, and, in its GTP-bound state, binds to the N-terminal regulatory domain of Ste20. Thus, Ste20 was the first member of the family of protein kinases known as PAKs (for p21-activated protein kinases) to be recognized. In addition, Ste20 is localized specifically near the rest of the pheromone response machinery at the plasma membrane because a motif near the C terminus of Ste20 binds to G$\beta\gamma$. The third component recruited to the plasma membrane by the released G$\beta\gamma$ complex is another scaffold protein (Far1) that carries the guanine nucleotide exchange factor (Cdc24) that stimulates conversion of Cdc42 from its GDP- to its GTP-bound state. Once activated via this phosphorylation cascade, Fus3 is released from Ste5, translocates to the nucleus, and relieves negative regulation of a transcription factor (Ste12) that is poised on the promoters of pheromone-responsive genes, thereby inducing the expression of those genes. Complete sequence analysis of the *S. cerevisiae* genome, accomplished in 1996, identified all of the genes that contain potential Ste12-binding sites in their promoter regions, subsequent chromatin immunoprecipitation demonstrated that many of these promoters are indeed occupied by Ste12 before induction, and now with the advent of DNA microarrays, all genes actually induced by pheromone have been identified. Not surprisingly,

this set of genes includes those needed for cell cycle arrest, agglutination, morphological changes, cell fusion, and nuclear fusion. Interestingly, many signaling components, including the pheromones and receptors, as well as additional gene products that function in adaptation (down-regulation) of the response are induced as part of the highly organized intercellular communication that occurs between mating cells. Collectively, these gene products control the spatial and temporal events of the mating process, as well as recovery from those changes if conjugation does not occur successfully (Figure 2).

Pheromone Receptors Sense Spatial Gradients

A key role played by pheromone receptors in conjugation is in sensing the position of the mating partner and providing proper spatial orientation for the subsequent morphogenesis that enables cells of opposite mating type to grow toward each other, thereby enhancing the probability of their encounter and subsequent fusion. The ability of a yeast cell to track a gradient of pheromone emanating from a cell of the opposite mating type requires dynamic interplay of signaling and adaptation, particularly at the level of the pheromones and receptors. For example, exposure of *MAT*α cells to **a**-factor increases transcription of the α-factor genes, whereas exposure of *MAT***a** cells to α-factor induces expression of an extracellular protease that degrades α-factor in the medium. Another aspect of this interplay involves removal of ligand-bound receptors by endocytosis and their replacement by newly synthesized receptors, which are deposited at the site on the surface immediately adjacent to the partner cell (because the oriented morphogenesis mentioned above directs secretory vesicles to their destination). This behavior sustains the highest degree of receptor activation in the region nearest to the site, on the surface that is exposed to the highest concentration of pheromone emanating from the closest potential partner. Such localized receptor signaling is thought to establish and then reinforce the spatial cues that stimulate properly oriented actin polymerization and other aspects of the directed morphogenesis necessary for conjugation.

Pheromone Receptors are Regulated at Several Levels

Control of pheromone receptor expression and function are key for proper intercellular communication and also for allowing cells to return to normal growth in the event that mating does not occur. These controls have been best studied for Ste2 (α-factor receptor). The C-terminal cytosolic domain of Ste2 is the target for several adaptation mechanisms (and similar mechanisms are known to regulate the **a**-factor receptor, Ste3). First, once ligand-bound, rapid phosphorylation of Ste2 within the C-terminal sequence appears to inhibit the ability of the receptor to continue to signal. It is most likely that the conformational change caused by pheromone binding makes the C-terminal segment of the receptor more accessible to certain protein kinases (casein kinase I family members) that are constitutive residents of the plasma membrane, once again due to the prenylation, carboxylmethylation, and palmitoylation of the C termini of these enzymes. Second, phosphorylation creates a determinant that leads to recognition by a ubiquitin ligase complex and the subsequent covalent addition of ubiquitin to Lys337 in the C terminus (Figure 3). This monoubiquitination triggers endocytosis and removal of the receptor from the cell surface. Third, receptors are also regulated by association with a protein (Afr1) that localizes to the neck of the growing projection in mating cells, prevents receptor-G protein coupling, and thereby restricts receptors that are competent to signal to the leading edge of the projection.

Other components of the pheromone signaling pathway also undergo pheromone-induced down-regulation. For example, induction of Sst2, the first regulator of G protein-signaling (RGS) protein to be recognized, promotes hydrolysis of the GTP bound to Gpa1, thereby deactivating Gα and promoting its reassociation with G$\beta\gamma$. Similarly, induction of Msg5, a dual-specificity MAPK-specific phosphatase, dephosphorylates and thereby inactivates Fus3 (Figure 2).

Pheromone Receptor Synthesis Requires the Secretory Pathway

In the description that follows, Ste2 will continue to be the model because it has been studied most extensively. Ste2 is inserted into the plasma membrane such that it spans the membrane seven times (Figure 3). Biogenesis of Ste2 commences with its import into the endoplasmic reticulum (ER) via a classical N-terminal signal peptide, with concomitant addition of two Asn-linked oligosaccharides, which are further modified and extended with mannose-rich outer chains during transport of Ste2 through the Golgi complex. Although this N-glycosylation does not seem to be critical for receptor function, it may direct or stabilize proper folding of Ste2. While still in the secretory pathway, Ste2 self-associates to form dimers. The interface is thought to include a region of the first transmembrane segment (TMD1) containing Gly56 and Gly60 (Figure 3), which form a GxxxG motif similar to one that mediates dimerization of the red

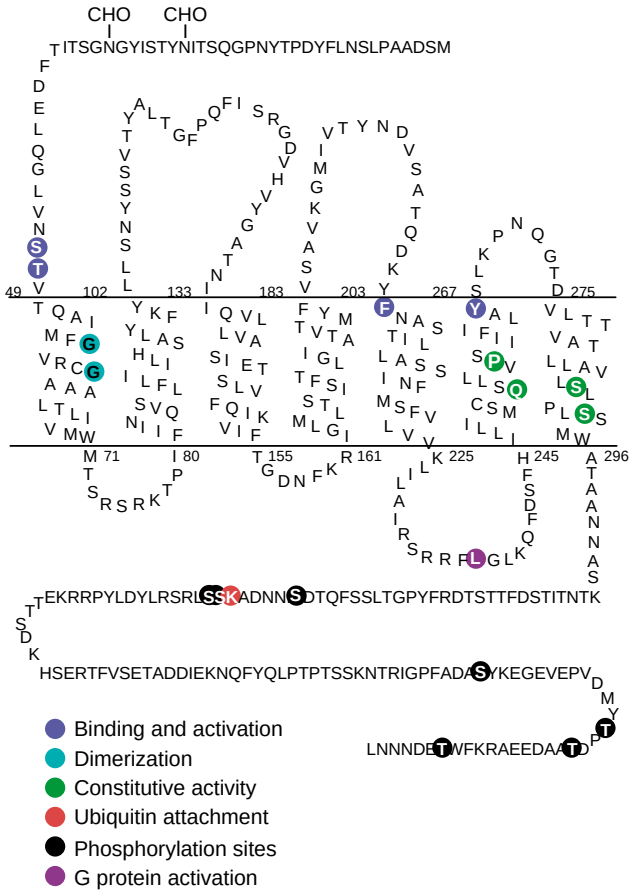

FIGURE 3 Primary structure of *S. cerevisiae* Ste2 (α-factor receptor). The amino acid sequence of Ste2, in the one-letter code, is arranged to represent the seven membrane-spanning elements in their presumed topology across the plasma membrane. Residues discussed in the text that have key functional properties in receptor signaling and adaptation are shaded according to their role in ligand recognition (blue), receptor dimerization (turquoise), conformational constraint (green), phosphorylation (black), and ubiquitination (red). Two sites in the extracellular amino terminus are modified by N-linked glycosylation (CHO). The consensus site for attachment of Asn-linked oligosaccharide (N-X-T or N-X-S) at residue 25 is used close to 100% of the time, whereas that at residue 32 is used only about 50% of the time, and that at residue 46 is not used at all, presumably because it is too close to the membrane for recognition by the eight-subunit oligosaccharyltransferase enzyme complex that transfers the mannose-rich core oligosaccharide from its membrane-bound dolichol carrier to N-X-T or N-X-S motifs in secreted and membrane-localized proteins. Certain naturally occurring neutral polymorphisms exist in the primary structure of Ste2, specifically: residue 269 is E in some *S. cerevisiae* strains, but K in others.

blood cell transmembrane protein, glycophorin A. Dimerization appears to be important for efficient trafficking of Ste2 to the plasma membrane and available evidence suggests that the native signaling-competent state of Ste2 is the dimer. Receptors that fold improperly in the ER are ultimately degraded by ER quality control-mechanisms; those misfolded receptors that make it to the Golgi are sorted to the vacuole (equivalent of the mammalian lysosome) for degradation. It is not clear where or when, properly folded and dimerized receptors first encounter and couple to the quiescent form of the G$\alpha\beta\gamma$ heterotrimer (Gpa1-Ste4-Ste18). However, receptors at the plasma membrane are associated with the heterotrimeric G protein in preactivation complexes primed for the arrival of their pheromone ligand.

Pheromone Receptors Bind Ligand via Contacts with the Extracellular Ends of the Transmembrane Segments

The ligand-binding site in the pheromone receptors (and in other seven-transmembrane segment, G protein-coupled receptors) are conceivably rather complex in that they have the potential to be composed of determinants that reside within the seven transmembrane segments, and/or the three extracellular loops, and/or the extracellular N-terminal extension (or combinations of these elements). The lipid modification of **a**-factor has prevented the application of standard methods for analyzing its binding to Ste3. Hence, the binding of α-factor to Ste2 has been examined in much greater detail. A combination of genetic and biochemical studies strongly implicates residues near the extracellular ends of the transmembrane segments (TMDs) as forming the α-factor-binding pocket. This conclusion suggests a model for receptor activation in which ligand binding to the ends of the TMDs could influence the overall packing or structure of part or all the seven-helix bundle. The resulting conformational change could then be relayed to the intracellular side, and thereby communicated to the associated G protein to promote its activation. Two residues in Ste2 that are necessary for pheromone-induced receptor activation are Phe204, situated near the end of TMD5, which is required for high-affinity α-factor binding, and Tyr266, located near the end of TMD6, which, although not important for binding affinity *per se*, is nonetheless needed for subsequent signaling. The extracellular ends of TMDs 5 and 6, are of course, directly connected to their intracellular ends, and the third intracellular loop of Ste2, which spans the intracellular ends of TMDs 5 and 6, has been implicated in G protein-activation. This situation provides a ready explanation for how conformational change upon pheromone binding could be directly coupled to the associated G protein. Residues (Ser47 and Thr48) near the end of TMD1 are also thought to contact α-factor and may constitute part of the ligand-binding pocket, but do not appear to play a significant role in activation.

Pheromone Receptor Activation may Involve Relief of Conformational Constraint

Current models for signaling by G protein-coupled receptors (GPCRs) suggest that, in the absence of ligand, the off-state is conformationally restricted and that conformational changes upon ligand binding are manifested as greater conformational flexibility. Insights about the conformational state of Ste2 that accompanies its activation have been provided by analysis of constitutively active mutants that signal in a ligand-independent manner. These mutations primarily alter residues within the TMDs, suggesting that constitutive activity can result from changes in the packing of the bundle of transmembrane α-helices. Genetic analysis of constitutive mutants suggests that one restraint may involve interaction between TMD6 and TMD7 mediated via H-bonding between Gln253 in TMD6 and both Ser288 and Ser292 in TMD7. Likewise, a high degree of constitutive receptor activity is caused by substitutions that alter Pro258 in TMD6. In an otherwise α-helical segment, Pro has the unique property of introducing a kink. Thus, substitution of Pro258 with other residues should affect the topology of TMD6. Moreover, TMD6 is the segment whose intracellular end is the most proximal to those residues in the third intracellular loop most strongly implicated in G protein-activation. Hence, the effect of substitution of Pro258 in TMD6 may reflect the conformational change induced within TMD6 that normally occurs only upon ligand binding. In this regard, it is noteworthy that the majority of mammalian receptors of this class also contain Pro at a similar position in TMD6. In those mammalian proteins where it has been examined, the Pro in TMD6 has been implicated in receptor activation, suggesting mechanistic similarities in the activation process from yeast to humans.

Pheromone Receptors Promote G-Protein Activation via the Third Intracellular Loop

The receptor residues on its cytoplasmic surface that contact the G protein and promote GDP–GTP exchange on the Gα-subunit have not been pinpointed precisely. Analysis of chimeras between Ste2 and Gpa1 indicate that merely bringing the receptor and G protein into close proximity is not sufficient to stimulate GDP–GTP exchange because ligand stimulation is still required for activation of downstream signaling by such receptor-Gα hybrids. As discussed above, current evidence suggests that pheromone binding promotes a conformational change at the extracellular ends of the transmembrane helical bundle in Ste2 that is propagated to the intracellular ends of the transmembrane segments, thereby probably exposing previously buried residues that promote G-protein activation. Mutagenesis indicates that, in Ste2, the third intracellular loop certainly plays a key role. Consistent with this view, biochemical studies have demonstrated conformational changes in the third intracellular loop that are induced upon ligand binding. Remarkably, functional ligand-dependent Ste2 can be reconstituted by co-expressing halves of the receptor that are split in the middle of the third intracellular loop. Thus, it is possible that the residues closest to where TMDs 5 and 6 exit, the plasma membrane boundaries are the most important for G protein activation, assuming that the residues closest to the cut ends of such split receptors are the least likely to remain in their native condition. However, substitution of Leu236 (with His) very near the "middle" (at least in terms of primary sequence) of the third loop, yields a Ste2 mutant that displays an essentially wild-type level of surface expression, an essentially wild-type ability to bind α-factor, and an essentially wild-type level of association with the G$\alpha\beta\gamma$ heterotrimer, yet is strongly defective in promoting signaling, suggesting it is specifically defective in activation of the associated G protein. Interestingly, Ste2(L236H) still undergoes ligand-stimulated endocytosis, indicating that the conformational changes and the determinants recognized by the endocytic machinery are distinct from those required for G-protein activation.

Further confounding understanding of the mechanism of G protein-activation is the fact that, although Ste2 and Ste3 both act through the same G protein (Gpa1-Ste4-Ste18), Ste2 and Ste3 do not share any recognizably significant tracts of sequence similarity, even at the intracellular ends of TMDs 5 and 6 or within the third intracellular loop. In this same regard, certain seven-transmembrane segment receptors from other organisms, including mammals, have been expressed in *S. cerevisiae* and in response to the appropriate agonist, are able to activate, albeit to different extents, the endogenous yeast G protein. Again, this cross-species functionality occurs even though the heterologous receptors do not share any obvious sequence identity with the yeast pheromone receptors. Although the ability of receptors from yeast to man to activate the same G protein suggests a common mechanism underlying receptor and G protein activation, the structural determinants of that common action are not readily apparent. Nevertheless, continued functional studies of the yeast pheromone receptors are likely to continue to shed light on how this important class of receptors operates.

See Also the Following Articles

Ubiquitin-Like Proteins • Ubiquitin System

Glossary

agonist A ligand that activates a receptor to transduce a signal.

ligand A substance, such as a mating pheromone, that binds to a receptor molecule.

mating projection A term used to describe the distinctive type of morphogenesis observed in yeast treated with mating pheromone. This structure is thought to form the conjugation bridge that connects mating cells. Commonly referred to as a shmoo.

transmembrane domain A region of a protein that spans a membrane bilayer. These domains are typically present in an ordered structure, such as an α-helix or β-sheet, which allows the polar carbonyl groups of polypeptide chains to be shielded from the hydrophobic membrane bilayer. In the case of the GPCRs the transmembrane domains are thought to form an α-helical structure.

Further Reading

Banuett, F. (1998). Signalling in the yeasts: An informational cascade with links to the filamentous fungi. *Microbiol. Mol. Biol. Rev.* **62**, 249–274.

Brown, A. J., and Casselton, L. A. (2001). Mating in mushrooms: Increasing the chances but prolonging the affair. *Trends Genet.* **17**, 393–400.

Dohlman, H. G., and Thorner, J. W. (2001). Regulation of G protein-initiated signal transduction in yeast: Paradigms and principles. *Annu. Rev. Biochem.* **70**, 703–754.

Elion, E. A. (2000). Pheromone response, mating and cell biology. *Curr. Opin. Microbiol.* **3**, 573–581.

Herskowitz, I. (1989). A regulatory hierarchy for cell specialization in yeast. *Nature* **342**, 749–757.

Kronstad, J. W., and Staben, C. (1997). Mating type in filamentous fungi. *Annu. Rev. Genet.* **31**, 245–276.

Leberer, E., Thomas, D. Y., and Whiteway, M. (1997). Pheromone signalling and polarized morphogenesis in yeast. *Curr. Opin. Genet. Dev.* **7**, 59–66.

Biography

James Konopka is a Professor in the Department of Molecular Genetics and Microbiology at the State University of New York, Stony Brook.

Jeremy Thorner is the William V. Power Professor of Biochemistry and Molecular Biology in the Department of Molecular and Cell Biology at the University of California, Berkeley. Konopka and Thorner's research laboratories are actively engaged in studying the molecular mechanisms that control yeast cell growth and development.

PHO Regulon

Bengt L. Persson
University of Kalmar, Kalmar, Sweden

The *PHO* (*pho*sphatase-encoding) regulon of the yeast *Saccharomyces cerevisiae* is a genetic regulatory circuit, involving structural and regulatory units, essential for controlled expression of phosphatase genes. The network consists of components encoded by ~30 genes which upon expression allow for a coordinated cellular response and adaptation to changes in availability of extracellular phosphate. When phosphate becomes limiting, the cells respond by an increase in the synthesis of high-affinity transporters and phosphatases in order to scavenge phosphate from the environment. Several of the *PHO* regulon components of *S. cerevisiae* are homologous to proteins that take part in the regulation of the eukaryotic cell cycle, including a cyclin-dependent kinase (CDK, Pho85), a cyclin, (Pho80) and a CDK inhibitor (Pho81). The regulator complex formed by these determines the transcription of executive genes encoding the phosphate transporters and phosphatases.

Background

Regulation of cellular activities in response to external nutrient levels is fundamental to all living cells. To achieve this, the cells make use of numerous and varied mechanisms by which changes in the extracellular conditions can be sensed.

Phosphate, an essential nutrient for all organisms, is required for the synthesis of many cellular components (nucleic acids, proteins, lipids, and sugars) as well as for metabolic needs (cellular metabolic pathways such as glycolysis and ATP production). In every cell, whether of prokaryotic or eukaryotic origin, phosphate acquisition plays a key role in maintaining cellular phosphate homeostasis. Therefore, these organisms have evolved regulatory mechanisms for acquisition, storage, and release of this molecule allowing them to respond and adapt to fluctuations in phosphate availability. Phosphate metabolism in the yeast *S. cerevisiae* has been extensively studied for many years and this unicellular organism has provided an excellent model system for understanding how a cell makes a coordinated response to environmental phosphate changes. This organism responds to a diverse array of signals, and many of the responses involve the regulation of gene expression. The transcriptional regulation results in a corresponding adjustment in signaling systems that are activated by a changed phosphate status. The signal transduction pathway involved in the regulation of phosphate-responsive genes is complex and involves at least 22 different genes. The regulation of cellular phosphate uptake activity as well as phosphate starvation responses are maintained by a phosphate signal transduction pathway, the so-called *PHO* regulon. The preferred phosphate source is inorganic phosphate (Pi). Carrier-mediated Pi transport across the plasma membrane, an essential step in the utilization of Pi by *S. cerevisiae*, is mediated by several specific plasma membrane transport systems allowing the cell to switch between a low-affinity and a high-affinity mode of phosphate acquisition. However, when Pi becomes limiting in the growth media, there is an increased production of a high-affinity transport system and of secreted phosphatases that scavenge Pi from a variety of organic compounds through the action of periplasmically located acid phosphatases and of alkaline phosphatases presumably involved in releasing Pi from intracellular substrates. The ability of yeast to utilize various Pi sources is thus highly regulated, and the expression of the genes required for the utilization has been a major topic of study for many years.

The *PHO* Genes and their Regulation

The expression of the *PHO* genes is under tight regulation of the *PHO* regulon. The status of the regulon is commonly genetically and biochemically monitored by use of the activity of a secreted acid phosphatase (the gene product of *PHO5*), which is transcriptionally induced in response to Pi starvation. Although secreted acid phosphatases are encoded by several genes, *PHO3*, *PHO5*, *PHO11*, and *PHO12*, the Pho5 protein is responsible for more than 90% of the acid phosphatase activity of the cells. Most of the information on *PHO5* regulation has been obtained by the isolation and characterization of *PHO* regulon mutants that are defective in Pi regulation of acid phosphatase synthesis.

Besides *PHO5* and its homologues, *PHO11* and *PHO12*, additional genes of the *PHO* regulon which are activated by a Pi-starvation signal include the vacuolar alkaline phosphatase gene, *PHO8*, the genes encoding high-affinity Pi transporters of the plasma membrane, *PHO84* and *PHO89*, the *PHO86* gene encoding an endoplasmatic reticulum (ER) resident protein required for the ER exit of the synthesized Pho84 protein, and the *PHO81* gene encoding an inhibitor (CKI) of a cyclin-dependent kinase (CDK).

At least five regulatory proteins of the *PHO* pathway are believed to be involved in the transcriptional regulation of the *PHO* genes: A complex of the Pho85 CDK and its cyclin Pho80, and the CKI Pho81, together with the transcription factors Pho4 and Pho2 constitute the core components of the regulation (Figure 1). By a yet unknown mechanism, Pi limitation initiates a signal transduction cascade that activates Pho81, the inhibitor of the phosphorylation activity of the cyclin–CDK, Pho80–Pho85.

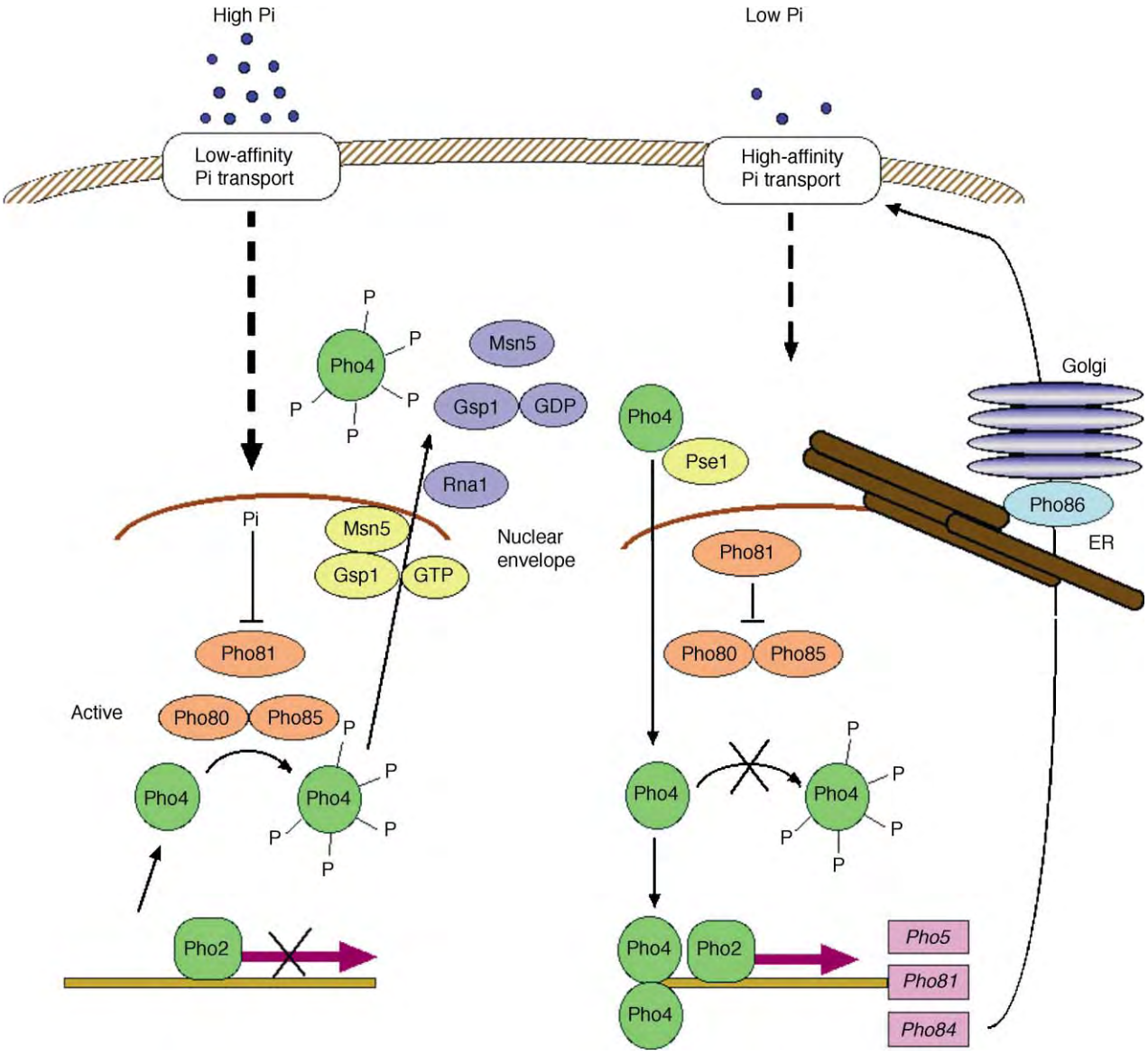

FIGURE 1 Transcriptional regulation of *PHO* genes through the *PHO* regulon at high (left) and low (right) external Pi concentrations. When Pi is abundant, the transcription factor Pho4 is phosphorylated by the Pho80–Pho85 cyclin–CDK complex, assembled with the Msn and Gsp1 proteins and exported to the cytoplasm resulting in a repressed transcription of the *PHO* genes. The CDK inhibitor, Pho81, is associated with the Pho80–Pho85 complex at both high and low Pi conditions, but exerts its inhibition on the complex under conditions of Pi limitations. Under these conditions, the Pho4 will be transported into the nucleus in unphosphorylated form via the Pse1 protein and together with Pho2 bind to the promoter regions and activate transcription of the *PHO* genes. Expression of *PHO*84, encoding a high-affinity Pi transporter results in synthesis and Pho86-mediated delivery of the Pho84 transporter via Golgi to the plasma membrane.

Pho2, Pho4, and Pho81 are positive regulators of *PHO5* and deletion of these genes confer an inability to induce *PHO5* expression upon Pi limitation. Deletion analysis of the *PHO5* promoter has revealed two distinct regulatory elements (upstream activator sequences, UAS), UAS1 and UAS2, to which the transcription factor Pho4 binds under Pi starvation, but not under high-Pi conditions. The binding sequences for Pho4, CACGTG or CACGTT, have been identified and the existence of at least one copy of these sequences has been shown in the immediate promoter region of all but one of the described *PHO* genes, suggesting that Pho4 is a transcriptional activator for all these genes. The structure of the DNA-binding domain of Pho4, resolved to 2.8Å, has revealed a folding of this domain into a C-terminal basic helix-loop-helix (bHLH) motif. A native cysteine residue in the bHLH motif is essential for Pho4 dimerization, binding of the homodimer to the UAS of *PHO5*, and for transcriptional activation of the *PHO* regulon. When localized to the nucleus, Pho4 binds to the two bHLH consensus sequences (CACGTG or CACGTT) in the *PHO* promoter sequences, and the transcriptional regulator Pho2, a homeobox DNA-binding protein, binds cooperatively with Pho4 to activate expression of target genes. As Pho2 binds to its consensus sequence (T/C)TAA(T/A)T(T/G)AAT with low affinity it interacts with several other proteins and participates in the regulation of a diverse array of genes. For its function in *PHO* regulation, Pho2 acts through multiple DNA-binding sites. At the *PHO5* promoter region, one of these sites significantly overlaps with the Pho4-binding site as UAS1, while another two sites flank the second Pho4-binding site, UAS2. As access of the transcriptional regulators Pho2 and Pho4 is aided or hindered by the chromatin structure, the nature of DNA packing is important for the regulation of gene expression. For a chromatin remodeling function in *PHO5* region, the participation of a nuclear-located inositol polyphosphate kinase, Arg82, has been proposed. Factors implicated in chromatin-packing arrangements are histone-DNA interactions in promoter regions of certain *PHO* genes, and acetylation, methylation, or phosphorylation of histones.

A central role in Pi regulation has been demonstrated for the Pho80 cyclin and the Pho85 cyclin-dependent kinase which upon complex formation allows for a differential hyperphosphorylation of the Pho4 transcription factor in the nucleus. Pho85 is one of five CDKs found in *S. cerevisiae*. Activation of CDKs requires binding of a cyclin. At least ten different cyclins involved in cell cycle and/or metabolic regulation are known to bind Pho85. In the Pi assimilation process, the kinase function of Pho85 is activated by interaction with Pho80 whereby the kinase activity of the Pho80–Pho85 cyclin–CDK complex phosphorylates Pho4. Protein phosphorylation has been found to play an important role in the control of diverse cellular processes, especially that of transcriptional factors in regulation of gene expression. The phosphorylated state of Pho4 is important for its localization in the cell and thus for its activity in transcriptional regulation of the *PHO* genes. The CKI Pho81 binds to the Pho80–Pho85 protein complex when cells are grown at both high and low Pi conditions but a pronounced inhibition of the kinase activity and hence an abolished hyperphosphorylation is seen only at Pi-limiting conditions. Under these conditions, the *PHO* genes, including *PHO81*, are activated. The unphosphorylated form of Pho4, which has a low affinity for the nuclear exportin receptor Msn5, is presumably transported into the nucleus through an import pathway that utilizes the importin Pse1. In contrast, the hyperphosphorylated form of Pho4, which is unable to bind to Pse1, is accessible for complex formation with Msn5 and Gsp1, a yeast Ran homologue, after which the complex is transported into the cytoplasm. Dissociation of the complex in the cytoplasm involves the participation of Rna1, a GTPase-activating protein responsible for the conversion of the GTP bound to Gsp1 in its complex active form to GDP. Thus, Pho4 is concentrated to the nucleus when yeast cells are starved for Pi and is predominantly cytoplasmic when yeast cells are grown at high, repressive Pi conditions. It has been proposed that also Pho2 can be phosphorylated by a kinase, possibly indicating a similar mechanism whereby the transcriptional activity of Pho2 may thus be regulated by a phosphate switch, not only enhancing the transcriptional activity but also facilitating the interaction between Pho2 and Pho4. Only when Pho2 is phosphorylated, the *PHO5* can be expressed under Pi limiting conditions. Transcription of *PHO* genes under Pi limitation would thus necessitate Pho4 dephosphorylation as well as Pho2 phosphorylation. Such a feedback Pi-controlled regulation of transcription ensures balanced levels of regulatory proteins and a swift response to changes in Pi concentrations.

The positive feedback-regulated inhibition of Pho85–Pho80 exerted by Pho81, makes Pho81 a key player in the *PHO* regulatory pathway. Pho81 harbors a tandem repeat of six ankyrin consensus regions, of which one is regarded to play an essential role in the CKI/CDK complex interaction. However, both the mechanisms by which the Pi limitation signal is transduced to Pho81 and where the signal originates are still unclear.

Due to a comprehensive identification and characterization of the *PHO*-regulated genes in the yeast genome, the late events in the *PHO* pathway are now well understood, an important step toward an understanding of the physiological regulation of Pi metabolism.

See Also the Following Articles

Diacylglycerol Kinases and Phosphatidic Acid Phosphatases • Mitochondrial Genes and their Expression: Yeast • Pentose Phosphate (Hexose Mono Phosphate) Pathway • Pentose Phosphate Pathway, History of

Glossary

ankyrin region Protein domains that contain 33-amino acid long sequences that often occur in tandem arrays and are involved in protein's molecular recognition.

CDK Cyclin-dependent kinases, a family of protein kinases that control cell cycle progression in all eukaryotes and require physical association with cyclins to achieve full enzymatic activity. CDK's are regulated by phosphoryation and dephosphorylation events.

CKI Cyclin-dependent kinase inhibitor, small protein that binds stoichiometrically to regulate the activity of CDKs.

cyclin Protein found in certain eukaryotic cells that helps regulate the cell cycle by causing cells to begin mitosis. Cyclins are regulatory subunits of the cyclin-dependent protein kinases.

homeobox genes Genes with a shared nucleotide segment that are involved in the formation of bodily segmentation during embryologic development.

***PHO* regulon** Genetic regulatory network of scattered genes involving structural and regulatory units active in phosphate signal transduction.

promoter A DNA sequence that enables a gene to be transcribed.

Further Reading

Carroll, A. S., and O'Shea, E. K. (2002). Pho85 and signaling environmental conditions. *Trends Biochem. Sci.* **27**, 87–93.

Lenburg, M. E., and O'Shea, E. K. (1996). Signaling phosphate starvation. *Trends Biochem. Sci.* **21**, 383–387.

Ogawa, N., DeRisi, J., and Brown, P. O. (2000). New components of a system for phosphate accumulation and polyphosphate metabolism in *Saccharomyces cerevisiae*. *Mol. Biol. Cell.* **11**, 4309–4321.

Oshima, Y. (1997). The phosphatase system in *Saccharomyces cerevisiae*. *Genes Genet. Syst.* **72**, 323–334.

Persson, B. L., Lagerstedt, J. O., Pratt, J. R., Pattison-Granberg, J., Lundh, K., Shokrollahzadeh, S., and Lundh, F. (2003). Regulation of phosphate acquisition in *Saccharomyces cerevisiae*. *Curr. Genet.* **43**, 225–244.

Torriani-Gorini, A., Silver, S., and Yagil, E. (1994). *Phosphate in Microorganisms: Cellular and Molecular Biology.* American Society for Microbiology, Washington DC.

Biography

Bengt L. Persson is a Professor in the Department of Chemistry and Biomedical Sciences at the University of Kalmar. His principal research interests are in molecular membrane biochemistry and cellular regulation of phosphate acquisition systems. He holds a Ph.D. from the University of Stockholm and received his postdoctoral training at the University of California, Los Angeles. He is presently conducting research on phosphate transport regulation at the Universities of Stockholm and Kalmar and has authored several papers on phosphate transporters of yeast.

Phosphatidylinositol Bisphosphate and Trisphosphate

Alex Toker
Harvard Medical School, Boston, Massachusetts, USA

Phosphatidylinositol (PtdIns) is a minor membrane phospholipid which is found in all eukaryotic cells. It is the precursor of a family of phosphorylated lipids which are collectively known as phosphoinositides, and rather than serving a structural role in cellular membranes, they act as functional second messengers to transduce biochemical signals in the cell. The article in detail discusses the synthesis, hydrolysis, and cellular functions of phosphotidylinosital bisphosphate and trisphosphate.

Phosphoinositides are composed of a water-soluble inositol ring which can be phosphorylated at each of three positions (D-3, D-4, and D-5), and a greasy fatty acid tail which is attached to a glycerol and linked to the inostol ring by a phosphodiester bond (Figure 1). The concerted actions of phosphoinositide kinases, phosphoinositide phosphatases, and phospholipases on phosphatidylinositol leads to the production of seven additional phosphoinositides which are known to exist in cells (Figure 2). Of these, phosphatidylinositol-4,5-bisphosphate (PtdIns-4,5-P_2) and phosphatidylinositol-3,4,5-trisphosphate (PtdIns-3,4,5-P_3) are the best understood and characterized. Both the synthesis and the degradation of PtdIns-4,5-P_2 and PtdIns-3,4,5-P_3 are tightly regulated, and this ensures efficient and coordinated signaling through these second messengers. Biochemical and genetic studies have implicated both PtdIns-4,5-P_2 and PtdIns-3,4,5-P_3 in numerous cellular responses, such as cell growth, cell survival, cell motility and modulation of the actin cytoskeleton, gene transcription and vesicle trafficking (Figure 3). The importance of these phosphoinositides in cell biology is exemplified by the fact that deregulation in the metabolism or mechanism of action of these lipids often results in human diseases such as cancer and type 2 diabetes.

Phosphatidylinositol-4,5-Bisphosphate

Synthesis

PtdIns-4,5-P_2 is often considered to be one of the most important functional lipids in eukaryotic cells, because it not only has a functional second messenger role *per se*, but can also serve as an intermediate for the production of additional lipid mediators. It can serve as a substrate for phosphoinositide 3-kinase (PI 3-K) to produce PtdIns-3,4,5-P_3, it can be hydrolyzed by phospholipases to produce diacylglycerol (DAG) and soluble inositol phosphates, and it can also be dephosphorylated by D-4 and D-5 lipid phosphatases (Figure 2). Although the bulk of PtdIns-4,5-P_2 is found at the plasma membrane, other distinct pools of PtdIns-4,5-P_2 have been reported. For example, there exists a nuclear phosphoinositide cycle where PtdIns-4,5-P_2 production has been detected. However, there are relatively modest, if any, changes in the total levels of PtdIns-4,5-P_2 upon cellular stimulation with agonists such as growth factors or hormones. This is difficult to reconcile with the second messenger hypothesis which dictates that a lipid mediator must rapidly accumulate to amplify downstream signaling. Therefore, it is likely that the constitutive levels of PtdIns-4,5-P_2 change locally at discrete intracellular sites, such that the accumulation of this lipid is regulated both spatially and temporally. In addition, there are two other isomers of phosphatidylinositol bisphosphate: PtdIns-3,4-P_2 and the recently discovered PtdIns-3,5-P_2. The function of these two phosphoinositides is not entirely clear, but they are likely to mediate certain responses downstream of PI 3-K.

The synthesis of PtdIns-4,5-P_2 is controlled by the sequential action of phosphoinositide 4-kinases, which use phosphotidylinositol (PtdIns) as substrate and produce PtdIns-4-P, and phosphoinositide phosphate kinases (PIPKs), which can use either PtdIns-4-P or PtdIns-5-P as substrates. In both cases, the product is PtdIns-4,5-P_2 (Figure 2). Much is known about the enzymes which produce PtdIns-4,5-P_2. There are two families of PIPKs, type I and type II. Type I kinases preferentially phosphorylate PtdIns-4-P at the D-5 position, and this appears to be the major route of PtdIns-4,5-P_2 synthesis. However, it was recently discovered that type II PIPKs can phosphorylate PtdIns-5-P at the D-4 position, and so it is likely that in some instances this represents an important pathway for the

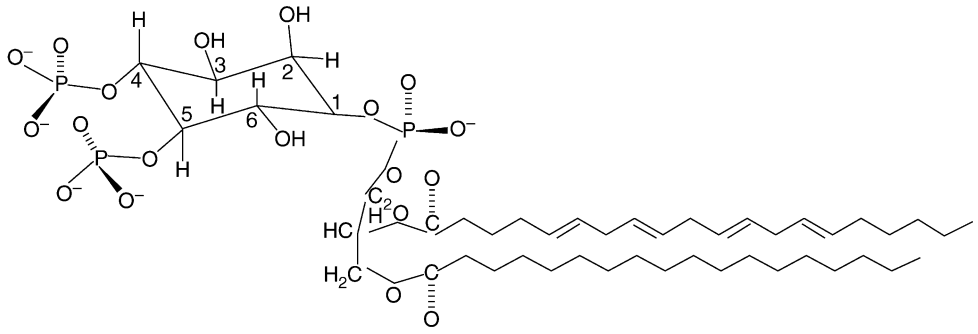

FIGURE 1 Structure of phosphatidylinositol-4,5-bisphosphate. The structure shows PtdIns-4,5-P_2\, which contains an inositol head group connected to a diacylglycerol via a phosphodiester linkage. The fatty acid moiety is typically stearoyl-arachidonyl. The inositol head group can be phosphorylated at one of three positions, D-3, D-4, and D-5. Shown are phosphate groups at the D-4 and D-5 position in PtdIns-4,5-P_2. Phosphoinositide 3-kinases phosphorylate the D-3 position of PtdIns-4,5-P_2 to produce PtdIns-3,4,5-P_3.

generation of PtdIns-4,5-P_2. Several forms of both type I and type II PIPKs exist in mammalian cells, and homologues are also found in lower eukaryotes such as yeasts, highlighting the importance of these enzymes in biology. The crystal structure of a type II enzyme has been solved, and has revealed an elongated, flat surface covered with highly basic, positively charged amino acids which are ideally positioned for interaction with the negatively charged phosphoinositides such as PtdIns-5-P. Finally, a separate route of synthesis for PtdIns-4,5-P_2 is the dephosphorylation of PtdIns-3,4,5-P_3 by D-3 phosphoinositide phosphatases, though it is not clear what fraction of the bulk PtdIns-4,5-P_2 pool is accounted for by this mechanism. Regardless, PIPKs represent the major pathway leading to the production of PtdIns-4,5-P_2, and as such their activities are tightly controlled.

Hydrolysis

PtdIns-4,5-P_2 is hydrolyzed by phosphoinositide-specific phospholipases. These enzymes, also known as type C phospholipases (PLC), hydrolyze PtdIns-4,5-P_2 into two important second messengers: the membrane-bound fatty acid moiety, also known as diacylglycerol (DAG), and the soluble portion which is an inositol trisphosphate (Ins-1,4,5-P_3, when PtdIns-4,5-P_2 is the PLC substrate). Each of these products has important roles

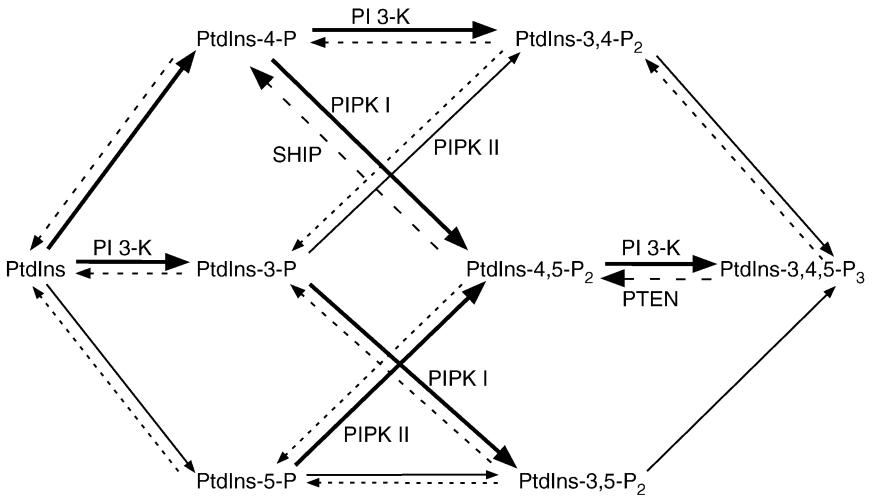

FIGURE 2 Phosphoinositide metabolism. The pathways responsible for the production of all known phosphoinositides are shown. The concerted actions of phosphoinositide kinases, such as PIPKs (type I and type II phosphoinositide 4-phophate and 5-phosphate kinases) and phosphoinositide 3-kinases (PI 3-K), as well as phosphatases (PTEN and SHIP) leads to the production of seven distinct phosphoinositides, from the precursor phosphatidylinositol (PtdIns). Although all of the forward (solid arrows, mediated by kinases) and reverse (broken arrows, mediated by phosphatases) reactions are possible, the pathways which are likely to predominate in cells are shown in bold arrows.

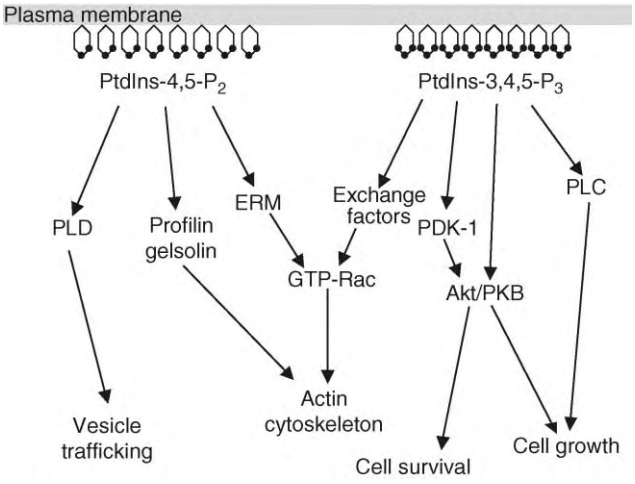

FIGURE 3 Targets of PtdIns-4,5-P_2 and PtdIns-3,4,5-P_3. A large number of proteins whose activities are directly regulated by either PtdIns-4,5-P_2 or PtdIns-3,4,5-P_3 exist. A few of these are depicted and serve to illustrate that the binding of the phosphoinositide to the protein can alter its cellular location as well as directly influencing catalytic activity when enzymes are the targets. These interactions are responsible for the activation of secondary signaling pathways, which ultimately lead to numerous physiological responses, as depicted. In many cases, PtdIns-4,5-P_2 and PtdIns-3,4,5-P_3 have overlapping functions, due to the activation of distinct effector molecules, such as the remodeling of the actin cytoskeleton which occurs as a consequence of both PtdIns-4,5-P_2- and PtdIns-3,4,5-P_3-dependent signaling.

in lipid signaling. DAG is the activator for members of the protein kinase C family of serine/threonine kinases, which are recruited to the membrane at the site of DAG production. Ins-1,4,5-P_3 plays an equally important role in lipid signaling as it is responsible for the release of Ca^{2+} from internal stores, such as the endoplasmic reticulum.

Although four distinct families of PLC exist in mammalian cells, they all share a similar catalytic mechanism employing calcium as a cofactor. All members of the PLC family use PtdIns-4-P and PtdIns-4,5-P_2 as substrates. PLCβ enzymes are regulated by binding to both $\beta\gamma$-as well as α-subunits of heterotrimeric GTP-binding proteins. PLCδ also appears to be regulated by G proteins, although the mechanism is unclear, and it is also reported that increases in Ca^{2+} alone are sufficient to activate PLCδ. Phospholipases belonging to the PLCγ family are activated by the binding of SH2 domains to phosphotyrosine-containing sequences in receptor tyrosine kinases, and as such participate in growth-factor-dependent responses such as cell growth. Tyrosine phosphorylation of PLCγ is also important in controlling catalytic activity. Very recently a new PLC subtype has been described, PLCε, and has shown to be a novel effector of the GTP bound form of the Ras GTPase. The diversity and complexity of the PLC family underscores the importance of PtdIns-4,5-P_2 hydrolysis and DAG/Ins-1,4,5-P_3 production in mediating cell proliferation, differentiation, and cell motility.

Cellular Function

In addition to serving as the substrate for additional lipid second messengers, PtdIns-4,5-P_2 is an important lipid mediator in its own right. Numerous studies have shown that PtdIns-4,5-P_2 can modulate the activity of proteins which regulate actin assembly, leading to rearrangements of the actin cytoskeleton (Figure 3). For example, PtdIns-4,5-P_2 has been shown to promote actin polymerization by directly interacting with actin-binding proteins such as profilin. Similarly, actin-capping proteins, such as CapZ, prevent spontaneous actin assembly by capping the free ends of actin filaments, and the binding to PtdIns-4,5-P_2 disrupts this capping event leading to filament assembly. The list of actin-binding proteins whose activities are also regulated by PtdIns-4,5-P_2 includes gelsolin, cofilin, filamin, and vinculin. The small GTPase Rac also plays an important role in the remodeling of the actin cytoskeleton, and in some instances this requires PtdIns-4,5-P_2. For example, the ERM family of proteins (*E*zrin, *R*adixin, and *M*oesin), a family of Rac effector molecules, are also PtdIns-4,5-P_2-binding proteins which regulate dynamic actin assembly, again linking PtdIns-4,5-P_2 function to the actin cytoskeleton. Rac, in the active GTP bound form, also interacts with PIP kinases, which are responsible for PtdIns-4,5-P_2 synthesis. Recent studies in cells have provided further evidence that PtdIns-4,5-P_2 is a critical regulator of the actin cytoskeleton. For example, expression of type I PIPK enzymes in cells leads to a dramatic reorganization of the actin cytoskeleton, and PIPK I appears to be targeted to focal adhesions, sites of cellular contact with the extracellular matrix. This targeting provides clear evidence for the localized accumulation of PtdIns-4,5-P_2 in the cell. Studies such as these, carried out in mammalian cells, have also been corroborated in yeasts, whereby genetic ablation of PIP kinases (such as Mss4p) leads to abnormalities in the actin cytoskeleton, which can be rescued by the introduction of human PIPK isoforms.

PtdIns-4,5-P_2 is also an important cofactor for the activity of a number of signaling enzymes. The best example is for *p*hospho*l*ipase *D* (PLD), an enzyme responsible for the production of *p*hosphotidic *a*cid (PA) in the cell. PLD requires PtdIns-4,5-P_2 for efficient catalytic function. Because certain PIP kinases also depend on PA for enzymatic activity, and PtdIns-4,5-P_2 stimulates PLD leading to PA production, the net result is a positive amplification loop which leads to amplification of PA and PtdIns-4,5-P_2 synthesis at specific intracellular compartment where these enzymes are located. Both PIPKs and PLD have been implicated in trafficking and secretion, and as such their products are

directly involved in controlling vesicle formation, as well as endocytosis (Figure 3).

Phosphatidylinositol-3,4,5-Trisphosphate

Synthesis

Unlike its substrate PtdIns-4,5-P_2, phosphotidylinositol-3,4-trisphosphate (PtdIns-3,4,5-P_3) is nominally absent in unstimulated cells and rapidly accumulates in response to virtually all known growth factors, hormones, cytokines, and other stimuli. In most cells, production of PtdIns-3,4,5-P_3 typically peaks within seconds to a few minutes after stimulation, and declines to near basal levels after 1–2 h. A second peak of PtdIns-3,4,5-P_3 has been observed in cells between 4 and 8 h after stimulation with mitogens such as platelet-derived growth factor (PDGF). This second peak of PtdIns-3,4,5-P_3 is responsible for efficient cell cycle progression in fibroblasts, specifically entry into the S phase where DNA synthesis occurs. Although the bulk of PtdIns-3,4,5-P_3 is produced at the plasma membrane, it is also known that there are discrete intracellular locations where this phosphoinositide is also found, particularly the nucleus. PI 3-Ks are responsible for the production of PtdIns-3,4,5-P_3 in higher eukaryotes. These enzymes phosphorylate the D-3 position of the inositol head ring, and depending on the substrate, four distinct products can result: PtdIns-3-P, PtdIns-3,5-P_2, PtdIns-3,4-P_2, and PtdIns-3,4,5-P_3 (Figure 1). Although different forms of PI 3-Ks exist, each with unique substrate selectivity, the class Ia enzymes are responsible for the production of PtdIns-3,4,5-P_3 in cells. These PI 3-Ks are composed of a p85 regulatory subunit and a p110 catalytic subunit. The regulatory subunit binds to specific phosphotyrosine-containing sequences in the cytosolic domains of activated receptor tyrosine kinases, via a tandem repeat of two Src-Homology 2 (SH2) domains. This interaction facilitates the activation of the catalytic subunit, whose activity is also increased by a direct interaction with the activated form of the small GTPase Ras. The newly activated PI 3-K converts PtdIns-4,5-P_2 to PtdIns-3,4,5-P_3. In addition, class Ib PI 3-Ks are also capable of producing PtdIns-3,4,5-P_3, and these kinases are typically activated downstream of heterotrimeric G protein-coupled receptors, such as the thrombin receptor in platelets. Class Ib enzymes are also composed of two subunits, a p120 catalytic subunit and a p101 regulatory subunit, which confers sensitivity to G$\beta\gamma$. Class Ib enzymes also require activated Ras for full catalytic function. Thus, the primary route of synthesis for PtdIns-3,4,5-P_3 in cells is through the activation of class I PI 3-Ks which use PtdIns-4,5-P_2 as substrate.

PtdIns-3,4,5-P_3 Phosphatases

Because the production of PtdIns-3,4,5-P_3 is critical for a number of physiological responses in cells, mechanisms exist which mediate the termination of PI 3-K and PtdIns-3,4,5-P_3 signaling. PI 3-K lipid products, including PtdIns-3,4,5-P_3, are not degraded by phospholipases, but instead are down-regulated by at least two different types of phosphoinositide phosphatases. SHIP1 and SHIP2 (*SH*2-containing *i*nositol 5′-*p*hosphatases) are lipid phosphatases which specifically remove the D-5 phosphate from both PtdIns-4,5-P_2 and PtdIns-3,4,5-P_3 (Figure 2). The action of SHIP1/2 on PtdIns-3,4,5-P_3 results in the production of PtdIns-3,4-P_2, and although this can impair signaling downstream of PI 3-K, PtdIns-3,4-P_2 is able to mediate certain responses which overlap with PtdIns-3,4,5-P_3. Despite this, loss of SHIP2 increases insulin sensitivity in responsive tissues such as muscle and fat. *P*hosphatase and *ten*sin (PTEN) homologue deleted on chromosome 1, is a D-3 phosphatase which dephosphorylates PtdIns-3,4,5-P_3 with PtdIns-4,5-P_2 as the product (Figure 2). PTEN is very effective at terminating PI 3-K and PtdIns-3,4,5-P_3 signaling, and this is evidenced by the fact that mutations in the PTEN gene have been detected in a large fraction of advanced human tumors. For this reason, PTEN is referred to as a tumor-suppressor gene. Thus, efficient termination of PtdIns-3,4,5-P_3 signaling is of critical importance for intracellular signaling, and deregulation of this signal can have adverse consequences for cellular responses, often leading to diseases such as diabetes and cancer.

PtdIns-3,4,5-P_3-Binding Proteins

The mechanism by which PI 3-K activates downstream secondary signaling pathway is by the recruitment of cytosolic proteins to the plasma membrane at the site of PtdIns-3,4,5-P_3 production. This recruitment can have a number of consequences; in addition to causing a change in the cellular location of the protein, it can induce a conformation change, and in the case of enzymes, it can increase (and sometimes decrease) enzymatic activity. Typically, a combination of these events results from the PtdIns-3,4,5-P_3-protein interaction. A number of protein domains have evolved which specifically recognize phosphoinositides, particularly PtdIns-3,4,5-P_3. The first described example is the *P*leckstrin *H*omology (PH) domain, a 100 amino acid sequence found in several signaling proteins which participate in PI 3-K responses. PH domains are found in both serine-threonine protein kinases (e.g., Akt/PKB and PDK-1), tyrosine kinases (e.g., Tec family kinases such as Btk), guanine nucleotide exchange factors of small GTP-binding proteins (e.g., SOS, Grp-1 and pREX), and GTPases themselves (e.g., dynamin). In some of these

cases, the PtdIns-3,4,5-P_3-protein interaction is well understood. For example, recruitment of Akt/PKB to the plasma membrane occurs in response to PtdIns-3,4,5-P_3 production. The PH domain of Akt/PKB directly binds to PtdIns-3,4,5-P_3 with high affinity and selectivity, and this leads to a conformational change in the protein kinase which leads to unfolding of the PH domain, revealing a sequence in the catalytic domain known as the activation loop. The PDK-1 kinase, which also has a PH domain and is recruited to the membrane simultaneously with Akt/PKB, can now phosphorylate Akt/PKB at a critical threonine residue in this loop. The phosphorylated Akt/PKB is now fully catalytically competent and can itself phosphorylate downstream protein substrates. This elegant mechanism is recapitulated in a large number of other protein kinases which are also regulated by PtdIns-3,4,5-P_3 or PDK-1, or both (e.g., protein kinase C and S6-kinases).

Recently, a distinct phosphoinositide-binding domain was described, and termed the *p*ho*x (PX)* domain. This 130 amino acid domain is also found in many important signaling proteins, and was originally described in the $p40^{phox}$ and $p47^{phox}$ subunit of the NADPH-oxidase superoxide-generating complex in phagocytic cells. Although PX domains do not appear to bind to PtdIns-3,4,5-P_3, they bind with high affinity to PtdIns-3-P and PtdIns-3,4-P_2, and thus are important in mediating signaling downstream of these PI 3-K lipids. Another domain which has been shown to bind PtdIns-3,4,5-P_3 is the SH2 domain. Although less well understood, binding of PtdIns-3,4,5-P_3 to the SH2 domain of the phospholipase PLCγ-1, for example, leads to an increase in its enzymatic activity. Thus, several domains have evolved in higher eukaryotic cells which have the ability to bind with distinct affinities and selectivity to PtdIns-3,4,5-P_3, and other phosphoinositides. This interaction has a profound effect on downstream signaling and cellular responses.

Cellular Function

Numerous biochemical, pharmacological, and genetic studies have demonstrated that PI 3-K, and its product PtdIns-3,4,5-P_3, regulates a multitude of cellular responses. These include cell growth, protection from cell death (apoptosis), remodeling of the actin cytoskeleton, cell migration and invasion, metabolism and insulin responses, cell cycle regulation, and gene transcription (Figure 3). It is beyond the scope of this article to discuss all of these in any detail, but some notable examples are given. Activation of the protein kinase Akt/PKB by the PI 3-K pathway regulates cellular survival mechanisms, as well as insulin-dependent metabolism. Most proteins which mediate Akt/PKB-dependent cellular survival are inhibited by the phosphorylation event. For example, phosphorylation of the Forkhead family of transcription factors (e.g., FKHR-L1) by Akt/PKB inhibits their translocation to the nucleus due to the creation of a binding site for 14-3-3, a family of molecular chaperones. This retention of FKHR-L1 in the cytoplasm inhibits the transactivation of genes intimately associated with cell death, and the net effect is an increase in survival. Similarly, Akt/PKB phosphorylation of the pro-apoptotic protein Bad also facilitates 14-3-3 binding, and this prevents Bad from binding to the anti-apoptotic proteins Bcl-2 and Bcl-X_L, effectively preventing apoptosis. Akt/PKB can also regulate both cell cycle progression and gluconeogenesis/glycolysis by phosphorylating *g*lycogen *s*ynthase *k*inase-*3* (GSK-3). This phosphorylation inhibits the elevated constitutive activity of GSK-3, which can no longer phosphorylate proteins such as Myc, the cell cycle regulator cyclin D, and glycogen synthase. Thus, Akt/PKB signaling results in the activation of several pathways which are normally inhibited by GSK-3.

Not all PI 3-K responses are mediated by Akt/PKB. In fact there are several other kinases which are activated by PtdIns-3,4,5-P_3 signaling, and which have important roles in cell physiology. For example, the S6-kinases, S6K-1 and S6K-2, regulate protein synthesis and insulin responses. The protein kinase C family of kinases can also be regulated by PtdIns-3,4,5-P_3-dependent mechanisms, and have been shown to mediate both cell growth and survival mechanisms, though these are not as well understood as the Akt/PKB pathway. The Tec family kinase *B*ruton's *t*yrosine *k*inase (Btk), which binds to PtdIns-3,4,5-P_3 via its PH domain, is important for B cell development, and importantly, genetic mutations within its PH domain have been shown to give rise to certain immunodeficiencies in humans.

Finally, regulation of the dynamics of the actin cytoskeleton is also achieved by PtdIns-3,4,5-P_3-dependent responses, and this leads to increased cell migration of many cell types (Figure 3). One important mechanism by which PtdIns-3,4,5-P_3 regulates such responses is by activating the small GTP-binding protein Rac, known to contribute to actin remodeling and directional migration in response to chemotactic stimuli. Small GTPases such as Rac are activated by binding to GTP, and this is stimulated by the activation of Rac-specific guanine nucleotide exchange factors, such as SOS, Vav and in particular, pREX. These exchange factors have PH domains which in some cases have been shown to bind to PtdIns-3,4,5-P_3, leading to an increase in exchange activity towards Rac. In summary, the diverse cellular responses attributed to PI 3-K signaling are explained by the fact that there exist numerous signaling proteins which interact with PtdIns-3,4,5-P_3. This binding has a profound

consequence on the function of the protein, leading to the activation of downstream pathways.

See Also the Following Articles

Diacylglycerol Kinases and Phosphatidic Acid Phosphatases • Inositol Lipid 3-Phosphatases • Inositol Phosphate Kinases and Phosphatases • Phosphatidylinositol-3-Phosphate • Phosphoinositide 3-Kinase • Phosphoinositide 4- and 5-Kinases and Phosphatases • Phosphoinositide-Dependent Protein Kinases • Phospholipase C • Phospholipase D

Glossary

phosphatidylinositol Membrane phospholipid which is a precursor to all known phosphoinositides and is composed of an inositol head ring and fatty acid tail.

phosphoinositide Phospholipid second messenger which is found in intracellular membranes and which can be phosphorylated on the inositol head ring at the D-3, D-4, and D-5 positions resulting in seven known phosphorylated species.

phosphoinositide kinase An enzyme which can use phosphoinositides as substrates, and can phosphorylate the inositol head ring at either the D-3, D-4, or D-5 positions.

phosphoinositide phosphatase An enzyme which can specifically remove the D-3, D-4, or D-5 phosphate from phosphorylated phosphoinositides.

phospholipase An enzyme which can hydrolyze the phosphodiester bond in phospholipids and produce soluble inositol lipids and membrane-bound diacylglycerol; type C phospholipases specifically use phosphoinositides as substrates.

PH domain A protein domain composed of approximately of 100 amino acids which can specifically bind to Ptdins-4,5-P_2 and Ptdins-3,4,5-P_3.

Further Reading

Anderson, R. A., Boronenkov, I. V., Doughman, S. D., Kunz, J., and Loijens, J. C. (1999). Phosphatidylinositol phosphate kinases, a multifaceted family of signaling enzymes. *J. Biol. Chem.* **274**, 9907–9910.

Cantley, L. C. (2002). The phosphoinositide 3-kinase pathway. *Science* **296**, 1655–1657.

Cullen, P. J., Cozier, G. E., Banting, G., and Mellor, H. (2001). Modular phosphoinositide-binding domains—their role in signalling and membrane trafficking. *Curr. Biol.* **11**, R882–R893.

Leslie, N. R., Biondi, R. M., and Alessi, D. R. (2001). Phosphoinositide-regulated kinases and phosphoinositide phosphatases. *Chem. Rev.* **101**, 2365–2380.

Rhee, S. G. (2001). Regulation of phosphoinositide-specific phospholipase C. *Annu. Rev. Biochem.* **70**, 281–312.

Toker, A. (2002). Phosphoinositides and signal transduction. *Cell Mol. Life Sci.* **59**, 761–779.

Vivanco, I., and Sawyers, C. L. (2002). The phosphatidylinositol 3-kinase AKT pathway in human cancer. *Nat. Rev. Cancer* **2**, 489–501.

Wishart, M. J., and Dixon, J. E. (2002). PTEN and myotubularin phosphatases: From 3-phosphoinositide dephosphorylation to disease. Phosphatase and tensin homolog deleted on chromosome ten. *Trends Cell Biol.* **12**, 579–585.

Biography

Alex Toker is an Associate Professor of Pathology at the Beth Israel Deaconess Medical Center, Harvard Medical School, Boston. His principal research interests are the role of lipid signaling pathways and protein kinases in regulating carcinoma cell growth, survival, and invasion. He holds a Ph.D. from the National Institute for Medical Research, London, and has done postdoctoral research first at Tufts University Medical School, then at Harvard Medical School, Boston. He joined the staff at the Boston Biomedical Research Institute, as a Staff Scientist in 1997, and in 2000 moved to the Department of Pathology, BIDMC.

Phosphatidylinositol-3-Phosphate

Joseph V. Virbasius and Michael P. Czech
University of Massachusetts Medical School, Worcester, Massachusetts, USA

Phosphatidylinositol is a polar phospholipid which comprises a small fraction of the total membrane lipids in cells. The hydroxyl moieties of the inositol head group may be reversibly modified by transfer of a phosphate group from ATP to one or more of three positions. This reaction is catalyzed by the class of enzymes referred to as phosphatidylinositol kinases (PI kinases). Specific PI kinases can produce three monophosphorylated phosphatidylinositols, PtdIns(3)P, PtdIns(4)P, and PtdIns(5)P in intact cells. These can be further phosphorylated by PI kinases to yield such polyphosphoinositides as PtdIns(4,5)P_2 and PtdIns(3,4,5)P_3, which function in regulating plasma membrane activities and cell signaling cascades, respectively. Although it is likely that PtdIns(4)P and PtdIns(5)P have important functions, molecular targets of these phosphoinositides have yet to be characterized. In contrast, through both genetic and biochemical studies our understanding of PtdIns(3)P functions and the PI 3-kinases which specifically produce PtdIns(3)P are well advanced. In recent years, a large number of proteins that interact with PtdIns(3)P have been discovered and their roles in various cellular processes including membrane trafficking and signaling have been elucidated.

Synthesis and Turnover of PtdIns(3)P

Although PtdIns(3)P synthesis is not known to be acutely activated by extracellular stimuli as is the case for certain other phosphoinositides, PtdIns(3)P content of membranes appears to be dynamically regulated and spatially restricted in intracellular compartments. Current data indicate that PtdIns(3)P is found primarily, and perhaps exclusively, in endosomal membranes (Figure 1). These membranes are vesicular structures which delimit compartments derived from endocytic internalization of patches of membrane from the cell surface. Mechanisms for generation of PtdIns(3)P must therefore be activated concurrently with or shortly after endocytosis, while turnover of PtdIns(3)P by hydrolysis or additional phosphorylation must occur during the progression of endosomes toward their cellular fates. These fates include recycling to the plasma membrane and fusion with lysosomes. Cellular proteins embedded in these membrane patches can likewise be targeted for recycling back to the plasma membrane where they may resume their functions, or for degradation in the lysosome. Recent discoveries indicate that PtdIns(3)P and its molecular targets play critical regulatory roles in such membrane trafficking pathways of endosomes, and thus help to determine the cellular distribution and fate of membrane proteins such as receptors for growth factors.

Synthesis of PtdIns(3)P by PI 3-Kinases

In the yeast genome, a single gene encoding a PtdIns 3-kinase has been identified. *VPS34* was originally identified in a screen for mutants that failed to properly direct a protein degradation enzyme to the vacuole, the organelle with functions similar to the lysosome of animal cells. The 100 kDa protein encoded by this gene, *Vps34p*, has a domain highly similar to mammalian PI 3-kinase and was subsequently shown to have PI 3-kinase activity. *Vps34p* exists in a complex with a 150 kDa serine/threonine kinase,Vps15p, which serves to target the Vps34p enzyme to membranes where its substrate phosphatidylinositol resides. Phosphorylation of Vps34p by the protein kinase activity of Vps15p is required for full activity of the Vps34p PI 3-kinase. A homologous PI 3-kinase complex exists in all eukaryotes studied. The mammalian Vps34 PI 3-kinase (also referred to as a class III PI 3-kinase) appears to be the predominant enzyme which produces PtdIns(3)P in cells. Although Class I and II PI 3-kinases are also capable of phosphorylating PI *in vitro*, their contribution to PtdIns(3)P production *in vivo* is not established. Additionally, other PtdIns(3)P-producing activities which differ from known enzymes in terms of inhibitor sensitivities have been reported to exist.

Dephosphorylation of PtdIns(3)P

PtdIns(3)P may be converted back to phosphatidylinositol by the action of a 3-phosphatase, an enzyme which catalyses the hydrolysis of the phosphate group on the 3′ position of the inositol ring. A number of

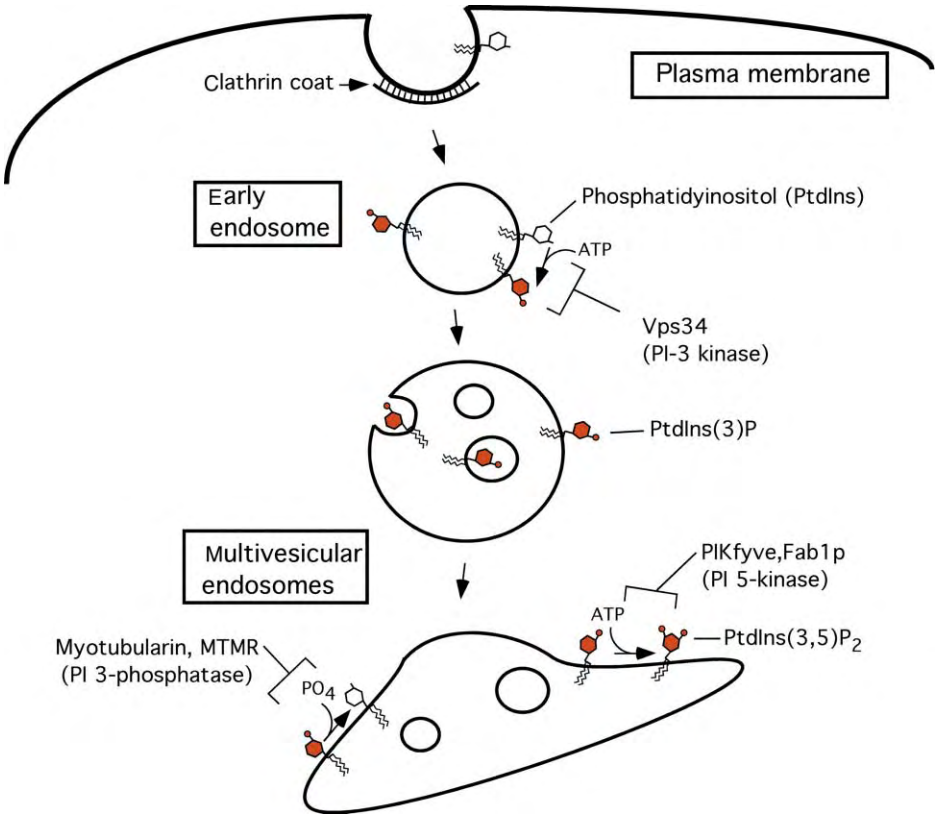

FIGURE 1 Production and turnover of PtdIns(3)P in endosomal membranes. In the process known as endocytosis patches of plasma membrane invaginate as the result of formation of clathrin coats. Subsequent scission from the plasma membrane and uncoating of these vesicles produce early endosomes where PtdIns(3)P is produced by the Vps34 PI 3-kinase. PtdIns(3)P also persists on the limiting membrane as well as intralumenal vesicles of the multivesicular endosome, a product of fusion of early endosomes. During subsequent maturation, the PtdIns(3)P may be hydrolyzed by the action of myotubularin family PI- phosphatases, or further phosphorylated by the PIKfyve/Fab1p PI 5-kinases to produce PtdIns(3,5)P2. These reactions may also take place in the intralumenal vesicles.

phosphoinositide phosphatases have been characterized in yeast and mammalian systems, but to date, activity against PtdIns(3)P has been attributed only to members of the myotubularin family. This family consists of at least 12 genes in humans with one putative homologue in yeast. Of the human proteins, eight have functional phosphatase domains, the others have similar protein sequences but apparently no catalytic activity. These proteins also have potential phosphoinositide-binding PH domains while two have FYVE domains likely to specifically target PtdIns(3)P. Details regarding the activity of myotubularin proteins in cells have yet to be reported. However, mutations in a number of human myotubularin genes have been linked to neuromuscular diseases pointing to significant roles in development or function of neural and muscle tissues.

Phosphorylation of PtdIns(3)P

In addition to hydrolysis of the 3-phosphate group by phosphatases, PtdIns(3)P levels may be modulated by additional phosphorylation. Recently, it was shown that significant levels of PtdIns(3,5)P_2 are present in yeast and mammalian cells. This phosphoinositide appears to be formed primarily by phosphorylation of PtdIns(3)P at the 5′ position of the inositol ring. The Fab1 protein of yeast and a mammalian homologue called PIKfyve possess this enzymatic activity. Both of these proteins are also able to bind specifically to PtdIns(3)P via a FYVE domain. Conversion of PtdIns(3)P to PtdIns(3,5)P_2 would serve to terminate PtdIns(3)P-dependent cellular functions, but may also contribute to cellular responses to osmotic stress or other signals as well as to maturation of endosomes. The relative contribution of phosphorylation versus hydrolysis to PtdIns(3)P turnover is as yet undetermined.

Molecular Targets and Cellular Functions of PtdIns(3)P

Protein Domains that Bind to PtdIns(3)P

Two structurally unrelated protein domains have been shown to bind to PtdIns(3)P. The first to be discovered

was the FYVE domain (named for the first four proteins in which it was recognized, Fab1p, YOTB, Vac1p, and EEA1). The domain is characterized by a RING finger structure which binds two Zn molecules. It is found in five yeast proteins and ~30 human proteins. Binding of FYVE domains to PtdIns(3)P-containing membranes relies on a combination of nonspecific membrane interactions and a groove which specifically accommodates the phosphate group of PtdIns(3)P while sterically excluding other phosphoinositide head groups. To date all FYVE domains studied bind exclusively to PtdIns(3)P.

The phox homology (PX) domain was first recognized in two components of the phagocyte NADPH oxidase (phox) complex (p40phox and p47phox). It is structurally unrelated to the FYVE domain except for a somewhat similar binding pocket which accommodates the inositol 3-phosphate head group. However, comparison of the crystal structures of the p40phox PX domain bound to dibutanoyl PtdIns(3)P and the FYVE domain of early endosome antigen-1(EEA1) bound to the head group inositol 1,3bisphosphate indicates that both proteins utilize basic residues to bind both phosphate and hydroxyl groups in the lipid head group. All 15 PX domains in yeast bind PtdIns(3)P with varying affinities. Of the mammalian proteins characterized, many bind PtdIns(3)P strongly, while several have lower affinity for other, and in some cases several, phosphoinositides.

PtdIns(3)P-Binding Proteins in Endosomal Membrane Trafficking

In accordance with the predominant localization of PtdIns(3)P to membranes of the endosomal system, several PtdIns(3)P binding proteins have been shown to function in various steps of endosome fusion, sorting, and maturation (Table I). In mammalian cells, a major function of these events is to direct membrane components to the lysosome whereas sorting of proteins to the vacuole is a major function in yeast.

Following internalization of plasma membrane patches to form small membrane vesicles denoted as early endosomes, a process of maturation is initiated which involves fusion of early endosomes into larger multivesicular bodies. These multivesicular bodies form specialized subdomains marked by the recruitment of different sets of proteins. Eventually these specialized domains and their cargo proteins form new compartments, which may then be returned to the plasma membrane or delivered to lysosomes or the trans-Golgi complex. This process is controlled in part by various members of the small GTPase Rab family. Rab5 in particular is required for fusion of early endosomes and it accomplishes this in part by stimulating the production of PtdIns(3)P via Vps34, with the resulting recruitment of PtdIns(3)P-binding proteins to the endosomes. Such proteins include EEA1 and rabenosyn-5, which both bind Rab5 itself as well as PtdIns(3)P via a FYVE domain. Once recruited to the endosome through these mechanisms, EEA1 and rabenosyn-5 appear to function in the tethering, docking, and ultimate fusion of early endosomes.

The sorting nexin (SNX) family containing up to 25 human proteins and the yeast homologues Mvp1p, Vps5p, Vps17p, and Grd19p all contain a PX domain. All of the yeast SNX proteins and some of the mammalian counterparts have been found to bind preferentially or specifically to PtdIns(3)P, and most characterized SNX proteins localize at least partially to endosomes. Consistent with the importance of PtdIns(3)P in vacuolar protein sorting in yeast, Vps5p and Vps17p have a role in the retrieval of the vacuolar protein sorting receptor Vps10p while Mvp1p and Grd19 participate in Golgi to vacuole trafficking. In mammalian cells, roles of the various SNX proteins are being assigned, and the emerging picture suggests that different sorting nexins may be required for regulating the distinct fates of endosomes, i.e., recycling to the cell surface, delivery to lysosomes, or delivery to the trans Golgi.

TABLE I

Cellular Functions of PtdIns(3)P and some Associated Proteins

Cellular function	Domain	PtdIns(3)P-binding proteins
Endosome fusion/maturation	FYVE	EEA1, rabenosyn-5, PIKfyve/Fab1p
Golgi-vacuole trafficking (yeast)	FYVE	Vps27p, Vac1p, Fab1p
	PX	Grd19p, Mvp1p, Vps5p, Vam7p
Receptor sorting/ targeting to lysosome	FYVE	Hrs
	PX	Sorting nexins
Signal transduction	FYVE	SARA
	PX	CISK
Phagosome function/maturation	FYVE	EEA1
	PX	$p40^{phox}$

PtdIns(3)P in Phagocytosis and Bacterial Invasion

Many of the PtdIns(3)P-binding proteins involved in the endocytic process are likely involved in the similar processes of phagocytosis and host cell invasion by bacteria and parasites. Phagosomes, like endosomes, form by invagination of patches of the plasma membrane followed by "pinching off" and sealing to form a

self-contained intracellular compartment. PtdIns(3)P appears transiently on phagosomes in a manner which parallels its appearance and disappearance in endosomes. Phagosomal PtdIns(3)P is apparently generated by the targeting and activation of the VPS34 PI 3-kinase. As in early endosomes, the PtdIns(3)P synthesized in phagosomes recruits FYVE- and PX-domain containing proteins including EEA1. Likewise, in the process of secretion-mediated invasion by *Salmonella*, the membrane vacuole which envelops the invading bacterial cells accumulates PtdIns(3)P. In certain cell types, recruitment of the NADPH oxidase to phagosomes may occur via PX domains in its p40 and p47 subunits. This mechanism may contribute to defense against pathogens since the NADPH oxidase produces reactive oxygen species toxic to invading bacterial cells. Disruption of this recruitment mechanism by pathogenic bacteria enhances their ability to escape host cell defenses.

PtdIns(3)P and Signaling from the Endosomal System

Recently it has become clear that the endosomal system is an essential component of signal transduction pathways regulating proliferation, survival, differentiation, and stress responses. Current evidence suggests that growth factor receptors, many of which are internalized into endosomes following binding of their ligands, can continue to generate signals to downstream effectors as they transit through the endosomal system. Furthermore, internalization and delivery of such receptors to lysosomes for degradation is an important mechanism for down-regulation of signaling in a variety of systems.

The FYVE-domain protein, SARA, localizes to early endosomes via its association with PtdIns(3)P. SARA also binds to Smad2, a downstream target of the transforming growth factor-β (TGFβ) receptor. Association of the SARA–Smad complex appears to be essential for efficient phosphorylation of Smad by the internalized receptor. Thus, PtdIns(3)P in endosomes can serve to assemble signaling complexes in which the local concentration of components is increased by association with specific intracellular membranes. The FYVE domain-containing protein homologue of the yeast protein Vps27p (Hrs) may function in a similar manner in the TGFβ signaling pathway. However, in other systems, Hrs may promote the internalization and ultimate degradation of growth factor receptors. Thus, there is precedent for the involvement of PtdIns(3)P-binding proteins in attenuation as well as enhancement of growth factor signals.

Endosomal localization via PtdIns(3)P binding may also serve to target or sequester components of signaling pathways several steps removed from the initial receptor signal. The PX domain-containing protein kinase CISK (also denoted SGK3) is localized to endosomes and may function in this way. Like its related family members Akt and SGK, CISK is activated by regulatory protein kinases in response to growth factor-mediated regulation of PI 3-kinases that produce PtdIns(3,4,5)P_3. Based on its endosomal disposition, it seems likely that the substrates of the CISK protein kinase are similarly localized. CISK may function to attenuate apoptosis or to promote other processes yet to be discovered based on this unique association with the endosomal compartment.

PtdIns(3)P may also serve as a component of the cellular stress response. In yeast and mammalian cells, PtdIns(3,5)P_2 is formed in response to osmotic stress by the FYVE-domain proteins Fab1p and PIKFYVE, respectively. Effectors of PtdIns(3,5)P specific for this function have not been identified.

See Also the Following Articles

Inositol Lipid 3-Phosphatases • Inositol Phosphate Kinases and Phosphatases • Phosphatidylinositol Bisphosphate and Trisphosphate • Phosphoinositide 4- and 5-Kinases and Phosphatases • Phosphoinositide-Dependent Protein Kinases

Glossary

endocytosis The process by which regions of plasma membrane and any embedded proteins are brought inside the cell by formation of a membrane-bound intracellular vesicle.

endosome The membrane-bound intracellular vesicle formed by the process of endocytosis.

phagocytosis Uptake of particles such as cell fragments or bacteria by engulfing and then internalizing them in a membrane vesicle.

phagosome The membrane-bound intracellular vesicle formed by the process of phagocytosis.

phosphatidylinositol (PtdIns) A membrane lipid consisting of a pair of membrane embedded fatty acid chains linked to a surface-exposed inositol head group. The hydroxyl groups of the inositol may be phosphorylated by PI kinases at the 3′, 4′, and 5′ positions.

Further Reading

Brumell, J. H., and Grinstein, S. (2003). Role of lipid-mediated signal transduction in bacterial internalization. *Cell. Microbiol.* **5**, 287–297.

Corvera, S. (2001). Phosphatidylinositol 3-kinase and the control of endosome dynamics: New players defined by structural motifs. *Traffic* **2**, 859–866.

Czech, M. P. (2003). Dynamics of phosphoinositides in membrane retrieval and insertion. *Annu. Rev. Physiol.* **65**, 791–815.

Ellson, C. D., Andrews, S., Stephens, L. R., and Hawkins, P. T. (2002). The PX domain: A new phosphoinositide-binding module. *J. Cell Sci.* **115**, 1099–1105.

Lemmon, M. A. (2003). Phosphoinositide recognition domains. *Traffic* **4**, 201–213.

Misra, S., Miller, G. J., and Hurley, J. H. (2001). Recognizing phosphatidylinositol 3-phosphate. *Cell* **107**, 559–562.

Raiborg, C., Rusten, T. E., and Stenmark, H. (2003). Protein sorting into multivesicular endosomes. *Curr. Opin. Cell Biol.* **15**, 446–455.

Stenmark, H., Aasland, R., and Driscoll, P. C. (2002). The phosphatidylinositol 3-phosphate-binding FYVE finger. *FEBS Lett.* **20**, 77–84.

Wishart, M. J., and Dixon, J. E. (2002). PTEN and myotubularin phosphatases: From 3-phosphoinositide dephosphorylation to disease. *Trends Cell Biol.* **12**, 579–585.

Worby, C. A., and Dixon, J. E. (2003). Sorting out the functions of sorting nexins. *Nat. Rev. Mol. Cell Biol.* **3**, 919–931.

Biography

Joseph Virbasius is an Assistant Professor and Dr. Michael Czech is a Professor and Chair of Molecular Medicine at the University of Massachusetts Medical School in Worcester. Their research interests include molecular mechanisms of insulin action and functions of PI 3-kinase and its downstream effectors in insulin-responsive cells. Dr. Virbasius holds a Ph.D. from Northwestern University and served as a postdoctoral fellow at the University of Massachusetts Medical School.

Michael Czech holds a Ph.D. from Brown University. He was a postdoctoral fellow in the Department of Biochemistry at Duke University Medical School from 1972 to 1974 and was a Professor of physiological chemistry at Brown University before coming to the University of Massachusetts Medical School as Chair of the Department of Biochemistry and Molecular Biology in 1981.

Phosphofructokinase-2/Fructose Bisphosphatase-2

Daniel M. Raben
The Johns Hopkins University School of Medicine, Baltimore, Maryland, USA

6-Phosphofructo-2-kinase/fructose-2,6-bisphosphatase (PFK-2/FBPase-2) is a bifunctional enzyme wherein a single polypeptide chain contains two enzymatic activities—PFK-2 and FBPase-2. PFK-2 catalyzes the transfer of phosphate from ATP to the second carbon (C-2) of fructose-6-phosphate (F6P), an intermediate in the glycolytic pathway, generating fructose-2, 6-bisphosphate (F2,6BP). Conversely, FBPase-2 catalyzes the dephosphorylation of F2,6BP resulting in the liberation of free inorganic phosphate and regeneration of F6P. In this manner, these two physically linked enzymes function to modulate the cellular concentration of F2,6BP. The importance of this regulation cannot be overstated as this sugar plays an essential signaling role in regulating glucose metabolism in a variety of tissues. Perhaps most importantly, it is largely responsible for regulating the balance between glycolysis and gluconeogenesis in the liver. This balance, critical for maintaining blood glucose levels within the normal range regardless of the nutritional state, principally results from the fact that F2,6BP activates a key regulatory glycolytic enzyme, PFK-1 (6-phosphofructo-1-kinase) and inhibits a regulatory enzyme in gluconeogenesis, FBPase-1 (fructose-1,6-bisphosphatase). Therefore, in the liver, when F2,6BP levels are high, glycolysis predominates and when F2,6BP levels are low, gluconeogenesis predominates. In other tissues, F2,6BP levels mainly serve to help regulate glycolytic flux. By regulating the level of this phosphorylated sugar, PFK-2/FBPase-2 activities play a central role in maintaining glucose homeostasis and utilization.

Discovery of PFK-2/FBPase-2

As with many discoveries, the identification of PFK-2/FBPase-2 was preceded by the discovery of its product F2,6BP. This sugar was first identified as the mediator responsible for stimulating hepatic gluconeogenesis. It had been known for some time that gluconeogenesis was induced in liver by elevated levels of glucagon. Emil van Shaftingen and Henri-Gery Hers demonstrated that rat liver lysates contained an acid-labile phosphoric acid ester that greatly stimulated PFK-1. The concentration of this compound in isolated hepatocytes was significantly increased by glucose and decreased by glucagon. They also showed that this molecule was F2,6BP. Following this discovery, Hers and Uyeda identified PFK-2/FBPase-2 in rat liver as the bifunctional enzyme responsible for the generation and degradation of F2,6BP.

General Structure of PFK-2/FBPase-2

In mammalian tissues, PFK-2/FBPase-2 is a single protein with the PFK-2 activity located at the N-terminal end and the FBPase-2 located at the C terminus. Structural analyses demonstrated that the catalytic domains are flanked by regulatory regions at both the N and C termini. The enzyme functions as a dimer with protein–protein contacts being made at the regulatory regions at the N terminus only. In contrast to this structure, the yeast PFK-2 and FBPase-2 enzymes are separate proteins, but most likely function as dimers.

Enzymology of PFK-2

While PFK-2 shares the same substrate as PFK-1, F6P, the reaction catalyzed by PFK-2 differs from that catalyzed by PFK-1 in four important aspects. First, PFK-1 catalyzes the transfer of the γ-phosphate of ATP to C-1 of F6P generating F1,6BP while PFK-2 catalyzes the transfer of this ATP phosphate to C-2 yielding F2,6BP. Second, PFK-1 is an α-anomer while PFK-2 prefers the β-anomer. Third, PFK-1 is strongly inhibited by ATP while PFK-2 is not sensitive to this nucleotide. Finally, PFK-2 is inhibited by both of its products, ADP and F2,6BP, which are activators of PFK-1.

The complete catalytic mechanism of PFK-2-mediated phosphorylation of F6P has not been elucidated. Important features of the reaction have, however, been identified. In general, PFK-2 activity is much

weaker than that of PFK-1. This may be due to the fact that specific residues involved in accelerating catalysis in PFK-1 are absent in PFK-2. The pH optimum of the enzyme-catalyzed reaction is between 8 and 9, requires magnesium, and prefers ATP as the phosphate donor, but will also use GTP. Inhibition studies indicate that the PFK-2-mediated transfer of phosphate from ATP to F6P occurs via a sequential-ordered mechanism with ATP binding prior to F6P binding. Binding sites for ATP and F6P have been identified as well as residues critical for catalysis.

Enzymology of FBPase-2

Much more is known about the reaction mechanism used for FBPase-2-mediated hydrolysis. The enzyme has a pH optimum between 5.5 and 6.5 and does not require divalent cations. FBPase-2 specifically hydrolyzes the phosphate on carbon 2 (C-2) of F2,6BP and will not hydrolyze C-6 of either F2,6BP, F1,6BP or glucose-1,6-bisphosphate. However, it is inhibited by both its substrate and product—F6P and F2,6BP. Interestingly, the FBPase-2 reaction mechanism involves an intermediate in which F6P is covalently bound to a histidine residue on the enzyme. This covalent intermediate has been useful in structural studies designed to elucidate the reaction mechanism, which appears to resemble, but is not identical to, the mechanism used by serine proteases. Both involve a "catalytic triad" in which three residues work together to form an intermediate in which the substrate is covalently bound to the enzyme followed by hydrolysis of this intermediate to release the product from the enzyme. In the case of serine proteases, a serine residue on the enzyme is covalently bound to the catalytic intermediate while in FBPase-2 a phosphohistidine is formed and F6P is released. The dissociation of the F6P product appears to be the rate-limiting step.

Isoforms of PFK-2/FBPase-2

Since the discovery of PFK-2/FBPase-2 mammalian tissues, a number of mammalian isoforms have been identified from four genes, which include alternatively spliced products. In all isoforms, the catalytic domains are highly conserved while the N and C termini are most divergent. Most tissues contain varying amounts of different isoforms, with one isoform predominating. For example, in liver ~10% of the total PFK-2/FBPase-2 is the skeletal muscle isoform. Even within the predominant liver isoform there are two different species, a 54–55 kDa species and a 58 kDa species with only the 58 kDa species being regulated by phosphorylation. In addition to these mammalian isoforms, yeast contain PFK-2 and FBPase-2 activities, but in this case the enzymes are monomeric although they likely work as dimers.

In addition to sequence differences, kinetic properties of the kinase and bisphosphatase activities also differ among the various isoforms. While the substrate affinities (measured as a K_m) and maximum velocities (V_{max}) vary between isoforms, there are some notable differences. Comparison of bovine brain, liver, and testes shows that these isoforms have similar kinetic properties for PFK-2 in terms of K_m for F6P, but the liver and muscle FBPase-2 enzymes have K_m values for F2,6BP that are approximately 100- to 1000-fold lower than the other isoforms. Based on V_{max}, the skeletal muscle also appears to have the lowest kinase activity and high-phosphatase activity, while the placental isoform has the highest kinase activity with very low-phosphatase activity.

Regulation and Physiological Roles of Specific Isoforms in Specific Tissues

PFK-2/FBPase-2 is exquisitely poised to regulate the levels of F2,6BP. F6P exerts a substrate level control over PFK-2 and is a product inhibitor of FBPase-2. The K_m of PFK-2 and K_i of FBPase-2 for F6P are within the physiological concentration ranges of this phosphorylated sugar in different tissues suggesting that small changes in the levels of F6P result in significant reciprocal alterations in these two enzymatic activities. Such alterations have different effects in different tissues, depending on the isoforms and relative level of the endogenous PFK-2/FBPase-2 activities.

Perhaps the best-studied form of PFK-2/FBPase-2 regulation involves the phosphorylation of the enzyme. Both the liver and heart isozymes are subject to regulation by phosphorylation. The brain isoform is phosphorylated, but this phosphorylation does not appear to affect enzymatic activities. Muscle and testis isoforms are not phosphorylated. A liver isoform (58 kDa) was the first one shown to be regulated by a PKA (protein kinase A)-mediated phosphorylation stimulated by the glucagon-induced second-messenger cyclic AMP (cAMP). Further studies showed that PFK-2/FBPase-2 is phosphorylated on a specific serine residue, serine-32, near the N terminus. This phosphorylation leads to inhibition of PKF-2 and activation of FBPase-2. For PFK-2 at physiological pH, this is primarily due to an increase in the K_m (i.e., lower affinity) for F6P, without affecting the K_m for ATP, and only slightly perturbing V_{max}. In contrast, this phosphorylation activates FBPase-2 by increasing the V_{max} of the enzyme without affecting the K_m for F2,6BP. It is believed that this effect is largely due to an increase in

the rate of F6P dissociation from FBPase-2, which enhances the rate at which the phosphohistidine intermediate is hydrolyzed. Consistent with the critical role of this enzyme in regulating liver carbohydrate metabolism, phosphorylation of the enzyme can be reversed by specific, regulated protein phosphatases (protein phosphatase 2A and 2C), which serves to activate PFK-2 while inhibiting FBPase-2. On the other hand, phosphorylation of the heart isoform modulates only the PFK-2 activity without affecting FBPase-2. Importantly, in stark contrast to the liver isoform, phosphorylation of the heart isoform activates PFK-2. In bovine and rat hearts, phosphorylation lowers the K_m (i.e., increases the affinity) for F6P. The bovine heart isoform may be phosphorylated by PKA, and the rat heart isoform can be phosphorylated and modulated by either PKA or the calcium/calmodulin-dependent protein kinase.

The fact that PKF-2 and FBPase-2 are located near the N and C termini respectively, on the same polypeptide begs the question as to how both activities of the liver enzyme are affected by a phosphorylation near the N terminus. While the exact mechanism underlying the reciprocal regulation of these two activities has not been resolved, a current view is that in the nonphosphorylated state, the N termini of two polypeptides interact and activate the kinase while the C-terminal regions are separated (Figure 1). This is consistent with the crystal structure of the rat testis PFK-2/FBPase-2. Phosphorylation is believed to induce a conformational change in the enzyme resulting in the separation of the N termini, which inactivates the kinase while activating the phosphatase.

The above regulation provides for short-term, acute regulation for rapid, transient responses. The enzyme is also subject to long-term regulation mediated by gene expression. Both insulin and dexamethazone stimulate an increase in the level of PFK-2/FBPase-2 gene expression. Consistent with this, levels of liver PFK-2/FBPase-2 are depressed during starvation or diabetes and increase upon re-feeding or administration of insulin, respectively. Additionally, levels of PFK-2/FBPase-2 decrease following partial hepatectomy and increase during liver regeneration.

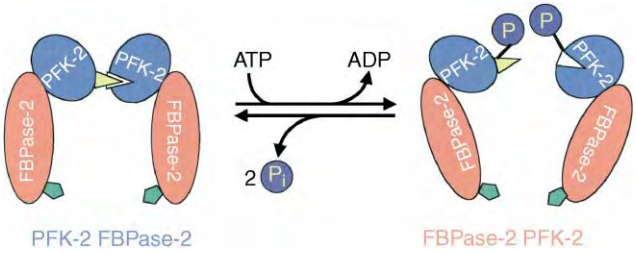

FIGURE 1 Reciprocal regulation of dimeric PFK-2/FBPase-2 in liver by phosphorylation. The blue indicates the N-terminal region containing PFK-2 activity and the red indicates the C terminus containing the FBPase-2 activity. The triangle at the N terminus and the pentagon at the C terminus represent regulatory regions.

The differences in isoforms and their regulation suggest different roles for each isoform. This is most dramatically seen when comparing the regulation of the liver isoform with that of the heart isoform. Liver not only consumes energy, it also stores energy mainly in the form of glycogen. It is also the only tissue, besides kidney to a small extent, which engages in gluconeogenesis to supply glucose to other glucose-dependent tissues in times of need. In that, as previously mentioned, the liver isoform is exquisitely poised to reciprocally regulate the level and activities of PFK-2/FBPase-2. This regulation is sensitive to glucose levels or hormones involved in regulating carbohydrate metabolism such as insulin, which stimulates glycolysis, and glucagons, which induces gluconeogenesis. On the other hand, heart muscle is a constant energy-consuming tissue, and, therefore, engages in glycolysis but not gluconeogenesis. Indeed, the heart does not respond to glucagon but does respond to another hormone that signals through PKA, epinephrine (adrenaline). Therefore, it is not surprising that the regulated heart isoform of PFK-2/FBPase-2 responds to phosphorylation by increasing PFK-2 activity, as this hormone would signal a need for increased glycolytic flux. The increased PFK-2 activity would lead to an increase in F2,6BP levels, thereby increasing glycolysis via activation of PFK-1. The regulation of liver and heart isoforms exemplifies how differential regulation of specific isoforms can serve different roles depending on the needs of various tissues in which they are expressed. This further illuminates the significant role PFK-2/FBPase-2 plays in appropriately regulating carbohydrate metabolism.

See Also the Following Articles

Enzyme Reaction Mechanisms: Stereochemistry • Glucagon Family of Peptides and their Receptors • Glycolysis, Overview • Pyruvate Carboxylation, Transamination and Gluconeogenesis

Glossary

anomer Stereoisomer (diastereoisomer) of sugars which differ with respect to their configuration about their anomeric carbon. The anomeric carbon is the carbon which forms a new stereocenter, when the sugar cyclizes on the former carbonyl carbon. The configuration may be α or β.

ATP Adenosine triphosphate, a molecule consisting of the nitrogenous base adenine linked to the sugar ribose, and containing three phosphate groups attached to the ribose. ATP, present in all living cells, serves as the principal energy source of energy for cells.

cAMP Cyclic adenosine monophosphate, a cyclic form of adenosine monophosphate where a single phosphate is attached to both

the third and fifth carbon of the ribose sugar linked to adenine. It is important in transmitting intracellular, as well as extracellular, signals induced by many agonists. cAMP binds to and activates the cAMP-dependent protein kinase, PKA.

gluconeogenesis The synthesis of glucose from noncarbohydrate sources occurring primarily in the liver and to a small extent in the kidney. It is stimulated during starvation or intense exercise.

glycolysis (glycolytic pathway) The anaerobic metabolism of glucose to pyruvate. This metabolism generates two molecules of ATP and one molecule of NADH per glucose molecule. The NADH may be used to generate energy in the form of ATP and the pyruvate may enter the tricarboxylic acid cycle to yield NADH for energy production under aerobic conditions.

GTP Guanosine triphosphate, a molecule consisting of the nitrogenous base, guanine, linked to the sugar ribose. The ribose contains three phosphate groups attached to the 5′ carbon. GTP is another source of metabolic energy and is involved in protein synthesis and a number of signal transduction cascades.

K_m A kinetic parameter that indicates the affinity of an enzyme for its substrate and often called the "Michaelis constant." It is defined as the concentration of substrate that results in half the maximal rate (V_{max}) of the enzyme-catalyzed reaction.

protein kinase A (PKA) An enzyme that catalyzes the phosphorylation of proteins on specific serine or theronine residues in response to cAMP.

V_{max} The maximal initial velocity of an enzyme-catalyzed reaction that occurs at saturating substrate concentrations.

Further Reading

Kurland, I. J., and Pilkis, S. J. (1995). Covalent control of 6-phosphofructo-2-kinase/fructose-2,6-bisphosphatase: Insights into autoregulation of a bifunctional enzyme. *Protein Sci.* **4**(6), 1023–1037.

Okar, D. A., Manzano, A., Navarro-Sabate, A., Riera, L., Bartrons, R., and Lange, A. J. (2001). PFK-2/FBPase-2: Maker and breaker of the essential biofactor fructose-2,6-bisphosphate. *TIBS* **26**(1), 30–35.

Pilkis, S. J., el-Maghrabi, M. R., and Claus, T. H. (1988). Hormonal regulation of hepatic gluconeogenesis and glycolysis. *Annu. Rev. Biochem.* **57**, 755–783.

Pilkis, S. J., Claus, T. H., Kurland, I. J., and Lange, A. J. (1995). 6-Phosphofructo-2-kinase/fructose-2,6-bisphosphatase: A metabolic signaling enzyme. *Annu. Rev. Biochem.* **64**, 799–835.

Biography

Daniel M. Raben is an Associate Professor in the Department of Biological Chemistry at the Johns Hopkins University School of Medicine. His principal research interests are in the broad fields of lipid biochemistry and chemistry, and signal transduction. He holds a Ph.D. from Washington University in St. Louis, Missouri and received his postdoctoral training at the University of California at Irvine. He is a well-published investigator, including several review articles on lipid-mediated signal transduction, and is on the editorial board of a number of biochemical journals.

Phosphoinositide 3-Kinase

Khatereh Ahmadi
PIramed Ltd., UK

Michael Waterfield
Ludwig Institute for Cancer Research, London, UK

The phosphoinositide 3-kinases (PI 3-kinases) are enzymes with intrinsic lipid kinase activity whose substrates are membrane phosphatidylinositol lipids. When activated by cell surface receptors, such as those that recognize growth factors, PI 3-kinases generate a PIP3 (phosphatidylinositol 3,4,5-triphosphate) second messenger lipid that binds and activates at the membrane, enzymes that control signal networks which control the life, death, and differentiated functions of cells. The loss of control of PI 3-kinase activity has been shown to be instrumental in causation or maintenance of major human diseases such as cancer, diabetes, and inflammation.

Identification of PI 3-Kinases as Signaling Molecules: A Historical Perspective

Signal transduction enables cells to communicate with each other and respond to their external environment through receptors on cell surfaces, which are activated by external ligands such as growth factors. Receptors send signals to the internal control systems of the cell and to internal organelles such as the mitochondria and the nucleus via a series of molecular cascades known as signaling pathways.

In the early 1990s, it was shown that ligand activation of receptors that have intrinsic tyrosine kinases (TK) causes autophosphorylation at specific sites on their kinase domains, initiating the formation of a signaling complex. Phosphoinositide (PI) 3-kinase activity was first found associated with the transforming complex of middle-T (mT) antigen and pp60c-src from polyoma virus-transformed cells and subsequently with the PDGF (platelet-derived growth factor) receptor, mediated by amino acid recognition sites around specific tyrosine residues. Since then it has become clear that PI 3-kinases are recruited to almost every receptor complex, including activated oncogenes and growth factor receptors, as well as heterotrimeric G proteins, a key effector of activated receptors.

PI 3-Kinases Phosphorylate Lipids

The discovery that the main product of these transforming protein-associated kinases was a PI that had a phosphate group on the D3 position of the inositol ring added a new second messenger to the armory of specific signal molecules used by cells. Three distinct signal molecules that are phosphorylated on the 3 position of the inositol ring can be generated by three classes of PI 3-kinase from specific phosphoinositol substrates. The signal molecules formed are phosphatidylinositol 3-phosphate or PI3P, PI(3,4)P2, and PI(3,4,5)P3 (see Figure 1).

A wide variety of receptor-mediated stimuli can lead to the rapid production of PI(3,4)P2 and PI(3,4,5)P3 in cells, whereas the intracellular levels of PI3P seem mostly unaffected by external cell stimulation. PI3P is used for internal cellular protein trafficking. The hydrolysis of these lipids occurs through the action of lipid phosphatases that remove the three phosphate groups from the inositol ring, thus regulating PI 3-kinase activity. The lipid signaling pathway initiated by PI 3-kinase is distinct from the classical pathway in which activation of phospholipase C causes to production of Ins(1,4,5)P3 and diacylglycerol, ultimately leading to mobilization of calcium and activation of protein kinase C.

Activation and Regulation of PI 3-Kinases

PI 3-kinase was first purified from bovine brain tissue as a lipid kinase activity and was shown, through a classical series of systematic biochemical analyses, followed by molecular cloning and expression of the recombinant proteins, to be a heterodimeric enzyme containing a

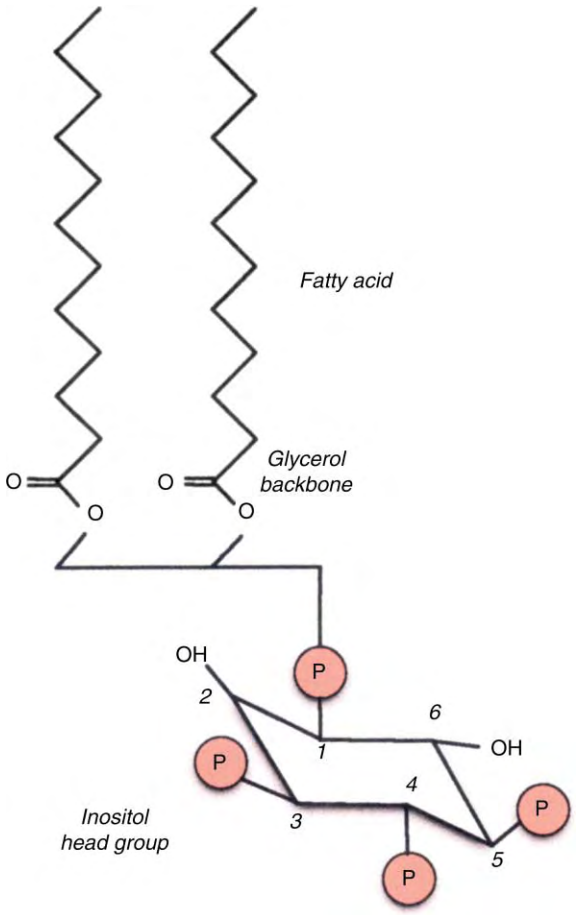

FIGURE 1 The signal molecule phosphatidylinositol 3-phosphate (PI 3-phosphate or PIP3).

110 kDa catalytic subunit (p110), and an 85 kDa adaptor subunit (p85). The primary structures of the p85 and p110 subunits were revealed through cDNA cloning using protein sequence data, thus shedding light on the mode of interaction between p85 and tyrosine phosphorylated proteins. The p85 subunit contains an N-terminal (src homology) SH3 domain, which binds to proline-rich sequences and two SH2 domains separated by an inter SH2 domain. SH2 domains have been found in many signaling proteins and bind phosphotyrosine residues within a specific polypeptide context, YXXM, where Y is a tyrosine, M is a methionine, and X can be any amino acid. The adaptor subunit also contains a breakpoint cluster region homology (BH) domain. These distinct functional domains make p85 an important interactive protein with a major regulatory role.

The p110 subunit was shown to contain an ATP-binding site, which is responsible for the catalytic activity of the enzyme. More recently the three-dimensional structure of a p110 (gamma) subunit revealed a modular structure comprising a Ras-binding domain (RBD), a C2 domain, a helical domain, and a catalytic domain. This structure has been invaluable in rationalizing the allosteric activation and regulation of PI 3-kinase, its ability to bind membranes, and its substrate specificity.

PI 3-kinases are recruited to activated receptors directly or to associated substrate scaffold molecules such as Grb3 or Shc through the binding of the SH2 domains of the p85 subunit to phosphorylated tyrosine residues. The current paradigm for the activation of PI 3-kinase is that interaction with the receptor brings the enzyme into close proximity to the membrane that contains the lipid substrates of PI 3-kinase. The p110 catalytic subunit is thus able to phosphorylate the lipids, which then act as second messengers, initiating a cellular signal that is carried to the cytoplasm, mitochondrion, or nucleus through a cascade of signaling molecules.

Down-Regulation of PI 3-Kinase Activity

The phosphatases SHIP (SH2 domain-containing inositol 5-phosphatase) and PTEN (phosphatase and tensin homologue deleted on chromosome 10) play a role in down-regulating PI 3-kinase activity by removing phosphate groups from the 3-phosphorylated lipid products of the enzyme. PTEN was identified as a tumor suppressor and tyrosine phosphatase. PTEN is now known to be the second most commonly mutated gene in all human cancers. SHIPs remove phosphate groups from the 5 position of the inositol ring and bind to diverse receptors and adaptor molecules.

PI 3-Kinases are a Family of Enzymes

Once the importance of PI 3-kinases in cell physiology was realized, several groups set out to purify and characterize PI-3 kinases from a variety of tissues. Eight PI 3-kinase isoforms are now known; they are divided into three classes based on their structure and *in vitro* substrate specificity.

Class I PI 3-Kinases

The class I molecules can use PI, PI(4)P, or PI(4,5)P2 as substrates *in vitro*. However, *in vivo*, they show a strong preference for PI(4,5)P2. The class I enzyme subtypes have been subdivided into class Ia and class Ib based on their mode of regulation (see Figure 2). The class Ia enzymes consist of three isoforms, p110α, p110β, and p110, which are encoded by three separate genes. The class Ia enzymes use p85 as their adaptor subunit, but this has at least seven adaptor variants, which are the alternative spliced products of three separate genes,

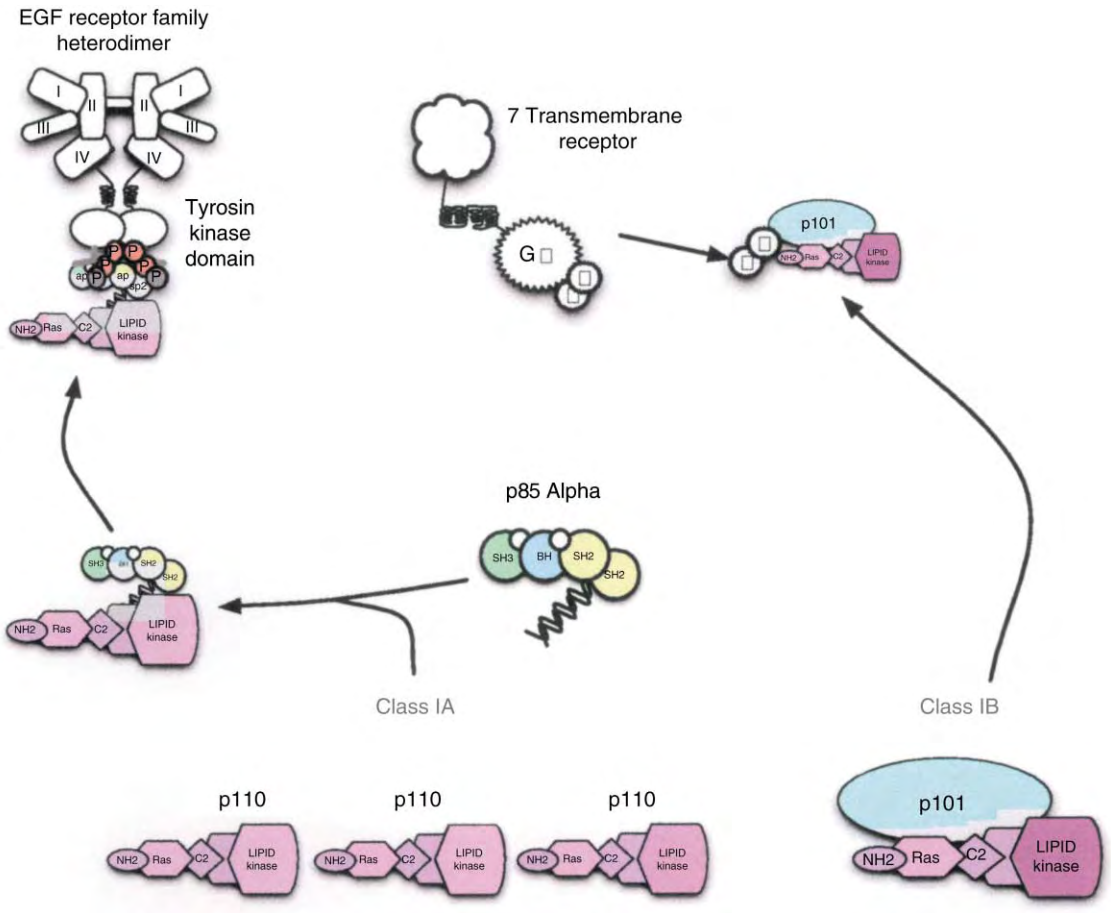

FIGURE 2 The class I PI 3-kinases are divided into groups Ia and Ib. Group 1a includes three catalytic subunits, p110α, β, and δ, which form heterodimers with their regulatory subunit p85. Class Ib includes the PI 3-kinase γ, which associates with the protein p101. The PI 3-kinases have amino-terminal (NH_2), Ras-binding, C2, and lipid kinase domains. The regulatory subunit p85 has an SH2 (src homology) region, which binds to phosphorylated sequences on growth factor receptors such as those of the EGF (epidermal growth factor) family, SH3, and BH domains. The PI 3-kinase γ is activated by G protein $\beta\gamma$ subunits that are released by signals from seven transmembrane receptors.

namely, p85α, p85β, and p55γ. The p110α and p110β subtypes are expressed ubiquitously, whereas p110δ has an expression pattern that is mainly restricted to hematopoietic cells. All mammalian cell types studied express at least one class Ia PI 3-kinase isoform class Ia PI 3-kinases are conserved in evolution and have been found and studied in *Drosophila melanogaster, Caenorhabditis elegans*, and *Dictyostelium discoideum*, as well as more recently in transgenic mice, with dramatic results.

Only one class Ib isoform exists, p110γ, which is activated by G protein-coupled receptors by binding to the G$\beta\gamma$ subunits of heterotrimeric G proteins. The p110γ catalytic subunit does not partner with the p85 adaptor subunits; instead, it forms a complex with a 101 kDa regulatory protein known as p101, which is not homologous to any known protein. The role of p101 is unresolved, although it may be involved in the interaction with G$\beta\gamma$. The p110γ/p101 complex has only been found in mammals and has a tissue distribution mainly restricted to hematopoietic cells. Some studies have shown that the class Ia isoform p110β can also bind to G$\beta\gamma$ and thus be activated by G protein-coupled receptors *in vitro*; however, the physiological significance of this interaction has not been established.

All class I subtypes bind to ras, a signaling molecule that is a key regulator of cell growth and transformation, which means that activated ras can turn on the PI 3-kinase pathway.

Transgenic mouse studies have helped to elucidate the functional specificity of the class I isoforms *in vivo*. For example, p110δ and p110γ clearly have a role in the regulation of the immune response, reflecting their restricted tissue distribution. P110γ knockout mice, in studies reported by three groups, had impaired neutrophil and macrophage chemotaxis and function and consequently were unable to mount an inflammatory response to bacterial infections. In another study, p110γ knockout mice were used to show that the enzyme acts as a negative regulator of heart muscle contractility.

The p110δ knockout mice have been described in studies by three groups, and the data have confirmed that p110δ functions primarily in B and T lymphocytes. The p110δ-deficient mice failed to raise an adequate immune response due to compromised B- and T-cell antigen receptor signaling. Deletion of the p110α gene gave an embryonic lethal phenotype, as did deletion of the p110β gene, which indicates that these isoforms play important roles in development.

Knockout studies of the adaptor subunits have shown that p85 is involved both in the cellular immune response and in the control of glucose metabolism Transgenic mice with deletions of all p85 isoforms resulted in perinatal lethality. Mice with were hypoglycemic, showed lower insulin levels, and had increased glucose tolerance. In addition, p85α knockout mice had diminished B-cell activity but functional T-cells, indicating that p85β but not p85α may be important in T-cell signaling.

Class II PI 3-Kinases

The class II enzymes have larger molecular weight catalytic subunits of 170 kDa, with a C-terminal C2 domain that can bind phospholipids *in vitro* in a Ca^{2+}-independent manner and possible amino-terminal protein interaction domains. The class II PI 3-kinases use mainly PI, and to a lesser extent PI(4)P and PI(4,5)P2, as substrates *in vitro*. However, the *in vivo* substrate specificity of class II PI 3-kinase is presently unknown. Three class II isoforms have been found in mammals, C2α, C2β, and C2γ. Only one isoform exists in *D. melanogaster*, and when it is mutated, developmental defects are induced. The function of PI 3-kinase class II in mammalian cells is far less characterized than that of the class I enzymes.

Class III PI 3-Kinases

The class III enzymes are homologues of the yeast enzyme vps34p; both enzymes use PI only as a substrate *in vitro*. Class III PI 3-kinases have a role in intracellular trafficking of proteins.

Signaling Downstream of PI 3-Kinases

The number of targets downstream of PI 3-kinase, which impinge on cellular functions as diverse as growth, apoptosis, glucose homeostasis, and heart muscle contractility, are ever expanding and comprise a vast area of research, a detailed account of which would be beyond the scope of this article.

The first direct target in downstream PI 3-kinase signaling is created by the interaction of their lipid products, the 3-phosphoinositides with proteins that have specific PI3P lipid-binding domains. Such proteins containing either a PH (pleckstrin homology) domain, such as AKT/PKB and PDK1, or a FYVE domain, named after the first four proteins shown to contain it, Fab1p, YOTB, Vac1p, and early endosome antigen 1 (EEA1). Both bind 3-phosphoinositides.

The protein AKT is a major player in PI 3-kinase signaling, lying directly downstream of PI 3-kinase in the pathway (see Figure 3). Both AKT and PDK contain PH domains and hence are brought to the membrane by binding to 3-phosphoinositides following PI 3-kinase activation. AKT activation is thought to occur via phosphorylation at two sites: Thr308 by PDK1 and S473 by a putative PDK2 molecule yet to be established. Once activated, AKT phosphorylates and regulates a diverse set of molecules. For example, AKT phosphorylates and inhibits the BCL-2 family member BAD and caspase 9, both of which promote apoptosis, and the forkhead transcription factors, which stimulate transcription of pro-apoptotic genes. These events have a combined antiapoptotic effect on the cell. AKT activation affects cell cycle activation by increasing cyclin D transcription and translation and by reducing levels of the cyclin-dependent kinase inhibitor p27kip1.

Studies of PI 3-kinase signaling in *D. melanogaster* have shown that overexpression of Dp110 in imaging disks increases cell growth and creates larger flies. The link between PI 3-kinase and cell growth is likely due to the fact the PI 3-kinase lies downstream of the insulin receptor and upstream of p70S6 kinase, which when activated phosphorylates the 40S ribosomal protein, S6. This process increases the translation of the 5′-TOP mRNAs, which encode ribosomal proteins and protein synthesis elongation factors. Another player in this pathway is mammalian target of rapamycin (mTOR), which lies downstream of PI 3-kinase and activates p70S6 kinase as well as the eukaryotic translation initiation factor (4E-BP1), promoting protein translation and ultimately cell growth.

The effects of PI 3-kinases on the regulation of the actin cytoskeleton occur not through AKT but via their interaction with guanosine nucleotide exchange factors (GEFs) and GTPase-activating proteins (GAPs) for small GTPases, such as Rac and members of the Arf family. These molecules are known to contain PH domains and thus are likely to be directly downstream of PI 3-kinases. The exact mechanism of the interaction of PI 3-kinase lipid products and GEFs has not been established, but it is clear that PI 3-kinase has at least a regulatory role in the organization of the cytoskeleton and thus cell motility.

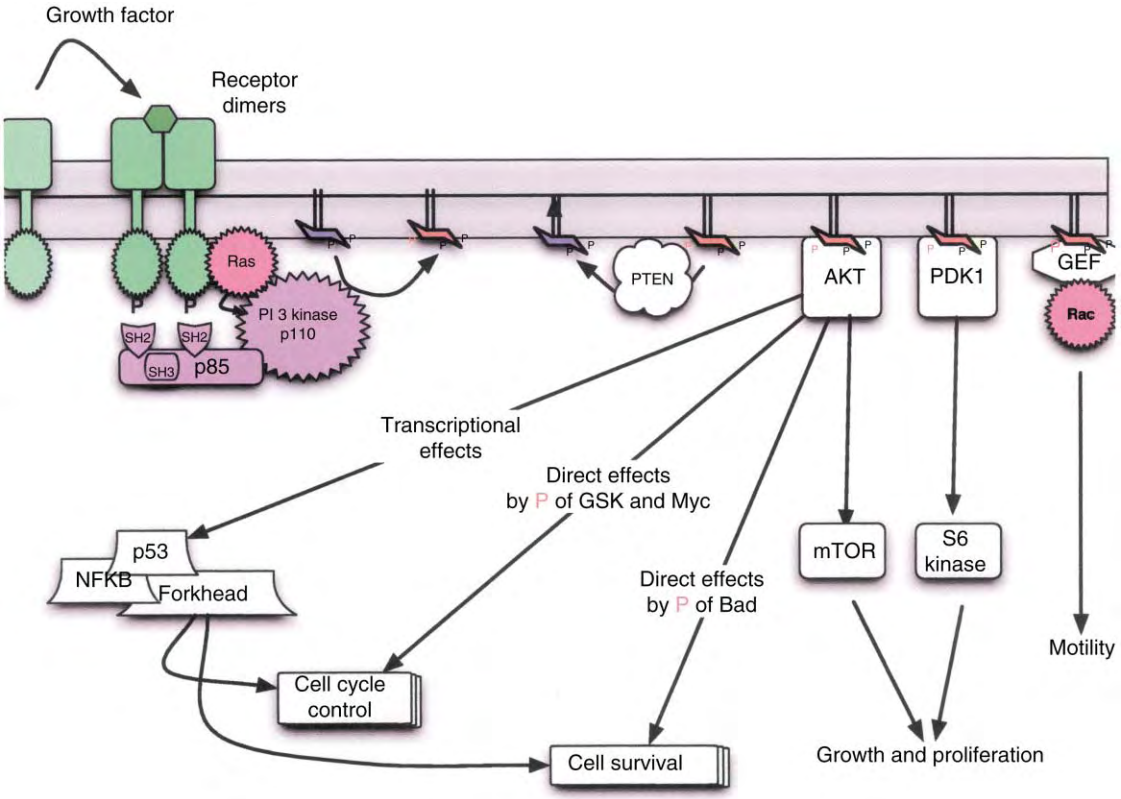

FIGURE 3 The PI 3-kinase signal pathways.

The Role of PI 3-Kinases in Human Disease

It is clear from the diverse role which PI 3-kinases plays in the cell that aberrations of the PI 3-kinase pathway are likely to perturb cellular homeostasis, leading to disease. Evidence has accumulated from transgenic manipulation studies of the PI 3-kinase genes in mice as well as from studies of disease models in nature. Interestingly, the transgenic studies in mice have revealed that the class I isoforms play important and distinct functions in cells of different tissue origin. Pharmaceutical companies have started to exploit the therapeutic potential of isoform selective PI 3-kinase inhibitors for various indications.

Cancer

The strongest link between PI 3-kinase and cancer is the tumor suppressor PTEN, which has been found to be the second most commonly mutated gene in cancer after p53 and a negative regulator of PI 3-kinase through its lipid phosphatase activity. Mutations that destroy function or the loss of PTEN are especially prevalent in prostate, brain (glioblastoma), and endometrial cancers. Increased PI 3-kinase activity associated either with lack of PTEN activity or mutation of the PI 3-kinase gene itself, as has been shown to occur in certain cancers, can promote the oncogenic action of this enzyme. Increased PI 3-kinase activity may lead to loss of the ability to regulate cell survival, loss of control of the cell cycle, and alterations in motility, which are some of the key events in cellular cancer progression. In addition, the enzyme PI 3-kinase lies downstream of the vascular endothelial growth factor (VEGF) receptor, a growth factor signal system that promotes angiogenesis in solid tumors, a key factor in supporting tumor growth. Therefore, inhibitors to PI 3-kinase would be suitable candidates for clinical evaluation in oncology.

Inflammatory Disease

Studies in transgenic mice either lacking or with mutated forms of the p110δ and p110γ isoforms have shown that these two enzymes have specific roles in regulating the immune response. Both isoforms have a tissue expression restricted mainly to hematopoietic cells. In addition, elegant studies in mice have allowed the differentiation of the role of these two isoforms. Thus p110γ has been shown to be involved in the innate immune response through regulation of macrophage and neutrophil function.

Knock-in mice with kinase-dead mutant versions of p110δ have been constructed, showing that this isoform regulated the development and function of B- and T-cell lymphocytes and thus the adaptive immune response. Several pharmaceutical companies have established programs to evaluate isoform-specific inhibitors to p110δ and p110γ in autoimmune and allergic disease.

Cardiovascular Disease

Tissue-specific knockout studies of PTEN have implicated the importance of PI 3-kinase enzymes in controlling both cardiac contractility and hypertrophy. Additional studies of these mice that involve the expression of dominant negative p110α and p110γ enzymes have given clues to the role of each isoform in the heart. The p110α isoform was found to be responsible for increases in the size of cardiomyocyte cells and p110γ to be associated with decreased heart contractility. Surprisingly, there were high levels of p110γ in total heart extracts of these mice, as this isoform was considered to be present primarily in leukocytes. Therefore, isoform selective inhibitors of PI 3-kinase may have therapeutic potential in treating heart failure.

See Also the Following Articles

Phosphatidylinositol Bisphosphate and Trisphosphate • Phosphatidylinositol-3-Phosphate • Phospholipase C • Protein Kinase C Family

Glossary

Akt A serine/threonine protein kinase that is activated by the lipid products of PI 3-kinase.

phosphatidylinositol 3,4,5-triphosphate (PIP3) A phosphatidylinositide that has three phosphate groups on the 3, 4, and 5 positions of the inositol ring that acts as a second messenger molecule in cells.

PI 3-kinase A family of enzymes that phosphorylate inositolphosphates on the 3 position of the inositol ring.

PTEN A lipid phosphatase that removes the phosphate from the 3 position of PIP3, thus down-regulating the growth and proliferation signal.

Further Reading

Leslie, N. R., and Downes, P. (2002). PTEN: The down side of PI 3-kinase signaling. *Cell. Signal.* **14**, 285–295.

Luo, J., Manning, B. D., and Cantley, L. (2003). Targeting the PI3K-Akt pathway in human cancer: Rationale and promise. *Cancer Cell* **4**, 257–262.

Vanhaesebroeck, B., Leevers, S. J., Ahmadi, K., Timms, J., Katso, R., Driscoll, P. C., Woscholski, R., Parker, P. J., and Waterfield, M. D. (2001). Synthesis and function of 3-phosphorylated inositol lipids. *Annu. Rev. Biochem.* **70**, 535–602.

Vivanco, I., and Sawyers, C. L. (2002). The phosphatidylinositol 3-kinase AKT pathway in human cancer. *Nat. Rev. Cancer* **7**, 489–501.

Walker, E. H., Pacold, M. E., Perisic, O., Stephens, L., Hawkins, P. T., Matthias, P., Wymann, T., and Williams, R. L. (2000). Structural determinants of phosphoinositide 3-kinase inhibition by wortmannin, LY294002, quercetin, myricetin, and staurosporine. *Mol. Cell* **6**, 909–919.

Wymann, M., Zvelebil, M., and Laffargue, M. (2003). Phosphoinositide 3-kinase signalling: Which way to target? *Trends Pharmacol. Sci.* **24**, 366–376.

Biography

Khatereh Ahmadi is Project Manager of the PI 3-kinase drug discovery program in oncology at Piramed, a start-up biotechnology company in the United Kingdom. She obtained a Ph.D. in immunology at Kings College London and was a postdoctoral Research Fellow at the Ludwig Institute for Cancer Research, working on PI 3-kinase biochemistry and molecular biology with Michael Waterfield. She managed the drug development program that led to the discovery of specific new inhibitors for these enzymes.

Michael Waterfield is Director of Research at the Ludwig Institute for Cancer Research at University College London where he is also Courtauld Professor of Biochemistry. With Peter Parker he first purified and characterized the PI 3-kinase enzymes and then co-developed specific inhibitors of these enzymes. Previously, he co-discovered the functional role of the sis oncogenes, and in studies of signal transduction with other colleagues, he purified and cloned the EGF receptor and found that when truncated it functioned as an oncogene. In 2003 he co-founded the Piramed company to develop PI 3-kinase inhibitors.

Phosphoinositide 4- and 5-Kinases and Phosphatases

Shawn F. Bairstow, Matthew W. Bunce and Richard A. Anderson
University of Wisconsin, Madison, Wisconsin, USA

Phosphoinositides are one of the many phospholipid families found within membrane bilayers of eukaryotic cells. Site-specific phosphorylation of phosphoinositides by lipid kinases results in the generation of multiple phosphatidylinositol phosphate isomers. These mono- or poly-phosphorylated isomers can be further modified by additional enzymes or can directly modulate numerous cellular functions. Because of the potential for phosphoinositides to alter a variety of cellular processes, their synthesis must be strictly regulated. A number of phosphoinositide kinases and phosphatases have been identified and characterized. By adding or removing phosphate groups at specific positions along the inositol ring, these kinases and phosphatases dictate the signaling capacity of phosphoinositides.

Phosphoinositides

Structure

The basic structure of phosphoinositides consists of a six-carbon inositol ring linked by a phosphodiester bond to diacylglycerol (DAG) (Figure 1). The two fatty acid tails of the DAG moiety anchor phosphoinositides into the various membrane structures throughout eukaryotic cells, such as the endoplasmic reticulum, Golgi apparatus, and plasma membrane. *In vivo*, phosphoinositides can be phosphorylated at the 3-, 4-, and 5-hydroxyl positions along the inositol ring in all possible combinations.

Nomenclature

Phosphatidylinositol (PI) is the initial substrate for a number of phosphoinositide kinases that phosphorylate the hydroxyl groups along the inositol ring. Mono- and polyphosphorylated phosphoinositides are named with respect to the positions of the inositol ring that are phosphorylated. Phosphorylation of PI at the 4-hydroxyl position generates phosphatidylinositol 4-phosphate (PI4P); a subsequent phosphorylation at the 5-hydroxyl position generates phosphatidylinositol 4,5-bisphosphate ($PI(4,5)P_2$). Phosphatidylinositol can be singly or severally phosphorylated at the 3-, 4-, and 5-hydroxyl positions to yield phosphatidylinositol mono-, bis-, or trisphosphate molecules.

Phosphatidylinositol 4-Kinases

Subfamilies

Phosphatidylinositol 4-kinases (PI 4-kinases) use PI as a substrate to generate PI4P. PI 4-kinases are classified as either type II or type III kinases based on their structural and kinetic properties. Two mammalian isoforms termed α and β have been identified for each PI 4-kinase subfamily. Type III PI 4-kinases are structurally and kinetically similar to PI 3-kinases. PI 3-kinases and type III PI 4-kinases have homologous catalytic domains, and type III PI 4-kinases are even inhibited by known PI 3-kinase inhibitors, such as wortmannin. Type II PI 4-kinases do not share these structural or catalytic similarities with PI 3-kinases.

Cellular Functions

The higher-order species such as $PI(4,5)P_2$ and $PI(3,4,5)P_3$ have received significant attention, whereas PI4P has typically been thought of simply as a metabolic intermediate in the synthesis of other phosphoinositides. However, a number of functional studies have demonstrated important roles for PI 4-kinases *in vivo*. Type II PI4-kinases have been linked to roles in both secretion and endocytosis. Type III PI4-kinases have been most thoroughly characterized in the budding yeast *Saccharomyces cerevisiae*. Stt4 and Pik1, the yeast homologues of mammalian type III α- and β-isoforms, respectively, are targeted to distinct subcellular locations and perform nonredundant functions. Pik1 is targeted to the nucleus and Golgi. The nuclear function of Pik1 is unknown, but several studies have indicated that Pik1 is required

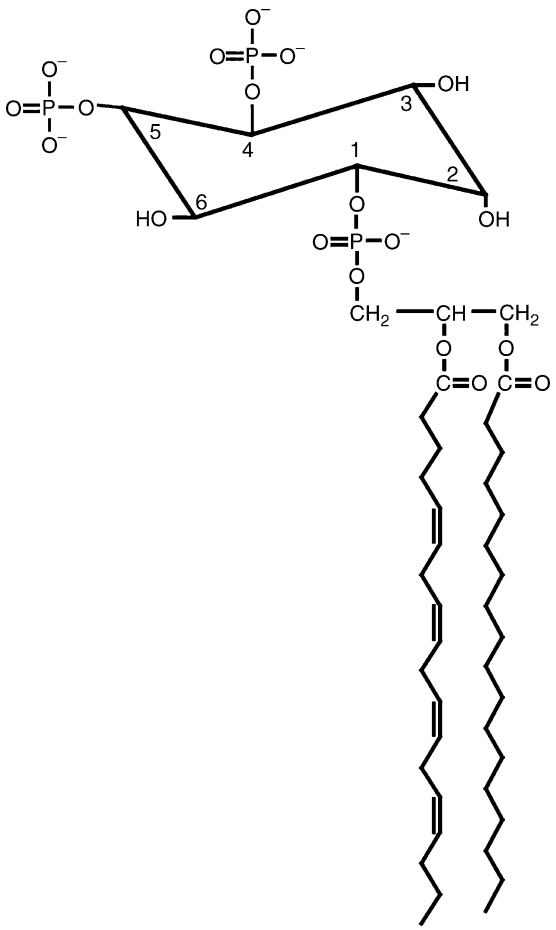

FIGURE 1 Phosphoinositide structure. Phosphoinositides are comprised of a six-carbon inositol ring linked by a phosphodiester bond to diacylglycerol. The inositol ring is numbered counterclockwise starting at the phosphodiester linkage. *In vivo*, phosphoinositides are phosphorylated at the 3, 4, and 5 positions of the inositol ring; phosphatidylinositol 4,5-bisphosphate ($PI(4,5)P_2$) is pictured.

for normal secretion from the Golgi. PI 4-kinase β, the mammalian homologue to Pik1, has also been implicated in Golgi function. Stt4 localizes primarily to the plasma membrane and ER and has been linked to actin cytoskeleton organization and cell wall stability. The PI4P generated specifically by Stt4 can be further phosphorylated by Mss4, the yeast homologue of type I phosphatidylinositol phosphate kinases, or dephosphorylated by the phosphoinositide phosphatase Sac1. The interplay between Stt4, Mss4, and Sac1 control actin dynamics in *S. cerevisiae*. As mentioned above, Pik1 and Stt4 are functionally nonredundant. A loss of activity in either PI 4-kinase causes a unique phenotype that cannot be rescued by increasing the activity of the other kinase. These observations suggest that Pik1 and Stt4 each generate discrete pools of PI4P at different subcellular locations, and that these pools of PI4P are utilized by unique sets of effectors.

Phosphatidylinositol Phosphate Kinases

Phosphatidylinositol phosphate kinases (PIP kinases) generate phosphatidylinositol bisphosphate (PIP_2) from phosphatidylinositol monophosphate isomers. PIP kinases are classified into type I, II or III subfamilies based on their structural and kinetic properties. Members of all three subfamilies have highly conserved kinase domains toward the C-terminus of the proteins, with more variable flanking sequences. Each PIP kinase subfamily has unique substrate specificity dictated by a region at the C-terminal end of the kinase domain named the activation loop. The activation loop is nearly identical for different isoforms within a subfamily but divergent between subfamilies (Figure 2).

Type I PIP Kinases

Type I PIP kinases are PI4P 5-kinases, i.e., they use PI4P as a substrate to generate $PI(4,5)P_2$. Three mammalian type I PIP kinase isoforms termed α, β, and γ have been identified. Type I PIP kinases modulate the organization of the actin cytoskeleton. $PI(4,5)P_2$ regulates the activity of many proteins that process actin at the plasma membrane. Mss4, the yeast homologue of mammalian type I PIP kinases, is required for proper actin cytoskeleton organization and cell wall integrity. Yeast lacking Mss4 activity can be rescued by expressing mammalian type I PIP kinase isoforms, illustrating that type I PIP kinases are functionally conserved in eukaryotes. Mammalian type I PIP kinases localize to sites of cortical actin dynamics, such as lamellipodia and focal adhesions, and modulate the assembly of these structures in a $PI(4,5)P_2$-dependent manner. The type Iγ isoform is targeted to focal adhesions by an association with the protein talin and is tyrosine phosphorylated in a focal-adhesion-kinase (FAK)-dependent manner. Kinase-dead PIP kinase Iγ mutants block focal adhesion assembly, reinforcing the requirement for $PI(4,5)P_2$ in focal adhesion signaling.

Type II PIP Kinases

Type II PIP kinases are PI5P 4-kinases, generating $PI(4,5)P_2$ from PI5P in a catalytically distinct reaction from type I PIP kinases. Like type I PIP kinases, the type II subfamily is comprised of α-, β-, and γ-isoforms. *In vivo* functions for type II PIP kinases have not been clearly defined. Although type I and type II PIP kinases both produce $PI(4,5)P_2$, the two subfamilies are functionally nonredundant. No homologues for mammalian type II PIP kinases have been identified in *S. cerevisiae*, so type II PIP kinases may have specialized functions in higher eukaryotes. One such function could be to modulate receptor-mediated signaling, as the type

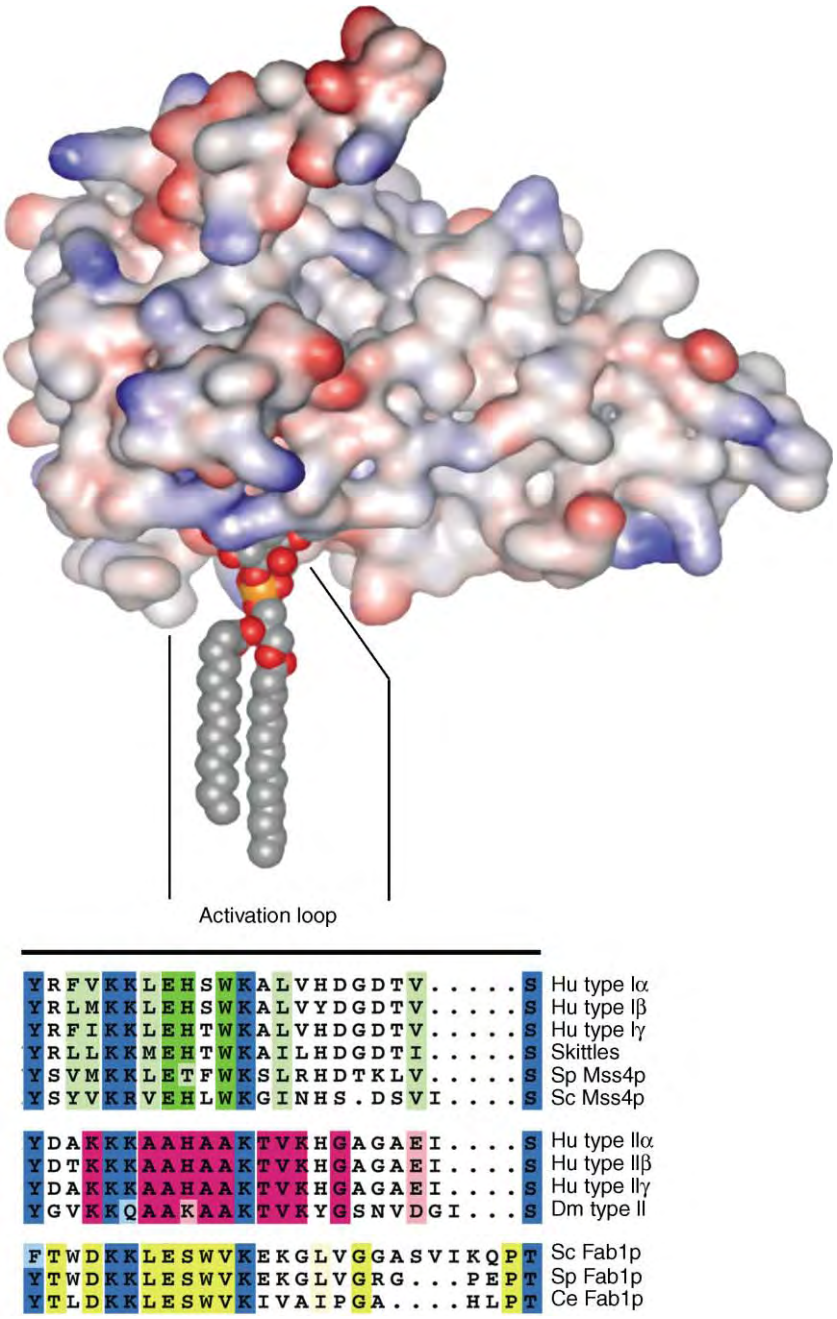

FIGURE 2 PIP kinase structure and the activation loop. The crystal structure for the human type IIβ PIP kinase isoform is shown above with PI5P modeled into the active site. Although the activation loop was not resolved in the crystal structure, its position relative to the active site is illustrated. A sequence alignment of type I, type II, and type III PIP kinase activation loops is shown below the crystal structure. The activation loop is highly conserved among members of each subfamily but divergent between subfamilies. Hu – human, Sp – *S. pombe*, Sc – *S. cerevisiae*, Dm – *D. melanogaster*, Ce – *C. elegans*.

IIβ-isoform has been identified in a complex with the p55 TNFα transmembrane receptor.

Type III PIP Kinases

Type III PIP kinases are PI3P 5-kinases, generating PI(3,5)P_2 from PI3P. The *S. cerevisiae* protein Fab1 was the first type III PIP kinase to be identified. In yeast, Fab1 and PI(3,5)P_2 are involved in vacuole morphology, membrane trafficking, and stress response. Type III PIP kinases were not initially identified in mammalian cells, and *in vitro* studies suggested that type I isoforms can generate PI(3,5)P_2 and thus may perform similar functions to those of Fab1 in yeast. More recently, however, proteins homologous to ScFab1 have been identified in mammalian cells. These mammalian enzymes have

similar *in vivo* substrate specificity to the *S. cerevisiae* Fab1 enzyme and appear to regulate membrane trafficking in a manner comparable to ScFab1.

Phosphatidylinositol Phosphatases

Phosphatidylinositol phosphatases are enzymes that can selectively dephosphorylate both lipid phosphoinositides and soluble inositol polyphosphates. As a family, they can be subdivided by their catalytic properties and substrate specificity.

Phosphoinositide 4-Phosphatases

The Phosphoinositide 4-Phosphatases (Inositol Polyphosphate 4-Phosphatases) are a family of enzymes that dephosphorylate the 4-position of the inositol ring in a magnesium-independent manner. The members of this family can utilize PI(3,4)P_2, Ins(3,4)P_2, and Ins(1,3,4)P_3 as substrates *in vitro*, generating PI3P, Ins3P, and Ins(1,3)P_2, respectively. Two genes have been identified in humans corresponding to type I and type II 4-phosphatases. These genes can be alternatively spliced, resulting in expression of several variant phosphatases. Both types share a 37% total sequence identity and a conserved CKSAKDRT consensus sequence. This C–X_5–R consensus sequence is consistent with other magnesium-independent phosphatases.

Cellular Functions of 4-Phosphatases

The PI-3 Kinase (PI3K) signaling pathway impacts cell growth, glucose metabolism, and apoptosis. Activation of the PI3K pathway results in the generation of PI(3,4,5)P_3 and PI(3,4)P_2, which stimulate downstream effectors such as protein kinase B/Akt and PI3K-dependent kinase 1. Phosphoinositide 4-phosphatases are thought to participate in regulation of the PI3K pathway by converting PI(3,4)P_2 to PI3P, thus attenuating the PI3K signal and subsequently deactivating PI3K effectors. An association identified between a PI 4-phosphatase and the PI3K p85 regulatory subunit supports this putative function for PI 4-phosphatases.

Phosphoinositide 5-Phosphatases

Phosphoinositide 5-phosphatases (inositol polyphosphate 5-phosphatases) dephosphorylate the 5-position of the inositol ring in a magnesium-dependent manner. This family collectively can utilize four substrates: PI(4,5)P_2, PI(3,4,5)P_3, Ins(1,4,5)P_3, and Ins(1,3,4,5)P_4. PI 5-Phosphatases contain a bipartite consensus sequence, (F/I)WXGDXN(F/Y)R, followed several amino acids downstream by (R/N)XP(S/A) (W/Y) (C/T)DR(I/V) (L/I). PI 5-phosphatases are classified into four groups based on their substrate specificity.

Group I 5-Phosphatases

Group I 5-phosphatases use Ins(1,4,5)P_3 and Ins(1,3,4,5)P_4 as substrates. Type I 5-phosphatase, one member of this group, is thought to play a role in the regulation of cellular calcium levels. Ins(1,4,5)P_3 (IP_3) is a pivotal regulator of cellular calcium levels and is generated by the cleavage of PIP_2 by phospholipase C. The resulting IP_3 binds to the IP_3 receptor, triggering a release of calcium ions from intercellular stores. Type I 5-phosphatase decreases this signal by dephosphorylating IP_3 into Ins(1,4)P_2.

Group II 5-Phosphatases

Members of group II 5-phosphatases can utilize all four of the substrates mentioned above. The synaptojanins, type II 5-phosphatase and the Oculocerebrorenal Syndrome of Lowe (OCRL) gene product, OCRL-1, are all members of this group. OCRL is an X-linked disorder resulting in mental retardation, renal dysfunction, and congenital cataracts. Although the pathogenesis for these symptoms is not currently known, OCRL-1 dysfunction results in an increase in PI(4,5)P_2 levels, as observed in cells cultured from individuals with this disorder. Interestingly, OCRL-1 shares 51% identity with type II 5-phosphatase. However, this enzyme cannot compensate for the lack of OCRL-1 activity, possibly due to a difference in substrate specificity or tissue localization. The synaptojanins have functions distinct from OCRL-1 and type II 5-phosphatase. Synaptojanin 1 has been shown to function in recycling of vesicles at neuronal synapses. Synaptojanin 2, on the other hand, is somewhat less characterized. This protein is alternatively spliced and some variants have been shown to have functions overlapping that of synaptojanin 1, while other variants have been localized to distinct cellular compartments, such as the outer mitochondrial membrane.

Group III 5-Phosphatases

Group III 5-phosphatases are active toward PI(3,4,5)P_3 and Ins(1,3,4,5)P_4, which have a 3-position phosphate group. Src homology domain containing inositol phosphatases (SHIPs), SHIP1 and SHIP2 are important members of this group. These proteins share 50% sequence identity and similar substrate specificity, but differ in their tissue expression levels. SHIP1 is primarily expressed in hematopoetic tissues while SHIP2 is expressed in nonhematopoetic tissues. Recent work has demonstrated an importance of SHIPs in signal

transduction. SHIP2 has been shown to associate with specific tyrosine kinase receptors, such as the EGF receptor. This places the phosphatase in an ideal location to attenuate the increased PI(3,4,5)P_3 and PI(3,4)P_2 levels generated by PI3K, which is also recruited to these receptors. SHIP2 mouse knockout experiments support SHIP2's role in PI3K signal termination and also suggest a link between SHIP2 activity and insulin resistance, a primary factor in type 2 diabetes.

Group IV 5-Phosphatases

Group IV phosphatases are the least-characterized of the four groups. One member, phosphoinositide 5-phosphatase type IV, has recently been identified. This phosphatase utilizes PI(3,4,5)P_3 as its primary substrate, but has also been shown to dephosphorylate PI(4,5)P_2 under certain conditions. Expression levels are highest in the brain for both humans and mice, with lower expression in other tissues. The cellular function of this phosphatase has yet to be determined.

See Also the Following Articles

Diabetes • Inositol Phosphate Kinases and Phosphatases • Phosphatidylinositol Bisphosphate and Trisphosphate • Phosphoinositide 3-Kinase • Phosphoinositide-Dependent Protein Kinases

Glossary

inositol A six carbon cyclic alcohol with hydroxyl residues present at each carbon.

kinase An enzyme that catalyzes the transfer of a phosphate group from adenosine triphosphate to a second substrate.

phosphatase An enzyme that hydrolyzes a phosphate group from a substrate.

phosphoinositide A phospholipid molecule composed of inositol and DAG.

Further Reading

Abel, K., Anderson, R. A., and Shears, S. B. (2001). Phosphatidylinositol and inositol phosphate metabolism. *J. Cell Sci.* **114**, 2207–2208.

Anderson, R., Boronenkov, I., Doughman, S., Kunz, J., and Loijens, J. (1999). Phosphatidylinositol phosphate kinases, a multifaceted family of signaling enzymes. *JBC* **274**, 9907–9910.

Cockcroft, S. (2000). *Biology of Phosphoinositides*. Oxford University Press, New York.

Majerus, P., Kisseleva, M., and Norris, F. (1999). The role of phosphatases in inositol signaling reactions. *JBC* **274**, 10669–10672.

Biography

Shawn F. Bairstow is a graduate student in the Department of Biomolecular Chemistry at the University of Wisconsin-Madison. His primary research focus is the spatial and temporal targeting of the type Iγ PIP kinase isoform and its involvement in focal adhesion assembly. He earned a B.S. in Biochemistry from the University of Illinois-Campaign/Urbana where he performed undergraduate research focusing on the catalytic mechanism of cytochrome P450.

Matthew W. Bunce earned a B.S. in Biochemistry at Virginia Tech and is currently a predoctoral graduate student in the lab of Dr. Richard Anderson at the University of Wisconsin-Madison. His research is focused on determining how PIP kinases interact with their substrates, and also on the identification and characterization of binding partners that direct PIP kinases to their unique subcellular compartments and modulate PIP kinase signaling.

Richard A. Anderson is Professor of Pharmacology and Director of Molecular and Cellular Pharmacology at the University of Wisconsin-Madison. His principal research interest is in cell signaling with an emphasis on phosphoinositide signal transduction mechanisms that modulate cancer development and metastasis. He holds a Ph.D. from the University of Minnesota and did his postdoctoral work at Yale University with Vincent T. Marchesi. He has authored numerous articles on the role of PIP kinases in signal transduction.

Phosphoinositide-Dependent Protein Kinases

Nick R. Leslie and C. Peter Downes
University of Dundee, Dundee, UK

The cells of multicellular organisms respond to external stimuli, such as growth factors, cytokines, neurotransmitters, and many hormones through regulated changes in the levels of cellular signaling molecules, termed second messengers. The inositol phospholipids (collectively known as phosphoinositides) are constituents of cell membranes that play important roles as second messengers in signal transduction and membrane trafficking. Many of the downstream effects of phosphoinositide signaling are mediated through reversible protein phosphorylation and in this article the principal focus will be upon protein kinases that function as downstream targets of the phosphoinositide 3-kinase (PI 3-kinase) lipid signaling pathway.

Phosphoinositide Signaling – An Overview

Phosphoinositides are a small family of differentially phosphorylated membrane-localized lipid second messengers. These lipids comprise the hydrophilic cyclic polyol, myo-inositol (Ins), linked via a diester phosphate in the 1-position to diacylglycerol, the hydrophobic membrane anchor. Several families of lipid kinases and phosphatases selectively insert and remove monoester phosphates in three of the remaining positions of the inositol ring, generating the eight currently known phosphoinositide species. This review focuses on some of the most intensively studied phosphoinositide signaling pathways initiated when growth factors, cytokines or insulin, and related hormones trigger the activation of one or more of the type I PI 3-kinases. These enzymes phosphorylate a small proportion of the cellular phosphatidylinositol 4,5 bisphosphate (PtdIns(4,5)P_2) to generate PtdIns(3,4,5)P_3 (often abbreviated to PIP_3). The latter is further metabolized by 5-phosphatases to PtdIns(3,4)P_2 or is returned to the PtdIns(4,5)P_2 pool by the tumor suppressor lipid phosphatase PTEN. PtdIns(3,4,5)P_3 activates downstream signaling through proteins which possess a phosphoinositide binding domain capable of distinguishing this target lipid within a membrane that contains at least 100-fold higher levels of the parent lipid PtdIns(4,5)P_2. Several modular protein domain families have now been identified that include members able to bind to specific phosphoinositides, such as pleckstrin homology (PH), Phox homology (PX), FYVE, and ENTH domains. Other domains, such as FERM, and PDZ domains may also function as phosphoinositide-binding motifs, although evidence for their selectivity between different phosphoinositides is currently lacking. In almost all cases presently identified, the PtdIns(3,4,5)P_3-specific-binding motifs mediating PI 3-kinase-dependent signaling are members of the PH domain family.

Protein Kinase B/Akt

Since the 1990s, it has become evident not only that PI 3-kinase signaling plays a pivotal role in regulating many diverse and significant cellular processes, including cellular proliferation, survival, size, and motility, but that many of the downstream effectors of PtdIns(3,4,5)P_3 are protein kinases. The best evidence for regulation by PtdIns(3,4,5)P_3 exists for three classes of kinase that carry PH domains able specifically to bind this lipid: the Ser/Thr kinases, PKB (or Akt), PDK1, and the Tec family Tyr kinases. Space limitations prevent us from addressing such enzymes as GSK3 or PAK, which can clearly be regulated by the PI 3-kinase pathway, though not by directly binding to PtdIns(3,4,5)P_3 and these enzymes can also be regulated by PI 3-kinase independent pathways. The PI 3-kinase signaling pathway has been dissected extensively using biochemical and genetic approaches. Significantly, the stimulated production of PtdIns(3,4,5)P_3 by PI 3-kinase enzymes is conserved in species from slime molds, through nematodes and flies to vertebrates. In species of all of these groups, genetic studies indicate that a principal (though not exclusive) cellular mediator of this signaling pathway is protein kinase B (PKB).

PKB, also known as Akt, has a C-terminal serine/threonine kinase domain and an N-terminal PH domain

that binds with high specificity to PtdIns(3,4,5)P_3 and PtdIns(3,4)P_2. The enzyme has been shown to be activated by phosphorylation of two key residues, threonine 308, in the activation loop (or T-loop) of the kinase domain, and serine 473 in the C-terminal tail. These phosphorylation events in turn are believed to alter the conformation of PKB greatly enhancing its activity, and although much of this work has focused on PKB, it now appears that a number of related kinases may be regulated by analogous mechanisms. Although PtdIns(3,4,5)P_3 and PI(3,4)P_2 do not directly enhance the activity of PKB *in vitro*, they play a critical role in the phosphorylation and activation of PKB, by recruiting PKB to the plasma membrane where it is activated, and by opening the conformation of the protein to allow phosphorylation. Thus it seems that in a normal cellular context the activity state of PKB is largely governed by cellular levels of PtdIns(3,4,5)P_3 and PI(3,4)P_2.

PDK1 and the Regulation of the AGC Kinases

3-Phosphoinositide dependent kinase 1 (PDK1) has been identified as the activating kinase that phosphorylates PKB in a PI 3-kinase dependent process at Thr 308 *in vitro* and *in vivo* (see Figure 1). This protein serine/threonine kinase also has a PH domain that specifically binds PtdIns(3,4,5)P_3 and PI(3,4)P_2 and is found both in the cytosol and on the plasma membrane. Significantly, after its initial identification as a PKB kinase, subsequent work has shown that it also phosphorylates and activates many other related kinases. A point of current controversy is whether the function of PDK1 itself is regulated through mechanisms such as phosphorylation or translocation to the plasma membrane. It has been proposed that PDK1 translocates to the plasma membrane in response to stimulated rises in cellular PtdIns(3,4,5)P_3 levels, as does PKB. However, this conclusion is not supported by other work, and as PDK1 has an affinity approximately tenfold greater for these lipids than does PKB, an alternative idea is that a pool of cellular PDK1 may be constitutively associated with the plasma membrane and that its activity is not normally regulated by changes in the levels of these lipids. It has also been proposed that PDK1 is activated in stimulated cells by tyrosine phosphorylation, possibly by a Src family kinase, although once more other work argues against this, and phosphorylation has not been observed in response to physiological stimuli, or in cells expressing physiological levels of the relevant kinases. Most of this work on the regulation of PDK1 function would suggest that if it is to be viewed as a phosphoinositide-regulated kinase, this regulation occurs through direct or indirect effects of PtdIns(3,4,5)P_3 on its substrates, rather than on PDK1 itself.

PKB exists as three isoforms in human cells (PKBα, β, and γ) but is itself a part of a diverse structurally-related

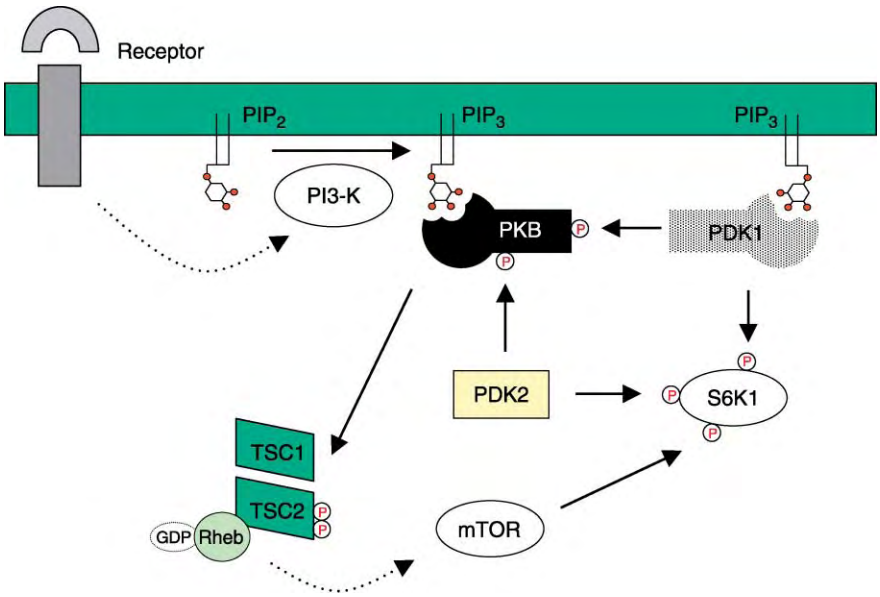

FIGURE 1 Mechanism of activation of PKB, mTOR, and S6K1 by PI 3-kinase. A model is shown for the activation of downstream kinases by a transmembrane receptor activating PI 3-kinase. Molecules are shown in the stimulated conformation. In unstimulated cells, PI3-kinase is less active, PIP_3 levels are low, PKB is cytosolic and along with TSC2 and S6K1, is unphosphorylated and inactive. Active TSC2 promotes the conversion of GTP to GDP by Rheb, although the mechanism by which this leads to the activation of mTOR signaling is unclear. Direct phosphorylation events are shown by bold arrows, indirect mechanisms of activation are represented by dotted arrows. Phosphates are represented by a circled letter P.

family of protein kinases, which are phosphorylated by PDK1 at a residue in the T-loop of each kinase. Although this PDK1-mediated phosphorylation plays a role in the activation of each of these kinases, in contrast to PKB, the phosphorylation of other family members is not directly responsive to cellular PtdIns(3,4,5)P_3 levels, and alternative signaling inputs seem to be required to activate these other kinases strongly. To allow efficient activation, most of these related kinases require the interaction of a hydrophobic motif, positioned C-terminal to their kinase domain, with a hydrophobic pocket on PDK1. In some cases, e.g., S6K1 and SGK, this hydrophobic motif contains a serine or threonine that must be phosphorylated to allow interaction with and activation by PDK1. In these cases, it appears that this phosphorylation is in turn mediated by an unknown PI 3-kinase-dependent kinase. In contrast, in place of this serine or threonine residue, PKCζ and PRK2 have an acidic residue which appears to mediate phosphorylation-independent interaction with, and activation by, PDK1. PKCζ, and probably the other atypical PKC kinases, PKCι and PKCλ, are also unusual in that there is some evidence for the direct activation of the kinase through interaction with PtdIns(3,4,5)P_3. However, these kinases lack a PH domain or other identified PtdIns(3,4,5)P_3-binding motif, and the mechanism and physiological relevance of this apparent activation is unclear.

PDK2 – The Unidentified Hydrophobic Motif Kinase

The term PDK2 was used originally to describe the unidentified kinase responsible for the phosphorylation of PKB at the hydrophobic motif serine 473. Since then, although several candidates have been proposed, such as ILK, MAPKAP-K2, NEK6, and both PKB and PDK1 themselves, the identity of PDK2 is still not clear. What is clear, however, is that most of the AGC family kinases become phosphorylated at a serine or threonine residue in a hydrophobic motif C-terminal to the kinase domain, and that this phosphorylation plays a critical role in the activation of each enzyme. It is quite possible that different PDK2s exist for different AGC family kinases, and it appears that a substantial component of the PI 3-kinase-dependent activation of kinases such as SGK and S6K1 may be mediated by an as yet unknown phosphoinositide-dependent hydrophobic motif kinase. As a consequence of the mechanisms of activation of this family of kinases, increases in cellular PtdIns(3,4,5)P_3 levels seem sufficient to activate PKB, since PtdIns(3,4,5)P_3 and PH domain-dependent colocalization of PKB and PDK1 appears to be the principal mechanism of regulation of this kinase. In contrast, most other PDK1-regulated kinases seem to require regulated docking with PDK1 through a protein–protein interaction to mediate activation in the cytosol, and it is this docking step that may be regulated by different upstream pathways, some of which may themselves involve phosphoinositide-dependent kinases.

Much of the interest in PKB stems from its role in mediating many of the effects of PI 3-kinase activation. Evidence now indicates that a substantial portion of the effects of elevated PtdIns(3,4,5)P_3 levels on cell-cycle progression, survival, growth, and insulin responses are mimicked by activation of PKB alone. In contrast, most PI 3-kinase-dependent cytoskeletal regulation appears to be PKB independent, but may rather result from the interaction of PtdIns(3,4,5)P_3 with the PH domains of guanine-nucleotide-exchange factors for Rho family GTPases. These findings go some way to explaining why isoforms of PKB have been found to be over-expressed in a range of human tumor types, and why activation of PKB activity appears to be an even more common feature of tumors.

Regulators of Cellular Growth – mTOR and S6K1

Work addressing the stimulation of cell growth by PtdIns(3,4,5)P_3 signaling implicates two protein kinases as key players in this process, the mammalian target of rapamycin (mTOR), and ribosomal protein S6 kinase 1 (S6K1, also known as p70S6K). While S6K1 seems to regulate translation through several mechanisms, mTOR has been proposed to play a central role in cellular growth control, as its activity is responsive to nutrients and ATP and is able to regulate a range of downstream processes related to cell growth, including transcription, tRNA and ribosome synthesis, autophagy, and nutrient transporter function. Although recent work has shed significant light on the regulation of both of these kinases, particularly the inputs from PtdIns(3,4,5)P_3 signaling, their regulation appears complex and many questions remain unanswered. mTOR activity now appears to be inhibited in nongrowing cells by the small GTPase Rheb, and a protein complex of two proteins, TSC1 and TSC2, the latter of which can function as a GTPase activating protein for Rheb. Upon activation of PI 3-kinase and PKB, TSC2 is phosphorylated by PKB, Rheb becomes inactive (in the GDP bound state) causing activation of mTOR. S6K1 is then believed to be stimulated through phosphorylation by activated mTOR (in addition to other activating

inputs such as PDK1). This model is represented in Figure 1.

The study of S6K1, and many other kinases that are affected by PtdIns(3,4,5)P_3 signaling, with the exception of PKB, highlights a possible role for the level of basal PtdIns(3,4,5)P_3 present in unstimulated growing cells in culture. For example, S6K1 can be potently activated by G protein-coupled receptors under conditions where PtdIns(3,4,5)P_3 levels do not increase. Thus, PtdIns(3,4,5)P_3 can play a permissive rather than stimulatory role in G protein-coupled receptor mediated S6K1 activation. Significantly, a similar role for basal PtdIns(3,4,5)P_3 has been proposed in the regulation of other molecules, such as Ras and PKCδ.

One important piece of evidence that cell growth responses stimulated by mTOR and S6K1 are downstream effectors specifically of PtdIns(3,4,5)P_3 is the sensitivity of PTEN null ES cells, MEFs, and tumors to the immunosuppressant rapamycin. Deletion of the PtdIns(3,4,5)P_3 specific phosphatase, PTEN, elevates PtdIns(3,4,5)P_3 levels and activates downstream PI 3-kinase dependent signaling without stimulating other pathways. Since these cells are unusually sensitive to growth inhibition by the mTOR (and thus S6K1) inhibitor rapamycin, this suggests that these pathways are significantly activated by increased PtdIns(3,4,5)P_3 levels, and that this is important for cell growth and tumor development.

Tec Family Kinases

The Tec family of tyrosine kinases has been implicated in signaling by lymphocyte antigen receptors. These kinases have an N-terminal PtdIns(3,4,5)P_3 binding PH domain and a C-terminal tyrosine kinase domain. They also contain a proline-rich region, and SH3 and SH2 domains in the central region of the proteins. It is believed that their activation requires recruitment to the plasma membrane by interaction of PtdIns(3,4,5)P_3 with the PH domain, and subsequent activation by members of the Src family of tyrosine kinases through phosphorylation of the kinase domain activation loop. These kinases are rather restricted in the range of tissues where they are expressed, most being hematopoietic specific, and appear to play a role most significantly in lymphocyte signaling. This picture has stemmed from the original identification of the first family member, Bruton's tyrosine kinase (Btk), as the gene mutated in a human immunodeficiency. The family is now known to include Btk, Tec, Itk, Bmx, and the slightly divergent Rlk. Interestingly, in Rlk, the PH domain has been replaced by an N-terminal palmitoylation and membrane targeting signal, leading to PI 3-kinase independent activation.

Perspectives

This article has focused largely upon well-studied kinases that are regulated through PtdIns(3,4,5)P_3 and PI(3,4)P_2 and the PI 3-kinase signaling pathway, and their roles in regulating cellular proliferation, survival, and growth. However, evidence for the regulation of kinases in these and other cellular signaling pathways by other phosphoinositides is emerging. For example, serum and glucocorticoid inducible protein kinase 3 (SGK3 or CISK) is localized to endosomes through a PX-domain-mediated interaction, probably via PtdIns(3)P. Although tethering to endosomes appears to be required for CISK to function, there is also evidence that its catalytic activity is controlled through stimulated type I PI 3-kinases and hence via a mechanism that also involves PtdIns(3,4,5)P_3. Since the human genome contains ~48 genes encoding proteins, many unstudied, with both a protein kinase domain, and a domain recognized as a potential phosphoinositide-binding domain (42 with PH domains and 6 with PX domains), it is quite possible that novel kinases exist that are regulated by any of the phosphoinositides and play a role in the regulation of quite distinct cellular processes.

See Also the Following Articles

Inositol Lipid 3-Phosphatases • Inositol Phosphate Kinases and Phosphatases • Phosphatidylinositol Bisphosphate and Trisphosphate • Phosphatidylinositol-3-Phosphate • Phosphoinositide 3-Kinase • Phosphoinositide 4- and 5-Kinases and Phosphatases • Protein Kinase B

Glossary

kinase An enzyme that catalyzes the transfer of a phosphate group from ATP onto another molecule.

phosphatase An enzyme that catalyzes the hydrolytic removal of phosphate from another molecule and its release as free phosphate.

phosphoinositide A phospholipid in which the polar head group is inositol or a phosphorylated derivative of inositol.

Further Reading

Biondi, R. M., and Nebreda, A. R. (2003). Signalling specificity of Ser/Thr protein kinases through docking-site-mediated interactions. *Biochem. J.* **372**, 1–13.

Kozma, S. C., and Thomas, G. (2002). Regulation of cell size in growth, development and human disease: PI3K, PKB and S6K. *Bioessays* **24**, 65–71.

Lawlor, M. A., and Alessi, D. R. (2001). PKB/Akt: A key mediator of cell proliferation, survival and insulin responses? *J. Cell Sci.* **114**, 2903–2910.

Leslie, N. R., and Downes, C. P. (2002). PTEN: The down side of PI 3-kinase signalling. *Cell Signal* **14**, 285–295.

Marygold, S. J., and Leevers, S. J. (2002). Growth signaling: TSC takes its place. *Curr. Biol.* **12**, R785–R787.

Vanhaesebroeck, B., and Alessi, D. R. (2000). The PI3K–PDK1 connection: More than just a road to PKB. *Biochem. J.* **346**, 561–576.

Vanhaesebroeck, B., Leevers, S. J., Ahmadi, K., Timms, J., Katso, R., Driscoll, P. C., Woscholski, R., Parker, P. J., and Waterfield, M. D. (2001). Synthesis and function of 3-phosphorylated inositol lipids. *Annu. Rev. Biochem.* **70**, 535–602.

Biography

Nick Leslie is a research fellow in the Division of Cell Signalling at the University of Dundee. He obtained his Ph.D. from Glasgow University (1995). Postdoctoral work at the Beatson Institute in Glasgow and the Division of Cell Signalling in Dundee University focused on mammalian signal transduction. His current projects involve phosphoinositide signaling and the tumor suppressor phosphatase PTEN.

Peter Downes is Director of the Inositol Lipid Signalling Laboratory in the Division of Cell Signalling, University of Dundee. He obtained his Ph.D. at the University of Birmingham, UK. After postdoctoral research in the MRC Neurochemical Pharmacology Unit in Cambridge, he worked for several years in the pharmaceutical industry before being appointed Professor of Biochemistry at the University of Dundee in 1989. He has been investigating the roles of inositol lipids in cell signalling for nearly 25 years.

Phospholipase A_2

Timothy R. Smith and Edward A. Dennis
University of California, San Diego, California, USA

Phospholipid membranes serve not only as structural components of the cell but are integral as a storage form for the precursors of numerous signaling molecules critically involved in a variety of inflammatory and immune responses including the production of the eicosanoids. Phospholipase A_2 (PLA_2) refers to a superfamily of enzymes that catalyze the hydrolysis of fatty acid esters from the *sn*-2 position of membrane phospholipids yielding a free fatty acid and a lysophospholipid. These enzymes have been shown to function both intra- and extracellularly and in some cases display molecular cross-talk between multiple family members. A classification system has been devised to subdivide the PLA_2 superfamily into 14 distinct groups based on sequence and structural homologies. Within these 14 groups, there are two distinct catalytic mechanisms employing either a catalytic serine or histidine, which the PLA_2 enzymes utilize to produce free fatty acids and lysophospholipids from membrane phospholipids. When the free fatty acid produced is an unsaturated one, such as arachidonic acid, it can be converted to the bioactive prostaglandins, leukotrienes and lipoxins by various downstream enzymes. Depending on the composition of the phospholipid precursor, the lysophospholipid can be converted to platelet activating factor (PAF), a potent inflammatory signaling molecule. While most PLA_2 enzymes function as signal initiators, the PAF acetyl hydrolases, which are actually PLA_2s, break down PAF and oxidized phospholipids to end the signaling process.

Phospholipase A_2 (PLA_2) Structures and Catalytic Mechanism

PLA_2 Enzymes Using a Catalytic Histidine ($sPLA_2$s)

The PLA_2 enzymes, initially described as small, secreted enzymes containing multiple disulfide bonds and a catalytic histidine, were first isolated and characterized from snake venoms and human pancreatic secretions. Based on their small size and the fact that they were secreted, these enzymes were referred to as $sPLA_2$s. The $sPLA_2$ enzymes are typically small, compact proteins held together by a network of integral disulfide bonds. These enzymes all contain an N-terminal signal peptide sequence that leads to them being secreted from cells and working extracellularly on membrane phospholipids. The only exception is that of the pancreatic group IB PLA_2 that is secreted with its propeptide intact and requires cleavage by trypsin in order to be catalytically active in the gut as a digestive enzyme. All of these enzymes share a requirement for millimolar levels of Ca^{2+}, which is necessary for catalysis. The catalytic core of the $sPLA_2$ enzymes is a His/Asp dyad made up of the catalytic histidine and a structurally adjacent aspartate residue. None of the $sPLA_2$ molecules show appreciable substrate specificity for saturated versus unsaturated fatty acids.

The structure and catalytic mechanism of *sn*-2 ester bond cleavage has been elucidated for the evolutionarily related Group I, II, V, and X PLA_2s. X-ray structures have been determined for the Group IA and IB, several of the Group II subfamily, the Group V and the Group X, and all of the members of these groups share a common protein fold and are 13–18 kDa in size. They all possess six common disulfide bond linkages. These disulfide bonds provide stabilization of the protein structure and allow the enzyme to remain functional in environmental extremes. There are up to two additional disulfide bonds that have been used to differentiate the groups from one another. Additionally they all share a common Ca^{2+} binding loop that includes the catalytically essential Asp. This residue acts to provide two coordinate interactions for the Ca^{2+} molecule that serves to stabilize the transition state of the PLA_2 reaction.

The first step in catalysis for any of the $sPLA_2$s is binding to the membrane interface. The Group I and II enzymes have been shown to preferentially bind to anionic vesicles that include phosphatidylserine or phosphatidylethanolamine while the group V and X PLA_2s are able to efficiently bind to zwitterionic vesicles, and are able to work on a phosphatidylcholine surface equally well. Once the enzyme is bound to the surface and Ca^{2+} is coordinated into the enzyme via the Asp, catalysis can occur. The catalysis is similar to

that observed with other lipase enzymes utilizing a histidine residue. The active site His recruits a water molecule and orients it for nucleophilic attack on the ester linkage of the *sn-2* fatty acid. The Ca^{2+} molecule is critical in positioning the catalytic water and the phosphate of the lipid. The result is the production of a free fatty acid and lysophospholipid coordinated to the Ca^{2+}. The catalytic mechanism for the other $sPLA_2$s (group III, IX, XI, XII, XIII, and XIV) is similar to that for the group I, II, V, and X, but with the exception of the group III enzyme, X-ray structures have not been reported to verify this.

PLA_2 Enzymes Utilizing a Catalytic Serine

In the mid-1980s, several laboratories discovered and characterized a cytosolic PLA_2 activity that utilized a catalytic serine as opposed to a histidine. Today, there are three classes of PLA_2 enzymes that utilize a catalytic serine, the $cPLA_2$s (group IV), the $iPLA_2$s (group VI), and the PAF-acetyl hydrolases (group VII and VIII).

$cPLA_2$

There are three PLA_2 enzymes classified as $cPLA_2$, group IVA, IVB, and IVC. The group IVA PLA_2 is the enzyme typically referred to as $cPLA_2$ and has been studied extensively. The group IVB and IVC enzymes have only recently been cloned and little is known about their structure, catalysis, or signaling roles.

The group IVA enzyme is an 85 kDa cytosolic enzyme initially cloned and purified from human neutrophils, platelets and monocytes. This enzyme contains two structurally distinct protein domains, a C2 domain and an α/β hydrolase PLA_2 catalytic domain. X-ray structure determination of the group IVA molecule by the Dessen and Somers group revealed that it possesses a novel fold unlike any other previously solved α/β hydrolase. The C2 domain controls the calcium-dependent enzyme translocation to the endoplasmic reticulum and nuclear envelope where the enzyme is catalytically active. The C2 domain and catalytic domain fold and can function independently, but the two domains together are required for biological activity. In addition to PLA_2 activity, the group IVA enzyme possesses both lysophospholipase and transacylase activity. There are several serine residues that are differentially phosphorylated on the group IVA enzyme; while none of these phosphorylation sites are critical for enzymatic activity, when modified they can increase the specific activity of the enzyme two to three fold. The group IVA enzyme utilizes micromolar levels of Ca^{2+} that binds to the C2 domain, but unlike the $sPLA_2$ enzymes the calcium functions in enzyme translocation and not for catalysis. Also unlike the $sPLA_2$s, the group IVA PLA2 shows a 10- to 20-fold specificity for arachidonic acid at the *sn-2* position over saturated or other unsaturated fatty acids.

The group IVA catalytic core is the Ser/Asp catalytic dyad with the serine in a Gly-Leu-Ser-Gly-Ser sequence similar to that of the classical lipase Gly-X-Ser-X-Gly motif found in other α/β hydrolases. The Ser/Asp dyad is unique among the α/β hydrolases and more closely resembles that of serine proteases, suggesting a novel catalytic mechanism. The proposed catalytic mechanism for the Group IVA PLA_2 enzyme is that once bound to the membrane bilayer, the side chain of an Arg stabilizes the phosphate head group of a membrane phospholipid in the active site. Once the enzyme-substrate complex is formed, the catalytic Asp activates the Ser side chain during nucleophilic attack of the *sn-2* acyl chain of the lipid. A serine acyl intermediate is formed, releasing a lysophospholipid, which then undergoes water mediated hydrolysis, releasing the free fatty acid chain. The oxyanion transition state is stabilized by the backbone amide protons of a Gly-Gly-Gly sequence.

$iPLA_2$

Like the group IV PLA_2 enzyme, the $iPLA_2$ enzyme has multiple group members, the group VIA PLA_2 and the group VIB PLA_2. These enzymes both localize in the cytosol and are unique from the group IV family of PLA_2s in that they are calcium-independent. The group VIA PLA_2 is most often referred to as $iPLA_2$ and was initially purified and characterized from the murine $P388D_1$ macrophage-like cell line. Of all of the $iPLA_2$ family members, the most is known about the enzymology and structural features of this enzyme. The group VIB enzyme has only recently been cloned and little is known about its enzymology or structure.

The group VIA enzyme is an 85–88 kDa cytosolic protein that is expressed as several distinct splice variants, only two of which are catalytically active (group VIA-1 and VIA-2). The enzyme contains a series of N-terminal ankyrin repeats, typically involved in the formation of protein–protein interactions, and the mouse group VIA-1 enzyme has been shown to function as a 340 kDa oligomeric complex. The group VIA-2 PLA2 has a 54 amino acid insertion in the eighth ankyrin repeat, likely a membrane-binding domain. The enzyme shows a consensus lipase motif, Gly-Thr-Ser-Thr-Gly. Other residues critical for catalysis have yet to be identified and the mechanism by which the $iPLA_2$ cleaves the *sn-2* linkage is still unclear, but it is likely to be an α/β hydrolase with a catalytic Ser/Asp dyad like the group IVA PLA_2. Like the group IVA enzyme, the group VIA PLA_2 exhibits both lysophospholipase and transacylase activities. Nucleotide di- and tri-phosphates have been shown to stabilize the purified enzyme and the nucleotides are not turned over during this process,

suggesting a structural role. Unfortunately at this time there is not a reported X-ray crystal structure of the group VIA PLA_2, so little is known about the overall fold or active site geometry.

PAF Acetyl-Hydrolase

The PAF acetyl-hydrolases are a family of enzymes first cloned in the mid-1990s that include members of both the group VII and group VIII PLA_2 enzymes. These enzymes are constitutively active, catalyzing the hydrolysis of short acyl chains at the *sn-2* position of 1-O-alkyl-2-acetyl phosphatidylcholine (PAF). They are unique among the PLA_2s in that they have little to no measurable activity on acyl chains longer than nine carbons.

The group VIIA PLA_2 is found in the blood plasma and is a 45 kDa monomeric enzyme of the α/β hydrolase family. This enzyme possesses a consensus lipase motif, Gly-His-Ser-Phe-Gly, with a catalytic serine residue. Unlike the group IV enzymes, the group VIIA proteins possess a classical hydrolase triad of Ser, Asp, and His, suggesting that its catalytic mechanism is similar to that of other α/β hydrolases. The group VIIA enzyme is the circulating form of the enzyme typically found associated with lipoproteins and binding to LDL causes an increase in PAF-AH activity through, as yet, an unknown mechanism. This enzyme has been reported to hydrolyze oxidized phospholipids in addition to PAF. The group VIIB enzyme is an intracellular monomeric 40 kDa protein closely related to the group VIIA enzyme with an identical active site lipase motif. Both of the group VII enzymes are able to hydrolyze PAF molecules with *sn-2* acyl chains as long as 5 carbons.

The group VIII enzyme is found most abundantly in brain tissues and is comprised of three subunits, α-1, α-2, and β, of which the α-1 and α-2 subunits both possess PAF-AH activity. The α-1 and α-2 subunits are 29 and 30 kDa respectively and share a 63% sequence identity between them. Both subunits contain a modified lipase motif of Gly-Asp-Ser-Met-Val and Gly-Asp-Ser-Leu-Val respectively. These enzymes both possess a classical Ser, Asp, His triad, again suggesting that their catalytic mechanisms is similar to that of other serine esterases. The β subunit does not possess any PLA_2 activity and is likely a structural or regulatory protein.

PLA_2 Cellular and Signaling Roles

The PLA_2 enzymes have been shown to be involved ubiquitously in almost all lipid signaling and metabolism functions within the cell. The group IVA and VIA enzymes have been shown to be linked to apoptosis. Additionally, the group VIA PLA_2 has been shown to be directly involved in cellular phospholipid remodeling. One of the most studied aspects of the mammalian PLA_2s, including the group II and V $sPLA_2$s and the group IVA $cPLA_2$, is their role in the production of arachidonic acid used in the production of the pro-inflammatory eicosanoids, including prostaglandins, leukotrienes, and lipoxins. These molecules play critical signaling roles in pathways as diverse as pain and inflammation, allergic responses, implantation and parturition, vasoconstriction and dilation, and renal function. Finally, the role of the group VII and VIII PLA_2 enzymes, the PAF acetyl hydrolases, is to break down the pro-inflammatory PAF molecule and terminate the signaling process. The group VIIA enzyme has also been shown to be associated with lipoproteins such as HDL and LDL and is thought to be critically involved in the breakdown of oxidized phospholipids.

See Also the Following Articles

Eicosanoid Receptors • Lysophospholipid Receptors • Phospholipid Metabolism in Mammals

Glossary

α/β hydrolase Superfamily of hydrolase enzymes containing a characteristic fold of 8 β-strands connected by α-helices commonly possessing a catalytic triad of Ser, Asp, and His.

eicosanoid Family of signaling molecules derived from the unsaturated fatty acid arachidonate that includes prostaglandins, leukotrienes, and lipoxins.

lysophospholipid Phospholipid in which either the *sn-1* or *sn-2* fatty acid has been removed.

PAF 1-O-alkyl-2-acetyl-*sn*-glycero-3-phosphocholine, a potent signaling molecule derived from 1-O-alkyl lysophospholipids involved in inflammation and allergic responses.

phospholipase A_2 Superfamily of enzymes which hydrolyze fatty acids from the *sn-2* position of membrane phospholipids.

phospholipid Major lipid component of biological membranes with an *sn*-glycerol-3-phosphate backbone, fatty acids on the *sn-1* and *sn-2* position, and a head group attached to the 3-phosphate.

Further Reading

Dessen, A., Tang, J., Schmidt, H., Stahl, M., Clark, J. D., Seehra, J., and Somers, W. S. (1999). Crystal structure of human cytosolic phospholipase A_2 reveals a novel topology and catalytic mechanism. *Cell* **97**, 349–360.

Nigam, S., Wilton, D. C., and Dennis, E. A (eds.) (2000). Molecular and cell biology of lipids phospholipase A_2 special issue. *Biochim. Biophys. Acta* **1488**, 1–2.

Singer, A. G., Ghomashchi, F., Le Calvez, C., Bollinger, J., Bezzine, S., Rouault, M., Sadilek, M., Nguyen, E., Lazdunski, M., Lambeau, G., and Gelb, M. H. (2002). Interfacial kinetic and binding properties of the complete set of human and mouse groups I, II, V, X, and XII secreted phospholipases A_2. *J. Biolog. Chem.* **277**, 48535–48549.

Biography

Edward A. Dennis is a Professor of Chemistry and Biochemistry at the University of California, San Diego. Since the 1970s, Dr. Dennis' laboratory has studied the structure and function of the phospholipase A_2 superfamily of enzymes, publishing over 250 articles on these topics. The Dennis laboratory was the first to purify and characterize the calcium independent PLA_2, has worked extensively on developing models for the action of PLA_2 enzymes at lipid interfaces, and explored the roles of individual PLA_2s in the eicosanoid cascade of macrophages.

Timothy Smith has been a Postdoctoral Associate in the Dennis laboratory since December 2000, working on the structural and biochemical characteristics of the calcium independent PLA_2 enzyme.

Phospholipase C

Fujio Sekiya, Yeun Ju Kim and Sue Goo Rhee
National Heart, Lung, and Blood Institute, Bethesda, Maryland, USA

Phospholipase C (PLC) is an enzyme that cleaves a glycerophospholipid at the phosphodiester bond between the glycerol backbone and the phosphate group. All known eukaryotic PLCs, including those implicated in calcium signaling in animal cells, utilize only phosphoinositides (phosphatidylinositol and its phosphorylated derivatives) as substrates, hence called phosphoinositide-specific PLC and frequently just referred to as PLC. The minor constituent of plasma membranes, phosphatidylinositol 4,5-bisphosphate (PIP2), appears to be the only physiological substrate of PLCs, though in test tubes other phosphoinositides can be hydrolyzed. PLC cleavage of PIP2 simultaneously generates two second messengers, inositol 1,4,5-trisphosphate (IP3) and 1,2-diacylglycerol (DAG). PLC is not a single entity but consists of members with various structures, and mechanisms to regulate PLC isozymes are also diverse. To date, 12 different mammalian PLCs have been identified, and they are grouped into 5 subfamilies based on their primary structures.

Biological Consequences of PLC Action

Early studies by Hokin and Hokin in the1950s revealed that stimulation of cells could induce rapid metabolism of inositol phospholipids, and in 1975 Robert Michell suggested the connection between phosphoinositide hydrolysis and calcium mobilization. Functions of IP3 and DAG as important second messengers were established in the mid-1980s by Michael Berridge and Yasutomi Nishizuka, respectively. It was these landmark discoveries that brought special attention to PLC as the key enzyme to generate the two second messengers.

The soluble part of PIP2 cleavage product, IP3, binds to its intracellular receptor present on the calcium storage site endoplasmic reticulum (ER), and the receptor constitutes a channel to gate calcium ions. IP3 ligation opens the channel, causing a transient increase in the cytoplasmic calcium concentration. The other cleavage product DAG stays in the plasma membrane and recruits protein kinase C (PKC) isozymes. Activation of certain PKC isozymes requires both binding to DAG and calcium ions. Activated PKC elicits a wide range of cellular responses through phosphorylation of many kinds of substrate proteins (Figure 1).

Increasing evidence indicates that PIP2 by itself participates in many cellular processes through binding to a number of proteins. First, the phospholipid is a focal point to bridge plasma membranes and networks of cytoskeletal proteins. It thus plays key roles in maintenance of cell morphology as well as in control of motility. Second, it can modify activities of various enzymes and channels; phospholipase D and capsaicin receptor (ion channel) are a few examples among many such PIP2 effectors. Third, it provides a platform to form functional signaling complexes, because many of those proteins participating in the complexes have lipid-binding modules, such as PH, FERM, and ENTH domains. Consistent with their physiological significance, cellular levels of PIP2 are maintained through strictly regulated production/destruction mechanisms involving many lipid kinases and phosphatases. Activation of PLC leads to a rapid reduction in cellular PIP2 level. Thus, both generation of IP3/DAG and destruction of PIP2 by PLC can dramatically affect the cell's physiology in many ways.

Given such diverse and profound consequences, PLC activation is one of central mechanisms of cellular signaling, and its activity is tightly controlled in cells. Indeed, a large number of hormones, growth factors, and neurotransmitters rely on PLC in transmitting their signals across plasma membranes.

Biochemistry of PLC

Structure of PLC

PLC has been found in yeasts, slime molds, plants, and animals, and is probably present in all taxa of eukaryotes. All eukaryotic PLCs appear to be evolved from a single archetype, and it is in the animal kingdom that PLC diversified. Eleven different genes encoding PLC isozymes have been identified in mammals, and they are grouped into four subfamilies, named as β, γ, δ, and ε. In addition, an isozyme named ζ, which has the simplest structure, has been found recently (Figure 2). Animals, from the nematode *Caenorhabditis elegans*

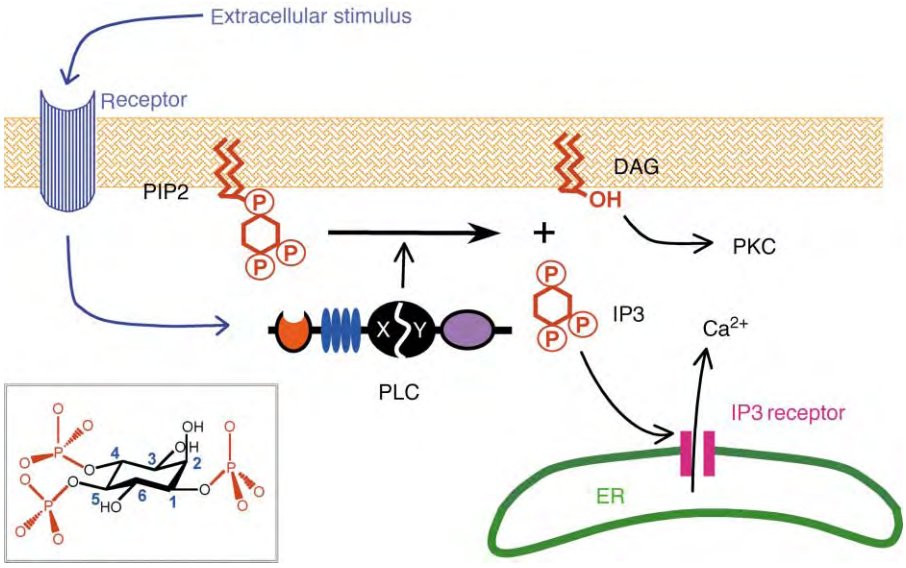

FIGURE 1 A scheme for the action of PLC in the cell. For abbreviations, see text. Inset shows chemical structure of IP3.

to the fly to the human, appear to have all subtypes, but only the primitive δ-like (or ζ-like) PLCs are found in other eukaryotes. The protein originally termed PLC-α was turned out to be a proteolytic fragment of PLC-δ1, and was thus eliminated from the nomenclature. Some isozymes have alternatively spliced variants at the mRNA level, and the total number of mammalian PLC polypeptides exceeds 20.

All PLC isozymes possess common structural features, indicating origination from a common ancestor. The δ-isozyme consists of an N-terminal PH (pleckstrin-homology) domain, four copies of EF-hands, regions called X and Y, followed by a C2 domain. Other three types of PLC isozymes are made up by additions (or replacements) of some regulatory domain structures to the δ-subtype (Figure 2). PH domains are ~120-residue units, which oftentimes function as membrane-binding sites through interaction with phosphoinositides. EF-hands are the calcium-binding motifs identified in calmodulin, but it is unclear whether PLC's EF-hands actually bind calcium ions. C2 domains (~120 residues) are the structures originally found in PKC that act as calcium-dependent lipid-binding modules. X and Y regions are unique to eukaryotic PLCs. Evidence shows that the two regions together form a discrete unit of catalyst, though they are separated by a linker in the primary structure.

Mechanism of Catalysis

Based on crystallographic structures of PLC-δ1 and biochemical data, the catalytic mechanism for PLC has been postulated. Calcium ion, which is required for all PLC isozymes, was seen in the catalytic center interacting with the IP3 moiety of PIP2; the cation activates the 2-hydroxy group of inositol ring that in turn attacks the 1-phosphate, cleaving off the head group to form a 1,2-cyclic phosphate intermediate and DAG. The cyclic derivatives are subsequently hydrolyzed to acyclic inositolphosphates. Several positive residues found in the active site pocket interact with the phosphate groups at the 4- and 5-positions of inositol ring, explaining the preference of enzyme for PIP2 over phosphatidylinositol or phosphatidylinositol 4-phosphate. The structure has also indicated that the pocket cannot accommodate phosphoinositides with phosphate at the 3-position (e.g., phosphatidylinositol 3,4,5-trisphosphate), explaining why 3-phosphorylated inositides are not substrates of PLC.

PLC Isozymes and their Regulation Mechanisms

PLC-β

Signals of many chemical and physical stimuli are received by cells via receptors that couple to heterotrimeric G proteins. A large portion of such stimulation induces PIP2 hydrolysis by activating PLC-β isozymes. Beta isozymes (β1 ~ β4; ~150 kDa) are unique in having long C-terminal extensions that are absent in other classes of isozymes (Figure 2).

Upon activation of receptor, the receptor-associated αβγ heterotrimer of G protein dissociates into α- and βγ-subunits. Both α-and βγ-subunits are able to transmit signals. The members of G_q family of α-subunits (αq, α11,

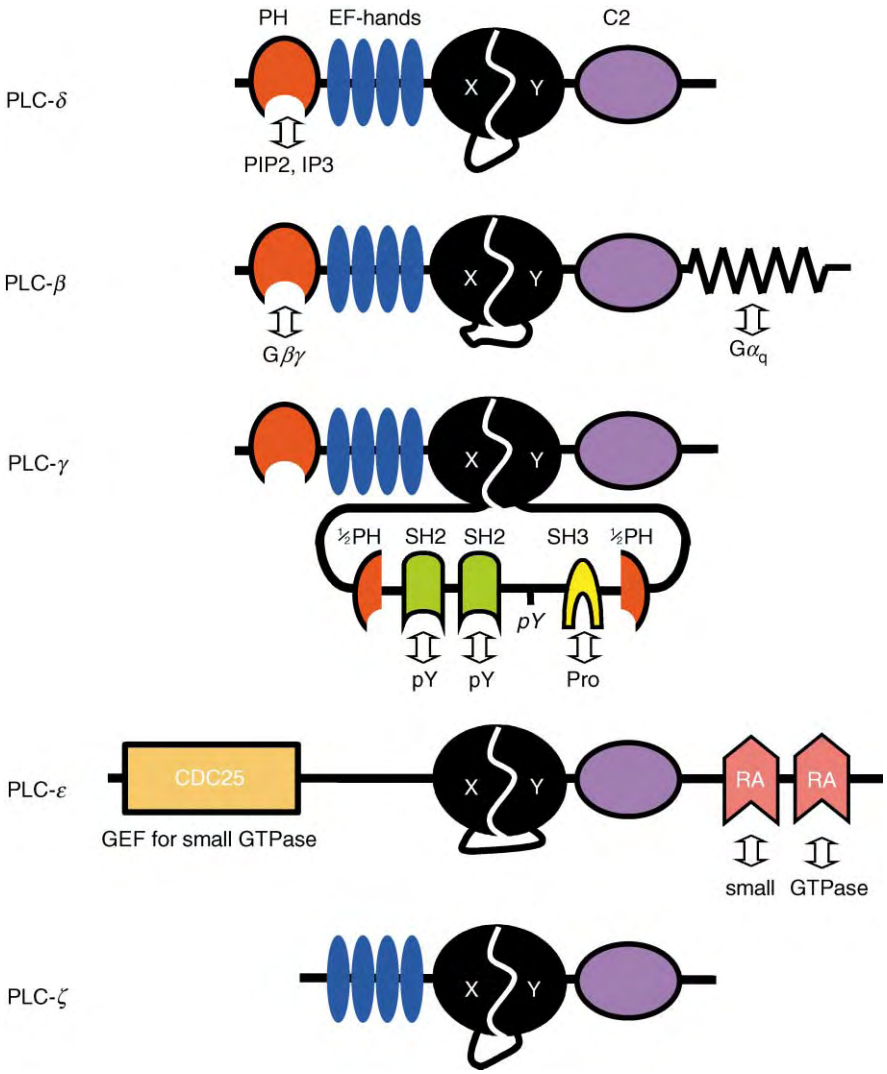

FIGURE 2 Structural organizations of PLC isozymes. Known ligands of domains of PLCs are shown. *p*Y, phosphotyrosine; Pro, proline-rich sequence.

α14, and α16) can activate PLC-β, but not PLC-δ and PLC-γ. In contrast, the α-subunits of other G protein subclasses (Gs, Gi, and G12/13) do not activate PLC-β. Also, $\beta\gamma$-complexes can specifically stimulate PLC-β. αq- and $\beta\gamma$-subunits appear to interact with different regions in the PLC-β molecule: αq is recognized by the C-terminal region unique to β-isozymes, whereas the $\beta\gamma$-subunit binds to the N-terminal PH domain. In most cells the Gi family of G protein is abundant compared to other classes. It is considered that only Gi-coupled receptors can provide significant amounts of $\beta\gamma$, and that agonists inducing activation of Gi are responsible for $\beta\gamma$-mediated activation of PLC-β.

Four isozymes of this subfamily appear to be expressed in different tissues and to have different sensitivities to the G protein subunits. PLC-β1 and β3 are widely expressed in various tissues and are more sensitive to the activation by αq compared to other isozymes. PLC-β2 expression is restricted to blood cells and is most sensitive to the activation by $\beta\gamma$ among the four PLC-βs. PLC-β4 expression is only seen in some parts of the brain and in the retina. Genes for all four β-isozymes have been disrupted in mice, and none of those single knockouts appeared to be fatal, probably because their functions overlap. Reported phenotypes of knockouts include: PLC-β1, epilepsy; PLC-β2, dysfunctions in neutrophils and platelets; PLC-β3, hyperresponse to opioid stimulation; and PLC-β4, ataxia and impairment in visual perception.

PLC-γ

Activation of PLC-γ is controlled by phosphorylation of its tyrosine residues, and the two isozymes of this subfamily (γ1 and γ2; $\sim$140 kDa) have a long linker sequence between the X and Y regions, which is indispensable for their regulation. The linker region consists of a half of a PH domain, two SH2

(Src-homology 2) domains, an SH3 (Src-homology 3) domain, and the remaining half of the split PH domain (Figure 2).

Binding of peptide growth factors (such as platelet-derived growth factor, epidermal growth factor, and nerve growth factor) to their cognate receptors results in activation of the intrinsic protein tyrosine kinase activity of the receptor and consequent autophosphrylation of their cytoplasmic tails, creating docking sites for phosphotyrosine-binding motifs. PLC-γ binds those phosphotyrosines using its SH2 domain and is then phosphorylated by the receptor protein tyrosine kinases. Tyrosine phosphorylation that occurs within the linker region leads to activation of PLC-γ by a mechanism not fully understood.

Immunoreceptors in blood cells, such as the T-cell receptor and the B-cell receptor for antigens, do not have intrinsic tyrosine kinase activity but are also able to activate PLC-γ. Ligand-induced clustering of immunoreceptors causes phosphorylation in the domain termed immunoreceptor tyrosine-based activation motif (ITAM) by receptor-associated Src-family tyrosine kinases (e.g., Lck, Lyn, and Fyn). Phosphorylated ITAMs recruit and activate Syk-family tyrosine kinases (Syk and ZAP-70), and the recruited Syk-kinases, in turn, phosphorylate many kinds of adaptor proteins, such as linker of activation of T cells (LATs) and B-cell linker protein (BLNK). PLC-γ then binds to and is phosphorylated by the resultant supermolecular complex consisting of aggregated immunoreceptors, Src kinases, Syk kinases, and adaptor proteins. Stimulation of blood cells, moreover, can activate another class of tyrosine kinase, Tec-family kinases (e.g., Btk), via a phosphoinositide 3-kinase-dependent mechanism. Tec-kinases are also implicated in PLC-γ activation.

PLC-γ1 is expressed ubiquitously and disruption of its gene is lethal at an early embryotic stage. PLC-γ2 is expressed in a set of hematopoietic lineages including B cells, platelets, neutrophils, and mast cells. Knockout of γ2 is not lethal but abolishes maturation of B cells, resulting in immunodeficiency, and causes dysfunctions of Fc-receptor-mediated signaling in platelets and mast cells.

PLC-δ

PLC-δ isozymes (δ1 ~ δ4; ~90 kDa) have simpler structures compared to other isozymes (Figure 2). They lack obvious regulatory domains that facilitate coupling to receptors. The exact nature of their activation mechanisms remains unclear, but probably they do not couple to hormone receptors directly. PLC-δ has greater calcium sensitivity compared to β- and γ-isozymes. It is proposed that PLC-δ can be secondarily activated when cytoplasmic calcium concentrations are elevated via PLC-β(or PLC-γ)/IP3-mediated mechanisms. The PH domain of PLC-δ binds to PIP2 and also recognizes IP3 with a higher affinity: this domain is thought to mediate tethering of PLC-δ to plasma membranes. When PIP2 hydrolysis occurs, generated IP3 causes dissociation of the enzyme from membranes, thus terminating the reaction. This mechanism constitutes a feedback negative regulation system for this isozyme.

Among four δ-isozymes known, gene targeting of δ1 and δ4 isozymes has been conducted. Both resulted non-fatal. PLC-δ1-deficient mice experienced progressive hair loss. The isozyme appears to be necessary for commitment of skin stem cells. Male homozygotes of PLC-δ4-deficient mice were infertile, and it was reasoned that the isozyme was required for the acrosome reaction of sperms.

PLC-ε

The ε-isozyme (>200 kDa) contains a CDC25-like domain in the N terminus, which has guanine nucleotide exchange factor (GEF) activity toward small GTPases, and two copies of Ras-binding motifs (RA domains) following the C2 domain, but neither a PH domain nor EF-hand is evident (Figure 2). It has been shown that (1) PLC-ε is capable of catalyzing PIP2 hydrolysis both *in vitro* and *in vivo*, (2) the CDC25-like domain can function as a GEF for Rap1A but not for Ras, and (3) the RA domains are able to bind to active forms of Ras and Rap1A. Because of the presence of domain structures that interact with small GTPase of Ras superfamily, it seems likely that PLCs-ε regulation utilizes these class of proteins. Whether they are regulators (upstream of PLC-ε) or effectors (downstream) or both is yet to be determined. Studies done so far are somewhat inconsistent with each other, and it is still premature to picture the exact mechanism by which this isozyme functions in the cell.

PLC-ζ

A novel type of PLC named PLC-ζ (~70 kDa) was recently identified as a sperm-specific isozyme. PLC-ζ has a very primitive structure. It even lacks the N-terminal PH domain (Figure 2) and rather resembles PLCs found in plants or yeasts. A phylogeny analysis revealed its least divergence from a hypothetical precursor among all mammalian PLCs. It has been shown that this sperm-specific isozyme is responsible to calcium oscillation in fertilizing eggs.

See Also the Following Articles

G_q Family • IP_3 Receptors • Phosphatidylinositol Bisphosphate and Trisphosphate • Phosphoinositide 3-Kinase • Protein kinase C Family

Glossary

diacylglycerol A product of PIP2 cleaved by PLC. It serves as a second messenger activating some members of PKCs, and is readily converted to phosphatidic acid in the cell by the action of diacylglycerol kinases.

IP3 The other product of PIP2 cleavage by PLC. IP3 is also a short-life second messenger due to inactivation either through dephosphorylation by specific phosphatases or through phosphorylation by the IP3 kinase.

pleckstrin homology (PH) domain A domain structure that occurs in a wide range of proteins involved in intracellular signaling or as constituents of the cytoskeleton. It was originally found in pleckstrin (platelet C-kinase substrate protein). It binds to phosphoinositides such as PIP2 and/or PIP3.

Src homology 2/3 (SH2/3) domain Domain structures that occur in various signaling proteins, initially identified in the protooncoprotein *src*. SH2 domain recognizes phosphorylated tyrosine residues in target peptides, whereas SH3 domain binds to peptide sequences rich in proline residues.

Further Reading

Carpenter, G., and Ji, Q.-S. (1999). Phospholipase C-γ as a signal-transducing element. *Exp. Cell Res.* **253**, 15–24.

Cockcroft, S. (1997). Phosphatidylinositol transfer proteins: Requirements in phospholipase C signaling and in regulated exocytosis. *FEBS Lett.* **410**, 44–48.

Fukami, K. (2002). Structure, regulation, and function of phospholipase C isozymes. *J. Biochem. (Tokyo)* **131**, 293–299.

Irvine, R. F. (2003). 20 years of Ins(1,4,5)P3, and 40 years before. *Nat. Rev. Mol. Cell Biol.* **4**, 586–590.

Rhee, S. G. (2001). Regulation of phosphoinositide-specific phospholipase C. *Annu. Rev. Biochem.* **70**, 281–312.

Williams, R. L., and Katan, M. (1996). Structural views of phosphoinositide-specific phospholipase C: Signaling the way ahead. *Structure* **4**, 21387–21394.

Biography

Fujio Sekiya is a Staff Scientist in the Laboratory of Cell Signaling at the National Heart, Lung, and Blood Institute (NHLBI), National Institutes of Health in Bethesda, Maryland. He received a Ph.D. from the Tokyo Institutes of Technology in 1991.

Yeun Ju Kim is a graduate student of the Ewha Womens University, Seoul, Korea, now staying at the Laboratory of Cell Signaling, NHLBI. She holds an M.Sc. degree from the Ewha Women's University.

Sue Goo Rhee is Chief of the Laboratory of Cell Signaling, NHLBI, NIH. He received a Ph.D. from the Catholic University of America in 1972.

Phospholipase D

Mary M. LaLonde and Michael A. Frohman
Stony Brook University, Stony Brook, New York, USA

The phospholipase D gene superfamily encodes a diverse array of enzymes that carry out phosphodiesterase actions on phospholipid and DNA substrates. All members share a structural domain known as the HKD catalytic motif. While bacterial PLD is constitutively active, eukaryotic PLDs are tightly regulated by signaling pathways. Mammalian PLD is synergistically regulated by PI4,5P_2, ARF, and Rho GTPases, and protein kinase C. Upon activation, eukaryotic PLDs, which are phsophatidylcholine-specific, cleave the substrate phosphatidylcholine to yield the pleiotropic lipid phosphatidic acid, which can serve as either a signal transducer, lipid anchor, signaling intermediate, or fusogenic lipid. *In vivo* roles for PLD consist of regulated membrane trafficking events including prospore membrane formation in yeast and regulated secretion in neuroendocrine cells, and cell shape dynamics.

Introduction

Phospholipase D (PLD) was the founding member of a superfamily that is now recognized to include phosphatidylserine synthase, a cardiolipin synthase, an atypical endonuclease, an enzyme that rescues covalently bound topoisomerase from DNA, a toxin from the black-death causative agent Yersinia pestis, a viral envelope protein required for pox virus (e.g., smallpox) pathogenesis, and many other gene products of unknown function. Despite the biologically diverse functional roles that these proteins undertake, they share a common catalytic mechanism that invariably targets a phosphodiester bond found in a varied set of substrates (see Figures 1 and 2). The phosphodiester-bond-containing substrates include several phospholipid species in which the phosphodiester bond forms a bridge between the lipid phosphate portion of the molecule and its headgroup; DNA, where the phosphodiester bond forms the link between individual nucleotides and a DNA-topoisomerase complex linked by the bond that occasionally inadvertently persists during DNA unwinding. Additional homologues that encode the PLD catalytic motif, but for which no function has been assigned, still await characterization. No doubt there are yet other interesting substrates and stories that will emerge from continued study of this superfamily.

PLDs found in yeast and animals catalyze hydrolysis of the phosphodiester bond found in the phospholipid phosphatidylcholine (PC). This generates soluble choline and the lipid phosphatidic acid (PA). Bacterial PLDs are promiscuous and will also use as substrate phospholipids with other headgroups, such as phosphatidylethanolamine or phosphatidylinositol. Although the hydrolysis of these phospholipids has been reported in mammals and yeast, the hydrolyzing proteins have not been identified and the eukaryotic PLDs have never been shown to perform these activities. Hence, additional genes of related function, if not sequence, may await discovery.

PLD Gene Families

The PLD gene families are relatively small in yeast (one member) and animals (generally one or two members). By contrast, plants encode up to a dozen PLDs, some of which are highly similar to the mammalian genes in structure. Two mammalian PLDs exist, PLD1 and PLD2, which are structurally similar and 55% identical on the amino acid level but are thought to be regulated somewhat differently and to carry out different cell biological roles. PLD1 has more commonly been shown to regulate vesicular trafficking events whereas PLD2 has been associated more often with regulation of cell shape. However, some overlap in function has also been described. Although many (but not all) cell types express both isozymes, the relative amounts of PLD1 and PLD2 expressed in individual tissues vary dramatically, suggesting that the enzymes carry out cell-type specific rather than universal constitutive roles.

PLD Structure

PLD superfamily members are defined by the presence of one or two copies of the consensus sequence, $HXK(X)_4D(X)_6GSXN$, denoted as the "HKD" domain, which encodes the key residues involved in catalysis (Figure 3). *Bona fide* PLD proteins also

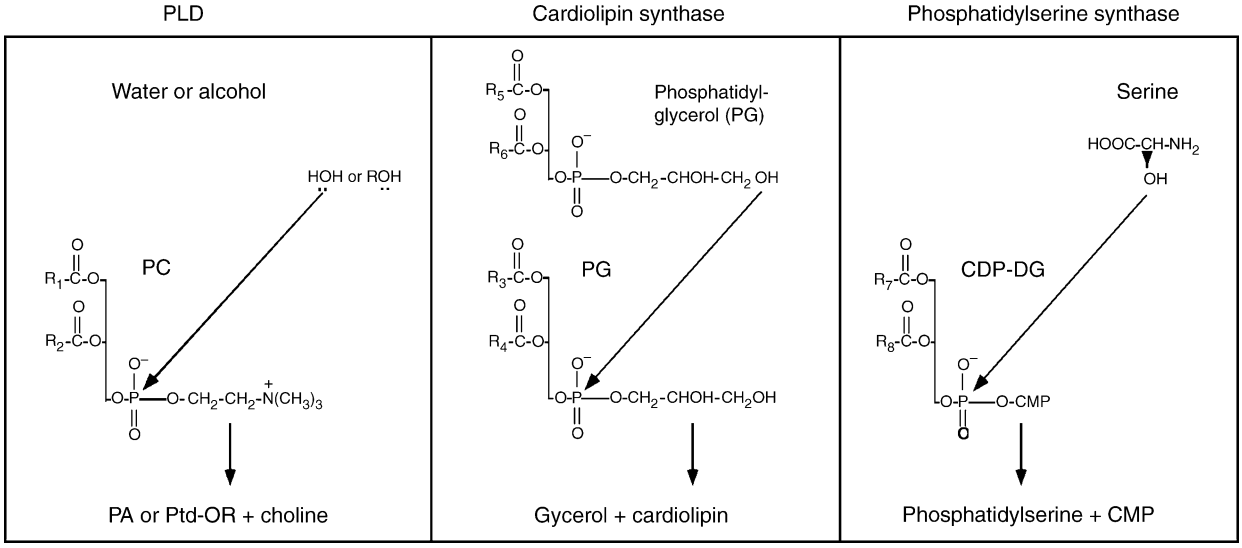

FIGURE 1 PLD, cardiolipin synthase, and phosphatidylserine synthase catalytic reactions. Each reaction involves nucleophile attack on a phosphate bond as shown. Two biochemical activities for PLD have been observed: phosphodiester bond hydrolysis and phospholipid transphosphatidylation. Using H_2O as an electron donor, PLD functions as a phospholipid hydrolysis enzyme, cleaving phosphatidylcholine (PC) to produce phosphatidic acid (PA) and choline. Through the same mechanism, but using alcohol instead of H_2O as the electron donor, PLD can generate phosphatidylalcohols. Nucleophiles that can be used by PLD include exogenously supplied butanol or endogenous diacylglycerol, yielding phosphatidylbutanol and bisphosphatidic acid, respectively. CLS and PSS only carry out synthetic reactions in which alcohols are used as the nucleophile, as shown. Reprinted from Sung, T. C., Roper, R., Zhang, Y., Rudge, S., Temel, R., Hammond, S., Morris, A., Moss, B., Engebrecht, J., and Frohman, M. (1997). Mutagenesis of phospholipase D defines a superfamily including a *trans*-Golgi viral protein required for poxvirus pathogenicity. *EMBO J.* **16**, 4519-4530, with permission of Oxford University Press.

invariably contain several additional conserved domains that assist in proper functioning of the catalytic site. The PLD catalytic core is comprised of two HKD motifs that juxtapose to create the active site, within which the histidine residues directly coordinate the transphosphatidylation reaction. This results in the formation of a covalent phosphatidyl-enzyme intermediate. Both HKD domains must be intact for PLD to be catalytically active. It has been suggested that protein modulators of mammalian PLD activity may influence activation by affecting the orientation of the HKD domains or their distance from the substrate. However, this remains hypothetical since only the mammalian isoforms are thusly regulated, and they have not yet been crystallized in a complex, with or even without their regulators.

Other domains universally found in animal and yeast PLD proteins include a PH domain, which is not essential for enzymatic activity but does regulate subcellular localization and translocation. A basic amino acid-rich phosphatidylinositol 4,5 bisphosphate ($PI4,5P_2$) binding site located near the center of the proteins is essential for catalysis, and plays an important but less conserved role in membrane association and subcellular localization. In addition to these domains, the proteins encode a Phox homology (PX) domain which also helps direct PLD subcellular localization. Finally, mammalian PLD1 is regulated not only by the phospholipid $PI4,5P_2$, but by at least three separate protein factors as well. These effectors (ARF GTPases, Rho GTPases, and PKC family members) act synergistically through binding at distinct sites in PLD1.

Regulation

Overview

Whereas bacterial PLD is constitutively active, eukaryotic PLD is generally activated during events associated with dynamic changes in cells. PLD in plants is activated by wounding and other external environmental cues. PLD in mammals has long been recognized to be activated in response to agonists that stimulate cells through G-protein-coupled or tyrosine kinase receptors. Examples of such agonists include neurotransmitters, serum-derived growth factors, hormones, and cytokines. Yeast PLD does not appear to be directly activated by receptor systems, but its transcription and its subcellular localization are tightly regulated by signaling pathways, which lead qualitatively to the same outcome.

Regulation of Mammalian Phospholipase D

Stimulation of mammalian PLD through G-protein-coupled or tyrosine kinase receptors is mediated principally by a phospholipid ($PI4,5P_2$) and three classes of proteins: ARF GTPases, Rho GTPases, and protein kinase C (PKC). The specific mechanism of

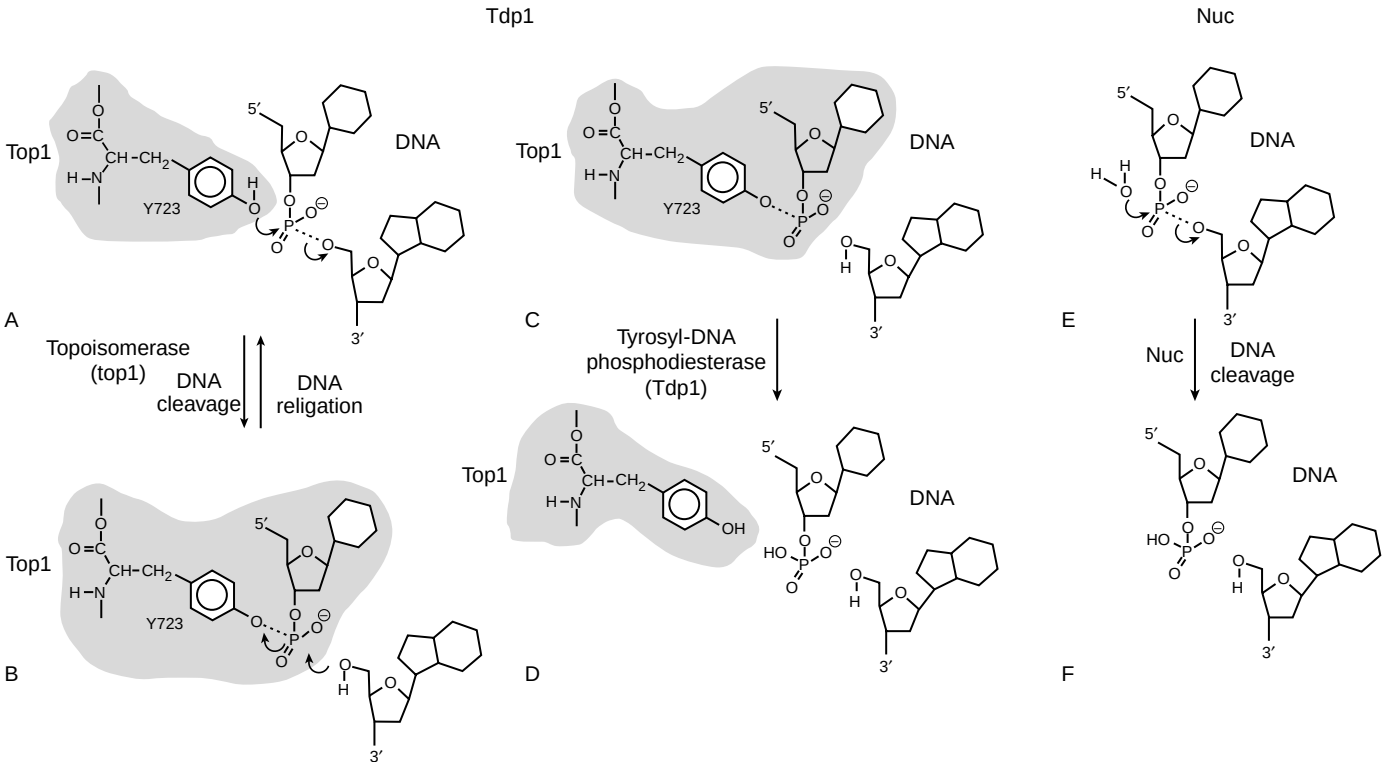

FIGURE 2 Schematic representation of mechanism of action of more divergent members of the PLD superfamily. (A) Topoisomerase I (top1) reversibly generates a cleavage complex by forming a covalent link between tyrosine 723 in top1 and the DNA backbone (B). (C, D) If top1 becomes stalled in the cleavage complex form, it is rescued by Tdp1 hydrolysis of the phosphotyrosyl (phosphodiester) bond (dotted line in (C)). (E,F) The bacterial endonuclease Nuc similarly uses water to attack the backbone phosphodiester bond in DNA to hydrolyze it. Cartoon adapted from Debethune *et al.* (2002).

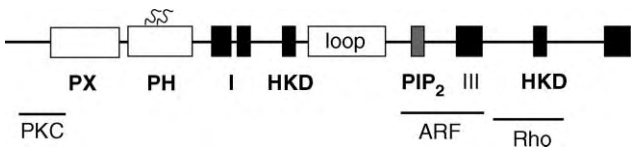

FIGURE 3 PLD structure. Mammalian PLD contains catalytic domains (HKD, I, III, and C-terminus), a $PI4,5P_2$ interacting motif (PIP_2), and PX and PH-membrane association domains. The PH domain is palmitoylated in PLD1. PLD1's activators Rho, ARF, and PKC interact with PLD1 within the regions depicted to activate it.

PLD activation varies with cell type and receptor system examined.

Phosphoinositides

A role for phosphoinositides in the regulation of PLD was first suggested by the finding that $PI4,5P_2$ was required for ARF stimulation of PLD in HL-60 cells and has since been confirmed using purified reagents in *in vitro* reconstitution systems. Activation of PLD1 by phosphoinositides is independent of the stimulatory effects of GTP-binding proteins and protein kinases. Phosphoinositides may function to anchor PLD to the phospholipid surface, thereby increasing the rate of catalysis by placing PLD in close proximity to its substrate.

Protein Kinase C

PKCα and PKCβ directly and indirectly mediate agonist-dependent activation of PLD. Overexpression of either PKC isoform potentiates PLD responses to agonists such as endothelin, thrombin, and PDGF. Down-regulation of PKC through long-term exposure to phorbol esters, antisense depletion of PKCα, or mutation of the site in PLD1 at which PKC interacts decreases agonist-stimulated PLD activity. PKC most commonly activates its targets through phosphorylation. Although PKC does phosphorylate PLD1, it has been shown convincingly that this is not the mechanism through which it activates the same. Activation by PKCα occurs in the absence of ATP (*in vitro*) and is not inhibited by staurosporine, a catalytic-site inhibitor. This non-kinase-dependent stimulatory activity resides within the regulatory domain of PKCα, and PKCα interacts directly with the amino terminus of PLD1. PKC also mediates activation of PLD through a kinase-dependent non-direct mechanism involving calcium influx into cells but which otherwise is not understood clearly. For both PLD isoforms, multiple kinase-dependent downstream consequences of PKC activation may also contribute to PLD activation. To give one such example, a major substrate for PKC subsequent to activation is the protein myristoylated alanine-rich C-Kinase substrate (MARCKS). Under basal conditions, MARCKS localizes to membrane surfaces through multiple low-affinity interactions with $PI4,5P_2$. Once phosphorylated by PKC, MARCKS relocates to the cytosol, making the previously sequestered $PI4,5P_2$ available for other interactions including PLD activation. Consistent with this idea, mutations to MARCKS that eliminate its phosphorylation decrease PKC-mediated PLD activation.

Rho Family of GTPases

The finding that a GTPγS-dependent factor required for PLD activity in neutrophils was removed by RhoGDI first suggested a role for Rho in PLD activation. Rho has since been shown to mediate agonist-dependent PLD activation downstream of numerous agonist-receptor combinations. Many studies on this topic have inhibited Rho using bacterial toxins such as C3 exotoxin from *C. botulinum* (inactivates Rho through ADP-ribosylation) or Toxin B from *C. difficile* (blocks Rho function through monoglucosylation). Dominant-negative Rho mutants have also been used and block phorbol ester-stimulated PLD activity in human adenocarcinoma A549 cells, suggesting that there is cross-talk between the Rho and PKC activation pathways. Direct activation of PLD1 by Rho through an interaction at the C-terminus has been demonstrated; this appears not to be the case, however, for PLD2. Indirect mechanisms of activation are also likely. Rho activates phosphatidylinositol 4-phosphate 5-kinase, which phosphorylates phosphatidylinositol-4-phosphate to generate $PI4,5P_2$, the cofactor required for PLD activity. Rho may also regulate PLD activity through activation of Rho kinase.

ADP-Ribosylation Factor Family of GTPases

ARF is the most potent activator of PLD activity *in vitro*. Activation of PLD by ARF is GTP-dependent, and appears to involve the N-terminus of ARF and the C-terminus of PLD. ARF proteins have been shown to mediate PLD activation by a number of agonists, including insulin, PDGF, angiotensin II, endothelin, N-FMLP, and glutamate. ARF-mediated activation of PLD is not believed to be specific to any particular ARF isoform. Overexpression of dominant-negative ARF1 and ARF6 mutants or BFA-mediated interference with ARF activation inhibits agonist-induced PLD activation in some settings.

Protein Phosphorylation

Both PLD isoforms appear to be phosphorylated by PKC. Recent studies indicate that PLD1 and PLD2 may be phosphorylated by serine/threonine kinases, including cyclic AMP-dependent protein kinase and calcium-calmodulin-dependent protein kinase, as well as by receptor and non-receptor tyrosine kinases. For example, mouse PLD2 associates with EGFR in a

ligand-independent manner and becomes tyrosine phosphorylated on Y11 in response to signaling by EGF. However, since mutation of Y11 to alanine does not affect PLD activation, and since this residue is not conserved in human PLD2, the physiological significance of the modification is not clear. Ultimately, the physiological relevance of phosphorylation on PLD activity and function has not yet been convincingly demonstrated.

Subcellular Localization of Mammalian Phospholipase D

Phospholipase D activity has been reported in almost every cellular compartment, including the plasma membrane, mitochondria, secretory granules, lysosomes, Golgi, endoplasmic reticulum membranes, and nuclear envelope. Immunolocalization of PLD protein presents a more restricted picture. PLD1 is found primarily on peri-nuclear vesicles in many cell types and on the plasma membrane in others; PLD2 is found primarily on the plasma membrane. However, the proteins may transit through multiple subcellular sites subsequent to cellular stimulation, leading to a record of PLD activity at a broader range of sites. The PLD1 PH domain is palmitoylated and this appears to play a role in targeting PLD1 to specific locations. Elimination of palmitoylation through mutation of key amino acids results in the redistribution of PLD1 from peri-nuclear vesicles to the plasma membrane. PLD2 contains one palmitoylation site. It is not known whether its subcellular localization is effected through lipid modification.

Function of PLD's Product

PA is a pleiotropic lipid. Four basic roles have been proposed for it.

Signal Transducer

PA has been shown to stimulate the activity of several different kinds of enzymes. One of these is phosphatidylinositol 4-phosphate 5-kinase, which phosphorylates the lipid phosphatidylinositol 4-phosphate (PI4P) to generate PI4,5P_2. PI4,5P_2 is well known for its roles in regulating trafficking of membrane vesicles in cells and for regulating cell shape and changes in morphology. PA also activates NADPH oxidase, which plays an important role as part of the neutrophil-mediated immunological response to infection. Another target has been identified recently as mTor, a key component in the regulation of protein translation and cell growth. Additional enzymes regulated by PA are likely to continue to emerge; current candidates include ARF GAPs, enzymes that deactivate ARF small G-proteins and thus are involved in regulating vesicular trafficking and cell shape.

Lipid Anchor

PA has also been reported to bind to and anchor a rapidly growing list of proteins involved in signaling, regulating vesicular trafficking and cell shape, or that have unknown functions. Although in some of these cases, PA may also be stimulating changes in the biochemical behaviors of the target proteins and thus act as a signal transducer, it seems likely that in many of the instances, it serves as a means to recruit effector molecules to a focused location in the cell. For example, at sites of budding from the Golgi or exocytosis at the plasma membrane. In another such example, Raf-1 kinase is activated by the oncogene Ras only at membrane surfaces, but Raf-1 is normally cytosolic and has been reported to become membrane associated only through interaction with PA, like the one which occurs subsequent to insulin receptor activation.

Signaling Intermediate

PA can also be dephosphorylated to yield diacylglycerol, a key lipid which activates protein kinase C (PKC), or monodeacylated to form lysoPA, a potent mitogen found in serum that mediates cell proliferation and shape change.

Biophysical Role

Space-filling models have suggested that with two acyl chains and a small headgroup, PA may act as a "hinge" lipid and promote membrane curvature towards the leaflet in which it is located. Conversely, lysoPA, which has the same headgroup but only one acyl chain, has been proposed to promote membrane curvature in the opposite direction. Since membrane vesicles undergoing budding from or fusion into planar membrane surfaces, pass through energetically unfavorable transition states as the membranes bend and fold at the neck of the vesicles, it is an attractive idea that conversion of PA into lysoPA, and vice versa, could make these events happen more efficiently (i.e., lower the activation energy). These models are supported by the observations that endophilin I, a protein that promotes endocytosis, is an enzyme that converts lysoPA into PA, and that adding PA to vesicles promotes accelerated rates of fusion in *in vitro* reconstitution assays.

Cell Biological Roles

Yeast

PLD function is best understood in yeast, where it was identified in a genetic screen for mutants unable to complete the late stages of meiosis. At the point in the meiotic process where PLD is required, duplication of the chromosomal DNA has been completed and individual sets of chromosomes are segregating to each pole of the four-lobed nucleus. The outer half of the spindle pole body found at each pole serves as a nucleating site for the formation of a new structure called the prospore membrane. The prospore membrane is built by aggregation and fusion of vesicles sent from the Golgi apparatus. These vesicles normally function in exocytosis and travel to the plasma membrane, but are redirected to the spindle pole body to build the prospore membrane during meiosis. As meiosis progresses, the prospore membranes grow in length and extend to cover each lobe of the nucleus (picture someone rolling socks onto their hands and feet), and eventually pinch off the nuclear lobes. This results in the "capture" of individual sets of chromosomes in their own nuclear envelopes. Each of these are immature spores, and the prospore membrane now surrounding them becomes the new plasma membrane. A cell wall eventually forms around each spore, making them ready for release from the original yeast cell.

When PLD is missing, the prospore membrane fails to form. PLD is distributed throughout the cell prior to meiosis but translocates to the spindle pole at the time when the prospore membrane needs to be built. PLD activity is not required for its translocation, indicating that it is not involved in the trafficking of membrane vesicles to the spindle pole body; however, the vesicles subsequently fail to aggregate and fuse when PLD is missing or catalytically inactive.

Although the precise mechanism mediated by PLD or its product PA in prospore membrane development remains unknown, this is the best-understood example of what is now recognized as a common theme for PLD function; regulation of vesicle production, trafficking, or fusion.

Mammals

Investigation of roles for PLD in mammals has been more challenging. Cells and animals lacking PLD have not yet been generated, and specific pharmacological PLD agonists and antagonists have not been identified. Nonetheless, an approach for probing PLD function exists that has been widely used, although interested readers need to keep in mind that it comes with significant caveats. This method involves exposing cells to moderately high levels of primary alcohols such as ethanol or 1-butanol. Short-chain primary alcohols can competitively substitute for water in the PLD hydrolysis reaction, leading to formation of phosphatidylalcohols at the expense of PA. Phosphatidylalcohols are believed to be relatively inert; that is, they do not activate the downstream pathways triggered by PA. Accordingly, diverting PA production to phosphatidylalcohol diminishes PLD-mediated activation of PA-dependent events. In addition, since phosphatidylalcohols are relatively metabolically inert, they serve as a history of PLD activation over the period during which the alcohols are present. Measuring accumulation of phosphatidylalcohols is very useful for quantitating PLD activity, since PA, in contrast, turns over rapidly once formed, and in fact can be generated through pathways other than PLD as well. Limitations of this approach include the facts that alcohols alter the fluidity of membranes, which affects many biological processes, and block activation of many tyrosine kinase receptors; for example, the insulin receptor. Moreover, at the concentrations of alcohol required to divert PA production effectively, levels of phosphatidylinositol lipids become significantly altered; for example, PIP levels decrease dramatically. Accordingly, although alcohol-mediated inhibition of PA production provides initial evidence for PA involvement in specific processes, it should not be considered definitive in the absence of other approaches. More recent approaches for manipulating PLD activity include overexpression or injection of wild-type PLD proteins to increase levels of activity or use of catalytically inactive PLD proteins to serve as dominant interfering mutants. Using such techniques, roles have been described for PLD in a number of settings.

Secretion

One of the better-characterized model systems involves regulated secretion from neuroendocrine cells, such as primary adrenal chromaffin cells. Exposure of these cells to the agonist nicotine stimulates receptors that activate PLD and triggers release of catecholamines through fusion of neurotransmitter-containing secretory granules with the plasma membrane. Analogous to the role of PLD in yeast meiosis, PLD in adrenal chromaffin cells is found on the acceptor membrane, in this case the plasma membrane. Increasing PLD activity through overexpression leads to increased regulated exocytosis and reducing PLD activity through any of the approaches described above leads to inhibition of catecholamine release. In this setting, PA appears to mediate the rate and efficacy of fusion of secretory granules into the plasma membrane as inhibition of PLD activity leads to individual granules fusing into the plasma membrane and disgorging their contents more slowly (Figure 4). Once again, the precise mechanism of PA function remains unknown, and could involve more than one of the possibilities described above. PLD activity has

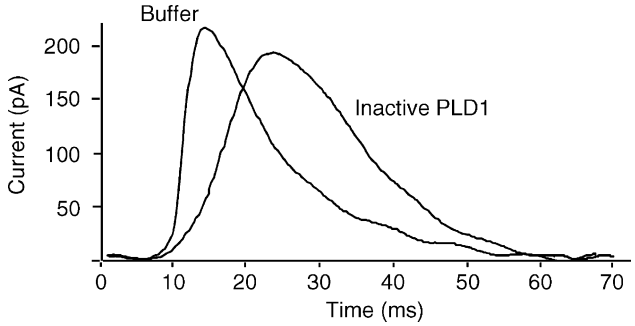

FIGURE 4 Catalytically inactive PLD1 inhibits nicotine-evoked catecholamine secretion from chromaffin cells, revealing a requirement for PA in the fusion of secretory granules into the plasma membrane. Chromaffin cells were microinjected with buffer or with catalytically inactive PLD1 protein which acts as a dominant negative mutant. Cells were stimulated 10–15 min later by a local application of nicotine for 5 s. Catecholamine secretion, which causes a change in local conductance due to its highly charged nature, was recorded using a carbon fiber electrode. Numerous spikes of current, representing fusion of individual granules of catecholamines with the plasma membrane are observed, but many fewer after injection of catalytically inactive PLD1 (not shown). Individual fusion events are shown above on the millisecond timescale. The fusion event observed for a normal (buffer-injected) cell occurs rapidly. The fusion event in the cell injected with catalytically inactive PLD1 protein occurs more slowly, indicated that the fusion pore formed between the secretory granule and the plasma membrane enlarges at a slower rate, causing the contents to be released more slowly as well. Reprinted from Vitale, N., Caumont, A. S., Chasserot-Golaz, S., Du, G., Wu, S., Sciorra, V. A., Morris, A. J., Frohman, M. A., and Bader, M. F. (2001). Phospholipase D1: a key factor for the exocytotic machinery in neuroendocrine cells. *EMBO J.* **20**, 2424–2434, with permission of Oxford University Press.

similarly been shown to promote or be required for fusion of histamine-containing secretory granules into the plasma membrane after IgE-triggered degranulation of mast cells, and for translocation of the Glut-4 glucose transporter from storage vesicles to the plasma membrane subsequent to insulin stimulation.

Finally, PLD activity has also been shown to promote the release of membrane vesicles from the trans-Golgi in endocrine cells. It may be that PLD promotes both budding and fusion of vesicles. Alternatively, the budding process could be facilitated by PLD-regulated fusion of vesicles into the trans-Golgi at an earlier step.

Morphology

The activators that stimulate mammalian PLD, i.e., ARF and Rho small G-protein family members and protein kinase C, are also well known for their roles in controlling changes in cell shape. Although, again, the precise role played by PA remains undefined, it is clear that inhibition of PLD activity blocks actin cytoskeleton-mediated cell shape changes in some settings (for example, formation of actin stress fibers in response to agonist stimulation) and that overexpression of PLD promotes them. At high levels of overexpression of the PLD2 isoform, cells undergo spontaneous changes in morphology, extending finger-like projections and undergoing continued ruffling. These sorts of responses indicate that PLD and PA play a role in regulating cell shape, although their role at normal levels of expression remains to be determined. Leading hypotheses include the possibilities that PLD activity increases levels of $PI4,5P_2$, a lipid known to be involved in reorganization of the actin cytoskeleton, or that it activates ARF GAPs, enzymes that deactivate ARF-stimulated pathways.

Other Roles

PLD-generated PA also promotes activation of Raf-1 kinase and mTor, key regulatory factors in cell growth, and NADPH-oxidase, a component of the respiratory burst response in inflammation and infection.

Summary

Phospholipase D, a lipid-modifying enzyme activated via complex regulation through G-protein and receptor tyrosine kinase signal transduction pathways, has roles in numerous cell biological settings including vesicular trafficking, cell shape modifications, and proliferation.

See Also the Following Articles

ARF Family • Phosphatidylinositol Bisphosphate and Trisphosphate • Phospholipid Metabolism in Mammals • Rho GTPases and Actin Cytoskeleton Dynamics

Glossary

phosphatidylalcohols Biologically inert, metabolically inactive compounds formed when primary alcohols are available to serve as the nucleophile instead of water in a PLD reaction.

phospholipases Enzymes that cleave phospholipids. Phospholipase A, C, and D each cleave distinct sites on phospholipids.

phospholipid A membrane lipid consisting of one or more fatty acid side chains linked to a glycerol phosphate backbone. The phosphate group frequently terminates in a "headgroup" such as choline or inositol via a phosphodiester bond that constitutes the target for PLD superfamily action.

Further Reading

Cockcroft, S. (2001). Signaling roles of mammalian phospholipase D1 and D2. *Cell Mol. Life Sci.* **58**, 1674–1687.

Exton, J. H. (2002). Phospholipase D-structure, regulation and function. *Rev. Physiol. Biochem. Pharmacol.* **144**, 1–94.

Frohman, M. A., Sung, T.-S., and Morris, A. J. (1999). Mammalian phospholipase D-structure and regulation. *Biochim. Biophys. Acta* **1439**, 175–186.

Jones, D., Morgan, C., and Cockcroft, S. (1999). Phospholipase D and membrane traffic: Potential roles in regulated exocytosis, membrane delivery and vesicle budding. *Biochim. Biophys. Acta* **1439**, 229–244.

Liscovitch, M., Czarny, M., Fiucci, G., and Tang, X. (2000). Phospholipase D: Molecular and cell biology of a novel gene family. *Biochem. J.* **345**, 401–415.

Rizzo, M., and Romero, G. (2002). Pharmacological importance of phospholipase D and phosphatidic acid in the regulation of the mitogen-activated protein kinase cascade. *Pharmacol. Therap.* **94**, 35–50.

Sung, T. C., Roper, R., Zhang, Y., Rudge, S., Temel, R., Hammond, S., Morris, A., Moss, B., Engebrecht, J., and Frohman, M. (1997). Mutagenesis of phospholipase D defines a superfamily including a *trans*-Golgi viral protein required for poxvirus pathogenicity. *EMBO J.* **16**, 4519–4530.

Biography

Mary LaLonde is a trainee in the Medical Scientist Training Program at Stony Brook who is exploring the role of Phospholipase D in Drosophila.

Michael A Frohman, M.D., Ph.D. is a Professor in the department of pharmacology and the Director of the Medical Scientist Training Program at Stony Brook. His group cloned the mammalian PLD genes and conducted many of the early molecular biological studies on them.

Phospholipid Metabolism in Mammals

Claudia Kent
University of Michigan, Ann Arbor, Michigan, USA

Phospholipids form the bilayer matrix of all natural biological membranes. In mammals, phospholipids take on additional importance as components of lipoproteins and as intermediates in signal transduction pathways. While the term "phospholipid" includes any lipid containing a phosphate moiety, in everyday usage the term has come to refer to glycerophospholipids, which are lipids containing glycerol phosphate as the "backbone," plus the phosphosphingolipid, sphingomyelin. These molecules are synthesized *de novo* in all mammalian cells, and actively degraded in those cells by multiple phospholipases. This article focuses on the metabolism of glycerophospholipids.

Biosynthesis of Phospholipids

Diacylglycerophospholipids

Major Glycerophospholipid Classes

The structures of the major classes of mammalian phospholipids are shown in Figure 1. Phosphatidate, or *sn*-1,2-diacylglycerol-3-phosphate, is a central intermediate in the biosynthesis of all phospholipids. In addition, this lipid has various functions in signal transduction pathways. Phosphatidylcholine is the major eukaryotic phospholipid, usually accounting for 40–50% of cellular phospholipids. Phosphatidylcholine plays a major structural role in biological membranes because of its excellent bilayer-forming properties. It is also found as a structural component of serum lipoproteins and pulmonary surfactant. In addition, phosphatidylcholine is a component of signal transduction pathways as a substrate for phospholipases that produce lipid mediators.

Phosphatidylethanolamine is also a major mammalian phospholipid, accounting for ~20–30% of cellular phospholipids. This lipid also plays a structural role in the bilayer, contributing to curvature stress because of its nonlamellar propensities, which in turn influences membrane–protein interactions. Phosphatidylserine represents roughly 10–15% of cellular phospholipids. This lipid plays a critical role in apoptosis, during which its exposure on the external leaflet of the plasma membrane is a recognition feature for engulfment by phagocytic cells.

Phosphatidylglycerol is found only in trace amounts in most mammalian cells, primarily in mitochondria. In lung, however, appreciable amounts of phosphatidylglycerol are found in type II alveolar cells and in their principal secretory product, pulmonary surfactant. The metabolic derivative of phosphatidylglycerol is diphosphatidylglycerol, commonly called cardiolipin; this lipid is found exclusively in mitochondria, where its role is to interact with proteins of the electron transport chain. Phosphatidylinositol is an important constituent of mammalian membranes, but is more widely appreciated as a substrate for kinases that convert it to multiply phosphorylated forms that participate in many signal transduction pathways.

Biosynthesis of the Central Intermediates

All mammalian glycerophospholipids, as well as triacylglycerols, are ultimately derived from phosphatidate. The main source of phosphatidate is the fatty acylation of *sn*-glycerol-3-phosphate (Figure 2), which in turn is formed by the reduction of dihydroxyacetone phosphate, a central intermediate of the glycolytic/gluconeogenic pathway. The first fatty acyl group is added by glycerol-3-phosphate acyltransferase, forming the product 1-acylglycerol-3-phosphate or lysophosphatidate. Two isoforms of glycerol-3-phosphate acyltransferase are found in mammals, one in the endoplasmic reticulum and the other in the mitochondrial outer membrane. The *sn*-2 position of lysophosphatidate is acylated by 1-acylglycerol-3-phosphate acyltransferase, a component of the endoplasmic reticulum. Fatty acyl-CoA serves as the donor for both acyltransferase reactions. Phosphatidate may also be formed by the action of phospholipase D, as is discussed in this article later, or by the action of diacylglycerol kinase; however, these last two enzymes do not participate in *de novo* phospholipid biosynthesis.

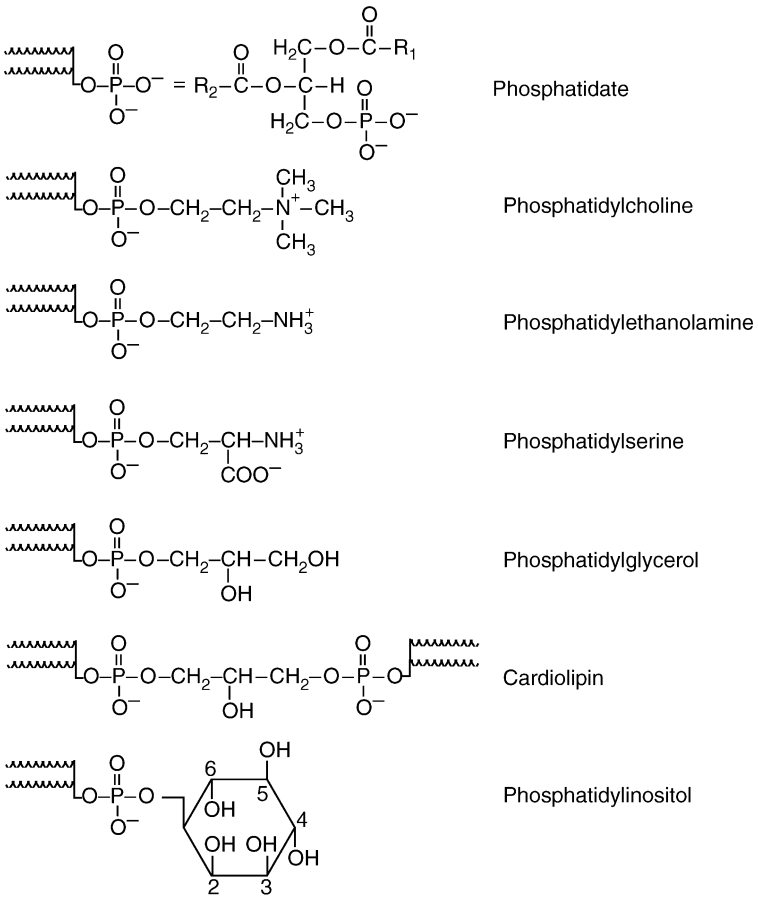

FIGURE 1 Structures of major glycerophospholipid classes. R_1 and R_2 refer to the different fatty acyl chains esterified to positions 1 and 2 of *sn*-glycerol-3-phosphate. The diacylglycerol moiety is represented by wavy horizontal lines connected to a vertical line.

Newly synthesized phosphatidate is channeled into two biosynthetic pathways, which are then used for the synthesis of different groups of phospholipids. In one pathway, phosphatidate phosphohydrolase converts its substrate to *sn*-1,2-diacylglycerol. Two isoforms of phosphatidate phosphohydrolase are found in mammalian cells; the one involved in glycerolipid biosynthesis appears to be both cytosolic and in the endoplasmic reticulum. The other isoform is plasma membrane-associated and functions primarily in signal transduction. The other pathway of phosphatidate utilization involves the formation of CDP-diacylglycerol, which takes place primarily in the endoplasmic reticulum.

The Diacylglycerol Pathway: Biosynthesis of Phosphatidylcholine, Phosphatidylethanolamine, and Phosphatidylserine

The biosynthetic pathways for all glycerophospholipids include at least one cytidylylated intermediate. The pathways for *de novo* biosynthesis of lipids that are derived from diacylglycerol involve the use of CDP-choline or CDP-ethanolamine (Figure 3). These nucleotide intermediates are made by the phosphorylation of choline and ethanolamine by choline/ethanolamine kinases, followed by transfer to the CMP moiety of CTP, catalyzed by phosphocholine and phosphoethanolamine cytidylyltransferases. The CDP-alcohols then react with diacylglycerol to form phosphatidylcholine and phosphatidylethanolamine.

The choline and ethanolamine kinases are soluble enzymes and are presumed to be cytosolic. Most of these enzymes can use either choline or ethanolamine as substrate but ethanolamine-specific kinases also exist. The cytidylyltransferases are specific for either phosphocholine or phosphoethanolamine and are regulatory for the CDP-choline and -ethanolamine pathways. There are nuclear and cytoplasmic isoforms of the phosphocholine cytidylyltransferase that are encoded by separate genes. These isoforms have an intriguing mode of regulation in which a membrane-binding segment of the enzyme "senses" the lipid composition and conveys a deficit of phosphatidylcholine to the active site of the enzyme, which is then activated in response to

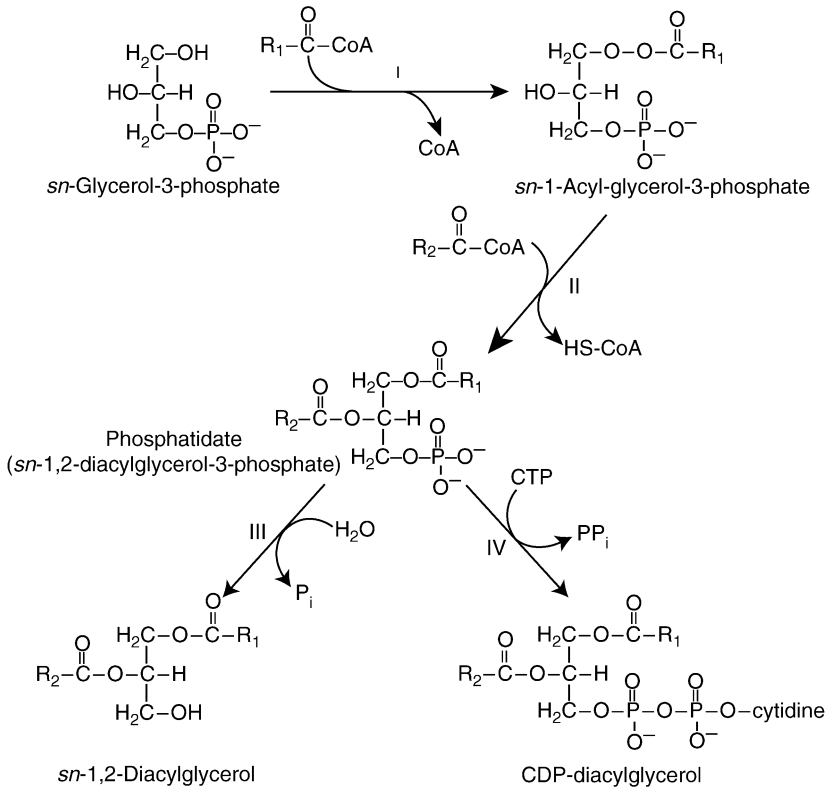

FIGURE 2 Biosynthesis of central intermediates of glycerophospholipid biosynthesis. Enzymes are I, glycerol-3-phosphate acyltransferase; II, 1-acylglycerol-3-phosphate acyltransferase; III, phosphatidate phosphohydrolase, and IV, CDP-diacylglycerol synthase.

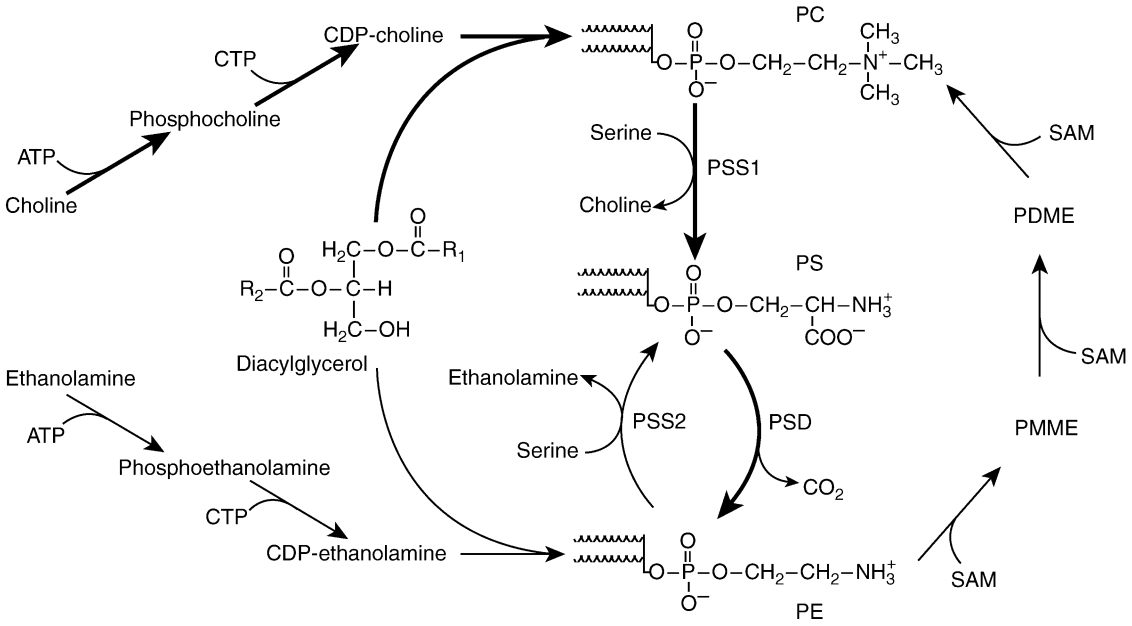

FIGURE 3 Synthesis of phospholipids derived from diacylglycerol. PC, phosphatidylcholine; PS, phosphatidylserine, PE, phosphatidylethanolamine; PMME, phosphatidylmonomethylethanolamine; PDME, phosphatidyldimethylethanolamine; SAM, S-adenosylmethionine. PSS1, phosphatidylserine synthase 1; PSS2, phosphatidylserine synthase 2; PSD, phosphatidylserine decarboxylase. Other enzymes are identified in the text. The thick arrows denote the major biosynthetic pathways.

the deficit. The phosphoethanolamine cytidylyltransferase is readily solubilized but appears to be associated with the endoplasmic reticulum. The alcohol phosphotransferases that catalyze the last steps, the formation of phosphatidylcholine and phosphatidylethanolamine, are embedded in the endoplasmic reticulum.

The CDP-choline pathway is the only mode for biosynthesis of phosphatidylcholine in most mammalian tissues. In liver, however, phosphatidylcholine is also made by the stepwise methylation of phosphatidylethanolamine, with S-adenosylmethionine as the methyl donor. In mammals, one phospholipid methyltransferase carries out all three steps; this methyltransferase activity is found in a specialized portion of the endoplasmic reticulum known as the mitochondria-associated membrane.

The CDP-ethanolamine pathway is important for the biosynthesis of ether lipids, but is a minor pathway for biosynthesis of diacyl ethanolamine phosphoglyceride. The predominant pathway for biosynthesis of the diacyl lipid is, rather, the decarboxylation of phosphatidylserine. The latter lipid in mammals is produced by exchange enzymes, in which serine exchanges with either the choline moiety of phosphatidylcholine, or ethanolamine of phosphatidylethanolamine, to form phosphatidylserine. The enzymes catalyzing these two exchanges are distinct; the choline exchange enzyme is responsible for bulk production of phosphatidylserine, which is then decarboxylated to form phosphatidylethanolamine. It is intriguing that the exchange enzymes are components of the endoplasmic reticulum, while the decarboxylase is mitochondrial. This dual location necessitates phospholipid transport systems that facilitate the transfer of phosphatidylserine and ethanolamine between these locations.

The CDP-Diacylglycerol Pathway: Synthesis of Phosphatidylglycerol, Cardiolipin, and Phosphatidylinositol

The nucleotide intermediate, CDP-diacylglycerol, is used for the biosynthesis of non-nitrogenous glycerophospholipids in mammals (Figure 4). In the pathway for the synthesis of the mitochondrial lipid, cardiolipin, CDP-diacylglycerol reacts with glycerol-3-phosphate to form phosphatidylglycerol-3-phosphate, which is then hydrolyzed to form phosphatidylglycerol. The usual fate of phosphatidylglycerol is to be converted to cardiolipin. In mammals that conversion involves reaction of phosphatidylglycerol with another molecule of CDP-diacylglycerol.

CDP-diacylglycerol is also used for the biosynthesis of phosphatidylinositol by reaction of the nucleotide lipid with free inositol. This reaction takes place predominantly in the endoplasmic reticulum. A number of phosphoinositide kinases have been identified that convert phosphatidylinositol to polyphosphoinositides.

Biosynthesis of Ether Glycerophospholipids

Ether phospholipids, in which the *sn*-1 acyl linkage is replaced by an ether bond, are major constituents of certain tissues, especially brain. They appear to play an

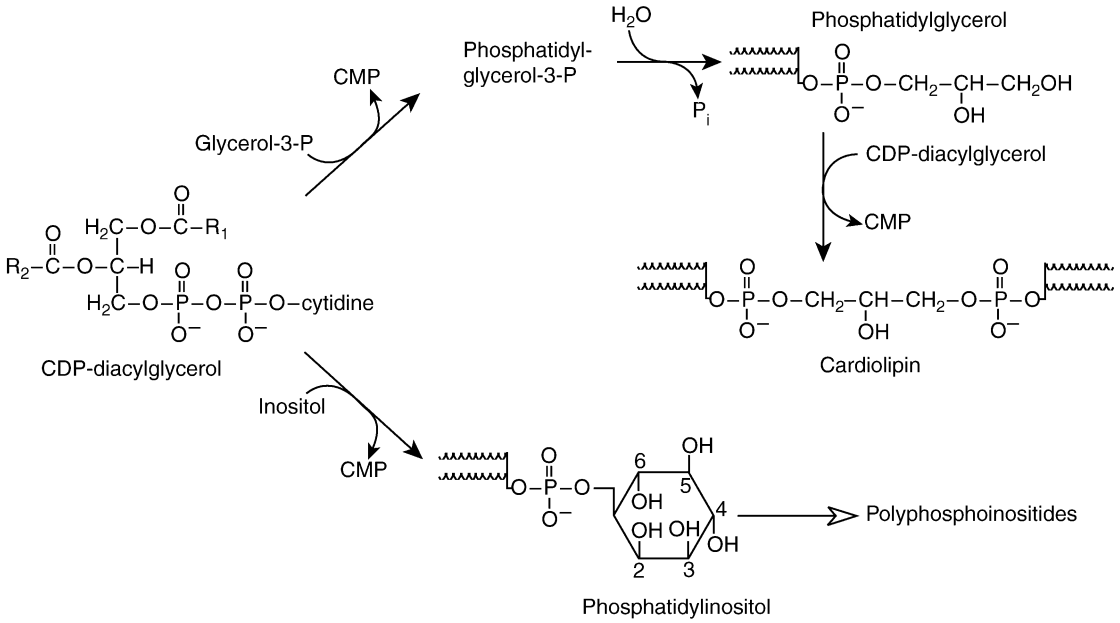

FIGURE 4 Synthesis of phospholipids derived from CDP-diacylglycerol. The open arrow in the lower right represents many phosphorylation steps leading to the polyphosphoinositides.

important role in mammalian physiology as judged by the severity of diseases resulting from abnormalities in their metabolism. These lipids are derived from dihydroxyacetone phosphate, which becomes fatty acylated at position 1 (Figure 5). The fatty acyl group is then replaced by a fatty alcohol to create the ether linkage. Reduction at C-2 followed by a second acylation produces 1-alkyl-2-acyl-glycerol-3-phosphate. This compound is then dephosphorylated, and the resultant free hydroxyl reacts with CDP-ethanolamine to produce 1-alkyl-2-acylglycerol-3-phosphoethanolamine, also known as plasmanylethanolamine. Introduction of a double bond at this stage into the fatty alcohol moiety results in the formation of the plasmalogen, plasmenylethanolamine. The mechanism of formation of plasmanyl/plasmenyl choline is not well established but may occur after hydrolysis of the ethanolamine ether lipids to 1-alkyl/alkenyl-2-acylglycerol, followed by reaction with CDP-choline. Ether lipid biosynthesis is unusual in that the first two enzymes are located in peroxisomes, the third step occurs in both peroxisomes and the endoplasmic reticulum, and the remaining steps occur in the endoplasmic reticulum.

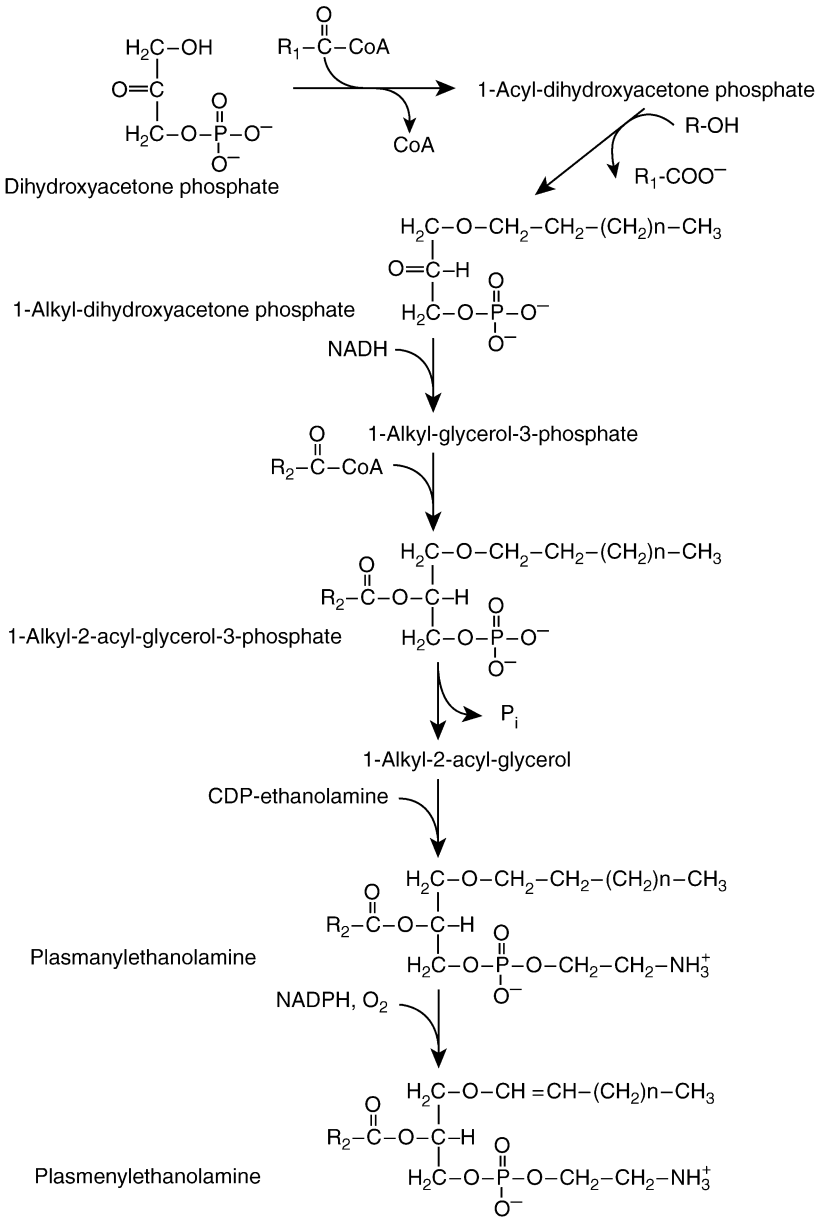

FIGURE 5 Biosynthesis of the ether lipids, plasmanylethanolamine, and plasmenylethanolamine. The ethanolamine ether lipids are precursors of choline ether lipids, but the conversion steps have not been firmly established.

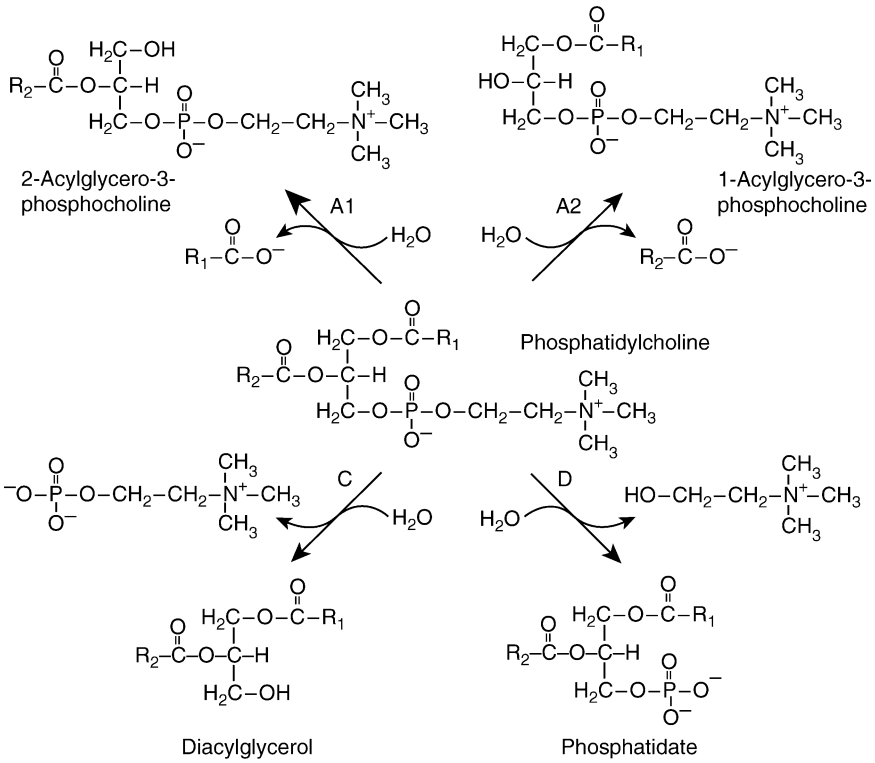

FIGURE 6 Specificity of phospholipases. A1, A2, C, and D refer to phospholipases of that specificity, as described in the text.

Catabolism of Phospholipids: Phospholipases

The degradation of phospholipids takes place during normal membrane turnover, as well as in response to the need for production of lipid mediators. The phospholipases that perform this degradation are divided into four general classes according to the reactions they catalyze (Figure 6). Hydrolysis of the fatty ester bond at C-1 is catalyzed by phospholipase A1. Multiple phospholipases A1 are found in mammals. Lysosomal phospholipase A1 functions in general phospholipid catabolism while phosphatidylserine-specific phospholipase A1 appears to generate the lipid-signaling molecule, 2-lysophosphatidylserine.

The best-studied phospholipases are phospholipases A2, which hydrolyze the ester bond at C-2. Mammalian phospholipases A2 function predominantly in the generation of free arachidonate, which is then converted by cyclooxygenases and lipoxygenases to a variety of eicosanoid-signaling molecules. Platelet-activating factor acetylhydrolase is a very specific phospholipase A2 that utilizes 1-alkyl-2-acetylphosphatidylcholine, also known as platelet activating factor, an important inflammatory lipid. Phospholipases A2 are also found in lysosomes where they play a more general catabolic role.

The phosphate ester bonds of phospholipids are hydrolyzed by phospholipases C, with the production of diacylglycerol, and D, with the production of phosphatidate. The best-studied phospholipases C are those involved in the hydrolysis of polyphosphoinositides, with the generation of diacylglycerol, which activates certain protein kinases, as well as inositol polyphosphates, which have many signaling functions. Phospholipases D mainly hydrolyze phosphatidylcholine and function both in signal transduction as well as in vesicular trafficking. Catabolism of sphingomyelin in mammals is carried out by neutral and acid sphingomyelinases that have a C-type specificity in that they generate ceramide and phosphocholine.

See Also the Following Articles

Phosphatidylinositol Bisphosphate and Trisphosphate • Phosphoinositide 3-Kinase • Phosphoinositide 4- and 5-Kinases and Phosphatases • Phosphoinositide-Dependent Protein Kinases • Phospholipase A_2 • Phospholipase D • Phospholipid Synthesis in Yeast • Sphingolipid Biosynthesis • Sphingolipid Catabolism

Glossary

ceramide The "backbone" of sphingolipids, consisting of sphingosine with an amide linkage to a fatty acid.

ether lipids Lipids containing a hydrocarbon chain in ether linkage to C-1 of the glycerol phosphate backbone.

glycerophospholipids Lipids composed of a backbone of *sn*-glycerol-3-phosphate, the first and second positions of which are fatty acylated.

phosphatidate *sn*-1,2-diacylglycerol-3-phosphate, also called phosphatidic acid.

phospholipase An enzyme catalyzing the hydrolysis of a phospholipid.

plasmalogen An ether lipid containing a *cis* double bond in the hydrocarbon chain, adjacent to the ether linkage.

polyphosphoinositide A phospholipid derived by phosphorylation of the inositol ring of phosphatidylinositol.

sphingomyelin A phospholipid consisting of ceramide linked to phosphocholine.

Further Reading

Nagan, N., and Zoeller, R. A. (2001). Plasmalogens: Biosynthesis and functions. *Prog. Lipid Res.* **40**, 199–299.

Vance, D. E. (2002). Phospholipid biosynthesis in eukaryotes. In *Biochemistry of Lipids, Lipoproteins, and Membranes* (D. E. Vance and J. E. Vance, eds.) 4th edition, pp. 205–232. Elsevier Science B.V., Amsterdam.

Voelker, D. R. (2000). Interorganelle transport of aminoglycerophospholipids. *Biochim. Biophys. Acta* **1486**, 97–107.

Biography

Claudia Kent is a Professor of Biological Chemistry at the University of Michigan. Her research interests have centered on phospholipid metabolism in eukaryotes and prokaryotes, with the principal focus being the enzymes that regulate phosphatidylcholine metabolism. She obtained a Ph.D. from Johns Hopkins University, and was a postdoctoral trainee at Washington University and a faculty member in biochemistry at Purdue University before moving to Michigan.

Phospholipid Synthesis in Yeast

Gil-Soo Han and George M. Carman
Rutgers University, New Brunswick, New Jersey, USA

Phospholipids are essential molecules that contribute to the structural definition of the cell. They also play a role as signaling molecules that participate in the regulation of cellular processes. The yeast *Saccharomyces cerevisiae* has been used as a model system to study phospholipid synthesis and its regulation in eukaryotes. Molecular, genetic, and biochemical studies have shown that phospholipid synthesis is regulated in a coordinated fashion. The mechanisms that govern this regulation mediate the mRNA and protein levels of the biosynthetic enzymes, as well as their activity and localization.

Phospholipid Composition

The major phospholipids found in the membranes of *S. cerevisiae* include phosphatidylcholine (PC), phosphatidylethanolamine (PE), phosphatidylinositol (PI), and phosphatidylserine (PS) (Figure 1). Mitochondrial membranes also contain phosphatidylglycerol (PG) and cardiolipin (CL). The composition of phospholipids in the cell can vary dramatically when culture conditions are altered. However, the average charge of the membrane phospholipids remains relatively constant. Genetic and biochemical regulation of the enzymes in the phospholipid biosynthetic pathways can compensate for changes in the levels of phospholipids of one charge by orchestrating parallel changes in the levels of phospholipids of the opposite charge.

Phospholipid Synthesis

Phospholipid synthesis is a complex process containing many branch points. A key molecule in this process is phosphatidate (PA). It plays a central role in phospholipid synthesis as the precursor of all phospholipids synthesized via the CDP–diacylglycerol (DAG), CDP–choline, and CDP–ethanolamine pathways (Figure 2). In the CDP–DAG pathway, PA is converted to CDP–DAG, which is then utilized for the synthesis of PS, PE, and PC. CDP–DAG is also utilized for the synthesis of PI and CL. In the CDP–choline and CDP–ethanolamine pathways, DAG is generated from the dephosphorylation of PA, and is utilized for the synthesis of PC or PE when cells are supplemented with choline or ethanolamine, respectively. The DAG derived from PA is also used for the synthesis of triacylglycerols. The nucleotide CTP is another important precursor in the synthesis of phospholipids. CTP, which is synthesized from UTP, is the direct precursor of the activated, energy-rich phospholipid pathway intermediates CDP–DAG, CDP–choline, and CDP–ethanolamine (Figure 2).

Synthesis of PA

PA is synthesized from glycerol 3-phosphate via two acylation reactions. The first acylation step, which results in the formation of lysoPA, is catalyzed by the *GAT1*- and *GAT2*-encoded glycerol 3-phosphate acyltransferases. Deletion of either gene does not affect cell viability, but deletion of both genes results in a lethal phenotype. Acylation of lysoPA, which is catalyzed by the *SLC1*-encoded lysoPA acyltransferase, generates PA. In addition to the *de novo* synthesis, PA can be produced from phospholipid turnover: (1) hydrolysis of PC by the *SPO14/PLD1*-encoded phospholipase D; (2) phosphorylation of DAG by CTP-dependent DAG kinase (whose structural gene is not yet known); and (3) dephosphorylation of diacylglycerol pyrophosphate (DGPP) by the *DPP1*- and *LPP1*-encoded lipid phosphate phosphatase enzymes.

CDP–DAG Pathway

PS, PE, and PC are synthesized via reactions in the CDP–DAG pathway. The committed step in this pathway is the synthesis of CDP–DAG from PA and CTP. This reaction is catalyzed by the essential enzyme CDP–DAG synthase, which is encoded by the *CDS1* gene. CDP–DAG is then converted to PS by the *PSS1/CHO1*-encoded PS synthase. This enzyme displaces the CMP moiety of CDP–DAG with serine. PS is then decarboxylated to PE by the *PSD1*- and *PSD2*-encoded PS decarboxylases. The *PSD1*-encoded PS decarboxylase is responsible for $>90\%$ of the cellular PS decarboxylase activity, while the *PSD2*-encoded enzyme is responsible for $\sim 10\%$ of the enzyme activity. Finally, PE is

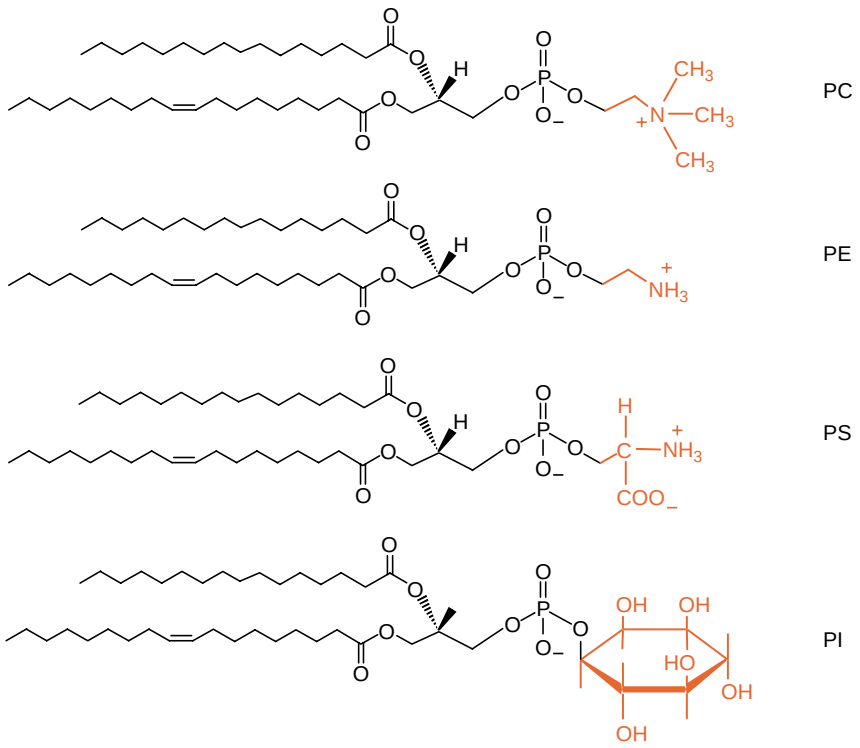

FIGURE 1 Major phospholipids in *S. cerevisiae*. The phospholipid headgroups (i.e., choline, ethanolamine, serine, and inositol) are shown in red.

converted to PC via three sequential methylation reactions. The first methylation reaction is catalyzed by the *PEM1/CHO2*-encoded PE methyltransferase, whereas the last two methylation reactions are catalyzed by the *PEM2/OPI3*-encoded phospholipid methyltransferase.

CDP–Choline and CDP–Ethanolamine (Kennedy) Pathways

When cells are supplemented with choline and ethanolamine, PC and PE are also synthesized via the CDP–choline and CDP–ethanolamine pathways, respectively. In the CDP–choline pathway, choline is phosphorylated with ATP to form phosphocholine by the *CKI1*-encoded choline kinase. Phosphocholine is then converted to CDP–choline by the reaction catalyzed by the *CCT1/PCT1*-encoded phosphocholine cytidylyltransferase. In the last step, PC is synthesized from CDP–choline and DAG by the *CPT1*-encoded choline phosphotransferase. The enzyme reactions in the CDP–ethanolamine pathway are similar to those in the CDP–choline pathway. The *EKI1*-encoded ethanolamine kinase catalyzes the phosphorylation of ethanolamine to phosphoethanolamine. Phosphoethanolamine is then converted to CDP–ethanolamine by the *ECT1*-encoded phosphoethanolamine cytidylyltransferase. In the last step, PE is synthesized from CDP–ethanolamine and DAG by the *EPT1*-encoded ethanolamine phosphotransferase. The Kennedy pathways become essential when the enzymes in the CDP–DAG pathway are defective or repressed. Mutants defective in the synthesis of PS, PE, or PC require choline for growth in order to synthesize PC via the CDP–choline pathway. Mutants defective in the synthesis of PS and PE can also synthesize PC if they are supplemented with ethanolamine. Ethanolamine is converted to PE via the CDP–ethanolamine pathway, and the PE is subsequently methylated to form PC via the CDP–DAG pathway. The CDP–choline pathway was once viewed as an auxiliary or salvage pathway used by cells when the CDP–DAG pathway was compromised. However, it is now known that the CDP–choline pathway contributes to PC synthesis even when wild-type cells are grown in the absence of exogenous choline. The PC synthesized via the CDP–DAG pathway is constantly hydrolyzed to form free choline and PA through the reaction catalyzed by the *SPO14/PLD1*-encoded phospholipase D. The free choline is incorporated back into PC via the CDP–choline pathway, and the PA is recycled into PC and other phospholipids via CDP–DAG and DAG.

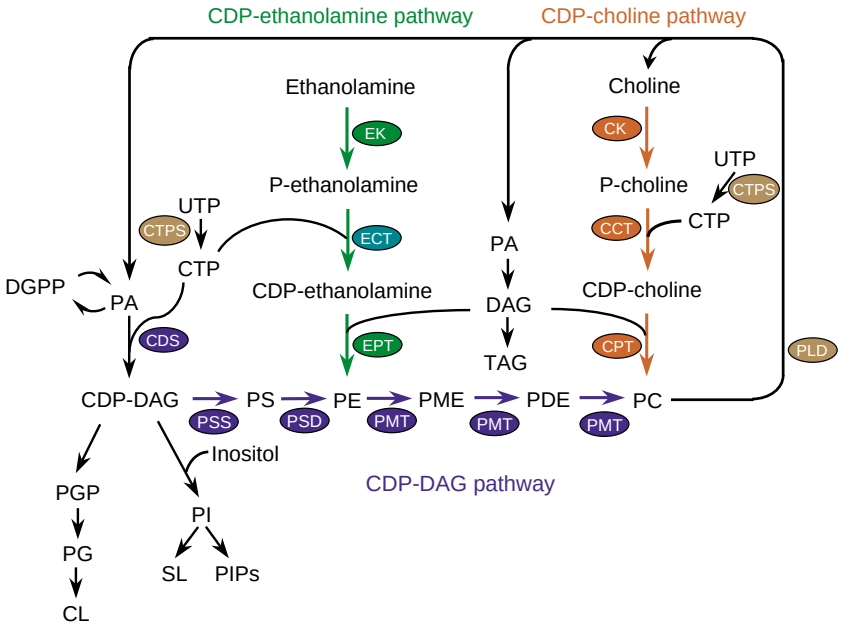

FIGURE 2 Pathways for the synthesis of the major phospholipids in *S. cerevisiae*. The pathways shown for synthesis of phospholipids include the relevant steps discussed in the text. The CDP–DAG, CDP–choline, and CDP–ethanolamine pathways are indicated. The enzymes CDP–DAG synthase (CDS), PS synthase (PSS), PS decarboxylase (PSD), and the PE methyltransferases (PMT) catalyze reactions that lead to the formation of PC by the CDP–DAG pathway (shown in blue). Choline kinase (CK), choline–P cytidylyltransferase (CCT), and choline phosphotransferase (CPT) catalyze reactions that lead to the formation of PC by the CDP–choline pathway (shown in red). Ethanolamine kinase (ET), ethanolamine-P cytidylyltransferase (ECT), and ethanolamine phosphotransferase (EPT) catalyze reactions that lead to the formation of PE by the CDP–ethanolamine pathway (shown in green). The reactions catalyzed by CTP synthetase (CTPS) and phospholipase D (PLD) are shown in brown. A more comprehensive description that includes the synthesis of PA and additional steps in these pathways may be found elsewhere. PA, phosphatidate; CDP–DAG, CDP–diacylglycerol; PS, phosphatidylserine; PE, phosphatidylethanolamine; PME, phosphatidylmonomethylethanolamine; PDE, phosphatidyldimethylethanolamine; PC, phosphatidylcholine; DAG, diacylglycerol; TAG, triacylglycerol; PGP, phosphatidylglycerophosphate; PG, phosphatidylglycerol; CL, cardiolipin; SL, sphingolipids; PIPs, polyphosphoinositides, DGPP, diacylglycerol pyrophosphate.

Other Pathways from CDP–DAG

The essential *PIS1*-encoded PI synthase enzyme catalyzes the displacement of the CMP moiety of CDP–DAG with inositol, resulting in the formation of PI. In this reaction, the water-soluble inositol is provided either by receptor-mediated transport from the growth medium or by *de novo* synthesis from glucose 6-phosphate. When cells are grown in the absence of inositol, glucose 6-phosphate is converted to inositol 1-phosphate, which is catalyzed by the *INO1*-encoded inositol 1-phosphate synthase. Inositol 1-phosphate is then dephosphorylated to form inositol by the *INM1*-encoded inositol monophosphatase. PI is itself a branch point in phospholipid biosynthesis: it is further converted to multiple phosphorylated forms (polyphosphoinositides) by PI kinases, or its phosphoinositol moiety is transferred to ceramide to form sphingolipids. In the CL pathway, CDP–DAG is converted to phosphatidylglycerolphosphate (PGP) by displacement of CMP from CDP–DAG with glycerol 3-phosphate. This reaction is catalyzed by the *PGS1/PEL1*-encoded PGP synthase. PGP is then converted to PG by PGP phosphatase whose structural gene has not yet been identified. In the last step, CL is synthesized from PG and CDP–DAG by *CLS1/CRD1*-encoded CL synthase.

Regulation of Phospholipid Synthesis

Phospholipid synthesis is regulated by a number of factors. These include water-soluble phospholipid precursors (e.g., inositol and choline), nucleotides (e.g., ATP and CTP), lipids (e.g., PA, CDP–DAG, and sphingolipids), growth phase, and phosphorylation. The regulation of phospholipid synthesis by these factors is complex and mediated not only by genetic mechanisms that control the synthesis of mRNA and protein, but also by biochemical mechanisms that modulate enzyme activity.

Genetic Regulation

The effect of inositol supplementation on phospholipid synthesis is a representative example of genetic regulation. When wild-type cells are grown in the presence of inositol, the levels of PS, PE, and PC decrease, while the level of PI increases. These changes in phospholipid composition result from the coordinated regulation of enzyme activities in phospholipid synthesis. Genetic regulation by inositol supplementation affects the enzyme activities by controlling protein content at the transcriptional level. Thus, inositol supplementation represses the transcription of *INO1* and other genes in the CDP–DAG and CDP–choline pathways, whereas inositol starvation stimulates the transcription of the coregulated genes. In many instances, the repressive effect of inositol is enhanced by the addition of choline or ethanolamine to the growth medium. All of the coordinately regulated genes contain a *cis*-acting element, UAS_{INO} (inositol-sensitive upstream activation sequence), in the promoter region. The UAS_{INO} element has the core consensus-binding site (CANNTG) for basic helix-loop-helix (bHLH) proteins. Ino2p and Ino4p are members of the bHLH family of DNA-binding proteins. They bind the UAS_{INO} element as a heterodimer and activate transcription. In addition, Ino2p (but not Ino4p) contains a transcriptional activation domain and is subject to autoregulatory control. Thus, levels of Ino2p appear to be limiting for the formation of the Ino2p/Ino4p heterodimer. In contrast, Opi1p represses the transcription of UAS_{INO}-containing genes. Opi1p contains a leucine zipper and two glutamine-rich domains that are required for Opi1p repressor activity. Opi1p mediates its negative regulatory activity through the UAS_{INO} element, but not by direct interaction. Instead, *in vitro* data indicate that Opi1p interacts with DNA-bound Ino2p within the leucine zipper domain of Opi1p. In addition, the global repressor Sin3p interacts with the N-terminal region of Opi1p. Studies using mutant alleles of *INO2*, *INO4*, *OPI1*, and *SIN3* support a model whereby these interactions play a role in the expression of UAS_{INO}-containing genes *in vivo*.

In addition to inositol, the transcription of the UAS_{INO}-containing genes is also regulated by growth phase. Cells entering stationary phase reveal the repression of the *INO1* gene expression even in the absence of inositol from the growth media. The stationary phase repression of *INO1* transcription is also controlled by Opi1p. Deletion of the *OPI1* gene results in the derepression of *INO1* transcription in stationary phase.

Some enzymes in phospholipid synthesis are regulated in an opposite fashion: they are up-regulated by inositol and derepressed in stationary phase. For example, inositol supplementation results in an increase in the level of DGPP phosphatase (encoded by *DPP1*) activity in both exponential and stationary phase cells. The activity is greater in stationary phase cells when compared with exponential phase cells, and the inositol- and growth phase-dependent regulation of DGPP phosphatase are additive. Analyses of DGPP phosphatase mRNA and protein levels indicate that transcriptional regulation is responsible for the control of the enzyme activity. This regulation is not mediated through a UAS_{INO} element, as the element does not exist in the *DPP1* promoter.

Biochemical Regulation

Alterations in phospholipid synthesis in response to environmental changes are also regulated by biochemical mechanisms. In addition to its role in regulating enzyme expression, inositol regulates the activity of phospholipid biosynthetic enzymes. Inositol inhibits PS synthase activity as a noncompetitive inhibitor, and regulates PI synthase activity through substrate availability. Since both enzymes share the common substrate CDP–DAG, inositol-mediated regulation of PS synthase activity contributes to the synthesis of PI at the expense of PS.

Phosphorylation is a mechanism by which an enzyme activity may be regulated, and indeed several phospholipid biosynthetic enzymes are phosphorylated. For example, the CTP synthetase, choline kinase, and PA phosphatase enzymes are phosphorylated and activated by protein kinase A, whereas the phosphorylation of PS synthase by protein kinase A results in the inhibition of activity. These phosphorylation reactions favor the synthesis of PC via the CDP–choline pathway.

Lipids regulate some phospholipid biosynthetic enzymes. For example, PS synthase activity is stimulated by PA and inhibited by CL and DAG. The PA phosphatase enzyme is stimulated by CL, CDP–DAG, PI, and DGPP. PS synthase and PA phosphatase are also inhibited by the sphingoid bases phytosphingosine and sphinganine.

Nucleotides regulate the activity of some phospholipid biosynthetic enzymes. For example, choline kinase is subject to allosteric regulation by its substrate ATP and its product ADP. ATP promotes the oligomerization of choline kinase, whereas ADP inhibits its activity by affecting the catalytic properties of the enzyme and the apparent affinity of the enzyme for substrates ATP and choline. CTP inhibits PS synthase activity by chelating its cofactor manganese ions. CTP synthetase is regulated by CTP product inhibition. The CTP-mediated inhibition of CTP synthetase activity increases the positive cooperativity of the enzyme for UTP. CTP synthetase with a mutation at Glu^{161} is less sensitive to CTP product inhibition, and cells carrying the mutant CTP synthetase accumulate elevated levels of CTP.

Because CTP inhibits PS synthase activity, the higher levels of CTP result in an increase in the utilization of the CDP–choline pathway at the expense of the CDP–DAG pathway.

In this article, we have only scratched the surface in discussing the complex mechanisms that govern the synthesis of membrane phospholipids. Moreover, once phospholipids are synthesized, they must be transported to the various organelles in the cell. These processes are complex, and in some cases, they regulate phospholipid synthesis. The availability of sequence information of the yeast genome continues to facilitate studies on the molecular genetic and biochemical mechanisms that regulate phospholipid synthesis.

See Also the Following Articles

Inositol Lipid 3-Phosphatases • Inositol Phosphate Kinases and Phosphatases • Lipid Bilayer Structure • Phosphatidylinositol Bisphosphate and Trisphosphate • Phosphatidylinositol-3-Phosphate • Phosphoinositide 3-Kinase • Phosphoinositide 4- and 5-Kinases and Phosphatases • Phosphoinositide-Dependent Protein Kinases • Phospholipase D

Glossary

biochemical regulation Process of controlling the activity of enzymes.

genetic regulation Process of controlling the expression of genes.

phospholipid A lipid molecule that contains two fatty acyl chains that are esterified to the *sn*-1 and *sn*-2 positions of a glycerol phosphate backbone. Different phospholipid molecules (e.g., PC, PE, etc.) are distinguished by the water-soluble head group (e.g., choline, ethanolamine, etc.) that is attached to the phosphate moiety of the molecule.

Saccharomyces cerevisiae A species of yeast that is commonly used in genetic and biochemical research. It serves as an excellent model eukaryotic organism because it is easily cultured and genetically manipulated.

Further Reading

Carman, G. M., and Henry, S. A. (1999). Phospholipid biosynthesis in the yeast *Saccharomyces cerevisiae* and interrelationship with other metabolic processes. *Prog. Lipid Res.* **38**, 361–399.

Daum, G., Lees, N. D., Bard, M., and Dickson, R. (1998). Biochemistry, cell biology and molecular biology of lipids of *Saccharomyces cerevisiae*. *Yeast* **14**, 1471–1510.

Greenberg, M. L., and Lopes, J. M. (1996). Genetic regulation of phospholipid biosynthesis in *Saccharomyces cerevisiae*. *Microbiol. Rev.* **60**, 1–20.

Henry, S. A., and Patton-Vogt, J. L. (1998). Genetic regulation of phospholipid metabolism: Yeast as a model eukaryote. *Prog. Nucleic Acid Res.* **61**, 133–179.

Wu, W.-I., and Voelker, D. R. (2002). Biochemistry and genetics of interorganelle aminoglycerophospholipid transport. *Semin. Cell Dev. Biol.* **13**, 185–195.

Biography

Gil-Soo Han is a Postdoctoral Associate in the Department of Food Science at Rutgers University. Dr. Han received B.S. and M.S. degrees from Sogang University in Korea, and a Ph.D. from Rutgers University. His research concerns the genetic and biochemical regulation of phospholipid biosynthetic enzymes in yeast.

George M. Carman is a Professor of Food Science at Rutgers University. He received a B.A. degree from William Paterson College, an M.S. degree from Seton Hall University, and a Ph.D. from the University of Massachusetts. His postdoctoral training was at the University of Texas Medical School in Houston. Dr. Carman's laboratory is recognized internationally for its work on the biochemical and molecular characterization of phospholipid metabolism in yeast. Dr. Carman is a Fellow of the American Academy of Microbiology.

Photoreceptors

King-Wai Yau
Johns Hopkins University School of Medicine, Baltimore, Maryland, USA

Photoreceptors are cells that can detect light by virtue of a light-absorbing pigment they contain. In most cases, photoreceptors are neurons in the nervous system, and they signal light to the organism for behavioral changes. In some cases, however, photoreceptors are simply modified epithelial cells, such as melanophores in lower animals that can change color by virtue of aggregation or dispersion of intracellular pigmented granules in response to illumination. In humans, all photoreceptors known to date are present in the retina of the eyes. In lower vertebrates such as birds and fish, photoreceptors are also present in the pineal gland and elsewhere in the brain (deep-brain photoreceptors). In some lizards and frogs, photoreceptors are present in the parietal eye (also called the third eye or the frontal organ). In invertebrates, photoreceptors are present in diverse locations either singly or in small or large clusters to form well- or ill-defined eyes. In this article, the discussion is confined to vertebrate photoreceptors in the nervous system.

Retinal Photoreceptors

The well-known retinal photoreceptors in all vertebrates are the rods and cones. Rods are extremely sensitive to light, being able to detect and signal the absorption of a single photon; they are responsible for dim-light vision. Cones are much less sensitive to light, and they also adapt to steady light much more effectively than rods; they are responsible for bright-light vision. In most animals, including humans, rods are predominant in the retina. In occasional diurnal species (such as ground squirrel), however, cones are very abundant.

Rods

In mammals, all rods in a retina are identical. Morphologically, they can be distinguished into the outer segment, the inner segment, the cell body, and the synaptic terminal (Figure 1).

Outer Segment

The outer segment is a modified cilium that has become a highly expanded structure, with hundreds of internalized membrane disks stacked on top of each other and oriented transverse to the longitudinal axis of the cell. The membrane disks are chock-full of the rod visual pigment, rhodopsin, a transmembrane protein. Rhodopsin consists of rod opsin, the apoprotein, covalently linked to the chromophore, 11-*cis*-retinaldehyde (a derivative of vitamin A). In the mammalian retina, there is a single class of rods, all with the same opsin. The wavelength of maximum absorption (λ_{max}) of rhodopsin is near 500 nm (blue-green monochromatic light).

Inner Segment

The inner segment contains much of the metabolic machinery of the cell, and gives rise to the outer segment. The part of the inner segment adjacent to the outer segment is packed with mitochondria, reflecting the heavy metabolic load on the cell.

Cell Body

The cell body contains primarily the nucleus of the cell.

Synaptic Terminal

The synaptic terminal contacts second-order retinal neurons, including the bipolar and horizontal cells. It releases glutamate as the neurotransmitter. The synapse has a ribbon structure that is typical of most sensory neurons.

Cones

In humans, there are three types of cones, each with a different cone opsin covalently linked to 11-*cis*-retinaldehyde. The three cone pigments have λ_{max} at ~430 nm (blue), 530 nm (green), and 560 nm (yellow), respectively. The functional interactions between the three cone types allow us to perceive colors. The morphology of cones is very similar to that of rods, except that the membrane disks in the outer segment are continuous with the plasma membrane.

Phototransduction

The process by which light triggers an electrical response (the signal that neurons use to communicate with each

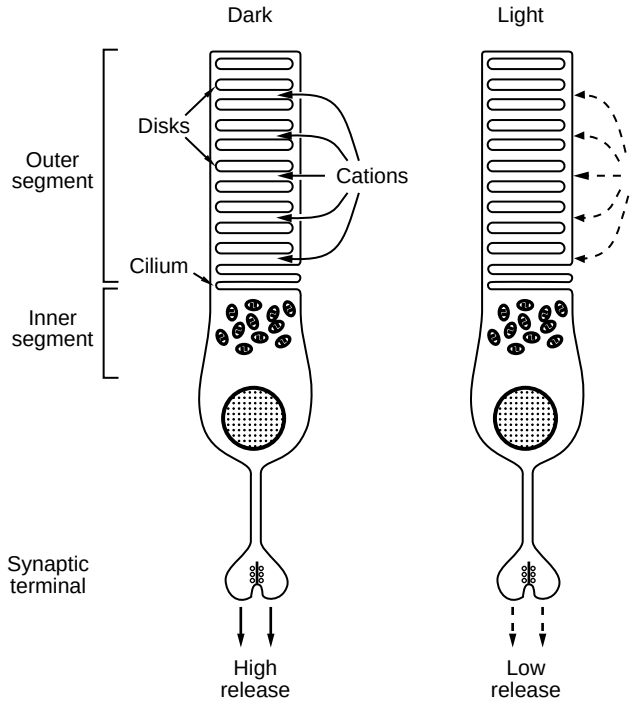

FIGURE 1 Diagram to show the overall morphology of a retinal rod photoreceptor and its response to light. See Figure 2 for the phototransduction mechanism underlying the response. Reproduced from Yau K.-W. (1994). Phototransduction mechanism in retinal rods and cones. The Friendenwald Lecture. *Invest. Ophthalmol. Vis. Sci.* **35**, 10–32, with permission through Copyright Clearance Center, Inc.

other) in rods and cones is called phototransduction. It is similar in both photoreceptor classes, and is now very well understood (Figure 2). There are nonselective cation channels on the plasma membrane of the outer segment that open (i.e., conduct ions) upon binding intracellular cGMP (cGMP-gated channels). In darkness, the free cGMP concentration in the outer segment is relatively high, thus keeping some of these cGMP-gated channels open. These open channels depolarize the cell and sustain a continuous release of glutamate from the synaptic terminal. Upon absorbing a photon, the 11-*cis*-retinaldehyde in a visual pigment molecule isomerizes to all-*trans*-retinaldehyde, as a result of which the opsin moiety undergoes several extremely rapid conformational changes, one of which (meta-II state) is catalytically active. It activates a G protein called transducin, which in turn stimulates a cGMP-phosphodiesterase to hydrolyze cGMP. As a result, the free cGMP concentration decreases, and the cGMP-gated channels close, producing a membrane hyperpolarization that reduces or completely stops neurotransmitter release from the synapse. This signal is picked up by the second-order retinal neurons. The inward, depolarizing membrane current through the open cGMP-gated channels in darkness in part involves Ca^{2+} (the rest is mostly Na^{+}), which is steadily pumped out of the cell by an antiporter involving exchange of external Na^{+} for internal Ca^{2+} and K^{+}. The dark Ca^{2+} influx decreases or stops in the light because the cGMP-gated channels close, but the Ca^{2+} efflux through the Na/Ca,K exchange continues, as a

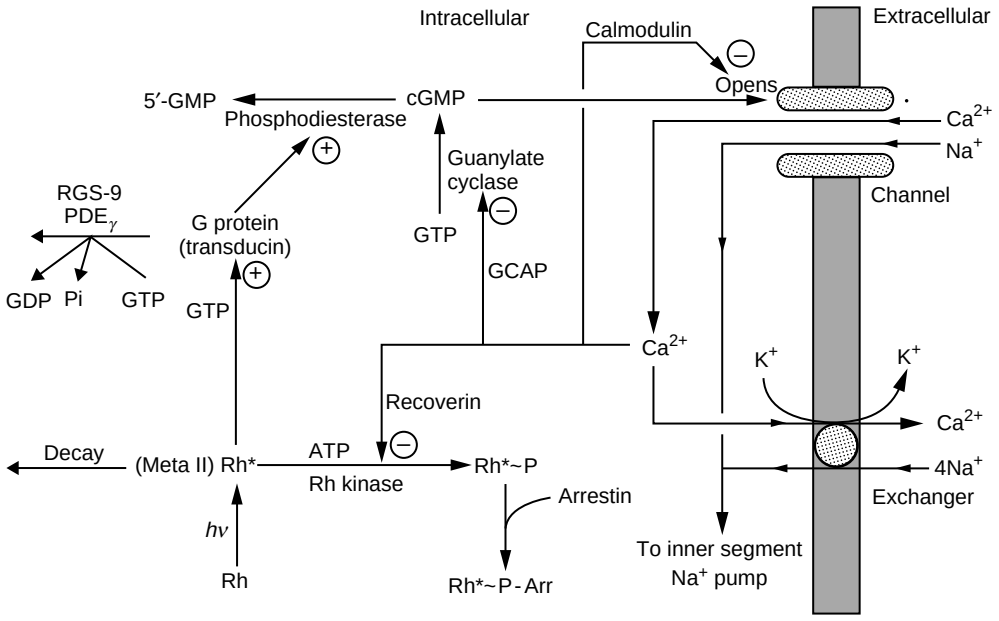

FIGURE 2 Phototransduction mechanism underlying the light response in rods. GCAP, guanylate-cyclase-activating protein; *hν*, photon; Rh, rhodopsin; Rh*, photoactivated rhodopsin; Rh* ~ P, phosphorylated form of rhodopsin; RGS-9, regulator of G protein-signaling isoform 9; PDE_{γ}, inhibitory (γ) subunit of the phosphodiesterase; +, stimulation or positive modulation; −, inhibition or negative modulation. Modified from Koutalos, Y., and Yau, K.-W. (1996). Regulation of light sensitivity in retinal rods. *Trends Neurosci.* **19**, 73–81, with permission from Elsevier.

result of which the free Ca^{2+} in the outer segment decreases. This Ca^{2+} decrease triggers negative feedback on multiple targets in the phototransduction machinery, leading to an attenuation of the initial cGMP decrease induced by light, and hence reopening of some of the cGMP-gated channels. This negative feedback constitutes the key mechanism for light adaptation by the photoreceptor, and is particularly important for cones because they function in bright light. The active, meta-II state of the pigment is deactivated by phosphorylation followed by binding of a protein called arrestin, which caps the pigment activity. After a delay, the meta-II decays into the inactive meta-III state and eventually splits into apo-opsin and all-*trans*-retinaldehyde (i.e, the pigment is bleached). The latter is reduced to all-*trans*-retinol (i.e., the corresponding alcohol), then leaves the photoreceptor to the neighboring retinal pigment epithelial cells, where all-*trans*-retinol is reisomerized/reoxidized to 11-*cis*-retinaldehyde. The 11-*cis*-retinaldehyde returns to the rod and cone outer segments, where it recombines with opsin to form a functional pigment molecule again.

Retinal Nonrod / Noncone Photoreceptors

Very recently, a different class of retinal photoreceptors has been discovered. These are a small subset of retinal ganglion cells, third-order retinal neurons that send light signals to the brain via their axons (optic-nerve fibers). The activity of the great majority of retinal ganglion cells is synaptically driven by the second-order retinal neurons, which in turn receive inputs from rods and cones. About 1% of the ganglion cells, however, are also intrinsically photosensitive. They express an opsin-like protein, melanopsin, which may or may not be the photopigment that makes these cells photosensitive (Figure 3). Light depolarizes these cells, leading to the firing of action potentials. The phototransduction mechanism underlying this depolarizing response is still unknown. While most retinal ganglion cells convey light information for image-forming vision, such as used in the detection and recognition of objects, the intrinsically photosensitive ganglion cells convey light information for nonimage-forming (accessory) visual functions, such as circadian photoentrainment and the pupillary light reflex. Accordingly, their axons project primarily to brain nuclei involved in these functions.

Parietal-Eye Photoreceptor

The parietal-eye photoreceptor bears remarkable morphological similarity to rods and cones (especially cones).

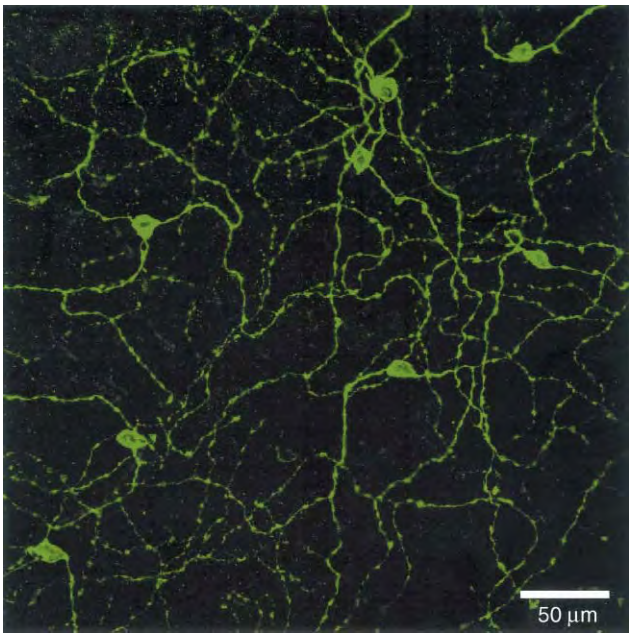

FIGURE 3 Immunofluorescent labeling of a flat-mounted rat retina with an antimelanopsin antibody. Green color shows the labeling. Stacked confocal images. (Reproduced from Hattar, S., Liao, H.-W., Takao, M., Berson, D. M., and Yau, K.-W. (2002). Melanopsin-containing retinal ganglion cells: Architecture, projections and intrinsic photosensitivity. *Science* **295**, 1065–1070, with permission.)

However, there are several interesting differences between them and rods and cones. First, even in isolation, the parietal-eye photoreceptor continues to respond to light after intense illumination, suggesting that there is a chromophore-recycling system within the cell that allows autonomous pigment regeneration. Second, there appear to be two pigments in the same cell, optimally responding to blue and green light, respectively. The green pigment when active depolarizes the cell, whereas the blue pigment when active hyperpolarizes the cell. The phototransduction mechanism is very similar to that in rods and cones, except that, although the blue pigment activates a cGMP-phosphodiesterase, the green pigment inhibits it. Thus, there is a chromatic antagonism in a given cell. Depending on the relative intensities of green and blue light, the cGMP level rises or falls, causing the cGMP-gated channels to open or close, hence a depolarization or hyperpolarization. The exact function of the parietal eye is unclear, but may also have to do with circadian photoentrainment.

Pineal Photoreceptors

In birds and fish, the pineal gland is photosensitive. Morphologically, the pineal photoreceptors roughly resemble rods and cones. Light elicits a hyperpolarizing response from these cells, with an underlying

transduction mechanism also similar to that in rods and cones.

Deep-Brain Photoreceptors

At least in birds, there is evidence that certain cells in the brain are intrinsically photosensitive. Also, immunocytochemistry and *in situ* hybridization studies suggest that opsin proteins are present in small populations/ clusters of neurons in the diencephalon. No other details are known at present.

See Also the Following Articles

G Protein-Coupled Receptor Kinases and Arrestins • The The Neuronal Calcium Signal in Activity-Dependent Transcription

Glossary

circadian photoentrainment The shifting of the (endogenous) circadian clock by light so that it is synchronized with the ambient light–dark cycle.

depolarization Phenomenon in which the electrical potential inside the cell relative to outside becomes more positive compared to the resting state.

hyperpolarization The electrical potential inside the cell relative to outside becomes more negative compared to the resting state.

nonselective-cation channel An ion channel that allows only cations (largely Na^+, K^+, and Ca^{2+}) to go through but does not discriminate much between them.

phototransduction The cellular mechanism that transduces light into an electrical signal in the photoreceptor.

Further Reading

Baylor, D. A. (1987). Photoreceptor signals and vision. The Proctor Lecture. *Invest. Ophthalmol. Vis. Sci.* **28**, 34–49.

Hattar, S., Liao, H.-W., Takao, M., Berson, D. M., and Yau, K.-W. (2002). Melanopsin-containing retinal ganglion cells: Architecture, projections and intrinsic photosensitivity. *Science* **295**, 1065–1070.

Koutalos, Y., and Yau, K.-W. (1996). Regulation of light sensitivity in retinal rods. *Trends Neurosci.* **19**, 73–81.

Vigh, B., Manzano, M. J., Zadori, A., Frank, C. L., Lukats, A., Rohlich, P., Szel, A., and David, C. (2002). Nonvisual photoreceptors of the deep brain, pineal organs and retina. *Histol. Histopathol.* **17**, 555–590.

Xiong, W. H., Solessio, E. C., and Yau, K.-W. (1998). An unusual cGMP pathway underlying depolarizing light response of the vertebrate parietal-eye photoreceptor. *Nat. Neurosci.* **1**, 359–365.

Yau, K.-W. (1994). Phototransduction mechanism in retinal rods and cones. The Friedenwald Lecture. *Invest. Ophthalmol. Vis. Sci.* **35**, 10–32.

Biography

King-Wai Yau is a Professor of Neuroscience Johns Hopkins University School of Medicine. His principal interest is in phototransduction in the retina and olfactory transduction in the nose. He received an A.B. (Physics) from Princeton and a Ph.D. (Neurobiology) from Harvard. He is a Fellow of the American Academy of Arts and Sciences.

Photosynthesis

Richard C. Leegood
University of Sheffield, Sheffield, UK

Photosynthesis involves the capture of the Sun's energy into biochemical energy that sustains all life on Earth. It is a massive process that has radically changed the composition of the atmosphere. Its scale can be judged from the fact that man's entire fossil fuel use from 1860 to 1988 was equivalent to only two years' global photosynthesis. Although photosynthesis occurs in a wide range of organisms (bacteria, cyanobacteria, algae, and plants), and about a third of it occurs in the oceans, the present discussion will concentrate on plants.

Photosynthetic Structures

Leaves contain many different types of cell, including stomata, which regulate gas exchange through the epidermis, and the photosynthetic palisade and mesophyll cells, which are thin-walled and have abundant air spaces for the diffusion of gases. Chloroplasts are the organelles which carry out photosynthesis within these cells. The chloroplast has a double-membrane envelope, which regulates transport of metabolites and proteins with the cytosol. It contains thylakoids, a system of membranes, which contain the components of photosynthetic light harvesting (including chlorophyll), electron transport, and ATP synthesis. The thylakoids form sacs with an internal lumen. Thylakoid sacs can occur singly or in stacks, called grana, which resemble a pile of coins. The soluble phase of the chloroplast is the stroma, which contains enzymes of a wide range of biosynthetic processes (Figure 1).

Harvesting Light

Light Harvesting

The first step in photosynthesis is light absorption by pigments. Besides various types of chlorophyll, these pigments include carotenoids, and open-chain tetrapyrrole bilin pigments found in, for example, cyanobacteria. Chlorophyll is a pigment based on a tetrapyrrole ring, rather like hemoglobin, except that it contains magnesium rather than iron. The ring is linked to a long side chain. Chlorophyll absorbs blue and red light, while it transmits the green, and hence appears green. In plants, two types of chlorophyll, *a* and *b*, increase the range of wavelengths absorbed. The light energy absorbed by chlorophyll molecules can either be lost as heat or fluorescence, or it can be transferred between adjacent chlorophyll molecules by resonance transfer. Chlorophyll and carotenoids associate with proteins in light-harvesting complexes. The light-harvesting complexes are doughnut shaped in bacteria, probably surrounding the reaction center. A light-harvesting complex acts like an antenna, similar to a satellite dish, feeding photons into the reaction centers, which contain a dimeric form of chlorophyll, where charge separation occurs. The concept of an antenna arose from the discovery in 1932, by Emerson and Arnold, that only one CO_2 molecule was produced from ~2500 chlorophyll molecules after a short flash of light.

At a higher level of organization, the leaf and its cells are also adapted to harvest light efficiently. In shade, the photosynthetic apparatus is spread out in large thin leaves, to increase the area of light capture and to allow light to penetrate adequately, and there is more light-harvesting chlorophyll per antenna. Within the leaf, epidermal cells can act to focus light, elongated palisade cells act as light guides, while mesophyll cells reflect light, acting like a "hall of mirrors" and increasing the distance that photons travel, thereby increasing the chance that they will hit an antenna complex.

Energy Capture

Reaction centers are multisubunit protein complexes situated in the photosynthetic membrane. These complexes contain the reaction center chlorophylls as well as other components involved in electron transfer. The reaction center is the core of the photosynthetic process, converting the energy of sunlight into a usable chemical form. Reaction centers carry out light-driven electron transfer reactions that result in charge separation across the photosynthetic membrane. Rapid electron transfer to secondary acceptors is necessary to prevent recombination of these separated charges. There are two classes of reaction center with different terminal electron acceptors: those with Fe_4S_4 clusters (type 1) and those

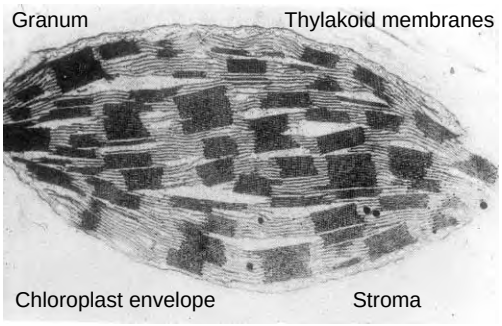

FIGURE 1 Electron micrograph of a chloroplast from maize.

with pheophytin/quinones (type 2). In plants, green algae and cyanobacteria, both reaction centers are present (in photosystems 1 and 2 respectively), while photosynthetic bacteria have only one type of reaction center (e.g., type 1 in green sulfur bacteria, type 2 in purple bacteria). In plants, photosystem 2 contains a chlorophyll dimer which, when in the excited state ($P680^*$), is an extremely strong reducing agent. An acceptor molecule, a quinone, Q, becomes reduced, leaving the positively charged chlorophyll dimer ($P680^+$). This is an extremely strong oxidant, so strong that it can extract electrons from water.

Water Oxidation

Water oxidation is a unique feature of photosystem 2. Water is the electron donor for photosynthetic electron transport. Each photon absorbed by P680 enables it to extract one electron from a manganese-containing enzyme, in an oxygen-evolving complex. Once four electrons have been extracted, this complex can, in turn, oxidize water, releasing O_2 to the atmosphere, as well as releasing $4H^+$ to the thylakoid lumen. Photosynthetic bacteria utilize other sources, such as H_2S or organic compounds, as electron donors.

Energy Dissipation and Repair

In addition to acting as accessory pigments in the antenna, carotenoids also have a photoprotective function. When there is an excess of light energy (e.g., when CO_2 uptake is limited by stomatal closure brought about by water stress), carotenoids can quench the excited triplet state of chlorophyll before it reacts with oxygen, forming destructive singlet state oxygen. Carotenoids can also regulate energy flow in the antenna by dissipating excitation of the chlorophylls as heat (nonphotochemical chlorophyll fluorescence quenching). Energy dissipation is associated with the accumulation of the carotenoid, zeaxanthin, which is interconverted with another carotenoid, violaxanthin, in the xanthophyll cycle. Physical changes, such as chloroplast movements within cells and heliotropic leaf movements, can also reduce or enhance light absorption, and photorespiration can dissipate excess photosynthetic energy. Photosystem 2 itself is very prone to photodamage, with one of its components, the D1 protein, undergoing constant turnover. The photosystem 2 complex is continuously disassembled and reassembled to insert repaired D1.

Electron Transport and ATP Synthesis

There are two photosystems, 1 and 2, involved in photosynthesis in plants, algae, and cyanobacteria. The structures of both have been determined. In 1960, Hill and Bendall published the "Z" scheme, which describes how the two photosystems and the electron carriers are organized with respect to their redox potentials (Figure 2). Electrons from photosystem 2 reduce a number of intermediate electron carriers, such as plastoquinone (PQ), the cytochrome *b/f* complex (including the Rieske iron-sulfur center) and plastocyanin (PC). The reaction center of photosystem 1 (P700) receives its electrons from photosystem II via these carriers and thus oxidizes Q. Photosystem 1 reduces an initial acceptor, A_o, then a series of Fe–S acceptors and ferredoxin (Fd, another iron–sulfur protein) and, finally, NADP is reduced to NADPH. Electrons may also cycle around photosystem 1, leading to ATP generation, as also occurs in some photosynthetic bacteria.

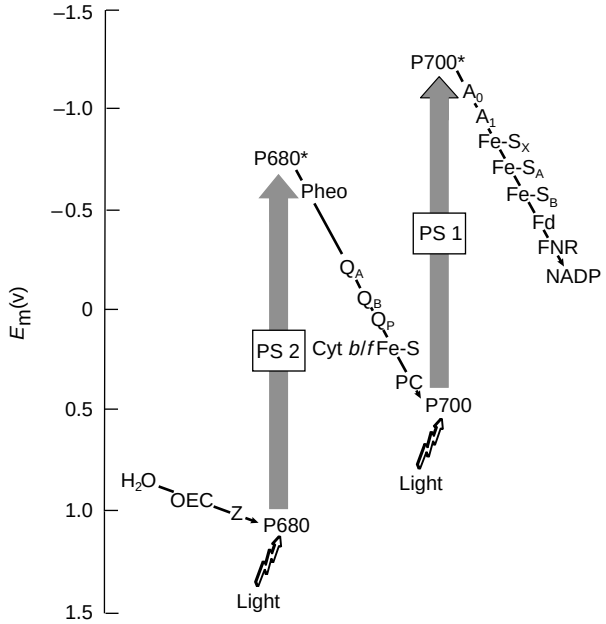

FIGURE 2 The Z-scheme of photosynthetic electron transport, showing the mid-point redox potentials of electron donors, acceptors, and carriers.

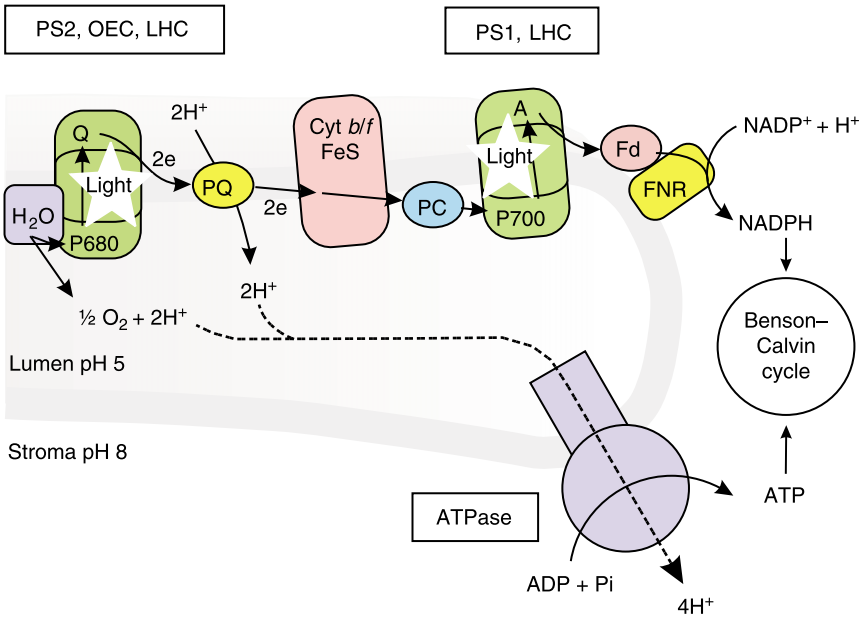

FIGURE 3 Organization of photosynthetic electron transport within the thylakoid membrane, showing how proton production and translocation generates a proton gradient between the thylakoid lumen and the stroma.

Electron transport components are organized within the thylakoid membrane so that, as electrons flow from water to NADP, protons are transferred from the stroma to the thylakoid lumen (Figure 3). This is possible because the key component linking the two photosystems is PQ which is a hydrogen carrier, carrying both an electron (e) and a proton (H^+). Electrons from photosystem II reducePQ, together with protons from the stroma, while oxidation of PQ releases electrons to the cytochome *b/f* complex and protons to the thylakoid lumen. This proton shuttle is driven by photosynthetic electron transport. Protons are also released to the thylakoid lumen when water is oxidized. These processes decrease the pH in the stroma (from pH 7 in the dark to pH 8 in the light) and acidifies the lumen (to ~pH 5). A pH gradient is therefore created which is used to drive ATP synthesis (chemiosmosis). For each molecule of ATP synthesized, $4H^+$ move from the lumen to the stroma. Movement of protons through the ATPase causes its central crankshaft-like core to rotate. This rotational movement causes conformational changes in the active sites of other subunits which result in the synthesis of ATP from ADP and Pi.

Carbon Fixation and Photorespiration

The chloroplast is one of the plant cell's most important factories. ATP and NADPH are utilized to drive biosynthetic processes in the chloroplasts, including the reduction of sulfate and nitrite and the synthesis of lipids and amino acids, in addition to CO_2 fixation.

Benson–Calvin Cycle

Although often termed the "dark reaction" of photosynthesis, CO_2 fixation can only proceed in the light, both because it requires photosynthetically-generated ATP and NADPH and because many of the enzymes which catalyze the process are themselves activated by light. The Benson–Calvin cycle (or Reductive Pentose Phosphate Pathway) is the only mechanism in plants and algae which can catalyze the net fixation of CO_2, although some bacteria have an alternative mechanism. The Benson–Calvin cycle (Figure 4) was discovered in the early 1950s by Melvin Calvin and co-workers, who supplied algae, such as *Chlorella*, with $^{14}CO_2$. The first product of photosynthesis, containing 100% of the radioactivity at zero time, was a three-carbon compound, glycerate 3-phosphate (hence the term C_3 plants). The primary acceptor was identified as ribulose 1,5-bisphosphate (RuBP). RuBP is a five-carbon sugar phosphate which is carboxylated to form two molecules of glycerate-3-P. The Benson–Calvin cycle comprises three phases: (1) carboxylation by ribulose 1,5-bisphosphate carboxylase-oxygenase (Rubisco); (2) reduction of glycerate-3-P to triose-P (which requires ATP and NADPH); and (3) regeneration of the acceptor, RuBP, from triose-P in a "sugar-phosphate shuffle," which requires ATP. Triose-P is a simple sugar phosphate produced by the Calvin cycle. Triose-P that is not

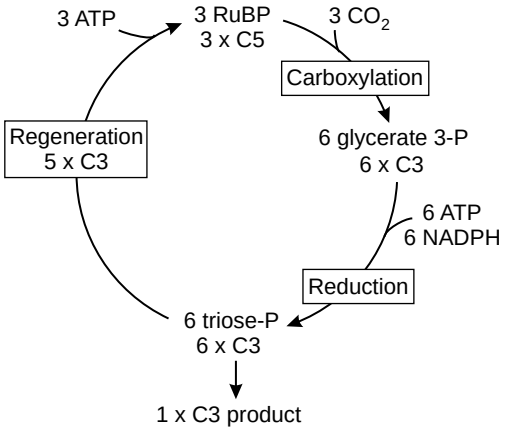

FIGURE 4 A simplified scheme for the Benson–Calvin cycle, showing the carboxylation of RuBP by Rubisco, reduction of glycerate 3-P to triose-P, and regeneration of the initial acceptor from triose-P.

needed for regeneration of RuBP can either be converted to starch in the chloroplast or it can be exported to the cytosol, via the phosphate translocator, to make sucrose.

Photorespiration

Rubisco is an inefficient enzyme. It has a slow catalytic turnover rate, and about half the soluble protein in leaves is Rubisco, making it the most abundant protein in nature.

$$\text{RuBP} + \text{O}_2 \xrightarrow{\text{RuBP oxygenase}} \text{glycerate-3-P} + \text{glycollate-2-P}$$

Rubisco also catalyzes a side-reaction with oxygen, an inevitable consequence of its reaction mechanism. Rubisco evolved in the photosynthetic bacteria in an atmosphere which was richer in CO_2 and depleted in O_2 by comparison with the present atmosphere. The ratio of oxygenation to carboxylation by Rubisco depends upon the relative concentrations of CO_2 and O_2 and oxygenation increases as the temperature increases. Photorespiration is the process by which two molecules of glycollate-2-P, which is not a metabolite of the Benson–Calvin cycle, are retrieved and converted into two molecules of an amino acid, glycine (C2), and then into one molecule of glycerate-3-P (C3). This involves shuttling of metabolites between the chloroplasts, cytosol, peroxisomes, and mitochondria. During this process, one quarter of the carbon in glycollate-2-P is lost as CO_2 and ammonia is liberated. Photorespiration is therefore a wasteful process because it both reduces carbon gain and dissipates photosynthetic energy (because CO_2 is fixed and released again). There is, therefore, a selection pressure on plants to reduce the rate of photorespiration by means of CO_2-concentrating mechanisms, so as to improve their carbon economy. This will be particularly strong when high rates of photorespiration are favored, as at high temperatures. However, a future doubling of ambient CO_2 will reduce photorespiration by ~50% and it would be completely eliminated by a 5-fold rise in atmospheric CO_2.

CO_2-Concentrating Mechanisms

C_4 Photosynthesis

C_4 plants include many tropical grasses and are among the world's most important crop species (maize, sugar cane). Although small in terms of total number of flowering plant species (3%), they constitute ~50% of the 10,000 grass species. Their productivity is high and C_4 grasses in savanna regions (15% of the Earth's vegetated surface) are responsible for ~20% of global photosynthesis. C_4 plants have a distinctive leaf anatomy (Kranz anatomy), with chlorophyll-containing mesophyll and bundle-sheath cells, which form a gas-tight cylinder surrounding the vascular bundle. A CO_2 pump (the C_4 cycle) takes CO_2 from the mesophyll and transfers it into the bundle-sheath, which contains Rubisco and the enzymes of the Benson–Calvin cycle (Figure 5). The process raises the concentration of CO_2 in the bundle-sheath, sufficient to saturate Rubisco with CO_2 and to eliminate photorespiration. Like all pumps, the C_4 cycle requires an input of energy in the form of ATP. Recently, two terrestrial plants have been shown to have single-celled C_4 photosynthesis.

The mechanism of photosynthesis in C_4 plants was elucidated in the 1960 s by Hatch and Slack in Australia. C_4 plants are so-called because the first product of CO_2

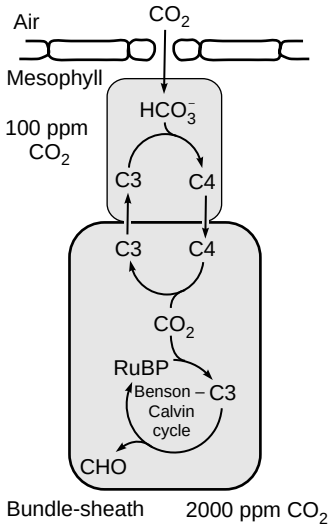

FIGURE 5 A simplified scheme for the mechanism of C_4 photosynthesis, showing how the C_4 cycle shuttles C_4 acids into to bundle-sheath, where they are decarboxylated to raise the CO_2 concentration in the vicinity of Rubisco and thereby suppress photorespiration.

fixation is a C4 organic acid, oxaloacetate, formed by the carboxylation of phosphoenolpyruvate (PEP) by PEP carboxylase. The oxaloacetate is converted to other C4 acids (malate or aspartate) and transferred to the bundle-sheath. Transport of metabolites between the mesophyll and bundle-sheath occurs by diffusion via plasmodesmata. In the bundle-sheath, the C4 acids are decarboxylated to generate CO_2, and a C3 compound returns to the mesophyll. The mechanism of decarboxylation differs, with NADP-malic enzyme in the chloroplast (maize), NAD-malic enzyme in the mitochondria (millet), or PEP carboxykinase in the cytosol (e.g., guinea grass).

C_4 plants are commonly found in warm-to-high temperature environments, such as tropical grasslands, where photorespiratory rates would be high in C_3 plants. C_4 plants have double the water-use efficiency of C_3 plants because photosynthesis can operate at low intercellular concentrations of CO_2, and hence lower stomatal conductances. Nitrogen-use efficiency is also improved because Rubisco is used more efficiently, due to the suppression of photorespiration.

Aquatic Photosynthesis

The aquatic environment poses serious problems for the acquisition of CO_2. First, the diffusion of CO_2 in water is 10 000 times slower than in air. Second, inorganic carbon is present in water as CO_2, HCO_3^- and CO_3^{2-}, the relative amounts of which depend upon the pH of the water. Most inorganic carbon in alkaline waters is therefore present as carbonate and bicarbonate. Photosynthesis by aquatic plants, algae, and phytoplankton may raise the local O_2 concentration and enhance photorespiration. Aquatic organisms (cyanobacteria, micro- and macro-algae, aquatic angiosperms) have developed means of taking up dissolved inorganic carbon (CO_2 and HCO_3^-) actively from their environment. They can concentrate it internally in Rubisco-containing structures, such as carboxysomes and pyrenoids, and thus suppress photorespiration.

Crassulacean Acid Metabolism

Leaves are faced with a difficult task. Leaf cells have thin walls and the intercellular spaces are saturated with water vapor. As leaves assimilate CO_2 (5 000 litres of air are needed to manufacture 1 g of sucrose), they need to restrict the amount of water lost from the leaf via the stomata. There is therefore a conflict between the requirements for CO_2 fixation and water conservation. Crassulacean acid metabolism (CAM) is a photosynthetic adaptation to periodic water supply, occurring in plants in arid regions (e.g., cacti) or in tropical epiphytes (e.g., orchids and bromeliads). CAM plants close their stomata during the day and take up CO_2 at night, when the air temperature is lower. Water loss can be lowered by an order of magnitude. CAM occurs in between 5% and 10% of plants and is always associated with succulence, at least at a cellular level.

Although the biochemistry is similar to that of C_4 plants, two carboxylations are now separated in time rather than in space. Malic acid is synthesized from carbohydrates, via PEP carboxylase, at night and is stored in the vacuole. During the day malate is decarboxylated, via PEP carboxykinase or NAD(P)-malic enzymes in the cytosol, CO_2 is refixed via the Benson–Clavin cycle, and carbohydrates are reformed. This process occurs behind closed stomata. The internal concentration of CO_2 is raised as high as 10 000 ppm, which also suppresses photorespiration. CAM plants show a high degree of metabolic flexibility. Seedlings and well-watered plants may show little or no CAM and perform C_3 photosynthesis, opening their stomata during the day. This allows increased carbon gain during periods of water availability or during seedling establishment. Water or salt stress can then induce CAM, switching on gene expression for synthesis of the component enzymes.

See Also the Following Articles

Chlorophylls and Carotenoids • Chloroplasts • Ferredoxin • Green Bacteria: The Light-Harvesting Chlorosome • Light-Harvesting Complex (LHC) I and II: Pigments and Proteins • Photosynthetic Carbon Dioxide Fixation • Photosystem I: F_X, F_A, and F_B Iron-Sulfur Clusters • Photosystem II Light Harvesting System: Dynamic Behavior • Photosystem II: Water Oxidation, Overview

Glossary

CO_2-concentrating mechanism A biochemical (in terrestrial plants) or biophysical pump (in many aquatic photosynthetic organisms), which concentrates CO_2 around Rubisco so as to reduce photorespiration.

photorespiration The wasteful process by which glycollate 2-phosphate, which results from the oxygenation reaction of Rubisco, is recycled to the Benson–Calvin cycle.

reaction center A multisubunit protein complex situated in the photosynthetic membrane. containing the reaction center chlorophylls as well as other components involved in electron transfer, which together convert the energy of sunlight into a usable chemical form.

Further Reading

Blankenship, R. E. (2002). *Molecular Mechanisms of Photosynthesis*. Blackwell Science, Oxford.

Capaldi, R. A., and Aggeler, R. (2002). Mechanism of the F_1F_0-type ATP synthase, a biological rotary motor. *Trends Biochem. Sci.* **27**, 154–160.

Chitnis, P. R. (2001). Photosystem I: Function and physiology. *Annu. Rev. Plant Physiol. Plant Mol. Biol.* **52**, 593–626.

Horton, P., Ruban, A. V., and Walters, R. G. (1996). Regulation of light-harvesting in green plants. *Annu. Rev. Plant Physiol. Plant Mol. Biol.* **47**, 655–684.

Kaplan, A., and Reinhold, L. (1999). CO_2 concentrating mechanisms in photosynthetic microrganisms. *Annu. Rev. Plant Physiol. Plant Mol. Biol.* **50**, 539–570.

Rutherford, A. W., and Faller, P. (2001). The heart of photosynthesis in glorious 3D. *Trends Biochem. Sci.* **26**, 341–344.

Sage, R. F., and Monson, R. K. (1999). *C_4 Plant Biology.* Academic Press, San Diego.

Spreitzer, R. J., and Salvucci, M. E. (2002). Rubisco: Structure, regulatory interactions, and possibilities for a better enzyme. *Annu. Rev. Plant Biol.* **53**, 469–475.

Walker, D. A. (1992). *Energy, Plants, and Man*. Oxygraphics, Brighton.

http://www.wkap.nl/prod/s/AIPH—All volumes in the series "Advances in Photosynthesis and Respiration" published by Kluwer Academic Publishers, Dordrecht.

Biography

Richard C. Leegood is a Professor of Plant Sciences in the Department of Animal and Plant Sciences and a member of the Robert Hill Institute for Photosynthesis Research at the University of Sheffield, U.K. His principal research interests are carbon and nitrogen metabolism and their regulation in plants. He holds a Ph.D. from the University of Cambridge. He has authored and edited several texts and many review articles in the field of photosynthesis and metabolism.

Photosynthetic Carbon Dioxide Fixation

Matthew J. Paul
Rothamsted Research, Harpenden, UK

Photosynthetic carbon dioxide fixation is the point of entry of carbon into organic molecules. Light provides the energy (ATP) and reducing power (NADPH) from electron flow in chloroplasts for CO_2 to be reduced to triose phosphate in reactions of the Calvin cycle. The cycle is the starting point for the synthesis of sugars, amino acids, and other plant products. Accompanying the provision of ATP and NADPH in light reactions of photosynthesis is the production of O_2. Thus, photosynthesis generates organic molecules that underpin all biology and agriculture and provides the necessary oxygen that also enables aerobic respiration to proceed for them to be metabolized in the growth and maintenance of all living things. In Earth's early history, photosynthesis enabled the evolution of complex multicellular life forms and continues till today to regulate the gas composition of the atmosphere and hence climate.

Light Provides Energy (ATP) and Reducing Power (NADPH) for CO_2 Fixation

Photons in the range 400–700 nm – except green light, which is reflected – drive photosynthesis through provision of ATP and NADPH. Light also regulates the Calvin cycle in other ways. Photons interact with electrons in chlorophylls of light-harvesting antenna in thylakoid membranes of chloroplasts. There are two light-absorbing photosystems that cooperate in the reduction of NADP by electrons derived from water. Energy is passed from these to reaction centers of photosystem II, where electrons are excited and passed to an acceptor and down an electron transport chain to photosystem I. Electrons and protons pass to NADP, yielding NADPH. The open reaction of photosystem II is filled with electrons from water, from which O_2 is evolved. A pH gradient across the thylakoid membrane from H^+ accumulation in the thylakoid lumen provides the impetus for ATP synthesis by ATP synthase (Figure 1).

The Path of Carbon in Photosynthesis

The sequence of reactions that fix CO_2 into triose phosphate using ATP and NADPH from these light reactions was determined using C14 radioisotopes by Melvin Calvin and colleagues, for which the Nobel prize for chemistry was awarded. This sequence of reactions is now known as the Calvin cycle, reductive pentose phosphate pathway, or photosynthetic carbon reduction cycle. It consists of three distinct phases. First, the fixation of CO_2 into 3-phosphoglyceric acid (3-PGA) (carboxylation). Second, the reduction of 3-PGA into the triose phosphate, glyceraldehyde-3-phosphate (GAP), which can be exported to the cytosol for sucrose synthesis or remain in the chloroplast for starch synthesis or the other biosynthetic reactions that occur there. Triose phosphate also has to remain in the cycle to allow regeneration of the CO_2 acceptor, ribulose 1,5-bisphosphate (RuBP), in the third, regenerative phase of the cycle (Figure 2).

Carboxylation Phase

Carboxylation is catalyzed by the Earth's most abundant protein, ribulose bisphosphate carboxylase/oxygenase (Rubisco), which can constitute up to 50% of the soluble protein in a leaf. The combination of CO_2 with RuBP, a five-carbon compound, yields two molecules of the three carbon compound 3-PGA. Many enzymes will bind molecules in addition to the ones they have primary affinity for, if they are present at high enough concentrations. Present-day atmospheric O_2 concentration is a thousand times higher than that of CO_2 and in ambient conditions oxygenation of RuBP also occurs. This produces phosphoglycolate which is metabolized in the glycolate pathway outside the chloroplast and returned to the Calvin cycle as 3-PGA in a process termed photorespiration because CO_2 is evolved in the process (Figure 1). Some plants have evolved a supplementary

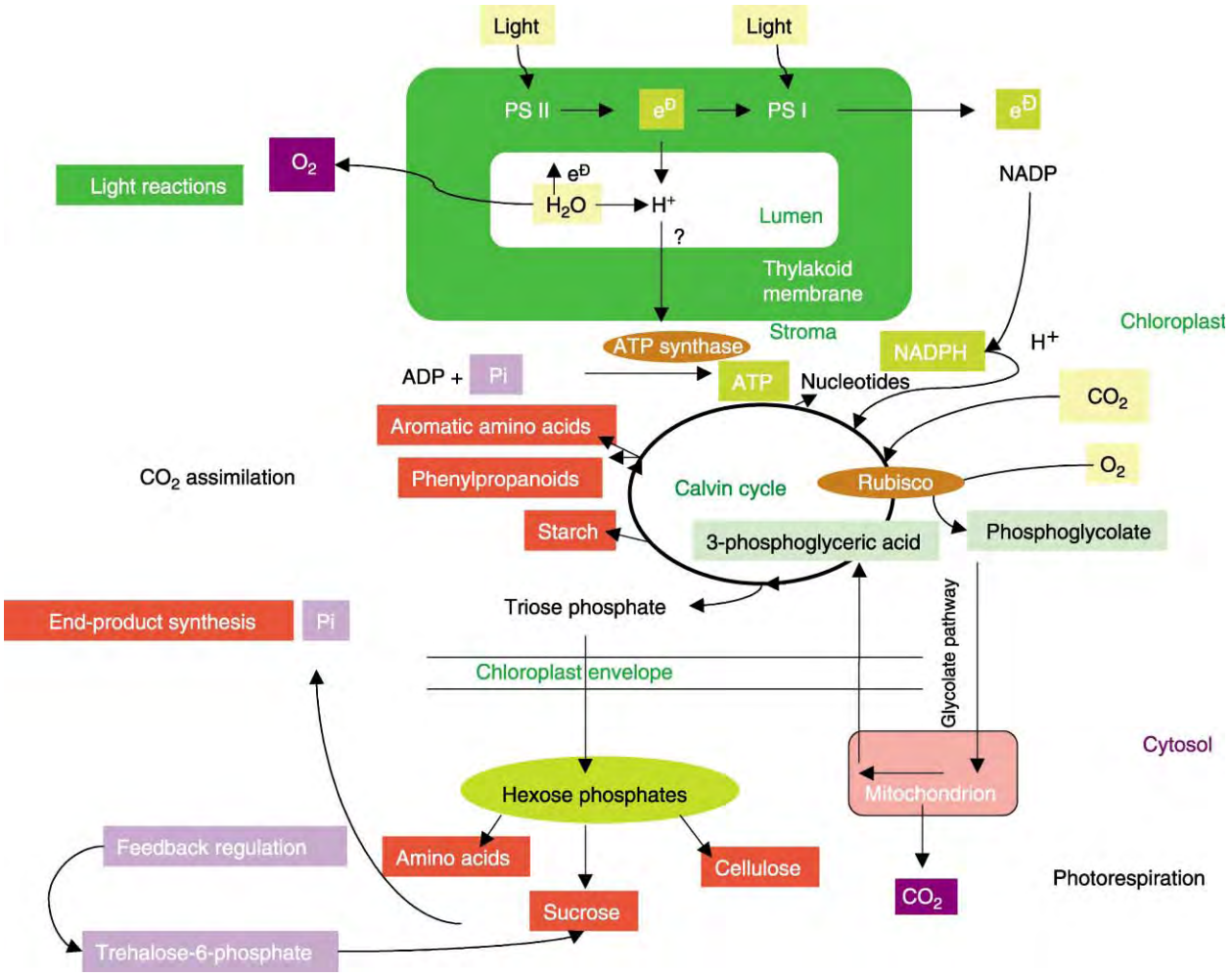

FIGURE 1 Schematic of photosynthetic metabolism summarizing the principal components of light reactions, CO_2 fixation into the Calvin cycle and the synthesis of end products.

carboxylation reaction catalyzed by phosphoenol pyruvate carboxylase where minimal oxygenation occurs. Such plants are known as C4 plants because the first products of CO_2 fixation are carboxylic acids containing four carbon atoms. A high concentration of CO_2 generated from the decarboxylation of these acids at the site of the Calvin cycle minimizes the oxygenation reaction of Rubisco and hence suppresses photorespiration. Other specialized plants known as Crassulacean acid metabolism (CAM) plants fix CO_2 into C4 acids at night. These metabolic adaptations of C4 and CAM ensure a high intercellular CO_2 concentration which maintains a small stomatal aperture, conserving water, an overriding selection force in some environments. In CAM plants stomata can be shut for much of the day and is observed in more extreme xerophytes such as cacti and succulents. C4 grasses are very common in Australia. More recent evolution has resulted in these adaptations rather than large modification of the properties of Rubisco to further favor carboxylation rather than oxygenation. Instead Rubisco has been the target of biotechnologists to improve photosynthesis. However, altering Rubisco properties more in favor of carboxylation has proved technically demanding and is being superseded by other strategies of enhancing photosynthesis.

Reduction Phase

The 3-PGA produced in the carboxylation phase (and returned from photorespiration) is reduced to triose phosphate, GAP, in two steps. The first, a phosphorylation step, requires ATP. The 1,3-bisphosphoglycerate formed is then reduced with NADPH to GAP. The high ATP and NADPH concentrations associated with photosynthesis shift these reactions in favor of triose phosphate.

Regeneration Phase

Triose phosphate is essentially the end product of photosynthesis as it is exported from the chloroplast.

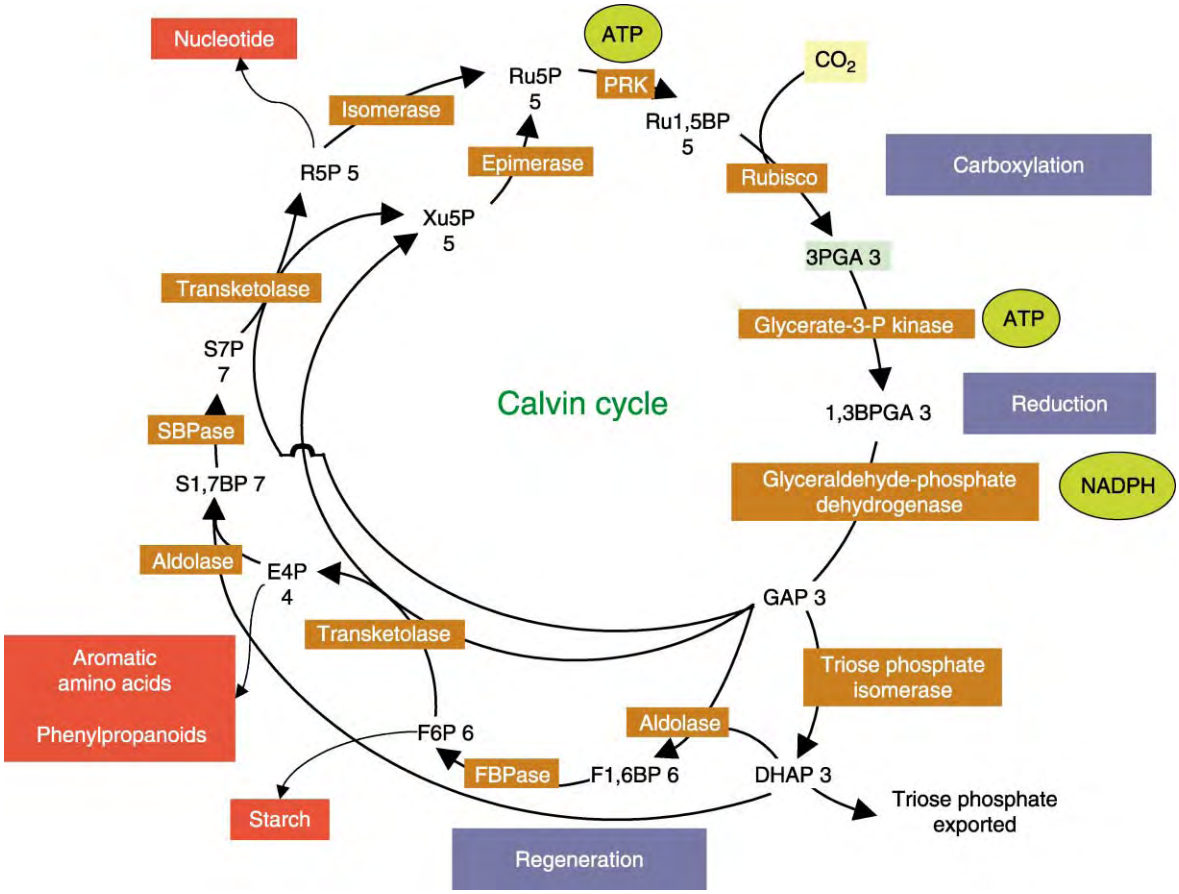

FIGURE 2 Calvin cycle of reactions that incorporate CO_2 into triose phosphate and which regenerate ribulose-1,5-bisphosphate (Ru1,5BP) for continued CO_2 fixation. Numbers after compounds indicate number of carbon atoms. 3-PGA, 3-phosphoglyceric acid; 1,3 BPGA, 1,3 bisphosphoglyceric acid; GAP, glyceraldehydes-3-phosphate; DHAP, dihydroacetone phosphate; F1,6BP, fructose-1,6-bisphosphate; F6P, fructose 6-phosphate; E4P, erythrose-4-phosphate; S1,7BP, sedoheptulose-1,7-bisphosphate; S7P, sedoheptulose-7-phosphate; R5P, ribose-5-phosphate; Ru5P, ribulose-5-phosphate; Xu5P, xylulose-5-phosphate. Enzymes are Rubisco, ribulose-1,5-bisphosphatase; FBPase, fructose-1,6-bisphosphatase; SBPase, sedoheptulose-1,7-bisphosphatase; PRK, phosphoribulokinase.

However, some must be retained in the cycle to resynthesize the acceptor molecule for CO_2 fixation, RuBP to keep the cycle going. In this series of reactions, five trioses are converted into three pentoses. The first part involves the conversion of GAP to fructose-6-phosphate (F6P). Then the carbon atoms in F6P, GAP, and dihydroxyacetone phosphate are rearranged into the pentose, ribulose-5-phosphate (Ru5P). In the final step Ru5P is converted to RuBP in an ATP-requiring step. Like the rest of the cycle this phase is highly regulated and can strongly affect the ultimate rate of CO_2 fixation. An important branch point in this segment of the cycle, catalyzed by transketolase links primary and secondary metabolism. The substrates and products of transketolase can supply carbon (erythrose-4-phosphate) for the synthesis of aromatic amino acids and phenylpropanoids (compounds important for flavor, texture, color), nucleotide synthesis (R5P), and starch (F6P) in addition to the regeneration of RuBP.

Regulation of the Calvin Cycle

Metabolic regulation enables the balance between substrate and product of enzyme-catalyzed reactions to be maintained so that ordered metabolic flow to sustain life can occur in response to developmental requirements and environmental constraints. The Calvin cycle is regulated by light which ensures its temporal separation and prevents competition with other reactions, such as the oxidative pentose phosphate pathway, also present in the chloroplast stroma. Light regulates the cycle through provision of ATP and NADPH, which regulate those steps dependent on them. Light also causes an increase in the pH of the chloroplast stroma to ~8, the pH optimum for Calvin cycle enzymes. Pumping of protons into the thylakoids is also coupled with flow of magnesium necessary for enzyme activity into the stroma. A further way that light regulates the cycle is through photosynthetic electron transport. Reducing equivalents from photosystem I via ferredoxin-thioredoxin reductase

reduce the thiol groups of GAP dehydrogenase (GAPDH), fructose-1,6-bisphosphatase (FBPase), sedoheptulose-1,7-bisphosphatase (SBPase) and phosphoribulokinase (PRK) increasing their activity. Rubisco is activated by CO_2 and magnesium in a process called carbamylation, a process promoted by an activating protein, Rubisco activase. Enzymes of the Calvin cycle are associated as enzyme complexes. For example GAPDH and PRK are linked by the protein CP12. The precise role of this association of such complexes is not yet known, but is likely to facilitate further regulation of metabolic flow.

Are Some Calvin Cycle Enzymes More Important in Regulating Carbon Flux than Others?

The equilibrium position of reactions catalyzed by Rubisco, SBPase, FBPase, and PRK as a consequence of their regulation lies very much in favor of the end-product. These enzymes are termed irreversible enzymes because of the large amount of energy that would be required to reverse the reaction. Such enzymes have traditionally been seen as key enzymes because of their importance in directing carbon flow. Since the early 1990s genetic modification has enabled individual enzymes to be targeted through use of antisense RNA to decrease the synthesis of target proteins. Lines of transgenic plants exhibiting progressive decreases in activity of an enzyme has enabled metabolic control analysis to be undertaken and flux control coefficients for individual enzymes assigned. For the Calvin cycle a change in enzyme activity can then be related to flux through the pathway by measuring CO_2 uptake by leaves using infra-red gas analysis. The flux control coefficient is given as $C = \delta J/J$, where J is original flux, and δJ is changed flux. This coefficient can also be written as $C = \delta E/E$, where E is original enzyme activity, and δE is changed enzyme activity.

So, if a 50% decrease in enzyme activity achieves a 25% decrease in CO_2 uptake then the flux control coefficient is 0.5 (25/50); essentially half the control of the pathway resides with that enzyme. If a 50% decrease achieves no change in flux then the flux control coefficient is zero and the enzyme is in excess under those conditions. Over the course of a day, and during the life cycle of a plant, an enzyme may exhibit a range of flux control coefficients. Variation during the course of a day will be caused largely by changes in illumination, whereas over the life cycle by nitrogen availability and changes in light environment. Both light and nitrogen affect the amount of enzyme synthesized and light affects enzyme activity to different extents for different enzymes, so relative contributions to flux control change. Other aspects of environment, for example temperature and phosphorus nutrition are also influential.

Calvin Cycle Enzymes that Most Limit Flux

The first enzyme for which detailed flux control analysis was conducted using transgenics was Rubisco. Quite surprisingly at the time, in view of the perceived importance of the enzyme, the first data showed that removing half of it with antisense resulted in little change in CO_2 fixation. However, when plants were grown at high light the flux control coefficient rose, and combined with low nitrogen, could reach 0.8. Rubisco is the enzyme that imposes the greatest potential limitation of Calvin cycle carbon fixation. SBPase is another enzyme with a potentially high flux control coefficient at high light. A major surprise was that nonregulated equilibrium enzymes, aldolase, and transketolase could have flux control coefficients around 0.3 under high light conditions. Other enzymes in the cycle when decreased up to 50% have showed no large impact on flux. The most extreme example of this is phosphoribulokinase, where a decrease up to 85% has no impact on CO_2 fixation.

The important message to come from this work is that both highly regulated and unregulated equilibrium enzymes could control flux. The work supported the von Caemmerer and Farquhar 1981 model, which proposed that photosynthesis was colimited between carboxylation (Rubisco activity) and the capacity to regenerate ribulose-1,5-bisphosphate. Control was seen as poised between carboxylation and regeneration, but under saturating light the balance would shift toward Rubisco and under low light toward regeneration. The research using antisense confirmed this assumption and gave useful indications as to which enzymes in the regeneration phase would be most likely to increase rates of CO_2 fixation if their activities could be increased. Thus, there would most likely be benefit if one or more of activities of SBPase, aldolase, or transketolase could be increased.

Genetic Modification of Photosynthesis to Improve Growth and Yield

Direct Targeting of Calvin Cycle

In support of the findings of flux control analysis, expression of a bifunctional SBPase/FBPase from a cyanobacterium resulted in increased photosynthesis and biomass production. This was the first report of an increase in activity of one or more Calvin cycle enzymes

benefiting photosynthesis and biomass production. There is also evidence that overexpressing the plant SBPase improves photosynthetic rates. Improved photosynthesis has also been achieved through expressing a cyanobacterial gene in plants involved in HCO_3^- accumulation which releases CO_2 within the leaf for CO_2 fixation and hence improves carboxylation. These former targets constitute direct targeting of the Calvin cycle. Another approach has been to target feedback mechanisms that regulate CO_2 fixation.

Feedback Regulation of the Calvin Cycle and its Targeting to Improve Photosynthesis

In addition to the sophisticated control mechanisms that relate CO_2 fixation to light availability (feedforward regulation), feedback mechanisms relate Calvin cycle activity to the demand for the end products of photosynthesis. Inorganic phosphate (Pi) is a component of phosphorylated intermediates in pathways and is liberated when end product, e.g., sucrose, is synthesized (sucrose contains no Pi). This recycling of Pi is necessary to ensure that metabolic flow can continue. Photophosphorylation and ATP synthesis are particularly sensitive to Pi supply. Slow recycling of Pi caused by low temperature, for example, can restrict the recycling of Pi and so limit photosynthesis.

Demand for end product is also determined by the genetic potential of the plant for growth and by other environmental factors, particularly nitrogen, which facilitates high growth rates. The assimilation of nitrogen into amino acids requires carbon skeletons derived from triose phosphates supplied by the Calvin cycle. An impairment of nitrogen supply slows growth, which can lead to a build of sugar in leaves, because photosynthates are no longer being used in growth and nitrogen assimilation. It was shown in 1990 that seven maize photosynthetic genes were repressed by glucose or sucrose in a maize protoplast system. Further evidence of control of photosynthetic gene expression by sugars has been obtained where sugars were made to accumulate in leaves due to genetic modification, environmental treatments (high CO_2 and low N, in particular), and through direct feeding of sugars to leaves. The exact mechanism through which this may operate is not clear, but it is likely to be part of a fundamental metabolic signaling process that links photosynthesis with requirement for sugar. Recently it has been shown that modification of such feedback mechanisms may be a way forward to improving photosynthesis. The trehalose pathway, once thought to have become largely extinct in plants, is now known to be ubiquitous with an indispensable role in regulating carbohydrate use. Modification of a key component of this regulation, trehalose 6-phosphate (T6P), has been shown to alter sugar metabolism in growth processes and alter photosynthesis. There is a close correlation between T6P, Rubisco content, and photosynthetic rate. Increasing amounts of T6P by genetic modification increased amounts of Rubisco and photosynthetic rate of leaves. It is thought that T6P links carbohydrate utilization to photosynthesis as part of a feedback loop that regulates photosynthesis in response to sugar use. Modification of this process provides a route toward increasing Rubisco activity and photosynthesis.

Photosynthetic CO_2 Fixation of Whole Plants

A central strategy of photosynthetic regulation of whole plants is to balance photosynthetic rate of leaves with the overall leaf area of the plant. Surveys of variations in photosynthesis per unit leaf area of many crops demonstrate a strong negative relationship with leaf area. Many environmental factors, particularly light, and the genetic make up of the plant determine this trade off. Growth rate and productivity are more closely related to leaf area than the photosynthetic rate of individual leaves. This is reflected in crop breeding for yield which has increased leaf area often at the expense of photosynthetic rate. Large leaf area combined with use of fertilizers and control of pests and diseases has maximized photosynthesis per unit of land for high crop yields. Improvements in yields in this way may be reaching a limit, so advances in improvement of photosynthetic rate combined with large leaf area may be the way forward to increasing photosynthesis and for future productivity gains. The complexity of photosynthetic regulation at the pathway and whole plant level show there are many things to consider in trying to genetically engineer photosynthesis and productivity. However, the nature of recent progress gives much room for optimism.

See Also the Following Articles

ATP Synthesis in Plant Mitochondria: Substrates, Inhibitors, Uncouplers • Chlorophylls and Carotenoids • Chloroplasts • Ferredoxin • Pentose Phosphate (Hexose Mono Phosphate) Pathway • Photosynthesis

Glossary

Calvin cycle, reductive pentose phosphate pathway or **photosynthetic carbon reduction cycle** Series of reactions that reduce CO_2 into triose phosphate in the chloroplast from which sugars, amino acids, and other plant products are synthesized.

chloroplast Organelle in which light reactions and Calvin cycle take place.

feedback regulation Regulates carbon flow through the Calvin cycle in response to the demand for photosynthate in end-product synthesis. It can operate at the level of recycling inorganic phosphate back to the Calvin cycle and at the level of gene expression of Calvin cycle enzymes by sugars and their metabolism.

feedforward regulation Enables the Calvin cycle to respond sensitively to light by affecting the synthesis of Calvin cycle enzymes and their activity.

light reactions They drive electron flow which leads to the reduction of NADP to NADPH and synthesis of ATP necessary for the operation of the Calvin cycle.

Further Reading

Calvin, M. (1961). The path of carbon in photosynthesis. In *Nobel Lectures, Chemistry 1942–1962*. Elsevier, Amsterdam.

Leegood, R. C., Sharkey, T. D., and von Caemmerer, S. (eds.) (2000). Advances in photosynthesis. In *Photosynthesis: Physiology and Metabolism*, Vol. 9, Kluwer Academic, Dordrecht.

Lieman-Hurwitz, J., Rachmileuitch, S., Mittler, R., Marcus, Y., and Kaplan, A. (2003). Enhanced photosynthesis and growth of transgenic plants that express ictB, a gene involved in HCO_3^- accumulation in cyanobacteria. *Plant Biotechnol.* **1**, 43–50.

Miyawaga, Y., Tamoi, M., and Shigeoka, S. (2001). Over expression of a cyanobacterial fructose-1,6-bisphosphatase/sedoheptulose-1,7 bisphosphatase in tobacco enhances photosynthesis and growth. *Nat. Biotechnol.* **19**, 965–969.

Pellny, T. K., Ghannoum, O., Conroy, J. P., Schluepmann, H., Smeekens, S., Andralojc, J., Krause, K.-P., Goddijn, O., and Paul, M. J. (2004). Genetic modification of photosynthesis with *E. coli* genes for trehalose synthesis. *Plant Biotechnol. J.* **2**, 71–82.

Raines, C. A. (2003). The Calvin cycle revisited. *Photosynthesis Res.* **75**, 1–10.

Von Caemmerer, S., and Farqhuar, G. D. (1981). Some relationships between the biochemistry of photosynthesis and the gas exchange of leaves. *Planta* **153**, 376–387.

Biography

Matthew Paul is a Research Leader at Rothamsted Research, grant aided by the Biological and Biotechnological Sciences Research Council of the United Kingdom. His principal research interests are the regulation of sugar metabolism and photosynthesis by metabolic signaling processes and in particular the role of the trehalose pathway in this regard. He holds a Ph.D. from the University of Leicester and worked as a Royal Society postdoctoral fellow at the University of Bayreuth, Germany.

Photosystem I, Structure and Function

Petra Fromme
Arizona State University, Tempe, Arizona, USA

Photosystem I (PS I) is a bio-solar energy converter that plays the key role in the first steps of oxygenic photosynthesis: the conversion of the light energy from the sun into chemical energy. It is a large membrane protein complex, consisting of 12 proteins, to which 127 cofactors (as chlorophylls, carotenoids, FeS clusters, and vitamin K1) are noncovalently bound. The function of PS I can be described as a bio-solar cell. It captures the light from the sun by a large antenna system (consisting of 90 chlorophylls and 22 carotenoids) and transfers the energy to the center of the complex, where the electron transfer chain is located. When the excitation energy reaches the center of the complex, charge separation takes place. An electron is ejected and transferred across the membrane to the terminal FeS cluster by a chain of six different electron carriers. In the next step of the reaction cycle, the electron is transferred from PS I to the soluble electron carrier protein ferredoxin leading finally to the reduction of $NADP^+$ to NADPH by the ferredoxin:NADP:reductase (FNR). The cycle is completed by the re-reduction of the donor site of PS I by either plastocyanin or cytochrome c_6.

Photosynthesis

Oxygenic photosynthesis is the main process on earth that converts the light energy from the sun into chemical energy. The process supplies all higher life on earth with food and produces all the oxygen in the atmosphere. Three different kinds of organisms are able to perform oxygen-evolving photosynthesis: plants, algae, and cyanobacteria. Whereas plants and algae are eukaryotic cells containing chloroplasts, cyanobacteria are prokaryotes. It was suggested that chloroplasts had been formed in early times of evolution by endosymbiosis. During this process an ancestor of the plant cell may have incorporated an early ancestor of cyanobacteria which subsequently lost its independent status and became a cell organelle in later stages of evolution. Whereas this process may have occurred billions of years ago, the primary steps of photosynthesis have been conserved and are still essentially the same in plants and cyanobacteria.

The initial steps of photosynthesis, the light reactions, occur on a membrane system, known as the thylakoids. Two large membrane protein complexes – the photosystems I and II (abbreviated as PS I and PS II, respectively) that are embedded in this membrane – catalyze the initial steps of photosynthesis, the light-induced charge separation. A pool of plastoquinones, the cytochrome b_6f complex, and plastocyanine or cytochrome c_6 functionally couple both photosystems. The thylakoid membrane is charged by this process (comparable to the charging of a battery) and a proton gradient develops across the membrane. Both the electrical gradient and the proton gradient (i.e., the electrochemical gradient) drive the synthesis of ATP. Reduced hydrogen for sugar formation is provided by reduction of $NADP^+$ and H^+ to NADPH. The reaction is driven by the electrons provided by PS I.

Function of PS I

PS I is a large membrane protein complex; in cyanobacteria it consists of 12 protein subunits to which 127 cofactors are noncovalently bound. It catalyzes the light-driven electron transfer from the soluble Cu-containing protein plastocyanine on the lumenal side (i.e., the inside of the thylakoids) to ferredoxin at the stromal side (outside) of the thylakoid membrane. Cyanobacteria can also use the hem containing soluble protein cytochrome c_6 as an alternate or unique electron donor to PS I. There is also some flexibility concerning the electron acceptor. In the case of iron deficiency, flavodoxin can act as the electron acceptor instead of ferredoxin.

In plants, the system contains at least four additional subunits whose functions are still under investigation. It is known that the main proteins, including all cofactor-binding sites, are well conserved between plants and cyanobacteria. However, detailed structural information is available only for the latter one from the X-ray structure of PS I from the thermophilic cyanobacterium *Synechococcus elongatus* at 2.5Å resolution. In cyanobacteria, PS I is a trimer with a molecular weight of more than 1000 kDa. Figure 1 shows the picture of the trimeric complex, pointing out the complex organization of this nano-bio-solar system. PS I is the largest and most complex membrane protein for which the structure has been determined.

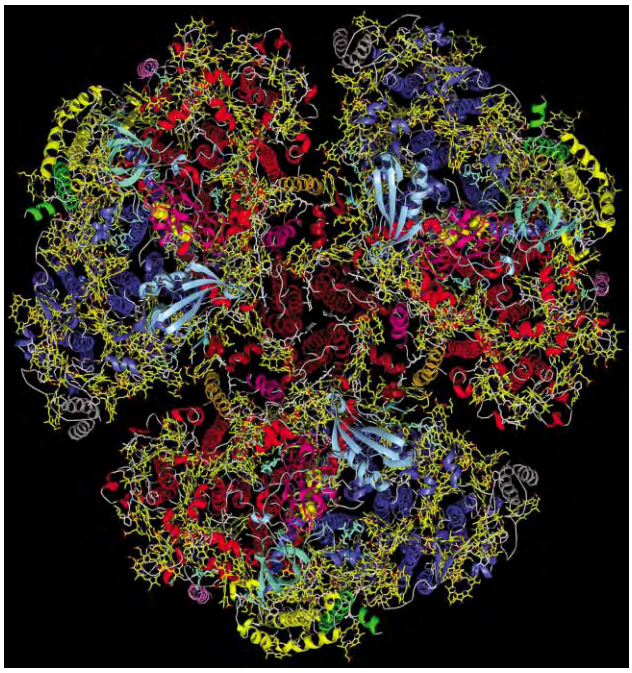

FIGURE 1 The trimeric structure of PS I from cyanobacteria; the view direction is from the stromal side onto the membrane plane. The 12 proteins are shown in a backbone representation (PsaA, blue; PsaB, red; PsaC, pink; PsaD, turquoise; PsaE, light blue; PsaF, yellow; PsaI, dark pink; PsaJ, green; PsaK, gray; PsaL, brown; PsaM, orange, and PsaX, light pink). The head groups of the chlorophylls are shown in yellow, their phytyl-tails have been omitted for clarity. The carotenoids are depicted in gray; the lipids, in dark turquoise.

Each monomeric unit contains 12 proteins, 96 chlorophylls (the pigments that give the plants the green color), 22 carotenoids (orange pigments, which become visible in autumn), 3 [4Fe–4S] clusters, 2 phylloquinone molecules, and 4 lipids.

The first step of the whole process is the light capturing, performed by the large antenna system, which consists of 90 antenna chlorophylls and 22 carotenoids. The energy is transferred to the center of the complex, where the electron transport chain is located. When the energy excites a special pair of two chlorophylls, located in the center of the complex, the "action" takes place and charge separation occurs. Due to its absorption maximum at 700 nm, this pair of chlorophylls was named P700. The electron is transferred from P700 across the membrane by a chain of electron carriers. These electron carriers were previously identified by spectroscopic investigations, and their historical names have been maintained. The electron transport chain consists of five steps. The electron is stepwise transferred from P700 to A (a chlorophyll *a* molecule), A0 (also a chlorophyll *a* molecule), A1 (a phylloquinone molecule) and from there to the three [4Fe–4S] clusters – FX, FA, and FB. After the docking of the soluble electron carrier ferredoxin, the electron is transferred from PS I to ferredoxin, which subsequently leaves the docking site responsible for bringing the electron to the ferredoxin-$NADP^+$-reductase, which then finally reduces $NADP^+$ to NADPH. After this process has occurred once, $P700^+$ has to be re-reduced to complete the reaction cycle. There is a docking site for soluble electron carrier proteins located at the lumenal site of the complex, just underneath P700. In plants reduced plastocyanine docks to this site and reduces $P700^+$, whereas cytochrome c_6 can substitute plastocyanine in cyanobacteria.

The Proteins

The structure and location of the proteins in PS I is shown in Figures 2A and 2B. Cyanobacterial PS I consists of 12 different protein subunits, which are named PsaA to PsaX, according to their genes. The two most important proteins are the large subunits PsaA and PsaB. They harbor most of the antenna system as well as most of the cofactors of the electron transport chain from P700 to the first FeS cluster, FX. The latter is a rare example of an inter-protein FeS cluster coordinated by four cysteines, two of them provided by PsaA and the other two cysteine ligands provided by PsaB. Each of the two large subunits consists of 11 transmembrane helices, connected by partially extended loops that also contain many secondary structural elements as α-helices and β-sheets. The docking site of plastocyanine/cytochrome c_6 is formed by two of these surface helices. The five C-terminal helices are located in the center of the PS I and surround the electron transfer chain, whereas the six N-terminal helices flank the inner core on both sites. They are arranged as a trimer of dimers and they coordinate a large part of the antenna pigments in PS I. The six smaller membrane-embedded proteins (PsaF, PsaI, PsaJ, PsaK, PsaL, and PsaX) surround the core formed by PsaA and PsaB. Their main function is the stabilization of the antenna complex. PsaL also has an important structural role, because it is involved in the formation of the trimer. A further function of the smaller subunits may be the interaction of PS I with external antenna complexes. Cyanobacteria contain large membrane-associated antenna complexes, called phycobillisomes, which are either connected to PS I or to PS II, depending on the light conditions. There is some indication from deletion mutants that PsaF may play an important role in the connection of PS I with the phycobillisomes. Under an environmental stress, such as iron deficiency, the phycobillisomes are degraded and PS I is supplied with additional energy by a ring of 18 subunits of a membrane integral antenna complex, which is named IsiA (for iron stress induced protein A). With a molecular weight of 43 kDa, this protein has homologies to the internal antenna protein of PS II (CP43) and is therefore also

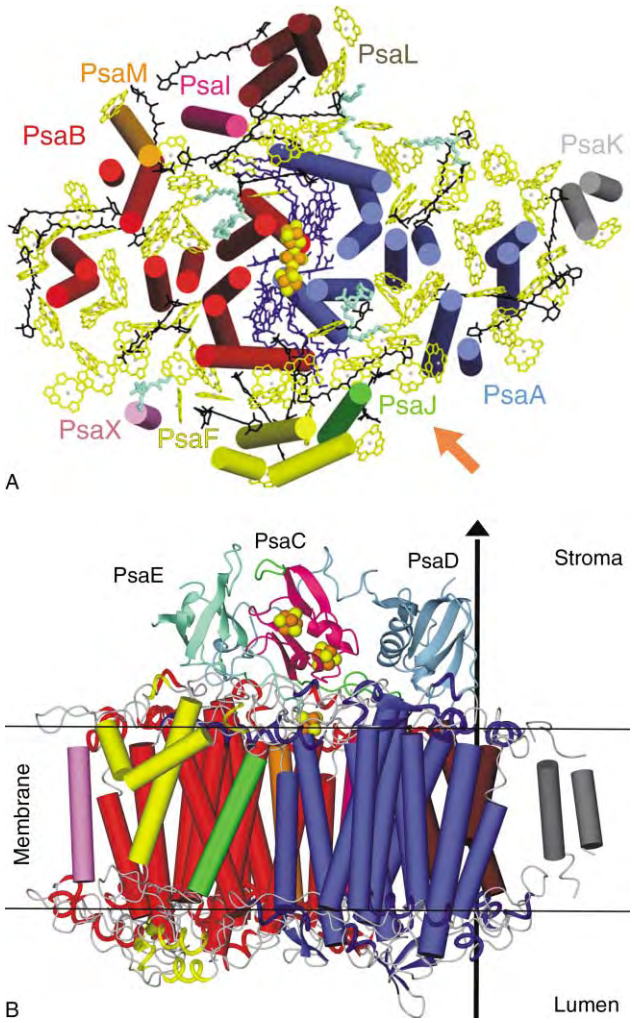

FIGURE 2 Arrangement of protein subunits and cofactors in one monomeric unit of PS I (A) view from the stromal side onto the membrane plane. The three stromal subunits have been omitted for clarity. Color coding of the membrane intrinsic subunits is as shown in Figure 1: PsaA, blue; PsaB, red; PsaF, yellow; PsaI, dark pink; PsaJ, green, PsaK, gray; PsaL, brown; PsaM, orange, and PsaX, light pink. Transmembrane α-helices of the membrane intrinsic subunits are represented as colored cylinders, the loops as well as the three stromal subunits PsaC, PsaD, and PsaE are omitted for clarity. (B) Side view of the monomer of the PS I complex. The view is parallel to the membrane plane. The orange arrow in (A) indicates the view direction in (B). All cofactors have been omitted except the three FeS clusters. For an explanation of the colors see legend to Figure 1. The three stromal subunits PsaE (light green), PsaC (violet), and PsaD (light blue) are located on top of the transmembrane α-helices.

called CP43′. The interaction with the IsiA ring may be performed by PsaF, PsaJ, PsaK, and PsaX.

Plant PS I is very homologous to its cyanobacterial sister, however the external antenna systems are quite different in plants and cyanobacteria. Plants do not have phycobillisomes, instead, the membrane intrinsic antenna proteins LHCI (light harvesting complex I) and LHCII (light harvesting complex II) can be connected to the monomeric core of PS I.

In addition, the plant system does not contain PsaM and PsaX but instead contains at least four additional proteins not found in cyanobacteria: PsaG, PsaH, PsaN, and PsaO. There is not any detailed structural information available on the plant PS I, but biochemical studies have shown that PsaH and PsaO may be located close to PsaL, and may interact with the LHC II complex, whereas the interaction with the LHC I complex is mediated by PsaF, PsaJ, and PsaK. PsaF is also involved in the docking of plastocyanine in plants by its lumenal N-terminal extension.

Both in plants and cyanobacteria, three extrinsic subunits, which do not contain any transmembrane helices, are located at the stromal site of the PS I complex. These three subunits (PsaC, PsaD, and PsaE) form a "stromal hump" that extends the membrane by 35Å and provides the docking site for the soluble electron carriers ferredoxin and flavodoxin. The central subunit PsaC thereby carries the terminal electron acceptors, the two [4Fe–4S] clusters named FA and FB.

The Electron Transport Chain

The electron transport chain is the heart of PS I. Figure 3 shows the structural organization of the cofactors of the electron transport chain. The organic cofactors of the electron transfer chain are arranged in two branches. They are named the A- and B-branches, because most – but not all – cofactors of the A-branch and B-branch are coordinated by PsaA and PsaB, respectively.

The pair of chlorophylls assigned to P700 is located close to the lumenal surface of PS I. It consists of two chemically different chlorophyll molecules. The chlorophyll on the B-branch is the common chlorophyll *a* molecule, chemically identical to all of the other 95 chlorophylls in PS I, whereas the chlorophyll at the A-branch is chlorophyll *a*′, the epimer at the C13 position of the chlorine ring system. The protein environment further enhances the asymmetry of the two chlorophylls: three hydrogen bonds are formed between the protein and the P700-chlorophyll *a*′ at the A-branch, whereas the P700 chlorophyll at the B-branch does not form any hydrogen bonds to the protein environment. The asymmetry could lead to significant differences in the redox potential of both chlorophylls, which may explain why more than 85% of the unpaired electron of $P700^+$ is located, on the B-branch chlorophyll. A possible function of the asymmetry may be a gating of electrons along the two branches but to date this suggestion has not been proven experimentally. From P700 the electron is transferred via one of the chlorophylls from the second pair chlorophylls, "A", to the first stable electron acceptor "A0," which may be located on one of the chlorophylls located in the middle of the membrane.

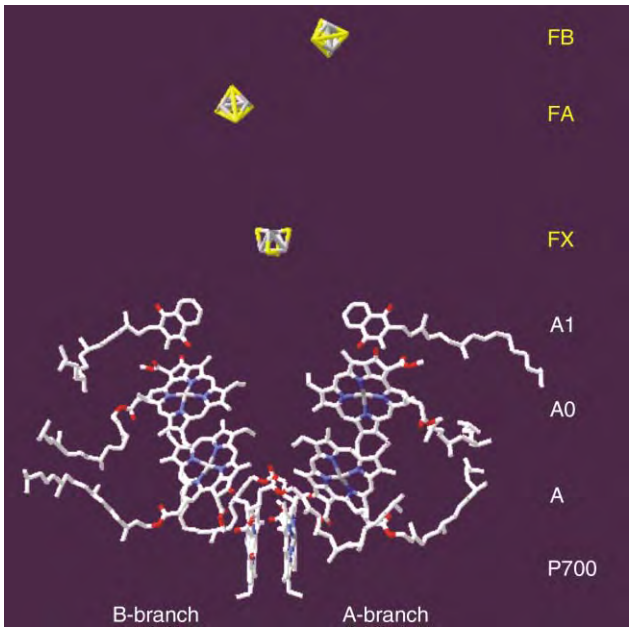

FIGURE 3 The electron transfer system of PS I. The view is parallel to the membrane plane. The organic cofactors of the electron transfer chain are arranged in two branches. The left branch is called the B-branch, whereas the right branch is the A-branch. The three [4Fe–4S] clusters FX, FA, and FB are located at the stromal side of the membrane (on top of the figure). At right margin the names of the cofactors are given as derived from spectroscopic investigations.

These first steps of electron transport occur in less than 3 ps (3/1000 000 000 parts of a second) so that the second pair of chlorophylls has not been detected by spectroscopy so far. The coordination of the chlorophylls of "A" and "A0" is very remarkable, because none of them is coordinated by histidine, the favorite side chain for providing the fifth ligand to the Mg^{2+} in a chlorophyll molecule. Instead, both chlorophylls of "A" are coordinated by a water molecule, which forms the second H-bond to two asparagine side chains of the opposite branch. That means that the first electron acceptor at the A-branch is coordinated by PsaB and *vice versa*. The coordination of the two chlorophylls of "A0" is even more remarkable. The sulfur atom of methionine in both cases provides the fifth ligand of the Mg^{2+}. This is very unusual, because there should be only a very weak interaction between sulfur as a weak acid and Mg^{2+} as a strong base. In can be suggested that the weak interaction hinders a strong base (like water) from entering the site, thereby leading to a chlorophyll which may behave as if it lacks a fifth ligand. There is not an example of a sulphur–Mg^{2+} ligandation in the whole realm of inorganic or organic chemistry. It may be responsible for the extreme negative redox potential of A0 of -1000 mV. The unusual ligandation is absolutely essential for the electron transport, because replacement of the Methionine by histidine, which provides a strong ligand to the chlorophyll, blocks electron transport at the level of A0. In the next step of the electron transfer chain; the electron is further transferred from A0 to one of the phylloquinones, which represent the electron acceptor "A1". The two phylloquinones, which may represent A1, are located at the stromal side of the membrane. The binding pockets are identical on both sites but differ significantly from all other quinone-binding pockets found in proteins so far. Both quinones are π-stacked with a tryptophane residue and both show asymmetric hydrogen bonding: only one of the two oxygen atoms forms an H-bond to an NH backbone group, whereas the other oxygen atom is not hydrogen bonded at all. This could lead to a protein-induced asymmetry in the distribution of the unpaired electron in the radical state $A1^{-\cdot}$, formed when one of the phylloquinones gets reduced. This may answer the question of why A1 has the most negative redox potential (-770 mV) of all quinones found in nature. The electron proceeds from A1 to the FeS cluster FX. This is the rate-limiting step of the electron transfer in PS I. Still, a lively scientific discussion is going on regarding the question of whether one or both branches are active.

There is now experimental evidence that this step can proceed on both branches, but with different rates. In the green algae *Chlamydomonas reinhardtii*, the electron transfer is about a factor of 50 slower on the A- than on the B-branch. This could be the result of a higher activation energy barrier on the A- compared to the B-branch. This finding raises the question of the reason for this difference. There is not a significant difference concerning the protein environment in both branches, but there are two lipid molecules located close to the pathway from A1 to FX that could be responsible for the asymmetry. A negatively charged phospholipid is located on the slower A-branch and the electron has to be transferred against this negative charge, whereas on the faster B-branch a neutral galactolipid has replaced the phospholipid. This is the most reasonable explanation for the higher activation energy barrier.

The Antenna System

The antenna system of PS I consists of 90 chlorophyll *a* molecules and 22 carotenes. The arrangement of the pigments is shown in Figure 4. The function of the antenna chlorophylls (shown in green) is to capture light and transfer the excitation energy to the center of the complex, where the electron transfer chain is located (pigments of the electron transfer chain are shown in blue). The efficiency of the energy transfer is very high. After excitation of any of the antenna chlorophylls the chance that the energy is successfully transferred to P700

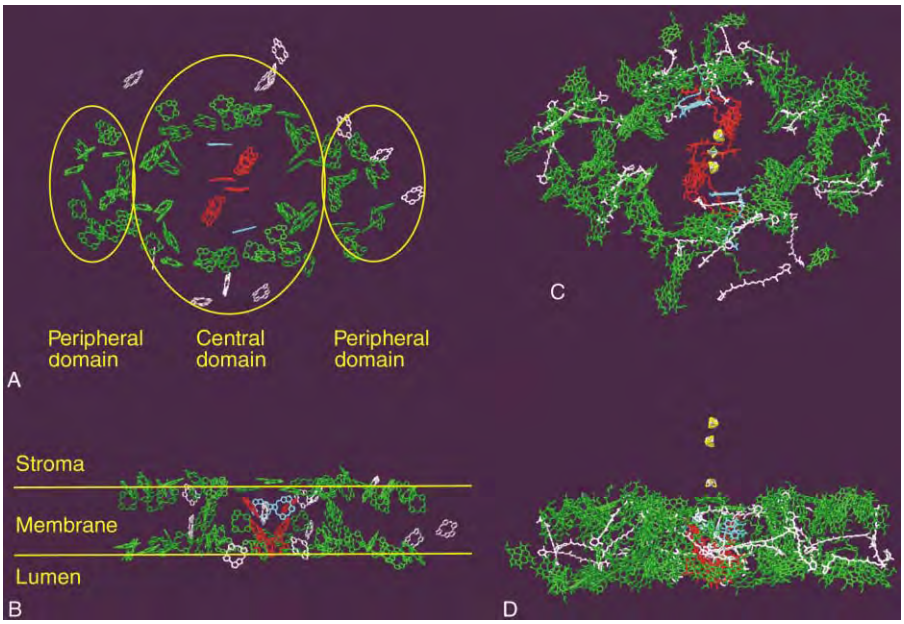

FIGURE 4 The antenna system of PS I (A) Organization of the chlorophylls. The view is from the stromal side onto the membrane plane. For clarity only the ring system of the chlorophylls is shown. The antenna chlorophylls that are coordinated by PsaA and PsaB are shown in green, the chlorophylls coordinated by the smaller membrane integral subunits are depicted in gray. The chlorophylls of the electron transport chain are highlighted in red and the two chlorophylls that may link the electron transport chain and the antenna system are depicted in turquoise. (B) Organization of the chlorophylls. Side view of the cofactors of PS I; the view direction is parallel to the membrane plane. The colors depicted are the same as shown in (A). (C) Complete depiction of the cofactors of the antenna system and the electron transfer chain. The view direction is as in (A). All antenna chlorophylls are shown in green, the carotenoids in white, the chlorophylls of the electron transfer chain in red and the FeS clusters in yellow/gray. (D) Complete depiction of the cofactors of the antenna system and the electron transfer chain. The view direction is as in (B) and the colors are identical to (C).

and subsequent charge separation occurs is 99.98% at room temperature.

The arrangement of the antenna system in PS I is unique. Instead of forming a symmetric ring surrounding the reaction center core, as it is in the light harvesting systems of purple bacteria, the chlorophylls form a clustered network. Each of the chlorophylls have several neighbors at a distance of less than 15Å, so energy can be efficiently transferred in multiple pathways to the center of the complex. The system can be, to some extent, compared to the nerve-network system in the brain where multiple connections are responsible for the high efficiency of information transfer. The antenna system in PS I is highly optimized for efficiency and robustness. The side view along the membrane plane shows that it can be divided into a central domain, which surrounds the electron transfer chain, and two peripheral domains, flanking the core on both sides. In the peripheral domains, the antenna chlorophylls are arranged in two layers, one close to the stromal surface of the membrane and the other close to the lumenal surface of the membrane. When a peripheral antenna chlorophyll is excited the energy will be first transferred from this "two-dimensional" layer to the central domain. In the central domain, chlorophylls are distributed over the full depths of the membrane, i.e., the excitation energy can be exchanged between the two layers. From the chlorophylls of the central domain the excitation energy is then transferred to the electron transfer chain. There are two chlorophylls that seem to structurally link the antenna system to the electron transfer chain (yellow in Figure 4), but the question as to whether they play a crucial role in energy transfer is still not solved.

The carotenoids fulfill three functions in PS I. They play a structural role, function as additional antenna pigments and prevent the system from damage by over-excitation caused by excess light (photoinhibition). The latter function is very critical for the whole system. Chlorophylls are in principle dangerous and reactive molecules. Over-excitation can lead to the formation of chlorophyll triplets (Chl^3), which can react with oxygen to form the highly toxic singlet oxygen, a very dangerous cell poison. Multiple interactions can be observed between the carotenoids and the chlorophylls of the antenna system. The carotenoids are distributed over the whole antenna system and prevent photo damage by the quenching of chlorophyll triplet states. The energy from the triplet chlorophylls is transferred to

the carotenoids that form the carotenoids' triplet state Car^3. The energy of the Car^3 is too low to react with O_2, this results in the carotenoids returning to the ground state by the dissipation of the energy just as heat, thereby preventing photodamage. The system works very efficiently, even under high-light conditions, as the Chl^3 triplet state cannot be detected in the intact PS I.

See Also the Following Articles

Chlorophylls and Carotenoids • Chloroplasts • Cytochrome *c* • Ferredoxin • Green Bacteria: Secondary Electron Donors (Cytochromes) • Photosynthesis • Photosystem I: F_X, F_A, and F_B Iron-Sulfur Clusters • Purple Bacteria: Electron Acceptors and Donors • Purple Bacteria: Photosynthetic Reaction Centers • The Cytochrome b_6f Complex

Glossary

chloroplast Organelle of the plant cell, where photosynthesis takes place.

electron donor/acceptor Molecules that donate or accept electrons in a redox reaction.

electron transfer chain Sequential arrangement of pigments within the PS I, which transports the electron across the membrane.

excitation energy transfer Transfer of the energy absorbed by the antenna pigments to the site of charge separation.

photosystem I and II Large membrane protein complexes that perform the first reaction of energy conversion, the light-induced charge separation.

thylakoid Membrane system, located inside the chloroplasts. The site where the proteins of the electron transfer chain are located and the primary processes of photosynthesis take place.

Further Reading

Bibby, T. S., Nield, J., and Barber, J. (2001). Iron deficiency induces the formation of an antenna ring around trimeric photosystem I in cyanobacteria. *Nature* **412**, 743–745.

Boekema, E. J., Hifney, A., Yakushevska, A. E., Piotrowski, M., Keegstra, W., Berry, S., Michel, K. P., Pistorius, E. K., and Kruip, J. (2001). A giant chlorophyll-protein complex induced by iron deficiency in cyanobacteria. *Nature* **412**, 745–748.

Brettel, K., and Leibl, W. (2001). Electron transfer in photosystem I. *Biochim. Biophys. Acta* **1507**, 100–114.

Fromme, P., Jordan, P., and Krauss, N. (2001). Structure of photosystem I. *Biochim. Biophys. Acta* **1507**, 5–31.

Gobets, B., and van Grondelle, R. (2001). Energy transfer and trapping in photosystem I. *Biochim. Biophys. Acta* **1507**, 80–99.

Jordan, P., Fromme, P., Witt, H. T., Klukas, O., Saenger, W., and Krauß, N. (2001). Three-dimensional structure of cyanobacterial photosystem I at 2.5Å resolution. *Nature* **411**, 909–917.

Scheller, H. V., Jensen, P. E., Haldrup, A., Lunde, C., and Knoetzel, J. (2001). Role of subunits in eukaryotic photosystem I. *Biochim. Biophys. Acta* **1507**, 41–60.

Biography

Petra Fromme is a Professor in the Department of Chemistry and Biochemistry at Arizona State University. Her principal research interest is in the broad field of the structure and function of membrane proteins, with a special focus on the proteins involved in the primary steps of photosynthesis. Her group and co-workers have determined the structures of both PS I and PS II. She holds a Ph.D. in chemistry from the Technical University Berlin and has authored several reviews and book chapters on the structure and function of PS I and PS II. She has received several awards, including the Hill Award from the Photosynthetic Society, the Lemberg Fellowship of the Australian National Academy of Science, and the Biology 2001 award of the Academy of Science of Goettingen. She is a fellow of the Biophysical Society and the Gesellschaft fuer Biologische Chemie.

Photosystem I: F_X, F_A, and F_B Iron–Sulfur Clusters

Mikhail L. Antonkine
Max-Planck Institut für Bioanorganische Chemie, Mülheim, Germany

John H. Golbeck
Pennsylvania State University, University Park, Pennsylvania, USA

Photosystem I is a membrane-bound pigment–protein complex found in photosynthetic organisms that converts the energy of light into chemical bond energy. It is classified as a type I reaction center because it uses iron–sulfur clusters as the terminal electron acceptors. Two variants of low-potential iron–sulfur clusters are employed in photosystem I. The membrane-spanning subunits PsaA and PsaB provide the binding site for F_X, which is a rare instance of an interpolypeptide [4Fe–4S] cluster ligated between the protein heterodimer. The stromal subunit PsaC provides the binding sites for F_A and F_B, which are [4Fe–4S] clusters located on a tightly bound, bacterial ferredoxin-like protein. F_X, F_A, and F_B serve as electron wires to vector the electron from the initial site of charge separation located deep in the membrane to soluble ferredoxin located on the stromal surface of the membrane. They provide good examples of how the physical and biochemical properties of iron–sulfur clusters can be adjusted to suit a specific function in electron transfer.

Photosynthesis

Photosynthesis is the process by which solar energy is converted into chemical bond energy by living organisms. This process can be conveniently divided into two parts, the light reactions and the dark reactions. The light reactions employ four major membrane-bound multisubunit complexes in the energy-conversion process: photosystem I, photosystem II, the cytochrome b_6f- Reiske iron–sulfur complex, and ATP synthase. NADPH is produced directly as a result of photosystem I, and molecular oxygen is produced directly as a result of photosystem II. A proton gradient is generated, in part, by the cytochrome b_6f- Reiske iron–sulfur complex and utilized by ATP synthase for the generation of ATP. During the dark reactions, carbon dioxide is enzymatically converted into carbohydrates at the expense of ATP and NADPH. The chemical bond energy of ATP and NADPH is also used by the organism for cellular processes such as metabolism, growth, and reproduction.

Types of Photosynthetic Reaction Centers

Two types of photosynthetic reaction centers have evolved that are capable of performing light-induced charge separation. Type I reaction centers utilize iron–sulfur clusters as terminal electron acceptors. This type is represented by the green-sulfur bacterial reaction center, the heliobacterial reaction center, and photosystem I in cyanobacteria, algae, and higher plants. Type II reaction centers utilize quinones as terminal electron acceptors. This type is represented by the purple bacterial reaction center, the green nonsulfur bacterial reaction center, and photosystem II in cyanobacteria, algae, and higher plants. Photosystem I is the best studied of the type I reaction centers and is considered the prototype for the entire class.

Photosystem I: The Best-Studied Type I Reaction Center

Photosystem I is a component of the photosynthetic electron transfer chain in all oxygen-evolving organisms. The X-ray crystal structure of cyanobacterial photosystem I has been solved at a resolution of 2.5Å. This large membrane-bound pigment–protein complex exists as a trimer in cyanobacteria; each monomer consists of 12 subunits, labeled PsaA through PsaF, PsaI through PsaM, and PsaX. Among the 127 cofactors are 96 chlorophylls, 2 phylloquinones, and 3 [4Fe–4S] clusters, referred to as F_X, F_A, and F_B. The majority of the electron transfer cofactors are bound to the two large, membrane-embedded subunits PsaA and PsaB. They form the heterodimeric core of photosystem I, and are related by a pseudo-C_2 symmetry axis that also includes the electron transfer cofactors (Figure 1A). The terminal

electron acceptors, iron–sulfur clusters F_A and F_B, are bound to the PsaC subunit on the stromal (cytoplasmic) side of the thylakoid membrane (Figure 1B). Light-induced charge separation occurs between the primary electron donor P700 ($E_m' \sim -1300$ mV), which is a chlorophyll a/a′ heterodimer located on the luminal (inner) side of the membrane, and the primary electron acceptor A_0 ($E_m' \sim -1000$ mV), which is a chlorophyll a monomer. The electron is quickly passed to A_1 ($E_m' \sim -800$ mV), which is a phylloquinone molecule, to F_X ($E_m' = -705$ mV), the interpolypeptide [4Fe–4S] cluster, and finally to F_A ($E_m' = -540$ mV) and F_B ($E_m' = -590$ mV), the [4Fe–4S] clusters bound to PsaC. The soluble protein ferredoxin accepts the electron from F_B on the stromal side of the membrane and interacts with NADP:ferredoxin oxidoreductase to generate NADPH. The initial charge-separated state between $P700^+$ and A_0^- is thus stabilized by the displacement of the electron through a series of acceptors arranged from the lumenal to the stromal side of the thylakoid membrane. The F_X, F_A, and F_B iron–sulfur clusters participate in this process by functioning as a molecular wire. This allows the charge-separated state to be separated in space and lengthened in time, thus permitting a high quantum yield. This strategy represents an excellent example of how Gibbs free energy, in the form of diminishing reductive power of every successive cofactor, is traded to gain time in the form of longer-lived charge-separated states.

Iron–Sulfur Clusters in Biology

Geometry and Oxidation States

Iron–sulfur clusters are one of the most common biological cofactors. They are employed in biological systems in many different roles. For example, iron–sulfur clusters can play a structural role (endonuclease III) as well as a functional role such as in catalysis (aconitase) and in the regulation of gene expression (SoxR). However, by far the most common function is in electron transfer. A few examples include relatively simple proteins such as plant and bacterial ferredoxins, and complex multisubunit proteins such as hydrogenase, complex I, and photosystem I. There are four basic prototypes of iron–sulfur clusters; each differs in the number of iron and sulfur atoms. These differences lead to a widespread variation in geometry, in reduction potential, and ultimately in biological function. (1) In a rubredoxin, a single iron is tetrahedrally coordinated by four cysteine ligands. (2) In a [2Fe–2S] cluster, the iron atoms are bridged by the sulfur atoms in a rhombic structure. Each of the iron atoms is ligated by two cysteines (although in the case of Rieske iron–sulfur proteins, one of the iron atoms is ligated by two histidines) that are positioned in a plane perpendicular to the bridging sulfur atoms. (3) In a [4Fe–4S] cluster, the iron and sulfur atoms alternate in corner positions of a cube (Figure 2). Each of the iron atoms is ligated by a cysteine (in rare instances by water or aspartate); the sulfur atoms form a tetrahedron around the cluster. (4) In a [3Fe–4S] cluster, one of the iron atoms is missing from the corner of the cube; hence, the overall geometry is nearly the same as that of a [4Fe–4S] cluster. Among these prototypes, the [4Fe–4S] clusters are unique because they can potentially exist in three different oxidation states 3+, 2+, and 1+. However, in any given protein, only one of the two different oxidation–reduction pairs is found: 3+/2+ or 2+/1+; the choice is determined by the surrounding protein matrix. In high potential iron–sulfur proteins (HiPIP), the 3+/2+ pair is used, and in low-potential iron–sulfur proteins, the 2+/1+ pair is used. Thus, the protein plays a crucial role in determining the oxidation–reduction pair employed by the cofactor, thereby determining the approximate range of its midpoint potential. The midpoint potential of a [4Fe–4S] cluster is further modulated by coulombic interaction with the protein, polarizability of the protein, and accessibility to solvent; these factors specify the biological function of the [4Fe–4S] cluster. In photosystem I, low-potential [4Fe–4S] clusters are found. In the reduced (+1) state there exist three Fe^{2+} ions and one Fe^{3+} ion, however, due to valence delocalization, only two pairs of iron atoms are observed. One is an equal-valence pair in which both iron atoms exist in a 2+ oxidation state, and the other is mixed-valance pair in which both iron atoms exist in a 2.5+ oxidation state. The position of both pairs, with respect to protein ligands, can change at room temperature, i.e., any iron atom can assume the 2+ or 2.5+ oxidation state at any time, and as a result, the mixed- and equal-valence pairs migrate around the cube. Since in proteins the [4Fe–4S] clusters are slightly distorted due to the interactions with a nonhomogeneous matrix, preferential positions for both pairs exist. The positions can be determined by studying temperature dependence of the NMR chemical shift of the αH and βCH_2 protons of the cysteines ligands of the [4Fe–4S] cluster in a biologically relevant temperature range. In the reduced (+1) state, low-potential [4Fe–4S] clusters are paramagnetic, i.e., the cluster as a whole has an unpaired electron. This property allows detection by electron paramagnetic resonance (EPR) spectroscopy, which is sensitive only to paramagnetic species. Thus, EPR spectroscopy focuses on the properties of the cofactor and not on the properties of the surrounding protein matrix, which is diamagnetic. However, the EPR spectrum is sensitive to changes in the environment of the cofactor caused by changes in surrounding protein. A combination of these properties makes EPR an indispensable tool in the investigation of protein

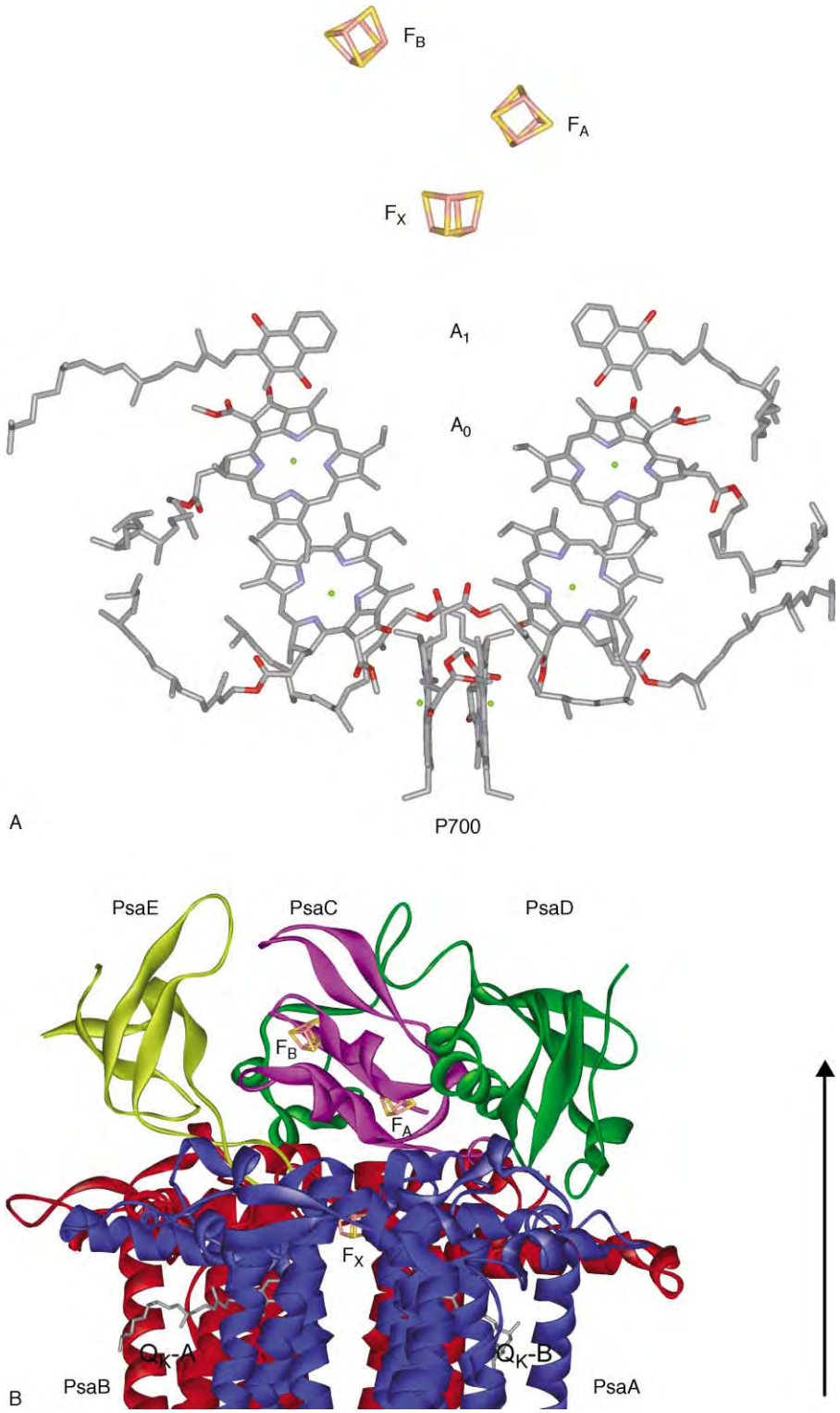

FIGURE 1 The X-ray structure of photosystem I at 2.5Å resolution (PDB entry 1JB0). Detail of the structural model of the photosystem I monomer. View parallel to the membrane plane. (A) Photosystem I cofactors involved in electron transfer. All cofactors are shown as "stick" models; the positions of the carbon, nitrogen, and oxygen atoms are indicated by light gray, blue, and red colors respectively. The positions of Mg^{2+} ions are indicted by green spheres. The [4Fe–4S] clusters F_X, F_A, and F_B are shown as cubes in which the yellow corners indicate the positions of sulfur atoms and the pink corners the position of iron atoms. Note the C_2-symmetric arrangement of cofactors P700, A_0, A_1, and F_X, all of which are bound by two core, membrane-spanning subunits PsaA and PsaB; as well as the symmetry-breaking arrangement of cofactors F_A and F_B, bound by stromal subunit PsaC. (B) The complete backbones of the stromal subunits PsaC, PsaD, and PsaE proteins, as well as their respective arrangement on the stromal surface of the PsaA/PsaB heterodimer. PsaA is shown in blue, PsaB in red, PsaC in magenta, PsaD in green, PsaE in olive; peripheral proteins are omitted for clarity; [4Fe–4S] iron–sulfur clusters F_X, F_A, and F_B are shown as cubes, in which the yellow corners indicate positions of

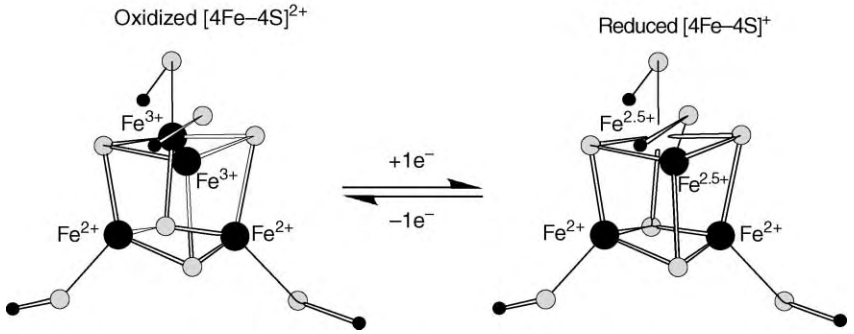

FIGURE 2 The structure of a [4Fe–4S] cluster. The presence of equal valence (Fe^{2+}) and mixed valence ($Fe^{2.5+}$) iron pairs in the reduced state is shown. The iron and sulfide atoms of the [4Fe–4S] clusters as well as sulfur and Cβ atoms of the cysteines ligating the [4Fe–4S] cluster are shown with iron atoms as large black spheres, sulfur atoms as light-gray spheres and Cβ as small black spheres. Reprinted from Vassiliev, I. R., Antonkine, M. L., and Golbeck, J. H. (2001). Iron–sulfur clusters in Type I reaction centers. *Biochim. Biophys. Acta* (special issue on Photosystem I), **1507**, 139–160, with permission from Elsevier.

cofactors in general, and iron–sulfur clusters in particular. This technique is especially advantageous for studying of cofactors in large protein complexes, in which it is difficult to apply other techniques due to the presence of interfering chromophores or to the size of the biomolecule.

Self-Assembly in Solution

Iron–sulfur clusters self-assemble in aqueous solutions under anaerobic (oxygen-free) conditions in presence of iron and sulfide ions along with a thiol-containing reductant. If an apoprotein with an iron–sulfur cluster-binding site is added to the solution, the clusters self-insert into the site via a thiol exchange mechanism. In the living cell the assembly of iron–sulfur clusters is tightly regulated and is performed by a set of special enzymes that act sequentially. However, iron–sulfur proteins with *in vitro* or *in vivo* inserted clusters have identical spectroscopic and biochemical properties. Thus, *in vitro* insertion of clusters is a useful preparative tool for investigation of iron–sulfur proteins.

The F_X, F_A, and F_B Clusters of Photosystem I

F_X, the Interpolypeptide [4Fe–4S] Cluster Bound by PsaA and PsaB

F_X in the interpolypeptide iron–sulfur cluster bound between the PsaA and PsaB subunits (Figure 1). EXAFS and Mössbauer spectroscopic studies unambiguously identified F_X as a [4Fe–4S] cluster. The midpoint potential of F_X was measured directly and was found to be -705 mV, making it one of the most reducing [4Fe–4S] clusters known in biology. The binding site of F_X was identified from amino acid sequences of the PsaA and PsaB polypeptides that comprise the membrane-bound core of photosystem I. The site consists of two identical amino acids sequences, FPCDGPGRGGTC, located in loops connecting helices *j* and *k* on PsaA and *j*′ and *k*′ on PsaB. Each of these sequences provides two conserved cysteine ligands to the cluster; thus, F_X represents a highly unusual instance of a [4Fe–4S] cluster bound between a protein heterodimer. The high-resolution crystal structure of cyanobacterial photosystem I shows that charged amino acids within the conserved F_X-binding sequences on PsaA and PsaB provide a set of ionic contacts for the binding of PsaC. The F_X-binding sequences on both PsaA and PsaB are parts of large, extramembrane loops that have a completely symmetric three-dimensional structure. In addition to providing ligands for F_X they serve several additional functions such as forming the ionic contacts with PsaC and shielding the F_X cluster from molecular oxygen. F_X is additionally shielded by α-helices that comprise the core of the PsaA/PsaB heterodimer. The iron protein of nitrogenase (e.g., protein data bank (PDB) entry 1CP2) and 2-hydroxyglutaryl-CoA dehydratase component A (PDB entry 1HUX) are the only other proteins that have both an interpolypeptide [4Fe–4S] cluster and a solved three-dimensional

sulfur atoms and light-brown corners the position of iron atoms; quinones Q_K-A and Q_K-B are shown as "stick" models, both represent the acceptor A_1 bound to PsaA and PsaB respectively. The position of the trimer C_3-symmetry axis is indicated by an arrow. Reprinted from Antonkine, M. L., Jordan, P., Fromme, P., Krauβ, N., Golbeck, J. H., and Stehlik, D. (2003). Assembly of protein subunits within the stromal ridge of Photosystem I. Structural changes between unbound and sequentially PS I-bound polypeptides and correlated changes of the magnetic properties of the terminal iron–sulfur clusters. *J. Mol. Biol.*, **327**, 671–697, with permission from Elsevier.

structure. However, the environments of these [4Fe–4S] clusters are significantly different in that each subunit of these homodimeric proteins has two fully conserved cysteines that are located far apart from each other in the amino acid sequence. Hence, in these proteins, there is no short consensus binding sequence for the [4Fe–4S] cluster as exists for F_X. It follows that properties of these interpolypeptide [4Fe–4S] clusters are also very different from F_X. They have midpoint potentials of -420 to -430 mV (i.e., 250–300 mV more oxidizing than F_X), which is more typical for low-potential [4Fe–4S] clusters in monocluster and dicluster bacterial ferredoxins. Moreover, the [4Fe–4S] clusters in nitrogenase and 2-hydroxyglutaryl-CoA dehydratase component A are highly oxygen sensitive, probably because the binding site of the interpolypeptide cluster is open and accessible. In contrast, F_X needs to be oxygen insensitive because it is probably assembled as an intermediate in the biogenesis of the photosystem I reaction center.

F_A AND F_B, THE [4Fe–4S] CLUSTERS BOUND BY PSAC

The Amino Acid Sequence of PsaC

F_A and F_B are iron–sulfur clusters bound to the PsaC subunit. A 9 kDa iron–sulfur protein, with an unusual EPR spectrum, was originally isolated by methanol/acetone extraction of spinach chloroplast membranes. Although at the time no function could be assigned, it was later shown to be identical to PsaC. When this protein was rebound to photosystem I cores, the characteristic EPR signals of F_A and F_B could be restored to that found in the wild type. The amino acid sequence of PsaC in a variety of organisms was deduced by direct amino acid sequencing of the protein and from the sequences of the *psaC* genes. The 80 amino acids are extremely well conserved both in cyanobacteria and in higher plants. PsaC has sequence similarity to bacterial ferredoxins, from which it is presumed to have evolved, in the regions surrounding the two [4Fe–4S] clusters (Figure 3). Similar to bacterial ferredoxins, PsaC contains two consensus [4Fe–4S] cluster-binding sites consisting of C(I)xxC(II)xxC(III)xxxC(IV)P, where C is cysteine, P is proline, and x is any other amino acid. Cysteines I, II, and III of the first binding site ligate the first [4Fe–4S] cluster, while cysteine IV ligates the second [4Fe–4S] cluster; cysteines I′, II′, and III′ of the second binding site ligate the second [4Fe–4S] cluster, while cysteine IV′ ligates the first [4Fe–4S] cluster. The distance between the two [4Fe–4S] clusters in the protein is predetermined by the distance between Cys(III) and Cys(IV) in the binding site because they always ligate different clusters. Through site-directed mutagenesis studies, it was shown that in PsaC cysteines 10, 13, 16, and 57 ligate F_B and cysteines 47, 50, 53, and 20 ligate F_A. F_B and F_A in PsaC are equivalent to cluster I and cluster II in bacterial ferredoxins, respectively. The similarity of PsaC to bacterial ferredoxins fostered the use of the three-dimensional structures of these proteins as models for PsaC. This is a valid approach, particularly if one is interested in the structure of the iron–sulfur core of the protein. However, there are several significant regions where their amino acid sequences differ. PsaC has a sequence insertion between the two consensus iron–sulfur binding sites and a sequence extension at the C-terminal end of the protein. Not surprisingly both of these sequences are involved in photosystem I-specific functions of PsaC. The sequence insertion, known as the Z-loop, participates in ferredoxin/flavodoxin binding and the C-terminal

```
                        10  13 16  20                          47 50 53  57
C. acidi urici  --AYVINEACISCGACEPECPVNAIS--------SGDDRYVIDADTCIDCGACAGVCPVD
C. pasteurianum --AYKIADSCVSCGACASECPVNAIS--------QGDSIFVIDADTCIDCGNCANVCPVG
P. aerogenes    --AYVINDSCIACGACKPECPVNIQ---------QG-SIYAIDADSCIDCGSCASVCPVG
Synechococcus   SHSVKIYDTCIGCTQCVRACPLDVLEMVPWDGCKAGQIASSPRTEDCVGCKRCETACPTD
                  .  * ..*. *  *   **.             *       .. *. *  *   **

C. acidi urici  APVQA---------------
C. pasteurianum APVQE---------------
P. aerogenes    APNPED-------------
Synechococcus   FLSIRVYLGAETTRSMGLAY
```

FIGURE 3 Sequence alignment of PsaC from *Synechococcus* sp. PCC 7002 and dicluster bacterial ferredoxins from *Clostridium pasteurianum*, *Clostridium acidi urici*, and *Peptococcus aerogenes*. The cysteines that coordinate the [4Fe–4S] clusters are indicated by bold underlined letters and their number in *Synechococcus* sp. PCC 7002 PsaC sequence is shown at the top. The sequences were aligned with CLUSTALW (1.60). Conserved amino acids are indicated by an asterisk, conservative substitutions by a dot. Reprinted from Antonkine, M.L., Bentrop, D., Bertini, I., Luchinat, C., Shen, G., Bryant, D. A., Stehlik, D., and Golbeck, J. H. (2000). Paramagnetic ^{1}H NMR spectroscopy of the reduced, unbound Photosystem I subunit PsaC: sequence-specific assignment of contact-shifted resonances and identification of mixed- and equal-valence Fe–Fe pairs in the [4Fe–4S] centers $F'_A$and F'_B. Reprinted from (2000). *J. Biol. Inorg. Chem.*, **5**, 381–392, with permission from Springer.

sequence extension is one of the key elements involved in binding to the photosystem I core. One of the interesting features of the amino acid sequence of PsaC that was not recognized immediately is the increased number of charged amino acids in the vicinity of the binding site of the F_A cluster, as compared both to the binding site of F_B and to the binding sites of clusters I and II in bacterial ferredoxins. The basic amino acids of the F_A site are now known to be responsible for binding PsaC; they form the majority of the contacts that anchor PsaC to the PsaA/PsaB heterodimer. This is achieved by formation of ionic bonds with acidic amino acids in the [4Fe–4S] cluster F_X-binding site.

The Three-Dimensional Structure PsaC

PsaC is tightly bound to the PsaA/PsaB stromal surface and is packed between the PsaD and PsaE subunits (Figure 1B). However, PsaC is also a highly soluble protein, a property that has allowed study of its structure in the unbound state. The biochemical and magnetic properties of the F_A and F_B iron–sulfur clusters are similar in unbound PsaC, while they are distinctly different in photosystem I-bound PsaC. Rebinding studies of PsaC, PsaD, and PsaE to the PsaA/PsaB core proteins have been aided by the availability of large amounts of recombinant PsaC, PsaD, and PsaE proteins from overexpression systems in *Escherichia coli*. The EPR properties of F_A and F_B change in three distinct steps during the assembly of photosystem I. The first is unbound PsaC in solution; the second is PsaC bound to photosystem I in the absence of PsaD; and the third is PsaC bound to photosystem I in the presence of PsaD. The presence or absence of PsaE has no effect on the EPR properties of F_A and F_B. Since EPR is highly sensitive to changing environment of the [4Fe–4S] clusters, these results were interpreted as a change in the conformation of PsaC in three distinct steps. PsaD does not bind any cofactors; rather, the binding of PsaD induces conformational changes in PsaC and locks it into its final state. The solution structure for unbound PsaC (PDB entry 1K0T) was solved by NMR. In the iron–sulfur core of PsaC, the [4Fe–4S] clusters F_A and F_B are connected by two short α-helices and assume a very similar geometry in both unbound and bound PsaC (Figure 4). As predicted from the amino acid sequence, this region shows structural features similar to those of bacterial ferredoxins. In particular, the position, distance and relative orientation of the two [4Fe–4S] clusters as well as the conformation of two-cluster consensus binding sites are similar in PsaC and bacterial ferredoxins. A comparison of the unbound PsaC structure with that in the X-ray structure of bound PsaC reveals significant differences that mainly concern the structure of the N, pre-C, and C termini. In unbound PsaC the C terminus assumes a disordered helical conformation, and is clearly different from the extended coil conformation in bound PsaC. Indeed, this is one of the structural elements required to anchor PsaC to the photosystem I core heterodimer. In solution, the N terminus of PsaC is in contact with the pre-C-terminal region (equivalent to the C terminus in bacterial ferredoxins). As compared to bound PsaC, the N terminus in unbound PsaC is bent and is located in between the pre-C-terminal region and the iron–sulfur core region of the protein. The same N- and pre-C-terminal regions are arranged as an antiparallel β-sheet and are much closer to F_A-binding site in bound PsaC. The antiparallel β-sheet arrangement of the N terminus and C terminus (equivalent to the pre-C terminus in PsaC) is typical for bacterial ferredoxins. Thus, PsaC assumes a ferredoxin-like conformation only in the photosystem I-bound form.

Assembly of the Stromal Subunits of Photosystem I

The changes in the structure of PsaC are caused by the sequential formation of multiple networks of ionic and hydrogen bond contacts with the PsaA/PsaB core proteins and with the other two proteins of the stromal side, PsaD, and PsaE. A comparison of the structure of unbound and bound PsaC, PsaD, and PsaE suggests a probable assembly scenario for the sequential binding of the stromal proteins. The assembly of F_X and the proper folding of the large loops that provide a binding site for F_X are preconditions for the binding of the stromal proteins. PsaC has a defined three-dimensional structure only after insertion of both [4Fe–4S] clusters. Therefore, the presence of the iron–sulfur clusters F_A and F_B is precondition for binding of the PsaC and the other stromal proteins. PsaC binds first. Its conformation changes after it binds to photosystem I; the binding of PsaD causes further conformational changes in PsaC, whereupon both assume their final structures. The biochemical and magnetic properties of [4Fe–4S] clusters F_A and F_B, typical for the photosystem I bound state of PsaC, are now established. PsaE probably binds last of the three stromal proteins, thereby completing the assembly process.

Resolution of the Sequence of Electron Transfer: $F_X > F_A > F_B$

Since the reduction potential of F_A (E_m' −540 mV) is higher than F_B (E_m' −590 mV), it was long assumed that F_A was the terminal electron acceptor in photosystem I. In this view, electron transfer in photosystem I is always thermodynamically favorable from $P700^*$ ($E_m' = -1300$ mV) to soluble ferredoxin ($E_m' = -420$ mV). However, EPR studies of PsaC

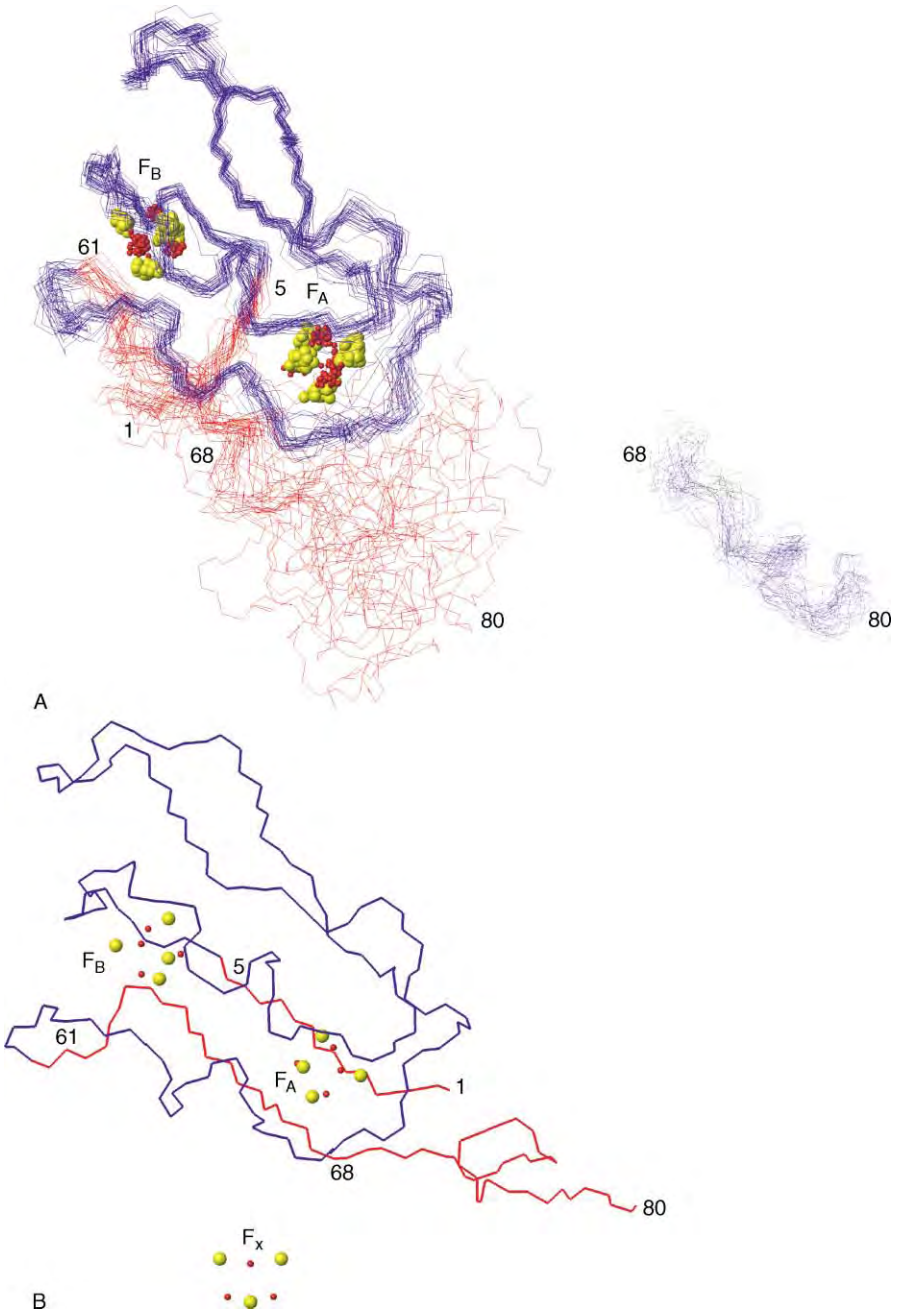

FIGURE 4 Comparison of the NMR solution structure of unbound PsaC (PDB entry 1K0T) with bound PsaC as part of the 2.5Å X-ray structure of Photosystem I (PDB entry 1JB0). The regions where the two structures show significant differences are identified by the red color. Iron atoms are represented by red circles, and sulfur atoms are represented by yellow circles. (A) Backbone drawing of the final family of 30 superimposed structures of unbound, oxidized PsaC from *Synechococcus* sp. PCC 7002 determined by solution NMR. Backbone of the family of 30 structures is shown in a superposition of residues 5–67. The iron and sulfur atoms of the [4Fe–4S] clusters of each of the 30 structures are shown. The view direction is equivalent to the membrane plane of the assembled photosystem I complex (see Figure 1). The inset shows the backbone of residues 68–80 in the same family of 30 PsaC structures. Superposition of solely the residues 68–80 reveals the helical secondary structure of the C-terminus. (B) Structure of photosystem I-bound PsaC taken from the PS I X-ray structure at 2.5Å X-ray resolution (PDB entry 1JB0). The polypeptide backbone and iron–sulfur clusters F_A and F_B are shown. F_X is included to indicate the position and the correct orientation of PsaC on PS I. This figure was prepared using MOLMOL. Reprinted from Antonkine, M. L., Jordan, P., Fromme, P., Krau*β*, N., Golbeck, J. H., and Stehlik, D. (2003). Assembly of protein subunits within the stromal ridge of Photosystem I. Structural changes between unbound and sequentially PS I-bound polypeptides and correlated changes of the magnetic properties of the terminal iron sulfur clusters. *J. Mol. Biol.*, **327**, 671–697, with permission from Elsevier.

mutants, in which cysteine II in the F_A or F_B consensus binding sequence was changed to glycine, alanine, serine, or aspartate, led to the assessment that F_B is the terminal electron acceptor in photosystem I. This was in agreement with EPR relaxation and optical spectroscopy data obtained, around the same time, on photosystem I samples with selectively destroyed F_B. The presence of this small, thermodynamically unfavorable electron transfer step has little consequence because overall, electron transfer remains highly thermodynamically favorable from the excited state of $P700^*$ to ferredoxin. Furthermore, each forward electron transfer step in photosystem I is sufficiently rapid such that charge recombination events are negligible, and this results in the extraordinary quantum yield of ~1.0.

See Also the Following Articles

Chlorophylls and Carotenoids • Ferredoxin • Iron–Sulfur Proteins • Photosynthesis • Photosystem I, Structure and Function • Quinones

Glossary

cofactor Organic or inorganic molecule bound (covalently or through non-covalent interactions) to the protein that is necessary for/or aiding its function. For example, chlorophylls, quinones, and iron–sulfur clusters are cofactors in photosystem I.

F_A A low potential [4Fe–4S] cluster bound by cysteines 20, 47, 50, and 53 of the PsaC subunit of photosystem I; it is equivalent to Cluster II in bacterial ferredoxins that contain two [4Fe–4S] clusters.

F_B A low potential [4Fe–4S] cluster bound by cysteines 10, 13, 16, and 57 of the PsaC subunit of photosystem I; it is equivalent to Cluster I in bacterial ferredoxins that contain two [4Fe–4S] clusters.

F_X A low potential interpolypeptide, [4Fe–4S] cluster bound by two consensus FPCDGPGRGGTC sequences on the PsaA and PsaB subunits of photosystem I.

high-potential iron–sulfur proteins (HiPIP) These contain [4Fe–4S] clusters that shuttle between oxidation states of 3+/2+ .

low-potential iron–sulfur proteins These contain [4Fe–4S] clusters that shuttle between oxidations states of 2+/1+ .

quantum yield The number of electrons transferred per photon absorbed.

type I Photosynthetic reaction centers that use a [4Fe–4S] cluster as the terminal electron acceptor.

type II Photosynthetic reaction centers that use a mobile quinone as the terminal electron acceptor.

Further Reading

Antonkine, M. L., Jordan, P., Fromme, P., Krauß, N., Golbeck, J. H., and Stehlik, D. (2003). Assembly of protein subunits within the stromal ridge of photosystem I. Structural changes between unbound and sequentially PS I-bound polypeptides and correlated changes of the magnetic properties of the terminal iron sulfur clusters. *J. Mol. Biol.* **327**, 671–697.

Antonkine, M. L., Liu, G., Bentrop, D., Bryant, D. A., Bertini, I., Luchinat, C., Golbeck, J. H., and Stehlik, D. (2002). Solution structue of the unbound, oxidized photosystem I subunit PsaC, containing [4Fe-4S] clusters F_A and F_B: a conformational change occurs upon binding to photosystem I. *J. Biol. Inorg. Chem.* **7**, 461–472.

Antonkine, M. L., Bentrop, D., Bertini, I., Luchinat, C., Shen, G., Bryant, D. A., Stehlik, D., and Golbeck, J. H. (2000). Paramagnetic ^{1}H NMR spectroscopy of the reduced, unbound photosystem I subunit PsaC: sequence-specific assignment of contact-shifted resonances and identification of mixed- and equal-valence Fe-Fe pairs in [4Fe-4S] centers F_A and F_B. *J. Biol. Inorg. Chem.* **5**, 381–392.

Bentrop, D., Capozzi, F., and Luchinat, C. (2001). Iron–sulfur proteins. In *Handbook on Metalloproteins* (Bertini, I., Sigel, A., and Sigel, H., Eds.) pp. 357–460, Marcel Dekker, New York.

Chamorovsky, S. K., and Cammack, R. (1982). Direct determination of the midpoint potential of the acceptor X in chloroplast photosystem I by electrochemical reduction and ESR spectroscopy. *Photobiochem. Photobiophys.* 4, 195–200.

Compendium of authors (2001). Type 1 photosynthetic reaction centers (P. Heathcote ed.), *Biochim. Biophys. Acta-Bioenerg.* 1507, 1–310.

Golbeck, J. H., Parrett, K. G., Mehari, T., Jones, K. L., and Brand, J. J. (1988). Isolation of the intact photosystem I reaction center core containing P700 and iron-sulfur center F_X. *FEBS Lett.* **228**, 268–272.

Golbeck, J. H. (1999). A comparative analysis of the spin state distribution of *in vivo* and *in vitro* mutants of PsaC. A biochemical argument for the sequence of electron transfer in Photosystem I as F_X -> F_A -> F_B -> ferredoxin/flavodoxin. *Photosynth. Res.* **61**, 107–149.

Golbeck, J. H. (1994). Photosystem I in cyanobacteria. In *The Molecular Biology of Cyanobacteria* (Bryant, D. A., Ed.) pp. 179–220. Kluwer Academic Publishers, The Netherlands.

Golbeck, J. H. (2003). The binding of cofactors to photosystem I analyzed by spectroscopic and mutagenic methods. *Annu. Rev. Biophys. Biomol. Struct.* **32**, 237–256.

Jordan, P., Fromme, P., Witt, H. T., Klukas, O., Saenger, W., and Krauß N. (2001). Three dimensional structure of cyanobacterial photosystem I at 2.5Å resolution. *Nature* **411**, 909–917.

Li, N., Zhao, J., Warren, P. V., Warden, J. T., Bryant, D. A., and Golbeck, J. H. (1991). PsaD is required for the stable binding of PsaC to the photosystem I core protein of *Synechococcus* sp. PCC 6301. *Biochemistry* **30**, 7863–7872.

Lippard, S. J., and Berg, J. M. (1994). *Principles of Bioinorganic Chemistry.* University Science Books, Mill Valley, California, USA.

Malkin, R., Aparicio, P. J., and Arnon, D. I. (1974). The isolation and characterization of new iron-sulfur protein from photosynthetic membranes. *Proc. Natl Acad. Sci. USA* **71**, 2362–2366.

Zhao, J., Li, N., Warren, P. V., Golbeck, J. H., Bryant, D. A. (1991). Site-directed conversion of a cysteine to aspartate leads to the assembly of a [3Fe-4S] cluster in PsaC of photosystem I – The photoreduction of F_A is independent of F_B. *Biochemistry* **31**, 5093–5099.

Biography

Mikhail L. Antonkine is Postdoctoral Fellow at Max-Planck Institut for Bioinoganic Chemistry. His principal research interests are the structure and function of iron–sulfur proteins including photosystem I. He holds a Ph.D. from the Pennsylvania State University and received postdoctoral training at The Free University of Berlin. He participated in determination of the solution structure of PsaC and in the

development of an assembly scenario for the stromal proteins of photosystem I.

John H. Golbeck is a Professor of Biochemistry and Biophysics at the Pennsylvania State University. His research interests are the structure, function, and organization of photosystem I and the biogenesis of iron–sulfur clusters. He holds a Ph.D. from Indiana University and received his postdoctoral training at Martin Marietta Laboratories. He developed methods to remove and reconstitute PsaC, PsaD, and PsaE in photosystem I, and he assigned the F_A and F_B clusters to the cysteine ligands on PsaC.

Photosystem II Light Harvesting System: Dynamic Behavior

Peter Horton and Alexander Ruban
University of Sheffield, Sheffield, UK

The light harvesting proteins of higher plants play a vital role in the regulation of photosynthesis. These proteins show striking structural and functional flexibility. This dynamic behavior provides a key physiological function to plants, which adapts them to continuously changing environmental conditions. In particular, dynamic properties of the light harvesting proteins of photosystem II promote the efficient collection of sunlight when the intensity is limiting photosynthesis and effective photoprotection when the intensity is excess.

Photosynthetic Light Harvesting

Photosystem II (PSII) is the multisubunit chloroplast membrane-associated pigment–protein complex that uses the energy of sunlight to drive the oxidation of water, evolving oxygen, donating electrons into the photosynthetic electron transfer chain, and depositing protons into the thylakoid lumen. Along with the photosystem I (PSI) it forms the electron–proton transfer chain, which drives the synthesis of ATP and NADPH (Figure 1). Vitally important components of both photosystems are the light-harvesting antennas, light-collecting units (mainly LHCI and LHCII for PSI and PSII, respectively) which ensure high rates of energy input into the photosynthetic reaction centers (RCI and RCII, respectively) by intercepting large numbers of light quanta of various energies/colors. The analogy of LHCs as funnels feeding the RCs with light energy is most appropriate.

Structure and Function of LHCII

The light-harvesting antenna of PSII consists of several proteins which together bind ~300 chlorophyll molecules. Associated tightly with the D1/D2 reaction center are the core antenna complexes CP47 and CP43. The remainder of the antenna consists of the Lhcb proteins, Lhcb1–6. These bind chlorophyll *a*, chlorophyll *b*, and xanthophylls to form several different complexes – LHCII, CP24, CP26, and CP29. LHCII is the main complex and contains ~40% of the PSII chlorophyll – it is the most abundant chlorophyll protein in nature.

Figure 2 depicts the current knowledge of LHCII structure on different levels of organization. The single monomeric unit is a relatively small protein, ~25–28 kDa, containing three transmembrane α-helical structures and binding 12 molecules of chlorophyll (seven chlorophyll *a* and five chlorophyll *b*). Three LHCII monomers are associated together into heterotrimers containing Lhcb1, Lhcb2, and Lhcb3. Additional pigments, carotenoids, are also present in LHCII. Two xanthophylls, luteins, are associated with the helices A and B. A third carotenoid, neoxanthin, is associated with the helix C and the trimer also binds peripherally the carotenoids violaxanthin or zeaxanthin. The xanthophylls play several important roles: (1) ensuring correct assembly of LHCII during biosynthesis; (2) protection of chlorophylls against photooxidation by quenching chlorophyll triplet states and scavenging oxygen radicals; (3) being structurally flexible molecules they allow dynamic behavior of LHCII leading to alteration in chlorophyll interaction and subsequent change in light collection efficiency; and (4) they modulate the interactions between LHCII trimers. Indeed, it was shown that extent of interaction between trimers depends on the type of peripherally bound carotenoid, violaxanthin, or zeaxanthin. *In vivo*, PSII unit is built on the stereo principle: two reaction center complexes build the dimeric PSII core complex, which binds four trimeric LHCII and six monomeric CP24, CP26, and CP29 (Figure 2C). In the photosynthetic membrane these PSII units are often seen as ordered arrays (Figure 2D). Here the LHCII antenna forms an entire network, or macrodomain, of monomeric and trimeric subunits, associated with each other and the reaction center complex. Associated with this macrostructure is the stacking of the complexes together in the characteristic grana membranes.

Three major parameters determine the efficiency of light harvesting: (1) cross-section or number of pigments and their ability to intercept light quanta with the broad

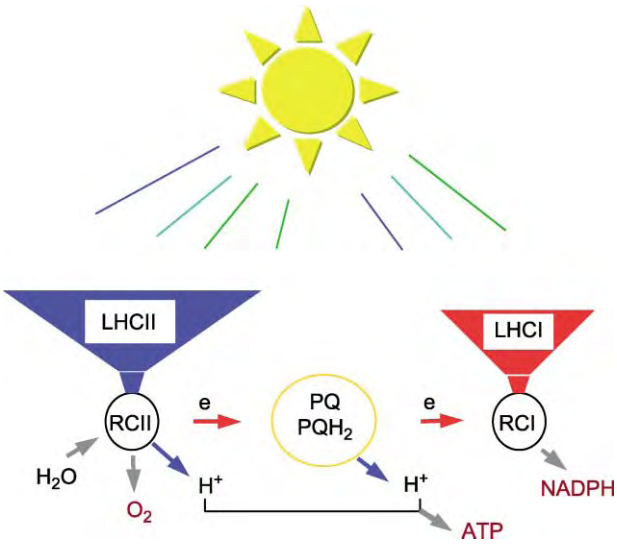

FIGURE 1 Photosynthetic electron transfer. LHCI and LHCII – light harvesting antenna of photosystem I and II, respectively; RCI and II – reaction centers; e – electrons; PQ and PQH_2 – intermediate electron carrier plastoquinone in oxidized and reduced form; H^+ – protons.

range of energy (color); (2) the time during which energy of light can be kept in antenna so it can be funneled into the reaction center; and (3) rate of the funneling. Thus, a large cross-section, long excitation energy lifetime, and high rate of energy transfer to the reaction center are the attributes of an efficient antenna and productive photosynthetic unit. Hence, the efficiency of light harvesting in PSII is determined by the number of LHCII subunits, the pigment order within them, the interaction between subunits and their closeness to the reaction center complex.

The Need for Control of the Light Reactions of Photosynthesis

The light and dark reactions of photosynthesis are tightly coupled, the ATP and NADPH provided by the electron-proton transfer system driving the fixation of CO_2 into carbohydrate. During a day, the light spectrum changes dramatically due to filtering by atmosphere, clouds and sometimes by other plants. Since LHCI and

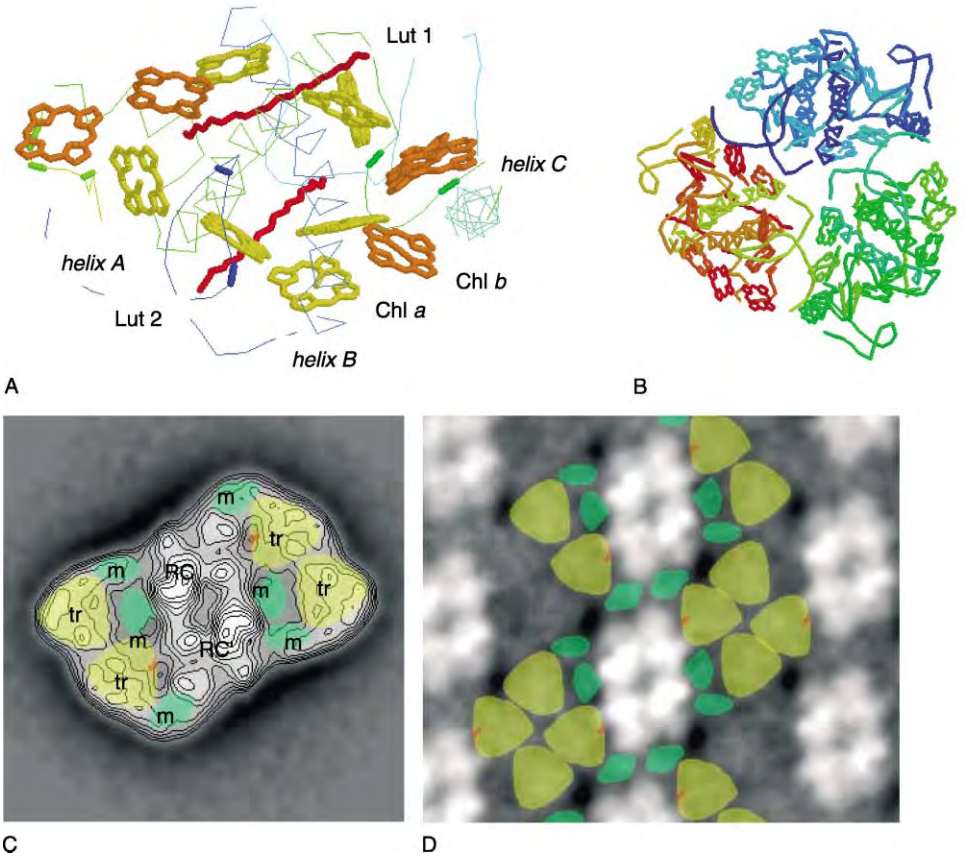

FIGURE 2 Structure of LHCII. (A) Atomic structure based on the electron diffraction analysis of 2D crystals of the isolated LHCII; Chl *a* and *b* – chlorophyll *a* and *b*; Lut 1 and 2 – luteins. (B) 3 monomeric LHCII forming the trimer. (C) Assembly of light harvesting complexes, monomers of CP26, CP29, and CP24 (m) and LHCII trimers (tr, highlighted light green) around two reaction center complexes (RC) in the photosystem II supercomplex. (D) Arrangement of ordered 2D arrays of photosystem II complexes in the photosynthetic membrane; highlighted structures: LHCII trimers – light green, monomers of CP24, CP26 and CP29 – dark green.

LHCII have different capacities to absorb light of different colors – the former preferring more red light than the latter – there will be a frequent imbalance in light energy input into reaction centers. This imbalance will decrease the electron transfer efficiency, hence the quantum yield of photosynthesis. The light intensity is also a very changeable parameter, sometimes varying 1000-fold. Whenever light input exceeds the capacity of electron transport and CO_2 assimilation, there is an excess of light, which may cause photoinhibition – the destabilization (by over-reduction and over-energization) and even damage (by photo-oxidation and generation of reactive oxygen species) to photosynthetic components, mainly in PSII. The effects of changes in light delivery can be amplified by alterations in photosynthetic capacity brought about by changes in other environmental factors, or by changes in metabolic demand, which result in variation in the rate of turnover and the stoichiometry of ATP and NADPH.

In order to achieve balance and stability of the photosynthetic process, regulatory mechanisms are necessary. The plant cell first has to assemble a chloroplast with the "correct" composition, and then various parts of the photosynthetic process need to be able to adjust their activities in response to internal and external information. Thus, the electron transport and carbon metabolism can be considered to be linked by a feedback and feed-forward control network. There is a compromise between maximizing the collection and utilization of light, and the avoidance of instability when light is in excess. The most appropriate way of looking at the regulatory mechanisms is, given a fixed composition and a fluctuating environment, that they extend the range of conditions over which photosynthesis can remain in balance – they provide homeostasis of excitation energy level, redox state, and ΔpH.

To optimize light harvesting function, two distinct regulatory strategies are required. The first aims to balance the input of light energy to PSI and PSII reaction centers in order to optimize electron transfer rate – this is called the state transitions. The second should regulate the amount of light energy directed to PSII – this is called nonphotochemical energy dissipation, or quenching (NPQ). As a result of evolution, both regulatory mechanisms have developed in the LHCII system and rely on its abilities to sense the "state" of the light energy balance and structurally respond, being capable of dynamic behavior.

State Transitions

The Lhcb1 and Lhcb2 polypeptides of LHCII are reversibly phosphorylated by a redox-regulated thylakoid-associated protein kinase. Phosphorylation at threonine residues near the N terminus of LHCII

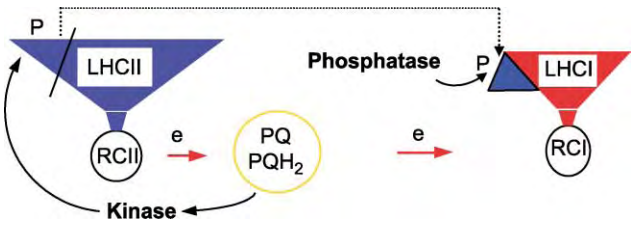

FIGURE 3 State transitions: the mechanism of compensation against imbalance of energy input into photosystems I and II. The redox controlled protein kinase phosphorylated LHCII when PQH_2 accumulates. A constitutive phosphatase activity dephosphorylates LHCII. This self-regulating system depends upon the different affinities of LHCII and phospho-LHCII for RCI and RCII.

weakens the association between PSII and LHCII, as a result of electrostatic and conformational changes. Phospho-LHCII partitions in favor of PSI, the association depending on the presence of the PSI-H subunit – in mutants without PSI-H phospho-LHCII remains associated with PSII. The kinase is activated when the plastoquinone pool is reduced, this being sensed by the quinone oxidation site on the cytochrome b_6f complex. The kinase therefore monitors the relative rates of delivery of excitation energy to PSII and PSI (Figure 3); overexcitation of PSII (state 1) activates the kinase, decreases delivery of excitation energy to PSII, and increases transfer to PSI (state 2). Levels of LHCII phosphorylation are lower at high light compared to low light, showing that the state transitions optimize photosynthesis in limiting light. This includes not only optimizing linear electron transport, but also the provision of optimal ΔpH and ATP/NADPH ratios by controlling the proportion of cyclic electron transfer around PSI.

Nonphotochemical Energy Dissipation

Energy-Dependent Quenching, qE

Dissipation, or quenching, of excess excitation energy absorbed by LHCII occurs by two processes, distinguished by the speeds with which they are induced upon exposure to illumination, their relaxation times in darkness and the light intensity threshholds. The major process under "normal" conditions is called qE, since it depends upon the energization of the thylakoid membrane as a result of ΔpH formation. Thus, the progressive increase in ΔpH that occurs as light saturation of photosynthesis is reached and is the trigger for energy dissipation. It can therefore be referred to as feedback de-excitation. The formation of qE occurs within seconds – minutes of exposure to excess light, and relaxes with a similar rate in darkness. In contrast, the sustained qI-type of quenching may take several

minutes or even hours to appear and relax, and under some conditions (such as low temperature) may be stable for days.

The Site of Quenching

Application of mathematical models for PSII energy transfer showed that quenching associated with qE occurred in the light harvesting antenna. Refinements of the analysis showed that qE is best explained by the transition between two states of the antenna, with different rate constants for energy dissipation. Subsequently, analysis of the chlorophyll fluorescence lifetimes provided direct support for this suggestion. Spectroscopic data and biochemical analysis confirmed that the PSII antenna was the site of quenching. A powerful way to determine which proteins are involved in qE is to investigate plants deficient in specific components. Experiments using plants deficient in all of the Lhcb proteins suggested that qE was not a property of the core antenna. However, plants in which Lhcb1 and 2, Lhcb4 and 5 have been separately reduced to less than 5% wild-type levels of protein by antisense technology show little or no change in qE, and in plants it has not proved possible to invoke a particular antenna complex as having an obligatory role. A major landmark in qE research was the identification of the *npq4* mutant, a mutant lacking qE and which is deficient in the Lhc-related protein PsbS. This four-helix protein is located in PSII, and contains protonatable amino acid residues which are thought to sense the thylakoid lumen pH.

The Xanthophyll Cycle

Under conditions of excess light, violaxanthin is de-epoxidized to zeaxanthin via the mono-epoxide antheraxanthin due to the activation of violaxanthin de-epoxidase, a thylakoid lumen enzyme. Another enzyme, zeaxanthin epoxidase, reverses the reaction in low light. A vast amount of data, from a wide variety of plant species under many different environments, showed correlations between the extent of qE and the de-epoxidation state of the xanthophyll cycle pool. Zeaxanthin is an activator of qE in that the apparent pK_a of the protonation reaction inducing qE shifts from near 4.5 to well over 5.0 in the presence of zeaxanthin. Since the ΔpH *in vivo* does not fall below 5.5, qE will depend completely on de-epoxidation of violaxanthin. Therefore, qE is an allosteric process, under the control of the interacting effects of protonation and zeaxanthin binding, similar to a regulated enzyme (Figure 4). This mode of regulation explained how the chloroplast could have a ΔpH high enough in limiting light to allow ATP synthesis without qE, yet in saturating light, how to have maximum electron transport rates and high qE simultaneously.

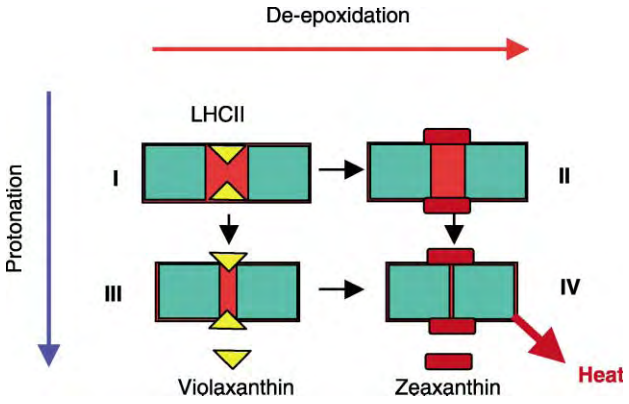

FIGURE 4 Model for the excess energy dissipation in the LHCII antenna. I – light-harvesting mode, a dark-adapted state; II – partially energy-dissipative, intermediate state; III – light "memory" mode, a dark-adapted mode after zeaxanthin was formed; IV – energy dissipative mode. The closeness of the boxes represents the extent of pigment interaction in LHCII and controls the level of quenching.

It has proved difficult to distinguish between the proposal that zeaxanthin was directly involved in quenching chlorophyll excited states by chlorophyll/zeaxanthin energy transfer, and the notion that zeaxanthin was working indirectly, modifying or inducing a quenching process intrinsic to the PSII antenna.

The Nature of the Quenched State of LHCII

Changes in the absorption spectra of chlorophyll and carotenoid occur upon formation of qE. A band with a maximum at 535 nm (ΔA_{535}) has attracted most attention, since its appearance is perfectly correlated to the amount of "quencher." Resonance Raman spectroscopy of leaves and chloroplasts has shown that ΔA_{535} is electronic in origin, and arises from a pool of one or two zeaxanthin molecules per PSII, which undergo a strong red shift in the presence of ΔpH. A similar red shift occurs when zeaxanthin binds to PsbS *in vitro*, and it is concluded that ΔA_{535} arises from this interaction.

Analysis of fluorescence lifetimes shows that the qE state of the PSII antenna has a lifetime of 0.4 ns, and the unquenched state 1.6 ns. Experiments with isolated light harvesting complexes have shown how such a change can arise. Detergent-solubilized LHCII has a lifetime of 4 ns, but reduction of the detergent concentration causes formation of oligomers with an average lifetime of 0.3 ns. This quenching has many features that are similar or identical to qE. The spectral changes in chlorophyll accompanying this *in vitro* quenching indicate that a particular LHCII domain is involved. The *in vitro* quenched state can also be investigated by reconstitution of light harvesting complexes with altered carotenoid content.

Substitution of lutein with zeaxanthin in LHCII causes partial chlorophyll fluorescence quenching.

In general, the ease with which LHCII *in vitro* can adopt a quenched state reflects the high density of pigment within it. Its design as a light harvesting complex means it maximizes the amount of chlorophyll per unit volume. Specific features of protein structure are needed to control the interactions between pigments, to promote energy transfer and to prevent formation of quenchers – dimers or excimers of chlorophylls and/or chlorophyll-xanthophyll associates. Therefore, only rather small changes in structure are needed to allow a quencher to form. Indeed, the activation energy for the formation of a quencher in LHCII is only 6 kcal mol^{-1}, indicative of the breakage of just a couple of H bonds. Thus, LHCII is uniquely poised to allow a switch between an unquenched state functioning in photosynthetic energy capture and a quenched state, dissipating excess energy as heat.

Biological Diversity of qE

The amount of qE in different plants is highly variable. High light grown plants may have 2–3 times more qE capacity and plant species adapted to growing in stressful environments have a much higher qE capacity than those inhabiting milder conditions. Genetic manipulation to increase the level of the PsbS protein results in an increase in qE, suggesting that the level of this protein is an important determinant of qE capacity.

Algae exhibit different qE properties as compared to higher plants. In *Chlamydomonas*, qE is smaller and forms more slowly, and mutation of an LHCII subunit decreases the capacity of qE, suggesting that here a less efficient process is controlled directly by the antenna and not by PsbS. In diatoms, which have light harvesting proteins of a different type, qE can be much larger than in higher plants, and its formation and relaxation totally depend upon the de-epoxidation of the violaxanthin analogue, diadinoxanthin. It seems that some features of the molecular mechanism for the regulation of light harvesting have diverged during evolution of classes of organisms.

Other Responses of LHCII to Excess Light

The sustained qI-type of quenching appears to also result, in part at least, from alteration in the antenna of PSII. At low temperature strong quenching is induced by light which has some features diagnostic of an increase in aggregation state of LHCII – formation of a red-shifted fluorescence emission band at 77 K. This state of LHCII seems to be semipermanent in some evergreen plants during winter. The mechanism by which such quenching is formed is currently unknown, although one possibility is that it arises from a direct effect of light on LHCII. Such an effect is well known for LHCII *in vitro*, and it appears to be triggered by a light-induced dissociation of trimers into monomers. At elevated temperature increased light-induced quenching arises from a different process – LHCII dissociates from PSII to be quenched by PSI, in a process that resembles the state transition, and in fact phosphorylation of LHCII and elevated temperature act synergistically.

When plants grown under low light are exposed to a sustained increase in light intensity, LHCII degradation is induced. Only monomers can be the substrates for proteolysis, and so this process must be preceded by a light-induced breakdown of trimers. Little is known about the biochemistry or regulation of this proteolytic process. Under extreme conditions, not only LHCII but complete photosystems are degraded as the plants seek to minimize oxidative damage.

The content of LHCII varies significantly depending on the light intensity under which the plants are grown. Typically, a low light grown plant may have 4–5 trimers per PSII core complex, whereas in high light this reduces to 1–2. The extra LHCII in low light plants appears to be present in membrane domains deficient in PSII core complexes. These LHCII domains can still be involved in efficient energy transfer, even transferring energy to pigments on opposite membranes in the grana.

The adjustment of the composition of photosystem II upon growth in high light compared to low light maintains the redox potential and ΔpH at the correct level, optimizing photosynthesis and avoiding oxidative stress. At higher growth irradiance, when LHCII cannot decrease any more, there are increases in the capacity for photoprotection (e.g., through an increase in xanthophyll cycle activity or PsbS content) and, eventually, decrease in the chlorophyll content of the leaf in order to lower light absorption. Even macroscopic events such as chloroplast movements or changes in leaf orientation can be similarly viewed as contributing to the optimization of light harvesting and counter-acting photodamage. Thus, plants do whatever they can, by a multitude of mechanisms, to limit the level of excitation energy in the PSII antenna, giving balance with the demands of photosynthesis, and optimising the redox state and ΔpH.

See Also the Following Articles

Chlorophylls and Carotenoids • Light-Harvesting Complex (LHC) I and II: Pigments and Proteins • Photosynthesis

Glossary

grana membrane The characteristic organization of the chloroplast thylakoids in which regions of membrane become tightly appressed together to form stacks of membranes, associated with the lateral segregation of the photosystems.

nonphotochemical quenching The quenching of chlorophyll fluorescence that arises because of an increase in thermal dissipation of excitation energy, contrasted to the photochemical quenching that arises because energy is used to drive photosynthetic electron transfer.

ΔpH The pH gradient, ~pH 7–8 outside and pH 5–6 inside, across the thylakoid membrane that results from light-induced proton uptake.

photoinhibition The inhibition of photosynthesis that arises during excess illumination, either from sustained quenching of antenna or reaction center complexes, or from accumulation of damaged photosystem II D1 proteins.

state transitions The reversible adaptation of the light harvesting system to differential excitation of PSI and PSII; in state 1, induced by overexcitation of PSI, energy transfer from LHCII to PSII is maximum, and in state 2, induced by overexcitation of PSII, energy transfer from LHCII to PSI is maximum.

xanthophyll cycle The reversible de-epoxidation of thylakoid bound violaxanthin to zeaxanthin, via the intermediate antheraxanthin.

Further Reading

Blankenship, R. E. (2001). *Molecular mechanisms of photosynthesis.* Blackwell Science, UK, p.328.

Demmig-Adams, B., and Adams, W. W. (2002). Antioxidants in photosynthesis and human nutrition. *Science* **298**, 2149–2153.

Green, B. R., and Dunford, D. G. (1996). The chlorophyll-carotenoid proteins of oxygenic photosynthesis. *Annu. Rev. Plant Physiol. Plant Molecul. Biol.* **47**, 685–714.

Haldrup, A., Jensen, P. E., Lunde, C., and Scheller, H. V. (2001). Balance of power: a view of the mechanism of photosynthetic state transitions. *Trends Plant Sci.* **6**, 301–305.

Hankamer, B., and Barber, J. (1997). Structure and membrane organization of photosystem II in green plants. *Annu. Rev. Plant Physiol. Plant Molecul. Biol.* **48**, 641–671.

Horton, P., Ruban, A. V., and Walters, R. G. (1996). Regulation of light harvesting in green plants. *Annu. Rev. Plant Physiol. Plant Molecul. Biol.* **47**, 655–684.

Horton, P., Ruban, A.V., Young, A.J (1999). Regulation of the structure and function of the light harvesting complexes of photosystem II by the xanthophyll cycle. In *The Photochemistry of Carotenoids: Applications in Biology* (H.A. Frank, A.J. Young and R.J. Cogdell, eds.) pp. 271-291, Dordrecht, The Netherlands, Kluwer Academic.

Horton, P., Murchie, E. H., Ruban, A. V., and Walters, R. G. (2001). Increasing rice photosynthesis by manipulation of the acclimation and adaptation to light. Rice biotechnology: improving yield, stress tolerance and grain quality. *Novartis Foundation Symposium,* **236**, 117–134.

Niyogi, K. K. (1999). Photoprotection revisited: genetic and molecular approaches. *Annu. Rev. Plant Physiol. Plant Molecul. Biol.* **50**, 333–359.

Muller, P., Li, X. P., and Niyogi, K. K. (2001). Non-photochemical quenching. A response to excess light energy. *Plant Physiol.* **125**, 1558–1566.

Biography

Peter Horton is a Professor of Plant Biochemistry in the department of Molecular Biology and Biotechnology at the University of Sheffield in the United Kingdom. His principal research interest is in photosynthesis and related aspects of plant biology. He holds a D.Phil. and D.Sc. from the University of York and received postdoctoral training at Purdue University. He has developed the concepts involved in the regulation of the light reactions of photosynthesis, establishing the role of LHCII phosphorylation in the state transitions, developing the methodology and framework of chlorophyll fluorescence analysis, and determining the basic mechanisms underlying nonphotochemical quenching.

Alexander Ruban is a Research Associate at the University of Sheffield where his principal research interest is in the biophysical aspects of photosynthesis. He holds a Ph.D. from the University of Kiev. Dr. Ruban has developed a number of spectroscopic approaches to investigate the dynamics of LHCII *in vitro* and *in vivo*.

Photosystem II: Assembly and Turnover of the D1 Protein

Eira Kanervo and Eva-Mari Aro
University of Turku, Turku, Finland

Photosystem II (PSII) is an integral membrane protein complex of ~25 subunits. It resides in the thylakoid membrane of organisms performing oxygenic photosynthesis, i.e., in chloroplasts of higher plants, mosses, ferns and algae, as well as in prokaryotic cyanobacteria. The synthesis and assembly of a new PSII complex in eukaryotic organisms require cooperation of both chloroplast and nuclear genomes. Besides structural protein subunits, PSII contains pigments and cofactors involved in the photochemistry of PSII. Most of the cofactors are ligated to the reaction center proteins D1 and D2. Such an arrangement together with the toxic nature of PSII photochemistry renders the reaction center prone to a photo-induced damage and accelerates the turnover rate of PSII subunits. The primary target of photodamage and the most rapidly turning-over subunit is the D1 protein. This protein has to be constantly replaced in order to maintain the PSII complex in an active state. This dynamic process, known as the PSII photoinhibition repair cycle, occurs in the thylakoid membrane at the rate depending on light intensity. The repair cycle is an absolute requirement for the maintenance of PSII complexes active in photosynthesis.

Biogenesis and Assembly of a New PSII Complex

Cooperation between Chloroplast and Nucleus

The PSII complex of eukaryotic organisms contains both nuclear and chloroplast-encoded gene products, as is the case with other photosynthetic protein complexes in the thylakoid membrane. This indicates that a tight cooperation exists between the organelle and nucleus in building up the PSII complex. From at least 25 genes encoding the PSII proteins, 15 genes reside in the chloroplast genome, rest of them locating in the nucleus.

Targeting the Chloroplast-Encoded PSII Proteins

The majority of the PSII core proteins are chloroplast encoded. These comprise the D1, D2, CP43, CP47, cyt $b559\alpha$, and cyt $b559\beta$ proteins encoded by the *psbA*, *psbD*, *psbC*, *psbB*, *psbE*, and *psbF* genes, respectively. In addition, the PSII core proteins include the *psbH*, *psbI*, *psbJ*, *psbK*, *psbL*, *psbM*, *psbN*, *psbTc*, and *psbZ* gene products of low molecular weight. Translation of the chloroplast-encoded PSII core proteins takes place on the surface of the thylakoid membrane. Initiation of translation of many chloroplast-encoded proteins is regulated by nuclear-encoded mRNA-binding proteins. To what extent these proteins are involved in targeting the ribosome–mRNA complexes to the thylakoid membrane is, however, unclear. Insertion of the chloroplast-encoded PSII proteins to the thylakoid membrane occurs both co- and posttranslationally, and several soluble and membrane proteins are involved in assisting these processes. Cotranslational membrane insertion is typical for the PSII core proteins with several transmembrane helices, such as the D1, D2, CP43, and CP47 proteins.

Targeting the Nuclear-Encoded PSII Proteins

The nuclear-encoded PSII core monomer proteins are three low-molecular-weight (LMW) subunits, namely the *psbW*, *psbX*, and *psbTn* gene products. In addition, proteins of the light-harvesting chlorophyll *a/b*-binding protein complex II (LHCII) and the oxygen-evolving complex (OEC) are nuclear encoded. All the nuclear-encoded proteins are synthesized as precursors on cytosolic ribosomes. These precursors are subsequently targeted to the chloroplast via an N-terminal transit peptide, which is proteolytically cleaved after import into the chloroplast. The nuclear-encoded precursor proteins targeted to the thylakoid lumen contain a bipartite N-terminal transit peptide, the last part of which is removed after the arrival of the transported protein into the lumen. The lumenal proteins, including those for the OEC, use both the Sec machinery and the ΔpH pathway in their insertion and translocation to the lumenal side of the thylakoid membrane. Integration of the LHCII proteins to the membrane is dependent on the presence of the thylakoid-located Alb3 protein.

Assembly of a New PSII Complex

General Features

Understanding of the assembly of the PSII complex is, so far, in its infancy. Besides purely biochemical approaches, the assembly of PSII has been studied using plant and cyanobacterial mutants. Such mutants have been deficient in a specific PSII subunit or they have carried a mutation in a nuclear gene that affects the expression or assembly of a structural PSII subunit. Also studies on plastid development from etioplast to chloroplast have contributed to the understanding of PSII assembly. Furthermore, research on the light-induced turnover of the PSII complex has produced information that can be applied also for the research on the assembly process of a new PSII center.

Sequence of the Assembly of PSII Core, OEC and LHCII Proteins

Light is required for maturation of etioplasts to chloroplasts and for synthesis and assembly of most of the PSII subunits. However, some of the PSII subunits do not need light for synthesis, since they exist already in etioplasts. This is the case particularly with cyt *b559* and the OEC proteins. In the assembly of the PSII core proteins, the two-subunit cyt *b559* functions as the first assembly partner for the D2 protein. All these together form an initial complex that functions as a receptor for the cotranslational assembly of the precursor-D1 protein. The assembly process then continues by association of the *psbI* gene product and the CP47 protein to the PSII subcomplex. Subsequently, the *psbH* gene product, the CP43 protein, and several LMW subunits attach to the growing PSII subcomplex. Assembly of the additional LMW subunits, namely the *psbJ* and *psbL* gene products, is essential for subsequent proper association of the OEC proteins to the lumenal side of the PSII core monomer. Finally, the rest of the LMW subunits, such as the *psbK*, *psbW*, and *psbZ* gene products, are required for the last events of the assembly process. These events include dimerization of the PSII core monomer and the attachment of LHCII to the PSII complex resulting in formation of a PSII supercomplex. An array of such PSII supercomplexes exists in the grana membranes of chloroplasts.

Regulation of the PSII Assembly

Light is required for an efficient translation elongation and accumulation of the D1 protein as well as for synthesis of the CP43 and CP47 core proteins. In addition to light, regulation of synthesis and assembly of the PSII complex involves the availability of a variety of factors, including the ligation of pigments and cofactors (chlorophyll *a*, pheophytin, β-carotene, Fe, Mn, plastoquinone) and the availability of the assembly partners.

The chloroplast-encoded core proteins D1, D2, CP43, and CP47 are cotranslationally inserted into the thylakoid membrane. Pigments are thought to bind to these proteins during their cotranslational membrane translocation and during the concomitant association of the protein with its assembly partner(s). Light is needed for the chlorophyll biosynthesis at the level of conversion of protochlorophyllide to chlorophyll *a*. Currently, we lack information on details of the pigment binding, even though the importance of this event as a regulative step in the PSII assembly has been known for a long time. It is clear, however, that the chlorophyll-binding proteins of PSII are stabilized by ligation of pigments. Most chlorophyll-binding proteins do not accumulate at all in a nonpigmented form.

Successful synthesis of the PSII core proteins requires the availability of assembly partners. Synthesis of the D2 protein is dependent on the presence of cyt *b559*. Furthermore, cyt *b559*/D2 subcomplex is indispensable for the synthesis of D1, and the cyt *b559*/D2/D1 subcomplex, in turn, functions as an assembly partner for CP47. From the PSII core proteins, CP43 seems to be synthesized quite independently.

Turnover of the D1 Protein of PSII

PSII Photoinactivation and the D1 Protein Damage

The PSII complex performs a remarkable task in splitting water molecules to oxygen and hydrogen (protons). Such oxidizing electron transfer reactions of PSII in an atmosphere containing oxygen readily lead to the formation of highly reactive radicals that are potentially harmful to the protein moiety. Conditions that lead to imbalance between the various steps during the linear electron transfer process can lead to photoinactivation of PSII. Thus PSII, when performing its normal function, is hazardous for itself.

Photoinactivation of PSII increases almost linearily with increasing light intensity. Under low light the rate of photoinactivation is also low. The rate of inactivation correlates with the amount of photons absorbed and mediated to the reaction center. Upon inactivation, the PSII complex becomes unable to transfer electrons and split water molecules. A constant repair of inactivated complexes is required to guarantee the maintenance of a sufficient level of active PSII complexes for photosynthesis. The efficiency of repair is affected negatively by environmental stress factors, such as high light and the extremes of temperature. If the repair process cannot keep up with the rate of photodamage, nonfunctional PSII complexes start to accumulate. This situation leads to the measurable decrease in the rate of total photosynthesis.

The primary target of the photo-induced PSII damage is the reaction center protein D1. This fact reflects the "grand design" of PSII: only one protein of the multi-subunit complex is primarily destroyed, the rest of the proteins being rescued for further use, i.e., reparation of the PSII complex. The primary photodamage is thought to include a conformational change and an oxidative damage to the D1 protein. These events, in turn, trigger the reaction center protein D1 to a substrate for proteolytic degradation. However, the actual nature of the primary photodamage is not yet properly understood.

PSII Photoinhibition Repair Cycle

Start of the Repair Process

Active PSII centers exist as dimers in the thylakoid membranes of grana stacks (Figure 1). After a light-induced damage to PSII, the LHCII antenna dissociates and monomerization of PSII occurs. PSII monomers then migrate from the grana to the stroma-exposed thylakoid membranes where a contact with the components acting in degradation and synthesis of the D1 protein is feasible. OEC dissociates from PSII and a partial disassembly of the PSII core proteins takes place. The stages from photodamage to degradation of the D1 protein are regulated by phosphorylation-dephosphorylation events of the PSII core proteins.

Degradation of the D1 Protein

Degradation of the light-damaged D1 protein is a proteolytic process that occurs in a well-coordinated manner on the stroma-exposed thylakoid membranes, leaving the closest partner, the D2 protein, most often

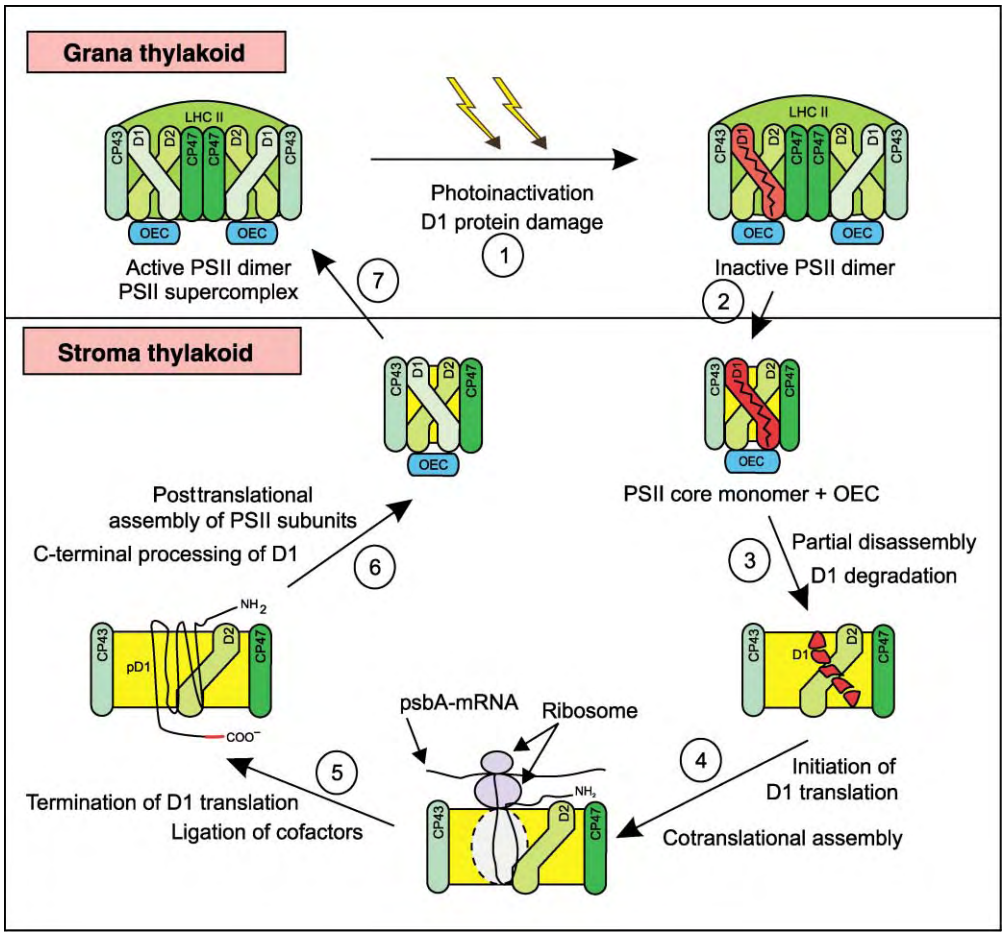

FIGURE 1 Model for the PSII photoinhibition repair cycle. 1) Photoinactivation of PSII and damage to the D1 protein. 2) Monomerization of the inactive PSII complex and its translocation from the grana thylakoids to the stroma-exposed thylakoids. 3) Partial disassembly of the PSII core proteins and proteolytic degradation of the D1 protein. 4) Initiation of D1 translation and cotranslational assembly of the nascent D1 chain into the D1-depleted PSII core monomer. 5) Ligation of cofactors during translation elongation and termination of D1 translation. 6) C-terminal processing of the pD1 protein; posttranslational assembly of the PSII core subunits and OEC. 7) Translocation of the repaired PSII monomer from the stroma-exposed thylakoids to the grana thylakoids; dimerization of PSII and the attachment of the LHCII antenna. D1, D2, CP43, CP47 = chlorophyll *a*-binding proteins of the PSII core; LHCII = light-harvesting chlorophyll *a*/*b* binding protein complex II; OEC = oxygen-evolving complex; pD1 = precursor-D1 protein.

intact. The D1 protein is an integral membrane protein with five transmembrane helices. Between helices there are loops both on the stromal and lumenal sides of the thylakoid membrane. The loops are the preferential sites of the primary cleavage of an integral membrane protein, in general, the stromal DE-loop being the most important one in the case of the D1 protein. The primary proteolysis of D1 produces fragments that are further degraded by the secondary proteolysis. Proteases from the DegP and FtsH families are known to act on the proteolysis of the D1 protein.

Synthesis of the D1 Protein

Synthesis of the D1 protein during the PSII repair cycle shares features with synthesis of the D1 protein in the assembly of a new PSII complex (see above). The D1 protein is encoded by the *psbA* gene residing in the chloroplast genome. The *psbA* mRNA-ribosome complex is targeted to the stroma-exposed thylakoid membrane, where elongation of the nascent D1 chain takes place. The nascent D1 chain is cotranslationally inserted into the thylakoid membrane, where the D2 protein and cyt *b559* act as the first association partners. Elongation is controlled by a variety of factors. Such factors include association of the nascent chain with a translocon, availability of the assembly partners, redox control of translation elongation and ligation of pigments. Resynthesis of the assembly partners is not needed, since they originate mainly from the existing PSII centers under repair.

When all the five transmembrane helices have been synthesized, the precursor D1 protein releases from the ribosome. The fifth transmembrane helix traverses the membrane, finally having its carboxy terminus in the thylakoid lumen.

Posttranslational Events of the D1 Synthesis and Reactivation of the PSII Complex

Posttranslational events of the D1 protein synthesis include several steps. First, during maturation of the D1 protein, the lumenal processing protease CtpA removes the extension of 9–16 amino acids from the carboxy terminus of the precursor D1 protein. This cleavage is necessary for ligation of the manganese cluster and reassociation of the OEC to the PSII complex. Before the OEC proteins can reassociate, the core proteins CP47, CP43 and most of the LMW subunits have to be reassembled to the PSII subcomplex. Finally, the properly assembled PSII monomer migrates back to the grana thylakoids, where PSII core dimerization and full reactivation of the PSII complex take place. The final reactivation stage also includes an association of the LHCII antenna proteins to the PSII dimer. These final stages in the grana thus accomplish the PSII photoinhibition repair cycle providing an active PSII dimer for photosynthesis.

See Also the Following Articles

Chloroplasts • Photosystem II Light Harvesting System: Dynamic Behavior • Photosystem II: Protein Components • Photosystem II: Water Oxidation, Overview

Glossary

D1 protein turnover Replacement of a nonfunctional D1 protein in the PSII complex.

photoinactivation Light-induced inactivation of the PSII electron transfer and water splitting.

PSII (photoinhibition) repair cycle Cycling of the PSII complexes between the grana- and stroma-exposed thylakoid membranes during the turnover of the D1 protein.

Further Reading

Andersson, B., and Aro, E.-M. (2001). Photodamage and D1 protein turnover in photosystem II. In *Regulation of Photosynthesis* (E.-M. Aro and B. Andersson, eds.) Vol. 11, pp. 377–393. Kluwer, Dordrecht, The Netherlands.

Baena-Gonzáles, E., and Aro, E.-M. (2002). Biogenesis, assembly and turnover of photosystem II units. *Phil. Trans. Roy. Soc. Lond. B* **357**, 1451–1460.

Herrmann, R. G., and Westhoff, P. (2001). Thylakoid biogenesis and dynamics: the result of a complex phylogenetic puzzle. In *Regulation of Photosynthesis* (E.-M. Aro and B. Andersson, eds.) Vol. 11, pp. 1–28. Kluwer, Dordrecht, The Netherlands.

Paulsen, H. (2001). Pigment assembly – Transport and ligation. In *Regulation of Photosynthesis* (E.-M. Aro and B. Andersson, eds.) Vol. 11, pp. 219–233. Kluwer, Dordrecht, The Netherlands.

Van Wijk, K. J. (2001). Proteins involved in biogenesis of the thylakoid membrane. In *Regulation of Photosynthesis* (E.-M. Aro and B. Andersson, eds.) Vol. 11, pp. 153–175. Kluwer, Dordrecht, The Netherlands.

Zerges, W. (2002). Does complexity constrain organelle evolution? *Trends Plant Sci.* **7**, 175–182.

Biography

Eva-Mari Aro is a Professor and Academy Professor in the Department of Biology at the University of Turku in Finland. Her principal interests are in the field of photosynthesis, including the photosystem II photoinhibition repair cycle, the assembly of PSII, and the redox regulation of thylakoid protein phosphorylation. Her scientific training abroad includes research visits to the University of California in Berkeley, USA, CEN Cadarache in France, the University of Stockholm in Sweden, and CSIRO in Canberra, Australia.

Eira Kanervo is a lecturer in the Department of Biology at the University of Turku in Finland. Her principal research interests include regulation of the D1 protein degradation and stress physiology of plants. She has been as a post-doc researcher at the National Institute for Basic Biology in Okazaki, Japan, and at the University of Linkoping, Sweden.

Photosystem II: Protein Components

James Barber
Imperial College, London, UK

Photosystem II (PSII) is a multisubunit protein complex embedded in the thylakoid membranes of oxygenic photosynthetic organisms: plants, algae, diatoms, and cyanobacteria. By using chlorophyll and several redox active cofactors, it captures and uses solar energy to split water into molecular oxygen and reducing equivalents.

$$2H_2O \xrightarrow[PSII]{4h\nu} O_2 + 4H^+ + 4e^-$$

To produce a dioxygen molecule, four photons ($h\nu$) are needed to provide the energy to split two water molecules The dioxygen released maintains our oxygenic atmosphere and provides an ozone layer which protects us from the damaging effects of UV radiation. The reducing equivalents which exit PSII as plastoquinol, are ultimately used, with the aid of additional light energy absorbed by photosystem I, to convert atmospheric carbon dioxide to the organic molecules that make up virtually all the biomass on our planet.

Morphology

Thylakoid Membrane

In chloroplasts of plants and green algae, the thylakoids are highly folded membranes having stacked (grana) and unstacked (stromal) lamellae regions. PSII is located mainly in the stacked regions. In cyanobacteria, diatoms, and other types of algae the thylakoids do not have a clear differentiation into stacked and unstacked regions and PSII is more evenly distributed along the plane of the membrane. In all cases the thylakoid membrane encloses an inner aqueous compartment known as the lumen while the outer compartment is either the stroma of the chloroplast or cytoplasm of cyanobacteria.

Reaction Center (RC)

RC is that part of a photosystem, like PSII, where light energy is converted to electrochemical potential energy. It is composed of protein-bound redox active cofactors that facilitate charge separation across the membrane.

Light-Harvesting Complexes

These pigment–protein complexes capture light energy and transfer it to the reaction center. They are often composed of several hundred pigment molecules, the exact number being dependent on growth conditions. Various pigments are used so as to fully utilize the solar spectrum and for PSII these are different types of chlorophyll, phycobilins, and carotenoids. Some light-harvesting complexes (LHCs) are contained within the thylakoid membrane (intrinsic) and some attach to the surface (extrinsic) of the membrane.

Redox Active Cofactors

P680

P680 is composed of a chlorophyll *a* molecule which, after excitation by the absorption of light to form $P680^*$, gives up an electron to an acceptor, converting it to $P680^{\cdot+}$. The redox potential of this radical cation is estimated to be 1.1 V or more, which is required to oxidize water. Its oxidation causes a bleach in its absorption spectrum centered at 680 nm. P680 is located on the lumenal side of the PSII RC. Recent work suggests that the excited state $P680^*$ is delocalized over four chlorophyll molecules and that upon oxidation the "hole" becomes localized on a single chlorophyll.

Pheophytin *A*

Pheophytin *a* (Pheo) is the primary electron acceptor of PSII located toward the stromal side of the RC. It receives an electron from $P680^*$ in a few picoseconds to form a radical pair $P680^{\cdot+}Pheo^{\cdot-}$. The reduction of Pheo can be detected as an optical absorption decrease at 422 nm and its reduction potential is ~ -600 mV.

Q_A

Q_A is a bound plastoquinone (PQ) molecule which undergoes a single reduction by $Pheo^{\cdot-}$ in $\sim$200 ps, forming the charge transport state $P680^{\cdot+}$ Pheo $Q_A^{\cdot-}$ where the redox potential of the semi-plastoquinone (Q_A^-) is ~ -150 mV.

Q_B

Q_B is also a plastoquinone (PQ) which can accept two electrons successively from $Q_A^{\cdot -}$ and together with two protons (H^+) from the stroma or cytoplasm to form plastoquinol (PQH_2). In this fully reduced form PQH_2 is released from the Q_B-binding site of the PSII RC and diffuses into the lipid matrix of the thylakoid membrane until it is oxidized by the cytochrome b_6f complex. The reducing equivalents are further "energized" by a second light reaction which occurs in photosystem I (PSI) so as to reach a redox potential sufficient to reduce carbon dioxide.

Y_Z

Y_Z is redox active tyrosine which reduces $P680^{\cdot +}$. In so doing, it loses an H^+ from its phenolic group and the resulting species is a neutral tyrosine radical $Y_Z^{\cdot}$.

$(Mn)_4$-Cluster

A cluster of four manganese atoms together with a Ca^{2+} atom, make the catalytic center (Mn_4Ca^{2+}-cluster), where the splitting of two substrate molecules occurs. The removal of 4e and $4H^+$ requires four successive oxidations of P680, and there is evidence that $Y_z^{\cdot}$ may act as an H^+ as well as an electron acceptor and therefore is directly involved in the water oxidation reaction.

Proteins

The RC core complex of PSII is composed of a large number of proteins encoded by Pcb genes (see Table I). The RC core is serviced by LHC proteins, the number and type of which varies between different types of organisms. Plants and green algae have their LHC proteins encoded by *cab* genes while red algae and cyanobacteria contain phycobiliproteins encoded by *apc* and *cpc* genes. Here we confine ourselves to PSII RC core proteins encoded by the *psb* genes (Figure 1).

PsbA-D1 Protein

After C-terminal posttranslational modification this protein has a molecular mass ~38 kDa and contains ~350 amino acids depending on species. It has five transmembrane α-helices (A–E), DE stromal surface α-helix, and CD lumenal surface α-helix. It binds the majority of the cofactors involved in PSII-mediated electron transport: Y_Z is Tyr161, $P680^{\cdot +}$ is chlorophyll *a* ligated by His198, Pheo is probably H-bounded by Tyr126 and Glu130, Q_B via interactions with His 215 and Ser 264. The Mn_4Ca^{2+}-cluster, is probably ligated by Asp170, Glu189, Ala344, His332, Glu 333, and His337. The D1 protein also binds a non-heme iron, which is normally redox inactive and positioned between Q_A and Q_B, and is ligated by His215 and His272.

Another important property of the D1 protein is that it turns over more rapidly than any other protein in the thylakoid membrane. This remarkable feature is linked to the fact that PSII is susceptible to photoinduced damage leading to photoinhibition and a lowering of photosynthetic efficiency. The degradation, synthesis, and reinsertion of this protein into the RC core complex represents a very important aspect of the dynamics of PSII.

PsbB-CP47

This highly conserved PSII RC protein consists of ~500 amino acids and has a molecular mass of ~56 kDa depending on species. It is often known as CP47 and has 6 transmembrane α-helices (I–VI) arranged in a ring consisting of 3 pairs with N and C termini exposed at the stromal surface. The lumenal loop joining transmembrane helices V and VI is large, consisting of 200 amino acids. It binds 16 chlorophyll *a* molecules and probably 3 β-carotenes. Most of the Chls are ligated to His residues located in the transmembrane helices and form an LHC system for the RC. The large lumenal loop functions indirectly in the water oxidation reaction by interacting with the D2 protein. Depletion of the *psb*B gene and a wide range of site-directed mutational studies have emphasized the absolute requirement of the PsbB protein in PSII assembly and function.

PsbC-CP43

After posttranslational processing the PsbC-CP43 protein, depending on species, contains ~470 amino acids and has a molecular mass of ~50 kDa. It is homologous with PsbB (CP47) in that it has 6 transmembrane α-helices arranged in the same way. It also contains a considerable number of histidine residues which are involved in ligating some of the 14 Chl*a* bound to this protein. Like CP47, CP43 probably binds 3 β-carotene molecules and has a large lumenal loop joining helices V and VI. However, this loop is slightly smaller, having ~150 amino acids. It also differs from CP47 in that in plants (but not in algae and cyanobacteria) the N-terminal threonine of CP43 can be reversibly phosphorylated. Moreover CP43 seems to be more weakly associated with PSII than with CP47, a feature which may be important when the D1 protein is degraded and replaced. Despite these differences, CP43, like CP47 acts as a LHC for PSII and its presence is also necessary for water splitting activity since it provides a ligand for the Mn_4Ca^{2+}-cluster.

TABLE I

Protein Subunits of PSII Core Reaction Center Complex

Gene	Subunit	Mass (kDa)	No. of transmembrane α-helices
*psb*A (c)	D1	38.021 (S)	5
*psb*B (c)	CP47	56.278 (S)	6
*psb*C (c)	CP43	50.066 (S)	6
*psb*D (c)	D2	39.418 (S)	5
*psb*E (c)	α-cyt b559	9.255 (S)	1
*psb*F (c)	β-cyt b559	4.409 (S)	1
*psb*H (c)	H protein	7.697 (S)	1
*psb*I (c)	I protein	4.195 (S)	1
*psb*J (c)	J protein	4.116 (P)	1
*psb*K (c)	K protein	4.283 (S)	1
*psb*L (c)	L protein	4.366 (S)	1
*psb*M (c)	M protein	3.755 (P)	1
*psb*N (c)	N protein	4.722 (T)	1
*psb*O (c)	33 kDa O protein	26.539 (S)	0
*psb*P (n)	23 kDa P protein	20.210 (S)	0
*psb*Q (n)	16 kDa Q protein	16.523 (S)	0
*psb*R (n)	R protein	10.236 (S)	0
*psb*S (n)	S protein	29.197 (S)	4
*psb*T (c)	T_C protein	3.849 (S)	1
*psb*T (n)	T_n protein	5.000 (A)	0
*psb*U	U protein	10.491 (Sy)	
*psb*V	V protein	15.121 (Sy)	0
*psb*W (n)	W protein	5.928 (S)	1
*psb*X (n)	X protein	4.225 (S)	1
*psb*Y (c)	Y protein	4202 (Sy)	1
*psb*Z (c)	Z protein	6.541 (S)	2

These proteins are products of the *psb*A to *psb*Z genes that occur in oxygenic organisms. In eukaryotic organisms the *psb* genes are located in either the chloroplast (c) or nuclear (n) genes. The molecular masses of the mature PsbA–PsbZ proteins are calculated from the protein sequences reported in the SwissProt database using the MacBioSpec program (Sciex Corp., Thornhill, ON, Canada) for spinach (S), pea (P), tobacco (T), *Arabidopsis* (A), and *Synechocystis* PCC6803 (Sy).

PsbD-D2 Protein

The PsbD-D2 protein is homologous to the D1 protein. Although it is slightly larger than the D1 protein, having in the region of 353 amino acids and a molecular mass of ~39.5 kDa, depending on species it has 5 transmembrane helical segments organized in the same way as the D1 protein. Compared with the D1 protein it is involved to a lesser extent in binding active cofactors. Another chlorophyll that forms a cluster constituting $P680^*$ is ligated to His197, while the binding of Q_A may involve at least His214, Phe261 and possibly Trp253 and Leu267. The D2 protein also provides ligands for the non-heme iron being His214 and His268. Normally the D2 protein does not turn over rapidly like the D1 protein but, under extreme conditions (e.g., irradiation with damaging UV light), it will be replaced by a repair process.

PsbE and PsbF

These are the α- and β-subunits respectively of cytochrome b559. After processing, the PsbE and PsbF contain 82 and 38 amino acids in most higher plants, and have molecular masses of ~9.3–4.4 kDa. Both subunits have a single transmembrane helix with their N termini exposed to the stromal surface.

The α-subunit is characterized by having a long C terminus of ~44 amino acid residues extending from the lumenal surface of the membrane while the β-subunit has essentially no lumenal domain. Of considerable importance is that each subunit contains a conserved

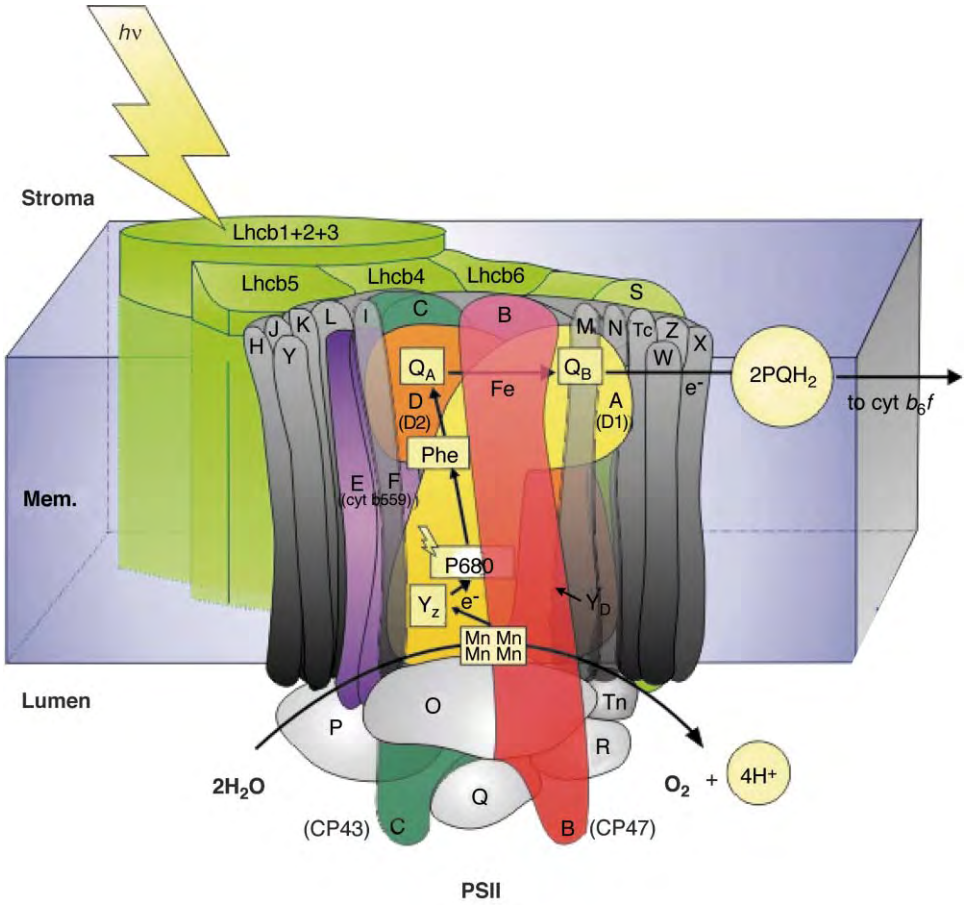

FIGURE 1 Cartoon showing the protein components of PSII of plants and algae, and the primary and secondary electron steps that occur in the reaction center D1 and D2 proteins. The RC core proteins are labeled according to their gene letter (e.g., *psb*A = A). Also shown are the Lhcb Chl*a*/Chl*b*-binding proteins encoded by *cab* genes that form the outer light-harvesting antenna system of higher plants and green algae.

histidine residue which is located within the membrane-spanning region towards the stromal surface. These two residues form axial ligands to the heme of the cytochrome. Although it had been argued by some that there are two cyt b559 per RC, there is strong evidence favoring a single copy of the cytochrome per RC. The deletion of the *psb*E gene results in a lack of assembly of PSII. On the other hand replacement of the His residue in the α-subunit can lead to an assembled and functionally active PSII complex even when no heme is ligated to the PsbE and PsbF proteins. Normally the heme has a high redox potential of $\sim$0.4 V but under some circumstances this potential is lowered to 0.15 V or less. The chemical basis of this redox shift and its significance, if any, is unclear. Under some circumstances, usually when the water splitting reactions are inhibited such as at low temperature, the heme of cyt b559 is oxidized by $P680^{+}$. According to recent structural models the heme is at least 40Å from P680, which is too far to account for the millisecond time constant for its oxidation. Accordingly it has been suggested that a β-carotene molecule bound within the D1/D2 heterodimer acts as a redox intermediate between the cyt b559 and $P680^{+}$. The reduction of the oxidized heme may involve Q_A^-, Q_B^-, or $Pheo^-$ but again there is a distance problem, with the required electron donation occurring over distances of 28Å or more, according to the recent X-ray structure. It seems likely that cyt b559 plays a protective role in minimizing photodamage of the RC.

PsbG

A chloroplast gene was initially called *psb*G but it was shown later that the product of this gene was not a PSII protein but rather a component of a chloroplast located NADPH/quinone oxidoreductase. This gene is now known as *ndh*K.

PsbH

In higher plants, the PsbH protein contains 72 amino acids and has a calculated mass of $\sim$7.7 kDa.

In cyanobacteria the protein is slightly smaller (~6.5 kDa) with a truncated N terminus and as such does not have the N-terminal threonine residue which is conserved in all higher plant and green algal sequences which is the site for reversible phosphorylation. The functional significance of the phosphorylation process is unclear. The higher plant protein is characterized by having a single transmembrane helix with a long N-terminal region consisting of ~41 amino acids at the stromal surface, which reduces to ~30 residues in the case of cyanobacteria. The *psb*H gene can be deleted from the cyanobacterium *Synechocystis* without impairing the assembly of PSII and photoautotrophic growth. The knockout mutant was, however, more sensitive to photoinhibition than the wild type. This sensitivity seemed to be due to the partial inhibition of the D1 protein repair process rather than to an increase in photochemical damage. In contrast, when the *psb*H gene was deleted in *Chlamydomonas reinhardtii*, PSII did not assemble.

PsbI

The PsbI protein has a molecular mass of ~4.2 kDa. In most eukaryotes this protein contains 35 amino acids and is predicted to have a single transmembrane helix with a short N-terminal region at its stromal end. It is located close to the D1/D2 heterodimer being adjacent to the B-helix of the D1 protein. Interestingly, the mature protein retains the initiating N-formyl group at its N-terminal methionine residue. The *psb*I gene has been deleted in the green alga *Chlamydomonas* and the cyanobacterium *Synechocystis*, without inhibiting PSII assembly and photoautotrophic growth. Thus, the function of the PsbI protein remains unknown.

PsbJ

In most organisms the *psb*J gene is located in a gene cluster also containing the *psb*E, *psb*F, and *psb*L genes. The PsbJ protein is highly conserved, consists of 39 amino acids and has a calculated molecular mass of 4.1 kDa. It is predicted to have one transmembrane helix. The *psb*J gene has been deleted in cyanobacteria to generate a knockout mutant which assembles PSII at a lower level than the wild type and consequently has a slower photoautotrophic growth rate.

PsbK

This ~43 kDa protein is highly conserved and has 37 amino acid residues. It is predicted to have a single transmembrane helix. Of particular note is that in higher plants, 24 amino acids are posttranslationally cleaved from the initial gene product. In cyanobacteria eight amino acids are removed after translation. These presequences probably bring about the insertion of the protein into the thylakoid membrane such that its N terminus is on the lumenal side. Deletion of the *psb*K gene in cyanobacteria has very little effect on photoautotrophic growth and PSII activity. In the case of green algae, however, the deletion of the gene destabilized the PSII complex and the transformant was unable to grow photoautotrophically.

PsbL

This highly conserved PSII protein contains 37 amino acids and has a calculated molecular mass of ~4.4 kDa. In most organisms its gene is located in the cluster together with *psb*E, *psb*F, and *psb*J. Hydropathy analysis suggests that it contains a single transmembrane helix. Inactivation of the *psb*L gene in cyanobacteria resulted in a loss of PSII-mediated oxygen evolution and the transformant was unable to grow photoautotrophically. It has also been reported that PsbL is required for normal functioning of the Q_A site based on studies with isolated PSII complexes. This conclusion was reinforced by the finding that PsbL is required for the oxidation of Y_Z by $P680^{+}$. As a consequence, the primary quinone acceptor is destabilized by the increased probability of rapid recombination between Q_A^- and $P680^{+}$.

PsbM

The PsbM protein is predicted to have one transmembrane helix with a very short N-terminal extension on the stromal side. It contains 33 amino acids and has a molecular mass of ~3.7 kDa. PsbM has been identified in PSII isolated from cyanobacteria and green algae. Together with PsbL and PsbTc this protein may function to stabilize PSII as a dimer.

PsbN

As in the case of PsbM, this protein is predicted to be in both cyanobacterial and plant PSII. However, it has not been detected directly in plant PSII although it has been identified in cyanobacteria. PsbN has a predicted single transmembrane helix. Deletion of both *psb*N and *psb*H genes from *Synechocystis* caused no effect other than those observed in the absence of *psb*H alone. Thus, the function and location of *psb*N are unknown.

PsbO

PsbO is a 33 kDa manganese stabilizing protein. Between higher plants and cyanobacteria this protein is

highly conserved containing, after processing, 241–247 residues. Although the mature PsbO protein is often referred to as the 33 kDa protein, its calculated molecular mass is ~26.5 kDa. It is an extrinsic protein with high β-sheet content and plays an important role in maintaining an optimal environment for water oxidation to occur. Various studies indicate that it does so by controlling Ca^{2+} and Cl^- levels at the catalytic site and by stabilizing the Mn_4-cluster, but it does not bind Mn directly. For this reason it is often called the "manganese stabilizing protein." Its deletion in cyanobacteria does not prevent water oxidation although the equivalent mutant in green alga does not assemble a functional PSII RC complex.

PsbP

PsbP is a 23 kDa extrinsic protein. After processing, this protein consists of ~186 amino acids with a calculated molecular mass of ~20 kDa. Although found in higher plants and green algae, it is not conserved in cyanobacteria. Like PsbO, its function seems to be to optimize the Ca^{2+} and Cl^- levels needed for the water oxidizing reaction and is located in the vicinity of the 33 kDa protein to which it binds.

PsbQ

The PsbQ mature protein contains ~49 amino acids and, like PsbP, is located close to the 33 kDa protein and the Mn_4-cluster. It is predicted to be an all α-protein and also seems to be involved in optimizing the ionic environment necessary for oxygen evolution. PsbQ, however, is not found in cyanobacterial PSII although a *psb*Q-like gene is present. Its binding to PSII requires the presence of PsbO and PsbP.

PsbR

The role of PsbR is unknown. It has a molecular mass of 10.2 kDa and consists of ~99 amino acids. It seems to be an extrinsic protein of plants, and is bound relatively tightly to the lumenal surface in the vicinity of the water splitting site. Whether it has a transmembrane helix is a matter for debate. It does not exist in cyanobacteria.

PsbS

The PsbS protein consists of ~205 amino acids and has an apparent molecular mass of 22 kDa although its calculated mass is ~29 kDa. It is predicted to have four transmembrane helices. Helices I and III, and II and IV, are homologous indicating that the protein is derived from internal gene duplication. Sequence homology studies suggest that PsbS is related to Chl*a*/Chl*b*-binding antenna Lhcb1–6 proteins (*cab* gene products) and is likely to be a chlorophyll-binding protein. A functional role for PsbS, therefore, could be to act as a pigment chaperonin which aids the incorporation of chlorophyll molecules into the various pigment-binding proteins of PSII. This protein has also been implicated in the protection of PSII against photoinduced damage (photoinhibition). It does not exist in cyanobacteria.

$PsbT_C$

The chloroplast-encoded $PsbT_C$ protein is also found in cyanobacteria. It contains 30–34 amino acids, has a molecular weight of ~3.9 kDa and retains the initiating N-formyl group on its N-terminal methionine residue. It is predicted to have a single transmembrane helix which is located in the N terminus of the protein. The *psb*T_C gene was formerly known as ycf8 and is located close to the *psb*B gene in the chloroplast genome. The first identification of this subunit was made by comparing wild type and a mutant of *Chlamydomonas* and lacked the *psb*T_C gene. This work also showed that the $PsbT_C$ is a PSII protein and is required for optimal activity under high-light conditions so as to prevent photoinhibition. It is located with PsbM and PsbL in the dimerization domain.

$PsbT_N$

A nuclear-encoded hydrophilic 5 kDa protein which copurifies with PsbO. Although its function is unknown, it seems to be an extrinsic protein located on the surface of PSII. The mature $PsbT_n$ protein consists of ~28 amino acids in higher plants and the presence of two cysteine residues suggests that it contains a disulfide bridge. It is not present in cyanobacteria.

PsbU

This is a cyanobacterial all α-protein reported to be extrinsically located on the lumenal surface of PSII close to the 33 kDa protein. It has an apparent molecular mass of ~11 kDa. It is also found in red algae but not in plants and green algae.

PsbV

PsbV is also known as cytochrome c550 and is found only in cyanobacteria and red algae. It has a molecular mass of 15 kDa and is an extrinsic protein found on the lumenal surface of PSII. It plays no direct role in water

oxidation although it does help to provide a Ca^{2+}/Cl^{-} environment at the catalytic site. It does not, however, bind directly to PsbO but indirectly via PsbU, which forms a bridge.

PsbW

The PsbW protein is found in higher plants and green algae. A cyanobacterial "PsbW-like" gene has also been documented which has a low homology with the eukaryotic equivalent, and therefore there is some uncertainty whether or not cyanobacteria contain the PsbW protein. In higher plants and green algae, it is nuclear-encoded and is processed to a mature protein having an apparent molecular mass of 6.1 kDa and consists of 54–56 amino acids. It is predicted to have one membrane-spanning region with its N terminus located on the lumenal side of the membrane. This orientation is consistent with the pre-sequence of the PsbW protein having characteristics of a target sequence typical for lumenal proteins. The function of PsbW is unknown.

PsbX

The PsbX protein is nuclear-encoded in higher plants and green algae, and consists of ~42 amino acids. In higher plants its synthesis is tightly regulated by light. The mature PsbX protein is reported to have a molecular mass of 4.1 kDa and predicted to have a single transmembrane helix. It has been detected in the oxygen-evolving PSII core complex of higher plants and cyanobacteria. The deletion of the *psb*X gene in cyanobacteria did not inhibit PSII assembly and photoautotrophic growth. However these studies suggest that PsbX may play a role in the function of Q_A and Q_B. It is located close to the B-helix of the D2 protein.

PsbY

This protein is located in PSII of plants, algae, and cyanobacteria. It has a molecular mass of ~4.2 kDa, consists of 36–39 amino acid residues, and has one transmembrane segment. The deletion of the *psb*Y gene in cyanobacteria did not impair the water oxidation process and is therefore likely to be located in a peripheral region of the PSII complex.

PsbZ

This 6.8 kDa protein contains 62 amino acids and forms two transmembrane helices. It is located at the peripheral edge of the PSII complex adjacent to PsbC (CP43) where, in plants and algae, it could be involved in binding the outer Chl*a*/Chl*b* light-harvesting systems.

Conclusion

Here 26 different Psb subunits have been described that are found in the PSII RC core. In a few cases, the subunits are either specific to plants and green algae or to red algae and cyanobacteria. In addition, there may be some other candidates which have yet to be characterized in detail. Recently X-ray structures of the cyanobacterial PSII RC core have been obtained and the resolution is now sufficient to unambiguously assign proteins to most electron densities. This has proved relatively easy for the D1, D2, CP43, CP47, PsbE, PsbF, and the extrinsic proteins. The most recent X-ray structure has identified the positions of 12 low-molecular-weight subunits in the cyanobacterial PSII complex.

See Also the Following Articles

Chlorophylls and Carotenoids • Chloroplasts • Light-Harvesting Complex (LHC) I and II: Pigments and Proteins • Photosystem II: Assembly and Turnover of the D1 Protein • Photosystem II Light Harvesting System: Dynamic Behavior • Photosystem II: Water Oxidation, Overview

Glossary

light-harvesting system Proteins that bind chlorophyll, carotenoids, and phycobilins which absorb light and transfer excitation energy to the reaction center.
oxidation The process of removing an electron to a chemical species.
photosystem Pigment–protein complex containing a light-harvesting system and a reaction center.
radical Reactive chemical species with an unpaired electron.
reaction center Protein subunits of the photosystem that bind redox active cofactors which use excitation energy to bring about charge transfer across the membrane.
reduction The process of donating an electron to a chemical species.

Further Reading

Barber, J. (2003). Photosystem: II. The engine of life. *Quart. Revs. Biophys.* **36**, 71–89.
Barber, J., Nield, J., Morris, E. P., Zheleva, D., and Hankamer, B. (1997). The structure, function and dynamics of photosystem two. *Physiol. Plant.* **100**, 817–827.
Blankenship, R. E. (2002). *Molecular Mechanisms of Photosynthesis*. Blackwell, Chichester, UK.
Ferreira, K., Iverson, T., Maghlaoui, K., Barber, J., and Iwata, S. (2004). Architecture of the photosynthetic oxygen-evolving centre. *Science* **303**, 1831–1838.
Hankamer, B., Morris, E. P., Nield, J., Carne, A., and Barber, J. (2001). Subunit positioning and transmembrane helix organisation in the core dimer of photosystem II. *FEBS Lett.* **504**, 142–151.

Kamiya, N., and Shen, J.-R. (2003). Crystal structure of oxygen-evolving photosystem II from *Thermosynechococcus vulcanus* at 3.7Å resolution. *Proc. Natl. Acad. Sci. USA* **100**, 98–103.

Ort, D. R., and Yocum, C. F. (1996). Oxygenic photosynthesis. In *The Light Reactions, Advances in Photosynthesis*, Vol 4, Kluwer, Dordrecht, The Netherlands.

Zouni, A., Witt, H. T., Kern, J., Fromme, P., Krauss, N., Saenger, W., and Orth, P. (2001). Crystal structure of photosystem II from *Synechococcus elongatus* at 3.8 Å resolution. *Nature* **409**, 739–742.

Biography

James Barber is the Ernst Chain Professor of Biochemistry and Former Dean of the Royal College of Science and Head of the Department of Biochemistry at Imperial College, London. His principal research interest is light absorption and utilization in photosynthesis, with special focus on photosystem II and the water oxidation process. He has published over 500 papers, edited many specialized books, and was elected to Academia Europaeae in 1989 and a Foreign Member of the Swedish Royal Academy of Sciences in 2003.

Photosystem II: Water Oxidation, Overview

Fabrice Rappaport and Pierre Joliot
Centre National de la Recherche Scientifique, Paris, France

The appearance of oxygen-producing organisms about three billions years ago is widely believed to be at the origin of the conversion of our atmosphere from anaerobic to its present oxygen rich composition. The switch from reduced carbon or sulfur compound oxidation to water oxidation and carbon dioxide reduction did not only result in a major change in the gas composition of the earth atmosphere, but also boosted the apparition of aerobic metabolism, which produces 18 times more energy per unit of substrate than anaerobic metabolism. Photosynthetic oxygen evolution, which accompanies the conversion of solar energy to biomass is thus rightly considered as the source of most of the energy available to life on Earth as well as a mandatory process to fuel the respiratory metabolism. Since the discovery by Priestley of the gas exchange (oxygen production and carbon dioxide assimilation), resulting from the photosynthetic process, till today, much insight into the mechanism of water splitting into dioxygen has been gained with an impressive acceleration in the last 30 years. The enzymatic machinery which drives water oxidation is identified, its three-dimensional structure has first been determined, by the groups of W. Saenger and H.T. Witt, with a resolution of 3.5Å, which has improved since then. Yet, the precise chemistry and energetics of water splitting remains to be clarified, if not understood.

Photosystem II and the Water Splitting Enzyme

The Photosystem II Complex

Water oxidation into dioxygen (O_2) follows the equation: $2H_2O \rightarrow O_2 + 4H^+ + 4e^-$, where H^+ and e^- stand for protons and electrons, respectively. Water is obviously a very stable compound and its oxidation requires the availability of strongly oxidizing species (at pH 7.0 the midpoint potential of the H_2O/O_2 couple is 810 mV). This oxidizing power is formed at the expense of light absorption and the conversion of light energy into electrochemical energy. The action spectrum of oxygen emission showed that it is sensitized by pigments associated with Photosystem II (PS II). Photosystem II is a large pigment protein complex located in the thylakoid membrane of the chloroplast, in green algae or higher plants or in the cytoplasmic membrane in cyanobacteria. As illustrated in Figure 1, the core of PS II is composed of two homologous polypeptides (D_1 and D_2, D for diffuse electrophoretic profile) each of which consists of five transmembrane helices. It bears various redox cofactors among which a chlorophyll dimer (P_AP_B), two chlorophyll monomers (B_A and B_B), two pheophytins (Ph_A and P_B), and two quinones Q_A and Q_B. Among the various photosynthetic reaction centers, PS II is unique since it bears a tetra manganese cluster which, coupled to a redox active tyrosine Y_Z, is responsible for water splitting into oxygen. The core of the reaction center is surrounded by pigment (chlorophyll and carotenoid)-binding proteins, which increase by a factor of ~200 its absorption cross-section. Thus, under normal solar radiance, one photon is absorbed by PSII every 10 ms or so. The absorption of a photon by one of the chlorophyll borne by the pigment-binding proteins results in the formation of an excited state of a chlorophyll, i.e., an electron jumps from the highest occupied molecular orbital to the lowest unoccupied orbital of higher energy. Provided other pigments are close enough, this excitation energy may hop from one pigment to another and then be funneled to the core of the reaction center and more precisely to the primary donor P (denoted P^* in the excited state). The singularity of P resides in the fact that in its close vicinity one finds an electron acceptor (Ph_A). The excitation energy, by weakening the binding energy of the electron by the energy of the transition between the two molecular orbital, allows the electron transfer reaction between P^* and this nearby acceptor to occur, yielding the "charge separated state" ($P^+Ph_A^-$). This state is then further stabilized by successive electron transfer step between the different redox compounds. At room temperature the first oxidized cofactor is essentially P_A. It is reduced in a few tens of nanoseconds by the redox active Y_Z (Y161 of the D_1 polypeptide), which is in turn reduced at the expense of the water

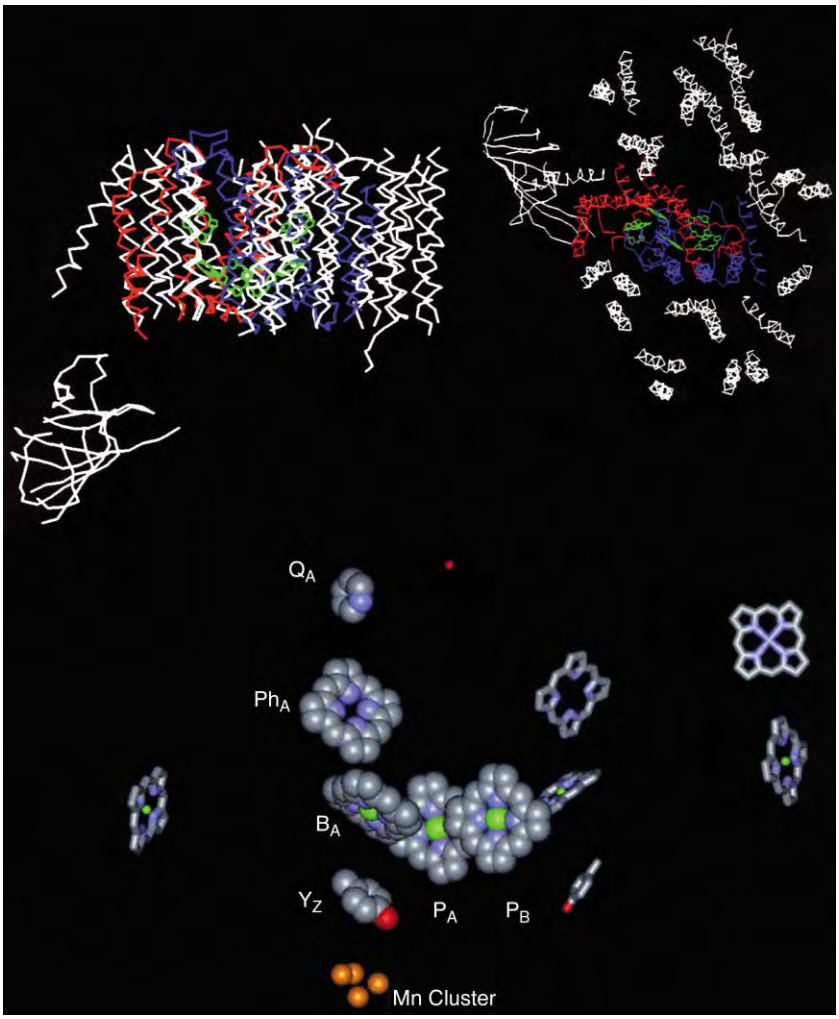

FIGURE 1 A structural model of Photosystem II based on X-ray diffraction studies by Zouni *et al.* (2001). *Nature* **409**, 739–743, with permission of Nature pdb: 1FE1. Top: parallel (left panel) and normal (right panel) views with respect to the membrane plane of the photosystem II complex. In red and blue are the D1 and D2 subunits which bear the main redox cofactors involved in water oxidation (shown in green). Bottom: The structural arrangement of the redox active components of photosystem II.

splitting enzyme. As shown in Figure 1, despite the arrangement of the various redox cofactors in two symmetrical branches with respect to a pseudo C_2 symmetry axis perpendicular to the membrane plane, electron transfer only proceeds down one of these two branches indicating that function does not strictly follow structure.

The Water Splitting Enzyme

As just described, conversion of light energy into electrochemical energy is a one-electron process. However, water oxidation into dioxygen is a four-electron process. Taking advantage of the possibility to trigger the light-induced electron-transfer reaction by short light flashes P. Joliot showed that the oxygen emission yield is maximum after the third, seventh, eleventh… flash of a series (Figure 2). This oscillating pattern with a periodicity of four was modeled by B. Kok who postulated, on this basis, the existence of a charge storing device allowing, in a single catalytic unit associated with PSII, the accumulation of the four oxidizing equivalent needed to split water into oxygen. In this model, illustrated in Figure 2, the catalytic center has five different oxidation states (S_0, S_1, S_2, S_3, and S_4). Four successive light-induced oxidation triggers the four successive transitions between the S_i and S_{i+1} states. Upon S_4 formation, oxygen is produced and released while S_0 is regenerated. The beauty of the Kok model resides in its ability to fully describe the function of the enzyme without any assumption neither on the chemical nature of the transient states it involves, nor on the precise mechanism underlaid by the successive transition between the S states. This accounts for its success as a working model ever since it was enounced. Simultaneously to the discovery of this charge-storing device,

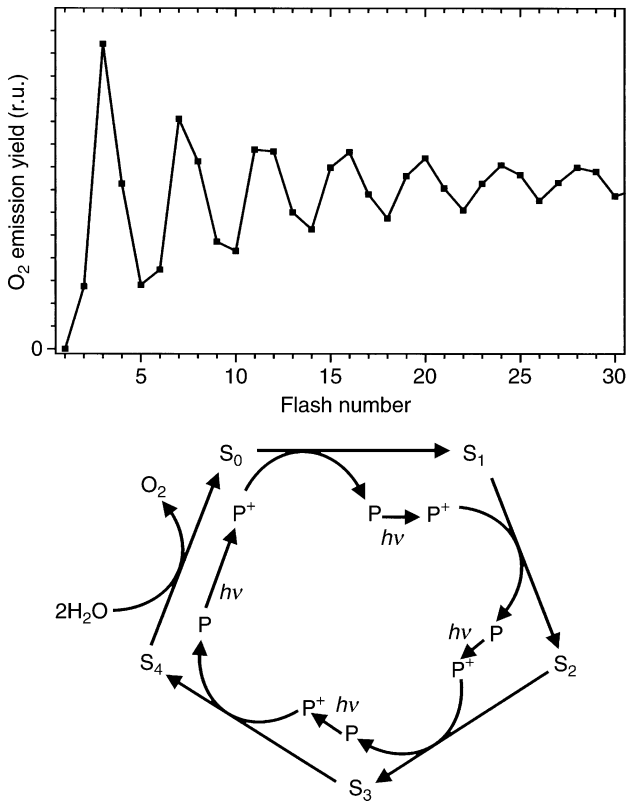

FIGURE 2 Top: The O_2 emission yield as a function of the flash number in a series. Note that this yield depends on the flash number with a periodicity of four. Bottom: The charge storing device allowing accumulation of the oxidizing power needed to split water as modeled by Kok.

Cheniae and co-workers evidenced the requirement for manganese atoms in water splitting. The determination of a stoichiometry of four Mn atoms per PSII complexes provided the chemical basis for the catalytic center where the accumulation of the oxidizing equivalent produced by light-induced charge separation occurs. Together with this manganese cluster, the catalytic center bears two ions, Ca^{2+} and Cl^-, which may be removed by various chemical treatments. In the absence of either one of these two ions, the lower S states (S_0 and S_1) may undergo oxidation but the advancement of the Kok cycle cannot be completed and water splitting is inhibited. The water splitting enzyme further comprises extrinsic polypeptides, which stabilizes the assembled tetranuclear cluster.

The Assembly of the Manganese Cluster

The ligands involved in the Mn cluster binding to the protein backbone are provided by the polypeptide D_1. They have not been all identified but amongst the good candidates are: three histidines, three carboxylic acids, and the C terminus alanine. The assembly of the Mn cluster requires Mn^{II}, in the $Mn(OH)^+$ or $Mn(OH)_2$ form, Ca^{2+}, Cl^- and light. The absorption of light by PSII produces the oxidant Y_Z^{ox},which oxidizes the Mn^{II} ions. The first oxidation of a Mn^{II} has a high quantum yield unlike the following steps which are needed for the oxidation-induced association of the stable tetra nuclear cluster.

The Thermodynamic and Kinetic Features of the Water Splitting Enzyme

Before attempting to address the mechanism of water oxidation one should question the thermodynamic and kinetic issues of this reaction. Obviously water is a very stable molecule under physiological condition, while its oxidation into molecular oxygen is likely to involve the transient formation of highly reactive species such as oxo-radicals, hydrogen peroxides, etc. The enzyme must meet the following requirements: accumulate enough oxidizing power to perform a very demanding reaction with respect to common biological redox potential but also prevent side reactions, which are thermodynamically made possible by the accumulation, in a single catalytic site, of such an oxidative power.

The Redox Potential of the Different S States

Until now, the redox potentials of the different S states have not been determined by direct redox titration. They could only be inferred from the redox potentials of other cofactors found in the PS II reaction centers combined with the free energy change associated with the electron transfer reaction between the S states and these cofactors. There are thus large error bars on the value, which can be found in the literature. The redox potential of the P^+/P couple, which drives the catalytic cycle, has been estimated to 1.1–1.3 V, making the P^+ species the strongest oxidant found in biology. With an estimated midpoint potential of $\sim$0.75 V, the S_1/S_0 couple lies $\sim$0.5 V below the P^+/P couple whereas the S_2/S_1, S_3/S_2, and S_4/S_3 midpoint potentials are estimated to $\sim$1 V. The overall free energy available to oxidize water is thus $\sim$3.75 V. This is sufficient to drive the reaction at neutral pH (the minimal driving force required to reversibly oxidize water at pH 7 is 0.81 V per electron) but becomes low when the reaction has to occur at a pH close to 5, a value often quoted when the photosynthetic chain is at work.

The Rates of Oxidation of the Various S States

The rates of the various electron transfer reactions between the oxidized tyrosine Y_Z^{ox} and the S-states S_i are in the tens or hundreds of microseconds for the three lower S states. The S_4 to S_0 transition is significantly slower, in the millisecond time range, and concomitant with O_2 production and release. Based on the distance between the electron acceptor Y_Z^{ox} and the Mn cluster (7Å) combined with the free energy changes associated with these reactions, these rates appear much too slow for the reaction to be kinetically limited by the electron transfer proper. This has been taken as an indication of either redox-induced structural changes or/and of a coupling with other processes than electron transfer such as proton transfer. Interestingly, a lag phase of a few tens of microseconds preceding the decay of S_4 into S_0, which is accompanied by O_2 release might evidence such events.

The Structure of the Catalytic Center and the Redox Events during the Reaction Cycle

Despite the tremendous amount of effort put into its elucidation, the structure as well as the valence of the Mn cluster are still matters of strong debate. Numerous sophisticated spectroscopic methods have been used to address this issue without completely succeeding to define a clear picture. Electron paramagnetic resonance (EPR) and X-ray absorption spectroscopy were by far the most productive methods and provided a set of possible structures. Recently, a low resolution crystallographic structure put additional constraints on the structures, which can be considered.

The Structure of the Manganese Cluster

The light-induced formation of the S_2 state results in a remarkable EPR signal which was first reported by Dismukes and Siderer. This signal shows very rich hyperfine structures (it is commonly referred to as the "multiline" signal), which have been taken as the spectroscopic signature of a mixed valence dinuclear Mn cluster. The multiline signal has provided experimental basis for modeling the structure and the valence state of the Mn cluster in the S_2 state. X-ray absorption spectroscopy (EXAFS), pioneered by M. Klein, has provided valuable data on the distances separating the heavy atoms such as Mn or Ca, which are found in the catalytic center. These data put severe constraints on the possible structures. From both the EPR and EXAFS data, a dimer of di-μ-oxo Mn dimers has long been favored. However, several other structures with oxo-bridged Mn atoms are compatible with the data. Although not settled yet, the debate seems to be converging to structures with three strongly coupled Mn and one weakly coupled Mn. Indeed the electron density map obtained by Zouni *et al*. can accommodate these structures but not the earlier favored dimers.

The Redox Events during the Catalytic Centers

As alluded to above, EPR and X-ray spectroscopies have also generously fed the debate on the valence state of the tetranuclear cluster during the catalytic cycle. Mn edge absorption spectroscopy has provided strong evidences for oxidation of an Mn atom during the S_0 to S_1 and S_1 to S_2 transitions. EPR and (less clearly) UV spectroscopies supported this view. Based on a kinetic analysis the S_4 is equivalent to the $[S_3Y_Z^{ox}]$ state. This seems to ground the accumulation of four oxidizing equivalents within the catalytic center (which would then include Y_Z as a partner), before water is oxidized. Yet, the assignment of the substrate of the oxidation associated with the S_2 to S_3 transition is still an open question. This ambiguity mainly comes from the fact that depending on the group involved in these studies, X-ray absorption spectroscopy shows either a shift in the absorption edge consistent with a Mn oxidation, or little, if any, shift in the absorption edges, ruling out this latter assignment and favoring the formation of a radical species. Unfortunately other spectroscopies such as EPR or UV absorption did not provide either unequivocal results. The disappearance upon S_3 formation of the EPR "multiline signal" arising from S_2 could be taken as a strong support for a Mn oxidation. However, this disappearance could be as well accounted for by a magnetic interaction between a radical species and the Mn cluster as argued by Styring, Rutherford, and Boussac.

The Mechanism of Water Oxidation

If indeed, the S_2 to S_3 transition involves the formation of a radical species, the possibility arises that a water molecule is oxidized during this step. If, on the contrary, the three successive steps leading to the formation of S_3 only involve Mn oxidation, an obvious conclusion is that water oxidation only takes place after the formation of S_4 (i.e., $S_3Y_Z^{ox}$). As just seen, this alternative could not be settled by spectroscopic approach. However, recent experiments on substrate binding tilt the scale toward

the latter and further constrain the inventiveness when attempting to draw possible mechanism for water splitting.

Substrate/Bulk Water Molecule Exchange

In a series of very elegant studies, Hillier and Wydrzynski have used isotopically labeled water ($H_2\ ^{18}O$) and measured the release of either O_2^{34} or O_2^{36} after a rapid mixing with PSII in the presence of unlabeled water. Most interestingly, they observed that substrate water may be exchanged with bulk water up to the S_3 state. This has been, until now, the strongest result in favor of a O–O bond-formation step occurring after S_3 is formed and thus during the S_4 to S_0 transition.

Proton Release during the Catalytic Cycle

The oxidation of two water molecules does not only release oxygen as a byproduct but also four protons. From the pioneering work of Fowler it is known that proton release accompanies the S_i to S_{i+1} transitions, which precedes the final S_4 to S_0 step during which O_2 is released. However, it is commonly agreed that these proton release events do not result from water chemistry. Indeed, proton transfers are often associated with redox changes either when the species which undergo the redox change is itself protonated or when the change in electrostatic potential resulting from the redox change shifts the affinity of a nearby acid group for proton. The two non-exclusive processes are likely to be at work, simultaneously or not, during the S_0 to S_1, S_1 to S_2, and S_2 to S_3 steps. The different groups which are deprotonated during these steps would be reprotonated by the protons produced during water oxidation. Although they most probably do not originate from water splitting, the proton release events occurring during the first three steps do play an important role in the overall water chemistry. They obviously compensate the charge accumulation which would otherwise result from three successive electron abstractions from a single catalytic unit. They control the thermodynamics of the enzyme by modulating the redox potential of the successive intermediate.

The Mechanisms for O_2 Formation

As discussed above, many issues regarding the catalytic cycle are still obscure. This may explain why there are almost as many mechanistic models for water splitting as groups studying this fascinating enzyme. It is beyond the scope of the present overview to present them all. As described Mn atoms are oxidized during some, if not all, transitions between S states. Obviously many models have incorporated these results and are based upon Mn-centered redox chemistry. There is a trend toward mechanisms in which only two among the four Mn atoms really participate in the water chemistry. The oxo or μ-oxo bridges which are thought to link the Mn atoms may also participate to the formation of the final O–O product. Last, the tyrosine Y_Z could play a crucial catalytic role. As discussed above, the S_4 state is equivalent to the $[S_3Y_Z^{ox}]$ state so that Y_Z may be considered as a full member of the catalytic center. The close proximity between Y_Z and the Mn cluster supports this view. Furthermore the phenolic oxygen of the tyrosine side chain is protonated when Y_Z is in the reduced state, whereas EPR spectra shows Y_Z^{ox} is deprotonated. Its reduction must thus be accompanied by its reprotonation. This led G. Babcock to propose that Y_Z could act as H atom abstractor undergoing a simultaneous reprotonation and reduction at the expense of water molecule. Although it seems to be agreed that this process does not occur on each step, as previously proposed, this model is largely resorted to for the higher S-states transitions.

Perspective

Obviously important questions such as when and how does water oxidation chemistry come into play are still unsettled. However, as illustrated by the recent release of new structural models by Shen or Iwata and Barber, the expected improvement in our knowledge of PSII at the atomic level should clarify if not solve some of the remaining ambiguities. Yet, it will not put an end to the sparkling development of models and concepts since identifying the different intermediate states during the overall reaction is a constantly renewed challenge, which is likely to be taken up by the field.

Glossary

chlorophyll excited state State that is formed after absorption by a chlorophyll molecule of a light quantum. At the molecular orbital level it corresponds to the hopping of an electron from the highest occupied molecular orbital to the lowest unoccupied molecular orbital.

oxidation De-electronation reaction or abstraction of an electron from a molecule.

reduction Electronation reaction. An electron transfer reaction occurs between an electron donor (which is oxidized) and an electron acceptor (which is reduced). In the case of photosynthetic water oxidation, two molecules of water (H_2O) are oxidized into molecular oxygen and serve as an electron source.

S_i states Successive states, as defined by B. Kok, formed during the accumulation in the catalytic center of the water-splitting enzyme of the oxidizing power required to split water into dioxygen. The transition from state S_i to state S_{i+1} reflects the abstraction of one electron from the catalytic center.

Further Reading

Cramer, W. A., and Soriano, G. M. (2000). Thermodynamics of energy transduction in biological membranes. Biophysics Textbook Online http://www.biophysics.org/btol/bioenerg.html#1.

Debus, R. J. (2000). The polypeptides of Photosystem II and their influence on mangano-tyrosyl-based oxygen evolution. In *Metal in Biological Systems* (H. Sigel and A. Sigel, eds.) Marcel Dekker, New York.

Diner, B. A., and Babcock, G. (1996). In *Oxygenic Photosynthesis: The Light Reactions* (D. R. Ort and C. F. Yocum, eds.), pp. 213–247. Kluwer Academic Publishers, Dordrecht, The Netherlands.

Goussias, C., Boussac, A., and Rutherford, A. W. (2002). Photosystem II and photosynthetic oxidation of water: An overview. *Philos. Trans. R. Soc. Lond. B Biol. Sci.* **357**, 1369–1381.

Hoganson, C. W., and Babcock, G. T. (1997). A metalloradical mechanism for the generation of oxygen from water in photosynthesis. *Science* **277**, 1953–1956.

Lavergne, J., and Junge, W. (1993). Proton release during the redox cycle of the water oxidase. *Photosynt. Res.* **38**, 279–296.

Lavergne, J., and Joliot, P. (2000). Thermodynamics of the excited states of photosynthesis. Biophysics Textbook Online http://www.biophysics.org/btol/bioenerg.html#2.

Nicholls, D. G., and Ferguson, S. J. (2002). *Bioenergetics 3*. Academic Press, London.

Nugent, J. (ed.) (2001). Photosynthetic water oxidation. *Biochim. Biophys. Acta* **1503**(1–2), 1–260.

Biography

Fabrice Rappaport joined Pierre Joliot's Lab in 1990 and holds a permanent position in the Centre National De La Recherche Scientifique. His principal interests are in proton and electron transfer in photosynthetic bioenergetic chain.

Pierre Joliot is a Professor Honoraire at the Collège De France And member of the French And United States Academies Of Science. He has developed tools to study the photosynthetic process *in vivo* and is mainly interested in the photosynthetic electron transfer chain with an emphasis on its supramolecular organization.

Plant Signaling: Peptides

Clarence A. Ryan and Gregory Pearce
Washington State University, Pullman, Washington, USA

Peptide hormones are extracellular signaling molecules that are found in animals, yeast, and plants. In animals, many physiological processes are regulated by peptide signals including, for example, metabolism, cell division, growth, pain, well-being, reproduction, and immunity. Before 1991, plants were thought to utilize small, non-peptide organic molecules called phytohormones, to regulate all physiological processes. Since then, over a dozen peptide hormones have been isolated from plants, or identified by genetic approaches, that regulate physiological processes, such as defense, cell division, growth and development, and reproduction.

Many similarities exist between some animal and plant peptide hormones, their receptors, and their signaling pathways, indicating that they may have evolved from common ancestral origins. Several plant peptide hormones and their precursor are shown in Figure 1. Plant peptide hormones and their receptors provide new approaches for improving crop yields and for the production of phytochemicals for industry and medicine.

Systemins

Tomato Systemin

The tomato systemin peptide $^{+}$AVQSKPPSKRD PPKMQTD^{-} is composed of 18 amino acids and is derived from a 200 amino acid precursor protein. The precursor, called, prosystemin, differs from animal peptide hormone precursors in that it lacks a signal sequence at its N terminus and is not synthesized through the secretory pathway. The potency of systemin is similar to animal peptide hormones, being active in the nanomolar range. The function of systemin as a primary signal for the activation of defense genes was confirmed by producing transgenic tomato plants that constitutively express an antisense prosystemin gene. The plants do not exhibit a systemic induction of proteinase inhibitors in response to *Manduca sexta* larval damage or to other mechanical wounding, and the larvae rapidly consume the plants in contrast to the less palatable wild-type plants.

Prosystemin genes are present in various solanaceous species, but not all, and its gene has not been identified in any other plant family. Why and how systemin evolved as a systemic wound signal only in some solanaceous species is not known. The mechanism for the release and transport of systemin through the plants is also not understood, but its long range signaling effects in response to wounds caused by attacking insects are thought to involve a mechanism for amplification of the signal. The presence of prosystemin in vascular bundle cells suggests that its localization there is important for long distance signaling. The proteolytic processing of prosystemin does not involve the typical dibasic sites usually found for processing of animal secretory prohormones. Processing enzymes that convert prosystemin to systemin have not been identified, nor have the initial cleavage sites.

Systemin exhibits only weak structural features in aqueous solutions, which reflect a poly(L-proline) II, 3_1 helix secondary structure that is due to the two proline doublets in the central region of the peptide. The resulting kinks in the peptide appear to be important for recognition by its receptor. The systemin receptor is a 160 kDa membrane-bound protein. It is a leucine-rich repeat (LRR) receptor kinase with a K_d of about 10^{-10} M, which is generally similar to many peptide-LRR receptor kinase interactions found in animals.

Systemin activates a complex signaling pathway that is analogous to the inflammatory response in animals. Early events following the systemin-receptor interaction include the activation of a MAP kinase and a phospholipase that cleaves linolenic acid from membranes, in much the same manner as arachidonic acid is released from animal membranes in response to cytokines. In plants, linolenic acid is converted to the oxylipin, jasmonic acid, a powerful inducer of defense genes, while in animals arachidonic acid is converted to the oxylipin prostaglandins, a mediator of inflammation.

Tomato and Tobacco Hydroxyproline-Rich Glycosylated Defense Signals

Other peptide signals have been associated with the activation of defense genes in response to herbivore attacks; two in tobacco leaves and three in tomato leaves. These peptides range from 15 amino acids to

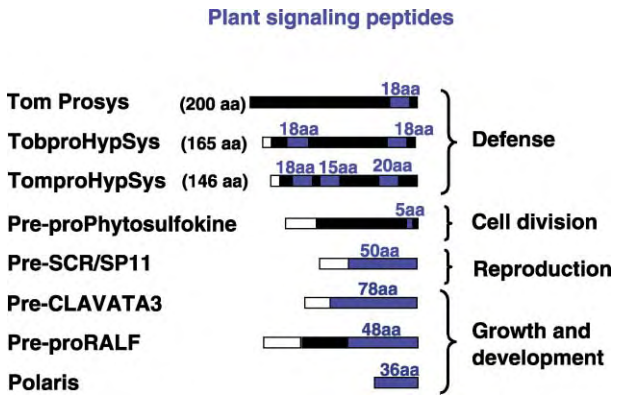

FIGURE 1 Box representations of plant peptide hormones and, where known, the precursor proteins from which they were derived. The locations of the peptides within the precursor are designated by the blue boxes.

20 amino acids in length and are structurally different from systemin in that they are hydroxyproline-rich and are glycosylated. This suggests that they are synthesized through the secretory pathway. The peptides activate proteinase inhibitor genes when supplied to plants at nMolar levels. Because of their sizes and their biological activites in signaling the activation of defense genes, they have been assigned to the systemin family, which is now a functionally defined family of peptide defense signals that are derived from plants.

The tobacco peptides are called Tobacco Hydroxyproline-rich Systemins, abbreviated to TobHypSys I and TobHypSys II. Wounding tobacco leaves results in a strong local response but a very weak systemic response, and these peptides are thought to be involved in signaling that is localized within the wounded leaves. The two tobacco systemins are derived from a single precursor protein of 165 amino acids that includes a signal sequence, with TobHypSys I sequence near the N terminus and TobHypSys II sequence near the C terminus.

The three tomato peptides, called TomHypSys I, II, and III, may also be localized signals, since prosystemin antisense tomato plants do not respond systemically to wounding but do generate a substantial localized wound response. As in tobacco, the localized defense response may result from the release of the TomHypSys peptides near the wound sites. The three TomHypSys peptides are derived from a single 146 amino acid precursor that has a leader peptide at its N terminus. Multiple peptide signals derived from a single precursor, as found with both TobHypSys and TomHypSys peptides is a scenario that is often found among precursors of peptide hormones in animals.

Standard protein–protein and nucleotide–nucleotide searches for cDNAs and pre-proproteins with homologies to the systemin precursor genes did not reveal homologues in other plant species, but short regions (less than 10 amino acids) in the N and C termini of the TomHypSys and TobHypSys precursors exhibit identity, suggesting that their genes may have evolved from a common ancestor.

Peptide Signals for Growth and Development

Phytosulfokine

A sulfated pentapeptide, called phytosulfokine (PSK), with the structure Tyr(SO_3H) -Ile-Tyr(SO_3H) -Thr-Gln, regulates plant cell proliferation. The peptide was initially found to cause low-density suspension cultured cells to proliferate rapidly. PSKs with identical structures are found in many plants, where they are derived from larger precursor pre-proproteins. The rice (*Orizae sativa) PSK* gene, for example, is a single-copy gene consisting of one large intron and two exons. The gene codes for a PSK pre-prohormone precursor of 89-amino acids including a leader peptide, suggesting that it is synthesized through the secretory pathway, where sulfation and processing occur. Sulfated tyrosines are often found in animal proteins, but to date PSK is the only example of a post-translational sulfated tyrosine in plants.

PSK is the ligand for a 150 kDa membrane-bound LRR receptor kinase with a K_d in the nMolar range. It plays *in vivo* functional roles in differentiation of cell cultures of zinnia into tracheary elements, in somatic embryogenesis in carrot, in the induction of adventitious root and bud formation in *Antirrhinum* callus, and in the formation of adventitious roots on cucumber hypocotyls. These effects of PSK require the presence of various levels of two small phytohormones, auxin, and cytokinin, indicating that PSK is part of a complex, but integrated, signaling network.

Clavata3

Clavata3 (CLV3) is an extracellular signaling polypeptide composed of 96 amino acids of which 18 residues comprise an N-terminal leader peptide. CLV3 and its receptor CLV1 have been studied extensively in *Arabidopsis thaliana*. CLV3 helps determine the fate of cells in shoot apical meristems (SAM). The identity and position of aerial organs in plants is initiated and established in the SAM, where a balance between the division of stem cells and differentiation is maintained as the plant grows. The stem cells divide slowly while the surrounding cells divide and differentiate.

No evidence is available to support any further processing of CLV3 after removal of the signal peptide, but dibasic or monobasic residues are present internally

that could be candidates for processing sites to produce smaller peptides that may have a role in signaling.

The CLV3 receptor, CLV1, is an 980 bp LRR receptor kinase that is associated with a 720-amino acid LRR receptor-like protein lacking a kinase domain. The CLV3-receptor complex results in autophosphorylation, leading to the binding of downstream signaling proteins as an early step in stem cell differentiation.

SCR/SP11: Signals for Self-Incompatibility

A family of intercellular signaling peptides of 47–60 amino acids in length play a central role in pollen self-incompatibility in the Brassicaceae family. The peptides are cumulatively called S-locus Cysteine Rich proteins (SCR) or S-locus Protein 11 (SP11), and are signals from the pollen that determine incompatibility when recognized by the appropriate receptor. During pollination, as pollen comes in contact with the papilli of the stigma, a self-recognition occurs that results in dehydration of the papilli and cessation of the pollenation process. SCR/SP11 peptides are found as a large gene family of 28 members that are derived from cysteine-rich pre-proteins of 74–83 amino acids in length that include leader peptides. In contrast to animal and plant leader peptides, the amino acid sequences of the SCR/SP11 leader peptides are highly conserved, while the mature SCR/SP11 peptides share only weak identities except at the eight cysteine positions that are conserved among most of the family members.

SCR/SP11 interacts with an S-locus Receptor Kinase (SRK). The receptor in Arabidopsis is composed of 858 amino acids including a 31 amino acid leader peptide. It is localized in membranes associated with the cell walls of stigma papillae. The SRK has a functional serine/threonine kinase at its C terminus with a transmembrane region in the middle and an extracellular cysteine-rich domain at its N-terminal region. An abundant soluble 60 kDa S-Locus Glycoprotein (SLG) appears to be associated with SRK and is often present in a 100-fold excess and appears to facilitate a functional SCR/SRK/SLG complex that results in signaling intracellular events leading to dehydration and incompatibility.

RALF, a Signal for Root Growth

The rapid alkalinization factor, called RALF, is a 49 amino acid peptide that is derived from the C terminus of a 115-amino acid precursor that contains a 25 amino acid leader peptide at its N terminus. RALF was named because of its ability to cause a rapid alkalinization of suspension cultures of tomato, tobacco, and alfalfa. Databases revealed the existence of RALF homologues in more than 15 plant species from nine families, present in a variety of tissues and organs. Two binding proteins of 120 and 25 kDa are thought to be part of a receptor complex that recognizes RALF to initiate a signaling pathway. The addition of micromolar solutions of tomato RALF to germinating tomato and Arabidopsis seedlings caused root growth to immediately cease. RALF inhibits both cell elongation and cell division. While its specific biochemical role in plants is not known, the ubiquity of the RALF peptides suggests that they have a fundamental physiological role in different organs and tissues of the plants. Nine RALF genes are present in Arabidopsis that contain highly conserved RALF sequences. The N-terminal amino acid sequences of each RALF precursor are much less conserved than the C-terminal sequences encoding the RALF peptide. The presence of two Arg residues just upstream from the putative N termini may be a recognition site for processing enzymes. The region just upstream of the dibasic site is rich in polar residues that are highly conserved among RALF precursors from different species and, as in animals, may be part of a recognition site for a RALF-processing proteinase.

Other Signaling Peptides

Several other peptides have been suggested to be hormone-like signaling molecules in plants with various roles related to growth, development, and differentiation. A small peptide of 36 amino acids lacking a signal peptide is translated from a 450 bp mRNA in Arabidopsis seedlings and root tips. This peptide, called POLARIS, is required for cytokinin and ethylene signaling during root growth, but its specific role in signaling is not known.

Several laboratories have looked for homologues of animal peptide hormone genes in plants, but none have been found.

Concluding Remarks

Since the discovery of insulin in 1922, hundreds of peptide hormones have been found in animals that regulate fundamental physiological processes. Over a dozen peptide hormones have now been identified in plants, establishing a new frontier for studies of plant growth, development, reproduction, defense, and responses to the environments. In many respects the properties of plant peptide hormones resemble those of animals, but several plant peptides have unique properties, indicating that the diversity of properties of peptide signals in plants may be the rule, rather than the exception. It is not clear whether all peptide signaling traces back to a common ancestral signaling system, or if

peptide signaling was reinvented many times by nature during the evolution of plants and animals. It is clear that peptide signaling has conferred a distinct advantage to the organisms, whether animal or plant. The recent discovery of peptide signals has laid to rest the long held hypothesis that all plant processes are regulated by small phytohormones.

To date, the receptors for peptide hormones appear to be either LRR receptor kinases or cysteine-rich receptor kinases (SRK). Although only a small number of plant peptide hormones and their receptors have been identified, peptide signaling in plants has become a focus of inquiry to gain a better understanding of plant signaling. Peptide signaling is a new area of research for the discovery of fundamental knowledge about plants. Such knowledge holds promise to reveal novel regulatory systems that can be used for biotechnological approaches to improve man's environment, to increase crop yields, and to provide nutraceuticals and medicines for human health.

See Also the Following Articles

G Protein-Coupled Receptor Kinases and Arrestins • Mitogen-Activated Protein Kinase Family• Glycoproteins, Plant

Glossary

Arabidopsis thaliana A small plant of the Cruciferae family with a very small genome that serves as a model for biochemical and genetic studies of plants.

leader peptides Short N-terminal amino acid sequences of nascent polypeptides that target the proteins to the Golgi for processing and secretion, and are removed by leader peptidases during transport across the Golgi membrane.

peptide hormones Intercellular signaling peptides.

phytohormones Small organic molecules that regulate numerous processes in plants. These hormones include auxins, gibberellins, cytokinins, ethylene, abscissic acid, and brassinolides.

shoot apical meristem The region of the growing tip of a plant shoot in which stem cells are produced and differentiate into plant organs as the plant grows.

systemins A functionally defined family of signaling peptides from plants that are released at sites of herbivore or pathogen attacks and activate defensive genes.

Further Reading

Bergey, D., Howe, G., and Ryan, C. A. (1996). Polypeptide signaling for plant defensive genes exhibits analogies to defense signaling in animals. *Proc. Natl Acad. Sci (USA)* **93**, 12053–12058.

Fletcher, J. C., Brand, U., Running, M. P., Simon, R., and Meyerowitz, E. M. (1999). Signaling of cell fate decisions by *CLAVATA3* in Arabidopsis shoot meristems. *Science* **283**, 1911–1914.

Kachroo, A., Nasrallah, M. E., and Nashallah, J. (2002). Self-incompatibility in the Brassicaceae: Receptor–ligand signaling and cell-to-cell communication. *Plant Cell* **14**, S227–S238.

Kende, H., and Zeevaart, J. A. D. (1997). The five "classical" plant hormones. *Plant Cell* **9**, 1197–1210.

Ryan, C. A., Pearce, G., Moura, D., and Scheer, J. (2002). Polypeptide hormones. *Plant Cell* **14**, S251–S264.

Suzuki, G., Kai, N., Hirose, T., Fukui, K., Nishio, T., Takayama, S., Isogai, A., Watanabe, B., and Hinata, K. (1999). Genomic organization of the S locus: Identification and characterization of genes in SLG/SRK region of S^9 haplotype of *Brassica campestris* (syn. rapa). *Genetics* **153**, 391–400.

Yang, H., Matsubayshi, Y., Hanai, H., and Sakagami, Y. (2000). Phytosulfokine-α, a peptide growth factor found in higher plants: Its structure, functions, precursor and receptors. *Plant Cell Physiol.* **41**, 825–830.

Biography

Clarence Ryan is a Professor of Biochemistry in the Institute of Biological Chemistry at Washington State University. He received a Ph.D. from Montana State University, Bozeman, MT, and was a postdoctoral fellow at Oregon State University, Corvallis, OR and at the USDA Pioneering Laboratory in Albany, CA.

Gregory Pearce is the Senior Laboratory Supervisor in the Ryan laboratory. He received his B.S. in Biochemistry and M.S. in Animal Nutrition at Washington State University.

Plasma-Membrane Calcium Pump: Structure and Function

Emanuel E. Strehler
Mayo Clinic College of Medicine, Rochester, Minnesota, USA

Plasma-membrane calcium pumps, also called plasma-membrane calcium ATPases (PMCAs), are integral membrane proteins responsible for the expulsion of ionized calcium (Ca^{2+}) from the cell interior to the extracellular milieu. They use adenosine triphosphate (ATP) as energy source to pump Ca^{2+} "uphill" against a large concentration gradient, thereby ensuring that the resting free intracellular Ca^{2+} concentrations remain low and that Ca^{2+} signaling can occur with fidelity and spatial precision.

Plasma-Membrane Calcium Pump Abundance and Isoforms

Plasma-membrane calcium pumps are ubiquitous in eukaryotic cells, although there are differences in expression during development in various tissues and even among different membrane domains within the same cell.

Isoforms

In mammals, multiple plasma-membrane calcium pumps are generated from multigene families and via alternative RNA splicing, giving rise to pump isoforms with distinct regulatory and functional properties. Humans, rats, mice, and other mammals express four distinct genes (human genome database nomenclature ATP2B1–ATP2B4) coding for PMCA isoforms 1–4. Alternative RNA splicing of the primary gene transcripts occurs at two major sites (called splice sites, A and C) and involves multiple exons that can either be spliced out or wholly or partially retained in the final mRNA (Figure 1). Combinatorial alternative splicing produces multiple splice variants of each PMCA isoform.

Expression

Development

Plasma-membrane calcium pumps are differentially expressed during mammalian development, though mouse embryonic stem cells express all four PMCA genes. In mice, PMCA1 is expressed from the earliest embryonic stage identified, and is ubiquitously present in all tissues. PMCA 2, 3, and 4 are first detected at ~12 days postcoitum and show a changing and restricted tissue distribution during embryonic development. PMCA2 is essentially confined to neuronal tissues, PMCA3 initially shows widespread expression but eventually becomes restricted to the nervous system and muscle, and PMCA4 is transiently expressed at high levels in the liver but then becomes less abundant and more evenly distributed in multiple tissues including the brain, heart, and intestine.

Tissues

In the adult, PMCA1 and PMCA4 are expressed in virtually all tissues, with PMCA1 normally being the most abundant isoform. PMCA2 is largely confined to nervous tissue as well as to epithelia of the breast and kidney, and PMCA3 is expressed at generally low levels and restricted to specific areas in the brain and to skeletal muscle.

Cells

Differential distribution of PMCA isoforms in different plasma membrane domains has been demonstrated in many cell types, notably in highly polarized cells such as retinal photoreceptors, auditory, and vestibular hair cells, cerebellar Purkinje cells, and epithelial cells. In cochlear hair cells, for example, PMCA2 is exclusively and highly expressed in the apical stereocilia, whereas PMCA1 may be concentrated along the basolateral membrane and close to synaptic terminals.

Plasma-Membrane Calcium Pump Structure

The overall structure of plasma-membrane calcium pumps resembles that of the calcium pump of the

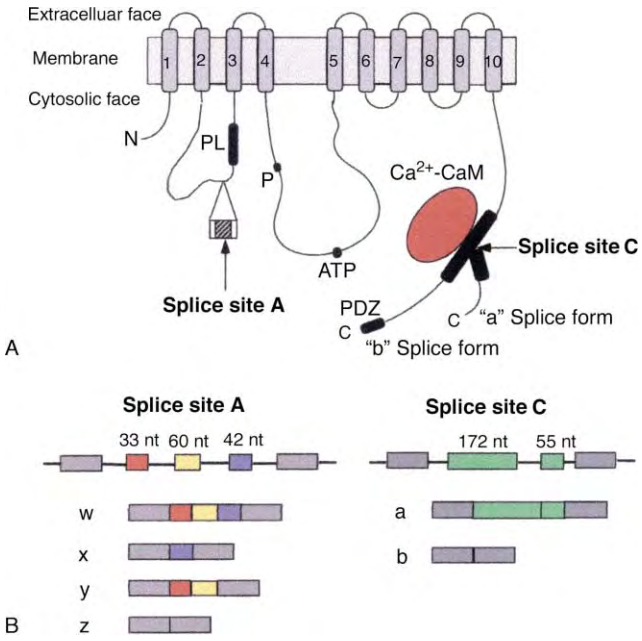

FIGURE 1 (A) Schematic model of the plasma membrane calcium pump, showing the major domain substructure. The ten transmembrane regions are numbered and indicated by shaded boxes. The cytosolic amino- (N) and carboxyl-terminal (C) ends are labeled, and a phospholipid-sensitive region (PL), the calmodulin-binding region and the C-terminal PDZ domain binding sequence of the "b" splice forms are shown as black boxes. P is the site (aspartate residue) of the obligatory aspartyl-phosphate formed during each Ca^{2+} transport cycle, and ATP denotes the specific residues involved in nucleotide (ATP) binding. The PMCA is shown in its active form, with Ca^{2+}-loaded calmodulin (Ca^{2+} -CaM, red oval) bound to the regulatory C-terminal tail. Arrows labeled "splice site A" and "splice site C" denote the regions affected by alternative splicing. At site A, the peptide segment encoded by alternatively spliced exon(s) is indicated by a hatched box, and at site C, the two major splice variants (a and b splice forms) created by alternative splicing are drawn as separate carboxyl-terminal tails. (B) Major alternative splicing options for the generation of PMCA splice variants. The example given is that of human PMCA2. At splice site A, three exons (shown as red, yellow, and blue boxes) can be all excluded or variably included to generate splice variants w, x, y, and z. At splice site C, two exons (green boxes) are either included or excluded to generate splice variants a or b, respectively. The sizes of the exons in human PMCA2 RNA are indicated in nucleotides (nt). Constitutively spliced exons are shown as dark gray boxes. Note that the combinatorial use of splicing options at sites A and C can generate a large number of different PMCA variants.

sarco/endoplasmic reticulum membrane. Major features include intracellular amino- and carboxyl-terminal ends, ten membrane-spanning domains, and three distinct intracellular domains involved, respectively, in ATP binding (N-domain), formation of an obligatory phosphorylated intermediate (P-domain), and actuating large conformational movements (A-domain) to complete the catalytic cycle that links ATP hydrolysis to transmembrane movement of Ca^{2+} (Figure 2).

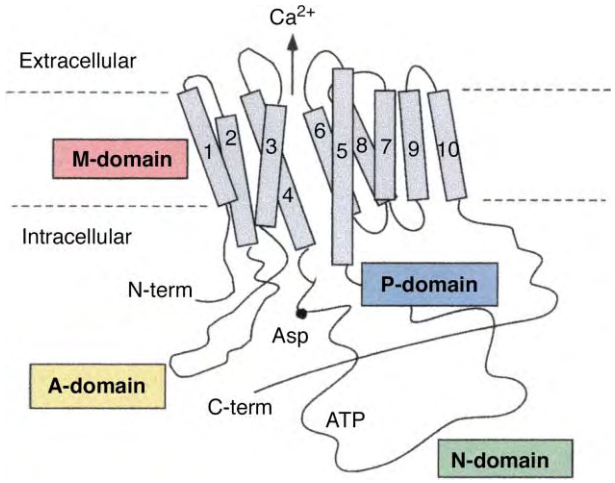

FIGURE 2 Folding and domain model of the PMCA based on structural homology to the sarco/endoplasmic reticulum calcium pump. The ten membrane-spanning regions are numbered and shown as gray cylinders forming the M-domain. The invariant aspartate residue (Asp) undergoing phosphorylation during the reaction cycle is indicated, as is the ATP-binding site (ATP). The three major cytosolic domains are labeled A (actuator), P (phosphorylation), and N (nucleotide-binding). The amino (N-term) and carboxyl ends (C-term) are indicated; the arrow shows the direction of Ca^{2+} pumping. The extended C-terminal tail is drawn to indicate its intramolecular interaction with other cytosolic domains as found in the autoinhibited state of the pump.

Mechanistic Aspects

The plasma-membrane calcium pumps belong to the superfamily of P-type ion-motive ATPases, where they are classified into the type II subfamily that also includes organellar Ca^{2+} ATPases, Na^+/K^+ ATPases, and H^+/K^+ ATPases. The salient feature of the P-type ATPases is the formation of a phosphorylated intermediate during the reaction cycle, whereby the γ-phosphate of ATP is transferred to an invariant aspartate residue in the central catalytic domain of the pump (see Figures 1 and 2). The basic reaction scheme for the stepwise cycling of the pump between conformational states which link ATP hydrolysis and ion translocation across the membrane is described by the E1–E2 model (Figure 3). In this scheme, the pump alternates between the E1 and E2 conformations, where the E1 state describes the pump with its ion (Ca^{2+}) sites facing the cytoplasmic side and the E2 state that of the pump having its ion sites facing the extracellular side. The energy of hydrolysis of one ATP molecule is required for each Ca^{2+} ion transported by the plasma membrane calcium pump. The Ca^{2+} transport cycle is accompanied by large conformational changes in the pump protein, whereby the reactions occurring at the cytoplasmic ATP binding and phosphorylation sites are coupled to the rearrangement of the membrane-spanning domains corresponding to the Ca^{2+} transport site. The positive charge

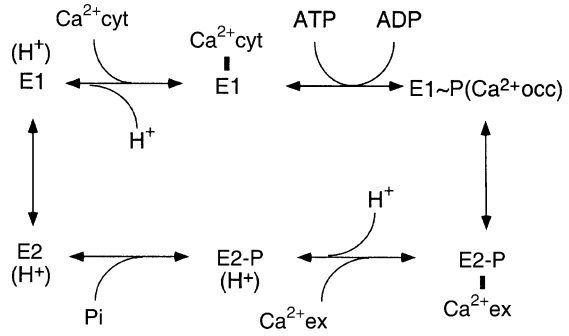

FIGURE 3 Reaction scheme of the plasma membrane calcium pump. The pump adopts two major states E1 and E2. The E1 state shows high affinity for Ca^{2+} on the cytosolic side of the membrane (Ca^{2+} cyt). Ca^{2+}-binding stimulates the ATPase activity of the pump, leading to the formation of the phosphorylated intermediate E1 ~ P and "occlusion" (occ) of the bound Ca^{2+} ion. Translocation of the Ca^{2+} ion across the membrane occurs concomitantly with the release of stored energy during the conformational transition from the E1 ~ P to the E2-P state. The Ca^{2+} affinity of the pump in the E2-P state is low and Ca^{2+} dissociates on the extracellular side of the membrane (Ca^{2+} ex). This is followed by hydrolysis of the phosphoenzyme and rearrangement of the E2 to the E1 state. The charge movement during Ca^{2+} transport is at least partially neutralized by countertransport of protons (H^+).

movement accompanying the transport of Ca^{2+} from the intracellular to the extracellular side of the membrane is at least partially compensated by countertransport of H^+ ions. When fully active, the turnover number of the PMCA is of the order of 50–100, i.e., a single PMCA molecule can pump about 50–100 Ca^{2+} ions per second across the membrane.

Domain Structure

The plasma-membrane calcium pumps can be divided into an N-terminal cytoplasmic domain followed by a first membrane-spanning hairpin loop, an intracellular loop making up most of the A-domain, a second membrane-spanning hairpin loop, the major cytosolic catalytic loop containing the nucleotide-binding and phosphorylation domains, three additional membrane-spanning hairpin loops and a final, cytosolic C-terminal domain containing multiple regulatory sequences (Figures 1 and 2). Based on structural homology to the sarco/endoplasmic reticulum calcium ATPase (SERCA) for which a high-resolution three-dimensional structure is available, the PMCAs consist of a compact membrane-embedded domain comprising the ten membrane-spanning regions, and of a large cytoplasmic domain that can be subdivided into the three well-separated A, N, and P domains (see Figure 2). The P (phosphorylation) domain of the PMCA assumes the structural-fold characteristic of haloacid dehalogenase. The three-dimensional structure of the C-terminal regulatory domain unique to the PMCAs is not yet known, but chemical cross-linking and proteolysis studies indicate that this domain is involved in extensive intramolecular interactions with the A and the N/P domains.

Plasma-Membrane Calcium Pump Regulation and Function

Plasma-membrane calcium pumps function to maintain and reset the low (~100 nM) intracellular Ca^{2+} concentrations required for effective Ca^{2+} signaling. Through multifaceted regulation, these pumps also participate in spatio-temporal Ca^{2+} signaling by restricting the spread of Ca^{2+} signals and reducing noise in local signal transduction.

Regulation

The calcium sensor protein calmodulin is a major regulator of the plasma-membrane calcium pumps. In general, the PMCAs are autoinhibited at very low cytosolic-free Ca^{2+} concentrations ($[Ca^{2+}]_i$ < 50–100 nM). Upon a rise in $[Ca^{2+}]_i$, Ca^{2+}-calmodulin activates the PMCAs by releasing the autoinhibition. Calmodulin binds to a specific binding site of varying length in the C-terminal tail of the PMCAs (Figure 1). Different PMCA isoforms and alternative splice variants show different affinities for Ca^{2+}-calmodulin, and hence are differently sensitive to rises in $[Ca^{2+}]_i$. The PMCAs are also regulated by phosphorylation. Protein kinases A and C phosphorylate specific residues in the C-terminal tail of various PMCAs downstream of and/or overlapping the calmodulin-binding domain. The effects of phosphorylation on PMCA activity are complex, involving both direct activation (by deinhibiting the pump) as well as interference with calmodulin regulation. Different PMCA isoforms and splice variants react differently to Ser/Thr phosphorylation in their C-terminal domains, depending on the specific sites of phosphorylation and the surrounding sequence context. Tyrosine phosphorylation also has been observed in some PMCAs and may lead to changes in the cellular distribution of the pumps. Additional regulatory mechanisms for the PMCAs involve activation by dimerization or oligomerization and stimulation by various acidic phospholipids (such as phosphatidic acid, phosphatidylinositol-phosphates). A phospholipid-sensitive region has been identified near the third membrane-spanning region in the A-domain (Figure 1). PMCA splice variants ending with the C-terminal amino acid sequence … GluThrSerVal or … GluThrSerLeu ("b" or CI splice variants, see Figure 1) bind directly to the PDZ (*PSD95/Dlg/ZO-1*) protein–protein interaction domain found in many scaffolding,

anchoring, and signaling proteins. These interactions may anchor the PMCAs to the submembraneous actin cytoskeleton and recruit them into multiprotein complexes with other membrane receptors, transporters, and signaling molecules.

Function: Resetting and Maintenance of Resting Calcium Levels

The primary function of the PMCAs has been traditionally linked to the maintenance of low resting levels of intracellular Ca^{2+}. In cell types such as human erythrocytes where the PMCA is the sole system for Ca^{2+} expulsion from the cytosol, the function of this pump is essential for Ca^{2+} homeostasis and normal cell physiology. Because of its low capacity (turnover number < 100) and low abundance in most membranes, the PMCA is not well suited to the mass evacuation of high Ca^{2+} loads that may occur after global Ca^{2+} influx (such as happens with every beat of a heart muscle). In these cases other, low-affinity but high-capacity systems such as the Na^+/Ca^{2+} exchangers are responsible for the bulk export of Ca^{2+} from the cell. However, with their high Ca^{2+} affinity in the fully activated state ($Kd_{Ca^{2+}} < 0.2\ \mu M$), the PMCAs are the only transport system of the plasma membrane capable of reducing cytosolic Ca^{2+} levels down to the required submicromolar and even nanomolar levels. The specific PMCA isoform and splice variant expression pattern enables each cell to fine-tune and maintain its $[Ca^{2+}]_i$, and to reset $[Ca^{2+}]_i$ to the resting level following transient increases generated by Ca^{2+} signals.

Function: Vectorial Calcium Transport And Local Calcium Signaling

In epithelia involved in transcellular Ca^{2+} transport, e.g., in the intestine and the distal kidney, the PMCAs are concentrated in the basolateral membrane of the cells where they play an important role in vectorial Ca^{2+} transport from the apical (intestinal lumen, kidney urinary lumen) to the basal (blood) side. In other tissues and cell types, e.g., in the choroid plexus and cochlear hair cells, specific PMCA isoforms are uniquely expressed in the apical plasma membrane where they are responsible for local Ca^{2+} transport into the cerebrospinal fluid and the endolymph, respectively. An important function of the PMCAs thus consists in their participation in localized Ca^{2+} transport to allow the selective enrichment of Ca^{2+} in a specific extracellular compartment. Besides their role in the maintenance of overall Ca^{2+} homeostasis, PMCAs also participate in Ca^{2+} signaling. Specific PMCA isoforms and splice variants are concentrated in multiprotein complexes localized in distinct membrane domains (e.g., in caveolae or at the neck of dendritic spines of hippocampal and cerebellar neurons). As part of "Ca^{2+} signalosomes," the PMCAs are involved in the spatial and temporal regulation of Ca^{2+} signaling. By preventing the spread of a local increase in Ca^{2+}, they contribute to the spatial resolution of Ca^{2+} signaling and suppress signaling "noise." By counteracting the local rise in Ca^{2+} following the temporary opening of influx channels, they also contribute to the termination of Ca^{2+} signaling and thus to its temporal regulation.

Diseases Linked to Plasma-Membrane Calcium Pumps

Specific human diseases linked to PMCA mutations or the lack of a particular PMCA isoform are not yet known. However, spontaneous mouse mutants called "deafwaddler" and "wriggle mouse Sagami" have been described in which mutations in the PMCA2 gene lead to a defective PMCA2 protein. Homozygous mutant mice are deaf and show an unsteady gait, underlining the importance of PMCA2 function in the auditory and vestibular hair cells. The same phenotype is observed in homozygous PMCA2 "knockout" mice, which are profoundly deaf and severely ataxic. By contrast, homozygous knockout mice lacking PMCA1 are embryonic lethal, as might be expected given the ubiquitous expression pattern of this PMCA. On the other hand, numerous disease conditions have been linked to abnormal expression of PMCAs. These include diabetes where a significant decrease in PMCA activity in erythrocytes has been described, and neurodegenerative disorders such as Alzheimer disease and stroke, where complex changes in PMCA isoform expression accompany or precede neuronal malfunction and death. Because of their large size (average > 100 kb), the human PMCA genes almost certainly suffer relatively frequent mutations. Many familial and "spontaneous" diseases with an incompletely understood etiology are therefore likely to be linked at least in part to abnormal PMCA expression and function.

See Also the Following Articles

ER/SR Calcium Pump: Function • ER/SR Calcium Pump: Structure

Glossary

alternative splicing Process in the cell nucleus whereby pieces of a primary gene transcript are optionally excised or included in the final messenger RNA. Translation of these differently spliced mRNAs normally leads to protein products that differ only in the region affected by the alternative splice.

apical membrane The part of the plasma membrane facing the lumen in polarized (asymmetric) epithelial cells separating two different extracellular compartments. The apical membrane is separated from the basolateral membrane by tight junctions formed between neighboring cells.

calcium signalosome Multiprotein complex of several functionally and physically linked proteins to allow the spatially defined generation and transmission of Ca^{2+} signals.

isoform A protein structurally and functionally similar to a given protein.

plasma membrane The lipid- and protein-rich structure defining the boundary between the extracellular space and the interior of a cell.

Further Reading

Andersen, J. P., and Vilsen, B. (1996). Primary ion pumps. In *Principles of Medical Biology* (E. E. Bittar and N. Bittar, eds.) Vol 4, pp. 1–66. Cell Chemistry and Physiology Part III, JAI Press, Greenwich, CT.

Axelsen, K. B., and Palmgren, M. G. (1998). Evolution of substrate specificities in the P-type ATPase superfamily. *J. Mol. Evol.* **46**, 84–101.

Carafoli, E. (1991). Calcium pump of the plasma membrane. *Physiol. Rev.* **71**, 129–153.

Dumont, R. A., Lins, U., Filoteo, A. G., Penniston, J. T., Kachar, B., and Gillespie, P. G. (2001). Plasma membrane Ca^{2+}-ATPase isoform 2a is the PMCA of hair bundles. *J. Neurosci.* **21**, 5066–5078.

Lehotsky, J., Kaplan, P., Murin, R., and Raeymaekers, L. (2001). The role of plasma membrane Ca^{2+} pumps (PMCAs) in pathologies of mammalian cells. *Front Biosci.* **7**, d53–d84.

Kozel, P. J., Friedman, R. A., Erway, L. C., Yamoah, E. N., Liu, L. H., Riddle, T., Duffy, J. J., Doeschman, T., Miller, M. L., Cardell, E. L., and Shull, G. E. (1998). Balance and hearing deficits in mice with a null mutation in the gene encoding plasma membrane Ca^{2+}-ATPase isoform 2. *J. Biol. Chem.* **273**, 18693–18696.

Moller, J. V., Juul, B., and leMaire, M. (1996). Structural organization, ion transport, and energy transduction of P-type ATPases. *Biochim. Biophys. Acta* **1286**, 1–51.

Pedersen, P. L., and Carafoli, E. (1987). Ion motive ATPase. I. Ubiquity, properties, and significance to cell function. *Trends Biochem. Sci.* **12**, 146–150.

Strehler, E. E., and Zacharias, D. A. (2001). Role of alternative splicing in generating isoform diversity among plasma membrane calcium pumps. *Physiol. Rev.* **81**, 21–50.

Street, V. A., McKee-Johnson, J. W., Fonseca, R. C., Temple, B. L., and Noben-Trauth, K. (1998). Mutations in a plasma membrane Ca^{2+}-ATPase gene cause deafness in deafwaddler mice. *Nature Genet.* **19**, 390–394.

Takahashi, K., and Kitamura, K. (1999). A point mutation in a plasma membrane Ca^{2+}-ATPase gene cause deafness in *Wriggle Mouse Sagami*. *Biochem. Biophys. Res. Commun.* **261**, 773–778.

Toyoshima, C., Nakasako, M., Nomura, H., and Ogawa H. (2000). Crystal structure of the calcium pump of sarcoplasmic reticulum at 2.6Å resolution. *Nature* **405**, 647–655.

Zacharias, D. A., and Kappen, C. (1999). Developmental expression of the four plasma membrane calcium ATPase (Pmca) genes in the mouse. *Biochim. Biophys. Acta* **1428**, 397–405.

Biography

Emanuel E. Strehler is a Professor in the Department of Biochemistry and Molecular Biology at the Mayo Clinic College of Medicine in Rochester, Minnesota. His principal research interest is in the molecular mechanisms of calcium regulation and calcium signaling, including calcium transport systems of the membrane and calcium sensor proteins. He holds a Ph.D. from the Swiss Federal Institute of Technology (ETH) in Zurich, Switzerland, and received his postdoctoral training at Harvard Medical School in Boston. He was involved in the first molecular cloning of a human plasma membrane calcium ATPase, and his laboratory has made seminal contributions to the characterization of the human plasma membrane calcium pump and calmodulin gene families.

Plastocyanin

Elizabeth L. Gross
Ohio State University, Columbus, Ohio, USA

The photosynthetic electron transport chain of higher plants, algae, and cyanobacteria consists of two light reactions (photosystem II (PSII) and photosystem I (PSI)) which act in series to produce molecular oxygen, reduce $NADP^+$ to NADPH, and synthesize ATP. The cytochrome b_6f complex is a large multi-subunit complex involved in the transfer of electrons from PSII to PSI. Plastocyanin is a ~10 kDa Cu-protein which acts as a mobile electron carrier, located in the lumen of the chloroplast thylakoid, which shuttles electron from cytochrome *f* (Cyt *f*) in the cytochrome b_6f complex to P700 in PSI. It can be replaced by an Fe-containing cytochrome (cytochrome c_6) in some green algae and cyanobacteria under conditions of copper deficiency.

Plastocyanin Structure

The Copper Center

Plastocyanin (PC) is a β-sheet protein (Figure 1) with a Cu atom that acts as the redox center. The Cu atom is coordinated to four amino acid residues (H87, H37, S84, and M92) in a distorted tetrahedral geometry. The distorted tetrahedral geometry of the Cu center together with the protein matrix promotes efficient electron transfer between Cyt *f* and P700. Electrons enter and leave PC via the H87 ligand to the copper which is located on the surface of the PC molecule (Figures 1 and 2A).

The Surface of the PC Molecule

Higher Plant and Green Algal PCs

Figure 2A depicts the surface of spinach PC which is a typical representative of higher plant and green algal PCs. There are two important features. The first is the patch of hydrophobic residues (green in Figures 2A and 2B) that surround the H87 ligand to the copper. These residues – including G10, L12, G34, F35, P36, L62, P86, G89, and A90 – are either conserved or replaced with similar residues in all PCs. They provide a hydrophobic binding surface for both Cyt *f* and PSI (see below). The second feature consists of two patches of negatively charged residues surrounding Y83 (yellow in Figures 2A and 2B). Negatively charged residues are shown in red and positively charged residues are shown in blue in Figure 2. The lower patch consists of anionic residues #42–44 and either #45 or #79. The upper patch consists of anionic residues #59–61 in most higher plant PCs. In a few higher plant species and in all green algae, one of the anionic residues in the upper patch is deleted and is replaced by a glutamate at position #85. Also, all higher plant and green algal PCs contain an additional anionic residue at either position #51 or #53. Thus, there are a total of eight anionic residues that contribute to large negatively charged electrostatic field surrounding Y83.

Cyanobacterial PCs

Cyanobacterial PCs are similar to those from higher plants and green algae in that a patch of hydrophobic residues surrounds the H87 ligand to the Cu (Figure 2B) (residues from cyanobacterial PCs are numbered so as to be consistent with those from higher plant PCs). However, the distribution of charged residues on their surface of cyanobacterial PCs is quite different than observed for higher plants and green algae. The only conserved anionic residue is D42. Instead, there are a series of positively charged residues on PC including R88, K44, and K51 that contribute to a positively charged electrostatic field surrounding Y83.

The Interaction of PC with Cyt *f*

The Structure of Cyt *f*

Cyt *f* is also a β-sheet protein with two domains. The heme is located on the large domain. The sixth ligand to the heme is the amino group of Y1 which may provide a pathway of electron transfer from the heme to H87 on PC. Y1 and the heme are surrounded by a patch of highly conserved hydrophobic residues. Cyt *f*s from higher plants and green algae have a highly conserved basic patch consisting of five residues (K58, K65, K66, K187, and R209 in turnip Cyt *f*). The negatively charged residues on higher plant and algal PCs are attracted to the positive patch on Cyt *f*. In contrast, Cyt *f* from

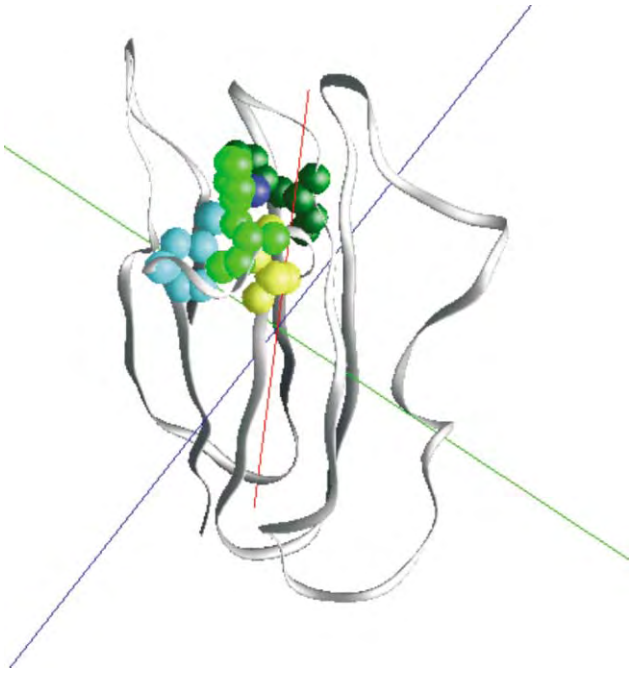

FIGURE 1 The structure of spinach plastocyanin: the copper center. The copper atom in PC (dark blue) is coordinated to two histidines (H87 – light green and H37 – dark green), C84 (yellow) and M92 (cyan). PC structures are taken from the Protein Data Bank from Berman H. M., Westboro, J., Feng, Z., Gilliland, G., Bhat, T. N., Weissig, H., Shindyalou, I. N. and Baume, P. E. (2000). The Protein Data Bank. *Nucleic Acids Res.* **28**, 235–242 and displayed using the Program GRASP (Nicholls, A., and Honig B. (1991). A rapid finite-difference algorithm, utilizing successive over-relaxation to solve the Possion-Boltzmann equation. *J. Comp. Chem.* 435–445).

the cyanobacterium *Phormidium lamanosum* has a large number of negatively charged residues on its surface that attract the positively charged residues on cyanobacterial PCs.

Complex Formation between PC and Cyt *f*

Figure 3 depicts a complex between spinach PC and turnip Cyt *f* determined by NMR. Two types of interactions are observed. First, there is an electrostatic attraction between cationic residues on Cyt *f* (blue) and the anionic residues surrounding Y83 on PC (red). These electrostatic interactions serve to bring the two molecules together and to orientate them properly. Evidence for electrostatic interactions come from cross-linking, chemical modification, and mutagenesis experiments. Second, hydrophobic residues surrounding the heme and Y1 on Cyt *f* interact with those surrounding the H87 ligand and the Cu on PC. These hydrophobic interactions anchor the two proteins in the proper orientation for efficient electron transfer from the heme and Y1 on Cyt *f* to H87 and the Cu on PC. Complexes formed between *Phormidium* Cyt *f* and *Phormidium* PC show a greater influence of hydrophobic as opposed to electrostatic interactions.

The Interaction of PC with PSI

The Structure of PSI

Recently, the structure of PSI from *Synechococcus elongatus* has been determined at a resolution of 2.5Å by X-ray crystallography. A simplified model of PSI is presented in Figure 4. Two regions of PSI have been implicated in PC binding. The first region includes the two largest subunits, PsaA and PsaB. These two subunits form a heterodimer containing P700 as well

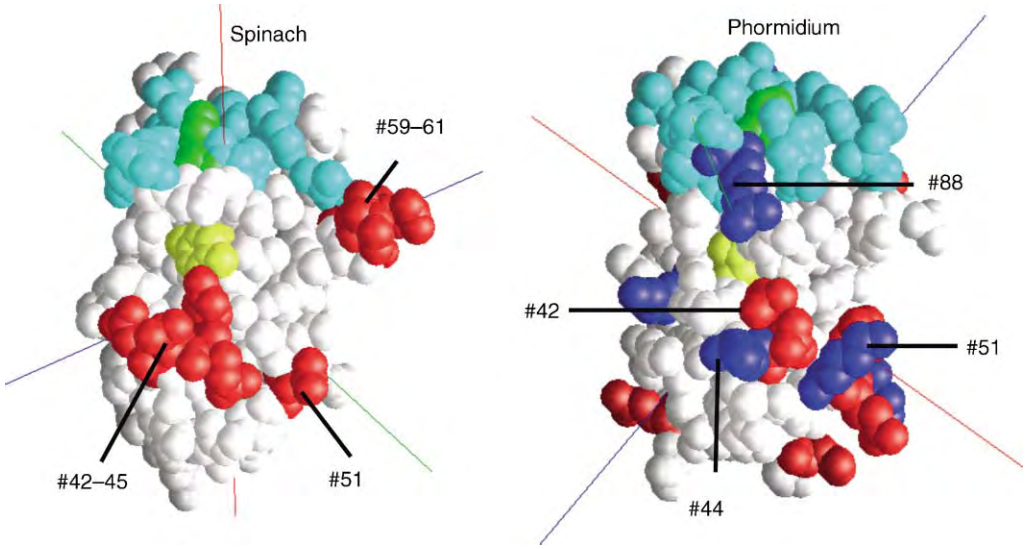

FIGURE 2 Surface residues on PC. H87, green; Y83, yellow; hydrophobic, cyan; cationic, blue; anionic, red: (A) spinach PC; (B) cyanobacterial PC from *P. lamanosum*. Other conditions were the same as for Figure 1.

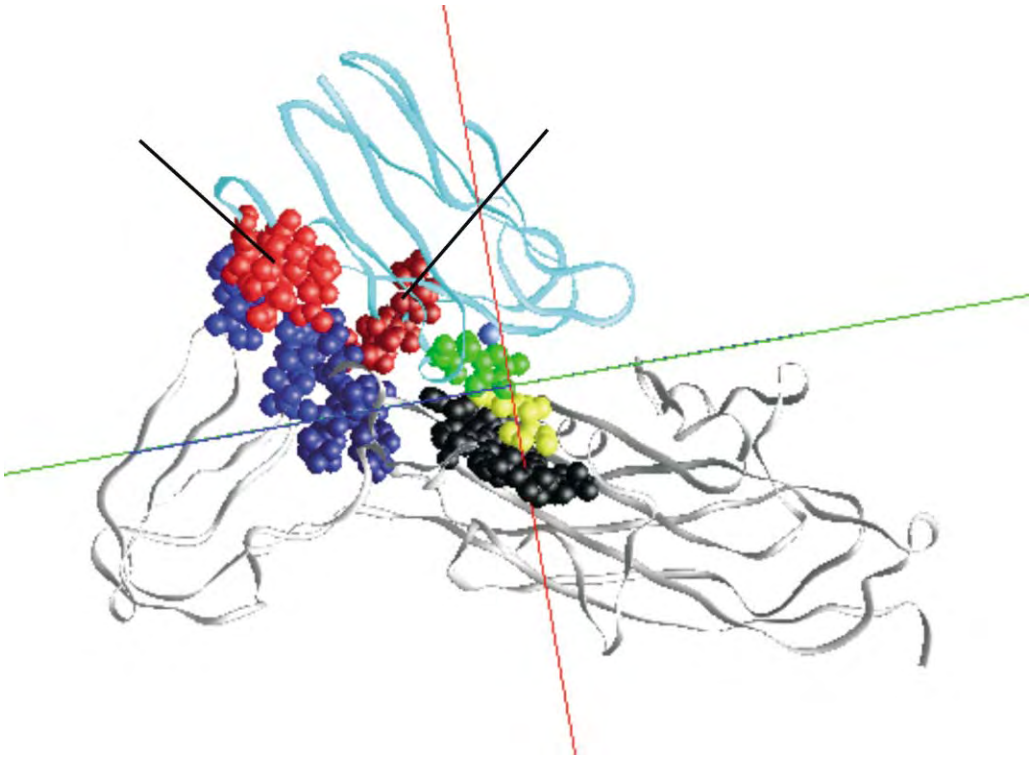

FIGURE 3 Complex formed between turnip Cyt *f* and spinach PC. Model 1 taken from Ubbink *et al.* (1988) *Structure* **6**, 323–335. Backbone of Cyt *f*, gray; backbone of PC, cyan. Other colors are the same as for Figure 2.

as the early electron acceptors A_0, A_1, and F_x. The second region includes the small subunit PsaF.

The Involvement of the PsaA and PsaB Subunits in Hydrophobic Interactions with PC

The PsaA–PsaB heterodimer has a 10Å depression which has been postulated to form a binding pocket for PC and cyt c_6 (Figure 4). Two surface-exposed hydrophobic helices line the binding pocket. One is part of PsaA and extends from residue #646 to residue #664; the second is located on PsaB and extends from residue #Y621 to residues #N639. Also, W655 on PsaA and W631 on PsaB are located in these helices and point toward the binding pocket. It has been postulated that these residues may be involved in the transfer of electrons from PC to P700. The observation that two mutants of residues located in the surface-exposed PsaB helix (W627F and E613N) caused significant inhibition of electron transport from PC to P700, support the hypothesis that these helices participate in the binding of PC to PSI.

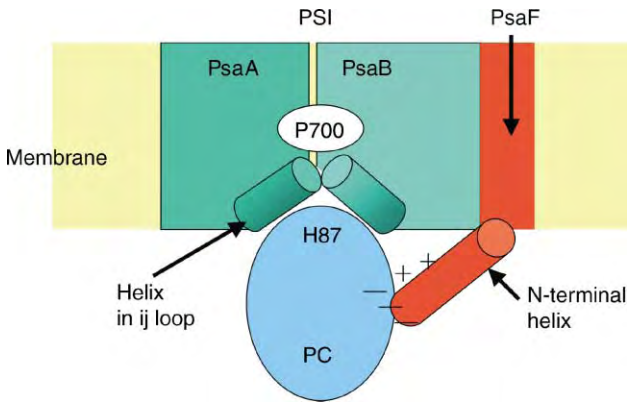

FIGURE 4 Model of the interaction of PC with PSI in higher plants and algae. The interactions of PC (blue) with: (1) the PsaA and PsaB subunits of PSI (green) and (2) the N-terminal positively charged helix of PsaF (red) are shown. The hydrophobic helices in the ij loops of PsaA and PsaB that have been postulated to be part of the binding pocket are also shown.

Involvement of the PsaF Subunit in Electrostatic Interaction between PC and PSI in Higher Plants and Green Algae

The PsaF subunit in green plants and algae has been implicated in PC binding to PSI (Figure 4). The evidence for this is as follows. First, removal of PsaF by either detergent treatment or mutagenesis inhibits the fast phase of electron transfer from PC to P700. This rapid phase has a half-time of ~11 ps and represents electron transfer from PC to P700 in preformed PC–PSI complexes. Second, mutagenesis of residues #42–45 in

the lower patch of PC inhibited the fast phase of electron transfer. In contrast, mutagenesis of the upper patch (residues #59–61) had very little effect. The N-terminal portion of PsaF consists of an amphipathic helix in which six lysine residues are lined up on one side of the helix. Third, mutagenesis of the lysine residues in this region of PsaF inhibited cross-linking and electron transfer from PC to P700; the greatest effect was observed for K23Q. Fourth, PC can be chemically cross-linked to PsaF. It was found that residues from the lower acidic patch of PC (#42–45) were cross-linked to residues #10–24 on PsaF, and residues from the upper acidic patch (#59–61) were cross-linked to residues #24–51 on PsaF.

The situation is different in cyanobacteria. Cyanobacteria show no rapid phase of electron transfer from PC to P700. In fact, the rate of electron transfer in cyanobacteria is approximately 2 orders of magnitude lower than that observed in green plants or algae. Also, removal of PsaF has no effect. An examination of PsaF in cyanobacteria shows that it lacks the N-terminal lysine-rich helix found in higher plant and green algae. However, when a chimeric PsaF, made up of the N-terminal sequence from *Chlamydomonas* PsaF and the C-terminal sequence from the cyanobacterium *Synechococcus*, was placed in *Synechococcus* cells, rapid electron transfer was observed between *Chlamydomonas* PC (and cyt c_6) and P700 which had the same characteristics as observed in *Chlamydomonas* cells. However, there is some evidence for electrostatic effects in cyanobacteria since removal of the negative charge of D42 on a cyanobacterial PC increased the rate of electron transfer to P700, whereas removal of the positive charge of R88 decreases it.

In conclusion, binding of PC to PSI in green plants and algae is similar to its binding to Cyt *f* in that electrostatic forces steer PC (and cyt c_6) to the hydrophobic binding sites on PSI (Figure 4) where electron transfer to P700 occurs in a rapid and efficient manner.

See Also the Following Articles

Cytochrome *c* • Photosystem I: F_X, F_A, and F_B Iron–Sulfur Clusters • Photosystem I, Structure and Function • Cytochrome b_6f Complex

Glossary

cytochrome b_6f complex Large multi-subunit complex located in the thylakoid membrane that mediates electron transport between plastoquinone and PC. Cyt *f*, a member of this complex, donates electrons directly to PC.

photosystem I Large multi-subunit complex located in the thylakoid membrane which accepts electrons from PC and donates them to ferredoxin. It contains the primary electron donor P700 and acceptors A_0, A_1, and Fx.

PsaA, PsaB, and PsaF Protein subunits of PSI.

P700 Chlorophyll dimer in the reaction center of PSI which is oxidized by light and reduced by PC.

thylakoid Portion of the inner membrane system of the chloroplast where the light reactions take place and where the cytochrome b_6f complex and PSI are located.

Further Reading

Berman H. M., Westboro, J., Feng, Z., Gilliland, G., Bhat, T. N., Weissig, H., Shindyalou, I. N. and Bourne, P. E. (2000). The Protein Data Bank. *Nucleic Acids Res.* **28**, 235–242.

Fromme, P., Jordan, P., and Krauss, N. (2001). Structure of photosystem I. *Biochim. Biophys. Acta* **1507**, 5–31.

Gross, E. L. (1996). Plastocyanin: structure, location, diffusion, and electron transfer mechanisms. In *Oxygenic Photosynthesis: The Light Reactions* (D. Ort and C. Yocum, eds.) pp. 413–429. Kluwer Academic Publishers, Dordrecht, The Netherlands.

Hippler, M., Reichert, J., Sutter, M., Zak, E., Altschmeid, L., Schroer, U., Herrmann, R. G., and Haehnel, W. (1996). The plastocyanin binding domain of photosystem I. *EMBO J.* **23**, 6376–6384.

Hippler, M., Drepper, F., Rochaix, J.-D., and Muhlenhoff, U. (1999). Insertion of the N-terminal part of PsaF from *Chlamydomonas reidhardtii* into photosystem I from *Synechococcus elongatus* enables efficient binding of algal plastocyanin and cytochrome c_6. *J. Biol. Chem.* **274**, 4180–4188.

Hope, A. B. (2000). Electron transfers amongst cytochrome *f*, plastocyanin and photosystem: I. Kinetics and mechanisms. *Biochim. Biophys. Acta* **1456**, 5–26.

Kannt, A., Young, S., and Bendall, D. S. (1996). The role of acidic residues of plastocyanin in its interaction with cytochrome *f*. *Biochim. Biophys. Acta* **1277**, 115–126.

Martinez, S. E., Huang, D., Szczepaniak, A., Cramer, W. A., and Smith, J. L. (1994). Crystal structure of the chloroplast cytochrome *f* reveals a novel cytochrome fold and unexpected heme ligation. *Structure* **2**, 95–105.

Nicholls, A., and Honig, B. (1991). A rapid finite-difference algorithm, utilizing successive over-relaxation to solve the Poisson-Boltzmann equation. *J. Comp. Chem.* **12**, 435–445.

Sigfridsson, K. (1998). Plastocyanin, an electron-transfer protein. *Photosynth. Res.* **57**, 1–28.

Ubbink, M., Ejdebäck, M., Karlsson, B. G., and Bendall, D. S. (1998). The structure of the complex of plastocyanin and cytochrome *f*, determined by paramagnetic NMR and restrained rigid-body molecular dynamics. *Structure* **6**, 323–335.

Biography

Dr. Elizabeth L. Gross is a Professor of Biochemistry and former Head of the Interdisciplinary Biophysics Graduate Program at the Ohio State University. Her research includes a study of chloroplast electron transport in general with an emphasis on plastocyanin using both experimental and computational methods. She has authored over 70 articles on the subject. She holds a Ph.D. in biophysics from the University of California, Berkeley and did postdoctoral work at the C. F. Kettering Research Laboratory in Yellow Springs, OH.

Platelet-Activating Factor Receptor

Katherine M. Howard and Merle S. Olson
University of Texas Health Science Center, San Antonio, Texas, USA

The platelet-activating factor (PAF) receptor is a member of the G protein-coupled seven transmembrane receptor superfamily. PAF receptor stimulation and the subsequent intracellular signaling events are involved in both physiological and pathophysiological processes but mainly participate in transcellular communication during inflammatory events. PAF receptor activation is instigated by the binding of PAF (1-*O*-alkyl-2-acetyl-sn-glycero-3-phosphocholine), a potent lipid mediator which produces biological responses at very low molar concentrations (10^{-10} M).

Platelet-Activating Factor

Although PAF was first identified in the 1970s as a soluble mediator responsible for platelet aggregation when IgE-sensitized basophils were challenged with antigen, researchers have since established that PAF has diverse and potent biological activities. In addition to platelet aggregation, PAF can activate monocytes/macrophages, induce hypotension and bronchoconstriction, stimulate glycogenolysis and participates in ovulation and ovoimplantation. In addition, PAF has a profound role in acute inflammation, allergic disorders, and endotoxic and anaphylactic shock. Unlike other cytokines and inflammatory mediators, PAF is not synthesized and stored in a preformed state; rather, it is rapidly synthesized in response to specific stimuli. Cells that participate in inflammatory reactions including monocytes/macrophages, polymorphonuclear neutrophils, eosinophils, basophils, and platelets all rapidly produce PAF upon stimulation. Most cells that produce PAF also express PAF receptors. Therefore, PAF can operate in an autocrine, paracrine, or juxtacrine fashion. For instance, stimulated monocyte/macrophages release a majority of the PAF synthesized into the fluid phase and this PAF can interact with PAF receptors on its own cell surface (autocrine) or can bind to PAF receptors on other inflammatory cells in the immediate vicinity (paracrine). In the case of endothelial cells and leukocytes, synthesized PAF remains partially cell associated. For endothelial cells, this PAF is presented on the cell surface for the juxtacrine activation of infiltrating leukocytes. The biological responses resulting from PAF receptor activation occur as a consequence of direct interactions of the mediator with receptors on target cells or through indirect secondary signaling effects.

In 1979, Hanahan and colleagues defined the chemical structure of this novel ether phospholipid and the chemical structure of the lipid is presented in Figure 1. The PAF molecule contains several specific structural features which are necessary for its potent biological activity. PAF contains an *O*-alkyl ether residue at the sn-1 position of the glycerol backbone. The ether-linked side chain can vary in chain length and degree of saturation but the 16:0 moiety is predominant. 18:0-, 17:0-, and 18:1-containing molecules also occur naturally but these molecules exhibit several orders of magnitude less biological activity. There is an acetyl moiety at the sn-2 position of PAF and removal of this acetate group by the enzyme PAF acetylhydrolase generates lyso-PAF which is biologically inactive. In addition to the strict structural requirements at the sn-1 and sn-2 positions, PAF requires a polar head group containing choline at the sn-3 position for specific PAF-binding and functional activation of the PAF receptor. Both PAF synthetic and degradative enzymes recognize these unique structural features of PAF.

There are two distinct synthetic routes for PAF production, a remodeling and a *de novo* pathway. The *de novo* pathway produces low levels of PAF and has been attributed to the formation of constitutive levels of PAF for normal physiological actions. The remodeling pathway is the predominant route of PAF production by cells and tissues in response to systemic or local injury and trauma. Such stimulants for PAF generation can be microbial agents like lipopolysaccharide (LPS) and zymosan or biological agents such as cytokines, chemotactic peptides, thrombin, and calcium ionophores.

Stimulating the remodeling pathway generates PAF in a two-step process. PAF synthesis begins with the activation of cytoplasmic phospholipase A_2 ($cPLA_2$). This enzyme preferentially cleaves membrane ether phospholipids with arachidonate at the sn-2 position. This reaction releases arachidonic acid during the formation of lyso-PAF. The arachidonic acid is converted

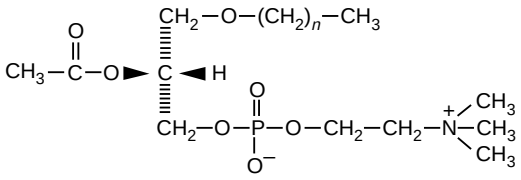

FIGURE 1 Chemical structure of PAF.

to eicosanoids via the lipoxygenase or cyclooxygenase pathways while the lyso-PAF is further converted to PAF by the actions of acetyl-CoA-lysoPAF acetyltransferase. Therefore, production of PAF occurs concomitant with the production of the eicosanoids which also contain far-reaching biological activities. The essential role of $cPLA_2$ in the synthesis of PAF has been confirmed from $cPLA_2$ knockout animals but little is known about the regulation of acetyl-CoA-lysoPAF acetyltransferase.

While the synthesis of PAF is tightly controlled, PAF-like species capable of binding and activating the PAF receptor can arise from the oxidation of unsaturated phosphatidylcholine. These ligands of the PAF receptor arising from oxidative damage of membrane phospholipids contribute to dysfunctional PAF receptor signaling and to the pathophysiological events associated with numerous disease entities.

Many of the biological and pathophysiological actions of PAF were initially investigated using specific PAF receptor antagonists. These PAF receptor antagonists include compounds with structural resemblance to PAF such as CV-3988 (phospholipid analogues) and nonstructural antagonists such as WEB 2086 and BN 50739. Classical ligand-binding experiments demonstrated specific PAF binding in numerous tissues and cells including platelets, neutrophils, macrophages, mononuclear leukocytes, eosinophils, Kupffer cells, epithelial cells, and endothelial cells.

The unique structural features of PAF, the existence of PAF receptor antagonists, and direct binding data utilizing radiolabeled PAF, as well as biochemical evidence for the diverse activation of second messenger signal cascades, all provided evidence for the existence of specific PAF receptors. Confirmation that PAF signaling occurs through receptor-mediated mechanisms was affirmed in 1991 with the molecular identification of the first receptor cloned for a lipid mediator by Shimizu and colleagues.

PAF Receptor Structure

Numerous attempts by investigators to isolate the PAF receptor proved unsuccessful. The eventual cloning of the PAF receptor was accomplished in an elegant strategy involving expression cloning of a guinea-pig lung cDNA library in *Xenopus laevis* oocytes. The initial cDNA library, constructed from size-fractionated poly (A) RNA, was converted *in vitro* into cRNA using the phage DNA as a template. Pools of cRNA were introduced into oocytes and a PAF-induced electrophysiological detection of G protein-coupled phosphatidylinositol (PI) turnover was assayed. A single PAF-receptor cDNA sequence isolated by the cloning strategy predicted a protein of 342 amino acids and a calculated molecular mass of ~39 kDa. However, immunological detection of the PAF receptor on Western blots revealed an apparent MW of 69 kDa suggesting the presence of posttranslational modifications of the receptor. In fact, two potential N-linked glycosylation sites were identified in the PAF receptor cDNA sequence. Hydropathy plot analyses of the deduced PAF receptor amino acid sequence predicted the presence of seven transmembrane-spanning domains within the PAF receptor. A schematic representation of the PAF receptor is presented in Figure 2. Through site-directed

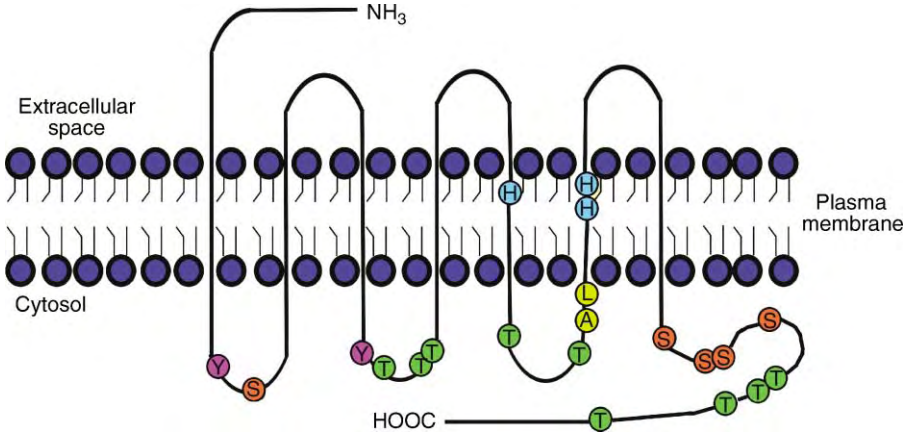

FIGURE 2 Schematic representation of the seven transmembrane spanning PAF receptor.

mutagenesis studies, several key features of the PAF receptor have been determined. Similar to other G protein coupled receptors, the ligand-binding site is defined in three dimensions by amino acids from several of the transmembrane-spanning regions. Mutations in membrane-spanning segments II (N58A, D63A), III (N100A, T101A, S104A), and VII (D289A) increased affinity of PAF binding while mutations in V (H188A), VI (H248A, H249A, Q289A), and VII (Q276A, T278A) lowered the affinity of PAF for the receptor. The third intracellular loop of the receptor is coupled to phosphatidylinositol turnover. The C-terminal cytoplasmic tail of the receptor containing a cluster of serine and threonine residues are candidate sites for phosphorylation by G protein receptor kinases, and are critical for agonist-induced desensitization.

Subsequent to the isolation of the guinea-pig cDNA, cDNA for numerous other species were isolated by cross hybridization. The PAF receptor maintains ~74% sequence identity between the various species identified to date. Because the PAF receptor mRNA is present in only subsets of cells, Northern blot hybridizations have limitations in detecting PAF receptor expression in some tissues. The relative tissue abundance among different species varies but in general lung, neutrophils, monocytes, macrophages, placenta, small intestine, heart, liver, kidney, brain, and spleen have detectable PAF receptor expression.

The isolation of human PAF receptor cDNAs identified two unique 5′-noncoding regions designated transcript 1 and transcript 2. The tissue- and cell-type distribution of these two transcripts are disparate. Transcript 1 can be found ubiquitously but is expressed abundantly in leukocytes, eosinophils, and monocytes/macrophages. Conversely, transcript 2 is found predominantly in heart, lung, spleen, kidney, and skin epithelial cells but not in leukocytes, eosinophils or monocyte/macrophages. Analysis of human genomic DNA sequence localized the PAF receptor to chromosome 1 and revealed other features of the PAF receptor gene. The PAF receptor gene contains no introns within the coding sequence of the gene (exon 3). Many G protein-coupled receptor genes also lack introns within their open reading frame. The first two exons of the PAF receptor gene are located entirely within 5′ -non-coding sequences and were identified by sequence comparisons to the human cDNAs. These two exons reside more than 20 kb upstream of exon 3 and each exon is spliced to the common exon encoding the PAF receptor protein thus creating PAF receptor transcript 1 and 2 (Figure 3). The two transcripts are controlled by distinct promoters immediately 5′ of the exons. Because transcript 1 was identified first, the exon further upstream was designated exon 2. Neither PAF receptor promoter region contains canonical TATA or CCAAT box regulatory sequences commonly found in the promoter regions of eukaryotic genes. Each PAF receptor promoter contains distinct regulatory features that reflect the requirement for PAF receptor expression in different target cells and tissues.

The promoter for transcript 1 contains three consensus transcription factor binding sites for nuclear factor-κB (NF-κB) and one for Sp1. The transcript 1 promoter also contains a pyrimidine-rich initiator sequence (Inr) which includes the transcriptional start site. Inr sequences aid in positioning the start site of transcription in many TATA-less genes. Functional analysis of the promoter region demonstrated that PAF and phorbol 12-myristate 13-acetate (PMA) increased PAF receptor transcript 1 levels through these three NF-κB sites. The NFκB transcription factor plays a crucial role in the regulation of many inflammatory response genes and is activated by various cytokines, PMA, and lipopolysaccharide (LPS).

The promoter for PAF receptor transcript 2 contains consensus sequences for AP-2 and Sp-1 that were demonstrated to control basal promoter activity. In addition to the basal promoter activity, a hormone responsive element (HRE) and a TGF-β inhibitory element function in regulating transcript 2 levels. Retinoic acid and thyroid hormone increase transcript 2 expression levels while TGF-β suppresses promoter activity. Thus, it is apparent that PAF receptor promoter 1 responds to inflammatory stimuli, whereas

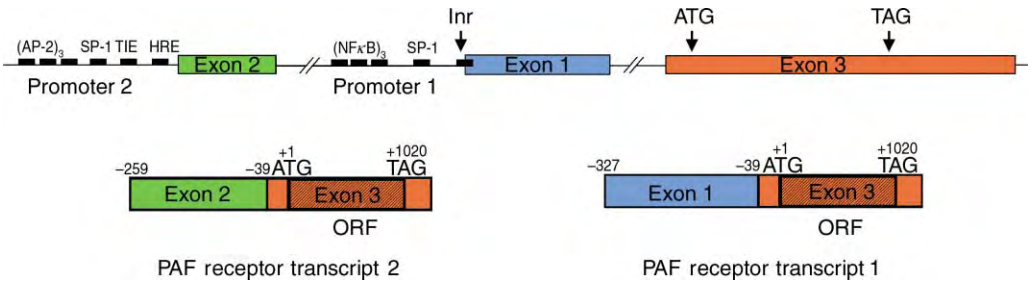

FIGURE 3 PAF receptor gene structure and transcript organization.

the PAF receptor transcript 2 expression is controlled by differentiation signals.

PAF Receptor Regulation

Because of the crucial role that PAF and PAF receptor activation plays in numerous physiological and pathophysiological events, PAF-instigated signaling is tightly controlled. The first manifestation of PAF receptor regulation is the expression in specific cells and tissues as already discussed. Another mechanism for tightly controlled regulation of PAF receptor signaling is controlling the availability of PAF. This mechanism includes regulation of both PAF synthesis and release, and the rapid inactivation of PAF by PAF acetylhydrolases. Other mechanisms of regulation of this signaling system are intrinsic to the PAF receptor and include homologous desensitization to repeated or sustained administration of PAF. Desensitization of the PAF receptor leads to decreased PAF-induced cellular responses in GTPase activity, IP_3 production, and calcium mobilization. The carboxy terminus of the PAF receptor is the target for phosphorylation required to desensitize the receptor. PAF receptor desensitization may occur by uncoupling of the receptor to G proteins and by ligand-induced internalization of the receptor.

As opposed to the fairly rapid process of controlling PAF availability and PAF receptor responsiveness, long-term regulation of the PAF receptor includes alterations in PAF receptor expression. Transient elevation of cyclic AMP (cAMP) reduces expression of the PAF receptor. This down-regulation is accompanied by a decreased responsiveness to a prolonged exposure of PAF. Conversely, priming of macrophages with low levels of LPS can induce a threefold increase in PAF receptor transcript levels thereby amplifying subsequent response to stimulation.

PAF Receptor Signal Transduction

The wide range of biological responses instigated by PAF receptor activation can be attributed to complicated intracellular signaling mechanisms. Calcium, cAMP, IP_3, and diacylglycerol (DAG) are all proven second messengers for PAF signaling. Figure 4 presents an overview of PAF receptor-mediated signaling pathways. Heterotrimeric G proteins are intricately involved in the signal transduction events generated by PAF receptor occupancy. G proteins bind guanine nucleotides, are activated by GTP and possess intrinsic GTPase activity. Binding of PAF activates the associated G protein by exchanging guanosine triphosphate for guanosine diphosphate. The PAF receptor is linked to more than one G protein because some processes are sensitive to pertussis toxin treatment while others are resistant. In fact, this G protein utilization also can differ in different cell types. The activated G proteins, in turn, activate polyphosphoinositide turnover mediated by phospholipase C (PLC). The subsequent generation of inositol 1,4,5-triphosphate (IP3) and diacylglcerol mobilizes intracellular Ca^{+2} and activates protein kinase C (PKC) respectively. PAF receptor associated G protein activation also leads to the activation of cytoplasmic phospholipase A_2 with the subsequent cleavage of arachidonic acid (AA) and the formation of leukotrienes (LT), prostaglandins (PG) and thromboxanes (TX). More recently, investigators demonstrated broader activation of kinases and phospholipases following PAF receptor activation. For instance, PAF receptor activation has been shown to activate mitogen-activated protein kinase (MAPK), phosphatidylinositol 3-kinases (PI3K), protein tyrosine kinases, and G protein receptor kinase.

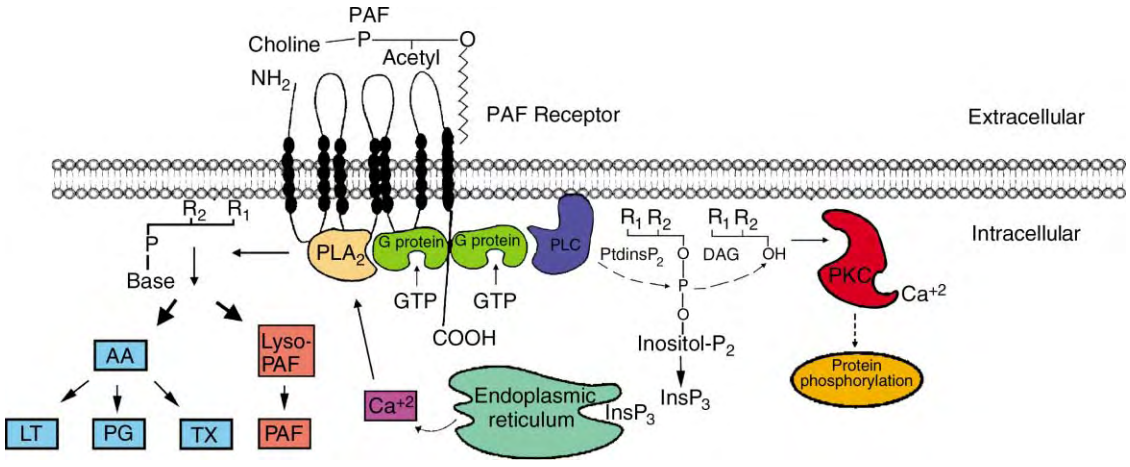

FIGURE 4 PAF receptor intracellular signaling pathways. See text for abbreviations.

Experiments in both PAF receptor knockout animals and transgenic animals overexpressing PAF receptors support the pathophysiological role attributed to PAF receptor signaling. Deletion of PAF receptors in mice drastically attenuates systemic anaphylactic responses after antigen challenge; whereas mice overexpressing PAF receptors exhibit hypersensitivity to bacterial endotoxin. It is not surprising then that PAF receptor activation is being investigated as a contributing factor in numerous disease entities including asthma, atherosclerosis, inflammatory bowel disease, ischemia-reperfusion injury, endotoxemia, and allergic disorders.

See Also the Following Articles

Eicosanoid Receptors • G Protein-Coupled Receptor Kinases and Arrestins • G_{12}/G_{13} Family • G_i Family of Heterotrimeric G Proteins • G_q Family • G_s Family of Heterotrimeric G Proteins

Glossary

autocoid Autopharmacologic substance that has potent local activity.

G protein-coupled receptor A class of receptors for a diverse set of ligands including hormones, lipid inflammatory mediators, and chemokines that use associated trimeric G proteins for intracellular signal transduction.

lipopolysaccharide A component of the cell wall of gram-negative bacteria containing both lipid and carbohydrate moieties that instigates many innate immune responses such as secretion of cytokines, activation of macrophages, and expression of leukocyte adhesion molecules. Synonymous with endotoxin.

platelet-activating factor (PAF) Lipid autocoid.

zymosan An insoluble protein–carbohydrate complex from the cell wall of yeast.

Further Reading

Chao, W., and Olson, M. S. (1993). Platelet-activating factor: Receptors and signal transduction. *Biochem. J.* **292**, 617–629.

Honda, Z., Nakamura, M., Miki, I., Minami, M., Watanabe, T., Seyama, Y., Okado, H., Toh, H., Ito, K., and Miyamoto, T. (1991). Cloning by functional expression of platelet-activating factor receptor from guinea-pig lung. *Nature* **349**, 342–346.

Ishii, S., and Shimizu, T. (2000). Platelet-activating factor (PAF) receptor and genetically engineered PAF receptor mutant mice. *Prog. Lipid Res.* **39**, 41–82.

Ishii, S., Kuwaki, T., Nagase, T., Maki, K., Tashiro, F., Sunaga, S., Cao, W. H., Kume, K., Fukuchi, Y., Ikuta, K., Miyazaki, J., Kumada, M., and Shimizu, T. (1998). Impaired anaphylactic responses with intact sensitivity to endotoxin in mice lacking a platelet-activating factor receptor. *J. Exp. Med.* **187**, 1779–1788.

Izumi, T., and Shimizu, T. (1995). Platelet-activating factor receptor: Gene expression and signal transduction. *Biochim. Biophys. Acta* **1259**, 317–333.

Nagase, T., Ishii, S., Katayama, H., Fukuchi, Y., Ouchi, Y., and Shimizu, T. (1997). Airway responsiveness in transgenic mice overexpressing platelet-activating factor receptor – Roles of thromboxanes and leukotrienes. *Am. J. Respir. Crit. Care Med.* **156**, 1621–1627.

Prescott, S. M., Zimmerman, G. A., Stafforini, D. M., and McIntyre, T. M. (2000). Platelet-activating factor and related lipid mediators. *Annu. Rev. Biochem.* **69**, 419–445.

Biography

Merle S. Olson is currently Dean of the Graduate School of Biomedical Science and former Chair of the Department of Biochemistry at the University of Texas Health Science Center, San Antonio. He received his Ph.D. from the University of Minnesota and has published over 200 articles in the field of PAF and hepatic mediators involved in intercellular communication.

Platelet-Derived Growth Factor Receptor Family

Marina Kovalenko and Andrius Kazlauskas
Harvard Medical School, Boston, Massachusetts, USA

Platelet-derived growth factor (PDGF) is a potent mitogen, chemoattractant, and survival factor for cells of mesenchymal origin (such as fibroblasts, smooth muscle cells (SMC), or glial cells). PDGF exists as a number of isoforms that initiate signaling via two closely related receptor tyrosine kinases (RTKs) named α- and β-receptors. PDGFs and their receptors (PDGFRs) are important for embryonic and postnatal development. Knockout mice lacking either PDGFs or receptors develop severe defects in various tissues and organs, and die before or shortly after birth. In adult organisms, PDGFs participate in wound healing, regulation of blood vessel tonus, and maintenance of the interstitial fluid pressure. PDGF signaling is also involved in the pathogenesis of various proliferative diseases (certain tumors, atherosclerosis and restenosis, fibrotic conditions). PDGFs and their receptors have been best characterized in mammals. However, there is evidence that PDGFR-like proteins are expressed in lower vertebrates, and PDGF-like growth factors have been found in molluscs, annelids, sea urchins (*Lytechinus pictus*), and *Drosophila*. Taken together, these findings indicate that PDGFs and their receptors play an important role in a variety of biological processes throughout eukaryotic species.

PDGF Isoforms

At present, four genes encoding different PDGF chains are known: A, B, C, and D. Biologically active PDGFs exist as disulfide-bonded homodimers designated AA, BB, CC, and DD. A and B chains form a heterodimeric PDGF AB (Figure 1). The history of the discovery of PDGFs dates back as early as 1974, when mitogenic activity of whole blood serum was linked to the presence of platelets. PDGF AB was the first to be purified and biochemically characterized a few years later, followed by PDGF BB and AA. Cloning of PDGF A and B cDNAs and determination of the structure of corresponding genes were completed in the 1980s.

New members of the PDGF family, PDGF C and PDGF D, were found only recently by searching the database of human-expressed sequences. PDGFs C and D have a 2-domain structure with N-terminal CUB domain and C-terminal PDGF/VEGF (core) domain, separated by a hinge region (Figure 1). No heterodimers involving C or D chains have been detected. The unique feature of these two new PDGFs is the requirement for proteolytic cleavage of the CUB domain upon secretion in order to achieve biological activity. Thus, latency may be the reason why these growth factors were not originally detected by functional assays.

PDGF Receptors

PDGFs exert their biological functions by binding to two isoforms of PDGF receptors, α and β, with different degrees of affinity. Both receptors are transmembrane tyrosine kinases, composed of extracellular, transmembrane, and intracellular parts. The extracellular part consists of five immunoglobulin-like domains that are involved in ligand binding (domains I–III) and receptor dimerization (domain IV). The intracellular kinase domain of the PDGF receptors is split into two by ~100-amino acid insert (Figure 1).

PDGF A chain binds specifically to α-receptor, and PDGF B can bind to both α and β. PDGF C was originally described as a ligand for PDGF α-, but not β-receptor, however, later it was shown to bind PDGF β-receptor in cells expressing both α- and β-isoforms. PDGF D has been reported to be a β-receptor ligand, but its ability to bind α-receptor in α/β-expressing cells remains controversial. Interactions of PDGFs with α- and β-receptors are summarized in Figure 1. A bivalent dimer, PDGF molecule binds to two receptor subunits causing them to dimerize. Upon dimerization, PDGF receptors become rapidly phosphorylated on multiple tyrosine residues. One of them ("regulatory tyrosine") is located in the second part of the kinase domain and is important for receptor kinase activity (Tyr857 in β-receptor and, by homology, Tyr849 in α-receptor). Most of other phosphorylation sites lie in noncatalytic parts of the receptor (Figure 2). The exact sequence of events during receptor activation and formation of signaling complex is unknown. By analogy to other RTKs, it is likely that

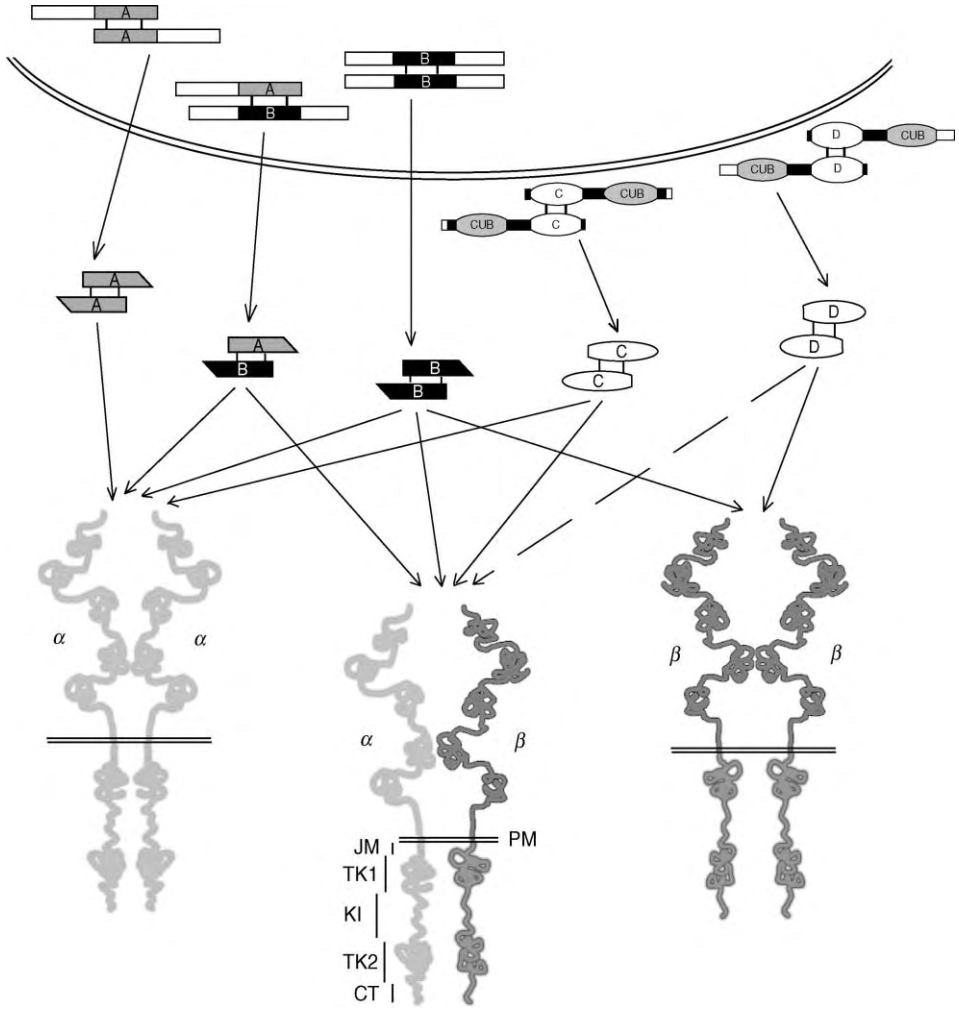

FIGURE 1 Platelet-derived growth factors and their receptors. PDGFs A and B are synthesized as precursors that are proteolytically processed before secretion. PDGFs C and D are secreted in latent form and activated by proteolytic cleavage of the CUB domain. All PDGF isoforms dimerize prior to the proteolytic cleavage. Specificity of binding of mature active PDGFs to their receptors is shown; dashed arrow indicates the lack of consensus regarding the ability of PDGF DD to cause the formation of a heterodimeric receptor. Domain structure of the PDGF receptor α-subunit (identical to that of β-subunit) is presented. The extracellular part of the receptor consists of 5 Ig-like domains. PM, plasma membrane; JM, juxtamembrane domain; TK1 and TK2, proximal and distal parts of tyrosine kinase domain; KI, kinase insert; and CT, carboxyl-terminal tail.

ligand binding and subsequent dimerization of the receptor induces a conformational change that facilitates transphosphorylation of regulatory tyrosine residues within the dimer. Importantly, the regulatory tyrosine lies within activation loop, the region that is conserved among receptor tyrosine kinases. As shown for the insulin receptor, the activation loop blocks the catalytic site in nonphosphorylated receptor, whereas upon ligand-induced phosphorylation it moves away providing access for substrate. It is possible that the PDGF receptor activation occurs via similar mechanism, although there is no direct evidence for this in the absence of crystal structure of the PDGF receptors.

Recently, ligand-bound dimerized PDGF β-receptor was found to be less susceptible to dephosphorylation by protein tyrosine phosphatases (PTPs) than the monomeric receptor. It is suggested that this "phosphatase protection" may contribute to maintenance of activated (phosphorylated) state of the receptor.

Proteins Associated with the PDGF Receptors and PDGF-Driven Signaling Pathways

A total of 13 tyrosine residues in β-receptor and 11 in α-receptor get phosphorylated upon PDGF stimulation. Phosphorylation of most of the tyrosines within PDGF receptors results in the creation of docking sites for a variety of proteins many of which in turn get phosphorylated upon association with the

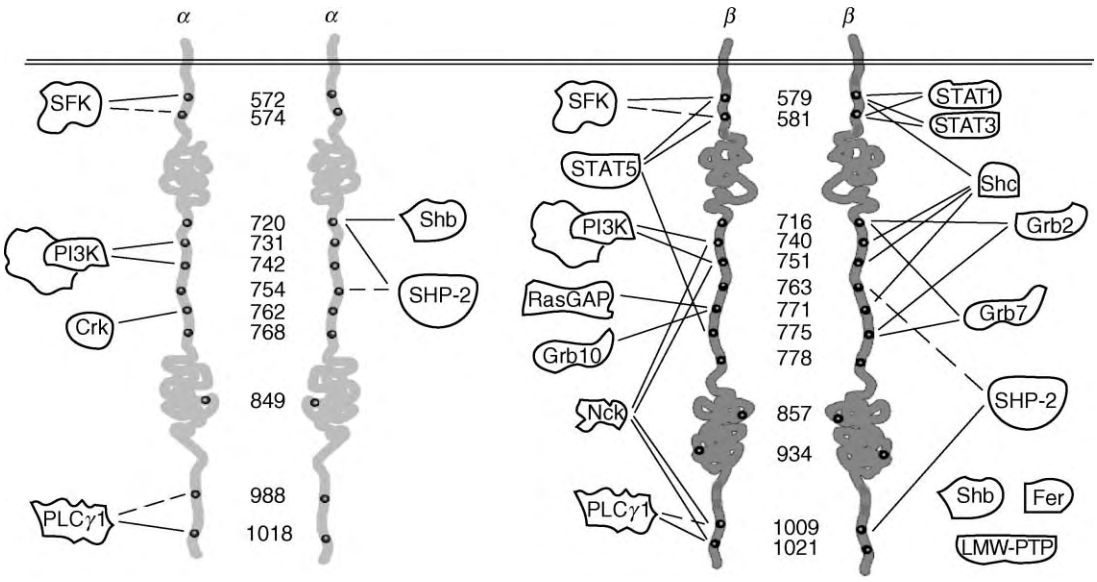

FIGURE 2 Intracellular domains of $\alpha\alpha$ and $\beta\beta$ homodimers of the PDGF receptor. Phosphorylated tyrosine residues are shown (dark circles). Numbers indicate their positions in the human PDGF receptor sequence. Association of signaling proteins with phosphorylation sites of the activated PDGF receptors is shown by solid lines (major binding sites) or dashed lines (additional sites). Proteins binding with high affinity (e.g., PI3-kinase, PLCγ1, RasGAP) bind to the receptor via one or two phosphotyrosine residues on the receptor, whereas low-affinity binding (e.g., Nck, Shc, or Shb binding to β-receptor) involves multiple sites. Shb was found to bind to most of the phosphorylated tyrosines on the PDGF β-receptor. Fer and LMW-PTP bind to as yet unidentified sites on the PDGF β-receptor.

receptors (Figure 2). These proteins include enzymes (phosphatidylinositol 3′-kinase (PI3-kinase), phospholipase C-γ1 (PLCγ1), SH2 domain-containing protein tyrosine phosphatase-2 (SHP-2), GTPase-activating protein of Ras (RasGAP), Src family kinases (SFKs), transcription factors (members of STAT family), or adaptor proteins, such as Grb2, Grb7, Shc, Shb, Nck, or Crk, linking the receptor to signaling proteins further downstream. Some proteins that are recruited to the PDGF receptors are both adaptors and enzymes, e.g., tyrosine phosphatase SHP-2 is able to recruit Grb2 via its phosphorylated C terminus. Association is mediated in most cases by SH2 (Src homology 2) domains of these proteins and is remarkably specific, each phosphorylation site having its own binding partner(s). This specificity is based on the ability of SH2 domains to differentially recognize amino acid sequence following the phosphorylated tyrosine. Many receptor-binding proteins also contain SH3 (Src homology 3), PTB (phosphotyrosine binding), or PH (pleckstrin homology) domains that may facilitate recruitment of other yet unidentified signaling molecules to the complex.

Cellular Responses Mediated by the PDGF Receptors

Assembly of the PDGF receptor complex initiates a number of signaling pathways leading to cellular responses (Figure 3): chemotaxis, proliferation, differentiation (in certain cell types), and protection from apoptosis. One pathway may lead to several different responses, whereas some of the pathways are redundant and converge on the same cellular effect.

Proliferation

Proliferation is the major and most well studied cellular effect induced by PDGFs. Virtually all signaling proteins binding to the receptors have been implicated in proliferation, but not all of them have to be present in the signaling complex at the same time to induce the response.

Ras-Dependent Pathway

The mitogenic pathway that involves Ras, a small GTPase, can be activated through multiple ways in response to PDGF. The complex of Grb2 (adaptor protein) and Sos1 (nucleotide exchange factor for Ras) can bind to the β-receptor either directly or via phosphorylated Shc or SHP-2. This association brings the complex to the plasma membrane where it activates Ras. Activated Ras GTPase interacts directly with Raf-1 serine/threonine kinase, in turn activating it. Raf-1 is the first kinase in MAP kinase cascade. Elevation of its activity is followed by sequential activation of MEK and MAP kinases Erk1 and 2, which are translocated to the nucleus and phosphorylate a number of transcription factors.

As for the PDGF α-receptor, Grb2 is able to bind to it via SHP-2, but there is no evidence of its involvement in

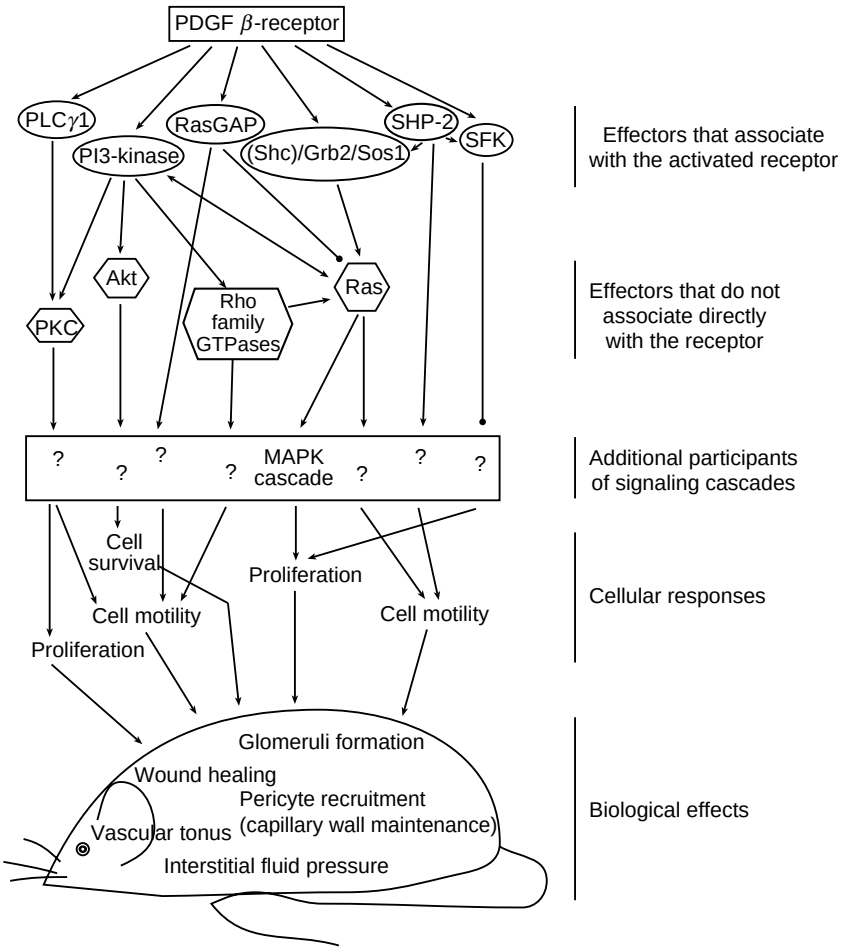

FIGURE 3 Major events initiated by the PDGF β-receptor and culminating in biological responses. Upon ligand binding, activated PDGF β-receptor recruits enzymes and adaptor proteins that start a number of distinct signaling pathways, some of which are shown on the figure. Note that not all of them are initiated by the same receptor dimer or in the same cell. Arrows represent either physical or functional interactions along the pathways. The least defined part of the signaling cascade is the one that bridges the receptor-proximal events with proteins that carry out cellular responses. PDGF is necessary but not sufficient to achieve biological effects. In a living organism, other growth factors and hormones, as well as cell–cell and cell–matrix interactions within tissues and organs make indispensable contributions.

Ras activation. Therefore, pathways other than the Ras-mediated one are likely to contribute to α-receptor-mediated proliferation.

The Ras pathway is believed to be counteracted by RasGAP that binds to the PDGF β-receptor (but not to α-receptor) and is able to enhance GTPase activity of Ras, thus converting it from active (GTP-bound) to inactive (GDP-bound) state. The extent to which this negative signaling affects proliferation may depend on many factors (cell type, environmental conditions).

Src

Src ($p60^{c\text{-}src}$) has been shown to be important for PDGF-driven mitogenesis. However, its association with the PDGF receptors and early PDGF-induced elevation of activity are dispensable for proliferative response and may have a different function. Yet, Src is required at multiple time points during PDGF-dependent cell-cycle progression. Thus, elevation of Src activity early in G1 leads to increase of *c-myc* expression, which is required for transition through G1. Importance of Src also has been confirmed for late G1 and for the exit from M-phase of the cell cycle.

PLCγ1

PLCγ1 binds to the PDGF receptors upon ligand stimulation and becomes phosphorylated and activated. Increasing the catalytic activity of PLCγ1 leads to production of inositol 1,4,5-trisphosphate (IP3) and diacylglycerol (DAG). IP3 is involved in regulation of cytoplasmic Ca^{2+} levels, which, together with direct action of DAG, can contribute to activation of certain members of the PKC family. In particular, DAG has been shown to activate protein kinase C-ζ (PKC-ζ) which then activates Raf-1 and, consequently,

the rest of MAP kinase cascade, leading to proliferation. PLCγ1 is involved in PDGF-stimulated proliferation mediated by β-receptor, whereas in the case of α-receptor, it is important mostly for the motility response.

PI3-Kinase

PDGF-dependent PI3-kinase activation is critical for mitogenesis in most cell types. Prolonged exposure to PDGF, needed to induce cell-cycle progression in quiescent cells, causes two distinct peaks of PI3-kinase activity, one within minutes and another following a delay of several hours. Only the second peak was found to be important for the cell-cycle progression, whereas the early increase of activity is required only for immediate responses to PDGF such as chemotaxis.

How this biphasic increase of PI3-kinase activity is linked to the cell-cycle machinery still remains an open question. Continuous treatment with PDGF can be substituted by two separate pulses of the growth factor, the first getting cells out of G0 to early G1 and the second pushing them through late G1 and into S phase. Early elevation of *c-myc* and sustained activation of the MAP kinase pathway can replace the first pulse of PDGF, but is not sufficient to drive the cell through late G1. To complete cell-cycle progression, a properly timed second peak of PI3-kinase activity (second pulse of PDGF or just the addition of PI3-kinase lipid products) is required. It is hypothesized that early *c-myc* and Erk activation trigger expression of new protein(s) whose interaction with the late PI3-kinase products is critical for S phase entry.

Chemotaxis

Most receptor-expressing cells exhibit chemotaxis upon exposure to PDGF. Migration of pericytes in response to SMC-released PDGF plays a critical role in capillary formation, which is particularly important during embryonic development. In the process of wound healing, PDGF causes chemotaxis of neutrophils and macrophages, as well as fibroblasts and SMC.

α- and β-PDGF receptors differ in their ability to mediate chemotaxis. PDGF β-receptor homodimer as well as α–β heterodimer potently stimulate it. However, the ability of α–α homodimer to drive chemotaxis remains controversial and may depend on the cell type. This difference may be explained by variations in composition of the signaling complex assembled by different receptor dimers, which may be cell-type specific.

PI3-Kinase and Ras Pathways

Chemotaxis involves dynamic remodeling of cytoskeleton, including rearrangement of actin filaments and microtubules, changes of focal adhesions, and formation of lamellipodia or filopodia. These processes are controlled, in part, by the Rho family of small GTPases (RhoA, Rac1 and Cdc42), that are activated by the PDGF receptors via different pathways. The PI3-kinase pathway is considered to be the major one. Activation of the Rho family of small GTPases is dependent on PI3-kinase lipid products. The Ras pathway that can be initiated by the PDGF receptor independently from PI3-kinase pathway, leads to chemotactic response via activation of Rac1, another small GTPase Ral, and in some cell types, MEK1 and stress-activated kinase p38. Interestingly, PI3-kinase is able to interact directly with Ras and activate it, whereas both Ras and Rho family GTPases can activate PI3-kinase, forming a positive feedback loop. Thus, reciprocal regulation of Ras and PI3-kinase provide an example of interaction between different PDGF-dependent pathways.

RasGAP, a negative regulator of Ras, has been shown to inhibit chemotaxis. However, in some cell types, RasGAP has also been shown to have a positive impact on motility that is most likely independent from Ras.

PLCγ1

PLCγ1 promotes chemotaxis in many cell types, but the knowledge about what happens downstream of PLCγ1 is only starting to emerge. Upon PDGF stimulation, PLCγ1 activates sphingosine kinase through IP3 formation and subsequent release of Ca^{2+} from intracellular stores. Sphingosine kinase product, sphingosine-1-phosphate (SPP), is a ligand for EDG-1, a G-protein coupled receptor (GPCR). Stimulation of EDG-1 by SPP leads to activation of Rho family GTPases, which, in turn, results in remodeling of actin cytoskeleton and cell–matrix adhesion sites. This is a new example of receptor crosstalk, where an RTK requires activation of a GPCR to achieve a cellular response.

PKC isoforms that are activated via both PI3-kinase and PLCγ1 pathways, are also involved in chemotactic signaling, as chemotaxis is reduced when PKCs are inhibited or downregulated.

SHP-2 and Low Molecular Weight Phosphatase (LMW-PTP)

Two other positive mediators of PDGF-induced chemotaxis are tyrosine phosphatases SHP-2 and LMW-PTP, both directly associated with the phosphorylated PDGF receptor and activated by PDGF-dependent phosphorylation. Involvement of SHP-2 in chemotactic signaling may occur via the Ras pathway, since SHP-2 can serve as

an adaptor protein for Ras binding. LMW-PTP is likely to act through dephosphorylating and inactivating one of its cellular targets, p190RhoGAP, a negative regulator of Rho GTPase, thus leading to increased activation of Rho and subsequent cytoskeletal rearrangements.

SFKs

The role of Src family kinases in PDGF-induced chemotaxis is not clear. A pathway leading to chemotaxis is initiated at SFK-binding sites in the juxtamembrane domain of the PDGF α-receptor, since mutating these tyrosines to phenylalanine residues results in chemotaxis inhibition. However, it is not yet clear whether it is Src family kinases or other signal transduction molecules binding to the same sites that are responsible for cell migration, since in triple SFK knockout cells PDGF-AA-dependent cell migration is intact.

It is necessary to note that $\alpha\alpha$- and $\beta\beta$-homodimers of the PDGF receptor cause different, although partially overlapping, cellular responses, due to the differences in their ability to bind signaling proteins (Figure 2). For instance, α-receptor homodimer has been found to send a less potent mitogenic signal than the β-receptor homodimer. Additionally, in some cell types (SMC, human foreskin fibroblasts), it fails to mediate a chemotactic response to PDGF AA and inhibits chemotaxis induced by other agents. PDGF β-receptor homodimer formation generally results in higher mitogenicity and chemotaxis. The heterodimeric $\alpha-\beta$ receptor is believed to have unique signaling properties, due to altered phosphorylation pattern of both α- and β-subunits, which results in recruitment of a different subset of signaling proteins. In particular, the heterodimer mediates a stronger mitogenic response than either $\alpha-\alpha$ or $\beta-\beta$ complexes. Distinct signaling properties of different PDGF receptor dimers are based not only on different intrinsic properties of receptor isoforms, but also on the type of cells where these receptors are expressed and on varying experimental conditions.

Negative Regulation of the PDGFR Signaling

Down-regulation mechanisms described for the PDGFR include internalization, ubiquitin-mediated proteolysis (degradation), and dephosphorylation by PTPs. Their relative contribution to the termination of signaling appears to be different.

Internalization and Degradation

Internalization of the PDGF receptors, mediated by clathrin-coated pits, occurs shortly after ligand stimulation and is dependent on the receptor kinase activity. Intracellular trafficking of the PDGF β-receptor involves PI3-kinase but is not entirely elucidated yet. Internalized receptors can be recycled and go back to the cell surface or can be directed to lysosomal degradation, which actually results in receptor down-regulation. However, before they are degraded, internalized receptors remain associated with downstream proteins and continue to signal. For this reason, internalization and subsequent trafficking can be considered a late signaling stage rather than the way of receptor inactivation only.

Additionally, PDGFRs can be targeted for cytoplasmic degradation in proteasomes via polyubiquitination. Ubiquitination of the receptors occurs upon ligand binding and is strictly dependent on receptor autophosphorylation. Generally, multi-ubiquitin chain is added to proteins by E3–E2 ubiquitin ligase system and after that ubiquitinated proteins are recognized by the 26S proteasome and degraded. c-Cbl, a E3 ubiquitin ligase, has been shown to be phosphorylated upon PDGF stimulation and is therefore likely to contribute to the PDGFR ubiquitination and subsequent proteolysis. Proteolytic degradation can be considered a true mechanism of receptor down-regulation that terminates signaling through decreasing the number of the PDGF receptor molecules.

Dephosphorylation by PTPs

PTP-dependent dephosphorylation of the PDGF receptors represents another level of regulation of PDGF-induced signaling. Thus, dephosphorylation of the regulatory site or non-specific removal of phosphate from all tyrosine residues would shut down all signaling, whereas site-specific dephosphorylation would selectively block corresponding signaling pathways. LMW-PTP, for instance, has been shown to act both ways. This PTP selectively interferes with two pathways initiated by the PDGF β-receptor: Src-dependent induction of *c-myc* and STAT1/3 mediated *c-fos* expression. It can also affect kinase activity of the PDGF β-receptor by dephosphorylating Tyr857, providing a general negative regulation of all downstream signals.

Unlike LMW-PTP that acts on membrane-bound PDGF β-receptor, PTP1B was found to dephosphorylate the receptor upon its internalization on the surface of the endoplasmic reticulum, shutting down signaling at a later time point, yet before the receptor gets degraded or recycled to the plasma membrane.

The ability of SHP-2 to act as both positive and negative regulator of PDGFR signaling puts it apart from other receptor-directed PTPs. It is able to dephosphorylate selectively, tyrosines 771 and 751 on the β-receptor, potentially turning off RasGAP and PI3-kinase pathways. On the other hand, SHP-2 can

serve as an adaptor for Grb2 binding, therefore initiating Ras-mediated signaling. Additionally, SHP-2 has been implicated as a positive regulator in the stimulatory effect of integrins on PDGF receptor signaling.

An increase of intracellular reactive oxygen species (ROS) is an early PDGF-dependent event mediated by PI3-kinase and Rac1, and it was shown to be important for mitogenic signaling. Since ROS reversibly inhibit PTPs, it is likely that this event helps to prevent the negative effect of PTPs on early stages of PDGF signaling.

Developmental Role of the PDGF Receptors

At very early stages of embryonic development (before gastrulation), both PDGF α-receptors and PDGF A chain are expressed throughout the embryo, suggesting that PDGF AA may be acting in autocrine manner to stimulate cell proliferation. At later stages, PDGF β-receptor and PDGF B chain appear, and both receptors and growth factor chains start to show distinct expression pattern. The expression of PDGF C largely overlaps with that of PDGF A, and information about PDGF D expression in embryo is still incomplete. PDGF receptors are found mainly in cells of mesodermal origin, with some exceptions (e.g., central nervous system), whereas PDGFs are present in adjacent ecto- and endodermal derivatives. This distribution indicates that, during morphogenesis, PDGFs act in a paracrine manner to induce migration of receptor-expressing mesenchymal cells.

As shown by genetic analysis in mice, interruption of PDGF signaling leads to morphogenic defects and embryonic or perinatal lethality. PDGFR α-null mice die before birth, many (but not all) at a very early stage. Those available for analysis have myotomal abnormalities, rib fusions, defects in neural crest derivatives, and incomplete cephalic closure. PDGF A knockouts demonstrate an emphysema-like lung condition characterized by the absence of mature alveoli. This defect originates due to a lack of migration of PDGF α-receptor expressing alveolar SMC progenitors in the walls of alveolar sacs. Both PDGF A and PDGFR α-null mice also display hypoplasia of skin mesenchyme and abnormal intestinal villi formation. The most pronounced phenotypic features of the PDGF B and PDGF β-receptor knockout mice are defects in kidney glomeruli and capillary microaneurisms. Both result from failure of capillary branching and dilation of capillary walls in the absence of PDGF-dependent recruitment of pericytes and kidney mesangial cells. Other abnormalities include dilation of heart and large arteries, thrombocytopenia, and anemia.

See Also the Following Articles

Chemotactic Peptide/Complement Receptors • Phospholipase C • Ras Family • Rho GTPases and Actin Cytoskeleton Dynamics • Src Family of Protein Tyrosine Kinases

Glossary

adaptor A protein linking together proteins that are otherwise unable to interact.

autocrine signaling Type of signaling in which the cell responds to a stimulus (e.g., growth factor) that is produced by the same cell.

cell cycle Tightly regulated sequence of events exhibited by dividing cells. Consists of the following phases: Gap 0 (G0; temporary or permanent quiescence), Gap 1 (G1; growth and preparation of the chromosomes for replication), S (synthesis of DNA), Gap 2 (G2; growth and preparation for mitosis) and M (mitosis).

chemotaxis The ability of cells to migrate toward a gradient of chemoattractant.

growth factor A substance that needs to be present in the environment of responsive cells in order for them to divide.

ligand A molecule (or ion) that can interact with a receptor.

mitogen A substance (e.g., growth factor) that can initiate cell division.

paracrine signaling Type of signaling in which the cell responds to a stimulus (e.g., growth factor) that is produced by a nearby cell.

pericytes Pluripotential cells surrounding blood vessels.

receptor A molecule (mostly of protein nature) able to detect the presence of a specific stimulus (ligand) and give rise to signaling events leading to physiological response(s).

transphosphorylation A phosphorylation event in which two protein kinases phosphorylate each other (e.g., within the dimer).

Further Reading

Betsholtz, C., Karlsson, L., and Lindahl, P. (2001). Developmental roles of platelet-derived growth factor. *BioEssays* **23**, 494–507.

Heldin, C.-H., Östman, A., and Rönnstrand, L. (1998). Signal transduction via platelet-derived growth factor receptors. *Biochim. Biophys. Acta* **1378**, F79–F113.

Östman, A., and Heldin, C.-H. (2001). Involvement of platelet-derived growth factor in disease: Development of specific antagonists. *Adv. Cancer Res.* **80**, 1–38.

Pietras, K., Östman, A., Sjöquist, M., Buchdunger, E., Reed, R. K., Heldin, C.-H., and Rubin, K. (2001). Inhibition of platelet-derived growth factor receptors reduces interstitial hypertension and increases transcapillary transport in tumors. *Cancer Res.* **61**, 2929–2934.

Rosenkranz, S., and Kazlauskas, A. (1999). Evidence for distinct signaling properties and biological responses induced by the PDGF receptor α and β subtypes. *Growth Factors* **16**, 201–216.

Smits, A., and Funa, K. (1998). Platelet-derived growth factor in primary brain tumours of neuroglial origin. *Histol. Histopathol.* **13**, 511–520.

Takehara, K. (2000). Growth regulation of skin fibroblasts. *J. Dermatol. Sci.* **24**(Suppl. 1), S70–S77.

Biography

Andrius Kazlauskas is currently a Senior Scientist at the Schepens Eye Research Institute, and Associate Professor at Harvard Medical School. He studies signal transduction pathways used by receptor tyrosine kinases to drive cell proliferation. He graduated from Cleveland State University with a Ph.D. in Chemistry in 1986, and

then studied signaling by tyrosine kinases as a postdoctoral fellow at the Fred Hutchinson Cancer Research Center from 1986 to 1990. He has held an independent research position from 1991.

Marina Kovalenko is a postdoctoral fellow in the lab of Andrius Kazlauskas. After graduating from Moscow State University, she earned her Ph.D. in Biochemistry from Friedrich Schiller University in Jena, Germany, in 1996. Then, she studied PDGF receptor-directed tyrosine phosphatases as a postdoctoral fellow at the Ludwig Institute for Cancer Research in Uppsala, Sweden. Both her thesis work and postdoctoral research were devoted to antagonists of the PDGF receptor tyrosine kinase.

Polysialic Acid in Molecular Medicine

Frederic A. Troy II
University of California School of Medicine, Davis, California, USA

Molecular medicine is an emerging new science that seeks to understand the complex interaction between genes (genomics), proteins (proteomics), carbohydrates (glycomics), and lipids (lipomics) in health and disease. Studies in this field are directed at elucidating the structure, synthesis, and function of these major classes of molecules in both normal and abnormal processes, including disorders in all organ systems of the human body. A major impact of molecular medicine is in the field of cancer metastasis, which is discussed in this article, with focus on the polysialic acid (polySia) molecule.

The cell surface of normal and cancer cells is decorated with a remarkable array of information-rich sugar molecules, usually attached to proteins (glycoproteins) and lipids (glycolipids). Surface expression of many of these complex sugars changes dramatically during the developmental life of a cell and with the onset of cancer. Importantly, these sugars carry specific information that determines the cell behavior at different stages in their life cycle, for example, when to detach and move to different locations and when to stop dividing and become adherent. A specific example of one class of these surface carbohydrates is "polysialic acid" (polySia), the focus molecule of this article.

The emerging importance of polySia in molecular medicine has given rise to a new sub-discipline of glycobiology, termed sialobiology. When polySia chains are attached to surface proteins designated neural cell adhesion molecules (N-CAMs), they help direct in a controlled way this "stop–go" signaling during development. During neural development, for instance, polySia is normally expressed on N-CAM during the embryonic stage, when cells need to avoid sticking together and must migrate to where their "zip code" has programmed them to go. When cells have reached their correct address and need to adhere, other molecular events signal the removal of the embryonic or polysialylated form of N-CAM (polySia-N-CAM) from the cell surface, thus facilitating N-CAM-mediated cell–cell adhesion. In this sense, polySia is an "anti-adhesive glycotope" that forbids cell adhesion and allows cell movement. But polySia is also an oncodevelopmental or oncofetal, tumor-associated antigen, which means that it can be re-expressed on the surface of adult cancer cells. When this re-expression occurs, polySia becomes a metastatic factor that promotes tumor cell detachment, invasion, and colonization at distant sites. Indeed, many human cancers that express polySia have a predilection for metastasis to the brain. How this re-expression occurs is not well understood, but the hereditary information or genes containing the "blueprint" for building the protein catalysts or enzymes required for synthesizing polySia (the polysialyltransferases (polySTs)) are reactivated in cancer cells, having been silenced at the end of embryonic development. The up-regulated polyST genes now allow the adult cancer cell to again synthesize the embryonic form of polySia-N-CAM, thus facilitating cell detachment and migration. This fundamental event may be key in allowing a number of polysialylated human cancer cells to detach from their original site and to spread or metastasize throughout the body. It is this metastatic property of cancer cells that is so feared and deadly, and that is the hallmark of malignancy.

In humans, the pathogenic neuroinvasive bacteria *Escherichia coli* (*E. coli*) K1 and *Neisseria meningitidis* (*N. meningitidis*) that cause meningitis express a surface capsule of polySia acid that is structurally identical to the polySia chains expressed on N-CAM. In this case, the capsule coats the entire surface of the bacterium and as such is a neurovirulent determinant that allows for the invasion and colonization of the brains (meninges) of neonates. Accordingly, the polySTs in both pathogenic bacteria and human cancer cells have become important targets for chemotherapeutic agents directed at treating meningitis and in slowing or stopping cancer cells from metastasizing. This article summarizes information related to the structure,

occurrence, function, synthesis, and glycopathology of polysialic acid in mammalian cells.

The Importance of Molecular Medicine in Health and Disease

The field of molecular medicine is important in human biology and medicine because of the new information it is providing towards the discovery, diagnosis, and treatment of known and emerging diseases. The discipline uses contemporary methodologies of biochemistry (molecular genetics, and molecular cell developmental and structural biology), to identify and analyze new information on the "molecule signature" and interaction of molecules, which are key molecular players in all aspects of health and disease. The outcome of studies in molecular medicine is already leading to a new generation of synthetic and biotechnology-based approaches for the diagnosis and treatment of a variety of health-related diseases.

Natural Occurrence and Structure of Oligo-Polysialic Acids

As shown in Figure 1, the polySia are linear sugar chains usually composed of one of the two most common sialic acid residues, N-acetylneuraminic acid (Neu5Ac) or N-glycolylneuraminic acid (Neu5Gc). Shorter chains of KDN (2-keto-3-deoxy-D-*glycero*-D-*galacto*-nonoic acid), the newest member of the class of sialic acids, occurs in some fish egg sialoglycoproteins and bacterial capsule polysaccharides. The sialic acids are unusual 9-carbon sugar acids that are joined internally by α2,8-, α2,9-, or alternating α2,8/α2,9-ketosidic linkages. The α2,8-linked chains are the most common, and are the principal polySia synthesized by mammalian cells. Their chain length, or degree of polymerization (DP) exceeds 200 Sia residues in *E. coli* K1 and 100 residues in some mammalian tissues. A striking feature of these chains is the bewildering degree of structural diversity and wide range of expression on the surface of both prokaryotic and eukaryotic cells. The operative paradigm is that this diversity in both structure and DP is related to the myriad of cellular functions regulated by polySia, including cell–cell adhesion, cell migration, neuronal development and regeneration, synaptic plasticity, neurotropism, and the possible activation of cell proliferation by initiating second messenger-related signaling pathways. A review of the structural and functional features of oligo-polySia has appeared in *Biology of the Sialic Acids*.

Polysialylated Neural Cell Adhesion Molecules

Embryonic and Adult Forms of N-CAM

N-CAMs are morphoregulatory glycoproteins that are members of the immunoglobulin gene superfamily. They represent a class of high-molecular-weight cell surface sialoglycoproteins that affect a number of cell adhesive and cell migration processes, including neurite fasciculation and neuromuscular interactions. N-CAMs are the most prevalent carrier proteins of polySia chains in mammalian cells and, as such, are the most thoroughly characterized. There are four different isoforms of N-CAM, which arise by alternative mRNA splicing. These include polypeptides with molecular masses of 180, 140, 120, and 110 kDa. The 180- and 140-kDa isoforms are linked to the plasma membrane via a transmembrane spanning domain, and each has a cytoplasmic domain. In contrast, the 120-kDa protein is attached to the membrane via a glycosylphosphatidylinositol anchor and thus lacks a cytoplasmic domain. The 110-kDa N-CAM is a secreted isoform. The 180-kDa isoform is expressed primarily on neurons but not on muscle cells, while the 140-kDa protein is expressed on both neural and muscle cells. A unique structural feature of N-CAM is the presence of α-(2,8)-linked polySia (polyNeu5AC) chains that posttranslationally modify the protein during embryonic development. These chains are attached to both N- and O-linked oligosaccharides that are located on the extracellular domain of N-CAM. No α2,9-ketosidic linkages, which characterize the polySia capsule in neuroinvasive

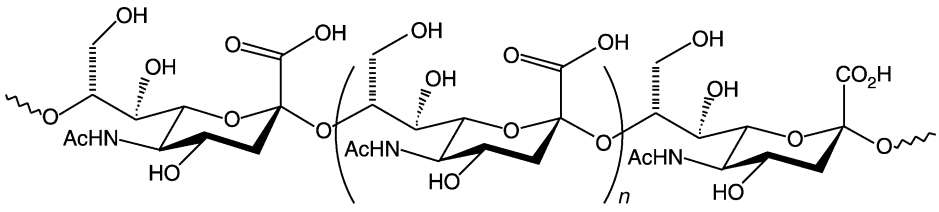

FIGURE 1 Structure of α2,8-polysialic acid.

N. meningitidis Gp. C, nor Neu5Gc or KDN residues have been reported as constituents of N-CAM. The covalent attachment of polySia chains to N-CAM, which characterizes the embryonic form of the molecule, decreases N-CAM-dependent cell adhesion in a variety of tissues, thereby acting as a negative regulator of cell–cell interactions. In contrast, cells expressing relatively low levels of polysialylated N-CAM, which characterizes the adult form, aggregate much more readily than those with high levels of polySia. Thus, polysialylation of N-CAM is an essential reaction that mediates cell recognition events that modulates cell migration and cell adhesion. As such, polysialylation plays a central role in regulating mammalian developmental processes, including neural cell differentiation, migration, and synaptic plasticity.

Temporal Expression of Polysialic Acid during Embryonic Neural Development

Maximal expression of the polysialylated form of N-CAM usually occurs in embryonic neural tissue, when cells are migratory, and is greatly reduced in adult tissue, where little cell migration occurs. The embryonic form of N-CAM has a high Sia content that undergoes a postnatal conversion to the adult form with a low Sia content. During development, the presence of polySia is closely correlated with axon pathfinding, synaptogenesis, and neuron–muscle formation. As the embryo develops, most of the N-CAM changes from the embryonic, or high-polySia form, to the adult, or low-polySia form. The adult form is postulated to help stabilize mature tissues. In this way, N-CAM plays a role in both facilitating two adjacent cells to form regions of contact and in inhibiting such contacts. If neighboring cells express the adult form of N-CAM, strong cell adhesion is promoted. In contrast, if cells express the polysialylated forms of N-CAM, cell adhesion is reduced. Thus, the polySia moiety on N-CAM is an anti-adhesive glycotope that has a regulatory effect on adhesion between living cells. The amount of this carbohydrate is important for normal development, and while the DP of polySia chains on N-CAM changes during embryonic chick brain development, the significance of this change is unknown.

Expression of Polysialic Acid in Adult Human Brain

Although polySia expression is most abundant during early stages of embryonic development in both neural and non-neural tissues, polysialylated N-CAM is also expressed in restricted parts of the adult brain that exhibit synaptic plasticity, and may be required for the rearrangement of neural cells or their interconnections. In rat brain and spinal cord, polysialylated N-CAMs are expressed in discrete regions of the hypothalamic and thalamic nuclei, the hippocampal dentate gyrus, mesencephalic central gray matter, the supraotic nucleus, and the olfactory bulb. It is also expressed on neurohypophysial astrocytes and on mesencephalic dopaminergic cells in the brain that persist throughout development. Functional studies on the role of polySia in adult brain suggest that its primary role is to promote plasticity in cell interactions, thus facilitating changes in the structure and function of the nervous system. PolySia therefore represents one of the few defined carbohydrate structures with an identifiable role in a morphogenic pathway.

Expression and Function of Polysialic Acid on Extraneural Cells

Roth and colleagues first showed that expression of the embryonic form of N-CAM was developmentally regulated in rat and human kidney, a mesodermally derived tissue. The polySia chains in kidney are maximally expressed early in development and, like brain, may regulate cell–cell adhesive interactions during kidney differentiation and development. The polySia chains are re-expressed in Wilms tumor, a highly malignant tumor of the kidney. Polysialylated N-CAM is also expressed on newborn heart and muscle tissue. In human, rat and chicken embryos polySia-N-CAM is expressed on cells derived from mesoderm (mesenchymal cells) and endoderm (pancreas, lung epithelium), and on neuroectoderm cells (neural or lung endocrine cells). In the thyroid gland, calcitonin-producing cells, which are endocrine derivatives of the neural crest, also express the embryonic form of polysialylated N-CAM. During the early stages of rat heart development, polySia-N-CAM is expressed on myocardial, endocardial, and some atrioventricular cells in the epicardium. Later during development, its appearance in the epicardium decreases. In the adult heart, the only significant expression of polysialylated N-CAM is during innervation. Polysialylated N-CAM is transiently expressed in developing chicken osteoblasts during osteogenesis and on dermal and smooth muscle cells in the chick during feather development. In *Drosophila melanogaster*, expression of α2,8-linked polySia chains is developmentally regulated, and occurs only during the early stages of development. The possible function of the polySia glycotope in prokaryotic and eukaryotic cells is summarized in Table I.

TABLE I

Possible Functions of the Polysialic Acid Glycotope

Bacterial polysialic acid capsules
- In neuroinvasive *E. coli* K1 and *N. meningitidis*, functions as a neurotropic determinant; facilitates invasion of the blood–brain barrier and colonization of the meninges of neonatal brains
- Polyanionic shield that masks the somatic O-antigen chains of lipopolysaccharide and renders cell resistant to immune detection and phagocytosis
- Receptor for binding K1-specific bacteriophages

Fish egg polysialoglycoproteins
- Implicated in regulating cell–cell interactions and cell migration during oogenesis
- May function as recognition markers for mediating egg–sperm interaction
- May protect the embryo from osmotic lysis, artificial activation, mechanical destruction, and bacterial infection by retaining Ca^{2+} around the embryo (KDN-gp has affinity for Ca^{2+} ions)
- *O*-Acetylation and KDN cosylation render polySia chains resistant to depolymerization by sialidases; consequence unknown (protective?)
- Expression of an $\alpha 2 \rightarrow 8$-polysialyltransferase is developmentally regulated

Polysialic acid-containing glycoproteins in the jelly coat of sea urchin eggs
- May mediate cell–cell interactions during gastrulation when endodermal cells interact with ectodermal cells
- May be involved in inducing the acrosome reaction in sperm
- Expression of an $\alpha 2,8$-polysialyltransferase is developmentally regulated

Polysialylated neural cell adhesion molecules (N-CAMs)
- Implicated in embryonic neural development and neuronal plasticity; mediates cell adhesive interactions including neurite fasciculation, neuromuscular interactions, and cell migration. Expression of polySia usually decreases N-CAM-mediated cell adhesion
- The amount of polySia on N-CAM is critical for normal morphogenesis and neural development
- Influences cell–cell apposition and regulates contact-dependent cell interactions. PolySia "shield" may simply increase the intercellular space between cells
- Participates in the establishment of neuronal connections and in modulating neurite outgrowth. May activate a second messenger pathway in primary neurons
- May influence the formation of new neural circuits in the dentate gyrus, and in reorganization of the piriform cortex in the adult rat
- Proposed to regulate intramuscular nerve branching during embryogenesis
- Implicated in the normal separation of secondary myotobes from primary myotobes during muscle development
- Influences the interaction of cells of the preimplantation mammalian embryo
- May couple the morphogenic effects of adhesion and synaptic activity-dependent processes
- In bone formation, may mediate the interaction of osteoblasts and regulate skeletogenesis
- May mediate the formation of fiber cell gap junctions and adherence junction during lens cell differentiation
- May control the migration and maturation of dopaminergic cells of the developing mesencephalon
- Participates in the internalization of the Antennapedia homeobox peptide involved in late expression of some homeogenes in the CNS

Expression on tumors
- In developing human kidney, brain (neuroblastomas), and plasma cells, polysialylated N-CAM is an oncodevelopmental antigen
- On some human cancers, e.g., natural killer-like and T-cell malignant lymphomas, acute myeloid leukemia, multiple myeloma, and some head and neck tumors, polySia expression may enhance neuroinvasive potential and metastases
- May protect malignant cells from immune surveillance

Sodium channel glycoproteins
- Function unknown. By analogy with bacterial polySia capsules, the polyanionic surface charge over the channel may maintain a solute reservoir and shield channel from toxins

Expression and Function of Polysialic Acid in Cancer

Prokaryotic-Derived Reagents for the Detection and Analysis of PolySia

α-(2,8)-Polysialylated N-CAM expression on a number of human cancers was revealed using anti-polySia and anti-N-CAM antibodies in combination with Endo-N-acylneuraminidase (Endo-N), a diagnostic enzyme specific for catalyzing the depolymerization $\alpha 2,8$-linked polySia chains. The ease with which these reagents can be used to discover and confirm the presence of polySia chains in mammalian cells and human cancers provides a way to study polysialylation that had not been previously possible. Using these specific molecular probes, α-(2,8)-polysialylated N-CAM expression was identified on a variety of human cancers, including high-grade tumors, e.g., medulloblastomas, neuroblastomas, pheochromocytomas, medullary thyroid carcinomas, small cell lung carcinomas, pituitary adenomas, and congenital

TABLE II

Human Tumors Expressing the $\alpha 2 \rightarrow 8$-Linked Polysialic Acid Glycotope

Neuroblastomas
Nephroblastomas (Wilms' tumor)
Medulloblastomas
Pheochromocytomas
Medullary thyroid carcinomas
Small-cell lung cancers
Lung carcinoid tumors
Pituitary adenomas
Congenital mesoblastic nephroma
Multiple myelomas
T-cell malignant lymphomas
Leukemias (AML)
Head and neck tumors (principally squamous cell carcinomas)
Malignant melanomas
Human tumor expression $(\rightarrow 9Neu5Ac\alpha 2 \rightarrow)_2$
Ovarian teratocarcinoma (PA1 embryonal carcinoma cells)

mesoblastic nephromas. Table II summarizes human cancers that have been shown to express the polySia glycotope. The human breast cancer cell line, MCF-7 and rat basophilic leukemia (RBL-1) cells are unique in that the $\alpha 2$,8-linked polySia chains are attached to O-linked oligosaccharides, suggesting that polysialylation of glycoproteins on tumor cells may be more prevalent than heretofore recognized. While few studies have been carried out to determine the length of polySia chains on cancer cells, polySia chains containing >55 Sia residues are expressed on human neuroblastoma cells. Because of methodological limitations, accurate DP values are difficult to obtain. Reported values thus represent minimum estimates, as some pre-hydrolysis of the polySia chains occurs during isolation and purification and/or derivitization procedures that are required for most chromatographic separation and detection methods.

Polysialic Acid as an Oncodevelopmental Antigen and its Relationship to Tumor Metastasis

Extended chains of polySia were first shown to be expressed on human neuroblastomas, some of which were metastatic to bone and brain. Concurrent studies showed that polySia was temporally expressed in human embryonic kidney, but not in adult kidney, and was re-expressed in malignant Wilms' tumors. These findings led to the important conclusion that polySia was an oncodevelopmental (oncofetal) antigen in human kidney and brain because the long-chain forms of polySia, which characterized the embryonic form of N-CAM, were infrequently expressed in adult brain. An exception to this paradigm, as noted above, is the hypothalamo-neurohypophysial system in the adult brain, where polySia-N-CAM is postulated to function in plasticity.

Evidence for the Role of Polysialic Acid in Cancer Metastasis

Several independent *in vivo* studies reveal a specific role for polySia in tumor metastasis. First, mice injected subcutaneously with polysialylated mouse leukemia cells develop tumors that are metastatic to the spleen. All of the metastatic tumors express polySia. Second, a significant correlation between the level of polySia-N-CAM expression and growth rate, invasion, hormone secretion, and metastasis occurs in rat pituitary tumors. Tumors showing the highest level of polySia-N-CAM expression show the highest level of metastasis. Third, human rhabdomyosarcoma cells expressing polysialylated N-CAM are able to form lung metastases in nude mice. Metastasis is decreased in mice receiving injections of Endo-N, the endo-sialidase that specifically removes polySia from the surface of the cancer cells.

Role of PolySia in Lung Cancer (Small-Cell Lung Carcinoma (SCLC) and Non-SCLC)

There is a positive correlation between polysialylated N-CAM expression and malignant behavior in SCLC and non-SCLC. This finding suggests that polySia functions to reduce cell–cell adhesion and cell–matrix interactions leading to tumor cell detachment, aggressive behavior, and a higher incidence of metastases. The overall survival of SCLC patients with polySia-negative cancers is higher than in patients with polySia-positive tumors. Thus, the polysialylated state of N-CAM may be a prognostic indicator in SCLC patients, corroborating earlier studies in which polySia-N-CAM is associated with poor differentiation and aggressive clinical behavior in patients with SCLC and other neuroendocrine lung tumors. The role of polySia in SCLC was confirmed by an analysis of surgically resected SCLC tumors. Patients with polySia-N-CAM-positive tumors have a significantly lower probability of survival than patients with polySia-negative tumors, again showing the prognostic value of polySia-N-CAM in SCLC. PolySia expression is also an important clinical marker in non-SCLC carcinomas, as patients with polySia-positive tumors have a poorer prognosis for survival. In non-SCLC patients, polySia expression shows a positive correlation with nodal and distant metastasis.

Biosynthesis of Polysialic Acid

The Polysialyltransferases

Molecular insight into the problem of how polySia is synthesized and how surface expression of oligo/polySia-containing glycoconjugates is controlled is currently an active area of investigation. These studies use a combination of biochemical, molecular genetic, and biophysical techniques. Two closely related polyST genes have been cloned, sequenced, and their encoded proteins shown to catalyze the biosynthesis of polySia chains. They are the CMP-Sia:α2,8-polySTs designated STX (ST8SiaII) and PST (ST8SiaIV). Both polySTs catalyze the transfer of sialic acid from the activated sugar nucleotide precursor, CMP-sialic acid, to endogenous or exogenous acceptor substrates. In mammalian cells, N-CAM is the most common endogenous acceptor. The catalytic domains of STX and PST are located in the lumen of the Golgi complex. The amino acid sequence of the human PST is 97% homologous with the hamster and mouse, and is encoded by a single gene (2.0 kb) that codes for a protein with a predicted molecular mass of 41.2 kDa. PST and STX show $\sim$60% homology at the protein level. The genomic structures and promoter activities of the mouse PST and STX genes have been reported, although there is little information about how transcription and translation of these genes are regulated. While the overall structure and genomic organization of STX and PST genes are similar, the 5′-flanking regions of PST and STX are distinctly different. The STX gene is about 80 kb long and consists of six exons, whereas the PST gene is $\sim$60 kb long and contains five exons. PST and STX can independently polysialylate N-CAM in transfected cell lines, where there are reports that the two enzymes may act cooperatively.

Autopolysialylation of the Polysialyltransferases

Soluble constructs of STX and PST both undergo "autopolysialylation" in cell lines transiently transfected with V5 epitope-tagged PST and STX cDNAs. The question of whether autopolysialylation is required for N-CAM polysialylation remains a point of some controversy, although it does not appear to be an obligatory requirement. STX is not autopolysialylated during neuronal development in embryonic chick brain, and it may not be so in cell lines that express no or low levels of N-CAM. It is possible that soluble constructs do not have the same catalytic properties as their membrane-bound counterparts, particularly in the presence of N-CAM. Soluble constructs of polySTs show reduced activity compared with the activity of the membrane-bound form, indicating that N-CAM may modulate polyST activity, and hence the extent and DP of N-CAM polysialylation.

How many Sialyltransferases does it take to Polysialylate?

Results from transfection experiments have been interpreted to support the hypothesis that only one enzyme is required for polySia chain synthesis, since individual cDNAs encoding for polySTs induce polySia expression in cell lines previously shown to be polySia negative. However, some transfected cell lines have pre-existing disialyl (Siaα2,8-Siaα2,3-) terminal residues that can serve as initiating sites for polySia chain polymerization. The presence of diSia in an acceptor substrate would obviate the need for an α2,8-monoST, or "initiase." Thus, while the transfection studies support the necessity of a PST or STX for polySia chain synthesis, they do not exclude the possibility that more than one enzyme may be involved. An alternative theory to the single-enzyme hypothesis is that more than one sialyltransferase is required to catalyze both chain initiation and polymerization. This hypothesis is based on structural studies of the cognate di-, oligo-, and polySia chains that are expressed at different stages of development in the rainbow trout. These studies show that at least two α2,8 sialyltransferases are required. The first, an "initiase," transfers the first α2,8-Sia residue to Siaα2,6/3Gal-acceptors forming the disialyl derivative, Siaα2,8Sia-. A separate polyST or "polymerase" is required to complete polySia chain elongation, based on the later appearance in the development of polysialylated glycoproteins.

Rationale for Chemotherapeutic Inhibition of PolySia Biosynthesis

The studies described above show that surface expression of polySia is positively correlated with increased metastasis in a number of human tumors. Accordingly, the design and synthesis of compounds that selectively inhibit the synthesis of polySia is an important area of research with direct impact on cancer metastasis and treatment of meningitis. The rationale for this idea is that if the oncofetal expression of polySia on the surface of human cancers can be inhibited, then the detachment and anti-adhesive properties of these cells may be diminished, and tumor metastasis may be slowed or stopped. The same rationale holds for treating neuroinvasive meningitis caused by the polysialylated *E. coli* K1 and *N. meningitidis* pathogens.

Selectivity of the PolySTs as Chemotherapeutic Targets

The specificity of chemotherapeutics to selectively inhibit the polySTs and not the monoST, which could have an effect on other tissues, is based on the fact that the two classes of enzymes are structurally and functionally distinct. They differ in the following key properties:

1. The polySTs, in contrast to the monoSTs, are oncodevelopmental enzymes that are selectively re-expressed in cancer. An exception, as noted above, is expression of polySia in the hypothalmo–neurohypophysial region of adult brain, the function/consequence of which is not known.
2. At the protein level, the two classes of enzymes are distinct and have different kinetic properties (K_m and V_{max} values). This is a key feature that favors the design of inhibitors to selectively target the polySTs.
3. The polySTs and monoSTs show limited structural homology and exhibit different structural properties. The polySTs, but not the monoSTs, contain a uniquely extended basic amino acid domain of 31 residues upstream of sialylmotif S. This cationic domain is essential for polysialylation, and thus provides a selective target for the polySTs.
4. The two classes of enzymes show differences in response to thiol reagents, thiol-directed alkylating reagents, and metal ion requirements. The polySTs contain a cystinyl residue required for polysialylation, while the monoSTs do not, and;
5. The polySTs catalyze a processive mechanism of synthesis while the monoSTs catalyze a distributive mechanism of synthesis.

The significance of these differences is two-fold. First, they provide new insight into the enzymatic basis of polysialylation. Second, they reveal for the first time structural features unique to the polySTs that are essential in the design of chemotherapeutic inhibitors to selectively target this class of glycosyltransferases. To our knowledge, no other family of mammalian glycosyltransferases exhibit such marked differences. As such, to use this new information to selectively target the polySTs represents a paradigm shift from the more conventional approaches and targets currently underway in the "glyco-drug" discovery field.

See Also the Following Articles

Glycoproteins, N-Linked • Glycoprotein-Mediated Cell Interactions, O-Linked • Oligosaccharide Chains: Free, *N*-Linked, *O*-Linked

Glossary

endo-N-acylneuraminidase (Endo-N) An endosialidase that catalyzes the depolymerization of polysialic acid chains and is a diagnostic enzyme for identifying **α**2,8-linked polysialic acid.

malignant Describing or referring to a tumor or cancer cell that is invasive and undergoes metastasis.

metastasis The process whereby malignant cancer cells spread from one location in the body to another.

monosialyltransferases (monoSTs) A family of sialyltransferases distinct from the polySTs that catalyze the addition of a single sialic acid residue to acceptor substrates.

neural cell adhesion molecules (N-CAMs) Cell surface glycoproteins that control cell adhesion and cell migration and are the major protein carriers of polysialic acid in mammalian cells.

oncodevelopmental/oncofetal antigens Glycoproteins or glycolipids that are most often expressed during embryonic development and are usually undetected in the differentiated adult. Many are then re-expressed in malignant cancer cells.

polysialic acid (polySia) Complex sugar molecules containing sialic acid that decorate the cell surface of neuroinvasive bacteria causing meningitis and some non-mammalian and mammalian cells. They are oncodevelopmental, tumor-associated antigens that regulate cell–cell interactions and allow some cancer cells to metastasize.

polysialyltransferases (polyST) A family of glycosyltransferases (enzymes) that catalyze the polymerization of multiple sialic acid residues forming polysialic acid.

sialobiology A sub-discipline of the field of glycobiology that focuses on the chemistry and biology of sialic acids in the molecular life sciences.

Further Reading

Close, B. E., Wilkinson, J. M., Bohrer, T. J., Goodwin, C. P., Broom, L. J., and Colley, K. J. (2001). The polysialyltransferase ST8Sia II/STX: Posttranslational processing and role of autopolysialylation in the polysialylation of neural cell adhesion molecule. *Glycobiology* **11**, 997–1008.

Fukuda, M. (1996). Possible roles of tumor-associated carbohydrate antigens. *Cancer Res.* **56**, 2237–2244.

Gluer, S., Schelp, C., von Schwenitz, D., and Gerardy-Schahn, R. (1998). Polysialylated neural cell adhesion molecule in childhood rhabdomyosarcoma. *Pediatric Res.* **43**, 145–147.

Inoue, Y., Lee, Y. C., and Troy, F. A., III (eds.) (1999). *Sialobiology and other novel forms of glycosylation.* Gakushin Pub. Co., Osaka, Japan, 307 pp.

Roth, J., Taatjes, D. J., Bitter-Suermann, D., and Finne, J. (1987). Polysialic acid units are spatially and temporally expressed in developing postnatal rat kidney. *Proc. Natl Acad. Sci. USA* **84**, 1969–1973.

Scheidegger, E. P., Lackie, P. M., Papay, J., and Roth, J. (1994). *In vitro* and *in vivo* growth of clonal sublines of human small cell lung carcinoma is modulated by polysialic acid of the neural cell adhesion molecule. *Lab. Investigation* **70**, 95–106.

Sevigny, M. B., Ye, J., Kitazame-Kawaguchi, S., and Troy, F. A., 2nd. (1998). Developmental expression and characterization of the α2, 8-polysialyltransferase activity in embryonic chick brain. *Glycobiology* **8**, 857–867.

Troy, F. A., II (1995). Sialobiology and the polysialic acid glycotope: Occurrence, structure, function, synthesis and glycopathology. In *Biology of the Sialic Acids* (A. Rosenberg, ed.) pp. 95–144. Plenum Press, New York.

Vimr, E. R., McCoy, R. D., Vollger, H. F., Wilkison, N. C., and Troy, F. A. (1984). Use of prokaryotic-derived probes to identify

poly (sialic acid) in neonatal membranes. *Proc. Natl Acad. Sci. USA* **81**, 1971–1975.

Biography

Frederic A. Troy II is professor and past chairman of the Department of Biochemistry and Molecular Medicine, University of California School of Medicine, Davis, California and a member of the UC Davis Cancer Center. His major area of research is glycoscience, cancer biology, and membrane chemistry. He received his Ph.D. in biological chemistry from Purdue University and carried out postdoctoral studies at Johns Hopkins University School of Medicine. He was a visiting professor in tumor biology at Karolinska Institute and has coedited two major texts in the field of Sialobiology.

Porphyrin Metabolism

Mark Shepherd and Harry A. Dailey
University of Georgia, Athens, Georgia, USA

Porphyrins are cyclic tetrapyrroles that perform critical roles in a variety of biological systems. Examples of important tetrapyrroles include heme and siroheme (both with chelated iron), chlorophyll (with chelated magnesium), coenzyme B_{12} (with chelated cobalt), and factor F_{430} (with chelated nickel). All of these are derived from a common precursor, δ-aminolevulinic acid (ALA). Heme, as a prosthetic group to various hemoproteins, is necessary for oxygen transport and storage as part of hemoglobin and myoglobin. It is essential for electron transport as part of various cytochromes and is also required by mixed function oxidases as a part of cytochrome P450. Additionally, heme is needed for the decomposition and production of hydrogen peroxide as a cofactor of catalase and peroxidase, respectively. Siroheme is the cofactor in both nitrite and sulfite reductases, and hence is not synthesized by mammals.

Several types of chlorophyll exist which differ with respect to the substituents on the tetrapyrrole ring. Chlorophylls are employed by photosynthetic organisms to absorb energy for photosynthesis. This process harnesses the vast majority of energy consumed by living organisms, and only chemolithotrophic bacteria are independent of this energy source. Chlorophylls are required in the first stage of photosynthesis, whereby visible radiation excites an electron in the porphyrin that, upon returning to a lower energy state, provides the energy needed for the synthesis of ATP and NAD(P)H.

Coenzyme B_{12} consists of cobalamin (vitamin B_{12}), a corrin ring, which is linked to dimethylbenzimidazole and 5′ deoxyadenosine via its central cobalt atom. The bond between the cobalt and the latter substituent is a weak cobalt–carbon bond, the only example known in biology, which catalyzes intramolecular rearrangements by cleaving homolytically to generate a free radical. Examples include methylations in methionine synthesis and the reduction of ribonucleotides to deoxyribonucleotides. Finally, there is a nickel (II) tetrapyrrole, factor F_{430}, which is found in methanogenic bacteria and is involved in methane metabolism.

Biosynthesis of Porphyrins

Figure 1 illustrates the first three steps of tetrapyrrole biosynthesis, which is common to all the tetrapyrroles mentioned above. All these molecules have a core structure of four pyrrole rings, designated A–D, as shown on the structure of heme in Figure 1. The carbon atoms are numbered 1–20 starting in ring A and ascending in a clockwise direction around the perimeter of the porphyrin ring.

Formation of δ-Aminolevulinic Acid

The first common intermediate in tetrapyrrole biosynthesis is δ-ALA. Two pathways for its synthesis are found in nature: the C_4 pathway in animals and some bacteria including *Rhodobacter sphaeroides*, and the C_5 pathway in plants, algae, and other bacteria including cyanobacteria. In the C_4, or Shemin pathway, ALA is formed by the condensation of glycine and succinyl coenzyme A in a reaction catalyzed by the enzyme ALA synthase. In the C_5 pathway an NADPH-dependent glutamyl-tRNA reductase produces glutamate 1-semialdehyde (GSA) from glutamyl-tRNA, which is subsequently converted to ALA by the replacement of the aldehyde moiety with an amide group. The C_5 pathway is thought to be ancestral to the Shemin pathway as bacteria with the former lack the α-ketoglutarate–dehydrogenase complex to make succinyl CoA. This group includes cyanobacteria such as *Synechocystis*, which may explain why plants today retain the C_5 pathway.

δ-Aminolevulinic Acid to Uroporphyrinogen III

In all organisms studied to date, the conversion of δ-aminolevulinic acid to uroporphyrinogen III proceeds via exactly the same steps. This process is summarized in Figure 1. The first step involves the condensation of two ALA molecules to form porphobilinogen with the release of two molecules of H_2O. This reaction is catalyzed by porphobilinogen synthase, also known as ALA dehydratase. Hydroxymethylbilane synthase, also known as porphobilinogen deaminase, catalyzes the condensation of four molecules of porphobilinogen in the order A, B, C, D

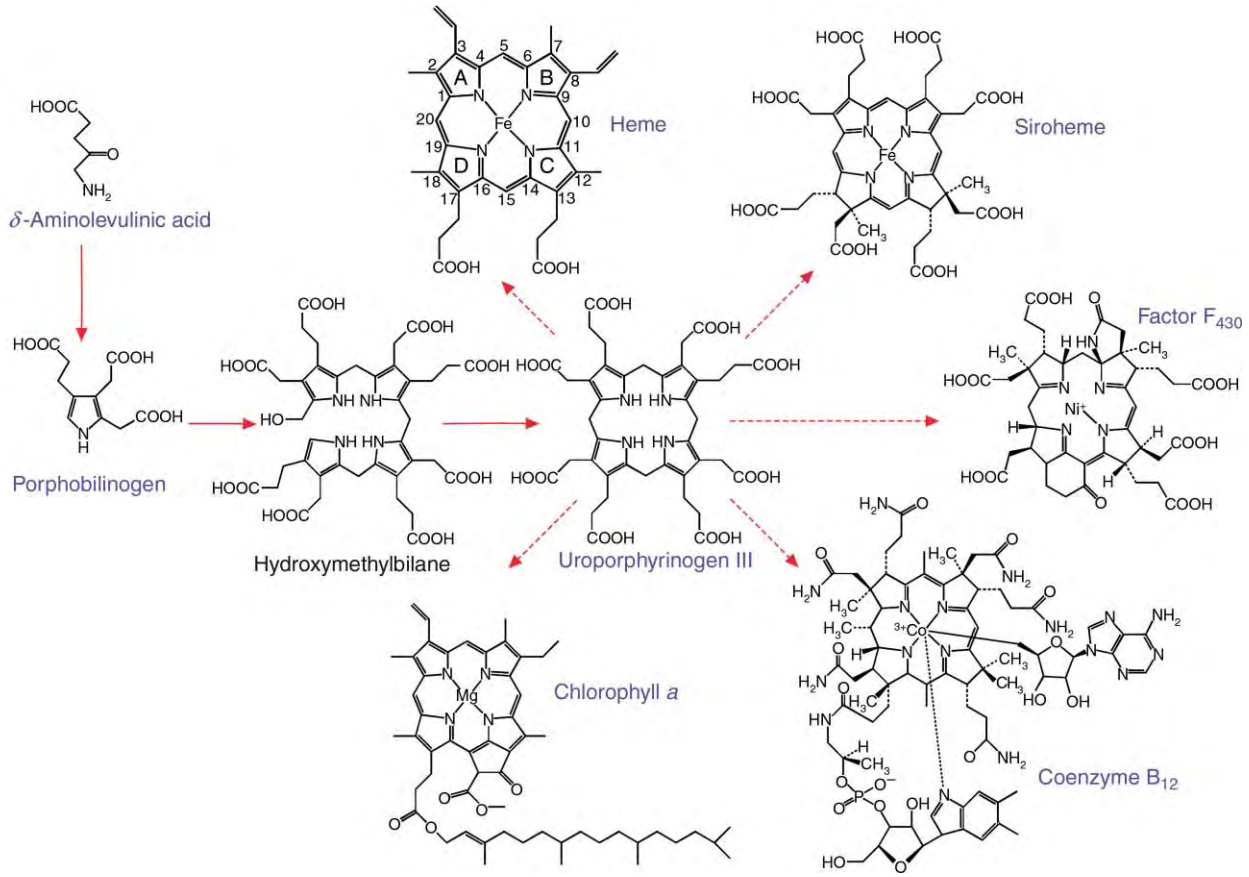

FIGURE 1 The porphyrins. The first three steps common to all porphyrin biosynthesis and the ultimate products of this branched metabolic pathway.

(the letters representing the rings of the ultimate tetrapyrrole product). This condensation gives rise to the first tetrapyrrole, hydroxymethylbilane, also known as preuroporphyrinogen, which is unstable and can close spontaneously, forming the biologically inactive isomer uroporphyrinogen I.

Several enzyme–substrate intermediates exist that are linked via a dipyrromethane cofactor (a modified dipyrrole). The dipyrromethane cofactor is posttranslationally attached to a cysteine residue of the enzyme. The first porphobilinogen molecule condenses with the cofactor and further porphobilinogen molecules are subsequently added to form hydroxymethylbilane. The enzymatic formation of the first macrocyclic tetrapyrrole, uroporphyrinogen III, is catalyzed by the enzyme uroporphyrinogen III synthase. During this reaction, the D pyrrole ring of hydroxymethylbilane undergoes an inversion, via a *spiro* intermediate. As free hydroxymethylbilane spontaneously reacts to form the biologically inactive isomer, uroporphyrinogen I, the enzyme must be present during or immediately after the release of hydroxymethylbilane from hydroxymethylbilane synthase to ensure that the correct isomer is formed.

Heme and Chlorophyll Biosynthesis

The biosynthesis of heme and chlorophyll proceeds along a common pathway until a branchpoint is reached at protoporphyrin IX (Figure 2). This pathway is conserved for almost all organisms studied, except *Desulfobrio vulgaris*, in which coproporphyrinogen III is formed from uroporphyrinogen III indirectly via precorrin-2. The formation of protoporphyrin IX from uroporphyrinogen III is achieved via a series of decarboxylation and oxidation steps. Uroporphyrinogen decarboxylase catalyzes the removal of a carboxyl group from each pyrrole ring to form coproporphyrinogen III. This is converted to protoporphyrin IX via the action of two enzymes, coproporphyrinogen oxidase and protoporphyrinogen oxidase. During aerobic growth both enzymes use oxygen as the terminal electron acceptor. However, anaerobic organisms have been shown to possess oxygen-independent isozymes and some facultative anaerobes encode both types of coproporphyrinogen oxidase.

The next step involves the insertion of a divalent cation into the porphyrin ring. Ferrochelatase catalyzes

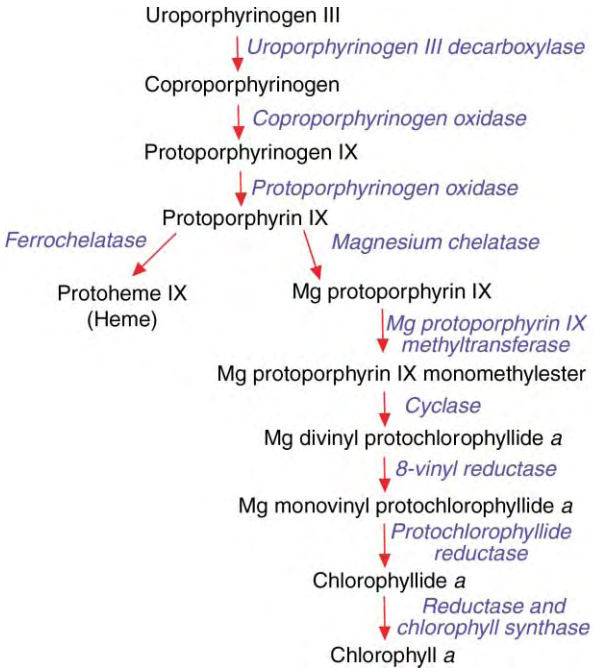

FIGURE 2 Heme and chlorophyll biosynthesis. The branching of the heme and chlorophyll biosynthetic pathways. The enzymes that catalyze the individual steps are shown in blue.

the insertion of an iron (II) ion whilst magnesium chelatase, as its name suggests, catalyzes the insertion of a magnesium (II) ion. It is thought that ferrochelatase distorts the porphyrin ring in such a way that allows the spontaneous insertion of iron (II). The insertion of magnesium requires the presence of MgATP and the participation of all three subunits of the heterotrimeric magnesium chelatase.

Subsequent steps of the chlorophyll biosynthetic pathway involve methylation and cyclization of the propionate group on ring C. After the reduction of the vinyl group on ring C, a light-dependent reaction takes place. This is catalyzed by protochlorophyllide reductase (POR) and is one of only two reactions known to be light dependent, the other being DNA photolyase. This reaction can also proceed via a light-independent reaction, catalyzed by dark protochlorophyllide reductase (DPOR). The formation of chlorophylls requires the addition of a hydrophobic tail to the propionate group on ring D via an esterification reaction. In the cases of chlorophyll and bacteriochlorophyll, these long chain alcohols are phytol and geranylgeraniol, respectively.

Coenzyme B_{12} and Factor F_{430} Biosynthesis

Figure 3 summarizes the synthesis of coenzyme B_{12} and factor F_{430} from uroporphyrinogen III. The first step

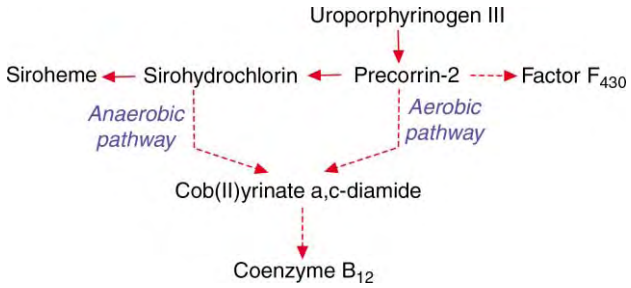

FIGURE 3 Coenzyme B_{12} and factor F_{430} biosynthesis. The branching of the coenzyme B_{12} and factor F_{430} biosynthetic pathways. The enzymes that catalyze the individual steps are shown in blue.

involves the methylation of uroporphyrinogen on rings A and B to form precorrin-2. Reduction to form sirohydrochlorin and subsequent ferrochelation yields siroheme, the prosthetic group for both nitrite and sulfite reductases. Factor F_{430} synthesis requires the cyclization of substituents on rings B and D and the chelation of nickel (II), which is bound to the pyrrole nitrogen on ring C. This final step is thought to be catalyzed by an ATP-dependent nickel chelatase.

The formation of coenzyme B_{12} involves a branched pathway consisting of several reactions. Figure 3 shows that the synthesis of cob(II)yrinate a,c-diamide can occur by either an anaerobic or an aerobic pathway. Both pathways involve the methylation, reduction, and isomerization of precorrin-2, along with the insertion of a central cobalt atom. The anaerobic chelatase has been compared to ferrochelatase as it is encoded by a single gene and does not require MgATP. The aerobic cobalt chelatase is similar to the magnesium chelatase involved in chlorophyll biosynthesis, as it is heterotrimeric and requires MgATP for catalysis. Coenzyme B_{12} is then formed via various alkylations, phosphorylation, an internal rearrangement, and the coordination of an adenosyl group to the central cobalt atom.

Regulation

As δ-ALA is the universal precursor for porphyrin synthesis, the supply of this metabolic intermediate ultimately governs whether or not porphyrin synthesis may take place. However, there are several examples where other key points in the pathway are subject to regulation. Heme plays a key role as a cofactor for many redox reactions in several different cell types and requires iron as a cofactor. From this it is clear that the regulation of heme biosynthesis must be dealt with on a global scale amongst different cell types and subcellular compartments. The model of negative feedback regulation mediated by a single regulator (heme) at a single site (ALA synthase) remained dogma for many years. Only after compelling evidence was generated to

support regulation at other sites, was it accepted that heme biosynthesis is subject to more complex control.

The biosynthesis of cofactor B_{12} or Factor F_{430} is more poorly understood. As mammals do not synthesize these cofactors, little work has been performed on the regulation of these pathways.

Regulation of Heme Biosynthesis

Role of ALA Synthase

In animal cells two ALA synthase (ALAS) genes exist that are classified by their histological localization. ALAS-E (or ALAS-2) is induced during erythroid differentiation and ALAS-1 encodes ALA synthase in other tissues. ALAS-1 is also referred to as ALAS-H (housekeeping) or ALAS-N (non-erythroid). The primary sequence of both ALAS proteins is highly conserved. However, significant differences exist between the regulatory regions of the genes and the untranslated regions of their respective mRNAs, which are manifested by the tissue-specific expression of the two enzymes.

Regulation at Sites Other than ALAS

Although it is accepted that ALAS is the major site of regulation, several examples of pathway control exist at the level of gene expression. In mammals, all the genes that encode heme biosynthetic enzymes possess both housekeeping and erythroid-specific promoter elements, although only ALAS is represented by two distinct genes.

A good example of regulation in response to an external stimulus is exhibited by the coproporphyrinogen oxidase of the nitrogen fixing bacterium *Azorhizobium caulinodans*. The enzyme responsible for nitrogen fixation, nitrogenase, requires the absence of oxygen to convert dinitrogen into ammonia. This organism is thought to possess both aerobic and anaerobic coproporphyrinogen oxidases and switches to the anaerobic isozyme in response to falling oxygen levels. Furthermore, the respiratory electron transport chain has been shown to act as the electron acceptor for protoporphyrinogen oxidase in anaerobically grown *E. coli*. This reaction is thought to be catalyzed by an enzyme distinct from the oxygen-dependent protoporphyrinogen oxidase.

Deficiencies in Porphyrin Synthesis

Porphyria

Porphyria is a mammalian disease caused by point mutations or deletions in the genes encoding heme biosynthetic enzymes. Individuals with this disorder are usually able to synthesize normal amounts of heme, but accumulate pathway intermediates that cause the clinical symptoms of porphyria. The disease can be divided into three groups: (1) cutaneous porphyrias, characterized by photosensitization; (2) acute porphyrias, where individuals experience abdominal pain, psychiatric disorders, constipation, vomiting, and paralysis; and (3) mixed porphyrias, which manifest themselves as a combination of both. Figure 4 illustrates the porphyrias that result from deficiencies in specific parts of the pathway.

Herbicides

The porphyrin biosynthetic pathway has been targeted for inhibition by certain herbicides to curtail the production of chlorophyll. Diphenyl ether-type herbicides, acifluorfen in particular, have been shown to act as potent inhibitors of protoporphyrinogen oxidase, the last enzyme before the branchpoint of heme and chlorophyll biosynthesis. These molecules compete for the tetrapyrrole-binding site on the enzyme, which impedes the binding of protoporphyrinogen. Hence, protoporphyrinogen production is inhibited, leading to reduced levels of heme and chlorophyll. As a result, plants treated with such herbicides appear chlorotic (yellow colored) due to their ability to produce

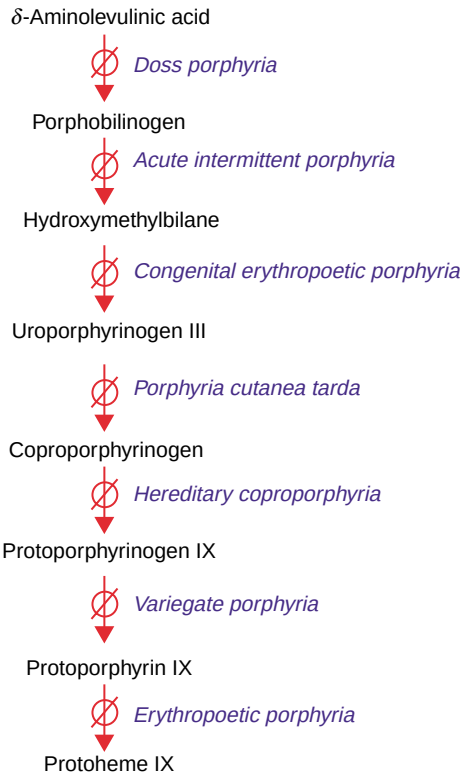

FIGURE 4 The porphyrias. The porphyric disorders that characterize deficiencies in specific parts of the heme biosynthetic pathway are shown in blue.

carotenoids but not chlorophylls. The action of these herbicides is characterized by the accumulation of protoporphyrinogen IX. This diffuses out of the plastids/mitochondria and is oxidized to protoporphyrin IX, either via non-enzymatic means or catalyzed by peroxidase. This mislocation of protoporphyrin IX leads to phototoxicity through the evolution of singlet oxygen species.

See Also the Following Articles

Chlorophylls and Carotenoids • Cytochrome P-450 • Heme Proteins • Heme Synthesis • Vitamin B_{12} and B_{12}-Proteins

Glossary

chelation The removal of free metal ions from solution by an organic chemical.

herbicide Chemical agent used to curtail plant growth.

plastid Generic name for chloroplasts and chloroplast precursors.

singlet oxygen A reactive oxygen radical with a single unpaired electron.

Further Reading

Beale, S. I. (1999). Enzymes of chlorophyll biosynthesis. *Photosyn. Res.* **60**, 43–73.

Bottomly, S. S., and Muller-Eberhard, U. (1988). Pathophysiology of heme synthesis. *Semin. Hematol.* **25**, 282–302.

Dailey, H. A. (1997). Enzymes of heme biosynthesis. *J. Biol. Inorg. Chem.* **2**, 411–417.

Falk, J. E. (1964). *Porphyrins and Metalloporphyrins: Their General, Physical and Coordination Chemistry, and Laboratory Methods*. Elsevier, Amsterdam.

Kadish, K. M., Smith, K., and Guilard, R. (2003a). The iron and cobalt pigments: Biosynthesis, structure, and degradation. In *The Porphyrin Handbook*, Vol 12. Academic Press, San Diego.

Kadish, K. M., Smith, K., and Guilard, R. (2003b). Chlorophylls and bilins: Biosynthesis, structure, and degradation. In *The Porphyrin Handbook*, Vol 13. Academic Press, San Diego.

Warren, M. J., and Scott, A. I. (1990). Tetrapyrrole assembly and modification into the ligands of biologically functional cofactors. *Trends Biochem. Sci.* **15**, 486–491.

Warren, M. J., Jay, M., Hunt, D. M., Elder, G. H., and Röhl, J. C. G. (1996). The maddening business of King George III and porphyria. *Trends Biochem. Sci.* **21**, 224–231.

Biography

Harry A. Dailey received a B.A. (bacteriology) in 1972 and a Ph.D. (microbiology) in 1976 from UCLA. He joined the Department of Microbiology at the University of Georgia in 1980 as an Assistant Professor following postdoctoral studies at the University of Connecticut Health Center. He served as Head, Department of Microbiology at UGA (1987–1996) and was appointed Director of the Biomedical and Health Sciences Institute in 2001. His research interests involve heme biosynthesis and the genetic diseases named porphyrias.

Mark Shepherd received a B.Sc. (1999) (Biochemistry) and a Ph.D. (2003) from the University of Sheffield. He then moved to the University of Georgia to perform postdoctoral research in the laboratory of Harry A. Dailey. His research interests involve the enzymology of heme and chlorophyll biosynthesis.

Pre-tRNA and Pre-rRNA Processing in Bacteria

Sidney R. Kushner
University of Georgia, Athens, Georgia, USA

In bacteria, tRNAs and rRNAs represent the large majority of RNA molecules found inside cells. rRNAs along with a variety of ribosomal proteins are the structural components of the ribosomes, the macromolecular complexes that carry out protein synthesis. In an exponentially growing bacterium such as *Escherichia coli*, there are 30 000–45 000 ribosomes per cell. tRNAs are also required for protein synthesis, being the molecules that bring individual amino acids to the ribosome for the process of peptide bond synthesis. Both of these types of RNA molecules are very stable and are essential for cell viability.

Interestingly, tRNAs and rRNAs are synthesized as parts of larger precursor molecules that must be processed to generate the mature forms that are either incorporated into ribosomes or that can be charged with amino acids. The processing of these RNA molecules is carried out by a series of ribonucleases that have very specific functions. These processing reactions, as described, have been studied extensively in *E. coli*, but may be significantly different in other bacteria.

tRNAs

Mature tRNAs are relatively small molecules that can range in length from 73 to 94 nucleotides (Figure 1). In order for them to be functional, they must contain the trinucleotide CCA at their 3′ termini (Figure 1) to which specific amino acids can be covalently attached. In some bacteria such as *E. coli* the CCA is encoded in the DNA. In others, the CCA has to be added posttranscriptionally to some of the tRNAs transcripts. In addition, there can be multiple tRNAs that can be charged with the same amino acid. For example, in *E. coli* there are 86 tRNA genes even though there are only 21 amino acids. Each tRNA folds into a characteristic cloverleaf structure (Figure 1), most likely during or even prior to the various processing events.

Primary Structure of tRNA Genes

Although there are large numbers of tRNA genes in each bacterium, they are not clustered in one specific region of the genome. Rather, they may exist as independent genes (Figure 2A), in a group of tRNA genes that are all transcribed from a single promoter (Figure 2B), in a group of genes that also include mRNAs or embedded in an operon that contains rRNA genes (Figure 2C). In all cases, the tRNA transcripts contain extra nucleotides (Figure 2, black lines) that must be removed to generate the mature, functional tRNAs that can be recognized by their respective aminoacyl transferases, the enzymes that specifically charge each of the tRNAs with the appropriate amino acid.

Enzymatic Processing of tRNA Precursors

Some features of tRNA processing have been universally conserved, while others may be specific to certain classes of bacteria. For example, the mature 5′ terminus of every tRNA is generated by an endoribonuclease called RNase P. This enzyme is composed of a catalytic RNA and a protein subunit, and is found in both prokaryotes and eukaryotes. However, at least in *E. coli*, RNase P cleavage requires prior processing at the 3′ terminus. Thus, in the initial processing step for most, if not all, *E. coli* tRNAs, RNase E cleaves endonucleolytically near the mature CCA sequence (1–3 nucleotides downstream, Figure 3, blue arrows). Cleavage by this enzyme is required whether the tRNA is a monocistronic transcript (Figure 3A) or exists as part of a polycistronic operon (Figure 3B).

Following RNase E processing, RNase P cuts at the 5′ end (Figure 3, red arrows), generating the mature terminus. Subsequently, the few extra nucleotides found at the 3′ terminus are removed exonucleolytically by a combination of RNase T, RNase D, RNase BN, RNase II, RNase PH, and possibly polynucleotide phosphorylase (Figure 3, dashed orange arrows). Based on the substrate preferences of these various 3′ → 5′ exonucleases, RNase T appears to be the most important of the various enzymes. In the case of organisms where the 3′ CCA nucleotides are not encoded in the DNA, an enzyme called tRNA nucleotidyltransferase is capable of

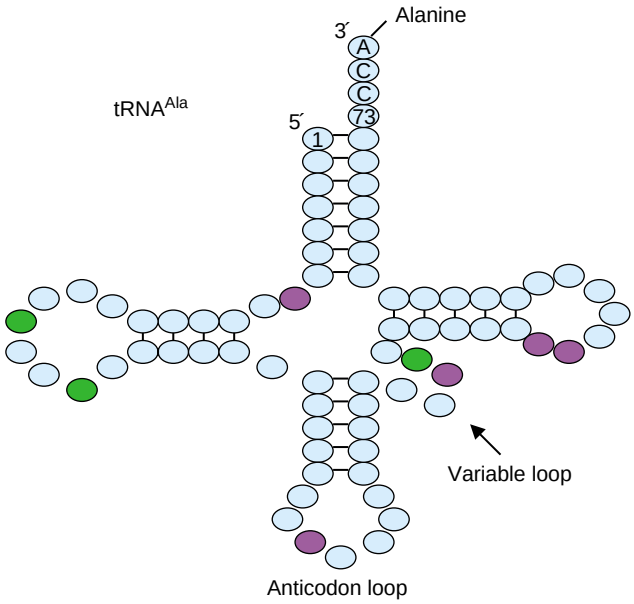

FIGURE 1 Schematic drawing of *Escherichia coli* alanine tRNA. This particular tRNA contains 76 nucleotides. The green ovals indicate positions at which one nucleotide may be deleted yielding tRNAs between 73–75 long or additional nucleotides can be added, yielding species up to 94 nucleotides in length. The magenta ovals indicate the locations of bases that are modified posttranscriptionally in this tRNA. Each tRNA has a unique pattern of base modification. The anticodon loop, used for reading the messenger RNA, as well as the CCA at the 3′terminus are indicated. The short black lines indicate positions of Watson–Crick base pairing.

adding the two Cs and one A, using CTP and ATP as substrates, to generate the mature 3′ terminus. Most bacteria contain this enzyme, which can also be used to repair 3′ termini that have been partially degraded during the exonucleolytic processing reactions (Figure 3A).

Modification of Individual Bases in tRNAs

Although tRNAs are synthesized using the standard nucleoside triphosphates containing either adenine, uracil, guanine or cytosine, each tRNA contains a number of modified bases that are generated posttranscriptionally (Figure 1). For example, a common modification involves the replacement of an oxygen atom at the 3 position of uracil with a nitrogen atom, generating a new base called pseudouracil. Additional alterations arise by the addition of methyl groups at specific locations. Some modifications occur through a single enzymatic step (methylation), while others require a series of biosynthetic steps (1-methylinosinic acid). Research has shown that only some of the modified bases are required for normal tRNA function. Many of the modifications are found not only in bacteria but in eukaryotic organisms as well.

rRNAs

rRNAs provide the structural core to which ribosomal proteins bind to form both the 30S and 50S bacterial ribosomal subunits. The 16S rRNA is found in the 30S subunit while the 23S and 5S species are located in the 50S ribosomal subunit. Numerous ribosomal proteins are associated with each subunit but recent crystallographic data suggest that it is the RNA component of the 50S subunit that catalyzes peptide bond formation. In bacteria all three rRNA species are transcribed as part of a single polycistronic transcript (30S) in the order of 16S, 23S, and 5S (Figure 2C). In addition, the rRNA genes are duplicated in most bacteria (seven copies in *E. coli*) and generally contain one or more tRNAs (Figure 2C).

Primary Processing

The primary 30S rRNA transcript is cleaved during its synthesis by the endoribonuclease RNase III. This enzyme recognizes specific stem-loop structures that are generated by inverted repeats within the RNA transcript. In bacteria, the 16S and 23S rRNAs form two adjacent stem-loop structures (Figure 4). RNase III

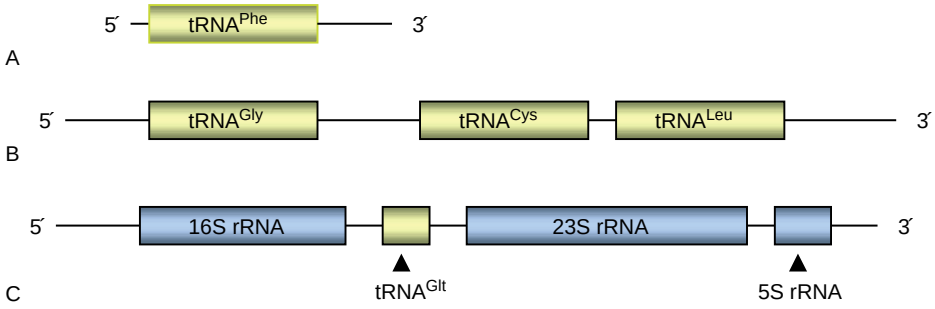

FIGURE 2 Organization of tRNA and rRNA genes. (A) The monocistronic phenylalanine tRNA gene from *E. coli*. (B) The polycistronic operon from *E. coli* containing glycine, cysteine, and leucine tRNA genes. (C) One of seven *E. coli* rRNA operons (*rrnB*) containing the sequences for 16S, 23S, and 5S rRNAs, as well as a glutamine tRNA. Colored boxes (yellow for tRNAs and blue for rRNAs) represent what will become the mature sequences. Black lines indicate sequences that will be removed by nucleolytic processing reactions.

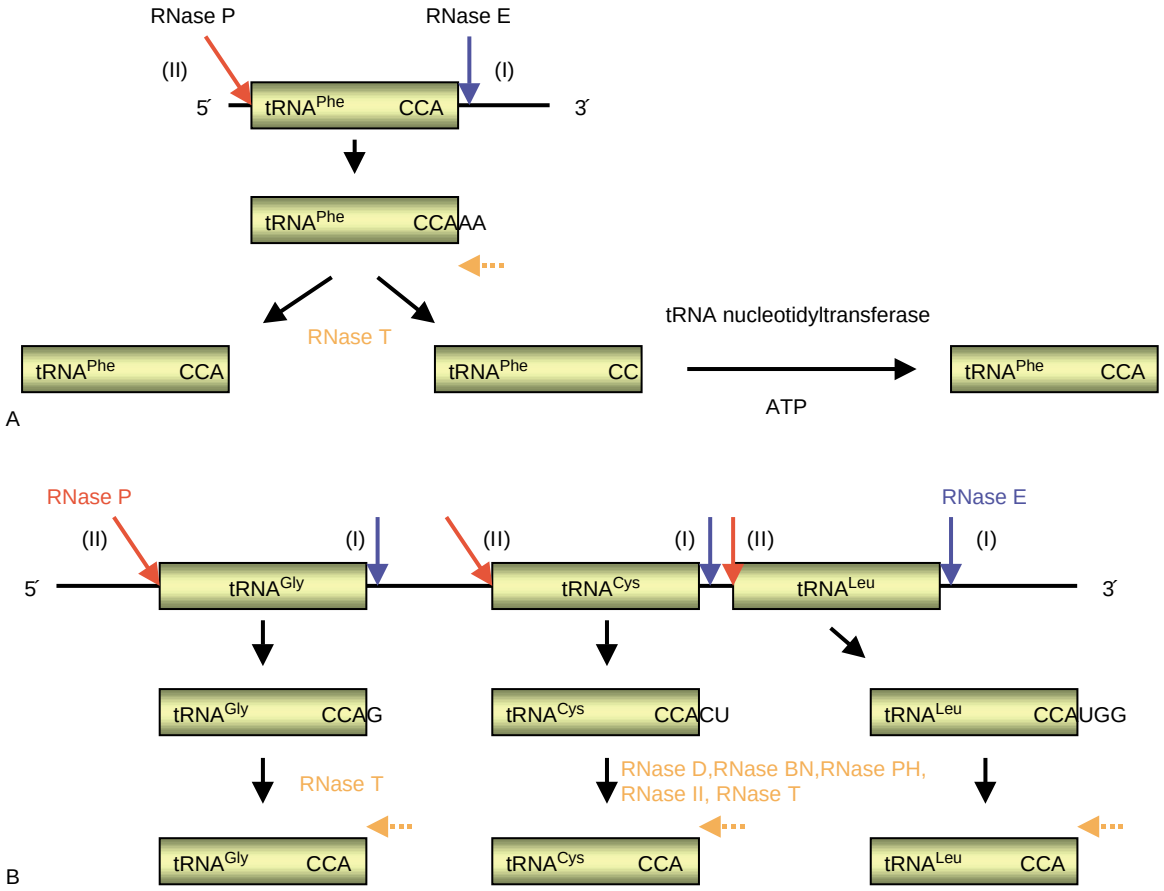

FIGURE 3 Processing of tRNAs in *E. coli*. (A) With a monocistronic operon, the initial cleavage (I) at the 3′ end is catalyzed by RNase E (blue arrow), followed by RNase P processing (red arrow) at the 5′ end (II). While RNase P cleavage generates the mature 5′ terminus, RNase E cleavage leaves a small number of extra nucleotides at the 3′ end. Based on extensive analysis of the various 3′ → 5′ exonucleases found in *E. coli*, it appears that RNase T (dashed orange arrow) is primarily responsible for processing the phenylalanine tRNA. If, however, RNase T removes one too many nucleotides, the A residue can be restored by the action of tRNA nucleotidyltransferase. (B) In the case of a polycistronic operon, the first series of cleavage reactions is again carried out by RNase E (blue arrows) (I). Subsequently, RNase P cuts (red arrows) at the 5′ end (II). Final processing normal involves RNase T (dashed orange arrow). In some cases, additional riboexonucleases, as indicated, are also required.

cleaves on both sides of each stem (Figure 4, magenta arrows). In one case, a 17S precursor of what will become the mature 16S rRNA is released. This molecule contains an extra 115 nucleotides at its 5′ terminus and 33 nucleotides at the 3′ terminus. In the case of the 23S rRNA, RNase III cleavage leaves an extra 3 or 7 nucleotides at the 5′ terminus and 7–9 nucleotides at the 3′ terminus. The RNase III cleavages release the 5S rRNA as part of a 9S precursor.

Generation of Mature rRNAs

16S rRNA

Recent studies have shown that the mature 5′ terminus of 16S rRNA is generated as a two-step process in which RNase E initially cuts endonucleolytically to remove 49 nucleotides from the immature 5′ end (Figure 4, blue arrow). Following this step RNase G cleaves to generate the mature 5′ end (Figure 4, green arrow). Removal of the extra 33 nucleotides at the 3′ end is thought to also occur endonucleolytically, even though the actual enzyme responsible for this processing event has not yet been identified (Figure 4, brown arrow).

23S rRNA

For the 3′ end of the immature 23S rRNA, experiments have indicated that a combination of polyadenylation and the activity of several exoribonucleases serve to generate the mature terminus (Figure 4, dashed orange arrows). In particular, RNase T appears to be the primary exonuclease involved in this process, but additional RNases such as RNase PH, RNase BN, RNase D and RNase II probably also participate. It is not known at this time how the extra nucleotides are removed from the 5′ end (Figure 4, brown arrow).

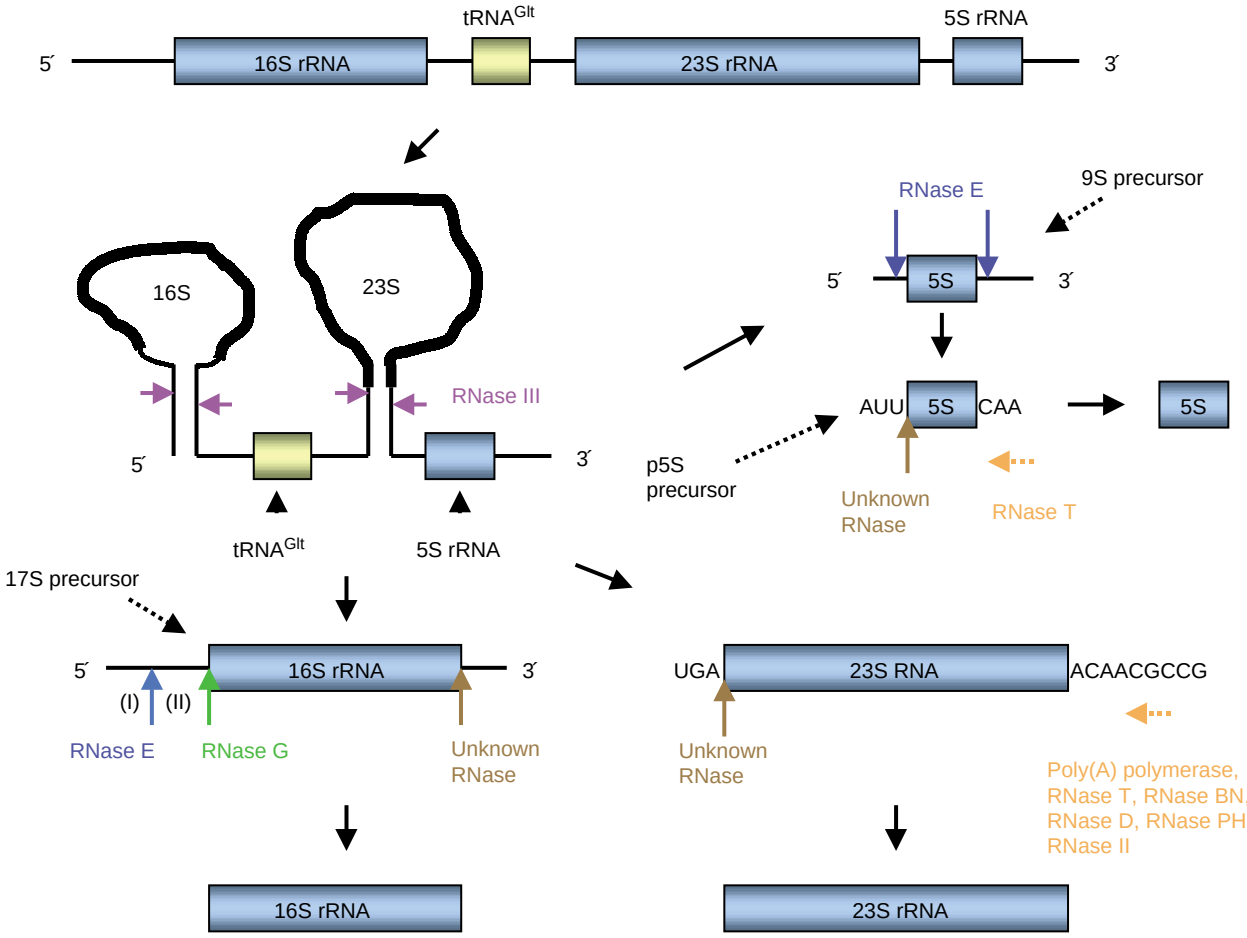

FIGURE 4 Processing of rRNA in *E. coli*. The polycistronic rRNA operon is shown initially in a linear form. Because of the presence of inverted repeats two double-stranded stems form, which loop out both the 16S and 23S rRNA sequences (thick lines). These stem-loop structures are recognized by RNase III (magenta arrows), which cuts on both sides of each stem to release pre16S (17S), 23S, and 9S species. The 17S species contains 115 extra nucleotides at the 5′end and 33 nucleotides at the 3′end. Processing at the 5′end involves a sequential series of reactions involving RNase E (blue arrow) first (I) followed by RNase G (green arrow) (II) to generate the mature 5′ end. An unknown endoribonuclease (brown arrow) is thought to generate the mature 3′ terminus. With the 23S rRNA, there are a few extra nucleotides at the 5′ end that are removed by an unidentified as yet RNase (brown arrow). At the 3′ end the extra 7–9 nucleotides are removed by a combination of polyadenylation and 3′ → 5′ exonucleases (dashed orange arrow). To generate 5S rRNA, RNase E (blue arrows) cuts the 9S precursor at both the 5′ and 3′ ends to release a p5S form that has three extra nucleotides at either end. RNase T (dashed orange arrow) processes the 3′ end, while the 5′ end is matured by an unknown ribonuclease (brown arrow). Processing of the glutamine tRNA is as described in Figure 3B.

However, since no 5′ → 3′ riboexonucleases have been identified in *E. coli*, it is presumed that this processing is carried out by an endoribonuclease.

5S rRNA

The 9S precursor, formed by RNase III cleavage of the 30S transcript, is cut twice by RNase E to release a p5S molecule (Figure 4, blue arrows). The p5S form contains three additional nucleotides at either end. In *E. coli*, RNase T has been shown to be essential for the removal of the extra nucleotides at the 3′ end (Figure 4, dashed orange arrow). It is not known how the 5′ end is processed (Figure 4, brown arrow).

Processing Differences among Various Bacterial Species

While the general genomic organization of the rRNA operons and tRNAs is conserved among bacterial species, it is not clear whether the processing reactions are identical in all organisms. For example, while certain enzymes such as RNase III and RNase P are highly conserved in large numbers of prokaryotes, others such as RNase G, RNase E, and RNase T, are found only in a limited number of bacteria. For example, RNase T homologues have been identified in gram-negative bacteria but have not been found in gram-positives. In addition, neither RNase E, RNase

G, nor RNase II exists in the Gram-positive organism *Bacillus subtilis*. Thus, while some aspects of processing are highly conserved in bacteria (RNase III cleavage of the 30S rRNA precursor and 5′ end processing of tRNAs by RNase P), there is probably considerable variation in the other aspects of processing.

What Happens when Processing is Defective?

Since mutations in either RNase E or RNase P lead to cell death, tRNA processing is essential for cell viability. This is not overly surprising because an immature 3′ terminus of a tRNA cannot be charged with the appropriate amino acid. Without charged amino acids, protein synthesis will not take place. This presumably is the reason for the presence of redundant enzymes (RNase T, RNase PH, RNase BN, RNase D, and RNase II) capable of removing the few remaining nucleotides at the 3′ terminus following RNase E cleavage. Loss of any one of these exoribonucleases does not compromise cell viability, as long as the others remain active. In addition, if processing happens to remove the 3′ terminal A, tRNA nucleotidyltransferase functions to restore a functional 3′ terminus (Figure 3A).

In contrast, the requirements for rRNA maturation are not as strict. Immature forms of 16S rRNA, 23S rRNA, and 5S rRNA can be incorporated into ribosomes that are biologically active. In addition, there are probably backup processing pathways for rRNA. For example, in RNase III mutants of *E. coli*, full-length 30S rRNA precursors are observed, but the cell is still viable. Under these circumstances, it is quite likely that alternative processing is carried out by either RNase G or RNase E. In *B. subtilis*, which lacks both these enzymes, RNase III is essential for cell viability.

See Also the Following Articles

Ribosome Assembly • Ribosome Structure

Glossary

polarity RNA molecules have 5′ and 3′ ends (termini) which are named for the orientation of the 5′ and 3′ carbon atoms of the ribose rings in the sugar/phosphate backbone.

riboendonuclease An enzyme that degrades a RNA molecule at internal locations.

riboexonuclease An enzyme that degrades an RNA molecule, one nucleotide at a time. If the enzyme initiates the degradation from the 3′ terminus it is called a 3′ → 5′ riboexonuclease.

sedimentation coefficient (*S*) Named after the Swedish scientist Svedberg, the *S* value is an indication of the size of a large macromolecule. It is based on the mobility of large molecules in a centrifugal field. Thus, the higher the number the larger the molecule.

Further Reading

Deutscher, M. P., and Li, Z. (2001). Exoribonucleases and their multiple roles in RNA metabolism. *Prog. Nucl. Acid Res. Mol. Biol.* **66**, 67–105.

Gopalan, V., Vioque, A., and Altman, S. (2002). RNase P: Variations and uses. *J. Biol. Chem.* **277**, 6759–6762.

Li, Z., and Deutscher, M. P. (1995). The tRNA processing enzyme RNase T is essential for maturation of 5S RNA. *Proc. Natl Acad. Sci. USA* **92**, 6883–6886.

Li, Z., Pandit, S., and Deutscher, M. P. (1999). Maturation of 23S ribosomal RNA requires the exoribonuclease RNase T. *RNA* **5**, 139–146.

Li, Z., Pandit, S., and Deutscher, M. P. (1999). RNase G (CafA protein) and RNase E are both required for the 5′ maturation of 16S ribosomal RNA. *EMBO J.* **18**, 2878–2885.

Ow, M. C., and Kushner, S. R. (2002). Initiation of tRNA maturation by RNase E is essential for cell viability in *Escherichia coli*. *Genes Develop.* **16**, 1102–1115.

Zuo, Y., and Deutscher, M. P. (2002). The physiological role of RNAse I can be explained by its unusual substrate specificity. *J. Biol. Chem.* **277**, 29654–29661.

Biography

Sidney Kushner is a Professor and former Head of the Department of Genetics at the University of Georgia. His research focuses on understanding the molecular mechanisms of RNA processing and decay, as well as polyadenylation in bacteria. He holds a Ph.D. from Brandeis University and was a Postdoctoral Fellow at the University of California, Berkeley and Stanford University. He is a Fellow of the American Association for the Advancement of Science and the American Academy of Microbiology.

Pre-tRNA and Pre-rRNA Processing in Eukaryotes

Hendrik A. Raué
Vrije Universiteit, Amsterdam, The Netherlands

The two most abundant stable RNA species in eukaryotic cells, tRNA and rRNA, are synthesized in the form of precursor molecules containing extra sequences not present in the mature molecules. By processing the ordered removal of these extra sequences by exo- and/or endonucleases is meant and, in the case of tRNA, covalent linkage of the fragments arising from removal of an internal region (splicing). In a wider sense, processing also encompasses various types of modification of particular nucleotides, as well as addition of nucleotides that are not encoded in the DNA (editing). This article describes the present knowledge of the mechanisms responsible for pre-tRNA and pre-rRNA processing. The emphasis is on the yeast *Saccharomyces cerevisiae*, where this processing has been studied in greatest detail. However, the general principles, and even many of the details, apply to most other eukaryotes as well.

Pre-tRNA Processing

Eukaryotic tRNAs are generally synthesized as individual precursor molecules that contain extra sequences at both the 5′- and 3′-end, called leader and trailer, respectively. Some, though not all, pre-tRNAs also contain an intron, which is always located directly downstream (i.e., 3′) from the anticodon. Consequently, the conformation of the mature domain of the tRNA is largely conserved in its precursor and structural features of this mature domain are in fact the major recognition elements for the various processing enzymes (Figure 1A).

Processing of eukaryotic pre-tRNA takes place in the nucleus and only fully processed tRNAs are recognized by the export machinery that transfers them to the cytoplasm (Figure 1B). However, there does not seem to be an obligatory order of the different steps leading from the pre-tRNA to the mature molecule.

Removal of Precursor-Specific Sequences

5′-End Processing

Removal of the 5′-leader region is normally the first event in eukaryotic pre-tRNA processing. It is carried out by the nuclear endonuclease RNase P, a ribonucleoprotein complex that has orthologues in eubacteria and archaebacteria, as well as in mitochondria and chloroplasts. RNase P contains a single, small RNA molecule the conformation of which, though not the sequence, has been strongly conserved from bacteria to man. This RNA molecule is associated with a variable number of proteins, depending on the organism, that show a lesser degree of conservation.

The substrate for RNase P is a complex of pre-tRNA and the La protein which binds to the 3′-end of the precursor immediately after termination of transcription. Substrate recognition is mainly based upon the consensus tertiary structure of the mature domain of the pre-tRNA, but the 3′-trailer region also contributes to efficient cleavage by RNase P.

In yeast 5′-end maturation of pre-tRNAs takes place mostly in the nucleolus, a specialized region of the nucleus not bound by a membrane that is also involved in the first stages of pre-rRNA processing (Figure 1B). However, 5′-end maturation can also occur in the nucleoplasm, though it is as yet unclear whether this applies to a small portion of all pre-tRNAs or only to a few specific pre-tRNA species. All subsequent steps in yeast pre-tRNA maturation occur in the nucleoplasm. In mammalian cells, the situation seems to be reversed with most 5′-end processing occurring in the nucleoplasm.

3′-End Processing

Removal of the 3′-trailer sequence follows cleavage by RNase P and is performed by, as yet, an unidentified endonuclease that acts upon the precursor/La-protein complex. In the absence of bound La-protein both the timing and the mechanism of 3′-end processing are altered. The naked pre-tRNA is first attacked by 3′ → 5′ exonucleases that remove the portion of the 3′-trailer not base-paired to the leader. Removal of the latter by RNase P, then exposes the remainder of the trailer to further exonucleolytic digestion.

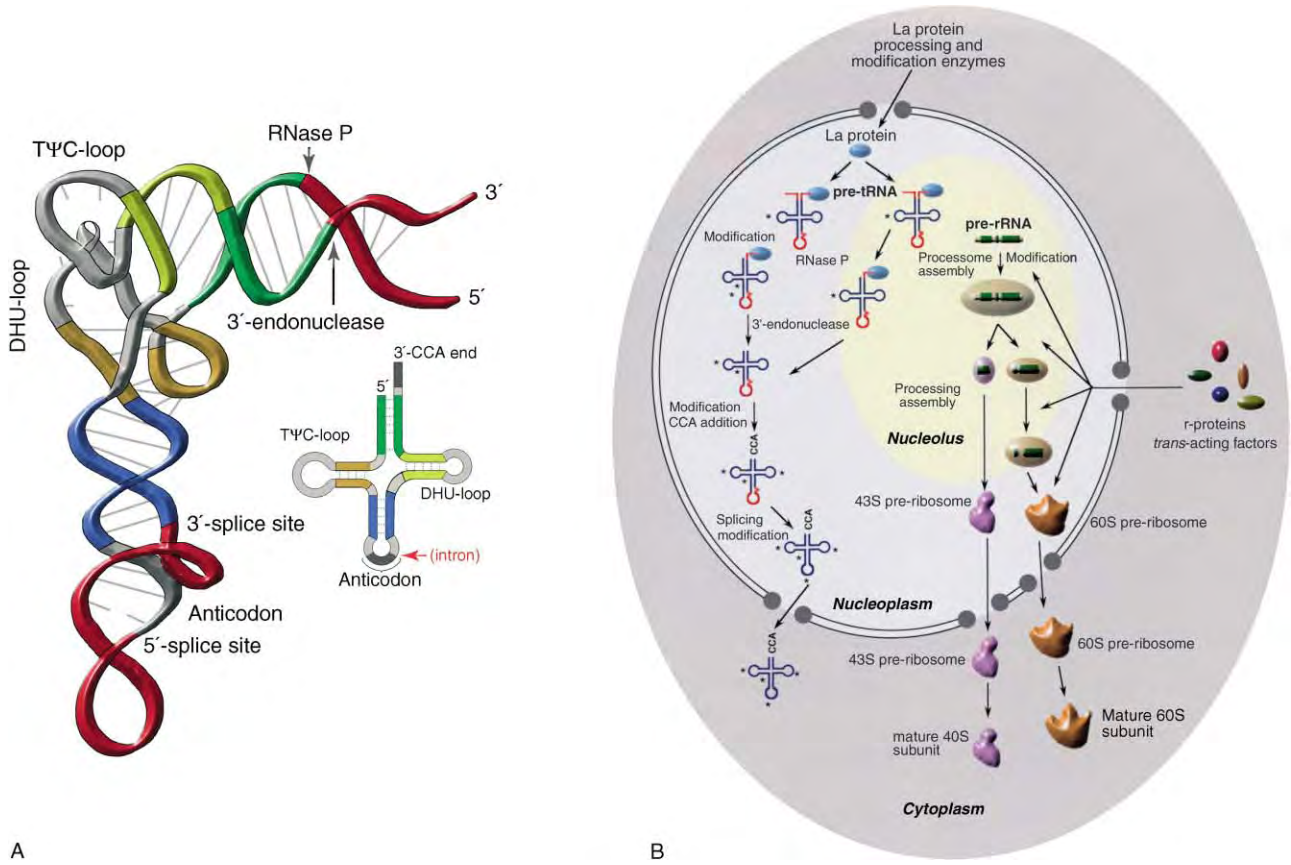

FIGURE 1 Overview of pre-tRNA processing and pre-rRNA processing/assembly in eukaryotic cells. (A) Conformation of pre-tRNA. The various regions are color-coded in the same manner as in the 2D model. Leader, trailer, and intron are in red. The mature domain of the precursor has essentially the same conformation before and after processing. (B) Subcellular localization. As discussed in the text pre-tRNA processing takes place in both the nucleolus and the nucleoplasm. Note that nucleotide modifications (indicated by asterisks) occur – in a specific order – at various stages. Pre-rRNA processing and its assembly with ribosomal proteins starts in the nucleolus with later stages taking place in the nucleoplasm. The finishing steps in formation of functional ribosomal subunits occur in the cytoplasm. In yeast this includes the final processing of 20S pre-rRNA into mature18S rRNA. In other eukaryotes the latter also occurs in the nucleoplasm. Export of tRNA and each of the two types of ribosomal subunits to the cytoplasm occurs by different pathways, which, however, do share some components. Note the nuclear pores are not selective for either the type of macromolecule to be transported or the direction of transport.

Removal of the Intron (Splicing)

Splicing is normally a late step in pre-tRNA processing, although under particular conditions it can occur prior to end maturation. Splicing involves the consecutive action of three enzymes. First, a splicing endonuclease cleaves the phosphodiester bonds at both ends of the intron. The yeast enzyme is a multi-subunit, integral membrane protein that may be located in the inner nuclear envelope. It contains two distinct active sites, one for each of the two splice sites. The enzyme selects the splice sites primarily by measuring their distance from specific structural features in the mature domain, using different features for each site. The intron, however, also contributes to this specific recognition.

The two, base-paired tRNA fragments left by the endonuclease are converted into a contiguous molecule by tRNA ligase in a complex three-step reaction that leaves a 2′-phosphate at the junction. This phosphate is removed by the third enzyme, an unusual NAD-dependent phosphotransferase.

Changes in Nucleotide Sequence of the Mature Domain

Addition of the 3′-CCA End

In contrast to their eubacterial counterparts, eukaryotic tRNA genes do not encode the 3′-CCA-end essential for tRNA function. These three nucleotides are added to the 3′-end formed after removal of the trailer by ATP[CTP]:tRNA nucleotidyltransferase. A cytoplasmic version of this enzyme is probably involved in repair of damaged CCA-ends.

Modification

tRNAs contain ~80 different types of modified nucleotide. All modifications are carried out by specialized

proteinaceous enzymes, that, depending upon their nature act on the primary precursor transcript, on one of the processing intermediates or possibly even on the cytoplasmic tRNA. Since in yeast most of the tRNA modifications studied are nonessential the presence of modified nucleotides probably serves to fine-tune tRNA function.

Pre-rRNA Processing

Each eukaryotic, cytoplasmic ribosome contains single copies of four different rRNA species. The18S rRNA (1500–2300 nucleotides, or nt) is part of the small (40S) subunit, while the large (60S) subunit contains 5S (~120 nt), 5.8S (~150 nt), and 25/28S rRNA (3400–5000 nt). The 18S, 5.8S, and 25/28S rRNAs are encoded by one or more sets of tandemly repeated rDNA units, each of which is transcribed by RNA polymerase I into a single long pre-rRNA molecule (35–45S), containing external transcribed spacers (ETS) at both ends (5′- and 3′-ETS) as well as two internal transcribed spacers (ITS1 and ITS2) that separate the coding regions (Figure 2). In *S. cerevisiae*, a single 5S rRNA gene is embedded in the DNA that separates two consecutive rDNA units, whereas in higher eukaryotes the 5S rRNA genes are scattered throughout the genome, often in clusters. All 5S rRNA genes are transcribed individually by RNA Polymerase III into a precursor carrying a short 3′-ETS.

Removal of the transcribed spacer sequences from the primary precursor transcript occurs in an ordered series of endo- and exonucleolytic steps, which, in the case of the 35–45S precursor, is preceded by modification.

Pre-rRNA transcription, a large portion of its maturation, i.e., modification and processing, as well as ordered association of the intermediate precursor species with most of the ribosomal proteins (r-proteins), takes place in the nucleolus. Later stages occur in the nucleoplasm and formation of functional ribosomal subunits is completed in the cytoplasm (Figures 1 and 3).

Modification of Pre-rRNA

Modification of pre-rRNA is limited to the mature 18S and 25/28S rRNA sequences and consists mostly of two types: conversion of U residues into Ψ (pseudouridylation) and 2′-*O*-methylation of the ribose moiety of nucleotides. A few nucleotides are base-methylated. The number of modified nucleotides increases with increasing complexity of the organism but most of the modifications found in lower eukaryotic cells (e.g., yeast) are conserved in higher eukaryotes, including man. 2′-*O*-Methylation and pseudouridylation take place on the primary pre-rRNA transcript and are carried out by two classes of small nucleolar ribonucleoprotein particles (snoRNPs). A collection of box C/D snoRNPs is responsible for methylation, whereas a similar collection of box H/ACA snoRNPs perform the U → Ψ conversions. The names refer to common primary and secondary structural features present in the RNA component of each member of that class. Each box C/D or box H/ACA snoRNA also contains at least one, and sometimes two, specific "guide" sequence(s) that are complementary to the rRNA region(s) containing the modification site. The specific rRNA/snoRNA base-pairing guides the modifying enzyme, which is an integral part of the snoRNP, to its target nucleotide. Base-methylation, occurs at later stages of ribosome formation and is carried out by conventional proteinaceous enzymes.

Experiments with yeast cells indicate that rRNA modification is not essential for ribosome formation or function but does strongly enhance functional efficiency of the ribosome.

Removal of the Spacer Regions

The Processing Pathway

In *S. cerevisiae*, the first detectable precursor of 18S, 5.8S, and 25S rRNA is called 35S pre-rRNA. This precursor has already lost most of the 3′-ETS due to endonucleolytic cleavage that occurs before its transcription has been terminated. The pathway by which the 35S precursor is subsequently converted into the mature rRNAs is depicted in Figure 2A.

Maturation of 35S pre-rRNA starts with the removal of the 5′-ETS by two successive cleavages, which produce first the short-lived 33S and then the 32S species. The latter is cleaved within ITS1 separating the small subunit 20S pre-rRNA from the 27SA2 large subunit intermediate. Processing of 20S pre-rRNA is completed in the cytoplasm by endonucleolytic cleavage at the mature 3′-end of 18S rRNA. So far none of the nucleases involved in these processing steps have been identified.

Processing of yeast 27SA2 pre-rRNA is more complicated and occurs via two separate pathways that produce the same 25S rRNA, but two distinct species of 5.8S rRNA whose 5′-ends differ by 6 nucleotides, in ratio of about 10:1 (Figure 2A). The physiological relevance of this phenomenon remains unclear.

As would be expected for such a vital process pre-rRNA processing shows considerable plasticity, which is revealed in cells in which a particular processing step is disturbed by a mutation in either the pre-rRNA or in an accessory factor. The 5′-ETS can be removed in a single step by cleavage at the 5′-end of the 18S rRNA sequence. Initial cleavage within ITS1 can occur at A3 instead of A2 giving rise to an aberrant 21S small subunit pre-rRNA that is still efficiently converted into 18S rRNA. When cleavage at A3 is prevented almost all of the 27SA2 pre-rRNA is processed via the "long" pathway

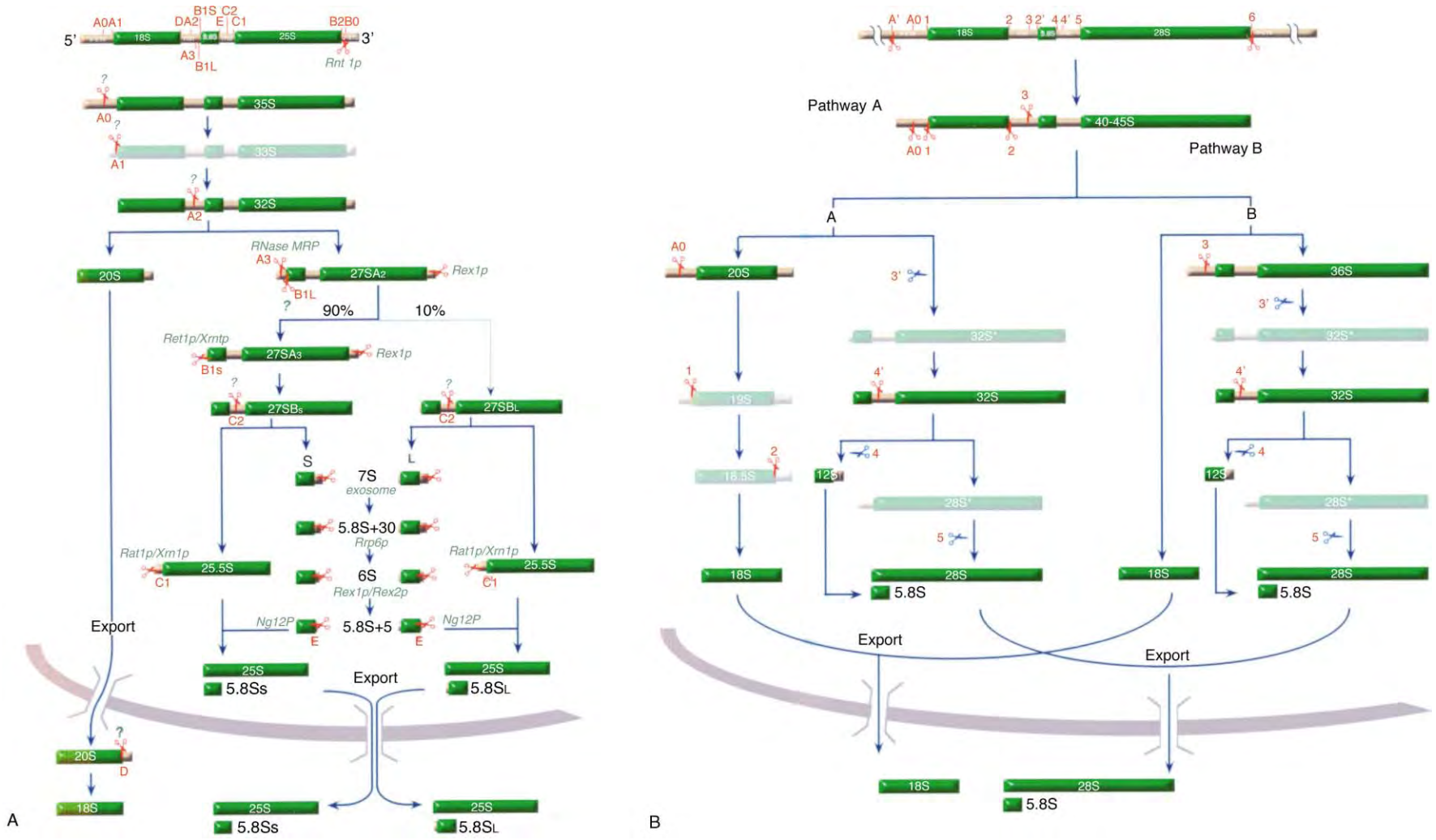

FIGURE 2 Pre-rRNA processing pathways in lower (panel A; *S. cerevisiae*) and higher (panel B) eukaryotic cells. The structure of the primary transcript including the processing sites is depicted at the top with the processing intermediates below. Regions encoding the mature rRNAs are in green, spacer regions are in brown. Light-colored intermediates are short-lived and not detectable under normal conditions. Vertical and horizontal scissors indicate endonucleolytic cleavages and exonucleolytic trimming, respectively. Blue scissors in panel B indicate that the nature of the processing step is unknown but, by analogy with yeast is likely to be exonucleolytic. Where known the enzyme(s) involved in a particular processing step is (are) identified. A question mark indicates that the enzyme is still unknown.

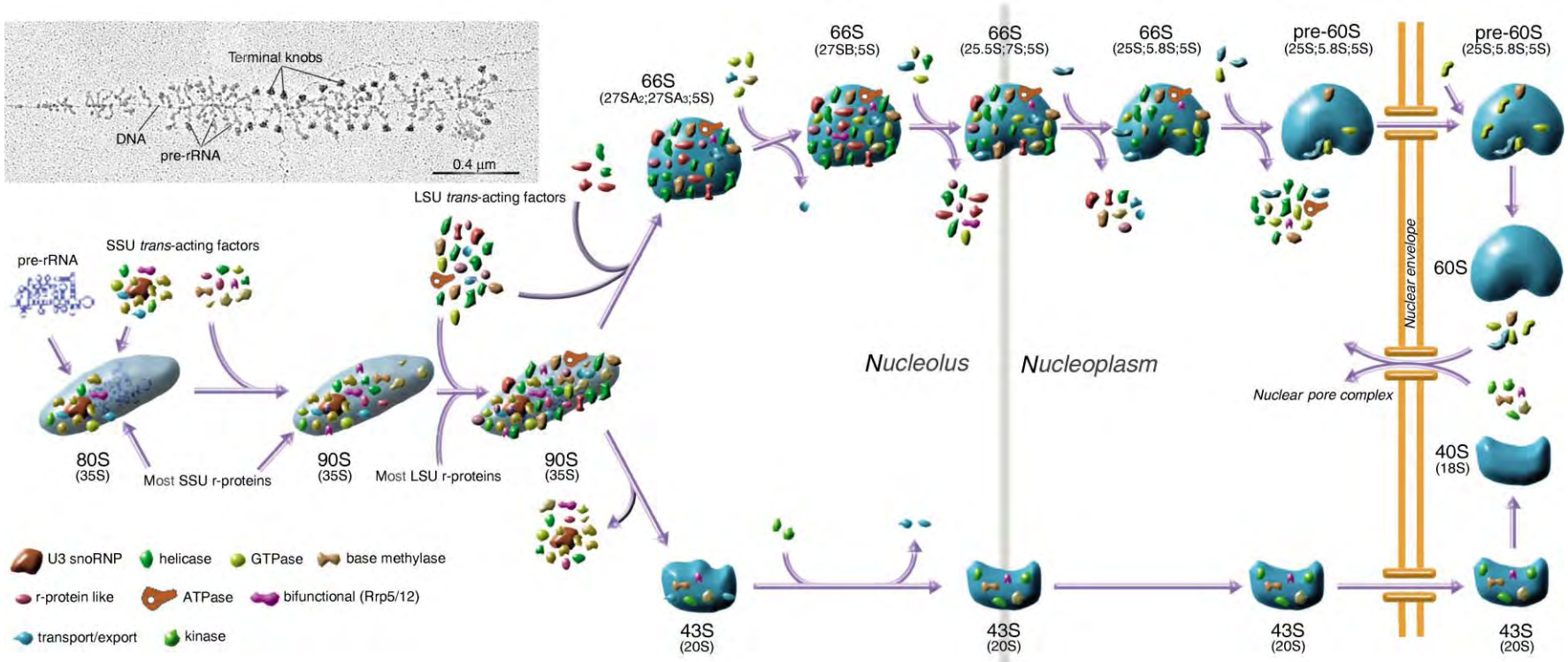

FIGURE 3 The pre-rRNA processing/assembly machinery in *S. cerevisiae*. The different intermediate pre-ribosomal particles so far identified are shown with their S value and, in parentheses, their pre-rRNA constituents. Note that the number of intermediates is tentative as is the nature of the components that associate or dissociate at the various stages. The inset shows an EM picture of the 'terminal balls' thought to correspond to the early stage in assembly of the 80S particle (photograph by Dr. Yvonne Osheim, University of Virginia).

producing 5.8S_L rRNA with little or no adverse effects on cell growth or maintenance.

Cleavage at site C2 is essential to initiate removal of ITS2 from either 27SB precursor but there is considerable redundancy among the exonucleases that remove the spacer nucleotides from the resulting 7S and 25.5S precursors.

Studies on pre-rRNA processing in other eukaryotes are limited mostly to *Drosophila*, *Xenopus laevis*, mouse and human and have not reached the same level of detail as those performed in *S. cerevisiae*. As shown in Figure 2B two pathways have emerged, of which the one labeled B is very similar, though not identical, to that of yeast. This pathway operates in *Xenopus* somatic cells, mouse and *Drosophila*. In *Xenopus* oocytes pre-rRNA processing can follow either pathway, even in the same cell, whereas pathway A occurs in human cells. In this pathway, cleavage at sites A0, 1, and 2 follows, rather than precedes processing at site 3.

Cis-Acting Elements

Correct and efficient processing of eukaryotic pre-rRNA is critically dependent upon structural features of the pre-rRNA (*cis*-acting elements). Such elements have been identified by *in vivo* mutational analysis, in particular in yeast, in both the mature and the spacer regions of the pre-rRNA. Some consist of short sequence elements, whereas for others their conformation, rather than their sequence, appears to be important. In only a few cases, the precise role of the element is known, e.g., the sequence spanning site A3, which constitutes the recognition element for RNase MRP.

Trans-Acting Factors

A large body of biochemical and molecular genetic studies, carried out mostly in yeast, have demonstrated that eukaryotic pre-rRNA processing and its assembly into functional ribosomes, apart from the ribosomal proteins, also requires a multitude of non-ribosomal factors. These *trans*-acting factors, whose number presently stands at ~200, include the modifying snoRNPs discussed before, a small number of additional snoRNPs (5 in yeast, including RNase MRP) and a large variety of proteins. Most have orthologues in other eukaryotes ranging from *C. elegans* to human, which underscores the strong evolutionary conservation of eukaryotic ribosome biogenesis.

Recent advances in the purification of large (ribonucleo) protein complexes by affinity chromatography (tandem-affinity-purification or TAP) and the identification of their constituents have clearly established that the *trans*-acting factors are the parts of two, essentially independent processing/assembly machineries (processomes) that govern formation of the small and large subunit, respectively. Both machineries are dynamic in nature, i.e., they lose particular components and acquire others in an ordered manner as subunit biogenesis progresses (Figure 3). Only two proteins have been found that are constituents of both the small and large subunit machinery.

Assembly of the small subunit (SSU) processome and the association of many of the SSU r-proteins on the pre-rRNA starts well before its transcription has been completed. The U3 box C/D snoRNP (which has no modification activity) plays a central role in the formation of the resulting 80S/90S pre-ribosome, the initial stages of which can be visualized as "terminal knobs" at the ends of the nascent transcripts by electron microscopy of an actively transcribed rDNA unit (inset in Figure 3). Actual processing is deferred, however, until the transcript has been released. Assembly of the large subunit (LSU) machinery starts a little later, immediately before cleavage at site A2 separates the 90S pre-ribosome into a 43S and a 66S particle, and many of the components of the LSU machinery may join only after this separation. Current, but definitely still incomplete, data indicate that the yeast 43S particle goes through at least two more stages before being exported to the cytoplasm, where cleavage at site D converts the 20S pre-rRNA into mature 18S rRNA. This final step requires several *trans*-acting factors that are coexported with the 43S particle and, after their release, are re-imported. The 66S pre-ribosome goes through at least five stages before an export-competent particle emerges that does contain the fully mature rRNA species but still has to undergo some structural rearrangement in the cytoplasm to acquire functionality. Again, some *trans*-acting factors needed for these finishing touches are already added in the nucleus and move back after having completed their task. Others may associate in the cytoplasm.

Studies on the specific function of the various *trans*-acting factors are still in their infancy. Comparative analysis, however, has identified several functional classes, whose role can at least be inferred (Figure 3). Nucleases constitute the most obvious, but also the most elusive, of these classes (Figure 2A). Remarkably, only one of the known processing nucleases (the $5' \rightarrow 3'$ exonuclease Xrn1p) has so far been detected in pre-ribosomes. A second class (19 members in yeast) is formed by proteins containing the signature motifs of RNA helicases. These proteins, therefore, could be involved in structural rearrangements of the pre-rRNA necessary for processing and assembly. Additional structural rearrangements may be carried out by a third class of proteins that show similarity to known GTPases or ATPases. A fourth class consists of proteins that may assist the association of particular r-proteins with the pre-ribosome. Circumstantial evidence points to the existence of at least two such assembly

chaperones for both the small and large subunit. Biochemical experiments have also identified several proteins involved in translocation of either the 43S or 66S pre-ribosome from the nucleolus to the nucleoplasm, while a considerable number has been implicated in export of either subunit to the cytoplasm. The latter include components of the generic nuclear export machinery as well as subunit-specific export factors. Four *trans*-acting factors have a structure strongly resembling that of a particular r-protein. It has been suggested that these rp-like proteins may play a role in timing the order of processing/assembly events by associating first and later giving way to their r-protein counterpart. A recent addition to this inventory are several protein kinases required for the final cytoplasmic step in 40S subunit formation.

This necessarily brief article leaves out the large majority of *trans*-acting factors for which little or no functional information is yet available. Obtaining this information and integrating it into a working model for the course of events in pre-rRNA processing/assembly is one of the major tasks for the future investigations into eukaryotic ribosome biogenesis.

See Also the Following Articles

Nucleolus, Overview • Ribosome Assembly • RNA Editing

Glossary

eukaryote Organism consisting of one or more cells containing a nucleus.

molecular genetics Changing the genetic make-up of an organism—often in a predetermined manner—by application of recombinant DNA technology.

nucleolus A distinct region within the nucleus where transcription of pre-rRNA and most of its processing and assembly with ribosomal proteins, as well as part of pre-tRNA maturation, takes place.

nucleoplasm The region of the nucleus not occupied by the nucleolus.

oocyte Unripe, unfertilized amphibian egg cell.

ribonucleoprotein A complex consisting of one or more RNA molecules associated with a number of proteins.

snoRNP Small nucleolar ribonucleoprotein particle.

somatic Of the body (somatic cell: differentiated body cell).

Further Reading

Abelson, J., Trotta, C. R., and Li, H. (1998). tRNA splicing. *J. Biol. Chem.* **273**, 12685–12688.

Fatica, A., and Tollervey, D. (2002). Making ribosomes. *Curr. Op. Cell Biol.* **14**, 313–318.

Kiss, T. (2002). Small nucleolar RNAs: An abundant group of noncoding RNAs with diverse cellular functions. *Cell* **109**, 145–148.

Kressler, D., Linder, P., and DeLaCruz, J. (1999). Protein *trans*-acting factors involved in ribosome biogenesis in *Saccharomyces cerevisiae*. *Mol. Cell. Biol.* **19**, 7897–7912.

Raué, H. A. (2003). Pre-ribosomal RNA processing and assembly in *Saccharomyces cerevisiae*. The machine that makes the machine. In *The Nucleolus* (M. O. J. Olson, ed.) Kluwer Academic/Plenum Publishers, New York, http://www.eurekah.com/chapter.php?chapid = 1223&bookid = 88&catid = 54.

Wolin, S. J., and Matera, A. G. (1999). The trials and travels of tRNA. *Genes Develop.* **13**, 1–10.

Biography

Hendrik A. Raué is a Professor of Biochemistry in the Faculty of Sciences at the Vrije Universiteit in Amsterdam, The Netherlands. He obtained his Ph.D. in Biochemistry at Groningen University, The Netherlands, and received his postdoctoral training at the National Institute of Child Health and Human Development in Bethesda, Maryland. His primary research interest is in eukaryotic ribosome biogenesis, using the yeast *S. cerevisiae* as a model organism.

Prions and Epigenetic Inheritance

Reed B. Wickner
National Institutes of Health, Bethesda, Maryland, USA

Just as nucleic acids can carry out enzyme reactions, it has now been found that proteins can be genes. The nonchromosomal genes [URE3], [PSI], and [PIN] of *Saccharomyces cerevisiae* and [Het-s] of the filamentous fungus *Podospora anserina* are self-propagating amyloid forms of normal cellular proteins Ure2p, Sup35p, Rnq1p, and HET-s, respectively. The phenotypes produced are due to the absence of the soluble forms in the [URE3] and [PSI] cases, but due to the presence of the amyloid forms in [PIN] and [Het-s]. The portions of the Ure2p, Sup35p, and Rnq1p molecules primarily responsible for prion formation and propagation (prion domains) are very rich in asparagine and glutamine residues, unlike the HET-s prion domain or the PrP molecule that plays a central role in the mammalian transmissible spongiform encephalopathies. The [Het-s] prion is of particular interest because it carries out a normal function for *Podospora*, namely, heterokaryon incompatibility. Chaperones play a critical role in prion propagation, by generating seeds for formation of the amyloid filaments.

Yeast and Fungal Prions: Genetic Criteria

The word "prion" means an infectious protein, by whatever mechanism. This idea arose from studies of the transmissible spongiform encephalopathies (TSEs) of mammals, believed to be due to an infectious form of a protein called PrP. Two nonchromosomal genes of *Saccharomyces cerevisiae*, called [URE3] and [PSI^+], were identified as prions because their unusual genetic properties were inconsistent with their being nucleic acid replicons, but were just what one would expect for a prion (Figure 1). First, each could be efficiently eliminated (cured) from cells, but from the cured cells could again arise at low-frequency cells carrying the nonchromosomal gene. Second, overproduction of the normal form of the protein was shown to increase the frequency with which the prion form arose *de novo*. And it was the protein whose overproduction induced the appearance of the nonchromosomal gene, not the RNA or the gene in high copy number. Finally, the chromosomal gene encoding the protein was of course necessary for the propagation of the prion, but the phenotype of mutants in the chromosomal gene was the same as that of the presence of the prion.

Known Prions of Yeasts and Fungi

[URE3] has each of these properties as a prion of the Ure2 protein, a regulator of nitrogen catabolism in yeast. Similarly, [PSI] has the properties expected of a prion of the Sup35 protein, a subunit of the translation termination factor. A prion of *Podospora anserina*, called [Het-s], is unique in performing a function for this fungus, being required for an antiviral defense mechanism called heterokaryon incompatibility. A third *S. cerevisiae* prion, called [PIN^+], was discovered by its ability to promote the *de novo* development of the [PSI^+] prion and is an altered form of Rnq1p. While [URE3] and [PSI^+] make their presence known by the absence of the normal form of Ure2p and Sup35p, respectively, both [Het-s] and [PIN^+] produce a phenotype by the presence of the abnormal forms of HET-sp and Rnq1p, respectively, similar to the case with the mammalian TSEs.

Prion Domains and Functional Domains

In Ure2p and Sup35p prion proteins, the C-terminal part of the protein carries out the normal function of the protein and the N-terminal segment is responsible for the prion properties (Figure 2). The prion domain can propagate the prion completely independent of the functional domain, and can even confer prion properties to a suitable unrelated reporter protein. The HET-s protein and Rnq1p also have special domains responsible for their prion properties. The Ure2p, Sup35p, and Rnq1p prion domains are all rich in asparagine or glutamine residues, and these runs of N or Q are important for the prion properties of the proteins. However, neither the HET-s protein nor mammalian PrP have regions rich in N or Q (Figure 2). The N-, Q-rich prion domains of Ure2p, Sup35p, and

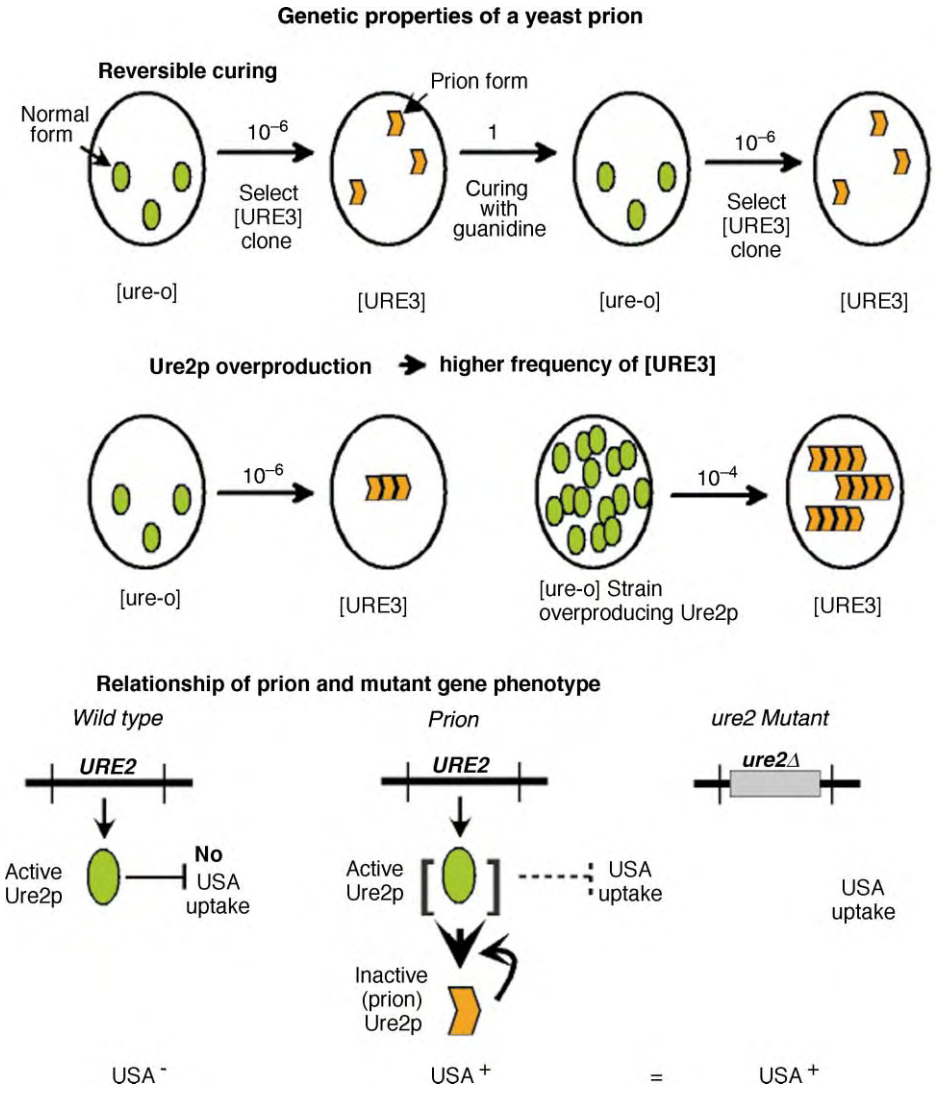

FIGURE 1 Genetic properties identify prions.

Rnq1 resemble the polyQ of Huntingtin whose amyloid formation is the central event in Huntington's disease.

In Ure2p, Sup35p, and HET-sp, the prion domain is stabilized by the rest of the molecule and largely prevented from converting into the prion form. This suggests that there is an interaction between the prion domains and the remainder of the molecule. In Ure2p, the prion domain helps with the nitrogen regulation function of Ure2p, although it is not essential for this activity.

Yeast, Fungal Prions [PSI$^+$], [URE3], and [Het-s] are Self-Propagating Amyloidoses

Amyloid is a special form of protein structure that is characteristic of a number of human diseases. Amyloid is a filamentous structure which is high in β-sheet structure, and which displays a characteristic yellow–green birefringence on staining with the aromatic dye Congo red. Amyloid filaments are partially resistant to protease digestion, probably reflecting their very stable β-sheet structure. Demonstration of aggregation is always simpler than that of amyloid structure, but it is evident that not all aggregates are amyloid. Amyloid formation by the Aβ peptide is the central event in Alzheimer's disease, while amyloid of amylin is a prominent feature of late-onset diabetes. Parkinson's disease features intracellular amyloid formation by α-synuclein, and amyloid of serum amyloid A protein is a complication of many long-term infectious and inflammatory processes.

Sup35p, Ure2p, and HET-sp each form amyloid *in vitro*. Moreover, the characteristics of the amyloid formed and the requirements for its formation closely reflect the corresponding properties and conditions of

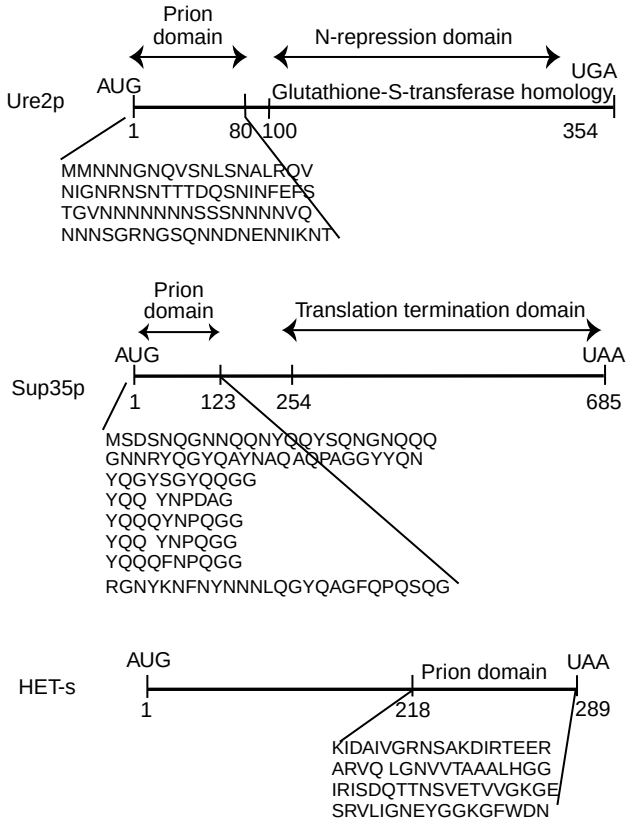

FIGURE 2 Prion domains of Ure2p, Sup35p, and HET-s. While the prion domains of Ure2p and Sup35p are rich in N and Q, that of HET-s is rich in neither.

prion formation *in vivo*. For example, extracts of [PSI$^+$] cells can prime the formation of amyloid by Sup35p much better than can extracts of normal cells. The prion domain of Ure2p induces amyloid formation by the full-length native Ure2p *in vitro* just as the prion domain produced *in vivo* induces *de novo* generation of the [URE3] prion (Figure 3). Indeed, filaments of the Ure2 protein have actually been visualized specifically in [URE3] cells.

Recombinant HET-s protein converted into amyloid *in vitro* efficiently transmits the [Het-s] trait to *Podospora* colonies when introduced by the "gene gun." The same protein, aggregated by heat denaturation or acid, or in its soluble form, has little or no such effect. This is a dramatic demonstration of the prion nature of [Het-s] which has not yet been accomplished in any of the yeast or mammalian systems.

The mechanism by which amyloid formation inactivates Ure2p is apparently not by a conformational change of the functional domain of the molecule. Fusion of the Ure2p prion domain to any of several enzymes shows no loss of their activity, but suggests that being in the amyloid filament sterically blocks access to binding Gln3p (the target of Ure2p action) or imposes a diffusion limitation.

The [HET-s] Prion Carries Out a Normal Function

Amyloidoses of humans are all associated with disease states, and the TSEs, in particular, are uniformly fatal. The [URE3] prion is associated with slow growth under most culture conditions. [PSI$^+$] and [PIN$^+$] do not confer any consistent phenotype on otherwise normal cells, although [PSI$^+$] is lethal in cells carrying a strong tRNA suppressor mutation. Searches by two groups for [PSI$^+$] in wild strains have failed to find it, supporting the notion that it is a disease, like the mammalian counterparts.

A colony of a filamentous fungus is not a pile of cells (as in yeast), but rather a syncytium – cells connected by cytoplasmic bridges. When two compatible colonies of *Podospora* or other filamentous fungi grow together, they fuse cellular processes (hyphae) thereby joining the two colonies into one, called a heterokaryon. This allows the colonies to share nutrients, but has the danger that a virus infecting one will spread by cytoplasmic mixing throughout the other. To minimize this risk, filamentous fungi have a system, called "heterokaryon incompatibility" which tests for identity between the partners at about a dozen polymorphic chromosomal loci. Nonidentity of alleles at a single locus is sufficient to abort the fusion process and a barrier to further fusion is formed. Most of these *het* loci are genetically unremarkable. The *het-s* locus of *Podospora* can have either of two alleles, *het-s* or *het-S*. A colony with the *het-s* allele is only incompatible with a *het-S* colony if the HET-s protein is in an amyloid form. This amyloid form is infectious and is the [Het-s] prion. The HET-S, which differs by only 14 amino acid residues from the HET-s protein, does not form amyloid, and residue 33 is critical in this difference.

Thus, the [Het-s] prion is the (so far) unique case of a prion that is necessary for a normal function, heterokaryon incompatibility. Consistent with this view is the fact that most wild strains of *P. anserina* with the *het-s* allele carry the [Het-s] prion.

Prion Generation

[PIN$^+$] was discovered as a nonchromosomal gene whose presence was necessary for the efficient induction of the *de novo* appearance of [PSI$^+$] by overexpression of Sup35p. [PIN$^+$] was found to be a prion of the Rnq1 protein, which had already been shown capable of a self-propagating aggregation *in vivo*. In fact, [URE3] was also capable of [PIN$^+$]-like activity. This showed that one prion could promote the generation of another. This may be because all of these prions ([PSI$^+$], [PIN$^+$], and [URE3]) are based on amyloid of asparagine-glutamine

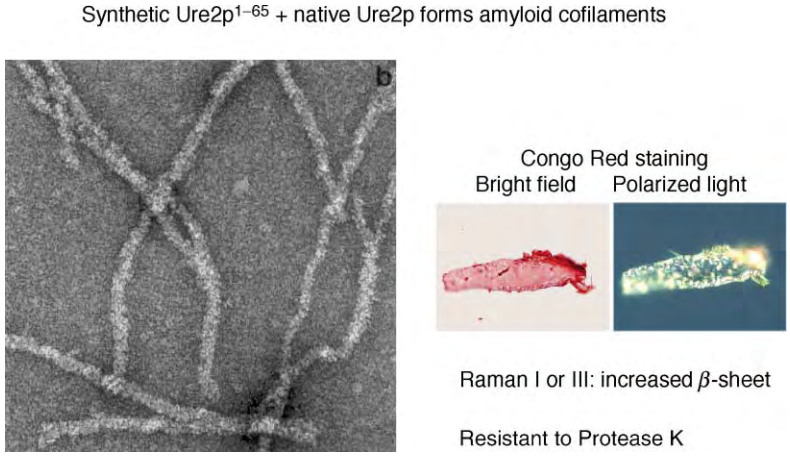

FIGURE 3 Amyloid and prions. The prion domain of Ure2p (for example) can form amyloid and can induce amyloid formation by the full-length native protein *in vitro*, just as overexpression of the prion domain *in vivo* induces prion formation by Ure2p.

rich segments. Although cross-priming of polymerization is not as efficient as self-priming (the usual propagation reaction), it is far more efficient than the truly spontaneous development of a prion. A similar, though weaker, effect of [PIN$^+$] on [URE3] generation has also been observed.

[URE3] has a very strong requirement for the Mks1 protein for *de novo* generation. Increasing or decreasing Mks1p levels dramatically increase or decrease the frequency of [URE3] arising. Although *mks1*Δ cells are nearly incapable of generating a new [URE3] prion, propagation of [URE3] is normal in such cells. Mks1p was discovered as a protein whose strong overproduction slows cell growth, but is inhibited in this activity by the Ras-cAMP pathway. Indeed, activation of Ras, like deletion of *MKS1*, dramatically diminishes [URE3] generation. Mks1p is also a regulator of glutamate biosynthesis, but the effects on [URE3] generation appear not to be mediated via glutamate levels. The detailed mechanisms of these effects remain to be elucidated.

Chaperones and Prion Propagation

Chaperones play a central role in the propagation of yeast prions (Table I). Hsp104 is a disaggregating chaperone critical in the cellular reaction to heat shock, and either increasing or decreasing its level adversely affects propagation of [PSI$^+$]. Overexpression of Hsp104 probably blocks propagation by completely disaggregating the Sup35p aggregates allowing return of the protein to its normal form. Elimination of Hsp104 interferes with seed formation. Amyloid aggregates are clumpy and may all remain in one of the daughter cells if they form a single lump in the mother cell. Modest levels of Hsp104 carry out the partial fragmentation of these filaments insuring that both daughter cells receive one or more seeds. [URE3] likewise requires Hsp104 for propagation, but unlike [PSI$^+$] is not cured by Hsp104 overproduction. Guanidine cures all the yeast prions and it has recently been shown that guanidine works by inhibiting Hsp104.

Different Hsp70s and Hsp40s have positive and negative functions with different prions as summarized in Table I. For example, overexpression of the Hsp40 protein, Ydj1, can cure [URE3]. Clearly, the detailed interactions of each prion with chaperones will be different, and this remains an important area to investigate. There is circumstantial evidence for a role of chaperones in the mammalian TSEs, but direct evidence has so far been limited to the yeast systems.

The importance of the discovery of the role of chaperones in yeast prions goes far beyond these systems and even the mammalian prion diseases. Amyloidoses are common (almost universal) diseases of old age, and one suspects that one of the primary roles of the heat-shock proteins is to defend against amyloid formation. It will be critical to learn how these systems can be marshaled to contend with the otherwise largely intractable human amyloidoses.

TABLE I

Chaperones and Prions

Chaperone	[PSI$^+$]	[URE3]	[PIN$^+$]
Hsp104	↑ → lost	↑ → OK	↑ → OK
	↓ → lost	↓ → lost	↓ → lost
Ssa1p (Hsp70)	↑ → OK	↑ → lost	
	↓ → lost		
Ssa2p	↑ → OK	↑ → OK	
Ydj1p (Hsp40)	↑ → OK	↑ → lost	
Sis1p (Hsp40)			↓ → lost

Conclusions

The ability of proteins to bear hereditary information recalls the earlier discovery by Sonneborn of cortical inheritance in *Paramecium*, in which the surgically altered arrangement of cilia on the surface of the cell was shown to be faithfully inherited by the progeny of the original cell. Self-propagating protein structures in the former case are closely analogous to self-propagating organellar structures in the latter. Efforts to find other self-propagating organellar structures have not yet met with any clear successes, and the mechanisms operating in the cortical inheritance phenomenon have not yet been elucidated.

All of the prions discussed here appear to be based on self-propagating amyloid of the corresponding protein. Of course, most amyloidoses are not prions, although nearly all have been shown to be self-seeding *in vitro*. Prion propagation requires both expansion of amyloid within one individual cell or compartment, but also a mode of transmission. There are indications that mature amyloid fibers may not be the infectious form of prions, and it is evident that the shorter the fiber, the higher the ratio of growing ends to mass of material. However, the *Podospora* studies show that amyloid itself can serve as the infectious material, and most infectivity assays with scrapie material show that the infectious material is relatively rapidly sedimenting.

The direct parallels between these yeast, fungal, and mammalian prions and amyloidoses have opened new areas for investigation of these very difficult human diseases.

A new prion (infectious protein) based on an enzyme whose active form is necessary *in trans* for activation of its inactive precursor has been described. This is the vacuolar protease B of *S. cerevisiae*. It is not news that a protease can activate its inactive precursor, but it is remarkable that such a protease can be a gene. Moreover, this suggests that other protein-modifying enzymes may prove to be prions under some circumstances.

See Also the Following Articles

Amyloid • Chaperones, Molecular • Prions, Overview

Glossary

amyloid A filamentous form that many proteins can assume characterized by high β-sheet content, protease-resistance and yellow-green birefringence on staining with Congo red.

chaperone A protein that aids the folding (or refolding or renaturation) of another protein.

prion A protein that transmits a trait or disease without the need for an accompanying nucleic acid.

prion domain Part of a protein that determines the prion properties of the full protein.

Further Reading

Chernoff, Y. O., Lindquist, S. L., Ono, B.-I., Inge-Vechtomov, S. G., and Liebman, S. W. (1995). Role of the chaperone protein Hsp104 in propagation of the yeast prion-like factor [psi+]. *Science* **268**, 880–884.

Kushnirov, V. V., and Ter-Avanesyan, M. D. (1998). Structure and replication of yeast prions. *Cell* **94**, 13–16.

Liebman, S. W., and Derkatch, I. L. (1999). The yeast [*PSI*+] prion: making sense out of nonsense. *J. Biol. Chem.* **274**, 1181–1184.

Masison, D. C., and Wickner, R. B. (1995). Prion-inducing domain of yeast Ure2p and protease resistance of Ure2p in prion-containing cells. *Science* **270**, 93–95.

Roberts, B. T., and Wickner, R. B. (2003). Heritable activity: a prior that propagates by covalent autoactivation. *Genes and Dev.* **17**, 2083–2087.

Saupe, S. J. (2000). Molecular genetics of heterokaryon incompatibility in filamentous ascomycetes. *Microbiol. Mol. Biol. Revs.* **64**, 489–502.

Serio, T. R., and Lindquist, S. L. (2001). [PSI+], SUP35, and chaperones. *Adv. Protein Chem.* **57**, 335–366.

Wickner, R. B. (1994). Evidence for a prion analog in *S. cerevisiae*: The [URE3] non-Mendelian genetic element as an altered *URE2* protein. *Science* **264**, 566–569.

Wickner, R. B., Edskes, H. K., Roberts, B. T., Pierce, M., and Baxa, U. (2002). Prions of yeast as epigenetic phenomena: High protein "copy number" inducing protein "silencing". *Adv. Genet.* **46**, 485–525.

Wickner, R. B., Liebman, S. W., and Saupe, S. J. (2004). Prions of yeast and filamentous fungi: [URE3], [PSI^+], [PIN^+] and [Het-s]. In *Prion Biology and Diseases* (S. B. Prusiner, ed.) Cold Spring Harbor Laboratory Press, pp. 305–372.

Biography

Reed B. Wickner, M.D. is Chief of the Laboratory of Biochemistry and Genetics in the National Institute of Diabetes Digestive and Kidney Diseases of the National Institutes of Health in Bethesda. He is interested in nonchromosomal inheritance, and has long studied yeast RNA viruses. He discovered yeast prions based on their unusual genetic properties and has studied the mechanisms of generation, propagation, and curing of the [URE3] prion, and the structure of the Ure2p amyloid that forms its basis.

Prions, Overview

Cedric Govaerts and Fred E. Cohen
University of California, San Francisco, California, USA

Prions are transmissible pathogens responsible for a series of fatal neurodegenerative diseases including, in humans, Creutzfeld–Jacob disease (CJD), Gerstmann–Straussler–Scheinker disease (GSS), fatal familial insomnia (FFI), and kuru. Other mammals succumb to prion diseases including sheep scrapie, bovine spongiform encephalopathy (BSE, also known as mad-cow disease), chronic wasting disease (CWD) in mule, deer, and elk, feline spongiform encephalopathy (FSE), and transmissible mink encephalopathy (TME). In each case the emergence of a misfolded form of the prion protein, PrP^{Sc}, is pathognomonic for the disease.

Misfolding Diseases

More than 20 human pathologies, including Alzheimer's, Parkinson's, Huntington's, and prion diseases, are associated with the "misfolding" of specific proteins or protein fragments. Under normal conditions, some newly synthesized proteins are folded and post-translationally modified in specific cellular compartments, called endoplasmic reticulum (ER), in an effort to deliver the protein to the appropriate cellular location in its native (physiologically relevant) conformation. However, occasionally, proteins can adopt an aberrant conformation either during the initial folding process or through a "conformational transition" from the native state. A misfolded protein, if not cleared by cellular or extracellular machinery, can cause disease. Two mechanisms of disease must be considered: loss of function and gain of function/dominant-negative effect. With loss of function, the misfolded protein cannot serve the biological function normally achieved by the native protein. Cystic fibrosis is a useful example where the quality control machinery prevents the misfolded mutant CFTR protein from reaching the cell surface. Conversely, pathology can arise from gain of function, when the aberrant conformation leads to a new and potentially harmful function of the protein. The prion diseases follow this paradigm. Invariably, misfolded forms of proteins have a strong propensity to aggregate into insoluble material. In several diseases, these aggregates adopt a fibrillar structure called "amyloid" and can form large deposits or plaques which are found in the affected tissue. Following proteolytic fragmentation, prions can form amyloid fibers and plaques. As with other amyloid-forming diseases, it remains unclear whether oligomers of the misfolded protein or much larger polymeric aggregates (or fibrils) injure cells and cause neurodegeneration.

Prion Protein and Diseases

PrP^{C} and PrP^{Sc}

The prion protein, or PrP, is a membrane anchored protein, expressed predominantly in neurons and lymphocytes. The biological function of the normally folded prion protein (cellular PrP, PrP^{C}) has yet to be identified, but PrP^{C} is known to bind copper and could be involved in its homeostasis. Prion diseases are associated with the emergence of a misfolded form of PrP^{C} called PrP^{Sc} (for scrapie form, the oldest known prion disease). A wealth of data suggest that PrP^{Sc} is the etiologic agent in the disease. While PrP^{C} and PrP^{Sc} have the same amino acid sequence, they differ in their structural characteristics, PrP^{C} is rich in α-helical structure while PrP^{Sc} has substantially more β-sheet structure. While PrP^{C} is monomeric and protease sensitive, PrP^{Sc} is resistant to degradation by protease and is multimeric.

Replication Cycle

The global mechanism of PrP^{Sc} production is fairly well understood. It involves the presence of an initial PrP^{Sc} multimer which can either be exogenous (infectious forms of the diseases) or endogenous (inherited or sporadic forms). This first prion will initiate PrP^{Sc} accumulation by sequentially converting PrP^{C} molecules, following a "replication cycle" (see Figure 1). As illustrated, PrP^{C} is thought to exist in equilibrium with a transient intermediate, PrP^{*}, which is normally in low abundance compared to PrP^{C}. Binding of a PrP^{Sc} molecule to PrP^{*} may lead to its conversion into a new PrP^{Sc} molecule, through structural templating. This newly formed PrP^{Sc} molecule can in turn convert neighboring PrP^{*} molecules and therefore amplify the replication cycle. Importantly, PrP^{C}, PrP^{*}, and PrP^{Sc} are

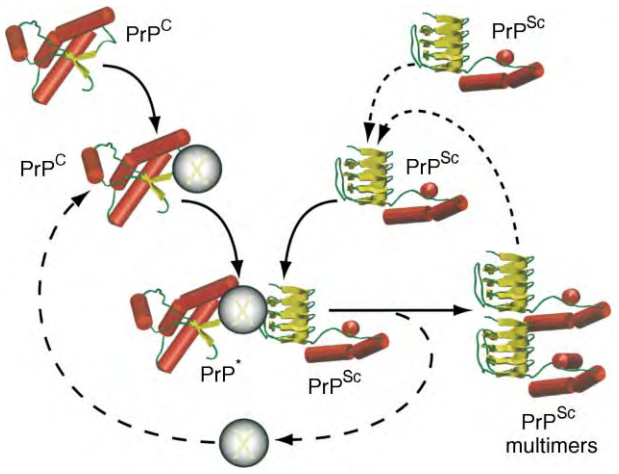

FIGURE 1 Exogenous or endogenous PrP^{Sc} initiates PrP^{Sc} synthesis by binding to a $PrP^{C/*}$/X complex. Facilitated by protein X and directed by the PrP^{Sc} template, PrP^{*} changes conformation and forms PrP^{Sc}. When PrP^{Sc} forms, the heteromultimeric complex dissociates, yielding recycled protein X and endogenous PrP^{Sc}. The newly generated PrP^{Sc} can then facilitate two replication cycles leading to an exponential rise in PrP^{Sc} formation.

not the only molecules involved in prion replication, as it has been demonstrated that at least one other protein is required for $PrP^{C} \rightarrow PrP^{Sc}$ conversion. This auxiliary protein remains to be identified and has been termed "protein X" (see Figure 1). Such additional complexity is probably responsible for the difficulties investigators have faced in building *in vitro* conversion protocols, leaving cell-based assays and animal systems (such as transgenic mice) as the only suitable experimental systems for the study of prion disease.

Transmission and Inheritance

Prion diseases are rare neurodegenerative disorders which affect approximately one person per million. Sporadic disease is the most common mechanism in humans and represents 85% of all cases. Individuals present in the sixth or seventh decade of life with a variety of cognitive defects. A rapidly progressive course leads to death in less than a year. Familial prion diseases (like GSS or FFI) represent 15% of all cases and are caused by mutations in the PrP gene. These mutations appear to favor the transition from the cellular form to the pathological form of PrP. PrP^{Sc} accumulates and neurodegeneration results.

In humans, infectious diseases are rare but have been a source of great concern, given the nature of the transmissible agent and its resistance to typical disinfection strategies. In the laboratory, disease can be readily transmitted to mice or hamster by intracranial injection of brain homogenate taken from prion-infected animals. Propagation of kuru disease in New Guinea Highlanders was due to ritualistic cannibalism involving ingestion of contaminated brain. Recently, it has been discovered that BSE had been transmitted to humans in Europe after consumption of infected beef, producing a variant of the CJD called vCJD (variant CJD). This constitutes a rare violation of the "species barrier," a term coined after observing that infectious material from one species inefficiently transmits to another species (this has presumably protected the human population from infection by scrapie-infected sheep).

Prion Strains

The various prion diseases are characterized by different incubation times and neuropathologic profiles, although in all cases the same misfolded protein (PrP^{Sc}) is responsible. This phenomenon has been attributed to the existence of various "prion strains." Although PrP^{Sc} molecules from different strains are chemically identical, they differ in their exact conformations. The structural characteristics of individual prion strains are propagated via the replication cycle. These characteristics appear to direct the precise tissue targeting, incubation time, and pathogenesis of the strain. For example, it has been established that consumption of BSE-infected meat has led to prion disease in over 100 people. Affected individuals suffer from a new form of CJD called vCJD, are drawn from a younger cohort and exhibit distinct clinical characteristics from CJD patients. The PrP^{Sc} molecules found in patients with vCJD can be conformationally distinguished from those of classical CJD, and have been shown to resemble PrP^{Sc} molecules from BSE-infected cattle. Therefore, vCJD is a different strain of prion from CJD, and is probably the human form of the bovine prion strain from BSE.

Physiopathology of Prion Diseases

Prions are neurodegenerative diseases, that induce neuronal dysfunction accompanied by neuronal loss with no inflammatory response. In most cases, the pathogenic process is characterized by vacuolar degeneration of the gray matter, which correlates with abundance of PrP^{Sc}. This vacuolation process creates spongiform change in the cerebral tissue. Prion diseases are therefore often referred to as transmissible spongiform encephalopathies (TSE). The precise location of tissue damage (e.g., cerebral cortex versus cerebellar cortex) may vary between the different prion diseases, but always correlates with the presence of PrP^{Sc}. In some forms, such as GSS, the disease is also characterized by the presence of amyloid plaques composed of PrP^{Sc} molecules. Although technological advances in medical imaging provide promising tools for the near

future, the definitive diagnostic for prion disease is currently achieved postmortem by histological analysis of brain tissue.

Structural Studies

As for any misfolding disease, the pathological form of the prion protein differs from the cellular one in its conformation. While no chemical difference is observed, biophysical and immunological measurements reveal important structural differences between the two isoforms. Notably, only a fraction of the specific antibodies targeted against PrP^{C} molecules are able to recognize the PrP^{Sc} isoforms. This suggests that the molecular structures of the two isoforms are significantly different.

The PrP^{C} molecule is soluble and its three-dimensional structure can be solved by classical techniques such as solution nuclear magnetic resonance (NMR). These experiments reveal that PrP^{C} fold is dominated by α-helices, tight helical structures found in a vast number of proteins with very little β-sheet, extended structures also commonly found (see Figure 2). While the structure of PrP^{Sc} cannot be probed by NMR due to its insolubility, biophysical measurements such as Fourier transform infrared spectroscopy (FT-IR) have deciphered important structural properties of PrP^{Sc}. These techniques have shown that the fold of PrP^{Sc} is composed of both β-sheet structures (40%), and α-helices (30%). Enrichment in β-sheet structure is commonly observed in proteins associated with misfolding diseases. This has led many to speculate that there are mechanistic similarities in the misfolding diseases. For a variety of technical reasons, resolving the atomic structure of PrP^{Sc} is extremely challenging. Recent advances include the discovery of two-dimensional crystals of PrP^{Sc} suitable for electron microscopic analysis. These data have led to the development of new models of the structure of PrP^{Sc}.

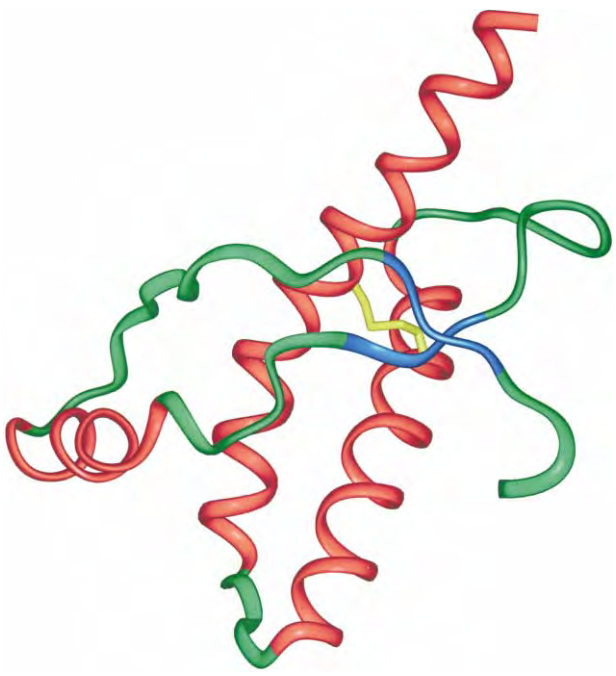

FIGURE 2 NMR structure of PrP^{C}. Ribbon representation of the globular structure of human PrP resolved by NMR, comprising residues 125–228. The three α-helices are colored in red and the small β-sheet is in blue.

Therapeutic Strategies

Currently, prion diseases are uniformly fatal illnesses. Diverse approaches are being taken to develop therapeutics for prion diseases. Compounds can be designed to specifically disrupt the replication cycle (illustrated in Figure 1), either by stabilizing the PrP^{C} conformation versus PrP^{*}, or by blocking interaction with the auxiliary partner protein X. Design of such compounds has proven successful in cell-based models of prion diseases but must now be extended to animal models and human clinical trials. Screenings of existing drugs that are known to penetrate the blood–brain barrier (and therefore potentially reach prion-infected tissues) have identified the drug quinacrine as being effective against PrP^{Sc} replication in cells. Quinacrine is currently approved for the treatment of giardiasis and has been used historically to treat malaria. Clinical trials are underway to determine its therapeutic utility in CJD patients. Similar approaches have identified a number of other potentially interesting compounds, but more efforts will be required to assess their therapeutic utility. Hopefully, one of these efforts will lead to potent antiprion drugs in the foreseeable future.

See Also the Following Articles

Amyloid • Glycosylation in Cystic Fibrosis • Prions and Epigenetic Inheritance • Protein Folding and Assembly

Glossary

amyloid fibers Fibrillar structures of misfolded protein aggregates, observed in human diseases such as prion diseases or Alzheimer's disease.

conformational transition Process during which the protein undergoes major structural change.

misfolding Process leading to an aberrant conformation of a protein, often linked to pathogenesis.

prion strains The subclassification of prions following their fine structural characteristics which appear to define their pathological profile.

PrP^{C} Cellular (normal) isoform of the PrP protein.

PrP^{Sc} Misfolded (pathological) isoform of the PrP protein.

replication cycle Mechanism by which PrP^{C} molecules are converted into PrP^{Sc} isoform with the help of pre-existing PrP^{Sc} molecules.

species barrier Apparent inability of prion from one species to infect organism from another species. Violations of the barrier have been observed.

Further Reading

Cohen, F. E., and Prusiner, S. B. (1998). Pathologic conformations of prion proteins. *Annu. Rev. Biochem.* **67**, 793–819.

DeArmond, S. J., and Bouzamondo, E. (2002). Fundamentals of prion biology and diseases. *Toxicology* **181–182**, 9–16.

Dobson, C. M. (1999). Protein misfolding, evolution and disease. *Trends Biochem. Sci.* **24**, 329–332.

Dobson, C. M. (2003). Protein folding and disease: A view from the first horizon symposium. *Nat. Rev. Drug Discov.* **2**, 154–160.

Prusiner, S. B. (ed.) (2004). *Prion Biology and Diseases*, 2nd edn. Cold Spring Harbor Laboratory Press, Cold Spring Harbor.

Prusiner, S. B., Scott, M. R., DeArmond, S. J., and Cohen, F. E. (1998). Prion protein biology. *Cell* **93**, 337–348.

Sacchettini, J. C., and Kelly, J. W. (2002). Therapeutic strategies for human amyloid diseases. *Nat. Rev. Drug Discov.* **1**, 267–275.

Biography

Fred E. Cohen is a Professor in the Departments of Cellular and Molecular Pharmacology and Biochemistry and Biophysics at the University of California, San Francisco. He holds a B.S. from Yale University, a D.Phil. from Oxford University and an M.D. from Stanford University. His fields of investigation include protein structure, protein folding, prion diseases, drug design against prions disease and parasitic diseases, and various aspects of computational biology.

Cedric Govaerts holds a B.S. and a Ph.D. from the Free University of Brussels. He is currently a postdoctoral fellow in the group of Fred Cohen and works on structural studies of prions.

Processivity Clamps in DNA Replication: Clamp Loading

Megan J. Davey and Mike O'Donnell
The Rockefeller University, New York, USA

DNA processivity clamps are ring-shaped proteins that encircle and slide freely along the DNA. These clamps tether replicative DNA polymerases to the DNA ensuring that they remain attached to the template for the many thousands of base pairs necessary to copy genomes. The stable toroidal structure of processivity clamps necessitates specialized machinery, termed a clamp loader, to open the clamp and place it onto DNA. Clamp loaders are hetero-oligomeric protein complexes that use the energy of ATP binding and hydrolysis for their function.

DNA Processivity Clamps

Chromosomal replicases are multi-subunit machines that use ATP to maintain a tight grip on DNA and thus are highly processive. Study of the T4 bacteriophage, *Escherichia coli*, and eukaryotic replisomes has demonstrated that these replicases consist of a polymerase and two accessory factors. Work on the *E. coli* system has identified the two accessory factors as a clamp and a clamp loader (Figure 1).

The first clue that one accessory protein acted alone as a ring-shaped sliding clamp was provided in the *E. coli* system. Biochemical experiments have shown that the *E. coli* DNA processivity clamp, β, binds tightly to circular DNA, yet slides freely along the duplex. Linearizing the DNA results in β sliding off the ends. This behavior led to the prediction that the clamp forms a topological link with DNA, independent of sequence and that it is shaped like a ring and encircles the duplex like a donut. This prediction was fulfilled by the crystal structure, which confirmed that β is ring shaped (Figure 2). Since that first structure, ring-shaped DNA processivity clamps have also been demonstrated in archaea, bacteriophage, and eukaryotes (Figures 1B and 2). These clamps share a common chain-fold; however, they employ slightly different strategies to achieve this structure. The *E. coli* β-clamp is composed of two crescent-shaped molecules that form a head-to-tail dimer. Each of the subunits is composed of three globular domains that lack sequence similarity yet have the same chain-folding pattern and are nearly superimposable. Thus, each β-clamp is composed of six globular domains arranged in a circle around a central channel (Figure 1A). The diameter of the central channel is $\sim$35 Å and is large enough to fit double strand DNA. The outside diameter of β is $\sim$80 Å. The structure contains 12 α-helices that are all positioned on the inside of the ring, lining the central channel. Although β has an overall negative charge, the helices carry a positive charge and are thought to contact the DNA phosphate backbone through nonspecific, water-mediated interactions, allowing the clamp to slide along DNA.

In eukaryotic cells the clamp is proliferating cell nuclear antigen (PCNA). PCNA shares very little sequence similarity with the β-clamp, yet the overall structure of PCNA is very similar to that of β (Figures 2A and 2C). The two structures have similar inner and outer diameters, and the domains have the same chain-folding pattern, making the molecules nearly superimposable. However, there is one major difference between the two clamps: PCNA is a trimer rather than a dimer. PCNA has two rather than three domains per monomer and trimerizes to form a six-domain ring. Eukaryotic PCNA is homologous to PCNA in archaea and, as expected, they share similar structures (Figure 2D). The replicase of bacteriophage T4 and the related phage RB69 also utilize a clamp and clamp loader. The T4 gene protein (gp) 45 has no sequence similarity with PCNA or β, but is a trimer, like PCNA, and the overall structure is quite similar to all the other clamps (Figure 2B).

Processivity Clamp Loaders

β and PCNA appear to be tightly closed rings. On circular DNA, β and PCNA remain associated with a half-life of 0.5–1 h at 37 °C, demonstrating that the interfaces between the protomers remain tightly associated. This tight association, while important for processivity, necessitates the use of a clamp loader to rapidly open and close the clamp.

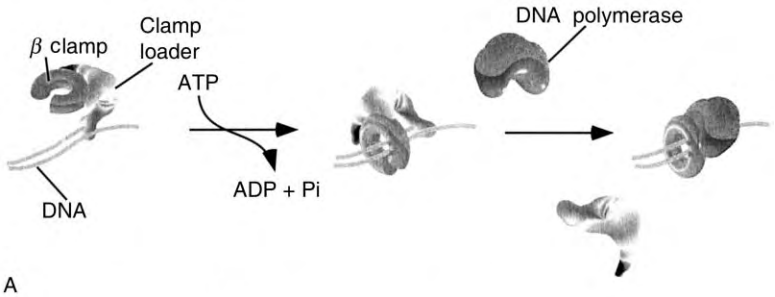

A

Organism	Clamp	Clamp loader
E. coli	Clamp (β_2)	γ-Complex ($\gamma_3^{\delta\delta'}\chi\psi$)
T4 bacteriophage	gp45 (trimer)	gp44/62 Complex
Eukaryotes	PCNA (trimer)	RFC *S. cerevisiae* Rfc 1-5 Human, p140, p37, p36, p40, p38
Archaea	PCNA (trimer)	RFC RFCS/RFCL

B

FIGURE 1 Components of a replicase. (A) Cellular replicases are composed of a ring-shaped clamp that is placed on DNA by a clamp loader. The clamp is utilized by DNA polymerase to remain tightly linked to DNA for highly processive replication. (B) Table of clamps and clamp loaders from different organisms.

Clamp loaders, both prokaryotic and eukaryotic, are hetero-oligomeric protein complexes, usually hetero-pentamers, that use the energy of ATP binding and hydrolysis to drive the loading of processivity clamps onto primed DNA. The loading process includes opening of the clamp, bringing the clamp to the DNA, and closing of the clamp around double-strand DNA. The different subunits within clamp loaders share sequence and/or structural homology. In addition, most of the clamp loader subunits from bacteria, T4 phage, eukaryotes, and archaea share sequence homology with each other, particularly within the sequences necessary for ATP binding and hydrolysis. Because of these similarities, clamp loaders from different systems are thought to function similarly. The clamp-loading mechanism has been most extensively studied in *E. coli*.

E. Coli Clamp Loader, γ-Complex

The clamp loader in *E. coli* is composed of five different subunits, γ, δ, δ', χ, and ψ. A complex composed of γ, δ, and δ' is sufficient for clamp loading and replication *in vitro*; χ and ψ are not absolutely required for clamp loading and their role will be discussed later in this entry.

The δ Subunit Opens the β Clamp

δ is the clamp loader subunit that binds β the tightest and is also capable of opening β on its own. Neither β nor δ can bind ATP, δ must open the clamp using the energy of protein–protein interaction. Only one δ subunit binds to one β dimer, suggesting that only one interface of β_2 is opened by δ. Furthermore, β_2 that has been cross-linked at one interface is capable of being loaded by γ complex, and therefore only one interface needs to be opened during the clamp-loading operation. Maintaining the integrity of one dimer interface ensures that β is easily reclosed.

Structure of the β_1–δ Complex Biochemical studies have shown that δ binds tightly to a mutant $\beta(\beta_1)$ that is rendered monomeric by mutating two hydrophobic residues at the dimer interface. This stable complex

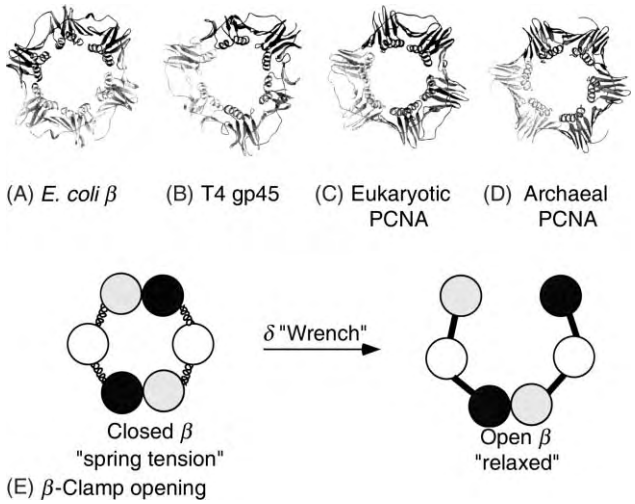

FIGURE 2 Similarity of clamp structures: The structures of (A) *E. coli* β-clamp, (B) T4 bacteriophage gp45, (C) *S. cerevisiae* PCNA, and (D) *P. furiousus* PCNA are shown. Each protomer in the ring is a different shade. Shown in (E) is a schematic of how β opens once it is cracked open by δ. Closed β is under spring tension, which is relieved when β is cracked, driving further opening of the ring.

enables the formation of a $\beta_1-\delta$ co-crystal. The crystal structure of $\beta_1-\delta$ suggests how δ may open β. δ contacts β in two different places. One contact is within a hydrophobic pocket between the middle and C-terminal domains of β and is thought to provide most of the binding energy. A second site of contact is between an α-helix in δ and a loop in β. This loop in β is near the dimer interface and is connected to an α-helix that contains hydrophobic core residues involved in formation of the β-dimer. In the $\beta_1-\delta$ structure the hydrophobic core residues are rotated out of the dimer interface. Perhaps, δ-binding to β forcibly disrupts the hydrophobic core of the dimer interface. Alternatively, there is a rapid exchange between open and closed forms of β, and δ simply stabilizes β in the open conformation. The stability of β on circular DNA suggests that the former case is more likely; however, the exact mechanism remains to be determined.

The β-Dimer is Under Spring Tension The distortion of the β_2-interface by δ may crack the ring, but does not explain how the edges of the crack open wide enough for passage of DNA. A striking difference in the shape of β_1 (with δ) and β_2 provides a strong clue as to how the ring opens up. The β-protomers within the β_2-structure have a higher degree of curvature than β_1. The change in curvature seems to result from rigid body motions between the three domains of the β-monomer. The largest of these changes occurs farthest away from the area of δ contact, suggesting that these rigid body motions are not a direct result of δ-binding β but are instead powered intrinsically within β itself. The increased curvature of β within β_2 suggests that β_2 is strained. Presumably, the two protomers come together and inward to form a ring due to the strength of the interaction. In other words, the free energy of forming the dimer interface is greater than the energy needed to bend the domains and form a closed ring. When the interface is disrupted by δ, the tension between the domains is allowed to relax and the ring opens (Figure 2E). This idea of a "spring-loaded" β-dimer is supported by molecular dynamics simulations that demonstrate that a protomer of β in the dimeric, strained conformation rapidly assumes the relaxed, monomeric conformation. When β_1 is modeled as a dimer, a gap at one interface is produced (as illustrated in Figure 2E).

Clamp Opening by γ Complex

Although δ is able to open the β-clamp in the absence of ATP, γ-complex requires ATP to open the β-clamp. γ is the only subunit that utilizes ATP and thus may be thought of as the motor that drives clamp loading. In the absence of ATP, γ-complex can no longer bind β, suggesting that other subunits occlude δ from binding β. In the presence of ATP, γ re-establishes a tight interaction between δ and β, suggesting that ATP binding (ATP hydrolysis is not necessary) powers a conformational change that exposes δ for interaction with β. Study of γ and δ' suggests that they interfere with $\delta-\beta$ interaction, implying that within the γ complex, δ' and γ may prevent $\delta-\beta$ contact in the absence of ATP.

$\gamma_3\delta\delta'$ Form a Heteropentameric Ring

The structure of the minimal $\gamma_3\delta\delta'$-clamp loader reveals that the subunits are arranged in a circle in which δ and δ' bracket three γ-subunits (Figure 3B). Each of the subunits shares a similar three-domain structure (Figure 3A). In fact, they share the exact same-chain-folding topology from head to tail. This similar structure was expected for γ and δ' since they are homologous to one another. However, this observation is somewhat surprising for δ since it shares no sequence similarity with δ' and γ. Most of the subunit contacts within $\gamma_3\delta\delta'$ are within the carboxy-terminal domains, which form a closed pentameric circle. However, when viewed from the amino-terminal face of the assembly, there is a gap between the amino-terminal domains of δ and δ'.

One of the striking features of this structure is the position of nucleotide-binding sites; they are located at the interfaces between subunits. There are three ATP-binding sites, one in each γ subunit, at the $\delta'-\gamma_1$, $\gamma_1-\gamma_2$, and $\gamma_2-\gamma_3$ interfaces. Each nucleotide-binding site seems to rely on residues from two different subunits for function. For example, the $\delta'-\gamma_1$ site is comprised of a canonical nucleotide-binding site in γ_1 and an arginine residue from δ'. The arginine residue is encoded by an SRC motif that is conserved in clamp loader residues from bacteria, phage, archaea, and eukaryotes.

Active and Inactive States of γ Complex The β-binding element in δ is located on the amino-terminal domain of δ, and is positioned in the gap between δ and δ'. This was somewhat surprising since the crystal structure was determined in the absence of ATP and thus should not be able to bind β. However, when β is modeled onto the $\gamma_3\delta\delta'$ assembly, using the $\beta_1-\delta$ structure as a guide, there is a severe clash between β and the clamp loader subunits. Thus, the complex would appear to be in an inactive state, unable to bind β.

What changes in the γ-complex structure occur, dependent on ATP binding, to accommodate interaction between δ and β? To dock β onto δ without clashing with other subunits, the N-terminal domain (domain I) of δ must be rotated outwards by at least 20–30° with respect to the C-terminal domain (domain III). Presumably, the binding of ATP to the γ subunits powers this change.

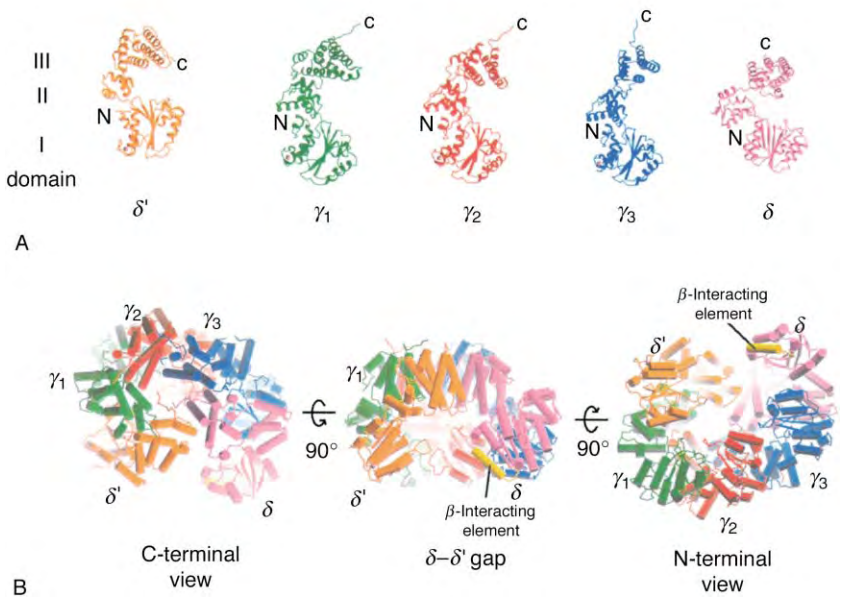

FIGURE 3 The structure of $\gamma_3\delta\delta'$ and individual subunits. Each of the clamp loader subunits is shown in (A). The three domains are indicated as well as the amino (N) and carboxy (C) terminal of each protein. In (B), the $\gamma_3\delta\delta'$-assembly is shown from three different views.

δ′ as a Stator All three subunits are present in different conformations, mainly due to the rigid body motion between domain III and domains I/II. Likewise, δ has a similar conformational difference upon comparing δ in $\beta_1-\delta$ and $\gamma_3\delta\delta'$-complexes. These observations suggest a flexibility between domain III and domains I/II in these protomers. However, the crystal structure of δ' alone is very similar to the structure of δ' in the $\gamma_3\delta\delta'$-assembly, implying that δ' is a more rigid protein than γ or δ. Examination of the structure of δ' reveals extra packing interactions between domains II and III, which may account for the apparent rigidity. Because of this seeming rigidity, δ' has been termed the stator (the stationary part of a motor against which other parts move). δ' can also be thought of as a backboard against which the ATP-dependent motions of the other subunits are braced.

Release of β and Closing of the Clamp

Once the γ-complex has bound to β and opened the clamp, it brings β to the primed site. The clamp loader-clamp complex binds tightly to primed DNA, which is, in fact, the best effector of ATP hydrolysis by γ-complex. When the clamp loader–clamp complex interacts with the primed site, the clamp loader hydrolyzes ATP and dissociates from β, leaving it on the primed site (Figure 4). It is proposed that the clamp loader is brought back to the inactive state upon hydrolysis of ATP (Figure 4). This presumably brings δ back into close proximity to γ and δ', pushing β off the δ wrench thereby releasing and allowing it to close around DNA.

The Role of χ and ψ

Neither χ nor ψ are required for clamp loading *in vitro*. However, when χ and ψ are missing from the clamp loader, both clamp loading and elongation become

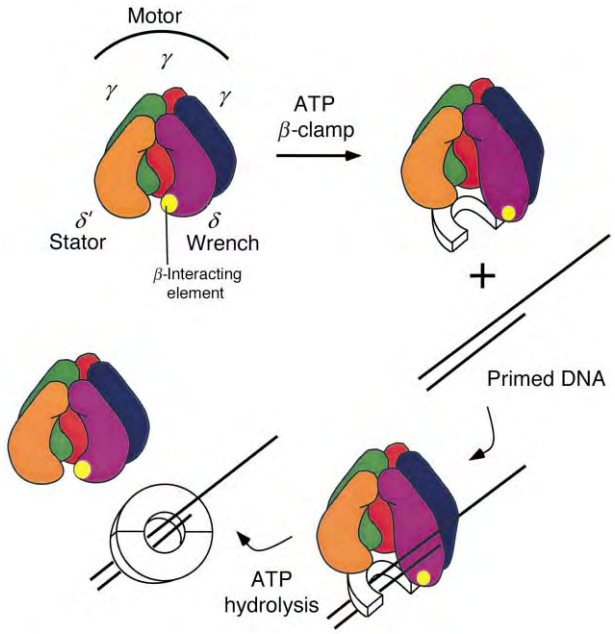

FIGURE 4 Clamp loading cycle by γ-complex. First, γ-complex binds ATP, which renders it capable of binding to and opening β. The clamp loader–clamp complex interacts with primed DNA which triggers ATP hydrolysis by γ-complex. ATP hydrolysis may cause γ-complex to release the clamp, allowing it to close around DNA.

sensitive to increased salt concentrations. This sensitivity is thought to arise from an interaction between χ and single strand DNA-binding protein, SSB. The contact between χ and SSB is important for the exchange of primase for both clamp loader and polymerase at the primed site. The role of ψ is somewhat less clear. It interacts with χ in a 1:1 complex. ψ also binds γ and forms a link between χ and the γ complex.

τ-Subunit and Interaction with DNA Polymerase III

The *dnaX* gene that encodes γ (47 kDa) also produces another protein, τ (71 kDa). A translational frameshift results in a stop codon to produce γ, whereas τ is the full-length protein. Therefore, τ is composed of γ plus 24 kDa of extra carboxy-terminal sequence. τ can fully substitute for γ in the clamp loader. Furthermore, while cells can survive in the absence of γ, they lack viability in the absence of τ. Thus, the carboxy-terminal residues unique to τ are essential. The carboxy-terminal sequences of τ interact with the DNA polymerase III core and with the replicative helicase, DnaB, providing a link between the clamp loader and the replisome. In the replicase, the clamp loader is thought to contain two τ subunits and one γ subunit, enabling this single clamp loader to cross-link two core polymerases for simultaneous synthesis of leading and lagging strands of the chromosome.

T4 Bacteriophage Clamp Loader

Although most viruses and bacteriophage do not employ a clamp and clamp loader machinery, T4 phage produces a clamp (gp45) and clamp loader for its chromosomal replicase (gp43). The clamp loader is composed of two different subunits, gp44 and gp62. Each clamp loader contains four copies of gp44 and one copy of gp62. Thus, the T4 phage clamp loader is a heteropentamer, like γ-complex. The gp44 subunit is homologous to γ and δ', and thus probably provides the motor function of the clamp loader. Gp62 has no known homologues.

In T4 bacteriophage, as in several eukaryotic DNA viruses, replication is tightly coordinated with late gene transcription (i.e., the early to late gene switch). Several elegant studies have revealed that the gp45 clamp slides along DNA and binds directly to RNA polymerase, specifically activating it at late gene promoters.

Archaeal RFC

Like the T4 bacteriophage clamp loader, archaeal cells contain only two different clamp loader subunits. These subunits are referred to as RFCL (L for large subunit) and RFCS (S for small subunit). Together these proteins form a complex that is capable of loading its cognate clamp onto DNA and stimulating the replicative DNA polymerase in several species of archaea. Initial characterization of the composition of these RFC complexes suggests a pentamer, with one or two copies of RFCL and three or four copies of RFCS, depending on the species. A structure of the small subunit from *Pyrococcus furiousus* has been solved. RFCS forms a dimer of trimers, and the trimer unit shares similar structure to the γ-trimer in γ-complex. In fact, RFCS has the same chain-fold and three-domain structure as γ, δ, and δ'.

Eukaryotic Clamp Loader

The eukaryotic clamp loader, termed replication factor C (RFC), is composed of five different subunits known as Rfc1-5 in *S. cerevisiae* and p140, p37, p36, p40, and p38 in human cells. All five subunits share sequence homology to each other and to the γ and δ' subunits of γ complex. Analogous to γ complex, the C termini of the RFC subunits are needed to form the pentamer. There is no crystal structure information on eukaryotic RFC; however, atomic force and electron microscope studies of RFC indicate a similarity to *E. coli* γ-complex. Atomic force microscope images of RFC indicate that the subunits are arranged in a circle similar to the C-terminal view of γ-complex. Electron microscope images of RFC in the presence of ATP show a gap in the circle similar to the amino-terminal face of γ-complex.

The results of biochemical experiments suggest that RFC may also function similarly to γ-complex. However, there are some important differences between γ-complex and RFC. For example, RFC has four rather than three ATP sites. This observation and the observation of five different subunits in RFC may reflect the greater complexity of eukaryotic cells compared to bacteria. It has been shown that PCNA interacts with numerous other proteins besides DNA polymerases. In addition, there are modified RFC assemblies in which one of the subunits has been substituted with a different protein. Hence, RFC (and modified RFCs) are thought to be involved in many different cellular processes such as DNA repair, cell cycle control/checkpoint, and chromosome segregation. PCNA can therefore be thought of as a "bull's eye," targeting proteins to DNA for specific events.

See Also the Following Articles

DNA Polymerase III, Bacterial • DNA Replication Fork, Bacterial • Eicosanoid Receptors • Sliding Clamps in DNA Replication: *E. coli* β-Clamp and PCNA Structure

Glossary

processivity The ability of an enzyme to catalyze more than one turnover before releasing the product or the substrate.

replicase Protein machinery that copies a strand of DNA. Chromosomal replicases typically contain a core polymerase, a processivity clamp, and a clamp loader.

replisome Protein machinery that copies DNA (both strands of DNA). Replisomes include the replicase (polymerase, clamp and clamp loader) as well as a helicase to unwind DNA. A priming activity is required for one strand.

Further Reading

Benkovic, S. J., Valentine, A. M., and Salinas, F. (2001). Replisome-mediated DNA replication. *Annu. Rev. Biochem* **70**, 181–208.

Jeruzalmi, D., Yurieva, O., Zhao, Y., Young, M., Stewart, J., Hingorani, M., O'Donnell, M., and Kuriyan, J. (2001). Mechanism of processivity clamp opening by the delta subunit wrench of the clamp loader complex of *E. coli* DNA polymerase III. *Cell* **106**, 417–428.

Lehninger, A. L., Nelson, D. L., and Cox, M. M. (2000). *Principles of Biochemistry.* Worth Publishing, New York.

O'Donnell, M., Jeruzalmi, D., and Kuriyan, J. (2001). Clamp loader structure predicts the architecture of DNA polymerase III holoenzyme and RFC. *Curr. Biol.* **11**, R935–R946.

Biography

Megan J. Davey is a Research Associate with Mike O'Donnell at The Rockefeller University, where she has pursued her interest in the assembly of replication–initiation complexes in bacterial and eukaryotic systems. Previously, Megan earned her Ph.D. studying plasmid segregation with Barbara Funnell at the University of Toronto.

Mike O'Donnell works in the area of DNA-replication mechanisms in several systems. He initially discovered the circular sliding clamp and the clamp–loader complex in the *E. coli* DNA-replication system in 1991. He obtained his Ph.D. from the Biological Chemistry Department at the University of Michigan, and then did postdoctoral training with Arthur Kornberg and Robert Lehman at Stanford University. He is now an Investigator at Howard Hughes Medical Institute (HHMI) and Professor at Rockefeller University in Manhattan, New York.

Propionyl CoA–Succinyl CoA Pathway

Wayne A. Fenton
Howard Hughes Medical Institute and Yale School of Medicine, New Haven, Connecticut, USA

The importance of the short metabolic pathway from propionyl CoA to succinyl CoA in humans was recognized in the 1960s with the description of newborns with severe, often fatal, metabolic acidosis accompanied by massive excretion of propionic or methylmalonic acid. It was established that these conditions resulted from deficiencies in the activity of propionyl CoA carboxylase or methylmalonyl CoA mutase, respectively, two of the enzymes in the pathway. These enzymes themselves were found to be defective in many cases. Because each requires a vitamin-derived coenzyme for activity, however, other cases resulted from defects in the transport or metabolism of the vitamins (biotin and vitamin B_{12}, respectively). Many of the proteins and enzymes involved in these steps have subsequently been described.

The Propionyl CoA–Succinyl CoA Pathway

The pathway involved is shown in eqn. [1]. Propionyl CoA is carboxylated by propionyl CoA carboxylase (EC 6.4.1.3), a biotin-containing enzyme, to form D-methylmalonyl CoA. This product is racemized by methylmalonyl CoA racemase (epimerase) (EC 5.1.99.1) to D,L-methylmalonyl CoA. The L-isomer is the substrate for methylmalonyl CoA mutase (EC 5.4.99.2), which carries out an adenosylcobalamin (coenzyme B_{12})-dependent rearrangement of the carbon backbone to form succinyl CoA. This product then enters the tricarboxylic acid cycle.

Propionyl CoA arises from a number of metabolic pathways, predominantly the catabolism of certain amino acids (isoleucine, methionine, threonine, and valine) and the β-oxidation of odd-chain fatty acids, with minor contributions from the degradation of thymine, uracil, and the side chain of cholesterol. Methylmalonyl CoA is produced essentially only from propionyl CoA. Gut bacteria produce a significant amount of propionic acid (and lesser amounts of methylmalonic acid); thus, propionyl CoA can also arise from this source by the action of cellular acyl CoA synthases.

The Enzymes

Propionyl CoA Carboxylase

Propionyl CoA carboxylase (PCC) is a large enzyme (~770 kDa) composed of two dissimilar subunits, α (72 kDa) and β (56 kDa), arranged in an $(\alpha\beta)_6$ quaternary structure. It is ubiquitously expressed and is localized to the mitochondrial matrix. The individual subunits are synthesized in the cytosol as larger precursors, which are proteolytically processed to their mature sizes and assembled after translocation into the mitochondrion. The α-subunit bears the lysine to which biotin is covalently bound via an isopeptide linkage to the ε-amino group and carries out the half-reaction in which carbon dioxide is activated to react with biotin, forming an enzyme-bound carboxyl-biotin intermediate. The β-subunit completes the reaction by transferring the carboxyl moiety to propionyl CoA to form methylmalonyl CoA.

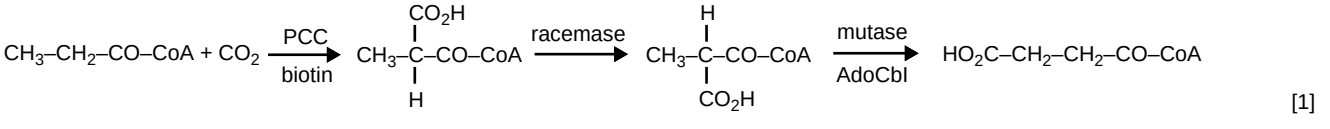

[1]

propionyl CoA | D-methylmalonyl CoA | L-methylmalonyl CoA | succinyl CoA

Methylmalonyl CoA Racemase

It is a dimer of identical subunits (~16 kDa) and is likely to be mitochondrially localized, but its expression pattern has not been established. The reaction mechanism appears to involve a simple abstraction/replacement of the labile proton on the α-carbon. In fact, racemization of methylmalonyl CoA occurs spontaneously in solution at a significant rate under physiologic conditions by exchange of this proton.

Methylmalonyl CoA Mutase

It is a dimer of identical subunits (78.5 kDa) and is expressed in all tissues examined. Its subunits are synthesized as larger precursors in the cytosol, translocated into mitochondria, and processed and assembled in the mitochondrial matrix. The coenzyme, adenosylcobalamin (AdoCbl), is very tightly bound to mutase; X-ray crystallography of the homologous enzyme from *P. shermanii* indicates that AdoCbl is buried in the interior of the enzyme. The reaction mechanism, while typical of AdoCbl-dependent enzymes, is unique in mammalian metabolism. In the presence of substrate, the carbon–cobalt bond of AdoCbl cleaves homolytically to form a free radical pair, Cbl^{II} and a deoxyadenosyl radical. The deoxyadenosyl radical abstracts hydrogen from the substrate to form a substrate radical that undergoes a rearrangement to form the product radical. This species recovers the hydrogen from deoxyadenosine to generate the final product and the original radical pair, which reverts to AdoCbl as the product leaves. Because these radical species are very labile to quenching by solvent, they appear to be highly protected in a buried active site. Crystal structures of the *P. shermanii* enzyme complexed with substrate analogues have been interpreted to suggest that the active site cleft opens to permit substrate entry, then closes until the reaction is completed, at which time it opens again to release the product.

The Cofactors

Biotin

Biotin is an abundant vitamin, available from a variety of plant and animal sources. It is used directly as a cofactor by four carboxylases in humans: acetyl CoA carboxylase, pyruvate carboxylase, β-methylcrotonyl CoA carboxylase, and PCC. Its metabolism is relatively uncomplicated, involving only two enzymes of note. One is biotinidase, a serum enzyme in man and other mammals, which specifically cleaves the isopeptide bond in biocytin (-biotinyl-lysine), the end product of proteolysis of biotin-containing enzymes, to release biotin for reuse. The other is holo-carboxylase synthase, the enzyme that forms the isopeptide bond between cellular biotin and the ε-amino group of the active site lysine in the apocarboxylases. Genetically determined defects in each of these have been described in humans, leading to a general deficiency of all of the carboxylases (multiple carboxylase deficiency) and pleiotropic metabolic effects, including propionic acidemia/aciduria (PA).

Vitamin B_{12} (Cobalamin)

In contrast to biotin, cobalamin is a rare vitamin that is available only from animal sources, which largely derive it in turn from gut bacteria. Plants, including yeast, do not synthesize the vitamin or use its cofactor forms. Although the daily requirement for vitamin B_{12} in humans is low (the current recommended dietary allowance, RDA, is 2.4 μg), an elaborate system of digestive enzymes and specific, high-affinity binding and transport proteins exists to ensure its efficient capture from dietary sources and delivery to cells throughout the body. Two distinct cofactor forms of the vitamin, methylcobalamin (MeCbl) and AdoCbl, are produced by a series of intracellular metabolic steps (eight have been recognized genetically) and are used by only two enzymes, methionine synthase and methylmalonyl CoA mutase, respectively. Deficiencies of many of these enzymes and proteins have been described. The most common are acquired defects in the activities of the digestive and gut transport proteins resulting from diseases of the digestive tract or surgical resection of these organs. These lead to a general vitamin B_{12} deficiency and the condition known as pernicious anemia. Genetic defects in these same proteins have been described, but are much rarer; they also lead to a form of pernicious anemia, generally at a much earlier age. Pernicious anemia is usually accompanied by methylmalonic acidemia/aciduria, although the hematologic defects are clinically more significant. Defects in cellular cobalamin metabolism lead to a variety of conditions, including methylmalonic acidemia/aciduria.

The Diseases

Propionic Acidemia/Aciduria (PA)

PA occurs in the setting of reduced activity of PCC (Figure 1). This can be due to biotin deficiency (very rare), biotin transport and activation defects (biotinidase or holocarboxylase synthase deficiency; sites 3 and 2, respectively), or defects in PCC itself (site 1). The first two of these lead to multiple carboxylase deficiency, in which all four biotin-dependent carboxylases are affected. This condition is characterized by neurologic symptoms, hypotonia, and failure to thrive, sometimes accompanied by skin rashes and allopecia. In genetically

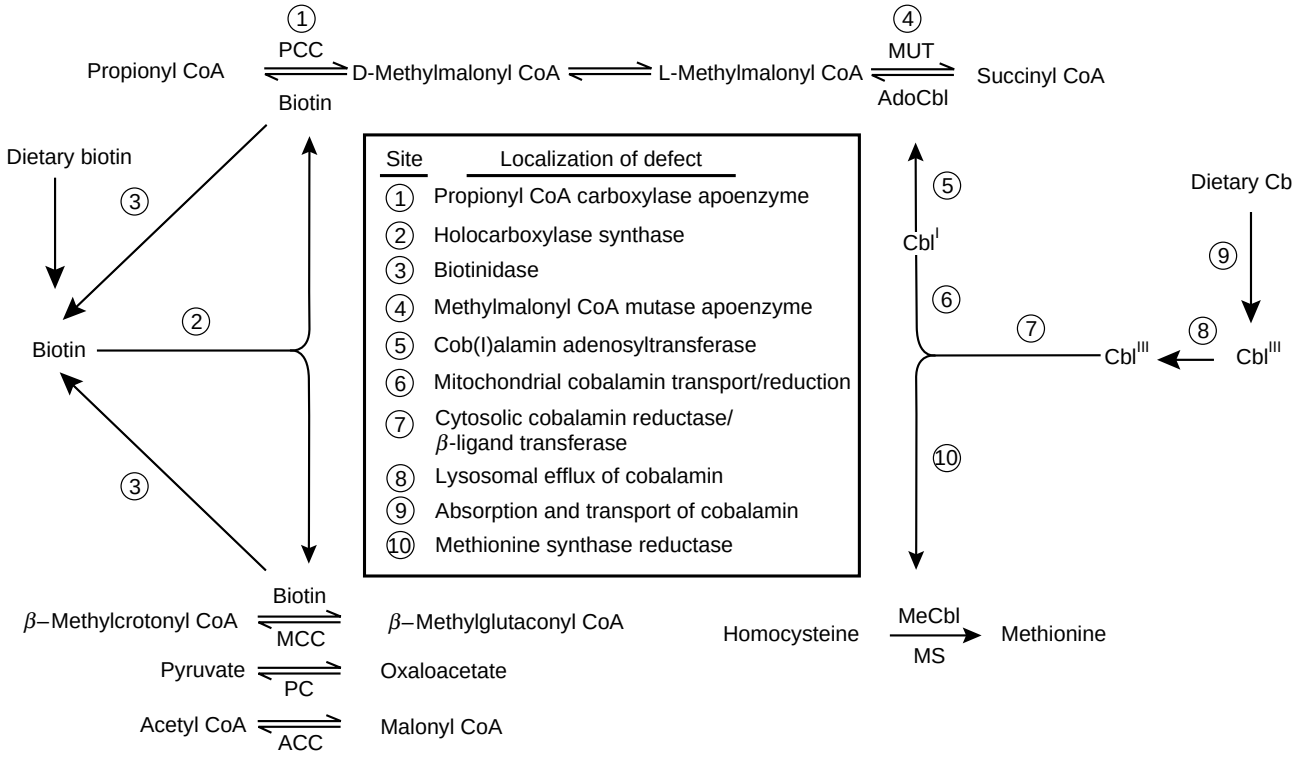

FIGURE 1 Sites of defects affecting the propionyl CoA–succinyl CoA pathway. A schematic of the biotin and cobalamin metabolism pathways is shown, along with their intersections with the propionyl CoA pathway. In several instances, the indicated sites encompass more than one enzyme or gene product. Genetic analysis suggests two gene products are involved at site 6; only one, of undefined activity, has been identified. Likewise, two gene products affect site 7 and the indicated metabolic activity. Defects in multiple gene products can contribute at site 9, including those in intrinsic factor, intrinsic factor receptor (megalin), and transcobalamin II, the serum cobalamin-carrying protein. Note that defects at site 10 and in methionine synthase (MS) affect a separate branch of cobalamin metabolism that has no impact on the propionyl CoA pathway. ACC, MCC, PCC, PC, acetyl CoA, β-methylcrotonyl CoA, propionyl CoA, and pyruvate carboxylase, respectively; MS, methionine synthase; MUT, methylmalonyl CoA mutase; Cbl, Cbl^{I}, Cbl^{III}, cobalamin and its 1+ and 3+ oxidation states, respectively; AdoCbl, MeCbl, adenosylcobalamin and methylcobalamin, respectively.

determined cases, onset of symptoms is often neonatal (synthase deficiency) or infantile (biotinidase deficiency), but may be delayed beyond the second decade. Biochemically, multiple carboxylase deficiency is marked by specific excretion of both propionic acid and methylcrotonic acid, their secondary metabolites (such as β-hydroxy propionic acid and tiglic acid), and glycine conjugates of these acids. Activities of the affected enzymes are low in serum (biotinidase) or cultured cells from patients, as are the activities of the carboxylases. At the genetic level, multiple carboxylase deficiency is an autosomal recessive trait, and mutations have been found in the genes for each of these enzymes. Treatment with high doses of biotin is usually effective in ameliorating these conditions.

PA arising from genetic defects in PCC itself is both more specific and often more severe. Neonatal onset is common, with vomiting, hypotonia, and neurologic symptoms resulting from an overwhelming metabolic acidosis. Massive excretion of propionic acid and its metabolites and conjugates is often accompanied by severe hyperammonemia. PCC activity is low or absent in cultured cells, but the other carboxylases are unaffected. PCC deficiency is inherited as an autosomal recessive trait, and causative mutations have been found in the genes for both the α- and β-subunits. Initially, treatment is supportive, seeking to reverse the profound metabolic acidemia and equally life-threatening hyperammonemia. Long-term therapy includes protein restriction using synthetic diets formulated to have reduced amounts of the metabolic precursors of propionate, such as branched-chain amino acids and odd-chain fatty acids, and antibiotic treatment to reduce the contribution of gut bacteria to the total metabolic load of propionate. Only a few patients with isolated PCC deficiency have responded to biotin supplementation. The long-term outcome for most patients has been poor, with many succumbing to acute metabolic decompensation triggered by infectious illnesses. However, a few have survived to adulthood and there are also a number of patients who have not been diagnosed until late into their second or even third decade. Although it has been suggested that genetic factors, such as the severity of the effects of a mutation on PCC activity, may

play a role in determining long-term survival, no clear genotype/phenotype correlation has been uncovered.

Methylmalonic Acidemia/Aciduria (MMA)

MMA arises from deficiencies in the activity of mutase. Although racemase deficiency would also be expected to produce MMA, no patients with this defect have been described. Environmental cobalamin deficiency, acquired and genetically determined cobalamin transport deficiencies, and cellular cobalamin activation defects, as well as defects in mutase itself, all of these contribute to the occurrence of this condition. Although environmental cobalamin deficiency is rare, it does occur in strict vegans and particularly in their breast-fed children. Much more common is acquired cobalamin deficiency resulting from disease processes affecting the stomach, including ulcers, alcoholism-induced destruction of the gastric mucosa, and surgical intervention including gastric bypass. All of these reduce the ability of the gastric parietal cells to produce intrinsic factor, a cobalamin transport protein that is essential for delivering ingested cobalamin to cells of the intestinal mucosa, where it is taken up and transported into the blood stream. The multi-step intestinal transport system for cobalamin (site 9) is also subject to genetic defects, although these are relatively rare. Clinically, the resulting cobalamin deficiency in all of these cases produces pernicious anemia, a characteristic megalobastic anemia. Biochemically, MMA can be demonstrated in these patients, although it is often mild, depending on the degree of cobalamin deficiency, and cellular mutase activity may be reduced. Therapeutically, the pernicious anemia and MMA resulting from cobalamin deficiency, whatever the underlying cause, can be treated effectively by injections of vitamin B_{12}.

Much more profound MMA occurs in patients with genetically determined defects in cellular cobalamin metabolism or in mutase itself. In these cases, severe neonatal metabolic acidosis is accompanied by massive excretion of methylmalonic acid, as well as lesser amounts of propionic acid and their metabolites. Because at least three of the eight cellular metabolic steps are common to AdoCbl and MeCbl production (sites 7 and 8), patients with defects in these steps also excrete homocystine, the oxidized form of homocysteine, the substrate of methionine synthase. Mutase activity is reduced or absent in cultured cells from patients with these disorders and from those with defects in the three metabolic steps that affect only AdoCbl metabolism (sites 5 and 6), although it can be restored in extracts of cells from patients by the addition of exogenous AdoCbl. Extracts from cells of patients with defects in mutase itself (site 4) generally do not show activity even with AdoCbl supplementation, except in rare cases where massive amounts of the coenzyme produce activity from a defective mutase enzyme with an abnormally high binding constant for AdoCbl. Genetically, all of these conditions appear to be inherited as autosomal recessive traits. In most cases, causative mutations in the individual genes for the affected enzymes have been found. Treatment of patients with defects in cellular cobalamin metabolism and in mutase has included symptomatic treatment of the severe metabolic acidosis, followed by protein restriction, synthetic diet, and antibiotic therapy, as with PA. Similarly, the long-term prognosis of these patients is poor, with one group of exceptions. In contrast to the lack of biotin-responsiveness in isolated PA, the clinical state of some MMA patients respond dramatically to supplementation with massive amounts of coenzyme in the form of injected hydroxocobalamin, with almost complete resolution of their clinical condition. Most of these patients have defects in one particular cobalamin metabolic enzyme (at site 6). The long-term prognosis of patients in this group seems very promising, although the effect of chronic MMA, which these patients still exhibit, remains unclear.

See Also the Following Articles

Biotin • Vitamin B_{12} and B_{12}-Proteins

Glossary

coenzyme/cofactor A small bio-organic compound, usually derived from a vitamin, that plays an essential role in assisting a specific enzyme to carry out its reaction.

hyperammonemia The condition of a high concentration of ammonium ion (ammonia) in the blood; ammonium ion is a common metabolic product and is normally found in significant amounts in the blood, but moderate elevations can damage the central nervous system if untreated.

metabolic acidosis A condition of reduced blood pH and bicarbonate ion concentration in response to the overproduction or decreased excretion of acidic metabolites.

pernicious anemia A distinctive blood disorder characterized by macrocytes in circulation and megaloblasts in bone marrow, generally due to a deficiency of either vitamin B_{12} (cobalamin) or folic acid.

propionic/methylmalonic acidemia The condition of excessive amounts of these metabolites in blood, where they are normally present in very small amounts.

propionic/methylmalonic aciduria The condition of excretion of very large amounts of these metabolites in the urine.

Further Reading

Banerjee, R. (ed.) (1999). *Chemistry and Biochemistry of B_{12}*. Wiley, New York.

Fenton, W. A., Gravel, R. A., and Rosenblatt, D. S. (2001). Disorders of propionate and methylmalonate metabolism. In *The Metabolic and Molecular Bases of Inherited Disease* (C. R. Scriver, A. L. Beaudet, W. S. Sly and D. Valle, eds.) 8th edition, pp. 2165–2193. McGraw-Hill, New York.

Rosenblatt, D. S., and Fenton, W. A. (2001). Inherited disorders of folate and cobalamin transport and metabolism. In *The Metabolic*

and Molecular Bases of Inherited Disease (C. R. Scriver, A. L. Beaudet, W. S. Sly and D. Valle, eds.) 8th edition, pp. 3897–3933. McGraw-Hill, New York.

Wolf, B. (2001). Disorders of biotin metabolism. In *The Metabolic and Molecular Bases of Inherited Disease* (C. R. Scriver, A. L. Beaudet, W. S. Sly and D. Valle, eds.) 8th edition, pp. 3935–3962. McGraw-Hill, New York.

Biography

Wayne A. Fenton is a Research Scientist in Genetics at Yale University School of Medicine. His general interests are in cobalamin metabolism and the mechanisms of protein folding and unfolding. He received a Ph.D. from Brandeis University and carried out postdoctoral work at Yale University.

Prostaglandins and Leukotrienes

William L. Smith
University of Michigan Medical School, Anna Arbor Michigan, USA

Robert C. Murphy
University of Colorado Medical School, Colorado, Denver, USA

Prostaglandins and leukotrienes are different types of eicosanoids – oxygenated, 20 carbon fatty acids synthesized from arachidonic acid (AA) (all *cis* 5,8,11,14-eicosatetraenoic acid). AA is a member of the n-6 family of fatty acids that are essential for mammals. There are three major groups of eicosanoids formed via three distinct pathways – the cyclooxygenase, lipoxygenase, and epoxygenase pathways. These pathways occur in higher eukaryotes that contain highly unsaturated fatty acids. Prostanoids, which include the prostaglandins (PGs) and thromboxanes (TXs), are formed through the cyclooxygenase pathway, leukotrienes and related hydroxy fatty acids come from the lipoxygenase pathway, and epoxy and dihydroxy acids are formed via epoxygenase (P450) pathways. Prostanoids and leukotrienes function through G protein-linked receptors, and there are one or more receptors for each prostanoid and leukotriene. These compounds act locally near their sites of synthesis without entering the circulation. They coordinate intercellular communication between the same (autocrine) and different (paracrine) cell types. Prostanoids promote inflammation and thrombosis and leukotrienes are involved in asthma. Nonsteroidal anti-inflammatory drugs such as aspirin, ibuprofen, and COX-2 inhibitors function by attenuating prostanoid synthesis while inhibitors of leukotriene synthesis and action such as zileuton and montelukast, respectively, are used to treat asthma.

Prostanoid Structures

Figure 1 shows the biosynthetic relationships among the prostanoids formed from arachidonic acid (AA). The letters following the abbreviation prostaglandins (PGs) indicate the nature and location of the oxygen-containing substituents present in the cyclopentane ring; the subscript indicates the number of carbon–carbon double bonds in the side chains. Greek subscripts denote the orientation of ring hydroxyl groups (e.g., $PGF_{2\alpha}$). Prostanoids known as isoprostanes are formed from AA by nonenzymatic autooxidation and consequently contain many stereoisomers. Interestingly, the amounts of isoprostane metabolites in urine are greater than prostanoids formed enzymatically.

Prostanoid Biosynthesis

Eicosanoids are not stored in cells but are formed on demand in response to extracellular hormonal stimuli (e.g., bradykinin, angiotensin, thrombin) that increase cell Ca^{2+} concentrations. Prostanoid formation requires three enzymatic steps: (1) mobilization of AA (or 2-arachidonylglycerol (2-AG)) from membrane phospholipids, (2) conversion of arachidonate (or 2-AG) to PGH_2 (or 2-PGH_2-glycerol), and (3) isomerization of PGH_2 (or 2-PGH_2-glycerol) to one of the major prostanoids by a terminal synthase. Mobilization of AA involves cytosolic phospholipase A_2 ($cPLA_2$) which translocates to the endoplasmic reticulum (ER) and nuclear membrane (NM) when intracellular Ca^{2+} concentrations rise and cleaves AA from a phospholipid on the cytosolic surface of the membrane. Newly released AA moves, methyl end first, to the luminal half of the bilayer where it enters the active site of a prostaglandin endoperoxide H synthase (PGHS) and is oxygenated to PGG_2 and its 15-hydroperoxyl group is then reduced to form PGH_2; PGHSs are also called cyclooxygenases (COX) and there are two isoforms (PGHS-1 and -2; COX-1 and -2). Once formed, PGH_2 is isomerized by a synthase located in the ER (e.g., TXA synthase, PGE synthase). Recently, 2-AG has been found to be converted to 2-PGH_2-glycerol by PGHS-2. This latter intermediate can be converted to the 2-prostanyl-glycerol derivatives but not 2-thromboxane-glycerol. 2-AG itself is probably formed from phosphatidylcholine by phospholipase C and monoacylglycerol lipase.

PGHS Catalysis and Inhibition

Figure 2 is a model of the cyclooxygenase and peroxidase active sites of ovine PGHS-1. To initiate oxygenation of AA at the cyclooxygenase site, the heme group at the peroxidase site must first be oxidized by a hydroperoxide. This causes formation of an oxidized

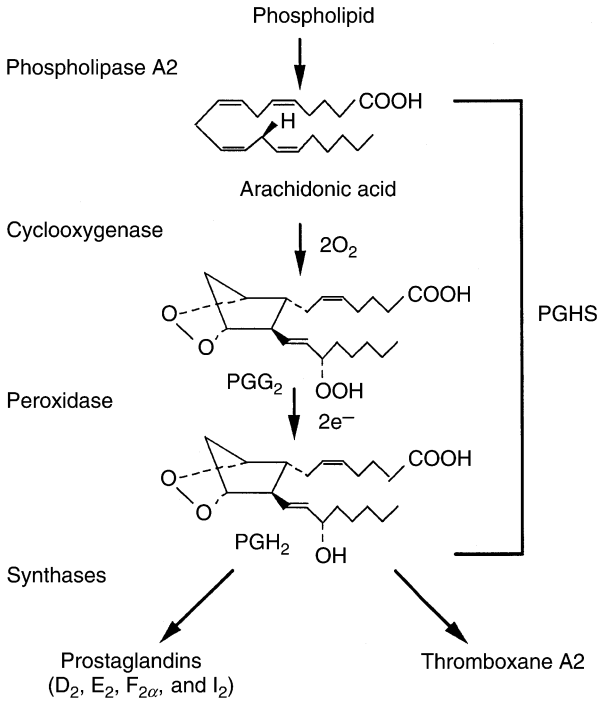

FIGURE 1 Biosynthesis of common prostanoids from AA.

heme intermediate that is reduced by an electron from Tyr385 thereby generating a Tyr385 radical. This radical abstracts a hydrogen from AA so that it can react with oxygen (Figure 1). The guanidino group of Arg120 binds to the carboxylate group of AA.

PGHS-1 is a constitutive enzyme purified in 1975 and its cDNA cloning has been reported in 1988. PGHS-2 is an inducible enzyme discovered in 1991 as an immediate early gene product in phorbol ester-activated murine 3T3 cells and in *v-src*-transformed chicken fibroblasts. PGHS-2 contains a unique 18 amino acid insert of as yet unknown function near its carboxyl terminus. The reason for the existence of the two PGHS isoforms is not known. Each protein functions as a homodimer with a monomer mass of 72 kDa. PGHSs are integral membrane proteins which instead of having transmembrane helices have a cluster of four amphipathic helices that interact with only one face of the lipid bilayer.

PGHSs are inhibited by nonsteroidal anti-inflammatory drugs (e.g., aspirin, ibuprofen, naproxen), which compete with AA for binding to the cyclooxygenase site of PGHSs. Prostaglandin synthesis mediated by PGHS-2 can be inhibited by anti-inflammatory steroids, which block the synthesis of PGHS-2 protein. Drugs called COX-2 inhibitors (e.g., rofecoxib and celecoxib) target PGHS-2 specifically and are used as anti-inflammatory and analgesic agents. Aspirin, acetylsalicylic acid, binds the cyclooxygenase site of PGHSs and acetylates Ser530 causing irreversible inhibition of PGHSs (Figure 2). Low doses of aspirin are used prophylactically to reduce coronary thrombosis; at low doses, aspirin inhibits PGHS-1 in platelets blocking thromboxane formation. PGHS inhibitors appear to reduce mortality from colon cancer.

PGHS-1 and PGHS-2 Gene Expression

There are separate genes for PGHS-1 and PGHS-2 located on different chromosomes. They have similar intron/exon structures but the PGHS-2 gene is 8 kb and the PGHS-1 gene is 22 kb. Little is known about the regulation of PGHS-1 gene expression. PGHS-2 gene transcription can be induced by cytokines and growth factors that function through multiple response elements in the PGHS-2 gene promoter. There is much interest in

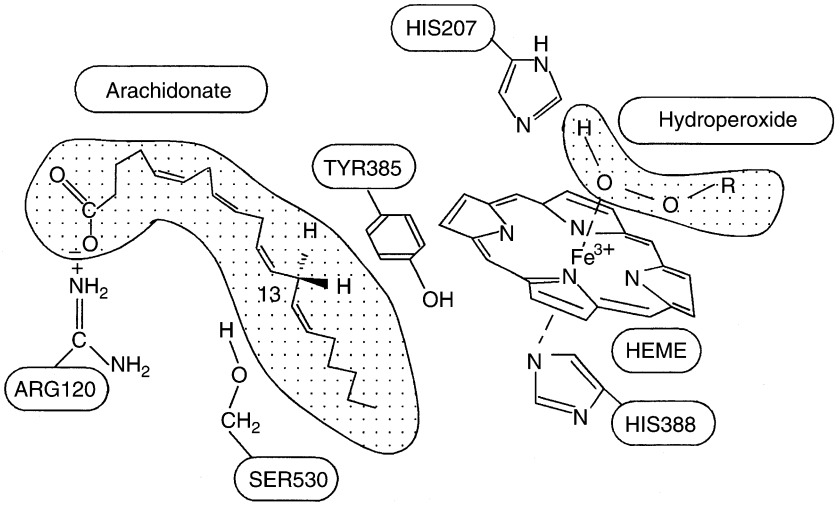

FIGURE 2 Model of the cyclooxygenase and peroxidase active sites of the ovine PGHS-1.

this because of the potential role of altered PGHS-2 expression in carcinogenesis.

PGH_2 Metabolism

Different cells form different prostanoids. PGE_2, PGD_2, PGF_2, PGI_2, and TXA_2 synthesis from PGH_2 is catalyzed by PGE synthase, PGD synthase, PGF synthase, PGI synthase, and TXA synthase, respectively; all of these enzymes catalyze isomerization reactions. PGF_2 formation involves a two-electron reduction of PGH_2. PGI synthase and TXA synthase are cytochrome P-450s. PGE synthase is a member of the MAPEG family of transmembrane ER proteins and requires reduced glutathione for activity. There are two PGD synthases; one is glutathione dependent and has been isolated from spleen and another is glutathione independent and occurs in brain.

Prostanoid Catabolism

The initial step in the inactivation of PGE_2 is oxidation of the 15-hydroxyl group to a 15-keto group catalyzed by 15-hydroxyprostaglandin dehydrogenase. Further catabolism involves reduction of the double bond between C-13 and C-14, β-oxidation, and ω-oxidation.

Prostanoid Actions

There are pharmacologically distinct receptors for each of the known prostanoids. In the case of PGE_2, four different prostaglandin E (EP) receptors have been identified and designated as EP1, EP2, EP3, and EP4 receptors. EP1 is coupled through G_q to the activation of phospholipase C, EP2 and EP4 are coupled via G_s to the stimulation of adenylate cyclase and EP3 receptors are coupled via G_i to inhibition of adenylate cyclase (16).

EP3 receptors are involved in the development of fever, EP2 and EP4 function in bone resorption and EP1 receptors are involved in chemically induced colon cancer. Prostanoids can activate some isoforms of peroxisomal proliferator activated receptors (PPARs). PGI_2 can be involved in PPARδ-mediated responses such as decidualization and apoptosis.

Leukotrienes and Lipoxygenase Products

Leukotrienes were discovered in 1979 during the search for the chemical structure of the "slow reacting substance of anaphylaxis." Leukotrienes are produced by the action of 5-lipoxygenase (5-LO) (Figure 3) which catalyzes both an oxygen insertion to form 5-HpETE and a dehydration reaction to form leukotriene A_4 (LTA_4). LTA_4 is converted to the biologically active leukotrienes LTB_4 and LTC_4 by LTA_4 hydrolase and LTC_4 synthase, respectively. LTB_4 is a potent chemotactic and chemokinetic agent for human polymorphonuclear leukocytes whereas LTC_4 constricts specific smooth muscle (e.g., bronchial smooth muscle) and mediates leakage of vascular fluid in the process of edema. The formation of LTC_4 versus LTB_4 is controlled by the expression of LTA_4 hydrolase or LTC_4 synthase by specific cell types. For example, the human neutrophil expresses LTA_4 hydrolase and produces LTB_4 while mast cells and eosinophils express LTC_4 synthase and produce LTC_4.

5-Lipoxygenase

Human 5-lipoxygenase (5-LO) (E.C.1.13.11.34) is a nonheme iron containing protein of 673 amino acids. It catalyzes the abstraction of a hydrogen atom from C-7 of AA and insertion of O_2 at C-5 to generate 5(S)-HpETE (Figure 3). The LTA_4 synthase activity of 5-LO then catalyzes removal of 10 pro-R hydrogen atoms from 5(S)-HpETE through a second redox cycle and an internal rearrangement of double bonds to form LTA_4. LTA_4, has a half-life of less than 10s at pH 7.4. Purified 5-LO requires Ca^{2+}, ATP, fatty acid hydroperoxide, and phosphatidylcholine in addition to the AA and O_2 substrates. Ca^{2+} facilitates the association of 5-LO with internal membranes. The need for an increase in intracellular Ca^{2+} concentrations differentiates 5-LO from other lipoxygenases. 5-LO oxygenates AA at the interface between membrane and cytosol. When Ca^{2+} concentrations increase in neutrophils and mast cells, 5-LO and cytosolic PLA_2 become associated with the nuclear membrane (NM) where another protein required for LTA_4 synthesis – 5-lipoxygenase activating protein (FLAP) – is found. In other cells 5-LO is constitutively associated with the NM while in alveolar macrophages 5-LO is present in the nucleus. The drug zileuton inhibits 5-LO.

The 5-LO gene is large (ca. 80 kb) and has 14 exons. It is on human chromosome 10. The human 5-LO gene promoter contains Sp1 and EGR-1 binding sites at -88 to -212 bp upstream of the translation start site. Genetic polymorphisms in humans are found in Sp1 binding sites.

5-Lipoxygenase Activating Protein (FLAP)

FLAP was discovered as a novel protein essential for leukotriene synthesis which was the target of an

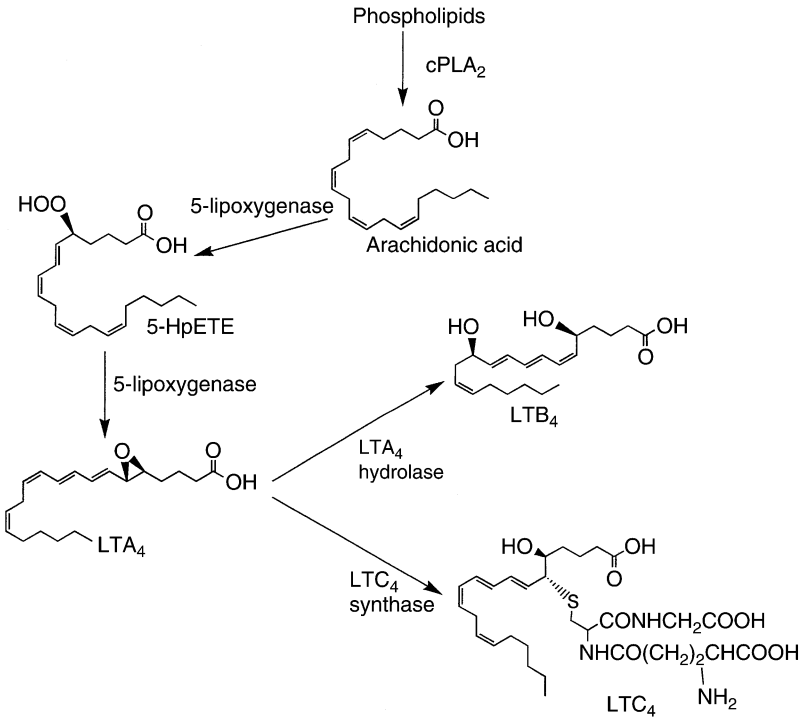

FIGURE 3 Biochemical pathway of the conversion of AA into the biologically active leukotrienes. AA released from phospholipid by $cPLA_2$ is metabolized by 5-LO to 5-hydroperoxyeicosatetraenoic acid (5-HpETE) and leukotriene A_4 (LTA_4) which is then converted to LTB_4 by LTB_4 hydrolase or conjugated to glutathione to form LTC_4 by LTC_4 synthase.

investigational drug from Merck (MK886). FLAP is an integral membrane protein of the NM containing 161-amino acids. The function of FLAP is unclear but it does bind AA analogues suggesting that it may transfer AA to 5-LO. LTC_4 synthase has 31% amino acid identity to FLAP with a highly conserved region putatively involved in AA binding.

LTA_4 Hydrolase and LTC_4 Synthase

LTA_4 hydrolase catalyzes the stereochemical addition of water to C-12 of LTA_4 to form the neutrophil chemotactic factor LTB_4. LTA_4 hydrolase contains 610 amino acids and one essential zinc atom. The enzyme is structurally related to zinc metalloproteases and exhibits protease activity; bestatin and captopril inhibit the enzyme. LTA_4 hydrolase is found in many cells including those which do not contain 5-LO, and it is felt that such cells function in transcellular LTB_4 synthesis. LTA_4 hydrolase is localized in the cytosol. To metabolize the unstable LTA_4, LTA_4 hydrolase must either come in contact with the NM during LTA_4 formation or a carrier protein must transfer LTA_4 to LTA_4 hydrolase. The crystal structure of LTA_4 hydrolase has been determined.

LTC_4 synthase (E.C.2.5.1.37) conjugates reduced glutathione (γ-glutamyl-cysteinyl glycine) to LTA_4. LTC_4 synthase is located on the NM. The enzyme has significant sequence homology to microsomal glutathione-S-transferases and FLAP. LTC_4 synthase is found predominantly in mast cells, macrophages, eosinophils, and monocytes. MK-886, which interacts with FLAP, also inhibits LTC_4 synthase. The gene for LTC_4 synthase is located on human chromosome 5.

Leukotriene Metabolism

LTB_4 can be oxygenated to 20-hydroxy-LTB_4 by specific cytochrome P-450s of the CYP4F family. 20-hydroxy-LTB_4 can be further metabolized to 20-carboxy-LTB_4 by CYP4F3 or to 20-oxo-LTB_4 by alcohol dehydrogenase then to 20-carboxy-LTB_4 by fatty aldehyde dehydrogenase. An alternative pathway involves an initial oxidation of the 12-hydroxy group to a 12-oxo moiety followed by reduction of the conjugated dienone and the 10,11 double bond. A secondary catabolic pathway, β-oxidation can occur from the C-1 carboxyl moiety of LTB_4 resulting in the loss of the C-5 hydroxyl group and from the 20-carboxy terminus of 20-carboxy-LTB_4. Individuals with genetic deficiencies in peroxisomal metabolism (Zellweger disease) that reduce β-oxidation or in aldehyde dehydrogenase (Sjogren–Larsson

syndrome) excrete intact LTB_4 and 20-hydroxy-LTB_4. LTC_4 catabolism involves peptide cleavage reactions involving glutamyl transpeptidase and various dipeptidases to yield LTD_4 and LTE_4, both of which have biological activity. The sulfur atom of sulfidopeptide leukotrienes can be oxidized by reactive oxygen species. More specific metabolic processing of the sulfidopeptide leukotrienes includes ω-oxidation by cytochrome P-450 followed by β-oxidation from the I terminus.

Leukotriene Biology and Leukotriene Receptors

LTB_4 functions in inflammatory processes through its chemotactic and chemokinetic affects human polymorphonuclear leukocytes. LTB_4 induces the adherence of neutrophils to vascular endothelial cells and enhances the migration of neutrophils (diapedesis) into extravascular tissues. The biological activity of LTB_4 is mediated through two specific G-protein coupled receptors termed BLT_1 and BLT_2. LTC_4 and its peptide cleavage products LTD_4 and LTE_4 mediate bronchial smooth muscle contraction in asthma and cause edema. There are two G protein-linked receptors for cysteinyl leukotrienes called $CysLT_1$ and $CysLT_2$. $CysLT_1$ is found in bronchial and intestinal smooth muscle; LTD_4 and LTC_4 activate $CysLT_1$. Montelukast, pranlukast, and zafirlukast inhibit the $CysLT_1$ receptor in humans. $CysLT_2$ receptors are abundant in the heart and in vascular endothelial cells.

See Also the Following Articles

Cytochrome P-450 • Eicosanoid Receptors • Phospholipase A_2 • Phospholipase C

Glossary

aspirin A nonsteroidal anti-inflammatory drug that inhibits cyclooxygenase by acetylating an active site serine residue and blocking productive binding of arachidonic acid.

cyclooxygenase Common name of the oxygenase enzyme that converts arachidonic acid and related 20 carbon essential fatty acids to prostanoids.

FLAP 5-lipoxygenase activating protein, an accessory protein that is required for 5-lipoxygenase functioning in intact cells.

leukotriene Those oxygenated derivatives of 20 carbon essential fatty acids formed through the action of 5-lipoxygenase and containing a conjugated triene system of double bonds.

5-lipoxygenase The oxygenase that converts arachidonic acid and related 20 carbon essential fatty acids to leukotrienes.

montelukast A drug used in the treatment of asthma that inhibits the binding of peptidoleukotrienes to the $CysLT_1$ receptor.

prostanoid Those oxygenated derivatives of 20 carbon essential fatty acids formed through the action of prostaglandin endoperoxide H synthase.

Further Reading

Kozak, K., Prusakiewicz, J., Rowlinson, S., Prudhomme, D., and Marnett, L. (2003). Amino acid determinants in cyclooxygenase-2 oxygenation of the endocannabinoid anandamide. *Biochemistry* **42**(30), 9041–9049.

Lam, B. K., and Frank Austen, K. (2000). Leukotriene C4 synthase. A pivotal enzyme in the biosynthesis of the cysteinyl leukotrienes. *Am. J. Respir. Crit. Care Med.* **161**(2 Pt 2), S16–S19.

Murphy, R. C., and Wheelan, P. (1998). Pathways of leukotriene metabolism in isolated cell models and human subjects. In *Five-Lipoxygenase Products in Asthma* (J. M. Drazen, ed.) pp. 87–123. Marcel-Dekker, New York.

Peters Golden, M., and Brock, T. G. (2000). Intracellular compartmentalization of leukotriene biosynthesis. *Am. J. Respir. Crit. Care Med.* **161**(2 Pt 2), S36–S40.

Smith, W. L., and Murphy, R. C. (2002). The eicosanoids: Cyclooxygenase, lipoxygenase and epoxygenase pathways. In *Biochemistry of Lipids, Lipoproteins and Membranes* (D. E. Vance and J. E. Vance, eds.) 4th edition., pp. 341–372. Elsevier Science B.V, Amsterdam.

Smith, W. L., DeWitt, D. L., and Garavito, R. M. (2000). Cyclooxygenases: Structural, cellular and molecular biology. *Annu. Rev. Biochem.* **69**, 149–182.

von der Donk, W., Tsai, A., and Kulmacz, R. (2002). The cyclooxygenase reaction mechanism. *Biochemistry* **41**(52), 15451–15458.

Biography

William L. Smith is a Professor of Biological Chemistry at the University of Michigan Medical School. His research interests are in the area of lipid mediators, particularly the enzymes involved in the biosynthesis of prostanoids. He has contributed to understanding the molecular basis for the actions of nonsteroidal anti-inflammatory drugs such as aspirin.

Robert C. Murphy is a Professor of Pharmacology at the University of Colorado Health Sciences Center in Denver. His research interests are in the area of lipids and lipid mediators particularly the metabolism of leukotrienes and related lipoxygenase products. Dr. Murphy determined the structures of the peptidoleukotrienes and has developed tools (mass spectrometry) for characterizing and quantifying lipids and lipid mediators.

Proteases in Blood Clotting

John D. Kulman and Earl W. Davie
University of Washington, Seattle, Washington, USA

Proteases are enzymes that hydrolyze peptide bonds within protein substrates. In vertebrates, proteases play an essential role in preventing the loss of blood by promoting hemostasis, a process that culminates in the formation of a platelet plug and the deposition of a polymerized fibrin network at sites of vascular injury. The mechanism of this process was first studied in the mid-1800s by a Scottish surgeon Andrew Buchanan, who proposed the existence of a clot-promoting factor that he called thrombin. This article discusses the coagulation cascade, and the structure and function of the blood clotting proteases.

The biochemical pathways leading to thrombin formation are now well understood, as are the mechanisms by which thrombin promotes and modulates hemostasis. In response to vascular damage, thrombin is generated from an inactive precursor by a series of biochemical reactions collectively known as the coagulation cascade (Figure 1). Thrombin subsequently catalyzes a series of reactions that lead to platelet aggregation, fibrin polymerization, and ultimately, feedback down-regulation of the coagulation cascade itself (Figure 2). The enzymes involved in these pathways are structurally and functionally related to trypsin, the prototypical serine protease of the digestive system. However, in contrast to trypsin, the coagulation proteases are characterized by a complex modular architecture that facilitates interactions with one another, with other protein substrates, as well as with protein cofactors. These interactions serve to restrict the proteolytic reactions of the blood coagulation cascade to coagulation-promoting surfaces at sites of vessel injury.

The Coagulation Cascade

The Extrinsic Pathway

Almost since the 1960s, the coagulation cascade has been envisaged as a series of stepwise reactions in which inactive forms of serine proteases are converted to active forms by limited proteolysis in a process known as zymogen activation. The coagulation cascade is initiated when tissue factor, an integral membrane protein located in the tissue adventitia, is exposed to circulating blood following a vascular injury (Figure 1). The binding of tissue factor to factor VII or to the active serine protease factor VIIa (trace amounts of which circulate in the blood) initiates the extrinsic pathway of coagulation. The tissue factor–factor VIIa complex converts factors IX and X to their active forms (IXa and Xa). Feedback amplification is achieved when inactive factor VII bound to tissue factor is converted to its active form (VIIa) by factors VIIa, IXa, and Xa, resulting in enhanced generation of factor Xa. The factor Xa thus produced generates thrombin from its inactive form (prothrombin) in the presence of calcium, the nonenzymatic cofactor factor Va, and anionic phospholipid (primarily phosphatidylserine (PS)) exposed on the surface of activated platelets or other cells. Thrombin generated in the extrinsic pathway initiates an additional feedback amplification loop by generating factors Va and VIIIa by limited proteolysis. These surface-bound protein cofactors serve as scaffolds for the assembly of complexes that facilitate the production of factors Xa and thrombin (the Xase and prothrombinase complexes, respectively).

The Intrinsic Pathway

Thrombin enhances flux through the coagulation cascade by activating the intrinsic pathway of coagulation. In this arm of the cascade, thrombin generates factor XIa from its zymogen form (XI) by limited proteolysis. Factor XIa then generates factor IXa by a similar mechanism. The precise physiological role of the intrinsic pathway has been the subject of considerable debate, particularly since defects or deficiencies of factor XI are mild, and are associated with a form of hemophilia that is quite distinct from classical hemophilia. Bleeding due to factor XI deficiency is typically associated only with major surgery or trauma, whereas deficiencies of factor VIII (hemophilia A) or factor IX (hemophilia B) give rise to spontaneous soft tissue and joint bleeding. Thus, whereas the extrinsic pathway is required in most cases of vessel injury, the intrinsic pathway appears to be necessary for sustained thrombin generation in response to severe hemostatic challenges.

The Role of Thrombin

Thrombin is a multifunctional enzyme that employs limited proteolysis to effect a variety of biochemical

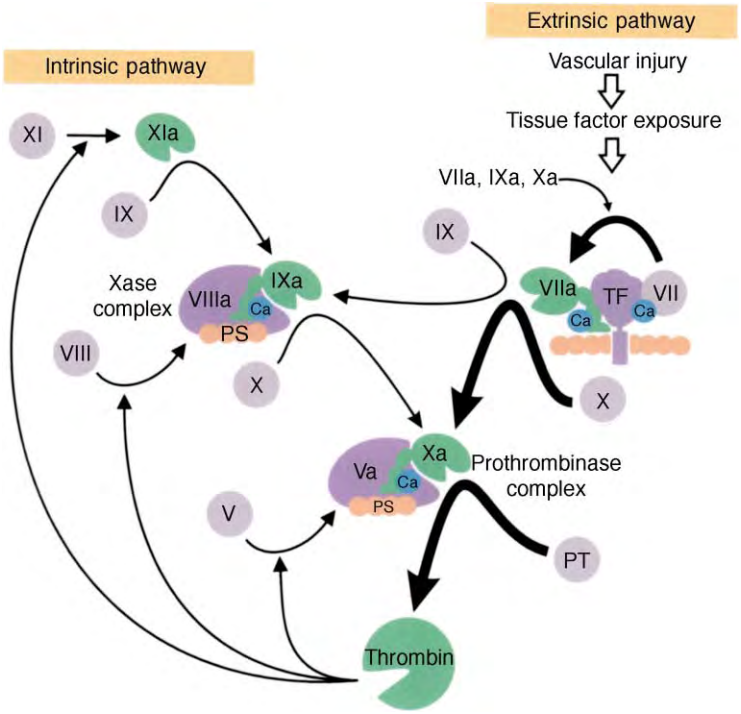

FIGURE 1 The blood coagulation cascade. Inactive cofactors and inactive (zymogen) forms of serine proteases are represented by gray circles. Active proteases are shown in green. Active protein cofactors are shown in purple. Phospholipid membranes are shown in orange. Proteolytic reactions are indicated by solid arrows. Ca, divalent calcium ions; PS, membrane surface-exposed phosphatidylserine; TF, tissue factor; PT, prothrombin.

reactions at the site of vascular injury (Figure 2). Thrombin has many physiological roles, such as promoting the formation of a cross-linked fibrin clot, the activation and aggregation of platelets, and ultimately, the attenuation of the clotting cascade.

Fibrin Polymerization

Fibrinogen is one of the more abundant proteins in the blood, circulating at a concentration of ~ 3 mg ml^{-1}. The fibrinogen molecule consists of six individual polypeptide chains arranged roughly in a dumbbell shape, with the amino termini localized to a central core and the carboxy termini located at each of the two ends. The carboxy terminal end comprises binding pockets that are unoccupied in the circulating fibrinogen molecule. Thrombin converts fibrinogen to fibrin by selectively cleaving short peptides (fibrinopeptides) from the central core region, thereby exposing new amino termini that interact with the carboxy terminal binding pockets on adjacent fibrin molecules (Figure 2, arrow A). In this way, fibrin monomers associate to form thin fibrils that thicken to form an insoluble fibrin clot.

Fibrin Cross-Linking by Factor XIIIa

When fibrin is formed, it accelerates the conversion of factor XIII to XIIIa in a reaction catalyzed by thrombin in the presence of calcium ions (Figure 2, arrow B). Factor XIIIa is unique among the coagulation enzymes in that it is not a serine protease. Rather, it is a transglutaminase that covalently links the side chains of lysine and glutamine residues present in the carboxy terminal regions of adjacent fibrin molecules. This cross-linking imparts structural integrity and rigidity to the clot.

Platelet Activation

Thrombin activates platelets by limited proteolysis of proteins called protease-activated receptors (PARs). PARs constitute a small subset of a much larger family of G protein-coupled receptors (GPCRs). GPCRs are seven-pass transmembrane proteins that transduce extracellular signals via intracellular activation of heterotrimeric G protein signaling pathways. The PARs are unique among the GPCRs in that they utilize a "tethered ligand" mechanism in which limited proteolysis within the extracellular region of the receptor unmasks a protein sequence that auto-activates the receptor itself (Figure 2, arrow C). In platelets, the proteolysis of PARs 1 and 4 by thrombin results in the expression of the hallmarks of platelet activation, namely, morphological change, degranulation, the expression of surface proteins required for aggregation, and the translocation of PS from the inner to the outer leaflet of the platelet membrane.

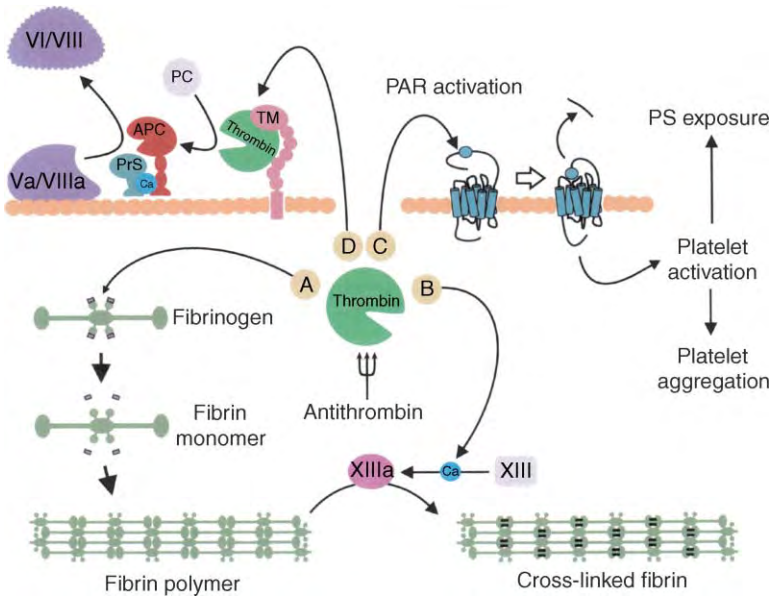

FIGURE 2 Effects of thrombin. Arrow A: Thrombin cleaves short fibrinopeptides from the central region of fibrinogen. The newly exposed termini spontaneously associate with the terminal domains of adjacent molecules allowing formation of polymeric fibrin. Arrow B: Proteolytic cleavage of factor XIII converts it into an active transglutaminase (XIIIa) that chemically cross-links adjacent fibrin molecules, providing structural integrity to the clot. Arrow C: Thrombin cleaves the extracellular region of protease-activated receptors (PARs) on the platelet surface. This modification exposes a tethered ligand that auto-activates the PAR, leading to platelet activation. Activated platelets aggregate to form a hemostatic plug and expose phosphatidylserine (PS), providing a pro-coagulant surface for the coagulation cascade. Arrow D: Feedback down-regulation of the coagulation cascade. Thrombin binds to thrombomodulin on the surface of endothelial cells. This association alters the substrate specificity of thrombin such that it cleaves protein C (PC) to form activated protein C (APC). In the presence of calcium and the cofactor protein S (PrS), APC promotes anticoagulation by proteolytically converting factors Va and VIIIa to their inactive forms (Vi and VIIIi).

The exposure of PS has dramatic consequences for amplification of the coagulation cascade. Under normal cellular homeostasis, PS is tightly restricted to the inner leaflet of the plasma membrane and, as such, is not exposed to the general circulation. However, the exposure of PS (whether through translocation on the platelet surface or by mechanical disruption of cells lining the vasculature) provides a surface for the recruitment of the components of the coagulation cascade, including the serine proteases and factors V and VIII. Viewed in this light, platelet activation and subsequent PS exposure provide yet another positive feedback loop for the generation of thrombin.

Attenuation of the Coagulation Cascade

The unregulated activation of the coagulation cascade would have serious consequences for an organism, including the occlusion of blood vessels and the formation of clots at locations other than the site of injury. Numerous serine protease inhibitors are present in the blood, and serve to restrict coagulation to sites of vessel injury. The most abundant among these is antithrombin, which is present at a concentration ~3 times that of prothrombin. Antithrombin rapidly and irreversibly inactivates thrombin, particularly in the presence of heparan sulfate, a proteoglycan present in the blood vessel wall. Antithrombin has also been shown to inhibit factors IXa, Xa, and XIa.

In an alternative mechanism for attenuating the coagulation cascade, thrombin initiates a pathway that leads to the destruction of factors Va and VIIIa. In this pathway, thrombin binds to thrombomodulin, an integral membrane protein located on the vascular endothelium (Figure 2, arrow D). As the name implies, thrombomodulin modulates the specificity of thrombin such that it generates activated protein C (APC), by limited proteolysis of protein C. APC then inactivates both factors Va and VIIIa by minor proteolysis in a reaction that requires calcium ions, anionic phospholipid, and the protein cofactor, protein S.

Structure and Function of the Blood-Clotting Proteases

Similarity to Trypsin

The proteases involved in blood coagulation are functionally and structurally related to trypsin, the

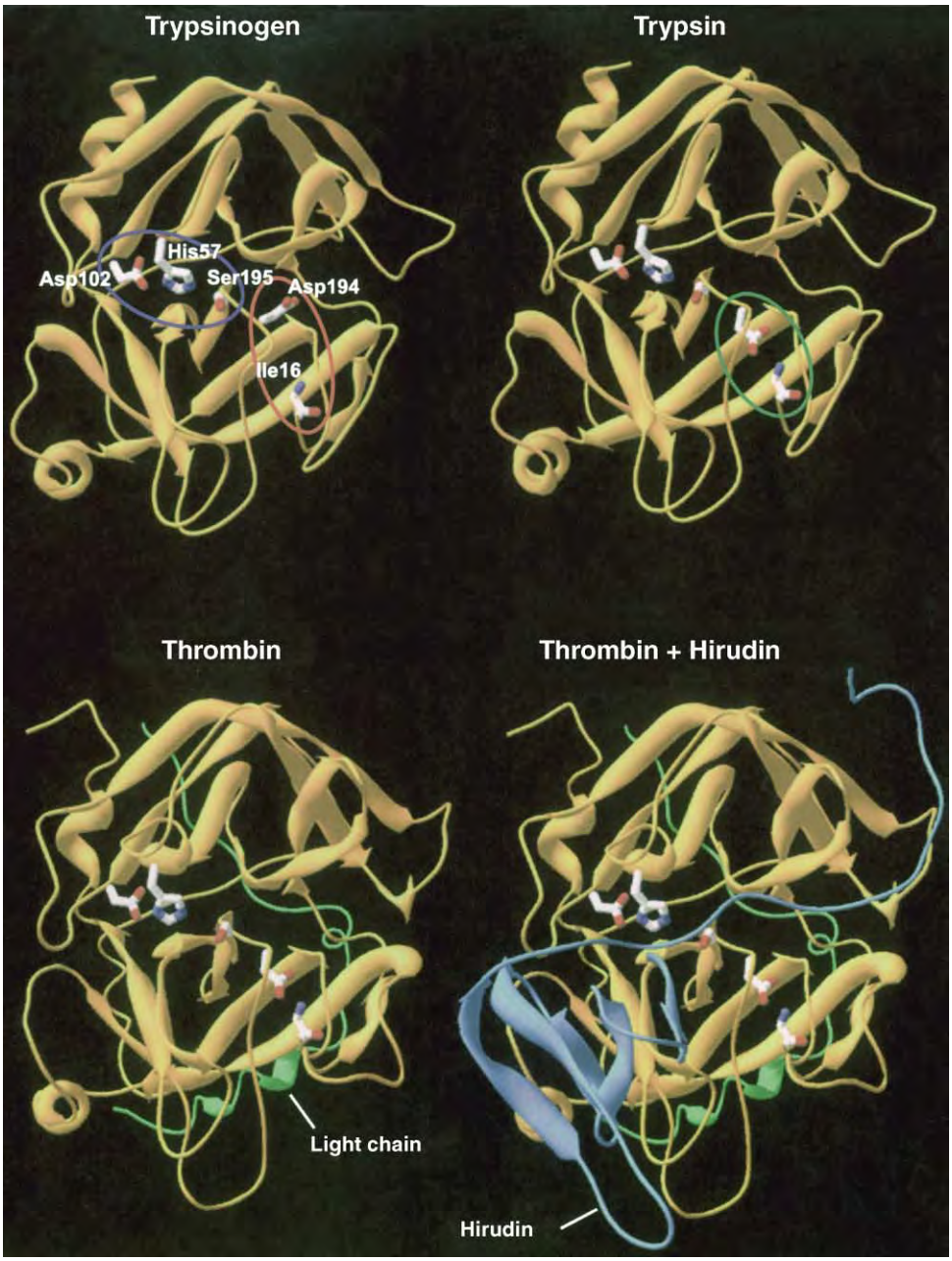

FIGURE 3 Related structures of trypsinogen, trypsin and thrombin. The structure of trypsinogen (upper left panel) reveals clamshell topology with a cleft harboring the active site. Residues His57, Asp102, and Ser195 constitute the catalytic triad (blue oval). In the inactive (zymogen) form of the enzyme the sidechain of Asp 194 does not contact the amide nitrogen (blue atom) of Ile16 (bounded by red oval). The preceding 15 residues have been omitted from the structure to provide ease of interpretation. The structure of trypsin (upper right panel) illustrates the structural change upon zymogen activation. Here the newly formed amino terminus at Ile16 forms a salt bridge with the side chain of Asp194. The structure of thrombin (lower left panel) illustrates its overall topological similarity with that of trypsin. The light chain of thrombin is shown in green. The structure of thrombin bound to the leech anticoagulant protein hirudin (lower right panel) demonstrates the molecular basis for hirudin's anticoagulant effect. Hirudin (depicted as a blue ribbon) blocks the active site of thrombin and extends an arm around thrombin to block its fibrinogen-binding exosite.

prototypical serine protease of the digestive system. Like trypsin, the proteases involved in blood coagulation (thrombin, APC and factors VIIa, IXa, Xa, and XIa) constitute a class of serine proteases that cleave their target proteins after basic (arginine and lysine) amino acid residues. However, trypsin cleaves nonspecifically after basic residues, whereas proteases of the coagulation cascade recognize and cleave only after basic residues surrounded by specific sequences within their targets. As is the case with the clotting proteases,

trypsin exists in a zymogen form (trypsinogen) that is activated by limited proteolysis. Thus, while trypsin does not possess the high degree of substrate specificity of the coagulation proteases, it shares the same general mode of zymogen activation and mechanism of catalysis.

The three-dimensional representation of trypsinogen solved by X-ray crystallography reveals a two-lobed structure resembling a clamshell with a cleft running between the two individual halves (Figure 3). The primary catalytic machinery of trypsin, the so-called "catalytic triad" consisting of histidine, aspartic acid, and serine residues, resides within this cleft. (It is the catalytic serine residue from which the serine proteases derive their name.) Trypsinogen is catalytically inactive until it is cleaved just prior to an isoleucine residue located near the amino terminus of the molecule. This proteolytic event triggers a subtle rearrangement of the molecule, driven by the generation of an electrostatic interaction between the positively charged amino group at the new amino terminus and a negatively charged aspartic acid residue adjacent to the catalytic serine residue. The formation of this salt bridge alters the structure of trypsin and renders it catalytically active.

The structure of thrombin is remarkably similar to that of trypsin (Figure 3), as are those of the other coagulation proteases. Thrombin shares with trypsin its overall clamshell structure, its catalytic triad, and its mode of zymogen activation upon limited proteolysis. However, in addition to the trypsin-like catalytic domain (heavy chain), thrombin possesses an additional polypeptide (the light chain)—a property shared by the other clotting proteases. In addition, thrombin possesses a secondary binding site on its surface that confers specificity for both fibrinogen and PAR1. The position of this so-called "fibrinogen-binding exosite" is illustrated in the structure of thrombin complexed with the leech

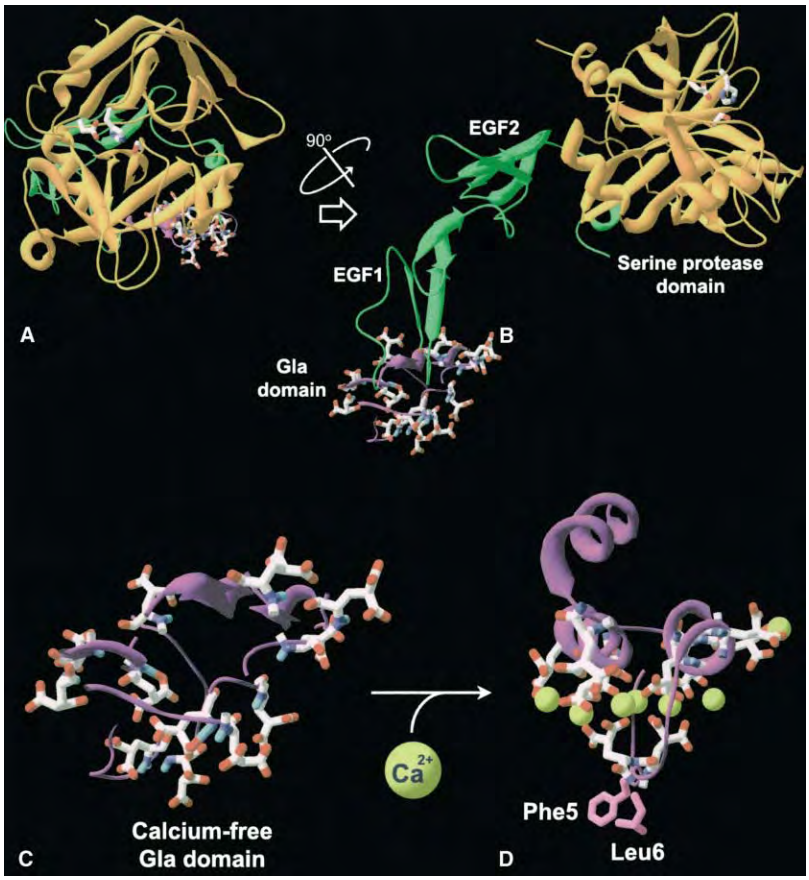

FIGURE 4 The role of Gla domains in the blood-clotting proteases. Panel A: Structure of factor IXa showing the serine protease domain with amino acid residues of the catalytic triad highlighted. In this view the light chain, consisting of a Gla domain and two tandem EGF domains is obscured. The factor IXa structure depicted was determined in the absence of calcium ions. Panel B: Rotation of the structure reveals the amino terminal Gla domain as well as the EGF domains. Panel C: Close-up of the Gla domain of calcium-free factor IXa. In the absence of calcium, the Gla domain is relatively disordered with the Gla residues projecting outward into solution. Panel D: The calcium-bound form of a Gla domain. The coordination of calcium ions by Gla residues within the core of the domain drives the exposure of a hydrophobic "thumb" consisting of a phenylalanine and a leucine residue. This region of the domain contacts the hydrophobic region of membranes. The nearly planar arrangement of positively charged calcium ions may provide specificity for negatively charged phospholipids such as PS.

salivary protein hirudin, which exerts its anticoagulant effect by simultaneously blocking access to the active site and occupying the fibrinogen-binding exosite with a long "arm" (Figure 3).

Gla Domains

The presence of both a catalytic heavy chain and a light chain is a common feature of the activated coagulation proteases. However, in contrast to thrombin, which has a relatively short light chain, the light chains of factors VIIa, IXa, Xa, and APC are longer and are characterized by the presence of multiple modular protein domains. (The crystal structure of factor IXa illustrates this arrangement—Figure 4, panel A.) When viewed in the same orientation as previously depicted structures of trypsinogen, trypsin and thrombin, the serine protease domain with its characteristic catalytic triad is clearly visible. However, this orientation obscures the light chain, which consists of an amino terminal Gla domain followed by two tandem modules that bear structural and sequence similarity to epidermal growth factor (EGF1 and EGF2). The modular structure of the factor IXa light chain is visible when the protein is rotated (Figure 4, panel B).

The Gla domain derives its name from a modification of glutamate residues that occur during the biosynthesis of factors VII, IX, and X, prothrombin, and protein C. The amino terminal 45 residues of these proteins contain between 9 and 13 glutamate (Glu) residues that are converted to γ-carboxyglutamate (Gla) residues in a reaction that requires vitamin K as a cofactor. Gla residues are capable of binding divalent ions, particularly calcium. The three-dimensional structure of factor IXa, determined in the absence of calcium, reveals an amino terminal Gla domain that is relatively disordered, with Gla residues projecting into solution. However, at physiological calcium levels found in the blood, the Gla residues coordinate with calcium and drive the Gla domain into its native conformation (Figure 4, panel C). In this form, the Gla domain is organized around a nearly planar array of calcium ions and projects a hydrophobic 'thumb' into solution. It is believed that the hydrophobic thumb associates with the hydrophobic regions of membranes, while the positively charged calcium ions associate electrostatically with the negatively charged head groups of PS exposed on coagulation-promoting surfaces such as the surface of activated platelets.

Gla domains are essential for localizing factors VIIa, IXa, and Xa, and APC, as well as their zymogen forms, to PS on the surface of activated platelets located at sites of vascular injury. (Thrombin is unique in that its Gla domain is removed from the light chain during the proteolytic activation of prothrombin.) The essential role of Gla domains and the Gla residues that they bear in directing the components of the coagulation cascade to PS-containing surfaces is underscored by the anticoagulant effect of warfarin, a potent vitamin K antagonist. Warfarin inhibits the conversion of Glu residues to Gla residues, rendering the clotting factors incapable of binding to the platelet surface. Originally employed at high doses as a rodent poison, warfarin is currently one of the most widely prescribed drugs for depressing the coagulation cascade in patients who are at risk of heart attack or stroke.

See Also the Following Articles

Platelet-Activating Factor Receptor • Vitamin K: Blood Coagulation and Use in Therapy

Glossary

Gla The amino acid gamma-carboxyglutamic acid.

hemophilia Any of several hereditary blood coagulation disorders in which the blood fails to clot normally.

hemostasis The stoppage of blood flow characterized by vasoconstriction and the formation of a platelet plug and polymerized fibrin.

platelet A small, non-nucleated, cell body found in the blood that functions to promote blood clotting.

protease Any of various enzymes that catalyze the hydrolytic breakdown of proteins into peptides or amino acids.

proteolysis The hydrolytic breakdown of proteins into smaller proteins, peptides, or individual amino acids.

transglutaminase Any of various enzymes that catalyze the covalent linkage of protein-bound glutamine and lysine amino acid side-chains.

vitamin K A fat-soluble vitamin that promotes blood coagulation and prevents hemorrhage.

warfarin A synthetic organic compound, derived from the natural product "coumarin," that antagonizes the effect of vitamin K.

zymogen The inactive precursor of an enzyme, converted into an active enzyme by proteolysis.

Further Reading

Brandstetter, H., Bauer, M., Huber, R., Lollar, P., and Bode, W. (1995). X-ray structure of clotting factor IXa: Active site and module structure related to Xase activity and hemophilia B. *Proc. Natl Acad. Sci. USA* **92**, 9796–9800.

Davie, E., Fujikawa, K., and Kisiel, W. (1991). The coagulation cascade: Initiation, maintenance, and regulation. *Biochemistry* **30**, 10364–10370.

Esmon, C. (2000). Regulation of blood coagulation. *Biochim. Biophys. Acta* **1477**, 349–360.

Fehlhammer, H., Bode, W., and Huber, R. (1977). Crystal structure of bovine trypsinogen at 1.8 angstrom resolution: II. Crystallographic refinement, refined crystal structure and comparison with bovine trypsin. *J. Mol. Biol.* **111**, 415–438.

High, K., and Roberts, H. (eds.) (1995). *Molecular Basis of Thrombosis and Hemostasis*. Marcel Dekker, New York.

Macfarlane, S., Seatter, M., Kanke, T., Hunter, G., and Plevein, R. (2001). Proteinase-activated receptors. *Pharmacol. Rev.* **53**, 245–282.

Scarborough, R., Naughton, M., Teng, W., Hung, D., Rose, J., Vu, T., Wheaton, V., Turck, C., and Coughlin, S. (1992). Tethered ligand agonist peptides. Structural requirements for thrombin receptor

activation reveal mechanism of proteolytic unmasking of agonist function. *J. Biol. Chem.* **267**, 13146–13149.

Soriano-Garcia, M., Padmanabhan, K., de Vos, A., and Tulinsky, A. (1992). The Ca^{2+} ion and membrane binding structure of the Gla domain of Ca-prothrombin fragment 1. *Biochemistry* **31**, 2554–2566.

Vitali, J., Martin, P., Malkowski, M., Robertson, W., Lazar, J., Winant, R., Johnson, P., and Edwards, B. (1992). The structure of a complex of bovine alpha-thrombin and recombinant hirudin at 2.8 angstrom resolution. *J. Biol. Chem.* **267**, 17670–17678.

Biography

John Kulman is a postdoctoral fellow in the Department of Biochemistry at the University of Washington. He earned an M.Phil. from the University of Cambridge where he studied biotin-dependent enzymes while in residence at Churchill College. He holds a Ph.D. from the University of Washington where he completed his doctoral research in the laboratory of Professor Earl W. Davie in the Department of Biochemistry. His principal research interests are in elucidating novel physiological roles of vitamin K and investigating the interplay between vitamin K-dependent proteins and cellular ubiquitination pathways.

Earl W. Davie received his Ph.D. from the Department of Biochemistry at the University of Washington, and then did postdoctoral studies with Professor Fritz Lipmann at Harvard University. After six years on the faculty at Case Western Reserve University, he joined the Department of Biochemistry at the University of Washington where he is a Professor. His research interests have focused mainly on the coagulation cascade and the proteins involved in fibrin formation.

26S Proteasome, Structure and Function

Peter Zwickl and Wolfgang Baumeister
Max Planck Institute of Biochemistry, Martinsried, Germany

The ubiquitin–proteasome pathway is the major route used by eukaryotic cells for disposing of misfolded or damaged proteins and for controlling the lifespan of regulatory proteins. The 26S proteasome is a huge molecular machine of ~2.5 MDa, which degrades protein substrates by an energy-dependent mechanism. It comprises two subcomplexes, the 20S-core particle and one or two regulatory complexes, the 19S caps. The 20S complex allows confining the proteolytic action to a nanocompartment, in which sequestered from the cellular environment substrates undergo degradation. The 19S regulatory complex recruits substrates targeted for degradation and prepares them for translocation into the 20S-core complex. The sequence of events encountered by a substrate until it is finally degraded is reflected by a linear arrangement of functional modules within the 45 nm long supramolecular assembly (Figure 1).

The 20S Proteasome

20S proteasomes are found in all domains of extant organisms in archaea, bacteria, and eukaryotes and share a highly conserved quaternary structure. Although their complexity in terms of subunit composition is surprisingly different, 20S proteasomes are generally built from two types of subunits, α and β, which segregate into seven-membered rings and collectively form a barrel-shaped complex with a network of internal cavities. These cavities or "nanocompartments" harbor the active sites and thus allow segregating the proteolytic action from the surrounding cytoplasm. This regulatory principle, referred to as "self-compartmentalization," is for prokaryotes, which lack membrane-bordered compartments, the only means of spatial confinement.

In addition to self-compartmentalization, proteasomes rely on another mechanism to prevent the uncontrolled breakdown of proteins that is not uncommon amongst proteases. The β-type subunits of 20S proteasomes, which bear the active site residues, are synthesized in an inactive precursor form; for the formation of the active sites, the propeptides must be removed posttranslationally. This process is tied in with the assembly of the 20S proteasome in such a manner that activation is delayed until assembly is complete and the active sites are sequestered from the cellular environment. In mature 20S proteasomes access to the inner proteolytic compartment is through narrow gates at the polar ends of the complex and thus restricted to small peptides and unfolded proteins. Therefore, the proteasome behaves, with respect to folded proteins, as a "latent" protease, which is dependent on regulatory complexes to assume its function. At the heart of the regulatory complexes, or "activators," are members of the AAA family of ATPases. In prokaryotes, members of this family form homohexameric complexes; in eukaryotes, six paralogs form heterohexameric complexes, which are integrated into the larger and multifunctional 19S regulatory complexes.

Subunit Composition

20S proteasomes from all three domains of life have a common overall architecture. They are built of 28 subunits arranged in a stack of four seven-membered rings. All subunits are members of the same superfamily of proteins, which group into two families, designated α and β. The two polar rings of the proteasome are formed by α-type subunits; the two equatorial rings are formed by β-type subunits (Figure 2A). Both families comprise a number of subfamilies. The sequence similarity between members of a subfamily, even from evolutionary distant species, is considerably higher than similarity between the members of different subfamilies from one species. While human and yeast proteins of the same subfamily have at least 50% similarity, there is only ~30% similarity between the seven subfamilies, and even less among the two families, α and β.

The main difference between eukaryotic and prokaryotic 20S proteasomes is one of complexity. Prokaryotic proteasomes are mostly composed of identical copies of 14 α-subunits and 14 β-subunits, eukaryotic proteasomes recruit α- and β-subunits out of 14 different subfamilies. Thus, the multiple axes of

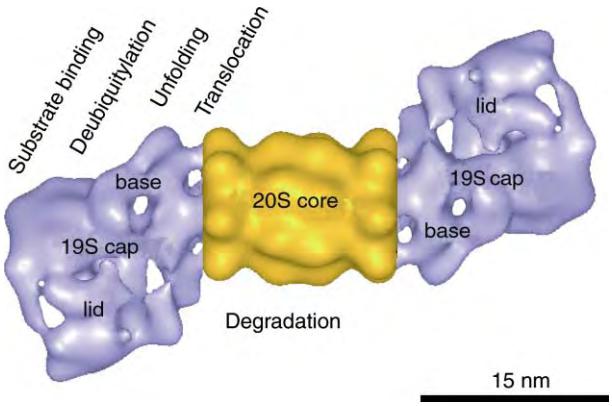

FIGURE 1 Composite model of the three-dimensional (3D) structure of the 26S proteasome combining a 3D reconstitution from electron micrographs of *Drosophila* 26S complexes and the crystal structure of the *Thermoplasma* 20S proteasome.

symmetry of the *Thermoplasma* proteasome are reduced to C2 symmetry in the eukaryotic proteasome; each of the 14 different subunits is found twice within the complex and occupies well-defined positions. According to their location within the α and β rings, yeast subunits are sequentially numbered $\alpha 1/\beta 1$ through $\alpha 7/\beta 7$, and those related by C2 symmetry are distinguished by the prime symbol ($\alpha 1'/\beta 1'$ through $\alpha 7'/\beta 7'$). The subunit topology in higher eukaryotes corresponds to that in yeast, i.e., members of the same subfamily occupy the same positions. Hence, that systematic nomenclature is generally applicable. While lower eukaryotes assume a stoichiometry of $(\alpha_1-\alpha_7)$ $(\beta_1-\beta_7)$ $(\beta_1-\beta_7)$ $(\alpha_1-\alpha_7)$, vertebrates have achieved an even higher degree of complexity. In addition to the 14 constitutive subunits, they contain 3 γ-interferon-inducible β-type subunits, which can replace their constitutive counterparts ($\beta 1$, $\beta 2$, and $\beta 5$) to form "immunoproteasomes."

Structure

On electron micrographs, 20S proteasomes from prokaryotes and eukaryotes are virtually indistinguishable, and also the crystal structures of *Thermoplasma* and yeast proteasomes are very similar. Proteasomes are barrel-shaped particles, with overall dimensions of 15 nm in length and 11 nm in diameter. A channel traverses the particle from end to end and widens into three internal cavities, each ~5 nm in diameter (Figure 2B). The two outer cavities are formed jointly by one α- and one β-ring; the central cavity is formed by the two adjacent β-rings. At a glance there appears to be one major difference between the crystal structures of the *Thermoplasma* and the yeast proteasome: In the archaeal proteasome 1.3 nm wide openings are visible at the center of the α rings, while in the yeast proteasome this channel appears to be closed. However, one has to keep in mind that in the crystal structure of the *Thermoplasma* proteasome the 12 N-terminal residues of the α-subunits remained invisible because of disorder; in yeast the corresponding residues plug the channel and act as a gate.

As expected from their sequence similarity, proteasome α- and β-subunits have the same fold (Figure 2C): a four-layer structure with two five-stranded antiparallel β-sheets (S1–S10) flanked on either side by α-helices, two on the one (H1 and H2), three on the other side (H3, H4, and H5). The β-sheet package is unusual in that one sheet is rotated relative to the other through a positive dihedral angle of +30°, in contrast to the value of the typical β-sheet twist, which is −30°. In the β-type subunits, the β-sheet sandwich is open at one end to form the active site cleft, and closed at the other end by four hairpin loops. In α-type subunits, however, an additional helix (H0) crosses the top of the β-sheet sandwich and fills the cleft. The fold of proteasome subunits was initially considered to be unique, but as it turned out, it is prototypical of a new family of proteins referred to as Ntn (N-terminal nucleophile) hydrolases.

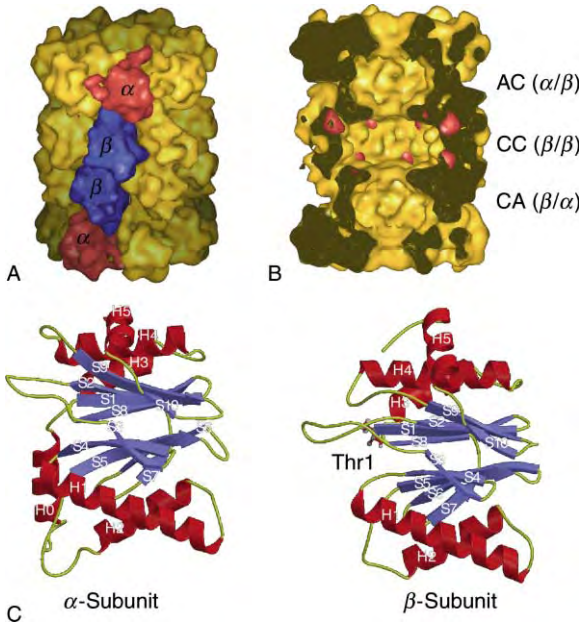

FIGURE 2 Structure of the 20S proteasome. (A) Low-resolution model (1 nm) of the 20S proteasome from the crystal structure of the *Thermoplasma* 20S proteasome. (B) The same structure as in (A) cut open along the sevenfold axis to display the two antechambers (AC and CA) and the central chamber (CC) with the 14 active sites (marked in red). The channel openings at the two ends of the cylinder are 1.3 nm in diameter. (C) Folds of the α and β-subunit from *Thermoplasma* 20S proteasomes. Helices are numbered H0 to H5 in the α-subunit, and H1 to H5 in the β-subunit; strands are numbered S to S10. H0 in the α-subunit occupies the cleft leading to the active site in the β-subunit. The active site threonine (Thr1) in the β-subunit is shown in ball-and-stick representation.

Currently known members of this family, whose primary structures have diverged beyond recognizable similarity, are aspartylglucosaminidase (AGA), glutamine phosphoribosyl pyrophosphate amidotransferase (GAT), penicillin acylase (PA), and L-aminopeptidase D-Ala-esterase/amidase (DmpA). Beyond the common fold, these enzymes share the mechanism of the nucleophilic attack and autocatalytic processing, but none of them has a quaternary structure similar to the proteasome.

The Active Site

A characteristic feature of Ntn hydrolases is a "single-residue" active site; both the nucleophile and the primary proton acceptor are provided by the same N-terminal residue of the proteins. The nucleophilic attack is initiated when the free N terminus, the primary proton acceptor, strips the proton off the catalytic side chain, the nucleophile; for steric reasons, a water molecule is supposed to mediate the proton shuttle, at least in the proteasome and in penicillin acylase. Different N-terminal residues are used as nucleophiles in Ntn hydrolases; serine in PA and DmpA, cysteine in GAT, and threonine in AGA and in the proteasome. In agreement with a catalytic mechanism that relies on a single residue, there is no consensus of residues in the vicinity of the active site. Nevertheless, several other residues are critical for activity of proteasomes, as consistently shown by site directed mutagenesis with archaeal, bacterial, yeast, and mammalian proteasomes. The exact roles of these residues, all highly conserved and in close proximity to Thr1, remain to be clarified. Lys33, which forms a salt bridge to Glu17, may lower the pK_a of the N terminus by electrostatic effects or may be part of the charge relay system in delocalization of the proton from the Thr1 hydroxyl group. Asp166 may be required for the structural integrity of the active site or directly be involved in catalysis.

Although all proteasome subunits have the Ntn-hydrolase fold, not all are actively involved in substrate cleavage. As mentioned above, in α-subunits, the active site cleft is occupied by an additional N-terminal α-helix, H0 (Figure 2C). Of the different eukaryotic β-type subunits, only three (β1, β2, and β5 and their interferon inducible counterparts) display proteolytic activity, whereas subunits β3, β4, β6, and β7 lack one or more of the critical residues and are inactive. This assignment, initially derived from the conservation pattern of the active site residues, has been confirmed by the crystal structure of yeast 20S proteasomes soaked in N-acetyl-Leu-Leu-norleucinal; only three subunits, β1/Pre3, β2/Pup1, and β5/Doa3, contain the inhibitor bound to Thr1. Since the backbone geometry is well conserved between all subunits, active or inactive, one would expect that introducing all residues regarded as critical would render inactive subunits active. However, this is not the case; the yeast subunits β3/Pup3, β6/Pre7, and β7/Pre4 remained unprocessed and consequently inactive, when the respective mutations were made.

The 26S Proteasome

Cellular Functions

In eukaryotic cells, the 20S proteasome assembles with one or two 19S regulatory complexes (RC) in an ATP-dependent manner to form the 26S proteasome. The 26S holoenzyme is the most downstream element of the ubiquitin–proteasome pathway. It is an abundant complex, both in the nucleus and in the cytoplasm, and studies with proteasome inhibitors indicate that the bulk of cellular proteins, 80–90%, are degraded via this pathway. It is not only used as a disposal machinery for misfolded proteins (termed DRiPs, for defective ribosomal products) and for proteins damaged by stress or aging, but also the lifespan of many short-lived regulatory proteins is controlled via this pathway. Interestingly, the 26S proteasome does not only degrade proteins completely, but also activates certain transcription factors by limited proteolytic processing of precursors, e.g., human NFκB and NFκB2, *Drosophila* Ci or yeast Spt23 and Mga2. In addition to its function in ubiquitin-dependent proteolysis, the 26S proteasome was also found to mediate ubiquitin-independent degradation of several proteins, e.g., ODC, c-Jun, IκBα, and $p21^{Cip1}$. Moreover, not yet fully understood nonproteolytic roles of proteasomes in nucleotide excision repair and transcriptional regulation have been described.

The 19S Regulator and its Subcomplexes

Slightly differing sets of RC subunits have been reported for different organisms and the abundance of factors that have been described to associate to the RC in a tissue- and development-specific manner and with variable affinities, makes it difficult to draw the line between interacting factors, transiently bound subunits or integral components of the RC. However, as the mass of the *Drosophila* RC, ~890 kDa, determined by scanning-transmission electron microscopy (STEM) measurements is in good agreement with the summed masses of the 18 individual subunits (932 kDa) identified on 2D gels, it seems likely that the catalogue of integral subunits is now complete. The catalogues of the *Drosophila* and yeast 19S subunits are identical, except for a single subunit (p37A), which seems to be absent from yeast 26S proteasomes.

The 19S regulator of the yeast proteasome can be dissociated into two subcomplexes, the "base" and the "lid," which are located proximally and distally with respect to the 20S core (Figure 1). The complex formed by the base and the 20S proteasome is sufficient for the ATP-dependent degradation of nonubiquitylated protein substrates, but does not mediate degradation of ubiquitylated substrate proteins. From the location of the base in the 26S complex, it had been inferred to have a role in substrate unfolding, acting as a "reverse chaperone," and in controlling the gate in the coaxial opposed α-rings of the 20S particle. A chaperone-like activity was demonstrated for the base, and likewise for the ancestral PAN complex. Both have the ability to recognize proteins destined for degradation, to unfold and to translocate them into the proteolytic-core complex in an ATP-dependent manner. The degradation signals remain to be defined, possibly some local unfolding and an exposure of hydrophobic segments is sufficient for targeting substrates. In one case, specific recognition of an ubiquitylated substrate by the Rpt5 ATPase subunit of the base was shown.

As only the 26S holoenzyme, but not the 20S-base complex degrades ubiquitylated proteins, it is likely that recognition, and binding of ubiquitin-tagged substrates is mainly mediated by the eight subunits of the lid subcomplex. Very little is known about the molecular mechanisms of substrate shuttling from the E3 ubiquitin–ligase complexes, where the final step of ubiquitylation takes place, to the lid subcomplex of the 26S proteasome. Free diffusion of ubiquitylated substrates to the 26S proteasomes would be consistent with the rather high-binding constants observed *in vitro*. On the other hand, subcomplexes or subunits of the RC, such as the lid or S5a/Rpn10, could serve as substrate carriers. Indeed, free-lid complexes exist and can be isolated from human erythrocytes as stable particles. Recently, it has been reported that E2 ubiquitin-conjugating enzymes, E3 ubiquitin-ligases, such as Ubr1 and Ufd4, and E3 ubiquitin-ligase complexes, such as SCF and APC, interact directly with subunits of the RC. In addition, adapter proteins such as Rad23 and Dsk2 proteins were shown to bind ubiquitylated proteins via their UBA (ubiquitin-pathway-associated) domain and to the S1 or S2 subunit of the base via their ubiquitin-like (UBL) domain. The latter findings imply that certain substrates may be first recognized and bound by uncomplexed adapter proteins, before the latter bind to the 19S regulator and transfer the substrate for degradation. Moreover, there is evidence that molecular chaperones were also involved in protein degradation by the 26S proteasome. It was found recently that the Hsp70 cochaperone CHIP has E3 ubiquitin-ligase activity and mediates degradation of certain substrate proteins by the 26S proteasome. Bag-1, another Hsp70-interacting protein, was also shown to stimulate substrate ubiquitylation and to bind directly to the 26S proteasome via its UBL domain. Thus, two distinct molecular machineries, the molecular chaperones and the 26S proteasome, seem to interact physically and cooperate in cellular protein quality control.

The molecular understanding of the steps involved in transferring ubiquitylated substrates from the lid to the base and eventually into the 20S core is crucial. One prerequisite for substrates to enter the proteolytic center is the removal of the multi-ubiquitin chain. In yeast, the deubiquitylating enzyme Doa4 was shown to interact physically and functionally with the proteasome supporting the model that Doa4 removes ubiquitin from proteolytic substrates en route to the 20S complex. Mammalian and *Drosophila* RCs were shown to contain a deubiquitylating subunit with a molecular mass of ~37 kDa. However, so far, this activity has only been reported to decrease substrate degradation rates, suggesting that it may have an editing function, rescuing incompletely ubiquitylated substrates. Very recently, Rpn11, a constituent subunit of the lid, was found to be essential for deubiquitylation and subsequent degradation of substrates. This suggests that coupling between deubiquitylation and degradation exists, which assures that a recognized substrate is irreversibly committed to destruction.

See Also the Following Articles

Chaperones, Molecular • Proteasomes, Overview • Ubiquitin-Like Proteins • Ubiquitin System

Glossary

AAA ATPases ATPases associated with a variety of cellular activities, comprising a Walker-type ATPase domain and a so-called second region of homology, as characteristic features.

base Subcomplex of the 19S regulator, which in the 26S proteasome is located proximal to the 20S proteasome and comprises the AAA ATPase subunits.

lid Subcomplex of the 19S regulator, which in the 26S proteasome is located distal to the 20S proteasome.

Ntn hydrolases N-terminal nucleophile hydrolases, enzymes with a similar fold and a single-residue N-terminal catalytic residue, threonine, serine, or cysteine, which mediates the nucleophilic attack on the substrate.

self-compartmentalizing A regulatory principle in which the quaternary structure creates inner compartments with limited access where degradation takes place.

UBA Ubiquitin-pathway-associated domain, responsible for ubiquitin binding.

ubiquitin A highly conserved eukaryotic protein of 76 amino acids, which is linked via its C-terminal carboxyl group to the ε amino group of a lysine residue in a protein destined for degradations.

UBL Ubiquitin-like domain similar in structure to ubiquitin, and which is mediating binding to the 26S proteasome.

Further Reading

Baumeister, W., Walz, J., Zühl, F., and Seemüller, E. (1998). The proteasome: Paradigm of a self-compartmentalizing protease. *Cell* **92**, 367–380.

Hershko, A., and Ciechanover, A. (1998). The ubiquitin system. *Annu. Rev. Biochem.* **67**, 425–479.

Rechsteiner, M., Realini, C., and Ustrell, V. (2000). The proteasome activator 11 S REG (PA28) and Class I antigen presentation. *Biochem. J.* **345**, 1–15.

Rock, K. L., York, I. A., Saric, T., and Goldberg, A. L. (2002). Protein degradation and the generation of MHC class I-presented peptides. *Adv. Immunol.* **80**, 1–70.

Varshavsky, A., Turner, G., Du, F. Y., and Xie, Y. M. (2000). The ubiquitin system and the N-end rule pathway. *Biolog. Chem.* **381**, 779–789.

Voges, D., Zwickl, P., and Baumeister, W. (1999). The 26S proteasome: A molecular machine designed for controlled proteolysis. *Annu. Rev. Biochem.* **68**, 1015–1068.

Biography

Peter Zwickl is a Research Group Leader in the Department of Structural Biology at the Max Planck Institute of Biochemistry. His principal research interest is the functional and structural characterization of ATP-dependent proteases. He holds a doctorate from the Technical University of Munich and received his postdoctoral training at Harvard Medical School, Boston.

Wolfgang Baumeister is Director at the Max Planck Institute of Biochemistry and Head of the Department of Structural Biology. His principal research interests are in the field of intracellular protein degradation and in the development of new techniques for structural studies, in particular electron tomography. He is an Honorary Professor of physics at the Technical University, Munich, and a member of several academies, including the German Academy of Sciences, Leopoldina and the American Academy of Arts and Sciences (Foreign Honorary Fellow). He has received several awards, most recently the Louis-Jeantet Prize for Medicine (2003).

Proteasomes, Overview

Martin Rechsteiner
University of Utah, Salt Lake City, Utah, USA

Proteasomes are cylindrical, multisubunit proteases found in eukaryotes, eubacteria, and archaebacteria. Eukaryotic proteasomes come in two sizes, the 20S proteasome and the considerably larger, ATP-dependent 26S proteasome formed when the 20S proteasome binds a regulatory complex. The 26S proteasome is the central protease in the ubiquitin (Ub)-mediated proteolytic pathway and is essential for a vast array of cellular processes including cell cycle traverse, transcription control, regulation of enzyme levels, and antigen presentation. Both 20S and 26S proteasomes can associate with protein complexes that activate peptide hydrolysis and may serve to localize the enzymes within cells.

The 20S Proteasome

Structure

The 20S proteasome is a cylindrical particle consisting of 28 subunits arranged as four rings of heptamers stacked upon one another (see Figure 1). The simpler archaebacterial enzyme is composed of just one kind of α-subunit and one β-subunit which form the end rings and the two central rings, respectively. Proteolysis is the province of the β-subunits, and their active sites face a central chamber within the cylinder. The α-subunit rings seal off the proteolytic chamber from the external solvent making the 20S proteasome a perfect protease to have among the critical proteins that comprise nucleus and cytoplasm. Unless a native protein is forced into the proteasome interior, it will be impervious to the enzyme. Moreover, proteasome β-subunits are not catalytically active unless they are present in the holoenzyme.

Eukaryotic proteasomes maintain the overall structure of the archaebacterial enzyme, but they exhibit a more complicated subunit composition. There are seven different α-subunits and at least seven distinct β-subunits. Although current evidence indicates that only three of its seven β-subunits are catalytically active, the eukaryotic proteasome cleaves a wider range of peptide bonds. The archaebacterial enzyme, with its 14 identical β-subunits, preferentially hydrolyzes peptide bonds following hydrophobic amino acids and is therefore said to have chymotrypsin-like activity. By contrast, the eukaryotic proteasome contains two copies each of trypsin-like, chymotrypsin-like, and post-glutamyl-hydrolyzing subunits. For this reason it is capable of cleaving almost any peptide bond having difficulty only with Pro-X, Gly-X, and to a lesser extent with Gln-X bonds. There is a further complication in higher eukaryotes. In immune tissues or after exposure to interferon γ, the three catalytically active β-subunits found in the proteasomes of most organs are replaced by β-subunits with differing substrate specificities. Thus, in higher vertebrates there are constitutive and immunoproteasomes. The latter are thought to play an important role in class I antigen presentation.

Enzyme Mechanism and Proteasome Inhibitors

Whereas most proteases use serine, cysteine, or metals to cleave peptide bonds, the proteasome employs N-terminal threonines in an unusual catalytic mechanism. The N-terminal threonines, generated by self-removal of short peptide extensions from the active β-subunits during assembly of the 20S particle, act as nucleophiles during peptide hydrolysis. There are highly specific inhibitors of the proteasome. The fungal metabolite lactacystin and the bacterial product epoxomicin covalently modify the active site threonines and inhibit the enzyme. Both compounds are commercially available; other inhibitors include vinylsulfones and various peptide aldehydes that are generally less specific.

The 26S Proteasome

Whereas bacteria may possess as many as five ATP-dependent proteases, the 26S proteasome is the only ATP-dependent protease discovered so far in the nuclear and cytosolic compartments of eukaryotic cells. As the 20S proteasome's internal cavities are inaccessible to intact proteins, openings must be generated in the enzyme's outer surface for proteins to be degraded. A number of protein complexes have been found to bind the proteasome and stimulate peptide hydrolysis. The most important of the proteasome-associated

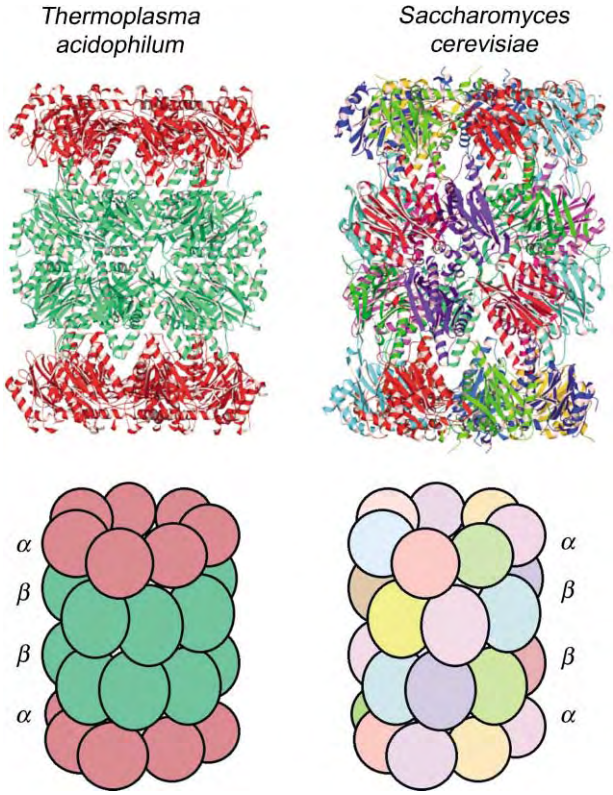

FIGURE 1 20S Proteasomes. At the top are ribbon diagrams of an archaebacterial proteasome (left) and a eukaryotic proteasome (right) as revealed by X-ray crystallography. Schematic representation of their subunit arrangements are shown below each crystal structure. Note that the archaebacterial proteasome is assembled from 14 copies of a single α-subunit and 14 copies of the same β-subunit. By contrast, the yeast 20S proteasome consists of two copies each of seven different α- and seven different β-subunits.

components is the 19S regulatory complex (RC) for it is a major part of the 26S ATP-dependent enzyme that degrades ubiquitylated proteins in eukaryotic cells (see Figure 2). As its name suggests, this 19S particle is roughly the same size as the 20S proteasome except that it is a more complex protein assemblage containing 18 different subunits. Among the RC subunits are six ATPases, an isopeptidase, a subunit that recognizes polyubiquitin chains, and a number of subunits whose functions are yet to be determined. RC subunits are arranged in two large subcomplexes, called the base and the lid. The ATPases and two other subunits comprise the base that sits directly on the end rings of the 20S proteasome; the lid is separated from the base by what appears to be a cavity. Overall the regulatory complex looks much like a Chinese dragon-head in negatively stained EM images.

Presumed Mechanism

The six ATPases in the 19S RC are members of the large family of AAA nucleotidases, whose members share the common property of altering the conformation or association state of proteins. In the case of the 19S RC ATPases, they are thought to act as "unfoldases" and translocases. Presumably ubiquitylated proteins are captured by the RC after which the ATPases unfold the bound substrate protein and thread it through the α ring of the 20S proteasome for its subsequent degradation in the central proteolytic chamber (see Figure 3). Most of the resulting peptide fragments are 5–10 residues in length, but fragments as long as 35 amino acids can be present. Furthermore, in some cases the 26S proteasome only partially degrades the substrate protein, releasing instead functionally processed domains.

How the 26S proteasome recognizes ubiquitylated proteins has not been firmly established. Ub chains containing four or more monomers are preferred substrates, and one RC subunit, called S5a, has been shown to bind polyUb. However, deletion of the gene encoding this subunit in budding yeast has only minor impact on intracellular proteolysis. Hence there must be other subunits or additional mechanisms by which the 26S enzyme recognizes polyUb-substrates. In this regard, there are recent reports that the 26S proteasome interacts directly with ubiquitin ligases or ligase-associated proteins that are ubiquitylated but not degraded. It should be noted that some non-ubiquitylated proteins are also degraded by the 26S proteasome.

Tissue and Subcellular Distribution of Proteasomes

Proteasomes are found in all organs of higher eukaryotes, but the degree to which the composition of proteasomes and its activators varies among tissues is largely unexplored territory. At the subcellular level 26S proteasomes are present in cytosol and nucleus where they appear to be freely diffusible. They are not found in the nucleolus or within membrane-bound organelles other than the nucleus. When large amounts of misfolded proteins are synthesized by a cell, they often accumulate around the centrosome in what are called "aggresomes". Under these conditions 26S proteasomes, chaperones, and proteasome activators also redistribute to the aggresomes presumably to refold and/or degrade the misfolded polypeptides.

Physiological Importance

Deletion of yeast genes encoding 20S proteasome and 19S RC subunits is usually lethal indicating that the 26S proteasome is required for eukaryotic cell viability. Known substrates of the 26S proteasome include transcription factors, cell cycle regulators, protein

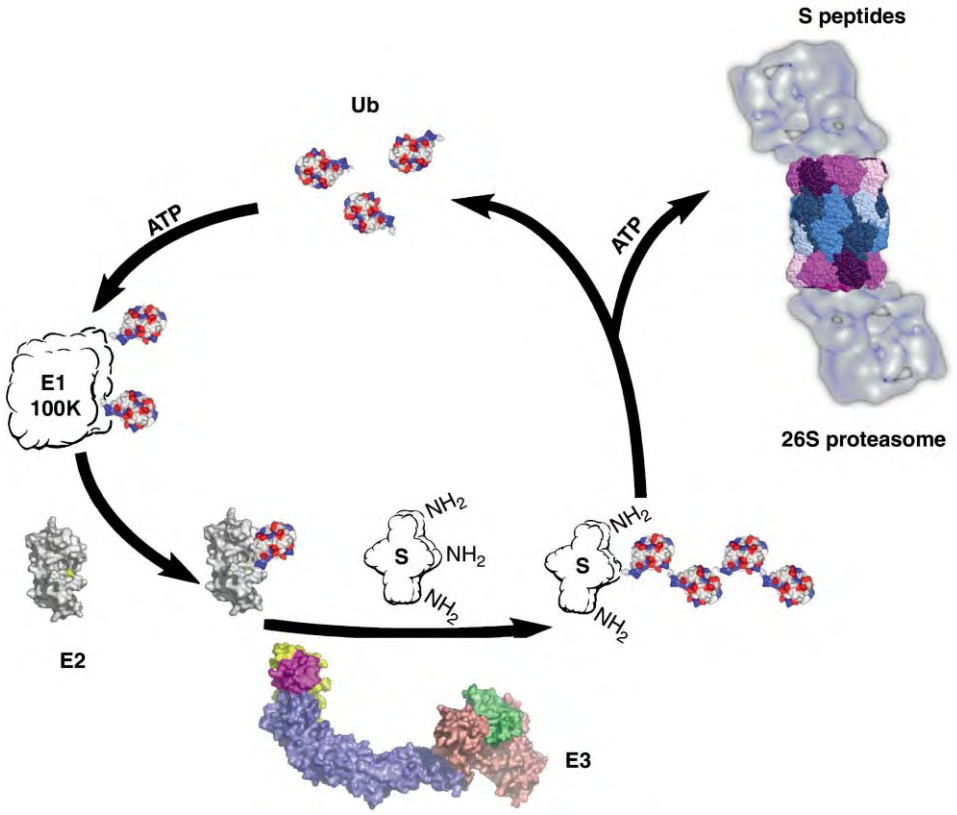

FIGURE 2 Schematic representation of ubiquitin activation and ATP-dependent proteolysis of conjugated substrates. Ubiquitin molecules are activated by an E1 enzyme in an ATP-dependent reaction, transferred to a cysteine residue (yellow) on an E2 or Ub carrier protein and subsequently attached to a substrate protein (S) by an E3 or ubiquitin ligase. Note that chains of Ub are generated on the substrate and these are recognized by the 26S proteasome depicted in the upper right at 1/20th scale.

kinases, etc., – essentially most of the cell's important regulatory proteins. Surprisingly even proteins secreted into the endoplasmic reticulum are returned to the cytosol for degradation by the 26S proteasome. Given the scope of its substrates, it is hardly surprising that in higher eukaryotes the ubiquitin-proteasome system affects a vast array of physiological processes ranging from cell cycle traverse to circadian rhythms to learning. The ubiquitin-proteasome system impacts a number of human neurological diseases that include Parkinson's, Huntington's, and Alzheimer's. Mutations in components of the ubiquitin-proteasome pathway also cause various other diseases.

Proteasome Activators

In addition to the RC there are two protein complexes, REG$\alpha\beta$ and REGγ, and a single polypeptide chain, PA200, that bind and stimulate peptide but not protein degradation by the proteasome (see Figure 4). A fourth protein, called ecm29 in yeast, associates with the proteasome. Like the RC, proteasome activators bind the ends of the 20S proteasome, and importantly, they can form mixed or hybrid 26S proteasomes in which one end of the 20S proteasome is associated with a 19S RC, and the other is bound to a proteasome activator. This latter property raises the possibility that proteasome activators serve to localize the 26S proteasome within eukaryotic cells. At present, we do not know whether activation, or targeting or something else is the primary function of proteasome activators.

REGs or PA28s

There are three distinct subunits of the 11S regulator (REG) called α, β, and γ. REGsα and β form hetero-heptamers found principally in the cytoplasm, whereas REGγ forms a homo-heptamer located in the nucleus. REGα and β are abundantly expressed in immune tissues while REGγ is highest in brain. In addition to their different locations the REGs differ in their activation properties. REG$\alpha\beta$ activates all three proteasome active sites; REGγ only activates the trypsin-like subunit. There is reasonably solid evidence that REG$\alpha\beta$ plays a role in class I antigen presentation, but we have no idea what REGγ does especially since REGγ knockout mice have almost no phenotype.

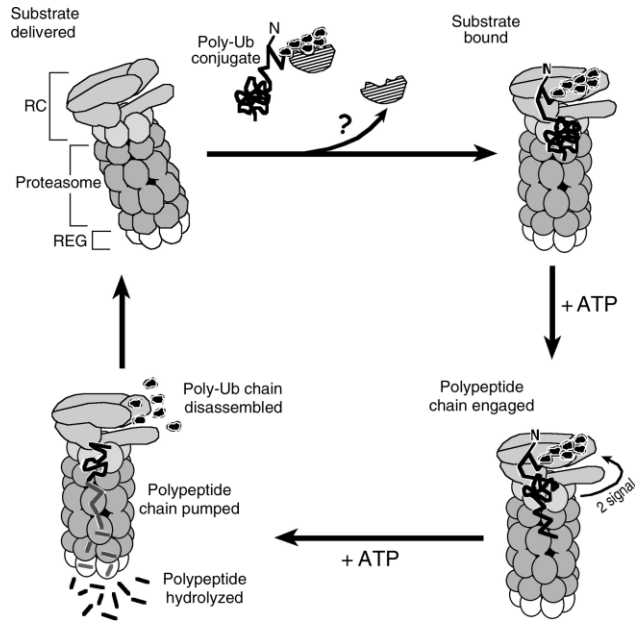

FIGURE 3 Hypothetical Reaction Cycle for the 26S Proteasome A polyubiquitylated substrate is delivered to the 26S proteasome possibly by chaperones (step 1). Substrate is bound by polyubiquitin recognition components of the regulatory complex (RC) until the end of the polypeptide chain is engaged by the ATPases (step 2). As the polypeptide chain is unfolded and pumped down the central pore of the proteasome, a signal is conveyed to the metallo-isopeptidase to remove the polyUb chain (step 3). The unfolded polypeptide is eventually degraded within the inner chamber of the proteasome (step 4) and peptide fragments exit the enzyme.

The crystal structure of REGα reveals seven subunits that form a donut-shaped structure with a central aqueous channel, and the structure of an REG–proteasome complex provides important insight into the mechanism by which REGα activates the proteasome. The carboxyl tail on each REG subunit fits into a corresponding cavity on the α-ring of the proteasome and loops on the REG subunits cause N-terminal strands on several proteasome α-subunits to reorient upward into the aqueous channel of the REG heptamer. These movements open a continuous channel from the exterior solvent to the proteasome central chamber.

PA200

A new proteasome activator, called PA200, was recently purified from bovine testis. Human PA200 is a nuclear protein of 1843 amino acids that activates all three catalytic subunits with some preference for the PGPH active site. Homologues of PA200 are present in budding yeast, worms, and plants. A single chain of PA200 can bind each end of the proteasome, and when bound, PA200 molecules look like volcanoes in negatively stained EM images. Mutation of yeast PA200 results in sensitivity to the DNA-damaging agent bleomycin, and evidence from both yeast and mammals indicates that PA200 is involved in DNA repair.

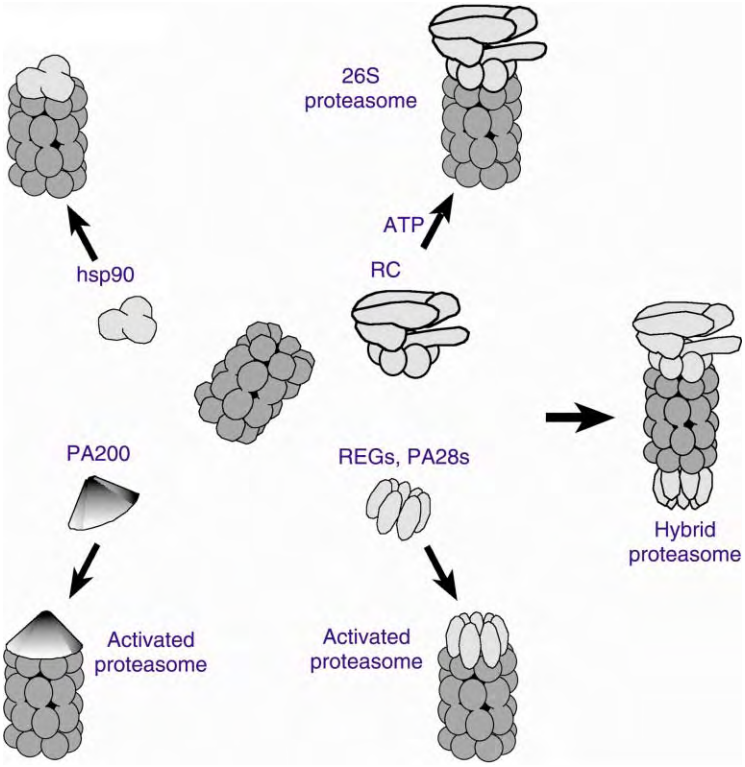

FIGURE 4 Schematic representation of the 20S proteasome assembling with various activator proteins (RC, REGs, PA200) and with the chaperone hsp90, a protein that inhibits the enzyme.

Ecm29

Another proteasome-associated protein, called ecm29p, has been identified in several recent proteomic screens. It has been reported that ecm29p serves to stabilize the yeast 26S proteasome, but the human homologue of ecm29p is found predominately associated with secretory and endocytic membranes, as per an unpublished observation by Gorbea and his associates, a location suggesting a role in secretion rather than 26S proteasome stability. Ecm29p clearly associates with the 26S proteasomes; whether it activates proteasomal peptide hydrolysis is unknown.

Protein Inhibitors of the Proteasome

Two proteins have been found to suppress proteolysis by the proteasome. One of these is PI31; the other is the abundant cytosolic chaperone, Hsp90. Both may affect how the proteasome functions in Class I antigen presentation. PI31 is a 30 kDa proline-rich protein that inhibits peptide hydrolysis by the 20S proteasome and can block activation by both RC and REG$\alpha\beta$. Although surveys of various cell lines show PI31 to be considerably less abundant than RC or REG$\alpha\beta$, when overexpressed, PI31 is reported to inhibit Class I antigen presentation by interfering with the assembly of immuno-proteasomes. A number of studies have shown that Hsp90 can bind the 20S proteasome and inhibit its chymotrypsin-like and PGPH activities. Interestingly inhibition by Hsp90 is observed with constitutive but not with immuno-proteasomes, a finding consistent with proposals that Hsp90 shuttles immuno-proteasome-generated peptides to the endoplasmic reticulum for Class I presentation.

Summary

The 20S proteasome was discovered in 1980 and its 26S version six years later. Since the 1980s, a great deal of knowledge has been gained about these two enzymes and their central importance in eukaryotic cell physiology. Still, there is much more to discover, e.g., the crystal structure of the 19S RC and the mechanism by which the 26S proteasome degrades its substrates; how the 26S proteasome is itself regulated; and the extent to which proteasomal components vary among tissues in higher eukaryotes.

See Also the Following Articles

26S Proteasome, Structure and Function • Chaperones, Molecular • Ubiquitin System • Ubiquitin-Like Proteins

Glossary

hybrid proteasome A 20S proteasome with an RC at one end and a proteasome activator at the other, essentially a 26S proteasome bound to a proteasome activator.

immuno-proteasome A 20S proteasome in which each of the three active β-subunits are replaced by interferon-γ inducible catalytic subunits.

proteasome activators Single polypeptide chains or small protein complexes that bind 20S proteasomes and stimulate peptide hydrolysis.

regulatory complex A particle containing 6 ATPases and 12 other subunits that binds the 20S proteasome to form the 26S proteasome, the eukaryotic cell's major ATP-dependent protease.

ubiquitin A small highly conserved protein that can be covalently attached to other proteins and to itself. Chains of ubiquitin target proteins for destruction by the 26S proteasome.

Further Reading

Bochtler, M., Ditzel, L., Groll, M., Hartmann, C., and Huber, R. (1999). The proteasome. *Annu. Rev. Biophys. Biomol. Struct.* **28**, 295–317.

Hampton, R. Y. (2002). ER-associated degradation in protein quality control and cellular regulation. *Curr. Opin. Cell Biol.* **14**, 476–482.

Hartmann-Petersen, R., Seeger, M., and Gordon, C. (2003). Transferring substrates to the 26S proteasome. *Trends Biochem. Sci.* **28**, 26–31.

Hershko, A., and Ciechanover, A. (1998). The ubiquitin system. *Annu. Rev. Biochem.* **67**, 425–479.

Hill, C. P., Masters, E. I., and Whitby, F. G. (2002). The 11S regulators of 20S proteasome activity. *Curr. Top Microbiol. Immunol.* **268**, 73–89.

Taylor, J. P., Hardy, J., and Fischbeck, K. H. (2002). Toxic proteins in neurodegenerative disease. *Science* **296**, 1991–1995.

Voges, D., Zwickl, P., and Baumeister, W. (1999). The 26S proteasome: A molecular machine designed for controlled proteolysis. *Annu. Rev. Biochem.* **68**, 1015–1068.

Yewdell, J. W., and Bennink, J. R. (2001). Cut and trim: Generating MHC class I peptide ligands. *Curr. Opin. Immunol.* **13**, 13–18.

Biography

Martin Rechsteiner is a Professor of Biochemistry at the University of Utah. Intracellular proteolysis has been his principal scientific interest since the 1980s. During this period, the laboratory discovered and functionally characterized the 26S proteasome as well as several proteasome activators, and also proposed that PEST sequences, regions rich in proline (P), glutamic acid (E), serine (S), and threonine (T), target proteins for rapid degradation.

Protein Carboxyl Esterification

Shilpa G. Lalchandani and Jeffry B. Stock
Princeton University, Princeton, New Jersey, USA

Carboxyl methylation is a reversible protein modification that regulates cellular responses to environmental stimuli. The present article describes this process in bacterial chemotaxis and eukaryotic signal transduction proteins.

Introduction

The methylation and demethylation reactions are catalyzed by two types of enzymes; methyltransferase (Mtase) and methylesterase (MEase). The Mtase transfers methyl groups from the universal methyl donor S-adenosylmethionine (SAM), to a carboxyl group in a target protein. This converts a negatively-charged carboxylate anion on the protein surface into a neutral methyl ester with concomitant formation of S-adenosylhomocysteine (SAH). The methyl group is subsequently removed by a MEase, that catalyzes the hydrolysis of the methyl ester to restore the carboxylate anion on the target protein with the concomitant production of methanol.

$$\text{MTase}: \text{SAM} + \text{Protein} \rightarrow \text{SAH} + \text{Methylated Protein}$$

$$\text{MEase}: \text{Methylated Protein} + H_2O \rightarrow \text{Methanol} + \text{Protein}$$

The central role of carboxyl methylation in sensory receptor function was first evidenced by the discovery, that membrane receptors proteins are methylated and demethylated during bacterial chemotaxis. The involvement of methylation in sensory regulation was extended to vertebrate systems by the finding that RAS related and heterotrimeric G proteins were subject to carboxyl methylation and demethylation. Finally, an exhaustive search for additional systems of carboxyl methylation revealed a second major regulatory locus in eukaryotic cells that involves methylation and demethylation of phosphoprotein phosphatase 2A (PP2A), the major phosphoprotein phosphatase in brain.

To understand how carboxyl methylation works to regulate cellular responses to extracellular signals, it is informative to consider the role of another type of protein modification chemistry, the phosphorylation, and dephosphorylation of protein side chains. As with carboxyl methylation, protein phosphorylation is controlled by two types of converter enzymes. A kinase catalyzes the transfer of a phosphoryl group from the universal phosphodonor, ATP, to an acceptor residue at the surface of a target protein with concomitant formation of ADP, and a phosphoprotein phosphatase catalyzes the hydrolysis of the protein phosphoester with concomitant production of inorganic phosphate. Phosphorylation generally acts as a switch to control the activity of a target protein. The first example of this regulatory mechanism was obtained through studies of the regulation of hormonal control of glucose metabolism in muscle and liver. There it is shown that the release of glucose from glycogen in response to epinephrine involves the activation of a specific kinase that turns on glycogen phosphorylase by transferring a phosphoryl group from ATP to a serine hydroxyl side chain in the enzyme. This modification is later reversed by a phosphoprotein phosphatase to turn off glycogen phosphorylase under resting conditions when glucose needs to be stored. Subsequent research has shown that regulation by phosphorylation and dephosphorylation is a ubiquitous mechanism. A typical vertebrate genome encodes upward of a thousand different protein kinases whose activities are controlled by different regulatory signals, and it has been estimated that a quarter of the proteins in a typical vertebrate cell are subject to regulation by phosphorylation and dephosphorylation.

One might suppose that carboxyl methylation and demethylation would provide the same type of switching mechanism as phosphorylation and dephosphorylation, however this is not the case. Whereas phosphorylation is quite common, carboxyl methylation is rare and present at only 2% of the level of phosphorylation. There appear to be only three MTase enzymes in living systems: one in prokaryotes that methylates chemotaxis receptors, and two in eukaryotes, the G protein and PP2A MTases. Moreover, in these instances carboxyl methylation does not function as an on/off switch, but serves instead to modulate the output of a regulatory network of kinase/phosphatase switches to optimize the response to a given stimulatory input. The global regulatory role of carboxyl methylation is best understood within the context of bacterial chemotaxis.

Carboxyl Methylation in Bacterial Chemotaxis

Virtually all motile prokaryotes use the same basic mechanism to control their motor activities in response to attractant and repellent stimuli. Generally, each cell has a signal transduction apparatus composed of a cluster of thousands of α-helical hair-like fibers that traverse the cytoplasmic membrane (Figure 1). The portion of each fiber located at the outside surface of the membrane acts as a sensory receptor, interacting with specific-attractant and -repellent stimuli in the extracellular medium. The portion of the fibrous array inside the cell controls the activity of an associated protein kinase that catalyzes the transfer of a phosphoryl group from ATP to a small protein in the cytoplasm, that subsequently interacts with the motor apparatus affecting a chemotaxis response. While the cytoplasmic domains of receptor fibers and their associated kinase/phosphatase signaling enzymes are highly conserved, the extracellular sensing domains are variable depending on the particular stimuli with which they interact. The number of different sensory receptor fibers encoded in a given genome ranges from just a few, e.g., five in the case of *Escherichia coli*, to a several dozen, e.g., 46 in *Vibrio cholera*.

Stimulus-response coupling through this phosphorelay signaling apparatus is modulated by carboxyl methylation. Sequences within the cytoplasmic portions of each fiber between the membrane spanning domain and the kinase regulatory domain contain a series of at least four glutamate residues that are subject to methylation and demethylation by specific MTase and MEase enzymes. The degree of methylation of the glutamyl carboxylate side chains control the link between stimulus binding to the extracellular sensory portions of the fibrous array and the intracellular kinase. In most bacteria lower levels of methylation act to increase the cell's sensitivity to attractant stimulation. The level of methylation is controlled by several parameters including the availability of SAM and feedback from the kinase, as well as by conformational changes in the fibers induced by stimulus interactions with the extracellular sensory receptor domains. Since changes in methylation occur at a much slower rate than changes in kinase activity, methylation provides an adaptive mechanism, whereby the sensory apparatus adjusts the phosphorylation response, to fit a given background stimulus intensity. The result is analogous to light–dark adaptation in vertebrate visual systems where sensitivity is shifted in response to background light intensity.

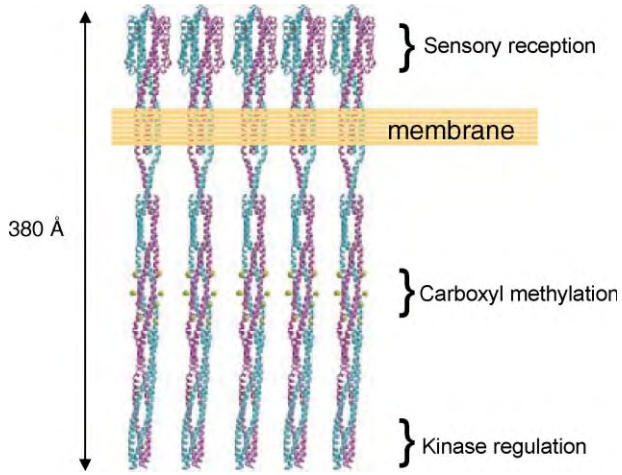

FIGURE 1 Model of the chemotaxis receptor fibers. Transmembrane methylatable receptors are employed as sensors in bacterial chemotaxis.

Carboxyl Methylation of Eukaryotic Signal Transduction Proteins

Responses of eukaryotic cells to extracellular signals is generally mediated by sensory receptor proteins that traverse the cytoplasmic membrane. Portions of these proteins at the cell surface interact with hormones and other stimuli. These interactions cause structural changes in portions of the proteins that extend into the cytoplasm, and these changes act in turn to cause associated G proteins to exchange bound GDP for GTP. The G proteins in their GTP-bound state are activated to produce second messengers such as cAMP that activate protein kinases that regulate key enzymatic activities by phosphorylating serine and threonine side chains. The phosphoryl groups are subsequently removed through the action of phosphoprotein phosphatases such as PP2A. These types of signal transduction pathways are modulated by carboxyl methylation and demethylation of alpha carboxyl groups at the C terminus of the G proteins and PP2A. Thus, although the chemistry is somewhat different, carboxyl methylation modulates receptor-mediated responses in eukaryotes just as it does in bacterial cells.

Ras-Related and Heterotrimeric G Protein

The majority of carboxyl methylated proteins in eukaryotic cells are Ras-related and heterotrimeric G proteins. These signal transduction proteins are targeted to membranes where they relay information from sensory receptors. Membrane targeting depends on a series of posttranslational modifications at the C terminus that includes prenylation, proteolytic cleavage and carboxyl methylation (Figure 2). The initial event, prenylation,

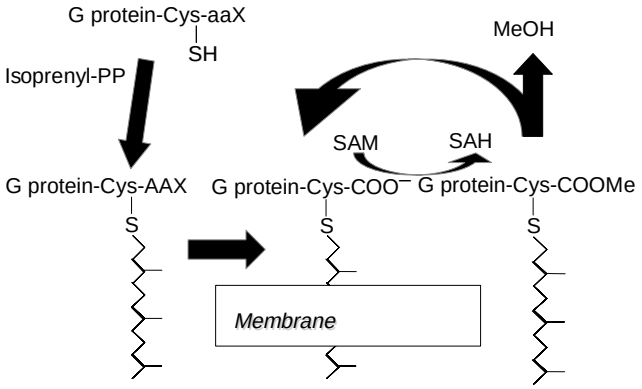

FIGURE 2 Sequence of processing events involved in isoprenylcysteine carboxyl methylation. The methylated molecules are soluble GTPases in the cytosol which are targeted to the membranes by a series of posttranslational modifications at the C-terminal that includes a prenylation, C-terminal proteolytic cleavage, and carboxyl methylation reactions.

depends on a characteristic C-terminal tetrapeptide, termed a CaaX motif, consisting of a cysteine, C, followed by two aliphatic amino acids, aa; and a final amino acid that is variable, X. The prenyl group is either a C-15, farnesyl, or C-20, geranylgeranyl, polyisoprenoid depending primarily on the nature of the C-terminal, X, residue. In either case, prenylation causes the G protein to become associated with Endoplasmic Reticulum (ER) membranes where a membrane-associated protease catalyzes the cleavage of the aaX sequence leaving a prenylcysteine alpha carboxyl group at the C terminus. This is the site of methylation by a specific MTase and demethylation by one or more MEase activities.

G protein methylation is catalyzed by an integral membrane protein that is localized in the ER. This MTase appears to have a broad specificity for prenylcysteine alpha carboxyl groups. It even catalyzes the methylation of amino acids such as N-acetyl-S-farnesylcysteine or N-acetyl-S-geranylgeranylcysteine. The rate of methylation is controlled at several levels. Whereas G protein activation leads to increases in methylation, elevated levels of SAH, feed back to inhibit MTase activity. Methylation is not required for receptor-mediated G protein signaling per se, but rather acts to modulate the stimulus response coupling. Mutant mice with MTase deletions die during early development.

Protein Phosphatase 2A

Protein phosphotase 2A (PP2A) is generally isolated as a trimeric complex consisting of three nonidentical subunits A, B, and C. The 65 kDa, A-subunit serves as a scaffold for the association of the 36 kDa catalytic C-subunit, and of regulatory B subunits. Although, AC dimers are abundant in tissue, ABC trimers of PP2A enzyme are prevalent *in vivo* and account for the main biological activities of the phosphatase. While only two isoforms of the A and C subunits have been reported so far in humans, there is a wide array of B-subunits and these B-subunits are reported to be in part responsible for the specificity of PP2A toward its numerous phosphoprotein substrates. It has been estimated that PP2A is responsible for roughly half of the total phosphoprotein phosphatase activity in vertebrate tissues. It is one of the most abundant enzymes in brain where it plays a critical role in the regulation of axonal microtubule assembly.

The PP2A catalytic subunit has a highly conserved C-terminal extension. The last six residues, TPDYFL being identical in all PP2As. The alpha carboxyl group of the C-terminal leucine residue is the site of methylation and demethylation (Figure 3). Methylation is essential for the assembly of PP2A holoenzymes. The discovery of the PP2A methylation system led to the purification and characterization of specific enzymes responsible for PP2A methylation and PP2A demethylation.

The PP2A MTase was initially purified from bovine brain as a soluble 38 kDa monomer. The enzyme appears to be completely specific for the methylation of PP2A AC dimers. PP2A methyl esters are hydrolyzed by the action of a specific MEase with similar specificity. The PP2A MEase has been purified from bovine brain as a soluble 46 kDa monomer. The MTase and MEase are highly conserved in species ranging from yeast to human.

Methylation has been demonstrated to function as a molecular switch that controls the assembly of the PP2A subunits. PP2A holoenzyme assembly could alter dephosphorylation of proteins due to changes in substrate targeting. Differential methylation of PP2A has been observed during cell cycle progression, suggesting that methylation might be altering the subcellular localization

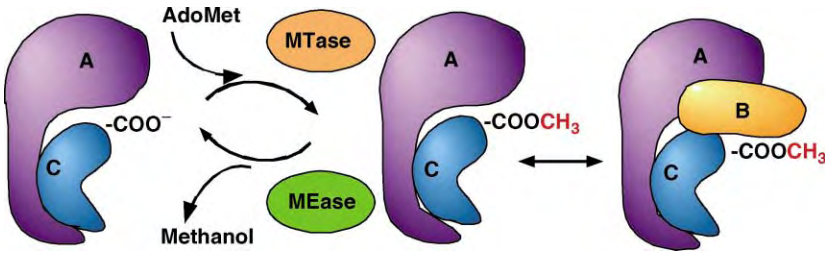

FIGURE 3 Carboxyl methylation regulates PP2A by controlling the association of regulatory B-subunits.

of PP2A. Selective microtubule-associated PP2A is differentially regulated during the cell cycle, implying that PP2A is regulated by methylation. The level of PP2A methylation is stimulated by cAMP and inhibited by SAH.

PP2A methylation seems to play an important role in growth control. Mutant yeasts that completely lack PP2A MTase activity are resistant to rapamycin and sensitive to antibiotics such as nacotazol that inhibit microtubule function. It has recently been proposed that in humans, inhibition of PP2A by SAH in brain may help explain why elevated homocysteine levels are a risk factor for Alzheimer's disease since homocysteine can condense with adenosine to generate SAH.

See Also the Following Articles

G Protein Signaling Regulators • G_{12}/G_{13} Family • G_q Family • G_s Family of Heterotrimeric G Proteins • Ras Family

Glossary

methylesterase Enzyme responsible for demethylating the target protein by hydrolysis of the methyl ester.

methyltransferase Enzyme that transfers a methyl group from the universal methyl donor S-adenosylmethionine, SAM, to a carboxyl group in a target protein.

Further Reading

Djordjevic, S., Stock, A. M., Chen, Y., and Stock, J. B. (1999). Protein methyltransferases in signal transduction. In *S-Adenosylmethionine-Dependent Methyltransferases: Structure and Functions* (X. Cheng and R. M. Blumenthal, eds.) pp. 149–183. World Scientific Publishing, Singapore.

Biography

Shilpa Lalchandani is a Postdoctoral Research Associate with Dr. Stock.

Jeffry B. Stock is Professor of Molecular Biology and Chemistry at Princeton University. His principal research interest is concerned with the biochemistry and biophysics of signal transduction with an emphasis on reversible methylation. He holds a Ph.D. in Biochemistry from Johns Hopkins University. Dr. Stock served as a postdoctoral research associate with Dr. D.E. Koshland, Jr., at the University of California, Berkeley. He is also on the editorial board of the *Journal of Biological Sciences* and serves as a member of Molecular Biophysics, Neuroscience and Materials Science Programs at Princeton University. He has authored and edited several books in his field and has over 150 peer-reviewed publications.

Protein Data Resources

Philip E. Bourne
University of California, San Diego, California, USA

Protein resources are defined here as Internet accessible data sources containing both primary data and interpretations of these data. Asking a bioinformatician to write about such resources is like asking a molecular biologist to write about cell signaling. Both are very broad and dynamic topics to which data and knowledge are constantly being added. To avoid providing a superficial view of protein resources, or a view that is going to be outdated before it is published, this article provides a description that will likely not change regardless of what new knowledge is acquired. Hence, this overview will focus on well-established resources of interest to the molecular and possibly cellular biologist. In short, the article addresses content associated with the sequence–structure–function triad, but does not address the significant amount of informatics and computational science research that goes into such resources. The number of protein resources addressing this triad is large and volatile – resources come and go. Emerging are resources that address proteins in the larger biological context through their role in biochemical pathways and in the functioning of a complete model organism. Examples of such resources are introduced to illustrate what can be expected in the future.

Primary and Secondary Resources

What are well-established resources? Well established implies the resource will likely be accessible in five years. That is, they are valuable enough to a broad community to warrant continuous financial support. Broadly speaking, established resources are of two types, primary and secondary. Primary resources are those which directly receive scientific input from the community in the form of protein sequences (usually translated from the DNA sequence), protein structures, expression data, NMR data, mass spectrometry data, measured binding constants, and so on. These data are usually annotated and curated either by humans, by machine, or by a combination of both. They form a backbone from which the study of the life sciences can proceed in an orderly way. Examples of primary resources are Genbank (primary sequences) and the protein data bank (PDB; macromolecular structure).

Secondary resources are derived using data from the primary resources and add value to this primary information either through expert opinion, computation or both. Examples of secondary resources include Swiss-Prot annotated protein sequences taken from TrEMBL and SCOP (Structure Classification of Proteins), which classifies structures from the PDB according to fold, family, and superfamily. Consider the process by which data enters and is processed by a primary and secondary resource so that the quality of these resources can be evaluated. Quality can be broadly judged by four criteria: amount, accuracy, completeness, and usability. This brief discussion does not consider usability.

The Process of Data Acquisition and Processing

We consider the PDB as an example of a primary data resource and Swiss-Prot as an example of a secondary data source.

Primary Data Acquisition – the PDB

The PDB is the single worldwide repository for data on the structure of biological macromolecules derived primarily by X-ray crystallography and NMR spectroscopy. Structural biologists submit depositions to the PDB almost exclusively through a web interface to one of three sites worldwide (Rutgers University, USA; the European Bioinformatics Institute, UK; and Osaka University, Japan). This submission comprises the final output of a program describing the atomic coordinates and any annotation provided by the depositor. The depositor immediately receives a PDB identifier which is the unique and immutable reference to that structure. The incentive to deposit comes from most journals not accepting a structure-based paper unless it includes a PDB identifier. Once received an annotator takes responsibility for processing this entry. A series of checks are performed to validate the integrity of this entry, these include the use of correct atom, residue and ligand naming, stereochemical correctness, and association of the structure with the nearest protein sequence derived

from the sequence databases. A completely annotated and validated entry is returned to the depositor usually within 1–2 working days for their approval. Either the depositor approves or a further round of refinement of the entry will ensue. Once finalized, the entry is released immediately, held until the primary paper associated with the structure is published and then released (the most common situation) or held for a maximum of 1 year. Every effort is made to make entries as complete, consistent, and accurate as possible based on the knowledge of the field at the time. The PDB in no way polices the data – the depositor always has the final say about what is released.

Secondary Data Acquisition – Swiss-Prot and TrEMBL

Swiss-Prot connects amino acid sequences with an annotated description of that protein. Each protein entry provides an interdisciplinary overview of relevant information, bringing together experimental results, computed features and sometimes even contradictory conclusions. Swiss-Prot provides annotated entries for all species, but concentrates on the annotation of entries from human and other model organisms. As a complement, TrEMBL strives to comprise all protein sequences that are not yet represented in Swiss-Prot, by incorporating a perpetually increasing level of mostly automated annotation. Consider the annotation steps associated with a Swiss-Prot entry, the source of which is TrEMBL. Much of this description is available from the Swiss-Prot web site.

The annotation steps are different depending on the source of the sequence. Sometimes scientists' isolate and then biochemically characterize the protein encoded by the gene they have sequenced. Other times they infer this information through similarity to other proteins within the same, conserved family. If it does not belong to a particular family they infer through purely sequence similarity. Finally there are the genome sequence data that often does not have an accompanying citation reporting any such classification. As a first step the sequence is aligned, using FastA or Blast, against all existing Swiss-Prot and TrEMBL entries. This determines whether the sequence can be related to existing families in Swiss-Prot. The next step is to read the article(s), assess the information given, and add relevant comments and features to the entry.

Often from reading the abstract of the paper and analyzing the FastA results the protein can be seen to belong to a particular family. In these cases, care is taken to look at other members of the family and to become familiar with the annotation that already exists. Any standard annotation that is common to the family, for example, the description line(s) and the keywords, can be added to the new entry. Other comments and features, specific to the family, can be added in conjunction with reading the paper. Any additional information from the paper, for example posttranslational modifications, is then added to the entry.

In the majority of articles reporting gene sequencing, the gene is translated to give the protein sequence but the *in vivo* protein is rarely isolated and characterized. Often a probe from a similar organism is used to pinpoint the gene and then the authors infer biochemical characteristics. In these cases, curators assess what the authors imply with the results of the alignments against Swiss-Prot and TrEMBL. When the sequence "hits" against a particular family the description line(s), the similarity comments, and keywords specific to the family, can be added to the new entry. More care is taken when looking at function, subunit, and sequence features. The annotation is then characterized as "probable," "potential," and "by similarity."

Genome sequencing has caused a massive influx of data into the nucleotide sequence databases and this has led to the same influx into TrEMBL giving thousands of entries waiting to go into Swiss-Prot. This sequence data is submitted to the nucleotide sequence databases and is reported in publications that show the entire genome sequence as well as genes that are predicted by a number of methods. Apart from these gene designations the papers rarely include experimental information about any of the predicted proteins from these analyses. By making use of what is reported coupled to the assessment of results from sequence alignments, that hit against both characterized and part-characterized protein sequences, Swiss-Prot makes an effort to add relevant biochemical information to these translated protein sequences.

In summary, established protein resources are generally staffed by knowledgeable scientists dedicated to the task of providing a worldwide community with accurate and timely information.

Data Dissemination

Currently the majority of access to protein resources is via the web, and the following sections provide details of access to a variety of resources. However, access via a web browser is by no means the only forms of access. Some resources provide bulk downloads either via ftp sites or through distribution of hard media, notably CDROM. For example, see http://www.rcsb.org/pdb/cdrom.html for receiving CDROMs of the PDB or contact datalib@ebi.ac.uk by email to receive copies of Swiss-Prot on CDROM. Users can also link to different resources from their own web pages and download data on demand, see for example, http://www.rcsb.org/pdb/

linking.html for linking to the PDB. The National Center for Biotechnology Information (NCBI) has an interesting service called Cubby to use with their Entrez integrated service. Cubby allows you to customize and store searches for future use. It is likely that in the future more protein resources will become more journal-like in that updates to the contents of the database will be provided by email in the same way the table or contents are provided by journals today. The sheer volume of data will require some prefiltering. One can imagine subscribing to a service that returns results of a user request such as "once per month send me a list of all serine/threonine kinase structures solved by X-ray crystallography to better than 2.5Å."

A Roadmap to Protein Data Resources

To anyone who has searched for protein data using a web browser it is immediately apparent there is an endless source of information, some good, some bad. Peer review is clearly needed and fortunately has been undertaken by the journal *Nucleic Acids Research* (NAR; http://nar.oupjournals.org/). NAR publishes both an annual database issue in January each year and a web server issue in July of each year. Resource developers strive to be included in these issues and reviewers carefully check the capabilities of the resource in the same way a scientific paper is considered for publication. The ever expanding list of quality resources are catalogued on-line at http://nar.oupjournals.org/cgi/content/full/31/1/1/DC1. This article considers a subset of those resources, which are considered most widely useful.

Primary Resources

As stated above, primary resources (Table I) are defined here as those that accept primary biological data through direct deposition from the author(s). These data may be supplemented by annotators adding data from the published literature and with some form of validation and cross checking. The vast majority of protein sequence data are derived from translation of DNA sequences. Sequence data ranges from data submitted on complete genomes via high throughput sequencing technologies to individual sequences submitted as part of a biochemical study to expressed sequence tags. A more complete list of resources can be found at the National Center for Biotechnological Information (NCBI; http://www.ncbi.nlm.nih.gov/Sitemap/index.html), perhaps the major keeper of biological information worldwide.

Structure data found in the PDB are derived both from high throughput structural genomics projects and more functionally driven conventional structural biology. The sequences of structures under consideration by the structural genomics projects can be found at http://targetdb.rcsb.org. The sequences of some structures awaiting release by the PDB can be found at http://www.rcsb.org/pdb/status.html.

TABLE I

Major Sources of Primary Data

Name	Description
Genbank	Primary source of DNA sequence information and coordinated with EMBL and DDBJ – http://www.ncbi.nlm.nih.gov/Genbank/index.html
PDB	Primary source of the 3D structures of biological macromolecules determined by X-ray crystallography and NMR – http://www.pdb.org
Entrez-Genome	Over 1000 genomes from bacteria, archea, and eukaryota – http://www.ncbi.nlm.nih.gov/entrez/query.fcgi?db = Genome
dbEST	Sequence data and other information on "single-pass" cDNA sequences, or Expressed Sequence Tags, from a number of organisms – http://www.ncbi.nlm.nih.gov/dbEST/

Secondary Sources

Secondary resources (Table II) in some way add value to data available through the primary resources. This occurs through processes such as provision of additional experimental data and/or additional annotation, validation, and checking, reductionism, computation of derived features, and provision of alternative views on the data. For example, for protein sequences, Swiss-Prot specializes in annotation, Pfam, SMART, and ProDOM are examples of resources that provide annotation at the level of the domain, whereas Prosite, Blocks and Prints use different methodologies to provide details at the level of short (usually functional) motifs.

For structure, PDBSum, MSD, and PDBj provide alternative views and mode of access to PDB primary data. A variety of structure classification tools exist as shown in Table II. SCOP is the most popular and classifies protein structures by fold, family (close sequence-structure-function relationship), and superfamily (structural and suggested evolutionary relationship).

Since proteins sequences outnumber structures by several orders of magnitude, yet structure provides an important linkage between sequence and function, there is a very significant effort to predict three-dimensional structure from sequence. Progress in this field is

TABLE II

Major Sources of Secondary Data

Sequence	
Swiss-Prot	Annotated protein sequence database – http://us.expasy.org/sprot/
TrEMBL	A computer-annotated supplement of Swiss-Prot that contains all the translations of EMBL nucleotide sequence entries not yet integrated in Swiss-Prot http://us.expasy.org/sprot/
Uniprot	The Universal Protein Knowledgebase is a central database of protein sequence and function by joining the forces of the Swiss-Prot, TrEMBL and PIR protein database activities – http://www.pir.uniprot.org/
Sequence – domains	
Pfam	Multiple sequence alignments and hidden Markov models covering many common protein domains and families – http://www.sanger.ac.uk/Software/Pfam/
SMART	A Simple Modular Architecture Research Tool which allows the identification and annotation of genetically mobile domains and the analysis of domain architectures – http://smart.embl-heidelberg.de/
ProDOM	A comprehensive set of protein domain families automatically generated from the SWISS-PROT and TrEMBL sequence databases – http://prodes.toulouse.inra.fr/prodom/current/html/home.php
Sequence – short sequence motifs	
Prosite	Protein families and domains with assigned functional motifs – http://us/expasy.org/prosite/
Blocks+	Blocks are multiply aligned ungapped segments corresponding to the most highly conserved regions of proteins – http://www.blocks.fhcrc.org/
Prints	A compendium of protein fingerprints – http://bioinf.man.ac.uk/dbbrowser/PRINTS/
Genomic sequence	
Ensembl	Genome browser for a number of model organisms – http://www.ensembl.org/
Structure	
PDBSum	Summaries for all protein structures including validation checks – http://www.biochem.ucl.ac.uk/bsm/pdbsum/
MSD	Database and tools for access and manipulation of PDB data – http://www.ebi.ac.uk/msd/
PDBj	Database and tools for access and manipulation of PDB data – http://pdbj.protein.osaka-u.ac.jp
Structure classification	
SCOP	The Structure Classification of Proteins – http://scop.mrc-lmb.cam.ac.uk/scop/
CATH	Class (C), Architecture (A), Topology(T), and Homologous superfamily (H) – http://www.biochem.ucl.ac.uk/bsm/cath_new/index.html
DALI	DALI Domain Dictionary – http://www.embl-ebi.ac.uk/dali/domain/
VAST	Vector Alignment Search Tool – http://www.ncbi.nlm.nih.gov/Structure/VAST/vast.shtml
CE	Polypeptide chain comparison – http://cl.sdsc.edu/ce.html
3Dee	Protein Domain Definitions – http://jura.ebi.ac.uk:8080/3Dee/help/help_intro.html
Structure prediction	
Eva	Evaluate of protein prediction servers – http://cubic.bioc.columbia.edu/eva/
LiveBench	Benchmarking of structure prediction servers – http://bioinfo.pl/LiveBench/
Protein–protein interactions	
DIP	Database of Interacting Proteins – http://dip.doe-mbi.ucla.edu/
BIND	The Biomolecular Interaction Network Database – http://www.bind.ca/

measured by the bi-annual Critical Assessment of Structure Prediction (CASP) meeting. CASP provides a blind test of how researchers worldwide are improving the ability to predict structure using comparative (homology) modeling, fold recognition (threading), and other more *ab initio* techniques. Progress in CASP is documented in a special issue of *Proteins, Structure, Function and Genetics*. A promising approach to the problem is the use of metaservers that provide a consensus view of prediction over a number of individual resources and approaches. Livebench and Eva are the most popular in this regard (Table II).

Data Reduction

The current wealth of proteomic data is both a blessing and a curse. It depends on what a user is trying to determine. If the results of a sequence search for

TABLE III
Reduced Data Subsets

Resource	Description
RefSeq	Curated, nonredundant set including genomic DNA contigs, mRNAs and proteins for known genes, mRNAs and proteins for gene models, and entire chromosomes – http://www.ncbi.nlm.nih.gov/RefSeq/
Astral	Nonredundant structure subsets at different levels of sequence identity – http://astral.stanford.edu/

homology returns hundreds of near identical sequences it may confuse the result rather than lead to a meaningful solution. Nonredundancy can assist in this regard by providing a filtered set of data. The issues then become the level of redundancy retained, the type of redundancy and the choice of a representative. Table III outlines the two common sources of reduced sequence and structure data. It should be noted that protein sequence redundancy is different than protein structure redundancy. Two protein sequences sharing a sequence identity of over 30% will likely share the same fold. However, structures with the same fold could have a sequence identity of less than 10% – the evolutionary drift of sequences is greater than that of structure. A key issue is then redundancy with respect to what. Table III describes two resources dealing with sequence redundancy, RefSeq provides a set of reference sequences and Astral a set of reference structures filtered by sequence identity and with an effort to select the most accurate structure as a representative. Some of the resources under structure classification in Table II provide a nonredundant set of structures with respect to the three-dimensional structure, not the sequence.

Consistent Annotation

Comparison of data, either within a given resource or certainly across resources, requires consistent annotation. This presents a very significant problem across molecular biology and thus with protein data. For example, there are issues of multiple common versus systematic names for proteins, lack of a singular systematic description at the time the protein was discovered and lack of the use of systematic nomenclature even when it exists. The use of International Union of Pure and Applied Chemistry (IUPAC; http://www.iupac.org) descriptors for chemical descriptions helps, as does the use of Enzyme Commission (EC; http://us.expasy.org/enzyme/) numbers for describing enzymes. Most recently, thanks to the work of database developers in recognizing the need for standardization, the Genome Ontology (GO) has been developed by the GO Consortium (http://www.geneontology.org/). GO provides consistent descriptions for biochemical process, molecular function, and cellular location in the form of a directed acyclic graph. That is, a node can have multiple parents, for example, a given protein can have multiple functions. Many of the resources described in Table I and II now assign GO annotation to their entries.

TABLE IV
Integrated Resources

Resource	Description
InterPro	InterPro is a database of protein families, domains and functional sites – http://www.ebi.ac.uk/interpro/
Entrez	Integrated scientific data and literature – http://www3.ncbi.nlm.nih.gov/Entrez/
Kegg	Kyoto Encyclopedia of Genes and Genomes – http://www.genome.ad.jp/kegg/kegg2.html
AfCS	The Alliance for Cell Signaling – http://www.afcs.org/
SRS	Sequence Retrieval System – http://srs.ebi.ac.uk
EcoCyc	Integrated description of *E. coli* – http://www.ecocyc.org

Integrated Resources

A number of cross-referenced resources which include primary and secondary protein data have been developed. Table IV provides a flavor of the wide variety of resources available. Usually this integration is achieved by sequence comparison between resources and subsequent cross checking of information like GO terms. Such cross checking also reveals errors in these databases. InterPro combines data from PROSITE, PRINTS, Pfam, SMART, TIGRFAMs, PIR SuperFamily, and SUPERFAMILY (sequence-motif methods) and ProDom (a sequence cluster method). Entrez combines a variety of sequence and structure data with the literature described mostly as abstracts in PubMed. SRS links a large variety of biological databases (over 200) and is a good place to start to explore resources in general, since the majority of major resources are cross referenced here.

The Future

A compendium of protein sequences or structures is not how a biologist thinks about a problem. Rather they often see a protein as part of a network of interactions with one or more roles that can be measured by a biochemical or phenotypic response, where the data associated with that response can be downloaded and further analyzed. Resources that place proteins as part of a pathway or more specifically in the correct biological

context are likely to be more common in the future. Several exist today (Table IV) and offer a window into what will become commonplace in the next five years. Ecocyc provides literature-based curation of the entire genome of *Escherichia coli* K12 MG1655 including transcriptional regulation, transporters, and metabolic pathways. The Alliance for Cell Signaling is modeling signaling pathways in several organisms and Kegg offers an integrated view of pathways and genomic data.

Clearly the challenge of the future is not having appropriate data, rather how to make the best use of the wealth of data in a way that it can be interpreted by those scientists who can gain most from it. At the same time traditional publishing models are changing through the use of the Internet and Open Access models. One can imagine a future in which the traditional journal article is merely one type of user interface to the data. Interesting times indeed!

See Also the Following Articles

Genome-Wide Analysis of Gene Expression • X-Ray Determination of 3-D Structure in Proteins

Glossary

curation The process of validating and annotating experimental or derived data.

data reduction The process of representing multiple data by a single representative data set based on some criteria of similarity.

integrated resource Single access point to data from multiple primary and secondary resources.

ontology Quantitative description of a field of study of defined scope.

primary resource Protein resource that accepts experimental data from the community.

protein resource Internet accessible information on protein sequence, structure, and function.

secondary resource Protein resource that post-processes experimental data to add derived data.

Further Reading

Ashburner, M., Ball, C. A., Blake, J. A., Botstein, D., Butler, H., Cherry, J. M., Davis, A. P., Dolinski, K., Dwight, S. S., Eppig, J. T., Harris, M. A., Hill, D. P., Issel-Tarver, L., Kasarskis, A., Lewis, S., Matese, J. C., Richardson, J. E., Ringwald, M., Rubin, G. M., and Sherlock, G. (2000). Gene ontology: Tool for the unification of biology. The gene ontology consortium. *Nat. Genet.* **25**, 25–29.

Baxevanis, A. D. (2003). The molecular biology database collection: 2003 update. *Nucleic Acids Res.* **31**, 1–12.

Benson, D. A., Karsch-Mizrachi, I., Lipman, D. J., Ostell, J., and Wheeler, D. L. (2003). GenBank. *Nucleic Acids Res.* **31**, 23–27.

Berman, H. M., Westbrook, J., Feng, Z., Gilliland, G., Bhat, T. N., Weissig, H., Shindyalov, I. N., and Bourne, P. E. (2000). The protein data bank. *Nucleic Acids Res.* **28**, 235–242.

Boeckmann, B., Bairoch, A., Apweiler, R., Blatter, M. C., Estreicher, A., Gasteiger, E., Martin, M. J., Michoud, K., O'Donovan, C., Phan, I., Pilbout, S., and Schneider, M. (2003). The SWISS-PROT protein knowledgebase and its supplement TrEMBL in 2003. *Nucleic Acids Res.* **31**, 365–370.

Gilman, A. G., Simon, M. I., Bourne, H. R., Harris, B. A., Long, R., Ross, E. M., Stull, J. T., Taussig, R., Arkin, A. P., Cobb, M. H., Cyster, J. G., Devreotes, P. N., Ferrell, J. E., Fruman, D., Gold, M., Weiss, A., Berridge, M. J., Cantley, L. C., Catterall, W. A., Coughlin, S. R., Olson, E. N., Smith, T. F., Brugge, J. S., Botstein, D., Dixon, J. E., Hunter, T., Lefkowitz, R. J., Pawson, A. J., Sternberg, P. W., Varmus, H., Subramaniam, S., Sinkovits, R. S., Li, J., Mock, D., Ning, Y., Saunders, B., Sternweis, P. C., Hilgemann, D., Scheuermann, R. H., DeCamp, D., Hsueh, R., Lin, K. M., Ni, Y., Seaman, W. E., Simpson, P. C., O'Connell, T. D., Roach, T., Choi, S., Eversole-Cire, P., Fraser, I., Mumby, M. C., Zhao, Y., Brekken, D., Shu, H., Meyer, T., Chandy, G., Heo, W. D., Liou, J., O'Rourke, N., Verghese, M., Mumby, S. M., Han, H., Brown, H. A., Forrester, J. S., Ivanova, P., Milne, S. B., Casey, P. J., Harden, T. K., Doyle, J., Gray, M. L., Michnick, S., Schmidt, M. A., Toner, M., Tsien, R. Y., Natarajan, M., Ranganathan, R., and Sambrano, G. R. (2002). Overview of the alliance for cellular signaling. *Nature* **420**, 703–706.

Kanehisa, M., Goto, S., Kawashima, S., and Nakaya, A. (2002). The KEGG databases at GenomeNet. *Nucleic Acids Res.* **30**, 42–46.

Karp, P. D., Riley, M., Saier, M., Paulsen, I. T., Collado-Vides, J., Paley, S. M., Pellegrini-Toole, A., Bonavides, C., and Gama-Castro, S. (2002). The EcoCyc database. *Nucleic Acids Res.* **30**, 56–58.

Mulder, N. J., Apweiler, R., Attwood, T. K., Bairoch, A., Barrell, D., Bateman, A., Binns, D., Biswas, M., Bradley, P., Bork, P., Bucher, P., Copley, R. R., Courcelle, E., Das, U., Durbin, R., Falquet, L., Fleischmann, W., Griffiths-Jones, S., Haft, D., Harte, N., Hulo, N., Kahn, D., Kanapin, A., Krestyaninova, M., Lopez, R., Letunic, I., Lonsdale, D., Silventoinen, V., Orchard, S. E., Pagni, M., Peyruc, D., Ponting, C. P., Selengut, J. D., Servant, F., Sigrist, C. J., Vaughan, R., and Zdobnov, E. M. (2003). The InterPro Database, 2003 brings increased coverage and new features. *Nucleic Acids Res.* **31**, 315–318.

Venclovas, C., Zemla, A., Fidelis, K., and Moult, J. (2003). Assessment of progress over the CASP experiments. *Proteins* **53**(Suppl. 6), 585–595.

Biography

Philip E. Bourne is a Professor in the Department of Pharmacology, University of California, San Diego and Co-Director of the Protein Data Bank. He is a former President of the International Society for Computational Biology and a Fellow of the American Medical Informatics Association. He received his Ph.D. from the Flinders University of South Australia. His research interests are broadly in the area of structural bioinformatics and the application of high performance computing technology to problems in the life sciences.

Protein Degradation

Tomo Šarić
Institute of Neurophysiology, University of Cologne, Cologne, Germany

Alfred L. Goldberg
Harvard Medical School, Boston, Massachusetts, USA

Nearly all proteins within cells and most in the extracellular space are in a state of continuous turnover, being synthesized from amino acids and, after varying life spans, broken down back to amino acids. The term "protein degradation" refers to several intracellular processes by which proteins are broken down to their basic constituents. Protein degradation occurs in all living species, from bacteria to humans, and is mediated by the sequential action of several endo- and exopeptidases.

Essential Biological Functions of Protein Degradation

Because cells use significant amount of energy for new protein synthesis, the continual destruction of proteins might appear highly wasteful. However, this process serves multiple important biological functions that are essential for life. The degradation of intracellular proteins is a highly selective and tightly regulated process that is required for removal of many regulatory proteins (transcription factors and signal transducers) and many key rate-limiting enzymes, whose rapid degradation is essential for maintaining cellular homeostasis.

Unlike most regulatory mechanisms (e.g., phosphorylation, ubiquitylation), peptide bond cleavage is an irreversible process, and proteases therefore act as unidirectional biological switches. The only way that cells can reduce the steady-state level of a particular protein is by proteolytic degradation, and removal of certain proteins permits cells to adapt to changes in cellular environment and new physiologic conditions. This kind of adaptation occurs in mammals, for example, in the liver during fasting when enzymes for glycogen production are removed and enzymes required for gluconeogenesis are up-regulated.

Under fasting conditions, protein breakdown also serves as a source of essential amino acids, especially in skeletal muscle, where it provides essential precursors for gluconeogenesis, protein biosynthesis, or energy production. Protein breakdown functions also as a quality control mechanism that selectively removes abnormal proteins resulting from mutation, chemical damage (e.g., oxidation), biosynthetic errors (e.g., premature termination of translation), or failure of normal folding or assembly (which may be a common event in cytosol and endoplasmic reticulum).

Most extracellular proteins (such as plasma proteins) also continuously turn over, mainly by uptake and degradation inside the cells. In higher vertebrates, protein degradation is critical for the function of the immune system. Proper defense against intracellular pathogens (e.g., viruses) or pathogens in the extracellular space (e.g., bacteria) is dependent on continual production of peptide antigens by intracellular proteolytic pathways. In eukaryotic cells, there are two principal pathways for complete degradation of proteins: endocytic–lysosomal and the ATP-dependent ubiquitin–proteasome pathway. The former occurs within the membrane-enclosed vesicles and the latter operates in the cytosol and nucleus. These pathways involve very different enzymes and serve different functions in the cell. Proteolytic systems are also present in some organelles (e.g., mitochondria). Bacteria and archaea do not have lysosomes or ubiquitin but, nevertheless, possess soluble or membrane-bound proteases, many of which are evolutionary precursors of more sophisticated eukaryotic enzymes. One critical feature of all these intracellular degradative systems is that they require metabolic energy, unlike the typical proteases functioning in the extracellular space. As explained in this article, energy-dependent processes help insure exquisite selectivity and allow regulation of the proteolytic enzymes.

Endocytic–Lysosomal Pathway

This pathway is responsible for degradation of extracellular proteins, most membrane proteins, some organelles, and some intracellular proteins. It is composed of heterogeneous groups of vesicles that differ in

morphology, function, and biochemical and biophysical properties. The principal component of this pathway where most protein degradation takes place is the lysosome (or the vacuole in yeast).

Lysosomes

Lysosomes are single membrane-bound spherical organelles in the cytoplasm. They were discovered by Christian de Duve and co-workers in the mid 1950s and are found in all mammalian cells except red blood cells. Lysosomes are not found in higher plants, but the plant cell vacuole performs some of their degradative functions. Lysosomes play an important role in innate immunity, adaptation to stress or starvation, recycling of cytoplasmic organelles, development, cell differentiation, and some forms of programmed cell death.

Uptake of Substrates

Lysosomes receive substrates for degradation by fusing with other intracellular vesicles that are formed by endocytosis (endosomes, pinosomes, phagosomes) or autophagy (autophagosomes). Endocytosis refers to the process of uptake of extracellular material or membrane proteins by invagination of the cell membrane, followed by formation of vesicles inside the cell. Before these vesicles reach the lysosomes (pH 4.5–5.0), ingested material moves from the less acidic early endosomes (pH 6.0–6.5) to the more acidic late endosomes (pH 5.0–6.0). There are three major forms of endocytosis: (1) receptor-mediated endocytosis (uptake of membrane proteins, such as cell surface receptors and their ligands), (2) pinocytosis (ingestion of extracellular liquid with its solute molecules), and (3) phagocytosis (engulfing of large particles such as bacteria or apoptotic bodies by specialized cells such as neutrophils, macrophages, or amoeba) (Figure 1). Pinocytosis and phagocytosis are nonselective bulk processes, but receptor-mediated endocytosis is a specific, regulated cellular process that is used, for example, by most cells to take up extracellular products (e.g., lipoproteins, transferin) or to reduce the levels of surface receptors (down-regulation) after receptors are occupied by ligands, or by some cells, such as B lymphocytes, to internalize antigens using antibodies on the cell surface as receptors. Autophagy is regulated, but nonselective, digestion of intracellular material (Figure 1). It serves an adaptive role in response to nutritional deprivation and stress and is responsible for digestion of some cytosolic proteins and redundant or damaged intracellular organelles, such as mitochondria and peroxisomes. In addition, some cytosolic proteins that contain specific amino acid motifs (e.g., KFERQ) are transported into lysosomes selectively through a specific energy-, chaperone-, and receptor-mediated process that is activated by nutrient deprivation (Figure 1).

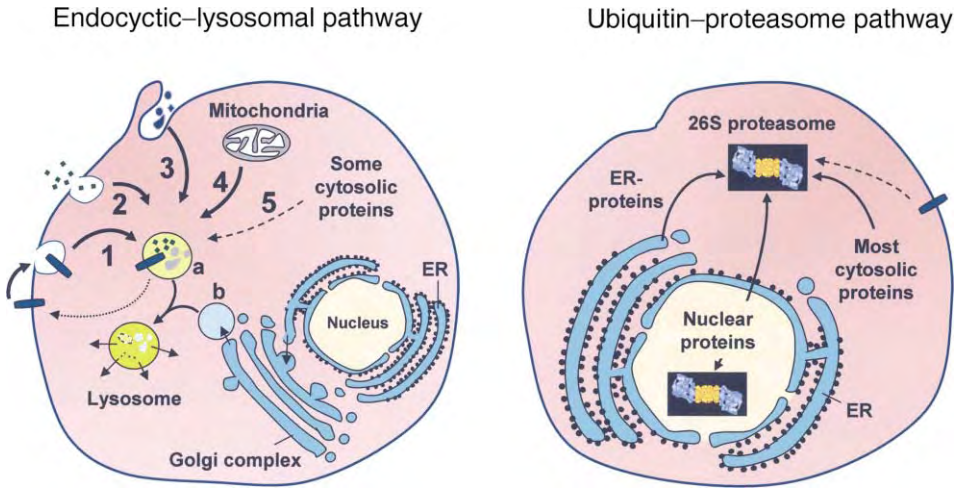

FIGURE 1 Pathways of protein breakdown in mammalian cells. Most intracellular proteins in the cytosol, nucleus, and endoplasmic reticulum (ER) are degraded by the ubiquitin–proteasome pathway (right panel). Extracellular and autophagocytized proteins and most membrane proteins are broken down within the endocytic–lysosomal compartment (left panel). Substrates are delivered to this pathway by receptor-mediated endocytosis (1), pinocytosis (2), phagocytosis (3), autophagy (4), and a selective process for some cytosolic proteins containing specific amino acid motifs (5). Some internalized membrane proteins are recycled back to the plasma membrane (dotted arrows). After the internalized material is enclosed in vesicles (a), the vesicle fuses with primary lysosomes (b), derived from the Golgi complex and ER, to form secondary lysosomes where final degradation takes place. Degradation products are transported across the lysosomal membrane into the cytosol. Some plasma membrane proteins are broken down by the ubiquitin–proteasome pathway, and some cytosolic proteins are degraded in lysosomes (dashed arrows). Although worn out mitochondria are cleared by autophagy, mitochondrial proteins are selectively broken down by their own ATP-dependent proteases.

Lysosomal Enzymes

Lysosomes contain at least 50 different hydrolytic enzymes, which catalyze the breakdown of proteins, nucleic acids, carbohydrates, and lipids into their components. Lysosomal hydrolases normally cannot escape into the cytoplasm and their isolation in this vesicular compartment is essential for protecting from nonspecific degradation of key cell constituents. However, during necrotic cell death, lysosomes release their content, which helps destroy the cell. Release of lysosomal enzymes outside of cells causes severe inflammation and contributes to the symptoms of some diseases (e.g., gout). Most lysosomal enzymes are optimally active at an acidic pH of 4–6, which is maintained by a cell membrane hydrogen ion ATPase. Many lysosomal proteases are traditionally called cathepsins, and most belong to the mechanistic family of cystein proteases. The most abundant proteases are cathepsins D and L (endopeptidases) and cathepsins B and H (exopeptidases). The acidic milieu in lysosomes not only keeps lysosomal enzymes at their most active state, but it also helps denature protein substrates, which enhances their susceptibility to proteolytic digestion. Once the protein substrates are degraded, the products of their digestion are transported across the membrane into the cytosol, where they are further metabolized.

Additional Roles of the Endocytic Pathway

The endocytic–lysosomal pathway plays an important role in maintaining the structural integrity of plasma membrane by continuously recycling internalized membranes and some membrane receptors back to the cell surface. In addition, in specialized antigen-presenting cells (macrophages, dendritic cells, and B cells), some peptides derived from breakdown of extracellular proteins escape complete destruction and are bound in late endosomes by specialized membrane receptors, called major histocompatibility (MHC) class II molecules. These complexes are transported to the cell surface for presentation to a subpopulation of T lymphocytes responsible for generation of humoral immune responses against non-native proteins, e.g., ones from pathogens.

Ubiquitin–Proteasome Pathway

Most cytosolic and nuclear proteins are degraded by the ubiquitin–proteasome pathway (Figure 2). This system catalyzes the breakdown of most normal long-lived proteins, which comprise the bulk of proteins in cells, and many short-lived proteins that regulate a wide variety of essential cellular processes, ranging from cell cycle progression to signal transduction and gene transcription. In addition, it catalyzes the selective and rapid elimination of damaged, misfolded, or mutated proteins, which are continuously produced due to imperfections of biosynthetic and folding machineries in the cell. The discovery of the ubiquitin–proteasome pathway resulted from the finding that the breakdown of intracellular proteins was ATP-dependent, which was surprising because the peptide bond cleavage *per se* does not require energy. Biochemical dissection of this pathway in the early 1980s revealed that it consists of two ATP-dependent processes: the conjugation of a small protein ubiquitin to proteins that marks them for degradation, and the hydrolysis of ubiquitylated proteins by the very large proteolytic machine, the 26S proteasome (Figure 2), (S refers to Svedberg – the unit of time used to measure velocity at which the protein sediments in a centrifuge).

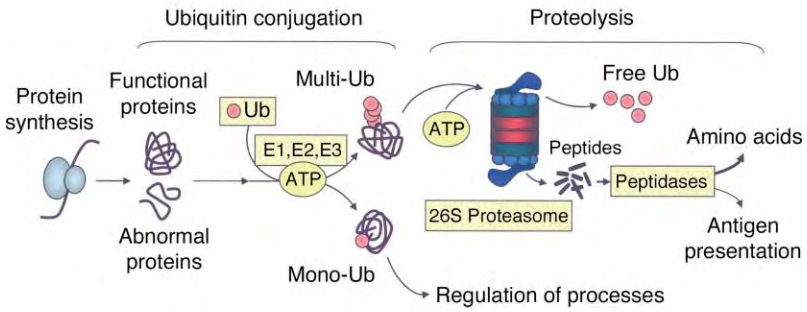

FIGURE 2 Ubiquitin–proteasome pathway for degradation of intracellular proteins. In eukaryotic cells, the site for degradation of most intracellular proteins is a large proteolytic particle, termed the 26S proteasome. Protein substrates destined for degradation by the 26S proteasome are first polyubiquitylated in ATP-dependent manner in a series of reactions involving at least three groups of enzymes (see text for details). Polyubiquitylated substrates are rapidly hydrolyzed by the 26S proteasome and monomeric ubiquitin is recycled by the action of deubiquitinating enzymes. The energy of ATP is required for ubiquitin conjugation, binding, and unfolding of a substrate and its translocation into the inner cavities of the proteasome. Most peptides produced by proteasomes are further degraded to amino acids by endo- and exopeptidases in the cytosol and nucleus, but a small fraction of peptides escapes complete hydrolysis and are utilized for MHC class I antigen presentation. Some proteins are conjugated to only a single ubiquitin molecule. This modification does not mark proteins for degradation by proteasomes but is utilized for regulation of cellular processes, such as endocytosis and transcription.

Ubiquitin Conjugation

Formation of Polyubiquitin Chains

In order to be degraded by 26S proteasomes, most intracellular proteins must be first conjugated to a chain of ubiquitin molecules. This process ensures that only selected substrates are degraded in a regulated manner and prevents the uncontrolled degradation of other cellular proteins. Ubiquitin is a 76-residue globular protein, which is present only in eukaryotic cells, and not in bacteria and archaea, where highly selective protein degradation is achieved through ATP-dependent proteolysis independent of ubiquitin. Ubiquitin conjugation to other proteins and the formation of polyubiquitin chains is mediated by the sequential action of three types of enzymes, called E1 (ubiquitin-activating enzyme), E2s (ubiquitin-conjugating enzymes or ubiquitin-carrier proteins) and E3s (ubiquitin-protein ligases). In this process, the single E1 enzyme activates ubiquitin in an ATP-dependent reaction by forming a highly reactive thiolester linkage between the C terminus of ubiquitin and the thiol group in the active site of the E1. The activated ubiquitin is then passed from the E1 to a sulfhydryl group on one of the cell's $\sim$30 E2s. Next, the activated ubiquitin molecules are linked to a lysine side chain or, in some cases, to the N-terminal amino group in the substrate protein, directly from the E2 (or in some cases after transfer of ubiquitin from the E2 to the E3). A single E2 may function with multiple E3s to provide specificity in a combinatorial fashion. Cells contain hundreds of distinct E3s. These enzymes are the main determinants of substrate specificity and are capable of recognizing a few or multiple substrates through specific degradation signals. E3s are soluble or membrane-bound proteins; some are monomeric enzymes containing distinct domains for binding a substrate and a specific E2 enzyme, while others are very complex oligomeric structures in which different subunits subserve different functions required for highly specific and efficient substrate recognition and ubiquitylation. A polyubiquitin chain is synthesized by linking new ubiquitin molecules to previously conjugated ubiquitin through its lysine residues. In most cases, proteasomal degradation requires formation of ubiquitin chain where ubiquitin molecules are linked to lysine 48, but other types of ubiquitin chains exist in cells and serve other regulatory roles distinct from proteolysis. Once conjugated to chains of four or more ubiquitins, proteins are degraded by 26S proteasomes. Ubiquitylation of certain cell surface receptors (e.g., growth factor receptors) results in their internalization and degradation in lysosomes, but not in proteasomes.

Mechanisms of Substrate Recognition

Ubiquitylation of proteins is triggered by various features of the substrates that act as signals (the so-called "degrons") that are recognized by the E3 and thus decrease the stability of the protein in the cell. These structural features can be constitutive elements in the substrate itself (e.g., a specific N-terminal amino acid residue or a short internal sequence of amino acids in a target protein) or can be acquired covalent modifications. Phosphorylation of substrates is one of the frequently employed acquired signals that regulate protein ubiquitylation. In many instances, this modification leads to direct recognition of a substrate by the specific E3, but, in some cases, phosphorylation of a substrate can inhibit ubiquitylation. Phosphorylation-dependent ubiquitylation is responsible for degradation of IκB during inflammatory response and of the various cyclins that control progression through the cell cycle. Other types of posttranslational protein modifications can either prevent or stimulate ubiquitylation, including acetylation, glycosylation, or attachment of small ubiquitin-like proteins, SUMO-1 or Nedd8. An interesting posttranslational modification that induces ubiquitylation of a substrate is hydroxylation of proline residues in the transcription factor HIF1-α, which plays an important role in transcriptional adaptation to hypoxia. Under normoxic conditions, two prolines in HIF1-α are readily hydroxylated, leading to its recognition and ubiquitylation by the specific E3. In yet another scenario for substrate recognition, association of the substrate with an adapter protein is required for its recognition and ubiquitylation by the specific E3 enzyme. This strategy is particularly exploited by some viruses. The best example is the E6/E6-AP-mediated ubiquitylation of p53. The selective degradation of unfolded proteins involves their initial recognition and binding by specific molecular chaperones and a chaperone-dependent E3, termed CHIP. For most substrates, degradation signals have not yet been defined. For example, it is unclear how cells recognize and selectively degrade abnormal proteins or normal myofibrilar proteins in skeletal muscle during muscle atrophy.

Deubiquitination

Ubiquitin conjugation to cellular proteins is a reversible process and is mediated by deubiquitinating enzymes, which are all cystein proteases. They catalyze the continuous disassembly of ubiquitin conjugates during degradation of ubiquitin-conjugated proteins by the 26S proteasome. They must play important roles in recycling monomeric ubiquitin for use in new conjugation reactions, and in preventing the accumulation of free polyubiquitin chains that could act as competitive inhibitors of the binding of ubiquitylated substrates to

the proteasome. These enzymes also probably serve as a proofreading system, which insures that no erroneous ubiquitylation of substrates takes place. Mutations in deubiquitinating enzymes can cause neuronal degeneration and may contribute to the occurrence of cancer.

Protein Degradation

The 26S Proteasome

Proteasomes are abundant evolutionarily highly conserved multimeric structures localized in the cytosol and nucleus of all eukaryotic cells. The proteasome complex responsible for degradation of ubiquitylated proteins is termed the 26S proteasome, which consists of the 20S core particle and one or two regulatory 19S particles (Figure 3).

The 20S Core Particle In eukaryotes, the 20S proteasome is a hollow cylinder and consists of four stacked rings, each containing seven homologous subunits. There are two identical outer α-rings and two identical inner β-rings (Figure 3). Three of the subunits in each inner β-ring contain the proteolytic active sites. The outer α-rings surround the narrow openings into the 20S particle at either end, through which substrates can enter into the inner proteolytic chamber. These openings are tightly regulated and protein access is enabled through the association of α-rings with different regulatory particles. This closed architecture with isolated active centers evolved to prevent the uncontrolled destruction of needed cell proteins. The proteasomal active sites in β-rings are confined to the interior of the cylinder where proteins are degraded. Each of the three active subunits has a different catalytic activity: one cleaves preferentially after basic amino acids in a protein substrate, one after large hydrophobic residues, and one after acidic residues. The active site nucleophile of the proteasome is the hydroxyl group of the threonine at the amino terminus of the β-subunit, and proteasomes thus belong to a novel mechanistic class of threonine proteases. The existence of this new type of proteolytic mechanism, not utilized by other known proteases, has enabled the synthesis of highly specific proteasome inhibitors. They are now an irreplaceable research tool and are very promising in clinical trials to treat myeloma and other cancers, and in animals have dramatic effect against diseases such as arthritis and stroke.

19S Regulatory Particle The 19S particle consists of at least 18 different subunits and associates with α-rings on one or both ends of the 20S proteasome. Two functionally different substructures of this complex have been distinguished: the base and the lid (Figure 3). The base, which touches the α-rings of the 20S core

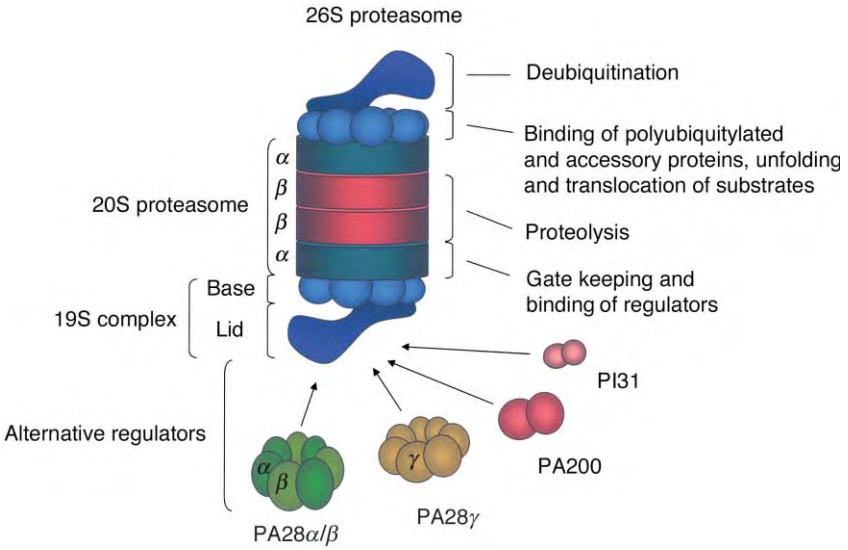

FIGURE 3 The 26S proteasome and its regulatory components. The 26S proteasome consists of the 20S core particle and one or two regulatory 19S particles. Different structures comprising the 26S proteasome carry out distinct functions (as detailed in the illustration). In addition to 19S regulators, eukaryotic 20S proteasomes can also associate with other ring-forming complexes, such as PA28α/β or PA28γ, or simpler proteins (PA200 or PI31). PA28α/β is a heptameric ring composed of α- and β-subunits. It promotes opening the channel enclosed by α-rings of 20S proteasomes. PA28γ is related to α- and β-subunits of PA28α/β and forms a homoheptameric complex that binds to 20S proteasomes and activates mainly the cleavages after charged residues in peptide substrates. It is predominantly found in the nucleus and, in some cells, is down-regulated by interferon γ. Its biological function is still not well understood. PA200 is a recently discovered 20S proteasome-interacting protein of 200 kDa that is localized in the nucleus. The mechanism of its association with proteasomes is not well understood, but like PA28, it activates only peptide hydrolysis by proteasomes. It appears to play a role in DNA repair by recruiting proteasomes to damaged DNA. PI31 is a homodimeric protein that was discovered by its ability to inhibit peptide hydrolysis by 20S proteasomes *in vitro*. Recent *in vivo* data suggest that this protein does not affect proteasome-mediated proteolysis but rather interferes with MHC class I antigen presentation by slowing maturation of immunoproteasomes.

particle, contains eight polypeptides including six ATPases that form a ring. These ATPases bind substrates and use the energy of the ATP to unfold protein substrates, open the gate in α-rings, and promote rapid translocation of substrates into the 20S core particle for degradation. The base of the 19S particle also contains surfaces responsible for transient binding of: (1) polyubiquitin chains, (2) deubiquitinating enzymes, and (3) ubiquitin-like domains of various adaptor proteins that may function in bringing ubiquitylated substrates to close proximity of proteasomes. The lid contains eight non-ATPase subunits of unknown function. This structure is required for proteolysis of ubiquitylated proteins, probably through interaction with the polyubiquitin chain.

Immunoproteasome and Hybrid Proteasome

In higher vertebrates that have an immune system, a small fraction of peptides generated by proteasomes is not completely degraded to free amino acids but instead transported into the ER, where they associate with specific membrane-bound MHC class I molecules and are subsequently transported to the cell surface. The immune system is continually surveying the surface of all cells for non-native peptides originating from viral or mutated proteins. If cells carrying such non-native peptides are encountered, they are rapidly destroyed by cytotoxic T-lymphocytes. Proteasomes found in most of the tissues (the so-called constitutive proteasomes) contribute to the generation of basal levels of antigenic peptides in the absence of infection. However, during inflammation, two additional types of proteasomes appear to play a major role in enhancing MHC class I antigen presentation and are termed immunoproteasomes and hybrid proteasomes. They are normally found in lymphoid tissues (e.g., spleen and thymus), but are induced in other tissues during infection in response to the cytokine interferon γ. Immunoproteasomes are formed by replacement of all three catalytic β-type subunits in constitutive proteasomes with alternative proteolytically active β-subunits. The alternative immunosubunits possess qualitatively different cleavage specificities than constitutive β-subunits and appear to play a major role in increasing the supply of appropriate peptides for MHC class I antigen presentation. Hybrid proteasomes are formed when 20S immunoproteasomes are capped on one side with the 19S particle and on the other side with an alternative protein complex, called PA28α/β (Figure 3). Most probably, in these hybrid particles, ubiquitylated substrates initially bind to the 19S regulator and peptide products are released at the opposite side through the PA28α/β that apparently promotes opening the channel enclosed by α-rings and allows generation of peptide fragments particularly suitable for MHC class I antigen presentation during inflammation.

Mechanism of Protein Degradation

Although the exact sequence of events in which proteins are degraded by 26S proteasomes is not fully understood, a rough outline of steps can be provided. Upon binding of the polyubiquitylated substrate by the proteasome, the substrate is first unfolded in an energy-dependent manner by the action of ATPases localized in the base of the 19S particle. Recent data suggest that proteins are unfolded prior to their translocation into the proteasome's inner cavity. Conformational changes induced by hydrolysis of ATP promote opening the gate in α-rings followed by translocation of the unfolded substrate into the inner chambers of the proteasome. Successful translocation of the substrate must follow disassembly of polyubiquitin chain by deubiquitinating enzymes attached to the 19S particle. Translocation can occur from its free amino or carboxyl terminus, depending on the substrate, or even internally by the process in which a polypeptide loop enters the axial channel to permit initial endoproteolytic cleavage. In some cases, proteasomes degrade substrates only partially, yielding biologically active protein fragments, like in the generation of the p50 subunit of the transcription factor NFκB from the larger precursor and in the processing and activation of some membrane-bound transcription factors. Once in the central chamber of the 20S particle, the substrate is cleaved by six catalytic subunits into small peptides ranging from 3 to 25 residues in length. Unlike traditional proteases, the proteasome does not simply cleave a protein and release the partially digested fragments; on the contrary, a protein substrate, once bound by the proteasome, is cut until small peptides are generated. This behavior ensures that partially digested proteins do not accumulate within cells. The product release may be facilitated in some cells by PA28α/β, as well as by hydrophobic products themselves which can trigger gate opening in α-rings. In eukaryotic cells, the products generated by proteasomes appear to be hydrolyzed into amino acids by the sequential actions of endopeptidases and aminopeptidases. The whole process of degradation of one molecule of the protein substrate requires several hundred molecules of ATP and is completed in a matter of seconds or minutes, depending on the size of a substrate. Generally, subtrates must be first ubiquitylated in order to be degraded by proteasomes. However, 26S proteasomes can degrade certain substrates *in vivo* (e.g., ornithin decarboxylase associated with cofactor antizyme) and many polypeptides *in vitro* (e.g., denatured casein, aged calmodulin) in ubiquitin-independent manner. It still remains uncertain whether *in vivo*

TABLE I

Disturbances of Ubiquitin-Dependent Proteolysis in Human Disease

Protein substrate	Disease	Mechanism
Increased proteolysis		
p53	Cervical carcinoma	E6/E6-AP-mediated degradation of p53
$p27^{Kip1}$	Colorectal/breast Ca.	Enhanced degradation of a cell cycle inhibitor
IκB	Inflammation	Activation of NFκB transcription factor
CFTR	Cystic fibrosis	Point mutation in CFTR, misfolding and degradation through ERAD
MHC class I heavy chain	Cytomegalovirus infection	Down-regulation of MHC class I by viral proteins
Most muscle proteins	Muscle atrophy, cachexia	Up-regulation of an SCF E3, Atrogin-1, and the RING finger E3, MurF-1
Decreased proteolysis		
HIF1-α	von Hippel–Lindau disease	Mutation in SCF E3, VHL
ENaC	Liddle syndrome	Mutation in HECT E3, NEDD4
Receptor tyrosine kinases	Cancer	Mutation in RING finger E3, c-Cbl
α-synuclein, unknown	Parkinson disease	Mutation in RING finger E3, Parkin
Unknown	Angelman syndrome	Mutation in HECT E3, E6-AP
α1-antitrypsin	Liver disease in some α1-antitrypsin deficient patients	Decreased degradation of mutated α1-antitrypsin by ERAD pathway
Epstein–Barr virus nuclear antigen 1 (EBNA1)	Epstein–Barr virus-associated malignancies	Immune evasion due to lack of EBNA1 degradation

there are more proteins that are degraded in ubiquitin-independent manner.

Endoplasmic Reticulum-Associated Degradation (ERAD)

Many newly synthesized proteins are translocated into the lumen of the ER or are inserted into the ER-membrane. They may remain in the ER or be exported into other organelles, or the cell surface membrane or be secreted into the extracellular space. The ER contains an abundant set of chaperones and enzymes that assist newly synthesized proteins in attaining their correct conformation and activity, but sometimes, this maturation process fails and misfolded proteins are generated. Such abnormal proteins are effectively removed so as not to aggregate and form potentially toxic inclusions and the process of their disposal is often called ER-associated degradation (ERAD). In this process, misfolded proteins are retrotranslocated from the ER back into the cytosol, where they are ubiquitylated and degraded by 26S proteasomes. This export is necessary because the ER does not contain proteolytic enzymes necessary for protein degradation. ERAD is used by some viruses to down-regulate MHC class I molecules in the ER (e.g., cytomegalovirus) as a means of viral evasion of the immune system. In addition, disturbances in ERAD pathway can cause serious human disease, such as cystic fibrosis or a form of α1-antitrypsin deficiency (Table I).

Proteolysis in Mitochondria

As in the cytosol and nucleus, proteins in mitochondria also have different half-lives and mitochondria can selectively degrade abnormal proteins. Although mitochondria as a whole can be degraded in lysosomes by autophagy, this process is nonselective and cannot account for different turnover rates of regulatory mitochondrial proteins. Since the matrix and the inner membrane of mitochondria are not accessible to cytosolic proteases, these sites harbor their own autonomous proteolytic system, which consists of several evolutionarily conserved ATP-dependent proteases. This system has dual functions; it mediates complete degradation of nonassembled or misfolded proteins, and it enables selective proteolysis of specific normal regulatory proteins that are important for the maintenance of mitochondrial functions. The matrix of mammalian mitochondria contains two kinds of soluble proteases that are homologous to eubacterial Lon and ClpXP proteases and responsible for degradation of matrix proteins. The mitochondrial inner membrane of all eukaryotic cells has two proteases that belong to the AAA superfamily of ATPases, termed *i*-AAA

(*i*, intermembrane) and *m*-AAA (*m*, matrix). These enzymes are complex structures with a native molecular mass of ~1 MDa composed of smaller subunits of 70–80 kDa. They expose their catalytic sites toward either the matrix or intermembrane space and have chaperone-like activity that is required for protein unfolding and subsequent degradation at proteolytic sites. Substrates of these proteases are proteins located in the inner membrane, and their degradation is essential for the maintenance of oxidative phosphorylation. Impaired function of these proteases causes neurodegeneration in humans and severe growth defects in yeast.

Proteolysis in Bacteria and Archaea

Roles of Proteolysis in Bacteria

Although bacteria and archaea do not have lysosomes, ubiquitin, or 26S proteasomes, they carry out very selective and highly regulated degradation of intracellular proteins. These prokaryotes contain several distinct ATP-dependent proteases that mediate initial steps in degradation of proteins in their cytoplasm. These enzymes serve functions similar to those in eukaryotic cells. Bacteria selectively destroy abnormal proteins, including those arising from mutations, gene fusions, misfolding, chemical damage, or genetic engineering. In fact, successful expression of many recombinant proteins in *Escherichia coli* (*E. coli*) has been hampered by the action of these enzymes, and several bacterial strains defective in some of these proteases have been developed to increase the stability of cloned foreign proteins. Exposure to harsh environmental conditions, such as high temperature (heat shock), induces the genes which encode several molecular chaperones and ATP-dependent proteases to refold or degrade unfolded proteins that may be generated and protect against the buildup of these potentially toxic polypeptides. During normal exponential growth, most normal bacterial proteins are quite stable entities. However, even during normal growth, certain polypeptides with major regulatory functions are degraded very rapidly. For example, the specific component of bacterial RNA polymerase, so-called sigma factor σ^{32}, has a half-life of 1–2 min in *E. coli* under normal conditions, but it becomes transiently stabilized during heat shock, when it mediates the heat shock response. A general enhancement of protein breakdown occurs in nongrowing cells deprived of nutrients in order to provide the starving organism with a source of amino acids for new protein synthesis or energy production. In many gram-positive bacteria, prolonged starvation triggers sporulation, which is also accompanied by the marked degradation of most normal cellular proteins to provide amino acids for the expression of spore-specific genes.

Bacterial ATP-Dependent Proteases

Many eubacterial and archaeal ATP-dependent proteases are ancestors of more complex eukaryotic enzymes. Archaea, for example, contain proteasomes that have similar architecture as eukaryotic 20S proteasomes, but are built only from single α- and β-subunits and function in protein breakdown in association with the ATPase PAN. This hexameric-ring structure is homologous to the six ATPases found in the 19S base of the eukaryotic proteasome and has the capacity to unfold globular proteins and promote their entry into the 20S particle. The major ATP-dependent proteases in eubacteria are the cytoplasmic serine proteases La/Lon, "caseinolytic serine proteases" ClpAP and ClpXP, the cytoplasmic threonine protease HslUV, and the inner membrane zinc-metalloprotease FtsH. The proteases La/Lon and caseinolytic proteases have their homologues in eukaryotic mitochondria. Bacterial ATP-dependent proteases are multimeric enzymes (400–700 kDa) that have distinct substrate specificities and subunit composition. They are composed of proteolytic domains and regulatory ATPase domains, which actually determine substrate specificities. The simpler proteases, La/Lon and FtsH, contain these two domains in a single polypeptide chain. Lon consists of four or eight identical 87 kDa protein subunits and was the first ATP-dependent protease described. Other proteases that are structurally related to the eukaryotic 20S proteasomes (such as HslUV and ClpAP) contain these domains in two separate structures. For example, the HslUV contains a central proteolytic chamber (HslV) composed of two hexameric rings with the active sites facing inward. Two ring-forming HslU complexes have ATPase activity and associate with proteolytic HslV cylinders on both ends to form a four-ring 20S proteasome-like particle capable of binding, unfolding, and degrading bacterial proteins. Besides proteases, the degradation of many proteins *in vivo* also requires chaperones of the Hsp70 and chaperonin (GroEL) families as cofactors that act in the recognition of unfolded substrates. ATP-dependent proteases generate short peptides of 10–40 amino acids, and they are degraded to amino acids by energy-independent peptidases.

Selection of Substrates

Bacteria lack ubiquitin and any homologous mechanism for covalent modification of substrates destined for proteolysis. The ATPase-ring components (e.g., HslU, ClpA or ClpX) of bacterial proteases determine the substrate specificity. With some exceptions, the exact recognition motifs on bacterial proteins are not well defined. However, special sequences on the N and C

termini of cell proteins have been identified that lead to recognition by ClpXP and may become particularly important in conditions when overall protein degradation is accelerated. All bacteria selectively degrade prematurely terminated proteins. A specific tRNA incorporates the tagging peptide SsrA (11-residue stretch of amino acids) into nascent polypeptide chain if ribosomes are stalled. The presence of an SsrA tag at the C terminus of a protein leads to its rapid hydrolysis by ClpXP and FtsH proteases. In addition to this recognition motif, in the case of multiprotein complexes, some proteins become substrates if present in cells without their natural binding partners because the motifs that are recognized may be more accessible. Finally, chaperones may also provide some assistance in increasing susceptibility of substrates to bacterial proteases.

Targeting Proteolysis for Drug Development

Although a number of lysosomal diseases are known, the major ones are not due to defects in lysosomal proteases but rather to failure to degrade polysaccharides or lipids due to lack of a specific lysosomal hydrolase. Commonly, these diseases are called lysosomal storage diseases because undegraded material progressively accumulates in lysosomes. One component of the endocytic–lysosomal pathway, the autophagy, has been reported to be disturbed in some malignancies, neurodegenerative, and cardiovascular disease; however, it is unknown if the impaired breakdown of a specific protein(s) is part of the underlying pathophysiological mechanism, or a secondary consequence. However, a number of major malignant, neurological, metabolic, and viral diseases are caused by the gain or loss of function of the ubiquitin–proteasome proteolytic system (Table I). Since the disturbances in the ubiquitin–proteasome system underlie the pathogenesis of many human diseases, drugs that target this system are being developed. The proteasome inhibitors are the first so far to be tested in animal models and are now in clinical trials for treatment of neoplastic disease. However, proteasome inhibition is not a very specific strategy to modulate stability of a specific protein and more selective approaches should prove to be more effective and have fewer side effects. A typical approach would be to develop small molecule inhibitors to target events upstream of proteasomes (e.g., ubiquitin ligation and substrate recognition).

See Also the Following Articles

Autophagy in Fungi and Mammals • Chaperones, Molecular • Endocytosis • Endoplasmic Reticulum-Associated Protein Degradation • N-End Rule • Proteasomes, Overview • 26S Proteasome, Structure and Function • Ubiquitin System • Ubiquitin-Like Proteins • Unfolded Protein Responses

Glossary

AAA ATPase (ATPases Associated with diverse cellular Activities) A distinct family of ATPases characterized by the presence of highly conserved domains in their primary sequence, hexameric structure, and protein unfolding activity.

ATPase Type of enzyme that hydrolyzes ATP and uses the energy released to drive biological processes such as pumping ions, unfolding proteins, and moving molecules.

folding A process in which newly synthesized polypeptides attain their native three-dimensional structures.

molecular chaperones Specialized proteins, many being ATPases, that prevent protein aggregation and may function to facilitate proteins attaining their native conformations; some can promote protein unfolding and solubilization of aggregated proteins.

Further Reading

Bryant, P. W., Lennon-Dumenil, A. M., Fiebiger, E., Lagaudriere-Gesbert, C., and Ploegh, H. L. (2002). Proteolysis and antigen presentation by MHC class II molecules. *Adv. Immunol.* **80**, 71–114.

Cuervo, A. M., and Dice, J. F. (1998). Lysosomes, a meeting point of proteins, chaperones, and proteases. *J. Molecul. Med.* **76**, 6–12.

Glickman, M. H., and Ciechanover, A. (2002). The ubiquitin–proteasome proteolytic pathway: Destruction for the sake of construction. *Physiol. Rev.* **82**, 373–428.

Goldberg, A. L., Cascio, P., Saric, T., and Rock, K. (2002). The importance of the proteasome and subsequent proteolytic steps in the generation of antigenic peptides. *Molecul. Immunol.* **39**, 147–164.

Gottesman, S. (1996). Proteases and their targets in *Escherichia coli*. *Annu. Rev. Genet.* **30**, 465–506.

Käser, M., and Langer, T. (2000). Protein degradation in mitochondria. *Semin. Cell Develop. Biol.* **11**, 181–190.

Kisselev, A. F., and Goldberg, A. L. (2001). Proteasome inhibitors: From research tools to drug candidates. *Chem. Biol.* **8**, 739–758.

Ogura, T., and Wilkinson, A. J. (2001). AAA + superfamily ATPases: Common structure–diverse function. *Genes Cells* **6**, 575–597.

Turk, V., Turk, B., and Turk, D. (2001). Lysosomal cysteine proteases: Facts and opportunities. *EMBO J.* **20**, 4629–4633.

Biography

Tomo Šarić is currently a Senior Scientist at the Institute for Neurophysiology, University of Cologne, Germany. His principal research interest is in intracellular proteolysis, especially in proteases acting downstream of proteasomes and their role in regulating immune responses. He holds an M.D. and a Ph.D. from the University of Zagreb in Croatia and received his postdoctoral training at the University of Texas and Harvard Medical School.

Alfred L. Goldberg is Professor of Cell Biology at Harvard Medical School in Boston. His principal research interests are in the field of protein degradation. His laboratory has contributed to many major discoveries in this field, such as the discovery of the ATP requirement for degradation of most intracellular proteins, discovery of the first ATP-dependent proteases in bacteria and proteasomes in eukaryotic cells, introduction of proteasome inhibitors and the role of the proteasome in antigen presentation, and muscle atrophy.

Protein Folding and Assembly

David P. Goldenberg
University of Utah, Salt Lake City, Utah, USA

In order to carry out their biological functions, most polypeptide chains must fold into stable three-dimensional (3D) structures, for it is the precise spatial distribution of chemical groups within a protein that gives the molecule its ability to interact specifically with other molecules and, in the case of an enzyme, catalyze a chemical reaction. In many cases, individual polypeptide chains must also assemble into larger structures containing additional proteins or nucleic acids. The folding of many proteins is reversible, so that the native structure can be disrupted by a change in temperature or addition of a chemical denaturant, and the unfolded protein can then be induced to refold and assemble by returning it to physiological conditions. Experiments of this type demonstrate that the information specifying the native structure of a protein resides in its amino acid sequence, and *in vitro* studies have provided important insights about the energetic factors that drive folding and assembly and the kinetic mechanisms of these processes. Folding *in vivo* is often facilitated by transient interactions with other proteins, molecular chaperones. Folding may also compete with the formation of aberrant aggregates *in vivo*, sometimes leading to pathological conditions such as amyloid diseases.

Thermodynamics of Protein Folding

The thermodynamic stability of a protein is defined by the equilibrium between the native folded form and the highly disordered unfolded state that is induced by elevated temperatures or chemical denaturants, such as urea or guanidinium chloride (GuHCl). Relatively small monomeric proteins, composed of 50–150 amino acid residues, typically unfold and refold efficiently and cooperatively, so that the process can be described as a simple equilibrium:

$$N \rightleftharpoons U$$

where N and U represent the native and unfolded states (Figure 1). While the native state usually has a well-defined 3D structure, the unfolded state is best thought of as a broad distribution of rapidly interconverting conformations.

Under physiological conditions, the change in free energy for unfolding (ΔG_u) for a small monomeric protein typically lies in the range of 5–15 kcal mol^{-1}. This relatively small preference for the native protein reflects a delicate balance between three major factors: (1) A large loss of entropy as the chain is converted from a highly disordered state to an ordered state, (2) the transfer of nonpolar groups from an aqueous environment to a nonpolar environment in the protein interior, and (3) the formation of stabilizing interactions within the protein, including hydrogen bonds, salt bridges, and van der Waals interactions.

During the 1980s and 1990s, a great deal of effort was devoted to measuring the stabilities of genetically modified proteins in which single amino acid residues were replaced so as to delete one or a few stabilizing interactions. Taken together, these studies revealed that proteins are surprisingly tolerant of amino acid replacements, so that most mutations destabilize the native state by only a few kcal mol^{-1}, and substitutions that completely prevent folding are quite rare. Substitutions that remove hydrogen bonds or nonpolar interactions cause, on an average, roughly similar degrees of destabilization (usually of the order of 1–3 kcal mol^{-1}), implying that both types of interactions play important roles in stabilizing native proteins.

Folding Kinetics and Mechanisms

Levinthal's Paradox

Much of the work on folding mechanisms, both experimental and theoretical, has been motivated by the realization that the number of possible conformations accessible to a polypeptide chain is so immense that random sampling to find the structure with minimum free energy would take a ridiculously long time. For instance, if a chain is composed of 100 residues, and each residue can take on ten possible conformations, then the total number of conformations is 10^{100}. If the various conformations are randomly sampled at a rate of 10^{13} s^{-1} (approximately the rate of rotation for a covalent bond), then the total time

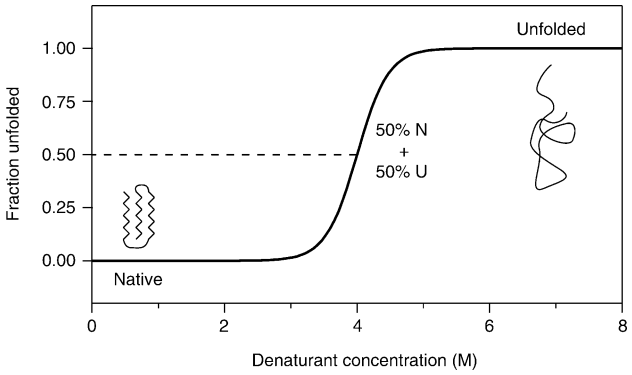

FIGURE 1 A cooperative protein unfolding–refolding transition. In a typical experiment, the native protein is incubated in solutions with increasing concentrations of denaturant such as urea or guanidinium chloride, and the fraction of unfolded molecules is determined by monitoring a spectroscopic signal, such as UV absorbance, fluorescence, or circular dichroism. For small monomeric proteins, the transition is usually highly cooperative, so that only the fully folded and unfolded forms are significantly populated and the fraction unfolded represents the relative concentrations of the two forms.

required to sample all of the conformations would be $\sim 10^{80}$ years!

The calculation outlined above is frequently identified as the "Levinthal Paradox," in recognition of an insightful 1969 paper by Cyrus Levinthal. Although this argument undoubtedly represents a great oversimplification, since many of the conformations assumed to be accessible to the chain will, in fact, be excluded by steric clashes among atoms in different residues, the calculation suggests that there must be some mechanism by which the search for the native conformation is limited.

Folding and Unfolding Rates

The rates at which different proteins fold and unfold vary tremendously. Even considering only relatively small proteins composed of a single domain, experimentally determined folding rate constants cover at least the range from 0.1 to $10^5\ s^{-1}$. While it might be expected that smaller and thermodynamically more stable proteins would fold the fastest, folding rates for unrelated proteins are poorly correlated with size or stability. Instead, a major determinant of folding rate appears to be the topological complexity of the native structure. While true topological knots are rarely found in folded proteins, different structures vary with respect to the relative prevalence of interactions formed between closely and distantly spaced residues, and faster folding in often associated with topologies in which short-range interactions are more prominent. The physical basis for this correlation is not yet fully understood, but it strongly suggests that the rate-determining step in folding is associated with formation of the correct topology, as opposed, for instance, to formation of a local structure that then nucleates rapid folding of the rest of the chain.

Unfolding rates also vary greatly among different proteins and under different solution conditions. For some proteins, unfolding may be a surprisingly common event, even under physiological conditions. For instance, if the stability of a protein, ΔG_u, is 5 kcal mol^{-1} at 25°C, and the folding rate is $10^3\ s^{-1}$, the unfolding rate is predicted to be about $0.5\ s^{-1}$, so that 99% of the molecules in a population will undergo an unfolding event over a period of 10 s. Since unfolded proteins are typically much more sensitive to proteolysis than folded proteins, spontaneous unfolding may be an important factor in determining the rate of protein turnover *in vivo*. Transient unfolding may also contribute to formation of aberrant structures, such as the amyloid fibers described below.

Folding Intermediates

Following the tradition of biochemists who have successfully dissected other processes by identifying and characterizing discrete intermediates, many investigators have studied kinetic intermediates that accumulate transiently before protein-folding reactions reach equilibrium. While there is considerable diversity in the intermediates observed in the folding of different proteins, there appear to be common features among many of them.

Generally, the most easily detected intermediates form very rapidly (on the ms timescale or faster) after the unfolded protein is transferred to conditions that favor the native state. Often, the intermediate appears to contain ordered secondary structure, especially α-helices, but there is little evidence of well-defined interactions between the side chains from different segments of the chain. The average dimensions of the chain in these intermediates typically lie between those of the native protein and the fully unfolded state in denaturants. Kinetic intermediates of this type also resemble partially unfolded states that can sometimes be generated under special solution conditions, including low pH for some proteins, or when a ligand (such as a metal ion or heme group) is removed from a native protein. These states, typically characterized by the presence of regular secondary structure but the absence of stable tertiary interactions, are described as "molten globules."

Because the most frequently observed partially folded states often interconvert rapidly with the fully unfolded protein, establishing whether or not these species are actually productive intermediates in folding, as opposed to products of side reactions, is quite difficult. As a consequence, there is presently a great deal of uncertainty and disagreement about the significance of these states for understanding folding mechanisms. Some authors believe that the formation of intermediates

is important for limiting the search for the native conformation, while others argue that they are simply compact forms of the denatured state and do not play any special role in directing the chain towards the native state.

Transition States

It might seem surprising that the concept of a transition state, derived from studies of simple chemical reactions, could be usefully applied to a process as complex as protein folding. However, the folding kinetics of many proteins can be well-described by a simple model in which the rate is determined by an equilibrium between the unfolded state and a higher energy state that is rapidly converted to the native conformation (Figure 2). The transition state can be envisioned as an ensemble of partially ordered conformations that collectively have an equal probability of being converted to either the native or fully unfolded states.

By their very nature, transition states cannot be characterized directly by spectroscopic or other physical methods. Instead, their properties must be inferred from the results of experiments in which the kinetics of folding and unfolding are compared after perturbing either the structure of the protein or its environment. For instance, replacing an amino acid residue that contributes to the stability of the transition state is expected to increase the free energy barrier for folding and, thereby, decrease the folding rate. On the other hand, a substitution that weakens an interaction that is present in the native protein but not the transition state is expected to increase the unfolding rate, without affecting the folding kinetics.

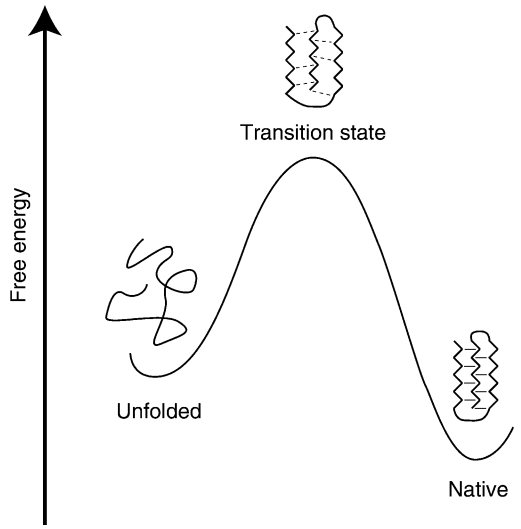

FIGURE 2 Hypothetical energy profile for a protein folding reaction. Currently available data, especially from mutational analyses of folding kinetics, suggest that the transition state for folding and unfolding is an ensemble of conformations that possess much of the topology of the native protein, but in which many of the native interactions are missing or weakened. The transition state ensemble is poised to fold completely or unfold rapidly.

Detailed mutational analyses of transition states have now been carried out for several proteins. In general, it has been found that substitutions that destabilize the native protein most often increase the unfolding rate more than they decrease the folding rate, suggesting that most interactions that are present in the native protein are significantly weakened in the transition state. Also, the relatively few residues that appear to play specific roles in stabilizing the transition state are often separated in the amino acid sequence but lie relatively close together in the native protein. These patterns suggest that the transition state ensemble may have a topology similar to that of the native protein, but not the network of cooperative interactions found in the fully folded structure (Figure 2). Poised with the correct topology, the molecules in the transition state can rapidly form these interactions, but can also unfold rapidly.

Collectively, studies of folding intermediates and transition states over the past decade generally support a view of folding in which there is considerable breadth in the distribution of conformations representing different stages of the process, a view that has also emerged from computational simulations of folding. The conformational heterogeneity of these states makes detailed structural analysis very difficult, and there is much about folding mechanisms that still remains hidden from experimental view. More detailed descriptions of folding can in principle be derived from computational simulations, and the rapidly increasing power of computers and the development of new algorithms is now making it possible to carry out detailed molecular dynamics simulations of folding reactions. The past several years have seen much more extensive collaborations between experimentalists and computational scientists working on protein folding, and this development is already leading to important new insights into both the details of specific folding reactions and the general principles of the process.

More Complex Folding Reactions

Although the great majority of protein-folding experiments and simulations have been carried out with small monomeric proteins, most proteins found in nature are larger and more complex structures. Most polypeptides form multiple domains when they fold, and many assemble into structures composed of multiple subunits. In addition, some proteins are stabilized by disulfide bonds, which are formed during the folding process, and others contain tightly bound ligands such as metal ions, heme groups, or cofactors required for enzyme activity.

Proteins with Multiple Domains

Early in the study of protein structure, it was recognized that most proteins composed of more than 100–200 amino acid residues are typically organized into domains in which segments of 50–150 residues are folded into compact structures that are relatively independent of one another. Although a precise definition of a domain is somewhat elusive, the organization of a protein into substructures is often quite apparent from inspection of the 3D structure or by computer analysis (Figure 3). Experimentally, domains can often be defined by limited treatment with a protease, since the polypeptide segments separating domains are usually much more sensitive to digestion than the regions within domains. The functions of larger proteins are often divided among their substituent domains, with different domains typically interacting with different molecules. It is clear from comparisons of protein structures and sequences that the same domains have frequently been exchanged among different proteins by genetic recombination, and the domain architecture of a protein can often be deduced by comparison of its sequence with those of known domains.

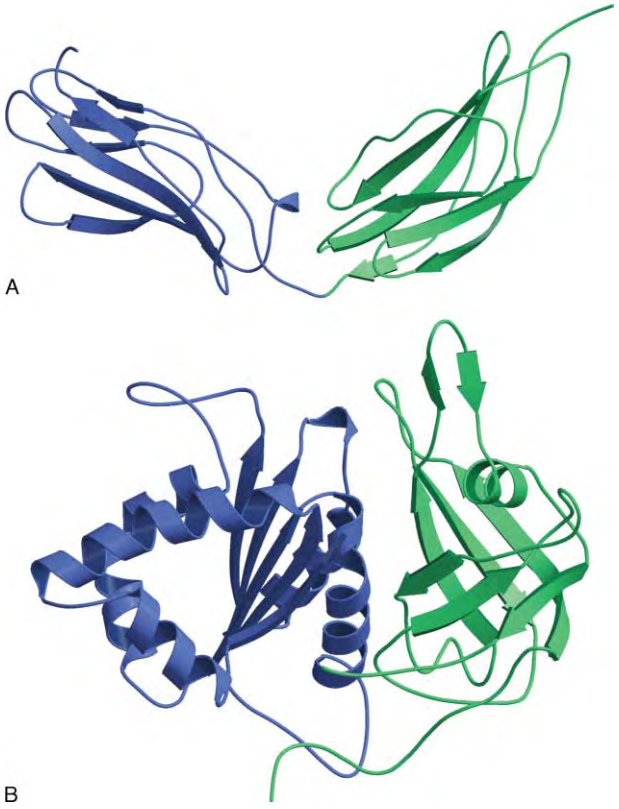

FIGURE 3 Domain structures of two proteins. In each drawing, the domains are distinguished by color. (A) Two domains of a cellular adhesion molecule, neuroglian from *Drosophila melanogaster*. The intact protein contains nine other domains, three of which are similar to the two shown here, which are members of the fibronectin III domain family. Drawn from the atomic coordinates of entry 1CFB in the Protein Data Bank (Huber, A. H., Wang, Y. M., Bieber, A. J., and Bjorkman, P. J. (1994). Crystal structure of tandem type III fibronectin domains from *Drosophila* neuroglian at 2.0Å. *Neuron* **12**, 717–731). (B) Ferrodoxin reductase from spinach chloroplasts. In this structure, the two domains do not resemble one another and interact much more extensively than the two fibronectin domains shown in (A). Drawn from the atomic coordinates of entry 1FNB in the Protein Data Bank (Bruns, C. M., and Karplus, P. A. (1995). Refined crystal structure of spinach ferredoxin reductase at 1.7Å resolution: Oxidized, reduced and 2′-phospho-5′-AMP bound states. *J. Mol. Biol.* 247, 125–145). The drawings in Figures 3 and 4 were made with the computer programs MOLSCRIPT and Raster3d.

When isolated from the rest of the protein, individual domains typically retain their native conformations and undergo cooperative unfolding transitions similar to those observed with smaller proteins. Furthermore, when the intact protein unfolds, the resulting spectroscopic signals often resemble a simple superposition of those for the isolated domains. In these cases, the domains appear to be truly independent, and studying their folding individually probably provides a good description of the folding mechanism for the intact protein. In other cases, however, the domains may interact more intimately, so that the entire structure unfolds cooperatively. The folding mechanism may also involve interactions among the domains before their individual structures are fully defined.

Disulfide-Coupled Folding

Many proteins, especially among those that function extracellularly, are stabilized by disulfide bonds, covalent bonds between the sulfur atoms of cysteine (Cys) residues that are formed by oxidation of the Cys thiol groups. *In vivo*, disulfide bonds are formed after the polypeptide is synthesized and translocated to either the endoplasmic reticulum in eukaryotes, or the periplasmic space in bacteria. In both types of cells, disulfides in the newly synthesized proteins are formed by exchange with disulfides present in special proteins that act as catalysts of the process.

In a landmark series of experiments in the early 1960s, C. B. Anfinsen and his colleagues demonstrated that the four disulfide bonds of bovine ribonuclease A could be induced to reform spontaneously *in vitro* after the protein had been fully reduced and unfolded in urea. The regeneration of active enzyme, even after the covalent constraints on the polypeptide chain had been broken, provided a vivid demonstration that the 3D structure was encoded by the amino acid sequence.

When refolding of a reduced protein is initiated, disulfides typically form quite randomly, leading to a distribution of molecules with different disulfide bonds that can rapidly interconvert. The formation of an initial disulfide, however, can often favor conformations that then bring other Cys residues together to form a second disulfide. These conformations can also be stabilized by

noncovalent interactions, leading to a high degree of cooperativity among the various interactions.

As more of the 3D structure forms and is stabilized by additional disulfides, the ability of the molecule to undergo additional disulfide formation and rearrangement steps can become severely constrained, leading to the accumulation of species that contain most or all of the native structure but lack one or more disulfides. *In vivo*, disulfide isomerase enzymes can catalyze the slow rearrangements necessary to convert the trapped molecules to the native form, or may promote alternative pathways that avoid the kinetic traps.

Ligand Binding

Yet another way in which folding can be influenced is through the binding of ligands such as metal ions or prosthetic groups. In most cases, ligands have little tendency to interact with unfolded proteins, so that the molecule must be at least partially folded before the interaction takes place. A thermodynamic consequence of this is that the stability of the folded protein is enhanced by the presence of ligand and depends on both the affinity of the interaction and the concentration of free ligand in solution. If the binding site is formed only when the protein is fully folded, binding may not greatly alter the folding process either *in vitro* or *in vivo*. On the other hand, interactions of ligands with partially folded species could favor some pathways over others and might prevent aberrant interactions with other molecules.

Proteins that require the binding of reactive metal ions such as those of iron, copper, or nickel present a particularly interesting problem during folding *in vivo*. Because these ions are highly toxic, their free concentrations are maintained at very low levels by transport and storage proteins that bind tightly to them. The ions must then be transferred to other proteins for which they are required for activity, such as catalysis. Although the details are not yet well-understood, it appears that quite elaborate systems involving multiple transfer proteins have evolved to facilitate the safe transfer of ions to their proper sites.

Some prosthetic groups, such as the heme group of cytochrome *c*, are covalently bonded to the polypeptide chain. For these proteins, the covalent modifications, and the enzymes that catalyze them, are likely to be intimately involved in the folding process.

Molecular Chaperones

While many proteins refold spontaneously and efficiently *in vitro*, it is now known that folding *in vivo* is often facilitated by molecular chaperones, proteins that interact transiently with the polypeptide chain and either promote folding or decrease the likelihood of nonproductive interactions. The best-characterized molecular chaperones include members of the GroEL/-GroES and HSP70 families. Members of both groups utilize the energy of ATP hydrolysis to couple conformational changes in the chaperone to a cycle of substrate protein binding and release, during which the substrate folds to its native conformation. Other examples of molecular chaperones include the catalysts of disulfide formation and exchange and the metal chaperones mentioned above. Although the chaperones can increase the efficiency of folding, it does not appear that they influence the final structure. Their discovery, therefore, has not required a revision of the fundamental idea that the folded structure of a protein is determined by the amino acid sequence. But, we now have a much greater appreciation of protein folding as a biological process that is intimately coupled to numerous other intracellular events.

Assembly of Oligomeric Proteins

Only a minority, perhaps 20%, of proteins contain a single polypeptide chain, the remainder being assemblies of multiple subunits. Dimeric and tetrameric complexes are the most common, but assemblies of 20–50 subunits are also known. The assembly of subunits into larger complexes can offer a variety of functional advantages, including mechanisms for regulating the activities of enzymes, the creation of novel binding sites at subunit interfaces and the coordination of multiple related functions in a single complex.

Multimeric proteins can be assembled from a single type of subunit, resulting in a homo-oligomer, or they can be hetero-oligomers composed of two or more different kinds of chains. Quite often, these structures are highly symmetrical. Dimers of identical polypeptide chains are especially common, and dimers are often the basic units of higher order structures, such as tetramers, hexamers, etc.

The types of interactions that hold the subunits of oligomers together are essentially the same as those found within monomeric proteins or the individual subunits themselves, including hydrogen bonds, ionic and van der Waals interactions. However, surveys of the distribution of different interaction types in various protein environments have revealed some differences between those found between and within subunits, with ionic interactions being more common in the interfaces between subunits.

Many oligomeric proteins have been successfully refolded and assembled *in vitro* after being unfolded in denaturants, though the reactions are often slower and less efficient than the folding of small monomeric proteins. In some cases, the rate of refolding is dependent on protein concentration, indicating that the rate is determined by intermolecular association

reactions. In other cases, the reaction kinetics are limited by intramolecular rearrangements that occur either before or after subunit association.

These differences in kinetic behavior suggest that oligomeric structures may form by a variety of mechanisms. In order to assure specificity, the initial interactions between two subunits presumably requires that one or both of them first takes on at least a partially folded conformation. In some cases, the interaction may only occur after the subunits are fully folded, so that folding and assembly are distinct processes. This mechanism requires that the individual subunits have compact self-contained structures similar to those of monomeric proteins, as epitomized by the four subunits of hemoglobin (Figure 4A). For some oligomers, however, the subunits form extensive interactions with one another along extensive interfaces that make it unlikely that the individual subunits could fold completely before assembling. In extreme cases, the subunits are actually wrapped around one another, as observed in the structure of the tailspike protein of bacteriophage P22 (Figure 4B). These more complex arrangements of subunits likely lend the structures a great deal of kinetic stability, but possibly at the cost of more complex folding mechanisms involving unstable intermediates that may be prone to aberrant misfolding or aggregation reactions.

Protein subunits can also form complexes with either RNA or DNA, as in ribosomes or the nucleosomes of eukaryotic chromatin. These interactions are often mediated by electrostatic interactions between Arg or Lys residues of the proteins and the negatively charged phosphate groups of the nucleic acids, but nonpolar interactions can also play a role. Just as protein subunits can associate with one another either before or after being fully folded, the formation of protein–nucleic acid complexes may involve folding processes that take place after association as well as before.

Protein Folding Pathologies

Over the past decade, defects in protein folding or assembly have become recognized as important factors leading to a variety of diseases. These include cystic fibrosis, some forms of emphysema and a large number of conditions associated with the formation of long fibrillar protein structures, the amyloid diseases. Mutations that destabilize the native protein may lead to premature degradation or the formation of aberrant assemblies, which, in turn, may lead to a deficiency for an important activity or the formation of structures that are actually toxic. At present, the amyloid diseases appear to be the most important category of folding pathologies. Diseases associated with amyloid formation include neurodegenerative conditions such as Alzheimer's and Parkinson's diseases and amyotrophic lateral sclerosis, as well as several systemic amyloid diseases. In an intriguing minority of diseases, particles of amyloid fibers from one individual can promote fibril

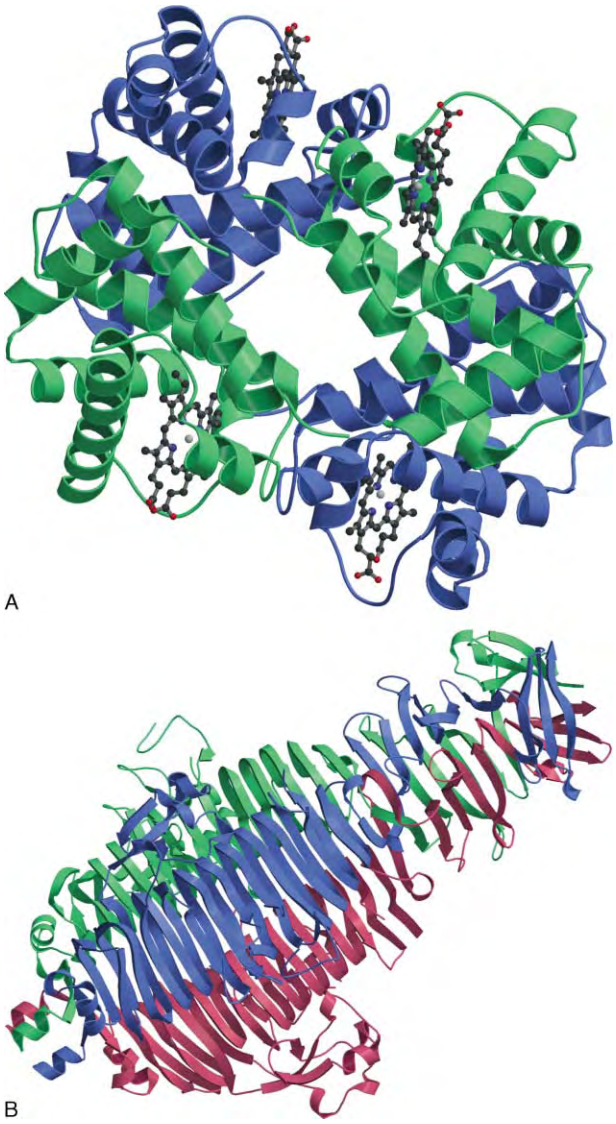

FIGURE 4 Subunit structures of two proteins. (A) Human hemoglobin, a tetramer formed of two types of subunits, colored green and blue in the drawing. Each of the subunits is a compact and self-contained structure. The heme groups associated with each of the four chains are also shown in a ball-and-stick representation. Drawn from entry 2HHB in the Protein Data Bank (Fermi, G., Perutz, M. F., Shaanan, B., and Fourme, R. (1984). The crystal structure of human deoxyhaemoglobin at 1.74Å resolution. *J. Mol. Biol.* 175, 159–174). (B) A fragment of the trimeric tailspike protein of bacteriophage P22. The intact protein includes an additional domain at the amino-terminus of the chain (at the lower left corner of the drawing), by which the tailspike binds the rest of the virus particle. In this structure, the individual subunits interact extensively with one another and are intertwined, requiring an assembly mechanism in which the chains do not fold completely until after they have associated. Drawn from entry 1TSP of the Protein Data Bank (Steinbacher, S., Seckler, R., Miller, S., Steipe, B., Huber, R., and Reinemer, P. (1994). Crystal structure of P22 tailspike protein: Interdigitated subnits in a thermostable trimer. *Science* **265**, 383–386).

formation in another, providing a mechanism of infectivity that does not involve either bacteria or viruses. These infectious agents have been named "prions" and the diseases they are associated with include scrapie (in sheep) and bovine spongiform encephalopathy (BSE or "mad cow disease"), as well as the human disease Kuru and a variant of Creutzfeld–Jacob disease that is believed to be derived from BSE. The transmission of an altered physiological state by a protein amyloid is not at all restricted to mammals, however, as a very similar process has been found in the unicellular yeast, *Saccharomyces cerevisiae*, and this discovery has provided an important experimental system for analyzing the prion phenomenon. A surprisingly large number of proteins are now known to form amyloid-like fibers under at least some *in vitro* conditions, and it may be that the ability to form these structures is a nearly universal property of polypeptide chains. Remarkably, there is a great deal of similarity among the structures of fibers formed from proteins with quite different native structures. The fibers are generally about 50–100Å in diameter and a fraction at least of the polypeptide chain has a β-strand conformation, with the strands oriented so that their backbones are approximately perpendicular to the fiber axis.

Fibril formation *in vitro* is typically favored by conditions that destabilize the normal folded conformation but do not fully unfold and solubilize the polypeptide. *In vivo*, conversion to the amyloid state may be promoted by inherited mutations, environmental stress or, as noted above, "seeding" by an existing fibril fragment. At present, it is difficult to establish a clear mechanistic link between fibril formation and the physiological changes associated with amyloid diseases. In some cases, the amounts of protein deposited in fibrils are so large, as much as several kg in some patients, that these structures are clearly able to interfere with normal organ function. Smaller fibrils may similarly be toxic at the cellular level. In other cases, it may be that diversion of essential proteins into fibrils leads to functional deficiencies.

Because amyloid fibril formation usually competes with normal folding, investigators are actively pursuing the possibility that these diseases might be prevented or treated by agents that favor productive folding or disfavor unfolding, for instance by binding to the native structure. These developments provide a vivid link between the basic science of protein folding and important medical problems.

See Also the Following Articles

Amyloid • Chaperones, Molecular • Disulfide Bond Formation • Glycoprotein Folding and Processing Reactions • Prions and Epigenetic Inheritance • Prions, Overview • Unfolded Protein Responses

Glossary

amyloid A polymeric and fibrous form of a protein, usually formed by polypeptides that have undergone unfolding or misfolding.

domain A compact structure composed of 50–150 amino acid residues that can fold independently of other parts of a protein.

folding intermediate A partially folded conformational state that may form transiently during the conversion of an unfolded protein to the native state.

molten globule A partially folded state that is characterized by the presence of regular secondary structure (usually α-helices), but lacking well-defined interactions between side-chains distant in the sequence.

native state The well-defined folded structure of a protein usually associated with biological activity.

unfolded state An ensemble of rapidly interconverting conformations with little or no stable structure, usually generated by incubating a native protein with a denaturant or at elevated temperature. *In vivo*, polypeptides that have not yet folded into their native conformations may resemble artificially unfolded proteins.

Further Reading

Bruns, C. M., and Karplus, P. A. (1995). Refined crystal structure of spinach ferredoxin reductase at 1.7Å resolution: Oxidized, reduced and 2′-phospho-5′-AMP bound states. *J. Mol. Biol.* **247**, 125–145.

Daggett, V., and Fersht, A. (2003). The present view of the mechanism of protein folding. *Nat. Rev. Mol. Cell Biol.* **4**, 497–502.

Dobson, C. M. (1999). Protein misfolding, evolution and disease. *Trends Biochem. Sci.* **24**, 329–332.

Englander, S. W. (2001). An amino acid code for protein folding. *Proc. Natl Acad. Sci. USA* **98**, 105–112.

Fermi, G., Perutz, M. F., Shaanan, B., and Fourme, R. (1984). The crystal structure of human deoxyhaemoglobin at 1.74Å resolution. *J. Mol. Biol.* **175**, 159–174.

Horwich, A. L. (ed.) (2002). Protein Folding in the Cell. In *Advances in Protein Chemistry*, Vol 59. Academic Press, New York.

Huber, A. H., Wang, Y. M., Bieber, A. J., and Bjorkman, P. J. (1994). Crystal structure of tandem type III fibronectin domains from *Drosophila* neuroglian at 2.0Å. *Neuron* **12**, 717–731.

Levinthal, C. (1969). How to fold graciously. In *Mossbauer Spectroscopy in Biological Systems* (J. T. B. DeBrunner and E. Munck, eds.) University of Illinois Press, Urbana, IL.

Matthews, C. R. (ed.) (2000). Protein Folding Mechanisms. In *Advances in Protein Chemistry*, Vol 53. Academic Press, New York.

Pain, R. (ed.) (2000). *Mechanisms of Protein Folding*, 2nd edition. Oxford University Press, Oxford, UK.

Steinbacher, S., Seckler, R., Miller, S., Steipe, B., Huber, R., and Reinemer, P. (1994). Crystal structure of P22 tailspike protein: Interdigitated subunits in a thermostable trimer. *Science* **265**, 383–386.

Biography

Dr. David Goldenberg is a Professor of biology at the University of Utah. He received his Ph.D. at the Massachusetts Institute of Technology and carried out postdoctoral research at the Medical Research Council Laboratory of Molecular Biology in Cambridge, UK. His research interests are in the areas of protein folding and dynamics, and he has worked extensively on the folding of disulfide-bonded proteins and the effects of mutations on folding energetics.

Protein Glycosylation Inhibitors

Alan D. Elbein
University of Arkansas for Medical Sciences, Little Rock, Arkansas, USA

Many proteins that are synthesized in eukaryotic cells undergo chemical modifications other than addition of amino acids, either while the protein is being synthesized, or after protein synthesis is finished. One of the major types of modifications that occur on many proteins is glycosylation, i.e., the covalent attachment of sugars to these proteins, to form glycoproteins. Proteins may be glycosylated either with O-linked sugars (sugars attached via hydroxyl groups of serine or threonine), or with N-linked-sugars (oligosaccharides attached to protein via the amide nitrogen of asparagine), or some proteins have both types of oligosaccharides. This article discusses the use of glycosylation inhibitors that either prevent the formation of N-linked oligosaccharides, or that modify the structure of the N-linked oligosaccharide chain after it is transferred to protein. The specific N-linked sugar structure on a particular protein may play an important role in protein folding, protein targeting, chemical recognition, and/or various disease processes. For this reason, inhibitors that alter the structure of the oligosaccharide can be valuable as tools to help decipher how specific carbohydrate structures are recognized by proteins that mediate these processes. In addition, this information can be utilized to prevent some of these processes, or to enhance those that are useful, and such a situation may be important in various therapies.

Mechanism of Action of Glycosylation Inhibitors

There are a number of glycosylation inhibitors that work on enzymes in the first series of reactions, i.e., the lipid-linked saccharide pathway that involves the participation of dolichyl-phosphate (see Figure 1). One of the most widely used and useful of these inhibitors is the antibiotic tunicamycin (Tun), a reversible tight-binding inhibitor of the GlcNAc-1-P transferase. This glycosyltransferase catalyzes the initial reaction in the assembly of N-linked oligosaccharides, i.e., the transfer of GlcNAc-1-P to dolichol-P to form GlcNAc-PP-dolichol. Since this inhibitor prevents this initial reaction, it essentially blocks the assembly of all N-linked oligosaccharide chains, and those proteins that normally have this type of glycosylation are synthesized in the unglycosylated form. As a result, many of these unglycosylated proteins do not fold properly in the ER, and are therefore degraded by the ubiquitin protein degrading system. In some cases, especially with hydrophobic membrane proteins, absence of the hydrophilic carbohydrate structure renders these proteins insoluble and causes them to aggregate into insoluble complexes. In most systems where N-linked glycoproteins are involved in recognition and binding interactions, Tun has dramatic effects. For example, this drug inhibits cell adhesion and spreading in various animal cell systems, and causes defects in the transport of glucose, uridine, and amino acids in chick fibroblasts. Treatment of mouse 3T13 fibroblasts with Tun inhibits their *in vitro* differentiation into adipose-like cells. This antibiotic also inhibited the fusion of myoblasts to form myotubes during muscle development. The difficulty with using tunicamycin in animal systems, or in chemotherapy against cancer or other diseases, is that it prevents glycosylation of all N-linked glycoproteins and therefore is quite toxic to most cells.

Amphomycin (Ampho) is a lipopeptide antibiotic that inhibits the formation of lipid-linked sugars in membrane fractions, but is not effective in whole cells, probably because it cannot cross the plasma membrane and get into the cells. This inhibitor blocked the formation of dolichyl-P-mannose (also refered to as mannosyl-P-dolichol), the donor of the last four mannose residues of the $Man_9GlcNAc_2$-PP-dolichol, resulting in the accumulation of $Man_5GlcNAc_2$-PP-dolichol in cell-free membrane preparations. Ampho has been a useful tool to demonstrate that the last four mannoses are donated by dolichyl-P-mannose, rather than by GDP-mannose.

Various sugar analogues, such as 2-deoxy-D-glucose (2-DG) and 2-deoxy-2-fluoro-D-glucose, also inhibit N-linked glycosylation and viral replication, as well as other processes that involve N-linked glycoproteins. This inhibition is probably due to the fact that these sugar analogues are incorporated by intact cells into various biosynthetic intermediates in place of the normal mannose residues, but these intermediates cannot be further elongated by addition of other sugars. These various inhibitors and others not reported here have been used in a variety of living systems to prevent

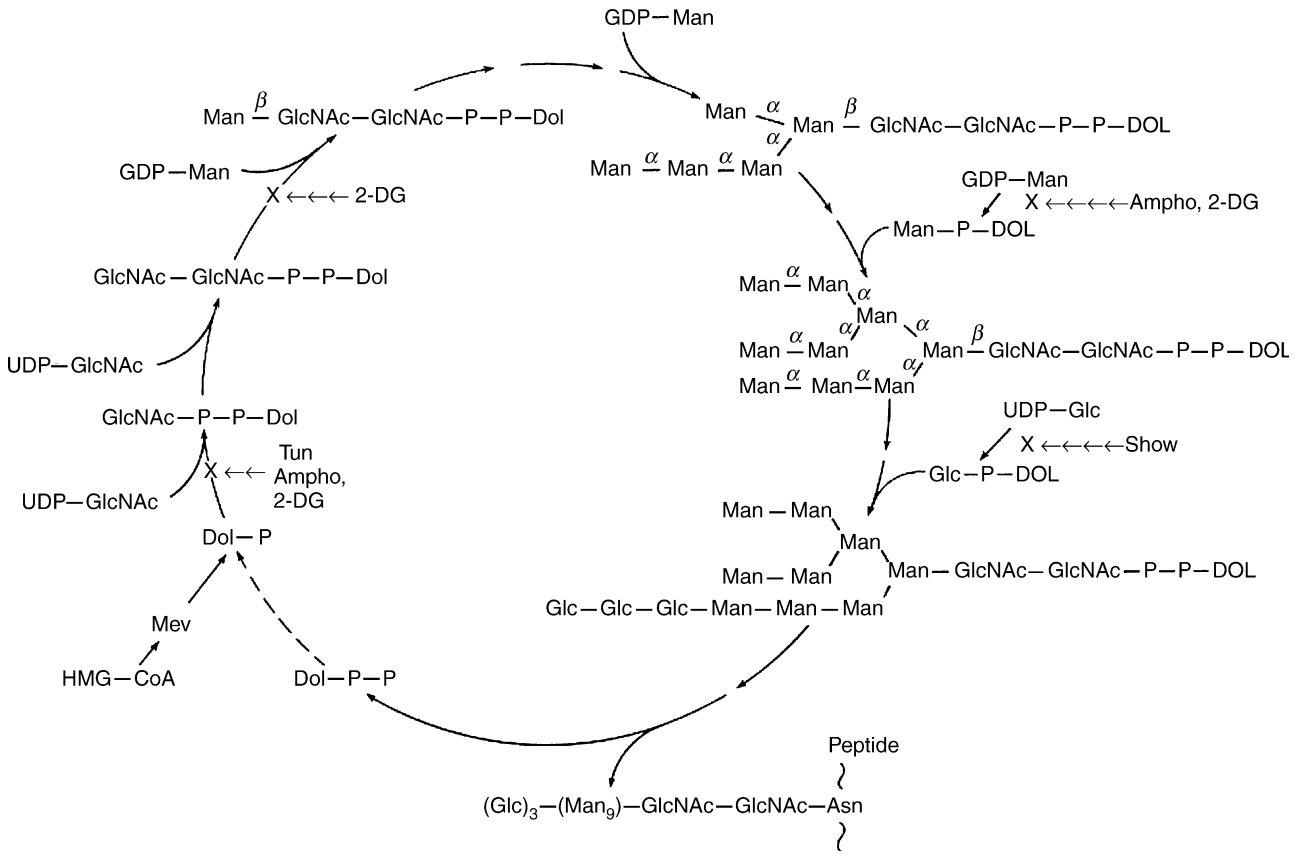

FIGURE 1 Inhibitors of N-linked oligosaccharide assembly. The biosynthesis of the N-linked oligosaccharides occurs on a dolichol carrier lipid in the endoplasmic reticulum. The individual sugars, N-acetylglucosamine (GlcNAc), mannose and glucose are sequentially added to the lipid from their activated form (i.e., UDP-GlcNAc, GDP-mannose or mannosyl-P-dolichol, UDP-glucose or glucosyl-P-dolichol) to form the 14 sugar oligosaccharide attached by a pyrophosphoryl bridge to the dolichol. Various compounds have been found to inhibit at specific sites in the pathway and these inhibitors have been useful tools to decipher and interrupt the biosynthetic pathway. Thus, tunicamycin (Tun), amphomycin (Ampho) and 2-deoxyglucose (2-DG) inhibit the first step in the assembly, i.e., the transfer of GlcNAc-1-P to dolichyl-P. Amphomycin and 2-deoxyglucose also inhibit the addition of the last four mannose residues by inhibiting the formation of mannosyl-P-dolichol (man-P-dol), while showdomycin (Show) inhibits formation of glucosyl-P-dolichol, the glucosyl donor for the three glucose units in the initial N-linked oligosaccharide.

glycosylation, and to show the necessary role of the N-linked oligosaccharides in key biological processes such as growth, cell–cell interactions, differentiation, development, and so on.

Mechanism of Action and Effect of Glycoprotein Processing Inhibitors

A number of plant alkaloids have a structure similar to that of the sugars glucose and mannose, but differ in having a nitrogen rather than an oxygen in the pyranose ring. These types of alkaloids have been found to be potent inhibitors of various glycosidases including those that are involved in the initial processing reactions that lead to the formation of complex N-linked oligosaccharides. The structures of several of these alkaloids and their sites of action in the processing pathway are shown in Figure 2. Castanospermine resembles glucose and inhibits both glucosidase I and glucosidase II, the ER glucosidases that remove all three glucose residues from the initial N-linked oligosaccharide. Castanospermine has been used in many cell culture systems, and in some whole animal studies to block the removal of glucose and prevent the formation of complex types of oligosaccharides. This has provided useful information on the function of specific glycoproteins. For example, in HepG2 cells, blocking the removal of glucoses from the N-linked oligosaccharides greatly reduced the rate of secretion of the serum protein, α_1-antitrypsin. Castanospermine also reduced the number of insulin receptors at the cell surface in IM-9 lymphocytes treated with this drug, and caused a significant decrease in the formation of new HIV viral particles, and in syncytium formation in cell culture. All of these effects were demonstrated to be attributable to the absence of glucose removal, leading to improper

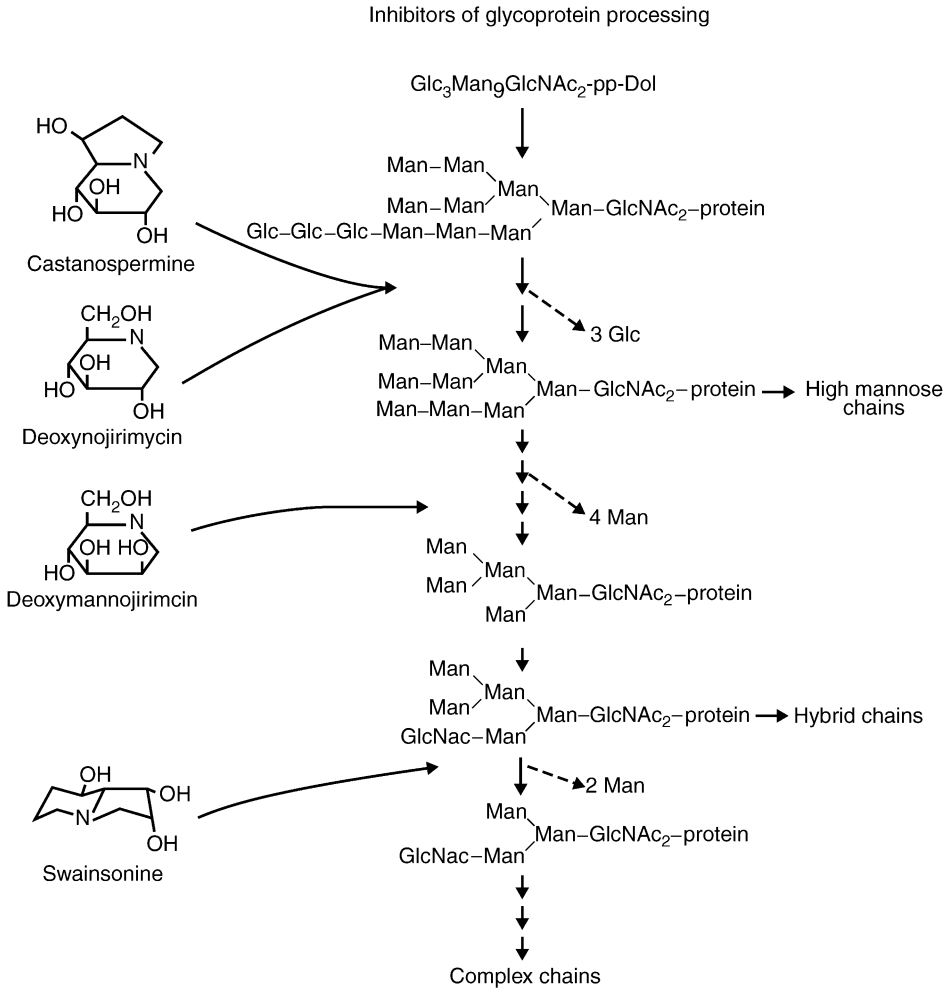

FIGURE 2 Inhibitors of glycoprotein processing. The processing of the oligosaccharide can be blocked at the very first step by the plant alkaloid, castanospermine, which inhibits α-glucosidases such as glucosidase I and glucosidase II. The trimming can also be stopped after the glucoses are removed by the α-mannosidase inhibitors, deoxymannojirimycin or kifunensine to cause accumulation of high mannose oligosaccharides. Finally the plant alkaloid swainsonine inhibits mannosidase II and causes the formation of hybrid structures.

protein folding and degradation of these proteins in the ER. Other glucosidase inhibitors have the same effect.

A second site of processing inhibition is at the stage of removal of the mannose residues. Deoxymannojirimycin (DMJ) is a chemically synthesized compound that resembles the structure of mannose, while kifunensine (KF) is a natural product that also resembles the mannose structure. Both of these compounds inhibit the Golgi α-mannosidase that releases four α1,2-linked-mannoses from the high mannose oligosaccharide. This is an essential step in the formation of complex chains, i.e., the addition of the first N-acetylglucosamine of the complex chains (structure 5 from top) requires a specific $Man_5GlcNAc_2$ structure. As far as formation or secretion of N-linked glycoproteins, these mannosidase inhibitors had essentially no effect on these processes. They also did not affect the formation in tissue culture cells of the influenza viral hemagglutinin, an N-linked glycoprotein coat protein that normally has 3 or 4 complex chains, nor the production of infectious influenza viral particles. These results suggest that the complex chain structures on this viral glycoprotein are not necessary for virus recognition or penetration in tissue culture cells.

DMJ has proven to be a useful tool to demonstrate that the initial removal of mannose residues from the high-mannose oligosaccharides in some cells occurs in the endoplasmic reticulum, and that there is also a mannosidase in the ER that removes a single mannose residue. That ER mannosidase is not susceptible to DMJ or KF. However, the next three mannoses are removed in the cis-Golgi compartment by another mannosidase which is inhibited by these two processing inhibitors. DMJ did inhibit the addition of L-fucose and sulfate into the N-linked oligosaccharides indicating that fucose and sulfate were added after the mannosidase I processing step. It is not clear whether DMJ and KF would affect the function of cell surface glycoproteins that are

involved in specific chemical recognition reactions, but one would expect that they should, since the specific carbohydrate structure should be involved.

A third site of inhibition is another mannosidase called mannosidase II that removes two mannoses from GlcNAc-Man_5-$GlcNAc_2$ to give a GlcNAc-Man_3-$GlcNAc_2$ structure, but this enzyme requires that the GlcNAc be added before it can release the two mannoses. Mannosidase II is not susceptible to DMJ or KF but is inhibited by swainsonine (SW), another plant alkaloid that has a structure related to mannose. Inhibition of mannosidase II by SW gives rise to hybrid structures like those found in humans with HEMPAS disease. In many systems, SW had little effect on functional aspects of the proteins in question, although it did cause the oligosaccharide structures to be of the hybrid type. However, SW did inhibit the attachment of osteoblasts to bone, and it also inhibited the interaction of the parasite *Trypanosoma cruzi* with macrophages when either the parasite or the macrophages were treated with this drug. This alkaloid also caused a dramatic decline in the ability of B16 melanoma cells to colonize the lungs of experimental animals. As a result of these studies, SW has been undergoing various tests to determine whether it will be useful as an anticancer drug.

See Also the Following Articles

Carbohydrate Chains: Enzymatic and Chemical Synthesis • GlcNAc Biosynthesis and Function, O-Linked • Glycosylation, Congenital Disorders of • Glycosylation in Cystic Fibrosis • Glycosylphosphatidylinositol (GPI) Anchors • Lectins • *N*-Linked Glycan Processing Glucosidases and Mannosidases • Oligosaccharide Chains: Free, *N*-Linked, *O*-Linked • Protein Glycosylation, Overview

Glossary

chemical recognition The chemical process by which molecules recognize other molecules and interact with or bind to them; in many cases of chemical recognition in living cells, a protein (called a lectin) on one cell recognizes a specific carbohydrate structure on another cell.

glycosidases Enzymes that cleave glycosidic bonds and release the monosaccharide from the nonreducing end of an oligosaccharide chain; these enzymes are specific for the sugar released and for the anomeric configuration.

glycosylation The process of addition of sugars to another molecule; in the context of this treatise it refers to the addition of sugars to proteins.

glycosylation inhibitors In the broadest context, this terminology refers to compounds that inhibit the formation of glycosidic bonds; in this treatise it refers to compounds that either prevent glycosylation of proteins or cause modifications in the oligosaccharide structure.

glycosyltransferases Enzymes that transfer sugars from their activated state to other sugars or to other molecules with the formation of a glycosidic linkage.

lectins Proteins that recognize specific carbohydrate structures and bind to these carbohydrates; they are frequently involved in recognition.

***N*-linked glycoproteins** Those proteins that have sugars (i.e., oligosaccharides) attached to the protein via an N-glycosidic linkage, which is to the amide nitrogen of asparagines.

Further Reading

Elbein, A. D. (1987). Inhibitors of the biosynthesis and processing of N-linked oligosaccharide chains. *Annu. Rev. Biochem.* **56**, 497–534.

Elbein, A. D. (1991). Glycosidase inhibitors: Inhibitors of N-linked oligosaccharide processing. *FASEB J.* **5**, 3055–3063.

Varki, A., Cummings, R., Esko, J., Freeze, H., Hart, G., and Marth, J. (1999). *Essentials of Glycobiology.* Cold Spring Harbor Laboratory Press.

Biography

Alan Elbein is Professor and Chairman of the Department of Biochemistry and Molecular Biology at the University of Arkansas for Medical Sciences in Little Rock. He received his Ph.D. in microbial biochemistry from Purdue University and did postdoctoral research at the University of Michigan and the University of California at Berkeley. He joined the faculty as an Assistant Professor of Biology at Rice University and then moved to the Department of Biochemistry at the University of Texas Health Science Center at San Antonio as Professor. His research focuses on the role of complex carbohydrates in glycoprotein function, and on novel carbohydrate target sites in chemotherapy of microbiol diseases.

Protein Glycosylation, Overview

Natasha E. Zachara and Gerald W. Hart
The Johns Hopkins University School of Medicine, Baltimore, Maryland, USA

Protein glycosylation is the enzymatically catalyzed attachment of glycans (carbohydrates) through a covalent bond to the polypeptide backbone of proteins. Protein glycosylation is a common co and/or posttranslational modification of eukaryotic proteins, and has now been found on a subset of proteins in both eubacteria and archaebacteria. Glycosylated proteins, termed glycoproteins, are distributed widely throughout the eukaryotic cell, being found in the extracellular space, on integral and peripheral membrane proteins, in the cytoplasm and nucleus, and in other subcellular organelles. Glycoproteins of prokaryotes (eubacteria and archaebacteria) are predominantly extracellular.

Basic Nomenclature

For small molecules, carbohydrates are complex! Carbohydrates gather their name from early studies which showed they had the chemical composition $(C(H_2O))_x$, or hydrated carbon. The carbons can be arranged in either an open conformation (less common) or one of two ring forms – the furanose (*f*) form (5 membered) or the pyranose (*p*) form (6 membered). Like amino acids, there is a dextrorotatory (D) and a levorotatory (L) enantiomer. The anomeric carbon, the carbon which forms the cyclic hemiacetal, is defined as carbon 1 (See Figure 1) and then the carbons are labeled two through six sequentially around the ring. Moreover, bonds formed by the hydroxyl group of the anomeric carbon can be in either of two conformations, leading to the α-sugar (axial bond), or β-sugar (equatorial bond). A nomenclature has evolved to describe all of these features accurately. For example, glucose or D-Glucopyranose, is abbreviated to D-Glc*p*. When defining the anomericity of the carbohydrate, the abbreviation (α,β) is included preceding the name of the sugar, for example the α-anomer of D-Glc*p* becomes D-αGlc*p*.

Carbohydrates can form covalent linkages through all of their hydroxyl groups to proteins, other carbohydrates or small molecules such as sulfate and phosphate. When sugars are linked together and then to a protein the structure is written from the nonreducing to reducing end (carbohydrate attached to the protein backbone). The position of the linkage is designated by the carbon residue to which the hydroxyl group forming the bond is linked. Thus, when the anomeric carbon of D-βGal*p* (galactose) is linked to the number 3 hydroxyl of D-αGalNAc*p* (*N*-acetylgalactosamine), which is then linked to protein, the resulting disaccharide is written D-βGal*p*1–3 D-αGalNAc*p*1-. Sometimes this is written as D-Gal*p*β1–3 D-GalNAc*p*α1-.

The Protein Carbohydrate Linkage

In the 1930s, Albert Neuberger and co-workers were able to demonstrate the first nonmucin protein carbohydrate linkage. These and subsequent studies showed that there was an amide bond between an asparagine (Asn) residue in chicken egg albumin (ovalbumin) and *N*-acetylglucosamine (GlcNAc). It is now known that of the 20 common amino acids, eight are involved in one of five chemically distinct covalent linkages to one of 13 different classes of carbohydrates. Variations in the covalent linkage, configuration of the linkage (α or β), the amino acid and the carbohydrate result in at least 41 different carbohydrate-protein linkages (Table I).

The five common covalent linkages between carbohydrates and proteins are:

1. *N-linked glycosylation*. This glycosylation typically refers to the amide bond formed between GlcNAc and Asn in the β-conformation. Less common amide bonds have been found between Asn and Glc, GalNAc and Rhamnose (Rham), and more recently between arginine (Arg) and Glc (Table I).
2. *O-linked glycosylation*. This glycosylation describes carbohydrates bound to the protein backbone through hydroxyl residues, such as those in serine (Ser), threonine (Thr), tyrosine (Tyr), hydroxylysine (Hly), and hydroxyproline (Hpr). O-linked sugars involve the greatest number of amino acids, sugars, and anomeric linkages (Table I), although in mammals the best characterized-O-linkage is to αGalNAc. As it was first characterized on mucins, it is often referred to as mucin-like glycosylation.

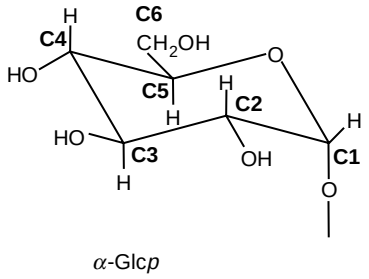

FIGURE 1 The hemiacetyl form of glucopyranose. Carbons are labeled from the anomeric carbon, C1.

3. *Glycosylphosphatidyl inositol (GPI)-anchors*. This is sometimes referred to as glypiation. GPI-anchors link the terminal residue of a protein through phosphoethanolamine to a core structure, which contains mannose (Man), glucosamine (GlcN), and inositol, to a lipid moiety, which anchors the protein in the lipid bilayer.

4. *C-mannosylation*. This is the attachment of an α-Man to carbon-2 of the indole ring of tryptophan (Trp). This form of protein glycosylation has been identified in eukaryotes on proteins such as RNAse2, interleukin-12 and properdin.

5. *Phosphoglycosylation*. This is the linkage of a carbohydrate through a phosphodiester bond to amino acids, such as Thr and Ser.

There are some posttranslational modifications of proteins that contain sugar, such as ADP-ribosylation that will not be discussed in this article. In addition, nonenzymatic glycation, the chemical reaction of reducing sugars with proteins, common in tissues and cells exposed to high levels of reducing saccharides, is not a form of protein glycosylation as (1) this reaction is not catalyzed by glycosyltransfereases; and (2) the Schiff base addition and subsequent Amadori rearrangement of the reducing sugar results in advanced glycation end products which can no longer be classified as carbohydrates.

Glycoprotein Synthesis

The extension of the first carbohydrate linked to the amino acid, sometimes referred to as the reducing terminal sugar, to form longer structures is typically performed in a stepwise manner. The exceptions are N-linked glycosylation and glypiation, where a core structure is added *en bloc* to the polypeptide chain and then remodeled.

Glycosyltransferases

The enzymatic addition of a carbohydrate to the protein backbone and the further modification of this carbohydrate is catalyzed by glycosyltransferases. These enzymes are typically type 2 membrane proteins that are situated in either the membrane of the endoplasmic reticulum (ER) or Golgi apparatus (Golgi), typically orientated toward the lumen of each organelle. Each different carbohydrate linkage is catalyzed by at least one glycosyltransferase.

Activated sugar nucleotide precursors, such as uridine diphosphate (UDP)- and guanosine diphosphate (GDP)-sugars, are necessary for the formation of all enzymatically synthesized glycosidic bonds. However, in some types of glycosylation, the sugar is transferred to a different intermediate donor, such as a lipid carrier, for example polyisoprenol monophosphate:dolichol phosphate (Dol-P), before transfer to the protein.

N-Linked Glycosylation

In eukaryotes, the initiation of N-linked glycosylation involves the synthesis of the core N-linked oligosaccharide, dolichol-diphosphate-$GlcNAc_2Man_9Glc_3$, on the cytosolic side of the ER membrane. After translocation to the lumen of the ER, the core structure is transferred *en bloc* to an Asn residue in the amino acid motif Asn-Xaa-Ser/Thr (Xaa $\neq$ Pro). Recently, it has been shown that when Cys is substituted for Ser/Thr, glycosylation may still occur in some cases. After transfer of the polypeptide to the Golgi, the core structure undergoes remodeling, resulting in three classes of N-linked glycosylation: high-mannose, hybrid, and complex (Figure 2).

High mannose structures contain more than the three mannose residues found in the core structure, and typically no other carbohydrate residues; while in complex structures both the terminal mannose residues in the core structure are typically modified by lactosamine (Gal1-4βGlcNAc) which can subsequently be modified further. Hybrid structures contain more than the three mannose residues in the core structure, as well as one or more lactosamine units.

O-Linked Glycosylation

Mammalian ER /Golgi Glycosylation

Unlike N-linked glycosylation, there is no single glycosylation motif that predicts the addition of O-linked carbohydrates to hydroxyl residues. O-glycosylation of cell-surface and secreted proteins in mammals appears to be initiated in the Golgi with the transfer of a monosaccharide residue from an activated sugar nucleotide to a hydroxyl residue. The reducing terminal sugar is further modified by stepwise addition of sugars from activated sugar nucleotides in the Golgi.

TABLE I

Different Types of Enzymatic Protein Glycosylation

Type	Reducing terminal linkage	Amino acid	Occurrence
N-linked	βGalNAc	Asn	Archaebacteria
	βGlc	Asn	Laminin only (Animals), Archaebacteria
	βGlcNAc	Asn	Common
	Rham	Asn	Eubacteria
	βGlc	Arg	Plants
O-linked	α Ara*f*	Hpr	Plants
	βAra	Hpr	Plants
	α Fuc	Ser, Thr	Animals
	αGal	Hpr	Plants, Eubacteria
	αGal	Ser, Thr	Plants, Eubacteria
	αGal	Hyp	Plants
	βGal	Hly	Collagen only (Animals)
	βGal	Tyr	Eubacteria
	αGalNAc	Ser, Thr	Common
	βGalNAc	Ser, Thr	Eubacteria
	αGlc	Tyr	Glycogen only (Animals)
	βGlc	Tyr	*C. thermohydrosulfuricum*
	βGlc	Ser, Thr	Eubacteria, Animals
	αGlcNAc	Ser, Thr	Protozoan
	βGlcNAc	Ser, Thr	Animals (cytoplasmic/nuclear)
	GlcNAc	Hyp	*D. discoideum*
	αMan	Ser, Thr	Animals, Fungi
	β FucNAc	Ser	*P. aeruginosa*
	β Xyl	Ser	Proteoglycans
	Diactrideoxyhexose	Ser, Thr	*N. meningitidis*
	αpseudaminic acid	Ser, Thr	*C. jejuni*
Phosphoglycosylation	β Fuc	Ser	*D. discoideum*
	αGlcNAc	Ser	*D. discoideum*
	αMan	Ser	*Leishmania mexicana*
	Xy1	Ser, Thr	*Trypanosoma cruzi*
C-mannosylation	αMan	Trp	Mammals
GPI-anchor	Conserved Core	C-terminal	Eukaryotic

Nonmammalian ER /Golgi Glycosylation

O-glycosylation of the protein backbone in fungi appears to be through lipid-P-donors. In yeast, addition of O-linked glycans is restricted to Dol-P-Man, although other fungi are capable of modifying the protein backbone with Glc and Gal. The study of prokaryotic glycosylation is an emerging field, and little information about the biosynthesis of prokaryotic glycosylation is available.

Cytosolic Glycosylation in Eukaryotes

Many nuclear and cytoplasmic proteins are glycoproteins, these proteins are modified with the simplest of the carbohydrate modifications, O-linked β-GlcNAc (*O*-GlcNAc). Unlike other forms of protein glycosylation, this modification is usually not further extended and occurs exclusively on cytoplasmic and nuclear proteins of metazoans. Consequently, the enzyme, which catalyzes the addition of *O*-GlcNAc, UDP-GlcNAc:polypeptide *O*-*N*-acetylglucosaminyl transferase, is not a type 2 membrane protein. Unlike other glycosyltransferases, this protein has tetratricopeptide repeat domains, which are protein–protein interaction domains and which have been shown to play a role in substrate recognition. Another form of intracellular protein glycosylation, involves the addition of GlcNAc to hydroxyproline of the ubiquitin ligase, Skp1, of the slime mold *Dictyostelium discoideum*. The enzyme has

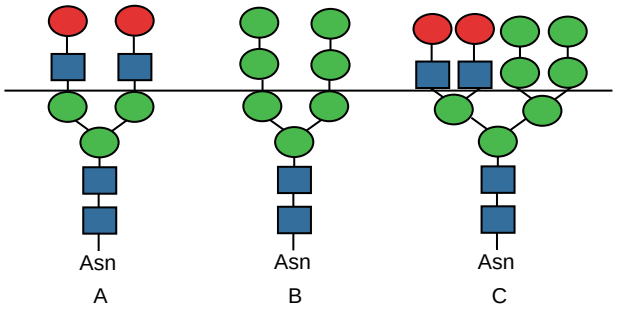

FIGURE 2 Different subgroups of N-linked oligosaccharides. (A) A complex-type oligosaccharide; (B) high-mannose-type oligosaccharide; (C) hybrid-type oligosaccharide. Structures below the solid line are common, while the structures above the line can vary. Further modification of the common structure with GlcNAc and Fuc is known. Different carbohydrates are represented by blue boxes (GlcNAc), green circles (Man), and red circles (Gal).

recently been cloned and appears unrelated to the metazoan GlcNAc transferase.

GPI-Anchors

There are several parallels between the biosynthetic pathways of GPI-anchors and N-linked oligosaccharides. Like the synthesis of N-linked glycosylation, a donor molecule is assembled on the cytosolic side of the ER membrane. Here, UDP-GlcNAc is first added to a phosphatidyl inositol ring, before the acetyl group is removed. Subsequent addition to the GlcN is via Dol-P-Man. Once complete, the structure is translocated through the ER membrane into the lumen, where it is attached to the completed polypeptide after a GPI-anchor consensus motif (C-terminal peptide) is cleaved off. During transit to the cell-surface the lipid component can be remodeled and the carbohydrate core structure can be further processed to give a range of glycoforms. While the core structure of all GPI-anchors appears to be identical, variations in structure appear to involve the nature of the lipid anchor and modification of the core carbohydrate structure with ethanolamine or other carbohydrate chains, the nature of which appear to be species and genera specific.

C-Mannosylation

C-mannosylation represents a linkage in which αMan is attached through a C-glycosidic linkage to the indole ring of Trp. Recently, it has been shown that this modification is added to the first Trp in the motif Trp-Xaa-Xaa-Trp, from a Dol-P-Man donor. This activity has been isolated in crude membrane preparations, suggesting ER/Golgi localization of this enzyme.

Phosphoglycosylation

First identified in *D. discoideum* in 1980 on the endopeptidase proteinase I, this modification, which involves the attachment of carbohydrate through a phosphodiester linkage to the protein backbone, has now been identified on a number of other proteins and in a number of different organisms, although the carbohydrate component differs. Recently, the *N*-acetylglucosamine-α-1-phosphate transferase from *D. discoideum* was partially purified from microsomal preparations and characterized.

Glycoforms of Glycoproteins

The carbohydrate components of proteins are by nature heterogeneous! Variations can occur in terms of the occupancy of potential sites of glycosylation (macroheterogeneity) or in the structures at sites of glycosylation (microheterogeneity), resulting in a variety of protein populations or glycoforms. One example of microheterogeneity is ovalbumin, which has one site of N-linked glycosylation, at which 22 different polysaccharides have been characterized.

Unlike proteins, the sequence of carbohydrates are not directly encoded for by the genome. The modification of proteins is dependent on the expression and regulation of different glycosyltransferases, sugar nucleotide levels, folding and transport of the polypeptide, and a myriad of other factors. Thus, different organisms, tissues and proteins are modified differently depending on the cellular environment, that is, the state of differentiation, development, disease, and cell cycle.

Glycosylation and Function

Deletion or mutation of glycosyltransferases results in predominantly severe to lethal phenotypes, underlying the importance of carbohydrates in the development and maintenance of organisms. While the inherent heterogeneity of carbohydrates has made defining the exact function of carbohydrate structures challenging, several clear roles have emerged from functional studies (Table II). Some examples are discussed below:

Protective

The epithelial surfaces of many organisms are coated with a mucous layer, one component of which are mucins. These high molecular weight glycoproteins are heavily glycosylated, and the carbohydrate component of these proteins are multifunctional. The negatively

TABLE II

Known Functions of the Carbohydrate Component of Glycoconjugates

Function
Stabilization of structure, protective
Modulation of biological activity
Antigenic determinants and modifiers of immune response
Cell-recognition and adhesion
Signal transduction
Protein folding
Protein trafficking and turnover
Hormonal actions

charged sugars in the oligosaccharides bind water tightly, preventing evaporation from the cell. In addition, the resulting gel protects cells from mechanical damage and bacterial attack, while providing specific binding sites for lectins.

Structural

Heavily glycosylated domains, that are reminiscent of mucins, are sometimes referred to as mucin-like domains. Here, hydration of the sugar residues appears to stiffen the protein backbone projecting different domains of proteins from each other and/or the plasma membrane.

Regulatory

The modification of nuclear and cytoplasmic proteins of metazoans with monosaccharides of O-Linked β-*N*-acetylglucosamine (*O*-GlcNAc) has been implicated in cellular control, playing an analogous role to protein phosphorylation. Like many forms of protein glycosylation, deletion of the *O*-GlcNAc transferase is lethal. While all of the functions of *O*-GlcNAc have not been elucidated, it is now clear that this modification alters protein–protein interactions, turnover rate of proteins and the phosphorylation state of proteins by competing with kinases for hydroxyl residues. Recently, perturbations in the regulation of *O*-GlcNAc have been implicated in the etiology of Type 2 diabetes.

Proteolysis and Stability

Carbohydrate modifications of proteins can affect the stability of proteins by several mechanisms. Carbohydrate modifications can reduce the availability of the protein backbone to proteolytic attack by steric hindrance, one example of this is seen on tissue plasminogen activator. Carbohydrates can stabilize protein structure by forming bonds, such as hydrogen bonds, with the protein backbone. Examples of this have been found in proteins such as CD2 and PMP-c protease inhibitor.

Intermolecular Interactions

Protein–protein interactions can be mediated by proteins through carbohydrate-binding domains. Proteins with such domains and which do not modify the carbohydrate are called lectins. There are several well-characterized families of lectins which are both intracellular and extracellular. Lectins mediate many important interactions within and between cells, possibly the best-characterized example are those of the selectins. Selectins mediate the interactions/movement between leukocytes and the endothelial surfaces of blood vessels.

Another key example of lectin–carbohydrate interactions are those that occur within the endoplasmic reticulum, between N-linked carbohydrates and the lectins, calnexin and calreticulin. If a protein folds properly, processing of N-linked glycosylation progresses, and calnexin and calreticulin fail to bind; improperly folded proteins are not processed, are bound by the lectins and presented to proteins such as Erp57, a protein disulphide isomerase, for refolding. Lectins are also involved in the export and degradation of misfolded proteins, as well and the transport of proteins from the ER to the Golgi.

See Also the Following Articles

Carbohydrate Chains: Enzymatic and Chemical Synthesis • GlcNAc Biosynthesis and Function, O-Linked • Glycosylation, Congenital Disorders of • Glycosylation in Cystic Fibrosis • Glycosylphosphatidylinositol (GPI) Anchors • Oligosaccharide Chains: Free, *N*-Linked, *O*-Linked • Protein Glycosylation Inhibitors

Glossary

glycoprotein A glycosylated protein.

glycosyltransferase An enzyme which transfers a sugar from a high energy donor to a protein, carbohydrate, or lipid.

reducing terminal sugar The carbohydrate linked directly to the protein backbone is often referred to as the reducing terminal saccharide or carbohydrate. This term is derived from early colorometric assay where the free hemiacetal form of sugars reduced ferric iron to ferrous iron.

saccharides Saccharide is derived from the Latin word for sugar, *saccharum*. A single sugar unit is referred to as a monosaccharide, two units as a disaccharide, three as a trisaccharides and several (2–10) as oligosaccharides and many (>10) as polysaccharides.

Further Reading

Fukuda, M., and Hindsgaul, O. (eds.) (2000). *Molecular and Cellular Glycobiology.* Oxford University Press, New York.

Furmanek, A., and Hofsteenge, J. (2000). Protein C-mannosylation: Facts and questions. *Acta Biochim. Pol.* **47**, 781–789.

Haynes, P. A. (1998). Phosphoglycosylation: A new structural class of glycosylation? *Glycobiology* **8**, 1–5.

Schaffer, C., Graninger, M., and Messner, P. (2001). Prokaryotic glycosylation. *Proteomics* **1**, 248–261.

Spiro, R. G. (2002). Protein glycosylation: Nature, distribution, enzymatic formation, and disease implications of glycopeptide bonds. *Glycobiology* **12**, 43R–56R.

Taylor, M. E., and Drickamer, K. (eds.) (2003). *Introduction to Glycobiology.* Oxford University Press, New York.

Varki, A. (1993). Biological roles of oligosaccharides: All of the theories are correct. *Glycobiology* **3**, 97–130.

Varki, A., Cummings, R., Esko, J., Freeze, H., Hart, G., and Marth, J. (eds.) (1999). *Essentials of Glycobiology.* Cold Spring Harbor Press, New York.

Zachara, N. E., and Hart, G. W. (2002). The emerging significance of O-GlcNAc in cellular regulation. *Chem. Rev.* **102**, 431–438.

Biography

Natasha E. Zachara received Bachelor of Technology (Biotechnology), Honours, from the School of Chemistry at Macquarie University (Sydney, Australia), in 1994. She completed her thesis entitled "Sequencing Proteins, Sequencing Sugars: A Unified Approach" at the Macquarie University Center for Analytical Biotechnology (Sydney, Australia), in 1998. She is currently working in the laboratory of Prof. G. W. Hart (Johns Hopkins University School of Medicine).

Gerald W. Hart is Director and DeLamar Professor of Biological Chemistry at the Johns Hopkins University School of Medicine. He received his Ph.D. in developmental biology at Kansas State University (USA) in 1977 and did his postdoctoral work with William J. Lennarz at Johns Hopkins, before joining the faculty in the Department of Biological Chemistry (1979). He was the founding editor-in-chief of *Glycobiology.*

Protein Import into Mitochondria

Johannes M. Herrmann and Walter Neupert
University of Munich, Munich, Germany

Mitochondria are essential organelles of eukaryotic cells that accommodate some 10–20% of the cellular proteome. They are made up by two membrane systems that divide the organelle into two aqueous subcompartments: the intermembrane space between the outer and the inner membrane, and the matrix which is enclosed by the inner membrane. The vast majority of mitochondrial proteins are encoded by the nuclear genome and synthesized on cytosolic ribosomes as precursors (also called preproteins). These proteins contain targeting information for specific sorting of each polypeptide to its respective mitochondrial subcompartment. Protein import into mitochondria is achieved by the concerted action of translocation complexes located in both membranes of the organelle.

Mitochondrial Targeting Signals

Targeting signals direct mitochondrial precursor proteins to their particular destination in the organelle. In addition, these sequences can prevent folding of precursor proteins in the cytosol and thereby maintain them in a transport-competent conformation. Proteins of the mitochondrial matrix and many inner membrane proteins are made with N-terminal extensions which are proteolytically removed by proteases following translocation into the mitochondrial matrix. These matrix targeting signals (MTSs) are referred to as presequences. Most mitochondrial proteins carry such N-terminal presequences. In addition, less defined internal signals are used for mitochondrial targeting, typically by proteins of the outer membrane, the intermembrane space, and by some inner membrane proteins.

Presequences

Presequences typically comprise 15–80 amino acid residues that have the potential to form amphipathic α-helices with one hydrophobic and one positively charged face. These signals are both necessary and sufficient for mitochondrial targeting. The addition of presequences to unrelated proteins typically leads to a targeting of the fusion proteins to mitochondria. The MTSs direct the extended polypeptide in an N-to-C-direction across both mitochondrial membranes. Examples were reported in which MTSs are located not at the N terminus, but at the C terminus or in the interior of a preprotein. In the latter case, the internal signal forms an amphipathic hairpin loop which precedes import of the N- and C-terminal parts of the preprotein. Typical N-terminal presequences can be detected by computer algorithms which predict the intracellular location of proteins.

Internal Targeting Signals

Many mitochondrial proteins contain less defined targeting signals which are a part of the mature polypeptide. These are referred to as internal signals. For example, proteins of the solute carrier family of the inner membrane are made up by modules of pairs of transmembrane domains which are imported as loop-like structures. The regions flanking these transmembrane domains are critical for the uptake of these proteins by the mitochondria. The nature of these signals and how they are deciphered is, however, not well understood.

Proteins of the outer membrane are often anchored in the lipid bilayer by terminal transmembrane domains. A moderate degree of hydrophobicity and flanking positive charges specify these proteins for mitochondria and differentiate them from other tail-anchored proteins of the cell.

Little is known about the targeting information that directs proteins into the intermembrane space of mitochondria. Many of these proteins are very small and bind cofactors such as metal ions or heme. The best-characterized example of the latter group of proteins is cytochrome *c*. Although many cytochrome *c* mutants were isolated that fail to be imported into mitochondria, a targeting signal of this protein was not identified so far.

Transport to and Across the Outer Membrane

A number of cytosolic factors were identified that bind to mitochondrial preproteins following their synthesis. Among these factors are members of the general chaperone system, such as Hsp70 and Hsp90,

and components that appear to play a more specific role in the targeting of mitochondrial proteins. These factors keep preproteins in an import-competent conformation and accompany them to the surface of mitochondria.

The TOM Translocase

The outer membrane harbors surface receptors that expose binding sites for MTSs to the cytosol (see Table I). These receptors are part of a multimeric protein translocase, called the *t*ranslocase of the *o*uter *m*embrane (TOM) complex. In fungi, the TOM complex comprises the receptor subunits Tom70, Tom22, and Tom20. These surface receptors direct preproteins to the so-called "general insertion pore" of the outer membrane, the main constituent of which is Tom40. Tom40 is thought to be present in a β-barrel structure in the outer membrane, similar to bacterial porin proteins, and

TABLE I

Components of the Mitochondrial Import Machinery

Components		
Fungi	**Mammals**	**Function**
Outer membrane, TOM complex		
Tom70, Tom71	Tom70	Surface receptor
Tom40	Tom40	Pore formation
	Tom34	Surface receptor, Tom70 homologue
Tom22	Tom22	Surface receptor
Tom20	Tom20	Surface receptor
Tom7	Tom7	Structural or regulatory component
Tom6		Structural component
Tom5		Receptor function
Intermembrane space		
Tim13	Tim13	Receptor and/or chaperone function
Tim12		Receptor and/or chaperone function
Tim10	Tim10 a, b	Receptor and/or chaperone function
Tim9	Tim9	Receptor and/or chaperone function
Tim8	DDP1, DDP2	Receptor and/or chaperone function
Inner membrane		
TIM23 complex		
Tim50	Tim50	Potentially receptor subunit
Tim44	Tim44	mtHsp70-binding
Tim23	Tim23	Receptor and channel activity
Tim17	Tim17	Function unclear
TIM22 complex		
Tim54		Function unclear
Tim22	Tim22	Channel activity
Tim18		Function unclear
Oxa1	Oxa1	Protein insertion from the matrix
Mba1		Protein insertion from the matrix
Imp1, Imp2	Imp1, Imp2	Sorting signal peptidases
Matrix		
Ssc1, Ecm10	mtHsp70	Chaperone, ATP-dependent precursor binding
Mge1	mtGrpE	Nucleotide exchange factor for mtHsp70
MPP	MPP	Processing of presequences
MIP	MIP	Processing of presequences
Mdj1	hTid (mtDnaJ)	Folding of imported proteins
Hsp60	Cpn60	Folding of imported proteins
Hsp10	Cpn10	Folding of imported proteins

by oligomerization forms protein-conducting channels. Three small additional subunits, Tom5, Tom6, and Tom7, appear to play a role as structural components and might be involved in regulating the interaction of the receptors with Tom40. In mammals, the TOM complex consists essentially of a similar set of homologous components. High-resolution electron microscopy of isolated TOM complexes revealed two membrane-traversing cavities of 2.2 nm, which most likely represent the preprotein-conducting channels in the outer membrane. Following translocation of preproteins through the general insertion pore, preproteins associate with the *trans* site of the TOM complex. This *trans*-binding site is formed by the intermembrane space domains of Tom40 and perhaps Tom22. An increasing binding affinity from *cis* to *trans* sites on the TOM complex was suggested to drive translocation of preproteins across the outer membrane into the intermembrane space.

Insertion into the Outer Membrane

In addition to its translocation function, the TOM complex facilitates the insertion of proteins into the lipid bilayer of the outer membrane (Figure 1, pathway 1). Although the molecular mechanism of this process is poorly understood, a critical role of the TOM complex was shown for membrane integration and assembly of TOM subunits, as well as for the insertion of other outer membrane proteins. The most abundant protein of the outer membrane, porin, and several tail-anchored proteins, like the apoptosis regulator bcl-2, require cytosolic receptor domains of TOM subunits for mitochondrial targeting. But, whereas integration of porin requires the general insertion pore in the TOM complex, bcl-2 was reported not to use the TOM channel.

Translocation into the IMS

The intermembrane space is a compartment of very small volume since the outer and inner membrane are ~ 8 nm apart which is about the diameter of a membrane. Only a rather small number of components of the intermembrane space are known most of which are required for mitochondrial biogenesis or have a function in respiration. A prominent example is cytochrome *c*, which plays a role in apoptosis apart from its function in shuttling electrons between complexes III and IV. Apocytochrome *c* is imported by the TOM complex and associates in the intermembrane space with the protein cytochrome *c* heme lyase (CCHL). CCHL represents a docking site for apocytochrome *c* and converts it to holocytochrome *c* by incorporation of a heme group. Holocytochrome *c* is not able to traverse the TOM channel and, thus, remains in the intermembrane space. Like cytochrome *c*, many intermembrane space proteins bind cofactors and may be imported by a similar mechanism (Figure 1, pathway 2).

A second group of intermembrane space proteins is synthesized with N-terminal presequences followed by sorting signals. These signals are proteolytically removed by the Imp1/Imp2 protease of the inner membrane and the mature parts of the precursors are released into the intermembrane space. These sorting signals can be transplanted to unrelated sequences and direct these into the intermembrane space. Examples for this type of proteins are cytochrome b_2 or cytochrome b_5 reductase.

Translocation into the Matrix

The mitochondrial matrix contains a large number of proteins, many of which fulfill important functions in metabolic processes, energy production or the replication and expression of the mitochondrial genome. These proteins typically contain N-terminal presequences and are imported on a common import route (Figure 1, pathway 4).

The TIM23 Complex

The TIM23 complex consists of the integral membrane proteins Tim50, Tim23, and Tim17, and the peripherally associated matrix protein Tim44. Tim23 and Tim17 are homologous to each other and form the translocation pore in the inner membrane. In yeast, the N terminus of Tim23 protrudes into the outer membrane and thereby may mediate close contact of the TOM and the TIM23 translocase. Tim50 exposes a large domain to the intermembrane space and might play a role in guiding preproteins from the TOM to the TIM23 complex. Binding of the presequence to the TIM23 complex leads to a membrane-potential-dependent gating of the channel, which allows the presequence to traverse the inner membrane. This translocation reaction is driven by the membrane potential which probably supports the movement of the positively charged presequences to the negatively charged matrix face of the inner membrane. In the matrix, the presequences are bound by the chaperone mtHsp70, which prevents backsliding of the translocation intermediate. MtHsp70 is recruited to the TIM23 translocase by the Tim44 subunit of the complex which warrants a high concentration of mtHsp70 at the exit of the TIM23 channel and, thus, the efficient trapping of the incoming polypeptide. The ATP-dependent interaction of mtHsp70 with the preprotein is regulated by a nucleotide exchange factor, mtGrpE/Mge1, and is responsible for the ATP dependence of the mitochondrial import process. Binding of the preprotein to mtHsp70 leads to the

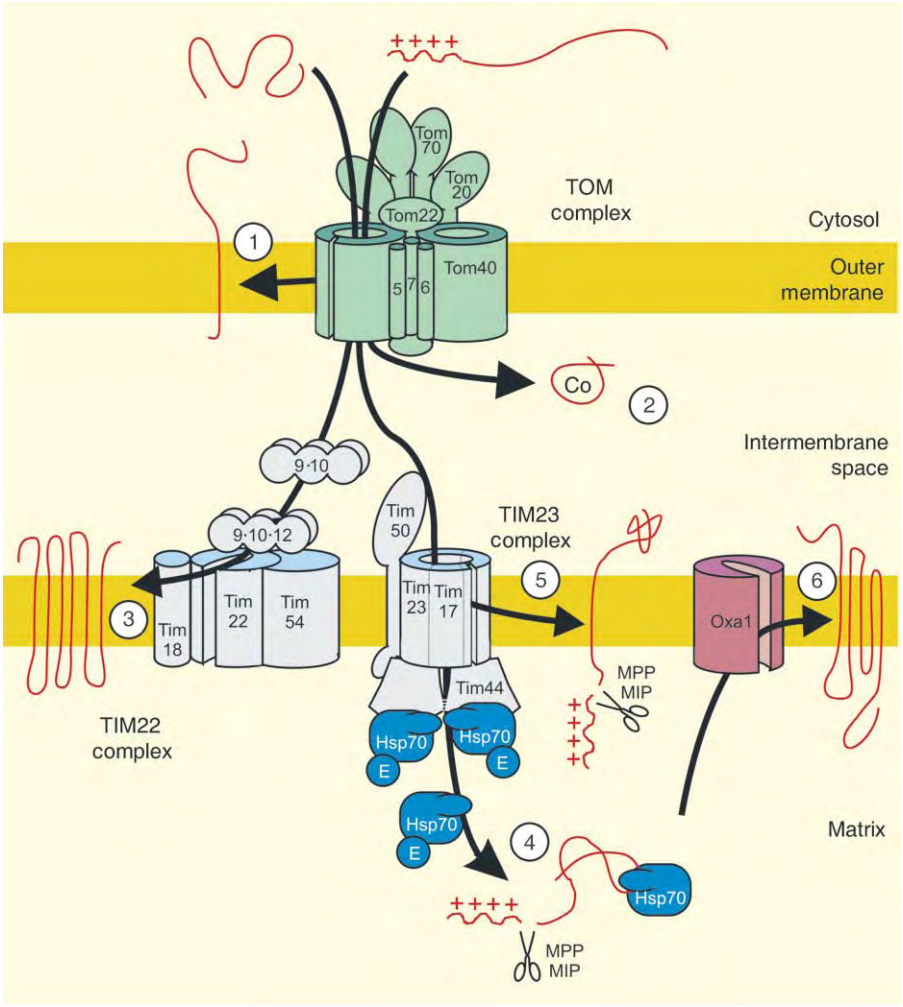

FIGURE 1 Protein import pathways in mitochondria. (1) Most outer membrane proteins bind to the receptor subunits of the TOM complex before they integrate into the membrane. The role of the general insertion pore in this process is not fully understood. (2) Proteins of the intermembrane space are often of small size and bind cofactors. These proteins are translocated through the general insertion pore of the TOM complex formed by Tom40. In the case of cytochrome c, the acquisition of the cofactor heme (Co) is required for efficient translocation of the protein. (3) Members of the solute carrier family and some Tim subunits traverse the outer membrane forming loop-like structures. They are escorted to the TIM22 translocase in the inner membrane by complexes of small Tim proteins in the intermembrane space. (4) Matrix proteins contain presequences that mediate translocation through the TOM channel and interact with the TIM23 complex in the inner membrane. The presequences are transported across the inner membrane in a membrane potential- and ATP-dependent manner, and removed by processing peptidases. After complete translocation across the inner membrane, matrix proteins fold under assistance of molecular chaperones. (5) Monotopic inner membrane proteins can be arrested at the TIM23 translocase and laterally integrated into the lipid bilayer of the inner membrane. (6) Conservatively sorted proteins are first transported into the matrix and form sorting intermediates bound by mtHsp70. Subsequently, these proteins are inserted into the inner membrane in a membrane potential-dependent reaction. The inner membrane protein Oxa1 is required for membrane integration of several of these proteins.

release of mtHsp70 from Tim44, and allows further translocation of the preprotein into the matrix driven by the Brownian movement of the polypeptide. Repeated binding cycles of mtHsp70 then lead to the vectorial import reaction. This mechanism is referred to as Brownian ratchet model as mtHsp70 would prevent backsliding of the preprotein. It was suggested that in addition to its trapping function, mtHsp70 undergoes an intramolecular conformational change and thereby mechanically pulls the bound preprotein into the matrix. The validity and significance of this motor model is still under debate.

Protein Folding and Assembly

In the matrix the presequences are typically removed by processing peptidases. The mitochondrial processing peptidase (MPP) consists of two conserved subunits which convert most matrix proteins into their mature form. In addition, some preproteins are further

processed by the mitochondrial intermediate peptidase, which removes another eight N-terminal amino acid residues. The mature proteins are then allowed to fold into their native structure. This process is facilitated by mtHsp70 which cooperates in this process with the DnaJ homologue Mdj1/hTid. Folding of some matrix proteins depends on the chaperonin complex formed by Hsp60 and Hsp10, which is homologous to the GroEL/GroES complex of the bacterial cytosol.

Protein Insertion into the Inner Membrane

The inner membrane contains a large number and diversity of proteins and belongs to the protein-richest membranes of eukaryotic cells. Inner membrane proteins reach their destination on several different insertion routes.

Insertion via the TIM23 Translocase

A number of monotopic inner membrane proteins are integrated into the inner membrane following translocation arrest at the level of the TIM23 complex (Figure 1, pathway 5). This sorting route was named the "stop-transfer" pathway. Most of these proteins are of $N_{in}-C_{out}$ topology, but some examples were reported which are oriented in a $N_{out}-C_{in}$ topology by internal loop-forming presequences.

Insertion from the Matrix

Alternatively, proteins can be inserted into the inner membrane following complete translocation into the matrix (Figure 1, pathway 6). This transport scheme was called conservative sorting, since the process employs a bacterial-like insertion reaction from the matrix. Examples for this sorting path are both mono- and polytopic inner membrane proteins of prokaryotic origin. Not only the direction of the membrane integration reaction resembles that in prokaryotes, but also the topogenic signals and the components that catalyze the insertion process. Conservatively sorted proteins adhere to the positive-inside rule according to which negative charges flanking the transmembrane segments are preferentially translocated across a membrane. A central player in the insertion process of these proteins is the inner membrane protein Oxa1 which forms the only translocation complex known to be conserved from bacteria to mitochondria. Besides its role in membrane integration of conservatively sorted proteins, the Oxa1 translocase mediates the insertion of mitochondrial translation products into the inner membrane.

Insertion via the TIM22 Translocase

The third group of inner membrane proteins is inserted by an alternative TIM complex, the TIM22 translocase (Figure 1, pathway 3). This pathway is used by members of the solute carrier family and by some TIM subunits. These proteins do not contain presequences but internal signals. Upon translocation through the TOM complex these proteins associate with the hexameric Tim9·Tim10 and Tim8·Tim13 complexes of the intermembrane space which belong to the family of "small Tim proteins." These complexes escort the hydrophobic precursor proteins from the TOM complex through the intermembrane space to the TIM22 complex. The TIM22 complex comprises the membrane-embedded subunits Tim54, Tim22, and Tim18 to which a Tim9·Tim10·Tim12 hexamer is associated. Tim22 is related to Tim17 and Tim23, and forms the translocation pore of the complex. Mutations in the human Tim8 homologue, DDP1, lead to the deafness dystonia (Mohr-Tranebjaerg) syndrome, a progressive, neurodegenerative human disorder.

See Also the Following Articles

Cytochrome *c* • Lipid Bilayer Structure • Membrane Fusion • Mitochondrial Membranes, Structural Organization • Mitochondrial Outer Membrane and the VDAC Channel • Protein Folding and Assembly

Glossary

Oxa1 translocase Protein complex of the inner membrane of mitochondria that facilitates membrane insertion of both nuclear and mitochondrially encoded proteins.

preprotein Precursor form of a mitochondrial protein; preproteins often contain presequences that have to be removed by mitochondrial processing peptidases.

presequence Typically N-terminal extension on a protein that serves as mitochondrial targeting signal (MTS).

TIM translocases Oligomeric translocation complexes of the inner membrane of mitochondria.

TOM translocase Multisubunit translocation complex of the outer membrane of mitochondria consisting of receptor subunits and a protein-translocating channel.

Further Reading

Herrmann, J. M. (2003). Converting bacteria to organelles: Evolution of mitochondrial protein sorting. *Trends Microbiol.* **11**, 74–79.

Hoogenraad, N. J., Ward, L. A., and Ryan, M. T. (2002). Import and assembly of proteins into mitochondria of mammalian cells. *Biochim. Biophys. Acta* **1592**, 97–105.

Koehler, C. M. (2000). Protein translocation pathways of the mitochondrion. *FEBS Lett.* **467**, 27–31.

Neupert, W. (1997). Protein import into mitochondria. *Annu. Rev. Biochem.* **66**, 863–917.

Neupert, W., and Brunner, M. (2002). The protein import motor of mitochondria. *Nat. Rev. Mol. Cell Biol.* **3**, 555–565.

Pfanner, N., and Geissler, A. (2001). Versatility of the mitochondrial protein import machinery. *Nat. Rev. Mol. Cell Biol.* **2**, 339–349.

Stuart, R. A. (2002). Insertion of proteins into the inner membrane of mitochondria: the role of the Oxa1 complex. *Biochem. Biophys. Acta* **1592**, 79–87.

Biography

Johannes Herrmann is a Group Leader in the Department of Physiological Chemistry of the University of Munich, Germany. He holds a Ph.D. from the University of Munich.

Walter Neupert is Chair of the Department of Physiological Chemistry in Munich. He holds a Ph.D. and an M.D. from the University of Munich.

Their principal research interest is the biogenesis of mitochondria, and especially the sorting and assembly of mitochondrial proteins.

Protein Kinase B

Bettina A. Dummler and Brian A. Hemmings
Friedrich Miescher Institute for Biomedical Research, Basel, Switzerland

Protein kinase B (PKB, also known as AKT) is an important mediator in intracellular signaling. Activation of PKB occurs in response to several cellular stimulants that act through receptor tyrosine kinases or G protein-coupled receptors. As a protein kinase, PKB catalyzes phosphorylation of proteins (the covalent linking of a phosphate group) on serine and threonine residues within a specific recognition sequence. Phosphorylation is a common mechanism in signal transduction to reversibly alter protein function, such as intrinsic activity, subcellular localization, half-life, or interaction of proteins with binding partners. Multiple PKB substrates have been identified and regulation of these molecules by phosphorylation plays an important role in the elaboration of physiological changes in a cell in response to extracellular signal molecules. Depending on cell type and stimulus, widely divergent cellular processes are regulated by PKB, including apoptosis, proliferation, differentiation, and metabolism.

Structure of PKB and Activation Mechanism

The AGC Family of Protein Kinases

Protein kinase B (PKB) is a member of a family of protein kinases that originally contained protein kinase *A*, cGMP-dependent protein kinase, and protein kinase *C*, termed the AGC family. Other members of the AGC family include p70 S6 kinase, protein kinase C-related kinase 2 (PRK2), and serum- and glucocorticoid-inducible kinase (SGK). The protein kinases of the AGC family show similarities in many structural and regulatory features. Highly similar in all AGC kinases is a flexible peptide loop (activation loop) proximal to the catalytic pocket of the kinase domain, and phosphorylation of this loop is required for the activation of virtually all AGC kinases.

Isoforms of PKB

There are three mammalian isoforms of PKB, PKBα (AKT1), PKBβ (AKT2), and PKBγ (AKT3). They are products of distinct genes but highly related, exhibiting greater than 80% sequence identity and sharing the same structural organization (see Figure 1A). The three genes are expressed differentially, with PKBα and PKBβ displaying fairly broad and PKBγ more restricted tissue distribution.

Structure of PKB

Each isoform possesses an amino-terminal pleckstrin homology (PH) domain that binds to 3-phosphoinositides, a central catalytic domain, and a carboxy-terminal regulatory domain (Figure 1A). Furthermore, all three isoforms possess two conserved phosphorylation sites, and phosphorylation of both sites is required for full activation of the kinase. The first one (Thr308 in PKBα) lies within the activation loop of the kinase domain and its phosphorylation induces a catalytically active conformation of the kinase. The second one lies within the regulatory domain in a six-amino-acid-long sequence termed the hydrophobic motif (FPQFS^{473}Y). Phosphorylation at Ser473 enables the hydrophobic motif to bind into a pocket within the small lobe (N-lobe) of the kinase domain and thereby it stabilizes the active conformation of PKB (Figure 1B). All PKB isoforms are assumed to have identical or similar substrate specificity. The minimal consensus sequence of preferred PKB *in vitro* phosphorylation sites has been defined as ArgXArgXXSer/Thr-Hyd, where X is any amino acid and Hyd is a bulky hydrophobic residue. Multiple PKB substrates have now been identified (Table 1).

The PI3K/PKB Signaling Pathway

Activation of receptor tyrosine kinases by ligands such as epidermal growth factor (EGF) and platelet-derived growth factor (PDGF) leads to autophosphorylation of specific tyrosine residues on the intracellular portion of the receptor (Figure 2). Recruitment of phosphoinositol 3-kinase (PI3K) then occurs, via binding of the Src homology 2 (SH2) domains of the regulatory subunit (p85) to specified phosphotyrosine residues on the receptor (in the case of insulin receptor this recruitment

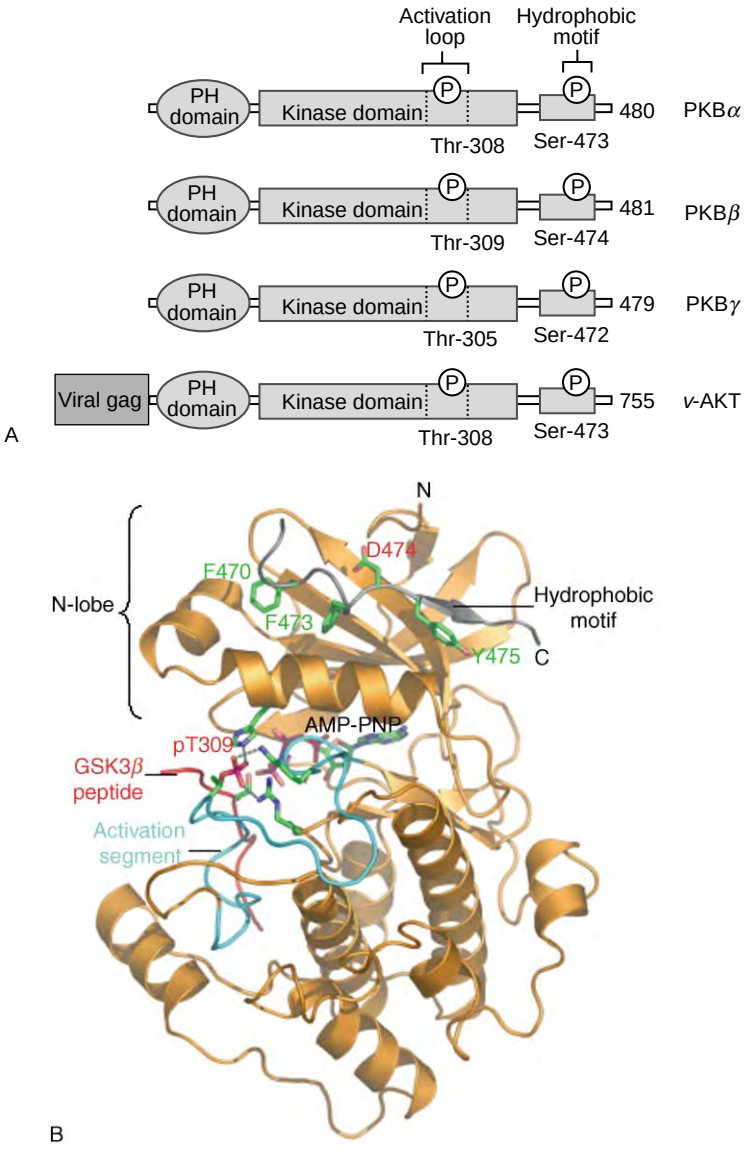

FIGURE 1 (A) Domain structure and regulatory phosphorylation sites of PKB. All isoforms contain a pleckstrin homology (PH) domain, a catalytic domain and a C-terminal regulatory domain. Phosphorylation of the activation loop and the hydrophobic motif (Thr308 and Ser473 in PKBα) are critical for kinase activation. v-Akt is the viral form of PKB and is a fusion between the viral Gag protein and mouse PKBα. (B) Structure of activated PKB. The ribbon diagram shows an activated PKBβ ternary complex with GSK3-peptide (red) bound in the substrate-binding site and AMP-PNP (a hydrolysis-resistant ATP analogue) bound in the ATP-binding site. To obtain an activated conformation, the hydrophobic motif of PKB was replaced with that of another AGC kinase, PRK2, and T309 in the activation segment (blue) was phosphorylated by PDK1. The hydrophobic motif of PRK2 contains an acidic residue (D474) in place of a phosphorylatable serine and binds constitutively to the N-lobe without needing phosphorylation. (Reproduced from Yang, J., Cron, P., Good, V. M., Thompson, V., Hemmings, B. A., and Barford, D. (2002). Crystal structure of an activated Akt/protein kinase B fernary complex with GSK3-peptide and AMP-PNP. *Nat. Struct. Biol.* **9**(12), 940–944, with permission.)

is largely mediated by the insulin receptor substrate (IRS) adapter proteins). This leads to a conformational change in PI3K and consequently to activation of the catalytic subunit (p110). Activated PI3K phosphorylates inositol-containing membrane lipids at the 3′-OH position of the inositol ring, generating phosphatidyl-inositol 3,4,5-trisphosphate (PI(3,4,5)P3). Subsequently, inactive PKB is recruited from the cytosol to the membrane via binding of its PH domain to PI(3,4,5)P3. Membrane recruitment brings PKB in close proximity to 3-phosphoinositide-dependent kinase (PDK1). PDK1 possesses a PH domain in its carboxy terminus, which binds PI(3,4,5)P3 and localizes PDK1 at the membrane. Co-localization of the two proteins and the conformational change induced in PKB upon lipid binding then enable PDK1 to phosphorylate PKB on Thr308 in the activation loop. For full kinase activation, PKB requires phosphorylation of an additional site,

TABLE I

PKB Substrates[a,b]

Protein	Biological effect
BAD	Phosphorylated BAD binds to 14-3-3 and is sequestered in the cytoplasm
BRCA1	Interferes with nuclear localization of BRCA1?
CREB	Increases association with CBP and p130
eNOS	Activates eNOS and leads to NO production
Forkhead family members (FKHR, FKHRL1, AFX)	Inhibits transcriptional activities of Forkhead family members
GSK3α/β	Inactivates GSK3 activity
IKKα	Activates transcriptional activity of NFκB
IRS-1	Positive regulation of IRS-1 function
Mdm2	Nuclear translocation of Mdm2, decreases p53 levels
Nur77	Inhibits transcriptional activity of Nur77
PFK-2	Activates PFK-2
Procaspase-9	Suppression of caspase-9-induced cell death
p21/Cip1	Cell cycle progression
p27/Kip1	Relieves inhibitory effect of p27/Kip1 on Cdk2
Raf1	Inhibition of Raf1 signaling
TSC2	Destabilizes TSC2 and disrupts its interaction with TSC1, leading to p70S6K activation

[a] Abbreviations: BAD, Bcl-2 pro-apoptotic family member; CBP, cAMP binding protein; Cdk2, cyclin-dependent kinase 2; CREB, cAMP responsive element binding protein; eNOS, endothelial nitric oxide synthase; GSK3, glycogen synthase kinase-3; IKKα, I-kB kinase α; IRS-1, insulin receptor substrate-1; NFκB, nuclear factor κB; NO, nitric oxide; PFK-2, phosphofructokinase-2; TSC2, tuberous sclerosis complex 2.

[b] Data supporting the *bona fide* nature of these substrates differs between proteins. Note also that because of space restrictions, not all published PKB substrates are included in the table.

Ser473, by an as yet unidentified Ser473 kinase. Following activation, PKB is detached from the plasma membrane and translocates to the cytosol and the nucleus to phosphorylate its substrates.

Negative Regulation of PKB Activity

Just as important as activation is the negative regulation of PKB activity, to avoid sustained signaling in absence of an appropriate extracellular signal. The key pThr308 and pSer473 residues in PKB have a relatively short half-life and become dephosphorylated by the action of phosphatases, such as PP2A, which returns PKB to its inactive conformation in the cytosol (see Figure 2). Another negative regulator of PKB activity is PTEN, a 3-phosphoinositide-specific phosphatase that dephosphorylates PI(3,4,5)P3, and thus antagonizes PI3K activity and recruitment of PKB to the membrane. Recently, a PKB-binding protein has been identified, carboxy-terminal modulator protein (CTMP), which appears to negatively regulate PKB by inhibiting its phosphorylation at Ser473 and thus maintaining the kinase in an inactive state.

Physiological Functions and Cellular Processes Regulated by PKB

Apoptosis and Cell Survival

The ability of a diverse array of physiological stimuli to promote cell survival can be attributed, at least in part, to the activation of the PI3K/PKB signaling pathway. Direct targets that PKB phosphorylates to protect cells from apoptosis include BAD, the Forkhead family of transcription factors, Mdm2, and the NFκB regulator IκB kinase (IKK) (Figure 3A). Each of these plays a critical role in cell death and by phosphorylation through PKB their pro-apoptotic function is inhibited and anti-apoptotic function promoted, respectively.

PKB Controls Subcellular Localization of BAD

The Bcl-2 protein family is a large family of structurally related proteins, of which some promote cell death and others survival. BAD is a pro-apoptotic member of this family that in its dephosphorylated form directly interacts with pro-survival Bcl-2 family

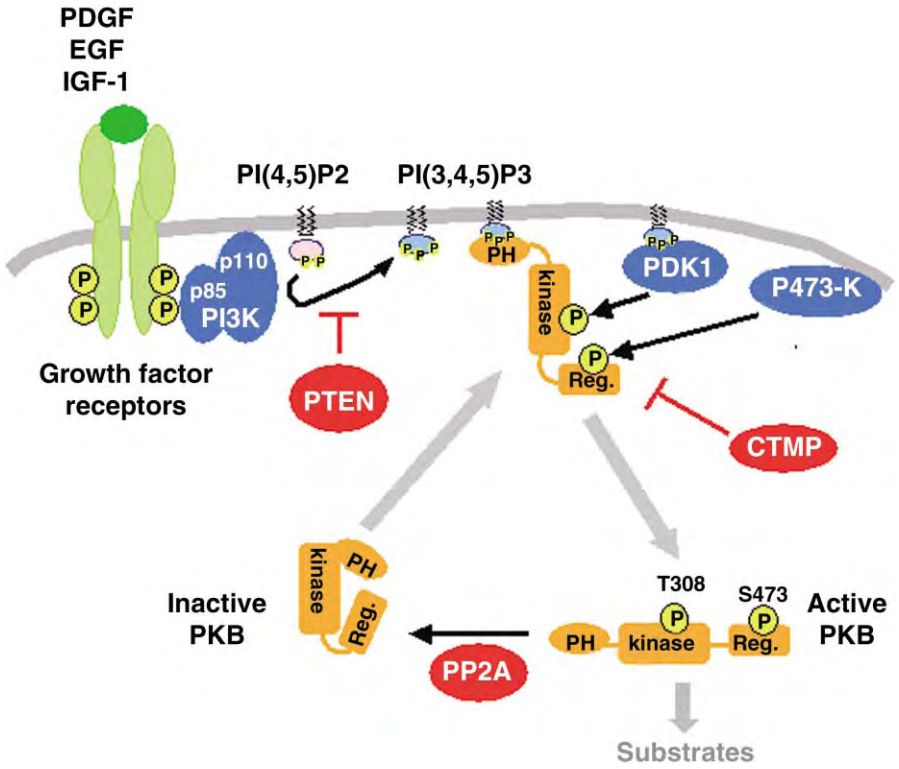

FIGURE 2 Current model for PKB regulation by receptor tyrosine kinases. Growth factor-mediated activation of PI3K leads to generation of PI(3,4,5)P3, which recruits inactive PKB to the plasma membrane. Residues Thr308 in the catalytic site and Ser473 in the hydrophobic motif are subsequently phosphorylated by PDK1 and by an as yet unidentified Ser473 kinase, respectively. Activated PKB can then phosphorylate substrates at the plasma membrane, in the cytosol, and in the nucleus. Activation of PKB is inhibited by the action of PTEN and presumably also by CTMP, which inhibits phosphorylation of PKB at Ser473. The kinase is deactivated by phosphatases such as PP2A.

members, such as Bcl-X_L. This interaction blocks pro-survival function of Bcl-X_L. Phosphorylation of BAD by activated PKB results in dissociation from Bcl-X_L and instead preferential association with cytoplasmic 14-3-3 proteins. The ability of BAD to bind to and inactivate Bcl-X_L is thereby disrupted and cell survival promoted.

PKB Controls Transcriptional Activity of Forkhead Transcription Factors

Many apoptotic stimuli also induce *de novo* gene expression of critical death genes and the Forkhead family of transcription factors mediates transcription of a defined subset of these genes. PKB-mediated phosphorylation of these transcription factors regulates their subcellular localization. In an unphosphorylated state, Forkhead family proteins translocate into the nucleus and activate transcription of their target (death) genes. But under conditions during which PKB is activated, these transcription factors are phosphorylated and are retained in the cytoplasm, potentially by interaction with 14-3-3 proteins, and are thus unable to mediate transcription.

PKB Controls p53 Levels in Cells via Mdm2 Phosphorylation

The p53 tumor suppressor protein is a short-lived protein, which is stabilized in response to cellular stress and promotes apoptosis. The ubiquitination and degradation of p53 are largely controlled by Mdm2, an E3 ubiquitin ligase. PKB can influence degradation of p53 through phosphorylation of Mdm2. Phosphorylation mediates translocation of Mdm2 to the nucleus, where it can bind to and modify nuclear p53, resulting in enhanced p53 degradation.

PKB Controls Transcriptional Activity of NFκB

Cell death is not only prevented by inhibition of apoptosis-promoting proteins on posttranslational and transcriptional level, but also through upregulation of survival-promoting genes. PKB is a signaling intermediate upstream of survival gene expression, which is dependent on the transcription factor NFκB (nuclear factor-κB). This transcription factor is retained in the cytoplasm by proteins of the IκB family. Phosphorylation of IκB by a specific IκB kinase (IKK) targets it for ubiquitination and proteosome-mediated degradation.

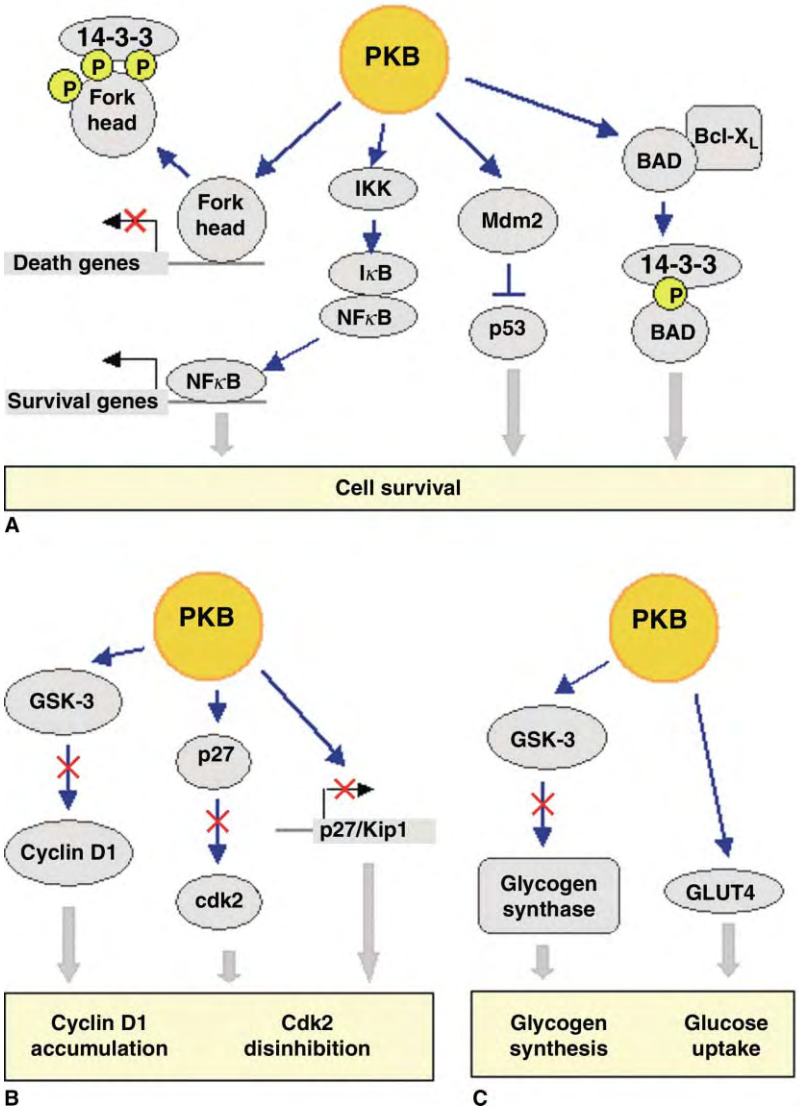

FIGURE 3 Physiological functions of PKB. PKB regulates (A) cell survival and apoptosis, (B) proliferation, and (C) glucose metabolism through phosphorylation of multiple substrates.

PKB regulates NFκB transcriptional activity through regulation of IKK activity. Activation of IKK leads to degradation of IκB and releases NFκB, allowing its nuclear translocation and subsequent activation of target genes.

Regulation of Proliferation

PKB may not be required for cell cycle progression *per se* but several downstream targets of PKB have an impact on the cell cycle machinery (Figure 3B). p27/Kip1 is a protein that blocks cell cycle. Anti-proliferative signals mobilize stored p27 and enable it to bind to and inhibit its nuclear target, cyclin-dependent kinase 2 (Cdk2), an important kinase for the initiation of DNA synthesis in the cell cycle. Phosphorylation of p27 on Thr157 by activated PKB relieves the inhibition on Cdk2. Thr157 lies within a nuclear localization signal and its phosphorylation impairs nuclear import of p27. Thus sequestered in the cytoplasm, p27 can no longer interact with Cdk2 and the kinase is allowed to remain active. In addition, PKB has been reported to downregulate transcription of p27. Another mechanism, by which PKB promotes cell proliferation, is the indirect regulation of cyclin D1 protein stability. The levels of cyclin D1 are important in G1/S phase transition in the cell cycle, and phosphorylation of cyclin D1 by glycogen synthase kinase-3 (GSK3) targets it for degradation by the proteosome. Active PKB can negatively regulate GSK3 activity by phosphorylation and thereby prevent cyclin D1 degradation. Subsequent accumulation of cyclin D1 promotes cell cycle progression.

Regulation of Glucose Metabolism

In skeletal muscle and adipocytes, PKB regulates insulin-stimulated glucose uptake and glycogen synthesis (Figure 3C). In both tissues PKBβ is the predominant isoform and becomes rapidly activated by insulin in a PI3K-dependent fashion. In unstimulated cells, glycogen synthase, the enzyme mediating incorporation of glucose from uridine diphosphoglucose into glycogen, is kept in an inactive state via phosphorylation through GSK3. Activated PKB phosphorylates and thereby inactivates GSK3, thus promoting dephosphorylation of glycogen synthase and increased glycogen synthesis. Another important PKB-dependent metabolic response to insulin is the translocation of GLUT4 from its intracellular storage pool to the plasma membrane. GLUT4 is an insulin-regulated glucose transporter in skeletal muscle and adipocytes, which in resting cells is present in intracellular endosome-like vesicles. Insulin-activated PKB triggers recruitment of these GLUT4-containing vesicles to the plasma membrane, which leads to a marked increase in the rate of glucose uptake.

Kinase-Independent Functions of PKB

In addition to acting as a kinase toward many substrates, PKB forms complexes with other proteins that are not substrates. Such proteins may serve to anchor PKB in different cellular compartments, to protect it from degradation and dephosphorylation, to regulate PKB kinase activity, or to recruit PKB substrates and/or upstream kinases. As an example, heat shock protein 90 (Hsp90) has been found to interact with PKB, possibly indirectly via the co-chaperone Cdc37, and this complex may stabilize active PKB, protecting it from dephosphorylation and degradation. Furthermore, Hsp90 might function as a scaffold protein that recruits the PKB substrate endothelial nitric oxide synthase (eNOS), an enzyme important in cardiovascular homeostasis and angiogenesis.

PKB and Cancer

PKB is the cellular homologue of the transforming oncogene v-Akt, which was found in a retrovirus termed AKT8. This retrovirus was originally isolated from mice with a high incidence of spontaneous lymphoma. v-Akt encodes a fusion protein between the viral protein Gag and full-length cellular PKBα (see Figure 1A). The viral gag domain in v-Akt possesses a myristoylation signal that mediates targeting to the plasma membrane and it thereby confers to v-Akt increased ligand-independent kinase activity as compared to cellular PKB. Deregulation of normal PKB signaling has been documented as a frequent occurrence in several human cancers. In a large number of cancers PTEN, which normally limits PKB activation, is mutated or deleted, resulting in elevated $PI(3,4,5)P_3$ levels and increased PKB activity. Furthermore, PKB gene amplification, mRNA upregulation or protein overexpression have also been reported. Aberrant elevated levels of PKB activity cause transformation of cells predominantly due to the anti-apoptotic function of PKB. Cells that have damaged DNA or are behaving in a discoordinated fashion will survive in this context instead of undergoing apoptosis, and can thus accumulate further mutations. Additionally, implication of PKB in angiogenesis and cell cycle control may contribute to cancer induction.

See Also the Following Articles

Cell Death by Apoptosis and Necrosis • Nuclear Factor kappaB • Phosphatidylinositol Bisphosphate and Trisphosphate • Protein Kinase C Family

Glossary

activation loop A short peptide loop present in protein kinases. Its conformation is altered by phosphorylation to increase or decrease catalytic activity.

apoptosis Programmed cell death, induced in cells when they are damaged (e.g., DNA damage), unnecessary, or harmful to the body.

extracellular signaling molecules Specific substances that are synthesized and released by signaling cells and produce a specific response in target cells, which have receptors for these molecules. Extracellular signaling molecules include hormones, growth factors, and neurotransmitters.

oncogene A gene whose product is involved in inducing cancer. Most oncogenes are mutant forms of normal genes involved in the control of cell cycle progression.

pleckstrin homology domain A sequence of about 100 amino acids that is present in many signaling molecules and has affinity for certain phospholipids.

Further Reading

Brazil, D. P., and Hemmings, B. A. (2001). Ten years of protein kinase B signalling: A hard Akt to follow. *Trends Biochem. Sci.* **26**, 657–664.

Brazil, D. P., Park, J., and Hemmings, B. A. (2002). PKB binding proteins: Getting in on the Akt. *Cell* **111**, 293–303.

Datta, S. R., Brunet, A., and Greenberg, M. E. (1999). Cellular survival: A play in three Akts. *Genes Develop.* **13**, 2905–2927.

Galetic, I., Andjelkovic, M., Meier, R., Brodbeck, D., Park, J., and Hemmings, B. A. (1999). Mechanism of protein kinase B activation by insulin/insulin-like growth factor-1 revealed by specific inhibitors of phosphoinositide 3-kinase–significance for diabetes and cancer. *Pharmacol. Ther.* **82**, 409–425.

Mayo, L., and Donner, D. (2002). The PTEN Mdm2, p53 tumor suppressor-oncoprotein network. *Trends Biochem. Sci.* **27**, 462–467.

Vivanco, I., and Sawyers, C. L. (2002). The phosphatidylinositol 3-kinase-Akt pathway in human cancer. *Nat. Rev. Cancer* **2**, 489–501.

Yang, J., Cron, P., Good, V. M., Thompson, V., Hemmings, B. A., and Barford, D. (2002). Crystal structure of an activated Akt/protein Kinase B Fernary complex with GSK3-peptide and AMP-PNP. *Nat. Struct. Biol.* 9(12), 940–944.

Biography

Brian Hemmings is Senior Group Leader at the Friedrich Miescher Institute. He has devoted a major part of his career to delineating the regulatory mechanisms utilized by protein kinases in signal transduction cascades.

Bettina Dummler is currently working on a Ph.D. thesis in Brian Hemmings' group at the Friedrich Miescher Institute.

Protein Kinase C Family

Alexandra C. Newton
University of California, San Diego, California, USA

Protein kinase C is a family of enzymes that has a central role in transducing information from external stimuli to cellular responses. Members of this family of serine/threonine kinases respond to signals that cause lipid hydrolysis. Protein kinase C isozymes phosphorylate an abundance of substrates, leading to both short-term cellular responses such as regulation of membrane transport and long-term responses such as memory and learning.

Historical Perspective

Protein kinase C was discovered in the late 1970s by Yasutomi Nishizuka and colleagues at Kobe University, Japan. Their initial discovery was of a constitutively active enzyme that required only Mg^{2+} for activity (and hence was named protein kinase M, PKM). Further studies revealed that PKM was a proteolytic product of a full-length enzyme; this enzyme was named protein kinase C because its enzymatic activity could be released by a Ca^{2+}-dependent protease. The subsequent discovery that protein kinase C is activated by the phospholipid hydrolysis product, diacylglycerol, was a major finding in biology: it provided the molecular mechanism for how lipid hydrolysis, discovered 25 years earlier to be triggered by stimuli such as acetylcholine, couples to cellular signaling pathways.

But the discovery that catapulted research on protein kinase C to the forefront of cellular signaling was the finding that it is the receptor for the potent tumor-promoting phorbol esters. Phorbol esters are present in the milky sap exuded from plants of the Euphorbiaceae family; the oil from the seeds of one member of this family, in particular croton tiglium, has particularly strong irritant properties and, as such, has been used over the millennia for purposes as varied as poison for hunting arrows to medicinal purposes. In the 1960s, the active ingredient in the oil was found to be a family of diesters of the tetracyclic diterpene phorbol. Phorbol esters were shown to be extremely potent tumor promoters, and classic studies revealed that painting phorbol esters on the skin of mice allowed otherwise subthreshold amounts of carcinogens to promote tumors. The finding that protein kinase C is the direct molecular target of phorbol esters placed this enzyme at the center of signaling pathways that control normal cell function and carcinogenesis.

Protein Kinase C Family Members

There are ten mammalian isozymes of protein kinase C that share in common a carboxyl-terminal kinase domain linked to an amino-terminal regulatory moiety (Figure 1). The regulatory moiety, in turn, contains a number of functional modules and it is the composition of these functional modules that further defines the three subfamilies of the protein kinase C isozymes. These modules are an autoinhibitory-pseudosubstrate sequence that maintains the enzyme in an inactive conformation, and one or two membrane-targeting modules that direct protein kinase C to the membrane following generation of the appropriate second messengers. Specifically, the C1 domain binds diacylglycerol and phorbol esters and the C2 domain binds Ca^{2+}; each event promotes the binding of the respective domain to membranes.

Conventional protein kinase C isozymes (α, βI, βII, and γ), have a C1 and a C2 domain and respond to both diacylglycerol and Ca^{2+}. Novel protein kinase C isozymes (δ, ε, η, and θ/L) have a C1 domain that binds diacylglycerol, but an impaired C2 domain that does not bind Ca^{2+}. These isozymes respond to cellular increases in diacylglycerol but not Ca^{2+}. Atypical protein kinase C isozymes (ζ and ι/λ) have an impaired C1 domain and no C2 domain and bind neither diacylglycerol nor Ca^{2+}. Thus, stimuli that elevate intracellular diacylglycerol activate conventional and novel protein kinase C family members, with conventional isozymes being additionally regulated by Ca^{2+}.

Protein Kinase C Phosphorylation

Before protein kinase C is competent to signal, it must first be processed by a series of ordered phosphorylations. The first is mediated by an upstream kinase, the phosphoinositide-dependent kinase, PDK-1.

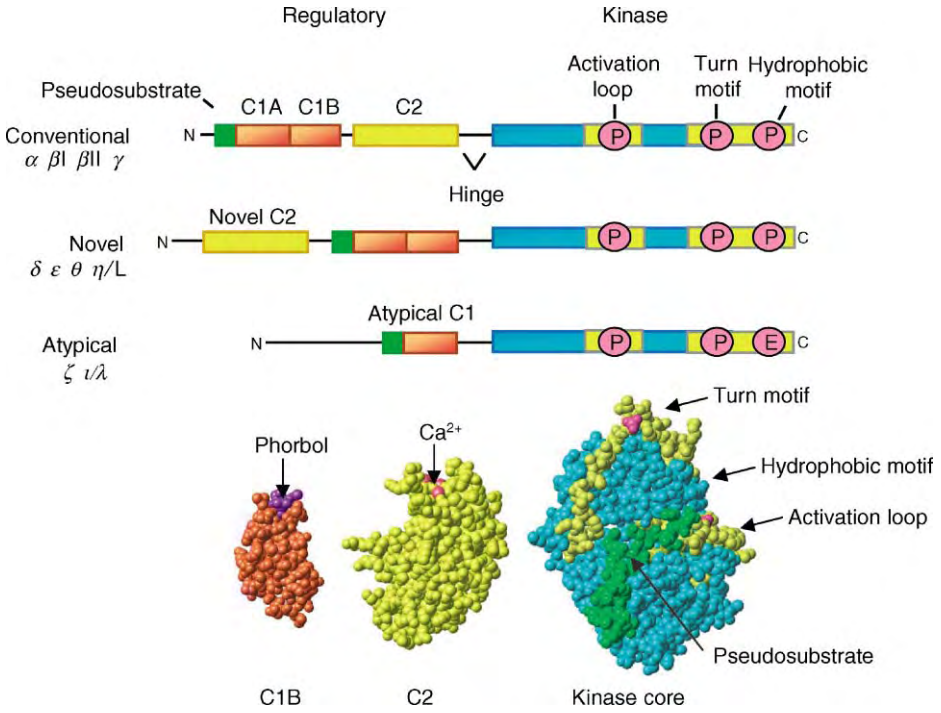

FIGURE 1 Primary structure and domain composition of protein kinase C family members. The amino terminal regulatory moiety contains the autoinhibitory pseudosubstrate sequence (green), the C1 domain, which binds diacylglycerol/phorbol esters (orange; present as a tandem repeat in conventional and novel protein kinase C isozymes), and the C2 domain, which binds Ca^{2+} (yellow). The C2 domain in novel protein kinase Cs and the C1 domain in atypical protein kinases are nonligand-binding variants. The carboxyl terminal catalytic moiety contains the kinase core which has two phosphorylation segments, the activation loop segment and the carboxyl-terminal segment (yellow), with a total of three phosphorylation sites (pink circles; the negatively charged amino acid glutamate (E) occupies the position of the phospho-acceptor position of the hydrophobic motif in atypical protein kinase Cs). The 3D structures of the domains are shown below the primary structure. Reproduced from Newton, A. C. (2003). Regulation of the ABC kinases by phosphorylation: Protein kinase C as a paradigm. *Biochem. J.* **370**, 361–371, by permission of the Biochemical Society.

This kinase has a pivotal position in cell signaling because it provides the activating phosphorylation to many other protein kinases, including the prosurvival kinase, Akt/protein kinase B. PDK-1 phosphorylates a conserved segment near the entrance to the active site referred to as the activation loop (Figure 1), an event that structures the active site for substrate binding and catalysis. The phosphorylation of the activation loop by PDK-1 triggers two intramolecular autophosphorylation reactions at two conserved positions in the carboxyl terminus, the turn motif, and hydrophobic motif (Figure 1). These phosphorylations lock protein kinase C in its mature and catalytically competent conformation. It is this species of protein kinase C that is activated by lipid hydrolysis and transduces signals.

Protein Kinase C Translocation

Mature (i.e., phosphorylated) protein kinase C is typically localized to the cytosol where it bounces on and off the membrane by diffusion-controlled mechanisms. It is maintained in an inactive conformation because the pseudosubstrate sequence occupies the substrate-binding cavity. For conventional protein kinase C isozymes, generation of Ca^{2+} and diacylglycerol target protein kinase C to the membrane by binding the C2 and C1 domains and thus tethering the enzyme to membranes. The membrane-bound species adopts an active conformation by removal of the pseudosubstrate from the substrate-binding cavity, allowing substrate binding, phosphorylation, and downstream signaling. Finding a membrane-embedded ligand (diacylglycerol) by diffusion from the cytosol is a low-probability event, and, in the case of conventional protein kinase Cs, nature has chosen a clever mechanism to increase the efficiency of this. Binding of Ca^{2+} to the C2 domain essentially pretargets protein kinase C to the membrane, where it can now initiate a much more effective search for its membrane-embedded ligand, diacylglycerol. As a consequence, conventional protein kinase Cs translocate to membranes ~1 order of magnitude faster than novel protein kinase C isozymes, which do not have the advantage of pretargeting by a Ca^{2+}-responsive C2 domain.

The advent of fluorescent methodologies has allowed imaging of protein kinase C translocation, and, most recently, activity in real time in living cells (Figure 2).

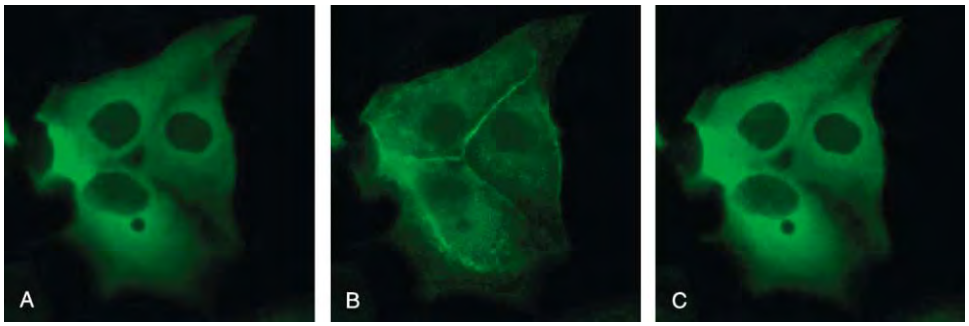

FIGURE 2 Protein kinase C was visualized in cells by expression of a construct of protein kinase C fused to a naturally fluorescent protein from the jellyfish *Aequorea victoria*, the green fluorescent protein (GFP). Panel A shows that protein kinase C is localized to the cytosol in unstimulated MDCK cells (diffuse fluorescence throughout the cell); panel B shows that protein kinase C translocates to the membrane (strong fluorescence intensity at cell peripheri) following 1 min of treatment with the agonist UTP, which induces phospholipid hydrolysis and generation of the two second messengers for protein kinase C:Ca^{2+} and diacyglycerol. Panel C shows that protein kinase C has redistributed back to the cytosol 5 min after UTP treatment; second messenger levels have returned to resting levels. Images courtesy of Jon Violin.

In general, protein kinase C translocation and activity mirrors the generation of its second messengers. For example, histamine stimulation of HeLa cells results in oscillations in protein kinase C substrate phosphorylation that are phase-locked with Ca^{2+} oscillations.

Protein Kinase C Scaffolds

Correct subcellular location is essential for normal signaling by protein kinase C. An abundance of scaffold proteins that tether protein kinase C near its substrates, activators, and regulatory proteins, such as phosphatases, has been described. The importance of correct subcellular location is perhaps best illustrated in the *Drosophila* visual cascade, where mutants lacking the protein kinase C-binding scaffold, InaD, are defective in visual transduction because components of the signaling cascade are mislocalized.

Protein Kinase C Downregulation

Prolonged activation of protein kinase C by treatment of cells with phorbol esters results in degradation of protein kinase C, a phenomenon referred to as down-regulation. In fact, prolonged treatment of cells with phorbol esters is a commonly used approach to deplete cells of all except atypical protein kinase Cs (these are resistant to phorbol ester-dependent down-regulation because they do not bind phorbol esters). The molecular mechanism of this down-regulation involves dephosphorylation of activated protein kinase C, followed most likely by ubiquitination and proteolysis. The molecular chaperone HSP70 has recently been shown to protect protein kinase C from down-regulation by allowing rephosphorylation of the enzyme and sustaining its signaling lifetime.

Protein Kinase C Signaling

Protein kinase C phosphorylates an abundance of substrates, including membrane proteins, cytoskeletal proteins, cytosolic proteins, and nuclear proteins. Yet identifying the precise cellular role and cellular targets of protein kinase C remains elusive. Genetic deletion of specific isozymes results in subtle phenotypic differences, suggesting functional redundancy of the isozymes. Nonetheless, sifting through the abundant studies on protein kinase C function reveals a few defined themes in addition to the general involvement in cell growth and proliferation. Notably, animals deficient in protein kinase C isozymes are deficient in adaptive responses. For example, mice lacking protein kinase C ε have reduced anxiety and have reduced tolerance to alcohol. Mice lacking protein kinase C γ have reduced pain perception, and mice lacking protein kinase C β II have reduced learning abilities and an impaired immune response. This theme carries over to the molecular level where many of the substrates of protein kinase C are receptors which become desensitized following phosphorylation by protein kinase C.

Isozyme-specific functions have been most clearly delineated for novel and atypical protein kinase C isozymes. For example, protein kinase C δ activation has been shown to play a role in apoptosis. Protein kinase C θ plays a key role in immune responses, and mice deficient in this isozyme have impaired T cell signaling and interleukin 2 production. Defined functions have also been established for protein kinase C ζ: this isozyme is required for maintenance of cell polarity and, in addition, regulates cell growth, DNA synthesis, and activation of the transcription factor, NFκB. Much less is known about defined physiological substrates and functions of conventional protein kinase C isozymes. Defining the precise raison d'etre for this

multi-membered class of kinases is one of the pressing issues in biological chemistry.

See Also the Following Articles

Calcium/Calmodulin-Dependent Protein Kinases • Glycine Receptors • Natriuretic Peptides and their Receptors • Neurotransmitter Transporters • Nicotinic Acetylcholine Receptors • Phosphoinositide 3-Kinase • Phospholipase C • Phospholipase D

Glossary

diacylglycerol The membrane-retained lipid backbone released from phospholipids following activation of appropriate phospholipases, enzymes that hydrolyze phospholipids. Diacylglycerol is considered a second messenger because it transfers information from stimuli such as hormones to protein kinase C, which transduces the signal by phosphorylating protein substrates.

kinase The class of enzymes that covalently transfer phosphate from ATP to hydroxyl groups of proteins.

phosphorylation The covalent attachment of phosphate from the cellular energy currency, ATP to hydroxyl residues of proteins, a modification that changes the properties of the protein.

Further Reading

Blumberg, P. M., Acs, G., Areces, L. B., Kazanietz, M. G., Lewin, N. E., and Szallasi, Z. (1994). Protein kinase C in signal transduction and carcinogenesis. *Prog. Clin. Biol. Res.* **387**, 3–19.

Kazanietz, M. G. (2002). Novel "nonkinase" phorbol ester receptors: The C1 domain connection. *Mol. Pharmacol.* **61**, 759–767.

Newton, A. C. (2000). Protein kinase C. In *Molecular Recognition* (P. M. Conn and A. R. Means, eds.) pp. 205–218. Humana Press, Totowa, NJ.

Newton, A. C. (2003). Regulation of the ABC kinases by phosphorylation: Protein kinase C as a paradigm. *Biochem. J.* **370**, 361–371.

Parker, P. J., and Parkinson, S. J. (2001). AGC protein kinase phosphorylation and protein kinase C. *Biochem. Soc. Trans.* **29**, 860–863.

Biography

Alexandra Newton is a Professor in the Department of Pharmacology at the University of California, San Diego, where her research team investigates the biology and chemistry of signaling by protein kinases, with particular focus on the molecular mechanisms of protein kinase C. She holds a Ph.D. in chemistry from Stanford University and received her postdoctoral training with Daniel E. Koshland, Jr., at the University of California, Berkeley.

Protein N-Myristoylation

Erica Dutil Sonnenburg and Jeffrey I. Gordon
Washington University School of Medicine, St. Louis, Missouri, USA

Protein N-myristoylation refers to the covalent attachment of myristic acid, a 14-carbon saturated fatty acid (C14:0), to the N-terminal glycine of proteins. Linkage occurs via an amide bond and takes place as proteins are being synthesized. N-myristoylproteins have varied intracellular destinations, and are involved in myriad cellular functions ranging from signal transduction to protein and vesicular trafficking. N-myristoylproteins are encountered in members of all Kingdoms of the eukaryotic domain (Protist, Fungi, Plant, and Animal) but are not produced by members of Bacteria or Archaea. MyristoylCoA:protein N-myristoyltransferase (Nmt), E.C. 2.3.1.97, a member of the GCN5 acetyltransferase (GNAT) superfamily, is responsible for catalyzing the transfer of myristate from myristoylCoA to proteins. While the acylCoA substrate specificity of Nmt has been highly conserved during evolution, its peptide substrate specificities have diverged among eukaryotes.

Protein N-myristoylation has relevance to a number of diseases. Genetic and pharmacologic studies have shown that Nmt activity is essential for the survival of a number of fungi that cause systemic infections in immunocompromised humans. These organisms include *Candida albicans* and *Cryptococcus neoformans*. Protein N-myristoylation is also critical to the life cycle of viruses, such as human immunodeficiency virus-1. Nmt levels are elevated in human gastrointestinal tract malignancies. Other pathogens, including *Plasmodium falciparum*, the parasite that causes malaria, have Nmts. Therefore, understanding the contributions of myristate to protein function, elucidating the structural basis for the divergent protein substrate specificities of orthologous Nmts, characterizing the myristoyl transfer reaction, and identifying biologically active, species-selective Nmt inhibitors may provide new therapeutic strategies and agents.

N-Myristoylproteins

Function of N-Myristoylation

Myristate exposed on the surface of a protein increases its lipophilicity, allowing transient, low-affinity interactions with cellular membranes or other proteins. This feature makes N-myristoylation an attractive choice for molecules involved in a variety of signaling cascades, such as protein kinases, kinase substrates, and protein phosphatases.

Myristate is not sufficiently hydrophobic to allow stable anchorage to cellular membranes. Therefore, most N-myristoylproteins utilize an additional mode of attachment. One supplementary membrane tether is provided by the reversible posttranslational covalent attachment of palmitate, a 16-carbon saturated fatty acid (C16:0), to cysteine (S-palmitoylation). Alpha subunits of heterotrimeric G proteins provide examples of this type of dual acylation. Other N-myristoylproteins, such as the protein tyrosine kinase Src, uses positively charged exposed residues to interact electrostatically with negatively charged groups in membrane lipids. Some N-myristoylproteins regulate their association with membranes through reversible exposure of their myristoyl moiety. Recoverin, a retinal photoreceptor protein involved in light adaptation, illustrates this "myristoyl-conformational switch": its myristoyl group is unfurled when the protein binds calcium; in the absence of calcium, the acyl chain is encased in a hydrophobic pocket.

Heterogeneous acylation is another device used by N-myristoylproteins to achieve regulated membrane association. Heterogenous acylation refers to Nmt-catalyzed linkage of tetradecanoate (C14:0), tetradecenoate (C14:1$^{\Delta 5}$), tetradecadienoate (C14:2$^{\Delta 5,8}$), or laurate (C12:0) to a substrate protein. At present, this phenomenon has only been described in retinal photoreceptor cells. Augmented production of these acyl-CoAs, and/or increased access of Nmt to these species, are among the mechanisms that have been invoked to account for the observed cell lineage-specificity of heterogenous acylation.

Examples of heterogeneously acylated proteins include recoverin, the α-subunit of the G protein transducin (Gtα), guanylyl cyclase activating protein, and the catalytic subunit of cAMP-dependent protein kinase. Lauric acid, and C14 fatty acids containing a *cis* double bond between C5–C6 (C14:1$^{\Delta 5}$) or C5–C6 and C8–C9 (C14:2$^{\Delta 5,8}$), have reduced hydrophobicity compared to C14:0. A less hydrophobic acyl chain may be required for these proteins to properly operate in photoreceptor cells,

either because of their extraordinarily high concentrations of membranes, and/or because the proteins require short-lived anchorage to membranes to rapidly transduce responses in visual signaling pathways.

Substrate Selection

Most proteins targeted for cotranslational N-myristoylation have an N-terminal consensus sequence of Met-Gly-X-X-X-Ser/Thr. The initiator methionine must first be removed from the nascent protein by another enzyme, methionylaminopeptidase, to expose the acceptor glycine. However, this consensus sequence is too general to allow definitive identification of Nmt substrates. Furthermore, in at least one case involving the pro-apoptotic protein BID, an internal myristoylation site is exposed after posttranslational proteolytic cleavage. Figure 1 provides a more detailed recognition consensus sequence that has been developed from an analysis of known N-myristoylproteins, as well as currently available X-ray crystal structures of Nmt.

There are a number of ways to establish that a protein is N-myristoylated, including metabolic labeling with tritiated or iodinated myristate, mass spectrometric analysis of the purified protein, or *in vitro* Nmt assays that contain the purified acyltransferase, myristoylCoA, and a peptide encompassing the N-terminal 8–15 residues of the candidate protein substrate. A current listing of experimentally confirmed as well as candidate N-myristoylproteins can be found at http://mendel.imp.univie.ac.at/myristate.

Escherichia coli containing a dual plasmid expression system has also been used widely to determine whether a protein is an Nmt substrate, and to study the functional significance of its myristoyl group. The system takes advantage of the fact that this bacterium is able to generate myristoylCoA but does not have any endogenous Nmt activity. The eukaryotic protein modification is recapitulated in this prokaryote by using one plasmid with an inducible promoter to direct expression of an Nmt, and another plasmid, containing a different inducible promoter, to express a candidate Nmt substrate. Production of Nmt is initiated first. Synthesis of the protein substrate is then turned on to allow for its cotranslational acylation. Incorporation of myristate can be verified by metabolic labeling or by mass spectrometry. The properties of the N-myristoylated protein can be compared and contrasted to that of the nonmyristoylated isoform produced in *E. coli* lacking the Nmt expression vector.

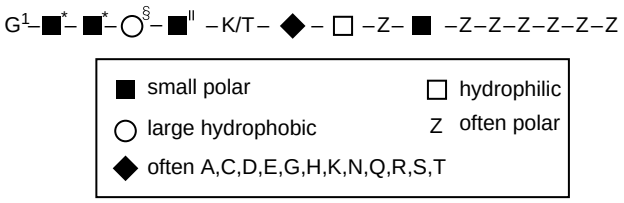

FIGURE 1 Consensus sequence for recognition of protein substrates by Nmt (*side chain volume compensation allowed; fungal Nmts allow hydrophobic residues; § some fungal Nmts prefer small residues; and ‖ often S or T). Figure based on Maurer-Strohl, S., Eisenhaber, B., and Eisenhaber, F. (2002). *J. Mol. Biol.* **317**, 523–540; 541–557.

N-Myristoyltransferase

Thus far, a total of 68 known and postulated Nmts have been identified from 63 species. Four mammalian genomes (*Homo sapiens*, *Mus musculus*, *Rattus norvegicus*, and *Bos Taurus*), plus a plant genome (the mustard weed *Arabidopsis thaliana*), contain two Nmt genes (designated type I and type II). Type I Nmts show a high degree of conservation among one another, as do the type II acyltransferases. Type I and II enzymes diverge most prominently at their N termini. These N-terminal domains are not required for catalytic activity *in vitro* but may help direct the acyltransferase to different intracellular sites. For example, the N terminus of type I human Nmt appears to be involved in its targeting to the ribosome.

Reaction Mechanism

The N-myristoyltransferase reaction mechanism has been characterized using the *Saccharomyces cerevisiae* enzyme as a model. *S. cerevisiae* Nmt contains 455 amino acids, is monomeric, and has no known cofactor requirements. Steady-state kinetics, isothermal titration calorimetrics, and X-ray crystallographic studies indicate that the enzyme has an ordered Bi–Bi reaction mechanism. The apo-Nmt first binds myristoylCoA to form a Nmt:myristoylCoA binary complex. MyristoylCoA binding allows subsequent binding of a nascent protein substrate to generate a Nmt:myristoylCoA:peptide ternary complex. Following the chemical transformation step (conversion of the enzyme:substrate complex to the enzyme:product complex), CoA and then myristoylpeptide are released. Pre-steady-state kinetic studies indicate that the rate determining step occurs after the chemical transformation, most likely involving release of myristoylpeptide.

Catalysis occurs through a classic nucleophilic addition–elimination reaction where the nucleophilic N-terminal Gly amine of the peptide substrate attacks the polarized thioester carbonyl of myristoylCoA. Several elements in the enzyme's active site facilitate this reaction. An oxyanion hole, formed by the backbone amides of two conserved residues, Phe170

and Leu171, polarizes the reactive carbonyl of myristoylCoA. The C-terminal carboxylate (Leu455 in the yeast enzyme) functions as a catalytic base to deprotonate the Gly1 ammonium to a nucleophilic amine. The amine rotates 180Å along Ψ to reduce its distance from the thioester carbonyl of myristoylCoA. H-bonding interactions between the Gly1 amine, Asn169, and Thr205 help direct the reaction trajectory, and facilitate nucleophilic attack of the polarized carbonyl. The oxyanion hole, together with the H-bonding network formed by Asn169 and Thr205, stabilizes the developing tetrahedral intermediate. With subsequent collapse of the intermediate, CoA is extruded. The Gly1 amine is deprotonated, while the thiolate leaving group of CoA is reprotonated (see www.jbc.org/cgi/content/full/276/43/39501/DC1 for an animated schematic of the reaction mechanism).

Three-Dimensional Structure of NMT: Insights about Substrate Recognition/Acquisition and Release

Presently, three X-ray crystal structures of *S. cerevisiae* Nmt have been reported: a binary complex containing bound myristoylCoA (Protein Data Bank (PDF) (www.rcsb.org/pdb/) accession 1IIC), plus two ternary complexes – one with a peptide substrate and S-(2-oxo)pentadecylCoA (a nonhydrolyzable myristoylCoA analogue containing a methylene interposed between the sulfur of CoA and the carbonyl of myristate; PDF 1IID), the other with S-(2-oxo)pentadecylCoA and a dipeptide inhibitor (PDB, 2NMT). In addition, three structures of *C. albicans* Nmt are available: the apo-enzyme (PDB, 1NMT), the enzyme with bound myristoylCoA and peptidic inhibitor (PDB, 1IYK), and the enzyme with a bound benzofuran inhibitor (PDB, 1IYL).

The Nmt fold consists of a large saddle-shaped β-sheet with several α-helices located on either side (Figure 2). There is pseudo-twofold symmetry. The N-terminal half forms the myristoylCoA binding site while the C-terminal half contributes to peptide recognition. The N terminus is disordered.

Binding of myristoylCoA induces two important conformational changes. A 3_{10} helix (A′ in Figure 2) is formed from part of the disordered N terminus, to complete the myristoylCoA binding site. There is also a change in the conformation of a loop connecting helix A and strand b (Ab loop), thereby opening a "lid" overlying the peptide binding site. The pantetheine group of CoA forms a key component of the peptide recognition site. Together, these observations indicate why myristoylCoA binding is a prerequisite for subsequent acquisition of a nascent protein substrate.

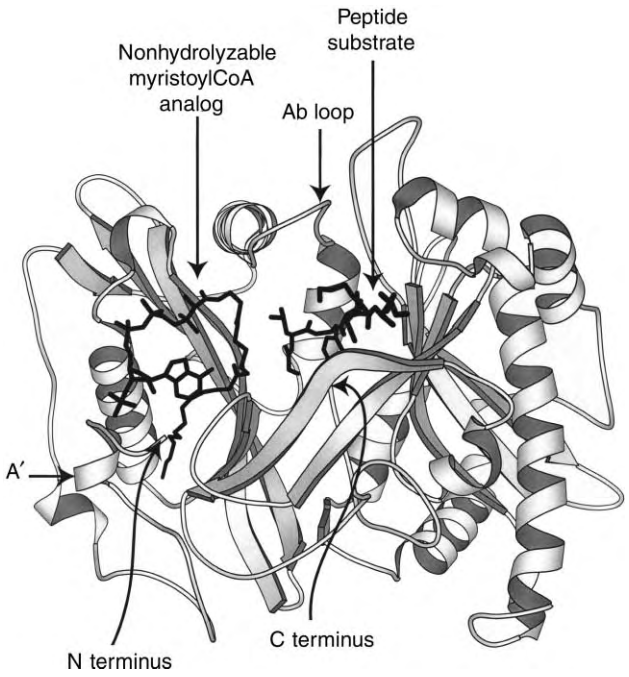

FIGURE 2 Ribbon diagram of *S. cerevisiae* Nmt. The enzyme is shown with a S-(2-oxo)pentadecylCoA, a non-hydrolyzable myristoylCoA analog and competitive inhibitor, and an octapeptide substrate (GlyLeuTyrAlaSerLysLeuAla) derived from the N terminus of ADP ribosylation factor 2 (Arf2). Binding of the myristoylCoA induces ordering of a 3_{10} helix (A′), a change in the conformation of the Ab loop, and completion of the peptide binding site. The C-terminal carboxylate (Leu455) functions as a catalytic base to deprotonate the Gly1 ammonium to a nucleophilic amine.

MyristoylCoA is bound to Nmt in a conformation that resembles a question mark (Figure 2). Nmt uses residues that produce bends at C1 and C6 of the bound myristoyl chain, as well as the floor of its acylCoA binding pocket, to measure and properly position myristoylCoA. Available X-ray structures indicate that the two additional methylenes present in palmitoylCoA cannot be accommodated by the enzyme without adversely affecting positioning of its thioester carbonyl within the oxyanion hole.

The X-ray structures suggest that the extent of ordering of the Ab loop may correlate with the overall catalytic efficiency of different Nmt peptide substrates, and that the rate limiting step in the Nmt reaction is an isomerization involving reversal of the conformational changes that take place when myristoylCoA is bound. In other words, disordering of the 3_{10} A′ helix and opening the lid formed by the Ab loop.

Therapeutics

Alignments of known Nmts disclose that their N-terminal halves are more conserved than

their C-terminal halves. This finding is consistent with their shared specificity for myristoylCoA, and with the divergent nature of their protein substrate specificities. Exploiting the differences in peptide recognition among Nmts may be key to developing species-specific inhibitors. This divergence, and the fact that genetic experiments have established that pathogenic fungi such as *C. albicans* and *C. neoformans* require Nmt for their survival, make N-myristoyltransferase an attractive target for developing new classes of fungicidal agents. The need for such agents is great given the limited number of existing drugs that effectively kill these organisms, and the increasing resistance being encountered to these available compounds.

Several classes of Nmt-targeted anti-fungal agents have been identified to date. Peptidomimetic inhibitors have been produced starting from an octapeptide substrate representing the N terminus of *S. cerevisiae* ADP ribosylation factor 2 (Arf2) (involved in vesicular trafficking). Benzofuran inhibitors have emerged from high throughput screens of chemical libraries. These benzofurans have several advantages over the Arf-derived compounds – smaller size, increased bio-availability, and resistance to degradation. Crystallographic studies of *C. albicans* Nmt revealed that one of the lead benzofurans was positioned in a hydrophobic pocket located within the enzyme's peptide substrate binding site. Using this structural information, a more biologically active derivative, substituted with difluorophenoxy- and pyridyl-terminated side chains, was created that inhibits fungal growth in a rat model of systemic Candidiasis. Further screens for compounds that display specificity for fungal compared to human Nmts are likely to yield additional classes of fungicidal compounds in the future.

See Also the Following Articles

Lipid Modification of Proteins: Targeting to Membranes • Src Family of Protein Tyrosine Kinases

Glossary

heterogeneous acylation Nmt-catalyzed attachment of the following acyl chains having somewhat lower hydrophobicity than C14:0: tetradecenoate (C14:1$^{\Delta 5}$), tetradecadienoate (C14:2$^{\Delta 5,8}$) or laurate (C12:0). At present, this modification is only known to occur in retinal photoreceptor cells.

N-myristoylproteins This diverse group of covalently modified proteins use their acyl chain to promote a variety of readily reversible interactions with various cellular membranes or with other proteins. The stability of their interactions can be regulated by other modifications, including conformational changes that affect the presentation of the myristoyl moiety, post-translational acylation at other sites with other lipids, or charge–charge interactions mediated by protein side chain atoms.

N-myristoyltransferase (Nmt) An enzyme that catalyzes the linkage of myristate, via an amide bond, to the N-terminal glycine amine of cellular proteins. Catalysis occurs through the nucleophilic addition–elimination reaction. The acyl chain length specificity of the enzyme has been highly conserved during evolution while its peptide substrate specificity has diverged among species. Nmt is a target for the development of drugs against fungal and other human pathogens.

protein N-myristoylation The covalent attachment of myristate, a 14-carbon saturated fatty acid (C14:0), to the N-terminal glycine residue of eukaryotic proteins.

Further Reading

Ames, J. B., Ishima, R., Tanaka, T., Gordon, J. I., Stryer, L., and Ikura, M. (1997). Molecular mechanics of calcium-myristoyl switches. *Nature* **389**, 198–202.

Devadas, B., Freeman, S. K., McWherter, C. A., Kishore, N. S., Lodge, J. K., Jackson-Machelski, E., Gordon, J. I., and Sikorski, J. A. (1998). Novel biologically active nonpeptidic inhibitors of myristoylCoA: Protein N-myristoyltransferase. *J. Med. Chem.* **41**, 996–1000.

Ebiike, H., Masubuchi, M., Liu, P., Kawasaki, K., Morikami, K., Sogabe, S., Hayase, M., Fujii, T., Sakata, K., Shindoh, H., Shiratori, Y., Aoki, Y., Ohtsuka, T., and Shimmma, N. (2002). Design and synthesis of novel benzofurans as a new class of antifungal agents targeting fungal N-myristoyltransferase. *Bioorg. Med. Chem. Lett.* **12**, 607–610.

Farazi, T. A., Manchester, J. K., Waksman, G., and Gordon, J. I. (2001). Pre-steady state kinetic studies of *Saccharomyces cerevisiae* myristoylCoA: Protein N-myristoyltransferase reveal that a step after chemical transformation is rate limiting. *Biochemistry* **40**, 9177–9186.

Georgopapadakou, N. H. (2002). Antifungals targeted to protein modification: Focus on protein N-myristoyltransferase. *Expert Opin. Invest. Drugs* **11**, 1117–1125.

Johnson, R. S., Ohguro, H., Palczewski, K., Hurley, J. B., Walsh, K. A., and Neubert, T. A. (1994). Heterogeneous N-acylation is a tissue- and species-specific post-translational modification. *J. Biol. Chem.* **269**, 21067–21071.

Lodge, J. K., Jackson-Machelski, E., Toffaletti, D. L., Perfect, J. R., and Gordon, J. I. (1994). Targeted gene replacement demonstrates that myristoylCoA: Protein N-myristoyltransferase is essential for the viability of *Cryptococcus neoformans*. *Proc. Natl. Acad. Sci. USA* **91**, 12008–12012.

Maurer-Strohl, S., Eisenhaber, B., and Eisenhaber, F. (2002). N-terminal N-myristoylation of proteins: prediction of substrate proteins from amino acid sequence. *J. Mol. Biol.* **317**(4): 541–547. N-terminal N-myristoylation of proteins: refinement of the sequence motif and its taxon-specific differences. *J. Mol. Biol.* **317**(4): 523–540.

Weinberg, R. A., McWherter, C. A., Freeman, S. K., Wood, D. C., Gordon, J. I., and Lee, S. C. (1995). Genetic studies reveal that myristoylCoA: protein N-myristoyltransferase is an essential enzyme in *Candida albicans*. *Mol. Microbiol.* **16**, 241–250.

Weston, S. A., Camble, R., Colls, J., Rosenbrock, G., Taylor, I., Egerton, M., Tucker, A. D., Tunnicliffe, A., Mistry, A., Mancia, F., de la Fortelle, E., Irwin, J., Bricogne, G., and Pauptit, R. A. (1998). Crystal structure of the antifungal target N-myristoyltransferase. *Nat. Struct. Biol.* **5**, 213–221.

Biography

Erica Dutil Sonnenburg is an Instructor in the Department of Molecular Biology and Pharmacology at Washington University School of Medicine in St. Louis. She holds a Ph.D. from the University

of California, San Diego in biomedical sciences and received her postdoctoral training at the Salk Institute for Biological Study in structural biology.

Jeffrey Gordon is the Dr. Robert J. Glaser Distinguished University Professor and Head of the Department of Molecular Biology and Pharmacology. He received his M.D. from the University of Chicago. In addition to characterizing the enzymology and biological significance of protein N-myristoylation, his laboratory uses mouse models to study gut development and the contributions of its indigenous microbial communities to health.

Protein Palmitoylation

Robert J. Deschenes
University of Iowa, Iowa City, Iowa, USA

Palmitoylation is the covalent modification of proteins with 16 carbon acyl chains related to palmitic acid. Protein palmitoylation was first described in the 1970s and is now recognized as a major form of posttranslational modification in all eukaryotes, with a few examples in prokaryotes as well. In many cases palmitoylation is a reversible modification, suggesting that the cell uses it to regulate protein function. This article will focus on the enzymology and functional significance of protein palmitoylation.

Covalent Modification of Proteins with Palmitoyl Groups

Palmitoylation refers to a family of protein modifications involving palmitic acid (Figure 1). The most common forms of palmitoylation are S-palmitoylation and N-palmitoylation. S-palmitoylation occurs on cysteine residues and involves a thioester linkage. In the cases where it has been investigated, S-palmitoylation is a reversible modification. Examples include receptors, signaling proteins, and scaffold proteins. N-palmitoylation reactions occur on the amino terminus or on the epsilon amino group of lysine. Reports of esterification of palmitate with serine and threonine residues (O-palmitoylation) have appeared for myelin proteolipids, however, other studies conclude that myelin proteolipids are S-palmitoylated. Protein palmitoylation is generally detected by labeling cells or cell extracts with [^{3}H]-palmitate. Identification of the covalently linked lipid is done by chemical or enzymatic cleavage followed by HPLC analysis. In most cases, palmitate is found, but in some cases unsaturated forms of palmitate are also detected. An estimate of the total extent of protein palmitoylation in the cell is difficult to obtain because of the rapid reversibility of palmitoylation and the chemical lability of thioesters. Proteomic methods that account for posttranslational modifications have begun, but application to lipid modifications needs further development. However, based on the growing list of palmitoylated proteins reported it is clear that palmitoylation is a significant posttranslational modification.

Palmitoyltransferases

There has been a debate concerning whether palmitoylation is spontaneous or enzyme mediated. The thiol of cysteine is capable of serving as a nucleophile in a spontaneous S-acylation reaction using palmitoyl-CoA as the acyl donor. However, it is difficult to know whether spontaneous palmitoylation occurs *in vivo*. It is more likely that protein acyltransferase(s) (PAT) are responsible for palmitoylation under physiological conditions. In fact, PAT activities have been reported that cofractionate with the plasma membrane and endomembranes suggesting that either there is ubiquitous expression of a single PAT or multiple PATs with distinct subcellular distributions. The recent discovery of protein PATs in model organisms has begun to shed light on this question.

Plasma membrane localization of Ras requires palmitoylation of a conserved cysteine located close to the C terminus. Palmitoylation is associated with the translocation of Ras from the endoplasmic reticulum (ER) to the plasma membrane where it functions in signaling. A genetic screen was carried out in yeast to identify mutants affecting Ras palmitoylation. Mutations in two genes, *ERF2* and *ERF4*, were identified. Lobo and co-workers found Erf2p and Erf4p form a complex that together carries out the enzymatic palmitoylation of Ras. The new enzyme is called Ras PAT. Erf2p has a conserved domain referred to as a DHHC–CRD motif (Pfam designation zfDHHC). Another yeast DHHC–CRD protein, Akr1p, has been shown to be the PAT for yeast casein kinase, Yck2p. Thus, Erf2p/Erf4p and Akr1p are founding members of a new class of S-PATs. The DHHC–CRD motif is found in six other yeast proteins, ~23 human proteins, and all other organisms examined.

Not all palmitoylated proteins are intracellular. The *Drosophila* secretes signaling molecules Hedgehog and Wnt, which are also palmitoylated. Again, genetic screens led to a candidate PAT. The gene goes by the names *skinny hedgehog* (*ski*), *sightless* (*sit*), *or rasp* depending on the group that isolated the mutation. A clue to the function came from a short region of sequence similarity with O-acyltransferases. Members

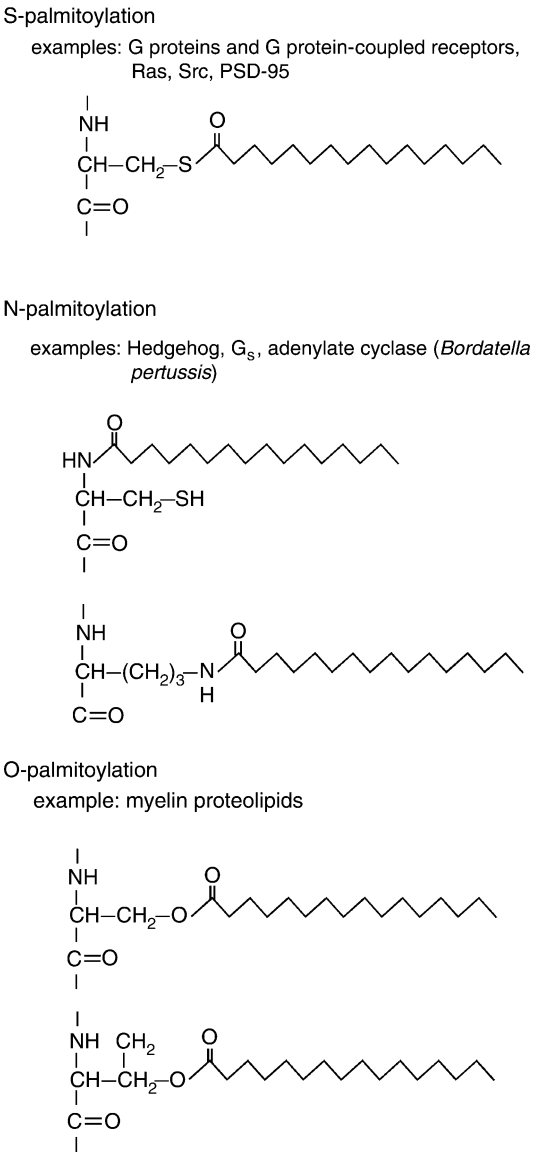

FIGURE 1 The three major classes of covalent attachment of palmitate in proteins. Representative examples of each type are listed.

of this family transfer fatty acids onto hydroxyl groups of nonproteinaceous targets. Mutation of residues in the conserved domain of *ski*/*sit*/*rasp* results in loss of Hedgehog palmitoylation and signaling. Biochemical studies are still needed to confirm that *ski*/*sit*/*rasp* is a PAT and to elucidate the mechanism.

The Wnt proteins are cysteine-rich secreted glycoproteins that have recently been shown to be palmitoylated on conserved cysteine. The modification could be removed by an acylprotein thioesterase (APT1) consistent with it being a thioester. Sequence alignment of Wnt family members reveals that this is the first cysteine residue in the sequence that is conserved in all family members. Thus, palmitoylation is likely to be found on all Wnt signaling proteins. Enzymatic depalmitoylation of purified Wnt3a protein results in the loss of its ability to stabilize β-catenin in mouse L cells, a measure of the Wnt signaling pathway. *porcupine* (*por*) is a segment polarity gene in *Drosophila* that is required for processing and secretion of Wingless (Wg). In *por* mutants, Wg is confined to cells where it is synthesized. Like *skinny hedgehog* (*ski*)/*sightless* (*sit*)/*rasp*, porcupine shares sequence homology with O-acyltransferases making it an excellent candidate for the Wnt PAT.

Palmitoylthioesterases

Given the reversible nature of protein palmitoylation, thioesterases are predicted to play an important regulatory role. However, the first protein thioesterases identified, PPT1 and PPT2, are apparently involved in protein turnover. PPT1 is found in lysosomes and mutations that reduce or eliminate its expression causes a severe neurodegenerative disorder, infantile neuronal ceroid lipofuscinosis (INCL). INCL is formally classified as a lysosomal-storage disorder. The neurological phenotype arising from a deficiency of PPT thioesterases is likely to be caused by the accumulation of palmitoyl peptides or palmitoylcysteine.

A cytosolic palmitoyl protein thioesterase, APT1, was discovered in rat liver extracts. APT1 was originally described as a lysophospholipase, but Duncan and Gilman showed that APT1 cleaves thioesters in acyl-CoAs and acylproteins, as well as oxyesters in lysolipids. In fact, APT1 exhibits a strong substrate preference for acylproteins over lipid substrates consistent with a role for APT1 as a regulator of protein thioacylation and not as a regulator of lipid metabolism. A number of substrates have been proposed for APT1 including G_α-subunits, Ras, and eNOS. APT1 orthologues have been identified in a large number of species, ranging from yeast to humans.

Palmitoylation and Protein Function

The functional significance of reversible palmitoylation depends on the protein under consideration. For peripheral membrane/cytosolic proteins lipid addition can be the primary determinant of membrane recruitment. It can also specify a particular membrane or microdomain of a membrane. A theme that has emerged from many studies is that palmitoylation operates along with other lipid modifications or membrane association sequences. Ras proteins are a case in point. Farnesylation of the C-terminal C*aaX* box targets H-Ras and N-Ras to the cytosolic surface of the ER membrane where it is further processed by a C*aaX* box protease

and methyltransferase. Plasma membrane localization of H-Ras requires palmitoylation by the Erf2p/Erf4p Ras PAT. Once at the plasma membrane, H-Ras reversibly associates with microdomains believed to be involved in signaling. There is intense interest in defining the nature of this microdomain and the role of palmitoylation in Ras signaling.

Reversible palmitoylation also influences the subcellular trafficking of integral membrane proteins. For example, receptor endocytosis and recycling is often controlled by palmitoylation status. In viral infected cells, palmitoylation directs Env proteins to lipid rafts where viral assembly occurs. In addition to surface expression and stability, palmitoylation has been proposed to play a role in signaling of some receptors. Palmitoylation can effect signaling by altering effector binding. For example, mutations in the palmitoylation site on the cytoplasmic tail of the β-adrenergic receptor leads to uncoupling of the receptor, its cognate G protein.

Palmitoylation also plays a role in vesicle trafficking and membrane fusion. Palmitoyl-CoA is required for efficient vesicle fusion in cell free assays. It is generally believed that palmitoylation of a specific protein or proteins accounts for this requirement. A possible candidate has emerged from the study of vacuole inheritance in yeast. Vac8p is a myristoylated and palmitoylated peripheral membrane protein that is required for vacuole inheritance. Palmitoylation, but not myristoylation, is required for Vac8p function. Palmitoylation of Vac8p may be involved in the interaction of Vac8p with vacuole specific SNARE complexes.

Not all palmitoylation is involved with membrane-mediated processes. Mitochondrial methylmalonyl semialdehyde dehydrogenase is covalently modified by palmitate on an active site cysteine residue. Insertion of [^{125}I]-labeled analogue of myristoyl-CoA at this site results in enzyme inhibition. This observation, together with other results that palmitoyl-CoA inhibits the activity of several mitochondrial enzymes suggests a regulatory role of S-acylation in metabolism.

Palmitoylation Inhibitors

The role of palmitoylation in cellular processes has been investigated using inhibitors such as 2-bromo or 2-fluoropalmitate, cerulenin, and tunicamycin. Each inhibits protein palmitoylation, but their mechanisms of action may differ. Cerulenin inhibits fatty acid synthase, but analogues with selectivity toward PATs are being developed and tested. Tunicamycin is a fatty acyl-CoA analogue and has been found to reduce protein palmitoylation without significantly affecting palmitoyl-CoA levels. In some cases 2-flouropalmitate has been shown to decrease uptake of [^{3}H]palmitate and thereby lower the levels of labeled palmitoyl-CoA levels and apparent protein palmitoylation. The recent identification of palmitoyltransferases should allow a more detailed characterization of these inhibitors and the development of new inhibitors with specificity toward the different classes of palmitoylated proteins.

Concluding Remarks

Protein palmitoylation has emerged as an important posttranslational modification used by cells to organize the subcellular distribution of proteins on membranes. The study of protein palmitoylation has entered a new phase with the identification of PATs in yeast and *Drosophila*. As the tools develop, the role of protein palmitoylation, in the cellular physiology, should come into better focus. PATs may be excellent targets for the design of drugs that alter the subcellular distribution of receptors and signaling molecules.

See Also the Following Articles

Fatty Acid Oxidation • Fatty Acid Receptors • Fatty Acid Synthesis and its Regulation • Lysophospholipid Receptors • Protein N-Myristoylation • Ras Family

Glossary

DHHC–CRD motif A protein sequence motif that is associated with the class of palmitoyltransferase that carries out the S-palmitoylation of proteins.

palmitoylation The process by which proteins become covalently modified by long-chain fatty acids related to palmitic acid.

palmitoylthioesterase An enzyme that cleaves palmitate from S-palmitoylated proteins.

protein acyltransferarse (PAT) An enzyme that carries out the palmitoylation of proteins.

Further Reading

Bijlmakers, M. J., and Marsh, M. (2003). The on–off story of protein palmitoylation. *Trends Cell Biol.* **13**, 32–42.

Chamoun, Z., Mann, R. K., Nellen, D., von Kessler, D. P., Bellotto, M., Beachy, P. A., and Basler, K. (2001). Skinny hedgehog, an acyltransferase required for palmitoylation and activity of the hedgehog signal. *Science* **293**, 2080–2084.

El-Husseini Ael, D., and Bredt, D. S. (2002). Protein palmitoylation: A regulator of neuronal development and function. *Nat. Rev. Neurosci.* **3**, 791–802.

Duncan, J. A., and Gilman, A. G. (1998). A cytoplasmic acyl-protein thioesterase that removes palmitate from G protein alpha subunits and p21 (RAS). *J. Biol. Chem.* **273**, 15830–15837.

Hancock, J. F. (2003). Ras proteins: Different signals from different locations. *Nat. Rev. Mol. Cell Biol.* **4**, 373–384.

Lee, J. D., and Treisman, J. E. (2001). Sightless has homology to transmembrane acyltransferases and is required to generate active Hedgehog protein. *Curr. Biol.* **11**, 1147–1152.

Linder, M. E. (2001). Reversible modification of proteins with thioester-linked fatty acids. In *The Enzymes: Protein Lipidation*, (F. Tamanoi and D. S. Sigman, eds.) Vol XXI, pp. 215–240. Academic Press, San Diego.

Linder, M. E., and Deschenes, R. J. (2003). New insights into the mechanisms of protein palmitoylation. *Biochemistry* **42**, 4311–4320.

Lobo, S., Greentree, W. K., Linder, M. E., and Deschenes, R. J. (2002). Identification of Ras palmitoyltransferase in *Saccharomyces cerevisiae*. *J. Biol. Chem.* **277**, 41268–41273.

Micchelli, C. A., The, I., Selva, E., Mogila, V., and Perrimon, N. (2002). Rasp, a putative transmembrane acyltransferase, is required for Hedgehog signaling. *Development* **129**, 843–851.

Nusse, R. (2003). Wnts and Hedgehogs: Lipid-modified proteins and similarities in signaling mechanisms at the cell surface. *Development* **130**, 5297–5305.

Resh, M. D. (1999). Fatty acylation of proteins: New insights into membrane targeting of myristoylated and palmitoylated proteins. *Biochim. Biophys. Acta* **1451**, 1–16.

Roth A. F., Feng, Y., Chen, L., and Davis, N. G. (2002). The yeast DHHC cysteine-rich domain protein Akrlp is a palmitoyl transferase. *J. Cell Biol.* **159**, 23-28.

Thompson, Jr. G. A., and Okuyama, H. (2000). Lipid-linked proteins of plants. *Prog. Lipid Res.* **39**, 19–39.

Biography

Robert Deschenes is a Professor in the Department of Biochemistry at the Carver College of Medicine, University of Iowa, Iowa City, Iowa. His research interests focus on signal transduction pathways that regulate eukaryotic cell growth, with an emphasis on the Ras oncogene. He holds a Ph.D. in biochemistry from Purdue University and was an Anna Fuller Cancer Fund Postdoctoral Fellow in the Molecular Biology Department of Princeton University. He is a member of the American Society of Biochemistry and Molecular Biology.

Protein Tyrosine Phosphatases

David J. Pagliarini, Fred L. Robinson and Jack E. Dixon
University of California, San Diego, California, USA

The process of reversible phosphorylation is perhaps the cell's most prevalent means of regulation at the molecular level. It has been estimated that up to 30% of all cellular proteins are phosphorylated, and phosphorylation has been shown to play a crucial regulatory role in such diverse cellular events as metabolism, growth and differentiation, vesicular transport, and gene transcription. Phosphorylation and dephosphorylation are carried out by kinases and phosphatases, respectively. There are currently predicted to be 518 kinases and ~125 phosphatases encoded in the human genome, further underscoring the overall importance of phosphorylation in molecular regulation. Phosphatases are generally divided into two main families based on their catalytic mechanism and substrate specificity: the protein phosphatases (PPs), which exclusively desphosphorylate serine and threonine residues, and the protein tyrosine phosphatases (PTPs), which can dephosphorylate tyrosine residues, and are the focus of this article. PTPs can be further classified into subfamilies based on (1) subcellular location (receptor versus intracellular), (2) substrate preference, and (3) three-dimensional topology. In this article, we describe the different subfamilies of PTPs and their conserved catalytic mechanism. In addition, human diseases that result from disrupted PTP signaling, and the pursuit of PTPs as drug targets are discussed.

Catalytic Mechanism of PTPs

PTPs, regardless of subfamily, are predicted to use similar mechanisms for catalyzing the removal of a phosphate group. All PTPs possess a catalytic domain that contains the active site signature motif cysteine-X_5-arginine (CX_5R; X = any amino acid), which constitutes the phosphate-binding pocket, or "P-loop". The dephosphorylation reaction is initiated when the thiol nucleophile of the active site cysteine attacks the phosphate group on the substrate molecule, forming a cysteinyl-phosphate intermediate (Figure 1). A conserved aspartic acid, usually residing outside of the P-loop, then acts as a general acid to aid in the ejection of the substrate molecule. In the second step of the reaction, the phosphoenzyme intermediate is hydrolyzed by a water molecule that has been activated by the aspartate, thereby releasing free phosphate and regenerating the active enzyme.

Classification of Protein Tyrosine Phosphatases

Intracellular PTPs

PTPs

PTPs can be classified as receptor-like (RPTPs) or intracellular based on their location within a cell. Whereas all RPTPs to date exhibit specificity towards phosphotyrosine substrates (referred to as "classic" PTPs), intracellular PTPs can be classic or dual-specific (DS-PTPs), having the ability to dephosphorylate serine/threonine, RNA, or inositol lipids in addition to pTyr (Figure 2). The major distinguishing factor between classic and dual-specific PTPs appears to be the depth of the substrate-binding pocket, with DS-PTPs having a shallower landscape less conducive to the binding of the long side chain of tyrosine. A series of structural studies over the past decade have revealed that all PTPs possess one of three distinct topologies (Figure 3). This first and largest topological family, referred to simply as PTPs, includes all of the RPTPs, such classic PTPs as PTP1B and the *Yersinia* PTP, and DS-PTPs such as VHR and PTEN, among others (Figure 2).

CDC25 family

The CDC25 family is a set of DS-PTPs involved in the regulation of the cell cycle. Each enzyme of this family is highly specific for a particular serine or threonine residue on a cyclin-dependent kinase/cyclin complex. Although presence of the signature CX_5R motif suggests a common catalytic mechanism, the PTP domains of these enzymes share little sequence homology with other PTPs (Figure 3).

LMW-PTPs

The third family of topologically distinct CX_5R phosphatases is the low-molecular-weight phosphatases

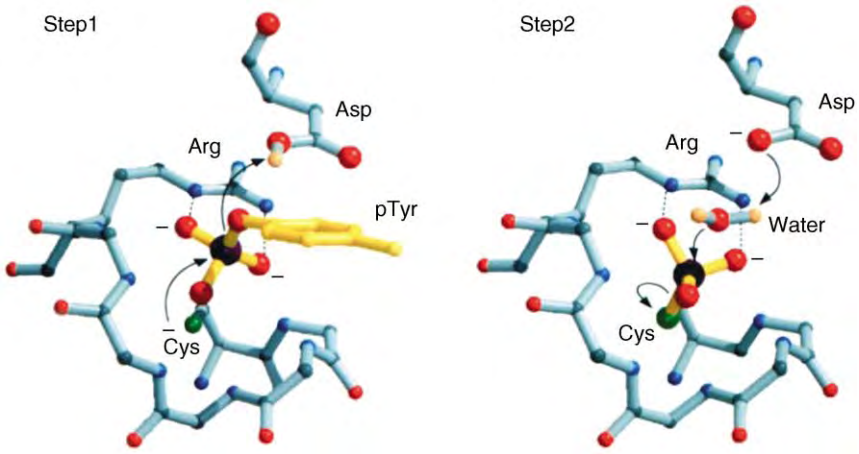

FIGURE 1 Catalytic mechanism of protein tyrosine phosphatases. Step 1: A thiolate anion of the active site cysteine performs a nucleophilic attack on the phosphate of phosphoryl-tyrosyl substrates, resulting in the formation a phospho-enzyme intermediate. An aspartic acid, acting as a general acid, donates a proton to the phosphate group, ejecting the tyrosine side chain. Hydrogen bonds between phosphate oxygen atoms and nitrogen atoms of the arginine guanido group promote phosphate binding and stabilize the transition state. Step 2: Acting as a general base, aspartate activates a water molecule for a nucleophilic attack on the phosphorous atom. The phosphorous–sulfur bond is hydrolyzed, thus regenerating the native enzyme. (Reproduced from Denu, J. M., Stuckey, J. A., Saper, M. A., and Dixon, J. E. (1996). Form and function in protein dephosphorylation. *Cell* **87**, 361–364.)

(LMW-PTPs). Conservation of the catalytic cysteine, arginine, and aspartic acid residues strongly suggests that these enzymes also utilize a similar catalytic mechanism. As with the CDC25 family, however, LMW-PTPs show no homology with other PTPs, and a lack of any other domains outside of their small (~150 amino acids) PTP domain provides few clues to their *in vivo* function. All LMW-PTPs examined to date have been specific for tyrosine-phosphorylated substrates.

Receptor-Like Tyrosine Phosphatases

Receptor-like tyrosine phosphatases (RPTPs) possess an extracellular receptor-like domain, a single transmembrane domain, and one or two intracellular classic tyrosine-specific PTP domains. Where two PTP domains exist, the membrane proximal domain accounts for the majority of catalytic activity. Based on their active site homology and common features of their extracellular domains, RPTPs can be further subdivided into eight subtypes: R1/R6, R2A, R2B, R3, R4, R5, R7, and R8 (Figure 2). The CD45 family (R1/R6) are expressed on nucleated hematopoietic cells and are thought to be involved in the positive regulation of antigen receptor signaling via dephosphorylation of the Src family kinases. RPTPs ρ, μ, κ, and λ (R2A) are marked by an extracellular MAM and an intracellular Cahedrin-like domains. They also possess extracellular fibronectin type III-like repeats and an immunoglobulin-like domain on their extracellular region that are involved in cell adhesion. The LAR-like PTPs (R2B) are primarily expressed in neuronal cells where they are thought to play an important role in neuronal development. They are marked by tandem repeats of immunoglobulin-like and fibronectin type III-like domains resembling neuronal adhesion molecules. Members of the R3 subfamily, e.g., the mammalian OST-PTP, possess multiple fibronectin type III repeats resembling cell adhesion molecules such as collagen type VII, fibronectin, and tenascin. PTP α and PTP ε (members of R4) are marked by their relatively small, highly glycosylated extracellular domains. PTP γ and PTP ζ represent the R5 subfamily, which have a carbonic anhydrase-like domain. RPTPs possessing a meprin domain in addition to immunoglobulin-like and fibronectin type III-like repeats comprise R6. Members of the R7 subfamily possess no additional extra- or intracellular domains, and the more evolutionarily distant R8 family members are predicted to be catalytically inactive.

PTPs and Human Disease

Involvement of PTPs in Mammalian Biology and Disease

At least 18 human protein tyrosine kinases (PTKs) have been shown to behave as oncoproteins when inappropriately activated by mutation. Given this, it was expected that PTPs, which can terminate tyrosine kinase signaling, might be found as genes frequently mutated in cancers. This has generally not proven to be the case. However, links between specific PTPs and human genetic diseases have been, and are continuing to be, established. In addition, numerous studies involving

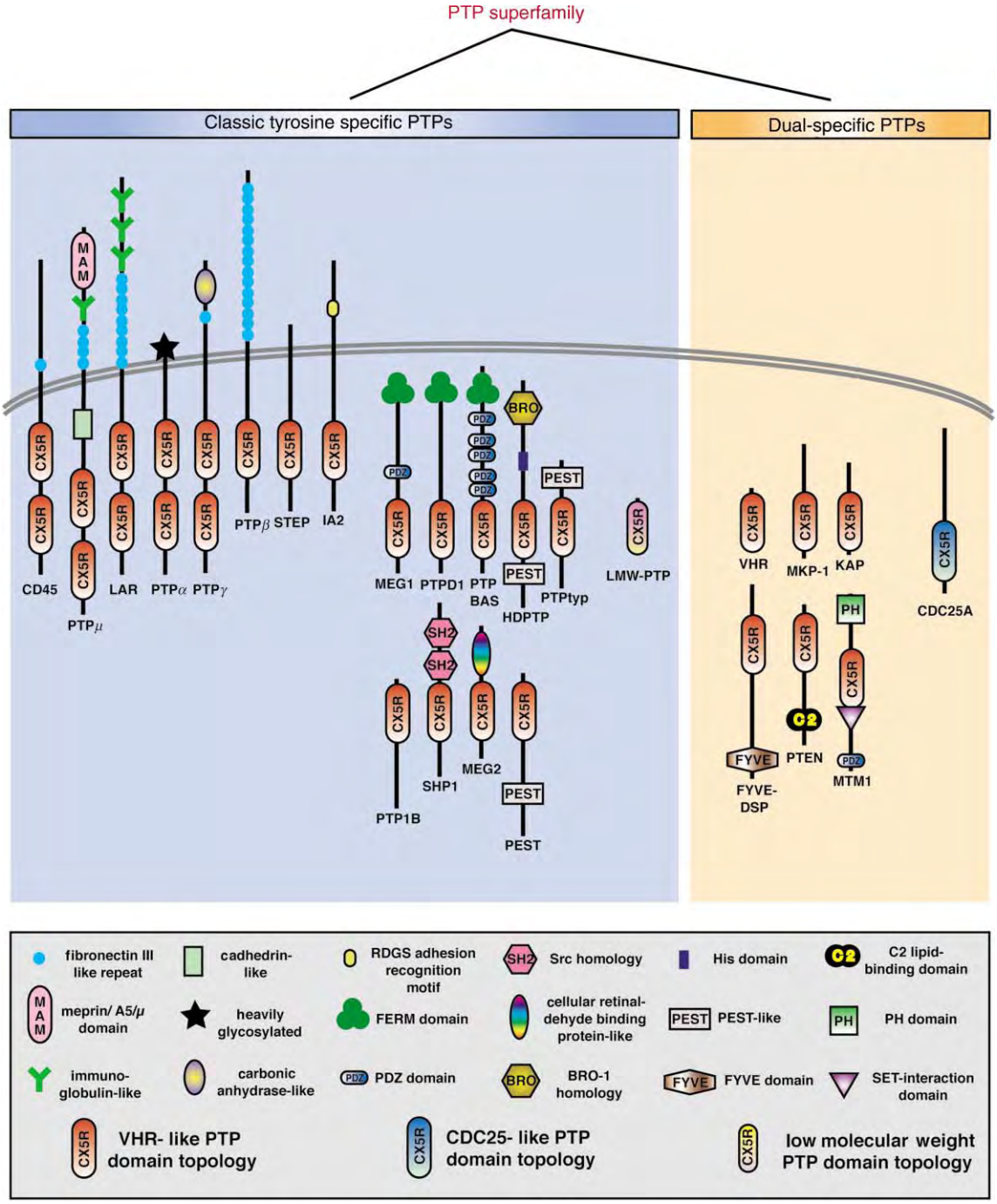

FIGURE 2 Schematic illustration of representative members of the PTP superfamily.

mice with targeted disruptions of individual PTP genes have provided *in vivo* evidence for the involvement of individual PTPs in specific biological processes. Abnormal PTP function has been implicated in a wide array of pathological conditions including diabetes, obesity, cancer, immune disease, neurodegeneration, and vascular disease. In this section, links between PTPs and human disease are briefly discussed. Studies of three PTPs that play essential roles in mammalian physiology are offered in examples. In addition, a summary of the results of PTP gene disruption experiments in mice is provided (Table I). Finally, the development of PTP inhibitors for use as therapeutics and research tools is discussed.

PTP-1B

A number of studies since the late 1990s have indicated that PTP-1B plays a specific role in down-regulating both insulin and leptin receptor signaling in mice.

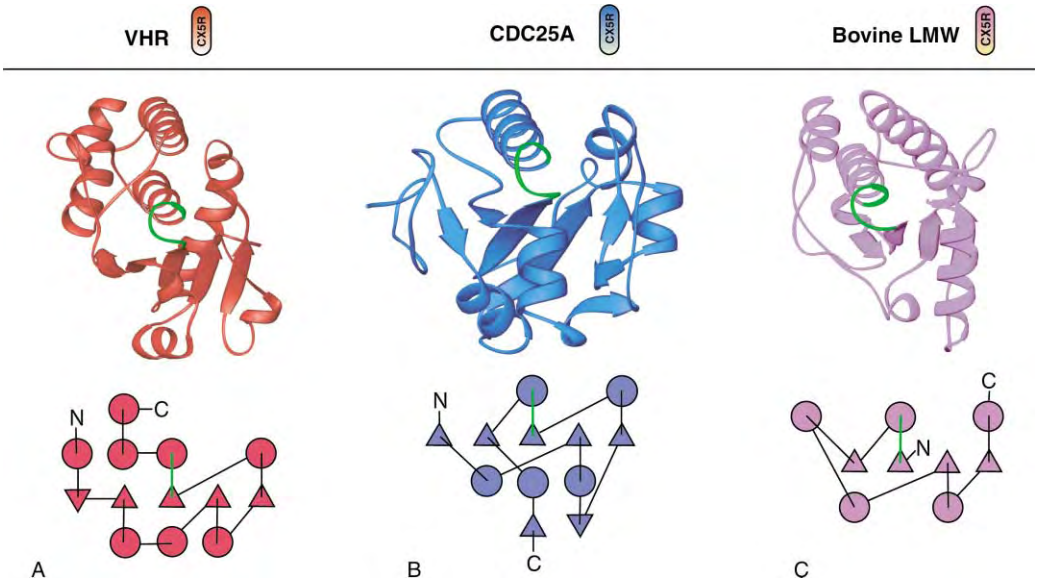

FIGURE 3 Crystal structures and topologies of representative members of each of the three topologically distinct PTP subfamilies. The amino (N) and carboxyl (C) termini of the proteins are indicated. Circles represent α-helixes; triangles represent β-strands. The location of the P-loop possessing the signature CX_5R motif is highlighted in green.

Studies from the laboratories of both Kennedy and Kahn have demonstrated that mice lacking PTP-1B are resistant to diabetes and diet-induced obesity, while displaying no other apparent physiological defects. Enhanced insulin sensitivity in PTP-1B-deficient mice likely results from hyperphosphorylation of the insulin receptor, as these mice display enhanced auto-phosphorylation of this protein in liver and muscle tissues. PTP-1B has been shown to associate with the insulin receptor PTK *in vivo* and both the insulin receptor and insulin receptor substrate 1 (IRS1) have been implicated as substrates for PTP-1B. Taken together, these data indicate a critical role for PTP-1B in turning off insulin signaling in sensitive mammalian tissues. The apparent *in vivo* specificity of PTP-1B function came as a surprise given the many other cellular processes in which this enzyme was thought to be involved. A number of pharmaceutical companies are attempting to generate specific inhibitors of PTP-1B for use as drugs to treat diabetes and obesity.

CD45

CD45 is an RPTP highly expressed in all nucleated hematopoietic cells. The extracellular portion CD45 contains fibronectin-like repeat sequences (Figure 2), is heavily glycosylated and is involved in the homodimerization of the molecule. Ligands for the extracellular domain of CD45 have not been identified, but this segment of the protein is important for the regulation of phosphatase activity. The cytoplasmic portion of CD45 contains two PTP domains; however, only the membrane proximal PTP domain is catalytically active and required for CD45 function. Homodimerization of CD45 is believed to maintain the phosphatase domain in a low activity state. CD45 mutations in either humans or mice result in a severe-combined immune deficient (SCID) phenotype, in which both B and T cells are affected (Table I). Consistent with the SCID phenotype, studies in CD45-deficient mice have indicated a role for this PTP as a critical positive regulator of immuno-receptor signaling in both B and T cells. In T cells, binding of an antigen to the extracellular portion of the T-cell receptor (TCR) results in the assembly of a cytoplasmic complex of TCR-associated signaling proteins. The PTKs Lck and Fyn phosphorylate a number of components of the assembled TCR signaling complex, leading to the recruitment and activation of the ZAP-70 PTK. Activated ZAP-70 participates in the transmission of stimulatory signals to downstream pathway components, ultimately leading to T-cell activation. The kinase activities of Lck and Fyn are negatively regulated by tyrosine phosphorylation on specific residues. By dephosphorylating these key inhibitory tyrosines, CD45 acts to prime Lck and Fyn for full activation, which is achieved through further phosphorylation. In this manner, CD45 is thought to function by setting an important threshold for T-cell activation.

Laforin

Mutations in the human gene for Laforin, a predicted DS-PTP, have been shown to cause Lafora disease, a progressive form of monoclonus epilepsy. The hallmark of Lafora disease is the accumulation of polyglucosan inclusions ("Lafora bodies") in the cytoplasm of cells of

TABLE I

Summary of PTP Gene Disruption Experiments in Mice

PTP	Mouse gene disruption phenotype and references
CD45	Severe-combined immunodeficiency (*1–3*)
CD148	Embryonic lethal (day 11.5); extensive vascular defects (*4*)
Cdc25b	Female sterility due to permanent meiotic arrest of oocytes (*5*)
Cdc25c	No phenotypic defects identified (*6*)
HePTP	Enhanced ERK activation in lymphocytes, but no physiological defects identified (*7*)
Laforin	Neurodegeneration and Lafora body accumulation; ataxia, epilepsy, and impaired behavioral responses (*8*)
LAR	Decreased basal forebrain cholinergic neuron size and hippocampal cholinergic innervation; delayed regenerative neurite outgrowth following nerve injury; impaired mammary gland development; abnormal glucose homeostasis (*9–14*)
PTP-1B	Enhanced sensitivity to insulin, leptin and growth hormone; obesity resistance (*15–19*)
PTPα	No gross phenotypic defects; reduced activation of Src and Fyn kinases; altered integrin signaling and cell migration (*20–23*)
PTPβ	No phenotypic defects identified (*24*)
PTPδ	Impaired learning; altered hippocampal long-term potentiation (*25*)
PTPε	No gross phenotypic defects; abnormal macrophage responsiveness; hypomyelination of sciatic nerve neurons; abnormal voltage-gated potassium channel function (*26*, *27*)
PTPσ	Neonatal or early lethality; developmental defects in neuronal and neuroendocrine cell lineages (*28–33*)
SHP-1	Early lethality ($<$12 weeks); severe hematopoetic dysregulation and autoimmunity (*34–37*)
SHP-2	Embryonic lethality (day 10.5) with gastrulation defects; enhanced MAP kinase activation (*38*, *39*)
TC-PTP	Early lethality ($<$*5* weeks); defective bone marrow function; impaired B and T cell function (*40–43*)

(1) Byth *et al.* (1996); (2) Mee *et al.* (1999); (3) Kishihara *et al.* (1993); (4) Takahashi *et al.* (2003); (5) Lincoln *et al.* (2002); (6) Chen *et al.* (2001); (7) Gronda *et al.* (2001); (8) Ganesh *et al.* (2002); (9) Van der Zee *et al.* (2003); (10) Xie *et al.* (2001); (11) Yeo *et al.* (1997); (12) Ren *et al.* (1998); (13) Schaapveld *et al.* (1997); (14) Van Lieshout *et al.* (2000); (15) Elchebly *et al.* (1999); (16) Klaman *et al.* (2000); (17) Cheng *et al.* (2002); (18) Zabolotny *et al.* (2002); (19) Gu *et al.* (2003); (20) Ponniah *et al.* (1999); (21) Su *et al.* (1999); (22) Zeng *et al.* (2003); (23) Zheng, D. Shalloway (2001); (24) Harroch *et al.* (2000); (25) Uetani *et al.* (2000); (26) Peretz *et al.* (2000); (27) Sully *et al.* (2000); (28) Batt, *et al.* (2003); (29) Meathre (2002); (30) McLean *et al.* (2002); (31) Batt *et al.* (2002); (32) J. Wallace *et al.* (1999); (33) Elchebly *et al.* (1999); (34) Kozlowski *et al.* (1993); (35) W. Tsui *et al.* (1993); (36) D. Shultz *et al.* (1993); (37) Kamata *et al.* (2003); (38) Saxton *et al.* (1997); (39) Arrandale *et al.* (1996); (40) Ibarra-Sanchez *et al.* (2001); (41) Dupuis (2003); (42) Galic *et al.* (2003); (43) You-Ten *et al.* (1997).

the brain, liver, kidney, skeletal and cardiac muscle, and skin. This human disease phenotype has recently been replicated in Laforin-deficient mice, through the work of Yamakawa and colleagues. In addition to its DS-PTP domain, Laforin possesses a carbohydrate-binding domain, which is required for its association with glycogen particles, and responsible for targeting the phosphatase to the same subcellular location as glycogen synthase. The cellular substrate(s) of Laforin have yet to be identified, but are actively being pursued.

PTPs as Drug Targets

Given the potential involvement of PTPs in many aspects of human biology and disease, there is considerable interest in the development of small molecule inhibitors of PTPs for use as therapeutics. In addition to their potential medical value, highly selective and potent PTP inhibitors would be powerful research tools for determining the functions of individual PTPs in mammalian cells. However, the development of specific PTP inhibitors has proved challenging. Like protein kinases, PTPs comprise a large family of enzymes that utilize a common chemical mechanism for catalysis. Accordingly, structure-based drug design is likely to be critical for the development of highly specific PTP inhibitors.

Structural studies have suggested a strategy by which inhibitor specificity for individual PTPs might be achieved. Investigations with PTPs have indicated that residues adjacent to the pTyr-binding site play essential roles in achieving substrate specificity and catalytic efficiency. Contemporary work has taken advantage of unique properties of the PTP-1B molecule to develop inhibitors with high selectivity. PTP-1B possesses a second phosphate-binding site on the protein surface, adjacent to its active site. Zhang and colleagues have designed small nonpeptide molecules containing two nonhydrolyzable phosphate moieties. Such molecules inhibit PTP-1B at nanomolar concentrations and are highly selective for this enzyme. High affinity and specificity are achieved by the combined action of the two phosphate moieties, with one binding in the active site and the other at the adjacent site. Such "bidentate" inhibitor compounds may serve as a model for the development of additional, highly specific PTP

inhibitors, as they target both the active site, which is highly conserved among PTPs, and adjacent portions of the structure, which are less highly conserved.

See Also the Following Articles

B-Cell Antigen Receptor • Serine/Threonine Phosphatases

Glossary

"classic" PTP (protein tyrosine phosphatase) These enzymes are specific for phosphotyrosine substrates.

DS-PTPs ("dual-specific" PTPs) In addition to having the ability to dephosphorylate phosphotyrosine substrates *in vitro*, DS-PTPs have been shown to utilize phosphoserine/threonine, RNA, or inositol lipids as their physiological substrate.

kinase Enzymes that work opposite of phosphatases by catalyzing the addition of phosphate group to a target substrate.

phosphatases Catalyze the removal of a phosphate group from a target substrate.

RPTP PTPs possessing a transmembrane domain and one or two classic, phosphotyrosine specific PTP domains.

Further Reading

Andersen, J. N., Mortensen, O. H., Peters, G. H., Drake, P. G., Iversen, L. F., Olsen, O. H., Jansen, P. G., Andersen, H. S., Tonks, N. K., and Moller, N. P. (2001). Structural and evolutionary relationships among protein tyrosine phosphatase domains. *Mol. Cell. Biol.* **21**, 7117–7136.

Arrandale, J. M., Gore-Willse, A., Rocks, S., Ren, J. M., Zhu, J., Davis, A., Livingston, J. N., and Rabin, D. U. (1996). Insulin signaling in mice expressing reduced levels of Syp. *J. Biol. Chem.* **271**, 21353–21358.

Batt, J., Asa, S., Fladd, C., and Rotin, D. (2002). Pituitary, pancreatic and gut neuroendocrine defects in protein tyrosine phosphatase-sigma-deficient mice. *Mol. Endocrinol.* **16**, 155–169.

Batt, J., Cutz, E., Fladd, C., and Rotin, D. (2003). Apparent normal lung architecture in protein tyrosine phosphatase-sigma-deficient mice. *Am. J. Physiol. Lung Cell. Mol. Physiol.* **284**, L214–L223.

Blume-Jensen, P., and Hunter, T. (2001). Oncogenic kinase signalling. *Nature* **411**, 355–365.

Byth, K. F., Conroy, L. A., Howlett, S., Smith, A. J., May, J., Alexander, D. R., and Holmes, N. (1996). CD45-null transgenic mice reveal a positive regulatory role for CD45 in early thymocyte development, in the selection of CD4 + CD8 + thymocytes, and B cell maturation. *J. Exp. Med.* **183**, 1707–1718.

Chen, M. S., Hurov, J., White, L. S., Woodford-Thomas, T., and Piwnica-Worms, H. (2001). Absence of apparent phenotype in mice lacking Cdc25C protein phosphatase. *Mol. Cell. Biol.* **21**, 3853–3861.

Cheng, A., Uetani, N., Simoncic, P. D., Chaubey, V. P., Lee-Loy, A., McGlade, C. J., Kennedy, B. P., and Tremblay, M. L. (2002). Attenuation of leptin action and regulation of obesity by protein tyrosine phosphatase 1B. *Dev. Cell* **2**, 497–503.

Denu, J. M., and Dixon, J. E. (1998). Protein tyrosine phosphatases: Mechanisms of catalysis and regulation. *Curr. Opin. Chem. Biol.* **2**, 633–641.

Denu, J. M., Stuckey, J. A., Saper, M. A., and Dixon, J. E. (1996). Form and function in protein dephosphorylation. *Cell* **87**, 361–364.

Dupuis, M., De Jesus lbarra-Sanchez, M., Tremblay, M. L., and Duplay, P. (2003). Gr-I + myeloid cells lacking T cell protein tyrosine phosphatase inhibit lymphocyte proliferation by an IFN-gamma- and nitric oxide-dependent mechanism. *J. lmmunol.* **171**, 726–732.

Elchebly, M., Payette, P., Michaliszyn, E., Cromliih, W., Collins, S., Loy, A. L., Normandin, D., Cheng, A., Himms-Hagen, J., Chan, C. C., *et al.* (1999a). Increased insulin sensitivity and obesity resistance in mice lacking the protein tyrosine phosphatase-1B gene. *Science* **283**, 1544–1548.

Elchebly, M., Wagner, J., Kennedy, T. E., Lanctot, C., Michaliszyn, E., Itie, A., Drouin, J., and Tremblay, M. L. (1999b). Neuroendocrine dysplasia in mice lacking protein tyrosine phosphatase sigma. *Nat. Genet.* **21**, 330–333.

Galic, S., Klingler-Hoffmann, M., Fodero-Tavoletti, M. T., Puryer, M. A., Meng, T. C., Tonks, N. K., and Tiganis, T. (2003). Regulation of insulin receptor signaling by the protein tyrosine phosphatase TCPTP. *Mol. Cell. Biol.* **23**, 2096–2108.

Ganesh, S., Delgado-Escueta, A. V., Sakamoto, T., Avila, M. R., Machado-Salas, J., Hoshii, Y., Akagi, T., Gomi, H., Suzuki, T., Amano, K., Agarwala, K. L., Hasegawa, Y., Bai, D. S., Ishihara, T., Hashikawa, T., Itohara, S., Cornford, E. M., Niki, H., and Yamakawa, K. (2002). Targeted disruption of the Epm2a gene causes formation of Lafora inclusion bodies, neurodegeneration, ataxia, myoclonus epilepsy and impaired behavioral response in mice. *Hum. Mol. Genet.* **11**, 1251–1262.

Gronda, M., Arab, S., Iafrate, B., Suzuki, H., and Zanke, B. W. (2001). Hematopoietic protein tyrosine phosphatase suppresses extracellular stimulus-regulated kinase activation. *Mol. Cell. Biol.* **21**, 6851–6858.

Gu, F., Dube, N., Kim, J. W., Cheng, A., Ibarra-Sanchez Mde, J., Tremblay, M. L., and Boisclair, Y. R. (2003). Protein tyrosine phosphatase 1B attenuates growth hormone-mediated JAK2-STAT signaling. *Mol. Cell. Biol.* **23**, 3753–3762.

Harroch, S., Palmeri, M., Rosenbluth, J., Custer, A., Okigaki, M., Shrager, P., Blum, M., Buxbaum, J. D., and Schlessinger, J. (2000). No obvious abnormality in mice deficient in receptor protein tyrosine phosphatase beta. *Mol. Cell. Biol.* **20**, 7706–7715.

Ibarra-Sanchez, M. J., Wagner, J., Ong, M. T., Lampron, C., and Tremblay, M. L. (2001). Murine embryonic fibroblasts lacking TC-PTP display delayed G1 phase through defective NF-kappaB activation. *Oncogene* **20**, 4728–4739.

Jackson, M. D., and Denu, J. M. (2001). Molecular reactions of protein phosphatases – insights from structure and chemistry. *Chem. Rev.* **101**, 2313–2340.

Kamata, T., Yamashita, M., Kimura, M., Murata, K., Inami, M., Shimizu, C., Sugaya, K., Wang, C. R., Taniguchi, M., and Nakayama, T. (2003). src homology 2 domain-containing tyrosine phosphatase SHP-1 controls the development of allergic airway inflammation. *J. Clin. Invest.* **111**, 109–119.

Kishihara, K., Penninger, J., Wallace, V. A., Kundig, T. M., Kawai, K., Wakeham, A., Timms, E., Pfeffer, K., Ohashi, P. S., Thomas, M. L. *et al.* (1993). Normal B lymphocyte development but impaired T cell maturation in CD45-exon6 protein tyrosine phosphatase-deficient mice. *Cell* **74**, 143–156.

Klaman, L. D., Boss, O., Peroni, O. D., Kim, J. K., Martino, J. L., Zabolotny, J. M., Moghal, N., Lubkin, M., Kim, Y. B, Sharpe, A. H., Stricker-Krongrad, A., Shulman, G. I., Neel, B. G., and Kahn, B. B. (2000). Increased energy expenditure, decreased adiposity, and tissue-specific insulin sensitivity in protein-tyrosine phosphatase 1B-deficient mice. *Mol. Cell. Biol.* **20**, 5479–5489.

Kozlowski, M., Mlinaric-Rascan, I., Feng, G. S., Shen, R., Pawson, T., and Siminovitch, K. A. (1993). Expression and catalytic activity of the tyrosine phosphatase PTP1C is severely impaired in motheaten and viable motheaten mice. *J. Exp. Med.* **178**, 2157–2163.

Li, L., and Dixon, J. E. (2000). Form, function, and regulation of protein tyrosine phosphatases and their involvement in human diseases. *Semin. Immunol.* **12**, 75–84.

Lincoln, A. J., Wickramasinghe, D., Stein, P., Schultz, R. M., Palko, M. E., De Miguel, M. P., Tessarollo, L., and Donovan, P. J. (2002). Cdc25b phosphatase is required for resumption of meiosis during oocyte maturation. *Nat. Genet.* **30**, 446–449.

McLean, J., Batt, J., Doering, L. C., Rotin, D., and Bain, J. R. (2002). Enhanced rate of nerve regeneration and directional errors after sciatic nerve injury in receptor protein tyrosine phosphatase sigma knock-out mice. *J. Neurosci.* **22**, 5481–5491.

Meathrel, K., Adamek, T., Batt, J., Rotin, D., and Doering, L. C. (2002). Protein tyrosine phosphatase sigma-deficient mice show aberrant cytoarchitecture and structural abnormalities in the central nervous system. *J. Neurosci. Res.* **70**, 24–35.

Mee, P. J., Turner, M., Basson, M. A., Costello, P. S., Zamoyska, R., and Tybulewicz, V. L. (1999). Greatly reduced efficiency of both positive and negative selection of thymocytes in CD45 tyrosine phosphatase-deficient mice. *Eur. J. Immunol.* **29**, 2923–2933.

Peretz, A., Gil-Henn, H., Sobko, A., Shinder, V., Attali, B., and Elson, A. (2000). Hypomyelination and increased activity of voltage-gated K(+) channels in mice lacking protein tyrosine phosphatase epsilon. *EMBO J.* **19**, 4036–4045.

Ponniah, S., Wang, D. Z., Lim, K. L., and Pallen, C. J. (1999). Targeted disruption of the tyrosine phosphatase PTPalpha leads to constitutive downregulation of the kinases Src and Fyn. *Curr. Biol.* **9**, 535–538.

Puius, Y. A., Zhao, Y., Sullivan, M., Lawrence, D. S., Almo, S. C., and Zhang, Z. Y. (1997). Identification of a second aryl phosphate-binding site in protein-tyrosine phosphatase 1B: A paradigm for inhibitor design. *Proc. Natl. Acad. Sci. USA* **94**, 13420–13425.

Ren, J. M., Li, P. M., Zhang, W. R., Sweet, L. J., Cline, G., Shulman, G. I., Livingston, J. N., and Goldstein, B. J. (1998). Transgenic mice deficient in the LAR protein-tyrosine phosphatase exhibit profound defects in glucose homeostasis. *Diabetes* **47**, 493–497.

Saxton, T. M., Henkemeyer, M., Gasca, S., Shen, R., Rossi, D. J., Shalaby, F., Feng, G. S., and Pawson, T. (1997). Abnormal mesoderm patterning in mouse embryos mutant for the SH2 tyrosine phosphatase Shp-2. *EMBO J.* **16**, 2352–2364.

Schaapveld, R. Q., Schepens, J. T., Robinson, G. W., Attema, J., Oerlemans, F. T., Fransen, J. A., Streuli, M., Wieringa, B., Hennighausen, L., and Hendriks, W. J. (1997). Impaired mammary gland development and function in mice lacking LAR receptor-like tyrosine phosphatase activity. *Dev. Biol.* **188**, 134–146.

Shen, K., Keng, Y. F., Wu, L., Guo, X. L., Lawrence, D. S., and Zhang, Z. Y. (2001). Acquisition of a specific and potent PTP1B inhibitor from a novel combinatorial library and screening procedure. *J. Biol. Chem.* **276**, 47311–47319.

Shultz, L. D., Schweitzer, P. A., Rajan, T. V., Yi, T., Ihle, J. N., Matthews, R. J., Thomas, M. L., and Beier, D. R. (1993). Mutations at the murine motheaten locus are within the hematopoietic cell protein-tyrosine phosphatase (Hcph) gene. *Cell* **73**, 1445–1454.

Su, J., Muranjan, M., and Sap, J. (1999). Receptor protein tyrosine phosphatase alpha activates Src-family kinases and controls integrin-mediated responses in fibroblasts. *Curr. Biol.* **9**, 505–511.

Sully, V., Pownall, S., Vincan, E., Bassal, S., Borowski, A. H., Hart, P. H., Rockman, S. P., and Phillips, W. A. (2001). Functional abnormalities in protein tyrosine phosphatase epsilon-deficient macrophages. *Biochem. Biophys. Res. Commun.* **288**, 184–188.

Takahashi, T., Takahashi, K., St John, P. L., Fleming, P. A., Tomemori, T., Watanabe, T., Abrahamson, D. R., Drake, C. J., Shirasawa, T., and Daniel, T. O. (2003). A mutant receptor tyrosine phosphatase, CD148, causes defects in vascular development. *Mol. Cell. Biol.* **23**, 1817–1831.

Tsui, H. W., Siminovitch, K. A., de Souza, L., and Tsui, F. W. (1993). Motheaten and viable motheaten mice have mutations in the haematopoietic cell phosphatase gene. *Nat. Genet.* **4**, 124–129.

Uetani, N., Kato, K., Ogura, H., Mizuno, K., Kawano, K., Mikoshiba, K., Yakura, H., Asano, M., and Iwakura, Y. (2000). Impaired learning with enhanced hippocampal long-term potentiation in PTPdelta-deficient mice. *EMBO J.* **19**, 2775–2785.

Van der Zee, C. E., Man, T. Y., Van Lieshout, E. M., Van der Heijden, I., Van Bree, M., and Hendriks, W. J. (2003). Delayed peripheral nerve regeneration and central nervous system collateral sprouting in leucocyte common antigen-related protein tyrosine phosphatase-deficient mice. *Eur. J. Neurosci.* **17**, 991–1005.

Van Lieshout, E. M., Van der Heijden, I., Hendriks, W. J., and Van der Zee, C. E. (2001). A decrease in size and number of basal forebrain cholinergic neurons is paralleled by diminished hippocampal cholinergic innervation in mice lacking leukocyte common antigen-related protein tyrosine phosphatase activity. *Neuroscience* **102**, 833–841.

Wallace, M. J., Batt, J., Fladd, C. A., Henderson, J. T., Skarnes, W., and Rotin, D. (1999). Neuronal defects and posterior pituitary hypoplasia in mice lacking the receptor tyrosine phosphatase PTPsigma. *Nat. Genet.* **21**, 334–338.

Xie, Y., Yeo, T. T., Zhang, C., Yang, T., Tisi, M. A., Massa, S. M., and Longo, F. M. (2001). The leukocyte common antigen-related protein tyrosine phosphatase receptor regulates regenerative neurite outgrowth in vivo. *J. Neurosci.* **21**, 5130–5138.

Yeo, T. T., Yang, T., Massa, S. M., Zhang, J. S., Honkaniemi, J., Butcher, L. L., and Longo, F. M. (1997). Deficient LAR expression decreases basal forebrain cholinergic neuronal size and hippocampal cholinergic innervation. *J. Neurosci. Res.* **47**, 348–360.

You-Ten, K. E., Muise, E. S., Itie, A., Michaliszyn, E., Wagner, J., Jothy, S., Lapp, W. S., and Tremblay, M. L. (1997). Impaired bone marrow microenvironment and immune function in T cell protein tyrosine phosphatase-deficient mice. *J. Exp. Med.* **186**, 683–693.

Zabolotny, J. M., Bence-Hanulec, K. K., Stricker-Krongrad, A., Haj, F., Wang, Y., Minokoshi, Y., Kim, Y. B., Elmquist, J. K., Tartaglia, L. A., Kahn, B. B., and Neel, B. G. (2002). PTP1B regulates leptin signal transduction in vivo. *Dev. Cell* **2**, 489–495.

Zeng, L., Si, X., Yu, W. P., Le, H. T., Ng, K. P., Teng, R. M., Ryan, K., Wang, D. Z., Ponniah, S., and Pallen, C. J. (2003). PTP alpha regulates integrin-stimulated FAK autophosphorylation and cytoskeletal rearrangement in cell spreading and migration. *J. Cell Biol.* **160**, 137–146.

Zheng, X. M., and Shalloway, D. (2001). Two mechanisms activate PTPalpha during mitosis. *EMBO J.* **20**, 6037–6049.

Zhang, Z. Y. (2002). Protein tyrosine phosphatases: Structure and function, substrate specificity, and inhibitor development. *Annu. Rev. Pharmacol. Toxicol.* **42**, 209–234.

BIOGRAPHY

Dave Pagliarini graduated with honors from the University of Notre Dame in 1999 with a B.S. in biochemistry, and is currently a doctoral candidate in Jack Dixon's lab at the University of California, San Diego. His thesis work deals with the novel mitochondrial phosphatase, PLIP.

Fred L. Robinson is a Postdoctoral Research Fellow in the laboratory of Jack E. Dixon at the University of California San Diego. He holds a Ph.D. from the University of Texas Southwestern Medical Center in Dallas. His primary research interests are protein tyrosine and lipid phosphatases.

Jack E. Dixon is a Professor of Pharmacology, Cellular and Molecular Medicine, and Chemistry and Biochemistry, as well as Dean for Scientific Affairs, at the University of California, San Diego. His principal research interests are protein tyrosine phosphatase signaling and molecular mechanisms of bacterial pathogenesis. He holds a Ph.D. from the University of California, Santa Barbara and was a postdoctoral fellow at the University of California, San Diego. He is a member of the American Academy of Arts and Sciences and the National Academy of Science.

Proteinase-Activated Receptors

Kristina K. Hansen and Morley D. Hollenberg
University of Calgary, Calgary, Alberta, Canada

Proteinase-activated receptors (PARs) are members of a recently discovered receptor family, belonging to the seven-transmembrane superfamily of cell-surface G-protein-coupled receptors. They are found in various organs across several species and have a number of physiological roles. To date, four members of this family have been cloned (PAR_1, PAR_2, PAR_3, and PAR_4). Their unique mechanism of activation involves enzymatic cleavage of the N-terminal domain. This cleavage then allows the newly unmasked N-terminal domain of the receptor to bind to another site of the receptor to start the signaling process. This process is an example of a tethered-ligand mechanism. Additionally, synthetic receptor-activating peptides (PAR-APs) of 5–6 amino acids can also bind to the receptor. Once the tethered ligand or PAR-AP binds to the receptor, a conformational change of the receptor leads to G-protein activation, which triggers the signal transduction cascade. This cascade is responsible for transcription, mitogenesis, growth, and differentiation.

Structure

Proteinase-activating receptors are composed of ~400 amino acids (Table I). All four PARs possess a number of potential N-linked glycosylation sequences on their extracellular domains. The sequence homology between all of the PARs is ~30%. The tethered ligand is revealed upon enzymatic cleavage at an arginine or lysine residue present in all of the PARs (Table I). Much evidence has supported the key role for extracellular loop 2 of PAR_1 and PAR_2 in the activation of PARs by PAR-APs. In PAR_1, a sequence of ~10 amino acids in the N-terminal extracellular domain (residues 83-93 in human PAR_1) is also involved in signaling by either the tethered ligand or by the PAR-AP. For activation by proteinases, however, the importance of extracellular loop 2 is less clearly understood. The human genes encoding PAR_1, PAR_2, and PAR_3 are all located on chromosome 5q13, while PAR_4 is located on chromosome 19p12. All of the PAR genes have similar overall structures.

Activating Proteinases

Thrombin was the first proteinase that was shown to activate PARs (Figure 1A). In fact, the original name for PAR_1 was thrombin receptor. It is now known that PAR_1, PAR_3, and PAR_4 are all targeted by thrombin. Thrombin is a key serine proteinase that regulates the blood coagulation cascade. Thrombin, however, does not activate PAR_2. The most common activator of PAR_2 is trypsin. Other serine proteinases that have been shown to target PARs include: cathepsin G, plasmin, granzyme A, factors VIIa/X/Xa/TF, mast cell tryptase, and the dust mite proteinases, Der p3 and Der p9. As already mentioned, the cleavage site that leads to activation for all of the PARs is adjacent to either an arginine or lysine residue ~40 amino acids from the N terminus (see Table I).

Inactivation

Once activated, the individual PAR receptor is no longer capable of producing another signal because it is rapidly desensitized and internalized by phosphorylation-dependent mechanisms, similar to other G-protein-coupled receptors. Another means of inactivation of PAR receptors is by cleavage of the receptor downstream (towards the C terminus) of the activation cleavage site (Figure 1D). For example, the neutrophil enzymes elastase, proteinase 3, and cathepsin G cleave PAR_1 on platelets and endothelial cells downstream of the thrombin cleavage site. The actions of these proteinases effectively inhibit thrombin from activating PAR_1.

Agonist Peptides

Specific agonist peptides (PAR-APs) modeled on the sequence of the tethered ligands can be used in place of proteinases to determine whether or not a certain PAR may be present and responsive in cells or tissues (Figure 1B). These receptor-selective peptide agonists can be used to help understand the physiological role of a particular PAR. Unlike thrombin and trypsin, which can act on various PARs, PAR-APs selective for PAR_1, PAR_2, and PAR_4 have been developed. The sequences of the selective PAR-APs for these three receptors, as designated by the one-letter codes for each amino acid are: TFLLR-NH_2 (PAR_1), SLIGRL-NH_2 (PAR_2), and

TABLE I

Summary of Human Protease-Activated Receptors

	PAR_1	PAR_2	PAR_3	PAR_4
Amino acid composition	425	397	374	385
Cleavage site for receptors	LDPR[41] ↓ SFLLRN	SKGR[36] ↓ SLIGKV	LPIK[38] ↓ TFRGAP	PAPR[47] ↓ GYPGQV
Proteinase activators	Thrombin	Trypsin, tryptase	Thrombin	Thrombin
Selective peptide agonists	TFLLR-NH_2	SLIGRL-NH_2	None known	AYPGKF-NH_2

AYPGKF-NH_2 (PAR_4), respectively (Table I). The peptide SFLLRN-NH_2, which matches exactly the tethered-ligand sequence of human PAR_1, activates both PAR_1 and PAR_2. Although SLIGRL is the tethered-ligand sequence of PAR_2 in both the rat and mouse but not the human, the peptide SLIGRL-NH_2 is a more potent agonist for human PAR_2 than SLIGKV-NH_2. Similarly, AYPGKF-NH_2 is 10 times as potent as a human PAR_4 agonist than the sequences GYPGQV-NH_2 or GYPGKF-NH_2, which represent the tethered ligands of the human and mouse receptors, respectively. The reasons for the improved selectivity and potency of the synthetic sequences versus the naturally occurring sequences have yet to be explained. At present, there is not a selective PAR_3 agonist peptide known.

Activation of PARs by Neighboring PARs

In addition to the ability of proteinases and agonist peptides to activate an individual PAR directly, one PAR can be activated via a neighboring PAR in the cell membrane. For example, it has been demonstrated that the proteolytically revealed tethered ligand of PAR_1 can in turn activate PAR_2 (Figure 1C). Thus, theoretically, PAR_2 can generate a response to thrombin without being directly activated by the enzyme. Further, by acting as a "docking site" for thrombin, PAR_1 and PAR_3 can potentially facilitate thrombin's ability to activate PAR_4. In this manner, the PARs are acting as coreceptors, the one for the other. To date, although able to act as a coreceptor for PAR_4, PAR_3 has not been found to generate an intracellular signal on its own.

Antagonists

To understand the physiological effects of the PARs fully, selective antagonists that inhibit activation of PARs by both activating proteinases and peptides will be of great use. Activation of PAR_1, by either thrombin or a PAR_1-AP, is inhibited by compounds 1 and 2 (Figure 2). Similarly, PAR_4 activation is inhibited by compound 3 (Figure 2). As yet, there are no known synthetic antagonists of PAR_2 or PAR_3.

Distribution

PARs have been detected in a variety of tissues by northern blot analysis. The brain, lung, heart, stomach, colon, kidney, small intestine, liver, pancreas, testes, prostate, uterus, placenta, trachea, thymus, lymph node, skeletal muscle, and adrenal gland have all been shown to have at least one of the PARs. Table II summarizes the tissues and cells in which each PAR is found. It is important to note, however, that cellular expression is not necessarily conserved across species. For example, human platelets express PAR_1 and PAR_4 while mouse platelets express PAR_3 and PAR_4.

Detection Methods

Reverse Transcriptase-Polymerase Chain Reaction (RT-PCR)

To see if known PARs are present in a given cell type or tissue, reverse transcriptase-polymerase chain reaction (RT-PCR) analysis, using the primers specific for each of the individual PARs, may be performed with the total RNA isolated from the cells or tissues. After complementary DNA purification by agarose gel electrophoresis and DNA sequence analysis, it can be concluded whether or not certain PARs are expressed in the sample tested. This method, however, does not guarantee that the PARs are present in their active states.

Northern Blot Analysis

In order to detect if any of the PARs are present in a tissue sample, northern blot analysis can also be performed. The total RNA is isolated from the tissue, separated by agarose gel electrophoresis, and transferred to a blotting membrane (i.e., nitrocellulose paper) via an electric field. The RNA of interest is identified by treatment of the blotting membrane with a complementary RNA or DNA probe that is labeled with ^{32}P or

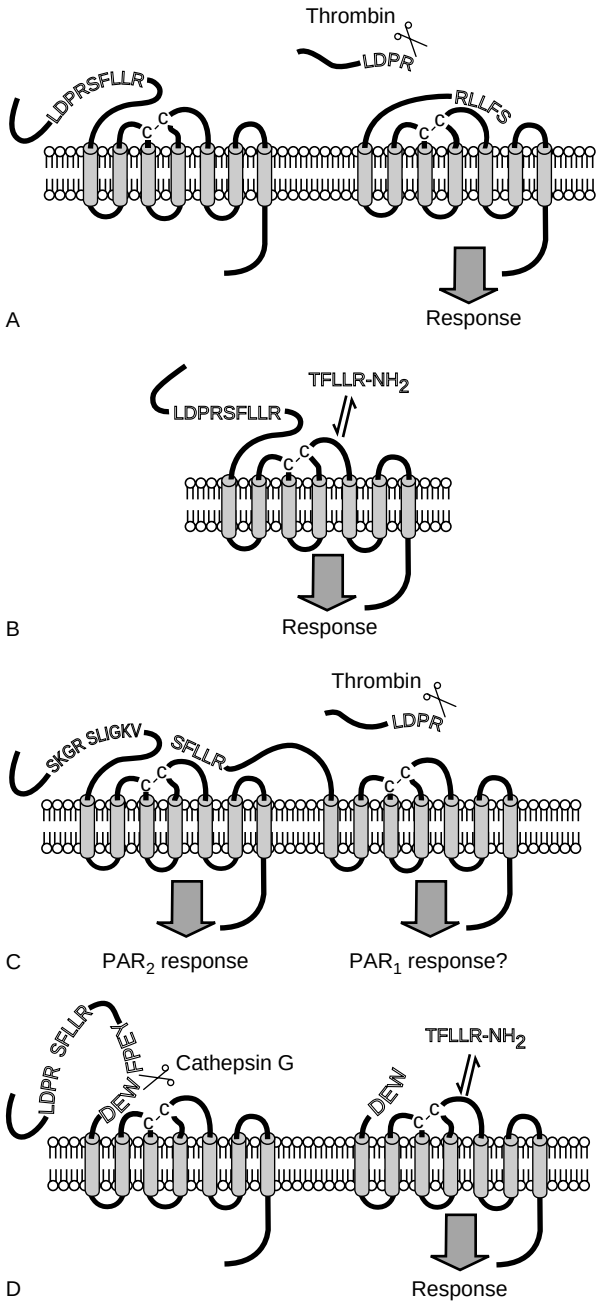

FIGURE 1 Mechanisms of activation and inactivation of PARs. (A) The functional PARs cloned to date contain within their receptor N terminus a serine protease cleavage/activation site that once cleaved by a serine protease, results in the unmasking of a cryptic tethered-ligand sequence. The revealed tethered-ligand sequence is believed to bind to and subsequently activate the receptor. The example provided (A) is for human PAR_1 activation by thrombin. (B) PARs may be activated independently of proteolytic unmasking of the tethered-ligand sequence by small synthetic peptides (PAR-APs) corresponding to the first five or six amino acids of the tethered-ligand sequence. Activation by the receptor-selective PAR_1AP, TFLLR-NH_2, is shown. (C) Intermolecular activation of PAR_1 or PAR_2 may occur following PAR_1 activation, whereby the unmasked tethered ligand of a PAR_1 receptor activates an uncleaved neighboring PAR_2 or PAR_1 receptor. (D) Inactivation of PARs may occur by proteases cleaving the receptor C-terminally of the tethered-ligand sequence, thus amputating the tethered ligand from the receptor body. These amputated receptors can no longer be activated by proteinases but are still responsive to exogenously applied PAR-APs. Note: a putative cysteine palmitoylation site in the C-terminal tail (present in all PARs except human PAR_4) may result in a fourth intracellular loop (not shown) that could play a role in receptor signaling. Reproduced with permission from Hollenberg, M. D., and Compton, S. J. (2002). International Union of Pharmacology XXVIII. Proteinase-activated receptors. *Pharmacol. Rev.* **54**, 203–217.

a fluorescent marker, followed by detection with the appropriate camera. One of the advantages of northern blot analysis is that the sequence of the probe does not need to be an exact match (e.g., from the same species).

Flow Cytometry

Flow cytometry is a technique for identifying and sorting cells that contain a component of interest by staining with a fluorescent dye and detecting the fluorescence by laser beam illumination. Cell-surface expression of PARs in a particular cell line can be identified by treatment of the cells first with anti-PAR antiserum (antibody) followed by the binding of fluorescein isothiocyanate-labeled goat antirabbit IgG that binds to the PAR antibody. Cell-surface expression of the PAR of interest can be quantified by fluorescence-activated cell sorting (FACS) analysis.

Immunocytochemistry/ Immunohistochemistry/ Immunofluorescence

These techniques take advantage of the strong interactions between antigens and their antibodies. The cells are immobilized by centrifugation onto slides using a cytospin machine or are grown directly on the slides, while tissues are embedded in paraffin, cut, and mounted on slides. The cell or tissue preparation is treated with anti-PAR antiserum (antibody) followed by a secondary antibody, which allows for detection. Antirabbit fluorescein isothiocyanate- or rhodamine-conjugated antibodies are examples of secondary antibodies used for fluorescence detection. An example of a visible detection approach is a sandwich streptavidin-conjugated peroxidase method using 3,3′diaminobenzidine as a substrate. These techniques detect the receptor directly.

In Situ Hybridization to Detect Receptor mRNA

In situ hybridization uses a complementary oligonucleotide, DNA, or RNA probe to detect a specific complementary mRNA sequence in intact tissue sections or cell preparations. This technique to locate PARs uses

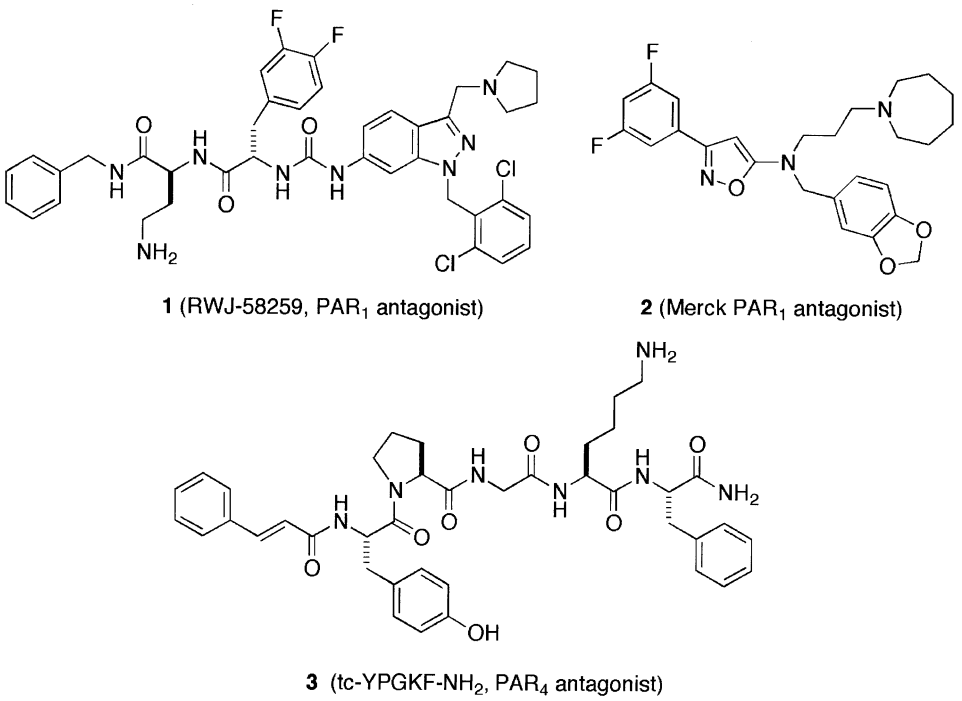

FIGURE 2 PAR antagonists.

the same principles used in northern blot analysis, except that the exact location of the mRNA can be identified. Immunohistochemistry techniques similar to those described above are used to detect the mRNA, instead of the receptor, to show where the receptor is being synthesized.

Bioassays

Measurement of Calcium Signaling Using Fluorescence Emission in Cultured Cells

As PARs are G protein-coupled receptors, once PARs are activated, the G protein undergoes a conformational change that activates phospholipase C (PLC), which then converts phosphatidyl inositol 4,5-bisphosphate (PIP_2) to inositol 1,4,5-trisphosphate (IP_3) and diacylglycerol (DAG). The IP_3 causes calcium to be released from the endoplasmic reticulum, thus increasing the intracellular calcium levels. This increase in intracellular calcium concentration can be measured in cells preincubated with a fluorescent calcium-sensitive dye (fluo-3 or fura-2) which is taken up into the cytoplasm. The fluorescence properties of the dye differ whether or not calcium is bound. For a calcium signaling assay, a fluorescence spectrophotometer measures the change in fluorescence at a defined wavelength versus time of a suspension or monolayer of cells preincubated with a fluorescent dye. When a specific PAR agonist is added to PAR expressing cells, a fluorescence peak is observed that reflects increased intracellular calcium. To confirm whether or not an unknown agonist or proteinase activates a certain PAR, cross-desensitization experiments can be performed. For example, PAR_1 and PAR_2 expressing HEK293 cells can be treated first with the PAR_1-specific agonist TFLLR-NH_2 (maximum dose) two times to desensitize PAR_1. This pretreatment is then followed by addition of the unknown agonist. If there is still a response, it can be concluded that the unknown agonist does not activate PAR_1. Likewise, to test for activation of PAR_2 by the same unknown agonist, the experiment can be repeated by exposing the cells first to the PAR_2-specific agonist SLIGRL-NH_2 to desensitize PAR_2. Alternatively, TFLLR-NH_2 may be added after two doses of the unknown agonist (maximum dose). If there is no response to TFLLR-NH_2, it can be concluded that the unknown agonist must have desensitized PAR_1 either by activation or another process.

Tissue Bioassays (Contraction or Relaxation)

To understand better how the activation of PARs leads to a biological response, blood vessels and smooth muscle strips may be treated with PAR-APs. The relaxation of rat aorta via the endothelium-dependent nitric oxide-mediated pathway can be measured. Similarly, contraction of the rat gastric longitudinal muscle can be assessed. For the bioassay experiment, a tissue is

TABLE II

Localization and Potential Roles of Human Proteinase-Activated Receptors

	PAR_1	PAR_2	PAR_3	PAR_4
Tissue distribution[a] (Northern blot analysis)	Brain, lung, heart, stomach, colon, kidney, testis	Prostate, small intestine, colon, liver, kidney, pancreas, trachea	Heart, kidney, pancreas, thymus, small intestine, stomach, lymph node, trachea	Lung, pancreas, thyroid, testis, small intestine, placenta, skeletal muscle, lymph node, adrenal gland, prostate, uterus, colon
Cellular expression	Platelets, endothelium, vascular smooth muscle, leukocytes, GI tract epithelium, fibroblasts, neurons, mast cells	Endothelium, leukocytes, GI tract epithelium and lung, airway and vascular smooth muscle, neurons, mast cells, keratinocytes, lung fibroblasts, renal tubular cells	Airway smooth muscle, platelets	Platelets, megakaryocytes
Known physiological role	Platelet activation			Platelet activation
Potential physiological roles	Pro-inflammatory, embryonic development, regulation of vascular tone	Pro-inflammatory, mediator of nocioception, airway protection, regulation of vascular tone	Cofactor for PAR_4	Platelet activation

[a] Information for PAR_2, PAR_3, and PAR_4 is provided for human tissues; for PAR_1, distribution is recorded in rat tissues, for which more extensive data are available than in human tissues.

GI, gastrointestinal.

Reproduced from Hollenberg, M. D., and Compton, S. J. (2002). International Union of Pharmacology XXVIII. Proteinase-activated receptors. *Pharmacol. Rev.* **54**, 203–217, with permission.

mounted under a resting tension in an organ bath. Changes in tension are detected using a force displacement transducer coupled to an amplifier and a data acquisition system. Known compounds that give a response are added to the organ bath to serve as a control. For example, acetylcholine is known to relax preconstricted aortic rings via an endothelium-dependent process, and potassium chloride is known to cause a large contractile response by acting directly on the smooth muscle present in the gastric or vascular preparation. PAR-APs are then added to the organ bath and the response is compared to the standards. As in the calcium signaling assay, cross-desensitization experiments can be performed to assess the potential contribution of each PAR to the biological response.

Platelet Aggregation

Platelets are known to express PARs. Activation of PARs on platelets causes aggregation. Using a light-transmission aggregometer, platelet aggregation can be monitored by measuring the turbidity of a suspension of platelets. Simply by adding agonists to a suspension of platelets, aggregation can be quantified either as a percentage increase in light transmission relative to that of the initial platelet suspension, or as a percentage of the maximal aggregation, versus time. This assay is commonly used to determine whether or not a compound is an agonist or an antagonist of PAR_1 and PAR_4. For example, if an antagonist is added before a specific PAR-AP, the aggregation of the platelets will be diminished.

Physiological Roles of PARs

PAR_1 plays an aggregatory and secretory role in human platelets and a role as a regulator of endothelial cell function. PAR_1 has also been shown to have an important role in the process of narrowing the arteries after vascular injury. PAR_2 has been suggested to be involved in the cardiovascular, pulmonary, and gastrointestinal systems, as well as having an important role in the settings of inflammation and pain sensation. Since the only role of PAR_3 shown to date is that it functions as a cofactor for thrombin-mediated activation of PAR_4, its physiological role is the same as for PAR_4. PAR_4, like PAR_1, has been shown to be responsible for the activation of platelets. There are many other physiological roles of PARs that have yet to be discovered.

See Also the Following Articles

PCR (Polymerase Chain Reaction) • Two-Dimensional Gel Electrophoresis

Glossary

agonist Compound that stimulates a cellular receptor to give a biological response.

antagonist Compound that binds to a cellular receptor which prevents a biological response from occurring.

antibody Protein produced by specialized B cells after stimulation by an antigen (foreign substance). Acts specifically against an antigen in an immune response.

glycosylation sequence Three amino acid sequence where the first amino acid is asparagine, the second is any amino acid except proline, and the third is serine or threonine.

proteinase Enzyme which selectively catalyzes the hydrolysis of peptide bonds.

PAR Acronym for proteinase-activated receptor. A G-protein-coupled receptor that is activated upon cleavage of the N-terminal domain by a proteinase.

PAR-AP Synthetic peptide that causes activation of a PAR.

Further Reading

Coughlin, S. R. (2000). Thrombin signalling and protease-activated receptors. *Nature* **407**, 258–264.

Déry, O., Corvera, C. U., Steinhoff, M., and Bunnett, N. W. (1998). Proteinase-activated receptors: Novel mechanisms of signaling by serine proteases. *Am. J. Physiol.* **274**, C1429–C1452.

Hollenberg, M. D., and Compton, S. J. (2002). International Union of Pharmacology XXVIII. Proteinase-activated receptors. *Pharmacol. Rev.* **54**, 203–217.

MacFarlane, S. R., Seatter, M. J., Kanke, T., Hunter, G. D., and Plevin, R. (2001). Proteinase-activated receptors. *Pharmacol. Rev.* **53**, 245–282.

O'Brien, P. J., Molino, M., Kahn, M., and Brass, L. F. (2001). Protease activated receptors: Theme and variations. *Oncogene* **20**, 1570–1581.

Biography

Kristina K. Hansen is a postdoctoral Fellow in the laboratory of Dr. Morley D. Hollenberg at the University of Calgary. In 2002, she received her Ph.D. in Organic Chemistry from the University of California, Berkeley.

Morley D. Hollenberg is a Professor in the Department of Pharmacology and Therapeutics and the Department of Medicine at the University of Calgary, Faculty of Medicine. His principal research interests focus on membrane receptors and signal transduction. He holds an M.D. from The Johns Hopkins University School of Medicine, Baltimore, Maryland and a D.Phil. From Oxford University, Oxford, UK.

Proteoglycans

Sara K. Olson and Jeffrey D. Esko
University of California, San Diego, La Jolla, California, USA

Proteoglycans (PGs) are glycoconjugates that contain glycosaminoglycans (GAGs) covalently attached to a protein core. They differ from glycoproteins by the unbranched, negatively charged GAG chains, which enables them to interact with numerous ligands, including growth factors, chemokines, cell adhesion proteins, protease inhibitors, and enzymes. This diverse group of molecules turns out to be essential for biological processes ranging from embryonic development to hemostasis and infection.

Proteoglycan Structure

Glycosaminoglycans

Proteoglycans (PGs) consist of two main structural components – the glycosaminoglycan (GAG) chains and the protein cores.

Three classes of GAG chains are covalently attached to PG core proteins: chondroitin sulfate (CS) /dermatan sulfate (DS), heparan sulfate (HS)/heparin, and keratan sulfate (KS) (Figure 1). Their structure, site of assembly, and pattern of sulfation and epimerization distinguish each of these types of GAGs. In addition, vertebrates contain a fourth class of GAGs called hyaluronan (hyaluronic acid, HA), but unlike the other GAGs, HA is not covalently bound to a protein core.

Building Blocks

Sugars used in GAG formation include xylose (Xyl), galactose (Gal), glucuronic acid (GlcA), N-acetylglucosamine (GlcNAc), and N-acetylgalactosamine (GalNAc). All of these sugars are hexoses (6-carbon sugars) except xylose, which contains five carbons. In order to build the chains, individual sugars are added in a stepwise manner. The enzymes that catalyze these reactions use activated sugar nucleotide donors, such as UDP-GlcNAc and UDP-GlcA for HA; UDP-GlcNAc or UDP-GalNAc, UDP-GlcA, UDP-Xyl, UDP-Gal and an activated form of sulfate called phosphoadenosine-5′phosphosulfate (PAPS) for HS/heparin and CS/DS; and UDP-Gal, UDP-GlcNAc, UDP-GalNAc, PAPS, and two additional sugar nucleotides for making keratan sulfate (GDP-Man and CMP-sialic acid). With the exception of UDP-xylose, which is derived from UDP-GlcA in the endoplasmic reticulum, all of the other sugar nucleotides assemble in the cytosol, and sugar nucleotide transporters shuttle them into the Golgi apparatus where they are used. The sugar and sulfate residues add to the growing chain, releasing UDP, PAP, GMP, or CMP for subsequent recycling in the cytoplasm.

Hyaluronan

Hyaluronan or HA is structurally the simplest GAG. It consists of repeating disaccharide units of GlcNAcβ1-4GlcAβ1-3, and does not undergo any further modification. HA is unique among the GAGs in that it does not assemble on a protein core and it is made at the plasma membrane instead of the Golgi apparatus. This orientation facilitates its extrusion from the cell into the surrounding extracellular matrix (ECM). The ECM is the network of polysaccharides and fibrous proteins that give strength, support, and structure to the cells embedded within it. HA chains are especially long, typically reaching 10^4 disaccharides. Due to their length they can intertwine to form a mesh-like material with interesting chemical properties, such as water retention and high viscosity. The turgor properties of the vitreous of the eye, the umbilical cord, and rooster combs reflect the high concentration of HA in these tissues. Several proteins, known as hyalectins, contain motifs that allow specific interactions with HA. HA helps to organize the extracellular matrix, and can bind to signaling and adhesion receptors on the cell surface, affecting growth and migration.

Chondroitin Sulfate/Dermatan Sulfate

Unlike HA, CS/DS (as well as HS/heparin) is synthesized while attached to a core protein. The chains initiate at Serine (Ser) residues of protein cores through the addition of Xyl from UDP-Xyl, followed by addition of two Gal residues, and finally GlcA from their corresponding sugar nucleotides. This linkage tetrasaccharide can undergo additional modifications, including sulfation of the Gal residues and phosphorylation of xylose, which may play a regulatory role in the assembly

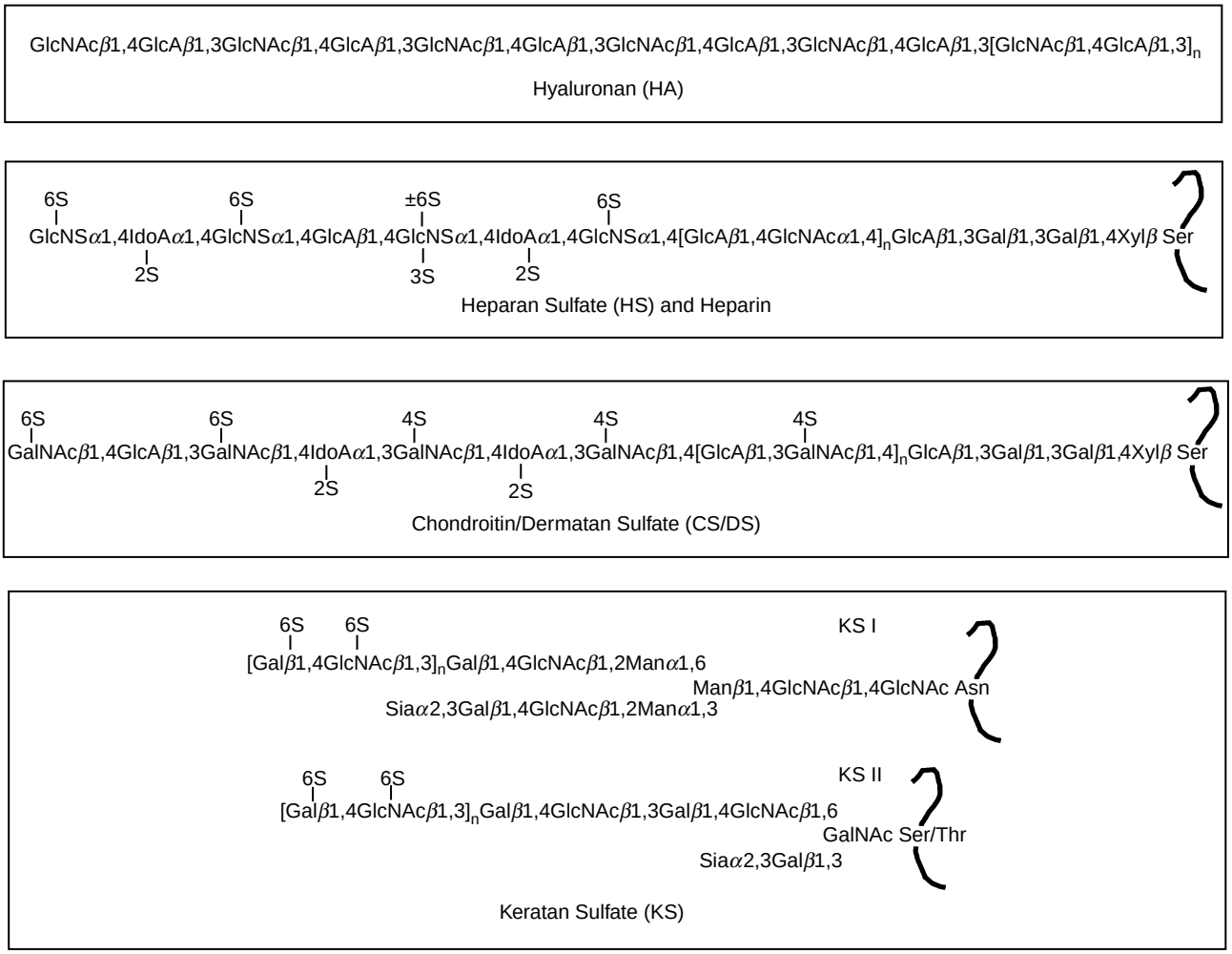

FIGURE 1 Classes of glycosaminoglycans. Hyaluronan (HA) is made up of repeating units of GlcNAc and GlcA. Heparan sulfate (HS) and chondroitin sulfate (CS) arise from a common linkage tetrasaccharide precursor linked to a protein core at serine (Ser) residues. HS consists of repeating GlcNAc and GlcA, while CS is composed of GalNAc and GlcA. Keratan sulfate (KS) is generated by the step-wise addition of GlcNAc and Gal residues. KS I is linked to the protein core via asparagine (Asn), whereas KS II is attached at Ser or threonine (Thr) residues.

process. Separate enzymes catalyze each step of the assembly of the linkage tetrasaccharide.

The growing chain is committed to become chondroitin by the addition of GalNAcβ1-4, and the chain then elongates by the assembly of the repeating units GalNAcβ1-4GlcAβ1-3, by the chondroitin synthase enzyme family. An average chain consists of $\sim$40 disaccharides, but the size varies in different tissues. The chondroitin backbone can be modified by sulfation of GalNAc units at the C-4 and/or C-6 positions, which tends to occur across the entire chain. In DS, a subset of D-GlcA units undergoes epimerization to L-IdoA, which can then be sulfated at C-2. Epimerization of GlcA to IdoA occurs by stereochemical inversion at C-5 (the proton is axial in D-GlcA but planar in L-IdoA).

CS/DS PGs are generally secreted into the extracellular matrix where they perform a variety of structural and developmental roles. The model organism *C. elegans* requires a nonsulfated form of chondroitin for the first embryonic cell division and the process of epithelial cell invagination in the vulva. In vertebrates, chondroitin sulfate plays numerous structural roles in cartilage, tendon, and other organized extracellular matrices. In the nervous system, it appears to affect axonal outgrowth and guidance. Very few binding proteins have been described, suggesting that some of chondroitin's properties may be related to its biophysical properties (hydrostatic and electrostatic effects). DS binds with growth factors and protease inhibitors involved in hemostasis.

Heparan Sulfate/Heparin

HS and heparin synthesis initiates in a manner similar to CS/DS by the assembly of the linkage tetrasaccharide.

The nascent chain becomes heparan upon addition of a GlcNAcα1-4 residue. Polymerization of the chain then ensues by the stepwise addition of GlcAβ1-4 and GlcNAcα1-4. As the chain elongates, it undergoes a number of modifications. Subsets of GlcNAc residues can be N-deacetylated, N-sulfated, and O-sulfated at the C-3 and C-6 positions. As in the case of CS/DS, epimerization of GlcA to IdoA can occur at residues neighboring GlcNS. Additionally, the uronic acids can be sulfated at C-2. HS chains are generally modified in sections, with highly sulfated blocks interspersed between nonmodified regions. Variable deacetylation, epimerization, and sulfation patterns give rise to specific binding sites for a large number of ligands, including growth factors (FGFs, Wnts, BMPs), anticoagulant proteins (antithrombin III, heparin cofactor II, which also binds DS, and thrombin), and matrix components (e.g., laminin, fibronectin, and some collagens). HS plays a vital role in numerous biological processes involved in cell growth, migration, and differentiation. A human disease called hereditary multiple exostosis (HME), characterized by bony outgrowths on the long bones, is caused by mutation of the enzymes responsible for polymerizing the HS chain (EXT-1 and EXT-2).

Heparin is a form of HS that has potent anticoagulant activity due to its ability to bind and activate antithrombin, a protease inhibitor, by way of a unique pentasaccharide sequence. In general, heparin is much more extensively modified compared to HS, containing as much as 85% GlcNS units and 75% IdoA, whereas HS contains 40–50% GlcNS and 25–40% IdoA. However, sections of HS chains can be extensively modified by sulfation and epimerization like heparin. Heparan sulfate is made by virtually all cells, whereas heparin is made selectively by connective tissue-type mast cells and stored in secretory granules. Therapeutic heparin derives from porcine and equine tissue digests. Commercial heparin Sepharose is often used to aid in the purification of proteins.

Keratan Sulfate

KS is classified as a glycoprotein as well as a PG. The chain consists of repeating Galβ1-4GlcNAcβ1-3 units (N-acetyllactosamine), containing sulfate groups in the C-6 positions of Gal and GlcNAc residues. Two forms of KS PGs vary by their linkage to core proteins. In KSI, the linkage of the polylactosamine is identical to conventional Asn-linked glycoproteins, whereas in KSII, the linkage is identical to that found in mucins (Figure 1). Like HS, the disaccharide units of KS can be unsulfated, monosulfated, or disulfated. KS is expressed in cartilage and a number of epithelial and neural tissues, playing a role in events as diverse as collagen fiber assembly, wound healing, and embryogenesis. They are also present in neurosecretory vesicles, suggesting unique roles in vesicle formation and neuronal activity.

Protein Cores

With the exception of HA, all GAGs are synthesized while attached to a protein core. Some PG cores serve functional roles by binding to other matrix molecules and bridging the extracellular matrix to the cytoskeleton. The number of GAG chains carried by individual PGs depends on the number of attachment sites, ranging from a single chain (decorin) up to 100 chains (aggrecan) (Table I). Most PGs contain multiple glycosylation sites, any or all of which may be used. A loose consensus sequence has been identified for HS and CS glycosylation sites on the protein core. Xylose is added to Ser residues that are followed by glycine (Gly), typically flanked by two or more acidic amino acids (Asp or Glu). The factors that regulate the efficiency of initiation are unknown. Evidence also exists that the presence of hydrophobic residues near the attachment sites, the density of attachment sites, as well as inhibitory sequences in the protein cores determine the selection of sites for the assembly of HS/heparin or CS/DS.

Proteoglycan Families

More than 25 PGs have thus far been identified in mammalian systems (Table I), and many fall into gene families based on sequence homologies. Some PGs carry a single type of GAG, whereas others can be hybrid molecules carrying HS and CS or CS and KS. Many PGs also carry other types of O-linked and N-linked glycans. Some PGs are large globular molecules reaching masses of 400 kDa, while others have small masses around 10 kDa. While structurally diverse, they can be classified into the following families based on location and homology.

Secreted and Matrix Proteoglycans

PGs secreted into the ECM can carry CS or DS chains. This group includes the small interstitial PGs, the aggrecan family, the basement membrane PG bamacan, and secretory granule PGs, such as serglycin. Perlecan and agrin are the only known HSPGs specifically secreted into the ECM. However, some membrane HSPGs can be shed from the cell surface and the ectodomains can become part of the ECM or accumulate in extracellular fluids.

TABLE I

Proteoglycan Families

Class	Family	Proteoglycan	Core mass (kDa)	Chain #	Chain type	Tissue
Matrix/secreted	Small interstitial	Decorin	36	1	CS	Connective tissue cells
		Biglycan	38	1–2	CS	Connective tissue cells
		Endocan	20	1	CS	Endothelial cells
		Epiphycan	35	2–3	CS	Cartilage
		Fibromodulin	42	2–3	KS	Broad
		Lumican	38	3–4	KS	Broad
		Keratocan	38	3–5	KS	Broad
		Mimecan/osteoglycin	25–35	2–3	KS	Broad, sulfated in cornea
		Osteoadherin	49	2–3	KS	Bone
	Aggrecan	Aggrecan	208–220	~100	CS/KS	Cartilage
		Versican	265	12–15	CS	Fibroblasts
		Neurocan	145	1–2	CS	Brain
		Brevican	96	0–4	CS	Brain
	Basement membrane	Bamacan	138	1–3	CS	Basement membranes
		Perlecan	400	1–3	HS	Basement membranes
		Agrin	212	2–3	HS	Basement membranes
	Intracellular storage	Serglycin	10–19	10–15	Heparin/CS	Mast cells
		SV2	80	1–3	KS	Synaptic vesicles
	Miscellaneous	Collagen α2 type IX	68	1	CS	Cartilage, vitreous humor
		Collagen type XVIII	150	1–3	HS	Epithelial cells, basement membranes
		Phosphacan	176		CS/KS	Brain
		Testicans 1–3	50	1–3	HS/CS	Testes, brain endothelium
Membrane bound	Syndecans	Syndecans 1–4	31–45	1–3	HS/CS	Epithelial cells, fibroblasts
	Glypicans	Glypicans 1–6	~60	1–3	HS	Epithelial cells, fibroblasts
	Miscellaneous	Betaglycan	110	1–2	HS/CS	Fibroblasts
		Thrombomodulin	58	1	CS	Endothelial cells
		CD44	37	1–4	CS	Lymphocytes
		NG2	251	2–3	CS	Neural cells
		Invariant chain	31	1	CS	Antigen-processing cells

Small Interstitial Proteoglycans (Small Leucine-Rich Proteoglycans)

This class of PGs includes proteins with leucine-rich repeats flanked by cysteines in their central domain. The family has over nine members, and all carry either CS/DS or KS GAG chains. Members include decorin and biglycan, which interact with collagen in the matrix. Much work to date has concentrated on understanding the role of these PGs in stabilizing and organizing collagen fibers. In decorin, this activity appears to be dictated by the PG core since removal of the GAG chains fails to disrupt fibrillogenesis. Mice lacking the decorin PG live to adulthood but show a fragile skin defect. Decorin mutants exhibit great variation in fibril diameter and spacing. In the cornea, KSPGs maintain the register of collagen fibers, which is required for transparency. Decorin is also able to bind TGF-β, serving as a sink to keep the growth factor sequestered.

Aggrecan Family

The Aggrecan family of PGs includes aggrecan, versican, brevican, and neurocan. All four members share these common features: the N-terminal domain is able to bind HA, the central region contains GAG attachment sites, and the C-terminal domain contains a C-type lectin domain (lectins are nonimmunoglobulin, nonenzymatic proteins that bind sugar chains). Aggrecan is the most well-known member of this family, since it is the

major PG present in cartilage. It contains by far the largest number of GAG chains, as many as 100 CS and KS chains per protein. It complexes with HA in the ECM and draws water into cartilage, thereby providing the ability to resist compressive forces. Versican is the largest member of the aggrecan family with a mass of 265 kDa, but it also undergoes alternative splicing events that generate smaller proteins. Roles in neural crest cell and axonal migration have been suggested. Neurocan and brevican are both localized to the brain. Neurocan is expressed in the late embryonic central nervous system (CNS) and acts to inhibit neurite outgrowth. Brevican is expressed in the terminally differentiated CNS, particularly in the perineuronal nets.

Basement Membrane Proteoglycans

The basement membrane is an organized layer of ECM that lies flush against epithelial cells and consists of laminin, collagen, nidogen, and PGs. Basement membranes contain three types of large PGs, each containing 1–3 GAG chains. Bamacan is the most recently cloned member of this family and has not yet been studied in detail. It carries predominantly CS chains. Perlecan and agrin, on the other hand, are HSPGs (though perlecan has been shown to carry CS on occasion). Perlecan is the largest known PG with a mass of 400 kDa and is a modular protein with multiple domains that serve numerous functions. It appears to play a role in embryogenesis and tissue morphogenesis. It is present in the pre-implantation blastocyst and endothelial cells. Agrin is a well-characterized PG that acts in the nervous system by aggregating acetylcholine receptors at the neuromuscular junction, and is additionally expressed in the renal tubules where it plays an important role in determining the filtration properties of the kidney. Homologues of the basement membrane PGs exists in flies and worms.

Secretory Granule Proteoglycans

Serglycin is the main PG localized to intracellular cytoplasmic secretory granules. It is synthesized by endothelial, endocrine, and hematopoietic cells, and it can carry CS, DS or heparin chains. Serglycin is stored in secretory granules until the host cell becomes activated, resulting in secretion of granular contents into the surrounding environment. Serglycin may play a role in packaging granular contents, maintaining proteases in an inactive state, and regulating activities after secretion, such as coagulation, host defense, and wound repair. Heparin, the highly sulfated form of HS, is made exclusively on serglycin present in mucosal mast cells.

Membrane-Bound Proteoglycans

Many PGs reside in cell membranes as type I transmembrane proteins (e.g. syndecan family) or glycosylphosphatidylinositol (GPI)-linked proteins (e.g. glypican family).

Syndecans

In syndecans, a short hydrophobic domain spans the membrane, linking the larger extracellular domain containing the GAG attachment sites to a smaller intracellular cytoplasmic domain. There are four members in mammalian systems, whereas lower organisms such as flies and worms contain only one homologue. They can carry HS and/or CS chains, which bind a wide range of extracellular ligands such as growth factors and matrix molecules. These interactions likely account for the requirement of syndecans at numerous stages of embryonic development and in the adult animal. Syndecans can additionally coordinate signals from the extracellular environment to the intracellular cytoskeleton via their cytoplasmic tails. For example, binding of a ligand to a GAG chain can induce oligomerization of syndecans at the cell surface. This leads to recruitment of factors at the cytoplasmic tail of syndecan, such as kinases (e.g. c-Src), PDZ-domain proteins, or cytoskeletal proteins. The recruitment of cytosolic proteins in turn triggers a signal that leads to actin filament assembly. Proteolytic cleavage of the syndecans occurs, resulting in release of the ectodomains bearing the GAG chains. These ectodomains can have potent biological activity.

Glypicans

The glypican family of cell-surface PGs is involved in numerous aspects of animal development. The C terminus is embedded in the membrane by a hydrophobic GPI-linked anchor, and thus the glypicans do not have a cytoplasmic tail like the syndecans. The N-terminal portion of the protein is globular and has been shown to carry only HS chains *in vivo*. The glypicans bind a wide array of factors that are essential for development and morphogenesis. Their roles in growth factor signaling potentially include both positive and negative regulation. HS chains are able to positively promote signaling by bringing a ligand and its receptor into close proximity. On the other hand, HS chains could negatively regulate signaling by binding a particular ligand and preventing its diffusion or interaction with a receptor.

Six glypican family members exist in mammals, two in flies and one in worms. Glypican-3 (GPC3) is the best-studied member of the family. Human patients lacking functional GPC3 exhibit Simpson–Golabi–Behmel Syndrome, which is characterized as an overgrowth

disorder. The overgrowth phenotype suggests that GPC3 normally functions to inhibit cell proliferation, likely mediated at the level of growth factor signaling at the cell surface.

Miscellaneous Membrane Proteoglycans

A number of membrane PGs do not show homology to syndecans or glypicans, but are expressed on the surface of many different cell types. The CSPG NG2 is a surface marker expressed on stem cell populations that are able to divide throughout an organism's life, including cartilage chondroblasts, myoblasts, endothelial cells of the brain, and glial progenitors. It has been shown to play a role in angiogenesis and inhibits neurite outgrowth. CD44 is a transmembrane cell surface receptor that plays a role in processes as diverse as immune function, axon guidance, and organ development. CD44 is considered a PG since it can carry GAG chains in certain cell types, such as lymphocytes. It is also an HA binding protein. The GAG chains allow CD44 to interact with ECM proteins and growth factors.

Processing

PGs are born in the endoplasmic reticulum (ER) and Golgi, but important steps of the PG life cycle also occur at the cell surface and other intracellular compartments.

Cell Surface Desulfation

The majority of sulfation reactions occur in the Golgi apparatus as the chains assemble prior to secretion. However, a family of cell surface sulfatases has been identified that removes sulfate groups from the C-6 position of glucosamine residues in HS. This sulfatase, called QSulf1 (first identified in quail), can promote Wnt growth factor signaling through HS in a finely tuned manner by desulfating HS at the appropriate time and place.

Turnover and Degradation

PGs are turned over on a continual basis (Figure 2). The syndecans undergo proteolytic cleavage and shedding at the cell surface, mediated by one of the matrix metalloproteases (MMP7). Additionally, some if not all membrane PGs are internalized by endocytosis. Enzymes called heparanases cleave the HS chains into fragments of a defined size, which then become localized to lysosomal compartments. Cells also endocytose HA, CS/DS, and KS proteoglycans, and sulfatases and exoglycosidases degrade the chains completely, while proteases degrade the core proteins. The liberated sugars (GlcNAc, GalNAc, Gal, and Man) and amino acids can then be recycled for the formation of new GAG chains and PGs, whereas the uronic acids and xylose are thought to undergo oxidative catabolism since no salvage pathway has been identified. The function of continuous turnover of the GAG chains and PGs is unclear. However, disruption of this pathway leads to lysosomal storage disorders with devastating health consequences.

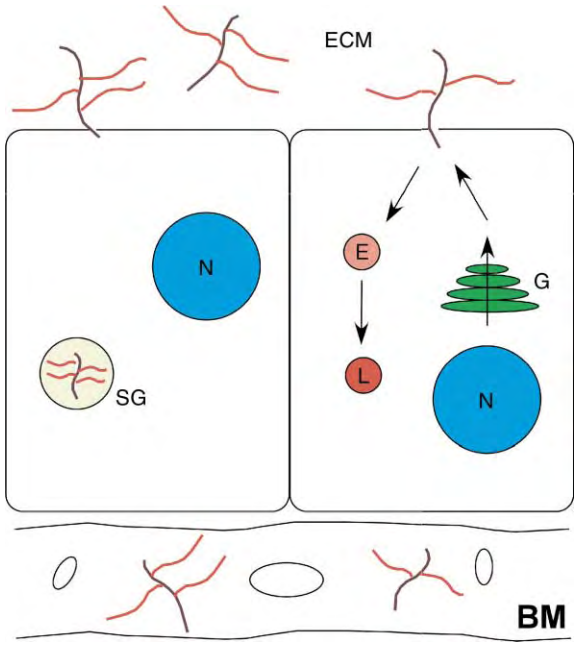

FIGURE 2 Life cycle of a proteoglycan. Proteoglycans are predominantly synthesized in the Golgi apparatus (G). A mature proteoglycan can be embedded in the plasma membrane, stored in secretory granules (SG), or secreted into the extracellular matrix (ECM) or basement membrane (BM). Degradation of proteoglycans begins with endocytic internalization, followed by cleavage of the GAG chains and protein core by glycosidases and proteases, respectively, in endosomes (E) and lysosomes (L). Nucleus (N).

See Also the Following Articles

Endoplasmic Reticulum-Associated Protein Degradation • Glycosylation, Congenital Disorders of • Glycosylation in Cystic Fibrosis • *N*-Linked Glycan Processing Glucosidases and Mannosidases • Protein Glycosylation, Overview • Protein Glycosylation Inhibitors

Glossary

chondroitin sulfate A type of glycosaminoglycan defined by the disaccharide unit (GalNAcβ1,4GlcAβ1,3)$_n$, modified with ester-linked sulfate at certain positions and typically found covalently linked to a PG core protein.

dermatan sulfate A modified form of chondroitin sulfate in which a portion of the β-glucuronic acid residues are epimerized to α-iduronic acid.

glycan Generic term for a sugar or assembly of sugars, existing either in free form or attached to another molecule.

glycosaminoglycan Polysaccharide side chains of PGs or free complex polysaccharides composed of linear disaccharide repeating units, each composed of a hexosamine and a hexose or a hexuronic acid.

glycosyltransferase An enzyme that forms a glycosidic linkage between a sugar and an acceptor.

heparan sulfate A glycosaminoglycan defined by the disaccharide unit $(GlcNAc\alpha1,4GlcA\beta1,4/IdoA\alpha1,4)_n$, containing N- and O-sulfate esters at various positions, and typically found covalently linked to a PG core protein.

heparin A type of heparan sulfate made by mast cells that has the highest amount of iduronic acid and of N- and O-sulfate residues.

hyaluronan A glycosaminoglycan defined by the disaccharide unit $(GlcNAc\beta1,4GlcA\beta1,3)_n$ that is neither sulfated nor covalently linked to protein, referred to in older literature as hyaluronic acid.

keratan sulfate A polylactosamine $(Gal\beta1,4GlcNAc\beta1,3)_n$ with sulfate esters at C-6 of GlcNAc and galactose residues found as a side chain of a keratan sulfate PG.

lectin A protein (excluding an antibody) able to bind glycans without causing modification of the glycan structure.

proteoglycan A protein with one or more covalently attached glycosaminoglycan chains.

sugar nucleotide Activated forms of monosaccharides, such as UDP-Xyl, UDP-Gal, UDP-GlcA, and UDP-GlcNAc, UDP-GalNAc, typically used as donor substrates by glycosyltransferases.

Further Reading

Bernfield, M., Gotte, M., Park, P. W., Reizes, O., Fitzgerald, M. L., Lincecum, J., and Zako, M. (1999). Functions of cell surface heparan sulfate proteoglycans. *Annu. Rev. Biochem.* **68**, 729–777.

Esko, J. D., and Selleck, S. B. (2002). Order out of chaos: Assembly of ligand binding sites in heparan sulfate. *Annu. Rev. Biochem.* **71**, 435–471.

Iozzo, R. (1998). Matrix proteoglycans: From molecular design to cellular function. *Annu. Rev. Biochem.* **67**, 609–652.

Song, H., and Filmus, J. (2002). The role of glypicans in mammalian development. *Biochim. Et. Biophys. Acta* **1573**, 241–246.

Varki, A., Cummings, R., Esko, J., Freeze, H., Hart, G., and Marth, J. (eds.) (1999). *Essentials of Glycobiology.* Cold Spring Harbor Laboratory Press, Cold Spring Harbor, New York.

Yoneda, A., and Couchman, J. (2003). Regulation of cytoskeletal organization by syndecan transmembrane proteoglycans. *Matrix Biol.* **22**, 25–33.

Biography

Sara Olson is a graduate student in the Biomedical Sciences Graduate Program in the School of Medicine at the University of California, San Diego (UCSD). She received her undergraduate education at Lawrence University where she developed an interest in developmental biology. She helped discover that vulval invagination in *C. elegans* depends on chondroitin biosynthesis.

Jeffrey D. Esko is a Professor of Cellular and Molecular Medicine and Co-director of the Glycobiology Research and Training Center at UCSD. He received his Ph.D. from the University of Wisconsin at Madison and was a Fellow of the Molecular Biology Institute at the University of California, Los Angeles. His principal research interests are in proteoglycan assembly and function using genetically altered cell lines and conditional mouse knockouts.

Pteridines

S. Colette Daubner and Paul F. Fitzpatrick
Texas A&M University, College Station, Texas, USA

The pteridines are a group of heterocyclic compounds containing a wide variety of substitutions on the basic compound pterin. Pterin itself is composed of a pyrazine ring and a pyrimidine ring; the pyrimidine ring has a carbonyl oxygen and an amino group. The biosynthesis of pterins begins with the molecule GTP; the enzyme which controls the conversion of GTP to pterin, GTP cyclohydrolase, is found in both prokaryotes and eukaryotes. Pterins were first discovered in the pigments of butterfly wings and perform many roles in coloration in the biological world. Pterins also function as cofactors in enzymatic catalysis. Folates, "conjugated" pterins which contain p-amino benzoic acid and glutamates in addition to the pterin ring system, are critical compounds in methyl transfer biochemistry. Tetrahydrobiopterin, the major unconjugated pterin in vertebrates, is involved in the hydroxylation of aromatic compounds and synthesis of nitric oxide. Molybdopterin, which contains pterin, a third heterocyclic ring containing an ether oxygen and two thiol substitutes, and molybdenum, is involved in biological hydroxylations, reduction of nitrate, and respiratory oxidation.

The name pteridine refers to the heterocyclic aromatic compound shown in Figure 1, composed of a pyrimidine ring fused to a pyrazine ring. However, the word pteridines has come to stand for an entire group of naturally occurring compounds. Their structures are based upon pteridine, but they have substituents on the pyrimidine ring: an amino group or a carbonyl at position 2 and a carbonyl group at position 4 (position numbers as shown in Figure 1). Pterin contains the amino substituent at position 2; all pterins are derivatives of this molecule. Most naturally occurring pteridines are pterins. The first pterins to be studied, leucopterin and xanthopterin, were pigments isolated from butterfly wings by Sir Frederich Gowland Hopkins at Cambridge University in the late nineteenth century. Their names are derived from the Greek words for wing, *pteron*, white, *leukos*, and yellow, *xanthos*.

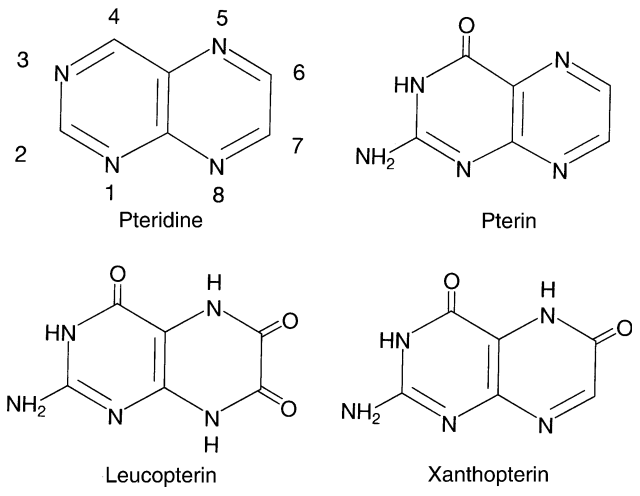

FIGURE 1 Structures of pteridine and three pteridines.

Pterins are referred to as being conjugated or unconjugated. The conjugated pterins are folates, derivatives of folic acid. They contain a *p*-aminobenzoate substituent at the 6-position and one or more glutamate residues. The folates are covered in a separate article in this series. As a general but not fast rule, folates are involved in one-carbon transfers in metabolism and pterins are involved in oxygenation reactions or in pigmentation.

Distribution of Pterins in Nature

Pterins are found in all living organisms, from bacteria, blue-green algae, and trypanosomes, to mammals; they have also been detected in the chloroplasts of spinach leaves and the cotyledons of pea sprouts. A wide variety of pterins exist in bacteria, such as the various pterins with three-carbon side chains of *Escherichia coli*, the glucuronidated pterins of *Bacillus subtilis*, the three ribityl pteridines of the marine bioluminescent bacterium *Photobacterium phosphoreum*, the molybdopterins of photosynthetic bacteria, and the tetrahydromethanopterin of methanogenic bacteria.

As pigments, pterins are not only found in butterfly wings, but also in moth heads, silkworm skin, grasshopper bodies, and honeybee larvae. A list of examples demonstrates the very wide use nature has made of pterins in coloration; diversity is found in species distribution, chemical structures, and hue. Unusual dimeric pterins are found in the eyes of the fruit fly, *Drosophila*. A blue pigment in the roundworm

Ascaris lumbricoides contains biopterin. Pterins are common in the skins of amphibians and fish, and photolabile pterins are found in some amphibians' eyes. The red color of some salmon, the Siamese fighting fish, and the red lizard *Anolis* is due to pterins, as is the green color of some snakes.

Clearly pterins serve widely in coloration, but they are also critical compounds in metabolic pathways. In the vertebrates the major pterin is tetrahydrobiopterin, which serves as a redox cofactor in enzymatic reactions utilizing molecular oxygen.

Biosynthesis of Neopterin and Biopterin

The synthesis of all pterins begins with the ring opening and reclosing of the nucleotide guanosine triphosphate (GTP) by the enzyme GTP cyclohydrolase (GTPCH). GTPCH has been isolated and sequenced from many sources. It is a decamer, each active site containing a zinc atom. As the rate-limiting enzyme of pterin biosynthesis, it is carefully regulated, both by transcriptional and posttranslational mechanisms. The catalytic domains of the *E. coli* and human enzyme are 37% identical in amino acid sequence, testifying to the ancient status of pterins in the living world.

The reaction catalyzed by GTPCH is shown in Figure 2. The purine ring system of guanine supplies all but two of the carbons in the ring system of pterin. The ribose moiety of GTP supplies the two new carbons for the pyrazine ring and the carbons of the erythrose side chain; one carbon from the guanine ring is released as formate. The pterin product is dihydroneopterin triphosphate. In eukaryotes, dihydroneopterin triphosphate is converted to dihydrobiopterin (Figure 3). In contrast, dihydrobiopterin is not formed in most bacteria.

The structures of biopterin and its reduced forms are shown in Figure 3. Reduction of the 7,8 double bond yields 7,8-dihydrobiopterin (a tautomer of 7,8-dihydropterin is quinonoid dihydropterin). Further reduction at the 5,6 double bond gives tetrahydrobiopterin.

Pterins in Metabolism

The Aromatic Amino Acid Hydroxylases (AAHs)

One of the most-studied processes involving biopterin is the hydroxylation of the aromatic amino acids. This is catalyzed by a small family of enzymes containing phenylalanine (PheH), tyrosine (TyrH), and tryptophan (TrpH) hydroxylase. They contain an iron atom and utilize tetrahydrobiopterin and molecular oxygen to hydroxylate a fairly unreactive entity, an aromatic ring. The AAHs are only active in the Fe^{II} state; one role of the tetrahydrobiopterin may be to keep the iron reduced. The major role of tetrahydrobiopterin is to activate the oxygen for eventual transfer to the aromatic amino acid

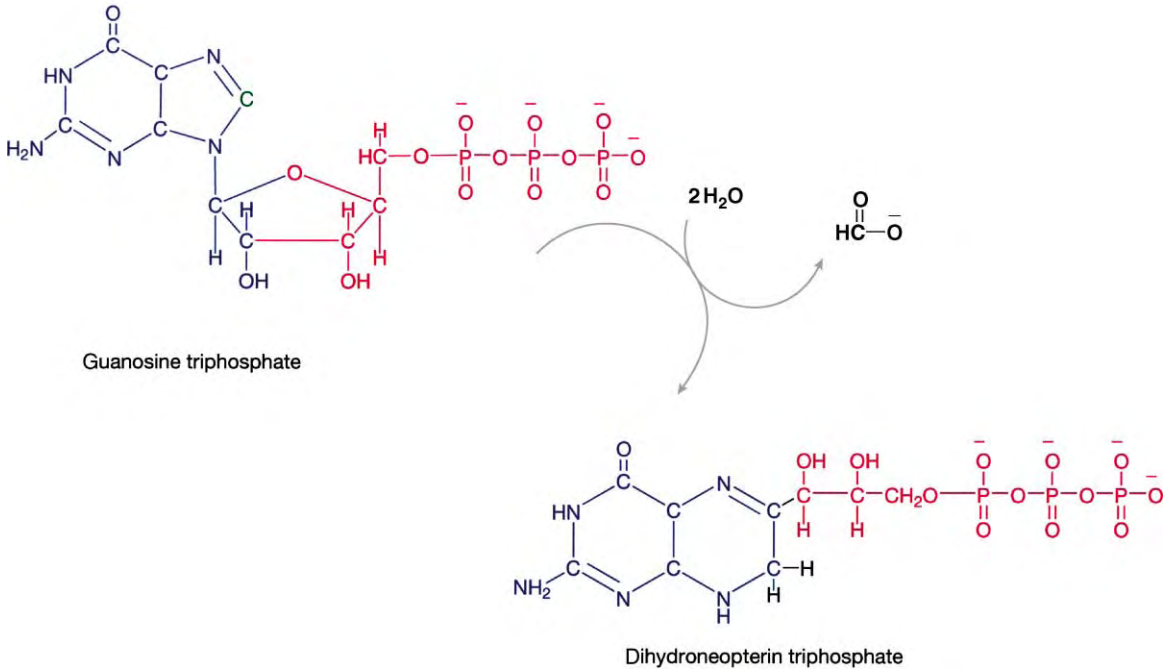

FIGURE 2 The first step in the synthesis of pterins from guanosine triphosphate. The atoms of GTP are color-coded to show their positions in the resulting neopterin molecule. Note that one carbon of GTP, colored green, is lost as formate.

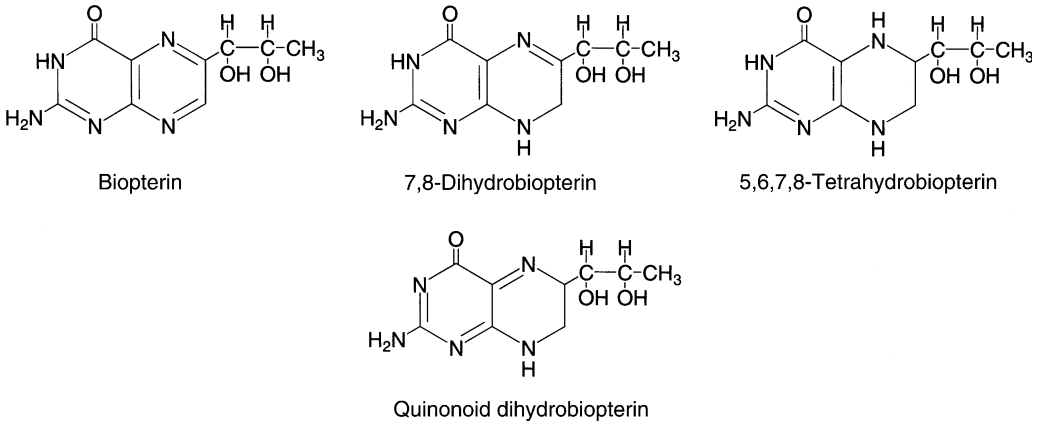

FIGURE 3 Structures of biopterin and its reduced forms.

substrate, probably through formation of a C4a-peroxy pterin intermediate (Figure 4).

Each of the AAHs catalyzes the rate-limiting step in its metabolic pathway: PheH in phenylalanine catabolism, TyrH in synthesis of the catecholamine neurotransmitters, and TrpH in serotonin synthesis. The three enzymes are homologous to a great extent in their catalytic domains (between any two there is 60% identity and 75% similarity). These enzymes as a rule are not found in bacteria, consistent with the general absence of biopterin from prokaryotes. However, PheH has been isolated from several prokaryotes, and from one, *Chromobacterium violaceum*, the sequence is 30% identical to the catalytic domain of human PheH. Two amino acid residues which bind tetrahydrobiopterin (in TyrH, F300 and E332) are conserved in all the aromatic amino acid hydroxylases studied, suggesting a central role for biopterin in the evolution of neurotransmitters and higher nervous systems.

The pterin product of the AAHs is C4a-carbinolamine dihydrobiopterin (Figure 4). It is released from the enzyme and is returned to the state needed for amino acid hydroxylation by the action of two more enzymes, C4a-carbinolamine dehydratase and dihydropterin reductase.

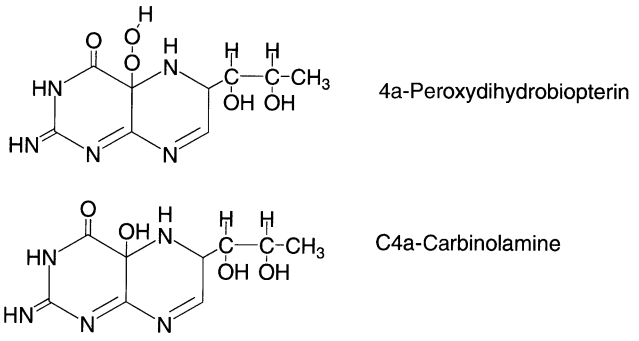

FIGURE 4 Peroxypterin and carbinolamine intermediates in the hydroxylation of aromatic amino acids.

Nitric Oxide Synthase

Nitric oxide synthase (NOS) is responsible for the synthesis of nitric oxide, NO. NOS utilizes tetrahydrobiopterin, NADPH, and molecular oxygen to convert L-arginine to L-citrulline and NO (Figure 5). Nitric oxide is a gas and a highly toxic compound. Because of its toxicity, its short half-life (1–5 s), and its diffusibility, NO serves the mammalian immune system as a killer of foreign intruders and cancer cells. It is also a cellular signal through its stimulation of cGMP synthesis.

NOSs are dimers of identical subunits. NOS contains flavin mononucleotide (FMN), flavin adenine dinucleotide (FAD), heme, and tetrahydrobiopterin. The tetrahydrobiopterin binding site is positioned close to the heme to facilitate electronic interaction between them. The tetrahydrobiopterin binding site is formed by residues in both subunits at the interface where the subunits associate; the pterin ring is sandwiched between a tryptophan residue from one subunit and a phenylalanine from the other. In contrast to the two-electron loss in AAHs, the tetrahydrobiopterin of NOS loses only one electron generating a biopterin radical. Biopterin remains bound to NOS before and after catalysis, another difference between NOS and the AAHs.

Molybdopterin-Containing Enzymes

A very large group of enzymes contain molybdenum (or in a few cases tungsten) in conjunction with a unique pterin, molybdopterin. These enzymes function in general to transfer oxygen to or from a physiological molecule. They can be assigned to two

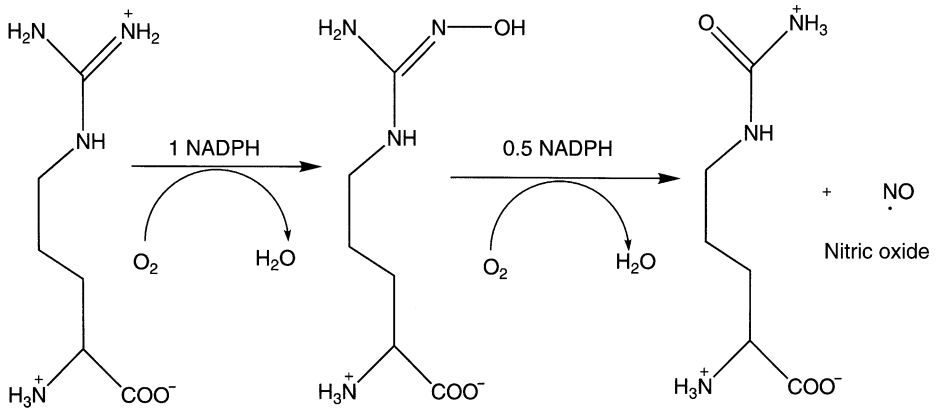

FIGURE 5 Reaction catalyzed by NOS.

categories based on the reaction catalyzed. The first group, the true hydroxylases, performs hydroxylation of aldehydes or aromatic rings; some of the enzymes in this category are milk xanthine oxidase, liver aldehyde oxidase, and bacterial enzymes such as formate dehydrogenase and nicotine dehydrogenase. The second category can be subdivided into: (1) sulfite oxidases and enzymes which reduce nitrate to enable a cell to utilize ammonia and (2) bacterial enzymes which function as terminal respiratory oxidases.

The structures of molybdopterin and the molybdenum cofactor are shown in Figure 6. The R group in prokaryotic systems can be guanine, cytosine, adenine, or hypoxanthine; in eukaryotes it is a hydrogen. The mode of binding the molybdenum cofactor to the protein differs from protein to protein in accord with the classification described above. The enzymes of the xanthine oxidase group contain one single molybdenum center per enzyme subunit, the sulfite oxidase family members are likely to have one molybdenum cofactor bound to a cysteine of the protein, and the final group can contain two molydopterins coordinated to one molybdenum, which can be coordinated to a selenium, sulfur, or cysteine. The biosynthetic pathways of these pterins have not been solved as yet.

The molybdenum enzymes are a vast enough group that a discussion of their properties is inappropriate here. In general, they contain other redox centers in addition to their pterin cofactor, such as heme, iron–sulfur clusters, and flavin. The role of the pterin is postulated to include mediation of electron transfer to the other redox active centers and modulation of the reduction potential of the molybdenum. The pterin is not thought to be itself oxidized and reduced during catalysis, a distinct difference between these enzymes and the NOSs and AHHs.

Tetrahydrobiopterin and Human Disease

Tetrahydrobiopterin deficiency is associated with a rare variant of hyperphenylalaninemia, which cannot be treated by the low phenylalanine diet successful for typical phenylketonuria (PKU) patients. It is characterized by a deficit of catecholamine neurotransmitters and serotonin as well (the products of the AAHs), affecting the nervous system as well as the liver. It can be caused by mutations in GTPCH or in the enzymes which recycle dihydrobiopterin. Decreased levels of tetrahydrobiopterin in cerebrospinal fluid have also

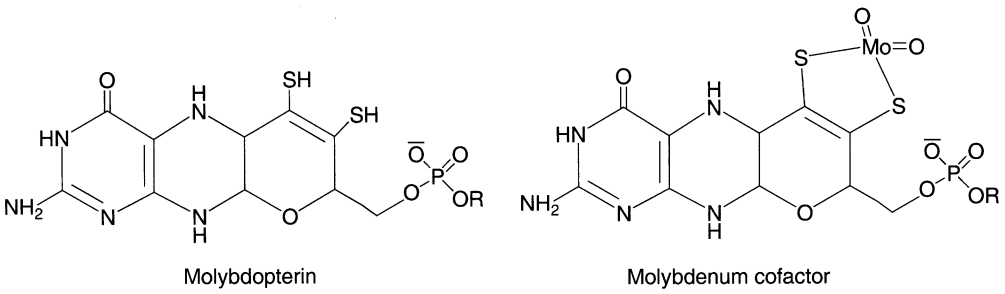

FIGURE 6 The structures of molybdopterin and the molybdenum cofactor.

been noted in such diseases as Parkinson's, autism, depression, and Alzheimer's.

See Also the Following Articles

Amino Acid Metabolism • Calcium Signaling: NO Synthase • Flavins • Heme Proteins

Glossary

aromatic amino acid Aromatic compounds are cyclic compounds containing double bonds so that their three-dimensional structure is planar. Amino acids are small molecules which consist of a central carbon atom, tetrahedrally bonded to a carboxylic acid group, an amino group, a hydrogen, and a fourth group, often called an R group; in the aromatic amino acids it is this R group which is aromatic.

heme A large planar heterocyclic compound consisting of four bridged pyrrole rings which binds Fe in biological systems for the transport or reactivity of oxygen.

heterocycle A ring-shaped compound made up of more than one kind of atom.

pyrimidine and pyrazine Organic heterocyclic compounds consisting of a six-membered ring with two nitrogen atoms separated by one carbon in pyrimidine and two carbons in pyrazine.

radical An atom or group of atoms possessing an odd (unpaired) electron.

Further Reading

Brown, G. M. (1985). Biosynthesis of pterins. In *Folates and Pterins, Chemistry and Biochemistry of Pterins* (R. L. Blakley and S. J. Benkovic, eds.) Vol 2, pp. 115–154. Wiley, New York.

Fitzpatrick, P. F. (2000). The aromatic amino acid hydroxylases. *Adv. Enzymol. Relat. Areas Mol. Biol.* **74**, 235–294.

Hille, R. (1996). The mononuclear molybdenum enzymes. *Chem. Rev.* **96**, 2757–2816.

Nixon, Jon C. (1985). Naturally occurring pterins. In *Folates and Pterins, Chemistry and Biochemistry of Pterins* (R. L. Blakley and S. J. Benkovic, eds.) Vol 2, pp. 1–42. Wiley, New York.

Rebel, J., Auerbach, G., Bader, G., Bracher, A., Nar, H., Hosl, C., Schramek, N., Kaiser, J., Bacher, A., Huber, R., and Fischer, M. (2003). Biosynthesis of pteridines. Reaction mechanism of GTP cyclohydrolase I. *J. Mol. Biol.* **326**, 503–516.

Thony, B., Auerbach, G., and Blau, N. (2000). Tetrahydrobiopterin biosynthesis, regeneration and functions. *Biochem. J.* **347**, 1–16.

Wei, C.-C., Crane, B. R., and Stuehr, D. J. (2003). Tetrahydrobiopterin radical enzymology. *Chem. Rev.* **103**, 2365–2383.

Biography

Colette Daubner and Paul Fitzpatrick have been working on the structure and function of the aromatic amino acid hydroxylases in the Department of Biochemistry and Biophysics at Texas A&M University since 1986. Dr. Daubner is a Research Scientist.

Paul Fitzpatrick is a Professor with joint appointment in Departments of Biochemistry and Biophysics and Chemistry. They received their Ph.D. at the University of Michigan and did postdoctoral research at The Pennsylvania State University.

P-Type Pumps: Copper Pump

Ilia Voskoboinik and James Camakaris
The University of Melbourne, Melbourne, Victoria, Australia

Copper pumps are copper-translocating P-type adenosinetriphosphatases (ATPases). Copper P-type ATPases, alongside other heavy-metal pumps, including silver, cadmium, lead, and zinc transporters, constitute group IB of the P-type ATPase family. Copper pumps are indispensable for maintaining copper homeostasis, including the delivery of copper to essential cuproenzymes and efflux of excess copper from the cell. P-type ATPases are the family of enzymes, which translocate a substrate across the lipid bilayer using the energy of ATP hydrolysis and which involve formation of an acyl-phosphate intermediate. P-type ATPases are ubiquitous proteins identified in most organisms, from bacteria to humans. These enzymes have evolved substrate specificity and regulatory mechanisms, which are essential for homeostasis of respective physiological or toxic substrates, amongst which are calcium, magnesium, sodium, potassium, protons, copper, and toxic heavy metals.

P-Type ATPases

Molecular and crystal structures of P-type ATPases have been revealed only in the last few years, despite massive efforts beginning in the early 1970s, to characterize the mechanisms of these enzymes. The best-studied molecules, at this stage, are calcium P-type ATPases, particularly the sarcoplasmic reticulum calcium pump. The catalytic mechanism, based on site-directed mutagenesis studies and the elegant studies by Toyoshima, who recently identified the crystal structure of sarcoplasmic reticulum calcium ATPase, consists of several fundamental steps (Figure 1): (1) Cation binding to high-affinity binding sites in the cation channel, which is formed by several transmembrane domains, leads to (2) conformational changes in the cytosolic ATP-binding domain, which acquire a conformation with high affinity for ATP. Subsequently, the terminal γ-phosphate is transferred to the invariant aspartate residue within the -DKTG- motif and forms a transient acyl-phosphate (aspartyl-phosphate) bond. The residual adenosine diphosphate dissociates from the cytosolic domain. These changes cause such significant conformational alterations within the transmembrane cation channel that its affinity for the cation is reduced and (3) the cation translocates across the membrane in a vectorial fashion. Subsequently, (4) the acyl-phosphate bond is hydrolyzed and (5) the enzyme returns to its original high-affinity cation-binding state. This model is generally accepted as a paradigm for P-type ATPases, including the copper pumps.

Copper

Copper is an essential trace element, whose redox properties (Cu^{2+}/Cu^{+}) are utilized by a number of enzymes catalyzing redox reactions. Cuproenzymes are found in various intracellular compartments, in the cytosol (e.g., Cu,Zn-superoxide dismutase), in the mitochondria (e.g., cytochrome *c* oxidase) and in the Golgi membranes (e.g., lysyl amine oxidase). At the same time, when present in excess, copper may exert its toxicity through the same redox properties. Thus, in the reduced intracellular environment copper undergoes redox cycling, which results in the generation of reactive oxygen species leading to oxidative stress, which, if not counterbalanced by antioxidant systems, may lead to cellular toxicity. In addition, copper, particularly copper(I), binds nonspecifically with high affinity to cellular proteins and can affect their physiological function. Biological systems accommodated both, the beneficial and potentially toxic roles of copper, through the evolution of the finely tuned machinery of copper homeostasis.

General Structure of Group IB P-Type ATPases

The first heavy-metal P-type ATPase was identified in 1989 through studies on cadmium-resistant bacteria. The predicted amino acid sequence analysis revealed little general similarity with other P-type ATPases, apart from some essential catalytic motifs. Since then, dozens of heavy-metal pumps, including copper, zinc, and cadmium transporters, as well as putative heavy-metal ATPases of unknown cation specificity, have either been identified through the predicted open reading frame

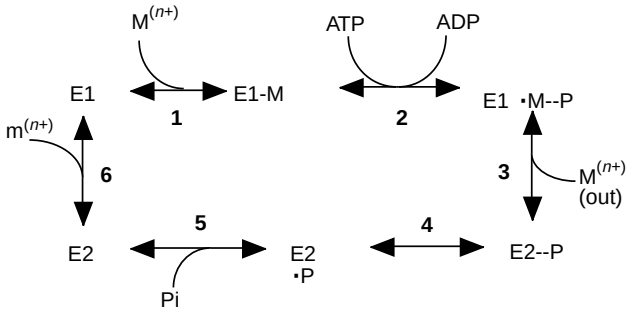

FIGURE 1 General concept of catalytic cycle of P-type ATPases, including copper transporters. $M^{(n+)}$ – cation to be translocated; $m^{(n+)}$ – counterion; P – terminal phosphate group of ATP forming an acyl-phosphate bond with invariant aspartate residue in the -DKTG- motif. (1) High-affinity cation binding; (2) high-affinity ATP binding and the transfer of the terminal γ-phosphate from ATP to the invariant aspartate residue, the formation of acyl-phosphate bond; (3) conformational change from the E1 to E2 state, translocation of the cation to the lumen; (4) transition to the low-energy acyl-phosphate bond; (5) dissociation of inorganic phosphate from the invariant aspartate residue; and (6) potential counterion translocation, transition from the E1 to E2 conformation. Reprinted from Voskoboinik, I., Camakaris, J., and Mercer, J. F. (2002). Understanding the mechanism and function of copper P-type ATPases. *Advances in Protein Chemistry* **60**, 123–150.

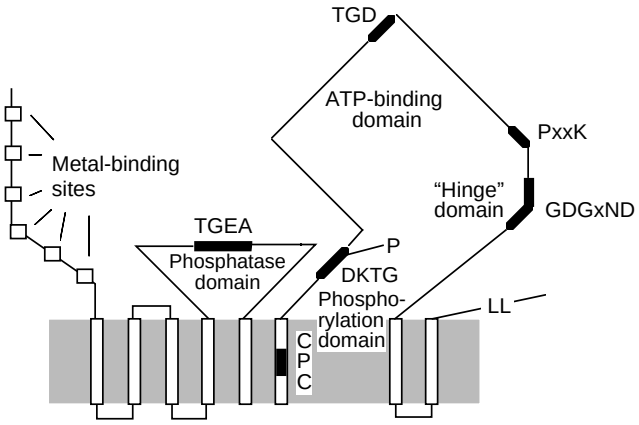

FIGURE 2 General structure of a heavy-metal P-type ATPase. "Metal-binding sites" are putative copper-binding motifs -GMxCxxC-; "phosphatase domain" – a cytosolic loop with conserved region(s), e.g., -TGEA-, essential for de-phosphorylation of the transient acyl-phosphate; P-DKTG is the phosphorylation domain, where P – indicates transient aspartyl-phosphate; "ATP-binding domain" and "hinge domain" – a large cytosolic loop with several conserved regions (e.g., -TGD-, -PxxK-, GDGxND) essential for ATP binding and the transfer of the terminal γ-phosphate of ATP to the invariant aspartate residue of the phosphorylation domain; the -CPC- motif is believed to constitute a part of the cation channel in heavy-metal P-type ATPases; -LL- motif is the internalization signal in ATP7A (position 1487/1488) and ATP7B (position 1454/1455). (Reprinted from Voskoboinik, I., Camakaris, J., and Mercer, J. F. (2002). Understanding the mechanism and function of copper P-type ATPases. *Advances in Protein Chemistry* **60**, 123–150.)

(ORF) analysis or characterized functionally in prokaryotes and eukaryotes. Heavy-metal transporters have eight predicted transmembrane domains (nonheavy-metal transporters contain ten) with an essentially invariant -CPC- motif in transmembrane domain 6 (Figure 2). The N terminus of these pumps generally contains up to six putative heavy-metal binding sites, with a common sequence GMxCxxC. Heavy metals have been shown to bind within this region with various affinities. The cytosolic ATP-binding loop contains the invariant acyl-phosphorylation motif -DKTG-, putative nucleotide and magnesium binding motifs -TGD- and -MVGDGIND-, yet lacks other conserved, among nonheavy-metal ATPases, regions. Furthermore, the phosphatase domain contains only one, TGE motif, out of three conserved regions (Figure 2). While additional functional motifs ought to be present in heavy-metal ATPases, they are yet to be identified and characterized.

Copper P-Type ATPases

Physiological Roles

Copper P-type ATPases have been identified in a variety of organisms, from bacteria to humans, which indicates their crucial importance for copper homeostasis. This has been proven experimentally in various experimental systems. Thus, the disruption of copper pumps in bacteria decreased their copper resistance, presumably through inability to efflux excess copper from the cell. In yeast, the plasma membrane copper pump, PcaI, also appears to be important for copper efflux. In contrast, the Golgi membrane copper P-type ATPase, Ccc2, has no direct role in copper resistance, but has been shown to be indispensable as a high-affinity copper transporter to the cuproenzyme, Fet3, which is required for high-affinity iron uptake. Similarly, in plants the Golgi membrane copper transporter, RAN1, has a crucial role in ethylene biosynthesis. Interestingly, plants appear to encode far more putative heavy-metal transporters than other organisms. However, their cation specificity and intracellular roles are yet to be identified. The analysis of the *Drosophila melanogaster* genome indicated the presence of a single copper P-type ATPase homologous to its human counterparts. However, the physiological role of this transporter has not been identified. In humans, two copper-translocating P-type ATPases have been identified and characterized: the ubiquitous (except the liver) Menkes protein (ATP7A), and the predominantly hepatic Wilson protein (ATP7B) which has ~65% homology with ATP7A. Unlike in unicellular organisms and in plants, these two transporters evolved a dual role in copper homeostasis, namely, the delivery of copper to cuproenzymes and the efflux of physiological or excess copper from the cell.

The latter function is essential for absorption of alimentary copper from the gastrointestinal tract and the reabsorption of copper in the kidney. The clinical symptoms of inherited genetic diseases, the X-linked recessive Menkes disease, and the autosomal-recessive Wilson disease, which are caused by detrimental mutations in the respective genes, demonstrate the essentiality of both proteins in copper homeostasis. Furthermore, the clinical features of Menkes and Wilson disease represent, respectively, the ultimate effects of systemic copper deficiency due to malabsorption, and toxicity due to copper hyperaccumulation.

Catalysis

Copper P-type ATPases vary in size from ~700 amino acids in bacteria to 1500 amino acids in humans. Nevertheless, they share significant structural similarity within regions, which have been postulated to be important for the catalysis of copper translocation. General elements of the catalytic cycle appear to be similar to those reported for calcium P-type ATPases (Figure 1). Thus, copper binding, presumably within the transmembrane cation channel, precedes the binding of ATP within the high-affinity cytosolic ATP-binding domain. This is followed by acyl-phosphorylation of the invariant, among all P-type ATPases, aspartate residue in the -DKTG- motif and subsequent copper translocation from the cytosolic to the lumenal side of the membrane. To complete the catalytic cycle the acyl-phosphate bond is hydrolyzed and the protein returns to its high-affinity copper-binding state. While copper pumps can be inhibited by orthovanadate, a classical inhibitor of P-type ATPases, the concentration required for such inhibition is considerably higher than the one observed for nonheavy-metal ATPases. Biochemical evidence suggests that copper ATPases can transport only reduced copper (Cu^+), which is the major form of copper in the reduced intracellular environment. The specificity of copper pumps for monovalent copper explains their silver (Ag^+) transporting activity and the lack of cross-specificity with divalent cations of heavy metals, e.g., cadmium, zinc, and lead. Copper ATPases investigated so far appear to be less catalytically active, with respect to cation translocation, than their non-heavy-metal transporting counterparts, as measured by the amount of ATPase-specific cation transported per minute. At the same time, the affinity of copper pumps for ATP is similar to the one determined for other P-type ATPases, consistent with conservation of essential ATP and magnesium-binding motifs in the ATP-binding cytosolic loop. The unique feature of copper P-type ATPases (as well as other heavy-metal pumps) is the presence of cytosolic N-terminal putative copper-binding sites with the sequence -GMxCxxC-. These conserved motifs bind copper(I) with higher affinity compared to copper(II) and other divalent heavy-metal cations. Furthermore, copper binding results in these motifs acquiring a conformation, which protects copper from being removed from these sites by nonspecific ligands, such as glutathione. The exact role of the N-terminal metal-binding sites is yet to be fully clarified, but they do not appear to play an essential role in cation translocation by copper ATPases. Yet these motifs have been shown to regulate the affinity of copper pumps for copper and may be particularly important in allowing its acquisition or delivery to a specific target under basal or copper-limited conditions. Similar findings were reported for the putative metal-binding sites of other heavy-metal P-type ATPases.

Regulation

The mechanisms of regulation of copper pumps vary considerably between prokaryotes and multicellular differentiated eukaryotic systems.

Prokaryotes

In prokaryotes, genes encoding copper ATPases are organized in an operon, which is regulated through a *trans*-acting repressor/activator system. Thus, in *Enterococcus hirae* under physiological or copper deficient conditions copper binds to a copper operon repressor, CopY, whose binding to the promoter region of the operon results in the suppression of copper ATPase synthesis. Conversely, in the presence of elevated copper concentrations, copper binding to a copper activator, CopZ, results in its overcompeting CopY–copper complex at the promoter region. This leads to overexpression of copper pumps, which, through efflux of excess copper, restores copper homeostasis. A member of the MerR family of DNA-binding metal-responsive transcriptional regulators, CueR, has been identified as a regulator of the copper export pump, CopA, in *Escherichia coli*. CueR binds in the promoter region of CopA and responds to elevated copper(I) or silver(I) concentrations by overexpression of CopA. The disruption of CueR causes the loss of CopA expression in bacteria.

Eukaryotes

Copper ATPases in yeast are represented by two pumps, which are localized at the cellular membrane, PcaI, and at the Golgi membrane, Ccc2. These transporters have defined functions: PcaI is presumed to function in copper efflux from the cell, while Ccc2 delivers copper to the multicopper ferroxidase, Fet3, and has no direct copper resistance function. Importantly, Ccc2 is a high-affinity transporter, which, under limited copper concentrations, receives copper from a low-molecular-weight copper chaperone, AtxI. This protein binds copper(I) within the high-affinity copper-binding site, GMxCxxC, and delivers it to the analogous site at the N terminus of Ccc2.

Copper does not appear to directly regulate the expression levels of PcaI or Ccc2. These protein–protein interactions between the copper chaperone Atx1 and the P-type ATPase permit copper transport under conditions where essentially no free ionic copper is available.

Mammals have evolved a novel system for regulating copper homeostasis via the Menkes (MNK; ATP7A) and Wilson (WND; ATP7B) P-type ATPases. These transporters exert a dual role in copper homeostasis by catalyzing efflux of copper from the cell at the plasma membrane and supplying copper to cuproenzymes of the secretory pathway in the Golgi compartment. These functions are achieved through copper-regulated vesicular trafficking of the transporters. Thus, under physiological copper concentrations both pumps are localized at the trans-Golgi network, where they supply copper to cuproenzymes. In the presence of elevated copper concentrations the proteins relocalize to the plasma membrane, they efflux excess copper from the cell. Once copper concentrations subside to physiological levels, the proteins relocate to the trans-Golgi network. Several signaling motifs have been shown to be responsible for regulation of the subcellular localization of ATP7A and ATP7B. These include the N-terminal putative copper-binding sites (important for exocytosis), and the C-terminal dileucine endocytic motifs (important for endocytosis). Importantly, under physiological concentrations copper is delivered to the copper-binding sites of ATP7A and ATP7B by a copper chaperone, ATOX1. The essentiality of such an interaction has been shown by using ATOX1 knock out mice. These transgenic animals have exhibited severe systemic copper deficiency, which has been associated with malabsorption of alimentary copper.

Two inherited diseases associated with mutations in copper P-type ATPases have been identified in humans and analogous disorders are found in other mammals. The systemic copper deficiency disorder, the X-linked Menkes disease, has been associated with detrimental mutations in the *ATP7A* gene, while the copper hepatotoxicity and neurotoxicity disorder, the autosomal-recessive Wilson disease, has been linked to mutations in the *ATP7B* gene. Importantly, the mutations which affect either the catalytic or the trafficking function of the pump can result in the disease phenotype. The nature and severity of the disease phenotype in Menkes and Wilson diseases can be explained for a number of mutations, based on predicted faulty localization/trafficking and magnitude of reduction in catalytic activity.

See Also the Following Articles

Chaperones for Metalloproteins • Chaperones, Molecular • Cytochrome *c* • Cytochrome Oxidases, Bacterial • Inorganic Biochemistry

Glossary

copper chaperone A small protein that binds, transports, and delivers copper to copper-requiring enzymes/proteins.

cuproenzyme An enzyme in which copper constitutes a core part of the active site; these enzymes usually utilize redox properties of copper to catalyze reactions of oxidation or reduction.

operon A cluster of genes that is coordinately regulated.

ORF (open reading frame) DNA sequence that contains features required for encoding a protein.

protein trafficking Relocalization of proteins from one part of the cell to another, normally via vesicles.

redox Chemical reaction involving oxidation and reduction.

Further Reading

Huffman, D. L., and O'Halloran, T. V. (2001). Function, structure, and mechanism of intracellular copper trafficking proteins. *Annu. Rev. Biochem.* **70**, 677–701.

Silver, S., and Phung, L. T. (1996). Bacterial heavy metal resistance: New surprises. *Annu. Rev. Microbiol.* **60**, 753–789.

Toyoshima, C., Nakasako, M., Nomura, H., and Ogawa, H. (2000). Crystal structure of the calcium pump of sarcoplasmic reticulum at 2.6 Å resolution. *Nature* **405**, 647–655.

Tumer, Z., Moller, L. B., and Horn, N. (1999). Mutation spectrum of ATP7A, the gene defective in Menkes disease. *Adv. Exp. Med. Biol.* **448**, 83–95.

Voskoboinik, I., Camakaris, J., and Mercer, J. F. (2002). Understanding the mechanism and function of copper P-type ATPases. *Adv. Protein Chem.* **60**, 123–150.

Biography

James Camakaris is an Associate Professor and Reader in Genetics and is also Head of the Department of Genetics, The University of Melbourne, and a research associate of the Murdoch Children's Research Institute. His primary research interest is in understanding the genes, proteins, and mechanisms of copper homeostasis with a current focus on structure–function aspects of the Menkes copper-translocating P-type ATPase.

Ilia Voskoboinik is a Postdoctoral Research Fellow in the Department of Genetics, The University of Melbourne. His primary research interest is in understanding structure–function of mammalian copper-translocating P-type ATPases, the Menkes, and the Wilson protein.

P-Type Pumps: H^+/K^+ Pump

Jai Moo Shin and George Sachs
University of California at Los Angeles and VA Greater Los Angeles Healthcare System, California, USA

The gastric H^+/K^+ pump is a member of the P_2-type ion-motive ATPase family and is responsible for the elaboration of HCl by the parietal cell of the gastric mucosa. The gastric H^+, K^+-ATPase catalyzes H^+ for K^+ exchange by an electroneutral exchange of cytoplasmic protons for extracytoplasmic potassium, while the protein undergoes phosphorylation and dephosphorylation related to ion binding and release. The gastric H^+, K^+-ATPase is composed of two subunits, the catalytic or α-subunit having ten transmembrane segments and the β-subunit having one transmembrane segment. The gastric H^+, K^+-ATPase α-subunit is a 100 kDa protein consisting of ~1034 amino acids and β-subunit is a glycoprotein with ~290 amino acids.

Structure of the Gastric H^+, K^+-ATPase

The α-Subunit of Gastric H^+, K^+-ATPase

The primary sequences of the α-subunits deduced from cDNA have been identified from pig, rat, and rabbit. The hog gastric H^+, K^+-ATPase α-subunit sequence deduced from its cDNA consists of 1034 amino acids with an M_r of 114 285 Da. The rat gastric H, K ATPase consists of 1033 amino acids with an M_r of 114 012 Da, and the rabbit gastric H, K ATPase consists of 1035 amino acids, showing an M_r of 114 201 Da. The degree of conservation among the α-subunits is extremely high (over 97% identity) among species. The gene sequence for human and the 5′ part of the rat H^+, K^+-ATPase α-subunits have been determined showing that the human gastric H^+, K^+-ATPase gene has 22 exons and encodes a protein of 1035 residues including the initiator methionine residue ($M_r = 114\,047$ Da). These H^+, K^+-ATPase α-subunits show high homology (~60% identity) with the Na^+, K^+-ATPase catalytic α-subunit. The putative distal colon H^+, K^+-ATPase α-subunit has also been sequenced and shares 75% homology with both the H^+, K^+- and Na^+, K^+-ATPases.

The gastric H^+, K^+-ATPase α-subunit has conserved consensus sequences along with the other P type ATPases, the sarcoplamic reticulum Ca^{2+}-ATPase and the Na^+, K^+-ATPase, for the ATP-binding site, the phosphorylation site, the pyridoxal 5′-phosphate-binding site and the fluorescein isothiocyanate-binding site. These sites are thought to be within the ATP-binding domain in the large cytoplasmic loop between transmembrane segments 4 and 5. Structurally, this enzyme can be divided into three domains, viz., cytoplasmic, membrane, and extracytoplasmic domains. The cytoplasmic domain contains four sub-domains, a stalk domain, N-domain, P-domain, and A-domain. The N-domain or nucleotide-binding domain is a large cytoplasmic domain between M4 and M5 where ATP binds. The P-domain or phosphorylation domain is a cytoplasmic domain near M4 where there is phosphorylation and dephosphorylation. The A-domain or activation domain is a cytoplasmic domain between M2 and M3, which moves depending on conformational changes. The stalk domain contains the extension of the transmembrane segments into the cytoplasmic region and forms a link for the passage of ions into the membranes and for transmission of conformational changes from the cytoplasm. The gastric α-subunit structure that is based on the 3D crystal of the SR Ca-ATPase structure is shown in Figure 1. Although this model is probably true in general, it is almost certainly incorrect in its detail.

There is much biochemical evidence showing the applicability of the ten transmembrane segment model to this ATPase. The C terminal amino acids of the α-subunit, tyr–tyr, are present in the cytoplasmic region, which was shown by a method of iodination with peroxidase-H_2O_2–^{125}I followed digestion with carboxypeptidase Y. Four transmembrane pairs connected by their luminal loop were detected in a tryptic digest of the hog gastric H^+, K^+-ATPase. A peptide fragment beginning at gln^{104} represents the H1/loop/H2 sector. The H3/loop/H4 sector was found at a single peptide peak beginning at thr^{291}, and the H5/loop/H6 sector at a peptide beginning at leu^{776}. The H7/loop/H8 region was found in a single peptide fragment of 11 kDa, beginning at leu^{853}. Surprisingly no peptide representing H9 and H10 was found in any enzyme digest procedure.

Antibody 95 inhibits ATP hydrolysis in the intact vesicles, and appears to be K^+ competitive. The sequence

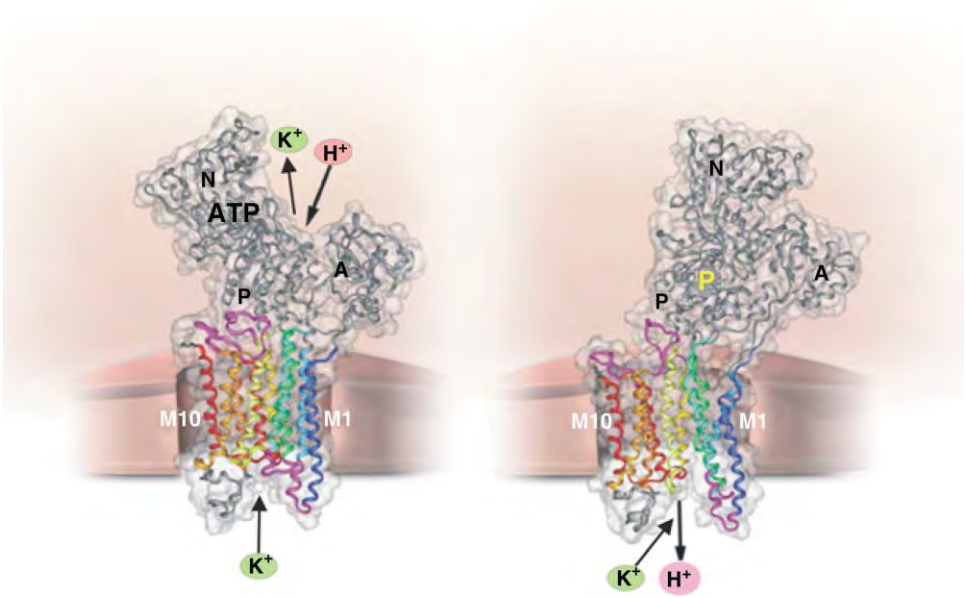

FIGURE 1 Proposed structure of the gastric H^+,K^+-ATPase α-subunit in E_1 (left) and E_2 (right) conformations. There are three lobes in the cytoplasmic domain: N (ATP binding), P (phosphorylation), and A (activation) regions. With binding of H^+ and MgATP to the E_1 form there is transient association of the N and P lobes with phosphorylation of asp386 and a conformational change to E_2P so that the A domain associates with the P domain. This change is transmitted to the membrane domain in the region of TM6 (dark yellow) and H^+ binding to the cation binding domain in the middle of the membrane domain is followed by release of H^+ and binding of K^+ from the luminal surface. There is then dephosphorylation and reformation of the E_1 conformation with release of K^+ to the cytoplasm.

recognized by this antibody was between amino acid positions 529 and 561. Since it inhibits the enzyme in intact cytoplasmic side out vesicles this epitope must be cytoplasmic and it is close to the region known to bind the cytoplasmic reagent, fluorescein isothiocyantate, FITC, a lysine reagent, namely in the loop between H4 and H5. Antibody 1218 was shown to have its major epitope between amino acid positions 665 and 689 in the same N domain. A second epitope for mAb 1218 was also identified to be between amino acid positions 853 and 907. Monoclonal antibody 146 epitope was defined to be between positions 873 and 877 of the hog α-subunit. This is on or close to the extra-cytoplasmic face of H7. The presence of H9 and H10 was shown by *in vitro* transcription/translation of cDNAs encoding these sequences. This technique also showed the presence of H1 through H4 but was unable to detect H5 or H6.

The β-Subunit of Gastric H^+, K^+-ATPase

The primary sequences of the β-subunits have been reported for rabbit, hog, rat, mouse, and human. The β-subunit with ~290 amino acids is a glycoprotein having one transmembrane segment located at the region between amino acid sequence positions 38 and 63 near the N terminus and six or seven N-linked glycosylation sites in the extracytoplasmic region. Using lectin affinity chromatography, the H^+, K^+-ATPase α-subunit was co-purified with the β-subunit, showing that the α-subunit interacts with the β-subunit. By cross-linking with low concentrations of glutaraldehyde, the β-subunit was shown to be closely associated with the α-subunit. In the extracytoplasmic domain, there are six cysteines which are linked through disulfide bonds. Reduction of the disulfides of the β-subunit inhibits the activity of the H^+, K^+-ATPase. In the case of the Na^+, K^+-ATPase, the effect of reducing agents on the ability of the enzyme to hydrolyze ATP and bind ouabain was quantitatively correlated with the reduction of disulfide bonds in the β-subunit. Seven putative N-glycosylated sites (AsnXaaSer and AsnXaaThr) are shown in rabbit H^+, K^+-ATPase β-subunit, which are conserved in rats and humans. Six putative N-glycosylation sites are found in the hog gastric β-subunit. The N-linked oligosaccharides of the β-subunit of rabbit gastric H^+, K^+-ATPase was identified. All N-linked AsnX(Ser/Thr) sequences at positions 99, 103, 130, 146, 193, and 222 were fully glycosylated. Asn 99 was modified exclusively with oligomannosidic-type structures, $Man_6GlcNAc_2$–$Man_8GlcNAc_2$, and Asn193 has $Man_5GlcNAc_2$–$Man_8GlcNAc_2$ and lactosamine-type structures. Asn 103, 146, 161, and 222 contain lactosamine-type structures. All the branches of the lactosamine-type structure

were terminated with Galα-Galβ-GlcNAc extensions. The role of the carbohydrate chains was studied using HEK-293 cells. The enzyme activity was not affected by removal of any one of seven carbohydrates of the β-subunit; however, removal of all carbohydrate chains resulted in the complete loss of activity. Except for the second glycosylation site, each site was essential for trafficking from Golgi to plasma membrane, but not for ER to Golgi movement.

The function of the β-subunit is not clearly known, but this subunit appears to be required for proper assembly and targeting of the catalytic subunit. Perhaps the β-subunit has a function in maintaining the structure of the α-subunit to enable effective binding of K^+ ion to the outside face of the α-subunit. The H^+, K^+-ATPase β-subunit has the sequence Phe-Arg-His-Tyr in its cytoplasmic domain. This tyrosine has been shown to be important for the retrieval of the H^+, K^+-ATPase from the apical membrane of the parietal cells and to ensure its return to the tubulo-vesicular compartment in order to terminate the process of acid secretion. The participation of a tyrosine-based signal in the retrieval of the H^+, K^+-ATPase suggests that this process involves interactions with adaptins and is mediated by clathrin-coated pit formation. In knockout mice deficient in the H^+, K^+-ATPase β-subunit, cells that express the H^+, K^+-ATPase α-subunit had abnormal canaliculi and were devoid of typical tubulo-vesicular membranes.

Regions of Association in the Oligomeric Structure

There has been much suggestive evidence that the $\alpha-\beta$ heterodimeric H^+, K^+-ATPase exists as an oligomer. Such evidence includes target size by irradiation and unit cell size of the enzyme in two-dimensional crystals. Using Blue native gel separation and cross-linking with Cu^{2+}-phenanthroline, it was shown that the enzyme did indeed exist as an $(\alpha\beta)_2$ heterodimeric dimer. Membrane-bound H^+, K^+-ATPase reacted with Cu-phenanthroline to provide an $\alpha-\alpha$ dimer. The site of Cu^{2+}-oxidative cross-linking was either at cys^{565} or cys^{616}. Hence, this region of the α-subunit is in close contact with its neighboring α-subunit. No evidence was obtained for $\beta-\beta$ dimerization. ATP prevents this Cu-phenanthroline-induced $\alpha-\alpha$ dimerization. The M7/loop/M8 sector of the α-subunit is tightly associated with the β-subunit. An antibody mAb 146-14 recognizes the region of the α-subunit at the extra-cytoplasmic face of the M7 segment as well as the β-subunit, a finding consistent with the association found by column chromatography. Using a yeast two-hybrid analysis, a fragment Leu855 to Arg922 of the α-subunit was identified to bind the β-subunit. This is at the entrance of the TM8 into the membrane domain.

Kinetics and Conformational Changes of the Gastric H^+, K^+-ATPase

The gastric H^+, K^+-ATPase exchanges intracellular hydrogen ions for extracellular potassium ions by consuming ATP. The H^+ for K^+ stoichiometry of the H^+, K^+-ATPase is not clear. There are reports of two different stoichiometries, one or two H^+ per ATP hydrolyzed. In ion-tight vesicles studied at pH 6.1, the stoichiometry is $2H^+$:1ATP but at full pH gradient where the pH reaches 1.0, this has to fall to 1:1. Probably protonation of a carboxylic acid at the lower luminal pH is then maintained.

There are several steps in the reaction scheme of the H^+, K^+-ATPase. The enzyme is phosphorylated by ATP at asp^{386}. The rate of formation of the phosphoenzyme (EP) and the K^+-dependent rate of phosphoenzyme breakdown are sufficiently fast to allow the phosphoenzyme to be an intermediate in the overall ATPase reaction. The initial step is the reversible binding of ATP to the enzyme in the absence of added K^+ ion, followed by an Mg^{2+} (and proton) dependent transfer of the terminal (gamma) phosphate of ATP to asp^{386} of the catalytic subunit (E_1-P·H^+). The Mg^{2+} remains occluded until dephosphorylation. The addition of K^+ to the enzyme-bound acyl phosphate results in a two-step dephosphorylation. The faster initial step is dependent on the concentration of K^+, whereas the slower step is not affected by K^+ concentration. The second phase of EP breakdown is accelerated in the presence of K^+ but, at K^+ concentration exceeding 500 μM, the ratio becomes independent of K^+ concentration. This shows that two forms of EP exist. The first form E_2P is K^+ sensitive and converts spontaneously in the rate-limiting step to E_1P, the K^+ insensitive form. ATP binding to the H^+, K^+-ATPase occurs in both the E_1 and the E_2 state, but with a lower affinity in E_2 state (2 000 times lower compared to E_1). The effects of H^+ and K^+ on formation and breakdown of phosphoenzyme were determined using transient kinetics. Increasing hydrogen ion concentrations on the ATP-binding face of the vesicles accelerate phosphorylation, whereas increasing potassium ion concentrations inhibit phosphorylation. Increasing hydrogen ion concentration reduces this K^+ inhibition of the phosphorylation rate. Decreasing hydrogen ion concentration accelerates dephosphorylation in the absence of K^+, and K^+ on the luminal surface accelerates dephosphorylation. Increasing K^+ concentrations at constant ATP decreases the rate of phosphorylation and increasing ATP concentrations at

constant K^+ concentration accelerates ATPase activity and increases the steady state phosphoenzyme level. Therefore, inhibition by cations is due to cation stabilization of a dephospho form at a cytosolically accessible cation-binding site. The reaction mechanism is similar to that of the Na^+, K^+-ATPase.

The ions transported from the cytoplasmic side are H^+ at high pH. Since Na^+ is transported as a surrogate for H^+, it is likely that the hydronium ion, rather than the proton per se is the species transported. The ions transported inwards from the outside face of the pump are Tl^+, K^+, Rb^+, or NH_4^+. Presumably the change in conformation changes a relatively small ion-binding domain in the outward direction into a larger ion-binding domain in the inward direction.

The E_1 conformation of the H^+, K^+-ATPase binds the hydronium ion from the cytoplasmic side at high affinity. With phosphorylation, the conformation changes from $E_1P{\cdot}H_3O^+$ to $E_2P{\cdot}H_30^+$ form, which has high affinity for K^+ and low affinity for H_3O^+ allowing release of H_3O^+ and binding of K^+ on the extra-cytoplasmic surface of the enzyme. The rapid breakdown of the E_2P form requires K^+ or its congeners on the outside face of the enzyme. With dephosphorylation, the E_1K^+ conformation is produced with a low affinity for K^+, releasing K^+ to the cytoplasmic side, allowing rebinding of H_3O^+.

Fluorescein isothiocyanate (FITC) binds to the H^+, K^+-ATPase, inhibiting ATPase activity but not pNPPase activity. Fluorescence of the FITC-labeled enzyme, representing the E_1 conformation, was quenched by K^+, Rb^+, and Tl^+. The quenching of the fluorescence by KCl reflects the formation of E_2K^+. FITC binds at lys^{516} in the hog enzyme sequence. This FITC-binding site apparently becomes less hydrophobic when KCl binds to form the $E_2{\cdot}K$ conformation. In the E_1 form, the FITC region is relatively closer to the membrane and the extra-cytoplasmic loop relatively hydrophilic. With the formation of the $E_2{\cdot}K^+$ form, the FITC region is more distant from the membrane. These postulated conformational changes are therefore reciprocal in the two major conformers of the enzyme. When the gastric H^+, K^+-ATPase was cleaved by Fe^{2+}-catalyzed oxidation under various ligand, cleavage patterns were different between the different conformations. There are two Fe^{2+} cleavage sites. In Fe^{2+} site1, the parallel appearance of the fragments at ^{230}ESE, near ^{624}MVTGD, and at ^{728} VNDS upon transition from E_1 to E_2(Rb) conformations were observed. Meanwhile, in Fe^{2+} site2, the fragment near ^{299} HFIH was cleaved independent of conformational changes. These cleavage patterns were the same as those of the Na^+, K^+-ATPase. The cleavage data showed that the structural organization and changes in the cytoplasmic domains, association with E_1/E_2 transitions, are essentially the same for the H^+, K^+-ATPase, the Na^+, K^+-ATPase, and sr Ca-ATPase. N-domain where ATP binds inclines nearly 90° with respect to the membrane and the A-domain rotates by about 110° horizontally during the E1 to E2 conformation.

Functional Residues of the H^+, K^+-ATPase

When the gastric H^+, K^+-ATPase was digested by trypsin in the presence of high concentration of KCl, the tryptic membrane digest showed the presence of Rb^+ occlusion, i.e., stable binding of Rb^+ in the membrane domain of the catalytic subunit as does the Na^+, K^+-ATPase. Some regions near the membrane such as the region between gly^{93} and glu^{104} near the M1 segment, the region between asn^{753} and leu^{776} near the cytoplasmic side of the M5 segment, and the region after the M8 segment, especially the region between ile^{945} and ile^{963} containing five arginines and one lysine, were K^+ protected against digestion. Furthermore, when K^+ was removed from this membrane digest, the M5/M6 hairpin was released from the membrane, showing that M5M6 membrane hairpin is stabilized by K^+ ions. Proton pump inhibitors such as omeprazole, pantoprazole, lansoprazole, and rabeprazole all bind to Cys813 of M5M6, giving inhibition of activity.

Using site-directed mutagenesis of the gastric H^+, K^+-ATPase transfected in HEK293 cells, M5M6 luminal loop was studied in terms of K^+ access to the ion-binding domain. Mutations of M5, M5–M6, and M6 regions such as P798C, Y802L, P810A, C813A or S, F818C, T823V, and mutations of M7–M8 and M8 such as E914Q, F917Y, G918E, T929L, F932L, reduced the affinity for SCH28080, a reversible proton pump inhibitor, up to tenfold without affecting the nature of the kinetics. The L809F substitution in the loop between M5 and M6 resulted in about 100-fold decrease in inhibitor affinity. C813T mutant showed ninefold loss of SCH28080 affinity. All these data suggest that the binding domain for SCH28080 contains the surface between L809 and C813, where M5–M6 loop and the luminal end of M6 locate. Mutations of C813 and I816 in M6 and M334 in M4 also showed that the inhibitor binds close to the luminal surface of the enzyme. Mutations of the negatively charged amino acid residue in the α-subunit showed that the carboxyl group of the membrane-spanning domain is important for cation binding. Mutation of E820Q showed decreased K^+ sensitivity and the dephosphorylation was not stimulated by either K^+ or ADP, indicating that E820 might be involved in K^+ binding and transition to the E_2 form of the H^+, K^+-ATPase. Mutation of E795 showed a decrease of the phosphorylation rate and the apparent ATP affinity, indicating that E795 is involved in both K^+ and H^+

binding. Mutation of E795 and E820 in M5 and M6 resulted in a K^+-independent, SCH28080-sensitive ATPase activity, caused by a high spontaneous dephosphorylation rate. Thus the sixth transmembrane (M6) segment of the catalytic subunit plays an important role in the ion recognition and transport in the type II P-type ATPase families. When all amino acid residues in the M6 segment of gastric H^+, K^+-ATPase α-subunit were singly mutated with alanine, four mutants, L819A, D826A, I827A, and L833A, completely lost K^+-ATPase activity. Mutant L819A was phosphorylated but barely dephosphorylated in the presence of K^+, whereas mutants D826A, I827A, and L833A were not phosphorylated from ATP. Amino acids involved in the phosphorylation are located exclusively in the cytoplasmic half of the M6 segment and those involved in the K^+-dependent dephosphorylation are in the luminal half. Several mutants such as I821A, L823A, T825A, and P829A partly retained the K^+-ATPase activity accompanying the decrease in the rate of phosphorylation. Substituting three residues in the Na^+, K^+-ATPase sequence with their H^+, K^+-ATPase counterparts (L319F, N326Y, T340S) and replacing the TM3–TM4 ectodomain sequence with that of the H^+, K^+-ATPase result in a pump that gives 50% of ATPase activity in the absence of Na^+ at pH 6. The cation selectivity of the Na^+, K^+- and H^+, K^+-ATPase would be generated through a cooperative effort between residues of the transmembrane segments and the flanking loops that connect these transmembrane domains. A model that results from these studies and the 3D structure of the SR Ca-ATPase suggests that ion transport occurs between TM4, 5, 6 and perhaps TM8 and that the vestibule around cys813 is the binding domain of both compounds such as omeprazole and SCH28080.

Acid Secretion and the Gastric H^+, K^+-ATPase

The H^+, K^+-ATPase is present only in the gastric parietal cell and the intercalated cell of the distal renal tubule. In the resting parietal cell, it is present in smooth surfaced cytoplasmic membrane tubules. Upon stimulation of acid secretion, the pump is translocated to the microvilli of the secretory canaliculus of the parietal cell. This morphological change results in a several fold expansion of the canaliculus. There are actin filaments within the microvilli and the subapical cytoplasm. In the cytoskeleton system, there is abundance of microtubules among the tubulovesicles. Some microtubules appeared to be associating with tubulovesicles. A large number of electron-dense coated pits and vesicles were observed around the apical membrane vacuoles in cimetidine-treated resting parietal cells, consistent with an active membrane uptake in the resting state. Cultured parietal cells also undergo morphological transformation under histamine stimulation, resulting in great expansion of apical membrane vacuoles. Immunogold labeling of H^+, K^+-ATPase was present not only on the microvilli of expanded apical plasma membrane vacuoles but also in the electron-dense coated pits.

There is activation of a K^+ and Cl^- conductance in the pump membrane which allows K^+ to access the extra-cytoplasmic face of the pump. This allows H^+ for K^+ exchange to be catalyzed by the ATPase.

The covalent inhibitors of the H^+, K^+-ATPase that have been developed for the treatment of ulcer disease and esophagitis depend on the presence of acid secreted by the pump. They are also acid activated prodrugs that accumulate in the acid space of the parietal cell. Hence their initial site of binding is only in the secretory canaliculus of the functioning parietal cell. These data show also that the pump present in the cytoplasmic tubules does not generate HCl.

The upstream DNA sequence of the α-subunit contains both Ca and cAMP responsive elements in the case of the rat H^+, K^+-ATPase. There are gastric nuclear proteins present that bind selectively to a nucleotide sequence, GATACC, in this region of the gene. These proteins have not been detected in other tissues. Stimulation of acid secretion by histamine increases the level of mRNA for the α-subunit of the pump. Elevation of serum gastrin, which secondarily stimulates histamine release from the enterochromaffin-like cell in the vicinity of the parietal cell, also stimulates the mRNA levels in the parietal cell. H_2 receptor antagonists block the effect of serum gastrin elevation on mRNA levels. It seems therefore that activity of the H_2 receptor on the parietal cell determines in part the gene expression of the ATPase. It might be expected therefore that chronic stimulation of this receptor would up-regulate pump levels whereas inhibition of the receptor would down-regulate levels of the ATPase.

However, chronic administration of these H2 receptor antagonists, such as famotidine, results in an increase in pump protein, whereas chronic administration of omeprazole (which must stimulate histamine release) reduces the level of pump protein in the rabbit. Regulation of pump protein turnover downstream of gene expression must account for these observations.

See Also the Following Articles

Actin Assembly/Disassembly • Actin-Capping and -Severing Proteins • Actin-Related Proteins • Amino Acid Metabolism • Membrane Transport, General Concepts

Glossary

gastric H^+, K^+-ATPase An enzyme, which is one of the P_2-type ionmotive ATPases, that allows an electroneutral exchange of cytoplasmic protons for extracytoplasmic potassium.

α-subunit of gastric H^+, K^+-ATPase Functional subunit consisting of 1034 amino acids with an M_r of 114 KDa, which has ten transmembrane segments.

β-subunit of gastric H^+, K^+-ATPase A glycoprotein consisting of ~290 amino acids having one transmembrane segment and six or seven N-linked glycosylation sites in the extracytoplasmic region.

Further Reading

Melle-Milovanovic, D., Lambrecht, N., Sachs, G., and Shin, J. M. (1998). Structural aspects of the gastric H,K ATPase: The M5/M6 domain and alpha beta association. *J. Physiol. Scand.* **163**(suppl. 643), 147–162.

Munson, K., Lambrecht, N., Shin, J. M., and Sachs, G. (2000). Analysis of the membrane domain of the gastric H^+, K^+-ATPase. *J. Exp. Biol.* **203**(Pt 1), 161–170.

Munson, K., Vagin, O., Sachs, G., and Karlish, S. (2003). Molecular modeling of SCH28080 binding to the gastric H,K-Atpase and MgATP interactions with SERCA- and Na,K-ATPases. *Ann. New York Acad. Sci.* **986**, 106–110.

Shin, J. M., Bayle, D., Bamberg, K., and Sachs, G. (1998). The gastric H,K-ATPase. In *Advances in Molecular and Cell Biology*, Vol 23A, pp. 101–142. JAI Press, Connecticut.

Vagin, O., Munson, K., Denevich, S., and Sachs, G. (2003). Inhibition kinetics of the gastric H,K-ATPase by K-competitive inhibitor SCH28080 as a tool for investigating the luminal ion pathway. *Ann. New York Acad. Sci.* **986**, 111–115.

Biography

George Sachs is a Professor in the Department of Medicine and Physiology at The University of California, Los Angeles and Wilshire Chair in Medicine, University of California, Los Angeles, and Co-Director, Center for Ulcer Research and Education, University of California, Los Angeles, and VA Greater Los Angeles Healthcare System.

Jai Moo Shin is an Associate Researcher in the Department of Physiology at The University of California, Los Angeles.

P-Type Pumps: Na^+/K^+ Pump

Peter L. Jorgensen
University of Copenhagen, Copenhagen, Denmark

The Na^+/K^+ pump transforms the chemical energy in ATP to electric or osmotic work and maintains electrochemical Na^+ and K^+ gradients across cell membranes. At rest, the pump converts 20–30% of the current ATP production in mammals to active Na^+/K^+-transport in kidney, intestine, muscle, heart, central nervous system, and other cells of the body where Na^+/K^+ gradients are required for maintaining membrane potential and cell volume. The Na^+/K^+ pump is the largest protein complex in the family of P-type cation pumps. The minimum functional unit is an $\alpha\beta$-heterodimer of the calytic α-subunit containing the Na^+/K^+, ATP, and phosphate binding sites, and the glycosylated β-subunit required for the correct folding of the complex in the endoplasmic reticulum. The $\alpha\beta$-unit can also be coexpressed with small ion transport regulators of the FXYD family. Individual genes of four α-isoforms and at least three β-isoforms of the Na^+/K^+ pump are expressed in a tissue- and cell-specific manner to cover the demands for the specific physiological functions in epithelia, skeletal and heart muscles, nerves, and the reproductive system.

The Na^+/K^+ Pump Reaction Cycle

The Na^+/K^+ pump is a molecular machine which binds ATP in the cytoplasmic protrusion and couples the scalar processes of phosphorylation and dephosphorylation to the vectorial extrusion of $3Na^+$ ions and uptake of $2K^+$ ions. The reaction is specifically inhibited by high-affinity binding of cardiac glycosides like digoxin or ouabain. The driving force of the reaction is the free energy of ATP hydrolysis, which depends on the cytoplasmic concentrations of ATP, ADP, and Pi. In normal cells containing mitochondria, the free energy of ATP hydrolysis is close to $-60\,kJ\,mol^{-1}$ and the electrical driving force of the Na^+/K^+ pump is close to -600 mV ($-\Delta G/F$; where F is Faradays constant ($96\,485\,C\,mol^{-1}$)). Most of the electrochemical work (~ 390 mV) is used for the outward translocation of three Na^+ ions per cycle against the inside negative membrane potential and the tenfold-steep chemical gradient for Na^+ ions. Less energy (~ 40 mV) is used for the inward transport of two K^+ ions per cycle since potassium in most cells is close to electrochemical equilibrium.

In the first step of the reaction cycle of the Na^+/K^+ pump in Figure 1, ATP acting with low affinity accelerates inward transport of $2K^+$ ions coupled to the E_2 [2K] $\leftrightarrow$ E_1ATP transition. After dissociation of $2K^+$ ions, binding of $3Na^+$ ions at sites oriented towards the cytoplasm promotes phosphorylation of Asp-369 from ATP and occlusion of $3Na^+$ ions in the E_1-P[3Na] form. Outward transport of $3Na^+$ ions is coupled to the E_1-P $\leftrightarrow$ E_2-P conformational transition. Binding of $2K^+$ ions at extracellularly oriented sites of the E_2P form activates dephosphorylation and $2K^+$ ions are stably occluded in the E_2 [2K] form.

In normal cells, the extracellular $[K^+]_e$ activities (4–5 mM) exceed those required for full activation, since the $K_{1/2}$ value is 1 mM. At cytoplasmic ATP concentrations of 2–3 mM, the rate of turnover depends on the $[Na^+]/[K^+]$ activity ratios. In most cells the $[Na^+]/[K^+]$ activity ratios in the cytoplasm are in the range of 10/140–30/120 mM and below the $K_{1/2}$ value for activation of the pump at 37/113 mM. For the renal $\alpha 1\beta 1\gamma$-Na^+/K^+ pump, the rate at 10 mM $[Na^+]_i$ and 140 mM $[K^+]_i$ in the cytoplasm is less than 5% of the maximum velocity ($V_{max} = 7500\,ATP\,min^{-1}$). Due to the cooperativity of Na^+ activation, the rate raises steeply with the $[Na^+]_i$ activity in the cytoplasm to 10% at 16 mM $[Na^+]_i$ and 134 mM $[K^+]_i$ or 20% of V_{max} at 22 mM $[Na^+]_i$ and 128 mM $[K^+]_i$ in the cytoplasm. This autoregulatory mechanism is very important since regulatory processes, in particular coexpression with FXYD proteins, can alter the affinity for Na^+ ions and thus become very efficient regulators of Na^+/K pump rate.

E_1- and E_2-Conformations of the Na^+/K^+ Pump

The E_1- and E_2-conformations differ with respect to orientation and specificity of intramembrane cation sites for Na^+ and K^+. In the E_2 [2K] form there is a 3000-fold preference for binding of K^+ over Na^+ at the extracellular surface and this requires that K^+ binding

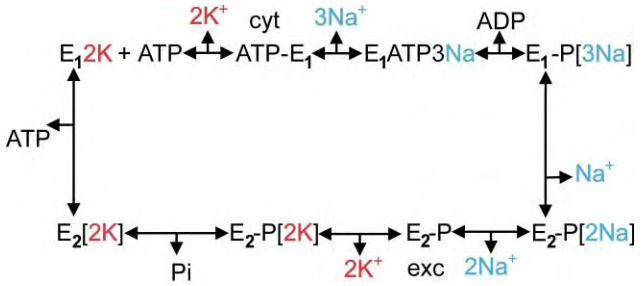

FIGURE 1 E_1–E_2 reaction cycle of the Na^+/K^+ pump with ping-pong sequential cation translocation. $[Na^+]$ or $[K^+]$ ions within brackets are occluded or tightly bound and prevented from exchanging with medium cations.

is 18 kJ mol^{-1} more stable than binding of Na^+. In the E_1ATP form, the affinity for Na^+ ions at the cytoplasmic surface is 16-fold higher than that for K^+ ions and this requires that binding of Na^+ is 6 kJ mol^{-1} more stable than binding of K^+. These adjustments of the cation sites are accompanied by changes of both the number of coordinating groups and their distances from the bound cations. The protein structure of the intramembrane domain of the Na^+/K^+ pump has not yet been solved at atomic resolution, but homology models based on the high-resolution structure of the Ca^{2+} pump of sarcoplasmic reticulum are efficient tools in interpretation of structure–function relationships of both the E_1- and E_2-conformations of the Na^+/K^+ pump, Figure 2. Modeling of the intramembrane domain shows that the structural changes accompanying the adjustments from an E_2-form with specificity for K^+ to an E_1-form with specificity for Na^+ can be achieved by twisting or tilting of the intramembrane helices to adapt the distances between the oxygen atoms of the coordinating groups of cation sites I and II in the intramembrane domain, Figure 2.

The overall structure of the α-subunit of the Na^+/K^+ pump is that the cation sites and transport path is made up of a bundle of transmembrane helices connected to a cytoplasmic protrusion consisting of three domains: the actuator or anchor (A), the phosphorylation (P) and the nucleotide-binding (N) domains. The N-domain is inserted between two Rossmann folds ($\alpha\beta\alpha\beta\alpha$) of the P-domain, which is directly connected to the extensions of the M4 and M5 transmembrane domains. The A-domain consists of the N-terminal portion of the α-subunit peptide chain and an insertion between M2 and M3. As seen from Figure 2, the $E_1P \rightarrow E_2P$ transitions are accompanied by large movements of the cytoplasmic A-, N-, and P-domains. The P-domain is rotated with reorientation of the catalytic site, including the important phosphorylated residue, Asp369, and the Mg^{2+} coordinating residue, Asp710. Movement of the N-domain is due mainly to the rotation of the P-domain. To stabilize the E_2P form, the A-domain rotates ~90°

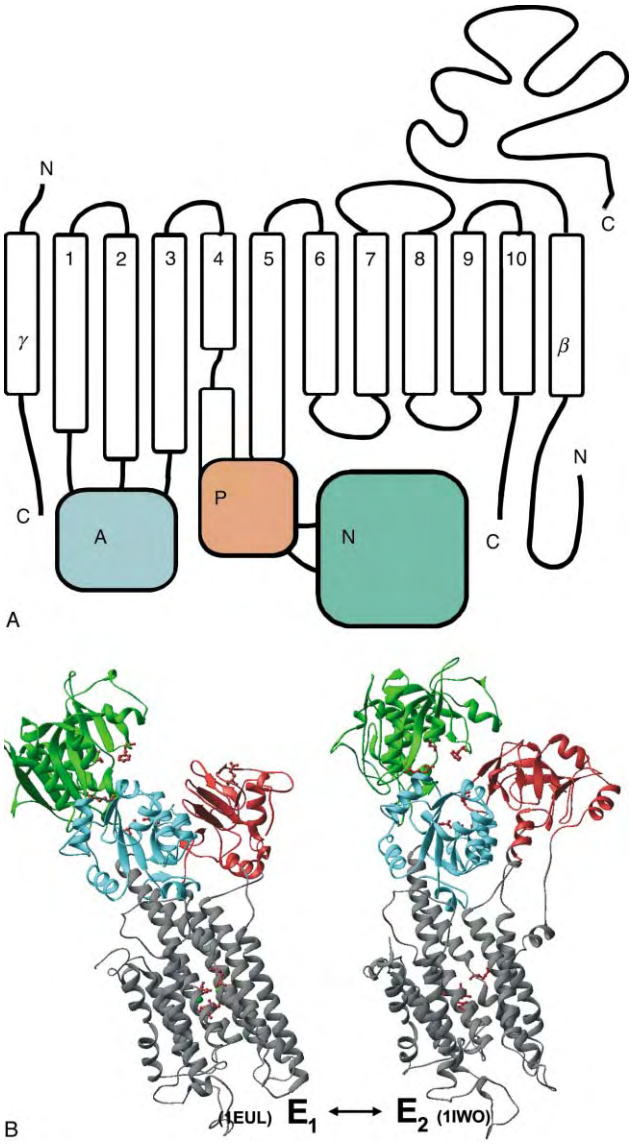

FIGURE 2 (A) Topology of the $\alpha\beta\gamma$-Na^+/K^+ pump. The β- and γ-subunits are single-pass membrane proteins. The α-subunit has ten transmembrane segments and the cytoplasmic protrusion is split in three domains: A, the anchor or attenuator domain; P, the phosphorylation domain, and N, the nucleotide binding site domain. (B) Models of E_1- and E_2-forms of the α-subunit of the Na^+/K^+ pump based on the high-resolution structure of Ca-ATPase in the E_1[2Ca] form (1EUL) and in the E_2-form (1IWO) stabilized by thapsigargin and Mg^{2+}. Side chains in ball and stick are shown for Phe475, Lys501, and Arg544 in the N-domain, for D369 and D710 in the P-domain, and for Glu327, Glu770, Asp804, and Asp808 in the cation binding domain. The position of the N-domain has been adjusted to allow spanning of an ATP molecule over the N- and P-domains.

about a vertical axis, thus docking the segment around Glu183 onto the P domain. These movements of the cytoplasmic domains are transmitted to tilting and twisting of the intramembrane helices and adjustment of the cation sites from a specificity for Na^+ in the E_1-form to a specificity for K^+ in the E_2-form.

Regulation of the E_1-E_2 Conformational Equilibrium

Physiological short-term regulation of the complex reaction cycle of the Na^+/K^+ pump is often directed towards rate limiting steps of the catalytic reaction, the long-range E_1-E_2 conformational changes which are linking the catalytic reactions to cation movements.

In the Na^+/K^+ pump, the conformational equilibria of both the phosphoforms (E_1P-E_2P) and dephosphoforms are poised heavily in direction of the E_2-forms. Thus in presence of K^+, the equilibrium constant (K_c) for the ratio E_2K/E_1K approaches a value of 1000. Changes of the conformational equilibrium may therefore have a strong influence on the turnover rate of the enzyme. Deletion of the N-terminal 30 residues by tryptic cleavage at 30Leu-Lys (T2) causes a 3–4-fold shift of the conformational equilibrium towards the E_1-form with reduction of Na^+/K^+ pump turnover to 45–50% of V_{max} values and the affinities for Na^+ or ATP are increased, while the apparent affinity for extracellular K^+ is reduced without interference with the capacity of the binding sites. Similar changes are seen after PKC mediated phosphorylation in the positively charged segment of the N terminus of the α1-subunit. The most pronounced structural variability between α-subunit isoforms occur at the N terminus. Comparison of the properties of α-isoforms shows that the maximum turnover rate is lower for the $\alpha2\beta1$-Na^+/K^+ pump ($4600\ min^{-1}$) than for the $\alpha1\beta1$-Na^+/K^+ pump ($7600\ min^{-1}$). The apparent affinities for Na^+ and ATP are two- and fourfold higher for α2- than for α1-isoforms, whereas the apparent affinity for K^+ is twofold lower for α2- than for α1-isoforms. These data are consistent with a shift of the E_1-E_2 conformational equilibrium toward E_1 in the α2-isoform. The properties of the α2-isoform are similar to those seen for the α1-isoform after deletion of 30 amino acid residues from the N terminus and they can be regarded as E_1-E_2 conformational isoforms. The rate of $\alpha3$-Na^+/K^+ pumps is about twofold lower than that of isoforms containing the α2-subunit.

Na^+/K^+ Pumps in Epithelial Cells of Kidney, Intestine, Lung, and Glands

The $\alpha1\beta1$-Na^+/K^+ pump is constitutively expressed in most cells and it maintains the Na^+ gradients driving the active transcellular transport in kidney, intestine, lung, and various glands. There is a close relationship between the capacity for reabsorption of Na^+ in these tissues and the abundance of $\alpha1\beta1$-Na^+/K^+ pumps in the basolateral membranes of the epithelial cells. The Na^+/K^+ pumps in human kidneys hydrolyze over 2 kg of ATP per day and over 600 g sodium is reabsorbed per day. Accordingly, ouabain binding data reveal 40–50 million Na^+/K^+ pumps per cell in thick ascending limbs of Henle (TALH) or distal convoluted tubules (DCT) as compared to a few hundred in red cells or a few thousand pumps in other nonpolarized cells. In all tubular cells the Na^+/K^+ pump maintains electrochemical gradients for sodium ($\Delta\mu Na^+$), the driving force for secondary active transport of other solutes and ions, such as H^+, Ca^{2+}, and Cl^-. In the TALH, the Na^+/K^+ pump functions in concert with the Na, K, $2Cl^-$ cotransporter and channels for K^+ or Cl^- to bring about transcellular NaCl transport, Figure 3. NaCl is reabsorbed at very high rates, while lumenal and cytoplasmic [Na^+] activities remain relatively high, 20–40 mM in the lumen of TALH.

The γ-subunit belongs to the FXYD family of small ion transport regulators. They are small single pass membrane proteins which share a 35 amino acid

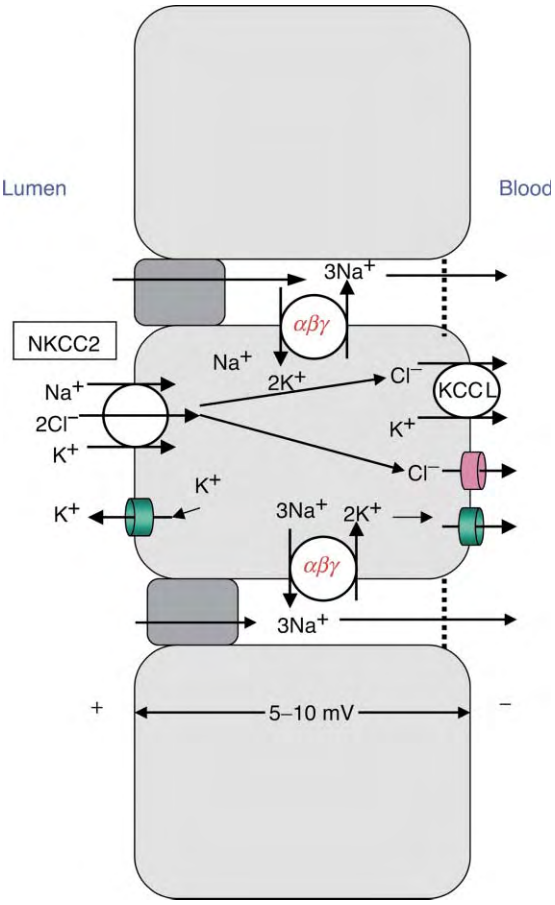

FIGURE 3 Mechanism of transcellular NaCl transport in thick ascending limb of Henle (TALH). The functions of the $\alpha1\beta1\gamma$-Na^+/K^+ pump are integrated with those of NKKCC2, the Na,K,Cl-cotransporter, KCCL, the K,Cl-cotransporter, and channels for K^+ and Cl^-.

TABLE I

Human Genes of Na^+/K^+ Pump Proteins: Isoforms of α and β Subunits are Expressed from Individual Genes[a]

Isoform	Gene	Human chromosome	Amino acid residues	Cell or tissue specific expression
$\alpha 1$	ATP1A1	1p13.1	1023	Constitutive, ubiquitous, dominant in epithelia of kidney, glands, and intestine
$\alpha 2$	ATP1A2	1q23.2	1020	Brain, muscle, heart
$\alpha 3$	ATP1A3	19q13.2	1013	CNS, brain
$\alpha 4$	ATP1A4	1q21–q23	1029	Testis, spermatozoa
$\beta 1$	ATP1B1	1q24.2	303	Ubiquitous, like the $\alpha 1$-subunit
$\beta 2$	ATP1B2	17p13.1	290	Brain, adhesion molecule (AMOG), liver
$\beta 3$	ATP1B3	3q23	279	Mostly in neural tissue, heart, kidney, lung

[a]Data from the genome database of National Center for Biotechnology Information.

signature sequence domain, beginning with the sequence FXYD and containing seven invariant and six highly conserved amino acids. The approved human gene nomenclature for the family is listed in Table I. Coexpression of the γ-subunit (FXYD2) with the $\alpha 1\beta 1$-Na^+/K^+ pump modifies the enzymatic properties with respect to the affinity for cytoplasmic $[Na^+]$. The $\alpha 1\beta 1\gamma$-Na^+/K^+ pump complex has a relatively low affinity for $[Na^+]_{cyt}$ and it is expressed at very high densities in the basolateral membranes of the TALH.

In the IMCD, the inner medullary collecting duct, Na^+/K^+ pump functions are integrated with those of the sodium channel, ENAC, and K^+-channels to drive reabsorption of Na^+ under the regulation of aldosterone. In the IMCD, the expression of FXYD4 or CHIF is stimulated by aldosterone and the CHIF-$\alpha 1\beta 1$-Na^+/K^+ pump complex has a relatively high affinity for $[Na^+]_{cyt}$, thus enabling the pump to reduce the activity of $[Na^+]$ to 2–5 mM in the tubular lumen and in the cytoplasm of the principal cells of the IMCD.

Aldosterone also regulates Na^+ reabsorption driven by the $\alpha 1\beta 1$-Na^+/K^+ pumps in epithelia of lung, glands, and colon, thus providing a major force in the regulation of Na^+ metabolism and extracellular fluid volume.

Na^+/K^+ Pump Isoform Expression and Regulation in Muscle and Central Nervous System

Extensive analyses have been performed to clarify the tissue specific gene expression and the molecular mechanisms of the regulation of the α- and β-subunit genes, Tables I and II. Experiments on animal models allow reverse genetic strategy to analyze the function of transport proteins. Targeted disruption of the $\alpha 1$- and $\alpha 2$-subunit isoforms in mice confirm that the Na^+/K^+ pump is essential for life of all mammalian cells. Egg cells lacking both copies of the ubiquitous $\alpha 1$-isoform do not pass the blastocyst stage. Homozygote knockouts of the $\alpha 2$-isoform results in death few minutes after birth of the mice apparently due to malformation of neural connections in the medulla oblongata. Knockout of one of

TABLE II

Human Genes of Na^+/K^+ Pump Proteins: Small Ion Transport Regulators of the FXYD Family

Isoform	Gene	Human chromosome	Amino acid residues	Cell or tissue specific coexpression with $\alpha\beta$-unit of Na,K-pump
FXYD1	PLM	19q13.1	92	Phospholemman coexpression with $\alpha 1\beta 1$ or $\alpha 2\beta$ suppress Na^+ affinity of Na,K-pump in muscle
FXYD2	ATP1G	11q23	66	Two splice variants, gamma(a) and gamma(b). Coexpression with $\alpha 1\beta 1$ reduces the Na^+ affinity of the Na,K-pump
FXYD3	MAT-8	19q13.11	87	
FXYD4	CHIF	10p11	89	In kidney and colon coexpression with $\alpha 1\beta 1$ increases the Na^+ affinity of the Na,K-pump
FXYD5	RIC	19q12–q13.1	178	
FXYD6	PHL	11q23.3	95	Phosphohippolin in brain and kidney
FXYD7		19q13.13	80	In brain, reduces K^+ affinity of Na,K-pump

the genes shows that α1- and α2-isoforms have different physiological functions. An increased force of contraction of the heart is seen in animals lacking one copy of the α2-isoform, whereas the force of contraction is reduced after elimination of one copy of the α1-isoform. There is a correlation between the expression of the α2-Na^+/K^+ pump and the Na^+/Ca^{2+} exchanger in plasma membrane domains overlaying the endoplasmic reticulum. Elevation of local activities of $[Na^+]_{cyt}$ may therefore increase the $[Ca^{2+}]_{cyt}$ activity in the space of the cytosol near the endoplasmic reticulum and thus amplify the force of contraction. This may explain the specific role of the α2-isoform as a regulator of calcium and the force of contraction in the heart.

In skeletal muscle, long-term regulation involves thyroid hormone-mediated changes of the expression level of Na^+/K^+ pumps. Short-term regulation of the Na^+/K^+ pump is mediated either by changes in intracellular Na^+ activity or by hormone-mediated protein kinase reactions leading to changes of the Na^+/K^+ pump transport properties or in its cell surface expression. Insulin causes translocation of α2-Na^+/K^+ pumps to the cell surface and the α2-Na^+/K^+ pumps in skeletal muscle are involved in specific regulation in response to hypokalemia. Exercise stimulates exocytosis of α1- and α2-Na^+/K^+ pumps to the plasma membranes of muscle cells and this response is important for recovery of K^+ after repetitive muscle contractions. Phospholemman (FXYD1) interacts with α1- and α2-isoform Na^+/K^+ pumps and modulates their properties to cause a decrease in the affinity to Na^+. The presence of Na^+/K^+ pumps with low affinity can also be important for the recovery process after muscle contractions. Skeletal muscles are the main intracellular store of K^+, and the Na^+/K^+ pumps in the sarcolemma are important for maintaining plasma K^+ along with H^+/K^+ pumps in kidney and colon.

All three α1-, α2-, and α3-isoforms are expressed in the central nervous system. During embryogenesis, the α2-Na^+/K^+ pumps are expressed in most regions of the brain and they are important in the modulation of neuronal activity in the neonate. In the adult, α2-Na^+/K^+ pumps are expressed primarily in astrocytes, where glutamate is transported in a sodium- and potassium-dependent fashion. FXYD7 has been identified as an isoform-specific regulator of the Na^+/K^+ pump in brain. The properties of α3-Na^+/K^+ pumps may allow reuptake of K^+ at low extracellular activities in the brain.

The α4-isoform is exclusively expressed in spermatozoa in the testis. In the mid-piece containing the flagellar motor, the α4-Na^+/K^+ pumps are tightly coupled to Na^+/H^+ exchange of primary importance for generation of ATP and thus for the mobility of spermatozoa.

See Also the Following Articles

Membrane Transport, General Concepts • Membrane Transporters: Na^+/Ca^{2+} Exchangers • Plasma-Membrane Calcium Pump: Structure and Function

Glossary

digoxin Cardiac glycoside, also known as digitalis. It is derived from the leaves of the foxglove plant (*Digitalis purpurea*) and is a classic drug which increases the force of contraction of the incompensated heart, probably by increasing the $[Ca^{2+}]$ activity in the cytoplasm of heart muscle cells.

E_1P The phosphorylated intermediate that is formed by Na^+-stimulated transfer of the γ-phosphate from ATP to form an acyl bond with the carboxylate group of Asp369 of the α-subunit. $E_1P[3Na]$ occludes $3Na^+$ ions and it is a high-energy intermediate as it can transfer its phosphate to ADP and form ATP.

E_2P It is formed in the conformational transition $E_1P \leftrightarrow E_2P$. The E_2P conformation has two cation sites with preference for K^+ over Na^+. The $E_2P[2Na]$ form may react with Na^+ and ADP to form ATP. In the forward reaction, K^+ will replace Na^+ and stimulate hydrolysis and release of inorganic phosphate. The $E_2P[2K]$ form is insensitive to ADP and can only react with water to release inorganic phosphate.

Na, K-ATPase The enzymatic equivalent of the Na^+/K^+ pump is the *in vitro* $Na^+ + K^+$ stimulated ATPase activity which is inhibited by ouabain.

ouabain Strophanthin G, a plant alkaloid from *Strophantus gratus*, a fast acting cardiac glycoside that binds with high affinity to the α-subunit of the Na^+/K^+ pump.

Further Reading

Blanco, G., and Mercer, R. W. (1998). Isozymes of the Na-K-ATPase: Heterogeneity in structure, diversity in function. *Am. J. Physiol.* **275**, F633–F650.

Feraille, E., and Doucet, A. (2001). Sodium-potassium-denosinetriphosphatase-dependent sodium transport in the kidney: Hormonal control. *Physiol. Rev.* **81**, 345–418.

Jorgensen, P. L., Hakansson, K. O., and Karlish, S. J. (2003). Structure and mechanism of Na,K-ATPase: Functional sites and their interactions. *Annu. Rev. Physiol.* **65**, 817–849.

Jorgensen, P. L., Karlish, S. J. D., and Maunsbach, A. B. (eds.) (2003) Na,K-ATPase and related cation pumps: structure, function and regulatory mechanisms. *Annu. New York Acad. Sci.* **896**.

Läuger, P. (1991). *Electrogenic Ion Pumps*. Sinauer Associates, Sunderland Massachusetts, USA.

Ogawa, H., and Toyoshima, C. (2002). Homology modeling of the cation binding sites of Na^+K^+-ATPase. *Proc. Natl Acad. Sci. USA* **99**, 15977–15982.

Toyoshima, C., and Nomura, H. (2002). Structural changes in the calcium pump accompanying the dissociation of calcium. *Nature* **418**, 605–611.

Toyoshima, C., Nakasako, M., Nomura, H., and Ogawa, H. (2000). Crystal structure of the calcium pump of sarcoplasmic reticulum at 2.6Å resolution. *Nature* **405**, 645–655.

Woo, A. L., James, P. F., and Lingrel, J. B. (2000). Sperm motility is dependent on a unique isoform of the Na, K-ATPase. *J. Biol. Chem.* **275**, 20693–20699.

Biography

Peter L. Jorgensen is a Professor of Molecular Physiology at the August Krogh Institute of the University of Copenhagen, Denmark. He holds a degree as medical doctor and a doctorate of medical sciences from the University of Aarhus, Denmark. He determined the physiological functions of the Na^+/K^+ pump in kidney and developed procedures for purification of the Na^+/K^+ pump from mammalian kidney and crystallization of the protein in the membrane plane. This led to detection of the distinct proteolytic cleavage patterns of the E_1- and E_2-conformations of the Na^+/K^+ pump and Ca^{2+} pump proteins. Recently, he contributed to solving the structure–function relationships of the binding sites for Na^+, K^+, Mg^{2+}, and ATP in the Na^+/K^+ pump protein.

P-Type Pumps: Plasma-Membrane H^+ Pump

A. Brett Mason and Carolyn W. Slayman
Yale University, New Haven, Connecticut, USA

Plasma-membrane H^+ pumps (also known as H^+-ATPases) are widely distributed throughout the fungal and plant kingdoms. They use the energy from ATP hydrolysis to generate a sizeable electrochemical gradient across the surface membrane, which in turn drives nutrient uptake into the cell via a series of H^+-coupled cotransporters (Figure 1A). The proton-pumping activity of the ATPase also contributes to the regulation of intracellular pH. Representative pumps have been cloned from budding (*Saccharomyces cerevisiae*) and fission (*Schizosaccharomyces pombe*) yeast, *Neurospora crassa*, several pathogenic fungi, and numerous plant species including *Arabidopsis thaliana*, *Nicotiana plumbaginifolia* (tobacco), and *Lycopersicon esculentum* (tomato).

Introduction

The fungal and plant plasma-membrane H^+-ATPases belong to a ubiquitous family of cation pumps known as P-type ATPases, so named because they hydrolyze ATP via a covalent aspartyl–phosphate reaction intermediate. When the P-ATPases are classified based on sequence alignments, membrane topology, and the nature of the transported cation(s), H^+-ATPases fall into a category designated as P_2 or type III.

Since 1986, when the *PMA1* genes of *S. cerevisiae* and *N. crassa* were cloned and sequenced, these two H^+-ATPases have served as prototypes for the group as a whole. Yeast in particular has proven to be an extremely useful model system. By virtue of the ease with which site-directed mutants can be made and analyzed, a large collection of *pma1* mutants has been generated which are providing molecular details as to the structure and function of the H^+-ATPase. The abundance of the ATPase in the yeast plasma membrane, where it may constitute up to 25% of total protein, is another feature of considerable value in the molecular characterization of the enzyme. Finally, the use of yeast as a vehicle for heterologous expression of other ATPases such as the individual isoforms of plant H^+-ATPase is providing information as to specific features of these enzymes that cannot be analyzed in their natural setting.

In addition to its utility in a comparative sense, the fungal ATPase has emerged as a potentially valuable target for the development of antifungal drugs. Most of the antifungals commonly used in the treatment of systemic fungal infections are either fungistatic compounds that inhibit the biosynthesis of ergosterol (the principal sterol in fungal membranes), or fungicidal compounds that interact with ergosterol directly, leading to disruption of the plasma membrane. Many pathogenic fungi are either innately resistant to existing antifungals, or are able to acquire resistance by developing mechanisms based on limitation of drug uptake, active drug efflux, or target resistance. In this regard, the H^+-ATPase has several properties that render it a promising new antifungal target: (1) it is an essential cell component, which favors the chances of fungicidal rather than fungistatic effect and simultaneously decreases the chances of resistance; (2) its cell surface location allows for targeting by drugs which do not enter the cell, thus avoiding multi-drug resistance (MDR) pumps and reducing the likelihood of toxic effects on host cells; and (3) it is structurally and functionally conserved across a wide range of fungal genera, promising broad-spectrum antifungal activity.

Structure

At the structural level, the fungal and plant plasma-membrane H^+-ATPases are composed of a 100 kDa polypeptide that is deeply embedded in the lipid bilayer, requiring detergents for solubilization. The predicted transmembrane topology of the 100 kDa polypeptide is shown in Figure 1B. As in other P_2-type ATPases, four hydrophobic segments at the N-terminal end of the polypeptide (M1–M4) and six hydrophobic segments at the C-terminal end (M5–M10) serve to anchor the ATPase in the membrane, while a large (340 amino acid) cytoplasmic loop in the center of the polypeptide

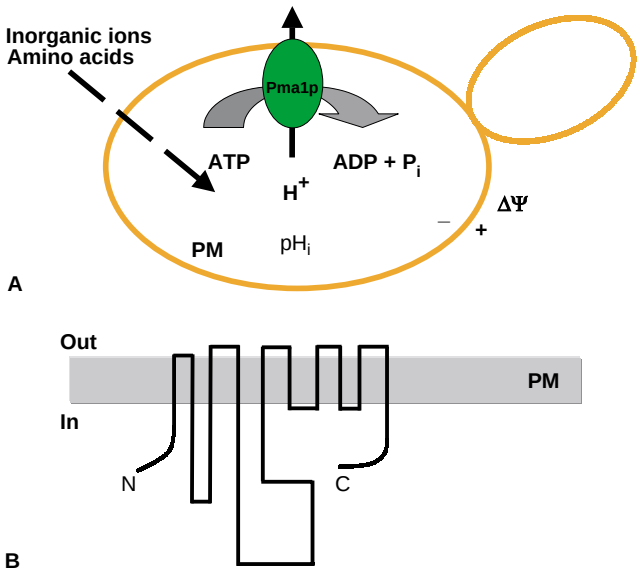

FIGURE 1 (A) The plasma membrane H^+-ATPase plays an essential role in yeast cell physiology. The pumping of protons (H^+) across the membrane at the expense of ATP hydrolysis establishes the membrane potential ($\Delta\Psi$) required for nutrient import and helps to regulate intracellular pH (pH_i). PM, plasma membrane. (B) Transmembrane topology of the fungal and plant H^+-ATPases. The ATPase has 10 transmembrane α-helices. Both N and C termini as well as the large catalytic domain of the enzyme are located in the cytoplasm. PM, plasma membrane.

contains the critical catalytic sites that bind ATP and form the aspartyl–phosphate intermediate.

The first three-dimensional glimpse of H^+-ATPase structure came from cryoelectron microscopic maps of the *Neurospora* enzyme at 8Å resolution. Ten transmembrane segments could be discerned clearly, connected by a narrow stalk to the multi-lobed, cytoplasmic headpiece of the enzyme. This low-resolution view has recently been confirmed and extended by comparison with X-ray crystallographic structures of the related mammalian sarcoplasmic reticulum Ca^{2+}-ATPase in two different conformations. In the first structure, with two Ca^{2+} ions bound, the headpiece of the Ca^{2+}-ATPase displayed a relatively open structure consisting of three well-separated domains: N (nucleotide-binding), P (phosphorylation), and A (actuator). In the second structure, obtained in the presence of a specific inhibitor known as thapsigargin, the three cytoplasmic domains had shifted towards one another to produce a relatively closed structure. Kühlbrandt and colleagues have demonstrated that the amino acid sequence of the *Neurospora* H^+-ATPase can be overlaid upon the Ca^{2+}-ATPase template to give a three-dimensional structure that agrees well with the earlier cryoelectron microscopic maps. Thus, structural information is now in hand that will serve as a valuable framework for mechanistic studies.

Reaction Mechanism

Like the intensively studied mammalian Na^+-, K^+-, and Ca^{2+}-ATPases, the fungal and plant plasma-membrane H^+-ATPases are considered to alternate between two major conformational states (E_1 and E_2) during their reaction cycle (Figure 2A). In E_1, the enzyme binds and hydrolyzes ATP to form a phosphorylated intermediate (E_1P), accompanied by protonation of the membrane-embedded transport site. It then undergoes a conformational change from E_1P to E_2P, during which the proton is extruded into the extracellular medium. After the release of inorganic phosphate, the E_2 conformation shifts back to E_1 to complete the cycle. The physical scale of these molecular movements can be appreciated by comparing the two crystal structures of Ca^{2+}-ATPase, where the top of the N-domain moves more than 50 Å and the A-domain rotates 90° to interact with the P-domain. A simple representation of this E_1 to E_2 conformational shift for a general P_2-type ATPase is depicted in Figure 2B. A stretch of 13 consecutive residues in stalk segment 4 of the yeast H^+-ATPase has

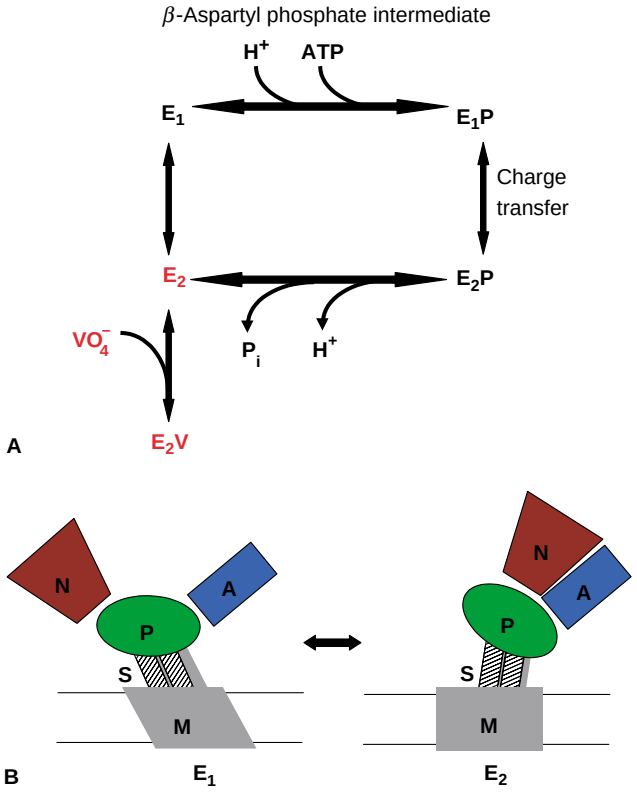

FIGURE 2 (A) The H^+-ATPase reaction cycle. See text for explanation. VO_4^-, vanadate, a potent P-type ATPase inhibitor. (B) Major domain movements that occur during conversion of the ATPase from the E_1 (cation-bound) to the E_2 (cation-free) conformation. N, nucleotide-binding domain; P, phosphorylation domain; A, actuator domain; S, stalk region; M, membrane sector formed by 10 transmembrane helices.

recently been shown to play a key role in the E_1-E_2 conformational change.

Given the similar arrangement of membrane-spanning α-helices (M1–M10) in the Ca^{2+}- and H^+-ATPase crystal structures, the cation pathway through the H^+-ATPase is probably formed by M4, M5, M6, and M8 as it is in the Ca^{2+}-ATPase. Consistent with this idea, site-directed mutations in three of these segments (M5, M6, and M8) have been shown to alter the stoichiometry of proton transport. These studies were carried out with inside-out secretory vesicles, using the fluorescence quenching of acridine orange to measure H^+ transport into the vesicle. When such measurements were made over a range of MgATP concentrations, and the initial rate of quenching was plotted as a function of the initial rate of ATP hydrolysis, wild-type ATPase and most mutant forms of the enzyme displayed a linear relationship, with a slope corresponding to a stoichiometry of $1H^+$ translocated per ATP hydrolyzed. By contrast, several mutants in M5, M6, and M8 exhibited a decreased slope indicating partial uncoupling, and two mutants in M8 exhibited an increased slope reflecting an apparent increase in transport stoichiometry.

Considerable efforts are currently being made to obtain higher-resolution crystal structures of the H^+-ATPase. Information from these studies, in combination with further site-directed mutagenesis experiments, will soon provide more insight into the proton's path across the membrane bilayer.

Biogenesis

Biogenesis of the H^+-ATPase begins with its synthesis in the rough endoplasmic reticulum (ER), from which it travels to the plasma membrane via the secretory pathway (Figure 3). Because of its abundance in the membrane, together with the ease of making site-directed mutants, the yeast H^+-ATPase has served as a valuable model for studying this process.

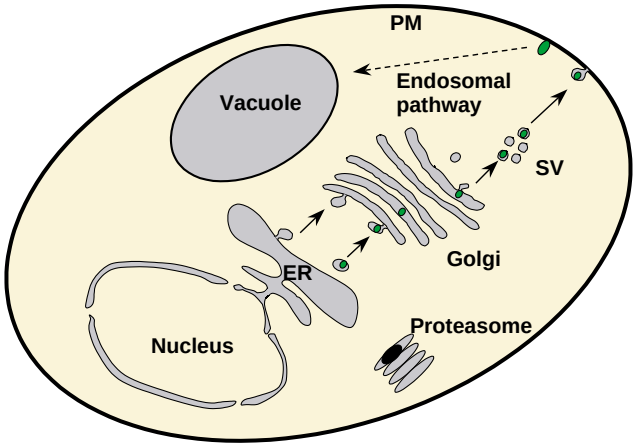

FIGURE 3 The yeast secretory pathway. ER, endoplasmic reticulum; SV, secretory vesicles; PM, plasma membrane.

While still in the ER, the ATPase adopts a fully folded structure that has the protease-resistant characteristics of the mature enzyme at the plasma membrane. The folded molecule is then incorporated into coat protein complex II (COPII) vesicles and shuttled to the *cis*-Golgi. Of considerable interest, a subpopulation of COPII vesicles has recently been identified that preferentially recruits and packages the H^+-ATPase by virtue of a specific coat protein, Lst1p. At least in principle, this mechanism provides a way to regulate biogenesis, underscoring the significance of the ATPase to the functioning of the cell as a whole.

Recent research has begun to shed light on the form of the ATPase as it exits the ER. Oligomeric forms of the *Neurospora* H^+-ATPase have been known for many years, and were originally thought to be by-products of detergent treatment. In the past several years, however, oligomers of the yeast H^+-ATPase have been detected early in biogenesis by three different methods: blue native gel electrophoresis, sucrose gradient centrifugation, and cross-linking of epitope-tagged polypeptides. In addition, oligomer formation provides a logical explanation for the existence of dominant negative *pma1* mutants, which cause coexpressed wild-type H^+-ATPase to be retained in the ER. The functional significance of the oligomers is not yet clear, given an earlier demonstration that the *Neurospora* H^+-ATPase is fully active when solubilized and reconstituted as a monomer. There has been speculation that the oligomers may play a special role in biogenesis and/or as a storage form of the ATPase, but further work will be required to test these ideas.

Parallel studies have been carried out recently to explore the association of the yeast H^+-ATPase with lipid rafts, sterol-, and sphingolipid-rich structures that are believed to segregate certain plasma-membrane proteins en route to the cell surface. Based on its insolubility in 1% Triton X-100 at 0°C, wild-type ATPase becomes associated with rafts prior to exiting the ER. Preventing the association by means of a mutation in sphingolipid biosynthesis does not block export, however, indicating that rafts do not play an obligatory role in this process.

Many mutations in the *PMA1* gene that lead to misfolding of the H^+-ATPase result in arrest of the polypeptide in the ER and massive accumulation of internal membranes. This represents the first level of quality control in biogenesis and, in most instances, is followed by redirection of the offending ATPase via the ER-associated degradation (ERAD) pathway for digestion in the proteasome. Quality

control screening is maintained, however, as the H^+-ATPase progresses through the secretory pathway. There are now several examples of mutant ATPases that escape the ER quality control mechanism only to be recognized as aberrant and differentially processed at later stages of the secretory pathway by vacuolar proteases.

Regulation

In addition to the major H^+-ATPase gene (*PMA*1), *S. cerevisiae* and *S. pombe* each have a second gene, *PMA2*, that encodes a nearly identical protein. The expression level of *PMA2* is so poor that it is unable to support growth, however, and the physiological function of the second ATPase remains unclear.

By contrast, plants possess multiple H^+-ATPase genes. In *A. thaliana*, for example, whole-genome sequencing has identified a family of 11 such genes, most or all of which are expressed in a tissue-specific way. Where tested, the corresponding H^+-ATPase isoforms differ detectably in their catalytic behaviors, suggesting that enzyme characteristics may be matched to the physiological requirements of individual tissues.

A diversity of environmental conditions and stress factors influence the biosynthesis and the activity of fungal and plant plasma-membrane H^+-ATPases (Figure 4). In yeast, two mechanisms have been identified, both resulting in up-regulation of the H^+-ATPase by glucose. At the transcriptional level, addition of glucose to the growth medium leads to a rapid increase in mRNA for the H^+-ATPase, and analysis of the promoter region of the *PMA1* gene has revealed active binding sites for several recognized transcription factors including Tuf1/Rap1/Grf1 and Gcr1. It is almost certainly significant that the same factors promote transcription of genes encoding glycolytic enzymes, pointing to a coordinated set of mechanisms that enable rapid, efficient growth on glucose.

Because the yeast H^+-ATPase has an unusually long half-life at the plasma-membrane (~11 h), posttranslational mechanisms are required to modulate its activity rapidly. Indeed, within minutes of glucose addition, the yeast ATPase displays an increased V_{max}, a lowered K_m, and a more alkaline pH optimum. There is growing evidence that this ensemble of changes results from posttranslational phosphorylation near the C terminus of the 100 kDa polypeptide. Truncation of the C terminus leads to constitutive activation, suggesting that the domain normally behaves in an autoinhibitory fashion. Detailed mutational analyses have linked the glucose-induced change in V_{max} with amino acids Arg^{909} and Thr^{912} and the change in K_m with Ser^{899} and Glu^{901}. Both pairs of residues constitute potential phosphorylation sites, and two novel phosphopeptides have been observed (though not yet sequenced) in proteolytic digests of H^+-ATPase from glucose-metabolizing yeast cells. Studies using site-directed mutagenesis of the yeast H^+-ATPase, coupled with suppressor analysis, suggest that the C terminus interacts with the stalk region near the cytoplasmic surface of the membrane and also with the ATP-binding (N) domain.

In plants, a variety of physiological conditions can affect the expression of specific ATPase isoforms, but

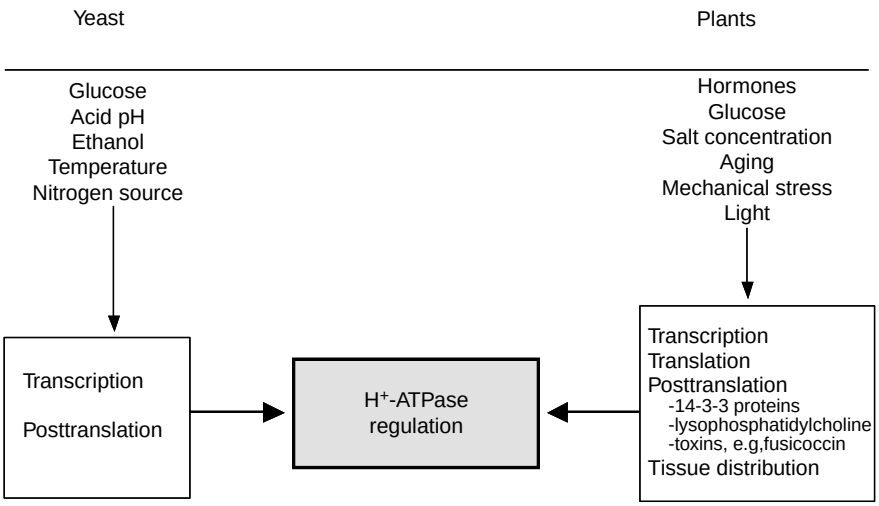

FIGURE 4 A comparison of the major environmental factors and mechanisms that regulate yeast and plant plasma membrane H^+-ATPase activity.

precise transcriptional mechanisms have not yet been elucidated. Translational mechanisms may also exist, possibly involving an untranslated leader sequence on the mRNA transcript that contains a short open reading frame (ORF). As in yeast, however, the primary modulator of plant H^+-ATPase activity is the C terminus of the enzyme, again acting in an autoinhibitory fashion. Growing evidence indicates that regulation is mediated by the binding of 14–3–3 proteins, a highly conserved family of acidic proteins expressed ubiquitously in eukaryotic cells. 14–3–3 proteins interact with many phosphoproteins, probably acting as dimers. A recent study of the Aha2p isoform of *Arabidopsis* H^+-ATPase expressed in yeast suggests that phosphorylation of Thr^{947} leads to the binding of 14–3–3 proteins, activating the enzyme. In the same study, the removal of two inhibitory sequences from the carboxyl terminus was also able to activate the Aha2p ATPase.

Regulation of H^+-ATPase activity is achieved through the coordinated action of multiple pathways. Our appreciation of the significance and complexity of this network will increase as our ability to explore cell physiology on a genome-, transcriptome-, and proteome-wide basis improves.

Summary

Research into the structure, function, biogenesis, and regulation of fungal and plant plasma-membrane H^+ pumps continues to provide a wealth of scientific information about the physiology of their host cells. Moreover, these pumps are invaluable as protein models not only for P_2-type ATPases but for complex integral membrane proteins in general.

And finally, with the continued increases in the incidence and variety of life-threatening fungal infections, particularly in immunocompromised patients, the fungal H^+-ATPase has assumed added significance as a viable target for the development of antifungal drugs.

See Also the Following Articles

Membrane Transport, General Concepts • Proteasomes, Overview

Glossary

fusicoccin A compound toxic to plants that is produced by the fungus *Fusicoccum amygdali*.

Gcr1 *G*ly*c*olysis *r*egulation 1. A yeast transcription factor that acts together with Rap1 to increase expression of some glycolytic enzymes.

lysophosphatidylcholine A phospholipid that activates plant plasma-membrane H^+-ATPases.

proteasome A large cytosolic protease complex that is responsible for intracellular protein degradation.

Tuf1/Rap1/Grf1 *T*ranslation *u*pstream *f*actor 1/*R*epressor *a*ctivator *p*rotein 1/*G*eneral *r*egulatory *f*actor 1. A yeast transcription factor involved in a variety of cellular processes including telomere regulation, chromatin silencing, glycolysis.

Further Reading

Ferreira, T., Mason, A. B., and Slayman, C. W. (2001). The yeast Pma1 proton pump: A model for understanding the biogenesis of plasma membrane proteins. *J. Biol. Chem.* **276**, 29613–29616.

Kühlbrandt, W., Zeelen, J., and Dietrich, J. (2002). Structure, mechanism, and regulation of the *Neurospora* plasma membrane H^+-ATPase. *Science* **297**, 1692–1696.

Morsomme, P., Slayman, C. W., and Goffeau, A. (2000). Mutagenic study of the structure, function and biogenesis of the yeast plasma membrane H^+-ATPase. *Biochim. Biophys. Acta* **1469**, 133–157.

Portillo, F. (2000). Regulation of plasma membrane H^+-ATPase in fungi and plants. *Biochim. Biophys. Acta* **1469**, 31–42.

Schekman, R. (2002). SEC mutants and the secretory apparatus. *Nat. Med.* **8**, 1055–1058.

Shimoni, Y., and Schekman, R. (2002). Vesicle budding from endoplasmic reticulum. *Meth. Enzymol.* **351**, 258–278.

Biography

Carolyn W. Slayman, Sterling Professor of Genetics and Cellular and Molecular Physiology at Yale University School of Medicine, has studied the plasma membrane H^+-ATPases of yeast and Neurospora for many years, focusing on the structure–function relationships that underlie proton transport.

A. Brett Mason, Associate Research Scientist in the Department of Genetics at Yale, began research on the yeast H^+-ATPase 10 years ago in New Zealand and joined the Slayman laboratory in 2000 to investigate the mechanism of ATPase biogenesis.

Purple Bacteria: Electron Acceptors and Donors

Evaldas Katilius and Neal W. Woodbury
Arizona State University, Tempe, Arizona, USA

Cyclic electron transport in the purple photosynthetic bacteria is facilitated by several soluble and integral membrane proteins. These proteins contain redox active cofactors serving as electron acceptors or donors. The cofactors are bacteriochlorophyll, bacteriopheophytin, quinone, or heme molecules. The electrochemical properties of these molecules are strongly affected by their protein environment allowing their midpoint potentials to be tuned to different values appropriate for their role in the cyclic electron transfer process.

General Description of the Cyclic Electron Transfer Chain

Generation of an electrochemical membrane gradient in purple nonsulfur bacteria involves light-driven electron transfer across the intracytoplasmic membrane followed by cotransport of electrons and protons in the opposite directions. The cycle starts with light-induced charge separation in the reaction center protein, where the electron transfer results in double reduction of a quinone molecule to quinol (see Figure 1) accompanied by proton uptake. Quinol then leaves the reaction center protein and is oxidized in the ubiquinol–cytochrome *c* oxidoreductase (also called cytochrome bc_1 complex). The quinol oxidation involves electron transfer both to a soluble cytochrome c_2 and to heme cofactors in the cytochrome bc_1 complex. This heme-mediated electron transfer in the cytochrome bc_1 complex results in the reduction of one quinone molecule bound in the Q_i site for every two quinol molecules oxidized in the Q_0 site (see Figure 1). The protons taken up from the cytoplasm during quinone reduction to quinol in the reaction center and cytochrome bc_1 are released to the periplasm during oxidation. Cytochrome c_2 in turn reduces the oxidized initial electron donor in the reaction center. The cyclic electron transfer results in the translocation of four protons from the cytoplasm to the periplasm for every two photons of light absorbed by the initial electron donor in the reaction center (Figure 1).

Reaction Center

The reaction center is an integral membrane protein, consisting of 3–4 protein subunits. In all species of purple bacteria, the reaction center contains two membrane-spanning protein subunits, called L (light) and M (medium), and the third subunit, called H (heavy), which is positioned on the cytoplasmic side of the membrane. Many species also contain a fourth subunit, a permanently associated cytochrome. The two membrane-spanning subunits bind the redox-active cofactors: four bacteriochlorophyll, two bacteriopheophytin, and two quinone molecules (see Figure 2). The protein also contains a redox inactive, nonheme iron atom and carotenoid molecule. Depending on the species, reaction centers contain either bacteriochlorophyll *a* or *b*, bacteriopheophytin *a* or *b*, and ubiquinone or menaquinone cofactors. The bacteriochlorophylls, bacteriopheophytins, and quinones are arranged in two nearly C_2 symmetric branches (see Figure 2). However, only one of these branches (usually called the A-branch), made up from cofactors mostly associated with the L protein subunit, is photochemically active *in vivo* (Figure 2). Upon the excitation with light, the initial electron donor P (a pair of bacteriochlorophyll molecules on the periplasmic side of the protein) donates an electron to a monomer bacteriochlorophyll, B_A, in ~3 picoseconds (ps), forming the charge-separated state $P^+B_A^-$, and then in ~1 ps the electron is further transferred to the bacteriopheophytin, H_A, forming the state $P^+H_A^-$. Electron transfer then proceeds to a primary quinone acceptor, Q_A, in ~200 ps, creating the charge-separated state $P^+Q_A^-$. From Q_A, the electron is transferred to a secondary quinone acceptor, Q_B, in 10–100 microseconds (μs). The semiquinone form of Q_B remains tightly bound to the reaction center. It is reduced to the quinol form after a second electron transfer event, which is coupled to proton uptake. The second electron transfer cycle is initiated when oxidized P^+ is reduced by cytochrome c_2, allowing light-induced charge separation to occur from P for a second

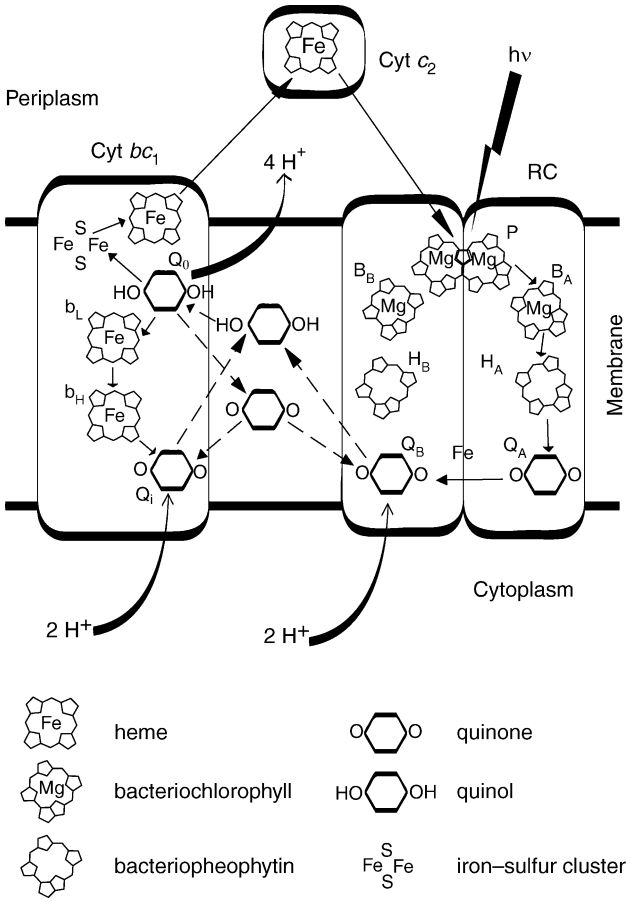

FIGURE 1 Cartoon diagram of the cyclic electron transfer reactions in photosynthetic purple bacteria. The main proteins involved in the reactions and their cofactors are shown schematically. RC stands for reaction center, Cyt c_2 – cytochrome c_2, Cyt bc_1 – cytochrome bc_1 complex. Q_0 and Q_i label two different quinone-binding sites in the cytochrome bc_1 complex. P, B_A, B_B, H_A, H_B, Q_A, Q_B label different cofactors in the reaction center (see Figure 2 for detailed explanation). Movement of the electrons is shown by solid arrows, dashed arrows depict movement of quinone and quinol cofactors.

time. The proton-coupled reduction of Q_B to a quinol occurs in ~1 millisecond (ms). The doubly reduced Q_B, Q_BH_2, then leaves the reaction center and enters the quinone pool (later binding to the cytochrome *bc*1 complex).

Properties of Reaction Center Cofactors

The initial electron donor, P, in purple bacteria consists of an excitonically coupled pair of bacteriochlorophyll molecules. The cation of P is a rather strong oxidant, with a P/P^+ midpoint potential of 0.50 V. On the other hand, the excited state of P, P^*, is a strong reductant with an estimated P^*/P^+ midpoint potential of ~ − 0.9 V, as the P to P^* transition energy is ~1.4 eV. The standard free energy of the first charge-separated state $P^+B_A^-$ is ~0.05 eV below P^* and the standard free energy of the state $P^+H_A^-$ is in the range of 0.15–0.25 eV below P^* (see Figure 2C). Further electron transfer from H_A to the quinone Q_A is driven by a larger free energy gap; $P^+Q_A^-$ is ~0.85 eV below P^*. The reduction potential of Q_A is ~ − 0.05 V, and therefore the free energy captured in the state $P^+Q_A^-$ is ~0.55 eV, or ~40% of the P to P^* transition energy (Figure 2C). The last charge-separated state $P^+Q_B^-$ is only slightly lower in free energy than $P^+Q_A^-$, given that the reduction of Q_B to the semiquinone has a midpoint potential ($E_m(Q_B/Q_B^-)$) of 0.02 V, while the reduction potential of semiquinone forming the quinol has an $E_m(Q_B^-/Q_BH_2)$ of ~0.1 V.

The fact that the reaction center has a symmetric arrangement of cofactors, yet an asymmetric electron transfer pathway, has intrigued researchers ever since the crystal structure was determined. Experimental results answering the question of what determines the electron transfer directionality have been presented over

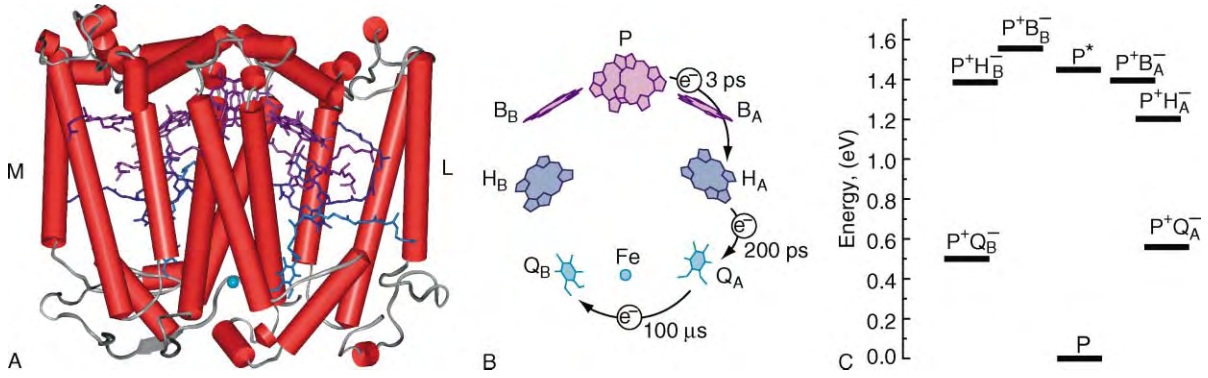

FIGURE 2 (A) Structure of the core subunits of the purple bacterial reaction center. The α-helices of the two subunits, L and M, are shown as red barrels. Bacteriochlorophyll, bacteriopheophytin, and quinone cofactors are shown inside the protein. This figure was created using the 1PCR entry from the Protein Data Bank. (B) Schematic arrangement of the symmetric branches of the bacteriochlorophyll (P and B), bacteriopheophytin (H), and quinone (Q) cofactors. The two branches, usually called A and B, are depicted as the subscripts. The asymmetric electron transfer reactions and their lifetimes are also shown. (C) The energetics of the charge-separated states in the reaction centers of purple bacteria. The free energies of the states are presented relative to the ground state of P, which was set at 0 eV.

the last few years. From site-directed mutagenesis studies, it has been deduced that the main factor limiting the electron transfer along the inactive B branch is the lower midpoint potential of the monomer bacteriochlorophyll cofactor B_B, which makes the standard free energy of the state $P^+B_B^-$ above the state P^* by ~ 0.1 eV (see Figure 2C). This high energetic barrier essentially blocks the electron transfer along the inactive branch, even though the standard free energy of the other charge-separated state, $P^+H_B^-$, is apparently slightly below P^*. The ability of the normally inactive branch (the B-side) to take part in charge separation has been demonstrated in various mutants of the reaction center in which the free energies of the charge-separated states involved were adjusted such that B-side electron transfer could effectively compete with A-side transfer.

Cytochromes

Light-induced charge separation in the reaction center generates both a reduced and an oxidized cofactor. While the doubly reduced quinone, Q_BH_2, has the ability to leave the reaction center to join the quinone pool, oxidized P (the cation free-radical P^+) has to be re-reduced to the neutral state by an external electron donor. This is accomplished by a *c*-type cytochrome. Purple bacteria can be categorized into two groups based on the type of the cytochrome *c* donor used and how it is associated with the reaction center.

The first and major group of bacteria has reaction centers that have permanently associated *c*-type heme-containing cytochrome subunits. These permanent RC-cytochrome complexes are best characterized in the purple bacteria *Blastochloris (Bl.) viridis* (previously named *Rhodopseudomonas viridis*), as this is the strain of bacteria from which the first crystal structure of reaction centers was determined. The cytochrome subunit, which is attached to the periplasmic side of the reaction center, is ~ 40 kDa and contains four heme cofactors. A separate water-soluble cytochome c_2 provides the electrons for the "fixed" cytochrome and mediates the cyclic electron flow between the reaction center and cytochrome bc_1 complex.

Another group of purple bacteria have simpler reaction centers with no permanently attached cytochrome subunit. Instead, a water-soluble cytochrome c_2 acts directly as the donor to oxidized P^+ as well as the acceptor of electrons from the cytochrome bc_1 complex. This group of bacteria includes such strains as *Rhodobacter (Rb.) sphaeroides* and *Rb. capsulatus*. Cytochrome oxidation and P^+ reduction in these strains occur through transient complexes that are formed between the reaction center and cytochrome c_2. The association of the two proteins is mediated mostly by electrostatic interactions, involving negatively charged residues on the periplasmic surface of the reaction center and positively charged residues on the surface of cytochrome c_2.

Properties of the Redox Active Centers in the Cytochromes

Cytochrome c_2 is a small protein containing only one covalently attached heme group. The redox potential of the heme cofactor ranges from 280 to 360 mV in various strains of purple bacteria. Electron transfer between cytochrome c_2 and P occurs with biphasic kinetics, with the major reaction phase having a reaction time constant of 1–4 μs and a slower phase with a 100–400 μs time constant. The first phase reflects the fast electron transfer from the cytochromes that are already associated with the reaction centers, while the slower phase represents the diffusion-limited second-order reaction.

Reduction of P^+ in the other group of the purple bacteria is performed by the permanently attached cytochrome. This cytochrome subunit contains two high and two low midpoint potential heme cofactors. As the best-studied example, the cytochrome from *Bl. viridis* has two hemes with low midpoint potentials of -60 and 20 mV and two high potential hemes, with midpoint potentials of 320 and 380 mV, respectively. The heme arrangement in the cytochrome is such that the heme with the highest midpoint potential is closest to the primary electron donor in the reaction center; the order (from proximal to distal) is: 380 mV → 20 mV → 320 mV → -60 mV. The reduction of P^+ in this cytochrome–reaction center complex is much faster than electron transfer between the soluble cytochrome c_2 and the reaction center. P^+ is reduced by the highest midpoint potential heme; the actual reaction rate depends on the redox state of the other hemes in the subunit and its time constant is on the order of a few hundred nanoseconds. Upon electron donation to P^+, the oxidation of heme 1 is followed by its reduction by heme 3 (with the midpoint potential of 320 mV) in several microseconds. The re-reduction of the oxidized hemes in the reaction center-associated cytochrome is again mediated by soluble cytochrome c_2; this reaction occurs in several hundred microseconds.

Ubiquinol–Cytochrome *c* Oxidoreductase (Cytochrome bc_1 Complex)

Ubiquinol–cytochrome *c* oxidoreductase (or the cytochrome bc_1 complex) is an integral membrane protein

involved in cyclic light-driven electron transfer as well as dark respiration. This complex both oxidizes and reduces quinones and reduces oxidized cytochrome c_2. The simplest of the cytochrome bc_1 complexes are found in the purple bacteria. In most species, this complex consists of only three subunits – cytochrome b, cytochrome c_1, and the "Rieske" iron–sulfur protein. Cytochrome b binds two redox-active heme molecules, called b_L and b_H, with the subscripts referring to the relatively low (~ -100 mV) and high (50 mV) redox midpoint potentials of the two hemes. Cytochrome c_1 binds only one heme molecule, which has a much higher midpoint potential of 290 mV. The "Rieske" iron–sulfur protein contains a $[Fe_2S_2]$ cluster with a relatively high midpoint potential of $\sim$280 mV.

The cytochrome bc_1 complex completes the electron transfer cycle in purple bacteria by re-reducing the cytochrome c_2 that was oxidized by the reaction center and performing the net oxidation of the quinol molecules released by the reaction center. First, the high potential iron–sulfur cluster is oxidized by cytochrome c_2 in $\sim$150–200 μs. Then, quinol binds to the Q_0 site at the interface of cytochrome c_1 and the "Rieske" protein on the complex and re-reduces the iron–sulfur cluster in a one-electron transfer. The second electron from the quinol is used to reduce the b_L cofactor and subsequently is transferred to b_H in $\sim$700 μs. The resulting oxidation of quinol in the Q_0 site results in release of two protons to the periplasmic side of the photosynthetic membrane. Heme b_H then reduces a quinone molecule bound in the second quinone-binding site Q_i, followed by proton uptake to form a semiquinone. This cycle repeats resulting in reduction of a second cytochrome c_2 and oxidation of a second quinol molecule in the Q_0 site, accompanied by release of two more protons on the periplasmic side of the membrane. The semiquinone molecule bound in the Q_i site is then reduced to quinol and released into the quinone pool. The reduction of the quinone molecule to quinol in the Q_i site results in uptake of two protons from the cytoplasmic side of the membrane. Thus, in total four protons are transferred from the cytoplasm to the periplasm, but the net number of quinol molecules oxidized in the cytochrome bc_1 complex is only one. This proton pumping creates the electrochemical gradient needed to drive ATPsynthase.

See Also the Following Articles

Chlorophylls and Carotenoids • Cytochrome bc_1 Complex (Respiratory Chain Complex III) • Cytochrome c • Purple Bacteria: Photosynthetic Reaction Centers • Quinones

Glossary

intracytoplasmic membrane A specially modified portion of the inner cell membrane made up of membrane invaginations which form tubes, vesicles, or flat lamellar membranes.

quinol (also dihydroquinone) Doubly reduced form of the ubiquinone.

quinone (also ubiquinone or coenzyme Q) Any member of a class of cyclic organic compounds containing two carbonyl groups, C = O, in a six-membered unsaturated ring. Widely distributed in plants, animals, and microorganisms, quinones function in oxidation–reduction processes.

semiquinone A stable anion free radical of the ubiquinone.

Further Reading

Berry, E. A., Guergova-Kurras, M., Huang, L., and Crofts, A. R. (2000). Structure and function of cytochrome *bc* complexes. *Annu. Rev. Biochem.* 69, 1005–1075.

Blankenship, R. E. (2002). *Molecular Mechanisms of Photosynthesis*. Blackwell Science, UK.

Hoff, A. J., and Deisenhofer, J. (1997). Photophysics of photosynthesis. Structure and spectroscopy of reaction centers of purple bacteria. *Phys. Rep.* 287, 1–247.

Scott, R. A., and Mauk, A. G. (eds.) (1996). *Cytochrome c: A Multidisciplinary Approach*. University Science Books, Sausalito, CA.

van Brederode, M. E., and Jones, M. R. (2000). Reaction centres of purple bacteria. In *Subcellular Biochemistry* (N.S. Scrutton and A. Holzenburg, eds.), Vol. 35: Enzyme-Catalysed Electron and Radical Transfer, pp. 621–676. Kluwer Academic/Plenum Publishers, New York.

Biography

Evaldas Katilius is a Faculty Research Associate in the Department of Chemistry and Biochemistry at Arizona State University in Tempe, Arizona. He holds a Ph.D. in chemistry from Arizona State University and M.S. in biophysics from Vilnius University, Lithuania.

Neal W. Woodbury is a Professor of Chemistry and Biochemistry at Arizona State University in Tempe, Arizona. He is the Director of the Center for BioOptical Nanotechnology in the AZBiodesign Institute and has a variety of interests in photochemistry and photobiology including energy and electron transfer in photosynthesis, single molecule spectroscopy of DNA/protein interactions, and optically directed molecular evolution. He holds a Ph.D. in biochemistry from the University of Washington, Seattle and performed postdoctoral study at the Carnegie Institution of Washington and Stanford University.

Purple Bacteria: Photosynthetic Reaction Centers

C. Roy D. Lancaster
Max Planck Institute of Biophysics, Frankfurt am Main, Germany

Located within photosynthetic membranes, reaction centers (RCs) are defined as the minimal functional units that can catalyze light-induced electron transfer reactions, thus stabilizing the separation of charged species across the membrane. The RC essentially functions as a ferrocytochrome c_2:quinone photo-oxidoreductase. The absorption of two photons of light leads to two one-electron oxidations of cytochrome c_2 in the periplasm and to the two-electron reduction of a quinone, which is coupled to the uptake of two protons from the cytoplasm. The resulting quinol then leaves its binding site, diffuses in the photosynthetic membrane and is reoxidized by a second membrane protein complex, the cytochrome bc_1 complex, which results in proton release to the periplasm. The electrons are transferred to re-reduce the cytochrome c_2 in the periplasm. This net proton transport produces a transmembrane electrochemical proton potential that can drive ATP synthesis through a third membrane-spanning complex, the ATP synthase.

Photosynthetic Reaction Centers

Virtually all life on Earth ultimately depends on the ability of photosynthetic organisms to convert solar energy into biochemically amenable energy. Photosynthesis is performed by higher plants, algae, and photosynthetic bacteria. Photosynthetic organisms absorb photons for the generation and storage of energy and for the production of biomass. A large proportion of photosynthetically active organisms consists of anoxygenic photosynthetic bacteria. In contrast to the higher plants, algae, and cyanobacteria of oxygenic photosynthesis, which contain the two membrane-bound photosystems I and II, each of the anoxygenic photosynthetic bacteria has only one type of reaction center. While the iron–sulfur type RCs of heliobacteria and anaerobic green sulfur bacteria resemble that of photosystem I, the pheophytin-quinone type RCs of purple bacteria are more similar to the RC of photosystem II.

Purple bacteria find their ecological niche in deeper layers of stagnant bodies of water. In all purple bacteria, the photosynthetic pigments and the photosynthetic apparatus are located within a more or less extended system of invaginated intracytoplasmic membranes. Unlike photosystem II, however, the purple bacterial RC is incapable of extracting electrons from water. Instead it must oxidize inorganic or organic molecules available in the environment. According to their electron donor requirements, sulfur and nonsulfur purple bacteria have traditionally been distinguished. In contrast to sulfur purple bacteria (*Chromatiaceae*, *Ectothiorhodospira*), nonsulfur purple bacteria (*Rhodospirillaceae*) do not require inorganic sulfur compounds, such as hydrogen sulfide, but instead use organic electron donors such as malate or succinate as electron donors. Most of what is known today about purple bacterial RCs results from studies on RCs from nonsulfur purple bacteria. These are currently the best-characterized membrane protein complexes.

Subunit Composition and Molecular Characterization

Most purple bacterial reaction centers contain four protein subunits (Figure 1), referred to as H, M, L, and C (a tetraheme cytochrome *c*). Some, however, such as the RCs of *Rhodobacter* (*Rb.*) *sphaeroides*, *Rb. capsulatus*, and *Rhodospirillum* (*Rs.*) *rubrum*, contain only the H, M, and L subunits. The related RC of the green aerobic thermophilic bacterium *Chloroflexus* (*Cf.*) *aurantiacus* lacks the H subunit.

Generally, RCs from purple bacteria have been isolated and characterized from *Rhodopseudomonas* (*Rp.*) *viridis* (suggested by Hiraishi in 1997 to be to referred to as *Blastochloris viridis*), *Rb. sphaeroides*, *Rb. capsulatus* and a number of other purple bacteria. Variant RCs have been created by site-directed mutagenesis as well as classical herbicide-resistance selection procedures and have been isolated and characterized from *Rb. capsulatus*, *Rb. sphaeroides*, and *Rp. viridis*.

RC preparations have a nonheme iron and four magnesium-containing bacteriochlorophyll cofactors

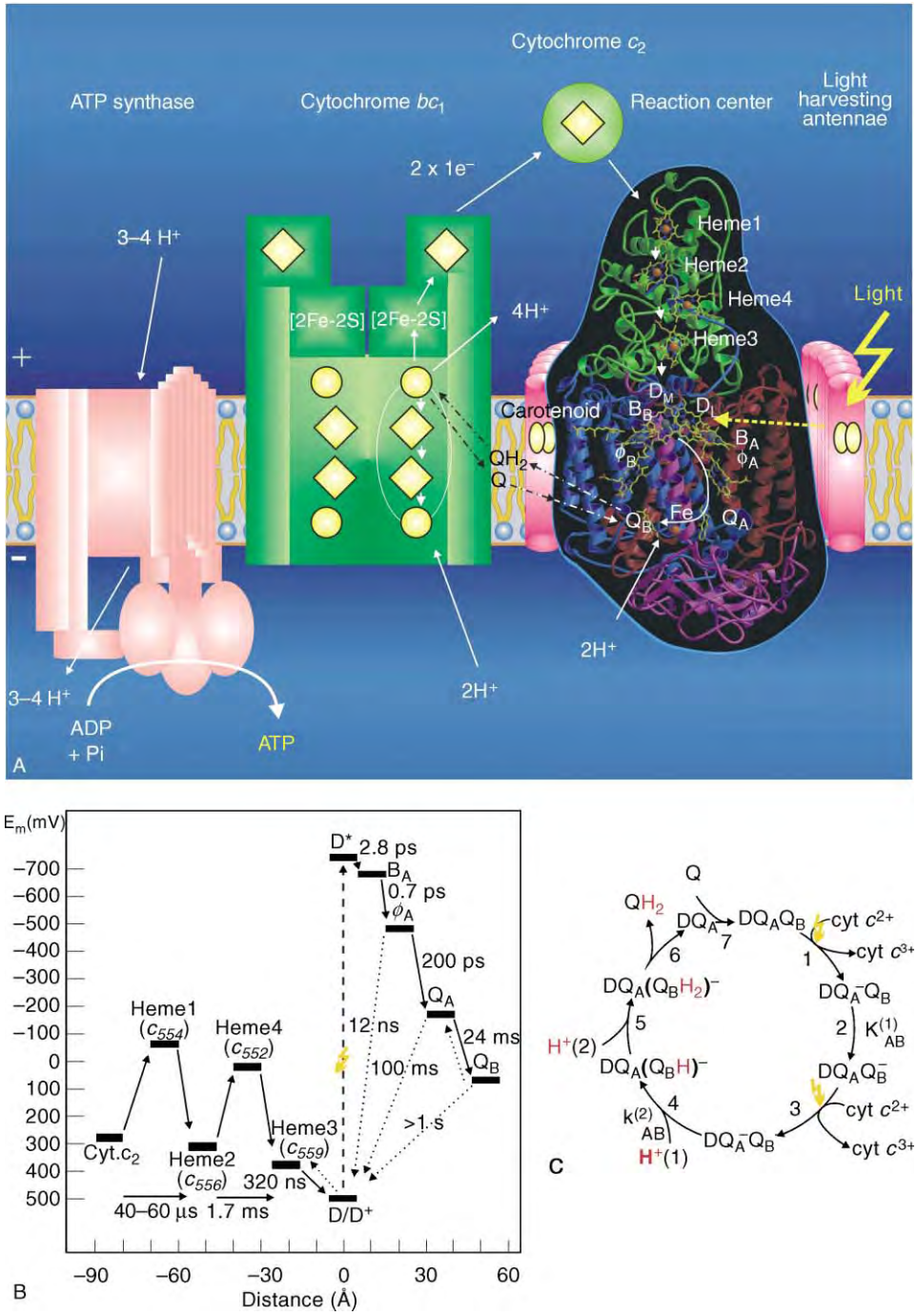

FIGURE 1 Structure and function of the photosynthetic RC. (A) Light-induced cyclic electron flow and the generation and utilization of a transmembrane electrochemical potential in the purple bacterium *Rp. viridis*. The structure of the *Rp. viridis* RC is represented schematically showing the heterotetramer of C, L, M, and H subunits as Cα traces in green, brown, blue, and purple, respectively, plus the fourteen cofactors, which have been projected on to the molecule for better visibility. Also for the sake of clarity, the quinone tails are truncated after the first isoprenoid unit and the phytyl side chains of the bacteriochlorophyll and bacteriopheophytin molecules have been omitted, as have those atoms of the carotenoid molecule, which were not observed in the electron density and assigned zero occupancy in the PDB entry 2PRC. Carbon, nitrogen, and oxygen atoms are drawn in yellow, blue, and red, respectively. (B) Equilibrium oxidation–reduction potentials of the *Rp. viridis* RC cofactors (as compiled by Lancaster, C. R. D., and Michel, H. (2001). Photosynthetic reaction centers. In *Handbook of Metalloproteins* (A. Messerschmidt, R. Huber, T. Poulos and K. Wieghardt, eds.) Vol 1, pp. 119–135. Wiley, Chichester, UK and references therein) as a function of inter-cofactor distance. The soluble electron donor protein cytochrome c_2 has been included as suggested in Figure 4A. Reaction halftimes indicated are taken from the references cited by Lancaster, C. R. D., and Michel, H. (2001). Photosynthetic reaction centers. In *Handbook of Metalloproteins* (A. Messerschmidt, R. Huber, T. Poulos and K. Wieghardt, eds.) Vol 1, pp. 119–135. Wiley, Chichester, UK. The photochemical excitation is indicated by a dashed arrow and unphysiological charge recombination reactions are shown as dotted arrows. (C) Quinone reduction cycle. Steps 2, 4, 5, and 6 are reversible. See text for details.

per RC, as measured by atomic absorption spectroscopy. In *Rb. sphaeroides* and *Rp. viridis*, these are bacteriochlorophyll *a* and bacteriochlorophyll *b*, respectively (Figures 1A and 2A). Those preparations with a tightly bound C subunit have four iron-containing heme groups, which are covalently bound to the protein via thioether bonds formed with the Cys residues of the heme attachment site sequences Cys-X-Y-Cys-His and the His is the fifth ligand to the heme iron. In the *Rp. viridis* RC, the sixth ligands to heme1, heme2, and heme3 are Met residues (His-Met-ligated hemes), whereas the sixth ligand to heme4 is a second His (*bis*-His ligation). Apart from these four hemes, all other cofactors are noncovalently bound by the L and M subunits. The six-coordinated nonheme ferrous iron is coordinated by the Nε atoms of four His residues and the two Oε atoms of a Glu residue. The fifth ligands to the five-coordinated bacteriochlorophyll-magnesium ions are provided by the Nε atoms of His side chains. In addition to these metal-containing cofactors, there are two bacteriopheophytin groups, a carotenoid, and two quinones bound by the RC. In *Rb. sphaeroides*, these are bacteriopheophytin *a*, spheroidene, and ubiquinone-10, respectively, whereas *Rp. viridis* contains bacteriopheophytin *b*, 1,2-dihydroneurosporene, menaquinone-9, and ubiquinone-9 (Figures 1A and 2A–2C).

Apart from the availability of high resolution crystal structures discussed, one major reason why, despite its complexity, the purple bacterial RC has become the "hydrogen atom of protein electron transfer" (W.W. Parson), is the richness of its characterization by optical absorption, electron paramagnetic resonance

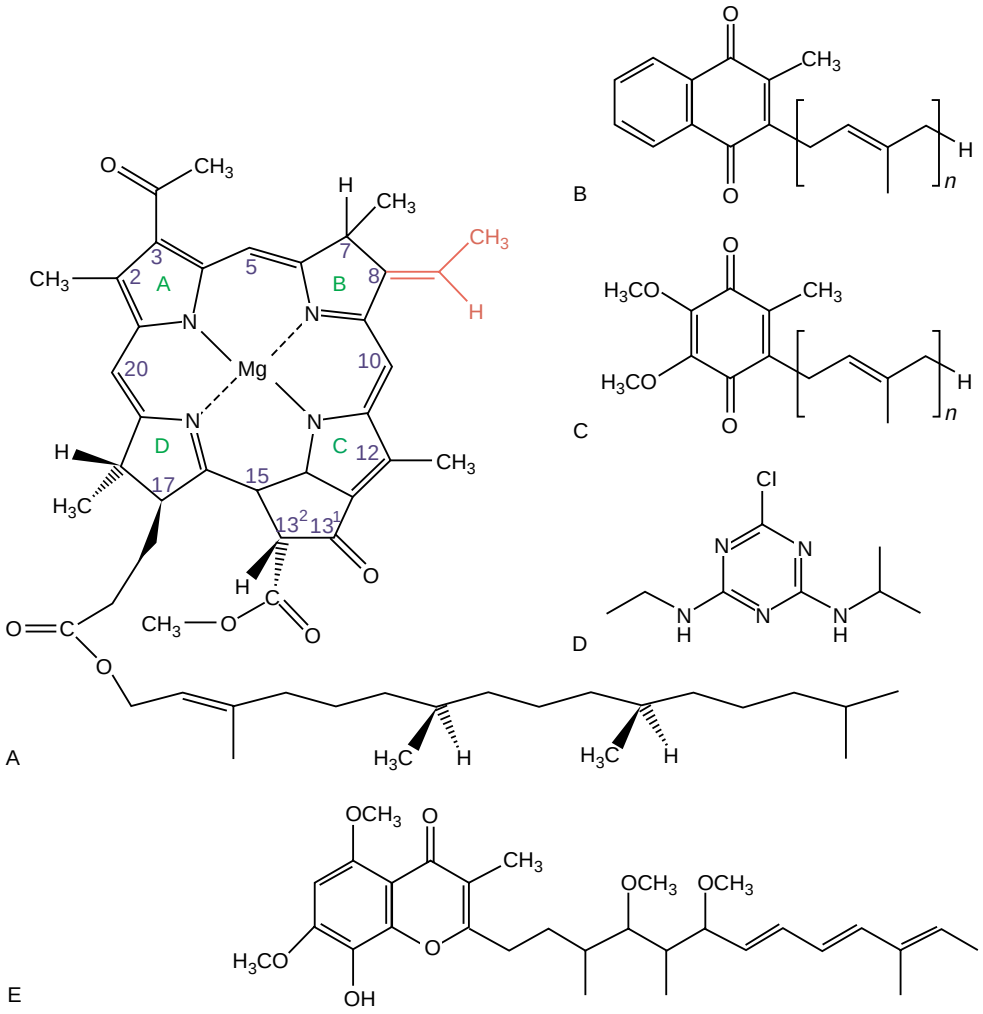

FIGURE 2 Chemical structures of RC cofactors (A–C) and inhibitors at the Q_B site (D–E). (A) Bacteriochlorophyll *b*, as bound in the *Rp. viridis* RC. The bacteriochlorophyll *a* bound in the *Rb. sphaeroides* RC differs by the presence of a C8 ethyl group instead of the C8 ethylidene group indicated in red. Bacteriopheophytins (*a* or *b*) are the metal-free variants of the bacteriochlorophylls (*a* or *b*) with two protons bonded to the nitrogens of the unsaturated pyrrole rings "A" and "C." (B) Menaquinone-n. The native Q_A in the *Rp. viridis* RC is menaquinone-9. (C) Ubiquinone-n. The native Q_A in the *Rp. viridis* RC is ubiquinone-9. In the *Rb. sphaeroides* RC, both Q_A and Q_B are ubiquinone-10. (D) Atrazine (2-chloro-4-ethylamino-6-isopropylamino-*s*-triazine). (E) Stigmatellin A.

(EPR), electron-nuclear double resonance (ENDOR), Fourier transform infrared (FTIR), Resonance Raman (RR), fluorescence, Stark effect, and other types of spectroscopy.

X-Ray Crystal Structures of RCs from Purple Bacteria

The photosynthetic RC from *Rp. viridis* was the first membrane protein complex for which an atomic structural model could be determined by X-ray crystallography (Protein Data Bank (PDB) entry 1PRC). The structure of the four-subunit *Rp. viridis* RC is shown schematically in Figure 1A. The structure of the RC from *Rb. sphaeroides* (not shown) would appear almost identical except for the C subunit at the top, which would be missing. The recently determined structure of the RC from the sulfur purple bacterium *Thermochromatium tepidum* (PDB entry 1EYS) is very similar in overall architecture to that of *Rp. viridis*.

The *Rp. viridis* RC has an overall length of 130Å in the direction perpendicular to the membrane. Parallel to the membrane, the maximum width is ~70Å. The central core of the RC is formed by the L subunit and the M subunit, which possess five membrane-spanning segments each. Both subunits are closely associated and noncovalently bind ten cofactors as detailed above and shown in Figure 1A. Large parts of the L and M subunits and their associated cofactors are related by a two-fold axis of symmetry perpendicular to the plane of the membrane. The H subunit is anchored to the membrane by a single membrane-spanning helix and is attached to the LM core on the cytoplasmic side. On the periplasmic side, the C subunit with its four covalently bound heme groups is attached. The N-terminal diacylglycerol moiety which, in addition to the interaction with the LM core, anchors the C subunit in the membrane is not visible in the electron density map.

The pigments form two symmetry-related branches, also shown in Figure 1A, each consisting of two bacteriochlorophylls, one bacteriopheophytin and one quinone, which both cross the membrane starting from the "special pair" D of two closely associated bacteriochlorophylls (D_M and D_L) near the periplasmic side, followed by the "accessory" bacteriochlorophyll, B, one bacteriopheophytin, ϕ, and a quinone, Q. As shown in Figure 1A, only the branch more closely associated with L subunit is used in the light-driven electron transfer. It is called the A-branch, the inactive one the B-branch. The active branch ends with the primary quinone Q_A, the inactive one with the secondary quinone Q_B. Halfway between both quinones, the nonheme iron is located. The carotenoid is in van der Waals contact with B_B and disrupts the twofold symmetry. In both species, the crystallographic temperature factors, which are a measure for the rigidity of the structure, are considerably higher along the B-branch than along the A-branch.

Functional Aspects

Oxidation–Reduction Potentials

The oxidation–reduction midpoint potentials, E_M, of the four heme groups follow the order low, high, high, low in the sequence or low, high, low, high if the hemes are ordered with decreasing distance (see Figure 1B) from the primary electron donor D. Theoretical analysis by the application of continuum electrostatics to the crystal structure of the C subunit has provided quantitative estimations of the factors contributing to the equilibrium E_M values of the four hemes. Specific residues and the propionic side chains on the hemes are calculated to strongly modulate the E_M values. The correct division into low and high potential hemes can be obtained by taking only the protein into account. Consideration of heme–heme interactions is required to reproduce the experimental data quantitatively.

The redox potentials of the other *Rp. viridis* RC cofactors are also included in Figure 1B. The potential of the excited state D^* is derived from the free energy difference between the lowest vibrational levels of D and D^*. Estimated from the wavelength of the absorption maximum, the dimer of bacterichlorophyll *b* in *Rp. viridis* provides an energy of 1240 meV between D and D^*, that of the bacteriochlorophyll *a* dimer in *Rb. sphaeroides* one of 1380 meV. The redox potential of *Rb. sphaeroides* D has been increased from 505 to 765 mV by the introduction of three additional hydrogen bonds to the special pair bacteriochlorophylls by site-directed mutagenesis, thus destabilizing the oxidized state of the donor, D^+.

The redox potential of Q_A is higher in the *Rb. sphaeroides* RC than in the *Rp. viridis* RC because of the different chemical nature of the quinones (ubiquinone versus menaquinone). However, it is still 67 mV lower than that of *Rb. sphaeroides* Q_B, even though both cofactors are chemically identical, thus requiring a role of the protein in tuning the *in situ* redox potentials of the quinones.

Kinetics

Figures 1A and 1B show schemes of the electron transfer steps that occur in the purple bacterial reaction center. Light absorption leads to an excited primary donor D^*, from which an electron is transferred via the monomeric bacteriochlorophyll B_A (reaction halftime: 2.8 ps) and the bacteriopheophytin ϕ_A (700 fs) to Q_A in 200 ps, leading to the formation of $D^+Q_A^-Q_B$. Re-reduction of

D^+ by cytochrome c_{559} (heme 3) occurs in 320 ns. These processes are much faster than the subsequent proton uptake and inter-quinone electron transfer reactions. Therefore, the first step of quinone reduction in the RC can be viewed as a "photochemical cytochrome oxidation," giving rise to the radical state $DQ_A^-Q_B$ (Figure 1C). Re-reduction of cytochrome c_{559}^+ by cytochrome c_{556} (heme 2) occurs in 1.7 μs. The second step of quinone reduction involves the transfer of the first electron to Q_B in 17–25 μs, resulting in the state $DQ_AQ_B^-$. The one-electron reduction of Q_B is not associated with direct protonation and the semiquinone species is anionic. However, the $Q_A^-Q_B \rightleftarrows Q_AQ_B^-$ equilibrium constant is pH-dependent, as electron transfer is accompanied by substoichiometric proton uptake due to the protonation of amino acid residues. Cytochrome c_{556}^+ is re-reduced by cytochrome c_2 in 40–60 μs. In species that lack the C subunit, e.g., *Rb. sphaeroides*, the photoxidized special pair is directly re-reduced by cytochrome c_2 in a biphasic reaction. The fast phase of ~1 μs is attributed to intermolecular electron transfer, the slow phase of 100 μs is limited by docking and reorientation of the cytochrome c_2-RC complex. After a second "photochemical cytochrome oxidation," the diradical state $DQ_A^-Q_B^-$ is formed at rates similar to those for the first electron transfer. Coupled transfer of the first proton and the second electron to Q_B^- leads to the monoprotonated, doubly reduced state $DQ_A(Q_BH)^-$. Transfer of the second proton for the formation of Q_BH_2 is kinetically indistinguishable from the first proton transfer in the wild-type RC and can only be resolved in the case of mutants with significantly retarded second proton transfer rates.

Functional Derivatives

Substrate Analogue and Inhibitor Complexes

In the original *Rp. viridis* RC structure (PDB entry 1PRC), the Q_B site was poorly defined because it was only partially occupied with the native ubiquinone-9 in the standard RC crystals. However, ubiquinone-2-reconstitution experiments have yielded crystals with full quinone occupancy of the Q_B site. Subsequent X-ray diffraction analysis and refinement has led to a well-defined Q_B-site model (2PRC), with the quinone bound in the "proximal" position, i.e., close to the nonheme iron (hydrogen-bonded to its ligand His L190, see Figure 3A). In the RC structure with a Q_B-depleted Q_B site (3PRC, Figure 3B), refined at 2.4Å, apparently five, possibly six, water molecules are bound instead of the ubiquinone head group, and a detergent molecule binds in the region of the isoprenoid tail. Using the structures 2PRC and 3PRC as references, the original data set 1PRC was re-examined. A more quantitative analysis of the original data resulted in 20% of the Q_B sites being occupied with quinone in the proximal site, 30% having quinone bound in a more distal site, not hydrogen-bonded to His L190 and further away from the nonheme iron (see Figure 3A), and half of the Q_B sites being empty or having the quinone unaccounted for. A further structure, the RC complex with the inhibitor stigmatellin (see Figure 2E), refined at 2.4Å, indicates that additional hydrogen bonds stabilize the binding of stigmatellin over that of ubiquinone-2 (4PRC, see Figure 3C). The binding pattern observed for the stigmatellin complex can be viewed as a model for the stabilization of a monoprotonated reduced intermediate (Q_BH or Q_BH^-). This indicates that the Q_B site is not optimized for Q_B binding, but for Q_B reduction to the quinol. In combination with the results of electrostatic calculations, these crystal structures can provide models for intermediates in the reaction cycle of ubiquinone reduction to ubiquinol, as discussed next.

The Q_B site is also a well-established site of herbicide action. Over half of the commercially available herbicides function by inhibition of higher plants at the QB site of the D1 polypeptide of the photosystem II RC. A commercially very important class of herbicides are the triazines, which were introduced by J.R. Geigy S.A. in the 1950s. A prominent example is atrazine (Figure 2D), first reported in 1957. According to statistics from 1995, atrazine was used on ~67% of all US corn acreage, 65% of sorghum acreage, and 90% of sugarcane acreage. Another well-known triazine is terbutryn (2-*t*-butylamino-4-ethylamino-6-methylthio-*s*-triazine). X-ray crystal structures of complexes of the RC with atrazine (PDB entry 5PRC) and terbutryn (PDB entry 1DXR) have been determined at 2.35Å and 2.00Å resolution, respectively. In both cases, three hydrogen bonds bind the distal side of the inhibitors to the protein, and four additional hydrogen bonds, mediated by two tightly-bound water molecules are apparent on the proximal side, as shown for atrazine in Figure 3D. In contrast to the proximal binding of stigmatellin (Figure 3C), the triazine inhibitor partially overlaps with both the distal- and the proximal ubiquinone-binding sites (Figure 3D).

Mutants

Work on site-directed mutagenesis of photosynthetic reaction centers started with the RC from *Rb. capsulatus*. This species is genetically very well characterized and able to grow non-photosynthetically under aerobic conditions, as well as under anaerobic conditions using e.g., dimethylsulfoxide as an electron acceptor. Most importantly, under these latter conditions, the photosynthetic apparatus is fully induced. Unfortunately, the RC from *Rb. capsulatus* could not be crystallized, thus thwarting proper inspection for structural changes.

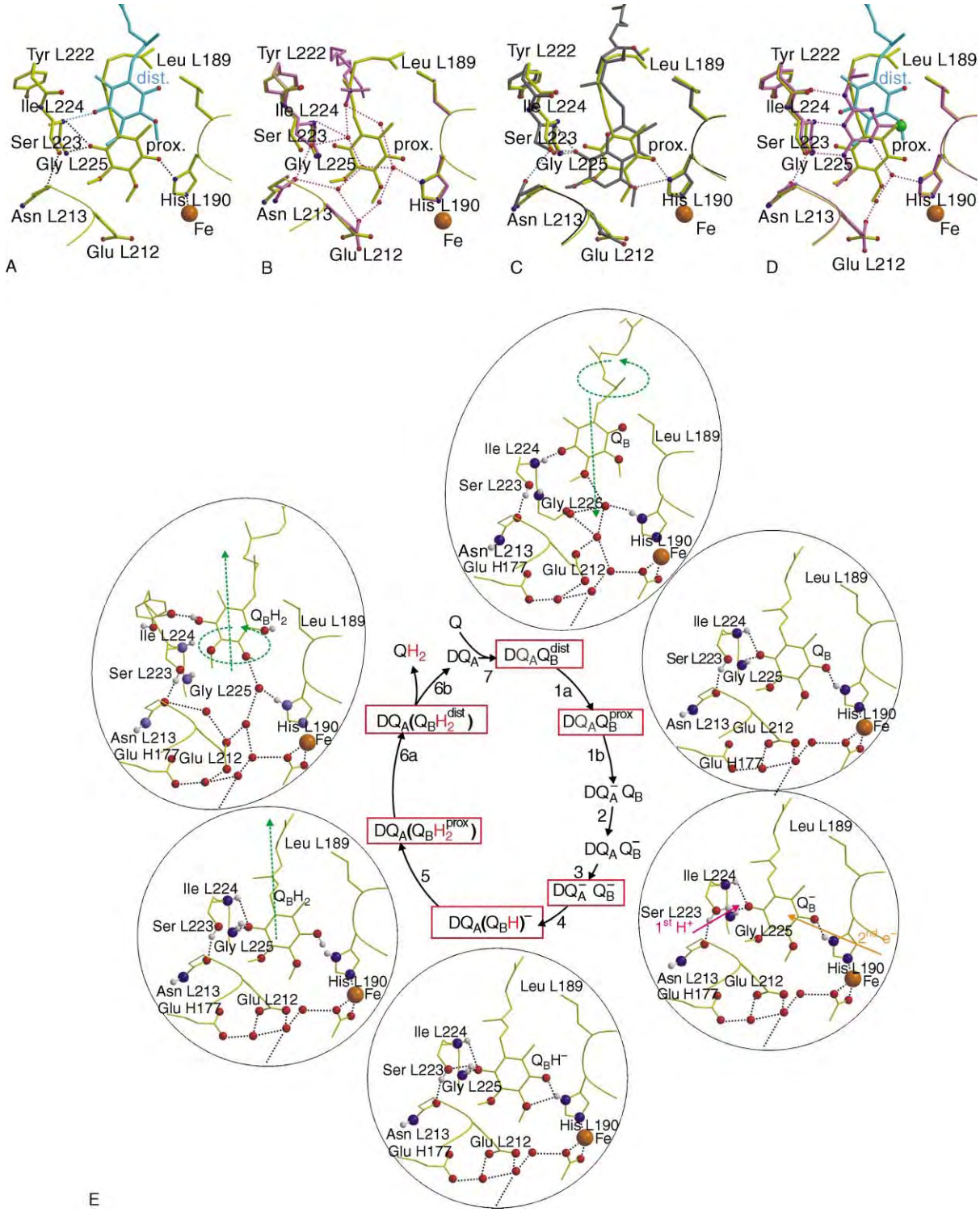

FIGURE 3 Derivatives at the Q_B site of the *Rp. viridis* RC. (A) Comparison of distal ($1PRC_{new}$, cyan) and proximal (2PRC, yellow) ubiquinone-binding sites. (B) Comparison of Q_B-depleted (3PRC, pink) and ubiquinone-2-occupied (2PRC, yellow) Q_B sites. (C) Comparison of stigmatellin binding (4PRC, gray) and ubiquinone-2 binding (2PRC, yellow). (D) Atrazine binding (5PRC, pink) compared to distal ($1PRC_{new}$, cyan) and proximal (2PRC, yellow) ubiquinone-binding sites. (E) Mechanistic implications of the structures 2PRC, 3PRC, 4PRC, and the revised model $1PRC_{new}$ for the events at the Q_B site within the reduction cycle of quinone to quinol. The numbering of the steps is analogous to that in Figure 1C. Hydrogen atoms are drawn as small light gray spheres. Dashed green arrows symbolize quinone movements.

The closely related *Rb. sphaeroides* can be grown under similar non-photosynthetic conditions, so that site-directed mutagenesis is also straightforward. As mentioned above, this RC is amenable to inspection by X-ray crystallography for structural changes. Many amino acids which were considered to be of importance for pigment binding, electron transfer or proton transfer were changed in *Rb. sphaeroides* RCs. In addition to mutagenesis, quinone or bacteriochlorin cofactors may be removed or replaced chemically with a wide range of similar compounds.

Site-directed mutagenesis of the RC from *Rp. viridis* is possible but more difficult. *Rp. viridis* can grow only under photosynthetic and, very slowly, under microaerophilic conditions. However, under microaerophilic conditions, the photosynthetic apparatus is hardly induced and photosynthetic growth conditions exert a selection pressure for revertants and suppressor mutants if the RCs are functionally impaired. On the other hand, very interesting herbicide-resistant mutants were obtained by classical selection procedures, with mutations some of which would not have been made by site-directed mutagenesis.

Some of these herbicide resistant mutants of the *Rp. viridis* RC have also been analyzed by X-ray crystallography. For instance, the mutation Tyr L222 → Phe unexpectedly leads to resistance against the herbicide terbutryn. In the wild type, Tyr L222 forms a hydrogen bond with the peptide carbonyl oxygen of Asp M43. Since this hydrogen bond is now missing, a stretch of the M subunit (M25–50) moves into a new position. The side chain of Phe L222 rotates by 90° into the herbicide binding site, thereby preventing the binding of terbutryn by steric hindrance, but at the same time introducing sensitivity to two other classes of photosystem II inhibitors normally inactive in bacterial RCs, the ureas and phenolics.

Using site-directed mutagenesis, the highly conserved Tyr L162, positioned halfway between D and the proximal heme3 (cytochrome c_{559}) in the *Rp. viridis* RC (see Figure 4A, below), was exchanged against a number of amino acids. All mutants grew photosynthetically. The redox potentials of D and c_{559} were changed by the mutations. The structures of two variant RCs (Tyr L162 → Phe and Tyr L162 → Thr) were determined and found not to differ significantly from the wild-type structure. Analysis of the kinetics of electron transfer led to the conclusion that the tyrosine residue at position L162 is not required for fast electron transfer from c_{559} to D^+.

Mutation of Arg C264 → Lys decreases the midpoint potential of heme3 (cytochrome c_{559}) from +380 mV to +270 mV, i.e., below that of heme2 (+320 mV, see Figure 1B). In the structure of the variant RC at 2.46Å resolution, no remarkable differences were found apart from the mutated residue itself. The halftime of electron transfer between heme2 and heme3 was the same as in the wild-type, indicating that the observed reaction rate is limited by the very uphill electron transfer from heme2 to heme4 (see Figure 1B).

Inter- and Intramolecular Electron and Proton Transfer and Catalytic Mechanism

Intramolecular Electron Transfer

The kinetics of light-induced electron transfer via Q_A to Q_B and of the re-reduction of the special pair have been detailed earlier. The reasons for the unidirectionality of electron transfer along the active A branch and not along the inactive B branch, despite the twofold pseudosymmetry of the LM core of the RC, have been the subject of numerous theoretical and experimental investigations. Slight differences in geometry, differences in rigidity, and differences in the amino acid composition of the L and M subunits have been suggested to contribute to unidirectionality. The latter aspect was specified by the theoretical identification of a large electrostatic field favoring charge separation along the A branch. A major contributor to the potential gradient is Arg L103, whose positive charge is stabilized by different sections of the polypeptide backbone. This dipolar stabilization leads to a much longer-range effect of the positive charge than if it were stabilized by a counter ion.

An experimental observation consistent with this electrostatic analysis is the finding that a site-directed double mutant in *Rb. capsulatus* RCs (Leu L212 → His; Gly L201 → Asp) appears to show significant electron transfer to ϕ_B. The first mutation leads to the incorporation of the β bacteriochlorophyll in the ϕ_A position and the second mutation introduces a negative charge close to B_A, thus making electron transfer down the A branch less favorable.

Quinone Reduction and Protonation

Both Q_A and Q_B sites are deeply buried within the photosynthetic reaction center complex, ~15Å from the cytoplasmic surface. Proton transfer to the reduced quinone within the Q_B site could occur by protons moving along a chain of proton donors and acceptors by a "proton wire," or hydrogen-bonded chain mechanism. Possible proton donors and acceptors are protonatable amino acid residues and water molecules. A number of the protonatable residues between the Q_B site and the cytoplasmic surface have been shown to be functionally relevant to the proton transfer process by analysis of site-directed mutations and second site revertants.

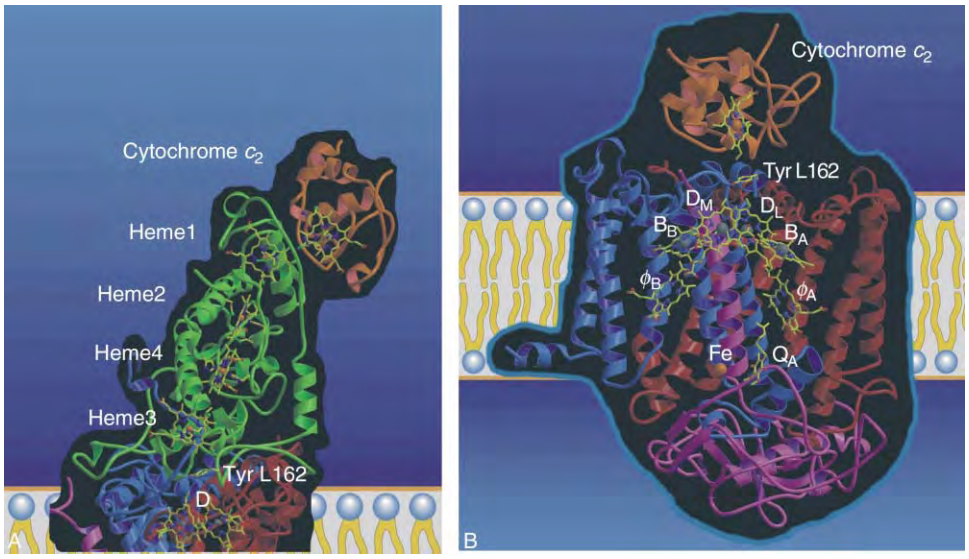

FIGURE 4 Cytochrome c_2 oxidation by the photosynthetic RCs of *Rp. viridis* and *Rb. sphaeroides*. (A) Reduction of the photo-oxidized tetraheme C subunit of the *Rp. viridis* RC (color-coding as in Figure 1A) by *Rp. viridis* cytochrome c_2 (orange). Theoretical docking as suggested from mutagenesis experiments. (B) Reduction of the special pair D in the *Rb. sphaeroides* RC (color coding of the L, M, and H subunits analogous to Figure 1A) by *Rb. sphaeroides* cytochrome c_2 (orange) as determined by X-ray crystal structure analysis (PDB entry 1L9B).

The observed effects can be due to the modification of the kinetics and thermodynamics of electron or proton transfer. Electrostatic calculations based on the X-ray structure coordinates of the RCs from *Rb. sphaeroids* and *Rp. viridis* led to the identification of residues that can contribute to the changes in equilibrium distributions of protons in the different redox states of the protein, thus helping to determine the role of the functionally important residues.

In combination with the results of electrostatic calculations, the crystal structures 3PRC, $1PRC_{new}$, 2PRC, and 4PRC already discussed (cf. Figures 3A–3D) can provide models for intermediates in the reaction cycle of ubiquinone reduction to ubiquinol (see Figure 3E). The binding of the incoming Q_B to the distal site displaces some of the water molecules present in the "empty" pocket. The quinone ring is flipped around the isoprenoid tail and further water molecules are displaced for the Q_B to occupy the proximal position (step 1a in Figure 3E). This is the position in which neutral Q_B accepts an electron from Q_A^-. The hydrogen bonds donated to the quinone will automatically lead to a tighter binding of the negatively charged semiquinone Q_B^- compared to the neutral Q_B (step 2). Additionally, the side chain of Ser L223 can reorient by rotation of its χ_2 (Cα–Cβ–Oγ–Hγ) torsional angle, thus establishing an additional hydrogen bond to Q_B^-. Coupled to the transfer of the second electron, the first proton is transferred, possibly via a transiently protonated Ser L223-OH_2^+, thus forming the monoprotonated, doubly reduced intermediate Q_BH^- (steps 3 and 4). After transfer of the second proton (step 5), movement of the quinol from the proximal to the distal position (step 6a) may be facilitated by increased stacking interactions of the aromatic ring systems with the Phe L216 ring and the diffusion of water molecules back into the pocket. The structures of these intermediates provide explanations for their relative binding affinities, as required for proper enzymatic function of the Q_B site. A rearrangement of hydrogen bonds, most prominently the reorientation of the Ser L223 side chain for Q_B reduction, as suggested by the scenario in Figure 3E, has also been calculated by Alexov and Gunner to be necessary to make Q_B reduction more favorable than Q_A reduction. These local rearrangements may constitute the conformational changes deduced to be required for function by a variety of experiments.

Cytochrome c_2 Oxidation

All four hemes of the *Rp. viridis* RC tetraheme C subunit are located close enough to the surface of the protein to accept electrons from soluble cytochrome c_2. Site-directed mutagenesis in another non-sulfur purple bacterium, *Rubrivivax gelatinosus*, has led to the identification of a patch of acidic residues immediately surrounding the distal low-potential heme1 of the tetraheme C subunit that apparently forms an electrostatically favorable binding site for soluble cytochromes. Thus all four hemes in the C subunit appear to be directly involved in the electron transfer toward the photo-oxidized special pair. Based on these findings, a model was proposed for the transient cytochrome c_2-RC complex for *Rp. viridis* (see Figure 4A).

In the case of the *Rb. sphaeroides* RC, which lacks the C subunit, the photo-oxidized special pair D^+ is directly re-reduced by cytochrome c_2. The structure of the co-complex of the *Rb. sphaeroides* RC and cytochrome c_2 has been determined by X-ray crystallography at 2.4Å resolution (cf. Figure 4B). In these crystals, D^+ is reduced by cytochrome c_2 at the same rate as measured in solution, indicating that the structure of the complex in the region of electron transfer is the same in the crystal and in solution. The binding interface can be divided into two domains. The first domain contributes to the strength and specificity of cytochrome c_2 binding and is a short-range interaction domain that includes Tyr L162 (cf. Figure 4B), and groups exhibiting non-polar interactions, hydrogen bonding, and a cation-π interaction. The second is a long-range, electrostatic interaction domain that contains complementary charges on the RC and cytochrome c_2. In addition to contributing to the binding, this domain may help steer the unbound proteins into the right orientation.

Relevance to Photosystem II

Based on the determined structure of the purple bacterial RC, very specific sequence homologies, and azidoatrazine labeling, the RC core of higher plant photosystem (PS) II was proposed to be similar to the LM core of the bacterial RC, with the D1 and D2 proteins corresponding to the L- and M subunits, respectively. This proposal could be verified experimentally. Recently, suitably designed, modified bacterial RCs have been shown to mimic tyrosine oxidation in PS II. In the absence of a high-resolution structure of the photosystem II RC, the purple bacterial RC still serves as the basis for models of PS II.

See Also the Following Articles

Cytochrome bc_1 Complex (Respiratory Chain Complex III) • Cytochrome *c* • Green Sulfur Bacteria: Reaction Center and Electron Transport • Heme Proteins • Heme Synthesis • Light-Harvesting Complex (LHC) I and II: Pigments and Proteins • Photosystem II: Protein Components • Purple Bacteria: Electron Acceptors and Donors • Quinones

Glossary

cytochrome c_2 A heme-containing hydrophilic protein that functions as an electron carrier in both photosynthesis and respiration.

photosynthetic reaction center A membrane-intrinsic protein complex that carries out the primary photochemical event, the charge separation process.

purple bacteria Prokaryotes that catalyze photosynthetic electron transfer. Divided into *Rhodospirillaceae* (nonsulfur) and *Chromatiaceae* (sulfur).

ubiquinone (formerly called coenzyme Q) A quinone derivative with a variable length side chain of isoprene units (mostly 8–10). It occurs in the lipid core of the eukaryotic inner mitochondrial membranes and of bacterial cytoplasmic membranes and functions as a mobile, lipophilic carrier of electrons (and protons).

Further Reading

Blankenship, R. E., Madigan, M. T., and Bauer, C. E. (eds.) (1995). *Anoxygenic Photosynthetic Bacteria*. Kluwer Academic Publishers, Dordrecht, NL.

Deisenhofer, J., and Michel, H. (1989). The photosynthetic reaction center from the purple bacterium *Rhodopseudomonas viridis* (Nobel Lecture). *EMBO J.* **8**, 2149–2170.

Hoff, A. J., and Deisenhofer, J. (1997). Photophysics of photosynthesis – structure and spectroscopy of reaction centers of purple bacteria. *Phys. Rep. Rev. Sect. Phys. Lett.* **287**, 1–247.

Lancaster, C. R. D. (1999). Quinone-binding sites in membrane proteins: What can we learn from the *Rhodopseudomonas viridis* reaction centre? *Biochem. Soc. Trans.* **27**, 591–596.

Lancaster, C. R. D., and Michel, H. (2001). Photosynthetic reaction centers. In *Handbook of Metalloproteins* (A. Messerschmidt, R. Huber, T. Poulos and K. Wieghardt, eds.) Vol 1, pp. 119–135. Wiley, Chichester, UK.

Michel-Beyerle, M. E. (ed.) (1996). *The Reaction Center of Photosynthetic Bacteria – Structure and Dynamics*. Springer-Verlag, Berlin.

Moser, C. C., Page, C. C., Cogdell, R. J., Barber, J., Wraight, C. A., and Dutton, P. L. (2003). Length, time, and energy scales of photosystems. *Adv. Prot. Chem.* **63**, 71–109.

Paddock, M. L., Feher, G., and Okamura, M. Y. (2003). Proton transfer pathways and mechanism in bacterial reaction centers. *FEBS Lett.* **555**, 45–50.

Parson, W. W. (2003). Electron donors and acceptors in the initial steps of photosynthesis in purple bacteria: A personal account. *Photosynth. Res.* **76**, 81–92.

Wraight, C. A. (2004). Proton and electron transfer in the acceptor quinone complex of photosynthetic reaction centers from *Rhodobacter sphaeroides*. *Front. Biosci.* **9**, 309–337. http://www.bioscience.org

Biography

C. Roy D. Lancaster is a Group Leader in the Department of Molecular Membrane Biology at the Max Planck Institute of Biophysics in Frankfurt am Main, Germany. He holds an M.Sc. from McMaster University, Hamilton, Ontario, Canada, and a Dr. phil. nat. degree from J. W. Goethe University, Frankfurt am Main. He teaches Biochemistry and Biophysical Chemistry at J. W. Goethe University. His principal research interests are in the structure and mechanism of action of selected membrane protein complexes, including photosynthetic reaction centers.

Pyridoxal Phosphate

David E. Metzler
Iowa State University, Ames, Iowa, USA

Pyridoxal phosphate (PLP) is one of several small organic molecules known as coenzymes, compounds that are essential to all forms of life. PLP, together with over 60 different enzymatic proteins, acts to catalyze a variety of specific chemical reactions, many of which are steps in chemical pathways of synthesis or degradation of amino acids or of other nitrogen-containing compounds. PLP is the phosphoric acid ester of pyridoxal, a form of vitamin B_6. This vitamin is synthesized by plants and by many microorganisms, but humans must obtain it from dietary sources. The major form of vitamin B_6 in plants (and in vitamin pills) is the alcohol pyridoxol (pyridoxine). In tissues of our bodies (as well as of other organisms) this is converted to pyridoxol 5′-phosphate, which can be dehydrogenated (oxidized) to the aldehyde PLP (Figure 1). Some enzymes can convert PLP reversibly to pyridoxamine phosphate (PMP) by a process known as transamination (Figure 2). All organisms contain PLP and PMP, much of which is bound to enzyme proteins. Excess PLP is rapidly dephosphorylated to pyridoxal and oxidized to the corresponding carboxylic acid, pyridoxic acid.

Transamination

Transamination is a biologically important process by which living cells exchange the oxygen atoms of α-oxoacids with amino groups (and associated hydrogen atoms) of amino acids such as glutamic acid (Figures 1 and 2). The process occurs via two half-reactions. In the first the amino group is transferred from the amino acid to PLP to form PMP. In the second the PMP that is formed transfers the amino group to the carbon skeleton of the original oxoacid (Figure 2). During the reactions the PLP or PMP is held tightly in the active sites of the enzymes where it reacts rapidly and reversibly to form intermediates known as aldimines (Figure 3) or ketimines (Figure 4). The coenzymes function many times before the less tightly bound PMP loses its hold on the active site or the coenzyme is inactivated by a side reaction.

In the human body transaminases (aminotransferases) catalyze numerous steps in biosynthesis or breakdown of amino acids. For example, glutamic acid from the diet can donate nitrogen to oxoacids to form such amino acids as alanine and aspartic acid. In plants and other autotrophic organisms glutamic acid also donates nitrogen to additional oxoacids to synthesize amino acids that cannot be made in the human body.

The Variety of PLP-Dependent Reactions

Transamination is only one of many reactions of amino acids and other amines that are catalyzed by PLP-dependent enzymes. Some of these are listed in Table I. Groups *a*, *b*, and *c* in this table are defined by the cleavage of one of three possible chemical bonds, *a*, *b*, or *c*, in an amino acid substrate (see Figure 3). The enzymes in group *a*, which includes transaminases, initiate the reaction by removing the α-hydrogen as H^+. In this way each enzyme creates an intermediate chemical species, the quinonoid-carbanionic form (Figure 3). For transaminases and several other enzymes this intermediate has been identified by spectroscopic studies and X-ray crystallography. The quinonoid-carbanionic form reacts in different ways that depend upon the individual enzymes. Transaminases catalyze addition of an H^+ ion at a new position to create a ketimine form as illustrated in Figure 4. Subsequent hydrolysis yields PMP and the oxoacid product of the transamination.

Racemases, after removal of the α-hydrogen of the aldimine as H^+, add an H^+ ion back to the same carbon atom but from the opposite side of the planar quinonoid-carbanionic structure (Figure 3). The effect is to catalyze the interconversion of the two stereoisomers known as the L- and D-forms of the amino acid. Many bacteria form D-alanine from the predominate "natural" L-alanine using a PLP-dependent racemase. Bacteria utilize the D-alanine, as well as D-glutamic acid, formed by a special aminotransferase, in construction of their cell walls. The D-amino acids help provide protection from enzymes that act on L-amino acids. In a similar way small amounts of D-serine, which functions in the brain, are formed from L-serine by a racemase. A third type of reaction of a quinonoid-carbanionic species (Figure 3) is formation of the cyclic

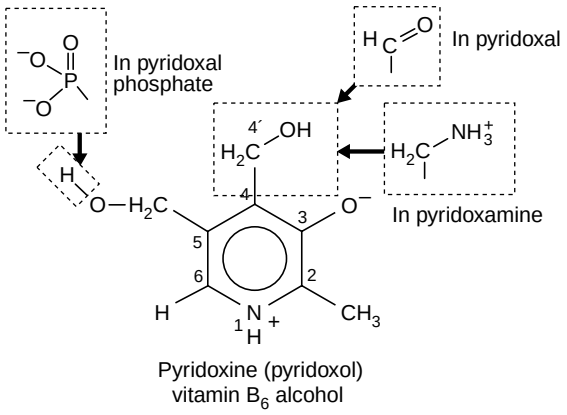

FIGURE 1 The vitamin B_6 (pyridoxine) family: pyridoxol, pyridoxal, pyridoxamine, and the coenzyme forms pyridoxal and pyridoxamine phosphates.

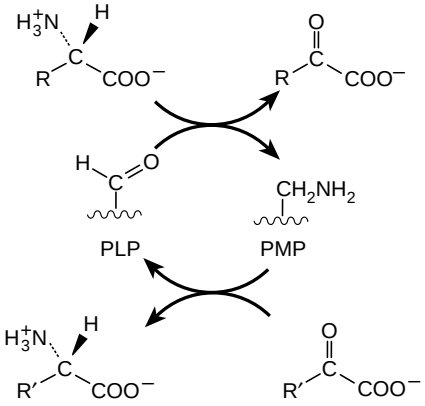

FIGURE 2 The transamination reaction by which amino groups are transferred from one carbon skeleton (in the form of an α-oxoacid) to another to form or to degrade an amino acid.

amino acid aminocyclopropane carboxylic acid, a precursor to the plant hormone ethylene. A large group of enzymes catalyze a fourth type of reaction, which involves elimination of a chemical group such as –OH, or –SH (designated – Y in Figure 3). This may be followed by a decomposition with liberation of NH_3 and other products or replacement of the eliminated group by a new group. These reactions play many roles in

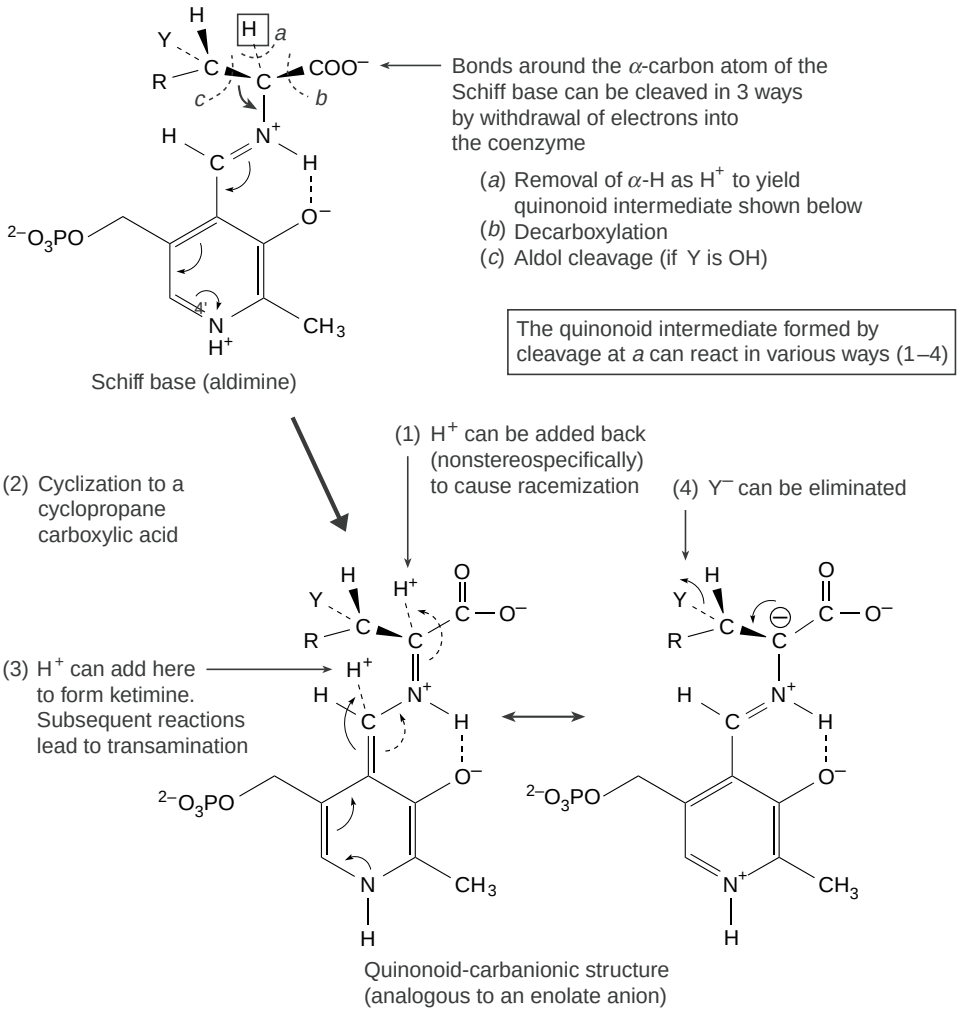

FIGURE 3 The action of pyridoxal phosphate in initiating catalysis of numerous reactions of α-amino acids. Completion of the various reactions requires a large variety of different enzyme proteins.

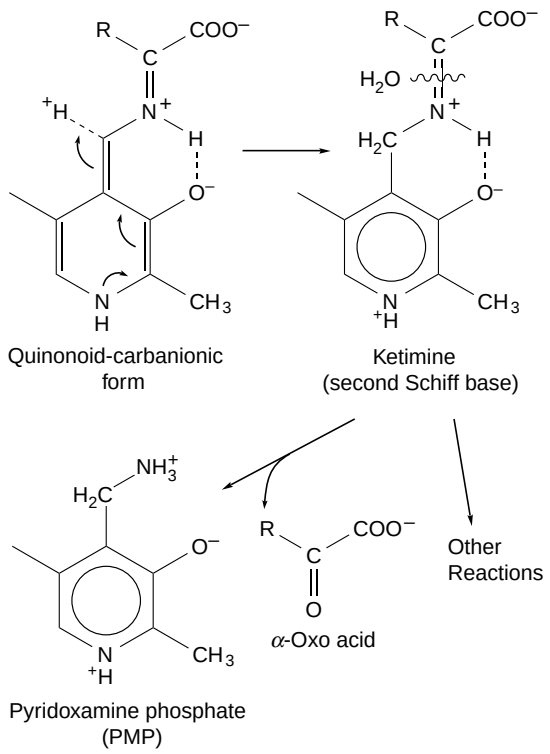

FIGURE 4 Conversion of the quinonoid-carbanionic intermediate into a ketimine which may give rise to PMP in a half-transamination reaction or may undergo alterations in the side chain (R–) to give other products.

TABLE I

Some Enzymes that Require Pyridoxal Phosphate as a Coenzyme

(a) Removing alpha hydrogen as H^+
- (1) Racemization
  - Alanine racemase
  - Serine racemase
- (2) Cyclization
  - Aminocyclopropane carboxylate synthase
- (3) Amino group transfer
  - Aspartate aminotransferase
  - Alanine aminotransferase
  - D-Amino acid aminotransferase
  - Branched chain aminotransferase
  - γ-aminobutyrate aminotransferase
  - ω-Amino acid:pyruvate aminotransferase
- (4) Beta elimination or replacement
  - D- and L-Serine dehydratases (deaminases)
  - Tryptophan indole-lyase (tryptophanase)
  - Alliinase
  - O-Acetylserine sulfhydrylase (cysteine synthase)
  - Tryptophan synthase

(b) Removal of alpha carboxylate as CO_2
- Diaminopimelate decarboxylase
- Glycine decarboxylase (requires lipoyl group)
- Glutamate decarboxylase
- Histidine decarboxylase
- Dopa decarboxylase
- Tyrosine decarboxylase

(c) Removal or replacement of side chain (or —H) by aldol cleavage or condensation
- Serine hydroxymethyltransferase
- δ-aminolevulinate synthase
- Serine palmitoyltransferase

(d) reactions of ketimine intermediates
- Aspartate γ-decarboxylase
- Selenocysteine lyase
- *Nif S* protein of nitrogen-fixing bacteria
- Gamma elimination and replacement
  - Cystathionine γ-synthase
  - Cystathionine γ-lyase
  - Threonine synthase

metabolism, both decomposing amino acids and forming new amino acids. A familiar example of such a decomposition reaction initiates the release of compounds giving the characteristic odor to crushed garlic.

A second major group of PLP-dependent enzymes (*b* in Figure 3 and Table I), the decarboxylases, remove a CO_2 molecule from a substrate. These enzymes also function in both catabolic and biosynthetic pathways. In each case the loss of CO_2 helps to drive the pathway in the needed direction. The most familiar decarboxylases participate in the formation of neurotransmitters such as γ-aminobutyrate, dopamine, adrenaline, and serotonin. A third major group of PLP-dependent enzymes (*c* in Figure 3 and Table I) catalyze cleavage or formation of carbon–carbon bonds in amino acids. These reactions resemble aldol-type reactions of organic chemistry. An example is formation of serine from glycine and formaldehyde. The latter, being a toxic compound, is carried as a derivative of another coenzyme tetrahydrofolic acid. The enzyme serine hydroxymethyltransferase (Table I), which catalyzes this reaction, allows bacteria and plants to form serine from glycine and also allows our bodies to form glycine from serine.

A fourth large group of enzymes (d in Table I) have more complex mechanisms that involve initial formation of ketimines followed by additional steps. One of these is a bacterial enzyme that converts the selenium-containing selenocysteine into L-alanine and elemental selenium (Se^0). Related enzymes in all organisms transfer sulfur, as S^0, into important metal–sulfur clusters such as Fe_4S_4 or the $MoFe_7S_9$ cluster, which participates in conversion of N_2 to HN_3 by nitrogen-fixing bacteria.

Chemical Mechanisms

Some details of mechanism have been indicated in Figures 3 and 4. However, many individual chemical steps performed in sequence are required of each enzyme. For several enzymes details have been established by use of spectroscopic techniques and by determination of

structures at atomic resolution by X-ray crystallography. In the first step of a reaction the enzymes must "recognize" a substrate molecule that repeatedly bumps against it as a result of the random movements of the molecules in the liquid environment in which it acts. Each protein, which is much larger than its substrate, contains a specifically constructed cavity that permits close contacts with the substrate molecule in the "active site." Close contact allows van der Waals attractive forces and electrostatic forces between oppositely charged ionic groups to hold the substrate if the latter has the appropriate structure. The PLP, which is also held by the protein, forms part of the binding cavity. In the free enzyme the PLP has a structure similar to that in Figure 3. However, the Schiff base linkage is not to the substrate, as in Figure 3, but to the $-NH_2$ group of a side chain of a lysine unit in the protein structure. This "internal aldimine" is the "resting form" of the PLP in the active site. Notice the positive charges provided by H^+ ions bound to the PLP at top and bottom and the negative charge provided by the oxygen atom attached to the ring (Figure 3). These charges provide electrostatic interactions that function both in the binding of substrates and in subsequent reactions. The reaction steps must occur rapidly, each step setting the stage for the next and permitting the whole sequence to be completed in a millisecond or less in some enzymes.

Recognition of a substrate often induces some movement in the protein. In some proteins a chemical group moves into a new position or a flap of protein folds over to partially cover the substrate. At some point in the sequence an H^+ ion must be removed from the $-NH_3^+$ group of the substrate. The resulting $-NH_2$ group, sometimes aided by a tilting of the bound PLP, moves toward the 4′-carbon atom of PLP and reacts via a chemical addition to form a transient geminal diamine (not shown here). Additional rapid steps release the lysine $-NH_2$ group and form the "external aldimine" shown at the top of Figure 3. The released lysine $-NH_2$ then serves as a "catalytic base" able to remove the α-H to form lysine $-NH_3^+$. In a transaminase the resulting lysine $-NH_3^+$ can place the H^+ that it carries onto the 4′ position of the PLP to form a ketimine (Reaction 3 of Figures 3 and 4). A water molecule then reacts to release the α-oxoacid product (Figure 3) and to leave PMP bound weakly to the protein. This represents the first of the two half reactions (Figure 2) occurring in transamination. The same sequence in reverse, using a different oxoacid, completes the transamination. This also illustrates the fact that every step catalyzed by transaminases is reversible, the overall reaction being driven by differences in concentration of reactants and products. The individual structures, chemical groups involved, and individual steps vary from one enzyme and one reaction type to another. Most do not form PMP as an intermediate. However, virtually all PLP-dependent enzymes use an active site lysine and multiple H^+ transfers.

The fundamental importance of the ring nitrogen at the bottom of the structure in Figure 3 lies in its action as an electron-attracting center. This is indicated by the curved arrows in the figure. The flow of electrons in this manner is thought to be coordinated with the major bond-breaking reactions catalyzed by these enzymes. In many of the enzymes a negatively charged carboxylate ($-COO^-$) side chain of the protein forms a hydrogen bond to the N^+-H at the bottom of the PLP ring. This carboxylate helps keep the H^+ on the ring and may also modulate the electron flow. At the same time the $-O^-$ group on the 3-position of the ring opposes the electron withdrawal from the substrate, perhaps assisting in other steps in the reaction. The $-O^-$ also helps to hold a proton onto the Schiff base nitrogen as shown in Figure 3. Each specific enzyme must hold its substrate in such a way that one of the bonds to the α-carbon atom (*a*, *b*, or *c* in Figure 3) is perpendicular to the plane of the pyridoxal phosphate ring. This is the bond that will be broken in the key step of the reaction sequence.

See Also the Following Articles

Amino Acid Metabolism • B_{12}-Containing Enzymes

Glossary

aldol-type reaction Biochemical reactions related in their chemical mechanisms to the classical aldol condensation and cleavage reactions of organic chemistry.

coenzymes Small organic molecules that function together with enzymes to catalyze specific types of chemical reactions.

lysine unit A lysine residue, a molecule of the amino acid lysine incorporated into a protein molecule.

substrate The substance which undergoes the reaction catalyzed by an enzyme.

tetrahydrofolic acid A coenzyme formed by reduction of the vitamin folic acid.

Further Reading

Anthony, C., John, R. A., and Wilmot, C (eds.) (2003). 3rd international symposium on vitamin B6, PQQ, carbonyl catalysis and quinoproteins. *Biochim. Biophys. Acta.* **1647**, 1–408.

Bender, D. A. (1999). Non-nutritional uses of vitamin B_6. *British J. Nutr.* **81**, 7–20.

Christen, P., and Metzler, D. E. (1985). *Transaminases*. Wiley, New York.

Cooper, A. J. L., and Meister, A. (1989). An appreciation of Professor Alexander E. Braunstein. The discovery and scope of enzymatic transamination. *Biochimie* **71**, 387–404.

Dolphin, D., Poulson, R., and Arramovic, O. (1986). Vitamin B_6 Pyridoxal Phosphate Chemical, Biochemical, and Molecular Aspects, 2 Vols. Wiley, New York.

Jansonius, H. (1998). Structure, evolution, and action of vitamin B_6-dependent enzymes. *Curr. Opin. Struct. Biol.* **8**, 759–769.

Mehta, P. K., and Christen, P. (1998). The molecular evolution of pyridoxal-5′-phosphate-dependent enzymes. *Adv. Enzymol. Relat. Areas Mol. Biol.* **74**, 129–184.

Metzler, D. E. (2001, 2003). *Biochemistry. The Chemical Reactions of Living Cells*. Academic Press, San Diego.

Snell, E. E. (1958). Chemical structure in relation to biological activities of vitamin B_6. *Vit. Horm.* **16**, 77–125.

Biography

David E. Metzler is Professor Emeritus in the Department of Biochemistry, Biophysics, and Molecular Biology at Iowa State University, Ames, Iowa. He holds a Ph.D. from the University of Wisconsin. His research area is the chemistry of coenzymes, mechanism of their reactions, and the chemistry and structures of transaminases.

Pyrimidine Biosynthesis

Monika Löffler and Elke Zameitat
Philipps-University, Marburg, Germany

Pyrimidines are structural components in many natural compounds, such as nucleotides, nucleic acids, vitamins, pterins, and antibiotics. In all organisms pyrimidine nucleotides serve essential functions in cell metabolism as well as in nucleic acids such as the activation of sugars for polysaccharide and phospholipid synthesis, and glycosylation of proteins and lipids. In mammals pyrimidines are crucial to detoxification reactions in the liver. They are regarded as modulators of blood flow and have functions in the peripheral and central nervous system. The size of the pyrimidine nucleotide pools in cells is determined by the relative contributions of *de novo* synthesis and the interconversion reactions, together with salvage and presence or absence of enzymes of catabolic degradation. Some inherited disorders of pyrimidine biosynthesis and degradation have been diagnosed. Synthetic pyrimidine analogs act as antimetabolites and by selective interference in metabolic pathways, RNA and DNA synthesis, these and synthetic or natural enzyme inhibitors can combat infection, virus, tumor, and autoimmune diseases.

De novo Synthesis

Formation of UMP

Chemically, pyrimidines are heterocyclic six-membered ring structures containing two nitrogen atoms. The pyrimidine bases of nucleic acids possess an amino or hydroxyl group at position 4, and always an oxygen function at position 2. Thymine, in addition, has a methyl group at position 5. This gives rise to tautomeric structures for the bases uracil, cytosine, and thymine. The first pyrimidine nucleotide in cells, uridine monophosphate (UMP), is synthesized from CO_2, the glutamine amide group, aspartate, and phosphoribosyl-1-pyrophosphate (PRPP) (Figures 1 and 2). In contrast to the biosynthesis of purine nucleotides, the pyrimidine ring is assembled first and then linked to ribose phosphate to form a pyrimidine nucleotide. In higher eukaryotes, the cytosolic enzyme catalyzing formation of carbamoyl phosphate, carbamoylphosphate synthetase II (CPSase, Figure 1, no. 1), is distinctly different from carbamoylphosphate synthetase I, which is found in mitochondria as the first reaction of arginine biosynthesis and urea cycle in mammalian liver, and thus CPSase II is the first step committed to pyrimidine metabolism in higher animals (Figure 2). The formation of N-carbamoylaspartate (ATCase, no. 2) is the committed step for pyrimidine synthesis in prokaryotes, but is unregulated in eukaryotes. Next, the pyrimidine ring is cyclized by dihydroorotase (DHOase, no. 3). In higher animals the first three enzymes together with glutaminase (which provides the amino group from the side-chain amide group of glutamine) have been fused together (exon shuffling) during evolution to form a single polypeptide, CAD. This protein is located mainly in the cytosol and to some extent in the nucleus. Plants, such as prokaryotes, possess these enzymes individually encoded and located in chloroplasts. Formation of orotate from dihydroorotate is catalyzed by the mitochondrial flavoenzyme dihydroorotate dehydrogenase (DHODH, no. 4) transferring the reducing equivalents to the proximal acceptor ubiquinone and final acceptor molecular oxygen in the respiratory chain. Thus, the energy of dihydroorotate oxidation can be stored in ATP. Orotate phosphoribosyltransferase (OPRTase, no. 5) and orotidine decarboxylase (ODCase, no. 6) are fused on one bifunctional polypeptide, UMP synthase, operating in the cytosol of higher eukaryotes except in plants. Thus, only three genes (chromosomal location in Man: 2p21(CAD), 16q22 (DHODH), and 3q13 (UMP synthase)) code for the enzymes catalyzing the reaction of *de novo* UMP synthesis.

Regulation

Pyrimidine *de novo* synthesis is a demonstration that compartmentation within different parts of the cell – cytosol, mitochondria, chloroplasts – enhances the mode of regulation and flexibility of a metabolic pathway. Because of gene duplication, eukaryotes now have the potential to compartmentalize the synthesis of carbamoylphosphate for either pyrimidines (cytosol), or arginine and urea (mitochondria). In humans, urea synthesis takes place in liver only. The location of DHODH (Figure 2) in the inner mitochondrial membrane and its connection to the functional respiratory chain ensures the most efficient oxidation of

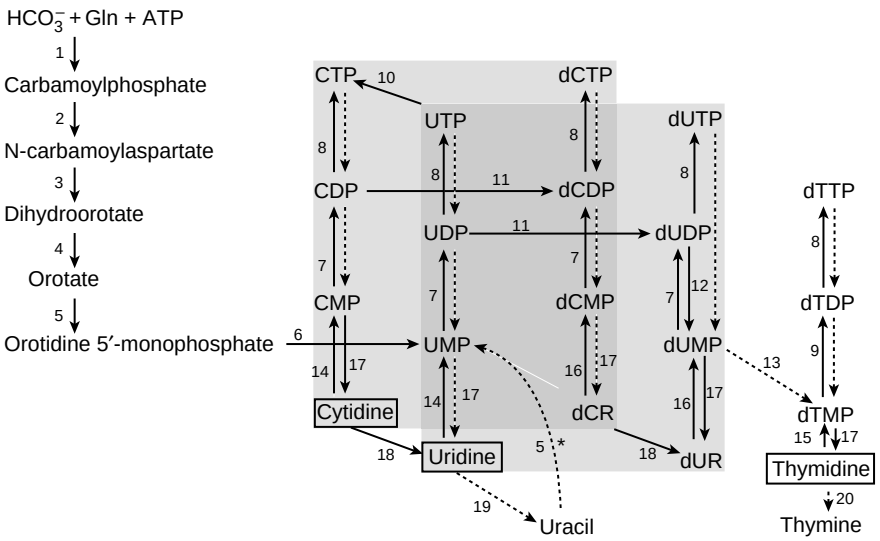

FIGURE 1 Biosynthesis and interconversion of pyrimidine nucleotides. The enzymes (given by numbers in the scheme) perform the *de novo* synthesis (1–6), interconversion of UMP to other ribonucleotides and deoxyribonucleotides (7–13), the salvage of preformed metabolites from dietary products or catabolism of nucleic acids (14–18), and the first steps of catabolism (19–20): 1, carbamoyl phosphate synthetase; 2, aspartate transcarbamoylase; 3, dihydroorotase; 4, dihydroorotate dehydrogenase; 5, orotate phosphoribosyltransferase; 6, orotidine 5′-monophosphate decarboxylase; 7, uridine(pyrimidine) monophosphate kinase; 8, pyrimidine diphosphate kinases; 9, thymidine monophosphate kinase; 10, cytidine triphosphate synthetase; 11, ribonucleoside diphosphate reductase; 12, dUDP phosphohydrolase; 13, thymidylate synthase; 14, uridine/cytidine kinase; 15, thymidine kinase; 16, deoxycytidine/uridine kinase; 17, 5′-nucleotidase; 18, (deoxy)cytidine deaminase; 19, uridine phosphorylase; and 20, thymidine phosphorylase. → (Pyro)Phosphohydrolases, not specified here. 5 * Uptake of 5′-fluoruracil by OPRTase.

dihydroorotate in aerobes. In turn, pyrimidine biosynthesis becomes a pacemaker for cell growth and proliferation under limited oxygen tension. Patients with acquired or inherited defects in mitochondria energetics, however, may suffer from a concomitant pyrimidine nucleotide starvation or imbalance. The two multienzyme polypeptides (CAD and UMP synthase) achieve a micro-compartmentation of pyrimidine *de novo* synthesis. Encoding five activities on two polypeptides simplifies the coordination and regulation of gene expression and activity. In addition, the direct transfer of a product from one active site to the next enzyme (channelling) considerably increases the efficiency of pyrimidine biosynthesis in higher eukaryotes. The first evidence for the location of CAD and UMP synthase close to the mitochondria surface has been obtained in a recent electron microscopic study. A metabolonlike complex facilitating the movement of substrate and product between cytosol and mitochondrion would allow a rapid increase in *de novo* synthesis when needed. The molecular regulation of pyrimidine *de novo* synthesis occurs at step 1 of CAD. The CPSase specific activity is low relative to that of the subsequent enzymes. It is allosterically activated by PRPP and feedback inhibited by UTP. The CAD activity is tuned by phosphorylation at two sites: MAP kinase action reduces the efficacy of UTP and increases that of PRPP, and phosphoylation by protein kinase A abolishes UTP inhibition but also makes PRPP less effective. Hence, by loosing feedback inhibition, carbamoyl phosphate synthesis is activated rapidly and sensitively in response to external growth-promoting signals. A modulation of ATCase activity is assured by a cooperative binding of carbamoyl phosphate and aspartate. An overflow into pyrimidine biosynthesis can occur from overabundant carbamoyl phosphate production in the case of urea cycle defects in liver: the carbamoyl phosphate leaves the mitochondria and is used by the ATCase of CAD. Under these conditions UMP synthase is the limiting enzyme, presumably because of an insufficient supply of PRPP for OMP synthesis, causing orotate to accumulate and to be excreted (secondary orotic aciduria).

Deficiency and Interference

The only hereditary but rare defect of pyrimidine *de novo* synthesis diagnosed so far in living humans is that of one or both activities in UMP synthase (OPRT domain or ODC domain) with different clinical manifestations, such as anemia or megaloblastic changes in bone marrow, immunodeficiency and gross orotate excretion in type 1 deficiency or orotidine plus orotic acid excretion, neurological deficits, and intellectual impairment, but no megaloblastic anemia in type 2 deficiency. There are

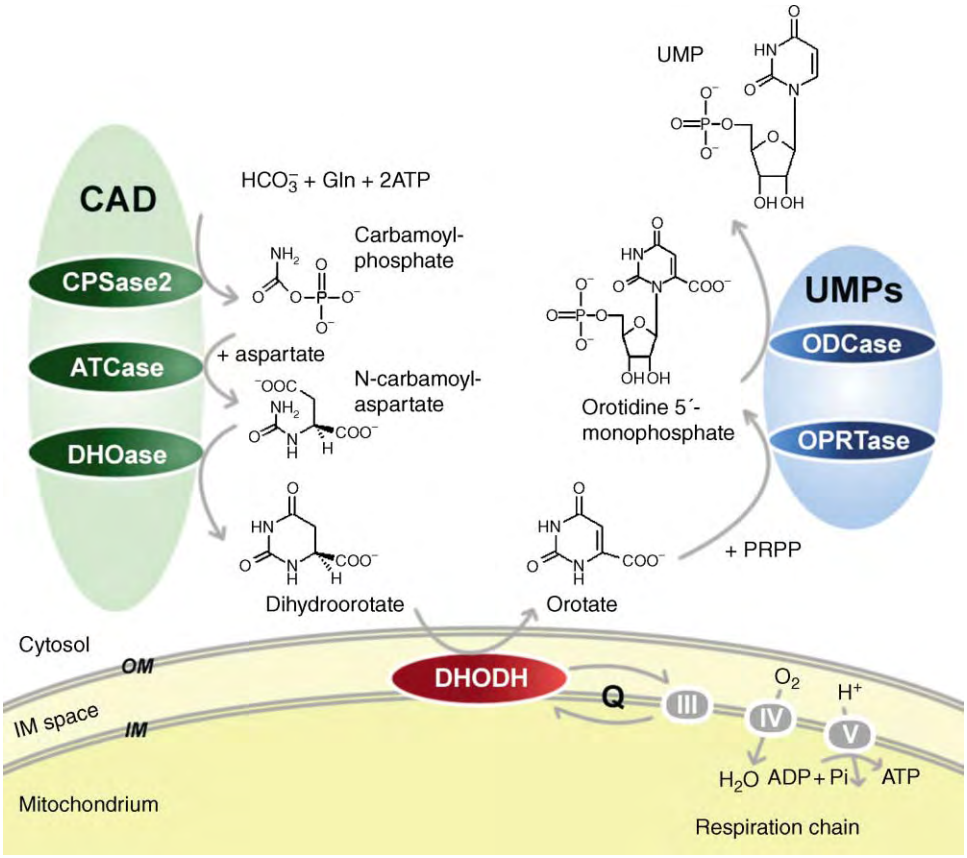

FIGURE 2 Compartmentation of pyrimidine *de novo* synthesis. In higher eukaryotes the multifunctional enzyme CAD (CPSase II + ATCase + DHOase, no. 1 + 2 + 3) and UMP synthase (OPRTase + ODCase, no. 5 + 6) are cytosolic, the monofunctional DHODH (no. 4) is in mitochondria and connected via ubiquinone (Q) to the functional respiratory chain at the stage of complex III (III). Electrons are transferred to oxygen via cytochrome oxidase (IV). ATP synthetase (V). Note that in plants no. 1,2,3 and no. 5 + 6 are in chloroplasts. In Gram-negative bacteria the quinone-dependent DHODH is attached to the plasma membrane. In Gram-positive bacteria and anaerobic yeasts all enzymes are cytosolic.

no specific inhibitors of CPSase of chemotherapeutic interest. N-phosphonoacetyl-L-aspartate (PALA), a model inhibitor of ATCase in prokaryotes, was clinically disappointing because gene amplification leading to overproduction of CAD caused resistance of human cancer cells. Current drug design for DHOase focuses on its Zn^{+2} center. Natural and chemical ubiquinone analogs, potent inhibitors against DHODH, failed to get clinical approval as anticancer drugs. The naphthoquinone atovaquone, a competitor for ubiquinone-dependent reactions, has been applied for treatment of opportunistic infections and malaria. The inhibition of DHODH by the isoxazol leflunomide, which was licenced recently, is central to the efficacy of this drug in treating rheumatoid arthritis and other autoimmune diseases. Antimetabolites of UMP synthase with anticancer activity but limited by toxicity at high dosage to patients (e.g., 6-azauracil, pyrazofurin) have been shown to suppress reproduction of *Toxoplasma gondii* and *Plasmodium falciparum*, because *de novo* pyrimidine synthesis is obligatory for these organisms to grow. Some widely used drugs, e.g., the calcium channel blockers nifedipine and nimodipine, were shown to suppress murine OMP decarboxylase and uridine kinase; barbiturates and aspirin interfered in the DHODH reaction. This emphasizes that the direct inhibition of pyrimidine biosynthesis is a potential side effect of drugs.

Interconversions in Pyrimidine Biosynthesis

Formation of Cytidine and Thymidine Nucleotides

Pyrimidine nucleotide di- and triphosphates are produced by ATP-dependent kinases (Figure 1, no. 7–9). CTP synthase (no. 10) catalyzes the formation of CTP from UTP using the amide group of glutamine – a GTP-dependent reaction (Figure 3A). Only at the time of DNA replication, do deoxynucleotide pools increase noticeably. Nucleoside 5′-diphosphate reductase

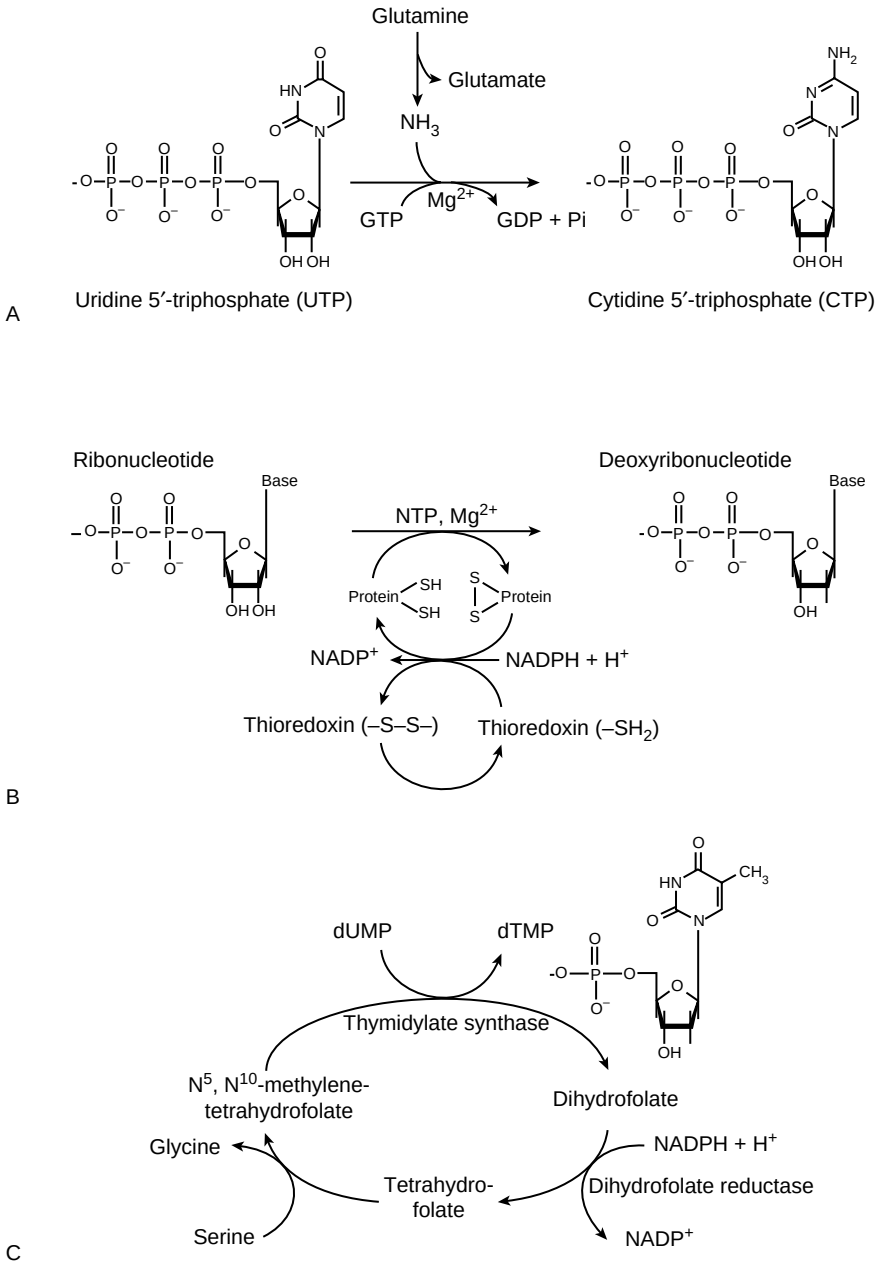

FIGURE 3 Formation of cytidine and thymidine nucleotides. (A) The synthesis of CTP from UTP by CTP synthase. (B) Conversion of UMP to dUMP by ribonucleotide reductase, schematic presentation of the enzyme. (C) The thymidylate synthase catalyzed reaction and regeneration of methylenetetrahydrofolic acid (THF) by means of dihydrofolate reductase.

(ribonucleotide reductase, no. 11) catalyzes the formation of deoxyribose (exchange of H for OH at C2′) of pyrimidine as well as purine ribonucleotides using NADPH and thioredoxin or glutaredoxin (Figure 3B). The product dUDP is dephosphorylated to dUMP (no. 12). In case of dUTP formation, this can effectively be reconverted to dUMP by the deoxyuridine triphosphate nucleotidohydrolase (pyrophosphohydrolase, Figure 1) in order to prevent its incorporation into DNA. dUMP is used by thymidylate synthase (no. 13) to form dTMP by means of (N^5, N^{10}-) methylenetetrahydrofolic acid (THF) as a one-carbon donor and reducing agent (Figure 3C).

Regulation

The enzymes of this part of pyrimidine synthesis are cytosolic. Their activity is strictly controlled by availability of substrates or by their products and other ribonucleotides and deoxyribonucleotides, respectively. This is a well-understood mechanism to ensure well-balanced pools of pyrimidine and purine

(deoxy)ribonucleotides in cells. For example, CTP is a negative effector of CTP synthase. This enzyme and CAD are connected with the cytoskeleton, hence are able to move around according to change in cell shape. Ribonucleotide reductase (no. 11) consists of two nonidentical protein subunits, one containing different effector binding sites, the other a nonheme iron and a tyrosyl radical generated by oxygen, giving the second control point for nucleic acid synthesis by O_2 in aerobes. This enzyme is subject to a sophisticated control mechanism, in which an excess of one deoxyribonucleotide inhibits reduction of all other ribonucleotides. Effective inhibition by dATP, dGTP, or dTTP explains the intrinsic toxicity of deoxyadenosine, deoxyguanosine, and thymidine to many organisms and the immunodeficiency in adenosine deaminase and purine nucleoside phosphorylase deficiency. dCTP and dTTP are major positive or negative effectors for the interconversion and salvage of deoxyribonucleosides. The key regulatory mechanism for thymidylate synthase is the delivery of THF by dihydrofolate reductase (Figure 3C). In plants and parasitic protozoa only, this enzyme is fused as a bifunctional polypeptide with thymidylate synthase.

Deficiency and Interference

Effective inhibitors of ribonucleotide reductase (e.g., hydroxyurea, HU) are potent inhibitors of DNA synthesis and hence of replication. HU also exerts a synergistic effect with nucleoside analogs used in the treatment of HIV-1. This is attributed to reduction in intracellular deoxyribonucleotides coupled with interference in antigen-dependent T-lymphocyte activation. However, the clinical application is disputed. It is noteworthy that healthy human lymphocytes do not pick up exogenous orotic acid, nor do they convert UTP to CTP. However, both these pathways are up-regulated in malignancy. Most of the CTP synthase inhibitors that have been developed and tested with experimental tumors are synthetic pyrimidine analogs (e.g., deazauridine and cyclopentenyl cytosine). Thymidylate synthase and dihydrofolate reductase are well-established target enzymes in cancer therapy using 5-F-UMP (from 5-fluoruracil which can be activated by OPRTase) and folate analogs (e.g., methotrexate) preventing THF regeneration.

Salvage

Phosphorylation and Dephosphorylation

The fact that hereditary orotic aciduria does respond to life-long supply with uridine but not to uracil indicated that pyrimidine nucleoside salvage can compensate for the lack of *de novo* synthesis in Man, if the dosage as food additive is in grams per day and increasing from child to adulthood. This is in direct contrast to purines where the gut mucosa contains a complement of enzymes which degrades all dietary purines to the end-product uric acid. Prominent salvage capacity is expressed in lymphoid cells, polymorphonuclear cells, and the central nervous system. Uridine, (deoxy)cytidine, and thymidine originating from daily nutrients or intracellular breakdown from nucleic acids are rescued from circulation by cytosolic (deoxy)ribonucleoside kinases that show a high level of specificity with respect to the base and sugar moieties, with ATP as the major phosphate donor (no. 14–16). In contrast to purines the salvage of free pyrimidine bases at the expense of PRPP does not occur in any mammalian tissue. Orotate as a natural component of dairy food is taken up and converted to UMP only by liver and erythrocytes. It can also stem from food additives such as zinc orotate and magnesium orotate, which are used for metal ion substitution therapy. Salvage of deoxycytidine is important in DNA repair. Deoxycytidine kinase is also responsible for activating some nucleoside analogs as well as natural deoxyribonucleosides – such as deoxyadenosine in adenosine deaminase deficiency. Pyrimidine and purine deoxyribonucleoside kinases seem to have evolved from a common progenitor multisubstrate kinase. Multisubstrate deoxyribonucleoside kinases were found in several insect species and shown to phosphorylate pyrimidines as well as purine (deoxy)nucleosides with high efficiency. The dephosphorylation of pyrimidine(deoxy)ribonucleoside monophosphates is catalyzed by 5′-nucleotidases (no. 17) which are found to occur as specific isoforms in different tissues. This reaction is a prerequisite for transport and delivery of pyrimidines by the circulation. In cells uridine and deoxyuridine can be formed from cytidine and deoxycytidine by cytidine deaminase (no. 18). The cleavage of uridine and thymidine by phosphorylases (no. 19–20) to the appropriate bases and ribose-1-phosphate would initiate the catabolic pathway.

Regulation

The balance between excretion and uptake is set by intracellular substrate cycles involving 5′-nucleotidases, kinases, and nucleoside transport through the plasma membrane of cells. Uridine is taken up effectively by a carrier-mediated concentrated transport process or by cotransport, by all human cells except erythrocytes.

Deficiency and Interference

Different mutants of the pyrimidine-5′nucleotidase are known causing enzyme deficiency. This is inherited as an

autosomal recessive trait. The symptoms include nonspherocytic hemolytic anemia, splenomegaly, and hepatomegaly; gross elevation in erythrocyte UTP/CTP are characteristic findings. A different deficiency of 5′-nucleotidase associated with hemolytic anemia has been described in patients with lead poisoning or thalassemia. Deficiency of the mitochondrial form of thymidine phosphorylase has major effects on many systems in humans. Patients with mutations in the mitochondria-specific thymidine kinase-2 develop myopathy and depletion of muscular mitochondrial DNA. Pyrimidine(deoxy)ribonucleoside kinases are critical constituents for interference by pharmacological agents: they are of key importance for the channelling of nucleoside analogs (such as arabinosyl cytosine, azidothymidine, 2′3′-dideoxycytidine) in cell metabolism of human and pathogens; mutants of thymidine kinases from virus and other organisms are proposed as "suicide agents" for gene therapy of cancers. On the other hand, strategies for inhibition of pyrimidine biosynthesis by drugs can be anticipated in cells with high activities in the salvage reactions. This aspect underlies current research on structure and function of pyrimidine (deoxy)ribonucleoside transporters in plasma and mitochondria membranes and their connection with salvage and biosynthesis of pyrimidines.

See Also the Following Articles

Membrane Transport, General Concepts • Urea Cycle, Inborn Defects of

Glossary

antipyrimidine A structural analog that is taken up by cells and interferes with normal metabolism.

flavoenzyme Enzyme containing a flavin group as redox cofactor.

metabolon Physically associated enzymes of a metabolic pathway to facilitate substrate channelling.

nucleoside Consists of [1 base + 1 (deoxy)ribose] such as uridine.

nucleotide Consists of [1 base + 1 (deoxy)ribose + 1–3 phosphate groups] such as dTTP or NTP (N, base not specified).

salvage Recycling of preformed nucleosides by cells.

Further Reading

Davidson, J. N., Carrey, E. A., Neuhard, J., and Franklin, C. (eds.) (1993–1999). *Path to Pyrimidines. An International Newsletter*, Vols 1–7, Chandler Medical Center, University of Kentucky, Lexington, USA.

Webster, D., Becroft, D. M. O., Van Gennip, A. H., and Van Kuilenburg, A. B. P. (2001). Hereditary orotic aciduria and other disorders of pyrimidine metabolism. In *The Metabolic and Molecular Bases of Inherited Disease* (C. R. Scriver, *et al.*, eds.) 8th edition, Vol II, pp. 2663–2702. McGraw-Hill, New York.

Biography

Monika Löffler is a Professor for Biochemistry at Philipps-University, Marburg, Germany. Her present research interest is enzymology of pyrimidine biosynthesis, its crosstalk to functional mitochondria. Further work of the group, metabolomics of pyrimidine metabolism in Man, is devoted to improve diagnosing and treating inherited and acquired disorders.

Elke Zameitat, having secured a diploma and degree in human biology, and presently a Ph.D. student, is involved in cloning, expression, and characterization of recombinant dihydroorotate dehydrogenase from different organisms, also for structure–activity relationship studies with inhibitors.

Pyruvate Carboxylation, Transamination, and Gluconeogenesis

Sarawut Jitrapakdee
Mahidol University, Bangkok, Thailand

John C. Wallace
University of Adelaide, Adelaide, Australia

The processes of transamination and pyruvate carboxylation combine to provide the pathway of gluconeogenesis with one of its principal substrates. For example, in transamination, a single amino acid (e.g., alanine) transfers its amine group to a ketoacid (typically α-ketoglutarate or oxaloacetate) to form their corresponding amino acids (i.e., glutamate and aspartate) while it is converted to its corresponding ketoacid (viz., pyruvate). Pyruvate carboxylation yields oxaloacetate, essential for gluconeogenesis in liver and kidney, for glyceroneogenesis in adipose tissue, and for the continuing operation of the Krebs tricarboxylic acid cycle. Gluconeogenesis is essential in maintaining normal blood glucose concentration during the postabsorptive state and especially in starvation, enabling brain, blood cells, and renal medulla to continue functioning properly.

Gluconeogenesis

Overview

Glucose occupies a central role in metabolism, both as a fuel for certain tissues and as a precursor of essential structural and other biomolecules in most tissues. The maintenance of a supply of glucose is essential for brain, renal medulla, and both red and white blood cells. These tissues rely exclusively on glucose as their energy source under normal circumstances, yet unlike liver and muscle do not store glucose as glycogen. When carbohydrate is not available from dietary sources in adequate amounts the blood glucose level is maintained within relatively narrow limits by a combination of glycogenolysis and gluconeogenesis. Liver glycogen can be broken down to release glucose into the blood circulation to other tissues, but it is usually depleted within 18–72 h after meals, depending on the species. Liver and kidney cortex cells circumvent this situation, especially during prolonged starvation, by having the pathway to synthesize glucose from substrates such as lactate derived from glycolytic tissues like skeletal muscle and red blood cells, glycerol from the breakdown of triglycerides stored in adipose tissue, and certain amino acids derived from the breakdown of muscle and other tissue proteins. The conversion of these precursor molecules to glucose is known as "gluconeogenesis." Gluconeogenesis, in part a reversal of glycolysis occurs exclusively in liver and kidney cortex utilizing most of the glycolytic enzymes except for three steps: (1) the conversion of pyruvate to phosphoenolpyruvate (PEP) via oxaloacetate, (2) fructose 1,6-bisphosphate to fructose-6-phosphate, and (3) glucose-6-phosphate to glucose. These reactions cannot be simply reversed by pyruvate kinase, phosphofructokinase and hexokinase, respectively, due to the large negative free energy changes in the direction of glycolysis. However, liver and kidney cortex cells overcome this situation by having another four enzymes including pyruvate carboxylase (PC) working in tandem with phosphoenolpyruvate carboxykinase (PEPCK) to form PEP, along with fructose-1,6-bisphosphatase and glucose-6-phosphatase which bypass the energy barriers as shown in Figure 1.

Control of Gluconeogenesis

As these three steps (often known as three "substrate cycles") are catalyzed by four separate enzymes, they are the targets to be controlled by short- and long-term mechanisms. Short-term regulation (seconds to minutes) of hepatic gluconeogenesis can be achieved through hormonal changes which in turn alter the enzymatic activities of the bifunctional enzyme 6-phosphofructo-2-kinase/fructose-2,6-bisphosphatase (PFK-2/F2,6BPase), and also of 6-phosphofructo-1-kinase (PFK-1), fructose-1,6-bisphosphatase (F1,6BPase) and pyruvate kinase (PK). Plasma glucagon and catecholamines, elevated during fasting, trigger an increase in cAMP levels leading to a rise in protein kinase A activity that results in the phosphorylation of pyruvate kinase and thus a

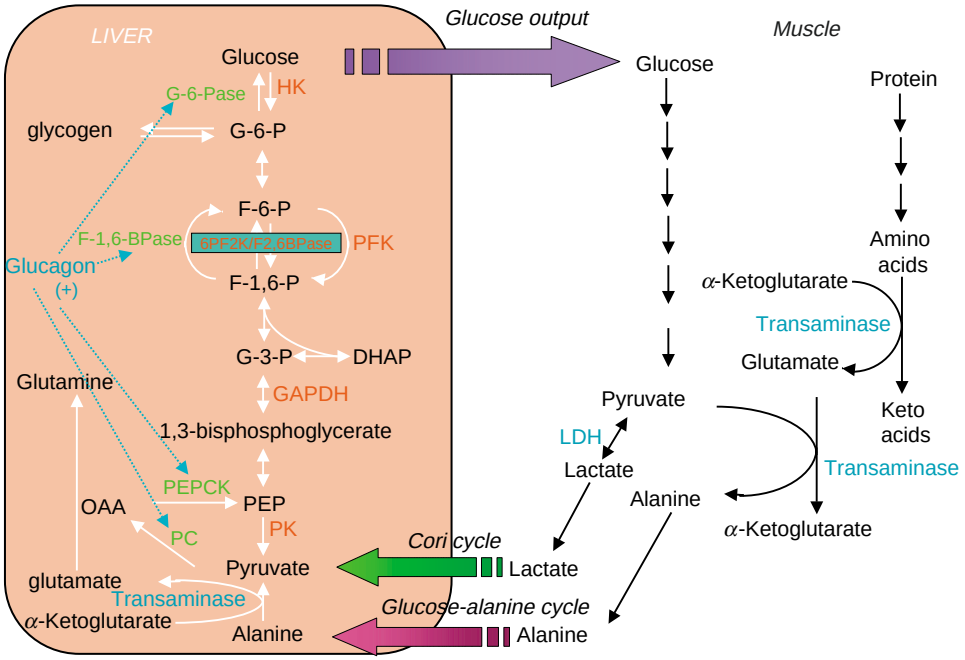

FIGURE 1 Glycolytic and gluconeogenic pathways. Also shown are the Cori cycle and glucose–alanine cycle. In glycolysis, glucose is oxidized by various enzymes to produce pyruvate, while in gluconeogenesis pyruvate is reconverted to glucose using most of the glycolytic enzymes plus four different enzymes, i.e., PC, PEPCK, fructose-1,6-bisphosphatase (F-1,6-BPase), and glucose-6-phosphatase (G-6-Pase). Lactate produced by anaerobic glycolysis in muscle can be converted to pyruvate by lactate dehydrogenase (LDH) in liver as part of the Cori cycle, while alanine produced by the breakdown of muscle protein can also be converted to pyruvate by transaminase in liver as part of glucose-alanine cycle. DHAP, dihydroxyacetone phosphate; HK, hexokinase; PFK, phosphofructokinase; GAPDH, glyceraldehyde-3-phosphate dehydrogenase; PC, pyruvate carboxylase; PEPCK, phosphoenolpyruvate carboxykinase.

decrease in its activity. Glucagon also exerts its effects on 6-phosphofructo-2-kinase/fructose-2,6-bisphosphatase through the same mechanism as for pyruvate kinase, resulting in the phosphorylation of this bifunctional enzyme. This leads to an increase in its F2,6BPase activity and a concomitant loss of its PFK-2 activity. The resulting reduction in the level of fructose-2,6-bisphosphate derepresses fructose-1,6-bisphosphatase activity while also reducing the activities of both phosphofructokinase and pyruvate kinase. These events therefore represent a major force in driving glucose metabolism in a gluconeogenic direction.

Long-term regulation (minutes to hours) of glucose metabolism can also be effected via hormonal changes. These occur when the dietary intake is low in carbohydrate, during starvation or prolonged exercise – all conditions which lead to low levels of insulin and high levels of plasma glucagon, catecholamines, and glucocorticoids. Glucagon and catecholamines act via cAMP to exert their effects by stimulating the transcription of genes encoding gluconeogenic enzymes. Therefore, it is not surprising to see the presence of cAMP-responsive elements in the promoters of the genes encoding PEPCK, fructose-1,6-bisphosphatase, and glucose-6-phosphatase. Glucocorticoids, acting via the glucocorticoid receptor, bind to the responsive element on promoters of PEPCK and glucose-6-phosphatase, and up-regulate transcription of both genes. These changes also drive glucose metabolism in the direction of gluconeogenesis. However, the opposite effect occurs when animals are fed a carbohydrate-rich diet that causes an increase in plasma insulin levels. The insulin signaling cascade results in the inhibition of transcription of genes encoding gluconeogenic enzymes. The very fine control of these enzymes' genes via hormones is a hallmark of long-term regulation in gluconeogenic tissues.

It is noteworthy that gluconeogenesis does not begin in the liver of rodents until immediately after birth as the maternal circulation provides glucose for the developing fetus. Of the four gluconeogenic enzymes present in liver, pyruvate carboxylase, PEPCK, and glucose-6-phosphatase are present in the liver at negligible levels before birth but appear rapidly after birth consistent with the onset of gluconeogenesis. The hormonal mechanism which mediates the increase in these three enzymes in liver at birth is not clearly defined. At least one of the following events that occur within a few hours after birth is likely to regulate gluconeogenesis: (1) a rapid and marked fall in the concentration of blood glucose which was hitherto supplied to the fetus from the maternal circulation via the placenta, and a low portal glucose concentration caused by a low

carbohydrate diet. This results in an increase in the cAMP level via elevated levels of glucagon and epinephrine and a low level of insulin. (2) An increased supply of plasma fatty acids to the liver caused by the hydrolysis of triglycerides in dietary milk.

Pyruvate Carboxylation

The carboxylation of pyruvate is a very important anaplerotic reaction to provide oxaloacetate for the Krebs cycle to operate continuously, as oxaloacetate and other intermediates are withdrawn from the cycle for a number of biosynthetic pathways including gluconeogenesis in liver and kidney, production of neurotransmitter substances in the glial cells of the brain, glyceroneogenesis in adipocytes, and fatty acid synthesis in liver, adipocytes and lactating mammary glands (see Figure 2). Therefore, oxaloacetate must be replenished at all times by the activity of PC (EC 6.4.1.1) that catalyzes the carboxylation of pyruvate to oxaloacetate as described in the following equation:

$$\text{Pyruvate} + HCO_3^- + \text{ATP} \overset{Mg^{2+},\text{acetyl-CoA}}{\rightleftharpoons} \text{oxaloacetate} + \text{ADP} + \text{Pi}.$$

PC contains covalently bound biotin as a prosthetic group that acts as a swinging arm to convey CO_2 between the two catalytic domains, i.e., the biotin carboxylation domain and the transcarboxylation domain. In mammals, PC is located in the mitochondrial matrix where its anaplerotic activity can be directly applied to the Krebs cycle. The control of pyruvate carboxylation can be achieved by three different ways: (1) control of substrate supply, (2) control by the enzyme's allosteric regulator(s), and (3) transcriptional/posttranscriptional control (see Table I).

Control by Substrate Supply

The first step to regulate pyruvate carboxylation is to control the availability of substrates to be converted to pyruvate and enter the mitochondria. These substrates are lactate, and gluconeogenic amino acids, principally alanine but also serine and several others indirectly. Due to a limiting O_2 supply to the muscle cells during intense exercise, skeletal muscle glycogen is metabolized anaerobically by the glycolytic pathway for ATP production. The pyruvate derived from glycolysis is reduced to lactate with the concomitant oxidation of NADH by the action of lactate dehydrogenase. This lactate is exported from muscle cells to the liver via the blood circulation. Lactate once taken up by liver cells is converted back to pyruvate and subsequently carboxylated to oxaloacetate for gluconeogenesis. In what is known as the Cori cycle, glucose produced from liver cells is then circulated to muscle to replenish its glycogen after the exercise. Therefore intense exercise enhances gluconeogenesis via pyruvate carboxylation. Breakdown of muscle protein during starvation yields gluconeogenic amino acids that also contribute to the supply of pyruvate. Glycerol derived from the hydrolysis of triglyceride in adipose tissue during prolonged fasting and in

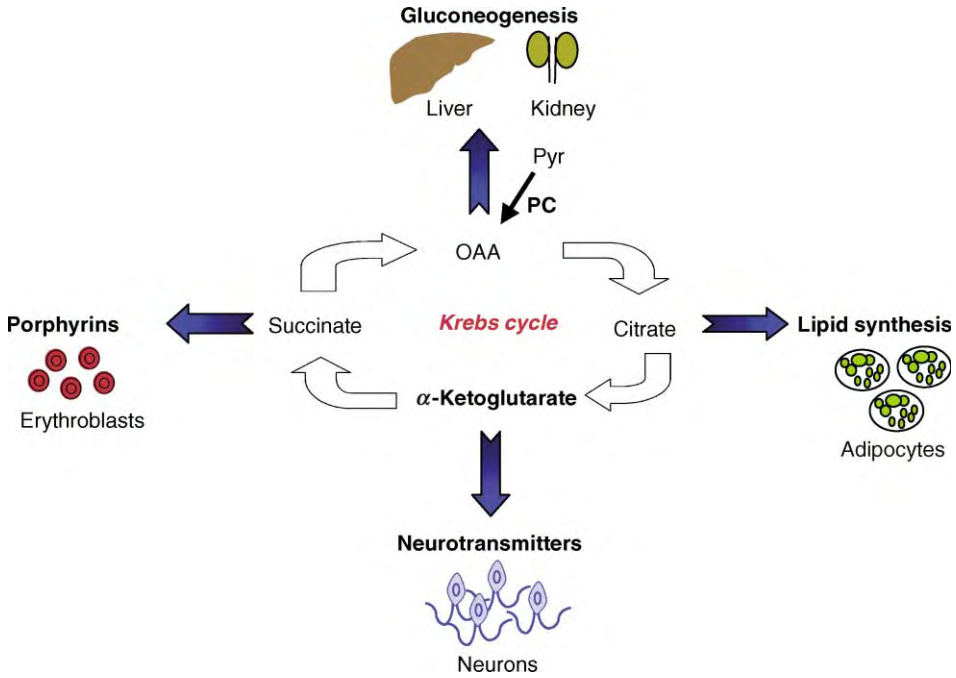

FIGURE 2 The anaplerotic function of PC in mammalian tissues in which oxaloacetate is withdrawn from the Krebs tricarboxylic acid cycle for various biosynthetic pathways. OAA, oxaloacetate; Pyr, pyruvate.

TABLE I

Factors Affecting Pyruvate Carboxylation

Factor	Mechanism of action
Insulin	Inhibits PC gene expression; inhibits protein breakdown and hence restricts substrate supply
Thyroid hormone	Stimulates PC synthesis
Glucocorticoids	Increases substrate supply
Glucagon	Increases ATP/ADP ratio
Acetyl-CoA	Allosteric activation

diabetes is another substrate that is converted to glucose. It has been estimated that ~15% of hepatic glucose production are derived from the Cori cycle while ~12% are derived from the glucose–alanine cycle. Glycerol accounts to only 2% of hepatic glucose production in the postabsorptive state but can become more significant (~10–15%) in prolonged fasting or in diabetes.

Control by Allosteric Regulator

Short-term regulation of pyruvate carboxylation is principally controlled by its allosteric activator, acetyl-CoA. The β-oxidation of free fatty acids during fasting results in an elevated level of acetyl-CoA in the mitochondria, and the binding of acetyl-CoA by PC results in its allosteric activation thereby enhancing pyruvate carboxylation.

Control by Transcriptional/ Posttranscriptional Mechanisms

Long-term regulation of pyruvate carboxylation is a slow response process taking several hours or days and involves alteration of transcriptional and posttranscriptional mechanisms. In rat, two tissue-specific promoters of the PC gene are activated differentially to mediate the production of mRNA transcripts bearing different 5′-noncoding regions with distinct translational efficiencies. Pathophysiological conditions including diabetes, hyperthyroidism, and obesity are known to affect pyruvate carboxylase activity in the long term.

Link between Pyruvate Carboxylation and Insulin Secretion

It is known that pancreatic islets contain high concentrations of PC mRNA and protein, and that the latter's specific activity is equivalent to that in liver and kidney. However, the islets lack PEPCK activity and its mRNA. This provides us with a clue that here PC does not serve the purpose of gluconeogenesis. It has been shown that there are two alternative routes for using oxaloacetate produced by PC, i.e., the pyruvate/malate and the pyruvate/citrate shuttles operating across the mitochondrial membrane. These routes are essential for glucose-induced insulin secretion as specific inhibition of PC activity also reduces the secretion of insulin in response to glucose, further suggesting a role for PC in insulin secretion.

Transamination

Breakdown of Amino Acids in Liver

Dietary proteins are digested by enzymes in the stomach and small intestine to yield various amino acids. This process provides both nitrogen and carbon sources for various biosynthetic pathways. Once transported to liver, these amino acids are subjected to a variety of enzymatic reactions, some are anabolic while others are catabolic. Of the latter the first is called "transamination." This process removes the NH_2 group from each amino acid to produce an α-keto acid. The α-amino group is most frequently transferred to α-ketoglutarate to form glutamate. This reaction is catalyzed by enzymes called a "transaminase" or an "aminotransferase." For example, alanine aminotransferase or aspartate aminotransferase transfers the α-amino group from alanine or aspartate to α-ketoglutarate:

$$\text{Alanine} + \alpha\text{-ketoglutarate} \leftrightarrow \text{pyruvate} + \text{glutamate}.$$

$$\text{Alanine} + \alpha\text{-ketoglutarate} \leftrightarrow \text{oxaloacetate} + \text{glutamate}.$$

Transaminases or aminotransferases are known to require pyridoxal phosphate (a derivative form of vitamin B6) as a cofactor of the reaction. Glutamate is then converted back to α-ketoglutarate by glutamate dehydrogenase in liver. This reaction yields NH_3, which enters the urea cycle.

Breakdown of Amino Acids in Muscle and the "Glucose–Alanine Cycle"

At rest, muscle can utilize fatty acids, ketone bodies, or blood glucose as carbon sources, depending on their availability, while during intense exercise muscle utilizes glycogen as an energy source via anaerobic glycolysis to produce lactate. However, vigorously contracting muscle or prolonged starvation triggers protein breakdown thereby producing amino acids which either can be oxidized or in some cases used as gluconeogenic substrates. As mentioned above, transamination of most amino acids prior to the oxidation of their ketoacid derivative produces

glutamate as the end product. The α-amino group of glutamate can be transferred to pyruvate, the readily available product of glycolysis in muscle, to form alanine. The alanine is then transported through the blood circulation to the liver where alanine is converted back to pyruvate by alanine aminotransferase. This reaction is exceptionally important in liver as it provides pyruvate to be used for gluconeogenesis. Glucose produced in liver is then circulated back to the muscle where it is utilized for glycogen synthesis or as an energy source during rest periods. The transfer of an amino group from glutamate to pyruvate to form alanine in muscle and the conversion of alanine back to glucose via pyruvate is known as "glucose–alanine cycle"(see Figure 1). The operations of the glucose–alanine cycle and the Cori cycle in liver provide an economic means to produce glucose from the end products of muscle metabolism.

See Also the Following Articles

Anaplerosis • Biotin • Biotinylation of Proteins • Branched-Chain α-Ketoacids • Fatty Acid Synthesis and Its Regulation • Gluconeogenesis • Phosphofructokinase-2/Fructose Bisphosphatase-2

Glossary

allosteric regulation Process by which enzyme activity is modulated by noncovalent binding of a specific chemical at a site other than the active site.

anabolic Promoting biosynthesis (opposite of catabolic).

anaplerotic Replenishing what has been removed (e.g., Krebs tricarboxylic acid cycle intermediates).

catecholamines Group of hormones including epinephrine and norepinephrine.

phosphorylation Process of adding a phosphate group from ATP to protein.

responsive element DNA sequence upstream of transcription initiation where a regulatory protein is bound and stimulates or represses transcription.

Further Reading

Brooks, G. A. (2002). Lactate shuttles in nature. *Biochem. Soc. Trans.* **30**, 258–264.

Corssmit, E. P. M., Romijn, J. A., and Sauerwein, H. P. (2002). Regulation of glucose production with special attention to non-classical regulatory mechanisms: A review. *Metabolism* **50**, 742–755.

Jitrapakdee, S., and Wallace, J. C. (1999). Structure, function and regulation of pyruvate carboxylase. *Biochem. J.* **340**, 1–16.

Magnuson, M. A., She, P., and Shiota, M. (2003). Gene-altered mice and metabolic flux control. *J. Biol. Chem.* **278**, 32485–32488.

Owen, O. E., Kalhan, S. C., and Hanson, R. W. (2002). The key role of anaplerosis and cataplerosis for citric acid cycle function. *J. Biol. Chem.* **277**, 30409–30412.

Roden, M., and Bernroider, E. (2003). Hepatic glucose metabolism in humans – its role in health and disease. *Best Practice Res. Clin. Endocrinol. Metabolism* **17**, 365–383.

Yang, D., and Brunengaber, H. (2000). Glutamate, a window on liver intermediary metabolism. *J. Nutr.* **130**, 991S–994S.

Biography

Sarawut Jitrapakdee has studied the regulation of pyruvate carboxylase in liver and pancreatic islets with particular reference to glucose-induced insulin secretion by β-cells and the relevance of this to obesity and type 2 diabetes. He has been awarded several distinguished prizes for his graduate studies at the University of Adelaide and subsequently since taking up a Faculty position at Mahidol University, Bangkok.

John C. Wallace undertook postdoctoral studies on gluconeogenesis with Sir Hans Krebs (Oxford), and with the codiscoverers of pyruvate carboxylase, Professor Merton Utter (Cleveland) and Dr. Bruce Keech (Adelaide). He has published 70 papers on structure/function studies of pyruvate carboxylase, and has been awarded the LKB Medal and the Lemberg Medal by the Australian Society for Biochemistry and Molecular Biology. His other research interests include the insulin-like growth factor system with 69 publications and several international patents in this area.

Pyruvate Dehydrogenase

Sam A. Johnson
Salk Institute, La Jolla, California, USA

James G. McCormack
OSI Pharmaceuticals Ltd., Oxford, UK

The Pyruvate dehydrogenase (PDH) complex (EC 1.2.4.1 + 2.3.1.12 + 1.8.1.4) is a multi-enzyme complex, which in eukaryotes is located within the mitochondrial matrix associated with the inner mitochondrial membrane. PDH catalyzes the oxidative decarboxylation of pyruvate with the concomitant formation of carbon dioxide, acetyl CoA, and NADH (reaction [1]), and thus forms the link between the glycolytic and Kreb's citric acid cycle (TCA) pathways.

$$\text{Pyruvate} + \text{CoA} + \text{NAD}^+ \rightarrow \text{Acetyl-CoA} + \text{NADH} + \text{H}^+ + \text{CO}_2 \quad [1]$$

This reaction is essentially irreversible ($\Delta G^{o'} = -39$ kJ) and, as it represents the "point-of-no-return" for carbohydrate utilization in mammals, it is highly regulated. This is primarily achieved by regulation of the amount of PDH in the active state by reversible phosphorylation by multiple dedicated kinases and phosphatases, and also by end-product inhibition.

Components and Structure of PDH

The known components of the PDH complex and its associated regulatory enzymes are listed in Table I. PDH complex isolated from mammalian tissues has an overall molecular weight of 7–10 MDa (i.e., ~2 times that of a eukaryotic ribosome) and can be visualized using an electron microscope.

The structure of the mammalian PDH complex is based around a core 60-mer of 6 E3-BP and 54 E2-subunits arranged as a pentagonal dodecahedron (E3-BP has previously been called component (or protein) X). The inner domains of the E2 and E3-BP-subunits interact to produce the core frame of the complex. The lipoyl domains protruding from the core contain flexible linkers allowing the outer domains some mobility with respect to the core. Both E2 and E3-BP have subunit-binding domains that bind other proteins in the complex and anchor them to the core 60-mer (see Figure 1). The lipoyl groups (covalently attached to E2 lysines) participate in catalysis and their flexibility relative to the core is essential for this function. The E3 component is also present in two similar complexes, the 2-oxo-acid dehydrogenase and the branched chain oxo-acid dehydrogenase complexes, as well as in the glycine-cleavage system, all of which are also located within the mitochondrial matrix.

It is thought that the six E3-BPs are located at the faces of the pentagons where they each bind an E3 homodimer. The $\alpha_2\beta_2$ heterotetramers of E1 (20–30 per complex) are thought to be localized to the edges of the pentagons. The regulatory kinases and phosphatases associate with the E2-subunits and act on serine residues in the E1α-subunits. The precise stoichiometry of the regulatory proteins in the complex is unknown but there are estimated to be approximately three molecules of kinase per complex. This is obviously fewer than the number of E1-subunits and it is thought the kinase moves over the surface of the core by utilizing the mobility of the lipoyl groups.

The structure of the bacterial form of PDH has been studied more extensively than the mammalian form; it is based on a 24-mer core of E2 with 24 E1 and 12 E3-subunits attached. No E3BP is present and the complex is not regulated by phosphorylation. The yeast *Saccharomyces cerevisiae* form of the complex is based on a 60-mer core, possibly with the E3-subunits located inside of the hollow E2 core at the 12 holes. The yeast complex, although more like the mammalian form in structure, is not regulated by reversible phosphorylation, a fact supported by the lack of homologues of PDK or PDP in the complete yeast genome sequence.

There are a number of inherited metabolic defects which have been described where various components of the PDH system, or their expression, have been shown to be defective, and interestingly, the auto-immune response which is thought to be the basis of primary biliary cirrhosis appears to be directed primarily against the E3BP and E2 components of the PDH complex.

TABLE I

Components of the PDH Complex and its Regulatory Enzymes

Components	EC reference	Full name	Subunit M_R (kDa)	Cofactors	Stoichiometry in mammalian complex
E1	1.2.4.1	Pyruvate dehydrogenase	α 42 β 36	TPP, Mg^{2+}	20–30 α_2 β_2 heterotetramers
E2	2.3.1.12	Dihydrolipoamide acetyltransferase	52	Lipoate	54
E3	1.8.1.4	Lipoamide dehydrogenase	55	FAD	6 homodimers
E3BP	None	E3 binding protein	51	Lipoate	6
PDK	2.7.1.99	Pyruvate dehydrogenase kinase	45–48 (4 isoforms)	Mg^{2+}	?Few
PDP	3.1.4.33	Pyruvate dehydrogenase phosphatase	cat 50	Mg^{2+}	?Few
			r 90	FAD?	

Mechanism of the Reaction Catalyzed by PDH

The multi-step reaction catalyzed by the PDH complex involves sequential reactions with the intermediates being relayed between the subunits via the flexible lipoyl domains.

E1 catalyzes the decarboxylation of pyruvate forming 2-(1-hydroxyethyldiene)-TPP bound to E1 (TPP is thiamin pyrophosphate). E1 also catalyzes the transfer of the intermediate as an acetyl group to the lipoyl moiety of E2. Each E2-subunit contains two flexible lipoyl groups. The acetyl group is shuttled between them to achieve the transfer between reaction centers that are too distant to be connected by one lipoyl group. E2 catalyzes the transfer of the acetyl group from the attached lipoyl group to CoA forming acetyl-CoA, leaving the lipoate group in the reduced form. E3 (and possibly E3-BP) catalyzes the transfer of electrons from the reduced lipoyl group attached to E2 to NAD^+ generating NADH and an oxidized lipoyl group. Thus, the overall reaction has been catalyzed and the PDH complex is returned to its original state.

Role of PDH in Metabolism

The reaction catalyzed by the PDH complex is central within metabolic pathways, most importantly linking glycolysis to the TCA cycle. Pyruvate has multiple sources and the acetyl-CoA produced has multiple

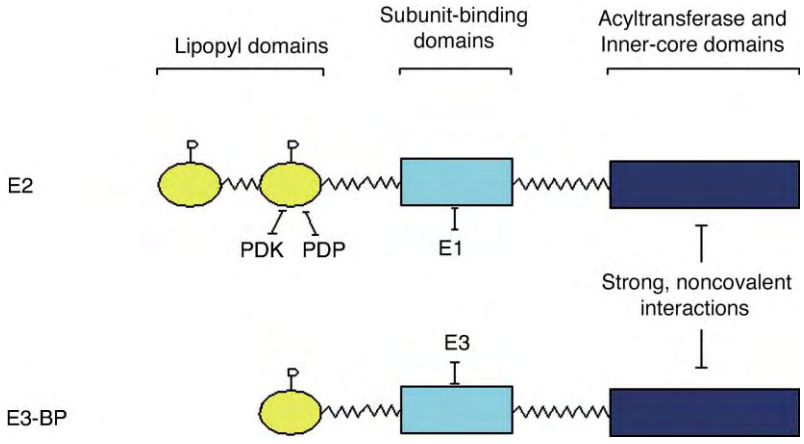

FIGURE 1 Schematic structures of the E2- and E3BP-subunits of the PDH complex. The acetyltransferase domains of the E2-subunits and the inner-core domains of the E3-BP-subunits interact to produce the dodecahedral core of the PDH complex. The subunit-binding domains and lipoyl domains (the majority of the proteins) are exterior to the core. The other major subunits (E1 and E3) are bound to the relevant subunit-binding domains. The regulatory proteins associate with the lipoyl domains of E2 and act to regulate the phosphorylation status of E1. Domains are linked by flexible linker regions composed of sequences rich in alanine and proline.

destinations, both catabolic and anabolic. The correct rate of flux through PDH is essential for the homeostasis of the cell. Coupled with the fact that the reaction catalyzed by PDH is irreversible in mammals and thus represents the point of commitment of carbohydrate metabolism, this means that the regulation of PDH is extremely important.

Regulation of PDH

Regulation of Activity by Phosphorylation

The major regulation of PDH is based on phosphorylation. The activity of the complex is modulated by phosphorylation of the E1α-subunits on three serine residues. The complex is inactive in the phosphorylated state (PDH-P) and active in the non-phosphorylated state (PDHa). The three phosphorylation sites (site 1 (S264), site 2 (S271), and site 3 (S203)) do not have equal importance in causing inactivation of the complex. Site 1 is the main inhibitory site and has been shown to account for at least 98% of the inhibition in rat heart mitochondria. Sites 2 and 3 are thought to reinforce the inactivating action of phosphorylation at site 1 and to make dephosphorylation more prolonged.

The phosphorylation status of PDH is regulated by dedicated kinases and phosphatases (Figure 2). The only other known phosphorylated protein within the mitochondrial matrix of mammalian cells is the related branched chain oxo-acid dehydrogenase complex which appears to have its own dedicated set of regulatory enzymes that are sequentially related to those for PDH.

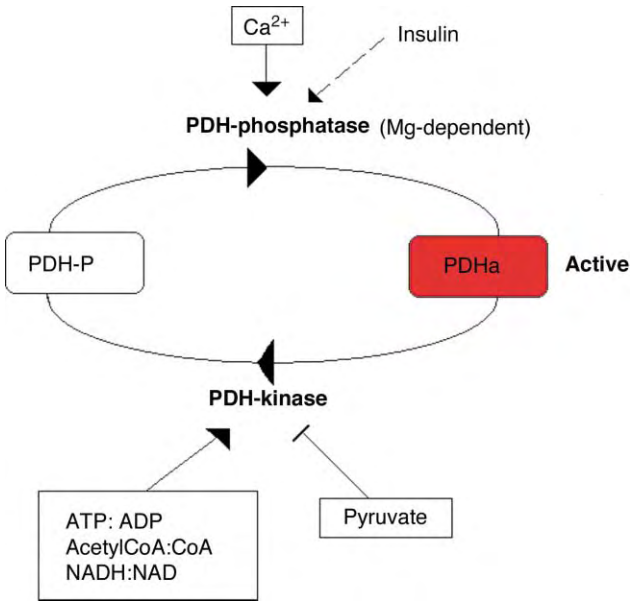

FIGURE 2 Regulation of PDH activity by phosphorylation-dephosphorylation. PDH is inactive in the phosphorylated form and active in the dephosphorylated form. Both intrinsic and extrinsic regulation is based on interconversion of the two forms by dedicated kinases and phosphatases.

Pyruvate Dehydrogenase Kinase

Currently, four isoforms of pyruvate dehydrogenase kinase (PDK) have been cloned from mammalian sources and studied (a fifth member of the family is present in the human genome sequence). These are expressed in a tissue-specific manner and differ substantially in their kinetics and allosteric modulation. Their expression is also altered differentially by hormones and nutritional status. The differences between the properties of the isoforms are substantial. For example, PDK3 has the highest specific activity and is virtually insensitive to NADH and acetyl-CoA inhibition, whereas PDK2 and PDK4 (which appears to be preferentially up-regulated in starvation and diabetes) have lower specific activities and are much more sensitive to NADH and acetyl-CoA. There is also evidence that different PDK isoforms have different activities towards the different phosphorylation sites in PDH E1α.

The kinases are strongly associated with the inner lipoyl domains of the E2-subunit of the PDH complex. The kinases act on the three serine residues on the E1α-subunit previously described. Their association with the E2-subunit increases the efficiency of phosphorylation of E1α.

The primary sequences of the PDKs are more like bacterial histidine kinases than eukaryotic serine/threonine kinases and evidence exists for the similarity of mechanism between PDK and a bacterial histidine kinase. However, the sites phosphorylated by the PDH kinases are situated in consensus sequences typical of eukaryotic serine/threonine phosphorylation sites. It is interesting to speculate that this situation arose by evolution from the endosymbiotic status of mitochondria in eukaryotic cells.

Pyruvate Dehydrogenase Phosphatase

Pyruvate dehydrogenase phosphatase (PDP) is a member of the PPM-family of phosphatases. PDP dephosphorylates the E1α-subunit and so causes the activation of PDH complex. PDP appears to act exclusively on PDH: no other substrates of PDP are known. PDP is also the only known phosphatase to act on PDH *in vivo*.

PDP has been cloned from a number of species. The phosphatase was originally cloned from bovine tissues, where the phosphatase is heterodimeric consisting of a catalytic (PDP_{cat}) and regulatory (PDPr) subunit. In rat, two isoforms of the catalytic subunit have been cloned, but as yet no regulatory subunit has been cloned.

The bovine phosphatase is the most extensively studied. It is Ca^{2+}-activated with Ca^{2+} causing a reduction in the $K_{0.5}$ for Mg^{2+}. Ca^{2+} also causes a reversible E2-PDP association and resultantly a 20-fold reduction in the $K_{0.5}$ of PDP for phosphorylated E1.

The two cloned rat isoforms of the phosphatase appear to differ in their regulation. PDP1 (orthologue of PDP_{cat}) is activated by Ca^{2+} but not by spermine. PDP2 has a much higher $K_{0.5}$ for Mg^{2+} (17.4 ± 2.7 mM versus 1.5 ± 0.5 mM for PDP1 in the absence of Ca^{2+}) and is not activated by Ca^{2+} but is activated by spermine. PDP1 appears to be the more strongly expressed form in skeletal muscle whereas PDP2 is the more strongly expressed in 3T3-L1 adipocytes and liver.

The role of the regulatory subunit of PDP is unclear. Studies in which recombinant PDP_{cat} and highly purified PDP are compared suggest several potential properties of PDPr. Firstly, it causes an increase in the $K_{0.5}$ of PDP_{cat} for Mg^{2+}. Secondly, the presence of PDPr confers spermine sensitivity to the phosphatase. Thirdly, differences in affinity of PDP to E2 were found with and without PDPr, so that it is likely that PDPr contributes to the binding and/or orientation with the core PDH complex via E2. PDPr was not found to have any native phosphatase activity and, despite the homology of PDPr to the enzyme dimethylglycine dehydrogenase, no enzymatic activity towards dimethylglycine or related molecules was found. Intriguingly, PDPr is a flavoprotein that binds a dissociable FAD, but it is not clear if this is involved in the function of the protein.

Intrinsic Regulation of PDH

Intrinsic regulation is predominantly based on the reversible phosphorylation mechanism of E1α-subunits as described above, and on end-product inhibition. Intrinsic regulation ensures that the rate of flux through PDH is appropriate for the metabolism of the cell. As illustrated in Figure 2, the kinase is activated by increased ratios of [ATP]/[ADP], [acetyl-CoA]/[CoA] and [NADH]/[NAD^+]. Thus, in the states where the ratios of [products]/[reactants] are high, the kinases are activated and so PDH is inactivated. This is reinforced by increased ratios of [acetyl-CoA]/[CoA] and [NADH]/[NAD^+] also causing end-product inhibition of the catalytic activity of PDH itself. This is also the principal regulatory mechanism by which the so-called glucose-fatty acid (or Randle) cycle operates, and ensures that carbohydrate is preserved when fatty acids are being oxidized (which will lead to increases in intramitochondrial NADH and acetyl-CoA levels). Conversely, high concentrations of pyruvate inhibit the kinase and so favor the active state of PDH where pyruvate will be metabolized. NADH also has an inhibitory effect on PDP, thus making the regulation more efficient by coordinate action on the activities of the kinase and phosphatase.

Extrinsic Regulation of PDH

Extrinsic (i.e., hormonal) regulation of PDH is also predominantly based on the modulation of complex activity by reversible phosphorylation. The localization of PDH exclusively within the mitochondrial matrix presents a problem to the cell in transmitting an extracellular signal to the PDH system: not only must the signal cross the plasma membrane, but also cross the largely impermeable mitochondrial inner membrane.

Calcium Regulation of PDH

Calcium has a physiological role in activating mitochondrial metabolism. For example, in muscle cells, increased cytosolic Ca^{2+} concentration stimulates contraction and so increases ATP usage. The increased cytosolic Ca^{2+} concentration is relayed into the mitochondrial matrix by a specific Ca^{2+}-uniporter in the inner membrane (where there are also specific Ca^{2+} export mechanisms). The increases in mitochondrial Ca^{2+} concentration cause activation of PDP and so an increase in PDHa as well as activation of two other intramitochondrial dehydrogenases that are sensitive to calcium (NAD^+-isocitrate dehydrogenase and 2-oxoglutarate dehydrogenase which are activated by Ca^{2+} causing decreases in their K_m values for isocitrate and 2-oxoglutarate respectively). The overall result is increased production of NADH for ATP generation by oxidative phosphorylation. This mechanism can thus override the intrinsic mechanisms described above and thereby increase metabolic flux whilst maintaining or even increasing key metabolite ratios such as [ATP]/[ADP] and [NADH]/[NAD^+]. Increases in cytosolic and mitochondrial Ca^{2+} can be brought about by several different hormones acting on several different tissues.

Insulin Regulation of PDH

Insulin causes an acute increase in the activity of PDH, so increasing the production of acetyl-CoA and the rate of lipogenesis in certain tissues. Insulin is not thought to cause an acute response in the PDKs, but long-term insulin stimulation down-regulates the transcription of these enzymes. Acutely, insulin acts via an increase in the activity of PDP. Insulin causes a reduction of the $K_{0.5}$ for Mg^{2+} and so an activation of PDP, and hence an activation of PDH. The precise mechanism by which insulin transduces a signal into the mitochondria to cause this effect is unknown.

See Also the Following Articles

Calcium Transport in Mitochondria • Glycolysis, Overview • Insulin Receptor Family • Tricarboxylic Acid Cycle

Glossary

extrinsic regulation Regulation of a component of a cell by an extrinisic factor, commonly a hormone (e.g., insulin activation of PDH).

intrinsic regulation Regulation of a component of a cell by factors within the cell to ensure homeostasis (e.g., the rate of flux through PDH is regulated by end-product feedback to ensure that the supply of acetyl-CoA is sufficient for the needs of the cell).

$K_{0.5}$ or K_m value Concentration of effector at which 50% of the observed effect occurs.

Further Reading

Harris, R. A., Bowker-Kinley, M. M., Huang, B., and Wu, P. (2002). Regulation of the activity of the pyruvate dehydrogenase complex. *Adv. Enzyme Regul.* **42**, 249–259.

Patel, M. S., and Harris, R. A. (1995). Mammalian alpha-keto acid dehydrogenase complexes: Gene regulation and genetic defects. *FASEB J.* **9**, 1164–1172.

Patel, M. S., and Korotchkina, L. G. (2001). Regulation of mammalian pyruvate dehydrogenase complex by phosphorylation: Complexity of multiple phosphorylation sites and kinases. *Exp. Mol. Med.* **33**, 191–197.

Popov, K. M., Hawes, J. W., and Harris, R. A. (1997). Mitochondrial alpha-ketoacid dehydrogenase kinases: A new family of protein kinases. *Adv. Second Messenger. Phosphoprotein Res.* **31**, 105–111.

Randle, P. J. (1998). Regulatory interactions between lipids and carbohydrates: the glucose fatty acid cycle after 35 years. *Diabetes Metab. Rev.* **14**, 263–283.

Robinson, B. H., MacKay, N., Chun, K., and Ling, M. (1996). Disorders of pyruvate carboxylase and the pyruvate dehydrogenase complex. *J. Inherit. Metab. Dis.* **19**, 452–462.

Roche, T. E., and Patel, M. S. (eds.) (1989). Alpha-keto acid dehydrogenase complexes: organization, regulation, and biomedical ramifications. *Ann. NY Acad. Sci.* **573**, 474.

Roche, T. E., Baker, J. C., Yan, X., Hiromasa, Y., Gong, X., Peng, T., Dong, J., Turkan, A., and Kasten, S. A. (2001). Distinct regulatory properties of pyruvate dehydrogenase kinase and phosphatase isoforms. *Prog. Nucl. Acids Res. Mol. Biol.* **70**, 33–75.

Yeaman, S. J., Kirby, J. A., and Jones, D. E. (2000). Autoreactive responses to pyruvate dehydrogenase complex in the pathogenesis of primary biliary cirrhosis. *Immunol. Rev.* **174**, 238–249.

Biography

Sam Johnson received his doctoral training in the laboratory of Professor Richard Denton at the University of Bristol, United Kingdom. He is currently undertaking postdoctoral work at the Salk Institute, La Jolla, California.

Jim McCormack also obtained his Ph.D. through Dick Denton's lab in Bristol, and later a D.Sc. from the same University. He is currently Vice President of UK Discovery for OSI Pharmaceuticals in Oxford, and was previously vice president for Scientific Affairs and for Target Cell Biology at Novo Nordisk in Denmark. Previously he was Director of Diabetes Discovery at Novo Nordisk, head of Biochemical Pharmacology at Syntex Research in Edinburgh, and a tenured lecturer in Biochemistry at Leeds University, where he was also a research fellow of the Lister Institute of Preventive Medicine.

Together, Sam and Jim estimate that the number of assays of PDH and its associated enzymes which they have carried out is well into six figures.

Pyruvate Kinase

Kosaku Uyeda
University of Texas Southwestern Medical School, Dallas, Texas, USA

Pyruvate kinase catalyzes the last step of glycolysis which is important for generating ATP. Mammals express four major pyruvate kinase isozymes, muscle (M1), liver (L), erythrocyte (R) and the ubiquitous M2 types. All but the M1 isozyme exhibit positive cooperative kinetic behaviors upon binding the allosteric activator fructose-1,6-diphosphate and in the presence of increasing phosphoenolpyruvate concentrations. All four isozymes are inhibited by phenylalanine. The L-pyruvate kinase isozyme activity also is inhibited by phosphorylation in response to glucagon. Consistent with its important role in regulating glucose metabolism and fat synthesis in liver, L-pyruvate kinase also is extensively regulated at the level of transcription. L-pyruvate kinase transcription increases in response to glucose and insulin and decreases in response to glucagon and high fat diets.

Pyruvate Kinase Reaction

Pyruvate kinase (PK) (EC 2.7.1.40) catalyzes the final step of glycolysis,

$$\text{P-enolpyruvate} + \text{ADP-Mg}^{2+} \rightarrow \text{Pyruvate} + \text{ATP-Mg}^{2+} + \text{H}^{+}$$

The enzyme requires two equivalents of divalent cation and K^+ for a full activity. One divalent cation complexes with ATP or ADP and the other cation binds to the protein and functional groups of pyruvate. The γ-phosphate of ATP bridges the two divalent cations.

Structure

All PKs from a variety of sources are tetramers (Mr = 240 kDa). Mammals express four isozymes designated as M1 and M2 for muscle type, L for liver, and R for erythrocytes. M1 muscle isozyme is the only PK exhibiting hyperbolic kinetics for phosphoenolpyruvate (PEP). However, in the presence of the allosteric ligand such as phenylalanine, it shows cooperative saturation for PEP. All other isozymes exhibit cooperativity with respect to PEP and are activated by fructose 1,6-diphosphate (Fru1,6-P_2) by lowering K_{PEP}.

PK has been isolated and characterized from a number of prokaryotes and from eukaryote tissues. Each consists of ~500 amino acid residues. Crystal structures of the enzymes from cat and rabbit muscle, yeast, *Escherichia coli* and *Leishmania mexicana* have been reported (1 and reviewed in 2). They all exhibit a very similar 3D structure (Figure 1A). Each subunit contains three domains: the A domain with the classic $(\alpha/\beta)_8$ structure; the B domain with an irregular fold; and the C domain with an α- and β-organization (Figure 1B). The eukaryotic enzymes contain additional short N-terminal peptides. The active site is situated on the C-terminal side of the A domain, facing the cleft between the A and B domains. The Fru 1,6-P_2 complex of yeast PK has revealed that the Fru 1,6-P_2-binding site is located in the C (regulatory) domain, which is 40Å away from the catalytic center.

Regulation of LPK *in vitro*

Effect of pH

In alkaline pH, LPK exhibits a sigmoidal saturation curve with PEP, but at lower pH the enzyme shows Michaelis–Menten kinetics. The transition between these two enzyme conformational states occurs at a narrow pH range between 6.8 and 7.3.

Allosteric Effectors

Fru 1,6-P_2 reduces the cooperative effects of PEP and converts the enzyme to a form exhibiting Michaelis–Menten kinetics with a higher affinity for the substrate. ATP and alanine are inhibitors of liver PK (LPK), and these ligands raise the apparent K_{PEP} to higher values. The inhibitory effect of ATP and alanine is counteracted by PEP and Fru 1,6-P_2. Pig LPK is inhibited by phenylalanine more strongly than alanine.

Phosphorylation/ Dephosporylation

LPK was first shown to be regulated by phosphorylation catalyzed by cAMP-dependent protein kinase (PKA), resulting in loss of the enzyme activity. The phosphate

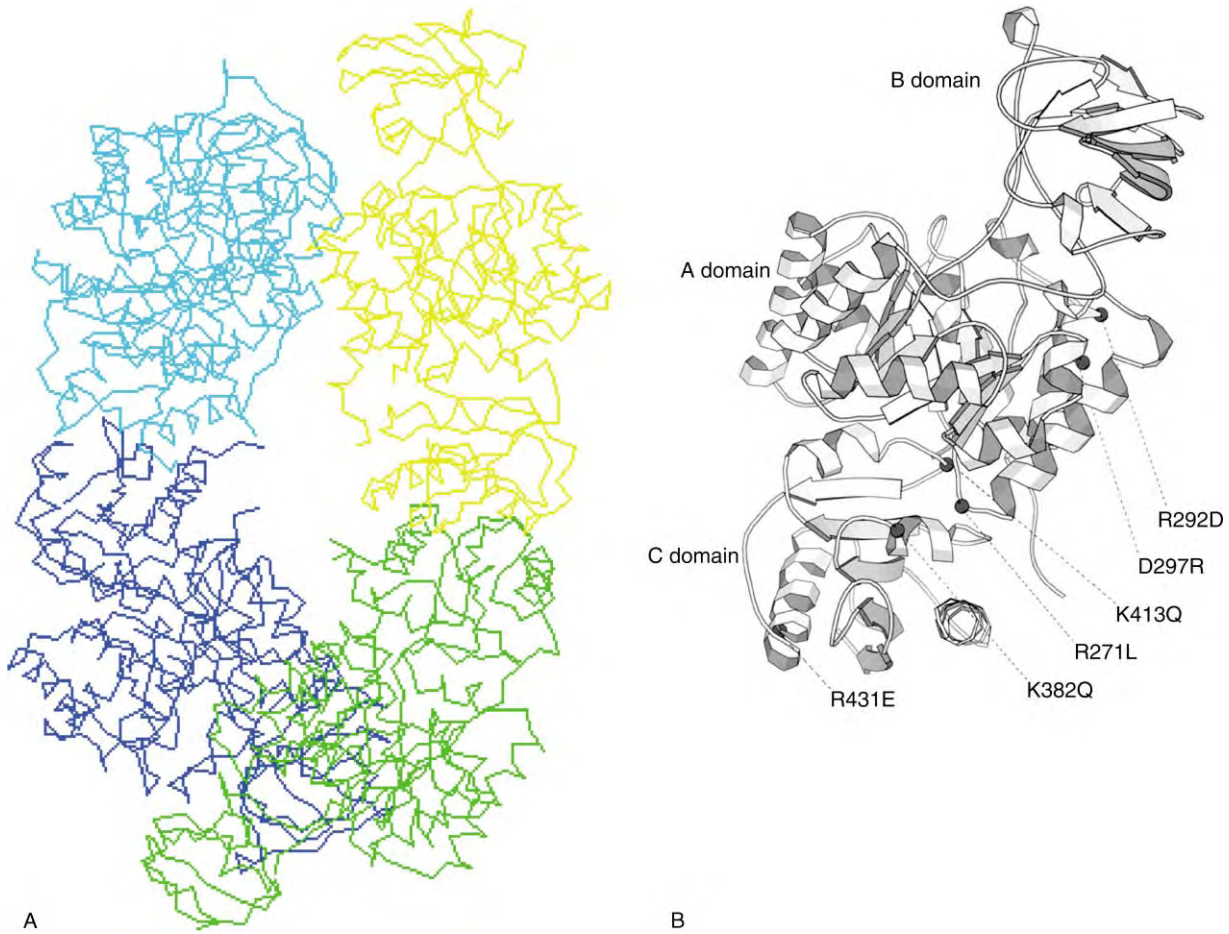

FIGURE 1 (A) Tetrameric *E. coli* PK in inactive T state. (B) *E. coli* PK subunit. The orientation is same as in A. (Reproduced from Valentini, G. *et al.* (2000). The allosteric regulation of pyruvate kinase. *J. Biol. Chem.* **275**, 18145–18152.)

incorporation is one mole phosphate per mole enzyme subunit on the N-terminal Ser within the consensus PKA target sequence (ArgArgAlaSerPVal). When the phosphorylated LPK was dephosphorylated by histone phosphatase, the enzyme recovered full activity.

The major effect of phosphorylation is to raise the apparent K_{PEP} approximately threefold (from 0.3 to 0.8 mM). It also increases the Hill coefficient from 1.1 to 1.5. V_{max} remains the same for both enzyme forms. This inhibitory effect of phosphorylation is counteracted by Fru 1,6-P_2 and H^+. Phosphorylation does not inhibit the rat LPK in the presence of 5 μM Fru 1,6-P_2 at pH 7.3, and the enzyme follows Michaelis–Menten kinetics with K_{PEP} of 0.04 mM. Phosphorylated LPK is more sensitive to inhibition by ATP and alanine than is the dephospho form.

Crystallographic Studies

Crystallographic and mutagenesis studies provided the mechanistic features for the allosteric transition in PK at the molecular level. The enzyme displays significant conformational changes involving all three domains of each subunit in the tetrameric enzyme in moving from the T- to R-state (Figure 2). This model is based on the X-ray structure determination of the allosteric *E. coli* PK in the inactive T-state and the M1 isozyme, which is an active R-conformation. In general, the allosteric transition involves two kinds of movements, (1) the rotation of the B and C domains (17° and 15°) within each subunit and, (2) a 16° rotation of each subunit within the tetramer. Thus, the allosteric activation of PK appears to involve rotation of both domain and subunit. This model is further supported by the observation that the 3D structure of each domain is not altered by their movement, suggesting that they rotate as rigid bodies connected by flexible hinges. The transition from R- to T-state also causes significant changes in the active site including distortion of the PEP-binding site, suggesting the poor substrate affinity of the T-state. It also shrinks the cleft between the A and C domains preventing effector binding.

These kinetic changes induced by various ligands and by phosphorylation are the acute regulation of PK activity by hormonal and nutritional states. Experiments performed on intact animals confirm the regulation of

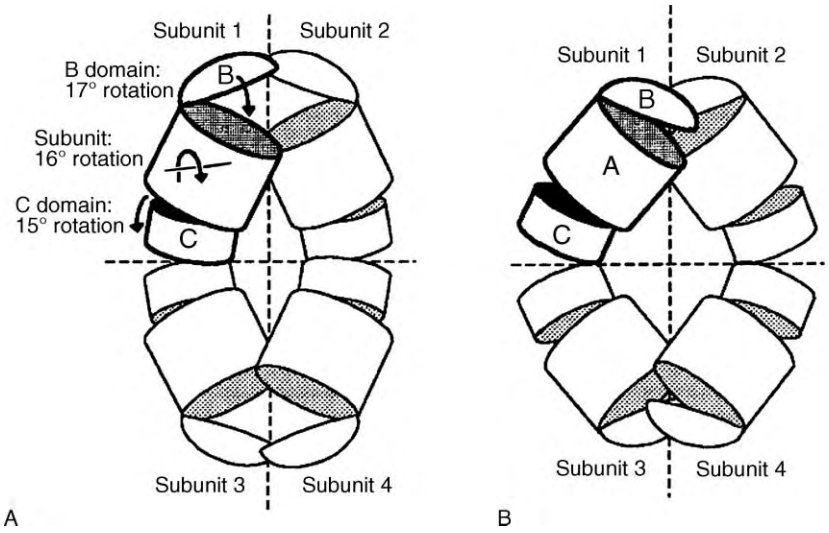

FIGURE 2 Schematic representation of the domain and subunit rotations in the T- and R-state transitions of PK.

PK *in vivo*. Intravenous administration of glucagon causes rapid inactivation of PK in liver. The effect of glucagon also raises cAMP concentration. Insulin causes rapid activation of PK.

Regulation of LPK Concentration by Gene Expression

Effect of Insulin, Glucagon, and Carbohydrate in Liver

In long-term regulation, LPK gene expression is controlled also by hormones and nutrients. Feeding mammals a diet rich in carbohydrate and low in fat leads to an increase in insulin levels and a fall in glucagon. Insulin and glucagon can activate and repress, respectively, the LPK transcription. These hormonal effects are mediated by direct response to the hormonal signals acting via membrane receptors.

In addition to increased insulin secretion, the excess glucose leads to activation of LPK gene transcription. This activation of gene expression is mediated by glucose, independent of insulin, and requires metabolism of glucose. Thus, glucose is not only a source of energy but also is able to stimulate glycolytic, and lipogenic enzyme genes.

Carbohydrate Response Element of LPK Promoter

The LPK gene promoter contains the glucose response element (−168 to −145 nucleotides upstream of open reading frame) and several other nuclear factor binding sites including nuclear factor (NF) and HNF4. The transcription factor binding to the glucose response element was identified recently and termed carbohydrate response element binding protein (ChREBP). In addition, it contains multiple phosphorylation sites, subject to regulation by protein kinase/phosphatase.

Carbohydrate Response Element Binding Protein

ChREBP is a large protein (Mr = 94.6 kDa) containing 846 amino acids. It consists of several functional domains including nuclear localization signaling (NLS) site, basic/helix-loop-helix/Zip region, polyproline, and Zip-like regions (Figure 3). ChREBP belongs to the MyoD family of transcription factors and binds to two consensus sequences (5′-CANNTG-3′) that are separated by five bases.

Regulation of ChREBP in Response to Glucose and cAMP

Inhibition by cAMP-Dependent Protein Kinase, PKA

ChREBP contains multiple phosphorylation sites including three sites for PKA, located at Ser196 (near NLS site), Ser626, and Thr666. ChREBP is controlled at two levels, nuclear entry and DNA binding. PKA-catalyzed

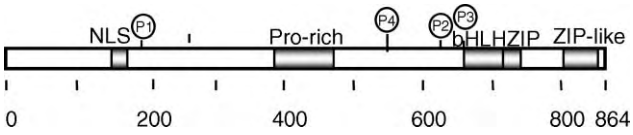

FIGURE 3 The domain structure of ChREBP. The locations of NLS, proline-rich stretch, bHLH/Leucine zipper, and Zip like domains are indicated. The locations of four phosphorylation sites of PKA are designated as P1, P2, and P3. The AMPK site is indicated as P4.

phosphorylation of Ser196 results in inhibition of nuclear import of ChREBP, while that of Thr666 leads to complete inhibition of the DNA binding. In low glucose, ChREBP is localized in the cytoplasm as the phosphorylated form, but in high glucose, it migrates to the nucleus as a dephosphorylated form.

Inhibition by AMP-Activated Protein Kinase, AMPK

Incubation of hepatocytes in fatty acids results in inhibition of glucose activated LPK transcription. This inhibition is mediated by phosphorylation of another site (Ser568) by AMPK. AMPK is activated by increased AMP generated by fatty acylCoA synthetase.

Activation by Glucose

Excess glucose activates the LPK gene expression by increased metabolism of glucose which activates ChREBP by dephosphorylation catalyzed by a specific protein phosphatase (PPase). A specific PP2A activated by Xu5P catalyzes the dephosphorylation and activation of phosphorylated/inactive ChREBP in liver in response to high carbohydrate. Xu5P is a metabolite in the pentose shunt pathway which increases with increased glucose metabolism, and serves as a glucose signaling compound. Thus, these results outline how glucagon/cAMP and high-fat diet repress ChREBP activity by phosphorylation. Glucose, however, activates the ChREBP activity and this activation of ChREBP leads to increased transcription of the LPK gene (and probably others), increasing glucose metabolism.

See Also the Following Articles

Gluconeogenesis • Glycolysis, Overview • Insulin- and Glucagon-Secreting Cells of the Pancreas • Insulin Receptor Family

Glossary

carbohydrate response element A DNA sequence within the promoter of a gene to which a specific transcription factor binds in response to excess carbohydrate.

gene promoter A region of a gene that responds to glucose, hormones, and other stimuli and binds a number of transcription factors that affect transcription.

liver pyruvate kinase An isoenzyme of pyruvate kinase that occurs mainly in liver.

transcription Synthesis of mRNA transcribed from a specific sequence of DNA of a gene.

Further Reading

Girard, J., Ferre, P., and Foufelle, F. (1997). Mechanism by which carbohydrates regulate expression of genes for glycolytic and lipogenic enzymes. *Annu. Rev. Nutr.* **17**, 325–352.

Mattevi, A., Bolognesi, M., and Valentini, G. (1996). The allosteric regulation of pyruvate kinase. *FEBS Lett.* **389**, 15–19.

Uyeda, K., Yamashita, H., and Kawaguchi, T. (2002). Carbohydrate responsive element – binding protein (ChREBP): A key regulator of glucose metabolism and fat storage. *Biochem. Pharmacol.* **63**, 2075–2080.

Valentini, G. *et al.* (2000). The allosteric regulation of pyruvate kinase. *J. Biol. Chem.* **275**, 18145–18152.

Wool, J. O., Friesen, R. H. E., White, M. A., Watowich, S. J., Fox, R. O., Lee, J. C., and Czerwinski, E. W. (2001). Structural and functional linkages between subunit interfaces in mammalian pyruvate kinase. *J. Mol. Biol.* **312**, 525–540.

Biography

Kosaku Uyeda is a Professor in the Biochemistry Department of University of Texas Southwestern Medical School in Dallas. His principal research interests are in mechanism of regulation of carbohydrate metabolism and lipogenesis. He holds a Ph.D. from the University of California, Berkeley. His laboratory codiscovered an important allosteric activator of glucose metabolism (fructose 2,6-P_2). In addition, they isolated and identified a new transcription factor (ChREBP) which stimulates glucose metabolism and conversion to fat in liver in response to excess carbohydrate.

Quinones

Giorgio Lenaz and Maria Luisa Genova
University of Bologna, Bologna, Italy

Chemistry of Quinones

Quinones are diketones derived by oxidation of dihydroxyarenes; the simplest quinones are those derived by benzenediols (1,2- and 1,4-dihydroxybenzene:

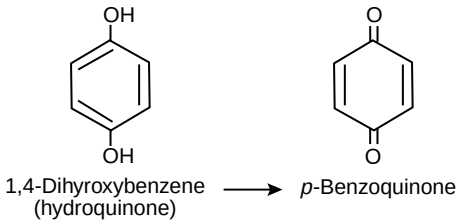

Also condensed arenes give quinones, e.g., the naphthoquinones:

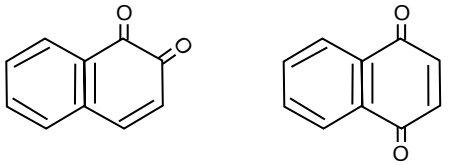

The reversible oxidation of dihydroxyarenes to the respective quinones is a two-electron process with the intermediate formation of the radical form of semiquinones, e.g.,

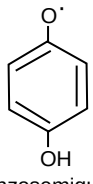

The redox systems quinone/diphenol (or quinol) are widely present in nature. Also known is the charge transfer complex quinhydrone, where quinone is the electron acceptor while diphenol is the electron donor:

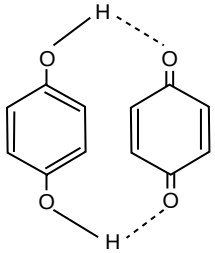

Biological Benzoquinones: Coenzyme Q and Plastoquinone

Chemistry and Distribution

Coenzyme Q was discovered in 1957 by F. L. Crane in Wisconsin as a yellow oily substance, extracted from bovine heart mitochondria, and having redox properties. It is also called ubiquinone, initially from the European nomenclature. The bovine compound is 2,3-dimethoxy-5-methyl-6-decaprenyl-1,4-benzoquinone (Coenzyme Q_{10}), but other homologues exist having polyprenyl chains of different lengths in the 6-position (Table 1). Also some analogues with different substitutions in the benzene ring have been found in nature or synthetized.

Coenzyme Q homologues were initially found in the inner membrane of mitochondria of eukaryotic cells and in the plasma membranes of aerobic and photosynthetic bacteria and they were discovered to be essential components of respiratory and photosynthetic chains. A different analogue, plastoquinone-9 (2,3-dimethyl-5-nonaprenyl-1,4-benzoquinone), was found in chloroplasts of higher plants and algae and in cyanobacteria and proven as an essential component of the photosynthetic apparatus (see structure below).

TABLE 1

Naturally Occurring Homologues and Analogues of Coenzyme Q

Homologue or analogue	Molecular weight	Occurrence
Coenzyme Q_6	590	*Saccharomyces cerevisiae* and other yeasts
Coenzyme Q_7	659	Minor component of some yeasts
Coenzyme Q_8	728	Some yeasts, *Escherichia coli*, and many other bacteria
Coenzyme Q_9	794	Rat, mouse, shark, some insects, protozoa, molds, yeasts, basidiomycetes, *Pseudomonas fluorescens*, and other bacteria
Coenzyme Q_{10}	862	Most mammals including man, birds, amphibia, most invertebrates, most photosynthetic bacteria, and some other bacteria
Rhodoquinone-10	847	*Rhodospirillum rubrum*
Ubichromenol-10	862	Accompanies Q_{10} in minor amounts as a cyclization product
Plastoquinone-9	747	Chloroplasts of higher plants and algae

See text for chemical structures.
Rhodoquinone-10 is 2-methoxy-3-amino-5-methyl-6-decaprenyl-1,4-benzoquinone.

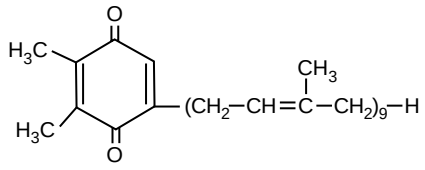

Plastoquinone-9

Soon after its discovery, Coenzyme Q was also found to be present in other cellular membranes of eukaryotic cells, including Golgi apparatus, lysosomes, and plasma membrane.

The major redox forms of Coenzyme Q, with their prevalent protonation states, are the following:

unit of the side chain forming the respective ubichromenols:

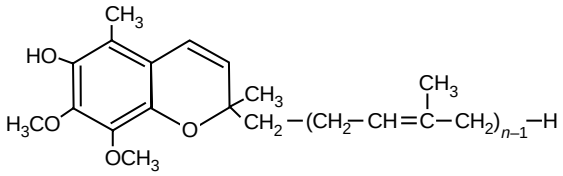

Ubichromenols

Coenzyme Q homologues 1–12 are soluble in most organic solvents but not in water due to their isoprenoid sidechains. Only homologues 6–12 are obtained in crystalline form at room temperature.

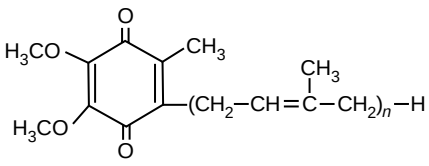

ubiquinone (Q)

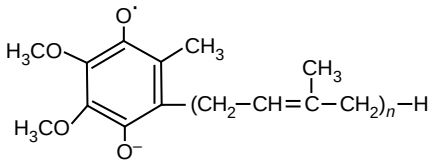

ubisemiquinone anion (Q·)

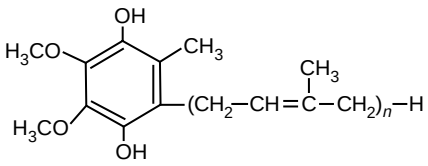

ubiquinol (QH_2)

The standard redox potential of the ubiquinone/ubiquinol couple at pH 7 is $\sim +100$ mV. The semiquinone radical is intermediate in most redox reactions of Coenzyme Q; however, it is very unstable and is rapidly dismutated to the quinone and quinol forms:

$$2Q\cdot + 2H^+ \longleftrightarrow Q + QH_2$$

Under some conditions, ubiquinones undergo cyclization between the ring and the first isoprenoid

In water, Coenzyme Q homologues form micelles or aggregates. They are soluble in lipids and disperse in monomeric form in phospholipid bilayers as well as in biological membranes.

Coenzyme Q absorbs light in the UV with a maximum at 275 nm in ethanol and at 270 nm in hydrocarbons when in oxidized form (extinction coefficient 15 $mM^{-1}\,cm^{-1}$), and with a maximum at 290 nm in all organic solvents when in reduced form (extinction coefficient 4 $mM^{-1}\,cm^{-1}$). The ubisemiquinone anion

has a maximum at 318 nm (extinction coefficient 10.7 mM^{-1} cm^{-1}) and minor peaks also in the visible spectrum. The semiquinones are best detected by electron spin resonance techniques.

The lateral mobility of Coenzyme Q in phospholipid bilayers is very high: using the method of collisional fluorescence quenching with membrane-bound fluorescent molecules, a lateral diffusion coefficient was calculated $\sim 10^{-7}$ cm^2 s^{-1}. Such mobility seems essential for the function of the quinone in electron transfer chains in energy-transducing membranes.

Functions of Coenzyme Q

Electron Transfer Chains of Mitochondria and Bacteria

The best known function of Coenzyme Q is as a redox component of the mitochondrial respiratory chain, localized in the inner membrane. A standard scheme of the respiratory chain is depicted in Figure 1.

Coenzyme Q was first described as a mobile diffusible component localized between Complex I (NADH Coenzyme Q reductase) or Complex II (succinate Coenzyme Q reductase) and Complex III (ubiquinol cytochrome *c* reductase); in these systems, Coenzyme Q is reduced by Complex I or II and reoxidized by Complex III; it was then found that Coenzyme Q is also reduced by other mitochondrial enzymes, such as glycerol-1-phosphate dehydrogenase, electron transfer flavoprotein (ETF) dehydrogenase (an enzyme involved in fatty acyl CoA oxidation), and dihydro-orotate dehydrogenase.

Due to its extremely hydrophobic nature, Coenzyme Q is localized in the hydrocarbon interior of the lipid bilayer of the inner mitochondrial membrane, where its diffusion rate may be very high. In such way it behaves as a common pool of molecules, so that any molecule would be randomly reduced by any Complex I or II and reoxidized by any Complex III.

Besides the Coenzyme Q pool dissolved in the lipid bilayer, Coenzyme Q molecules bound to the individual complexes have also been described. These bound quinones may be important for the mechanism of outward proton translocation, required in the chemiosmotic mechanism of oxidative phosphorylation. The best-known mechanism is the Q-cycle, first proposed by the Nobel laureate Peter Mitchell (Figure 2).

Tight Coenzyme Q binding to proteins (Q-binding proteins) in the respiratory complexes is required to stabilize the semiquinone form that is an essential intermediate in the mechanism of proton translocation.

Moreover, a well-known example of bound quinones is represented by the reaction center of photosynthetic bacteria that has been crystallized and resolved by X-ray diffraction together with its bound prosthetic groups (Figure 3). In bacteria, besides ubiquinone, also menaquinone (a naphthoquinone) may participate in electron transfer.

In chloroplasts of photosynthetic algae and higher plants, the function of ubiquinone is exploited by plastoquinone, present in bound form in photosystem II and free as a pool in the lipid bilayer.

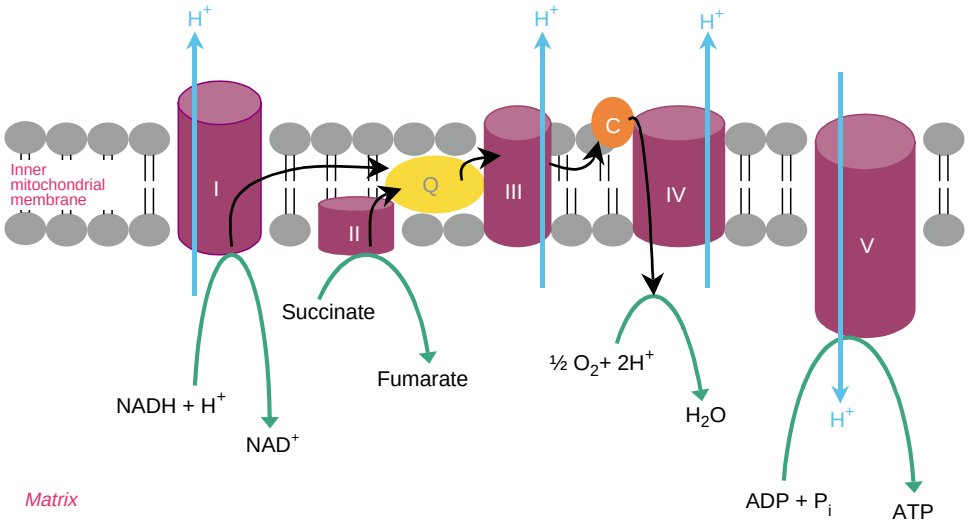

FIGURE 1 Schematic view of the mitochondrial oxidative phosphorylation system, showing the role of Coenzyme Q as a shuttle of electrons between Complex I or Complex II and Complex III. Other dehydrogenases using Coenzyme Q as acceptor are not shown for simplicity. Roman numbers refer to the respective enzyme complexes. Black arrows indicate the flux of electrons, green arrows indicate chemical reactions, and blue arrows indicate proton translocation. During redox reactions catalyzed by Complex I, III, and IV, protons are extruded forming a transmembrane gradient that is used by Complex V (ATP synthase) for synthesizing ATP.

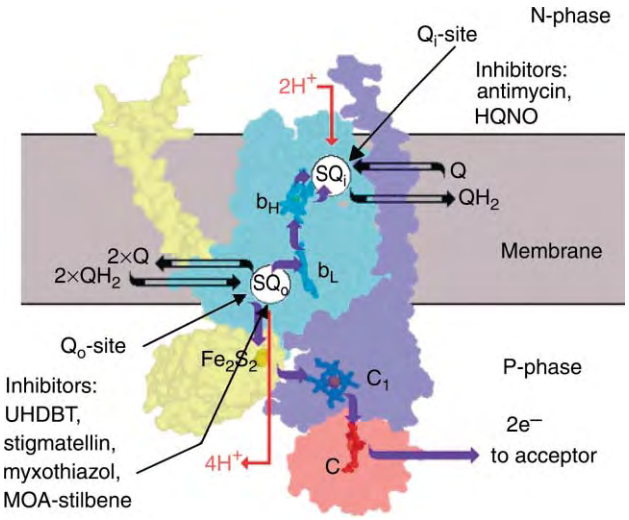

FIGURE 2 The Q-cycle as a mechanism of proton translocation in complex III of the mitochondrial respiratory chain. The scheme shows the Q-cycle in the context of the enzyme structure where the catalytic subunits are shown by their surfaces and made transparent so as to show the redox centers (cyan: cytochrome *b*; yellow: iron-sulfur protein; blue: cytochrome c_1). Quinol (QH_2) is oxidized in a bifurcated reaction at the Q_o-site of the complex located at the outer positive side of the membrane (P-phase): one electron is transferred to the high-potential chain, consisting of the Fe_2S_2 center and cytochrome c_1, and then to cytochrome *c* (red) that carries the electron to Complex IV. Since the semiquinone formed (SQ_o) is unstable, another electron is transferred through the low-potential chain of cytochrome hemes (b_L and b_H) to the Q_i-site where a quinone molecule is fully reduced to quinol. In order to provide the two electrons required at the Q_i-site, located at the inner negative side of the membrane (N-phase), the Q_o-site oxidizes two equivalents of quinol ($2 \times QH_2$) in successive turnovers. Information about inhibitor specificity of the above-mentioned reactions is shown in the figure. The integration of the redox reactions with the release or uptake of protons in the aqueous phases (red arrows) allow the complex to pump protons across the membrane. With permission of Dr. A. R. Crofts, University of Illinois at Urbana-Champaign, IL, USA.

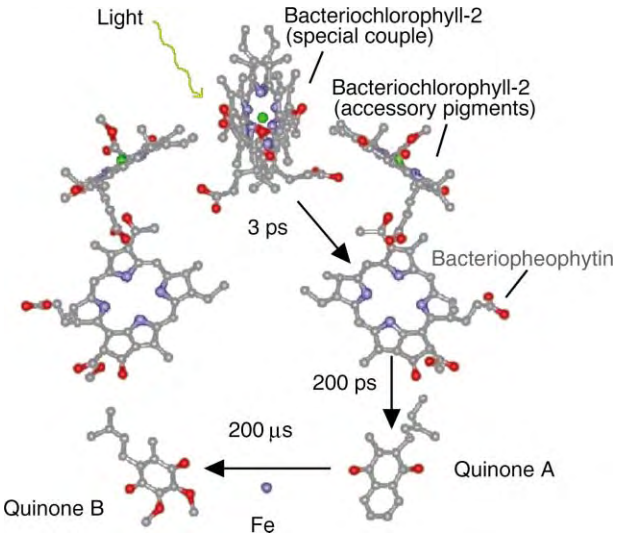

FIGURE 3 Bound quinones in the photosynthetic reaction center of Rhodopseudomonas viridis. Following excitation, the special pair of bacteriochlorophyll molecules donates an electron to a nearby bacteriopheophytin pigment (time constant: 3 ps). Subsequent transfer to the primary quinone (QA, a bound menaquinone) occurs with a half-time of 200 ps. Further electron transfer occurs from QA to the quinone acceptor QB, a bound ubiquinone occupying an active site near the cytoplasmic surface of the protein. QB accepts two electrons and two protons, then it undergoes exchange with the mobile pool of quinones in the lipid bilayer. With permission of Dr. R. Baxter, University of Chicago, IL, USA.

Other Electron Transfer Chains

Coenzyme Q of eukaryotic cells is present in most intracellular membranes and in the plasma membrane as well. Its function in these systems is better known in the plasma membrane oxidoreductase (PMOR) where the quinone appears to participate in transmembrane electron transfer between intracellular NADH or NADPH and extracellular acceptors including the ascorbic acid free radical, derived from the partial oxidation of ascorbic acid. This system may be involved in the antioxidant defenses of the cell since it regenerates ascorbic acid, an antioxidant.

Coenzyme Q as an Antioxidant

Coenzyme Q and other quinones are powerful antioxidants in their reduced form. The ubiquinol reacts with peroxide radicals, such as the lipid peroxide radical LOO·:

$$QH_2 + LOO\cdot \longrightarrow QH\cdot + LOOH$$

where LOOH is a lipid hydroperoxide.

In addition, it may be used to regenerate the reduced antioxidant form of vitamin E (α-tocopherol, T-OH) from the tocopheroxyl radical TO·:

$$T\text{–}OH + LOO\cdot \longrightarrow T\text{–}O\cdot + LOOH$$

$$T\text{–}O\cdot + QH_2 \longrightarrow T\text{–}OH + QH\cdot$$

The semiquinone form of Coenzyme Q, originated from its antioxidant action, is readily converted to the oxidized form by another radical:

$$QH\cdot + X\cdot \longrightarrow Q + XH$$

The cell contains several enzymatic systems to reduce oxidized Coenzyme Q (Q) back to its antioxidant form (QH_2). Among these are the cytosolic enzyme DT-diaphorase (NAD(P)H dehydrogenase (quinone) E.C.1.6.99.2), also found bound to the plasma membrane, a cytosolic NADPH quinone reductase, and microsomal NADH cytochrome b_5 reductase.

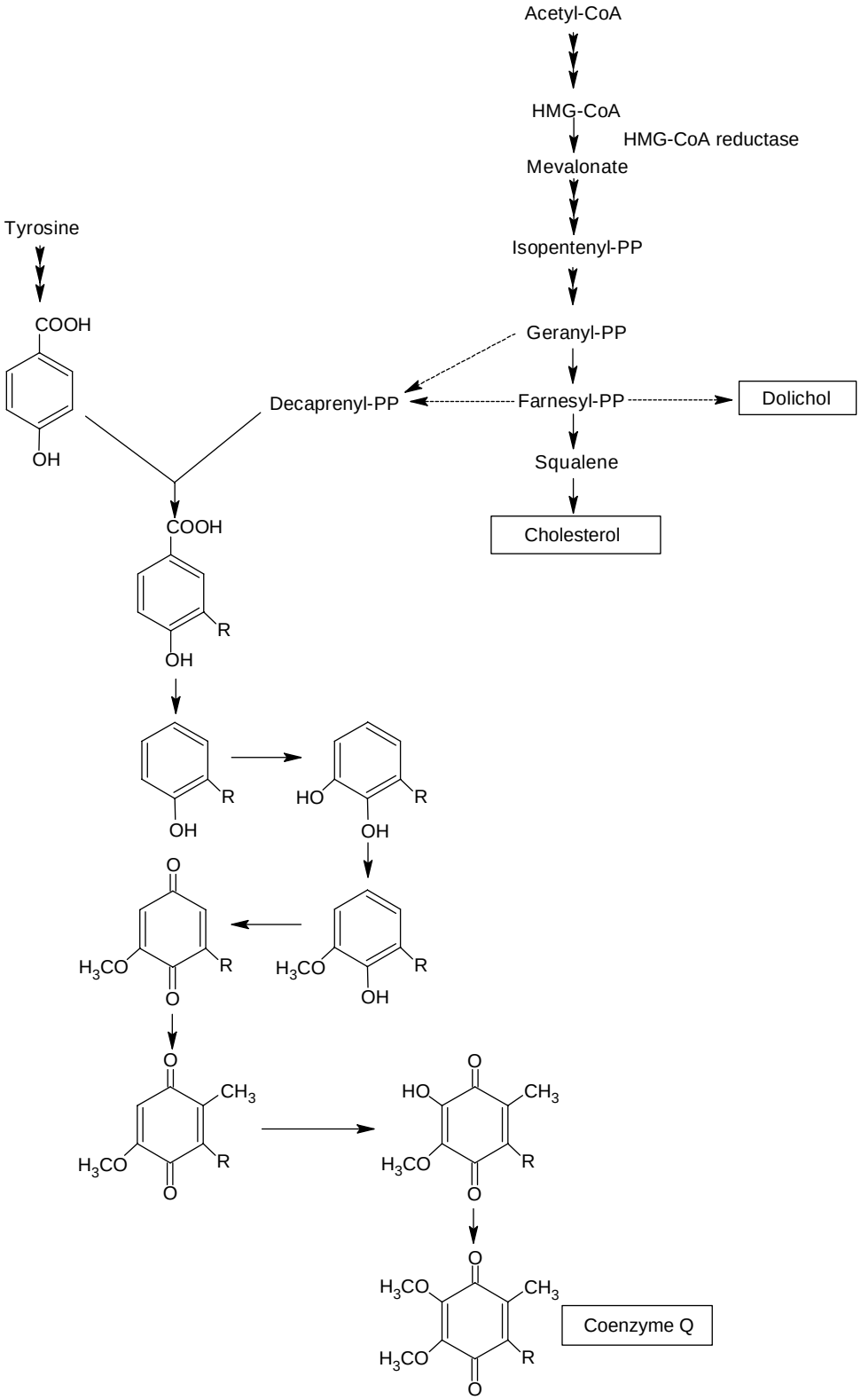

FIGURE 4 Simplified scheme of the biosynthesis of Coenzyme Q. R = isoprenoid side chain; HMG-CoA = 3-hydroxy-3-methyl-glutaryl Coenzyme A.

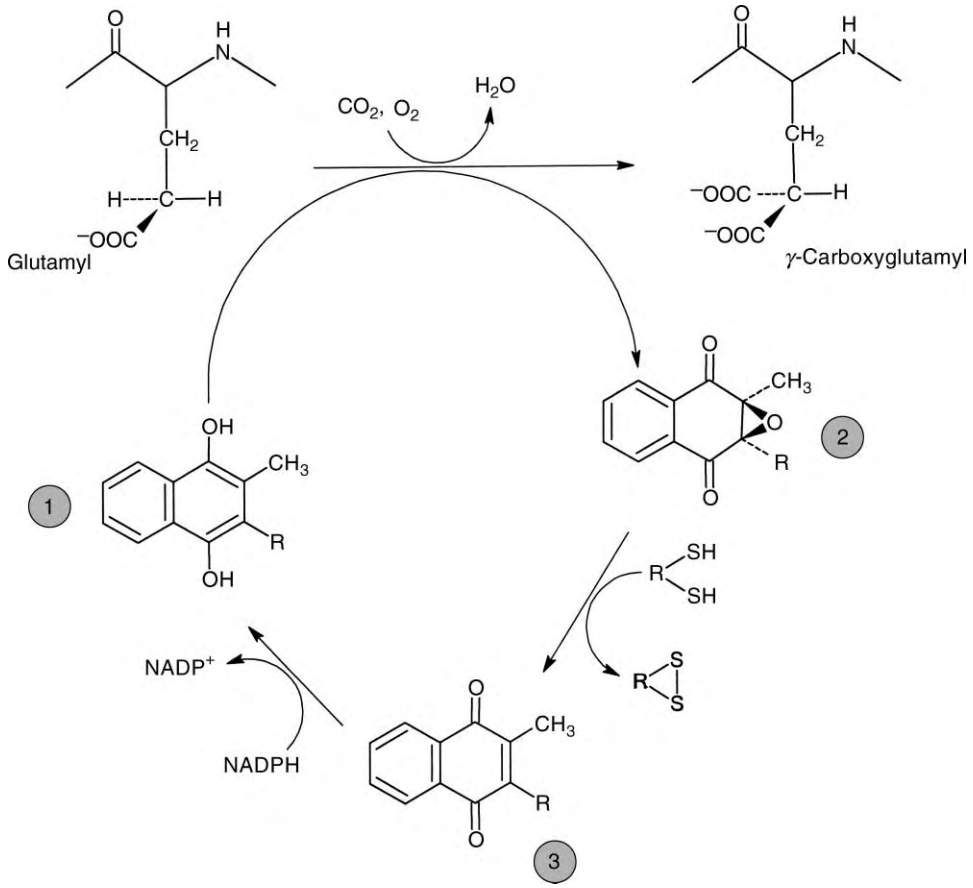

FIGURE 5 Mechanism of action of vitamin K in protein carboxylation. The γ-carboxylation reaction of protein-bound glutamate requires molecular oxygen and the reduced form of vitamin K (1); the hydroquinone is converted to the vitamin K epoxide (2) during the reaction. The vitamin K epoxide must be reconverted to the hydroquinone; this happens in two steps: in the first step the epoxide is converted to the quinone form (3) using the coenzyme thioredoxin [$R(SH)_2$]; the quinone is then reduced to the hydroquinone in an NADPH-dependent reaction.

Biosynthesis of Coenzyme Q

Coenzyme Q is synthetized by animals starting from the amino acid tyrosine which is converted to *p*-hydroxybenzoate; after insertion of the isoprenoid side chain in the 6-position, the ring is completed by a complex series of reactions involving hydroxylations and O-methylations. The isoprenoid side chain is synthesized starting from acetyl CoA through the mevalonate pathway and isopentenyl pyrophosphate, which is common to the synthesis of cholesterol, dolichol, and other polyprenyl compounds (Figure 4). It was found that cholesterol-lowering agents acting on the enzyme 3-hydroxy-3-methyl-glutaryl CoA reductase, which converts 3-hydroxy-3-methyl-glutaryl CoA to mevalonate, besides lowering plasma cholesterol, also lower Coenzyme Q levels, suggesting caution in the use of these agents.

The biosynthesis of Coenzyme Q requires several vitamin-derived coenzymes and appears to be easily limiting on the normal levels of the quinone in the body. For this reason dietary intake of Coenzyme Q, as a vitamin-like supplement, has been recommended by many authors.

Biological Naphthoquinones: Menaquinone and Vitamin K

Menaquinone is the quinone used for electron transfer by many bacteria, either alone or together with ubiquinone (Figure 3).

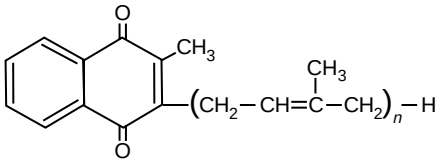

Menaquinones ($n = 7–9$)

Vitamin K exists in two natural forms, phylloquinone (K1) and menaquinone (K2), with 4 and 6 isoprenoid units, respectively. In phylloquinone, three isoprenoid units are hydrogenated. Menadione (K3), without an

isoprenoid chain, is a synthetic derivative.

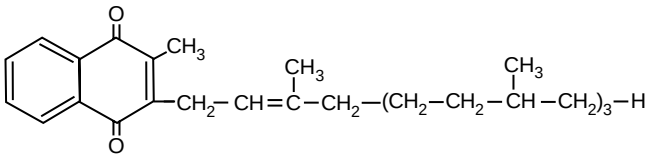

Vitamin K1

Vitamin K is involved in the process of blood coagulation, being required for the synthesis of prothrombin and factors VII, IX, and X. Vitamin K is involved in posttranslational modifications of these proteins consisting in the γ-carboxylation of glutamate residues. Vitamin K is the coenzyme of the carboxylase enzyme and acts in its reduced hydroquinone form. The mechanism of action is shown in Figure 5.

See Also the Following Articles

Purple Bacteria: Electron Acceptors and Donors • Respiratory Chain Complex II and Succinate: Quinone Oxidoreductases • The Cytochrome b_6f Complex • Vitamin K: Biochemistry, Metabolism, and Nutritional Aspects • Vitamin K: Blood Coagulation and Use in Therapy

Glossary

antioxidants Molecules capable of preventing the propagation of free radicals and hence protecting cellular and extracellular biomolecules from free-radical-induced damage, such as lipid peroxidation and genetic mutations in DNA. There are water-soluble antioxidants, such as ascorbic acid (vitamin C), and lipid-soluble antioxidants such as α-tocopherol (vitamin E). Ubiquinol belongs to this latter category.

chloroplasts Organelles present in photosynthetic higher plants and in eukaryotic algae that carry out the process of oxygen-evolving photosynthesis by extracting electrons from water, in a complex electron transfer chain containing plastoquinone among other components, and reducing CO_2, thus yielding carbohydrates by a complex synthetic process (Calvin cycle).

coenzyme A nonprotein compound required for the catalytic action of an enzyme that can be strongly bound to the enzyme itself as a prosthetic group or participate as a substrate to the enzyme-catalyzed reaction. Several coenzymes cannot be synthetized *de novo* and derive from nutritionally supplied vitamins.

free radical An atom or molecule having one or more unpaired electrons. For this reason free radicals are usually very reactive, in the attempt to donate or receive an electron, and may damage biological molecules by establishing a chain reaction of propagation followed by permanent chemical modification of the attacked molecules. Among free radicals are some of the so-called reactive oxygen species, derived by partial reduction of molecular oxygen during mitochondrial respiration and other biological processes.

mitochondria Organelles present in most eukaryotic cells carrying out the process of oxidative phosphorylation and several other metabolic pathways. Mitochondria consist of two membranes, the inner membrane being the site of the respiratory chain, delimiting two aqueous compartments (called the intermembrane space and the matrix).

vitamin A biological molecule, acting in small amounts (therefore not a structural component), that cannot be synthetized by the body and therefore requires dietary supplementation. Many vitamins are part of coenzymes. Vitamins are classified as water soluble and lipid soluble.

Further Reading

Ebadi, M., Marwath, J., and Chopra, R. (eds.) (2001). *Mitochondrial Ubquinone (Coenzyme Q_{10}): Biochemical, Functional, Medical, and Therapeutic Aspects in Human Health and Diseases*, **2 vols.** Prominent Press, Scottsdale, AZ.

Kagan, V. E., and Quinn, P. J. (eds.) (2001). *Coenzyme Q: Molecular Mechanisms in Health and Disease*. CRC Press, Boca Raton, FL.

Lenaz, G. (ed.) (1985). *Coenzyme Q: Biochemistry, Bioenergetics and Clinical Applications of Ubiquinone*. Wiley, London.

Many authors (1999). *BioFactors* 9. Special Issue dedicated to the First Conference of the International Coenzyme Q_{10} Association.

Many authors (2002). *Free Radical Research* 36(4). Special Issue dedicated to the Second Conference of the International Coenzyme Q_{10} Association.

Website of the International Coenzyme Q_{10} Association – http://www.csi.unian.it/coenzymeQ.

Biography

Giorgio Lenaz is a Professor of biochemistry at the Medical School of the University of Bologna, Italy. After his medical degree at the University of Bologna he was a postdoctoral fellow at the University of Wisconsin. His main research interest is mitochondrial bioenergetics in health and pathology, in particular mitochondrial encephalomyopathies and aging. He is an expert in Coenzyme Q and related compounds and has published many experimental papers and reviews in leading journals on the subject. He is a member of the executive committee of the International Coenzyme Q_{10} Association.

Maria Luisa Genova is a postdoctoral fellow in biochemistry at the University of Bologna. She holds a Ph.D. in biochemistry, and was trained at Rice University in Houston, Texas; she has published several papers on the subject of Coenzyme Q and mitochondrial bioenergetics.

Rab Family

Mary W. McCaffrey and Andrew J. Lindsay
University College, Cork, Republic of Ireland

Rab proteins are monomeric small GTPases that function as key regulators of eukaryotic membrane trafficking. Specifically, they have been implicated in the budding, transport, docking, and fusion of lipid bilayer vesicles. The Rabs form the largest and most diverse branch of the Ras protein superfamily. They are evolutionarily conserved and are present in all eukaryotes investigated, localizing to specific organelles of the secretory and endocytic pathway. The human genome project has demonstrated the existence of at least 60 members in the human Rab family, which can be divided into 10 subfamilies. Members of each subfamily have similar subcellular localization and some functional overlap. Most Rab proteins are ubiquitously expressed; however, a number such as Rab3A, which is expressed neurons, and Rab27, expressed in melanocytes and platelets, are cell-type specific. Rab proteins are characterized by their functional cycle. As their name suggests they bind GTP, which results in their activation. The GTP can then be hydrolyzed to GDP resulting in the Rab adopting an inactive (GDP-bound) conformation and leading to its subsequent membrane dissociation. Several Rab-interacting proteins have been identified, which regulate either the Rab nucleotide-bound state, its localization, or act as "effectors" of Rab function.

Discovery

The first Rab GTPases were discovered in the late 1980s, through the pioneering work of the Tavitian group, in Paris, which set out to identify homologues of the Ras oncogenes. They screened a brain cDNA library with degenerate oligonucleotides designed against the most conserved regions of G proteins (the G boxes). Besides known G proteins, new ras-related genes were identified in this screen. These were sufficiently different from Ras and Rho to be placed in a new family of the Ras superfamily and were named the Rabs–*Ra*s homologue from *b*rain.

Sequencing revealed that these new Rab genes bore greatest similarity to two previously described yeast secretory mutant genes, *sec4* and *ypt1*. The fact that these two yeast orthologues had previously been implicated in membrane trafficking provided the first clues that the members of the Rab GTPase family function in membrane trafficking in higher eukaryotes. In the years that followed, several research groups (notably the Zerial group) extended the family to 11 then to between 30 and 40 distinct members. With the aid of information from the human genome project, 60 distinct human Rab GTPases have now been identified.

Primary Structure and Evolution

The Rab family members are the most divergent and extensive branch of the ras superfamily. They contain ~200 amino acids with a molecular mass between 20 and 25 kDa, and are hydrophilic in nature (see Figure 2 for a schematic representation of Rab functional domains). Like all G proteins, they contain well-conserved guanine nucleotide binding domains (G-boxes) but otherwise are quite divergent – particularly in their carboxy-terminal region. This region is known to be critical for specifying membrane localization.

Their extreme carboxy termini also possess a characteristic conserved CC or CXC motif (C = cysteine, X = any amino acid). This motif is post-translationaly modified, in a process known as isoprenylation, by the addition of geranyl groups. The addition of a hydrophobic moiety on the cysteine results in a protein that is chemically competent for insertion into the lipid bilayer (further details on post-translational modifications are discussed later in this article).

By analogy with the Ras proteins, a further domain has been identified in the Rabs – the "effector" domain. This domain of ~10 amino acids was found to be critical for transmission of the Ras signal to its downstream machinery. Mutation of this effector domain abolishes growth signaling, independent of Ras GTP binding. Thus, this region was named the effector domain of ras. The equivalent region in the Rabs, also termed the effector domain, is frequently mutated in studies that investigate Rab function.

By analogy with the oncogenic Ras mutants, a number of Rab mutations have been generated. The most frequently utilized activating mutant for the

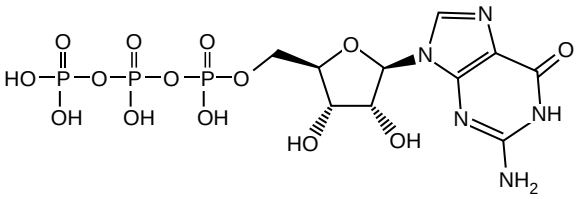

FIGURE 1 The structure of GTP.

Rabs is at amino acid position ~70 and is generated by the conversion of a glutamine (Q) to a leucine (L) at this position. Such Rab mutants are deficient in GTPase activity and thus remain in the 'activated' GTP-associated state (see Figure 1 for GTP structure). A serine (S) to asparagine (N) mutation, near amino acid 20, generates a dominant negative Rab mutant, that is constitutively GDP-bound and therefore inactive. Expression of these mutants in mammalian cells has revealed important Rab functional data.

In a study of the evolution and complexity of the core protein machinery involved in intracellular trafficking (coat complexes, Rab GTPases, SNAREs, and Sec1s) by the Scheller group, 60 distinct Rab genes were identified in humans. It was noted that there was a significant expansion of the Rab family from yeast to worms, and a further expansion from worms to mammals. A phylogenetic tree of the human Rab family is reproduced from Bock *et al.* (see Figure 3). Of the four core membrane-trafficking families compared, the Rabs were the only family that underwent such a significant expansion. It is likely that the higher degree of complexity in multicellular organisms is reflected by the greater requirement for Rabs, not only for more intricate regulation of intracellular trafficking but also for tissue specialization of membrane-trafficking functions.

The Rab family can be divided into ~10 subfamilies. Representative members of these subfamilies are Rab1, Rab3, Rab4, Rab5, Rab6, Rab8, Rab11, Rab22, Rab27, and Rab40.

Post-translational Modifications

Rab proteins are hydrophilic, thus, in order for membrane binding they must possess one, or two, C20 geranyl–geranyl lipid groups at their carboxy terminus. The process by which they gain these lipid moieties is known as isoprenylation. Newly synthesized, unprenylated, Rab GTPases are bound by Rab escort protein (REP) and delivered to Geranylgeranyl Transferase (GGTase). GGTase catalyzes the attachment of the lipid groups to two carboxy-terminal cysteine residues present on all Rab GTPases. REP appears to be a specialized Rab GDI that can deliver newly synthesized, GDP-bound, Rab proteins to GGTase for isoprenylation, and then transport the modified protein to its target membrane. It is thought that Rab-GDP binds its host membrane via a protein receptor, which 'senses' the Rab carboxy-terminal domain, however, very little evidence currently exists in the literature regarding the identity of such Rab receptors. Thus, while the amino acid sequence in the C-terminal region confers membrane specificity to a given Rab, the isoprenoid group confers chemical compatibility with the membrane, anchoring the otherwise hydrophilic protein in the hydrophobic lipid bilayer.

Cellular Localization

Rab proteins have now become standard markers for organelles of the secretory and endocytic pathways. Not all 60 human Rab GTPases have yet been sufficiently characterized such that the entire Rab localization pattern is known. However, for those that have been characterized, it is clear that they localize to distinct membrane organelles. For example, Rab1 localizes to the ER/*cis*-Golgi and Rab3 localizes to synaptic vesicles/chromaffin granules of the neuroendocrine system, while Rab5, Rab4, and Rab11 localize to distinct early endosomal membranes, Rab6 is located

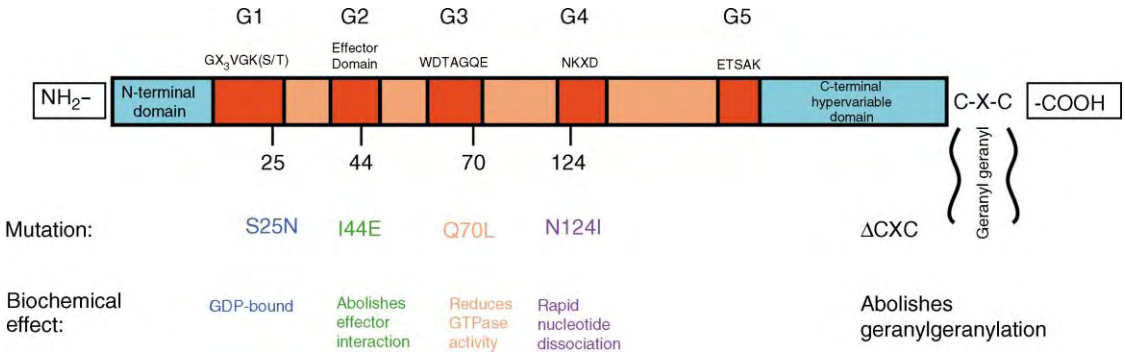

FIGURE 2 Schematic diagram of the general domain structure of Rab GTPases. Indicated are the commonly used Rab11 mutations and their biochemical consequences.

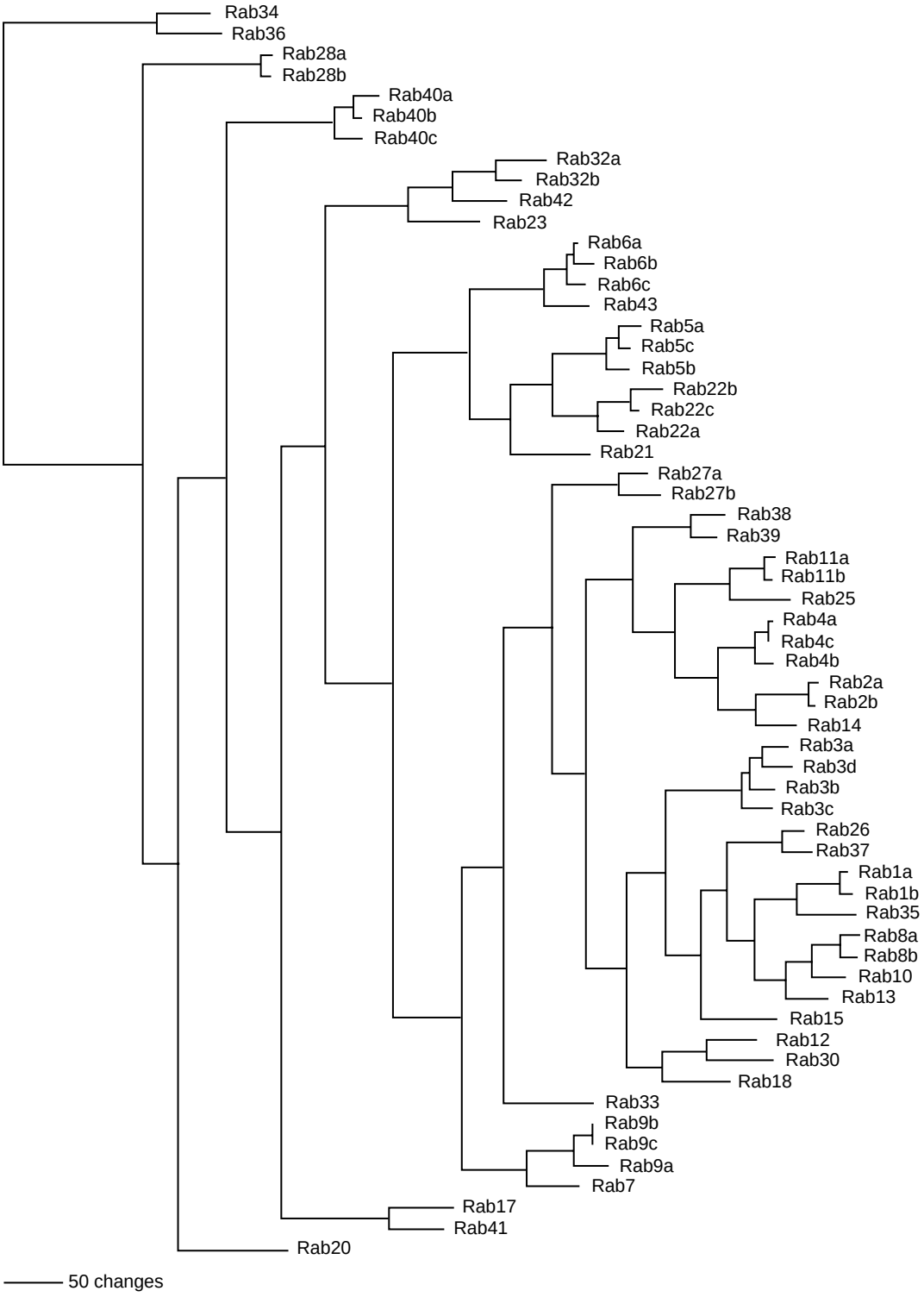

FIGURE 3 Phylogenetic tree of the human Rab GTPases. (Reprinted from Bock, J. B., Matern, H. T., Peden, A. A., and Scheller, R. H. (2001). A genomic perspective on membrane compartment organization. *Nature* **409**, 839– 841, by permission of Nature.)

on the Golgi apparatus, Rab7 is on late endosomes, Rab22 localizes to endosomes and the Golgi and Rab27 to melanosomes and lytic granules. Figure 4 and Table I indicate the known localization and trafficking steps controlled by Rabs characterized to date.

Functional Cycle

The functional cycle of Rab5 has been extensively characterized and is used here as a paradigm of all Rabs (see Figure 5 for generalized Rab GTPase cycle).

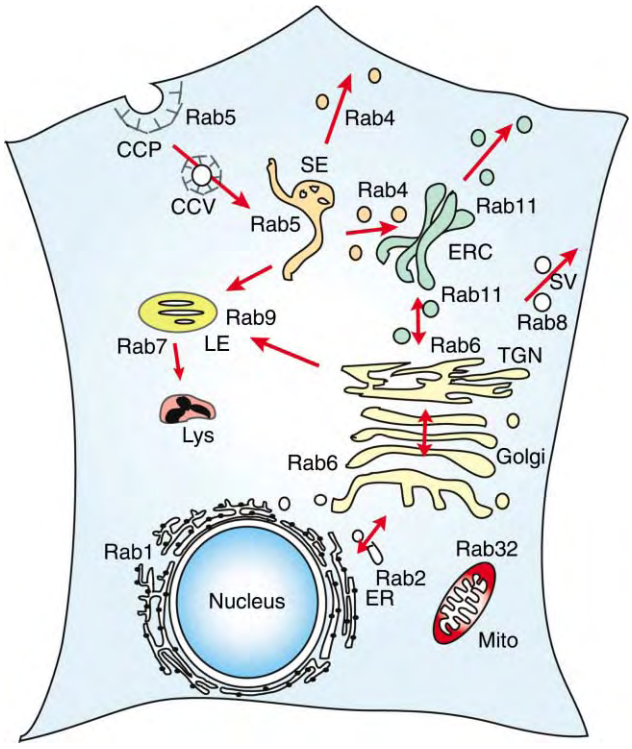

FIGURE 4 Localization of selected Rab GTPases and the membrane-trafficking pathways they regulate. The endocytic pathway involves internalization of cargo in clathrin-coated vesicles (CCV) and delivery to the early/sorting endosome (SE). Cargo is then either sorted for transport along the degradative pathway to the late endosomes (LE) and lysosomes (Lys), or directly recycled back to the plasma membrane from the SE, or indirectly, via the endocytic recycling compartment (ERC). The biosynthetic pathway transports proteins from the endoplasmic reticulum (ER) through the Golgi complex from where they are delivered to the cell surface in secretory vesicles (SV). The endocytic and secretory pathways communicate through the *trans*-Golgi network (TGN).

GDP-bound Rab5 is delivered to its target membrane by Rab guanine nucleotide dissociation inhibitor (Rab GDI). Rab guanine nucleotide exchange factor (Rab GEF) then catalyzes the exchange of the GDP for GTP, allowing Rab5 to adopt its active conformation. The GTP-bound Rab is now resistant to extraction by Rab GDI. Once membrane associated and in its active conformation the Rab protein is now competent to exert a controlling function on membrane trafficking. Rab5 mediates its function by recruiting a repertoire of specific effector proteins necessary for fusion of early endosomes. Upon completion of Rab function the GTP is hydrolyzed by the Rab GTPase enzymatic activity, releasing inorganic phosphate and resulting in an inactive Rab bound to GDP. This GTPase activity is stimulated by Rab GTPase *a*ctivating *p*rotein (Rab GAP).

Rabs have been variously implicated in vesicle budding from the donor membrane, transport along the cytoskeleton, docking to, and fusion with, the acceptor membrane. Though there is evidence for various Rabs of their involvement in these distinct events in membrane trafficking, it is not clear whether some Rabs function in vesicle budding exclusively, while others function in vesicle transport or docking, or whether a given Rab, in association with one specific set of effector proteins, functions in budding and in combination with other sets of effector proteins functions in transport, docking, or fusion.

Effectors

Several putative Rab effectors have been identified – primarily by two-hybrid library screening with GTPase deficient (dominant-positive) Rab mutants. While a survey of all of the Rab effectors reported in the literature is beyond the scope of this review, it is clear that there are likely to be many more Rab effectors than Rab GTPases. The GTP-bound form of Rab5 has been shown to interact specifically with at least 20 different proteins. Several Rab effectors have coiled-coil and/or phospholipid-binding domains (such as FYVE or C2 domains), while some are enzymes, or cytoskeletal (actin or tubulin) motor proteins. Identification of Rab effectors, and regulatory proteins, is a very important approach towards understanding the function of Rab GTPases and is likely to be an area of continued research for several years to come.

Rabs and Diseases

Sequencing of the human genome has revealed that a substantial number of disease-causing genes are involved in membrane trafficking. A proportion of these genetic diseases are the result of mutations in Rab GTPases, or their interacting proteins. Griscelli syndrome is an autosomal recessive disorder that results in pigmentation defects. There are two variants of this disease, one that results in immunological defects, and the other is associated with neurological dysfunction. The former is caused by missense mutations in the Rab27a gene, and the latter is the result of mutations in its putative effector, myosin Va. Both are located side-by-side on chromosome 15. Rab27a functions to regulate the transport of melanosomes to the periphery of melanocytes, also regulating the secretion of lytic granules in cytotoxic T lymphocytes. Hence, the lack of functional Rab27a results in the loss of pigmentation and in the uncontrolled activation of T lymphocytes. Mutation of myosin Va causes pigmentation defects, but since it is not involved in lytic granule movement, it does not cause immunological defects. Choroideremia is an X-linked disease that results in the degeneration of the pigment epithelium of the eye. It is caused by a defect in the REP-1 gene. REP-1 is one of the two

TABLE I

Localization, Tissue Distribution, and Function of the Human Rab GTPases

Rab GTPase	Localization	Tissue expression	Function
Rab34	Golgi	Ubiquitous	Lysosome positioning
Rab36	Golgi	Unknown	Unknown
Rab28	Unknown	Unknown	Unknown
Rab40	Unknown	Unknown	Unknown
Rab32	Mitochondria	Ubiquitous	A-kinase anchoring protein
Rab42	Unknown	Unknown	Unknown
Rab23	Unknown	Brain	Negative regulator of Sonic hedgehog pathway in mouse
Rab6	Golgi	Ubiquitous	Retrograde Golgi transport
Rab43	Unknown	Unknown	Unknown
Rab5	Plasma membrane, CCVs, and early endosomes (EE)	Ubiquitous	Transport from the plasma membrane to EE
Rab22	EE, LE, Golgi	Ubiquitous	Communication between biosynthetic and endocytic pathways
Rab21	Apical vesicles	Ubiquitous	Unknown
Rab27	Melanosomes and granules	Melanocytes, platelets, and lymphocytes	Transport of melanosomes and lytic granules
Rab38	Melanosomes	Melanocytes	Melanosome sorting
Rab39	Golgi-associated organelles	Ubiquitous	Endocytosis
Rab11/Rab25	Recycling compartment (RC) and TGN	Ubiquitous	Endocytic recycling and transport to TGN
Rab4	EE	Ubiquitous	Endocytic recycling and degradation
Rab2	Golgi	Ubiquitous	Golgi to ER transport
Rab14	ER/Golgi/Endosomes	Ubiquitous	Transport between Golgi endosomes
Rab3	Synaptic vesicles (SV)	Neurons	Regulation of neuro-transmitter release
Rab26	Secretory granules	Parotid gland	Regulated secretory pathway
Rab37	Secretory granules	Mast cells	Mast cell degranulation
Rab1	ER/*cis*-Golgi	Ubiquitous	ER to Golgi transport
Rab35	Unknown	Unknown	Unknown
Rab8	Transport vesicles	Ubiquitous	Regulates polarized membrane transport
Rab10	Golgi	Ubiquitous	Unknown
Rab13	Junctional complexes	Epithelial cells	Regulation of structure and function of tight junctions
Rab15	EE and RC	Ubiquitous	Inhibitor of endocytic recycling
Rab12	Granules/Golgi	Ubiquitous	Unknown
Rab30	Golgi	Unknown	Unknown
Rab18	Apical dense tubules	Epithelial cells	Unknown
Rab33	Unknown	Unknown	Unknown
Rab9	LE	Ubiquitous	LE to TGN transport
Rab7	Late endosomes (LE)	Ubiquitous	Transport from LE to lysosomes
Rab17	Epithelial cells	Apical RC	Transport through apical RC
Rab41	Unknown	Unknown	Unknown
Rab20	Apical dense tubules in kidney tubule epithelial cells	Epithelial cells	Unknown

isoforms of GGTase that prenylate Rab GTPases. It is essential for the prenylation of Rab27a in the retinal pigment epithelium. REP-2 appears to be sufficient for the efficient geranyl-geranylation of all other Rab GTPases. Thus, the lack of functional REP-1 results in nonfunctional Rab27a and the onset of the disease. The pathology of this disease may be caused by the degeneration of the retinal epithelium due to deficient melanosome transport, and hence lack of protection during light exposure.

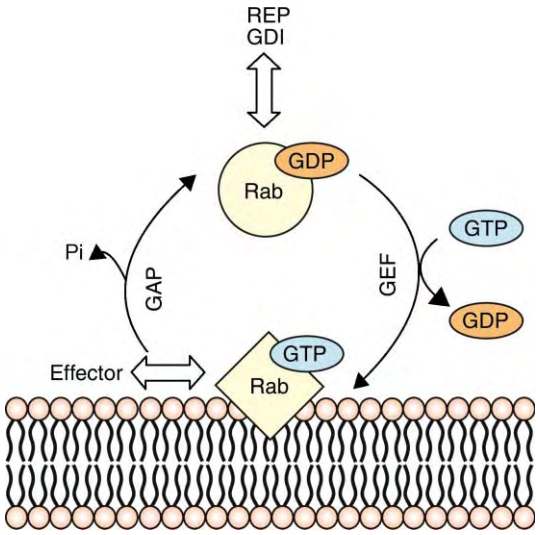

FIGURE 5 The Rab GTPase cycle. Rab GTPases cycle between GTP- and GDP- bound forms, allowing the Rab to adopt active and inactive conformations. The cycle is mediated by various accessory factors. A guanine-nucleotide exchange factor (GEF) exchanges the GDP for GTP. Conversion from the GTP- to the GDP-bound form is mediated by a GTPase-activating protein (GAP) which stimulates the Rab to hydrolyze bound GTP. The active GTP-bound form mediates its function through specific effector molecules. Newly synthesized cytosolic, GDP-bound Rab, interacts with Rab escort protein (REP) for membrane delivery. Subsequently, after each functional round, the GDP-bound Rab is extracted by the GDP dissociation inhibitor (GDI) from its host membrane and delivered to a new membrane location for another functional round.

Tuberin is a tumor suppressor protein that interacts with Rabaptin-5 and negatively regulates endocytosis by acting as a Rab5-GAP. Its inactivation causes tuberous sclerosis, a disease that results in malformations and tumors of the central nervous system. Finally, mutations in the GDI1 gene, which encodes GDI-α have been found in a subgroup of patients with X-linked nonspecific mental retardation. GDI-α is particularly abundant in brain tissue, thus defective membrane recycling of one or more Rab GTPases in brain synapses is likely to be the cause of this condition.

See Also the Following Articles

Ras Family • Rho GTPases and Actin Cytoskeleton Dynamics • Small GTPases

Glossary

effectors Proteins that are necessary to effect small GTPase function. Many (putative) effectors of the Ras superfamily have been described in the past decade.

GTPases Proteins capable of hydrolyzing GTP by cleavage of its terminal phosphate. This reaction results in the protein being switched to the inactive state, i.e., associated with GDP.

Ras Monomeric GTPases, first identified as oncogenes/oncoproteins, which function as central players in mitogenic signalling pathways.

Rho The first ras homologue to be identified, Rho proteins control actin cytoskeleton organization and structure.

Further Reading

Aridor, M., and Hannan, L. A. (2002). Traffic jams II: An update of diseases of intracellular transport. *Traffic* **3**, 781–790.

Bock, J. B., Matern, H. T., Peden, A. A., and Scheller, R. H. (2001). A genomic perspective on membrane compartment organization. *Nature (London)* **409**, 839–841.

Stenmark, H., and Gillooly, D. J. (2001). Intracellular trafficking and turnover of phosphatidylinositol 3-phosphate. *Semin. Cell Dev. Biol.* **12**, 193–199.

Woodman, P. (1998). Vesicle transport: More work for the Rabs? *Curr. Biol.* **8**, R199–R201.

Zerial, M., and McBride, H. (2001). Rab proteins as membrane organisers. *Nat. Rev. Mol. Cell Biol.* **2**, 107–119.

Biography

Mary W. McCaffrey is a Lecturer in Biochemistry and Science Foundation Ireland (SFI) Investigator in the National University of Ireland, Cork. Her principal research focus involves the functional characterization of Rab proteins in mammalian endosomal trafficking. She holds a Ph.D. from the University of London, England and received postdoctoral training in the Pasteur Institute, Paris, France. Her group is a world leader in the identification and characterization of the Rab11 effector machinery.

Ran GTPase

Mary Shannon Moore
Baylor College of Medicine, Houston, Texas, USA

Ran (Ras related nuclear protein) is a 25 kDa member of the Ras superfamily of small GTPases. To date, a Ran homologue has been found in every nucleated cell of every eukaryotic organism on Earth, and Ran is essential for the viability of all those cells. During interphase, Ran plays an essential role in driving and regulating the active transport of cargo between the nucleus and cytoplasm. Ran also has critical functions during mitosis when Ran is essential for mitotic spindle assembly and placement as well as re-assembly of the nuclear envelope.

Small GTP-Binding Proteins as "Molecular Switches"

Ran is called a GTPase because it binds and hydrolyzes GTP. All small GTPases of the Ras superfamily cycle between GTP- and GDP-bound states, and undergo a marked conformational change upon conversion from one state to the other. Thus, GTPases in the GTP-bound form can bind proteins that the GDP-bound form cannot, and vice versa. This key property confers on small GTPases the ability to function as "molecular switches" that cycle between active and inactive states, the GTP-bound form generally being the active form.

Ran represents its own family of small GTP-binding proteins in the Ras superfamily, of which it is the only member. The other families include the Ras, Rab, Arf, Rac, and Rho families that regulate signal transduction, vesicular transport, cytoskeletal organization, and cell proliferation. Ran's role is to act as a "switch" to regulate nuclear transport during interphase and spindle, and nuclear envelope assembly during mitosis.

Nucleocytoplasmic Transport

A basic necessity of the eukaryotic cell is the ability to transport macromolecules bidirectionally between the nucleus and cytoplasm. The traffic between these two compartments is both heavy and complex with multiple classes of cargo being actively transported in both directions (Figure 1). Nuclear proteins such as transcription factors and histones are, like all proteins, made in the cytoplasm and must cross the nuclear envelope into the nuclear interior to carry out their function. Conversely, ribosomal subunits, tRNAs, and mRNAs produced inside the nucleus must cross the nuclear envelope in the opposite direction into the cytoplasm in order to be used for protein translation.

Nucleocytoplasmic traffic is restricted to nuclear pore complexes (NPCs), which are large proteinaceous structures that bridge the double membrane of the nuclear envelope to form aqueous channels linking the cytoplasm and nucleoplasm. The vertebrate NPC is composed of ~30 different proteins and a HeLa cell contains ~3000 NPCs. At present, all NPCs appear to be functionally identical with the same NPC capable of carrying out both import and export virtually simultaneously. While molecules up to ~50 kDa can diffuse through the NPC, the majority of nuclear proteins (both larger and smaller than 50 kDa) as well as the other classes of transport cargo appear to undergo signal-mediated active transport rather than diffusion.

There are two types of nuclear transport signals, NLSs (nuclear localization sequences) that mediate nuclear import and NESs (nuclear export sequences) that mediate nuclear export. There are multiple types of NLSs and NESs found on different types of cargo, and, in general, each type of signal is recognized by a different nuclear receptor/carrier. Most nuclear carriers are members of the karyopherin-β superfamily and there are over twenty members of this family in human cells. During nuclear import, a soluble carrier binds the NLS-containing cargo in the cytoplasm, then moves the cargo through the NPC and releases it in the nuclear interior. Nuclear export works essentially the same way in reverse, with an NES-containing cargo being recognized by its specific carrier inside the nucleus, movement of the export complex through the NPC, and disassembly of the complex and release of the cargo upon reaching the cytoplasm.

The Ran GTPase

The Cellular Gradient of RanGTP

A key player in the majority of the known nuclear transport pathways is the small GTPase Ran and, not

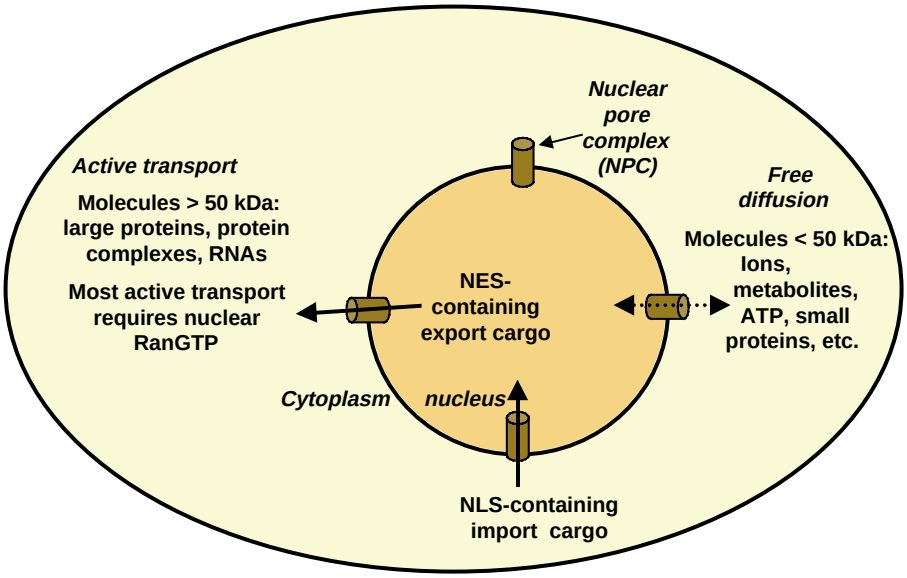

Some NLS-containing import cargo:	Some NES-containing export cargo:
Nuclear proteins	Shuttling proteins
Shuttling proteins	Newly formed ribosomal subunits
	tRNAs
	mRNAs

FIGURE 1 Overview of nucleocytoplasmic transport. Most nuclear transport requires nuclear RanGTP, however mRNA export does not. Carriers of the NTF2 family mediate mRNA export, and this transport pathway is Ran-independent. Active transport of the rest of the cargo listed does require nuclear RanGTP.

incidentally, the main region of homology between all the karyopherin-β nuclear carriers is a RanGTP-binding domain. Inside the cell, Ran is primarily nuclear in spite of the fact it does not appear to contain an NLS in its sequence. This is because Ran is actively imported into the nucleus by a small protein called p10/NTF2, which is a member of a second class of nuclear carriers, the NTF2 family.

Importantly, whether Ran is in the cytoplasm or nucleus determines whether it is RanGTP or RanGDP (Figure 2). Inside the nucleus, Ran is converted to the GTP-bound form by the RanGEF (guanine nucleotide exchange factor), which stimulates RanGDP to release GDP and bind GTP. In contrast, the RanGAP (GTPase-stimulating protein) is located in the cytoplasm. The RanGAP rapidly converts any RanGTP entering the cytoplasm to RanGDP by stimulating Ran to hydrolyze its bound GTP.

The resulting concentration gradient of low RanGTP in the cytoplasm to high RanGTP in the nucleus is vitally important for controlling the directionality of nuclear transport by regulating the assembly and disassembly of karyopherin-β containing transport complexes. Also, because the RanGEF is bound to chromatin, the concentration of RanGTP is highest near the chromatin where it is produced (Figure 2C). This location becomes important during mitosis, when chromatin-localized RanGTP stimulates mitotic spindle and nuclear envelope assembly in the correct location around chromatin.

Cellular Functions of Ran

Nuclear Transport

The increasing RanGTP concentration from the cytoplasm to the nuclear interior is the primary factor that triggers the disassembly of transport complexes at their correct final destination. Members of the karyopherin-β family preferentially bind RanGTP with a much lower affinity for RanGDP, and upon binding RanGTP, the karyopherin-β carrier undergoes a conformational change that alters its cargo-binding domain. NLS receptors of the karyopherin-β family can only bind their cargo when they do not have bound RanGTP, which is their probable state in the cytoplasm. After movement across the NPC into the nuclear interior where the import complex encounters RanGTP,

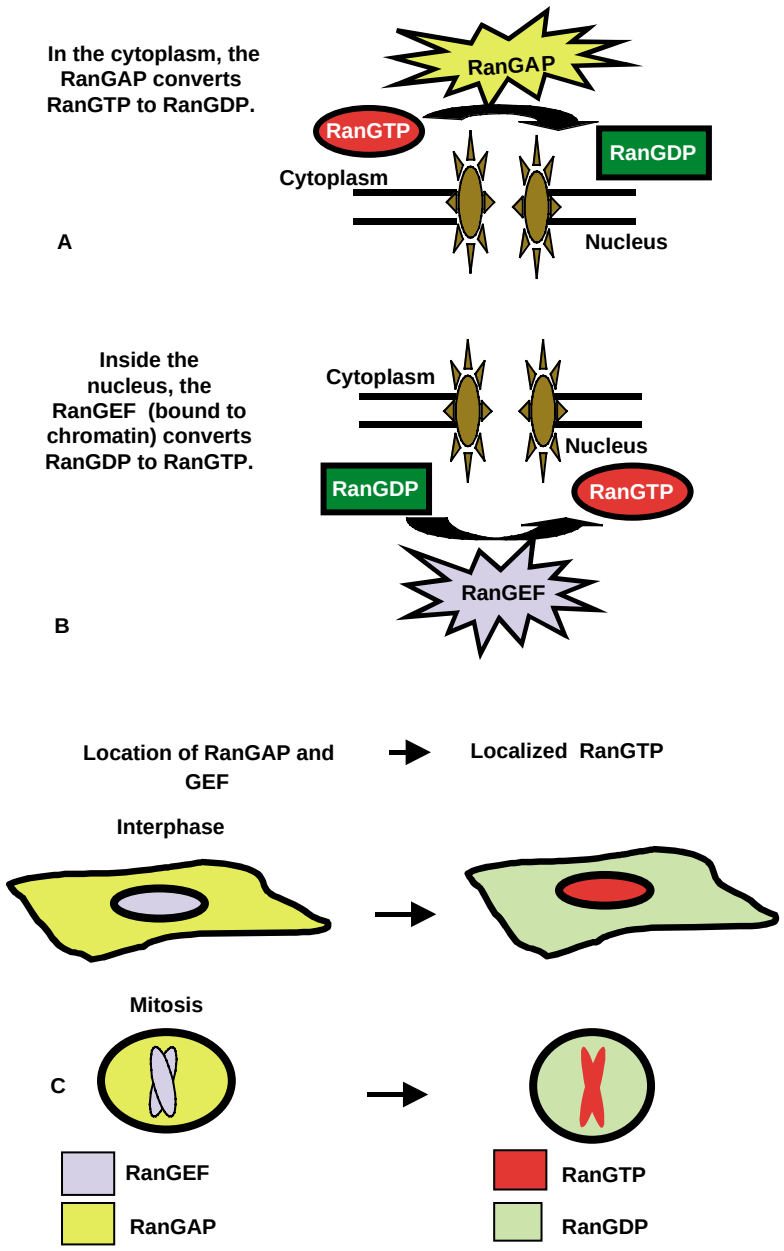

FIGURE 2 Establishment of the RanGTP gradient between the cytoplasm and nucleoplasm. (A) The RanGAP, which stimulates Ran to hydrolyze its bound GTP, is restricted to the cytoplasm. (B) The RanGEF, which stimulates Ran to release bound GDP and take up GTP, is found inside the nucleus bound to chromatin. (C) Restricting the RanGAP and the RanGEF to different compartments results in high levels of RanGTP inside the nucleus and low levels of RanGTP in the cytoplasm during interphase (top). The resulting gradient of RanGTP concentration between the cytoplasm and nucleoplasm is the key regulatory mechanism controlling the assembly and disassembly of nuclear import and export complexes in the correct cellular location (see Figure 3). Also, the RanGEF remains bound to chromatin throughout the cell cycle, and production of RanGTP at the chromatin surface in mitotic cells is required for proper placement of the mitotic spindle and re-assembly of the nuclear envelope around chromatin at the end of mitosis (bottom).

the carrier binds RanGTP, and as a result, releases its cargo into the nuclear interior (Figure 3A).

Export carriers of the karyopherin-β family behave just the opposite. These export carriers, in order to simultaneously bind their export cargo, must first bind RanGTP. After movement through the NPC, the cargo:export carrier:RanGTP complex encounters the RanGAP in the cytoplasm. Ran is stimulated to hydrolyze its bound GTP, and after hydrolysis, becomes RanGDP. The export carriers have a low affinity for RanGDP and, as a result, both RanGDP and an export cargo dissociate from the export carrier in the cytoplasm.

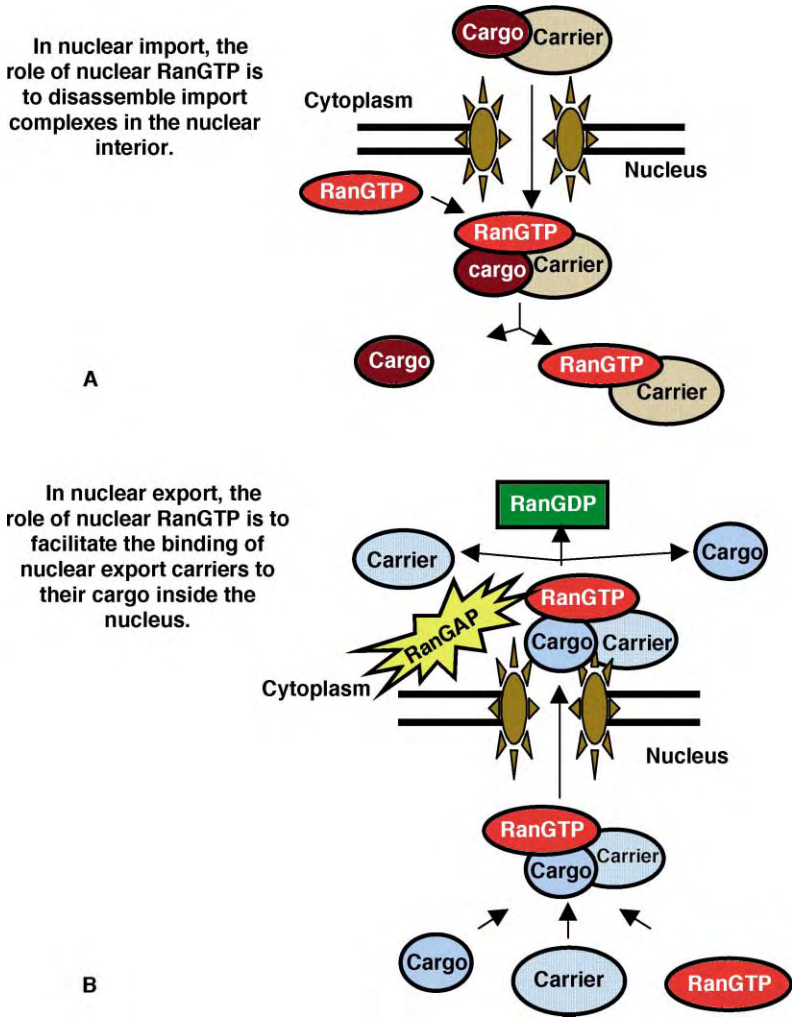

FIGURE 3 The RanGTP gradient across the NPC controls the assembly and disassembly of nuclear transport complexes. (A) Nuclear import carriers cannot bind import cargo and RanGTP simultaneously. After import of the import carrier:cargo complex through the nuclear pore complex (NPC), the carrier binds nuclear RanGTP. As a result of binding RanGTP, the import carrier releases the import cargo in the nuclear interior. (B) In contrast to nuclear import carriers, nuclear export carriers require bound RanGTP in order to bind their export cargo with high affinity. After export through the NPC, the export complex (RanGTP:export carrier:cargo) encounters the RanGAP in the cytoplasm that stimulates Ran to hydrolyze its bound GTP. Conversion of RanGTP to RanGDP results in the release of RanGDP and export cargo from the export carrier into the cytoplasm.

Regulation of Spindle and Nuclear Envelope Assembly at Mitosis

The nuclear envelope vesiculates and breaks apart during mitosis in vertebrate cells, and then reforms after the daughter cells are divided. Accordingly, no nuclear transport occurs during this time because there is no nuclear envelope and the cytoplasmic and nuclear contents are mixed. Ran however has additional functions critical to this period. Nuclear proteins containing an NLS are once again exposed to the NLS receptors and can be re-bound by them. However, as during nuclear import, RanGTP can break this complex apart, releasing the proteins.

Many of the proteins responsible for assembly of the mitotic spindle at mitosis are nuclear during interphase and contain an NLS. To be active for spindle assembly, RanGTP must first release these spindle assembly factors from NLS receptors. Because the concentration of RanGTP is highest, close to the chromatin due to the RanGEF located there; active spindle assembly factors (as opposed to inactive factors complexed with NLS receptors) are also most concentrated there. RanGTP is thus essential for spindle formation; both to release spindle assembly factors from NLS-binding carriers and for correct orientation of the spindle around chromatin.

As stated above, when a human cell enters mitosis at the beginning of cell division, the nuclear envelope fragments into vesicles. At the end of mitosis, after the two daughter cells have separated, these membrane vesicles bind to the decondensing chromatin and then

fuse together laterally to re-form an intact nuclear envelope. RanGTP is essential for this fusion step, as is one particular nuclear carrier of the karyopherin-β family (importin-β), however the exact mechanism is not yet known.

Other Roles of Ran

In addition to the cellular roles for Ran discussed above, Ran has also very recently been implicated in prevention of re-replication of chromatin during S phase and in regulation of kinetochore function throughout the cell cycle. It should be noted that in all of the multiple pathways in which Ran has been implicated, the general nature of the biochemical reaction carried out by Ran remain constant. Switching between RanGDP and RanGTP controls Ran's association with different proteins, and Ran's association with assorted proteins has different downstream effects depending on the protein involved, the cellular location where the interaction occurs, and the stage of the cell cycle when the interaction occurs. In summary, the Ran GTPase plays a powerful and irreplaceable role in the eukaryotic cell, both for constitutive viability and for cell division.

See Also the Following Articles

ARF Family • Mitosis • Nuclear Pores and Nuclear Import/Export • Ras Family

Glossary

GDP Guanosine 5′-diphosphate, a nucleotide analogous to ADP that is composed of guanine linked to ribose and two phosphates.

GTP Guanosine 5′-triphosphate, an energy-rich nucleotide analogous to ATP that is composed of guanine linked to ribose and three phosphates.

GTPase A protein that can bind and hydrolyze GTP.

interphase A period or stage between two successive mitotic divisions of a cell nucleus.

mitosis The sequential differentiation and segregation of replicated chromosomes in a cell nucleus that precedes complete cell division.

nuclear pore complex (NPC) Large organelles of the nuclear envelope through which passage of proteins and RNAs between the cytoplasm and nuclear interior occurs.

Further Reading

Arnaoutov, A., and Dasso, M. (2003). The Ran GTPase regulates kinetochore function. *Dev. Cell* **5**, 99–111.

Dasso, M. (2002). The Ran GTPase: theme and variations. *Curr. Biol.* **12**, R502–R508.

Kunzler, M., and Hurt, E. (2001). Targeting of Ran: Variation on a common theme? *J. Cell Sci.* **114**, 3233–3241.

Steggerda, S. M., and Paschal, B. M. (2002). Regulation of nuclear import and export by the GTPase Ran. *Int. Rev. Cytol.* **217**, 41–91.

Talcott, B., and Moore, M. S. (1999). Getting across the nuclear pore complex. *Trends Cell Biol.* **9**, 312–318.

Weis, K. (2003). Regulating access to the genome: nucleocytoplasmic transport throughout the cell cycle. *Cell* **112**, 441–451.

Yamaguchi, R., and Newport, J. (2003). A role for Ran-GTP and Crm1 in blocking re-replication. *Cell* **113**, 115–125.

Biography

Mary Shannon Moore is an Assistant Professor in the Department of Molecular and Cellular Biology at Baylor College of Medicine, Houston. Her principal research interests are nuclear structure and function and nucleocytoplasmic transport. She received her Ph.D. from UT Southwestern Medical Center at Dallas, and did her postdoctoral work in Dr. Günter Blobel's laboratory at Rockefeller University in New York. In 1993, Drs. Moore and Blobel published the first paper showing a role for Ran in nucleocytoplasmic transport.

Ras Family

Lawrence A. Quilliam
Indiana University School of Medicine, Bloomington, Indiana, USA

Since the discovery of Ras activity in a cancer-causing retrovirus in 1964, it has become the prototype of a superfamily of over 100 GTP-binding proteins that regulate a myriad of biological functions in eukaryotic cells. This superfamily can be subdivided based on primary sequence or biological function into five major subfamilies; Ras, Rho, Rab, Ran, and ARF. This article will focus on the Ras subfamily of proteins that are primarily responsible for regulating cell proliferation and differentiation. These proteins function as molecular switches that alternate between active GTP and inactive GDP-bound conformations. Acquisition of the active GTP bound state and its hydrolysis to GDP are tightly regulated by guanine-nucleotide-exchange factors (GEFs) and GTPase activating proteins (GAPs) that in turn receive direction from the signal transduction pathways that are elicited by hormone and growth factor binding to cell surface receptors. Upon activation, Ras proteins bind specific downstream effector proteins, promoting their subcellular relocalization or conformational changes that result in their activation and transmission of a signal to induce events that include gene expression and cytoskeletal rearrangement. Mutations that prevent GTP hydrolysis result in constitutive signaling to downstream effectors and promote uncontrolled cell growth. These mutations are found in several common human cancers and can be used by researchers to understand their mechanism of action.

Physical Properties

Ras family proteins are often referred to as small or low-molecular weight GTPases. This is due to their 20–25 kDa size being smaller than the 38–52 kDa α-subunits of the heterotrimeric G proteins, another class of cell signaling molecules that bind and hydrolyze GTP. Ras proteins consist of a core GTP-binding/GTPase domain that encompasses ~160 amino acids, followed by a hypervariable domain that is thought to act as a flexible linker, and a C-terminal CAAX (cysteine-aliphatic-aliphatic-other amino acid) motif that is the signal for posttranslational lipid modification, see Figure 1. Addition of a 15 carbon farnesyl or 20 carbon geranylgeranyl isoprene group to the Cys, cleavage of the three C-terminal (AAX) residues, and methylation of the C-terminal COO- group help promote the membrane targeting of most Ras subfamily GTPases. Additional palmitylation of nearby cysteine(s) or presence of many basic (arginine, lysine) residues in the hypervariable region help maintain tight membrane association. Membrane association is essential for Ras protein function and mutation of the CAAX cysteine, preventing the series of posttranslational modifications, disables Ras function. Most of the Ras superfamily proteins are modified by a geranylgeranyl transferase that adds the 20 carbon lipid. However, H-, K-, and N-Ras are modified by a farnesyl transferase that recognizes a different CAAX sequence that adds a 15 carbon farnesyl lipid instead. Because of this specificity, drugs that mimic the C terminus of Ras and/or the farnesyl lipid can block posttranslational modification and clinical trials are being performed to evaluate their use in cancer chemotherapy.

The GDP/GTP Cycle and Ras Mutations

Ras binds GTP and GDP, but not GMP, with very high affinity. The intrinsic rates of nucleotide exchange and GTP hydrolysis by Ras *in vitro* are very slow (on the order of minutes to hours) and not practical for a signaling molecule that needs to rapidly respond to stimuli. However, this is by design. Each Ras protein is tightly regulated by one or more guanine-nucleotide-exchange factors (GEFs) that help turn it on and GTPase activating proteins (GAPs) that subsequently help to inactivate it, see Figure 2.

Ras GEFs contain a CDC25 homology domain that shares similarity with the yeast RAS1/2 GEF, CDC25. There are over 30 CDC25 homologues in the human genome. Some are highly specific for one Ras protein while others catalyze nucleotide exchange and multiple family members. GEFs promote the release of GDP, then stabilize the nucleotide-free protein until GTP can bind and displace them. This occurs very rapidly *in vivo* due to the high affinity of Ras for GTP. Also because GTP is in a 10–20-fold excess over GDP, the GEF is predominantly

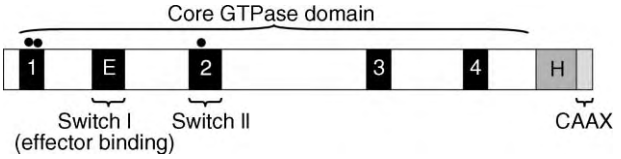

FIGURE 1 Linear diagram of Ras protein highlighting key sequences. Black areas are highly conserved across the entire Ras superfamily and form the guanine-nucleotide-binding pocket. Closed circles indicate sites of activating mutations found in human cancers. Switch I and II domains change conformation upon GDP versus GTP binding. E = effector binding loop that associated with downstream effectors. H = hypervariable domain, a 10–20 amino acid linker that also contributes to membrane binding. CAAX represents the terminal four residues that signal for posttranslational lipid modification of the cysteine residue. The identity of residue X dictates whether the G protein receives a 15 or 20 carbon lipid tail.

displaced by GTP. Because of the ability of nucleotide-free Ras to bind tightly to GEFs, dominant inhibitory mutants have been designed that have low affinity for nucleotide. These bind tightly to GEFs and prevent them from activating the endogenous wild type Ras, so blocking signaling pathways. These are useful tools for implicating Ras proteins or Ras pathways in the control of cellular events.

Although Ras is a GTPase, it has a poorly designed catalytic site. However, GAPs help stabilize the catalytic site and contribute a critical arginine residue that greatly accelerated nucleophilic attack of the GTP. One reason the α-subunits of heterotrimeric G proteins are bigger than Ras proteins is that they have an extra domain that contributes an "arginine finger" resulting in their typically having a higher intrinsic GTPase activity than Ras. Mutations that block intrinsic and GAP-stimulated GTP hydrolysis result in Ras proteins being locked in their active GTP-bound state. Such mutations at residues 12, 13, and 61 are found in H-, K-, or N-Ras in various human tumors. To date only ~10 Ras subfamily GAPs have been characterized. These fall into two structurally distinct families; those that regulate Rap/Rheb and those that regulate Ras and other GTPases. One of the Ras GAPs, neurofibromin, is the product of the NF1 tumor suppressor and, upon its loss, Ras GTP levels become elevated contributing to increase signaling that results in cancer and other proliferative diseases. Information on the better-characterized Ras subfamily members is discussed next.

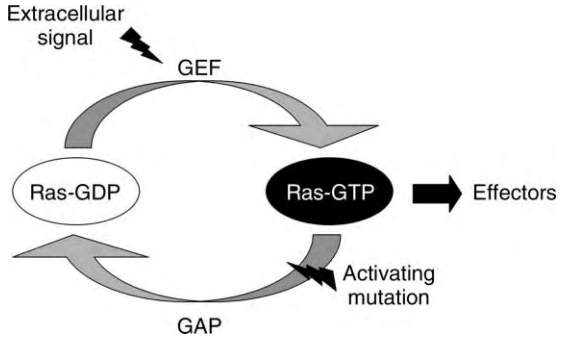

FIGURE 2 GDP/GTP cycle activity of Ras family GTPases. Ligand binding induce receptor-mediated activation or membrane-recruitment of guanine-nucleotide-exchange factors (GEFs) which promote the release of GDP from Ras and acquisition of GTP from the cytosol. GTP binding promotes a conformational change permitting Ras to associate with downstream effector proteins to elicit a biological response. GTPase activating proteins (GAPs) also recognize Ras-GTP and their binding promotes rapid acceleration of Ras' intrinsic GTPase activity. This converts Ras back to its inactive GDP-bound state from which the cycle can begin again. Mutations that block the intrinsic and GAP-stimulated GTPase activity lock Ras in its active, GTP-bound state.

H-, K-, and N-Ras

H-, K-, and N-Ras represent the original and best-studied/understood Ras proteins. Mutations of each of these proteins are found in human tumors with those in K-Ras being the most prevalent. K-Ras can have alternate splicing of its fourth exon with the 4B version being the most predominant.

It was long known that Ras was involved in growth control downstream of growth factor receptors and in 1993 an entire pathway from cell-surface receptor to the nucleus was delineated. The binding of growth factors to their protein tyrosine kinase receptors leads to phosphorylation of the receptors on tyrosine residues. This enables the binding of various adapter proteins that contain modular Src homology 2 or SH2 domains that recognize specific primary sequences that contain phospho-tyrosine. One such molecule is Grb2 that also has two SH3 domains that bind to proline-rich sequences like those found in the Ras GEF, Sos. Binding of a preformed Grb2-Sos complex to receptor tyrosine kinase results in recruitment of Sos to the plasma membrane where it promotes GTP-loading of Ras. In its active GTP-bound state, Ras now adopts a conformation that enables it to bind to the serine/threonine protein kinase, Raf. This in turn recruits Raf to the membrane, promotes a conformational change, and enables Raf to be phosphorylated by nearby kinase(s). Raf then phosphorylates MEK, which phosphorylates extracellular signal-regulated kinases (ERKs) 1 and 2. Phospho-ERKs dimerize and translocate into the nucleus where they phosphorylate transcription factors such as Elk1, leading to increased gene expression. It is now known that a number of additional signals activate Ras. For example, Ras GEFs (such as GRF1 in brain and GRP1 in T cells) and GAPs (Capri, Rasal) can be activated by Ca^{2+} elevation and/or diacylglycerol. Additionally, G protein-coupled receptors can trigger tyrosine phosphorylation to regulate the Grb2/Sos complex.

Ligand receptors reside on the plasma membrane and Ras also localizes there. However, recent studies indicate that Ras is also found on the Golgi membrane and that many of the events mediated by Ras occur at this intracellular site. One mechanism whereby activation of cell-surface receptors might signal to Ras at a remote intracellular membrane is via Ca^{2+} elevation, resulting in the activation of a $Ca2^{+}$-regulated exchange factor. This has been reported in T cells.

Binding of GTP triggers a conformational change in Ras in two regions called switch I and II. Switch I, which encompasses residues ~32–40 is the main determinant for effector binding. Conformation of this and switch II dictate which targets various Ras subfamily members associate with. A number of putative Ras effectors have been described however three have been best characterized. These include the protein kinase Raf, phosphatidylinositol 3 kinase, and RalGDS, an exchange factor for the Ras-related GTPase, Ral. There are several isoforms of each of these effectors that have different tissue distribution and affinities for various Ras family members. Each of these effectors has a related ~60 residue Ras association (RA) or Ras-binding domain (RBD). Since RA domains bind specifically to Ras-GTP, the isolated domains (typically fused to glutathione S-transferase and immobilized on glutathione-conjugated beads) can be used to precipitate Ras-GTP from cell lysates to gauge intracellular Ras activity. The Raf RBD is typically used to detect H-, K-, or N-Ras activity. While most Ras activity is associated with increasing cell growth and transformation, several recently characterized Ras targets that include RASSF1 appear to have tumor-suppressing properties.

Ral

As indicated above, a family of four Ral GEFs (RalGDS, Rgl, Rgl2/Rlf, Rgl3/RPM) possess Ras-binding domains and are downstream effectors of Ras. The primary function of Ras here is in recruiting Ral-GEFs to the membrane where they can activate Ral. In addition to being regulated by Ras/RalGDS, Ral is activated by Ca^{2+}, possibly due to its ability to bind calmodulin and by a second class of GEFs (the RalGPS or RalGEF2 family) that lack an RA domain.

Due to its regulation by Ras, initial studies focussed on its ability to regulate transformation. Recently RalGDS was found to be an important mediator of Ras-induced transformation in human epithelial cells. However, the downstream target(s) responsible for this effect remain to be identified. Ral or its GEFs have been reported to regulate various transcription factors including c-Fos, c-Jun, STAT3, and AFX (a member of the forkhead family). Interestingly, Ral-GEFs are often more potent at inducing biological effects than activated (GTPase-defective) Ral mutants. This may be because GTP/GDP cycling is required for Ral function or that binding of Ral-GEFs to additional proteins such as the serine/threonine kinase PDK1 or the scaffold protein, β-arrestin contributes to their biological activity.

Studies on Ral-binding proteins revealed the involvement of this GTPase in additional cellular functions that include vesicle sorting. This is not surprising since much of the Ral protein localizes to intracellular vesicles in both endocytic and exocytic compartments. Ral binds to and may assist in the formation of the exocyst, a complex of at least eight proteins, which directs vectorial targeting of vesicles from the Golgi to the basolateral but not apical membrane of epithelial cells. Ral is essential for this process in higher eukaryotes but, puzzlingly, Ral is not present in yeast where the exocyst was first identified. Ral also regulates receptor-mediated endocytosis but this is achieved via a distinct effector, RalBP1/RLIP76. RalBP1 binds to proteins associated with endocytosis but also contains a GAP-like domain for the Rho family GTPase, CDC42. It is via this activity that it may also regulate cell morphology. Given these myriad functions it is not surprising that Ral can contribute to cell proliferation and cancer.

R-Ras 1, 2, and 3

R-Ras, TC21 (R-Ras2), and M-Ras (R-Ras3) are closely related to Ras (Figure 3) and have overlapping signaling and biological function. However, although some activating mutations have been found in cultured cell lines, these GTPases appear to seldomly if ever be mutated in human cancers despite the transforming activity of laboratory-engineered mutants. R-Ras activates PI3K but does not regulate the Raf/ERK or RalGDS pathway. Distinct from H-Ras, it has been implicated in "inside-out" signaling, increasing the ability of integrin to bind extracellular matrix. This results in increased cell attachment and spreading. One study has implicated Rap1 as a mediator of R-Ras action, another example of a Ras protein cascade. The binding of R-Ras to focal adhesion kinase has also recently been reported, providing another avenue for it to regulate integrins and/or cell adhesion. Like R-Ras, TC21 and M-Ras also effectively activate PI3K. M-Ras preferentially activates B-Raf over the more common Raf-1 isoform. While M-Ras is most abundant in brain, the exact function of either M-Ras or TC21 is unclear.

Rap1 and 2

There are five members of the Rap cluster: Rap1A and 1B and Rap2A, 2B, and 2C. Rap1A/Krev-1 was isolated in 1988 due to sequence homology with Ras

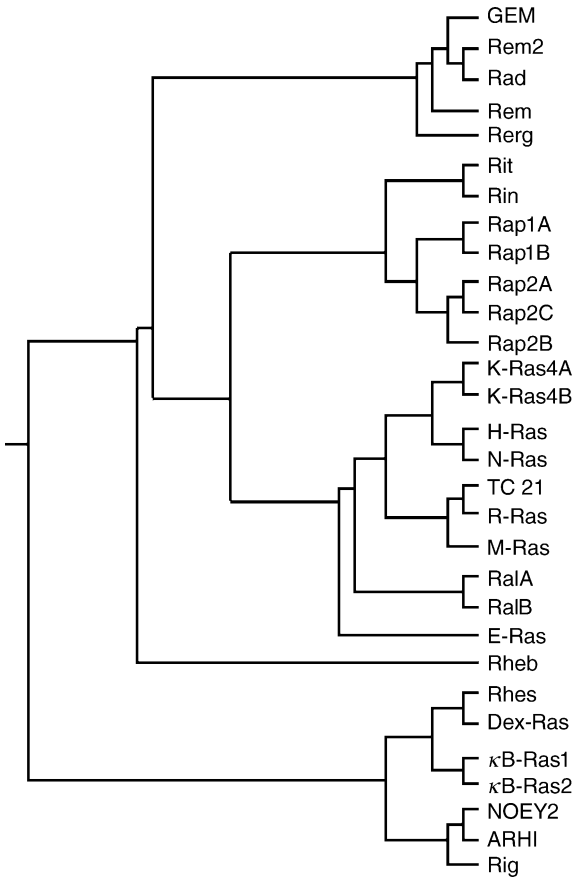

FIGURE 3 Dendrogram showing the relatedness of mammalian Ras subfamily GTPases.

(Ras proximate) and also due to its ability to revert the transforming activity of K-Ras. The revertant activity was believed due to Rap1A binding to Ras effectors and acting as a competitive antagonist of Ras. This indeed may be the true function of Rap in, e.g., T cells where Rap needs to be turned off by a costimulatory receptor such as CD28 in order for T cell receptor-induced activation of Ras to have its desired effect. However, the main role of Rap1 appears to be in the inside-out regulation of integrins. A Rap1 effector RAPL has recently been described in leukocytes that is responsible for promoting integrin clustering but how Rap regulated adhesion of cells in solid tissues has yet to be determined. While early studies described Rap1 and 2 localization to endocytic and Golgi membranes, recent studies have found Rap1 on epithelial cell junctions. It is likely that Rap1 and 2 plays multiple cell type-specific roles.

Rap1 and 2 are regulated by the same GEFs and GAPs. Strikingly, at least ten of the CDC25 family as well as the unrelated Smg GDS and DOCK4 proteins act as Rap GEFs suggesting that Raps play fundamental roles in cell biology that are triggered by a broad spectrum of extracellular stimuli. Signals from Ca^{2+}, diacylglycerol, receptor and nonreceptor protein tyrosine kinases, and cyclic AMP can all activate Rap. Indeed the protein kinase A-independent effects of cyclic AMP are due to activation of two Rap GEFs, Epac1 and 2 that contain cyclic nucleotide-binding domains. Several Rap GEFs contain RA domains, suggesting that they are recruited to membranes as downstream effector of other GTPases. This suggests that Rap activation may be a requisite for other Ras family members to execute their biological functions.

Rheb

Despite its name (Ras homologue expressed in brain), Rheb is found in many tissues. However it was discovered in 1995 as a protein whose expression was induced by synaptic stimulation. Although no Rheb GEFs have been found to date, Rheb's GTPase activity is regulated by TSC2, a tumor suppressor whose C terminus resembles Rap GAPs. Following loss of TSC2 or mutation of its GAP domain, the loss of GAP activity results in the accumulation of Rheb GTP. This activates a kinase cascade involving mTOR and ribosomal S6 kinase that promotes protein synthesis. Interestingly, Rheb is posttranslationally farnesylated similarly to H, K-, and N-Ras. It is therefore possible that Rheb represents an additional target of farnesyl transferase inhibitors designed to block Ras action and that these drugs might have use in the treatment of the proliferative disorders associated with tuberous sclerosis (TSC).

Other Ras Family Members

A number of additional GTPases exist (Figure 3) that are less well characterized but help exemplify the diversity of GTPase functions. These include ARHI/NOEY, Rig, and Rerg that have each been shown to play inhibitory roles. Critical conserved residues within their GTP-binding pockets diverge from those of most other Ras family members suggesting that these G proteins are constitutively GTP bound. The expression of these proteins can be induced by various agonists suggesting that they are regulated at the level of gene expression rather than by GEFs and GAPs. Further, it is their loss rather than mutation that contributes to cellular proliferation/transformation. Regulation at the level of transcription is not limited to these proteins; for example Dex-Ras expression is induced by corticosteroids, Rhes by thyroid hormone and as noted above Rheb by synaptic stimulation. Expression of many Ras family GTPases is also regulated by growth factors. Another branch of the Ras subfamily regulates transcription: κB-Ras binds to the IκB/NFκB complex and helps mask a nuclear localization sequence so that this transcription factor complex cannot translocate to the

nucleus and induce gene expression. The function of the Rad/Gem branch of the Ras family has until recently eluded investigators. However, they were recently shown to be negative regulators of the Rho–Rho kinase pathway, helping to explain their ability to modulate the actin cytoskeleton. Finally, several of the Ras family proteins lack the characteristic C-terminal CAAX box required for their posttranslational lipid modification. These include the closely related Rit and Rin proteins as well as Rerg and κB-Ras. While the former two proteins have been reported to regulate PC12, pheochromocytoma, cell differentiation, an event regulated by several Ras proteins via Raf and/or PI3K, Rit, and Rin appear to act via some alternative pathway(s). Interestingly, although Rit lacks any known recognition signal for C-terminal lipidation, Rit-transformed cell growth and survival in low serum is dependent on a farnesylated protein. Since most prenylated proteins are G proteins this suggests, once again, the existence of crosstalk between members of this subfamily of GTPases.

See Also the Following Articles

Rab Family • RAN GTPase • Small GTPases

Glossary

effector Proteins (typically enzymes) that GTP-bound Ras proteins bind to elicit a biological response.

GTPase Describes the intrinsic GTP hydrolyzing enzymatic activity of Ras. Binds GDP or GTP with high affinity and catalyzes the hydrolysis of GTP to GDP and phosphate.

GTPase activating proteins (GAPs) Negative regulators of Ras that bind the GTPase and accelerate its ability to hydrolyze bound GTP.

Guanine-nucleotide-exchange factors Upstream positive regulators of Ras proteins that promote increased nucleotide exchange so that Ras can bind to GTP.

isoprenylation Process of irreversible post-translational covalent modification of the C terminus of proteins by 15 carbon farnesyl or 20 carbon geranylgeranyl isoprene-derived lipids.

Ras A high-affinity guanine nucleotide-binding protein with intrinsic GTPase activity that acts as a molecular switch or bio-timer by cycling between inactive GDP- and active GTP-bound states.

Further Reading

Berg, J. M., Tymoczko, J. L., and Stryer, L. (2002). *Biochemistry*, 5th edition. W. H. Freeman, New York.

Bos, J. L., de Rooij, J., and Reedquist, K. A. (2001). Rap1 signalling: Adhering to new models. *Nat. Rev. Mol. Cell Biol.* **2**, 369–377.

Caron, E. (2003). Cellular functions of the Rap1 GTP-binding protein: A pattern emerges. *J. Cell Sci.* **116**, 435–440.

Feig, L. A. (2003). Ral-GTPases: Approaching their 15 minutes of fame. *Trends Cell Biol.* **13**, 419–425.

Hancock, J. F. (2003). Ras proteins: Different signals from different locations. *Nat. Rev. Mol. Cell Biol.* **4**, 373–384.

Quilliam, L. A., Rebhun, J. F., and Castro, A. F. (2002). A growing number of guanine nucleotide exchange factors is responsible for activation of ras family GTPases. *Prog. Nucl. Acid Res. Mol. Biol.* **71**, 391–444.

Takai, Y., Sasaki, T., and Matozaki, T. (2001). Small GTP-binding proteins. *Physiol. Rev.* **81**, 153–208.

Biography

Lawrence Quilliam received his Ph.D. from the University of Sheffield, England and obtained postdoctoral training at the Scripps Research Institute, La Jolla, CA. He is currently an Associate Professor of biochemistry and molecular biology at Indiana University School of Medicine and a member of the Walther Oncology Center. His research focuses on the delineation of cellular signaling pathways involved in cancer with particular emphasis on Ras family proteins and their guanine nucleotide exchange factors.

Recombination: Heteroduplex and Mismatch Repair *in vitro*

Leroy Worth Jr.
National Institute of Environmental Health Sciences, Research Triangle Park, North Carolina, USA

The methyl-directed repair pathway of *Escherichia coli* ensures genome stability by testing for the occurrence of mismatched base pairs. In addition to rectifying biosynthetic errors that occur through misincorporation during DNA biosynthesis, this pathway also controls the level of recombination between closely related sequences.

Mismatch Repair in Genetic Exchange

Early indications of the role of mismatch repair in genetic exchange were initially provided by the observation that null mutations in *mutS*, *mutL*, *mutH*, or *uvrD* genes result in a hyper-rec phenotype. Thus, in addition to replication error, DNA mismatches that arise during recombination are subject to the action of these activities. Specifically, the formation of hybrid or heteroduplex DNA during genetic exchange results in mispaired bases, which are formed at regions of sequence divergence between two homologous chromosomes. However, unlike mismatches produced during DNA replication, these mispairs are not necessarily promutagenic, but rather substrates for repair.

Homeologous recombination is defined as the genetic exchange between DNA sequences that are nearly identical. During this type of exchange, newly formed heteroduplex that failed to escape mismatch repair results in non-reciprocal exchange (gene conversion; non-Mendelian segregation), as one allele is replaced by the other.

Several studies have shown that as the level of divergence between DNAs decreases, so does the frequency with which they will recombine. Mismatch repair provides an efficient homology-sensing tool that assists in maintaining an energetic barrier to exchange between closely related sequences. Conversely, the low level of mismatches that happen to escape repair does not appear to be detrimental, but rather favors the appearance of newly formed recombinants, which may or may not be beneficial. Certainly, during meiotic recombination, a process required for proper chromosome segregation, a possible intolerable outcome of genetic exchange is imprecise chromosome disjunction.

The barrier to recombination caused by sequence divergence is most likely manifested at two distinct stages of recombination: the formation of heteroduplex joints and subsequent action of mismatch repair. The molecular steps of genetic recombination have been studied extensively in *Escherichia coli* and *Saccharomyces cerevisiae* and to a lesser extent in other systems. In *E. coli*, initial processing of the donor DNA is necessary to produce free single-stranded tails. The RecBCD enzyme unwinds and digests double-stranded DNA until a characteristic chi (χ) sequence (octanucleotide: 5′-GTCGGTGG-3′) is encountered. Once bound to chi, a cascade of events ensues, resulting in a free single-stranded 3′-end that is the substrate for RecA strand transfer. This free end is invasive and is able to displace one of the recipient strands in a RecA-dependent fashion.

In fact, no homologue of the RecD protein, which is necessary for DNA cleavage, is observed in *Bacillus*. All subsequent recombination functions are dependent on the function of RecA. The recombinant joint is subject to strand extension, branch migration mediated by the RuvAB (branch migration activity) complex, and editing. In *E. coli*, the editing process involves the methyl-directed mismatch repair system, controlled by the MutS and MutL proteins. In *Streptococcus pneumoniae*, the editing function is carried out by the homologous, nick-directed HexAB repair system. If mismatches are detected, the repair system may reject the entire donor strand and abort the recombination process.

RecA Strand Transfer

The level of homeologous recombination depends upon the degree of sequence divergence between the recombining sequences. It is known that independent of sequence identity, the degree of exchange is at least an order of magnitude lower than that between completely

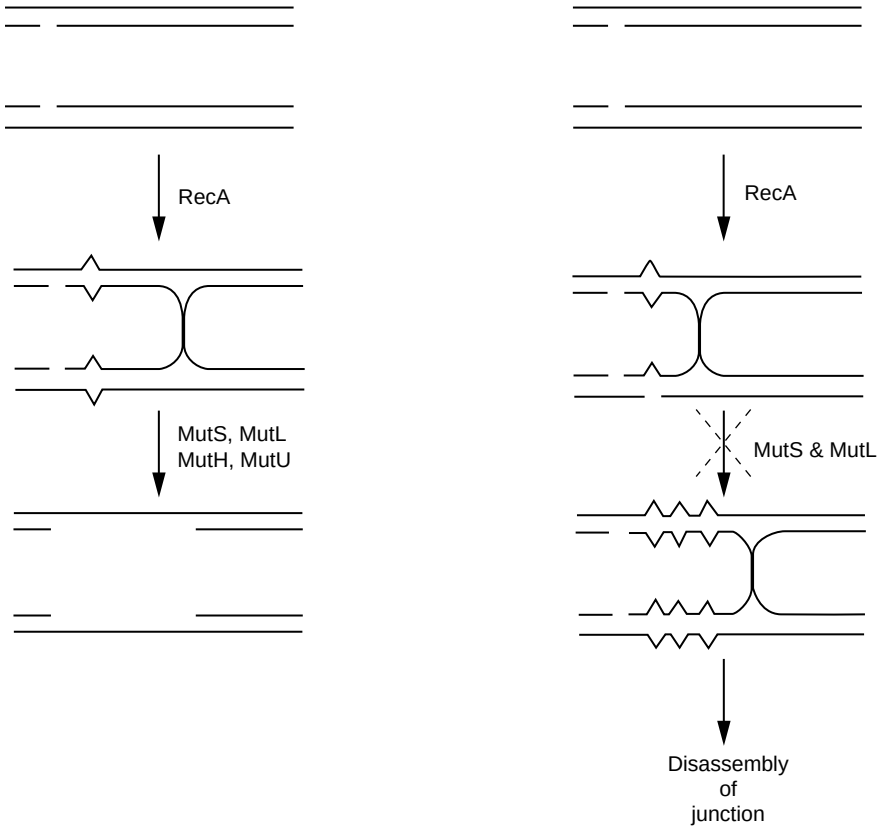

FIGURE 1 Potential mechanisms of DNA mismatch repair in modulating heteroduplex formation between divergent DNAs.

identical DNAs. This effect is remarkably independent of mismatch correction and can only be alleviated by the overproduction of proteins involved in recombination, specifically RecA protein.

The process of heteroduplex formation by RecA is associated with the initiation step of recombination and involves the formation of branched joints that proceed in a polarity-dependent fashion (Figure 1, top). These branched intermediates are stable and possess the ability to move through regions of lower sequence identity, thus the introduction of DNA mismatches. That near-perfect sequence identity is required for initiation is probably due to RecA-mediated homology search and the subsequent stability of the recombinant joint within the filament.

Mismatch Repair Mediates Heteroduplex Formation

DNA mismatch repair is able to recognize incorrect base pairs in DNA, but it is less known mechanistically as to how this pathway controls recombination between nearly identical DNAs. In terms of possible modes that could be envisioned, one might imagine that, as in replication fidelity, activities such as MutS and MutL could be involved in recognizing mismatches that are generated in newly formed heteroduplex. Indeed, these activities could act as a "mismatch sensing" and recognize regions of sequence divergence once they are encountered during the strand exchange process (Figure 1). Biochemical evidence for such a possibility was first demonstrated by studies of Worth *et al.* using purified *E. coli* repair activities. Both MutS and MutL proteins were shown to block RecA-mediated strand transfer between DNAs that shared more than 96% sequence identity. Specifically, using filamentous bacteriophage DNAs M13 and fd, whose DNAs share approximately 97% sequence identity, and the model three-strand *in vitro* transfer reaction, this study was able to show that RecA catalyzes the complete transfer of the complement strand, beginning with the 3′-end originating from a linear duplex molecule. The transfer of the complement results in a displaced linear single-strand that is formed from the 5′-end of the opposite strand, which in this case is identical in nature to the recipient DNA and the formation of full-length heteroduplex (Figure 1). This reaction requires the presence of single-stranded binding protein (SSB) and ATP. SSB acts to remove any secondary structure that might form and to aid in strand transfer by binding the growing displaced single-stranded DNA. Strand exchange between these DNAs (M13–fd) is not as efficient as those reactions carried out between identical DNAs

(e.g., M13–M13). This reduction in full-length heteroduplex suggests that the formation of mismatches, an indication of sequence divergence, acts as an energetic barrier to recombination.

MutS Inhibits Strand Exchange

Further data demonstrating the role of MutS in this process were provided by titration studies, which showed that increasing concentrations of this activity completely abolished heteroduplex formation between M13–fd DNAs. This process was shown to be dependent upon the formation of mismatches, as MutS had no effect on exchange reactions between identical DNAs. Because MutS is a known ATPase, and ADP is known to cause RecA to dissociate from DNA, it was thought that this inhibition could be due to an equilibrium shift in nucleotide, as more hydrolysis would occur for heteroduplex formation and therefore higher ADP pools. This possibility was shown not to be the case, however, as an ATP-regenerating system alleviated the potential to build up ADP and thus caused RecA to dissociate. Indeed, subsequent studies showed that mismatch recognition alone could act to block the heterologous reaction and thus partly explain the role of these activities in recombination.

MutL Enhances Inhibition

To test other components in the pathway, an additional *in vitro* study evaluated the role of MutL, if any, in this block. Studies involving equimolar MutS and MutL revealed an attenuated block of strand transfer between M13–fd DNAs beyond that exhibited by MutS alone. Although high concentrations of MutL alone failed to block strand transfer between these phage DNAs, it stimulated the inhibition afforded by MutS, as lower concentrations of this activity were required in eliminating full-length heteroduplex formation. This level of inhibition by mismatch repair was afforded when these individual activities were present in a 1:1 stoichiometry. Again, these activities did not inhibit DNA exchange as catalyzed by RecA when the donor and recipient DNAs were identical. This inhibition of the heterologous reaction thus demonstrates an act of synergy between these activities in sensing for the occurrence of DNA mismatches. Similar to replication fidelity, these components appear to act in concert to impose their anti-recombinogenic activity.

Recent studies have evaluated the role of mismatch repair in mediating downstream components of recombination, specifically RuvAB complex. These activities are involved in branch migration and are more efficient than RecA in extending newly recombinant DNA. Recent studies have shown that MutS and MutL also act to mediate branch migration as a consequence of the activities, which are not subject to the polarity restrictions associated with RecA. This observation suggests that mismatch repair might have a role in the resolution of DNA joints that are in the vicinity of DNA sequence divergence.

Alternative Role of Repair in Recombination

A second possibility to explain mismatch repair anti-recombination activity, which should not be viewed as mutually exclusive, is the removal of the invading strand through the recruitment of downstream components of the repair pathway (Figure 1). Indeed, similar to the proposed role of the *E. coli* system, these activities could react to the recombination intermediates by a mechanism similar to that for replication fidelity. The excision system could eradicate the newly formed intermediates by mismatch-dependent loading on the invading strand. In this case, mismatch detection along with a 3′-end would suffice as normal repair signals and thereby act to abort the recombining event through removal of the invading strand and full recovery of the recipient DNA through DNA synthesis. This process would require the unwinding activity of helicase II, which drives orientation-specific loading of the proper excision machinery.

The role of DNA repair in modulating heteroduplex formation is ongoing, and continued studies will seek to define how these activities regulate the frequency of genetic exchange as a function of sequence divergence.

See Also the Following Articles

DNA Mismatch Repair: *E. coli* Vsr and Eukaryotic G–T Systems • DNA Mismatch Repair in Bacteria • Recombination: Strand Transferases

Glossary

filamentous bacteriophage Viral non-lytic ssDNA encapsulated in coat protein (capsid).

full-length heteroduplex A process involving the complete transfer of an invading (donor) single-strand DNA to the recipient complement.

heteroduplex The joining or annealing of two single strands originating from differing origins.

homeologous Similar but non-identical in nature.

homoduplex The joining or annealing of two single strands originating from identical origins.

recombination A combining of nucleotide sequences or genes different from what they were in the parents.

transformation The heritable conversion in properties of a competent bacterium by DNA from another bacterial strain.

Further Reading

Au, K. G., Welsh, K., and Modrich, P. (1992). Initiation of methyl-directed mismatch repair. *J. Biol. Chem.* **267**, 12142–12148.

Abdulkarim, F., and Hughes, D. (1996). Homologous recombination between the tuf genes of *Salmonella typhimurium*. *J. Mol. Biol.* **260**, 506–522.

Burdett, V., Baitinger, C., Viswanathan, M., Lovett, S. T., and Modrich, P. (2001). *In vivo* requirement for RecJ, ExoVII, ExoI, and ExoX in methyl-directed mismatch repair. *Proc. Natl. Acad. Sci. USA* **98**, 6765–6770.

Datta, A., Adjiri, A., New, L., Crouse, G. F., and Jinks Robertson, S. (1996). Mitotic crossovers between diverged sequences are regulated by mismatch repair proteins in *Saccaromyces cerevisiae*. *Mol. Cell. Biol.* **16**, 1085–1093.

Fabisiewicz, A., and Worth, L., Jr. (2001). *Escherichia coli* MutS,L modulate RuvAB-dependent branch migration between diverged DNA. *J. Biol. Chem.* **276**, 9413–9420.

Humbert, O., Prudhomme, M., Hakenbeck, R., Dowson, C. G., and Claverys, J. P. (1995). Homeologous recombination and mismatch repair during transformation in *Streptococcus pneumoniae*: Saturation of the Hex mismatch repair system. *Proc. Natl. Acad. Sci. USA* **92**, 9052–9056.

Modrich, P., and Lahue, R. (1996). Mismatch repair in replication fidelity, genetic recombination, and cancer biology. *Annu. Rev. Biochem.* **65**, 101–133.

Petit, M. A., Dimpfl, J., Radman, M., and Echols, H. (1991). Control of large chromosomal duplications in *Escherichia coli* by the mismatch repair system. *Genetics* **129**, 327–332.

Selva, E. M., New, L., Crouse, G. F., and Lahue, R. S., (1995). Mismatch correction acts as a barrier to homeologous recombination in *Saccharomyces cerevisiae*. *Genetics* **139**, 1175–1188.

Stambuk, S., and Radman, M. (1998). Mechanism and control of interspecies recombination in *Escherichia coli*. I. Mismatch repair, methylation, recombination and replication functions. *Genetics* **150**, 533–542.

Worth, L. J. Jr, Clark, S., Radman, M., and Modrich, P. (1994). Mismatch repair proteins MutS and MutL inhibit RecA-catalyzed strand transfer between diverged DNAs. *Proc. Natl. Acad. Sci. USA* **91**, 3238–3241.

Worth, L., Jr., Bader, T., Yang, J., and Clark, S. (1998). Role of MutS ATPase activity in MutS,L-dependent block of in vitro strand transfer. *J. Biol. Chem.* **273**, 23176–23182.

Zahrt, T. C., and Maloy, S. (1997). Barriers to recombination between closely related bacteria: MutS and RecBCD inhibit recombination between *Salmonella typhimurium* and *Salmonella typhi*. *Proc. Natl. Acad. Sci. USA* **94**, 9786–9791.

Biography

Leroy Worth, Jr., is a Scientific Review Administrator at the National Institute of Environmental Health Sciences (NIEHS), in the Division of Extramural Research Training. He was previously a researcher in the NIEHS Laboratory of Molecular Genetics. Dr. Worth holds a B.S. in chemistry from the University of North Carolina and a Ph.D. in biochemistry from the University of Maryland. He did post-doctoral training with Dr. Paul Modrich at Duke University. Dr. Worth's major research interest is in DNA replication/repair mechanisms and oxidative stress.

Recombination: Strand Transferases

Floyd R. Bryant
The Johns Hopkins University, Baltimore, Maryland, USA

The recombination of homologous DNA molecules plays a central role both in gene rearrangement reactions and in the repair of damaged DNA. Genetic and biochemical studies have established that homologous recombination proceeds via the formation of intermediate structures in which the two recombining DNA molecules are joined together by single-stranded crossover connections. A continuing strand exchange between the two polynucleotide chains can then occur, leading to the generation of heteroduplex DNA. The formation of the recombinational intermediates is carried out by a class of proteins known as recombination strand transferases or DNA recombinases.

DNA Recombinases

The most well-studied members of this class of proteins are the bacterial RecA proteins and the eukaryotic Rad51 proteins. Other members of this class include the archaeal RadA proteins and the bacteriophage T4 UvsX protein.

Bacterial RecA Proteins

The prototypical DNA recombinase is the RecA protein of *Escherichia coli* (*E. coli*). Genetic studies have shown that the RecA protein is involved in virtually all aspects of homologous recombination in *E. coli*. Moreover, *E. coli recA* mutants are highly susceptible to DNA damaging agents (e.g., ultraviolet light or chemical mutagens), and in recent years the central role played by the RecA protein in recombinational DNA repair has been more clearly defined.

The *E. coli* RecA protein is composed of 352 amino acids (37 842 Da). The purified RecA protein binds to DNA, is a DNA-dependent ATPase, and promotes a variety of ATP-dependent DNA strand transfer reactions that are presumed to reflect *in vivo* recombination functions. In addition to its strand transfer activities, the RecA protein also promotes the autocatalytic cleavage of several proteins that are involved in the bacterial response to DNA damage. Although the *E. coli* RecA protein is the best characterized of the bacterial RecA proteins, RecA-like genes have been identified in all bacterial species that have been examined and RecA protein homologues have been analyzed from several other bacterial species, including *Bacillus subtilis* and *Streptococcus pneumoniae*.

Eucaryotic Rad51 Proteins

Eucaryotic homologues of the RecA protein, the Rad51 proteins, have been isolated and characterized from yeast and from human cells. The Rad51 proteins have been shown to play an essential role in DNA recombination and repair in eucaryotic cells.

The human and yeast Rad51 proteins are composed of 339 amino acids (36 966 Da) and 400 amino acids (42 961 Da), respectively. Although not as extensively investigated as the *E. coli* RecA protein, the human and yeast Rad51 proteins have been shown to promote ATP-dependent strand exchange reactions that are generally similar to those of the *E. coli* RecA protein.

A second group of eucaryotic RecA homologues which function specifically during meiosis, the Dmc1 proteins, has been isolated and characterized from yeast and human cells. However, the DNA strand exchange properties of the Dmc1 proteins have not yet been fully evaluated.

Other RecA Homologues

RecA-like proteins, known as the RadA proteins, have also been isolated and characterized from various archaeal cells, including *Sulfolobus solfataricus* and *Archaeoglobus fulgidus*. In addition, a RecA-like protein, the UvsX protein, is encoded by *E. coli* bacteriophage T4. The universal presence of RecA-like proteins suggests that functionally related homologous recombination and recombinational DNA repair systems are operative in all organisms.

Structure

The RecA and Rad51 proteins have been analyzed by a variety of structural methods. X-ray crystallography and electron microscopy have been especially useful in identifying the functional form of these proteins.

X-Ray Crystallography

The three-dimensional structure of the *E. coli* RecA protein has been determined by X-ray crystallography. The RecA protein consists of a central core domain (amino acids 34–240) which contains the ATP-binding site and possibly the DNA-binding site(s), and a smaller amino-terminal domain (amino acids 1–33) and carboxy-terminal domain (amino acids 241–352). Sequence comparisons indicate that a structurally similar central core domain is present in the Rad51 proteins. The Rad51 proteins, however, lack the carboxy-terminal domain found in the RecA protein, and have an extended amino-terminal domain that is not present in the RecA protein.

Electron Microscopy

Electron microscopy studies have shown that RecA protein monomers assemble on single-stranded DNA (ssDNA) in the 5′ to 3′ direction to form a right-handed helical nucleoprotein filament with one RecA monomer per three nucleotides of ssDNA, and approximately six RecA monomers per helical turn of the filament (Figure 1). The RecA protein forms a structurally similar filament on double-stranded DNA (dsDNA), with one RecA monomer per three base pairs of dsDNA.

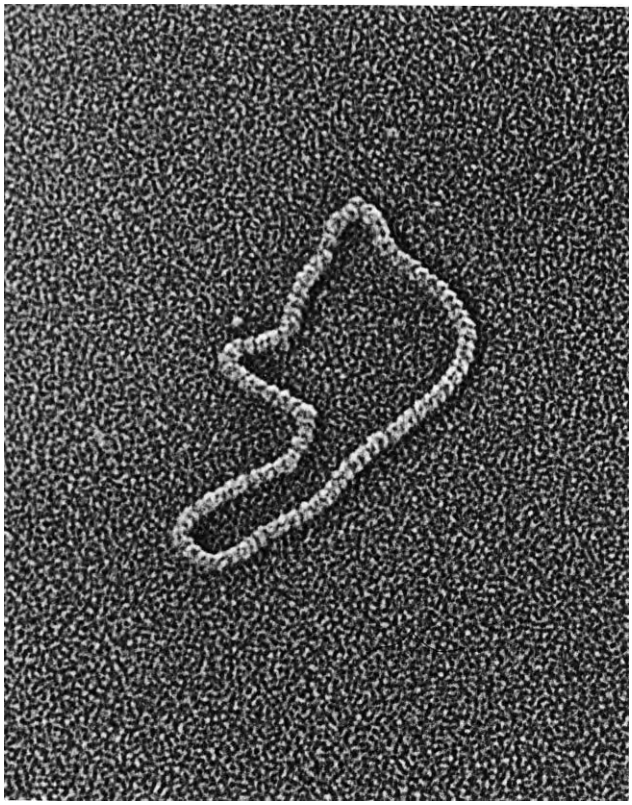

FIGURE 1 Circular ssDNA molecule covered by a helical filament of *E. coli* RecA protein (electron micrograph by Dr. Jack Griffith).

However, the binding to dsDNA is much slower than to ssDNA, and occurs only in the presence of ATP, whereas the binding to ssDNA occurs in either the presence or absence of ATP.

The conformation of the nucleoprotein RecA-DNA filament changes in response to the binding of nucleotide cofactors. In the absence of nucleotide cofactor, or in the presence of ADP, the filament adopts a compressed conformation with a helical pitch of ~70–85Å (seen on ssDNA only). In the presence of ATP, however, the filament assumes a more extended conformation with a helical pitch of 95Å (seen on ssDNA or dsDNA). In the ATP-activated state, the DNA inside the filament is stretched to 5.1Å per base/base pair (compared to 3.4Å per base pair in free dsDNA), and untwisted to 18.6 bases/base pairs per turn (compared to 10.5 base pairs per turn in free dsDNA).

The Rad51 proteins form filaments on DNA that are structurally similar to those formed by the RecA protein. This indicates that the altered conformation that is imposed on DNA in the ATP-activated state of the nucleoprotein filament is integral to the mechanism of action of the RecA and Rad51 proteins.

Model Reactions

The RecA and Rad51 proteins promote a variety of ATP-dependent DNA strand transfer reactions with defined DNA substrates. These reactions include D-loop formation and the three-strand exchange reaction.

D-Loop Formation

The RecA and Rad51 proteins can promote the pairing of a ssDNA with the complementary strand of a homologous covalently closed circular dsDNA to form a three-stranded structure known as a D-loop. However, because the dsDNA substrate lacks a free end, the invading ssDNA and the complementary strand from the dsDNA are unable to fully interwind, and the amount of strand transfer that can occur in this reaction is limited.

Three-Strand Exchange Reaction

The most extensively studied DNA strand transfer reaction is the three-strand exchange reaction, in which a circular ssDNA and a homologous linear dsDNA (typically from bacteriophage ϕX174 or M13 DNA; 5000–10 000 bases/base pairs in length) are recombined to yield a nicked circular dsDNA molecule and a linear ssDNA molecule. This reaction is a convenient model reaction for mechanistic studies because the substrates and products can be easily separated by agarose gel electrophoresis. Most of our understanding of the mechanism of action of the RecA

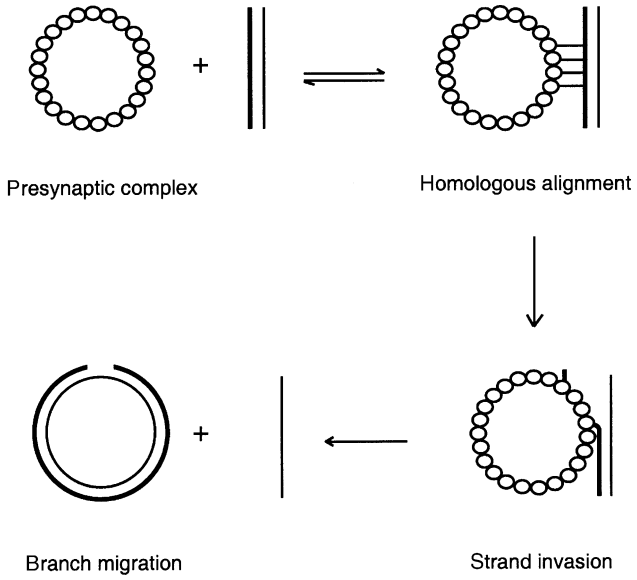

FIGURE 2 Schematic representation of the three-strand exchange reaction. A presynaptic complex (consisting of a circular ssDNA covered with a filament of RecA or Rad51 protein) interacts with a homologous linear dsDNA to produce a nicked circular dsDNA and a linear ssDNA. See text for details.

and Rad51 proteins has been derived from the study of this model reaction.

The three-strand exchange reaction proceeds in three distinct phases (Figure 2). In the first phase, stoichiometric amounts of RecA or Rad51 protein assemble onto the circular ssDNA substrate, forming a nucleoprotein filament known as the *presynaptic complex*. In the second phase, the presynaptic complex interacts with the linear dsDNA substrate, the homologous regions of the ssDNA and dsDNA are brought into register (*homologous alignment*), and new base-pairing interactions are formed between the circular ssDNA and the complementary strand of the linear dsDNA (*strand invasion*). In the third phase, strand exchange continues in a unidirectional manner, leading to the complete transfer of the complementary strand from the linear dsDNA to the circular ssDNA (*branch migration*).

ATP Hydrolysis

The RecA and Rad51 protein-promoted three-strand exchange reactions are absolutely dependent on ATP (or dATP) as a nucleotide cofactor. Curiously, however, the rate of ATP hydrolysis by the Rad51 protein ($0.1–1\ min^{-1}$) is much lower than that by the RecA protein ($20–30\ min^{-1}$). The mechanistic role of ATP hydrolysis in DNA strand exchange reactions is still poorly understood, and the functional significance of the difference between the RecA and Rad51 proteins is not clear. However, studies with nonhydrolyzable ATP analogues, and with mutant RecA proteins which bind but do not hydrolyze ATP, suggest that the homologous alignment and strand invasion reactions require ATP binding but not ATP hydrolysis, whereas the subsequent branch migration reaction may be coupled to the hydrolysis of ATP. These and other findings have led to the suggestion that the RecA protein may use the energy of ATP hydrolysis to actively drive branch migration. The Rad51 protein, in contrast, may stabilize the heteroduplex DNA formed by spontaneous branch migration in a process that is largely independent of ATP hydrolysis. Consistent with this view, it has been shown that RecA protein-promoted strand exchange proceeds uniquely in a 5′ to 3′ direction relative to the invading ssDNA (as expected for a coupled process), whereas the Rad51 protein-promoted reaction can proceed in either the 5′ to 3′ or 3′ to 5′ direction (as expected for a spontaneous process).

Accessory Proteins

The strand exchange activities of the RecA and Rad51 proteins are influenced by a host of recombination accessory proteins. These accessory proteins include the ssDNA-binding proteins and specialized recombination mediator proteins.

Single-Stranded DNA-Binding Proteins

The three-strand exchange activity of the RecA protein is stimulated by the *E. coli* SSB protein, a homotetrameric, non-sequence-specific, ssDNA-binding protein that is involved in many aspects of DNA biochemistry. SSB protein stimulates the strand exchange reaction both presynaptically (by removing secondary structure in the ssDNA substrate which otherwise impedes RecA binding) and postsynaptically (by binding to the displaced strand that is generated when the ssDNA substrate invades the homologous dsDNA). The strand exchange activity of the Rad51 protein is similarly stimulated by the heterotrimeric eucaryotic ssDNA-binding protein, replication protein A(RPA).

Mediator Proteins

The activities of the RecA and Rad51 proteins are also regulated by recombination mediator proteins. In bacterial systems, these mediator proteins include the RecO, RecR, and RecF proteins. The RecO and RecR proteins facilitate the binding of RecA protein to SSB protein-covered ssDNA and stabilize the resulting RecA-ssDNA filament, whereas the RecF and RecR proteins limit the extension of the RecA filament from an ssDNA gap or tail into an adjacent region of dsDNA. The best characterized

mediator of Rad51 protein activity is the Rad52 protein. The Rad52 protein, which may be a functional analogue of the bacterial RecO protein, stimulates Rad51 filament formation by facilitating the displacement of RPA protein from ssDNA.

Biological Reactions

The characterization of the biochemical activities of the RecA and Rad51 proteins has served to identify the mechanistic pathways that may occur in the cell during homologous recombination and recombinational DNA repair. The likely biological roles of the RecA and Rad51 proteins can be illustrated using the double-strand break repair model, which has emerged as a favored model for both the recombinational repair of fragmented DNA molecules and for programmed gene rearrangement reactions (Figure 3).

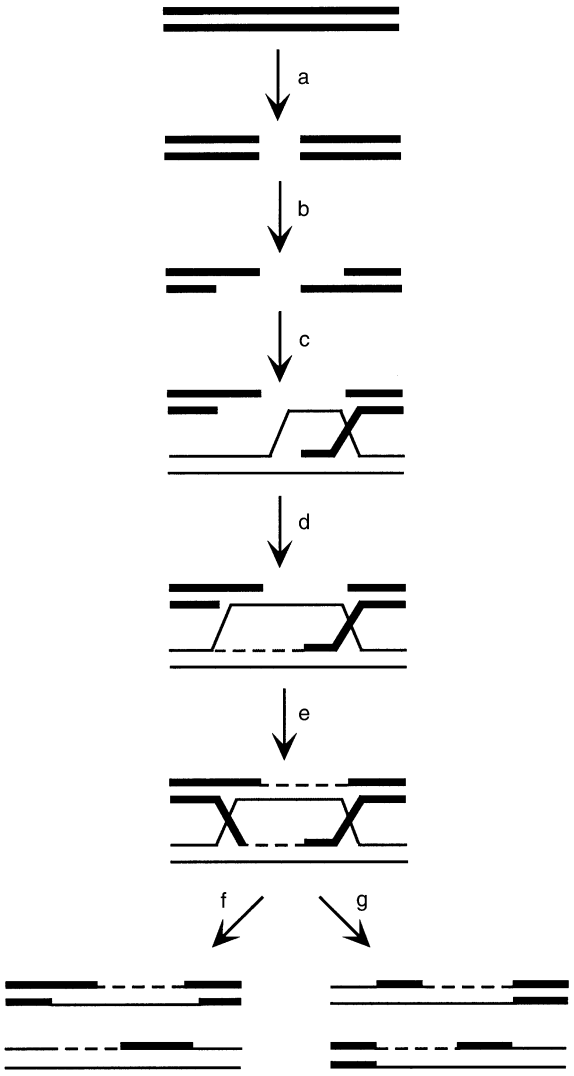

FIGURE 3 Schematic representation of the double-strand break repair model. The bold lines indicate a dsDNA undergoing a double-strand break, the thin lines indicate an intact homologous dsDNA, and the dashed lines indicate newly synthesized DNA. See text for details.

In this model, a double-strand break is introduced into a dsDNA molecule, either by a DNA-damaging agent or by a recombination-specific nuclease (*step a*). The ends of the two dsDNA fragments are then processed by specific nucleases so as to produce 3′-single-stranded "tails" (*step b*). RecA or Rad51 protein then assembles onto each of the single-stranded tails (with the assistance of various accessory proteins) to form active presynaptic nucleoprotein filaments. The single-stranded tail from one DNA fragment then pairs with an intact homologous dsDNA molecule (*step c*), forming a D-loop structure. The ssDNA tail from the second DNA fragment then pairs with the resulting displaced strand (*step d*). This sequence of strand transfer steps links the DNA molecules together by two single-stranded crossover connections, known as "Holliday junctions." A continuing strand exchange reaction, together with the synthesis of new DNA, results in the formation of regions of heteroduplex DNA in the linked DNA molecules (*step e*). Finally, cleavage of the crossover connections by a DNA junction-specific nuclease results in the separation or resolution of the two DNA molecules. Depending on direction of cleavage, the resolution step can produce either two DNA molecules that have been rejoined in the original linkages (*step f*), or two DNA molecules in new recombinant linkages (*step g*).

See Also the Following Articles

Cell Cycle: DNA Damage Checkpoints • DNA Mismatch Repair and Homologous Recombination • DNA Mismatch Repair and the DNA Damage Response • Homologous Recombination in Meiosis • Recombination: Heteroduplex and Mismatch Repair *in vitro* • X-Ray Determination of 3-D Structure in Proteins

Glossary

adenosine triphosphate (ATP) A nucleoside triphosphate whose hydrolysis to adenosine diphosphate (ADP) and phosphate can be coupled to various energy-requiring processes in the cell.

ATPase An enzyme that catalyzes the hydrolysis of ATP to produce ADP and phosphate.

heteroduplex DNA Double-stranded DNA formed from complementary single strands derived from two different DNA molecules.

homologous recombination Recombination between two DNA molecules with similar sequences.

nuclease An enzyme that catalyzes the hydrolysis of phosphodiester bonds in DNA or RNA.

Further Reading

Bianco, P. R., Tracy, R. B., and Kowalczykowski, S. C. (1998). DNA strand exchange proteins: A biochemical and physical comparison. *Front. Biosci.* **3**, d570–d603.

Cox, M. M. (2001). Historical overview: Searching for replication help in all of the rec places. *Proc. Natl Acad. Sci. USA* **98**, 8173–8180.

Egelman, E. H. (2003). A tail of two polymers: New insights into helical filaments. *Nat. Rev. Mol. Cell. Biol.* **4**, 621–630.

Lusetti, S. L., and Cox, M. M. (2002). The bacterial RecA protein and the recombinational DNA repair of stalled replication forks. *Annu. Rev. Biochem.* **71**, 71–100.

West, S. C. (2003). Molecular views of recombination proteins and their control. *Nat. Rev. Mol. Cell. Biol.* **4**, 1–11.

Biography

Floyd Bryant is a Professor in the Department of Biochemistry and Molecular Biology at the Johns Hopkins University, Bloomberg School of Public Health. He holds a Ph.D. from the Pennsylvania State University and received his postdoctoral training at Stanford University. His principal research interests are in the mechanistic analysis of bacterial RecA proteins and in the role of DNA recombination in the development of antibiotic resistance in pathogenic bacteria.

Recombination-Dependent DNA Replication

Kenneth N. Kreuzer
Duke University Medical Center, Durham, North Carolina, USA

Over the last several decades, the processes of homologous genetic recombination and DNA replication have largely been studied in isolation from one another. However, beginning with a few studies of bacteriophages in the 1960s and 1970s, the possibility emerged that extensive DNA replication can sometimes be triggered by homologous genetic recombination. Over the last several years, scientists working with diverse organisms have shown that recombination-dependent DNA replication (RDR) is very common and that this process provides an important back-up mechanism for completing DNA replication when replication forks fail. Mutational inactivation of certain proteins that are involved in RDR or related processes can lead to genome instability and a predisposition to cancer in higher organisms.

Early Models of Homologous Recombination Invoke RDR

One of the early molecular models for homologous recombination, called break-and-copy, invoked *r*ecombination-*d*ependent DNA *r*eplication (RDR). One simple version of this model invoked a break in one molecule, with a resulting 3′ broken end being used as primer for DNA replication. Another DNA molecule, of different parentage, is used as the template, resulting in a genetic crossover in the resulting DNA molecule.

As the field progressed, evidence accumulated in a number of systems for break-and-rejoin models, without extensive DNA replication, and break-and-copy models fell into disrepute. We now understand that there are indeed many pathways of homologous recombination that do not involve extensive DNA replication, but also some very important recombination pathways that trigger extensive replication, as in the original break-and-copy models.

Modern versions of the break-and-rejoin model, such as the Meselson–Radding and double-strand-break repair (DSBR) models, invoke limited DNA replication events (e.g., gap filling) to fill in missing information. Such limited replication will not be considered here as RDR. Rather, the definition of RDR will be restricted to those events that are dependent on homologous recombination proteins and capable of replicating large portions of a chromosome.

RDR Pathways in Bacteriophage

Most of the early data arguing for the existence of RDR came from studies of bacterial viruses. For example, recombination-deficient mutants of well-known bacteriophages such as T4, T7, and lambda were found to be partially defective in DNA replication. The interpretation of that replication defect has not been straightforward, because recombination reactions can play indirect roles in viral DNA replication. For example, if recombination links multiple bacteriophage genomes together into a linear concatamer, a single initiation event from a conventional replication origin can result in much more DNA replication than if the genomes are not linked. Furthermore, recombination proteins might play a role in converting a theta-form replication intermediate into a rolling circle, resulting in numerous replication products rather than just two.

Studies with bacteriophage T4, however, demonstrated that the involvement of homologous recombination proteins in DNA replication is very direct. At early times of infection, T4 DNA replication initiates at replication origins by a mechanism that involves a persistent RNA–DNA hybrid (R-loop), but this origin-dependent replication is turned off after several minutes. For the remainder of the infection cycle, all DNA replication initiates by an RDR mechanism in which a fully functional replication complex is assembled on a displacement loop (D-loop; Figure 1). The D-loop is formed when the 3′ single-stranded end of one phage DNA molecule invades a homologous region of another phage DNA molecule, or the other end of the same molecule (since T4 DNA is terminally redundant).

Most or all D-loop formation depends on the phage-encoded UvsX and UvsY proteins, acting in concert with the T4 single-stranded DNA binding protein gene

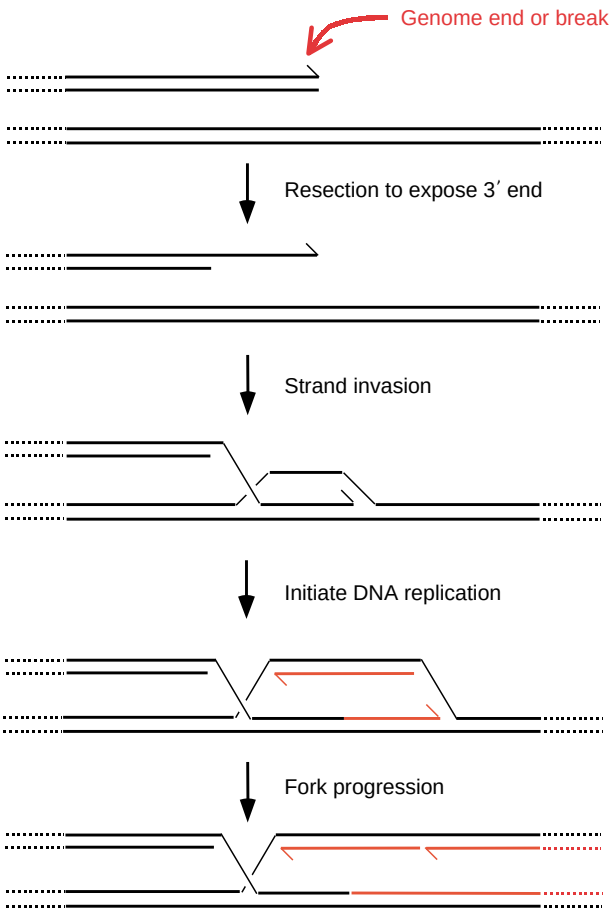

FIGURE 1 Model for bacteriophage T4 RDR. A single-stranded 3′ end is generated from a genomic end or break in the first step, either by exonuclease resection or by prior DNA replication up to the end (not shown in the figure). The strand invasion step creates a D-loop, upon which replication is initiated after assembly of the replication complex. The dotted lines indicate extended regions of the phage chromosome, and all newly replicated DNA is in red.

*p*roduct 32 (gp32). UvsX is a strand invasion protein, homologous to bacterial RecA and eukaryotic Rad51 protein, while UvsY plays the key role of loading UvsX onto gp32-coated single-stranded DNA (i.e., the 3′ end).

Once a D-loop is formed, the phage protein gp59 is the critical component that directs the replication machinery to the D-loop. The gp59 protein preferentially binds branched DNA and also gp32-coated DNA, and one or both of these preferences are thought to explain D-loop recognition. Gp59 has been first identified based on its ability to stimulate the loading of the replicative helicase (gp41) onto DNA during *in vitro* replication reactions. Once the replicative helicase is loaded, more extensive template unwinding, loading of additional replication proteins, and extensive DNA replication becomes possible. Proteins that allow the loading of replicative helicases onto recombination intermediates are central to the process of RDR, and the corresponding bacterial proteins will be discussed below.

There is now quite convincing experimental evidence for the T4 RDR pathway. A variety of physical and genetic experiments support the proposal that genome ends trigger DNA replication after a strand-invasion reaction. Furthermore, artificially introduced double-strand breaks (DSBs) dramatically stimulate the replication of homologous DNA *in vivo*. Finally, a robust *in vitro* system of RDR has been established using the T4 system, and recapitulates the major features of *in vivo* RDR.

Demonstration of RDR in *Escherichia coli* and Yeast

An apparent cellular RDR pathway, called inducible stable DNA replication (iSDR), was first uncovered by the late Tokio Kogoma and colleagues. They found that *E. coli* cells deficient in normal origin-directed replication can nonetheless replicate if their SOS system for DNA damage response is activated. This DNA replication required the strand invasion protein RecA, and a variety of results led to the proposal that iSDR also required chromosomal DNA breaks induced by some component of the SOS system. The simplest model is that the induced DNA breaks lead to invasive 3′ ends, and that resulting D-loops become the sites of assembly of new replication complexes (much like in Figure 1). More recent experiments have demonstrated that artificially induced DSBs can indeed trigger DNA replication in *E. coli*, providing strong support for a cellular pathway of RDR.

A key protein for *E. coli* RDR is PriA, which like T4 gp59, allows the loading of the replicative helicase (DnaB in this case) onto D-loop structures. Several other *E. coli* proteins, including DnaC, PriB, and PriC, can also participate in this reaction. The importance of PriA in the survival of *E. coli* will be discussed later, when we consider the role of RDR in completing genome replication. It is interesting to note at this point, however, that mutational inactivation of PriA dramatically reduces phage P1-mediated generalized transduction and also conjugal recombination. Therefore, these seemingly well-studied genetic pathways, which had been thought for decades to occur by a break-and-rejoin-like mechanism, may actually occur by a mechanism similar to RDR.

RDR is apparently not limited to prokaryotic systems such as T4 and *E. coli*. Indeed, genetic experiments have provided very strong evidence that RDR is a legitimate pathway of DNA break repair in the yeast *Saccharomyces cerevisiae*. Several different genetic approaches have revealed RDR in yeast. One approach used a diploid cell with a site that can be cleaved to create a DSB on one of the two copies of a particular chromosome (Figure 2). The arms of the two

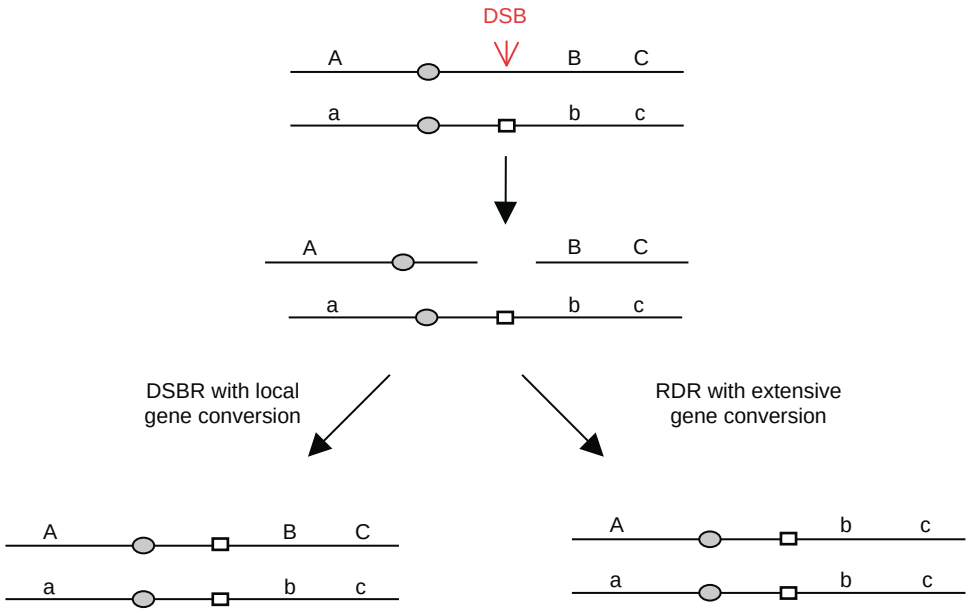

FIGURE 2 Two pathways for repair of a chromosomal DSB in yeast. Repair of a DSB occurs by a localized DSBR pathway on the left side; this pathway involves the reattachment of the two broken arms and a small region of DNA replication to replace any missing DNA near the break site. In the pathway on the right side, the smaller chromosomal fragment (containing alleles B and C) is lost. However, an intact chromosome is regenerated by an RDR reaction in which the broken end of the larger chromosomal fragment invades the intact homologous chromosome, and then triggers a DNA replication fork that travels to the end of the intact chromosome. This duplicates the chromosomal arm that contains alleles b and c, and with Holliday junction resolution, provides the cell with two complete and intact chromosomes to fulfill the diploid state. In this figure, each solid line is a DNA double helix, and gray ovals indicate centromeres. The downward pointing arrow indicates the site for the DSB, while the empty box indicates the DNA sequence at the corresponding site on the noncleavable chromosome (the sequences in this region of the two chromosomes are different from each other). Based on Malkova *et al.* (1996). *Proc. Natl Acad. Sci. USA* **93**, 7131–7136.

chromosomes were marked with a series of heteroalleles (indicated by the letters A/a, B/b and C/c in Figure 2). In wild-type cells, when the DSB is induced on the top chromosome, the diploid that resulted from DSB repair usually maintained each of the three pairs of heteroalleles, indicating a local DSBR event that caused gene conversion at the site of the DSB and that reattached the broken distal arm of the chromosome (Figure 2; left). At a low frequency, however, the resulting diploid cell experienced an extensive gene conversion event in which all alleles in the arm distal to the DSB had been converted to the form that was originally located on the unbroken (homologous) chromosome (Figure 2; right). Apparently, the distal chromosomal fragment with the "B" and "C" alleles had been lost, and replaced with a newly replicated copy of the distal arm from the unbroken chromosome.

While these RDR products were normally quite rare in wild-type cells, they became predominant when the cells had a mutation that inactivated the Rad51 protein (strand invasion protein, homologous to RecA/UvsX). Also, when the experimental setup was altered so that the distal fragment of the broken chromosome had no homology to the intact chromosome, wild-type cells efficiently utilized this RDR pathway to regenerate an intact chromosome. The only general mechanism to explain this extensive gene conversion of a large portion of a chromosome is that the centromere-proximal chromosomal end undergoes a strand-invasion reaction with the homologous chromosome, and the resulting D-loop triggers a new replication fork just as in the RDR pathways.

RDR as a Backup Mechanism to Complete DNA Replication

Nearly 30 years ago, Ann-Marie Skalka proposed that recombination could provide a mechanism for creating new replication forks after a previous fork encountered a template nick. Her proposal dealt with the complexities of phage lambda DNA replication, and has not been ascribed any broader significance for some time. However, many years later, scientists realized that a similar mechanism provides a means of restarting a replication fork that has been destroyed by a template nick. As diagrammed in Figure 3, when a replication fork encounters a template nick, one of the two arms can be broken off and replication thereby terminated. The broken end can be reconfigured into a replication fork by first forming a D-loop using a strand-invasion

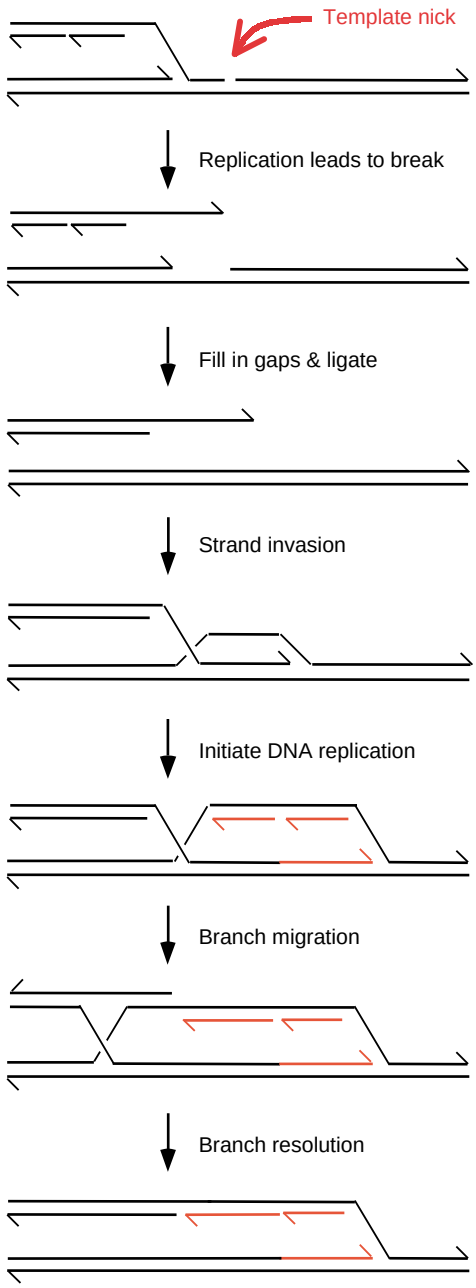

FIGURE 3 Replication fork breakage at a nick and restart by recombination. A template nick leads to a broken fork, which is then restarted by RDR. Note that one DNA strand has been flipped to the top in the molecule immediately after the arrow indicating branch migration (because DNA is a double helix but the drawing depicts only parallel lines, this flipping is just a convenience to make the drawing simpler).

reaction, and then assembling a replication complex onto the D-loop. Subsequent branch migration and junction resolution can thereby regenerate a simple replication fork and allow the completion of replication and normal segregation of the products at the next cell division (Figure 3).

We now believe that this pathway explains why many recombination-deficient mutants of bacteria and yeast grow poorly – they have great difficulty completing DNA replication due to problems at the fork. Notably, PriA-deficient mutants of *E. coli*, whose primary defect is in replication fork restart, are nearly inviable and quickly accumulate suppressor mutations that improve their viability.

In vivo experiments have demonstrated that replication forks are indeed broken when they encounter a template nick. It is not clear how often replication forks encounter template nicks, but broken replication forks also arise by another pathway that could be even more common. In bacterial and phage systems, it has been demonstrated that certain stalled or blocked replication forks are prone to breakage. This breakage depends on the branched-DNA-specific nucleases that normally resolve Holliday junctions (i.e., *E. coli* RuvC and T4 endonuclease VII). Results in eukaryotic systems also suggest that some blocked forks are broken, although the identity of the cleaving nuclease is uncertain.

It may seem strange that blocked replication forks would be actively cleaved by recombination nucleases, and this is indeed a dangerous reaction. However, this cleavage is apparently under strict control, and may only be used as a "last resort" when a stalled or blocked replication fork cannot be restarted by other mechanisms. By coupling fork cleavage with an RDR reaction, the replication fork can potentially be restarted and the cell saved from the dire consequences that result from trying to segregate a partially replicated DNA molecule in the next cell division.

With this new view that recombination provides a back-up mechanism to restart broken replication forks, it is worth reconsidering an interesting question from evolutionary biology—how and why did homologous recombination evolve? It is now clear that homologous recombination can play an important role at the level of single cell survival, namely the completion of DNA replication. Furthermore, it seems likely that DNA replication was even more prone to failure early in the evolution of cells, before very sophisticated replication machineries and repair pathways have been fully developed. Therefore, many scientists in the field now believe that homologous recombination first evolved as a means to complete cellular DNA replication, and that all the other wonderful benefits of recombination came later.

Replication Fork Failure and Direct Restart Pathways

The above description of replication fork restart is incomplete, focusing only on the restart of forks that end up being broken. As might be expected, other pathways

are able to directly restart stalled or blocked replication forks without the dangerous step of breaking the fork. Indeed, bacterial cells have multiple pathways for directly restarting forks. Although these pathways need not involve any recombination of the DNA molecules, some of the proteins that are involved in direct restart pathways are nonetheless recombination proteins that play roles in recombinational restart or other homologous recombination pathways.

One of the important unanswered questions is the fate of the various components of the replication machinery when forks are blocked or stall. It is clear that replication fork restart pathways require proteins that can load the replicative helicase, and so by inference, the replicative helicase seems to be lost when forks stop prematurely. We don't know which other components of the replication machinery are lost upon fork failure. Because the replicative helicase is thought to encircle the lagging-strand template, it is presumably lost whenever that strand is broken. In other cases (e.g., breakage of the leading strand and fork arrest without breakage), it remains to be determined how exactly the helicase is lost, and for that matter, whether the helicase is lost in only a subset of replication fork failures.

There are many possible reasons why a replication fork might stop prematurely. For example, a particular nucleotide might be temporarily limiting, a noncovalently bound protein might be encountered on the template duplex, or one of the key proteins of the replication machinery might become damaged or displaced from the replication fork. Sidestepping the question of how and why the replicative helicase and other proteins might be lost from such a fork, it is easy to see how direct restart pathways can solve the immediate problem and allow a completion of DNA replication.

However, the true complexities and benefits of replication fork restart pathways only become obvious when we consider other problems that a replication fork can encounter, particularly the many different forms of template DNA damage. The most obvious problem is when the replication machinery encounters a damaged base on the leading-strand template. In this case, one can easily see the advantage of disassembling the normal replication machinery—namely that an appropriate DNA repair complex can be recruited to fix the template damage or, if that fails, a translesion DNA polymerase can be recruited to incorporate something opposite the damaged base (Figure 4; left). After the repair or translesion synthesis event, the normal replication machinery would need to be assembled to resume replication, hence the need for a direct restart pathway (or an RDR event if the fork has become broken). This description of the behavior of the replication fork at sites of template DNA damage is very superficial and incomplete, in part because there are many forms of damage and multiple pathways of repair. The more serious limitation at this time, however, is that the field is just beginning to investigate what promises to be a very rich area, this interface where DNA replication, repair and recombination all intersect at troubled replication forks.

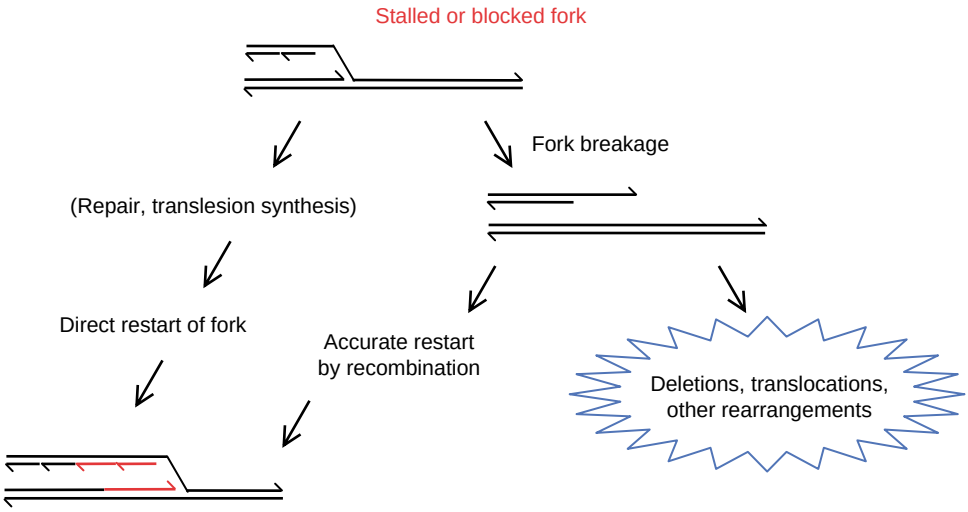

FIGURE 4 Pathways for restarting replication forks. Replication forks may stall due to the absence of nucleotides or problems with the replication machinery, or may be blocked due to template damage or bound proteins ahead of the fork. If the fork is blocked by template damage, repair of the damage or translesion synthesis may precede direct fork restart. If the fork is simply stalled, direct fork restart can occur without repair. In either case, some or all of the replication proteins need to be reassembled on the fork to reinitiate replication. In the pathway on the right, the stalled or blocked fork is broken, for example, by a recombination nuclease. Accurate restart of the fork by RDR (as in Figure 3) can lead to a normal cell without any genetic damage, but failure of this accurate pathway can lead to chromosomal rearrangements.

Disturbances in Fork Processing Lead to Genome Instability and Cancer Predisposition

DNA breaks are inherently dangerous. A broken fragment of a chromosome that lacks the centromere may be lost during mitosis to generate a terminal chromosomal deletion (assuming that the centromere-containing fragment acquires a new telomere). A broken end might engage in a non-homologous end joining reaction, or if the end is located within a repeat region, might undergo homeologous recombination with another copy of the repeat. In both cases, chromosomal deletions, inversions, and translocations can result.

With an understanding that DNA replication can lead to DNA breaks, it is therefore not surprising to find a strong association between disturbances in replication fork processing and genome instability. For example, studies in *S. cerevisiae* have shown that mutational inactivation of genes involved in the recombinational restart of replication forks (RDR) leads to genome instability. Apparently, when the normal pathway of restarting broken forks is disturbed, the broken DNA can result in chromosomal rearrangements (Figure 4).

Cells from individuals who suffer from certain human cancer predisposition syndromes (Werner's, Bloom's, and Rothmund–Thomson syndrome) show increased genome instability. Genetic analysis has traced these defects to genes that encode proteins that are suspected to be involved in replication fork integrity, recombinational restart of broken forks, and/or direct restart pathways. All three of these proteins belong to the RecQ family of DNA helicases (named after the founding member, bacterial RecQ). The precise role of any of these proteins is presently unclear, but it is easy to imagine that genome instability could result from a defect in recombinational restart of broken forks, or from a higher incidence of replication fork breakage. Increased fork breakage could potentially arise from a defect in a protein that is involved in direct restart pathways, or from any mutation that leads to more frequent fork arrest.

In summary, the period since the early 1990s has seen a remarkable merger of studies of DNA replication, recombination, and repair. These three processes apparently participate in an intricate choreography that is necessary for the accurate and complete replication of the genome, which in turn is important for genome stability and for the prevention of cancer in humans.

See Also the Following Articles

DNA Replication Fork, Bacterial • DNA Replication Fork, Eukaryotic • Phosphoinositide 3-Kinase • Protein Kinase B

Glossary

direct restart pathways Pathways that restart replication forks that are intact but have become stalled or blocked.

gene conversion Nonreciprocal recombination event in which one allele is converted into the form of the second allele.

homeologous recombination Recombination between two nearly identical sequences that are not allelic (i.e., not at the same corresponding position on the chromosome).

recombination-dependent replication (RDR) Extensive replication of a chromosome that is dependent on homologous genetic recombination and recombination proteins.

recombinational restart The restart of replication forks by an RDR reaction.

Further Reading

Cox, M. M., Goodman, M. F., Kreuzer, K. N., Sherratt, D. J., Sandler, S. J., and Marians, K. J. (2000). The importance of repairing stalled replication forks. *Nature* **404**, 37–41.

Haber, J. E. (1999). DNA recombination: The replication connection. *Trends Biochem. Sci.* **24**, 271–275.

Hickson, I. (2003). RecQ helicases: Caretakers of the genome. *Nat. Rev. Cancer* **3**, 169–178.

Kogoma, T. (1997). Stable DNA replication: Interplay between DNA replication, homologous recombination, and transcription. *Microbiol. Mol. Biol. Rev.* **61**, 212–238.

Kowalczykowski, S. C., and von Hippel, P. H. (2000). Special issue: The DNA replication—recombination interface. *Trends Biochem. Sci.* **25**, 155–206.

Malkova, A., Ivanov, E. L., and Habes, J. E. (1996). Double-strand break repair in the absence of RAD51 in yeast: a possible role for break induced DNA replication. *Proc. Natl Acad. Sci. USA* **93**, 7131–7136.

McGlynn, P., and Lloyd, R. G. (2002). Genome stability and the processing of damaged replication forks by RecG. *Trends Genet.* **18**, 413–419.

Radding, C. (2001). Links between recombination and replication: Vital roles of recombination. *Proc. Natl Acad. Sci. USA* **98**, 8172. (This is the introductory article for a special colloquium issue, and is followed by numerous articles on the same topic.)

Skalka, A.-M. (1974). A replicator's view of recombination (and repair). In *Mechanisms in Recombination* (R. F. Grell, ed.), Plenum Press, New York, pp. 421–432.

Biography

Kenneth N. Kreuzer is a Professor of Biochemistry and Microbiology at Duke University Medical Center in Durham, North Carolina. He was trained as an undergraduate at MIT, earned his Ph.D. from the University of Chicago, and received his postdoctoral training at the University of California, San Francisco. The research interests in his laboratory include mechanisms of DNA replication, recombination and repair, and the mechanism of action of antitumor agents that target DNA topoisomerases.

recQ DNA Helicase Family in Genetic Stability

Mary A. Risinger and Joanna Groden
University of Cincinnati College of Medicine, Cincinnati, Ohio, USA

Helicases are enzymes that use nucleoside triphosphate (usually ATP) hydrolysis to unwind nucleic acid duplexes (DNA–DNA, RNA–RNA, or DNA–RNA). Most helicases exclusively unwind either DNA or RNA duplexes, although some can unwind DNA duplexes and RNA duplexes as well as DNA–RNA hybrids. Because virtually all forms of DNA metabolism (including transcription, replication, recombination, and repair) require the unwinding of double stranded DNA (to allow access to the bases which encode the genetic information), DNA helicases are essential to the function and maintenance of the genome. This article deals with one family of DNA helicases, the recQ family, named for the similarity of family members to the prototype *Escherichia coli* recQ helicase, which participates in the recF genetic recombination pathway. Loss of recQ helicase function results in a loss of genomic stability that can be manifested in various ways. In humans, loss of function of certain recQ helicases results in cancer predisposition and variable degrees of premature aging. The study of these ubiquitous and highly conserved proteins promises to yield important information concerning tumorigenesis and the aging process.

Classification of Helicases

By primary structure comparisons helicases are divided into five superfamilies. The recQ family belongs to superfamily II (Sf2), one of the largest of the superfamilies. All Sf2 helicases contain seven conserved helicase motifs designated I, Ia, II, III, IV, V, and VI. Motifs I and II are the Walker A and B sequences characteristic of ATPases. Motif II of recQ helicases contains the DEXH motif (single-letter amino-acid code) that is a major characteristic of this family and is essential for ATP hydrolysis and, consequently, for helicase activity.

In *E. coli*, recQ is the sole member of its family. Most lower eukaryotic organisms also have a single recQ helicase. Examples are sgs1 from the budding yeast, *Saccharomyces cerevisiae*, and rqh1 from the fission yeast, *Schizosaccharomyces pombe*. However, higher organisms generally have multiple recQ helicases, presumably needed to maintain more complex genomes. Humans have at least five recQ helicases encoded by the *BLM*, *RECQ1* (also referred to as *RECQL*), *RECQ4*, *RECQ5*, and *WRN* genes.

Human Genetic Disorders Resulting from Defects in recQ Helicases

Defects in three of the five human recQ helicases result in defined clinical disorders known as chromosome breakage syndromes (autosomal recessive human disorders characterized by spontaneous genomic instability). Bloom syndrome, Rothmund–Thomson syndrome, and Werner syndrome are caused by germ-line defects in the *recQ* genes *BLM*, *RECQ4*, and *WRN*, respectively. Hallmarks of these rare diseases are genomic instability (apparent at the cellular level), cancer predisposition, and variable characteristics of premature aging.

Bloom Syndrome

Bloom syndrome (BS) persons (who lack the BLM protein due to various mutations in the *BLM* gene) are proportional dwarfs with sun-sensitive facial erythema (redness), impaired fertility, immune deficiency, and a high incidence of almost all forms of cancer with a very early age of onset (average 24 years). This makes BS a particularly interesting model for the study of tumorigenesis since most other hereditary cancer predisposition disorders result in the development of site-specific cancers. Cells cultured from BS persons demonstrate genomic instability in the form of a higher rate of the same types of chromosomal aberrations detected in cells cultured from normal individuals. Chromosomal breaks and rearrangements that are a result of increased homologous recombination are frequently observed. The classic feature of BS cells, which is considered diagnostic of the disease, is a several-fold increase in the frequency of sister chromatid exchanges (SCEs; reciprocal exchanges of DNA between sister

chromatids by homologous recombination). BS cells also demonstrate an abnormal profile of DNA replication intermediates.

Rothmund–Thomson Syndrome

Rothmund–Thomson syndrome (RTS) persons have progressive poikiloderma (a variegated hyperpigmentation and telangiectasia of the skin, followed by atrophy) that is apparent in early childhood. Common characteristics include numerous skeletal abnormalities, thin hair, cataracts, hypogonadism, and short stature. RTS persons are primarily susceptible to a single type of cancer, osteosarcoma (median age of onset 12 years), but skin malignancies and other forms of cancer have also been reported. Cells isolated from RTS persons reveal genomic instability in the form of chromosome translocations, rearrangements, and deletions.

Werner Syndrome

Werner syndrome (WS) is a hallmark premature aging disease. It is generally not detected until adolescence when WS persons fail to undergo the usual growth spurt and begin to display symptoms of premature aging including graying and thinning of the hair, wrinkling of the skin, cataracts, type II diabetes mellitus, osteoporosis, and atherosclerosis. WS persons are short in stature due to lack of the adolescent growth spurt and often have reduced fertility. They demonstrate a high incidence of malignancies, particularly sarcomas. The major causes of death are malignancy and vascular disease (average lifespan 47 years). Cells isolated from WS persons have a reduced replicative lifespan (they divide fewer times before becoming senescent) and are marked by increased genomic instability in the form of chromosomal alterations including chromosome translocations, rearrangements, and large deletions.

Structural Characteristics of recQ Helicases

In recQ family members, the helicase domain containing seven helicase motifs (I, Ia, III–VI) is generally centrally located (Figure 1). Most recQ helicases also have an recQ family C terminal (RQC) domain located just C terminal to the helicase domain. Since mutations of conserved residues in this region severely decrease ATPase activity, helicase activity, and single stranded DNA binding, it has been suggested that this domain may be involved in coupling DNA binding to ATP hydrolysis. More distal to the helicase domain is another conserved C-terminal domain designated as the helicase RNase D C-terminal (HRDC) domain. The HRDC domain is thought to be an auxiliary DNA binding domain. Unlike the RQC domain that is characteristic of recQ helicases, the HRDC domain is also found in other types of DNA-binding proteins (including other helicases, recombinases, and polymerases). With the exception of a nuclear localization signal identified in some recQ helicases, there is little additional C-terminal homology among recQ helicases. N-terminal domains vary greatly in length among recQ family members and there is generally little homology in this region. Several family members have N-terminal acidic regions and some have C-terminal acidic regions, which may be involved in protein–protein interactions.

Functional Characteristics of recQ Helicases

All recQ helicases studied to date are ATP- and Mg^{2+}-dependent 3–5′ helicases, i.e., they translocate along the DNA strand to which they bind in the 3–5′ direction as they unwind duplex DNA. Human *WRN* helicase and frog *FFA-1* helicase are unique in that they also have a 3–5′ exonuclease activity. It has been difficult to define the functions of recQ helicases at the molecular level *in vivo*. Since higher organisms have multiple recQ helicases and the loss of function of a single recQ helicase is compatible with survival, it is likely that recQ helicases have some overlapping functions where the remaining helicases can partially compensate for the loss. (RecQ helicases must also have some independent functions since diseases associated with the loss of a particular helicase have distinct characteristics.) The processes in which recQ helicases are likely involved (replication, recombination, and repair) are also closely intertwined. Clues to the *in vivo* functions of recQ helicases are provided by associated clinical syndromes (described above), *in vitro* studies, and *in vivo* localizations and associations.

Functional Clues Provided by *in vitro* Studies

RecQ helicases are unusual among helicases in their DNA substrate preferences. Although they are generally unable to unwind blunt-ended duplex DNA (unless a bubble is present), they efficiently unwind such non-Watson–Crick DNA structures as G-quadruplexes (extremely stable DNA secondary structures that can form in guanine-rich regions of DNA) and Holliday junctions (four-way crossover structures formed by DNA strand exchange during homologous recombination). They also unwind displacement loops (D-loops; intermediates formed during the strand invasion step of recombination).

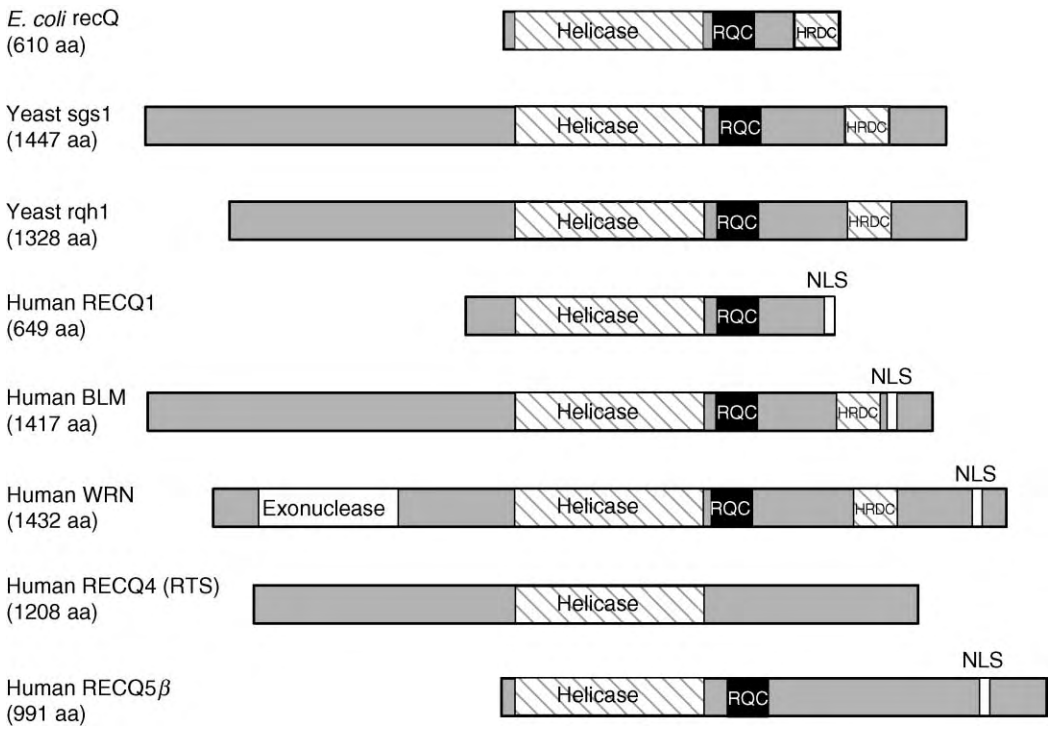

FIGURE 1 Schematic representation of domain structure of several recQ helicases. The names and sizes (numbers of amino acids) of the helicases are listed on the left. The positions of the conserved helicase, RQC (RecQ family C terminal), and HRDC (Helicase RNase D C terminal) domains are indicated on each diagram. The locations of the known nuclear localization signals (NLS) and the exonuclease domain of human WRN are also indicated.

Functional Clues Provided by Localizations and Associations

RecQ helicases undergo subnuclear relocalizations under various conditions. For instance, BLM generally has a punctate distribution within the nucleus that is at least partially associated with PML bodies (named for the presence of promyelocytic leukemia tumor suppressor protein). After treatment of cells with DNA damaging agents or inhibitors of DNA replication, BLM becomes associated with sites of DNA repair (defined by the presence of RAD51, required for the initial DNA strand pairing and invasion of homologous recombination). BLM directly binds to RAD51. BLM also associates with other proteins involved in DNA repair including ATM (ataxia telangiectasia mutated; serine/threonine kinase which phosphorylates BLM and other proteins involved in DNA damage repair), RPA (Replication Protein A; single stranded DNA binding protein involved in replication, recombination, and repair), BRCA1 (breast cancer susceptibility gene product), and MLH1 (mismatch repair protein). BLM (and most recQ helicases from lower organisms) binds topoisomerase III (relaxes negatively supercoiled DNA) and stimulates its activity. The tumor suppressor p53 binds to BLM and regulates its helicase activity.

WRN is generally associated with the nucleolus and/or is nucleoplasmic but undergoes translocation to DNA replication foci when DNA synthesis in inhibited. Potential roles for WRN in DNA replication, recombination, and repair are suggested by its association with a number of proteins involved in these processes including: RPA, FEN 1 (flap endonuclease 1; 5–3′ DNA structure-specific nuclease implicated in replication, recombination, and repair), EXO-1 (exonuclease 1; member of the RAD2 family of nucleases implicated in replication, recombination, and repair), pol-δ (DNA polymerase-δ; major DNA polymerase involved in replication), PCNA (Proliferating Cell Nuclear Antigen; pol-δ accessory factor), pol-β (DNA polymerase-β; major DNA polymerase involved in both short and long patch base excision repair), RAD52 (mediator of homologous recombination), the DNA-PK holoenzyme (DNA-PK_{CS} plus Ku70/80; serine/threonine kinase which phosphorylates WRN and other DNA repair proteins) and p53.

Potential Functions for recQ Helicases in Replication-Associated DNA Repair

Although loss of recQ helicase function leads to a number of phenotypic cellular changes, two consistent features are abnormal DNA replication and an increased occurrence of recombination. Distinctive characteristics of recQ helicases include their unusual substrate preferences

(G-quadruplexes, structures which resemble Holliday junction recombination intermediates, and D-loops) and their associations with other proteins implicated in replication, recombination, and repair. They also associate with what are presumed to be stalled replication forks after replication has been interrupted or DNA damage has occurred. These data suggest that the major function of recQ helicases is to maintain genomic stability by restarting stalled replication forks, although more than one mechanism could be responsible for this function. RecQ helicases may resolve DNA secondary structures such as G-quadruplexes ahead of the replication fork to allow the replication fork to proceed unimpeded. Indeed, WRN and *E. coli* recQ enable DNA polymerase-δ to traverse DNA tetraplex and hairpin structures *in vitro*.

RecQ helicases also may reset replication forks when they stall after encountering an area of DNA damage. One model that explains how this might occur is the "chickenfoot" model (Figure 2). In this case, leading strand synthesis is blocked by a lesion in the template while lagging strand synthesis continues for a short distance (Figure 2B). When replication stops, positive supercoiling surrounding the replication fork favors the formation of a four-way junction, the so-called chickenfoot that is analogous to a Holliday junction (Figure 2C). The shorter leading strand can now be extended to the end of the longer lagging strand with which it is now paired, past the lesion in the template (Figure 2D). RecQ helicases might then unwind these structures to restart the replication fork past the area of damage (Figure 2E). In the absence of a recQ helicase, the chickenfoot could be resolved by homologous recombination to re-establish the replication fork. RecQ helicases also may have a role in DNA repair by homologous recombination as suggested by their ability to unwind D-loops *in vitro* (disrupting less productive or inappropriate recombination intermediates). This could partially explain the observation of increased homologous recombination in cells lacking the BLM recQ-like helicase.

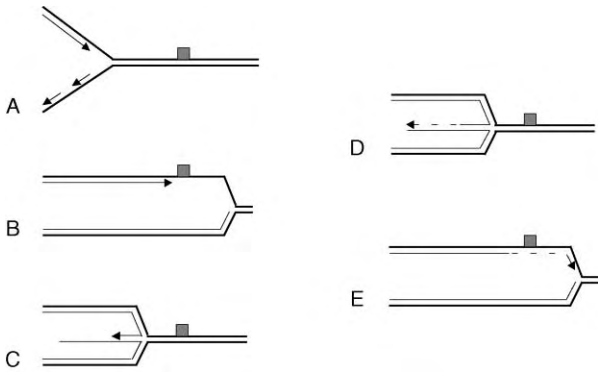

FIGURE 2 Chickenfoot model for the role of recQ helicases in restarting replication forks stalled by DNA damage. A replication fork is shown with the leading strand on top and the lagging strand on bottom (A). The long arrow represents leading strand synthesis, while the short arrows indicate lagging strand synthesis. When the fork encounters a lesion in the template on the leading strand (gray square), leading strand synthesis is halted but lagging strand synthesis can proceed for a short distance (B). When replication stops, positive supercoiling surrounding the replication fork favors the formation of a four-way junction, the chickenfoot (C). The shorter leading strand can now be extended to the end of the longer lagging strand with which it is now paired, past the lesion in the template (D). RecQ helicases would then unwind these structures to restart the replication fork past the area of damage (E).

Potential Function for recQ Helicases in Telomere Maintenance

Telomeres are structures composed largely of G,C-rich DNA repeat sequences that cap the ends of eukaryotic chromosomes and are required for chromosome stability. Telomeres become shorter each time a cell replicates its chromosomes. Stem cells and most immortal tumor cells overcome telomeric shortening using telomerase (a reverse transcriptase) to extend telomere ends. A relatively small proportion of human cancers use a telomerase-independent mechanism called alternative lengthening of telomeres (ALT) to extend telomeres and allow for continued cell division. Through recombination, long stretches of telomeric-repeat DNA are added to telomeres. Budding yeast strains that lack telomerase use a telomere maintenance pathway that resembles ALT and requires the recQ helicase sgs1. The human recQ helicases BLM and WRN have been localized to telomeres in ALT cells; both helicases bind to the telomere-associated protein TRF2 (Telomeric Repeat Factor 2). These data suggest that recQ helicases might have a role in telomere maintenance, at least in ALT cells. Since telomeres are G,C-rich structures in which G-quadruplexes are likely to form, recQ helicases might unwind these structures prior to replication of telomeric DNA. Additionally (or alternatively), recQ helicases might have a more direct role in the recombination process used for telomere lengthening.

See Also the Following Articles

DNA Helicases: Dimeric Enzyme Action • DNA Helicases: Hexameric Enzyme Action • DNA Polymerases: Kinetics and Mechanism • Exonucleases, Bacterial • Telomeres: Maintenance and Replication

Glossary

chromosome breakage syndromes Autosomal recessive human disorders characterized by spontaneous genomic instability and including Bloom, Rothmund–Thomson, and Werner syndromes.

D-loops Displacement loops; intermediates formed during the strand invasion step of recombination.

G-quadruplexes Extremely stable DNA secondary structures that can form in guanine-rich regions of DNA.

helicases Enzymes that use nucleoside triphosphate (usually ATP) hydrolysis to unwind nucleic acid duplexes (DNA–DNA, DNA–RNA, or RNA–RNA).

Holliday junctions Four-way crossover structures formed by DNA strand exchange during homologous recombination.

sister chromatid exchanges Reciprocal exchanges of DNA between sister chromatids by homologous recombination.

Further Reading

Cox, M. M. (2001a). Historical overview: Searching for replication help in all of the rec places. *Proc. Natl. Acad. Sci.* **98**, 8173–8180.

Cox, M. M. (2001b). Recombinational DNA repair of damaged replication forks in *Escherichia coli*: Questions. *Annu. Rev. Genet.* **35**, 53–82.

Gorbalenya, and Koonin (1993). Helicases: amino acid sequence comparisons and structure–function relatinship. *Curr. Opin. Struct. Biol.* **3**, 419–429.

Haber, J. E. (1999). DNA recombination: The replication connection. *Trends Biochem. Sci.* **24**, 271–275.

Hickson, I. D. (2003). RecQ helicases: Caretakers of the genome. *Nat. Rev. Cancer* **3**, 169–178.

Higgins, N. P., Kato, K., and Strauss, B. (1976). A model for replication repair in mammalian cells. *J. Mol. Biol.* **101**, 417–425.

Moheghegh, P., and Hickson, I. D. (2002). Premature aging in RecQ helicase-deficient human syndromes. *Int. J. Biochem. Cell Biol.* **34**, 1496–1501.

Nakayama, H. (2002). RecQ family helicases: Roles as tumor suppressor proteins. *Oncogene* **21**, 9008–9021.

Oakley, T. J., and Hickson, I. D. (2002). Defending genome integrity during S-phase: Putative roles for RecQ helicases and topoisomerase III. *DNA Repair* **1**, 175–207.

Singleton, M. R., and Wigley, D. B. (2002). Modularity and specialization in Superfamily 1 and 2 helicases. *J. Bacteriol.* **184**, 1819–1826.

Soultanas, P., and Wigley, D. B. (2001). Unwinding the "Gordian knot" of helicase action. *Trends Biochem. Sci.* **26**, 47–54.

Umezu, K., Nakayama, K., and Nakayama, H. (1990). *Escherichia coli* RecQ protein is a DNA helicase. *Proc. Natl. Acad. Sci.* **87**, 5363–5367.

Biography

Joanna Groden is a Professor in the Department of Molecular Genetics, Biochemistry, and Microbiology at the University of Cincinnati College of Medicine, and an Assistant Investigator of the Howard Hughes Medical Institute. Her principal research interest is inherited susceptibility to cancer. She holds a Ph.D. from Cornell University and received her postdoctoral training at the University of Utah. Her work resulted in the cloning and characterization of two human disease genes that determine cancer susceptibility, the *APC* tumor suppressor and the *BLM* helicase.

Regulated Intramembrane Proteolysis (Rip)

Jin Ye, Michael S. Brown and Joseph L. Goldstein
University of Texas Southwestern Medical Center, Dallas, Texas, USA

Regulated intramembrane proteolysis (Rip) is a newly recognized mechanism for signal transduction that involves the generation of regulatory molecules from membrane proteins. Such cleavage liberates cytoplasmic or lumenal/extracellular fragments from transmembrane precursor proteins, allowing the cleaved fragments to function at a new location. Rip influences processes as diverse as cellular differentiation, lipid metabolism, and the response to unfolded proteins, as originally addressed in a review article by Brown *et al.*. In addition to its occurrence in animal cells, Rip has been observed in bacteria, and, remarkably, the bacterial proteases are related evolutionarily to the ones used in animal cells. Proteins that are known to undergo Rip, span all the membrane bilayer at least once. In nearly all cases, the intramembrane cleavage does not take place until the bulk of the protein on the extracytoplasmic (lumenal or extracellular) face has been removed by a primary cleavage. This primary cleavage shortens the extracytoplasmic segment to less than 30 amino acids, which is a prerequisite for the secondary intramembrane cleavage. At least ten membrane proteins are currently known to undergo Rip, and their intramembrane cleavage is mediated by four different families of membrane-bound proteases (Figure 1).

Rip Mediated by Site-2 Protease (S2P) Family

S2P is a polytopic membrane protein with the characteristics of a membrane-embedded zinc metalloprotease (Figure 2). Genes similar to the one encoding mammalian S2P have been identified in DNA sequences from multiple species, including archaea, bacteria, plants, and animals. The encoded proteins share a similar hydrophobicity profile that predicts a highly hydrophobic structure with multiple membrane-spanning regions (Figure 2). The NH_2-terminal portion of all of these proteins contains a sequence conforming to the HE*xx*H consensus that is found in a large subfamily of zinc metalloproteases (where *x* is typically a noncharged amino acid). In these proteins, the two histidines of the HE*xx*H motif coordinate with a zinc atom, and the glutamate activates a water molecule, allowing it to make a nucleophilic attack on the peptide bond. Unlike its location in hydrophilic domains of classic zinc metalloproteases, the HE*xx*H sequence of S2P is embedded in a highly hydrophobic segment (Figure 2).

In addition to the HE*xx*H motif, classic zinc metalloproteases contain a remote residue (tyrosine or aspartate) that provides an additional coordination bound for the zinc. In the S2P-like proteins, this function is believed to be filled by the aspartate of the sequence LDG, which resides in a hydrophobic segment that shows a characteristic double peak in hydrophobicity plots and is located near the COOH terminus (Figure 2). The hydrophobic nature of S2P is consistent with its postulated role in cleaving a peptide bond that is located within a membrane bilayer.

Five membrane proteins, two in animals and three in bacteria, are known to be cleaved by the S2P family (Figure 2). In animal cells, both S2P substrates (SREBP and ATF6) contain one conserved asparagine and one conserved proline residue in the middle of the transmembrane domain, located about ten residues COOH-terminal to the cleavage site. Single amino acid substitution of either the asparagine or proline reduces cleavage only slightly, but substitution of both residues abolishes cleavage. The asparagine–proline sequence may serve as an NH_2-terminal cap that allows a portion of the transmembrane α-helix to unwind partially to expose the peptide bond for cleavage by S2P.

Sterol Regulatory Element-Binding Proteins (SREBPs)

SREBPs are membrane-bound transcription factors that regulate the synthesis of cholesterol, a major component of membranes in mammalian cells. As shown in Figure 1, SREBP is inserted in membranes of the endoplasmic reticulum (ER) in a helical hairpin fashion. The cytosolic NH_2-terminal domain is a transcription factor of the basic-helix-loop-helix-leucine zipper family. The COOH-terminal domain, also cytosolic, forms a

Membrane protein	Organism	Primary cleavage enzyme	Enzyme mediating Rip	Regulator of cleavage	Sites of cleavage	Function or consequence of cleaved protein
					Extracytosolic / Membrane / Cytosolic	
Rip by S2P family of proteases						
SREBP	Mammals/ *Drosophila*	S1P	S2P	Sterols/ phospholipids		Activates genes for lipid metabolism
ATF6	Mammals	S1P	S2P	Unfolded proteins		Activates genes for ER chaperones
RseA	*E.coli*	DegS	YaeL	Unfolded proteins		Releases σ^E, which activates stress induced genes
cAD1	*E. faecalis*	Signal peptidase	Eep	?		Stimulates mating
pro-σ^k	*B. subtilis*	None	SpoIVFB	SpoIVB		Activates genes for sporylation
Rip by γ-Secretase (Presenilin)						
APP	Mammals	β-Secretase	γ-Secretase	?		Generates Aβ peptide
Notch	Mammals/ *Drosophila*	TACE	γ-Secretase	Delta		Activates genes for differentiation
ErbB-4	Mammals	TACE	γ-Secretase	Heregulin		Phosphorylates nuclear proteins that inhibit cellular growth
Rip by Other Proteases						
MHC, class I	Mammals	Signal peptidase	Signal-peptide peptidase	?		Generates peptide for antigen presentation by HLA-E
Spitz	*Drosophila*	None	Rhomboid	Star		Generates ligand for EGF receptor

FIGURE 1 Membrane proteins that undergo regulated intramembrane proteolysis (Rip) categorized according to the Rip protease. The cleaved protein fragments are highlighted in red. For simplicity, proteins are not drawn to scale, and we do not show the alternate pathway for APP processing, which involves cleavage by TACE. For Notch, we show only the transmembrane subunit.

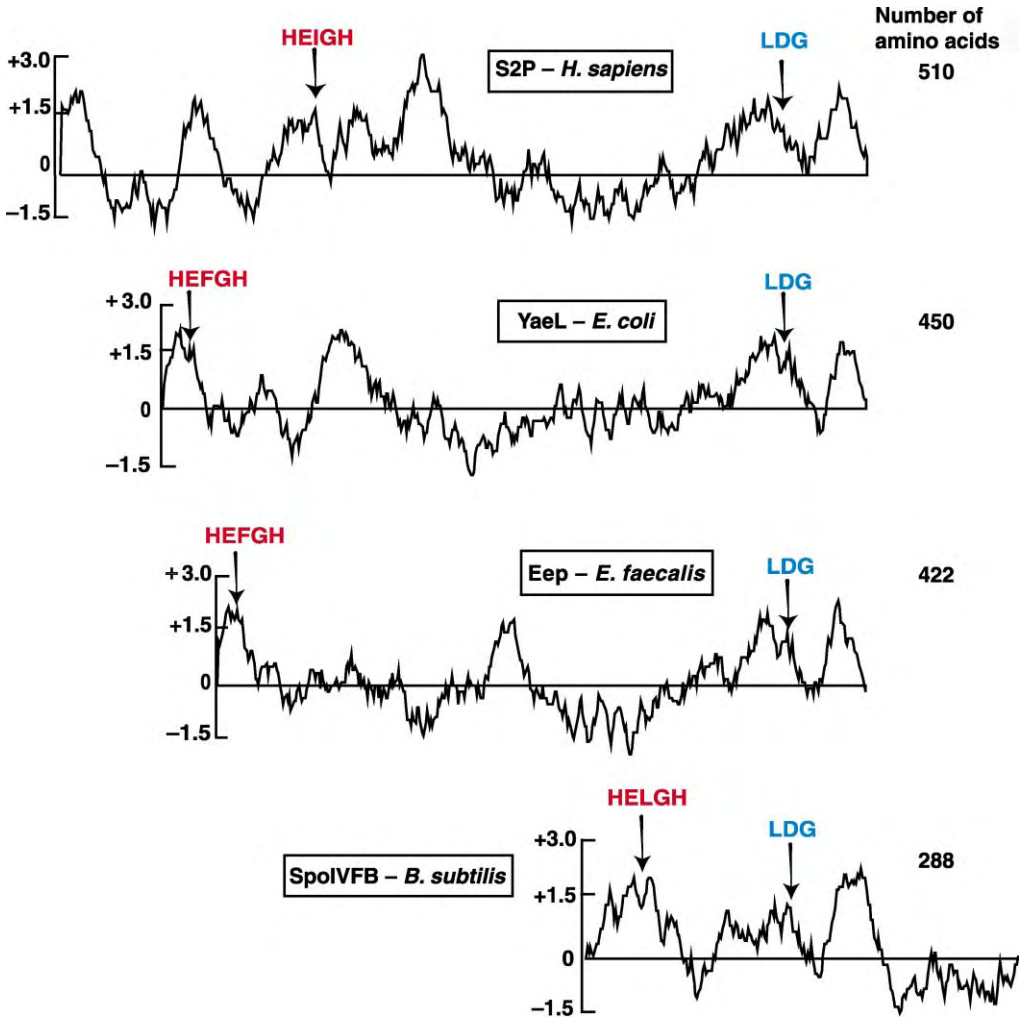

FIGURE 2 Hydropathy plots of human S2P and its bacterial family members. The HE*xx*H and LDG motifs (discussed in the text) are highlighted in red and blue, respectively. Each plot is drawn on the same scale and aligned by the position of the LDG motif. GenBank Accession numbers for the amino acid sequences are as follows: S2P, AAC51937; YaeL, AAC73287; Eep, AAD47948; and SpoIVFB, p26937.

complex with a polytopic membrane protein called SCAP. Upon deprivation of sterols, SCAP transports SREBP from ER to Golgi, where cleavage occurs. When cells are overloaded with sterols, the SCAP/SREBP complex is trapped in the ER and cleavage cannot occur. Inasmuch as SREBPs activate genes encoding enzymes of cholesterol synthesis, this sterol-mediated block in transport allows cholesterol to inhibit its own synthesis in a classic feedback fashion.

The first cleavage of SREBP is catalyzed by site-1 protease (S1P), a membrane-bound serine protease that is oriented with its active site in the lumen of the Golgi complex. Cleavage by S1P separates the two transmembrane helices of SREBP, but the NH_2-terminal fragment remains membrane-bound until it is cleaved by S2P at a site that is three residues within the transmembrane segment (Figure 1). Even though the activity of S2P is not regulated directly by sterols, S2P does not act until the two transmembrane segments have been separated by S1P, which effectively brings this reaction under cholesterol control.

In *Drosophila*, orthologues of SREBP, SCAP, S1P, and S2P are all expressed even though *Drosophila* cells do not produce sterols. *Drosophila* SREBP is processed by S1P and S2P in a reaction that requires SCAP and presumably requires ER to Golgi transport. The major SREBP targets in *Drosophila* S2 cells are enzymes required for synthesis of saturated fatty acids, which are incorporated into the major phospholipid, phosphatidyl ethanolamine (PE). PE, rather than sterols, is the feedback regulator of SREBP cleavage in these cells.

ATF6 AND RSEA

ATF6 is a type 2 membrane protein with a single transmembrane domain (Figure 1). Its NH_2-terminal

cytosolic domain is a transcription factor of the bZIP family. When mammalian cells produce unfolded endoplasmic reticulum (ER) proteins, ATF6 translocates from ER to Golgi, where it is cleaved sequentially by S1P and S2P, the same proteases that process SREBP. The intramembrane proteolysis carried out by S2P liberates the NH_2-terminal domain of ATF6 from the membrane, allowing it to activate transcription of *BiP/GRP78* and other genes whose products assist the folding of ER proteins. This regulatory pathway, called the unfolded protein response, helps cells to survive conditions of ER stress.

In *E.coli*, σ^E is the transcription factor that regulates extracytoplasmic stress response. Under nonstress conditions, σ^E is negatively regulated by RseA, an inner membrane protein with one transmembrane domain (Figure 1). The NH_2-terminal cytosolic domain of RseA binds to σ^E and is sufficient to inhibit σ^E activity. When unfolded proteins accumulate in the periplasmic space (similar to ER lumen in eukaryotic cells), RseA is first cleaved by DegS, a membrane-bound serine protease with its active site projecting into the periplasmic space. Cleavage by DegS removes the majority of the COOH-terminal periplasmic domain of RseA. YaeL, an orthologue of S2P, then cleaves the remaining part of RseA, after which RseA is rapidly degraded. This frees σ^E to associate with RNA polymerase and direct transcription of its target genes.

The similarity between mammalian and bacteria unfolded-protein response suggests that S2P-mediated Rip has been selected to cope with extracytoplasmic stress during evolution, although individual organisms use the mechanism in different ways: in mammalian cells Rip directly releases the active transcription factor from its substrate, whereas in bacteria Rip leads to degradation of a membrane-bound inhibitor of the responsible transcription factor.

Other Bacterial Proteins

Enterococcus faecalis, a Gram-positive bacterium, secretes an 8-amino acid peptide pheromone called cAD1, which induces a mating response in other enterococci that harbor a plasmid called pAD1 (Figure 1). Genomic sequencing revealed that the octapeptide pheromone is derived from a 143-amino acid precursor that contains a signal peptide at the NH_2-terminus and is inserted into the plasma membrane with a type 2 orientation. The pheromone corresponds to the COOH-terminal 8 amino acids of the signal peptide (Figure 1). The octapeptide is generated by cleavage of the precursor at two sites, at the extracellular side of the membrane in a reaction carried out by signal peptidase and at a site in the middle of the transmembrane signal peptide by Eep, an S2P orthologue. This system differs from the others in that the active fragment is released by S2P into the extracellular space rather than the cytosol.

Another prokaryotic relative of S2P is a *B. subtilis* protein called spoIVFB. This protein contains an HE*xx*H motif in a hydrophobic segment near the NH_2 terminus and an LDG motif in a double-peaked hydrophobic segment toward the COOH terminus (Figure 2). The overall hydrophobicity profile of SpoIVFB differs from those of the other family members. SpoIVFB is a much smaller protein, and it contains a hydrophilic extension on the COOH-terminal side of the hydrophobic LDG segment. SpoIVFB is the protease that removes a membrane-embedded NH_2-terminal hydrophobic peptide from a transcription factor, pro-σ^K, thereby releasing the factor into the cytosol and allowing it to activate gene transcription. This process is necessary for completion of spore formation in response to nutrient deprivation. The membrane orientation of pro-σ^K is opposite to the type 2 orientation of other known S2P substrates, and it is the only S2P substrate that does not require a primary cleavage (Figure 1). These differences in catalytic requirements may account for the differences in structure between SpoIVFB and the other members of the S2P family.

Rip Mediated by γ-Secretase

γ-Secretase is a membrane-bound complex consisting of several proteins, including presenilin and nicastrin. Presenilin contains two conserved aspartate residues that are located in 2 of its 8 transmembrane helices at positions that are predicted to place them at the same depth in the membrane. This property is reminiscent of soluble aspartyl proteases, which contain two closely apposed aspartates that are required for activity. Experiments with active-site-modifying agents specific for aspartyl proteases provide evidence that presenilin contains the active proteolytic site. The second component of γ-secretase, also required for catalytic activity, is a membrane protein called nicastrin. Nicastrin is believed to present substrates to presenilin, regulate its stability, and deliver it to the cell surface.

Several membrane proteins are believed to be cleaved by γ-secretase, but only three have been well characterized, as discussed here.

Amyloid Precursor Protein (APP)

APP is a type 1 membrane protein with an NH_2-terminal extracellular domain and a COOH-terminal cytosolic tail (Figure 1). Processing of APP generates a toxic amyloid β peptide that is responsible for Alzheimer's disease. APP is first cleaved at a site that is 28 amino acids from the transmembrane helix by β-secretase, a membrane-bound aspartyl protease with an extracytoplasmic active

site. This cleavage shears off the bulk of the extracellular domain of APP, which then allows the protein to be cleaved within the membrane by γ-secretase. Intramembrane cleavage can occur at either of the two sites separated by two amino acids, leading to two different amyloid β peptides, designated $A\beta_{1-40}$ and $A\beta_{1-42}$, which accumulate extracellularly. After the intramembrane γ-secretase cleavage, the cytosolic tail of APP enters the nucleus where it may affect transcription of genes that are not yet identified.

In addition to cleavage by β-secretase, APP can be cleaved by TNFα converting enzyme (TACE), a membrane-bound metalloprotease whose active site faces the extracellular surface. TACE cuts the extracytosolic domain of APP even closer to the membrane, leaving only 12 amino acids on the external surface. Like the β-secretase cleavage, TACE cleavage is followed by γ-secretase cleavage. In this case, the liberated fragment is too short to form an amyloid deposit, and thus cleavage by TACE does not lead to Alzheimer's disease.

Notch

The cell surface receptor Notch is synthesized as a type 1 membrane protein (Figure 1) that is processed constitutively by a furin-like enzyme in the secretory pathway. The enzyme cleaves the precursor to generate two subunits: an extracellular subunit and a transmembrane subunit, which remain associated as a noncovalent heterodimer. The heterodimer travels to the cell surface and remains intact until it binds its ligand Delta, a membrane protein that resides on the surface of an adjacent cell. Binding leads to cleavage of the transmembrane subunit of Notch by TACE, the same enzyme that cleaves APP. TACE cleavage releases most of the extracellular portion of the transmembrane subunit of Notch along with the attached extracellular subunit. The shortened transmembrane subunit is then cleaved by γ-secretase within the membrane-spanning helix, liberating a cytosolic fragment. The cytosolic fragment translocates to the nucleus where it activates several genes whose products influence the fate of cells during development.

ErbB-4

ErbB-4 is a transmembrane receptor tyrosine kinase that regulates cell proliferation and differentiation. It adopts a type 1 orientation with an NH_2-terminal extracellular ligand-binding domain and a COOH-terminal cytosolic tyrosine kinase domain (Figure 1). Upon binding to its ligand, heregulin, the ErbB-4 ectodomain is cleaved by TACE, followed by intramembrane proteolysis carried out by γ-secretase. The intramembrane cleavage results in the release of the cytosolic fragment, which travels to the nucleus where it phosphorylates substrates that regulate cell growth.

Rip Mediated by Signal-Peptide Peptidase (SPP)

SPP, a resident ER protein with 7 transmembrane domains, contains two conserved aspartate residues, each within adjacent transmembrane helices. As discussed above, such motifs are characteristic of the presenilin-type of aspartic protease. Similar to S2P, cleavage by SPP requires helix-breaking residues within the transmembrane domain of its signal peptide substrates.

The best-studied example of Rip mediated by SPP is the proteolytic processing of signal peptides from MHC class I molecules such as HLA-A, -B, -C, and -G. These molecules are expressed with a typical signal sequence for targeting to the secretory pathway. During their translocation through the ER membrane, the signal sequences are cleaved off from the pre-protein by signal peptidase. The cleaved signal peptides, which remain membrane-bound with a type 2 orientation, are then cleaved by SPP in the middle of the membrane to liberate the NH_2-terminal half of the signal peptides into the cytosol (Figure 1). These cytosolic fragments are then transported into the ER lumen where they bind to HLA-E, a nonclassical MHC class I molecule. The HLA-E/peptide complexes travel to the cell surface where they bind to CD94/NKG2A receptors on natural killer (NK) cells and inhibit NK cell-mediated lysis. This pathway protects cells expressing normal MHC class I molecules from killing by NK cells.

Rip Mediated by Rhomboid

Rhomboid, a Golgi membrane protein with 7 transmembrane domains, is a serine protease whose catalytic triad is buried within the membrane bilayer. Rhomboid belongs to a large gene family that is conserved throughout archaea, bacteria, yeast, plants, and animals, including humans. To date, rhomboid has only been characterized in *Drosophila* where it initiates epidermal growth factor receptor (EGFR) signaling.

Spitz is the main ligand for *Drosophila* EGFR. It is synthesized as a transmembrane precursor with an NH_2-terminal extracellular EGF-like domain and a short COOH-terminus cytosolic tail (Figure 1). Spitz is confined to the ER and is inert until it binds to another protein named star. Star escorts spitz from ER to Golgi where spitz is cleaved by rhomboid. The intramembrane cleavage liberates the extracellular

EGF-like domain from the membrane, allowing it to be secreted out of the cell.

Unlike Rip mediated by other proteases, a primary cleavage that sheds the extracytoplasmic domain of spitz is not required for the action of rhomboid, as rhomboid itself is directly responsible for the release of the extracellular domain of spitz (Figure 1). It remains unclear why spitz is subjected to Rip rather than being cleaved by an extracellular protease such as TACE.

See Also the Following Articles

Amyloid • Cholesterol Synthesis • Secretases

Glossary

regulated intramembrane proteolysis (Rip) A process of signal transduction in which a membrane-bound protease cleaves its substrate within the lipid bilayer, thus allowing the cleaved protein fragment to function at a new location.

rhomboid An intramembrane serine-protease involved in the Rip of Spitz.

γ-secretase A protein complex containing an intramembrane aspartyl-protease catalytic subunit involved in the Rip of APP, Notch, and ErbB-4.

S2P An intramembrane metalloprotease involved in the Rip of SREBPs and ATF6.

SPP An intramembrane aspartyl-protease involved in the Rip of signal peptides released from certain MHC class I molecules.

Further Reading

Alba, B. M., Leeds, J. A., Onufryk, C., Lu, C. Z., and Gross, C. A. (2002). DegS and YaeL participate sequentially in the cleavage of RseA to activate the σ^E-dependent extracytoplasmic stress response. *Genes Develop.* **16**, 2156–2168.

Brown, M. S., Ye, J., Rawson, R. B., and Goldstein, J. L. (2000). Regulated intramembrane proteolysis: A control mechanism conserved from bacteria to humans. *Cell* **100**, 391–398.

Haze, K., Yoshida, H., Yanagi, H., Yura, T., and Mori, K. (1999). Mammalian transcription factor ATF6 is synthesized as a transmembrane protein and activated by proteolysis in response to endoplasmic reticulum stress. *Molecul. Biol. Cell* **10**, 3787–3799.

Lee, J. R., Urban, S., Garvey, C. F., and Freeman, M. (2001). Regulated intracellular ligand transport and proteolysis control EGF signal activation in *Drosophila*. *Cell* **107**, 161–171.

Lemberg, M. K., and Martoglio, B. (2002). Requirements for signal peptide peptidase-catalyzed intramembrane proteolysis. *Molecul. Cell* **10**, 735–744.

Ni, C.-Y., Murphy, M. P., Golde, T. E., and Carpenter, G. (2001). γ-Secretase cleavage and nuclear localization of ErbB-4 receptor tyrosine kinase. *Science* **294**, 2179–2181.

Rawson, R. B., Zelenski, N. G., Nijhawan, D., Ye, J., Sakai, J., Hasan, M. T., Chang, T-Y., Brown, M. S., and Goldstein, J. L. (1997). Complementation cloning of *S2P*, a gene encoding a putative metalloprotease required for intramembrane cleavage of SREBPs. *Molecul. Cell* **1**, 47–57.

Rudner, D. Z., Fawcett, P., and Losick, R. (1999). A family of membrane-embedded metalloproteases involved in regulated proteolysis of membrane-associated transcription factors. *Proc. Natl Acad. Sci. USA* **96**, 14765–14770.

Selkoe, D. J., and Podlisny, M. B. (2002). Deciphering the genetic basis of Alzheimer's disease. *Annu. Rev. Genomics Hum. Genet.* **3**, 67–99.

Ye, J., Rawson, R. B., Komuro, R., Chen, X., Dave, U. P., Prywes, R., Brown, M. S., and Goldstein, J. L. (2000). ER stress induces cleavage of membrane-bound ATF6 by the same proteases that process SREBPs. *Molecul. Cell* **6**, 1355–1364.

Biography

The authors are members of the Department of Molecular Genetics at the University of Texas Southwestern Medical Center in Dallas. Dr. Ye is a postdoctoral fellow in the Department of Molecular Genetics at the University of Texas Southwestern Medical Center in Dallas. He delineated the role of S2P in cleaving membrane-bound SREBPs and ATF6 and advanced a provocative hypothesis to explain the mechanism by which intramembrane proteases cleave transmembrane proteins.

Brown and Dr. Goldstein are Professors in the Department of Molecular Genetics at the University of Texas Southwestern Medical Center in Dallas. They have worked together for 30 years on the genetics and regulation of cholesterol metabolism. They received the Nobel Prize in Physiology or Medicine in 1985 and the Albany Medical Center Prize in Medicine and Biomedical Research in 2003.

Respiratory Chain and ATP Synthase

David G. Whitehouse and Anthony L. Moore
University of Sussex, Brighton, UK

The respiratory chain and ATP synthase are, in eukaryotic cells, located in the inner membrane of mitochondria. Mitochondria are oval-shaped organelles, typically 1–2 μm long and 0.5 μm in diameter, whose principal cellular functions are to generate energy, in the form of ATP and carbon skeletons for biosynthetic purposes. The shape and appearance of mitochondria vary considerably and these organelles appear to be most numerous in mammalian tissues with a high-energy demand (heart, liver, muscle, and brain and in rapidly dividing plants cells). The respiratory chain functions to oxidize NADH ($+H^+$) and $FADH_2$ and reduce molecular oxygen to water. These functions are electron transfer (electronmotive) processes and result in a substantial release of energy, which generates a protonmotive force, that is used to drive the ATP synthase in the forward direction thereby synthesizing ATP for use in cellular reactions.

Components of the Respiratory Chain

The conversion of the electronmotive force (NADH and FADH oxidation) into a protonmotive force is carried out by three electron-driven proton-pumping respiratory chain complexes. These large transmembrane complexes contain numerous reduction–oxidation (redox) components that include flavins, iron–sulfur proteins, cytochromes, ubiquinone, and metal ions.

Flavins

Flavin mononucleotide (FMN) and flavin dinucleotide (FAD) are tightly bound (to their enzymes) cofactors that can accept (or donate) two electrons and two protons (to become fully reduced) or a single electron and proton to form the semiquinone intermediate.

Iron–Sulfur Proteins

Iron–sulfur (or nonheme iron proteins) contain iron atoms covalently bound to the apo-protein by cysteine sulfurs and to other iron atoms via acid labile sulfur bridges. In general, there are three types of Iron–sulfur proteins namely a single iron atom coordinated to the sulphydryl groups of four cysteine residues of the protein, a protein containing two irons and two inorganic sulfides (2Fe–2S) and four irons and four inorganic sulfides (4Fe–4S). Similar to the single iron cluster, both are coordinated by four cysteine residues. All three types of Iron–sulfur proteins can act as single electron carriers.

Cytochromes

Cytochromes are proteins containing a prosthetic group called a heme. The basis of the heme is a porphyrin, which consists of four pyrrole rings linked in a cyclic manner by methene bridges with a central coordinated iron atom that acts as a single electron carrier. There are at least four classes of cytochromes (cytochrome A–D) differentiated from each other by the ability to absorb light at different wavelengths (due to differences in the side chains on the porphyrin).

Ubiquinone

Ubiquinone or coenzyme Q is a hydrophobic quinone derivative that in mammalian mitochondria has a side chain of ten 5-carbon isoprene units (Q_{10}). Ubiquinone can be fully reduced to the quinol form by the acceptance of $2H^+$ and $2e^-$ (or the semiquinone derivative can be formed through the acceptance of a single proton and electron).

Respiratory Chain Complexes

The following respiratory chain complexes (I, III, and IV) are associated with proton translocation across the inner mitochondrial membrane.

Complex I (NADH-Ubiquinone Oxidoreductase)

NADH-ubiquinone oxidoreductase is the largest (750 kDa) and most complicated of the respiratory

chain complexes, having ~43 subunits. Although it is well established that complex I contains FMN and numerous Iron–sulfur proteins as redox centers, the exact route of electron transfer is uncertain. What is certain, however, is that the enzyme transfers two protons and two electrons from NADH ($+H^+$) to ubiquinone, and electron transfer is accompanied by the translocation of protons across the membrane with a stoichiometry of $4H^+/2e^-$. Enzyme activity is potently inhibited by rotenone and piercidin A. Electron microscopic studies suggest that complex I has an L-shape with the majority (if not all) of the redox centers being located within the peripheral part of the enzyme. The exact mechanism whereby protons are translocated across the membrane is uncertain.

Complex III (Ubiquinone–Cytochrome *c* Oxidoreductase or the bc_1 Complex)

Complex III is a large (250 kDa) multicomponent complex that catalyzes the oxidation of ubiquinol and the reduction of cytochrome c_1 and results in the vectorial transport of protons across the inner mitochondrial membrane. Redox centers include a 2Fe-2S protein (the Rieske center), two *b* cytochromes (cytochrome b_L and b_H) and cytochrome c_1. X-ray crystallography studies reveal that the enzyme is dimeric, with each of the two monomers being composed of at least 11 subunits (8 of which appear to have no catalytic role). Crystallography has also revealed that the monomers do not function independently but cooperate during electron transfer. Structural studies have also shown that the Rieske center shuttles between the quinone-binding site (of one of the monomers) in its oxidized state and cytochrome c_1 (of the second monomer) in its reduced state. Although the pathway of electron flow through complex III (known as the Q-cycle) is complicated, the net equation is:

$$QH_2 + 2\text{cyt}c_{1(\text{oxidized})} + 2H^+_N = Q + 2\text{cyt}c_{1(\text{reduced})} + 4H^+_P$$

where N and P refer to the negative and positive sides of the membrane (Figure 1).

The Q-cycle accommodates the fact that there is a mixture of two and one electron carriers and hence there must be a switch between ubiquinol (a two electron carrier), the cytochromes, and Rieske center (all of which are single electron carriers). It also explains the well-documented observation that the H^+/e^- stoichiometry for the bc_1 complex is 4. Complex III is inhibited by antimycin A, myxothiazol, and stigmatellin.

Complex IV (Ferrocytochrome *c* – Oxygen Oxidoreductase or Cytochrome *c* Oxidase)

Complex IV is a third large transmembrane enzyme (204 kDa) that catalyzes the oxidation of reduced cytochrome *c* and the reduction of molecular oxygen to water. It is also associated with the translocation of protons across the membrane and has at least 13 subunits of which only subunits I and II appear to play

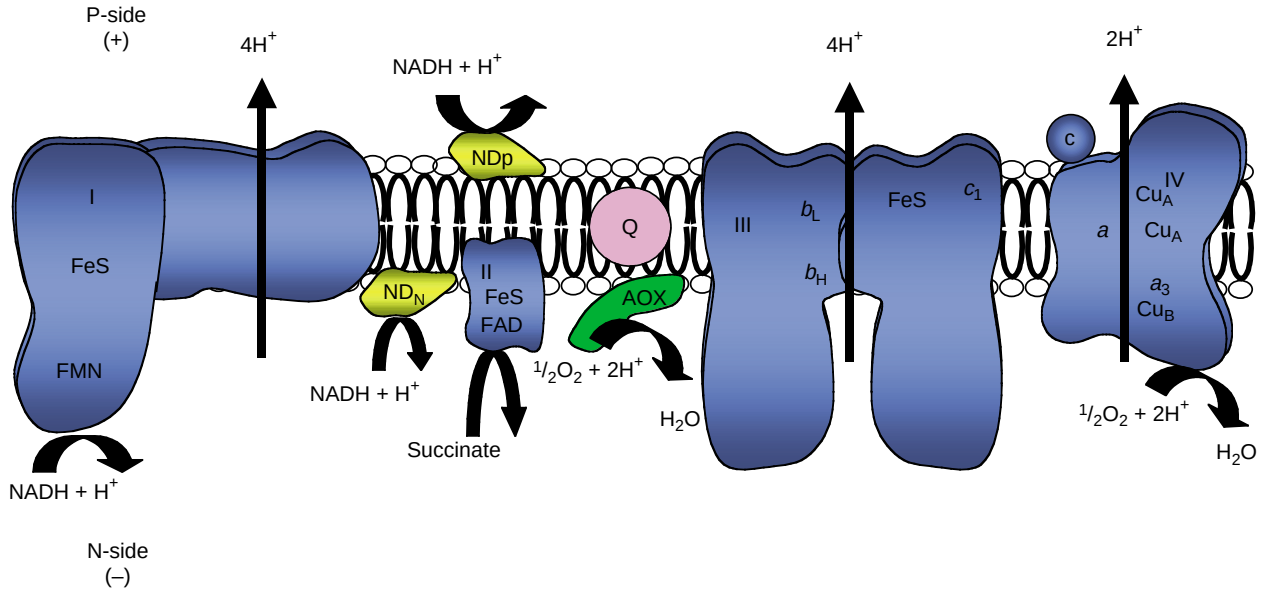

FIGURE 1 A schematic representation of the respiratory chain. The P- and N-sides of the membrane refer to the intermembrane space (positive) and matrix (negative), respectively. ND_P and ND_N refer to NADH dehydrogenases (such as the ETF, glycerol-3-phosphate and externally located NADH dehydrogenases) located on the P- and N-sides, respectively. AOX is the alternative oxidase.

a role in catalysis. The complex contains three Cu atoms and two heme *a* (cytochrome *a* and cytochrome a_3). High-resolution structural studies reveal that subunit II contains two of the Cu atoms complexed with sulfur atoms to form a binuclear center (known as Cu_A center). Subunit I contains the two cytochromes and the third Cu atom (Cu_B), which is closely associated with cytochrome a_3 forming a second binuclear center. Electron transfer through complex IV is from cytochrome *c* to the Cu_A center (which acts as a single electron receptor), then to heme *a* (which is slightly closer to the Cu_A center than heme a_3) onto the heme a_3–Cu_B center and finally onto oxygen bound to heme a_3. For every four electrons passing through the complex, one molecule of oxygen is reduced to two molecules of water, four protons are consumed from the matrix, and four protons are translocated across the membrane. It should be noted that the four electron reduction of molecular oxygen occurs as four single electron events and hence it is important that the potentially dangerous partially reduced intermediates such as superoxide anion are not released but remain tightly bound until completely reduced to water. Cytochrome *c* oxidase is potently inhibited by cyanide, azide, and carbon monoxide, which bind at the oxygen-binding site. Nitric oxide is also a reversible inhibitor of this complex.

Other Ubiquinone-Reducing Enzymes

Animal, plant, and a number of protest mitochondria also contain a number of membrane-bound enzymes that can reduce ubiquinone. These enzymes do not transfer charge across the membrane, i.e., protons are not vectorially transported across the inner mitochondrial membrane and are detailed in the following section.

Succinate Dehydrogenase

Succinate dehydrogenase is the only membrane-bound enzyme of the citric acid cycle that interacts directly with the respiratory chain. Succinate dehydrogenase is much smaller than complex I (140 kDa) being composed of four subunits. The two larger of these subunits are peripheral proteins that contain covalently bound FAD (on subunit I) and three Iron–sulfur centers (on subunit II). These two large subunits are anchored to the inner surface of the inner membrane by two integral membrane polypeptides (subunits III and IV) in which a single heme *b* is located. Although the exact route of electron transfer from succinate to ubiquinone is uncertain, it is known that the reduction of ubiquinone by succinate is not associated with any charge movement.

Electron-Transferring Flavoprotein (ETF)-Ubiquinone Reductase

The ETF-ubiquinone oxidoreductase is a globular protein located on the inner surface of the inner membrane and contains FAD, an Fe–S center and a ubiquinone-binding site. The enzyme can accept reducing equivalents from a variety of dehydrogenases including those involved in fatty acid oxidation or amino acid and choline catabolism.

Glycerol-3-phosphate Dehydrogenase

Glycerol-3-phopshate dehydrogenase is located on the outer surface of the inner membrane and catalyzes the oxidation of glycerol-3-phosphate to dihydroxyacetone phosphate and the reduction of ubiquinone. Although little is known about the structure or the route of electron transfer to ubiquinone, redox centers include FAD and probably an Iron–sulfur center.

External NADH Dehydrogenase

There are a number of rotenone-insensitive NADH dehydrogenases located on the outer and inner surface of the inner mitochondrial membrane in plant and yeast mitochondria. Again there is little structural information apart from the presence of FAD and possibly an Iron–sulfur center. Electron transfer is probably similar to that described for the ETF-ubiquinone oxidoreductase since the enzyme catalyzes the oxidation of NADH and the reduction of ubiquinone. In plants, the external NADH dehydrogenase (on the outer surface of the inner membrane) is regulated by cytosolic Ca^{2+}. These enzymes are not associated with proton pumping across the mitochondrial membrane.

Other Ubiquinol Oxidizing Enzymes (The Alternative Oxidase)

Although mammalian mitochondria do not possess any other ubiquinol-oxidizing enzymes apart from cytochrome oxidase (complex IV), most plants, some yeasts, fungi, and trypanosomes possess a cyanide- and antimycin-insensitive alternative oxidase that catalyzes the oxidation of ubiquinol and reduces molecular oxygen to water. Unlike cytochrome *c* oxidase, electron transfer does not result in proton translocation and redox energy is released as heat. Although no structural information is available, the enzyme is believed to contain two nonheme iron atoms linked by an oxygen atom as its only redox carrier (di-iron protein) and is probably globular with two of its amphiphilic helices lying parallel to the membrane plane. Enzyme activity is insensitive to all complex IV inhibitors but can be potently inhibited by salicylhydroxamic acid and the alkyl gallates.

Organization of the Respiratory Chain

The respiratory chain complexes in mammalian and plant mitochondria are generally considered to be free to diffuse laterally and independently of each other within the plane of the membrane. They are connected electronically to each other by ubiquinone and cytochrome *c* with electron transfer occurring by diffusion-based collisions between these components. There is also evidence to suggest that the numbers of complexes within the membrane are unequal with the following ratio: complexes I:II:III:IV: cytochrome *c*: ubiquinone = 1:2:3:7:14:63. Both cytochrome *c* and ubiquinone are considered to function as common pools and hence act as mobile carriers mediating electron transfer between freely diffusible large respiratory complexes.

For every $2e^-$ passing from NADH ($+H^+$) to oxygen to produce one molecule of water a total of ten protons are released at the P-side of the membrane. Since four protons are required to synthesize and export one ATP, then the amount of ATP formed by the oxidation of NADH is 2.5 (1.5 for succinate).

The ATP Synthase

The ATP synthase (or F_1F_0 ATPase and also referred to as complex V) uses the free energy of an electrochemical gradient of protons (or sodium ions) generated by the respiratory chain to synthesize ATP. The ATP synthases comprise a very large group of highly conserved enzymes that are found in the bacterial cytoplasmic membranes, the thylakoid membranes of chloroplasts, and the inner membranes of mitochondria. Most members of the group use H^+ as the coupling ion (the *Propionigenium modestum* enzyme is an example of the few ATP synthases that can use Na^+ as the physiological coupling ion).

Structure of the ATP Synthase

The ATP synthase is a miniature rotating motor and the simplest or prototype enzyme is that isolated from *E. coli*. The enzyme has a bipartite structure composed of a membrane-bound (hydrophobic) F_0 component crossing the inner mitochondrial membrane and a water-soluble (hydrophilic) F_1 component that protrudes into the mitochondrial matrix.

The F_0 Component

The F_0 entity is composed of three subunits (*a*, *b*, and *c*) with a stoichiometry of: *a*:2*b*:9–12*c* and it functions as a proton channel. The proton channel is a ring of 9–12 *c* subunits (the number of subunits may depend on the carbon source used for growth) positioned in the membrane and tightly bound to one *a*-subunit plus two *b*-subunits of F_0 and also bound to the γ, δ, and ε subunits of the F_1 component of the synthase.

The F_1 Component

The F_1 component has five types of subunits (α, β, γ, δ, and ε) with a stoichiometry of $3\alpha{:}3\beta{:}\gamma{:}\delta{:}\varepsilon$. The $\alpha_3\beta_3$ subunits are arranged as a hexamer of alternating α- and β-subunits with the γ-subunit projecting into the central cavity of this hexamer. The β-subunits contain the catalytic site for ATP synthesis/hydrolysis and bind the adenylates and inorganic phosphate.

ATP synthases from other sources all have very similar structures to the *E. coli* synthase except the mitochondrial enzyme. It contains an inhibitor protein and a mitochondrial oligomycin-sensitivity-conferring protein (OSCP factor). The mitochondrial δ-subunit is related to the ε-subunit of the *E. coli* synthase (Figure 2).

Mechanism of ATP Synthesis

ATP synthesis is driven by the rotation of the single γ-subunit, which extends into the center of the α_3/β_3 hexamer that contains the catalytic sites. As the single γ-subunit rotates so it alternately alters the conformation (and hence binding characteristics) of the catalytic sites. Changes in nucleotide affinity occur in the three β-subunits and arise from their interactions with the γ-subunit. This results in the sequential binding of ADP and Pi, followed by ATP synthesis and ATP release. This concept recognizes that the β-subunit can exist in three conformations: open, tight, or loose forms. These forms correspond to the binding, synthesis, and release of ATP and are driven by the rotation of the γ-subunit. The hydrolysis of ATP will drive the rotation of the γ-subunit in the opposite direction to that of synthesis.

Subunits c_{9-12}, γ, and ε constitute the rotor (rotating unit) and subunits α_3, β_3, δ, *a*, and b_2 constitute the stator (stationary unit). The protonmotive force drives rotation of the oligomeric ring of the *c*-subunits and of the γ-subunit in F_0 (since the γ-subunit is attached to the *c*-oligomer). Thus, protons moving from the P-side to the N-side of the inner membrane (i.e., down the electrochemical gradient are converted into rotational torque of γ, which alters nucleotide binding at the β-catalytic site and results in the synthesis/hydrolysis of ATP. It is not the synthesis of ATP but its release from the synthase that is driven by the protonmotive force. Subunits γ and ε rotate relative to the $\alpha_3\beta_3$ hexamer to alter the nucleotide affinities (and hence binding) in the β-catalytic sites. Probably subunit γ of F_1 and two copies of subunit *b* in F_0 stabilize the synthase complex.

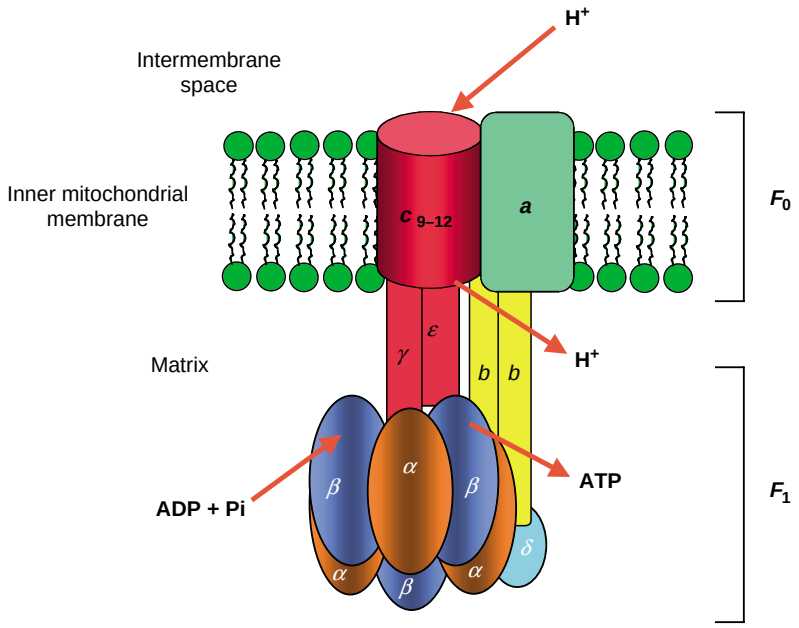

FIGURE 2 Diagram of the ATP synthase. Note that during ATP synthesis, subunits *c*, γ, and ε rotate as a complete unit with respect to the other (fixed) subunits.

A simplified mechanism suggests that it is the flow of protons through *c* via *a* channel (or two half channels) that protonates an aspartate residue and the proton is released through the channel (or second half channel). Conformational changes during this cycle of protonation–deprotonation provide the basis to explain rotation. This protonated *c* subunit then rotates through 360° during ATP synthesis/hydrolysis and both the subunits γ and ε rotate by 120° for each ATP synthesized (or hydrolyzed) with the rotation being coupled to the protonation-deprotonation of three–four *c* subunits.

See Also the Following Articles

ATP Synthesis in Plant Mitochondria: Substrates, Inhibitors, Uncouplers • Cytochrome bc_1 Complex (Respiratory Chain Complex III) • Cytochrome *c* • Flavins • Iron–Sulfur Proteins

Glossary

binuclear center A binuclear center comprises two redox-active components in close proximity, e.g., copper and cytochrome *a* or two iron atoms linked by an oxygen atom that function as a single entity to mediate electron transfer.

proton pump A transmembrane protein which mediates the active transport of protons across the inner mitochondrial membrane/thylakoid membrane.

protonmotive force The energy contained in an electrochemical gradient of protons across the inner mitochondrial membrane/thylakoid membrane and composed of two components, the membrane potential and pH gradient. It is the driving force for the transport of substrates across the membrane and for the synthesis of ATP.

respiratory chain An assemblage of electron carriers normally arranged as a multicomponent complex and located in the inner mitochondrial membrane.

Further Reading

Abrahams, J. P., Leslie, A. G., Lutter, R., and Walker, J. E. (1994). The structure of F_1-ATPase from bovine heart mitochondria determined at 2.8 Å resolution. *Nature (London)* **370**, 621–628.

Boyer, P. D. (1997). The ATP synthase: A splendid molecular machine. *Annu. Rev. Biochem.* **66**, 717–749.

Mitchell, P. (1979). Keilin's respiratory chain concept and its chemiosmotic consequences. *Science* **206**, 1148–1159.

Nelson, D. L., Cox, M. M., and Lehninger, A. L. (2000). In *Principles of Biochemistry*, 3rd Edition. Worth Publishers, New York.

Nicholls, D. G., and Ferguson, S. J. (2002). In *Bioenergetics 3*. Academic Press, London.

Biography

Anthony L. Moore is a professor in the Department of Biochemistry at the University of Sussex, United Kingdom. His principal research interests are in the structure and function of plant mitochondrial respiratory chain proteins. He holds a Ph.D. from the University of Aberdeen and received his postdoctoral training at the University of Pennsylvania. He developed a procedure for measuring the steady-state redox poise of the ubiquinone pool in isolated mitochondria, which his laboratory has used to investigate the regulation of the alternative oxidase.

David G. Whitehouse is a research fellow in the Department of Biochemistry at the University of Sussex, United Kingdom. His principal research interests are in the structures and functions of both the plant mitochondrial and the chloroplast electron transport chains. He holds a Ph.D. from the University of London and received his postdoctoral training at Imperial College, London. He has published a number of research articles and chapters on the regulation of mitochondrial electron transport.

Respiratory Chain Complex I

Ulrich Brandt
Johann Wolfgang Goethe-University, Frankfurt, Germany

Complex I (EC 1.6.5.3) is a multi-subunit respiratory chain NADH:ubiquinone oxidoreductase that is found in the inner mitochondrial membrane of almost all eukaryotes and in the plasma membrane of many bacteria. It contains one molecule of flavine mononucleotide (FMN) and eight to nine iron–sulfur clusters as redox prosthetic groups.

Mammalian complex I couples the transfer of two electrons to the pumping of four protons across the mitochondrial inner membrane and thereby provides up to 40% of the driving force for ATP generation by oxidative phosphorylation (OXPHOS). Complex I is the target of numerous pathological human mutations in both the mitochondrial and the nuclear genomes. Since single electron transfer is part of its catalytic cycle and semiquinone radicals are natural intermediates, complex I is also considered a major source for reactive oxygen species that have been implicated in the etiology of neurodegenerative disorders and in aging.

Complex I Structure

Overall Shape and Subcomplexes

Till date there is no detailed structural information available for complex I. Electron microscopic analysis using single particles and 2D crystals have demonstrated that the enzymes from bovine heart mitochondria, the eubacterium *Escherichia coli*, and the fungi *Neurospora crassa* and *Yarrowia lipolytica* are L-shaped with a hydrophobic membrane integral arm and a hydrophilic peripheral arm that protrudes into the mitochondrial matrix (Figure 1).

When *N. crassa* is grown in the presence of the mitochondrial protein synthesis inhibitor chloramphenicol, a small form of complex I is made which consists of hydrophilic proteins only. Chaotropic agents such as NaBr or detergents can separate the two arms of complex I and also dissociate them further. Subcomplexes have been studied extensively for bovine heart, *N. crassa*, and *E. coli* complex I (Table I).

Central Subunits and Redox Clusters

A minimal form of complex I, consisting of 14 subunits, is found in bacteria such as *E. coli*. Seven of these make up the peripheral arm and contain all the known redox prosthetic groups, namely, one molecule of FMN and eight to nine iron–sulfur clusters. The remaining seven are hydrophobic proteins located in the membrane arm. All these 14 central subunits are also present in eukaryotic complex I. In most eukaryotes, the seven central subunits of the membrane arm (ND1-6, ND4L) are encoded by the mitochondrial genome (Figure 1).

Accessory Subunits

Eukaryotic complex I also contains a large number of additional subunits, resulting in a total number of more than 35 subunits in fungi and at least 45 subunits in mammals. While some may simply serve as a scaffold to increase the stability of the enzyme, there are indications that others may confer additional features specific to eukaryotic complex I. One such example is the acyl carrier protein (ACP) that carries a phosphopantheteine prosthetic group and may function in mitochondrial lipid biosynthesis. The AQDQ subunit seems to be involved in regulation. Phosphorylation at a cAMP-dependent protein kinase consensus site (RVS) was found to stimulate complex I activity. The B16.6 kDa subunit is identical with the programmed cell death regulatory GRIM19 protein and may link complex I function to apoptosis. The MWFE subunit of the membrane arm seems to be involved in complex I assembly. Overall very little is known about the function of the accessory subunits.

A nomenclature established for the bovine enzyme by John Walker and co-workers has been generally accepted for the subunits of complex I. Apart from some of the nuclear-coded subunits that were originally named by their molecular masses, the first four amino acids of the mature protein are used (see Table I). If the mature protein is N-terminally blocked, a number indicating the molecular mass preceded by the letter B identifies the subunit.

Assembly Factors

Two proteins, named CIA30 and CIA84 (for complex I associated), were found to be associated with peripheral

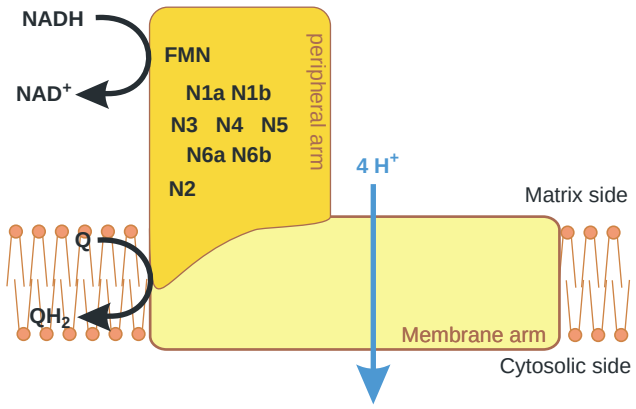

FIGURE 1 Schematic representation of mitochondrial complex I. The peripheral arm contains the seven nuclear-encoded central subunits and harbors all known redox prosthetic groups. The membrane arm contains the seven mitochondrially encoded subunits which are all highly hydrophobic. Eukaryotic complex I contains a number of additional "accessory" subunits distributed over both arms. The mechanism by which the transfer of electrons from NADH to ubiquinone is linked to proton translocation is essentially unknown. Q, ubiquinone; QH_2, ubiquinol.

arm subcomplexes in complex I mutants of *N. crassa*, but are not present in the fully assembled enzyme. Deletion of CIA30 or CIA84 led to complex I assembly defects in *N. crassa*. A CIA30 homologue is also present in mammalian genomes.

Complex I Evolution

Complex I was assembled from at least three pre-existing structural and functional modules during evolution. The homology to [NiFe] hydrogenases from various archae- and eubacterial sources has been especially useful for the understanding of complex I.

The Hydrogenase Module

Water-soluble hydrogenases from *Desulfovibrio* species consist of a large subunit which carries the [NiFe] site and is homologous to the 49 kDa subunit of complex I, and a small subunit which carries three iron–sulfur clusters and is homologous to the PSST subunit of complex I. In membrane-bound [NiFe] hydrogenases, exemplified by the enzyme encoded by the *ech* operon in *Methanosarcina barkeri*, the PSST homologue has suffered a C-terminal deletion abolishing two iron–sulfur clusters. Instead, an additional subunit carrying two iron–sulfur clusters in a ferredoxin-like fold has been acquired in this type of hydrogenase that is homologous to the TYKY subunit of complex I. It has been proposed that the hydrogenase structural fold has been conserved and shaped the catalytic core of complex I. According to this hypothesis, a significant part of the ubiquinone binding site of complex I has been derived

TABLE I

The Fourteen Central Subunits of Complex I and their Evolutionary Relationship to [NiFe] Hydrogenase Subunits; Eucaryotic Complex I Contains a Large Number (31 in Heart) of Additional "Accessory" Subunits

Subunit symbol			Location in[a]			Homologous subunit in [NiFe] hydrogenases	
Bovine	*Y. lipolytica*	*E. coli*	*Bovine*	*E. coli*	Redox prosthetic groups[b]	Water-soluble, e.g., *D. fructosovorans*	Membrane-bound, e.g., *M. barkeri*
75 kDa	NUAM	NuoG	Iλ	PA-DF	N1b N5 N4		
51 kDa	NUBM	NuoF	Iλ	PA-DF	FMN, N3		
49 kDa	NUCM	NuoD[c]	Iλ	PA-CF		Large subunit	EchE
30 kDa	NUGM	NuoC[c]	Iλ	PA-CF			EchD
24 kDa	NUHM	NuoE	Iλ	PA-DF	N1a		
TYKY	NUIM	NuoI	Iλ	PA-CF	N6a, N6b		EchF
PSST	NUKM	NuoB	Iλ	PA-CF	N2	Small subunit	EchC
ND1	ND1	NuoH	Iγ	MA			EchB
ND2[d]	ND2[d]	NuoN	Iγ	MA			EchA
ND3	ND3	NuoA	Iγ	MA			
ND4[d]	ND4[d]	NuoM	Iβ	MA			EchA
ND4L	ND4L	NuoK	Iγ	MA			
Nd5[d]	Nd5[d]	NuoL	Iβ	MA			EchA
ND6	ND6	NuoJ	?	MA			

[a] In *bovine* and *E. coli* complex I. Iλ, Iβ, Iγ, different subcomplexes of bovine heart complex I; PA-DF, peripheral arm, dehydrogenase fragment; PA-CF, peripheral arm, connecting fragment; MA, membrane arm.

[b] Compiled from EPR studies of the bovine heart (N1–N5) and the *N. crassa* enzymes (N6a, N6b). N1a and N1b are binuclear clusters, N2, N3, N4 and N5 are tetranuclear clusters. N6a and N6b are EPR-silent tetranuclear clusters in a ferredoxin-like arrangement.

[c] NuoC and NuoD are fused to a single polypeptide in *E. coli*.

[d] These subunits are similar to each other and to a family of Na^+/H^+ or K^+/H^+ antiporters.

from the [NiFe] site in the large subunit, while cluster N2 corresponds to the proximal iron–sulfur cluster in the small subunit of water-soluble hydrogenases. Based on known X-ray structures of water-soluble [NiFe] hydrogenases, a structural model for the catalytic core of complex I was deduced by Brandt and co-workers and validated by site-directed mutagenesis in the yeast *Y. lipolytica*.

The Na^+/H^+ Transporter Module

One of the two transmembrane subunits of the Ech hydrogenase is homologous to the complex I subunit ND1, while the other exhibits similarities to the three complex I subunits ND2, ND4, and ND5. These three subunits are in turn related to a particular type of Na^+/H^+ or K^+/H^+ antiporter, exemplified by the MrpA and MrpD proteins of *Bacillus subtilis*. Recruitement of this transmembrane module by the water-soluble [NiFe] hydrogenases clearly was an important step toward development of complex I as it provided a component most likely critical for the development of a proton translocation machinery.

The NADH Dehydrogenase Module

The "electron input device" of complex I is related to the NAD^+-reducing [NiFe] hydrogenase from *Ralstonia eutropha*, encoded by the *hox* operon. The 24 and 51 kDa subunits are homologous to HoxF and the first 200 residues of the 75 kDa subunit are homologous to HoxU. The C-terminal half of the 75 kDa subunit shows sequence similarity to a formate dehydrogenase from *Methanobacterium formicicum*.

Variants of Complex I

Interestingly, several complex I variants are known that lack the 75, 51, and 24 kDa subunits of the NADH dehydrogenase module. Two archaebacterial proton pumping enzymes, $F_{420}H_2$:methanophenazine oxidoreductase from *Methanosarcina mazei* and $F_{420}H_2$:menaquinone oxidoreductase from *Archaeoglobus fulgidus*, accept electrons from coenzyme F_{420}, which is specific for methanogenic archaebacteria. The metabolic function of complex I from cyanobacteria and the chloroplasts of higher plants is not known. It may catalyze electron transfer from either NADH, NADPH, or ferredoxin to plastoquinone.

Complex I from the bacteria *Helicobacter pylori* and *Campylobacter jejuni* lack the 51 and 24 kDa subunits and contain a modified version of the 75 kDa subunit. Therefore, it is likely that the electron donor to these enzymes is also not NADH.

Complex I Function

The overall reaction of respiratory chain complex I is the transfer of electrons from NADH to ubiquinone or menaquinone in some bacteria and the concomitant buildup of chemiosmotic membrane potential that in mammalian mitochondria contributes ~40% to the total proton-motive force generated during oxidative phosphorylation.

Electron Transfer and Redox Centers

The physiological reaction of complex I involves electron transfer from NADH via FMN onto a series of iron–sulfur clusters with E_{m7} values between −370 and −250 mV. The tetranuclear iron–sulfur cluster N2 (E_{m7} −150 mV) is generally regarded as the last redox center in this electron transfer chain and there is evidence that it is the immediate electron donor for ubiquinone. Electron transfer from NADH to artificial acceptors such as ferricyanide or hexaammineruthenium(III) chloride does not involve the quinone binding site and can also be observed with a three-subunit subcomplex (flavoprotein, FP) of bovine heart complex I which consists of the peripheral arm subunits 51, 24, and 10 kDa.

Proton Pumping

Experimental data with intact mitochondria and submitochondrial particles indicate that complex I pumps protons with a stoichiometry of 4 $H^+/2\,e^-$. The mechanism how proton translocation is coupled to redox chemistry is still unknown. A large number of concepts and more or less detailed hypothetical mechanisms have been proposed over the last decades, but even the fundamental issue, whether there is just one integrated pumping device or two pumps transporting 2 $H^+/2e^-$ each are operational in complex I, remains unsolved. While FMN could be ruled out as a component of the proton pump, most researches in the field consider iron–sulfur cluster N2 as probable candidate to be directly involved in ubiquinone reduction and proton translocation. This view is supported by experimental evidence for the most part obtained by Tomoko Ohnishi and co-workers demonstrating for this redox center a pH-dependent midpoint potential and magnetic coupling to ubisemiquinone species. However, all known redox centers of complex I reside in the peripheral arm and it remains obscure how electron transfer drives proton translocation across the membrane part. In recent years, different directly linked mechanisms essentially inverting the proton-motive ubiquinone cycle of the cytochrome bc_1 complex have been put forward, but emerging

evidence seems to favor a more indirect mechanism based on conformational coupling.

Na^+ Pumping by Bacterial Complexes I

In some bacteria, complex I pumps sodium ions in addition or instead of protons across the plasma membrane generating a sodium motive force rather than a proton motive force. For the purified and reconstituted complex I of *Klebsiella pneumonia*, a pump stoichiometry of 1 Na^+/e^- was determined.

Inhibitors of Complex I

A plethora of structurally diverse hydrophobic compounds have been reported to inhibit complex I and are considered to interfere with ubiquinone binding. Among these inhibitors are naturally occurring antibiotics as well as synthetic insecticides and acaricides. Also a number of drugs such as amytal and meperidine, neurotoxins related to 1-methy-4-phenylmeperidinium, and even detergents such as Triton X-100 and Thesit inhibit complex I. Kinetic studies suggested that these inhibitors can be grouped into three different classes that are represented by the well known and widely used inhibitors DQA (2-decyl-4-quinazolinyl amine) and piericidin A (class I/A-type), rotenone (class II/B-type), and capsaicin (C-type). Except for capsaicin, all these inhibitors exert their inhibitory potential at I_{50} values in the nanomolar range. Competition experiments demonstrated that these inhibitors share one common binding domain with partially overlapping sites. In agreement with this observation, cross-resistance between DQA/piericidin A and rotenone is observed in inhibitor resistant mutants.

Complex I in Disease

Genetic defects in complex I typically result in multisystem disorders with a wide spectrum of severities ranging from adult onset exercise intolerance to fatal infantile lactic acidosis. Disease is often progressive.

Mitochondrial Mutations

Deletions within the mitochondrial genome or point mutations in mitochondrial tRNA genes affect the function of several respiratory chain complexes simultaneously. Skeletal muscle biopsies from such patients typically show ragged red fibers caused by mitochondrial hypertrophy. The typical clinical phenotype of mitochondrial point mutations in the ND genes is Leber's Hereditary Optic Neuropathy (LHON), characterized by optic nerve atrophy or LDYT (LHON plus dystonia), characterized by additional lesions in the caudate and putamen. Ragged red fibers are not commonly observed in patients with isolated complex I defects.

Nuclear Mutations

Due to the large number of potential target genes, mutations affecting nuclear-coded subunits of complex I have been described only recently. The typical clinical picture is Leigh syndrome, a severe, early onset neuromuscular disorder, associated with lactic acidosis, ataxia, hypotonia, spasticity, developmental delay, optic atrophy, and, in the terminal stage, degeneration of the basal ganglia. Sometimes, this is accompanied by hypertrophic cardiomyopathy. Such mutations were found in the 75 kDa, 51 kDa, 49 kDa, PSST, TYKY, and AQDQ homologues.

Mechanisms of Complex I Pathology

Complex I dysfunction has several biochemical consequences which may be relevant for producing disease symptoms. (1) Feedback inhibition of the NADH-producing citric acid cycle and pyruvate dehydrogenase complex results in elevated blood lactate levels. (2) Lowered OXPHOS efficiency will reduce ATP production. OXPHOS defects often show a remarkable degree of tissue- and organ specificity. This has been explained by assuming different energetic thresholds, in descending order for optic nerve, neuronal cells, heart muscle, skeletal muscle, and liver. (3) Increased generation of reactive oxygen species. Oxidative stress is evident from the induction of MnSOD mRNA in complex I patients. ROS damage of complex I and the ND genes in the mitochondrial genome may result in a vicious cycle of mitochondrial damage. (4) Reduced mitochondrial energy production and elevated oxidative stress may lead to the opening of the mitochondria permeability transition pore, release of pro-apoptotic factors, and apoptotic cell death.

Poisoning of Complex I

The neurotoxin 1-methyl-4-phenyl 1,2,3,6 tetrahydropyridine (MPTP), a synthetic meperidine analogue, is able to rapidly and persistently induce symptoms of acute Parkinsonism in humans and other primates. MPTP is metabolized to 1-methyl-4-phenylpyridinium (MPP^+) by the action of glial cell monoamine oxidase B. Since MPP^+ is a substrate for the dopaminergic re-uptake pathway, it accumulates in the nigrostriatal dopaminergic neurons, where it causes a specific reversible inhibition of complex I. Strikingly, highly selective neurodegeneration of the nigrostriatal dopaminergic system was also observed

following chronic exposure of rats to the common complex I inhibitor rotenone. These results support the view that complex I deficiency may also be involved in the etiology of idiopathic Parkinsonism.

See Also the Following Articles

Cytochrome bc_1 Complex (Respiratory Chain Complex III) • Mitochondrial DNA • Mitochondrial Genome, Overview • Photosystem I: F_X, F_A, and F_B Iron–Sulfur Clusters • Respiratory Chain Complex II and Succinate: Quinone Oxidoreductases • Respiratory Chain Complex IV

Glossary

iron–sulfur clusters Nonheme iron prosthetic groups found in a wide range of redox enzymes. The reduced forms of binuclear and tetranuclear iron–sulfur clusters are paramagnetic and can be studied by electron-paramagnetic-resonance (EPR) spectroscopy.

mitochondrial DNA Small genome that codes for 13 subunits of the respiratory chain complexes and ATP synthase. A typical mammalian cell contains several hundreds of mitochondria and several thousands of mitochondrial genomes that are inherited exclusively through the oocyte cytoplasm.

oxidative phosphorylation (OXPHOS) "Fuel cell" of aerobic metabolism. Process by which redox energy derived from NADH or $FADH_2$ is converted into the phosphorylation potential of ATP. Electron transport and ATP synthesis are energetically coupled through an electrochemical proton potential across the inner mitochondrial membrane.

reactive oxygen species (ROS) Superoxide ($O_2^{\cdot-}$), hydrogen peroxide (H_2O_2), and hydroxyl radical ($OH^{\cdot}$) that may cause severe damage to lipids, proteins, and DNA. In mitochondria ROS are generated by side reactions of the respiratory chain complexes.

Further Reading

Brandt, U. (1997). Proton-translocation by membrane-bound NADH:ubiquinone-oxidoreductase (complex I) through redox-gated ligand conduction. *BBA-Bioenergetics* **1318**, 79–91.

Brandt, U., Kerscher, S., Dröse, S., Zwicker, K., and Zickermann, V. (2003). Proton pumping by NADH:ubiquinone oxidoreductase. A redox driven conformational change machanism? *FEBS Lett.* **545**, 9–17.

Complex I website: http://www.scripps.edu/mem/biochem//CI/MITOMAP: A Human Mitochondrial Genome Database: http://www.mitomap.org.

Degli Esposti, M. (1998). Inhibitors of NADH-ubiquinone reductase: An overview. *BBA-Bioenergetics* **1364**, 222–231.

Friedrich, T., and Scheide, D. (2000). The respiratory complex I of bacteria, archaea and eukarya and its module common with membrane-bound multisubunit hydrogenases. *FEBS Lett.* **479**, 1–5.

Hirst, J., Carroll, J., Fearnley, I. M., Shannon, R. J., and Walker, J. E. (2003). The nuclear encoded subunits of complex I from bovine heart mitochondria. *Biochim. Biophys. Acta* **1604**, 135–150.

Ohnishi, T. (1998). Iron–sulphur clusters/semiquinones in complex I. *BBA–Bioenergetics* **1364**, 186–206.

Schulte, U., and Weiss, H. (1995). Generation and characterization of NADH:ubiquinone oxidoreductase mutants in *Neurospora crassa*. *Methods Enzymol.* **260**, 1–14.

Smeitink, J., Sengers, R., Trijbels, F., and van der Heuvel, L. (2001). Human NADH:ubiquinone oxidoreductase. *J. Bioenerg. Biomembr.* **33**, 259–266.

Steuber, J. (2001). Na^+ translocation by bacterial NADH:quinone oxidoreductases: An extension to the complex-I family of primary redox pumps. *BBA-Bioenergetics* **1505**, 45–56.

Yagi, T., Yano, T., Di Bernardo, S., and Matsuno-Yagi, A. (1998). Procaryotic complex I (NDH-1), an overview. *Biochim. Biophys. Acta* **1364**, 125–133.

Biography

Ulrich Brandt is Professor at the Gustav-Embden Center for Biological Chemistry of the Johann Wolfgang Goethe-University in Frankfurt am Main, Germany. His principal research interest is the structure and function of respiratory chain complexes and the molecular causes of mitochondrial disorders. He holds a Ph.D. from the University of Munich and received his postdoctoral training at the Dartmouth Medical School, New Hampshire and the Glynn Research Institute, Cornwall, United Kingdom. He has studied the mechanism by which mitochondrial cytochrome bc_1 complex is inhibited by strobilurins, a family of compounds now widely used as potent fungizides in agriculture. He serves as the General Secretary of the German Society for Biochemistry and Molecular Biology.

Respiratory Chain Complex II and Succinate: Quinone Oxidoreductases

C. Roy D. Lancaster
Max Planck Institute of Biophysics, Frankfurt am Main, Germany

Succinate:quinone oxidoreductases (SQORs) are enzymes that couple the two-electron oxidation of succinate to fumarate [Eq. (1)] to the two-electron reduction of quinone to quinol [Eq. (2)]:

$$\text{succinate} \leftrightarrows \text{fumarate} + 2H^+ + 2e^- \quad (1)$$

$$\text{quinone} + 2H^+ + 2e^- \leftrightarrows \text{quinol} \quad (2)$$

They can also catalyze the opposite reaction, the coupling of quinol oxidation to the reduction of fumarate. Depending on the direction of the reaction catalysed *in vivo*, the members of the superfamily of SQORs can be classified as either succinate:quinone reductases (SQR) or quinol:fumarate reductases (QFR). SQR and QFR complexes are anchored in the cytoplasmic membranes of archaebacteria, eubacteria, and the inner mitochondrial membrane of eukaryotes with the hydrophilic domain generally extending into the cytoplasm and the mitochondrial matrix, respectively. SQR (respiratory complex II) is involved in aerobic metabolism as part of the citric acid cycle (Krebs cycle) and of the aerobic respiratory chain (Figure 1A). QFR participates in anaerobic respiration with fumarate as the terminal electron acceptor (Figure 1B) and is part of the electron transport chain catalyzing the oxidation of various donor substrates (e.g., H_2 or formate) by fumarate. These reactions are coupled via an electrochemical proton potential (Δp) to ADP phosphorylation with inorganic phosphate by ATP synthase.

Succinate:Quinone Oxidoreductases Classification

Functional Classification

Succinate:quinone oxidoreductases (SQORs) can be divided into three functional classes based on the quinone substrate and the *in vivo* function of the enzyme. Subclass 1 contains those enzymes that oxidize succinate (with an oxidation–reduction potential at pH 7, $E_{M7,}$ of +25 mV) and reduce a high-potential quinone, e.g., ubiquinone ($E_{M7} = +90$ mV) or caldariella quinone ($E_{M6.5} = +103$ mV). The succinate:quinone reductases (SQRs) from mammalian mitochondria (respiratory complex II) and many prokaryotes belong to this group. Subclass 2 comprises those enzymes that catalyze the oxidation of a low-potential quinol, e.g., menaquinol ($E_{M7} = -74$ mV) or rhodoquinol ($E_{M7} = -63$ mV), and the reduction of fumarate. All quinol:fumarate reductases (QFRs) studied so far belong to this subclass. Subclass 3 includes those enzymes that catalyze the oxidation of succinate and the reduction of a low-potential quinone, e.g. menaquinone or thermoplasmaquinone. These subclass 3 enzymes are found in gram-positive bacteria (e.g., *Bacillus subtilis*, *Paenibacillus macerans*, *Bacillus licheniformis*) and archaebacteria (e.g., *Thermoplasma acidophilum*).

Structural Classification

SQORs generally contain four protein subunits, referred to as A, B, C, and D. Subunits A and B are hydrophilic, whereas subunits C and D are integral membrane proteins. Among species, subunits A and B have high sequence homology, while that for the hydrophobic subunits is much lower. Most of the SQR enzymes of gram-positive bacteria and the QFR enzymes from ε-proteobacteria contain only one larger hydrophobic polypeptide (C), which is thought to have evolved from a fusion of the genes for the two smaller subunits C and D. While subunit A harbors the site of fumarate reduction and succinate oxidation, the hydrophobic subunit(s) contain the site of quinol oxidation and quinone reduction.

Based on their hydrophobic domain and heme *b* content, SQORs are divided into five types (Figure 2A). Type A enzymes contain two hydrophobic subunits and two heme groups, e.g., SQR from the archaea *Archaeoglobus fulgidus*, *Natronomonas pharaonis*, and *T. acidophilum*. Type B enzymes contain one hydrophobic subunit and two heme groups, as is the case for SQR from the gram-positive bacteria *B. subtilis* and *P. macerans* and for QFR from the ε-proteobacteria *Campylobacter jejuni*, *Helicobacter pylori*, and

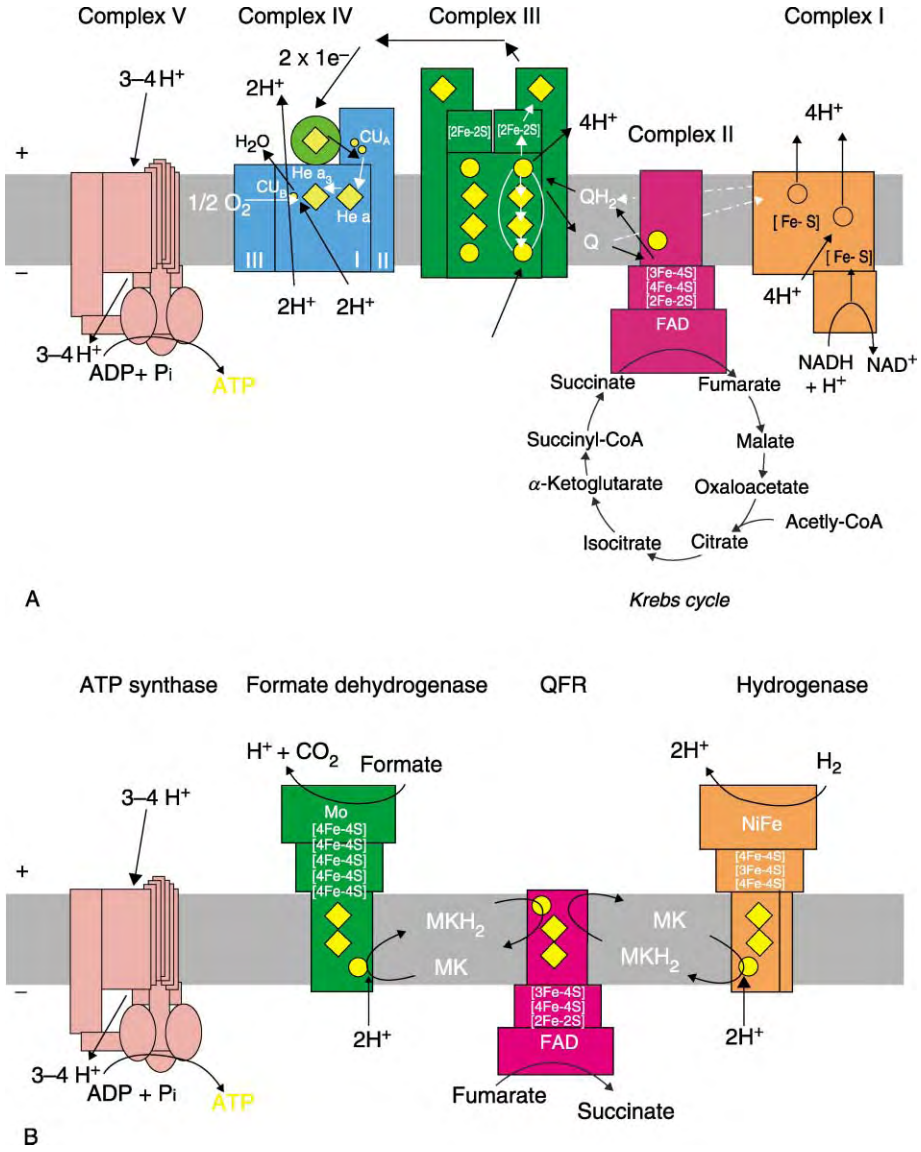

FIGURE 1 Electron flow and the generation and utilization of a transmembrane electrochemical potential in aerobic respiration (A) and anaerobic respiration (B). Modified from Lancaster, C. R. D. (2003). The role of electrostatics in proton-conducting membrane protein complexes. *Adv. Protein Chem.* **63**, 131–149. *FEBS Lett.* **545**, 52–60.

Wolinella succinogenes. Examples for type C enzymes, which possess two hydrophobic subunits and one heme group, are SQR from mammalian mitochondria and from the proteobacteria *Paracoccus denitrificans* and *Escherichia coli*, and QFR from the nematode *Ascaris suum*. The QFR of *E. coli* is an example of a type D enzyme, which contains two hydrophobic subunits and no heme group. Finally, type E enzymes, such as SQRs from the archaea *Acidianus ambivalens* and *Sulfolobus acidocaldarius*, but also from the proteobacterium *C. jejuni* and the cyanobacterium *Synechocystis*, also contain no heme, but have two hydrophobic subunits very different from the other four types and more similar to those of heterodisulfide reductase from methanogenic archaea.

SQOR Structure and Function

Overall Description of the Structure

The currently available crystal structures of SQORs (Figure 2B–2D) are those of two prokaryotic QFRs, both from 1999, and one prokaryotic SQR, from 2003. The *E. coli* QFR (Figure 2D), determined at 3.3Å resolution, belongs to the type D enzymes, and the QFR of *W. succinogenes* (Figure 2B), refined at 2.2Å resolution, is of type B. The structure of the SQR from *E. coli* (Figure 2B) was reported at 2.6Å resolution. Interestingly, *E. coli* QFR appears to be a monomeric complex of one copy each of the A, B, C, and D subunits, whereas

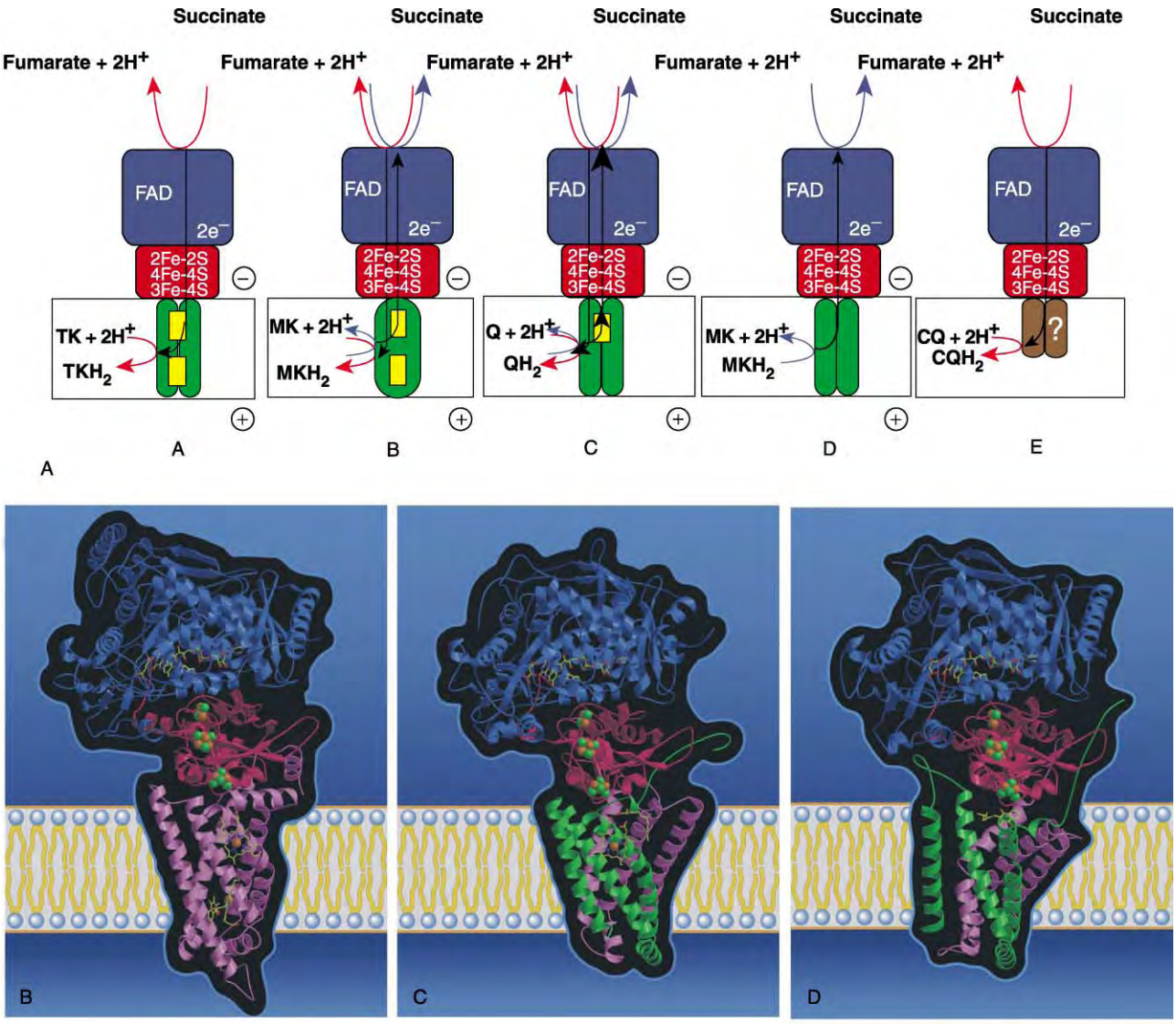

FIGURE 2 (A) Classification (A to E) of succinate:quinone oxidoreductases based on their hydrophobic domain and heme content. The hydrophilic subunits A and B are drawn schematically in blue and red, respectively; the hydrophobic subunits C and D in green. Heme groups are symbolized by small yellow rectangles. The directions of the reactions catalyzed by SQR and QFR are indicated by red and blue arrows, respectively. White rectangles symbolize the respective cytoplasmic or inner mitochondrial membrane bilayer. The positive (+) and negative (−) sides of the membrane are indicated. In bacteria, the negative side is the cytoplasm ("inside"), the positive side the periplasm ("outside"). For mitochondrial systems, these are the mitochondrial matrix and the intermembrane space, respectively. The type of quinone transformed in vivo is not necessarily unique for each type of enzyme. The examples given are thermoplasma-quinone (TK), menaquinone (MK), ubiquinone (Q), and caldariella quinone (CQ).(-B-D) Three-dimensional structures of *W. succinogenes* QFR, a B-type SQOR (B) (determined by Lancaster, C.R., Kroger, A., Auer, M., and Michel, H. (1999). Structure of fumarate reductase from *Wolinella succinogenes* at 2.2Å resolution. *Nature* **402**, 377–385), *E. coli* SQR, a C-type SQOR (C) (determined by Yankovskaya, V., Horsefield, R., Tornroth, S., Luna-Chavez, C., Miyoshi, H., Leger, C., Byrne, B., Cecchini, G., and Iwata, S. (2003). Architecture of succinate dehydrogenase and reactive oxygen species generation. *Science* **299**, 700–704), and *E. coli* QFR, a D-type SQOR (D) (determined by Iverson, T. M., Luna-Chavez, C., Cecchini, G., and Rees, D. C. (1999). Structure of the *Escherichia coli* fumarate reductase respiratory complex. *Science* **284**, 1961–1966). The Cα traces of the A subunits are shown in blue, those of the B subunits in red, those of the C subunits in pink, and those of the D subunits in green. The atomic structures of the prosthetic groups are superimposed for better visibility. From top to bottom, these are the covalently bound FAD, the [2Fe–2S], the [4Fe–4S], and the [3Fe–4S] iron–sulfur clusters, and (where present) the proximal and the distal heme *b* groups. Atomic color coding is as follows: C, N, O, P, S, and Fe are displayed in yellow, blue, red, light green, green, and orange, respectively. Figures with atomic models were prepared with a version of Molscript (Kraulis, P. J. (1991). MOLSCRIPT: a program to produce both detailed and schematic plots of protein structures. *J. Appl. Crystallogr.* **24**, 946–950) modified for color ramping (Kraulis, P. J. (1997). Esnouf Rm. An extensively modified version of MolScript that includes greatly enhanced coloring capabilities. *J. Mol. Graphics Mod.* **15**, 132–134) and rendered with the program Raster3D (Merrit, E. A. and Bacon, D. J. (1997). Raster 3D: Photorealistic molcecular graphics. *Meth. Enzymol.* **277**, 505–524).

W. succinogenes QFR is apparently a homodimer of two sets of A, B, and C subunits, and *E. coli* SQR is a homotrimer of three sets of A, B, C, and D subunits. For the *Wolinella* enzyme, analytical gel filtration experiments have shown that the homodimer is apparently also present in the detergent-solubilized state of the enzyme, implying that it is unlikely to be an artifact of crystallization. However, functionally all three enzymes appear to act as monomers, which is why only the monomeric complexes are shown in Figure 2B–2D.

The Relative Orientations of Soluble and Membrane-Embedded SQOR Subunits

The structures of all three enzymes shown in Figure 2B–2D can be superimposed on the basis of the Cα positions of the conserved hydrophilic subunits A and B. In this superimposition, large parts of the membrane-embedded subunits can be aligned in the case of *W. succinogenes* QFR and *E. coli* SQR, but not for *E. coli* QFR. However, as demonstrated by Lancaster and coauthors, in an alternate orientation the transmembrane subunits of *E. coli* QFR and of *W. succinogenes* QFR can be overlaid in spite of the respective absence and presence of the two heme groups. Consequently, the relative orientations of the hydrophilic subunits and the transmembrane subunits is similar in *W. succinogenes* QFR and *E. coli* SQR and different in *E. coli* QFR.

Subunit A and the Site of Succinate Oxidation/Fumarate Reduction

The flavoprotein or A subunit (64–73 kDa) of all described membrane-bound SQOR complexes contains a flavin adenine dinucleotide (FAD) prosthetic group covalently bound to a conserved His residue as an 8α-[Nε-histidyl]-FAD. The two most important domains of subunit A are the bipartite FAD-binding domain and the "capping" domain, which is inserted between the two parts of the FAD-binding domain. The capping domain contributes to burying the otherwise solvent-exposed FAD isoalloxazine ring from the protein surface.

The binding site of succinate/fumarate is located between the FAD-binding domain and the capping domain next to the plane of the FAD isoalloxazine ring. The structures and results from site-directed mutagenesis suggest that the *trans*-dehydrogenation of succinate to fumarate occurs via the combination of a hydride ion transfer from one succinate methylene group to the N5 position of the FAD and a proton transfer from the other succinate methylene group to the side chain of a conserved Arg residue of the capping domain (Figure 3). All residues implicated in substrate binding and catalysis are conserved throughout the superfamily

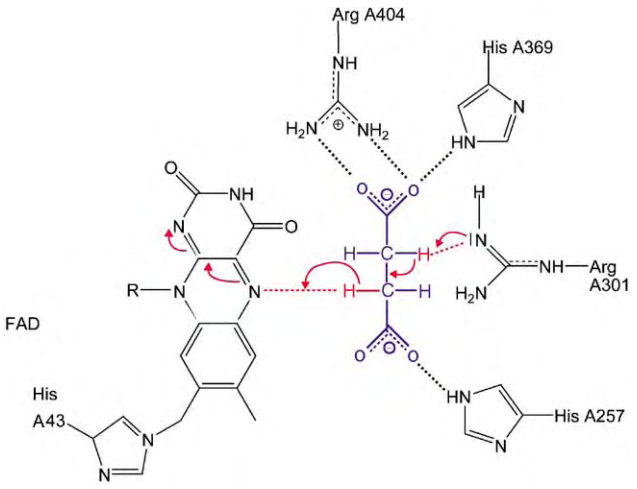

FIGURE 3 Possible mechanism of succinate oxidation. Modified from Lancaster C. R. D. (2001). *Eur. J. Biochem.* **268**, 1820–1827.

of SQORs, so that this reversible mechanism is considered generally relevant for all SQORs. Release of the product could be facilitated by movement of the capping domain away from the dicarboxylate site.

Subunit B: The Iron–Sulfur Protein

Generally, SQORs contain three iron–sulfur clusters, which are exclusively bound by the B subunit of 26–30 kDa. Enzyme types A–D contain one [2Fe–2S]$^{2+,1+}$, one [4Fe–4S]$^{2+,1+}$, and one [3Fe–4S]$^{1+,0}$ cluster, whereas an additional [4Fe–4S]$^{2+,1+}$ cluster apparently replaces the [3Fe–4S]$^{1+,0}$ in the type E enzyme. This subunit consists of two domains, an N-terminal plant ferredoxin domain, in contact with subunit A and binding the [2Fe–2S] cluster, and a C-terminal bacterial ferredoxin domain, in contact with the hydrophobic subunit(s) and binding the [4Fe–4S] and the [3Fe–4S] clusters. In general, these iron–sulfur clusters are coordinated by conserved Cys residues, although one of the ligands to the [2Fe–2S] cluster in *E. coli* SQR is an Asp. At the position corresponding to the fourth Cys of the [4Fe–4S] cluster, the [3Fe–4S] cluster contains a Leu (*W. succinogenes* QFR), Ile (*E. coli* SQR), Val (*E. coli* QFR), or Ser (*B. subtilis* SQR). Whereas the introduction of a Cys into *E. coli* QFR could replace the native [3Fe–4S] by a [4Fe–4S] cluster, this was not the case for *B. subtilis* SQR.

The Integral Membrane Subunit(s) C (and D) and the Sites of Quinol Oxidation/Quinone Reduction

Type A, C, and D SQOR enzymes contain two hydrophobic polypeptides with three membrane-spanning

helices each (numbered I, II, and III and IV, V, and VI, respectively). According to an evolutionary model proposed by C. Hägerhäll and L. Hederstedt, the large single hydrophobic polypeptides of type B SQOR enzymes with five membrane-spanning helices are thought to have evolved from the fusion of the genes for the two small hydrophobic polypeptides with concomitant loss of transmembrane helix III. This view is supported by the structural superpositions previously discussed. To a varying degree, all transmembrane segments are tilted with respect to the membrane normal.

The planes of both heme molecules bound by *W. succinogenes* QFR are approximately perpendicular to the membrane surface, and their interplanar angle is 95°. The His axial ligands to the proximal heme b_P, located toward the cytoplasmic surface of the membrane, and thus toward the [3Fe–4S] cluster, are located on transmembrane helices II and V. Residues of the two other transmembrane helices I and IV interact with the propionate groups of heme b_P via hydrogen bonds and salt bridges; this underscores the structural importance of the bound heme. The axial ligands to the distal heme b_D are located on helices I and IV. The binding of the two heme *b* molecules by an integral membrane protein four-helix bundle described here is very different from that described for other diheme-binding membrane protein complexes, such as the cytochrome bc_1 complex, where only two transmembrane segments provide two axial heme *b* ligands each, and also the membrane-bound hydrogenases and formate dehydrogenases, where one transmembrane helix provides two axial His ligands and two others provide one His ligand each. One consequence of this difference is that the distance between the two heme iron centers is distinctly shorter in *W. succinogenes* QFR (15.6Å) than it is in the mitochondrial cytochrome bc_1 complex (21Å) and in *E. coli* formate dehydrogenase-N (20.5Å). The mode of heme binding for the single (proximal) heme of *E. coli* SQR is analogous to that described for heme b_P of *W. succinogenes* QFR.

The sites of quinol oxidation/quinone reduction have been localized in all three enzymes of known three-dimensional structure by a combination of X-ray crystallography, site-directed mutagenesis, functional characterization of resulting variant enzymes, and/or inhibitor-binding studies, respectively. In *E. coli* QFR, the menaquinol oxidation site is located proximally, close to the [3Fe–4S] cluster. In *E. coli* SQR, this position is occupied by the heme *b* group, but the ubiquinone reduction site is also located proximally, close to the [3Fe–4S] cluster, at an alternate position. In *W. succinogenes* QFR, the menaquinol oxidation site is located distally, close to heme b_D.

Electron and Proton Transfer

Electron Transfer

For the function of QFR, electrons have to be transferred from the quinol-oxidizing site in the membrane to the fumarate-reducing site, protruding into the cytoplasm. Conversely, for the function of SQR, electrons have to be transferred from the succinate oxidation site in subunit A to the quinone reduction site in the membrane. The linear arrangement of the prosthetic groups in the complexes shown in Figure 2B–2D therefore provides one straightforward pathway by which electrons could be transferred efficiently between the two sites of catalysis. It has been shown for other electron transfer proteins that physiological electron transfer between prosthetic groups occurs if the edge-to-edge distances relevant for electron transfer are shorter than 14Å, but does not occur if they are longer than 14Å. In all three cases, this indicates that physiological electron transfer can occur between the prosthetic groups of one heterotrimeric or heterotetrameric complex, but not between the two (*W. succinogenes* QFR) or three (*E. coli* SQR) complexes in the respective homodimer or homotrimer.

Prior to the determination of the three-dimensional structures, because of its very low midpoint potential ($E_m < -250$ mV), it had been suggested that the [4Fe–4S] cluster does not participate in electron transfer. However, the determined low potential may be an artifact due to anti-cooperative electrostatic interactions between the redox centers. The position of the [4Fe–4S] cluster as revealed in the structures is highly suggestive of its direct role in electron transfer between the [3Fe–4S] cluster and the [2Fe–2S] cluster. Despite this major thermodynamically unfavorable step, the calculated rate of electron transfer is on a microsecond scale, demonstrating that this barrier can easily be overcome by thermal activation as long as the electron transfer chain components are sufficiently close to promote intrinsically rapid electron tunneling.

The positioning of the heme in *E. coli* SQR is puzzling because it does not seem to be required for electron transfer between the catalytic sites. A possible explanation for this also explains why SQR is favored over QFR in *E. coli* when oxygen is present. Under aerobic conditions, reduced *E. coli* QFR produces large amounts of reactive oxygen species (ROS), including superoxide radical (O_2^-) and hydrogen peroxide (H_2O_2), which has been suggested to be caused by electron accumulation around the FAD. In sharp contrast, *E. coli* SQR reacts poorly with molecular oxygen, producing modest amounts of O_2^- and no H_2O_2. On the basis of their crystal structure, Yankovskaya *et al.* (2003) argued that the heme group

in SQR provides an electron sink when the quinone site is not occupied, thus preventing buildup of electrons around the FAD and subsequent ROS generation. However, this electron-sink mechanism is predicted to be less effective for mitochondrial SQRs because heme *b* has a lower redox potential than in *E. coli* SQR.

Electron-Coupled Proton Transfer

In addition to the transfer of electrons, two protons are bound at the site of reduction and two protons are liberated at the site of oxidation [see Eqs. (1) and (2)]. An overview of the current status of discussion of electron and proton transfer in succinate:quinone oxidoreductases is shown in Figure 4A–4D. In mitochondrial complex II and other C-type enzymes such as SQR from *P. denitrificans* and *E. coli*, electron transfer from succinate to ubiquinone does not lead to the generation of a transmembrane electrochemical potential, Δp, since the protons released by succinate oxidation are on the same side of the membrane as those consumed by quinone reduction (Figure 4A). Similarly, in *E. coli* QFR, the protons released by proximal quinol oxidation are balanced by the protons consumed by fumarate reduction (Figure 4B). Succinate oxidation by menaquinone, an endergonic reaction under standard conditions, is catalyzed by a B-type SQOR in gram-positive bacteria, e.g., *B. subtilis*. There is experimental evidence indicating that the menaquinone reduction site in *B. subtilis* SQR is close to the heme b_D in a position analogous to the menaquinol oxidation site of *W. succinogenes* QFR. This arrangement of the catalytic sites of succinate oxidation and menaquinone reduction would allow succinate oxidation by menaquinone in *B. subtilis* to be driven by the electrochemical proton potential (Figure 4C), and there is indeed experimental evidence that this is the case. This reaction is analogous to that suggested by the arrangement of the catalytic sites for *W. succinogenes* QFR, but in the opposite direction. Experimental results do indicate that *B. subtilis* SQR generates a proton potential when functioning as a QFR. However, the experimental results on intact bacteria, with inverted vesicles or liposomes containing *W. succinogenes* QFR, indicate that the oxidation of menaquinol by fumarate as catalyzed by *W. succinogenes* QFR is an electroneutral process. In order to reconcile these experimental findings with the arrangement of the catalytic sites in the structure, it has been proposed that transmembrane electron transfer in dihemic QFRs is tightly coupled to the compensatory, parallel transfer of protons across the membrane, thus balancing the protons released to the periplasm upon menaquinol oxidation and the protons bound from the cytoplasm upon fumarate reduction (Figure 4D). A key residue in this proposed proton transfer pathway is a Glu residue located in the middle of the membrane that is conserved only in dihemic menaquinol:fumarate reductases, but not in dihemic succinate:menaquinone reductases. The first experimental results supporting this E-pathway hypothesis have recently been obtained.

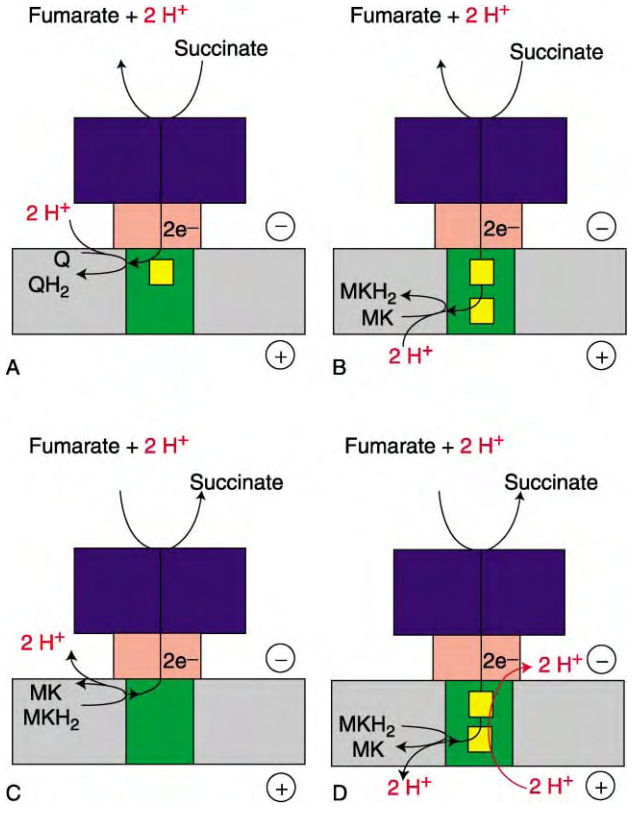

FIGURE 4 The coupling of electron and proton flow in succinate: quinone oxidoreductases in aerobic (A, B) and anaerobic respiration (A, C), respectively. Positive and negative sides of the membrane are as described for Figure 2 (A and B). Electroneutral reactions as catalyzed by C-type SQR enzymes (A) and D-type *E. coli* QFR (C). (B) Utilization of a transmembrane electrochemical potential Δp as possibly catalyzed by A-type and B-type enzymes. (D) Electroneutral fumarate reduction by B-type QFR enzymes with a proposed compensatory E-pathway.

See Also the Following Articles

Ferredoxin • Ferredoxin-NADP$^+$ Reductase • Flavins • Iron–Sulfur Proteins • Photosystem I: F_X, F_A, and F_B Iron–Sulfur Clusters

Glossary

flavin adenine dinucleotide (FAD) A riboflavin-containing hydrogen acceptor molecule in the Krebs cycle and a coenzyme of some oxidation–reduction enzymes.

fumarate A dicarboxylate anion ($^{-}OOC-CH{=}CH-COO^{-}$) that occurs as an intermediate compound in metabolic processes, most importantly in the citric acid cycle (Krebs cycle).

heme group A complex organic red iron-containing pigment used by proteins to bind oxygen and/or electrons.

His ligand A histidine residue that participates in forming a complex around a central atom or ion, e.g., the central iron of a heme group.

succinate A dicarboxylate anion ($^{-}OOC-CH_2-CH_2-COO^{-}$) that occurs as an intermediate compound in metabolic processes, most importantly in the citric acid cycle (Krebs cycle).

Further Reading

Ackrell, B. A. C., Johnson, M. K., Gunsalus, R. P., and Cecchini, G. (1992). Structure and function of succinate dehydrogenase and fumarate reductase. In *Chemistry and Biochemistry of Flavoenzymes* (F. Mueller, ed.) Vol 3 pp. 229–297. CRC Press, Boca Raton, FL.

Cecchini, G. (2003). Function and structure of complex II of the respiratory chain. *Annu. Rev. Biochem.* **72**, 77–109.

Hägerhäll, C. (1997). Succinate:quinone oxidoreductases: Variations on a conserved theme. *Biochim. Biophys. Acta Bioenerg.* **1320**, 107–141.

Hederstedt, L. (1999). Respiration without O_2. *Science* **284**, 1941–1942.

Hederstedt, L. (2003). Complex II is complex too. *Science* **299**, 671–672.

Lancaster, C. R. D. (2001). Succinate:quinone oxidoreductases. In *Handbook of Metalloproteins* (A. Messerschmidt, R. Huber, T. Poulos and K. Wieghardt, eds.) Vol 1, pp. 379–401. John Wiley & Sons, Chichester, UK.

Lancaster, C.R.D (ed.) (2002). Special issue on fumarate reductases and succinate dehydrogenases. *Biochim. Biophys. Acta* **1553**, 1–176.

Lancaster, C. R. D. (2003). The structure of *Wolinella succinogenes* quinol:fumarate reductase and its relevance to the superfamily of succinate:quinone oxidoreductases. *Adv. Protein Chem.* **63**, 131–149.

Ohnishi, T., Moser, C. C., Page, C. C., Dutton, P. L., and Yano, T. (2000). Simple redox-linked proton-transfer design: New insights from structures of quinol-fumarate reductase. *Structure* **8**, R23–R32.

Biography

C. Roy D. Lancaster is a Group Leader in the Department of Molecular Membrane Biology at the Max Planck Institute of Biophysics. He teaches biochemistry and biophysical chemistry at J.W. Goethe University, Frankfurt am Main. His principle research interests are in the structure and mechanism of action of membrane protein complexes. He holds an M.Sc. degree from McMaster University and a Dr. phil. nat. degree from J.W. Goethe University. His postdoctoral training was at the Max Planck Institute of Biophysics. He has determined the highest resolution structure to date of a succinate:quinone oxidoreductase and has authored and edited key texts in the field.

Respiratory Chain Complex IV

Hartmut Michel
Max Planck Institute of Biophysics, Frankfurt, Germany

Located within the inner membranes of mitochondria, or within the cytoplasmic membranes of aerobic bacteria, complex IV is the terminal enzyme of aerobic respiratory chains. It belongs to the superfamily of heme/copper containing terminal oxidases and catalyzes the reduction of oxygen to water. Typical representatives of this enzyme superfamily, as those found in mitochondria, use reduced cytochrome *c* as electron donor and are therefore also called cytochrome *c* oxidases. Cytochrome *c* provides its electrons from the outer side of the membrane, whereas the protons required for water formation access the active site from the inner ("matrix") side of mitochondria or from the cytoplasm of bacteria. As a result of the different spatial origin of the electrons and protons consumed in the reaction, four elementary charges per oxygen molecule reduced are translocated across the inner mitochondrial (or bacterial) membrane. In addition, four protons are transported ("pumped") from the mitochondrial matrix (or bacterial cytoplasm, respectively) to the outside of mitochondria or bacteria. Therefore the reaction can be written as

$$4e^- + O_2 + 8H_i^+ \rightarrow 2H_2O + 4H_o^+,$$

where H_i^+ stands for protons originating from the matrix (cytoplasmic) space and H_o^+ for protons released at the external side.

The proton transport produces a transmembrane electrochemical proton potential that drives the synthesis of adenosine-5′-triphosphate ("ATP") from adenosine-5′-diphosphate ("ADP") and inorganic phosphate through another membrane-spanning complex, the ATP synthase, which is also called complex V of the respiratory chain.

Background

Aerobic, oxygen-consuming respiration is the major means of producing energy in animals, fungi, many yeasts and bacteria. Oxygen itself is a side product of the oxygenic photosynthesis occuring in plants, algae, and cyanobacteria. These organisms produce reduced coenzymes (NADPH, quinols) and ATP in the course of the photosynthetic light reaction. NADPH is used to fix carbon dioxide and to synthesize carbohydrates and other organic compounds during the photosynthetic dark reactions. This organic matter is consumed by heterotrophic organisms. NADH and quinols are formed during the degradation of foodstuff and oxidized in the respiratory chain. In the typical mitochondrial respiratory chain (Figure 1) NADH is oxidized by complex I (NADH dehydrogenase). The electrons are transferred onto ubiquinone, the ubiquinol formed is oxidized by complex III (cytochrome bc_1 complex, also called ubiquinol-cytochrome *c* oxidoreductase) which reduces cytochrome *c*. This electron carrier is oxidized again by complex IV (cytochrome *c* oxidase). The latter uses the electrons to reduce oxygen and to form water, thus closing the cycle. Complex II (succinate dehydrogenase) constitutes a parallel entry into the respiratory chain and is also part of the citric acid cycle.

The respiratory chains from aerobic bacteria contain many more membrane-protein complexes and are often branched. They may contain up to four different terminal oxidases reacting with molecular oxygen. The electron donating substrates for the individual terminal oxidases may be cytochromes of the *c* type, various quinols, or even high-potential iron sulfur proteins. Most of them belong to the family of heme/copper containing terminal oxidases. The exception is cytochrome *bd*, which is a ubiquinol oxidase and not related to the heme/copper containing terminal oxidases. Cytochromes *bd* do not pump protons, however, electrons and protons, as in the heme/copper containing oxidases, enter the active site of this enzyme from opposite sides of the membrane leading to a net translocation of four charges per oxygen molecule consumed.

Astonishingly, the superfamily of the heme/copper containing terminal oxidases appears to be rather old. Family members are found in bacteria, as well as in archaea. The splitting into these lineages during evolution predates the conversion of the atmosphere from a reducing one to an oxidizing one, which dates back to ~2 billion years, when cyanobacteria developed the water-splitting, oxygen-releasing photosystem II. It turned out that the nitric oxide reductase (nitrogen monoxide reductase, NO reductase) is closely related to the heme/copper containing terminal oxidases. An iron atom in the NO reductases replaces a copper atom

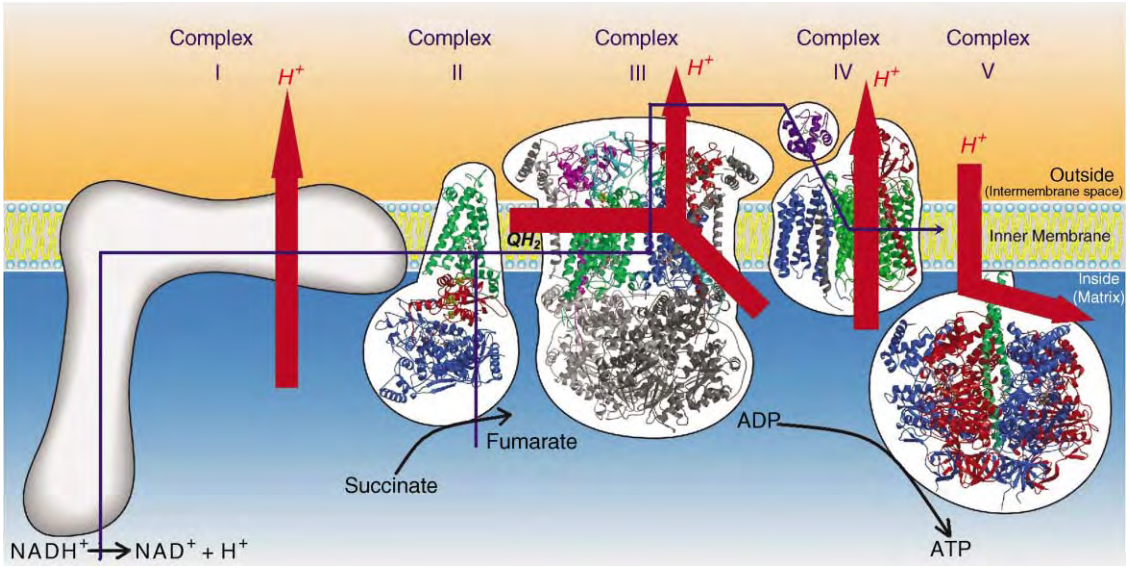

FIGURE 1 The mitochondrial respiratory chain. The five complexes of the respiratory chain are presented with their known structures in a functional context. The atomic structure of complex I or NADH dehydrogenase (left) is not known, but its shape has been determined by electron microscopy. It reduces ubiquinone to ubiquinol and pumps protons. Complex II (succinate dehydrogenase) is represented by a chain model. It also produces ubiquinol (QH_2). Ubiquinol is oxidized by complex III (cytochrome bc_1 complex). The cytochrome bc_1 complex releases protons at the outside and uses a quinone cycle to translocate additional protons across the membrane. The cytochrome bc_1 complex from yeast is shown. It reduces cytochrome *c*, which is oxidized by cytochrome *c* oxidase. The bacterial cytochrome *c* oxidase from *Paracoccus denitrificans* is shown. Cytochrome *c* oxidase pumps protons. The pumped protons flow back via the membrane part of complex V (ATP synthase). The backflow leads to a rotation of a subunit in the extramembraneous part of the ATP synthase, which is coupled to the synthesis of ATP. Proton flows are indicated by the red arrows. Figure drawn by P. Lastrico and E. Olkhova.

which is a part of the active site in the heme/copper containing terminal oxidases. NO reductases appear to be unable to pump protons. The original task of both the heme/copper containing terminal oxidases (which are OO reductases) and the NO reductases might have been detoxification. Molecular oxygen, being toxic for the organisms living under the reducing atmosphere, might have been created by photolysis of water by ultraviolet light and had to be destroyed.

Prosthetic Groups

The heme/copper containing terminal oxidases minimally contain two heme groups and one copper atom as prosthetic groups. One of the heme groups is a high-spin heme. A copper atom, called Cu_B, is found in ~5Å distance. Cu_B and the high-spin heme form the so-called binuclear center. During turnover, molecular oxygen is bound to the central iron atom of the high-spin heme between the heme and Cu_B and reduced there during the catalytic cycle of the enzyme. The second heme is a low-spin heme and acts as an intermediate electron carrier.

The optical absorbance spectra have been the signature for the cytochrome *c* oxidases. In the mitochondrial cytochrome *c* oxidases both hemes are of the A type (see Figure 2), which give rise to characteristic absorbance maxima at around 600 nm. The high-spin heme of the active site is called heme a_3, the low spin one heme *a*. The term cytochrome aa_3 was used for the terminal oxidase of mitochondria. In many bacteria, the low-spin heme is a heme B, giving rise to a terminal oxidase of the ba_3 type. One ubiquinol oxidase of *Escherichia coli* contains heme O as the high-spin heme, therefore it is also called cytochrome *bo* or bo_3.

Cytochrome *c* oxidases contain another copper center, which is called Cu_A. It is actually formed by two copper atoms, which share one electron upon reduction. During turnover of the enzyme, Cu_A receives the electron from cytochrome *c* and transfers it to the low-spin heme. Ubiquinol oxidases do not possess this Cu_A center. Several terminal oxidases also contain a covalently bound cytochrome *c*. Depending on the nature of the other hemes these enzymes are called caa_3, or *cbo*, or cbb_3 oxidases. The terminal oxidases of the cbb_3-type operate at rather low-oxygen concentrations and, for example, are required for the nitrogen fixation in *Rhizobia* in order to keep the oxygen levels very low.

Cytochrome *c* oxidases also contain a magnesium or manganese atom close to the periplasmic (intermembrane) face of the enzyme. It is missing in the ubiquinol

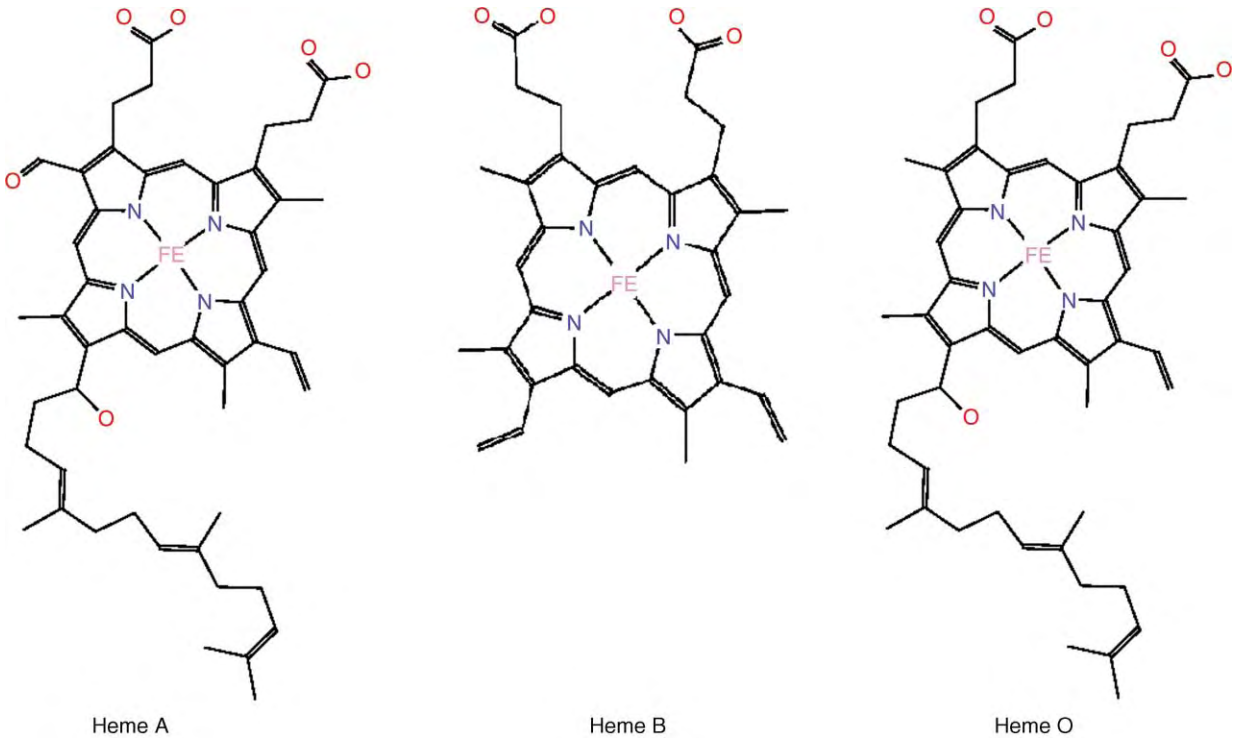

FIGURE 2 Chemical structures of the noncovalently bound hemes found in terminal oxidases. The structures of heme A, heme B, and heme O (from left to right) are shown.

oxidases and does not appear to be involved in electron transfer.

Protein Composition

The mitochondrial cytochrome *c* oxidases possess a core consisting of three protein subunits. These subunits are encoded by the mitochondrial genome. Subunit I is the largest subunit and possesses between 500 and 600 amino acid residues. It binds heme *a* as well as the heme a_3-Cu_B binuclear center and is the major catalytic subunit. Subunit II provides the binding site for the Cu_A-center and is anchored to the membrane by two N-terminal membrane-spanning helices. Subunit III possesses seven membrane-spanning helices but no prosthetic groups. Its function is unknown; it is not required for the catalytic activity. If its gene is deleted in bacteria, an active two-subunit enzyme is still found, albeit at a reduced level. If subunit III is removed the enzyme becomes rather unstable under turnover conditions.

The mitochondrial cytochrome *c* oxidases contain up to eight additional smaller subunits, which are encoded by the nuclear genome. For some of the subunits, organ specific subtypes exist; for example, there are liver and heart types of the so-called subunit VIa in the mammalian cytochrome *c* oxidase. It has been suggested that the presence of the liver or heart type determines the efficiency of proton pumping, and that only two protons per oxygen molecule are pumped by cytochrome *c* oxidase in liver, but four in heart. Subunit VIa also seems to be responsible for the dimer formation of cytochrome *c* oxidase from bovine heart mitochondria.

The bacterial cytochrome *c* oxidases of known structure contain one additional small protein subunit, called subunit IV. It has no counterpart in the mitochondrial enzyme and its function is not known.

X-Ray Crystal Structures of Cytochrome *c* Oxidases and Other Terminal Oxidases

Protein Structure

Until now atomic structures, determined by X-ray crystallography, have been presented for the cytochrome *c* oxidases from the soil bacterium *Paracoccus denitrificans*, from the purple photosynthetic bacterium *Rhodobacter sphaeroides* and from bovine heart mitochondria. These are rather typical closely related enzymes. Both *Paracoccus* and *Rhodobacter* are grouped within the α-proteobacteria, and the symbiotic ancestor of the mitochondria belonged to this group. In addition, the structure of the aberrant ba_3 type cytochrome *c* oxidase (e.g., it does not possess a

homologue of subunit III) from the bacterium *Thermus thermophilus*, and that of the ubiquinol oxidase (cytochrome bo_3) from *E. coli* have been determined.

In the cytochrome *c* oxidases the subunits I, II, and III form the core, which, viewed parallel to the membrane, has a trapezoidal shape, when seen from above it looks oval. The length of the trapezoid is about 90Å, its height 55Å. It comprises 21 membrane-spanning helical segments. The globular polar domain of subunit II is attached to the narrow, periplasmic (intermembrane, respectively) side of the trapezoid (see Figures 1 and 3). Subunit I contains twelve membrane-spanning helices which are arranged in a threefold symmetric manner. In this kind of arrangement three "pores" are formed. One contains the heme *a* with two histidine residues as axial iron ligands, another heme a_3 with one axial histidine ligand and Cu_B, and the third one is blocked by aromatic residues. Subunit II contains two N-terminal membrane-anchoring transmembrane helices. The globular domain contains a ten-stranded β-barrel similar to the copper proteins plastocyanin and azurin. The copper-binding site is in the same position, but to subunit II two copper atoms instead of one are bound. Subunit III possesses seven transmembrane helices. They form two bundles, one of five, the other of two transmembrane helices. Between them a V-shaped cleft exists, which is partially filled by lipid molecules. In the cleft at the center of the membrane, an entrance to a hydrophobic channel can be seen which leads to the active site. It has been proposed that this channel is a diffusion channel for oxygen because it leads to the active site, and because the solubility of oxygen in the hydrophobic center of the membrane is considerably higher than in the aqueous phase. Subunit III of the ubiquinol oxidase (cytochrome bo_3) from *E. coli* consists of five transmembrane helices only. The loss is compensated by the addition of two transmembrane helices to the twelve of subunit I.

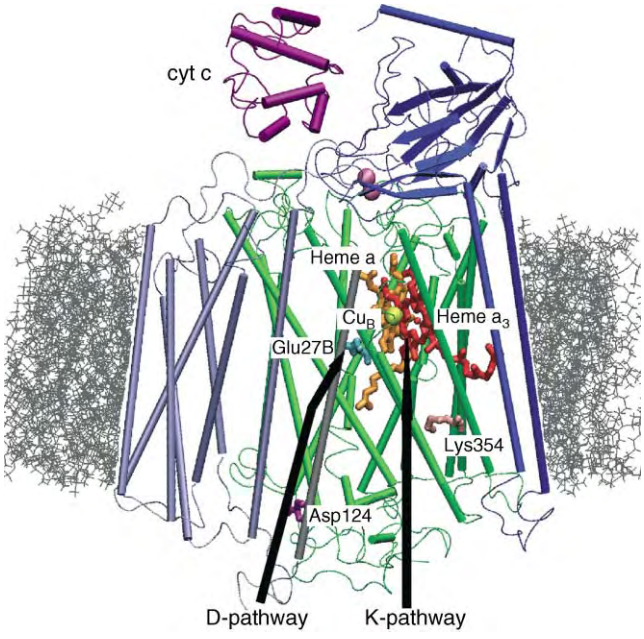

FIGURE 3 Cytochrome *c* oxidase in a bilayer membrane. The four subunits containing cytochrome *c* oxidase from *Paracoccus denitrificans* is shown together with its substrate cytochrome *c* (purple, top). Helices are represented as columns, β-strands as ribbons with arrows. Green: subunit I; dark blue: subunit II; iceblue: subunit III; gray: subunit IV; heme *a* is shown in orange, heme a_3 in red, Cu_B in yellow, and Cu_A in mauve. The lipid bilayer is represented in gray as atomic model. Figure prepared by E. Olkhova using the program vmd.

Arrangement of the Prosthetic Groups

Cu_A receives an electron from cytochrome *c* at the periplasmic (intermembrane) surface of the membrane. Tryptophan 121 (*Paracoccus* numbering) appears to play an important role in the electron transfer. From Cu_A the electron is transferred to heme *a*, the distance of the lower Cu-atom to the iron atom of heme *a* is ~20Å. Heme a_3 lies in the membrane in the same height, so that electron transfer from heme *a* to heme a_3 occurs parallel to the membrane. The center-to-center distance of both hemes is 13–14Å. The propionate side chains of both heme groups are oriented towards the external (periplasmic or intermembrane) side. Their charges are partially compensated by the formation of ion pairs with two arginine residues.

Cu_B is ~5Å away from the heme a_3 iron, so that a very rapid electron transfer between heme a_3 and Cu_B has to be expected. It is a general problem in cytochrome *c* oxidase research that Cu_B is silent and there is no spectroscopic technique available which allows determining the redox state of Cu_B. Cu_B possesses three histidine ligands. One of them is covalently linked to a nearby tyrosine. The existence of a covalent histidine-tyrosine cross-link was unknown prior to the X-ray crystallographic structure determinations.

Proton Transfer Pathways

The structural knowledge combined with the results of previous site-directed mutagenesis experiments lead to the identification of two proton transfer pathways. One, called the K-pathway because of the existence of an essential lysine residue as a component of this pathway, leads straight from the cytoplasmic (matrix) surface into the binuclear site. The cross-linked tyrosine is a part of it. Mutation of the essential lysine residue to other residues prevents the initial reductions of the binuclear site during the catalytic cycle.

A second proton transfer pathway has been called the D-pathway because an aspartic residue at the protein surface is a part of it. A change of this aspartate residue to an asparagine still allows a (reduced) turnover of the enzyme, but proton pumping is abolished. The D-pathway is wider than the K-pathway, and many water molecules are involved. It leads straight up first, then changes direction at a water filled cavity, which leads to a glutamate residue (E278 in *Paracoccus* numbering). The further pathway is unclear. There must be a possibility for proton transfer to the active site, because the reaction cycle can be started from an artificially fully reduced enzyme in K-pathway mutants, proceeds quite normally and water is formed in the active site. Proton transfer using a temporarily established chain of water molecules is a possibility. Alternatively, pumped protons can be transferred to the heme propionates and stored there in some parts of the catalytic cycle.

The existence of a third pathway, called H-pathway, has been suggested for the bovine heart mitochondrial cytochrome *c* oxidase. However, there is no evidence for it on the basis of mutagenesis experiments in bacterial enzymes and the proposal has met with a lot of skepticism.

The Catalytic Cycle and Proton Pumping

The catalytic cycle starts with a fully oxidized enzyme (O-state). All four prosthetic groups (Cu_A, heme *a*, heme a_3 and Cu_B) are oxidized. In cytochrome *c* oxidases an electron is first transferred from cytochrome *c* to Cu_A, and then to heme *a* with a time constant of 20–50 μs. The published values for the electron transfer to heme a_3 from heme *a*, vary greatly and most likely this electron transfer requires proton uptake via the K-pathway first. Most likely in this E-state, the single electron equilibrates over all prosthetic groups. A second electron has to be provided by cytochrome *c*. When the binuclear site is doubly reduced, an oxygen molecule can be bound to the iron atom of heme a_3, thus the oxygenated form, called compound A, corresponding, for example, to oxygenated myoglobin, is formed. This reacts to an intermediate state called P, which is characterized by an absorption maximum at 607 nm. P stands for peroxy because the original (incorrect) belief was that this form contains a peroxide dianion. After the input of a third electron into the enzyme a state absorbing visible light at 580 nm is formed. This was believed to be the oxoferryl state and called F. After the fourth reduction step the iron-bound oxygen atom was thought to be converted to a second water molecule under consumption of two protons and the O-state is formed again. Such a simple catalytic cycle is presented in Figure 4A.

In recent years much of the accepted knowledge had to be revised. First, it is clear now that there are two P- and F-states each, one each in the two-electron reduced enzyme, and one each in the three-electron reduced enzyme. It cannot be excluded that all of them are part of the catalytic cycle (Figure 4). Second, it has been convincingly demonstrated by resonance Raman spectroscopy and chemical experiments that in the P-state the O=O double bond is already broken and that an oxoferryl state already exists. This finding causes the problem that four electrons are required to split the O=O double bond, but only three (two from the Fe^{II} to Fe^{IV} transition upon formation of the oxoferryl state, and one from Cu_B) are available from the prosthetic group. Although definite proof could not be presented yet, it is the general belief that the fourth electron (and a proton) is provided by the cross-linked tyrosine, which becomes a neutral tyrosine radical. The existence of the cross-link which most likely is a side product formed by a tyrosine radical in one of the first turnovers, has to be considered as a hint for the occurrence of a tyrosine radical. Also most likely, a hydroxide as a Cu_B-ligand is generated, and may cause the difference of the optical absorbance spectra between the P- and the F-states. The F-state in the three-electron reduced enzyme is most likely to contain water instead of the hydroxide, and the tyrosine radical has become a neutral tyrosine.

The question, which of the electron transfer steps are coupled to proton pumping, is currently a matter of intense debate. The already generally accepted proposal that only the P to F-, and F to O-transitions are linked to proton pumping with two protons pumped each, could not be maintained. There is good evidence that one proton is pumped upon the input of the second electron into the oxidized enzyme in the absence of oxygen, and it has also been proposed that under turnover conditions already the first reduction step is connected to proton pumping. For a final answer, further experiments are required. It is a general problem in cytochrome *c* oxidase research that many kinetic experiments are started from a fully reduced enzyme (all four prosthetic groups are artificially reduced). However, this state is not part of the catalytic cycle and the value of the conclusions drawn is limited.

As long as it is unknown, when proton pumping occurs in the catalytic cycle, it is very difficult to find out the mechanism of proton pumping. A rather general mechanism of proton pumping, that has found many supporters, is based on the charge-compensation principle. This principle states that each electron transfer into the membrane to heme *a* is

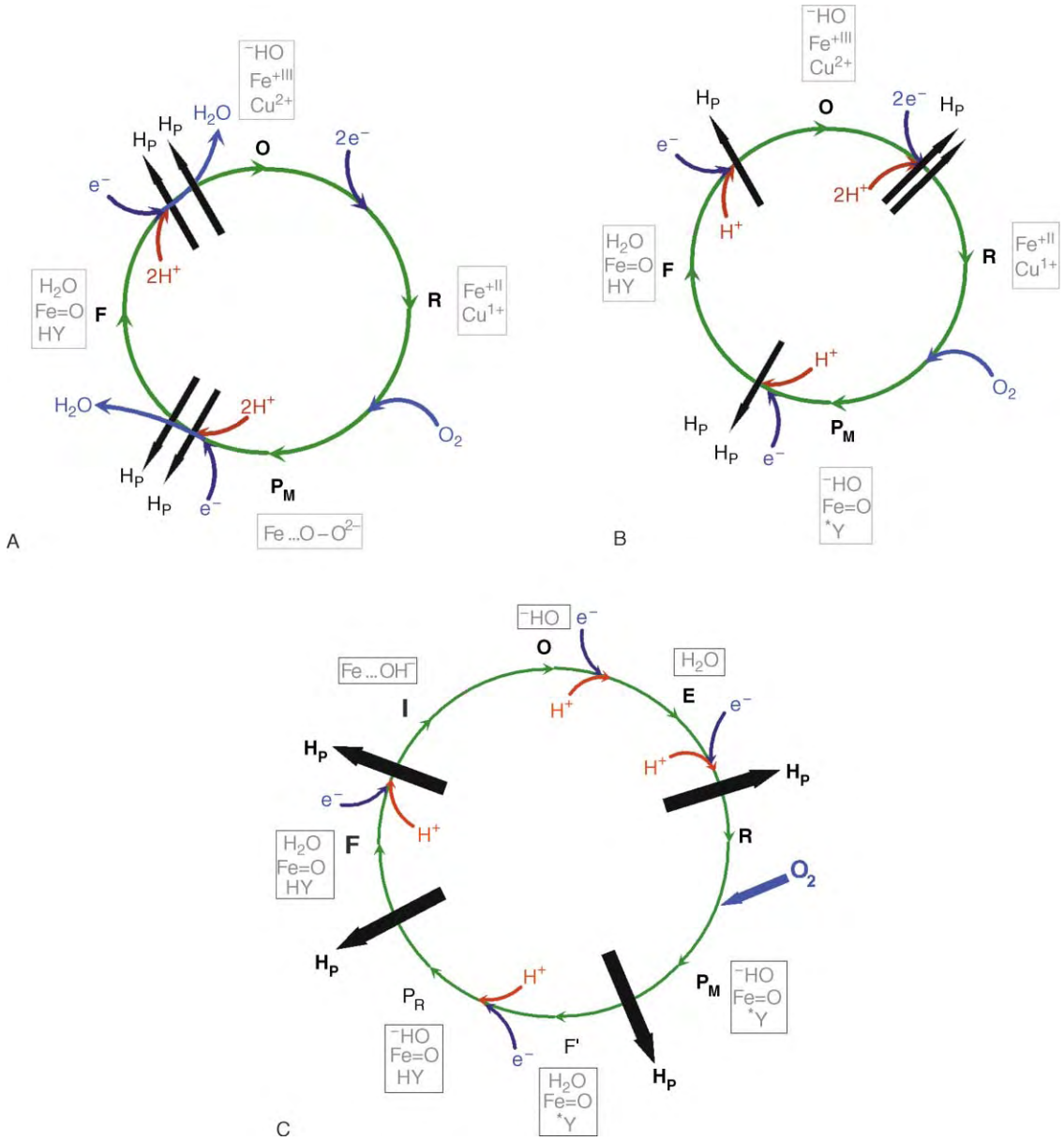

FIGURE 4 Catalytic cycles of cytochrome *c* oxidase. Classical, now obsolete cycle with only four states. The P-state erroneously has a peroxide anion bound to the heme a_3-iron; two protons are pumped during the P to F-, and during the F to O transitions under consumption of two protons each. It is clear now, that only one proton is consumed during each transition. (A) Adaptation of the classical cycle to recent findings. Two protons are taken up already during the initial two-electron reduction of the enzyme, and two protons are pumped in this phase (under turnover conditions). The P_M-state contains a oxoferryl-iron, a tyrosine radical and a hydroxide in the binuclear center, only one proton is pumped during the P to F-, and during the F to O transitions. (B) A recent cycle with two P and two F-states. The protonations of the hydroxides in the binuclear sites of the P-states leads to proton pumping, each electron uptake is accompanied by a charge compensating proton uptake. Tyrosine radicals are present in the two-electron reduced states, tyrosines in the three-electron reduced states. One proton is pumped during the second reduction step, which could now be experimentally demonstrated. One electron is pumped during the F to O-transition as a result of the protonation of the oxo-group at the heme a_3 iron. (C)

charge-compensated by uptake of one proton from the opposite side of the membrane and not consumed in water formation. This proton is supposed to be electrostatically repelled and thus pumped by those protons, which are later taken up and consumed in water formation. The mechanism requires storage of the charge-compensating protons in a way that they cannot be used for water formation.

It is evident that still many experiments are required before the mechanism of proton pumping by cytochrome *c* oxidases can be considered to be known.

See Also the Following Articles

Cytochrome bc_1 Complex (Respiratory Chain Complex III) • Cytochrome *c* • Heme Proteins • Heme Synthesis

Glossary

α-proteobacteria A group of eubacteria containing many well characterized.

bacterial species The evolutionary ancestor of mitochondria is most likely a close relative of the *Rickettsiaceae* which belong to the this group of bacteria.

cyanobacteria Prokaryotes that perform oxygenic photosynthesis. They developed the water-splitting system converting the atmosphere to an oxidizing one. They are considered to be the evolutionary ancestor of chloroplasts.

cytochrome *c* A heme-containing hydrophilic protein that functions as an electron carrier in respiration.

ubiquinol A hydrophobic coenzyme which carries hydrogen atoms in membranes. It can release protons and electrons separately. It forms ubiquinone upon oxidation.

Further Reading

Ferguson-Miller, S., and Babcock, G. T. (1996). Heme/copper terminal oxidases. *Chem. Rev.* **96**, 2889–2907.

Jünemann, S. (1997). Cytochrome *bd* terminal oxidase. *Biochim. Biophys. Acta* **1321**, 107–127.

Michel, H. (1999). Cytochrome *c* oxidase: Catalytic cycle and mechanism of proton pumping – a discussion. *Biochemistry* **38**, 15129–15140.

Michel, H., Behr, J., Harrenga, A., and Kannt, A. (1998). Cytochrome c oxidase: Structure and spectroscopy. *Annu. Rev. Biophys. Biomol. Struct.* **27**, 329–356.

Ostermeier, C., Harrenga, A., Ermler, U., and Michel, H. (1997). Structure at 2.7 angstrom resolution of the Paracoccus denitrificans two-subunit cytochrome c oxidase complexed with an antibody F-V fragment. *Proc. Natl. Acad. Sci. USA* **94**, 10547–10553.

Pereira, M. M., Santana, M., and Teixeira, M. (2001). A novel scenario for the evolution of haem-copper oxygen reductases. *Biochim. Biophys. Acta* **1505**, 185–208.

Ruitenberg, M., Kannt, A., Bamberg, E., Fendler, K., and Michel, H. (2002). Reduction of cytochrome *c* oxidase by a second electron leads to proton translocation. *Nature* **417**, 99–102.

Saraste, M. (1999). Oxidative phosphorylation at the fin de siecle. *Science* **283**, 1488–1493.

Saraste, M., and Castresana, J. (1994). Cytochrome-oxidase evolved by tinkering with denitrification enzymes. *FEBS Lett.* **341**, 1–4.

Yoshikawa, S., Shinzawa-Itoh, K., Nakashima, R., Yaono, R., Yamashita, E., Inoue, N., Yao, M., Fei, M. J., Peters Liebeu, C., Mizushima, T., Yamaguchi, H., Tomizaki, T., and Tsukihara, T. (1998). Redox-coupled structural changes in bovine heart cytochrome *c* oxidase. *Science* **280**, 1723–1729.

Biography

Hartmut Michel is a Director at the Max Planck Institute of Biophysics and Head of the Department of Molecular Membrane Biology in Frankfurt am Main, Germany. He received a Diploma (equivalent to M.Sc.) in Biochemistry at the University of Tübingen and a Dr. rer. nat degree from the University of Würzburg. His principal research interest is to understand the mechanism of action of selected membrane–protein complexes based on accurately known structures. The focus of his current research lies on the complexes of the respiratory chain and on G protein-coupled receptors. Dr. Michel received the Nobel prize in chemistry in 1988 "for the determination of the three-dimensional structure of a photosynthetic reaction center." This was the first structure determination of a membrane protein or of a membrane–protein complex.

Respiratory Processes in Anoxygenic and Oxygenic Phototrophs

Roberto Borghese and Davide Zannoni
University of Bologna, Bologna, Italy

Phototrophic microrganisms include "*anoxygenic phototrophs,*" which are bacteria capable of growing photosynthetically with no oxygen generation, and *Cyanobacteria* which are "*oxygenic phototrophs*" because their photosynthetic apparatus generates oxygen. Several genera of anoxygenic phototrophs are capable of obtaining energy also from *aerobic* and *anaerobic respiration* in darkness; conversely, only a few filamentous cyanobacteria can grow in the dark on glucose or other sugars using the organic material as both carbon and energy source. The latter observation suggests that besides the bioenergetic aspect, respiration in cyanobacteria plays other roles such as to control the redox balance or to act as a scavenger for O_2 during nitrogen fixation. Facultative phototrophs (capable of both respiration and photosynthesis) contain a photosynthetic apparatus whose synthesis is repressed by oxygen; an exception to this rule is the group of aerobic-anoxygenic phototrophs, mainly marine microorganisms, requiring the presence of oxygen to synthesize their photosynthetic apparatus.

Anoxygenic Phototrophs

On a phylogenetic basis (16S rRNA analyses) phototrophic bacteria and their relatives are grouped in a class, the Proteobacteria, which is formed by several subclasses, named α, β, γ, δ, and ε. Facultative photosynthetic bacteria belong to α and β subclasses, e.g., genera *Rhodobacter*, *Rhodospirillum*, *Rhodocyclus*, *Rubrivivax*, and *Erytrobacter.*

Metabolic Aspects of Facultative Anoxygenic Bacteria

Facultative phototrophs are probably the most metabolically flexible organisms of the microbial world. Species such as *Rhodobacter* (*Rba.*) *capsulatus* and *Rba. sphaeroides* can grow by aerobic respiration and photosynthesis using either organic or inorganic substrates but also by anaerobic respiration with trimethylamine-N-oxide (TMAO) or dimethyl sulfoxide (DMSO) as electron acceptors. Further, some strains of the species *Rhodopseudomonas* (*Rps.*) *palustris*, *Roseobacter* (*Rsb.*) *denitrificans* and *Rba. sphaeroides* can reduce nitrate (NO_3^-) into dinitrogen (N_2) via nitrite (NO_2^-), and, in some cases, also nitric oxide (NO) and nitrous oxide (N_2O). These energy generating processes are catalyzed by oxido-reduction protein complexes forming composite electron transport chains. Apparently not all the above summarized metabolic options are activated or can be available simultaneously in a single species; however, cells of *Rba. capsulatus* or *Rba. sphaeroides* grown photosynthetically in the presence of low oxygen tension ($<1\%$) contain both photosynthetic and respiratory apparatuses.

Electron Transport Chains

Respiration in facultative phototrophs involves numerous redox carriers, namely: (1) transmembrane protein complexes such as NADH- and succinate-quinone oxidoreductases (NQR and SQR, respectively), cytochrome (cyt) bc_1 or hydroquinone-cytochrome *c* oxidoreductase (QCR), quinol oxidase(s) (QOX), and cyt cbb_3 and/or aa_3 oxidases (COX); (2) electron and/or proton carriers such as ubiquinones (UQ), cyt c_2, HiPIP, and cyt c_y; (3) enzymes of the periplasmic space such as NO_3^-, NO_2^-, N_2O, and DMSO reductases. With O_2 as final electron acceptor, the NQR, QCR, and COX enzymes constitute three main coupling sites where the potential energy between the initial donor and the final acceptor molecules is released in small steps, that are controlled by the differences between the redox midpoint potentials (E_m) of the redox couples involved, and efficiently coupled to the generation of an electrochemical proton gradient ($\Delta\mu_{H+}$). Photosynthesis converts the radiant energy into chemical energy at the level of the photochemical reaction center (RC). This transmembrane protein complex generates a charge separation that is followed by a cyclic electron transfer involving quinone molecules (UQ-10), cyt bc_1 complex, and soluble cyt c_2 in addition to the membrane-bound cyt c_y, in the case of *Rba. capsulatus*. Under dark aerobic

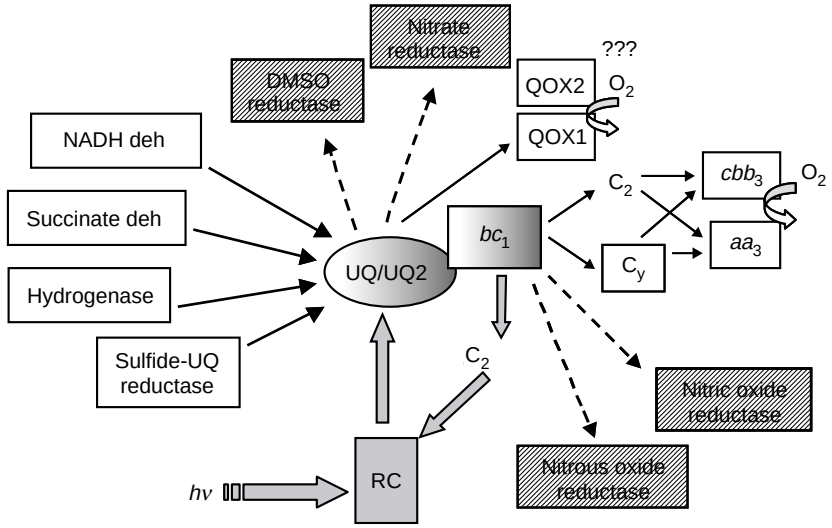

FIGURE 1 Block scheme illustrating the complex network of electron transport chains in *Rba. sphaeroides*. Black arrows indicate the influx of reducing equivalents and the efflux of electrons leading to the membrane-bound oxidases. Dashed black arrows indicate output of electrons involved in anaerobic respiration. Gray-colored redox components and arrows are those specifically involved in photocyclic electron transfer while those shaded off are shared by photosynthesis and respiration. RC, photochemical reaction center; *hν*, radiant energy; C_2, soluble cyt c_2; C_y, membrane-attached cyt c_y; QOX1, functional ubiquinol oxidase (*qxtAB* operon); QOX2, not functional ubiquinol oxidase (*qoxBA* operon).

conditions, facultative phototrophs use a respiratory chain, closely related to that present in mitochondria. The last step of O_2 reduction into H_2O is catalyzed by two oxidases (not always present in a single species): a cyt *c* oxidase (of cbb_3 and/or aa_3 type), inhibited by μM cyanide, and a quinol oxidase (of *bo* type), inhibited by mM cyanide, branching the electron flow at the level of the UQ-10 pool. Figure 1 shows a block scheme of the different electron transport pathways operating in *Rhodobacter sphaeroides*.

Interaction between the Diverse Electron Transport Chains

The interaction between the different bioenergetic chains of photosynthetic bacteria occurs by two nonexclusive mechanisms, namely: (1) an indirect mechanism, exerted by the proton motive force (PMF) as a "back pressure" on the rate of electron transport catalyzed by redox complexes, and (2) a direct mechanism of interaction between electron carriers, e.g., UQ-10 or cyt c_2, that are engaged in multiple bioenergetic processes. In this way, the activity of a given bioenergetic chain would affect the redox state of the components in common and, consequently, the functioning of the other chains.

Respiratory and photosynthetic apparatuses are localized in different parts of the internal bacterial membrane (CM); this implies the diffusion of some electron carriers such as UQ, in the lipid phase, or cyt c_2, in the periplasmic space. However, the diffusion of these elements does not occur on the entire internal membrane; thus, the different redox chains are not necessarily in thermodynamic equilibrium. For example, two functional pools of soluble cyt c_2 exist in *Rba. sphaeroides* and *Rba. capsulatus*. Further, the membrane-bound cyt c_y is a direct electron donor to the cbb_3-type oxidase of *Rba. capsulatus* or to the cbb_3/aa_3 type oxidases of *Rba. sphaeroides*. Consequently, the redox chain containing cyt c_y must be organized in *supramolecular* complexes and operate independently of the redox state of the other respiratory pathways.

Genetic Regulation of Respiration and Photosynthesis in Facultative Phototrophs

Oxygen is the key factor in the coordinated regulation of respiratory and photosynthetic activities since it participates, directly or indirectly, in determining the levels of expression of all components involved in these processes (Figure 2). The main regulatory element in *Rba. capsulatus* is the RegA/RegB couple (PrrA/PrrB in *Rba. sphaeroides*), which is able to sense the change in O_2 partial pressure in the environment, and to transform this information into a regulatory response. Within this couple, RegA is the effector component while RegB is the sensor partner. This sensor-effector couple functions according to a widespread regulatory model in which the sensor protein (RegB) detects changes in the environment, in this case variations in O_2 tension, and modifies the effector protein (RegA) by phosphorylating it. Depending on its phosphorylated or dephosphorylated status, the effector can regulate the expression of

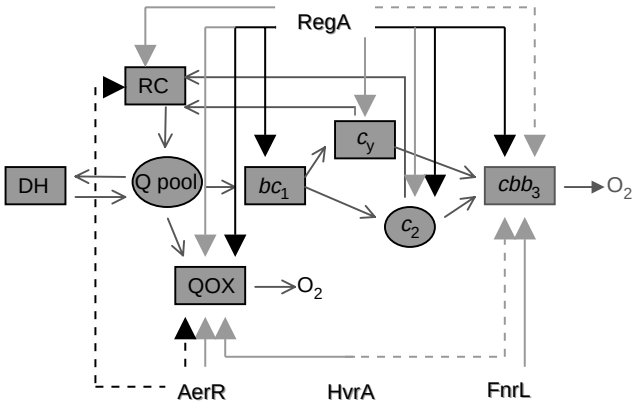

FIGURE 2 Genetic regulatory network of respiratory and photosynthetic activity in *Rhodobacter capsulatus*. Black and gray arrows indicate regulation under aerobic and anaerobic conditions, respectively. Straight lines are for positive regulation (induction), dotted lines are for negative regulation (repression). Genetic regulators are written in black while respiratory/photosynthetic components, connected by thin arrows, symbolising electron flow, are in dark gray. DH, NADH dehydrogenase; RC, photosynthetic reaction center; Q pool, ubiquinone-10 pool; bc_1, transmembrane cyt bc_1 complex; c_y, membrane-anchored cyt c_y; c_2, periplasmic (soluble) cyt c_2; cbb_3, membrane-bound cyt *c* oxidase; QOX, membrane-bound quinol oxidase. See text for further details.

a number of genes. RegA/RegB is a general aerobic/anaerobic regulatory couple that influences the expression of many processes in addition to respiration and photosynthesis: N_2 fixation, CO_2 fixation, and H_2-ase activity. The electron transport chain (ETC) genes that have been shown to be regulated by RegA/RegB are the ones coding for COX and QOX, which are specific for the respiratory chain, and those coding for the *bc*1 complex, cyt c_2 and cyt c_y which participate in both respiration and photosynthesis (Figure 2). RegA/RegB also regulate the level of the RC. Other regulatory elements that participate in the regulation of respiratory ETC components are AerR, that operates in the presence, as well as in the absence, of O_2; HvrA and FnrL are anaerobic regulators only (Figure 2). Although the interaction of all the aforementioned regulatory elements is quite complex, it allows the fine tuning and controlled interplay of respiratory and photosynthetic activities.

Oxygenic Phototrophs

Cyanobacteria are capable of oxygenic photosynthesis, differing in that from anoxygenic phototrophs. Cyanobacteria form one of the major phila of *Bacteria* and they were most likely the first oxygen-evolving organisms on Earth changing the atmosphere from anoxic to oxic. Oxygenic phototrophs are grouped into several morphological groups; however, most of the available biochemical and genetic data concern mainly unicellular genera such as *Synechococcus* and *Synechocystis*.

Respiration is by definition a membrane-bound process; in this respect, cyanobacteria contain three different types of membranes: (1) the outer membrane, typical of Gram negatives, which has no specific role in respiration; (2) the cytoplasmic membrane (CM); and (3) the intracytoplasmic membranes (ICMs) or thylakoids. Both CM and ICM contain respiratory redox complexes; electron microscopy also indicates that CM and ICM might be connected, at least in *Synechococcus* sp. strain PCC 6301, although a correct picture of the membrane arrangement *in vivo* is lacking at present.

Electron Transport Pathways in Oxygenic Phototrophs

Respiratory and photosynthetic electron transports are intimately connected in two distinct bioenergetically active membranes, ICM and CM. All photosynthetic electron transport is located in the ICM, where photosynthesis and respiration share components (Figure 3). In addition, ample experimental evidences indicate the presence of respiratory chain(s) in the CM. Cyanobacterial respiratory terminal oxidases (RTOs) have no direct function in photosynthesis and therefore can be considered the key enzymes of respiration. All cyanobacteria (investigated so far) contain several respiratory branches ending in different RTOs but their actual location in the membrane cell (ICM, CM, or both) is far from being assessed. The best-characterized species is *Synechocystis* sp. strain PC 6803, for which the complete genomic sequence is available. Three sets of genes for RTOs were found, the well-characterized aa_3-type cyt *c* oxidase (COX, encoded by *coxBAC*), a related set of genes also belonging to the heme-copper oxidase superfamily, termed alternate RTO (ARTO; encoded by *ctaCII-ctaDIIEII*), and two genes (*cydAB*) encoding a putative cyt *bd*-type quinol oxidase (Cyd).

The CM forms the inner boundary of the periplasmic space and is known to contain proteins typically associated with respiratory electron transport, such as NAD(P)H dehydrogenase, cyt b_6/f (homologous of the bc_1 complex), and terminal oxidases (presumably, ARTO). Two types of NAD(P)H dehydrogenase have been found. One is a NADPH-type I dehydrogenase (NDH-1), that is encoded by *ndh* genes, which consists of about 12 subunits and contributes to a proton gradient ($\Delta\mu_{H+}$) across the membrane. The second type of dehydrogenase is a NADH-type II dehydrogenase (NDH-2) consisting of a single subunit and probably not contributing to energy transduction.

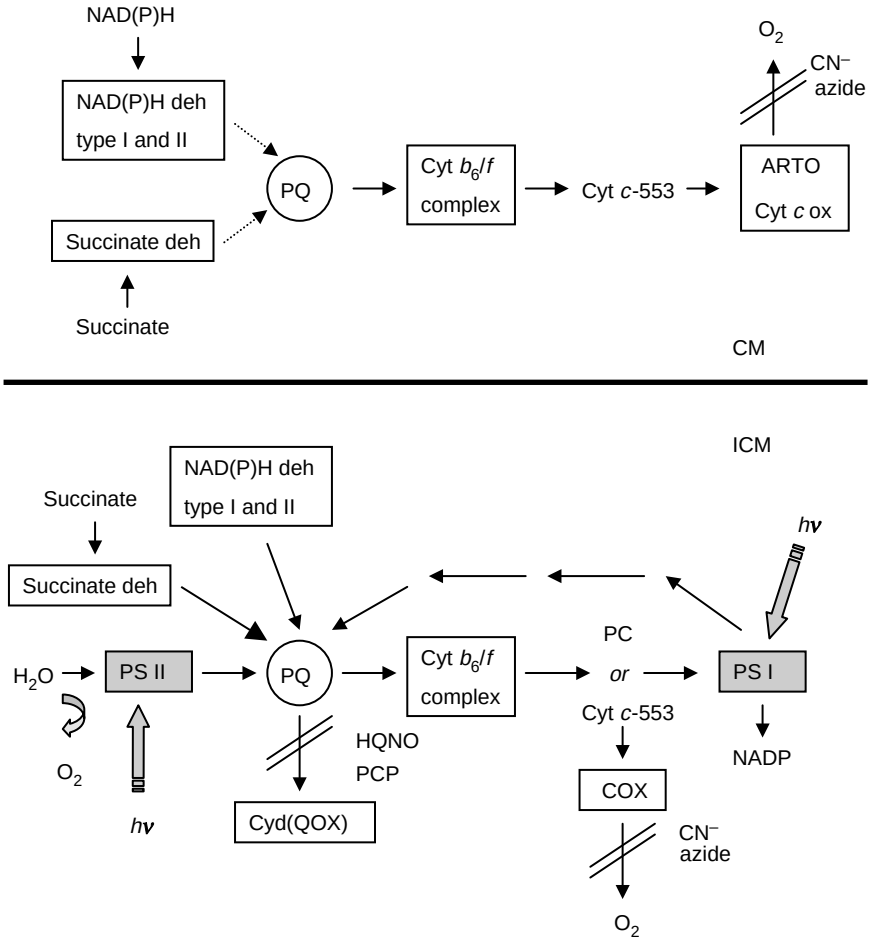

FIGURE 3 Working model of photosynthetic and respiratory electron transport chains in *Synechocystis* sp. strain PCC 6803 in CM and ICM. Membrane-bound redox complexes are indicated as rectangular boxes. Dotted arrows (CM redox chain) symbolize the lack of evidence for electron flow while the thickness of arrows (ICM redox chain) symbolize their relative activities. HQNO, 2-heptyl-4-hydroxy-quinoline-N-oxide; PCP, pentachlorophenol; CN^-, cyanide anion; PC, plastocyanin; PQ, plastoquinone pool; *hν*, radiant energy; see text for further details.

In *Synechocystis* sp. strain PCC 6803, three genes coding for NDH-2 (*ndbA,B,C*) are found.

Three intermingling pathways are dominant in *Synechocystis* sp. strain PCC 6803 thylakoids (ICM), namely: (1) a linear electron transport from H_2O to NADPH, catalyzed by photosystems I and II (PSI/PSII), (2) a respiratory transport from NAD(P)H and succinate to both COX and QOX, and (3) a cyclic electron flow around PSI, i.e. electrons at the acceptor side of PSI returning to the PQ pool (Figure 3). However, as generally seen in facultative anoxygenic phototrophs, electrons can move from one pathway to another at the level of the PQ pool, b_6/f complex, and/or soluble carriers such as plastocyanin (PC) or cyt *c*-553 (Figure 3). For example, in the absence of PSI, reducing equivalents generated by PSII are fed into COX, while in darkness, respiratory electrons are used to reduce the acceptor side of PSII if terminal oxidases are blocked. Results with mutants of *Synechocystis* sp. strain PCC 683 impaired in several combinations of respiratory and photosynthetic redox complexes indicate that succinate dehydrogenase (SDH) is the main electron transfer pathway into the PQ pool and that type I and II NAD(P)H dehydrogenases might simply operate as regulators of NADP and NAD reduction levels. This indicates that respiration in cyanobacteria plays an important role in the control of the intracellular redox balance.

In general, the genes for components of the respiratory chain(s) are present in only one copy per chromosome even in those species having two respiratory chains (Figure 3). How one gene directs its gene product into two different membranes (CM and ICM) is an intriguing yet unanswered question. Further, the amounts of several components of the respiratory chain(s) are regulated by external factors such as the concentration of Cu^{2+} for synthesis of cyt *c*-553 and plastocyanin or the ionic strength for cyt aa_3-type oxidase synthesis. Unfortunately, the mechanisms of gene regulation are largely unknown at present and they will be important topics for future studies in respiration of oxygenic phototrophs.

See Also the Following Articles

Cytochrome bc_1 Complex (Respiratory Chain Complex III) • Photosynthesis • Respiratory Chain Complex II and Succinate:Quinone Oxidoreductases

Glossary

cytochromes Redox proteins with an iron-containing porphyrin ring (heme).

electrochemical proton gradient It defines the membrane energized state in terms of electrical units.

genetic regulatory element A molecule that regulates gene expression by interacting with DNA.

phototroph An organism that converts radiant energy into chemical energy.

proton motive force An energized state of the membrane resulting from the separation of charges across the membrane.

respiration The process in which a compound is biologically oxidized by an electron acceptor (O_2 or an O_2 substitute) linked to generation of a proton motive force.

Further Reading

Schmetterer, G. (1995). Cyanobacterial respiration. In *The Molecular Biology of Cyanobacteria* (D. A. Bryant, ed.) Vol. 1, pp. 409–435. Kluwer, Dordrecht.

Vermeglio, A., Borghese, R., and Zannoni, D. (2004). Interaction between photosynthesis and respiration in facultative phototrophs. In *Respiration in Archaea and Bacteria* (D. Zannoni, ed.) Kluwer, Dordrecht, Vol. 16.

Zannoni, D. (1995). Aerobic and anaerobic electron transport chains in anoxygenic phototrophic bacteria. In *Anoxygenic Photosynthetic Bacteria* (R. E. Blankenship, M. T. Madigan and C. E. Bauer, eds.) Vol. 2, pp. 949–971. Kluwer, Dordrecht.

Biography

Davide Zannoni is Professor of General Microbiology in the Department of Biology at the University of Bologna, Italy. His main research interests are in the broad field of microbial physiology and biochemistry of facultative phototrophic and aerobic bacteria. He holds a degree in biology from the University of Bologna and received postdoctoral training at the St. Louis University School of Medicine. He carried out pioneering studies on bioenergetics of bacterial respiration and interaction between photosynthetic and respiratory redox complexes in facultative phototrophs.

Roberto Borghese is Research Associate and Lecturer of General Microbiology in the Department of Biology at the University of Bologna, Italy. He holds a degree in biology from the University of Bologna and a Ph.D. from the University of Missouri – Columbia. His main research interest is in genetics of anoxygenic photosynthetic bacteria.

Retinoblastoma Protein (pRB)

Nicholas Dyson and Maxim Frolov
Massachusetts General Hospital Cancer Center, Boston, Massachusetts, USA

The retinoblastoma protein (pRB) is the product of the retinoblastoma tumor susceptibility gene (*RB1*). The gene takes its name from the discovery that mutation of both copies of *RB1* is the critical rate-limiting event in the development of retinoblastoma, a rare form of cancer that affects very young children. Mutation of *RB1* is also found in a variety of cancers and pRB is thought to be functionally inactivated in most tumor cells. pRB is a nuclear protein, present in most cell types, that functions as a general negative regulator of cell proliferation. It is a member of a family of proteins (the pRB family) that have overlapping functions and are regulated by cyclin-dependent kinases. pRB is generally thought to function by controlling gene expression, and its best known target is the E2F transcription factor.

The pRB Family of Proteins

pRB-related proteins are conserved in plants and animals. Mammalian cells contain three pRB-family members (pRB, p107, and p130) that share a similar domain structure and a low, but significant, degree of primary sequence homology. All three proteins contain a conserved pocket domain that provides binding sites for E2F proteins, and complexes that repress transcription. In addition pRB, p107, and p130 contain many sites for phosphorylation by cyclin-dependent kinases (cdks). p130 is most highly expressed in differentiated cells, whereas p107 is highly expressed in populations of proliferating cells.

Although pRB, p107, and p130 are currently studied for their roles in the control of cell proliferation, they were first discovered as proteins that associate with the viral oncoprotein Adenovirus E1A. The binding sites for pRB, p107, and p130 map to the regions of E1A that are needed for its oncogenic properties. Similar sequences are also present in the E7 proteins of human papilloma viruses and large T antigens of several polyoma viruses. In each case, genetic studies show that the ability of the viral proteins to bind to pRB/p107/130 allows them to interfere with control of cell proliferation. The viruses are thought to use these interactions to create a cellular environment that is favorable for viral replication.

The RB Tumor Suppressor

The *RB1* gene was the first tumor suppressor gene to be identified and it is often described as a prototype for this class of cancer-related genes. Unlike oncogenes, whose activation promotes tumorigenesis, it is the inactivation of tumor suppressor genes that is linked to the development of cancer.

Individuals inheriting a mutant allele of *RB1* are very highly predisposed to develop retinoblastoma within the first two years of life. Patients, successfully treated for the eye cancer, often develop osteosarcoma in later life. Inactivation of *RB1* appears to be essential for the development of both familial and sporadic retinoblastoma, and also occurs in many osteosarcomas. *RB1* mutation is common in small cell lung cancers and has also been found in other tumors including bladder, prostate, and breast carcinomas. Although *RB1* is mutated in only a subset of tumors, it is thought that pRB is functionally compromised in most tumor cells. pRB is broadly expressed and thought to control the proliferation of most cell types. Precisely why people who inherit a mutant allele of *RB1* are only predisposed to certain types of cancer is still largely unclear. Studies with mice suggest that variations in the extent of functional overlap between pRB and other pRB family members may be important. Animals carrying a mutant allele of the murine *Rb* gene do not develop retinoblastoma but develop pituitary and thyroid tumors instead. However, the combined mutation of *Rb* and the related *p107* gene allows tumors to develop in the retina. This suggests that p107 is able to compensate for the absence of pRB in the developing mouse retina, and it may do so in other cell types.

In addition to its role in E2F regulation, which occurs in many diverse cell types, pRB also interacts with cell-type specific factors. These additional functions may explain why the inactivation of pRB has a greater effect on some cell types than others. For example, pRB interacts with the osteoblast transcription factor CBFA1 to promote the expression of bone specific genes. This role, particularly when combined with its functions in E2F regulation, may explain why pRB is important for suppression of osteosarcoma.

The Cellular Function of pRB

pRB function is often viewed through the prism of the cellular changes that occur when pRB is removed. pRB-deficient cells are smaller than wild-type cells and have defective cell cycle control. In tissue culture assays *Rb-/-* cells are generally less responsive to signals that cause wild-type cells to stop proliferating, and they are more readily driven from quiescence into the cell cycle. *Rb-/-* cells fail to arrest in G1, or S-phase, in response to DNA damage, and they show a reduced sensitivity to $p16^{INK4}$-induced cell cycle arrest and ras-induced senescence. Studies in primary cultures of mouse embryonic fibroblasts show that *Rb-/-* cells are genetically unstable and prone to polyploidy and aneuploidy.

Rb-deficient mice die fairly early in development (day 13–15 of embryogenesis) and display elevated levels of apoptosis, inappropriate cell proliferation, and developmental defects in several tissues. Studies of the murine pRB-family have revealed an extensive degree of redundancy and compensation between family members. Each of the pRB family members has been inactivated in the mouse by homologous recombination. Animals lacking two pRB family members are more severely affected than the single knockouts, and the inactivation of all three family members renders cells unresponsive to most types of G1 control. Triple knockout cells differentiate poorly, are readily immortalized, and easily transformed.

Remarkably and unexpectedly, the early lethality of *Rb-/-* animals has recently been shown to be an indirect consequence of a placental defect. When pRB is expressed specifically in the placenta, the rescue of placental function allows *Rb*-mutant embryos to survive close to birth. Although these mutant animals have defects in cell cycle control, and in skeletal muscle development, the development of these animals is surprisingly normal. Experiments in tissue culture using cells derived from the knockout animals have shown that the sudden removal of pRB causes more severe cell cycle control defects than those seen in cells derived from *Rb-/-* animals. This difference is due, at least in part, to an up-regulation of p107 that occurs in the sustained absence of pRB and appears to allow p107 to compensate for the loss of pRB function.

Regulation of pRB Activity

pRB is a long-lived protein (half-life > 16 h) and its activity is controlled by phosphorylation. When normal cells proliferate, pRB is inactivated by cdks, the kinases that drive progression through the phases of the cell division cycle. When cells cease to proliferate, the loss of cdk activity allows pRB to accumulate in its active form. Inactivation of pRB is not achieved by the phosphorylation of a single site but by the accumulation of phosphorylated residues at multiple sites that are scattered throughout the protein. A cluster of phosphorylation sites is found in the C-terminal fragments of pRB, p107, and p130 and the accumulation of negative charge in this domain is believed to drive a large conformation shift.

As quiescent cells enter the cell cycle pRB is sequentially phosphorylated by a series of cyclin-dependent kinases. Cyclin D/cdk4 is believed to be the first kinase to act on pRB with cyclin E/cdk2, and perhaps cyclin A-dependent kinases completing the process. Phosphorylation of pRB causes it to migrate slowly on SDS-PAGE gels. This mobility shift is often used as an indicator of pRB activity, but it is an unreliable measure; pRB inactivation appears to involve the cumulative effects of multiple phosphorylation events, and some modifications have no effects on the migration of the protein, whereas changes at others sites have a major effect.

Microinjection experiments on cultures of synchronized cells revealed that the ability of pRB to prevent cells from entering S-phase is restricted to a window within G1 phase of the cell cycle. Once cells progressed beyond a point in G1, ~ 2–4 h prior to S-phase, the introduction of pRB had no effect. The loss of a pRB-induced arrest correlates with the accumulation of cdk activity, and corresponds approximately to the "restriction point," a point in G1 where cells become irreversibly committed to progress through a complete cell cycle.

pRB that has been phosphorylated by cdks *in vitro* is unable to arrest cells in G1. *In vivo*, pRB is abruptly dephosphorylated at metaphase of mitosis and, presumably, reactivated. Phosphorylation is not the only type of posttranslational modification of pRB. Recent studies have shown that pRB is also acetylated on lysine residues but the functional significance of pRB aceylation is not well established at present.

The Rb Pathway

It has been proposed that pRB is a component of a critical regulatory pathway that is functionally inactivated in most tumor cells. This pathway comprises pRB, cyclin D/cdk4 (the kinase that phosphorylates pRB in G1), and $p16^{INK4}$ (a cdk inhibitor that antagonizes cyclin D/cdk4 activity and is induced in response to certain cellular stresses). Molecular studies have shown that the overexpression of cyclinD/cdk4 phosphorylates pRB and prevents it from arresting the cell cycle. In addition, cells lacking pRB are largely insensitive to $p16^{INK4}$-induced cell cycle arrest.

The $p16^{INK4}$/cyclin D/cdk4/pRB pathway is disrupted in a variety of ways in tumor cells. Retinoblastoma cells, for example, contain mutations in *RB1*. Many cervical cancers, on the other hand, express HPV E7 proteins that bind and inactivate all three of the pRB family members. Other cells contain lesions that elevate the activity of the cyclin D/cdk4 kinase (overexpression of cyclin D1, loss of the $p16^{INK4}$ cdk inhibitor, or mutations of cdk4 that are resistant to $p16^{INK4}$). Although most tumor cells contain one of these changes, these lesions primarily occur in a mutually exclusive manner. This may mean that there is no further selection for changes in this group of genes once the $p16^{INK4}$/cyclin D/cdk4/pRB pathway is disrupted. However, it is also true that several types of tumors are associated with specific types of mutations (e.g., pRB mutations are the only types of lesions in this pathway found in retinoblastoma, while most breast cancers contain elevated levels of cyclin D1), hence the relative importance of individual components of the pathway varies greatly between cell types.

Molecular Functions of pRB

Over 120 proteins have been reported to associate with pRB and many of these have been proposed to contribute to its tumor-suppressing properties. Most of these pRB-associated proteins are transcription factors and, although the list is diverse, in general pRB has been proposed to inhibit the activity of factors that are needed for cell proliferation, but to augment the activity of factors that promote cell differentiation.

The best-characterized property of pRB is its ability to repress E2F-dependent transcription. The E2F transcription factor allows the periodic expression of many proliferation-related genes to be tightly coupled with cell cycle position. E2F controls the expression of an extensive network of genes that includes essential components of the DNA synthesis machinery, and proteins needed for cell cycle progression, Mitosis, checkpoint responses, as well as regulators of apoptosis. pRB blocks cell proliferation, at least in part, by blocking the expression of E2F-regulated genes.

E2F complexes act as strong repressors of transcription in quiescent cells and during G1 phase of the cell cycle. As cells progress towards S-phase, these repressor complexes are disrupted and replaced by E2F activator complexes in a cdk-regulated process. All three pRB-family members associate with E2F proteins. In wild type cells, p107 and p130 associate primarily with E2F4 and E2F5 and are components of E2F repressor complexes. In these complexes the pRB-family members act as adapter proteins: binding to E2F with one surface, and to chromatin remodeling proteins through a second binding site (the LXCXE-binding cleft). In doing so, they allow a variety of enzymatic activities to be recruited to E2F regulated promoters. In a similar way, pRB also interacts with E2F4 and has the potential to recruit repressor complexes to DNA. In addition, pRB has the important ability to regulate E2F1, E2F2, and E2F3, the activator forms of E2F. pRB binds to an element that is buried within the transcriptional activation domain of the E2Fs, preventing them from activating transcription. Biochemical studies have also shown that pRB that is recruited to DNA by its association with E2F is also able to prevent adjacent DNA-bound transcription factors from interacting with the basal transcription machinery.

Chromatin immuno-precipitation experiments have given a detailed picture of the sequential binding of E2F and pRB-family members to E2F-regulated promoters during cell cycle progression. Surprisingly, p107 and p130 are the pRB-family members that are most easily detected at most E2F targets in proliferating cells. While some studies have found pRB at E2F-regulated promoters in cultures of proliferating cells, others have shown that pRB is most clearly recruited to E2F targets in response to specific signals, such as p16-induced cell cycle arrest, or ras-induced senescence. Under these circumstances pRB is thought to recruit histone deacetylase and/or histone methylase activities to DNA. These complexes repress transcription through modification of histone tails, changing the local chromatin structure to a form that is non-conducive to gene expression.

Genetic interactions between *Rb* and *E2F* genes have been demonstrated in multiple experimental systems and in species as diverse as mice and fruit flies. However, precisely how much of pRB's functions in development and tumor suppression are mediated through its interaction with E2F is uncertain. In addition to the many transcription factors that can bind to pRB, pRB has also been reported to relocalize to origins of replication following DNA damage and to interact with a diverse collection of chromatin-associated complexes. Further studies are needed to demonstrate the functional significance of almost all of pRB's proposed binding partners.

See Also the Following Articles

Cell Cycle Controls in G_1 and G_0 • Cell Death by Apoptosis and Necrosis • Chromatin Remodeling • Chromatin: Physical Organization

Glossary

apoptosis Programmed cell death.

cell cycle The complete sequence of events needed for the production of a new daughter cell. A mitotic cell cycle has two major landmarks, S-phase and Mitosis, which are separated by two gap phases, G1 (the period before DNA synthesis) and G2 (the period between the S and M-phases).

cell proliferation The overall increase in cell number that occurs when the rate of cell division is greater than the rate of cell death.

compensation A change in function that allows one type of gene product to perform a function that is normally carried out by another type of gene product.

redundancy The situation that occurs when two or more genes have a similar function and either gene is sufficient for a biological process.

Further Reading

Dyson, N (1998). The regulation of E2F by pRB-family proteins. *Genes Dev.* **12**, 2245–2262.

Goodrich, D. W., Wang, N. P., Qian, Y. W., Lee, E. Y., and Lee, W. H (1991). The retinoblastoma gene product regulates progression through the G1 phase of the cell cycle. *Cell* **67**, 293–302.

Harbour, J. W., and Dean, D. C. (2000). The Rb/E2F pathway: Expanding roles and emerging paradigms. *Genes Dev.* **14**, 2393–2409.

Robanus-Maandag, E., Dekker, M., van der Valk, M., Carrozza, M. L., Jeanny, J. C., Dannenberg, J. H., Berns, A., and te Riele, H. (1998). p107 is a suppressor of retinoblastoma development in pRb-deficient mice. *Genes Dev.* **12**, 1599–1609.

Sage, J., Mulligan, G. J., Attardi, L. D., Miller, A., Chen, S., Williams, B., Theodorou, E., and Jacks, T. (2000). Targeted disruption of the three Rb-related genes leads to loss of G(1) control and immortalization. *Genes Dev.* **14**, 3037–3050.

Sage, J., Miller, A. L., Perez-Mancera, P. A., Wysocki, J. M., and Jacks, T. (2003). Acute mutation of retinoblastoma gene function is sufficient for cell cycle re-entry. *Nature* **424**, 223–228.

Sherr, C. J. (1996). Cancer cell cycles. *Science* **274**, 1672–1677.

Thomas, D. M., Carty, S. A., Piscopo, D. M., Lee, J. S., Wang, W. F., Forrester, W. C., and Hinds, P. W. (2001). The retinoblastoma protein acts as a transcriptional coactivator required for osteogenic differentiation. *Mol Cell.* **8**, 303–316.

Weinberg, R. A. (1995). The retinoblastoma protein and cell cycle control. *Cell* **81**, 323–330.

Wu, L., de Bruin, A., Saavedra, H. I., Starovic, M., Trimboli, A., Yang, Y., Opavska, J., Wilson, P., Thompson, J. C., Ostrowski, M. C., Rosol, T. J., Woollett, L. A., Weinstein, M., Cross, J. C., Robinson, M. L., and Leone, G. (2003). Extra-embryonic function of Rb is essential for embryonic development and viability. *Nature* **421**, 942–947.

Biography

Nicholas Dyson and Maxim Frolov are members of the Massachusetts General Hospital Cancer Center. Their research interests are focused on the control of cell proliferation by RB and E2F family members. Dr. Dyson is a Professor of Medicine at Harvard Medical School.

Retinoic Acid Receptors

Martin Petkovich
Queen's University, Kingston, Ontario, Canada

Retinoic acid receptors (RARs) are nuclear transcription factors that, once activated by retinoic acid (RA), regulate the expression of RA target genes, leading to changes in cell differentiation, cell proliferation, and apoptosis. The discovery of the first RAR in 1987 defined for the first time the mechanism of action of vitamin A outside of the visual cycle. Three RAR subtypes have been identified in the vertebrate genome and have been named RARα, RARβ, and RARγ.

RA and RA Signaling

Retinoic acid (RA) is a signaling molecule derived from vitamin A (retinol) that is essential for normal embryonic development and health in the adult. RA is produced in a two-step enzymatic process involving the alcohol dehydrogenase-mediated conversion of retinol to retinaldehyde and, in a subsequent retinaldehyde dehydrogenase-catalyzed step, to RA. RA signaling is mediated by retinoic acid receptors (RARs).

RARs belong to the superfamily of nuclear receptors and bear conserved structural similarities to other members of this family, including estrogen and androgen receptors, glucocorticoid receptor, thyroid hormone receptor, and vitamin D receptor. In general, members of this family can be distinguished by the linear arrangement of six more or less conserved functional domains labeled A through F. Key functional domains of RARs include the RA-binding domain, the DNA-binding domain, and two separate transcription activation domains (see Figure 1). While the DNA- and RA-binding domains of the RARs are similar between subtypes, the transcription activation domains vary considerably, possibly reflecting target gene-specific interactions. Several regions within RAR domains mediate specific interactions with retinoid-x-receptor subtypes (RXRα, RXRβ, or RXRγ), forming an obligatory heterodimeric partnership required for activation of RA target genes. RAR/RXR heterodimers bind to specific DNA elements called retinoic acid response elements (RAREs) usually found in the promoters of such genes. The unique expression patterns of each RAR subtype in the embryo and the adult also support the specific functional role that each of the RARs fulfills. Murine knockout studies have revealed that although there is functional redundancy between RARs, each receptor is essential for normal physiology.

RAR Structure and Function

RARs share structural similarities with other members of the nuclear receptor family. The key functional domains of RARs include the RA-binding domain, the DNA-binding domain, transcriptional activation domains, and amino acid sequence motifs that are necessary for interactions between RARs and other transcription factors, including RXRs. RARs form heterodimeric complexes with RXRs in order to regulate gene expression.

DNA-Binding Domain

The hallmark of all nuclear receptors is the DNA-binding domain (domain C), which comprises a highly conserved, 66–68 amino acid stretch encoding two zinc-binding fingers labeled C1 and C2. The RARs' DNA-binding domain is 66 amino acids in length, and its structure has been determined by X-ray crystallographic studies. The two zinc fingers fold into a globular domain such that residues of the first zinc-binding finger (C1) make specific contacts with DNA through interactions between three conserved amino acid residues (P-box) with specific base residues in the major groove of the DNA double helix. The second zinc finger (C2) is more basic in nature, making contacts with the negatively charged phosphate backbone of DNA. This helps to stabilize the interaction between RARs and the DNA motifs to which they bind, RAREs. RARs do not bind to RAREs independently but rather as a heterodimeric complex formed between an RAR and an RXR. Residues in C2 are critical for heterodimer formation.

Retinoic Acid-Binding Domain

The retinoic acid-binding domain (domain E) fulfills several important functions, including, of course, retinoic acid binding, transcription activation, and nuclear localization. The RA-binding domain binds

FIGURE 1 Domain structure of RARs. All RARs and RXRs have domain structures similar to other members of the nuclear receptor family. Domains A–F are shown. DNA-binding domain (C) and ligand-binding domain (E) are highly conserved. Transcription activation functions are found in E (AF-2) and A (AF-1) domains.

both *all-trans* and 9-*cis* isomers of RA with high affinity. In contrast, the ligand-binding domain of RXRs bind only the 9-*cis* RA isomer. These ligand-binding domains possess a series of 12 α-helical structures (H1–H12) that fold together to form the ligand-binding pocket. H12 contains the transcription activation domain AF-2. From X-ray crystallographic studies, it has been proposed that conformational changes occurring with the binding of RA alter the position of H12 and thus the ability of the AF-2 to interact with transcription factors that repress or activate gene transcription. In the "mouse-trap" model of ligand activation, H12 is extended into the solvent in the absence of RA but snaps shut once ligand enters the RA-binding pocket. These dynamic conformational reconfigurations result in differential interactions with cofactors that functionally link the receptor complex with the transcription initiation complex.

Other Functional Regions of RARs

The N terminus of RARs, comprising domains A and B, contains another region important for transcriptional activation. Interestingly, differential splicing/alternate promoter usage can give rise to multiple A domains for each subtype. This multiplicity of RAR isoforms and their potential to form partnerships with RXR subtypes creates, at least conceptually, a remarkable number of combinatorial possibilities that may each have subtly different yet important contributions to RA target gene regulation. Domain D, or the hinge region, has been described as a tether that connects DNA and ligand-binding functions. This domain also appears to posses a nuclear localization motif required to sequester receptors in the nucleus. Unlike steroid hormone receptors, which reside in the cell cytoplasm bound to heat-shock proteins that are released to the nucleus upon ligand binding, RARs and RXRs are complexed with DNA in their unliganded state. The role of the F-domain located at the extreme C terminus of RAR is not known.

Retinoic Acid Response Elements

RAREs are DNA motifs to which RAR/RXR heterodimers can bind with high affinity. In most cases, these motifs comprise a direct repeat of the half-site consensus, PuGGTCA, separated by five base pairs; however, other configurations are also possible. These elements can be found in variations of number and orientation from within a few base pairs of transcription initiation sites to several thousand base pairs (usually upstream). These elements concentrate RAR/RXR heterodimers, which are normally in very low abundance, near transcription complexes.

RA Transcriptional Activation

RARs act as biosensors to detect RA in the local environment. The binding affinity of these receptors for RA is on the order of 10–30 nM. Once RAR-expressing cells are exposed to RA, changes in the pattern of gene transcription will occur. The role of transcription activators is to increase the efficiency of RNA polymerase II binding to the promoter and engage the successful transcription of a gene – and in the case of RARs, to do so only in the presence of RA. In unliganded form, the RAR/RXR heterodimer, when bound to an RARE on a target gene, can act to repress transcription (Figure 2). This complex recruits a specific type of transcription factor called a corepressor. The first such nuclear receptor corepressor found to interact with unliganded RAR was N-CoR/SMRT. The presence of RA causes allosteric modulation of the ligand-binding domain, shifting the cofactor binding preference from corepressor to coactivator. Thus, release of N-CoR/SMRT by RA results in the complex having increased affinity for coactivators such as p140 and p160. Many coregulators that interact with RAR/RXRs and that also have other chromatin-remodeling functions, such as histone-deacetylase activity, kinase activity, or methylase activity, have been isolated. In addition to chromatin-remodeling functions, some of these cofactors correspond to factors critical for establishing a stable transcription initiation complex. The net effect of these interactions is increased or decreased transcription of target genes, depending on the promoter sequence, the local concentrations of factors binding to the promoter, and whether other signaling pathways are regulating the activities of any of these factors. In this way, RA signal is processed in a manner that integrates the activities of many pathways of a given cell type.

Retinoic Acid Receptor Function

Each of the murine RAR and RXR subtypes has been knocked out by homologous recombination in order to determine their functions during embryonic development and in the adult. Although there are multiple receptor isoforms, there are distinct roles for each defined by spatiotemporal distribution and

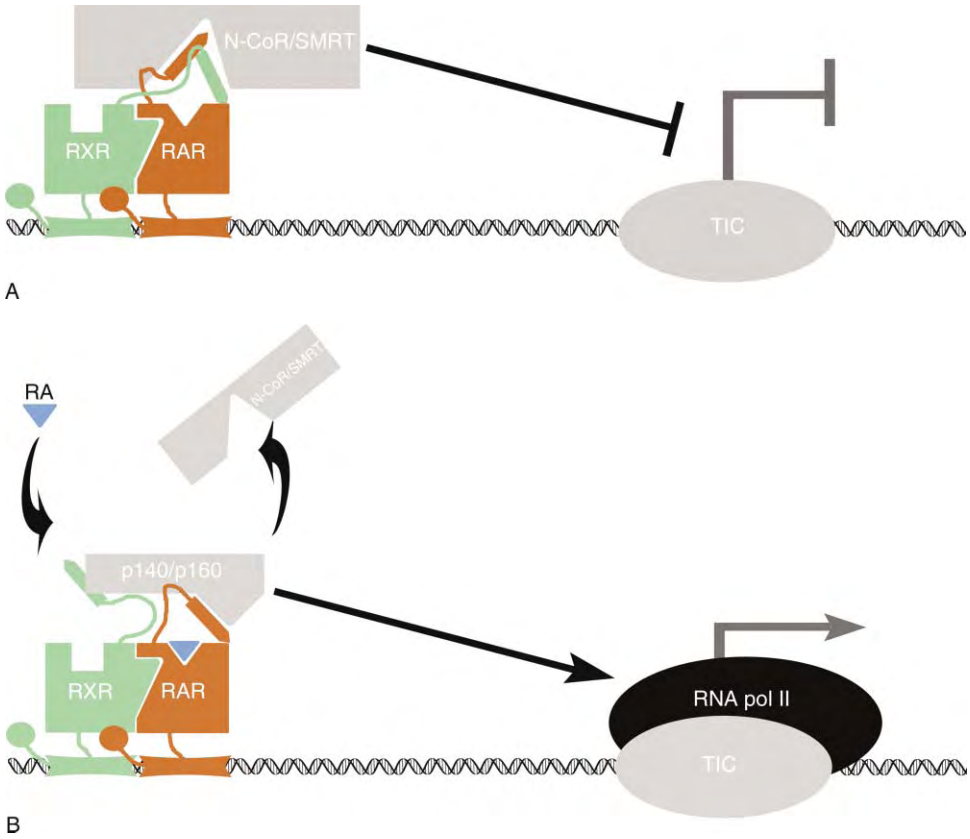

FIGURE 2 The RAR/RXR complex regulates transcription. (A) Transcriptional repression occurs when unliganded RAR/RXR heterodimer binds to an RARE in the promoter region upstream of the transcription start site of an RA-responsive gene. Unliganded receptors bind to corepressor factors such as N-CoR/SMRT that act to limit the function of the transcription initiation complex (TIC) through reorganization of chromatin structure. (B) Binding of RA ligand to the RXR/RAR complex induces a conformational change in the ligand-binding domain of RAR, causing the release of N-CoR/SMRT and allowing the recruitment of transcriptional coactivators such as the p160 complex. This coactivator complex promotes the binding of transcription accessory factors essential for the efficient engagement of RNA pol II activity.

promoter-specific activities. Throughout the murine life cycle, RARα is ubiquitously expressed and may play a role in some general housekeeping functions. In contrast, RARβ transcript distribution indicates that this receptor may be involved in ontogenesis of the central nervous system during development and differentiation of epithelia in the adult. Similarly, the expression patterns of RARγ are spatiotemporally regulated, suggesting that this receptor is involved in embryonic tail bud development, craniofacial morphogenesis, chondrogenesis, and maintenance of squamous epithelia. Among RXRs, RXRα is ubiquitously expressed, whereas RXRβ and RXRγ are more restricted during embryogenesis.

Gene knockout studies confirmed distinct roles for each RAR and RXR subtype and also revealed a high level of functional redundancy. Whereas the RARα- and RARβ-null mutants display some of the postnatal defects observed in vitamin A-deficient (VAD) mice (poor viability, growth deficiency, and male sterility), most of the RAR- or RXR-null single mutants exhibit only subtle or, in some cases, undetectable developmental abnormalities. In contrast, RAR double mutants exhibit reduced viability and recapitulate most symptoms of VAD.

RXR$\beta^{-/-}$RXR$\gamma^{-/-}$RXR$\alpha^{+/-}$ triple-mutant mice exhibit marked growth deficiency but, surprisingly, display no obvious congenital or postnatal abnormalities. However, mutation of both RXRα alleles is lethal. Therefore, RXRα may carry out most of the vital developmental and postnatal functions of the RXRs.

See Also the Following Articles

RNA Polymerase II and Basal Transcription Factors in Eukaryotes • RNA Polymerase II Elongation Control in Eukaryotes • RNA Polymerase II Structure in Eukaryotes • Zinc Fingers

Glossary

retinoic acid The derivative of the fat-soluble vitamin A that is active in the regulation of gene expression by activating nuclear retinoic acid receptors.

transcription The process by which RNA polymerase II is recruited to the promoter of a gene and enzymatically copies the base sequence of a gene into an RNA transcript.

transcription factor A protein or collection of proteins that are involved in altering the efficiency of RNA polymerase II activity in transcribing a gene.

Further Reading

Chambon, P. (1996). A decade of molecular biology of retinoic acid receptors. *FASEB J.* **10**, 940–954.

Clagett-Dame, M., and DeLuca, H. F. (2002). The role of vitamin A in mammalian reproduction and embryonic development. *Annu. Rev. Nutr.* **22**, 347–381.

Rosenfeld, M. G., and Glass, C. K. (2001). Coregulator codes of transcriptional regulation by nuclear receptors. *J. Biol. Chem.* **276**, 36865–36868.

Ross, S. A., McCaffery, P. J., *et al.* (2000). Retinoids in embryonal development. *Physiol. Rev.* **80**, 1021–1054.

Biography

Martin Petkovich is a Professor of Biochemistry and Pathology in the Cancer Research Institute at Queen's University in Kingston, Ontario. His research interests include molecular genetics of retinoid signaling and metabolism in embryonic development and pattern formation. He discovered the first nuclear receptor for retinoic acid and has also identified key enzymes involved in regulating RA levels in tissue.

Reverse Transcriptase and Retroviral Replication

Laura Tarrago-Litvak, Marie-Line Andréola and Simon Litvak
Réplication et Expression des Génomes Eucaryotes et Rétroviraux (REGER), Bordeaux, France

Since its discovery, reverse transcriptase (RT) has been associated with retroviruses. In the following years this RNA-dependent DNA polymerase was found in eukaryotes, prokaryotes, retrotransposons, hepadnaviruses, retrons, and even humans. The role of RT in all retroviruses is to synthesize double-stranded DNA copying the retrovirus single-stranded RNA genome. This DNA is then integrated into the host cell's chromosomes as a provirus. Transcription then leads to copies of the viral RNA genome, from which the virus's own proteins and enzymes are formed. New viral particles then bud from the membrane of the cell. Thus, reverse transcriptase is essential for viral replication.

RT performs a remarkable feat, reversing the normal flow of genetic information. The polymerases synthesizing DNA and RNA in cells are very accurate and make very few mistakes. This is essential because they are the caretakers of our genetic information, and mistakes may be passed on to the offspring. RT, on the contrary, makes mistakes very often by incorporating a non-complementary nucleotide. One might think that this would cause severe problems to the virus. But, in fact, this high error rate turns out to be an advantage for the virus. The errors allow the retrovirus to mutate rapidly in order to fit new conditions and escape, for instance, the immunological response of the host or the effect of therapeutic agents.

Discovery of Reverse Transcriptase

The publication of the presence of reverse transcriptase (RT) in retroviruses in 1970 by the groups of Howard Temin and David Baltimore in the same issue of *Nature* must be considered as a landmark in the story of biological sciences in the second half of the twentieth century. The presence of a DNA polymerase able to copy RNA into DNA (contrary to all the enzymes of this family described before which copy a DNA template into DNA), violated the so-called central dogma of molecular biology which stated that genetic information always flowed from DNA to RNA to protein. It is of interest to point out that while the laboratory of Baltimore came to this conclusion by searching for the mechanisms used by polymerases, involved in the replication of different viruses, the findings of Temin's group came as a strong support of his earlier experiments, which showed that the replication of retroviruses was sensitive to inhibitors of DNA-dependent polymerases. Since the early 1960s Temin had proposed the idea, widely rejected at that time, that the replication of RNA oncoviruses, as they were called, had to go via a DNA intermediate that may be integrated in the host genome. Years later, after the discovery of RT, the finding in 1983 that the cause of AIDS was a retrovirus, the human immunodeficiency virus type 1 (HIV-1), and the consequent emotion provoked by the AIDS pandemics led to an explosive burst of research on this virus. It can be considered that very few organisms have provided so much information on their structure and function in such limited time as in the case of HIV-1. Most of the information on retroviral replication since the early 1980s has come from the work on this human retrovirus.

Retrovirus Genome

All retroviral genomes consist of two identical molecules of RNA, which are single-stranded, (+) sense and have a 5′-end cap and a 3′-end pol (A) as in the case of eukaryotic messenger RNAs (mRNAs). Retroviral genomes vary in size from 8 to 11 kb. Some distinctive features of the retrovirus genomes concern the fact that they are the only RNA viruses which are not only truly diploid but also whose genome is produced by the cellular transcriptional machinery, without the involvement of a viral-encoded polymerase (Figure 1). Moreover, they are the only (+) sense RNA viruses whose genome does not serve directly as mRNA immediately after infection. The two RNA genomic molecules are physically linked as a dimer by hydrogen bonds. In addition, another nucleic acid is present in all viral particles, a specific transfer RNA (tRNA) required for the initiation of replication. Most, if not all, DNA polymerases require a primer carrying

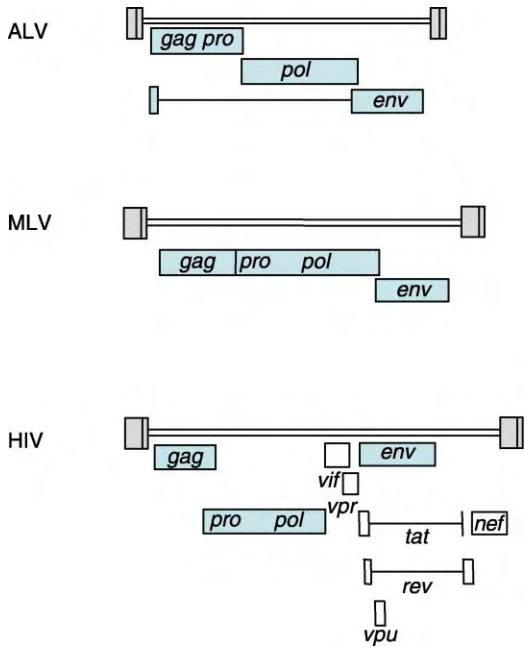

FIGURE 1 Genetic organization of prototypic retroviruses. An open rectangle indicates the open reading frame for the gene marked. Gag, pol, and env, common to all retroviruses, are shown in blue. *Gag*: encodes a polyprotein (Gag), whose cleavage products are the major structural proteins (matrix [MA], capsid [CA], and nucleocapsid [NC]) of the virus core; *pro*: encodes part of a polyprotein (Gag-Pro, or Gag-Pro-Pol), whose cleavage products include protease (PR); *pol*: encodes part of a polyprotein (Gag-Pro-Pol), whose cleavage products include reverse transcriptase (RT) and integrase (IN); *env*: encodes a polyprotein (Env), whose cleavage products SU (surface) and TM (transmembrane) are the structural proteins of the viral envelope; *tat*: an accessory gene encoding for a low-molecular-weight protein (trans activator) that activates transcription by binding to TAR; *rev*: an accessory gene encoding a protein that regulates splicing and RNA transport; *nef*: an accessory gene encoding a protein that reduces the level of CD4 on the cell surface, and also stimulates some infected cells to divide; *vpu*: an accessory gene encoding a protein (viral protein u) that triggers CD4 degradation. Enhances virion release; *vif*: an accessory gene encoding a protein (virion infectivity factor) that affects infectivity of viral particles; *vpr*: an accessory gene encoding a protein (viral protein r) that causes infected cells to arrest in G_2 and may also promote transport of the preintegration complex into the nucleus after reverse transcription. Horizontal lines indicate that this segment is spliced out. ALV: avian leukemia virus; MLV: murine leukemia virus; HIV: human immunodeficiency virus.

a free 3′-end OH from where DNA synthesis is initiated. In the case of retroviruses, this primer is a cellular tRNA, which is able to anneal partially to a region near the 5′-end of the RNA viral genome, the "primer-binding site" (PBS). Examination of the sequences of several retroviruses has shown that the PBS is complementary to the 3′-end of a given tRNA: $tRNA^{Trp}$ in avian retroviruses, $tRNA^{Pro}$ in murine viruses and $tRNA^{Lys3}$ in HIV-1. The mechanism involved in the selection of a specific tRNA is not fully understood. While the role of the viral genome has been ruled out, early results with avian retroviruses suggested that RT was involved in tRNA packaging. Very recent work seems to indicate that in the case of HIV-1, the lysine aminoacyl-tRNA synthetase may encapsidate the cognate tRNA primer in the retroviral particle. The small basic nucleocapsid (NC) protein encoded in the C-terminal region of the *gag* gene seems to play an important role in the annealing of primer tRNA to the PBS region, thus allowing the initiation of retroviral replication. The gene order in all retroviruses is invariant: 5′-gag-pol-env-3′. However, some complex retrovirus, like HIV-1, encode several other small regulatory proteins.

Activities Associated with the Reverse Transcriptase

With the exception of some murine retroviral polymerases, most RTs are heterodimeric enzymes. The retroviral-encoded protease cleaves a polyprotein precursor leading to an RT subunit that is further cleaved by the same protease (Figure 2). Thus, RTs are formed by two subunits where the smallest one carries the same sequence as the largest. Retroviral DNA synthesis is

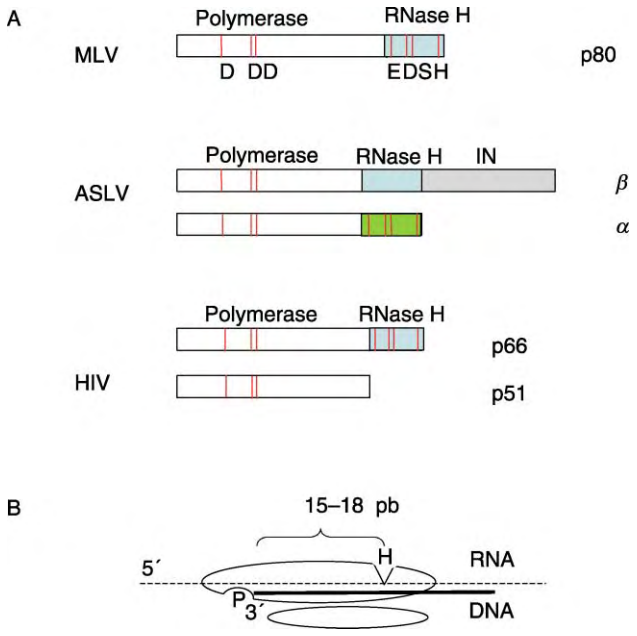

FIGURE 2 (A). Subunit structure of various retroviral RT. The MLV RT is a monomer. The ASLV RT is a heterodimer, the cleavage at the RT-IN boundary is incomplete. In HIV, the IN is produced as a separate protein. Vertical lanes show the positions of the active site residues in the polymerase and RNase H domains. (B). Mode of HIV-1 RT positioning for synthesis and RNase H cleavage. The 3′-end of the DNA directs RT positioning for optimal RNase H cleavage.

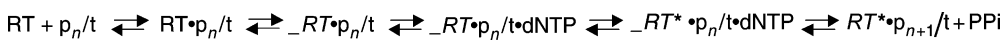

FIGURE 3 Model for the kinetic mechanism of the polymerase reaction. Asterisks distinguish structural states of the system. p_n: primer containing n nucleotides; p_{n+1}: primer containing $n + 1$ nucleotides; t: template; PPi: pyrophosphate.

absolutely dependent on the two enzymatic activities associated with RT: a DNA polymerase that can use either RNA or DNA as a template, and a nuclease, named ribonuclease H (RNase H), that is specific for the RNA strand of RNA·DNA hybrids. All of the enzymatic functions required to complete the series of steps involved in the generation of a retroviral DNA can be attributed to either the DNA polymerase or the RNase H of RT as described below. However, it cannot be ruled out that certain viral proteins, such as the nucleocapsid protein, may increase the efficiency of reverse transcription.

Reverse transcription of the retroviral genome depends on the coordination of the polymerase and RNase H activities of RT. The spatial arrangement between the two active sites of the enzyme (corresponding to ~15–18 bases in the template) contributes to the coordination of these two activities. While the 3′-OH of the primer strand is positioned close to the RT amino acid residues important in the DNA polymerase active site, the template strand is positioned close to RT residues important for RNase H activity.

Biochemistry of Reverse Transcriptase

Mechanism of Action

The study of the mechanism of the RNA- and DNA-dependent DNA polymerase activity has led to a model involving a two-step binding mechanism. DNA polymerization catalyzed by RT is a multistep reaction, requiring the binding of the primer·template duplex and a deoxynucleoside triphosphate (dNTP) to RT prior to deoxy-nucleoside-5′-monophosphate addition to the 3′ end of the primer. Kinetic experiments have established the order of binding of the substrates. The primer·template duplex binds prior to binding of the deoxynucleoside triphosphate substrate to form the catalytically competent ternary complex. The rate-limiting step for nucleotide incorporation prior to dissociation of the enzyme is a conformational change. Following pyrophosphate liberation, the elongated product is released. Small changes in the rates and equilibrium constants have been observed for RNA- versus DNA-dependent DNA synthesis. All these mechanisms have been derived from pre-steady-state or steady-state kinetic assays using short primer·templates and do not always reflect the true nature of reverse transcription, although they are necessary in determining the kinetics and affinity of substrate binding to RT (Figure 3).

Processivity

The elongation phase of DNA synthesis by DNA polymerases may be processive or distributive. A processive DNA polymerase is able to synthesize long DNA stretches without dissociation of the enzyme from the primer·template duplex, while a distributive polymerase dissociates easily after incorporation of few nucleotides. Reverse transcriptase is considered to be poorly processive as compared with replicative DNA polymerases. However, a higher processivity of RT may be observed when copying specific regions of the viral genome or in the presence of some viral proteins.

Fidelity

All RTs show poor fidelity when compared to host DNA polymerases in *in vitro* systems. The lack of a proofreading function as well as the enzyme ability to extend mismatched primer termini probably explains much of this high error rate. The tendency of RT to switch templates, paired with its ability to extend mismatches by incorporating "wrong" nucleotides may be a significant source of replication errors. The error rates of various RTs estimated in different types of assays can be significantly affected by altering the parameters of the reaction. The error rate is quite dependent on sequence context and "hot spots," where errors occur frequently, and may differ according to the particular RT used in the assay. In addition, error rates may be different on RNA and DNA templates. As a consequence, it is not possible to define the error rate as a single number. These studies, taken together, do suggest that the overall error rate is high: about one per genome in a reverse transcription cycle. Cellular factors may alter error rates and some studies suggest that somewhat lower error rates occur *in vivo*. However, the *in vitro* data lead to the generally accepted impression that the average retroviral DNA genome differs from its parent by at least one mutation, and have provided the evidence for the existence of retroviral "quasi-species."

Replication Errors *in Vivo* and the Emergence of Antiviral Resistance

The rates at which mutations accumulate in retroviral and host genomes are very different since the viral genomes are found to evolve at rates perhaps a million-fold higher than the genomes of their hosts. The lack of RT fidelity and the accumulation of nonlethal mutations are closely related to the emergence of resistance towards antiviral therapeutic agents. This effect is especially dramatic in the case of HIV-1, the causal agent of AIDS. After short spans of treatment, viral quasi-species appear with mutations in the viral target proteins (the most used targets against HIV-1 are RT and protease). The introduction of the so-called combination therapy against AIDS has greatly improved the possibility to keep the seropositive patients for several years with a low or undetectable viral charge. The combination of several anti-proteases and anti-RTs makes it possible that if a given mutation leads to the apparition of resistance against a specific drug, the other antivirals are still effective, giving time to replace the one to which the target enzyme has become resistant.

Inhibitors of Reverse Transcriptase

Emphasis in the search of RT inhibitors has been obviously focused on the HIV-1 enzyme but some of the inhibitors developed against this agent may be useful in arresting retroviruses involved in other pathologies. Inhibitors of HIV-1 RT were the first therapeutic agents described against AIDS. The protease inhibitors appeared later, and currently inactivating agents against several viral targets (viral entry, integrase, etc.) are actively being studied. As mentioned elsewhere in this article the combined use of anti-proteases and anti-RTs has led to a great improvement in the control of HIV-1 proliferation in AIDS patients. Two main families of HIV-1 RT inhibitors are used against AIDS, the nucleoside analogue inhibitors of RT (NRTI) and the non-nucleoside inhibitors of RT (NNRTI). The first one is recognized and incorporated by RT in the newly synthesized DNA but as they lack or have a modified group in the 3′ position of the ribose they cannot be linked to the following dNTP precursor and thus they act as chain terminators. To be active *in vivo* the putative NRTI, which are active against all retroviral RTs, must be triphosphorylated by cellular kinases. The first NRTI described was azidothymidine or zidovudine but currently more than a dozen of these inhibitors have been approved by the US FDA and are used in clinics. The second family, the NNRTIs, is specific of the HIV-1 RT since they inhibit the viral polymerase after binding to a hydrophobic region of this enzyme. They do not have a typical nucleoside structure but belong to a variety of different chemical families of compounds and in contrast to NRTIs they do not need to be metabolized inside the cell to display their antiviral effect.

Recombination

Since retroviruses ordinarily carry two identical or nearly identical RNAs, the genetic consequences of using only one RNA versus portions of both of the RNAs to template DNA synthesis are usually the same. However, under certain conditions, two genetically distinct RNAs can be encapsidated. Portions of each template can be used to generate a single DNA, producing a recombinant. Recombination does occur in virions produced by a single cell that has been co-infected by two different viruses demonstrating that recombination requires co-packaging of two viral genomes into the same particle. During reverse transcription in such heterozygous virion particles, the DNA product can be generated containing portions of each of the two genomic sequences in one molecule.

The Role of RT in Reverse Transcription

Reverse transcription catalyzed by RT begins when the viral particle enters the cytoplasm of a target cell. DNA synthesis using the RNA retroviral genome as template takes place in the cytoplasm leading to a linear double-stranded DNA (dsDNA), co-linear with the viral RNA template, the proviral DNA. However, proviral DNA contains terminal duplications known as the long terminal repeats (LTRs) that are not present in viral RNA (Figure 4).

The following scheme is widely accepted to reflect the process of retroviral DNA synthesis catalyzed by RT:

1. Minus-strand DNA synthesis starts from the 3′ end of a tRNA partially annealed to the primer-binding site (PBS) in genomic RNA. Minus-strand DNA synthesis proceeds until the 5′-end of genomic RNA is reached, generating a short DNA intermediate termed minus-strand strong-stop DNA (−sssDNA). Since the PBS is near the 5′end of viral RNA, the length of this strong-stop DNA is ~100–150 nucleotides.
2. Following RNase H-mediated degradation of the RNA strand of the RNA·(−sssDNA) duplex, the first strand transfer involves the annealing of the −sssDNA to the 3′-end of a viral genomic RNA. This transfer is allowed by the presence of identical sequences known as the repeated (R) sequences, present at the 5′- and 3′-ends of the RNA genome. The 3′-end of (−sssDNA) is copied from the R sequences at the 5′-end of the viral genome and therefore contains sequences

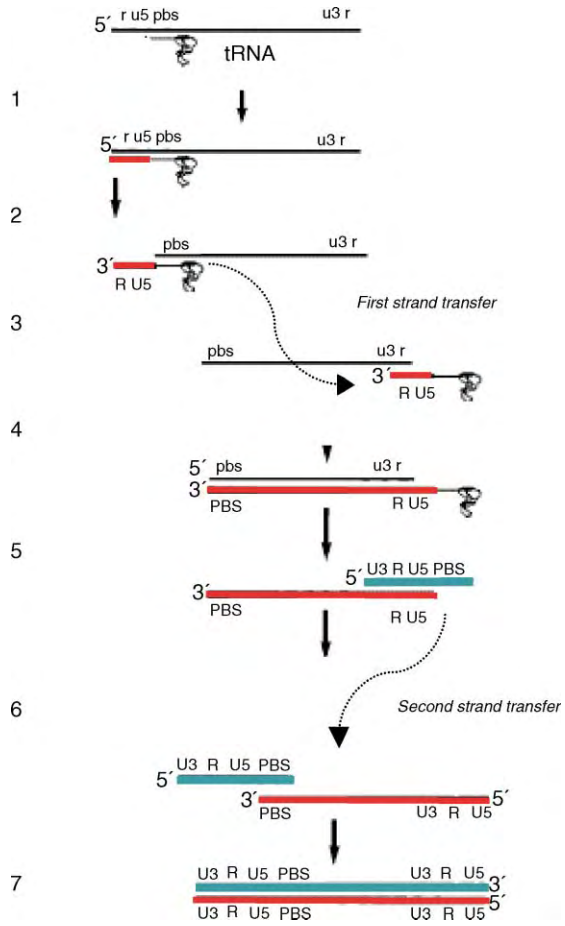

FIGURE 4 Process of reverse transcription. Thick lane, DNA; thin lane, RNA.

complementary to R. After the RNA template has been removed, the (− sssDNA) can anneal to the R sequences at the 3′-end of the RNA genome. The annealing reaction related to the first strand transfer, appears to be facilitated by the NC protein.

3. Once the (− sssDNA) has been transferred to the 3′ R region on viral RNA, minus-strand DNA synthesis may start again, followed by RNase H digestion of the template strand.

4. RNase H degradation is not complete since some hybrid regions seem to be more resistant to the nuclease. The RNA genome contains a short polypurine tract (PPT) that is relatively resistant to RNase H degradation. A defined RNA segment derived from the PPT primes plus-strand DNA synthesis. Plus-strand synthesis is halted after a portion of the primer tRNA is reverse-transcribed, leading to a DNA called plus-strand strong-stop DNA (+sssDNA). Some retroviruses generate more than one plus-strand primers from the RNA genome.

5. RNase H removes the primer tRNA, exposing sequences in (+sssDNA) that are complementary to sequences at or near the 3′ end of plus-strand DNA.

6. Annealing of the complementary PBS segments in (+sssDNA) and minus-strand DNA constitutes the second strand transfer.

7. Plus- and minus-strand syntheses are then completed, with the plus and minus strands of DNA each serving as a template for the other strand.

Integration and Retroviral Replication

As proposed by Temin since the early 1960s, retrovirus replication is performed via a DNA intermediate, the proviral DNA is synthesized by the RT in the cytoplasm. Integrase (IN), the third retroviral encoded enzyme in addition to RT and protease, is involved in the integration of the proviral DNA in the nuclear DNA of the infected cell. Integration is a crucial step in viral replication since retroviral DNA molecules are not ordinarily able to replicate autonomously and they depend on integration for stable maintenance in dividing cells. Once integrated the proviral DNA is recognized by the host-cell enzymatic machinery for efficient transcription of viral DNA into new copies of the viral genome and mRNAs that encode viral proteins. Moreover, integration also stabilizes the viral DNA against degradation and allows its genetic transfer as an integral element of the host genome.

Role of Reverse Transcriptase in Modern Biology

It is now well known that RT is present not only in animal retroviruses but also plays a crucial role in DNA replication of prokaryotic and eukaryotic cells, in the replication of some plant and animal DNA viruses, as well as in the function of several classes of transposable elements. As mentioned in the remarkable book *Retroviruses* "it should be remembered that RT has had a critical role in the development of modern biology. The ability to convert RNA into DNA has been as important to molecular biologists as it has been to retrovirologists. It is worth taking a moment to reflect on how much more difficult it would have been to solve the puzzles posed by the organization and expression of genes in higher eukaryotes if RT did not exist."

See Also the Following Articles

HIV-1 Reverse Transcriptase Structure • Non-Homologous Recombination: Retro-Transposons

Glossary

cap The structure at the 5′-end of eukaryotic mRNA introduced after transcription. It results from adding a methylated G to the terminal base of the mRNA.

DNA polymerase An enzyme that systhesizes a daughter strand of DNA under direction from a DNA or an RNA template.

hot spot A site at which the frequency of mutation (or recombination) is increased significantly.

LTR An abbreviation for long-terminal repeat, a sequence directly repeated at both ends of a retroviral DNA.

primer A short sequence (often of RNA) that provides a free 3′-OH end at which a DNA polymerase starts synthesis of a deoxyribonucleotide chain.

retrovirus An RNA virus that propagates *via* conversion into duplex DNA.

template A polynucleotide which furnishes the instructions for the sequence of nucleotides to be added to the primer strand during DNA polymerization.

Further Reading

Arts, E. J., and Le Grice, S. F. (1998). Interaction of retroviral reverse transcriptase with template-primer duplexes during replication. *Prog. Nucleic Acid Res. Mol. Biol.* **58**, 339–393.

Baltimore, D. (1970). RNA-dependent DNA polymerase in virions of RNA tumor viruses. *Nature* **226**, 1209–1211.

Coffin, J. M., Hughes, S. H., and Varmus, H. E. (eds.) (1997). *Retroviruses*. Cold Spring Harbor Laboratory Press, New York.

Darlix, J. L., Lapadat-Tapolsky, M., de Rocquigny, H., and Roques, B. P. (1995). First glimpses at structure–function relationships of the nucleocapsid protein of retroviruses. *J. Mol. Biol.* **254**, 523–537.

De Clercq, E. D. A. (ed.) (2001). *Antiretroviral Therapy*. ASM Press, Washington, DC.

Skalka, A. M., and Goff, S. P. (eds.) (1993). *Reverse Transcriptase*. Cold Spring Harbor Laboratory Press, New York.

Tarrago-Litvak, L., Andreola, M. L., Nevinsky, G. A., Sarih-Cottin, L., and Litvak, S. (1994). The RT of HIV-1: From enzymology to therapeutic intervention. *FASEB J.* **8**, 497–503.

Temin, H. M. (1993). Retrovirus variation and reverse transcription: Abnormal strand transfers result in retrovirus genetic variation. *Proc. Natl Acad. Sci. USA* **90**, 6900–6903.

Temin, H. M., and Mizutani, S. (1970). RNA-dependent DNA polymerase in virions of Rous sarcoma virus. *Nature* **226**, 1211–1213.

Verma, I. M. (1997). The reverse transcriptase. *Biochim. Biophys. Acta.* **473**, 1–38.

Waters, L. C., and Mullin, B. C. (1997). Transfer RNA into RNA tumor viruses. *Prog. Nucleic Acid Res. Mol. Biol.* **20**, 131–160.

Biography

Laura Tarrago-Litvak was born in Santiago, Chile. She did her university undergraduate studies at the University of Chile and obtained her Ph.D. at the University of Bordeaux, France. Her current research interest is in the field of retroviruses, mainly in two retroviral enzymes, reverse transcriptase and integrase.

Marie-Line Andréola was born in Sainte-Foy-la-Grande, France. She did her university undergraduate studies and obtained her Ph.D. at the University of Bordeaux, France. Her current research interest is in the field of retroviruses, focused on the mechanism of action and search of inhibitors of two retroviral enzymes, reverse transcriptase (RNase H activity) and integrase.

Simon Litvak was born in Valparaiso, Chile. He did his university undergraduate studies at the University of Chile at Santiago and obtained his Ph.D. at the University of Paris, France. He is affiliated to the CNRS as Principal Investigator and is currently the Director of the REGER Laboratory (UMR-5097. CNRS – University of Bordeaux 2) and former Director of the Institut Federatif des Recherches "Pathologies Infectieuses et cancers," Bordeaux, France. His current research interest is in the field of retroviruses. Research in his group is focused on the mechanism of action of two key HIV-1 enzymes: reverse transcriptase and integrase. He has also contributed in the search for specific inhibitors of HIV-1 RT and IN (small ligands and oligonucleotides).

Rho GTPases and Actin Cytoskeleton Dynamics

Priam Villalonga and Anne J. Ridley
Ludwig Institute for Cancer Research and University College London, UK

The dynamic regulation of the actin cytoskeleton plays a crucial role in the control of cell shape and movement, and therefore has a profound impact on the biology of multicellular organisms. Accordingly, actin cytoskeleton regulators modulate a broad array of cellular processes such as cell migration, tissue morphogenesis, inflammation, vesicular trafficking, secretion, and cancer cell invasion and metastasis, just to name a few of them. Members of the Rho family of small GTPases have emerged as major regulators of the actin cytoskeleton in all eukaryotic cells. Like other small GTPases, these proteins are molecular switches that are exquisitely regulated by several positive and negative regulators that can either "switch" them on or off. Once activated, they bind to and activate a number of downstream effectors, most of them directly implicated in the regulation of actin-related biochemical events (e.g., actin polymerization). This enables Rho GTPases to act as key players in processes that require the dynamic regulation of the actin cytoskeleton.

Rho GTPase Family: Overview and Regulation

Rho GTPases constitute a separate family within the larger Ras superfamily of small GTPases. In mammalian cells, the prototypical Rho family members are RhoA, Rac1, and Cdc42, which have been the most extensively characterized. However, there are many other members in this family including Rho, Rac, and Cdc42 isoforms and several other proteins that are more or less related to these three in terms of sequence homology, thereby defining subfamilies within the Rho family (Figure 1). Some Rho family members show a tissue-specific pattern of expression, although most of them are expressed in the vast majority of mammalian cells, localizing to different cellular membranes as a consequence of lipid modifications at their carboxy termini. Like other GTPases, Rho proteins bind to guanine nucleotides and, except for members of the Rnd subfamily, cycle between an active GTP-bound state and an inactive GDP-bound state. Three different types of regulators can modulate the activation levels of these GTPases: guanine-nucleotide-exchange factors (GEFs), GTPase-activating proteins (GAPs), and guanine-nucleotide-dissociation inhibitors (GDIs), as illustrated in Figure 2.

Guanine-Nucleotide-Exchange Factors

GEFs promote the release and exchange of bound nucleotides on the GTPase, effectively leading to an increase in the number of GTP-bound molecules due to the higher intracellular concentration of GTP. GEFs are, therefore, positive regulators of Rho GTPases that promote their activation. In mammalian cells, a large number of GEFs have been described, all sharing a highly conserved exchange factor domain termed Dbl-homology (DH), named after the first GEF identified, Dbl. They also have other conserved domains such as the phospholipid-binding domain PH (Pleckstrin homology), involved in the localization of GEFs in the vicinity of the GTPases on membranes, providing a mechanism for GEF regulation. In addition to their regulation by phospholipid binding, GEFs can be regulated by binding to other proteins or by phosphorylation. Rho GEFs exhibit different degrees of specificity *in vitro* towards Rho GTPases, but it still has not been clearly established which GEFs regulate each of the Rho GTPase members *in vivo*.

GTPase-Activating Proteins

GAPs act by binding to the GTPase and enhancing hydrolysis of GTP, an otherwise slow and inefficient process, and by promoting the conversion of GTP to GDP they are negative regulators of Rho GTPases. Rho GAPs share in common a 140 amino acid domain, termed the RhoGAP domain, that confers GAP activity. However, they are usually large

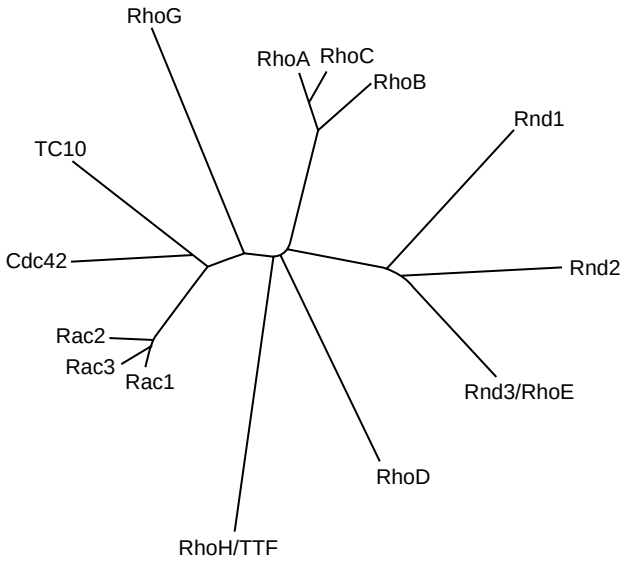

FIGURE 1 Phylogenetic tree of the Rho GTPase family. Rho GTPase family members can be grouped into subfamilies according to their sequence similarity.

proteins containing other domains involved in signaling and lipid and protein binding. Although these domains are thought to influence GAP function in cells, very little is known concerning how these proteins are regulated *in vivo*, although it has been reported that some of them can be regulated by tyrosine phosphorylation.

Guanine-Nucleotide-Dissociation Inhibitors

GDIs bind to Rho GTPases in the cytosol and prevent their interaction with the membranes, and with both GEFs and GAPs. For these reasons they are considered to be negative regulators of Rho GTPases that sequester them in an inactive form in the cytoplasm. Signals that activate Rho GTPases will disrupt the GTPase/GDI complex and localize the GTPase to membranes. It has been reported that GDIs can be phosphorylated by protein kinase C, leading to their dissociation from GTPases and consequently to GTPase activation. There are three RhoGDIs in mammalian cells that show differences in their pattern of expression, activity, and specificity.

Rho GTPase Family Activity: Downstream Targets

Rho GTPases exert their function by binding to and modulating the activity of an array of downstream effectors. Here the manner in which Rho GTPases activate some of their most relevant targets in terms of actin cytoskeleton control will be described (Table 1).

Rho Effectors

The archetypical responses elicited by Rho activation in cells are the assembly of bundles of filamentous actin

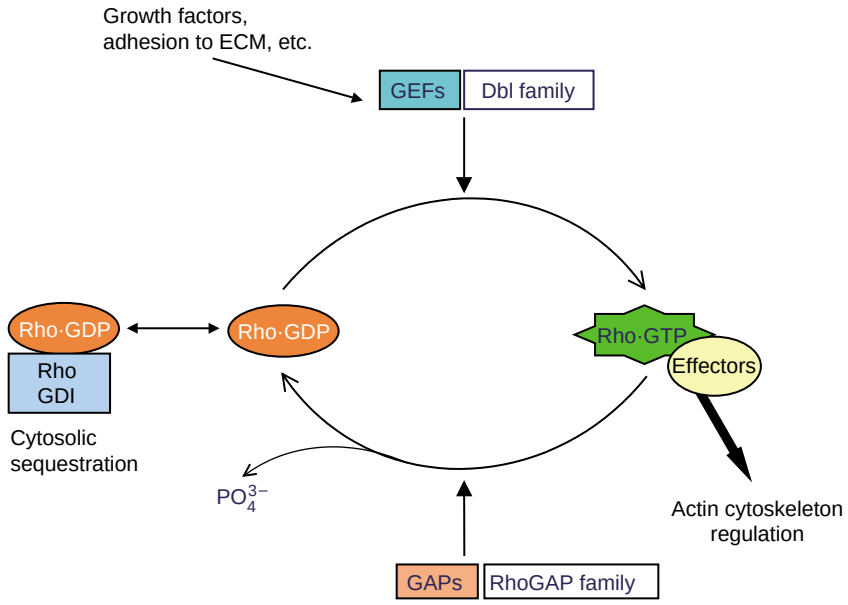

FIGURE 2 Rho GTPase regulation. Rho GTPases cycle between a GDP-bound, inactive state, and a GTP-bound active state. When GDP-bound, Rho GTPases can bind to RhoGDIs and remain sequestered in the cytoplasm. Extracellular signals induce the exchange of GDP for GTP, which is regulated by GEFs, thereby activating Rho GTPases and localizing them on membranes. In their GTP-bound form, Rho GTPases interact with their downstream effectors and regulate the actin cytoskeleton. Inactivation is achieved through GTP hydrolysis, which is often promoted by GAP binding to Rho GTPases.

TABLE 1

Rho GTPase, Downstream Effectors, and their Functions

Rho GTPase	Downstream effectors	Function in cell biology
RhoA, B, C	ROCK I, II	Actomyosin contractility: Stress fiber and focal adhesion formation. Tail retraction and new focal adhesion formation in cell migration
	mDia	Actin filament formation
Rac1, 2, 3	IRSp53	Actin polymerization, through WAVE activation, and Lamellipodia formation. Driving force in cell migration
	PAK1, 2, 3	Actin polymerization through LIMK-induced cofilin inhibition
Cdc42	WASP/N-WASP	Actin polymerization and filopodia formation. Sensor role in cell migration
Rnd1, 2, 3/RhoE	Unknown (RhoE binds to ROCK I)	Antagonizing RhoA effects: Disassembly of actin stress fibers and focal adhesions
RhoH/TTF	Unknown	Antagonizes some aspects of RhoA signaling in lymphocytes
TC10	WASP	Actin polymerization, filopodia formation

and myosin, termed stress fibers, and the formation of multimolecular complexes at the end of those fibers at sites of integrin-mediated cell adhesion, termed focal adhesions. Both effects can be largely attributed to one Rho effector, the serine/threonine kinase, Rho-kinase (ROCK). Rho-GTP binding to ROCK unfolds and relieves its kinase domain from an otherwise closed, autoinhibited, conformation. The two isoforms of ROCK phosphorylate a number of proteins involved in regulating the actin cytoskeleton, including the myosin-binding subunit of myosin light-chain phosphatase, thereby inhibiting its phosphatase activity and enhancing myosin light-chain phosphorylation and actomyosin-based contractility. Other Rho effectors contribute to Rho-mediated actin cytoskeleton regulation, such as mDia, which binds to the actin-binding protein profilin and stimulates actin filament formation.

Cdc42 Effectors

Activation of Cdc42 in most cells promotes the formation of filopodia, spike-like membrane protrusions induced by actin polymerization in parallel bundles. As with Rac-induced lamellipodia, these structures are associated with the leading edge of migrating cells. A clear model has emerged in which a Cdc42 effector, WASP (Wiskott Aldrich syndrome protein), directly controls actin polymerization to extend filopodia in response to extracellular signals. The hematopoietic-specific WASP or its widely expressed isoform, N-WASP, induce *de novo* actin polymerization through their binding to the Arp2/3 (actin-related protein) complex. Binding of active Cdc42 to WASP changes its conformation, relieving it from an autoinhibited state and exposing a previously masked domain, the VCA domain (verprolin-homology, cofilin-homology and acidic region). Once exposed, this domain binds to G-actin through the V-domain and to the Arp2/3 complex through the CA-domain, strongly activating Arp2/3 complex-induced actin nucleation and polymerization. WASP also binds to the actin-binding protein profilin, which further enhances WASP-mediated actin filament formation through its ATP/ADP exchange activity towards actin. Activation of WASP family proteins by Rho GTPases, such as WASP activation by Cdc42, is a typical example of downstream effector activation by binding to active GTPases (Figure 3).

Rac Effectors

In most mammalian cells, activation of Rac induces lamellipodia and membrane ruffles, both being plasma membrane protrusions that extend over the substratum or upwards, respectively. These protrusions are driven by a branching network of actively polymerizing actin filaments, and are usually found at the leading edge of migrating cells. The Rac effector pathway that leads most directly to actin polymerization involves WAVE proteins (wasp/verprolin homologous protein). WAVEs are members of the WASP family that are crucial mediators of actin polymerization mediated by the Arp2/3 complex. WAVE1 and WAVE2 have been shown to be activated downstream of Rac, although Rac does not bind directly WAVEs and the mechanism of activation is different to Cdc42 stimulation of WASP, but with similar consequences: activation of Arp2/3 complex-mediated actin polymerization (see Figure 3). Other Rac effectors also contribute to actin polymerization and to extension of lamellipodia and membrane ruffles. For example, PAKs (p21-activated

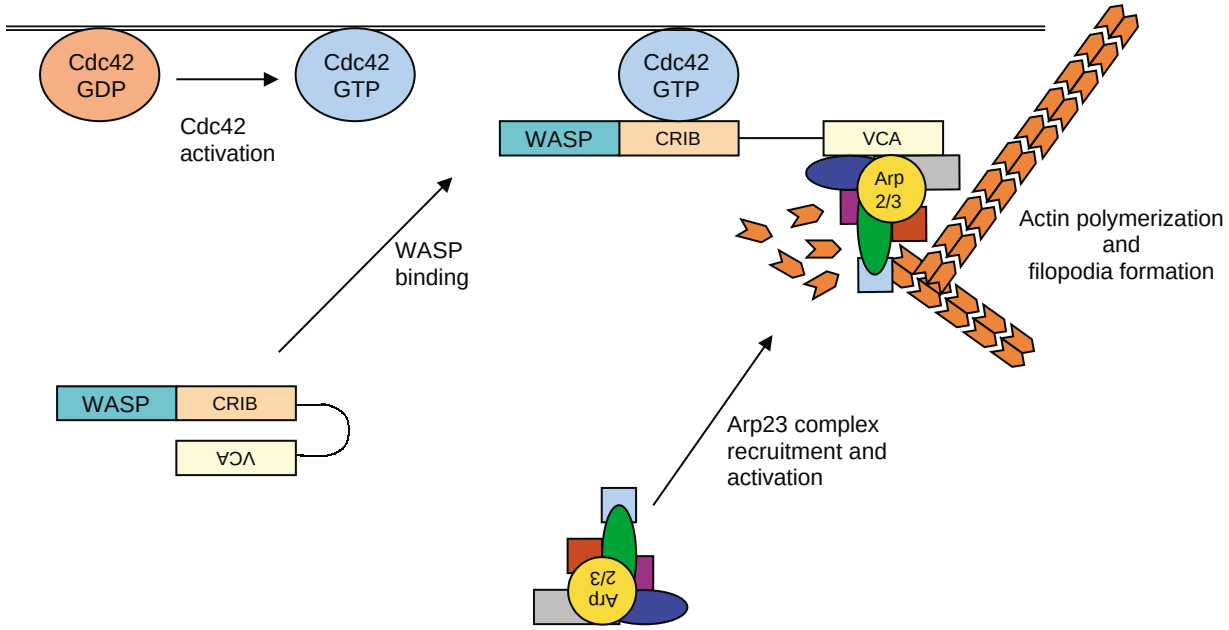

FIGURE 3 Model of effector activation by Rho GTPases: Cdc42-induced WASP activation promotes filopodia. When Cdc42 is inactive, WASP is in an auto-inhibited conformation. Upon Cdc42 activation, inactive WASP binds to Cdc42-GTP through its CRIB domain, relieving its inhibitory conformation and exposing its VCA domain. The VCA domain is now available to recruit and activate the Arp2/3 complex, stimulating actin polymerization and formation of filopodia.

kinases) are a family of kinases that can be activated by Rac and Cdc42 and contribute to actin reorganization, for instance through phosphorylation of LIM kinase, which phosphorylates and inhibits the actin-depolymerizing protein cofilin, and thus promotes actin polymerization.

Other Members

Although RhoA, Rac1, and Cdc42 are the most-extensively studied members of the Rho family, evidence is now accumulating that they are not alone in their regulatory roles on the actin cytoskeleton. First of all, it is not yet clear what the specific roles are of closely related isoforms of these proteins such as RhoB or Rac2, and other less-characterized members of the family are only starting to be investigated. The Rnd proteins are an exciting new subfamily that have been shown to be unusual examples of GTP-binding proteins as they do not cycle between an active GTP-bound state and an inactive GDP-bound state. Among these proteins, Rnd1 and Rnd3/RhoE have been shown to antagonize RhoA in its effects on the actin cytoskeleton, promoting stress fiber and focal adhesion disassembly in several different types of mammalian cells. Similarly to Rnd proteins, RhoH/TTF seems to antagonize some of the RhoA GTPase functions, but it is only expressed in hematopoietic cells. Other members have more similar effects to those of the prototypical Rho GTPases: RhoG signals in parallel to Rac and Cdc42, whereas TC10 is more related to Cdc42 and induces filopodia.

Rho GTPase Family: Functions in Cell Biology

The ability to regulate the actin cytoskeleton dynamically enables Rho GTPases to be involved in many cellular processes, the most obvious of them being cell migration. However, there are many other processes that require Rho GTPases, such as secretion, endocytosis, and cell proliferation.

Cell Migration

Cell movement requires an orchestrated spatio-temporal regulation of the actin cytoskeleton, which involves coordinated activation of several members of the Rho GTPase family. Rac isoforms are important to induce actin polymerization in the leading edge of the cell, in the form of lamellipodia and membrane ruffles, pushing forward the plasma membrane and generating the driving force for cell motility. Cdc42 has shown to be essential for directionality, for instance in macrophage chemotaxis, through the formation of filopodia that are believed to sense the extracellular environment. Rho, in turn, contributes to cell motility by providing actomyosin-based contractility necessary for cell body contraction and tail retraction. Rac activity is also crucial to form adhesions as cells move forward and interact with new extracellular matrix. In addition, Rho GTPases affect microtubule dynamics, which is also important for cell migration. Although the principal

roles of Rho GTPases in cell migration have been already established, there are important differences in the role that these proteins have in different cell types, such as epithelial cells versus macrophages. Furthermore, it is not yet fully understood how these proteins and their effectors are spatially and temporally regulated, and how such an exquisite level of coordination in their functions is achieved in cell migration.

Secretion and Endocytosis

Vesicle trafficking requires both the actin cytoskeleton and the microtubule network, and Rho GTPases have been shown to affect different aspects of vesicle trafficking. Activation of Rho, Rac, and Cdc42 enhance secretion in mast cells, and conversely, their inhibition reduces secretion induced by different agents in these cells. Although it has been established that secretion is accompanied by Rho GTPase-dependent actin reorganization, it is not clear how each Rho GTPase specifically contributes to this process. Rho GTPases have also been shown to modulate endocytosis, and interestingly, two less-studied Rho family members, RhoB and RhoD, have been found to localize to endosomes, and RhoD has been shown to modulate endosome dynamics, fuelling the concept that these proteins may play an important role in endocytosis.

Proliferation and Transformation

Both Rho and Rac isoforms have been shown to be necessary for cell proliferation. Although Rho effectors are important for the actin ring contraction that drives cytokinesis, it is in the G_1 phase of the cell cycle where Rho GTPase function seems to be essential in cell cycle progression. Activation of both Rho and Rac have been linked to the activation of cyclin-dependent kinases through the expression of D-type cyclins and the inhibition of the expression of cyclin-dependent kinase inhibitors, such as $p21^{cip1}$ and $p27^{kip1}$. However, the downstream effectors that lie between Rho GTPases and cell cycle regulators remain completely unknown. Interestingly, Rho GTPases also contribute to cell transformation. Active mutants of Rho, Rac, and Cdc42 all have positive effects on cell transformation and anchorage-independent growth, although they are not considered to be true oncogenes when compared to mutant forms of Ras or Src, for example. However, their biological effects on cell proliferation and actin cytoskeleton place them as potentially important mediators of neoplastic transformation. For instance, their crucial role in cell motility has been shown to influence the loss of epithelial polarity and invasiveness of cancer cells.

See Also the Following Articles

Actin Assembly/Disassembly • Actin-Capping and -Severing Proteins • Actin-Related Proteins • Cell–Matrix Interactions • Endocytosis • Small GTPases

Glossary

cell transformation A complex alteration of cellular behavior that is characteristic of cancer cells. It involves a reduction in the dependence on soluble mitogens and anchorage to the extracellular matrix in order for the cells to proliferate, together with loss of the ability to respond to growth-inhibitory signals both from the extracellular environment or arising from intracellular checkpoint controls.

cytoskeleton Filaments consisting of protein polymers that are responsible for giving the cell mechanical strength, controlling its shape and driving cell movement. Three types of filaments are found in animal cells: actin filaments, microtubules, and intermediate filaments.

leading edge The front of an actively migrating cell, which generally displays a fan-shaped meshwork of actin filaments that push forward the plasma membrane as they polymerize and grow.

small GTPases Monomeric GTP-binding proteins, as opposed to the transmembrane receptor-coupled family of heterotrimeric G proteins, that bind guanine nucleotides and have different conformations when bound to GTP or GDP. This enables them to act as molecular switches and transiently activate several effector proteins.

Further Reading

Bishop, A. L., and Hall, A. (2000). Rho GTPases and their effector proteins. *Biochem. J.* **348**, 241–255.

Etienne-Manneville, S., and Hall, A. (2002). Rho GTPases in cell biology. *Nature* **420**, 629–635.

Peck, J., Douglas, G. I. V., Wu, C. H., and Burbelo, P. D. (2002). Human RhoGAP domain-containing proteins: Structure, function and evolutionary relationships. *FEBS Lett.* **25**(528), 27–34.

Ridley, A. J., and Hall, A. (1992). The small GTP-binding protein rho regulates the assembly of focal adhesions and actin stress fibers in response to growth factors. *Cell* **70**, 389–399.

Sahai, E., and Marshall, C. J. (2002). Rho-GTPases and cancer. *Nat. Rev. Cancer* **2**, 133–142.

Zheng, Y. (2001). Dbl family guanine nucleotide exchange factors. *Trends Biochem. Sci.* **26**, 724–732.

Biography

Priam Villalonga completed his M.Sc. in Pharmacy (Biochemistry) in the University of Barcelona, and then obtained his Ph.D. working on Ras signaling and cell cycle in the School of Medicine in Barcelona. He is now a postdoctoral fellow working on RhoE and its role in cell proliferation and transformation in Anne Ridley's laboratory in the Ludwig Institute for Cancer Research in London.

Anne Ridley studied biochemistry in Cambridge, then carried out her Ph.D. research in London, studying the role of Ras in cell transformation. She worked as a postdoctoral fellow in Cambridge, Massachusetts and then in London, investigating the functions of Rho and Rac proteins. She is now a Laboratory Leader at the Ludwig Institute for Cancer Research, studying the molecular basis for eukaryotic cell migration, concentrating on intracellular signaling processes involving the Rho family of GTPases.

Ribosome Assembly

John L. Woolford
Carnegie Mellon University, Pittsburgh, Pennsylvania, USA

The assembly of ribosomal proteins with rRNAs to form ribosomes is a major metabolic pathway in cells. Because ribosomes are central to the growth and proliferation of cells, many cellular functions have evolved to ensure a steady and regulated supply of ribosomes. Ribosomes consist of two ribonucleoprotein particles that catalyze protein synthesis through translation of the genetic code in mRNA. This is an essential step in the expression of genes in all organisms. The smaller (30S to 40S) subunit of the ribosome serves as a platform to bring together messenger RNA, aminoacylated transfer RNAs, and translation factors. The larger (50S to 60S) ribosomal subunit provides peptidyl transferase activity to catalyze peptide bond formation in nascent polypeptides.

Introduction

The 30S ribosomal subunit of prokaryotes and archaea contains ~20 different proteins (depending on the species), and a 16S ribosomal RNA (rRNA), while the 50S ribosomal subunit contains 30–40 proteins, a 5S rRNA, and a 23S rRNA. Eukaryote ribosomes are more complex. The 40S subunit contains ~32 proteins and the 18S rRNA, while the 60S subunit contains ~47 proteins and the 5S, 5.8S, and 25S (or 28S in metazoans) rRNAs. The structure and function of these ancient multimolecular machines have been explored in great detail. Each ribosomal subunit contains an intricate structural core of RNA decorated on its surface with the ribosomal proteins. A significant fraction of the nucleotides in the RNA contact ribosomal proteins or base pair with other sequences in the RNA.

How these multiple, dynamic protein–RNA, RNA–RNA, and protein–protein interactions are established and rearranged during the assembly of ribosomes is a central question in ribosome biology. In eukaryotes, ribosome assembly occurs primarily in the nucleolus, a subcompartment of the nucleus where the rDNA genes are actively transcribed. There are several major steps in ribosome assembly: synthesis, modification, and nucleolytic processing of the pre-rRNAs, ordered assembly of ribosomal proteins with the pre-rRNAs, and in eukaryotes, release of the nascent ribonucleoprotein particles from the nucleolus to the nucleoplasm, and subsequent export to the cytoplasm, where the mature ribosomes catalyze protein synthesis.

Model Systems

Much has been learned about ribosome biogenesis from studies of bacterial ribosome assembly *in vitro* and from analysis of yeast ribosome synthesis *in vivo*. Analysis of the nucleotide sequence of genomes from prokaryotic and eukaryotic model organisms demonstrates that ribosomes and the RNAs, and proteins necessary for their production are highly conserved. Thus, the principles and mechanisms of ribosome assembly learned from bacteria and yeast will be applicable to other organisms.

Assembly of Bacterial Ribosomes *in vitro*

Functional bacterial 30S and 50S ribosomal subunits can be reconstituted *in vitro* from rRNA plus each of the ribosomal proteins. These studies provide useful paradigms to understand the mechanism of assembly of ribosomes *in vivo*. For example, reconstitution studies defined an "assembly map" for the order of association of each ribosomal protein with rRNA (Figure 1). Ribosomal proteins can be divided into three obligatory binding classes. Primary binding proteins associate directly with the rRNA, often requiring or inducing changes in the conformation of the RNA. Secondary binding ribosomal proteins bind only after a primary protein has assembled and create a binding site for the next protein. Tertiary proteins assemble upon association of the primary and secondary proteins, to complete the pathway of assembly. Despite its hierarchical, interdependent nature, ribosome assembly is not completely cooperative. Three nucleation sites assemble independently to form three structurally separate domains of the 30S subunit: the body, platform, and head. The body assembles around the 5′ structural domain of 16S rRNA, the platform with the central domain, and the head around the 3′ major domain of

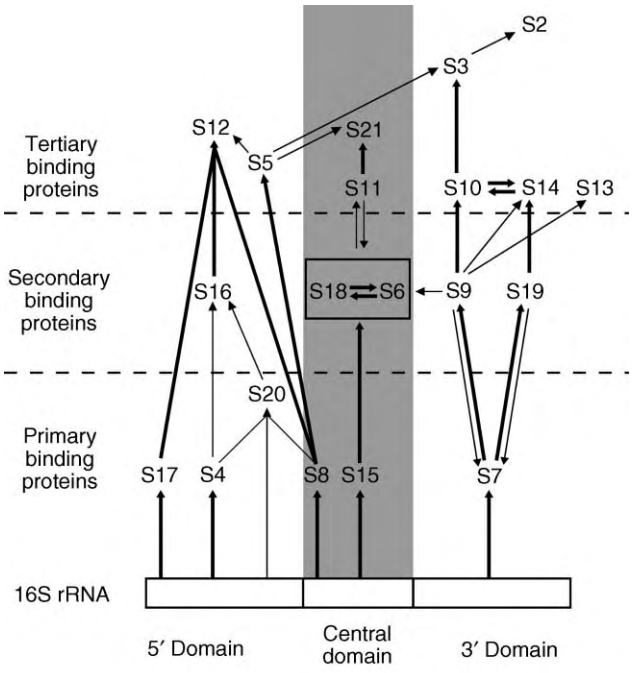

FIGURE 1 Assembly map for reconstitution of *E. coli* 30S ribosomal subunits from 16S rRNA and 20 ribosomal proteins. Each of the three structural domains of the 16S rRNA independently assembles with a subset of ribosomal proteins in a defined order. Primary ribosomal proteins bind first, then secondary proteins, and finally tertiary proteins. The thick or thin arrows represent the relative strength of binding or the relative facilitating effect on binding of one protein to another protein or to RNA.

16S rRNA (Figure 1). Each domain can be independently reconstituted *in vitro*. Formation of the central platform nicely illustrates details of assembly. First, the primary protein S15 binds to a particular conformer of the junction of rRNA helices 20, 21, and 22. Binding is stabilized by additional contacts between S15 and a tetraloop at the end of helix 23a, and by an interhelical RNA–RNA base pairing. The latter is required for binding of secondary proteins S6 and S18, which first form a heterodimer. Their association with the growing platform may establish a conformation of helix 23b, required for assembly of the tertiary binding protein S11. Bound S11 is further stabilized through interactions with S18.

Self-assembly of 30S ribosomal subunits *in vitro* suggests that extrinsic factors are not required to build a ribosome. However, several other results indicate otherwise. First, *in vitro* assembly is temperature dependent. At low temperatures, 16S rRNA binds to a subset of ribosomal proteins to form a 21S–26S assembly intermediate. Subsequent heating is required for conformational rearrangements to create an activated intermediate that can bind the remaining ribosomal proteins. The requirement for this heat-sensitive step can be circumvented by addition of the DnaK, DnaJ, and GrpE proteins plus ATP. This molecular chaperone system may recognize exposed hydrophobic surfaces of incompletely folded proteins or RNA in the assembling ribosome and either prevents misfolding and aggregation into nonproductive intermediates or promotes productive conformational changes. Second, a number of bacterial mutants have been identified that are deficient in production of ribosomes. Such mutants, including a *DnaK* mutant of *E. coli*, may be defective in assembly due to loss of function of a *trans*-acting assembly factor. As described below, a large number of *bona fide trans*-acting factors involved in ribosome biogenesis have been identified in eukaryotes.

Eukaryotic Ribosome Biogenesis *in vivo*

Synthesis, Modification, and Processing of rRNA

The 18S, 5.8S, and 25S/28S eukaryotic rRNAs are derived from a single 35S (47S in metazoans) transcript synthesized by RNA polymerase I (Figure 2). The 5S rRNA is transcribed from separate genes by RNA polymerase III. The genes for rRNA are tandemly repeated (100 to 10,000 copies – depending on the organism) at one or a few chromosomal loci. In yeast and a few other eukaryotes, the 5S and 35S genes are interspersed, comprising one repeat unit, although in most organisms the two classes of genes (5S and 35S/47S) are unlinked. The high copy number of these genes enables cells to produce large quantities of ribosomes when necessary, e.g., ~40 ribosomes per second in rapidly dividing yeast cells.

Immediately following transcription, the 35S pre-rRNA is covalently modified. In yeast cells, rRNA undergoes 2′-O-ribose methylation at 55 positions, pseudouridylation (rotation of a uridine) at 45 positions, and methylation of 12 bases. The sites of modification are located within conserved, functionally important domains of the mature rRNA. Although base methylations are catalyzed by individual proteins, most of the modification sites are identified and modified by a large collection of small nucleolar RNAs (snoRNAs). Each snoRNA contains sequences complementary to one of the modified rRNA sequences and thus functions as a "modification guide" to identify a potential target. The snoRNAs are associated with a small set of proteins, in small nucleolar ribonucleoprotein particles (snoRNPs). One class of snoRNP proteins is associated with the "C + D" class of snoRNAs responsible for methylation, and a different set of snoRNP proteins is present in the "H + ACA" snoRNPs catalyzing pseudouridylation.

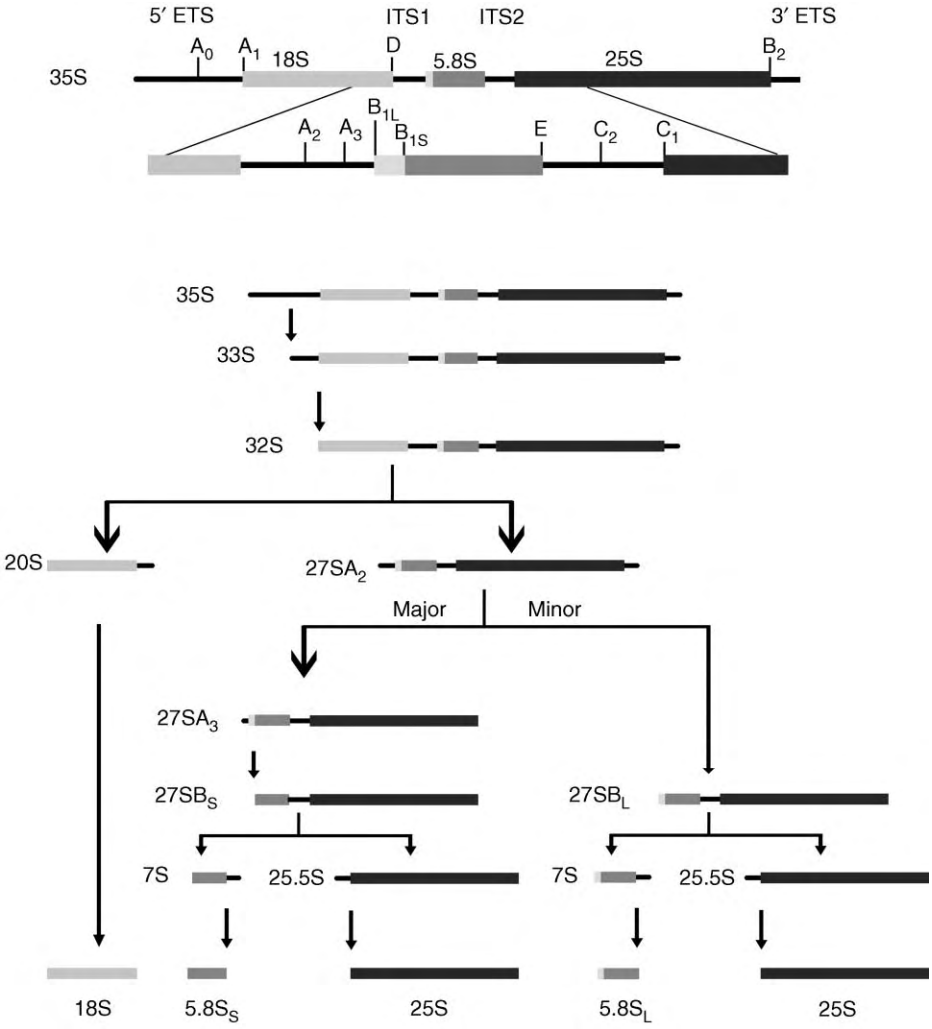

FIGURE 2 (A) Structure of the 35S pre-rRNA primary transcript. The external and internal transcribed spacers are indicated by thin lines, and the mature rRNA sequences by thick lines. Locations of the known processing sites are indicated. (B) Pathway of processing of 35S pre-rRNA to produce the mature 18S, 5.8S, and 25S rRNAs. Each pre-rRNA processing intermediate in the pathway is shown. The ordered set of processing steps is indicated.

Among these snoRNP proteins are the potential rRNA 2′-O-methyl transferase Nop1p and the putative pseudouridine synthase Cbf5p. Although snoRNPs associate with nascent rRNA, modification does not occur until transcription is completed. It is not clear what triggers these modifications, or how the snoRNPs are released from the assembly complex. Also, the function of the modifications is not known.

Eukaryotic rRNA precursors contain two internal transcribed spacers, ITS1 and ITS2 separating the 18S, 5.8S, and 25S/28S rRNA sequences, respectively. Additionally, there are 5′ and 3′ external transcribed spacers, 5′ETS and 3′ETS flanking the mature rRNA sequences (Figure 2). The predicted secondary structures of the mature rRNAs are highly conserved, although their lengths vary slightly among species. However, these features are somewhat less conserved for the transcribed spacer RNAs. The spacers are removed from the 35S–47S primary transcript to produce the three mature rRNAs by a series of conserved endonucleolytic and exonucleolytic processing steps (Figure 2). The secondary structures of the excised spacers are important for their removal. The pathways of rRNA processing appear to be quite similar among the best-studied eukaryotes – yeast, *Drosophila*, Xenopus, mouse, rat, and humans. However, certain ambiguities still exist concerning the precise locations of processing sites and whether sites are generated exo- or endonucleolytically (or by a combination).

In yeast, the first detectable precursor is the 35S pre-rRNA, which has already undergone cleavage by the Rnt1p endonuclease near the 5′ end of the 3′ ETS. The 5′ ETS of 35S pre-rRNA is then removed by rapid sequential endonucleolytic cleavages at the A_0 and A_1

sites to generate the 33S and 32S intermediates. The biosynthetic pathway then bifurcates upon cleavage at the A_2 site to generate the 20S and $27SA_2$ pre-rRNAs. The remainder of ITS1 is removed from the 20S pre-rRNA by processing at site D to generate the mature 18S rRNA. The $27SA_2$ pre-rRNA undergoes a more complex series of processing reactions to produce mature 5.8S and 25S rRNAs. The majority of $27SA_2$ is cleaved at site A_3 by the endonuclease activity of the MRP RNP, immediately followed by $5' \rightarrow 3'$ exonucleolytic trimming of $27SA_3$ to the B_{1S} site by Rat1p or Xrn1p exonucleases to generate $27SB_{1S}$. Alternatively, a small fraction of $27SA_2$ is processed to $27SB_{1L}$, by a mechanism yet to be determined. The two 27SB pre-rRNAs are endonucleolytically cleaved at the C_2 and perhaps C_2' sites, to create the 7S and 25.5S pre-rRNAs. The $3'$ end of 7S is removed by the exosome complex of $3' \rightarrow 5'$ exonucleases to generate the $5.8S_L$ and $5.8S_S$ rRNAs. The $5'$ end of the 25.5S pre-rRNA undergoes rapid $5' \rightarrow 3'$ trimming to the C_1 site by the Rat1p or Xrn1p exonucleases, generating mature 25S rRNA.

Endonucleolytic cleavage at the A_0, A_1, and A_2 sites requires the U3, U14, snR10, and snR30 snoRNPs as well as several individual proteins. Cleavage at A_0 requires base pairing between the U3 snoRNA and sequences in the $5'$ ETS ~140 nucleotides, $5'$ of the A_0 site. Likewise, base pairing between U14 snoRNA and rRNA is necessary for U14 function. The exact roles of these molecules are not known; no endonucleases have been identified that cleave the A_0, A_1, and A_2 sites. The interdependence observed for these three processing reactions may reflect a complex series of rearrangements of the architecture of the processing rRNA, mediated by the snoRNPs and protein factors.

Ribosome Assembly

Initial studies revealed a crude outline of the assembly pathway. 35S pre-rRNA is present in a 90S rRNP that is converted to 43S and 66S rRNP assembly intermediates. These precursor particles are then converted to the mature 40S and 60S ribosomal subunits, respectively (Figure 3). The 43S assembly intermediate contains the 20S pre-rRNA. There are at least six 66S assembly intermediates containing the $27SA_2$, $27SA_3$, $27SB_{1L}$, $27SB_{1S}$, 25.5S + 7S, and 25S + 5.8S rRNAs, respectively. Each of these rRNPs contains a subset of the ribosomal proteins found in mature subunits, plus a number of nonribosomal proteins not present in mature functioning ribosomes. More than 150 such *trans*-acting factors required for assembly of ribosomes have been identified in yeast, using genetic screens or selections to identify mutants defective in ribosome biogenesis or using proteomic approaches to purify and characterize assembly intermediates. Recently, metazoan counterparts of most of these proteins have been identified by mass spectrometry of proteins from purified nucleoli.

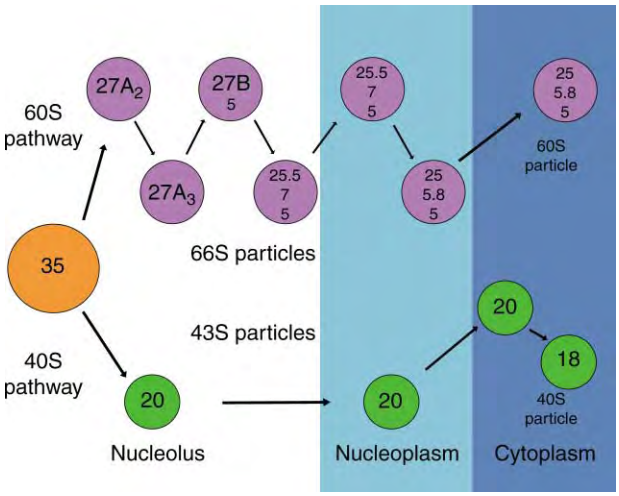

FIGURE 3 Pathway of ribosome assembly. The earliest ribosome precursor particle is the 90S rRNP, which is converted to 43S and 66S rRNP assembly intermediates. Each 66S rRNP intermediate contains a unique successive pre-rRNA processing intermediate. Most steps in assembly occur in the nucleolus. However, the 43S rRNP undergoes final maturation in the cytoplasm, and the 66S rRNP undergoes late maturation steps in the nucleoplasm and the cytoplasm. The pre-rRNA intermediates present within each rRNP are indicated.

The earliest defined step in ribosome assembly is association of the U3 snoRNP with the $5'$ ETS of the nascent 35S pre-rRNA. Electron microscopy of chromatin spreads reveals "terminal knobs" present near the $5'$ ends of nascent rRNA, which contain the U3 snoRNP. During or immediately after completion of transcription, 20–30 nonribosomal proteins plus the U14, snR10, and snR30 snoRNPs also associate with the 35S pre-rRNA. At the same time, a large number of ribosomal proteins destined for the 40S subunit, as well as a few destined for the 60S subunit, assemble into the nascent rRNP. Thus, upon termination of its transcription, the 35S rRNA is packaged into a rapidly changing, short-lived, and heterogeneous collection of RNPs ~90S in size. Cleavage at the A_0, A_1, and A_2 sites occurs within these rRNPs.

The 43S and 66S rRNPs are generated from the 90S rRNP by cleavage of the A_2 site. All but seven of the nonribosomal molecules present in the 90S rRNP are absent from the 43S rRNP or 66S rRNPs. The 43S pre-rRNP travels rapidly from the nucleolus through the nucleoplasm to the cytoplasm, where it undergoes final steps in maturation, including cleavage of 20S pre-rRNA at site D, to form the functional 40S subunit. Several of the ribosomal and nonribosomal proteins present in the 43S rRNP are required for this step, which is likely to involve the reconfiguration of the 20S pre-rRNA and the 43S rRNP into conformations favoring cleavage.

Late assembling ribosomal proteins associate with the 43S rRNP in the nucleoplasm and in the cytoplasm.

While most of the nonribosomal proteins necessary for production of 40S ribosomal subunits assemble with the 35S pre-rRNA in 90S rRNPs, only a few factors involved in 60S subunit biogenesis have been found in association with 35S pre-rRNA. The mechanism of transition from the 90S rRNPs to 66S rRNPs is less clear than that for the 43S rRNP. The first defined 66S rRNP contains $27SA_3$ pre-rRNA and several dozen nonribosomal proteins necessary for 60S subunit production. It is not clear whether these 60S assembly factors associate weakly with the 90S rRNP and therefore cannot be detected in the purified particle, or else assemble into early 66S complexes during or immediately after processing at the A_2 site.

What functions must occur to produce mature ribosomal subunits from the precursor particles and what kinds of molecules carry out these functions? Clues come not only from the paradigms of bacterial ribosome assembly *in vitro*, but also from functions suggested by the amino acid sequence motifs within the nonribosomal proteins implicated in assembly. For example, a number of nonribosomal proteins necessary for ribosome assembly contain RNA-binding motifs. Such proteins may function as RNA chaperones to help fold the pre-rRNA or to prevent misfolding. In addition to nucleases that catalyze rRNA processing, ribosome biogenesis requires cofactors necessary to remodel the rRNA and rRNPs into configurations necessary for the processing. Dynamic rearrangement of the nascent RNPs most likely also creates binding sites for the many ribosomal proteins (and nonribosomal proteins) added to the growing subunit. Such rearrangements must also enable dissociation of processing or assembly factors. Seventeen putative RNA-dependent helicases/ATPases, six potential GTPases, and an AAA-type ATPase are involved in production of ribosomal subunits. These RNA helicases are thought to catalyze winding or unwinding of RNA helices as well as rearrangement of protein conformations in the rRNP. As observed for the prototype GTPase translation factor G, the nucleotidases may also reconfigure the RNP. In addition, they have been hypothesized to serve as checkpoint or quality control factors, for successfully monitoring assembly of functional ribosomal precursors. The assembly factors Rlp7, Rlp24, and Mrt4p are ribosome-like proteins, close relatives of the ribosomal proteins, Rpl7, Rpl24, and RpP0, respectively. They may function as "stunt-doubles" to form or maintain a potential ribosomal protein assembly site. Alternatively, the exchange of such an Rlp protein with the corresponding ribosomal protein may provide another "structural proofreading" function in the assembly pathway. A number of potential scaffolding proteins are present in assembly intermediates; they may function as platforms for assembly of multimolecule-subassembly complexes. Several proteins associated with 90S, 66S, and 43S rRNPs are implicated in triggering release of 43S and 66S rRNPs from the nucleolus to the nucleoplasm. It is not known whether these proteins help make subunits competent for nucleolar exit by (1) serving as receptors or tags to "mark" subunits for exit, (2) reconfiguring the nascent subunits to expose such a tag, or (3) helping overcome mechanisms of retention in the nucleolus or nucleoplasm. Nuclear export of pre-60S RNPs involves binding of ribosomal protein rpL10 to the adaptor protein Nmd3p. Nmd3p binds to the export receptor Xpo1p/Crm1p which links ribosomes to Ran GTP and nuclear pore proteins. Likewise, 43S rRNPs require Ran GTP for export to the cytoplasm.

Integration of Ribosome Biogenesis with Cell Growth and Proliferation

Regulation of the biogenesis and function of ribosomes appears to play a critical role in mechanisms that couple cell growth and cell proliferation. However, few details are clear for how this occurs. A number of proteins necessary for ribosome assembly are also involved in cell growth and proliferation. These include not only nonribosomal proteins, but also ribosomal proteins. For example, several of the ribosome assembly factors interact with the origin recognition complex (ORC) and are required for DNA replication. Some are required for exit from Go and entry into the cell cycle, or for progression through other steps of the cell cycle. A recent screen for yeast mutants with abnormally small or large cell volumes identified 15 proteins, previously implicated in ribosome biogenesis. It will be of great interest to learn whether and how these molecules help couple growth and proliferation.

Another important question remaining to be explored is how ribosome synthesis is coupled with cell cycle progression. Cyclin-dependent kinases are thought to govern formation and maintenance of the nucleolus during the cell cycle. A number of protein phosphatases and protein kinases are localized to the nucleolus or copurify with ribosome assembly factors, but their functions in ribosome biogenesis remain to be explored.

See Also the Following Articles

Nucleolus, Overview • Ribosome Structure • RNA Polymerase I and RNA Polymerase III in Eukaryotes • RNA Polymerase II and Basal Transcription Factors in Eukaryotes

Glossary

nucleolus Nuclear subcompartment of eukaryotic cells defined by the location of actively transcribing rDNA genes. Most, but not all steps of ribosome assembly occur in the nucleolus.

pre-rRNA rRNA primary transcript or processing intermediate; precursor to mature rRNA.

ribosomal protein Protein stably associated with mature, functional ribosomes.

rRNA RNA molecule present in mature, functional ribosomes.

rRNP Ribosomal ribonucleoprotein particle; ribosome assembly intermediate containing pre-rRNAs, ribosomal proteins, and nonribosomal proteins involved in assembly.

Further Reading

Balakin, A. G., Smith, L., and Fournier, M. J. (1996). The RNA world of the nucleolus: Two major families of small RNAs defined by different box elements with related functions. *Cell* **86**, 823–834.

Eichler, D. C., and Craig, N. (1994). Processing of eukaryotic ribosomal RNA. *Prog. Nucl. Acid Res. Molecul. Biol.* **49**, 197–239.

Fatica, A., and Tollervey, D. (2002). Making ribosomes. *Curr. Opin. Cell Biol.* **14**, 313–318.

Nomura, M. (1989). History of ribosome research: A personal account. In *The Ribosome: Structure, Function and Evolution* (W. E. Hill, A. Dahlberg, R. A. Garrett, P. B. Moore, D. Schlessinger and J. R. Warner, eds.) pp. 3–55. American Society for Microbiology, Washington, DC.

Recht, M. I., and Williamson, J. R. (2001). Thermodynamics and kinetics of central domain assembly. In *The Ribosome*, Cold Spring Harbor Symposia on Quantitative Biology LXVI, pp. 591–598. Cold Spring Harbor Laboratory Press, Woodbury, NY.

Traub, P., and Nomura, M. (1968). Structure and function of *E. coli* ribosomes, V. Reconstitution of functionally active 30S ribosomal particles from RNA and proteins. *Proc. Natl. Acad. Sci. USA* **59**, 777–784.

Warner, J. R. (2001). Nascent ribosomes. *Cell* **107**, 133–136.

Biography

John Woolford is a Professor of Biological Sciences at Carnegie Mellon University in Pittsburgh, Pennsylvania. His principal research interests are in the regulation of expression of ribosomal protein genes and the mechanism of ribosome assembly. He holds a Ph.D. in biochemistry from Duke University and was a postdoctoral fellow at Brandeis University. His laboratory has made several important contributions towards the understanding of coordinate expression of ribosomal protein genes, and was one of the first groups to purify and characterize intermediates in the assembly of eukaryotic ribosomes.

Ribosome Structure

Brian T. Wimberly
Rib-X Pharmaceuticals, Inc., New Haven, Connecticut, USA

The ribosome is the large and complex polymerase responsible for translation, the synthesis of protein according to genetic instructions encoded in a mRNA template. Ribosomes make proteins by joining amino acids delivered by its substrates, the aminoacyl tRNAs. The most important activities of the ribosome are accurate substrate selection, catalysis of peptide bond formation, and movement of the substrate–template complex through the ribosome. Understanding and exploiting these activities will require determination of three-dimensional structures of this universal and uniquely complex macromolecular machine in its many different functional states.

Ribosome Function

Overview

In all organisms, template-directed protein synthesis is performed by the ribosome. The ribosome translates genetic information contained within its template, messenger RNA (mRNA), by joining amino acids carried by its substrate, transfer RNA (tRNA). The mRNA template is a linear sequence of non-overlapping three-nucleotide codons, each of which codes for a single amino acid to be added to the protein chain. There are 20 different tRNA substrates, one for each kind of amino acid. Each is a fairly large, L-shaped macromolecule with functionally important ends. One end, the 3′ CCA terminus, is the site of covalent attachment of the amino acid, while the other end features a three-nucleotide anticodon that forms base-pairing interactions with a complementary mRNA codon while in the ribosome. As the base-paired tRNA–mRNA complex passes through the ribosome, each tRNA adds its amino acid to the growing peptide chain. After passing through the ribosome, tRNAs dissociate from the mRNA template, since their triplet base-pairing interaction is only marginally stable.

The chemistry of peptide bond formation originally suggested that the ribosome should contain binding sites for mRNA and two tRNAs. In fact, the ribosome contains three distinct binding sites for substrate tRNAs, as well as a path for mRNA (Figure 1A). The three tRNA-binding sites are named after the distinguishing amino acid or peptide group attached to their resident tRNAs. The A site binds an incoming aminoacyl tRNA, which carries a single amino acid, the next to be added to the growing peptide chain. The P site contains the peptidyl tRNA, to which the nascent peptide chain is covalently attached. The E site contains an "empty" or exiting tRNA, which has already donated its amino acid to the growing chain and is therefore deacylated (not esterified by an amino acid or peptide). As translation proceeds, the tRNA–mRNA complex moves in concert through the ribosome, from right to left, while the growing peptide chain exits the ribosome through a separate tunnel.

Fundamental Activities of the Ribosome

All of the most important ribosomal functions are exemplified during the elongation cycle of translation. At the beginning of the cycle, a candidate aminoacyl tRNA binds to the A site. The ribosome then determines whether the candidate tRNA is a correct (or cognate) tRNA, or one of the more numerous incorrect (noncognate) tRNAs. This gate-keeping function, known as decoding, is crucial for maintaining the accuracy of translation. Decoding is a multistep process that requires testing the fit of the aminoacyl tRNA in the A site. Although not all of the details are known, it is clear that decoding depends on the ribosome's ability to monitor both the geometry and the affinity of the three base-pairing interactions between the aminoacyl tRNA anticodon and the A-site mRNA codon.

Once an incoming aminoacyl tRNA has been accepted in the A site, its amino acid must be added to the peptide chain attached to the P-site tRNA. Catalysis of the formation of the new peptide bond, known as peptidyl transfer, is the second fundamental ribosomal activity. The reaction occurs when the α-amino group of the A site amino acid attacks the C-terminal carbonyl of the growing peptide (Figure 1B). This results in the transient attachment of the now slightly longer peptide chain to the tRNA in the A site and the transient presence of a deacylated tRNA in the P site. Subsequent movement of the tRNA–mRNA complex relative to the

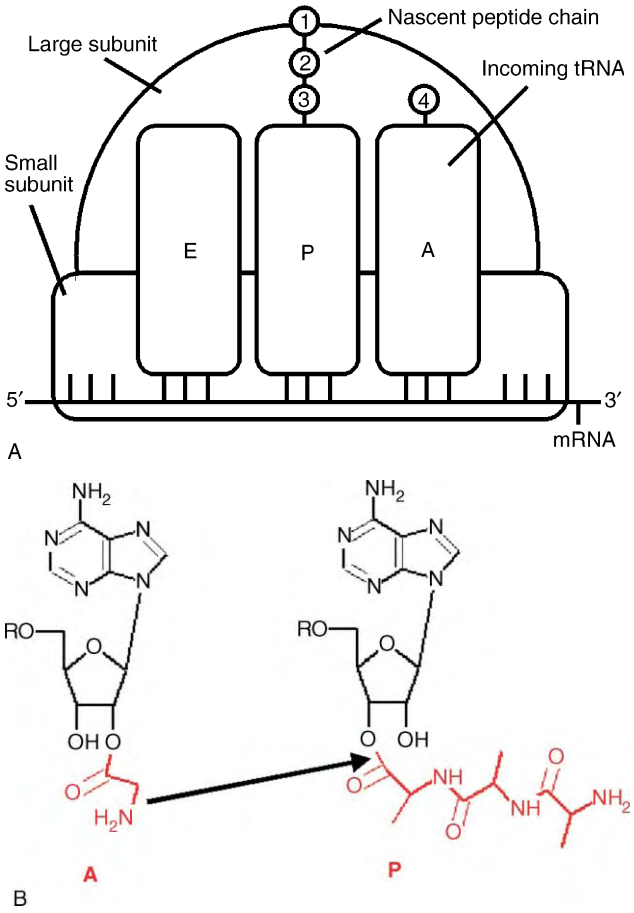

FIGURE 1 (A) Schematic view of a translating ribosome. Three amino acids (circles numbered 1–3) have already been joined to form the nascent peptide chain, whose C-terminal end is covalently attached to the tRNA (center rectangle) in the P site. The N-terminal end of the peptide is traversing a tunnel in the large ribosomal subunit. The next amino acid to be added (circle 4) is attached to an aminoacyl tRNA (right rectangle), which has just bound the ribosomal A site. A deacylated tRNA (left rectangle) is in the E site and will soon exit the ribosome. Vertical triplet bars represent codons in the mRNA, which base-pair to complementary anticodons in the tRNAs. The tRNA–mRNA complex moves through the ribosome from right to left, with each tRNA donating its covalently attached amino acid to the growing peptide chain as it passes through the peptidyltransferase site. See text for further details. (B) The chemistry of peptide bond formation. The 3′-terminal aminoacylated adenosine of an incoming aminoacyl tRNA in the A site (left) and the 3′-terminal peptidyl adenosine of the P-site tRNA (right) are shown at the moment of peptide bond formation. The peptidyl and aminoacyl moieties are highlighted in red. The N terminus of the A-site amino acid attacks the esterified C-terminal end of the peptidyl moiety. This reaction results in addition of a new amino acid to the peptide chain and transient attachment of the chain to the tRNA in the A site.

ribosome (from right to left in Figure 1A) restores a peptidyl tRNA in the P site and places a deacylated tRNA in the E site. This movement, known as translocation, is a third crucial ribosomal activity. The mechanism of translocation is still not well understood. It is thought to proceed in at least two steps, with movement of the tRNA CCA ends preceding movement of the anticodon ends. Because the tRNA substrates are so large, translocation requires large tRNA displacements of tens of Angstroms. Thus the ribosome is not only an enzyme; it is also a molecular machine.

The need for translocation also highlights an additional requirement seemingly at odds with the need for ligand movement. During translocation, the ribosome must prevent slippage of the tRNA substrates relative to the mRNA template. In other words, the reading frame must be maintained. Such a slippage, known as a frameshift event, results in the synthesis of an incorrect and usually prematurely terminated protein, which is usually detrimental to the organism. Because translocation must involve releasing and reforming of ribosome–ligand contacts, whereas maintaining the reading frame requires keeping such contacts, the structural basis of translocation is of particular interest.

This simplified summary of elongation neglects the important contributions of the nonribosomal protein elongation factors, which vastly accelerate translation rates and are essential for translation *in vivo*. Moreover, like other polymerization processes, translation also has distinct initiation and termination phases, each of which normally requires nonribosomal initiation and termination factors. Nevertheless, the fundamental ribosomal functions – decoding, peptidyltransferase, translocation, and maintenance of the reading frame – have been shown to be intrinsic to the ribosome itself.

Ribosome Structure

Distinguishing Structural Features of the Ribosome

Ribosomes have functions more complex than virtually any other enzyme, so it is not surprising that ribosomes have a unique and complex structure. The ribosome's most striking and distinguishing structural feature is its great size. The simplest ribosomes from bacteria have a mass of some 2.5 million Da, which is many times larger than a typical monomeric enzyme that catalyzes a reaction between small-molecule substrates. However, because the ribosomal substrates are themselves macromolecules – tRNAs have a mass of 25 kDa and measure some 75Å end to end – the size of the ribosome is, in fact, in normal proportion to the size of its substrates. When one considers that the ribosome must accommodate not one but three substrate tRNAs, as well as the mRNA template and large-scale movements of all of these ligands, the ribosome begins to look like a marvel of structural efficiency.

A second distinguishing feature of the ribosome is its unusual and complex composition. All ribosomes

consist of an RNA core and a large number of small proteins. Bacterial ribosomes, for example, are about two-thirds RNA by mass and contain approximately 50 different proteins, while ribosomes from eukaryotic organisms contain relatively more protein. It does not appear to be an accident that the ribosome is an RNA-based enzyme, whereas most other enzymes are made entirely of protein. After all, if proteins were made by a hypothetical ribosome composed entirely of protein, then it would be hard to imagine how this protein-only ribosome could have evolved. An RNA-based ribosome solves this "chicken-and-egg" problem, and jibes well with speculations about an "RNA world" preceding the existence of large proteins and DNA.

Subunit Organization and Nomenclature

All ribosomes consist of two loosely associated subunits of unequal size. In the well-studied bacterial ribosome, the larger subunit is denoted 50S, the smaller subunit 30S, and the entire ribosome 70S, according to their rates of sedimentation during ultracentrifugation. The bacterial small subunit RNA is the 16S RNA of approximately 1500 nucleotides, while the large subunit contains two RNAs, the 23S RNA (about 2900 residues) and the 5S RNA (about 120 residues). All eukaryotic cells contain both cytoplasmic and mitochondrial ribosomes; plants also have chloroplast ribosomes. The mitochondrial and chloroplast ribosomes are very similar to the bacterial ribosome, although the mitochondrial ribosome has a much smaller RNA component and an expanded number of proteins. The eukaryotic cytosolic ribosome is denoted 80S, with a 60S large subunit and a 40S small subunit. The RNA of the 40S subunit is the 18S RNA, and the large subunit RNAs are denoted 5S, 28S, and 5.8S (the last two of which are homologous to the bacterial 23S RNA). In all ribosomes, the large subunit interacts with the CCA end of the tRNAs and contains the active site that catalyzes peptide bond formation (the peptidyltransferase center). The small subunit binds the anticodon end of the tRNAs, both monitoring (during decoding) and maintaining (during translocation) the tRNA–mRNA base-pairing interactions. The ribosomal proteins are numbered and assigned to a subunit using a prefix of S (small) or L (large), so that individual proteins are denoted S1, S2, …, S21, L1, L2, and so forth.

Struggling with Ribosome Structure

The great size and complex composition of ribosomes have been enormous barriers to efforts to determine the structural basis of ribosome function. The ribosome is of an inconvenient size for structural biology: it has been until very recently too large for X-ray crystallography, but also rather too small for traditional electron microscopy (EM) methods. EM played a crucial role in the discovery and early structural characterization of ribosomes. However, negatively stained EM images were of very low resolution, allowing identification of only the largest structural features. During the 1970s and 1980s, many ingenious new genetic, biochemical, and biophysical methods were developed to probe ribosome structure, and an enormous amount of data was obtained. Combination of these data with EM-derived structures allowed the low-resolution assignment of a variety of functional sites. A complementary "divide and conquer" strategy to determine high-resolution structures of ribosomal fragments began to bear fruit in the 1980s and early 1990s, when a number of X-ray and NMR-derived structures of individual ribosomal proteins and ribosomal RNA fragments began to appear. Such data provided valuable insights into ribosome function and were useful guides for the design of new experiments, but it was not clear how such methods could ever result in a complete structure of a subunit, let alone the entire ribosome, at a resolution that would reveal the chemical basis of protein synthesis. However, in the mid-1990s, new techniques combining EM with single particle reconstruction revealed higher resolution images, including the first direct visualization of tRNAs and elongation factors bound between the ribosomal subunits. Ultimately, however, these new EM methods did not win the race to the long-sought goal of high resolution. In 2000, the first near-atomic resolution structures of ribosomal subunits were determined by X-ray crystallography methods, and in 2001 a medium-resolution crystal structure of the bacterial 70S ribosome was determined.

Why do we need to know the structure of the ribosome at high resolution? One motivation is the desire to determine the fundamental physical mechanisms of translation. Understanding exactly how ribosomes work will enrich and advance understanding of other aspects of biology in ways that are difficult to predict. Because the ribosome has many distinct functional states, a complete understanding of translational mechanisms will require many different structures – in other words, a "movie" of translation. Moreover, these structures must be of atomic or near-atomic resolution in order to identify the substrate–ribosome interactions that suggest mechanisms, and to direct additional experiments (for example, site-directed mutagenesis) to test these mechanistic hypotheses. The other reason to determine high-resolution ribosome structures is the more practical need to exploit fundamental knowledge

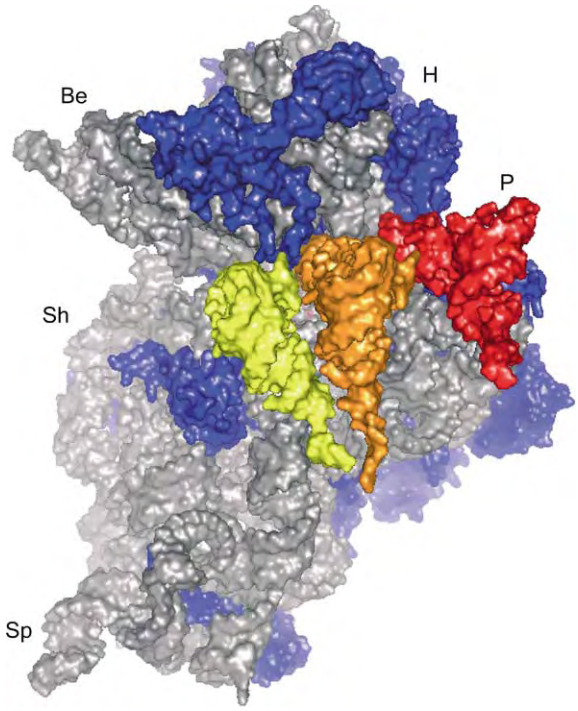

FIGURE 2 The high-resolution structure of the bacterial small ribosomal subunit, as determined by X-ray crystallography. The view is from the large subunit. Ribosomal RNA is gray, and ribosomal proteins are blue. Landmark features previously known from lower resolution methods are labeled: H (the head domain), Be (the beak), P (the platform), Sh (the shoulder), and Sp (the spur). The A-site (yellow), P-site (orange), and E-site (red) substrate tRNAs are also shown, in positions determined from the crystal structure of the entire bacterial 70S ribosome. The mRNA template (not visible in this view) is buried in the neck region, a crevice between the head, shoulder, and platform. Note the proximity of the CCA ends of the A- and P-site tRNA substrates (foreground), as required for peptide bond formation.

of biological mechanisms. Because the ribosome is the target of many clinically useful antibiotics, high-resolution ribosome structures will have a very practical use: structure-based design of improved new antibiotics that overcome the increasingly serious problem of antibiotic resistance mutations. It is also possible that a detailed structural understanding of human translation could be used to treat diseases caused by defects in normal human translation.

General Features of Ribosomal Architecture Revealed from the Subunit Structures

After more than 40 years of only low-resolution ribosome structures, the crystal structures of the large and small subunits, reported within a few months of each other in 2000, suddenly revealed almost all of the details of ribosomal architecture, as well as many fundamental new insights into the structural basis for translation mechanisms. Both its overall architecture and the composition of its functional centers reveal the ribosome to be essentially an RNA-based machine. The overall shape of both subunits is determined by the RNA component: only one of the landmark features visible at low resolution (the L7/L12 stalk) is composed only of protein (Figures 2 and 3). Moreover, the overall distribution of the proteins is not uniform: the proteins are concentrated on the back and sides of the subunits, away from the most functionally important regions at the subunit interface. The protein component is also concentrated on the surface, rather than buried in the middle of the subunits; the ribosome thus literally has an RNA core. Many of the proteins contain both a globular component on the periphery of the subunits, and one or more narrow extended peptide "tails" that penetrate deeply into crevices of the RNA core. Many of the proteins are found to interact with RNA multistem junctions and tight bends in the RNA, which suggests particular functional roles in subunit assembly. In the case of the 30S subunit, there are extensive biochemical data on the mechanisms of assembly, and an analysis of the crystal structure is in good overall agreement with these data. The subunit crystal structures have provided an enormous boost to the understanding of RNA–protein interactions, since relatively few

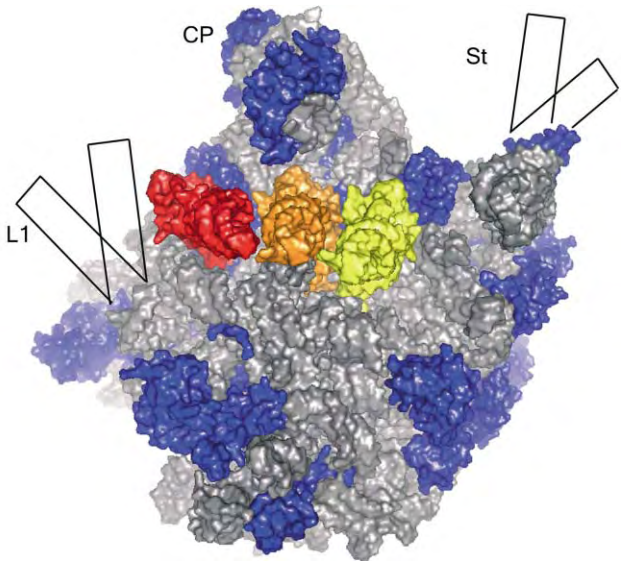

FIGURE 3 The high-resolution structure of the large ribosomal subunit from *Haloarcula marismortui*, as determined by X-ray crystallography. The view is from the small subunit, and the color scheme is as in Figure 2. The central protuberance (CP), a landmark feature previously known from lower resolution methods, is labeled. Two additional landmark features (the L1 arm and the L7/L12 stalk) are partially disordered in the crystal structure; their approximate locations and range of motions are schematically indicated. Substrate tRNAs are also shown, in positions determined from the crystal structure of the entire bacterial ribosome.

structures of RNA–protein complexes were available prior to 2000. Even less was known about RNA tertiary structure, and the subunit structures have revealed several new principles of RNA higher order structure. A common strategy for packing RNA helices makes use of patches of adenine residues, whose bases and 2′ OH moieties pack favorably against the minor groove of another RNA helix. Four different classes of this A-minor motif were defined, some of which had been previously observed in other structures. Another common RNA structural motif is the kink-turn, a tight bend that is often stabilized, although in various ways, by a bound protein. There is also a special role for G-U pairs in mediating some helix–helix packings. Analysis of the structures is continuing, and may lead to improvements in the prediction of RNA tertiary structure. The resolution of the *Haloarcula marismortui* 50S structure – at 2.4Å, significantly higher than any of the other subunit structures, and much higher than that of the 70S structures – allows reliable identification of metal ions and water molecules, which play important roles in stabilizing RNA structure. The relatively high resolution also allows the finer details of the conformation of RNA and protein to be determined. The *H. marismortui* 50S structure therefore serves as the "gold standard" for ongoing efforts to mine the recently vastly expanded RNA structure database.

There is one difference between the large-scale architectures of the 30S and 50S subunits that is probably functionally important. Whereas the secondary structure domains of the 23S rRNA interact closely to form a single, nearly hemispherical mass, the 16S rRNA secondary structure domains are for the most part independent globular entities – i.e., true three-dimensional domains – that have relatively few interactions with each other. One domain of the 16S rRNA constitutes the head, another the platform, and another the bulk of the body (Figure 2). This architecture suggests that independent movement of one or more of the domains (e.g., the head or platform domains, as has been observed in cryo-EM work) may be functionally important. For example, several groups had previously suggested that rotation of the head may accompany translocation; this hypothesis now seems probable.

High-Resolution Structure of the Small Subunit

The crystal structure of the 30S subunit from the thermophilic bacterium *Thermus thermophilus* has been determined at 3Å resolution (Figure 2). The refined structure includes virtually all of the 16S rRNA and almost all of the small subunit proteins, except for protein S1, which can be considered an initiation factor. The structure was determined in the absence of any explicitly added tRNA or mRNA ligands. However, the relatively high affinity of the 30S subunit for an RNA stem-loop in its P site resulted in a crystal packing arrangement that provides a high-resolution model for how the P-site tRNA and mRNA interact with the P site of 30S subunit. Helix 6, which constitutes the spur feature, was found to pack into the P site of a neighboring 30S subunit in a manner that mimics how the P-site tRNA anticodon stem-loop would bind. In addition, the hairpin loop of this helix was found to base-pair with a segment of single-stranded RNA – a mimic of the P-site mRNA. For several reasons, this model is only approximate, but it is nevertheless in good agreement with the lower resolution view of tRNA/mRNA–30S interactions seen in the 70S crystal structures from Noller and co-workers (see later discussion).

The 30S subunit plays a crucial role in decoding, by directly monitoring base-pairing interactions between the tRNA anticodon and the mRNA codon in the A site. The role of 30S in decoding has been investigated by determining several crystal structures with a cognate, near-cognate, or noncognate tRNA oligonucleotide analogues bound to the 30S subunit. In the presence of a cognate A-site tRNA anticodon stem-loop, several conformational changes occur in the 16S rRNA. First, Gua-530 and Ade-1492/Ade-1493 (*Escherichia coli* numbering) swing out and dock into the minor groove of the A-site codon-anticodon minihelix. Together with other conserved elements of the head (helix 34) and body (the 530 loop) previously implicated in decoding, these mobile 16S rRNA residues directly sense the "correctness" of the codon–anticodon interaction. Second, in the presence of a cognate tRNA substrate there is a more global conformational change, movement of the head and shoulder elements, resulting in a tightened grip on the A-site tRNA–mRNA helix. This larger scale conformational change from an open to a closed form has been proposed to be the signal for GTP hydrolysis by EF-Tu, the elongation factor that delivers the incoming candidate tRNAs to the A site.

Interestingly, binding of error-inducing antibiotics of the aminoglycoside family induces some of these conformational changes, such as the swinging out of A1492-3. These aminoglycosides were thus proposed to induce miscoding by stabilizing a conformation very similar to the "closed" form adopted during normal translation. Structures of the *Thermus thermophilus* 30S subunit bound to many other antibiotics (streptomycin, spectinomycin, tetracycline, hygromycin B, pactamycin, edeine) and two different initiation factors (IF-1 and IF-3) have also been reported.

High-Resolution Structures of the 50S Subunit

The structure of the 50S subunit from the halophilic archaeon *H. marismortui* was determined by Moore, Steitz, and co-workers. Despite the presence of many RNA insertions and an expanded protein repertoire, this archaeal 50S subunit is sufficiently similar to the *E. coli* subunit to allow exploitation of the vast literature describing the bacterial subunit. The 50S subunit features several protuberances, two of which are particularly disordered in the crystal structure (Figure 3). Both features are known to be functionally important. The L1 arm is thought to play a role in release of the E-site tRNA from the ribosome, while the L7/L12 stalk plays an important but poorly understood role in stimulating the GTPase activity of the elongation factors. A better understanding of how the 50S subunit interacts with these factors will come from studies on whole ribosomes. The 50S structure is more useful in understanding the nature of the peptidyl transferase activity. There is no protein at all within 18Å of the peptidyl transferase site, which was localized crystallographically by soaking in a transition-state analogue: definitive proof at last that the ribosome is an RNA enzyme, or ribozyme. This structural work and supporting biochemical data were also used to propose a mechanism for peptidyltransferase activity, with a catalytic role for nucleotide Ade-2486 (Ade-2451 in the *E. coli* numbering). However, subsequent genetic and biochemical experiments cast doubt on the proposed role of Ade-2486 as a general acid or base. More work is needed to nail down the details of the peptidyl transferase mechanism.

In 2001, a structure of the 50S subunit from the bacterium *Deinococcus radiodurans* was reported by Yonath, Franceschi, and co-workers at lower resolution. Most of the structural results are in good agreement with the *H. marismortui* structure. Interestingly, however, there are significant differences in the positioning of the L1 arm and in the conformation of RNA residues surrounding the peptidyltransferase center. The *D. radiodurans* 50S subunit structure has also been solved in the presence of five different antibiotics, four macrolides and chloramphenicol, at reported resolutions of 3.1–3.5Å. Structures of the *H. marismortui* 50S subunit bound to a variety of different antibiotics have also been reported. Such high-resolution structures of 50S–antibiotic complexes will be of great utility in the rational design of improved antibacterial drugs.

Medium-Resolution Structure of the 70S Ribosome

Structures of the *T. thermophilus* 70S ribosome with tRNA and mRNA ligands were reported by Noller, Cate, Yusupov, and colleagues in 2001, at resolutions as high as 5.5Å. This apparently rather modest resolution is in fact a phenomenal achievement, given the even greater biochemical and crystallographic difficulties of the 70S system. At this resolution, it is possible to trace RNA (but not protein) chains, albeit with errors in registry, if there are additional data to constrain the chain tracing. Once available, the high-resolution 30S structures were used to correct errors in the registry of the 16S rRNA trace and as a source for the structures of the small subunit proteins. Similarly, the high-resolution *H. marismortui* 50S structure was also invaluable for interpretation of the electron density for the large subunit in the 70S maps, although the many differences between the archaeal and eubacterial 50S subunits limited the extent to which the *T. thermophilus* 50S proteins could be built. The 70S crystal structures are largely complementary to the higher resolution subunit structures described previously. The 70S system is clearly more relevant for an understanding of the structure of the entire ribosome; thus, the 70S structures can be used to confirm the relevance of certain aspects of the higher resolution subunit structures. On the other hand, the 70S structures suffer from a lack of resolution. Thus, the high-resolution structures are of crucial importance in maximizing the utility of the 70S structures.

Comparison of the high-resolution subunit crystal structures with their structures in the context of the 70S particle reveals many small but significant differences, many of which can be ascribed to the effects of crystal packing in the "naked" high-resolution subunit structures. Some of the functionally important protein and RNA features that protrude from the 50S subunit, and that were partly disordered in one or both of the 50S structures, are found to be well ordered in the 70S structure by virtue of their interactions with the 30S subunit or tRNA ligands. Indeed, the most exciting aspects of the 70S structure are the identification of the 30S–50S contacts and the ribosome–tRNA contacts. The core of the 30S–50S contact region consists of RNA–RNA contacts, with a more peripheral ring of RNA–protein and protein–protein contacts. As with the overall architecture of each subunit, this RNA-based manner of subunit association once again emphasizes the overriding functional importance of the RNA component. Analysis of the tRNA–ribosome interactions is equally fascinating. The three tRNA substrates are intimately cradled by intersubunit bridges in the intersubunit space (Figure 4), in such a way that relative movement of the subunits, as seen in cryo-EM experiments, could effect translocation of the tRNAs.

Clearly, a more complete understanding of translational mechanisms will require more, and higher resolution, structures of distinct functional states of the

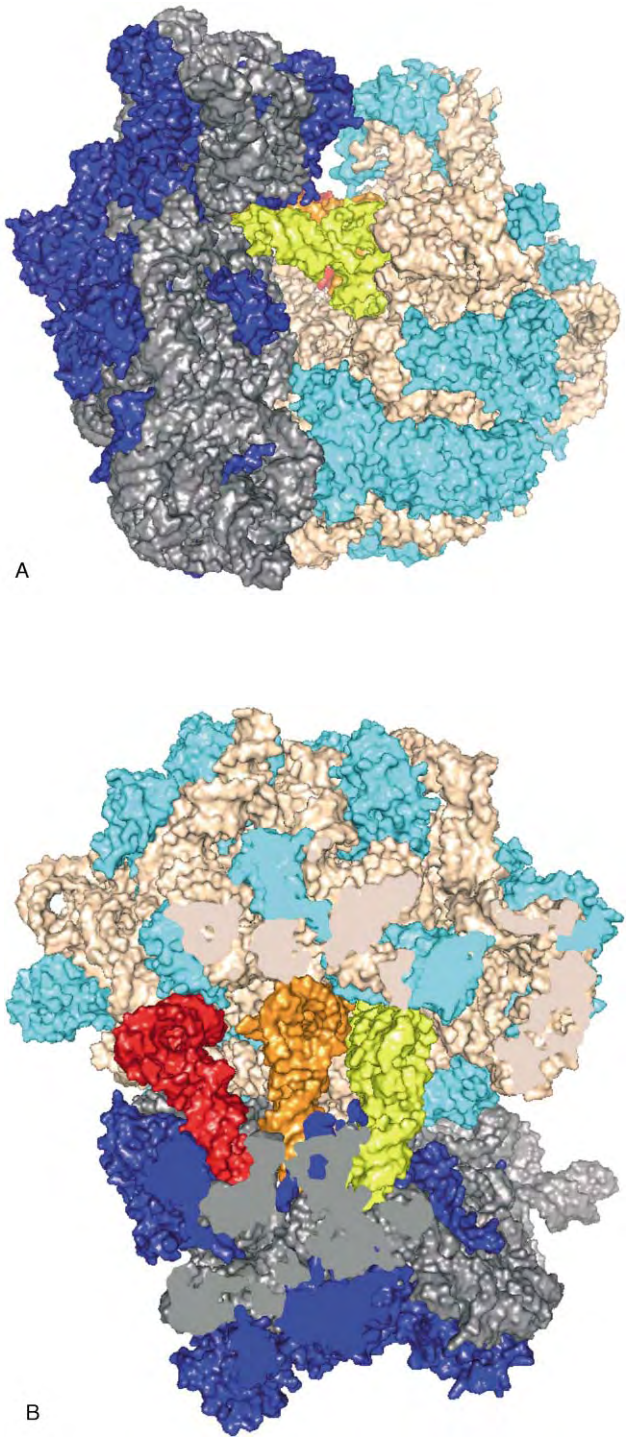

FIGURE 4 (A) The medium-resolution structure of the entire ribosome, as determined by X-ray crystallography. The view is from the A-site side, with the small subunit on the left and the large subunit on the right. For clarity, the small subunit RNA is gray, the small subunit proteins are blue, the large subunit RNA is salmon, and the large subunit proteins are light blue. The tRNAs (colored as in Figure 2) bind between the 50S and 30S subunits, with the tRNA anticodons base-paired with mRNA (not visible here), and the aminoacyl ends of the A- and P-site tRNAs are located in the peptidyltransferase site on the 50S subunit. (B) Cutaway view of the substrate tRNAs in the ribosome, with the color scheme as in A.

ribosome. Both X-ray crystallography and cryoelectron microscopy will be used toward these ends. Equally importantly, the structures now available are being used to design new genetic, biochemical, and kinetic experiments. Thus, this burst of structural information is by no means the end of the story; it is instead a new beginning.

See Also the Following Articles

Multiple Sequence Alignment and Phylogenetic Trees • Nucleolus, Overview • Ribosome Assembly • Translation Elongation in Bacteria • Translation Initiation in Bacteria: Factors and Mechanisms • Translation Termination and Ribosome Recycling

Glossary

A site The ribosomal binding site for the incoming aminoacyl tRNA, whose covalently bound amino acid will be the next addition to the growing peptide chain.

decoding The multistep process in which the ribosome decides whether an incoming tRNA carrying the next amino acid to be added is correct or incorrect. If incorrect, the tRNA is rejected.

E site The ribosomal binding site for the exiting tRNA, which has already donated its amino acid to the peptide chain.

messenger RNA (mRNA) A transient RNA copy of the DNA instructions coding for the protein to be synthesized, hence the genetic template for protein synthesis on the ribosome.

peptidyltransfer The chemical reaction between the free amino group of an amino acid and the esterified carboxy terminus of a peptide, which results in the formation of a new peptide bond. The RNA-based ribosomal activity that catalyzes this reaction is referred to as peptidyltransferase.

P site The ribosomal binding site for the peptidyl tRNA, which is covalently attached to the growing peptide.

ribosome The macromolecular complex of several large RNAs and about 50 small proteins that performs translation.

translation The synthesis of protein, as determined by a messenger RNA template; it is catalyzed by ribosomes and ribosome-associated proteins, such as the initiation, elongation, and termination factors.

transfer RNA (tRNA) The substrate for the ribosome. One end of the L-shaped tRNA base pairs with mRNA, which allows ribosomal decoding, while the other end bears a covalently attached amino acid, which is added to the growing protein in the ribosome.

translocation The movement of tRNAs and associated mRNA through the ribosome, from A site to P site, and from P site to E site.

Further Reading

Frank, J. (2003). Toward an understanding of the structural basis of translation. *Gen. Biol.* **4**, 237.

Jenni, S., and Ban, N. (2003). The chemistry of protein synthesis and voyage through the ribosomal tunnel. *Curr. Opin. Struct. Biol.* **13**, 212–219.

Moore, P. B., and Steitz, T. A. (2003). The structural basis of large ribosomal subunit function. *Ann. Rev. Biochem.* **72**, 813–850.

Ogle, J. M., Carter, A. P., and Ramakrishnan, V. (2003). Insights into the decoding mechanism from recent ribosome structures. *Trends Biochem. Sci.* **28**, 259–266.

Ramakrishnan, V., and Moore, P. B. (2001). Atomic structures at last: The ribosome in 2000. *Curr. Opin. Struct. Biol.* **11**, 144–154.

Ramakrishnan, V. (2002). Ribosome structure and the mechanism of translation. *Cell* **108**, 557–572.

Steitz, T. A., and Moore, P. B. (2003). RNA, the first macromolecular catalyst: The ribosome is a ribozyme. *Trends Biochem. Sci.* **28**, 411–418.

Van Heel, M. (2000). Unveiling ribosomal structures: The final phases. *Curr. Opin. Struct. Biol.* **10**, 259–264.

Wilson, D. N., and Nierhaus, K. (2003). The ribosome through the looking glass. *Angew. Chem. Int. Ed.* **42**, 3464–3486.

Yonath, A. (2002). The search and its outcome: High-resolution structures of ribosomal particles from mesophilic, thermophilic, and halophilic bacteria at various functional states. *Ann. Rev. Biophys. Biomol. Struct.* **31**, 257–273.

BIOGRAPHY

Brian T. Wimberly is Associate Director of Structure-Based Drug Design at Rib-X Pharmaceuticals, where he leads the X-ray crystallography part of the effort to discover new antibiotics active against bacterial ribosomes. He holds a Ph.D. from the University of California at Berkeley. During his postdoctoral training with Venki Ramakrishnan, he played a leading role in the determination of the high-resolution crystal structure of the bacterial 30S ribosomal subunit.

Ribozyme Mechanisms

John Hsieh and Carol A. Fierke
University of Michigan, Ann Arbor, Michigan, USA

RNA-catalyzed reactions are ubiquitous and important in many processes. RNA enzymes, or ribozymes, enhance chemical reaction rates using a variety of catalytic strategies, similar to those used by protein enzymes, to stabilize the transition state of the reaction. RNA and protein enzymes both use acid–base groups and metal ions to activate nucleophiles and to stabilize developing charge in the leaving group. Although limited by the ranges of functional groups and naturally occurring structure motifs, RNA enzymes can function as well as protein enzymes. The catalytic mechanisms of several well-characterized RNA enzymes, including ribonuclease P, *Tetrahymena* group I self-splicing intron and hammerhead ribozyme are discussed in detail.

Introduction

A class of naturally occurring RNA molecules, called ribozymes, enhance the speed and specificity of biologically important phosphodiester bond cleavage and peptide bond synthesis reactions, with rates that are increased by many orders of magnitude. Ribozymes have been discovered in all types of organisms from viruses to humans. Additionally, many new ribozymes that catalyze a broad range of chemical reactions have been identified in laboratory experiments called *in vitro* selection experiments. These observations have given credibility to the hypothesis of an ancient RNA World, where RNA initially served both as the genetic material and the principal cellular catalyst. During evolution, the catalytic functions of many RNA molecules were taken over by proteins. The remaining ribozymes catalyze essential biological reactions and often form complexes with proteins.

Today, many important biological processes in organisms from bacteria to humans are still carried out by RNA–protein (ribonucleoprotein, or RNP) complexes (Table I). These complexes vary greatly in size and function. For example, more than 40 protein and several RNA components are present in the ribosome, the protein synthesis machinery. Recently, the RNA components in the ribosome have been proposed to be the site responsible for catalytic activity. The spliceosome, which catalyzes the removal of noncoding sequences (introns) from pre-messenger RNA (pre-mRNA), consists of 30–100 proteins and several RNA species. Additionally, in most eukaryotes, the ends of chromosomes (the telomeres) are replicated by an enzyme called telomerase, in which an RNA subunit acts as a template, and a protein subunit catalyzes the synthesis of telomeric DNA. These examples demonstrate the importance of RNA catalysts in biology.

To understand the chemical repertoire and limitations of RNA-catalyzed reactions, this review will focus on several topics: the chemical structure of RNA, the folding of RNA molecules, and examples of the mechanism of specific ribozyme-catalyzed reactions.

Chemical Structure of RNA

Similar to DNA, RNA is made of repeating units of ribonucleotides. Each ribonucleotide consists of a five-carbon sugar in ring form (the ribose), a phosphate group, and a nitrogenous base (a pyrimidine or a purine). The same two purines, adenine (A) and guanine (G), are found in RNA and DNA. The two pyrimidines found in RNA are cytosine (C) and uracil (U); in DNA, thymine is incorporated instead of uracil. The polymer is formed by linking the monomer units via a phosphodiester bond between the 3′-hydroxyl group on one ribose unit and the 5′-phosphate group on its neighbor. Hence, the RNA polymer exhibits 5′ to 3′ directionality. The 2′-hydroxyl group on the ribose moiety of the ribonucleotide can react with the adjacent 3′-phosphodiester group to cleave the RNA polymer. This reaction is accelerated by the interaction of metal ions with the 2′-hydroxyl. The reactivity of the 2′-hydroxyl group is important for the activity of many catalytic RNAs but this moiety also makes RNA less stable in solution than DNA, which lacks a 2′-hydroxyl group.

Similar to DNA, the nucleotide bases of RNA can interact with complementary bases by hydrogen bonds. However, base pairing in RNA does not strictly obey the Watson–Crick base-pairing scheme observed in DNA, where A/T and G/C pairing occurs through hydrogen

TABLE I

Naturally Occurring Ribozymes

Ribozyme	Catalytic function	Biological function
Ribosome	Peptide bond formation	Protein synthesis
Ribonuclease P	Phosphodiester bond hydrolysis	Maturation of transfer RNA
Spliceosome Self-splicing group I and group II introns	Phosphodiester bond hydrolysis and ligation	Remove introns from precursor messenger RNA
Hairpin ribozyme Hammerhead HDV *Neurospora* Varkud Satellite	Phosphodiester bond hydrolysis	RNA virus replication pathway

bonding. In addition, since single-stranded RNA is more flexible than DNA, complementary RNA strands or different regions of the same strand can base-pair to form complex secondary and tertiary structures. This process is called RNA folding, and the stable compact structure of an RNA polymer is often referred to as its native structure. Because of the high density of negative charges when the RNA strands are brought into proximity with each other, the folding of RNA is accompanied by the binding of positively charged cations to prevent charge repulsion between the backbone phosphate ions. Therefore, RNA folding can be stimulated by the presence of cations (monovalent or divalent) as well as interactions with basic proteins. In many cases, divalent cations such as magnesium are strictly required for RNA to fold into a functional conformation; in a few cases, monovalent cations, such as potassium and ammonium ions, may make important contributions.

Catalytic Requirements of RNA and Protein Enzymes

In many aspects, protein and RNA enzymes face the same main challenge in catalysis: stabilizing the most unstable species formed during the chemical reaction, called the transition state. Like protein enzymes, RNA catalysis requires the formation of a specific tertiary structure and is sensitive to mutations in the RNA. Under optimized conditions, ribozymes can be as efficient as protein enzymes. For example, the hepatitis delta virus (HDV) ribozyme carries out phosphodiester bond cleavage ($10^2 - 10^4\ s^{-1}$) as fast as the protein enzyme RNase A ($1.4 \times 10^3\ s^{-1}$) at room temperature. However, catalysis by RNA enzymes differs from protein enzymes in several ways. First, since RNA contains only four unique nucleotide bases while proteins are composed of 20 different amino acids, RNA lacks the diverse functional groups characteristic of protein enzymes. This fact potentially limits the range of mechanisms that can be catalyzed by RNA. Nonetheless, small RNAs that can catalyze diverse chemical reactions have been selected in the laboratory from large pools of RNA molecules, in experiments termed *in vitro* selection. Second, the amino acid side chains are mainly located on the outside of protein secondary structures (α-helices or β-sheets) where they can form tertiary and quaternary contacts, while the chemical groups of the RNA bases are largely on the interior of base-paired duplexes. The third way that RNA and protein enzymes differ is that the proteins fold around a central hydrophobic core, whereas RNA usually folds by the packing of domains around a central conserved region. The high density of negative charges and the flexibility of the phosphate backbone of RNA could prevent RNA from forming stable active-site pockets. These differences affect how RNA and protein enzymes function.

The lack of diverse functional groups in RNA molecules and the propensity for RNA to bind metal ions led to the early hypotheses that all ribozymes require bound divalent metal ions to catalyze chemical reactions. However, small ribozymes, such as the hairpin and hammerhead ribozymes, can both fold and catalyze phosphodiester bond cleavage in the presence of monovalent ions (i.e., Na^+, Li^+, and NH_4^+) without any divalent cations. These small enzymes perform site-specific strand scission reactions using base-pairing and other interactions to align the cleavage site to the ribozyme active site. Current data indicate that cleavage reactions catalyzed by RNA enzymes use diverse mechanisms.

The examples of RNA enzymes described below are those whose catalytic mechanisms are among the best characterized. There are still many RNA reactions in which the catalytic mechanisms have not yet been elucidated.

Metalloribozymes

Ribonuclease P

Ribonuclease P (RNase P) catalyzes site-specific hydrolysis of precursor tRNA substrates to produce 5′-phosphate and 3′-hydroxyl end groups. This reaction is essential for the formation of mature tRNA required for protein translation. In bacteria, RNase P consists of one catalytically active RNA and one protein subunit. RNase P enzymes in eukaryotes contain multiple protein subunits. The bacterial RNA component alone is capable of catalyzing the cleavage of multiple substrate tRNAs in the presence of high salt. The protein

component is required for cleavage by RNase P *in vivo* and increases the catalytic efficiency *in vitro*. Evidence that RNase P is a metalloenzyme comes from several experimental observations. First, catalytic activity is observed only in the presence of divalent cations such as Mg^{2+} or Mn^{2+}, even though the RNA component forms a native-like structure in the absence of divalent cations. Second, the substitution of phosphate oxygen atoms with sulfur atoms at the phosphodiester bond that is cleaved in precursor tRNA leads to a significant decrease in catalytic activity in the presence of Mg^{2+}, which prefers to coordinate oxygen atoms. The decrease in the catalytic activity is less in the presence of Mn^{2+} or Cd^{2+} which can more readily coordinate the sulfur atom, suggesting that a metal ion may directly coordinate to the phosphate oxygen to enhance catalysis. These observations have led to a model for the RNase P catalyzed cleavage reaction (Figure 1A). In this model, a hydroxide ion, or metal-coordinated hydroxide, attacks the phosphate atom at the same time as the phosphate–oxygen bond begins to break. In the transition state, the phosphate atom has trigonal-bipyramidal geometry. This model is very similar to the catalytic mechanism of phosphoryl transfer reactions catalyzed by many protein enzymes. The essential metal ion(s) have been proposed to play multiple roles, including activation of the water nucleophile and stabilization of the developing negative charge in the transition state. The exact position and function of the catalytic metal ions in this reaction have not been completely elucidated.

Self-Splicing Introns

Introns are small segments of noncoding RNA that are interspersed among the regions of mRNA that code for protein. Prior to translation, these segments must be removed to form a mature mRNA. Certain intron sequences contain a common secondary structure core and use a common mechanism to catalyze excision of the RNA, termed self-splicing. This self-splicing reaction is a two-step transesterification reaction. In group I introns, self-splicing is initiated by nucleophilic attack of an exogenous molecule of guanosine. In a second type of reaction used by group II introns, the 2′-hydroxyl group of a specific adenosine within the intron acts as the nucleophile. Metal ions, Mg^{2+} and/or Mn^{2+}, are essential for the self-splicing reaction catalyzed by group I and II introns. A recent model for the transition state of the group I intron from *Tetrahymena*, based on kinetic assays of metal-dependent activity in introns containing single sulfur atom substitutions, suggests that up to three metal ions are catalytically important. In addition to promoting the formation of the correct active site structure, the catalytically important metal ions are proposed to correctly position the substrates with respect to the catalytic groups, activate the nucleophilic attack by deprotonating the 2′ hydroxyl group of the guanosine, and stabilize the developing negative charge in the transition state (Figure 1C).

Small Ribozymes that do not Require Divalent Metals

A number of small, virally encoded ribozymes have been identified, including the hammerhead, the hairpin, the HDV, and the *Neurospora* Varkud satellite (VS) ribozymes. These ribozymes are distinguished from each other by different secondary and tertiary structures. However, they all catalyze the nucleophilic attack of a 2′-hydroxyl on the neighboring 3′ phosphate to form a 2′–3′ cyclic phosphate (Figure 1B). Since this is not an irreversible reaction, these ribozymes are also observed to catalyze religation. This class of ribozymes retains significant catalytic activity with high concentrations of monovalent cations and no divalent cations, suggesting a mechanism that is different than that used by RNase P and self-splicing introns. In these ribozymes, the phosphoryl transfer reaction is proposed to be catalyzed by a general acid–base mechanism, similar to reactions catalyzed by protein RNases. The 2′-hydroxyl adjacent to the scissile phosphate is activated for nucleophilic attack by abstraction of a proton by a basic group. Concurrently, a proton is donated to stabilize the developing negative charge on the leaving group oxygen (Figure 1B).

Acid–base chemistry was not initially considered for RNA-catalyzed reactions, since there are no functional groups in ribonucleotides that can be protonated near neutral pH. In RNA, the pK_a values of the ring nitrogens of adenine and cytosine are between 3.5 and 4.1. However, in the folded RNA, the environment around the ionizing group can significantly alter the pK_a of a group. The first evidence of acid–base catalysis was observed in the HDV ribozyme when the catalytic activity of a mutant ribozyme could be partially rescued by the addition of exogenous imidazole, proposed to function as a general acid–base catalyst. A similar function has been proposed for a conserved and catalytically important guanosine of the hairpin ribozyme based on its proximity to the 2′ hydroxyl group near the scissile phosphodiester bond in the active site, as observed in the X-ray crystallographic studies. Therefore, general acid–base catalysis may be a common mechanism for RNA-mediated reactions. However, it is difficult to test this mechanism unambiguously since chemical modification or mutations of the nucleotides may perturb both chemical interactions and the structure of the RNA.

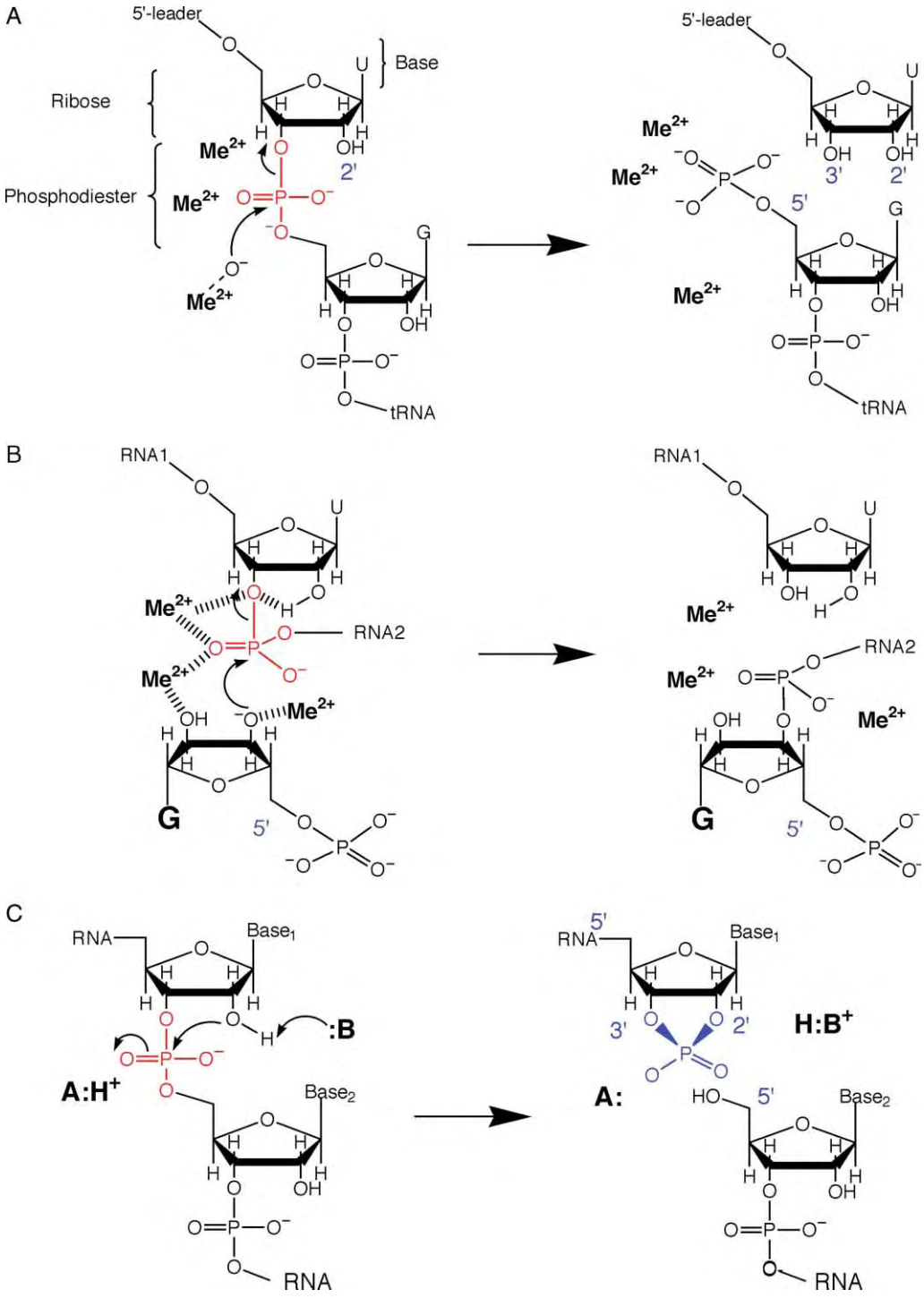

FIGURE 1 Models for ribozyme-catalyzed reactions. The phosphodiester bond is colored red. (A) Metal-mediated reaction catalyzed by RNase P. As many as four metal ions (Me) are proposed to enhance this reaction. One of the products has a 3′ hydroxyl group and the mature tRNA product contains a 5′ phosphate group. (B) General acid–base mechanism proposed for the reaction catalyzed by hammerhead or HDV ribozyme. The 2′-hydroxyl adjacent to the scissile phosphodiester is activated by a base (:B) for nucleophilic attack. Concurrently, a proton is donated to stabilize the developing negative charge on the leaving group oxygen. Note that one of the products is a 2′–3′ cyclic phosphate (in blue), and the other, a 5′ hydroxyl group. (C) Proposed metal-catalyzed mechanism for RNA cleavage catalyzed by the *Tetrahymena* group I intron.

Summary

RNA-catalyzed reactions are ubiquitous and important in many processes. Due to the limited range of functional groups and naturally occurring structure motifs, it is surprising that RNA enzymes can function as well as protein enzymes. The general catalytic strategies used by both biological catalysts appear to be similar; RNA and protein enzymes both use acid-base groups and metal ions to activate nucleophiles and to stabilize developing charge on the leaving group. Both types of enzymes use a variety of strategies to stabilize the transition state and thereby enhance the reaction rate.

See Also the Following Articles

Ribosome Assembly • Ribosome Structure • Ribozyme Structural Elements: Group I Introns • Ribozyme Structural Elements: Hairpin Ribozyme • Ribozymes and Evolution • RNA Editing • RNA Polymerase I and RNA Polymerase III in Eukaryotes • RNA Polymerase II and Basal Transcription Factors in Eukaryotes • RNA Polymerase II Elongation Control in Eukaryotes • RNA Polymerase II Structure in Eukaryotes • RNA Polymerase Reaction in Bacteria • RNA Polymerase Structure, Bacterial • T7 RNA Polymerase • Translation Termination and Ribosome Recycling

Glossary

catalysis Process by which the speed of a chemical reaction is enhanced by stabilization of unstable species formed during the reaction.

introns Regions in the precursor messenger RNA that do not code protein sequences.

***in vitro* selection** Process in which a large pool of different RNA molecules is prepared and RNAs with specific properties (such as catalytic activity) are selected based on these properties.

phosphodiester A functional group containing two alcohols attached to an oxygen atom in a single phosphate group. A phosphodiester bond links adjacent nucleotides in both DNA and RNA.

ribonuclease P A ribonucleoprotein complex that catalyzes cleavage of the 5′ end of the precursor transfer RNA to form mature tRNA.

ribonucleoprotein (RNP) Cellular particles consisting of both RNA and protein components. Known RNP's include the ribosome, ribonuclease P, and the spliceosome.

ribosome A cellular complex made up of ribosomal RNA and proteins that carries out protein synthesis using messenger RNA sequences as templates.

ribozyme An RNA molecule that catalyzes biological reactions.

RNA folding The process by which an RNA molecule forms a compact, tertiary structure through formation of specific interactions, including hydrogen-bond interaction between bases.

RNA World A hypothetical time in the early evolution of life when RNA functioned both as the sole genetic material, and as catalyst for biological reactions.

spliceosome Complexes made up of small nuclear RNA and protein that remove noncoding regions from precursor messenger RNA.

telomere A noncoding, repetitive DNA sequence located at the terminus of a chromosome.

transition state The highest energy species formed during the chemical transformation of a substrate into a product.

Further Reading

Cech, T. R. (2002). Ribozymes, the first 20 years. *Biochem. Soc. Trans.* **30**, 1162–1166.

DeRose, V. J. (2002). Two decades of RNA catalysis. *Chem. Biol.* **9**, 961–969.

Doudna, J. A., and Cech, T. R. (2002). The chemical repertoire of natural ribozymes. *Nature* **418**, 222–228.

Fedor, M. J. (2002). The role of metal ions in RNA catalysis. *Curr. Opin. Struct. Biol.* **12**, 289–295.

Orgel, L. F. (1994). The origin of life on earth. *Sci. Am.* **October**, 77–83.

Steitz, T. A., and Moore, P. B. (2003). RNA, the first macromolecular catalyst: The ribosome is a ribozyme. *Trends Biochem. Sci.* **28**, 411–418.

Biography

John (Chang-tai) Hsieh holds a Ph.D. from Washington University in Saint Louis, and is a postdoctoral research fellow at the University of Michigan. His research interests have been in the catalytic properties of enzymes in nucleic acid metabolisms. With Dr. Fierke, his research focuses on the elucidation of the kinetic properties of the ribonuclease P.

Carol Ann Fierke received her Ph.D. from Brandeis University and was an NIH postdoctoral fellow at the Pennsylvania State University. She was appointed as an Assistant Professor of Biochemistry at Duke University Medical Center and was promoted to associate professor. She then moved to the University of Michigan, where she is appointed as the Jerome and Isabella Karle Collegiate Professor of Chemistry and Professor of Biological Chemistry. Her research focuses on mechanisms of biological catalysis in metalloenzymes and ribozymes.

Ribozyme Structural Elements: Group I Introns

Barbara L. Golden
Purdue University, West Lafayette, Indiana, USA

Many eukaryotic genes are interrupted by segments of DNA called intervening sequences or introns. These introns are transcribed into RNA along with the coding segments of gene, called exons. In most cases, the introns are removed from the RNA by a cellular apparatus called the spliceosome. In the presence of biologically relevant concentrations of magnesium and guanosine nucleoside, some introns, called group I introns, are capable of self-splicing: excising themselves from the flanking RNA, and religating the RNA exons to form a functional RNA. Group I introns are the relics of selfish genetic elements that carried with them genes encoding enzymes capable of integrating the entire genetic element into cellular DNA. The self-splicing activity of the RNA transcript allowed the element to have minimal impact upon the host gene. Group I introns are found within a diverse variety of genes including those encoding the energy transducing machinery in mitochondria, ribosomal RNAs, tRNAs, and phage genes. By appropriate engineering, a group I intron can be converted into a multiple turnover RNA enzyme, or ribozyme, capable of cleaving single-stranded RNA substrates. The catalytic activity of these molecules depends on accurate folding into a three-dimensional structure that precisely positions both functional groups on the RNA and divalent metal ions to catalyze a specific phosphotransesterification reaction.

The Self-Splicing Reaction

The self-splicing reaction of group I introns is accomplished by two sequential phosphotransesterification reactions (Figure 1A). In the first step of splicing, a guanosine nucleoside substrate (guanosine, GMP, GDP, or GTP) is bound by the intron and positioned for nucleophilic attack at the 5′ splice site. The 3′-OH of the guanosine attacks at the phosphorus of the 5′ splice site and displaces the 3′-OH of the 5′ exon. This reaction results in release of the 5′ exon, and covalent attachment of the guanosine molecule to the intron. In the second step of splicing (Figure 1A), a conserved guanosine at the 3′ end of the intron (called ωG) is positioned by the intron in a manner similar to binding of the exogenous guanosine substrate in the first step of splicing. In a reaction chemically analogous to the reverse of the first step of splicing, the 3′-OH of the 5′ exon displaces the 3′-OH of ωG from the phosphate at the 3′ splice site. Ligation of the 5′- and 3′ exons, and release of the intron results.

Secondary Structure

Structured RNAs, such as tRNAs, ribosomal RNAs, and ribozymes do not have extended linear structures; they are folded. While not completely double-stranded-like genomic DNA, they have short base-paired regions formed from self-complementary sequences within the primary structure of the RNA. Group I introns have a conserved secondary structure consisting of a series of double-stranded regions labeled P1–P9 (Figure 2). These helical regions are linked by "single-stranded," or joining, stretches of RNA labeled for the two helices that they connect (e.g., J8/7) and are capped by loops designated with an "L." While most joining and loop regions are not involved in forming Watson–Crick base pairs, they usually form well-defined structures, including base pairs. These helices, loops, and joining nucleotides are organized into three domains designated P1–P2, P3–P9, and P4–P6 (Figure 2).

The P1–P2 domain, or substrate domain, spans the 5′ end of the molecule and contains the 5′ splice site, which is located within the short helix P1. The final nucleotide in the 5′ exon is a uridine, which is base-paired to guanosine on the complementary RNA strand of the intron, forming a G·U wobble base pair. The P3–P9 domain immediately follows the P1–P2 domain in the primary structure of the intron. This domain contains the helix P7 that binds to an exogenous guanosine substrate in the first step of splicing, and to ωG in the second step of splicing. The P3–P9 domain also contains a single-stranded stretch of 5–6 nucleotides called J8/7 that is involved in binding and positioning the P1 helix, and thereby the 5′ splice site. The P3–P9 domain is interrupted by the P4–P6 domain. The P4–P6 domain folds together with the P3–P9 domain, to comprise most, if not all, of the catalytic core of the intron.

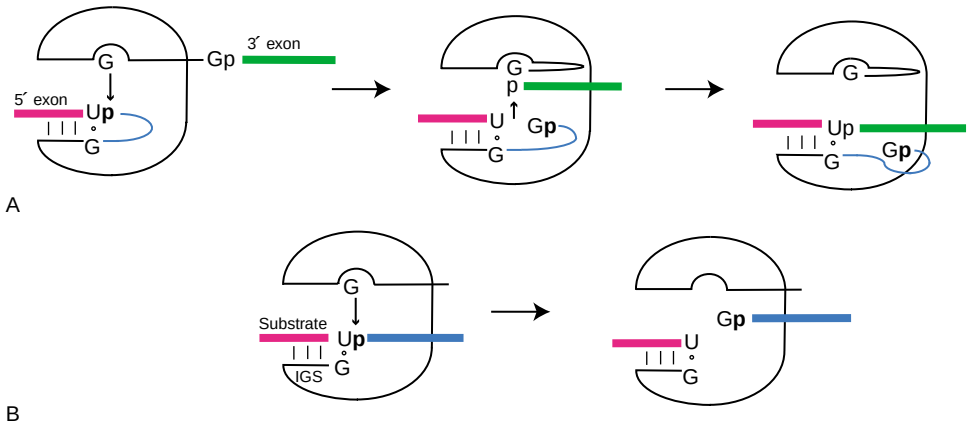

FIGURE 1 Reactions of group I intron RNAs. A. The self-spicing reaction is initiated by binding of a guanosine nucleoside. The 3′-OH of the nucleoside is activated for attack at the 5′ exon–intron junction. In the first step of splicing the guanosine becomes covalently attached to the intron, and the 5′ exon (pink) is cleaved from the intron (blue). In the second step of splicing, the 3′-OH of the 5′ exon attacks at the junction of the intron and the 3′ exon (green). This reaction links the 5′ and 3′ exons and releases the intron. B. The intron can be converted into a ribozyme capable of cleaving an RNA substrate using a guanosine nucleoside. The substrate RNA, like the 5′ exon in the self-splicing molecule, can base-pair to the 5′ end of the ribozyme that is called the IGS (G = guanosine, GMP, GDP, or GTP).

This domain also participates in splice-site recognition by binding the guanosine within the G·U wobble base pair at the 5′ splice site.

Tertiary Structure

The secondary structures in the intron fold in a magnesium-dependent manner to form a compact tertiary structure much like a globular protein enzyme (Figure 3). Formation of the folded structure is absolutely dependent on divalent metal ions, usually Mg (II), which serve to stabilize the structure by neutralizing the negative charges of the phosphate groups on the RNA backbone and by organizing the RNA into specific structures required for proper folding. In crystal structures of group I intron domains, magnesium ions are seen bound within the major groove, mediating the close approach of RNA helices, and stabilizing unusual conformations that allow the formation of intramolecular RNA–RNA contacts. Folding of the RNA creates binding sites for the P1 helix and the guanosine nucleotide cofactor described below.

The tertiary structure of group I introns has been investigated from two opposite directions. Fragments of group I introns have been crystallized to generate models of the three-dimensional structure. These studies have provided high-resolution structural information for one of the domains, medium-resolution structural information for a second domain, and no structural information for the third domain. Complementary work has been performed to elucidate contacts between individual atoms within the ribozyme as it approaches the transition state. These data can be put together to help elucidate the structural basis for group I intron catalysis.

The crystal structure of the P4–P6 domain of a group I intron reveals many of the strategies used by RNAs to form tertiary structures. Perfectly double-stranded helical RNAs do not tend to form stable tertiary structures. The structural information encoded by the RNA sequence is sequestered within the base pairs of a perfect helix, and the exposed, accessible surface is limited to the backbone and the shallow minor groove.

To facilitate tertiary structure formation, "flaws" in the helices are often present, containing base pairs other than the standard Watson–Crick A–U and G–C base pairs. These can readily form in between helices and, when present, they distort the major and minor grooves of the double-stranded helix to create distinct shapes and to expose hydrogen-bonding groups on the bases. This forms complementary surfaces that allow RNA domains to pack together. Loops, particularly four nucleotide sequences called tetraloops, which cap helices can also form distinct structures that mediate long-range tertiary interactions. These interactions are further stabilized by hydrogen bonds that can form between the 2′-OH groups of the ribose backbone. These tertiary structures are termed "ribose zippers."

Substrate Recognition

Group I introns have binding sites for two substrates: a guanosine nucleophile and a short duplex containing a G·U wobble base pair.

The Guanosine-Binding Site

The guanosine cofactor (in the ribozyme reaction and in the first step of splicing) and ωG (in the second step of

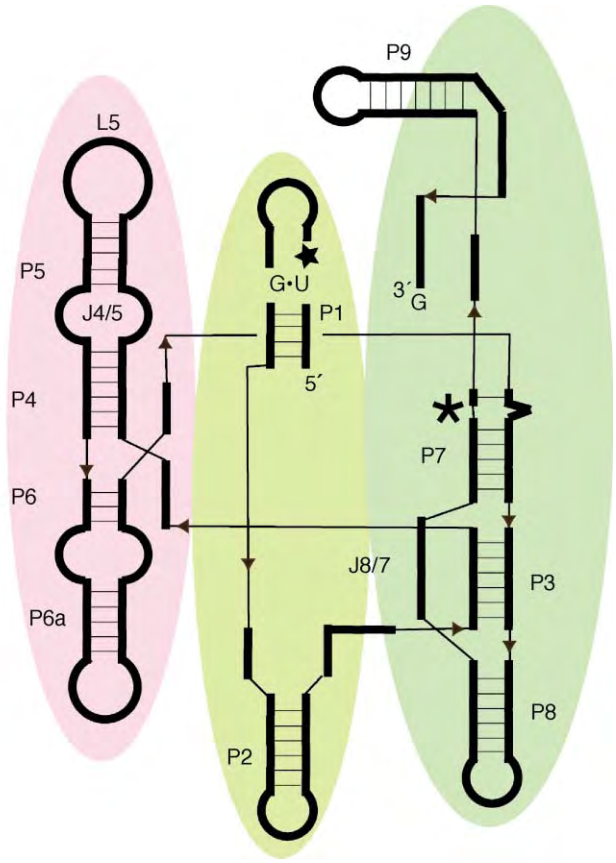

FIGURE 2 Secondary structure of a group I intron. The sequence of a group I intron folds into a secondary structure containing a series of base-paired regions called P1–P9. These short duplexes are linked by "single-stranded" nucleotides designated "J" and capped with loop sequences designated "L." These secondary structural elements are organized into three domains termed P1–P2, P3–P9, and P4–P6 that are shaded yellow, green, and pink, respectively. The P1 helix is formed by base pairing between the 5′ end of the ribozyme and the 5′ intron. Folding of the ribozyme brings the 5′ splice site (★) and the guanosine substrate binding site (∗) into proximity.

splicing) are recognized by a single guanosine-binding site located in the major groove of helix P7, a distorted double helix with a narrowed major groove. A G–C base pair near the "top" of the P7 helix provides significant specificity for the guanosine base. Recognition of the guanosine base can largely be described as a base triple. Additional orientation of the ribose group of the guanosine comes from magnesium ions bound at the intron's active site (Figure 4).

Helix P1 and 5′ Splice-Site Recognition

The 5′ splice site is recognized in the context of a short double-stranded region called P1. In self-splicing introns, helix P1 is formed by intramolecular base pairing between the 5′ exon and a complementary sequence near the 5′ end of the intron, creating a stem-loop structure (Figure 2). The helix is 3–6 bp in length, depending on the specific intron, and the final base pair is a G·U wobble pair composed of the last nucleotide in the 5′ exon, and a guanosine near the 5′ end of the intron. G·U wobble pairs, like A–U base pairs, contain two hydrogen bonds between the two bases (Figure 4), but the geometry of the pair is slightly altered compared to a Watson–Crick base pair: the guanosine base is pushed slightly into the minor groove and the uridine base is pushed slightly into the major groove. This base pair can be readily incorporated into an RNA double helix and is about as stable as an A–U base pair.

The intron may be converted into a ribozyme by splitting the P1 helix into two molecules (Figure 1). The first strand is formed from the very 5′ end of the ribozyme and is called an internal guide sequence (labeled IGS in Figure 1). The second strand serves as

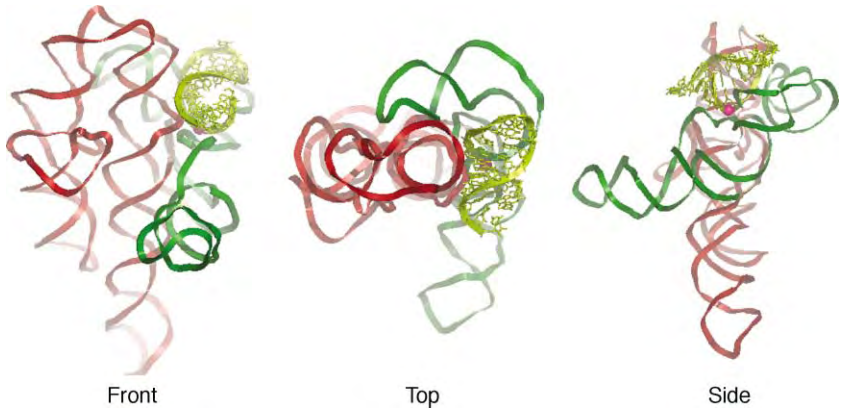

FIGURE 3 The three domains of a group I intron packed closely together to create an active site made of RNA. The model consists of the crystal structure an RNA spanning the P4–P6 (red) and P3–P9 (green) domains of a group I intron from *Tetrahymena* ribosomal RNA. Docked into the active site is a model of helix P1 that contains the 5′ splice site helix (yellow). The phosphorus atom at the 5′ splice site is drawn as a magenta sphere. The P1 helix is bound and positioned by cooperative action of the P4–P6 and P3–P9 domains.

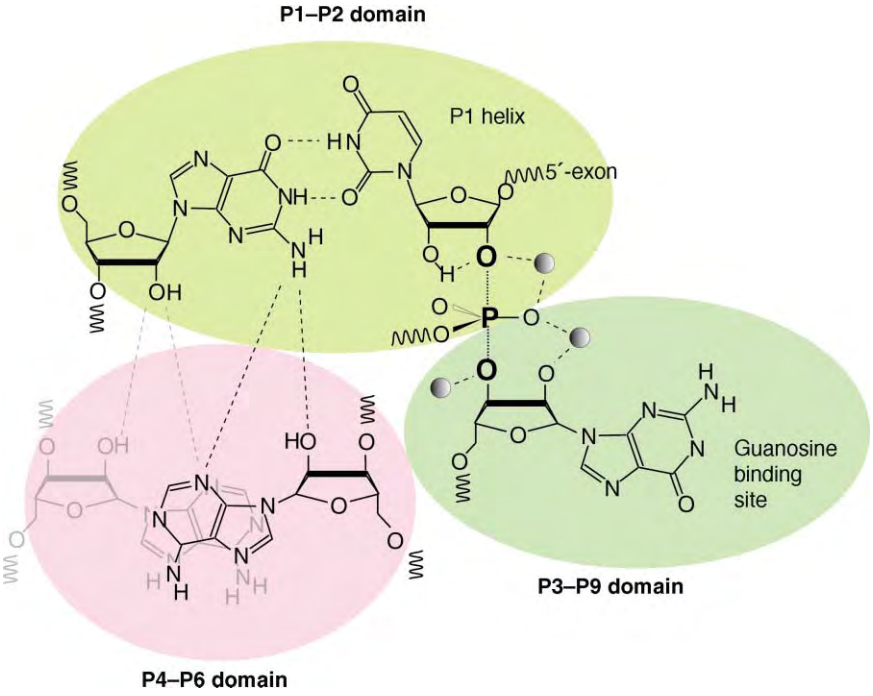

FIGURE 4 Interactions between the three domains in the transition state. Near the transition state for the ribozyme reaction, the bond between the 5′ exon and the intron is partially broken and the bond between the guanosine substrate and the intron is partially formed. Three magnesium ions help orient the substrates and stabilize the transition state, facilitating catalysis. The G·U wobble at the 5′ splice site is shaded yellow. The guanosine bound in the guanosine-binding site is shaded green. Adenosines within the P4–P6 domain involved in positioning the G·U wobble are shaded pink. Magnesium ions that participate in catalysis are drawn as spheres. Hydrogen bonds and metal interactions are indicated by dashed lines, and partial bonds are indicated by dotted lines.

a substrate for the ribozyme. It is complementary to the first strand, maintains the G·U wobble base pair, and extends for at least one nucleotide beyond the cleavage or splice site.

P1, whether composed of a hairpin in the self-splicing intron or composed of an intermolecular duplex in a ribozyme form, docks into the active site of the ribozyme. Docking is stabilized by interactions between the single-stranded region J8/7 and the minor groove of P1. These contacts are primarily hydrogen bonds to the ribose backbone and, therefore, are sequence independent. Except for the G·U wobble base pair, identity of base pairs within the P1 helix is not critical for recognition. Thus, by appropriate variation of the nucleotides in the IGS, almost any RNA substrate containing a uridine can be recognized and cleaved by a group I ribozyme.

The guanosine of the G·U wobble base pair is recognized by the J4/5 region of the P4–P6 domain. The J4/5 region contains tandem A·A non-Watson–Crick base pairs that interact with the exocyclic amine and the 2′-OH of the guanosine in the wobble pair (Figure 4). With the ribozyme "pinched" down upon the guanosine in the wobble pair, the phosphate that follows the uridine is placed in an optimal position to interact with the guanosine nucleophile and the intron's active site. The requirement for a G·U instead of a G–C Watson–Crick base pair at this position can be attributed to two characteristics of this special base pair. First, the exocyclic amine of the guanosine is displaced into the minor groove, allowing it to hydrogen bond to the J4/5 region. The exocyclic amine of a guanosine within a G–C base pair is involved in hydrogen bonding to the cytosine and is, therefore, sterically occluded from this interaction. Second, if the guanosine base in a G·U base pair is superposed on the guanosine G–C base pair, the position of the pyrimidine (U or C), and therefore the phosphate at the 3′ position, is quite different in the two structures. Displacement of the uridine towards the major groove as occurs in a wobble base pair is required to place the phosphate at the 5′ splice site into the active site of the intron.

In summary, group I introns may be thought of as RNA restriction endonucleases, capable of recognizing double-stranded RNA and specific for cleavage at G·U wobble base pairs. The catalytic activity of group I introns is dependent on proper folding of the RNA into a stable three-dimensional structure containing three domains. The three domains act cooperatively to position the 3′-OH of the guanosine nucleophile, the 5′ splice-site phosphate, and at least three magnesium

ions bound in the heart of the ribozyme (Figure 4), and thereby promote catalysis.

See Also the Following Articles

Ribozyme Mechanisms • Ribozymes and Evolution • Spliceosome

Glossary

exons Segments within a gene that encode a functional cellular protein or RNA.

introns Noncoding DNA sequences that interrupt functional genes and are removed by splicing once the gene has been transcribed into RNA.

RNA splicing Process by which intervening sequences are removed from a transcribed RNA and the flanking exons are joined to make a functional cellular RNA.

Further Reading

Cate, J. H., Gooding, A. R., Podell, E. R., Zhou, K., Golden, B. L., Kundrot, C. E., Cech, T. R., and Doudna, J. A. (1996). Crystal structure of a group I ribozyme domain: Principles of RNA packing. *Science* **273**, 1678–1685.

Golden, B. L., and Cech, T. R. (1999). Building a catalytic active site using only RNA. In *The RNA World* (R. F. Gesteland, T. R. Cech and J. F. Atkins, eds.) 2nd edition, pp. 321–349. Cold Spring Harbor Laboratory Press, Cold Spring Harbor, NY.

Golden, B. L., Gooding, A. R., Podell, E. R., and Cech, T. R. (1998). A preorganized active site in the crystal structure of the *Tetrahymena* ribozyme. *Science* **282**, 259–264.

Shan, S.-O., Kravchuk, A. V., Piccirilli, J. A., and Herschlag, D. (2001). Defining the catalytic metal ion interactions in the *Tetrahymena* ribozyme reaction. *Biochemistry* **40**, 5161–5171.

Strobel, S. A., and Doudna, J. A. (1997). RNA seeing double: Close-packing of helices in RNA tertiary structure. *TIBS* **22**, 262–266.

Biography

Barbara Golden is an Associate Professor in the Department of Biochemistry at Purdue University. Her research interests include the structural biology of catalytic RNAs and RNA-binding proteins. She holds a Ph.D. from Duke University and received postdoctoral training at the University of Colorado.

Ribozyme Structural Elements: Hairpin Ribozyme

Adrian R. Ferré-D'Amaré
Fred Hutchinson Cancer Research Center, Seattle, Washington, USA

The hairpin ribozyme is an RNA that catalyzes sequence-specific cleavage and ligation of the phosphate backbone of its RNA substrate. Two short irregular double helices, stems A and B, dock to form the active RNA. The scissile phosphate is in stem A. The reaction catalyzed by this RNA requires that the reactive groups adopt an in-line conformation. Prior to docking, the conformation of stem A is such that the reaction cannot take place. Docking of stems A and B results in a dramatic rearrangement that produces a reactive, in-line substrate conformation. Comparison of structures of the hairpin ribozyme in complex with a noncleavable substrate mimic, a transition-state mimic, and the cleavage products shows that the ribozyme has an active site with a rigid arrangement of purine bases that make more hydrogen bonds to the transition state than to the precursor or products, thus lowering the activation energy of the reaction. Because RNAs have less chemical diversity than proteins, catalytic strategies such as precise reactive group orientation and transition state stabilization are important for ribozyme function.

Biological Context

Four RNAs that catalyze RNA cleavage and ligation through transesterification have been identified from natural sources: the hammerhead, hairpin, hepatitis delta virus (HDV), and Varkud satellite (VS) ribozymes. In nature, all four function in the life cycle of satellite RNAs of viruses, or a replication intermediate of a plasmid (VS). In all cases, the ribozyme domain is part of a larger circular RNA that is replicated through a rolling-circle mechanism by host RNA polymerases. The linear concatamers produced by rolling-circle replication self-cleave into unit-length RNA molecules. These can then be ligated (either by the RNA itself or by a different catalyst) into circles. These circles, which are complementary in sequence to the infecting circular RNA, undergo an equivalent replication/self-cleavage/ligation cycle to produce copies of the original RNA.

The domain responsible for cleavage and ligation of the minus strand of the satellite of tobacco ringspot virus (-sTRSV) was mapped by deletion analysis. When synthesized *in vitro*, this RNA domain can act as a multiple turnover catalyst. This is the hairpin ribozyme. Because of its small size (constructs less than 60 nucleotides in length are active *in vitro*) the hairpin ribozyme has been amenable to extensive genetic, biochemical, and structural analysis, and constitutes one of the paradigms of catalytic RNA.

Primary and Secondary Structures

The minimal sequence elements required for hairpin ribozyme activity *in vitro* are contained in two helical segments, stems A and B (Figure 1). Each stem comprises a central portion of conserved nucleotides that engage in nonstandard base pairing or are unpaired (these are referred to as loops A and B in the older literature), flanked on both sides by canonical Watson-Crick base-paired duplexes. As long as base pairing is maintained, the sequences of these flanking duplexes can be varied arbitrarily.

One of the strands of stem A is the substrate RNA. As indicated in Figure 1, the cleavage site can be preceded by any nucleotide (position − 1), but must be followed (position + 1) by a G residue. Three other residues on the substrate strand are conserved at positions − 2, +2, and + 3. As long as these four nucleotides are present in the correct order in a substrate, a hairpin ribozyme can be engineered to cleave it by making the sequence of the Watson–Crick segments of the other strand of stem A complementary to the sequence of the target RNA.

Tertiary Structure

Stems A and B can be synthesized as separate molecules, and mixed to reconstitute activity in the test tube. The two stems associate with modest affinity to form the active species. In the biological RNA, stems A and B are connected to each other as part of a four-helix junction. The four-helix junction increases the

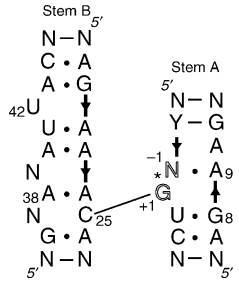

FIGURE 1 Schematic secondary structure of the core of the hairpin ribozyme. Two irregular double helices, stems A and B, dock to form the active ribozyme. One of the strands of stem A is the substrate, and carries the scissile phosphate (* , flanked by the two nucleotides shown in outline letters). Nucleotides whose identity is essential to function are identified in single letter code (A, C, G, U), those that can be varied freely without compromising activity, as N. Y denotes either pyrimidine. Thin lines denote Watson–Crick pairs, black circles, noncanonical pairs. Numbering is according to convention. Note the interhelical Watson–Crick base pair between G + 1 (in the substrate strand of stem A) and C25 (stem B).

local concentration of stems A and B and places the two stems in the optimal orientation relative to each other. Constructs that incorporate the junction are much more active *in vitro* than the two isolated stems, or even the two stems connected by a flexible linker. Four-helix junction constructs of the hairpin ribozyme bind two equivalents of divalent metal ions with high affinity and, upon metal ion binding, undergo a conformation rearrangement at the junction that brings the conserved, noncanonical segments of stems A and B into close spatial proximity.

The three-dimensional structure of a four-helix junction form of the hairpin ribozyme was determined by X-ray crystallography. Stems A and B were revealed to be highly irregular (with stem B particularly overwound), and to associate through their minor groove faces (Figure 2). The interhelical interface buries $\sim 1600 Å^2$ of solvent accessible surface area, implying that considerable binding energy is available from docking of the stems. The scissile phosphate lies at the interface of the two stems, surrounded by the purine bases of residues 8, 9, 10, and 38. These four nucleotides are all highly conserved (Figure 1) and have been shown by mutagenesis experiments to be essential for catalysis.

The structures of the isolated stems A and B were determined by nuclear magnetic resonance spectroscopy. Comparison of their free and docked structures shows that both stems undergo dramatic conformation rearrangements upon association. Only two out of nine noncanonical base pairs that constitute the core of the docked ribozyme are present in the free stems. Of particular importance is the extrusion of the base of G + 1 from the stem-A helical stack upon assembly of the ribozyme. As can be seen in Figure 2B, this base forms part of an interhelical pair in the docked

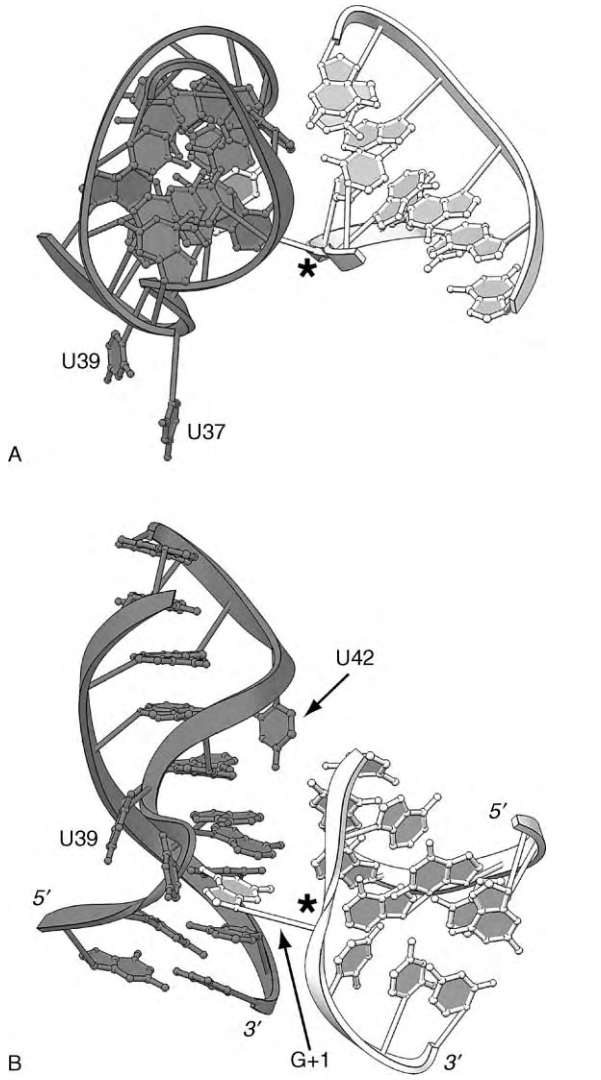

FIGURE 2 Simplified representation of the three-dimensional structure of the hairpin ribozyme. The RNA backbone is depicted as a ribbon; nucleotide bases are shown in ball-and-stick representation. Stem A is in white; stem B in dark gray. The position of the scissile phosphate is indicated byasterisk. Panel A is a view orthogonal to panel B. The scissile phosphate is buried in the interface of the two irregular helices.

ribozyme. G + 1 forms a Watson–Crick pair with C25 (from stem B; see also Figure 1).

The S_N2 (bimolecular nucleophilic substitution) reaction catalyzed by the hairpin ribozyme requires that the 2′-OH nucleophile and the 5′-oxo leaving groups be aligned with the phosphorus of the scissile phosphate. Prior to docking, the conformation of stem A is such that the reaction cannot take place. Extrusion of G + 1 from stem A concomitant with docking results in a reactive, in-line substrate conformation. The ribozyme uses the energy resulting from formation of the interhelical interface to properly orient its substrate.

Catalytic Mechanism

Although divalent metal ions are essential for activity of the hairpin ribozyme, biochemical and structural studies have shown that these ions play a structural role, rather than acting as cofactors in the active site. The hairpin ribozyme is active in a variety of divalent cations. The ribozyme is also active when the divalent cations are replaced by the complex ion cobalt (III) hexammine. The amine ligands that coordinate the cobalt in this complex do not exchange with solvent ions. While cobalt hexammine mimics hydrated magnesium ion (with its six water ligands), it is incapable of making direct metal to RNA interactions (inner sphere coordination), or to bind water and activate it to act as a base. Full activity of the hairpin ribozyme in cobalt hexammine implies that the RNA does not need to make direct coordination with its bound metal ions, nor does it use the cations as cofactors for generating hydroxyl ions. The crystal structure of the docked hairpin ribozyme shows the locations of several bound metal ions. These are in the narrow major groove of stem B, not in the wide minor groove where the active site lies.

Crystal structures have been determined of the hairpin ribozyme in complex with a noncleavable substrate mimic, a transition-state mimic (Figure 3), and the cleavage products. Comparison of these structures shows that the ribozyme has an active site with a rigid arrangement of purine bases that make more hydrogen bonds to the transition state than to the precursor or products, thus lowering the activation energy of the reaction. Although this has not been demonstrated directly, it appears that the pK_a of one of the active site adenosines (A38, Figure 3) is shifted towards neutral pH, resulting in protonation of its N1 imino nitrogen. The positive charge thus acquired by this active-site adenosine may also aid in catalysis.

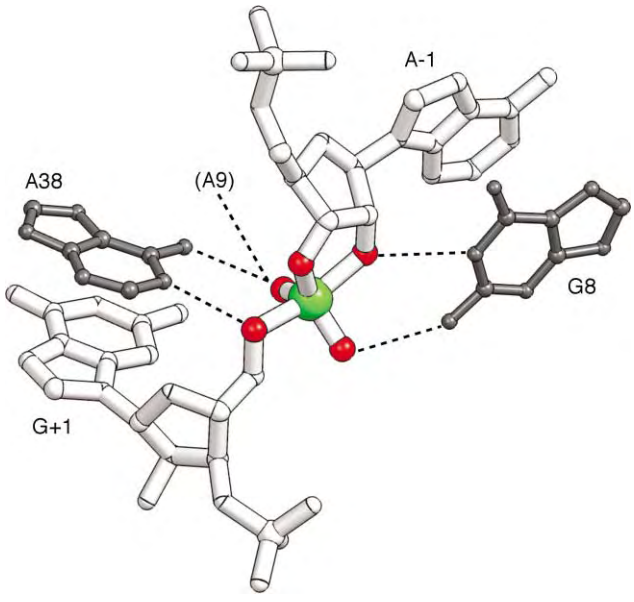

FIGURE 3 Structure of the active site of a transition-state mimic complex of the hairpin ribozyme. Vanadate (vanadium coordinated to five oxygens, three of which are provided by the RNA) mimics the trigonal bipyramidal coordination geometry of the scissile phosphate, which is pentavalent in the transition state. The vanadium atom is colored green, and the five oxygen atoms to which it coordinates are red.

Comparison with Other Ribozymes

Whereas protein enzymes can use 20 chemically varied amino acids to construct their active sites, ribozymes are limited to four nucleotides with limited functional group diversity. Studies on the group I intron, the first catalytic RNA discovered, demonstrated that this ribozyme overcomes the chemical limitations of RNA by recruiting multiple divalent cations into its active site. The group I intron uses these to orient reactive moieties, to activate water (to generate basic hydroxyl ions), and as sources of positive charge to stabilize negatively charged transition states. Early work on ribozymes assumed that RNA catalysts would always use cations as active-site cofactors.

We now know that ribozyme mechanisms can be more varied. Although isolated nucleotides do not have functional groups with near-physiologic pK_a, intricately folded RNA structures are capable of perturbing the acidities of purine and pyrimidine bases. For instance, the HDV ribozyme uses a cytosine whose pK_a is shifted from 4.2 to ~7 as a general acid catalyst (analogous to His119 in RNase A, a protein enzyme that catalyzes the same transesterification reaction as the hairpin ribozyme; see Figure 4). The hairpin ribozyme demonstrates

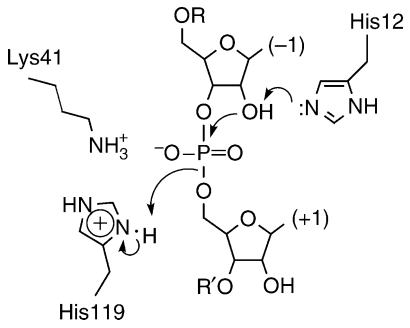

FIGURE 4 Catalytic mechanism of ribonuclease A. Histidine is particularly well suited to act as a general acid–base catalyst because its p*Ka* is close to physiologic pH. In RNase A, histidines 12 and 119 act as general base and acid, deprotonating the nucleophile and protonating the leaving group of the transesterification, respectively. Deprotonation of the 2′-OH makes it a better nucleophile, and protonation of the 5′-oxo leaving group lowers the energy of the product state. Lysine 41 (which has a positively charged side chain at physiologic pH) counteracts the increased negative charge at the scissile phosphate during the transition state, and thus helps lower the activation energy of the reaction.

another way in which a catalytic RNA can achieve catalysis: selective hydrogen bonding to one state of the reaction. Nucleotide bases are well suited for hydrogen bonding, and the ribozyme provides a rigid structure to orient them precisely. It appears that the ribosome also achieves catalyses (protein synthesis in this case) by precise orientation of functional groups, rather than general acid-base catalysis.

See Also the Following Articles

Ribozymes and Evolution • Ribozyme Mechanisms • Ribozyme Structural Elements: Group I Introns

Glossary

acid dissociation constant (pK_a) pH at which half the acid exists in the protonated form and the other half in the deprotonated, or conjugate-base, form.

four-helix junction Nucleic acid structure in which four double helices abut, and are connected by sharing of the strands between adjacent helices.

general acid–base catalysis Mode of chemical catalysis in which a functional group that is not water accelerates a chemical reaction by facilitating proton transfer.

minus strand The anti-sense strand of a single-stranded circular RNA. For infectious RNAs, the infecting strand is the plus strand. This gets copied into its complement (minus strand), which in turn is copied to regenerate the original species.

ribozyme Ribonucleic acid that acts as a catalyst, accelerating the rate of a chemical transformation without itself undergoing a permanent chemical change.

specific acid–base catalysis Chemical catalysis in which water functions as a base (in the form of the hydroxyl ion) or an acid (as a hydronium ion) to increase the rate of a reaction.

Further Reading

Fedor, M. (2002). The role of metal ions in RNA catalysis. *Curr. Opin. Struct. Biol.* **12**, 289–295.

Klostermeier, D., and Millar, D. P. (2002). Energetics of hydrogen bond networks in RNA: Hydrogen bonds surrounding G + 1 and U42 are the major determinants for the tertiary structure stability of the hairpin ribozyme. *Biochemistry* **41**, 14095–14102.

Murchie, A. I., Thomson, J. B., Walter, F., and Lilley, D. M. J. (1998). Folding of the hairpin ribozyme in its natural conformation achieves close physical proximity of the loops. *Molecul. Cell* **1**, 873–881.

Raines, R. T. (1998). Ribonuclease A. *Chem. Rev.* **98**, 1045–1065.

Rupert, P. B., and Ferré-D'Amaré, A. R. (2001). Crystal structure of a hairpin ribozyme–inhibitor complex with implications for catalysis. *Nature* **410**, 780–786.

Rupert, P. B., Massey, A. P., Sigurdsson, S. Th., and Ferré-D'Amaré, A. R. (2002). Transition state stabilization by a catalytic RNA. *Science* **298**, 1421–1424.

Ryder, S. P., and Strobel, S. A. (2002). Comparative analysis of hairpin ribozyme structures and interference data. *Nucleic Acids Res.* **30**, 1287–1291.

Biography

Adrian R. Ferré-D'Amaré is a Faculty Member in the Division of Basic Sciences of the Fred Hutchinson Cancer Research Center in Seattle. His principal research interests are in RNA catalysis and RNA–protein interactions. He received his Ph.D. from the Rockefeller University, and was a postdoctoral fellow at Yale University. He has developed procedures that facilitate the crystallization of RNA, and his laboratory was the first to obtain crystallographic "snapshots" of a catalytic RNA as it carries out its reaction.

Ribozymes and Evolution

Niles Lehman
Portland State University, Portland, Oregon, USA

Ribozymes, also known as ribonucleic acid (RNA) enzymes, have been known since the early 1980s when it was first discovered that RNA could catalyze chemical reactions. Previously it had been thought that all enzymes were proteins, but it is now clear that RNA-directed catalysis plays many important cellular functions, and that numerous ribozymes can be found in organisms spanning the tree of life. Notably, for example, we now realize that the catalytic core of the ribosome itself, the cellular machinery for protein synthesis, consists of RNA such that peptide-bond formation is catalyzed by ribosomal RNA. These findings suggest strongly that RNA, or some RNA-like molecule, was an integral piece of the earliest biochemical processes to evolve on the Earth. In 1986 Walter Gilbert coined the phrase "RNA World" to invoke a time during the coalescence of life when RNA was responsible for most if not all of the genetic transformations of the planet's first organisms. Ribozymes have thus played an important role in biological evolution and have recently been used to perform evolution experiments in the laboratory.

RNA

RNA is a polymer of ribonucleotides. RNA differs from DNA in three basic respects. First, RNA employs uracil as a nitrogenous base, in place of the thymine used in DNA. Second, RNA nucleotides possess a hydroxyl group at the 2′ position, while DNA is deoxygenated at that position to a proton. And third, RNA is more often found single stranded than DNA, which is typically completely base paired into a double helix. All three of these features help engender RNA with catalytic capabilities, although they also tend to make RNA chains less chemically stable than DNA. From an informational point of view, both DNA and RNA have the capability to store and transmit biological information through complementary base paring: C with G, and T(U) with A.

Catalytic RNA

RNA as an Enzyme

Enzymes are molecules that can catalyze a chemical reaction by lowering the activation energy needed to transit from reactants to products. Proteins, built up from amino acids of twenty or more varieties, are well known to perform catalysis in biological systems. RNA is built up from only four nucleotide varieties but still can perform catalysis. Similar to protein-directed catalysis, the basis for this is the acquisition of a three-dimensional structure that contains a catalytic pocket. Many ribozymes can speed up the rate of reaction 10^3- to 10^{11}-fold over the corresponding uncatalyzed rate, and can behave as true enzymes by "turning over," catalyzing more than one reaction event.

Chemistry

In the catalytic pocket, RNA usually relies on metal-ion coordination and one or more chemical strategies to accomplish catalysis. In some cases, the 2-hydroxy group itself can serve as a nucleophile to attack a chemical bond in the substrate molecule. In other cases, the chemical moieties on the nitrogenous bases (adenine, guanine, uracil, or cytosine) can act as acids or bases to stimulate a reaction. For example, it is now thought that peptide-bond formation in the heart of the ribosome is promoted by some type of interaction between amino acids and a phylogenetically invariant adenosine residue in the ribosomal RNA. In most cases, RNA must bind divalent metals such as magnesium to help properly position the substrate molecules in order to stabilize the transition state.

Classes of Natural Ribozymes

Since 1982, several types of naturally occurring ribozymes have been discovered (Figure 1). With the notable exception of the ribosome, these ribozymes are generally limited in their capacity to making and/or breaking phosphoester bonds that hold nucleic acids together. In addition to the list below, RNA plays an important role in the catalytic events promoted by ribonucleoproteins such as telomerases, spliceosomes, and editosomes. Other natural ribozyme will undoubtedly be discovered in the near future.

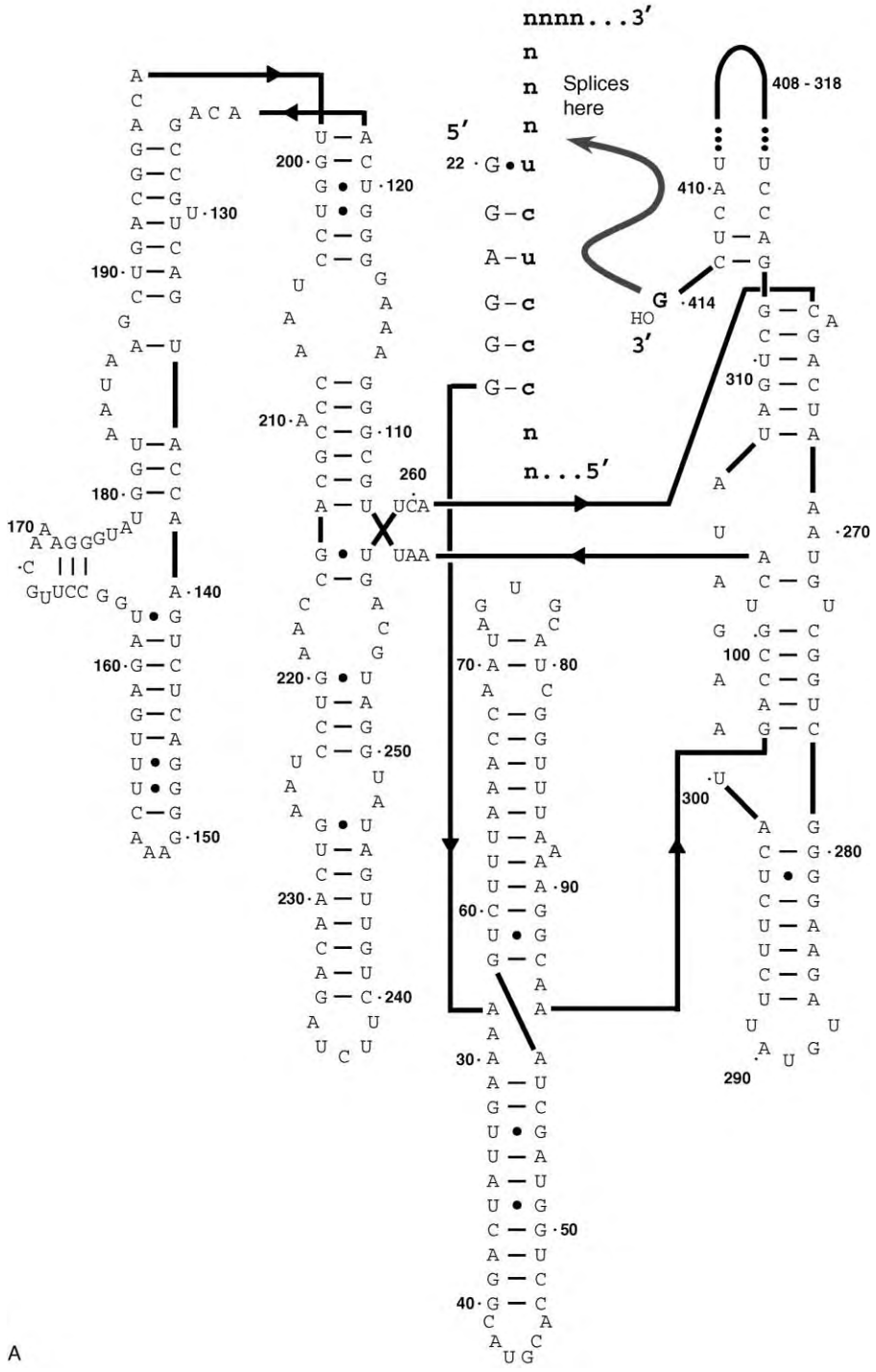

FIGURE 1 Some known ribozymes. (A) The group I intron from the ciliate *Tetrahymena thermophila*. Shown is the shortened version of the natural rRNA intron; this 414 nucleotide ribozyme binds a complementary RNA substrate (lower case letters) via complementary base pairing and catalyzes phosphoester bond cleavage and ligation reactions at the site indicated by the arrow. (B) One possible hammerhead ribozyme. This ribozyme self-cleaves at the site indicated by the arrow.

Group I and Group II Introns

These are large (>200 nucleotides) self-splicing introns: rRNA or tRNA introns that excise themselves from nascent RNA transcripts via ribozyme activity.

RNase P

RNase P is a large ribozyme that allows maturation of nascent tRNA transcripts and a few other small RNAs by removing the 5′-leader portion of those transcripts.

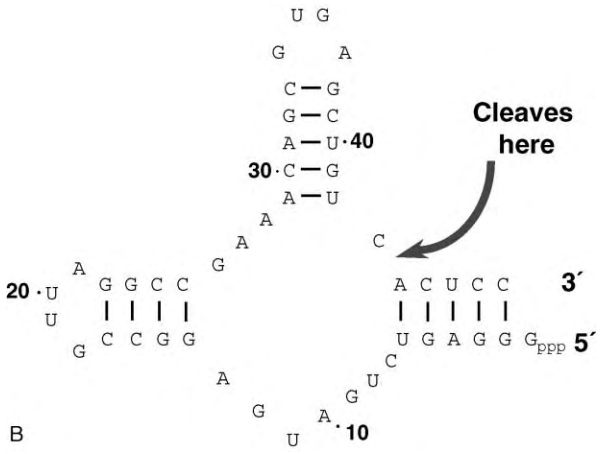

FIGURE 1 (*continued*)

Hammerhead

These small ribozymes, of which there are many throughout nature, possess three base-paired stems and catalyze self cleavage of a RNA phosphodiester bond.

Hairpin

Like the hammerheads, hairpin ribozymes, originally found in a tobacco RNA virus, self-cleave an RNA bond, but unlike the hammerheads, consist of four stems in two general domains.

Hepatitis Delta Virus

The HDV ribozyme is another viral-derived small ribozyme that catalyzes RNA bond cleavage, but it is slightly more complex, having a "pseudoknot" folded structure.

VS

The VS motif is another small self-cleaving ribozyme, found first in a satellite plasmid of *Neurospora* mitochondria. This ribozyme, as is the case for all RNA enzymes, can also catalyze the reverse reaction, which here would be ligation of two RNA strands.

Unnatural Ribozymes

Using the techniques of SELEX, *in vitro* selection, and *in vitro* evolution, many novel catalytic RNA sequences have been discovered (Figure 2), many of which promote chemistries not yet seen in natural ribozymes. The existence of these ribozymes demonstrates not only that RNA has a wide repertoire of catalytic capabilities, but that evolutionary forces are quite adept at molding RNA-based catalysis.

Ligase Ribozymes

Isolated from random pools of RNA sequences, the ligase ribozymes were one of the first type of unnatural ribozymes to be fashioned. These RNAs catalyze phosphoester-bond formation between themselves and an exogenous oligoribonucleotide. Several classes of ligase ribozymes exist, with differing RNA folds. Ligases catalyze bond formation by a chemistry that is distinct from that of known natural ribozymes, but which is remarkably similar to the chemistry used by the protein enzyme RNA polymerase. In fact some ligases can be engineered to behave as rudimentary RNA polymerases.

Diels-Alderase Ribozymes

To move from phosphoester chemistry to carbon–carbon bond chemistry, it was necessary to derivatize one of the four bases, uridine, with a pyridyl moiety. This allowed the selection *in vitro* of a Cu^{2+}-dependent ribozyme that could catalyze a Diels-Alder cycloaddition reaction.

Three- and Two-Base Ribozymes

Recently ribozymes have been selected that use only three (i.e., A, G, and U) nucleotides to perform catalysis. Also, if only U and 2,6-diaminopurine are available, a 2-base ligase ribozyme can be constructed through *in vitro* evolution.

Other Unnatural Ribozymes

Many other unnatural ribozymes exist and more are being constructed. These ribozymes can catalyze amide bond formation, N-alkylation, porphyrin metallation, thioester bond formation, and a host of other chemical reactions.

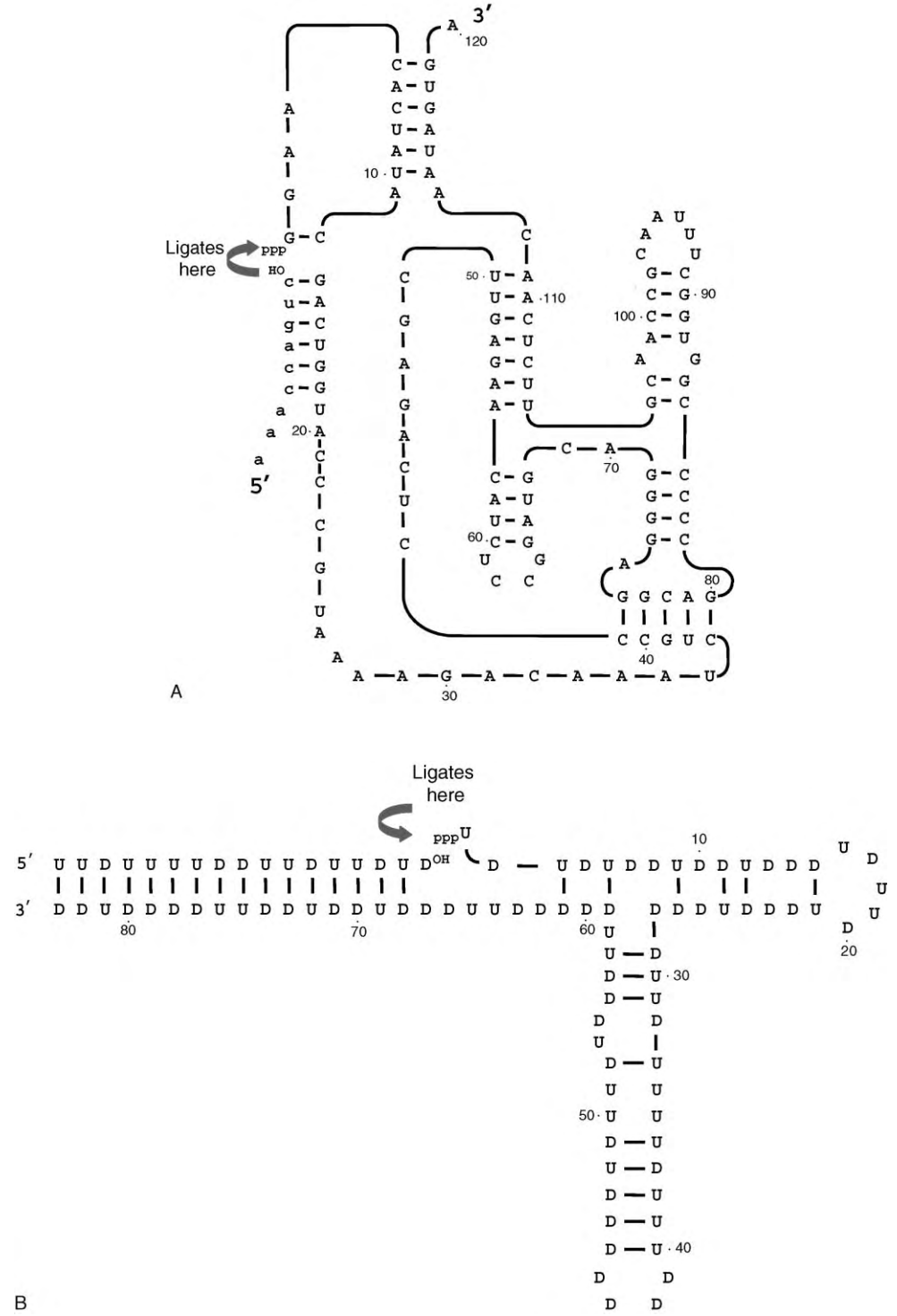

FIGURE 2 Some known unnatural ribozymes. (A) The b1-207 ligase ribozyme selected *in vitro* from a random pool of RNA sequences. This ribozyme binds a complementary RNA substrate (lower case letters) via complementary base pairing and catalyzes a ligation to form a new phosphoester bond. (B) A ligase ribozyme evolved *in vitro* to function with only two nucleotides: D = 2,6-diaminopurine and U = uridine.

Phylogenetic Distribution of Ribozymes

Judging from the phylogenetic distribution of natural ribozymes (Figure 3) and from the central nature of the reactions that they catalyze, it is clear that catalytic RNA was likely present in the last common universal ancestor (LUCA) of contemporary life. Group I ribozymes for example, are present in eukaryotes (e.g., the ciliated protozoan *Tetrahymena*) and in eubacteria, including some bacteria thought to occupy basal lineages in the tree of life (e.g., the hyperthermophilic bacterium *Thermatoga*). Ribozymes are wide spread in RNA viruses, group II introns have been recently isolated from deep-sea hydrothermal vent bacteria, and small ribozymes have been isolated from genomes in organelles such as mitochondria and chloroplasts. Also, the RNase P ribozyme is present in a variety of archaeal species.

RNA and the Origins of Life

In addition to the inference that ribozymes were a feature in the LUCA, there is much evidence and corresponding speculation that RNA, in particular catalytic RNA, was critical in the earliest life forms on the Earth. RNA, or an RNA-like molecule, could even have been the basis for the origins of life itself. Initially this postulate was based on the observation that RNA was the only known polymer to possess simultaneously a genotype and a phenotype. Subsequently, more direct evidence of the antiquity of RNA has come to light. These data include the realization that, the ribosome is a ribozyme, RNA can catalyze a diverse array of reactions, a ligase-derived RNA can catalyze rudimentary RNA polymerization, RNA can catalyze recombination, and, importantly, populations of RNA can evolve in a test tube and respond to environmental pressures in manners quite analogous to natural populations of organisms. Moreover, much is now known about plausible abiotic synthetic routes to RNA precursors such as purines, pyrimidines, carbohydrates, and phosphorylated compounds. For example, cationic clays such as montmorillonite can promote the polymerization of RNA-like monomers into RNA chains of 50 or more nucleotides in length.

In vitro Evolution of RNA

SELEX

Systematic evolution of ligands by exponential enrichment (SELEX) is a powerful method to isolate RNA sequences that bind to particular substrates without necessarily reacting with them. Random pools of RNA, typically 40–100 nucleotides in length, are created such that billions of possible sequences are represented. These pools are challenged to bind a target substrate, such as a

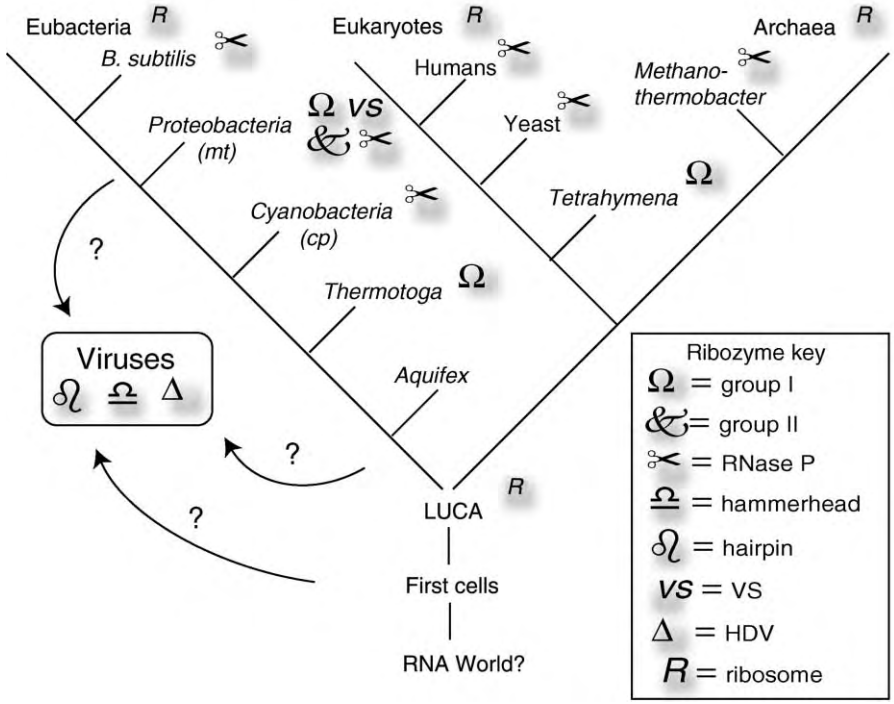

FIGURE 3 Distribution of ribozymes in the tree of life. The examples shown here are not exhaustive; branch lengths are not indicative of extinction events or amount of evolutionary change. Mitochondria (mt) and chloroplasts (cp) are included with their bacterial precursors.

particular protein or small molecule such as an amino acid, and the successful binders are separated from the failures and amplified. Repetition of this process 5–10 times often generates a small subset of RNA sequences, called aptamers that have a high-binding affinity toward the substrate.

Selection *in vitro*

Selection *in vitro* (in a test tube) follows the same basic strategy as SELEX, only RNAs are isolated that catalyze a target chemical reaction (Figure 4). These RNAs must bind one or more substrates and then promote a reaction in such a way that the RNA is modified or "tagged" for amplification. In this technique, the initial pool can either be a set of random RNA sequences, or a set of mutants based on a particular known wild-type sequence.

Evolution *in vitro*

Evolution *in vitro* follows the strategy of selection *in vitro* except that in each round, mutations are deliberately introduced into the RNA population to provide additional variation on which natural selection can operate (Figure 4). The mutation can come from error-prone protein polymerase enzymes, from mutagenic PCR, or from sexual PCR. Evolution *in vitro* can in principle be carried out for an indefinite number of rounds, but in principle convergence on a particular catalytic solution, if one exists, typically occurs after 10–20 rounds and will occur in general accordance to the principles of population genetics.

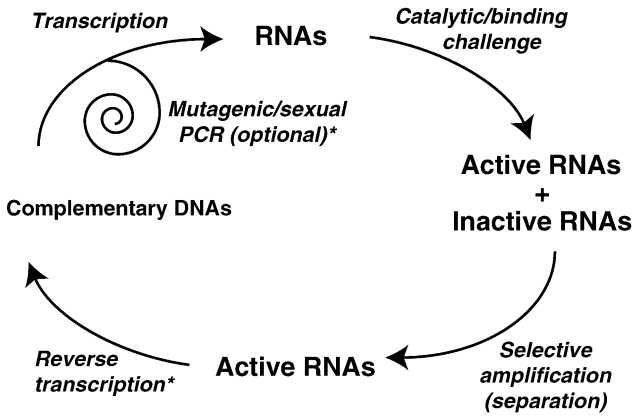

FIGURE 4 *In vitro* selection/evolution. A pool of RNA molecules, partially or completely randomized in nucleotide sequence, is challenged to perform a novel binding and/or catalytic event. As a result of successfully performing that event, RNA molecules become physically tagged in such a manner that they can be separated from unsuccessful RNA molecules. The successful RNAs then get converted to a corresponding DNA sequence through reverse transcription and back into RNA by forward transcription. A complete cycle is called a round, or a generation, and may or may not include mutagenic steps (indicated by asterisks) to introduce an evolutionary element into the process.

Continuous Evolution *in vitro*

The most recent modification of these RNA evolution techniques is to mimic a prebiological milieu in which all the components of evolution – the RNA, the nucleotides, the salts, the oligonucleotides, and the protein enzymes, if any – are simultaneously present in a single test tube. In this fashion several rounds of evolution occur autonomously before equilibrium is reached. Serial dilution and fresh additions of reagents can result in the extremely rapid evolution of RNA populations.

See Also the Following Articles

Ribozyme Mechanisms • Ribozyme Structural Elements: Group I Introns • Ribozyme Structural Elements: Hairpin Ribozyme • Spliceosome

Glossary

abiotic Formed in the absence of life.
nucleotide A chemical subunit of nucleic acids (A = adenosine, C = cytidine, G = guanosine, U = uridine).
phylogeny A tree-like representation of the ancestral–descendant relationships among species.
polypeptide A polymer of amino acids that forms a protein.
ribozyme An enzyme made of RNA.
RNA Ribonucleic acid, a polymer of nucleotide subunits.

Further Reading

Bartel, D. P., and Unrau, P. J. (1999). Constructing an RNA world. *Trends Cell Biol.* **9**, M9–M13.
Bittker, J. A., Phillips, K. J., and Liu, D. R. (2002). Recent advances in the *in vitro* evolution of nucleic acids. *Curr. Opin. Chem. Biol.* **6**, 367–374.
Breaker, R. R., and Joyce, G. F. (1994). Inventing and improving ribozyme function: Rational design versus iterative selection methods. *Trends Biotech.* **12**, 268–275.
Gilbert, W., and de Souza, S. J. (1999). Introns and the RNA world. In *The RNA World* (R. F. Gesteland, T. R. Cech and J. F. Atkins, eds.) 2nd edition, pp. 221–231. Cold Spring Harbor Press, Cold Spring Harbor, NY.
Joyce, G. F. (1992). Directed molecular evolution. *Sci. Am.* **267**, 90–97.
Lilley, D. M. (2003). The origins of RNA catalysis in ribozymes. *Trends Biochem. Sci.* **28**, 495–501.
Wilson, D. S., and Szostak, J. W. (1999). In vitro selection of functional nucleic acids. *Ann. Rev. Biochem.* **68**, 611–647.

Biography

Niles Lehman is an Associate Professor in the Department of Chemistry at Portland State University in Portland, Oregon. His principal research interests are in molecular evolution and the origins of life on the Earth. He holds a Ph.D. from the University of California, Los Angeles and received postdoctoral training at The Scripps Research Institute and the University of Oregon. He is an associate editor of the *Journal of Molecular Evolution*, and his laboratory has pioneered the studies on RNA-directed recombination of RNA.

RNA Editing

Charles E. Samuel
University of California, Santa Barbara, California, USA

RNA editing is the posttranscriptional modification of an RNA nucleotide sequence at one or more positions. There are two general types of RNA editing, viz., substitution editing and insertion/deletion editing. RNA editing of either type leads to the formation of transcripts whose sequence differs from that found in the genome. Such RNA sequence differences between mature transcript and encoding genome represent a form of genetic recoding. The sequence changes generated by RNA editing are different from those arising from 5′-capping, 3′-polyadenylation, and splicing, processing events that also may occur as part of mRNA biogenesis. RNA editing is widely observed in eukaryotic organisms and their viruses. Editing, like splicing, represents a form of processing that has the capacity to amplify genetic diversity and product function by altering the information transfer process at the posttranscriptional level of gene expression.

Discovery of RNA Editing

RNA editing was discovered in a unicellular protozoan. The frameshifted cytochrome oxidase *coxII* transcript of trypanosome mitochondria was found to contain four inserted uridines that were not encoded by the genomic DNA. Then editing by nucleotide substitution was found in two mammalian RNAs. The apolipoprotein B (apoB) mRNA in mouse intestine had a translation stop codon at a position in the mature mRNA, where the genomic DNA specified the amino acid glutamine, and the glutamate-gated ion channel (GluR-B) mRNA in mouse brain had the amino acid arginine in place of the genome-encoded glutamine at the same position. Several biochemical mechanisms account for the RNA editing identified in mRNA transcripts. These include A-to-I substitution editing; C-to-U substitution editing; U insertion/deletion editing; C insertion editing; and G insertion editing. In addition, 2′-O-methyl ribose nucleotide modification and uridine to pseudouridine conversion represent editing events mediated by complexes of small nucleolar RNA (snoRNA) cofactor guides and associated proteins that modify ribosomal RNAs and other RNAs. This article will focus on A-to-I and C-to-U RNA editing that occur by selective RNA-specific deamination reactions that lead to nucleotide substitutions. Genetic recoding by such substitution editing can create gene products with altered sequence and hence altered function.

Adenosine-to-Inosine Substitution RNA Editing

RNA Substrates that Undergo A-to-I Editing

RNA editing by adenosine (A) to inosine (I) substitution is catalyzed by C6-adenosine deaminases that act on double-stranded RNA substrates (Figure 1A). A-to-I editing occurs in several eukaryotes including *Caenorhabditis* (nematode worm), *Drosophila* (fruit fly), and *Xenopus* (frog) in addition to mammals and their viruses. Among mammalian RNAs, transcripts encoding glutamate-receptor (GluR) channels of the α-amino-3-hydroxy-5-methyl-isoxaole-4-propionate (AMPA) and kainate GluR receptor subtypes represent one of the best-understood cases of A-to-I editing. This is illustrated by the AMPA receptor subunit B (GluR-B), one of four GluR subunits. Exon 11 possesses a genome-encoded glutamine (Q) codon (CAG) in unedited GluR-B transcripts. This exon codes for a hydrophobic domain (TM2) that loops into the cytoplasmic membrane. The edited GluR-B mRNA possesses an arginine (R) codon (C*I*G) at the same codon position, because I is recognized as G by decoding ribosomes during the translational process. Editing at this site, known as the Q/R site, occurs almost completely in the brain of adult rodents. Q/R editing of GluR-B affects channel subunit assembly in a manner that results in reduced permeability to Ca^{++} ions. A second A-to-I editing site in GluR RNA, termed the R/G site, involves the conversion of a genome-encoded arginine (R) codon (*A*GA) to a glycine (G) codon (*I*GA) in exon 13 of edited GluR-B, -C, and -D subunit transcripts. Editing at the R/G site controls the kinetic properties of AMPA receptor channels and leads to faster recovery rates from receptor desensitization.

Editing of GluR-B occurs at the pre-mRNA level within the nucleus, prior to splicing. RNA elements

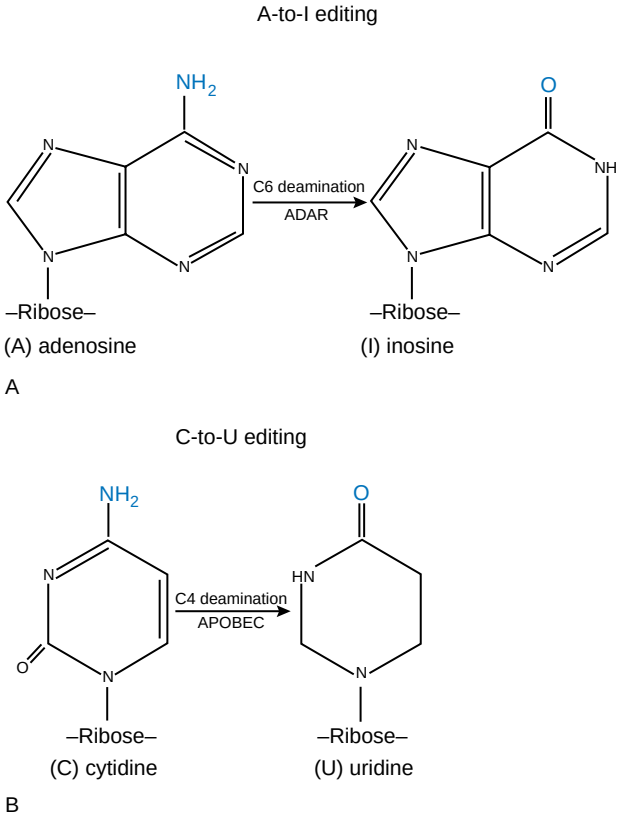

FIGURE 1 Substitution RNA editing by hydrolytic deamination. (A) A-to-I RNA editing involves the C6 deamination of adenosine to generate inosine catalyzed by ADAR enzymes. (B) C-to-U RNA editing involves the C4 deamination of cytidine to generate uridine catalyzed by APOBEC enzymes.

dictate the specificity of editing at the Q/R and R/G sites. The elements consist of unique *cis*-acting complementary inverted repeat sequences that are present in the intron adjacent to the exon possessing the edited adenosine. For the Q/R site in exon 11, the inverted repeat in intron 11 is predicted to form an imperfect duplex structure spanning the edited "A" at the Q/R site. A similar duplex RNA structure also exists within exon 13 containing the R/G site and the proximal portion of the adjacent intron 13. These exon–intron double-stranded RNA structures are absolutely essential for efficient editing at the Q/R and R/G sites of GluR-B.

The serotonin (5-hydroxytryptamine)-2C receptor (5-HT_{2c}R) provides another example of a neurotransmitter receptor whereby A-to-I editing of the pre-mRNA prior to splicing leads to amino acid substitutions in the encoded protein that alter activity. In the case of rat 5-HT_{2c}R pre-mRNA, four selective A-to-I editing sites denoted A, B, C, and D have been identified in exon 3 that specify three amino acid substitutions. The 5-HT_{2c}R genomic sequence specifies the sequence …AUA CGU AAU CCU AUU… that encodes …*ile*-arg-*asn*-pro-*ile*… in the unedited RNA. Editing of the four sites leads to the sequence …IUI CGU AIU CCU IUU… in fully edited RNA that encodes …*val*-arg-*ser*-pro-*val*… The three amino acid substitutions created by A-to-I editing of 5-HT_{2c}R transcripts occur in the putative intracellular loop II of the receptor and they cause an ~tenfold reduction in G protein-mediated signaling. Here again, the selective editing of 5-HT_{2c}R pre-mRNAs is dictated by imperfect inverted repeat sequence that forms an RNA duplex between the 3′-end of exon 3 spanning the four editing sites and the 5′-end of the adjacent intron-3.

One of the challenges of A-to-I editing is to identify additional substrates. The GluR-B and 5-HT_{2c}R substrates in rodents and humans were identified serendipitously. In *Drosophila*, a comparative genomics approach has identified 16 new targets for A-to-I editing; all were voltage-gated ion channels, ligand-gated ion channels, or part of the synaptic release machinery.

Adenosine Deaminases that Act on RNA

A-to-I editing events of substrates such as GluR-B and 5-HT_{2c}R are catalyzed by a multigene family of enzymes known as ADARs, *a*denosine *dea*minases that act on *R*NA. Two mammalian genes are known to encode catalytically active deaminases, *ADAR1* and *ADAR2*, that efficiently deaminate both synthetic and naturally occurring double-stranded RNA substrates (Figure 2). The ADAR1 and ADAR2 enzymes show different activities for the different sites in the GluR-B and 5-HT_{2c}R transcript RNAs. The ADAR2 deaminase efficiently edits the Q/R site of GluR-B, but the ADAR1 enzyme possesses little editing activity at Q/R. Both ADAR1 and ADAR2, however, are capable of editing the R/G site of GluR-B. For 5-HT_{2c}R, ADAR1 very efficiently edits the A site but is inactive for the D site, whereas ADAR2 efficiently edits the D site. ADAR1 and ADAR2 possess multiple copies of a canonical double-stranded RNA-binding motif (R, dsRBM) that are located in the central region of the protein. The interferon inducible form of ADAR1 possesses, in addition to the R motifs, two copies of a Z-DNA-binding motif (Zα and Zβ) in the N-terminal region of the protein. The dsRNA- and Z-DNA-binding motifs of ADAR1 are distinct from the deaminase catalytic domain located in C-terminal region of the ADAR proteins (Figure 2). The dsRNA-binding motifs are presumed to play a role in the binding of substrate RNAs, but it is also possible that they too play a role in regulation of enzymatic activity. For example, adenovirus VA_I RNA, a small and highly structured viral gene product transcribed by cellular RNA polIII, efficiently antagonizes ADAR deaminase activity.

The expression of ADAR enzymes in cells is a complex process. For example, in the case of the

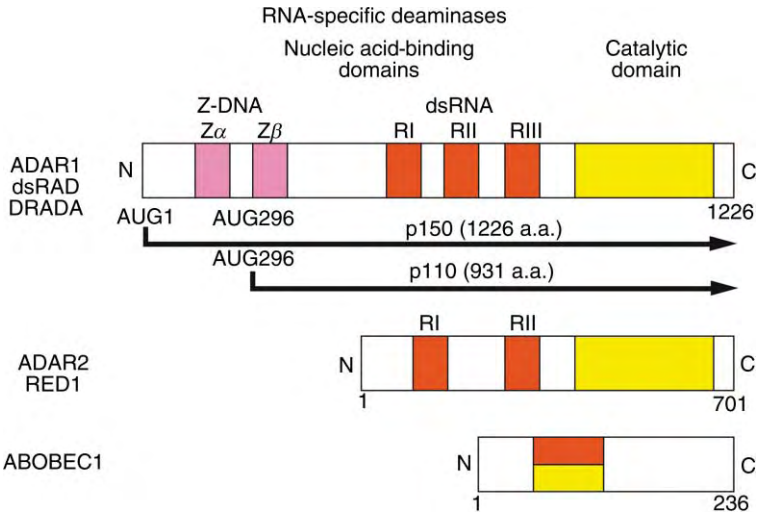

FIGURE 2 Schematic structure of mammalian RNA-specific deaminases. ADAR1 and ADAR2 possess double-stranded RNA-binding (R) motifs (red) and Z-DNA-binding motifs (pink). The RNA-binding motif of APOBEC1 overlaps with the catalytic domain. The catalytic domains of ADAR and APOBEC are shown in yellow. Two size forms of ADAR1 are expressed, the larger p150 interferon inducible form and the smaller constitutive p110 form. ADAR2 and APOBEC1 are not known to be regulated by cytokines or growth factors.

human *ADAR1* gene, alternative promoters including one inducible by interferons together with alternative exon 1 splicing give rise to two differently sized enzyme isoforms, p150 and p110 (Figure 2). The interferon inducible form of ADAR1, p150, is found in both the cytoplasm and nucleus of cells. The constitutive p110 form, which lacks the N-terminal 295 amino acids that includes the Zα-binding motif, is found predominantly if not exclusively in the nucleus. Additional ADAR protein multiplicity is achieved by alternative splicing involving downstream exons, both in the case of ADAR1 and ADAR2. The physiological significance of the splice variants of ADAR is not known; one possibility may relate to the substrate selectivity of the enzymes.

Cytidine-to-Uridine Substitution RNA Editing

RNA Substrates that Undergo C-to-U Editing

Cytidine (C) to uridine (U) substitutional RNA editing is catalyzed by C4-cytidine deaminases that act on single-stranded RNA substrates (Figure 1B). C-to-U editing has been characterized in both plants and mammals. One of the best-understood examples is the mammalian mRNA transcript that encodes apolipoprotein B (apoB) that functions in lipid metabolism. There are two forms of apoB. The larger form (apoB100) is synthesized in the liver and assembled into lipoprotein particles that are secreted into the bloodstream. The carboxyl terminal region of apoB100 interacts with the low-density lipoprotein receptor to remove LDL from circulation. Editing of apoB mRNA by deamination of a single cytidine changes a genome-encoded glutamine codon (*CAA*) to a translation termination codon (*UAA*). This C-to-U editing happens in the small intestine but not the liver. ApoB RNA editing causes the synthesis of a truncated intestinal lipoprotein known as apoB48 that lacks the C-terminal region of apoB100, but otherwise is identical to the N-terminal 48% of apoB100. While apoB100 is associated with LDL protein particles, apoB48 is associated with chylomicron and lacks receptor-binding activity.

Editosome Complex

C-to-U editing of apoB mRNA occurs in the nucleus and is selective for spliced transcripts rather than pre-mRNAs. Deamination is mediated by a multiprotein complex as illustrated by the schematic diagram shown as Figure 3. This complex, called an editosome, includes a protein that possesses catalytic activity (*Apo*lipoprotein *B E*diting Catalytic subunit 1, APOBEC-1) together with one or more associated proteins that include an *a*pobec-1 *c*ompetence *f*actor (ACF), which possesses RNA-binding activity. Unlike the ADARs, APOBEC does not possess a separate canonical RNA-binding motif, but rather RNA-binding activity overlaps with the catalytic domain residues (Figure 2). A tripartite RNA motif that includes efficiency elements, spacer, and a mooring sequence surrounds the edited nucleotide C6666 of apoB mRNA and appears sufficient to confer the required specificity in the C-to-U editing reaction. ACF protein binds apoB RNA selectively at the region of the editing site and interacts with APOBEC-1 deaminase to mediate C-to-U editing activity. Multiple

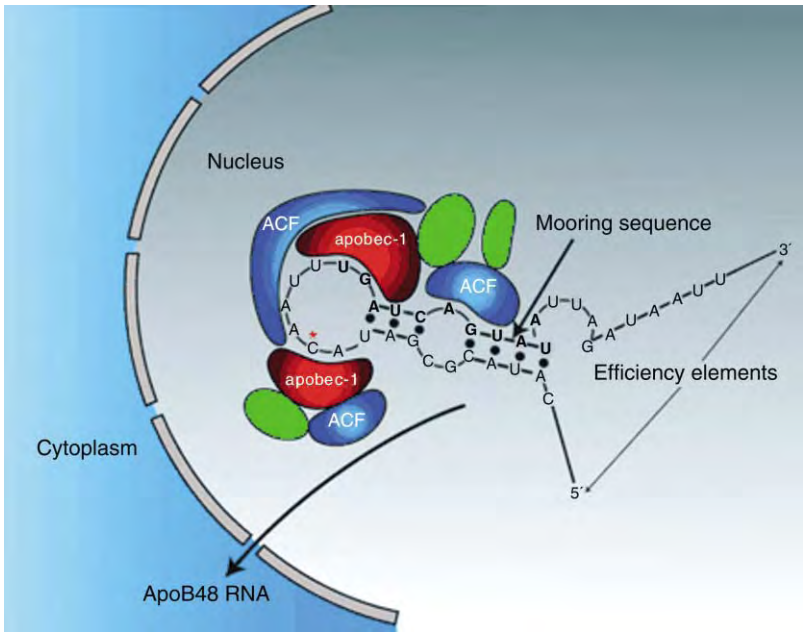

FIGURE 3 Model for C-to-U editing of apolipoprotein B mRNA. The schematic representation shows the APOBEC-1 enzyme (red) and ACF competence factor (blue) binding to the apoB RNA both 5′ and 3′ to the edited C. Additional proteins (green) may modulate assembly of the editosome complex. The mooring sequence is shown in bold font. (Reprinted from Blanc, V., and Davidson, N. O. (2003). C-to-U RNA editing: Mechanisms leading to genetic diversity. *J. Biol. Chem.* **278**, 1395–1398, with permission of the American Society for Biochemistry & Molecular Biology.)

splice variants of the ACF protein are found in different human tissues, but their functional significance remains unknown. Likewise, several homologues of the APOBEC-1 catalytic deaminase have been identified including ARCD1/APOBEC-2, AID, and phorbolin/ARCD2-7/APOBEC-3A to G. The target substrates and physiologic roles of the many APOBEC homologue proteins in RNA editing are not yet well defined.

The existence of multiple APOBEC-1 homologues and ACF variants points to the existence of primary substrates beyond apoB mRNA that may undergo C-to-U editing. One candidate for site-specific cytidine deamination is the cellular mRNA for the neurofibromatosis type 1 (NF1) protein encoded by NF1 tumor suppressor gene. This protein, neurofibromin, functions as a Ras-GTPase-activating protein (GAP). Site-specific deamination of a cytidine (nucleotide C3916) in NF1 mRNA converts a genome coded arginine codon (*C*GA) to a translation termination codon (*U*GA). The shortened NF1 open reading frame that results from this C-to-U editing has been observed in neuronal tissue from NF1 patients and is predicted to give rise to a truncated neurofibromin protein product deficient in GAP activity.

Substitution Editing of Viral RNAs

RNA editing may play a significant role in viral pathogenesis and affect the host response to viral infection. A number of viral RNAs, including those of avian leukosis virus (ALV), hepatitis delta virus (HDV), measles virus, parainfluenza virus 3, polyoma virus, respiratory syncytial virus, and vesicular stomatitis virus, all show codon changes under certain infection conditions that are consistent with A-to-I editing. The best-characterized viral RNA substrate is that of HDV. Both ADAR1 and ADAR2 convert an amber translation stop codon (UAG) to a tryptophan codon (UIG) in HDV antigenomic RNA. This editing allows for the synthesis of two delta virus antigen forms, a short form used in viral replication and a long form necessary for assembly of viral particles. A viral RNA candidate for A-to-I editing is that of measles virus (MV), where viral RNAs isolated from brains of persistently infected subacute sclerosing panencephalitis (SSPE) patients, possess multiple sequence differences from the viral RNA genome that correspond to A-to-G and U-to-C substitution mutations. Because MV, a negative-strand RNA virus, replicates in the cytoplasm, it is presumed that ADAR1 is the responsible enzyme. The DNA virus vaccinia that also replicates in the cytoplasm of cells encodes a protein product (E3L) that efficiently antagonizes ADAR1 deaminase activity, and mutations in E3L are known to affect viral pathogenesis in the mouse model.

Finally, C-to-U RNA editing like A-to-I editing may play a role in the interactions between viral pathogens and their hosts. Among the homologues of APOBEC-1, the APOBEC-3G gene product has been shown to possess broad anti-retroviral activity. The antiviral effects of APOBEC-3G appear to result from the generation of biased G to A hypermutations that impair

virus replication in a manner that, in the case of human immunodeficiency virus, is modulated by an accessory protein of the virus known as Vif.

Editing by Nucleotide Insertion/Deletion

A second general type of RNA editing, in addition to base substitution editing, is nucleotide insertion/deletion editing. Among the best-characterized examples of insertion/deletion editing is that of U-insertion and U-deletion. Uridine insertion/deletion editing occurs by an enzymatic cleavage-ligation mechanism. The specificity of U-insertion/deletion editing is determined by RNA–RNA base pairing between a complementary guide RNA (gRNA) and the target RNA (mRNA) substrate. The base-paired RNA complex serves to position the enzymatic machinery at the site of U insertion or deletion, thereby "guiding" the modification process. Much has been learned from the trypanosome mitochondrial system about the features and requirements of the complimentary gRNAs that act in trans to target enzyme complexes to the mRNA site of uridine insertion/deletion editing. The enzymatic cleavage-ligation mechanism of U insertion/deletion editing involves hybridization of gRNA to mRNA to form a gRNA:mRNA anchor duplex, after which the mRNA is specifically cleaved by a gRNA-dependent ribonuclease at the site of the gRNA:mRNA mismatch. For U-insertion editing, a 3′-terminal uridylyl transferase (TUTase) then adds U's to the 3′-end of the 5′-fragment guided by base pairing with the gRNA, followed by ligation of the two fragments by an RNA ligase. For U-deletion editing, a U-specific 3′-5′ exonuclease removes the bulged U residues, followed by ligation of the two RNA fragments. Finally, in addition to U-insertion editing as exemplified by the cytochrome oxidase mRNA in trypanosome mitochondria, C-insertion editing and G-insertion editing also are known to occur as illustrated by Physarum mitochondria and by negative-strand RNA viruses, respectively. In the case of paramyxoviruses such as Sendai virus, G-nucleotide insertion occurs during the RNA transcription process to generate edited P/C mRNA that includes nontemplated Gs.

Roles of RNA Editing

Altering the information transfer process at the post-transcriptional level of gene expression by RNA editing represents an important strategy for amplifying genetic diversity and modifying the functions of products encoded by an organism's genome. Some of the mechanistic roles that substitution editing through A-to-I and C-to-U deamination play, or are anticipated to play, in biological processes are summarized in Figure 4. These biochemical mechanisms include effects of editing on mRNA translation, pre-mRNA splicing, RNA degradation, RNA replication, and RNA structure that result from nucleotide substitution via deamination or nucleotide insertions. Site-specific editing may change the coding potential of mRNA transcripts, leading to proteins with altered function due to amino acid substitutions following A-to-I editing. This is exemplified

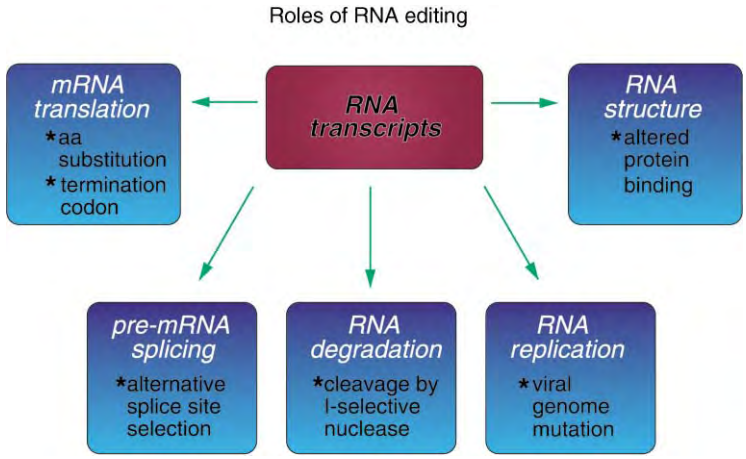

FIGURE 4 Established and potential roles of RNA editing by deamination. Edited RNA transcripts (A-to-I; C-to-U) possess different sequences than their unedited transcript counterparts, and hence may display different functional activities than that shown by the unedited transcripts. Editing may alter processes including mRNA translation, by changing codons and hence coding potential; editing may alter pre-mRNA splicing patterns by changing splice site-recognition sequences; editing may affect RNA degradation by modifying RNA sequences involved in nuclease recognition; editing may affect viral RNA genome stability by changing template and hence product sequences during RNA replication; and, editing potentially may affect RNA structure-dependent activities that entail binding of RNA by proteins. (Reprinted from Samuel, C. E. (2003). RNA editing minireview prologue. *J. Biol. Chem.* **278**, 1389–1390, with permission of the American Society for Biochemistry & Molecular Biology.)

by the GluR-B and serotonin-2c receptor proteins. Introduction or removal of translation termination codons may also occur, as exemplified by apoB and NF1 mRNAs where C-to-U editing generates UAA and UGA translation termination codons respectively, and HDV RNA where A-to-I editing converts an amber UAG stop to a tryptophan codon. ADAR2 edits its own transcript, to create an alternative splice acceptor site; and, a novel ribonuclease selective for inosine-containing RNAs has been described, consistent with the notion that A-to-I edited transcripts may be degraded preferentially relative to the unedited transcripts. For viral RNAs, deaminations in either the plus- or minus-strand RNA could lead to mutations in the encapsidated viral genome sequence. Finally, sequence changes resulting from editing may subsequently affect RNA structure and function, including protein–RNA interactions (Figure 4).

See Also the Following Articles

Nuclear Pores and Nuclear Import/Export • Pre-tRNA and Pre-rRNA Processing in Eukaryotes • Ribozyme Mechanisms • tRNA Synthetases

Glossary

adenosine-to-inosine (A-to-I) editing The deamination of adenosine (A) to yield inosine (I), which is recognized as G rather than A, and hence represents a kind of base substitution RNA editing.

cytidine-to-uridine (C-to-U) editing The deamination of cytidine (C) to yield uridine (U), which is a kind of base substitution RNA editing.

deamination editing The replacement of the amino group of adenosine (A) with oxygen from water to generate inosine (I), or in the case of cytidine (C) to generate uridine (U).

edited RNA RNA transcript in which the RNA nucleotide sequence differs from that of the encoding genome sequence at one or more sites, either by base substitution or by nucleotide insertion/deletion.

RNA editing The posttranscriptional modification of an RNA nucleotide sequence by base substitution or by nucleotide insertion/deletion.

unedited RNA RNA transcript in which the nucleotide sequence corresponds to that encoded by the genome.

Further Reading

Bass, B. L. (2002). RNA editing by adenosine deaminases that act on RNA. *Annu. Rev. Biochem.* **71**, 817–846.

Blanc, V., and Davidson, N. O. (2003). C-to-U RNA editing: Mechanisms leading to genetic diversity. *J. Biol. Chem.* **278**, 1395–1398.

Decatur, W. A., and Fournier, M. J. (2003). RNA-guided nucleotide modification of ribosomal and other RNAs. *J. Biol. Chem.* **278**, 695–698.

Gott, J. M., and Emeson, R. B. (2000). Functions and mechanisms of RNA editing. *Annu. Rev. Genet.* **34**, 499–531.

Maas, S., Rich, A., and Nishikura, K. (2003). A-to-I RNA editing: Recent news and residual mysteries. *J. Biol. Chem.* **278**, 1391–1394.

Reenan, R. (2001). The RNA world meets behavior: A to I pre-mRNA editing in animals. *Trends Genet.* **17**, 53–56.

Samuel, C. E. (2001). Antiviral actions of interferons. *Clin. Microbiol. Rev.* **14**, 778–809.

Samuel, C. E. (2003). RNA editing minireview prologue. *J. Biol. Chem.* **278**, 1389–1390.

Seeburg, P. H., and Hartner, J. (2003). Regulation of ion channel/neurotransmitter receptor function by RNA editing. *Curr. Opin. Neurobiol.* **13**, 279–283.

Simpson, L., Sbicego, S., and Aphasizhev, R. (2003). Uridine insertion/deletion RNA editing in trypanosome mitochondria: A complex business. *RNA* **9**, 265–276.

Biography

Charles Samuel is the C. A. Storke II Professor and Chair of the Department of Molecular, Cellular, and Developmental Biology at the University of California, Santa Barbara. His research concerns the mechanisms of interferon action, including the modification of RNA by editing. He holds a Ph.D. in biochemistry from the University of California, Berkeley, was a Damon Runyon Scholar at Duke University Medical School, and has authored more than 150 research publications in the fields of virology and biochemistry.

RNA Polymerase I and RNA Polymerase III in Eukaryotes

Robert J. White
University of Glasgow, Glasgow, UK

RNA polymerases are the enzymes responsible for synthesizing RNA, in a process called transcription. They use DNA as a template, and the RNA they produce carries a faithful copy of the genetic information contained in the template. Whereas bacteria use a single RNA polymerase to transcribe all their genes, the nuclei of eukaryotes contain three. Each is responsible for transcribing a unique set of essential genes. RNA polymerase I synthesizes most of the rRNA, RNA polymerase II synthesizes the protein-encoding mRNA and most snRNA, while RNA polymerase III synthesizes a variety of small untranslated RNAs, including tRNA and 5S rRNA. An additional RNA polymerase is present in mitochondria, which carry a small DNA molecule of their own. This division of labor could have become necessary as genomic complexity increased during evolution. In actively growing cells, RNA polymerase I can be responsible for ~70% of all nuclear transcription, whereas RNA polymerases II and III contribute ~20% and 10%, respectively.

Genes Transcribed by RNA Polymerases I and III

Despite its very high activity, RNA polymerase I only transcribes a single type of gene, which encodes the large rRNA precursor molecule. This precursor is then processed into the mature 5.8S, 18S, and 28S rRNA components of ribosomes. A single molecule of each of these rRNAs, along with a 5S rRNA molecule and ~85 proteins, is incorporated into each ribosome. The pre-rRNA is encoded by multiple gene copies, the number of which varies between different organisms; mammals have ~150–200 copies arranged in tandem head-to-tail arrays.

The genes transcribed by RNA polymerase III are invariably very short, rarely exceeding 300 bp in length. Many of their products have essential functions, such as the 5S rRNA and tRNAs (required for protein synthesis), 7SL RNA (involved in intracellular trafficking of proteins as part of the signal recognition particle), and the U6, MRP, and H1 RNAs (involved in the processing of mRNA, rRNA, and tRNA, respectively). Mammalian genomes also contain large numbers of short interspersed repeats (SINEs) that are transcribed by RNA polymerase III, such as the Alu family in man. In addition, certain viruses carry genes that are transcribed by RNA polymerase III, such as the VA genes of adenovirus and the EBER genes of Epstein–Barr Virus. The products of these viral genes can subvert the translational machinery of an infected cell, diverting it towards the more effective production of viral proteins.

Nucleoli

Within the nucleus, the most obvious landmarks under a light microscope are nucleoli, because of their high density. These form around the actively transcribed rRNA gene repeats and contain closely packed molecules of transcribing RNA polymerase I, each with a nascent pre-rRNA attached. Furthermore, ribosomal proteins assemble on the nascent transcript whilst it is being made. Although nucleoli have the appearance of organelles, they are in fact dynamic structures without membranes that disappear when transcription stops (e.g., during the general suppression of gene expression that accompanies mitosis). Transferring rRNA genes to a novel chromosomal location can result in the appearance of an ectopic nucleolus. When cells become very old, their nucleoli fragment; it has been suggested that nucleolar degeneration may be an important aspect of cellular aging.

The RNA Polymerase Molecules

RNA polymerases I, II, and III are large and complex proteins, consisting of 14, 12, and 17 subunits, respectively. Five of these subunits are shared, and a further two are found in RNA polymerases I and III, but not in RNA polymerase II. The two largest subunits of each enzyme are unique, but share substantial homology with each other and also with bacterial RNA polymerases;

they fold together to provide the catalytic site of the enzyme. Besides these, RNA polymerases I, II, and III each have an additional set of unique subunits. Although most of the subunits are required for cell viability, their precise roles remain poorly characterized.

The RNA Polymerase I and III Transcription Apparatus

Despite their complexity, the nuclear RNA polymerases require considerable assistance to locate their genetic templates. Sets of transcription factor proteins assemble at promoter DNA sequences near the initiation sites of genes and then serve as molecular beacons which recruit the appropriate RNA polymerase.

For the large rRNA genes, promoter recognition is achieved by the homodimeric factor UBF that binds across the promoter region upstream of the transcription start site. UBF bends the DNA and wraps it around itself to create a three-dimensional nucleoprotein structure that is recognized by SL1, the factor responsible for polymerase recruitment. RNA polymerase I is pre-assembled with a polypeptide called Rrn3 that serves as an essential bridge between the polymerase and SL1 (Figure 1A). Several additional transcription factors are also associated with RNA polymerase I and are recruited with it in a concerted manner. Although these principles apply to mammals and frogs, the machinery required for rRNA synthesis is rather different in yeast. Indeed, the RNA polymerase I transcription apparatus is much less well conserved through evolution than those of RNA polymerases II or III; whereas human proteins can transcribe a yeast tRNA gene, they will not even recognize the large rRNA genes from mouse.

In the case of RNA polymerase III, two key transcription factors, TFIIIB and TFIIIC, play central roles in both yeast and man (Figure 1B). The former is responsible for recruiting RNA polymerase III and positioning it over the transcription initiation site; it also helps separate the two strands of the DNA helix, thereby facilitating the start of RNA synthesis. However, TFIIIB is unable to recognize the DNA sequences of most RNA polymerase III promoters, but must be brought into position through protein-protein interactions with DNA-bound TFIIIC. An unusual feature of this system is that the promoter sequences recognized by TFIIIC are located downstream of the transcription start site, within the transcribed region. Although in most cases TFIIIC binds directly to DNA, this is not possible for the 5S rRNA genes which have a distinct promoter arrangement. In these cases, an additional polypeptide, TFIIIA, binds along the DNA and provides a protein scaffold to which TFIIIC binds (Figure 1C). TFIIIA contains nine tandem copies of the zinc finger DNA-binding domain. Indeed, it was the

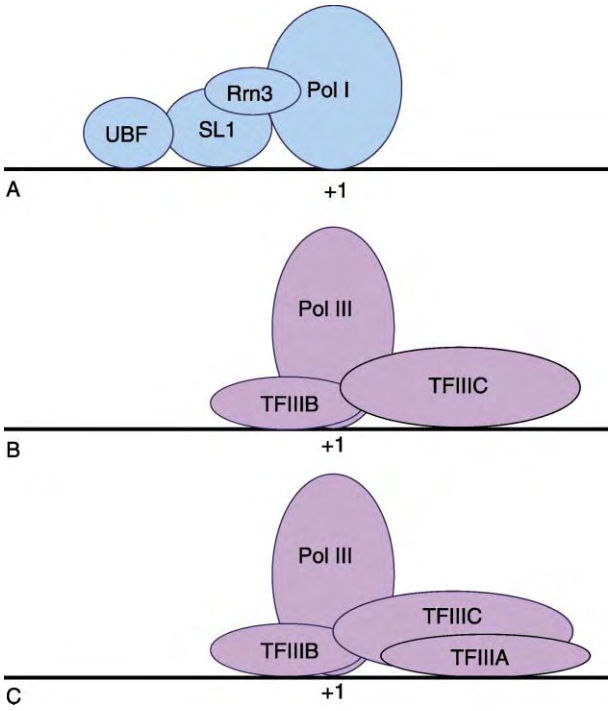

FIGURE 1 Simplified model of the transcription complexes used by RNA polymerases I and III. (A) UBF and SL1 assemble at the promoters of large rRNA genes and then recruit a preassembled complex containing Rrn3 and RNA polymerase I (Pol I), as well as additional factors not shown. (B) TFIIIC binds directly to the promoters of most genes transcribed by RNA polymerase III, e.g., tRNA genes. TFIIIB is recruited by protein/protein interactions with TFIIIC and then serves to bring RNA polymerase III (Pol III) to the transcriptional start site. (C) Similar events occur at 5S rRNA genes, but these are initiated by TFIIIA, which binds promoter DNA and provides a scaffold for TFIIIC assembly. + 1 denotes where transcription initiates.

founder member of the zinc finger family, the largest group of transcription factors in organisms ranging from yeast to man (~900 members in humans).

Alu Genes and Retrotransposition

The human genome carries over a million copies of the Alu gene, which provides ~10% of our total DNA. Despite their abundance, only small numbers of Alu genes are actually transcribed, the remainder being silenced through epigenetic mechanisms, including methylation and incorporation into repressive chromatin. SINEs propagate by retrotransposition, in which their RNA transcripts are copied into DNA and then inserted into novel genomic sites. These insertions occur preferentially into areas of active transcription, perhaps because of their more open and accessible chromatin structure. This increases the danger that integrating SINEs will disrupt genes at the recipient loci, thereby having a mutagenic effect. Indeed, cases of haemophilia,

neurofibromatosis, and breast cancer are believed to have arisen in this way. It is estimated that Alu insertions account for ~0.1% of all human genetic disorders. In contrast, retrotransposition is much more active in mice, where it may contribute ~10% of mutations.

RNA Polymerases I and III and Tumor Suppression

The RNA polymerase I and III transcription systems are both targeted directly by two key tumor suppressor products, p53 and RB. Both these proteins bind to TFIIIB and block its interactions with TFIIIC and RNA polymerase III, thereby repressing transcription. RB also binds to UBF to inhibit synthesis of large rRNA, whereas p53 inactivates SL1. The ability of RB and p53 to suppress the output of RNA polymerases I and III may contribute to their capacity to restrain cell growth. RB has been described as a gatekeeper that only allows cells to grow and proliferate when conditions are propitious. Inherited mutations in RB can cause the paediatric eye cancer retinoblastoma. Indeed, it is widely believed that RB function must be compromised in some way before any tumor can develop. The most commonly mutated gene in human cancer is p53, which is famous as "the guardian of the genome." If a cell's DNA gets damaged, for example, through exposure of skin to excessive doses of UV light, p53 gets activated and triggers a protective response; this can involve halting growth and cell cycle progression until the damage has been mended or, under extreme circumstances, apoptotic death. These responses ensure that DNA carrying potentially harmful mutations are not passed on to further generations of cells.

Links between Human Disease and RNA Polymerases I and III

RNA polymerases I and III together may contribute ~80% of nuclear transcription and provide ~95% of the total RNA in cells. This very high level of production is necessary to make the several million new ribosomes that are needed per generation to maintain protein synthetic capability. Because they are such major determinants of biosynthetic capacity, the activities of RNA polymerases I and III are closely linked to the rate of cellular growth. In hyperproliferative diseases such as cancer, there is generally an elevated rate of transcription by these polymerases. Indeed, pathologists use enlarged nucleoli (a sign of accelerated rRNA synthesis) as a diagnostic indicator of tumor formation. To a large degree, the elevated activity of RNA polymerases I and III in cancer cells is likely to reflect the inactivation of p53 and/or RB; since these tumor suppressors play a major role in restraining transcription by RNA polymerases I and III in healthy cells, their inactivation during cancer development will remove a major restraining influence and allow deregulated gene expression. These effects must be extremely widespread, since p53 is mutated in ~50% of human tumors and RB function may be compromised in all forms of malignancy. In addition to their release from these transcriptional repressors, the output of RNA polymerases I and III is also increased in some cancers through the action of certain oncogenic proteins. An example is c-Myc, which is deregulated in many tumor types and is believed to contribute to one in seven US cancer deaths. TFIIIB is bound and activated by c-Myc, leading to elevated rates of RNA polymerase III transcription. Certain types of cancer also produce abnormally high levels of the transcription factors used by RNA polymerases I and III. For example, UBF is frequently overexpressed in hepatocellular carcinomas, whereas TFIIIC is unusually abundant in ovarian tumors.

Epstein–Barr Virus is associated with gastric and nasopharyngeal carcinomas, Burkitt's lymphoma, Hodgkin's disease, and AIDS-associated lymphoma. Its most highly expressed gene products are the EBER RNAs, which are synthesized by RNA polymerase III. The presence of these transcripts is used diagnostically as a test for Epstein–Barr Virus. Indeed, very few other viral genes are expressed in Burkitt's lymphomas. Recent studies have shown that the EBER1 transcript can be sufficient for oncogenic transformation, a remarkable fact since it is only 167 nucleotides long. This provides the first reported example of an untranslated RNA that can transform cells.

An inherited-developmental disorder has been shown to result from mutations in the MRP gene that is transcribed by RNA polymerase III to produce a short RNA that is required for mitochondrial replication and for the processing of large rRNA. Families afflicted with this condition suffer from cartilage–hair-hypoplasia, a complex syndrome involving short stature (adult heights of 104-149 cm), abnormal cartilage, and hypoplastic hair, sometimes with a compromised immune system. This disorder is especially common amongst the Old Order Amish of Pennsylvania.

See Also the Following Articles

Nucleolus, Overview • RNA Polymerase II and Basal Transcription Factors in Eukaryotes

Glossary

chromatin The DNA wrapped up with proteins, as found in chromosomes.

promoter A stretch of DNA located near the transcription start site that influences the efficiency of transcription.

RNA polymerase The enzyme responsible for synthesizing RNA.

transcription The process using DNA as template to synthesize a complementary RNA.

transcription factor Protein that influences the ability of RNA polymerase to carry out transcription.

Further Reading

Batzer, M. A., and Deininger, P. L. (2002). Alu repeats and human genomic diversity. *Nat. Rev. Genet.* **3**, 370–380.

Carmo-Fonseca, M., Mendes-Soares, L., and Campos, I. (2000). To be or not to be in the nucleolus. *Nat. Cell Biol.* **2**, E107–E112.

Felton-Edkins, Z. A., Kenneth, N. S., Brown, T. R. P., Daly, N. L., Gomez-Roman, N., Grandori, C., Eisenman, R. N., and White, R. J. (2003). Direct regulation of RNA polymerase III transcription by RB, p53 and c-Myc. *Cell Cycle* **2**, 181–184.

Geiduschek, E. P., and Kassavetis, G. A. (2001). The RNA polymerases II transcription apparatus. *J. Molecul. Biol.* **310**, 1–26.

Moss, T., and Stefanovsky, V. Y. (2002). At the center of eukaryotic life. *Cell* **109**, 545–548.

Paule, M. R. (1998). *Transcription of Ribosomal Genes by Eukaryotic RNA Polymerase I*. Landes Biosciences, Austin.

Paule, M. R., and White, R. J. (2000). Transcription by RNA polymerases I and III. *Nucleic Acids Res.* **28**, 1283–1298.

Schramm, L., and Hernandez, N. (2002). Recruitment of RNA polymerase III to its target promoters. *Genes Develop.* **16**, 2593–2620.

White, R. J. (2001). *Gene Transcription: Mechanisms and Control*. Blackwell Science, Oxford.

White, R. J. (2002). *RNA Polymerase III Transcription*. Landes Biosciences, Austin, http://www.eurekah.com.

Biography

Robert J. White is Professor of Gene Transcription at the Institute of Biomedical and Life Sciences at the University of Glasgow, UK. His principal research interests concern transcription by RNA polymerases I and III, and how this is regulated in health and disease. Most noted for his work on RNA polymerase III and cancer, he was chosen by the European Association for Cancer Research as the Young Cancer Researcher of 2003.

RNA Polymerase II and Basal Transcription Factors in Eukaryotes

Joan Weliky Conaway and Ronald C. Conaway
Stowers Institute for Medical Research, Kansas City, Missouri, USA

In eukaryotes from yeast to man, synthesis of messenger RNA is catalyzed by the 12 subunit enzyme RNA polymerase II, with the assistance of a set of five basal transcription factors designated TFIIB, TFIID, TFIIE, TFIIF, and TFIIH. The basal transcription factors function together to promote proper binding of RNA polymerase II to the promoter-regulatory regions of genes and synthesis of the first few phosphodiester bonds of new transcripts.

Structure and Catalytic Activity of RNA Polymerase II

RNA polymerase II (pol II) is a DNA-dependent RNA polymerase that is responsible for transcription of protein-coding genes in the nucleus of eukaryotic cells. Pol II transcription results in synthesis of an RNA copy of the protein-coding DNA strand of genes. This primary RNA transcript is referred to as pre-mRNA and is subsequently spliced and polyadenylated to form mature mRNA, which can then be exported to the cytoplasm to direct translation of its protein products by the ribosomes. Pol II is capable of initiating transcription in a promoter-independent fashion on single-stranded DNA templates and of elongating transcripts on single- or double-stranded DNA templates without assistance from auxillary transcription factors. To initiate transcription from the promoters of protein-coding genes, however, pol II requires the assistance of a set of auxillary transcription factors referred to as the "basal" factors.

Pol II carries out initiation and synthesis of pre-mRNA by catalyzing DNA template-directed addition of single nucleotides to the 3′-end of growing transcripts. Pol II accomplishes this by catalyzing formation of phosphodiester bonds between the 3′-nucleotide of the transcript and incoming ribonucleoside triphosphates specified by the DNA. Phosphodiester bonds are formed by nucleophilic attack of the 3′-hydroxyl of the transcript on the α-phosphorus of the incoming ribonucleoside triphosphate, with the release of pyrophosphate. A remarkable feature of transcribing pol II is the enormous stability of the pol II–DNA–RNA ternary elongation complex, which can synthesize transcripts as long as the two-million-nucleotide *dystrophin* pre-mRNA without dissociating from the DNA.

Pol II is a multisubunit enzyme composed of ~12 subunits designated Rpb1–Rpb12, with sizes ranging from ~220 to ~10 kDa, respectively. Pol II is highly evolutionarily conserved from yeast to man. High-resolution X-ray crystal structures of free and transcribing *Saccharomyces cerevisiae* pol II have revealed that the two largest pol II Rpb1 and Rpb2 subunits associate with one another to form the core of the enzyme, with the remaining pol II subunits positioned on the outer surface of the Rpb1–Rpb2 core. The pol II catalytic site is contained within a positively charged cleft formed at the Rpb1–Rpb2 interface. The cleft extends from the enzyme's outer surface to the catalytic Mg^{2+} ion buried deep in the enzyme. The cleft is of sufficient size to accommodate as many as 20 bp of DNA. The catalytic Mg^{2+} ion participates directly in formation of phosphodiester bonds, most likely by coordinating the phosphates of the incoming ribonucleoside triphosphate in preparation for nucleophilic attack by the oxygen of the 3′-hydroxyl of the nascent transcript.

The X-ray crystal structure of the transcribing pol II–DNA–RNA ternary complex has revealed features of the complex that provide insights into the mechanism of pol II transcription. Approximately nine nucleotides of RNA at the 3′-end of the nascent pre-mRNA transcript are base-paired to the DNA in a DNA–RNA hybrid that holds the transcript's 3′-hydroxyl properly positioned with respect to the catalytic Mg^{2+} ion. Approximately 4 bp of DNA ahead of the 3′-end of the nascent transcript are unwound, providing the incoming ribonucleoside triphosphates with access to the single-stranded DNA template to ensure proper base-pairing with the template. The pre-mRNA is physically separated from the DNA–RNA hybrid ~10 nucleotides upstream of the transcript's 3′-end and exits the pol II catalytic site through a discrete RNA-binding groove in the enzyme. Finally, a large ~50 kDa clamp comprising portions

of the Rpb1, Rpb2, and Rpb3 subunits closes tightly around the DNA–RNA hybrid, providing a molecular explanation for the great stability and high processivity of the pol II–DNA–RNA ternary elongation complex.

Mechanism of Transcription Initiation by RNA Polymerase II

Synthesis of eukaryotic pre-mRNA by pol II requires that the enzyme finds and binds selectively to promoters located upstream of the protein-coding genes they control and, in most cases, buried amid thousands of base pairs of DNA separating adjacent genes on the chromosomes. Unlike most bacterial RNA polymerases, which are capable of recognizing and binding their promoters and initiating transcription pol II requires a minimum set of five basal transcription factors designated as TFIIB, TFIID, TFIIE, TFIIF, and TFIIH, which are necessary to direct selective binding of the enzyme to its promoters and to support transcription initiation. Like pol II, the basal factors exhibit a high degree of evolutionary conservation from yeast to man. The basal factors assemble with pol II at promoters into a stable preinitiation complex that can initiate transcription when provided with an ATP or dATP cofactor and the ribonucleoside triphosphates needed for RNA synthesis.

Pol II Promoters

Pol II promoters vary considerably from gene to gene and can include as little as a few hundred to many thousands of base pairs of DNA located upstream and even within or downstream of the genes they control. All pol II promoters include a "core" element, which surrounds the transcriptional start site and is sufficient to direct synthesis of accurately initiated transcripts. Core promoters include some combination of three types of promoter element: (1) an ~7 bp, degenerate motif called the TATA box, which is found from ~24 to ~30 bp upstream of the transcriptional start site and has the consensus sequence TATAAAA, (2) an initiator element (Inr), which surrounds the transcriptional start site and has the consensus sequence Y_{4-5}CANTY_{4-5} (where Y is a pyrimidine, and N can be any of the four bases A, C, G, or T), and (3) a 5 bp downstream promoter element or DPE, which is positioned at residues 28–32 bp downstream of the conserved A residue within the Inr. The consensus sequence for the *Drosophila melanogaster* DPE, which has been most thoroughly studied, is (A/G)G(A/T)Y(G/A/C).

In metazoans, a recognizable TATA element is found in a little less than half of the promoters examined, while Inr elements are included in ~70% of promoters. Some promoters have both a TATA element and an Inr, and others have only one or the other of these elements. DPEs are most commonly found in promoters that lack TATA boxes. Unlike the TATA or Inr elements, DPEs cannot function independently of other core promoter elements, but must be precisely positioned downstream of an Inr.

In addition to a core promoter, pol II promoters include additional DNA sequence motifs that serve as binding sites for one or more of the large number of DNA-binding transcriptional regulatory proteins that control the frequency of pol II transcription initiation from the core promoter. Among these DNA motifs are upstream promoter elements (UPEs), enhancers, and silencers. UPEs are typically clustered a few hundred base pairs upstream of the core promoter. Enhancers and silencers can be located thousands of base pairs upstream or downstream of the core promoter. Estimates suggest that as many as 10 000 human genes encode UPE, enhancer, and silencer DNA-binding proteins that function alone and in combination to fine tune the levels of pol II transcription of eukaryotic protein-coding genes.

Roles of the Basal Factors in Transcription Initiation by Pol II

Transcription initiation by pol II is a multistep process that begins with assembly of the enzyme with the basal factors at the core promoter to form a stable preinitiation complex and culminates with ATP (dATP)-dependent unwinding of core promoter DNA at the transcriptional start site, synthesis of the first few phosphodiester bonds of the nascent transcript, and escape of polymerase from the promoter. In the first step, the basal factor TFIID binds to the core promoter to form the nucleoprotein recognition site for pol II on the DNA. TFIID is a multisubunit protein composed of the TATA-box binding protein (TBP) and as many as 13 additional proteins designated TBP-associated factors (TAFs). The TBP subunit of TFIID binds directly to the TATA box and is capable of recognizing and binding stably to TATA boxes not only with the consensus TATAAA sequence, but also with a large number of divergent TATA-box sequences. The TFIID subunit TAF2 can bind in a sequence-specific manner to the Inr element surrounding the transcriptional start site. Although it is not yet clear how the DPE is recognized, some evidence suggests that the TFIID subunits TAF6 and TAF9 are located close to the DPE and may make sequence-specific contacts with it.

Once TFIID has bound the core promoter, the basal factor TFIIB recruits pol II to the TFIID–core promoter complex through specific protein–protein interactions with both the TBP subunit of TFIID and pol II. TFIIB is a small, modular protein of ~30 kDa with distinct

protein–protein interaction domains capable of interacting independently with TBP and pol II. Once pol II and TFIIB have bound to the TFIID–core promoter complex, TFIIF can enter the preinitiation complex. TFIIF is a two-subunit protein that strongly stabilizes binding of pol II to the core promoter. TFIIF is also required for stepwise entry of TFIIE and TFIIH into the pol II complex to form the fully assembled preinitiation complex. TFIIE is a two-subunit protein, and TFIIH is a nine-subunit protein possessing both DNA helicase and protein kinase activities. As a component of the preinitiation complex, the TFIIH DNA helicase catalyzes ATP(dATP)-dependent unwinding of core promoter DNA at the transcriptional start site to provide pol II access to a short stretch of single-stranded DNA to allow initiation of pre-mRNA synthesis.

See Also the Following Articles

DNA Helicases: Dimeric Enzyme Action • DNA Helicases: Hexameric Enzyme Action • RNA Polymerase I and RNA Polymerase III in Eukaryotes • RNA Polymerase II Elongation Control in Eukaryotes • RNA Polymerase II Structure in Eukaryotes

Glossary

basal transcription factors Minimal set of auxillary transcription factors required to support promoter-specific transcription initiation by pol II.

DNA helicase Enzyme that uses the energy of ATP(dATP) hydrolysis to unwind the two strands of DNA.

DNA template DNA that is transcribed by RNA polymerases.

promoter DNA sequences that direct RNA polymerases to transcribe genes.

RNA polymerase Enzyme that catalyzes synthesis of RNA.

Further Reading

Conaway, J. W., and Conaway, R. C. (1997). General transcription factors for RNA polymerase II. *Prog. Nucleic Acid Res. Mol. Biol.* **56**, 327–346.

Coulombe, B., and Burton, Z. F. (1999). DNA bending and wrapping around RNA polymerase: A "revolutionary" model describing transcriptional mechanisms. *Microbiol. Mol. Biol. Rev.* **63**, 457–478.

Cramer, P., Bushnell, D. A., and Kornberg, R. D. (2001). Structural basis of transcription: RNA polymerase II at 2.8 Angstrom resolution. *Science* **292**, 1863–1876.

Dvir, A., Conaway, J. W., and Conaway, R. C. (2001). Mechanism of transcription initiation and promoter escape by RNA polymerase II. *Curr. Opin. Genet. Develop.* **11**, 209–214.

Gnatt, A. L., Cramer, P., Fu, J., Bushnell, D. A., and Kornberg, R. D. (2001). Structural basis of transcription: An RNA polymerase II elongation complex at 3.3 Angstrom resolution. *Science* **292**, 1876–1882.

Smale, S. T., and Kadonaga, J. T. (2003). The RNA polymerase II core promoter. *Annu. Rev. Biochem.* **72**, 449–479.

Biography

Joan Weliky Conaway and Ronald C. Conaway are investigators at the Stowers Institute for Medical Research in Kansas City, Missouri. Research in their laboratory is aimed at contributing to an understanding of the molecular mechanisms that control the synthesis of eukaryotic messenger RNA. They hold Ph.D.s from the Stanford University School of Medicine.

RNA Polymerase II Elongation Control in Eukaryotes

David H. Price
University of Iowa, Iowa City, Iowa, USA

During the 1990s, it became clear that the elongation properties of RNA polymerase II are regulated and the factors responsible play a critical role in controlling gene expression in eukaryotic cells. One set of factors helps RNA polymerase II to negotiate pause and arrest sequences in the template and to maintain an elongation rate of 1000–1500 nucleotides per minute. The initiation factor TFIIF reduces RNA polymerase II pause times and stimulates the rate of elongation. The elongation factor S-II or (TFIIS) rescues polymerase molecules that are blocked from further elongation at arrest sites. Another set of factors is responsible for an elongation control process that regulates the fraction of initiated polymerases that enter productive elongation to generate mRNAs. Negative transcription elongation factors (N-TEFs), such as DSIF and NELF, slow the rate of elongation and restrict the polymerase to promoter proximal sequences. The positive transcription elongation factor, P-TEFb, overcomes the effect of the negative factors and allows the production of full length transcripts. The function of P-TEFb is regulated through interactions with many other transcription factors and the amount of active P-TEFb in the cell is precisely regulated through a reversible inhibition by the small cellular RNA, 7SK.

Historical Perspective

It has been clear for some time that much of the regulation of prokaryotic gene expression is accomplished by controlling the elongation potential of RNA polymerase, but only recently has it become apparent that eukaryotic gene expression is similarly regulated. Early work in John Lis's lab showed that there was an RNA polymerase II molecule engaged in transcription of the major *Drosophila* heat shock gene, HSP70, under conditions where no full length mRNAs were being produced. Only after heat shock were the polymerases allowed to continue elongation and produce mRNAs. Similarly, regulated premature termination of transcription was seen on a number of viral genes, most notably from HIV, as well as on cellular genes, including oncogenes such as c-myc and c-fos. In the early 1990s *in vitro* systems were beginning to reproduce the elongation control process and ultimately these systems allowed the identification and purification of some of the specific factors involved. The current model of RNA polymerase II elongation control has the look and feel of models of prokaryotic antitermination, but there are important differences in mechanistic details.

Positive and Negative Elongation Factors

Elongation Maintenance Factors

During transcription, RNA polymerase II is aided by specific factors as it encounters numerous blocks to elongation inherent in a template sequence. During normal transcription *in vivo*, each nucleotide addition to an RNA chain requires ~50 ms on average. However, *in vitro* RNA polymerase II may pause for seconds or minutes at specific sites in the absence of any accessory factors. TFIIF, a factor required for RNA polymerase II initiation, can also decrease the time that the polymerase spends at pause sites. This has the effect of increasing the overall elongation rate because, for the most part, the elongation rate is determined by how long the polymerase stops at the strongest pause sites. It has been hypothesized that the mechanism utilized by TFIIF involves an interaction-induced change in the polymerase from the paused conformation to the elongation competent form. Other factors that belong in this same class are ELL and elongin, but TFIIF has the most dramatic elongation stimulatory activity. The elongation factor S-II functions by a completely different mechanism. At some sites a fraction of RNA polymerase II molecules fall into an arrested conformation from which they cannot escape unaided. At these sites the 3′ end of the nascent transcript is removed from the active site of the polymerase as the polymerase "backslides" along the template while maintaining an RNA:DNA hybrid. When this happens, the polymerase may remain engaged for hours or days without extending the transcript. S-II stimulates an intrinsic ribonuclease activity of the

polymerase that removes the unpaired 3′ end of the transcript and puts the new 3′ end in register with the active site of the polymerase. This reactivates elongation and the polymerase has a second chance to pass the arrest site. Eventually, all polymerases can pass the arrest site although many may require several rounds of S-II-mediated transcript cleavage. Through the combined function of both classes of factors, the elongation rate of RNA polymerase II is maintained between 1000 and 1500 nucleotides per minute.

Elongation Control

In addition to the factors that maintain efficient elongation, there is another set of factors responsible for regulating the efficiency of initiated polymerases to reach the 3′ end of genes. This process has been termed RNA polymerase II elongation control and is best viewed as an obligatory event mediated by the default action of negative factors, N-TEFs, and the regulated action of a positive factor, P-TEFb (Figure 1). The process was demonstrated *in vitro* by first showing that the transcription inhibitor 5,6-dichlororibofuranosyl benzamidizole (DRB) could block the production of long, but not short transcripts. Elongation control was further characterized by the separation of N-TEFs, which direct polymerases to generate only short promoter proximal transcripts, from a positive factor, ultimately identified as P-TEFb, which reverses the action of the N-TEFs. A combination of the action of the N-TEFs and the activity of transcription termination factor 2 (TTF2) results in a process called abortive elongation characterized by the premature termination of transcripts before the mature 3′ end of the gene is reached. P-TEFb plays a key role in that it is responsible for the transition into productive elongation. Stated in another way, the ability to produce mRNAs is directly linked to the activity of P-TEFb. Elongation control machinery exists in all eukaryotic species that have been examined and the current evidence suggests that P-TEFb is required for transcription of most genes.

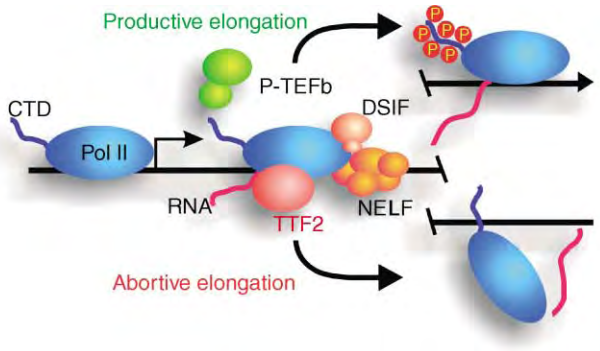

FIGURE 1 RNA polymerase II elongation control. After initiation pol II enters abortive elongation by default because of the action of N-TEFs, such as DSIF and NELF. Phosphorylation of the CTD of the large subunit of RNA polymerase II by P-TEFb causes the transition into productive elongation. If P-TEFb does not act, transcription is prematurely terminated by TTF2.

N-TEFs and Termination Factors

The evidence gathered so far points to the existence of two factors (DSIF and NELF) that play a negative role in elongation control. DSIF, the DRB sensitivity-inducing factor, was discovered as a protein required for DRB sensitive transcription *in vitro*. It is comprised of two subunits with strong sequence similarity to the yeast proteins SPT4 and SPT5. DSIF has almost no function on RNA polymerase II alone. The negative elongation factor (NELF) also has no effect on RNA polymerase II alone, but the combination of NELF and DSIF is able to slow the elongation rate and cause the polymerase to reside longer at pause sites. In this way, NELF and DSIF act in exactly the opposite way as TFIIF, which reduces pause time. NELF is comprised of four subunits, including a putative RNA-binding protein called RD. A defined elongation control system comprised of isolated RNA polymerase II elongation complexes (NELF, DSIF, and P-TEFb) displays many of the properties of elongation control seen when transcription is carried out in nuclear extract. DSIF is involved in controlling transcription from the HSP70 locus in *Drosophila*, but the generality of its function has not been demonstrated. Although removal of DSIF in *C. elegans* using RNAi techniques relieved most of the requirements of P-TEFb at a heat shock locus, similar results were not found in expression of several other genes. These facts along with the fact that homologues of NELF subunits have not been identified in many organisms suggest that other negative factors, which operate at a wide variety of genes, remain to be discovered.

So far only one transcription termination factor, TTF2 (formerly and uninformatively called factor 2), has been identified. It is a member of the SWI2/SNF2 family of proteins that are generally involved in disrupting protein nucleic acid interactions. It binds to both single- and double-strand DNA and has a strong dsDNA-dependent ATPase activity that is required for termination activity. The termination activity of TTF2 is inhibited by TFIIF, and while the mechanism of this inhibition is unknown, it provides a possible method to control the activity of TTF2 during transcription. The role of TTF2 seems to operate outside of the elongation control process in that its negative effect is not directly reversed by P-TEFb. However, a role for the factor in abortive elongation (premature termination) or in normal termination associated with mature 3′ end formation has not been ruled out.

P-TEFb

Subunits and Activity

P-TEFb is a cyclin-dependent kinase comprised of Cdk9 and one of several cyclin subunits. Three genes in humans – T1, T2, and K – encode cyclin subunits that can associate with and activate Cdk9. Two cyclin T genes have been found in *C. elegans*, but only one in *Drosophila*. Supporting a broad role in gene expression, knockout of Cdk9 in *C. elegans* causes loss of gene expression and death at the same early stage as knockout of one of the subunits of RNA polymerase II. The same lethal phenotype is observed when both cyclin T's are knocked out. The carboxyl terminal domain (CTD) of the large subunit of RNA polymerase II is phosphorylated by P-TEFb and this domain has been shown to be required for the function of P-TEFb in the transition into productive elongation. The CTD is comprised of multiple repeats of the heptapeptide YSPTSPS, and P-TEFb predominately phosphorylates the second serine. P-TEFb had been shown to have broad substrate specificity *in vitro* and will phosphorylate the large subunit of both DSIF and TFIIF. Although the CTD is phosphorylated by P-TEFb and is required for the function of P-TEFb in transcription, there may be other important functional phosphorylation targets. The effect of DRB on transcription is explained by the fact that it inhibits the kinase activity of P-TEFb. All P-TEFb inhibitors reduce the production of mRNAs *in vivo* and are lethal at high concentrations. Flavopiridol, the most potent P-TEFb inhibitor found, is in clinical trials against cancer.

Recruitment of P-TEFb

P-TEFb interacts in a functional way with a number of important transcription factors. Cyclin T1 interacts with the HIV transactivator Tat, and P-TEFb containing cyclin T1 can be recruited to elongation complexes on the HIV template through the interaction of Tat and cyclin T1 with a stem loop structure that forms in the nascent HIV transcript called TAR. This recruitment of P-TEFb activates transcription of the HIV genome. A cellular factor, CIITA, which is involved in activating transcription of the MHC class II genes, has also been shown to function through interaction with P-TEFb. That interaction is blocked in the presence of Tat suggesting that the binding site is similar for the viral and cellular protein and providing a mechanism for inhibition of MHC class II gene expression during HIV infection. Other transcription factors and enhancer binding proteins – including NFκB, c-myc, MCEF, and the androgen receptor – have been demonstrated to various degrees to have functional interactions with P-TEFb.

Recruitment of P-TEFb through artificial targeting to promoter DNA or to nascent RNA has revealed several important aspects of its function. First, when a protein is expressed in which Cdk9 or cyclin T1 or T2 is tethered to the DNA-binding domain of a yeast protein (Gal4) and the binding sites for that protein are placed close to a human promoter, transcription is stimulated from that promoter. Besides the core promoter elements, SP1 binding sites are also required to see an effect of the recruited P-TEFb in this system. This is consistent with the model for P-TEFb function because P-TEFb only affects polymerases that have already initiated and SP1 increases the initiation efficiency. Expression of Cdk9, cyclin T1, T2, or K tethered to an RNA-binding domain (e.g., HIV rev) activates transcription of a gene containing the appropriate RNA element. In both tethering experiments, the untethered component of P-TEFb is also recruited due to the inherent interaction between P-TEFb subunits. Cyclin K does not work when tethered to DNA elements because it lacks a CTD present on both cyclin T1 and T2 that plays another role by interacting with the CTD of the large subunit of RNA polymerase II.

Control of P-TEFb by 7SK

Very recently, the laboratories of Olivier Bensaude and Qiang Zhou simultaneously discovered the small cellular RNA, 7SK, in association with a fraction of P-TEFb in cells. The large complex containing P-TEFb and 7SK was relatively inactive compared to the free P-TEFb (Figure 2). Addition of small amounts of compounds that inhibit elongation by RNA polymerase II causes a reduction in the large form of P-TEFb *in vivo* and a concomitant increase in the small active form. Evidently, a cell will try to compensate for reduced production of mRNAs by activating more P-TEFb. The change in large to small form of P-TEFb can occur within minutes and is reversible. The significance of the large form of P-TEFb was demonstrated using a mouse model of cardiac hypertrophy. Heart cells that were stimulated to grow in size had an increase in P-TEFb activity, but no increase in the amount of P-TEFb. It was shown that all hypertrophic signals tested caused a release of 7SK. The signal transduction pathways involved in hypertrophy of cardiac cells at least partially routes through the elongation control pathway.

Integration of Elongation Control and Gene Expression

Elongation control may play a very significant role in controlling eukaryotic gene expression. Most RNA polymerase II molecules found transcribing human genes require the prior function of P-TEFb. Recruitment

FIGURE 2 Control of P-TEFb by 7SK. The amount of P-TEFb activity in the cell can be quickly adjusted by the reversible association of 7SK RNA. The large form with 7SK bound is inactive.

of P-TEFb by transcription factors allows specific genes to be targeted, and both the targeted and the untargeted functions of P-TEFb may allow global regulation of mRNA production. Regulating the conversion of the large to small P-TEFb form by signal transduction pathways is another global means to regulate mRNA levels. Overall, the combined action of negative and then positive factors results in a kinetic delay of the progression of polymerases down the gene. This may provide a window of opportunity for RNA processing machinery to function or associate with the elongating polymerase, ensuring a truly productive elongation event resulting in a complete, functional mRNA. The human capping enzyme is functionally coupled to transcription and guanylates the nascent transcript before P-TEFb acts. However, some components of the polyadenylation and splicing machinery have been shown to associate with the phosphorylated CTD. Perhaps the processing machinery is functionally coupled to transcription through interactions provided by elongation control and scans the nascent transcript for processing sites as it is being made. Many mechanistic details of how RNA polymerase II elongation control is accomplished and the ramifications of the process on subsequent events remain to be determined.

See Also the Following Articles

RNA Polymerase II and Basal Transcription Factors in Eukaryotes • RNA Polymerase II Structure in Eukaryotes

Glossary

DRB The P-TEFb inhibitor 5,6-dichlororibofuranosyl benzamidizole.

DSIF DRB sensitivity inducing factor, an N-TEF.

NELF Negative elongation factor, an N-TEF.

N-TEFs Negative transcription elongation factors.

P-TEFb Positive transcription elongation factor b composed of Cdk9 and a cyclin partner.

Further Reading

Marshall, N. F., and Price, D. H. (1992). Control of formation of two distinct classes of RNA polymerase II elongation complexes. *Mol. Cell Biol.* **12**, 2078–2090.

Nguyen, V. T., Kiss, T., Michels, A. A., and Bensaude, O. (2001). 7SK small nuclear RNA binds to and inhibits the activity of CDK9/cyclin T complexes. *Nature* **414**, 322–325.

Price, D. H. (2000). P-TEFb, a cyclin-dependent kinase controlling elongation by RNA polymerase II. *Mol. Cell Biol.* **20**, 2629–2634.

Sano, M., Abdellatif, M., Oh, H., Xie, M., Bagella, L., Giordano, A., Michael, L. H., DeMayo, F. J., and Schneider, M. D. (2002). Activation and function of cyclin T-Cdk9 (positive transcription elongation factor-b) in cardiac muscle-cell hypertrophy. *Nat. Med.* **8**, 1310–1317.

Shim, E. Y., Walker, A. K., Shi, Y., and Blackwell, T. K. (2002). CDK-9/cyclin T (P-TEFb) is required in two postinitiation pathways for transcription in the *C. elegans* embryo. *Genes Dev.* **16**, 2135–2146.

Zhu, Y., Pe'ery, T., Peng, J., Ramanathan, Y., Marshall, N., Marshall, T., Amendt, B., Mathews, M. B., and Price, D. H. (1997). Transcription elongation factor P-TEFb is required for HIV-1 tat transactivation in vitro. *Genes Dev.* **11**, 2622–2632.

Biography

David Price, Ph.D., is a Professor of Biochemistry at the University of Iowa. His interest is in understanding the basic mechanisms controlling eukaryotic gene expression. His laboratory focuses on postinitiation activities of RNA polymerase II, including elongation and termination, and how RNA processing and transcription are functionally coupled. The discovery of P-TEFb and its involvement in HIV in his laboratory is currently being extended by mechanistic studies concerning how HIV controls P-TEFb during infection.

RNA Polymerase II Structure in Eukaryotes

Patrick Cramer
University of Munich, Munich, Germany

RNA polymerase II (pol II) carries out transcription of protein-coding genes by catalyzing DNA-directed synthesis of messenger RNA. Detailed three-dimensional structures are now available for yeast pol II in free form, in form of a minimal elongation complex with bound nucleic acids, in an inhibited form with the bound toxin α-amanitin, and in complex with two additional subunits, Rpb4 and Rpb7. Together with functional data, these structures provide many insights into the mechanism of mRNA transcription.

Architecture

A ten-polypeptide pol II core enzyme is sufficient to elongate the RNA transcript. For transcription initiation, an additional two-subunit Rpb4/7 complex, and several general transcription factors are required. In the crystal structures of the pol II core, the two large subunits, Rpb1 and Rpb2 (Table I), form the central mass of the enzyme, and opposite sides of a positively charged "cleft" that contains the active center (Figure 1). The two large subunits are bridged on one side by a module of subunits Rpb3, Rpb10, Rpb11, and Rpb12. Around the periphery of the enzyme, Rpb5, Rpb6, and Rpb8 bind to Rpb1, and Rpb9 binds to both Rpb1 and Rpb2. The structures lack subunits Rpb4 and Rpb7, which form a stable heterodimer that can dissociate from the yeast pol II core. The structure of an archaeal Rpb4/7 counterpart revealed that Rpb7 spans the elongated heterodimer and is organized in two domains. The Rpb4 homologue forms a conserved hydrophobic interface with the Rpb7 homologue at the connection between the two Rpb7 domains. Recent structures revealed that the Rpb4/7 complex binds to the pol II core via subunit Rpb7 and that it protrudes from the pol II core surface near subunit Rpb6.

Structural Elements

The Rpb1 side of the pol II cleft is formed by a mobile clamp, whereas the Rpb2 side consists of the lobe and protrusion domains. The entrance to the cleft is formed between the upper and the lower jaw, which include subunits Rpb9 and Rpb5, respectively. The end of the cleft is blocked by a protein wall. The active center is at the floor of the cleft, between the protrusion, the wall, and the clamp. Before the active center and opposite of the wall, a long bridge helix spans the cleft. The bridge partially lines a pore in the active center, which widens toward the other side of the enzyme, creating an inverted funnel. The rim of the pore includes the highly conserved aspartate loop of Rpb1 that binds a catalytic Mg^{2+} ion, termed metal A. A second metal ion, metal B, is weakly bound next to metal A further in the pore. Both metal ions are accessible from one side.

The clamp is trapped in two different open states in the free core structures, but is rotated and closed in the structure of the pol II transcription–elongation complex that comprises template DNA and the RNA transcript. In this structure, the clamp binds the DNA template strand with three out of five switch regions. The switch regions form the base of the clamp, connecting to the remainder of pol II. Upon clamp closure, the switches change conformation or undergo folding transitions. The closed conformation of the clamp is also observed in the complete pol II that contains the Rpb4/7 complex. The Rpb4/7 complex appears to form a wedge between the clamp and subunit Rpb6, thus preventing clamp opening.

The Rpb1 polypeptide chain protrudes below the Rpb4/7 complex on the outside of pol II, and gets disordered after a few residues. These residues of Rpb1 constitute the beginning of a flexible linker that connects to the mobile C-terminal repeat domain (CTD). The CTD, a unique feature of pol II, consists of repeats of a heptapeptide with the consensus sequence Tyr-Ser-Pro-Thr-Ser-Pro-Ser. A total of 26 and 52 CTD repeats are found in yeast and human Rpb1, respectively.

Mechanism

Transcription Cycle

The transcription cycle is divided into three phases: initiation, elongation, and termination. Steps during

TABLE I

Polypeptide Composition of Cellular RNA Polymerases

Pol I	Pol II	Pol III	Archaea	Bacteria	Class[a]
A190	Rpb1	C160	$A' + A''$	β'	Core
A135	Rpb2	C128	B ($B' + B''$)	β	Core
AC40	Rpb3	AC40	D	α	Core
AC19	Rpb11	AC19	L	α	Core
Rpb6	Rpb6	Rpb6	K	ω	Core, common
Rpb5	Rpb5	Rpb5	H		Common
Rpb8	Rpb8	Rpb8			Common
Rpb10	Rpb10	Rpb10	N		Common
Rpb12	Rpb12	Rpb12	P		Common
A14	Rpb4	C17	F		Rpb4/7
A43	Rpb7	C25	E		Rpb4/7
A12.2	Rpb9	C11	X		Specific
A34.5					Specific
A49					Specific
		C82			Specific
		C34			Specific
		C31			Specific

[a] Core, sequence partially homologous in all RNA polymerases; common, shared by all eukaryotic RNA polymerases; Rpb4/7, Rpb4/7 heterodimer and its structural counterparts.

initiation include promoter binding, DNA melting, and synthesis of short RNA transcripts. The transition from initiation to elongation is referred to as promoter escape, and results in a stable elongation complex that is characterized by an open DNA region, the transcription bubble. The bubble contains the DNA–RNA hybrid, a heteroduplex of eight or nine base pairs. The growing RNA 3′-end is located at the end of the hybrid that is engaged with the pol II active site. Pol II alone can maintain an open transcription bubble, translocate along the DNA template, synthesize RNA, and detect errors in the nascent RNA. For all other steps, however, pol II requires the help of additional proteins.

Several steps of the transcription cycle are accompanied by phosphorylation or dephosphorylation of the pol II CTD. During initiation, the CTD gets phosphorylated, and the CTD phosphorylation pattern changes during elongation. CTD phosphorylation patterns govern specific interaction with RNA processing factors, thereby coupling transcription to RNA processing. The CTD is flexibly linked to a region beyond the saddle, from which RNA exits, consistent with its role in coupling transcription to mRNA processing. Several kinases and at least one phosphatase control the phosphorylation state of the pol II CTD.

Initiation

To bind and melt promoter DNA, pol II assembles on DNA with the general transcription factors TFIIB,

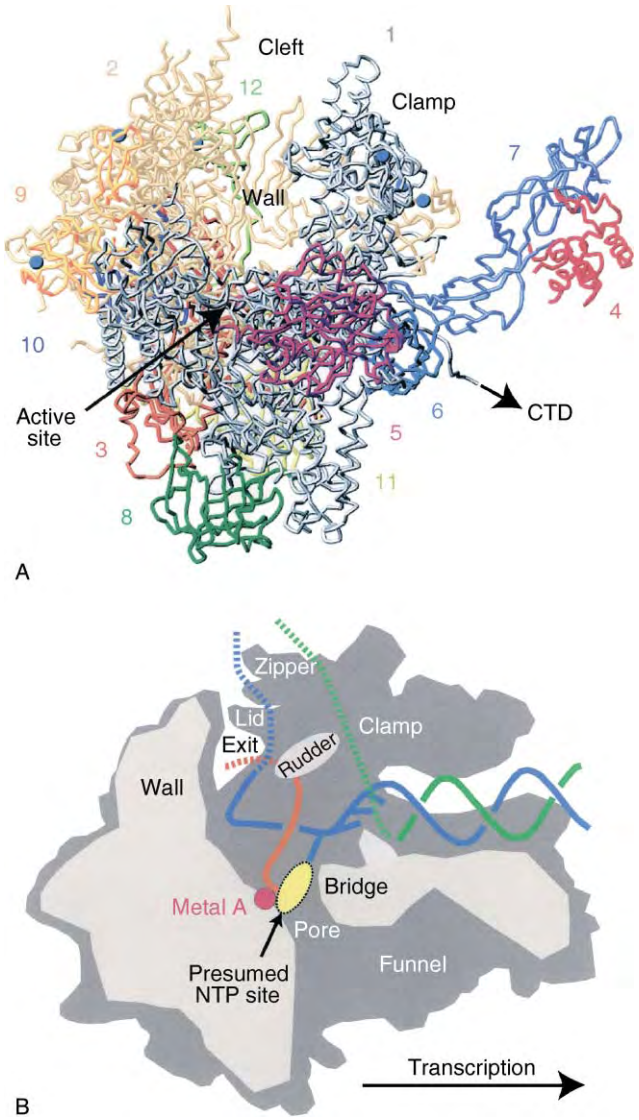

FIGURE 1 RNA polymerase II structures. (A) Ribbon model of yeast RNA polymerase II. The 12 subunits are shown in different colors. The active site metal ion A is depicted as a pink sphere. Zinc ions are shown as cyan spheres. (B) Schematic cut-away view of the pol II core elongation complex. The view is related to the one in (A) by a 90° rotation around a vertical axis. The DNA template and nontemplate strands are in blue and green, respectively, and the RNA is in red. Four of the bases in the DNA template strand are indicated as sticks protruding from the backbone. The yellow oval depicts the presumed binding site for the incoming nucleoside triphosphate substrate.

-D, -E, -F, and -H. The general factors are involved in sequence-specific promoter recognition (TFIIB, TFIID), prevention of nonspecific DNA binding (TFIIF), and DNA melting and CTD phosphorylation (TFIIE, TFIIH). RNA synthesis initiates within the bubble. The early transcribing complex is functionally unstable. Short RNAs are frequently released and pol II has to restart transcription (abortive cycling). There is a decline in abortive transcription when the RNA reaches a length of about four nucleotides, a transition

termed "escape commitment." RNA that has grown to a length of at least four nucleotides is generally not contacted by pol II anymore and is held in the elongation complex by base pairing with the DNA template strand. A second barrier in the transition from initiation to elongation has to be overcome when the RNA reaches a length of about ten nucleotides. At this length, the 5′-end of the RNA is detached from the DNA template strand, and is redirected to the pol II "saddle" and an exit tunnel. A third transition of the early elongation complex is reflected in the continued requirement for ATP and TFIIH until the RNA is about 15 nucleotides long. This transition may reflect successful positioning of all bubble-maintaining structural elements of pol II with respect to the bubble, and detachment of RNA from the pol II surface. Two possible RNA exit grooves have been suggested beyond the saddle, and binding of RNA to the saddle and to one of the exit grooves could account for an additional gain in stability of the elongation complex. Successful passage of early pol II elongation complexes through all three transitions has been referred to as "promoter clearance."

Elongation

During elongation, downstream DNA enters pol II at two mobile "jaws," and extends through the cleft toward the active site. Beyond the active site, a nine base pair DNA–RNA hybrid extends upward, toward the wall. The axes of the downstream DNA duplex and the DNA–RNA hybrid heteroduplex enclose an angle of ~90°. The growing RNA 3′-end is located above the pore, which allows entry of nucleoside triphosphate substrates from below. In the crystal structure of the pol II elongation complex, the incoming DNA duplex is mobile and badly ordered. However, three nucleotides before the active site, the DNA template strand becomes well-ordered by binding to the bridge helix and to two "switch" regions at the base of the clamp. A 90° twist between subsequent nucleotides orients a DNA base toward the active site for base pairing with an incoming nucleotide.

The property of the polymerase to stay attached to the template, even during transcription of long genes, is often referred to as processivity. The major cause of processivity is the high stability of the pol II elongation complex, caused by tight binding of the DNA–RNA hybrid. This stability can be accounted for by the highly complementary hybrid-binding site on pol II, which is partially created upon clamp closure and folding of the switches. Several pol II structural elements are predicted to maintain the hybrid and the transcription bubble during elongation, including the fork loops, the top of the wall, and three loops protruding from the edge of the clamp, called rudder, lid, and zipper.

The nucleotide addition cycle during RNA chain elongation begins with entry of the nucleoside triphosphate (NTP) substrate, maybe together with metal B, and its binding between the bridge helix and the end of the hybrid, to form a base pair with the coding DNA base. Correct orientation of the substrates and metal ions would lead to synthesis of a new phosphodiester bond and to the release of pyrophosphate, maybe together with metal B. The resulting complex adopts the pre-translocation state, which was apparently trapped in the pol II elongation complex structure, with the RNA 3′-terminal nucleotide occupying the NTP-binding site. Subsequent translocation of nucleic acids would align the new RNA 3′ end with metal A, and would free the NTP-binding site, preparing pol II for another cycle of nucleotide addition.

Specificity for synthesizing RNA rather than DNA is achieved by at least three mechanisms. First, the discriminating 2′-OH group of the incoming NTP may be hydrogen-bonded by a conserved pol II residue. Second, 2′-OH groups of the last few nucleotides that were incorporated into the growing RNA are directly hydrogen-bonded by pol II residues. Finally, the active center of pol II is complementary to the resulting DNA–RNA hybrid duplex that adopts a conformation intermediary between canonical A- and B-forms.

It is a mystery of the transcription mechanism how rapid translocation of nucleic acids can be achieved while nucleic acids are bound tightly by pol II. Hints for understanding translocation are, however, provided by the pol II structures. First, nucleic acids are only contacted via their backbones; base interactions that would impede translocation are not observed. Second, long-range electrostatic attraction of the nucleic acid backbones by positively charged protein groups in a "second shell" may enable tight binding of nucleic acids without restricting their movement. Finally, translocation may be accompanied by conformational changes in pol II that could maintain some of the protein–nucleic acid contacts during translocation. Structural comparisons suggest that one such conformational change may be bending of the bridge helix.

Pol II elongation is inhibited by the cyclic octapeptide α-amanitin, the toxin of the "death cap" mushroom. α-Amanitin does not greatly influence NTP binding, and a phosphodiester bond can still be formed when the toxin is added to an elongation complex. However, the rate of transcription is dramatically reduced. Only several nucleotides are incorporated per minute. In the structure of a pol II core–α-amanitin complex, α-amanitin binds to the bridge helix, and could restrain a possible movement of this helix, thereby blocking conformational changes that are important for translocation. However, the exact mechanism of pol II inhibition by α-amanitin is not understood.

Pol II does not move along the DNA template in a unidirectional manner, it rather oscillates between movements forward and backward ("backtracking"). During backtracking, RNA is extruded through the pol II pore into the funnel. Backtracking can lead to transcriptional pausing and arrest. Pausing is defined as a temporary block to elongation, from which pol II can escape by itself. In contrast, pol II cannot escape from arrest without the help of the transcript cleavage factor TFIIS, which stimulates a weak intrinsic nuclease activity of pol II, which cleaves RNA. Access of TFIIS to the pol II active site is apparently provided via the funnel and pore. Backtracking and TFIIS action may also underlie "proofreading" of the nascent transcript. During proofreading, a misincorporated nucleotide results in a mismatch base pair within the DNA–RNA hybrid. The induced distortion of the hybrid destabilizes the elongation complex and can lead to immediate cleavage of a mononucleotide, or it can trigger in backtracking, which results in threading of a short stretch of RNA (comprising the misincorporated nucleotide) into the pore and cleavage with the help of TFIIS. Any proofreading reaction creates a new RNA 3′-end at the active site, from which transcription can resume.

Termination

Transcription termination occurs in a reaction coupled to RNA 3′-end processing. Most eukaryotic mRNA precursors are cleaved in a site-specific manner in the 3′-untranslated region, followed by polyadenylation of the upstream cleavage product. A large number of proteins is involved in these reactions. The exact mechanism of coupling between 3′-end processing and transcription termination remains unclear. Termination is accompanied by dephosphorylation of the pol II CTD, but the precise timing of pol II dephosphorylation is also unclear. Dephosphorylation is required for the reinitiation of transcription, since pol II can only join an initiation complex in its unphosphorylated form. The CTD phosphatase Fcp1 plays a key role in pol II dephosphorylation and recycling. Fcp1 binds to pol II via Rpb4. Rpb4 apparently recruits Fcp1 to the vicinity of the CTD since the Rpb4/7 complex binds near the linker that connects the pol II core to the CTD.

Conservation

Pol II belongs to the family of cellular RNA polymerases, which also includes the two other eukaryotic RNA polymerases, pol I and pol III, and the bacterial and archaeal RNA polymerases. All three eukaryotic RNA polymerases share five common subunits (Table I). Four core subunits of pol II, Rpb1, Rpb2, Rpb3, and Rpb11, as well as subunit Rpb9, all have close homologues in pol I and pol III. Recent studies show that the Rpb4/7 complex of pol II also has structural and functional counterparts in pol I and pol III, and in the archaeal RNA polymerase. Since the 12 subunits of pol II are either identical or homologous in all three eukaryotic enzymes, the pol II structure is a good model for all eukaryotic RNA polymerases. Comparison of pol II with a bacterial RNA polymerase structure revealed that five core subunits underlie a general RNA polymerase architecture with an active center cleft. Twenty-two regions of sequence homology cluster around the active site and generally adopt the same structure in all cellular RNA polymerases. The structurally conserved core includes the functional elements of the active center, indicating that all cellular RNA polymerases share common mechanistic features. Homologues for all pol II subunits (except Rpb8) are found in archaeal RNA polymerases. Thus the overall structure of archaeal RNA polymerases is very similar to that of pol II except several external domains.

The pol II structure is strikingly different from structures of the many single subunit DNA and RNA polymerases. However, in functional complexes of these diverse enzymes, nucleic acids take a similar course through the active center. The entering DNA duplex encloses an angle of $\sim 90°$ with the exiting template–product duplex. At the location of the bend, subsequent DNA template bases are twisted. This twist aligns the coding base with the binding site for the incoming nucleoside triphosphate substrate. The nucleoside triphosphate enters through an opening that is found in all polymerases, and generally binds between an α-helix and two catalytic metal ions. The exiting template–product duplex is bound from the minor groove side in all polymerases. Conformational changes upon nucleic acid binding have been detected for several different polymerases, but the nature of this "induced fit" differs.

See Also the Following Articles

Recombination: Heteroduplex and Mismatch Repair *in vitro* • RNA Polymerase I and RNA Polymerase III in Eukaryotes • RNA Polymerase II and Basal Transcription Factors in Eukaryotes • RNA Polymerase II Elongation Control in Eukaryotes

Glossary

backtracking Reverse movement of pol II along DNA and RNA.
DNA–RNA hybrid 8–9 base pair double-stranded heteroduplex formed between the DNA template strand and the RNA transcript within the transcription bubble.
downstream DNA DNA that is going to be transcribed.
Rpb1–Rpb12 RNA polymerase B (II) polypeptide subunits 1–12.

transcription bubble Open DNA region in the active center of pol II.
translocation Movement of pol II by a step of one base pair along the DNA template.
upstream DNA DNA that has been transcribed.

Further Reading

Armache, K.-J., Kettenberger, H., and Cramer, P. (2003). Architecture of the initiation-competent 12-subunit RNA polymerase II. *Proc. Natl. Acad. Sci. USA* **100**, 6964–6968.

Bushnell, D. A., and Kornberg, R. (2003). Complete 12-subunit RNA polymerase II at 4.1Å resolution: Implications for the initiation of transcription. *Proc. Natl. Acad. Sci. USA* **100**, 6969–6973.

Cramer, P. (2002). Multisubunit RNA polymerases. *Curr. Opin. Struct. Biol.* **12**, 89–97.

Cramer, P., Bushnell, D. A., Fu, J., Gnatt, A. L., Maies-Davis, B., Thompson, N. E., Burgess, R. R., Edwards, A. M., David, P. R., and Komberg, R. D. (2000). Architecture of RNA polymerase II and implications for the transcription mechanism. *Science* **288**, 640–649.

Cramer, P., Bushnell, D. A., and Kornberg, R. D. (2001). Structural basis of transcription: RNA polymerase II at 2.8 angstrom resolution. *Science* **292**, 1863–1876.

Gnatt, A. L., Cramer, P., Fu, J., Bushnell, D. A., and Kornberg, R. D. (2001). Structural basis of transcription: An RNA polymerase II elongation complex at 3.3Å resolution. *Science* **292**, 1876–1882.

Woychik, N. A., and Hampsey, M. (2002). The RNA polymerase II machinery: Structure illuminates function. *Cell* **108**, 453–463.

Biography

Patrick Cramer is Assistant Professor of Biochemistry at the Institute of Biochemistry and Gene Center of the University of Munich. His research interest is in the structural biology of the eukaryotic mRNA transcription machinery. He obtained a Ph.D. from Heidelberg University and the European Molecular Biology Laboratory, and carried out postdoctoral research at Stanford University. For his work on the structure determination of RNA polymerase II, he was elected EMBO Young Investigator in 2000 and received the GlaxoSmithKline Science Award in 2002.

RNA Polymerase Reaction in Bacteria

Arkady A. Mustaev and Alexander D. Goldfarb
Public Health Research Institute, Newark, New Jersey, USA

The expression of genetic information encoded in DNA requires the production of an RNA molecule (known as transcription) using DNA as a template. The resulting RNA (the transcript) represents an exact copy of the transcribed DNA segment, or the gene. Information in RNA is encoded using a four-letter alphabet of nitrous bases, the same as in DNA, with the difference that uracil (U) is used in RNA instead of thymine (T). In addition to the copying of the DNA sequence into RNA, the transcription process involves the selection of the beginning (promoter) and the end (terminator) of each gene.

Transcription: Basic Mechanism

RNA synthesis requires base-pairing interactions between the single-stranded DNA template and ribonucleoside-5′-triphosphate (NTP) substrates. Thus, transcription involves unwinding of a small section (10–13 nucleotide residues) of the DNA double helix at which point one of the two DNA strands acts as a template for RNA synthesis. The unwound portion of DNA is called the transcription bubble; it contains a DNA–RNA hybrid of 8–9 base pairs. Each elementary step of transcription constitutes the incorporation of an NTP at the 3′ terminus of the growing RNA chain, so that the bubble propagates stepwise along the template accompanied by unwinding of the DNA duplex ahead, peeling of the transcript from the hybrid, and closing of the DNA duplex behind.

The nucleotide addition is accomplished through the formation of a phosphodiester bond and the release of pyrophosphate (PPi). It is a highly energetically favorable reaction ($\Delta G \cong 7$ kcal/mol), which is practically irreversible under physiological conditions but may be reversed *in vitro* by excess of PPi. As the result, a linear RNA polymer is built in the 5′ to 3′ direction. Selection of the substrates is achieved through hydrogen bonding between complementary bases, adenine to thymine (or uracil), and guanine to cytosine.

The enzyme that performs transcription of cellular DNA is called DNA-dependent RNA polymerases (RNAPs). The best characterized RNAP is that from the bacterium *Escherichia coli*. RNAP's catalytic core enzyme contains five subunits (α_2, β, β', and ω) and has an M_r of 390 kDa. The sixth interchangeable subunit, σ, is derived from a group of related polypeptides of different size. The σ-subunit is a specificity factor, which transiently associates with the core enzyme to form the holoenzyme that is capable of recognition of and specific binding to the promoter. The most common σ-factor in the bacterial cell is σ70. In contrast to DNA polymerase, the RNAP holoenzyme is able to initiate RNA synthesis starting from NTP and does not require a primer. Transcription is completely processive, i.e., RNAP is associated with the transcription bubble at all times in a ternary complex in which the nucleic acid scaffold slides through the protein as the bubble propagates. At the termination site, the ternary complex dissociates, the bubble collapses, and single-stranded RNA product is released.

Thus, synthesis of a particular transcript can be divided into three distinct steps: initiation, elongation, and termination, which jointly constitute the transcription cycle (Figure 1). Each step of the transcription cycle is subject to regulation either by factors external to the transcriptional apparatus or by signals encoded in the DNA sequence.

Transcription Initiation

The search for a promoter occurs through occasional collision and sliding of RNAP along DNA. Sliding greatly accelerates the search, which is concluded by establishment of specific contacts between RNAP and a promoter in a relatively unstable closed complex. In bacteria, the RNAP holoenzyme binds to the promoter region from -70 to -40 to $+30$ nucleotides relative to the transcription start site. Within the promoter, RNAP usually recognizes two relatively short sites centered around the positions -35 and -10 (Figure 2A), which are contacted by the σ-subunit. Some of the promoters contain an additional recognized sequence, the so-called UP element, which spawns the register -60 to -40 and interacts with the α-subunit of RNAP.

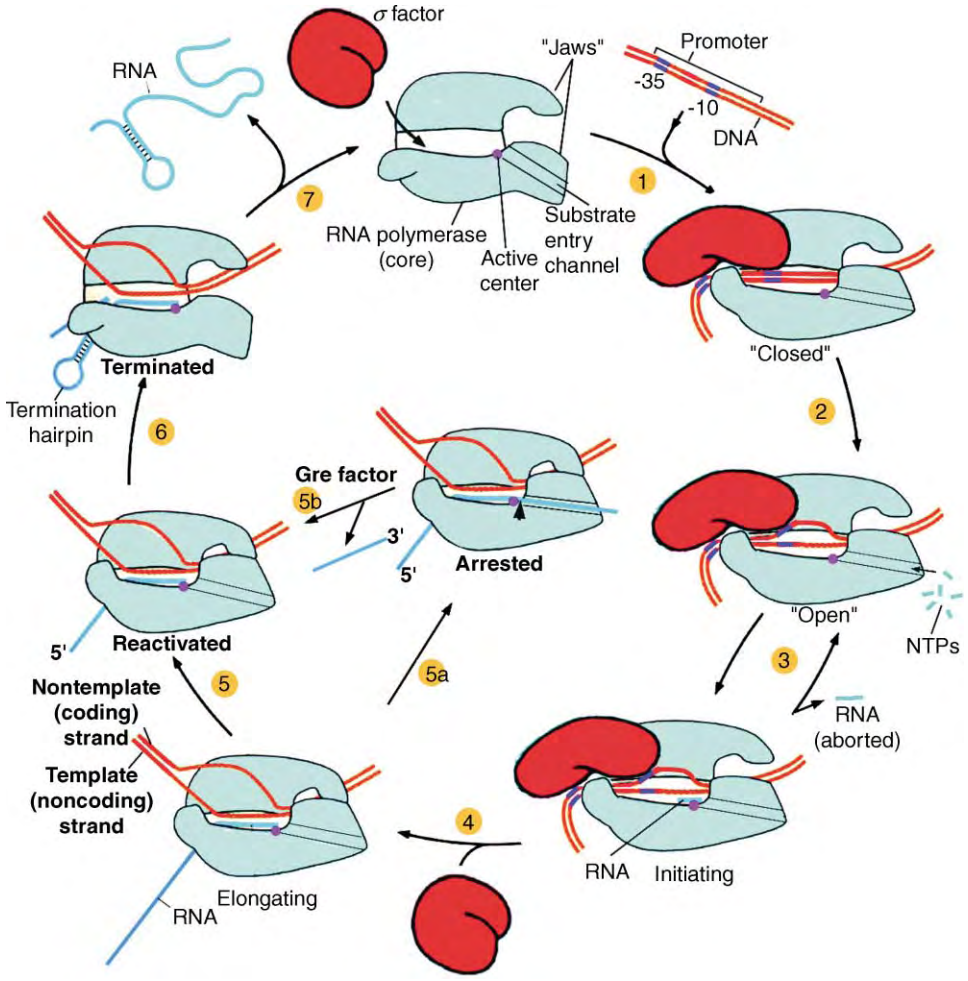

FIGURE 1 The transcription cycle. The RNAP core enzyme associates with the σ-factor and recognizes a promoter (step 1). RNAP locally melts the DNA duplex and starts RNA synthesis on the template strand of DNA (steps 2 and 3). The enzyme is still anchored to the promoter due to specific contacts with the recognition sequence, which impede the promoter escape, causing premature dissociation of short RNA products and their resynthesis in the cyclic reaction of abortive initiation. Occasionally, some RNA products that have reached a critical size (approximately 8–10 nucleotides) enter the RNA exit channel and displace the σ-factor. This leads to the stabilization of the transcription complex and relinquishing of the contacts between the σ-subunit and the promoter (step 4). The ternary elongating complex is highly processive. At certain sequences, RNAP occasionally backtracks, losing its grip on the growing RNA end, which extrudes beyond the active center, rendering the complex inactive (step 5a). The transcription factor GreB assists with cleavage of the extruded RNA, reactivating the enzyme (step 5b). Eventually, the elongating complex encounters a terminator, which causes the enzyme to stop and release the transcript due to a conformational change induced by the RNA hairpin. The RNAP core enzyme can rebind σ-factor and perform another cycle of transcription.

Even though the sequence of promoters is not strictly conserved (which accounts for variations in their efficiency), there are certain nucleotides that are found with high frequency at each position of a consensus sequence. The consensus sequences for the -35 and -10 positions are TTGACA and TATAAT, respectively. Some promoters have an extended -10 recognition region with the invariant dinucleotide TG just one nucleotide upstream of the main consensus sequence. The typical length of the nonspecific spacers between the -35 and -10 regions and from the -10 region to the first transcribed nucleotide are 17 and 7 nucleotides, respectively, with slight variations (Figure 2B).

Much of the regulation of gene expression occurs at the level of promoter recognition. Promoters can be subdivided into two groups, constitutive promoters, whose activity always remains constant, and regulated promoters, in which RNAP has to be recruited by an auxiliary protein factor or the promoter is blocked by bound repressor. For example, cAMP receptor protein activates promoters for the production of enzymes involved in the metabolism of some sugars, whereas Lac repressor blocks transcription of the genes for utilization of lactose.

After promoter recognition, the DNA double helix unwinds locally, resulting in the formation of the open

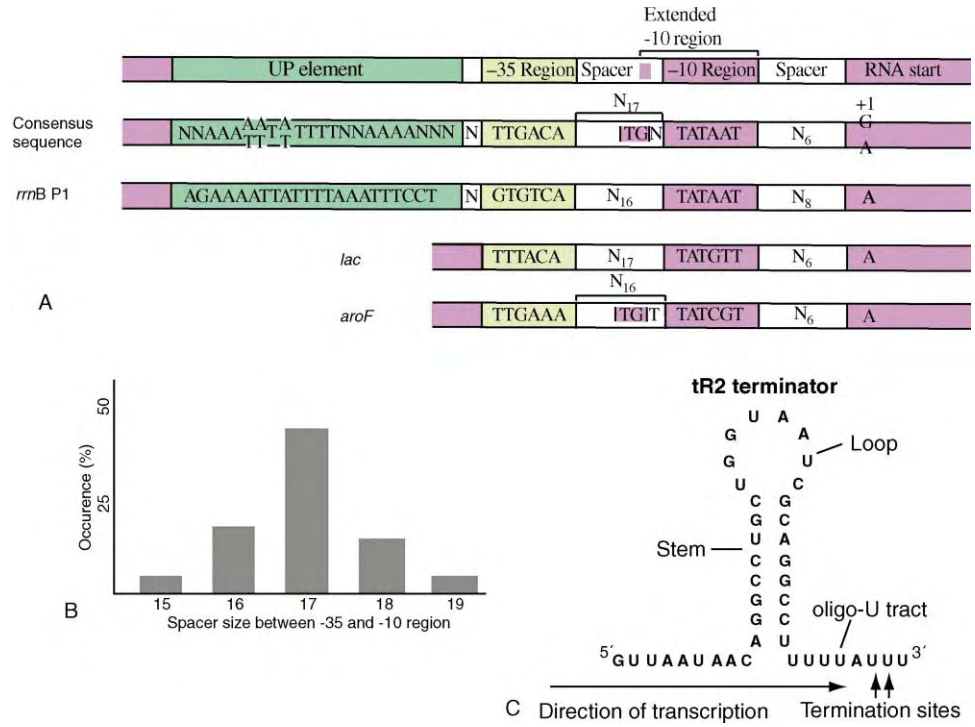

FIGURE 2 Bacterial promoters and terminators. (A) Typical promoters recognized by the RNAP holoenzyme containing σ70. Sequences of the nontemplate strand at the recognition sites are shown in the direction from 5′ to 3′. The structure of the promoters is variable, which is consistent with the wide range of their efficiency. The recognition sequences are highlighted. (B) Variation in the spacer size between the −10 and −35 regions in natural promoters. (C) The structure of a typical ρ-independent terminator. The tR2 terminator shown contains two self-complementary G-C reach regions followed by oligo-U tracts. The termination site is usually located 7–8 nucleotides downstream from the stem of the RNA hairpin.

complex (Figure 1, step 2). At this point, the active center of the RNAP enzyme can initiate synthesis. The initial short RNA molecules are poorly retained at the active center and dissociate into solution in a phenomenon called abortive synthesis (Figure 1, step 3). After each abortion cycle, the enzyme remains promoter bound, and it reinitiates and releases RNA again until it eventually escapes the promoter. This escape to the elongation phase occurs after the size of the transcript reaches 7–11 nucleotides. Transition from initiation to elongation (promoter clearance) (Figure 1, step 4) is accompanied by the relinquishing of the sequence-specific interactions between DNA and the σ-subunit complex and often by dissociation of σ. In some cases, however, the subunit remains associated with RNAP.

Transcription Elongation

Even though the ternary elongation complex (TEC) is exceptionally stable to dissociation, it is maintained only by topological contacts between protein, DNA, and RNA, which allow free sliding of the enzyme along the template. During elongation, TEC acts as a powerful motor, generating a force (25 pN) greatly exceeding that for conventional cellular motors such as kinesin and myosine. The relative force generated by RNAP is about 10^6 times greater than that generated by the space shuttle carrier.

The principal nucleic acid–protein interactions in TEC occur at three crucial operationally defined sites (Figure 3): the DNA-binding site that holds on to the downstream DNA duplex and acts as a sliding clamp, and the front and rear zip-locks at the ends of the RNA–DNA hybrid-binding site that accommodates the RNA–DNA heteroduplex (Figure 3B). The rear zip-lock ensures displacement of RNA product from the template during elongation. The front zip-lock coincides with the RNAP active center and also enables peeling of RNA from DNA upon TEC's occasional backtracking, a process in which the bubble propagates backward while extruding the 3′ terminus of RNA (Figure 1, step 5a).

In the X-ray crystal structure of TEC (Figure 3A), the DNA-binding site is seen as a deep trough formed by the β'-subunit, which is topped by a "roof" formed by a domain of the β-subunit. The RNA–DNA hybrid is enclosed in the main channel formed by the β- and β'-subunits of the enzyme, between the active center at its downstream end and the rudder loop of the β'-subunit at its upstream end, corresponding to the front and rear zip-locks, respectively. The active center, which contains

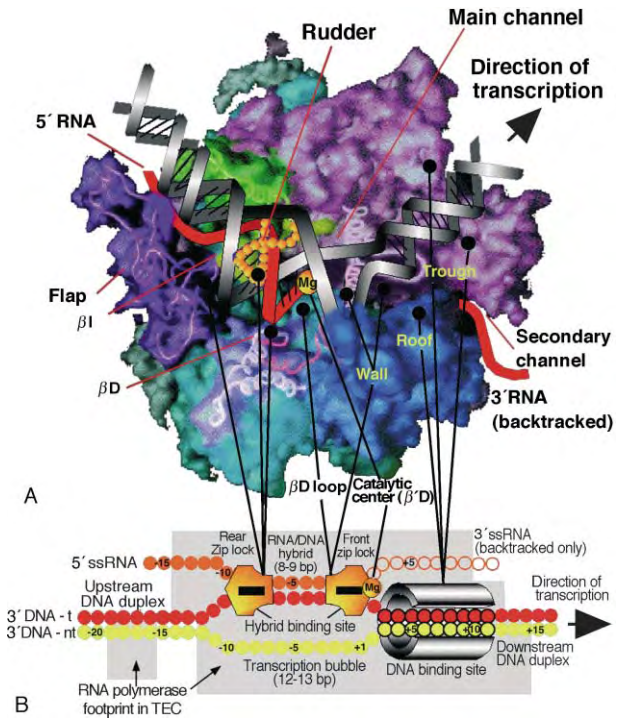

FIGURE 3 A structure–function model of the ternary elongating complex (TEC). (A) A model of TEC based on the X-ray crystal structure of RNAP. White lines show the correspondence between the operationally defined functional elements and the structural features of TEC. (B) The nucleic acid scaffold and its interactions with RNAP protein in TEC. The five elements are the upstream and downstream DNA duplexes, the 8–9 bp RNA–DNA hybrid, the single-stranded region of DNA in the transcription bubble, and the nascent single-stranded RNA upstream of the hybrid. In the "backtracked" complex, an additional segment of RNA appears downstream of the bubble. Filled circles represent the DNA (red, template strand; yellow, nontemplate strand); the DNA-binding site is represented by the sliding clamp that encloses 9 bp of the downstream DNA duplex. The hybrid-binding site that accommodates the RNA–DNA heteroduplex is flanked by the two zip-locks that hold on to the edges of heteroduplex and either zip or unzip the hybrid, maintaining its constant size during lateral movement of RNAP. The gray area shows the RNAP footprint on DNA.

the stably bound catalytic Mg^{2+} ion, marks the beginning of the secondary channel, which is used for the supply of NTP substrates and which accommodates the 3′-terminal end of single-stranded RNA upon RNAP backtracking. The secondary channel is branched from the main channel by the wall. The 5′ segment of the nascent transcript exits through the channel underneath the flap, which is a long flexible loop of the β-subunit.

The rate of RNA synthesis in elongation is sequence dependent, usually about 10 to 50 nucleotides per second, but can slow down to a full stop at points called pausing sites. One of the reasons for pausing is the energetics of base-pairing in the DNA–RNA scaffold of TEC. The energy of base-pairing is not equal for different nucleotides (ranging from 0.9 to 3.2 kcal/mol), so that TEC translocation is strongly suppressed at certain sites. In extreme cases, this causes reversible backtracking or even irreversible transcriptional arrest. The GreB protein rescues the arrested complex by stimulating RNA cleavage activity intrinsic to the RNAP active center, releasing the extruded 3′ RNA segment, and allowing RNA synthesis to continue (Figure 1, step 5b). A homologous GreA protein facilitates RNA cleavage in slightly backtracked TECs (by 1 or 2 nucleotides), thus preventing the arrest pathway.

Pausing, backtracking, and excision regulate elongation rate and serve to correct errors of elongation, which occur at a rate of one per every 10^4–10^5 nucleotides (compare with the fidelity of replication—one misincorporation per 10^7 nucleotides).

The RNA synthesis in bacteria is sensitive to inhibitors. The most important are rifampicin, streptolydigin, and microcin J-25. Rifampicin plugs the RNA exit channel in TEC, streptolydigin inhibits RNAP translocation, and microcin J-25 most likely blocks the NTP entry into the active center.

The Unified Catalytic Mechanism of RNA Synthesis and Degradation

The principal enzymatic activity of RNAP is the transfer of nucleotidyl moiety from the NTP substrate to the 3′ hydroxyl of the RNA terminus. Thus, the RNAP active center (Figure 4) *a priori* includes the binding site for the RNA terminus (i site) and the site for the NTP donor of the nucleotidyl residue (i + 1 site). The formation of the phosphodiester bond is followed by translocation of the newly formed RNA terminus from the i + 1 to the i site. The reaction and the movement are reversible: excess of PPi stimulates processive degradation of RNA (pyrophosphorolysis) with the release of 3′-terminal RNA residues in the form of NTPs. The RNAP active center can also perform hydrolysis of RNA in backtracked and arrested complexes. Central to these reactions is a symmetrical pair of Mg^{2+} ions that switch their roles in synthesis and degradation (Figure 4). One ion is retained in RNAP permanently (I) while the other is recruited for each act of catalysis (II). In polymerization reactions, it is recruited by incoming NTP (Figure 4A), whereas in cleavage reactions it is recruited by carboxylate residues of the Gre factors (Figure 4B).

Transcription Termination

Termination signals are encoded in the DNA sequence. There are two classes of termination signals in bacteria: one in which termination is assisted by a protein factor ρ, and another in which termination is ρ independent. The ρ-independent terminators (Figure 2C) contain

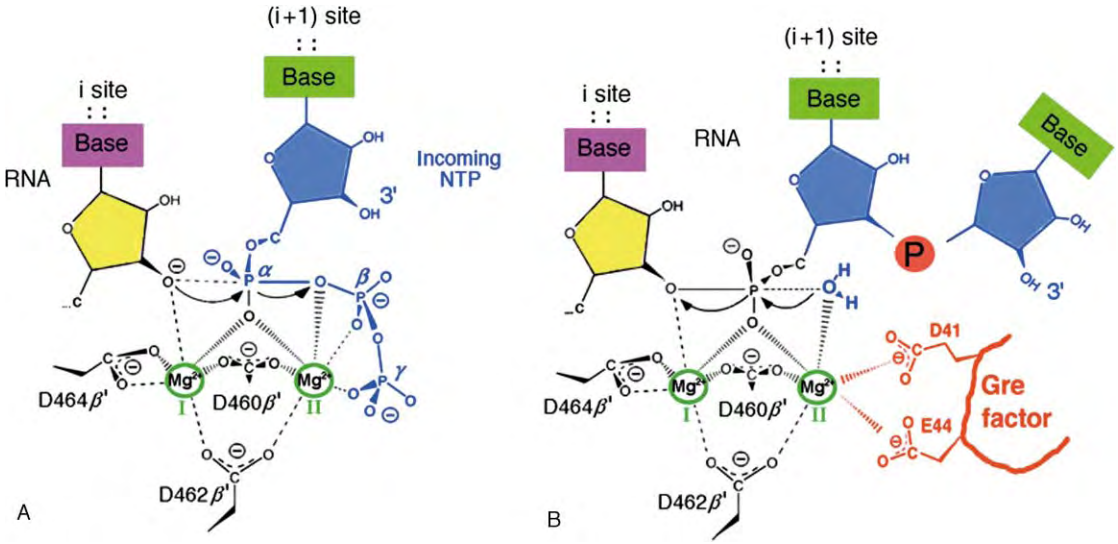

FIGURE 4 Catalytic mechanism of in RNA synthesis and degradation by RNAP. (A) The nucleotidyl transfer reaction. Two Mg^{2+} ions coordinated by three aspartate residues of the active center are enclosed in green circles. The tightly bound Mg-I activates the 3′ hydroxyl of the terminal RNA residue, promoting its attack on the α-phosphorus of the incoming NTP, and stabilizes the penta-coordinated transition state, while Mg-II facilitates the release of PPi during the phosphodiester bond formation. (B) The transcript cleavage reaction, assisted by the Gre factor. The Gre protein recruits the weakly bound Mg-II by providing residues for additional coordination. Mg-II orients and activates the attacking water molecule for hydrolytic cleavage of the phosphodiester bond. Mg-I coordinates the 3′ hydroxyl group of the RNA residue occupying the i site of the active center, making it a better leaving group. The disengaged 3′ RNA terminus is tilted to reflect the loss of base-pairing with DNA through backtracking.

short self-complementary GC-rich sequences followed by an oligo-A tract. Transcription of such sequences is accompanied by pausing of RNAP due to backtracking, which ensures the formation of a hairpin-like RNA structure (Figure 1, step 6). The RNA hairpin destroys the nucleic acid contacts in the rear zip-lock, forcing the rudder and the flap to open, which leads to collapse of the transcription bubble and disintegration of the transcription complex (Figure 1, step 7).

The ρ-dependent termination also requires pausing, but entails sequences without oligo-A tracts. The ρ protein loads onto RNA at some distance behind TEC and moves along the transcript toward RNAP, using the energy of ATP hydrolysis. Eventually, the factor bumps into the enzyme and pulls out RNA from the complex, causing the release of the transcript and dissociation of RNAP from DNA.

See Also the Following Articles

DNA Polymerase I, Bacterial • DNA Polymerase II, Bacterial • DNA Polymerase III, Bacterial • T7 RNA Polymerase • Transcription Termination

Glossary

operator A short segment of DNA in a bacterial chromosome that controls the transcription of an adjacent gene.

operon In the bacterial chromosome, a group of adjacent genes that are transcribed to a single mRNA molecule.

transcription factor Any protein required to initiate or regulate transcription.

Further Reading

Borukhov, S., and Nudler, E. (2003). RNA polymerase holoenzyme: Structure, function and biological implications. *Curr. Opin. Microbiol.* **6**, 93–100.

Darst, S. A. (2001). Bacterial RNA polymerase. *Curr. Opin. Struct. Biol.* **11**, 155–162.

Gnatt, A. L., Cramer, P., Fu, J., Bushnell, D. A., and Kornberg, R. D. (2001). Structural basis of transcription: An RNA polymerase II elongation complex at 3.3 A resolution. *Science* **292**, 1876–1882.

Korzheva, N., Mustaev, A., Nudler, E., Nikiforov, V., and Goldfarb, A. (1998). Mechanistic model of the elongation complex of *Escherichia coli* RNA polymerase. *Cold Spring Harbor Symp. Quant. Biol.* **63**, 337–345.

Korzheva, N., Mustaev, A., Kozlov, M., Malhotra, A., Nikiforov, V., Goldfarb, A., and Darst, S. A. (2000). Structural model of transcription elongation. *Science* **289**, 619–625.

Korzheva, N., and Mustaev, A. (2001). Transcription elongation complex: Structure and function. *Curr. Opin. Microbiol.* **4**, 119–125.

Losick, R., and Chamberlin, M. (eds.) (1976). *RNA Polymerase*. Cold Spring Harbor, New York.

Murakami, K. S., and Darst, S. A. (2003). Bacterial RNA polymerases: The wholo story. *Curr. Opin. Struct. Biol.* **13**, 31–39.

Sosunov, V., Sosunova, E., Mustaev, A., Bass, I., Nikiforov, V., and Goldfarb, A. (2003). Unified two-metal mechanism of RNA synthesis and degradation by RNA polymerase. *EMBO J.* **22**, 2234–2244.

Biography

Arkady A. Mustaev is a Research Associate at the Public Health Research Institute in Newark, New Jersey. He holds a Ph.D. from the Novosibirsk Institute of Bioorganic Chemistry (Russia). His principal research interest is studies of the catalytic mechanism of RNA polymerase. He developed superselective affinity labeling and fast mapping of the cross-linking sites in proteins, use of which allowed the design of a high-resolution model of the transcription elongation complex.

Alex Goldfarb is a Professor at the Public Health Research Institute. He holds a Ph.D. from the Weizmann Institute of Science in Israel. His principal research interest is the molecular mechanisms of transcription.

RNA Polymerase Structure, Bacterial

Michael Anikin, Dmitri Temiakov and William T. McAllister
State University of New York, Downstate Medical Center, Brooklyn, New York, USA

The first step in gene expression, transcription of genetic information in the DNA into messenger RNA, is carried out by DNA-dependent RNA polymerase (RNAP). Understanding how this enzyme carries out RNA synthesis and responds to regulatory signals is of fundamental importance to the comprehension of gene regulation. Extensive studies over the past decade (i.e., since 1990s) have probed the nature of the machinery that carries out this process. These approaches have involved genetics (identification and characterization of the genes that encode the protein subunits of the RNAP and the transcription factors that interact with the RNAP) and biochemical approaches (such as cross-linking experiments to characterize the trajectory of the nucleic acid components within the transcription complex). More recently, structural studies using methods such as NMR, X-ray crystallography, and fluorescence resonance energy transfer (FRET) have been brought to bear in an attempt to characterize the transcription complex in greater detail. The past few years have seen unprecedented breakthroughs in our understanding of the organization and function of the transcription complex, resulting in high resolution structures that may be interpreted in light of the abundant genetic and biochemical data. An overview of our understanding of the organization of bacterial RNAPs, and the relationship of structure to the mechanism of polymerase action is provided in this article.

Organization of the Transcription Complex

In a bacterium such as *E. coli* (the paradigm for studies of bacterial RNAPs), the minimal configuration needed for transcript elongation is a "core" complex that consists of five subunits, ($\alpha_2\beta\beta'\omega$) having an aggregate molecular weight of ~400 kDa and an additional factor, σ, is required for recognition of the promoter during initiation, and other factors may regulate the ability of the polymerase to clear the promoter, enhance processivity, or modulate termination. RNAPs from eukaryotic cells also have multiple subunits, and many of these subunits are homologous to the core subunits found in the bacterial RNAP. Thus, much of the information that comes from the study of bacterial RNAPs has direct relevance to studies of RNAPs from higher organisms.

Unlike DNA polymerases (DNAPs), which extend a primer and leave the polynucleotide product in association with the template, RNAPs must displace the RNA product from the template and restore the DNA to duplex form after the passage of the enzyme. To accomplish this, the polymerase establishes a locally unwound transcription bubble of ~12–14 bp which encloses an RNA:DNA hybrid that extends ~8 bp upstream from the growing end of the RNA chain. As the polymerase moves downstream, the two DNA strands are separated at the leading edge of the bubble and reannealed at the trailing edge, where the RNA is displaced (see Figure 1).

Extensive biochemical and genetic experimentation anticipated the essential elements that are required for RNA synthesis, and a general understanding of the organization of the complex (Figure 1). A central cavity encloses the active site and the short RNA:DNA hybrid where the nascent transcript is found before its displacement from the template (T) strand of the DNA. Leading into this cavity are pores and channels for the entrance and exit of the duplex DNA, an exit channel for the RNA product, and a substrate entrance pore. Another channel is required to accommodate the locally displaced nontemplate (NT) strand of the DNA in the transcription bubble.

Structure of the Core Enzyme

For a number of reasons, RNAPs from thermophilic organisms such as *Thermus aquaticus* (*Taq*) have proven more amenable for crystallographic analysis than the *E. coli* enzyme. A high resolution structure of the *Taq* core RNAP is shown in Figure 2. The overall organization of the enzyme resembles that of a crab claw which surrounds an open cleft in which the DNA is bound. The active site (which involves coordination of two Mg^{++} ions that are essential for the phosphoryl transferase reaction) is located at the back of this cleft. Many of the features that are important for the catalytic steps and processivity described above may be visualized

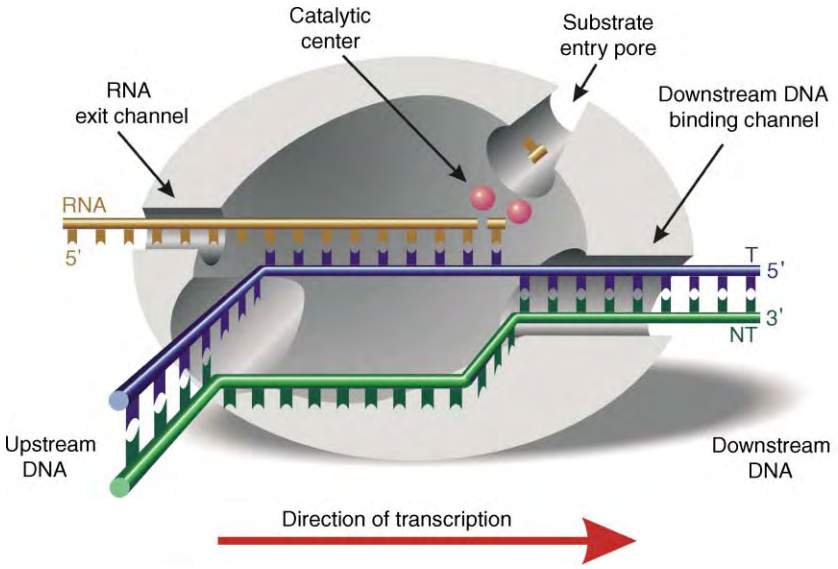

FIGURE 1 Organization of the transcription complex. The elongating RNA is found in the interior of the protein as an 8 bp RNA:DNA hybrid (RNA yellow, DNA blue). The nontemplate strand of the DNA (green) is displaced from the template strand at the leading edge of the transcription bubble and reannealed at the trailing edge. Channels that lead to the interior cavity allow for entry and exit of the duplex DNA, exit of the RNA product, and entrance of substrate. Elongation of the RNA chain occurs at the active site (catalytic center) where the phosphoryl transferase reaction is catalyzed by a pair of magnesium ions (purple spheres).

in this structure. Although the structure of an elongation complex of the bacterial RNAP in association with all of the nucleic acid components has not yet been determined, the structure of a yeast RNAP elongation complex has been solved. The organization of the eukaryotic complex is remarkably similar to that of the bacterial enzyme.

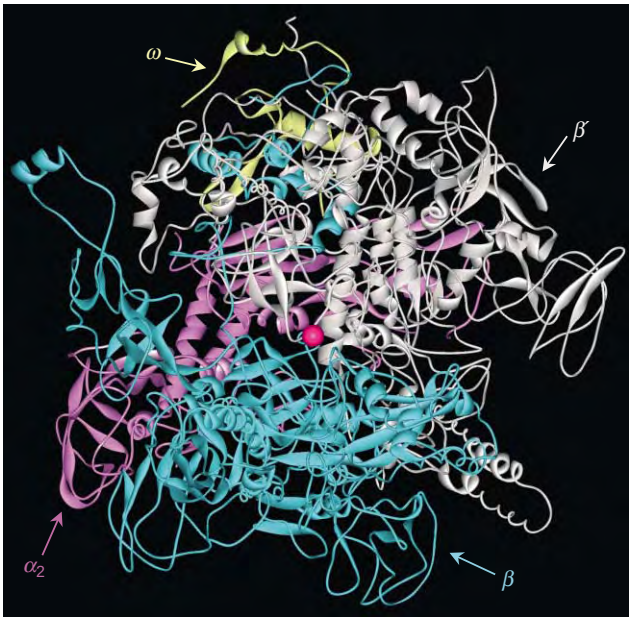

FIGURE 2 Structure of the *Taq* core enzyme. The core subunits are color coded as indicated. A magnesium ion in the active site is indicated by a purple sphere.

The bacterial RNAP structure is supported, and is made interpretable, by the results of previous biochemical and genetic experiments that identified important functional regions of the various subunits, and the nature of their interactions with nucleic acid components. In addition to the general features described in Figure 1, more details concerning the mechanism of transcription are revealed by the structure. These include upstream and downstream "zippers" for unwinding and rewinding the duplex DNA and displacing the product, and the organization of the active site. Nevertheless, more information will be required to understand other aspects of transcription, such as the mechanism of substrate selection and discrimination (ribo- versus deoxyribonucleotides), and how the movement of the RNAP along the template (translocation) is controlled.

Structure of the Holoenzyme

One of the key events during the transcription process is the transition from an unstable initiation complex to a processive elongation complex, which is accompanied by release of the promoter contacts and movement of the RNAP away from the promoter. The σ factor is intimately involved in promoter recognition and in the early stages of transcription. Association of σ with the core enzyme results in the formation of the "holoenzyme", which carries out the early stages of transcription. The structure of the holoenzyme from *Thermus thermophilus* (*Tth*) is shown in Figure 3.

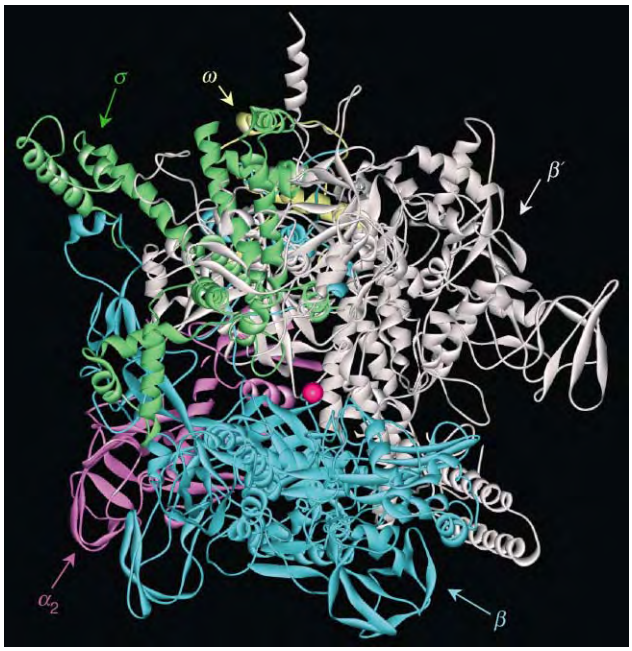

FIGURE 3 Structure of the *Tth* holoenzyme. The subunits of the core enzyme are colored as in Figure 2; (σ factor is green). The surface-exposed components are available for binding to the promoter DNA in a specific manner; a portion of σ is embedded in the hybrid binding cleft, and must be displaced during initiation.

In this structure, the regions of σ that are known to be involved in promoter recognition are displayed on the surface of the enzyme, where they would be able to interact with the upstream regions of the promoter. However, a flexible loop segment of σ is buried within the core enzyme, and occupies part of the RNA exit channel and the RNA:DNA hybrid binding cavity. This portion of σ would need to be displaced during initiation, perhaps precipitating the loss of σ that occurs during the transition to the elongation phase.

Structure of a Single Subunit Phage RNAP

Although the multisubunit RNAP described above is responsible for transcription of cellular DNA under normal growth conditions, there are occasions in which other RNAPs may also be operative within the bacterial cell. For example, certain viruses that infect bacteria encode a new RNAP that is responsible for transcription of the viral genome. The paradigm of this is the RNAP encoded by bacteriophage T7, which consists of a single subunit of ~100 kDa. Although this enzyme does not exhibit any amino acid sequence conservation with the bacterial enzymes, it is related to mitochondrial polymerases and with many organellar RNAPs from higher cells and plants (e.g., chloroplasts). It thus appears to be an evolutionarily conserved RNAP that arose at a different time from the multisubunit RNAPs. Interestingly, the phage RNAPs are also related to bacterial DNAPs and to reverse transcriptases. They are therefore members of a superfamily of nucleotide polymerases that is distinct from the multisubunit RNAPs.

Despite the differences in the sequence and detailed structure of the phage RNAP versus the bacterial RNAP, the phage RNAP nevertheless carries out all of the steps in the transcription cycle in an identical manner to the multisubunit RNAPs, including promoter recognition, elongation, and termination.

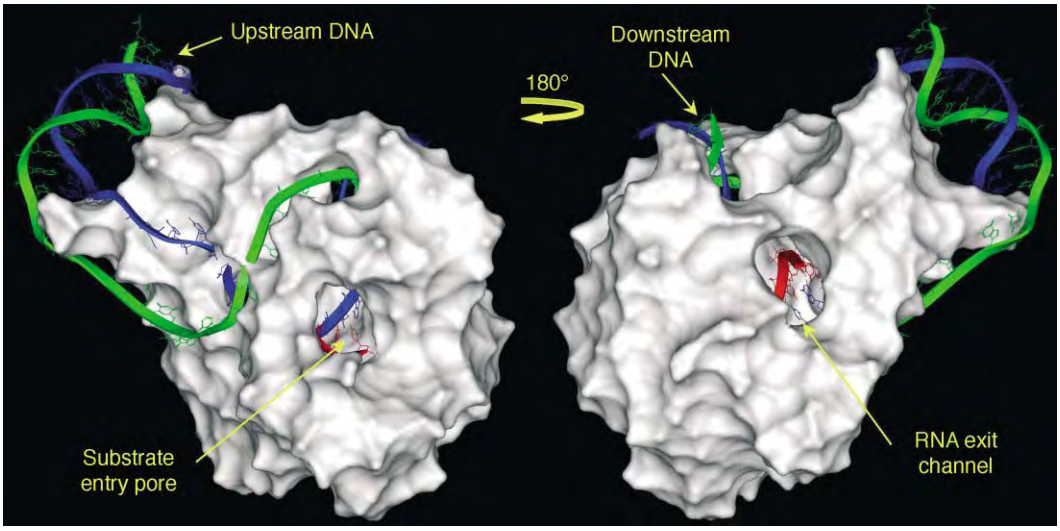

FIGURE 4 Model of a T7 RNA polymerase elongation complex just prior to promoter release. The RNAP maintains contacts with the upstream region of the promoter until it enters a fully processive elongation mode; potential interactions of the promoter with the RNAP at this stage of initiation are shown (DNA template strand, blue; nontemplate strand, green; RNA, red). The substrate entry and RNA exit channels are indicated.

Characterization of phage RNAP structures is more comprehensive than that of the bacterial RNAPs. Structures have now been solved for the free enzyme, the enzyme in association with its promoter, an early initiation complex, and elongation complexes in the presence and absence of substrate. Thus, many of the events in the overall transcription cycle have been captured in atomic detail for the phage RNAP.

The transition from an initiation complex to an elongation complex by T7 RNAP is accompanied by a massive reorganization of the amino terminal one-third of the enzyme (Figure 4). Remarkably, after the transition to an elongation complex, the overall organization of T7 RNAP resembles the organization of the bacterial RNAP, having an RNA:DNA hybrid of ~8 bps, pores for substrate entry and exit, a channel for the displaced NT strand, and regions for binding of upstream and downstream DNA. More detailed examination of the phage RNAP reveals elements that are involved in displacing the RNA product and for reannealling the T and NT strands at the upstream edge of the bubble, as well as mechanisms for substrate selection and translocation control. Due to the conservation in the overall mechanism of transcription, many of the findings from the phage RNAPs are likely to inform experimental approaches in the multisubunit RNAPs.

Future Prospects

Until the past few years, characterization of transcription complexes had relied largely upon biochemical and genetic approaches. The merger of structural methods with biochemical and genetic methods now affords the opportunity to determine the organization of the complexes at each stage of the transcription cycle with atomic resolution, and to correlate this structure with mutational and biochemical analyses.

See Also the Following Articles

RNA Polymerase II and Basal Transcription Factors in Eukaryotes • RNA Polymerase II Structure in Eukaryotes • RNA Polymerase Reaction in Bacteria • Sigma Factors • T7 RNA Polymerase

Glossary

initiation The first step in transcription, in which the RNAP forms an unstable initiation complex before clearing the promoter and entering into the elongation phase.

processive elongation RNAP continuously extends the RNA chain without dissociating from the template.

promoter Specific sequence in the DNA that directs RNAP to bind to the template and to begin transcription.

termination RNAP recognizes a specific signal in the template that causes it to release the RNA and to dissociate from the template.

Further Reading

Borukhov, S., and Nudler, E. (2003). RNA polymerase holoenzyme: Structure, function and biological implications. *Curr. Opin. Microbiol.* **6**, 93–100.

Cheetham, G. M., and Steitz, T. A. (2000). Insights into transcription: Structure and function of single-subunit DNA-dependent RNA polymerases. *Curr. Opin. Struct. Biol.* **10**, 117–123.

Darst, S. A. (1988). Two-dimensional crystals of Escherichia coli RNA polymerase holoenzyme on positively charged lipid layers. *J. Mol. Biol.* **203**, 269–273.

Murakami, K. S., and Darst, S. A. (2003). Bacterial RNA polymerases: The whole story. *Curr. Opin. Struct. Biol.* **13**, 31–39.

Murakami, K. S., Musada, S., and Darst, S. A. (2002). Structural basis of transcription initiation: RNA polymerase holoenzyme at 4Å resolution. *Science* **296**, 1280–1284.

Murakami, K. S., Musada, S., Campbell, E. A., Muzzin, O., and Darst, S. A. (2002). Structural basis of transcription initiation: An RNA polymerase holoenzyme-DNA complex. *Science* **296**, 1285–1290.

Tahirov, T. H., Temiakov, D., Anikin, M., Patlan, V., McAllister, W. T., Vassylyev, D. G., and Yokoyama, S. (2002). Structure of a T7 RNA polymerase elongation complex at 2.9Å resolution. *Nature* **420**, 43–50.

Vassylyev, D. G., Sekine, S.-I., Laptenko, O., Lee, J., Vassyleva, N., Borukhov, S., and Yokoyama, S. (2002). Crystal structure of a bacterial RNA polymerase holoenzyme at 2.6Å resolution. *Nature* **417**, 712–719.

Yin, Y. W., and Steitz, T. A. (2002). Structural basis for the transition from initiation to elongation transcription in T7 RNA polymerase. *Science* **298**, 1387–1395.

Zhang, G., Campbell, E. A., Minakhin, L., Richter, C., Severinov, K., and Darst, S. A. (1999). Crystal structure of *Thermus aquaticus* core RNA polymerase at 3.3Å resolution. *Cell* **98**, 811–824.

Biography

Michael Anikin received his Ph.D. in Bioorganic Chemistry from the Moscow Institute of Fine Chemical Technology.

Dmitri Temiakov received his Ph.D. in Molecular Biology from the Institute for Genetics and Selection of Microorganisms, Moscow.

William McAllister, Professor and Chair, received his Ph.D. from the University of New Hampshire, and postdoctoral training at the University of Heidelberg.

The authors are in the Morse Institute for Molecular Genetics, Department of Microbiology and Immunology, SUNY Downstate Medical Center, Brooklyn, NY. The research interests of the laboratory focus upon the structure and function of the single subunit bacteriophage T7 RNA polymerase.

Editors-in-Chief

William J. Lennarz

State University of New York at Stony Brook, Stony Brook, New York, USA

Section: Lipids, Carbohydrates, Membranes and Membrane Proteins

WILLIAM J. LENNARZ received his B.S. in Chemistry from Pennsylvania State University and a Ph.D. in Organic Chemistry from the University of Illinois. Subsequently he carried out postdoctoral work at Harvard with Konrad Bloch on fatty acid biosynthesis. In 1962 he was appointed Assistant Professor at Johns Hopkins in the Department of Physiological Chemistry. After promotion to Associate Professor in 1967, and full Professor in 1971, he remained at Hopkins until 1983. At that time, he was appointed Robert A. Welch Professor and Chair of the Department of Biochemistry and Molecular Biology at the University of Texas Cancer Center, M.D. Anderson Hospital. In 1989 he became a Leading Professor and Chair of the Department of Biochemistry and Cell Biology at SUNY at Stony Brook. In 1990 he founded and became Director of the Institute for Cell and Developmental Biology at Stony Brook.

Dr. Lennarz has served on many national and international committees. He has served as President of the Biochemistry Chairman's Organization, President of the American Society for Biochemistry and Molecular Biology and President of the Society for Glycobiology. He was a member of the Executive Committee of the International Union of Biochemistry and Molecular Biology for almost a decade.

He has presented special lectures at the University of Notre Dame, the NIH, the University of West Virginia, Johns Hopkins University, Florida State University, the University of California at San Diego, the University of Arkansas, Indiana University and the Medical College of Virginia.

He is a member of the National Academy of Sciences. The focus of his early work was on lipids and bacterial cell surfaces. More recent efforts have been in the structure, biosynthesis and function of cell surface glycoproteins. The biosynthesis studies initially were carried out in liver and oviduct, but these efforts now are focused in yeast. The functional studies have concentrated on the role of cell surface glycoproteins in fertilization and early development in the sea urchin and, more recently, the frog. For over 30 years Dr. Lennarz' research has been supported by federal sources, primarily the National Institutes of Health. Recently he was appointed Distinguished Professor and Chair of his department.

M. Daniel Lane

The Johns Hopkins University, School of Medicine, Baltimore, Maryland, USA

Section: Metabolism, Vitamins and Hormones

M. DANIEL LANE received B.S. and M.S. degrees in 1951 and 1953 from Iowa State University and a Ph.D. in 1956 from the University of Illinois. He was a Senior Postdoctoral Fellow with Professor Feodor Lynen at the Max-Planck Institute Fur Zellchemie in Munich. Following faculty positions at Virginia Polytechnic Institute and New York University School of Medicine, he joined the faculty at the Johns Hopkins University School of Medicine in 1969 and served as DeLamar Professor and Director of the Department of Biological Chemistry from 1978 to 1997. He is presently Distinguished Service Professor at Johns Hopkins. In 2002 he received an honorary degree, Doctor of Humane Letters, from Iowa State University.

Dr. Lane was elected to membership in the National Academy of Sciences (in 1987) and was elected as a Fellow of the American Academy of Arts and Sciences (in 1982) and of the American Society of Nutritional Sciences (in 1996). He received the Mead Johnson Award from the American Society for Nutritional Sciences in 1966 for his research on biotin-dependent enzymes and in 1981, the William C. Rose Award from the American Society for Biochemistry and Molecular Biology for his work on the insulin receptor. In 1990–1991 Lane served as President of the American Society of Biochemistry and Molecular Biology. He has presented many named lectureships (including the

Feodor Lynen Lecture in Germany in 1999) and served on numerous editorial boards including the Journal of Biological Chemistry and the Annual Reviews of Biochemistry. Currently he is Associate Editor for Biochemical and Biophysical Research Communications.

Dr. Lane has published 280 research papers in major scientific journals. His early work focused on various enzymatic CO_2 fixation reactions, notably the mechanisms by which the B-vitamin, biotin, functions in enzymes to catalyze carboxylation. Dr. Lane's work on the regulation of acetyl-CoA carboxylase, the key regulatory enzyme of fatty acid synthesis, led him to his present interests which are to understand the basic mechanisms of lipogenesis, adipogenesis and the consequence of aberrations in these processes, most notably obesity. Research currently underway in his laboratory focuses on: (1) the genes that signal stem cell "commitment" to the adipocyte lineage and subsequent differentiation into adipocytes, and (2) the mechanisms by which the region of the brain, known as the hypothalamus, monitors and controls the drive to eat.

Associate Editors

Ernesto Carafoli

Università degli Studi di Padova, Padova, Italy
Section: Bioenergetics

ERNESTO CARAFOLI earned his M.D. degree at the University of Modena in Italy in 1957. After postdoctoral studies in the Laboratory of Albert L. Lehninger at Johns Hopkins University in the mid 1960s he returned to his home institution in Italy where he worked until 1973, when he was appointed Professor of Biochemistry at the Swiss Federal Institute of Technology (ETH) in Zurich. He returned to Italy in 1998 as a Professor of Biochemistry at the University of Padova, where he now also directs the newly founded Venetian Institute of Molecular Medicine (VIMM).

Dr. Carafoli became interested in calcium as a signaling agent during his post-doctoral days at Johns Hopkins. When he arrived there his main interests were in mitochondrial bioenergetics and it was thus natural for him to expand them to the newly discovered area of mitochondrial calcium transport. He was involved in most of the early discoveries in the field, and he continued to work on mitochondria and calcium after his return to Italy and until he moved to the ETH. There his interests still remained focused on calcium, but the emphasis shifted to the proteins that transport it across membranes and to those that process its signal. His favorite object of study became the calcium pumps, especially that of the plasma membrane, an enzyme which is essential to the regulation of calcium homeostasis and thus to the well being of cells. His contributions on the enzyme, especially after he purified it in 1979, have helped establishing most of its properties and have clarified important problems of mechanism, regulation and structure.

Dr. Carafoli has authored or co-authored about 450 peer-reviewed articles and reviews, and has edited or co-edited about 20 books. He has served on the Editorial or Advisory Boards of several periodicals and has organized about 30 International Workshops and Symposia. He has been featured as a plenary or honorary lecturer at numerous events ranging from specialized Workshops to International Symposia and Congresses. Dr. Carafoli's honors and awards include several international prizes and medals, memberships in several Academies, and three honorary degrees.

Don W. Cleveland

University of California, San Diego, La Jolla, CA, USA
Section: Cell Architecture and Function

DON W. CLEVELAND has been a longstanding contributor to the elucidation of regulation of assembly of mitotic spindles and chromosome movement and how errors in these contribute to the chromosome loss characteristic of human tumors. He discovered the tubulin gene families encoding the major subunits of microtubules and the first mammalian example of control of gene expression through regulated RNA instability. He identified components required for microtubule nucleation and anchoring during spindle assembly. He identified the first human centromeric protein (CENP-B). He then discovered CENP-E, the centromere-associated, microtubule-motor that he showed to be essential for chromosome attachment and for activation and silencing of the mitotic checkpoint, the cell cycle control mechanism that prevents errors of chromosome segregation in mitosis.

Dr. Cleveland has also been a leading force in dissecting the disease mechanism for major human neurodegenerative disorders. He initially purified and characterized tau, the microtubule-associated protein that assembles aberrantly in human dementias including Alzheimer's disease and Pick's disease. He established that the extreme asymmetry of neurons acquired during development is achieved with a deformable array of interlinked neurofilaments, microtubules and actin. He showed that disorganization of neurofilament arrays caused selective death of motor neurons in mice and humans. He also demonstrated that neuronal death could also arise by a toxicity of mutant superoxide dismutase unrelated to its normal activity, thereby uncovering the mechanism underlying the major genetic form of amyotrophic lateral sclerosis. He showed that this toxicity could be

sharply ameliorated by lowering the content of neurofilaments.

Dr. Cleveland is currently Head, Laboratory for Cell Biology in the Ludwig Institute for Cancer Research and Professor of Medicine, Neurosciences and Cellular and Molecular Medicine at the University of California at San Diego. He is also the Editor of the Journal of Cell Biology and Current Opinion in Cell Biology.

Jack E. Dixon

University of California, San Diego School of Medicine,
La Jolla, CA, USA
Section: Protein/Enzyme Structure, Function, and Degradation

JACK E. DIXON earned his Ph.D. in Chemistry at the University of California, Santa Barbara in 1971 and did his postdoctoral training in Biochemistry at the University of California, San Diego.

Dr. Dixon is a pioneer and leader in the structure and function of the protein tyrosine phosphatases (PTPases). He demonstrated that the unique catalytic mechanism of the PTPases proceeds via a novel cysteine-phosphate intermediate. He discovered the first dual-specificity phosphatase, which led to the identification of the cell cycle protein, $p80^{cdc25}$, as a phosphatase. He also showed that the bacteria responsible for the plague or "black death" harbor the most active PTPase ever described. He and his colleagues went on to demonstrate that this PTPase gene product is essential for the pathogenesis of the bacteria. Dr. Dixon and his colleagues determined X-ray structures for both tyrosine and dual specificity phosphatases. Dr. Dixon also found that sequences outside of the PTPase catalytic domain could function to direct the subcellular localization of the PTPases and to restrict their substrate specificity. This is now a widely acknowledged regulatory paradigm for the PTPases. Recently, his laboratory demonstrated that the tumor suppressor gene, PTEN, which shares sequence identity with the PTPases, catalyzes the dephosphorylation of a lipid second messenger, phosphatidylinositol 3,4,5-trisphosphate (PIP3). This represents the first example of a PTPase dephosphorylating a lipid second messenger. PIP3 activates the protein kinase, AKT, which plays a critical role in controlling the balance between apoptosis and cell survival. The loss of the PTEN gene elevates PIP3 levels leading to constitutive activation by AKT and oncogenesis. Recently, Dr. Dixon in collaboration with Nikola Pavletich determined the X-ray structure of PTEN. Their structure–function studies explain the PIP3 substrate specificity of PTEN and also provide a rationale for many of the mutations seen in human cancers. Earlier in his career, Dr. Dixon adopted the tools of molecular biology as they became available in the 1970s, and his laboratory was among the first to use synthetic oligonucleotides to isolate and extensively characterize cDNAs encoding peptide hormones.

Dr. Dixon is Professor of Pharmacology, Cellular and Molecular Medicine and Chemistry and Biochemistry and Dean of Scientific Affairs at the University of California, San Diego. He is a member of the National Academy of Sciences, the Institute of Medicine and the American Academy of Arts and Sciences. Dr. Dixon was the recipient of the 2003 William C. Rose Award from the American Society for Biochemistry and Molecular Biology.

John H. Exton

Howard Hughes Medical Institute, Vanderbilt University School of Medicine, Nashvillie, TN, USA
Section: Signaling

JOHN H. EXTON was born and educated in New Zealand where he received his medical training and a Ph.D. in Biochemistry from the University of Otago in 1963. He did postdoctoral work at Vanderbilt University under Charles R. Park and Earl W. Sutherland, and became an Investigator of the Howard Hughes Medical Institute in 1968 and Professor of Physiology in 1970. He is presently Professor of Molecular Physiology and Biophysics, Professor of Pharmacology and a Hughes Investigator at Vanderbilt.

Dr. Exton's research initially focused on the changes in carbohydrate metabolism in liver during diabetes and treatment with various hormones using the perfused rat liver as the experimental system. His work concentrated on gluconeogenesis and identified the enzymatic reactions that were under control by insulin, epinephrine (adrenaline), glucagon and glucocorticoids, and demonstrated the importance of cyclic AMP in the regulation of these reactions. The role played by the supply of substrates, especially of alanine, was also shown.

Dr. Exton then turned his attention to the action of epinephrine (adrenaline) and demonstrated that many of its actions were not mediated by cyclic AMP but by calcium ions. This led to study of the breakdown of inositol phospholipids by phospholipase C that underlay the increase in calcium. Later this resulted in the discovery of G_q, a novel G protein that activated phospholipase C. Further studies demonstrated that agonists caused the breakdown of another phospholipid (phosphatidylcholine) by another phospholipase (phospholipase D). Current work is focused on the physiological role of phospholipase D.

Dr. Exton has authored over 350 scientific articles and is presently an Associate Editor of the Journal of Biological Chemistry. He has served on many scientific review groups and as a reviewer for many journals. He has won numerous awards, most notably the Lilly

Award of the American Diabetes Association, Fellow of the American Association for the Advancement of Science and election to membership in the National Academy of Sciences.

Paul Modrich

Duke University Medical Center, Durham, NC, USA
Section: Molecular Biology

PAUL MODRICH is an Investigator of the Howard Hughes Medical Institute and James B. Duke Professor of Biochemistry at Duke University Medical Center. He received his undergraduate degree from M.I.T. and his Ph.D. in Biochemistry from Stanford University. His current research addresses the mechanisms of DNA repair. He has served on the editorial boards of the Journal of Biological Chemistry, Biochemistry, Proceedings of the National Academy of Sciences, and DNA Repair. His honors include election to National Academy of Sciences and the Institute of Medicine, the Pfizer Award in Enzyme Chemistry, the General Motors Mott Prize in Cancer Research, and the Pasarow Foundation Award in Cancer Research.

Preface

Biological Chemistry is defined as the chemistry of the compounds and processes that constitute living organisms. The ultimate goal, of course, is to understand and define biology at a mechanistic level. This was aptly stated in an historical treatise on the founding of the *Journal of Biological Chemistry*, where John Edsall quoted a statement in a letter from J. L. Loeb (in Berkeley), "The future of biology lies with those who attack its problems from a chemical point of view." What was an emerging field in 1900 with its origins in physiology, nutrition and chemistry has broadened and expanded to include numerous other fields including mechanistic enzymology, molecular biology, structural biology, cell biology, genomics, proteomics, bioinformatics, metabolomics and others, that were not defined as discrete fields at that time.

Modern biochemistry (biological chemistry) began with the accidental discovery by Eduard Buchner in 1897 that a cell-free yeast extract could carry out fermentation of glucose to alcohol and CO_2 *in the absence of intact cells*. He named the dissolved substance responsible for this process zymase, the substance(s) we now refer to as enzymes. Importantly, Buchner recognized the significance of his discovery. This ended the dogma of the time, perpetuated by Pasteur, the concept of *vitalism*; i.e., that fermentation (and presumably other complex biological phenomena) required the action of intact cells. Thus, serendipity and a prepared mind ushered in a new era of discovery. Now it became possible to dissect complex physiological processes and to study them with preparations free of the constraints of intact cells. Once a metabolic pathway/process was established, it became possible to purify the enzymes, cofactors and substrates involved, to reconstitute the process with purified components and to characterize the components chemically. What followed was an information explosion in the field of biochemistry and progression through a series of trends, each "in vogue" in its time. The identification of the dietary essentials, the hunt for the vitamins/cofactors, the hormones, identification of metabolic pathways and the enzymes involved, oxidative phosphorylation, protein synthesis, molecular biology—each developed as a primary focus.

The need to associate chemistry with function came early and was evident in the naming of departments and journals. Over time names changed from Agricultural Chemistry to Physiological Chemistry to Biochemistry to Biological Chemistry. An example is the Department of Biochemistry at the University of Wisconsin, which began in 1883 as the Department of Agricultural Chemistry.

Where are we headed? We have reached the point where the borders of these areas have become blurred. What constitutes cell biology, molecular biology/genetics, developmental biology, physiology, immunology—ultimately reduces to chemistry. To understand these processes we must know what the molecules are and understand how they interact, i.e. the basic chemistry. That is what this encyclopedia is about.

The breadth of content of this encyclopedia aims to cover major topics of modern biochemistry, each authored by an expert in the area. We feel that the coverage is broad and we have been inclusive in choice of topics. The encyclopedia is a reference work encompassing four volumes containing over 500 articles with more than 750 authors or coauthors. Each article/topic covers an important area of the field which reflects the point of view of the authors. Together the articles cover virtually every aspect of biology for which we have "mechanistic" information. For those who wish to probe more deeply into a topic, references to further readings are included at the end of each article. The editorial board that made decisions on coverage consists of seven members, each an expert representing a major area in the field of biochemistry. A dedicated effort was made to provide coverage that is as complete as possible. The content is presented at a level that we hope will be interpretable to interested individuals with some background in chemistry and biology. It is intended for such individuals rather than specialists with extensive scientific backgrounds in specific areas. It is aimed at the generalist as opposed to the specialist.

Finally, we would like to single out Gail Rice and Dr. Noelle Gracy for their enormous contribution in putting this encyclopedia together. They, in fact, were a driving force that brought this major work to completion.

Notes on the Subject Index

Abbreviations used in subentries without explanation:

CoA	coenzyme A
DAG	diacylglycerol
ELISA	enzyme-linked immunosorbent assay
ERK	extracellular-signal regulated kinase
GlcNAC	N-Acetylglucosamine
HPLC	high-pressure liquid chromatography
IP_3	inositol 1,4,5-triphosphate
MAP	mitogen-activated protein
MMP	matrix metalloproteinase
mtDNA	mitochondrial DNA
NADPH	nicotinamide-adenine dinucleotide phosphate
PFK-2/ FBPase-2	6-phosphofructo-2-kinase/fructose-2,6-bisphosphatase
PI3K	phosphatidylinositol 3-kinase
PIP_2	phosphatidylinositol 4,5-bisphosphate
PIP_3	phosphatidylinositol-3,4,5-triphosphate
PPAR	peroxisome proliferator-activated receptor
RPLC	reversed-phase high-performance liquid chromatography

Volume 1

Volume 2

Inorganic Biochemistry, Pages 417-420, Robert J. P. Williams

Inositol Lipid 3-Phosphatases, Pages 421-426, Gregory S. Taylor and Jack E. Dixon

Inositol Phosphate Kinases and Phosphatases, Pages 427-429, Stephen B. Shears

Insulin- and Glucagon-Secreting Cells of the Pancreas, Pages 430-435, Franz M. Matschinsky

Insulin Receptor Family, Pages 436-440, Paul F. Pilch and Jongsoon Lee

Integrin Signaling, Pages 441-445, Lawrence E. Goldfinger and Mark H. Ginsberg

Interferon Receptors, Pages 446-451, Christopher P. Elco and Ganes C. Sen

Intermediate Filament Linker Proteins: Plectin and BPAG1, Pages 452-457, Peter Fuchs and Gerhard Wiche

Intermediate Filaments, Pages 458-464, Kelsie M. Bernot and Pierre A. Coulombe

Intracellular Calcium Channels: cADPR-Modulated (Ryanodine Receptors), Pages 465-468, Antony Galione

Intracellular Calcium Channels: NAADP+-Modulated, Pages 469-472, Armando A. Genazzani and Marcella Debidda

Ion Channel Protein Superfamily, Pages 473-477, William A. Catterall

IP3 Receptors, Pages 478-481, Colin W. TaylorEdward Morris and Paula da Fonseca

Iron-Sulfur Proteins, Pages 482-489, Helmut Beinert

JAK-STAT Signaling Paradigm, Pages 491-496, Edward Cha and Christian Schindler

Keratins and the Skin, Pages 497-504, Pierre A. Coulombe and Kelsie M. Bernot

Ketogenesis, Pages 505-507, Janos Kerner and Charles L. Hoppel

Melanocortin System, Pages 617-620, Roger D. Cone

Membrane Fusion, Pages 621-626, Joshua Zimmerberg and Leonid V. Chernomordik

Membrane Transport, General Concepts, Pages 627-630, Stanley G. Schultz

Membrane Transporters:Na+/Ca2+ Exchangers, Pages 631-636, Jonathan Lytton

Membrane-Associated Energy Transduction in Bacteria and Archaea, Pages 637-645, Gunter Schafer

Metabolite Channeling: Creatine Kinase Microcompartments, Pages 646-651, Uwe Schlattner and Theo Wallimann

Metalloproteases, Pages 652-656, David S. Auld

Metalloproteinases, Matrix, Pages 657-665, Hideaki Nagase and Gillian Murphy

Metaphase Chromosome, Pages 666-671, Sharron Vass and Margarete M. S. Heck

Methyl-CpG-Binding Proteins, Pages 672-675, David G. Skalnik

Microtubule-Associated Proteins, Pages 676-682, Nobutaka Hirokawa and Reiko Takemura

Mitochondrial Auto-Antibodies, Pages 683-688, Harold Baum

Mitochondrial Channels, Pages 689-692, M. Catia Sorgato and Alessandro Bertoli

Mitochondrial DNA, Pages 693-696, Gottfried Schatz

Mitochondrial Genes and their Expression: Yeast, Pages 697-702, Piotr P. Slonimski and Giovanna Carignani

Mitochondrial Genome, Evolution, Pages 703-708, B. Franz Lang, Dennis V. Lavrov and Gertraud Burger

Mitochondrial Genome, Overview, Pages 709-715, Douglas C. Wallace

Mitochondrial Inheritance, Pages 716-719, Eric A. Shoubridge

Mitochondrial Membranes, Structural Organization, Pages 720-724, Carmen A. Mannella

Volume 3

Volume 4

Lipids, Carbohydrates, Membranes and Membrane Proteins

Carbohydrate Chains: Enzymatic and Chemical Synthesis; Vol.1 - Pages 307-313, Thomas J. Tolbert and Chi-Huey Wong

Cell–Matrix Interactions; Vol.1 - Pages 362-366, Janet A. Askari and Martin J. Humphries

Detergent Properties; Vol.1 - Pages 577-581, Darrell R. McCaslin

Endocytosis; Vol.2 - Pages 16-19, Julie G. Donaldson

Flippases; Vol.2 - Pages 123-127, Charles J. Waechter

Galectins; Vol.2 - Pages 171-174, R. Colin Hughes

GlcNAc Biosynthesis and Function, O-Linked; Vol.2 - Pages 189-192, Kaoru Sakabe and Gerald W. Hart

Glycation; Vol.2 - Pages 229-236, Suzanne R. Thorpe and John W. Baynes

Glycolipid-Dependent Adhesion Processes; Vol.2 - Pages 261-265, Senitiroh Hakomori

Glycoprotein Folding and Processing Reactions; Vol.2 - Pages 272-276, Armando J. Parodi

Glycoprotein-Mediated Cell Interactions, O-Linked; Vol.2 - Pages 277-282, Robert S. Haltiwanger

Glycoproteins, N-Linked; Vol.2 - Pages 283-292, Mark A. Lehrman

Glycoproteins, Plant; Vol.2 - Pages 293-296, Carolyn J. Schultz

Glycosylation in Cystic Fibrosis; Vol.2 - Pages 297-301, Andrew D. Rhim, Thomas F. Scanlin and Mary Catherine Glick

Glycosylation, Congenital Disorders of; Vol.2 - Pages 302-307, Hudson H. Freeze

Glycosylphosphatidylinositol (GPI) Anchors; Vol.2 - Pages 308-311, Anant K. Menon

Ion Channel Protein Superfamily; Vol.2 - Pages 473-477, William A. Catterall

Lectins; Vol.2 - Pages 535-540, Nathan Sharon and Halina Lis

Lipases; Vol.2 - Pages 571-575, Howard L. Brockman

Lipid Bilayer Structure; Vol.2 - Pages 576-579, Erwin London

Lipid Rafts; Vol.2 - Pages 584-587, Deborah A. Brown

Lipoproteins, HDL/LDL; Vol.2 - Pages 588-593, Fayanne E. Thorngate and David L. Williams

MDR Membrane Proteins; Vol.2 - Pages 605-609, Nathan C. Rockwell

Membrane Fusion; Vol.2 - Pages 621-626, Joshua Zimmerberg and Leonid V. Chernomordik

Mucin Family of Glycoproteins; Vol.2 - Pages 758-764, Juan Perez-Vilar and Robert L. Hill

Mucins in Embryo Implantation; Vol.2 - Pages 765-769, Daniel D. Carson

Neoglycoproteins; Vol.3 - Pages 11-15, Y. C. Lee and Reiko T. Lee

N-Linked Glycan Processing Glucosidases and Mannosidases; Vol.3 - Pages 46-49, Linda O. Tremblay and Annette Herscovics

Oligosaccharide Chains: Free, N-Linked, O-Linked; Vol.3 - Pages 161-164, Tadashi Suzuki

Phospholipid Metabolism in Mammals; Vol.3 - Pages 314-320, Claudia Kent

Phospholipid Synthesis in Yeast; Vol.3 - Pages 321-325, Gil-Soo Han and George M. Carman

Prostaglandins and Leukotrienes; Vol.3 - Pages 452-456, William L. Smith and Robert C. Murphy

Protein Glycosylation Inhibitors; Vol.3 - Pages 500-503, Alan D. Elbein

Proteoglycans; Vol.3 - Pages 549-555, Sara K. Olson and Jeffrey D. Esko

Secretory Pathway; Vol.4 - Pages 11-16, Karen J. Colley

Siglecs; Vol.4 - Pages 38-40, Ajit Varki

Sphingolipid Biosynthesis; Vol.4 - Pages 76-81, Martina Leipelt and Alfred H. Merrill, Jr.

Sphingolipid Catabolism; Vol.4 - Pages 82-87, Akira Abe and James A. Shayman

Sugar Nucleotide Transporters; Vol.4 - Pages 127-129, Carlos B. Hirschberg

Trehalose Metabolism; Vol.4 - Pages 251-255, Alan D. Elbein

Metabolism, Vitamins and Hormones

Amino Acid Metabolism; Vol.1 - Pages 90-95, Luc Cynober

Anaplerosis; Vol.1 - Pages 105-110, Raymond R. Russell, III and Heinrich Taegtmeyer

Bile Salts and their Metabolism; Vol.1 - Pages 159-163, Ulrich Beuers and Thomas Pusl

Biliary Cirrhosis, Primary; Vol.1 - Pages 164-169, Marshall M. Kaplan

Branched-Chain -Ketoacids; Vol.1 - Pages 186-191, David T. Chuang

Carnitine and -Oxidation; Vol.1 - Pages 314-318, Janos Kerner and Charles L. Hoppel

Cholesterol Synthesis; Vol.1 - Pages 451-455, Peter A. Edwards

Diabetes; Vol.1 - Pages 582-592, David W. Cooke

Fat Mobilization: Perilipin and Hormone-Sensitive Lipase; Vol.2 - Pages 85-89, Constantine Londos and Alan R. Kimmel

Fatty Acid Oxidation; Vol.2 - Pages 90-94, Horst Schulz

Fatty Acid Synthesis and its Regulation; Vol.2 - Pages 99-103, Steven D. Clarke and Manabu T. Nakamura

Gluconeogenesis; Vol.2 - Pages 197-203, Richard W. Hanson and Oliver E. Owen

Glucose/Sugar Transport in Bacteria; Vol.2 - Pages 204-207, Lan Guan and H. Ronald Kaback

Glucose/Sugar Transport in Mammals; Vol.2 - Pages 208-212, Silvia Mora and Jeffrey Pessin

Glycogen Metabolism; Vol.2 - Pages 244-248, Peter J. Roach

Glycogen Storage Diseases; Vol.2 - Pages 249-254, George H. Sack, Jr.

Glycolysis, Overview; Vol.2 - Pages 266-271, Robert A. Harris

Hexokinases/Glucokinases; Vol.2 - Pages 372-377, Emile Van Schaftingen

Insulin- and Glucagon-Secreting Cells of the Pancreas; Vol.2 - Pages 430-435, Franz M. Matschinsky

Ketogenesis; Vol.2 - Pages 505-507, Janos Kerner and Charles L. Hoppel

Ornithine Cycle; Vol.3 - Pages 172-177, Malcolm Watford

Pentose Phosphate (Hexose Mono Phosphate) Pathway; Vol.3 - Pages 211-215, Bernard R. Landau

Pentose Phosphate Pathway, History of; Vol.3 - Pages 216-225, John F. Williams

Phosphofructokinase-2/Fructose Bisphosphatase-2; Vol.3 - Pages 277-280, Daniel M. Raben

Photosynthesis; Vol.3 - Pages 330-335, Richard C. Leegood

Photosynthetic Carbon Dioxide Fixation; Vol.3 - Pages 336-341, Matthew J. Paul

Porphyrin Metabolism; Vol.3 - Pages 415-419, Mark Shepherd and Harry A. Dailey

Propionyl CoA–Succinyl CoA Pathway; Vol.3 - Pages 447-451, Wayne A. Fenton

Pyruvate Carboxylation, Transamination, and Gluconeogenesis; Vol.3 - Pages 606-610, Sarawut Jitrapakdee and John C. Wallace

Pyruvate Dehydrogenase; Vol.3 - Pages 611-615, Sam A. Johnson and James G. McCormack

Pyruvate Kinase; Vol.3 - Pages 616-619, Kosaku Uyeda

Starvation; Vol.4 - Pages 99-110, Oliver E. Owen and Richard W. Hanson

Tricarboxylic Acid Cycle; Vol.4 - Pages 256-262, Richard L. Veech

Urea Cycle, Inborn Defects of; Vol.4 - Pages 326-330, Marsha K. Fearing and Vivian E. Shih

Vitamin A (Retinoids); Vol.4 - Pages 354-359, Joseph L. Napoli

Vitamin B12 and B12-Proteins; Vol.4 - Pages 360-366, Bernhard Krautler

Vitamin C; Vol.4 - Pages 367-371, Robert B. Rucker and Francene Steinberg

Vitamin D; Vol.4 - Pages 372-377, Hector F. DeLuca and Margaret Clagett-Dame

Vitamin E; Vol.4 - Pages 384-388, Ute C. Obermuller-Jevic and Lester Packer

Vitamin K: Biochemistry, Metabolism, and Nutritional Aspects; Vol.4 - Pages 389-393, J. W. Suttie

Vitamin K: Blood Coagulation and Use in Therapy; Vol.4 - Pages 394-398, Matthew D. Stone and Gary L. Nelsestuen

Cell Architecture and Function

Chromosome Organization and Structure, Overview; Vol.1 - Pages 469-474, Elena Gracheva and Sarah C. R. Elgin

Cytokinesis; Vol.1 - Pages 556-561, Masanori Mishima and Michael Glotzer

Desmosomes and Hemidesmosomes; Vol.1 - Pages 569-576, Rachel L. Dusek, Jonathan C. R. Jones and Kathleen J. Green

Dynactin; Vol.1 - Pages 823-826, Trina A. Schroer

Dynein; Vol.1 - Pages 827-831, K. Kevin Pfister

Endoplasmic Reticulum-Associated Protein Degradation; Vol.2 - Pages 20-23, Maurizio Molinari

Focal Adhesions; Vol.2 - Pages 128-133, Eli Zamir and Benjamin Geiger

Golgi Complex; Vol.2 - Pages 312-315, Mark Stamnes

Heat/Stress Responses; Vol.2 - Pages 343-347, Davis T. W. Ng

Inositol Lipid 3-Phosphatases; Vol.2 - Pages 421-426, Gregory S. Taylor and Jack E. Dixon

Intermediate Filament Linker Proteins: Plectin and BPAG1; Vol.2 - Pages 452-457, Peter Fuchs and Gerhard Wiche

Intermediate Filaments; Vol.2 - Pages 458-464, Kelsie M. Bernot and Pierre A. Coulombe

Keratins and the Skin; Vol.2 - Pages 497-504, Pierre A. Coulombe and Kelsie M. Bernot

Kinesin Superfamily Proteins; Vol.2 - Pages 508-516, Nobutaka Hirokawa and Reiko Takemura

Kinesins as Microtubule Disassembly Enzymes; Vol.2 - Pages 517-521, Susan L. Kline-Smith and Arshad Desai

Meiosis; Vol.2 - Pages 610-616, Neil Hunter

Metalloproteinases, Matrix; Vol.2 - Pages 657-665, Hideaki Nagase and Gillian Murphy

Microtubule-Associated Proteins; Vol.2 - Pages 676-682, Nobutaka Hirokawa and Reiko Takemura

Mitosis; Vol.2 - Pages 743-747, Patricia Wadsworth and Nasser M. Rusan

Myosin Motors; Vol.2 - Pages 778-781, Roy E. Larson

N-End Rule; Vol.3 - Pages 6-10, Alexander Varshavsky

Neuronal Intermediate Filaments; Vol.3 - Pages 21-25, Ronald K. H. Liem

Nuclear Compartmentalization; Vol.3 - Pages 87-91, Kelly P. Smith and Jeanne B. Lawrence

Nuclear Envelope and Lamins; Vol.3 - Pages 92-95, Bryce M. Paschal

Nuclear Pores and Nuclear Import/Export; Vol.3 - Pages 109-114, Anita H. Corbett

Peroxisomes; Vol.3 - Pages 246-250, Suresh Subramani

26S Proteasome, Structure and Function; Vol.3 - Pages 469-473, Peter Zwickl and Wolfgang Baumeister

Protein Glycosylation, Overview; Vol.3 - Pages 504-509, Natasha E. Zachara and Gerald W. Hart

Rho GTPases and Actin Cytoskeleton Dynamics; Vol.3 - Pages 714-718, Priam Villalonga and Anne J. Ridley

Septins and Cytokinesis; Vol.4 - Pages 22-26, Makoto Kinoshita and Christine M. Field

SUMO Modification; Vol.4 - Pages 130-134, Frauke Melchior and Andrea Pichler

Tight Junctions; Vol.4 - Pages 187-189, Shoichiro Tsukita

Transcriptional Silencing; Vol.4 - Pages 200-203, Ann Sutton and Rolf Sternglanz

Tubulin and its Isoforms; Vol.4 - Pages 272-276, Eva Nogales

Unfolded Protein Responses; Vol.4 - Pages 319-325, David Ron

Vacuoles; Vol.4 - Pages 331-336, Christopher J. Stefan and Scott D. Emr

Protein/Enzyme Structure Function and Degradation

Allosteric Regulation; Vol.1 - Pages 68-73, Barry S. Cooperman

Aminopeptidases; Vol.1 - Pages 96-98, Ralph A. Bradshaw

Amyloid; Vol.1 - Pages 99-104, Ronald Wetzel

Aspartic Proteases; Vol.1 - Pages 123-127, Ben M. Dunn

B12-Containing Enzymes; Vol.1 - Pages 145-151, Vahe Bandarian and Rowena G. Matthews

Biotin; Vol.1 - Pages 174-178, Steven W. Polyak and Anne Chapman-Smith

Biotinylation of Proteins; Vol.1 - Pages 179-181, Ronald A. Kohanski

Calpain; Vol.1 - Pages 300-306, Hiroyuki Sorimachi and Yasuko Ono

Chemiluminescence and Bioluminescence; Vol.1 - Pages 399-404, Thomas O. Baldwin

Coenzyme A; Vol.1 - Pages 475-477, M. Daniel Lane

Collagenases; Vol.1 - Pages 478-481, Kenn Holmbeck and Henning Birkedal-Hansen

Collagens; Vol.1 - Pages 482-487, Darwin J. Prockop

Cysteine Proteases; Vol.1 - Pages 516-520, David J. Buttle and John S. Mort

Disulfide Bond Formation; Vol.1 - Pages 598-602, Hiram F. Gilbert

Elastin; Vol.2 - Pages 10-12, Judith Ann Foster

Enzyme Inhibitors; Vol.2 - Pages 31-37, Vern L. Schramm

Enzyme Kinetics; Vol.2 - Pages 38-44, Irwin H. Segel

Enzyme Reaction Mechanisms: Stereochemistry; Vol.2 - Pages 45-50, Ming-Daw Tsai, Li Zhao and Brandon J. Lamarche

Flavins; Vol.2 - Pages 118-122, Barrie Entsch and David P. Ballou

Heme Proteins; Vol.2 - Pages 354-361, Johannes Everse

HIV Protease; Vol.2 - Pages 384-387, Ben M. Dunn

Kinetic Isotope Effects; Vol.2 - Pages 522-527, Justine P. Roth and Judith P. Klinman

Lipid Modification of Proteins: Targeting to Membranes; Vol.2 - Pages 580-583, Marilyn D. Resh

Low Barrier Hydrogen Bonds; Vol.2 - Pages 594-598, Perry A. Frey

Metalloproteases; Vol.2 - Pages 652-656, David S. Auld

Peptide Amidation; Vol.3 - Pages 226-230, Mark J. Niciu, Richard E. Mains and Betty A. Eipper

Phage Display for Protein Binding; Vol.3 - Pages 251-255, Henry B. Lowman

Prions, Overview; Vol.3 - Pages 437-440, Cedric Govaerts and Fred E. Cohen

Proteases in Blood Clotting; Vol.3 - Pages 457-463, John D. Kulman and Earl W. Davie

Proteasomes, Overview; Vol.3 - Pages 464-468, Martin Rechsteiner

Protein Carboxyl Esterification; Vol.3 - Pages 474-477, Shilpa G. Lalchandani and Jeffry B. Stock

Protein Degradation; Vol.3 - Pages 484-492, Tomo ari and Alfred L. Goldberg

Protein Folding and Assembly; Vol.3 - Pages 493-499, David P. Goldenberg

Protein N-Myristoylation; Vol.3 - Pages 527-531, Erica Dutil Sonnenburg and Jeffrey I. Gordon

Protein Palmitoylation; Vol.3 - Pages 532-535, Robert J. Deschenes

Pteridines; Vol.3 - Pages 556-560, S. Colette Daubner and Paul F. Fitzpatrick

Pyridoxal Phosphate; Vol.3 - Pages 595-599, David E. Metzler

Regulated Intramembrane Proteolysis (Rip); Vol.3 - Pages 665-670, Jin Ye, Michael S. Brown and Joseph L. Goldstein

Secretases; Vol.4 - Pages 7-10, Robert L. Heinrikson

Selenoprotein Synthesis; Vol.4 - Pages 17-21, August Bock

Substrate Binding, Catalysis, and Product Release; Vol.4 - Pages 123-126, W. Wallace Cleland

Two-Hybrid Protein–Protein Interactions; Vol.4 - Pages 290-293, Ilya Serebriiskii and Erica A. Golemis

Tyrosine Sulfation; Vol.4 - Pages 294-297, Denis Corbeil and Wieland B. Huttner

Ubiquitin System; Vol.4 - Pages 299-303, Aaron Ciechanover and Michael H. Glickman

Ubiquitin-Like Proteins; Vol.4 - Pages 304-307, Edward T. H. Yeh

Zinc Fingers; Vol.4 - Pages 435-439, Mark Isalan

Bioenergetics

Calcium/Calmodulin-Dependent Protein Kinase II; Vol.1 - Pages 274-280, Andy Hudmon and Howard Schulman

Calcium-Binding Proteins: Cytosolic (Annexins, Gelsolins, C2-Domain Proteins); Vol.1 - Pages 287-293, Joachim Krebs

Calcium-Modulated Proteins (EF-Hand); Vol.1 - Pages 294-299, Robert H. Kretsinger

Cell Death by Apoptosis and Necrosis; Vol.1 - Pages 352-355, Pierluigi Nicotera

Chemiosmotic Theory; Vol.1 - Pages 405-412, Keith D. Garlid

Chemolithotrophy; Vol.1 - Pages 419-424, Alan B. Hooper

Chlorophylls and Carotenoids; Vol.1 - Pages 430-437, Hugo Scheer

Chloroplast Redox Poise and Signaling; Vol.1 - Pages 438-445, John F. Allen

Chloroplasts; Vol.1 - Pages 446-450, Nicoletta Rascio

Cytochrome b6f Complex; Vol.1 - Pages 521-527, Gunter A. Hauska and Thomas Schodl

Cytochrome bc1 Complex (Respiratory Chain Complex III); Vol.1 - Pages 528-534, Bernard L. Trumpower

Cytochrome c; Vol.1 - Pages 535-538, Hans Tuppy and Gunther Kreil

Cytochrome Oxidases, Bacterial; Vol.1 - Pages 539-543, Peter Brzezinski and Pia Adelroth

Cytochrome P-450; Vol.1 - Pages 544-549, Rita Bernhardt

Energy Transduction in Anaerobic Prokaryotes; Vol.2 - Pages 24-30, Gottfried Unden

ER/SR Calcium Pump: Function; Vol.2 - Pages 56-60, Giuseppe Inesi

ER/SR Calcium Pump: Structure; Vol.2 - Pages 61-65, Chikashi Toyoshima and Yuji Sugita

F1–F0 ATP Synthase; Vol.2 - Pages 73-79, Donata Branca

Ferredoxin; Vol.2 - Pages 104-106, Giuliana Zanetti and Vittorio Pandini

Luft's Disease; Vol.2 - Pages 599-601, Salvatore DiMauro

Membrane Transport, General Concepts; Vol.2 - Pages 627-630, Stanley G. Schultz

Membrane Transporters:Na+/Ca2+ Exchangers; Vol.2 - Pages 631-636, Jonathan Lytton

Membrane-Associated Energy Transduction in Bacteria and Archaea; Vol.2 - Pages 637-645, Gunter Schafer

Metabolite Channeling: Creatine Kinase Microcompartments; Vol.2 - Pages 646-651, Uwe Schlattner and Theo Wallimann

Mitochondrial Auto-Antibodies; Vol.2 - Pages 683-688, Harold Baum

Mitochondrial Channels; Vol.2 - Pages 689-692, M. Catia Sorgato and Alessandro Bertoli

Mitochondrial DNA; Vol.2 - Pages 693-696, Gottfried Schatz

Mitochondrial Genes and their Expression: Yeast; Vol.2 - Pages 697-702, Piotr P. Slonimski and Giovanna Carignani

Mitochondrial Genome, Evolution; Vol.2 - Pages 703-708, B. Franz Lang, Dennis V. Lavrov and Gertraud Burger

Mitochondrial Genome, Overview; Vol.2 - Pages 709-715, Douglas C. Wallace

Mitochondrial Inheritance; Vol.2 - Pages 716-719, Eric A. Shoubridge

Mitochondrial Membranes, Structural Organization; Vol.2 - Pages 720-724, Carmen A. Mannella

Mitochondrial Metabolite Transporter Family; Vol.2 - Pages 725-732, Ferdinando Palmieri and Martin Klingenberg

Mitochondrial Outer Membrane and the VDAC Channel; Vol.2 - Pages 733-736, Marco Colombini

Neuronal Calcium Signal; Vol.3 - Pages 16-20, Hilmar Bading

Nicotinamide Nucleotide Transhydrogenase; Vol.3 - Pages 50-56, Jan Rydstrom

Nuclear Genes in Mitochondrial Function and Biogenesis; Vol.3 - Pages 100-104, Alexander Tzagoloff and Carol L. Dieckmann

Oncocytes; Vol.3 - Pages 165-166, Bernard Tandler and Charles L. Hoppel

Oxygenases; Vol.3 - Pages 178-182, Osamu Hayaishi

Periplasmic Electron Transport Systems in Bacteria; Vol.3 - Pages 231-238, David J. Richardson, Gary Sawers and Rob J. M. Van Spanning

Phosphatidylinositol-3-Phosphate; Vol.3 - Pages 272-276, Joseph V. Virbasius and Michael P. Czech

Photosystem I, Structure and Function; Vol.3 - Pages 342-347, Petra Fromme

Photosystem I: FX, FA, and FB Iron–Sulfur Clusters; Vol.3 - Pages 348-356, Mikhail L. Antonkine and John H. Golbeck

Photosystem II Light Harvesting System: Dynamic Behavior; Vol.3 - Pages 357-362, Peter Horton and Alexander Ruban

Photosystem II: Assembly and Turnover of the D1 Protein; Vol.3 - Pages 363-366, Eira Kanervo and Eva-Mari Aro

Photosystem II: Protein Components; Vol.3 - Pages 367-374, James Barber

Photosystem II: Water Oxidation, Overview; Vol.3 - Pages 375-380, Fabrice Rappaport and Pierre Joliot

Plasma-Membrane Calcium Pump: Structure and Function; Vol.3 - Pages 385-389, Emanuel E. Strehler

Plastocyanin; Vol.3 - Pages 390-393, Elizabeth L. Gross

Protein Import into Mitochondria; Vol.3 - Pages 510-515, Johannes M. Herrmann and Walter Neupert

P-Type Pumps: Copper Pump; Vol.3 - Pages 561-564, Ilia Voskoboinik and James Camakaris

P-Type Pumps: H+/K+ Pump; Vol.3 - Pages 565-570, Jai Moo Shin and George Sachs

P-Type Pumps: Na+/K+ Pump; Vol.3 - Pages 571-576, Peter L. Jorgensen

P-Type Pumps: Plasma-Membrane H+ Pump; Vol.3 - Pages 577-581, A. Brett Mason and Carolyn W. Slayman

Purple Bacteria: Electron Acceptors and Donors; Vol.3 - Pages 582-585, Evaldas Katilius and Neal W. Woodbury

Purple Bacteria: Photosynthetic Reaction Centers; Vol.3 - Pages 586-594, C. Roy D. Lancaster

Pyrimidine Biosynthesis; Vol.3 - Pages 600-605, Monika Loffler and Elke Zameitat

Quinones; Vol.3 - Pages 621-627, Giorgio Lenaz and Maria Luisa Genova

Respiratory Chain and ATP Synthase; Vol.3 - Pages 671-675, David G. Whitehouse and Anthony L. Moore

Respiratory Chain Complex I; Vol.3 - Pages 676-680, Ulrich Brandt

Respiratory Chain Complex II and Succinate: Quinone Oxidoreductases; Vol.3 - Pages 681-687, C. Roy D. Lancaster

Respiratory Chain Complex IV; Vol.3 - Pages 688-694, Hartmut Michel

Respiratory Processes in Anoxygenic and Oxygenic Phototrophs; Vol.3 - Pages 695-699, Roberto Borghese and Davide Zannoni

Spastic Paraplegia; Vol.4 - Pages 61-66, Elena Irene Rugarli and Andrea Ballabio

Store-Operated Membrane Channels: Calcium; Vol.4 - Pages 117-122, Indu S. Ambudkar

Superoxide Dismutase; Vol.4 - Pages 135-138, Irwin Fridovich

Uncoupling Proteins; Vol.4 - Pages 313-318, Daniel Ricquier and Frederic Bouillaud

V-ATPases; Vol.4 - Pages 349-353, Michael Forgac

Voltage-Dependent K+ Channels; Vol.4 - Pages 399-404, Ramon Latorre and Francisco J. Morera

Voltage-Sensitive Ca2+ Channels; Vol.4 - Pages 405-408, Harald Reuter

Voltage-Sensitive Na+ Channels; Vol.4 - Pages 409-415, William J. Brammar

Molecular Biology

DNA Restriction and Modification: Type I Enzymes; Vol.1 - Pages 767-771, David T. F. Dryden

DNA Restriction and Modification: Type II Enzymes; Vol.1 - Pages 772-777, Darren M. Gowers and Stephen E. Halford

DNA Restriction and Modification: Type III Enzymes; Vol.1 - Pages 778-781, Desirazu N. Rao and S. Srivani

DNA Secondary Structure; Vol.1 - Pages 782-787, Albino Bacolla and Robert D. Wells

DNA Sequence Recognition by Proteins; Vol.1 - Pages 788-793, Arabela A. Grigorescu and John M. Rosenberg

DNA Supercoiling; Vol.1 - Pages 794-797, Tao-shih Hsieh

DNA Topoisomerases: Type I; Vol.1 - Pages 798-805, James J. Champoux

DNA Topoisomerases: Type II; Vol.1 - Pages 806-811, Renier Velez-Cruz and Neil Osheroff

DNA Topoisomerases: Type III–RecQ Helicase Systems; Vol.1 - Pages 812-816, Rodney Rothstein and Erika Shor

EF-G and EF-Tu Structures and Translation Elongation in Bacteria; Vol.2 - Pages 1-5, Poul Nissen and Jens Nyborg

Exonucleases, Bacterial; Vol.2 - Pages 66-72, Susan T. Lovett

HIV-1 Reverse Transcriptase Structure; Vol.2 - Pages 388-392, Kalyan Das, Stefan G. Sarafianos, Eddy Arnold and Stephen H. Hughes

Homologous Recombination in Meiosis; Vol.2 - Pages 393-397, Nancy M. Hollingsworth

lac Operon; Vol.2 - Pages 529-534, Liskin Swint-Kruse and Kathleen S. Matthews

LexA Regulatory System; Vol.2 - Pages 546-550, Veronica G. Godoy, Penny J. Beuning and Graham C. Walker

Metaphase Chromosome; Vol.2 - Pages 666-671, Sharron Vass and Margarete M. S. Heck

Methyl-CpG-Binding Proteins; Vol.2 - Pages 672-675, David G. Skalnik

mRNA Polyadenylation in Eukaryotes; Vol.2 - Pages 748-752, Mary Edmonds

mRNA Processing and Degradation in Bacteria; Vol.2 - Pages 753-757, Deborah A. Steege

Non-Homologous End Joining; Vol.3 - Pages 66-70, Penny A. Jeggo

Nonhomologous Recombination: Bacterial Transposons; Vol.3 - Pages 71-79, Bao Ton Hoang and Michael G. Chandler

Nonhomologous Recombination: Retrotransposons; Vol.3 - Pages 80-86, Siew Loon Ooi and Jef D. Boeke

Nuclear Organization, Chromatin Structure, and Gene Silencing; Vol.3 - Pages 105-108, Lori L. Wallrath, John R. Danzer, Oya Yazgan and Pamela K. Geyer

Nucleoid Organization of Bacterial Chromosomes; Vol.3 - Pages 115-118, Charles J. Dorman

Nucleolus, Overview; Vol.3 - Pages 119-122, Thoru Pederson

Nucleotide Excision Repair and Human Disease; Vol.3 - Pages 123-129, James E. Cleaver

Nucleotide Excision Repair in Eukaryotes; Vol.3 - Pages 130-133, Laura A. Lindsey-Boltz and Aziz Sancar

Nucleotide Excision Repair, Bacterial: The UvrABCD System; Vol.3 - Pages 134-142, Bennett Van Houten and Lawrence Grossman

Nucleotide Excision Repair: Biology; Vol.3 - Pages 143-147, Errol C. Friedberg

PHO Regulon; Vol.3 - Pages 262-265, Bengt L. Persson

Pre-tRNA and Pre-rRNA Processing in Bacteria; Vol.3 - Pages 420-424, Sidney R. Kushner

Pre-tRNA and Pre-rRNA Processing in Eukaryotes; Vol.3 - Pages 425-431, Hendrik A. Raue

Prions and Epigenetic Inheritance; Vol.3 - Pages 432-436, Reed B. Wickner

Processivity Clamps in DNA Replication: Clamp Loading; Vol.3 - Pages 441-446, Megan J. Davey and Mike O'Donnell

Recombination: Heteroduplexand Mismatch Repair in vitro; Vol.3 - Pages 645-648, Leroy Worth, Jr.

Recombination: Strand Transferases; Vol.3 - Pages 649-653, Floyd R. Bryant

Recombination-Dependent DNA Replication; Vol.3 - Pages 654-659, Kenneth N. Kreuzer

recQ DNA Helicase Family in Genetic Stability; Vol.3 - Pages 660-664, Mary A. Risinger and Joanna Groden

Reverse Transcriptase and Retroviral Replication; Vol.3 - Pages 708-713, Laura Tarrago-Litvak, Marie-Line Andreola and Simon Litvak

Ribosome Assembly; Vol.3 - Pages 719-724, John L. Woolford

Ribosome Structure; Vol.3 - Pages 725-732, Brian T. Wimberly

Ribozyme Mechanisms; Vol.3 - Pages 733-737, John Hsieh and Carol A. Fierke

Ribozyme Structural Elements: Group I Introns; Vol.3 - Pages 738-742, Barbara L. Golden

Ribozyme Structural Elements: Hairpin Ribozyme; Vol.3 - Pages 743-746, Adrian R. Ferre-D'Amare

Ribozymes and Evolution; Vol.3 - Pages 747-752, Niles Lehman

RNA Editing; Vol.3 - Pages 753-758, Charles E. Samuel

RNA Polymerase I and RNA Polymerase III in Eukaryotes; Vol.3 - Pages 759-762, Robert J. White

RNA Polymerase II and Basal Transcription Factors in Eukaryotes; Vol.3 - Pages 763-765, Joan Weliky Conaway and Ronald C. Conaway

RNA Polymerase II Elongation Control in Eukaryotes; Vol.3 - Pages 766-769, David H. Price

RNA Polymerase II Structure in Eukaryotes; Vol.3 - Pages 770-774, Patrick Cramer

RNA Polymerase Reaction in Bacteria; Vol.3 - Pages 775-780, Arkady A. Mustaev and Alexander D. Goldfarb

RNA Polymerase Structure, Bacterial; Vol.3 - Pages 781-784, Michael Anikin, Dmitri Temiakov and William T. McAllister

Sigma Factors; Vol.4 - Pages 41-44, John D. Helmann

Sliding Clamps in DNA Replication: E. coli -Clamp and PCNA Structure; Vol.4 - Pages 45-47, Eric R. Goedken and John Kuriyan

Spliceosome; Vol.4 - Pages 88-92, Timothy W. Nilsen

T7 RNA Polymerase; Vol.4 - Pages 147-151, Rui Sousa

Telomeres: Maintenance and Replication; Vol.4 - Pages 174-179, Alessandro Bianchi and David Shore

Transcription Termination; Vol.4 - Pages 195-199, Thomas J. Santangelo and Jeffrey W. Roberts

Transcription-Coupled DNA Repair, Overview; Vol.4 - Pages 204-208, Isabel Mellon

Translation Elongation in Bacteria; Vol.4 - Pages 214-223, Oliver Vesper and Knud H. Nierhaus

Translation Elongation in Eukaryotes; Vol.4 - Pages 224-229, William C. Merrick and Anton A. Komar

Translation Initiation in Bacteria: Factors and Mechanisms; Vol.4 - Pages 230-236, Cynthia L. Pon and Claudio O. Gualerzi

Translation Initiation in Eukaryotes: Factors and Mechanisms; Vol.4 - Pages 237-241, Tatyana V. Pestova and Christopher U. T. Hellen

Translation Termination and Ribosome Recycling; Vol.4 - Pages 242-246, Nadja Koloteva-Levin and Mick F. Tuite

Translesion DNA Polymerases, Eukaryotic; Vol.4 - Pages 247-250, Alexandra Vaisman and Roger Woodgate

tRNA Synthetases; Vol.4 - Pages 263-266, Karla L. Ewalt and Paul Schimmel

trp Operon and Attenuation; Vol.4 - Pages 267-271, Paul Gollnick

UmuC, D Lesion Bypass DNA Polymerase V; Vol.4 - Pages 308-312, Zvi Livneh

XPV DNA Polymerase and Ultraviolet Damage Bypass; Vol.4 - Pages 419-421, Alan R. Lehmann

Yeast GAL1–GAL10 System; Vol.4 - Pages 429-433, Dennis Lohr and Ralph Bash

Signaling

Cyclic AMP Receptors of Dictyostelium; Vol.1 - Pages 488-493, Dale Hereld and Peter N. Devreotes

Cyclic GMP Phosphodiesterases; Vol.1 - Pages 494-500, Sharron H. Francis and Jackie D. Corbin

Cyclic Nucleotide Phosphodiesterases; Vol.1 - Pages 501-505, Vincent C. Manganiello and Eva Degerman

Cyclic Nucleotide-Dependent Protein Kinases; Vol.1 - Pages 506-511, Sharron H. Francis and Jackie D. Corbin

Cyclic Nucleotide-Regulated Cation Channels; Vol.1 - Pages 512-515, Martin Biel and Franz Hofmann

Cytokines; Vol.1 - Pages 550-555, Andrea L. Wurster and Michael J. Grusby

Cytokinin; Vol.1 - Pages 562-567, Thomas Schmulling

Diacylglycerol Kinases and Phosphatidic Acid Phosphatases; Vol.1 - Pages 593-597, Stephen M. Prescott and Matthew K. Topham

Dopamine Receptors; Vol.1 - Pages 817-822, Kim A. Neve

Eicosanoid Receptors; Vol.2 - Pages 6-9, Richard M. Breyer and Matthew D. Breyer

Endocannabinoids; Vol.2 - Pages 13-15, Daniele Piomelli

Epidermal Growth Factor Receptor Family; Vol.2 - Pages 51-55, Denis Tvorogov and Graham Carpenter

FAK Family; Vol.2 - Pages 80-84, Steven K. Hanks

Fatty Acid Receptors; Vol.2 - Pages 95-98, Christer Owman and Bjorn Olde

Fibroblast Growth Factor Receptors and Cancer-Associated Perturbations; Vol.2 - Pages 112-117, Marko Kornmann and Murray Korc

G Protein Signaling Regulators; Vol.2 - Pages 147-151, John H. Exton

G Protein-Coupled Receptor Kinases and Arrestins; Vol.2 - Pages 152-157, Jeffrey L. Benovic

G12/G13 Family; Vol.2 - Pages 158-161, Stefan Offermanns

GABAA Receptor; Vol.2 - Pages 162-166, Richard W. Olsen and Gregory W. Sawyer

GABAB Receptor; Vol.2 - Pages 167-170, S. J. Enna

Gi Family of Heterotrimeric G Proteins; Vol.2 - Pages 181-185, Maurine E. Linder

Glucagon Family of Peptides and their Receptors; Vol.2 - Pages 193-196, Laurie L. Baggio and Daniel J. Drucker

Glutamate Receptors, Ionotropic; Vol.2 - Pages 213-219, Derek B. Scott and Michael D. Ehlers

Glutamate Receptors, Metabotropic; Vol.2 - Pages 220-223, P. Jeffrey Conn

Glycine Receptors; Vol.2 - Pages 237-243, Bodo Laube and Heinrich Betz

Glycogen Synthase Kinase-3; Vol.2 - Pages 255-260, James R. Woodgett

Gq Family; Vol.2 - Pages 316-320, Wanling Yang and John D. Hildebrandt

Gs Family of Heterotrimeric G Proteins; Vol.2 - Pages 337-341, Susanne M. Mumby

Hematopoietin Receptors; Vol.2 - Pages 348-353, Barbara A. Miller and Joseph Y. Cheung

Hepatocyte Growth Factor/Scatter Factor Receptor; Vol.2 - Pages 367-371, Selma Pennacchietti and Paolo M. Comoglio

Histamine Receptors; Vol.2 - Pages 378-383, Stephen J. Hill and Jillian G. Baker

Immunoglobulin (Fc) Receptors; Vol.2 - Pages 411-416, Mark Hogarth

Inositol Phosphate Kinases and Phosphatases; Vol.2 - Pages 427-429, Stephen B. Shears

Insulin Receptor Family; Vol.2 - Pages 436-440, Paul F. Pilch and Jongsoon Lee

Integrin Signaling; Vol.2 - Pages 441-445, Lawrence E. Goldfinger and Mark H. Ginsberg

Interferon Receptors; Vol.2 - Pages 446-451, Christopher P. Elco and Ganes C. Sen

JAK-STAT Signaling Paradigm; Vol.2 - Pages 491-496, Edward Cha and Christian Schindler

Leptin; Vol.2 - Pages 541-545, Thomas W. Gettys

Lysophospholipid Receptors; Vol.2 - Pages 602-604, Gabor J. Tigyi

Melanocortin System; Vol.2 - Pages 617-620, Roger D. Cone

Mitogen-Activated Protein Kinase Family; Vol.2 - Pages 737-742, Hidemi Teramoto and J. Silvio Gutkind

Muscarinic Acetylcholine Receptors; Vol.2 - Pages 775-777, Neil M. Nathanson

Natriuretic Peptides and their Receptors; Vol.3 - Pages 1-5, Lincoln R. Potter

Neuropeptide Y Receptors; Vol.3 - Pages 26-31, Eric M. Parker

Neurotensin Receptors; Vol.3 - Pages 32-36, William Rostene, Patrick Kitabgi and Didier Pelaprat

Neurotransmitter Transporters; Vol.3 - Pages 37-40, Aurelio Galli, Randy D. Blakely and Louis J. DeFelice

Neurotrophin Receptor Signaling; Vol.3 - Pages 41-45, Jennifer J. Gentry and Bruce D. Carter

Nicotinic Acetylcholine Receptors; Vol.3 - Pages 57-61, Nivalda O. Rodrigues-Pinguet and Henry A. Lester

Nitric Oxide Signaling; Vol.3 - Pages 62-65, Michael A. Marletta

Nuclear Factor kappaB; Vol.3 - Pages 96-99, Thomas D. Gilmore

Olfactory Receptors; Vol.3 - Pages 149-154, Sigrun I. Korsching

Opioid Receptors; Vol.3 - Pages 167-171, P. Y. Law and Horace H. Loh

P2X Purinergic Receptors; Vol.3 - Pages 183-187, Annmarie Surprenant

P2Y Purinergic Receptors; Vol.3 - Pages 188-191, George R. Dubyak

p53 Protein; Vol.3 - Pages 192-195, Jamie Hearnes and Jennifer Pietenpol

p70 S6 Kinase/mTOR; Vol.3 - Pages 196-200, Christopher G. Proud

Parathyroid Hormone/Parathyroid Hormone-Related Protein Receptor; Vol.3 - Pages 201-207, Thomas J. Gardella

Peroxisome Proliferator-Activated Receptors; Vol.3 - Pages 239-245, Mary C. Sugden, Edward A. Sugden and Mark J. Holness

Pheromone Receptors (Yeast); Vol.3 - Pages 256-261, James B. Konopka and Jeremy W. Thorner

Phosphatidylinositol Bisphosphate and Trisphosphate; Vol.3 - Pages 266-271, Alex Toker

Phosphoinositide 3-Kinase; Vol.3 - Pages 281-286, Khatereh Ahmadi and Michael Waterfield

Phosphoinositide 4- and 5-Kinases and Phosphatases; Vol.3 - Pages 287-291, Shawn F. Bairstow, Matthew W. Bunce and Richard A. Anderson

Phosphoinositide-Dependent Protein Kinases; Vol.3 - Pages 292-296, Nick R. Leslie and C. Peter Downes

Phospholipase A2; Vol.3 - Pages 297-300, Timothy R. Smith and Edward A. Dennis

Phospholipase C; Vol.3 - Pages 301-305, Fujio Sekiya, Yeun Ju Kim and Sue Goo Rhee

Phospholipase D; Vol.3 - Pages 306-313, Mary M. LaLonde and Michael A. Frohman

Photoreceptors; Vol.3 - Pages 326-329, King-Wai Yau

Plant Signaling: Peptides; Vol.3 - Pages 381-384, Clarence A. Ryan and Gregory Pearce

Platelet-Activating Factor Receptor; Vol.3 - Pages 394-398, Katherine M. Howard and Merle S. Olson

Platelet-Derived Growth Factor Receptor Family; Vol.3 - Pages 399-406, Marina Kovalenko and Andrius Kazlauskas

Protein Kinase B; Vol.3 - Pages 516-522, Bettina A. Dummler and Brian A. Hemmings

Protein Kinase C Family; Vol.3 - Pages 523-526, Alexandra C. Newton

Protein Tyrosine Phosphatases; Vol.3 - Pages 536-542, David J. Pagliarini, Fred L. Robinson and Jack E. Dixon

Proteinase-Activated Receptors; Vol.3 - Pages 543-548, Kristina K. Hansen and Morley D. Hollenberg

Rab Family; Vol.3 - Pages 629-634, Mary W. McCaffrey and Andrew J. Lindsay

Ran GTPase; Vol.3 - Pages 635-639, Mary Shannon Moore

Ras Family; Vol.3 - Pages 640-644, Lawrence A. Quilliam

Retinoblastoma Protein (pRB); Vol.3 - Pages 700-703, Nicholas Dyson and Maxim Frolov

Retinoic Acid Receptors; Vol.3 - Pages 704-707, Martin Petkovich

Serine/Threonine Phosphatases; Vol.4 - Pages 27-32, Thomas S. Ingebritsen

Serotonin Receptor Signaling; Vol.4 - Pages 33-37, Paul J. Gresch and Elaine Sanders-Bush

Small GTPases; Vol.4 - Pages 48-54, Adam Shutes and Channing J. Der

Somatostatin Receptors; Vol.4 - Pages 55-60, Agnes Schonbrunn

Src Family of Protein Tyrosine Kinases; Vol.4 - Pages 93-98, Jonathan A. Cooper

Steroid/Thyroid Hormone Receptors; Vol.4 - Pages 111-116, Ramesh Narayanan and Nancy L. Weigel

Syk Family of Protein Tyrosine Kinases; Vol.4 - Pages 139-145, Andrew C. Chan

Tachykinin/Substance P Receptors; Vol.4 - Pages 152-157, Mark D. Richardson and Madan M. Kwatra

Taste Receptors; Vol.4 - Pages 158-161, John D. Boughter, Jr. and Steven D. Munger

T-Cell Antigen Receptor; Vol.4 - Pages 162-168, Andrea L. Szymczak and Dario A. A. Vignali

Tec/Btk Family Tyrosine Kinases; Vol.4 - Pages 169-173, Shuling Guo and Owen N. Witte

Thyroid-Stimulating Hormone/Luteinizing Hormone/Follicle-Stimulating Hormone Receptors; Vol.4 - Pages 180-186, Deborah L. Segaloff, Dario Mizrachi and Mario Ascoli

Toll-Like Receptors; Vol.4 - Pages 190-194, Himanshu Kumar, Kiyoshi Takeda and Shizuo Akira

Transforming Growth Factor-β Receptor Superfamily; Vol.4 - Pages 209-213, Mark de Caestecker

Tumor Necrosis Factor Receptors; Vol.4 - Pages 277-283, Karen G. Potter and Carl F. Ware

Vascular Endothelial Growth Factor Receptors; Vol.4 - Pages 337-342, Kenneth A. Thomas

Vasopressin/Oxytocin Receptor Family; Vol.4 - Pages 343-348, Michael J. Brownstein

Vitamin D Receptor; Vol.4 - Pages 378-383, Diane R. Dowd and Paul N. MacDonald

Von Hippel-Lindau (VHL) Protein; Vol.4 - Pages 416-418, Ronald C. Conaway and Joan Weliky Conaway

Techniques and Methodology

Affinity Chromatography; Vol.1 - Pages 51-56, Pedro Cuatrecasas and Meir Wilchek

Affinity Tags for Protein Purification; Vol.1 - Pages 57-63, Joseph J. Falke and John A. Corbin

Genome-Wide Analysis of Gene Expression; Vol.2 - Pages 175-180, Karine G. Le Roch and Elizabeth A. Winzeler

HPLC Separation of Peptides; Vol.2 - Pages 398-403, James D. Pearson

Imaging Methods; Vol.2 - Pages 405-410, Gyorgy Szabadkai and Rosario Rizzuto

Inorganic Biochemistry; Vol.2 - Pages 417-420, Robert J. P. Williams

Multiple Sequence Alignment and Phylogenetic Trees; Vol.2 - Pages 770-774, Russell F. Doolittle

Oligosaccharide Analysis by Mass Spectrometry; Vol.3 - Pages 155-160, Andrew J. Hanneman and Vernon N. Reinhold

PCR (Polymerase Chain Reaction); Vol.3 - Pages 208-210, Michael J. Brownstein

Polysialic Acid inMolecular Medicine; Vol.3 - Pages 407-414, Frederic A. Troy, II

Protein Data Resources; Vol.3 - Pages 478-483, Philip E. Bourne

Secondary Structure in Protein Analysis; Vol.4 - Pages 1-6, George D. Rose

Spectrophotometric Assays; Vol.4 - Pages 67-75, Britton Chance

Two-Dimensional Gel Electrophoresis; Vol.4 - Pages 284-289, Gerhard Schmid, Denis Hochstrasser and Jean-Charles Sanchez

X-Ray Determination of 3-D Structure in Proteins; Vol.4 - Pages 422-428, Martha L. Ludwig

ENCYCLOPEDIA OF
Biological Chemistry

Editors
William J. Lennarz
M. Daniel Lane